2013 Abstracts

Thirty-Fifth Annual Meeting of the American Society for Bone and Mineral Research

Baltimore Convention Center in Baltimore, Maryland, USA October 4–7, 2013

The *Journal of Bone and Mineral Research* (ISSN: 0884-0431 [print]; 1523-4681 [online]) provides a forum for papers of the highest quality pertaining to bone, muscle, and mineral metabolism. Manuscripts are published on the biology and physiology of bone and muscle, relevant systems biology topics (e.g., osteoimmunology), and the pathophysiology and treatment of sarcopenia, and disorders of bone and mineral metabolism. All authored papers and editorial news and comments, opinions, findings, conclusions or recommendations in the *Journal* are those of the author(s) and do not necessarily reflect the views of the *Journal* and its publisher, nor does their publication imply any endorsement.

The JOURNAL OF BONE AND MINERAL RESEARCH (ISSN: 0884-0431), is published monthly on behalf of the American Society for Bone and Mineral Research by Wiley Subscription Services, Inc., a Wiley Company, 111 River St., Hoboken, NJ 07030-5774. Periodical Postage Paid at Hoboken, NJ and additional offices.

Postmaster: Send all address changes to JOURNAL OF BONE AND MINERAL RESEARCH, Journal Customer Services, John Wiley & Sons Inc., 350 Main St., Malden, MA 02148-5020. **Information for subscribers:** The *Journal of Bone and Mineral Research* is published in 12 issues per year. Institutional subscription prices for 2013 are: Print & Online: US$1024 (US), US$1086 (Rest of World), €787 (Europe), £671 (UK). Prices are exclusive of tax. Asia-Pacific GST, Canadian GST and European VAT will be applied at the appropriate rates. For more information on current tax rates, please go to www.wileyonlinelibrary.com/tax-vat. The price includes online access to the current and all online back fi les to January 1st 2009, where available. For other pricing options, including access information and terms and conditions, please visit www.wileyonlinelibrary.com/access. **Commercial Reprints:** Beth Ann Rocheleau, Reprints and Eprints Manager, Rockwater, Inc., PO Box 2211, Lexington, SC 29072, USA; Tel: +00 (1)803 359-4578; Fax: +00 (1)803-753-9430; E-mail: asbmr@rockwaterinc.com. For submission instructions, subscription and all other information, visit: http://onlinelibrary.wiley.com/journal/10.1002/%28ISSN%291523-4681

The *Journal of Bone and Mineral Research* is the official journal of the American Society for Bone and Mineral Research, 2025 M Street, NW, Suite 800, Washington, DC 20036-3309, USA. **Advertising:** Address advertising inquiries to Stephen Donohue, Advertising Sales Executive, Wiley Blackwell, 350 Main Street, Malden, MA 02148, (781) 388-8511 (Tel); sdonohue@wiley.com (email). Advertisements are subject to editorial approval and must adhere to ASBMR's advertising policy as specified here: http://onlinelibrary.wiley.com/journal/10.1002/%28ISSN%291523-4681/homepage/advertising_policy.htm. Publication of the advertisements in JBMR is not an endorsement of the advertiser's product or service or the claims made for the product in such advertising. **Disclaimer:** No responsibility is assumed, and responsibility is hereby disclaimed, by the American Society for Bone and Mineral Research, the *Journal of Bone and Mineral Research,* and the Publisher for any injury and/or damage to persons or property as a matter of products liability, negligence or otherwise, or from any use or operation of methods, products, instructions or ideas presented in the *Journal*. Independent verification of diagnosis and drug dosages should be made. Discussions, views and recommendations as to medical procedures, choice of drugs and drug dosages are the responsibility of the authors. Advertisers are responsible for compliance with requirements concerning statements of efficacy, approval, licensure, and availability. The *Journal of Bone and Mineral Research* is a **Journal Club™** selection. The Journal is indexed by *Index Medicus, Current Contents/Life Science, CABS (Current Awareness in Biological Sciences), Excerpta Medica, Cambridge Scientific Abstracts, Chemical Abstracts, Reference Update, Science Citation Index,* and Nuclear Medicine Literature Updating and Indexing Service.

GUIDELINES FOR ABSTRACT READERS

The *JBMR*® Supplement 1 Abstracts serves as a compiled version of the Abstracts. Authors submit their own abstracts and are charged a fee to do so. Each abstract must be sponsored by a current ASBMR member. Authors are responsible for the accuracy of the content that they post. Authors are responsible for ensuring compliance with applicable human subject and animal subject procedures. When an abstract is submitted, one person is identified as the Presenting Author, the person who is expected to present the abstract at the ASBMR Annual Meeting.

The ASBMR depends upon the honesty of the authors and presenters and relies on their assertions that they have had sufficient full access to the data to be and are convinced of its reliability. The ASBMR expects that authors and presenters:

- Will disclose any conflicts of interest, real or perceived.
- Should disclose any relationship that may bias one's presentation or which, if known, could give the perception of bias.
- Will affirm, for any study funded by an organization with a proprietary or financial interest, that they had full access to all the data in the study.
- Are responsible for the content of abstracts, presentations, slides, and reference materials.
- Keep the planning, content and execution of abstracts, speaker presentations, slides, abstracts and reference materials free from corporate influence, bias or control.
- Should give a balanced view of therapeutic options by providing several treatment options, whenever possible, and by always citing the best available evidence.
- Should disclose when any commercial product is not labeled for the use under discussion or that the product is still investigational.

The ASBMR:

- Will note those speakers who have disclosed relationships, including the nature of the relationship and the associated commercial entity.
- Will peer-review the abstracts according to categories, but only to determine which will be selected for oral presentation, for poster presentations or for any awards. Abstracts are not otherwise subject to any quality or content review by ASBMR or *JBMR*®.
- Expects the audience for the Abstracts to be researchers, physicians and other health and allied health professionals.
- Protects the Abstracts by copyright, and prohibits the reproduction, distribution or transmission of the abstracts without the express written permission of ASBMR.
- Embargoes the Abstracts for public release in written, oral and electronic communications until one hour after the abstract has been presented.

Disclaimer. All authored abstracts, findings, conclusions, recommendations or oral presentations are those of the author(s) and/or speaker(s) and do not reflect the views of the American Society for Bone and Mineral Research or imply any endorsement. No responsibility is assumed, and responsibility is hereby disclaimed, by the American Society for Bone and Mineral Research for any injury and/or damage to persons or property as a matter of products' liability, negligence or otherwise, or from any use or operation of methods, products, instructions or ideas presented in the abstracts or at the ASBMR Annual Meeting. Independent verification of diagnosis and drug dosages should be made. Discussions, views and recommendations regarding medical procedures, choice of drugs and drug dosages are the responsibility of the authors and presenters.

TABLE OF CONTENTS

JBMR® Editorial Board

AMERICAN SOCIETY FOR BONE AND MINERAL RESEARCH (ASBMR)

OFFICERS

Lynda F. Bonewald, Ph.D., President
Roberto Civitelli, M.D., President-Elect
Keith Hruska, M.D., Past-President
Brendan Boyce, M.D., Secretary-Treasurer
Dolores Shoback, M.D., Secretary-Treasurer Elect

COUNCILORS

Robert Adler, M.D.	*Term expires 2015*
Peter Ebeling, MBBS, M.D., FRACP	*Term expires 2014*
Dana Gaddy, Ph.D.	*Term expires 2014*
Nancy Lane, M.D.	*Term expires 2013*
Deborah V. Novack, M.D, Ph.D.	*Term expires 2015*
Eric S. Orwoll, M.D.	*Term expires 2013*
Roberto Pacifici, M.D.	*Term expires 2014*
G. David Roodman, M.D., Ph.D.	*Term expires 2013*
Eileen M. Shore, Ph.D.	*Term expires 2015*
Juliet E. Compston, M.D., FRCP	*Ex-Officio 2017*

ASBMR STAFF

Sarah Alcock, *Accountant*
Moira Andersen, *Meetings Associate*
William Braun, *Marketing Associate*
Angela Cangemi, *Program Manager*
Jenny Cano, *Registration Associate*
Sarah Dickey, *Associate*
Ann L. Elderkin, P.A., *Executive Director*
Douglas Fesler, *Associate Executive Director*
Bethel Habte, *Senior Associate*
Melissa Huston, *Director, Event Services*
Jessica Klapstein, *Housing and Ancillary Meetings Manager*
Deborah Kroll, *Director of Development*
Earline Marshall, *Senior Grants Administrator*
Brenda Malottke, *Director of Finance*
Kirsten Mills, *Operations Manager*
Lindsay Pullen, *Marketing Coordinator*
Lindsay Schoenle, *Program Coordinator*
Daniel Tadesse, *Registration Manager*
Natasha Verna, *Exhibits Coordinator*
Amanda Wood, *Marketing Director*

ASBMR BUSINESS OFFICE

2025 M Street, NW
Suite 800
Washington, DC 20036-3309
USA
Tel: +1 (202) 367-1161
Fax: +1 (202) 367-2161
E-mail: asbmr@asbmr.org
Internet: http://www.asbmr.org

2013 PROGRAM COMMITTEE

President: Lynda F. Bonewald, Ph.D.
Program Co-Chair: Laurie K. McCauley, D.D.S., Ph.D.
Program Co-Chair: Richard Eastell, M.D., FRCP

2013 ABSTRACT REVIEWERS

Robert Adler, M.D.
Andrea Alford, Ph.D.
Matthew Allen, Ph.D.
Catherine Amara, Ph.D.
Laleh Ardeshirpour, M.D.
Teresita Bellido, Ph.D.
Rajib Bhattacharya, M.D.
Neil Binkley, M.D.
Susan Bloomfield, Ph.D.
Jean-Philippe Bonjour, M.D.
Edith Bonnelye, Ph.D.
Mary Bouxsein, Ph.D.
Robert Brommage, Ph.D.
Marco Brotto, BSN, MS, Ph.D.
Ernesto Canalis, M.D.
Jane Cauley, Ph.D.
Bart Clarke, M.D.
Thomas Clemens, Ph.D.
Gregory Clines, M.D., Ph.D.
Martine Cohen-Solal, M.D.
Patricia Collin-Osdoby, Ph.D.
Peter Croucher, Ph.D.
Steven Cummings, M.D.
Bess Dawson-Hughes, M.D.
Anne Delany, Ph.D.
Maureen Devlin, Ph.D.
Jean-Pierre Devogelaer, M.D.
Paola Divieti Pajevic, M.D., Ph.D.
Robert Downs, M.D.
Matthew Drake, M.D., Ph.D.
Marc Drezner, M.D.
Patricia Ducy, Ph.D.
Gustavo Duque, M.D., Ph.D.
Michael Econs, M.D.
John Eisman, MBBS, Ph.D.
Klaus Engelke, Ph.D.
Karyn Esser, Ph.D.
Eric Everett, Ph.D.
Mary Farach-Carson, Ph.D.
Charles Farber, Ph.D.
Colin Farquharson, Ph.D.
Howard Fink, M.D., MPH
Pierrick Fournier, Ph.D.
Renny Franceschi, Ph.D.
Seiji Fukumoto, M.D., Ph.D.
Dana Gaddy, Ph.D.
Deborah Galson, Ph.D.
Thomas Gardella, Ph.D.
Jürg Gasser, Ph.D.
Louis Gerstenfeld, Ph.D.
Matthew Gillespie, Ph.D.
Francis Glorieux, M.D., Ph.D.
Agi Grigoriadis, Ph.D.
Gloria Gronowicz, Ph.D.
Ted Gross, Ph.D.
Nuria Guanabens, M.D.
Marian Hannan, DSc, MPH
Stephen Harris, Ph.D.
Tamara Harris, M.D., M.S.
Geoffrey Hendy, Ph.D.
Eric Hesse, M.D., Ph.D.
Martin Hewison, Ph.D.
Lorenz Hofbauer, M.D.
Keith Hruska, M.D.
Karl Insogna, M.D.
Karl Jepsen, Ph.D.
Mark Johnson, Ph.D.
Deborah Kado, M.D.
Hiroshi Kaji, M.D.
Ivo Kalajzic, M.D., Ph.D.
David Karasik, Ph.D.
Tony Keaveny, Ph.D.
Gordon Klein, M.D., MPH
Robert Klein, M.D.
David Kohn, Ph.D.
Stavroula Kousteni, Ph.D.
Christopher Kovacs, M.D.
Kenneth Kozloff, Ph.D.
Richard Kremer, M.D., Ph.D.
Tae-Geon Kwon, D.D.S., Ph.D.
Beate Lanske, Ph.D.
Meryl LeBoff, M.D.
E. Michael Lewiecki, M.D., FACP, FACE
Xin Li, Ph.D.
Robert Lindsay, MBChB, Ph.D., FRCP
Fei Liu, D.D.S, Ph.D.
Anne Looker, Ph.D.
Joseph Lorenzo, M.D.
Pierre Marie, Ph.D.
Joan Marini, M.D., Ph.D.
Michael McClung, M.D.
Salvatore Minisola, M.D.
Madhusmita Misra, M.D., MPH
Subburaman Mohan, Ph.D.
Elise Morgan, Ph.D.
Leslie Morse, D.O.
Mark Nanes, M.D., Ph.D.
Tuan Nguyen, Ph.D.
Charles O'Brien, Ph.D.
Claes Ohlsson, M.D., Ph.D.
Regis O'Keefe, M.D.
Eric Orwoll, M.D.
Merry Jo Oursler, Ph.D.
Roberto Pacifici, M.D.
Serk In Park, D.D.S., Ph.D.
Eleftherios Paschalis, Ph.D.
Munro Peacock, M.D.
Robert Pignolo, M.D., Ph.D.
Carol Pilbeam, M.D., Ph.D.
Lilian Plotkin, Ph.D.
Ling Qin, Ph.D.
Yi-Xin Qin, Ph.D.
David Reid, M.D., FRCP
Lars Rejnmark, M.D., Ph.D.
F. Patrick Ross, Ph.D.
Janet Rubin, M.D.
Clinton Rubin, Ph.D.
Ernestina Schipani, M.D., Ph.D.
Markus Seibel, M.D., Ph.D.
Deborah Sellmeyer, M.D.
Eileen Shore, Ph.D.
Anna Spagnoli, M.D.
Rene St-Arnaud, Ph.D.
Jan Stepan, M.D., Ph.D.
Elsa Strotmeyer, Ph.D., MPH
Larry Suva, Ph.D.
Sakae Tanaka, M.D., Ph.D.
Anna Teti, Ph.D.
Andre van Wijnen, Ph.D.
Peter Vestergaard, M.D., Ph.D.
Dennis Villareal, M.D.
Michael Wacker, Ph.D.
Noah Weisleder, Ph.D.
Bart Williams, Ph.D.
Yingzi Yang, Ph.D.

ASBMR COMMITTEE MEMBERS AND REPRESENTATIVES

ADVOCACY/SCIENCE POLICY COMMITTEE

Dwight Towler, M.D., Ph.D., *Chairperson*
Laura R. McCabe, Ph.D.
Paola Divieti Pajevic, M.D., Ph.D.
Kenneth G. Saag, M.D., MSc
Robert S. Weinstein, M.D.
Bart O. Williams, Ph.D.
Sylvia Christakos, Ph.D., *Ex-Officio*
Suzanne M. Jan De Beur, M.D., *Ex-Officio*
Robert A. Adler, M.D., *Council Liaison*
Ann L. Elderkin, P.A., *Staff Liaison*
Douglas Fesler, *Staff Liaison*

EDUCATION COMMITTEE

Marian T. Hannan, D.Sc., MPH, *Chairperson*
Charles R. Farber, Ph.D.
Louis C. Gerstenfeld, Ph.D.
Erik A. Imel, M.D.
Yebin Jiang, M.D., Ph.D.
Stavroula Kousteni, Ph.D.
Bruno Camargos, M.D., *Ad Hoc*
Nicola Napoli, M.D., *Ad Hoc*
Nancy Lane, M.D., *Council Liaison*
Angela Cangemi, *Staff Liaison*
Lindsay Schoenle, *Staff Liaison*

ETHICS ADVISORY COMMITTEE

Michael J. Econs, M.D., *Chairperson*
Kristina Akesson, M.D., Ph.D.
Maria-Grazia Ascenzi, Ph.D.
Douglas P. Kiel, M.D., MPH
Laurie K. McCauley, D.D.S., Ph.D.
Tamara J. Vokes, M.D.
Keith A. Hruska, M.D., *Ex Officio*
Lynda F. Bonewald, Ph.D., *Ex Officio*
Eileen M. Shore, Ph.D., *Council Liaison*
Ann L. Elderkin, P.A., *Staff Liaison*
Earline Marshall, *Staff Liaison*
Kirsten Mills, *Staff Liaison*

FINANCE COMMITTEE

Brendan F. Boyce, M.D., *Chairperson*
Daniel D. Bikle, M.D., Ph.D.
Robert D. Blank, M.D., Ph.D.
Mark C. Horowitz, Ph.D.
Majd Zayzafoon, M.D., Ph.D., *Ad Hoc*
Lynda F. Bonewald, Ph.D., *Ex Officio*
Roberto Pacifici, M.D., *Council Liaison*
Ann L. Elderkin, P.A., *Staff Liaison*
Brenda Malottke, *Staff Liaison*

MEMBERSHIP ENGAGEMENT COMMITTEE

Wenhan Chang, Ph.D., *Chairperson*
Cheryl L. Ackert-Bicknell, Ph.D.
Gustavo Duque, M.D., Ph.D.
Deborah L. Galson, Ph.D.
Martin Hewison, Ph.D.
David Karasik, Ph.D.
Robert R. McLean, DSc
Kristy M. Nicks, Ph.D.
Babatunde O. Oyajobi, MBBS, Ph.D.
Lilian I. Plotkin, Ph.D.
Peter R. Ebeling, MBBS, M.D., FRACP, *Council Liaison*
Kirsten Mills, *Staff Liaison*
Bethel Habte, *Staff Liaison*
Sarah Dickey, *Staff Liaison*

MINORITY SUBCOMMITTEE

Sherri-Ann M. Burnett-Bowie, M.D., MPH, *Chairperson*
Jacqueline P. Akech, Ph.D.
Sunday Akintoye, D.D.S.
Sylvia Christakos, Ph.D.
Jeanette N. Keith, M.D.
Kristy M. Nicks, Ph.D.
Roger Zebaze, M.D.
Kirsten Mills, *Staff Liaison*
Bethel Habte, *Staff Liaison*
Sarah Dickey, *Staff Liaison*

YOUNG INVESTIGATOR SUBCOMMITTEE

John R. Hawse, Ph.D., *Co-Chairperson*
Meghan E. McGee-Lawrence, Ph.D., *Co-Chairperson*
Jodi Dowthwaite, Ph.D.
Jessica A. Fowler
Anne Gingery, Ph.D.
Francesco Grassi
Kristie Kapinas
Kristi Milley
Kenneth Philbrick
Benjamin Sinder
Kirsten Mills, *Staff Liaison*
Bethel Habte, *Staff Liaison*
Sarah Dickey, *Staff Liaison*

PROFESSIONAL PRACTICE COMMITTEE

Suzanne M. Jan De Beur, M.D., *Chairperson*
Susan V. Bukata, M.D.
Matthew T. Drake, M.D., Ph.D.
Julie Glowacki, Ph.D.
Robert Pignolo, M.D., Ph.D.
Deborah E. Sellmeyer, M.D.
Emily Margaret Stein, M.D.
G. David Roodman, M.D., Ph.D., *Council Liaison*
Dana Gaddy, Ph.D., *Council Liaison*
Douglas Fesler, *Staff Liaison*
Ann L. Elderkin, P.A., *Staff Liaison*

PUBLICATIONS COMMITTEE

Philip Osdoby, Ph.D., *Chairperson*
Matthew Allen, Ph.D.
Carlos M. Isales, M.D.
Robert L. Jilka, Ph.D.
Moustapha Kassem, M.D., Ph.D.
Paul D. Miller, M.D., FACP
Dolores Shoback, M.D.
Anna Spagnoli, M.D.
Juliet E. Compston, M.D., FRCP, *Ex Officio*
Clifford J. Rosen, M.D., *Ex Officio*
Eric S. Orwoll, *Council Liaison*
Lynn King, *Staff Liaison*

PAST PRESIDENTS

Louis V. Avioli, M.D.	*1979–1980*	Gregory R. Mundy, M.D.	*1996–1997*
Lawrence G. Raisz, M.D.	*1980–1981*	Michael Rosenblatt, M.D.	*1997–1998*
Claude D. Arnaud, M.D.	*1981–1982*	Jane E. Aubin, Ph.D.	*1998–1999*
Stephen M. Krane, M.D.	*1982–1983*	David Goltzman, M.D.	*1999–2000*
William A. Peck, M.D.	*1983–1984*	Robert Marcus, M.D.	*2000–2001*
Paula H. Stern, Ph.D.	*1984–1985*	Robert R. Recker, M.D.	*2001–2002*
B. Lawrence Riggs, M.D.	*1985–1986*	Clifford J. Rosen, M.D.	*2002–2003*
Norman H. Bell, M.D.	*1986–1987*	Robert A. Nissenson, Ph.D.	*2003–2004*
Gideon A. Rodan, M.D., Ph.D.	*1987–1988*	Sylvia Christakos, Ph.D.	*2004–2005*
John G. Haddad, Jr., M.D.	*1988–1989*	Elizabeth Shane, M.D.	*2005–2006*
Armen H. Tashjian, Jr., M.D.	*1989–1990*	Steven R. Goldring, M.D.	*2006–2007*
Frederick R. Singer, M.D.	*1990–1991*	Barbara Kream, Ph.D.	*2007–2008*
Mark R. Haussler, Ph.D.	*1991–1992*	Marc Drezner, M.D.	*2008–2009*
Steven L. Teitelbaum, M.D.	*1992–1993*	Jane B. Lian, Ph.D.	*2009–2010*
Henry M. Kronenberg, M.D.	*1993–1994*	Sundeep Khosla, M.D.	*2010–2011*
Ernesto Canalis, M.D.	*1994–1995*	Keith Hruska, M.D.	*2011–*2012
John P. Bilezikian, M.D.	*1995–1996*		

PAST SECRETARY-TREASURERS

Norman H. Bell, M.D.	*1977–1985*	Andrew F. Stewart, M.D.	*2000–2004*
Gregory R. Mundy, M.D.	*1985–1991*	Marc K. Drezner, M.D.	*2004–2007*
Arnold J. Kahn, Ph.D.	*1991–1997*	Keith A. Hruska, M.D.	*2007–2009*
Steven R. Goldring, M.D.	*1997–2000*	Lynda F. Bonewald, Ph.D.	*2008–2011*

PAST COUNCILORS

John S. Adams, M.D.,	*2009–2012*	Maxine Gowen, Ph.D.	*2000–2003*
Constantine Anast, M.D.	*1980–1982*	Susan Greenspan, M.D.	*2002–2005*
Claude D. Arnaud, M.D.	*1979–1980*	Theresa Guise, M.D.	*2004–2007*
Andrew Arnold, M.D.	*1999–2002*	John G. Haddad, Jr., M.D.	*1982–1985*
Jane E. Aubin, Ph.D.	*1991–1994*	Mark R. Haussler, Ph.D.	*1982–1985*
Roland Baron, D.D.S., Ph.D.	*1991–1994*	Hunter H. Heath III, M.D.	*1985–1988*
Teresita Bellido, Ph.D.	*2008–2011*	Helen L. Henry, Ph.D.	*1985–1988*
Daniel Bikle, M.D., Ph.D.	*2003–2006*	Mark C. Horowitz, Ph.D.	*2005–2008*
John P. Bilezikian, M.D.	*1987–1990*	Keith A. Hruska, M.D.	*1989–1992*
Dennis M. Black, Ph.D.	*2001–2004*	Arnold J. Kahn, Ph.D.	*1986–1989*
Lynda F. Bonewald, Ph.D.	*1995–1998*	Frederick S. Kaplan, M.D.	*1997–2000*
Maria Luisa Brandi, M.D., Ph.D.	*2006–2009*	Sundeep Khosla, M.D.	*2002–2005*
Arthur E. Broadus, M.D., Ph.D.	*1990–1993*	Douglas P. Kiel, M.D., MPH	*2008–2011*
Ernesto Canalis, M.D.	*1989–1992*	Stephen M. Krane, M.D.	*1979–1981*
Janet M. Canterbury, M.D.	*1981–1984*	Barbara E. Kream, M.D.	*1985–1988*
Jane Cauley, Ph.D.	*2003–2006*	Henry M. Kronenberg, M.D.	*1986–1989*
Sylvia Christakos, Ph.D.	*1989–1992*	Meryl S. Leboff, M.D.	*2007–2010*
Roberto Civitelli, M.D.	*2006–2009*	Joseph Lorenzo, M.D.,	*2008–2011*
Thomas L. Clemens, Ph.D.	*1998–2001*	Barbara Lukert, M.D.	*2001–2004*
Jack W. Coburn, M.D.	*1981–1984*	Jane B. Lian, Ph.D.	*1991–1994*
David V. Cohn, Ph.D.	*1982–1985*	Robert Marcus, M.D.	*1995–1998, 1999–2002*
Cary W. Cooper, Ph.D.	*1980–1981*	Thomas J. Martin, M.D.	*1987–1990*
Steven R. Cummings, M.D.	*1996–1999*	Stephen Marx, M.D.	*1983–1986*
Bess Dawson-Hughes, M.D.	*1996–1999*	Toshio Matsumoto, M.D.	*1999–2002*
Hector F. DeLuca, Ph.D.	*1979–1980*	Laurie K. McCauley, D.D.S., Ph.D.	*2007–2010*
Marie Demay, M.D.	*2000–2003*	Gregory R. Mundy, M.D.	*1983–1985, 1995–1997*
Richard Eastell, M.D., F.R.C.P.	*2000–2003*	Masaki Noda, M.D., Ph.D.,	*2009–2012*
Michael Econs, M.D.	*2005–2008*	Robert Nissenson, Ph.D.	*1993–1996*
John Eisman, MBBS, Ph.D.	*1994–1997*	Anthony W. Norman, Ph.D.	*1980–1982*
Murray J. Favus, M.D.	*1992–1995*	Philip A. Osdoby, Ph.D.	*1997–2000*
David Feldman, M.D.	*1982–1986*	Susan M. Ott, M.D.	*1988–1991*
Lorraine A. Fitzpatrick, M.D.	*1998–2001*	A. Michael Parfitt, M.D.	*1990–1993*
Francis Glorieux, M.D., Ph.D.	*1988–1991*	Nicola C. Partridge, Ph.D.	*1993–1996*
Julie Glowacki, Ph.D.	*1999–2002*	William A. Peck, M.D.	*1979–1981*
Steven R. Goldring, M.D.	*1993–1996*	John T. Potts, Jr., M.D.	*1979–1981*
Ralph S. Goldsmith, M.D.	*1980–1983*	Paul A. Price, Ph.D.	*1986–1989*
David Goltzman, M.D.	*1984–1988*	Stuart H. Ralston, MBChB, M.D.	*2007–2010*

Robert R. Recker, M.D.	*1995–1998*	René St-Arnaud, Ph.D.	*2006–2009*
Pamela G. Robey, Ph.D.	*1992–1995*	Paula H. Stern, Ph.D.	*1980–1983*
Gideon A. Rodan, M.D., Ph.D.	*1984–1986*	Andrew F. Stewart, M.D.	*1994–1997*
Sevgi B. Rodan, Ph.D.	*1990–1993*	Gary Stein, Ph.D.	*2002–2005*
René Rizzoli, M.D.	*2004–2007*	Gordon J. Strewler, M.D.	*1992–1995*
Vicki Rosen, Ph.D.	*2003–2006*	Larry Suva, Ph.D.	*2001–2004*
Michael Rosenblatt, M.D.	*1988–1991*	Armen H. Tashjian, Jr., M.D.	*1979–1982*
Janet Rubin, M.D.	*2005–2008*	John D. Termine, Ph.D.	*1984–1987*
Elizabeth Shane, M.D.	*1994–1997*	Robert Wasserman, Ph.D.	*1984–1987*
Dolores M. Shoback, M.D.	*1998–2001*	Jennifer J. Westendorf, Ph.D.,	*2009–2012*
Ethel Siris, M.D.	*1996–1999*	Glenda Wong, Ph.D.	*1984–1987*
Eduardo Slatopolsky, M.D.	*1980–1983*	Marian F. Young, Ph.D.	*1997–2000*
Thomas Spelsburg, Ph.D.	*2004–2007*		

THE WILLIAM F. NEUMAN AWARD

Gerald D. Aurbach, M.D.	*1981*	Steven L. Teitelbaum, M.D.	*1998*
Paul L. Munson, Ph.D.	*1982*	Gregory R. Mundy, M.D.	*1999*
D. Harold Copp, M.D., Ph.D.	*1983*	R. Graham Russell, M.D.	*2000*
Roy V. Talmage, Ph.D.	*1984*	Harold M. Frost, M.D.	*2001*
Hector F. DeLuca, Ph.D.	*1985*	B. Lawrence Riggs, M.D.	*2002*
Lawrence G. Raisz, M.D.	*1986*	Henry M. Kronenberg, M.D.	*2003*
John T. Potts, Jr., M.D.	*1987*	Jane E. Aubin, Ph.D.	*2004*
Louis V. Avioli, M.D.	*1988*	Mark R. Haussler, Ph.D.	*2005*
Stephen M. Krane, M.D.	*1989*	Jane Lian, Ph.D., and Gary Stein, Ph.D.	*2006*
Robert H. Wasserman, Ph.D.	*1990*	Lance Lanyon, Ph.D., BVSc	*2007*
Claude D. Arnaud, M.D.	*1991*	David Baylink, M.D.	*2008*
Herbert A. Fleisch, M.D.	*1992*	Roland Baron, DDS, Ph.D.	*2009*
Gideon A. Rodan, M.D., Ph.D.	*1993*	Michael A. Parfitt, M.D.,	*2010*
Thomas John Martin, M.D., D.Sc.	*1994*	Gerard Karsenty, M.D., Ph.D.	*2011*
Anthony W. Norman, Ph.D.	*1995*	Sundeep Khosla, M.D.	*2012*
Melvin Jacob Glimcher, M.D.	*1996*	John A. Eisman, MBBS, Ph.D.	*2013*
Tatsuo Suda, D.D.S., Ph.D.	*1997*		

THE FULLER ALBRIGHT AWARD

Michael F. Holick, M.D., Ph.D.	*1980*	René St-Arnaud, Ph.D.	*1997*
Mark R. Haussler, Ph.D.	*1981*	Shigeaki Kato, Ph.D.	*1998*
Stephen Marx, M.D.	*1982*	Theresa A. Guise, M.D.	*1999*
Gregory R. Mundy, M.D.	*1982*	Dwight Towler, M.D., Ph.D.	*2000*
Edward M. Brown, M.D.	*1983*	Charles H. Turner, M.D.	*2001*
Helen L. Henry, Ph.D.	*1984*	Nobuyuki Udagawa, M.D.	*2002*
Henry M. Kronenberg, M.D.	*1985*	Patricia Ducy, Ph.D.	*2003*
Michael Rosenblatt, M.D.	*1986*	Hiroshi Takayanagi, Ph.D.	*2004*
Michael P. Whyte, M.D.	*1987*	Mary Bouxein, Ph.D.	*2005*
Rajiv Kumar, M.D.	*1988*	Hong-Wen Deng, Ph.D.	*2006*
Timothy Chambers, M.D.	*1989*	Kenneth White, Ph.D.	*2007*
Michael A. Levine, M.D.	*1990*	Kurt Hankenson, D.V.M., Ph.D.	*2008*
Dean T. Yamaguchi, M.D., Ph.D.	*1991*	Jennifer Westendorf, Ph.D.	*2009*
Andrew Arnold, M.D.	*1992*	Natalie A. Sims, Ph.D.	*2010*
Pamela G. Robey, Ph.D.	*1993*	Alexander G. Robling, Ph.D.	*2011*
Roberto Civitelli, M.D.	*1994*	Laura Calvi, M.D.	*2012*
Roberto Pacifici, M.D.	*1995*	Stavroula Kousteni, Ph.D.	*2013*
Clinton T. Rubin, Ph.D.	*1996*		

THE FREDERIC C. BARTTER AWARD

Jack Coburn, M.D.	*1986*	A. Michael Parfitt, M.D.	*1995*
Constantine Anast, M.D.	*1987*	C. Conrad Johnston, Jr., M.D.	*1996*
Charles Y.C. Pak, M.D.	*1988*	Robert Lindsay, MBChB, Ph.D.	*1997*
Arthur E. Broadus, M.D., Ph.D.	*1989*	B.E. Christopher Nordin, M.D., Ph.D.	*1998*
B. Lawrence Riggs, M.D.	*1990*	Pierre Meunier, M.D.	*1999*
Eduardo Slatopolsky, M.D.	*1991*	John P. Bilezikian, M.D.	*2000*
Norman H. Bell, M.D.	*1992*	Joseph Melton, III, M.D.	*2001*
Francis H. Glorieux, M.D., Ph.D.	*1993*	Ego Seeman, M.D., FRACP	*2002*
Robert P. Heaney, M.D.	*1994*	Robert R. Recker, M.D.	*2003*

Pierre Delmas, M.D., Ph.D.	*2004*	Juliet Compston, M.D., FRCP	*2009*
John Kanis, M.D.	*2005*	Ian Reid, M.D., MBChB	*2010*
Sundeep Khosla, M.D.	*2006*	Jane Cauley, Ph.D.	*2011*
Michael Whyte, M.D.	*2007*	Michael Econs, M.D.	*2012*
Steven Cummings, M.D., FACP	*2008*	Elizabeth Shane, M.D.	*2013*

THE LOUIS V. AVIOLI FOUNDERS AWARD

Stavros Manolagas, M.D., Ph.D.	*2000*	G. David Roodman, M.D., Ph.D.	*2007*
Gerard Karsenty, M.D.	*2001*	Rajiv Kumar, M.D.	*2008*
Roland Baron, D.D.S., Ph.D.	*2002*	Rajesh Thakker, M.D., FRCP	*2009*
Edward Brown, M.D.	*2003*	Pierre Marie, Ph.D.	*2010*
Ernesto Canalis, M.D.	*2004*	Roberto Pacifici, M.D.	*2011*
Gino Segre, M.D.	*2005*	J. Wesley Pike, Ph.D.	*2012*
Andrew Arnold, M.D.	*2006*	Thomas L. Clemens, Ph.D.	*2013*

THE SHIRLEY HOHL SERVICE AWARD

Louis V. Avioli, M.D.	*1997*	Julie Glowacki, Ph.D.	*2005*
Norman H. Bell, M.D.	*1998*	Paula Stern, Ph.D.	*2006*
Murray J. Favus, M.D.	*1999*	Philip Osdoby, Ph.D.	*2007*
Arnold J. Kahn, Ph.D.	*2000*	Elizabeth Shane, M.D.	*2008*
Lawrence G. Raisz, M.D.	*2001*	Robert Nissenson, Ph.D.	*2010*
Nicola C. Partridge, Ph.D.	*2002*	Joan A. McGowan, Ph.D.	*2011*
Marc K. Drezner, M.D.	*2003*	Janine Danks, BSc, MSc, Ph.D.	*2012*
Jane B. Lian, Ph.D.	*2004*		

THE LAWRENCE G. RAISZ AWARD

David Goltzman, M.D.	*2010*	Ernesto Canalis, M.D.	*2012*
Hiroshi Kawaguchi, M.D., Ph.D.	*2011*	Clifford J. Rosen, M.D.	*2013*

THE PAULA STERN ACHIEVEMENT AWARD

Laurie McCauley, D.D.S., Ph.D.	*2010*	Theresa Guise, M.D.	*2012*
Marie Demay, M.D.	*2011*	Nancy E. Lane, M.D.	*2013*

THE GIDEON A. RODAN EXCELLENCE IN MENTORSHIP AWARD

Gideon A. Rodan, M.D., Ph.D.	*2001*	Lawrence Raisz, M.D.	*2008*
Sylvia Christakos, Ph.D.	*2002*	John Bilezikian, M.D.	*2009*
Webster S. Jee, Ph.D.	*2003*	David Burr, Ph.D.	*2010*
Claude Arnaud, M.D.	*2004*	Henry Kronenberg, M.D.	*2011*
Barbara Kream, Ph.D.	*2005*	Steven Teitelbaum, M.D.	*2012*
B. Lawrence Riggs, M.D.	*2006*	Gary S. Stein, Ph.D.	*2013*
Thomas John Martin, M.D., D.Sc.	*2007*		

ASBMR EARLY CAREER EXCELLENCE IN TEACHING AWARD

Sharon Nickols-Richardson, Ph.D., R.D.	*2006*	Lora M. Giangregorio, Ph.D.	*2010*
Catherine Gordon, M.D.	*2007*	Stuart J. Warden, Ph.D.	*2011*
Rachel Davey, Ph.D.	*2008*	Robert Pignolo, M.D., Ph.D.	*2012*
Babette Zemel, Ph.D.	*2009*	Suzanne M. Cadarette, Ph.D.	*2013*

ASBMR CAREER ENHANCEMENT AWARDS

Supported by an educational grant from Lilly USA, LLC

Roberta Faccio, Ph.D.	*2005*	Elizabeth Samelson, Ph.D.	*2007*
David Karasik, Ph.D.	*2005*	Tamim Diab, Ph.D.	*2008*
Baojie Li, Ph.D.	*2005*	Ivo Kalajzic, M.D., Ph.D.	*2008*
Jiake Xu, M.D., Ph.D.	*2005*	Tatsuya Kobayashi, M.D.	*2008*
Anja Nohe, Ph.D.	*2006*	Jie Song, Ph.D.	*2008*
Deborah Novack, M.D., Ph.D.	*2006*	Claire M. Edwards, Ph.D.	*2009*
Matthew Stewart, Ph.D.	*2006*	Kenneth Kozloff, Ph.D.	*2010*
Shoshara Yakar, Ph.D.	*2006*	Lin Qin, Ph.D.	*2011*
Gregory Adam Clines, M.D.	*2007*	Despina Sitara, Ph.D.,	*2012*
Adi Cohen, M.D.	*2007*	Warren Grayson, Ph.D.	*2013*
Lorena Havill, Ph.D.	*2007*		

RAISZ-DREZNER FIRST AUTHOR JOURNAL AWARDS

James R. Cavey, B.Sc. *2005*
Xuesong Chen, Ph.D. *2005*
Claudia Riedt, Ph.D. *2005*
Jennifer L. Fiori, Ph.D. *2006*
Guillaume E. Beranger, Ph.D. *2006*
Xiaojing Wang, Ph.D. *2007*
Kuan-Ping Yu, Ph.D. *2007*
Romain Voide, Ph.D. *2008*
Susannah J. Sample, MS *2008*
Mei Zhu, Ph.D. *2009*
Daniel Toben, M.D. *2010*
Erica Homan *2012*
Glenn Rowe *2012*

JUNIOR FACULTY OSTEOPOROSIS RESEARCH AWARD

Supported by an educational grant from Merck & Co., Inc

Roy Morello, Ph.D. *2010*
Beatrice Jara-Almonte Edwards, M.D., MPH *2010*
Emily Stein, M.D., MS *2011*
Eve Donnelly, Ph.D., *2012*
Susan Krum, Ph.D., *2012*
Ling Qin, Ph.D. *2013*
Shivani Sahni, Ph.D. *2013*

2013 ASBMR MOST OUTSTANDING BASIC ABSTRACT AWARD

Aruna Kode, Ph.D.

2013 ASBMR MOST OUTSTANDING CLINICAL ABSTRACT AWARD

Thomas O. Carpenter, M.D.

2013 ASBMR PRESIDENT'S AWARD

Aude-Helene Capietto, Pharm.D., Ph.D.

2013 ASBMR FELIX BRONNER YOUNG INVESTIGATOR AWARD

Joel Jules, Ph.D.

2013 ASBMR YOUNG INVESTIGATOR AWARD RECIPIENTS

Supported by educational grants from Pfizer, Inc., Lilly USA, LLC and Merck & Co., Inc.

Rana Abou-Khalil, Ph.D.
Lindsay A. Bashur, Ph.D.
Miranda Boggild, M.D.
Wafa Bouaziz
Sandrine P.G. Bours, M.D.
Lauren A. Burt, Ph.D.
Pamela Cabahug, MSc
Jingjing Cao, Ph.D.
Didier Chalhoub, M.D., M.P.H.
Abhishek Chandra, Ph.D.
Julia C. Chen, Ph.D.
Paul G. Daft
Agnese Di Rocco, Ph.D.
Danielle M. Frechette, M.S.
Alejandro J. Garcia, Ph.D.
Joseph D. Gardinier, Ph.D.
Sarah A. Hardcastle, MBChB, BSc
Leigh Gabel, MSc
Denise H.M. Heppe, MSc
Anna Idelevich, Ph.D., MBA
Aaron W. James, M.D.
Ha-Neui Kim, Ph.D.
Hiroshi Kobayashi, M.D.
Keiji Kobayashi, M.D.
Carole Le Henaff, Ph.D.
Joshua R. Lewis, Ph.D.
Susan Li
Tieshi Li, Ph.D.
Xianwen Liu, D.D.S.
Aimee-Lee Anne Luco
Kelsey M. Mangano, Ph.D., R.D.
Takamitsu Maruyama, Ph.D.
Kazuhiko Matsuoka, Ph.D.
Yuki Matsushita, D.D.S., Ph.D.
Kyla L. Naylor, B.H.K., MES.
Toru Nishikawa, D.D.S., Ph.D.
Kyle Nishiyama, Ph.D.
Yasuhisa Ohata, M.D.
Karla J. Oldknow, BSc (Hons)
Perla C. Reyes Fernandez, B.Sc.
Jörg H. Schilcher, M.D.
Zeynep Seref-Ferlengez, MSc
Barbara C. C. Silva, M.D., Ph.D.
Lachlan J. Smith, Ph.D.
Fabiana N. Soki, D.D.S.
Courtney A. Sprouse, B.S.
Ryan E. Tomlinson, Ph.D.
Konstantinos A. Toulis, M.D., M.Sc., MRes
Christophe Travert, Ph.D.
Julia T. Warren

2013 SUPPORTERS

The ASBMR gratefully acknowledges the following companies for their support:

DIAMOND LEVEL

Lilly
Answers That Matter.

PLATINUM LEVEL

MERCK AMGEN

BRONZE LEVEL

ucb WARNER CHILCOTT Pfizer

FRIEND LEVEL

NOVARTIS ALEXION KYOWA KIRIN

2013 EXHIBITORS

Active Life Scientific, Inc.
Alexion Pharmaceuticals
ALPCO
American Society for Nutrition
Amgen
Atlantic Bone Screen
Biomedica Medizinprodukte GmbH & Co KG
BIOQUANT Image Analysis Corporation
BioVendor Laboratorni medicina a.s.
Bose Corporation
Bruker BioSpin Corp.
Canadian Institutes of Health Research - Institute of Musculoskeletal Health and Arthritis
Charles River
Clinical Endocrinology News
DIAsource ImmunoAssays S.A.
Elsevier
EMD Millipore Corporation
The Endocrine Society
European Calcified Tissue Society
Everidis Health Sciences
FASEB MARC Program
Faxitron
Hologic
Immundiagnostik AG
Immunodiagnostic Systems (IDS)
Immutopics International
International Bone & Mineral Society
International Society for Clinical Densitometry
Kubtec Digital X-ray
Lilly USA, LLC.
Lone Oak Medical Technologies
medimaps group
Medtronic
Merck
Micro Photonics, Inc.
Mindways Software, Inc.
Mission Pharmacal Company
National Bone Health Alliance (NBHA)
NIH Osteoporosis & Related Bone Diseases ~ NRC
Orthometrix, Inc.
OsteoMetrics, Inc.
PerkinElmer
PharmaLegacy Laboratories (Shanghai) Co., Ltd.
Quidel Corporation – Specialty Products
R&D Systems, Inc.
Rare Bone Network
Ratoc System Engineering Co., Ltd.
Research Diets, Inc.
Roche Diagnostics Company
Scanco Medical
Springer
Vidara Therapeutics Inc.
Warner Chilcott
Wiley

Continuing Medical Education Credits

This educational activity has been planned and implemented in accordance with the Essential Areas and policies of the Accreditation Council for Continuing Medical Education (ACCME) through the joint sponsorship of the Institute for the Advancement of Human Behavior (IAHB) and the American Society for Bone and Mineral Research (ASBMR). The IAHB is accredited by the ACCME to provide continuing medical education for physicians.

AMA PRA Statement

The *IAHB designates this educational activity for a maximum of 32.25 AMA PRA Category 1 Credits*™ Physicians should only claim credit commensurate with the extent of their participation in the activity.

Online Evaluation to Receive CME

The online evaluation to receive CME will be available beginning Thursday, October 10. *Please Note*: There will be a $50 fee per application. This fee can be paid when you register for the Annual Meeting or added during the Meeting at the Registration Desk. Should you have questions regarding the online CME evaluation, contact Jillian Davis at +1 (651) 789-3722 or jillian@cmehelp.com.

Meeting Objectives

Upon returning home from the meeting, participants should be able to:

- Discuss the most current and significant advances in biomedical and clinical research in bone and mineral metabolism, specifically in the areas of cancer and bone, personalized medicine, chronic kidney disease, osteoporosis, metabolic bone diseases and therapeutics.
- Better understand the interrelationship among basic research, clinical research and patient care.
- Improve their ability to treat and care for patients through an enhanced knowledge of osteoporosis, other diseases of bone, basic bone biology and its correlation to mineral metabolism.
- Develop new and enhanced strategies for the diagnosis and treatment of patients with disorders of bone and mineral metabolism.

Target Audience

The program is designed for researchers, physicians and other health and allied health professionals with interests in biomechanics, cell biology, dentistry, endocrinology, epidemiology, genetics, internal medicine, metabolism and musculoskeletal research, molecular biology, molecular genetics, nephrology, orthopaedics, pathology, pharmacology, physiology and rheumatics.

Disclosure Policy

The American Society for Bone and Mineral Research is committed to ensuring the balance, independence, objectivity and scientific rigor of all its individually sponsored or industry-supported educational activities. Accordingly, the ASBMR adheres to the requirement set by ACCME that audiences at jointly sponsored educational programs be informed of a presenter's (speaker, faculty, author or planner) academic and professional affiliations, and the disclosure of the existence of any significant financial interest or other relationship a presenter or their spouse has with any proprietary entity over the past twelve months producing, marketing, re-selling or distributing health care goods or services, consumed by, or used on patients, with the exemption of non-profit or government organizations and non-health care related companies. When an unlabeled use of a commercial product, or an investigational use not yet approved for any purpose, is discussed during the presentation, it is required that presenters disclose that the product is not labeled for the use under discussion or that the product is still investigational. This policy allows the listener/attendee to be fully knowledgeable in evaluating the information being presented. The *On-Site Program* book will note those speakers who have disclosed relationships, including the nature of the relationship and the associated commercial entity.

Disclosure should include any relationship that may bias one's presentation or which, if known, could give the perception of bias. This includes relevant financial relationships of a spouse or partner. Disclosures will be printed in the program materials. These situations may include, but are not limited to:

DISCLOSURE KEY

1) stock options or bond holdings in a for-profit corporation or self-directed pension plan
2) research grants
3) employment (full or part-time)
4) ownership or partnership
5) consulting fees or other remuneration
6) non-remunerative positions of influence such as officer, board member, trustee, or public spokesperson
7) receipt of royalties
8) speaker's bureau
9) other

ABSTRACT-BASED AWARDS

2013 ASBMR Most Outstanding Basic Abstract Award

1005	Leukemogenic Transformation of Hematopoietic Stem Cells by Constitutive Activaton of Canonical Wnt signaling in Osteoblasts	Aruna Kode, Columbia University Medical Center, USA

2013 ASBMR Most Outstanding Clinical Abstract Award

1048	A First-in-Human, Randomized, Double-Blind, Placebo-Controlled, Single-Dose Study of Human Monoclonal Anti-FGF23 Antibody (KRN23) in X-linked Hypophosphatemia	Thomas O. Carpenter, Yale University School of Medicine, USA

2013 ASBMR President's Award

1058	Downregulation of PLCy2/β-catenin Pathway Promotes Activation and Expansion of Myeloid-Derived Suppressor Cells in Cancer	Aude-Helene Capietto, Washington University School of Medicine, USA

2013 ASBMR Felix Bronner Young Investigator Award

1092	Conditional ablation of Cbfβ in different stages of skeletogenesis results in a novel cleidocranial dysplasia mouse model revealing a new role of Cbfβ in postnatal skeletal and tooth development	Joel Jules, University of Alabama at Birmingham, USA

2013 ASBMR Young Investigator Awards

1002	The Cardiovascular Safety of Calcium Supplementation With or Without Vitamin D in Elderly Women: A Collaborative Meta-analysis of Published and Unpublished Trial Level Evidence from Randomised Controlled Trials.	Joshua R. Lewis, University of Western Australia, Sir Charles Gairdner Hospital, Australia
1003	Risk of Non-spine Fractures Among Men and Women with Sarcopenia, Low Bone Mass or Both	Didier Chalhoub, University of Pittsburgh, USA
1004	PTH Release during Exercise Regulates Trabecular Bone Adaptation	Joseph D. Gardinier, University of Michigan, USA
1008	Role Of Muscle Stem Cells During Bone Regeneration	Rana Abou-Khalil, INSERM U781 Colnot Group, France
1010	Loss of Material Properties Due to Diffuse Microdamage in Rat Living Bone Recovers without Osteoclastic Bone Remodeling	Zeynep Seref-Ferlengez, City College of New York, USA
1012	Satellite Cell Populations in Skeletal Muscle, Compromised by Ovariectomy, are Rescued by Daily Bouts of Low Intensity Vibration	Danielle M. Frechette, Stony Brook University, USA
1015	Primary Cilia of Bone Marrow Stromal Cells Mediate Mechanically Induced Osteogenesis	Julia C. Chen, Columbia University, USA

1021	Teriparatide Is Associated with Improved Microarchitecture and Estimated Bone Strength in Premenopausal Women with Idiopathic Osteoporosis: An HR-pQCT Study	Kyle Nishiyama, Columbia University, USA
1024	Systemic Administration of NELL-1, a Wnt/β-Catenin Regulator, Induces Bone Formation in Osteoporotic Mice via Integrinβ1	Aaron W. James, University of California, Los Angeles, USA
1032	Miglustat Normalizes Bone Mass And Improves Bone Microarchitecture In F508del Cystic Fibrosis Mice Through Beneficial Effects on Bone Formation and Resorption	Carole Le Henaff, Inserm Unit 606 and University Paris Diderot, France
1035	The Role of Macrophage Efferocytosis in Prostate Cancer Skeletal Metastasis	Fabiana N. Soki, University of Michigan School of Dentistry, USA
1041	PHOSPHO1: Recognition of roles beyond skeletal mineralization	Karla J. Oldknow, The Roslin Institute, The University of Edinburgh, United Kingdom
1043	Inhibition of AP-1 in specific hypothalamic neurons increases both energy expenditure and bone density in mice	Anna Idelevich, Harvard University, USA
1045	Fetal Stage-Specific Mineral Metabolism in *Hyp* Mice Is Associated with Effects of FGF23 on Placenta	Yasuhisa Ohata, Osaka Medical Center and Research Institute for Maternal and Child Health, Japan
1054	3D-XA-Based Vertebral Finite Element Model for Strength Evaluation in Osteoporosis	Christophe Travert, Arts et Metiers ParisTech, France
1056	Wnt Production of Signaling in Fate Determination and Differentiation of the Skeletal Precursors	Takamitsu Maruyama, University of Rochester Medical Center, USA
1057	Wnt16 Deletion Differentially Affects Cortical and Trabecular Bone: Increased Cortical Bone Resorption, Porosity and Fracture in Wnt16 Knockout Mice	Xianwen Liu, Harvard School of Dental Medicine, USA
1061	Parathyroid Hormone-related Peptide (PTHrP) blockade inhibits the development of bone metastasis and potentiates the effect of zoledronic acid in vitro and in vivo in a mouse model of breast tumor progression	Aimee-Lee Anne Luco, McGill University, Canada
1068	Sclerostin Preserves Cartilage Integrity in Murine Osteoarthritis	Wafa Bouaziz, INSERM U606, France
1073	Osteoclast-secreted Complement Component 3a Stimulates Osteoblast Differentiation	Kazuhiko Matsuoka, National Center for Geriatrics and Gerontology, Japan
1074	RANKL increase ROS and Bone Resorption by Inhibiting FoxO-mediated Catalase Expression	Ha-Neui Kim, University of Arkansas for Medical Sciences, USA
1076	HIF-1α Regulates Bone Formation Following Osteogenic Mechanical Loading	Ryan E. Tomlinson, Washington University in St. Louis, USA
1079	Histology of Atypical Femoral Fractures	Jörg H. Schilcher, Linköping University, Sweden
1082	A Five-Year Longitudinal Study of Site-Specific Changes in Bone Quality in the Calgary Population-Based Cohort: an HR-pQCT Study	Lauren A. Burt, University of Calgary, Canada
1085	Associations of Fetal and Childhood Growth with Bone Mass in School Age Children. The Generation R Study.	Denise H.M. Heppe, Erasmus MC, The Netherlands

1093	NF-κB Family Member Rela/p65 in Chondrocytes Controls Skeletal Growth and Osteoarthritis Development by Inhibiting Chondrocyte Apoptosis	Hiroshi Kobayashi, The University of Tokyo Hospital, Japan
1094	TGF-beta Signaling Regulates Interleukin-36 alpha in Joint Development and Osteoarthritis.	Tieshi Li, University of North Carolina at Chapel Hill, USA
1100	Neonatal Enzyme Replacement Therapy Improves Cervical Spine Bone Architecture and Mineralization in Mucopolysaccharidosis I Dogs	Lachlan J. Smith, University of Pennsylvania, USA
1101	The Transcriptional Cofactor Jab1 is Essential for Mouse Limb Development	Lindsay A. Bashur, Case Western Reserve University, USA
1106	Wnt5a and Wnt5b in osteoblastic niche differentially regulate HSC maintenance and differentiation	Jingjing Cao, Shanghai Jiao Tong University, People's Republic of China
1108	Assessment of Vertebral Fractures in Patients Older than 50 Years with a Recent Non Vertebral Fracture Before and After Introduction of Systematic Vertebral Fracture Assessment (VFA)	Sandrine P.G. Bours, Maastricht University Medical Centre, The Netherlands
1111	β-adrenergic Receptor Antagonists and Fracture Risk: A Meta-analysis of Selectivity, Dose, Gender and Site-specific Effects	Konstantinos A. Toulis, Aristotle University of Thessaloniki, Greece
1113	Alleviation of Radiotherapy-Induced Bone Loss by Parathyroid Hormone Treatment is Associated with Improved DNA Repair in Osteoblasts	Abhishek Chandra, University of Pennsylvania, USA
1114	Manipulation of RANK monomer assembly as a novel anti-resorptive strategy	Julia T. Warren, Washington University in St. Louis School of Medicine, USA
1117	GATA4 Regulates Bone Mineralization Via Estrogen Receptor-Dependent and -Independent Pathways	Alejandro J. Garcia, University of California, Los Angeles, USA
FR0012	Protein Intake is Protective Against Grip Strength Loss in Adults: The Framingham Osteoporosis Study	Kelsey M. Mangano, Institute for Aging Research, Hebrew SeniorLife, Harvard Medical School, USA
FR0104 SA0104	CCN3 Participates in Bone Regeneration as an Inhibitory Factor	Yuki Matsushita, Tokyo Medical and Dental University, Japan
FR0172 SA0172	Beneficial Effects of PTH(1-84) in Hypoparathyroidism as Determined by Microarchitectural Texture Assessment (TBS): a 4-year Experience	Barbara C. C. Silva, Columbia University Medical Center, USA
FR0192 SA0192	Selective RARγ agonist blocks heterotopic ossification and promotes skeletal muscle repair	Agnese Di Rocco, Children's Hospital of Philadelphia, ARC, USA
FR0194 SA0194	CKMM Polymorphism Is Associated with Physical Fitness Test Scores In Military Recruits	Courtney A. Sprouse, Children's National Medical Center, USA
FR0196	Effect of 1 year of whole-body vibration therapy on muscle density and volume in postmenopausal women: the Vibration Study	Miranda Boggild, University of Toronto, Canada
FR0283 SA0283	Inhibition of Osteocyte Apoptosis Prevents Extensive Trabecular Bone Loss Caused by Unloading in the Long Bone of Mice	Pamela Cabahug, City College of New York, USA

FR0366	Muscle Power and Force may Contribute to Cortical Bone Strength Through Distinct Mechanisms: Findings from a Cross-sectional Study of High Bone Mass Cases and Controls	Sarah A. Hardcastle, University of Bristol, United Kingdom
FR0437 SA0437	FRAX Predicts Fracture Risk in Kidney Transplant Recipients	Kyla L. Naylor, Western University, Canada
SU0033	Relationships between Muscle Power, Force, Density and Bone Quality in Children, Adolescents and Young Adults	Leigh Gabel, University of British Columbia, Canada
SU0284	Osteocyte Specific Deletion of Superoxide Dismutase2 Induces Osteocyte Loss Resulting in Bone Loss Associated with Impairment of Bone Remodeling	Keiji Kobayashi, Chiba University, Japan
SU0447	Duodenal Ca Absorption Increases to Compensate for the Loss of Vitamin D Receptor (VDR) from the Large Intestine and Kidney of Mice	Perla C. Reyes Fernandez, Purdue University, USA
MO0002	Characterization of Age-related Skeletal Muscle Regenerative Function and Gait Performance Recovery in Hindlimb Injured Fibroblast Growth Factor-2 Null Mice	Toru Nishikawa, University of Connecticut Health Center, USA
MO0261	RBP-J imposes a requirement for ITAM-mediated co-stimulation of RANKL and TNF signaling during osteoclastogenesis	Susan Li, Hospital for Special Surgery, USA
MO0470	Tumor-initiating Stem Cells are Regulated by α-CaMKII-induced VEGF in Human Osteosarcoma	Paul G. Daft, The University of Alabama at Birmingham, USA

ABSTRACT PRESENTATION KEY	
1001-1118	Distinguished and Concurrent Oral Presentations
FR#	Friday Poster Presentations
SA#	Saturday Poster Presentations
SU#	Sunday Poster Presentation
MO#	Monday Poster Presentations
*	Denotes Abstract Presenting Author

1001

Dietary and Supplemental Calcium Intake and the Risk of Mortality in Older Men: the MrOS Study. Douglas Bauer*[1], Stephanie Harrison[2], Peggy Cawthon[3], Elizabeth Barrett-Connor[4], James Shikany[5], Kristine Ensrud[6], Eric Orwoll[7], Steven Cummings[2]. [1]University of California, San Francisco, USA, [2]San Francisco Coordinating Center, USA, [3]California Pacific Medical Center Research Institute, USA, [4]University of California, San Diego, USA, [5]University of Alabama at Birmingham, Birmingham, AL, USA, [6]Minneapolis VA Medical Center / University of Minnesota, USA, [7]Oregon Health & Science University, USA

Controlled trials suggest that calcium supplement use might increase cardiovascular events and mortality, and one recent observational study also implicated high intake of dietary calcium. As data are scarce in men we assessed dietary calcium intake, use of calcium supplements and mortality among men >65 in MrOS.

At baseline, MrOS participants (N=5967) completed an extensive survey that included dietary calcium intake (Block Food Frequency Questionnaire). Calcium supplements, including multivitamins, were verified by review of pill bottles by trained staff. Mortality during follow-up was confirmed by contacting relatives and blinded central review of death certificates. Calcium intake was analyzed a priori across quartiles. Hazard ratios for total and cardiovascular mortality were estimated with proportional hazards models; final models were adjusted for age, ethnicity, education, BMI, walking speed, total energy intake, health habits, calcium supplement use and clinical center. Additional analyses were stratified by supplement use.

At baseline the mean age ($\pm$ SD) was 74 $\pm$ 6 yr., mean dietary calcium intake was 1142 $\pm$ 590 mg/d, and 65% reported use of calcium supplements. Compared to those with lower total calcium intake (diet plus supplements), men with higher intake were older, thinner, better educated, more likely to be Caucasian, less likely to smoke, and had higher gait speed (p trend<0.05 for all). During 10 years of follow-up 2,022 men died; 687 deaths were attributed to cardiovascular disease. In base models adjusted for age, energy intake and calcium supplement use, those in the lowest quartile of total intake (<621 mg/d) had higher total mortality (RH = 1.19, CI: 1.02, 1.39) compared to those in the highest quartile (>1565 mg/d). After additional adjustment for other potential confounding factors, calcium intake was not associated with total (Figure) or cardiovascular mortality (p trend = 0.51 and 0.79, respectfully). Calcium supplement use was not associated with total (RH = 1.06, CI: 0.96, 1.18) or cardiovascular mortality (RH = 1.00, CI: 0.83, 1.20). Results were similar in analyses stratified by calcium supplement use, and there was no evidence that supplements increased the risk of mortality among those with the highest dietary calcium intake (interaction p value = 0.84)In this large prospective study of older men, total calcium intake, use of calcium supplements and the combination of high dietary calcium intake and supplement use were not associated with total or cardiovascular mortality.

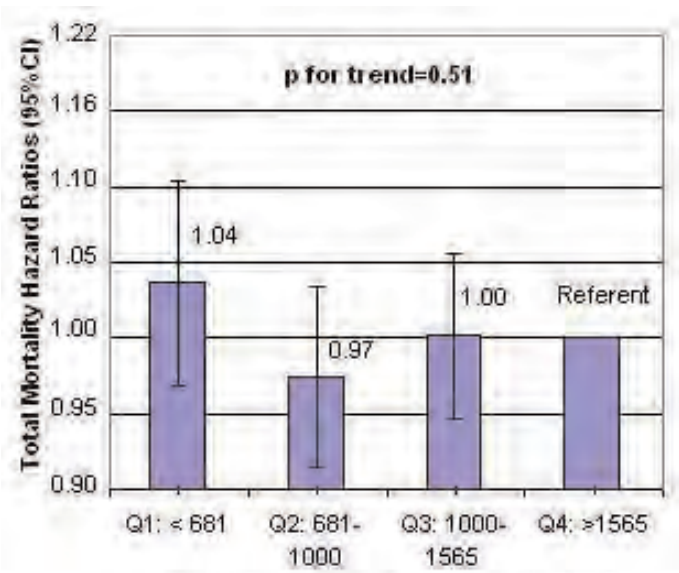

Figure. Adjusted total mortality by quartile of total calcium intake (dietary plus supplements)

***Disclosures: Douglas Bauer**, None.*

1002

The Cardiovascular Safety of Calcium Supplementation With or Without Vitamin D in Elderly Women: A Collaborative Meta-analysis of Published and Unpublished Trial Level Evidence from Randomised Controlled Trials. Joshua Lewis*[1], Lars Rejnmark[2], Kerry Ivey[3], Ross Prentice[4], Richard Prince[5]. [1]University of Western Australia, Sir Charles Gairdner Hospital, Australia, [2]Aarhus University Hospital, Denmark, [3]University of Western Australia, School of Medicine & Pharmacology, Australia, [4]Public Health Sciences Division, Fred Hutchinson Cancer Research Center, USA, [5]Sir Charles Gairdner Hospital, Australia

The use of calcium supplements, predominantly with vitamin D, is an important therapy for the prevention of osteoporosis and its clinical consequences in older women. However the clear benefit on reduction of osteoporosis risk in clinical fracture has been complicated by meta-analyses of cardiovascular disease (CVD) adverse events occurring in RCT's using events that were not properly adjudicated, leading to the concern that more patients on calcium supplements were misreporting more CVD events than the placebo groups, possibly due to reporting stomach ache not heart ache (Lewis et al. JBMR 2012:27; 719–722). This is in addition to concerns over the analysis of different outcomes and the combination of event data from men and women who have different CVD epidemiology presentation and outcomes. The incidence of ischemic heart disease in elderly women lags behind men by up to 20 years for myocardial infarction and is relatively uncommon even in elderly women (Lloyd-Jones D, et al. Circulation 2010;121:e46-e215). To address these concerns we have undertaken a collaborative pre-planned meta-analysis of trials of calcium supplementation with or without vitamin D with primary outcomes of a) all-cause mortality b) adjudicated ischemic heart disease (IHD) hospitalizations or death that include angina, myocardial infarction and chronic ischemic heart disease and adjudicated myocardial infarction as a secondary outcome. MEDLINE, EMBASE and Cochrane Library databases were searched until January 2013, using PRISMA guidelines and we identified19 studies that met the inclusion criteria of; a) randomised controlled trials published in the English language b) women over 50 years of age c) calcium supplementation > 1 year and d) reported all-cause mortality and / or adjudicated cardiovascular outcomes. The trial level relative risk (RR) data for the 4,646 deaths in 59,844 participants yielded a RR of 0.96 (0.91-1.02), P = 0.18 with low heterogeneity (I^2 = 0%) for those randomized to supplements. The trial level RR for the 3,334 ischemic heart disease events in 46,843 participants was 1.02 (0.96-1.09), P = 0.53 (I^2 = 0%) while the trial level RR for the 1,097 myocardial infarction events in 49,048 participants was 1.09 (0.89-1.33), P = 0.21 with low heterogeneity (I^2 = 28%).

The data from this meta-analysis does not support the concept that calcium supplementation with or without vitamin D increase the risk of ischemic heart disease or total mortality in elderly women.

***Disclosures: Joshua Lewis**, None.*

1003

Risk of Non-spine Fractures Among Men and Women with Sarcopenia, Low Bone Mass or Both. Didier Chalhoub*[1], Peggy Cawthon[2], Kristine Ensrud[3], Marcia Stefanick[4], Deborah Kado[5], Eric Orwoll[6], Jane Cauley[7]. [1]University of Pittsburgh, USA, [2]California Pacific Medical Center Research Institute, USA, [3]Minneapolis VA Medical Center / University of Minnesota, USA, [4]Stanford University School of Medicine, USA, [5]University of California, San Diego, USA, [6]Oregon Health & Science University, USA, [7]University of Pittsburgh Graduate School of Public Health, USA

The combination of both sarcopenia (low lean mass and poor muscle function) and low bone mass together on fracture risk has not been studied. We examined the risk of non-spine fractures in older men and women based on both sarcopenia and osteopenia/osteoporosis.

The prospective, longitudinal study data consisted of 1,204 white and black women (mean age=77.6 years) from the Study of Osteoporotic Fractures (SOF) and 5,729 white, black, and Hispanic men (mean age=73.7 years) from the Osteoporotic Fractures in Men (MrOS) study. BMD and appendicular lean mass (ALM) were assessed by DXA (Hologic 2000 for women, Hologic 4500 for men); grip strength by Jamar dynamometry; and walking speed over 6 m. Sarcopenia was based on European Working Group on Sarcopenia in Older Persons definition and included: 1) slowness (gait speed ≤0.8 m/s); 2) weakness (grip strength <30 kg men, <20 kg women); and 3) low lean mass (ALM corrected for height and total fat mass; <20%,"sarcopenic"); ''sarcopenia'' was defined as low lean mass plus either slowness or weakness. Osteopenia/osteoporosis was based on the WHO definition (femoral neck T-score <-2.5, with T-score based on young Caucasian women). Participants were classified into four groups: normal BMD and lean mass (normals) (N=3398 men, 312 women); sarcopenia with normal BMD (N=153 men, 45 women); osteopenia/osteoporosis and no sarcopenia (N=1972 men, 621 women); and sarcopenia with osteopenia/osteoporosis (N= 205 men, 139 women). Non-spine fractures were confirmed by central review of radiographic report over 8 years for women and 9 years for men. Cox proportional-hazards modeling was used to compare the risk of fracture across the four groups. Age adjusted incidence rates of non-spine fractures were calculated.

Men with sarcopenia and osteopenia/osteoporosis had the highest incidence rate of fracture (table). Sarcopenia alone was associated with an increased risk of fracture in men but not women. In men and women, osteopenia/osteoporosis alone was

associated with an increased risk of facture. Women with osteoporosis alone or sarcopenia and osteopenia/osteoporosis had a similar risk of fracture.

Men with both sarcopenia and osteopenia/osteoporosis had almost a two fold higher risk of fracture compared to men with either sarcopenia alone or osteopenia/osteoporosis alone suggesting that the combination of both of these factors may identify men at highest risk.

Table: Hazard ratios (95% confidence interval) and incidence rates (95% confidence interval) per 1000 person years for non-spine fractures in older individuals by sarcopenia, osteopenia/osteoporosis, and sarcopenia-osteopenia/sarcopenia-osteoporosis.

	Normal BMD and lean mass	Sarcopenia alone	Osteopenia/ Osteoporosis alone	Sarcopenia osteopenia/ Sarcopenia osteoporosis
Men				
Hazard ratios				
Age adjusted	1.00	1.6 (1.1, 2.5)	1.8 (1.5, 2.1)	3.2 (2.4, 4.3)
MV adjusted	1.00	1.5 (1.0, 2.3)	1.7 (1.4, 2.0)	3.0 (2.2, 4.0)
Incidence rates				
Age adjusted	9.9 (8.8, 10.9)	15.7 (9.4, 21.9)	17.4 (15.6, 19.3)	30.5 (22.1, 38.8)
Women				
Hazard ratios				
Age adjusted	1.00	1.6 (0.7, 3.6)	3.0 (2.0, 4.4)	3.0 (1.9, 4.8)
MV adjusted	1.00	1.6 (0.7, 3.7)	3.0 (2.0, 4.5)	3.1 (1.9, 5.1)
Incidence rates				
Age adjusted	10.9 (6.9, 14.9)	17.3 (4.5, 30.2)	32.6 (27.9, 37.4)	32.8 (22.9, 42.6)

MV= Multivariate model: Adjusted for age, previous fracture, current smoking, steroid intake, rheumatoid arthritis, alcohol consumption, physical activity, and bisphosphonate (in males).

Hazard ratios and incidence rates for fractures in older individuals by bone and body composition

***Disclosures: Didier Chalhoub**, None.*

1004

PTH Release during Exercise Regulates Trabecular Bone Adaptation. Joseph Gardinier*, David Kohn, Fatma Mohamed. University of Michigan, USA

The ability to enhance the structural integrity of bone at a young age reduces the risk of bone fracture as well as the development of musculoskeletal diseases. The structural integrity of bone is constantly adapting in response to dynamic loading and parathyroid hormone (PTH). Although the combination of dynamic loading and intermittent PTH(1-34) treatment can enhance bone adaptation, their distinct influence on bone adaption during exercise has yet to be established. The purpose of this study was to first establish that PTH is released during exercise, and second test our hypothesis that PTH released during exercise regulates bone adaption. In the first experiment, systemic PTH levels were measured following a single bout of exercise. In a second experiment, mice were assigned to sedentary or exercise groups, which were treated for 21 consecutive days with either PTH(7-34), PTH(1-34) or vehicle to determine the influence of PTH on bone adaptation during exercise. In both experiments 16 week old male mice were used and an exercise regimen involving treadmill running at 12 m/min on a 5˚ incline for 30 minutes under approval by the University Committee on Use and Care of Animals. Ex-vivo micro-CT scans of the tibia were taken for trabecular bone analysis, while cortical bone histomorphometry was measured at the tibia mid-diaphysis. Plasma levels of PTH were significantly greater 30 minutes after exercise and returned to baseline 1hr after exercise. Compared to sedentary controls, 3 weeks of exercise significantly increased trabecular bone volume (BV/TV) and thickness, but decreased the structure model index (SMI). PTH(7-34) treatment prior to exercise significantly decreased BV/TV and increased SMI compared to exercise alone. PTH(1-34) treatment alone had no effect on SMI, but significantly increased BV/TV along with the mineralizing surface (MS) and mineral apposition rate (MAR) of cortical bone at the endosteum and periosteum. PTH(1-34) treatment prior to exercise significantly increased endosteal MS and MAR, but periosteal MS was significantly attenuated compared to PTH(1-34) treatment alone. Overall, there is an immediate increase in systemic PTH levels in response to exercise that regulates an increase in trabecular BV/TV and shift in structure. The significant attenuation in BV/TV due to PTH(7-34) treatment prior to exercise demonstrates that bone adaptation during exercise is not only a function of the dynamic loading, but also the release of PTH.

***Disclosures: Joseph Gardinier**, None.*

1005

Leukemogenic Transformation of Hematopoietic Stem Cells by Constitutive Activation of Canonical Wnt signaling in Osteoblasts. Aruna Kode*[1], Sanil J Manavalan[1], Ioanna Mosialou[1], Chozha V Rathinam[1], Govind Bhagat[1], Murty Vundavalli[1], Naomi Galili[1], Siddhartha Mukherjee[1], Azra Raza[1], Julie Teruya Feldstein[2], Ellin Berman[2], Stavroula Kousteni[1]. [1]Columbia University Medical Center, USA, [2]Memorial Sloan-Kettering Cancer Center, USA

Osteoblasts have been implicated in self-renewal and expansion of hematopoietic stem cells (HSCs) and the fate of malignant stem cells. However, the molecular basis of these functions remain poorly understood. Here we show that constitutive activation of the Wnt/b-catenin signaling pathway in osteoblast precursors in mice ($\beta cat(ex3)_{osb}$) disrupts hematopoiesis by shifting the differentiation potential of HSC progenitors to the myeloid lineage. As a result, there is accumulation of granulocyte/monocyte progenitors and development of acute myeloid leukemia (AML). This AML phenotype is associated with clonal evolution at the cytogenetic level since common clonal abnormalities could be detected in leukemic blasts from all $\beta cat(ex3)_{osb}$ mice examined. In addition, transplantation of bone marrow cells derived from $\beta cat(ex3)_{osb}$ mice to lethally irradiated wild-type mice recapitulates hematopoietic deregulation with increased myeloid activity and decreased B-lymphopoiesis in recipient animals. A full fledge AML was seen in these mice within 6 weeks following $\beta cat(ex3)_{osb}$ bone marrow transplantation, demonstrating progression towards cells autonomous AML, a hallmark of leukemia. In addition, b-catenin-activated osteoblasts increased proliferation of human HSCs in co-cultures, increased the percentage of early myeloid cells (CD34+/CD33+) but decreased the percentage of late differentiated myeloid cells (CD34+/CD11b+/CD14+) suggesting maturation arrest of the myeloid lineage and accumulation of immature myeloid cells. Consistent with these observations obtained from mice and human cell cultures, malignancy-inducing osteoblasts, detected by nuclear accumulation of β-catenin in bone marrow biopsies, were identified in 38% of patients with myelodysplasia (MDS) or AML. Specifically, β-catenin localized to the nucleus of osteoblasts in 15 of 44 patients with MDS (34%), 9 of 26 patients with AML (34.61%), and 12 of 26 patients (46.1%) with AML that arose from prior MDS. In contrast, β-catenin localized to the cell membrane of osteoblasts of all healthy controls examined. Activation of b-catenin signaling was detected specifically in osteoblasts from the patients with nuclear accumulation of β-catenin in osteoblasts. These findings demonstrate that genetic alterations in osteoblast precursors can induce AML in mice and are associated with AML development in humans. They also provide a molecular basis for the leukemogenic transformation.

***Disclosures: Aruna Kode**, None.*

1006

***WNT1* Mutations in Early-Onset Osteoporosis and Osteogenesis Imperfecta Identify a Key WNT Ligand Regulating Bone Mass.** Brendan Lee[1], Christine Laine[2], Kyu-Sang Joeng[3], Philippe Campeau[3], Kati Tarkkonen[4], Monica Grover[5], James Lu[6], Minna Pekkinen[2], Maija Wessman[7], Terhi Heino[8], Vappu Nieminen-Pihala[9], Tero Laine[10], Heikki Kroger[11], William Cole[12], Anna-Elina Lehesjoki[13], Deborah Krakow[14], Cynthia Curry[15], Daniel Cohn[16], Richard Gibbs[3], Riku Kiviranta[17], Outi Makitie*[18]. [1]Baylor College of Medicine & Howard Hughes Medical Institute, USA, [2]Folkhälsan Institute of Genetics, Finland, [3]Molecular & Human Genetics, Baylor College of Medicine, USA, [4]Department of Medical Biochemistry & Genetics & Department of Medicine, University of Turku, Finland, [5]Department of Molecular & Human Genetics, Baylor College of Medicine, USA, [6]Human Genome Sequencing Center, Baylor College of Medicine, USA, [7]Folkhälsan Institute of Genetics & Institute for Molecular Medicine Finland, University of Helsinki, Finland, [8]Department of Cell Biology & Anatomy, University of Turku, Finland, [9]Department of Medical Biochemistry & Genetics, University of Turku, Finland, [10]Department of Orthopaedics, Sahlgrenska University Hospital, Sweden, [11]Department of Orthopaedics & Traumatology, Kuopio University Hospital, Finland, [12]Division of Pediatric Surgery, University of Alberta, Canada, [13]Folkhälsan Institute of Genetics & Neuroscience Center, University of Helsinki, Finland, [14]Departments of Orthopaedic Surgery & Human Genetics, University of California-Los Angeles, USA, [15]Genetic Medicine Central California, University of California San Francisco, USA, [16]UCLA, USA, [17]Department of Medical Biochemistry & Genetics & Department of Medicine, Finland, [18]Folkhälsan Institute of Genetics & Children's Hospital, Helsinki University Central Hospital & University of Helsinki, Finland

The role of the WNT pathway in skeletal maintenance has been extensively studied since the identification of mutations in key signaling WNT mediators (LRP5 and sclerostin) in high and low bone mass phenotypes. However, the identity of the key WNT ligand that signals via LRP5/6 has remained unknown. This study aimed to identify genes with a major effect on the skeleton by studying individuals and families with early-onset osteoporosis or osteogenesis imperfecta (OI). We recruited a Finnish family with severe early-onset and dominantly inherited osteoporosis, characterized by low BMD and vertebral fractures, in 10 individuals. Histomorphometry showed severe low-turnover osteoporosis with low bone formation in two adults and reduced bone remodeling in a 14-year-old boy. A genome-wide microsatellite scan, fine-mapping and targeted next-generation sequencing of the linkage region identified a single novel variant in *WNT1* (p.C218G) segregating with the phenotype. We also ascertained a Laotian Hmong family with two severely affected daughters suffering from recessive OI. After exclusion of mutations in the known OI genes we performed whole-exome sequencing and identified a homozygous nonsense mutation in *WNT1* (p.Ser295*) in both affected children. The mutant $WNT1^{C218G}$ and $WNT1^{S295*}$ proteins were stable and exhibited similar cellular distribution to the wild type (wt) WNT1. In contrast with wt-WNT1, $WNT1^{C218G}$ and $WNT1^{S295*}$ did not induce significant accumulation of active β-catenin in the nucleus. Accordingly, $WNT1^{C218G}$ and $WNT1^{S295*}$ showed significantly reduced capacity to induce canonical WNT signaling in a superTOPFLASH reporter assay. They also had impaired capacity to induce the WNT target gene expression and osteoblast differentiation in vitro. In

expression profiling by RT-PCR we detected *Wnt1* expression in mouse brain, femur and spleen but not in calvarial osteoblasts, osteoclasts or human mesenchymal stromal cells. *Wnt1* was clearly expressed in bone marrow, especially in B-cell lineage and hematopoietic progenitors. Using a Wnt1-Cre crossed with a reporter mice Wnt1 expression was also detected in a subset of osteocytes. Our results suggest altered cross-talk of WNT signaling between hematopoietic and osteoblast lineage cells as the pathogenetic mechanism. These findings indicate that loss-of-function heterozygous or bi-allelic mutations in *WNT1* result in early-onset osteoporosis or OI and identify WNT1 as a key WNT ligand in the regulation of bone mass.

***Disclosures: Outi Makitie**, None.*

1007

Whole Exome Sequencing Reveals a Pathogenic Mutation in a Kindred with Congenital Kyphosis and Anterior Fontanelle Patency. Philip Giampietro[1], David Sweetser[2], Alex Stoddard[3], Robert Blank*[4], Mark Stephan[5], Cathleen Raggio[6], Kristen Rasmussen[7], Michael Pickart[8], Sarah Sund[4], Ulrich Broeckel[3]. [1]University of Wisconsin Madison/Department of Pediatrics, USA, [2]Massachusetts General Hospital, USA, [3]Medical College of Wisconsin, USA, [4]University of Wisconsin, USA, [5]Madigan Army Medical Center, USA, [6]Hospital for Special Surgery, USA, [7]Marshfield Clinic, USA, [8]Concordia University, USA

Congenital vertebral malformations (CVM) represent defects in formation and segmentation of somites and have an estimated incidence of 0.13-0.50 per 1000 live births. Extreme genetic heterogeneity and the rarity of large families with CVM limit the ability to identify mutations in patterning genes associated with CVM by traditional genetic study designs. We therefore used whole exome sequencing (WES) to study a kindred in which a man and his two daughters suffered from kyphoscoliosis, vertebral body hypoplasia, short lumbar spinal pedicles, and prolonged anterior fontanelle patency. WES was performed using Agilent SureSelect hybridization-based exome capture methodology. Results were filtered to excude all except heterozygous nonsynonymous coding variants with minor allele frequency $< 1\%$. This strategy yielded 21 candidates, with *TLE4* harboring a c.A1318G:p.T440A variant. The functional significance of the *TLE4* variant was demonstrated by a mouse knockout of *Tle4*, the murine homolog. *Tle*$^{-/-}$ mice displayed a profound impairment of bone formation, while Tle$^{+/-}$ mice displayed a similar phenotype to the affected humans, including shortened vertebral pedicles and delayed mineralization of the skull. *TLE4* encodes a transcription factor in a gene family that participates in the determination of hematological cell fate in response to Notch signaling, a critical signaling pathway in somitogenesis. These findings highlight the potential of deep sequncing approaches, particularly when coupled with functional studies in appropriate models, to identify novel genetic determinants of uncommon disorders. While much work remains to be done to fully define the mechanisms by which *TLE4* mutations produce the observed phenotypes, these data nevertheless demonstrate the ability of a deep sequncing strategy to discover previously unknown skeletal genes.

***Disclosures: Robert Blank**, None.*

1008

Role Of Muscle Stem Cells During Bone Regeneration. Rana Abou-Khalil*[1], Frank Yang[2], Catia Pereira[1], Shirley Lieu[2], Frederic Relaix[3], Theodore Miclau[2], Ralph Marcucio[4], Celine Colnot[1]. [1]INSERM U781, Université Paris Descartes-Sorbonne Paris Cité, Institut Imagine, Hôpital Necker Enfants Malades, France, [2]Department of Orthopaedic Surgery, University of California at San Francisco, USA, [3]INSERM, UMR-S 787, UPMC Paris VI, Institut de Myologie, Faculté de Médecine Pitié-Salpétrière, France, [4]University of California, San Francisco, USA

Bone has a remarkable and sustained ability to regenerate following injury. Bone regeneration is a highly orchestrated process involving the activation of skeletal stem cells and various other cellular components as well as molecular pathways to insure proper healing. The identity of endogenous skeletal stem cells that contribute to bone regeneration has not yet been greatly elucidated. Periosteum plays an indispensible role in bone regeneration and is a major source of stem cells for cartilage and bone formation. Besides, surrounding soft tissues, such as skeletal muscle, may also procure a source of stem cells and play other functional roles during bone regeneration. Here, we provide evidence for a supporting role for skeletal muscle during bone regeneration specifically through the contribution of satellite cells, the adult muscle stem cells that primarily support muscle regeneration. Using a periosteal graft model, we showed that muscle enhanced periosteal contribution to bone regeneration. Conversely, muscle obstruction, using a porous filter, impaired bone regeneration by decreasing the periosteal activation. We showed the direct cellular contribution of muscle to bone regeneration by transplanting a whole GFP- actin muscle adjacent to a fracture site. By 10 days of bone regeneration, GFP+ chondrocytes were observed within the facture callus. To dissect the identity of muscle-derived stem cells during bone regeneration, we performed lineage analyses using Pax3Cre;R26RLacZ mice (Pax3 being a marker of myogenic lineage) and observed LacZ+-Pax3 derived chondrocytes within the fracture callus, indicating that satellite cells contribute to bone regeneration. Next, we showed that satellite cells are functionally involved in fracture repair. We assessed bone regeneration in Pax7 KO mice that lack Pax7+ satellite cells. We also used tamoxifen inducible Pax7CreER mice crossed with Diphtheria Toxin (DTA$^{f/f}$) mice, therefore ablating Pax7+ satellite cells and causing satellite cell suicide. Satellite cell loss as well as satellite cell depletion severely impaired bone regeneration with a delay in both cartilage and bone deposition. Therefore, for the first time, our results demonstrate the functional role of skeletal muscle during bone regeneration, via the direct contribution of satellite cells, the muscle stem cells, in the process of endochondral ossification in vivo.

***Disclosures: Rana Abou-Khalil**, None.*

1009

Osteocytes, but not osteoblasts, provide the RANKL required for bone remodeling in adult mice: novel insights from Sost-Cre;RANKLf/f mice. Jinhu Xiong*[1], Rajamani Selvam[2], Yiying Wang[2], Marilina Piemontese[2], Melda Onal[3], Priscilla Baltz[2], Stavros Manolagas[1], Charles O'Brien[1]. [1]Central Arkansas VA Healthcare System, Univ of Arkansas for Medical Sciences, USA, [2]University of Arkansas for Medical Sciences, USA, [3]university of wisconsin, USA

The cytokine RANKL is essential for osteoclastogenesis and recent studies have shown that RANKL expressed in Dmp1-Cre transgene-expressing cells is required for cancellous bone remodeling in adult mice. However, the Dmp1-Cre transgene used in those studies is active in both osteocytes and matrix-synthesizing osteoblasts, leaving open the possibility that either or both cell types produce the RANKL required for osteoclast formation in cancellous bone. To distinguish between osteocytes and osteoblasts as sources of RANKL, we created transgenic mice expressing the Cre recombinase under the control of regulatory elements of the Sost gene, which is expressed in osteocytes but not osteoblasts in murine bone. Activity of the Sost-Cre transgene in vivo was determined by crossing Sost-Cre mice with Rosa26R reporter mice, which express LacZ only in cells expressing Cre recombinase. LacZ staining of long bones and vertebrae of these mice, which had also been injected with calcein to identify surfaces undergoing active bone formation, demonstrated that the Sost-Cre transgene is active in osteocytes but not osteoblasts. We then crossed Sost-Cre mice with mice harboring a RANKL conditional allele (RANKLf/f) to delete the gene in osteocytes but not osteoblasts. Quantitative real-time PCR using genomic DNA isolated from osteocyte-enriched cortical bone confirmed that the RANKL gene was reduced by 70% in osteocytes of Sost-Cre;RANKLf/f mice, which displayed normal tooth eruption and were not grossly osteopetrotic. However, at 5 weeks of age, a small increase in spinal bone mineral density (BMD) was observed by DEXA in Sost-Cre;RANKLf/f mice compared with control littermates, and this difference increased progressively with age, so that at 22 weeks there was a 20% increase in vertebral BMD. Analysis by micro-CT at 22 weeks revealed that cancellous bone volume was much higher in femurs and L4 vertebra of Sost-Cre;RANKLf/f mice compared to control littermates. However, femoral cortical thickness was not affected. Consistent with the increase in cancellous bone, osteoclast number on vertebral cancellous bone was dramatically reduced in Sost-Cre;RANKLf/f mice compared with littermates. Moreover, the results obtained in Sost-Cre;RANKLf/f mice were comparable to those observed in Dmp1-Cre;RANKLf/f mice. These findings demonstrate that osteocytes, but not osteoblasts, provide the majority of the RANKL required for cancellous bone remodeling in adult murine bone.

***Disclosures: Jinhu Xiong**, None.*

1010

Loss of Material Properties Due to Diffuse Microdamage in Rat Living Bone Recovers without Osteoclastic Bone Remodeling. Zeynep Seref-Ferlengez*[1], Claudy Philemon[1], Oran Kennedy[2], Mitchell Schaffler[1]. [1]City College of New York, USA, [2]New York University, Hospital for Joint Diseases, USA

Introduction: Recent studies show that wear and tear causes bone microdamage at different hierarchical levels, and these have different biological consequences. Typical, linear microcracks are repaired by remodeling that removes and replaces the damaged bone region. Clusters of large numbers of submicron-sized cracks deemed Diffuse damage (DDx) also occur frequently. DDx is not remodeled, thus its long-term consequences are not known. Our recent results show that DDx induced in living bone is reduced over time, suggesting the intriguing idea that small cracks in living bone might be repaired directly. In these studies, we tested this hypothesis by examining whether the microscopic mechanical function list due to DDx is recovered in vivo.

Methods: Under IACUC approval, ulnae of 2 groups of adult female SD rats (n=12, 4-5m.o.) were subjected to in vivo creep loading to a predetermined displacement to induce solely DDx in the diaphyseal cortex. Group 1 rats were euthanized immediately after damage induction in order to assess the 'Acute' effect of DDx on bone elastic modulus (Ei). Group 2: one ulna was damaged with creep loading and rats returned to their cages for 14 days to test whether modulus recovered in DDx regions over time. Cross-sections were cut from DDx regions or equivalent levels from Non-loaded Control ulnae and tissue level Ei was measured within each DDx and Non-Dx Zone using microindentation.

Results: In Controls, Ei was equivalent in all cortex regions (Table 1). In Acute-Loaded ulnae, Ei in DDx Zones was reduced 15.2 $\pm$ 4% compared to non-damaged regions of the same ulna. Ei of cortical regions without damage was the same as

Control bone. After the 14-Day survival period, Ei in previously damaged areas had returned to normal.

Conclusion: The current studies reveal that diffuse damage (clusters of submicron-size cracks) in bone causes a marked and highly localized loss of bone stiffness. Recently we showed histologically that content of diffuse damage induced in living bone is reduced over time. Whether this reduction in microdamage translates to restoration of tissue integrity was not known. Here, we found that local material properties in diffuse damage areas of living bone recovered by 14 days after damage induction. Further studies are needed to elucidate the mechanisms by which this direct repair occurs. Nevertheless, our studies reveal that living bone directly repairs small matrix cracks both structurally and mechanically.

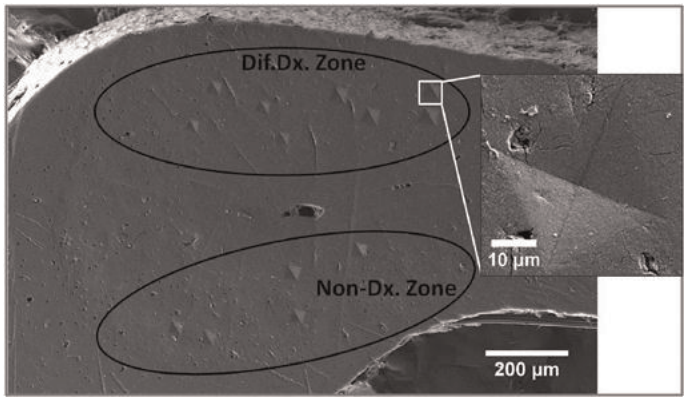

SEM image of 14D Survival ulnar cortex-resdiual indentation profiles in the DDx and Non-Dx zones

	Non-Dx Zone	Diffuse Dx Zone	p-Value
Control	14.8±1.7	14.3±1.3	>0.6
Acute-Loaded	14.8±1.1	12.6±1.0 *	<0.002
14-Day Survival	14.9±1.4	14.7±1.1	>0.6

Ei values for groups in GPa (mean ± s.d., *:$p<0.002$ vs Control)

***Disclosures: Zeynep Seref-Ferlengez**, None.*

1011

A Myostatin Inhibitor (propeptide-Fc) Increases Muscle Mass but Does Not Alter Bone Density or Strength in Aged Mice. Phonepasong Arounleut[1], Peter Bialek[2], Mohammed Elsalanty[3], Sunil Upadhyay[4], Carlos Isales[4], William Hill[5], Xing-Ming Shi[3], Mark Hamrick*[3]. [1]Georgia Regents University (formally Georgia Health Sciences University), USA, [2]Pfizer Inc., USA, [3]Georgia Health Science University, USA, [4]Georgia Regents University, USA, [5]Georgia Regents University & Charlie Norwood VAMC, USA

Myostatin deficiency is associated with increased muscle mass in mice, dogs, cows, sheep and humans, and mice lacking myostatin have also been observed to show increased bone density in the limb, spine, and jaw. Transgenic overexpression of myostatin propeptide, which binds and inhibits the active myostatin ligand, also increases muscle mass and bone density in mice. We therefore sought to test the hypothesis that inhibition of myostatin using an injectable myostatin propeptide (GDF8 propeptide-Fc) would increase both muscle mass and bone density in aged (24 mo) mice. Mice were injected weekly (20 mg/kg body weight) with recombinant myostatin propeptide-Fc (PRO) or vehicle (VEH; saline) for four weeks. There was no difference in body weight between the two groups after the treatment period but PRO treatment significantly increased mass of the tibialis anterior muscle (+7%) and increased muscle fiber diameter of the extensor digitorum longus (+16%) and soleus (+6%) muscles. Bone volume relative to total volume (BV/TV) of the femur calculated by microCT did not differ significantly between PRO and VEH, and ultimate force (Fu), stiffness (S), toughness (U) measured from three-point bending tests also did not differ significantly between groups. These data suggest that while developmental perturbation of myostatin signaling through either gene knockout or transgenic inhibition may alter both muscle and bone in mice, pharmacological inhibition of myostatin in aged mice has a more pronounced effect on skeletal muscle than on bone. Funding for this research was provided by the Department of the Army (CDMRP093619).

***Disclosures: Mark Hamrick**, None.*

1012

Satellite Cell Populations in Skeletal Muscle, Compromised by Ovariectomy, are Rescued by Daily Bouts of Low Intensity Vibration. Danielle Frechette*, Divya Krishnamoorthy, M. Ete Chan, Benjamin Adler, Clinton Rubin. State University of New York at Stony Brook, USA

The ability of skeletal muscle to regenerate itself following injury is highly dependent on the activation of satellite cells (SC) in the muscle tissue. Chronic disease conditions, including obesity and type II diabetes, experience significant adipose infiltration which can disturb muscle homeostasis and compromise the regenerative process through disrupting SC populations. While the increase in adiposity that parallels menopause is thought to disrupt SC, it has also been proposed that mechanical stimulation suppresses fat accumulation, potentially allowing SC populations to recover. We hypothesized that adipose accumulation in a post-menopausal model (OVX) will decrease SC proportions in muscle, while low intensity vibration (LIV) will provide physical signals anabolic to muscle, reducing adiposity and protecting SC populations. 8w female C57BL/6 mice underwent either OVX or sham surgery (AC, n=10). OVX mice were subject to LIV (V, n=10) for 0.3g at 90Hz for 15min/d and 5d/w, or sham vibrated (O, n=10). At 6w, μCT analysis of the abdomen showed O had greater total abdominal (+43%, $p<0.001$) and visceral (+125%, $p<0.001$) adiposity compared to baseline scans, while LIV treated animals only increased 21% ($p\leq0.05$) and 70% ($p\leq0.005$), respectively. Rate of adipose accretion was significantly higher in O compared to AC ($p<0.005$), but not in V, demonstrating LIV's ability to mitigate adipose accumulation. PPARγ and PPARδ gene expression, mediators of preadipocyte proliferation and adipogenesis activation, were measured in the muscle. Compared to AC, expression levels in O increased 78% and 120%, respectively ($p\leq0.001$), while LIV suppressed expression in V relative to O essentially by half (-52% and -42%, respectively; $p<0.001$). Adipose gene expression was inversely related to the percentage of total SC and activated SC in the hind limb muscles, with total and activated SC populations declining in O compared to AC (-21%; -28%, respectively; $p<0.01$), while V mitigated these declines (-11%, -17%, respectively; $p>0.05$). These results indicate the potential damage of ovariectomy to SC differentiation and/or proliferation. Further, mechanical signals stand as a potential antagonist of adipogenesis in skeletal muscle, which could improve overall muscle homeostasis through maintaining SC populations and improving their ability to respond to detriment.

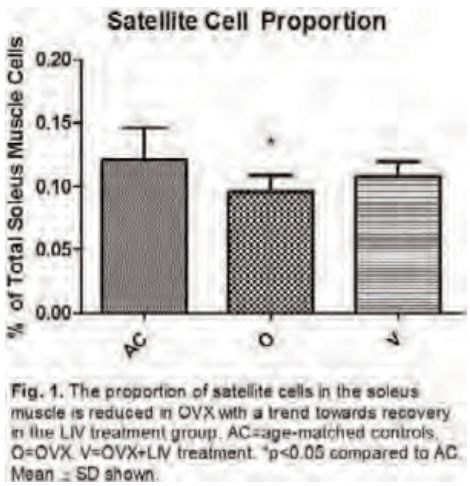

Fig. 1. Satellite Cell Proportion

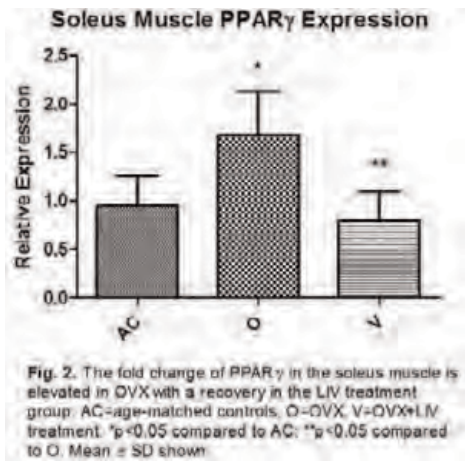

Fig. 2. Soleus Muscle PPARgamma Expression

***Disclosures: Danielle Frechette**, None.*

1013

ERα Signaling in Osterix1 and Prx1 Expressing Cells, Respectively, Mediates the Anabolic Effect of Mechanical Loading in the Murine Periosteum and the Protective Effects of Estrogens on Endocortical Resorption. Srividhya Iyer*[1], Li Han[1], Ha-Neui Kim[2], Semahat Serra Ucer[2], Shoshana Bartell[1], Aaron Warren[3], Julie Crawford[2], Robert Skinner[4], Mark Dallas[5], Mark Johnson[6], Robert Weinstein[1], Robert Jilka[1], Charles O'Brien[1], Maria Jose Almeida[1], Stavros Manolagas[1]. [1]Central Arkansas VA Healthcare System, Univ of Arkansas for Medical Sciences, USA, [2]University of Arkansas for Medical Sciences, USA, [3]Univ. Arkansas for Medical Sciences, & Central Arkansas Veterans Healthcare System, Little Rock, AR, USA, [4]Department of Orthopaedic Surgery, Center for Orthopaedic Research, Univ. Arkansas for Medical Sciences, Little Rock, AR, USA, USA, [5]Department of Oral & Craniofacial Sciences, University of Missouri, Kansas City, MO, USA, [6]University of Missouri, Kansas City Dental School, USA

Targeted deletion of the estrogen receptor (ER) α from pluripotent mesenchymal osteoblast progenitors (using a Cre recombinase driven by Prx1), bi-potential osteoblast precursors (using a Cre recombinase driven by Osx1), or mature osteoblasts and osteocytes (using a Cre recombinase driven by Col1 or Dmp1) has revealed that ERα signaling in Osx1 cells potentiates Wnt/β-catenin signaling and periosteal cell proliferation independently of estrogens. This signaling pathway is required for optimal cortical bone accrual at the periosteum. In addition, ERα signaling in Prx1 expressing cells and their descendants is required for the protective effect of estrogens in the endocortical surface. On the other hand, ERα signaling in Col1 or Dmp1 expressing cells has no effect on bone mass or the effect of mechanical loading. Based on this and evidence that the periosteal response to mechanical loading is compromised in mice with global deletion of the ERα, we investigated here whether ERα signaling in Osx1 cells is indeed required for the osteogenic response of the periosteum to mechanical stimulation. To do this, the right ulnae of 5 month old female ERα-flox;Osx1-Cre and Osx1-Cre littermate control mice (5 animals per group) were loaded at ~2500 microstrains for 3 weeks. At the end of the experiment, bone formation was determined in undecalcified bone sections from the loaded ulnae and the unloaded contralateral ulnae. Loading induced a 2.5 fold increase in mineralizing surface at the periosteum of the loaded, as compared to the unloaded ulnae. The response to loading was completely abrogated in the ERα-flox;Osx1-Cre mice. In addition, we have ovariectomized (OVX) 5 month old ERα-flox;Osx1-Cre mice and examined the effects of OVX 6 weeks later. In difference to the finding that ERα-flox;Prx1-Cre are protected from the loss of cortical bone caused by OVX, ERα-flox;Osx1-Cre and their littermate control mice exhibited indistinguishable loss of femoral BMD by DEXA. These results indicate that the effect of mechanical loading on the periosteum and the protective effects of estrogens on endocortical resorption are mediated by ERα signaling in two distinct cell types of the osteoblast lineage: Osx1 and Prx1 expressing cells, respectively. In the former, ERα is activated by mechanical loading and in the latter by estrogens. Furthermore, these results strongly suggest that Osx1 progenitors residing in the periosteum have mechanosensing properties.

***Disclosures: Srividhya Iyer**, None.*

1014

Conditional Disruption of the miR17-92 Cluster in Osteoblasts Impairs Skeletal Growth and Periosteal Response to Mechanical Loading. Chandrasekhar Kesavan*, Jon Wergedal, Subburaman Mohan. Jerry L. Pettis Memorial VA Medical Center, USA

While the role of osteoblast (OB) produced IGF-I in regulating skeletal growth has been well established from mouse conditional knock out (cKO) studies, little is known about the immediate downstream targets of IGF-I signaling in regulating skeletal growth. Because of the established importance of microRNA (miR) in posttranscriptional gene regulation, we evaluated expression levels of several miRs in the bones of IGF-I cKO and WT mice and found reduced expression (2-3 fold, $P<0.05$) of miR20a and 92 in the miR17-92 cluster in the OB-specific cKO mice. Accordingly, treatment of serum-free cultures of OBs with IGF-I caused a 2-3 fold ($P<0.05$) increase in miR20a and 92. Based on these data and the finding that targeted deletion of the miR17-92 cluster produced widespread skeletal defects in E.18.5 embryos and perinatal lethality in mice, we proposed the hypothesis that the miR17-92 cluster is important for skeletal development. MiR17-92 cKO mice were generated by crossing floxed miR17-92 mice with collagen type I Cre mice. At 4 and 8 weeks of age, total body BMC measured by DEXA was reduced by 29% and 24% (both $P<0.01$) respectively in cKO females compared to wild type (WT) control mice. This reduction in BMC was maintained at 12 weeks and was caused by reductions in bone length (10%, $P<0.05$) and cross sectional area (CSA, 18%, $P<0.05$) but not by a vBMD change as measured by pQCT. Male mice also exhibited significant reductions in total body BMC at 4 and 8 weeks of age. Since mechanical loading (ML) by 4 point bending induced a 2-fold increase in miR20a expression and miR17-92 cKO mice showed reduced bone size, we next tested if the miR 17-92 cluster was required for a normal periosteal response to ML. Nine and 7 N (to produce an equivalent amount of mechanical strain) were applied to the right tibia of WT and cKO female mice for a period of 2 weeks (6 days/week) at a 2Hz frequency for 36 cycles once per day by a 4 point bending method which produces a robust periosteal response at the diaphysis. The left tibia was used as an internal control. Two weeks of ML produced a 28%, 38% and 13% increase in CSA, BMC and vBMD, respectively in WT mice. ML-induced changes were significantly less (45-62%) in the cKO mice compared to WT mice. Based on our data, we conclude that the miR17-92 cluster expressed in osteoblasts is regulated by IGF-I and exerts an important role in periosteal bone formation during skeletal development and in response to mechanical strain.

***Disclosures: Chandrasekhar Kesavan**, None.*

1015

Primary Cilia of Bone Marrow Stromal Cells Mediate Mechanically Induced Osteogenesis. Julia Chen*[1], David Hoey[2], Christopher Jacobs[1]. [1]Columbia University, USA, [2]University of Limerick, Ireland

Osteoporosis is a disease of low bone mass and occurs when the activity of bone-forming osteoblasts is insufficient to counteract that of bone-resorbing osteoclasts. *In vitro* studies have shown that physical stimulation influences the differentiation of bone marrow stromal cells (BMSCs) into osteoblasts. One potential mechanosensor is the primary cilium, which is an antennae-like organelle extending into the extracellular space. Previous *in vitro* studies demonstrate that the osteogenic response of BMSCs to fluid flow is mediated by primary cilia. The objective of this study was to investigate the contribution of BMSCs to bone formation *in vivo,* and the role of primary cilia. Deletion of Kif3A, a subunit of an intraflagellar transport protein, disrupts primary cilia formation, but is embryonic lethal. Therefore, chimeric animals were generated with impaired primary cilia formation only in BMSCs. First, $Kif3A^{fl/fl}$;GFP;$Cre\text{-}ER^{T2}$ donor mice were generated where Kif3A could be deleted by tamoxifen induction of Cre. Wild type mice were irradiated, depleting their original BMSCs, and transplanted with BMSCs from either $Kif3A^{fl/fl}$;GFP (control) or $Kif3A^{fl/fl}$;GFP;$Cre\text{-}ER^{T2}$ (experimental) donors. Injection with tamoxifen induced Cre recombination in animals receiving $Kif3A^{fl/fl}$;GFP;$Cre\text{-}ER^{T2}$ cells, resulting in chimeric experimental animals. Right ulnae were axially loaded at 3N for 120 cycles for 3 days, and left ulnae remained non-loaded. Calcein and alizarin dyes were injected to mark new bone formation. After sacrifice, ulnae were prepared for histological analysis and dynamic histomorphometry. Donor-derived GFP-positive osteocytes were detected in loaded ulnae, indicating that transplanted BMSCs contributed to bone formation. Mineralizing surface (MS/BS), mineral apposition rate (MAR), and bone formation rate (BFR/BS) were measured using dynamic histomorphometry. Mechanical loading resulted in increases in the MS/BS, MAR, and BFR/BS in loaded ulnae compared to non-loaded ulnae for both experimental and control groups. Relative (r) rates were calculated by subtracting nonloaded from loaded values. Compared to controls, animals with disrupted primary cilia in BMSCs had significant reductions in rMS/BS and rBFR/BS of 46% ($p<0.05$) and 53% ($p<0.001$), respectively (Fig. 1). These results demonstrate that BMSCs contribute to mechanically induced bone formation, and primary cilia are important for this process.

Keywords: primary cilia, bone formation, mechanical loading

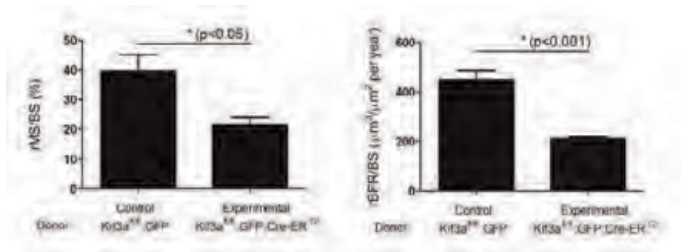

Fig. 1 Disruption of primary cilia formation in BMSCs affects mechanically induced bone formation.

***Disclosures: Julia Chen**, None.*

1016

Live Imaging of Collagen Assembly and Cell Membrane Dynamics in Osteoblasts and Acceleration of Collagen Assembly by Wnt3a. Erica Perryn*, Patricia Veno, Yongbo Lu, Sarah Dallas. University of Missouri - Kansas City, USA

Type I collagen, the major bone extracellular matrix protein, is composed of heterotrimers of two α1(I) chains and one α2(I) chain, encoded by the COL1A1 and COL1A2 genes. Although the post-translational modifications and intracellular assembly of collagen chains into trimers are well defined, the dynamic processes by which collagen assembles extracellularly are less clear. Previously we described the generation/validation of transgenic mice expressing α2(I)-collagen-GFP driven by the 3.6kb Col1A1 promoter.To gain further insight into collagen assembly, widefield and

confocal live cell imaging were performed on osteoblasts from α2(I)-col-GFP mice. The mice were also crossed with mice expressing a membrane-targeted TdTomato reporter to examine collagen assembly simultaneously with cell membrane dynamics. Live cell imaging showed that collagen assembly is a highly dynamic process involving extensive cell motions which stretched and contracted the fiber network during assembly. A subpopulation of osteoblasts was more active in collagen assembly compared to other cells. Upon addition of ascorbate, GFP-collagen translocated to the periphery of these cells into vesicle-like structures. These vesicles showed extensive intracellular movement to localized regions within the cell and appeared to be involved in the assembly process. Dual imaging of α2(I)-col-GFP/TdTomato osteoblasts showed that early collagen assembly occurred at the cell periphery and that the cell margins extended much further than previously appreciated from DIC imaging, with cell projections extending up to 2-3 cell diameters. Live imaging of α2(I)-col-GFP/mem-TdTomato osteoblasts seeded at low densities on wild type osteoblasts showed GFP-collagen deposition only in areas in which the cell body or cell processes had been, suggesting active placement of collagen by cells rather than diffusion of collagen away from the producing cell. Some cells were able to physically reshape the collagen fiber network by pushing collagen outwards to generate holes resembling lacunae. Treatment with Wnt3a accelerated the collagen assembly process, likely in part through its effect on increasing cell motility and mitosis. These data suggest that collagen assembly is a highly dynamic process involving internal movement of collagen to localized areas of the cell, exertion of forces on the developing fibers via cell motion and physical reshaping of the collagen via cell generated forces.

***Disclosures: Erica Perryn**, None.*

1017

Further Reduction in the Nonvertebral Fracture Rate Is Observed Following 3 Years of Denosumab Treatment: Results With Up to 7 Years in the FREEDOM Extension. Serge Ferrari*[1], Jonathan D. Adachi[2], Carol Zapalowski[3], Paul D. Miller[4], Jean-Yves Reginster[5], Ove Törring[6], Nadia Daizadeh[3], Andrea Wang[3], Cynthia O'Malley[3], Rachel B. Wagman[3], E. Michael Lewiecki[7]. [1]Geneva University Hospital, Switzerland, [2]McMaster University, Canada, [3]Amgen Inc., USA, [4]Colorado Center for Bone Research, USA, [5]University of Liège, Belgium, [6]Karolinska Institutet, Södersjukhuset, Sweden, [7]New Mexico Clinical Research & Osteoporosis Center, USA

Purpose: Some antiresorptives reduce nonvertebral fracture incidence in the first 3 years of treatment; however, evidence for further reduction of nonvertebral fractures with prolonged therapy is limited. The effects of denosumab (DMAb) treatment for up to 10 years are being evaluated in the 3-year FREEDOM study and its 7-year extension. Here we compare the nonvertebral fracture rate during the first 3 years of DMAb with that in the following 4 years of treatment.

Methods: During the extension, all subjects received 60 mg DMAb Q6M. Here, long-term subjects received 7 years of DMAb (3 years in FREEDOM followed by 4 years in the extension); subjects from the cross-over group received 4 years of DMAb (3 years of placebo in FREEDOM followed by 4 years of DMAb in the extension). Nonvertebral fracture rates for the first 3 years of DMAb were compared with rates in the 4th year of DMAb in each group separately and combined. For the long-term group only, the nonvertebral fracture rate in the first 3 years of DMAb was also compared with the fracture rate during the subsequent 4 years. Adjusted rate ratios (95% CIs) between observational periods were computed via generalized estimating equation (GEE) Poisson regression.

Results: Of 5928 women eligible for the extension, 4550 (77%) enrolled (N=2343 long-term; N=2207 cross-over). In the long-term group, the nonvertebral fracture rate was 1.98 per 100 subject-years during years 1–3 of DMAb (FREEDOM). This rate decreased during year 4 (extension) to 1.43 (rate ratio=0.73; P=0.096), and the rate remained low at 1.45 during years 4–7 (rate ratio=0.74; P=0.016; Table). Similarly for the cross-over group, the fracture rate was 2.20 during years 1–3 of DMAb (extension) and decreased to 1.03 at year 4 (rate ratio=0.48; P=0.004). Combining the long-term and cross-over groups yielded a fracture rate of 2.08 during the first 3 years of DMAb (FREEDOM or extension) that decreased to 1.27 at year 4 (rate ratio=0.62; P=0.002).

Conclusion: Three years of DMAb treatment significantly reduced the nonvertebral fracture rate compared with placebo. When DMAb was continued for an additional 4 years, the fracture rate remained low and was significantly lower than that in the first 3 years of treatment. Contributing factors that might explain this observation include sustained reduction in bone resorption, continued gains in hip BMD and bone mass, decrease in cortical porosity, and increases in cortical/trabecular strength observed with DMAb.

Table. Comparison of Nonvertebral Fracture Rates up to 7 Years of DMAb Treatment

	First 3 Years of DMAb Treatment	4th Year of DMAb Treatment	Years 4–7 of DMAb Treatment
Long-term Subjects (N=2343)	140 Fractures	33 Fractures	119 Fractures
Fracture Rate (95% CI)	1.98 (1.67–2.35)	1.43 (1.02–2.01)	1.45 (1.21–1.74)
Rate Ratio (95% CI)	Referent	0.73 (0.50–1.06)	0.74 (0.59–0.95)
P-value		*P*=0.096	*P*=0.016
Cross-over Subjects (N=1730)	114 Fractures	17 Fractures	
Fracture Rate (95% CI)	2.20 (1.82–2.66)	1.03 (0.64–1.66)	
Rate Ratio (95% CI)	Referent	0.48 (0.29–0.79)	
P-value		*P*=0.004	
Long-term and Cross-over Subjects Combined (N=4073)	254 Fractures	50 Fractures	
Fracture Rate (95% CI)	2.08 (1.83–2.36)	1.27 (0.96–1.67)	
Rate Ratio (95% CI)	Referent	0.62 (0.46–0.83)	
P-value		*P*=0.002	

N = number of subjects who completed FREEDOM (ie, completed their 3-year visit and did not discontinue IP), did not miss >1 dose of IP in FREEDOM, and who enrolled in the extension. In addition, cross-over subjects completed 3 years of the extension and did not miss >1 dose of DMAb during the first 3 years of the extension. Fracture rates and rate ratios were obtained using GEE Poisson models; fracture rates are per 100 subject-years. Rate ratios relative to the first 3 years of DMAb treatment were adjusted for age, total hip BMD T-score, weight, and history of nonvertebral fracture. In addition, the treatment group variable was included in the model for the combined analysis only.

Table

***Disclosures: Serge Ferrari**, Amgen, GSK, Lilly, MSD; Novartis, 9; Bioiberica, 2; Amgen, MSD, 6*
This study received funding from: Amgen Inc.

1018

Denosumab Significantly Increases Bone Mineral Density Compared With Ibandronate and Risedronate in Postmenopausal Women Previously Treated With an Oral Bisphosphonate Who Are at Higher Risk for Fracture. Jacques P. Brown*[1], Michael A. Bolognese[2], Pei-Ran Ho[3], Jesse Hall[3], Christian Roux[4], Henry G. Bone[5], Sydney Bonnick[6], Joop van den Bergh[7], Irene Ferreira[8], Prayashi Ghelani[9], Paula Dakin[3], Rachel B. Wagman[3], Christopher Recknor[10]. [1]CHU de Quebec Research Centre & Laval University, Canada, [2]Bethesda Health Research Center, USA, [3]Amgen Inc., USA, [4]Paris Descartes University, France, [5]Michigan Bone & Mineral Clinic, USA, [6]Clinical Research Center of North Texas, USA, [7]VieCuri Medical Centre & Maastricht University, Netherlands, [8]Amgen Inc., United Kingdom, [9]Ovatech Solutions, United Kingdom, [10]United Osteoporosis Centers, USA

Purpose: Low bone mineral density (BMD) is an important and modifiable risk factor for fracture in postmenopausal women with osteoporosis. Denosumab (DMAb), which has a unique mechanism of action, has demonstrated a stronger relationship between BMD increases and antifracture efficacy (new or worsening vertebral and nonvertebral fracture) than bisphosphonate (BP) therapies. There is a clinical need to treat subjects who remain at higher risk for fracture despite current BP therapy. In 2 open-label studies, DMAb significantly increased BMD and decreased bone turnover markers vs a BP, specifically ibandronate (IBN) or risedronate (RIS), in subjects previously treated with, though suboptimally adherent to, a BP. Here we evaluate the effects of DMAb vs a BP (IBN and RIS) to increase BMD in a subset of subjects at higher risk for fracture.

Methods: Both studies were multicenter, randomized, open-label, parallel-group designs in which postmenopausal women ≥55 years were randomized 1:1 to DMAb 60mg subcutaneously every 6 months or a BP 150mg orally every month for 12 months. In this combined post-hoc analysis, higher-risk subjects were identified by meeting ≥1 risk criteria (advanced age, low BMD, prior osteoporotic fracture, high baseline sCTX-1; Table) and the BMD percentage change from baseline in total hip, femoral neck, and lumbar spine at month 12 was calculated.

Results: Subjects from these 2 studies (852 DMAb; 851 BP) had a mean (SD) age of 67 (7.4) years, and mean (SD) T-score at the total hip, femoral neck, and lumbar spine of –1.7 (0.8), –2.0 (0.7), and –2.4 (1.0), respectively. For subjects at higher risk for fracture, denosumab significantly increased BMD at 12 months compared with a BP (IBN and RIS) at the total hip (2.2% vs 0.8%, respectively), femoral neck (1.8% vs 0.3%), and lumbar spine (3.8% vs 1.4%) (p<0.0001 for all; Figure). These results are consistent with the overall study population (treatment-by-risk subgroup interaction p>0.05). In general, AEs and SAEs were similar between DMAb and the comparator BP group.Conclusion: For subjects previously or suboptimally treated with a BP who remain at higher risk for fracture, transitioning to DMAb led to significantly greater increases in BMD at month 12 compared with cycling to another BP. These results in higher-risk subjects are consistent with those obtained in the overall population and support DMAb as an alternative therapeutic option for women at higher risk for fracture.

Table. Identification of Subjects at Higher Risk for Fracture

	BP N = 851	DMAb N = 852	All N = 1703
Higher-risk subjects, n (%)	469 (55.1)	475 (55.8)	944 (55.4)
1. Age ≥75 years	150 (17.6)	160 (18.8)	310 (18.2)
2. Baseline BMD T-score ≤–2.5 at total hip or femoral neck	250 (29.4)	245 (28.8)	495 (29.1)
3. Baseline BMD T-score ≤–1.0 at total hip or femoral neck and with prior osteoporotic fracture	256 (30.1)	265 (31.1)	521 (30.6)
4. Baseline sCTX-1 >0.9 ng/mL and BMD T-scores ≤ –2.0 at total hip or femoral neck	17 (2.0)	10 (1.2)	27 (1.6)
Subjects remaining at risk*	319 (37.5)	319 (37.4)	638 (37.5)
Subjects with unknown risk status due to missing data	63 (7.4)	58 (6.8)	121 (7.1)

N=number of subjects randomized. *Subjects who did not meet any of the higher-risk criteria. BP=ibandronate and risedronate; DMAb=denosumab.

Table

Figure. BMD Percentage Change From Baseline at Month 12

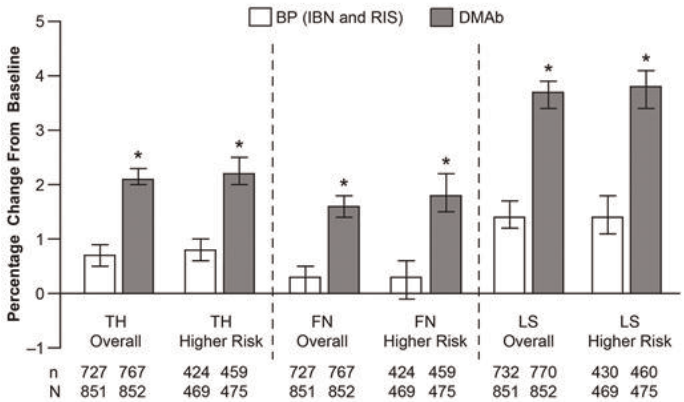

Data are least-squares means and 95% CI. Results are based on ANCOVA model adjusting for treatment, time of BMD assessment (study day), treatment by time interaction, baseline BMD value, DXA machine type, and baseline BMD value by DXA machine-type interaction. *p<0.0001 for DMAb vs BP (IBN and RIS). N=number of subjects randomized. n=number of subjects with available baseline and postbaseline BMD data. At risk subjects were subjects who did not meet any of the higher-risk criteria. Higher risk=age ≥75 years, baseline T-score ≤–2.5 at TH or FN, baseline T-score ≤–1.0 at TH or FN and with prior OP fracture, or baseline sCTX-1 >0.9 ng/mL and BMD T-score ≤–2.0 at TH or FN. BP=ibandronate and risedronate; DMAb=denosumab; TH=total hip; FN=femoral neck; LS=lumbar spine.

Figure

Disclosures: Jacques P. Brown*, Amgen, Eli Lilly, Merck, Novartis, Sanofi-Aventis, Warner Chilcott,; Abbott, Amgen, Bristol-Myers Squibb, Eli Lilly, Merck, Novartis, Pfizer, Roche, Sanofi-Aventis, Servier, Warner Chilcott, Takeda, 6; Amgen, Eli Lilly, Novartis, Merck, 9*
This study received funding from: Amgen Inc.

1019

The DATA Extension Study: 2 Years of Combined Denosumab and Teriparatide in Postmenopausal Women with Osteoporosis: A Randomized Controlled Trial. Benjamin Leder*[1], Alexander Uihlein[2], Joy Tsai[2], Robert Neer[2], Erica Siwila-Sackman[2], Yuli Zhu[2], Katelyn Foley[2], Hang Lee[2], Sherri-Ann Burnett-Bowie[2]. [1]Massachusetts General Hospital Harvard Medical School, USA, [2]Massachusetts General Hospital, USA

Background: Current osteoporosis medications increase bone mineral density (BMD) modestly and reduce, but do not eliminate, fracture risk. Attempts to improve treatment efficacy by combining anabolic agents with bisphosphonates (BPs) have been unsuccessful. In contrast, we recently reported that 12 months of combined denosumab (DMAB) and teriparatide (TPTD) increases BMD more than either drug alone. We now report the effects of this combination over 24-months of treatment.

Methods: 100 postmenopausal women at high fracture risk (age 51-91) who had not used oral BPs in the past 6 months or ever taken parenteral BPs or TPTD were randomized to receive TPTD (20 mcg SC daily), DMAB (60 mg SC every 6 months), or both for 24 months. BMD of the hip, spine and 1/3 distal radius were assessed by DXA. All subjects completing at least 1 post-baseline visit were included in our modified intention-to-treat analysis (n=94) and between-group differences were examined by a longitudinal linear mixed-effects model.

Results: At baseline, subjects were well matched for all clinical characteristics, including BMD at all measured sites. Of the 94 subjects completing at least 1 post-baseline visit, 83 completed all study visits. The 24-month changes in BMD are shown in the figure. PA spine BMD (mean ± SD) increased more in the combination group (12.7 ± 5.1%) than in either the TPTD (9.5 ± 5.9%, P<0.001) or DMAB (8.3 ± 3.4%, P<0.001) groups. Femoral neck BMD also increased more in the combination group (6.4 ± 3.8%) than in the TPTD (2.8 ± 3.6%, P=0.002) and DMAB (4.1 ± 3.8%, P=0.028) groups. Similarly, total hip BMD increased more in the combination group (6.1 ± 2.7%) than in either the TPTD (2.0 ± 3.0%, P<0.001) or DMAB groups (3.2 ± 2.5%, P<0.001). BMD at the 1/3 distal radius increased similarly in the DMAB (2.0 ± 3.7%) and combination groups (2.4 ± 3.1%) but decreased -1.7 ± 4.6% in the TPTD group (P<0.001 for both between-group TPTD comparisons). DMAB alone and TPTD alone produced similar changes at the spine (P=0.831) and femoral neck (p=0.194) but DMAB increased total hip BMD more than TPTD (p=0.005).

Summary and Conclusions: While the improvements in BMD observed after 1 year of therapy are extended in year 2 in all treated groups, the combination of TPTD and DMAB continues to demonstrate superior efficacy compared to TPTD or DMAB treatment alone. DMAB-TPTD co-administration may prove to be an important treatment option in patients at high risk of fracture.

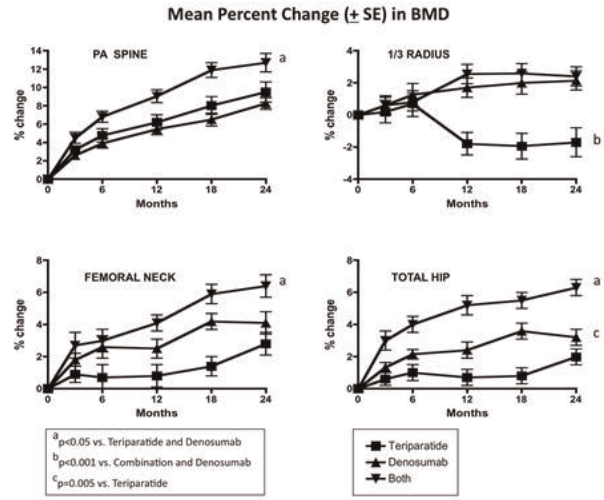

Figure

Disclosures: Benjamin Leder*, Amgen, 6; Lilly, 6; Merck, 2*
This study received funding from: Amgen, Lilly

1020

A longitudinal study of Skeletal Histomorphometry in subjects On Teriparatide (TPTD) or Zoledronic acid (ZOL), the SHOTZ study. David Dempster*[1], Hua Zhou[2], Robert Recker[3], Jacques P. Brown[4], Michael Bolognese[5], Christopher Recknor[6], David Kendler[7], E. Michael Lewiecki[8], David Hanley[9], Sudhaker Rao[10], Paul Miller[11], Grattan Woodson[12], Robert Lindsay[2], Neil Binkley[13], Jahangir Alam[14], Valerie A Ruff[14], Boris Janos[15], Kathleen A Taylor[14]. [1]Columbia University, USA, [2]Helen Hayes Hospital, USA, [3]Creighton University, USA, [4]CHU de Québec Research Centre, Canada, [5]Bethesda Health Research, USA, [6]United Osteoporosis Center, USA, [7]Associate Professor University of British Columbia, Canada, [8]University of New Mexico School of Medicine, USA, [9]University of Calgary, Canada, [10]Henry Ford Hospital, USA, [11]Colorado Center for Bone Research, USA, [12], USA, [13]University of Wisconsin, Madison, USA, [14]Lilly USA, LLC, USA, [15]Eli Lilly Canada Inc., Canada

Purpose: Few studies have evaluated progressive effects of osteoporosis therapy using histomorphometric indices; no previous study has directly compared effects of an anabolic vs an antiresorptive agent on bone remodeling in the same individuals over time. Previously we reported contrasting effects of TPTD, an established anabolic agent, and ZOL, a prototypical antiresorptive agent, on bone remodeling based on histomorphometric analysis of bone biopsies after 6 months' therapy. Using a paired-biopsy design, we now extend these observations to month 24.

Methods: SHOTZ is a 2-year trial to assess the biological effects of TPTD and ZOL based on histomorphometric indices and material properties in postmenopausal women with osteoporosis. Subjects from the 12-month randomized study were eligible to enroll in a 12-month extension and assigned open label to their original treatment regimen: TPTD 20 µg/d (sc injection) or ZOL 5 mg/y (IV infusion). Transiliac crest bone biopsies were obtained after tetracycline labeling at month 6 and 24. Here we report dynamic histomorphometric results.

Results: Nineteen subjects had biopsies at both month 6 and 24 (TPTD, n=10; ZOL, n=9). The proportion of samples with tetracycline labels was higher in the TPTD group vs ZOL in all 3 bone envelopes at month 24 and the cancellous envelope at month 6; a similar trend was seen on the endocortex (Table). Mineralizing surface/bone surface (MS/BS), a robust indicator of bone formation especially at low remodeling rates, was significantly higher in the TPTD group in all 3 envelopes at month 6 and 24, except the periosteum at month 6 (Figure). In the cancellous envelope, bone formation rate/BS (BFR/BS) and activation frequency (Ac.f) remained significantly higher at month 24 in the TPTD group. Within-group analyses showed no significant changes in the proportion of samples with labels from month 6 to 24 in either treatment group. No appreciable shifts in dynamic indices were seen in the ZOL group over time. In the TPTD group, MS/BS, BFR/BS and Ac.f remained constant in the cancellous envelope at month 6 and 24 but were reduced in the endocortex at month 24.

Conclusions: This is the first analysis to compare progressive effects of TPTD vs ZOL on bone histomorphometry using paired biopsies. These data reveal histomorphometric characteristics of anabolic vs antiresorptive agents over time and show that the marked difference in the mechanism of action of TPTD and ZOL was maintained for 2 years.

	Month 6			Month 24		
	TPTD n=10	ZOL n=9	P value	TPTD n=10	ZOL n=9	P value
CANCELLOUS						
Any Label, n (%)	10 (100) n=10	3 (33) n=9	0.003	10 (100) n=10	5 (56) n=9	0.033
MAR, μm/d	0.53 (0.45, 0.62) n=10	0.37 (0.30, 0.51) n=3	0.151	0.43 (0.37, 0.52) n=10	0.30 (0.30, 0.34) n=5	0.084
BFR/BS, $mm^3/mm^2/y$	0.0067 (0.0040, 0.0193) n=10	0.0006 (0.0002, 0.0014) n=3	0.022	0.0057 (0.0022, 0.0061) n=10	0.0005 (0.0002, 0.0011) n=5	0.032
Ac.f, per year	0.22 (0.16, 0.56) n=10	0.02 (0.01, 0.05) n=3	0.022	0.18 (0.08, 0.20) n=10	0.02 (0.01, 0.04) n=5	0.032
ENDOCORTICAL						
Any Label, n (%)	7 (100) n=7	5 (56) n=9	0.088	9 (100) n=9	3 (38) n=8	0.009
MAR, μm/d	0.44 (0.42, 0.57) n=7	0.30 (0.30, 0.40) n=5	0.033	0.42 (0.37, 0.45) n=9	0.44 (0.30, 0.52) n=3	0.926
BFR/BS, $mm^3/mm^2/y$	0.0334 (0.0159, 0.0411) n=7	0.0009 (0.0008, 0.0054) n=5	0.009	0.0090 (0.0049, 0.0100) n=9	0.0027 (0.0004, 0.0051) n=3	0.096
Ac.f, per year	0.92 (0.46, 1.09) n=7	0.03 (0.02, 0.13) n=5	0.009	0.24 (0.14, 0.29) n=9	0.07 (0.01, 0.13) n=3	0.064
PERIOSTEAL						
Any Label, n (%)	5 (71) n=7	2 (22) n=9	0.126	8 (89) n=9	2 (25) n=8	0.015
MAR, μm/d	0.30 (0.30, 0.30) n=5	0.32 (0.30, 0.34) n=2	0.809	0.30 (0.30, 0.32) n=8	0.30 (0.30, 0.30) n=2	0.872
BFR/BS, $mm^3/mm^2/y$	0.0014 (0.0008, 0.0021) n=5	0.0022 (0.0006, 0.0038) n=2	1.000	0.0021 (0.0017, 0.0028) n=8	0.0040 (0.0013, 0.0067) n=2	0.896

Ac.f was not measured in the periosteum.
Mineral apposition rate (MAR) was measured on double labels or assigned a value of 0.3 μm/d if only single labels were present; if no label was present MAR was treated as missing.
All indices are shown as medians (interquartile range).
P values are for between-group differences for TPTD vs ZOL, using Wilcoxon Rank sum tests.

Table

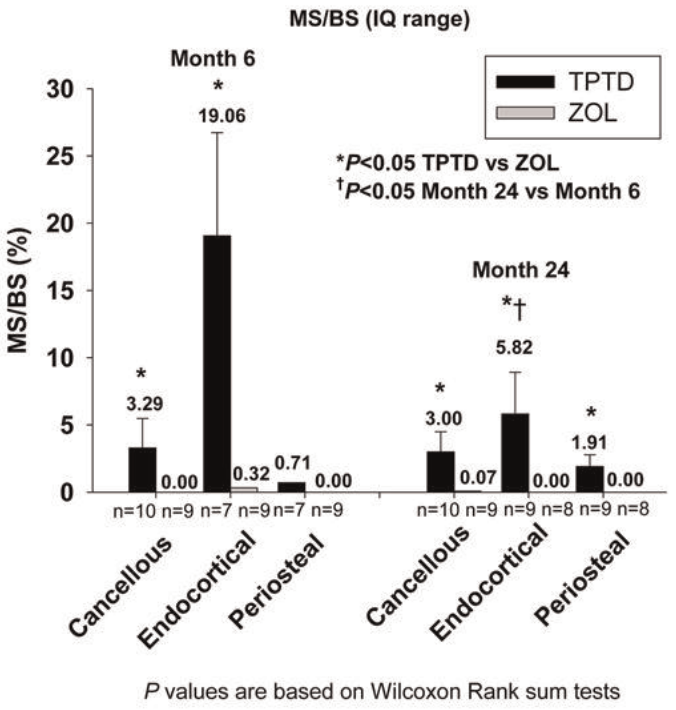

Figure

***Disclosures: David Dempster**, Eli Lilly, Amgen, Novartis, P&G, Merck,; Eli Lilly, Amgen, Merck, 2; Eli Lilly, 6*
This study received funding from: Eli Lilly and Company

1021

Teriparatide Is Associated with Improved Microarchitecture and Estimated Bone Strength in Premenopausal Women with Idiopathic Osteoporosis: An HR-pQCT Study. Kyle Nishiyama*[1], Ji Wang[1], Polly Young[1], Robert Recker[2], Joan Lappe[3], Serge Cremers[1], X Guo[1], Elizabeth Shane[4], Adi Cohen[5]. [1]Columbia University, USA, [2]Creighton University, USA, [3]Creighton University Osteoporosis Research Center, USA, [4]Columbia University College of Physicians & Surgeons, USA, [5]Columbia University Medical Center, USA

In premenopausal women with idiopathic osteoporosis (IOP), we have previously reported that teriparatide (TPTD; 20 mcg SC daily for 18-24 months) is associated with improved bone density and quality at the central skeleton. In this regard, we documented increases in areal BMD by DXA at the lumbar spine (LS; mean ± SD: 10.8 ± 8.3%) and femoral neck (FN; 7.6 ± 3.4%) as well as in trabecular bone volume fraction measured on paired transiliac biopsies (48 ± 65%). In this analysis, we examined whether TPTD was also associated with improvements in volumetric BMD, bone microarchitecture and estimated bone strength of the peripheral skeleton as assessed by high-resolution peripheral quantitative computed tomography (HR-pQCT, Scanco Medical AG). Premenopausal women (N=20, age 41 ± 5 yrs) with IOP (low-trauma fractures and/or T-scores ≤ 2.5) were scanned with HR-pQCT at the distal radius and tibia at baseline and after 18-months of TPTD. Cortical (Ct) and trabecular (Tb) volumetric BMD and microarchitecture were measured by both standard and individual trabecula segmentation (ITS) techniques, and bone strength was estimated by micro finite element analysis (μFEA). Tb vBMD increased significantly by 2.6% at the radius and 2.5% at the tibia (Table). While Tb number and thickness did not change overall, ITS analysis revealed significant increases in Tb plate bone volume fraction, plate number and thickness at both radius and tibia. While Ct thickness and density did not change, Ct porosity increased at the radius by 17.1%, but not at the tibia. Despite this increase in porosity, whole bone stiffness and failure load estimated by μFEA increased at both radius and tibia and Tb stiffness and failure load increased at the tibia. At the radius, increases in bone volume fraction were associated with increases in LS aBMD (r=0.49, p=0.03) and total hip aBMD (r=0.51, p=0.03). At the tibia, increases in bone volume fraction were associated only with increases in total hip aBMD (r=0.46, p=0.02). In summary, in premenopausal women with IOP, 18-months of TPTD was associated with increases in Tb vBMD, mainly due to improvements in Tb plate microarchitecture. Although cortical porosity increased, cortical density and thickness did not change and estimated bone strength also improved at both radius and tibia. We conclude that TPTD has beneficial effects on both the central and peripheral skeleton in premenopausal women with IOP.

Table: Percent changes [Median (Interquartile Range)] between baseline and 18-months for trabecular (Tb) and cortical (Ct) HR-pQCT measurements.
* p<0.05, ** p<0.01

	Radius	Tibia
vBMD (mgHA/cm^3)	0.6 (0.0, 2.9)*	1.5 (0.1, 3.3)**
Tb vBMD (mgHA/cm^3)	2.6 (1.8, 6.2)**	2.5 (1.1, 3.6)**
Ct vBMD (mgHA/cm^3)	0.4 (-1.0, 0.8)	0.2 (-0.6, 1.3)
Tb BV/TV (%)	3.9 (2.6, 4.4)**	2.1 (1.1, 3.1)**
Tb Number (1/mm)	3.4 (-1.8, 5.8)	1.1 (0.0, 2.2)
Tb Thickness (mm)	0.0 (-1.9, 5.9)	1.8 (-1.5, 3.6)
Tb Separation (mm)	-3.2 (-6.0, 2.0)	-1.3 (-2.1, 0.1)*
Tb Plate BV/TV (%)	9.1 (2.1, 17.1)**	7.6 (1.0, 9.7)**
Tb Rod BV/TV (%)	3.4 (-0.7, 4.7)*	0.3 (-2.0, 1.1)
Tb Plate Number (1/mm)	2.3 (0.6, 4.7)**	1.4 (0.5, 2.2)**
Tb Rod Number (1/mm)	1.1 (-0.8, 1.9)	-0.1 (-1.1, 0.3)
Tb Plate Thickness (mm)	1.0 (-0.2, 1.5)*	0.2 (0.0, 1.0)**
Tb Rod Thickness (mm)	0.4 (-1.3, 1.6)	0.2 (-0.3, 0.7)
Ct Porosity (%)	17.1 (8.3, 34.1)**	-1.5 (-5.1, 7.1)
Ct Thickness (mm)	0.0 (-0.5, 1.0)	1.0 (-0.6, 1.9)
Stiffness (N/mm)	1.3 (0.6, 1.9)**	2.0 (0.8, 2.4)**
Failure load (N)	1.1 (0.2, 2.8)*	1.6 (1.0, 2.7)**
Tb Stiffness (N/mm)	0.9 (-0.2, 2.8)	1.5 (0.6, 2.9)**
Tb Failure load (N)	0.6 (-1.3, 2.8)	1.9 (0.8, 3.3)**

Table

***Disclosures: Kyle Nishiyama**, None.*
This study received funding from: Eli Lilly

1022

Effect of Romosozumab on Lumbar Spine and Hip Volumetric Bone Mineral Density (vBMD) as Assessed by Quantitative Computed Tomography (QCT). HK Genant*[1], S Boonen[2], MA Bolognese[3], C Mautalen[4], JP Brown[5], C Recknor[6], S Goemaere[7], K Engelke[8], Y-C Yang[9], M Austin[9], A Grauer[9], C Libanati[9]. [1]USCF & Synarc Inc., USA, [2]Leuven University Division of Geriatric Medicine, Belgium, [3]The Bethesda Health Research Center, USA, [4]Centro de Osteopatias Medicas, Argentina, [5]CHU de Québec Research Centre & Laval University, Canada, [6]United Osteoporosis Centers, USA, [7]Ghent University Hospital, Belgium, [8]Synarc Germany, Germany, [9]Amgen Inc., USA

Purpose: Sclerostin is an osteocyte-derived inhibitor of osteoblast activity. Romosozumab, a monoclonal antibody to sclerostin, stimulated bone formation, decreased bone resorption, and increased BMD in postmenopausal women with low bone mass. Here we describe the 12-month effect of romosozumab on lumbar spine (LS) and total hip (TH) BMD, and bone mineral content (BMC) as measured by QCT.

Methods: This international, randomized, placebo (Pbo)-controlled, phase 2 study enrolled postmenopausal women of 55–85 years with LS, TH, or femoral neck T-score ≤–2.0 and ≥–3.5. Measurements with QCT were performed at the "total" LS (mean of L1 & L2 entire vertebral bodies) and TH. Percentage change from baseline in integral and cortical vBMD and BMC, and trabecular vBMD was evaluated for Pbo, subcutaneous teriparatide (TPTD; 20 µg QD), and romosozumab (210 mg QM) at 12 months. Subjects with baseline and ≥1 post-baseline QCT measurements were included in the analyses.

Results: Treatment with romosozumab resulted in significant increases in integral vBMD and BMC at the "total" LS and TH from baseline, and compared with Pbo and TPTD (Figure). TPTD and Pbo were not different at the TH. Differences between romosozumab and TPTD were also observed in the trabecular and cortical bone compartments. Trabecular vBMD increased from baseline with romosozumab and TPTD at the LS and TH (both $p<0.05$). These gains were similar with romosozumab and TPTD at the LS (18.3% vs 20.1%, respectively), but were significantly larger with romosozumab at the TH (10.8% vs 4.2%, $p<0.05$). At the LS, treatment with romosozumab also resulted in significant increases from baseline in cortical vBMD compared with TPTD (13.7% vs 5.7%, $p<0.0001$) and cortical BMC (23.3% vs 10.9%, $p<0.0001$). At the TH, increases with romosozumab treatment from baseline were observed in cortical vBMD (1.1%) and cortical BMC (3.4%), but not with TPTD (–0.9% [cortical vBMD] and 0.0% [cortical BMC]); increases in cortical BMC with romosozumab were significant vs TPTD ($p<0.05$).

Conclusion: Romosozumab significantly increased vBMD and BMC at the "total" LS and TH compared with Pbo and TPTD as assessed by QCT in postmenopausal women with low bone mass. The gains, observed in the trabecular and cortical compartments, support the continued clinical investigation of romosozumab as a potential therapeutic agent for the treatment of women with postmenopausal osteoporosis with established BMD deficits and at increased fracture risk.

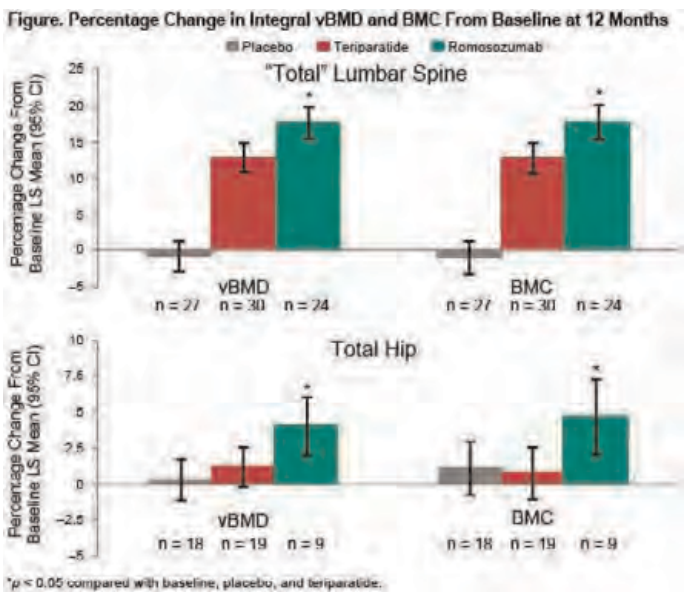

Figure

***Disclosures: HK Genant**, Amgen, Merck, Lilly, Pfizer, Janssen, Servier, Novartis, Radius,; Synarc, 2; Synarc, 7; Novartis, Merck, 9; Synarc, 8*
This study received funding from: Amgen Inc. & UCB Pharma

1023

Effects of Blosozumab on Estimated Spine and Hip Strength in Postmenopausal Women with Low Bone Mineral Density: Finite Element Analysis of a Phase-II Dosing Study. Tony Keaveny*[1], Stephen Myers[2], Alan Chiang[2], Jahangir Alam[2], Deborah Robins[2], John Krege[2], Adrien Sipos[2], Bruce Mitlak[2], Charles Benson[2]. [1]University of California, Berkeley, USA, [2]Eli Lilly & Company, USA

Blosozumab is a humanized monoclonal antibody targeted to inhibit sclerostin and promote new bone. To determine the effects of subcutaneous blosozumab treatment on non-invasive estimates of spine and hip strength, finite element analysis was performed longitudinally on quantitative CT images in postmenopausal women with low areal BMD (lumbar spine T-score -3.5 to -2.0). These women, mean age 62 years, were a subgroup of patients enrolled in a double-blind, placebo-controlled, randomized, multicenter, 1-year Phase-II dosing study of four treatment groups (all with calcium and vitamin D): placebo, blosozumab 180 mg every 4 weeks, blosozumab 180 mg every 2 weeks, or blosozumab 270 mg every 2 weeks. The study was conducted in accordance with the Declaration of Helsinki and was approved by an ethics committee at each center. To estimate spine and hip strength, finite element analyses were performed for all patients (n=42) who had spine and/or hip CTs at baseline and at either 24 or 52 weeks, using the VirtuOst software (O.N. Diagnostics, Berkeley, CA). A mixed-effect model was used for the statistical analyses. CTs that were technically adequate for interpretation were included in the statistical analyses. After confirming uniformity of the groups at baseline, we found for the placebo group that neither spine nor hip strength changed significantly from baseline. By contrast, in the treated groups, there were statistically significant increases in both spine and hip strength, at both 24 and 52 weeks ($P<0.05$ at least; Table). These effects were substantial in the highest dose group: at the spine, blosozumab increased strength compared to baseline by up to 29.6 % at Week 24 and 37.0% at Week 52, and at the hip, blosozumab increased strength by up to 9.6% at Week 24, and 12.6% at Week 52. At both the spine and hip, these strength changes were associated with statistically significant increases in volumetric BMD of both the trabecular and cortical compartments. Other than mild injection site reactions that were more frequent with blosozumab than placebo, adverse events were similar across all groups. In conclusion, in this Phase-II study, blosozumab increased finite element-estimated spine and hip strength in postmenopausal women with low BMD, displaying a statistically significant positive dose response at both sites.

Change in Finite Element-Estimated Spine and Hip Strength
Percent Change from Baseline; LS Mean, (95% C.I.)

	Placebo	Blosozumab 180 mg every 4 weeks	Blosozumab 180 mg every 2 weeks	Blosozumab 270 mg every 2 weeks
Spine				
24 weeks	-0.4 (-7.1, 6.3) n = 10	12.0†* (5.5, 18.4) n = 11	27.5†* (21.4, 33.7) n = 12	29.6†* (21.3, 37.9) n = 7
52 weeks	0.7 (-7.0, 8.5) n=7	13.7†* (6.3, 21.2) n=8	32.0†* (25.0, 38.9) n=10	37.0† (26.8, 47.2) n=3
Hip				
24 weeks	-0.4 (-2.3, 1.4) n = 11	0.7 (-1.1, 2.5) n = 12	3.1†* (1.3, 4.9) n = 12	9.6†* (7.1, 12.1) n = 6
52 weeks	0.3 (-1.9, 2.4) n=8	1.4* (-0.6, 3.5) n=9	5.4†* (3.4, 7.4) n=10	12.6†* (9.3,15.9) n = 3

$P < 0.05$ at least, as compared with placebo (†) or baseline (*); n = number of patients

Change in Finite Element-Estimated Spine and Hip Strength

***Disclosures: Tony Keaveny**, O.N. Diagnostics, 2; Amgen, 2; Amgen, 6; O.N. Diagnostics, 7; O.N. Diagnostics, 8; Novartis, 6; Merck, 6; Eli Lilly and Company, 6; Wright Medical Technology, 2; J&J, 6; Wright Medical Technology, 6; Pfizer, 6; Merck, 2; GSK, 6; UC Berkeley, 8*
This study received funding from: Eli Lilly and Company

1024

Systemic Administration of NELL-1, a Wnt/β-Catenin Regulator, Induces Bone Formation in Osteoporotic Mice via Integrinβ1. Aaron James*[1], Jia Shen[1], Omar Velasco[2], Greg Asatrian[2], Choon G Chung[2], Kevork Khadarian[3], Yulong Zhang[4], Le Chang[2], Raghav Goyal[2], Jung Kim[3], Xinli Zhang[1], John Adams[1], Kang Ting[1], Chia Soo[5]. [1]University of California, Los Angeles, USA, [2]Division of Associated Clinical Specialties & Section of Orthodontics, School of Dentistry, USA, [3]Department of Pathology & Laboratory Medicine, David Geffen School of Medicine, USA, [4]Department of Bioengineering, UCLA, USA, [5]Division of Plastic & Reconstructive Surgery, Department of Surgery, University of California, Los Angeles, USA

NELL-1 is a secreted protein that binds Integrinβ1 with known roles in craniofacial development. Nell-1 has recently been implicated in the pathoetiology of osteoporosis, as our laboratory recently described an osteoporotic phenotype of

Nell-1 haploinsufficient mice. While normal during development, senile *Nell-1*$^{+/-}$ mice manifest significant osteoporotic bone loss, with a reduction in the ratio of osteoblast-to-osteoclast cell number and activity, and reduced Wnt/β-catenin signaling.

This study expands on the association between NELL-1 and bone maintenance. First, the expression of Nell-1 was assessed during skeletal aging by qRT-PCR and immunohistochemistry. Next, recombinant human (rh)NELL-1 was systemically delivered by tail vein injection in a mouse model to treat ovariectomy-induced osteoporosis (1.25 ug/mg rhNELL-1 q48 hours, N=6-9 mice per group). Analyses included radiographic (DXA, CT/F18-PET, and postmortem microCT), and histological methods. Finally, MSC and pre-osteoclast cell lines were treated with rhNELL-1 in the setting of Integrinβ1 knockdown, in order to determine the necessity of Integrinβ1 for NELL-1 function.

Results showed that Nell-1 expression levels were inversely associated with skeletal aging – as Nell-1 gene and protein was high in early postnatal development, and decreased with aging (Fig. 1). Next, intravenous injection of rhNELL-1 was performed after induction of osteoporosis. We found that NELL-1 remained detectable in the blood for 24 hours post injection. After osteoporotic induction, intravenous rhNELL-1 was delivered every 48 hours for one month. DXA analysis of the lumbar spine and femur showed that rhNELL-1 injection resulted in a 10% increase in BMD in comparison to control, both osteoporotic and non-osteoporotic animals (Fig. 2). Next, we observed that rhNELL-1 activated Wnt/β-catenin associated gene expression in both osteoblast (M2-10B4) and osteoclast (RAW264.7) cell lines (Fig. 3). Moreover, rhNELL-1 activation of Wnt signaling required expression of the cell surface protein Integrinβ1, as Integrinβ1 siRNA abrogated rhNELL-1 induced Wnt signaling.

In summary, NELL-1 is a pro-osteogenic, anti-resorptive cytokine whose expression is lost with skeletal aging. Our studies suggest that systemic rhNELL-1 treatment is both safe and effective for osteoporotic condition. Moreover, NELL-1 treatment activates Wnt/β-catenin signaling in both osteoblast and osteoclast cell types in an Integrinβ1 dependent manner.

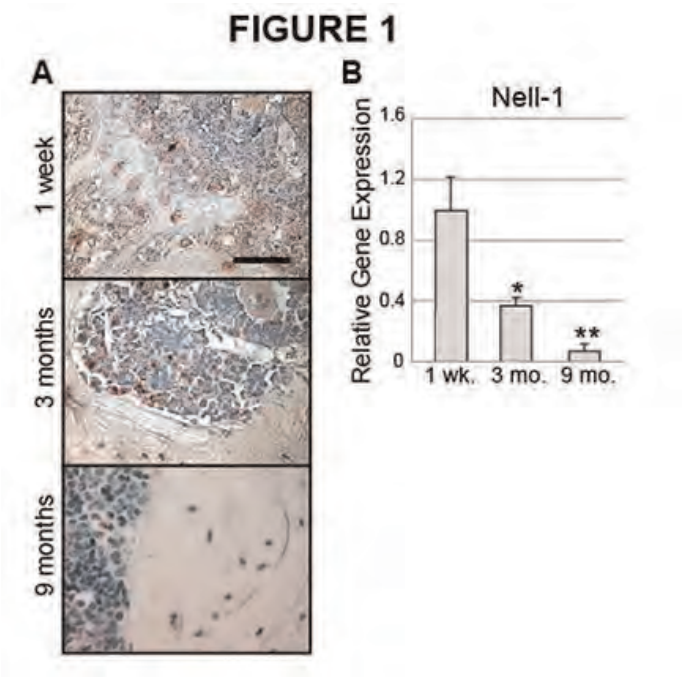

Figure 1

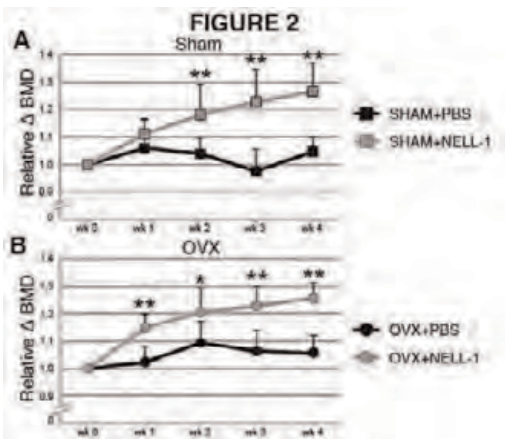

Figure 2

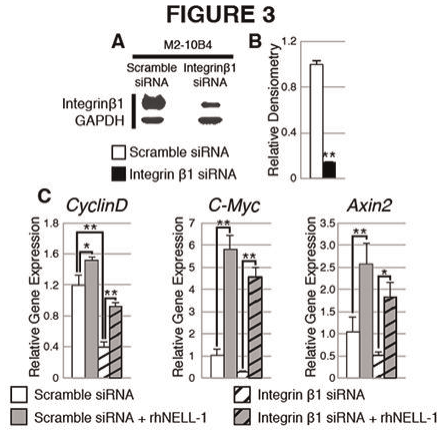

Figure 3

***Disclosures: Aaron James**, None.*

1025

Against All Odds: Results from the ZEST Trial in Long Term Care Residents. Susan Greenspan*, MaryAnne Ferchak, Subashan Perera, David Nace, Neil Resnick. University of Pittsburgh, USA

Background: Although nearly 85% of long term care (LTC) residents have osteoporosis, the pivotal osteoporosis trials have systematically excluded frail, functionally-impaired women. As a result, the vast majority are not treated even though they are at the greatest risk for fracture. The goal of the ZEST trial (Zoledronic acid in frail Elders to STrengthen bone) was to examine the safety and efficacy of a single dose of zoledronic acid in LTC residents.

Methods: This 2-year, double-blind, randomized controlled trial included women residents of a nursing home or assisted living facility, who were not on an antiresorptive agent despite having osteoporosis (BMD or fracture), a vitamin D level >20 ng/dL, and life expectancy of ⩾2 years. We included residents with cognitive impairment, immobility, and multiple diseases and medications. All subjects (or their proxies) provided informed consent, and all received a single dose of zoledronic acid 5 mg or placebo IV, in addition to daily calcium (1200 mg) and vitamin D (800 IU). The primary outcomes were 12-month BMD changes of the hip and spine. Secondary outcomes were 24 month BMD changes, safety and bone turnover markers. We measured BMD in a mobile unit and collected serious adverse events (AE) with an electronic surveillance system. We used linear mixed models for BMD and bone marker analyses.

Results: 181 women were randomized. Mean age was 85.4 and there were no baseline differences between groups in age, BMI, calcium/vitamin D intake, BMD, activities of daily living, or cognitive or mental health status. The active treatment group included more women with diabetes, falls history, anti-seizure medications, and slow gait speed. 92% of subjects completed 12 months; 67% completed 24 months. BMD percent changes at the total hip, femoral neck and spine were significantly greater in the active treatment group compared with the placebo group at 12 and 24 months (all p< 0.01, table), with 12 month absolute differences of 3.2 percentage points at the total hip and 1.8 at the spine. There were no significant differences in serious AEs or deaths.

Conclusions: This trial of single dose zoledronic acid for osteoporosis in cognitively impaired, frail osteoporotic women is the first to demonstrate that it is safe and effective in preserving/improving skeletal integrity over 2 years. Future studies are needed to determine if BMD improvement translates into fracture reduction.

Table: Percent change ± standard error in bone mineral density at the spine, total hip and femoral neck

Skeletal site	Month	Active (N=89)	Placebo (N=92)	P-value (between group difference)
Spine	12	2.9±0.4 **	1.0±0.4 *	<0.01
	24	4.2±0.8 **	0.6±0.5	<0.01
Total hip	12	2.7±0.5 **	-0.6±0.4	<0.01
	24	2.4±0.6 **	-1.6±0.7 *	<0.01
Femoral neck	12	2.1±0.7 **	-1.4±0.6 *	<0.01
	24	0.0±0.7	-3.3±0.8 **	<0.01

*p<0.05, ** p< 0.01 within group change from baseline

Table

***Disclosures: Susan Greenspan**, None.*

1026

The Platelet-inhibitor Clopidogrel Increases Risk of Bone Fractures in Stroke Patients. Niklas Jorgensen*[1], Peter Vestergaard[2], Peter Schwarz[3], Helle K. Iversen[4]. [1]Copenhagen University Hospital Glostrup, Denmark, [2]Aalborg University Hospital, Denmark, [3]Glostrup Hospital, Denmark, [4]The Stroke Unit, Department of Neurology, Glostrup Hospital, Denmark

Stroke is one of the leading causes of mortality and morbidity worldwide. In the surviving stroke patient the increased functional dependence and cognitive decline often leads to immobilization. Nearly three-quarters of all strokes occur in people over the age of 65, adding to the risk of osteoporosis in these patients. Balance is often impaired after a stroke increasing the risk of falls and in combination with immobilization and advanced age stroke patients have multiple risk factors for fractures. Finally, most stroke patients receive treatment with the platelet (ADP, $P2Y_{12}$) inhibitor Clopidogrel (Plavix®) which is shown to be associated with increased risk of fractures. The aim of the current study was to investigate the risk of fractures in stroke patients, and to determine whether clopidogrel treatment further increases the risk of fractures.

We investigated the association between clopidogrel use and fracture incidence in a nation-wide cohort study performed within the Danish population of approximately 5.3 million individuals. All subjects who were prescribed clopidogrel during the years 1996 to 2008 were included as exposed subjects (n=77,503), and for each exposed subject three subjects of the same age (same birth year) and gender were randomly selected from the background population as controls (n=232,510). Study endpoint was occurrence of stroke or transient ischaemic attack (TIA). Information on fracture occurrence and a number of confounders was obtained through different registers.

In the clopidogrel treated group 1.2% had a prior haemorrhagic stroke, 9.3% an ischemic stroke and 7.2% a TIA. In the non-clopidogrel treated group the percentages were 0.9% haemorrhagic stroke, 2.6% ischemic stroke and 2.3% TIA. Stroke patients had a significantly increased risk of fractures, both in the group of haemorrhagic stroke (HR: 1.34, $p<0.001$) and ischemic stroke (HR: 1.54, $p<0.001$). Interestingly, also patients with TCI patients had increased risk of fractures (HR: 1.28, $p<0.001$). Clopidogrel users also had an increased risk of fractures, though the contribution of the clopidogrel-treatment (HR: 1.05, p=0.001) was much less than the contribution of the stroke itself.In conclusion, stroke patients have increased risk of fractures due to a number of factors. One of these, treatment with the platelet-inhibitor clopidogrel, is associated with an increase in risk of fractures, though the contribution is minor compared to the stroke itself.

***Disclosures: Niklas Jorgensen**, None.*

1027

Effects of TZD Use and Discontinuation on Fracture Rates in ACCORD. Ann Schwartz*[1], Haiying Chen[2], Walter Ambrosius[3], Ajay Sood[4], Robert Josse[5], Denise Bonds[6], Adrian Schnall[7], Eric Vittinghoff[1], Douglas Bauer[1], Mary Ann Banerji[8], Robert Cohen[9], Bruce Hamilton[10], Tamara Isakova[11], Deborah Sellmeyer[12], Debra Simmons[13], Monica Stiles[14], Jeff Williamson[2], Karen Margolis[15]. [1]University of California, San Francisco, USA, [2]Wake Forest University Health Sciences, USA, [3]Wake Forest University School of Medicine, USA, [4]Case Western Reserve University, USA, [5]St. Michael's Hospital, University of Toronto, Canada, [6]National Institute of Health, USA, [7]University Suburban Health Center, USA, [8]SUNY Downstate Medical Center & Kings County Hospital, USA, [9]University of Cincinnati College of Medicine, USA, [10]VA Medical Center & University of Maryland School of Medicine, USA, [11]University of Miami, USA, [12]Johns Hopkins School of Medicine, USA, [13]University of Arkansas for Medical Sciences, USA, [14]University of Minnesota, USA, [15]HealthPartners Research Foundation, USA

Trials indicate that thiazolidinediones (TZD) increase fracture risk in women but not men. The fracture effect of discontinuing TZDs is not known. To assess whether TZD use increases fracture risk in men and women and to determine if TZD discontinuation affects fracture risk, we used data from the Action to Control Cardiovascular Risk in Diabetes (ACCORD) trial designed to test the effect of intensive versus standard glycemia therapy on cardiovascular disease. At participating clinics (54 of 77), non-spine fractures were reported at annual visits and centrally adjudicated. Rosiglitazone was included in the original treatment algorithm for the intensive and standard glycemia therapy groups, and pioglitazone was added in Fall 2007. The intensive glycemia intervention was stopped in February 2008, and the trial ended in June 2009. Participants attended clinic visits every 2-4 months before and after the intensive glycemia intervention was stopped. At each visit, staff recorded the participant's use of diabetes medications, including TZDs, at visit entry and prescribed medications at visit exit. Mean age of the 6,865 included participants was 62.4 (SD 6.6) years; mean BMI was 32.6 (SD 5.3) kg/m^2; and mean duration of diabetes was 11.1 (SD 7.8) years. During mean follow-up of 4.8 (SD 1.5) years, 549 participants experienced at least one confirmed fracture. In proportional hazards models adjusted for age and glycemia randomization assignment, non-spine fracture rate was increased with TZD use and decreased with discontinuation in women, but not men (Table). To our knowledge, this is the first report to assess the effects of TZD discontinuation on fracture. These results confirm previous reports from clinical trials that TZD use increases fracture risk in women, but not men. Attenuation of increased fracture risk in women occurs after TZD use is discontinued.

Table. Adjusted hazard ratios (HR) for non-spine fracture by duration of TZD use and discontinuation

	Women		Men	
	HR	(95% CI)	HR	(95% CI)
Duration of TZD use				
TZD use ≤1yr vs None	1.70*	(1.11, 2.61)	1.44	(0.94, 2.22)
TZD use >1yr vs None	2.18*	(1.56, 3.06)	1.15	(0.82, 1.62)
Time since last TZD use				
Discontinued TZD ≤ 1yr vs Current user	0.70	(0.48, 1.04)	1.22	(0.83, 1.80)
Discontinued TZD >1yr vs Current user	0.58*	(0.39, 0.86)	1.04	(0.69, 1.55)
*p<0.05				

Table

***Disclosures: Ann Schwartz**, None.*

1028

Estrogen Reduces Bone *sost* mRNA and Circulating Sclerostin Levels in Postmenopausal Women. Matthew Roforth*[1], Koji Fujita[1], Susan Demaray[1], Ulrike McGregor[2], Salman Kirmani[1], Louise McCready[1], James Peterson[1], Matthew Drake[3], David Monroe[4], Sundeep Khosla[5]. [1]Mayo Clinic, USA, [2]King's College, London UK, United Kingdom, [3]College of Medicine, Mayo Clinic, USA, [4]Mayo Foundation, USA, [5]Mayo Clinic College of Medicine, USA

Studies in postmenopausal women have shown that estrogen (E) reduces circulating sclerostin levels (JBMR 26:27, 2011). However, recent studies in mice (JBMR 28:618, 2013) found no significant effects of ovariectomy on serum sclerostin levels and lack of a relationship between circulating sclerostin and *sost* mRNA levels in various bones. To resolve this issue in humans, we measured serum sclerostin and bone *sost* mRNA levels in needle biopsies (1-2 mm diameter) from 20 postmenopausal women (71 ± 5 yr) treated with transdermal estradiol (0.05mg/d) for 3 weeks and 20 untreated control women (73 ± 7 yr). Serum sclerostin levels were 29% lower ($P = 0.008$) in the E-treated compared to the control women. Concomitantly, bone *sost* mRNA levels were reduced by 48% ($P = 0.03$) in the E-treated women. Interestingly, bone *sost* mRNA levels were significantly correlated with serum sclerostin levels in the E-treated ($r = 0.57$, $P = 0.008$), but not in the control women ($r = -0.25$, $P = 0.280$). In addition, mRNA levels of the sclerostin domain-containing protein 1 (*sostdc1*), a sclerostin-related protein that is another Wnt/BMP inhibitor, were also reduced in the bones of the E-treated compared to the control women (by 54%, $P = 0.01$).

We further extended these studies using customized, in-house QPCR analyses to examine the mRNA expression of genes in other pathways related to bone metabolism, as well as the expression of 71 genes linked to SNPs from GWAS studies (Nat Genet 44:491, 2012). Consistent with studies in mice showing that ovariectomy upregulated components of NFκB signaling, leading to impaired osteoblastic bone formation (Nat Med 15:682, 2009), we found significantly reduced mRNA levels of both *NFκB2* and *relB*, along with an overall trend ($P = 0.028$ by cluster analysis) for lower mRNA levels of multiple inflammatory markers in the bone biopsies of the E-treated compared to the control women. Of the 71 GWAS-related genes examined, 14 were modulated *in vivo* by E treatment.

In summary, our studies demonstrate that, in humans, E reduces both bone *sost* mRNA and circulating sclerostin levels. Further, since bone loss following E deficiency is associated with impaired bone formation relative to bone resorption, our findings point to increases in two key inhibitors of Wnt/BMP signaling, sclerostin and sostdc1, along with increased NFκB signaling, as mediating this relative deficit in bone formation in E-deficient postmenopausal women.

***Disclosures: Matthew Roforth**, None.*

1029

Efficacy of a Tissue-nonspecific Alkaline Phosphatase Inhibitor in a Mouse Model of Severe Medial Vascular Calcification. Campbell Sheen*[1], Thangchanthida N. Chhea[1], Anthony B. Pinkerton[2], Michael R. Jackson[2], Jose Luis Millan[3]. [1]Sanford Burnham Medical Research Institute, USA, [2]Conrad Prebys Center for Chemical Genomics, Sanford Burnham Medical Research Institute, USA, [3]Sanford-Burnham Medical Research Institute, USA

Upregulation of tissue-nonspecific alkaline phosphatase (TNAP) in the vasculature occurs in a variety of disorders which manifest medial vascular calcification (MVC). We have previously described a mouse model that overexpresses human TNAP in vascular smooth muscle cells, in an X-linked manner, and consequently causes extensive MVC. Hemizygous overexpressor male mice ($Tagln^{Cre/WT}$; $HprtALPL^{flox/Y}$) exhibit severe cardiac hypertrophy and have a median age of death

of 44 days, whereas the hypertrophy is less pronounced and life expectancy is normal in heterozygous females (*Tagln*$^{Cre/WT}$; *HprtALPL*$^{flox/WT}$). Through medicinal chemistry efforts, we have developed inhibitors of TNAP with drug-like characteristics that have efficacy *in vitro*. Here, we tested one of these inhibitors of TNAP, named SBI-425, to determine whether the compound had efficacy in our *in vivo* model of MVC.

Mice were i.p. injected once daily with either 10 mg/kg SBI-425 or vehicle-only control. Male and female mice were treated from day 7 to day 30 and day 60, respectively. Aortic calcium deposition was measured using acid leeching and a cresolphthalein complexone assay, which showed a significant decrease in calcification in female, but not male, mice. Heart weight to body weight ratios were significantly lower in both male and female treated mice, indicating improvement in cardiac hypertrophy. A separate group of male mice was treated with 10 mg/kg of SBI-425 or control from day 7 until death. This showed that SBI-425 treatment significantly increased the median life expectancy of affected male mice from 44 to 68 days. Possible toxic effects on bone were also evaluated by static and dynamic histomorphometry.Together, these results indicate that SBI-425 can effectively reach and inhibit TNAP in the vasculature, which suggests that it may be an effective treatment for MVC.

***Disclosures: Campbell Sheen**, None.*

1030

PTH 1-84 Targets Bone Vascular Structure and Perfusion in Mice: Impacts of its Administration Regimen and of Estrogen Deficiency. Bernard Roche*, Arnaud Vanden-Bossche, Martin Jannot, Robin Chaux, Luc Malaval, Laurence Vico, Marie-Hélène Lafage-Proust. INSERM U1059-Université de Lyon-Université Jean Monnet, France

Bone vessels functions during bone remodeling are poorly understood. They depend on both vessel network structure and vasomotor regulation. Parathyroid hormone (PTH) is a systemic vasodilator and may modulate microvascularisation. Moreover, while intermittent PTH is anti-osteoporotic, PTH continuous administration can be catabolic for bone. Finally, ovariectomy (OVX) reduces bone perfusion and vessel density in mice. In this context, our working hypotheses were that PTH effects on bone vascularisation 1) depend on its administration regimen and 2) may be impacted by estrogen deficiency. We used 4 month-old female C57BL/6 mice (n=15/group). Tibia bone perfusion was measured in vivo with a Laser Doppler device while systemic blood pressure (BP) and heart rate were monitored. After barium infusion, bone and vascular quantitative histomorphometry was performed on the same tibia. First, a 100µg/kg daily dose of PTH 1-84 was administered for 15 days either as daily Sc injection (iPTH) or continuously (ALZET minipump, cPTH). Compared to untreated controls (CT), iPTH and cPTH both increased bone formation but had opposite effects on bone resorption. iPTH increased bone perfusion (27% vs CT, $p<0.001$), with no difference in BP, while cPTH did not. Although both i- and cPTH were slightly angiogenic, iPTH increased microvessel size by 48%, while cPTH decreased it by 29% ($p<0.001$, vs CT). Second, the vascular effects of a 15d-iPTH treatment (100µg/kg/d) were analysed in OVX mice and compared to sham-operated and OVX CT. In order to asses specificity of PTH effects on vessels, two other anti-osteoporotic drugs were tested in OVX mice: zoledronate which is potentially anti-angiogenic (ZOL, 1 single injection, 70µg/kg) and propranolol (PROP), an anti hypertensive β-blocker, at a dose known to protect bone mass in rodents (5mg/kg/d). No change in bone mass occurred in this time frame. iPTH stimulated bone formation and fully prevented OVX-induced reduction in bone perfusion and vessel density, but with no change in vessel size. ZOL and PROP strongly lowered bone turnover. Surprisingly, ZOL did not further reduce bone vessel density below OVX levels and it prevented, like iPTH, OVX-induced reduction in bone perfusion, while PROP did not. Thus, our integrative approach demonstrates that PTH effects on bone vessel network microstructure and function depend on its mode of administration as well as estrogen status, and that OVX-induced vascular changes are prevented by iPTH.

***Disclosures: Bernard Roche**, None.*

1031

Parathyroid Hormone Rescues Impaired Tooth Extraction Healing Associated with Bisphosphonates. Junro Yamashita*[1], Laurie McCauley[2], Shinichiro Kuroshima[3]. [1]University of Michigan, USA, [2]University of Michigan School of Dentistry, USA, [3]Nagasaki University, Japan

Osteonecrosis of the jaw (ONJ) is a rare and devastating condition that has emerged in association with antiresorptive therapy. The pathophysiology of ONJ is unknown and no established cure currently exists. The purpose of this study was to determine whether daily PTH administration after tooth extractions would prevent the development of ONJ-like lesions in bisphosphonate-treated rats. Rats were ovariectomized and the combination of alendronate and dexamethasone (Aln/Dex) administered for 12 wks. Tooth extractions (maxillary 2nd molars) were performed and bony defects created in the proximal tibiae to compare osseous healing between the jaw and long bones. Half of the rats received daily PTH injections and the other half saline as vehicle control (VC). Healing of the extraction sites and tibial defects was assessed at 2 wks by microCT and histomorphometric analyses. All rats in the Aln/Dex-VC group developed ONJ-like lesions, while only 30% of rats in the Aln/Dex-PTH group developed ONJ-like lesions. Histomorphometrically, ONJ-like lesions were characterized by the retention of necrotic bone and severe PMN infiltration, while in PTH-treated rats healing occurred with new bone and increased collagen apposition in the extraction wounds. These findings suggest that daily PTH administration prevented the development of ONJ-like lesions. No differences in gross healing in the tibiae were noted between groups. Although the Aln/Dex-VC treatment was not associated with compromised gross healing of the tibiae as found in the oral cavity, histomorphometric analysis showed significantly more necrotic bone in Aln/Dex-VC vs. Aln/Dex-PTH tibiae. PTH administration increased bone mass significantly in the tibial defects regardless of bisphosphonate pretreatment. However, its anabolic effect on osseous wounds was significantly less in the Aln/Dex pretreatment group compared to control. Thus in both the extraction wounds and tibial defects PTH therapy promoted healing by suppressing necrotic bone and increasing bone mass. In this study ONJ-like lesions developed in the tooth extraction wounds but not in the tibial defects in rats on bisphosphonates and steroids. PTH therapy prevented the development of ONJ-like lesions and was more effective in building bone in the absence of bisphosphonate and steroid. These findings suggest daily PTH administration could be effective to prevent ONJ in patients on combination antiresorptive and steroid therapy.

***Disclosures: Junro Yamashita**, None.*

1032

Miglustat Normalizes Bone Mass And Improves Bone Microarchitecture In F508del Cystic Fibrosis Mice Through Beneficial Effects on Bone Formation and Resorption. Carole Le Henaff*[1], Eric Haÿ[2], Caroline Marty[2], Pierre J. Marie[2], Jacky P. Jacquot[1]. [1]EA 4691, SFR CAP-Santé (FED 4231), Université Reims Champagne Ardenne, France, [2]Inserm Unit 606 & University Paris Diderot, France

Male and female patients with cystic fibrosis (CF) show CF-related bone disease characterized by brittle bones. CF patients with the F508del mutation in the transmembrane conductance regulator (*Cftr*) gene display vertebral fractures and subsequent kyphosis, thus accelerating the course of the disease. We recently showed that mice with the F508del mutation in *Cftr* display a severe osteopenic phenotype early on. Using this mouse model, we tested the effect of N-butyldeoxynojyrimicin (miglustat, Zavesca, Actelion), an approved drug for treating bone pathology in type I Gaucher disease which was found to normalize CFTR-dependent sodium and chloride transport in nasal mucosa of F508del cystic fibrosis mice. To this goal, we treated male F508del mice and wild type (WT) littermates by oral administration (gavage) with a low dose (120 mg/kg/day) of miglustat for 28 days. At sacrifice, bone mass and bone microarchitecture were determined by micro-CT analysis, and bone formation and resorption were assessed by histomorphometric analyses in lumbar vertebrae and long bones (femur) after double tetracycline/calcein labelling. At 10 weeks of age, F508del mice showed decreased bone volume, reduced trabecular number and thickness, and increased trabecular separation compared to age-matched WT mice. This phenotype resulted from decreased mineral apposition rate and increased osteoclast surface and number at the two skeletal sites, reflecting decreased osteoblast function and increased bone resorption. Treatment of F508del mice with miglustat normalized trabecular bone volume and microarchitecture parameters in the lumbar spine and femur. This effect was related to correction of the osteoblast function evaluated by the mineral apposition rate, associated with decreased osteoclast surface and number at the two bone sites. Interestingly, miglustat treatment decreased serum IGF-1 level in WT mice, but not in F508del mice. In contrast, miglustat treatment increased serum 17ß-estradiol level in F508del (male) mice but not in WT mice, suggesting that the beneficial effect of miglustat on bone may in part be linked to 17ß-estradiol but not to IGF-1 production. This study provides evidence that miglustat at low dose normalizes bone mass by increasing bone formation and decreasing bone resorption in F508del cystic fibrosis mice and suggests the potential interest of miglustat to treat bone loss in patients with cystic fibrosis related bone disease.

***Disclosures: Carole Le Henaff**, None.*

1033

Parathyroid Cyp27b1 Mediates Skeletal Effects of Hyperparathyroidism by Controlling Serum 1,25-dihydroxyvitamin D_3 and Calcium Levels in Mice. Zhiqiang Cheng, Chia-Ling Tu, Alfred Li, Rachel Roston, Nathan Liang, Hanson Ho, Tsui-Hua Chen, Nehal Naik, Daniel Bikle, Dolores Shoback, Wenhan Chang*. Endocrine Unit, VA Medical Center, University of California, San Francisco, USA

Mechanisms underlying skeletal effects of hyperparathyroidism (HPT) remain unclear. Primary HPT (1° HPT) can have anabolic effects on trabecular (Tb) bone whereas secondary HPT (2° HPT) due to 1,25-dihydroxyvitamin D_3 (1,25D) and Ca^{2+} deficiencies is catabolic to bone, suggesting that the skeletal action of PTH depends on changes in 1,25D and Ca^{2+} status. To determine whether increased serum 1,25D (s1,25D) and Ca^{2+} (sCa) levels contribute to skeletal anabolism in 1° HPT, we studied CaSR-Het mice, a 1° HPT mouse model due to heterozygous knockout (KO) of the Ca^{2+}-sensing receptor (CaSR) gene in parathyroid cells (PTCs); Cyp-KO mice, a novel 2° HPT mouse model due to homozygous deletion of Cyp27b1 gene in PTCs; and double KO (CaSR-Het/Cyp-KO) mice. The Cyp-KO mice develop 2° HPT due to a profound reduction in s1,25D (by >70%) and sCa levels (see Table). We compared

serum PTH (sPTH), sCa, and s1,25D levels and Tb bone mass and structural parameters, by micro-computed tomography, in distal femurs of these 3 mouse strains. PTC-specific gene deletion in the mice was confirmed by PCR analyses of genomic DNA and RNA from various tissues. As anticipated, sPTH, sCa, and s1,25D levels were significantly ($p<0.01$) increased in CaSR-Het vs control (Cont) mice (see Table), indicative of 1° HPT. These changes were accompanied by a significantly ($p<0.01$) increased ratio of Tb bone volume (Tb.BV)/total tissue volume (TV) (Tb.BV/TV), Tb number (Tb.N), and Tb thickness (Tb.Th) in CaSR-Het vs control (Cont) mice (see Table), reflecting anabolic effects of 1° HPT. In contrast, Cyp-KO mice developed 2° HPT, as indicated by reduced s1,25D and sCa levels, when compared to Cont mice. Their increased sPTH levels were comparable to those of CaSR-Het mice (see Table). These serum changes were accompanied by catabolic bone effects, reflected by reduced Tb.BV/TV, Tb.N, and Tb.Th (see Table). In CaSR-Het//Cyp-KO double KO mice, concurrent ablation of parathyroid Cyp27b1 significantly ($p<0.01$) decreased sCa and s1,25D levels, despite the presence of their higher levels of sPTH vs those in CaSR-Het mice, and these reduced sCa and s1,25D levels severely blunted the anabolic effects of 1° HPT due to CaSR KO. Our data suggest that the parathyroid Cyp27b1 activity critically mediates skeletal actions of PTH by controlling s1,25D and sCa levels in mice.

Genotype	sPTH, ng/mL	sCa, mg/dL	s1,25D, pM	Tb.BV/TV	Tb.N	Tb.Th, μm
Cont	112 ± 8	9.78 ± 0.04	109.1 ± 14.7	8.7 ± 0.3	3.36 ± 0.11	30.6 ± 0.7
CaSR-Het	218 ± 27	11.01 ± 0.20	219.4 ± 13.9	11.8 ± 1.0	5.13 ± 0.17	40.9 ± 1.2
Cyp-KO	369 ± 71	9.45 ± 0.08	42.0 ± 3.3	6.9 ± 0.6	2.54 ± 0.11	24.9 ± 1.6
Cyp-KO// CaSR-Het	380 ± 49	10.22 ± 0.08	31.7 ± 1.0	8.1 ± 0.5	2.92 ± 0.18	27.8 ± 0.8

Table

***Disclosures: Wenhan Chang**, None.*

1034

Suppression of Sclerostin by PTH in Osteocytes Contributes to the Coupling of Formation to Resorption in Trabecular Bone in Mouse Models of Primary and Secondary Hyperparathyroidism. Robert Jilka*, Annick DeLoose, Kanan Vyas, Leslie Climer, Robert Weinstein, Charles O'Brien, Stavros Manolagas. Central Arkansas VA Healthcare System, Univ of Arkansas for Medical Sciences, USA

Osteocytes play a central role in the choreography of bone remodeling by controlling rate-limiting steps of both resorption and formation. However, the role of this cell type in the pathologic bone remodeling associated with primary or secondary hyperparathyroidism is not fully understood. Nonetheless, it is well documented that PTH acts on osteocytes to increase the production of RANKL and suppress the expression of sclerostin. To investigate the contribution of reduced sclerostin production to remodeling balance in hyperparathyroidism, we used C57BL/6 mice overexpressing human sclerostin in osteocytes under the control of a PTH-insensitive DMP1 promoter (DMP1-Sost mice). Administration of a Ca-deficient diet for 4 weeks to 9-mo-old males raised circulating PTH in both genotypes. However, the magnitude of the loss of vertebral BMD by DEXA in DMP1-Sost mice was greater than in wild type (WT) mice (-13.6 ± 3.8% vs. -6.1 ± 5.2%, $P<0.05$). This difference was due, at least in part, to a greater loss of trabecular bone, as determined by μCT. Loss of femoral DEXA BMD was also greater in DMP1-Sost mice, but μCT did not reveal a differentially sensitive site. Ca deficiency caused an equivalent increase in osteoclasts in both genotypes, as evidenced by expression of cathepsin K mRNA in tibial extracts. In contrast, there was no detectable increase in osteocalcin mRNA in DMP1-Sost mice whereas it increased by 2-fold in WT mice, suggesting an increase in osteoblast number in the latter. Hence, the greater bone loss in DMP1-Sost mice may be due to inadequate osteoblastogenesis. Hyperparathyroidism is also associated with peritrabecular fibrosis, thought to be caused by increased numbers of osteoprogenitors that are arrested prior to terminal differentiation. To explore the role of sclerostin in this pathology, we administered 400 ng/g/day of PTH(1-34) by infusion for 5 days. Extensive fibrosis was present in the vertebrae and femora of 9-mo-old wild type mice, but was barely detectable in DMP1-Sost mice. Finally, PTH-induced expression of Wnt target genes including Axin2, Nkd2, and Cx43 was attenuated in DMP1-Sost mice. Collectively, these results reveal that in hyperparathyroid states suppression of sclerostin production by osteocytes and the resulting increase in Wnt signaling contributes to the coupling of bone formation to bone resorption – at least in the cancellous compartment – as well as to the development of peritrabecular fibrosis.

***Disclosures: Robert Jilka**, None.*

1035

The Role of Macrophage Efferocytosis in Prostate Cancer Skeletal Metastasis. Fabiana Soki*[1], Yeo Won Kim[2], Amy Koh[2], Payam Entezami[2], Sun Wook Cho[3], Serk In Park[4], Sudha Sud[2], Kenneth Pienta[2], Laurie McCauley[1]. [1]University of Michigan School of dentistry, USA, [2]University of Michigan, USA, [3]Seoul National University Hospital, South Korea, [4]Vanderbilt University, USA

Macrophages are implicated in both skeletal homeostasis and tumorigenesis; yet their role in skeletal metastasis is unclear. Macrophage phagocytosis of apoptotic cells is referred to as efferocytosis, and is an integral process by which harmful by-products of dead and dying cells are removed to create a pro-resolving environment. Rapidly growing tumors are accompanied by extensive apoptosis, of which the clearance mechanisms and implications remain unclear. The purpose of this study was to determine the role of macrophages and efferocytosis in prostate cancer skeletal metastasis. *In vivo* experimental approaches employed a chemically inducible macrophage ablation model (i.e. MAFIA mice) in which AP20187 (AP) injections result in fas-induced apoptosis of c-fms (CSF-1 receptor)-positive macrophage lineage cells. Macrophage depletion was optimized, and reduction in mature bone marrow macrophages was validated by FACS analysis ($GR1^{lo}F4/80^{+}CD115^{+}SSC^{int/lo}CD11b^{hi}$ cells ~2.5% in control vs 0.2% in AP-treated). When tumors were co-implanted with neonatal murine vertebrae (vossicles) in AP-treated mafia mice, there was a significant increase in TUNEL positive apoptotic cells (due to inefficient clearance). A significant reduction in tumor growth was noted in tibiae after intratibial tumor inoculations when macrophages were ablated. To evaluate macrophage efferocytosis *in vitro*, immunofluorescence staining was performed to validate and quantify bone marrow macrophage efferocytosis of cobalt chloride-induced apoptotic RM-1 and PC-3 prostate cancer cells. Efferocytosis was increased and to a greater extent when macrophages were co-cultured (5hrs) with prostate cancer cells that were highly apoptotic (>40%) versus low apoptotic (<20%). Concomitantly, milk fat globule-EGF factor 8 (MFG-E8), an efferocytosis facilitator protein, was also increased. Downstream of MFGE8, the SOCS3 (suppressor of cytokine signaling 3) pathway was activated. In addition, CD206+ pro-tumorigenic macrophages (M2) and *IL10* gene expression (encoding interleukin 10) were increased when macrophage lineage cells encountered apoptotic tumor cells. In conclusion, depletion of macrophages hindered tumor growth in bone and phagocytosis via MFG-E8 modulated polarization to M2 tumor associated macrophages. These studies identify a new mechanism by which tumor associated macrophages support prostate cancer growth, and a potential therapeutic target in skeletal metastasis.

***Disclosures: Fabiana Soki**, None.*

1036

Altered TGF-beta signaling contributes to skeletal and extraskeletal manifestations in the Crtap-/- model of recessive Osteogenesis Imperfecta. Ingo Grafe*[1], Tao Yang[2], Stefanie Alexander[3], Erica Paige Homan[3], Caressa Lietman[3], Elda Munivez[3], Ming-Ming Jiang[3], Terry Bertin[3], Yuqing Chen[3], Gautam Sule[3], Mary Ann Weis[4], Yoshihiro Ishikawa[5], Brian Dawson[3], Kuber Sampath[6], Hans Peter Bächinger[5], David Eyre[7], Brendan Lee[8]. [1]Department of Molecular & Human Genetics, Baylor College of Medicine, USA, [2]Van Andel Research Institute, USA, [3]Baylor College of Medicine, USA, [4]University of Washington, USA, [5]Shriners Hospital for Children, USA, [6]Genzyme Corporation, USA, [7]University of Washington Orthopaedic Research Labs, USA, [8]Baylor College of Medicine & Howard Hughes Medical Institute, USA

Osteogenesis Imperfecta (OI) is characterized by low bone mass, fractures and extraskeletal manifestations. Treatment options are limited to symptomatic therapies since the underlying molecular pathomechanisms of OI are not completely understood. Recently, we have shown that mutations in *CRTAP* cause recessive OI. Interestingly, the phenotype of *Crtap-/-* mice overlaps with phenotypes resulting from increased TGFb signaling, including decreased bone mass and increased alveolar airway space in lungs. We hypothesize that the alteration of collagen post-translational modifications in *Crtap-/-* mice results in a dysregulation of matrix-cell signaling which contributes to phenotype manifestation.

Here we show dysregulated TGFb activity in *Crtap-/-* mice, as evidenced by an increased ratio of pSmad2/Smad2 protein and increased expression of TGFb target genes in calvarial bone. Consistent with this, *Crtap-/-* mice carrying a TGFb-luciferase reporter transgene show increased bioluminescence in skeletal tissue compared to WT mice. Furthermore, increased immunostaining of pSmad2 in lungs of *Crtap-/-* mice shows similarly dysregulated TGFb activity in extraskeletal tissues.

To block the increased TGFb activity, we utilized a pan-TGFb neutralizing antibody (1D11, Genzyme) to treat 8 week old *Crtap-/-* mice for 8 weeks (10mg/kg,IP,3x/week). Control antibody treated *Crtap-/-* and WT mice served as controls. MicroCT analysis of L4 vertebrae showed that compared to control *Crtap-/-* mice, 1D11 treatment significantly improved trabecular bone parameters including BS (+91%) and Tb.N (+88%); BV/TV (+193%), Tb.Th (+57%) and Tb.Sp (-58%) were no longer statistically different than WT mice. Similarly significant improvements were also observed at the trabecular bone of femurs. In addition, 1D11 treatment ameliorated the lung phenotype, as demonstrated by a significant reduction of the alveolar airway space.

In summary, we show that dysregulated TGFb signaling is a novel molecular mechanism and important contributor to the bone and lung defects in the *Crtap-/-* model of recessive OI. Given the phenotypic overlap between recessive and dominant forms of OI this mechanism may also contribute to the phenotypes in dominant OI as a common mechanism of disease. These findings could shed new light on the molecular mechanisms of human OI, and potentially may be translated into signaling based therapies to alleviate skeletal as well as extraskeletal manifestations in patients with OI.

***Disclosures: Ingo Grafe**, None.*

1037

NOS-Mediated Vasodilation Causes Immediate Increases in Blood Flow Rate Following Osteogenic Mechanical Loading in Rats. Ryan Tomlinson*[1], Kooresh Shoghi[1], Matthew Silva[2]. [1]Washington University in St. Louis, USA, [2]Washington University in St. Louis School of Medicine, USA

The vascular response following osteogenic mechanical loading is poorly understood. Here, either damaging (WBF) or non-damaging (LBF) axial compression was used to generate woven or lamellar bone formation, respectively, in the adult rat forelimb.

PET imaging was used to evaluate blood flow and fluoride kinetics at the site of bone formation. As early as a few hours after WBF loading, the blood flow rate increased approximately 30%; this significant increase was maintained for 14 days. In contrast, fluoride uptake peaked 7 days after WBF loading, and declined sharply between days 7 and 14. There were no significant changes in blood flow rate or fluoride uptake following LBF loading.

To quantify vasodilation, the area of the anterior interosseous artery was measured following loading. WBF loaded limbs had significantly increased arterial area (+50%) compared to non-loaded limbs at days 1 and 3. By day 7, arterial area was not different between loaded and non-loaded limbs. Similarly, there were no significant differences in arterial area following LBF loading. Since mast cells are a possible effector of vasodilation, mast cell infiltration and Nos2 expression were quantified following loading. Nos2+ mast cells in WBF loaded limbs were significantly increased on days 1 and 3. By day 7, there were no differences between loaded and non-loaded limbs. LBF loading was not associated with increases in Nos2+ mast cells.

L-NAME (N^{ω}-nitro-L-arginine methyl ester), a NOS inhibitor, prevented the expression of Nos2 in mast cells following WBF loading. Additionally, L-NAME treatment abolished the increase in blood flow rate at days 1 and 3, and decreased fluoride uptake at day 3. Finally, L-NAME treatment decreased woven bone formation, with significant decreases in woven bone area (-23%), volume (-27%), and BMD (-26%), compared to vehicle controls.

In summary, WBF loading was associated with a rapid and persistent increase in blood flow rate. This increase was mediated by vasodilation associated with mast cells positive for Nos2 in the expanded periosteal region. Treatment with L-NAME blocked the expression of Nos2 as well as the increase in blood flow rate, and ultimately impaired woven bone formation. In contrast, LBF loading was not associated with increases in blood flow rate, vasodilation, or Nos2 expression in mast cells.

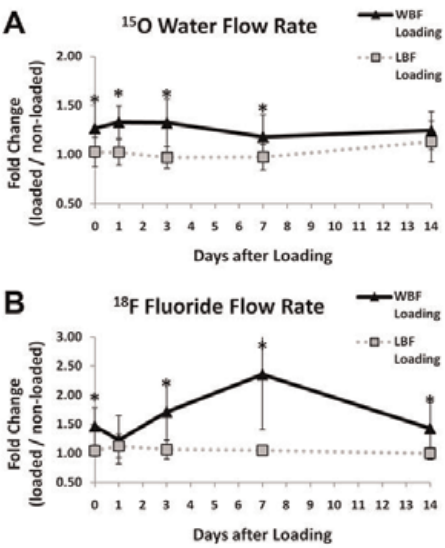

15O Water and 18F Fluoride flow rates are temporally regulated following mechanical loading

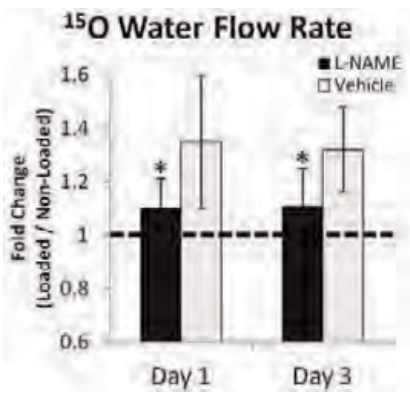

L-NAME treatment inhibited early increases in blood flow rate following WBF loading

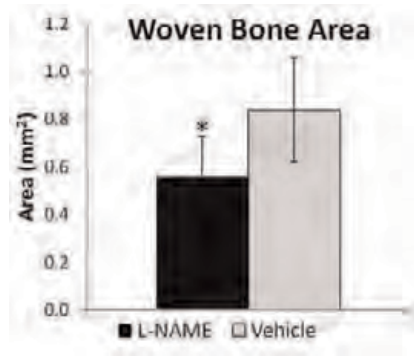

L-NAME treatment was associated with decreased woven bone area by dynamic histomorphometry

***Disclosures: Ryan Tomlinson**, None.*

1038

Interactions Among Cortical and Trabecular Traits During Growth Provide Insight Into Establishing Whole Bone Mechanical Function in the Lumbar Vertebral Body. Melissa Ramcharan*[1], Meghan Faillace[2], Zoe Guengerich[1], Valerie Williams[1], Karl Jepsen[3]. [1]Mount Sinai School of Medicine, USA, [2]GE Inspection Technologies, USA, [3]University of Michigan, USA

Studying bone as a complex adaptive system will benefit efforts to understand how interactions among cortical and trabecular traits define whole bone mechanical function and to identify genetic and environmental factors that contribute to reduced bone strength. Much is known about cortical and trabecular bone separately, but very little is known about how these traits co-develop during growth to establish bone strength. To study this, we adopted a paradigm which postulates that early variation in one trait is followed by adaptive changes in other traits. We examined temporal changes in bone traits during growth in the vertebral body of three inbred mouse strains, A/J(AJ), C3H/HeJ(C3H) and C57BL/6J(B6). Strains range from a slender to a robust bone phenotype each with widely varying adult trait sets.

Female mice were sacrificed at 1, 4, 7, 10, 14, 28, and 105 days of age (n=10/age/strain). Histological sections of plastic embedded vertebral bodies were imaged along the L3 mid-transverse or L4 mid-coronal plane using fluorescent microscopy. Morphological traits quantified in the transverse plane included total cross-sectional area and cortical area (CtAr). Traits quantified in the coronal plane included percent trabecular bone area (%TBA), trabecular thickness, and anisotropy. Differences in traits relative to age and genotype were determined using a one-way ANOVA and a Tukey's posthoc test ($p<0.05$).

Inter-strain differences in trabecular %TBA and anisotropy observed at 15weeks of age were established as early as 7 days of age. %TBA was highest in B6 mice followed by AJ then C3H mice. Trabecular anisotropy was highest in C3H mice followed by B6 then AJ mice. Also, by 7 days of age, a decrease in %TBA was accompanied by an increase in trabecular anisotropy. This suggests an early restructuring of the trabecular architecture to increase the efficiency of load transfer through the vertebral body. The inter-strain variation in %TBA was retained throughout growth. In contrast, cortical area was highly variable with C3H showing a 135% increase in Ct.Ar between 4 and 15 weeks of age. This suggests an adaptive response of cortical area to the low %TBA present at 4 days of age.

Our results suggest variation in the cortical trait arises from an adaptive response to early genetic variation in trabecular traits. This insight is important for understanding functional bone adaptation and interpreting adaptive changes in bone due to genetic or environment perturbations.

***Disclosures: Melissa Ramcharan**, None.*

1039

Osteocyte Pericellular Matrix Density Regulates Bone's Anabolic Response to Mechanical Loading. Christopher Price*[1], Tonima Quabili[1], Wei-Ju Tseng[2], X. Sherry Liu[2], Catherine Kirn-Safran[1], Liyun Wang[1]. [1]University of Delaware, USA, [2]University of Pennsylvania, USA

Osteocytes are responsible for detecting mechanical loading and orchestrating the bone's remodeling process. Using fluorescence recovery after photobleaching (FRAP), we have demonstrated significant interstitial fluid flows (50um/s) around the osteocyte cell processes in bone under moderate loading. However, the apparatus by which the osteocyte senses these signals remains unclear. We believe that pericellular matrix (PCM) fibers, which tether the osteocyte cell processes to lacunar wall, constitute the cells' ''sensing antennae''. PCM fibers can be deformed by fluid flow, much like trees are bent under the wind, and may thus allow the transfer of external loading signals to the cells interior and the initiation of biochemical responses. Further, we recently found that the density of the PCM was reduced -34% in mice with deficiency of perlecan (a PCM constituent). We hypothesized that a

reduction in PCM fiber density would reduce bone's sensitivity and anabolic response to mechanical loading.

In this study, we subjected the right tibiae of 3.5-month old perlecan deficient mice (Hypo, N=7) and age-matched control mice (CTL, N=8) to compressive uniaxial-tibial loading (peak load 8.5N at 4 Hz, 5 sessions over 10 days, 5 min/day). The left tibiae served as non-loaded control. Tibiae were scanned in a micro-CT scanner at a resolution of 6um^3/voxel, followed by three-point bending testing.The microCT data showed no significant differences in cortical bone morphology between control tibiae in the CTL and Hypo mice, except for a slightly higher tissue mineral density in the Hypo mice. Loading resulted in an increase in cortical bone polar moment inertia (+6.5%, p=0.02) and a reduction in the cortical porosity (-3.1%, p=0.04) relative to non-loaded tibiae in CTL mice, while no such effects were seen in the Hypo mice (Table 1). Loading also significantly increased tibial stiffness in CTL mice (+ 13.4%, p=0.01), but failed to reach significance in Hypo mice (p=0.19, Table 2). Overall, the hypo mice demonstrated diminished anabolic response to mechanical loading compared with control mice, supporting our original hypothesis. We are currently investigating how the altered PCM fiber density affects bone responses to disuse challenge. These studies will help elucidate the cellular mechanisms underlying bone's intrinsic (in-) sensitivity to mechanical loading, and may provide potential targets to promote bone formation and prevent bone loss.

Table 1 Micro-CT Data (Tibial Cortical Mid-Shaft)

	Control Mice (n=8)			Hypo Mice (n=6)			p values (Control vs. Hypo)	
	Left (unloaded)	*Right (loaded)*	*p value (R vs. L)*	*Left (unloaded)*	*Right (loaded)*	*p value (R vs. L)*	*Left (unloaded)*	*Right (loaded)*
Ct.Th (mm)	0.199±0.012	0.203±0.004	0.38	0.207±0.007	0.210±0.006	0.19	0.22	0.02
Ct.Por (%)	5.2%±0.3%	5.1%±1.2%	**0.04**	5.1%±0.5%	5.6%±1.4%	0.5	0.65	0.27
Ct.Ar (mm^2)	0.64±0.08	0.66±0.06	0.12	0.67±0.08	0.67±0.06	0.68	0.51	0.62
Ct.pMoI (mm^2)	0.17±0.04	0.18±0.03	**0.02**	0.18±0.05	0.18±0.04	0.93	0.69	0.95
Ct.TMD (mgHA/mm^3)	1194.84±12.26	1194.36±11.02	0.92	1209.15±10.03	1208.80±6.89	0.94	**0.04**	**0.02**

Table 1

Table 2 Mechanical Properties by Three Point-Bending (Tibiae)

	Control Mice (n=7)			Hypo Mice (n=5)			p values (Control vs. Hypo)	
	Left (unloaded)	*Right (loaded)*	*p value (R vs. L)*	*Left (unloaded)*	*Right (loaded)*	*p value (R vs. L)*	*Left (unloaded)*	*Right (loaded)*
Stiffness (N/mm)	151.5±15.8	171.1±16.5	**0.01**	128.98±25.11	152.47±33.35	0.19	0.08	0.23
Max Load (N)	18.9±1.8	20.3±1.9	0.31	16.5±3.0	17.7±2.2	0.27	0.12	**0.05**
Disp@Max Load (mm)	0.22±0.04	0.28±0.05	**0.04**	0.28±0.06	0.24±0.04	0.08	0.07	0.19
Yield Load (N)	13.9±2.3	13.4±2.4	0.78	11.8±1.5	14.5±2.8	0.09	0.11	0.48
Post Yield Disp (mm)	0.23±0.18	0.25±0.23	0.85	0.43±0.21	0.45±0.17	0.83	0.09	0.12

Table 2

***Disclosures: Christopher Price**, None.*

1040

Genotypic and Phenotypic Muscle-Bone Interactions During Unloading/ Reloading. Stefan Judex*[1], Weidong Zhang[2], Leah Rae Donahue[2], Engin Ozcivici[3]. [1]Stony Brook University, USA, [2]Jackson Laboratory, USA, [3]Izmir Institute of Technology, Turkey

The concept of a muscle-bone unit tuned to the magnitude of contractile forces has intuitive appeal, however there is little direct evidence that the relatively few, large-magnitude muscle contractions arising during daily activities dominate skeletal adaptation. Here, we produced a genetically heterogeneous mouse population with large individual differences in mechanosensitivity and tested muscle-bone interactions during 3wk of hindlimb unloading and subsequent 3wk reambulation. Each of the 352 adult mice of the F2 cross of BALB/cByJ and C3H/HeJ were μCT scanned in vivo at baseline and after the two experimental phases. Muscle cross-section area of the upper hindlimb as well as trabecular and cortical morphology of the distal femur and middiaphysis were quantified. DNA was extracted from each mouse and genome wide scans determined quantitative trait loci (QTL) for unloading and reambulation induced changes in tissue quantity of muscle, trabecular, and cortical bone. As expected from this specific mouse population specifically bred for a large range in musculoskeletal mechanosensitivity, the response of all three tissues to the two experimental regimes varied greatly across individuals; from small to large losses during unloading and from continued deterioration to full recovery during reambulation. For instance, unloading resulted in losses of BV/TV between 15-71% while changes during reambulation ranged from -18% to +56%. Averaged across mice, muscle recovered greater losses during reambulation than either trabecular or cortical bone. Changes in muscle area during unloading and reambulation were not correlated with changes in trabecular and cortical quantity (R^2<12%); individuals with the greatest changes in muscle area did not coincide with those that showed the greatest changes in bone. QTL that regulated the magnitude of the response of any given tissue to unloading and reambulation showed little overlap between muscle and trabecular/ cortical bone. These data emphasize the strong influence of genetic variations on the response of the musculoskeletal tissues. The low correlations between morphological changes in muscle and bone, together with the distinct genetic regulation of the response, provide evidence against the hypothesis that bone's response to (un)loading is modulated by muscle forces. They also suggest that the development of physical interventions for musculoskeletal ailments may have to be optimized independently for bone and muscle.

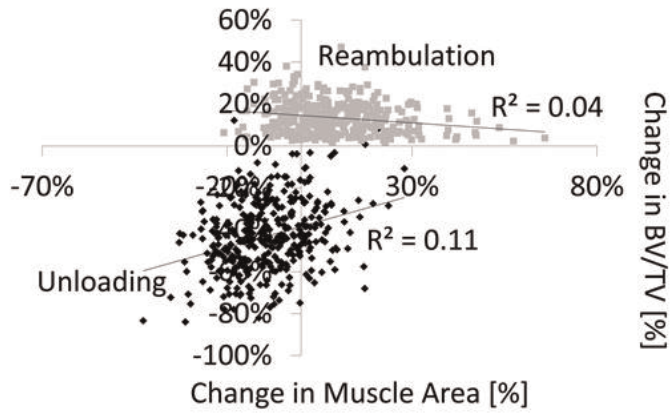

Correlation between muscle area and trabecular BV/TV during unloading and reambulation

***Disclosures: Stefan Judex**, None.*

1041

PHOSPHO1: Recognition of roles beyond skeletal mineralization. Karla Oldknow*[1], Nik Morton[2], Manisha Yadav[3], Sophie Rajoanah[2], Carmen Huesa[4], Lutz Bunger[5], Derek Ball[6], Mathieu Ferron[7], Gerard Karsenty[8], Vicky MacRae[4], Jose Luis Millan[9], Colin Farquharson[10]. [1]The Roslin Institute, The University of Edinburgh., United Kingdom, [2]QMRI, The University of Edinburgh, United Kingdom, [3]Burnham Institute for Medical Research, USA, [4]The Roslin Institute, The University of Edinburgh, United Kingdom, [5]SRUC, United Kingdom, [6]Heriot-Watt University, United Kingdom, [7]Institut de recherches cliniques de Montreal, Canada, [8]Columbia University, USA, [9]Sanford-Burnham Medical Research Institute, USA, [10]Roslin Institute, University of Edinburgh, United Kingdom

Advances in genetic approaches to bone physiology have expanded our understanding of the mechanisms by which bone and energy homeostasis interact. PHOSPHO1, a bone specific phosphatase is essential for the initiation of bone mineralization. Here we now show that *Phospho1* ablation confers a remarkable protection against obesity and diabetes in mice. To understand the mechanism whereby *Phospho1* impacts metabolism, microarray analysis of osteoblasts, the primary site of *Phospho1* expression was performed. *Esp* (encoding the phosphatase OST-PTP) which controls hormonally active osteocalcin secretion, was 20-fold more highly expressed in *Phospho1*$^{-/-}$ osteoblasts ($p<0.05$). Conversely, *Esp* mRNA was decreased in *Phospho1* overexpressing osteoblasts ($p<0.001$). Unexpectedly, serum levels of uncarboxylated and undercarboxylated osteocalcin were normal suggesting an osteocalcin-independent mechanism of PHOSPHO1 regulated energy metabolism. 120 day-old *Phospho1*$^{-/-}$ mice were hypoglycaemic (wild-type (WT) 9.48 ± 0.31 mmol/L, *Phospho1*$^{-/-}$ 8.30 ± 0.26 mmol/L; $p<0.01$) and showed improved glucose and insulin tolerance compared to WT mice ($p<0.05$). These observations were consistent with the finding of smaller (mg/g BW) subcutaneous (WT 4.51 ± 0.37, *Phospho1*$^{-/-}$ 2.79 ± 0.42; $p<0.01$), mesenteric (WT 13.2 ± 1.34, *Phospho1*$^{-/-}$ 5.56 ± 1.61; $p<0.01$) and epididymal (WT 13.7 ± 1.81, *Phospho1*$^{-/-}$ 6.96 ± 0.58; $p<0.001$) fat deposits noted in *Phospho1*$^{-/-}$ mice at necropsy and confirmed by MRI and CT. Remarkably, *Phospho1*$^{-/-}$ mice resisted the pronounced weight gain (WT 38.0 ± 1.54 g, *Phospho1*$^{-/-}$ 32.4 ± 1.26 g; $p<0.05$) and diabetes (WT 10.3 ± 0.53 mmol/L, *Phospho1*$^{-/-}$ 9.27 ± 0.77 mmol/L; $p<0.05$) exhibited by WT mice when fed a chronic high fat diet (HFD; 14 weeks, 58% kcal as fat) and this was not explained by altered activity. Circulating levels of total and high molecular weight adiponectin were decreased in *Phospho1*$^{-/-}$ mice on both control and HFD, whereas leptin levels were decreased on HFD only ($p<0.05$). Histology revealed smaller epididymal adipocytes, decreased fat content, decreased pancreatic islet number and increased mitochondria number in brown fat ($p<0.05$). However, no differences were observed in brown fat specific genes including *Ucp1* suggesting canonical thermogenesis does not underlie metabolic protection. Our findings indicate *Phospho1* deficiency improves the metabolic profile of mice in vivo and confers resistance to obesity and diabetes most likely through a primary effect on bone metabolism/turnover.

***Disclosures: Karla Oldknow**, None.*

1042

Loss of Cbl PI3K Interaction Alters the Composition of Hematopoietic Stem Cells and Osteoclast Precursor Cells in Bone Marrow in Association with Increased SDF-1 Production by CAR Cells. Naga Suresh Adapala[1], Sierra Root[2], Joseph Lorenzo[3], Hector Aguila[3], Archana Sanjay*[3]. [1]Department of Orthopedic Surgery, University of Connecticut Health Center, USA, [2]Department of Immunology, University of Connecticut Health Center, USA, [3]University of Connecticut Health Center, USA

Cbl functions as E3 ubiquitin ligase and adaptor protein in osteoclasts (OCs) and osteoblasts. One major function of Cbl involves the regulation of phosphatidyl inositol kinase (PI3K) activity. Tyrosine phosphorylation in the Y^{737}EAM motif is essential for Cbl-PI3K interaction. Substitution of phenylalanine for tyrosine 737 (YF) abrogates Cbl-PI3K interaction. We reported that mice harboring the YF mutation (YF mice) have increased OC numbers with defective bone resorption. This results in mild osteopetrosis, possibly due to perturbed spatiotemporal distribution of PI3K activity. To explore the origin of the increased OCs in YF mice, we performed FACS analysis and found that YF mice had 2-fold more OC precursors ($CD3^-CD45R^-NK.1.1^-CD11b^{lo}$ $CD115^{hi}$) in their bone marrow (BM). The granulocyte macrophage progenitors (GMP) progenitors which give rise OCPs were increased by 1.2 fold in YF mice while the numbers of common myeloid progenitors (CMP) and megakaryocyte-erythroid progenitors (MEP) were comparable to wild type. We have previously shown that levels of a chemokine, stromal derived factor-1 (SDF-1) are increased in YF BM. SDF-1 plays a crucial role in the initiation and maintenance of hematopoietic niches, and promotes OCP recruitment. By FACS analysis we demonstrated that expression of SDF-1 and its receptor CXCR4 is increased in YF derived GMPs and OCPs. Additionally, migration of YF derived OCPs towards a SDF-1 gradient was increased (WT 10.2% + 1.5; YF 17.8% + 1.8 $p < 0.0008$). Together, these data provide a mechanism for the increase in the number of OCPs in YF mice. Further analysis of the non-hematopoietic compartment revealed that the number of CXC12 abundant reticular (CAR) cells, which are the major source of SDF-1 in BM was significantly increased in YF mice and treatment of BM cells with a PI3K inhibitor attenuated SDF-1 expression. SDF-1 promotes B-cell development and selective ablation of SDF-1 in adult BM stromal cells resulted in expansion of hematopoietic stem cells (HSCs). We found that YF BM had a 1.6 fold decrease in HSCs ($Lin^-Sca1^+c\text{-}Kit^+$) as well as a decrease in common lymphoid progenitors (CLP) and T cells (CD3+) but an increase in B cells (B220+). These results demonstrate that the composition of the BM milieu in the YF mice is perturbed by their increased production of SDF-1. We conclude that Cbl-PI3K interaction has an important role in maintaining the balance of cellular components within the BM microenvironment.

***Disclosures: Archana Sanjay**, None.*

1043

Inhibition of AP-1 in specific hypothalamic neurons increases both energy expenditure and bone density in mice. Anna Idelevich*[1], Kazusa Sato[2], Glenn Rowe[3], Francesca Gori[4], Roland Baron[5]. [1]Harvard University, USA, [2]Harvard School of Dental Medicine, USA, [3]Harvard Medical School, USA, [4]Harvard School of Dental Medicine, Massachusetts General Hospital, USA, [5]Harvard School of Medicine & of Dental Medicine, USA

It has been recognized that the regulation of bone homeostasis and energy metabolism, once thought to be self-governing, may be coordinated by common neuronal relays. ΔFosB, a natural splice isoform of FosB and antagonist of AP1 transcriptional activity, increases both energy expenditure and bone formation, in a transgenic mouse model or following viral-mediated gene delivery into the ventral hypothalamus (VHT). Several VHT neurons forming the Ventromedial and Arcuate nucleai, have been previously implicated in the regulation of energy metabolism including AgRP, CART, POMC, NPY and SF1 neurons. The aim of the present study was to identify the individual AP-1 responsive VHT neuronal circuits that mediate the metabolic, skeletal or both effects.For this purpose,we generated Cre-inducible lentiviral vectors that express AP1 antagonists: ΔFosB, Δ2ΔFosB and DNJunD, as well as AP-1 agonist: FosB. The expression of these factors was restricted to specific neuronal types via stereotaxic delivery into the VHT of transgenic mice expressing Cre-recombinase under the control of the neuron-specific promoters, including AgRP-Cre, CART-Cre and SF1-Cre. Energy expenditure was assessed using calorimetric and monitoring system (CLAMS), whereas bone density was evaluated by micro-CT. Despite the classically divergent functions of anorexigenic CART and orexigenic AgRP neurons in feeding behavior and energy balance, AP-1 inhibition in either CART or AgRP neurons resulted in a consistent increase in energy expenditure and bone density. Moreover, all AP-1 antagonists in either of the three neuron-specific expression systems displayed a similar phenotype of lower weight gain and smaller fat pads with smaller adipocytes. Stimulation of AP-1 transcriptional activity via overexpression of full length FosB reversed the metabolic phenotype induced by AP-1 blockade, resulting in contrastingly lower energy expenditure and higher fat gain.

This study demonstrates that: 1) The induction of high energy expenditure and high bone density by ΔFosB in the VHT results from its antagonistic activity to AP-1 and 2) Selective inhibition of AP-1 in only one of AgRP, CART or SF1 neuron subtypes is sufficient to stimulate total body metabolism, decrease fat and increase bone density. These findings suggest that bone and energy are at least in part under common neuronal control and these effects are mediated by a central factor common to and/or affecting several hypothalamic neurons.

***Disclosures: Anna Idelevich**, None.*

1044

Expression of Glucose Transporter-4 by the osteoblast is required for global glucose metabolism. Zhu Li*[1], Julie Leslie[2], Guang William Wong[1], Barbara Kahn[3], Ryan Riddle[1], Thomas Clemens[2]. [1]Johns Hopkins University School of Medicine, USA, [2]Johns Hopkins University, USA, [3]Harvard Medical School, USA

Recent studies have identified the osteoblast as a major insulin responsive cell that regulates global energy metabolism by secreting hormones such as osteocalcin that alter insulin secretion and sensitivity. However, little is known of the major fuel requirements of osteoblasts. In this study, we examined the oxidation of glucose and fatty acids after insulin stimulation. Whereas oxidation of ^{14}C-oleate was decreased by insulin treatment, metabolism of ^{14}C-glucose was dose-dependently increased. Classical insulin responsive cells express glucose transporters (Glut) that facilitate the uptake of hexoses to be stored or metabolized. Primary mouse osteoblasts expressed Glut1 and Glut3 at low levels whereas Glut4 mRNA increased 6-fold during the course of osteoblast differentiation, compatible with the increased uptake of glucose during matrix production and mineralization. Insulin treatment induced Glut4 translocation to the plasma membrane in association with increased 2-deoxy-glucose uptake. Disruption of this transporter in osteoblasts *in vitro* eliminated insulin-stimulated glucose uptake, reduced proliferation and diminished measures of osteoblast maturation (Alkaline phosphatase and Alizarin red staining). *In vivo*, Glut4 was expressed by osteoblasts, osteocytes and chondrocytes at levels approaching those observed in adjacent skeletal muscle. To determine the importance of Glut4 in bone, we generated mice lacking Glut4 in osteoblasts/osteocytes (Glut4 Ob-KO). Glut4 Ob-KO mice were viable, exhibited normal linear growth, and had cortical and trabecular bone architecture indistinguishable from control littermates. Remarkably, however, Glut4 Ob-KO mice exhibited increased peripheral adiposity in association with mild hyper-insulinemia but marked insulin resistance measured by ITT. Quantitative PCR analysis of gene expression profiles in the liver and adipose of Glut4 Ob-KO mice revealed that insulin sensitivity was not altered in these tissues, suggesting that resistance to insulin was the result of decreased Glut4-mediated uptake of glucose in bone. Based on these observations, we conclude that the osteoblast-lineage contributes to the clearance of glucose in response to insulin and likely functions in the regulation of whole body metabolism beyond the secretion of osteocalcin.

***Disclosures: Zhu Li**, None.*

1045

Fetal Stage-Specific Mineral Metabolism in *Hyp* Mice Is Associated with Effects of FGF23 on Placenta. Yasuhisa Ohata*[1], Miwa Yamazaki[1], Masanobu Kawai[1], Kanako Tachikawa[1], Tomoko Koinuma[1], Kazuaki Miyagawa[2], Akihito Kimoto[1], Masahiro Nakayama[1], Noriyuki Namba[3], Hironori Yamamoto[4], Keiichi Ozono[5], Toshimi Michigami[1]. [1]Osaka Medical Center & Research Institute for Maternal & Child Health, Japan, [2]Osaka University, Japan, [3]Osaka University Graduate School of Medicine, Japan, [4]University of Jin-ai, Japan, [5]Osaka University Graduate School of Medicine, Japan

We previously reported that human placenta expresses α-Klotho, which is required for fibroblast growth factor (FGF)23 signaling. Here we investigated the roles of FGF23 in mineral metabolism at the fetal stage using *Hyp* mice with high levels of circulating FGF23. *Hyp* and wild-type (WT) females were mated with WT males, and the mothers and their male fetuses were analyzed. Despite hypophosphatemia in *Hyp* mothers, serum phosphate (Pi) levels in fetuses were comparable among the 3 groups: *Hyp* and WT fetuses from *Hyp* mothers and WT fetuses from WT mothers. FGF23 levels in *Hyp* mothers were elevated. FGF23 levels were about 20-fold higher in *Hyp* fetuses than in *Hyp* mothers. WT fetuses from *Hyp* mothers exhibited low levels of FGF23, as did fetuses from WT mothers, suggesting that FGF23 does not cross the placenta or is rapidly degraded after its transfer. In kidneys of *Hyp* fetuses, although the expression of *Slc34a1* and *Slc34a3* was decreased and that of *Cyp24a1* was increased, the levels of Pi in amniotic fluids were comparable among the 3 groups. The feto-maternal interface of the placenta both in WT mouse and normal human expressed FGFR1 as well as α-Klotho. An antibody against the phosphorylated

FGFR (Y653/Y654) positively immunostained the interface, and so did an antibody against early growth response-1 (EGR-1), a target gene of FGF signaling. These observations indicated that these areas seemed to be receptive to FGF signaling. The expression of FGFR1 and α-Klotho in the placenta led us to hypothesize that FGF23 may exert its effects on the placenta and regulate mineral metabolism at the fetal stage. To test this hypothesis, we compared placental gene expression among WT fetuses from WT mothers and WT and *Hyp* fetuses from *Hyp* mothers. In *Hyp* fetuses, *Cyp24a1* expression was elevated in the placenta. To examine whether this increase in the placental expression of *Cyp24a1* was caused by an elevated level of FGF23, we performed *ex vivo* experiments using an organ culture of placentas from WT mice. In the organ culture of placentas, treatment with the plasma from *Hyp* mothers increased the expression of *Cyp24a1*, which was abolished by the addition of the anti-FGF23 neutralizing antibody. The direct injection of recombinant FGF23 into WT placentas induced the placental expression of *Cyp24a1* and *Egr-1*. These results indicate that the placenta is a target of FGF23, which may play a role in fetal vitamin D metabolism.

***Disclosures: Yasuhisa Ohata**, None.*

1046

Bone Marrow Adipogenesis. Mark Horowitz*[1], Ryan Berry[2], Jackie Fretz[1], Tracy Nelson[2], Chris Church[2], Casey Doucette[3], Nancy Troiano[2], Joshua VanHoutan[2], Ormond MacDouglad[4], Clifford Rosen[5], Matthew Rodeheffer[2]. [1]Yale University School of Medicine, USA, [2]Yale University, USA, [3]Maine Medical Center Research Institute, USA, [4]University of Michigan, USA, [5]Maine Medical Center, USA

Adipocytes were identified in the bone marrow (BM) more than a century ago, but unlike adipose tissue in other depots, these cells have never been considered more than ''fillers'' for other ''more important'' BM cells. ''Yellow'' fatty marrow replaces ''red'' hematopoietic/osteogenic marrow within the long bones of humans. However, little is known about the origin, differentiation and function of BM adipocytes or their relationship to adipocytes in other depots.We have found that both rosiglitazone feeding and BM reconstitution following irradiation induces BM adipogenesis. BM adipocytes can be visualized through new techniques using osmium staining with quantitation by micro-CT or confocal imaging of BM plugs or frozen sections to assess morphology and expression of adipocyte genes.Experiments show that B6 mice, which have low BMD have few marrow adipocytes, which increase with calorie restriction and high fat diet (HFD). In contrast, C3H mice have high BMD and many adipocytes, which increase with HFD.Lineage tracing shows that BM adipocytes express adiponectin as rosiglitazone feeding of adiponectin-cre:mT/mG mice; in which expression of Cre recombinase from a promoter of interest (adiponectin) results in permanent removal of the targeted dTomato (mT) cassette and expression of the membrane targeted eGFP (mG) cassette, resulting in flipping from a dTomato+ to an eGFP+ cell; results in eGFP+ BM adipocytes. Using Vav1-cre:mT/mG mice we show that hematopoietic BM cells are Vav+, while none of the adipocytes express Vav. In contrast, using Pdgfra-cre:mT/mG mice we show that a subpopulation of BM adipocytes are Pdgfra+.Reconstitution of irradiated mice with mT/mG, Vav1-cre:mT/mG, Pdgfra-cre:mT/mG, or adiponectin-cre:mT/mG BM yields unlabeled LipidTox+ adipocytes, indicating that BM adipocytes do not arise from donor cells. Supporting this finding, white adipose tissue progenitors (Lin-Pdgfra+CD29+CD34+Sca-1+CD24+) are not found in isolated BM cells by FACS. Reconstitution of mT/mG mice with B6 BM results in dTomato+ adipocytes, indicating that BM adipocyte progenitors (AP) are present in the irradiated host. These experiments suggest that: A non-hematopoietic precursor cell resides in a BM ''niche'' giving rise to BM adipocytes; MAT can contribute to systemic metabolism through expression of adiponectin; BM AP are different than AP in other depots; These data are the first to define genetic markers in BM adipocyte progenitors *in vivo*.

***Disclosures: Mark Horowitz**, None.*

1047

Bone Specific Deletion of *Fgfr1* in Hyp Mice Partially Corrects the Hypophosphatemic Rickets Phenotype. Zhousheng Xiao*, Jinsong Huang, Li Cao, Yingjuan Liang, L. Darryl Quarles. The University of Tennessee Health Science Center, USA

Osteoctyes regulate phosphate and vitamin D homeostasis through the release of the Fgf23 hormone. Recent studies suggest that activation of Fgfr1 signaling underlies the increased Fgf23 levels in *Phex* mutant *Hyp* mice. To directly test the role of Fgfr1 in osteocytes, we conditionally deleted *Fgfr1* in *Hyp* osteocytes by crossing male *Dmp1*-Cre;*Fgfr1*$^{null/+}$ mice with female *Fgfr1*$^{flox/flox}$;*Hyp* mice. We characterized ''wild-type'' littermates (*Fgfr1*$^{flox/+}$), conditional homozygous *Fgfr1* null (*Fgfr1*$^{Dmp1\text{-}cKO}$) mice with intact *Phex* lacking *Fgfr1*, *Hyp* mice with intact *Fgfr1* lacking *Phex*, and conditional homozygous *Fgfr1* knockout mice lacking *Phex* (*Fgfr1*$^{Dmp1\text{-}cKO}$;*Hyp*). Mice were born with the expected Mendelian frequency. T*here were no differences in survival between these 4 genotypes*. *Dmp1*-Cre resulted in a 70% decrease of *Fgfr1* transcripts in bone. The gross appearance, *bone mineral density (BMD), periosteal mineral apposition rate (MAR), trabecular bone volume (BV/TV) and cortical thickness (Ct.Th) of Fgfr1*$^{Dmp1\text{-}cKO}$ mice were *indistinguishable from wild-type mice. However,* loss of *Fgfr1* in osteocytes resulted in a 30% reduction in *Fgf23* transcripts and a significant decrease in *Phex*, *Mepe*, *Sost* and *Dmp1*, but not *Ocn* or *Opn* transcripts in bone of *Fgfr1*$^{Dmp1\text{-}cKO}$ mice. Serum Fgf23 concentrations were reduced 2-fold, but no alterations in serum PTH, calcium, or phosphate concentrations were observed *in Fgfr1*$^{Dmp1\text{-}cKO}$ mice. In contrast, the tail length and body size of compound *Fgfr1*$^{Dmp1\text{-}cKO}$;*Hyp* mice were intermediate to wild-type and *Hyp* mice. In addition, compared to Hyp mice, compound *Fgfr1*$^{Dmp1\text{-}cKO}$;*Hyp* mice showed significant increments in *BMD, BV/TV, Ct.Th, and MAR,* suggesting partial rescue of the *Hyp* phenotype. *Concordant with the improved bone parameters, s*erum Fgf23 decreased from 3899 to 885 pg/ml and serum phosphate increased from 7.2 mg/dl to 10.2 mg/dl in *Hyp* and *Fgfr1*$^{Dmp1\text{-}cKO}$;*Hyp* mice, respectively. The reductions in circulating FGF23 levels were greater than the decrease in FGF23 mRNA expression in bone of *Fgfr1*$^{Dmp1\text{-}cKO}$;*Hyp* mice. In conclusion, conditional deletion of *Fgfr1* in osteocytes results in significant reductions of serum Fgf23 concentrations in both wild-type and *Hyp* mice, indicating that Fgfr1 signaling plays a role in regulating Fgf23 production in bone. Further studies are needed to determine the mechanisms underlying the residual FGF23 transcription and disproportionate reductions in circulating concentrations in *Fgfr1*$^{Dmp1\text{-}cKO}$;*Hyp* mice.

***Disclosures: Zhousheng Xiao**, None.*
This study received funding from: NIAMS

1048

A First-in-Human, Randomized, Double-Blind, Placebo-Controlled, Single-Dose Study of a Human Monoclonal Anti-FGF23 Antibody (KRN23) in X-linked Hypophosphatemia. Thomas Carpenter*[1], Erik Imel[2], Mary Ruppe[3], Thomas Weber[4], Mark Klausner[5], Margaret Wooddell[6], Tetsuyoshi Kawakami[6], Takahiro Ito[6], Xiaoping Zhang[6], Jeffrey Humphrey[6], Karl Insogna[1], Munro Peacock[7]. [1]Yale University School of Medicine, USA, [2]Indiana University School of Medicine, USA, [3]The Methodist Hospital, USA, [4]Duke University Medical Center, USA, [5]Kyowa Hakko Kirin, USA, [6]Kyowa Hakko Kirin Pharma Inc, USA, [7]Indiana University Medical Center, USA

Purpose: X-linked hypophosphatemia (XLH) is an inherited metabolic bone disease characterized by short stature and skeletal deformities. XLH is caused by mutations of *PHEX* resulting in abnormally elevated serum FGF23, which causes low serum phosphorus (P) and inappropriately normal 1,25 dihydroxyvitamin D (1,25D) levels. A Phase 1 study was conducted with a human monoclonal anti-FGF23 antibody (KRN23) to measure changes in biochemical markers and to assess its safety and tolerability in adult patients with XLH.

Methods: Thirty-eight adults with XLH and baseline FGF23 ⩾ 30 pg/mL were randomized to receive single doses of KRN23 or placebo via intravenous (IV) (0.003 to 0.3 mg/kg) or subcutaneous (SC) (0.1 to 1.0 mg/kg) routes. Dose-escalation occurred after establishing safety of the prior dose. Biochemistry, pharmacokinetics, pharmacodynamics, and immunogenicity were assessed at baseline and at various time points up to Day 50 postdosing. Changes from baseline values for each dose level were compared with placebo as least squares means.

Results: Twenty-two subjects were in the IV arm (17 KRN23, 5 placebo), and 16 in the SC arm (12 KRN23, 4 placebo). Baseline age, sex, weight, and height were comparable in all groups. Serum P and renal threshold maximum for phosphate reabsorption (TmP/GFR) were lower than reference ranges in all subjects. Single doses of either IV or SC KRN23 increased serum P, TmP/GFR and 1,25D compared to placebo for higher doses. Peak serum P effects occurred later with SC (8-15 days) than with IV dosing (0.5-4 days). Duration of effect on P was dose-related, greater with SC than IV, and persisted beyond 29 days with SC. No meaningful changes in serum calcium, serum parathyroid hormone, or urinary calcium excretion occurred. Adverse events (AEs) occurred with higher frequency in patients receiving KRN23 (82% IV and 83% SC) compared to those receiving placebo (40% IV and 50% SC). AEs considered related to the study drug occurred in 6 patients (4 in IV dose groups [24%] and 2 in SC groups [17%]). There were no SAEs, and no changes in safety biochemistries, ECGs, or renal sonograms. Single-dose administration of KRN23 was safe and well-tolerated; no patient developed anti-KRN23 antibodies.

Conclusions: Blocking FGF23 activity with KRN23 is a novel treatment for XLH. Single IV or SC doses increased serum P and TmP/GFR, with effects lasting for more than 4 weeks with SC dosing.

***Disclosures: Thomas Carpenter**, Kyowa Hakko Kirin Inc., 6; Kyowa Hakko Kirin Inc., 2*
This study received funding from: Kyowa Hakko Kirin Pharma Inc.

1049

Fracture Patterns with use of Selective Serotonin Receptor Inhibitors, Proton Pump Inhibitors and Glucocorticoids in a Large International Observational Study: GLOW. Jonathan Adachi*[1], Allison Wyman[2], Gordon FitzGerald[2], Silvano Adami[3], Steven Boonen[4], Roland Chapurlat[5], Juliet Compston[6], Cyrus Cooper[7], Adolfo Diez-Perez[8], Stephen Gehlbach[9], Susan Greenspan[10], Andrea Lacroix[11], Robert Lindsay[12], Lyn March[13], Coen Netelenbos[14], Johannes Pfeilschifter[15], Maurizio Rossini[16], Christian Roux[17], Kenneth Saag[18], Ethel Siris[19], Stuart Silverman[20], Nelson Watts[21]. [1]St. Joseph's Hospital, Canada, [2]UMASS Medical School, USA, [3]University of Verona, Italy, [4]Center for Metabolic Bone Disease & Division of Geriatric Medicine, Bel, [5]E. Herriot Hospital, France, [6]University of Cambridge School of Clinical Medicine, United Kingdom, [7]University of Southampton, United Kingdom, [8]Autonomous University of Barcelona, Spain, [9]University of Massachusetts, USA, [10]University of Pittsburgh, USA, [11]Fred Hutchinson Cancer Research Center, USA, [12]Helen Hayes Hospital, USA, [13]Royal North Shore Hospital, Australia, [14]VU Medical Center, The Netherlands, [15]Alfried Krupp Krankenhaus Steele, Germany, [16]University of Verona, Italy, [17]Hospital Cochin, France, [18]University of Alabama at Birmingham, USA, [19]Columbia University College of Physicians & Surgeons, USA, [20]Cedars-Sinai/UCLA, USA, [21]Mercy Health Osteoporosis & Bone Health Services, USA

Introduction: Selective serotonin receptor inhibitors (SSRIs), proton pump inhibitors (PPIs) and glucocorticoids (GCs) are associated with increased fracture risk. The objective of this study is to assess patterns of fractures over 5 years among GLOW participants.

Methods: GLOW comprises women ⩾55 years of age, enrolled in 615 primary care practices (17 sites, 10 countries). Self-administered surveys, mailed at baseline, 12, 24, 36 and 60 months, sought data on patient characteristics, risk factors, and use of estrogens, SSRIs, PPIs, GCs and anti-osteoporosis medication (AOM). Multivariable regression calculated odds ratios (ORs) and 95% confidence intervals (CIs). Adjustment was made for age, fracture between age 45 and enrollment into the study (baseline), and baseline use of anti-osteoporosis medication.

Results: 9347 subjects were never treated with SSRIs, GCs, PPIs, estrogen or AOM; 2715 women were on PPIs, 5304 on GCs and 1149 on SSRIs at some point between baseline and year 2. SSRI use was the only therapy associated with a statistically significant increase in overall, clinical spine and non-hip-non-vertebral (NHNV) fractures (Table). GCs were significantly associated with spine fractures. PPIs, while not statistically significant, were associated with NHNV fractures.

Introduction: Selective serotonin receptor inhibitors (SSRIs), proton pump inhibitors (PPIs) and glucocorticoids (GCs) are associated with increased fracture risk. The objective of this study is to assess patterns of fractures over 5 years among GLOW participants.

Methods: GLOW comprises women ⩾55 years of age, enrolled in 615 primary care practices (17 sites, 10 countries). Self-administered surveys, mailed at baseline, 12, 24, 36 and 60 months, sought data on patient characteristics, risk factors, and use of estrogens, SSRIs, PPIs, GCs and anti-osteoporosis medication (AOM). Multivariable regression calculated odds ratios (ORs) and 95% confidence intervals (CIs). Adjustment was made for age, fracture between age 45 and enrollment into the study (baseline), and baseline use of anti-osteoporosis medication.

Results: 9347 subjects were never treated with SSRIs, GCs, PPIs, estrogen or AOM; 2715 women were on PPIs, 5304 on GCs and 1149 on SSRIs at some point between baseline and year 2. SSRI use was the only therapy associated with a statistically significant increase in overall, clinical spine and non-hip-non-vertebral (NHNV) fractures. GCs were significantly associated with spine fractures. PPIs, while not statistically significant, were associated with NHNV fractures.

Conclusions: SSRIs were associated with the greatest risk for fracture (any fracture, vertebral fracture and NHNV), followed by GCs (vertebral only).

Table 1. Multivariable regression model predicting year 3/year 5 fracture, based on medication use (vs no medication use)

Medication Use	SSRI	GC	PPI
Any fracture*			
Odds ratio	1.66	1.06	1.16
95% CI	(1.31–2.11)	(0.91–1.23)	(0.97–1.40)
p-value	<0.0001	0.46	0.11
Hip fracture			
Odds ratio	0.65	1.13	0.57
95% CI	(0.20–2.09)	(0.71–1.79)	(0.28–1.17)
p-value	0.47	0.60	0.13
Spine fracture			
Odds ratio	2.18	1.63	1.43
95% CI	(1.12–4.26)	(1.08–2.47)	(0.86–2.38)
p-value	0.022	0.021	0.17
NHNV fracture†			
Odds ratio	1.66	0.99	1.19
95% CI	(1.29–2.15)	(0.84–1.17)	(0.98–1.45)
p-value	<0.0001	0.90	0.08

*Self-reported fracture of any of the following bones: collar bone or clavicle, upper arm, wrist, spine, rib, hip, pelvis, ankle, upper leg, or lower leg.
† Self-reported fracture of any of the following bones: collar bone or clavicle, upper arm, wrist, rib, pelvis, ankle, upper leg, or lower leg.

Table 1

***Disclosures: Jonathan Adachi**, Warner Chilcott Company, 6; sanofi-aventis , 6*
This study received funding from: Warner Chilcott Company, LLC, sanofi-aventis

1050

Prevention of Bone Loss in Breast Cancer Survivors on Aromatase Inhibitors: Results of the REBBeCA II Trial. Susan Greenspan*[1], Subashan Perera[1], Karen Vujevich[1], Gisberta van Londen[2], Adam Brufsky[2], Barry Lembersky[2], Shannon Puhalla[2]. [1]University of Pittsburgh, USA, [2]Magee-Womens Hospital, USA

Background: Aromatase inhibitors (AIs) including anastrozole, letrozole, and exemestane are routinely used for adjuvant treatment of postmenopausal women with hormone receptor positive breast cancer. Because AIs inhibit peripheral conversion of androgens to estrogen, women have a marked reduction in estrogen leading to accelerated bone loss and fractures. Little data are available on the impact of an oral bisphosphonate in women with low bone mass (not osteoporosis) who are on these commonly used AIs. The goal of the REBBeCA II trial (Risedronate's Effect on Bone in women with Breast CAncer II) was to examine the prevention of bone loss with the oral bisphosphonate risedronate in breast cancer survivors on an AI.

Methods: This 2-year randomized, double-blind, placebo-controlled trial included postmenopausal women over age 55 with breast cancer on an AI who had low bone mass, were not treated with a bisphosphonate in the previous year, and had no illness or were on no medications known to affect bone and mineral metabolism. Subjects provided informed consent and were randomized to risedronate 35 mg once weekly or placebo. All received daily calcium (up to 1200 mg daily) and vitamin D (800 IU). The primary outcomes were 24 month changes in spine, total hip and femoral neck bone mineral density (BMD), analyzed using linear mixed models.

Results: Of the 109 randomized, 77% were on anastrozole, 15% on letrozole and 8% on exemestane. Mean age was 64.2 years and there were no baseline differences between the groups in age, BMI, calcium/vitamin D intake or BMD. 87% completed 24 months. The BMD percent changes at the spine, total hip, and femoral neck showed significant increases in the active treatment group compared to the placebo group at 12 and 24 months (table), with 24 month absolute difference of 3.9 percentage points at the spine and 3.2 at the total hip. The medication was well tolerated and there were no significant differences in serious adverse events or deaths.

Conclusions: The oral bisphosphonate risedronate maintained/improved skeletal integrity over 2 years during a time of accelerated bone loss in breast cancer survivors on AIs.

Table: Percent change ± standard error in bone mineral density at the spine, total hip and femoral neck

Skeletal site	Month	Active (N=55)	Placebo (N=54)	P-value (between group difference)
Spine	12	2.0±0.5**	-1.2±0.5 *	<0.01
	24	2.3±0.6**	1.7±0.6**	<0.01
Total hip	12	0.5±0.4	-1.6±0.4**	<0.01
	24	0.6±0.4	-2.7±0.5 **	<0.01
Femoral neck	12	-0.3±0.5	-1.7±0.5 *	NS
	24	0.4±0.6	-2.1±0.6 **	<0.01

*p≤0.05, ** p≤0.01 within group change from baseline

Table

***Disclosures: Susan Greenspan**, None.*
This study received funding from: Warner Chilcott

1051

Pathogenesis of Cortical Deficits and Decreased Bone Stiffness after Kidney Transplantation. Kyle Nishiyama[1], Sapna Iyer[2], Lucas Nikkel[3], Chiyuan Zhang[1], Elzbieta Dworakowski[1], Serge Cremers[1], Bin Zhou[1], Donald McMahon[4], X Guo[1], Elizabeth Shane[4], Thomas Nickolas*[4]. [1]Columbia University, USA, [2]University of California San Diego, USA, [3]Columbia University Medical Center, USA, [4]Columbia University College of Physicians & Surgeons, USA

Fracture risk is more than 4-fold higher after kidney transplantation than in the general population. We reported that hyperparathyroidism (HPT) is associated with progressive cortical (Ct) losses in patients with chronic kidney disease. As HPT commonly persists after kidney transplantation, we hypothesized that Ct deficits would worsen, would be directly associated with HPT and elevated bone turnover markers, and would lead to impaired bone strength. We scanned the distal radius and tibia by high-resolution peripheral quantitative CT (HRpQCT, Scanco Medical) in 31 patients (22 men, 9 women; age 52±13 years) within 2 weeks of, and 1 year after transplantation. Ct porosity (CtPo) was quantified by indexing the Ct region of interest to the baseline image and endocortical losses at follow-up were quantified as CtPo. Whole bone stiffness and failure load were estimated using finite element analysis. Intact PTH and markers of bone formation (BSAP, osteocalcin, P1NP) and resorption (CTX and Trap5b) were measured at 3, 6 and 12 months post-transplantation and were time-averaged. Mixed linear models adjusted for baseline bone measures were used to determine longitudinal changes. At 1 year, 74% of patients had HPT (PTH>65 pg/mL). At the radius, Ct density decreased by 2.2±1.8%, thickness by 2.2±0.8% and area by 2.5±0.8% (all $p<0.05$); CtPo increased by 78±9% ($p<0.01$) and trabecular area by 0.4±1.8% ($p=0.06$). Stiffness and failure decreased by 3.1±1.3% and by 3.4±1.4% (both $p<0.05$) respectively. At the tibia, Ct density decreased by 1.9±0.6% and thickness by 1.1±0.5% (both

p<0.05); CtPo increased by 30±5% (p<0.05). Changes in stiffness and failure load were not significant. At 1 year, greater CtPo was significantly associated with lower Ct density, thickness and area, and whole bone stiffness and failure load (all p<0.001). Correlations between bone metabolic markers and changes in Ct measures, stiffness and failure load were strongest at the radius (Table). Decreases in stiffness and failure load were strongly associated with higher levels of PTH (r= -0.45, p<0.05) and remodeling markers (Osteocalcin and Stiffness r= -0.70; Osteocalcin and Failure Load r= -0.64, both p<0.001). In conclusion, persistent HPT and elevated bone turnover after transplantation drive progressive Ct deterioration and decreased bone stiffness. Further studies are needed to determine whether mitigating the adverse effects of HPT on cortical bone will protect against fracture.

Correlations between Cortical Measures and Bone Stiffness and Failure Load at 1-year follow-up and Biomarkers of Bone Metabolism*

	PTH	BSAP	Osteocalcin	P1NP	CTX	Trap5b
			Radius			
Ct Density	-0.55 (<0.01)	-0.59 (<0.01)	-0.59 (<0.01)	-0.53 (<0.01)	-0.71 (<0.001)	-0.39 (0.06)
Ct Thickness	-0.30 (0.2)	-0.52 (<0.01)	-0.55 (<0.01)	-0.44 (<0.05)	-0.47 (<0.05)	-0.26 (0.2)
Ct Area	-0.25 (0.2)	-0.55 (<0.01)	-0.68 (<0.001)	-0.59 (<0.01)	-0.53 (<0.01)	-0.45 (<0.05)
Tb area	0.25 (0.2)	0.09 (0.7)	-0.12 (0.6)	-0.15 (0.5)	0.06 (0.8)	-0.27 (0.2)
Ct Porosity	0.64 (<0.001)	0.62 (<0.01)	0.54 (<0.01)	0.50 (<0.05)	0.64 (<0.001)	0.40 (<0.05)
Stiffness	-0.24 (0.3)	-0.45 (<0.05)	-0.70 (<0.001)	-0.60 (<0.01)	-0.58 (<0.01)	-0.41 (<0.05)
Failure Load	-0.12 (0.6)	-0.37 (0.07)	-0.64 (<0.001)	-0.56 (<0.01)	-0.45 (<0.05)	-0.35 (0.1)
			Tibia			
Ct Density	-0.29 (2)	-0.18 (0.4)	-0.39 (0.05)	-0.15 (0.5)	-0.41 (0.04)	-0.22 (0.29)
Ct Thickness	-0.13 (0.5)	-0.41 (<0.05)	-0.39 (0.06)	-0.34 (0.09)	-0.22 (0.3)	-0.17 (0.4)
Ct Area	-0.18 (0.4)	-0.51 (<0.01)	-0.61 (<0.01)	-0.54 (<0.01)	-0.43 (<0.05)	-0.38 (0.06)
Tb area	0.08 (0.7)	-0.20 (0.3)	-0.33 (0.1)	-0.33 (0.1)	-0.25 (0.2)	-0.44 (<0.05)
Ct Porosity	0.298 (0.2)	-0.08 (0.8)	0.18 (0.4)	-0.10 (0.6)	0.17 (0.4)	0.03 (0.9)
Stiffness	-0.00 (1)	-0.35 (0.09)	-0.50 (<0.05)	-0.45 (<0.05)	-0.33 (0.1)	-0.33 (0.1)
Failure Load	0.06 (0.8)	-0.30 (0.2)	-0.42 (<0.05)	-0.54 (<0.01)	-0.38 (0.06)	-0.32 (0.1)

* data is represented as r (p-value)

Table

***Disclosures: Thomas Nickolas**, None.*

1052

Circulating Sclerostin is Negatively Associated with Cortical BMD, PINP, Estradiol and IGF-1. Jennifer Walsh*, Fatma Gossiel, Margaret Paggiosi, Richard Eastell. University of Sheffield, United Kingdom

Sclerostin is produced by osteocytes and inhibits osteoblast function through the Wnt signalling pathway. It may be an important mediator of the skeletal response to loading.

We measured serum sclerostin in 170 healthy men and women ages 16-18, 30-32 and over 70, to determine 1) how sclerostin varies with age and gender, 2) whether it correlates with BMD by DXA and BMD and microarchitecture assessed by HR-pQCT, 3) whether it correlates with bone formation markers and IGF-1.

Sclerostin was measured using an ELISA from BioMedica (Austria). Sclerostin was not normally distributed so non-parametric tests were used (Kruskal-Wallis for group comparisons and Spearman's rank for correlation).

Sclerostin did not differ between men and women (mean (95% CI); men 27.9 (25.0 to 30.9), women 25.1 (22.4 to 27.8) pmol/l). It was higher in adults aged over 70 than in younger adults (mean (95% CI); ages 16-18 22.0 (17.8 to 26.3), ages 30-32 22.6 (20.8 to 24.5), ages 70+ 35.5 (32.5 to 38.5) pmol/l (p<0.001)).

Sclerostin was not correlated with BMD by DXA at the spine or hip. At the distal radius, sclerostin was negatively correlated with total BMD (r -0.30, p <0.001), cortical BMD (r -0.32, p<0.001), cortical thickness (r -0.35, p<0.001) and trabecular thickness (r -0.17, p<0.05), but positively correlated with total area (r 0.20, p<0.01). At the distal tibia, sclerostin was negatively correlated with total BMD (r -0.17, p <0.05) and cortical BMD (r -0.24, p<0.001).

Sclerostin was negatively correlated with PINP (r -0.23, p <0.001), and IGF-1 (r -0.47, p <0.001). It was negatively correlated with estradiol in women (r -0.51, p<0.001), but not in men.

These results support the role of sclerostin as an inhibitor of bone formation. The DXA and HR-pQCT result suggest that it is more strongly associated with cortical bone density than trabecular properties. Estradiol may influence sclerostin secretion through direct actions on osteocytes, and previous studies show that estrogen receptors interact with mechanical strain to control the skeletal response to loading. IGF-1 is an important regulator of bone formation and muscle mass. It is possible that IGF-1 is associated with sclerostin via muscle mass and hence bone loading, or that it influences sclerostin secretion directly.

***Disclosures: Jennifer Walsh**, None.*

1053

Serum Estradiol Levels are Inversely Associated with Cortical Pore Size in Older Men – The MrOS Sweden Study. Liesbeth Vandenput*[1], Maria Nilsson[2], Daniel Sundh[3], Magnus Karlsson[4], Mattias Lorentzon[5], Dan Mellstrom[6], Claes Ohlsson[7]. [1]University of Gothenburg, Sweden, [2]Department of Clinical Chemistry, Sahlgrenska University Hospital, Sweden, [3]Centre for Bone & Arthritis Research, Institute of Medicine, Sahlgrenska Academy, University of Gothenburg, Sweden, [4]Skåne University Hospital Malmö, Lund University, Sweden, [5]Geriatric Medicine, Center for Bone Research at the Sahlgrenska Academy, Sweden, [6]Sahlgrenska University Hospital, Sweden, [7]Center for Bone & Arthritis Research at the Sahlgrenska Academy, Sweden

It has been firmly established that estradiol (E2) plays a fundamental role in the maintenance of skeletal health in men. Serum E2 levels associate not only with bone mineral density (BMD) and BMD loss but are also predictors of incident fracture risk in older men. Yet, the role of E2 for trabecular and cortical bone microstructure, measurable by high-resolution peripheral quantitative computed tomography (HRpQCT), still remains unknown.

Therefore, we examined the associations between serum levels of E2, testosterone (T) (both analyzed by gas chromatography-mass spectrometry) and sex hormone-binding globulin (SHBG) and HRpQCT-derived bone parameters at the tibia in older men (n=438, mean 80.1 years of age) participating in the prospective population-based MrOS Sweden cohort.

In regression analyses adjusted for age, height and weight, serum E2 associated inversely with both cortical porosity (standardized beta= -0.11, p<0.05) and cortical pore diameter (beta= -0.14, p<0.01). Serum T associated only moderately with cortical pore diameter (beta= -0.10, p=0.04), whereas SHBG was not associated with any of these cortical microstructural parameters. Interestingly, multiple linear regression models including serum E2, T, and SHBG and adjusted for age, height and weight demonstrated that only serum E2 associated independently with both cortical porosity (beta= -0.11, p=0.01) and cortical pore diameter (beta= -0.14, p<0.01). In addition, serum E2 associated with the cortical pore diameter distribution (beta= -0.13, p<0.01). In similar analyses, serum E2, T and SHBG were not associated with any of the trabecular microstructural parameters such as trabecular bone volume/total volume (BV/TV), trabecular number and trabecular thickness.

In conclusion, serum E2 levels are inversely associated with cortical pore size in older men. This might indicate, as previously suggested, that serum E2 is more important for cortical than trabecular bone structure in older subjects. A recent study indicated that bone loss in elderly subjects is mainly due to loss of cortical and not trabecular bone. In addition, it has been proposed that the age-related increase in cortical porosity is a major determinant of cortical bone strength. We propose that serum E2 may modulate cortical bone strength by affecting the cortical pore size, and, thus, indirectly may influence fracture risk.

***Disclosures: Liesbeth Vandenput**, None.*

1054

3D-XA-Based Vertebral Finite Element Model for Strength Evaluation in Osteoporosis. Christophe Travert*[1], Anabela Darbon[2], Nicolas Vilayphiou[3], Helene Follet[4], Jean-Baptiste Pialat[5], Wafa Skalli[6]. [1]Arts et Metiers ParisTech, France, [2]EOS imaging, France, [3]INSERM UMR1033, Université de Lyon & Hospices Civils de Lyon, France, [4]INSERM, UMR1033; Universite De Lyon, France, [5]INSERM U1033, Team1, Université de Lyon & Hospices Civils de Lyon, France, [6]Arts et Metiers ParisTech, Fra

CT-scan-based Finite Element Models (FEM) have been proposed to evaluate vertebral strength and fracture risk. The main limitation of such approach in routine osteoporotic diagnosis is the cost of CT-scan. Developing an accurate FEM which is deployable at a large scale is still a challenge. Approaches have been proposed to build a FEM using 2D Bone Mineral Density (BMD) measurements, such as DXA or the EOS system in dual energy. However, specific algorithms are required to estimate the BMD distribution in such models.

The purpose of this study is to develop a method to estimate 3D BMD distribution from 2D BMD measurements and evaluate its impact on vertebral strength estimation.

Lumbar spine segments (6 donors aged 80 ± 9 years) have been imaged with the EOS low dose X-ray device in dual energy to provide frontal and lateral BMD images of the spine segments, and to build 19 3D-XA vertebral FEMs (fig. 1). In addition, they have been scanned with a calibration phantom to build CT-based FEMs. In the CT FEM, geometry was obtained by segmentation. A specific meshing technic was developed to obtain regular hexahedral meshes while respecting shape accuracy. Material properties were assigned to each element of the model using published relationship between volume BMD and Young modulus. A convergence analysis was performed to select appropriate mesh refinement. For the 3D-XA FEM, 3D geometry was reconstructed using the pair of EOS images and the same meshing technic was used. A generic BMD distribution was first associated to this mesh from an independent vertebral model database, then element BMD values were adjusted to insure image similarity between the dual energy images and virtual images derived from this estimated BMD distribution. Average vertebral body volume BMD and

BMD distribution in 27 areas of the 3D-XA FEMs were compared to CT-scan. Vertebral strength was estimated in anterior compression on CT and 3D-XA FEM for comparison.

Average vertebral body BMD was estimated by the EOS model with a root mean square error (RMSE) of 13mg/cm^3 with no significant bias. In the 27 areas, RMSE was 40mg/cm^3. The failure load of the CT and 3D-XA FEM were 3217 $\pm$ 1294 N and 3346 $\pm$ 1337 N respectively, with R^2 = 0.91 and RMSE = 409 N between the two FEMs (fig. 2).Although these results should be confirmed by experimentations *in vitro* and *in vivo*, 3D-XA FEM appears as a good alternative to CT-based FEM. They could help osteoporotic fracture risk assessment in clinical routine.

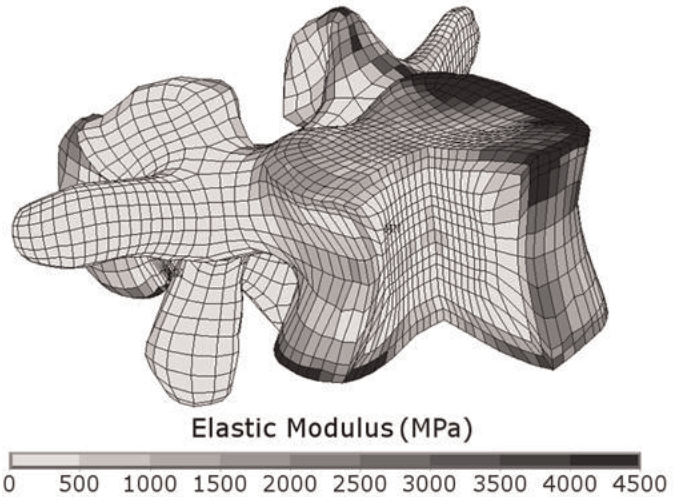

Figure 1: Low-dose finite element model (cut view)

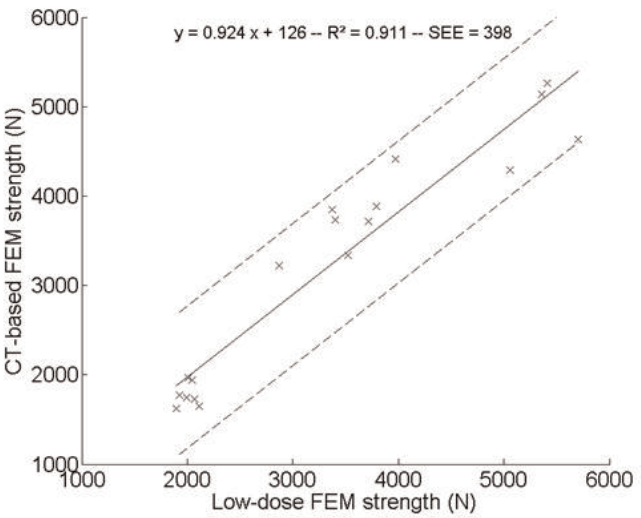

Figure 2: Comparison of the low-dose and CT-based models

***Disclosures: Christophe Travert**, None.*

1055

Bone gain with unexpected elevated bone resorption by activating canonical Wnt/βcatenin signaling in osteocytes. Xiaolin Tu*[1], Kevin McAndrews[1], Meloney Cregor[1], Munro Peacock[2], Makoto M. Taketo[3], Lilian Plotkin[1], Teresita Bellido[1]. [1]Indiana University School of Medicine, USA, [2]Indiana University Medical Center, USA, [3]Department of Pharmacology, Graduate School of Medicine, Kyoto University, Japan

Osteocytes orchestrate the response of osteoblasts and osteoclasts to mechanical and hormonal stimuli by modulating Wnt signaling. Moreover, deletion from osteocytes of βcatenin, the obligatory transducer of canonical Wnt signaling, leads to low bone mass and high resorption. However, the consequences of activating canonical Wnt/βcatenin signaling in osteocytes are unknown. To address this question, we generated mice expressing a dominant active (da) form of βcatenin in these cells (daβCat^{Ot}), by crossing Catnb$^{lox(ex3)}$ mice, in which the phosphorylation sites required for βcatenin degradation are flanked by loxP sites, with DMP1-8kb-Cre mice. daβcat^{Ot} mice display no gross skeletal abnormalities at birth, exhibit tooth eruption, and live up to 1 year. These features contrast with those of daβcat$^{Ob/Ot}$ mice expressing the same da βcatenin in both osteoblasts and osteocytes (Col1-2.3kb-Cre), which lack tooth eruption due to decreased resorption and die after weaning. At 4 months, daβcat^{Ot} mice showed denser bones by X-ray and increased total, spinal, and femoral BMD (142, 152 and 128%, compared to control Catnb$^{lox(ex3)}$ littermates). Distal femur μCT revealed increased BV/TV and trabecular number (499 and 469%), decreased trabecular separation (71%), with no changes in trabecular thickness. In contrast to daβcat$^{Ob/Ot}$ mice that exhibit decreased bone resorption, daβcat^{Ot} mice display high resorption with 4.3- and 2.5-fold increase in CTX at 2 and 4 months, respectively, vs controls. Circulating alkaline phosphatase was also increased 4- and 3-fold at 2 and 4 months, respectively; but osteocalcin was similar to controls. Gene expression analysis of bones (L4) revealed the expected upregulation of Wnt target genes (lef1, BMP4, Cx43, axin2 and Smad6). Similar to daβcat$^{Ob/Ot}$ mice, OPG expression in daβcat^{Ot} mice was high (>4-fold). However, RANKL expression was also high (>9-fold) resulting in increased RANKL/OPG ratio; and MCSF expression was also increased. Moreover, Runx2 and alkaline phosphatase expression was markedly increased in daβcat^{Ot} mice, but osteocalcin expression was not different. Thus, activation of canonical Wnt/βcatenin signaling in osteocytes increases bone remodeling with a positive balance in favor of bone gain. These findings establish unexpected converse changes in resorption by activating canonical Wnt/βcatenin signaling in osteocytes vs osteoblasts/osteocytes; and high resorption by either activating or deleting βcatenin in osteocytes.

***Disclosures: Xiaolin Tu**, None.*

1056

Wnt Production of Signaling in Fate Determination and Differentiation of the Skeletal Precursors. Wei Hsu, Takamitsu Maruyama*, Ming Jiang. University of Rochester Medical Center, USA

The Wnt signal transduction pathway controls development of various stem cell types essential for proper formation of multiple organs. In the skeleton, Wnt signaling regulates bone formation and remodeling through modulation of osteoblasts, chondrocytes and osteoclasts. Genetic inactivation of *CTNNB1* encoding β-catenin further indicates its important function in the determination of mesenchymal cell fate. We have recently identified *Gpr177*, the mouse orthologue of *Drosophila Wls*/*Evi*/*Srt* essential for Wnt sorting and secretion. The protein encoded by *Gpr177* exhibits an ability to regulate the intracellular trafficking of Wnt proteins in signal-producing cells. Human genetic analysis further reveals that *Gpr177* is a susceptibility locus for bone-mineral-density and osteoporosis. To determine the unknown function of this gene in skeletogenesis, we have generated four different mouse models with Gpr177 deficiency in various skeletal cell types. The loss of Gpr177 severely impairs development of the craniofacial and body skeletons, demonstrating its requirement for intramembranous and endochondral ossifications, respectively. Defects in the expansion of skeletal precursors and their differentiation into osteoblasts and chondrocytes suggest that Wnt production and signaling mediated by Gpr177 cannot be substituted. Mesenchymal but not osteoblast production of Wnt is essential for development of the skeletal precursors into osteoblast lineage. However, Wnt proteins produced by chondrocytes are necessary for the chondrogenic lineage. Our findings not only identify the sources of Wnt essential for osteogenesis and chondrogenesis, but also reveal the function of Gpr177 in modulating the interplay of Wnt signals across distinct cell types. However, the disruption of Wnt secretion does not result in mesenchymal cell fate change. The discrepancy is likely attributed to the dual role of β-catenin in cell adhesion and signaling as the loss of Gpr177 would not interfere with cell-cell interaction. To test the possible involvement of β-catenin-mediated cell adhesion regulating the lineage commitment of mesenchymal cells, we have created mice with disruption of only the transcriptional activity of β-catenin required for Wnt signal transduction. Without interfering with cell adhesion, these mutants permit a definitive assessment of β-catenin as a master transducer of Wnt signaling, leading to a new mechanism underlying mesenchymal cell fate determination mediated by β-catenin.

***Disclosures: Takamitsu Maruyama**, None.*

1057

Wnt16 Deletion Differentially Affects Cortical and Trabecular Bone: Increased Cortical Bone Resorption, Porosity and Fracture in Wnt16 Knockout Mice. Xianwen Liu*[1], Kenichi Nagano[2], Hiroaki Saito[2], Roland Baron[3], Francesca Gori[4]. [1]Harvard School of Dental Medicine, Sichuan University, USA, [2]Harvard School of Dental Medicine, USA, [3]Harvard School of Medicine of Dental Medicine, USA, [4]Harvard School of Dental Medicine, Massachusetts General Hospital, USA

Wnt16 has recently emerged as a determinant of cortical bone thickness, bone mineral density, bone strength, and fracture risk in several GWAS studies (Medina-Gomez *et al.* PLoS Genet. 2012, Zheng *et al.* PLoS Genet. 2012). Decreased cortical bone density is associated with non-vertebral osteoporotic fractures but the mechanisms by which cortical bone mass is regulated remain largely unknown. To examine the role of Wnt16 in bone homeostasis, we analyzed Wnt16$^{-/-}$ mice. Micro-CT and bone histomorphometry show a marked decrease in cortical bone thickness in both Wnt16$^{-/-}$ male (-22.73% $\pm$7.21%) and female (-25.62% $\pm$4.75%) compared to WT littermates. Notably, cortical bone porosity was significantly increased in both male (+29.11%$\pm$15.32%) and female (+38.56%$\pm$14.19%) Wnt16$^{-/-}$ mice compared to WT littermates and approximately 30% of Wnt16$^{-/-}$ mice developed spontaneous long

bone fractures. The endocortical surface showed a marked increase in osteoclast numbers and surface, with no changes in osteoblast (OB) numbers. In sharp contrast with the changes in cortical bone, a small but significant increase in trabecular bone volume was observed in Wnt16$^{-/-}$ mice, with no changes in other histomorphometric parameters. Analysis of femur cortical bone showed that the decrease in cortical bone mass was associated with a significant increase in sclerostin and a decrease in OPG, leading to a marked increase in the RANKL/OPG ratio. Accordingly, Wnt16 deletion results in a marked increase in osteoclastogenesis in vitro. Importantly, Wnt16 is a potent regulator of non-canonical Wnt signaling as indicated by the significant reduction in JNK and c-JUN phosphorylation levels seen with Wnt16 deletion. The opposite was true in Wnt16 treated osteoblasts. Furthermore, activation of Topflash reporter assay, increased expression of Wnt target genes including TCF1 and Axin2, ß-catenin and phosphorylated LRP6 levels seen in OBs treated with Wnt16 protein, imply that Wnt16 also signals via or indirectly affects canonical Wnt signaling. These data demonstrate that Wnt16 has a crucial role in cortical bone homeostasis. Deletion of Wnt16 specifically affects cortical bone in mice, increasing sclerostin and RANKL/OPG ratio and leads to increased resorption and porosity and decreased thickness. These findings provide a novel insight into the mechanism by which cortical bone homeostasis is regulated in mice and may help explain the link between Wnt16, bone mass and fractures in humans.

***Disclosures: Xianwen Liu**, None.*

1058

Downregulation of PLCγ2/β-catenin pathway promotes activation and expansion of Myeloid-Derived Suppressor cells in cancer. Aude-Helene CAPIETTO*[1], Seokho Kim[2], Deborah Novack[2], Roberta Faccio[2]. [1]Washington University School of Medicine, USA, [2]Washington University in St Louis School of Medicine, USA

Myeloid-derived Suppressor Cells (MDSC) promote tumor dissemination by mainly suppressing anti-tumor T-cell responses in many cancers. Although the mechanism of T-cell inhibition is well-established, the pathways leading to MDSC accumulation in bone marrow and secondary lymphoid organs remain unclear. We found that downregulation of PLCγ2 signaling in tumor-bearing mice induces aberrant expansion of MDSC in the bone marrow, spleen and tumor site. To analyze whether MDSC promote tumorigenesis in PLCγ2-/- mice, we adoptively transferred MDSC isolated from PLCγ2-/- or WT mice into subcutaneous tumor-injected WT mice. Animals receiving PLCγ2-/- MDSC displayed greater expansion of MDSC in the spleen and increased tumor burden compared to mice receiving WT MDSC. Furthermore, PLCγ2-/- MDSC were more efficient than WT cells to suppress CD8+ T-cell proliferation, via increased ROS and NO production. Mechanistically, PLCγ2-/- MDSC display reduced β-catenin levels and its rescued expression decreases MDSC expansion and tumor growth in PLCγ2-/- mice. In addition, the deletion of β-catenin in myeloid cells (LysM-Cre/β-cat.cKO), including MDSC, led to enhanced tumor growth and a 2-fold increase in MDSC compared to control mice. By contrast, constitutive β-catenin activation in myeloid cells (LysM-Cre/β-cat.CA) decreased tumor growth while MDSC percentage was reduced compared to control mice. Consistent with a role for β-catenin in MDSC during tumor progression, its expression was reduced in tumor-bearing WT mice compared to tumor-free animals. The relevance of the PLCγ2/β-catenin axis is further documented in MDSC from pancreatic cancer patients which show reduced phospho-PLCγ2 and β-catenin expression levels compared to healthy controls. Importantly, aberrant expansion of MDSC in tumor bearing hosts is also likely to contribute to bone metastatic dissemination, even in the context of osteoclast blockade. Consistent with this hypothesis, PLCγ2-/- mice display increased bone tumor burden compared to WT animals despite reduced osteoclast differentiation and function. The elevated rate of tumor growth in bone is due to impaired CD8+ T-cell responses and correlates with greater accumulation of MDSC in spleen of PLCγ2-/- mice. In conclusion, we show that downregulation of PLCγ2/β-catenin pathway occurs in mice and humans, leading to MDSC-mediated tumor expansion. Our data also implicates MDSC as new modulators of bone metastases.

***Disclosures: Aude-Helene CAPIETTO**, None.*

1059

Adult-onset deletion of β-catenin in 10kbDmp1-expressing cells prevents intermittent PTH-induced bone gain. Alexander Robling[1], Rajendra Kedlaya*[1], Paola Divieti Pajevic[2]. [1]Indiana University, USA, [2]Massachusetts General Hospital & Harvard Medical School, USA

PTH is a potent calcium-regulating factor with anabolic and catabolic properties. Bone cells express PTH receptors, but the cellular responses to PTH in bone are incompletely understood. Wnt signaling has recently been implicated in the osteoanabolic response to the hormone. Whereas downstream nodes of the canonical Wnt pathway itself, and canonical Wnt-responsive transcriptional mechanisms are altered by PTH treatment, it is less clear whether the Wnt pathway is required for the anabolic action of PTH. We have found that the Wnt co-receptor Lrp5 is not required for intermittent PTH (iPTH) effects, and others have reported that the cytoplasmic tail of Lrp5 does not undergo phosphorylation in response to PTH treatment, whereas that of Lrp6 does. Whether Lrp6 is required for PTH effects in bone is less clear, partly because Lrp6$^{-/-}$ mice die at birth and are precluded from study. We sought to better understand the role of Wnt signaling in iPTH-induced bone metabolism by targeting and disabling β-catenin—a downstream facilitator of canonical Lrp5/Lrp6 signaling—during iPTH treatment. Male mice homozygous for the floxed loss-of-function β-catenin allele (loxP in introns 1 and 6) were raised with and without the tamoxifen-inducible 10kbDmp1-CreERt2 transgene. At 12 wks of age, the mice were given DEXA scans then treated with 3 doses of tamoxifen (20 mg/kg) or corn oil, spaced 7 days apart, to induce recombination of the β-catenin alleles. Two days after beginning tamoxifen/oil treatment, the mice were given daily injection of 30 ug/kg human PTH 1-34 or vehicle control. After 4 wks of treatment, the mice were given a second DEXA scan and sacrificed. Tamoxifen treatment in had a small but significant effect on bone mass in the presence of PTH or vehicle. PTH increased whole body BMD by 7.5% in control (oil-treated) mice, compared to a 1.6% increase in BMD among control mice receiving vehicle. In mice receiving tamoxifen (conditional β-catenin KO), BMD was unchanged by vehicle treatment. PTH treatment in these mice was not effective in improving bone mass, and significantly exacerbated bone loss in the spine. In summary, the anabolic action of iPTH appears to require funcitonal β-catenin in Dmp1-expressing cells. Because signaling pathways other than Wnt/Lrp5/6 effects β-catenin (e.g., PKA, mTor), it is unclear whether the deficit in PTH signaling observed in β-catenin mutant mice extends from Wnt or from an alternate pathway.

***Disclosures: Rajendra Kedlaya**, None.*

1060

Continuous PTH Infusion Increases Trabecular but Not Cortical Bone in Cyclooxygenase-2 Knockout Mice. Shilpa Choudhary*[1], Ernesto Canalis[2], Adam Harris[1], Douglas Adams[1], Renata Rydzik[1], Carol Pilbeam[1]. [1]University of Connecticut Health Center, USA, [2]St. Francis Hospital & Medical Center, USA

Intermittent PTH *in vivo* increases bone mass, while continuous PTH infusion causes bone loss. *In vitro,* continuous PTH inhibits osteoblast differentiation in marrow stromal cells but can stimulate differentiation if COX-2 expression or activity is absent. We examined the impact of COX-2 knockout (KO) on continuous PTH infusion *in vivo*. Three-mo old male wild type (WT) and KO mice (n=6-7/group) were infused with vehicle or hPTH 1-34 (40 μg/kg/d) via ALZET pump for 21 days. Measurements included % change in femur BMD; distal femur trabecular and midshaft femur cortical morphometry by μCT; distal femur trabecular histomorphometry; serum analyses; and tibial mRNA expression. Data were analyzed by 2-way ANOVA. Both WT and KO mice were hypercalcemic after infusion but did not lose weight. PTH infusion decreased femur bone mineral density (BMD) in WT mice and increased BMD in KO mice. By μCT, PTH decreased femur trabecular bone volume fraction (BV/TV) 50% in WT mice and increased BV/TV 60% in KO mice. In addition, PTH decreased trabecular connectivity density 73% in WT femurs and increased connectivity density 100% in KO femurs. In WT femurs, PTH decreased trabecular number 34% and increased trabecular spacing 56%. In KO femurs, PTH increased trabecular number 16% and decreased spacing 14%. Similarly, by histomorphometry, PTH decreased trabecular BV/TV 54% in WT femurs and increased trabecular BV/TV 68% in KO femurs. In contrast to the effects seen in trabecular bone, no statistical difference was observed in cortical parameters with PTH. There was a trend for PTH to increase cortical porosity 2-fold in KO but not WT femurs. Consistent with its effects on trabecular bone, PTH increased serum osteocalcin, a marker of bone formation, only in KO mice (7.6-fold). CTX, a serum marker of bone resorption, was increased by PTH similarly in WT (1.9-fold) and KO mice (1.7-fold). PTH also increased *Osteocalcin* mRNA only in KO tibiae (8.6-fold) but increased *Rankl*/*Opg* expression similarly in WT and KO tibiae (3.8-fold and 3.0-fold, respectively). In addition, expression of inhibitors of Wnt signaling, *Dkk-1* and *Sost,* was significantly lower in KO compared to WT tibiae after PTH infusion. In summary, COX-2 absence prevented trabecular, but not cortical, bone loss secondary to PTH infusion. These data suggest that prostaglandins produced by COX-2 do not enhance PTH-stimulated resorption but can suppress PTH-stimulated osteoblast differentiation.

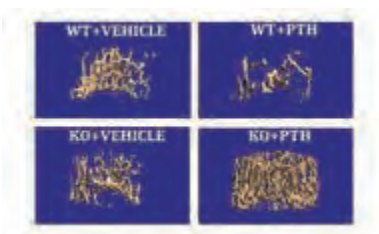

Continuous PTH-Choudhary etal

***Disclosures: Shilpa Choudhary**, None.*

1061

Parathyroid Hormone-related Peptide (PTHrP) blockade inhibits the development of bone metastasis and potentiates the effect of zoledronic acid in vitro and in vivo in a mouse model of breast tumor progression. Aimee-Lee Luco*[1], Jiarong Li[1], Benoit Ochietti[2], Ibtihal Fadhil[2], Anne Camirand[2], Monzur Murshed[1], Andrew Karaplis[1], Richard Kremer[3]. [1]McGill University, Canada, [2]McGill University Health Center, Canada, [3]McGill University, Royal Victoria Hospital, Canada

Using conditional ablation of PTHrP in mammary epithelial cells in the PyVMT model of breast tumor progression, we previously demonstrated that PTHrP has a major role in breast cancer initiation, growth and metastasis outside the skeleton. Here we investigated its role on the development of skeletal metastasis alone and in combination with the potent bisphosphonate zoledronic acid (ZA).First isolated tumor cells from control (PyVMT-PTHrP$^{flox/flox}$-Cre^{-}) and homozygous (PyVMT-PTHrP$^{flox/flox}$-Cre^{+}) animals were examined *in vitro and in vivo* in the presence of a monoclonal antibody (mAb) against PTHrP1-33 and ZA alone or in combination. *In vitro* cell growth was reduced by over 80% in PTHrP ablated cells or by mAb treatment of control cells (IC50 2µg/ml).Treatment with ZA resulted in a dose dependent inhibition of growth(IC50 $5x10^{-5}$M) and the combination of the mAb and ZA was additive .Next we examined the effect of PTHrP inhibition alone and in combination with ZA following intra-tibial injection of isolated tumor cell into the right tibia.500 000 control or PTHrP ablated breast tumor cells were injected intra-tibially in 8 week old wild type female FVB mice and treated with either control IgG, mAb(200 ug subcutaneously, every 2 days), ZA (2.5 µg/week) or a combination(n=10/group). Three weeks following tumor cell injections the mice were sacrificed, blood collected, X-rays(Faxitron) taken for osteolysis scoring and tumor weight determined by subtracting weight of the injected limb from weight of the contro-lateral limb. Bones were embedded in plastic for histomorphometric analysis of tumor burden. Mice injected with control cells had the largest tumor weight, tumor burden and osteolytic score. Animals injected with PTHrP ablated cells had over 80% reduction in tumor weight and volume compared to control animals($p<0.001$). Combination of ZA and PTHrP ablation or ZA combined with mAb administration resulted in an almost complete inhibition of tumor growth within bone and was significantly superior than PTHrP ablation or ZA alone($p<0.05$). In summary our data demonstrate that PTHrP blockade has a direct effect on tumor growth of breast cancer cells *in vitro and in vivo* and potentiates the effect of ZA with almost complete inhibition of tumor growth within bone. Our data lend support to the "seed and soil" hypothesis and the rational of targeting both the tumor cells and the bone microenvironment in order to eradicate the development of skeletal metastasis.

***Disclosures: Aimee-Lee Luco**, None.*

1062

Continuous PTH Treatment Induces Bone Loss through T Cells Produced IL17. Jau-Yi Li*, Michael Reott, Qun Dai, Jonathan Adams, M. Neale Weitzmann, Roberto Pacifici. Emory University School of Medicine, USA

Hyperparathyroidism in humans and continuous PTH treatment (cPTH) in mice stimulate bone resorption and cause bone loss by regulating RANKL/OPG production by stromal cells (SCs) and osteoblasts. Reports have shown that T cells markedly potentiate the bone catabolic effect of cPTH by inducing CD40 signaling in SCs through their surface receptor CD40L. In addition, cPTH stimulate T cells to secrete the osteoclastogenic cytokine TNF, a factor that potentiates the osteoclastogenic activity of RANKL. A search for additional mechanisms by which T cells potentiate cPTH induced bone loss revealed that in vivo cPTH treatment for 2 weeks increased by ~2-3 fold the frequency of Th17 cells in the BM. Th17 are a highly osteoclastogenic population of CD4+ cells defined by the capacity to produce IL-17, a potent inducer of RANKL and TNF production. Accordingly, we found cPTH to cause a 2-3 fold increase in intracellular IL-17A and a 4 fold increase in the expression of the Th17-inducing transcription factors RORα and RORt, in BM CD4+ T cells. To investigate the contribution of Th17 to cPTH induced bone loss 16 week-old WT mice were treated with vehicle or cPTH (80mg/kg/day subcutaneously for 2 weeks) alone or in combination with mouse IL-17 neutralizing antibody (mIL-17 Ab) or isotype matched irrelevant Ab (Irr.Ig). We found that treatment with mIL-17 Ab decreased by ~ 50% the loss of trabecular bone volume (as measured by mCT), the increase in bone resorption (as measured by serum CTX) and the formation of osteoclasts in cultured of bone marrow cells induced by cPTH treatment. By contrast, treatment with Irr Ig did not antagonize the bone catabolic effects of cPTH. Measurement of serum P1NP, a marker of bone formation, showed that neither mIL-17 Ab nor Irr.Ig blunted the increase in serum P1NP (a marker of bone formation) induced by cPTH. Furthermore, mIL-17 Ab completely blocked the increase in SC production of TNFa and RANKL induced by cPTH, while Irr. Ig had no effects, thus demonstrating that cPTH stimulates SC osteoclastogenic function through T cell produced IL17. In summary, these findings demonstrate that cPTH polarizes the differentiation of CD4+ cells toward the Th17 subset. Moreover, increased T cell production of IL-17 is a novel mechanism by which cPTH stimulates bone resorption and causes bone loss.

***Disclosures: Jau-Yi Li**, None.*

1063

Marked Increases in Cortical Porosity After Kidney Transplantation Especially Near the Endocortical Surface: An HR-pQCT Study. Kyle Nishiyama*[1], Yves Pauchard[2], Lucas Nikkel[3], Sapna Iyer[4], Steven Boyd[5], Elizabeth Shane[6], Thomas Nickolas[6]. [1]Columbia University, USA, [2]University of Western Ontario, Canada, [3]Columbia University Medical Center, USA, [4]University of California San Diego, USA, [5]University of Calgary, Canada, [6]Columbia University College of Physicians & Surgeons, USA

We reported that hyperparathyroidism (HPT) in chronic kidney disease patients results in progressive increases in cortical porosity (Ct.Po), which may contribute to their increased fracture risk. While most kidney transplant patients have persistent HPT, it is unclear whether Ct.Po worsens after transplant or whether changes in Ct.Po are confined to specific cortical (Ct) regions, such as the endocortex. Defining the Ct region of interest (ROI) in longitudinal high-resolution peripheral quantitative CT (HRpQCT) studies with current analytical methods is challenging since changes at the Ct surface may confound changes in Ct.Po. Our objective was to compare image registration methods for assessment of changes in Ct.Po in patients undergoing first time kidney transplant. We assessed post-transplant bone resorption with CTX and used HRpQCT (Scanco Medical) to scan the distal radius and tibia in 31 patients (22 men; age: 52 ± 13yrs) at transplant and after 1 year. Baseline and 1 year images were aligned using a fully automated, intensity-based image registration framework. We compared 3 methods to define the Ct ROI and quantify changes in Ct.Po: (1) Ct bone was independently defined in baseline and 1 year scans; (2) Ct bone was defined as the common ROI in baseline and 1 year scans; and (3) Ct ROI for both baseline and 1 year scans was indexed to the baseline cortex. Data are expressed as median percent change (IQR) and all are significant ($p<0.01$). By independently defined ROI, Ct.Po increased 10.4% (3.8, 26.0) at the radius and 10.3% (0.6, 14.4) at the tibia. By common ROI, Ct.Po increased 10.8% (0.6, 22.8) at the radius and 4.8% (0.0, 17.5) at the tibia. By indexed ROI, Ct.Po increased 74.6% (38.8, 112.1) at the radius and 27.1% (16.8, 35.4) at the tibia. The increase in Ct.Po with indexed ROI was significantly greater than for other methods ($p<0.001$). In contrast to other methods, indexed ROI was the most sensitive at detecting resorption-associated changes in Ct.Po, even at low CTX levels (Figure). These results indicate that intracortical porosity increases throughout the cortex after transplant. This increase is particularly marked at the endocortical surface, likely through endocortical cancellization, and is driven by increased resorption rates. These results demonstrate that image registration is essential to quantify regional changes in Ct.Po. The effects of increased Ct.Po on skeletal fragility in transplant recipients require further study.

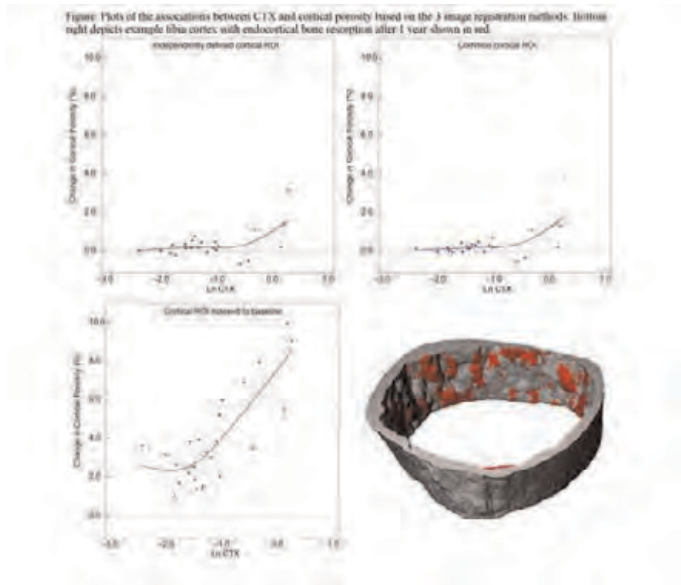

Figure

***Disclosures: Kyle Nishiyama**, None.*

1064

Fracture History of Healthy Premenopausal Women is Associated with a Prevailing Reduction of Cortical Microstructural Components at the Distal Radius. Thierry Chevalley*[1], Jean-Philippe Bonjour[2], Bert van Rietbergen[3], Serge Ferrari[4], Rene Rizzoli[4]. [1]University Hospitals of Geneva Division of Bone Diseases, Switzerland, [2]University Hospital of Geneva, Switzerland, [3]Department of Biomedical Engineering, Netherlands, [4]Geneva University Hospital & Faculty of Medicine, Switzerland

Purpose: To determine in healthy premenopausal women which bone structural components of distal radius are the most closely associated with a history of fracture. Methods: Measurement of radial areal bone mineral density (aBMD) by DXA, microstructural components by high-resolution quantitative peripheral computerized tomography (HR-pQCT) and strength variables by micro Finite Element Analysis (μFEA) were made in 196 healthy premenopausal women aged 45.9±3.7 (±SD) years with (FX, n=96) and without (NO-FX, n=100) a history of fracture.

Results: In the whole group the mean radial metaphysis aBMD T-Score was not significantly different from zero. In the FX as compared to the NO-FX group, the differences in T-Scores after adjustment for age, height, weight, menarcheal age, calcium and protein intakes, and physical activity were for: radial metaphysis aBMD, -0.24 (P=0.005); for distal radius microstructure components: cortical volumetric (v) BMD, -0.38 (P=0.0009); cortical thickness, -0.37 (P=0.0001); cross-sectional area (CSA), +0.24 (P=0.034); endosteal perimeter, +0.28 (P=0.032); for strength estimates: stiffness: -0.15 (P=0.030); failure load: -0.14 (P=0.044); apparent modulus: -0.28 (P=0.006). T-scores of trabecular volumetric BMD and thickness did not significantly differed between the FX and the NO-FX groups. Differences in T-scores for cortical vBMD and cortical thickness remained significant after further adjustment to radial metaphysis aBMD (P=0.035 and P=0.003, respectively) and to CSA (P=0.009 and P=0.0007, respectively). The Figure below illustrates the fracture risks (OR, 95% CI) for 1 SD decrease in various radius measurements, after adjustment for all confounding factors. After additional adjustment to radial metaphysis aBMD, ORs for cortical vBMD and cortical thickness remained significant: 1.63 (CI: 1.05-2.54, P=0.031) and 2.58 (CI: 1.36-4.86, P=0.004), respectively.

Conclusions: In healthy premenopausal women, a history of fracture is associated with reduced T-Scores in the distal radius, the greatest deficit being measured in cortical thickness. A reduction of one SD in cortical thickness is associated with about 2.5 fold increased risk of fracture. This finding strengthens the notion that, in healthy women, fractures occurring before the menopause are associated with a substantial degree of bone structural fragility. The strategy of individual prevention of postmenopausal osteoporosis should take into acount this important risk factor.

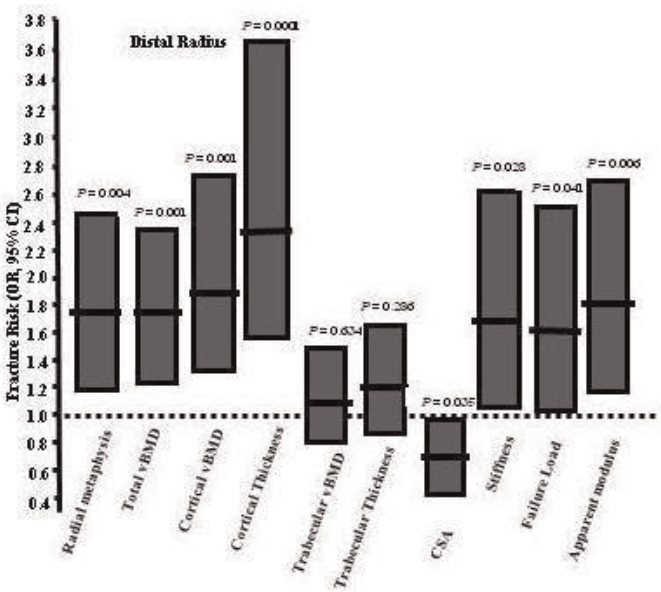

Figure

***Disclosures: Thierry Chevalley**, None.*

1065

Denosumab Reduces Hip Cortical Porosity in Women With Osteoporosis. Roger M Zebaze*[1], Cesar Libanati[2], Michael R McClung[3], Jose R Zanchetta[4], David L Kendler[5], Arne Høiseth[6], Andrea Wang[2], Ali Ghasem-Zadeh[1], Ego Seeman[1]. [1]Austin Health, University of Melbourne, Australia, [2]Amgen Inc., USA, [3]Oregon Osteoporosis Center, USA, [4]Instituto de Investigaciones Metabólicas, Argentina, [5]University of British Columbia, Canada, [6]Curato Røntgen, Norway

Purpose: Cortical thickness, area, mass, and porosity are determinants of bone strength and so, contribute to nonvertebral fracture risk. Cortical porosity is a marker of structural decay associated with an exponential worsening in bone fragility and is the result of unbalanced and accelerated intracortical remodeling upon Haversian canal surfaces. Canals enlarge, coalesce, and fragment the cortex. Reducing remodeling will limit worsening of porosity but for individuals already at increased risk for fracture, reducing porosity is preferred. Using multi detector computer tomography (MDCT) hip images from the FREEDOM study, we previously reported that hip cortical mass and thickness improved over 3 years of denosumab (DMAb) administration. We postulated that this could be explained by infilling of porosity in the inner cortical region adjacent to the medullary canal. Here, we used a subset of these images to evaluate changes in hip porosity.

Methods: FREEDOM was a 3-year, randomized, double-blind trial that enrolled postmenopausal women with a lumbar spine or total hip T-score <–2.5 but not <–4.0 at both sites. Women received placebo (Pbo) or 60 mg DMAb every 6 months. Percentage porosity in both the compact and the trabecularized (outer and inner transitional zones) cortical volumes of the subtrochanter region were measured using StrAx1.0 software (Zebaze et al., *Bone* 2013) from MDCT hip images obtained at baseline and year 3 (Pbo n=22; DMAb n=28).

Results: The percentage volume occupied by porosity at baseline was 72% in the inner transitional zone adjacent to the medullary compartment, 37% in the outer transitional zone, and 29% in the compact-appearing cortex. Cortical porosity correlated positively with serum CTX (p=0.017) and negatively with hip strength estimated using finite element analysis (p=0.027). DMAb reduced porosity compared with baseline and Pbo at year 3 across the entire cortex (Figure) and in each compartment, reaching treatment effect (DMAb–Pbo) improvements of –1.8% (inner transitional zone), –5.6% (outer transitional zone), and –7.9% (compact-appearing cortex) (all p<0.001).

Conclusions: This is the first report of the response of hip porosity *in vivo* to pharmacological therapy. Since reductions in cortical porosity equate to increased mineralized bone matrix mass and both are relevant to strength, these improvements are expected to contribute to the observed reductions in nonvertebral fractures associated with DMAb administration.

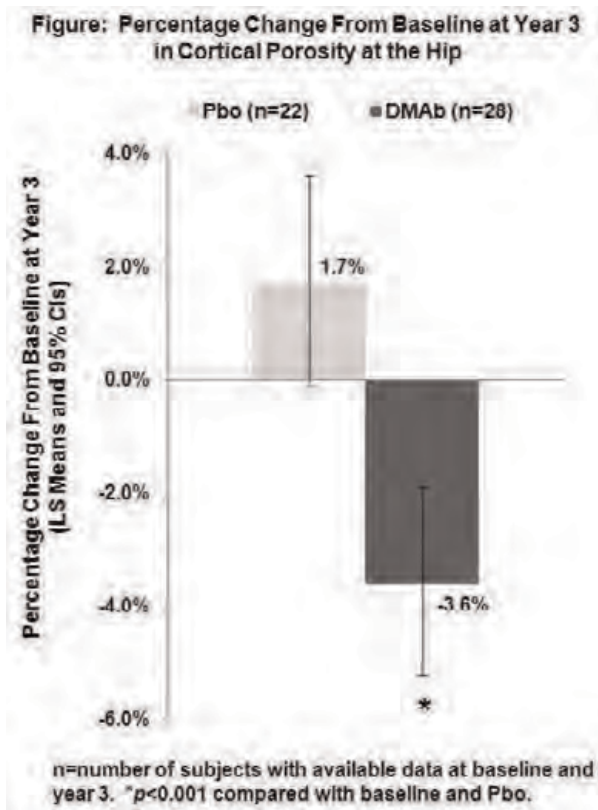

Figure

***Disclosures: Roger M Zebaze**, None.*
This study received funding from: Amgen Inc.

1066

Total Body Lean Mass and Fat Mass Differentially Affect Hip BMD and Strength Index in Women and Men But Are Not FRAX Independent Risk Factors for Fracture: A Large Clinical Cohort Study. William Leslie*[1], Eric Orwoll[2], Carrie Nielson[2], Suzanne Morin[3], Sumit Majumdar[4], Helena Johansson[5], Eugene McCloskey[6], Anders Oden[7], John Kanis[8]. [1]University of Manitoba, Canada, [2]Oregon Health & Science University, USA, [3]McGill University, Canada, [4]University of Alberta, Canada, [5]Swedish University of Agricultural Sciences, The Biomedical Center, Sweden, [6]University of Sheffield, United Kingdom, [7]Consulting statistician, Sweden, [8]University of Sheffield, Belgium

Background: Although increasing body weight has been regarded as protective against osteoporosis and fractures, there is accumulating evidence that fat adversely affects skeletal health compared with lean tissue.

Objective: To examine skeletal health parameters in women and men as a function of estimated total body lean and fat mass.

Methods: 40,050 women and 3,600 men age ⩾50 y at the time of baseline DXA testing (Lunar Prodigy; GE Healthcare) with FRAX probabilities were identified in a clinical database from Manitoba, Canada. Major osteoporosis fractures (MOF) and hip fractures (HF) were obtained via linkage to a population-based repository. Total body lean and fat mass in kg and kg/m^2 were estimated using non-linear prediction equations based on weight, sex and DXA fat percent from abdomen and hip (modified from Leslie WD: JCD 2009;12:428). Hip BMD, strength index (SI), cross sectional area (CSA) and cross sectional moment of inertia (CSMI) were calculated using Advanced Hip Analysis (enCore version 13.6; GE Healthcare). Generalized additive models (cubic splines with 4 df) and Cox proportional hazards models with multivariable adjustments were used to study the independent contributions of lean and fat mass on BMD, SI and fracture risk.

Results: During mean 5-years observation, incident MOF occurred in 2505 women and 180 men (626 and 45 HF). Increasing lean mass was associated with near-linear increases in hip BMD, CSA and CSMI for both women and men, while increasing fat mass showed a minor initial increase that plateaued without further gain. In contrast, SI was relatively unaffected by increasing lean mass but showed a continuous linear decline with increasing fat mass (predicting higher fracture risk). All findings were similar in men and women, without significant sex interactions. There was no evidence that lean mass, fat mass or SI consistently affected risk of MOF or HF after adjustment for FRAX covariates or FRAX scores (with or without BMD).

Conclusions: Skeletal adaptation to increasing lean mass was associated with greater BMD but neutral effects on SI, whereas increasing fat mass had neutral effects on BMD but adversely affected SI. Despite predictions of higher fracture risk, greater fat mass was not independently associated with an observed increased risk of fractures. FRAX robustly predicted fractures and was not affected by variations in body composition.

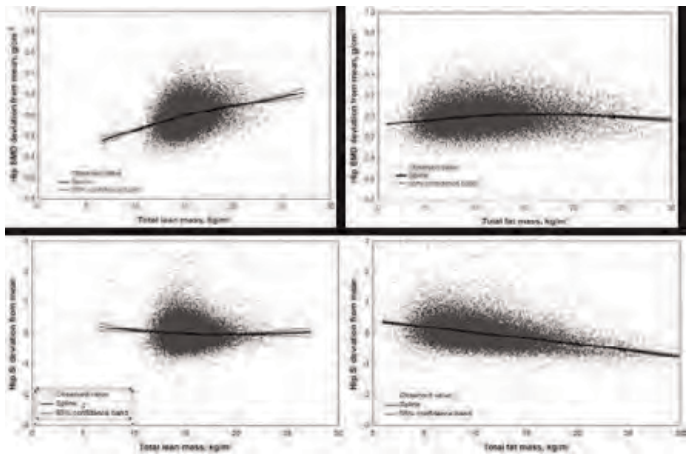

Hip BMD (upper) and SI (lower) for lean mass index (left) and fat mass index (right) in women

***Disclosures: William Leslie**, None.*

1067

Protein-Coding Less-Common Variants Are Associated with BMD: An Exome-Chip Meta-Analysis of Adult Caucasians. Karol Estrada[1], Ching-Ti Liu[2], Chia-Ho Cheng[3], Carolina Medina-Gomez[4], Yanhua Zhou[2], Ling Oei[5], Albert Hofman[5], Carola Zillikens[5], David Karasik[6], Andre Uitterlinden[7], L. Adrienne Cupples[2], Douglas Kiel[8], Fernando Rivadeneira[9], Yi-Hsiang Hsu*[10]. [1]Analytic & Translational Genetics Unit, Massachusetts General Hospital, USA, [2]Dept. Biostatistics, School of Public Health, Boston Univ., USA, [3]Hebrew SeniorLife Institute for Aging Research, USA, [4]Erasmus Medical Center, The Netherlands, [5]Erasmus University Medical Center, The Netherlands, [6]Hebrew SeniorLife; Bar Ilan University, USA, [7]Rm Ee 575, Genetic Laboratory, The Netherlands, [8]Hebrew SeniorLife, USA, [9]Erasmus University Medical Center, The Netherlands, [10]Hebrew SeniorLife Institute for Aging Research & Harvard Medical School, USA

We previously reported 56 novel genome-wide significant loci for BMD, but these loci focus on common (MAF>5%) SNPs and only explain 5% of the BMD variance. Recent studies suggest that less-common variants in protein-coding and regulatory regions may contribute to the susceptibility of common disorders. The availability of the "exome-chip" with 235,933 less-common protein-coding variants (with functional implication as non-synonymous, splice sites and stop altering SNPs) provides a feasible way to identify less-common coding variants of diseases. We conducted an exome-chip meta-analysis for BMD to identify (1) novel coding variants (with predicted deleterious function) that associated with BMD; and (2) coding variants (with predicted deleterious function) that may responsible for the 56 BMD loci. 6,348 Framingham Heart Study (FHS) participants and 2,427 Rotterdam Study (RS) Caucasian participants (58.7% female) were genotyped with Illumina exome-chip. We found 78% of genotyped variants with MAF $\leq$ 1% and 16% monomorphic. To identify novel less-common coding variants (MAF $\leq$ 1%) associated with BMD, we performed two gene-based burden tests (allele-count and "SKAT" tests) in each study, adjusting for age, age^2, sex, weight, genetic ancestry and estrogen use (in FHS females only). A meta-analysis was then used to combine results from two studies. We identified novel associations ($p < 5x10^{-5}$) with LS BMD (*DYRK4, KIAA1324L, SGM2*) and FN BMD (*PPP4R2*), although none of them achieved genome-wide significance ($p < 4.2x10^{-6}$, Bonferroni correction). To identify functional coding variants that may responsible for the 56 BMD loci, we performed regression analyses in each study adjusting for the same set of covariates and followed by an inverse-variance fixed-effect meta-analysis. The most significant association was found for a reported missense SNP V667M in the *LRP5* gene ($p < 8.9x10^{-4}$ with LS BMD). Other strongly associated missense deleterious SNPs were also found (i.e. N501H in *LRP4* and A745V in *LRP5* with LS BMD). In summary, this is the first exome-chip meta-analysis conducted for BMD in which we focus on less-common coding variants with functional implication. We identified novel less-common coding variants associated with BMD as well as deleterious variants in previously identified BMD loci. A large-scale exome-chip meta-analysis with an additional ~20,000 samples is underway to increase the statistical power of identifying less-common coding variants for BMD.

***Disclosures: Yi-Hsiang Hsu**, None.*

1068

Sclerostin Preserves Cartilage Integrity in Murine Osteoarthritis. Wafa Bouaziz*[1], Thomas Funck-Brentano[2], Hilène Lin[3], Caroline Marty[2], Dominique Come[2], Eric Hay[4], Martine Cohen-Solal[5]. [1]INSERM U606, France, [2]Univ Paris Diderot, Sorbonne Paris Cité, Lariboisière Teaching Hospital, France, [3]INSERM UMR-606, France, [4]INSERM 4606, France, [5]Centre Viggo Petersen, France

Purpose: Sclerostin is a Wnt inhibitor produced by mineralizing cells such as osteocytes and hypertrophic chondrocytes. Sclerostin may regulate cartilage homeostasis by inhibiting Wnt pathways in osteoarthritis. Here, we assessed the effect of Sclerostin in osteoarthritic cartilage using Sost-deficient mice.

Methods: 10 week-old Sost-KO and wild type (WT) mice underwent partial transsection of the meniscus (Mnx). Mice were sacrificed at 4, 6 or 9 weeks after Mnx to analyze 1) bone volume (BV/TV) at the medial femoral condyle, 2) osteophyte volume (microCT), 3) cartilage damage (OA score) and 4) expression of matrix proteins. The role of Sclerostin in chondrocyte metabolism was analyzed in primary murine chondrocyte cultured with Wnt3a and Sclerostin (RT-PCR and WB). Proteoglycan content was quantified in the culture supernatant by a colorimetric assay and GAG accumulation by Alcian blue staining. We further investigated the role of JNK pathway using SP600125 inhibitor.

Results: Sclerostin was only expressed in the calcified cartilage and osteocytes and was enhanced in OA. At any time, cartilage was preserved in Sost-KO mice despite a markedly high BV/TV. Mnx resulted in a higher OA score in Sost-KO mice than in WT at Week 4 (6.66 $\pm$ 0.57 vs 3.25 $\pm$ 0.95, $p<0.05$) and Week 6 (11 $\pm$ 1 vs 7 $\pm$ 0,81, $p<0.05$), along with increased type X collagen and Adamts-4 expressions, suggesting an enhanced chondrocyte catabolism. However, osteophyte volume was not affected by the lack of Sclerostin at Week 4 (0.033 $\pm$ 0.019 vs 0.024 $\pm$ 0.01, p: NS) and at Week 6 (0.023 $\pm$ 0.01 vs 0.02 $\pm$ 0.01, p: NS).In primary chondrocytes, Wnt3a reduced the proteoglycan release and this was rescued by Sclerostin. Wnt3a increased

the expression of Adamts-4 & -5, MMP-3 & -13 and type X collagen, while this effect was totally abolished by Sclerostin through a mediation of the canonical pathway. Moreover, Wnt3A promoted the phosphorylation of JNK which was inhibited by Sclerostin. We further investigated whether Sclerostin-induced inhibition of JNK affects chondrocyte anabolism. Interestingly, in Wnt-induced chondrocytes, Sclerostin rescued the accumulation of GAG and the expression of the anabolic genes when JNK pathway was inhibited.

Conclusions: Lack of Sclerostin results in cartilage damage and disrupts the anabolic/catabolic balance in OA. Sclerostin inhibits both Wnt canonical and non canonical JNK pathway preserving the chondrocyte metabolism. These data suggest an important role of Sclerostin in cartilage integrity in OA.

***Disclosures: Wafa Bouaziz**, None.*

1069

Acute Increase in Bone Formation Following Sclerostin Antibody Treatment Is Consistent With Activation of Bone Lining Cells in Aged Ovariectomized Rats. Michael S Ominsky*, Steve Kaufman, Dave Cordover, Gwyneth Van, Irene Soto, Qing-Tian Niu, Rogely W Boyce. Amgen Inc., USA

To investigate if the acute increase in bone formation in response to sclerostin antibody (Scl-Ab) is associated with an increase in osteoblast number, unbiased stereological methods were used to estimate the total number of RUNX2-positive (RUNX2+) cells immediately adjacent to the cancellous bone surface (lining cells and osteoblasts) and in the peritrabecular stroma (osteoprogenitors) in vertebrae from rats following a single dose of Scl-Ab.

Aged ovariectomized (OVX) rats were given a single dose of vehicle (Veh) or 100 mg/kg Scl-Ab (Scl-Ab VI) (n = 5/group) and vertebrae (L6 and T9) were collected at 168 hours post-injection. Xylenol orange, calcein green, and alizarin were given on days –3, 2, and 5, respectively. L6 vertebrae were processed undecalcified and osteoid (OS/BS) and mineralizing (MS/BS) surfaces were estimated based on calcein and alizarin labels. The physical fractionator, a stereological estimator not previously applied to bone, was used to estimate the total number of RUNX2+ cells in T9 vertebrae. The physical fractionator provides estimates of total cell number independent of size, shape, or orientation using physical disectors, paired consecutive thin sections constituting a 3-dimensional probe in which cells are counted. T9 vertebrae were decalcified; processed in paraffin; exhaustively sectioned at 3 μm, collecting $1/80^{th}$ of the sections as disector pairs; and immunostained for RUNX2. Using AutoDisector® software (Visiopharm), sections were aligned and $1/50^{th}$ of the cancellous tissue area was sampled as matched fields of view in the paired sections; cells were then counted using the disector counting principle.

Despite a 280% and 65% increase in OS/BS and MS/BS, respectively, after Scl-Ab treatment, the total number of RUNX2+ cells directly adjacent to the bone surface was not increased compared with Veh treatment (Scl-Ab = 269,200 ± 65,293; Veh = 251,600 ± 29,711). The total number of peritrabecular RUNX2+ osteoprogenitor cells was also similar in both groups (Scl-Ab = 57,600 ± 9,633; Veh = 60,000 ± 18,547).

These data indicate that the acute increase in bone formation following Scl-Ab treatment is not associated with an increase in surface-associated RUNX2+ cells or osteoprogenitor cells. These data are consistent with Scl-Ab-mediated activation of lining cells into matrix-producing osteoblasts.

***Disclosures: Michael S Ominsky**, Amgen, 7; Amgen, 3*
This study received funding from: Amgen Inc. and UCB Pharma

1070

An End-product of Tryptophan Degradation is a Potential Anabolic Treatment for Osteoporosis. Christopher Vidal*[1], Sandra Bermeo[1], Wei Li[2], Krishanthi Gunaratnam[3], Chai Lim[4], Guilles Guillemin[4], Gustavo Duque[5]. [1]University of Sydney, Australia, [2]University of Sydney, Nepean Clinical School, Australia, [3]Sydney Medical School-NepeanLevel 5 South Block, Australia, [4]Mcquarie University, Australia, [5]Ageing Bone Research Program, University of Sydney, Australia

New anabolic treatments for osteoporosis are highly needed. Inhibiting gut-derived serotonin increases bone formation in oophorectomized mice. However, the role of the alternative pathway of tryptophan degradation, the kynurenine pathway(KP), in bone metabolism has not been explored. Stimulation of KP with interferon gamma in mesenchymal stem cells (MSC) has an osteogenic effect. Similar effect is observed in MSC treated with picolinic acid(PA), an end product of KP. In this study, we investigated the effect of PA treatment to rescue osteoporosis in vivo. Nine-month-old oophorectomised (OVX) and SHAM C57BL/6 mice (n=24/group) were treated with PA(0.25, 0.5 and 1 g/kg/day) in drinking water for 6 weeks. Mice treated with water were used as controls. After treatment, we performed bone phenotyping using μ-*CT,* histology and histomorphometry. Serum was collected for analyses of minerals, calciotropic hormones, and pharmacokinetics. RNA and proteins were assessed for osteogenic markers and MSC cultured ex vivo. Serum PA reached therapeutic levels in the treated groups in a dose-dependent manner, with no difference in body weight or water consumption. Serum concentrations of nine minerals, duodenal Zn, PTH and VitD did not differ between the groups showing that the effect of PA on bone is independent of Zn absorption in the gut or changes in calciotropic hormones. Quantitative μCT showed a significant increase in bone volume (~+5% femoral BV/TV; $p<0.05$) and trabecular number (~+20%; $p<0.05$) with a decrease in trabecular separation (~-15%; $p<0.05$) in PA treated SHAM and OVX mice. Similar gains were observed at the lumbar spine. Histology showed a significant increase in Ob number in PA-treated mice ($p<0.01$). Mineral apposition rate(MAR) was higher in both trabecular and cortical bone with higher mineralization being observed in PA treated mice. Ex-vivo MSC in osteogenic conditions showed higher mineralization and bone forming units in treated mice compared to controls. Higher levels of the osteogenic genes Runx2 (~+2.5 fold) and osteocalcin (~+2.0 fold) were observed in all the PA-treated groups ($p<0.05$). In conclusion, PA treatment improves bone mass and microarchitecture in both OVX and SHAM mice. PA had an osteo-anabolic effect through the expression of osteogenic genes with no cross-related effects on mineral absorption or calciotropic hormones. PA was well tolerated and absorbed without any side effects making it an ideal treatment for osteoporosis.

***Disclosures: Christopher Vidal**, None.*

1071

High Fat Diet Rapidly Suppresses B Lymphopoiesis by Diminishing the Supportive Capacity of the Bone Marrow Niche. Benjamin Adler*[1], Danielle Green[1], M. Ete Chan[1], Clinton Rubin[2]. [1]Stony Brook University, USA, [2]State University of New York at Stony Brook, USA

The bone marrow (BM) niche is the primary site of hematopoiesis, and cues from this microenvironment are critical to the normal maintenance and mobilization of hematopoietic stem cells as well as the differentiation of their progeny such as B lymphocytes. Obesity increases lifetime susceptibility to a host of chronic diseases, and has been linked to defects in leukocyte differentiation and function. The central role of BM health in B lymphopoiesis and the changes BM experiences due to obesity lead us to hypothesize that a high fat diet (HFD: 60% Kcal from fat) will impair B cell development. Seven week old male C57Bl/6J mice were fed either a high fat (HFD) or regular chow (RD) diet. Bone marrow was analyzed using flow cytometry after 2 days, 1 week and 6 weeks to characterize B cells (B220+) in the early stages of obesity (n=10). B cells were not changed after 2d of HFD, but within 1w B cell proportions were reduced by -10% and by 6w by -25% in HFD compared to RD ($p<0.05$). Using RT-PCR, BM RNA was evaluated for the expression of Il-7, Ebf1 and Pax5, representing sequential stages of commitment to the B cell lineage. At 2d, despite no decrease in B220+ cells, the expression of Il-7 and Ebf1 were reduced by -20% ($p=0.08$) and -11% ($p=0.06$), strong trends indicating the initiation of B cell suppression occurs at the early stages of B cell development. Pax5, which is expressed in cells further along in B cell commitment, was not significantly impacted at 2d (-9%). Meanwhile the expressions of Il-7, Ebf1, and Pax5 were reduced by -19%, -20% and -16% after 1w, and -23%, -29% and -34% after 6w in HF animals ($p<0.05$ for all). Il-7 is a critical factor in the early B lineage which is secreted by supportive cells in the BM niche, and whose binding to IL-7r+ common lymphoid progenitors initiates Ebf1 expression and B cell commitment. Here we report for the first time that BM Il-7 expression, and by extension B cell differentiation, are rapidly impaired by HFD. The trend towards suppressed expression of Il-7 following only 2d of HFD demonstrates how susceptible the BM niche is to changes in diet and fat phenotype. Ultimately, it is still unclear whether this susceptibility is to the dietary insult itself, rapid accretion of adiposity, or both. These data provide developmental insight into the etiology of obese leukocyte defects and are striking for the speed with which B lymphopoiesis is harmed following initiation of HFD.

***Disclosures: Benjamin Adler**, None.*

1072

Inflammatory and Non-inflammatory Actions of Activated NLRP3 Inflammasome Culminate in Skeletal Abnormalities. Sheri Bonar[1], Cynthia Brecks[1], Sung Yeop Jeong[2], Marcus Watkins[3], Matthew McGeough[4], Chang Yang[5], Deborah Novack[3], Ernestina Schipani[6], Hal Hoffman[4], Roberto Civitelli[3], Gabriel Mbalaviele*[3]. [1]Washington University in St. Louis, USA, [2]Washington University School of Medicine, USA, [3]Washington University in St. Louis School of Medicine, USA, [4]University of California, San Diego, USA, [5]Washington University in St Louis School of Medicine, USA, [6]Indiana University School of Medicine, USA

Activating missense mutations in the NOD-like receptor (NLR) family, pyrin domain-containing 3 gene (*NLRP3*) in humans is associated with skeletal manifestations, including abnormal growth plate development, low bone mass and short stature. Accordingly, knock-in mice globally expressing a constitutively active NLRP3 allele exhibit growth plate dysplasia, severe osteopenia, and stunt growth. To gain insights into the cellular mechanisms of NLRP3 actions, we employed Cre/*LoxP* technology to generate mice expressing active NLRP3 in myeloid cells using LysM-Cre ($NLRP3^{LysM}$). $NLRP3^{LysM}$ mice are phenotypically undistinguishable from mice globally expressing active NLRP3, as they develop systemic inflammation, are significantly smaller, and are osteopenic due to increased osteoclastogenesis relative to wild type (WT) mice. To further characterize the impact of NLRP3 activation specifically in the osteoclast cell lineage, we engineered mice in which the active *Nlrp3* mutant is driven by cathepsin K-Cre ($NLRP3^{CatK}$). Intriguingly, $NLRP3^{CatK}$ mice also exhibit low bone mass, but there is no systemic inflammation and no evidence of

increased osteoclastogenesis. Interestingly, osteoclasts from NLRP3^{CatK} bone marrow macrophages form more resorption pits on bone slices *in vitro* than WT cells, suggesting a role of the NLRP3 inflammasome in osteoclast bone-resorbing activity. Intriguingly, growth plate development is normal in NLRP3^{LysM} mice and NLRP3^{CatK} mice, suggesting that NLRP3 activation in myeloid cells does not affect growth plate development. Consistent with a chondrocyte autonomous action, activation of NLRP3 in chondrocytes driven by type II collagen-Cre (NLRP3^{Col2}) does not cause systemic inflammation, but leads to disorganized growth plate associated with massive chondrocyte death in the center of the epiphysis. Collectively, these data indicate that the NLRP3 inflammasome regulates skeletal development and remodeling in inflammatory and non-inflammatory conditions.

***Disclosures: Gabriel Mbalaviele**, None.*

1073

Osteoclast-secreted Complement Component 3a Stimulates Osteoblast Differentiation. Kazuhiko Matsuoka*[1], Masako Ito[2], Kyoji Ikeda[1], Sunao Takeshita[1]. [1]National Center for Geriatrics & Gerontology, Japan, [2]Nagasaki University Hospital, Japan

In bone remodeling, "coupling" of resorption to subsequent formation plays a pivotal role; however, information on the mechanisms and signaling molecules that link osteoclasts to osteoblasts is scarce. The objective of the present study is to identify a candidate coupling factor from the conditioned medium (CM) of mature osteoclasts.

We have established a co-culture system in which increasing number of osteoclasts stimulates the differentiation of calvaria-derived primary osteoblasts, as determined by alkaline phosphatase (ALP) activity. The stimulation of ALP activity was mimicked by adding the CM from mature osteoclasts in a dose-dependent manner. The ALP-stimulating activity was purified through several steps of ion chromatography, and was identified as complement component 3a (C3a) by LC-MS/MS.

The results of microarray and qRT-PCR analyses revealed the expression of C3 gene markedly increased during osteoclast differentiation, and the cleavage product C3a was detected by ELISA in the CM of mature osteoclasts, but not of bone marrow macrophages. Retroviral expression of C3a itself stimulated osteoblast differentiation, while an antagonist of the C3a receptor (SB290157) inhibited the stimulation of ALP activity by the osteoclast CM.

The involvement of C3a in the coupling process in vivo was investigated in OVX model, where bone formation is stimulated secondarily to accelerated resorption. We reasoned that since coupling of resorption to formation is stimulated in OVX (with a net decrease in bone mass), if C3a is involved, the secondary stimulation of bone formation is inhibited when blocked C3a receptor by SB290157, resulting in an acceleration of net bone loss. Ten-week-old *ddY* mice, sham or OVX operation, were given daily i.p. injections of SB290157 for 6 days. OVX was associated with significant increases in the expression of C3 gene in bone as well as C3a concentrations in the bone marrow. Bone histomorphometic analysis at the proximal tibia revealed the stimulation of BFR/BS following OVX was completely suppressed by simultaneous administration of SB290157. This was associated with an exacerbation of bone loss following OVX, as determined by microCT scanning.We conclude that mature osteoclasts express C3 gene and secrete C3a, that acts on osteoblast lineage cells to stimulation their differentiation. Thus, osteoclast-secreted C3a may function in the relay from osteoclasts to osteoblasts as a candidate of coupling factor.

***Disclosures: Kazuhiko Matsuoka**, None.*

1074

RANKL increase ROS and Bone Resorption by Inhibiting FoxO-mediated Catalase Expression. Ha-Neui Kim*[1], Shoshana Bartell[2], Li Han[2], Aaron Warren[3], Srividhya Iyer[2], Julie Crawford[4], Haibo Zhao[2], Charles O'Brien[2], Stavros Manolagas[2], Maria Jose Almeida[2]. [1]Univ. Arkansas for Medical Sciences, USA, [2]Central Arkansas VA Healthcare System, Univ of Arkansas for Medical Sciences, USA, [3]Univ. Arkansas for Medical Sciences, & Central Arkansas Veterans Healthcare System, Little Rock, USA, [4]Univ. Arkansas for Medical Sciences, Little Rock, USA

RANKL stimulates reactive oxygen species (ROS) formation, which in turn promotes osteoclast differentiation, activity, and survival. In several cell types, the FoxO family of transcription factors decreases ROS by up-regulating the expression of several antioxidant enzymes. Here, we investigated the role of FoxOs in osteoclastogenesis and bone resorption. We report that serum starvation of bone marrow-derived osteoclast progenitors promoted nuclear translocation of FoxOs and FoxO-mediated transcription. On the other hand, treatment of the osteoclast progenitors with RANKL for 1 h abrogated the nuclear translocation of FoxOs, as determined in Western blot of nuclear extracts. Stimulation of FoxO-mediated transcription by serum depletion or transfection of FoxO1, FoxO3 or FoxO4 plasmids was also inhibited by RANKL, as measured by the activity of a FoxO-luc reporter plasmid in Raw264.7 macrophages. In addition, RANKL decreased protein levels of FoxO1, FoxO3, and FoxO4. To determine the significance of these findings to the in vivo situation, we used mice in which FoxO1,3,4 were specifically deleted (FoxO1,3,4ΔOc) or FoxO3 was overexpressed (FoxO3TgOc) in the osteoclast lineage, using LysM-Cre knock-in mice. Bone marrow-derived macrophages from FoxO1,3,4ΔOc mice exhibited greater proliferation, higher ROS levels and osteoclastogenesis in response to RANKL, and decreased expression of the FoxO-target gene catalase as compared to cells from FoxO1,3,4 flox littermate controls. Cells from the FoxO3TgOc mice exhibited the opposite phenotype when compared to their respective LysM-Cre controls. Moreover, FoxO1,3,4ΔOc mice had higher levels of ROS in the bone marrow and lower vBMD and cancellous bone volume in vertebrae and femora, as well as decreased femoral cortical thickness. The low bone mass phenotype was associated with increased CTx levels in the serum and high mRNA expression of TRAP and catK in bone, as well as with high osteoclast number in histological sections of vertebrae. Administration of catalase to 4 week old FoxO1,3,4ΔOc mice for 6 weeks prevented the decrease in bone mass. Once again, FoxO3TgOc mice had the opposite phenotype to that of the FoxO1,3,4ΔOc mice: increased bone mass associated with decreased resorption markers and osteoclast numbers in bone. These results demonstrate that attenuation of FoxO activation and thereby catalase expression is a seminal mechanism by which RANKL increases ROS generation and bone resorption.

***Disclosures: Ha-Neui Kim**, None.*

1075

Connective Tissue Growth Factor (Ctgf) is a Novel Notch Target Gene in Osteoblasts and Osteocytes. Ernesto Canalis*, Anna Smerdel-Ramoya, Stefano Zanotti. St. Francis Hospital & Medical Center, USA

Ctgf, a member of the CCN family of proteins, is required for skeletal development and adult skeletal homeostasis. Ctgf regulates the activity of signaling molecules in the bone environment, and previous studies revealed newly discovered interactions between Ctgf and Notch, a molecule with a key role in osteoblastic cell fate and function. In the present study, we explored whether Notch regulated Ctgf expression in the skeleton. Calvarial osteoblasts were obtained from *Rosa^{Notch}* mice, where the Notch intracellular domain is expressed under the control of the *Rosa26* promoter following the excision of an intervening *loxP* flanked STOP cassette. Osteoblasts from *Rosa^{Notch}* mice were transduced with an adenoviral vector expressing Cre under the control of the CMV promoter to activate Notch or with a control vector. Activation of Notch signaling induced canonical target genes of the *Hes* and *Hey* families. Furthermore, Notch increased Ctgf mRNA by ~7 fold, an effect that was sustained for up to 2 weeks of culture. Notch induced the newly transcribed Ctgf hnRNA nearly 3 fold indicating a transcriptional level of regulation. The half-life of Ctgf transcripts was 2.5 hours in transcriptionally arrested *Rosa^{Notch}* control osteoblasts, and in the context of Notch activation, indicating that Ctgf mRNA stability was not altered by Notch. The effect of Notch on Ctgf transcription was mediated by canonical signaling, since it was lost in the context of Rbpjk/Csl (required for canonical signaling) downregulation by RNAi. Downregulation of *Hes* and *Hey* genes did not preclude the induction of Ctgf by Notch suggesting that *Ctgf* is a direct Notch target gene. To ensure that the induction of Ctgf by Notch was physiological, wild type osteoblasts were cultured on wells coated with the Notch ligand Delta-like 1 (Dll1), which induced Ctgf mRNA and hnRNA by 1.5 to 2 fold. In addition, Notch induced Ctgf mRNA by 2 to 9 fold in femurs and calvariae from *Rosa^{Notch}* mice crossed with transgenics expressing Cre under the control of the *Osterix*, *Osteocalcin*, *Type I a1 collagen* or *Dentin matrix protein 1* promoter. This demonstrates that Notch induced Ctgf in undifferentiated and differentiated osteoblasts and osteocytes *in vivo*. These results establish Ctgf as a new and direct target of Notch signaling in osteoblasts and osteocytes suggesting that Ctgf may mediate selected actions of Notch in osteoblasts.

***Disclosures: Ernesto Canalis**, None.*

1076

HIF-1α Regulates Bone Formation Following Osteogenic Mechanical Loading. Ryan Tomlinson*[1], Matthew Silva[2]. [1]Washington University in St. Louis, USA, [2]Washington University in St. Louis School of Medicine, USA

HIF-1α is a factor typically associated with angiogenic gene transcription under hypoxic conditions. In addition, HIF-1α has been shown to associate with β-catenin, potentially inhibiting downstream activation of Wnt target genes. Importantly, both angiogenesis and Wnt signaling are differentially regulated following osteogenic mechanical loading. To clarify the role of HIF-1α in this process, mice lacking HIF-1α in the osteoblast lineage (ΔHIF-1α) or wild type (WT) mice were subjected to damaging or non-damaging mechanical loading, producing woven or lamellar bone, respectively.

ΔHIF-1α mice produced less woven bone than WT mice 7 days after damaging mechanical loading, with significant decreases in woven bone volume (-22%) and extent (-21%), but no changes in woven bone BMD. These decreases in woven bone formation were precipitated by a significant decrease in vascularity (-35%), as measured by immunohistochemistry against vWF. Additional immunohistochemistry was used to show that osteocytes, rather than osteoblasts, are the main bone cell expressing HIF-1α following damaging loading.

Following non-damaging mechanical loading, both ΔHIF-1α and WT mice had increased lamellar bone formation in loaded limbs compared to non-loaded limbs, with significant increases in Ec.MS/BS, Ps.MS/BS, Ps.MAR, and Ps.BFR/BS. Importantly, loaded limbs from ΔHIF-1α mice had greater increases in both Ps.MAR and Ps.BFR/BS than WT loaded limbs. However, ΔHIF-1α mice also had increased baseline mineralization, demonstrated by increased periosteal bone formation in non-loaded limbs compared to WT non-loaded limbs.

In summary, ΔHIF-1α mice produced less woven bone following damaging mechanical loading, but generated additional lamellar bone following non-damaging mechanical loading. The diminished response to damaging loading was attributed to the role of HIF-1 as a pro-angiogenic transcription factor, since angiogenesis is required for optimal bone formation after stress fracture. The increased bone formation following non-damaging loading was attributed to decreased binding of HIF-1α to β-catenin, a process that disrupts Wnt signaling associated with periosteal bone apposition. These results demonstrate that HIF-1α is a factor that regulates bone formation following osteogenic mechanical loading.

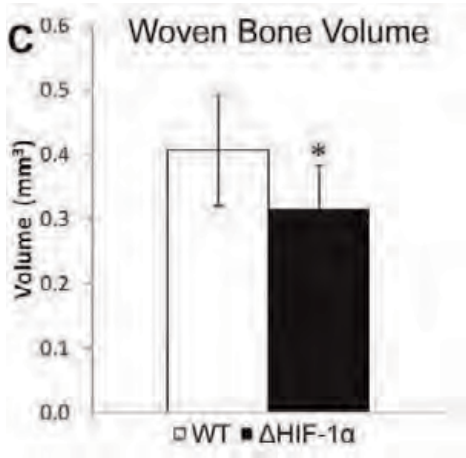

Figure 1 – Loading-induced woven bone formation is impaired in dHIF-1a mice

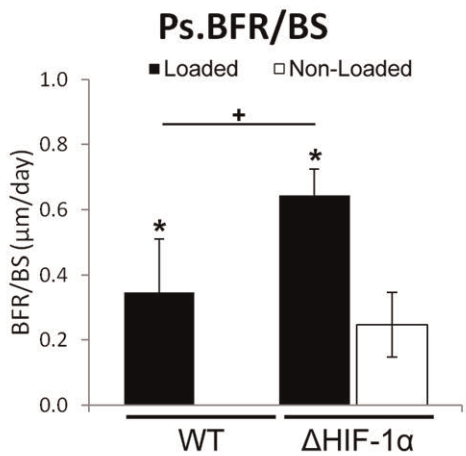

Figure 2 – Loading-induced lamellar bone formation is increased in dHIF-1a mice

***Disclosures: Ryan Tomlinson**, None.*

1077

R-spondin 3 Is a Negative Regulator of Bone Formation. Kei Yamana*[1], Hiroaki Saito[1], Kenichi Nagano[1], Riku Kiviranta[1], Francesca Gori[2], Roland Baron[3]. [1]Harvard School of Dental Medicine, Harvard Medical School, USA, [2]Harvard School of Dental Medicine, Massachusetts General Hospital, USA, [3]Harvard School of Medicine & of Dental Medicine, USA

Wnt ligands function with an entourage of receptors, co-receptors, agonists and antagonists that either enable or prevent Wnt signaling activation. Although activation of canonical Wnt signaling exerts a positive action on bone homeostasis, not all aspects of how it regulates bone homeostasis are clear. R-spondins (Rspos) consist of 4 cysteine-rich secreted glycoproteins essential in development. Although the mechanism of action of these proteins in mammals is not clear, the general consensus is that they potentiate canonical Wnt signals and thereby should exert a positive influence on bone formation and bone mass.

To test this hypothesis, and since Rspo3 is highly expressed in skeletal elements during development and is associated with bone density in GWAS studies, we investigated the biological function of Rspo3 in bone. Rspo3 is expressed in MEFs and in primary calvarial osteoblasts (OBs) and its expression increases during OB differentiation. While global deletion of Rspo3 results in embryonic lethality, Rspo3+/- mice develop normally and are healthy. In contrast to our expectations, Rspo3 haplo-insufficiency led to a striking increase (11X) in bone formation rate (BFR) and a 3X increase in mineral apposition rate in both female and male mice and at several time points. Accordingly, trabecular bone mass was significantly increased. Preliminary studies indicate that Rspo1 null mice develop high bone mass as well, suggesting that the increase in bone mass also apply to other members of the R-spondin family. In vitro studies in MEFs and calvarial OBs confirm that deletion and haplo-insufficiency of Rspo3 results in increased OB differentiation. Remarkably, lack of Rspo3 leads to activation of canonical Wnt signaling as indicated by reporter gene activity and increased expression of canonical Wnt target genes, activated β-catenin and phosphorylated LRP5/6. In addition, Wnt3a decreases while Dkk1 increases Rspo3 expression suggesting a feedback loop regulating Rspo3 and thereby canonical Wnt signaling. Finally, deletion of one allele of Dkk1 or overexpression of Dkk1 in Rspo3+/- mice aggravates or normalizes the Rspo3+/- bone phenotype, respectively, confirming activation of canonical Wnt signaling in these mice.

Thus, although R-spondins are believed to potentiate canonical Wnt signaling, our findings reveal a novel and unexpected function of this component of the Wnt signaling pathway as negative regulators of bone formation and homeostasis.

***Disclosures: Kei Yamana**, None.*

1078

Fracture Healing Via Periosteal Callus Formation Requires Macrophages for Both Initiation and Progression of Endochondral Ossification. Allison Pettit[1], Liza Raggatt*[1], Martin Wullschleger[2], Kylie Alexander[3], Roland Steck[4], Simranpreet Kaur[5], Andy Wu[5]. [1]Mater Medical Research Institute, Australia, [2]The University of Queensland & RBWH, Australia, [3]Center for Clinical Research, Australia, [4]Queensland University of Technology, Australia, [5]The University of Queensland, UQ-CCR, Australia

The importance of inflammation to the initiation of fracture repair is established. Macrophages have been implicated in these inflammatory events but there has been little consideration of their possible roles beyond this. Our discovery that bone tissues contain resident macrophages (osteomacs) that exert pro-anabolic influence exposed a novel role for macrophages in bone biology. This included demonstration of a critical role for osteomacs in promoting intramembranous ossification during bone healing. Macrophage distribution throughout fracture healing was investigated using immunohistochemical staining with a panel of macrophage and bone cell marker antibodies in samples collected from a clinically relevant fracture model (MouseFix) that repairs via endochondral callus formation. Macrophage functional contributions during endochondral callus formation were determined using inducible in vivo macrophage depletion (Mafia transgenic mice) in the same fracture model. We confirmed macrophages were prominent during both the inflammatory and early anabolic phases and extended this through identification of 3 macrophage subpopulations including inflammatory macrophages and osteomacs. We showed that macrophages persist throughout later healing phases, but at reduced frequency, with enrichment of osteomacs at sites of bone formation. Notably, inflammatory macrophages were scattered within foci of mesenchymal condensation during the initiation of endochondral ossification. They were also located at the chondro-osseous junction, preceding osteoclast invasion into cartilage matrix. Depletion of macrophages initiating at the time of surgery resulted in catastrophic failure of fracture healing including persistence of hematoma and absence of granulation tissue. Delayed macrophage depletion commencing at the transition to early anabolism resulted in significant reduction in soft callus area (greater than 50%, $p = 0.002$). A significant positive correlation was observed between residual callus size and efficiency of macrophage depletion ($r = 0.6$). These observations provide the most compelling evidence to date regarding the necessity of macrophages in the initiation of fracture repair and establish their direct functional contribution to anabolic mechanisms during endochondral callus formation. Our accumulating data implicating macrophages in both endochondral and intramembranous ossification mechanism solidifies this pathway as a key cellular mechanism in bone biology.

***Disclosures: Liza Raggatt**, None.*

1079

Histology of Atypical Femoral Fractures. Jörg Schilcher*[1], Per Aspenberg[1], Olof Sandberg[2]. [1]Linköping University, Sweden, [2]Department of clinical & experimental medicine, Linköping University, Sweden

Background: The pathophysiology behind bisphosphonate-associated atypical femoral fractures remains unclear. Histological findings at the fracture site itself might provide important clues. So far only one case has been published describing the histological appearance of the fracture.

Methods: Between 2008 and 2013, bone biopsies from the fracture sites were collected from 8 patients with 4 displaced and 4 undisplaced atypical femoral fractures. Seven female patients reported continuous bisphosphonate use for an average of 10 years. One patient was a man, not using bisphosphonates. Laboratory parameters were obtained, and the patients were followed until union. The bone biopsies were evaluated histologically and with micro-computed tomography.

Results: The 4 undisplaced fractures engaged the whole cortical thickness and comprised a 160 to 200 μm wide, meandering fracture gap filled with amorphous necrotic material. Active resorption and remodeling was common in the close vicinity of the fracture, but seldom reached into the fracture gap. In some areas, the bone adjacent to the gap appeared to undergo fragmentation and disintegration, possibly due to abrasion. Loose bone fragments could be found in the fracture gap in all cases. Where fragments had loosened, defects occurred in the underlying bone. Woven bone was common adjacent to the fracture gap, and appeared to have been formed in the

defects caused by abrasion. Periosteal and endosteal callus was found in all cases. Far away from the fracture, large areas of osteonal bone with only empty osteocyte lacunae were found in some samples.

Figure 1 shows a fracture gap (x) with amorphous material (+). A fragment of lamellar bone is about to loosen. White arrows indicate a thin layer of amorphous material between this fragment and the intact bone. Black arrows indicate resorption cavities near the fracture.

Discussion: Atypical femoral fractures show signs of increased remodeling in the vicinity of the fracture gap. The narrow width of the gap and its necrotic contents suggest that micromotion leads to strains between the fracture fragments that precludes survival of ingrowing cells. Moreover, there seemed to be continuous mechanical fragmentation of the bone at the crack, and replacement of fragmented areas with woven bone. Thus, it appears that the fracture line is not static, but moves in the bone over time, like the changes in the course of a meandering river.

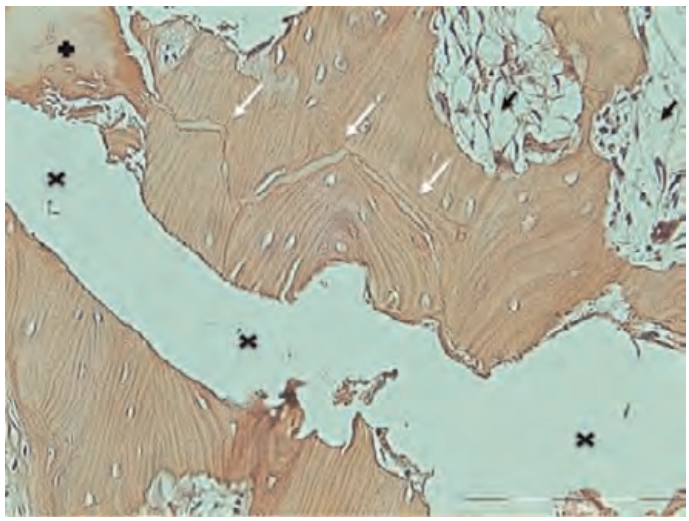

Figure 1. See text

***Disclosures: Jörg Schilcher**, None.*

1080

Effect of Teriparatide on Healing of Incomplete Atypical Femur Fractures. Angela M. Cheung*[1], Jonathan Adachi[2], Aliya Khan[3], Robert Bleakney[4], Earl Bogoch[5], Rowena Ridout[6], Heather McDonald-Blumer[7], Lianne Tile[8], Savannah Cardew[9], Khalid Syed[8], Jessica Chang[8], Judite Scher[8], Hanxian Hu[8], Suzanne Morin[10], Alexandra Papaioannou[11], Sophie Jamal[12], Robert Josse[13]. [1]University Health Network-University of Toronto, Canada, [2]St. Joseph's Hospital, Canada, [3]McMaster University, Canada, [4]Mount Sinai Hospital, Canada, [5]St. Michael's Hospital, Canada, [6]Toronto Western Hospital, Canada, [7]University of Toronto, Canada, [8]University Health Network, Canada, [9]Women's College Hospital, Canada, [10]McGill University, Canada, [11]Hamilton Health Sciences, Canada, [12]The University of Toronto, Canada, [13]St. Michael's Hospital, University of Toronto, Canada

Background: With increased awareness of atypical femur fractures (AFFs), incomplete non-displaced AFFs are diagnosed more frequently. Optimal therapy for these fractures is unclear. We describe a case series of 22 patients with incomplete AFFs treated with teriparatide (TPD) therapy.

Methods: These 22 patients are part of our larger Ontario AFF Cohort Study. All satisfied the criteria set forth by the ASBMR Task Force for the definition of AFF. Baseline demographic characteristics including BMD at the lumbar spine, total hip and femoral neck were collected. We assessed radiographic fracture healing using CT scans and plain radiographs, measuring depth of the lucency line through the cortex and degree of extension around the circumference every 6 months for up to 2 years (recommended duration of TPD therapy for osteoporosis in Canada). Progression / regression of fracture line up to last follow-up were noted. Pain, mobility and any surgical intervention were noted. We summarized our results using descriptive statistics.

Results: All 22 patients were postmenopausal women (68% Caucasian, 32% Southeast/South Asian): mean age 65.9 years (range 26.0 - 80.8 yrs), mean BMI 28.4 kg/cm2 and mean serum 25-hydroxyvitamin D 110 nmol/L at diagnosis. All had normal ionized calcium and intact PTH. 17 (77%) had bilateral AFFs (12 had a complete AFF surgically fixed on the contralateral side and 5 had bilateral incomplete AFFs), and 5 (23%) had unilateral incomplete AFF. Average length of bisphosphonate use was 12.0 years (range 3.4-28.7 yrs). Mean BMD T-scores at the LS, TH and FN were -1.76, -1.16 and -1.78, respectively. Average duration of TPD was 18.8 months (range: 1-36 months). Of the 22 patients, 3 underwent prophylactic surgical repair (2 due to debilitating pain/progression and 1 due to patient/physician preference). Of the remaining 19 patients, follow-up imaging was available for 15 patients with 19 incomplete AFFs. Of these 19 incomplete AFFs, 2 had healed, 5 were healing, 12 were stable, and none had worsened at last follow-up. However, 4 patients developed new lucency lines in the same femur as their original incomplete AFF despite teriparatide therapy.

Conclusions: Teriparatide may promote healing of incomplete non-displaced AFFs. However, a randomized placebo-controlled trial is urgently needed to definitively answer this question.

***Disclosures: Angela M. Cheung**, Eli Lilly, 9; Amgen, 9; Eli Lilly, 6; Amgen, 5; Eli Lilly, 5; Merck, 9; Amgen, 6; Merck, 6; Warner Chilcott, 5; Warner Chilcott, 2*

1081

Beyond 10 yrs Prediction of Fragility Fracture by DXA in Women. The OFELY study. Elisabeth Sornay-Rendu, François Duboeuf, Stephanie Boutroy, Roland Chapurlat*. INSERM UMR1033, Université de Lyon, France

Low bone mineral density (BMD) is a major determinant of fragility fractures (Fx) but its very long term prediction is poorly documented. In the OFELY study, we analyzed the risk of Fx over 20 yrs and more particularly beyond 10 yrs in women aged 40 yrs and more at the inclusion. BMD was measured at baseline at the spine, hip and forearm in 868 women (mean age 59 $\pm$ 10 years, 78% postmenopausal) using dual-energy X-ray absorptiometry (DXA). All peripheral and vertebral fragility Fx, were confirmed by radiographs and prospectively registered. During a median follow-up of 19.7 yrs (IQ :2.8), 245 women sustained one or more incident fragility Fx (first Fx: vertebral n=65, peripheral n=180). Each SD decrease of BMD at the femoral neck (FN) , total hip, spine and ultradistal (UD) radius was associated with an increased risk of fragility Fx with an odds ratio [95% CI] of 1.49 [1.23-1.79], 1.54 [1.32-1.82], 1.47 [1.28-1.67] and 1.72 [1.45-2.04] respectively, after adjustment for age, prior Fx, parental hip Fx, treatment at baseline or during follow-up (hormone replacement therapy, bisphosphonates, etc ...) and duration of follow-up. Women who sustained Fx beyond 10 years (Fx 10-20, n=109) were younger compared with those in the first10 years (Fx 0-10, n=136) ($p<0.0001$). After adjusting for age, Fx 10-20 had greater grip strength and spine BMD and used more often HRT, compared with Fx 0-10 ($p=0.01$ to 0.02). The risk of Fx 10-20 was significantly increased with adjusted OR of 1.35 [1.06-1.72], 1.39 [1.12-1.72], 1.30 [1.09-1.56] and 1.67 [1.32-2.08] for each SD decreased of FN, total hip, spine and UD, in the same order of Fx 0-10 (OR 1.61 [1.25-2.08], 1.69 [1.37-2.13], 1.67 [1.39-2.00] and 1.79 [1.45-2.17] respectively). Parental hip Fx was associated with an increased risk of Fx 10-20 but contrasting with Fx 0-10, Fx 10-20 were not associated with lower grip strength, falls and previous Fx at baseline after adjusting for age. In conclusion, low BMD in women aged 40 yrs or more is significantly associated with an increased risk of fracture beyond 10 years independently of age and other predictors of fractures. The prediction conferred by baseline BMD did not decline with time.

***Disclosures: Roland Chapurlat**, None.*

1082

A Five-Year Longitudinal Study of Site-Specific Changes in Bone Quality in the Calgary Population-Based Cohort: an HR-pQCT Study. Lauren Burt*[1], Anne-Laure Ménard[2], Heather Macdonald[3], David Hanley[1], Steven Boyd[1]. [1]University of Calgary, Canada, [2]Ecole Polytechnique of Montréal, CHU Ste-Justine Research Center, Canada, [3]University of British Columbia, Canada

Age-related bone loss measured by dual-energy X-ray absorptiometry (DXA) occurs at a rate of 1-2% per year, but the age at which bone loss occurs varies with skeletal sites and imaging modalities. Age-related bone loss measured with high-resolution peripheral quantitative computed tomography (HR-pQCT) may differ from DXA measurements. In our population-based cohort we aimed to compare subject-specific longitudinal age-related bone changes in different skeletal sites using two imaging modalities.

Women (N=112, 60-85 yrs) from the Calgary cohort of the Canadian Multicentre Osteoporosis Study (CaMos) participated in a 5-year follow-up study. Areal bone mineral density (aBMD) at the lumbar spine (LS), femoral neck (FN) and total hip (TH) were obtained from DXA (Hologic, USA) scans of L1-L4 and the left hip. The non-dominant radius and left tibia were scanned using HR-pQCT (Scanco Medical, Switzerland). Total volumetric BMD (Tt.BMD), cortical BMD (Ct.BMD), trabecular BMD (Tb.BMD) and cortical porosity (Ct.Po) were assessed using standard and automated segmentation methods. Finite element analysis (FEA) estimated apparent bone strength. Repeated measures ANOVA assessed age-related bone change over time. T-tests compared differences between skeletal sites and imaging modalities.

Over 5-years, DXA-derived aBMD decreased between 4% (FN) and 6% (TH) whereas HR-pQCT-derived Tt.BMD declined between 3% (tibia) and 7% (radius) ($p<0.05$). At the radius, Tb.BMD decreased 6% and Ct.BMD 4% ($p<0.01$). However, at the tibia Tb.BMD did not change significantly ($p>0.05$) and Ct.BMD decreased by 5% ($p<0.01$). The greatest age-related change was in Ct.Po; Ct.Po increased by 53% at the radius and 33% at the tibia ($p<0.01$). Preliminary FEA results revealed a loss in radial apparent bone strength of 3% ($p<0.05$). Comparisons between skeletal sites indicated that age-related changes in Tt.BMD and Ct.Po were larger at the radius than tibia ($p<0.05$). Similarly, age-related aBMD changes were greater at the TH than LS ($p<0.01$).

Our 5-year longitudinal HR-pQCT study is the longest population-based cohort study, demonstrating age-related skeletal changes in women over 60 yrs. Age-related changes differed according to imaging modality (DXA vs HR-pQCT) and skeletal sites: more bone loss occurred at the radius than tibia. Whether this holds true for men will be the subject of our continued study. Further understanding of age-related changes bone quality will enhance our ability to assess bone health with HR-pQCT.

***Disclosures: Lauren Burt**, None.*

1083

Inflammatory Markers and Risk of Hip Fracture in Older Women: The Study of Osteoporotic Fractures. Kamil Barbour*[1], Li-Yung Lui[2], Kristine Ensrud[3], Teresa Hillier[4], Marc Hochberg[5], Jane Cauley[6]. [1]CDC, USA, [2]California Pacific Medical Center Research Institute, USA, [3]Minneapolis VA Medical Center / University of Minnesota, USA, [4]Kaiser Center for Health Research, USA, [5]University of Maryland School of Medicine, USA, [6]University of Pittsburgh Graduate School of Public Health, USA

Cytokines play a major role in bone remodeling *in vitro* and in animal models, with evidence supporting the involvement of inflammatory markers in the pathogenesis of osteoporosis. Moreover, there is evidence showing that high levels of inflammatory makers may increase bone loss in predominantly older women. However, few studies have examined the association between inflammatory marker levels and risk of hip fracture, the most serious consequence of osteoporosis. We used a case-cohort design nested in a cohort of 4709 white women from the Study of Osteoporotic Fractures at year 10 (1997-1998) to determine if high levels of inflammation increase the risk of hip fracture, and whether this association is mediated by frailty, physical function, calciotropic hormones, renal function, and bone mineral density (BMD). We randomly selected 1171 to serve as the random subcohort (mean age 80.1 $\pm$ 4.2 years) plus the first 300 women with incident hip fracture after the Year 10 examination. The median (interquartile range (IQR)) study follow-up time was 6.3 (3.7, 6.9) years. We examined inflammatory marker levels in quartiles as their distribution was shown to be skewed. In multivariable models, the hazard ratio (HR) of hip fracture for participants with the highest levels (quartile 4) of 4 inflammatory markers compared with those with lower levels (quartiles 1, 2, and 3) was 1.33 (95% confidence interval [CI], 0.97-1.82) for interleukin-6 (IL-6), 1.13 (95% CI, 0.83-1.54) for IL-6 soluble receptor (SR), 1.52 (95% CI, 1.11- 2.08) for tumor necrosis factor (TNF) SR1, and 1.05 (95% CI, 0.75-1.45) for TNF SR2. Among participants with 2 and $\geq$3 of 4 markers in the highest quartile, the HR of hip fracture was 1.50 (95% CI, 1.06-2.11) and 1.42 (95% CI, 0.87-2.31), in comparison with participants with 0 or 1 marker(s) (p trend = 0.03). After individually adjusting for 6 potential mediators, cystatin-C (a biomarker of renal function) attenuated the dose-response relationship the most (p trend=0.24); even greater than BMD (p trend=0.16). Based on findings from this and our prior study, older women with higher levels of inflammatory markers are at increased risk of hip fracture in part due to their reduced renal function.

Table. Hazard ratios (95% CIs) of hip fracture, according to number of high* inflammatory markers

	0, 1 (Ref)	2	≥3	P trend
Base analysis†	ref	1.50 (1.06, 2.11)	1.42 (0.87, 2.31)	0.03
Base analysis† + frailty	ref	1.47 (1.05, 2.08)	1.35 (0.83, 2.22)	0.06
Base analysis† + walking speed	ref	1.39 (0.97, 1.99)	1.31 (0.79, 2.16)	0.11
Base analysis† + cystatin-C	ref	1.41 (1.00, 2.01)	1.14 (0.63, 2.07)	0.24
Base analysis† + 25(OH)D	ref	1.47 (1.04, 2.08)	1.32 (0.80, 2.18)	0.07
Base analysis† + PTH	ref	1.50 (1.06, 2.12)	1.42 (0.87, 2.32)	0.03
Base analysis† + BMD	ref	1.44 (1.00, 2.08)	1.22 (0.73, 2.02)	0.16

*Number of inflammatory markers in the top quartile according to the distribution of inflammatory markers among women in the random subcohort
†Base analysis controlled for age, BMI, self-reported health, diabetes, prevalent history of fracture, vitamin D, and steroid use.

Table

***Disclosures: Kamil Barbour**, None.*

1084

Bone Material Strength Measured by *In Vivo* Microindentation is Compromised in Postmenopausal Women with Type 2 Diabetes Mellitus. Joshua Farr*[1], Shreyasee Amin[1], L. Joseph Melton[1], Louise McCready[1], Sundeep Khosla[2]. [1]Mayo Clinic, USA, [2]Mayo Clinic College of Medicine, USA

Type 2 diabetes mellitus (T2DM) is an established, independent risk factor for fracture. Moreover, recent evidence suggests that fracture risk is higher for a given femoral neck BMD T-score and age in patients with T2DM as compared to non-diabetics (JAMA 305:2184, 2011). These observations have led to the notion that bone "quality" (i.e., bone material properties) is abnormal in T2DM, leading to reduced bone strength for a given bone mass. To rigorously test this hypothesis *in vivo*, we used an innovative hand-held microindentation instrument (Osteoprobe®) to directly measure the bone material strength (BMS) of the midshaft of the tibia in a case-control study of 30 postmenopausal women (mean age $\pm$ SD: 65.5 $\pm$ 8.1 yrs, range: 50–80 yrs) diagnosed with T2DM for at least 10 yrs and 30 age-matched, non-diabetic women. In addition, we measured serum hemoglobin A1c (HbA1c) as well as bone density at the radius, spine, hip, and total body by DXA and microarchitecture at the distal radius and tibia by HRpQCT. Compared to controls, women with T2DM had significantly lower tibial BMS, both unadjusted and following adjustment for BMI (–10.5%, P<0.001), but showed no differences in cortical or trabecular bone microarchitecture at the distal radius and tibia as well as in BMD at any site. Importantly, BMS of the tibia was negatively correlated with HbA1c in women with T2DM (r=–0.41, P=0.026; Fig. A) but not in controls (r=–0.09, P=0.626; Fig. B). BMS of the tibia was not significantly correlated with any of the DXA- or HRpQCT-derived bone parameters.

These findings represent the first demonstration, using a direct *in vivo* measure of BMS, of compromised bone quality in women with T2DM. By contrast, HRpQCT and DXA were not able to differentiate between women with or without T2DM. Given the lack of associations between BMS and bone density or microarchitecture, our data suggest that these BMS measures may reflect a unique component of bone quality that could serve to better identify individuals at risk for fragility fractures. Our finding of an inverse relationship between HbA1c and BMS in women with T2DM supports this possibility, and may reflect the detrimental effects of prolonged hyperglycemia on bone material properties. Our study also points to the need to further define the factors that regulate bone material properties in T2DM, which could lead to novel insights into the pathophysiological basis and possible prevention of the fractures observed in these patients.

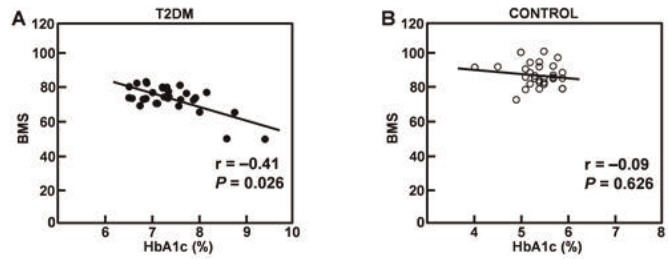

Figure

***Disclosures: Joshua Farr**, None.*

1085

Associations of Fetal and Childhood Growth with Bone Mass in School Age Children. The Generation R Study. Denise Heppe*[1], Carolina Medina-Gomez[2], Albert Hofman[3], Fernando Rivadeneira[4], Vincent W.V. Jaddoe[5]. [1]Erasmus MC, The Netherlands, [2]Erasmus Medical Center, The Netherlands, [3]Department of Epidemiology Erasmus Medical Center, Netherlands, [4]Erasmus University Medical Center, The Netherlands, [5]Generation R Erasmus Medical Center, Netherlands

Fetal growth restriction, as indicated by low birth weight, leads to lower bone accrual in children and peak bone mass acquisition in adults. We aimed to assess how different patterns of fetal and childhood growth influence bone properties at school age. In 5,431 children, participating in a prospective birth cohort study, we measured fetal growth by ultrasound during the second and third trimesters, and childhood growth at birth, 1, 2, 3 and 4 years of age. We measured total body bone mineral density (BMD) by dual-energy x-ray absorptiometry (DXA) at the median age of 6.0 (IQR 0.37) years and analyzed bone parameters after body size correction. As compared to children born with normal birth weight, the bone mineral content (BMC) and bone area (BA) were all lower in small (<10^{th} percentile) for gestational age (SGA) children and higher in large (>90^{th} percentile) for gestational age (LGA) children. SGA children with normal postnatal growth in the first two years had -0.30 SD (95%CI -0.42, -0.18) lower BMC, -0.35 SD (95%CI -0.47, -0.24) lower BA and -0.21 SD (95%CI -0.36, -0.06) lower BMD than children born with normal birth weight and normal growth in the first 2 years. No differences in BMD, BMC or BA were seen in SGA children with catch-up growth in the first two years (>0.67 SD increase in weight) and LGA children with catch-down growth (<-0.67 SD decrease in weight). Conditional growth analysis showed that all fetal and childhood growth measures, except birth length, were positively associated with BMC, BA and BMD (all with P <0.05). Birth length was positively associated with BMC and BA, not BMD (both with P <0.001). Overall, childhood growth exerted a larger influence on bone parameters than fetal growth did. The strongest effect of growth during the first years of life was seen for weight and height on BMC (ß 0.25 SD, 95%CI 0.23, 0.27 and ß

0.31 SD, 95%CI 0.29, 0.33 per SD increase, respectively). Results were less prominent on BMD, probably due to positive relations with both BMC and bone size (BA). We conclude that fetal and childhood growth influence bone mineral accrual, particularly in the first postnatal years. Compensatory growth in the first postnatal years may eradicate the consequences of slower fetal growth rates on bone development.

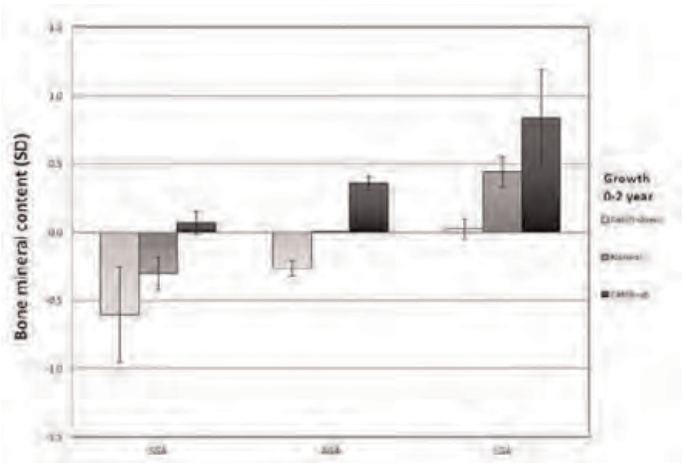

BMC by Growth periods

***Disclosures: Denise Heppe**, None.*

1086

The Oral Small Molecule Phenamil Regulates BMP Signaling and Prevents Ovariectomy-Induced Osteoporosis. Aaron James*[1], Choon G Chung[2], Greg Asatrian[2], Omar Velasco[2], Daniel Halperin[3], Kye Won Park[4], Georgina Bayani[2], Kevork Khadarian[2], Xinli Zhang[1], Kang Ting[1], Peter Tontonoz[3], Chia Soo[5]. [1]University of California, Los Angeles, USA, [2]Division of Associated Clinical Specialties & Section of Orthodontics, UCLA School of Dentistry, USA, [3]Department of Pathology & Laboratory Medicine, David Geffen School of Medicine, USA, [4]Sunkyunkwon University, Korea, Korea, democratic people's republic of, [5]Division of Plastic & Reconstructive Surgery, Department of Surgery, University of California, Los Angeles, USA

Introduction: Phenamil is a non-toxic, small molecule that induces *in vitro* osteogenesis via downregulation of the BMP (bone morphogenetic protein) antagonist Smurf1 (SMAD ubiquitin regulatory factor 1). Moreover, phenamil plays a role in regulating the balance of osteogenesis versus adipogenesis via Trb3 (Tribbles homolog 3)-dependent promotion of BMP action. No prior studies have reported anabolic effects of phenamil *in vivo*. Here, we sought to determine if oral administration of phenamil would induce bone formation in osteoporotic and non-osteoporotic mice.

Methods: Wildtype mice underwent ovariectomy (OVX) or SHAM surgery, followed immediately by feed supplemented with Phenamil (50 mg / kg diet) or control. Analysis was performed by weekly Dual-energy X-ray absorptiometry (DXA), post-mortem high-resolution micro computed tomography (microCT), histology and immunohistochemistry. N=20 mice in total were split evenly into treatment groups and were followed for four weeks post-OVX. All analyses were performed on the lumbar spine.

Results: As expected, OVX induced significant bone loss among mice treated with control feed. Remarkably, maintenance of bone mineral density (BMD) was observed when OVX mice were treated with Phenamil feed (*$p<0.01$ in comparison to control feed) (Fig. 1A). MicroCT showed a significant increase in bone volume (BV) (Fig. 1B) and fractional bone volume (BV/TV) when either sham or OVX mice were treated with Phenamil feed (*$p<0.05$ in comparison to control feed), also observed in microCT 3D coronal reconstructions (Fig. 1C). Non-significant trends toward increased trabecular bone thickness and trabecular bone number were observed among Phenamil treated groups.

Conclusions: This study shows for the first time that the small molecule phenamil induces bone formation *in vivo*, and helps to counteract ovariectomy induced bone loss. As phenamil is a non-toxic derivative of amiloride (an FDA approved potassium sparing diuretic), these finding are highly translatable to clinical use.

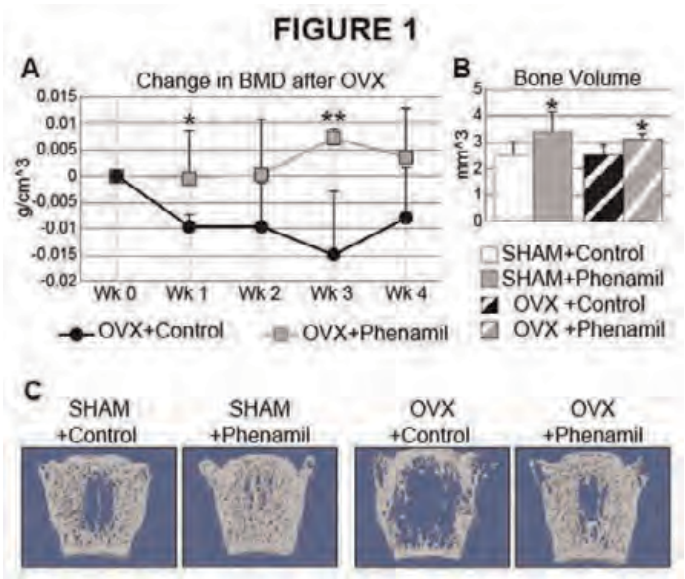

Figure 1

***Disclosures: Aaron James**, None.*

1087

Bone Marrow Stromal Cell Proliferation in Mice Lacking NFATc1 in Mature Osteoclasts. Julia Charles*[1], Jonathan Quang[2], Kelly Tsang[3], Antonios Aliprantis[4]. [1]Brigham & Women's Hospital & Harvard School of Medicine, USA, [2]Boston University School of Medicine, USA, [3]Brigham & Women's Hospital, USA, [4]Brigham & Women's Hospital & Harvard School of Public Health, USA

Nuclear Factor of Activated T Cells c1 (NFATc1) is a key transcription factor in osteoclast (OC) differentiation where it drives expression of osteoclast-specific genes in precursor cells. Although the role of NFATc1 in OC formation is well described, little is known about the function of NFATc1 in mature OCs. To address this, $Nfatc1^{fl/fl}$*Ctsk-Cre*$^{+}$ ($Nfatc1^{\Delta OC/\Delta OC}$) mice were generated, in which *Nfatc1* is deleted in mature OCs. These mice were compared to $Tnfrsf11a^{fl/fl}$*Ctsk-Cre*$^{+}$, in which the gene encoding Receptor activator of nuclear factor kB (RANK) is knocked out in OCs ($Rank^{\Delta OC/\Delta OC}$). Both $Nfatc1^{\Delta OC/\Delta OC}$ and $Rank^{\Delta OC/\Delta OC}$ mice are runted and toothless with an increase in calcified cartilage in the long bones. In contrast to $Rank^{\Delta OC/\Delta OC}$ mice, which largely lack OCs, abnormally large, multinucleated OCs are present in the bones of $Nfatc1^{\Delta OC/\Delta OC}$ mice. Strikingly, in $Nfatc1^{\Delta OC/\Delta OC}$ mice, bone marrow hematopoietic elements are replaced with spindle shaped stromal cells. In contrast, $Rank^{\Delta OC/\Delta OC}$ mice do not display expansion of stromal cells and normal appearing hematopoietic cells occupy the residual marrow space. The expanded bone marrow stromal cells in $Nfatc1^{\Delta OC/\Delta OC}$ mice are likely of the osteoblast (OB) lineage, as they differentiate into OBs ex vivo and support osteoclastogenesis. To exclude that the stromal cell proliferation phenotype could be due to unanticipated deletion of the conditional *Nfatc1* allele by *Ctsk-Cre* in OBs, we also crossed $Nfatc1^{fl/fl}$ with *Osx-Cre* and *Prx1-Cre*, which are expressed in OBs and limb mesenchymal progenitors, respectively. Neither $Nfatc1^{fl/fl}$*Osx-Cre*$^{+}$ nor $Nfatc1^{fl/fl}$*Prx1-Cre*$^{+}$ recapitulates the $Nfatc1^{\Delta OC/\Delta OC}$ phenotype. To test if OCs are required for the stromal proliferative phenotype, mice doubly deficient for *Nfatc1* and *Rank* in mature OCs ($Nfatc1^{\Delta OC/\Delta OC}Rank^{\Delta OC/\Delta OC}$) were examined. RANK-deficiency completely rescued the stromal proliferative phenotype, with $Nfatc1^{\Delta OC/\Delta OC}Rank^{\Delta OC/\Delta OC}$ mice demonstrating an identical bone phenotype to $Rank^{\Delta OC/\Delta OC}$ mice. In summary, deficiency of NFATc1 in mature OCs results in a high bone mass phenotype with effacement of the marrow space by OB lineage stromal cells and enlarged OCs, a constellation of pathologic findings reminiscent of fibrous dysplasia. We hypothesize that NFATc1 in mature OCs regulates the expression of a factor that either promotes stromal cell proliferation or drives stromal cells to differentiate into OBs.

***Disclosures: Julia Charles**, None.*

1088

Absence of the αvβ3 Integrin and the ITAM Protein, DAP12, Causes Severe Osteopetrosis. Wei Zou*[1], Jean Chappel[2], Steven Teitelbaum[1]. [1]Washington University in St. Louis School of Medicine, USA, [2]Washington University School of Medicine, USA

Osteoclastic bone resorption depends upon the cell's ability to organize its cytoskeleton via the αvβ3 integrin and osteoclastogenic cytokines. Ligand occupancy of αvβ3 induces phosophorylation of the ITAM-bearing adaptor protein, DAP12, which we have established is essential for osteoclast function, in vitro. Like those deleted of only αvβ3, however, DAP12-/- mice exhibit only a slight increase in bone mass. Alternatively, DAP12-/- mice, also lacking another ITAM protein, FcRγ, are severely osteopetrotic, establishing that FcRγ compensates for DAP12 deficiency in the bone-resorbing polykaryons. Here we show that despite the mild phenotype of single gene deletion, β3/DAP12 double-deficient (β/D) mice are severely osteopetrotic. In contrast, mice with combined deletion of β3 and FcRγ exhibit no skeletal abnormalities. Bone marrow macrophages, derived from β/D mice, precursors normally express osteoclast differentiation markers when exposed to M-CSF and RANKL but the derivative TRAP+ cells fail to multinucleate and have a more severe phenotype than those lacking either αvβ3 or DAP12. β/D mice also express normal endogenous FcRγ , indicating that absence of the integrin precludes compensation for DAP12 deficiency by FcRγ. Consistent with this hypothesis, overexpression OSCAR, the co-receptor which activates FcRγ, rescues spreading and function of DAP12-/-, but not β/D osteoclasts. These data indicate αvβ3 is an essential partner of FcRγ/OSCAR and in fact, the three proteins associate under the influence of cytoskeleton-organizing cytokines. OSCAR, activated in bone-residing osteoclasts also phosphorylates Syk, a tyrosine kinase which is essential for organization of the osteoclast cytoskeleton. We found that MCSF induces Syk phosphorylation in DAP12 deficient osteoclast transduced with OSCAR, but not in β/D osteoclasts. Thus αvβ3, FcRγ and OSCAR form a cytoskeleton-activating complex required to compensate for DAP12 deficiency.

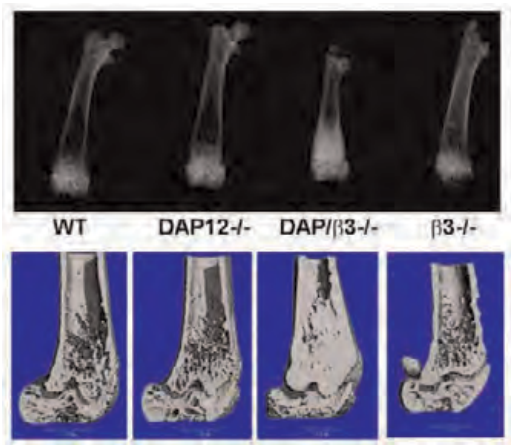

bone phenotype

***Disclosures: Wei Zou**, None.*

1089

CSF-1 in Osteocytes and Late Osteoblasts Controls Major Aspects of Bone Remodeling. Sherry Abboud Werner*[1], Diane Horn[1], Yves Gorin[1], Roberto Fajardo[2], Jean Jiang[1], Marie Harris[1], Stephen Harris[1]. [1]University of Texas Health Science Center at San Antonio, USA, [2]UT Health Science Center, San Antonio, USA

CSF-1 is a key factor in regulating bone remodeling. The precise source of CSF-1 that controls this remodeling process is unknown. Osteocytes express CSF-1 and its receptor. Viable osteocytes are essential for bone remodeling through cell-cell contact and secretion of factors that regulate osteoblasts and osteoclasts. Increased oxidative stress contributes to osteocyte death and correlates with bone loss during aging. The NADPH oxidase Nox4 is constitutively active and is a major source of reactive oxygen species (ROS) in bone. CSF-1 decreases Nox4 expression, suggesting that CSF-1 protects against oxidant stress. Little is known regarding the role of CSF-1 and Nox4 in osteocytes and oxidant stress-induced alterations in skeletal tissues. To examine CSF-1/Nox4 biologic effects, DMP1Cre-CSF-1cKO (CSF-1cKO) mice that lack CSF-1 in late osteoblasts/osteocytes were generated. Bones from WT and CSF-1cKO mice were examined for bone phenotype using μCT and histomorphometry; Nox4 and 4-HNE (marker of oxidant stress) expression were determined using immunohistochemistry. In parallel, bones from CSF-1KO mice with global CSF-1 deficiency were examined and enriched osteocytes from CSF-1KO mice were analyzed for apoptosis, gap junction function, NADPH oxidase activity and Nox4 protein by Western blot. WT osteocytes were treated with CSF-1 and examined for NADPH oxidase activity. CSF-1cKO bone phenotype showed a modest increase in bone mass, decreased osteoclasts and elevated Nox4 and 4-HNE expressing osteocytes. CSF-1cKO mice also showed reduced bone formation rate that would predispose to bone loss/fracture with age. Similarly, osteopetrotic CSF-1KO mice showed osteocyte defects including apoptosis, associated with increased Nox4 expression/activity as well as 4-HNE and DHE fluorescence and reduced Cx43 expression required for osteocyte function. Cultured CSF-1KO osteocytes were also predisposed to apoptosis and showed elevated NADPH oxidase activity/Nox4 protein and reduced gap junction function compared to WT osteocytes. Notably, CSF-1 inhibited NADPH oxidase activity in WT osteocytes. Taken together, studies indicate a novel link between CSF-1, Nox4-derived ROS and osteocyte survival/function and that CSF-1 deficiency in osteocytes regulates bone remodeling. Results reveal new mechanisms by which CSF-1/oxidative stress regulate osteocyte homeostasis and suggest therapeutic targets for improving osteocyte viability crucial for bone strength and longevity.

***Disclosures: Sherry Abboud Werner**, None.*

1090

Deletion of ERβ in Early Osteoprogenitor Cells Leads to a Doubling of Trabecular Bone Volume. Kristy Nicks*[1], Koji Fujita[1], Daniel Fraser[1], Ulrike McGregor[2], Meghan McGee-Lawrence[1], Jennifer Westendorf[1], David Monroe[3], Sundeep Khosla[4]. [1]Mayo Clinic, USA, [2]King's College, London UK, United Kingdom, [3]Mayo Foundation, USA, [4]Mayo Clinic College of Medicine, USA

While the role of ERα in regulating bone metabolism has been extensively studied, ERβ has been largely dismissed as a relevant modulator of bone mass. However, all previous studies have used an ERβ KO mouse that expressed transcript variants of ERβ and also involved global deletion of ERβ; the latter resulted in systemic hormonal changes (e.g., increased IGF-I levels) that confounded interpretation of the skeletal phenotype. Thus, we used a mouse model with flox sites ($ER\beta^{fl/fl}$) that, upon cleavage with Cre, led to a complete deletion of ERβ (Antal et al. PNAS 105:2433, 2008) specifically in mature osteoblasts (Col 2.3 Cre) or in early osteoprogenitors (Prx-1 Cre). In 3-month old female mice, ERβ deletion using the Col 2.3 Cre resulted in a 9% increase in spine ($P < 0.05$) and 7% increase in femur ($P < 0.01$) BMD relative to control (Cre alone) mice. More detailed studies using the Prx-1 Cre mice revealed that ERβ deletion in early osteoprogenitor cells resulted in a 93% increase ($P < 0.001$) in trabecular BV/TV by μCT at the femoral metaphysis; by contrast, cortical thickness at the femur mid-shaft was unchanged in the KO mice. Bone histomorphometric analysis demonstrated a 54% increase in osteoblast numbers ($P = 0.001$) but no changes in osteoclast numbers or eroded surfaces in the ERβ KO mice, consistent with ERβ deletion in osteoblasts leading to enhanced bone formation. To determine potential underlying mechanism(s), we isolated RNA from the femur metaphysis of $PrxCre//ER\beta^{fl/fl}$ and controls and utilized customized, in-house QPCR analyses of 240 genes related to bone metabolism, including genes reflecting 17 pre-specified pathways. Genes in the pathways were analyzed using a cluster analysis (O'Brien Umbrella Test) which tests for concordant changes in multiple genes in the pathway. Highly regulated pathways in the ERβ KO mice included adipogenesis (decreased, $P = 0.007$), autophagy (decreased, $P = 0.0008$), and oxidative stress (decreased, $P = 0.005$), suggesting that deletion of ERβ resulted in modulation of several pathways related to bone formation. In summary, our data demonstrate that deletion of ERβ in osteoblast lineage cells, in the absence of all splice variants, results in increased trabecular bone mass associated with increased osteoblast numbers and modulation of multiple pathways related to bone formation. These findings also suggest that pharmacological inhibition of ERβ in bone may provide a novel anabolic approach to treat osteoporosis.

***Disclosures: Kristy Nicks**, None.*

1091

Deletion of gp130 in Osteocytes Blocks PTH Anabolic Effect. Therese Standal*[1], Rachelle Johnson[2], Narelle McGregor[2], T. John Martin[2], Natalie Sims[2]. [1]St Vincent's Institute for Medical Research, Melbourne & Department of Cancer Research & Molecular Medicine, Trondheim, Norway, [2]St. Vincent's Institute of Medical Research, Australia

In exerting its anabolic effect on bone, PTH acts via its receptor (PTH1R) to increase osteoblast proliferation and differentiation and to inhibit apoptosis. Members of the IL-6/gp130 superfamily of cytokines are rapidly upregulated by PTH in the osteoblast lineage, and share similar gene targets, such as inhibiting osteocytic sclerostin. This study addresses whether gp130 signaling in osteocytes is needed for PTH's anabolic effect.

Male mice with conditional deletion of gp130 in osteocytes (Dmp1-Cre gp130f/f) and littermate controls (Dmp1-Cre gp130w/w) were treated with PTH(1-34) (30ug/kg s.c. 5x/week for 5 weeks). In w/w mice this treatment doubled osteoblast number / bone perimeter (p=0.001), and significantly increased osteoid surface / bone surface (BS) (p=0.009), osteoblast surface /BS (p=0.001) and mineralizing surface /BS (p=0.03). However in f/f mice, PTH treatment changed none of these parameters. Serum N-terminal propeptide of type I collagen (P1NP) levels were increased by 30% (p= 0.006) with PTH treatment in w/w mice, but were not modified in PTH-treated f/f mice. The only effect of PTH common to both w/w and f/f mice was to increase trabecular mineral apposition rate to the same extent in each. This suggests that the mineralization response to PTH is retained in some differentiated osteoblasts in f/f mice, but that PTH does not increase osteoblast proliferation and differentiation in

the absence of osteocytic gp130. Osteoclast number neither differed in number or size between the two groups, nor changed in response to PTH.

Since the PTH-induced increase in osteoblast number was completely blocked in the f/f mice, we investigated whether knockdown of gp130 in osteocytes influenced PTH1R expression in bone. Indeed, in f/f femurs gp130 mRNA levels were reduced by 44% ($p < 0.001$) and PTH1R mRNA reduced by 47% compared to w/w femurs ($p=0.03$). This was supported by *in vitro* data, where C57Bl/6 and gp130f/f primary osteoblasts were infected with lentiviral cre. In cre-infected gp130f/f osteoblasts both gp130 and PTH1R mRNA were 52% ($p=0.008$) and 84% ($p=0.03$), respectively, lower than in infected C57Bl/6 cells.In conclusion, osteocytic gp130 is required for PTH to increase osteoblast number and bone forming surfaces, and to maintain PTH1R expression in the osteoblast lineage.

***Disclosures: Therese Standal**, None.*

1092

Conditional ablation of Cbfβ in different stages of skeletogenesis results in a novel cleidocranial dysplasia mouse model revealing a new role of Cbfβ in postnatal skeletal and tooth development. Joel Jules*, Mengrui Wu, Wei Chen, Junqing Ma, Guochun Zhu, Fei Tian, Matthew McConnell, Christie Paulson, Yi-Ping Li. University of Alabama at Birmingham, USA

RUNX/Cbfβ complexes are critical for skeletogenesis, but not only is the role of Cbfβ in postnatal bone formation and disease unclear, but also the pathogenesis of cleidocranial dysplasia (CCD), a human disease of Runx2 deficiency characterized by short stature and defective cranial bones and clavicle, is largely unknown due to the embryonic lethality of Cbfβ deficiency. Toward this end, we used the Cre-loxp system to delete Cbfβ by conditional knockout (CKO) at different stages of differentiation and in different tissues. First, we used the Twist2-Cre mice to restrict Cbfβ in mesenchymal progenitors. Twist2-Cre;$Cbf\beta^{f/f}$ mice died at birth and were dwarfism with defective skeleton. Notably, Runx2 expression was not affected by Cbfβ CKO, but osteoblast and chondrocyte genes were repressed. To explore the role of Cbfβ in cartilage, we used Col2a-Cre mice to excise Cbfβ in chondrocytes. Col2a-Cre;$Cbf\beta^{f/f}$ mice lived to adulthood with dwarfism and severe bone defects but normal cranial bones. There was drastic reduction in the expression of Indian hedgehog (Ihh), critical for chondrocyte differentiation, and its target gene cyclin D1, and chondrocyte genes in these mice, indicating that Cbfβ regulates chondrocyte biology during postnatal cartilage development partly by regulating chondrocyte genes. We then explored the role of Cbfβ in bone formation by restricting its expression in the osteoblast lineage using Col1-Cre mice. Col 1-Cre;$Cbf\beta^{f/f}$ mice lived to adulthood with dwarfism and severe bone defects. Osteoblast, but not chondrocyte, genes were repressed in Col1 CKO mice, indicating that Cbfβ regulates osteoblastogenesis during postnatal skeletogenesis partly by regulating osteoblast genes. Given the separate effects of Cbfβ in chondrocytes and osteoblasts, we used the Osx-Cre mice to collectively excise Cbfβ in odontoblasts/osteoblasts/chondrocytes. Osx-Cre;$Cbf\beta^{f/f}$ mice also lived to adulthood with severe bone defects but recapitulated the clinical features of CCD. Notably, Osx-Cre;$Cbf\beta^{f/f}$ also had defective mandible, mandibular and teeth, critical CCD features. We then revealed that Cbfβ interacted with Runx1 and Runx2 in distinct regions of the growth plate to mediate postnatal skeletogenesis. Overall, we showed that Cbfβ regulates both osteoblasts and chondrocytes during postnatal skeletogenesis, and its deletion via Osx-Cre leads to a novel CCD mouse model mimicking human CCD. Significantly, these findings may assist in developing new therapies for CCD.

***Disclosures: Joel Jules**, None.*

1093

NF-κB Family Member Rela/p65 in Chondrocytes Controls Skeletal Growth and Osteoarthritis Development by Inhibiting Chondrocyte Apoptosis. Hiroshi Kobayashi*[1], Makoto Hirata[2], Shozo Itoh[2], Taku Saito[3], Haruhiko Akiyama[4], Ung-Il Chung[5], Hiroshi Kawaguchi[6]. [1]The University of Tokyo Hospital, Japan, [2]The University of Tokyo, Japan, [3]University of Tokyo, Graduate School of Medicine, Japan, [4]Kyoto University, Japan, [5]University of Tokyo Schools of Engineering & Medicine, Japan, [6]University of Tokyo, Faculty of Medicine, Japan

The NF-κB family of transcription factors plays crucial roles in a variety of cell functions. Here we examined the role of NF-κB family member Rela/p65 in chondrocytes during skeletal growth and osteoarthritis (OA) development. In the mouse limb cartilage, Rela/p65 was expressed ubiquitously in chondrocytes of various differentiation stages. We then examined the skeletal growth of conditional knockout mice at several differentiation stages by mating *Prx1-Cre*, *Col2a1-Cre,* and *Col10a1-Cre* transgenic mice, respectively, with mice homozygous for a floxed *Rela* allele (*Rela*$^{fl/fl}$). *Prx1-Cre*;*Rela*$^{fl/fl}$ and *Col2a1-Cre*;*Rela*$^{fl/fl}$ mice exhibited limb shortening, whereas *Col10a1-Cre*;*Rela*$^{fl/fl}$ mice exhibited normal skeletal growth, suggesting an important role of Rela/p65 at the early stage of chondrocyte differentiation. Expressions of the early differentiation markers: *Sox9, Col2a1, aggrecan* in the culture of *Prx1-Cre*;*Rela*$^{fl/fl}$ articular chondrocytes were comparable to those of the control *Rela*$^{fl/fl}$ littermates. However, the cell number was decreased in the *Prx1-Cre*;*Rela*$^{fl/fl}$ chondrocyte culture, as well as by the *Rela* knockdown through siRNA in the mouse chondrogenic ATDC5 cell culture. Although the growth plate chondrocytes of *Col2a1-Cre*;*Rela*$^{fl/fl}$ mice showed normal proliferation determined by BrdU uptake, they exhibited enhanced apoptosis determined by Tunel staining. Next, to examine the function of Rela/p65 in the OA development, time-specific conditional knockout mice of *Rela* in cartilage were generated by mating tamoxifen (TM)-inducible *Col2a1-Cre* transgenic mice (*Col2a1-Cre*^{TM}) with the *Rela*$^{fl/fl}$ mice. TM was injected to 7-week-old mice, and the OA model was created surgically in knee joints one week after the injection. Eight weeks after the surgery, OA development was enhanced in *Col2a1-Cre*^{TM};*Rela*$^{fl/fl}$ mice as compared to the control *Rela*$^{fl/fl}$ littermates, with acceleration of chondrocyte apoptosis at the frontline of degraded articular cartilage. In the *ex vivo* culture of *Prx1-Cre*;*Rela*$^{fl/fl}$ articular chondrocytes, the TNF-α-induced apoptosis was more enhanced than in the *Rela*$^{fl/fl}$ culture. Microarray analysis between the two genotype chondrocytes predicted 10 anti-apoptotic genes under the TNF-α induction, in which expressions of Traf2 and c-Iap1,2 were confirmed to be suppressed in the *Prx1-Cre*;*Rela*$^{fl/fl}$ chondrocytes by real-time RT-PCR. In conclusion, Rela/p65 in chondrocytes controls skeletal growth and OA development by inhibiting chondrocyte apoptosis.

***Disclosures: Hiroshi Kobayashi**, None.*

1094

TGF-beta Signaling Regulates Interleukin-36 alpha in Joint Development and Osteoarthritis. Tieshi Li*[1], Lara Longobardi[1], Timothy Myers[2], Joseph Temple[1], Alessandra Esposito[1], Anna Spagnoli[1]. [1]University of North Carolina at Chapel Hill, USA, [2]University of North Carolina, USA

TGF-β type II receptor (Tgfbr2) signaling plays an essential role in joint development and homeostasis. By combining laser-capture microdissection for RNA sampling with microarrays we found that in the joint interzone of mice in which the Tgfbr2 signaling is conditionally inactivated in limb mesenchyme (Tgfbr2Prx1KO), the inflammatory cytokine interleukin-36 alpha (IL36α) is up-regulated more than 40-fold compared to control (Tgfbr2flox/flox). The upregulation of IL36α in Tgfbr2Prx1KO was confirmed by immunohistochemistry and evaluated throughout joint development. IL36α has been reported to be involved in psoriasis and more recently, increased levels have been found in the inflamed joints of patients with different forms of arthritis. To determine the interplay between IL36α and Tgfbr2 signaling in osteoarthritis (OA) we have generated mice in which we have induced a conditional inactivation of Tgfbr2 in post-natal life (tamoxifen-induced inactivation at P3) named Prx1CreERT2;Tgfbr2lox/lox mice. We have found that Prx1CreERT2;Tgfbr2lox/lox mice progressively develop severe knee OA starting as early as P31, at P3M they show loss of Safranin O staining and by P14 months they demonstrate total loss of knee articular cartilage, severe subchondral bone sclerosis, osteophytes formation and severe synovitis. We found that in Prx1CreERT2;Tgfbr2-lox/lox mice, IL36α was up-regulated in articular cartilage, subchondral bone, superficial layer of meniscus and synovial membrane, such expression proceeded along with the progression of OA and was especially found in areas affected by OA. Elevated expression of IL36α was also found in the arthritic knee joints of mice subjected to a destabilization of medial meniscus (DMM) as a murine model of post-traumatic OA. In DMM, expression of IL36-α correlated with the severity of OA progression although interestingly up-regulation seems to be lower than the one found in Prx1CreERT2;Tgfbr2lox/lox mice. Furth more, the expression of IL36α showed an age-dependent increase in knee articular cartilage and this trend appeared opposite to Tgfbr2's expression that decreased with age. Our findings indicate that inactivation of Tgfbr2 signaling in pre-natal and postnatal limbs induces up-regulation of the inflammatory cytokine IL36α and such up-regulation was associated with severe OA progression. Our studies open novel perspective for the prevention and treatment of OA by manipulating the TβRII/ IL36 α axis.

***Disclosures: Tieshi Li**, None.*

1095

Lower Limb Geometrical Parameters in the Pathogenesis of Bisphosphonate-Associated Atypical Femur Fractures. Suzanne Morin*[1], Benoit Godbout[2], Michelle Wall[3], Laetitia Michou[4], Andrew Karaplis[1], Etienne Belzile[5], Louis-Georges Ste-Marie[6], Thomas Moser[7], Jacques deGuise[8], Jacques P. Brown[9]. [1]McGill University, Canada, [2]Centre de Recherche du Centre Hospitalier de l'Université de Montreal, Canada, [3]McGill University Health Center Research Institute, Canada, [4]Université Laval, Canada, [5]Laval University, Canada, [6]CHUM, Canada, [7]Université de Montreal, Canada, [8]Centre de Recherche du Centre Hospitalier Université Montreal, Canada, [9]CHU de Québec Research Centre, Canada

Background: Atypical femur fractures (AFF) arise in the subtrochanteric and diaphyseal regions. Because of this unique distribution, we hypothesized that patients with AFF demonstrate specific geometrical variations of their lower limb whereby baseline tensile forces applied to the lateral cortex are higher and might favor the appearance of these rare stress fractures, when exposed to bisphosphonates.

Methods: Subjects exposed to bisphosphonates who sustained AFF, as defined by the ASBMR task force, were recruited. Using the EOS™ low irradiation 2D-3D X-Ray scanner, bilateral lower extremities examinations were obtained in the upright weight-bearing position. EOS™ permits 3D surface images of high resolution from simultaneous two-plane images. We compared the participants' leg geometrical

parameters to those of reference cohorts and also examined differences between women who sustained diaphyseal versus subtrochanteric AFF. For each subject with AFF, we are currently enrolling age- (± 5 yrs), sex-, height- (± 6 cm) and cumulative bisphosphonate exposure- (±2 yrs) matched controls without femur fracture. Conditional logistic regression models will be constructed to estimate the effect of selected geometric parameters on AFF.

Results: We identified 25 subjects (21 women; mean age 67 SD [9] yrs; 23 Caucasian) with AFF and an average cumulative duration of use of bisphosphonate of 10.6 SD [4.6] yrs). There were 40 AFF: 15 subjects had bilateral AFF; 15 AFF were complete and 25 were incomplete; 28 were diaphyseal and 12 subtrochanteric. Bilateral AFF occurred in the identical region of the femurs in 75% of subjects. We documented differences in geometrical parameters of the lower limb in subjects with AFF compared to those reported in normal populations (Table 1). Compared to women with diaphyseal fractures (n=11), those with subtrochanteric fractures (n=5) had a lesser femur neck-shaft angle (123.0˚ SD [3.3] versus 129.2˚ SD [7.1]; $p < 0.05$), longer femoral offset (4.2 SD [0.2] cm versus 3.7 SD [0.6] cm; $p < 0.05$), and tended to have less pronounced femur bowing in frontal plane (- 2.7˚ SD [5.6] cm versus -4.2˚ SD [3.3]; p= 0.60).

Conclusion: Our analyses, though limited by sample size, support that subjects with AFF exhibit femur geometry that results in higher tensile mechanical load on the lateral femur, particularly in women with subtrochanteric fractures; this may play an important role in the pathogenesis of AFF.

Table 1 Clinical characteristics of subjects with AFF, and measures of geometrical parameters compared to normal reference values, measured with EOS 2D-3D system

Characteristic	AFF (n=25)	
Age *(years) (SD)*	66.7 (9.2)	
Women *n (%)*	21 (84.0)	
Height *(cm) mean (SD)*	157.9 (6.7)	
BMI *(kg/m²) mean (SD)*	26.6 (3.7)	
Caucasian Ethnicity *n (%)*	23 (92)	
Comorbid Count *mean (SD)*	4 (1.6)	
Bone Mineral Density *mean (SD)*		
Femoral Neck T-score	-1.8 (0.5)	
Spine T-score	-1.7 (1.3)	
Geometrical Parameter	**AFF**	**Reference***
Femur length *(cm) mean (SD)*	39.9 (2.2)	42.9- 44.4 (3.1)
Tibia length *(cm) mean (SD)*	33.9 (2.2)	37.1- 38.2 (2.8)
Femoral Neck Shaft angle (˚) *mean (SD)*	125.6 (6.5)	128- 133 (6.5)
Femoral Torsion (˚) *mean (SD)*	15.1 (10.8)	11.5- 17.1 (8.0)
Hip Knee Shaft angle (˚) *mean (SD)*	7.0 (1.8)	4.8-5.8 (2.0)
Femorotibial rotation (˚) *mean (SD)*	7.7 (5.8)	2.3 (7.2)
Varus/Valgus at knee (˚) *mean (SD)*	-2.8 (3.6)	-0.8 (3.1)
Tibia Mechanical angle (˚) *mean (SD)*	85.5 (3.1)	88.0 (3.6)

*Than P et al, *Int Orthop* 2012; 36: 1291-7 and Chaibi Y et al, *Comput Methods Biomech Biomed Engin*. 2012;15: 457-66

Table 1 Clinical characteristics of subjects with AFF, and measures of geometrical parameters compar

***Disclosures: Suzanne Morin**, Merck, 2; Novartis, 2; Eli Lily, 2; Amgen,; Amgen, 6; Novartis,; Amgen, 2*

1096

Early Diagnosis of Atypical Femoral Fracture Using DXA by Extending Femur Length. Malachi McKenna*[1], Susan van der Kamp[2], Eric Heffernan[2]. [1]St. Michael's Hospital, Ireland, [2]St. Vincent's University Hospital, Ireland

Introduction: The Task Force Report of the ASBMR 2010 listed five major criteria, all of which must be present, to make a diagnosis of AFF: located on the femoral shaft anywhere between lesser trochanter and the supracondylar flare, non-comminuted, transverse or short oblique, incomplete on lateral surface only or complete with a medial spike, and as a consequence of minimal or no trauma. The Task Force also listed minor criteria, such as: localized periosteal reaction of lateral cortex with ''beaking'' or ''flaring''. Since AFF often have a prodrome of pain and tenderness at the fracture, there is window of opportunity for early detection. McKiernan has demonstrated that incomplete AFF may be detected using DXA scan by extending the length of the femur image.

Methods: Patients over 50 years of age presenting for routine DXA who had been taking bisphosphonates therapy in excess of 5 years had an extended hip scan performed bilaterally using an array mode. We extended femur length from default of approximately 15.3 cm up to 22 cm, in order to view the extra length of the femoral shaft. Images were viewed independently by two observers. If abnormalities were noted in the lateral aspect of the femur, namely ''flare'' or ''beaking'', then patients were referred for a plain X-ray of pelvis with imaging of lateral femur.

Results: Over 16 month spell, 257 patients had an extended DXA imaging. Patients were predominantly women; Alendronate and Risedronate accounted for 89% of treatments. At the time assessment, the prevalence of DXA-based diagnosis of osteoporosis at any site was 56%. A suspected abnormality on the DXA was noted in 19 of 257 (7.4%). On X-ray, 7 (2.7%) showed no abnormality, 7 (2.7%) showed evidence of AFF, and 5 (2.0%) showed an additional abnormality (an osteochondroma, an abnormal lucency, and 3 cases of cortical thickening). Of the 7 cases with X-ray evidence of AFF, 5 had a periosteal flare and 2 had a visible fracture line. The latter patients were referred for orthopedist opinion, and both subsequently had elective insertion of an intramedullary nail. On multivariable analysis, duration of bisphosphonate therapy was the only factor associated with diagnosis of AFF (OR=1.35, 95%CI=1.04-1.76, p=0.026).

Conclusion: Extended DXA imaging of the lateral femur shaft permits early detection of AFF. We noted a prevalence of AFF of 2.7% in patients on bisphosphonate therapy over 5 years.

***Disclosures: Malachi McKenna**, None.*

1097

Pamidronate Treatment of Pediatric Burns Attenuates Muscle Breakdown. Elisabet Borsheim[1], David Herndon[1], Matthew Cotter[1], Gordon Klein*[2]. [1]University of Texas Medical Branch & Shriners Burns Hospital, USA, [2]University of Texas Medical Branch, USA

Acute intravenous administration of pamidronate to burned children has been shown to preserve bone mass for up to 2 yr. However, inasmuch as these children also suffer from muscle wasting, likely a result of elevated production of endogenous glucocorticoids, it is unclear whether treating the bone with pamidronate is associated with any secondary benefits to muscle. To address this question we studied burned pediatric patients who were enrolled in a double-blind placebo-controlled study of acute pamidronate infusion and its effect on bone mass who also underwent infusion with deuterated phenylalanine tracer alone and on the same day in combination with unlabelled amino acids and who also had a vastus lateralis muscle biopsy and arterial and venous blood sampling. All studies were done during the acute hospitalization. We measured incorporation of tracer into muscle and calculated fractional synthetic rate (FSR), rate of appearance of phenylalanine from muscle into the blood (Ra), and net balance (NB) of phenylalanine in muscle as arterio-venous difference X blood flow/100 ml leg volume. FSR rose in response to amino acid infusion in placebo subjects (n=3) but did not rise in those receiviing pamidronate (n=4), F=11.55, p=0.014 by one-way ANOVA. Ra, a measure of muscle breakdown, was 246.8 + 166.4 (SD) nmol/min/100 ml leg volume in the controls (n=7) and 112.1 + 53.9 in the pamidronate group (n=10), p=0.0375 by two-tailed t test. NB was -61.7 + 73.2 nmol/min/100 ml leg volume in the controls (n=7) and 132.6 + 190.5 in the pamidronate group (n=10), p=0.024 by two-tailed t test. Thus pamidronate treatment not only prevents post-burn bone loss but these data suggest that it may also indirectly attenuate muscle breakdown and that treatment of bone loss may confer indirect muscle-sparing effects.

***Disclosures: Gordon Klein**, None.*

1098

Incidence of Vitamin D Toxicity: A Population-Based Study in Olmsted County, Minnesota. Daniel Dudenkov*[1], Barbara Yawn[2], Sara Oberhelman[1], Philip Fischer[1], Ravinder Singh[1], Steven Cha[1], Julie Maxson[1], Stephanie Quigg[1], Tom Thacher[1], Tom Thacher[1]. [1]Mayo Clinic, USA, [2]Olmsted Medical Center, USA

Background: Hypervitaminosis D and associated toxicity may complicate vitamin D supplement use. The initial finding in almost all reported cases of vitamin D toxicity is hypercalcemia. Our objective was to determine the incidence trend of hypervitaminosis D and its association with hypercalcemia in Olmsted County, Minnesota.

Methods: We identified all serum 25-hydroxyvitamin D [25(OH)D] measurements >50 ng/ml (hypervitaminosis D) in persons residing in Olmsted County, MN during a 10-year interval (2002-2011), through the Rochester Epidemiology Project databases. The date of the first value >50 ng/ml was considered the index date for incidence determination. Hypercalcemia (serum calcium >10.1 mg/dl or ionized calcium >5.3 mg/dl) was considered associated with hypervitaminosis D if measured within 3 months of 25(OH)D measurement.

Results: Of 20,308 total 25(OH)D measurements, 1885 (9.3%), 133 (0.7%), and 44 (0.2%) unique persons had 25(OH)D values >50, ⩾80, and ⩾100 ng/ml, respectively. The incidence of hypervitaminosis D increased from 10 per 100,000 in 2002 to 260 per 100,000 in 2011. The increase in incidence was greater in persons age ⩾65 years and in females. The proportion of 25(OH)D values >50 ng/ml increased from 2002 to 2011, but the proportion of 25(OH)D values ⩾80 and ⩾100 ng/ml did not increase. Of 960 with serum calcium measured within 3 months of 25(OH)D value, 180 (19%) had hypercalcemia. The greatest serum 25(OH)D of 364 ng/ml was associated with the greatest serum calcium of 17.5 mg/dl. This person had been taking vitamin D 50,000 IU four times daily for several weeks. When this subject was excluded, serum 25(OH)D values were not significantly related with serum calcium values (r=-0.01; p=0.70) or with the risk of hypercalcemia [OR=0.93 (95% CI 0.50-1.7) for 25(OH)D⩾80, and OR 0.94 (0.35-2.5) for 25(OH)D ⩾100 ng/ml]. The incidence of hypercalcemia between 2002 and 2011 did not change.

Conclusion: The incidence of hypervitaminosis D has increased between 2002 and 2011 without an increase in extreme 25(OH)D values. Hypercalcemia was common but its relationship with hypervitaminosis D was not established.

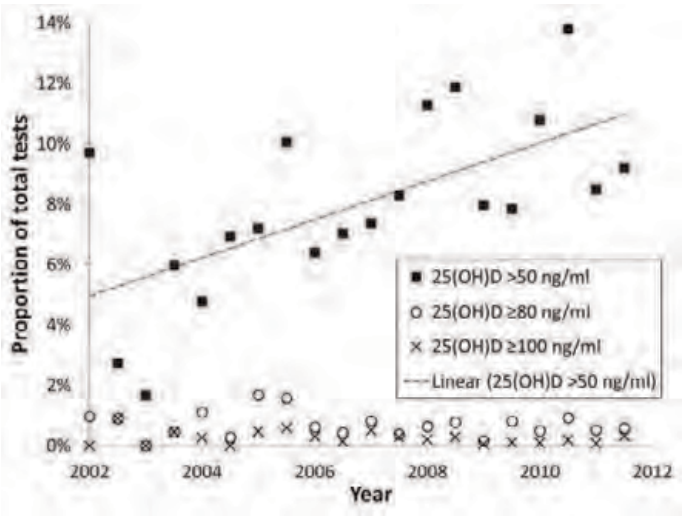

Hypervitaminosis D in Olmsted County, MN from 2002-2011

***Disclosures: Daniel Dudenkov**, None.*

1099

Bone Turnover Markers and Prediction of Fracture in a 15-year Follow-Up Study of Elderly Women. Kaisa Ivaska*[1], Fiona McGuigan[2], Karl Obrant[3], Paul Gerdhem[4], Kristina Akesson[5]. [1]University of Turku, Finland, [2]University of Lund, Malmö, Skane University Hospital, Malmö, Sweden, [3]University Hospital, Sweden, [4]Karolinska Institutet, Sweden, [5]Skåne University Hospital, Malmö, Sweden

High level of bone turnover is associated with increased fracture risk, but the information on how long time markers can predict fractures is limited. The aim of this study was to investigate whether bone markers are associated with long-term fracture risk in the elderly.

Fracture prediction was evaluated in the population-based OPRA cohort of 1044, 75-year-old women. Bone turnover markers (CTX, PINP, TRACP5b, bone-specific ALP, serum and urinary osteocalcin) were measured at baseline and prospective fractures were recorded and verified for the mean of 15.0 years (range 13.4 – 17.0 years). The ability of baseline bone markers to predict fracture was estimated by Cox proportional hazard ratios for 5 years, 10 years and for the entire follow up of mean 15 years.

The number of women who sustained at least one fracture of any type was 214 at five years, 399 at ten years and 524 at the end of the follow-up. By the end of the follow-up 195 women sustained a hip fracture, 214 women a vertebral fracture and 453 women a FRAX fracture (hip, spine, forearm or shoulder). Mortality at five, ten and fifteen years was 10%, 29% and 57%, respectively. During the 5-year follow up, women in the highest tertile for bone markers (particularly CTX and urinary osteocalcin) had significantly higher risk for sustaining any fracture, FRAX fracture or vertebral fracture when compared to women in the lowest tertile. The hazard ratios for fracture were 1.5 - 2.0 ($p<0.05$), depending on the marker. Baseline bone markers were not significantly associated with fracture risk for the follow-up period of 10 years, and the predictive ability of bone markers was further attenuated when the follow-up time was continued for up to 15 years. However, women in the middle tertile of baseline formation markers appeared have lower long term risk for sustaining vertebral fractures than those in the low or high tertile (hazard ratios 0.6-0.7, $p<0.05$). Baseline bone markers were not associated with the risk for hip fracture at any of the evaluated time points.

In conclusion, increased levels of bone turnover markers are associated with increased probability of fracture, particularly in first five years following the measurement. The ability of a single measurement of bone marker to predict fractures in elderly women attenuates over time and is not significant for long follow-up time of 10 - 15 years.

***Disclosures: Kaisa Ivaska**, None.*

1100

Neonatal Enzyme Replacement Therapy Improves Cervical Spine Bone Architecture and Mineralization in Mucopolysaccharidosis I Dogs. Lachlan Smith*[1], Joseph Chiaro[1], Patricia O'Donnell[1], Eileen Shore[1], Neil Malhotra[1], Dawn Elliott[2], Katherine Ponder[3], Mark Haskins[1]. [1]University of Pennsylvania, USA, [2]University of Delaware, USA, [3]Washington University in St Louis, USA

Mucopolysaccharidosis I (MPS I) is a lysosomal storage disorder characterized by deficient α-L-iduronidase activity, leading to the accumulation of poorly degraded dermatan and heparan sulfate glycosaminoglycans (GAGs). Clinical presentation includes significant cervical spine disease, leading to spinal cord compression and kypho-scoliosis. Using the authentic MPS I canine homolog, we showed previously that MPS I dogs have significantly lower trabecular bone volume and mineralization in the cervical vertebrae from as early as 3-months-of-age, and abnormal persistence of growth plate cartilage at 12-months-of-age. The purpose of this study was to determine whether neonatal enzyme replacement therapy (ERT, currently in clinical use), alone or in combination with oral simvastatin (ERT+S), could attenuate cervical spine bone disease in MPS I.

Four groups were studied (all n=5): normal controls; MPS I untreated; MPS I ERT treated; MPS I ERT+S treated. Treatments commenced at 1-week-of-age, and all animals were euthanized at 12-months-of-age. C2 vertebrae were excised, trabecular bone imaged using microCT, and standard morphometric parameters and BMD determined. Vertebrae were processed for paraffin histology to evaluate presence of growth plate cartilage.

Untreated MPS I dogs had significantly reduced BV/TV (49% of normal), Tb.Th (74% of normal), and BMD (61% of normal), and increased Tb.Sp (1.5-fold normal) (all $p<0.05$, Figure). ERT treated dogs had improved BV/TV (85% of normal), Tb.Th (95% of normal), Tb.Sp (1.2-fold normal), and BMD (89% of normal), none significantly different from normal and all significantly greater the untreated MPS I. ERT+S treated dogs showed similar, but not greater, improvements. Histological assessment of GAG and collagen revealed growth plate remnants in all five untreated MPS I vertebrae, in two ERT treated vertebrae, and in one ERT+S treated vertebra. In all normals, growth plates were absent.

These results show that neonatal ERT effectively attenuates vertebral bone disease in MPS I dogs. There is evidence that simvastatin has anti-inflammatory properties and can stimulate BMP signaling, however, in this study supplementation with simvastatin provided minimal additional benefits over ERT alone. Future work will seek to further elucidate the underlying pathogenesis of bone and disc disease in MPS, with the goal of developing new therapeutic strategies.

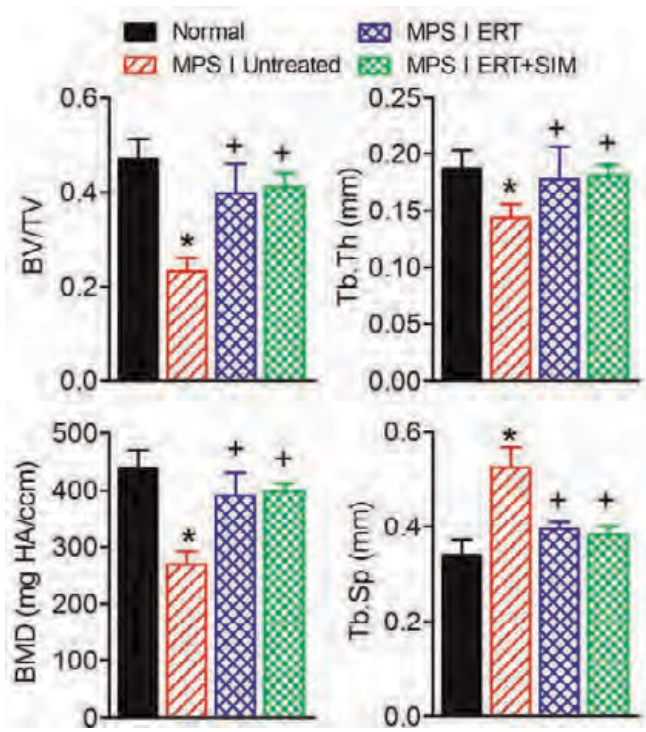

Figure: MicroCT analysis results. *$p<0.05$ vs normal; +$p<0.05$ vs untreated MPS I

***Disclosures: Lachlan Smith**, None.*

1101

The Transcriptional Cofactor Jab1 is Essential for Mouse Limb Development. Lindsay Bashur*, Dongxing Chen, Bojian Liang, Zhijun Chen, Shunichi Murakami, Guang Zhou. Case Western Reserve University, USA

The transcriptional cofactor Jab1 controls cell proliferation, apoptosis, and differentiation in many developmental processes by regulating the activity of various transcription factors. However, the physiological role of Jab1 in skeletal development is still poorly understood. To determine the role of Jab1 during early limb development, we developed a novel *Jab1^{floxlflox};Prx1-Cre* conditional knockout (*cKO*) mutant mouse model in which *Jab1* was deleted specifically in the osteochondroprogenitor cells of limb buds. *Jab1 cKO* mutant mice displayed drastically shortened limbs at birth, strikingly mirroring phocomelia, a devastating human birth defect with severe limb truncation. Real time RT-PCR analysis revealed no significant changes in the expression of chondrocyte differentiation markers *Sox9* and *Col2a1* in E11.5 *Jab1 cKO* mutant limb buds. At E12.5, *Jab1 cKO* mutant mice and wild-type littermates exhibited no gross morphological differences. However, the short limb defect became apparent in *Jab1 cKO* mutants at E14.5 and increasingly worsened thereafter. By E18.5, *Jab1 cKO* mutant mice exhibited significantly shorter limbs with: very few hypertrophic chondrocytes, disorganized chondrocyte columns, much smaller primary ossification centers, significantly increased apoptosis, but normal proliferation. The expression of *Sox9*, *Col2a1*, and *Col10a1* were all down-regulated in E15.5 and E18.5 *Jab1 cKO* mutant long bones by real time RT-PCR, indicating impaired chondrogenesis. Immunohistochemistry revealed decreased expression of both Sox9 and BMP signaling downstream effector phopho-Smad1/5, in *Jab1 cKO* mutants. Furthermore, in a well-established micromass culture model of early limb mesenchyme cells, Alcian blue staining showed a significant decrease in chondrogenesis in *Jab1 cKO* micromasses. The expression of Sox9 and its downstream targets *Col2a1* and *Aggrecan*, and also the BMP downstream targets *Col10a1*, *Ihh* and *Id1*, were all significantly decreased in *Jab1 cKO* micromasses. This suggests that Jab1 positively regulates Sox9 and BMP signaling during early limb development. In conclusion, the deletion of *Jab1* in early limbs inhibits chondrocyte differentiation and cell survival, consequently leading to a phocomelia-like phenotype in mice. Thus, Jab1 is a novel and essential regulator of limb development *in vivo*, and our *Jab1 cKO* mice can serve as an excellent model for elucidating the pathogenesis of and developing therapeutic interventions for phocomelia.

***Disclosures: Lindsay Bashur**, None.*

1102

TAK1 Regulates SOX9 Expression and is Essential for Postnatal Development of the Growth Plate and Articular Cartilages. Jennifer Jonason[1], Lin Gao*[1], Tzong-Jen Sheu[1], Yufeng Dong[1], Michael Zuscik[2], Edward Schwarz[1], Matthew Hilton[3], Regis O'Keefe[1]. [1]UNIVERSITY OF ROCHESTER, USA, [2]University of Rochester School of Medicine & Dentistry, USA, [3]University of Rochester Medical Center, USA

TGF-β-activated kinase 1 (TAK1) is a MAP3K that mediates non-canonical TGF-β and BMP signaling. During the embryonic period, TAK1 is essential for cartilage and joint development as deletion of *Tak1* in chondro-osteo progenitor cells leads to severe chondrodysplasia with defects in both chondrocyte proliferation and maturation. Here, we designed experiments to address the role of TAK1 in committed chondrocytes during early postnatal development. Using the *Col2a1-CreER^{T2}; Tak1$^{f/f}$* mouse model, we induced deletion of *Tak1* at postnatal day 7 and characterized the skeletal phenotypes of these mice at one and three months of age. Mice with chondrocyte-specific *Tak1* deletion exhibited severe growth retardation and disorganized growth plate cartilage with reduced chondrocyte proliferation. Strikingly, the articular cartilage of these mice exhibited reduced proteoglycan and Type II Collagen content in zones of uncalcified cartilage. Consistent with these observations, we found reduced *Col2a1* and *Acan* gene expression, but increased *Mmp13* and *Adamts5* gene expression, in articular chondrocytes isolated from the *Tak1*-deficient mice as well as in *Tak1$^{f/f}$* primary sternal chondrocytes infected, *in vitro*, with adenovirus encoding Cre recombinase. Additionally, expression of the SOX trio of transcription factors, SOX9, SOX5, and SOX6, was decreased in chondrocytes both *in vivo* and *in vitro* upon deletion of *Tak1*. It is well established that BMP signaling regulates SOX9 expression in chondrocytes, but the precise mechanism by which it does so is unclear. We, therefore, designed experiments to determine whether TAK1 is a downstream effector of BMP-mediated SOX9 expression. We found that BMP2 induced *Sox9* gene expression and promoter activation in chondrocytes, but that these effects were suppressed upon deletion of *Tak1* or inhibition of TAK1 kinase activity. TAK1 affects both canonical and non-canonical BMP signal transduction and we found that both of these pathways contributed to BMP2-mediated *Sox9* promoter activation. Specifically, *Smad1* or *Atf2* gene silencing via siRNA suppressed *Sox9* promoter activation in response to BMP2 treatment. Finally, we found that ATF2 directly binds the *Sox9* promoter in response to BMP2 signaling and that this effect is dependent upon TAK1 kinase activity. These novel findings establish that TAK1 is essential for BMP2-mediated *Sox9* gene expression and the postnatal development of normal growth plate and articular cartilages.

***Disclosures: Lin Gao**, None.*

1103

***Hox* genes, critical regulators of embryonic skeletal development, are required for adult fracture healing.** Danielle Rux*[1], Ilea Swinehart[1], Aleesa Schlientz[1], Kenneth Kozloff[2], Steven Goldstein[3], Deneen Wellik[4]. [1]University of Michigan, USA, [2]University of Michigan Department of Orthopaedic Surgery, USA, [3]University of Michigan Orthopaedic Research Lab, USA, [4]University of Michigan Medical Center, USA

The *Hox* genes are critical regulators of embryonic skeletal development. Loss of function mutations in any one of the 13 paralogous groups (*Hox1-13*) leads to regionally-restricted malformations of the axial skeleton and the limbs. Specifically, loss of *Hox11* function results in severe mispatterning of the sacrum and of the skeletal elements of the limb zeugopod (tibia/fibula, radius/ulna). We show that *Hox11* is expressed in the mesenchyme of the developing limb bud, but is surprisingly excluded from the condensing chondrocytes that will become the zeugopod elements. Instead, it is expressed highly in the perichondrium and periosteum up to E18.5. Previous studies have suggested that *Hox* genes may continue to function after embryonic development. Our lab shows significant evidence that this is the case. First, we show that *Hox11* expression persists in periosteal fibroblast populations of the limb skeleton during post-natal and adult stages. Further, we demonstrate that cell populations expressing *Hox* increase dramatically after fracture injury. Expression is especially high in the fibroblast cells expanded from the periosteal surface of the bone to encase the fracture callus suggesting a role for *Hox* in early mesenchymal differentiation. Using *Hox11* compound mutants (mutant for three of four alleles that function in zeugopod development), we show that loss of *Hox* function disrupts the endochondral ossification process during fracture repair. In contrast, intramembranous bone formation appears to proceed normally. Loss of *Hox11* function leads to significant perturbation of the fracture healing process. In *Hox11* compound mutants, the fracture gap is not bridged until several weeks after controls are fully bridged, and remodeling is incomplete even five months after fracture. Cartilage formation is decreased in *Hox11* compound mutants during early stages of repair, but osteoblast and osteoclast formation is comparable to controls. These results indicate a novel role for *Hox* genes in fracture repair. Further study may shed new light on the differential patterning of mesencymal progenitor cells during fracture repair and the role *Hox* genes play in this process.

***Disclosures: Danielle Rux**, None.*

1104

Cells Expressing Type 2 Collagen Are Self-renewing Multipotent Mesenchymal Progenitors during Postnatal Bone Development. Noriaki Ono*, Wanida Ono, Henry Kronenberg. Massachusetts General Hospital, USA

In skeletal development, matrix-producing osteoblasts and hematopoiesis-supporting stromal cells are constantly generated to drive bone growth. Although cells expressing osterix (Osx) in the embryonic perichondrium (PC) are implicated as the transient source of these cells, how they are replenished during postnatal bone development is not well understood. Type 2 collagen (Col2) is expressed by chondrocytes within and at the periphery of the growth cartilage adjacent to the PC. To test the hypothesis that Col2$^+$ cells are earlier progenitors upstream of Osx$^+$ cells, we first performed fate mapping using a Col2-cre recombinase that activates a Rosa26 tomato reporter. The majority of osteogenic perichondrial cells at embryonic day 13.5 (E13.5) were descendants of Col2$^+$ cells. Furthermore in postnatal bone, a great majority of osteocalcin (Oc)-GFP$^+$ osteoblasts and Cxcl12-GFP^{high} stromal cells were derived from Col2$^+$ cells. Second, to unravel the difference between Col2$^+$ and Osx$^+$ cells at specific points during embryogenesis, a pulse-chase experiment was conducted using an inducible cre recombinase (Col2-CreER, Osx-CreER) with a single tamoxifen injection. Col2$^+$ cells appeared earlier than Osx$^+$ cells, and only Col2$^+$ yielded a number of red cells at postnatal day 0 (P0) upon E11.5 injection. Next, the mice received tamoxifen at E13.5 and were analyzed a week later at birth. While initially present within the PC, Osx-descendants disappeared from newly generated PC. In contrast, although initially absent from the PC, Col2-descendants robustly contributed to the PC. The majority of Osx-descendants disappeared by P21. Third, to test whether postnatal Col2$^+$ cells also behave as early progenitors, the mice received tamoxifen at P3 and were chased for up to 6 months. Osx$^+$ cells gave rise to osteoblasts for the first month. However, as the chase extended, they disappeared from the metaphysis, while they became increasingly present as stromal cells in the diaphysis. In contrast, Col2$^+$ cells continued to yield osteoblasts for the entire chase period. The fraction of Col2-descendants among Oc-GFP$^+$ osteoblasts increased progressively from 4.3% to 46% during the first month of chase. Col2$^+$ cells also became Cxcl12^{high} stromal cells and adipocytes in bone marrow. These data indicate that both embryonic and postnatal Col2-expressing cells are self-renewing multipotent progenitors that continue to become chondrocyte, osteoblast and stromal lineage-cells during bone development.

***Disclosures: Noriaki Ono**, None.*

1105

Progenitor-Derived VEGFA Regulates the Fate and Population Dynamics of Osteoblast Precursor Cells in Bone Development and Maintenance. Agnes Berendsen*, Bjorn Olsen. Harvard School of Dental Medicine, USA

Vascular endothelial growth factor A (VEGFA) is expressed by multiple cell types in the skeleton and is most commonly known as an important regulator of angiogenesis. We previously reported a novel function for VEGFA in controlling the balance between osteoblast/adipocyte differentiation in osteoblast precursor cells. Here, we further uncovered the cellular and molecular mechanisms involved in the VEGF-dependent regulation of the fate and population dynamics of osteoblast precursor cells. Conditional deletion of *Vegfa* in osteolineage cells using the *Osx* promoter to drive expression of Cre recombinase resulted in a reduced size and thickness of the craniofacial as well as the long bones in mice at birth. This loss of bone mass progressively worsened with age and furthermore a dramatic increase in marrow fat was detected in bones of 6-week-old *Vegfa* CKO mice. Use of the Cre reporter transgene tdTomato revealed that the marrow adipocytes were derived from osterix-expressing progenitor cells, thus pointing towards cell autonomous mechanisms of VEGF-dependent control of cell fate. Conditional knockdown of VEGF receptor 2 in addition to knockdown of VEGFA in osterix-expressing progenitor cells further reduced the bone density in adult mice, confirming that VEGF signaling in progenitor cells is required for their differentiation into mature osteoblasts. Interestingly, reduced expression of VEGF receptor 2 in addition to VEGFA in progenitor cells did not affect the marrow fat content in bones of 6-week-old mice, suggesting differential VEGF-dependent molecular mechanisms controlling the differentiation into osteoblast and adipocyte cell lineages. Immunohistochemistry revealed that the number of osterix-expressing cells during vascular invasion into the primary ossification centers of developing bones was reduced in the limbs of *Vegfa*-CKO mice. As elegant pulse-chase studies recently demonstrated that the turnover of osteoblast progenitor cells and mature osteoblasts in bones is a highly dynamic process, our data therefore suggest that VEGFA is one of the key mediators in regulating the fate and dynamics of the osteoblast precursor cell population serving the demands of both development and maintenance of the skeleton.

***Disclosures: Agnes Berendsen**, None.*

1106

Wnt5a and Wnt5b in osteoblastic niche differentially regulate HSC maintenance and differentiation. Jingjing Cao*, Yong Wan, Zhengju Yao, Xizhi Guo. Bio-X Institutes, Shanghai Jiao Tong University, China

The hematopoietic stem cells (HSC) are mostly maintained in the endosteal and vascular niche in bone marrow. Osteoblasts are key components of the endosteal niche for HSC. Recent studies have indicated that non-canonical Wnt signaling from N-cad^{+} osteoblasts maintains HSCs quiescence in the endosteal niche. However which non-canonical Wnt ligand from osteoblastic cells performs the role is still unknown. To address this question, we first blocked the Wnt secretion from osteoblasts through conditional inactivation of *Wntless* using *Col1 (3.6kb)-Cre*. We found that blocking Wnts from the osteoblasts resulted in higher proportion of HSC, impaired B cell development and increased percentage of myeloid cells in bone marrow. Our study showed that *Wnt5a* and *Wnt5b* were highly expressed in osteoblasts of the postnatal bones. When *Wnt5b* was overexpressed in osteoblasts by generating transgenic mice *Col1a1-Wnt5b*, the frequency and number of HSC were decreased in bone marrow while HSC subsequent differentiation was not disturbed compared to the control. In contrast, overexpression of *Wnt5a* in osteoblasts of transgenic mice *Col1a1-Wnt5a* led to defective B lymphopoiesis and augmented myeloid development. Although the HSC frequency was not changed in the *Col1a1-Wnt5a* mice, the absolute HSC number was decreased due to the decline of bone marrow cellularity. Taken together, these results indicate that non-canonical Wnts in osteoblasts are important in HSC maintenance and differentiation. Wnt5a prefers to regulate HSC differentiation including B lymphopoiesis and myeloid differentiation, and Wnt5b intends to regulate HSC maintenance rather than HSC differentiation.

***Disclosures: Jingjing Cao**, None.*

1107

Prediction of vertebral fracture by Trabecular Bone Score in elderly women of The Rotterdam Study. Biljana Atanasovska*[1], Ling Oei[2], Carolina Medina-Gomez[3], Natalia Campos[1], Karol Estrada[4], Albert Hofman[5], Berengere Aubry-rozier[6], Carola Zillikens[7], Andre Uitterlinden[8], Edwin Oei[9], Didier Hans[6], Fernando Rivadeneira[2]. [1]Erasmus MC, The Netherlands, [2]Erasmus University Medical Center, The Netherlands, [3]Erasmus Medical Center, The Netherlands, [4]Analytic & Translational Genetics Unit, Massachusetts General Hospital, USA, [5]Department of Epidemiology, Erasmus Medical Center, Netherlands, [6]Lausanne University Hospital, Switzerland, [7]Department of Internal Medicine, Department of Epidemiology, Netherlands, [8]Rm Ee 575, Genetic Laboratory, The Netherlands, [9]Department of Radiology, Netherlands

Aim: The trabecular bone score (TBS) reflects the microarchitecture of the vertebral bones and can be extracted from dual-energy X-ray absorptiometry (DXA) images of the lumbar spine. We aimed to examine the ability of TBS to predict the risk of prevalent and incident vertebral fracture in a large population based study of Dutch elderly women.

Methods: This study included a selection of 2760 women from the three Rotterdam Study cohorts (RS-I, RS-II and RS-III). DXA scans (GE-Lunar Prodigy, Madison) and BMD of the lumbar spine were measured in RS-I during the third follow-up (mean age 75.5 SD=6.0 years), in RS-II during the first follow-up (mean age 69.2 SD=7.4 years) and RS-III during the baseline visit (mean age 58.0 SD=7.1 years). TBS were calculated centrally by Lausanne University Center blinded to clinical parameters and outcomes using the TBS iNsight software (Medimaps, Pessac). Radiographic vertebral fractures were available for RS-I (McCloskey-Kanis; n=845, 53 cases) and RS-III (Optasia quantitative morphometry; n=1272, 221 cases). Incident clinical vertebral fractures occurring during follow-up (mean 3.0 SD 0.1 years) after DXA were extracted from computerized records of the general practitioners and hospital registries for RS-I (mean age 76.6 SD=5.4 years) and RS-II (mean age 69.2 SD=7,3 years) participants, (combined n=1484, 21 events). Logistic- and Cox-regression models corrected for age, height and weight were used to obtain risk estimates per SD decrease in TBS for prevalent and incident vertebral fractures, respectively.

Results: Correlation between TBS and LS-BMD was low (Pearson rho 0.25-0.30) across studies ($p<0.001$). Both TBS and BMD mean levels are significantly lower in fracture cases than non-cases ($P<0.05$). Lower TBS scores were associated with increased risk for prevalent vertebral fractures in both RS-I (OR 1.71 95%CI [1.29-2.27]; P=0.0002) and RS-III (OR 1.27 95%CI [1.08-1.48]; P=0.004), respectively per SD decrease. The combined analysis of incident vertebral fractures in RS-I and RS-II was also suggestive of increased risk per SD decrease in TBS score (HR 1.48 95%CI [0.96-2.29]; P=0.08). Adjustment for lumbar spine BMD did not affect the risk estimates.

Conclusion: Trabecular bone scores are strongly associated with prevalent vertebral fractures independent of BMD. Despite the borderline statistical significance our results are indicative of TBS being also predictive for incident vertebral fractures in women.

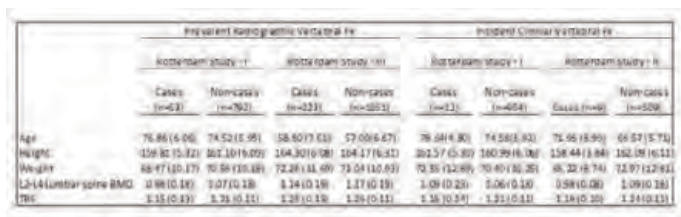

Table

***Disclosures: Biljana Atanasovska**, None.*

1108

Assessment of Vertebral Fractures in Patients Older than 50 Years with a Recent Non Vertebral Fracture Before and After Introduction of Systematic Vertebral Fracture Assessment (VFA). Sandrine Bours*[1], Piet Geusens[2], Willem Lems[3], Robert Van der Velde[4], Tineke Van Geel[5], Joop Van Den Bergh[6]. [1]Maastricht University Medical Centre, The Netherlands, [2]University Hasselt, Belgium, [3]Vrije Universiteit Medical Centre, The Netherlands, [4]Viecuri MC, Netherlands, [5]Maastricht University, The Netherlands, [6]VieCuri MC Noord-Limburg & Maastricht UMC, The Netherlands

Purpose: To compare the prevalence of vertebral fractures (VF) in patients evaluated at fracture liaison services (FLS) in the Netherlands because of a recent non-vertebral fracture, before and after the implementation of the new (2011) Dutch CBO guideline (1) for osteoporosis and fracture prevention.

Material and methods: This study was performed at the FLS of 3 hospitals in the Netherlands (VU MC Amsterdam, Maastricht UMC, VieCuri MC). DXA measure-

ments were performed at the lumbar spine and hip. Patients were classified according to the lowest value of T-score in total hip, femoral neck, or lumbar spine: osteoporosis as a T-score of -2.5 or less, osteopenia as a T-score between -2.5 and -1.0, and normal BMD as a T-score of -1.0 or higher. Non-vertebral fractures were classified according to Center in hip, major, minor and finger/toe fractures (2). Vertebral fractures were diagnosed using VFA (or spine X-ray) according to the method described by Genant (3). A VF was diagnosed if impression was > 20% at the anterior, mid or posterior location of the vertebral body.

Results: We evaluated 1400 patients, 730 pre- and 670 post-guideline (mean age 65.9 and 66.5 years; 71.6% and 73.6% women respectively). The percentage of patients with a normal BMD, osteopenia and osteoporosis were not significantly different (16.9%, 56.0%, 27.1% pre- and 18.2%, 51.6%, 30.2% post-guideline). Imaging of the spine increased from 16.5% in the pre- to 95.4% in the post-guideline group ($p<0.0001$). In the pre-guideline group, 8.4% had a VF and in 8.1% a VF could be excluded, in the post-guideline group, these percentages were 25.8% and 69.6% ($p<0.0001$). Of the fully assessed patients in the post-guideline group (n=639), 27.1% had one or more newly diagnosed VFs; 42.2% of the patients with a hip fracture, 34.1% with a major fracture, 23.0% with a minor fracture and 26.8% with finger/toe fractures. 33.2% of patients with osteoporosis had a VF, 26,6% of patients with osteopenia and 18.5% of patients with a normal BMD.

Conclusion: Overall, systematic implementation of VFA revealed a newly diagnosed VFs in 25% of all patients that present with a non-vertebral fracture at the FLS, which was significantly higher than before introduction of the guideline. VFs were more prevalent in patients with hip and major fractures and in patients with osteoporosis but were newly diagnosed in all subgroups, regardless of non-vertebral fracture classification or BMD result.

References

1. www.cbo.nl

2. Center JR, Bliuc D, Nguyen TV, Esiman JA. Risk of subsequent farcture after low-trauma fracture in men and women. JAMA 2007 297;387;387-394

3. Genant, HK, Wu, CY, van, KC, Nevitt, MC. Vertebral fracture assessment using a semiquantitative technique. JBone MinerRes 1993; 8;9;1137-1148

***Disclosures: Sandrine Bours**, None.*
This study received funding from: Eli Lilly

1109

Differentiating Osteoporotic Vertebral Fractures from Scheuermann's Disease using Different Radiological Assessment Methods for Osteoporotic Vertebral Fractures: The Rotterdam Study. Ling Oei*[1], Stephan Breda[2], Guirong Jiang[3], Salih El Saddy[2], Ater Makurthou[2], Felisia Ly[2], Martha Castano-Betancourt[1], Albert Hofman[2], Erwin Waarsing[2], Dennis Black[4], John Schousboe[5], Frank van Rooij[2], Joyce Van Meurs[1], Andre Uitterlinden[6], Maria Zillikens[2], Fernando Rivadeneira[1], Edwin Oei[2]. [1]Erasmus University Medical Center, The Netherlands, [2]Erasmus MC, Netherlands, [3]University of Sheffield, United Kingdom, [4]University of California, San Francisco, USA, [5]Park Nicollet Clinic University of Minnesota, USA, [6]Rm Ee 575, Genetic Laboratory, The Netherlands

Osteoporotic vertebral fractures are a major health issue and should be diagnosed accurately. An important radiological differential diagnosis is Scheuermann's disease. The radiographic assessment of osteoporotic vertebral fractures with quantitative morphometry (QM) evaluates vertebral height loss and is unable to distinguish fractures from non-fracture deformities with vertebral height loss, such as Scheuermann's disease. In contrast, it is said that vertebral fracture assessment with the algorithm based qualitative (ABQ) method is able to systematically rule out non-fracture deformities. Our aim was to evaluate how ABQ and QM assessments perform on independently ascertained cases of radiological Scheuermann's disease. Two independent groups of trained research assistants applied the algorithm based qualitative (ABQ) or software-assisted QM (SpineAnalyzer® software to measure vertebral height ratios which includes Genant's classification of shape and severity of deformities). These methods for osteoporotic vertebral deformities were compared on cases of radiological Scheuermann's disease, which were diagnosed by an independent third reader group who applied the criteria by Sørensen and Sachs (three or more adjacent wedged vertebral bodies each of at least 5 degrees, endplate irregularities [including Schmorl's nodes] and thoracic kyphosis greater than 45 degrees). Complete data was available for 2,311 lateral spine radiographs (T4-L4) from the population-based Rotterdam Study (42.7% men, age 46-89). Radiographic Scheuermann's disease was present in 4.2% (95% CI: 3.4%-5.0%; n=96) of the sample. Of these participants with radiographic Scheuermann's disease, QM scored 71.9% (95% CI: 62.9%-80.9%; n=69) as having osteoporotic vertebral deformities, while ABQ classified only 8.3% (95% CI: 2.8%-13.8%; n=8) as having osteoporotic fractures. Although we cannot exclude that radiographic Scheuermann's disease and osteoporotic vertebral fractures may co-exist, general consensus is that radiographic Scheuermann's disease and osteoporotic vertebral fractures are two different entities that should be diagnosed differentially. In conclusion, accurate vertebral fractures diagnosis is needed to identify patients with high risk for future fractures to optimize patient management. The inability of QM to rule out non-fracture deformities explains in part the higher number of osteoporotic vertebral deformities misclassified when applying QM as scoring method compared to ABQ.

***Disclosures: Ling Oei**, None.*

1110

Incidence of and Risk Factors for Clinical Fractures in Patients with Systemic Lupus Erythematosus and Matched Controls: a Population-based Study in the United Kingdom. Irene Bultink*[1], Nicholas Harvey[2], Arief Lalmohamed[3], Cyrus Cooper[4], Willem Lems[5], Tjeerd Van Staa[6], Frank De Vries[7]. [1]VU University Medical Center, The Netherlands, [2]MRC Lifecourse Epidemiology Unit, University of Southampton, United Kingdom, [3]Division of Pharmacoepidemiology & Clinical Pharmacology, Utrecht University, Netherlands, [4]University of Southampton, United Kingdom, [5]Vrije Universiteit Medical Centre, The Netherlands, [6]Clinical Practice Research Datalink, United Kingdom, [7]Pharmacoepidemiology & Clinical Pharmacology, Utrecht University, Netherlands

Background: Systemic lupus erythematosus (SLE) has been associated with an increased risk of low bone mineral density and fractures. However, data on absolute fracture risk and risk factors associated with clinical fractures are very scarce.

Objective: To estimate incidence rates of clinical fractures in patients with SLE and relative risks compared with matched controls, and to evaluate risk factors associated with fractures in SLE.

Methods: We conducted a population-based cohort study using the Clinical Practice Research Datalink (from 1987 to 2012). Each SLE patient (n=4343) was matched with up to 6 controls (n=21780) by age and gender. Fracture type was stratified according to WHO definitions into osteoporotic fracture (clinical spine, hip, forearm, or humerus) and non-osteoporotic fracture. Cox proportional hazards models were used to calculate relative rates (RR) of fracture, and time interaction terms to evaluate fracture timing patterns. Incidence rates of fractures in SLE patients, stratified by age, gender, type of fracture, disease duration, and therapy variables, were compared with fracture rates in controls.

Results: Mean age was 46.7 years. Follow-up duration was 6.4 years in SLE patients and 6.6 years in matched controls. Overall, SLE patients had an increased risk of any fracture compared to controls, after adjustment for confounders (adj RR 1.22; 95% confidence interval (CI) 1.05-1.42, and the risk further increased with a longer disease duration. Glucocorticoid (GC) use in the previous six months raised the risk of any fracture (adj RR 1.27; 95% CI 1.02-1.58), but was not further increased with higher cumulative GC exposure. A similar pattern was found for osteoporotic fracture, but did not reach statistical significance (adj RR 1.23; 95% CI 0.91-1.67). Cerebrovascular events, seizures, and (as expected) previous osteoporotic fractures were identified as significant predictors for any and osteoporotic fractures (table 1).

Conclusions: SLE patients in the United Kingdom have an increased risk of clinical fractures compared to age- and sex-matched controls. GC use in the previous six months and longer disease duration are important factors associated with the increased fracture risk in SLE. In addition, special attention should be paid to lupus patients with neuropsychiatric organ damage or a history of osteoporotic fractures since these subgroups of patients are at high risk of the occurrence of (subsequent) fractures.

Table 1. Risk of fracture within SLE patients (n=4343), stratified according to organ damage. (reference = no risk factor)

	Any fracture		Osteoporotic fracture	
	Events	Adj RR (95% CI)*	Events	Adj RR (95% CI)*
Cognitive impairment	5	1.67 (0.68-4.08)	4	2.25 (0.82-6.16)
Seizures	34	**2.01 (1.41-2.86)**	22	**2.81 (1.80-4.40)**
Cerebrovascular event	55	**1.49 (1.12-2.00)**	35	**1.77 (1.22-2.57)**
Renal disease	54	1.30 (0.96-1.75)	32	1.35 (0.91-2.00)
Previous osteoporotic fracture	172	**4.26 (3.49-5.18)**	95	**3.85 (2.92-5.07)**
Diabetes	21	1.39 (0.89-2.17)	11	1.33 (0.72-2.45)
Malignancy	50	1.23 (0.91-1.68)	28	1.22 (0.81-1.84)

*Adjusted for: previous fracture, use of glucocorticoids, antimalarials, calcium/vitamin D supplements, benzodiazepines, and proton pump inhibitors in the previous 6 months.

Table 1

***Disclosures: Irene Bultink**, None.*
This study received funding from: The Division of Pharmacoepidemiology

1111

β-adrenergic Receptor Antagonists and Fracture Risk: A Meta-analysis of Selectivity, Dose, Gender and Site-specific Effects. Konstantinos Toulis*[1], Karla Hemming[2], Stavros Stergianos[3], Krishnarajah Nirantharakumar[2], John Bilezikian[4]. [1]Aristotle University OF Thessaloniki, Greece, [2]Department of Public Health, Epidemiology & Biostatistics, University of Birmingham, Birmingham, UK, United Kingdom, [3]Department of Internal Medicine, Sundsvall Hospital, Sweden, [4]Columbia University College of Physicians & Surgeons, USA

Aim: To determine by meta-analysiswhether β-adrenergic blockers (βBs) reduce fracture risk and whether the effect, if demonstrable, is dependent upon selectivity, dose, gender, or fracture site.

Methods: A literature search was performed in electronic databases MEDKINE, EMBASE and reference sections of relevant articles to identify eligible studies. Adjusted estimates of fracture risk (ES) were pooled across studies using fixed or random-effects (RE) meta-analysis as appropriate. Dose-related effects were evaluated using meta-regression. To explore the relative efficacy of β1-selective blockers in comparison to non-selective βBs, adjusted indirect comparison was performed.

Results: A total of sixteen studies (seven cohort and nine case-control studies), involving 1,644,570 subjects, were identified. The risk of any fracture was found to be significantly reduced in subjects receiving βBs as compared to control subjects (16 studies, RE pooled effect size (ES) = 0.86, 95% CI: 0.78 - 0.93, I^2 = 87%). In a sensitivity analysis limited to those studies deemed to be most robust, the βB effect to reduce fracture risk was sustained (4 studies, pooled ES = 0.79, 95% CI: 0.67 - 0.94, I^2 = 96%). The risk of a hip fracture was lower in both women and men receiving βBs [women: pooled ES = 0.86, 95% CI: 0.80 - 0.91, I^2 = 1 % and men: pooled ES = 0.80, 95% CI: 0.71 - 0.90, I^2 = 0%). Similar risk reductions were found for clinical vertebral and forearm fractures, although statistical significance was not reached. The reduction in risk did not appear to be dose-related (test for a linear trend *p*-value: 0.150). Using adjusted indirect comparisons, it was estimated that β1-selective agents were significantly more effective than non-selective βBs in reducing the risk of any fracture (6 studies, β1-selective blockers versus non-selective βBs: RE pooled ES = 0.82, 95% CI = 0.69 - 0.97).

Conclusions: The findings suggest thatthe risk of fracture is approximately 15% lower in patients treated with βBs compared to controls independent of gender, fracture site, and dose. This risk reduction might be attributable to the effects of β1-selective blockers. Assuming that the lifetime risk of any osteoporotic fracture at the age of 50 is approximately 30%, 1 osteoporotic fracture would have been prevented with every 30 patients treated with βBs.

***Disclosures: Konstantinos Toulis**, None.*

1112

Aging Alters Bone-Fat Reciprocity and MPC Engraftment In Vivo. Lakshman Singh, Elizabeth Russell, Jung-Hoon Kim, Qijun Chen, Frederick Johnson, Robert Pignolo*. University of Pennsylvania, USA

Bone marrow derived mesenchymal progenitor cells (MPCs) play an important role in bone homeostasis. Age-related changes occur in bone resulting in a decrease in bone density and a relative increase in adipocity. Although *in vitro* studies suggest the existence of an age-related lineage switch between osteogenic and adipogenic fates, stem cell and microenvironmental contributions to this process have not been elucidated *in vivo*. In order to study the effects of MPC and microenvironmental aging on functional engraftment and lineage switching, bone marrow transplantation (BMT) was performed under non-myeloablative conditions in young and old recipients, with donor MPCs derived from young and old green fluorescent protein (GFP) transgenic mice. Our results from syngeneic transplantations show that engraftment of MPCs was primarily a function of cell intrinsic aging. Robust engraftment by young MPCs was observed in the marrow, bone-lining region and in the matrix of young recipients. No engraftment, however, was observed in young recipients transplanted with MPCs derived from old GFP transgenic mice and significantly lower engraftment was seen at the same sites in old recipients transplanted with old MPCs. The absence of engraftment observed in old into young transplants was mitigated by myeloablation with concomitant reversal of splenic sequestration, resulting in engraftment of old MPCs in as little as 4 hours post-transplantation. Differentiation of transplanted MPCs strongly favored adipogenesis over osteogenesis in old recipients irrespective of MPC donor age, suggesting that microenvironmental alterations that occur with aging in vivo are predominately responsible for MPC lineage switching. These data indicate that aging alters bone-fat reciprocity and engraftment of mesenchymal progenitors, with important implications for the treatment of age-related osteoporosis as well as transplant biology.

***Disclosures: Robert Pignolo**, None.*

1113

Alleviation of Radiotherapy-Induced Bone Loss by Parathyroid Hormone Treatment is Associated with Improved DNA Repair in Osteoblasts. Abhishek Chandra*[1], Tiao Lin[1], Ji Zhu[2], Beom Huh[1], Allison Altman[1], Sarah Hagan[1], Keith Cengel[1], Xiaowei Liu[1], Ling Qin[1]. [1]University of Pennsylvania, USA, [2]University of Pennsylvania, School of Medicine, USA

Radiation damage to tumor-adjacent bones is a well-recognized late effect of radiotherapy, resulting in a spectrum of bone changes from mild osteopenia to osteoradionecrosis. Since radiation primarily causes bone atrophy, we propose that PTH, an anabolic agent for bone formation, should preserve bone structure and strength against radiation damage. In this study, 3-month-old rats were focally irradiated at the proximal metaphyseal region of right tibiae by a unique SARRP irradiator that replicates clinical focal radiotherapy with an accuracy of 1 mm resolution(8 Gy at day 1 and 3), designed to mimic the dose to the hip during hypofractionized radiation protocols for prostate cancer. Rats were then administered daily with vehicle (n=9) or PTH(1-34, 60 μg/kg, n=9) for 4 weeks. μCT scans revealed a significant 20% decrease in trabecular bone volume (BV) in irradiated tibiae compared to the contralateral tibiae in the vehicle group, mainly due to a 17% decrease in trabecular number (Tb.N). 3D registration of μCT images before and after radiation confirms that some trabecular elements were lost after radiation while almost all elements were preserved and thickened after 4 weeks in non-irradiated tibiae. Finite element analysis indicates that this microstructural deterioration resulted in a 57% decrease in trabecular bone stiffness. Conversely, PTH injections remarkably increased BV,Tb.N, and stiffness in both non-irradiated and irradiated trabecular bone to a similar level and preserved all trabecular elements in the irradiated bone. Histological analysis indicates that radiation caused apoptosis in osteoblasts, leading to 70% fewer viable and functional osteoblasts on the trabecular bone surface compared to the non-irradiated control, while PTH injections increased their number and protected them from cell death. In vitro experiments replicated in vivo observations that a single dose (8 Gy) of X-ray radiation resulted in an 18% apoptotic rate in osteoblastic cells after 2 days and that PTH treatment abolished this deleterious effect via a beta-catenin-dependent pathway. PTH did not affect the production of reactive oxygen species (ROS) by radiation. Using a gamma-H2AX foci assay that detects DNA double-stranded breaks (DSBs), we demonstrate that PTH promotes DSB repair in osteoblasts. Taken together, our data demonstrate a strong radioprotective effect of PTH on bone integrity and a novel role of PTH in regulating DSB repair machinery and chromatin remodeling.

***Disclosures: Abhishek Chandra**, None.*

1114

Manipulation of RANK monomer assembly as a novel anti-resorptive strategy. Julia Warren*[1], Christopher Nelson[2], Lawrence Yu[2], Daved Fremont[2], Steven Teitelbaum[1]. [1]Washington University in St. Louis School of Medicine, USA, [2]Washington University in St. Louis, USA

The interaction of receptor activator of NF-kB ligand (RANKL) with its receptor RANK is essential for the differentiation and function osteoclasts (OCs). RANKL exists as a homotrimer, with classical models of receptor activation assuming trimeric clustering of receptor as necessary for signal transduction. We have designed a novel single-chain RANKL (scRANKL) construct to test the assumption that trimeric clustering of RANK is necessary for downstream signaling, and to function as a competitive antagonist of this pathway. scRANKL consists of all three RANKL monomers connected by short protease-resistant linkers, enabling individual manipulation of each RANK binding site and assessment of the receptor clustering state necessary for downstream signaling. We used our co-crystal structure of RANK/RANKL to design mutations in RANKL that abolish binding to RANK. After inserting these variants at one scRANKL site, to create a single-blocked ligand capable of recruiting only two RANK receptors, we still observe OC formation, although only at high ligand concentration. In contrast, double-blocked scRANKL does not form OCs. Hence, dimeric engagement of RANKL by RANK is sufficient and necessary for downstream signaling in the OC. Although double-blocked scRANKL may potentially antogonize RANK/RANKL signaling, it competes poorly with endogenous RANKL due to loss of receptor avidity. Therefore, we identified mutations in RANKL, using yeast surface display, that dramatically increase its affinity for RANK. Concurrently, we sorted for loss of binding to OPG, the RANKL endogenous decoy receptor, with the hypothesis that this trait would allow scRANKL to more efficiently function as a competitive antagonist, in vivo. When inserted at the intact RANK binding sites in single- or double-blocked scRANKL (termed "single-blocked, RANK-high" or "double-blocked, RANK-high"), these novel constructs are highly efficient competitive antagonists of wild-type RANKL-induced osteoclastogenesis. Our work demonstrates that the manipulation of RANK receptor oligomerization, and the subsequent blockade in signaling, may provide a novel avenue to develop anti-resorptive drugs. Additionally, the design of single-chain TNFSF ligands with individually manipulated receptor binding sites can more broadly inform our knowledge of how these receptors, with diverse biological functions, initiate signal transduction.

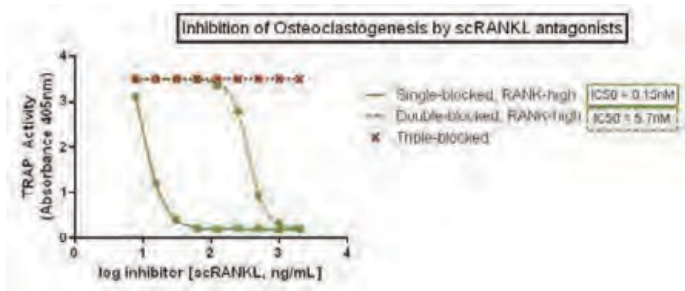

Inhibition of Osteoclastogenesis by scRANKL Antagonists

***Disclosures: Julia Warren**, None.*

1115

WNT16 is a Novel Osteoblast-Derived Paracrine Regulator of Osteoclastogenesis, Cortical Bone Mass and Fracture Susceptibility. Sofia Moverare Skrtic*[1], Petra Henning[2], Anna Börjesson[2], Klara Sjögren[2], Sara Windahl[3], Hanna Isaksson[4], Emma Eriksson[5], Farasat Zaman[5], Lars Sävendahl[6], Ulf Lerner[7], Claes Ohlsson[1]. [1]Center for Bone & Arthritis Research at the Sahlgrenska Academy, Sweden, [2]Centre for Bone & Arthritis Research, Institute of Medicine, Sahlgrenska Academy, University of Gothenburg, Sweden, [3]Center for Bone & Arthritis Research, Sahlgrenska Academy, Sweden, [4]Division of Solid Mechanics, & Department of Orthopedics, Lund University, Lund, Sweden, [5]Karolinska Institutet, Sweden, [6]Department of Women's & Children's Health, Karolinska Institutet, Pediatric Endocrinology Unit, Stockholm, Sweden, [7]University of Umea, Sweden

We have previously identified a missense variant in the *WNT16* gene associated with cortical bone thickness and forearm fracture risk in humans. To determine the mechanisms of action for WNT16 in the regulation of cortical bone mass, *Wnt16*$^{-/-}$ mice were evaluated. Although *Wnt16*$^{-/-}$ mice were born healthy, 46% exhibited spontaneous tibia diaphyseal fractures before 11 weeks of age.

Computed tomography (CT) analyses of tibia revealed a pronounced reduction of cortical volumetric BMD (-21.4 $\pm$ 1.2%, $P < 0.01$) and cortical bone thickness (-13.1 $\pm$ 1.9%, $P < 0.01$) in *Wnt16*$^{-/-}$ mice compared to wild type (WT) mice. Analysis of cortical bone composition using Fourier Transform Infrared Spectroscopy demonstrated reduced mineral to matrix ratio (-18.6 $\pm$ 4.0%, $P < 0.01$) and collagen maturity (-7.3 $\pm$ 2.3%, $P < 0.05$). In contrast, the trabecular bone volume (BV/TV) as analyzed by μCT was normal in *Wnt16*$^{-/-}$ mice. *Wnt16* mRNA measurements and immunohistochemistry of WT mice revealed abundant and specific WNT16 expression in cortical bone. Primary cultured osteoblasts, but not osteoclasts, expressed high *Wnt16* mRNA levels.

Cell cultures isolated from *Wnt16*$^{-/-}$ mice did not show any major differences in osteoblast differentiation, nor was RANKL induced osteoclastogenesis in bone marrow macrophages from *Wnt16*$^{-/-}$ mice affected, suggesting that WNT16 does not exert cell autonomous effects. Importantly, recombinant WNT16 protein dose-dependently inhibited RANKL induced osteoclastogenesis associated with decreased mRNA levels of the osteoclast specific genes *Acp5, Ctsk* and *Nfatc1* and decreased bone resorption measured by CTX release. These findings are consistent with that the number of osteoclasts was increased in the cortical bone of *Wnt16*$^{-/-}$ mice ($P < 0.01$).

Endogenous *Wnt16* mRNA levels in calvarial osteoblasts were increased by Oncostatin M (+273 $\pm$ 61%, $P < 0.01$). Oncostatin M induced osteoclastogenesis in co-cultures of calvarial osteoblasts and bone marrow macrophages was enhanced when the osteoblast were from *Wnt16*$^{-/-}$ mice, suggesting that WNT16 is involved in a negative feed-back loop of Oncostatin M induced osteoclastogenesis.In conclusion, WNT16 is a novel osteoblast-derived regulator of osteoclastogenesis, cortical bone mass and fracture susceptibility. We propose that WNT16 is expressed by osteoblasts in cortical bone and is a crucial regulator of cortical bone mass, and thereby fracture susceptibility, acting as a paracrine inhibitor of osteoclastogenesis.

***Disclosures: Sofia Moverare Skrtic**, None.*

1116

Treatment With Anti-sclerostin Antibody Restores Endosteal Osteoblasts in Osteocyte-specific Gsα-KO Mice. Keertik Fulzele*[1], Christopher Dedic[2], Xiaolong Liu[2], Paola Divieti Pajevic[1]. [1]Massachusetts General Hospital; Harvard Medical School, USA, [2]Endocrine Unit, Massachusetts General Hospital & Harvard Medical School, USA

Intermittent PTH and sclerostin antibodies are potent anabolic agents for osteoporosis treatment, both of which increase osteoblasts numbers to build new bone. How the new osteoblasts are recruited in response to these treatments is not clear. Previously, in-vivo lineage tracing experiments showed that intermittent PTH administration increases osteoblast numbers by converting bone lining cells (BLC) into mature osteoblasts (JBMR; 27(10):2075–84). Histological analysis of mice lacking the stimulatory subunit of G-proteins (Gsα) in osteocytes (DMP1-GsαKO), unexpectedly revealed lack of endosteal osteoblast (endo-OB) those could be observed under light microscope. Gsα-deficient osteocytes also showed a dramatic increase in sclerostin expression as assessed by quantitative PCR and immunohistochemistry. Because PTH is a potent suppressor of sclerostin expression and can also convert BLC into mature osteoblasts, we hypothesized that treatment with anti-sclerostin antibody may restore the endo-OB in the mutant mice. To confirm the contribution of Gsα signaling in osteocytes in the maintenance of endo-OB, we also generated mice lacking Gsα in mature osteoblasts using osteocalcin-Cre (OC-GsαKO). OC-GsαKO mice also showed increased sclerostin expression in osteocytes. Interestingly endo-OB were present in OC-GsαKO mice but were fewer, thinner, and disorganized as compared to control littermates. Taken together this data indicated that Gsα signaling in osteocytes plays an important role in the maintenance of endo-OB. We next treated DMP1-GsαKO and control mice with anti-sclerostin antibody (25 mg/kg, 2 times per week) for 4-weeks. Upon the antibody treatment, the endo-OB reappeared in the DMP1-GsαKO mice to a comparable level to that of the vehicle treated control littermates. In control mice, E11/gp38 positive osteocytes were observed in parallel with the endo-OB with higher dendrite density towards the endo-OB. In DMP1-GsαKO mice, E11/gp38 positive osteocytes were lacking dendrites and were randomly scattered throughout the bone matrix. After treatment with anti-sclerostin antibody, DMP1-GsαKO mice showed increased E11/gp38 positive osteocytes near the endosteal bone surface and endo-OB. However, whether the appearance of E11/gp38 positive osteocytes is a cause or effect of appearance of endo-OB is not clear. Taken together, this data suggest that young osteocytes regulate endo-OB, at least in part, by secretion of sclerostin.

***Disclosures: Keertik Fulzele**, None.*

1117

GATA4 Regulates Bone Mineralization Via Estrogen Receptor-Dependent and -Independent Pathways. Alejandro Garcia*[1], Miriam Guemes[2], Stephanie Runke[2], Diana Rigueur[2], Gustavo Miranda-Carboni[2], Karen Lyons[1], Susan Krum[2]. [1]University of California, Los Angeles, USA, [2]UCLA, USA

Osteoporosis is a disease characterized by low bone mass that leads to an increased risk of fragility fractures. The biggest risk factor for osteoporosis is being a post-menopausal woman. Estrogens play a role in almost all cells and tissues in the body, but how tissue specificity occurs is largely unknown. We have identified GATA4 as a transcription factor expressed in osteoblasts and recruited to estrogen receptor alpha (ERα) binding sites near osteoblast-specific genes that control differentiation and tissue specificity. GATA4 binding precedes that of ERα and is necessary for histone modifications associated with recruitment of ERα to binding sites. Bone mineralization decreases in calvarial osteoblasts following GATA4 knockdown are both dependent and independent of 17β-estradiol (E2*)* activity. Microarray analysis, followed by qPCR and immunoblots, of wildtype vs. GATA4 knockdown showed that GATA4 regulates TGFβ and BMP signaling. GATA4 knockdown decreases the expression of BMPs -3, -4, and -6 and R-SMADs -3 and -5, proteins known to induce osteoblast differentiation. Furthermore, there is an increase in I-SMAD expression, especially Smad6. In the absence of GATA4, TGF-β signaling, which has been shown to inhibit expression of bone-specific genes, is increased. *In vivo* deletion of GATA4, driven by Cre-recombinase in osteoblasts (Col2.3-Cre, 2.3 kb fragment of the rat Col1a1 gene) results in low birth weight, stunted intrauterine long bone growth and perinatal lethality. Taken together, the data support that GATA4 has both E2-dependant and independent effects regulating osteoblast function and bone development. Understanding of the role of GATA4 to regulate the tissue specificity of estrogen-mediated osteoblast gene regulation and estrogen-independent bone differentiation may help in therapeutics of post-menopausal osteoporosis.

***Disclosures: Alejandro Garcia**, None.*

1118

Glucocorticoids Stimulate Osteocyte Autophagy in Mice but Suppression of Autophagy in Osteocytes does not Accentuate their Negative Impact on the Skeleton. Marilina Piemontese*[1], Melda Onal[2], Jinhu Xiong[3], Yiying Wang[1], Rajamani Selvam[1], Stuart Berryhill[1], Li Han[3], Erin Hogan[1], Robert Weinstein[3], Stavros Manolagas[3], Charles O'Brien[3]. [1]University of Arkansas for Medical Sciences, USA, [2]university of wisconsin, USA, [3]Central Arkansas VA Healthcare System, Univ of Arkansas for Medical Sciences, USA

Glucocorticoid excess decreases bone mass and strength but the mechanisms remain unclear. Autophagy is a lysosome-based recycling pathway that promotes the turnover of cellular components and can promote cell survival under stressful conditions. Recent studies have shown that glucocorticoids stimulate autophagy in an osteocytic cell line. These studies suggest the possibility that autophagy may oppose the negative actions of glucocorticoids on osteocytes and that in the absence of autophagy, the impact of glucocorticoids on the skeleton might be increased. To address this possibility, 6-month-old mice lacking the Atg7 gene, which is essential for autophagy, specifically in osteocytes (Dmp1-Cre;Atg7f/f) and their control littermates (Atg7f/f) were implanted with pellets releasing vehicle or prednisolone and examined after 28 days. Prednisolone elevated conversion of LC3 form I to form II in osteocyte-enriched cortical bone of Atg7f/f mice, demonstrating that glucocorticoids stimulate autophagic flux in osteocytes in vivo. However, prednisolone did not stimulate LC3 conversion in cortical bone in Dmp1-Cre;Atg7f/f mice, confirming suppression of autophagy in the osteocytes of these mice. Comparison of the vehicle treated groups revealed that suppression of autophagy in osteocytes reduced cortical bone thickness, cancellous bone volume, osteoblast number, and osteoclast number but increased cortical bone porosity as well as oxidative stress in the bone microenvironment. In Atg7f/f mice, prednisolone reduced femoral cortical thickness, increased cortical porosity, reduced bone strength, reduced osteoblast number and increased oxidative stress. Similar changes were observed in Dmp1-Cre;Atg7f/f mice with the exception that prednisolone did not reduce osteoblast number, which was already reduced by Atg7deletion. Similarly, prednisolone reduced the bone formation rate in Atg7f/f mice, but not in Dmp1-Cre;Atg7f/f mice, which already displayed a significant reduction in this parameter. Taken together, these results demonstrate that although glucocorticoids stimulate autophagy in osteocytes, suppression of autophagy in this cell type does not accentuate the negative impact of glucocorticoids on the skeleton. Thus stimulation of autophagy in osteocytes does not appear to be an important defense mechanism opposing the negative effects of glucocorticoids on the skeleton.

***Disclosures: Marilina Piemontese**, None.*

FR0010

Effects of Age on Molecular Pathways Regulating Bone Formation in Humans: A Key Role for Notch and Rorβ Signaling. Matthew Roforth*[1], Koji Fujita[1], Ulrike McGregor[2], Salman Kirmani[1], Louise McCready[1], James Peterson[1], Matthew Drake[3], David Monroe[4], Sundeep Khosla[5]. [1]Mayo Clinic, USA, [2]King's College, London UK, United Kingdom, [3]College of Medicine, Mayo Clinic, USA, [4]Mayo Foundation, USA, [5]Mayo Clinic College of Medicine, USA

Despite extensive studies in mice, there is currently little information on the molecular pathways contributing to age-related bone loss in humans. In part, this stems from the difficulty of obtaining trephine bone biopsies (~5-7 mm diameter) in normal volunteers. Thus, we used the standard clinical approach hematologists employ for bone marrow aspirates and biopsies to obtain needle biopsies (1-2 mm diameter) from the posterior iliac crest in 20 young (30±5 yr) and 20 old (73±7 yr) women. We coupled this to customized, in-house QPCR analyses of 288 genes related to bone metabolism, including genes reflecting 17 pre-specified clusters/pathways (e.g., Wnt targets) and 71 genes linked to SNPs from GWAS studies (Nat Genet 44:491, 2012). Genes in pre-specified pathways were analyzed using a cluster analysis (O'Brien Umbrella Test) which tests for concordant changes in multiple genes in the pathway.

One of the most highly upregulated pathways in the old women was Notch (P = 0.003), which is known to modulate age-related bone loss in mice (Nat Med 14:306, 2008). Individual significant (P<0.05) gene changes in this pathway were *hes1* (1.6x), *hey1* (1.8x), *heyL* (1.5x), and *Jag1* (1.2x). In addition, recent studies have identified retinoic acid receptor-related orphan receptor β (*Rorβ*) as an important regulator of osteogenesis that is markedly upregulated in bone marrow mesenchymal cells from aged versus young mice (JBMR 27:891, 2012). *Rorβ* itself (1.6x) as well as multiple *Rorβ* target genes (P = 0.001 for the pathway) were also upregulated in the biopsies from the old women. Both Notch and Rorβ signaling inhibit runx2 activity, thereby potentially blocking osteoblast differentiation. Interestingly, a panel of stem cell markers was significantly upregulated with aging (P = 0.022), including *nestin* (2.0x), *CD146* (1.4x), and *nanog* (1.3x), suggesting that activation of Notch and Rorβ signaling may result in a block in osteoblast differentiation with resultant expansion of the stem cell pool within bone.Of the 71 GWAS genes, 11 were significantly altered with aging, most notably *mmp7* (4.0x). Other individual gene changes of interest with aging included *rankl* (1.6x) and *fgf23* (2.0x).In summary, we describe a novel approach coupling needle biopsies of bone to customized QPCR analyses to study genes/pathways regulating bone metabolism in humans. Our work validates, in humans, several pathways associated with age-related bone loss in mice, including Notch and Rorβ signaling.

***Disclosures: Matthew Roforth**, None.*

FR0011

Low trunk muscle density is associated with prevalent vertebral fractures in older adults. Dennis Anderson*[1], Brett Allaire[1], Alexander Bruno[2], Serkalem Demissie[3], Douglas Kiel[4], Mary Bouxsein[1]. [1]Beth Israel Deaconess Medical Center, USA, [2]Harvard-MIT, USA, [3]Boston University School of Public Health, USA, [4]Hebrew SeniorLife, USA

Low x-ray attenuation (low density) of muscles in CT scans, indicative of fat accumulation within muscle, has been associated with reduced strength and physical performance in older adults. In addition, low density of the trunk muscles is associated with increased prevalence of back pain and increased hyperkyphosis, while low density of the thigh muscles is associated with increased risk of incident hip and non-vertebral fractures, independent of BMD. However, the association of muscle density with vertebral fractures (VF) has not been previously examined.

To test whether density of the trunk muscles is associated with prevalent VF we conducted a cross-sectional study of 267 subjects (44 with moderate/severe prevalent VF, 223 with no VF) ⩾50 years old from the community-based Framingham Heart Study CT cohort. Muscle density (in Hounsfield Units) was determined from axial CT scans at the L3 level of the spine. Logistic regression models were performed to determine the associations between prevalent VF and muscle density, adjusting for age, sex and vertebral body integral vBMD. Odds ratios for VF were calculated for overall muscle density (weighted average of all muscles), and for specific muscle groups.

Cases with prevalent VF were similar in age to controls without VF (68.3±9.7 vs. 66.2±10.1 yr, p=0.209), but had lower vertebral vBMD (0.130±0.040 vs. 0.163±0.044 g/cm^3, p<0.001) and lower overall trunk muscle density (34.3±9.5 vs. 39.4±8.2 HU, p=0.003). After adjusting for age, sex, and BMD, 1 SD lower trunk muscle density was associated with more than double the odds for prevalent VF (Table). When examined individually, lower density of the rectus abdominis, latissimus dorsi and external oblique muscle groups were associated with prevalent VF (p<0.05), while lower density of erector spinae and multifidus did not achieve significance (p<0.10).

Low trunk muscle density is associated with prevalent VF, independent of age, sex and BMD. Overall muscle density had the strongest association, while some muscle groups had weaker associations, which may indicate that VF is associated with a general loss of muscle quality or function rather than declines in a specific muscle group. These results, in conjunction with previous reports that low muscle density is an independent risk factor for incident non-vertebral fractures, provide strong motivation for future studies examining the contribution of trunk muscle density to the risk of incident VF.

Table. Association between muscle density at L3 and prevalent VF, expressed as odds ratio per 1SD reduction, adjusted for age, sex and vertebral BMD.

	OR (95% CI)	p-value
Overall Muscle Density (All Muscles Combined)	2.16 (1.23-3.99)	**0.009**
Rectus Abdominis	1.69 (1.04-2.77)	**0.034**
Latissimus Dorsi	2.08 (1.39-3.19)	**<0.001**
External Oblique	1.64 (1.08-2.54)	**0.023**
Erector Spinae	1.49 (0.99-2.24)	0.054
Multifidus	1.48 (0.93-2.39)	0.097

Table

***Disclosures: Dennis Anderson**, None.*

FR0012

Protein Intake is Protective Against Grip Strength Loss in Adults: The Framingham Osteoporosis Study. Kelsey Mangano*[1], Robert McLean[2], Marian Hannan[3], Douglas Kiel[4], Virginia Casey[4], Shivani Sahni[2]. [1]Institute for Aging Research, Hebrew SeniorLife, Harvard Medical School, USA, [2]Hebrew SeniorLife Institute for Aging Research & Harvard Medical School, USA, [3]HSL Institute for Aging Research & Harvard Medical School, USA, [4]Hebrew SeniorLife, USA

Rationale: Muscle function is progressively lost with aging and has been linked to unfavorable health outcomes. Previously, dietary protein intakes were associated with improved lean muscle mass; however, the role of protein with muscle strength remains unclear. Further, the relation between type of dietary protein and muscle function has yet to be elucidated. Objective: To determine the longitudinal associations of types of dietary protein with grip strength among Framingham Offspring participants. Methods: Grip strength (kg) was measured by isometric hand dynamometer (3 trials/hand) and the maximum value across trials was used at baseline (1999-2002) and at follow-up (2005-2007) among 1,564 men and women. Longitudinal change in grip strength, presented as % change per year, was calculated from baseline to follow-up. Usual intakes (g/d) of total, animal and plant protein were assessed in 1995-98 via food frequency questionnaire. Multivariable linear regression was used to assess the association of dietary protein (energy adjusted; residual method) with change in grip strength. Least squares-adjusted mean strength was calculated for quartiles of energy-adjusted protein intake and linear trend was tested. Models were adjusted for baseline age, sex, height, BMI, health status (self-reported: excellent, good, fair; poor), physical activity (PASE) menopause status (>1y post-menopausal y/n), baseline grip strength (kg) and total energy intake (kcal/d). Animal and plant protein were adjusted for each other. Results: Mean age was 59.5±9.3y (range 29-86). Mean protein intakes (g/d) were 79±28 (total), 55±23 (animal) and 24±9 (plant); mean baseline grip strength was 32.6 ± 12.7kg. Average follow up was 5.8±1.1y; mean grip strength loss was -0.08±6.0% per year (absolute change: -0.3±1.6kg/y). A positive association between dietary protein and % change grip strength was observed for all dietary protein types (total protein: β=0.020, p=0.03; animal protein: β=0.019, p=0.04; plant protein: β=0.089, p=0.002); where for 1g greater intake of total protein grip strength increased 0.65kg per year. Similar protective trends were observed with protein quartiles; however, only results for plant protein reached statistical significance (Figure). Conclusions: Similar protective patterns were observed across type of dietary protein with change in grip strength. These results suggest greater intake of dietary protein may be beneficial in preventing muscle strength loss over time.

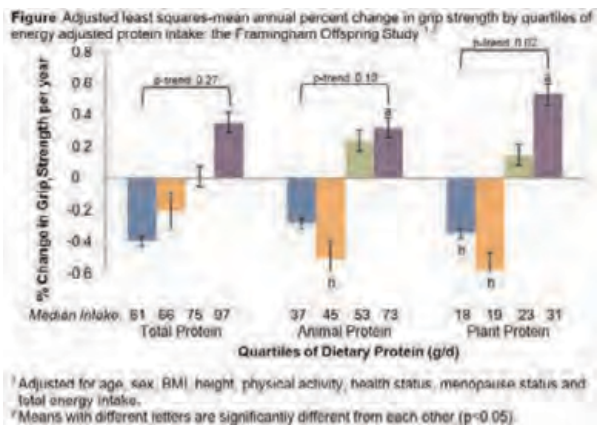

Figure. Annual Percent Change in Grip Strength by Quartiles of Dietary Protein

***Disclosures: Kelsey Mangano**, None.*
This study received funding from: General Mills Bell Institute for Health and Nutrition

FR0022

Exercise During Growth as an Independent Predictor of Cortical Bone Size and Strength in Older Swedish Men. Martin Nilsson*[1], Claes Ohlsson[1], Magnus Karlsson[2], Dan Mellstrom[3], Mattias Lorentzon[4]. [1]Centre for Bone & Arthritis Research At the Sahlgrenska Academy, Sweden, [2]Skåne University Hospital Malmö, Lund University, Sweden, [3]Sahlgrenska University Hospital, Sweden, [4]Geriatric Medicine, Center for Bone Research at the Sahlgrenska Academy, Sweden

Purpose: We have previously reported an association between exercises during youth and increased areal bone mineral density in older men (Nilsson, M. et al. Ost. Int. Nov, 2008). The aim of this study was to investigate if exercise during growth was associated with cortical bone geometry and whole bone strength in weight-bearing bone in older men.

Methods: Cortical bone geometry at the tibia and radius was measured by peripheral quantitative computed tomography (pQCT) (XCT-2000, Stratec), whereas finite element analysis of the ultra distal tibia and radius was performed, using measurements from a high-resolution 3D pQCT device (XtremeCT, Scanco). The study was performed in 600 men, 79.9 ± 3.4 (mean ± SD) years old, from the Gothenburg part of the MrOS Sweden five-year follow-up study. A standardized questionnaire was used to collect information about previous and current exercise.

Results: A linear regression model (including age, height, weight, calcium intake, smoking, levels of exercise during growth, and current exercise) revealed that levels of exercise during growth (10-20 years) was independently associated with periosteal circumference (β=0.09, $p<0.01$), cortical thickness (β=0.15, $p<0.001$) at the tibia and total bone strength (estimated ultimate failure load (β=0.13, $p<0.01$) and stiffness (β=0.13, $p<0.01$)) at the ultra distal tibia. Current exercise was independently associated with endosteal circumference (β=-0.11, $p<0.01$), cortical thickness (β=0.13, $p<0.01$) at the tibia and total bone strength (estimated ultimate failure load (β=0.09, $p<0.05$) and stiffness (β=0.09, $p<0.05$)) at the ultra distal tibia. Current or previous exercise was not associated with the corresponding measurements at the radius.

Conclusion: In this large cohort of elderly men, exercise during growth was independently associated with larger periosteal circumference, and higher bone strength, whereas current exercise was independently associated with lower endosteal contraction and bone strength at the tibia. These findings indicate that exercise during growth can increase the cortical bone size via periosteal expansion while exercise at old age can decrease endosteal bone loss in weight-bearing bone in older men.

***Disclosures: Martin Nilsson**, None.*

FR0023

Long-term Exercise Intervention in Older Adults: 4-Year Follow-up of a Randomized Controlled Trial of Music-Based Multitask Training (Jaques-Dalcroze Eurhythmics). Andrea Trombetti*, Mélany Hars, François Herrmann, René Rizzoli. Division of Bone Diseases, Geneva University Hospitals & Faculty of Medicine, Switzerland

Long-term prospective controlled data supporting the efficacy of exercise to prevent physical decline in old age are scarce. In a 1-year randomized controlled trial [1], we showed that a 6-month music-based multitask exercise program (i.e., Jaques-Dalcroze eurhythmics) improved gait and balance, and reduced falls in older adults. We conducted a 4-year extension of this trial aimed at assessing the effects of long-term practice of the multitask exercise regimen.

We planned a long-term follow-up extension of a 1-year randomized controlled trial in which 134 community-dwellers aged ⩾65 years at increased risk of falls received an immediate or a delayed 6-month music-based multitask exercise program, with outcomes assessed at baseline, 6-month, and 1-year. Four years following original trial enrolment, 52 subjects (baseline mean ± SD age, 75 ± 8 years) who i) have maintained exercise program participation through the 4-year follow-up visit (long-term "intervention group", n=23) or ii) have discontinued participation following original trial completion ("control group", n=29) were studied. They were reassessed in a blind fashion, using the same procedures.

At 4 years, linear mixed-effects models showed significant gait (gait speed, P=0.006) and balance (unipodal stance time, P=0.015) improvements in the intervention group, compared with the control group. Also, intervention subjects did better on Timed Up & Go, Five-Times-Sit-to-Stand and hand grip strength tests, than controls ($P<0.05$, for all comparisons). Furthermore, the exercise program had a protective effect on falls (relative risk, 0.69; 95% confidence interval, 0.5 to 0.9; P= 0.008).

This 4-year extension of a randomized controlled trial suggests that long-term maintenance of a music-based multitask exercise program later in life is a promising strategy to prevent age-related physical decline. This exercise regimen promotes both compliance and adherence in older adults.

References

[1] Trombetti et al. Effect of music-based multitask training on gait, balance, and fall risk in elderly people: a randomized controlled trial. Arch Intern Med. 2011;171(6):525-33.

***Disclosures: Andrea Trombetti**, None.*

FR0024

Height Age Correction of Pediatric DXA: Illustration of its Importance. Katherine Madson*[1], Gary S Gottesman[1], Fan Zhang[2], Michael Whyte[1]. [1]Shriners Hospital for Children-Saint Louis, USA, [2]Shriners Hospital for Children, USA

Pediatric bones change size and shape with growth, and this dynamism poses challenges when measuring bone mineral density (BMD) in children by dual-energy x-ray absorptiometry (DXA). Additionally, DXA measures "areal" BMD (gm/cm^2), not true volumetric BMD (gm/cm^3), and is therefore influenced significantly by bone size (length and width). Age-, gender-, and race-specific healthy control ranges help to interpret pediatric BMD, but DXA BMD Z scores still under- or over-estimate bone density in children who have less or more than average height, respectively. Until recently, a simple way to correct pediatric BMD for height was unavailable. Then, in 2012, one equation each for pre-teenage boys and girls was published[(1)] that corrected for height variation thus improving pediatric DXA interpretation.

Here, beginning July, 2012, we prospectively analyzed our DXAs for all pre-pubertal patients to assess the importance of height correction. Our Hologic Discovery-A densitometer software uses the normative data of Kelly et al[(2)] and Kalkwarf et al[(3)]. We studied 61 consecutive patients (boys n=30) undergoing DXA and interpreted the BMD Z scores for both chronologic age (CA-Z) and then "height age" (HA-Z). Interpretable data were available for L1-L4 spine CA-Z n=61 and HA-Z n=59, and for total hip CA-Z n=50 and HA-Z n=48. In the total hip, non-usable data occurred from surgical metal and an older age reference range. Most patients had metabolic bone disease, thus heights were shorter than in the normal population.

Individual spine and hip BMD Z score differences were defined as HA-Z minus CA-Z. We pooled the data for boys and girls after no gender difference was identified by ANCOVA (spine p=0.77; hip p=0.27). Next, linear regression for the patients with height Z score (HT-Z) within -2 to +2 was used to evaluate the correlation between BMD Z score difference versus HT-Z for spine and hip, respectively. We found negative correlations: Spine HA-Z – CA-Z = -0.40 x HT-Z, r^2=0.75 ($p<0.0001$) and total hip HA-Z – CA-Z = -0.407 x HT-Z, r^2=0.879 ($p<0.0001$). Thus, the further the HT-Z deviated from average (Z=0), the greater the HA-Z correction (Figure).

Our data illustrate how height correction can have importance when interpreting pediatric DXA.

1) Zhang et al J Clin Densitom 2012 p 267.
2) Kelly et al Bone 2005 p s30.
3) Kalkwarf et al J Clin Endocrinol Metab 2007 p 2087

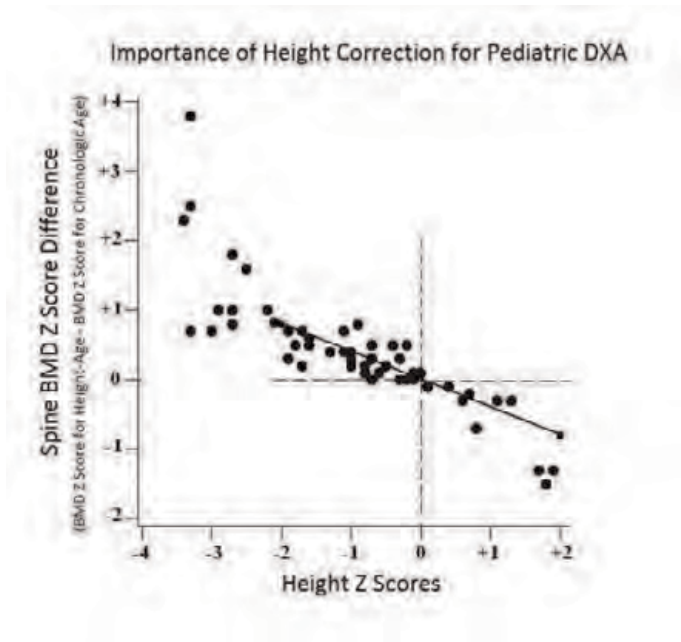

Importance of Height Correction for Pediatric DXA

***Disclosures: Katherine Madson**, None.*

FR0025

RANKL Inhibition Improves Long Bone and Vertebral Bone Properties in Moderately Severe Type IV Osteogenesis Imperfecta Brtl Mice. Patricia Collin-Osdoby*[1], Tarpit Patel[2], Michael Brodt[2], Linda Rothe[2], Chun Ya Han[3], Marina Stolina[4], Matthew Silva[5], Paul Kostenuik[4], Joan Marini[6], Philip Osdoby[1]. [1]Washington University in St. Louis, USA, [2]Washington University, USA, [3]Amgen, USA, [4]Amgen Inc., USA, [5]Washington University in St. Louis School of Medicine, USA, [6]National Institute of Child Health & Human Development, USA

Brtl mice contain a glycine substitution (G349C) in half of their type I collagen a1(I) chains and exhibit key characteristics typical of moderately severe human Type IV osteogenesis imperfecta (OI). Thus, Brtl mice have a smaller body size, reduced cortical and trabecular bone volumes, abundant osteoclasts, matrix insufficiency, and brittle bones prone to fracture. While bisphosphonates have proven useful as anti-resorptive drugs to reduce the severity of OI-related bone loss in humans and animal models, new therapeutics are being sought for improved OI skeletal management. Here, we investigated the potential benefits of inhibiting RANKL-stimulated osteoclast bone resorption in the Brtl OI mouse. Male littermate Brtl and wild-type (WT) mice were injected with RANK-Fc (10 mg/kg) twice weekly from 5 to 8 weeks of age (the time of peak OI phenotype in Brtl mice), after which serum and bones were collected for analysis. Serum CTXI and OC bone turnover marker levels, which were significantly higher in Brtl vs. WT mice, were markedly reduced along with TRACP5b by RANK-Fc treatment in both Brtl and WT mice. Consistent with this, microCT analysis of femoral and tibial bones showed that RANK-Fc treatment had little effect on cortical bone but dramatically suppressed trabecular bone resorption and increased BV/TV, Tb Th, BMD, and TMD. Bone marrow compartments were noticeably smaller due to excess bone present in RANK-Fc treated Brtl and WT mice. Similarly, microCT analyses of BV/TV, Tb. N, and BMD in vertebral bones (L4, L5), which all were lower in Brtl vs. WT mice, were each significantly increased following RANK-Fc treatment. Biomechanical 3-point bending tests of long bones revealed that RANK-Fc increased the rigidity (stiffness) and brittleness of WT and/or Brtl femoral bones, and produced only slight improvements in Brtl bone toughness or resistance to fracture. Vertebral crush tests of L4 and L5 vertebrae demonstrated that stiffness, resistance to deformation, and maximal force to crush, which all were lower in Brtl vs. WT vertebral bone, increased in Brtl and WT vertebrae following RANK-Fc treatment. We conclude that RANK-Fc inhibition of osteoclast-mediated bone turnover improves multiple structural and biomechanical properties of vertebral and long bones in Brtl OI mice. Further studies may indicate if RANKL inhibition will be a useful therapeutic alternative to bisphosphonates for improving bone properties and limiting bone loss in human OI.

***Disclosures: Patricia Collin-Osdoby**, Amgen, 6*
This study received funding from: Amgen

FR0066

Treatment with a soluble bone morphogenetic protein Type 1A receptor (BMPR1A) fusion protein increases bone formation and bone mass in a mice subjected to hindlimb unloading. Miranda Van Vliet*[1], Rachel Ellman[1], Daniel Grasso[1], Daniel Brooks[1], Christine Conlon[1], Jordan Spatz[2], Mary Bouxsein[1]. [1]Beth Israel Deaconess Medical Center, USA, [2]Harvard-MIT Division of Health Sciences & Technology (HST), USA

Previous work has shown that RAP661, a soluble murine BMPR1A–fusion protein, binds to BMP2/4 BMP2 and BMP4 with high affinity, preventing downstream signaling. Further, Baud'huin et al (PNAS 2012) showed that treatment of intact and ovariectomized mice with RAP661 led to increased bone mass, improved bone microarchitecture and strength, via increased bone formation and reduced resorption. In this study, we tested the effects of RAP661 on disuse-induced bone loss caused by 21 days of hindlimb unloading (HLU) via tail suspension vs. cage controls (CON). Adult female C57BL6/J mice (12 wks old) were assigned to one of four groups (n=10 each): CON-VEH; CON-RAP661; HLU-VEH; and HLU-RAP661. Mice were injected subcutaneously with VEH or RAP661 (4.5 mg/kg, Acceleron Pharma, Cambridge, MA) 2x/week for duration of study. Leg BMD declined in the HLU-VEH group (-5.3 $\pm$ 1.3%), whereas it was unchanged in HLU-RAP661 (-0.3 $\pm$ 0.9%, $p<0.05$ vs HLU-VEH). Additionally, leg BMD increased significantly more in CON-RAP661 than CON-VEH (10.2$\pm$0.6% vs 4.4$\pm$0.8%). In the femur, trabecular and cortical bone microarchitecture was worse in the HLU-VEH compared to CON-VEH mice, whereas RAP-661 treatment led to improved Tb.BV/TV, Tb.Th and midshaft Ct.Th in both the HLU and CON groups ($p<0.05$). In 3-pt bend testing, both CON and HLU animals treated with RAP661 showed either no change or increases in mechanical properties. Specifically, HLU-RAP661 had 21% greater failure load ($p<0.05$) compared to their VEH-treated counterparts. Dynamic histomorphometry indicated that treatment with RAP661 led to significant increases in mineralizing surface and mineral apposition rate, resulting in a 3.5-fold and 5-fold increase in bone formation rate in the RAP661-treated CON and HLU animals vs. VEH groups, respectively. RAP661-treated mice had a similar number of osteoblasts but significantly fewer osteoclasts than VEH-treated animals in both the CON and HLU groups. Altogether these findings suggest that treatment with the soluble BMPR1A fusion protein RAP661 may be useful for maintenance of skeletal integrity in the setting of disuse-induced bone loss.

Keywords: disuse, treatment, bone morphogenetic proteins, mechanical loading, hindlimb unloading, tail-suspension

***Disclosures: Miranda Van Vliet**, None.*
This study received funding from: Acceleron Pharma

FR0081

Cartilage-specific RUNX2 Activity Regulates Endochondral Bone Formation and Articular Cartilage Homeostasis. Jennifer Jonason[1], Donna Hoak*[1], Tzong-Jen Sheu[1], Fanxin Long[2], Regis O'Keefe[1], Matthew Hilton[3]. [1]University of Rochester, USA, [2]Washington University School of Medicine, USA, [3]University of Rochester Medical Center, USA

RUNX2 is a transcription factor critical for normal endochondral bone formation. *In vivo* and *in vitro* evidence suggest that RUNX2 is required for chondrocyte maturation and terminal differentiation. To date, however, *in vivo* studies have been limited to global deletion of *Runx2* or RUNX2 overexpression in chondro-osteoprogenitor cells preventing investigation of RUNX2 function solely in chondrocytes. Here, we examined the effects of RUNX2 gain-of-function (GOF) specifically in committed chondrocytes during endochondral bone development and in postnatal articular chondrocytes using the tamoxifen-inducible *Col2a1-CreER^{T2}* transgene in combination with *Rosa-Runx2^{flf}* alleles. Overexpression of RUNX2 was induced at E13.5 for all developmental studies and at P14 for all postnatal studies. Histological examination and in situ hybridization analyses of the humeri at E14.5 and E15.5 reveal an early onset of hypertrophy and terminal maturation in the RUNX2 GOF mutants compared to controls. By E15.5, the overall length of the mutant limbs is significantly shorter than that of the controls and by E18.5, the length of the mutant hypetrophic zone is decreased compared to controls suggestive of accelerated progression through terminal differentiation. Additionally, at E18.5, the RUNX2 GOF mutants have enhanced TUNEL staining indicative of increased chondrocyte apoptosis throughout all regions of the growth plate. Surprisingly, no histopathological signs of osteoarthritis (OA) are observed four months following induction of RUNX2 overexpression in postnatal animals. The amount of uncalcified cartilage is reduced, however, in the RUNX2 GOF mutants compared to controls and the number of hypertrophic chondrocytes in the calcified cartilage zone is increased. RUNX2 GOF articular cartilage exhibits decreased *Col2a1* and *Prg4* expression, however, there is no evidence of cartilage fibrillation, cell cloning, chondrophyte/osteophyte formation or subchondral bone sclerosis in these mice. This mild phenotype was unpredicted since it has been well documented that RUNX2 expression is increased in both mouse and human osteoarthritic cartilage and is a target of many signaling pathways known to be dysregulated in OA. Altogether, these data confirm a role for RUNX2 in chondrocyte maturation and terminal differentiation during endochondral bone development and in the maintenance of the articular cartilage, but suggest that overexpression of RUNX2 alone is insufficient to cause OA.

***Disclosures: Donna Hoak**, None.*

FR0083

Forkhead protein FoxC1 regulates chondrogenic genes expression by modulating Ihh/Gli2 signaling. Michiko Yoshida*[1], Kenji Hata[2], Sachiko Iseki[3], Teruko Takano-Yamamoto[4], Toshiyuki Yoneda[5], Riko Nishimura[2]. [1] Division of Orthodontics & Dentofacial Orthopedics, Graduate School of Dentistry, Tohoku University, Japan, [2]Osaka University Graduate School of Dentistry, Japan, [3]Section of Molecular Craniofacial Embryology, Graduate School, Tokyo Medical & Dental University, Japan, [4]Tohoku University, Japan, [5]Indiana University School of Medicine, USA

Endochondral ossification is a unique and complex biological event that is harmoniously and sequentially regulated by several transcription factors. However, the mechanism by which these transcriptional networks control endochondral ossification is still elusive. To address this, we attempted to identify a novel chondrogenic transcription factor(s) by performing gene-cloning by combination of mouse genetics and microarray. As a result, we isolated FoxC1 as a specific transcription factor in cartilage development. In situ hybridization analysis revealed a strong expression of FoxC1 in resting and proliferating chondrocytes. Mutations in FOXC1 cause Axenfeld-Rieger syndrome (ARS), which is associated with skeletal malformations including developmental delay and cleft palate. Furthermore, FoxC1 deficient mice showed impaired cartilage development. We therefore examined the effects of FoxC1 on the expression of chondrogenic genes. We found that FoxC1 overexpression in mouse primary chondrocytes up-regulated Ihh target genes such as PTHrP and Gli1. ChIP assay and DNA pull-down assay showed that FoxC1 directly bound to FoxC1 consensus binding site (CTAAATAAC) present in PTHrP and Gli1 gene promoter. Interestingly, FoxC1 enhanced PTHrP and Gli1 expression induced by Ihh or Gli2, an Ihh signaling transcriptional mediator. In contrast, dominant negative-Foxc1 inhibited expression of PTHrP, Gli1, Col10a1, Osx and ALP induced by Ihh. Co-immunoprecipitation experiment showed a physical interaction between FoxC1 and Gli2. Moreover, FoxC1 significantly increased the DNA binding of Gli2 to the Ihh target gene promoter as determined by ChIP assay. These data collectively suggest that FoxC1 controls expression of chondrogenic genes through stimulating Ihh/Gli2 function.

We next investigated the pathological role of *FOXC1* mutations using F112S mutant identified in ARS. F112S inhibited the transcriptional activity of wild-type FoxC1 and Ihh- dependent PTHrP expression. Of note, F112S retained binding activity to PTHrP gene promoter but lost the function interacting with Gli2. Consistently, F112S diminished Gli2 function compared with wild-type FoxC1. These data suggest the possibility that loss of functional interactions with Gli2 partially account for the pathophysiology of ARS caused by F112S mutation. In conclusion, FoxC1 regulates expression of chondrogenic genes in association with Gli2, and consequently modulates chondrogenic action of Ihh/Gli2 signaling.

***Disclosures: Michiko Yoshida**, None.*

FR0094

Sirt6 regulate proliferation and differentiation of the postnatal growth plate chondrocyte via Ihh signaling. Jinying Piao*[1], Kunikazu Tsuji[2], Hiroki Ochi[3], Morita Sadao[4], Daisuke Koga[5], Atsushi Okawa[5], Shu Takeda[6], Yoshinori Asou[2]. [1]Graduate School, Tokyo Medical & Dental University, Japan, [2]Tokyo Medical & Dental University, Japan, [3]Laboratory of Veterinary Microbiology, Nippon Veterinary & Life Science University, Japan, [4]Department of Rehabititation Medecine, Tokyo Medical & Dental Univrsity, Japan, [5]Department of Orthopedics Surgery, Tokyo, Medical & Detal University, Japan, [6]Keio University, Dept. of Nephrology, Endocrinology & Metabolism, Japan

Members of the sirtuin family of NAD-dependent deacetylases promote longevity in multiple organisms. Sirt6 null mice exhibit growth retardation, and aging-like phenotypes, including osteopenia and lordokyphosis. However, as Sirt6 null mice die young, the role of Sirt6 in cartilage metabolism is unclear. The aim of this study was to investigate the Sirt6 signal pathway in cartilage metabolism. Sirt6 gene was shown to be expressed in primary epiphyseal chondrocytes (EC) and the chondrocyte-like cell line ATDC5. At birth, Sirt6 null mice showed dwarfism. Two weeks after birth, growth retardation was more apparent in Sirt6-/-, with reduced proliferating zone and hypertrophic zone in the growth plate (GP), delayed ossification of secondary ossification center and decreased primary spongiosa. PCNA expression was reduced in GP chondrocytes in Sirt6-/- mice. When Sirt6 expression was knocked down by siRNA in vitro, mRNA expression of cyclin D1 and D2 was reduced in both EC and ATDC5 cells. In contrast, the expression of these genes was enhanced by overexpression of Sirt6 in ATDC5 cells. The number of TUNEL positive cells was comparable in GP between Sirt6-/- and littermates. Immunohistological analysis revealed the expression of Col2 and Col10 was reduced in GP with impaired expression of Indian hedgehog (Ihh) in Sirt6-/- mice. mRNA expression of these genes was also reduced in EC derived from Sirt6-/- mice. When Sirt6 was knocked down in EC and ATDC5 cells, the expression of Col2al, Col10a1, Ihh and its downstream genes were also reduced. We further examined the action of Sirt6 on chondrocyte biology using ATDC5 cells to determine the status of Hh signaling activity. Impaired expression of Col2a1 and Col10a1 by Sirt6 silencing was rescued by administration of purmorphamine, a Hh signal agonist. Conversely, the administration of nicotinamide mononucleotide, a key NAD+ intermediate, enhanced Col10a1 expression together with increased expression of Ihh and Gli1, and these effects were clearly cancelled by Sirt6 silencing. The effect of Sirt6 knockdown was partially ameliorated by activation of ATF4, the positive regulater of Ihh expression. ChIP assay using EC revealed that ATF4 binding to the Ihh promoter was markedly decreased by Sirt6 knockdown. In conclusion, Sirt6 directly controls proliferation and differentiation of chondrocytes. Furthermore, Sirt6 positively regulates chondrocyte differentiation via the ATF4 -Ihh axis.

***Disclosures: Jinying Piao**, None.*

FR0096

β-catenin Signaling Regulates Endochondral Ossification through Bmp2 Signaling. Jennifer Jonason[1], Yongchun Zhang*[1], Debbie Dao[2], Donna Hoak[1], Tzong-Jen Sheu[1], Matthew Hilton[3], Regis O'Keefe[1]. [1]University of Rochester, USA, [2]University of San Francisco, USA, [3]University of Rochester Medical Center, USA

The Wnt/β-catenin signaling pathway regulates endochondral bone formation and is essential for skeletal development. Genetic models using β-catenin gain-of-function (GOF) and loss-of-function (LOF) in mesenchymal progenitor cell populations have shown that β-catenin promotes osteoblast differentiation while inhibiting chondrogenesis. For this reason, the role of β-catenin signaling in committed chondrocytes during endochondral bone formation is only more recently emerging. The current studies used a tamoxifen-inducible *Col2Cre^{ERT2}* transgene in combination with *β-catenin$^{f(exon3)/+}$* and β-*catenin$^{f/f}$* alleles to induce chondrocyte-specific either β-catenin GOF and LOF following administration of tamoxifen at stage E13.5. In the gain of function model chondrocytes had increased expression of BMP-2 and the MAP3K TAK1. These mice had accelerated development of the secondary ossification center, early cartilage vascular canal formation, and enhanced perichondrial bone formation. The opposite phenotype was observed in the LOF model. *In vitro* assay shows that Bmp2 transcription and BMP-2 secretion are increased in the β-catenin GOF chondrocytes. The differentiation of osteoprogenitors was accelerated in co-cultures with β-catenin GOF chondrocytes further showing that chondrocyte secreted factors regulate bone formation. We also performed experiments *in vivo* to examine the potential role for chondrocyte β-catenin GOF in growth plate chondrocyte maturation, terminal differentiation and primary bone formation. In the growth plate, chondrocyte β-catenin GOF resulted in delayed terminal chondrocyte differentiation and reduced formation of the primary medullary bone center. To examine a potential role of non-canonical BMP signaling, β-catenin GOF chondrocytes were crossed with TAK1$^{f/f}$ mice. We observed partial rescue of the delayed chondrocyte terminal differentiation. Altogether our findings suggest that β-catenin expression in chondrocytes has important effects on the terminal differentiation of chondrocytes. Furthermore, we show that the effects are context specific with acceleration of terminal differentiation in the secondary center and delay in the growth plate.

***Disclosures: Yongchun Zhang**, None.*

FR0104

CCN3 Participates in Bone Regeneration as an Inhibitory Factor. Yuki Matsushita*[1], Kei Sakamoto[1], Kiyoshi Harada[1], Tokutarou Minamizato[2], Akira Yamaguchi[1]. [1]Tokyo Medical & Dental University, Japan, [2]Graduate School of Biomedical Science, Nagasaki University, Japan

To explore the expression profile of genes involved in bone regeneration, we conducted microarray analysis using a bone regeneration model in mice, and identified CCN3 as one of the most upregulated genes at the early stage of bone regeneration. CCN3 is a matricellular protein that belongs to the CCN family of genes. CCN3, a member of the CCN protein family, inhibits osteoblast differentiation *in vitro*. However, the role of CCN3 in bone regeneration has not been well elucidated. In this study, we investigated the role of CCN3 in bone regeneration. We identified *Ccn3* gene by microarray analysis as a highly expressed gene at the early phase of bone regeneration in a mouse bone regeneration model. We confirmed the upregulation of *Ccn3* at the early phase of bone regeneration by RT-PCR, western blot, and immunofluorescence analyses. *Ccn3* transgenic mice, in which *Ccn3* expression was driven by 2.3-kb *Col1a1* promoter, showed osteopenia compared with wild-type mice, but *Ccn3* knockout mice showed no skeletal changes compared with wild-type mice. We analyzed bone regeneration process in *Ccn3* transgenic mice and *Ccn3* knockout (KO) mice by microcomputed tomography and histological analyses. Bone regeneration in *Ccn3* KO mice was accelerated compared with that in wild-type mice. The mRNA expression levels of osteoblast-related genes (*Runx2, Sp7, Col1a1, Alpl, Bglap*) in *Ccn3* KO mice were upregulated earlier than those in wild-type mice, as demonstrated by RT-PCR. Phosphorylation of Smad1/5 was highly upregulated at bone regeneration sites in *Ccn3* KO mice compared with wild-type mice. The number of CFU-Alpl significantly increased in cultures of *Ccn3* KO mice compared with that in wild-type mice, suggesting that the number of osteoprogenitors was greater in the bone marrow of *Ccn3* KO mice than that of wild-type mice. Bone regeneration in *Ccn3* transgenic mice showed no significant changes compared with that in wild-type mice. Collectively, the present study demonstrates that CCN3 appears at an early stage of bone regeneration, and that it participates in bone regeneration as an inhibitory factor. These results indicated that the use of counteracting agents against CCN3 is a potential strategy to develop new bone regeneration therapies.

***Disclosures: Yuki Matsushita**, None.*

FR0109

Loss of the E3 Ubiquitin Ligase Von Hippel Lindau (VHL) in Limb Bud Mesenchyme causes dwarfism and tumors of the soft tissue. Laura Mangiavini*[1], Christophe Merceron[2], Tremika Leshan Wilson[1], Rita Gerard-O'Riley[1], Amato J Giaccia[3], Ernestina Schipani[1]. [1]Indiana University School of Medicine, USA, [2]Indiana University School of Medicine; Inserm, UMRS 791-LIOAD, Centre for Osteoarticular & Dental Tissue Engineering, Group STEP ''Skeletal Tissue Engineering & Physiopathology'', Nantes, France, USA, [3]Stanford University, USA

Adaptation to low oxygen tension is a critical event in fetal development. The hypoxia inducible factor-1 (HIF-1) and HIF-2 are essential mediators of the homeostatic responses that allow hypoxic cells to survive and differentiate. Our working hypothesis is that gradients of oxygen control organ size and shape during development by regulating the HIF signaling pathway. Along these lines, we have demonstrated that HIF-1 is an indispensable survival and differentiation factor for fetal chondrocytes, whereas HIF-2 is not necessary for fetal growth plate development. VHL is the E3 ubiquitin ligase that targets HIFs to the proteasome for degradation in normoxia, and it is also a tumor suppressor gene. In this study we analyzed the role of VHL in the context of endochondral bone formation.

We conditionally deleted VHL in whole limb bud mesenchyme by using the Cre-loxP system. Mutant mice were born with the expected mendelian frequency, but they died three-four weeks later. Prenatally, mutant cartilaginous elements lacking VHL were short and misshapen. This phenotype was due, at least in part, to a delayed transition from proliferation to hypertrophy, and from hypertrophy to bone marrow cavity formation. Moreover, chondrocyte proliferation rate was impaired.

Postnatally, VHL deficient chondrocytes underwent massive cell death that eventually caused to the collapse of the growth plate, and was paradoxically associated to a dramatic increase of trabecular bone, expansion of the bone marrow stroma and dilated bone marrow blood vessels.

In addition, VHL deficiency caused massive fibrosis in the synovial space associated to partial destruction of articular surface cartilage. More strikingly, in about 70% of the analyzed mice, loss of VHL led to the formation of fibroblastic

tumors of the soft tissue, which aggressively invaded and destroyed the surrounding cartilaginous, muscular and bony structures.

In double mutant mice lacking both VHL and HIF-2 in limb bud mesenchyme, synovial fibrosis was partially corrected; though fibroblastic tumors were still detectable in at least 46% of the cases. Conversely in VHL/HIF-1 double mutants, these tumors were no longer present.

Taken together, our findings demonstrate that loss of VHL in mesenchymal cells controls size and shape of the skeletal elements, and its loss causes HIF-1 dependent aggressive fibroblastic tumors of the soft tissue.

***Disclosures: Laura Mangiavini**, None.*

FR0113

Osteonectin/SPARC Single Nucleotide Polymorphism (SNP) Alters Trabecular Bone and is Targeted by miRNA-433. Neha Dole*[1], Kristina Kapinas[2], Catherine B Kessler[1], Anne Delany[1]. [1]University of Connecticut Health Center, USA, [2]University of Massachusetts, Worcester, USA

Osteonectin is an extracellular matrix protein that regulates collagen fibril organization and promotes osteoblast differentiation and survival. Osteonectin-null and haploinsufficient mice are osteopenic. Genetic factors impact bone mass, and polymorphisms in selected genes involved in bone remodeling have been associated with bone density. Previously, haplotypes consisting of 3 SNPs in the 3' untranslated region (UTR) of osteonectin, at cDNA bases 1046C/G, 1599G/C and 1970T/G, were associated with bone mass in a cohort of men with idiopathic osteoporosis. Specifically, haplotype A (1046C_1599G_1970T) was found at a higher frequency in severely affected osteoporosis patients, whereas haplotype B (1046C_1599C_1970T) was found at a higher frequency in less affected patients and healthy controls. We postulated that SNPs in the osteonectin 3' UTR modulate its expression and may affect bone mass.

To determine whether SNPs affected gene expression, Luciferase reporter constructs containing 6 different human osteonectin 3' UTR haplotypes were transfected into hFOB1.19 cells (human fetal osteoblast cell line). Constructs containing haplotype A had the lowest reporter gene expression, whereas constructs containing haplotype B had higher expression. Since the difference between haplotypes A and B is SNP 1599G/C, our results suggest that SNP 1599G, in haplotype A, could decrease osteonectin expression and may impact bone mass.

We found that SNP 1599 was within a potential binding site for microRNA (miR)-433. In hFOB1.19 cells transfected with haplotype A or B reporter constructs and miR-433 inhibitor, an increase in luciferase activity was observed for the haplotype A construct, but not for haplotype B. This suggests that 1599G, in haplotype A, allowed targeting of osteonectin by miR-433, whereas 1599C, in haplotype B, interfered with miR-433 targeting.

To determine whether the SNP at 1599 could affect skeletal phenotype in vivo, we replaced the mouse osteonectin 3' UTR with the human osteonectin haplotype A or B 3' UTR, using a knock-in strategy. Western blot analysis demonstrated that long bones from haplotype A mice had 3 fold less osteonectin compared with haplotype B. Preliminary microCT data suggest that trabecular thickness in the femur of haplotype A mice is less than that in haplotype B. Overall, SNP 1599 in the osteonectin 3' UTR regulates its expression and affects trabecular bone. miR-433 targeting of osteonectin likely plays a role in this process.

***Disclosures: Neha Dole**, None.*

FR0118

The Novel Interplay of Anemia and Hypoxia in the Control of FGF23 Expression. Erica Clinkenbeard*[1], Taryn Cass[2], Tim Lahm[3], Mircea Ivan[3], Kenneth White[4]. [1]Indiana University-Purdue University Indianapolis, USA, [2]Department of Medical & Molecular Genetics, Indiana University, USA, [3]Department of Medicine, Indiana University, USA, [4]Indiana University School of Medicine, USA

Patients with autosomal dominant hypophosphatemic rickets (ADHR) carry either R176Q/W or R179Q/W mutations within the FGF23 $_{176}$RXXR$_{179}$/S$_{180}$ proteolytic cleavage motif, resulting in the stabilization of the bioactive hormone. We previously found that hypophosphatemia with elevated FGF23 can be induced through iron deficiency anemia in ADHR knock-in mice, which parallels the late onset disease observed in some ADHR patients. Low iron can cause hypoxic responses due to decreased oxygen delivery, leading to activation of hypoxia inducible factor 1 (HIF1α) and adaptive changes in gene expression. We now show that during iron deficiency, erythropoietin (EPO), a known HIF target, was significantly up-regulated in ADHR and WT mice, and rats placed in a hypobaric chamber for two weeks maintained normal iron, but had increased serum total FGF23 (6-fold; $p<0.05$). Based upon these data, we hypothesized that during anemia/hypoxia, FGF23 is stimulated via a common pathway involving HIF1α. By chelating iron with deferoxamine (DFO) in UMR106 cells, HIF1α protein increased and translocated to the nucleus. This activation in UMR106 and also in U2OS cells, coincided with 6-fold and 3-fold increases in FGF23 ($p<0.05$) and VEGF mRNAs, respectively. To determine whether cis-regulatory elements were responsible for induction of FGF23, the FGF23 promoter was cloned into a luciferase vector (FGF23-pGL4). Cotransfection of this construct with a constitutively active HIF1α increased luciferase activity versus controls: 4-fold in UMR106 ($p<0.001$); 5-fold in U2OS ($p=0.003$); and 8-fold in HEK293 ($p=0.02$) cells. Further, HIF1α knockdown using both siRNA and shRNA prevented the accumulation of cellular HIF1α protein upon treatment with DFO. In HIF1α knockdown cells, or upon transfection of an FGF23 promoter construct with targeted mutation of proximal HIF response elements (native: 5′-[A/G]CGTG-3′ to: 5′-CAATG-3′), DFO- or HIF1α-dependent FGF23 expression was abolished. In summary, our data demonstrate that FGF23 expression increases during anemia/hypoxia are downstream of HIF1α activation. Taken together, these findings provide a novel mechanism for FGF23 induction arising in rare and potentially in common disorders of phosphate metabolism.

***Disclosures: Erica Clinkenbeard**, None.*

FR0119

Characterization of FGF23-dependent Egr-1 Cistrome in the Mouse Renal Proximal Tubule. Martin Zhang, Anthony Portale, Farzana Perwad*. University of California San Francisco, USA

The transcription factor, early growth response 1 (egr-1), is a biomarker for activation of the extracellular signal regulated kinase 1/2 (ERK1/2) signaling pathway by fibroblast growth factor 23 (FGF23). In the *Hyp* mouse, ERK1/2 signaling is constitutively activated by excess circulating FGF23. We and others have shown in *Hyp* mice that blockade of FGF23-dependent ERK1/2 signaling suppresses egr-1 expression, improves hypophosphatemia,and reverses1,25-dihydroxyvitamin D ($1,25(OH)_2D$) deficiency. To test whether egr-1 itself mediates the renal phosphaturic response to FGF23, we administered FGF23 to egr-1 null and normal mice. In mice lacking egr-1 expression, the hypophosphatemic response to FGF23 was blunted by 78% when compared to FGF23-treated normal mice. Using genome-wide chromatin-immunoprecipitation (ChIP) and sequencing, we demonstrated rapid binding of egr-1 to regulatory DNA elements in the kidney of FGF23-treated normal mice. We identified egr-1 binding to 8,708 specific genomic regions (active regions) that were unique in FGF23-treated mice compared with 114 active regions in vehicle-treated mice. Using in-depth *in silico* analysis, specific active regions were assigned to several genes responsible for sodium-dependent phosphate (Na/Pi) cotransport (*Npt2a, Npt2c, NHERF1, NHERF2*) and for $1,25(OH)_2D$ metabolism (*cyp27b1,cyp24a1,Vdr*). Binding of egr-1 protein to these specific active regions occurred only in FGF23-treated mice. These data suggest that the phosphaturic effect of FGF23 is mediated, atleast in part, by activation of the transcription factor, egr-1. Thus, we have identified novel FGF23-dependent egr-1 cistromes associated with specific genes that mediate Na/Pi cotransport and $1,25(OH)_2D$ synthesis in the kidney.

***Disclosures: Farzana Perwad**, None.*

FR0120

Genetic Rescue of Glycosylation-deficient Fgf23 in the Galnt3-null Mouse. Shoji Ichikawa*[1], Amie Gray[1], Erica Clinkenbeard[2], Kenneth White[1], Michael Econs[1]. [1]Indiana University School of Medicine, USA, [2]Indiana University-Purdue University Indianapolis, USA

Fibroblast growth factor 23 (FGF23) is a peptide hormone that inhibits renal reabsorption of phosphate and biosynthesis of 1,25-dihydroxyvitamin D. The subtilisin-like proprotein convertase recognition sequence (^{176}RHTR$^{179}\downarrow$) in FGF23 is protected by *O*-glycosylation through activity of ppGalNAc-T3 (GALNT3). Thus, inactivating GALNT3 mutations make mature FGF23 more susceptible to proteolysis, thereby reducing levels of circulating intact hormone and leading to hyperphosphatemic familial tumoral calcinosis.

However, it is unknown whether glycosylation is only necessary for FGF23 secretion or also affects FGF23 activity. To delineate the role of glycosylated Fgf23, we used two mutant mice for the present study: Galnt3 knockout mice, a model of familial tumoral calcinosis, and autosomal dominant hypophosphatemic rickets (ADHR) knock-in mice carrying a human ADHR FGF23 mutation (R176Q). The two lines of mice were crossed to generate five genotypes: wild type, Galnt3 knockout mice, ADHR mutant mice, and ADHR/Galnt3 double mutant mice that are Galnt3 null and either heterozygous or homozygous for the R176Q ADHR mutation.

Compared to same-sex wild-type controls, serum intact Fgf23 was significantly lower in all mice lacking Galnt3, regardless of Fgf23 genotype; however, Fgf23 levels were not affected in the ADHR mutant mice with normal Galnt3. In contrast to intact Fgf23 levels, total Fgf23 production at the mRNA and protein (13-16 fold) levels were significantly higher in Galnt3 knockout mice with wild-type Fgf23 alleles. However, the increase in total Fgf23 protein was almost completely normalized in the ADHR/Galnt3 double mutants (1-2 fold). Serum phosphorus levels were higher in Galnt3 knockouts, but lower in ADHR mutant mice. Interestingly, serum phosphorus levels in ADHR/Galnt3 double mutant mice remained normal even with lower intact Fgf23.

Thus, the Fgf23 ADHR mutation biologically 'cancelled out' the need for glycosylation by Galnt3 in vivo and was sufficient to maintain normal phosphorus levels in the absence of Galnt3, suggesting that glycosylation is only necessary for proper secretion of Fgf23. Furthermore, the ability of ADHR mutant mice to regulate phosphorus with less intact Fgf23 suggests that the mutant protein may be more potent.

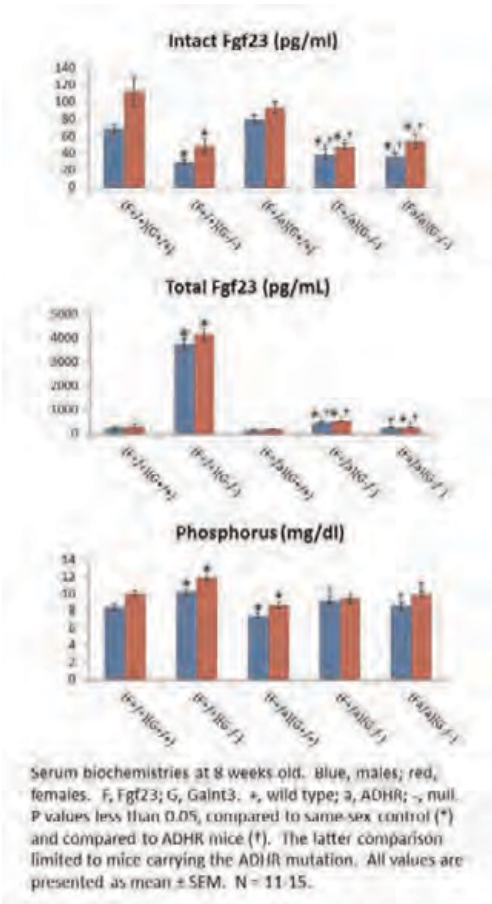

Figure

***Disclosures: Shoji Ichikawa**, None.*

FR0121

Phosphate Restriction Extends the Life of Uremic Rats with Established Vascular Calcification. Eduardo Slatopolsky[1], Jane Finch*[2], Sarah Zhang[2], Helen Liapis[2], Cynthia Ritter[2]. [1]Washington University in St. Louis School of Medicine, USA, [2]Washington University School of Medicine, USA

Numerous studies have demonstrated the role of hyperphosphatemia in the pathogenesis of secondary hyperparathyroidism, cardio-vascular disease and the progression of renal failure. The purpose of this study was to determine if, in rats with chronic kidney disease (CKD) and severe vascular calcification, a significant reduction in phosphate intake could prolong the life of these animals. CKD was induced by 5/6th nephrectomy. A group of normal rats served as control (NC). All rats were fed a high phosphate diet containing 1.4% phosphorus (P) and 0.8% calcium (Ca). After 3 months, a portion of rats from both groups were sacrificed. Compared to NC rats, the serum P in uremic rats increased from 5.9 $\pm$ 0.34 to 10.3 $\pm$ 0.76 mg/dl; the Ca x P increased from 56.7 to 94.3 mg^2/dl^2. Aortic calcium content also increased from 0.5 $\pm$ 0.06 (NC) to 46.2 $\pm$ 14.2 mg/mg dry wt (uremic). Uremic rats also exhibited positive aortic staining for von Kossa, RUNX2 and osteopontin. The remaining uremic rats were divided into the following 3 groups: uremic+1.4%P diet (UHP-6M); uremic+1.4%P+4%sevelamer (a phosphate binder; UHP+Sev); and uremic+a very low P diet (0.1%P, 0.3%Ca; ULP). After 3 additional months, the serum P in the UHP-6M group was 12 $\pm$ 1.35 vs 6.96 $\pm$ 0.82 (UHP+Sev), 3.69 $\pm$ 0.23 (ULP) and 3.9 $\pm$ 0.3 mg/dl (NC-6M). Mortality in the UHP group was 71.4%, and was reduced to 37.5% by treatment with sevelamer, and further reduced to 5.9% by the low P diet. Positive staining for aortic von Kossa, RUNX2 and osteopontin was increased in UHP-6M rats. P-restriction inhibited this. PTH decreased from 6574 $\pm$ 1641(UHP) to 289 $\pm$ 70 pg/ml in the ULP rats. FGF-23 also decreased from 22,244 $\pm$ 4049 (UHP) to 1079 $\pm$ 162 pg/ml (ULP). Cardiac perivascular fibrosis, cardiomyocyte size were significantly reduced by the low phosphate diet. In addition, glomerulosclerosis, renal interstitial fibrosis and severe interstitial inflammation were also greatly reduced in rats on the low phosphate diet compared to the high phosphate diet. These studies clearly demonstrate that a significant reduction in mortality in uremic rats with severe vascular calcification can be achieved by intensive control of phosphate restriction.

***Disclosures: Jane Finch**, Genzyme/Sanofi, 6*
This study received funding from: Genzyme/Sanofi

FR0125

Role of PTH/PTHrP Receptor Signaling in Osteocytes in Ovariectomy-Induced Osteopenia. Jenna Garr*[1], Dean Marengi[1], Vaibhav Saini[2], Xiaolong Liu[1], Paola Divieti Pajevic[3]. [1]Massachusetts General Hospital, USA, [2]MGH, Harvard Medical School, USA, [3]Massachusetts General Hospital & Harvard Medical School, USA

Over 200 million women worldwide suffer from post-menopausal osteoporosis; understanding the cellular and molecular mechanisms of this disease will aid development of better treatments. Parathyroid Hormone (PTH), an endogenous regulator of skeletal homeostasis, is the only FDA-approved anabolic agent to treat osteoporosis. Using microCT and histomorphometric analyses, we previously reported that mice lacking PTH receptor (PTHR1) expression in osteocytes (OcyPPRKO) have a significant increase in trabecular and cortical bone parameters as compared with control at 12 weeks of age. Moreover, when subjected to intermittent or continuous PTH injections, OcyPPRKO failed to display anabolic or catabolic effects, respectively. To investigate the role of PPR signaling in osteocytes in ovariectomy-induced osteopenic mice, ovariectomy (OVX) was performed on 10-week-old OcyPPRKO and control females. The skeletal phenotype of OcyPPRKO was compared to control at two and four weeks post OVX. MicroCT analysis of the distal femur showed a significant decrease in trabecular bone following OVX in both OcyPPRKO and control mice, as compared to sham-operated. These results indicate that PTHR1 signaling in osteocytes does not play a role in OVX-induced osteopenia. As expected, cortical parameters were not changed in either group following OVX. To investigate the role of PTHR1 signaling in osteocytes in the anabolic effect of PTH, we subjected OcyPPRKO and control OVX groups to intermittent PTH administration. Briefly, mice were injected daily with 80 ug/Kg hPTH(1-34) for 4 weeks. At the end of the treatment period, bones were collected and analyzed both histologically and by microCT. Interestingly, PTH induced an anabolic response, as assessed by a significant increase in BV/TV%, conn-density and Tb thickness, in both control and OcyPPRKO mice. Our data suggest that the mechanism of action of PTH in the setting of OVX-induced osteopenia is distinct from its anabolic effect in gonadal-intact animals. Further studies are ongoing to elucidate the cellular and molecular mechanisms of the anabolic effects of PTH.

***Disclosures: Jenna Garr**, None.*

FR0126

EphrinB2 reverse signaling in osteoblasts is required for normal bone material strength and increased bone formation in response to parathyroid hormone (PTH). Farzin Takyar[1], Christina Vrahnas[1], Stephen Tonna[1], Blessing Crimeen-Irwin[1], Patricia Ho[1], T J Martin[1], Natalie Sims*[2]. [1]St. Vincent's Institute, Australia, [2]St. Vincent's Institute for Medical Research, Australia

PTH stimulates osteoblastic expression of ephrinB2, and pharmacological inhibition of its interaction with EphB4 impairs late stage osteoblast differentiation. EphrinB2/EphB4 signals can occur in two directions and it remains unknown whether the effect of this interaction is mediated by ephrinB2 (reverse) or EphB4 (forward) signaling. Osteoblastic EphB4 signaling may also inhibit osteoblast differentiation due to activation by ephrinB2 expressed in the osteoclast lineage. To define the role of osteoblastic ephrinB2 signaling in bone formation we assessed the response to anabolic PTH in mice with osteoblast-specific deletion of the ephrinB2 signaling domain (Osx1Cre+EfnB2f/f) compared to littermate controls.

8-week-old male Osx1Cre+EfnB2f/f and control mice (n=7-12) were treated with PTH (30μg/kg; 5x/week) or vehicle for 4 weeks and samples, including flushed femora for RNA analysis, were collected 1 hr after the last injection. Femora were analyzed by microCT, quantitative real time PCR and reference point indentation; tibiae were analyzed by dynamic histomorphometry.

In untreated mice, while osteoblast numbers were not significantly altered in Osx1Cre+EfnB2f/f mice compared to controls, collagen1α1 and runx2 mRNA levels were significantly higher in Osx1Cre+EfnB2f/f femoral cortical bone compared to controls (2-fold and 6-fold, respectively). Conversely, mRNA levels of osteocalcin and sclerostin were significantly lower (both <50% of control) confirming a block in osteoblast differentiation, as previously reported in female Osx1Cre+EfnB2f/f mice. In addition, cortical thickness, cortical tissue mineral density and bone material stiffness were all significantly lower (each by ~10%, $p<0.05$) in OsxCre+EfnB2f/f mice compared to controls.

PTH treatment of control mice significantly increased osteoblast surface (by 244%), increased trabecular and periosteal mineral apposition rates (by 26% and 96%), and decreased sclerostin mRNA levels (to <50%), as expected. However, in Osx1Cre+.EfnB2f/f mice, the PTH-induced increase in osteoblast surface was significantly reduced to 50% of that observed in control mice. No increase in periosteal or trabecular MAR was observed in Osx1Cre+EfnB2f/f mice, nor was any reduction in sclerostin mRNA detected.

These data indicate that ephrinB2 reverse signaling is required for normal cortical growth, and that PTH-induced osteoblast differentiation and mineralization requires ephrinB2 reverse signaling within the osteoblast lineage.

***Disclosures: Natalie Sims**, None.*

FR0153

Pdlim7 (LMP) Knock-Out Mice Display a Significant Decrease in Trabecular Bone Volume. Manjula Viggeswarapu*[1], Matthew Gary[2], Colleen Oliver[3], Mesfin Teklemariam[4], Sreedhara Sangadala[1], F. Louisa Titus[5], Scott. D. Boden[6]. [1]Emory University School of Medicine, USA, [2]Department of Neurosurgery, Emory University, USA, [3]VA Medical Center, USA, [4]Department of Orthopaedics, Emory University, USA, [5]VA Medical Center, Decatur, USA, [6]Department of Orthopaedics, Emory University School of Medicine, USA

Rat and human LMP-1 were described by our group as osteoinductive proteins whose overexpression induces bone formation in rats and rabbits and enhances BMP-2 efficacy in vitro. In order to understand the systemic role of LMP during development and maturation, Knock-out (KO) mice were generated using ES cell technology. To characterize the skeletal phenotype, mice were sacrificed at 18 or 26 weeks. Weight and height were measured at euthanasia. Cardiac puncture was performed to obtain serum for analysis of serum chemistry. To assess trabecular and cortical bone structure we analyzed femurs and spines from WT, Heterozygous (Het) and KO LMP mice by micro computed tomography. In vitro osteoblastogenesis was performed using whole bone marrow stromal cells (BMSCs) from femurs of WT, Het and KO LMP mice.

The LMP KO mice weighed significantly less at 18 and 26 weeks-old and were shorter in length at 18 weeks-old compared to their WT counter parts (p= 0.001). Compared to WT, 18 week female KO mice, had a significant decrease in trabecular BV of 25% (p=0.04) and Tb.Th of 11% (p=0.02); there was a trend for decreased trabecular BV/TV of 23% (p=0.06) and cortical volume of 6% (p=0.06). In the 26 week female KO mice, there was a decrease in the trabecular BV of 45% (p=0.001), BV/TV of 41% (p=0.001), and Th.N. of 9% (p=0.04) and cortical volume of 8% (p=0.001). At the spine, the 26 week Female KO mice, had a significant decrease in vertebral trabecular BV/TV of 25% (p=0.001) and Tb.Th of 8% (p=0.005) in the KO mice. In the male KO mice, there was no statistically significant difference in any of the analyses of the femora or vertebrae at 18 or 26 weeks. The 26 week KO mice had normal serum chemistries; serum turnover markers were unchanged compared with WT. BMSC cultures from 18 week Het mice grown under osteogenic conditions formed a reduced area of mineralization (AOM) compared with cells from WT mice (p=0.04); cells from KO mice also formed less AOM.

We present here the development of the first LMP KO mouse. We conclude that LMP is an important determinant of mouse weight and length, female bone density and marrow stromal cell propensity for mineralization. We speculate that these may be due to altered responsiveness to BMP-2, an important determinant during development. Further research is needed to elucidate other phenotypic differences as well as to determine the mechanism causing the reduced body size and gender specific bone loss of LMP KO mice.

***Disclosures: Manjula Viggeswarapu**, None.*

FR0154

SH3BP2 "Cherubism" Gain-of-Function Mutation Exacerbates Inflammation and Bone Erosion in Murine Collagen-Induced Arthritis Model. Tomoyuki Mukai*[1], Shu Ishida[1], Teruhito Yoshitaka[2], Yoshitaka Morita[3], Keiichiro Nishida[4], Yasuyoshi Ueki[2]. [1]University of Missouri - Kansas City, USA, [2]University of Missouri-Kansas City, School of Dentistry, USA, [3]Kawasaki Medical University, Japan, [4]Okayama University, Japan

SH3BP2 is a signaling adapter protein in which gain-of-function mutations result in cherubism. Cherubism is an autosomal dominant craniofacial disorder in children characterized by the extensive growth of fibrous lesions containing a large number of TRAP-positive multinucleated cells, resulting in facial swelling and jaw bone destruction. Analysis of the mouse model of cherubism demonstrated that homozygous mutants exhibit TNF-α-dependent inflammatory bone destruction in joints due to enhanced TNF-α production in macrophages as well as to increased RANKL-induced osteoclastogenesis. However, it remains unclear whether SH3BP2 is involved in the pathogenesis of other common forms of inflammatory bone diseases than cherubism. In this study, we examined the role of SH3BP2 gain-of-function mutation in the development of arthritis using murine collagen-induced arthritis (CIA) model. Wild-type (WT) and SH3BP2 "cherubism" mutation heterozygous knock-in (KI/+) mice on C57BL/6 background were immunized with chicken type II collagen in complete Freund's adjuvant. Clinical arthritis scores (max=16) were evaluated by visual inspection of the paws up to 56 days. Synovial inflammation and bone erosion were evaluated by histological analysis. To analyze focal bone erosion and systemic bone loss, bone properties of talus and proximal tibia were examined by micro CT. The incidence of arthritis was increased in KI/+ mice compared to WT mice (50.0% vs. 27.3%, n=10–11). Arthritis score in KI/+ mice was higher than WT mice (7.20 ± 4.09 vs. 4.33 ± 0.58 at day 28). The higher arthritis score in KI/+ mice continued toward the end of inspection (8.00 ± 4.00 vs. 1.00 ± 1.73 at 56 days). Histological analysis showed that synovial inflammation and bone erosion in KI/+ mice were more severe than those in WT mice. Micro CT analysis revealed that bone volume reduction of talus in KI/+ was greater than that in WT mice (6.81 ± 8.85% and 1.73 ± 3.34% reduction from control mice of each genotype, respectively). Furthermore, bone volume/tissue volume of tibia was more reduced in KI/+ compared with WT (57.9 ± 15.0% and 23.8 ± 19.0% reduction from control mice of each genotype, respectively). Taken together, gain-of-function mutation in SH3BP2 increased the incidence and severity of arthritis accompanied by more severe bone destruction in murine CIA model. These data suggest a potential role of SH3BP2 in the pathogenesis of common inflammatory bone diseases such as rheumatoid arthritis.

***Disclosures: Tomoyuki Mukai**, None.*

FR0155

In Vivo Pharmacologic Modulation of Bone Marrow Microenvironmental Signals Promotes Long-Term Hematopoietic Stem Cell Function. Julianne Smith*[1], Alexandra Goodman[2], Laura Calvi[1]. [1]University of Rochester School of Medicine, USA, [2]University of Rochester School of Medicine & Dentistry, USA

Osteolineage cells (OBs) and the bone marrow (BM) vasculature constitute hematopoietic stem and progenitor cell (HSPC) niches. We previously demonstrated that OB-activation by Parathyroid Hormone (PTH) expands HSPCs. To test if the vasculature is also modulated by PTH, we assessed whether PTH expands BM endothelial structures. In a murine model of intermittent PTH treatment, PTH increased microvessels and vascular area in hindlimb BM as well as CD31+ Sca1+ BM endothelial cells (ECs). This PTH effect is OB-dependent since ECs were increased in transgenic mice with osteoblastic activation of the PTH receptor. PTH increased expression of the proangiogenic signal VEGF-A in OBs in vitro and strongly increased VEGF-A protein within endosteal cell populations in vivo. To determine the functional relevance of VEGF-A signaling in PTH-dependent microenvironmental activation and HSPC regulation, we used the anti-VEGF-A monoclonal antibody bevacizumab (αVEGF) in combination with PTH in vivo. αVEGF significantly decreased the PTH-mediated expansion of ECs, restoring it to control, without blocking the bone anabolic action of PTH, suggesting that PTH-dependent EC expansion in the BM is VEGF-A mediated. Surprisingly, αVEGF further increased the PTH-induced expansion of phenotypic and functional BM HSPCs. This effect persisted and was further enhanced by secondary transplantation. To examine whether co-administration of PTH and αVEGF expands long term HSPCs at the expense of hematopoietic progenitor and precursor maturation, acute hematopoietic recovery from chemotherapeutic injury was measured. The peripheral blood of PTH and αVEGF treated mice recovered similarly to that of controls and was restored to normal levels, suggesting no impairment of the short term HSPC compartment. Together our data demonstrate that blocking VEGF-A in PTH-initiated vascular remodeling enhances expansion of long-term HSPCs. Both fibroblast growth factor 2 (FGF2) and VEGF-A are proangiogenic signals involved in bone remodeling. VEGF-A promotes endothelial sprouting and permeability while FGF2-stimulated blood vessels are less cell-permeable. Moreover, FGF2 is reported to expand marrow HSPCs. PTH simultaneously increased FGF2 and VEGF-A in OBs in vitro. We speculate that αVEGF therapy permits dominance of PTH-induced FGF2 actions leading to preferential long-term HSPC expansion. These data also demonstrate the validity of niche manipulation for therapeutic targeting of specific HSPC subsets.

***Disclosures: Julianne Smith**, None.*

FR0156

EphrinB2/EphB4 Mediates the Actions of IGF-I Signaling in Regulating Vascularization during Endochondral Bone Formation. Yongmei Wang*[1], Alicia Menendez[2], Chak Fong[3], Daniel Bikle[4]. [1]Endocrine Unit, University of California, San Francisco/VA Medical Center, USA, [2]Endocrine Unit, University of California, San Francisco/San Francisco VA Medical Center, USA, [3]Endocine Unit, University of California, San Francisco/San Francisco VA Medical Center, USA, [4]Endocrine Research Unit, Division of Endocrinology UCSF & VAMC, USA

Ephrin B2 and its receptor EphB4 are critical in regulating vessel morphogenesis as well as mediating osteoblast (OB) and osteoclast differentiation and communication. Our previous studies demonstrated that both global insulin-like growth factor-I (IGF-I) knockout (KO) mice and cartilage-specific IGF-I receptor (IGF-IR) KO mice had impaired vascular invasion during endochondral bone formation, but the mechanism remained unknown. In the current study, we investigated the role of IGF-I signaling in regulating the vascularization process in endochondral bone formation with particular attention to the role of ephrin B2/EphB4.

Immnohistochemical localization demonstrated that ephrin B2 was expressed in the endothelial cells and pericytes in the vessels in the long bones. IGF-I treatment (50 mg/kg BW/day, 2 weeks) increased the number of vessels and the expression of ephrin B2 in the vessels of the chondro-osseous junctions in the tibia of wild-type mice (WT, 12W). In the global IGF-I KO mice, the expression of ephrin B2 was significantly decreased in the vessels of the tibia when compared to the WTs. To further investigate the role of IGF-I signaling in regulating vascularization, we generated mice with IGF-IR null mutation in the prehypertrophic chondrocytes (PHC), osteoprogentors and perichondium (osxIGF-IRKO, floxed IGF-IR mice X osterix promoter driven cre-recombinase). Histology showed that osxIGF-IRKO (3W) had delayed secondary ossification center (SOC) formation and fewer vessels in the (SOC) and chondro-osseous junctions in the tibia compared to controls. This was further confirmed by immunohistochemistry (IHC) using an antibody against CD31. IHC further showed

that ephrin B2 was expressed in chondrocytes, OBs, endothelial cells and pericytes in the tibia of the controls, but the expression was abolished in the tibia of the osxIGF-IRKO as was that of VEGF in these cellsThese results were confirmed by qRTPCR demonstrating that the mRNA (long bones, marrow flushed out) levels of ephrin B2 and EphB4 were significantly decreased in the osxIGF-IRKO (45% and 42% of the control, respectively). Our data indicate that IGF-I signaling in PHC, osteoprogenitors and perichondrium stimulates ephrin b2 production, which in turn to promotes vascularization in the primary and secondary ossification centers during endochondral bone formation.

***Disclosures: Yongmei Wang**, None.*

FR0157

IGF-I – Estrogen Cross Talk is Essential for Cortical Bone Response to Mechanical Loading in Mice. Bhat Chetan*[1], Subburaman Mohan[2], Jon Wergedal[2], Chandrasekhar Kesavan[2]. [1]JLP VA Medical Center, USA, [2]Jerry L. Pettis Memorial VA Medical Center, USA

The adaptive remodeling of the skeleton to mechanical strain is predicted to be mediated by the integrated actions of a number of signaling pathways including IGF-I, Wnt, integrin and estrogen. We recently demonstrated that osteoblast (Ob)-derived IGF-I is essential for mechanical loading (ML) induced new bone formation (BF) in mice. Based on the findings that estrogen receptors are involved in Ob mechanotransduction and based on the well established cross talk between estrogen and IGF-I signaling pathways to modulate biological responses, we proposed the hypothesis that the ML induced increase in IGF-I expression functionally interacts with estrogen signaling pathway to determine the amount of new BF in response to ML. To test this, we performed sham or partial-ovariectomy (p-OVX) on a 5 week-old heterozygous IGF-I knockout (H-IGF-I KO) mice in which one copy of the IGF-I gene is disrupted in type I collagen producing Obs by Cre/loxP technology and corresponding wild type (WT) littermate controls. At 10 weeks, a 10N axial load was applied on the right tibia of WT or H-IGF-I KO sham or p-OVX mice for a period of 2 weeks (3 days/week). The left tibia was used as an internal control. Partial estrogen loss in the WT mice resulted in a (5%) reduced BMD at the mid-diaphysis (P=0.08, ANOVA, LSD Pos-hoc test) when compared to the sham group. Micro-CT analysis of the loaded region revealed that 2 weeks of ML caused a 8-10% and a 11-12% ($p<0.05$ vs. unloaded bones) increase in cortical vBMD and cortical thickness (Cth), respectively, in the WT sham, WT p-OVX and H-IGF-I KO sham groups. In contrast, the magnitude of cortical vBMD (4%, P=0.11) and Cth (6%, $P<0.05$) responses were reduced by >50% in H-IGF-I KO p-OVX mice compared to the other 3 groups ($p<0.05$, LSD Post- Hoc test). The interaction between genotype and estrogen deficiency on the ML-induced cortical bone response was significant ($p<0.05$) by two-way ANOVA. 2 weeks of axial loading (AL) also induced trabecular (secondary spongiosa site) bone response as reflected by significant increases in trabecular BV/TV (15-18%) and thickness (18-23%) in all four groups of mice. Conclusions: 1) Partial loss of estrogen or IGF-I did not affect the ML induced cortical or trabecular bone response to AL 2) Partial loss of both estrogen and IGF-I significantly reduced cortical but not the trabecular bone response to ML, thus suggesting that IGF-I and estrogen cross talk to regulate the cortical bone response to ML.

***Disclosures: Bhat Chetan**, None.*

FR0160

Ovariectomy Induces Short-Term Hemopoietic Stem Cell Expansion through T Cells. Jau-Yi Li*[1], Jonathan Adams[1], Laura Calvi[2], M. Neale Weitzmann[1], Roberto Pacifici[1]. [1]Emory University School of Medicine, USA, [2]University of Rochester School of Medicine, USA

Estrogen deficiency expands bone marrow (BM) hemopoietic stem and progenitor cells (HSPCs) and mature blood lineages but neither the involved mechanism nor the affected HSPC populations are known. Since T cells contribute to ovariectomy (ovx) induced bone loss, we investigated the role of T cells in the HSPC expansion induced by ovx. Ovx increased the number of HSPCs (Lin-Sca-1+c-Kit+ cells) by ~2 fold and host survival after BM transplantation by ~4 fold in WT mice and T cell reconstituted-T cell deficient mice. By contrast ovx had no effects on HSPCs expansion and survival after BM transplantation in T cells deficient mice. Analysis of SLAM receptor expression on HSPCs and competitive repopulation assays demonstrated that ovx specifically expands short-term HSCs (ST-HSCs) without exhausting long-term HSCs (LT-HSCs) in T cell replete mice but not in T cell null mice. To determine whether the capacity of estrogen deficiency to induce HSPC expansion might be exploited in a clinical setting, we assessed the effects of the complete estrogen antagonist ICI 182,780 on the survival of mice undergoing myeloablative BM transplantation using limiting number of donor cells. We found that treatment of either donor or recipient mice with ICI 182,780 improved by 2-3 fold host survival after BM transplantation. Mechanistic studies revealed that ovx expands ST-HSPCs and improves host survival after BM transplantation through a dual role of the T cell costimulatory molecule CD40L. This surface receptor is required for ovx to stimulate T cell production of Wnt10b, a Wnt ligand that activates Wnt signaling in HSPCs and stromal cells (SCs). Moreover, CD40L is required for ovx to increase SC production of the hemopoietic cytokines IL-6, IL-7 and GM-CSF. Attesting to the relevance of CD40L and Wnt10b, ovx failed to expand ST-HSPCs and survival after BM transplant in CD40L null mice and in animals lacking global or T cell expression of Wnt10b. In summary, T cell expressed CD40L and the resulting increased production of Wnt10b and hemopoietic cytokines by T cells and SCs respectively, play a pivotal role in the mechanism by which ovx regulates hemopoiesis. The data suggest that anti-estrogens may represent pharmacological targets for promoting HSPC expansion and survival after BM transplant.

***Disclosures: Jau-Yi Li**, None.*

FR0162

Inhibition of TGF-β Signaling in Osteoblasts Leads to Activation of SOST and AXIN, Scoliosis-like Pathological Defects in Mice. Hsin-chiu Ho*[1], Shen-chin Hsu[2], Shanshan Shi[3], Eric Beier[3], Yongchun Zhang[3], Tzong-Jen Sheu[3], Mo Chen[4], Min-jon Lin[5], Wei Hsu[3], J. Edward Puzas[6]. [1]Wan-Chuan Clinics, Fangliao General Hospital, Taiwan, [2]Chung Shan Medical University Hospital Dept of Pharmacy, Taiwan, [3]University of Rochester, USA, [4]Columbia University, USA, [5]Chung Shan Medical University Dept of Biomedical Sciences, Taiwan, [6]University of Rochester School of Medicine, USA

TGF-β signaling can regulate Wnt/β-catenin pathways, which is crucial in modulating chondrocyte maturation during endochondral bone formation. Previously, using TGF-β receptor II conditional knockout mice with different skeletal tissue-specific targeting cre mice, they all showed skeletal malformation. However, the genetic evidence between WNT and TGF-β pathways cross-talk remains undefined. In this study, we used TGF-β reporter SBE-lucRT mice and WNT reporter TOP-GAL mice to identify what tissues had the active TGF-β and Wnt signals. Interestingly, we found the strongest TGFβ and Wnt reporter activity converges in Calvaria and spine. To delineate the coordination of TGF-β and Wnt signaling in these tissues, we generated Col-1 cre Tgfbr2 conditional knockout mice ($Tgfbr2^{Col1}$) and analyzed changes in histology, gene expression and bone density. Deletion of the Tgfbr2 gene in osteoblasts resulted in up-regulation of SOST, Mmp13, and Axin expression. Histological analysis showed end-plate cartilage degradation, vertebral distortion, scoliosis-like, and decreased vetebral bone mass in 2-month-old Tgfbr2Col1 mice. To determine if up-regulation of SOST and Axin expression is responsible for $Tgfbr2^{Col1}$-induced scoliosis, we generated Tgfbr2/SOST and Tgfbr2/Axin2 double KO mice. Deletion of the SOST gene significantly alleviates scoliosis-like pathological changes observed in 1- and 2-month-old $Tgfbr2^{Col1}$ mice, while deletion of the Axin2 gene reversed scoliosis-like phenotype in 2-month-old $Tgfbr2^{Col1}$ mice. These changes were confirmed by histomorphometric analysis and μ-ct imaging evaluation. In this study, we demonstrate that inhibition of TGF-β signaling and downstream WNT signaling in osteoblast leads to a progressive Scoliosis-like phenotype in mice and. SOST and Axin2 are critical downstream target genes of TGF-β signaling during scoliosis development.

***Disclosures: Hsin-chiu Ho**, None.*

FR0163

Atypical Femoral Fractures: Radiographic and Histomorphometric Features in 19 Patients. Aliya Khan*[1], Angela M. Cheung[2], O. Ahmed Khan[3], Zohair Rahman[4], Ken Pritzker[5], Brian Lentle[6]. [1]McMaster University, Canada, [2]University Health Network-University of Toronto, Canada, [3]Oakville Bone Centre, Canada, [4]McMaster, Canada, [5]University of Toronto, Canada, [6]University of British Columbia, Canada

Purpose: This study describes characteristics and histomorphometric and radiographic features of atypical femoral fractures (AFF) as seen in 19 cases referred for evaluation.

Methods: All patients referred for evaluation of AFF were reviewed. Patients meeting the ASBMR criteria for AFF were further evaluated and tetracycline labelled bone biopsies were completed. Radiographs were reviewed by a musculoskeletal radiologist.

Results: All fracture lines were transverse or short oblique and 15 of 19 patients demonstrated thickened cortices on xray. We report 19 cases of AFF in patients on long term bisphosphonate (BP) therapy. 14 of 19 fractures occurred without a fall or direct trauma to the femur with 5 cases occurring after a fall from standing height. All patients were female; average age was 65 years (range 23-80 years). 4 of the 19 cases were of Chinese descent, 4 were East Indian, with 11 being Caucasian. Average BP durations of use was 9.8 years (range 6-15 years). 9 of 19 patients were on alendronate alone, 2 patients were on risedronate alone, 6 patients on a combination and 1 patient on a combination of pamidronate and alendronate. 1 patient was on a combination of alendronate and denosumab. Prodromal thigh or groin pain was seen in 12 of the 19 patients for 1 to 15 months prior to fracture. Proton pump inhibitor use was present in 6 patients. 2 patients were on prednisone for rheumatoid arthritis and 2 patients on prednisone for asthma. 1 patient had a diagnosis of osteogenesis imperfecta type IV with a history of multiple fragility fractures and had experienced a femoral fracture after 12 years of IV pamidronate with features consistent with an AFF. All patients had 25OH Vit D levels > 50nmol/L. 18 of the patients with radiographic features of AFF had been on a bisphosphonate for > than 6 years. 1 patient had been on alendronate for 5 months. 8 of 19 patients had bilateral femoral fractures.

Summary: A large number of patients with radiographic features of an AFF had evidence of mineralization abnormalities on tetracycline labelled bone biopsy. Decreased osteoid surface and mean mineralized trabecular width was seen in 6 of 11 biopsies. Diffuse label was noted in 5 of 11 biopsies. Mineralization abnormalities

were noted in a significant number of patients with radiographic features of AFF (See Table 1). All of the women had normal or mildly reduced serum vitamin D levels.Conclusion: Histomorphometric features seen on bone biopsy in women sustaining an AFF in association with long term bisphosphonate use included evidence of mineralization abnormalities and decreased bone formation. 1 patient had features of decreased bone formation and mineralization abnormalities with only 5 months of bisphosphonate exposure. Improved understanding of the pathophysiology leading to these fractures may be gained with further histomorphometric data in larger numbers of patients.

11 Tetracycline labeled bone biopsies completed at the time of diagnosis of AFF: Histomorphemetric Data

Name	OS 16-23 (N)	MOW 9-11 (N)	MMTW 120-170 (N)	ES/TS	Label seen Y – Yes N- No	Type of tetracycline Bands Seen
NR	15% ↓	6 um ↓	115 um ↓	4%	N	None
DM	N/A	N/A	N/A	N/A	Y	Double - Distinct
AC	N/A	N/A	N/A	N/A		Necrosis is present
EP	22%	11 um	136 um	4%	Y	Double - Diffuse
WL	2% ↓	13 um	188 um	1%	Y	Double - Diffuse
KSC	26%	9 um	171 um	2%	Y	Single - Distinct
PW	36%	8 um ↓	169 um	2%	Y	Mix - Diffuse
JI	7% ↓	5 um ↓	129 um	2%	Y	Double - Diffuse
JD	9% ↓	6 um ↓	110 um ↓	5%	Y	Mix –Distinct
MSC	4% ↓	7 um ↓	134 um	5 %	Y	Double - Distinct
CD	7% ↓	8 um ↓	195 um	0%	Y	Single

Legend

OS - Osteoid surface
MOW – Mean Osteoid Width
MMTW – Mean Mineralized Trabecular Width
ES/TS – Eroded Surface/Trabecular Surface

Bone Biopsies Table

***Disclosures: Aliya Khan**, AMGEN, Merck, NPS, 6*

FR0165

FGF23 neutralization improves bone quality and osseointegration of titanium implants in chronic kidney disease mice. Ningyuan Sun*[1], shiwen zhang[2], Huawei Zou[2], Victoria Shalhoub[3], Reinhold Erben[4], Quan Yuan[5], Beate Lanske[5]. [1]Chn, [2]State Key Laboratory of Oral Diseases, West China Hospital of Stomatology, Sichuan University, China, [3]Amgen Inc., USA, [4]University of Veterinary Medicine, Austria, [5]Harvard School of Dental medicine, USA

Chronic kidney disease (CKD) has become a worldwide public health problem with its growing prevalence. FGF23, a phosphaturic hormone, increased significantly at the very early stage of CKD, and was found to be independently associated with the mortality and morbidity of CKD patients, including chronic kidney disease–mineral and bone disorder (CKD-MBD) and increased bone fracture risk. Our previous study showed that CKD impairs the osseointegration of titanium implants. The aim of this study was to evaluate whether FGF23 neutralization could improve the bone quality and osseointegration of titanium implants. Chronic renal insufficiency was induced by 5/6 nephrectomy in adult female mice. They were treated with FGF23 neutralizing antibody (FGF23 Ab 5mg/kg body weight) 3 times a week. Experimental titanium implants were inserted in the distal end of the femurs 2 weeks later. After 2-week healing, mice were sacrificed for samples collection. All mice were survived during the experimental period. FGF23 neutralization did not alter serum BUN, but significantly decreased serum PTH, and increased the Vitamin D and calcium levels. Histomorphometric analysis of the tibiae showed a significantly improvement of bone parameters. FGF23 neutralization also increased the fracture toughness of the tibiae as qualified by a three-point bending test. Although there is no significant change of bone-implant contact ratio, the strength of osseointegration, as evaluated by a biomechanical push-in test, was significantly improved by FGF23 neutralization. In summary, our findings indicate that FGF23 neutralization improves bone quality and osseointegration of titanium implants in chronic kidney disease mice, suggesting FGF23 is a key factor in the CKD related bone diseases.

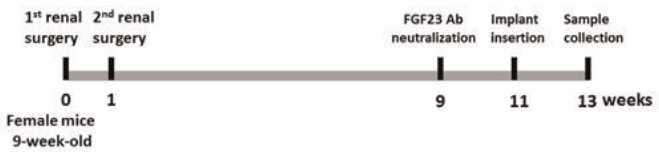

Illustration of the work flow

***Disclosures: Ningyuan Sun**, None.*

FR0172

Beneficial Effects of PTH(1-84) in Hypoparathyroidism as Determined by Microarchitectural Texture Assessment (TBS): a 4-year Experience. Barbara Silva*[1], Natalie Cusano[2], Chiyuan Zhang[3], Dinaz Irani[1], Jim Sliney Jr[1], Zachary Lenane[3], Laura Beth Anderson[3], Stephanie Boutroy[4], Didier Hans[5], Mishaela Rubin[3], John Bilezikian[2]. [1]Columbia University Medical Center, USA, [2]Columbia University College of Physicians & Surgeons, USA, [3]Columbia University, USA, [4]INSERM U1033 & Université de Lyon, France, [5]Lausanne University Hospital, Switzerland

We have shown that PTH(1-84) is a safe and effective treatment of hypoparathyroidism (HypoPT) for up to 4 yrs. BMD increases at the lumbar spine (LS) and remains unchanged at the hip. Yet, the effect of PTH(1-84) on skeletal microstructure over 4 yrs of PTH exposure is unknown. Trabecular bone score (TBS) is a quantitative estimate of trabecular microarchitecture that correlates with measures of bone microstructure by μCT and HRpQCT. In this study, we examined the effect of PTH(1-84) on TBS over a 4-yr period, with attention also to the possibility of sex-specific differences.

We studied 39 HypoPT subjects treated with PTH(1-84) for at least 2 and up to 4 yrs. Site-matched LS TBS data were extracted from the DXA image (Hologic) using TBS iNsight software. Linear mixed model for repeated measures was performed to assess the % change in TBS relative to baseline. Sex-specific differences were evaluated by using sex as a covariate in the model.

The mean age was 48 ± 2 yrs. Study subjects were pre- (PreM; n=18) and postmenopausal (PostM; n=10) women and men (n=11). PreM women were younger (PreM: 38 ± 2; PostM: 59 ± 2; Men: 54 ± 4 yrs; $p<0.001$) and had lower calcium levels (PreM: 8.2 ± 0.2; PostM: 9.0 ± 0.2; Men: 8.5 ± 0.2 mg/dl; p=0.06). Men had a longer duration of the disease (PreM: 12 ± 3; PostM: 16 ± 5; Men: 28 ± 5 yrs; p=0.02). At baseline, mean TBS was normal at 1.429 ± 0.020 (normal ≥ 1.35). TBS, while within normal limits, was lower in PostM (1.358 ± 0.036) than in PreM women (1.441 ± 0.032; p=0.09) or men (1.473 ± 0.034; p=0.04). In the entire cohort, PTH improved TBS at 2 yrs ($+1.4 \pm 0.7\%$; p=0.057), which plateaued after this time point, reaching a mean gain of $1.5 \pm 0.8\%$ at 4 yrs (p=0.04). Differences in the % change of TBS among the groups were seen at 18 months (p=0.04). While TBS remained unchanged in PostM women and men, it increased in PreM women by $2.1 \pm 1.0\%$ (p=0.04) at 18 months, and $2.6 \pm 1.0\%$ (p=0.01) at 2 yrs, plateauing thereafter (Fig). A positive correlation between the % change in TBS and LS BMD was noted at 6, 12, 30 and 36 months (r= 0.3-0.5; $p<0.05$).

TBS is normal in HypoPT subjects. Treatment of HypoPT with PTH(1-84) for up to 4 yrs improves TBS in PreM women, and preserves it in PostM women and men. The results suggest that microstructural improvements due to PTH(1-84) treatment of HypoPT can be monitored by TBS, that they are more apparent in younger individuals, and provide additional confirmation of the safety of the long-term treatment with PTH(1-84).

Figure: Percent change in TBS in PreM (A) and PostM (B) women, and Men (C) on PTH(1-84) therapy for 4 years
Mean ± SEM; *<0.05 relative to baseline

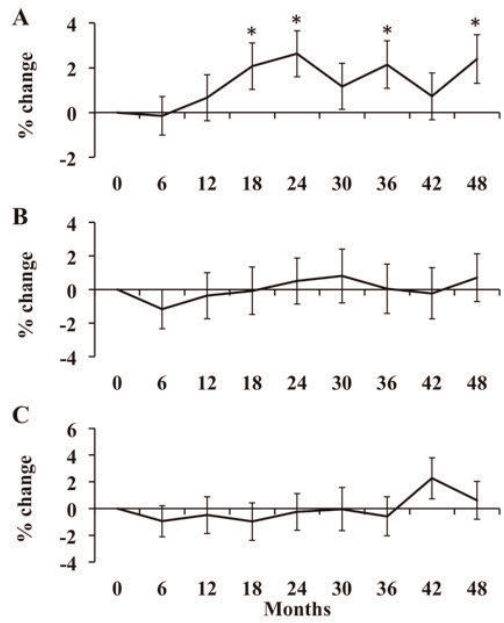

Figure

***Disclosures: Barbara Silva**, None.*

FR0174

CDC73/HRPT2 mutations and parafibromin immunohistochemistry in a large series of sporadic parathyroid carcinomas and atypical adenomas. Filomena Cetani*[1], Chiara Banti[2], Elena Pardi[2], Liborio Torregrossa[3], Simona Borsari[2], Federica Saponaro[2], Massimo Rugge[4], Gianmaria Pennelli[4], Mariarosa Pelizzo[5], Mauro Papotti[6], Marco Volante[6], Guido Gasparri[7], Paolo Miccoli[3], Claudio Marcocci[1]. [1]University of Pisa, Italy, [2]Department of Clinical & Experimental Medicine, University of Pisa, Italy, [3]Department of Surgical, Medical & Molecular Pathology, University of Pisa, Italy, [4]Department of Medicine, University of Padova, Italy, [5]Department of Medical & Surgical Sciences, Italy, [6]Department of Clinical & Biological Sciences, University of Torino, Italy, [6]Department of Clinical & Biological Sciences, University of Torino, Italy, [7]Department of Surgical Sciences, University of Torino, Italy

The histological diagnosis of parathyroid carcinoma (PC) is restricted to lesions showing perineural invasion, full thickness capsular invasion with growth into adjacent tissues, vascular invasion or metastasis. A subset of parathyroid tumors (atypical adenomas, AA) show pathologic features of PC, such as trabecular growth, fibrous bands, marked cellular atypia, increased mitotic activity, without the above criteria of malignancy. In some cases the distinction between AA and PC may be difficult at histology, and it might be that AA could be an early stage of PC.

Mutations of the *CDC73*/*HRPT*2 gene and/or loss of expression of its protein product, parafibromin (PF), have been detected in up to 70% of metastatic PC. To further investigate the involvement of *HRPT2*/*CDC73* gene in the pathogenesis of PC and AA we studied 80 patients with apparently sporadic primary hyperparathyroidism (PHPT) (58 PC and 22 AA). Mutational analysis of the *CDC73*/*HRPT*2 coding and splite site regions was performed in 40/58 PC and all 22 AA, and PF immunostaining in all PC and 21/22 AA.

Parathyroid cancer. CDC73/*HRPT2* mutations were found in 13 out of 40 (32.5%) PC, 5 were germline. Loss of PF staining (<5% positive cells) was observed in 11 of 13 mutated and 7 of 27 (25.9%) non-mutated samples. Of the 18 samples not tested for *CDC73*/*HRPT2* mutations 7 were negative and 11 positive at PF staining. Long term follow up was available in 35 patients: Twenty-one died because of PC and 12 of them carried a *CDC73*/*HRPT2* mutation; of the 11 patients still alive only 1 carried a *CDC73*/*HRPT2* mutation (p=0.01). By combining the different patterns of *CDC73*/*HRPT*2 mutation and PF staining we found that 18 out of 21 who died for PC had *CDC73*/*HRPT2* mutation and/or loss of PF staining; on the other hand 10 out 11 patients with PC who are still alive showed neither the mutation nor loss of PF staining (P<0.0001).

Atypical adenoma. A *CDC73*/*HRPT2* germline mutation associated with loss of PF staining was found in 1 out of 22 (4.5%) AA; loss of PF staining was observed in 14/21 (66.7%) non-mutated samples. Twenty-one patients, including the one carrying the mutation (with a follow up of 9 yrs), have been cured by surgery, and 2 have persistent/recurrent PHPT. The latter patient's tumors showed retained PF staining.

The present data suggest that patients with PC, whose primary tumor carry a *CDC73*/*HRPT2* mutation and/or loss of PF staining might have a more aggressive PC, since all but three died for the disease. Conversely, the absence of the mutation and the retained PF staining suggest a more being course of PC, since 10 of the 11 patients with these histologic features are still alive.

***Disclosures: Filomena Cetani**, None.*

FR0175

Changes in Bone Turnover Markers and Bone Mineral Density with Recombinant Human Parathyroid Hormone, rhPTH(1-84), in Hypoparathyroidism: Potential Utility as Surrogate Endpoints for Monitoring - the REPLACE Study. John Bilezikian*[1], Tamara Vokes[2], Jeffrey Rothman[3], Bart Clarke[4], Michael Mannstadt[5], Hjalmar Lagast[6], Dolores Shoback[7]. [1]College of Physicians & Surgeons, Columbia University, USA, [2]University of Chicago, USA, [3]Staten Island University Hospital, USA, [4]Mayo Clinic College of Medicine, USA, [5]Massachusetts General Hospital & Harvard Medical School, USA, [6]NPS Pharmaceuticals, Inc., USA, [7]University of California-San Francisco Veterans Affairs Medical Center, USA

Hypoparathyroidism is a rare disorder characterized by hypocalcemia and absent or inappropriately low levels of PTH. Bone mineral density (BMD) is abnormally increased while bone turnover is very low. A phase III, randomized, multicenter, double-blind, placebo (PBO)–controlled study (REPLACE) was performed to determine whether treatment with rhPTH(1-84) could restore mineral homeostasis and lead to reduction of the large doses of oral calcium (Ca) and active vitamin (Vit D) generally required for management. Patients were randomized to receive daily subcutaneous injections of 50 µg rhPTH(1-84), which could be increased to 75 µg and then to 100 µg if needed, or PBO for 24 weeks. Responders were defined as patients whose oral Ca and active Vit D could be reduced by ≥50% from baseline at Week 24 while maintaining serum Ca levels: 53.3% of patients in the rhPTH(1-84) group vs. 2.3% in the PBO group ($P<0.001$) achieved this primary endpoint. We now report the effects of rhPTH(1-84) on bone turnover markers (BTMs) and BMD according to whether or not patients achieved the primary endpoint.

At baseline, mean BTMs were low normal and BMD was above average in both rhPTH(1-84) and PBO groups. At Week 24, BTMs rose to significantly higher levels after rhPTH(1-84) as compared to the PBO group, regardless of whether patients met the primary endpoint, ($P\leq0.001$ vs. PBO; Table). At Week 24, all BTMs were higher in patients who met the primary endpoint vs those who did not. BMD was reduced more towards normal in both groups of patients treated with rhPTH(1-84) than in those given PBO.

Results indicate that in patients with hypoparathyroidism, treatment with rhPTH(1-84) leads to an increase in bone remodeling, as indicated by increased BTMs and a decrease towards normal in BMD. This endpoint was reached even in those patients who did not meet the primary endpoint of the REPLACE trial (≥50% reduction in Ca and active Vit D). The results suggest that BTMs and BMD may serve as surrogate endpoints and might prove useful for monitoring bone remodeling activity in patients who receive rhPTH(1-84) for the treatment of hypoparathyroidism.

Table. Mean Change From Baseline in BTMs at Week 24†

	rhPTH(1-84)		Placebo
	Primary Endpoint Achieved n=40	Primary Endpoint Not Achieved n=42	n=44
BTMs:			
BSAP (µg/L)	23.9*	16.2*	0.23
s-CTx (ng/L)	874*	702*	9.70
Osteocalcin (µg/L)	27.1*	24.2*	−0.44
P1NP (µg/L)	348*‡	238*	2.48

BSAP, bone-specific alkaline phosphatase; s-CTx, serum carboxy-terminal telopeptide of type I collagen; P1NP, procollagen type I amino-terminal propeptide.
*P≤0.001 vs. Placebo.
‡P=0.03 vs. subjects who did not achieve primary endpoint.
†Post-hoc analysis.

Table - Mean Change From Baseline in BTMs at Week 24

***Disclosures: John Bilezikian**, NPS Pharmaceuticals, Inc., 6; NPS Pharmaceuticals, Inc., 2*
This study received funding from: NPS Pharmaceuticals, Inc.

FR0179

Parathyroid Hormone Regulates Bone Microstructure: Reciprocal Changes After Treatment of Hyper- and Hypoparathyroid Subjects. Natalie Cusano*[1], Mishaela Rubin[2], Barbara Silva[3], Chiyuan Zhang[2], Wen-Wei Fan[1], Megan Romano[1], Laura Beth Anderson[2], Jim Sliney Jr[3], John Bilezikian[1]. [1]Columbia University College of Physicians & Surgeons, USA, [2]Columbia University, USA, [3]Columbia University Medical Center, USA

In primary hyperparathyroidism (PHPT) and hypoparathyroidism (HypoPT), improvements are seen in some abnormal bone indices after parathyroidectomy (PTX) and PTH therapy, respectively. However, direct comparisons *between* hyper- and hypoparathyroid microskeletal parameters following reversal of the abnormal parathyroid state have not yet been made. To this end, we studied 11 subjects with PHPT and HypoPT at baseline and 1 yr after intervention with high resolution peripheral quantitative computed tomography (HRpQCT, Scanco Medical AG). Subjects were matched for sex, race and menopausal status. There were 7 postmenopausal women and 4 men in both cohorts, all Caucasian. The mean age (± SD) was similar (PHPT: 63 ± 15 vs HypoPT: 57 ± 13 yrs; p=0.3). Baseline (10.8 ± 0.7 vs 8.7 ± 0.8 mg/dL; p<0.001) and 1 yr (9.3 ± 0.5 vs 8.3 ± 0.7 mg/d; p<0.001) serum calcium were higher in PHPT subjects. There was a trend toward longer duration of disease in the HypoPT subjects (7 ± 11 vs 19 ± 17 yrs; p=0.07), but no differences between groups with respect to height, weight, BMI, or 25-hydroxyvitamin D.

At baseline, at the radius, total volumetric (vBMD), cortical (Ct), and trabecular (Tb) density as well as Ct area and thickness (Ct.Th), Tb bone volume fraction and Tb number were all lower in the PHPT cohort, while Tb separation was higher. At the tibia, vBMD, Ct vBMD, inner Tb density (Dinn), and Tb thickness were lower in PHPT subjects (see Table for all results). One yr after PTX in PHPT subjects and initiation of PTH(1-84) in HypoPT subjects, there were significant *within group* differences at the tibia in both cohorts and at the radius in the HypoPT cohort. Comparing the response *between groups*, in general there were reciprocal changes at both the radius and tibia with the tibia showing the greatest change: total (p=0.004), cortical (p=0.005), and trabecular area (p=0.002), total vBMD (p=0.003), Ct.Th (p=0.004), Ct vBMD (p=0.007), and Dinn (p=0.03).

We have demonstrated reciprocal changes in bone density and geometry in PHPT and HypoPT subjects before and after therapy using high resolution imaging. The changes are mostly present at the weight-bearing site of the tibia. These results suggest that correction of PTH excess or deficiency is associated with a reversal of abnormalities and gives further direct evidence for PTH's critical role in regulating skeletal microstructure.

Table. Baseline and 1 year changes in cortical (Ct) and trabecular (Tb) HRpQCT parameters in subjects with PHPT and HypoPT after intervention (PTX and start of PTH therapy, respectively)

	PHPT (n=11)		HypoPT(n=11)	
Radius	***Baseline***	***1 year (%)***	***Baseline***	***1 year (%)***
Ct Area	47 ± 18[a]	2.1 ± 6	66.4 ± 18	-2.5 ± 4
Ct Thickness	0.64 ± 0.2[a]	2.3 ± 6	0.93 ± 0.2	-2.5 ± 4
Tb Area	239.5 ± 63	-0.2 ± 1	212.5 ± 78	0.7 ± 1[b]
Total vBMD	247 ± 74[a]	0.6 ± 4	363 ± 82	1.8 ± 3[b]
Ct vBMD	795 ± 79[a]	-0.3 ± 3	906 ± 55	-1.3 ± 3
Tb vBMD	113 ± 38[a]	1.4 ± 4	163 ± 50	0.2 ± 3
Inner Tb density	68 ± 40[a]	0.8 ± 15	120.3 ± 57	0.1 ± 4
Meta Tb density	178 ± 38[a]	0.9 ± 3	224.4 ± 43	0.3 ± 3
BV/TV	0.09 ± 0.03[a]	1.3 ± 4	0.14 ± 0.04	0.2 ± 3
Tb Number	1.67 ± 0.4[a]	0.8 ± 9	2.09 ± 0.3	-1.6 ± 7
Tb Separation	0.60 ± 0.2[a]	-0.2 ± 9	0.43 ± 0.1	1.8 ± 7
Tibia	***Baseline***	***1 year (%)***	***Baseline***	***1 year (%)***
Total area	811 ± 166	0.1 ± 0.3[c]	758.5 ± 167	-0.2 ± 0.1[b]
Ct Area	92 ± 47	6.7 ± 8[b,c]	121.0 ± 37	-2.4 ± 3[b]
Ct Thickness	0.82 ± 0.3	7.3 ± 9[b,c]	1.11 ± 0.3	-3.1 ± 4[b]
Tb Area	719 ± 167	-0.5 ± 0.3[b,c]	638 ± 160	0.2 ± 0.5
Total vBMD	236 ± 51[a]	1.9 ± 3[b,c]	296 ± 59	-1.6 ± 2[b]
Ct vBMD	730 ± 102[a]	0.4 ± 2[c]	855 ± 62	-2.2 ± 2[b]
Inner Tb density	108 ± 33[a]	2.5 ± 4[b,c]	142.8 ± 43	-0.5 ± 2
Tb Thickness	0.06 ± 0.01[a]	4.5 ± 7	0.08 ± 0.02	-0.8 ± 7

Mean ± SD; vBMD, volumetric bone mineral density; BV/TV, Tb bone volume fraction; [a]p<0.05 comparison between groups at baseline, [b]p<0.05 comparison *within* group at 1 year, [c]p<0.05 comparison between groups at 1 year

Table

Disclosures: Natalie Cusano*, None.*
This study received funding from: NPS Pharmaceuticals

FR0180

Assessment of Osteovascular Interactions by HR-pQCT: Links Between Lower Leg Arterial Calcifications and Renal Osteodystrophy. Janina Patsch*[1], Mafo Kamanda-Kosseh[2], Serge Cremers[2], Elzbieta Dworakowski[2], Chiyuan Zhang[2], Donald McMahon[3], Elizabeth Shane[3], Thomas Nickolas[3]. [1]Medical University of Vienna, Austria, [2]Columbia University, USA, [3]Columbia University College of Physicians & Surgeons, USA

Vascular calcifications (VC) are common in patients with chronic kidney disease (CKD) and are associated with increased risk of cardiovascular disease and fracture. Methods typically used to quantify severity of VC are associated with considerable radiation doses, which limits clinical investigation of bone-vascular interactions. High-resolution peripheral quantitative CT (HR-pQCT, SCANCO Medical AG) measures true volumetric BMD (vBMD) and trabecular and cortical microarchitecture at the distal radius and tibia with low radiation dosages (3 μSv per scan), and can also detect VC. We hypothesized that peripheral arterial calcifications detected by HR-pQCT would be inversely associated with vBMD and microarchitecture in patients with CKD. We enrolled patients with CKD stages 2+3 (n=18), 4+5 (n=14), hemodialysis (HD, n=16) and an age-, sex- and race- matched reference group with normal kidney function (n=21). Tibia HR-pQCT scans were reviewed for lower leg arterial calcifications (LLAC) and a semi-automated, image-processing algorithm was applied. This included image downscaling, removal of bone volume, and detection of remaining focal hyperdense areas by dual threshold seed-point segmentation. LLAC mass was expressed in mg hydroxyapatite (mgHA). Relationships between LLAC and eGFR, cortical and trabecular vBMD and microarchitecture, PTH, and markers of bone formation (BSAP, osteocalcin, P1NP) and resorption (CTX, TRAP5b) were assessed. Analyses were adjusted for kidney function. Mean age was 65 ± 9 (± SD) years, 57% were male and 45% were Black. Compared to the reference group, LLAC was 3.2 mgHA higher in patients with CKD stages 4+5 and 8.8 mgHA higher in patients on HD (both $p<0.05$). LLAC was inversely associated with total density (r= -0.30, $p<0.05$) and trabecular thickness (r= -0.30, $p<0.03$) at the radius, and with total (r= -0.30, $p<0.05$) and cortical density (r= -0.30 $p<0.05$), and cortical thickness (r= -0.20, $p<0.05$) at the tibia. LLAC was positively associated with BSAP (r= 0.40, $p<0.05$). In summary, LLAC measured by HR-pQCT was higher in patients with advanced CKD, was inversely associated with vBMD at both radius and tibia, and was directly associated with the bone formation marker, BSAP. These findings suggest that HR-pQCT may prove to be a useful technology to investigate the pathogenesis of associations between the cardiovascular system and the skeleton in CKD and other diseases.

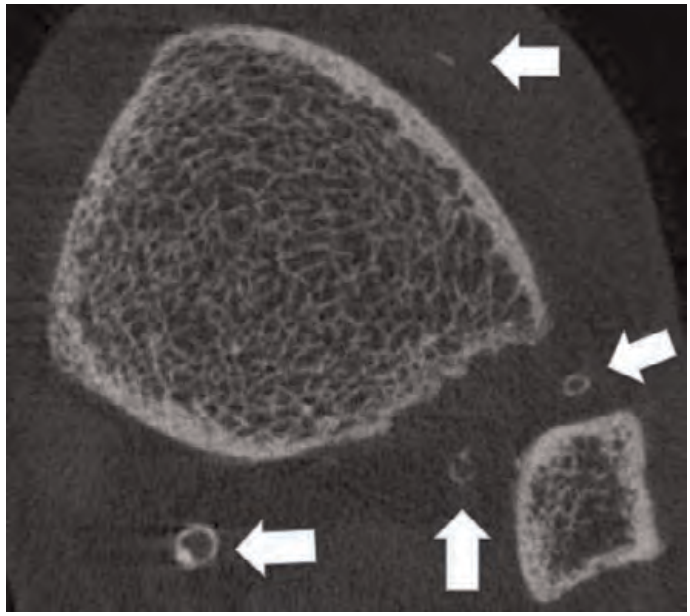

Vascular calcifications in a CKD patient visualized by HR-pQCT

Disclosures: Janina Patsch*, None.*

FR0181

Does a Progressively Hostile Marrow Microenvironment Ossify Bone Marrow Blood Vessels and Contribute to Bone Microvascular Dysfunction?. Rhonda Prisby*[1], Ashley Bice[2], Arun Kumar[3]. [1]University of Delaware, USA, [2]University of Delaware, Department of Kinesiology & Applied Physiology, USA, [3]University of Delaware, Department of Medical Laboratory Sciences, USA

BACKGROUND: With aging, diaphyseal blood flow transitions from a centrifugal to a centripetal direction. In old rats, reduced vasodilator capacity of the femoral principal nutrient artery (PNA) coincided with diminished bone and marrow blood flow (Prisby et al., 2007; Dominguez et al., 2010). However, can declines in nutrient artery function solely account for the age-related reversal in direction of diaphyseal flow? Atherosclerosis occurs in bone marrow arteries (Brenneise & Squier 1985). Yet, it is presumed that systemic atherosclerosis and arteriosclerosis contribute to declines in skeletal perfusion (Brenneise & Squier 1985; Shao et al., 2011). We examined diaphyseal bone marrow blood vessels and assessed the influence of the marrow microenvironment on vascular function.

METHODS: Femoral bone marrow blood vessels and PNAs were isolated from young (4-6 mon; n=7) and old (22-24 mon; n=7) male Fischer-344 rats. Bone and bone marrow blood vessels (n=3-4/age) were analyzed by FT-IR. In addition, femoral PNAs were cannulated to assess vasodilation to acetylcholine (10^{-9} – 10^{-4} M) in the presence and absence of marrow.

RESULTS: Body mass was higher ($p<0.05$) in old (429 ± 14 g) vs. young (363 ± 12 g) rats while marrow mass did not differ between groups (58 ± 15 mg & 35 ± 10 mg, respectively). Bone marrow blood vessel ossification seemed evident at both ages, but accounted for the majority of the microvascular network in old rats. Morphologically, these vessels resembled bone tissue such that osteocyte lacunae appear present on the vessel surface (see Figure). FT-IR analysis revealed that old bone marrow blood vessels have FT-IR spectra which show that the mineral-to-matrix ratio, carbonate-to-phosphate ratio area and crystallinity peak area are similar to old bone. As expected, endothelium-dependent vasodilation was diminished ($p<0.05$) in old age. Strikingly, in the presence of the marrow, vasodilation was reduced by 41% ($p<0.05$) and 39% ($p=0.07$) in young and old rats, respectively.

CONCLUSION: These data suggest that bone marrow presumably represents a progressively toxic microenvironment, whereby it induces vascular dysfunction and ossification. Ossification of bone marrow blood vessels may result in "microvascular dead space" and coupled with reduced vasodilator capacity of the nutrient arterial system may account for the age-related declines in bone perfusion and centripetal nature (i.e., from the cortices towards the marrow) of diaphyseal flow.

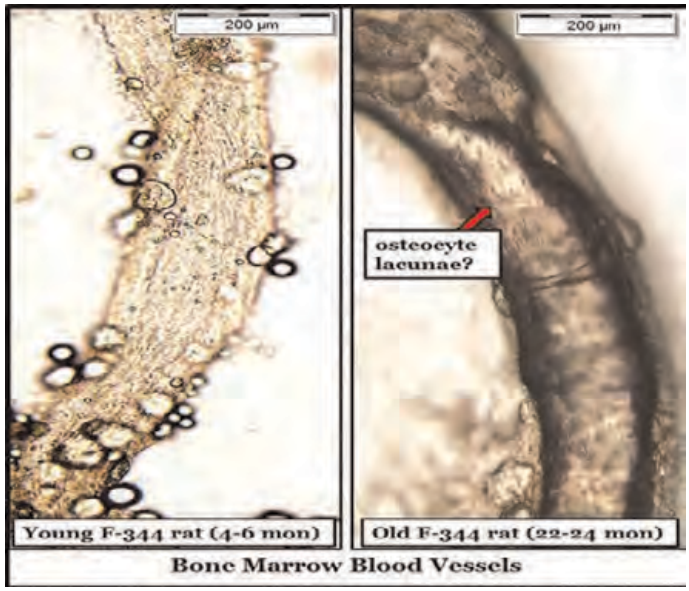

ossified bone marrow vessel

***Disclosures: Rhonda Prisby**, None.*
This study received funding from: NIH

FR0186

Potential Role of Leptin and BMP2 in Osteocyte Regulation of Muscle Mass and Function in the Adult Skeleton and With Age. Jeffrey Gorski*[1], Nichole T. Huffman[1], Leticia Brotto[1], Mark Dallas[1], Anne Breggia[2], Sridar V. Chittur[3], Jian Huang[1], Chenglin Mo[4], Ying Liu[1], Nabil G. Seidah[5], Clifford Rosen[2], Marco Brotto[1], Lynda Bonewald[1]. [1]University of Missouri - Kansas City, USA, [2]Maine Medical Center, USA, [3]Center for Functional Genomics, University of Albany, SUNY, USA, [4]University of Missouri-Kansas City, USA, [5]Clinical Research Institute of Montreal, Canada

MBTPS1 (SKI-1 or S1P) is a serine protease that regulates the transcription of genes in cultured bone cells such as *COL11* and *FBN* and osteocyte markers *PHEX* and *DMP1* by activating membrane bound transcription factors like SREPB-1, ATF-6, and CREB-H. To determine the role of this protease in vivo, cKO mice were generated by crossing floxed MBTPS1 with DMP1 Cre mice. We previously showed that at 15-20 wks, cKO mice have a 20% higher body weight compared to controls (p=0.034). But, no significant differences were found in bone size and morphology, BMC, and ash weight, or in whole body or abdominal fat. MBTPS1 cKO mice are larger due to a general gain in skeletal muscle mass (for example, +12.3% for cKO soleus muscles, p=0.03). MBTPS1 cKO muscles also contracted with more force and histologically exhibited features of regenerating muscle. To identify the mechanism responsible, MBTPS1 protein analyses, food intake measurements, osteocyte microarray data, and serum biomarker analysis on blood samples were performed at 40 wks of age. Immunoblotting of muscle extracts revealed that MBTPS1 protein was unchanged in knockouts and controls (n=3). Despite differences in body mass, cKO and control littermates had equivalent food intake. Whole genome arrays of isolated bone cells enriched for osteocytes (n=4) showed that MBTPS1 deficiency significantly reduced expression of 230 genes including osteocyte markers such as *PHEX*, *DMP1, MEPE,* and *SOST* as well as *BMP2*, *BMP3*, *BMP4*,*TGFb2* and *TGFb3*. Leptin was significantly increased in serum in cKO mice compared with littermate controls (7176 vs. 3575 pg/ml, p=0.018). Interestingly, serum leptin and BMP2 in cKO mice correlated directly (leptin, r^2=0.89, p=0.001) and inversely (BMP2, r^2=0.58, p=0.028) with overall body weight when analyzed by linear regression (Fig. 1). These data provide new evidence of bone-muscle crosstalk and suggest that osteocytes play a key role in regulating muscle mass and contractile force. We propose a model in which osteocytes normally inhibit the growth and differentiation of skeletal muscle by secreting BMPs, negative regulators of myogenic differentiation of primary satellite cells. With reduction of MBTPS1 in osteocytes, this repressive signaling is abrogated and elevated circulating leptin stimulates differentiation of muscle precursor cells. Further characterization should prove useful in identifying targets for the treatment of sarcopenia, muscle atrophy, and muscle myopathies.

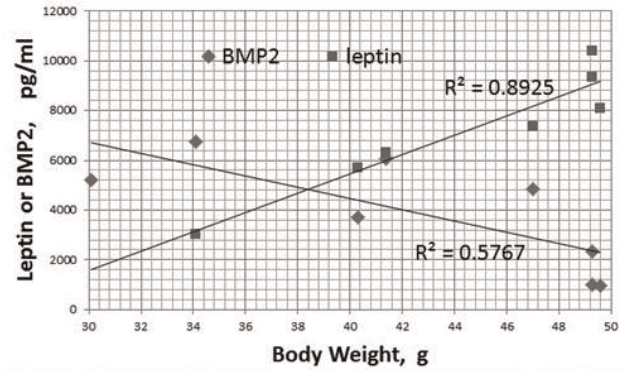

Figure 1: Serum leptin and BMP2 correlate directly and inversely, respectively, with body weight of MBTPS1 conditional knockout mice.

Fig. 1: Serum leptin and BMP2 correlate directly and inversely, respectively, with body weight

***Disclosures: Jeffrey Gorski**, None.*

FR0187

Neuroskeletal Signaling In The Regenerating Zebrafish Fin: Remote Inhibition of Osteoblast Function via Disruption of Cholinergic Signaling. Anthony Recidoro, Amanda Roof, Brandon Ausk, Sundar Srinivasan, Edith Gardiner, Ted Gross, Steven Bain, Christopher Allan, Ronald Kwon*. University of Washington, USA

Disruption of the nervous system (e.g., via brain, spinal cord, or peripheral nerve injury) has been widely associated with aberrant bone function. Zebrafish are small, optically accessible, genetically manipulable vertebrates whose tail fins possess a remarkably simple neuroskeletal structure (~18 bone rays each with several intra-/inter-ray nerves, Fig 1A). The capacity for zebrafish to undergo rapid bone regeneration following fin amputation confers unique opportunities to examine neuroskeletal signaling within a highly tractable experimental system.

In this study, we developed a model of cholinergic disruption in the regenerating tail fin using intramuscular injections of Botuliunum toxin B (BTxB). The tail fin is muscularized only at the base. By administering BTxB into the base, we were able to examine remote effects of BTxB at the distal tip while minimizing the influence of impaired muscle near the regenerate (Fig 1B). BTxB resulted in multi-faceted effects on bone regeneration in adult zebrafish (9dpa, ~30mm S.L.). For example, BTxB fish exhibited a significant decrease in the % length of bone regrowth compared to saline controls (sal: 74.8±8.1%, btx: 35.2±4.6%, $p<0.001$ for treatment, n=5). The degree of inhibition was significantly more pronounced in the middle of the regenerate compared to the dorsal/ventral regions ($p<0.05$ for region:treatment), suggesting that the trophic influence of fin base nerves can be spatially focused to distinct fin regions. We also found that bone ray bifurcations were significantly reduced in BTxB fish (sal: 9.4±1.0, btx: 6.7±0.3 $p<0.05$), indicating a role for the nervous system in guiding bone patterning. Finally, when fish were calcein stained, we found that BTxB dramatically decreased osteoblast activity in regenerating bone. Interestingly, the effects of BTxB appeared to be spatially restricted within individual rays, as evidenced by marked differences in osteoblast activity between adjacent rays (Fig 1C). This suggests a potential role for intra- and/or inter-ray nerves in mediating the effects of nerve disruption in the fin base on osteoblast activity in the distal tip. Collectively, these studies demonstrate the capacity for focal cholinergic disruption to remotely alter bone regeneration in a multi-faceted manner. Given the genetic and optical tools for dissecting neural pathways in zebrafish, this model provides a powerful platform for identifying novel mechanisms underlying neural control of bone growth.

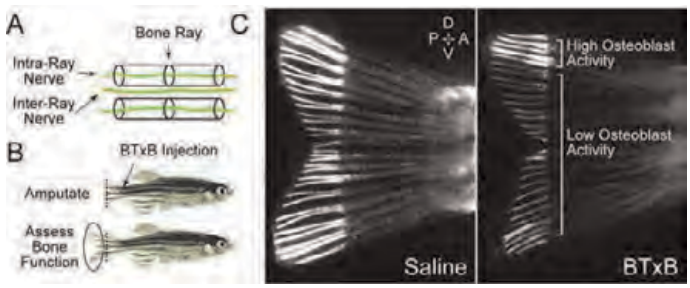

Figure 1

***Disclosures: Ronald Kwon**, None.*

FR0189

Muscle-Bone Interactions during Multiple Hindlimb Unloading and Reambulation Cycles. Sarah Manske*[1], Surabhi Vijayaraghavan[1], Alyssa Tuthill[1], Jean Olivier Brutus[1], Shikha Gupta[2], Stefan Judex[1]. [1]Stony Brook University, USA, [2]State University of NY, Stonybrook, USA

Exposure to single and multiple bouts of hindlimb unloading (HLU) causes rapid deterioration of the musculoskeletal system. We recently showed that after single or multiple exposures to 2wk HLU and 4wk of reambulation (RA), neither hindlimb muscle cross-sectional area (MCSA) nor distal femur bone volume fraction (BV/TV) recovered to the level of age-matched controls, regardless of the previous number of exposures to unloading. Here, we hypothesized that extending the RA period between multiple bouts of HLU can mitigate the loss of muscle and bone upon subsequent unloading cycles and enhance long-term recovery. Ninety 16wk-old female mice (double cross of BALB and C3H strains) were exposed to 3x(3wk HLU and 3wk RA) (3W), 3x(3wk HLU and 9wk RA) (9W) or no unloading (C). *In vivo* micro-CT scans tracked changes in distal femur bone and upper hindlimb MCSA through each HLU/RA cycle and long-term recovery at 62wk. Finite element models of the metaphyseal region were constructed to assess stiffness. Animal activity was monitored pre- and post-HLU via infrared beams over 24h periods. We found that increasing the RA period yielded greater recovery between HLU bouts, however 9W had greater rates of loss in the final two HLU periods than 3W for MCSA, BV/TV and stiffness (Figure 1). Due to these differences in rates of loss, 3W and 9W mice reached similar absolute values of MCSA, BV/TV and stiffness at the end of each HLU period after adjusting for initial values indicating that lengthened RA periods did not protect the musculoskeleton when exposed to multiple bouts of HLU. Long-term, MCSA fully recovered in both groups at 62wks. In contrast, BV/TV did not normalize to control levels over the same duration ($p<0.05$ for 3W and trend for 9W). Stiffness also reflected this trend. The lack of BV/TV recovery was consistent with the drop in the percent load carried by trabecular bone in 3W vs C. Mean loss of stiffness moderately correlated with MCSA over all three HLU periods ($R^2 = 0.32$), similar to stiffness vs MCSA in the first two RA periods ($R^2 = 0.31$). Addition of activity levels did not enhance the association between muscle and bone. These results indicate that both muscle and bone desensitize in response to multiple bouts of HLU. As the magnitude of the muscle and bone response to HLU and RA across individuals did not correlate well and activity levels were a poor predictor for recovery, it is unlikely that bone changes were primarily a result of muscle loading.

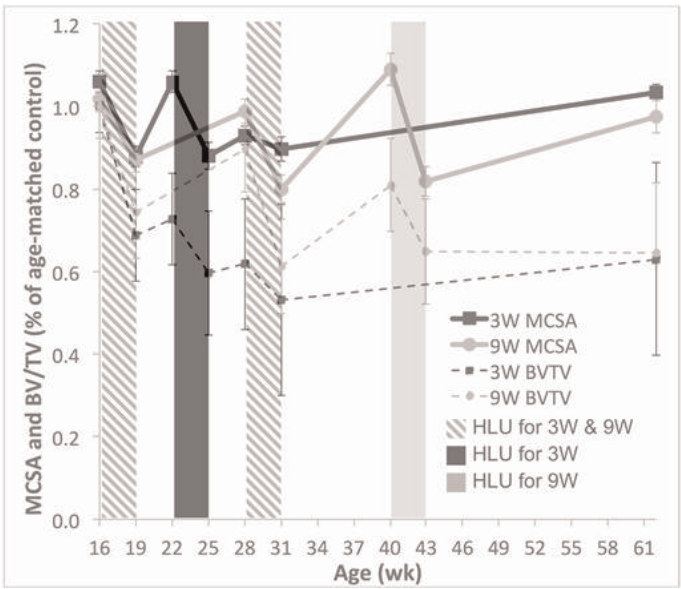

Figure 1

***Disclosures: Sarah Manske**, None.*

FR0190

Visualizing the Skeletal Response to Resistance Exercise. Thomas Lang*[1], Isra Saeed[2], Julio Carballido-Gamio[2], Roy Harnish[2], Lynda Frassetto[2], Tim Streeper[2], Jean Sibonga[3], Stuart Lee[3], Joyce Keyak[4], Peter Cavanagh[5]. [1]University of California, San Francisco, USA, [2]UC San Francisco, USA, [3]NASA, USA, [4]Department of Radiological Sciences, University of California, Irvine, USA, [5]University of Washington, USA

Understanding the skeletal effects of resistance exercise depends on our ability to delineate the spatially heterogeneous response of bone to the load distributions from contractions of different muscles. Densitometric analyses may obscure these patterns by averaging data from tissues that vary in their mechano-responses. To quantify heterogeneity in the response of the hip to resistance exercise, we carried out pre- and post-training quantitative computed tomography (QCT) (GE vCT 64, 120 kVp/150 mAs, 2.5 mm slice thickness) in 15 subjects (age range 25-55 years, 6 males, 9 females) performing two different types of resistance training for 16 weeks. Group A (N=7) performed 4 sets each of squats and deadlifts (SQDL) and Group B (N=8) performed 4 sets each of standing hip abductions and adductions (ABADD). Subjects exercised three times weekly, and the daily load was adjusted to their maximum effort. To examine the exercise-related changes on a per voxel basis, we used voxel-based morphometry (VBM) (1). Briefly, all vQCT images were registered onto an anatomic template, creating a single atlas of pre- and post-exercise images. The BMD change was computed per voxel in the atlas, and a cluster of voxels was tested for statistically significant pre- to post-training change (paired t-test) if it included 25 contiguous voxels which changed by ≥ 10 mg/cm^3. We also computed whole bone strength using finite element modeling (FEM) with stance and fall loading conditions (2), and cortical and trabecular BMD and cortical tissue volume using analytic techniques published previously (3). Figure 1 shows the effects of SQDL and ABADD exercise detected by VBM. For both groups, there were only changes in cortical bone. SQDL produced focal regions of increased BMD in the femoral neck, which were localized to the trochanter for ABADD. Table 1 shows results for FEM and vQCT. While SQDL increased femoral neck cortical vBMD and volume, as well as hip strength in stance loading, ABADD increased only trochanteric cortical volume. In conclusion, we observed differential patterns of proximal femoral response to SQDL and ABADD exercise. This study suggests that VBM and vQCT can quantify the subtle and spatially heterogeneous effects on bone of different types of muscle contractions.

1) Carballido-Gamio et al J Bone Miner Res. 2013 Mar;28(3):537-46
2) Keyak et al Clin Orthop Relat Res. 2005 Aug;(437):219-28
3) Lang et al J Bone Miner Res. 2004 Jun; 19(6):1006-12

Table 1: Percent changes in vQCT and FEM bone variables for ABADD and SQDL exercise groups. FN=femoral neck;cBMD=cortical BMD ;iBMD=integral BMD;cVOL=cortical volume. Pre- to post-training within group paired t-test *: p<0.05;**:p<0.01

	FN cBMD	FN iBMD	FN cVOL	Troch cBMD	Troch iBMD	Troch cVOL	Strength FALL	Strength STANCE
ABADD	0.0	0.8	3.8 (p=0.07)	0.2	0.4	4.4**	0.5	0.4
SQDL	1.6 **	1.6 *	4.4*	0.2	0.0	0.0	1.0	9.2*

Table 1

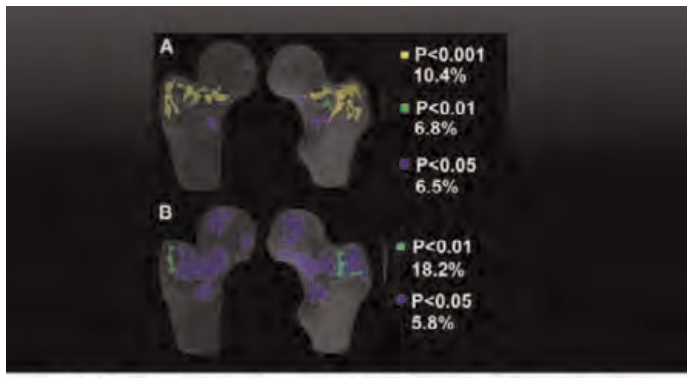

Figure 1: Voxel clusters meeting criteria for statistically significant change (at least 25 contiguous voxels with BMD change ≥ 10 mg/cm^3). A) ABADD B) SQDL

Figure 1

***Disclosures: Thomas Lang**, Amgen, 2*

FR0192

Selective RARγ agonist blocks heterotopic ossification and promotes skeletal muscle repair. Agnese Di Rocco*, Kenta Uchibe, Maurizio Pacifici, Masahiro Iwamoto. Children's Hospital of Philadelphia, ARC, USA

Skeletal muscles can be damaged or injured for a variety of reasons such as overuse and trauma. Repair/regeneration of severely damaged and/or degenerated muscle tissue is still quite challenging and often result loss of functionality of the muscle tissue.

Heterotopic ossification (HO) is a pathological bone formation in the soft tissue. Since majority of HO occurs in the skeletal muscle, HO has been linked with muscle degeneration for a long time. We have recently reported that selective agonists for retinoic acid receptor gamma (RARγ agonist) effectively blocks HO in the fibrodysoplasia ossificans progressiva like model mouse (FOP like model). In this model, we locally injected cardiotoxin as an inducer of inflammation and muscle degeneration. In control, skeletal muscle tissue around HO was heavily degenerated. Interestingly, RARγ agonist not only blocked HO but also prevented muscle degeneration. The observation suggests that the beneficial effect of RARγ agonist on skeletal muscle could be an indirect effect by blocking HO or direct effect on skeletal muscle tissue. We tested the latter possibility.

In the first experiment, we created a critical round-shape defect in tibialis anterior-muscle of 6 weeks old wild type mice and examined the effect of RARγ agonist. In control, the defects were mostly filled with scar and adipose tissues. In contrast,

RARγ agonist treatment not only reduced the size of the defect but also decreased adipose and fibrous tissue in the defect.

To study the role of RARγ in muscle repair, we injected carditoxin into tibialis anterior-muscles of RARγ-null or wild type littermates and analyzed histology at 2 weeks. In wild type, the initially damaged region was completely replaced with new muscle fibers. RARγ-null mice however still contained necrotic tissue and inflammatory cells. To further study the role of retinoid signaling in muscle regeneration, we examined distribution of retinoid signaling in RARE-Lac-Z reporter mice after muscle laceration. Lac-Z positive area started to appear 4 days after injury, and it can still be detected at day 7.

All together our results indicate that (1) RARγ is an endogenous regulator of muscle repair and (2) its activation using a selective agonist not only decreases skeletal muscle degeneration, but also accelerates muscle regeneration. Thus, selective RARγ agonists may be useful to treat variety of muscle problems ranging from local injury to systemic myopathy.

***Disclosures: Agnese Di Rocco**, None.*

FR0194

CKMM Polymorphism Is Associated with Physical Fitness Test Scores In Military Recruits. Courtney Sprouse*[1], Laura Tosi[1], Jason Lipof[2], Mai Abdel-Ghani[3], Hugo Clifford[2], Kirsten Norrell[2], Nathanael Leo[2], Victoria Rentas[4], Heather Gordish-Dressman[1], Joseph Devaney[1], Karen Kelly[5]. [1]Children's National Medical Center, USA, [2]George Washington University, USA, [3]George Mason University, USA, [4]Howard University, USA, [5]Naval Health Research Center, USA

Introduction: Muscle-specific Creatine Kinase (CKMM), an isozyme of creatine kinase, is abundant in skeletal muscle. CKMM is thought to play an integral role in maintaining energy homeostasis by providing a steady supply of creatine phosphate, which is critical for sustaining the Ca^{2+}-ATPase channel in the sarcoplasmic reticulum. It has been suggested that a genetic variant in the 3'-untranslated region of CKMM gene, rs8111989, contributes to individual differences in physical performance. We hypothesized that rs8111989 might be predictive of physical fitness test (PFT) scores in military recruits.

Methods: We studied 172 male military infantry recruits undergoing basic training. PFT measures included three-mile run-time and number of pull ups/sit-ups achieved in two minutes. BMI, body weight, smoking status and a total PFT score were calculated. DNA extracted from whole blood was genotyped using a Taqman genotyping assay from Life Technologies. Statistical analysis: Hardy- Weinberg equilibrium (HWE) was determined using a ^{2}-test to compare the observed genotype frequencies to those expected under HWE. Normality of each quantitative trait was tested using the Shipiro-Wilk normality test. Mean measurements were compared to SNP genotypes (dominant model: TT vs. CT/CC) using analysis of covariance (ANCOVA) methods, followed by Sidak post hoc analysis to control for multiple comparisons.

Results: Participants with two copies of the TT allele had higher PFTS for all three measures of physical fitness: run time, pull ups, and total physical fitness test score. Specifically run time scores were TT [n = 97]: 82 $\pm$ 10 PFTS versus CC/CT [n = 79]: 78 $\pm$ 11 PFTS; p = 0.0370, pull-ups scores were TT [n = 97]: 78 $\pm$ 11 PFTS versus CT/CC [n = 79]: 65 $\pm$ 21; p=0.0496. Total physical fitness scores were TT [n = 97]: 250 $\pm$ 31 PFTS versus CC/CT [n = 79]: 238 $\pm$ 31PFTS; p=0.0173. There was no association with BMI, body weight, number of sit-ups, and smoking status.

Discussion: We demonstrated an association between physical performance and variation in the CKMM gene (rs8111989). Two copies of the common allele were associated with faster run time PFT score, number of pull-ups, and total PFT score. Our study supports the findings of Heled et al. (2007) who found that individuals with the TT genotype were more likely to be high responders to exercise protocols.

***Disclosures: Courtney Sprouse**, None.*

FR0195

Effects of Vitamin D Supplementation on Neural Plasticity, Serum Brain-derived Neurotrophic Factor (BDNF) and Functional Performance in Older Adults: A 10-week Double-Blinded, Placebo Controlled Randomised Trial. Robin Daly*, Stephanie Pirotta, Dawson Kidgell. Centre for Physical Activity & Nutrition Research, Deakin University, Australia

Vitamin D has direct effects on muscle modulated by specific VDRs present in muscle tissue, but VDRs are also located in the brain and CNS, including the primary motor cortex (M1) which is responsible for controlling movement. Thus it is possible that the beneficial effects of Vit D on neuromuscular function may be mediated by changes in neural plasticity (eg. the ability of the brain to adapt and strengthen neural connections). Transcranial magnetic stimulation (TMS) is a non-invasive technique that allows an objective assessment of neurophysiological changes such as corticomotor plasticity and altered synaptic activity, and thus provides direct evidence of changes in the responsiveness of the human corticospinal tract. The aim of this 10-wk double-blinded, placebo controlled trial was to examine the effects of Vit D on: 1) corticomotor excitability and plasticity; 2) serum brain-derived neurotrophic factor (BDNF), a neurotrophin involved in regulating synaptic plasticity and neurogenesis, and 3) muscle strength, power and function. Healthy adults aged 60+ yrs with serum 25OHD <60 nmol/L were randomized to 2000IU/d Vit D3 (n=13) or a matched placebo group (n=13). Single and paired-pulse TMS applied over the M1 was used to assess changes in motor evoked potentials (MEPs) and short-interval intracortical inhibition (SICI), as a measure of corticomotor excitability and inhibition, respectively, by recording EMG responses to stimulation from the wrist extensors. Muscle strength (leg extension), power (stair climb), function (TUG, four square step test), serum 25OHD and BDNF were assessed. 96% of the participants completed the trial; supplement compliance was similar between the groups (98% Vit D; 89% placebo, P=0.13). Serum 25OHD increased by 34 nmol/L in the Vit D group with no change in the controls (-1.2 nmol/L). After 10-weeks, treatment with Vit D resulted in an increase in muscle strength (8-11%) and a reduction in cortical excitability (MEP amplitude) and intracortical inhibition (all $P<0.05$). However, these changes were not significantly different from those observed in the controls. There was no effect of Vit D on muscle power, function or serum BDNF. While the lack of significant between group differences may relate to the sample size, the reduction in excitability and inhibition suggests that Vit D may improve the efficacy of neural transmission within the corticospinal pathway, and thereby facilitate motor output and improve muscle performance.

***Disclosures: Robin Daly**, None.*

FR0196

Effect of 1 year of whole-body vibration therapy on muscle density and volume in postmenopausal women: the Vibration Study. Miranda Boggild*[1], Marta Erlandson[2], George Tomlinson[1], Eva Szabo[1], Lubomira Slatkovska[2], Lora Giangregorio[3], Cathy Craven[1], Shabbir Alibhai[1], Angela M. Cheung[5]. [1]University of Toronto, Canada, [2]University Health Network, Canada, [5]University Health Network-University of Toronto, Canada

Purpose: Whole-body vibration (WBV) therapy has been proposed as a potential therapy for reducing sarcopenia (or age-related skeletal muscle loss) and its negative consequences (such as frailty, functional impairment and increased risk of fracture). Previous meta-analyses suggest WBV therapy may improve muscle strength and balance in the elderly. The purpose of this study was to explore whether WBV therapy increases muscle density and volume as measured by high-resolution peripheral quantitative computed tomography (HR-pQCT) in the Vibration Study.

Methods: The Vibration Study is a 1-year 1: 1: 1 randomized controlled trial comparing 0.3g 30-Hz WBV, 0.3g 90-Hz WBV and control in 202 healthy postmenopausal women with low bone density (T-score -1 to -2.5). The WBV intervention groups were asked to stand on a 30- or 90-Hz WBV platform daily for 20 minutes; all participants received calcium and vitamin D. The primary outcome of the study was trabecular volumetric bone density at the distal tibia. For this secondary research question, we analyzed muscle density and volume in HR-pQCT distal tibia scans at baseline and 1-year in a blinded fashion. Our primary analysis was intention-to-treat, run separately for muscle density and volume; using linear regression, we compared change from baseline between WBV groups, adjusting for the baseline measurement.

Results: Compared to no WBV therapy, 0.3g 30- or 90-Hz WBV therapy had no significant effect on muscle density or muscle volume at the distal tibia after 1 year. The mean change in muscle density from baseline to 1 year was 0.39 (SD 1.5) mgHA/cm^3 in the 30-Hz WBV group, 0.18 (SD 1.6) mgHA/cm^3 in the 90-Hz WBV group, and 0.38 (SD 1.5) mgHA/cm^3 in the control group (p = 0.8). The mean change in muscle volume from baseline to 1 year was 77.6 (SD 550) mm^3 in the 30-Hz WBV group, 209.2 (SD 796) mm^3 in the 90-Hz WBV group, and 79.4 (SD 675) mm^3 in the control group (p = 0.5). Per-protocol, sensitivity, and subgroup analyses revealed no significant effects of WBV on muscle density or volume.

Conclusion: In this secondary exploratory analysis, one year of daily low magnitude whole-body vibration therapy at 30- or 90-Hz had no significant effect on muscle density or volume at the distal tibia in postmenopausal women.

Keywords: sarcopenia, whole-body vibration, muscle density, muscle volume, postmenopausal women, HR-pQCT

***Disclosures: Miranda Boggild**, None.*
This study received funding from: Juvent, Jamieson Laboratories,

FR0202

Intermittent PTH Increases Bone Formation but Not Bone Mass in Osteopenic Mice Lacking Gsa in Osteoblasts. Rhiannon Chubb[1], Partha Sinha[1], Piia Aarnisalo[2], Rachelle Johnson[3], Ingrid Poulton[3], Min Chen[4], Lee Weinstein[4], Natalie Sims[3], Henry Kronenberg[1], Joy Wu*[5]. [1]Massachusetts General Hospital, USA, [2]University of Helsinki & Helsinki University Central Hospital, Finland, [3]St. Vincent's Institute of Medical Research, Australia, [4]National Institute of Diabetes & Digestive & Kidney Diseases, USA, [5]Stanford University School of Medicine, USA

Parathyroid hormone is an important regulator of osteoblast function and is in clinical use as the only anabolic therapy currently approved for the treatment of osteoporosis. The parathyroid hormone (PTH) receptor (PPR) is a G protein-coupled receptor that signals via multiple G proteins including Gsα. Ablation of Gsα in the osteoblast lineage during embryonic development using osterix-driven Cre recombinase (GsαOsxKO mice) resulted in fractures at birth. GsαOsxKO mice do not survive past weaning, but administration of doxycycline to delay expression of Cre recombinase until birth yields mice with postnatal ablation of Gsα in the osteoblast

lineage (P-GsαOsxKO mice). We have previously reported that P-GsαOsxKO mice have markedly reduced trabecular and cortical bone, with normal serum calcium, phosphate, and PTH levels. Furthermore, expression of sclerostin, a canonical Wnt inhibitor that is suppressed by PTH and upregulated in the absence of Gsα, is significantly increased in P-GsαOsxKO osteocytes, suggesting efficient removal of Gsα in the osteoblast lineage. To determine the role of Gsα in the anabolic response to recombinant PTH administration, we administered daily PTH(1-34) (80 mg/kg/day) to male and female P-GsαOsxKO mice and controls, beginning at 8 weeks of age. Vehicle-treated P-GsαOsxKO mice had markedly reduced trabecular bone volume and cortical thickness relative to controls. After 4 weeks of PTH treatment, trabecular bone volume was increased in female control mice, but this was completely abrogated in P-GsαOsxKO mice. In both male and female mice, PTH treatment significantly increased trabecular thickness (measured by both microCT and histomorphometry); this effect was also observed in P-GsαOsxKO mice. In addition, osteoblast surface, osteoblast numbers and bone formation rate were each significantly increased to a similar extent in both P-GsαOsxKO and control mice treated with PTH. Osteoclast surface was slightly increased by PTH treatment only in P-GsαOsxKO mice, and while this did not reach statistical significance, trabecular number was significantly reduced in P-GsαOsxKO but not control mice treated with PTH, suggesting a bone resorption response. Together these data indicate that the anabolic effect of intermittent PTH treatment on overall trabecular bone volume is blunted by deletion of Gsα in osteoblasts. Surprisingly, however, PTH is capable of stimulating osteoblast differentiation and bone formation even in the absence of osteoblastic Gsα. This suggests a Gsα-independent pathway of PTH anabolic action on osteoblast differentiation.

***Disclosures: Joy Wu**, None.*

FR0210

Semaphorin 3A regulates bone homeostasis through sensory nerve system. Toru Fukuda*[1], Ren Xu[2], Hiroki Ochi[1], Satoko Sunamura[1], Tsuyoshi Sato[3], Shinsuke Shibata[1], Chenshan Ma[2], Cheng Xu[2], Ayako Kimura[2], Yoshinori Asou[2], Mitsuhiro Enomoto[2], Hideyuki Okano[1], Atsushi Okawa[2], Hiroshi Ito[1], Shu Takeda[1]. [1]Keio University School of Medicine, Japan, [2]Tokyo Medical & Dental University, Japan, [3]Saitama Medical University, Japan

Semaphorin 3A (Sema3A) is a secreted and membrane bound proteins originally discovered in the nervous system, which are involved in repulsive axon guidance during nervous system development. Previous studies have demonstrated that global Sema3A-knockout (KO) mice have multiple developmental defects including low bone mass due to bone-anabolic action of Sema3A. However, osteoblast-specific Sema3A-KO mice had normal bone mass, even though the expression of Sema3A in bone was substantially decreased. In contrast, mice lacking Sema3A in neurons had low bone mass similar to global Sema3A-KO mice, indicating that neuron-derived Sema3A is responsible for the bone abnormalities independent of the local effect of Sema3A in bone. Indeed, sensory innervations of trabecular bone were significantly decreased in neuron specific Sema3A-KO mice, whereas sympathetic innervations of trabecular bone were unchanged. Moreover, ablating sensory nerves decreased bone mass in wild-type mice, whereas it did not deteriorate low bone mass phenotype in neuron specific Sema3A-KO mice, further indicating the essential role of sensory nervous system in normal bone homeostasis. In summary, this study demonstrates that Sema3A regulates bone remodelling indirectly by modulating sensory nerve development and sensory neurons are indispensable for bone development and homeostasis.

***Disclosures: Toru Fukuda**, None.*

FR0211

TSC1 Deletion in Neural Crest-derived Cells Leads to Excess Craniofacial Bone Formation through the Expansion of Osteoblast Lineage Cells. Fang Fang*[1], Dongye Yang[1], Yuan Zhu[1], Fei Liu[2]. [1]University of Michigan, USA, [2]University of Michigan School of Dentistry, USA

Conflicting *in vitro* results were reported about the regulation of mTOR on osteogenesis. To study the role of mTOR signaling in bone homeostasis *in vivo*, we deleted TSC1, a negative regulator of mTOR signaling, with P0-Cre, which targets neural crest-derived (NCD) cells that generate majority of the craniofacial bones. Despite the low deletion efficiency (43%) in NCD bones shown by qPCR, μCT analysis demonstrated strikingly increased bone mass in all NCD bones such as frontal, nasal, and zygomatic bones. This mimicked the sclerotic lesions in craniofacial region of 40% of the Tuberous Sclerosis patients, in which mutations in TSC1 or TSC2 cause the disease. The thickness of frontal but not parietal (mesoderm derived) bone in conditional knockout (CKO) mice dramatically increased (1.25, 1.8, 2.09 and 2.83 folds at 1, 2, 3 and 12 month respectively, $p<0.05$, n=5-13) comparing to their control littermates (CTR). TRAP staining showed comparable osteoclast number in the frontal bone of CKO mice, which excluded the contribution of altered osteoclastogenesis. After the IP injection of rapamycin, inhibitor of mTOR, at 1mg/kg every the other day from 1 to 8.5 week, calvaria thickness increase in CKO mice was completely rescued. To perform lineage-tracing experiment, we crossed CTR and CKO mice to R26 reporter mice and found 3-fold increase in P0-Cre targeted NCD cells (lacZ positive) in both metopic suture and frontal bone of 7-day-old CKO mice. Importantly, rapamycin treatment (from birth to day 7) rescued the increase in lacZ staining in CKO bone. Interestingly, osteocyte density in CKO mice frontal bone was significantly higher than that of CTR at one month of age (1547 *vs.* 1072 cells/mm^2, $p<0.05$, n=5-6). In addition, mRNA expression of osteocalcin (OCN), an osteoblast specific marker, increased 50% in the frontal bone of 7-day-old CKO mice, further suggesting an increase in osteoblast lineage cells. *In vitro*, although we observed increased phospho-S6 and -4EBP1 expression, indication of enhanced mTOR signaling, in primary frontal osteoblasts of CKO mice, osteoblast differentiation was not affected, shown by the comparable Alkaline Phosphatase/Alizarin Red Staining and expression of osteoblast markers (OCN, BSP, Col1A1 and Runx2). Altogether, our findings suggest that enhanced mTOR signaling in NCD cells can increase bone mass through the enlargement of osteoblast population, which may be responsible for the hyperostosis observed in Tuberous Sclerosis patient.

***Disclosures: Fang Fang**, None.*

FR0212

The Presence of Either Cdc42 or Rac1 is Required for the Crosstalk between Osteoblasts and Adipocytes. Carina Wuerfel, Carla Sens, Christine Hoffmann, Inaam Nakchbandi*. Max-Planck Institute of Biochemistry & University of Heidelberg, Germany

Both RhoGTPase cdc42 and rac1 regulate cell division, migration and polarization, and are involved in the transfer of extracellular signals into the cells. Because of its importance knockout mice die during embryonal development. Because both RhoGTPases mediate effects required for osteoblast differentiation we examined their roles in osteoblasts.

Using the cre-lox*p* system we evaluated the effect of deleting cdc42 using the osterix promoter. There was a significant decrease in BMD in 3-week-old conditional knockout (cKO) mice (15%). Bone histomorphometry revealed a significant decrease in osteoblast numbers (29%). Isolated calvarial osteoblasts showed decreased differentiation. Interestingly, the number of adipocytes was significantly increased in the bone marrow (9-fold). This was not due to deletion of cdc42 in bone marrow cells because transplantation of cKO bone marrow into CT mice did not result in increased adipocytes. Coculturing cKO osteoblasts and CT bone marrow resulted in increased adipocytes. In line with these findings markers of adipocyte differentiation were significantly increased in cKO bone marrow (1.5 to 4-fold). These data suggest a direct effect of cdc42 in osteoblasts on adipocyte differentiation. In order to determine whether this was due to an upregulation of rac1 we first deleted rac1 in osteoblasts using the osterix promoter. This resulted in a significant decrease in BMD associated with a decrease in osteoblast numbers on bone histomorphometry (11 and 40%). Isolated osteoblasts showed significantly decreased differentiation *in vitro*. Cocultures of cKO osteoblasts with CT bone marrow resulted in a significant increase in adipocytes. This suggests that the absence of rac1 decreases osteoblast and increases adipocyte differentiation. In double cKO animals however, the decrease in BMD as well as osteoblast number *in vivo* and differentiation *in vitro* were not associated with an increase in adipocyte. Neither Runx2 nor a change in osteocyte numbers seemed to be responsible for this effect.

These data suggest that both rac1 and cdc42 are required for osteoblast differentiation, but that adipocyte differentiation is increased only if one of these two molecules is still present. Thus, the signals originating from the osteoblasts and resulting in adipocyte differentiation require the expression of at least one of these two molecules. This establishes a role for RhoGTPases in the crosstalk between osteoblasts and adipocytes.

***Disclosures: Inaam Nakchbandi**, None.*

FR0226

N-cadherin Restrains the Anabolic Action of Parathyroid Hormone via Interference with Lrp6/β-catenin Signaling. Leila Revollo*[1], Jin Norris[2], Gabriel Mbalaviele[3], Roberto Civitelli[3]. [1]Washington University, Division of Bone & Mineral Diseases, USA, [2]Washington University in St Louis, USA, [3]Washington University in St. Louis School of Medicine, USA

Interaction between PTHR1 and Lrp6 has been linked to the anabolic action of PTH. Since N-cadherin negatively regulates Wnt/β-catenin signaling by interaction with Lrp5/6 in osteoblasts, we hypothesized that N-cadherin may affect PTH-induced anabolic response by interfering with Lrp6 signaling. We tested our hypothesis in mice with a deletion of the N-cadherin gene (*Cdh2*) in osteoblasts ($Cdh2^{flox/flox}$*::Osx-Cre;* cKO). $Cdh2^{flox/flox}$ *and Osx-Cre* mice were used as control. Mice were treated with human PTH (80μg/kg bw, sc, 5x/week, 4 weeks) and changes in bone mass and architecture determined by μCT imaging. PTH increased trabecular thickness and bone volume/tissue volume in cKO to a significantly larger extent than in either control group, suggesting that N-cadherin restrains PTH anabolic effect. Co-immunoprecipitation experiments with bone marrow stromal stem cells (BMSC) from control mice show that PTHR1 interacts with Lrp6 but not Lrp5 or N-cadherin. Intriguingly, this interaction is sharply enhanced by exposure to PTH in cKO BMSC; whereas PTH has minimal effect on Lrp6/PTHR1 complexes in control cells. Confirming β-catenin activation, PTH stimulates Tcf/Lef transcriptional activity and pharmacological inhibition of PKA attenuates this effect. PTH stimulation of Tcf/Lef target genes is enhanced in N-cadherin-ablated BMSC compare to control cells. We have previously shown β-catenin up-regulation by PTH in bone. Indeed, in BMSC PTH promotes β-catenin phosphorylation at the C-terminus, an event shown to favor β-catenin stabilization and Tcf/Lef transcription. Accordingly, this phosphorylation is

hindered by a PKA inhibitor, suggesting that PTH activates β-catenin via PKA. Importantly, cKO BMSC exhibit larger and prolonged β-catenin C-terminus phosphorylation in response to PTH relative to control cells. Thus, absence of N-cadherin in osteoblasts enhances PTHR1/Lrp6 interaction in response to PTH, and leads to larger PTH-induced β-catenin stabilization via PKA-dependent phosphorylation at C-terminus sites. As others have shown that LRP6 is involved in PTH anabolic effect, we propose that N-cadherin modulates PTH-induced bone formation by functioning as a "buffer" for Lrp6, thus modulating Lrp6/PTHR1 interaction and consequently the intensity and duration of β-catenin signaling by PTH. Since N-cadherin is down-regulated as osteoblasts differentiate, this action may serve as a mechanism to restrain osteoblast precursor recruitment from uncommitted cells.

***Disclosures: Leila Revollo**, None.*

FR0230

Trabecular bone loss in Gα11 transgenic mice is characterized by decreased bone formation and increased osteoclastogenesis. Ariana Dela Cruz*[1], Michael Mattocks[1], Kim S. Sugamori[1], Marc Grynpas[2], Jane Mitchell[1]. [1]University of Toronto, Canada, [2]Samuel Lunenfeld Research Instituteof Mount Sinai Hospital, Canada

$G\alpha_{11}$ is a member of the heterotrimeric Gq protein family that mediates phospholipase C-dependent signaling downstream of G protein-coupled receptors including the parathyroid hormone 1 receptor (PTH1R). We previously demonstrated that the potent glucocorticoid dexamethasone increases $G\alpha_{11}$ protein expression in osteoblasts and can therefore enhance parathyroid hormone (PTH) signaling through the phospholipase C pathway. To identify how increased osteoblastic expression of $G\alpha_{11}$ affects bone, we generated transgenic mice that overexpress $G\alpha_{11}$ in osteoblasts (G11-Tg) driven by the 3.6kb Col1A1 promoter.

We found that G11-Tg mice overexpressed $G\alpha_{11}$ by 2-6 fold selectively in calvaria, vertebrae, long bone, and bone marrow stromal cells (BMSCs) compared to WT controls. DEXA scans revealed significant reductions in BMD in male and female G11-Tg mice aged 3- to 20-weeks. Furthermore, microCT scans showed that bone volume and microarchitecture parameters were decreased in 8-week old G11-Tg mice trabecular bone, while cortical bone was not changed. The functional consequence of decreased G11-Tg trabecular bone was assessed by vertebral compression testing, showing that G11-Tg vertebrae exhibited reduced biomechanical strength. Consistent with our microCT data, three-point bending tests displayed no differences in normalized cortical bone strength from G11-Tg mice compared to WT controls. These data indicate that $G\alpha_{11}$ over-expression preferentially affects the trabecular bone compartment.

To explore the cellular basis for the trabecular bone loss seen in G11-Tg mice, static and dynamic histomorphometry were performed. Bone resorption parameters including osteoclast number and surfaces were significantly increased, whereas osteoblast numbers were not altered. However, we found that G11-Tg rates of mineral apposition and bone formation were significantly decreased. In an *in vitro* assay to assess osteoblast differentiation, we assessed osteoblasts derived from BMSC cultures of G11-Tg mice and found increased expression of mRNA encoding osteoclast inducting proteins, M-CSF and RANKL, as well as the gene encoding MMP-13, a collagen degrading enzyme.

In summary, our results suggest that osteoblastic over-expression of $G\alpha_{11}$ results in a dual mechanism of trabecular bone loss by promoting induction of bone-resorbing osteoclasts and decreasing bone formation rate.

***Disclosures: Ariana Dela Cruz**, None.*

FR0241

Prostaglandin E2 Regulates Osteoblastic Niche Selectively for Hematopoietic Progenitors through Induction of Osteopontin via EP4 Receptor. Yuko Kawano*[1], Mari Sato[1], Noboru Asada[1], Chie Fukui[1], Kanako Wakahashi[1], Hiroki Kawano[1], Kentaro Minagawa[1], Akiko Sada[1], Satoshi Uematsu[2], Shizuo Akira[2], Toshimitsu Uede[3], Shuh Narumiya[4], Toshimitsu Matsui[1], Yoshio Katayama[5]. [1]Hematology, Department of Medicine, Kobe University Graduate School of Medicine, Japan, [2]Laboratory of Host Defense, WPI Immunology Frontier Research Center, Osaka University, Japan, [3]Division of Molecular Immunology, Institute for Genetic Medicine, Hokkaido University, Japan, [4]Department of Pharmacology, Kyoto University Graduate School of Medicine, Japan, [5]Hematology, Dept. Med., Kobe Univ., Japan

The regulation of osteoblastic niche in bone marrow (BM) microenvironment is crucial for the maintenance of hematopoietic stem/progenitor cells (HSCs/HPCs). The mobilization of HSCs/HPCs to the circulation is triggered by their release from the niche, and the cytokine G-CSF is widely used for this purpose in clinic. Because G-CSF administration causes fever and back pain and because these symptoms are ameliorated with NSAIDs, we investigated the role of PGE2 in osteobalstic niche regulation. First, HPC mobilization by G-CSF (125μg/kg/dose, every 12 hours, 8 divided doses) was significantly augmented in PGE syntase-1-deficient mice (42% increase), and strongly inhibited by exogenous administration of PGE2 (6mg/kg/day for 2 weeks) to wild-type (WT) mice (by 52%). The inhibitory effect of PGE2 was completely abrogated in PGE2 receptor EP4-deficient mice, and the chimeric model generated by the reciprocal BM transplantation revealed it was EP4 in microenvironment, but not in hematopoietic cells, that was critical for this effect. Since PGE2 did not change the CXCL12 behavior, we speculated that PGE2 increased another anchor in the niche, osteopontin (OPN). Immunofluorescence staining demonstrated clear upregulation of OPN by PGE2 and/or G-CSF in endosteum, which was abolished in EP4-/- mice. Indeed, the inhibitory effect of PGE2 on HPC mobilization was canceled partially in OPN-/- mice and almost completely in anti-OPN antibody-treated WT mice. To confirm the induction of OPN by PGE2 directly, we fractionated non-hematopoietic (CD45-CD31-Ter119-) cells isolated from femur into three populations, i.e. Sca-1+ALCAM- immature mesenchymal cells, Sca-1-ALCAM- preosteoblasts, and Sca-1-ALCAM+ mature osteoblasts that are most potent to maintain quiescent HSCs in vitro. PGE2 upregulated OPN protein 2-fold in Sca-1+ALCAM- immature mesenchymal cells in cultures, and more dramatically (6-fold) in Sca-1-ALCAM- preosteoblasts, as assessed by flow cytometry. In sharp contrast, no OPN induction was observed in Sca-1-ALCAM+ mature osteoblasts. In contrast to HPCs, the mobilization of long-term repopulating HSCs was not altered in PGE2-treated WT mice, indicating that PGE2 does not modulate HSC niche. Collectively, the results suggest that PGE2 regulates osteoblastic niche selectively for HPCs through the induction of OPN via EP4 receptor. Thus, PGE2/EP4/OPN pathway may be an important pharmacological target to modulate the function of BM microenvironment.

***Disclosures: Yuko Kawano**, None.*

FR0242

Rejuvenating Bone Fracture Repair. Gurpreet Baht*[1], Benjamin Alman[2]. [1]University of Toronto, Hospital for Sick Children, Canada, [2]Hospital for Sick Children, Canada

The capacity for tissues to repair and regenerate diminishes with age. In vivo bone repair and in vitro differentiation of bone marrow stromal cells to osteoblasts is more efficient in young animals than old animals. We sought to determine the effect of animal age, cell age, and matrix age on bone regeneration and osteoblast differentiation. Fracture repair and osteoblast differentiation were more efficient and more robust in young mice (4 months) than in old mice (18 months). Exposure to a youthful circulatory system by via heterochronic parabiosis rejuvenated aged fracture repair and aged osteoblast differentiation. When osteoblasts were ablated in the old heterochronic host, bone regeneration capacity and osteoblastogenesis were completely ablated. Conversely, removal of osteoblasts from young partners did not affect rejuvenation of old, heterochronic mice. Transplantation of young bone marrow rescued fracture repair and osteogenic potential in a mechanism which again required osteoblasts from the host animal but not osteoblasts from the donor animal. Tissue culture methods were used to rescue the age-dependent decrease in osteogenic potential. Western blot analysis from cell lysates identified a decrease in β-catenin during rescue. In vivo, β-catenin was found to be elevated upon fracture; however, β-catenin was elevated further in old calluses relative to young calluses and remained elevated throughout repair. Because β-catenin regulation is critical during mesenchymal commitment to an osteochondral lineage, its dysregulation in old bone may be contributing to the impaired fracture healing observed. Transplantation of young, wildtype bone marrow was not able to rejuvenate fracture repair in old mice in which β-catenin levels could not be modulated. Pharmacologic reduction of β-catenin during early fracture repair improved bone regeneration in old mice. These data demonstrate that the circulatory system carries within it a "youth factor" which originates, in part, from the bone marrow. This youth factor is able to rejuvenate bone repair and osteoblast differentiation through modulation of β-catenin. Agents which modulate β-catenin can improve the quality of fracture repair and osseous integration of implants in the aging population.

***Disclosures: Gurpreet Baht**, None.*

FR0243

Sirt1 in osteoblast progenitors expressing Osterix1 promotes cortical bone mass accrual. Srividhya Iyer*[1], Li Han[1], Shoshana Bartell[1], Aaron Warren[1], Julie Crawford[2], Rafael de Cabo[3], Stavros Manolagas[1], Maria Jose Almeida[1]. [1]Central Arkansas Veterans Healthcare System, University of Arkansas for Medical Sciences, USA, [2]University of Arkansas for Medical Sciences, USA, [3]Experimental Gerontology, NIA, NIH, Baltimore, MD, USA

Sirt1, a nicotinamide adenine dinucleotide+ class III histone deacetylase, associates with several non-histone regulatory proteins in mammalian systems and regulates age-related processes including, cancer, glucose metabolism, apoptosis, mitochondrial biogenesis, and defense against oxidative stress. Sirt1 deletion in mesenchymal cells expressing Prx1 attenuates their differentiation and decreases both cortical and cancellous bone in aged mice. In contrast, Sirt1 deletion in mature Col1a1 expressing osteoblasts decreases only cancellous bone. Notably, in either model, the bone phenotype is restricted to females. Here we have deleted the Sirt1 floxed (f) allele in osteoprogenitors and their descendants using the Osx1-Cre transgene. Sirt1 mRNA was reduced by ~90% in Osx1-Cre expressing cells from the $Sirt1^{f/f}$;Osx1-Cre mice compared to Osx1-Cre littermate controls. Bone marrow cultures from the $Sirt1^{f/f}$;Osx1-Cre mice had decreased numbers of colony forming unit of osteoblasts and adipocytes. High density cultures of adherent bone marrow cells exhibited reduced mineralization and decreased expression of osx1, runx2, col1 and osteocalcin. In addition, osteoprogenitor cells from $Sirt1^{f/f}$;Osx1-Cre mice exhibited increased apoptosis, as determined by caspase 3 activity. Stimulation of Sirt1 by two synthetic compounds (provided by GlaxoSmithK-

line), on the other hand, increased osteoblast differentiation in Sirt1 replete, but not deficient, bone marrow cultures. Strikingly, stimulation of osteoblast differentiation in bone marrow-derived osteoprogenitor cells by the Sirt1 activators was attenuated in cells lacking ERα, consistent with published evidence that Sirt1 and ERα interact in other cell types. Furthermore, female, but not male, $Sirt1^{f/f}$;Osx1-Cre mice had reduced cortical thickness in femur as well as in vertebra, as determined by microCT at 3 months of age. The vertebral cancellous bone volume (BV/TV) was unaffected; albeit, there was a small decrease in trabecular thickness in both femur and vertebra at this age. In addition, markers of oxidative stress, including reactive oxygen species levels in bone marrow, as well as phospho-$p66^{shc}$ in vertebral lysates were elevated in $Sirt1^{f/f}$;Osx1-Cre mice. Collectively, these results demonstrate that Sirt1 in Osx1 cells (not mesenchymal progenitors or mature osteoblasts) promotes accrual of cortical bone in females, perhaps in part by potentiating ERα signaling.

***Disclosures: Srividhya Iyer**, None.*

FR0244

Analysis of αSMA-labeled Progenitor Cell Commitment Identifies Notch Signaling as an Important Pathway in Fracture Healing. Brya Matthews*[1], Danka Grcevic[2], Liping Wang[3], Yusuke Hagiwara[3], Douglas Adams[3], Ivo Kalajzic[3]. [1]University of Connecticut Health Center, Department of Reconstructive Sciences, USA, [2]University of Zagreb, Croatia, [3]University of Connecticut Health Center, USA

Fracture healing is a complex process that involves coordinated cellular responses, but characterization of specific cell populations in this process has been limited. We identified alpha smooth muscle actin (αSMA) as a marker of periosteal progenitor cells that contribute to fracture healing.

To identify and trace cells in periosteum we used αSMA promoter-driven inducible Cre (αSMACreERT2) combined with a Cre-activated fluorescent reporter Ai9 to generate SMA9 mice. Tibial fractures were performed after tamoxifen-induced labeling of cells, and the SMA9+ population was characterized during the early stages of fracture healing by histology, flow cytometry and gene expression profiling.

Histology indicated that SMA9+ periosteal cells expanded after fracture, and by day 6 were contributing to chondrocytes and osteoblasts within the callus. Periosteal cells from labeled unfractured bone, or periosteum/fracture callus from fracture day 2 and 6 were isolated for flow cytometry or cell sorting for RNA extraction. Over 95% of SMA9+ cells were negative for hematopoietic and endothelial lineage markers. The frequency of mesenchymal stem cell markers such as Sca1 increased after fracture (9% unfractured SMA9+ cells, 26% at day 6). Gene expression profiling showed that proliferation genes and cytokines/chemokines were upregulated 2 days after fracture. By fracture day 6, genes involved in matrix production and remodeling, including chondrocyte markers Col2a1 and aggrecan, and osteoblast markers alkaline phosphatase and bone sialoprotein were elevated. Genes associated with muscle contraction and Notch signaling were downregulated after fracture. Given that Notch signaling is an important developmental pathway in bone, but its role in fracture healing is undefined, we examined the effect of forced Notch activation in SMA9+ mesenchymal progenitor cells *in vitro*. Cre-mediated activation of Notch signaling in SMA9+ cells from periosteal or bone marrow stromal cell cultures reduced or blocked differentiation into osteogenic, chondrogenic and adipogenic lineages.

This is the first study to characterize a defined population of mesenchymal progenitor cells that actively participate in bone repair. We found that down-regulation of Notch signaling may be important for commitment of SMA9+ cells to mature lineages. Further characterization of these cells could potentially reveal mechanisms for recruitment or expansion of progenitor cells to improve bone healing.

***Disclosures: Brya Matthews**, None.*

FR0245

Combined Deficiency of Prolyl Hydroxylase (PHD) 1 and PHD3 Increases Mesenchymal Stem Cell Number and Regulates the Hematopoietic Stem Cell Niche. Steve Stegen*[1], Satish Khurana[2], Nick van Gastel[1], Sophie Torrekens[1], Karen Moermans[1], Peter Carmeliet[3], Catherine Verfaillie[2], Geert Carmeliet[4]. [1]Laboratory of Clinical & Experimental Endocrinology, KU Leuven, Belgium, [2]Interdepartmental Stem Cell Institute, KU Leuven, Belgium, [3]Laboratory of Angiogenesis & Neurovascular Link, Vesalius Research Center, VIB, & Laboratory of Angiogenesis & Neurovascular Link, Vesalius Research Center, KU Leuven, Belgium, [4]Katholieke Universiteit Leuven, Belgium

Several distinct cell populations of the bone microenvironment are critical for hematopoietic stem cell (HSC) maintenance including mesenchymal stem cells (MSC), osteolineage cells and endothelial cells. Pharmacological block of the 3 prolyl hydroxylase domain enzymes (PHD), which regulate hypoxia signaling, has recently been reported to increase the number of quiescent HSCs. These compounds have previously been described to enhance bone mass by increasing the number of blood vessels. In this study we investigated the specific contribution of PHD1 and PHD3 on bone as well as HSC niche by genetic means.

Inactivation of both PHD1 and PHD3 (*Phd1/3* dKO) has no effect on most of the skeletal parameters including bone length, growth plate morphology, mineralized bone mass or the number of osteoblasts or osteoclasts, suggesting that PHD2 can compensate for these functions. However, several observations indicate that PHD1 and PHD3 specifically regulate the HSC niches in the bone/bone marrow. First, *Phd1/3* dKO osteoblasts produce more unmineralized bone matrix *in vivo*, without a change in dynamic mineralization parameters. Moreover, sorted osteoblasts ($Lin^-CD45^-CD31^-Sca1^-CD51^+$) displayed increased expression of genes coding for HSC supporting factors, including Osteopontin, CXCL12, Annexin A2, VCAM-1 and Angiopoietin-1. Secondly, *Phd1/3* deletion increases the number of MSC shown by a higher number of $Lin^-CD45^-CD31^-Sca1^+$ or $Lin^-CD45^-Nestin^+$ cells and supported by increased osteoblast colony forming units detected *in vitro*. In addition, sorted MSC ($Lin^-CD45^-CD31^-Sca1^+$) expressed increased levels of Osteopontin, CXCL12, Annexin A2, VCAM-1 and Angiopoietin-1. Thirdly, the number of blood vessels is increased shown by immunohistochemistry and the number of $Lin^-CD45^-CD31^+$ cells. Of note, opposite to the general accepted paradigm, the increased vascularity in *Phd1/3* dKO mice was not associated with increased bone mass, further supporting the concept that the primary role of PHD1 and PHD3 in bone is related to the control of the HSC niche by influencing multiple cell types. The changes in the HSC niches were linked to an increase in the frequency of primitive HSCs ($CD150^+CD48^-KLS$ cells) expressing more CXCR4 and showing improved competitive repopulation ability.

Taken together, this study indicates that PHD1 and PHD3 regulate the number and expression profile of osteolineage and endothelial cells constituting the HSC niche and control HSC number without affecting bone mass.

***Disclosures: Steve Stegen**, None.*

FR0246

Effects of Blockade of Endogenous Gi Signaling in Endothelial Lineage Cells on Bone Formation in a Heterotopic Ossification Model. Liping Wang*[1], Dylan O'Carroll[2], Xuhui Liu[3], Theresa Roth[2], Abbott Marcia[2], Hubert Kim[3], Bernard Halloran[4], Robert Nissenson[5]. [1]VA Medical Center, San Francisco, USA, [2]Endocrine Unit, VA Medical Center & Departments of Medicine & Physiology, University of California, USA, [3]Orthopedic Surgery, UCSF, USA, [4]VA Medical Center (111N), USA, [5]VA Medical Center & University of California, San Francisco, USA

Heterotopic ossification (HO) recapitulates normal endochondral bone formation in atypical locations. However, the precise lineage of progenitor cells forming HO lesions remains unknown. Current studies have revealed that endothelial lineage cells (ECLs) are a likely cellular source that contributes to HO through an endothelial-mesenchymal transition (EMT) mechanism. Since signaling through the G protein Gi is required for ECL motility, we hypothesized that blockade of endogenous Gi signaling in ECLs would prevent HO formation. We induced HO by injecting rhBMP-2 (1.5 μg in hydro gel) in quadriceps muscle in 12-16 week old littermate control and Tie2.PTX mice that expression of pertussis toxin (PTX) gene, driven by the endothelial-selective Tie2 promoter. Bone formation within HO lesions was evaluated by μCT 2 weeks after BMP injection. A sexually dimorphic responsiveness to BMP was observed. BMP-induced HO was detectable by uCT in about 50% of male mice (control, 7/14; Tie2.PTX, 8/20) and in about 90% of female mice (control, 10/11; Tie2.PTX, 8/9). Moreover, expression of PTX in ECLs significantly reduced the bone volume (BV) of HO lesions by 77.1% in male mice (control, 0.35 ± 0.14 mm^3; Tie2.PTX, 0.08 ± 0.03 mm^3, $p<0.05$) and by 76.7% in females (control, 0.90 ± 0.31 mm^3; Tie2.PTX, 0.21 ± 0.08 mm^3, $p<0.05$). In addition, the orthotopic bones were assessed by μCT and histomorphometry at the distal femur. Expression of PTX in ECLs did not change bone mass and structure in male Tie2.PTX mice, but significantly increased trabecular BV/TV by 31.6% ($p<0.01$), trabecular thickness by 13.6% ($p<0.01$), mineral appositional rate by 30.6% ($p<0.05$), and bone formation rate by 65.2% ($p<0.01$) in females. This result is strikingly similar to previous findings that blockade of Gi signaling in mature osteoblasts stimulates trabecular bone formation in female but not male mice. Lineage tracing of ECLs in adult Tie2.GFP mice showed that the GFP^+ cells appeared both inside and at the surfaces of bone tissue within the BMP-induced HO lesions and in the orthotopic bones. Collectively, the above findings suggest that ECLs are an important source of osteogenic cells during bone formation. Blockade of endogenous Gi signaling in ECLs prevents formation of ectopic bone and stimulates osteogenesis in orthotopic bones. Targeting of Gi protein coupled receptors in ECLs may be a novel therapeutic strategy in states of abnormal bone formation such as osteoporosis and HO.

***Disclosures: Liping Wang**, None.*

FR0248

Vinculin Regulates Osteoclast Function. Tomohiro Fukunaga*, Wei Zou, Steven Teitelbaum. Washington University in St. Louis School of Medicine, USA

Osteoclastic bone resorption depends upon the cell's ability to form sealing zones (actin rings) by organizing its cytoskeleton via the αvβ3 integrin and osteoclastogenic cytokines. Because vinculin is an actin-binding cytoskeletal protein, we asked if it participates in skeleton degradation. Thus, we mated Vinculin(fl/fl) mice with those expressing cathepsin K-Cre (CtsK-*VCL*) to delete the gene in mature osteoclasts or with lysozyme M-Cre (LysM-*VCL*) mice to delete Vinculin in all osteoclast lineage cells. Vinculin-deficient precursors normally express osteoclast differentiation markers when exposed to M-CSF and RANKL. However, vinculin-deficient osteoclasts, expressing either Cre recombinase, cultured on bone, are small and have the "crenated" appearance characteristic of those with dysfunctional cytoskeletons. In

keeping with this conclusion, the same cells form small actin-rings and fail to effectively resorb bone as demonstrated by pit formation and CTx analysis. In keeping with inhibited resorptive function, both of CtsK-*VCL* and LysM-*VCL* mice exhibit an approximate doubling of bone mass with no change in osteoclast number *in vivo*. Vinculin functions by interacting with other proteins. To clarify the mechanism how vinculin regulate osteoclast function, we transduced WT and various mutant vinculin into LysM-*VCL* macrophages and differentiated them into osteoclast. While WT vinculin completely rescues osteoclast spreading and actin-ring formation on bone, mutant P878A which lose the ability to bind Arp2/3, also completely rescues LysM-*VCL* osteoclast function. Surprisingly, actin and paxillin binding site deletion (VCL 1-880) mutant significantly increases actin-ring area ($P<.01$). However, (VCL A50I) which blocks binding with Talin and Talin binding site deletion (VCL 811-1066) mutants fail to rescue osteoclast spreading and actin-ring formation. Thus, vinculin binding Talin, but not Arp2/3 and paxillin, is critical for osteoclast function.

***Disclosures: Tomohiro Fukunaga**, None.*

FR0249

Deletion of the Glycoprotein130 Co-Receptor in Osteoclasts Reduces Cortical Bone Formation. Rachelle Johnson*, Narelle McGregor, Holly Brennan, Ingrid Poulton, T John Martin, Natalie Sims. St. Vincent's Institute of Medical Research, Australia

The glycoprotein130 (gp130) co-receptor transduces signals in response to Interleukin-6 (IL-6) family cytokines. It is abundantly expressed in bone cells, including osteoclasts, osteoblasts and osteocytes. Studies have suggested that IL-6 signalling stimulates osteoclast activity through direct action on the osteoclast, but the role of osteoclastic gp130 in bone remodeling is not known. To determine the contribution of osteoclastic gp130 signalling to bone turnover, the gp130 transmembrane domain was conditionally deleted in osteoclasts under the control of CathepsinK-Cre recombinase and the bone phenotype of male and female mice was assessed.

Prior to phenotypic analysis, osteoclasts from *CtkCre.gp130w/w* and *CtkCre.gp130fl/f* mice were generated *in vitro* and significant knockdown (by 31%, $p<0.0001$) was confirmed in floxed cells by qPCR. Significantly longer femora were detected in *CtkCre.gp130fl/f* male mice at 6, 12 and 26 weeks of age. This was associated with increased growth plate width at 6 weeks, which could relate to gp130 deletion due to CtkCre expression in hypertrophic chondrocytes, as previously reported.

Femoral and vertebral trabecular bone volumes were normal in *CtkCre.gp130fl/f* mice compared to *CtkCre.gp130w/w* controls at 6, 12 and 26 weeks. However, histomorphometric analyses revealed a significant reduction in trabecular osteoblast number (by 38%, $p<0.05$) and mineralising surface (by 17%, $p<0.05$) in 12-week old male *CtkCre.gp130fl/f* mice, and increased osteoclast length ($p<0.05$) in both males (13%) and females (22%).

In cortical bone, osteoclastic deletion of gp130 significantly inhibited periosteal bone formation rate (by 68%, $p<0.0001$), reducing both double-labeled surface (by 75%, $p<0.008$) and mineral apposition rate (by 45%, $p<0.05$) resulting in reduced cortical thickness at 12 weeks. This lower level of bone formation was associated with reduced cortical bone size ($p<0.01$) on the periosteal (8%) and endocortical surfaces (11%) in male but not female mice at 26 weeks, contrary to the larger cortical bone phenotype reported with osteocytic deletion of gp130. Since IL-6 and IL-11R global knockout mice exhibited a similar reduction in cortical width, we also assessed these strains for periosteal bone formation, which was reduced in similar extent (by 94% in IL-6, $p<0.01$; by 65% in IL-11R, $p<0.05$) to the *CtkCre.gp130fl/f* mice. These data suggest that IL-6 and IL-11 signalling maintain periosteal growth in male mice through osteoclastic gp130.

***Disclosures: Rachelle Johnson**, None.*

FR0253

The Rho GEF Def6 is a Novel, RANKL-independent in vivo Suppressor of Osteoclastogenesis and Bone Resorption under Inflammatory Conditions. F. Patrick Ross, Nikolaus Binder*, Benjamin Schatz, Alessandra Pernis, Steven Goldring. Hospital for Special Surgery, USA

Differentially Expressed in FDPC6 cells (Def6) is a guanine nucleotide exchange factor (GEF) for Rho family GTPases. Def6 null mice are osteoporotic, with 50% lower TV/BV than wild-type (WT) animals. Treatment of *Def6*$^{-/-}$ bone marrow macrophages (BMMs) with low levels of M-CSF and RANKL induces rapid formation of many large TRAP-positive osteoclasts (OCs); under similar conditions WT cells yield only TRAP-positive mononuclear precursors. Thus, Def6 suppresses osteoclastogenic (OCg) signals. In line with this hypothesis, expression of the OC marker genes *NFATc1, CathK and CTR* is up-regulated earlier and more robustly in *Def6*$^{-/-}$ cultures. Retroviral transduction of Def6 into *Def6*$^{-/-}$ BMMs reverses enhanced OC formation and gene expression, while its over-expression in WT precursors suppresses their capacity for OCg. When mice lacking *Def6*$^{-/-}$ are bred with TCR transgenic animals the progeny develop inflammatory arthritis with marked bone erosions and raised levels of IL-17 and IL-21, potent inducers of TNFα. Given these facts, we studied the impact of TNFα on OCg by *Def6*$^{-/-}$ BMMs. Treatment of *Def6*$^{-/-}$ precursors with TNFα alone results in robust OC formation and raised mRNA levels of prototypical OC genes, while WT counterparts developed few mature OCs, with smaller increases in expression of the same genes. To exclude the potential presence in the cultures of stromal cells, which express RANKL in response to TNFα, we repeated the studies, including BMM isolation and culture, in the continuous presence of osteoprotegerin (OPG), an endogenous high affinity RANKL-binding protein. As expected, presence of the inhibitor completely abolished RANKL-induced OCg by WT and *Def6*$^{-/-}$ BMMs. Critically, OPG presence failed to alter TNFα-induced OC formation in *Def6*$^{-/-}$ BMMs, confirming that the cytokine's ability to induce OCg is RANKL independent. Supracalvarial TNFα injections in WT and *Def6-/- mice* confirmed the enhanced capacity of TNFα to induce bone resorption in vivo. Next, we asked if TNFα regulates Def6 expression and found that, like RANKL, it reduces levels of the GEF. Finally, since Def6 has cytoplasmic and nuclear actions in T-cells, we expressed HA-tagged Def6 retrovirally in BMMs to study its cellular localization during OCg and find the protein in both locations in BMMs and OCs. In summary, Def6, likely via a combination of cytoplasmic and nuclear actions, acts as a novel, RANKL-independent suppressor of OCg under inflammatory conditions in vitro and in vivo.

***Disclosures: Nikolaus Binder**, None.*

FR0258

High Bone Mass in Mice Lacking Cx37 Due to a Cell-autonomous Defect in Osteoclast Differentiation and Fusion. Rafael Pacheco Da Costa*[1], Drew M Brown[2], Iraj Hassan[2], Surajudeen Bolarinwa[2], Meloney Cregor[2], Rejane Reginato[3], Angela Bruzzaniti[4], Teresita Bellido[4], Matthew Allen[4], Lilian Plotkin[4]. [1]Indiana University/Universidade Federal de Sao Paulo - Brazil, Brazil, [2]Dept. Anatomy & Cell Biology, USA, [3]Department of Morphology & Genetics, Federal University of São Paulo, Brazil, [4]Indiana University School of Dentistry, USA

Connexin (Cx) 37 is a gap junction protein expressed in osteoblasts, osteocytes and osteoclasts. However, the role of Cx37 on bone cell function has not been investigated. Newborn Cx37$^{-/-}$ or Cx37$^{+/-}$ mice exhibit normal cartilage and calcified tissue compared to wild type Cx37$^{+/+}$ mice, as evidenced in histological whole body preparations stained with alcian blue/alizarin red. However, Cx37$^{-/-}$ male mice (N=10-14) exhibit increased spinal BMD (10-12%) at 3-5 months of age. Femoral BMD was also increased (7-10%) at 3-4 months of age. In addition, Cx37$^{-/-}$ mice exhibit higher BV/TV and trabecular number, and lower trabecular thickness in L4, measured by μCT at 5 months of age. On the other hand, Cx37 deletion did not affect cortical bone geometry at the femoral midshaft. *Ex vivo* cultures of non-adherent bone marrow cells from Cx37$^{-/-}$ mice in the presence of sRANKL and MCSF for 5 days showed a 5-fold decrease in osteoclasts compared to cultures established with Cx37$^{+/+}$ cells. In addition, Cx37$^{-/-}$ osteoclasts are 5.6-fold smaller and exhibit lower number of nuclei per cells (10.5 versus 6.6 for Cx37$^{+/+}$ and Cx37 $^{-/-}$, respectively). Moreover, expression of cathepsinK, TRAP, RANK, and calcitonin receptor, markers of osteoclast number and activity, were decreased in Cx37$^{-/-}$ cells. Cx37 absence also decreased expression of DC-STAMP, NFATc1, and Atp6v0d2, genes associated with osteoclast fusion and function. On the other hand, non-adherent bone marrow cells from Cx37$^{-/-}$ mice exhibit a 2-fold increase in the expression of CD11b, a marker of osteoclast precursors. However, the ability of MLO-Y4 osteocytic cells to support osteoclast differentiation was not reduced by silencing Cx37 using shRNA. These results are consistent with a direct effect of Cx37 deletion on the differentiation of osteoclast precursors. The mineralization potential of bone marrow cells cultured in the presence of 50μg/ml ascorbic acid and 10mM β-glycerophosphate for 14d was not changed, as evidence by similar alizarin staining. Further, osteocalcin levels were similar in vertebrae bone lysates or in the circulation in Cx37$^{+/+}$ or Cx37$^{-/-}$ mice. These results suggest that Cx37 deletion does not alter osteoblast function. Thus, Cx37 deletion increases bone mass by inhibiting osteoclast differentiation, raising the possibility that intercellular communication via Cx37 channels among mononuclear osteoclast precursors is required for triggering cell fusion and differentiation.

***Disclosures: Rafael Pacheco Da Costa**, None.*

FR0259

Cx43 Scaffolding Cytoplasmic Domain Restrains Bone Resorption but is Dispensable for the Anabolic Action of Intermittent PTH Administration. Rafael Pacheco Da Costa*[1], Iraj Hassan[2], Xiaolin Tu[3], Rejane D Reginato[4], Eduardo Katchburian[4], Teresita Bellido[3], Lilian Plotkin[3]. [1]Indiana University/Universidade Federal de Sao Paulo - Brazil, Brazil, [2]Dept. Anatomy & Cell Biology, USA, [3]Indiana University School of Medicine, USA, [4]Department of Morphology & Genetics, Federal University of São Paulo, Brazil

Connexin (Cx) 43 channels mediate intercellular communication in bone. In addition, through its cytoplasmic domain, Cx43 serves as a scaffold, facilitating intracellular signaling. Loss-of-function studies showed that mice lacking Cx43 in osteoblastic cells exhibit high RANKL/OPG expression and increased osteoclasts, reduced Sost and increased bone formation, and a defective anabolic response to intermittent PTH. However, Cx43 domains responsible for these functions have not been identified. To investigate the role of Cx43CT domain, we generated Cx43$^{stop/fl}$ mice, in which one allele of the gene is truncated at aminoacid 258 rendering a mutant that forms functional channels but lacks the scaffolding ability; and the other allele is the full length Cx43flox (fl). Female 18-week-old Cx43$^{stop/fl}$ mice exhibit 30% lower

cancellous (L5) BV/TV, decreased trabecular number and increased trabecular separation (μCT) compared to $Cx43^{fl/fl}$ control littermates, suggesting that truncated Cx43 acts as dominant negative for the full length molecule. To explore the molecular basis of this phenotype, we examined gene expression by qPCR in vertebral bone (L6). OPG level was decreased without changes in RANKL, leading to a 6-fold higher RANKL/OPG ratio in $Cx43^{stop/fl}$ mice than in controls. MCSF levels were also 2-fold higher. Consistently, calcitonin receptor expression was 4-fold increased and TRAP expression was also higher but without reaching significance. On the other hand, osteocalcin and alkaline phosphatase levels were not changed and collagen1a1 expression was 2-fold higher. Further, circulating levels of CTX were 30% higher in $Cx43^{stop/fl}$ mice than in controls. Remarkably, loss of osteocytic Cx43flox allele by crossing $Cx43^{stop/fl}$ mice with DMP1-8kbCre mice reversed the effect of truncated Cx43. Thus, $Cx43^{stop/fl}$;DMP1-8kbCre mice have higher BV/TV and trabecular number and lower trabecular separation, associated with reduced Sost expression; and reduced RANKL/OPG ratio, calcitonin receptor, and CTX, compared to $Cx43^{stop/fl}$ littermates. In spite the differences under basal conditions, all mice responded in similar fashion to daily PTH injections (100ng/g for 14d) with increased BMD, BV/TV, and osteocalcin and collagen1a1 expression in the spine. Thus, Cx43 scaffolding cytoplasmic domain is responsible for Cx43 antiresorptive function and for maintaining Sost levels that restrain bone formation, but is dispensable for the skeletal anabolic action of intermittent PTH.

***Disclosures: Rafael Pacheco Da Costa**, None.*

FR0263

Induction of osteoclast-rich osteopetrosis leads to uncoupled formation and resorption, while induction of osteoclast-poor osteopetrosis does not. Christian Thudium*[1], Carmen Flores[2], Ilana Moscatelli[2], Annemarie Brüel[3], Jesper Thomsen[4], Karoline Natasja Stæhr Gudmann[1], Ellen Hauge[5], Morten Karsdal[1], Johan Richter[2], Kim Henriksen[1]. [1]Nordic Bioscience A/S, Denmark, [2]Lund University, Sweden, [3]University of Aarhus, Denmark, [4]Aarhus University, Denmark, [5]Aarhus University Hospital, Denmark

Osteopetrosis due to lack of acid secretion by osteoclasts is characterized by abolished bone resorption, increased osteoclast numbers, but normal or even increased bone formation. In contrast, osteoclast-poor osteopetrosis appear to have less osteoblasts and reduced bone formation, indicating that osteoclasts are important for bone formation.

To shed light on the role of the osteoclast in mediating bone formation in adult mice, we transplanted irradiated skeletally mature three-month old wt mice with hematopoietic stem cells (HSCs), to generate either an osteoclast rich or osteoclast poor osteopetrosis model. We used HSCs from 1) oc/oc mice (acidification deficient and non-resorbing), 2) HSCs from RANK KO (osteoclastogenesis impaired) mice, and 3) compared to wt control HSCs.

Briefly, 12 weeks old mice were lethally irradiate with 950 cGy and transplanted with 2x106 fetal live cells from either oc/oc, RANK KO or wt mice. The mice were followed for 15 weeks and serum samples were drawn every two weeks and analyzed for TRACP5b and CTX-I. At termination bones were isolated analyzed using μCT, dynamic histomorphometry, and mechanical testing.

TRACP5b, a marker of osteoclast number, showed an increase (125%) in oc/oc and a 50% decrease in Rank KO recipients, while the bone resorption marker CTX-I was similarly decreased (20%) in both groups. Both oc/oc and Rank KO recipients developed a mild osteopetrotic phenotype, however, the osteoclast-rich oc/oc recipients showed a higher trabecular bone volume (40%), and increased bone strength (66%) in trabecular bone, while RANK KO recipients showed a trend (16% and 19%) towards an increase compared to wt recipients. In cortical bone, similar but smaller effects on bone volume and strength were observed in both osteopetrosis groups. Furthermore, oc/oc recipients had increased bone formation rate in the trabecular compartment of the vertebrae (54%) compared to wt recipient controls, and these changes were not observed in RANK KO recipients.

In summary, we here present in vivo data showing that maintaining non-resorbing osteoclasts, as opposed to removing the osteoclasts, leads to increased bone formation, bone volume and ultimately higher bone strength *in vivo*. These data strongly indicate that the osteoclasts are sources of anabolic molecules for the osteoblasts, and thereby play an important role in maintaining bone turnover independently of their resorptive capacity.

***Disclosures: Christian Thudium**, None.*

FR0264

Novel Models Of Osteoporosis In Transgenic Mice Overexpressing Human RANKL. Vagelis Rinotas[1], Alexandra Niti[1], Romain Dacquin[2], Nicolas Bonnet[3], Serge Ferrari[4], Pierre Jurdic[5], Eleni Douni*[6]. [1]BSRC Alexander Fleming, Greece, [2]ENS de Lyon, France, [3]University Geneva Hospital-Department of Internal Medecine Specialities, Switzerland, [4]Geneva University Hospital & Faculty of Medicine, Switzerland, [5]Ecole Normale Superieure de Lyon, France, [6]Agricultural University of Athens/ BSRC Al. Fleming, Greece

Receptor activator of nuclear factor-κB ligand (RANKL) is a central regulator of bone remodeling by mediating osteoclast-induced bone resorption. Overproduction of RANKL is implicated in a variety of degenerative bone diseases such as osteoporosis and its specific inhibition effectively reduces the incidence of fractures in postmenopausal women. We have recently generated transgenic mice overexpressing human RANKL (TghuRANKL) in order to model human RANKL-mediated pathologies. To achieve a correct pattern of human RANKL expression in the mouse, a 200kb genomic fragment containing the whole human RANKL gene was used as a transgene. Quantitative bone analysis revealed a mild phenotype in the low copy number Tg5516 line displaying trabecular bone loss as well as reduced biomechanical properties at 3 months of age. A more severe osteoporotic phenotype was identified in the high copy Tg5519 line developing trabecular bone loss, severe cortical bone porosity, and decreased bone strength by the age of 3 months. The numbers of osteoclasts at the cortical surfaces as well as serum markers of bone turnover were significantly increased in Tg5519 mice. Moreover, this transgenic line also displayed active bone formation and significantly increased serum alkaline phosphatase levels, indicating increased bone remodeling. The observed phenotypes developed in both sexes, whereas the levels of human RANKL expression were correlated with bone resorption and disease severity. Notably, TghuRANKL mice rescued the osteopetrotic phenotype of mutant mice expressing an inactive form of endogenous RANKL, showing that the human RANKL protein is fully active in the mouse. Interestingly, treatment of TghuRANKL mice with known anti-resorptive drugs effectively inhibited bone resorption proving the significance of such mice in preclinical evaluation studies of novel anti-osteoporotic compounds. These novel human RANKL transgenic models of osteoporosis represent a unique tool for understanding the pathogenic mechanisms in bone resorption as well as for the preclinical evaluation of novel inhibitors that target human RANKL and osteoclasts.

***Disclosures: Eleni Douni**, None.*

FR0270

Comparative Analysis of the Specificity of Available Osteoclast Lineage Cre-Drivers and Identification of Novel Osteoclast Lineage Selective Genes. Megan Weivoda*[1], Katharina Jähn[2], Matt Prideaux[3], Ming Ruan[1], Sundeep Khosla[4], Lynda Bonewald[5], Merry Jo Oursler[1]. [1]Mayo Clinic, USA, [2]University Medical Center Hamburg-Eppendorf, Germany, [3]University of Missouri-Kansas City, USA, [4]Mayo Clinic College of Medicine, USA, [5]University of Missouri - Kansas City, USA

Osteocytes express certain osteoclast genes including cathepsin K (CTSK) and tartrate resistant acid phosphatase (TRAP) to remodel mineralized matrix in response to lactation. The CTSK and TRAP promoters are commonly used to drive Cre recombinase (Cre) expression to knockdown genes in osteoclasts. Activation of these promoters in osteocytes by lactation may lead to Cre expression and subsequent gene deletion in osteocytes, complicating the findings in osteoclast specific knockdown experiments. The goal of this study was to assess the tissue specificity of genes used to drive Cre expression in the osteoclast lineage and to identify novel gene candidates to selectively target osteoclasts. Expression of genes used to drive Cre in the osteoclast lineage was compared in osteocytes isolated from lactating female mice to virgin female osteocytes, bone marrow, and bone marrow-derived osteoclasts. Microarrays performed on virgin and lactating mouse osteocytes were analyzed in comparison to osteoclasts to reveal potential candidate genes for new osteoclast specific Cre models; identified targets were validated by qPCR. Osteoclast specificity of Cre driver genes and novel targets were assessed in a cDNA tissue library. Consistent with published data, lactation increased CTSK and TRAP expression in osteocytes. Osteoclasts expressed 7-fold and 8-fold higher levels of CTSK and TRAP, respectively, as compared to osteocytes isolated from lactating mice. Lactation did not significantly alter expression of CD11b, cFms, LysM, RANK, or Vav1, promoters of which have been used to drive Cre expression in the osteoclast lineage. Analysis of these genes in a cDNA tissue library showed that CD11b, cFms, and CTSK have greater specificity for the osteoclast lineage. In contrast, LysM, RANK, TRAP, and Vav1 revealed more heterogeneity in tissue expression. Microarray identified OSCAR and OC-STAMP as highly expressed in osteoclasts compared to virgin or lactating osteocytes. Validation by qPCR showed 20 and 54-fold increases, respectively, in comparison to lactating osteocytes. Moreover, OSCAR and OC-STAMP were highly restricted to the osteoclast lineage. These data suggest that although lactation induces CTSK expression in osteocytes, CTSK remains a good model for gene knockdown in the osteoclast lineage in virgin mice. This work also suggests that the development of OSCAR and OC-STAMP Cre models may be promising tools for highly specific gene deletion in the osteoclast lineage.

***Disclosures: Megan Weivoda**, None.*

FR0271

Deletion of the cell-adhesion mediator PODXL in early osteoclast precursors leads to a high bone mass phenotype in female, but not male mice: A role for PODXL in the localization of active Rac1 in osteoclasts. Megan Weivoda*[1], Muzaffer Cicek[1], Ashok Kumar[2], Ming Ruan[1], Larry Pederson[1], Christine Hachfeld[1], Michael Hughes[3], Kelly McNagny[3], Merry Jo Oursler[1]. [1]Mayo Clinic, USA, [2]Mayo Clinic College of Medicine, USA, [3]University of British Columbia, Canada

Podocalyxin (PODXL) is a mediator of cell adhesion expressed by the hematopoietic lineage. Due to the role of PODXL in adhesion, we hypothesized that PODXL may regulate osteoclast precursor fusion. We crossed PODXL floxed mice with Vav-Cre mice to obtain male and female mice with PODXL deleted in early osteoclast progenitors (Vav/PODXL^{del}). L4 vertebrae from 17-week mice were assessed by μCT and histomorphometry; femurs were assessed by pQCT. Bone marrow was cultured with RANKL and M-CSF and examined for osteoclast differentiation and cell signaling. Bones from Vav/PODXL^{del} mice exhibited increased osteoclast numbers. Unexpectedly, female, but not male, Vav/PODXL^{del} mice exhibited a high bone mass phenotype. Female L4 vertebrae had significant increases in BV/TV, TbN, and TbTh, and decreased TbSp. BMD and CTh were significantly increased in female femurs as measured by pQCT. To uncover the reason for the high bone mass despite elevated osteoclast numbers, we examined osteoclast functions *in vitro*. Vav/PODXL^{del} bone marrow cultured on tissue culture plastic produced TRAP^{+}, multinucleated osteoclasts. Although Vav/PODXL^{del} osteoclasts were capable of adhering to bone surfaces, they failed to form resorption pits on bovine bone chips *in vitro*; this was true of osteoclasts derived from both male and female mice. The fact that osteoclasts derived from male Vav/PODXL^{del} mice fail to resorb bone *in vitro* similarly to female derived Vav/PODXL^{del} osteoclasts suggests that the lack of an altered bone phenotype in males is due to endocrine influences. Consistent with the retained ability to bind bone surfaces, activation of the integrin $\alpha_v\beta_3$ was not impaired. While active Rac1 was localized to discrete membrane regions in wild type osteoclasts, Vav/PODXL^{del} osteoclasts exhibited diffuse Rac1 activation. Adenoviral infection of osteoclast precursors with constitutively active Rac1 restored resorption pit formation by Vav/PODXL^{del} osteoclasts *in vitro*. Together, these data suggest that PODXL is required for optimal Rac1 activity in the osteoclast and PODXL deletion leads to impaired osteoclast bone resorption due to improper localization of active Rac1. This phenotype may be evident in female mice due to estrogen-mediated decreases in Rac1 activity. Resolution of the mechanism by which PODXL regulates localization of active Rac1 in osteoclasts may provide new avenues to pursue to suppress bone resorption while preserving the anabolic influences of osteoclasts.

***Disclosures: Megan Weivoda**, None.*

FR0272

Diacylglycerol kinase ζ (DGKζ) is a critical regulator of bone homeostasis via modulation of DAG levels in osteoclasts. Ali Zamani*[1], Pamela Hesker[2], Roberta Faccio[3]. [1]Department of Orthopedics, Washington University, St. Louis, Missouri, USA, [2]Washington University in St Louis School, USA, [3]Washington University in St Louis School of Medicine, USA

Osteoclasts (OCs) are instrumental component in the pathogenesis of rheumatoid arthritis (RA) and osteoporosis. Our lab has previously shown that PLCγ2 is a critical modulator of OC differentiation and inflammation. Despite the critical role of PLCγ2 in both bone and immune cells in the context of RA, its high homology with the more ubiquitously expressed PLCγ1, rendering PLCγ2 specific targeting difficult. In contrast, diacylglycerol (DAG), a downstream product of PLCγ2 catalytic activity to control PLCγ2-mediated events in OC, is strictly controlled by tissue specific diacylglycerol kinases (DGKs). This high level of specificity makes DGKs an attractive target for therapeutic interventions. Among 10 different DGK isoforms, our data indicate that DGKζ is the most highly expressed isoform in macrophages and OC. Consistent with the role of DAG in PLCγ2-mediated events in OC, DGKζ deficiency, which leads to DAG accumulation, results in a substantial osteoporotic bone phenotype in vivo. 6 week old DGKζ -/- mice exhibit a very sparse trabecular pattern with 5 fold less trabecular volume/bone volume (BV/TV), along with thinning and erosion of the cortical bone, compared to WT mice. The number of periosteal OCs is also significantly increased in DGKζ -/- mice (nOC WT 8 ± 3; nOC DGKζ-/- 25 ± 2). This in vivo phenotype is maintained with age. Similarly, in vitro, DGKζ -/- bone marrow macrophages form more numerous OC than WT with high or low doses of RANKL stimulation. DGKζ-/- cells express higher levels of early OC differentiation markers (NFATc1, TRAP and CTSK) and display significant upregulation of fusion markers (DC-STAMP and ATP6V0D2). In addition, DGKζ-/- OC also show enhanced resorption activity when equal numbers of WT and KO DGKζ OC plated on bone for 24hrs. These data indicate that DGKζ is a critical regulator of bone homeostasis in vitro and in vivo. Mechanistically, DGKζ-/- OC precursors exhibit enhanced proliferation in response to M-CSF stimulation, which is reflected by increased CyclinD1 and p-pRb levels. Furthermore, the osteoclastogenic transcription factor c-Fos is also elevated in DGKζ-/- cells in response to M-CSF. To our knowledge, this is the first report that implicates the lipid kinase DGKζ as a novel critical regulator of bone homeostasis via modulation of DAG levels in the osteoclasts and positions DGKζ as a potential new therapeutic target for pathological bone loss.

***Disclosures: Ali Zamani**, None.*

FR0273

Novel Role of the Alternative NF-κB Pathway in Regulating Osteoclast Mitochondrial Biogenesis Distinct from Osteoclast Differentiation. Rong Zeng*[1], Chang Yang[2], Deborah Novack[2]. [1]Washington University in St. Louis, USA, [2]Washington University in St Louis School of Medicine, USA

Osteoclasts (OCs) are mitochondria-rich multinucleated cells specialized for the energy-intensive role of degrading bone matrix. We have previously shown that the alternative NF-κB pathway, controlled by the kinase NIK and mediated by the transcription factor subunit RelB, regulates OC differentiation and function. However, direct functional target genes of RelB controlling OC resorption have not been identified. In skeletal muscle, an unknown stimulus activates the alternative NF-κB pathway, and allows RelB to positively and directly regulate its target, PGC-1β, a transcription co-factor to PPARγ, important for controlling metabolism and mitochondria biogenesis in many metabolically active cell types, including OCs. Thus we hypothesize that the RANK-activated alternative NF-κB pathway in OCs directly controls mitochondrial biogenesis and its associated metabolic roles via PGC-1β, but may be independent from OC differentiation. In our studies, OC precursors from relb-/-, nik-/-, and CatK.NT3 (constitutively active NIK transgene driven by the Cathepsin K promoter) mice were cultured under osteoclastogenic conditions (in the presence of M-CSF and RANKL). Expression of PGC-1β and mitochondrial oxidative phosphorylation genes (for ATP synthesis) were significantly impaired in relb-/- and nik-/- OCs, as measured by qRT-PCR and immunoblotting. Furthermore, when total DNA (nuclear and mitochondrial) was extracted to quantitate relative mitochondrial copy numbers (CN), relb-/- and nik-/- OCs had deficient mitochondrial CN compared to WT. Examination of mitochondrial function with a Seahorse XF Flux Analyzer revealed that relb-/- and nik-/- OCs had a reduction in basal and maximum oxygen consumption rates. CatK.NT3 OCs showed increased mitochondrial CN and respiration rate. CatK.NT3 and relb-/- mutants showed abnormal mitochondrial morphologies by transmission EM. Mechanistically, Chromatin IP and luciferase assays suggest that RelB directly regulates PGC-1β transcription in OCs, making PGC-1β the likely mediator of the mitochondrial phenotypes. Retroviral overexpression of PGC-1β in relb-/- cells rescues mitochondrial defects but not OC differentiation or function, while overexpression of NFATc1 rescues OC differentiation but not mitochondrial or bone resorption defects. We conclude that mitochondrial biogenesis in OCs is regulated by the alternative NF-κB pathway, via PGC-1β, in a pathway distinct from osteoclastogenesis that contributes to bone resorption.

***Disclosures: Rong Zeng**, None.*

FR0274

RANKL/M-CSF-PI3K-Akt signaling in osteoclast differentiation and function is regulated via the direct interaction between G protein α subunit and Class IA PI3K. Mengrui Wu*, Wei Chen, Yi-Ping Li. The University of Alabama at Birmingham, USA

Current bone resorption inhibitors are effective but far from ideal because of side effects (*e.g.,* jaw osteonecrosis and increased bone fragility). Thus, there is a compelling need for better therapeutic agents in osteoclast-related bone diseases. The critical role of Phosphatidylinositol 3-kinase (PI3K), especially class IA PI3K, in osteoclast differentiation and function, has been established. Class IA PI3K is comprised of a regulatory subunit (p85/p55) and a catalytic subunit (p110α/β/δ). p110α is more abundant and important than p110β or δ in osteoclasts. Thus, we searched for candidate regulators of PI3K using an anti-p110α antibody co-immunoprecipitation approach. By co-immunoprecipitation, we demonstrated that guanine nucleotide binding protein α 13 (Gna13) was interacting with p110α, but not p85 or Csf1r. Knockdown of Gna13 *in vitro* and osteoclast-specific knockout of Gna13 *in vivo* increased osteoclast differentiation and function via PI3K/Akt signaling. The Gna13 mutant mice exhibit severe osteoporosis phenotype. Gna13 deficiency increased the formation of huge osteoclasts with more nuclei and larger actin rings. The average nuclei number of osteoclasts and the average size of actin rings were increased in the absence of Gna13 (by 100% and 300%, respectively). On the other hand, overexpression of the constitutively active form of Gna13 (Gna13 Q226L) in monocytes/macrophages blocked pre-osteoclast fusion by 85% and disturbed actin ring formation. Osteoclast-specific genes, Ctsk and NFATc1, were increased in Gna13-deficient osteoclasts (by 50% and 200%, respectively)and decreased in Gna13 Q226L-overexpressed osteoclasts (by 70% and 90%, respectively). Gna13 deficiency increased AKT phosphorylation and overexpression of Gna13 Q226L inhibited AKT activation, but the phosphorylation of Erk1/2, c-jun and p38 was not affected. Ctsk secretion and bone resorption were also increased in Gna13-deficient osteoclasts (by 200% and 200%, respectively) and decreased in Gna13 Q226L-overexpressed osteoclasts (by 80% and 90%, respectively). In summary, we demonstrated that Gna13 negatively regulates RANKL/M-CSF Class IA PI3K/AKT signaling by interacting with p110α, so as to inhibit osteoclast fusion and function. This is the first report of an endogenous interaction between G protein α subunit and PI3K and its biological role. Our study indicates that the constitutively active form of Gna13 could be a new therapeutic target of osteoclast-related bone diseases.

***Disclosures: Mengrui Wu**, None.*

FR0275

Activation of intracortical resorption in mouse long bone by acute placement of focal microdamage by in vivo indentation is controlled by osteocyte apoptosis. Oran Kennedy*[1], Anaya Philip[2], Jelena Basta Pljakic[2], Mitchell Schaffler[2]. [1]New York University, Hospital for Joint Diseases, USA, [2]City College of New York, USA

Introduction: Intracortical remodeling in bone removes and replaces microdamage. This process is known to include osteocyte apoptosis near sites of damage. In vivo fatigue loading of rat ulnae has been widely used to study this phenomenon [1,2]. The ability to scale down this approach for use in mice, and take advantage of genetic technologies, would be very valuable. However, this has proven difficult due to size issues. We previously showed that indentation which places microdamage in living cortical mouse bone, can activate a focal remodeling response [3]. Here, we use a pan-caspase inhibitor (QVD) to test whether the remodeling response is mediated by osteocyte apoptosis in this system.

Methods: We used a 50 µm conical indenter (Reference Point Indentation, Active Life Scientific, CA) to generate acute focal microdamage beneath the indenter tip in C57Bl/6 mouse tibiae [4]. Mice (n=6/group, IACUC approved) were assigned to 1 of 3 groups: Control, Indent+VEH or Indent+QVD. Under anesthesia, focal damage was placed on the anterior surface of the right limb at the level of the tibiofibular junction. The cortex at this site is sufficiently thick for indentation. Animals were sacrificed at 14 days – the resorption phase for the remodeling response to microdamage. Tibiae were examined by histology and IHC staining for apoptosis (Caspase 3).

Results and Discussion: Focal damage sites were highly consistent among all groups. Indentation/focal microdamage did not evoke a periosteal woven bone response, nor was there evidence of focal soft tissue inflammation. Intracortical remodeling was activated in the microdamage zone below indentation sites in Indent+VEH animals (Fig 1B). Such remodeling sites were absent from Indent+QVD and Control bones (Fig 1A,C). IHC analyses showed strong positive staining for caspase-3 in osteocytes at the indentation-remodeling sites in Indent+VEH animals (Fig 1E), but not in Indent+QVD and Control animals (Fig 1D,F).

Conclusion: We show that remodeling can be activated in mouse bone by acute focal microdamage placement with in vivo microindentation. Moreover, this remodeling response was completely abrogated when osteocyte apoptosis is inhibited by a pan-caspase inhibitor. These results show the damage-remodeling pathway in this acute microdamage model is the same as for fatigue microdamage, and identifies a powerful new approach for using mouse models to interrogate the regulatory role of osteocyte apoptosis in bone remodeling.

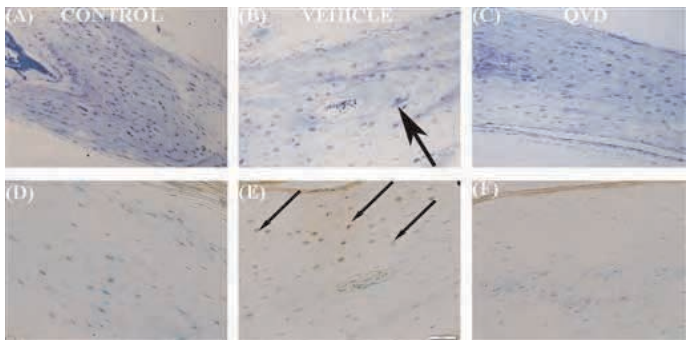

Sections stained either with toluidine blue (A-C) or for caspase-3 (D-F) from each treatment group

***Disclosures: Oran Kennedy**, None.*

FR0277

Disruption of Connexin 43 Channel Function in Osteocytes Differentially Reduces Bone Mass and Impairs the Tibial Anabolic Response to Load. Jean Jiang*. University of Texas Health Science Center at San Antonio, USA

Connexin (Cx) 43 plays an important role in bone function and development. Targeted deletion of Cx43 in osteoblasts or osteocytes results in increased osteocyte apoptosis, osteoclast recruitment, and reduced bone mass and strength. We and others have shown that the Cx43 hemichannel (HC) in osteocytes is a major portal for the release of bone-modulating factors (i.e. prostaglandins, ATP, etc) in response to mechanical stimulation. Interestingly, recent studies showed that knocking out Cx43 enhanced the anabolic responses of the bone to mechanical loading. Cx43 forms both gap junctions (GJ) and HCs; however, a significant amount of Cx43 is also retained in the cytoplasm of osteocytes. In order to determine the relative contributions of Cx43 GJs versus HCs in osteocytes, two transgenic mouse models driven by a 10 kb-DMP-1 promoter with the overexpression of dominant negative Cx43 mutants were generated - the Cx43 (R76W) mutant which blocks GJ but not HC function and the Cx43(?130-136) mutant that inhibits both GJ and HC activity. Immunohistochemistry showed predominant expression of these two mutants in osteocytes in situ. Dye transfer and dye uptake analyses confirmed the dominant negative function of these two Cx43 mutants on GJs and HCs in osteocytes isolated from transgenic mice. Both Cx43(R76W) and Cx43(?130-136) mice ranging from 2 to 6 month old showed a decrease in BMD, compared to wild-type controls. Fifteenweek-old mice subjected to tibial loading (11N, 1800 cycles at 2 Hz and 5 days/week for 2 weeks)showed a significant increase in BV/TV in wild-type control mice; however, this anabolic effect was completely abolished in both Cx43 transgenic mouse models. Moreover, after mechanical loading, tibia of R76W mice showed lower BV/TV thannon-loaded controls, suggesting non-coupling of resorption and formation. The compromised anabolic response to mechanical loading in transgenic mice was further confirmed by an increased osteoclast number by histomorphometry analyses, while a reduced osteoclast number was observed, as expected, for wild-type control mice. These results suggest that Cx43 GJs in osteocytes are critical for maintaining normal bone mass, but that HCs or overexpression of HCs as in the R76W mutant may increase resorption. In summary, normal expression of both GJs and HCs are responsible for mediating the anabolic response of mechanical loading on bone tissues by reducing osteoclast numbers.

***Disclosures: Jean Jiang**, None.*

FR0280

Osteocytes release microvesicles that regulate osteoblast function. Patricia Veno*, Matt Prideaux, Vladimir Dusevich, Lynda Bonewald, Sarah Dallas. University of Missouri - Kansas City, USA

Microvesicles (100-1000nm) and exosomes (50-100nm) are membrane-bound particles released by cells that provide a novel mechanism for intercellular communication through targeted delivery of their contents including proteins, mRNAs and microRNAs. We have developed transgenic mice expressing a membrane-targeted GFP in osteocytes, driven by the Dmp1 promoter (Dmp1-mem-GFP), which allows visualization of microvesicle shedding. Confocal microscopy showed abundant spherical GFP+ve microvesicles deposited around osteocytes in the calvaria, long bones and alveolar bone of neonatal and adult Dmp1-mem-GFP mice. GFP-positive microvesicles persisted in adult bone matrix even after osteocytes had stopped expressing Dmp1-GFP. Live imaging of Dmp1-mem-GFP positive osteocytes in situ within their bone matrix in calvarial organ cultures revealed shedding of vesicles from the cell body and dendrites. Some osteocytes appeared to extend their dendrites beyond the limits of their canaliculi to shed microvesicles into vascular channels. To further understand their function in bone, microvesicles were purified from osteocyte-enriched primary cultures of Dmp1-mem-GFP calvarial cells and from IDG-SW3 cells (a late osteoblast cell line that differentiates into mature osteocyte-like cells) for characterization by TEM and Western blotting. Western blotting showed that the contents of the microvesicles reflected the differentiated state of the parent cells, with microvesicles from 7 day cultures of IDG-SW3 and primary Dmp1-mem-GFP calvarial cell cultures expressing early osteocyte markers (E11/gp38 and a high MW form of MEPE) and microvesicles from 4 week old cultures expressing these early markers as well as the late osteocyte marker, sclerostin. Sclerostin was enriched in the microvesicle compartment compared to whole cell lysate and was strongly down regulated by PTH treatment. Treatment of undifferentiated IDG-SW3 cells or Dmp1-mem-GFP calvarial cells with microvesicles from late differentiated (mature osteocyte-enriched) cultures resulted in a strong induction of alkaline phosphatase and induction of Dmp1-GFP expression within 48h as well as increased expression of E11/gp38, suggesting regulation of osteoblast function and acceleration of differentiation towards an early osteocytic phenotype. These data suggest that osteocytes shed microvesicles containing bone regulatory proteins which may induce differentiation of osteoblasts and potentially have effects on distant tissues.

***Disclosures: Patricia Veno**, None.*

FR0283

Inhibition of Osteocyte Apoptosis Prevents Extensive Trabecular Bone Loss Caused by Unloading in the Long Bone of Mice. Pamela Cabahug*[1], Robert Majeska[1], Damien Ladier[2], Alyssa Tuthill[3], Stefan Judex[3], Mitchell Schaffler[1]. [1]City College of New York, USA, [2]The City College of NY, USA, [3]Stony Brook University, USA

Osteocyte apoptosis is required to activate bone remodeling in fatigue microdamage, estrogen withdrawal and disuse. In cortical bone, inhibition of apoptosis prevents the onset of osteoclast resorption due to these challenges, showing that regulated osteocyte death controls remodeling. Bone loss in mouse compact bone during estrogen loss or disuse is small and confined to endocortical surfaces, but trabecular bone loss due to disuse is extensive. We asked whether inhibiting osteocyte apoptosis (OtAp) would be effective in preventing such major bone loss. Our goals were to evaluate the effects of unloading on the trabeculae of long bone and determine if inhibition of OtAp prevents the onset of bone resorption due to unloading. Methods: C57BL/6J mice (4 mo-male, n=6/group) were hindlimb unloaded (HLU) by tail suspension. A group was HLU for 5 days to find acute effects on OtAp. Treatment groups were HLU for 14 days. These were: 1) HLU+Vehicle, 2) HLU+Ap inhibitor (ApInh = pan caspase inhibitor, QVD), 3) Veh and 4) ApInh treated cage control (CC) groups. Analyses were performed from distal femurs. Ot Ap was assessed using IHC staining for activated caspase-3. The proportion of positively stained Ots were expressed as a percentage of total Ot numbers (%Casp+Ot). Corresponding regions of contralateral femurs were scanned with a µCT to evaluate changes in bone architecture. The same femurs were sectioned undecalcified and used to measure resorption activity (% eroded surface, %ErS). ANOVA with post-hoc Mann-Whitney U test were used and significance reported at $p<0.05$. Results: %Casp+Ot after 5 days of HLU nearly quadrupled from baseline, and remained highly elevated at 14 days of HLU. This increase was prevented in HLU mice given the apoptosis inhibitor (Fig 1).

For the HLU+Veh animals, %ErS more than doubled. However, apoptosis inhibition prevented this increase (Fig 2). Most significantly, apoptosis inhibition completely prevented the loss of bone volume caused by 14 days of HLU (Fig 3). Conclusion: Our results show that apoptosis inhibition prevents the dramatic and rapid cancellous bone loss caused by disuse. Inhibiting OtAp was highly effective in preventing cancellous bone loss caused by hindlimb unloading thus indicating that selectively targeting osteocyte death may be a powerful strategy in combating disuse osteoporosis.

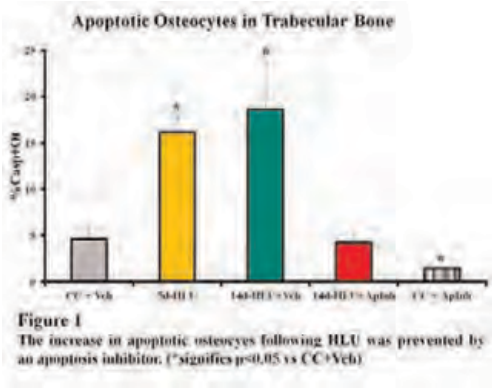

Figure 1
The increase in apoptotic osteocyes following HLU was prevented by an apoptosis inhibitor. (*signifies p<0.05 vs CC+Veh)

Fig 1

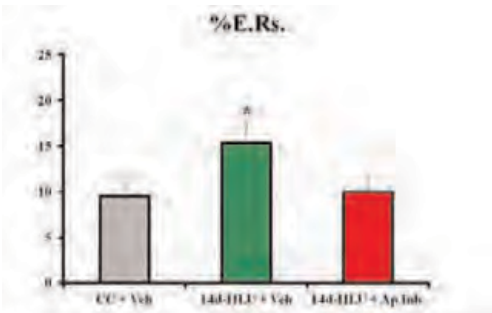

Figure 2
The increase in resorptive surface following HLU was at baseline levels when animals were given an apoptosis inhibitor. (*signifies p<0.05 vs CC+Veh)

Fig 2

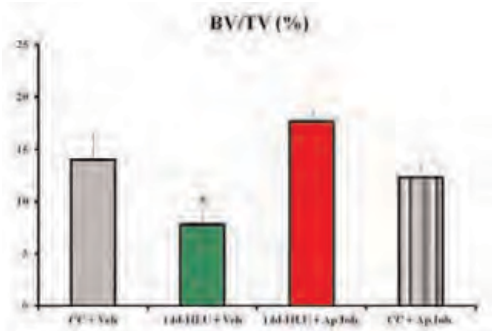

Figure 3
The significant decrease in the BV/TV of the trabeculae of the distal femur following HLU was prevented by an apoptosis inhibitor. (* signifies p<0.05 vs CC+Veh)

Fig 3

***Disclosures: Pamela Cabahug**, None.*

FR0285

PTH upregulates RANKL and MMP13 expression through direct actions on osteocytes, but MMP13 is derived from non-osteocytic cells. Jesus Delgado-Calle*, Xiaolin Tu, Amy Sato, Meloney Cregor, Kevin McAndrews, Lilian Plotkin, Teresita Bellido. Indiana University School of Medicine, USA

Activation of PTH receptor signaling in osteocytes is sufficient to increase bone mass and the rate of bone remodeling, two recognized skeletal actions of PTH. Whereas increased bone mass can be explained by downregulation of the osteocyte-specific bone formation inhibitor SOST, the mechanism by which osteocytes mediate bone resorption induced by PTH remains unclear. We report here that the expression of RANKL and MMP13, two genes involved in PTH-induced resorption, is elevated in transgenic mice with constitutive activation of the PTH receptor in osteocytes (DMP1-8kb-caPTHR1 mice). RANKL and MMP13 expression is also increased in bones (L4) from 4 month-old control mice injected with PTH (100ng/g) daily for 1 month. In contrast, PTH elevation did not increase RANKL or MMP13 expression in bones from mice with conditional deletion of the PTHR1 in osteocytes (cKO-PTHR1^{Ot} mice), generated by crossing PTHR1flox mice with DMP1-8kb-Cre mice. These findings demonstrate that regulation of RANKL and MMP13 requires direct actions of PTH on osteocytes. Osteocytes are the main source of RANKL; however, this cytokine is also expressed in other cells of the osteoblastic lineage. And, MMP13 is expressed by cells of both osteoblastic and osteoclastic lineage. Therefore, we next examined whether PTH regulates these genes directly in osteocytes using ex vivo and in vitro approaches. Long bone diaphyses of 1 month old mice devoid of marrow were digested with collagenase to remove bone surface cells. Remaining bone pieces were enriched in osteocytes as evidenced by 50-100 fold increase in Sost expression compared to undigested bones. Addition of PTH (100 nM) for 4h to these bone organ cultures increased the expression of RANKL in littermate control bones but not in bones from cKO-PTHR1^{Ot} mice. In contrast, PTH did not change MMP13 expression in osteocyte-enriched bones from either mouse strain. Moreover, PTH (or the stable cAMP analog DBA) also increased RANKL but not MMP13 expression in MLO-A5 osteocytic cells. These results demonstrate that PTH regulates the expression of RANKL but not of MMP13 in osteocytes. Taken together, these findings demonstrate that PTH regulation of the RANKL and MMP13 genes is exerted through direct hormonal actions on osteocytes. However, the origin of these pro-resorptive genes differs. Whereas RANKL is derived from osteocytes, the source of MMP13 is of non-osteocytic nature and must require crosstalk between osteocytes and other bone cells.

***Disclosures: Jesus Delgado-Calle**, None.*

FR0288

Osteocytes are Key to the Formation and Maintenance of Mineralized Bone. Yinshi Ren*[1], Shuxian Lin[2], Xianglong Han[3], Baozhi Yuan[4], Yan Jing[1], Ying Liu[1], Marc Drezner[4], Paul Dechow[2], Min Liu[5], Jian Feng[6]. [1]Baylor college of dentistry, Texas A&M Health Science Center, USA, [2]Baylor College of Dentistry, USA, [3]Baylor College of Dentistry, Texas A&M University, Biomedical Sciences, USA, [4]University of Wisconsin, USA, [5]Amgen Inc., USA, [6]Texas A&M Health Science Center, USA

The theory that osteoblasts (Obs) regulate mineralized bone formation is a cornerstone of bone biology. However, the role that the osteocyte (Ocy), the most abundant bone cell, may play in bone formation remains speculative. Thus, we tested if the Ocy does, in fact, have a role in this vital function. Using SEM and FITC (a fluoresce dye filling in Oycs and dendrites), we documented a close association between Ocy maturation and the degree of bone mineralization. Quantitative data revealed that the mature Ocy cell volume was 50% reduced, and the volume vacated by the reduced cell body in the matrix was replaced by mineral. Confocal microscopic examination of DAPI nuclear stained bone, previously labeled with calcein/alizarin red revealed not only mineral deposition surrounding Ocy matrix, but also at the mineralization front surrounding cananiculae. For the Ocy to play such a central role in formation of mineralized bone, access to a mineral source is critical. Yet, it is widely believed that there are few blood vessels in bone. However, we demonstrated high vessel density and numerous dendritic connections between the vessels and Ocys. Moreover, a dye injection into the rabbit abdominal aorta revealed dye in the Ocy bodies and their dendrites in < 2 minutes, indicating a rapid exchange and delivery of mineral between capillaries and Ocys. The vital Ocy role in mineralization was further demonstrated in *Dmp1* mice, where Obs failed to form Ocys; where b-catenin levels are >10-fold higher than WT; and the mice are osteomalacic. Moreover, in the offspring of mice obtained by crossing *Dmp1*-Cre and *Catnb*$^{\Delta ex3}$ mice, the elevated b-catenin levels recaptured an osteomalacia phenotype similar to*Dmp1* KO mice except without the FGF-23 abnormalities.

Currently, imbalances of Obs and osteoclasts are implicated in osteoporosis, although neither cell is embedded in bone matrix where Ocys likely play a key pathological role. To test this hypothesis, we evaluated patients with osteoporosis and ovariectomized (OVX) rats demonstrating distinct Ocy changes from a spindle to a round shape with >50% increase in Ocy volumes and reductions of Ocy numbers. Unexpectedly, there were sharp reductions of blood vessels in Ovx rat bones. Administration of Sclerostin antibody to Ovx rats reversed these changes, leading to bone mineral recovery. Our studies suggest that the Ocys, but not Obs, are the key cells building and maintaining bone mineralization, as such, defective Ocy function may underlie osteomalacia and possibly osteoporosis.

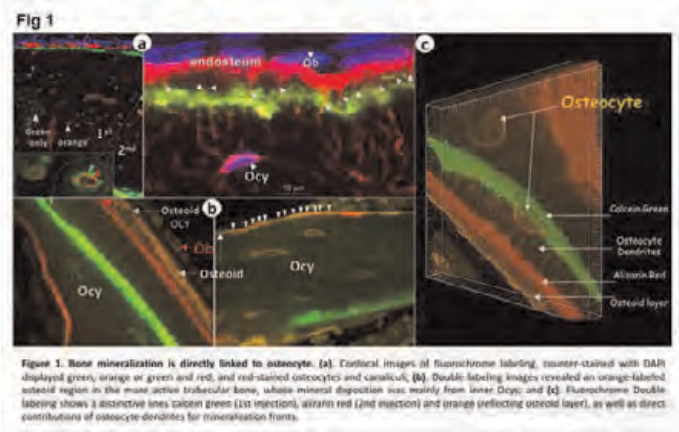

Fig-1

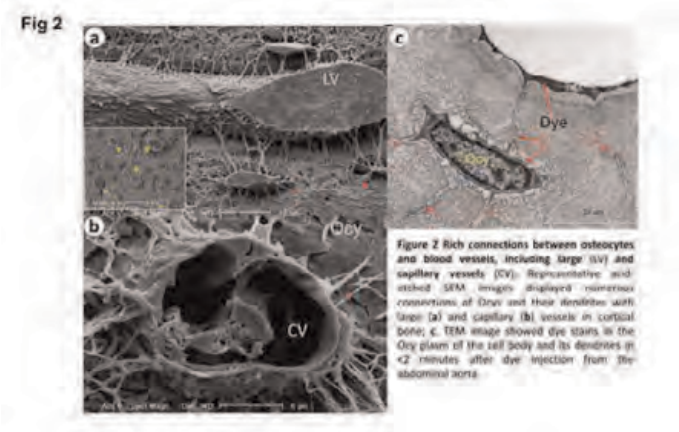

Fig-2

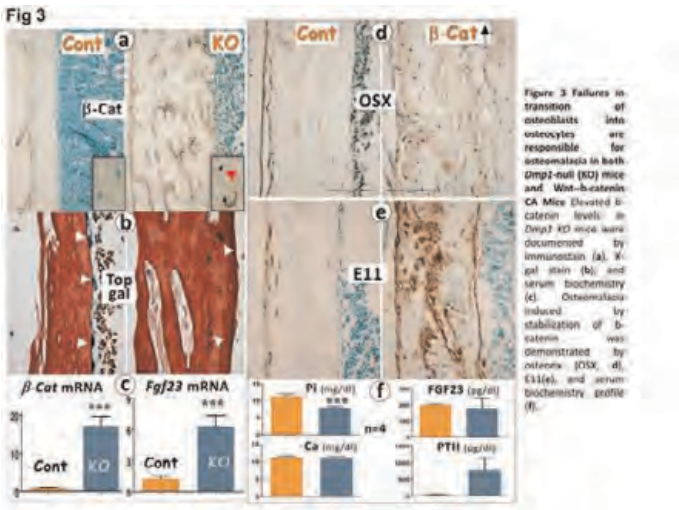

Fig-3

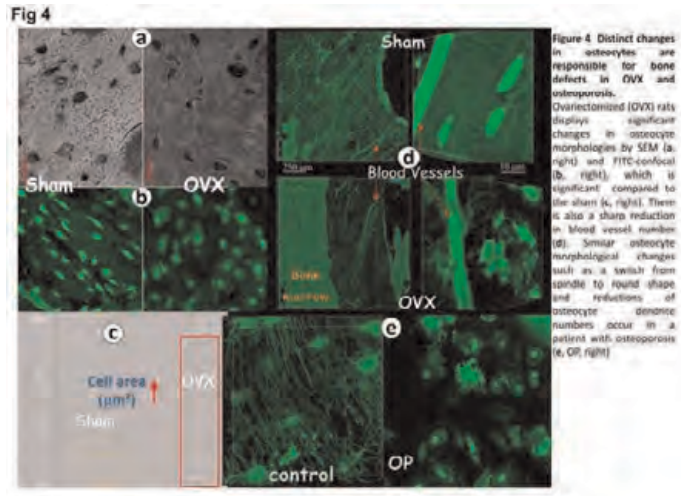

Fig-4

***Disclosures: Yinshi Ren**, None.*
This study received funding from: Amgen Inc.

FR0299

Quantification of Lower Leg Arterial Calcifications by High-Resolution Peripheral Quantitative Computed Tomography. Janina M Patsch*[1], Martin A. Zulliger[2], Nicolas Vilayphiou[3], Elizabeth Samelson[4], Daniel Cejka[1], Danielle Diarra[1], Gundula Berzaczy[1], Thomas Link[5], Michael Weber[1], Christian Loewe[1]. [1]Medical University of Vienna, Austria, [2]Former employee of SCANCO MEDICAL AG, Switzerland, [3]SCANCO MEDICAL AG, Switzerland, [4]Hebrew SeniorLife, Harvard Medical School, USA, [5]University of California, San Francisco, USA

High resolution peripheral quantitative computed tomography (HR-pQCT) is an in-vivo research tool primarily designed for the assessment of bone geometry, bone mineral density and bone microarchitecture of the ultradistal extremities. Vascular calcifications are frequently observed as incidental findings on HR-pQCT images and the interplay between vasculature health and bone health, is an emerging field of research. Nevertheless, quantitative analysis of vascular calcifications captured by HR-pQCT has not been performed yet. The objectives of our study were therefore to validate a quantitative tool for the assessment of lower leg arterial calcifications (LLAC) found in HR-pQCT scans and to test method reliability in the clinical setting. For validity assessment of our novel method, we recruited forty-six subjects with chronic kidney disease on hemodialysis with a mean age of 59 ± 13 years to undergo HR-pQCT of the ultradistal lower leg. As a standard of reference for quantitative assessment of vascular calcifications, we acquired MDCT scans of the heart and performed Agatston, mass, and volume scoring. HR-pQCT scans were graded for motion artifacts. The presence or absence of vascular calcifications in HR-pQCT scans was determined by visual assessment. If calcifications were detected in HR-pQCT scans, images were downscaled to a voxel size of 250µm to enhance comparability with MDCT. Subsequently, tibial and fibular bone volume was subtracted and lower leg arterial calcifications (LLAC) were detected and outlined by a semi-automated, dual-threshold seed-point segmentation. LLAC mass was calculated as the product of voxel-based LLAC volume and mean LLAC density. We used two-way random intra-class correlation (ICC) for reliability assessment of LLAC analyses by HR-pQCT on repeated image analysis of fourteen scans. Comparing lower leg arterial calcifications (LLAC) by HR-pQCT and coronary artery calcifications (CAC) by MDCT, there were significant positive correlations between LLAC mass and CAC as measured by Agatston score, mass score, and volume score (Spearman's rho=0.6;$p<0.01$). The ICC was 1.0. Our study indicates that lower leg arterial calcifications (LLAC) are quantifiable by HR-pQCT, which should facilitate quantitative research on osteo-vascular interactions. Associations with coronary artery calcifications (CAC) need to be confirmed in patients with normal kidney function, functional cardiovascular parameters and clinical outcomes.

***Disclosures: Janina M Patsch**, None.*

FR0305

Trait variances capture the micro-structural basis of bone fragility better than trait means. Yohann Bala*[1], Sandra Iuliano-Burns[2], Ali Ghasem-Zadeh[2], Xiao-Fang Wang[3], Qingju Wang[2], Roger Zebaze[2], Ego Seeman[2]. [1]University of Melbourne, Dept. of Medicine, Australia, [2]Austin Health, University of Melbourne, Australia, [3]University of Melbourne, Austin Health, Australia

High Resolution peripheral Quantitative Computerised Tomography (HR-pQCT) is a noninvasive method of image acquisition that quantifies cortical and trabecular microstructure. However, the use of fixed thresholds introduces errors as most voxels contain both bone and void. The void lowers the threshold which allocates porous cortical bone to the trabecular compartment underestimating cortical porosity and mass, and over estimated trabecular bone mass and so underestimates an individuals fracture risk. Non-threshold based segmentation allocates voxels by their anatomical location, not attenuation, and quantifies all voxel void and matrix volumes, rather than erroneous disregarding voxels 'tainted' by partial volume effects. We hypothesized that expressing microstructure as a continuum or frequency distribution curve of voxels containing differing volumes of void and bone matrix better discriminates women with and without forearm fracture and controls.

HR-pQCT images obtained in 33 women (57 ± 9 years) with forearm fractures and 53 aged-matched controls were analysed using Strax 1.0 and a DEXA scans of the lumbar spine (LS) and the femoral neck (FN). StrAx1.0 automatically segments bone from background and cortex into its compact appearing cortex, outer and inner transitional zones. Voxels were classified according their relative bone matrix and void volumes. Sensitivity and specificity was evaluated using the area under a receiver-operating curve (AUC).

aBMD did not discriminate cases from controls (AUC = 0.58 at LS, 0.53 at FN. Ct. and Tb.vBMD discriminated with AUCs of 0.69 and 0.63, respectively, $p<0.05$. However, the proportion of voxels containing 50-70%, 70-95% and >95% mineralized bone was the best discriminant (AUC 0.63 to 0.87) with the voxels containing 50-70% of mineralized bone in the outer transitional zone the most sensitive discriminant (AUC 0.87 and $p<0.05$ vs. Ct.vBMD and Tb.vBMD) associated with an OR (95% CI) for fracture of 11.20 (2.77-52.65) (Fig).

Fragility fractures are associated with heterogeneous abnormalities in cortical microstructure quantifiable by analysing trait variance, not means and expressing this as a frequency distribution of individual voxel contents.

References: 1) Khosla *et al.* JBMR 2006, 2) Boutroy *et al.* JCEM 2005, 3) Seeman *et al.* JBMR 2010, 4) Stein *et al.* JBMR 2010, 5) Zebaze *et al.* Bone 2013.

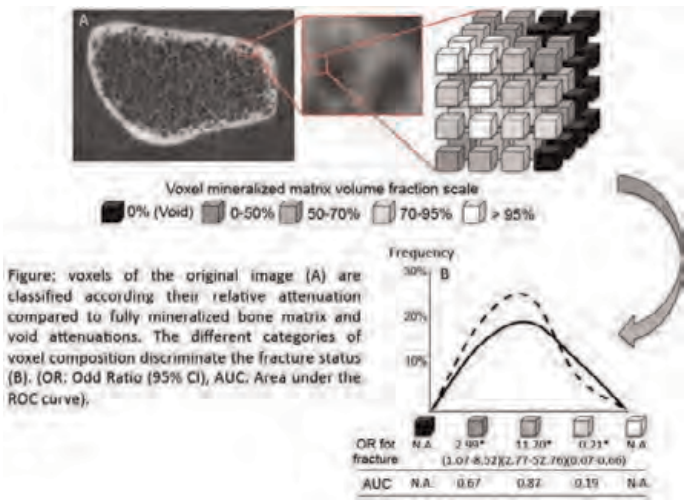

Figure

***Disclosures: Yohann Bala**, None.*

FR0313

Associations Between Biomarker-Calibrated Protein Intake and Bone Health in the Women's Health Initiative. Jeannette Beasley*[1], Andrea Lacroix[2], Joseph Larson[2], Charles Eaton[3], Marian Neuhouser[2], Lesley Tinker[2], Ying Huang[2], Rebecca Jackson[4], Karen Johnson[5], Linda Snetselaar[6], Ross Prentice[2]. [1]Einstein College of Medicine, Yeshiva University, USA, [2]Fred Hutchinson Cancer Research Center, USA, [3]MHRI, USA, [4]The Ohio State University, USA, [5]University of Tennessee Health Science Center, USA, [6]University of Iowa, USA

OBJECTIVE: The effects of dietary protein intake on bone health are controversial. This study examined the relation between protein intake with bone mineral density (BMD) and fracture within the Women's Health Initiative (WHI).

METHODS: The WHI recruited 161,806 women aged 65-79 into the WHI-Observational Study (OS) and WHI-Clinical Trial (CT) between 1993 and 1998. Fractures were collected annually (WHIOS) or semi-annually (WHI-CT) by questionnaire through 2011. BMD was measured at baseline and 6 years among 10,833 women using dual-energy x-ray absorptiometry. Protein and energy intake were assessed via the WHI Food Frequency Questionnaire and calibrated using regression equations established based on biomarkers of protein and energy intake. Cox (fracture) and linear (BMD) regression models were adjusted for confounders including age, race/ethnicity, and body mass index.

RESULTS: Median calibrated protein intake was 14% of energy. Women consuming 20% higher calibrated protein were 9% less likely to have a hip fracture (95% CI= 1%-15%). Each 20% increase in calibrated protein was associated with higher BMD for total body (mean 6-year change 0.004 g/cm2, 95% CI = 0.001- 0.007 g/cm2) and hip (0.003 g/cm2, 95% CI= 0.001-0.005 g/cm2). CONCLUSION: Higher protein intake was associated with reduced risk of hip fracture and better maintenance of BMD over time. These data suggest higher protein intake may be an intervention target for preserving bone health.

***Disclosures: Jeannette Beasley**, None.*

FR0315

Low Serum Concentration of Vitamin E Is Associated With Increased Risk of Hip Fracture in the Elderly. A NOREPOS Case-Cohort Study. Kristin Holvik*[1], Clara Gjesdal[2], Grethe Tell[3], Guri Grimnes[4], Ellen Apalset[3], Berit Schei[5], Rune Blomhoff[6], Karl Michaelsson[7], Haakon E. Meyer[8]. [1]Norwegian Institute of Public Health, Norway, [2]Department of Rheumatology, Haukeland University Hospital, Norway, [3]Department of Global Public Health & Primary Care, University of Bergen, Norway, [4]University Hospital of Northern Norway, Norway, [5]Department of Public Health & General Practice, Norwegian University of Science & Technology, Norway, [6]Department of Nutrition, Institute of Basic Medical Sciences, University of Oslo, Norway, [7]Uppsala Clinical Research Center, Sweden, [8]Norwegian Institute of Public Health/ University of Oslo, Norway

The increased oxidative stress associated with ageing influences the formation and survival of bone forming and bone resorbing cells. Vitamin E, of which α-tocopherol is the most abundant form in human tissues, is a plant-derived lipid soluble substance with potent antioxidant properties. The relation between vitamin E concentrations in blood and risk of hip fracture has not previously been investigated in a population-based study. We aimed to study the association between α-tocopherol levels in serum and risk of hip fractures in elderly men and women in Norway, the population with the world's highest hip fracture incidence.

In the Norwegian Epidemiologic Osteoporosis Studies (NOREPOS), we performed a case-cohort analysis in 21,774 men and women aged 65-79 years (mean 72 y) who underwent baseline examinations in four population-based health studies during 1994-2001. Data on incident hip fractures occurring up to 10.7 years of follow-up were retrieved from electronic patient administrative systems. Frozen serum samples from baseline were analyzed in participants who suffered a hip fracture during follow-up (n=1179; 307 men and 872 women) and in sex-stratified random samples from baseline (n=1447, including 89 of those who later suffered a hip fracture). α-tocopherol in serum was determined by high pressure liquid chromatography (HPLC)-fluorescence detection. Cox proportional hazards regression adapted for the case-cohort design was performed with adjustment for age, sex, and study center.

Median (25, 75-percentile) serum α-tocopherol concentration was 30.0 (22.6, 38.3) µmol/l. A linear inverse relation between serum α-tocopherol levels and hip fracture was observed, with hazard ratio (HR) 1.12 (95% CI 1.04-1.20) per 10 µmol/l lower serum α-tocopherol. HR of hip fracture in the lowest (<22.6 µmol/l) compared with the highest (>=38.3 µmol/l) quartile of serum α-tocopherol was 1.53 (95% CI 1.18-1.97). The trend was linear across quartiles ($p<0.001$). Additional adjustment for body mass index, cigarette smoking, month of blood draw, and length of education yielded similar results.

In conclusion, low serum concentrations of α-tocopherol were associated with increased risk of hip fracture in both men and women.

***Disclosures: Kristin Holvik**, None.*

FR0327

Markers of Bone Turnover for Prediction of Fracture: a Meta-analysis. Eugene McCloskey*[1], Anders Odén[2], John Kanis[3], Helena Johansson[4]. [1]University of Sheffield, United Kingdom, [2]WHO Collaborating Centre, University of Sheffield, United Kingdom, [3]University of Sheffield, Belgium, [4]Swedish University of Agricultural Sciences, The Biomedical Center, Sweden

The IOF/IFCC has recently recommended s-PINP and s-CTX as the primary candidates for markers of bone turnover. The aim of this analysis was to update and summarise the clinical performance of these two markers in the prediction of fracture.

The study comprised an updated systematic review to document the performance characteristics of s-PINP and s-CTX in fracture risk prediction in untreated

individuals in prospective cohort studies. Cross-sectional and case-control studies were excluded as were studies that did not provide separate data for incident hip fractures. Eight potentially eligible publications were identified and six included in meta-analysis, since one publication did not have numerical info and two publications studied the same cohort. Three publications were available for the meta-analysis of s-PINP and six for the meta-analysis of s-CTX.

Higher values of both markers were associated with future fracture risk, with no differences between genders so that data in men and women were combined. For example, the hazard ratio per SD increase in s-PINP (gradient of risk: GR) was 1.23 (95% CI: 1.09-1.39) for any fracture. There was also a significant association between s-CTX and risk of any fracture, GR 1.18 (95% CI: 1.08-1.29). For the outcome of hip fracture, association between s-CTX and risk of fracture was slightly higher 1.23 (95% CI: 1.04-1.47).

There is a modest but significant association between bone turnover markers and risk of future fractures. Whether this predictive ability remains significant following adjustment for other risk factors is unknown.

***Disclosures: Eugene McCloskey**, None.*

FR0342

Atypical Femoral Fracture Risk Factors: A Population-based Case-control Study. Annette Adams*[1], Fei Xue[2], Jean Wang[1], Richard Dell[3], Cathy Critchlow[2]. [1]Kaiser Permanente Southern California, USA, [2]Amgen, Inc., USA, [3]Kaiser, USA

Purpose: To identify risk factors for atypical femoral fractures (AFF) among women enrolled in a large integrated health care organization.

Methods: Subjects in this population-based case-control study were female, aged ⩾45 years, had a qualifying fracture between 2007-2011, and ⩾6 months enrollment in the health plan prior to fracture/index. Cases had an AFF, as validated by physician review, and were compared to subjects comprising 2 control groups: 1) other subtrochanteric/diaphyseal fractures (subtroch group), and 2) "classic" femoral neck or intertrochanteric hip fractures (hip group). Cases and controls were optimally matched 1:1 on index date ±6 months and medical center. Potential risk factors included demographic characteristics, clinical factors, bisphosphonate (BP) use characteristics, and other pharmacologic exposures up to 3 years prior to index.

Results: Overall, 115 AFF cases were matched to 107 subtroch and 115 hip fracture control subjects. Compared to the subtroch group, AFF cases were younger (median age 70 vs. 80 years, $p<0.01$), more likely to be Asian (vs. White, OR 13.0; 95% CI 3.1-54.8), to have an osteoporosis diagnosis prior to index (OR 2.5; 95% CI 1.2-4.9), and to be using BPs at index (OR 6.4; 95% CI 3.0-13.4). AFF cases also used BPs for longer durations (median 6.6 vs. 2.0 years, $p<0.01$), with risk increasing monotonically from OR 5.8 (95% CI 1.9-17.2) for use <4 years to OR 13.3 (95% CI 4.2-42.2) for use ⩾8 years (p for trend<0.01). Compared to the hip group, younger age (median age 70 vs. 83 years, $p<0.01$), Asian race (vs. White, OR 11.7; 95% CI 3.6-37.9), osteoporosis diagnosis (OR 2.1; 95% CI 1.1-3.9), active use of BPs at index (OR 6.8; 95% CI 3.2-14.2), and longer duration of use of BPs (median 6.6 vs. 2.4 years, $p<0.01$) were independent predictors of AFF status. AFF risk increased from OR 3.3 (95% CI 1.3-8.8) for <4 years of BP use to 10.5 (95% CI 3.6-30.8) for ⩾8 years use (p for trend<0.01).

Conclusion: Our findings suggest that subjects with AFF differ from subjects with other subtroch and classic hip fractures with regard to age, race, and patterns of BP use prior to fracture. The pathophysiology of AFF fractures continues to be investigated, and our findings may provide additional insight into the role of potentially modifiable risk factors such as BP use.

***Disclosures: Annette Adams**, Amgen, Inc., 6*
This study received funding from: Amgen, Inc.

FR0350

Long-Term Height Loss and Low BMI Strongly Predict Hip Fracture among 16,009 Women and Men Aged 70-79 Years. A NOREPOS Study. Haakon E. Meyer*[1], Siri Forsmo[2], Grethe S. Tell[3], Kristin Holvik[4], John Eisman[5], Anne Johanne Søgaard[6]. [1]Norwegian Institute of Public Health/University of Oslo, Norway, [2]Norwegian University of Science & Technology, Norway, [3]University of Bergen, Norway, [4]University of Oslo, Norway, [5]Garvan Institute of Medical Research, Australia, [6]Norwegian Institute of Public Health, Norway

We aimed to study the predictive power of height loss and low body mass index (BMI) on the risk of hip fracture in elderly women and men.

We used data from seven regional population based health studies carried out in the period 1995- 2002. All studies were part of the Cohort of Norway (CONOR) collaboration with similar data collection, including standardized height and weight measurements. The current analysis was restricted to women and men aged 70-79 years at examination (mean 73.9 ±2.5 years). The majority of the participants (86%) also had measured height and weight collected in a nationwide tuberculosis screening program during 1963-75 at mean age 44.6 ±3.6 years, enabling the calculation of height loss during a mean period of 29.3 ±2.9 years. They were followed with respect to incident hip fracture from the last examination throughout 2008. We estimated hazard ratios (HR) for hip fracture according to height loss (between the two examinations) and BMI (from the last examination) by Cox proportional hazards regression, adjusting for age and initial height.

During follow-up, 844 of 7,398 women and 461 of 8,611 men suffered a hip fracture. Height loss was positively and BMI inversely related to the risk of hip fracture. Independent of BMI, women with a height loss of 5 cm or more (13%) had HR = 1.95 (95% CI 1.57-2.42) for hip fracture compared to those with a height loss of less than 2 cm. The corresponding figure in men with ⩾5 cm height loss (7.6%) was HR = 2.45 (95% CI 1.82-3.30).

The highest risk of hip fracture was found in those who had both the greatest height loss (⩾5 cm) and the lowest BMI (< 24 kg/m^2) [HR 4.24 (95% CI 2.94-6.11) in women and 3.96 (95% CI 2-36-6.64) in men] compared to those with height loss < 2 cm combined with BMI ⩾ 27 kg/m^2. The probability of hip fracture in women is shown in the figure. For example, after five years of follow up it was ~9% in women with a BMI < 24 kg/m^2 and a height loss ⩾5 cm, and less than 2% in women with a BMI ⩾ 27 kg/m^2 and a height loss < 2 cm. Those with intermediate levels of the risk factors had an intermediate risk (data not shown).

In conclusion, both height loss and a low BMI were strong and independent predictors of hip fracture in elderly women and men. Those with both risk factors had a four-fold risk of hip fracture compared to those with neither risk factor. Including height loss in addition to BMI or weight has the potential to enhance fracture risk prediction in a clinical setting

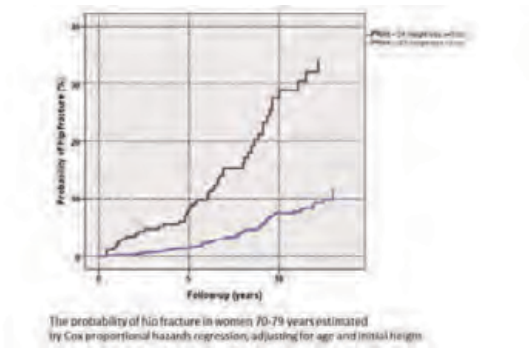

Figure

***Disclosures: Haakon E. Meyer**, None.*

FR0356

Vitamin D Insufficiency Sustained Over 5 Years Contributes to Increased 10-year Fracture Risk in Elderly Women. David Buchebner*[1], Fiona McGuigan[2], Paul Gerdhem[3], Kaisa Ivaska[4], Martin Ridderstråle[5], Kristina Akesson[6]. [1]Halmstad Hospital, Sweden, [2]University of Lund, Malmö, Skane University Hospital, Malmö, Sweden, [3]Karolinska Institutet, Sweden, [4]University of Turku, Finland, [5]University of Lund, Sweden, [6]Skåne University Hospital, Malmö, Sweden

BACKGROUND: Vitamin D insufficiency among the elderly is common and has been shown to contribute to increased risk of osteoporotic fractures through increased bone turnover, bone loss and mineralization defects as well as non-skeletal effects. Previous studies have used single Vitamin D measurements to investigate effects on bone. However, in elderly women, relatively little is known about the effects of long-term hypovitaminosis D on bone health. In this study we investigated sequential assessment of serum vitamin D to determine if sustained hypovitaminosis D leads to increased 10-year fracture incidence in elderly women.

METHODS: Study participants were Swedish women from the population based OPRA cohort. 1044 women, all aged 75 attended at baseline (BL), 715 attended at 5 year follow-up. Serum 25-hydroxy vitamin D (25OHD) levels (nmol/l) were classified as Low (<50), Intermediate (50-75) and High (>75) and were available for 987 (BL), and 640 (5y) women. Women with values in the same 25OHD category at both samplings were considered to have consistently low, intermediate or high levels. Fracture data was followed for 10 years through X-rays at the Radiology Department.

RESULTS: The incidence of hip fractures within 10 years was significantly lower in those women who were 25OHD sufficient (⩾50nmol/l) at baseline and maintained this level at 5 years (6.9% (H) and 9.9% (Int) vs 20.6% (L); p=0.005 and 0.031).

The proportion of women sustaining FRAX fractures was 26.2% and 30% in the consistently high and intermediate 25OHD groups compared to 45.6% in the consistently low group. (p=0.004 and 0.022). The incidence of shoulder, radius and vertebral fractures was not associated with 25OHD status in our study. The majority of fractures occurred between 5 and 10 years after baseline (hip 77%; FRAX 64%) however the time to first fracture (hip and FRAX) did not significantly differ between the 3 categories of 25OHD using either a single or serial measurement.

CONCLUSIONS: In this population sample of elderly women, 25OHD insufficiency sustained over 5-years was associated with increased 10-year risk of osteoporotic fracture.

***Disclosures: David Buchebner**, None.*

FR0363

Decrease in Bone Strength Due to Reduced Total Density and Content is Not Completely Compensated by Increase in Bone Area: Prospective pQCT Evidence from Distal Radius and Tibia in Postmenopausal Women. Saija Kontulainen*, Chantal Kawalilak, Andrew Frank, Wojciech Olszynski, James Johnston. University of Saskatchewan, Canada

Introduction: Prospective evidence from studies using 2 dimensional (2D) measurement techniques has provided conflicting evidence regarding whether bone mineral loss at the distal radius is compensated by an increase in bone width (an estimate of periosteal expansion) in postmenopausal women; a population prone to osteoporotic wrist fractures (Ahlborg et al. NEJM 2003, Szulc et al. JBMR 2006). In addition, cross-sectional evidence has indicated that intracortical remodelling and related trabecularization of the cortex could be the main source of bone loss in older women (Zebaze et al. Lancet 2010). Our objective was to characterize 3D-changes in estimated bone strength, density, content and area in the distal radii and tibiae of postmenopausal women. We tested three hypotheses: 1) bone strength would decrease; 2) the increase in bone area would compensate for bone mineral loss; and 2) increase in trabecular area would provide evidence of cortical trabecularization.

Methods: Participants (N=114) were from a randomized sample of community dwelling postmenopausal women (Saskatoon cohort of the Canadian Multicentre Osteoporosis Study, CaMos) with a mean age of 74.3 (SD7.7) years at baseline. We obtained bone scans from the distal radius and tibia using peripheral quantitative computed tomography (pQCT) at baseline and 1-year follow-up. We assessed changes in total and trabecular densities (ToA, TrD, mg/cm3), contents (ToC, TrC, mg/cm) and areas (ToA, TrA, mm2), respectively. We estimated bone strength in compression (BSIc, mg2/mm4) by multiplying ToA with squared ToD. We used paired t-test to assess bone changes. We report mean percent and absolute changes with 95% confidence intervals and p-values (significance set $p<0.05$).

Results: At the distal radius, bone strength decreased 4.6%, and decreases in ToD (-3.4%) and ToC (-1.5%) were accompanied by increases in ToA (2%) and TrA (3.5%) (Table 1). Changes in tibia were similar but seemed less in magnitude (Table 1).

Discussion: These unique prospective changes indicated that a 1-year decrease in bone strength, observed with a concomitant decrease in total density and content, was partially compensated by periosteal bone formation (increase in bone area) in postmenopausal women supporting previous longitudinal 2D evidence (Ahlborg et al. NEJM 2003). Increased trabecular area suggests trabecularization of the cortex which agrees with earlier cross-sectional evidence (Zebaze et al. Lancet 2010).

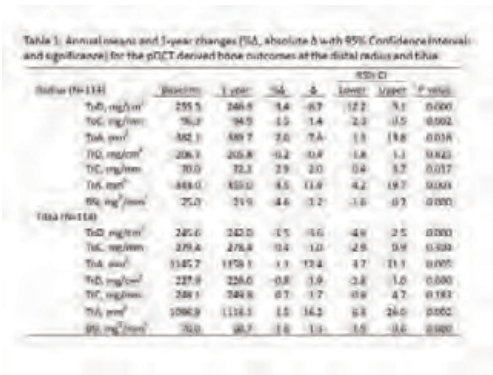

Table 1.

***Disclosures: Saija Kontulainen**, None.*

FR0364

Differences in Cortical and Trabecular Microstructure in Chinese and Caucasian Females originate during Peripubertal Growth. Xiao-Fang Wang*[1], Ali Ghasem-Zadeh[2], Qingju Wang[2], Jia Wei Teo[2], Sandra Iuliano-Burns[2], Yohann Bala[3], Roger Zebaze[2], Ego Seeman[2]. [1]University of Melbourne, Austin Health, Australia, [2]Austin Health, University of Melbourne, Australia, [3]University of Melbourne, Dept. of Medicine, Australia

Chinese women have fewer hip and forearm fracture rates despite having more slender bones. As remodelling is surface dependent, and the endocortical surface (lining the medullary canal) and the intracortical surface (formed by osteonal Haversian and Volkmann canals) are contiguous, we speculated that Chinese have lower resorptive remodelling and excavate a smaller medullary canal producing relatively the thicker cortex, and excavate fewer or smaller intracortical canals producing less porous cortices, than in Caucasians.

Distal radius images acquired using high-resolution peripheral quantitative computed tomography (HR-pQCT, XTreme CT, Scanco) were quantified for 34 healthy Chinese and 81 Caucasian females aged 7 to 46 years using Strax 1.0, a non-threshold based image analysis algorithm that segments the mineralized matrix and void volumes of the compact-appearing cortex, the transitional and trabecular regions. The proportion of void (porosity) was quantified as the average of void spaces in each voxel. The 1st CT slice commenced at the 4% of the radius length in children (under 18 years old) to adjust for any effects of bone length on scan region.

There was no detectable structural difference between races before puberty. After puberty, in Chinese, medullary area was lower, though to significantly so (97.4 vs.110.8 mm^2) while porosity of the compact-appearing cortex, outer and inner transitional zones were lower than Caucasians, respectively (35.9 vs. 45.6%; 45.0 vs. 53.1%; 74.5 vs. 78.8%. all $p<0.05$). Correspondingly, in pre-menopausal women, medullary area (101.2 vs. 130.6 mm^2, $p<0.001$), porosity of the compact-appearing cortex and outer transitional zone was lower than in Caucasians (21.2 vs. 23.3%; 31.6 vs. 33.6%. both $p<0.05$) but the racial differences appeared attenuated compared to postpubertal girls. The porosity of the inner transitional zone was similar between races (77.0 vs. 77.9%, NS).

Modelling and remodelling assemble a more robust skeleton in Chinese than Caucasian women. The smaller bone has a relatively thicker and less porous cortex perhaps attributed to excavation of a smaller medullary canal and fewer osteons. These morphological features may contribute to the lower fracture risk in Chinese women.

***Disclosures: Xiao-Fang Wang**, None.*

FR0365

Hip Cortical Porosity Predicts Fragility Fractures in Postmenopausal Women with Normal Hip Bone Mineral Density and Osteopenia. Luai A Ahmed*[1], Rajesh Shigdel[1], Ragnar Joakimsen[1], Petter Eldevik[2], Erik Fink Eriksen[3], Roger Zebaze[4], Ashild Bjornerem[1]. [1]University of Tromsø, Norway, [2]University Hospital North Norway, Norway, [3]Oslo University Hospital, Norway, [4]Austin Health, University of Melbourne, Australia

The majority of women with fractures exhibit normal areal bone mineral density (aBMD) or osteopenia. Thus, current methods based mainly on bone densitometry do not identify women at risk for fracture with high sensitivity and specificity. We hypothesized that women with fractures are better distinguished from controls by measures of microarchitecture, particular cortical porosity, or the combination of cortical porosity and aBMD, than either risk factors alone.

Using a nested case-control design we quantified microarchitecture using StrAx 1.0 software in computed tomography images of the subtrochanteric femoral site in 180 postmenopausal women aged 54-94 years with fractures (hip, humerus and forearm) and 209 age-matched controls, from the Tromsø Study, Norway. Total hip aBMD was measured using densitometry. The fracture risk was assessed using logistic regression analyses adjusted for age, height and weight, and prediction of fracture was assessed using the area under receiver operator curve (AUC).

In women with fractures, 61 (34%) had normal aBMD, 97 (54%) had osteopenia and 22 (12%) had osteoporosis. While in controls, 129 (62%) had normal aBMD, 73 (35%) had osteopenia and 7 (3%) had osteoporosis. Women with fractures exhibited 3.5% higher cortical porosity and 0.08 g/cm^2 lower aBMD than controls (both $p < 0.001$). Porosity predicted fracture independently of aBMD, in the whole cohort, in women with normal aBMD, as well as in women with osteopenia. In the whole cohort, each standard deviation (SD) higher porosity increased the risk of fracture (Odds ratio (OR) 2.13 (95% CI 1.64-2.76)), while each SD higher aBMD protected against fracture (OR 0.47 (95% CI 0.37-0.61)) both $p < 0.001$. AUC was 0.69 for porosity alone, 0.69 for aBMD alone and increased to 0.76 for the combination of porosity and aBMD. So after inclusion of cortical porosity there was an increase in AUC of 0.07 (95% CI 0.03-0.11) $p < 0.001$. In women with normal aBMD, each SD higher porosity increased fracture risk (OR 2.20 (95% CI 1.49-3.26), $p < 0.001$). In women with osteopenia, each SD higher porosity also increased fracture risk (OR 2.04 (95% CI 1.40-2.96) $p < 0.001$), while each SD higher aBMD protected against fracture (OR 0.30 (95% CI 0.12-0.76) $p = 0.01$).

In this general population, cortical porosity predicted fracture risk in women with normal aBMD and osteopenia independently of aBMD, improving the diagnostic sensitivity.

***Disclosures: Luai A Ahmed**, None.*

FR0366

Muscle Power and Force may Contribute to Cortical Bone Strength Through Distinct Mechanisms: Findings from a Cross-sectional Study of High Bone Mass Cases and Controls. Sarah Hardcastle*[1], Celia Gregson[1], Joern Rittweger[2], Kate Ward[3], Jon H Tobias[4]. [1]University of Bristol, United Kingdom, [2]Institute of Aerospace Medicine, German Aerospace Center, Cologne, Germany, [3]MRC Human Nutrition Research, United Kingdom, [4]Musculoskeletal Research Unit, School of Clinical Sciences, University of Bristol, United Kingdom

Background: Relationships between muscle function and bone have been examined using a range of techniques, with conflicting results. We aimed to determine these associations within an adult population comprising individuals with high bone mass and family controls.

Methods: Recruitment was from 3 UK sites within the High Bone Mass (HBM) study; cases and unaffected family controls were pooled. Peak ground reaction force and peak power, during a multiple one-leg jump and single two-leg jump respectively, were recorded using a Leonardo Mechanography Ground Reaction Force Platform. Total hip BMD was determined by DXA scanning. In addition, a subgroup had mid-tibial pQCT performed (Stratec XCT2000L). Linear regression analysis adjusted for age, gender, height and weight. Force and power were log transformed.

Results: Matching jump plate and hip DXA data was available in 189 participants comprising 70 males (mean age 58y) and 119 females (mean age 56y). Median jump power was 2.25 kW (IQR 1.78,2.93) and force 1.95 kN (1.68,2.39). Jump power was positively related to hip BMD (standardised β [95% CI] 0.29 [0.07,0.51], p=0.01), but jump force was not (0.03 [-0.16,0.22], p=0.74). In 113 participants with force and pQCT data, power was positively associated with tibial SSI (0.26 [0.09,0.44], p<0.01) and with cortical thickness (0.33 [0.06,0.60], p=0.02) but not with total bone area (0.10 [-0.10,0.30], p=0.33). Force was also positively associated with SSI (0.24 [0.07,0.42], p=0.01), but in contrast to power was associated with total bone area (0.22 [0.03,0.42], p=0.02) but not with cortical thickness (0.05 [-0.22,0.32], p=0.72).

Conclusion: Muscle power and force are both positively associated with cortical bone strength. However, distinct mechanisms appear to be involved, since power was primarily associated with reduced endosteal expansion (reflected by cortical thickness and hip BMD), whereas force was associated with increased periosteal expansion (reflected by total bone area). Based on these findings, the greatest increases in cortical bone strength may be achieved by interventions targeting both muscle force and power.

***Disclosures: Sarah Hardcastle**, None.*

FR0371

Bone Remodeling and Structure in the Proximal Femur. Felicia Cosman*[1], David Dempster[2], Jeri Nieves[3], Hua Zhou[1], Catherine Roimisher[1], Yvonne Houle[4], Robert Lindsay[1], Mathias Bostrom[4]. [1]Helen Hayes Hospital, USA, [2]Columbia University, USA, [3]Columbia University & Helen Hayes Hospital, USA, [4]Hospital for Special Surger, USA

Little is known about bone remodeling in the proximal femur. We designed a double blind placebo controlled trial to evaluate histomorphometry of the femur in patients scheduled for total hip replacement (THR) for severe osteoarthritis. To date, 19 samples have been fully analyzed (13 postmenopausal women, mean age 72; 6 men, mean age 70). Participants were randomized to receive teriparatide (TPTD) or Placebo by daily injection for 6 weeks. After 3 weeks, tetracycline label was administered following a standard protocol. During the THR, specimens of the femoral neck (FN) and trochanter (Troch) were procured and subsequently sectioned with division of the FN into superior, inferior, anterior and posterior regions (Figure). The Troch sample consisted of cancellous bone with a superior cortex. Investigators remain blinded to treatment and results are not separated by group. In the FN (Table), mineralized surface (MS/BS) and bone formation rate (BFR/BS) varied across bone envelopes, with a broad range of values among subjects (up to 60 fold). MS/BS and BFR/BS were overall highest in the periosteum. There was substantial variability across FN regions within each bone envelope, with overall lower MS/BS and BFR/BS in the inferior FN in all but the periosteal envelope. MAR varied to a much lesser degree (<3 fold), was consistent across the FN regions within each envelope, and highest in the periosteum. In Troch, MS/BS and BFR/BS in all 4 envelopes were consistently lower than in the FN, but varied broadly. Cortical width was similar in the superior, anterior and posterior FN and Troch (means 612-802 um), but higher in the inferior FN (mean 1246 um). Cancellous bone volume was also highest in the inferior FN (20.8% of total volume) and 3.8-18.3% in other regions. Osteophytes were seen in 15/19 subjects and woven bone was seen in 18/19 subjects, though it varied widely in extent and distribution. We conclude that histomorphometric examination of the proximal femur is feasible in patients who have received tetracycline label before THR. MS/BS and BFR vary broadly among subjects in different bone envelopes of the FN and Troch regions after TPTD or Placebo. Notably, the highest BFR was seen in the periosteum. Structural indices also vary by FN region. This study might provide the first evidence of where and to what extent TPTD stimulates bone formation in the proximal femur. Table: Bone Formation Indices in the Femoral Neck. Mean + SD (Range)

	MS/BS (%)	MAR (um/d)	BFR/BS (mm³/mm²/yr)
Cancellous			
Superior	7.74±7.66(0.46,31.5)	0.676±0.08(0.49,0.80)	0.021±0.02(0.001,0.09)
Inferior	4.85±4.00(0.22,15.0)	0.684±0.09(0.54,0.85)	0.014±0.01(0.001,0.04)
Anterior	7.54±7.11(0, 24.4)	0.646±0.1(0.47, 0.85)	0.019±0.02(0.00,0.063)
Posterior	7.38±8.6(0.49,37.7)	0.662±0.1(0.48, 0.89)	0.020±0.02(0.001,0.10)
Intracortical			
Superior	19.1±11(2.4,42.7)	0.780±0.1(0.57,1.00)	0.058±0.03(0.004,0.13)
Inferior	11.3±7 (0.8, 22.50)	0.736±0.1(0.37,0.88)	0.034±0.02(0.0, 0.07)
Anterior	16.4±12 (0.0, 47.96)	0.719±0.15(0.45,1.0)	0.045±0.03(0.0, 0.111)
Posterior	15.7±14 (1.0, 50.95)	0.753±0.18(0.44, 1.1)	0.047±0.041(0.0,0.137)
Periosteal			
Superior	18.87±12(4.2, 48.9)	0.850±0.24(0.59,1.46)	0.073±0.05(0.01,0.19)
Inferior	28.08±19 (2.3, 61.7)	0.946±0.20(0.63,1.45)	0.126±0.08(0.0,0.27)
Anterior	24.87±17 (0.6, 49.9)	0.765±0.16(0.52, 1.1)	0.102±0.056(0.04,0.20)
Posterior	21.12±19(0.0,54.2)	0.897±0.24(0.63,1.4)	0.092±0.071(0.0,0.21)
Endocortical			
Superior	17.76±12 (0.8, 46.5)	0.697±0.11(0.47,0.86)	0.052±0.046(0.0, 0.13)
Inferior	10.14±8 (0.7, 25.4)	0.669±0.14(0.44,0.92)	0.031±0.030(0.0, 0.08)
Anterior	14.23±15 (0.0, 45.3)	0.697±0.17(0.36,0.9)	0.042±0.047(0.0,0.15)
Posterior	10.61±12 (0.0, 48.4)	0.636±0.17(0.29,0.9)	0.027±0.030(0.0,0.12)

Table

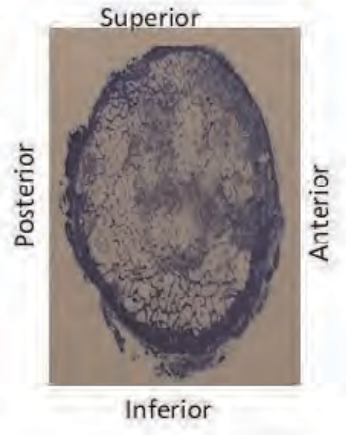

Figure

***Disclosures: Felicia Cosman**, Eli Lilly, Amgen,; Eli Lilly, Novartis, Amgen, 6; Eli Lilly, Amgen, Merck, Zosano, GSK, Unigene, Tarsa, 2*

FR0372

Comparative Effects of Teriparatide, Denosumab, and Combination Therapy on Peripheral Compartmental Bone Density and Microarchitecture: the DATA-HRpQCT Study. Joy Tsai*[1], Alexander Uihlein[1], Yuli Zhu[1], Katelyn Foley[1], Nicholas Derrico[1], Hang Lee[1], Sherri-Ann Burnett-Bowie[1], Robert Neer[1], Mary Bouxsein[2], Benjamin Leder[3]. [1]Massachusetts General Hospital, USA, [2]Beth Israel Deaconess Medical Center, USA, [3]Massachusetts General Hospital Harvard Medical School, USA

Background: In postmenopausal women, 12 months of combination therapy with denosumab (DMAB) and teriparatide (TPTD) increased bone mineral density at the spine and hip more than either drug alone. The effect of combined DMAB and TPTD therapy on peripheral compartmental bone density and microarchitecture, however, is unknown.

Methods: We randomized 100 postmenopausal women ages 51-91 at high fracture risk to 1 of 3 treatments: TPTD 20-ug SC QD, DMAB 60-mg SC Q6 months, or both (COMBO) for 12 months. Women were excluded if they had ever used parenteral bisphosphonates (BPs) or oral BPs in the past 6 months. Total, trabecular, and cortical density (DTot, DTrab, DCort); trabecular thickness, spacing, and number (Tb.Th, Tb.Sp, Tb.N); and cortical thickness and porosity (Ct.Th, Ct.Po) were measured by high-resolution peripheral quantitative CT (HR-pQCT) of the distal radius and tibia. Subjects completing at least 1 post-baseline visit were included in our longitudinal mixed-effects model analysis of between-group differences.

Results: As shown in the table, at both sites, DTot, DTrab, DCort and Ct.Th increased in the DMAB and COMBO groups but not the TPTD group. Ct.Po in the TPTD group increased at the radius but not the tibia. DTot increased more at the tibia in the COMBO group (3.1 ± 2.1%) than both the TPTD (0.0 ± 2.3%, P<0.0001) and DMAB groups (2.2 ± 2.0%, P=0.011) whereas radius DTot increased more in the COMBO group than the TPTD group only. DCort increased more in the

COMBO group than the TPTD group at both the radius and the tibia (P<0.001). At the tibia, Ct.Th increased significantly more in the COMBO group (5.4 ± 3.8%) than both other groups whereas at the radius, Ct.Th increased more in the COMBO group than the TPTD group only. At the tibia, cortical porosity increased more with TPTD (5.6 ± 10.3%) than both other treatments (DMAB -2.0 ± 10.6%, COMBO -1.0 ± 10.0%). At the radius, cortical porosity also increased more with TPTD (18.0 ± 36.4%) than both other treatments (DMAB 2.9 ± 18.8%, COMBO 3.0 ± 18.7%). but the TPTD vs. COMBO comparison was not significant (P=0.069). No between-group differences in trabecular microarchitecture were observed.

Conclusions: DTot and Ct.Th of the tibia increased more with combined therapy than with DMAB or TPTD alone. Moreover, the TPTD-induced changes in DCort and Ct.Po were prevented by DMAB co-administration. Combined DMAB-TPTD therapy appears to result in the most favorable changes in cortical bone parameters.

Table. Mean percent change (SD) from baseline in bone density and microarchitecture at 12 months.

	Radius (% change)			Tibia (% change)		
	TPTD (n=30)	DMAB (n=30)	Combination (n=76)	TPTD (n=29)	DMAB (n=30)	Combination (n=76)
DTot	-0.8 (3.7)	1.6 (2.0) [*,§]	2.0 (2.7) [*,§]	0.0 (7.3)	2.2 (2.0) [*,§]	3.1 (2.1) [*,§,¶]
DTrab	1.0 (2.9)	1.4 (2.8) [*]	2.5 (3.2) [*]	1.2 (3.8)	2.1 (3.0) [*]	1.6 (2.8) [*]
DCort	-1.9 (2.9) [*]	0.6 (1.4) [*,§]	1.0 (1.6) [*,§]	-1.5 (1.9) [*]	0.9 (1.7) [*,§]	1.5 (1.5) [*,§]
Th.Th	1.1 (7.4)	2.0 (7.1)	2.8 (7.8)	4.1 (12.4)	8.4 (10.7) [*]	5.0 (11.5)
Tb.Sp	0.3 (8.2)	0.5 (7.7)	0.1 (8.1)	3.0 (12.6)	2.1 (11.1)	1.6 (12.6)
Tb.N	0.5 (8.6)	0.0 (7.5)	0.3 (8.1)	-1.6 (12.1)	-1.9 (9.5)	-0.2 (13.0)
Ct.Th	-1.1 (6.5)	2.4 (4.9) [*,§]	2.1 (4.4) [*,§]	-0.2 (4.9)	3.6 (3.3) [*,‡]	5.4 (3.8) [*,§,¶]
Ct.Po	18.0 (36.4) [*]	2.9 (18.8) [§]	3.0 (18.7)	5.6 (10.3)	-2.0 (10.6) [*]	-1.0 (10.0) [*]

[§] p value <0.05 versus teriparatide (TPTD) alone
[‡] p value <0.05 versus denosumab (DMAB) alone
[*] p value <0.05 versus baseline

Table. Mean percent change (SD) from baseline in bone density and microarchitecture at 12 months

***Disclosures: Joy Tsai**, None.*
This study received funding from: Eli Lilly, Inc and Amgen, Inc

FR0374

Cortical Thickness and Density Changes Over the Proximal Femur Resulting From Switching To or Combining With Teriparatide After Prior Treatment With Raloxifene or Alendronate. Tristan Whitmarsh*, Graham Treece, Andrew Gee, Kenneth Poole. University of Cambridge, United Kingdom

For osteoporotic women undergoing treatment with an antiresorptive drug, such as Raloxifene (RLX) or Alendronate (ALN), a following treatment of Teriparatide (TPT) is sometimes recommended. In this case, a decision has to be made to either switch to or add TPT to the current treatment. The effects of adding versus switching to TPT have been previously studied by examining aBMD changes from DXA (Cosman, J Clin Endocrinol Metab 2009) and vBMD changes from QCT (Cosman, JBMR 2012.). These indicated a significant increase in density for all treatment groups, which was of greater magnitude when adding than when switching in that trial. However, previous studies have not separated cortical mass and thickness effects, nor assessed the distribution and extent of more localised changes.

In previous work, a method was presented to map the cortical thickness and mass from clinical CT over the surface of the proximal femur, accurate down to a thickness of 0.3mm (Treece, Med Image Anal 2010, 2012). We use this technique to analyse changes in cortical mass and thickness from QCT scans acquired 18 months after switching to TPT after 12 months prior treatment with RLX (25 women aged 69±9 years) or ALN (40 women aged 69±8 years) and 18 months after combining a previous treatment of RLX (28 women aged 67±8 years) and ALN (41 women aged 67±10 years) with TPT. Fig. 1 shows the mean thickness and mass changes compared to baseline, and the significance of such changes, for each of the four treatment groups.

Averaging these results over the entire proximal femur reveals global mass increases for the add group (2.8% RLX, 1.6% ALN) which are significantly (p<0.001) greater than for the switch group (0.7% RLX, -0.8% ALN). For cortical thickness, the increases for the add group (3.7% RLX, 1.9% ALN) are not significantly different from the switch group (1.7% RLX, 3.0% ALN).

These results are broadly in agreement with previously published work, though we here reveal significant mass increases for the add compared to the switch groups, which are primarily located at the posterior side of the trochanter. Hence this study provides new insights into the effects of switching versus adding Teriparatide on the cortical thickness and mass changes.

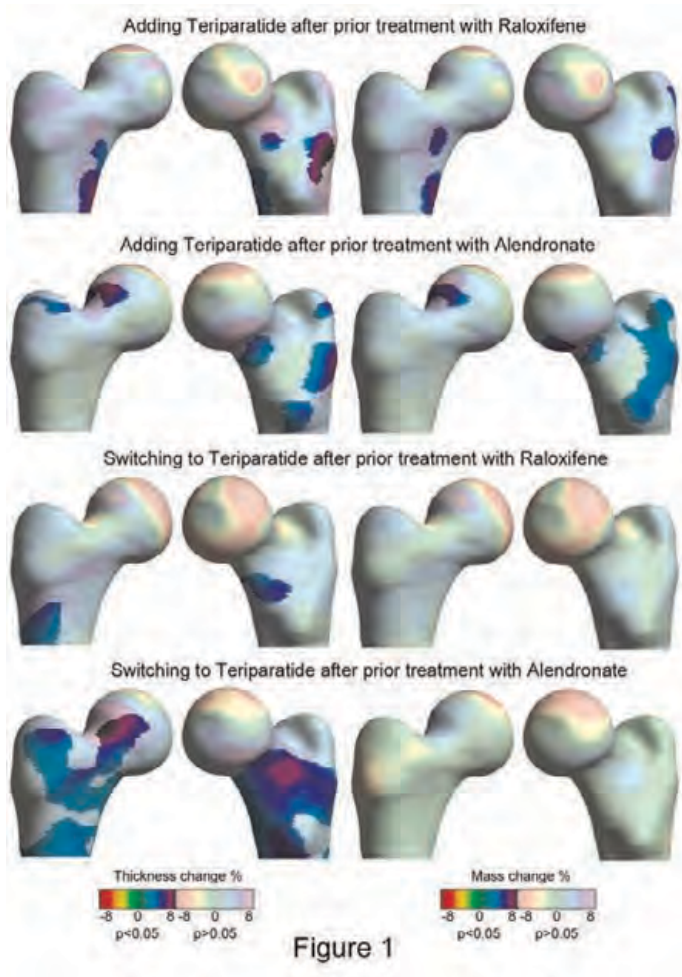

Figure 1

***Disclosures: Tristan Whitmarsh**, None.*
This study received funding from: Eli Lilly

FR0376

Once-weekly Teriparatide Reduces Vertebral Fracture Risk – Subgroup Analysis from the Teriparatide Once Weekly Efficacy Research (TOWER) Trial. Toshitsugu Sugimoto*[1], Masataka Shiraki[2], Tetsuo Nakano[3], Hideaki Kishimoto[4], Masako Ito[5], Masao Fukunaga[6], Hiroshi Hagino[7], Teruki Sone[6], Toshitaka Nakamura[8]. [1]Shimane University School of Medicine, Japan, [2]Research Institute & Practice for Involutional Diseases, Japan, [3]Tamana Central Hospital, Japan, [4]Nojima Hospital, Japan, [5]Nagasaki University Hospital, Japan, [6]Kawasaki Medical School, Japan, [7]Tottori University, Japan, [8]University of Occupational & Environmental Health, Japan

Introduction: We analyzed the effects of once-weekly teriparatide (human parathyroid hormone 1-34) injection on incident vertebral fracture in various subgroups using data from the TOWER trial (2012 JCEM).

Methods: Anti-fracture efficacy with weekly 56.5 μg teriparatide injection was examined in a randomized, double-blind, placebo-controlled trial of 542 Japanese patients with osteoporosis (65-95 years). Patients were divided by baseline age, number or deformity grade of prevalent vertebral fractures, BMD level, bone turnover marker levels (osteocalcin; N-terminal propeptides of type 1 procollagen; N-terminal crosslinking telopeptides of type 1 collagen; deoxypyridinoline), and level of renal function using estimated glomerular filtration rate (eGFR). Relative risk (RR) was calculated using Cox regression analysis.

Results: Incident vertebral fracture occurred in 2.7% (7/261) subjects in the teriparatide group and 13.2% of subjects (37/281) in the placebo group. The RR for incident vertebral fracture in teriparatide group was 0.20 (p<0.001), compared to placebo group. Significant fracture risk reductions were observed in the subgroup of subjects <75 years (RR, 0.06; p=0.007) and ⩾75 years (RR, 0.32; p=0.015). For prevalence of vertebral fractures, a significant risk reduction was observed in the subgroup with 1 vertebral fracture (RR, 0.08; p=0.015) and in those with ⩾2 vertebral fractures (RR, 0.29; p=0.009). In the subgroup based on deformity of vertebral fracture, a significant risk reduction was observed in subjects with grade 3 deformity

(RR, 0.26; p=0.003). Significant risk reduction was observed in the subgroup with lumbar BMD <-2.5SD (RR, 0.25; p=0.035). No incident vertebral fracture was observed in the subgroups with no prevalent vertebral fractures, with vertebral deformity grade 0 to 2, and with lumbar BMD ⩾-2.5 SD in the teriparatide group. Significant risk reductions were observed in the subgroups over/under the median value for each bone turnover marker. The subgroups over/under the eGFR levels: 70 ml/min/1.73m^2 showed a significant reduction in fracture risk (RR, 0.13, p=0.001; RR, 0.31; p=0.004, respectively).

Conclusion: Once-weekly injection of 56.5 μg teriparatide reduced vertebral fracture risk in subgroups divided by age, number and deformity of vertebral fractures, bone turnover levels, and eGFR levels. These results indicate a consistent anti-fracture efficacy of teriparatide in patients with various degrees of fracture risk.

***Disclosures: Toshitsugu Sugimoto**, None.*
This study received funding from: Asahi Kasei Pharma Corporation

FR0378

Teriparatide Delivered Orally with Novel Drug Delivery Technology - First in Humans Results. Hillel Galitzer*[1], Naifang Wang[2], Gregory Burshtien[3], Phillip Schwartz[1], Yoseph Caraco[4], Ehud Arbit[5]. [1]Entera Bio, Israel, [2]Entera Bio & Align Bioscience, USA, [3]Entera Bio Ltd., Israel, [4]Hadassah Hospital Jerusalem, Israel, [5]Entera Bio & NYU-Poly, USA

Teriparatide (PTH_{1-34}) is currently the only marketed anabolic agent for the treatment of osteoporosis. Its effect is mediated by an increase in osteoblast number and activity, leading to increased bone formation, bone mass and, as a consequence, substantial reduction in the risk for vertebral and non-vertebral fractures. A major obstacle to the broader adoption of teriparatide, as first line therapy in the treatment of osteoporosis, is its route of administration by s.c. (subcuatneous) injection. An oral dosage form will likely result in broader clinical use and foster compliance and adherence. In previous preclinical studies (Galitzer et. al. ASBMR 2012), we have demonstrated the utility of our proprietary drug delivery technology for delivering teriparatide orally. Here we present data from our first- in-human studies focusing on safety, tolerability and the absorption dynamics of oral teriparatide.

Methods: 12 healthy volunteers were given a single dose of s.c. teriparatide (20ug), as a comparator. One week following the s.c. dose a 200ug dose of Entera Bio's oral teriparatide was given to the same subjects. A full panel of safety parameters were measured following drug administration. Blood samples were taken at predetermined intervals and analyzed for PTH_{1-34} and a full set of standard of safety parameters.

Concentration of Human PTH_{1-34} in blood plasma was analyzed using a high sensitivity chemiluminescent immunoassay. Values were checked and normalized to known teriparatide standards.

Results: Oral PTH_{1-34} was well tolerated with no abnormal laboratory values or incidence of adverse events observed.

The absorption pattern was similar to that observed in SC injections and known to be therapeutically effective. The PTH_{1-34} increased rapidly followed by a slightly less rapid decrease.

[Graph attached]

Conclusion: This first in human study has demonstrated potential therapeutically relevant PTH_{1-34} systemic exposure after administration of Entera's proprietary oral PTH_{1-34} . These preliminary clinical studies have shown that volunteers manifest a pharmacokinetic profile similar to that observed with the SC injection. With additional research and development Entera's oral formulation of teriparatide may have the potential to serve as a viable alternative to currently used injectable forms of PTH.

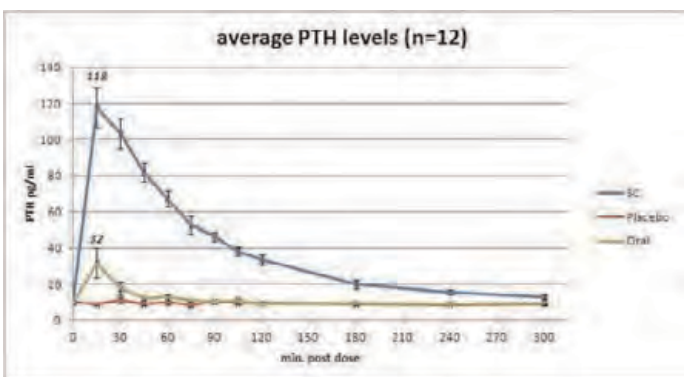

results for abstract

***Disclosures: Hillel Galitzer**, Entera Bio Ltd., 3*
This study received funding from: Entera Bio Ltd.

FR0379

Calcium plus Vitamin D supplementation: a Meta-analysis of Risk and Benefit. Steven Frost*[1], Nguyen Nguyen[2], Jacqueline Center[2], John Eisman[2], Tuan Nguyen[2]. [1]University of Western Sydney, Australia, [2]Garvan Institute of Medical Research, Australia

Background and Aim — Supplements of calcium and vitamin D have been suggested to be associated with an increased risk of cardiovascular disease (CVD) and stroke. However, calcium and vitamin D have also been suggested to reduce fracture risk. In this study, we sought to simultaneously examine the risk and benefit of calcium and vitamin D (CaD) supplementation.

Methods — This study is a meta-analysis of randomized controlled trials (RCTs). We identified 9 primary RCTs on the efficacy of CaD on fracture risk, and 3 post-hoc analyses of RCT on the association between CaD and CVD outcomes. The data were synthesized by both traditional and Bayesian random-effects meta-analysis, in which the risk of an outcome in individuals on CaD was compared with those on placebo. In addition, we used the Bayesian approach with non-informative priors to estimate the probability that CaD supplements increase or decrease the risk of an outcome by more than 10% - a level of difference usually deemed to be clinically meaningful. A meta-regression analysis was also conducted to identify the level of risk that is associated with the outcomes.

Results — CaD supplements reduced the risk of fragility fracture by 11% (RR 0.89; 95%CI 0.80-0.97), and the reduction was observed in nonvertebral fractures (RR 0.90; 0.79-0.99) and clinical vertebral fracture (RR 0.86; 0.75-0.99), but not in hip fracture (RR 0.88; 0.71-1.06). There was 48% chance that CaD supplements reduced fracture risk by at least 10%. Meta-regression analysis suggested that the anti-fracture benefit of CaD supplements was more likely observed in individuals with 2% and greater risk of fracture per year. CaD supplements were not significantly associated with any CVD outcome: myocardial infarction (RR 1.18; 0.73-1.74), stroke (RR 1.17; 0.75-1.70), myocardial infarction or stroke (RR 1.14; 0.74-1.64), and death (RR 1.01; 0.67-1.58). The probability that CaD supplements increase the risk of CVD outcomes by more than 10% was 0.34. The number needed to treat to reduce a fracture was 85, and the number needed to incur a CVD event was 170. Thus, the ratio of benefit over potential risk was 2.

Conclusions — These results confirm that CaD supplements reduce the risk of fracture, but the effect size is likely modest. The results also indicate that there is likely to be no significantly increased risk of CVD outcomes associated with CaD supplements.

Risk ratio of fracture and CVD outcomes associated with CaD supplements

Outcome	Relative Risk (RR) and 95% CI	Probability of RR<0.90 (for fracture) or RR>1.10 (for CVD outcomes)
All fractures	0.89 (0.80 – 0.97)	0.48
Vertebral fracture	0.86 (0.75 – 0.99)	0.59
Non-vertebral fractures	0.90 (0.79 – 0.99)	0.46
Hip fracture	0.88 (0.71 – 1.06)	0.47
Myocardial infarction (MI)	1.18 (0.73 – 1.74)	0.63
Stroke	1.17 (0.75 – 1.70)	0.62
MI or stroke	1.14 (0.74 – 1.64)	0.59
Death	1.01 (0.67 – 1.58)	0.30

Table

***Disclosures: Steven Frost**, None.*

FR0380

Bisphosphonates, Glucocorticoids, and Suffering from Collagen Diseases were Risk Factors for Developing Atypical Femoral Fractures in Japan. Yoshitomo Saita*, Muneaki Ishijima, Masashi Nagao, Kazuo Kaneko. Department of Orthopaedics, Juntendo University School of Medicine, Japan

Purpose: The long-term treatment of osteoporosis with anti-resorptive drugs may be associated with an increase in atypical femoral fractures (AFFs). However, the risk factors for Asian populations have not been fully elucidated.

Methods: In this retrospective observational cohort study, the clinical characteristics of patients with AFFs and typical femoral fractures (TFFs) treated from 2005 to 2010 in our hospitals were analyzed. A fracture location-, age- and gender-matched (1:3) case-control study was conducted to examine the risks for developing AFFs. The odds ratios of taking BPs, GCs, vitamin D analogues and proton pump inhibitors, and for suffering from collagen diseases and diabetes, were analyzed. The significance of the differences in the data was evaluated using the Mann-Whitney U-test. Odds ratios (ORs) and their 95% confidence intervals (CIs) between the patients with TFFs and those with AFFs in terms of several parameters, including BP exposure and comorbid conditions, were estimated by the Chi-square test. A p value < 0.05 was considered to be statistically significant. These analyses were performed using the SPSS ver.17 statistical software package (SPSS Inc., Chicago, IL).

Results: Fourteen AFFs were found in ten patients (four bilateral fractures) among all 2,238 hip and femoral shaft fractures, as we previously reported in annual meeting of ASBMR in 2011. The patients with AFFs (66.0 years) were significantly

younger than those with TFFs (78.8 years, p<0.0001). Nine (90%) and six (60%) of the ten patients with AFFs were using bisphosphonates and glucocorticoids (GCs), while 9.4% and 4.8%, respectively, of the patient with TFFs were using these agents. The case-control study showed that a high proportion of patients with AFFs used BPs and GCs and were suffering from collagen diseases (CDs)(odds ratios; 36.0, 13.0 and 9.0, respectively). On the other hand, no significant differences in the frequencies of using PPIs, vitamin D analogues, and suffering from diabetes were observed between the patients with AFFs and those with TFFs.

Conclusion: The prevalence of AFFs in the Japanese population was similar to that of Western countries. BPs, GCs, and suffering from CDs were the major risk factors for developing AFFs. To the best of our knowledge, this is the first report describing the case-control study of AFFs in East Asian countries.

***Disclosures: Yoshitomo Saita**, None.*

FR0388

Microdamage analysis of the cortical bone of fracture site in the patient with atypical femoral fracture. Ken Iwata*[1], Tasuku Mashiba[2], Takeshi Manabe[3], Toshiaki Hitora[1], Yoshiki Yamagami[1], Tetsuji Yamamoto[1]. [1]Kagawa University School of medicine, Japan, [2]Kagawa University Faculty of Medicine, Japan, [3]Kinashi Ohbayashi Hospital, Japan

In recent years, case reports of atypical femoral fracture (AFF) caused by minor trauma in patients receiving long-term bisphosphonate therapy have been makledly increased. Little is known regarding their etiology and mechanism. While report of a task force of the ASBMR suggests the possibility that microdamage accumulation due to severely suppressed bone turnover by long-term bisphosphonate treatment could cause AFF, few microdamage evaluations have been done in the fracture site. We report a case of AFF receiving long-term intravenous bisphosphonate therapy and the result of microdamage analysis in the cortical bone of fracture site.

A 56-year-old Japanese woman was admitted with non-traumatic subtrochanteric fracture of right femur. She was diagnosed with right breast cancer and taken radical mastectomy at the age of 35. Because multiple rib metastases were found 12 years after surgery, she was put under intervenous incadronic acid for 3 years, pamidonic acid for 1 year, then zoledronic acid for 3 years. At the age of 52, she suffered from spontaneous left subtrochanteric femoral fracture and treated with an intramedullary nail. However, because it was recognized as pathological fracture due to bone metastasis at that time, she had continued zoledoronic acid therapy for 3 years further. This time, she was diagnosed with right AFF (Fig 1.) and the fracture was osteosynthesised also using an intramedullary nail. Because there were no evidences of bone metastasis in her whole skeleton at the time of surgery, zoledronic acid was stopped after the surgery and complete radiological fracture healing was obtained 6 months after surgery.

At the surgery, a bone biopsy was performed at the thickened cortical bone of fracture site for bone histology and microdamage measurement. For microdamage analysis, bone sample was bulk stained with 1% basic fuchsin. There were no histological evidences of metastatic cancer, however, tremendous amount of microcracks were observed in the thickened cortical bone of fracture site (Fig. 2, Table 1). Although there is a limitation that microdamage can be overestimated due to the bone biopsy site adjacent to fracture, this is the first report demonstrated that marked accumulation of bone microdamage was clearly observed in the hypertrophic cortical bone of atypical femoral fracture site.

Microdamage parameter		
Cr.Dn (#/mm2)	Cr.Le (μm)	Cr.S.Dn (μm/mm2)
5.8	91.6	553.4

Table 1. Microdamage parameter

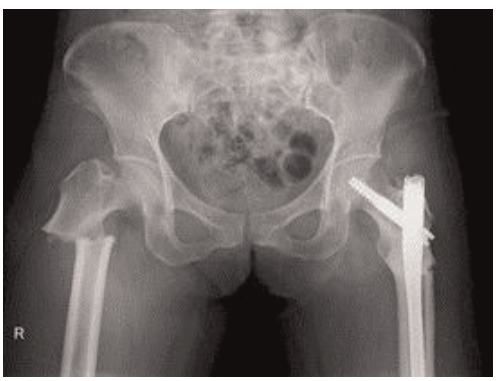

Figure 1. X-rey image of hip joint

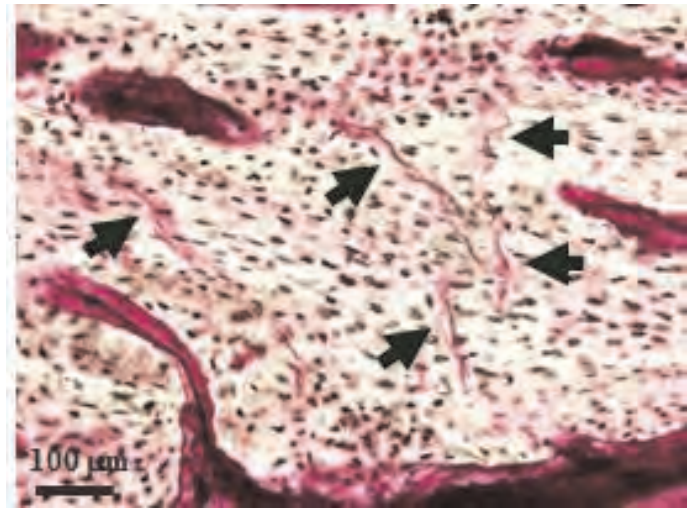

Figure 2. Histology and microdamage measurement

***Disclosures: Ken Iwata**, None.*

FR0391

Adherence to Oral Bisphosphonate Therapy in a Fracture Liaison Service: A Randomised Controlled Trial. Kirtan Ganda*[1], Markus Seibel[2], Andrea Schaffer[3], Sallie Pearson[3]. [1]Concord Hospital, Australia, [2]Bone Research Program, ANZAC Research Institute, University of Sydney, Australia, [3]Pharmcoepidemiology & Pharmaceutical Policy Ressearch Group, Faculty of Pharmacy, School of Public Healht, Sydney Medical School, The University of Sydney, Australia

Background: Fracture Liaison Services (FLS) are known to increase the proportion of patients initiated on osteoporosis medication following a minimal trauma fracture. However, little is known about long-term therapeutic adherence in patients managed by such fracture prevention programs.

Methods: This 2-year randomised controlled trial included 102 patients, all of whom had suffered an incident osteoporotic fracture prior to attending the FLS. After initiation of oral weekly bisphosphonate treatment, patients were randomised to either six-monthly follow-up visits with the FLS (Group A) or referral to their primary care physician with a single follow-up visit at the FLS after 24-months only (Group B). All patients received treatment subsidised through the Australian Pharmaceutical Benefits Scheme (PBS). Adherence was measured using pharmaceutical claims data extracted from the PBS database. Subjects with missing PBS data were excluded from the analysis (n=4 in each group). Patients with complete PBS data who attended at least one clinic appointment were included in the intention-to-treat (ITT) analysis (n=94). Subjects who attended all appointments were included in the per protocol (PP) analysis (n=74). Compliance (medication possession ratio, MPR) and persistence as well as predictors of adherence were analysed and compared between Group A and B. Associations between adherence and changes in bone mineral density (BMD) or bone turnover were determined at 24-months.

Results: Baseline characteristics were well matched across groups in both the ITT and PP populations. In the ITT analysis, median MPR over 24 months was 0.78 (IQR 0.50-0.93) and 0.79 (IQR 0.48-0.96) in Group A and B, resp. (p=0.68). Persistence at 24-months was 64% and 61% in Group A and Group B, resp. (p=0.75). After adjusting for confounders, patients in Group A were not more likely to be compliant (OR 1.06, 95%CI 0.46-2.47, p=0.89) or persistent (HR 0.83, 95%CI 0.27-1.67, p=0.61) than those in Group B. Results were nearly identical in the PP analysis. Ethnicity was a significant predictor of adherence. Neither compliance nor persistence were associated with changes in bone turnover markers or BMD over 24-months.

Conclusion: Once treatment has been initiated within the setting of a dedicated FLS, patient adherence to oral bisphosphonate therapy over 24 months remains high, independent of whether follow-up occurs through the primary care physician or the specialist service.

***Disclosures: Kirtan Ganda**, None.*

FR0401

Does Calcitonin-Salmon Cause Cancer?. George Wells[1], David Krause*[2], Jonathan Chernoff[3], James Gilligan[4]. [1]Universtiy of Ottawa, Canada, [2]Tarsa Therapeutics Inc., USA, [3]Fox Chase Cancer Center, USA, [4]Tarsa Therapeutics, USA

BACKGROUND: Calcitonin-salmon (sCT) is a 32 AA peptide hormone in birds, fish and mammals. Its mechanism of action is mediated via coupling to G protein-coupled receptors. sCT is a more potent antiresorptive agent than human calcitonin,

and has been used for > 30 yrs for the treatment of postmenopausal osteoporosis. Recently sCT was withdrawn from the market in EU because of a putative association with prostate cancer identified in an interim analysis of a large trial of oral sCT in osteoarthritis in adults. Subsequently a metanalysis of 17 clinical trials of intranasal (IN) sCT was reported to confirm an increased risk of any cancer, although final data from the OA trial did not ultimately reveal an increased risk of prostate cancer. This association would not have been predicted by previously performed carcinogenicity and mutagenicity studies or sCT's mechanism of action, and no signal was apparent in postmarketing surveillance data. METHODS: Data from 17 controlled IN studies and 3 large studies of an investigational orally administered sCT (Novartis) were obtained from publically available information, and combined with data from a different oral sCT product (Tarsa). An additional 2 studies of IN CT were obtained from the literature. Only data from female subjects were included. In IN studies the dose ranged from 8.3 mcg to 66.6 mcg/day, and the duration from 0.5 to 5 years. In oral studies the dose ranged from 200 mcg/day to 800 mcg BID, and the duration from 1 to 3 years. Adverse events (AEs) were recorded at periodic intervals. In all studies cancer was recorded as an AE; no study included prospective case definitions or blinded adjudication of cases. RESULTS: Almost 11,000 women were exposed to oral or nasal CT, or placebo. No AEs of malignancy were recorded in 4 trials, and results were heavily influenced by one trial (CT320). More than 20 types of malignancy were represented. Using the Mantel-Haenszel method with adjusted continuity correction for those trials with no cases, the, the odds ratio (OR) for the reporting of any malignancy, calcitonin: placebo, was 1.16 (95% CI: 0.925, 1.458). The Fig. shows the point estimate of OR and 95% CI for each trial. CONCLUSIONS: There is little biological plausibility to the thesis that sCT causes cancer or is tumor promoting. A meta-analysis of all available trials of IN and oral sCT trials in women yielded a narrow OR close to unity. sCT does not appear to cause cancer.

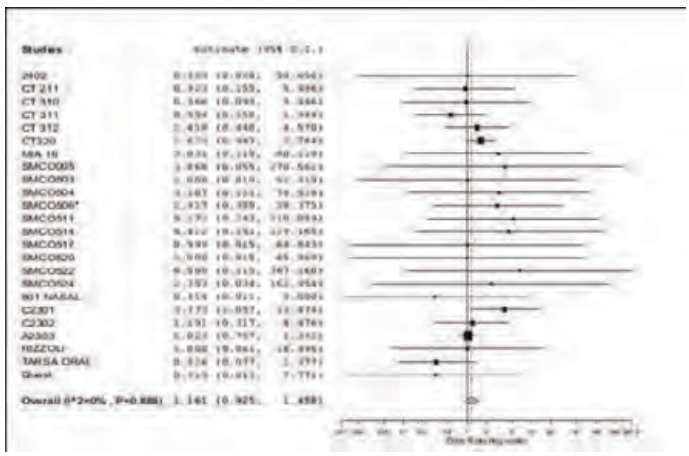

Figure

***Disclosures: David Krause**, Tarsa, 2*
This study received funding from: Tarsa Therapeutics

FR0404

Characteristics, Treatments, and Quality Of Life of Patients In a Swedish Osteoporosis Patient Registry. Dan Mellstrom[1], Arun Krishna*[2], Zhiyi Li[3], Chun-Po Steve Fan[4], Stina Salomonsson[5]. [1]Sahlgrenska University Hospital, Sweden, [2]Merck, USA, [3]AsclepiusJT LLC, USA, [4]AsclpeiusJT LLC, Canada, [5]MSD, Sweden

Objective: To describe patient characteristics, use of drug treatments, and quality of life on subjects in a Swedish patient registry database.

Methods: A descriptive analysis using a Swedish patient registry collected in an outpatient clinic in the region of Göteborg from 1991 to 2009 (study period). Included subjects were referred to the clinic for DXA scan for bone mineral density (BMD) measurement and osteoporosis (OP) diagnosis. Subjects were invited for a follow-up DXA scan every 2 years if the prior scan showed low BMD/OP diagnosis. This study analyzed subjects' current and previous OP treatments, fracture risk related to characteristics at enrollment, and Quality of life (QoL). QoL was collected post-2004 and measured by EQ-5D-3L covering dimensions of mobility, self-care, usual activities, pain/discomfort and anxiety/depression. Current and previous OP treatments were reported among subjects diagnosed with OP at the first visit. Means and standard deviations (SD) were reported for continuous measures; percentages were reported for categorical measures.

Results: 9,312 subjects were enrolled in the registry. 91% were female, with average age of 64.1 [SD=11.8] years. Average weight and height were 66.1 [SD=20.6] kg and 161.4 [SD=22.3] cm, respectively. 23% of subjects reported fractures at age >40, 35% had family history of fractures, 28% had back pain, and 33% were currently smokers. At the first visit, 3,292 (35%) subjects had a T-score (either hip or lumbar spine) ≤ -2.5 and 3,897 (42%) between -1 and -2.5. 3,587 (38.5%) were diagnosed with OP and 4,031 (43%) with osteopenia. EQ-5D was available for 1,570 subjects whose first visit was post-2004. The average scores were as follow: mobility: 1.37 [SD=0.49], self-care: 1.11 [SD=0.35], usual activities: 1.34 [SD=0.56], pain/discomfort: 1.91 [SD=0.60], and anxiety/depression: 1.52 [SD=0.57]. Among 2,101 diagnosed with OP at first visit and having ⩾1 follow-up visit, 1,146 (55%) received bisphosphonates (BIS) (alendronate, optinate, and etidronate), 259 (12%) received non-BIS (raloxifene and teriparatide), 1,651 (79%) received calcium+vitamin D, and 542 (26%) received estrogen.

Conclusion: This analysis provided an overview of the characteristics in a Swedish registry. In this Swedish population, more than 1/3 of subjects receiving DXA scan were diagnosed with OP or having T-score≤ -2.5; however, approximately one-third received no OP drug treatment (BIS or non-BIS) despite OP diagnosis.

***Disclosures: Arun Krishna**, None.*
This study received funding from: Merck & Co. Inc

FR0407

CaMKK2 Inhibition as a Novel Bone Anabolic Strategy in the Prevention of Post-Menopausal and Therapy-Induced Osteoporosis. Zachary Pritchard*[1], Rachel Cary[2], Deborah Novack[3], Michael Voor[4], Uma Sankar[1]. [1]Department of Pharmacology & Toxicology, University of Louisville, USA, [2]University of Louisville, USA, [3]Washington University in St. Louis School of Medicine, USA, [4]Department of Orthopedic Surgery, University of Louisville, USA

Osteoporosis is often detected only after the patient has sustained significant bone loss or a fracture, revealing acritical clinical need for anabolic bone therapies. We recently identified Ca^{2+}/calmodulin (CaM)-dependent protein kinase kinase 2 (CaMKK2) as a novel bone anabolic target in anti-osteoporosis therapy, as it plays key roles in both the anabolic and catabolic pathways of bone remodeling. Genetic ablation of CaMKK2 or its inhibition using the highly selective and cell permeable inhibitor STO-609 enhances osteoblast differentiation and bone growth while suppressing osteoclast differentiation, in vivo and in vitro. In vivo administration of STO-609 in ovariectomized (OVX) mice confers significant protection from osteoporosis.

Bilateral orchiectomy (ORX) or surgical castration triggers hypogonadism in male mice, resulting in bone loss similar to that following androgen-deprivation therapy (ADT) in men undergoing treatment for prostate cancer. To test whether pharmacological inhibition of CaMKK2 will protect against ADT-induced bone loss, we performed ORX in male WT mice with half of the mice receiving tri-weekly i.p. injections of STO-609 (10 μmol/kg body weight) or saline for 6 weeks post-surgery. STO-609 treatment conferred significant protection from ORX-induced bone loss as indicated by the significantly higher % of trabecular bone volume (BV/TV) and lower % of trabecular separation (Tr. Sp.), compared to saline treated controls. Subsequent studies have explored the utility of using STO-609 as a bone strengthening therapy and assessed the toxicity involved with the use of the drug in normal WT mice. Following a six-week regimen of STO-609 administration, long bones isolated from younger (6 week-old) and older (6 month-old) male and female mice indicate enhanced trabecular bone formation that translates into increased strength. Further, no differences were observed in weight,complete blood countprofile, serum inflammatory cytokine profile or hepatic biochemistry following drug administration. Furthermore, pharmacokinetic analyses did not detect the presence of the inhibitor in the brain homogenates from treated mice, indicating that STO-609 does not cross the blood-brain barrier. Taken together, our findings highlight the potential for therapeutic inhibition of CaMKK2 as a highly efficacious and safe bone anabolic strategy that also inhibits osteoclast differentiation in the treatment of age- and therapy-induced osteoporosis.

***Disclosures: Zachary Pritchard**, None.*

FR0409

Long Term effect of BA058, a Novel Human PTHrP Analog, Restores Bone Mass in the Aged Osteopenic Ovariectomized Cynomolgus Monkey. Nancy Doyle*[1], Aurore Varela[1], Susan Y. Smith[1], Gary Hattersley[2]. [1]Charles River Laboratories, Canada, [2]Radius, USA

BA058 is an analog of hPTHrP (1-34) undergoing clinical development for the treatment of osteoporosis. The purpose of this study was to evaluate the effects of BA058 for 16 months on bone markers and bone mineral density (BMD) measured by DXA and pQCT in the aged osteopenic, ovariectomized cynomolgus monkey. Female cynomolgus monkeys, ⩾9 years of age, were randomly assigned to 5 groups based on whole body bone mineral content. Four groups of 16 animals were ovariectomized (OVX) and an additional group underwent Sham surgery. Treatment commenced after a 9-month bone depletion (BD) period. Animals received daily subcutaneously injection of either vehicle (Sham and OVX controls), or BA058 at 0.2, 1 or 5 μg/kg for 16 months. Blood and urine samples were analyzed for NTx, CTx, BAP and P1NP. DXA and pQCT were performed prior to surgery, at the end of the BD period, and after 4, 6, 12 and 16 months of treatment. DXA scans were obtained for the lumbar and thoracic spine, and proximal femur. Peripheral QCT scans were obtained at the proximal tibia metaphysis and diaphysis. At the end of the BD period, increases in bone markers and decreases in BMD by DXA/pQCT were observed for OVX controls compared to pre-OVX or Sham controls, consistent with estrogen deprivation. Daily administration of BA058 for 16 months resulted in marked bone anabolic effects at all dose levels, with complete reversal of the OVX-induced osteopenia with 1 and 5 μg/kg/day after only 4 months. This was associated with increases in P1NP, without changes in resorption markers. DXA values were comparable to or above pre-surgery levels at the spine and femoral neck, by 4 months of treatment, with 4 to 9% increases after 12

months of treatment, which were sustained at 16 months, relative to changes in OVX controls. Total tibia metaphysis BMD (pQCT) increased at all doses, 3 to 6% from end of BD at 4 months, 8 to 11% after 12 months of treatment, and was sustained after 16 months of treatment. Daily administration of BA058 for 16 months resulted in marked bone anabolic effects with complete reversal of OVX-induced osteopenia at all sites evaluated by DXA and pQCT, at all doses. Serum calcium levels remained within physiological ranges. BA058 potentially offers important advantages as a new treatment for post-menopausal osteoporosis, including the ability to rapidly build new bone and sustain gains over time.

***Disclosures: Nancy Doyle**, None.*
This study received funding from: Radius Health

FR0410

Role of paraoxonase-1 in bone anabolic effects of parathyroid hormone in hyperlipidemic mice. Jinxiu Lu[1], Henry Cheng[2], Elisa Atti[1], Diana Shih[1], Linda Demer[3], Yin Tintut*[4]. [1]UCLA, USA, [2]Johns Hopkins, USA, [3]David Geffen School of Medicine At University of California Los Angeles, USA, [4]University of California, Los Angeles, USA

Hyperlipidemia blunts anabolic effects of intermittent parathyroid hormone (PTH) on cortical bone, and the responsiveness to PTH are restored in part by oral administration of the antioxidant ApoA-I mimetic peptide, D-4F. To evaluate the mechanism of this rescue, mice overexpressing the high-density lipoprotein-associated antioxidant enzyme, paraoxonase 1 (Ldlr-/-PON1tg) were generated, and daily PTH injections were administered to Ldlr-/-PON1tg and to littermate Ldlr-/- mice. Expression of bone regulatory genes was determined by realtime RT-qPCR, and cortical bone parameters of the femoral bones by micro-computed tomographic analyses. PTH-treated Ldlr-/-PON1tg mice had significantly greater expression of PTH receptor (PTH1R), activating transcription factor (ATF4), and osteoprotegerin (OPG) in femoral cortical bone, as well as significantly greater bone mineral content, thickness, and area in femoral diaphyses compared with untreated Ldlr-/-PON1tg mice. In contrast, in control mice (Ldlr-/-) without PON1 overexpression, PTH treatment did not induce these markers. Calvarial bone of PTH-treated Ldlr-/-PON1tg mice also had significantly greater expression of osteoblastic differentiation marker genes as well as BMP-2-target and Wnt-target genes. Untreated Ldlr-/-PON1tg mice had significantly greater expression of PTH1R than untreated Ldlr-/- mice, whereas sclerostin expression was reduced. In femoral cortical bones, expression levels of transcriptional factors, Fox1 and ATF4, were also elevated in Ldlr-/-PON1tg mice, suggesting enhancement of cellular protection against oxidants. These findings suggest that PON1 restores responsiveness to PTH through effects on oxidant stress, PTH receptor expression, and/or Wnt signaling.

***Disclosures: Yin Tintut**, None.*

FR0414

Effects of the Novel Cathepsin K Inhibitor, SCI-629, on Bone Resorption in in vitro and in vivo Assays. Yoshitaka TANAKA*, Toshiaki Fujii. SEIKAGAKU CORPORATION, Japan

SCI-629 is a next generation analog newly designed and synthesized based on SI-591, a unique peptidomimetic compound. It is orally bioavailable and inhibits the lysosomal cysteine protease cathepsin K involved in bone loss processes.

In an enzyme inhibition assay, SCI-629 inhibited human cathepsin K with an IC50 value of 0.61 nM, and its inhibitory effect was 18- to 7900-fold more selective for cathepsin K than other members of the human cathepsins. SCI-629 inhibited human osteoclast-mediated bone resorption with an IC50 value of 39 nM.

To study the preventive effects of SCI-629 on the ovariectomized (OVX) rat as a model of postmenopausal osteoporosis, adult female F344 rats underwent OVX surgery and were treated with a vehicle or SCI-629 (0.8-100 mg/kg p.o., s.i.d. or 0.4-50 mg/kg, b.i.d.) for 4 weeks. In either case, SCI-629 dose-dependently inhibited the urinary C-terminal cross-linking telopeptide of Type I collagen (CTX-I) release and prevented bone mineral density (BMD) loss in the lumber vertebrae. To further investigate the preventive effect of SCI-629 on OVX, cynomolgus monkeys (aged 9-10 years) underwent OVX surgery and were treated with a vehicle or SCI-629 (0.9-8 mg/kg p.o., s.i.d.) for 4 weeks. The OVX resulted in increases in both urine N-terminal cross-linking telopeptide of type I collagen (NTX) levels and serum bone gla protein (BGP) levels, when compared with pre-OVX values. Although no significant changes were noted in either parameter up to 2.7 mg/kg, SCI-629 at 8 mg/kg continuously suppressed the OVX-induced increase in urinary NTX levels during the 4-week dosing period. SCI-629 up to 8 mg/kg did not have any significant effects on serum BGP levels.

In addition, to evaluate the safety of SCI-629, the effects on the cellular accumulation of cathepsin B were evaluated. SCI-629 did not increase the cellular protein levels of cathepsin B in HepG2 cells even at a concentration of 10 μM. This result suggests that SCI-629 is a non-lysosomotropic molecule and potentially has a lesser risk of producing the adverse effects associated with the inhibition of the off-target cathepsins.

In summary, these results suggest that SCI-629 is a novel, safe and orally bioavailable inhibitor of cathepsin K. We decided to develop this compound as a preclinical candidate for postmenopausal osteoporosis.

***Disclosures: Yoshitaka TANAKA**, None.*

FR0425

Transplantation of Hemopoietic Cells Engineered to Constitutively Produce Wnt10b Leads to Massive Bone Anabolism – A New Potential Strategy for Bone Regeneration and Fracture Repair. Jau-Yi Li*, Jonathan Adams, M. Neale Weitzmann, Roberto Pacifici. Emory University School of Medicine, USA

Wnt10b is a potent osteogenic Wnt ligand produced by bone cells and hemopoietic cells. Wnt10b activates Wnt signaling in stromal cells (SCs) and osteoblasts (OBs) leading to increased osteoblastogenesis and decreased adipogenesis. In addition, production of Wnt10b by bone marrow (BM) T cells is required for intermittent PTH treatment to increase bone formation and exert its bone anabolic activity. We generated retroviral transgenic mice (also known as retrogenic mice) that express a constitutively active (ca) form of Wnt10b by hemopoietic and immune cells to determine whether Wnt10b might be used as a bone anabolic agent either alone or in combination with iPTH. BM cells from caWnt10b retrogenic mice produced levels of Wnt10b ~ 10 fold higher than controls. BM cells were then harvested from the retrogenic mice and transplantation into additional lethally irradiated WT mice. Changes in indices of bone volume and structure were followed by in vivo μCT scanning. Eight weeks after transplantation of caWnt10b BM cells, recipient mice exhibited a ~3 fold increase in trabecular metaphyseal bone volume and a dramatic development of new trabecular bone in the shaft of the femoral diaphysis, a region lacking trabecular bone in control mice. Serum levels of P1NP (a marker of bone formation) were higher in caWnt10b retrogenic mice than in controls, while levels of CTX (a marker of bone resorption) were similar in the two groups. In a second experiment, caWnt10b T cells were purified from the spleen of caWnt10b retrogenic mice and adoptively transferred into T cell deficient mice. μCT analysis revealed that 8 weeks after the T cell transfer mice reconstituted with caWnt10b T cells had a metaphyseal BV/TV 1.7 fold higher than mice reconstituted with control T cells. However, adoptive transfer of caWnt10b T cells induced no new trabecular bone formation in the diaphysis. These findings demonstrate that the production of large amounts of Wnt10b by all hemopoietic cells has a potent bone anabolic effect and leads to "de novo" formation of trabecular bone in the femoral diaphysis. By contrast, over production of Wnt10b by T cells only induce a more modest increase in trabecular BV/TV without de novo diaphyseal bone growth. Delivery of Wnt10b by transduced BM cells may thus represent a novel therapeutic approach for bone regeneration and fracture repair.

***Disclosures: Jau-Yi Li**, None.*

FR0428

A Randomized Controlled Trial of Exercise to Prevent Bone Loss and Adverse Cardiovascular changes in Premenopausal Women with Breast Cancer. Deborah Sellmeyer*[1], Susan Stewart[2], Joan Bloom[3]. [1]The Johns Hopkins Bayview Medical Center, USA, [2]University of California, Davis, USA, [3]University of California, Berkeley, USA

Increasing numbers of premenopausal women diagnosed with breast cancer are becoming long-term survivors, creating challenges regarding the long term consequences of successful breast cancer therapy such as bone loss and cardiovascular changes. In this randomized, controlled trial, we recruited 206 women age < 55 years at diagnosis who were within two years of receiving adjuvant chemotherapy. Complete data are available for 184 women. Women were randomized, stratified by tamoxifen use, to a 12 month exercise program with resistance training and cardiovascular activities implemented by a YMCA based personal coach. Women in the control group received a monthly health newsletter. Bone mineral density (BMD) and body composition were measured by dual energy x-ray absorptiometry at baseline and after one year of exercise; blood was drawn for skeletal and cardiovascular markers. The change in each parameter from baseline to end of study was compared within and between treatment groups using t-tests. Overall, lumbar spine BMD declined in both treatment groups with no significant difference between treatment groups (-0.008 g/cm^2 + 0.003 g/cm^2 treatment group vs. -0.014 g/cm^2 + 0.003 g/cm^2 control group, p=0.24). However, among the women who did not lose lean mass during the study (n=100, 54 control, 46 exercise), the exercise intervention was effective in preventing lumbar spine bone loss (0.001 g/cm^2 + 0.005 g/cm^2 treatment group vs. -0.014 g/cm^2 + 0.005 g/cm^2 control group, p=0.03). Bone turnover markers decreased significantly in both groups with no significant differences between groups. Among the metabolic parameters, HOMA-IR increased in both groups, but fructosamine increased only in the control group (p=0.06). Additionally, cholesterol/HDL ratio increased in the control group (p=0.03), but was unchanged in the exercise group. In summary, premenopausal women with breast cancer continue to lose bone density more than two years after diagnosis and treatment. Among women who maintained lean mass, our exercise intervention prevented ongoing bone loss; however, our intervention did not prevent bone loss among women who lost muscle mass. Adverse changes in metabolic parameters such as increased fructosamine and cholesterol/HDL ratio were also prevented by the exercise regimen. Additional investigation into exercise regimens that can prevent both bone and muscle loss may help prevent long term consequences of premenopausal breast cancer treatment.

***Disclosures: Deborah Sellmeyer**, None.*

FR0430

Bone loss and microarchitectural deterioration continue despite cessation of weight loss after bariatric surgery. Emily Stein*[1], Polly Young[2], Mariana Bucovsky[2], Chiyuan Zhang[2], Angela Carrelli[3], Marcella Walker[2], Elizabeth Shane[1], Shonni Silverberg[2]. [1]Columbia University College of Physicians & Surgeons, USA, [2]Columbia University, USA, [3]Columbia University Medical Center, USA

The long-term effects of bariatric surgery on bone are unknown, as few studies have evaluated changes beyond one year and none have used any modality other than DXA. We evaluated annual changes in cortical (Ct) and trabecular (Tb) volumetric BMD (vBMD) and microarchitecture using high resolution peripheral computed tomography (HRpQCT) in addition to areal BMD by DXA [lumbar spine (LS), total hip (TH), femoral neck (FN), 1/3 (1/3R) and ultra distal radius (UDR)]. We previously reported that aBMD at the TH and FN declined in association with weight loss 1 year after surgery. HRpQCT showed significant cortical bone loss at the tibia but no change at the radius. We now report on changes in the 2nd year following Roux-en-Y gastric bypass. Ten women (mean baseline age 45 ± 10 yrs, BMI 45 ± 7kg/m^2, 20% Caucasian, 70% Latina) have been followed for 2 years. In year 2, there were no further declines in weight (Yr1:-28%; Yr2:-1%) or aBMD at the TH and FN (Yr1:-7-8%; Yr2:-1%). LS and 1/3R BMD did not change. At the UDR, a decline in BMD that began in Yr 1 (-2.9%) became significant in Yr 2 (-4.5%;$p<0.05$). HRpQCT indices changed significantly in year 2 (Table). At the radius, Ct area declined and Tb area increased. Total, Ct and Tb vBMD declined. Tb BMD declined in both the sub-cortical and inner Tb compartments. Tb heterogeneity increased. At the tibia, the declines in Ct bone observed in year 1 continued, with further loss of Ct area, density, and thickness. Total density declined, and new changes in Tb bone were observed: Tb area increased, Tb density decreased in both the inner and sub-cortical compartments and there was a trend toward increased Tb separation. Thus, in the 2nd year following bariatric surgery, weight loss plateaus as do the associated declines in hip BMD. Meanwhile, cortical bone deterioration progresses, with declines in Ct density and thickness. The decrease in Ct area and increase in Tb area suggests endocortical resorption. Tb bone loss also becomes prominent in the 2nd year after surgery. UDR BMD declines, as does Tb density, while Tb separation and network heterogeneity increase. Total vBMD declines. In summary, prominent cortical and trabecular deterioration occur in the 2nd year after surgery. While the association of these findings with skeletal fragility and fracture is unknown, these preliminary data raise concern that bariatric surgery may have significant long-term detrimental effects on the skeleton even after cessation of weight loss.

Microarchitectural Changes After Roux-en-Y Gastric Bypass

Variable (%change)	RAD Yr 0-1	RAD Yr 1-2	RAD Yr 0-2	TIB Yr 0-1	TIB Yr 1-2	TIB Yr 0-2
Ct Area	2.3	3.5*	5.9**	3.0+	5.0*	8.0**
Tb Area	0.6	1.3*	1.9**	0.5	1.1**	1.6**
Total density	-1.1	-5.7**	-6.8**	-1.1	-5.4**	-6.5**
Ct density	-0.2	-3.2+	-5.2*	-1.7+	-2.4*	-4.1**
Tb density (total)	0.6	-9.8**	-9.3**	1.1	-6.1+	-5.1*
Tb density (sub-Ct)	0.7	-7.5**	-6.8**	0.1	-4.9**	-4.8*
Tb density (inner)	0.6	-13.3**	-12.7*	2.4	-7.9*	-5.5
Tb Number	0.4	-7.0	-6.6	1.4	-4.2	-2.8
Tb Separation	0.4	9.6	9.9*	-0.8	4.7+	3.9
Heterogeneity	-1.9	10.8*	8.9	-2.6	4.2	1.6

+p<0.10, *p<0.05, **p<0.01

Table HRpQCT After Bariatric Surgery

***Disclosures: Emily Stein**, None.*

FR0431

Denosumab for Elderly Men with Osteoporosis: A Cost-effectiveness Analysis from the US Payer Perspective. Anju Parthan[1], Morgan Kruse[1], Irene Agodoa*[2], Stuart Silverman[3], Eric Orwoll[4]. [1]OptumInsight, USA, [2]Amgen, USA, [3]Cedars-Sinai/UCLA, USA, [4]Oregon Health & Science University, USA

Purpose: To evaluate cost-effectiveness of denosumab (Dmab) versus other osteoporotic treatments (txt) in male osteoporosis (MOP) patients ⩾75 years (yrs) from a US 3rd party payer perspective.

Methods: A lifetime cohort Markov model previously developed for post-menopausal osteoporosis (PMO) was used for the study. During each 6-month cycle, patients could experience a hip, vertebral or other osteoporotic fracture (fx), remain in a non-fx state, remain in a post fx state or die (Figure 1). Background fx risks, mortality rates, persistence rates, health utilities, medical and drug costs were derived from published sources. Bone mineral density (BMD) improvements have shown to be similar between MOP and PMO populations. A recent fx trial showed zoledronate (Zol) to have effects in men similar to those reported previously in women; therefore fx efficacy data from PMO were used. Lifetime expected costs and quality-adjusted life-yrs (QALYs) were estimated for Dmab, generic alendronate (Alen), risedronate, ibandronate, teriparatide, and Zol. Rates of non-persistence for oral and injectable drugs were taken from published reports. Patients in the model were 78 yrs-old, with BMD T-score≤-2.12 and prevalent vertebral fx of 23%, based on the ⩾75 yr-old sub-group population in the ADAMO trial comparing 1 yr of Dmab vs. placebo.

In the base-case, model assumed patients received txt effects up to 2 yrs after discontinuing (offset time). Costs and QALYs were discounted 3% annually. One-way and probabilistic sensitivity analyses were conducted.

Results: Total lifetime costs and QALYs for all txts are shown in Table 1. Dmab had an incremental cost-effectiveness ratio (ICER) of $16,888 compared to Alen and dominated all other txts. Results were most sensitive to changes in drug costs of Dmab and relative risks of hip fx. The probability of Dmab being cost-effective compared to other txts was 75% at a threshold of $50K/QALY and 88% at a threshold of $100K/QALY.

In a sensitivity analysis using offset time of 5 yrs for all txts except Dmab (2 yrs) and teriparatide (2.5 yrs), Dmab had an ICER of $21,963 compared to Alen and dominated all other txts. Anticipating the availability of generic Zol, when the price was reduced by 35% and 65% of the brand price (to $705 and $379 annually, respectively), Dmab remained dominant compared to Zol.

Conclusion: Dmab is cost-effective compared to other osteoporotic txts in the US elderly male osteoporosis population.

Keywords: male osteoporosis, denosumab, cost-effectiveness analysis, elderly

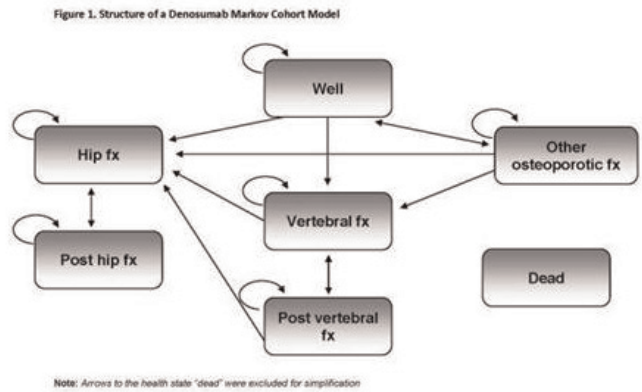

Figure 1

Table 1. Base-case Cost-effectiveness Results

Intervention	Total Costs	Total QALYs	Incremental Costs	Incremental QALYs	ICER
Generic Alendronate	$31,456	5.9866			
Denosumab	$32,334	6.0386	$878	0.0520	$16,888
Zoledronate	$35,138	6.0037	$2,804	-0.0350	Dominated
Risedronate	$35,232	5.9760	$2,899	-0.0626	Dominated
Ibandronate	$35,550	5.9663	$3,216	-0.0723	Dominated
Teriparatide	$48,828	6.0279	$16,495	-0.0107	Dominated

Table 1

***Disclosures: Irene Agodoa**, Amgen, 2*
This study received funding from: Amgen, Inc.

FR0432

Discrepant Areal and Volumetric BMD of the Spine and Hip in HIV-infected Postmenopausal Women. Polly Young*[1], Michael Yin[1], Ivelisse Colon[2], Mariana Bucovsky[1], Chiyuan Zhang[1], Susan Olender[1], Thomas Lang[3], Isra Saeed[3], David Ferris[4], Cosmina Zeana[5], Donald McMahon[6], Elizabeth Shane[6]. [1]Columbia University, USA, [2]Columbia University Medical Center, USA, [3]University of California, San Francisco, USA, [4]St Lukes Hospital Center, USA, [5]Bronx Lebanon Hospital Center, USA, [6]Columbia University College of Physicians & Surgeons, USA

HIV infection and antiretroviral therapy have been associated with low areal bone mineral density (aBMD) by dual energy xray absorptiometry (DXA). Some investigators have argued that BMD differences between HIV-infected and controls are largely attributable to group differences in weight. Previously, we reported that while aBMD by DXA was lower at the forearm in HIV-infected versus uninfected postmenopausal women, volumetric (vBMD) by High Resolution peripheral Quantitative CT (QCT) did not differ. We therefore assessed aBMD by DXA and

central QCT at the spine and hip to determine whether these measures were also discrepant at the central skeleton in 39 HIV-infected and 55 uninfected postmenopausal African American and Hispanic women from an established HIV cohort study of bone metabolism. HIV-infected women were of comparable age (58±5 vs 59±7, p=0.45) and height (158±8 vs157±8 cm, p=0.56) to uninfected women, but had lower weight (69±16 vs 79±21 kg, p=0.01), BMI (27.6±5 versus 32±7, p=0.001), %Total Body Fat (35.5±8 vs 42.8±6 p<.0001) and % Trunk Fat 34.9±8 vs 41.6±7, p<.0001). aBMD by DXA was lower at all sites in HIV-infected women (Table). In contrast, integral and trabecular vBMD and compressive strength did not differ at the spine (Table) or total hip (not shown). At the FN, cortical vBMD was higher and trabecular vBMD lower in the HIV-infected women, with no difference in Integral vBMD or compressive strength. In summary, although aBMD by DXA was lower in HIV-infected than uninfected postmenopausal women, true volumetric BMD by cQCT and compressive strength did not differ. We conclude that the lower areal BMD we previously observed in HIV-infected postmenopausal women could be an artifact of differences in body fat between HIV-infected and uninfected women. The lack of detectable differences in vBMD and microarchitecture is surprising given emerging data on increased fracture risk in older HIV-infected individuals.

Table	HIV+ (n=39)	HIV- (n=55)	p value
Areal BMD by DXA (g/cm2)			
Lumbar spine	0.87±0.13	0.93±0.17	0.03
Total Hip	0.85±0.15	0.92±0.14	0.02
Femoral Neck	0.72±0.12	0.81±0.17	0.006
Volumetric BMD by QCT (g/cm3) and Estimated Strength			
Lumbar spine Integral	0.21 ± 0.03	0.22 ± 0.03	0.11
Lumbar spine Avg Trab L1L2	0.21 ± 0.03	0.22 ± 0.03	0.06
Lumbar spine Compressive Strength Index	0.19 ± 0.08	0.21 ± 0.09	0.36
Femoral Neck Integral	0.284 ± 0.04	0.275 ± 0.04	0.32
Femoral Neck Cortical	0.50 ± 0.04	0.48 ± 0.04	0.02
Femoral Neck Minimal Cross-section	9.5 ± 1.4	10.1 ± 1.6	0.07
Femoral Neck Cortical Index	0.45 ± 0.06	0.43 ± 0.07	0.13

cQCT Abstract Table

***Disclosures: Polly Young**, None.*

FR0437

FRAX Predicts Fracture Risk in Kidney Transplant Recipients. Kyla Naylor*[1], William Leslie[2], Anthony Hodsman[1], David Rush[3], Amit Garg[4]. [1]Western University, Canada, [2]University of Manitoba, Canada, [3]Department of Medicine, University of Manitoba, Canada, [4]Division of Nephrology, Western University, Canada

Purpose: The WHO Fracture Risk Assessment Tool (FRAX) estimates the 10-year probability of fracture and has been validated in the general population. However, the utility of FRAX in the kidney transplant population is unknown. We assessed the prognostic value of FRAX in kidney transplant recipients (KTR).

Methods: We identified all adult KTRs from 1996 to 2011 undergoing baseline dual energy X-ray absorptiometry (DXA) examinations within 5 years of transplantation (median 5 months) in a large clinical database for the Province of Manitoba, Canada. FRAX probabilities were calculated from baseline information (age; sex; clinical risk factors; bone mineral density [BMD]). Incident fractures were determined through linkage with a population-based data repository. Change in BMD was examined as a secondary outcome (N=806 follow up DXA scans with 328 2nd DXA, 198 3rd DXA, 129 4th DXA, 80 5th DXA).

Results: Of 458 KTRs, 64% were men with an average age of 45 years. Mean BMD at baseline was only slightly below expected (mean Z-scores: lumbar spine -0.3; femoral neck -0.7; total hip -0.7). Based on National Osteoporosis Foundation criteria, only 19.0% of KTRs would be designated high risk (16.0% osteoporotic T-score; 2.2% prior spine/hip fracture; 1.5% high major osteoporotic fracture [MOF] probability [>20%]; 6.5% high hip fracture probability [≥3%]). Twenty-one (4.6%) recipients experienced a MOF over a mean follow-up of 6 years. The 10-year FRAX MOF probability was higher in fracture compared with non-fracture KTRs (8.3% versus 5.5%, $\rho<0.01$ FRAX with BMD; 6.8% versus 4.9%, $\rho<0.05$ FRAX without BMD). Mean total hip T-score was significantly lower in fracture compared with non-fracture KTRs (-"1.2±0.9 versus -0.6±1.3, $\rho<0.05$). Area under the curve (AUC) for incident MOF discrimination was similar to the general population (AUC: FRAX without BMD 0.62 [95% CI: 0.49-0.75]; FRAX with BMD 0.62 [95% CI: 0.50-0.74]; total hip T-score 0.64 [95% CI: 0.53-0.75]). The observed 10-year MOF fracture risk of 6.3% (95% CI: 3.4-9.2%) was concordant with FRAX predictions (5.0% with BMD, 5.6% without BMD). Mean BMD measurements at all sites increased over time (lumbar spine) or remained stable (femoral neck and total hip).

Conclusions: FRAX scores categorized most KTRs as a low risk group for fracture, and the low observed fracture rates were consistent with the ten-year fracture predictions. The WHO FRAX tool may serve as a useful prognostic aid for treatment decision-making in KTRs.

***Disclosures: Kyla Naylor**, None.*

FR0439

Clinical outcome with long-term bisphosphonate therapy in Paget's disease of Bone: The PRISM-EZ study. Kirsteen Goodman[1], Graeme MacLennan[2], Peter Selby[3], William Fraser[4], Stuart Ralston*[1]. [1]University of Edinburgh, United Kingdom, [2]University of Aberdeen, United Kingdom, [3]Manchester University, United Kingdom, [4]University of East Anglia, United Kingdom

Paget's disease of bone (PDB) is a common metabolic bone disease characterised by increased and disorganised bone remodelling. Bisphosphonates are highly effective at suppressing bone turnover in PDB are considered to be the treatment of choice. While aminobisphosphonates can normalise bone turnover in a high proportion of patients, it remains unclear whether this prevent complications. In the PRISM study we previously reported that bone pain, quality of life and complications of PDB were similar in patients randomised to ''intensive'' treatment in which the aim was to normalise alkaline phosphatase (ALP) versus ''symptomatic'' treatment in which treatment was given only if symptoms were present. Here we report upon the results of a three year extension to PRISM (PRISM-EZ) in which zoledronic acid was used as the bisphosphonate of choice in the ''intensive'' arm. The study group comprised 502 patients; 270 continued with intensive treatment and 232 with symptomatic treatment. The average total duration of follow up was about 6 years. The treatment groups were well matched at entry to PRISM-EZ for age, previous fracture, previous orthopaedic surgery, bone deformity and quality of life scores, but those in the intensive group had lower ALP levels (mean ± sem, 0.85±0.04 *vs.* 1.04± 0.06, p=0.012, where 1.0 is the upper limit of normal). During PRISM-EZ, ALP values decreased further in the intensive group and were consistently lower than in the symptomatic group throughout follow up (0.71±0.04 *vs.* 1.01± 0.06, p<0.0001). Despite the lower ALP, no differences were observed between the groups in quality of life scores or bone pain. Fractures were more common during follow up within the intensive group (8.2% *vs.* 4.7%; OR = 1.80 [0.87-3.71] but the difference between groups was not significant (p = 0.11). Fractures through Pagetic bone were also more common in the intensive group (1.4% *vs.* 0.8%), one of which was a subtrochanteric fracture occurring at the site of a pseudofracture in affected bone. We conclude that long term suppression of ALP with bisphosphonates including zoledronic acid did not improve clinical outcome in this group of patients with PDB and there was a slight increase in the risk of fracture.

***Disclosures: Stuart Ralston**, None.*

FR0440

IGF1 Contributes to the Increased Bone Formation Induced by Measles Virus Nucleocapsid Protein Expressed by Osteoclasts in Paget's Bone Disease. Noriyoshi Kurihara*[1], Jumpei Teramachi[2], Yukiko Kitagawa[1], Jolene Windle[3], G. David Roodman[1]. [1]Indiana University, USA, [2]The University of Tokushima, USA, [3]Virginia Commonwealth University, USA

We reported that 70% of patients with Paget's bone disease (PD) expressed Measles Virus Nucleocapsid Protein (MVNP) in their osteoclasts (OCLs) and that MVNP is not expressed in their osteoblasts (OBs). Further transgenic mice with targeted expression of MVNP to cells in the OCL lineage form pagetic-like bone lesions and display both increased bone resorption and rapid new bone formation. In contrast, mice with knock-in of the p62P394L mutation (p62-KI) linked to PD have increased bone resorption but do not have increased bone formation in vivo. EphrinB2 and EphB4 were identified as key coupling factors for OCL and OB. Since EphrinB2 is produced by OCL and dramatically enhances OB function and bone formation through specific interactions with EphB4 on OB, we determined if EphrinB2/EphB4 play a role in the effects of MVNP on bone formation. Therefore, we tested for expression of ephrins and Ephs in OCLs, OBs and total bone from 8 months old WT, MVNP and p62-KI mice. MVNP induced expression of both ephrinB2 and EphB4 in total bone lysates. Increased EphrinB2/EphB4 expression was only detectable in older MVNP mice (8-12 months), consistent with our previously findings that pagetic lesions are not detectable in these mice until 8-12 months of age. In contrast, total bone lysates from p62-KI mice did not express increased levels of EphrinB2 or EphB4. Only OCL derived from CD11b+ cells of MVNP or MVNP/p62-KI but not WT or p62-KI expressed increased EphrinB2. The enhanced EphB4 expression correlated with increased Runx2 expression in OBs from MVNP mice. Another coupling factor Semaphorin 3A had similar levels of expression between WT and MVNP. These results demonstrate that MVNP induces expression of EpherinB2/EphB4 coupling factors known to enhance OB activity. We then determined if other factors induced by MVNP enhanced EphrinB2/EphB4's coupling activity using gene-expressing profiling studies of highly purified OCLs derived from MVNP, p62-KI, p62-knockout and WT mice. IGF1 gene expression was significantly enhanced in MVNP expressing OCL precursors compared to other three genotypes. IGF1 expression by OCL from MVNP was confirmed at the protein level. These results suggest that EphrinB2/EphB4 enhances bone formation in vitro and in vivo in MVNP mice and IGF1 contributes to increased bone formation induced by MVNP by enhancing EphrinB2 expression.

***Disclosures: Noriyoshi Kurihara**, None.*

FR0443

ERα Expression in Non-Hematopoietic Cells is Required for the Protective Effects of Estrogen on Bone. Petra Henning[1], Cecilia Engdahl[2], Helen Farman[1], Andree Krust[3], Pierre Chambon[3], Hans Carlsten[4], Sara Windahl[2], Claes Ohlsson[5], Marie Lagerquist*[6]. [1]Centre for Bone & Arthritis Research, Institute of Medicine, Sahlgrenska Academy, University of Gothenburg, Sweden, [2]Center for Bone & Arthritis Research, Sahlgrenska Academy, Sweden, [3]Institut de Génétique et de Biologie Moléculaire et Cellulaire (CNRS, INSERM, UdS, Collège de France), Illkirch, Strasbourg, France, [4]Centre for Bone & Arthritis Research, Department of Rheumatology & Inflammation Research, Institute of Medicine, Sahlgrenska Academy, University of Gothenburg, Sweden, [5]Center for Bone & Arthritis Research at the Sahlgrenska Academy, Sweden, [6]Centre for Bone & Arthritis Research, USA

Estrogen has positive effects on both trabecular and cortical bone, but the exact mechanism behind this anti-osteoporotic effect is still not fully understood. To determine the relative importance of ERα expression in hematopoietic and non-hematopoietic cells, we have created chimeric mice with selective inactivation of ERα in hematopoietic (donor) or non-hematopoietic (recipient) cells using bone marrow (bm) transplantation.

12-week-old ovariectomized wild-type (wt) or ERα knock-out ($ER\alpha^{-/-}$) mice were lethally irradiated and reconstituted with hematopoietic stem cell (hsc)-enriched bm from wt or $ER\alpha^{-/-}$ females and, after two weeks, implanted with a 17β-estradiol (E2; 167ng/day) or placebo pellet. Four weeks after start of treatment, the mice were terminated and the bones were analyzed using computed tomography. Successful bm transplantations were verified by real-time PCR measurements of ERα gene expression, demonstrating significantly reduced ERα expression in wt/$ER\alpha^{-/-}$ mice (defined as recipient/donor) in blood, bm and spleen (-96%, -93% and -82%, respectively, $p<0.05$), while normal ERα expression was seen in $ER\alpha^{-/-}$/wt mice compared to wt/wt mice.

E2 treatment increased trabecular bone mineral density (BMD) in wt/wt mice ($507\pm36\%$, $p<0.001$) and wt/$ER\alpha^{-/-}$ mice ($370\pm39\%$, $p<0.001$), while no significant E2 effect was seen in $ER\alpha^{-/-}$/wt ($7\pm11\%$) or $ER\alpha^{-/-}$/$ER\alpha^{-/-}$ ($6\pm7\%$) mice compared to placebo treatment. E2 increased cortical thickness in wt/wt mice ($91\pm14\%$, $p<0.001$) and wt/$ER\alpha^{-/-}$ mice ($42\pm9\%$, $p<0.001$), while no cortical E2 effects were detected in $ER\alpha^{-/-}$/wt ($0\pm1\%$) or $ER\alpha^{-/-}$/$ER\alpha^{-/-}$ ($1\pm1\%$) mice. These data demonstrate the requirement of ERα expression in non-hematopoietic cells for the positive effects of E2 on bone mass. The E2 effects on trabecular BMD and cortical thickness were slightly, but significantly, reduced in wt/$ER\alpha^{-/-}$ mice compared to wt/wt mice (-27%, $p<0.05$ and -54%, $p<0.01$, respectively), suggesting that ERα expression in hematopoietic cells is involved in the estrogenic regulation of bone mass.

In conclusion, ERα expression in non-hematopoietic cells, but not in hematopoietic cells, is required for the protective effects of estrogen on both trabecular and cortical bone. However, our results indicate that ERα expression in hematopoietic cells may enhance the positive effect of E2 on bone in the presence of ERα expression in non-hematopoietic cells.

***Disclosures: Marie Lagerquist**, None.*

FR0444

Estrogen Receptor α36 Mediates the Anti-apoptotic Effect of Estradiol *in vitro* and Associates with Clinical Outcome *in vivo*. Reyhaan Chaudhri*[1], Agreen Hadadi[2], Barbara Boyan[3], Zvi Schwartz[1]. [1]Georgia Institute of Technology, USA, [2]School of Biology, Georgia Institute of Technology, USA, [3]Virginia Commonwealth University, USA

In breast cancer cells, 17β-estradiol (E_2) rapidly increases protein kinase C activity, which is associated with increased breast tumorigenicity, and promotes cancer cell survival, metastatic potential, and osteolytic activity by acting through the ERα variant, ERα36. The aims of this study were to elucidate the mechanism by which ERα36 promotes cancer cell survival and determine if ERα36 is associated with clinical outcome. Using signaling inhibitors and activators, we evaluated the role of specific proteins on the protective effect of E_2 against taxol-induced apoptosis. In order to evaluate these effects, we used MTT to measure cell viability, TUNEL to measure cell death, and caspase-3 activity to measure apoptotic phenotype. Inhibition of phosphatidyl-choline specific phospholipase D (PC-PLD) with wortmannin, lysophosphatidic acid signaling with VPC32183S, and phosphoinositide-3-kinase (PI3K) with LY294002, blocked the inhibitory effect of E_2 against taxol-induced caspase-3 activity, while activation of LPA signaling with exogenous LPA and PI3K signaling with 740 Y-P, inhibited the apoptotic effect of taxol. To determine if ERα36 may be a potential target in cancer, a tissue microarray containing tumors from 40 breast cancer patients were assayed for presence of ERα36 and vascular endothelial growth factor (VEGF) by immunohistochemistry (IHC) and blindly scored by three independent observers to quantify number of positive cells, intensity, and subcellular localization. We used fisher's exact test to determine correlations of several variables with ERα36 or VEGF, and found that ERα36 intensity was positively associated with age ($p=.0450$) and VEGF ($p=.0226$). We also performed Kaplan-Meier survival analysis and the log-rank test to evaluate the significance of variables associated with mortality. When all patients were evaluated, we found HER2 status, tumor stage, and lymph node metastasis were associated with mortality. However, when we stratified our analysis to patients with high ERα36 levels and cytosolic ERα36, we found that progesterone receptor status and tumor size were also associated with mortality. Our results indicate ERα36 mediates the anti-apoptotic effect of E_2. These effects were mediated by activation of PC-PLD, LPA and PI3K. Our TMA results suggest ERα36 as a predictor of outcome *in vivo*. These data suggest that ERα36 may be a potential target for diagnosis or treatment in breast cancer.

***Disclosures: Reyhaan Chaudhri**, None.*

FR0445

Mice Lacking Estrogen Receptor α in Hypothalamic Pro-opiomelanocortin (POMC) Neurons Display Enhanced Estrogenic Response on Bone Mass. Helen Farman*[1], Sara Windahl[2], Deborah Clegg[3], Shang Kui Xie[3], John-Olov Jansson[4], Lisa Hahner[3], Jordan Zehr[3], Marie Lagerquist[5], Claes Ohlsson[6]. [1]University of Gothenburg, Sweden, [2]Center for Bone & Arthritis Research, Sahlgrenska Academy, Sweden, [3]Department of Internal Medicine, UT Southwestern, Dallas, USA, USA, [4]Department of Internal Medicine, UT Southwestern, Dallas, USA, Sweden, [5]Centre for Bone & Arthritis Research, USA, [6]Center for Bone & Arthritis Research at the Sahlgrenska Academy, Sweden

Estrogen is an important endocrine regulator of bone and exerts its physiological effect on bone mainly via estrogen receptor α (ERα). The CNS is also a major target for estrogen and ERα is widely distributed in the brain with a high expression in some hypothalamic nuclei including the arcuate nucleus (ARC) and the ventral medial nucleus (VMN). In a previous study, we demonstrated that loss of central ERα expression results in increased bone mass, indicating an inhibitory role of central ERα signaling on bone mass. However, the primary ERα expressing target cell type that mediates the central negative effect of estrogen on bone mass has not yet been identified. We here tested the hypothesis that ERα in hypothalamic Pro-opiomelanocortin (POMC) neurons, located in ARC, is involved in the central effects of estrogen on bone mass.

POMC-Cre mice were crossed with ERαlox/lox mice to generate mice lacking ERα expression specifically in POMC neurons (ERαlox/loxPOMC-Cre). Six-month-old female ERαlox/loxPOMC-Cre and littermate wild type mice were ovariectomized (ovx) and treated with either vehicle or estradiol (E2; 0.5μg/day) for six weeks. Cortical and trabecular bone parameters were analyzed by quantitative computed tomography.

As expected, E2-treatment increased the trabecular volumetric BMD (vBMD) in the distal metaphyseal region of the femur and several cortical bone parameters (cortical bone mineral content, cortical bone area and cortical thickness) in the mid-diaphyseal region of the tibia in ovx wild type mice ($p<0.01$). Importantly, the estrogenic responses were substantially increased in ovx ERαlox/loxPOMC-Cre mice compared with the estrogenic responses in ovx wild type mice on trabecular vBMD ($+42\pm9\%$, $p<0.01$), cortical bone mineral content ($+127\pm27\%$, $p<0.01$), cortical bone area ($+158\pm34\%$, $p<0.01$) and cortical bone thickness ($+233\pm53\%$, $p<0.01$).

In conclusion, mice lacking ERα in POMC neurons display enhanced estrogenic response on bone mass. This finding supports the notion that central ERα expression has an inhibitory effect on bone mass. In addition, it demonstrates that ERα in POMC neurons regulates bone mass. We propose that the balance between inhibitory effects of central ERα activity in POMC neurons in ARC and stimulatory peripheral ERα-mediated effects directly in bone determines bone homeostasis and, thereby, bone mass.

***Disclosures: Helen Farman**, None.*

FR0446

Unlike the estrogen receptor α, the androgen receptor in osteoblast progenitors is dispensable for optimal cortical bone accrual. Semahat Serra Ucer*[1], Aaron Warren[2], Shoshana Bartell[3], Srividhya Iyer[3], Li Han[3], Julie Crawford[1], Charles O'Brien[3], Maria Jose Almeida[3], Stavros Manolagas[3]. [1]University of Arkansas for Medical Sciences, USA, [2]Central Arkansas Veterans Healthcare System, University of Arkansas for Medical Sciences, USA, [3]Central Arkansas VA Healthcare System, Univ of Arkansas for Medical Sciences, USA

Androgens are required for optimal cancellous and cortical bone acquisition and maintenance in males. However, whereas the androgen receptor (AR) in mature osteoblasts and osteocytes is required for cancellous bone mass accrual, it is dispensable for the effects of androgens on cortical bone. On the other hand, signaling via the osteoblast progenitor estrogen receptor (ER) α is needed for optimal bone apposition at the periosteum of male mice during puberty. Here, we have explored the possibility that the AR expressed in osteoblast progenitors contributes to the well-documented anabolic effects of androgens on periosteal bone apposition and cortical bone mass. To do this, we generated mice with conditional deletion of an AR allele in pluripotent mesenchymal progenitor cells expressing Prx1 (AR flox;Prx1-Cre). AR mRNA in osteoblasts from the AR flox;Prx1-Cre mice was decreased by 80%, but unaffected in osteoclasts, seminal vesicles, soleus, and kidneys. There was no difference in seminal vesicle and total body weight among wild-type controls, AR flox,

Prx1-Cre, and AR flox;Prx1-Cre mice, confirming the specificity of the deletion in cells of the osteoblast lineage. AR flox;Prx1-Cre male mice exhibited a decrease in trabecular bone volume (30%), volumetric BMD (25%), trabecular number (37%) and connectivity (60%), whereas trabecular thickness was unaltered. Periosteal perimeter, endosteal perimeter, and cortical thickness at the femoral midshaft were unaffected by the AR deletion. The differentiation of progenitors from AR flox;Prx1-Cre mice to the osteoblast lineage was also unaltered as measured by Alizarin red staining of mineralized bone marrow cell cultures. Female AR flox;Prx1-Cre mice had no changes in bone mass. These results demonstrate that the anabolic effects of androgens on periosteal bone formation and cortical bone mass are not mediated via activation of the AR in cells of the osteoblast lineage. Instead, they are mediated via estrogens acting on the ERα present in osteoblast progenitors and perhaps indirect effects of androgens resulting from their stimulatory effects on growth factor production and/or muscle size, which in turn can increase mechanical strains on bone. On the other hand, the identical phenotype of mice with AR deletion in Prx1 cells or mature osteoblasts and osteocytes establishes that AR signaling in the latter cell types is responsible for the effect of androgens on cancellous bone.

***Disclosures: Semahat Serra Ucer**, None.*

FR0447

1, 25 dihydroxyvitamin D Regulates Tumor Growth through NF Kappa B in a Mouse Model of Breast Cancer Progression. Jiarong Li*[1], Aimee-Lee Luco[1], Ben Ochietietti[1], Rene St-Arnaud[2], Timothy Reinhardt[3], Anne Camirand[1], William Muller[1], Richard Kremer[4]. [1]McGill University, Canada, [2]Shriners Hospital for Children & McGill University, Canada, [3]National Animal Disease Center, USDA, ARS, USA, [4]McGill University, Royal Victoria Hospital, Canada

The transgenic PyVMT mouse model reproduces the various phases of human breast cancer from hyperplasia to adenocarcinoma in 100% of animals. We disrupted CYP27B1, the enzyme responsible for the conversion of 25 hydroxyvitamin D to 1, 25-dihdroxyvitamin D (1, 25(OH) 2D) in the mammary epithelium of female PyVMT mice using the Cre/LoxP recombination system. The lack of local production of 1, 25(OH) 2D resulted in accelerated mammary tumor growth. *In vitro* isolated PyVMT-CYP27B1$^{flox/flox}$-Cre^{-} cells treated with 25OHD showed dose dependent(10^{-9} -10^{-6}) growth inhibition but 25OHD had no effect on cell growth in isolated PyVMT-CYP27B1$^{flox/flox}$-Cre^{+} cells. Tumors and isolated tumor cells from control (PyVMT-CYP27B1$^{flox/flox}$-Cre^{-}) and homozygous (PyVMT-CYP27B1$^{flox/flox}$-Cre^{+}) animals were analyzed by real time quantitative PCR expression arrays (Qiagen), confocal microscopy and Western Blots. Tissue concentrations of 1, 25(OH)2D were reduced by over 80% in homozygous ablated tumors compared to tumors from control animals. Comparative analysis revealed that key components of NFKappa B signaling were upregulated in tumors from CYP27B1 ablated animals compared to controls($p<0.05$).In contrast isolated breast tumor cells from PyVMT-CYP27B1$^{flox/flox}$-Cre^{-} animals treated with 1, 25(OH)2D were characterized by downregulation of NFKappa B signaling at the gene and protein levels.Furthermore,confocal microscopy analysis of the VDR and NFKappa B regulatory protein p65 revealed that treatment of isolated cells with 1, 25(OH)2D induced retention of p65 in the cytoplasmic compartment and its co-localization with the VDR preventing activation of NFKappa B.Western Blot analysis of cytoplasmic and nuclear extracts confirmed the retention of p65 in the cytoplasmic compartment following 1, 25(OH)2D treatment.siRNA knockdown of p65 significantly reduced the growth inhibitory effect of 1, 25(OH)2D on isolated PyVMT-CYP27B1$^{flox/flox}$-Cre^{-} cells further supporting the role of NFKappa B signaling in 1, 25(OH)2D mediated growth inhibition. In summary our data demonstrate that local production of 1, 25(OH)2D by breast tumor cells plays an important role on breast tumor growth and that its effect is mediated at least in part through critical components of the NFKappa complex.

***Disclosures: Jiarong Li**, None.*

FR0448

Appropriately Directed Expression of a Human Ligand Binding-Defective Vitamin D Receptor Rescues Hair Cycling Defects But Not Mineral Homeostasis in Humanized VDR-Null Mice. Seong Min Lee*[1], Erin Riley[1], Charles O'Brien[2], J. Pike[1]. [1]University of Wisconsin-Madison, USA, [2]Central Arkansas VA Healthcare System, Univ of Arkansas for Medical Sciences, USA

The identification of specific VDR mutations in hereditary 1,25-dihydroxyvitamin D_3 ($1,25(OH)_2D_3$) resistant rickets (HVDRR) together with studies of directed expression of the VDR in the VDR-null mouse model have shown that VDR-mediated mineral homeostasis requires activation by $1,25(OH)_2D_3$, whereas VDR-mediated hair cycle regulation is hormone independent. A signature mutation that supports this premise is the L233S VDR mutation that abrogates $1,25(OH)_2D_3$ binding activity. Patients with this mutation do not, however, exhibit alopecia. Indeed, directed expression of the human L233S VDR mutant to the skin rescues the alopecic phenotype in the VDR null mouse. However, effect of the mutation on mineral homeostasis *in vivo* has not been elucidated. We have recently generated a humanized transgenic mouse strain with a modified wildtype hVDR BAC minigene that contained both the natural regulatory components of the gene and the VDR transcription unit as well. VDR expression from this transgene recapitulated endogenous VDR expression in the mouse, restored normal gene expression patterns and fully rescued the biological phenotype of the VDR null mouse. In the present study, we recreated the L233S-mutation in the hVDR BAC clone, introduced it as a transgene into mice and then crossed this strain into the VDR null mouse to assess whether the mutant could rescue the aberrant mineral homeostasis, the alopecia, or both. Like the wildtype transgene, the mutated transgene recapitulated the tissue-specific expression pattern of the endogenous mouse VDR. To test the transcriptional activity of the L233S mutation *in vivo*, we administered an IP injection of 10 ng $1,25(OH)_2D_3$/g body weight, collected tissues after 6 hr and evaluated the RNA for target gene expression by RT-PCR. While the wildtype transgene induced both *Trpv6* and *S100g* in the intestine, the mutant transgene was inactive. The L233S mutant also failed to upregulate *Cyp24a1* and to downregulate *Cyp27b1* in the kidney; it was similarly unable to modulate *Cyp24a1*, *Tnfsf11*, *Spp1* and *Fgf23* expression in the calvaria. Thus, the mutant L233S hVDR failed to rescue the aberrant mineral homeostasis characteristic of the VDR null mouse. Importantly, however, alopecia was not observed in these humanized L233S mutant mice. This study confirms that loss of ligand-binding activity of the VDR compromises regulation of mineral homeostasis but not of the hair cycle *in vivo*.

***Disclosures: Seong Min Lee**, None.*

FR0450

Deletion of vitamin D receptor in mature osteoblasts and osteocytes, but not osteoclasts, impairs bone turnover in growing mice. Howard Morris*[1], Paul Anderson[2], Yolandi Starczak[3], Jackson Ryan[3], Helen Tsangari[3], Rebecca Sawyer[4], Kate Barratt[3], Andrew Turner[3], Gerald Atkins[5], Rachel Davey[6]. [1]SA Pathology, Australia, [2]Musculoskeletal Biology Research, University of South Australia, Australia, [3]School of Pharmacy & Medical Sciences, University of South Australia, Australia, [4]Chemical Pathology Directorate, SA Pathology, Australia, [5]University of Adelaide, Australia, [6]University of Melbourne, Australia

Direct activities of vitamin D through $1,25(OH)_2D_3$, on the skeleton have previously been reported to include catabolic, anabolic and inhibitory actions. These varied findings suggest multiple, complex roles for VDR mediated within the bone micro-environment. We have previously shown that vitamin D activity within mature osteoblasts and osteocytes enhances bone formation. In addition, vitamin D activity within osteoclasts modulates resorptive activity. It is unclear however as to the dominant activity of VDR in osteoblasts and osteoclasts in the *in vivo* setting. To address this question, we crossed the floxed-VDR (VDR-loxP) mouse with osteocalcin-Cre mice to inactivate VDR in osteoblasts and osteocytes (ObVDRKO). In addition, we crossed VDR-loxP mice with cathepsin K-Cre mice to inactivate VDR in osteoclasts (OcVDRKO). At 6 weeks of age, both male and female ObVDRKO mice demonstrated significant increases in both cortical bone volume and metaphyseal BV/TV% (Male ObVDRKO, 21% increase, $p<0.05$; Female ObVDRKO, 23% increase, $p<0.05$) when compared to VDR-loxP control littermates. The increase in bone volume in young ObVDRKO mice was associated with a marked decrease in RANKL mRNA expression, decreased metaphyseal osteoclast surface and serum Crosslaps. In addition, metaphyseal osteoblast surface and bone formation rate were both modestly reduced associated with marked reductions of mRNA for several key osteoblastic genes such as *Alkaline phosphatase*, *Osteocalcin* and *Sost*. At 6 weeks of age, both male and female OcVDRKO mice however exhibit unaltered bone volume. At 12 weeks of age, cortical bone volume in ObVDRKO mice was no longer different from levels in control mice. Metaphyseal BV/TV% was attenuated in male mice (6% increase, $p<0.05$) but remained significantly greater in female ObVDRKO mice (28% increase, $p<0.05$). By 26 weeks of age, metaphyseal BV/TV% in female ObVDRKO mice was no longer significantly different from bone levels in control mice. These data suggest that while VDR in osteoclasts appears to have no major role in regulating bone resorption in young mice, VDR in mature osteoblast and osteocytes promotes RANKL-mediated osteoclast activity, at least when RANKL is up-regulated during periods of growth.

***Disclosures: Howard Morris**, None.*

FR0453

The Vitamin D Receptor Promotes Human Breast Cancer Cell Growth via a Ligand Independent Cytoplasmic Function. Trupti Trivedi*[1], Yu Zheng[1], Pierrick Fournier[2], Colin Dunstan[3], Khalid Mohammad[2], Hong Zhou[1], Markus Seibel[1], Theresa Guise[2]. [1]Bone Research Program, ANZAC Research Institute, The University of Sydney, Australia, [2]Indiana University, USA, [3]University of Sydney, Australia

Previous reports show that vitamin D deficiency promotes human breast cancer growth in bone. In the current study we aimed to define the role of the vitamin D receptor (VDR) in breast cancer cell growth. We hypothesized that VDR knockdown enhances human breast cancer cell growth.

In vitro: Using stable shRNA expression and single cell clonal selection, VDR expression was knocked down by ~85% in MCF-7 cells (MCF-7$^{VDR-/-}$). Compared to parental (PA) and non-target (NT) controls, induction of CYP24 mRNA expression

by $1,25(OH)_2D_3$ was completely abrogated in MCF-$7^{VDR-/-}$ clones, confirming effective disruption of VDR signaling.

Treatment of PA & NT cells with $1,25(OH)_2D_3$ reduced cell growth by 32% compared to untreated cells ($p< 0.001$). In ligand-free culture, surprisingly, the growth of MCF-$7^{VDR-/-}$ clones was reduced by up to 34%, with a 6-fold increase in cell apoptosis compared to controls ($p< 0.001$), suggesting that VDR might have a ligand-independent effect in promoting cell growth. Treatment of MCF-$7^{VDR-/-}$ clones with $1,25(OH)_2D_3$ had no additional effect on cell growth and apoptosis.

In vivo: To investigate the putative effect of VDR on tumor growth *in vivo*, MCF-$7^{VDR-/-}$ and NT cells were xenografted orthotopically into the mammary fat pad of nude mice. VDR knockdown resulted in reduced tumor growth from day 18 to 51 ($p<0.001$). Intra-tibial implantation of NT cells into nude mice resulted in significant osteosclerosis as assessed by microCT (trabecular bone volume:+38%; trabecular number: +500%; compared to sham-injected tibia; $p<0.001$). Tumor-induced osteoblastic bone lesions were significantly less pronounced ($p< 0.001$ compared to NT cells) following implantation of MCF-$7^{VDR-/-}$ clones (trabecular volume: +9%; trabecular number: +30% compared to sham-injected tibia), indicating that VDR knockdown is associated with significantly retarded tumor growth.

Overexpression of a mutant VDR deficient in the nuclear localization signal (mVDR) in NT and MCF-$7^{VDR-/-}$ cells restored cell growth in MCF-$7^{VDR-/-}$ cells to the same level as seen in controls. This was associated with cytoplasmic accumulation of mVDR.Conclusion: The VDR has ligand-independent functions promoting breast cancer cell growth which contrast with its ligand-dependent, anti-proliferative effects.

***Disclosures: Trupti Trivedi**, None.*

FR0455

Vitamin D Is a Regulator of Endothelial Nitric Oxide Synthase and Arterial Stiffness in Mice. OLENA ANDRUKHOVA*[1], Svetlana Slavic[2], Ute Zeitz[2], Sabine Riesen[3], Tamas Ambrisko[3], Mato Markovic[3], Wolfgang Kuebler[4], Reinhold Erben[5]. [1]INST. OF PHYSIOLOGY, PATHOPHYSIOLOGY & BIOPHYSICS, Austria, [2]Department of Biomedical Research, University of Veterinary Medicine, Austria, [3]Department for Companion Animals & Horses, University of Veterinary Medicine, Austria, [4]Institute of Physiology, Charité, Germany, [5]University of Veterinary Medicine, Austria

Epidemiological data in humans have shown that vitamin D insufficiency is associated with hypertension, left ventricular hypertrophy, and increased arterial stiffness. However, the pathophysiological mechanisms underlying the association between vitamin D insufficiency and cardiovascular diseases remain largely unexplained. To elucidate further the role of vitamin D in the regulation of cardiovascular function we examined male 3-and 9-month-old mice with a nonfunctioning vitamin D receptor ($VDR^{\Delta/\Delta}$). To normalize mineral homeostasis, the mice were kept on a rescue diet enriched with calcium, phosphate, and lactose. Elderly but not young $VDR^{\Delta/\Delta}$ mice showed increased heart/body weight ratio and left ventricular muscle mass. Mean arterial pressure as well as renal renin expression and serum aldosterone were unchanged in young and older $VDR^{\Delta/\Delta}$ mice on rescue diet. However, arterial catheterization revealed profoundly increased arterial pulse pressure together with increased arterial stiffness, increased aortic impedance, structural remodeling of the aorta, and impaired systolic and diastolic heart function in elderly, but not in young $VDR^{\Delta/\Delta}$ mice. Furthermore, young and older $VDR^{\Delta/\Delta}$ mice were characterized by lower bioavailability of the vasodilator nitric oxide (NO), and showed decreased aortic expression of endothelial NO synthase (NOS3), the main regulator of vascular NO levels. Conversely, incubation of mouse aortic rings with $1,25(OH)_2D_3$ increased *NOS3* mRNA abundance *in vitro.* Treatment of $VDR^{\Delta/\Delta}$ mice with the NO donor sodium nitroprusside acutely reduced the elevated arterial stiffness to levels similar to those observed in wild-type controls. To analyze the direct effects of vitamin D signaling on *NOS3* transcriptional activity, we double transfected HEK cells with human *VDR* and *NOS3* plasmids. Stimulation of transfected cells with $1,25(OH)_2D_3$ significantly increased NOS3 expression in a VDR dependent manner. These results suggest that VDR signaling regulates NO production by enhancing the transcription of its main endothelial synthetizing enzyme, NOS3. Our data demonstrate the importance of intact VDR signaling in the preservation of vascular function, and may provide a mechanistic explanation for epidemiological data in humans showing that vitamin D insufficiency is associated with hypertension and endothelial dysfunction.

***Disclosures: OLENA ANDRUKHOVA**, None.*

FR0456

Anti-PTHrP monoclonal antibodies are potent proliferation inhibitors in triple negative human breast cancer cells and potentiate the effects of taxol and doxorubicin. Richard Kremer*[1], Benoit Ochietti[2], Ibtihal Fadhil[2], Anne Camirand[2]. [1]McGill University, Royal Victoria Hospital, Canada, [2]McGill University, Canada

Approximately 15% of breast cancer cases present tumors that lack progesterone, estrogen and Her2/neu receptors. The majority of these triple-negative breast cancer types (TNBC) progress rapidly due to lack of effective drugs and resistance to chemotherapy. In this study, we targeted parathyroid hormone-related protein (PTHrP) using the blocking monoclonal antibody (mAb) M158 (directed against its N-terminus) to determine its effects on *in vitro* proliferation as a single agent, and in combination with standard chemotherapeutic agents taxol (Tax) and doxorubicin (Dox). TNBC cell lines MDA-MB-468, BT 549, MDA-MB-231 and MDA-MB-435 were treated with increasing concentrations of Dox, Tax, and the anti-PTHrP mAb M158 as single agents or in combination, and cell survival assayed with Presto-Blue (InVitrogen/Life Technologies). As a single agent, the anti-PTHrP M158 mAb significantly inhibited proliferation in a dose-dependent fashion in all cell lines (see table), as compared to control IgG, except in MDA-MB-468 cells which are PTHrP-negative. Tax and Dox as single agents caused dose-dependent growth inhibition in all lines tested compared to vehicle (see table). Importantly, in PTHrP-positive TNBC cells, M158 mAb enhanced the growth inhibition of Tax and Dox in additive (for MDA-MB-231 and -435) or synergistic fashion (for BT-549). In summary, all PTHrP-positive TNBC cells were significantly inhibited by the blocking mAb as a single agent, and M158 also enhanced the anti-proliferative effect of chemotherapeutic agents, suggesting that the use of an anti-PTHrP mAb in combination therapy could be beneficial to TNBC patients.

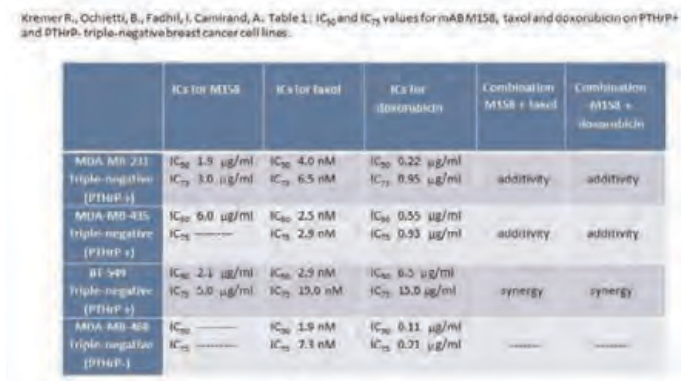
Kremer R., Ochietti, B., Fadhil, I. Camirand, A. Table 1 : IC_{50} and IC_{75} values for mAB M158, taxol and doxorubicin on PTHrP+ and PTHrP- triple-negative breast cancer cell lines.

	IC$_x$ for M158	IC$_x$ for taxol	IC$_x$ for doxorubicin	Combination M158 + taxol	Combination M158 + doxorubicin
MDA-MB-231 Triple-negative (PTHrP +)	IC_{50} 1.9 µg/ml IC_{75} 3.0 µg/ml	IC_{50} 4.0 nM IC_{75} 6.5 nM	IC_{50} 0.22 µg/ml IC_{75} 0.95 µg/ml	additivity	additivity
MDA-MB-435 Triple-negative (PTHrP +)	IC_{50} 6.0 µg/ml IC_{75} ———	IC_{50} 2.5 nM IC_{75} 2.9 nM	IC_{50} 0.55 µg/ml IC_{75} 0.93 µg/ml	additivity	additivity
BT-549 Triple-negative (PTHrP +)	IC_{50} 2.1 µg/ml IC_{75} 5.0 µg/ml	IC_{50} 2.9 nM IC_{75} 15.0 nM	IC_{50} 6.5 µg/ml IC_{75} 15.0 µg/ml	synergy	synergy
MDA-MB-468 Triple-negative (PTHrP -)	IC_{50} ——— IC_{75} ———	IC_{50} 1.9 nM IC_{75} 7.3 nM	IC_{50} 0.11 µg/ml IC_{75} 0.21 µg/ml	———	———

IC50 and IC75 values for mAB M158, tax and dox on PTHrP+ and PTHrP- TNBC cells

***Disclosures: Richard Kremer**, None.*

FR0457

Biological characterization of PTHrP(12-48): Novel biomarker of breast cancer bone metastasis or new active peptide?. Larry Suva[1], Archana Kamalakar*[1], Dana Gaddy[1], Charity Washam[2], Frances Swain[2], Bethany Allen[2], Nisreen Akel[1], Kim Leitzel[3], Alan Lipton[3]. [1]University of Arkansas for Medical Sciences, USA, [2]UAMS Orth Surgery, USA, [3]Penn State Hershey Cancer Institute, USA

Bone metastasis (BM) is a common occurrence in breast cancer. Approximately 20% of adjuvant breast cancer patients will relapse and die from distant metastasis; of these over 75% will develop BM. Despite intensive research in both the metastatic and early breast cancer setting, there is currently no clinically-approved biomarker that can identify or predict the development of BM. Our discovery of PTHrP(12-48) as a circulating biomarker significantly correlated with BM has the potential to change this paradigm and become the basis for a predictive BM assay that will personalize therapy for adjuvant breast cancer BM prevention. Although PTHrP(12-48) circulates at detectable concentrations ($\sim 103 \pm 46$ng/mL) in breast cancer patients with BM compared with 53 ± 23ng/mL in patients without BM (n=42), there is no evidence for any specific biologic activity. To address this question, we utilized *in silico*, biochemical and immunohistochemical approaches. First, a *de novo* structural model of PTHrP(12-48) was derived and compared to all known PTHrP (and PTH) structures. The model predicted PTHrP(12-48) to be an alpha helix followed by an unstructured region after residue 42. Structural alignments suggested that PTHrP(12-48) is unlikely to have any biological interactions with the PTH1 receptor. PTHrP(12-48) was synthesized for use as an immunogen and for biologic characterization. Supporting the model prediction, PTHrP(12-48) did not induce cAMP accumulation or phosphorylate PKC in hPTH1 receptor-expressing SaOs2 cells. Nor was any biologic function of PTHrP(12-48) detected, such as stimulation of ALP in osteoblasts or the enhancement of RANKL-induced osteoclastogenesis. Interestingly, using a polyclonal PTHrP(12-48)Ab, negatively selected against PTHrP(1-15) and PTH(1-34), we observed tissue- and breast cancer–specific immunostaining of PTHrP(12-48). The polyclonal Ab detected PTHrP(12-48), PTHrP(1-139) but not PTHrP(1-37) or PTH. Classic N-terminal PTHrP target tissues (breast, placenta, cartilage) were positive for PTHrP(1-15) as expected, but negative for PTHrP(12-48). We next examined 15 archival paired primary human breast cancer and BM specimens. Interestingly, 11/15 primary cancers that were PTHrP(1-15) negative were PTHrP(12-48) positive. Of the 15 BM examined, 10 were PTHrP(12-48) positive. These data suggest that PTHrP(12-48) not only circulates at detectable levels in breast cancer patients, but may be commonly expressed by both primary breast tumors and BM

***Disclosures: Archana Kamalakar**, None.*

FR0458

Function of ERRa in Mediating Mixed Metastatic Bone Lesion from Prostate Cancer Cells: Implication of Endothelin 1 and Wnt/periostin pathway. Anais Fradet[1], Akeila Bellahcene[2], Vincent Castronovo[2], Philippe A.R. Clezardin[1], Edith Bonnelye*[3]. [1]INSERM & University of Lyon, France, [2]University of Liège, GIGA-CANCER, Belgium, [3]Faculte de Medecine RTH Laennec, France

Up to 80% of patients dying from prostate carcinoma have developed bone metastases that are incurable. We had shown that the orphan nuclear receptor ERRa (Estrogen receptor related receptor alpha) is involved in skeletal development and in bone metastases from breast cancer cells. Because we found ERRa also expressed in bone metastases from prostate cancer patients, we decide to modulate its expression in PC3 cells and investigate its role in the development of bone metastases from prostate cancer cells. We show that human PC3 cells over-expressing wild-type ERRa (PC3-ERRaWT) induced osteolytic bone lesions in SCID mice (n=10) that were increased (51,5 ± 6,7* for Bone volume (BV/TV)(%) and 18,5 ± 5,4** for skeletal tumor burden (TB/STV)(%)) compared to that observed with PC3-CT cells (59,5 ± 2,75 (BV/TV) and 2 ± 0,73 (TB/STV)). Surprisingly bone destruction was combined with new bone formation, as 70% of the metastatic limbs that were bearing PC3-ERRaWT cells had mixed lesions compared with CT-PC3 that only developed osteolytic lesions. Osteoclasts were not directly affected *in vivo* and *in vitro*. On the other hand, a statistical stimulation of bone nodules number (calvaria culture) was observed when cells were treated with conditioned medium extracted from PC3-ERRaWT compared with PC3-CT which was combined with the up-regulation of BSP, OCN expression and a decrease of RANKL in MC3T3 cells. Interestingly, microenvironment was impacted by PC3-ERRaWT cells, as mouse periostin (POSTN), that is known to contribute to the metastatic niche, is over-expressed *in vivo* suggesting the implication of the stroma in the tumor progression in bone mediated by ERRa. Finally, PC3-ERRaWT cells stimulated tumor growth after subcutaneous injection. Pro-osteolytic factors such as TGFβ1, MMP1, Runx2 and Cathepsin K were found to be up-regulated in PC3-ERRaWT compared with CT-PC3 tumors. The expression of pro-osteoblastic factors Wnt3a, 5a, 10b, 11 and ET1 was also stimulated *in vivo* which may explain the occurrence of bone formation in these skeletal lesions. The direct regulation of Wnt3a and 5a, ET1, OPG, MCP1, CK and Runx2 was confirmed by using the inverse agonist XCT790 (10^{-6}M) on PC3 cells during 24h. In conclusion, our data suggest that ERRa can promote both osteolysis and osteosclerosis in animal models of prostate cancer bone metastases and suggest an implication of ERRa in cancer stem cells maintenance and metastatic niche via the POSTN/ Wnt signaling.

***Disclosures: Edith Bonnelye**, None.*

FR0459

PGE2 receptor EP4 regulates breast cancer metastasis and bone resorption through osteoblastic RANKL production. Satoshi Yokoyama[1], Kenta Watanabe[1], Michiko Hirata[1], Chiho Matsumoto[1], Takayuki Maruyama[2], Chisato Miyaura[1], Masaki Inada*[1]. [1]Tokyo University of Agriculture & Technology, Japan, [2]Ono Pharmaceutical Co., Ltd., Japan

Bone metastasis of breast cancer is accompanied by severe bone destruction. We identified that prostaglandin E2 (PGE2)-induced osteoclast formation was mediated by RANKL production in osteoblasts, and that EP4 is the most effective PGE receptor rather than the other EP subtypes (EP1, EP2, EP3). Here, we examined the effects of EP4 antagonist in the model of *in vivo* inoculation of breast cancer into bone. First, we have identified the expression profiles of EPs in mouse breast cancer cell 4T1, and found the expression of EP1 and EP4 in 4T1 cells. PGE2-induced 4T1 proliferation was suppressed by both EP1 and EP4 antagonist in the cells, suggesting the 4T1 has a diversity to respond multiple PGE2 signaling channels for the proliferation. To examine the mechanism of 4T1 induced-bone resorption, 4T1 cells were co-cultured with bone marrow cells and osteoblasts to evaluate the supporting capacities of osteoclast formation. We newly employed the experimental system to evaluate cell-cell interaction by the contact adhesion, co-cultured bone cells on fixated cancer cell with cell membrane. Contact with fixed-4T1 cell strongly induced RANKL expression and PGE2 production in osteoblasts. Osteoclast formation was induced in the co-culture of osteoblasts and bone marrow cells on fixed-4T1 cells, and only EP4 antagonist completely inhibited the osteoclast formation. When 4T1 cells were co-cultured with mouse calvaria to evaluate bone resorbing activities, 4T1 cells attachment to bone surface markedly induced the number of osteoclast and following bone resorption. In the organ culture, adding EP4 antagonist attenuated 4T1-induced bone resorption. By 3D-micro CT analyses, the resorbing trail was detected on calvarial bone surface and suppressed by the treatment of EP4. Finally, *in vivo* experiments using the tibial inoculation model of 4T1 cells, the oral administration of EP4 antagonist clearly protected the 4T1-induced bone destruction in both cancerous and cortical bone of tibia. These results suggest that the EP4 specifically regulates RANKL production in osteoblast that leads osteoclast differentiation and following osteolysis. EP4 antagonist is a candidate for the therapy of breast cancer with bone metastases.

***Disclosures: Masaki Inada**, None.*

FR0460

Presence of Giant Osteoclasts in Zoledronic Acid Treated Prostate Cancer Bone Metastasis. Martine P Roudier*[1], Colm Morrissey[1], Alexander Dowell[2], Eva Corey[1], Celestia HIGANO[3], Lawrence TRUE[3], Robert Vessella[3]. [1]University of Washington, USA, [2]University of Alabama at Birmingham, USA, [3]UW, USA

Zoledronic acid (ZOL), a new generation bisphosphonate, reduces skeletal-related events in patients with prostate cancer (PCa) bone metastases. We have shown previously that bisphosphonates significantly increased bone volume in PCa bone metastases with no apparent reduction in osteoclast numbers. In the present study we aimed to characterize responses of osteoclasts in PCa bone metastases to ZOL treatment. We measured number of osteoclasts/13.55 mm2 in bone biopsies obtained from 27 ZOL-treated and 10 ZOL-untreated patients with PCa bone metastases (total of 357 TRAP stained plastic sections). We found no difference in osteoclast numbers between ZOL-treated (n=257) versus ZOL-untreated (n=100) PCa bone metastases per surface area (average 7.2 ± 8.6 vs 6.2 ± 9, p=0.143). To compare the morphology of osteoclasts in ZOL-treated and ZOL-untreated patient biopsies, we selected biopsies which had more than two TRAP-positive osteoclasts/bone surface (n=37), and counted the number of osteoclasts per section (total area 95 mm2). We did not detect differences between ZOL-treated and ZOL-untreated biopsies: no ZOL (n=10), 36.7 ± 61; ZOL-treated (n=27), 44.3 ± 49, (p=0.143). In the biopsies from patients treated with ZOL for less than 1 year and more than 3 years, we found an average of two giant osteoclasts with > 20 nuclei per section. No giant osteoclasts were observed in sections from untreated patients. In all ZOL-treated biopsies we found an average of three osteoclasts with >13 nuclei per section, none in untreated sections, and a global average of 45 osteoclasts with up to 12 nuclei per section in all metastatic biopsies that were included in the analysis. In corresponding H&E on paraffin embedded biopsies, we counted osteoclast number/section, selected the sections with more than two osteoclasts/section and performed a TUNEL assay. In 41 ZOL-treated and 65 ZOL-untreated sections, we found averages of 11 ± 9.7 and 10 ± 12.5 osteoclasts/section respectively, averages of 40 and 33 nuclei/section, and averages of 7 and 6 TUNEL-positive nuclei/section. None of these parameters were significantly different between the groups (p=0.405). In summary, our results show that osteoclasts are present in high numbers in PCa bone metastases, and the ZOL treatment does not reduce their numbers. Our results also did not reveal any differences in apoptosis of osteoclast associated with ZOL treatment in patients with advanced PCa bone metastases. However, our results indicate that ZOL treatment results in development of giant osteoclasts. Biological significance of this finding for PCa metastases and effects of ZOL on bone will require further detailed analyses.

***Disclosures: Martine P Roudier**, None.*

FR0461

Integrin-beta 3 is required for breast tumor cell response to bone rigidity. Jonathan Page*[1], Nazanin Ruppender[1], Shellese Cannonier[1], Ushashi Dadwal[1], Alyssa Merkel[1], Scott Guelcher[1], Julie Sterling[2]. [1]Vanderbilt University, USA, [2]Department of Veterans Affairs (TVHS)/Vanderbilt University Medical Center, USA

The importance of the bone microenvironment in the regulation of tumor cell behavior is increasingly recognized. While many aspects of this environment have been explored, we have demonstrated that the physical rigidity of bone can regulate *Pthrp* and *Gli2* expression in bone metastatic cells. This response was dependent on Rho-associated protein kinase (ROCK), as ROCK shRNA or a dominant negative ROCK construct blocked the rigidity-mediated increase in *Pthrp* expression, while a dominant active construct increased *Pthrp* expression. Since studies in soft tissue tumors have demonstrated that $\alpha_v\beta_3$ integrin mediates tumor response to rigidity, we hypothesized that the tumor response to bone rigidity was also integrin-dependent. LM609, a $\alpha_v\beta_3$ inhibitory antibody, reduced the expression of *Pthrp* and *Gli2* by 2.8 and 10-fold respectively ($p \leq 0.01$), and reduced *Pthrp* expression in the ROCK dominant active cells by 9-fold ($p \leq 0.005$) in MDA-MB-231 cells grown on rigid polyurethane (PUR) films. To further determine the importance of integrin β_3, we stably transfected MDA-MB-231 cells with β_3 shRNA (90%), and measured the cells' ability to respond to mechanical cues using PUR films with tunable rigidity. Integrin β_3 knock-down reduced *Pthrp* expression by 54-fold in cells grown on rigid PUR films ($p \leq 0.001$), but not on compliant films. Since we have previously shown that TGF-β Receptor type II (RII) is required for the mechanotransduction response of MDA-MB-231 cells, we investigated whether integrin and RII interacted. Using immuno-precipitation, we found that integrin β_3 and RII co-localized as a function of increasing rigidity, suggesting pathway cross-talk. Finally, since p38 MAPK is known to play an important role in mechanotransduction and the MAPK inhibitor SB202190 reduced *Pthrp* expression on rigid films by 4-fold ($p \leq 0.01$), we investigated whether rigidity alone, in the absence of exogenous TGF-β, could upregulate p38 MAPK phosphorylation. Phosphorylation of p38 MAPK was increased on rigid films compared to compliant films by Western blot, while no changes were observed in the expression of non-phosphorylated p38 MAPK. Additionally, no increase in p38 MAPK phosphorylation was observed in the ROCK dominant negative cells. Taken together these data indicate that integrin β_3, via a pathway involving RII, ROCK and p38, is required for tumor cells to sense the rigidity of the bone microenvironment.

***Disclosures: Jonathan Page**, None.*

FR0462

Combined TGF-β and Proteasome Inhibition Improves Bone Architecture and Reduces Tumor Burden in Myeloma Bone Disease. Jeffry Nyman*[1], Alyssa Merkel[1], Barbara Rowland[2], Alexander Makowski[3], Julie Sterling[4]. [1]Vanderbilt University Medical Center, USA, [2]Department of Veterans Affairs (TVHS), USA, [3]Department of Veterans Affairs, Vanderbilt University, USA, [4]Department of Veterans Affairs (TVHS)/Vanderbilt University Medical Center, USA

Myeloma patients often develop tumor-induced bone destruction where bone volume is reduced as tumor cells expand. While there are available therapies to treat the bone disease, none eliminate the tumor or fully reverse the bone loss. Previous studies indicate that TGF-β inhibition improves bone volume and reduces tumor growth in several solid tumor models. Since elevated TGF-β signaling could also be involved in myeloma-related bone loss, we hypothesized that TGF-β inhibition would reduce tumor growth and improve bone architecture in myeloma-bearing mice. First, 5TGM1 myeloma cells were inoculated into the immune compromised, Rag 2-/- (Taconic), mice. Mice were treated with 10 mg/kg, 3x/week, of the anti-TGF-β antibody (1D11, Genzyme, n=12) or the control antibody (13C4, n=12) beginning at the time of tumor injection for 4 weeks. Surprisingly, 8 out of 12 Rag 2 -/- mice treated with 1D11 developed plasmacytomas, compared to 1 in the 13C4 group. Furthermore, 1D11 treatments did not alter IgG2bκ or spleen weights (tumor burden) in the myeloma-bearing Rag2 -/- mice, indicating no effect on tumor burden. However, 1D11 had a beneficial effect on bone architecture in that it increased trabecular BV/TV, connectivity density, and tissue mineral density ($p \leq .001$) as determined by μCT analysis of the femur metaphysis. In addition, 1D11 reduced the resorption-related increase in cortical porosity of the metaphysis. In order to determine if combining an anti-myeloma drug with 1D11 could both reduce tumor burden and improve bone architecture, we performed co-treatments with Velcade (.5 mg/kg, 3xs a week). For this study, we used the immune competent KaLwRij model inoculated with 5TGM1 cells ($n \geq 8$ per group) to avoid confounding interactions with immune deficiency. In this study, we found that Velcade + 1D11-treated mice, but not 1D11-alone, reduced spleen weight (49%, $p \leq .001$) and reduced IgG2bκ (40%, $p \leq .05$) compared to the vehicle treated mice. Furthermore, this combined therapy group displayed a reduction in μCT-derived cortical porosity (66%, $p \leq .05$) and an increase in trabecular BV/TV (50%, $p \leq .001$), whereas Velcade alone did not affect bone architecture. While 1D11 did not inhibit tumor growth and promoted plasmacytomas in immune compromised mice, combination therapy with proteasome and TGF-β inhibition improved bone architecture and inhibited tumor growth, and thus, it may be a promising strategy for treating patients with myeloma-induced bone disease.

***Disclosures: Jeffry Nyman**, None.*

FR0463

Hypoxia upregulates calpain-6 expression in osteosarcoma cells: implication in cancer stem cells. Imene Kaci[1], Rafik MANSOURI[2], Pierre Marie[3], Dominique Modrowski*[4]. [1]Unité 606 INSERM, France, [2]INSERM, France, [3]Inserm Unit 606 & University Paris Diderot, France, [4]INSERM U606, France

We previously showed that calpain-6 overexpression in osteosarcoma cells is involved in chemoresistance. Here we characterized the mechanisms driving the abnormal expression of calpain-6 in bone tumours. Human primary bone tumours express higher calpain-6 mRNA levels compared to cultured osteosarcoma cells, suggesting a role of the microenvironment. Immunohistochemistry showed that within the tumours, calpain-6 was strongly expressed in hypoxic areas labelled by a hypoxia marker (pimonidazole). Calpain-6 promoter sequence displays functional hypoxia response elements (HRE) and consensus sites for NFkB, as assessed by ChIP analysis. Culturing human osteosarcoma cell lines in hypoxic conditions (3% O2) increased calpain-6 mRNA and protein levels, and this effect was strongly reduced when HIF-1a was silenced using siRNA. Hypoxia also activated NFkB, as shown by reporter assays, and promoted the endothelin-1/NFkB pathway by increasing endothelin-1 receptor expression. In addition to HRE, the regulatory sequence of calpain-6 displays functional sites for Oct4, Nanog and Sox2 stem cell transcription factors which were up-regulated by hypoxia. Silencing Oct4, Nanog or Sox2 strongly reduced the increase of calpain-6 induced by hypoxia, suggesting a relationship between calpain-6 and the stem cell phenotype. To test this hypothesis, we prepared stem-like cells performing sphere forming assays. Different osteosarcoma cell lines showed a various potential to form floating spherical colony-like structures that grew in anchorage-independent conditions in serum-free medium and resisted to enzymatic dispersion. The number of spheres increased when the cells were cultured under hypoxic conditions, indicating that hypoxia promotes the stem cell phenotype. Interestingly, the spheres expressed higher levels of Oct4, Nanog, Sox2 and calpain-6 than parental cells. Calpain-6 overexpression using a lentiviral vector in U2OS osteosarcoma cells did not change sphere number but increased cell survival upon cell passages, indicating that calpain-6 plays a role in stem cell renewal. Altogether, our results demonstrate that hypoxia controls calpain-6 expression in osteosarcoma cells through direct and indirect pathways involving HIF-1a and NFkB effectors. Moreover, the induction of calpain-6 by hypoxia depends on stem cell factors, suggesting a particular regulation of calpain-6 in the tumour inducing cells that may be related to its role in chemoresistance.

***Disclosures: Dominique Modrowski**, None.*

FR0465

Potent induction of bone formation in myeloma bone lesions by the cathepsin K inhibitor KK1-300-01 in combination with the proteasome inhibitor bortezomib. Keiichiro Watanabe*[1], Masahiro Abe[2], Hiroshi Mori[3], Ryota Amachi[4], Masahiro Hiasa[5], Takeshi Harada[6], Shiro Fujii[6], Shingen Nakamura[6], Hirokazu Miki[6], Kumiko Kagawa[6], Itsuro Endo[7], Eiji Tanaka[4], Toshio Matsumoto[7]. [1]Tokushima University Hospital, Japan, [2]University of Tokushima, Japan, [3]Ono Pharmaceutical Co., Ltd., Japan, [4]Department of Orthodontics & Dentofacial Orthopedics, The University of Tokushima Graduate School, Japan, [5]University of Tokushima Graduate School, Japan, [6]Department of Medicine & Bioregulatory Sciences, The University of Tokushima Graduate School, Japan, [7]University of Tokushima Graduate School of Medical Sciences, Japan

Multiple myeloma (MM) enhances osteoclastogenesis while suppressing osteoblastogensis to develop devastating bone destruction. Restoration of bone in osteolytic lesions in MM still remains an important clinical issue in the present therapeutic strategies. Unlike other anti-bone resorptive agents, cathepsin K inhibitors potently suppress bone resorption while sparing cytotoxic damage in osteoclasts (OCs). In the present study, we explored the effects of cathepsin K inhibition on bone destruction in MM. The cathepsin K inhibitor KK1-300-01 (KK1) potently suppressed pit formation enhanced in the cocultures of rabbit bone cells with MM cells. However, KK1 did not affect the viability of OCs and osteoclastogenesis, and allowed OCs to facilitate in vitro mineralized nodule formation by MC3T3-E1 cells, suggesting the preservation of OC-driven osteoblastogenesis by KK1. We next examined the in vivo effects of KK1 using human INA6 MM-bearing SCID-rab models, which exhibit tumor progression with osteolytic lesions in implanted rabbit bones. Oral dosing of KK1 prevented bone destruction with marked increase in bone trabecular size and BMD in the rabbit bones and tumor reduction within their bone marrow cavity. Histological analyses showed increased bone volume/total volume with a marginal change in OC numbers in the treated mice. Of note, combinatory treatment with KK1 and bortezomib sq at 0.5 mg/kg twice a week almost completely eradicated MM cells and resumed bone formation achieving the highest BMD, while bortezomib alone showed only partial suppression of tumor growth and bone destruction. Given OC-derived ''coupling'', KK1 is suggested to spare the damage in OCs to retain the ''coupling'' for bone formation while inhibiting bone resorption, leading to robust bone formation and thereby MM contraction in bone. It can be envisaged that KK1 effectively induces bone restoration and tumor reduction in combination with anti-MM proteasome inhibitors with anabolic actions.

***Disclosures: Keiichiro Watanabe**, None.*
This study received funding from: ONO Pharmaceutical Co., LTD

SA0001

***In Vitro* Bone to Muscle Cell Signaling is Negatively Affected by Aging and Common Non-steroidal Anti-inflammatory Drugs (NSAIDs).** Asmaa Alsousi*[1], Marco Brotto[1], Chenglin Mo[1], Mostafa Badr[1], Lori Wetmore[2], Lynda Bonewald[1], Julian Vallejo[1]. [1]University of Missouri - Kansas City, USA, [2]William Jewell College, USA

Myogenic differentiation is not only critical during development, but also during adult life, since it allows muscle repair and regeneration. Previously, we demonstrated that conditioned media (CM) from the osteocyte-like MLO-Y4 osteocytes (MLO-Y4) accelerated myogenic differentiation of murine C2C12 myoblasts. We have now expanded these studies to test the effects of CM from murine primary osteocytes (MPO) on C2C12 myoblasts. Our morphological studies indicated that a low concentration of 1% CM from MPO is able to accelerate myogenic differentiation of C2C12 myoblasts. To refine our quantification and data fidelity we have used flow cytometry (FC) to more objectively quantify the effects of bone cell CM on muscle cells. C2C12 cells were cultured in growth medium (CGM: Dulbecco's modified Eagle's medium with 10% fetal bovine serum, 70% confluence). In order to arrest cell cycle differentiation, cells were synchronized with 1% FBS CGM. Medium was switched to DMEM with 2% horse serum (Differentiation medium DM). At day 5-7 of treatment, cells were trypsinized, fixed with ethanol and then treated with propidium iodide (1mg/ml) for FC analyses. In myoblasts treated with CM from young mice, cells percentage that entered the G0/G1 phase decreased by 10% in comparison with the control, which indicated an acceleration of myogenesis. This effect correlated with a significant decrease of approximately 8% in the subG population. Osteoporosis is an aging-related condition, and osteocytes from aged mice might secrete less or different factors when compared to young mice. FC revealed that CM from aged mice increased the percentage of cells entering the G0/G1 phase by 5% compared to young CM. Thus, a higher percentage of cells become arrested after treatment with aged CM, suggesting that effects of primary osteocytes CM are influenced by aging. Last, since our group has previously shown that PGE2 treatment partially mimics the acceleration of myogenesis effects of MLO-Y4 CM effects in C2C12 myoblasts, we have begun studying the effects of commonly used non-steroidal anti-inflammatory drugs (NSAIDs), Acetylsalicylic acid (Aspirin) and Acetaminophen on C2C12 myogenesis. We observed an increase of 10-15% in cells that entered the G0/G1 phase, suggesting potentially detrimental effects on myogenesis. We are currently focusing on deciphering the cellular mechanisms underlying the effects of aging and NSAIDs on myogenesis.

***Disclosures: Asmaa Alsousi**, None.*

SA0002

Age-associated Changes in MicroRNA Expression Affects Differentiation Potential in Human Mesenchymal Stem Cells. Sudharsan Periyasamy-Thandavan*[1], Sergi Mas[2], Sadanand Fulzele[3], Xingming Shi[3], Norman Chutkan[3], Randy Ruark[3], John Hinson[3], Monte Hunter[3], Raymond Corpe[3], Hongyan Xu[3], Carlos Isales[3], Mark Hamrick[4], William Hill[1]. [1]Georgia Regents University & Charlie Norwood VAMC, USA, [2]Universitat de Barcelona, Spain, [3]Georgia Regents University, USA, [4]Georgia Health Sciences University, USA

Age-associated osteoporosis is largely accepted as an emerging stem cell disease in recent times. Maintenance of the local bone marrow (BM) microenvironment extracellular matrix and signaling factors is critical in regulation of proliferation, and differentiation, of the multipotent BM mesenchymal stromal/stem cell (MSC) population with age. Recently, the role of microRNAs (miRNAs) in modulating the BM microenvironment along with the proliferation and differentiation of MSCs has been recognized. Here, we examined the role of miRNAs with age-associated changes in MSC osteogenic potential. To avoid artifacts introduced with standard MSC isolation and cell culturing techniques, we directly isolated CD271+ MSCs (that are CD90, 105, 73+ and CD14, 20, 34, 45-) from human surgical bone marrow aspirates of patients, isolated the total RNA and performed a microarray analysis (Affymetrix GeneChip® miRNA 2.0 Array) of young vs old CD271+ MSCs using the Partek Genomics Suite and Functional Hierarchical Clustering. The miRNAs identified as differentially expressed with age were validated by qRT-PCR. The predicted targets were clusters of genes associated with bone formation, extracellular matrix components, as well as osteogenic signaling pathways. The overexpressed miRNAs were predicted to target multiple osteogenic genes, including SDF-1 and BMP2; while targets of the underexpressed miRNAs included adipogenenic genes such as PPAR-gamma, and AP2-alpha. Specific miRNA mimics and inhibitors of miRNAs that were differentially expressed with age were transfected in cultured CD271+ MSCs from young patients. ELISA, quantitative Real-Time PCR (qRT-PCR), migration assay and differentiation assays were performed. Mimics of the overexpressed miRNAs significantly downregulated the mRNA expression of SDF-1-CXCR4 axis and osteogenic genes; while silencing the underexpressed miRNAs significantly upregulated PPAR-gamma mRNA expression. Similarly, ELISA analysis demonstrated the significant reduction of SDF-1 protein secretion in the cell culture medium. In addition, migration assay confirmed the reduced migration of MSCs towards the respective cell culture medium. Differentiation assays showed transfection of these miRNA mimics and inhibitors in the MSCs, reduced osteogenesis and increased adipogenic markers. Overall, these findings confirm that differential expression of miRNA shift the differentiation potential of MSCs from an osteogenic to an age-associated adipogenic lineage.

***Disclosures: Sudharsan Periyasamy-Thandavan**, None.*

SA0003

Swedish mutant APP suppresses osteoblast differentiation and causes osteoporotic deficit, which are ameliorated by n-acetyl-l-cysteine. Wen-Cheng Xiong*, Wen-Fang Xia, Jiung Jung, Shun Cui, Shan Xiong, Lei Xiong. Georgia Regents University, USA

Reduced bone mineral density and hip fracture are frequently observed in patients of Alzheimer's disease (AD). However, mechanisms underlying their association remain poorly understood. Amyloid precursor protein (APP) is a transmembrane protein that is ubiquitously expressed, including bone marrow stromal cells (BMSCs), osteoblasts (OBs), macrophages (BMMs), and osteoclasts (OCs). Mutations in APP gene identified in early-onset AD patients are believed to cause AD. But, little is known about APP's role in bone remodeling. Here, we present evidence for Swedish mutant APP (APPswe) in suppression of OB differentiation and function in culture and in mouse. APP expression in BMSCs increases during ageing. Ubiquitous expression of APPswe in young adult Tg2576 (under the control of prion promoter) recaptured skeletal "ageing-like" deficits, including decreased OB genesis and bone formation, increased adipogenesis and bone marrow fat, enhanced OC genesis and bone resorption. Remarkably, selective expression of APPswe in mature OB-lineage cells in TgAPPswe-Ocn mice [under the control of osteocalcin (Ocn) promoter driven Cre] also decreased OB genesis and increased OC formation, resulting in a trabecular bone loss. These results thus suggest a cell autonomous role for APPswe in suppressing OB formation and function, but a non-autonomous effect on OC genesis. Notably, increased adipogenesis and elevated bone marrow fat were detected in young adult Tg2576, but not TgAPPswe-Ocn, mice, implicating that APPswe in BMSCs and/or multi-cell types in bone marrow promotes bone marrow adipogenesis. Intriguingly, the skeletal ageing-like deficits in young adult Tg2576 mice were prevented by treatment with NAC (n-acetyl-l-cysteine), an anti-oxidant, suggesting that reactive oxygen species (ROS) may underlie APPswe-induced osteoporotic deficits. Taken together, these results demonstrate a role for APPswe in suppressing OB differentiation and bone formation, implicate APPswe as a detrimental factor for AD associated osteoporotic deficit, and reveal a potential clinical value of NAC in the treatment of osteoporotic deficits.

***Disclosures: Wen-Cheng Xiong**, None.*

SA0004

Testosterone Modulates Inflammation-Induced Periodontal Bone Loss. Luis Carlos Spolidorio*[1], Leila Santana Coimbra[2], Carlos Rossa Jr[2], Alpdogan Kantarci[3], Thomas E Van Dyke[3], João Paulo Steffens[4]. [1]Campus of Araraquara, Brazil, [2]Department of Physiology & Pathology*, Dental School of Araraquara, State University of São Paulo (UNESP), Araraquara, São Paulo, Brazil, Brazil, [3]The Forsyth Institute, Department of Applied Oral Sciences, USA, [4]Department of Physiology & Pathology*, Dental School of Araraquara, State University of São Paulo (UNESP), Brazil

Abnormal testosterone levels result from several physiological, pathological and pharmacological conditions. Periodontitis is an inflammatory condition that leads to alveolar bone loss. The purpose of this study was (i) to evaluate the impact of sub- and supraphysiologic doses of testosterone (T) on experimental periodontitis, and (ii) to assess the actions of T on osteoclastogenesis in vitro. Forty male Holtzman rats were subjected to orchiectomy to suppress T production (Ocx). Twenty of the rats received 250mg/kg T. An additional twenty rats served as sham-operated controls. Experimental periodontitis was induced in ten animals in each group by ligature placement around the lower first molar teeth 30 days post-surgery and maintained for 15 days. The remaining animals served as controls. Changes in alveolar bone height were radiographically quantified. Serum levels of cytokines and chemokines were measured. In vitro, RAW 264.7 cells were used as osteoclast (OC) precursors and OC RANKL-mediated differentiation and activity were evaluated in the presence of 1nM-1μM doses of testosterone. Flutamide (100nM) was used as a specific blocker to assess the role of androgen receptors. In the absence of periodontitis, there was significant bone loss in the T group (0.74 ± 0.04 mm) when compared to Ocx (0.49 ± 0.07) or Sham (0.55 ± 0.05; $p<0.05$). Ocx alone increased serum IL-2 levels (+90%) and T increased IL-1β (+174%), IL-2 (+200%) and IFN-γ (+73%). Periodontitis resulted in significantly higher bone loss in the Ocx group (1.69 ± 0.14) compared to Sham controls (1.32 ± 0.09; $p<0.05$), and also led to a significant reduction in IL-10 (-44 and -47%) in Ocx and T groups, respectively. A decrease in IL-4 (-52%) and an increase in IL-1β (+173%) accompanied these changes in the T group. In vitro, T dose-dependently inhibited OC numbers and area ($p<0.05$), although the highest dose resulted in an increase in OC formation. The addition of flutamide rescued the 100nM T inhibition restoring the number of OC. In conclusion, sub- and supraphysiologic T levels predispose to inflammatory changes with a significantly higher periodontal destruction in rats. These clinical observations are accompanied by

cytokine/chemokine and ALP modulation. T presents an optimal range (10/100nM) to reduce OC formation and activity in vitro, which is mediated, at least in part, via the androgen receptor.

***Disclosures: Luis Carlos Spolidorio**, None.*
This study received funding from: FAPESP- Fundação de Amparo à Pesquisa do Estado de São Paulo - Brasil and Conselho Nacional and Conselho Nacional de Desenvolvimento Científico e Tecnológico CNPq Brasil

SA0005

The Role of Inflammation in Senescence of Human MSCs. Julie Glowacki*, Shuanhu Zhou. Brigham & Women's Hospital, USA

Skeletal aging is characterized as a gradual loss of bone mass to the point of osteopenia or osteoporosis, and eventually bone fracture. We reported that human marrow-derived stromal cells (hMSCs), with potential to differentiate to osteoblasts, show reproducible declines in proliferative and osteoblast potential with the age of the subject from whom the cells were obtained. They also show an age-related increase in biomarkers of cell senescence, including the % Senescence-Associated-β-galactosidase (SA-β-gal)-positive cells and expression of p53 and its target p21; furthermore there is an age-related increase in their constitutive secretion of pro-inflammatory interleukins. Our previous unsupervised miRNA cluster comparison showed NF-κB dysregulation in cells from elders; Westerm immunoblotting showed increased phosphorylated NF-κB/p65 in cells from elders. These observations raise the possibility that inflammation can be a mechanism of cell senescence in hMSCs. Tumor necrosis factor-α (TNF-α) is a key inflammatory mediator implicated in the onset of several diseases. TNF-α interacts with two receptors (TNFR1 and TNFR2) that are differentially expressed on cells and tissues and initiate both distinct and overlapping signal transduction pathways. In this study, we tested the mechanistic hypothesis that TNF-α induces senescence of human MSCs.

We examined the effects of TNF-α on hMSCs from a 17-year-old man. There was a dose-dependent increase in phosphorylation of NF-κB/p65 and on sensecence markers. TNF-α (10 ng/mL) increased the number of SA-β-gal-positive cells by 11-fold and decreased proliferation to 29% of control; there was a dose-dependent decrease in osteoblast differentiation, assessed by Alkaline phosphatase (ALP) activity after 7 days in osteoblastogenic medium (Figure). We used groups of hMSCs from 4 young (*Y*; <45 y) and 4 older (*O*; >65 y) subjects to evaluate constitutive expression of TNF receptors; expression of TNFR2 in *O*-hMSCs was 21% of that in *Y*-hMSCs (p=0.03), with no difference in TNFR1.

These studies show that TNF-α induced a senescent phenotype in hMSCs from a 17-year old man: increased SA-β-gal and decreased proliferation and osteoblast differentiation. Age effects on TNF receptors do not appear to account for senescence of hMSCs. In sum, these observations add evidence that intrinsic age-associated inflammatory processes can contribute to decreased osteoblast differentiation and skeletal aging.

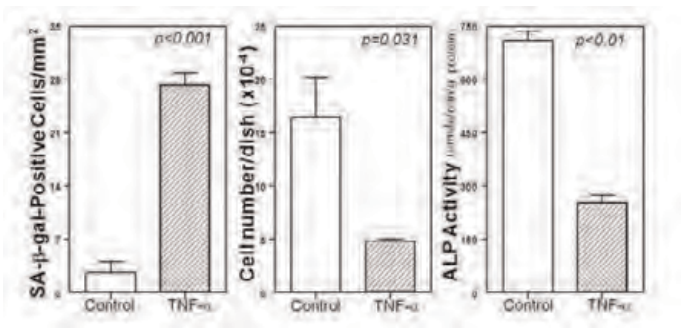

Figure

***Disclosures: Julie Glowacki**, None.*

SA0006

Baseline serum markers of adiposity driven immune/endocrine perturbations are not significantly correlated with longitudinal changes in lean mass in postmenopausal women. Andriene Grant[1], Jennifer H Stern[2], Cynthia A Thomson[3], Robert Kaplan[4], Todd Manini[5], Charles Eaton[6], Lesley Tinker[7], Erin LeBlanc[8], Scott Going[1], Oleg Zaslavsky[9], Zhao Chen*[1]. [1]The University of Arizona, USA, [2]University of Arizona Cancer Center, USA, [3]University of Arizona College of Public Health, USA, [4]Albert Einstein College of Medicine, USA, [5]University of Florida Aging Rehabilitation Research Center, USA, [6]Division of Biology & Medicine, Brown University, USA, [7]Fred Hutchinson Cancer Research Center, USA, [8]The Center for Health Research, Kaiser Permanente, USA, [9]Faculty of Health Science & Social Welfare, University of Haifa, Israel

Background: Sarcopenic obesity, a combination of obesity and low muscle mass, has recently been defined as an epidemic. While it is possible that these pathophysiological states may simply coexist, there is a causal link between obesity and sarcopenia that has yet to be fully understood. Total body fat is associated with higher circulating pro-inflammatory cytokines, decreased growth hormone (GH) production, and altered circulating levels of adiponectin and leptin. These hormonal and inflammatory perturbations have been implicated as determinants of sarcopenia. This study investigates the association between adiposity driven immune/endocrine biomarkers and the trajectory of change in lean mass (ΔLM), with special consideration to the trajectory of change in fat mass (ΔFM) in postmenopausal women (PMW).

Methods: Utilizing a cohort of PMW from the Women's Health Initiative, we investigated the relationship between baseline circulating levels of inflammatory cytokines (CRP, IL-6, IL-1, TNF-α), GH, adiponectin, and leptin with longitudinal changes in DXA-derived total body lean mass (LM) and fat mass (FM). ΔLM and ΔFM were determined from measures collected at baseline, y3 and y6 of the study. Fasting blood samples were collected to assess baseline circulating biomarker concentrations. Multiple linear regression analysis was used to determine the association between the slope of ΔLM and biomarkers.

Results: Mean LM declined from 36.61±4.99 kg at baseline to 36.26±4.97kg at year 6 ($p<0.05$), while mean FM and body weight (BW) increased with time (FM: 29.55±10.78kg at baseline to 30.10±10.49kg at year 6, BW: 69.67±15.05kg at baseline to 70.23±14.91kg at year 6, $p<0.05$ for FM and BW). Although GH (p=0.024), leptin (p=0.041) and the leptin to adiponectin ratio (LAR) (p=0.024) were crudely associated with ΔLM in linear regression models, when the ΔFM was added to the model as a covariate, this was no longer statistically significant (p=0.05, 0.088, and 0.121 for GH, leptin, and LAR, respectively).

Conclusion: After controlling for longitudinal changes in fat mass, baseline circulating markers of adiposity driven hormonal and inflammatory perturbations were not associated with longitudinal changes in lean mass in this population of postmenopausal women. The association of growth hormone, leptin and LAR with ΔLM observed in this study may be mediated by ΔFM and thus, these biomarkers may not be reliable predictors of longitudinal changes in lean mass in PMW.

***Disclosures: Zhao Chen**, None.*

SA0007

Components of sarcopenia and the risk of co-morbidity among postmenopausal women – 10 year follow-up of the OSTPRE study. Juha Suuronen*[1], Samu Sjöblom[1], Toni Rikkonen[1], Marjo Tuppurainen[2], Risto Honkanen[1], Heikki Kröger[3], Joonas Sirola[4]. [1]University of Eastern-Finland, Finland, [2]Kuopio University Hospital, Finland, [3]Kuopio University Hospital, UEF, Finland, [4]University of Eastern Finland / Kuopio, Finland

Introduction: Muscle strength and physical performance level are measures of sarcopenia. The aim of the present study was to investigate the effects of grip strength and physical capability on postmenopausal co-morbidity.

Methods: 2735 Finnish Caucasian women from the OSTPRE cohort were measured with grip strength (GS) dynamometer at baseline (1994) and at 10-year follow-up (2004) and categorized into quartiles. Physical capability (PC) was assessed with questionnaires and categorized into: 1) Full PC (n=1487) 2) Able to walk over 1 km but not to run (n=1000) and 3) Able to walk less than 1 km (n=248). Osteoporosis was defined as 10-year follow-up FN or LS T-score under -2.5 SD or under -2.0 SD + low trauma energy follow-up fracture. Information on co-morbidities was based on self-reports. Effects of Grip strength and physical capability on prediction for morbidities were analyzed disease specifically during 10-year follow-up. At baseline, women with end-point morbidity were excluded from the analysis. The risk of co-morbidity related to sarcopenia at 10-year the follow-up was estimated with multivariate logistic regression, adjusting for age, BMI, HT use, alcohol intake and smoking.

Results: The prevalence of co-morbidities at the end of follow-up were: hypertension (HT) 25.7 %, cardiac insufficiency (CI) 6.2 %, coronary artery disease (CAD) 10.3 %, stroke (ST) 5.0 %, diabetes mellitus (DM) 7.3 %, osteoarthritis (OA) 22.3 %, breast cancer (BC) 2.8 %, depression 2.8 %, osteoporosis (OP) 8.2 %, chronic back pain (BP) 17.1 % and poor self-rated health (SRH) 4.3 %. Women within the lowest grip strength quartile had lower risk of HT (OR 0.74, $p<0.05$), higher risk of ST (OR 1.74, $p<0.05$) and OA (OR 1.45, $p<0.02$) in comparison to women within the highest GS quartile in multivariable model. Women with the poorest PC had a higher risk of CI (OR 2.56, $p<0.01$), CAD (OR 2.19, $p<0.001$) and OP (OR 2.51, $p<0.001$).

Conclusions: Grip strength and Physical capability predict different co-morbidities among postmenopausal women. Physical capability is a better predictor of clinical osteoporosis than GS in multivariable model. These findings support the concept of including different measures of sarcopenia in its diagnostics. The role of muscle mass and quality to predict the morbidity remains unclear.

***Disclosures: Juha Suuronen**, None.*

SA0008

Dairy intake is not associated with quadriceps muscle strength in adults: The Framingham Offspring Study. Shivani Sahni*[1], Kelsey Mangano[2], Robert McLean[1], Douglas Kiel[3], Xiaochun Zhang[4], Marian Hannan[5]. [1]Hebrew SeniorLife, Institute for Aging Research & Harvard Medical School, USA, [2]Institute for Aging Research, Hebrew SeniorLifeHarvard Medical School, USA, [3]Hebrew SeniorLife, USA, [4]Institute for Aging Research, Hebrew SeniorLife, USA, [5]HSL Institute for Aging Research & Harvard Medical School, USA

Rationale: Previous studies have shown that dairy intake can aid in weight loss while retaining lean muscle mass, possibly because dairy foods are high in protein, which has been linked with muscle mass and strength. Furthermore, dairy foods provide other nutrients beneficial for muscle health such as vitamin D. Thus health effects of dairy foods on muscle may be due to more than a single nutrient. Yet, it's unclear if dairy food groups may play a direct role in muscle strength.

Objective: To determine the cross-sectional association of dairy food group with quadriceps muscle strength among Framingham Offspring participants. We further examined if these associations vary by BMI levels considering the role of dairy foods in weight loss.

Methods: 2,548 men & women completed a food frequency questionnaire to determine dairy food groups (milk, yogurt, cheese, cream, total dairy in servings/week) and had isometric quadriceps strength measured by a hand-held dynamometer (kg, max of 2 trials, 1995-98). We used linear regression to calculate beta estimates and *P* values (for dairy food groups in servings/week) as well least squares adjusted means for dairy food groups (in categories) adjusting for age, sex, height, BMI, physical activity, menopause status, and total energy intake (kcal/d). These associations were further examined by BMI levels [$<$ 25 (normal), $\geqslant$25-30, $\geqslant$30 kg/m^2 (obese)].

Results: Mean age was 59.6$\pm$9.3y (range 26-85). Mean intakes (servings/week) were 5.7$\pm$6.2 (milk), 1.0$\pm$2.0 (yogurt), 2.7$\pm$3.1 (cheese); 4.0$\pm$6.2 (cream) and mean quadriceps strength was 20.1$\pm$6.4kg. No significant association was observed between number of servings and quadriceps muscle strength for any dairy food group (*P* range: 0.26-0.96). Upon stratification by BMI groups, cream intake was inversely associated with muscle strength in normal BMI group (β: -0.054$\pm$0.03, P=0.10) while milk intake was positively associated with muscle strength in obese group (β: -0.071$\pm$0.04, P=0.08). Though these associations were not statistically significant. No significant associations were observed for any other dairy food group (P range for BMI $<$25: 0.26-0.96, BMI $\geqslant$25-30: 0.22-0.93; BMI $\geqslant$30 kg/m^2: 0.32-0.90). Similar non-significant associations were observed when dairy food groups were analyzed in categories.

Conclusions: Dairy food intake may not be associated with quadriceps strength in this cohort of adult men and women. Possible reasons for null associations may include insufficient power or other factors in the pathway may contribute more to the muscle stength.

***Disclosures: Shivani Sahni**, from the General Mills Bell Institute for Health and Nutrition, 6*

SA0009

Genetic variants in *CAPN3* and *ACVR2B* are associated with lean body mass in postmenopausal women. Yann Klimentidis*[1], Patricia Thompson[2], Walter Klimecki[3], Chengcheng Hu[1], Guanglin Wu[4], Jennifer Bea[5], J. Skye Nicholas[6], CHARGE Consortium Musculoskeletal Working Group[7], David Allison[8], Zhao Chen[9]. [1]University of Arizona Mel & Enid Zuckerman College of Public Health Epidemiology & Biostatistics, USA, [2]University of Arizona Cellular & Molecular Medicine, USA, [3]University of Arizona Pharmacology & Toxicology, USA, [4]University of Arizona, USA, [5]University of Arizona College of Medicine, USA, [6]University of Arizona Mel & Enid Zuckerman College of Public Health, USA, [7]USA, [8]University of Alabama at Birmingham, USA, [9]University of Arizona College of Public Health, USA

Background: Loss of lean body mass is a major cause of disability and diminished quality of life. Twin and family studies have demonstrated that lean body mass is a heritable trait. However, relatively few specific genetic factors have been identified as potentially influencing this trait.

Methods: In this study, we selected 1,493 single-nucleotide polymorphisms (SNPs) in 155 candidate genes and examined their association with lean body mass in a sample of 2,406 non-Hispanic and Hispanic white postmenopausal women from the Women's Health Initiative (WHI) Observational Study. Lean body mass was assessed using dual energy x-ray absorptiometry.

Results: We identified 43 SNPs with evidence for a significant association (consistently by subgroup and by anatomical site for $p<0.05$) to lean mass in the WHI cohort. To assess the reproducibility of our findings, we replicated our findings using data from the CHARGE Consortium Musculoskeletal Working Group that performed a genome wide association study of lean mass in twenty cohorts. Considering the results from both the discovery and replication stages, genetic variation in the calpain 3 (*CAPN3)* at SNP rs12439003 and the activin A receptor, type IIB (*ACVR2B) at* SNP rs2276541 were significantly associated with lean body mass ($p<1 \times 10^{-4}$). Calpain 3 is a muscle-specific member of the family for which mutations have previously been associated with a form of muscular dystrophy. ACVR2B is known to be involved in the regulation of myostatin signaling and has previously been identified in a candidate gene study as a determinant of skeletal muscle mass in men but not women.

Conclusion: Our findings support a previously proposed role of ACVR2B allelic variation as a determinant of muscle mass and extend prior findings in men to women. To our knowledge, this is the first observation for a role of allelic variation in CAPN3 as a determinant of lean body mass. Additional large-scale studies will be needed to confirm our findings, including analyses to assess their association in different populations.

***Disclosures: Yann Klimentidis**, None.*

SA0010

Low protein intake is one of the correctable risk factors of sarcopenia in Korean men(KNHANES IV, 2008-2009). JO EUN KIM*[1], Kwang Joon Kim[2], Sihoon Lee[3], Yumie Rhee[4], Sung-Kil Lim[5]. [1]Yonsei University Health System, South Korea, [2]Severance Hospital, South Korea, [3]Gachon University School of Medicine, Rok, [4]Department of Internal Medicine, College of Medicine, Yonsei University, South Korea, [5]Yonsei University College of Medicine, South Korea

Sarcopenia is a syndrome characterized by the progressive loss of skeletal muscle mass and strengths and associated with increased risk of falls and fractures, loss of independence and increased risk of death. However, there are few studies about curable or non curable identification of the country specific risk factors for sarcopenia. The aim of this study is to determine the correctable risk factors for sarcopenia in Korean elderly.

We analyzed 940 men and 1,324 women aged 65 years and older who completed the analysis of body composition using a dual energy X-ray absoprtiometry (DXA) in Fourth Korean National Health and Nutrition Examination Surveys IV (2008-2009). Sarcopenia was defined as the apendicular muscle mass divided by height square of less than one standard deviation below the sex-specific normal mean for the young reference group.

In univariate analysis, age, BMI, HOMA-IR, limitation of day-to-day activities, regular exercise, frequency of high risk drinking, family income, femur neck BMD, total hip BMD, lumbar spine BMD, total energy intake and protein intake were associated with sarcopenia in men (*p* value$<$0.05, respectively), and age, BMI, limitation of day-to-day activities, regular exercise, occupation, total hip BMD and total energy intake were associated with sarcopenia in women (*p* value$<$0.05, respectively). In multiple logistic regression analysis of subgroup, sarcopenia was strongly associated with osteoporosis of femur neck (OR = 9.45, 95% CI = 1.26-70.60) and negatively associated with highest quartile of protein intake (OR = 0.003, 95% CI = 0.00004-0.32) in men.

In conclusion, osteoporosis of femur neck and low protein intake are independent risk factors for low muscle mass in Korean. Correction of common etiology related to sarcopenia and osteoporosis with encouraging sufficient protein intake might be one of good approaches to prevent sarcopenia in Korean elderly men.

***Disclosures: JO EUN KIM**, None.*

SA0011

See Friday Plenary Number FR0011.

SA0012

Sarcopenia and health-related quality of life over five years in community-dwelling older adults. David Scott*[1], Kerrie Sanders[2], Laura Laslett[3], Alan Hayes[4], Peter Ebeling[1], Graeme Jones[5]. [1]The University of Melbourne, Australia, [2]NorthWest Academic Centre, The University of Melbourne, Western Health, Australia, [3]Menzies Research Institute, University of Tasmania, Australia, [4]Institute of Sport, Exercise & Active Living, College of Health & Biomedicine, Victoria University, Australia, [5]Menzies Research Institute, Australia

Purpose: Sarcopenia may be diagnosed according to operational definitions based on low muscle mass or function. It is unclear whether differing associations exist for sarcopenia with health-related quality of life (HRQOL) according to the definition applied. The aim of this study was to examine effects of low muscle mass and strength on HRQOL over five years in community-dwelling older adults.

Methods: 1028 community-dwelling volunteers (62.9$\pm$7.5 [mean$\pm$SD] years; 50% female) completed baseline assessments and 832 and 731 participants completed follow-up assessments 2.6$\pm$0.4 and 5.1$\pm$0.5 years later. The validated Assessment of Quality of Life (AQoL-4D) was completed at all time-points and health utility scores were calculated on a scale where 0 = death and 1 = full health. Quality-adjusted life years (QALYs) were calculated as mean utility scores multiplied by time between each measurement. Low muscle mass and strength at baseline were categorised according to the lowest sex-specific tertiles of height-adjusted lean mass (assessed by dual-energy X-ray absorptiometry) and lower-limb strength (assessed by dynamometer). Linear mixed model regression analyses adjusting for age, sex and comorbidity examined associations of sarcopenia at baseline with HRQOL over five years.

Results: Utility scores were significantly poorer for sarcopenic compared with non-sarcopenic participants at baseline, according to both muscle mass (median [Interquartile Range] 0.79 [0.69, 0.89] vs 0.82 [0.71, 0.91]; $P = 0.026$) and strength (0.71 [0.58, 0.84] vs 0.79 [0.72, 0.91]; $P < 0.001$) definitions. Non-sarcopenic participants according to muscle strength accumulated more QALYs over five years than sarcopenic individuals (4.03 [3.60, 4.58] vs 3.62 [3.09, 4.23]; $P < 0.001$), and this difference was significant after adjustment for age, but no significant differences were observed according to muscle mass. Similarly, sarcopenia according to muscle strength was a significant independent predictor of reduced utility after 2.6 years (β [95% CI] -0.05 [-0.07, -0.04]) and 5.1 years -0.05 [-0.07, -0.02]), but no associations were observed for sarcopenia according to muscle mass.

Conclusions: Low muscle strength, but not low muscle mass, is associated with a biologically meaningful reduction in HRQOL over five years in community-dwelling older adults. These findings suggest that clinical sarcopenia assessments and interventions should preferentially target muscle strength rather than mass alone.

***Disclosures: David Scott**, None.*

SA0013

The Frequency of Hypothyroidism in Older Patients Presenting with Acute Thoracic and Lumbar Spine Fractures. Alison Dittmer*[1], Osa Emohare[1], David Wright[2], Charles Ledonio[1], Robert Morgan[1], David Polly[1], Julie Switzer[3]. [1]University of Minnesota, USA, [2]Regions Hospital, USA, [3]University of Minnesota Physicians, USA

Introduction: Thyroid function is intertwined with bone metabolism, and both hyperthyroidism and hypothyroidism can increase the risk of fracture. The most recent study evaluating baseline levels in patients age 65 and over found 15% had subclinical and 1.6% had overt hypothyroidism. One of the characteristic spine features in older patients can be the presence of compression fractures at levels of significant axial loading; axial loading of impaired bone can predispose to fractures. This study aims to assess both the frequency of concomitant hypothyroidism in patients with thoracic and lumbar spine fractures, and the impact of advancing age on this specific complication.

Methods: Following Institutional Review Board approval, patients who presented to our facility with acute fractures of the thoracic and lumbar spine were reviewed and stratified by age (younger than 65 vs. 65 and older). Patients presenting with spine injuries that did not include an acute fracture were excluded. Electronic medical records were reviewed for clinical evidence of hypothyroidism and for previous diagnosis and treatment with levothyroxine.

Results: A total of 169 patients were included in this study. Eighty-three were younger than 65 with a mean age of 41.7 (range 18-64), and 86 were 65 or older with a mean age of 78.6 (range 65-96). In the younger cohort, a minority of 24 patients (29%) were female; this increased to a majority of 52 (60%) in the older cohort. In those $<$ 65, 2 patients (2%) were either hypothyroid or being treated for hypothyroidism; in patients $\geqslant$ 65, this increased to 22 (26%) ($p<0.001$). A further comparison was performed between the hypothyroidism rate in our older cohort of fracture patients with historical data outlining the rate in US patients over 65 ($p=0.006$).

Discussion: These results showed a tenfold difference in the proportion of hypothyroid patients when a comparison was made between those under age 65 and those age 65 and over. The magnitude of this difference suggests that impaired thyroid function critically impacts the maintenance of appropriate bone function, especially in older patients. A further comparison with US population level data showed a significantly higher incidence for both subclinical and overt hypothyroidism in our fracture cohort. This study indicates that hypothyroidism is significantly associated with agerelated impairment in bone quality and thus impacts the management of fracture risk in older patients.

***Disclosures: Alison Dittmer**, None.*

SA0014

Atsttrin Primer, an Engineering Protein Derived from Progranulin Growth Factor, Binds to TNF-α Receptors and is Therapeutic Against Inflammatory Arthritis. Qingyun Tian*[1], Yunpeng Liu[2], Chuanju Liu[2]. [1]NYU Hospital for Joint Diseases, USA, [2]New York University, USA

Progranulin (PGRN) is a multifunctional growth factor which is composed of seven-and-a-half repeats of a cysteine-rich motif in the order P-G-F-B-A-C-D-E. We previously reported that PGRN directly bound to TNF-α receptors (TNFR), and inhibited TNF-α activity (Tang, W, et al, Science. 2011). Atsttrin, an engineered protein composed of three PGRN fragments (1/2F-1/2A-1/2C), exhibited selective TNFR binding, and potently prevented inflammation in multiple arthritis mouse models (Tang, W, et al, Science. 2011). It is well established that TNF family ligands bind to receptors in a heterohexameric 3:3 complex. We created a novel engineering protein, Atsttrin primer, which comprised the same fragments as Atsttrin but in a different sequence (1/2A-1/2C-1/2F). The purpose of this study is to determine (1) whether the three fragments of Atsttrin (i.e. 1/2A, 1/2C and 1/2F) act independently for interacting with TNFR; and if so, (2) whether Atsttrin primer is able to block the binding of TNF-α to TNFR, and has therapeutic effect in inflammatory arthritis, as does Atsttrin. Molecular mechanistic studies through Yeast-two hybrid screening and Solid-phase binding assay revealed that Atsttrin primer had stronger binding affinity to TNFR compared with Atsttrin, and effectively inhibited TNF-α from binding to TNFRs. To define the role of Atsttrin primer in inflammatory arthritis, we induced collagen-induced-arthritis (CIA) model in DBA-1 mice. Clinical arthritis score showed that Atsttrin primer treatment delayed CIA development and ameliorated arthritis severity. Furthermore, micro-CT showed that Atsttrin primer protected against bone erosion in CIA model. In addition, Safranin O staining showed that Atsttrin primer protected loss of cartilage matrix. Besides, we used spontaneous inflammatory arthritis model in TNF-α transgenic (TNF-Tg) mice, and treatment of Atsttrin primer significantly attenuated arthritis severity in this model. Taken together, these data indicate that as a novel engineering protein derived from PGRN, Atsttrin primer has high affinity to bind TNFR and antagonize TNF-α action, and plays a protective role in murine inflammatory arthritis models. This study not only testified that the three fragments which comprise Atsttrin and Atsttrin primer function independently for binding to TNFR and antagonizing TNF-α action, but may also provide us with additional interventions for treating inflammatory musculoskeletal diseasess clinically in the future.

***Disclosures: Qingyun Tian**, None.*

SA0015

Bone Mass and Cartilage Traits among Asymptomatic Postmenopausal Women and those with Mild Knee Osteoarthritis. Juhani Multanen*[1], Miika Nieminen[2], Arja Häkkinen[3], Urho Kujala[4], Hannu Kautiainen[5], Eveliina Lammentausta[6], Ilkka Kiviranta[7], Ari Heinonen[4]. [1]University of Jyväskylä, Finland, [2]Department of Diagnostic Radiology, Oulu University Hospital & Department of Radiology, University of Oulu, Finland, [3]Department of Health Sciences, University of Jyväskylä, & Department of Physical Medicine & Rehabilitation, Central Finland Central Hospital, Finland, [4]Department of Health Sciences, University of Jyväskylä, Finland, [5]Unit of Family Practice, Central Finland Central Hospital, & Unit of Primary Health Care, Kuopio University Hospital, Finland, [6]Department of Diagnostic Radiology, Oulu University Hospital, Finland, [7]Department of Orthopaedics & Traumatology, University of Helsinki, & Helsinki University of Central Hospital, Finland

The purpose of this study was to determine the association of the degree of osteoarthritis (OA) to (i) femoral neck BMC and (ii) knee cartilage biochemical composition in a sample of asymptomatic postmenopausal women and those with mild knee OA.

78 postmenopausal women (mean age: 58 (SD 4) yrs, height: 163 (6) cm, weight: 71 (11) kg) with early knee OA were examined. Women with Kellgren–Lawrence (K/L) radiographic grading of knee OA 1 (n=25) and 2 (n=53) were included for a related intervention study (ISRCTN58314639). In addition, age adjusted convenience sample of 12 radiographically confirmed asymptomatic voluntary women (mean age: 58 (SD 3) yrs, height: 161 (6) cm, weight: 67 (11) kg) were included. The femoral neck BMC was measured by DXA from the higher K/L grade knee side. In asymptomatic subjects the average BMC value of both femoral neck sites was calculated for the analysis. Biochemical composition of cartilage was evaluated using delayed gadolinium-enhanced MRI of cartilage (dGEMRIC) sensitive to cartilage glycosaminoglycan (GAG) content. Perceived knee pain, stiffness, and self-rated physical functioning were assessed with the Western Ontario and McMaster Universities Arthritis Index (WOMAC). As risk factors of falling maximal isometric knee extension and flexion forces were measured with a dynamometer. The statistical significance for linearity between K/L grades was calculated by using linear regression analysis.

The results are presented in Table 1. In femoral neck there was a significant linearity showing that BMC adjusted for age, weight and height increased with higher OA grades of the knee joint. There were no linear relationships in knee cartilage indices at any anatomical sites, or in muscle force according the K/L grades. In WOMAC subscales there were linear trends showing that the higher the OA grade was, the more the subjects experienced knee pain, stiffness and physical disability.

Our bone results show that there is an inverse relationship between BMC and mild knee OA. However, the anomalous findings of dGEMRIC indices at different radiographic OA stages suggest that a more complex pattern of GAG behavior may occur at early stages of disease.

Table 1. Bone and cartilage traits and clinical outcomes according the Kellgren-Lawrence (K/L) grades.

	K/L 0 (n=12)	K/L 1 (n=25)	K/L 2 (n=53)	P for linearity
Bone mineral content (BMC), g	4.183 (0.836)	4.463 (0.874)	4.726 (0.575)	0.019
dGEMRIC index, msec				
MEDIAL CONDYLE				
posterior part of central femur	446 (60)	461 (55)	456 (78)	0.78
central tibia	362 (67)	412 (72)	402 (58)	0.18
LATERAL CONDYLE				
posterior part of central femur	474 (67)	512 (75)	469 (59)	0.27
central tibia	426 (107)	433 (82)	437 (77)	0.61
WOMAC, range 0-100				
Pain	2 (5)	6 (5)	8 (8)	0.008
Stiffness	5 (10)	8 (9)	11 (12)	0.036
Physical function	2 (4)	4 (4)	5 (5)	0.033
Strength, N				
extension	381 (49)	384 (79)	417 (82)	0.059
flexion	172 (44)	174 (53)	184 (54)	0.35

Table

***Disclosures: Juhani Multanen**, None.*

SA0016

Deficiency of epidermal growth factor receptor (EGFR) signaling enhances cartilage destruction in mouse experimental osteoarthritis. Xianrong Zhang[1], Ji Zhu[1], Yumei Li[2], Abhishek Chandra[3], Frank Beier[4], Motomi Enomoto-Iwamoto[5], Ling Qin*[3]. [1]University of Pennsylvania, School of Medicine, USA, [2]Shanghai Municipal Hospital of Traditional Chinese Medicine, Shanghai University of Traditional Chinese Medicine, China, [3]University of Pennsylvania, USA, [4]University of Western Ontario, Canada, [5]Children's Hospital of Philadelphia, USA

Osteoarthritis (OA) is a progressive joint degenerative disease characterized by destruction of articular cartilage. We have previously demonstrated a critical role of EGFR signaling in growth plate development during endochondral ossification. However, its role in the pathogenesis of OA is largely unknown. In this study, we induced experimental OA in two mouse models with deficient EGFR activity at 12 weeks of age by destabilization of the medial meniscus (DMM) of the right knees. In the first model, wild type 129/SvEv (n=17) received gefitinib (100 mg/kg/dose) every other day following DMM to specifically inhibit EGFR activity. The second model uses a genetically modified mice with a dominant-negative mutant of EGFR (Wa5/+, n=19). Twelve weeks post surgery, knee joints were isolated for histological analysis. Scoring of cartilage destruction by Mankin's method indicated that both OARSI scores for medial tibial plateau and medial femoral condyle were significantly increased in gefitinib-treated mice and Wa5/+ mice compared to their respective controls, indicating that decreased EGFR activity leads to more severe cartilage destruction after DMM. TUNEL assay revealed that chondrocyte apoptosis increased by more than 60% in the articular cartilage of gefitinib-treated mice and Wa5/+ mice, suggesting that EGFR signaling protects chondrocytes from destabilization-induced apoptosis. Furthermore, immunohistochemistry showed that aggrecan degradation products, along with their cleavage enzymes, MMP13 and Adamts5, were strongly elevated in the articular cartilage of EGFR-deficient mice after DMM. Interestingly, while Adamts5 amount was similarly increased in the sham-operated left knees of EGFR-deficient mice, MMP13 amount was significantly decreased in these knees, which is consistent with our previous report that EGFR signaling stimulates MMP13 expression in primary chondrocytes from neonatal animals. Further studies revealed that the amount of HIF-2a, a transcription factor for MMP13 in chondrocytes, was also stimulated in the cartilage of EGFR-deficient mice after DMM. Activation of EGFR by TGFa in primary chondrocytes inhibited the expression of Adamts5 and HIF-2a. Taken together, our studies demonstrate that EGFR signaling plays a significant role in OA development by stimulating chondrocyte survival and preventing articular cartilage degradation and our data also implicate this signaling pathway as a potential therapeutic target for OA treatment.

***Disclosures: Ling Qin**, None.*

SA0017

Femoral Neck Structural Traits among Asymptomatic Postmenopausal Women and Those with Mild Knee Osteoarthritis. Ari Heinonen*[1], Juhani Multanen[2], Miika Nieminen[3], Arja Häkkinen[4], Urho Kujala[1], Hannu Kautiainen[5], Eveliina Lammentausta[6], Ilkka Kiviranta[7]. [1]Department of Health Sciences, University of Jyväskylä, Finland, [2]University of Jyväskylä, Finland, [3]Department of Diagnostic Radiology, Oulu University Hospital & Department of Radiology, University of Oulu, Finland, [4]Department of Health Sciences, University of Jyväskylä, & Department of Physical Medicine & Rehabilitation, Central Finland Central Hospital, Finland, [5]Unit of Family Practice, Central Finland Central Hospital & Unit of Primary Health Care, Kuopio University Hospital, Finland, [6]Department of Diagnostic Radiology, Oulu University Hospital, Finland, [7]Department of Orthopaedics & Traumatology, University of Helsinki, & Helsinki University Central Hospital, Finland

Many studies have found increased BMD in patients with osteoarthritis (OA). However there are sparse information of the relationship between bone structural traits and OA. The purpose of this study was to examine the relationship between radiographic knee OA and femoral neck structural traits in a sample of asymptomatic postmenopausal women and those with mild knee OA.

78 postmenopausal voluntary women (mean age: 58 (SD 4) yrs, height: 163 (6) cm, weight: 71 (11) kg) with early knee OA were recruited via newspaper advertisement. Women with Kellgren–Lawrence (K/L) radiographic grading of knee OA 1 (n=25) and 2 (n=53) were included for a related intervention study (ISRCTN58314639). In addition, age adjusted convenience sample of 12 radiographically confirmed asymptomatic women (mean age: 58 (SD 3) yrs, height: 161 (6) cm, weight: 67 (11) kg) were included. Proximal femur was scanned with DXA at the narrowest femoral neck section from the higher K/L grade knee side in the subjects with mild knee OA. Femoral neck cross-sectional area (CSA, [mm^2], the surface area of bone in the cross-section after excluding all trabecular and soft tissue space) the section modulus (Z, [mm^3], an index of bending strength), and subperiosteal width (W, [mm]) were calculated with advanced hip structural analysis (AHA). In asymptomatic subjects the average bone traits values of both femoral neck sites was calculated for the analysis. Perceived knee pain, stiffness, and self-rated physical functioning were assessed with the Western Ontario and McMaster Universities Arthritis Index (WOMAC). The statistical significance for linearity between K/L grades (0-2) was calculated by using linear regression analysis.

The results are presented in Table 1. In femoral neck there was a significant linear association showing that bone structural traits adjusted for age, weight and height increased significantly with higher OA grades of the knee joint. Also, in WOMAC subscales there were significant linear trend showing that the higher the OA grade was, the more the subjects experienced knee pain, stiffness and physical disability. Our results show that there was an inverse relationship between femoral structural traits and mild radiographic knee OA.

Table 1. Bone structural traits and clinical outcomes according the Kellgren-Lawrence (K/L) grades.

	K/L 0 (n=12)	K/L 1 (n=25)	K/L 2 (n=53)	P for linearity
Bone structure				
Section modulus (Z), mm^3	543 (98)	611 (170)	628 (101)	0.033
Cross sectional area (CSA), mm^2	135 (22)	142 (28)	150 (19)	0.019
Width (W), mm	46.8 (3.2)	48.4 (3.3)	49.4 (4.9)	0.022
WOMAC, range 0-100				
Pain	2 (5)	6 (5)	8 (8)	0.008
Stiffness	5 (10)	8 (9)	11 (12)	0.036
Physical function	2 (4)	4 (4)	5 (5)	0.033

Table

***Disclosures: Ari Heinonen**, None.*

SA0018

NELL-1 Protects Articular Cartilage from the Effects of IL-1β Induced Arthritis. Jie Jiang*[1], Felipe Ituarte[1], Dahae Shim[1], Varsha Gupta[1], Dang Tran[1], Frank Petrigliano[1], Benjamin Bengs[2], Kang Ting[1], Chia Soo[1]. [1]University of California, Los Angeles, USA, [2]UCLA, USA

Introduction: Arthritis is the leading cause of disability in the United States. Existing clinical options are limited to either symptomatic relief or total joint replacement. Both of these options have considerable limitations and have thus prompted significant interest in biological agents which may serve as treatment for arthritis. NELL-1 is a potent, stage-specific factor that enhances anabolic activity while inhibiting catabolic activity in articular cartilage. Nell-1 is normally expressed in articular cartilage, and its loss results in abnormal cartilage development. We have recently demonstrated the utility of NELL-1 protein for cartilage regeneration in both *in vitro* and *in vivo* models. The purpose of this study was to evaluate the therapeutic benefit of NELL-1 in the treatment of arthritic cartilage. We *hypothesized* that NELL-1 would reduce the inflammatory and catabolic response of IL-1β stimulation in articular chondrocytes.

Methods: To examine the beneficial effect of NELL-1, we used a well-established IL-1β induced arthritis model. Specifically, chondrocytes (ATDC5 and primary rabbit articular chondrocytes) were grown to confluence in 24 well plates. Prior to treatment, the cells were serum starved for 24 hours. Cells were then treated with NELL-1 for 2 hours prior to the addition of IL-1β. After 24 hours, cells were harvested and the effects of NELL-1 were examined using qPCR and immunohistochemistry.

Results: IL-1β treatment significantly increased inflammation and catabolic activity of both ATDC5 and articular chondrocytes. The addition of NELL-1 diminished the inflammatory effect of IL-1β stimulation. Specifically, in ATDC5 cells, NELL-1 treatment down-regulated inflammation (IL-6) expression after IL-1β stimulation while it had no effect in catabolic gene expression (Mmp13, Adamts4). In primary rabbit articular chondrocytes, NELL-1 significantly down regulated both IL-6 and catabolic gene expression. Additionally, NELL-1 was also able to up-regulate anabolic gene expression in articular chondrocytes (Col2a1, Agg).

Conclusion: Our data shows that NELL-1 holds potential for the treatment of arthritis. In this study, NELL-1 down-regulated both inflammation and catabolic genes, and up-regulated anabolic activity in articular chondrocytes. Future studies will focus on the effects of NELL-1 using articular cartilage explants and *in vivo* effects of NELL-1 in arthritic animal models.

***Disclosures: Jie Jiang**, None.*

SA0019

Raman spectroscopy reveals evidence for early bone changes in osteoarthritis. Jemma Kerns*[1], Panagiotis Gikas[2], Kevin Buckley[3], Helen Birch[4], Ian McCarthy[4], Jonathan Miles[5], Tim Briggs[5], Richard Keen[5], Anthony Parker[3], Pavel Matousek[3], Allen Goodship[4]. [1]UCL, United Kingdom, [2]UCL, Institute of Orthopaedics, United Kingdom, [3]Central Laser Facility, STFC Rutherford Appleton Laboratory, United Kingdom, [4]UCL Institute of Orthopaedics & Musculoskeletal Science, Royal National Orthopaedic Hospital, United Kingdom, [5]Royal National Orthopaedic Hospital, United Kingdom

Osteoarthritis (OA) is a common, debilitating disease of joints involving degeneration of cartilage and bone. There are two competing theories for bone as the primary site for initiation of osteoarthritis. Firstly, increased load on the joint leads to increased subchondral bone stiffness1. Secondly, composition of the subchondral bone changing towards homotrimeric collagen2.

The aim of the study is to explore the hypothesis: there are chemical differences in the bone matrix of OA subchondral bone compared to matched individuals unaffected by OA. Samples were acquired (with ethical approval) from human tibial plateaus with established medial compartment osteoarthritis (n=10), non-OA from amputees (n=5) and non-OA aged-matched cadaveric tissue (n=5). Subchondral bone samples were analysed with Raman spectroscopy (830nm excitation wavelength, Renishaw, UK)3,4, peripheral quantitative computed tomography (pQCT; for bone mineral density) and chemical analysis (collagen alpha chain ratios). Mineralisation ratios were calculated from spectra and multivariate analysis performed to assess variance across the spectral range (750–1800 cm-1)5.

Results showed that medial subchondral bone of the OA samples had a greater vBMD (p=0.05) and was thicker than the lateral side. The non-OA specimens had the same thickness on both sides of the tibial plateau with some differences in density. The Raman results showed no spectral differences between medial and lateral areas of the plateau in OA or in the non-OA samples (Figure 1). However, regardless of compartment, there were significant differences in Raman spectra between the OA and non-OA samples (p=0.02), and differences in type I collagen chemistry with medial OA samples exhibiting higher than normal levels of homotrimeric collagen.

These results support the theory that there is a biochemical difference between OA and non-OA subchondral bone. Future efforts will assess Raman spectroscopy for both characterising and detecting osteoarthritis during its early subclinical phase.

The results suggest that Raman spectroscopy could be further developed as a screening tool for early detection of joint degeneration based on detecting molecular modifications in the subchondral bone.

1. Radin EL (2004).J.Rheum., 31,suppl 7.
2. Bailey AJ et al (2002). Int J.Biochem.Cell Biol., 34(2),176-82.
3. Buchwald T et at (2012). Biomed.Optics 17(1),017007.
4. Draper ER et al (2005).JBMR, 20(11),1968-72.
5. Martin F et al (2010).Nat.Prot.,5(11),1748-1760.

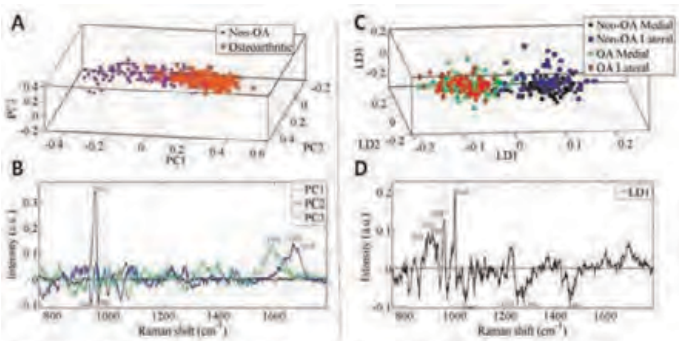

Figure 1: [A] PCA scores plot: non-OA medial (black square), non-OA lateral (blue circle), OA medial (green triangle), OA lateral (red diamond); [B] Corresponding loadings plot revealing wavenumbers responsible for the segregation in [A]) to [A]; [C] PCA-LDA scores plot for non-OA (black square) vs. OA (blue circle); [D] corresponding loadings plot to [C].

Figure and Legend

***Disclosures: Jemma Kerns**, None.*

SA0020

Subchondral Bone Turnover and Osteophyte Formation Are Key aspects in the Progression of Osteoarthritis (OA) and May Be Assessed and Predicted by α-CTX. Morten Karsdal*[1], Janet Huebner[2], Virginia Kraus[2], Diana Leeming[3], R Edward Coleman[2], Gary McDaniel[2], Kim Huffman[2], Anne-Christine Bay-Jensen[4], Kim Henriksen[1]. [1]Nordic Bioscience A/S, Denmark, [2]Department of Medicine, Duke University, USA, [3]Nordic Bioscience & University of Copenhagen, Denmark, [4]Nordic Bioscience, Denmark

Osteoarthritis (OA) is the most common form of arthritic disease. It is characterized by pathological changes in both bone and cartilage turnover as well as structure in which subchondral bone remodeling is speculated to be both an initiator and driver of OA.

The aim of the current study was to evaluate a biomarker of high localized bone resorption, a-CTX, previously used for bone metastasis. OA patients were characterized by; radiographic knee OA, severity, progression and localized knee bone turnover as assessed by bone scintigraphy, a dynamic and sensitive indicator of symptomatic knee OA.

Methods: A total of 149 participants (111 women, 38 men) were included who met ACR criteria for symptomatic OA and had the presence of Kellgren Lawrence (K/L) grade 1-4 radiographic OA in at least one knee. Late-phase bone scan images of both knees were obtained 2 hours after administration of ^{99m}Tc-MDP. The intensity of uptake was scored semi-quantitatively and summed for each joint site. Radiographic knee OA severity, based on the summed scoring of osteophytes (OST) and joint space narrowing (JSN) was assessed using the standardized OARSI radiographic atlas. Progression status was determined by calculating the sum of the change score in either JSN or OST between baseline and the 3-year follow-up assessment. The concentrations of urinary αCTX and CTX-II were determined by ELISA and normalized to creatinine concentration.

Results: a-CTX was related to OST formation independent of the effects of age, gender, BMI, and HRT (p=0.009). α-CTX did not correlate with severity of knee OA based on OST and JSN, but did correlate with bone turnover assessed by intensity of ^{99m}Tc-MDP uptake in the medial knee compartment. Concentrations of urinary CTX-II were strongly associated with knee OA severity based on osteophyte, intensity of total knee ^{99m}Tc-MDP uptake, and joint space narrowing.

Discussion: αCTX was associated with subchondral bone turnover, and osteophyte formation, both central features of the pathogenesis of OA. CTX-II was correlated to JSN, and burden of disease as previously reported. The significant and strong association of αCTX to bone turnover in the subchondral region suggests that this marker may be a non-invasive surrogate for active bone turnover in knee OA. Such markers may assist in the identification patients whom may benefit from strong anti-resorptives which inhibit bone and subchondral bone turnover.

***Disclosures: Morten Karsdal**, nordic Bioscience, 7; Nordic Bioscience, 3*

SA0021

α5 Integrin Deficiency Attenuates Osteoarthritic Changes in Mouse Knee Joints. Maria Elena candela*[1], Leslie Cantley[1], Motomi Enomoto-Iwamoto[1], Arjan van der Flier[2], Richard O. Hynes[2]. [1]Children's Hospital of Philadelphia, USA, [2]Howard Hughes Medical Institute, USA

α5 integrin is a major fibronectin receptor. Previous studies have demonstrated that α5 integrin is involved in regulation of synovial joint development and chondrocyte survival and matrix degradation in articular cartilage. Expression of α5 integrin was high in the superficial layer and down-regulated in the deeper zones of articular cartilage. It remains unclear whether control of α5 integrin expression is important for articular cartilage development and whether α5 integrin mediates protective or harmful actions in articular chondrocytes for maintenance of articular cartilage. To ask these questions, we generated compound mice (GDF5Cre;α5fl/-) lacking α5 integrin expression specifically in synovial joints.

The GDF5Cre;α5fl/-mice, α5 conditional knock out (α5 CKO), lacked alpha5 expression in articular cartilage and mice were born normally and had an overall appearance similar to the control (α5fl/fl or α5fl/-) mice. Histological analysis of the knee joints of the α5 CKO mice did not show significant abnormalities in the structure of synovial joints including articular cartilage. Next we compared the osteoarthritic changes between α5 CKO and the control mice after hemisectomy of the medial meniscus in the knee joint. Interestingly, we observed significantly milder histological osteoarthritic changes in the tibial medial plateaus of the α5 CKO mice than those in the control mice as determined by Mankin's score and OARSI score methods. The α5 CKO group contained a smaller number of TUNEL-positive cells as the control group, while the expression levels of MMP13 were similar between these two groups. The epiphyseal chondrocytes were isolated from the wild type mice and sorted by FACS to divide them into two groups that showed high levels of α5 integrin expression (high α5 group) and low or undetectable levels of α5 integrin expression (low α5 group). Chondrocytes in the low α5 group maintained polygonal cell morphology even at a low density in culture whereas chondrocytes in the high α5 group readily became fibroblastic and contained a much lower amount of highly sulfated proteoglycans than the low α5 group culture. These findings indicate that α5 integrin may not be essential for synovial joint development and articular cartilage organization, but participates in induction of cell apoptosis and osteoarthritic changes in articular cartilage and that down-regulation of α5 integrin could be important for stabilization of chondrocyte phenotype.

***Disclosures: Maria Elena candela**, None.*

SA0022

See Friday Plenary Number FR0022.

SA0023

See Friday Plenary Number FR0023.

SA0024

See Friday Plenary Number FR0024.

SA0025

An Examination of the Dose Response of Bone Consolidation to Docosahexaenoic Acid (DHA) in Young Female Sprague-Dawley Rats. Marie Freundorfer*[1], Hope Weiler[2]. [1]McGill University, Canada, [2]McGill University, USA

Recent animal studies have shown that DHA helps maintain bone mineral density (BMD) during aging, however little is known of the effects of DHA on growing bone. Since optimizing bone mass accumulation during growth can help prevent osteoporosis later in life, there is value to examining the effects of DHA on the development of peak bone mass. The purpose of this study was to determine the effects of increasing doses of DHA on consolidation of bone in young female rats during and after sexual maturation. Sixty female Sprague-Dawley rats (7wk at baseline) were randomized into the control (AIN93-M with 6% fat) or 1 of 4 experimental diets (n=12/diet) fed over 10 wk. The experimental diets contained increasing doses of DHASCO (0.1%, 0.4%, 0.8% and 1.2% DHA as % total diet), mixed with soybean oil to provide 6% fat in all diet groups. Blood was collected (unfed-am-state) at baseline, mid-way and end of study to measure biomarkers. Bone mineral content (BMC), bone area (BA), areal BMD and volumetric BMD were measured at baseline, mid-way and endpoint using dual-energy x-ray absorptiometry (DXA) and microcomputed tomography (μCT). Groups were not different at baseline for weight, length, BMC or BMD. Weight, length, and calcium homeostasis were not altered by the diets. Preliminary results for DXA and μCT regional lumbar spine scans show a significant increase in aBMD for 0.1% and 0.4% DHA groups, and a significant increase in vBMD for the 0.4% and 1.2% DHA groups (Table 1). Whole femur regional scans aBMD and vBMD were not different among the groups (Table 1). Whole body scans showed a significant increase in aBMD for the 0.4% and 1.2% DHA groups ($p<0.05$), however no significant differences in vBMD between the diet groups (data not shown). Further research including blood biochemistry, higher resolution μCT scanning and biomechanical testing is planned to clarify these preliminary results.

Scan region	Percent DHA in diet (%)				
	0	0.1	0.4	0.8	1.2
Lumbar spine					
aBMD[1](L1-L4)	0.303(0.005)	0.332(0.005)*	0.340(0.005)*	0.325(0.005)	0.324(0.005)
vBMD[2](L2-L4)	520.36(8.18)	546.81 (8.62)	561.48 (8.48)*	555.10 (8.55)	565.08(8.35)*
Whole femur					
aBMD	0.416 (0.011)	0.426 (0.011)	0.427 (0.011)	0.420 (0.011)	0.446 (0.011)
vBMD	696.27(11.95)	704.48 (10.15)	717.63 (11.24)	717.63 (5.63)	736.76(7.44)‡

*p<0.05 compared to controls, ‡p<0.06, [1]aBMD measured in g/cm², [2]vBMD measured in mg/cm³.

Table 1. Lumbar spine and femoral BMD (mean ±SE) for 17 wk old female Sprague-Dawley rats

***Disclosures: Marie Freundorfer**, None.*

SA0026

Bone Mineral Density Variation In Children Across Different Ethnic Backgrounds Is Partially Explained By Genetic Profiling. The Generation R Study. Carolina Medina-Gomez*[1], Denise H.M. Heppe[2], Karol Estrada[3], Ling Oei[4], Claudia J. Kruithof[2], Albert Hofman[5], Vincent V.W. Jaddoe[2], Andre Uitterlinden[6], Fernando Rivadeneira[4]. [1]Erasmus Medical Center, The Netherlands, [2]The Generation R Study Group, Erasmus Medical Center, Netherlands, [3]Analytic & Translational Genetics Unit, Massachusetts General Hospital, USA, [4]Erasmus University Medical Center, The Netherlands, [5]Department of Epidemiology, Erasmus Medical Center, Netherlands, [6]Rm Ee 575, Genetic Laboratory, The Netherlands

Aim: Ethnic differences in BMD variation are documented. To study genetically-determined differences in BMD in children across ethnicities, we compared total body BMD (TB-BMD) and examined the behavior of a genetic risk score (GRS), constructed from variants from 56 loci associated with BMD in adults, predicting total body BMD (TB-BMD) across children from multiple ethnic background.

Methods: We included 4,009 children from The Generation R study, a single center prospective birth cohort in Rotterdam, The Netherlands, with GWAS data and TB-BMD measured by DXA at a mean age of 6.2 years. The children come from a wide spectrum of ethnic origins including blends between continental groups. Clustering based on genetic data (using ADMIXTURE) was employed assigning children to one of three transcontinental ancestral groups: predominantly European (n=3,513), Asian (n=159) and African (n=337). Differences in TB-BMD were assessed by least-squares means using European population as reference and adjusting for age, sex, fat mass, lean mass and height. GRS consisted of the sum of BMD-increasing alleles (0,1,2) in each of the 63 genetic variants reported and analyzed across quintiles.

Results: As compared to Europeans (0.552 g/cm^2) age and sex corrected TB-BMD was higher in Africans (0.585 g/cm^2; P<1E-6) and lower in Asians (0.54 g/cm^2; P=0.002). Further adjustment for height, fat and lean mass resulted in children of both African (0.575 g/cm^2; P<1E-6) and Asian (0.559 g/cm^2;P=0.03) descent having higher BMD than Europeans (0.552 g/cm^2). Overall the GRS explained 5.2% of the variance (P<1E-6). As compared to children in the middle quintile (54% of the population; n=2,179), individuals in the highest quintile (2.6% of the population; n=106) had 0.69 SDs higher BMD (P<1E-6), while those in the lowest quintile (1.9% of the population; n=77) had 0.53 SDs (P=4E-6) lower BMD. Overrepresentation (65%) of the children of African descent was present in the two highest quintiles.

Conclusions: Ethnic differences in BMD are already evident at childhood. Apparent lower BMD in Asians is consequence of smaller skeletal frame size and adaptation to loading; correction for height, fat and lean mass results in relatively higher BMD in Asian children as compared to Europeans. Children of African descent have a higher frequency of BMD-increasing alleles. Ethnic differences in bone accrual are thus partially explained by allele frequency differences in variants from known BMD loci.

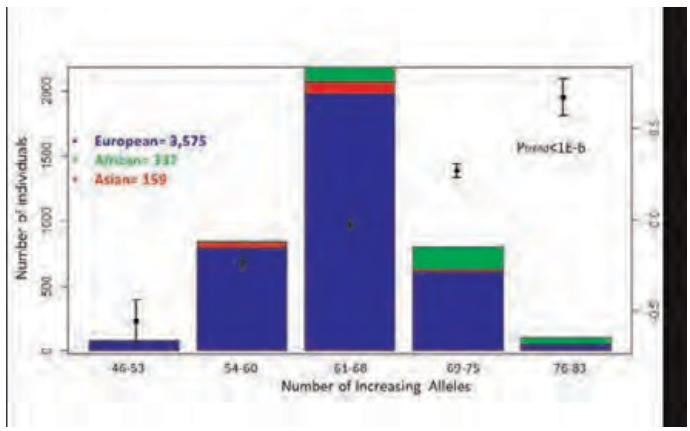

Combined effect of BMD-increasing alleles modelled in three ancestral groups

***Disclosures: Carolina Medina-Gomez**, None.*

SA0027

Does Insulin Initiate a Toxicity to the Bone Marrow Microenvironment Eliminating the Developmental Benefit of Bone Marrow Adipose Tissue?. Krista Casazza*[1], Lynae Hanks[2], Anna Newton[1], Stephenie Wallace[1]. [1]UAB, USA, [2]University of Alabama at Birmingham, USA

There is growing interest in understanding the physiology and function of adipose tissue within the bone marrow. Bone marrow adipose tissue (BMAT) is a metabolically distinct tissue from other peripheral fat depots, hypothesized to locally contribute to bone metabolism and hematopoiesis, and has been inversely associated with measures of bone strength and structure. Primarily in the long bones, BMAT replaces hematopoietic/osteogenic marrow at a rapid yet predictable and progressive rate during puberty, a well-established critical period for long-term bone health. Though a specific cue has not been elucidated, this conversion is thought to respond to hormonal trigger(s). Perturbed hormonal milieu as described in the obese state may accelerate normative conversion altering marrow composition properties, and may potentially provoke long-term consequences. The objective of this study was to evaluate the relationship between glucose and lipid metabolism and femoral BMAT in forty-six early pubertal girls ages seven to eleven years. Femoral BMAT was assessed by MRI, bone and fat mass by DXA and glucose, insulin and lipid profile by venipuncture while fasted. We observed a positive relationship between BMAT and body fat ($p=0.05$), bone mass ($p<0.001$) and fasting insulin ($p<0.05$). When the sample was stratified by adiposity using 30% body fat or BMI greater than 85th percentile as a cut-point, the relationship of BMAT with bone ($p<0.05$) and insulin ($p=0.06$) was only apparent in obese girls. Insulin, a known potent growth factor responsible for glucose handling commonly dysregulated in the obese state, may initiate toxicity within the bone marrow microenvironment eliminating the developmental benefit, provoking the pathogenesis attributed to BMAT in adulthood. While animal and human data demonstrate an inverse association between BMAT and measures of bone health, understanding the functional significance and role in skeletal maturation will be critical to better understanding pathophysiology of bone.

***Disclosures: Krista Casazza**, None.*

SA0028

Implications of Mild vs Moderate Trauma Childhood Distal Forearm Fractures for Peak Bone Mass Acquisition: The Two Faces of Growth.
Joshua Farr*[1], Sundeep Khosla[2], L. Joseph Melton[1], Elizabeth Atkinson[1], Salman Kirmani[1], Louise McCready[1], Shreyasee Amin[1]. [1]Mayo Clinic, USA, [2]Mayo Clinic College of Medicine, USA

Growth is the most opportune period to modify bone structure. We recently found that children who sustain a distal forearm fracture (DFF) due to mild, but not moderate, trauma have cortical thinning and deficits in bone microarchitecture at the radius and tibia. However, whether these skeletal deficits track into adulthood is unknown. Therefore, we used HRpQCT to examine cortical and trabecular bone parameters at the distal radius and tibia in 150 subjects (75 women; 75 men), age 20–40 yrs, who had a childhood (<18 yrs) DFF and 150 sex- and age-matched non-fracture controls. None used medications, or had diseases, affecting bone metabolism. We used the Landin classification (Acta Orthop Scand 202:1, 1983) to assign trauma levels, blind to the bone imaging results. None had a severe trauma DFF (e.g., traffic accident).

Adult women (Fig. A) and men (Fig. B) with a mild trauma (e.g., fall from standing height) DFF in childhood had significant deficits in cortical area (–10.2% and –9.2%, respectively; P<0.05) at the radius as compared to controls. Women with a mild trauma DFF in childhood also had significantly lower cortical volumetric BMD (vBMD, –1.7%; P=0.002), whereas men with a mild trauma DFF in childhood had significantly lower trabecular bone volume fraction (BV/TV, –9.0%; P=0.008) compared to controls. By contrast, adult women and men with a moderate trauma (e.g., sport-related collision) DFF in childhood both had higher radial cortical areas as compared to controls, although only the difference in men was statistically significant (+8.6%; P=0.041). Importantly, skeletal deficits in the mild trauma DFF cases were generalized, as these subjects tended to have similar changes at the tibia, as well as significantly lower DXA-derived areal BMD at the radius, lumbar spine, hip and total body regions as compared to their controls (all P<0.05).

In conclusion, a mild trauma DFF during childhood presages deficits in bone structure and density in adulthood. By contrast, as hypothesized by Parfitt ("The Two Faces of Growth: Benefits and Risks to Bone Integrity", Osteoporos Int 4:382, 1994), children who suffer a moderate trauma DFF may be paying the price of risk-taking behaviors (e.g., sports) in childhood that optimize cortical bone structure during growth. Therefore, children with a mild trauma DFF should be identified and targeted for lifestyle interventions that encourage achievement of their full skeletal genetic potential.

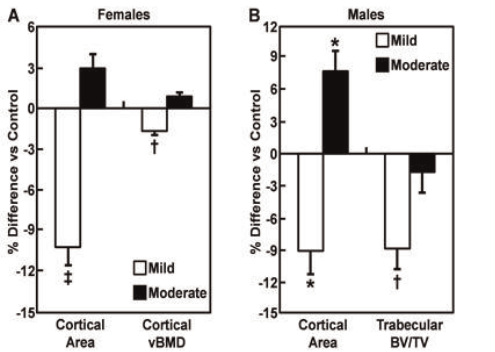

Figure

***Disclosures: Joshua Farr**, None.*

SA0029

Influence of Age and Gender on Spine Bone Density and TBS Microarchitectural Texture Parameters in Infants.
Renaud Winzenrieth*[1], Catherine Cormier[2], Silvana DiGregorio[3], Luis Del Rio[4]. [1]Med-imaps, Hôpital X. Arnozan, PTIB, Pessac, France, France, [2]AP-HP Groupe Hospitalier Cochin, France, [3]Cetir Grup Mèdic, Spain, [4]Cetir Centre Medical, Spain

Children bone knowledge is relatively sparse. This is especially true for infant and for bone microarchitecture data. We have investigated, in this study, the age-related modifications of spine microarchitectural texture, as assessed by TBS, on male and female infants during their two first years of life.

The study group was composed of 143 and 109 healthy female and male infants aged between 0 and 2 years. Height and weight Z-scores were normal for age (-0.61 and -0.65 for female; -0.62 and -0.77 for male) relative to The WHO Child Growth Standards. The areal BMD (aBMD) was assessed at spine L1-L4 using a prodigy densitometer (GE-LUNAR, USA). TBS was evaluated using TBS iNsight v2.0 (Medimaps, France). The LMS statistical method proposed by Cole and Green (Stat Med, 1992) was used to construct aBMD and TBS age-related curves for each gender using R software (v2.15.3).

Female and male infant shave the same mean age, height and weight Z-score and TBS (p>0.3) whereas female infants have higher aBMD than male (p=0.01). Before and after 12 months of age, TBS and aBMD correlations in both female and male infants were low (r^2<0.20).We have observed a first TBS decreasefrom birth to 12-15 months (for female and male infants respectively) followed by a TBS increasing without reaching the mean birth TBS value. In parallel, the aBMD always increases (see figure 1).

To date, our study is the first which has evaluated the modification of spine microarchitectural texture occurring in infants. Results obtained showed similar aBMD and TBS evolution shapes for both male and female infants. Surprisingly, TBS evolution exhibits a decreasing/increasing pattern. We can hypothesis that this pattern correspond to the infants bed-rest phase (no weight loads on the spine-> trabecular structure adaptation using minimum energy adaptation rule-> TBS decreasing) and the stand/walking phase (weight loads on spine->mechanical stress increasing -> trabecular structure positive adaptation -> TBS increasing). Further studies have to be conduct to confirm these first findings.

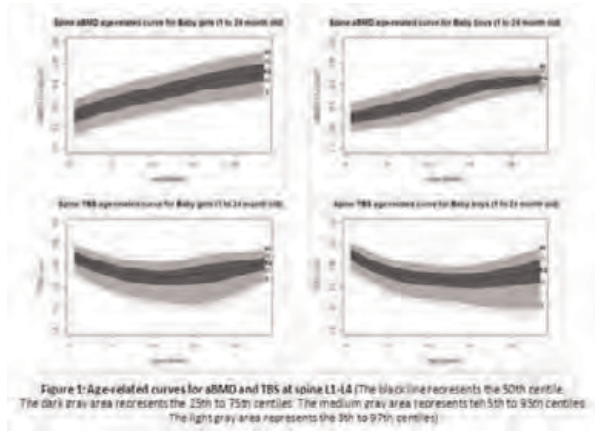

Figure 1

***Disclosures: Renaud Winzenrieth**, Med-Imaps, 3*

SA0030

Perinatal Epigenetic Marking at The CDKN2A Promoter Is Associated With Postnatal Bone Development: Results From The Southampton Women's Survey.
Nicholas Harvey*[1], Rebecca Clarke-Harris[2], Robert Murray[2], Paula Costello[2], Emma Garratt[2], Joanna Holbrook[3], Ai-Ling Teh[3], Johnny Wong[3], Shaillay Dogra[3], Sheila Barton[1], Lucy Davies[1], Hazel Inskip[1], Mark Hanson[2], Peter Gluckman[4], Cyrus Cooper[1], Keith Godfrey[5], Karen Lillycrop[2]. [1]MRC Lifecourse Epidemiology Unit, University of Southampton, United Kingdom, [2]Institute of Developmental Sciences, University of Southampton, United Kingdom, [3]Singapore Institute for Clinical Sciences, Singapore, [4]Liggins Institute, University of Auckland, & Singapore Institute for Clinical Sciences, Singapore, New Zealand, [5]MRC Lifecourse Epidemiology Unit, University of Southampton, & NIHR Southampton Biomedical Research Centre, University of Southampton & University Hospital Southampton NHS Foundation Trust, United Kingdom

We used a population-based mother-offspring cohort to investigate relationships between methylation status of the CDKN2A gene locus in umbilical cords at birth, and bone size, mineralisation and density measured by DXA in childhood.

Based on differentially methylated sites identified as having strong associations with offspring bone mass from a MeDIP-CHIP methylation array (Agilent) in 19 subjects, we used pyrosequencing to perform in-depth analysis of the methylation status of 9 CpGs within a region of CDKN2A in umbilical cords of 292 children assessed by DXA (Hologic Discovery) at 4 and 6 years old from the Southampton Women's Survey. Appropriate institutional ethics committee approval and participants' informed consent were obtained.

There was a wide variation in percentage methylation. After adjustment for age and sex, there were inverse associations between CDKN2A methylation at 5 of 9 CpG sites and bone measures in childhood (all p<0.05). At one of these sites, consistently strong inverse associations between percentage methylation and offspring whole body BA, BMC and BMD at both 4 and 6 years were observed. Thus BMC decreased by 1.0g at age 4 years and 1.8g at age 6 years (p=0.005 and 0.008 respectively) for each 1 percentage point increase in CpG methylation. Inclusion of percentage methylation at RXRA promoter sites, maternal parity, and maternal smoking, triceps skinfolds and physical activity in late pregnancy (all previously associated with offspring bone mass) in the models did not alter these relationships.

In this study, perinatal methylation status of CpG dinucleotides within the CDKN2A gene locus was inversely associated with bone size, mineral content and areal density in childhood. If replicated in other cohorts, these findings might suggest a specific role for CDKN2A in skeletal development and the potential for its use as a novel biomarker for later osteoporosis risk.

Acknowledgements: The EpiGen Consortium.

***Disclosures: Nicholas Harvey**, None.*

SA0031

Soluble Corn Fiber Increases Calcium Absorption in Free Living Adolescent Girls. Claire Macdonald-Clarke*[1], Berdine Martin[1], Corrie Whisner[2], George McCabe[1], Linda McCabe[1], Kimberly Ziarko[1], Claire Murphy[1], Connie Weaver[3]. [1]Purdue University, USA, [2]Cornell University, USA, [3]Purdue University, Dept of Nutrition Science, USA

Prebiotics have the potential to improve calcium nutrition through increasing calcium absorption which can benefit bone health. Previously, we demonstrated efficacy of Soluble Corn Fiber (SCF) in adolescent boys and girls with a 12% increase in calcium absorption after consuming 12 g fiber via SCF for 21 days compared to a control period in a crossover design using a controlled feeding metabolic balance approach (Whisner *et al* 2012). The objectives of the current study were to evaluate the dose response of 0, 10 and 20 g fiber/d via SCF supplementation on calcium absorption and biochemical bone properties in free-living adolescents. Twenty six females aged 11-14 y with habitual calcium intakes ≤ 800 mg/d and BMI <90th percentile for age, were randomized into this 3-phase, double blind, crossover study. For 4 weeks participants consumed a daily muffin and beverage containing a total of 0, 10 or 20 g fiber from PROMITOR® SCF (Tate & Lyle) followed by a 3-day clinical visit and 3-week washout phase. During the clinical visit, participants consumed a controlled basal diet containing 800 mg/d calcium, 15 g/d fiber and adequate nutrients and calories using the Harris-Benedict equation. Fractional calcium absorption was measured using a dual stable isotope method from pooled urinary Ca excretion at 12, 24, 36, and 48 hours following the test meal. Isotope enrichment was measured by ICP-MS. To determine the effects of SCF on calcium absorption over time, a mixed model was used based on sequence, ID nested within sequence, and treatment, at each 12 hour time point. Calcium absorption increased significantly, with dose ($p=0.016$) and with time ($p<0.001$), consistent with lower gut absorption. In summary, fermentable, non-digestible oligosaccharide carbohydrate SCF, given in snack products, can increase calcium absorption in free-living adolescent females. Food supplementation with SCF is well tolerated and an effective method to increase calcium absorption and bone health in populations where calcium intake is low. This study was sponsored by Tate & Lyle Health & Nutrition Sciences.

***Disclosures: Claire Macdonald-Clarke**, None.*
This study received funding from: Tate & Lyle Health & Nutrition Sciences

SA0032

The Relationship Between Intramuscular Fat and Cortical Bone Development from Age 11 to 19 Years. Natalie Glass*, Kathleen Janz, Elena Letuchy, James Torner, Trudy Burns, Julie Eichenberger Gilmore, Steven Levy. University of Iowa, USA

Purpose: Limited cross-sectional data suggest a relationship between intramuscular fat and cortical bone development. However, the direction of that relationship has varied among studies. The purpose of this study was to evaluate the longitudinal association between intramuscular fat and cortical bone development at the tibia throughout adolescence.

Methods: Iowa Bone Development Study participants who attended at least two measurement visits were included. Visits took place every 2 years from age 11 to 19 years. Cortical bone mineral density, mineral mass (BMC, mg) and area, periosteal and endosteal circumference, cortical thickness, strength-strain index (SSI, mm^3), muscle density (mg/cm^3) and muscle cross-sectional area were measured by peripheral quantitative computed tomography (Stratec XCT 2000/3000, Pforzheim, Germany) at the 66% site of the tibia. Muscle density was used to estimate intramuscular (IM) fat. Lower muscle density indicates greater IM fat. Anthropometric measurements were taken and maturity offset (years from peak height velocity) was estimated. The relationship between muscle density and cortical bone parameters was modeled using sex-specific multilevel regression models adjusted for age, limb length, muscle cross-sectional area and maturity status (pre/post peak height velocity).

Results: 249 girls and 243 boys attended at least two measurement visits. In multilevel linear regression models adjusted for covariates, muscle density was positively associated with cortical bone parameters but only reached statistical significance for BMC and SSI in girls (regression coefficient beta=15.3 ± 4.6 mm^3, $p=0.001$) and SSI in boys (beta=12.1 ± 4.9 mm^3, $p<0.05$). At age 13, this represented, for an individual with an average SSI, 3% greater SSI in girls and 2.3% greater SSI in boys in the 90th compared with the 10th percentile of muscle density. There was also a statistically significant interaction effect between muscle density and age ($p<0.001$) as well as maturity status ($p<0.01$) for BMC in girls.

Conclusions: Cortical bone strength generally increased as the amount of intramuscular fat within adjacent skeletal muscle decreased independent of muscle cross-sectional area and this relationship was sustained throughout adolescence. Because analyses controlled for differences in muscle size, these results suggest that greater fat content within muscle may not be beneficial to weight-bearing cortical bone during adolescence.

***Disclosures: Natalie Glass**, None.*

SA0033

Tracking of Bone Mass from Age 8 to 15 Years and Factors Associated with Tracking Deviations. Elena Letuchy, Julie Eichenberger Gilmore*, Kathleen Janz, Trudy Burns, James Torner, Steven Levy. University of Iowa, USA

Purpose: The purpose of this research is to determine the effects of body composition (whole body lean mass [LM] and fat mass [FM]), physical activity and health (asthma, medication use and bone fractures) on consistently high and increasing, or consistently low and decreasing hip and spine bone profiles.

Methods: DXA scans were obtained (Hologic 2000 and Hologic 4500) for 200 girls and 189 boys at baseline (age 8) and again at age 15. Measurements included bone mineral content (BMC) and density (BMD) for hip and spine, LM and FM. Translational equations were applied to account for machine differences. Minutes of daily moderate to vigorous intensity physical activity (MVPA) was measured using accelerometry (ActiGraph). Gender-specific tracking of bone outcomes was determined by correlation of residuals from models adjusted for height, weight, and scan age. Further analysis concentrated on tracking (remaining in the upper [lower] tertile) or deviation from tracking (moving to a higher [lower] tertile) for participants with consistently high [low] or increasing [decreasing] BMC/BMD, respectively. Body composition and MVPA changes were investigated as determinants of the tracking deviations. Associations with asthma, corticosteroid use and bone fractures were also explored to investigate the interrelation of health status and BMC/BMD tracking. Gender-specific logistic regression modeling was conducted for all association analyses.

Results: Residuals for all four bone outcomes demonstrated high levels of tracking during adolescence; r=0.73-0.79 for girls and 0.68-0.74 for boys in correlation analysis. Larger increases in LM and consistently high physical activity levels over time were associated with consistently high or movement to a higher tertile of BMC/BMD in both girls and boys. For example, for hip BMC OR 1.4, 95% CI (1.3, 1.6) and 1.3, 95% CI (1.2, 1.4) per 1 kg of LM increase, respectively. Greater FM increase had the opposite effect. For girls, low or relatively decreasing spine BMC was associated with bone fracture. For boys, corticosteroid use was associated with low or a relative decrease in hip and spine BMC/BMD.

Conclusion: Greater lean mass [fat mass] increase is a strong determinant of high [low] or movement to higher [lower] BMC/BMD. Physical activity and other environmental factors are also associated with the tracking of bone measures.

***Disclosures: Julie Eichenberger Gilmore**, None.*

SA0034

Disruption of Shp2 in Osteoblasts Causes Skeletal Abnormality in Mice Resembling of Human Noonan Syndrome. Jun Zheng*[1], Jay Cao[2], Kehong Ding[1], Nianlan Yang[3], Thomas Clemens[4], Mark Hamrick[1], Carlos Isales[3], Xing-Ming Shi[1]. [1]Georgia Health Sciences University, USA, [2]USDA ARS, USA, [3]Georgia Regents University, USA, [4]Johns Hopkins University, USA

Noonan syndrome (NS), characterized by skeletal malformations such as kyphosis and scoliosis, is a relatively common autosomal dominant disorder occurring between 1 in 1,000 and 1 in 2,500 children worldwide. 50% of all cases of NS are caused by mutations in the PTPN11 gene. PTPN11 encodes Src homology-2 domain-containing tyrosine phosphatase 2 (Shp2), a protein expressed ubiquitously in mammalian tissues. Shp2 gene KO is embryonic lethal, the role of Shp2 in skeletal development is not clear. We generated conditional Shp2 KO mice using Ocn2.3-Cre and we show here, for the first time, that disruption of Shp2 in osteoblasts is sufficient to cause skeleton abnormalities in mice resembling that of human NS (Fig. 1). All Shp2 cKO mice develop kyphosis and scoliosis, and a rapid reduction of body weight (-17%, $p<0.05$), at about 2.5mo of age. This phenotype manifests at 3mo of age and becomes worse thereafter. u-CT analysis of 3-mo-old femurs showed that the BV/TV, Cort. Th and Tb. N are all decreased dramatically (-50%, -44% and -29%, respectively), but the Tb.Sp is increased significantly (+46%) in Shp2 KO mice. DXA analysis of 3-mo-old femurs showed that while the BMD is decreased (-8.0%, $p<0.01$), the BMC is increased significantly (+14%, $p<0.05$) in Shp2 KO mice due to the increase in femoral size (length +8%, $p<0.01$; width +37%, $p<0.001$). Histological studies show that at 3 months of age, the growth plate of the cKO mice is markedly enlarged (distal femur: +114%; L5 vertebrae: +190%; and T5/6: +296%). While the BrdU labeling experiment showed no difference in cell proliferation between cKO and WT mice, TUNEL assays revealed a remarkable increase of apoptosis in both cortical and trabecular bones (femur, lumbar and thoracic vertebrae) in cKO mice. In line with the increased apoptosis, in vitro cell culture studies showed a significantly decreased osteogenic differentiation capacity of primary bone marrow cells from Shp2 cKO mice. To gain insight into the underlying molecular mechanisms by which Shp2 in osteoblasts regulates skeletal development, we examined the signaling pathways controlled by Shp2 and found that the level of pERK and pSTAT3 are reduced significantly in Shp2 KO osteoblasts. Together, our results have demonstrated that disruption of Shp2 signaling in osteoblasts is sufficient to cause NS, suggesting that targeting Shp2 signaling in osteoblasts is a potential therapeutic approach for correcting the skeletal abnormalities of children with NS.

***Disclosures: Jun Zheng**, None.*

SA0035

The Role of the Systemic Micro-Environment in DMD Bone Abnormalities. Nicholas Greco*[1], Johnny Huard[2], Hongshuai Li[2], Bing Wang[2], Ying Tang[2]. [1]University of Pittsburgh, USA, [2]Orthopaedic Surgery, USA

Introduction: Duchenne muscular dystrophy (DMD) is a genetic disorder causing skeletal muscle deterioration in affected children; however, there are also disturbances of osseous structure and function that have a significant impact on patient mobility and quality of life. In this study we determined whether providing a DMD animal model with a systemic milieu from a young, healthy animal through the technique of parabiosis could improve their osseous phenotype.

Methods: previous parabiotic method [1] was applied in a dystrophin/utrophin knockout (dKO) murine model of DMD [2]. In the first experiment, the parabiosis groups consisted of an old dKO-heterozygous mouse (dys-/-, utr-/+; age 12-14 mo) paired with a young mdx mouse (age 3-5 mo), while the control was a pair of old dKO-hetero mice. Bone quality was then evaluated via microCT (morphometric) and histomorphometic analysis after 5 months. In the second experiment, the groups consisted of a dKO-homozygote (dys-/-, utr-/-) mouse paired with a wild type mouse, while the control was a pair of dKO-homo mice. Two weeks after parabiosis, a tibial defect was created. The healing dynamics of the bone defect were evaluated via microCT and the content of bone marrow and hematopoietic stem cells were also compared between groups.

Results: After pairing with young mdx mice, Herovici staining and micro-CT analysis showed significantly less bone loss and greater trabeculae in the lumbar vertebrae and proximal tibia of the old dKO-hetero mice. Likewise, after pairing with wild type mice, there was a significantly increased rate of bone healing during the second and third weeks after the bone defect procedure in the dKO-homo mice (Figure 1). Furthermore, hematopoietic stem cell quantity was significantly increased with no significant difference in the bone marrow-derived stem cells in dKO-homo mice paired with wild type mice.

Discussion: Sharing of the vascular supply between an animal model with severe DMD pathology and one without disease burden as well as sharing between an aged DMD model with a young DMD model improved the osseous DMD phenotype. Furthermore, there was an increase in the hematopoietic stem cell population. This data implicates factors within the systemic milieu in the regulation of bone homeostasis, thus presenting a novel avenue to explore and improve osseous deficiencies in DMD patients.

Reference:
1. Boban et al. J Cell Physiol. 214:1, 2008
2. Isaac et al. J Orthop Res. 31:3, 2013

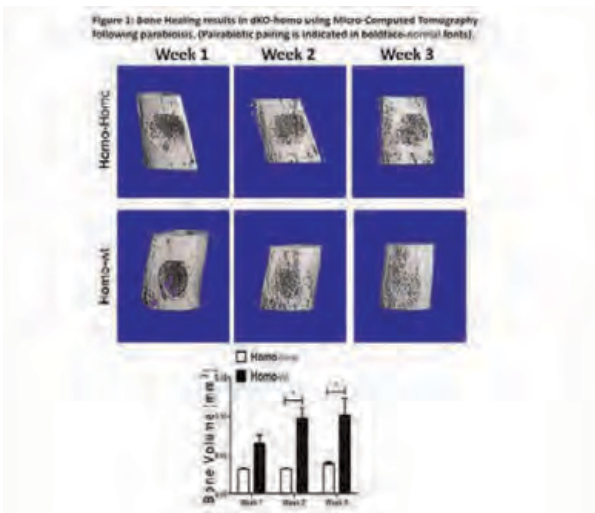

Figure 1

***Disclosures: Nicholas Greco**, None.*

SA0036

A Randomized, Double-blind, Placebo-controlled Trial of Alendronate Treatment for Fibrous Dysplasia of Bone. Alison Boyce*[1], Marilyn Kelly[2], Beth Brillante[2], Harvey Kushner[3], Shlomo Wientroub[4], Mara Riminucci[5], Paolo Bianco[5], Pamela Robey[6], Michael Collins[7]. [1]Children's National Medical Center, USA, [2]Clinical Skeletal Diseases Branch, National Institute of Dental & Craniofacial Research, National Institutes of Health, USA, [3]BioMedical Computer Research Institute, USA, [4]Dana Children's Hospital, Israel, [5]University La Sapienza, Italy, [6]National Institute of Dental & Craniofacial Research, USA, [7]National Institutes of Health, USA

Fibrous dysplasia (FD) is a benign skeletal disease caused by somatic activating mutations of $G_s\alpha$. These mutations lead to formation of abnormal and mechanically unsound bone and fibrotic tissue. Clinical sequelae include deformity, fracture, and pain. Studies in bisphosphonates have shown improvement in bone pain and inconsistent effects on FD mineralization; however interpretation has been limited by a lack of controlled trials. Objective: To determine the efficacy of oral alendronate for treatment of FD. Methods: Forty subjects with FD (15 children, median age 10, range 6-16, and 23 adults, median age 40, range 20-57) were enrolled in a randomized, double-blind placebo-controlled trial of alendronate (1 subject in each group withdrew prior to treatment). The co-primary efficacy endpoints were the change from baseline in N-telopeptide and osteocalcin at 18 months. Secondary endpoints included effects on pain, and bone mineral density at FD and non-FD sites. Subjects received drug or placebo for 6 months, followed by 6 months off, 6 months on, and 6 months off. Dosing was stratified as follows: 40 mg/day for subjects >50 kg, 20 mg for 30-50 kg, and 10 mg for 20-30 kg. Results: Compared to placebo at baseline, at 18 months alendronate use was associated with a decrease in the resorption marker N-telopeptide (p=0.001), with no significant effect on the formation marker osteocalcin (p=0.7). Subjects in the alendronate group did not show significant changes in pain as compared to placebo. At FD sites there was no significant change in bone mineral density at affected femora or humeri. At non-FD sites there was a significant increase in bone mineral density (p=0.003). Three subjects in the placebo and three in the alendronate group sustained fractures during the study period. One alendronate-treated subject with an undisclosed history of reflux developed an esophageal stricture. Conclusions: Alendronate at four times the osteoporosis dose decreased bone resorption markers, but did not improve FD mineralization or bone pain. These data support findings from previous open-label studies which demonstrated a lack of effect of bisphosphonates on FD mineralization, and suggest that oral bisphosphonates may be ineffective for FD-related bone pain.

***Disclosures: Alison Boyce**, None.*
This study received funding from: National Institutes of Health

SA0037

Exome Sequencing Reveals a Novel Nonsense Mutation in *MMP13* as a New Cause of Autosomal Recessive Metaphyseal Anadysplasia Type 1. David Weber*[1], Dong Li[1], Matthew Deardorff[1], Hakon Hakonarson[1], Michael Levine[2]. [1]The Children's Hospital of Philadelphia, University of Pennsylvania, USA, [2]Children's Hospital of Philadelphia, USA

Background: Metaphyseal anadsyplasia (MAD) is an uncommon chondrodysplasia characterized by early onset short stature, bowing of the legs, and abnormal growth plates. Because the metaphyseal dysplasia improves with age, the diagnosis of MAD is usually made retrospectively. MAD is caused by mutations in the genes encoding matrix metalloproteinase (MMP) 9 and 13. Type 1 MAD shows more severe skeletal defects and has been associated with dominant negative mutations, while the milder type 2 form is due to autosomal recessive (AR) missense mutations. Here we describe the molecular characterization of skeletal dysplasia in two brothers of Albanian descent who presented with marked short stature, metaphyseal dysplasia, and musculo-skeletal complaints. Heights of mother (-1.7 SD) and father (-1 SD) were below average; there was no history of consanguinity.

Methods: Peripheral blood mononuclear cell genomic DNA from the affected brothers was subjected to whole exome sequencing (WES) and identity by descent (IBD) analysis. The exome variant profile was considered under the assumption of an AR model based on family history. Variants with minor allele frequency>1%, found in our in-house database, or not present in the IBD regions were excluded. Validation was performed by Sanger sequencing in all family members.

Results: WES identified a homozygous C>T transition mutation in exon 2 of *MMP13* (c.325C>T) on chromosome 11q22.2 resulting in a premature stop codon (p.R109X) that is predicted to result in a markedly truncated protein. Sanger sequencing confirmed that the affected brothers were homozygous, while the parents were heterozygous. IBD analysis identified a 2.22 Mb homozygosity block around the *MMP13* gene in the affected brothers supporting a founder effect from a common ancestor.

Conclusions: We report a novel c.325C>T nonsense mutation in *MMP13* leading to an AR form of MAD type 1. The phenotype of our patients is more severe than was reported in the previous case of AR MAD type 2 due to a c.722C>A (p.H213N) missense mutation in exon 5 of *MMP13*. The mutation is in the catalytic region of MMP13 and results in a stable secreted protein; by contrast, the R109X mutation we identified occurs just after the pro-domain and is unlikely to result in a functional secreted protein. Given the mild short stature in the heterozygous parents of our patients, we hypothesize that there is a unique *MMP13* gene dosage effect on the growth plate that affects final adult height.

***Disclosures: David Weber**, None.*

SA0038

Serum Vitamin D Level can Affect the Treatment Outcome of Whole-body Vibration (WBV) for Osteopenia in Girls with Adolescent Idiopathic Scoliosis (AIS). Tsz Ping Lam*[1], Franco Tsz Fung Cheung[1], Queenie Wah Yan Mak[1], Fiona Wai Ping Yu[1], Kwong Man Lee[2], Bobby Kin Wah Ng[1], Ling Qin[3], Jack Chun Yiu Cheng[1]. [1]Department of Orthopaedics & Traumatology, The Chinese University of Hong Kong, Hong Kong, [2]Lee Hysan Clinical Research Laboratories, The Chinese University of Hong Kong, China, [3]Chinese University of Hong Kong, Hong Kong

INTRODUCTION: AIS was associated with systemic osteopenia which, apart from being an important health issue that could persist into adulthood, was also found to be a significant prognostic factor for curve progression in AIS. Our group has conducted a randomized controlled trial on WBV and reported its effect on increasing femoral neck areal bone mineral density(aBMD) mainly at the dominant leg. The objective of this study was to evaluate the role of Vit-D in moderating and enhancing the anabolic bone effect of WBV.

METHODS: This was a study nested within the randomized, controlled trial just mentioned, with enrolment of 122 skeletally mature (15-25 years old) girls with AIS and all with BMD Z-scores < -1. They were randomly allocated to the Treatment or Control group. In the Treatment group, subjects were treated by standing on a low-magnitude high-frequency WBV platform 20 mins/day, 5 days/week (acceleration 0.3g, frequency 35 Hz). Subjects in the Control group received observation alone. The study period was one year. aBMD at both femoral necks was measured with Dual-Energy X-ray Absorptiometry at baseline and at 12-month. Serum 25(OH)Vit-D level by liquid chromatography tandem mass spectrometry (LCTMS) was measured at 6-month within the treatment period.

RESULTS: The mean age was 17.8 (SD=1.5) years old and mean Cobb angle was 29.4 (SD=8.8) degrees. Subgroup analysis for those with serum 25(OH)Vit-D>40nmol/L revealed not only the positive effects of WBV were greater at both sides, treatment effects were explicitly also noted at the non-dominant leg (Table 1). In addition, the positive correlation between serum 25(OH)Vit-D and percentage increase in femoral neck aBMD that was not present in the control group was explicitly detectable in the WBV-treated group at the non-dominant leg (p=0.004) (Fig 1a and 1b).

CONCLUSIONS AND DISCUSSION: The results strongly suggested the treatment effect of WBV could be enhanced through its synergistic factor interaction with Vit-D. The study carried significant clinical implication in that Vit-D insufficiency could affect negatively the treatment outcome of WBV for osteopenia in girls with AIS.

Table 1: Percentage change in femoral neck aBMD from baseline to 12-month follow up for the Treatment and Control group

	Percentage change				
	Treatment group		Control group		
	Mean	SD	Mean	SD	p
All cases n=61(Treatment group), n=61 (Control group)					
Dominant femoral neck aBMD (g/cm^2)	2.15	4.32	0.14	3.67	0.007*
Non-dominant femoral neck aBMD (g/cm^2)	2.11	3.95	1.97	3.29	0.835
For those with serum 25(OH)Vit-D level <= 40 n=46 (Treatment group), n=42 (Control group)					
Dominant femoral neck aBMD (g/cm^2)	1.50	4.11	-0.17	3.37	0.039*
Non-dominant femoral neck aBMD (g/cm^2)	1.40	3.36	2.26	3.39	0.238
For those with serum 25(OH)Vit-D level > 40 n=15 (Treatment group), n=19 (Control group)					
Dominant femoral neck aBMD (g/cm^2)	4.14	4.48	0.83	4.28	0.035*
Non-dominant femoral neck aBMD (g/cm^2)	4.27	4.01	1.33	3.04	0.040*

(SD: standard deviation, p from Independent samples t-test, *: $p<0.05$)

Table 1

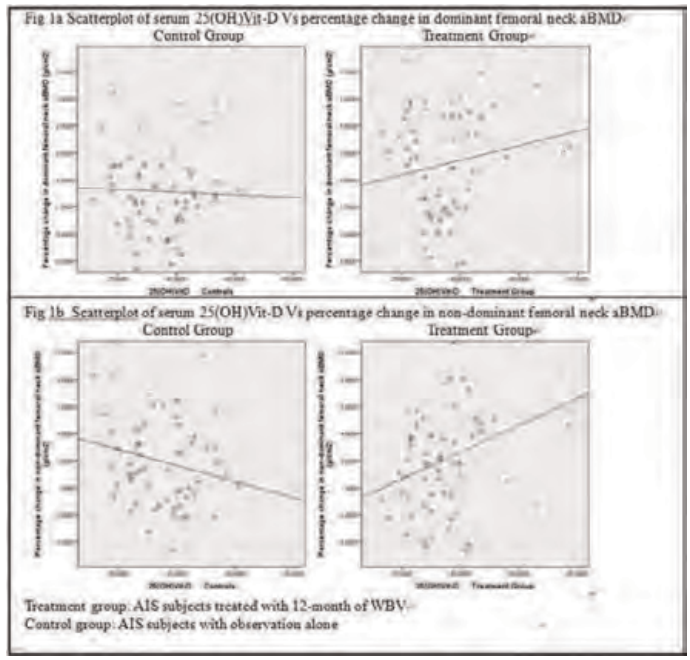

Fig 1a and 1b

***Disclosures: Tsz Ping Lam**, None.*

SA0039

Accuracy of QCT-Based Finite Element Models of the Vertebra. Amira Hussein*[1], Ginu Unnikrishnan[1], Glenn Barest[2], Elise Morgan[1]. [1]Boston University, USA, [2]Boston University Medical Center, USA

Introduction: Patient-specific quantitative computed tomography (QCT)-based finite element (FE) models of vertebrae have tremendous promise for non-invasive prediction of bone strength. However, these models have not yet been fully validated. Differences between FE-computed and experimentally measured values of vertebral strength can differ by more than two-fold, and few studies have assessed how well these models predict the deformation of the vertebra. Experimental measurements of deformation throughout the vertebral body are possible with digital volume correlation (DVC). The goal of this study was to evaluate the accuracy of QCT-based FE models generated using two common modeling approaches: voxel-based and geometry-based.

Methods: Fresh-frozen, human, L1 functional spine units (age: 80 ± 10, 2 female, 3 male) were scanned via QCT (0.3125x0.3125x0.625 mm/voxel) and then compressed axially in stepwise fashion to failure (1 mm/step applied at 0.25mm/sec). A micro-computed tomography (μCT) scan was performed at each step (37 μm/voxel). A validated DVC technique was applied to the μCT images to quantify displacements and strains throughout the vertebral body. Voxel-based FE models were generated from coarsened QCT images (hexahedral elements ~1.25mm in side length). Geometry-based FE models were created by meshing a solid geometric representation of the vertebral body (created from the QCT images) with tetrahedral elements. Linear, orthotropic elastic properties estimated from the local value of bone mineral density. Axial compression was simulated by applying displacements across the endplates that corresponded to the DVC-measured values at the yield point.

Results: Good agreement was found between the experimental and FE results in terms of the locations of large displacements and large strains (Figure 1). Greater spatial variations in strain were observed in the FE vs. experimental results.Conclusions: The two FE approaches yielded reliable and comparable results. Differences between FE and experimental strain distributions may be due to the relatively low spatial resolution of the experimental displacement fields. The non-uniformity in endplate displacements observed in the experiments suggests that FE models may benefit from accounting from factors such as intervertebral disc health that affect the load distribution across the endplate. This modification may provide even greater fidelity of QCT-based FE analyses for predicting vertebral failure.

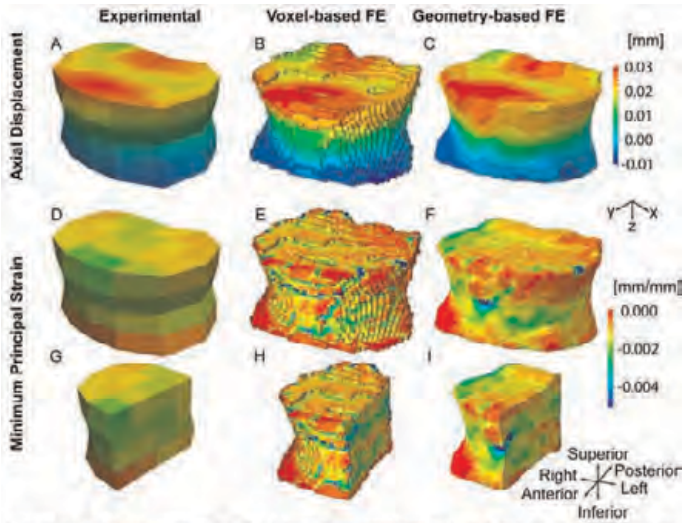

Figure 1. (A-C) Experimental and FE axial displacement fields (z-direction) at the yield point; (D-F) Experimental and FE minimum principal strain at the yield point; (G-I) mid-sagittal cut-away views of D-F

Figure 1

***Disclosures: Amira Hussein**, None.*

SA0040

Advanced Glycation End Product Accumulation in Cortical and Cancellous Bone Predicts Vertebral Load Share and Vertebral Fracture Behavior. Catalina Bravo*, Robert Hoy, Deepak Vashishth. Rensselaer Polytechnic Institute, USA

Vertebral fractures disproportionately affect the elderly and osteoporotic poulations. Computational models show the complexity of vertebral fracture and predictload sharing between cortical and cancellous bone[1]. Matrix modifications of bone collagen by Non enzymatic Glycation (NEG) vary with age in cortical and cancellous bone[2]. However, the differential accumulation of advanced glycation end products (AGEs) in vertebral cortical vs cancellous bone and its role in load sharing and eventual vertebral fracture is unknown. Using a mouse model, we conducted experimental biomechanical and biochemical analysis of whole vertebrae. Our results show for the first time that load sharing between vertebral cortical and cancellous bone varies with AGE accumulation and AGE accumulation in cortical and cancellous bone is associated with different aspects of vertebral fracture.

L1 to L3 vertebrae from 6 month old WT mice were randomly divided into three groups. Group 1 was separated into cortical and trabecular samples for biochemical analysis. AGE content was measured via fluorometric assay. Group 2 (intact) was compression tested to failure at a crosshead speed of .02 mm/s using an ELF 3200 and custom made self-aligning compression plates. Using established procedures [3], a cut was made on the cortical shell of vertebrae in Group 3 (cored) and the cancellous bone was extracted. Similar to intact, the cored vertebrae were loaded to failure. Load values at yield were compared to estimate the extent of load sharing between cortical and cancellous bone.

Our results show the load bearing by cancellous bone at yield decreased with an increase in the AGE content for cancellous bone (r= -0.94; p=0.02). In contrast, load bearing by cortical bone in vertebrae at yield increased with an increase in cortical AGE content (r=0.81; p=0.09). AGE accumulation in cortical and cancellous bone was not different (p=0.90) but was associated with different aspects of vertebral fracture. Cancellous bone AGEs predicted stiffness and yield vertebral properties ($r > 0.80$, $p < .05$). Cortical bone AGEs predicted energy to fracture (r=0.70, p=.07) (Fig 1). These finding suggest that the relative accumulation of AGEs in cortical and cancellous bone determines extent of load sharing and fracture of whole vertebrae.

[1] Eswaran et al, JBMR 2006
[2] Karim et al, Ost Intl, 2013
[3] Deal et al, 2013 Trans. ORS

Grants: NIH AG 20618, NIGMS 5T32GM067545

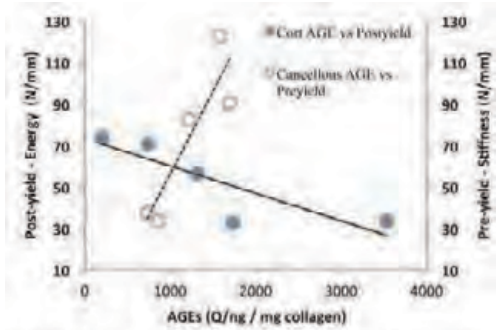

Fig 1: Pre and post yield fracture properties correlated against AGEs
Cortical bone predicts Energy to Fracture. Cancellous predicts Pre yield Stiffness and Yield properties

Fig1: PreYield and PostYield Properties vs AGEs

***Disclosures: Catalina Bravo**, None.*

SA0041

Bone Structure and Strength in Three Mouse Crosses as a Function of Strain. Mohammed Akhter*[1], John Danforth[2], Donald Kimmel[3], Josh McElwee[4], Matthew Furia[4], Brenda Pennypacker[5], Le Thi Duong[5], Robert Recker[2], Greg Opiteck[4]. [1]Creighton University Osteoporosis Research Center, USA, [2]Creighton University, USA, [3]Kimmel Consulting Services, USA, [4]Merck & Co., USA, [5]Merck Research Laboratories, USA

To identify new genes controlling bone density, structure, and strength, we undertook a series of large-scale mouse F2 crosses. The purpose is to report bone geometric and mechanical strength in femurs from young adults (age 20 weeks) of three of these F2 mouse crosses; 1) B6129 [C57BL/6Jx129S1vImJ] [N=427], 2) B6A [C57BL/6JxA/J] [N=472], and 3) B6D2 [C57BL/6JxDBA/2J] [N=282].

The distal metaphysis volume of interest (VOI) was 0.5mm inside the endocortical surface and 1.5-3.0mm proximal to the growth cartilage-metaphyseal junction. The diaphysis VOI was the central 1.5mm of the femur. Both were scanned @12µm pixel resolution (MicroCT, ScanCo40). Distal femur [df] bone volume (df.BVTV), trabecular number (df.TbN) and thickness (df.TbTh), apparent volumetric bone mineral density (df.vABMD), central femur [cf] cortical area (cf.CtAr.), and moment of inertia (cf.MOI) were determined. After MicroCT, a three point bending test of the mid-shaft (3mm/min displacement rate) was done (Instron 5534). Ultimate load (cf.ULd) was derived from the load deformation curve. Ultimate stress (cf.UStr) was calculated from cf.MOI. Data were analyzed by Kruskal-Wallis ANOVA with PLSD post-hoc testing. Multiple regression analysis was done for ULd vs. cortical geometric properties by gender and cross.

Gender differences exist within all crosses for each endpoint. df.BVTV and df.vBMD were similar in B6129 and B6A female mice, but lower in B6D2 mice. dfTbN, cf.CtAr, cf.MOI, and cf.ULd were lower in B6A and B6D2 than in B6129 mice. The strongest determinant of cf.ULd was cf.CtAr (R^2=~0.66), with occasional contribution by cf.MOI.

Significant variation exists among the crosses in bone microarchitecture and strength, as a function of mouse strain. Female B6129 mice, the basis of many genetically-altered mice, have rather low trabecular bone volume, making evaluation of further bone loss difficult. Cross-related microarchitectural differences are related to trabecular number, rather than thickness. Geometric properties are important determinants of cortical bone strength, confirming the ability of quantitative CT to improve bone strength prediction, when added to bone mass.

Variable	B6129 (223)	B6A (236)	B6D2 (140)
df.BV/TV	0.081±0.040	0.084±0.040	0.056±0.031[ab]
df.vABMD (mg/cm^3)	137.3±41.5	134.4±40.0	108.5±37.1[ab]
df.TbN (#/mm)	3.07±0.57	2.80±0.58[a]	2.54±0.5[ab]
df.TbTh (mm)	0.058±0.007	0.060±0.006	0.058±0.005
cf.ULd (N)	25.22±3.25	24.05±3.34[a]	21.71±2.83[ab]
cf.UStr (N/mm^4)	129.9±14.7	150.1±18.1[a]	133.4±13.4[b]
cf.CtAr (mm^2)	1.023±0.098	0.933±0.097[a]	0.965±0.082[ab]
cf.MOI (mm^4)	0.166±0.03	0.131±0.032[a]	0.125±0.023[ab]

[a]diff from B6129 (P<.001); [b]diff from B6A (P<.001)
Mean±SD (Number of animals))

TABLE

***Disclosures: Mohammed Akhter**, None.*

SA0042

Characterization of Bone Mineralization in a Rat Model of Chronic Kidney Disease. Hiromi Kimura-Suda*[1], Kyosuke Kanazawa[1], Sachio Kobayashi[2], Mieko Kuwahara[3], Teppei Ito[1], Naoya Sakamoto[2], Makoto Kajiwara[4], Hideyuki Yamato[3], Kuniharu Ijiro[5], Hisayoshi Yurimoto[6]. [1]Chitose Institute of Science & Technology, Japan, [2]CRIS, Hokkaido University, Japan, [3]Kureha Corporation, Japan, [4]Kureha Special Laboratory, Japan, [5]RIES, Hokkaido University, Japan, [6]Department of Natural History Science, Hokkaido University, Japan

One of the most important functions of the kidneys is to maintain calcium and phosphorus homeostasis in a body. Therefore, chronic kidney disease (CKD), which is characterized by an irreversible deterioration of kidney functions, causes bone and mineral disorder (MBD). CKD-MBD patients are characterized to reduce bone strength due to abnormal bone turnover. We have previously characterized bone quality of femur in rat 5/6 nephrectomy (5/6-Nx) model of CKD by Fourier transform infrared (FTIR) imaging, Raman spectroscopy and SEM with EDX. We have succeeded in showing that both cortical and trabecular bone in the femur of rat 5/6-Nx model of CKD was reduced, and also found that mineral/collagen matrix ratio in trabecular bone is lower than that in the cortical bone, and the center of cortical bone is calcified rather than the each side of cortical bone, namely, the endosteum side and the periosteum side. In this work, we characterize bone mineralization in CKD rat by FTIR imaging, Raman spectroscopy and isotope imaging. Thirteen-week male rats induced 4/5-nephrectomy (4/5-Nx) and sham-operated rats (Sham) were kept for 15 weeks to produce a rat model of CKD and a control, and then the CKD and the control rats were fed a diet containing at least one of stable calcium isotope (40Ca, 42Ca or 44Ca) for a week, and after that each femur in the rats was extirpated and embedded by poly (methyl methacrylate) (PMMA) to make longitudinal sections for each measurement. FTIR images of distribution of phosphate show that both cortical and trabecular bone in femur of rat 4/5-Nx model of CKD is also reduced; however, mineral/collagen matrix ratio of rat 4/5-Nx model of CKD is slightly higher than that of rat 5/6-Nx model of CKD. In isotope imaging, the stable calcium isotopes, 40Ca, 42Ca and 44Ca, were observed in both trabecular and cortical bone in the femur of the control rat and the rat of 4/5-Nx model of CKD. The stable calcium isotopes were observed in the area of low mineral to matrix ratios such as the endosteum side and the periosteum side.

***Disclosures: Hiromi Kimura-Suda**, None.*

SA0043

Characterization of Cancellous and Cortical Bone Strain in the Mouse Tibia During Axial Compression Loading Using Micro-CT Finite Element Analysis: A Sensitivity Study. Haisheng Yang*[1], Kent Butz[2], Daniel Duffy[3], Glen Niebur[4], Eric Nauman[2], Russell Main[1]. [1]Purdue University, USA, [2]School of Mechanical Engineering, Purdue University, USA, [3]Weldon School of Biomedical Engineering, Purdue University, USA, [4]The University of Notre Dame, USA

Characterization of the load-induced strain environment is critical to understanding the mechanobiological response of bone tissue to mechanical loading. Increasing use of the mouse tibial loading model in skeletal mechanobiological studies has produced a growing dataset of empirical strain measures and finite element analyses (FEA) for the tibia during compression loading. Despite this wealth of data, the strain distribution and factors affecting accurate strain assessment in cancellous tissues remain poorly understood. The objective of this study was to quantify tissue-level strain using micro-CT FEA, while considering the influence of multiple model parameters on the resulting analyses.

FE models of one representative 16wk old female C57Bl/6 tibia were created from micro-CT scans and loaded in simulated axial compression at -7N to mimic the *in vivo* tibial loading configuration. Strains in the proximal metaphyseal cancellous and midshaft cortical bone were calculated. A sensitivity analysis was performed according to Cotter's Method to evaluate the importance of 7 model parameters on the outcome strain measures: scan resolution, cancellous bone threshold, bone tissue heterogeneity, mesh refinement, element type, inclusion of the fibula, and horizontal constraint of the proximal tibia. This required 16 FE simulations for specified combinations of the lower and upper levels of each model parameter.Across all FE simulations, the range for the average longitudinal strain modeled on the medial midshaft surface exhibited good agreement with experimental strain gauge measures from the same bone (857-1998με vs. 1340με). The cut-offs for the upper 95th percentile of the minimum principal strain in the cancellous and cortical bone ranged from -2249με to -785με and -4959με to -1712με, respectively. Bone tissue heterogeneity had a strong influence on cancellous strain while cortical strain was mainly affected by the presence of the fibula and the proximal boundary conditions (Figs.1 & 2). Our results suggest that using a finer scan resolution, a cancellous-based threshold for cancellous tissues, density-based heterogeneous material properties, and inclusion of the fibula could improve the accuracy of FEA for addressing cancellous tissue-level strain environments in the mouse tibia. The validated model will be critical for relating detailed strain distributions in cancellous and cortical bone tissue in the tibia to the biological response to mechanical load.

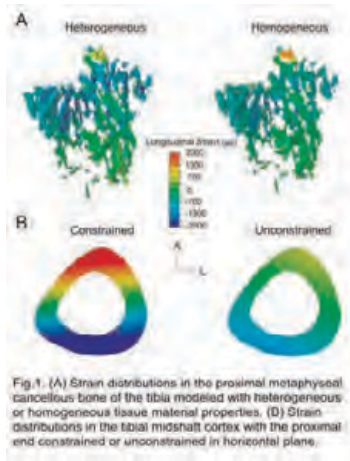

Fig.1. (A) Strain distributions in the proximal metaphyseal cancellous bone of the tibia modeled with heterogeneous or homogeneous tissue material properties. (B) Strain distributions in the tibial midshaft cortex with the proximal end constrained or unconstrained in horizontal plane.

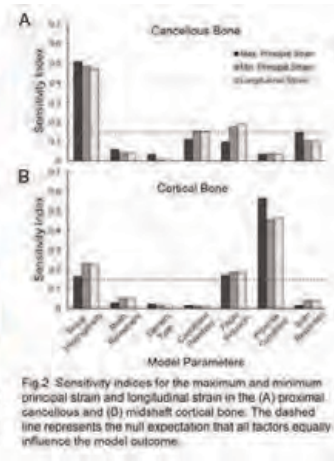

Fig.2. Sensitivity indices for the maximum and minimum principal strain and longitudinal strain in the (A) proximal cancellous and (B) midshaft cortical bone. The dashed line represents the null expectation that all factors equally influence the model outcome.

Figs.1 & 2

***Disclosures: Haisheng Yang**, None.*

SA0044

Combined effects of botulinum toxin injection and hindlimb unloading on bone and muscle. Rachel Ellman*[1], Daniel Grasso[1], Miranda Van Vliet[1], Daniel Brooks[1], Jordan Spatz[2], Christine Conlon[1], Mary Bouxsein[1]. [1]Beth Israel Deaconess Medical Center, USA, [2]Harvard-MIT Division of Health Sciences & Technology (HST), USA

Bone receives mechanical stimulation from two primary sources, muscle contractions and external gravitational loading, but the relative contribution of each to bone maintenance is not well studied. Thus, we investigated the relative effects of paralysis and unloading on changes in muscle mass, bone mass and microarchitecture.

Adult female C57Bl/6J mice (12 wks old) underwent one of the following (n=10/group): botulinum toxin A (BTX) injection, hindlimb unloading (HLU), both HLU and BTX (HLU+BTX), or no intervention. BTX-treated groups received a unilateral IM injection to the quadriceps and calf muscle groups (2U/100g total dose) three days before HLU; all mice were sacrificed after 21 days.

HLU, BTX and HLU+BTX all led to significant loss of leg muscle mass, hindlimb BMD and bone microarchitecture relative to controls, while generally the combined HLU+BTX intervention had the most detrimental changes in bone and muscle. As an example, controls gained BMD (+4.6%, $p<0.001$ vs. baseline, Figure) while HLU mice lost BMD (-4.9%, $p<0.01$). BTX-treated mice lost even more BMD in their injected leg (-19.1%, $p<0.001$), and the most severely affected were the HLU+BTX group with a -30.2% loss of BMD in their injected leg ($p<0.001$) – or 6-fold more than with HLU alone. Unexpectedly, we found a strong systemic effect of BTX affecting the uninjected (contralateral) leg that led to large BMD losses (-5.2% and -17.8% for BTX and HLU+BTX, respectively, $p<0.05$) and significant deficits relative to untreated controls in muscle mass (-25.2% BTX vs. control; -30.3% HLU+BTX vs. HLU) and trabecular bone volume (-24.0% BTX vs. control; -52.8% HLU+BTX vs. HLU). The magnitude of this indirect effect was comparable to the direct effects of BTX treatment and HLU alone. This confounding factor hinders our ability to conclude whether muscle forces or external gravitational forces contribute more to bone maintenance, but it appears that BTX-induced muscle paralysis was more detrimental to muscle and bone than hindlimb unloading. In light of this, untreated controls should be included in future BTX studies to gauge the presence of indirect effects on the uninjected leg that would otherwise go undetected. Our data indicate that BTX may affect bone through mechanisms other than direct loading.

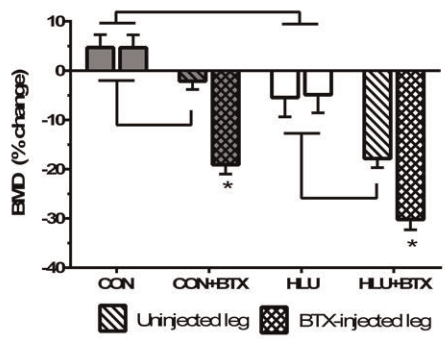

Figure

***Disclosures: Rachel Ellman**, None.*

SA0045

Comparative Study on the Effects of PTH(1-84) and Strontium Ranelate on Bone Biomechanics in Orquidectomized Rats. David Guede*[1], María Permuy[2], Marta Martín-Fernández[3], Mónica López-Peña[2], Concepción de la Piedra[3], Antonio González-Cantalapiedra[2], José R. Caeiro[4]. [1]Trabeculae, S.L., Spain, [2]Departamento de Ciencias Clínicas Veterinarias, Universidade de Santiago de Compostela, Spain, [3]Bioquímica Investigación, Instituto de Investigación Sanitaria Fundación Jiménez Díaz, Spain, [4]Servicio de Cirugía Ortopédica y Traumatología, Complexo Hospitalario Universitario de Santiago de Compostela, Spain

INTRODUCTION: Strontium ranelate (SrR) and PTH(1-84) have demonstrated their efficacy in the treatment of postmenopausal osteoporosis in experimental studies and clinical trials, being able to improve BMD and microarchitecture, significantly reducing the risk of fracture. The effects of these treatments on male osteoporosis are less well studied.

OBJECTIVES: To evaluate the effects of PTH(1-84) and SrR on bone strength in an experimental model of male osteoporosis (orchidectomized rats).

MATERIAL AND METHODS: Sixty 6-month-old male Sprague-Dawley rats were divided into 6 groups: SHAM (simulated operation); OQX (orchidectomized); OQX+PTH50 (OQX treated with PTH 50 µg/kg/day VO); OQX+PTH10 (OQX treated with PTH 10 µg/kg/day VO); OQX+SrR600 (OQX treated with strontium ranelate 600 mg/kg/day SC); and OQX+SrR250 (OQX treated with strontium ranelate 250 mg/kg/day SC). Treatments lasted 3 months (starting 6 months after orchiectomy). After sacrifice, the right femora were subjected to three-point bending mechanical testing while L5 vertebrae to compression assays.

RESULTS: In the vertebrae, orchiectomy caused a general worsening of the intrinsic and extrinsic mechanical properties, particularly noticeable in the values of work to failure and toughness. In the femurs, however, the variable showing the greatest decrease in the OQX group versus SHAM group is extrinsic stiffness.

SrR treated groups showed similar values to OQX group in all determined mechanical parameters, not being able to improve the biomechanical strength in compression or bending. The lower dose of PTH has not been able to cause remarkable changes in mechanical properties compared to OQX group. However, the dose of 50 µg of PTH increased the values of many mechanical parameters even significantly exceeding the values of SHAM group in work to failure and toughness of the lumbar vertebrae ($p<0.05$).

CONCLUSIONS: None of the tested doses of SrR neither the lower dose of PTH were able to significantly modify the negative effects of orchiectomy on mechanical properties in this model of male osteoporosis. However, the group treated with the highest dose of PTH have demonstrated the ability to considerably improve femoral and lumbar mechanical properties, reaching values even higher than SHAM group.

***Disclosures: David Guede**, None.*

SA0046

Crack Accumulation and Strength Loss in Fatigue-damaged Bone Increase when Osteoclasts Are Stimulated and Decrease when Osteoclasts Are Inhibited. Nicolas Bonnet*[1], Maude Gerbaix[2], Paul Kostenuik[3], Mike Ominsky[4], Serge Ferrari[5]. [1]University Geneva Hospital-Department of Internal Medecine Specialities, Switzerland, [2]Service of Bone Diseases, Hôpitaux Universitaires, Switzerland, [3]Amgen Inc., USA, [4]Metabolic disorders, Amgen Inc., Switzerland, [5]Geneva University Hospital & Faculty of Medicine, Switzerland

Antiresorptives consistently improve bone mass and structural strength in normally- and under-loaded bones, but concerns have been raised regarding potential effects on skeletal adaptation to fatigue loading, including damage accumulation and atypical fractures. We thus inhibited or activated osteoclasts with OPG-Fc or RANKL, respectively, and evaluated bone damage and strength after fatigue. Adult male mice were treated with RANKL (2mg/kg/d), OPG-Fc (5mg/kg 2/wk) or PBS (Veh) for 35 days. At day 28 of treatment, one tibia was fatigue loaded for 20 min by in vivo axial compression (14N, 4Hz), with animals sacrificed one week later. In another study, axial compression was applied 2 days after initiating OPG-Fc or RANKL, with treatments continuing for 28 more days (n=6 per group). We assessed cortical damage, bone mass, microarchitecture, and axial compressive strength. In mice treated 28 days before fatigue, tibial aBMD, trabecular and cortical parameters were all significantly higher with OPG-Fc and lower with RANKL, compared to Veh. One week post-fatigue, crack number per bone area (CrN/BA) was higher with RANKL ($368\pm48/mm^2$) compared to Veh ($205\pm29/mm^2$) or OPG-Fc ($233\pm47/mm^2$), both $p<0.05$. CrN/BA and total aBMD were respectively negatively and positively associated with peak load ($r^2=0.13$, $p<0.05$; $r^2=0.73$, $p<0.0001$). Tibial ultimate force was significantly higher with OPG-Fc ($29.8\pm0.8N$) and lower with RANKL ($16.9\pm1.0N$) compared to Veh ($25.8\pm1.9N$, both $p<0.05$). When fatigue was induced 2 days after initiating treatment, i.e., prior to changes in bone mass, CrN/BA at 28 days post-fatigue was higher with RANKL ($265\pm26/mm^2$) and lower with OPG-Fc ($78\pm17/mm^2$, $p<0.05$) vs Veh ($158\pm19/mm^2$; $p<0.01$). Reactive callus size was greater with 28 days of post-fatigue OPG-Fc administration ($0.098\pm0.009mm^3$) than with vehicle ($0.045\pm0.005mm^3$, $p<0.05$), and was unaffected by RANKL ($0.043\pm0.002mm^3$). Post-fatigue OPG-Fc administration led to the greatest bone strength, followed by vehicle and RANKL groups. In summary, bone mass exerted a dominant positive influence on the strength of post-fatigued bone, while cracks had a modest negative influence. OPG-Fc decreased cracks, likely due to increased bone volume and improved strength, whether or not bone mass had improved at the time of fatigue. RANKL had the opposite effects. We provide evidence that osteoclasts can weaken bone in the pre- and post-fatigue settings, possibly by compromising structure and predisposing to new cracks.

CrN/BA (1/mm²)	Veh	OPG-Fc	RANKL
28days treatments + 7days post-fatigue	205 ± 29	233 ± 47	368 ± 48
2days treatments + 7days post-fatigue	114 ± 7	119 ± 11	160 ± 12
2days treatments + 28days post-fatigue	158±19	78±17	265±26

Effects of OPG-Fc and RANKL on crack number per bone area in response to fatigue loading

***Disclosures: Nicolas Bonnet**, Amgen, 6*
This study received funding from: Amgen Inc

SA0047

Fetal Exposure to Selective Serotonin Reuptake Inhibitors has Long-Term Adverse Effect on Bone Properties in Rats. Maryam Badv*, Zahra Hosseini, Nicole De Long, Alison Holloway, Gregory Wohl. McMaster University, Canada

Introduction: Selective Serotonin Reuptake Inhibitors (SSRIs) are a class of antidepressant drugs that are commonly prescribed to treat depression during pregnancy. SSRI use during pregnancy has been associated with shorter birth length and congenital deformities including anencephaly. However, the effects of maternal SSRI use on the development of the appendicular skeleton in the offspring have not been investigated. The purpose of this study was to assess, in rats, the effects of fetal exposure to an SSRI (sertraline, Zoloft®) on postnatal bone properties.

Methods: Nulliparous female Wistar rats (200-250g) were randomly assigned to receive either SSRI (10 mg/kg/day; N=8) or vehicle (N= 5) from the confirmation of mating until parturition. Tissues were collected at necropsy from one male and one female pup per litter at 3, 7 and 26 weeks of age. Left femurs were scanned by microCT (23 µm resolution) and then loaded in three-point bending. Cross-sectional area properties were determined from microCT scans. Structural properties (maximal load, stiffness) were determined from mechanical tests. Maximal stress was calculated using areal properties. Groups were compared by two-way ANOVA with sex and treatment as the independent variables ($\alpha=0.05$).

Results: At 3 weeks of age, femurs of SSRI exposed female rats had larger cross-sectional area than controls (Fig 1). At 3 and 7 weeks of age, femurs of SSRI exposed animals had significantly lower maximal load (Fig 2), and at 7 weeks of age lower stiffness (Fig 3) compared to controls. At 3 weeks of age, femurs of SSRI exposed rats had significantly lower maximal stress (Fig 4) but there was no difference in older ages. At 26 weeks of age there was no main effect of either sex or SSRI exposure, However there was a significant interaction between sex and treatment; while femurs in the female rats from SSRI dams tended to be stronger than the controls, the femurs from males SSRI rats tended to be weaker.

Discussion: The bones of offspring born to SSRI-exposed dams are weaker compared to controls until 7 weeks of age (i.e., the peripubertal period). The fact that SSRI-exposed female offspring regain bone strength by 26 weeks of age an effect not seen in males, suggests that male bones are more susceptible to persistent effects of fetal SSRI exposure. Taken together these data indicate that fetal exposure to an SSRI antidepressant has long-term adverse effects on the development of the appendicular skeleton.

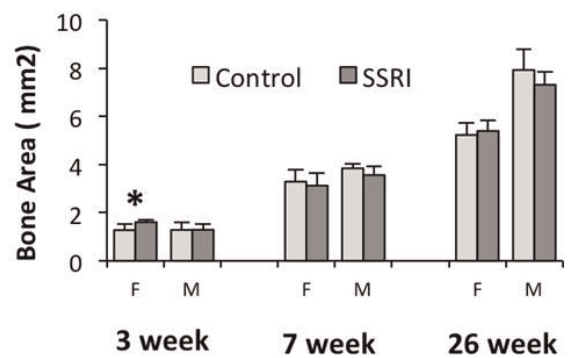

Figure 1. Cross-sectional area of femurs calculated from µCT scans. * SSRI < control ($p<0.05$).

Fig1

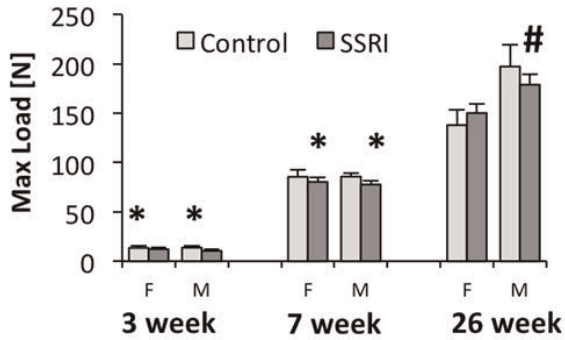

Figure 2. Maximal load of femurs tested in three point bending. * SSRI < control ($p<0.05$). # Significant sex X SSRI interaction (SSRI female vs SSRI male)

Fig2

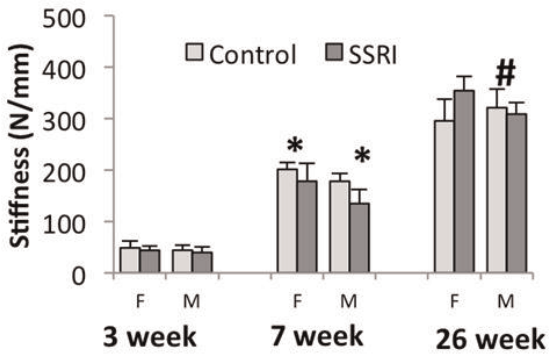

Figure 3. Stiffness of femurs tested in three point bending. * SSRI < control ($p<0.05$). # Significant sex X SSRI interaction (SSRI female vs SSRI male)

Fig3

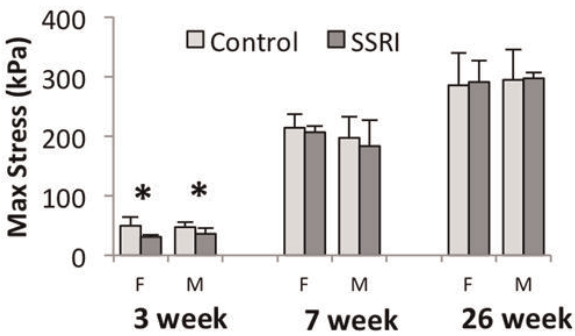

Figure 4. Maximal stress for femurs tested in three point bending. * SSRI < control ($p<0.05$).

Fig4

***Disclosures: Maryam Badv**, None.*

SA0048

High Resolution Imaging of Reference Point Indentations in Control and Type II Diabetic Bone. Connor Randall*, Kevin Hoffseth, Daniel Bridges, Henry Yang, Paul Hansma. University of California, Santa Barbara, USA

Individuals with type 2 diabetes (T2D) have an increased risk of bone fracture; however, bone mineral density is typically normal in these patients, suggesting the desirability of measuring bone fracturability directly. Reference Point Indentation has this capability. Though only a clinical study could determine if it is indeed useful for this application, we were able to obtain tibia from two 83 year old female cadavers, one with and one without T2D, to investigate with Reference Point Indentation, conventional four-point bending tests, and high resolution imaging of the induced micro-fractures.

Reference Point Indentation works by creating micro-indentations in the bone and measures the bone's ability to resist deformation. Recently Reference Point Indentation has been shown clinically to distinguish patients with and without fracture (JBMR 25: 1877, 2010). This technique does not require excised bone specimens and destructive sample preparation. Here, however, we do use excised bone specimens and destructive sample preparation to investigate microscopic mechanisms behind differences in the Bone Material Strength (BMS), a normalized measure of a bone's resistance to micro-indentations deep enough to cause microscopic fractures (Rev. Sci. Instrum. 83: 044301, 2012). BMS was measured with a new hand-held Reference Point Indentation instrument, the Osteoprobe®. The BMS of the healthy sample was 99.4 ± 4.3 (N=5), while the T2D sample had a BMS of 83.6 ± 2.2 (N=9). High resolution Scanning Electron Microscopy revealed dense collagen-fibril bridging across the microscopic fractures created by the Reference Point Indentations for the healthy bone, but not for the T2D bone. This is a toughening mechanism (Phys. Today 62: 41, 2009) that could be compromised by T2D. Four-point bending test confirmed that the toughness of the T2D sample, 3.1 mJ/mm^3, was indeed lower than the healthy sample, 5.0 mJ/mm^3. This is in qualitative agreement with a recent Reference Point Indentation study with animal models (Bone 53: 301, 2013)

The conclusion suggested from this case study is based on specimens from only two cadavers. It would, of course, be premature to conclude that this is a general characteristic of human T2D compared to control bone without further research.

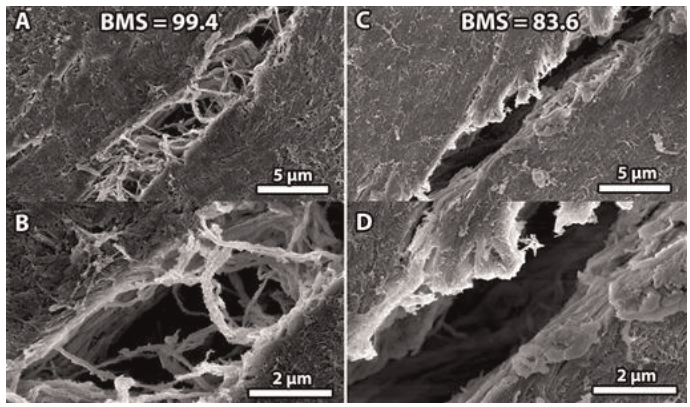

Fig 1: SEM images of a micro-fracture created by the Osteoprobe® on control (A,B) and T2D (C,D)

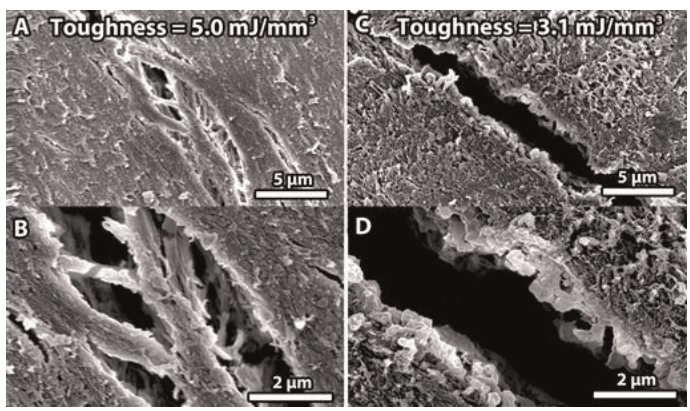

Fig 2: SEM images of a micro-fracture created by four-point bending on control (A,B) and T2D (C,D)

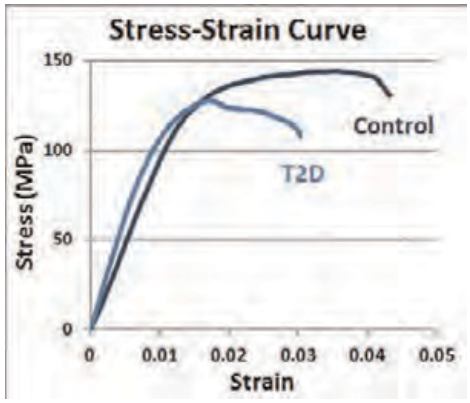

Fig 3: Stress-Strain curves of control and T2D bone

Material Properties	Control	T2D
Bone Material Strength (BMS)	99.4±4.3	83.6±2.2
Ultimate Stress (MPa)	146.4	130.3
Yield Stress (MPa)	123.7	109.3
Modulus (GPa)	9.7	12.4
Toughness (mJ/mm^3)	5.0	3.1

Table 1: Parameters obtained by the Osteoprobe® and four-point bending test

***Disclosures: Connor Randall**, Active Life Scientific, Inc., 5*

SA0049

Inhalant Lung Injury following Complex Organic Dust Extracts Results in Systemic Bone Loss and Disease in Mice. Anand Dusad*[1], Geoffery M. Thiele[2], Lynell W. Klassen[2], Angela M. Gleason[2], Christopher Bauer[2], Ted R. Mikuls[2], Michael J. Duryee[2], William W. West[2], Debra J. Romberger[2], Jill A. Poole[2]. [1]University of Nebraska Medical Center, USA, [2]UNMC, USA

Purpose. Skeletal health consequences associated with chronic inflammatory respiratory diseases, particularly chronic obstructive pulmonary disease (COPD), contribute to overall disease morbidity. Agriculture environmental exposures induce significant airway diseases including COPD. However, animal models to understand inhalant exposures-induced lung injury and bone disease have not been described.

Methods. Male C57BL/6 mice (6-8week old) were exposed to repetitive intranasal inhalation of sterile saline (PBS), complex organic dust extracts (ODE, 12.5%), lipopolysaccharide (LPS, 100 ng) and peptidoglycan (PGN, 100µg). Mice were treated daily for 3 weeks and euthanized 24 hours following the final exposure. Right hind limbs were collected for micro-CT and histology to analyze bone quantity and quality parameters. Analysis was focused on the trabecular bone of distal calcaneus. Whole lungs were also excised, inflated to preserve architecture and semi-quantitatively assessed for the degree of inflammation, as per published scoring system.

Results. As shown in Table 1, three weeks of repetitive ODE, LPS and PGN inhalation exposure lead to a significant loss of bone mineral density and trabecular bone volume fraction along with deteriorating microarchitecture changes in the trabecular bone as compared to saline control animals (Figure 1). Torsional resistance was also significantly reduced in these groups as compared to saline. Findings were not secondary to animal distress, and not entirely dependent upon the degree of induced lung parenchymal inflammation. Repetitive ODE and PGN treatment resulted in significant increases, while LPS treatment showed subtle but non-significant increase in all inflammatory parameters, compared to saline treated animals (Figure 2).

Conclusions. Overall this information suggests that inhalation of varying microbial motifs might be impacting lung (localized) versus systemic consequences differently. This animal model might substantially contribute to understanding mechanisms and evaluate therapeutics associated with adverse skeletal health consequences following chronic airway injury and can also be expanded to include other environmental exposure agents that might affect skeletal health. Future lines of epidemiologic research might be needed to determine links between occupational exposures and bone loss or fractures.

Table 1. Quantitative overview of bone loss using micro-CT

Parameter	Saline (n=3)	ODE (n=4)	LPS (n=4)	PGN (n=4)	ANOVA (*p*)
Bone mineral density (BMD, g/mm^3)	0.63 ± 0.03	0.48 ± 0.04 *	0.43 ± 0.02 * #	0.53 ± 0.06 *	0.000
Percent bone volume (BV/TV, %)	51.38 ± 2.54	38.40 ± 2.80 *	34.65 ± 1.86 * #	43.50 ± 5.46 *	0.000
Specific bone surface (BS/BV, mm^{-1})	39.95 ± 4.13	48.07 ± 4.21	52.76 ± 1.26 * #	43.79 ± 7.57	0.027
Trabecular pattern factor (Tb Pf, mm^{-1})	-0.83 ± 1.93	4.75 ± 0.20 *	4.75 ± 1.92 *	2.81 ± 2.57 *	0.008
Structural model index (SMI)	0.53 ± 0.27	1.09 ± 0.07 *	0.95 ± 0.15 *	0.96 ± 0.22 *	0.012
Trabecular thickness (Tb Th, mm)	0.091 ± 0.007	0.080 ± 0.008	0.073 ± 0.002 * #	0.087 ± 0.011	0.042
Trabecular number (Tb N, mm^{-1})	5.64 ± 0.16	4.76 ± 0.19 *	4.73 ± 0.26 *	5.01 ± 0.40 *	0.005
Trabecular separation (Tb Sp, mm)	0.11 ± 0.007	0.13 ± 0.005	0.12 ± 0.004	0.12 ± 0.014	0.094
Polar moment of inertia (MMI, mm^4)	0.0030 ± 0.00010	0.0020 ± 0.00017 *	0.0017 ± 0.00008 * #	0.0022 ± 0.00027 *	0.000

Table 1. *, #, & represents statistical significance ($p < 0.05$) from saline, PGN and ODE, respectively; using LSD as post-hoc for multiple comparisons within the groups. Data represented as mean ± SD.

Table 1

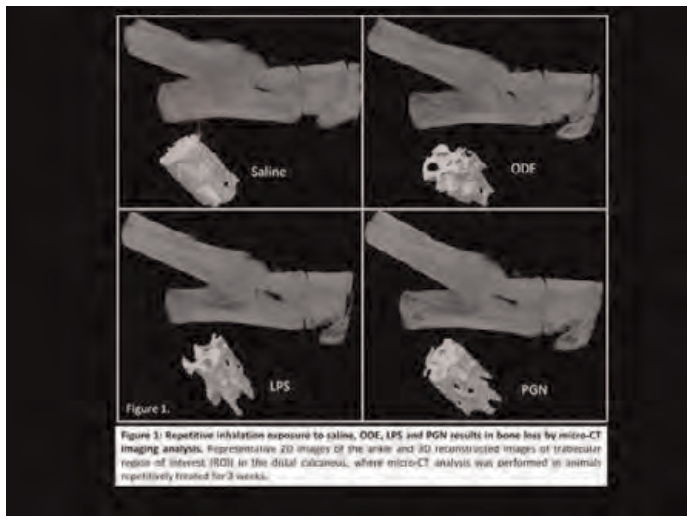

Figure 1: Repetitive inhalation exposure to saline, ODE, LPS and PGN results in bone loss by micro-CT imaging analysis. Representative 2D images of the ankle and 3D reconstructed images of trabecular region of interest (ROI) in the distal calcaneus, where micro-CT analysis was performed in animals repetitively treated for 3 weeks.

Figure 1

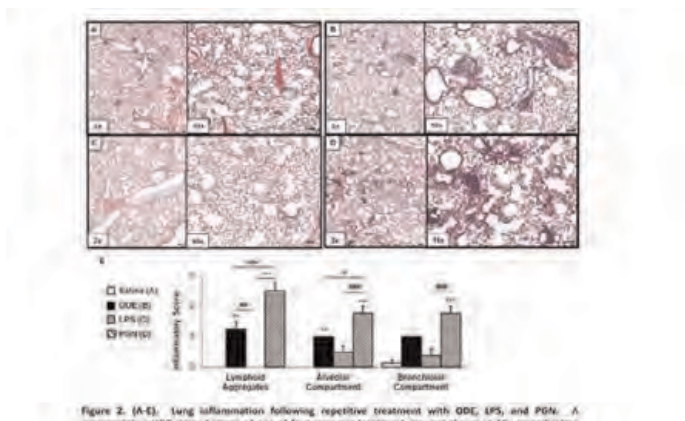

Figure 2: (A-E). Lung inflammation following repetitive treatment with ODE, LPS, and PGN. A representative H&E stained image of one of four mice per treatment group is shown at 10× magnification (A-D). E. Mean semiquantitative distribution of inflammatory score of Lungs in mice from different groups. Error bars represent SE. Statistical significance differences denoted by asterisks (*p<0.05, **p<0.01, ***p<0.001) compared to saline. #p<0.05, ##p<0.01, ###p<0.001 denotes significant differences between groups as indicated. One-way ANOVA with Tukey's post-hoc test comparison. Unit scale represents 50µm.

Figure 2

***Disclosures: Anand Dusad**, None.*

SA0050

Life-long Western Style Diet has Greater Adverse Affects on Cancellous Bone in Adult Female Wistar Rats Compared to Male Rats. Cheryl Druchok*, Alison Holloway, Andrew Don-Wauchope, Gregory Wohl. McMaster University, Canada

Introduction: A high-fat diet has been shown to adversely affect bone properties in rats, but most of these dietary interventions have been short-term. Generally, in humans, poor dietary habits occur over a period of time, they are not short-term insults. The purpose of this study was to examine cortical and cancellous bone properties in rats fed a life-long Western style diet (HF) or normal control (NC) diet.

Methods: At weaning (3 weeks of age), male and female Wistar rats were randomly assigned to receive a NC diet (NC–17% fat; N=8 male, 11 female) or HF diet (HF–41% fat; N=10 male, 9 female) until termination (39 weeks of age). Post-mortem, femoral cross-sectional area properties were determined by microCT. Femurs were loaded in three-point bending, to failure, to determine mechanical properties. L6 vertebrae were scanned by micro-CT to determine trabecular bone volume (BV/TV), trabecular number (Tb.N), thickness (Tb.Th) and spacing (Tb.Sp.).

Results: Body mass was significantly greater in HF males beginning at 14 weeks and females at 4 weeks compared to NC ($p < 0.05$) (Fig. 1). Cross-sectional area properties (bone area, moment of inertia) of the femoral mid-diaphysis were significantly greater in HF femurs vs. NC, for both sexes ($p < 0.05$). The HF diet did not adversely affect cortical bone mechanical properties (maximal load, bending stiffness, deformation and energy) ($p > 0.05$) in males. The only difference in females was significantly greater bending stiffness in HF femurs vs. NC ($p < 0.05$). Elastic modulus, calculated from deformation data, did not differ between HF and NC femurs ($p > 0.05$) for either sex. Female HF L6 vertebrae had a significantly lower BV/TV and Tb.N compared to NC ($p < 0.05$). There were no differences between male HF and NC vertebrae ($p > 0.05$).

Conclusions: Based on these data, a life-long Western style diet does not appear to adversely affect cortical bone mechanical properties in male or female rats, but it does diminish cancellous bone properties in females. It is not surprising that the HF diet affects cancellous bone, as it is more responsive to diet interventions than cortical bone. These results suggest that female rats are more sensitive to a HF diet than male rats over a life-long exposure and further work is required to elucidate the mechanisms that are involved.

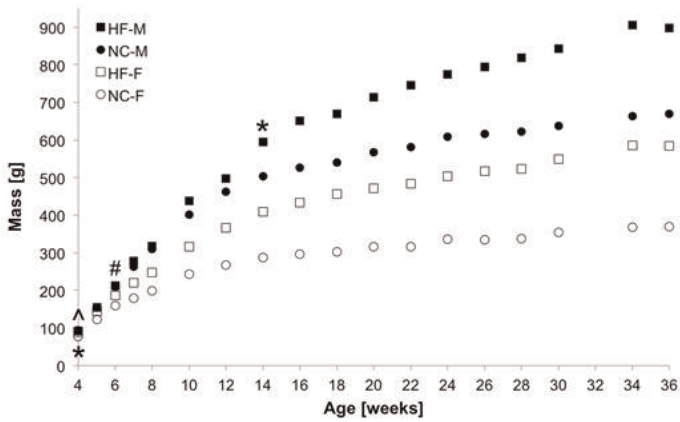

Figure 1. Body mass (g) over 36 weeks. Body mass was significantly greater in HF males beginning at 14 weeks (*p = 0.004) and females at 4 weeks (*p = 0.029) compared to NC. The males had significantly greater body masses than the females beginning at 4 weeks for NC (^p = 0.027) and at 6 weeks for HF (#p = 0.036).

Figure 1

Table 1. Cortical and cancellous bone properties (mean ± SD).

	Male		Female	
	NC (n=8)	HF (n=8)	NC (n=11)	HF (n=8)
XSA (mm²)	9.4 ± 0.7	[a] 10.5 ± 0.9	[b] 7.0 ± 0.5	[a,b] 7. 7 ± 0.8
Maximal Load (N)	257 ± 21	273 ± 30	[b] 189 ± 13	[b] 204 ± 23
Bending Stiffness (N/mm)	873 ± 112	991 ± 112	[b] 638 ± 68	[a,b] 713 ± 54
Calculated Elastic Modulus (GPa)	3.3 ± 0.8	2.8 ± 0.8	3.8 ± 0.5	3.5 ± 0.8
BV/TV (%)	22.4 ± 2.4	21.3 ± 2.3	[b] 29.8 ± 2.6	[a,b] 26.4 ± 2.4
Tb.Th (μm)	12.3 ± 0.7	12.5 ± 0.4	[b] 11.6 ± 0.4	[b] 11.2 ± 0.6
Tb.Sp (μm)	46.2 ± 3.4	48.2 ± 4.5	[b] 38.8 ± 15.0	[b] 39.9 ± 4.0
Tb.N (1/μm)	0.018 ± 0.001	0.017 ± 0.002	[b] 0.026 ± 0.002	[a,b] 0.024 ± 0.002

[a] Significant differences between diet groups (p < 0.05).
[b] Significant differences between male and female for same diet (p < 0.05).

Table 1

***Disclosures: Cheryl Druchok**, None.*

SA0051

Reference Point Indentation Detects Changes in Rat Bone Induced by In Vitro Sodium Fluoride Incubation. Lamya Karim*, Mamadou Diallo, Mary Bouxsein. Beth Israel Deaconess Medical Center, USA

The mechanical behavior of whole bone is determined by its mass, geometry, and tissue mechanical properties. Assessment of cortical bone tissue mechanical properties is now possible by in vivo and ex vivo reference point indentation (RPI), which measures cortical bone indentation properties resulting from cyclic loading. Our goal was to determine the ability of RPI and whole bone testing to detect changes in rat cortical bone tissue mechanical properties induced by in vitro sodium fluoride (NaF) incubation, which alters the physico-chemical structure of bone mineral.

Forty-two ulnae from adult rats were randomly divided into 5 groups (vehicle, 0.05M NaF, 0.25M NaF, 0.75M NaF, 1.5M NaF). Bones were washed in a detergent solution to remove organic barriers to ion exchange and incubated in respective treatment solutions (12hrs, 23℃). Cortical tissue mineral density (TMD) and geometry at the mid-diaphysis were determined by microCT. RPI was performed on the posterior surface of the distal diaphysis (9N, 2Hz, 10 cycles), and then bones were tested in 3-point bending until failure to assess stiffness and failure load. MicroCT data were used to compute apparent elastic modulus.

NaF-treated bones had significantly greater creep indentation distance (CID) and total indentation distance (TID) than vehicle treated bones ($p<0.05$). Specifically, TID increased with NaF dose until a plateau at 0.75M (Fig 1). Whole bone apparent elastic modulus, stiffness, and maximum load were also lower in NaF treated bones than in vehicle treated bones ($p<0.05$), with values decreasing with increasing NaF dose until a plateau at 0.75M (Fig 1). CID and TID were negatively correlated ($p<0.01$) with apparent elastic modulus (r= -0.68 and r= -0.73), stiffness (r= -0.50 and r= -0.61), and maximum load (r= -0.57 and r= -0.65), respectively. TID was independent of cortical TMD, but CID was negatively correlated with TMD (r=-0.27, p=0.09).

In conclusion, in vitro exposure to NaF dose-dependently led to reduced whole bone and tissue-level mechanical properties, as seen by higher indentation distances. Indentation distances correlated moderately with several whole bone mechanical properties. These results suggest that RPI can detect physico-chemical changes in cortical bone tissue that have a deleterious effect on mechanical behavior and that are independent of bone remodeling status.

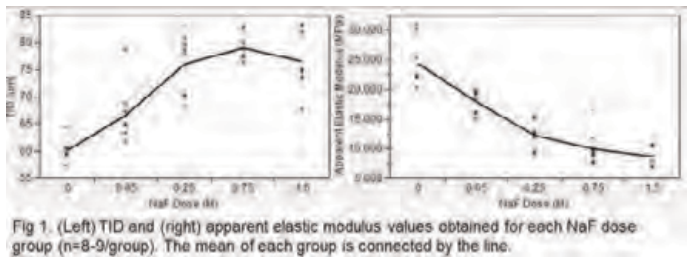

Fig 1. (Left) TID and (right) apparent elastic modulus values obtained for each NaF dose group (n=8-9/group). The mean of each group is connected by the line.

Figure 1

***Disclosures: Lamya Karim**, None.*

SA0052

Relationships between Cortical Bone Quality and Serum FGF23 in Growing Mice Challenged by Low Calcium and High Fructose in the Diet. Edek Williams*[1], Veronique Douard[1], Devendra Bajaj[2], Yves Sabbagh[3], Ronaldo Ferraris[1], JC Fritton[1]. [1]Rutgers/NJMS, USA, [2]NJMS, USA, [3]Genzyme, A Sanofi Company, USA

Serum levels of calcium, phosphate and $1,25(OH)_2$ Vitamin D_3 ($1,25(OH)_2D_3$) have long been known to affect fracture risk. More recently, fibroblast growth factor 23 (FGF23), produced primarily by osteoblasts and osteocytes, has demonstrated potent regulation of phosphate and $1,25(OH)_2D_3$ homeostasis [1]. The intake of these minerals and synthesis of these hormones have changed along with the Western diet. Fructose intake, in particular, has increased 10 fold over the past 30 years. Few studies have investigated the effects of fructose on bone growth [2]. To study these effects, thirty-six, 3-week-old C57BL/6 mice (n=9/group) were fed a combination of normal-calcium (0.5%) / low-calcium (0.02%) and glucose (43%) / fructose (43%) diets for 5 weeks. Humerii were tested in 3-point bending (Bose ElectroForce LM1 TestBench) and femurs were scanned for bone mineral density (Skyscan 1172 μCT), sectioned (Buehler 5000) and imaged for histomorphometry (Nikon A1 Confocal). Measured whole bone and calculated tissue-level mechanical properties were reduced with the calcium-deficient diet (ultimate strength: -40%, elastic modulus: -50%, $p<0.01$). FGF23 was positively correlated with stiffness for both glucose-fed and fructose-fed ($R^2=0.44$) groups. However, the positive correlation between FGF23 and bone tissue mineral density in glucose-fed mice ($R^2=0.52$; $p<0.05$) was not observed in the fructose-fed mice ($R^2=0.12$; ns). Several pathological conditions involving disruption of bone mineralization may be related to inappropriate, fructose-induced increases of FGF23 that reduce synthesis of $1,25(OH)_2D_3$, eventually decreasing intestinal calcium uptake [3]. Our next steps will determine if the dietary effects of fructose and calcium on FGF23 during bone growth are direct and regulated at the individual cell level or influenced by osteocyte density. By challenging mice with a calcium-deficient, fructose-excessive diet, we uncovered surprising relationships between serum levels of

FGF23, and the mineral quality of cortical bone. Following up on this work may lead to better serum readouts for bone quality during growth that include FGF23.

[1] Lu et al. Curr Osteoporos Rep 9:103, 2011. [2]Tsanzi et al. Bone 42:960, 2008.[3] Douard et al. FASEB J 26:707, 2012.

***Disclosures: Edek Williams**, None.*

SA0053

Running decreases marrow adipose tissue in chow and high fat fed mice. Maya Styner*[1], Sanjay Kadari[1], Kornelia Galior[2], Gunes Uzer[3], William Thompson[3], Natasha Case[1], Zhihui Xie[3], Buer Sen[4], Andrew Romaine[5], Martin Styner[5], Gabriel Pagnotti[6], Clinton Rubin[7], Mark Horowitz[8], Janet Rubin[1]. [1]University of North Carolina, Chapel Hill, School of Medicine, USA, [2]UNC-CH School of Medicine, USA, [3]University of North Carolina, USA, [4]University of North Carolina At Chapel Hill, USA, [5]University of North Carolina, departments of computer science & psychiatry, USA, [6]Stony Brook University, USA, [7]State University of New York at Stony Brook, USA, [8]Yale University School of Medicine, USA

The contribution of marrow adipose tissue (MAT) to states of low (osteoporosis, anorexia) and high bone mass (obesity) is unknown. A challenge in understanding the MAT: Bone relationship has been the quantification of marrow fat. We sought to measure volumetric MAT in both chow-fed and high fat diet (HFD)-fed mice treated with an exercise intervention. We hypothesized that MAT would increase with HFD and would decrease with running. 8-wk old female C57BL/6 mice were chow or HFD fed and divided into ± exercise groups consisting of voluntary access to running wheels (n= 5/group). Femoral MAT was quantified after infusing the lipid binder osmium tetroxide to assess osmium mm^3/bone volume by μCT with a volumetric semi-automated approach; the method employed rigid co-alignment, regional bone masks and normalization for total bone volume. Perigonadal fat pad weight was normalized to body weight. Bone quantity was assessed via tibial μCT. After 6 wk, weights of HFD and chow fed mice were similar, but perigonadal fat pads were 30% larger in HFD (p=0.005). Chow and HFD mice ran equivalent distances and times/day (11 km/320min). Running did not alter perigonadal fat within diet groups. In chow-runners compared with non-runners, distal femoral MAT was 118% less (p=0.036, quantified as % osmium, see Figure 1). In HFD, MAT was 62% greater than in chow fed (p=0.002, see Figure 1). Despite the significantly increased MAT due to HFD, running was associated with 122% less MAT as compared with HFD non-runners (p=0.018, see Figure 1). Triglyceride/femur protein correlated with volumetric osmium data for MAT. Bone quantity inversely correlated to MAT: Trabecular BV/TV and Ct.Th were higher in chow-run compared with nonrunners (27% and 13%, p=0.01 for both). HFD had lower trabecular BV/TV (p=ns) and showed reduction in Ct.Th of 8% compared to chow fed mice (p=0.004). HFD-runners had trabecular BV/TV that was 32% greater than HFD-nonrunners (p=0.01). There was a trend for greater cortical bone in HFD runners compared with nonrunners. In conclusion, applying a novel method for quantification of MAT that used osmium labeling along with volumetric μCT image analysis, we find that MAT is meaningfully increased in the setting of HFD, prior to onset of obesity. Distinct from white adipose tissue, MAT is highly sensitive to 6wk of running exercise in both chow and HFD-fed mice. As such, running exercise enhances the reciprocal relationship between MAT and bone quantity.

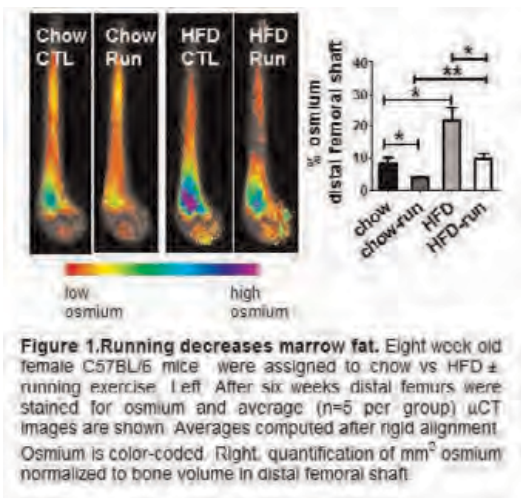

Figure 1.Running decreases marrow fat. Eight week old female C57BL/6 mice were assigned to chow vs HFD ± running exercise. Left: After six weeks distal femurs were stained for osmium and average (n=5 per group) μCT images are shown. Averages computed after rigid alignment. Osmium is color-coded. Right: quantification of mm^3 osmium normalized to bone volume in distal femoral shaft.

Figure 1

***Disclosures: Maya Styner**, None.*

SA0054

Small-angle X-ray Scattering Analysis of Bone Mineral in a Type 2 Diabetes Mouse Model. Silvia Pabisch*[1], Tsuguno Yamaguchi[2], Yasushi Koike[2], Shoko Tanaka[2], Shinsuke Kataoka[2], Wolfgang Wagermaier[3], Richard Weinkamer[3], Michiaki Murakoshi[2], Peter Fratzl[4]. [1]Max Planck Institute of Colloids & Interfaces, Potsdam, Germany, [2]Life Science Research Laboratories, LION Corporation, Japan, [3]Max Planck Institute of Colloids & Interfaces, Department of Biomaterials, Germany, [4]Max Planck Institute of Colloids & Interfaces, Germany

Metabolic diseases may influence bone formation and resorption processes, thereby reducing the mechanical performance of the material, which is known to crucially depend on the amount, size and distribution of mineral particles in the organic matrix. In this study, we investigate thickness (T-parameter) and degree of alignment (rho-parameter) of mineral particles in bone of a mouse model for type 2 diabetes mellitus (T2DM) using small-angle scattering of x-rays and synchrotron radiation. Resin-embedded bone sections from femur of 5, 15 and 22 weeks old animals as well as mandible (22 weeks old animals) were obtained from obese diabetes KKAy mice, as well as from C57BL/6 controls. Mineral particles were characterized at multiple sites within the femur and the mandible. For the latter, scans with 30 μm resolution (beam- and stepsize) were made to study the dependence of alveolar bone mineral on the distance from tooth cementum. Both T and rho were found to increase with age in the femoral cortex with a tendency for a lower rho in the KKAy mice. There was also a variation of T inside the cortex, with generally larger values on the periosteal side. In alveolar bone, there was an interesting gradient in mineral characteristics, where T decreases from both the medial and the lateral sides towards the tooth. Close to cementum, the mineral particles in alveolar bone were generally much thinner than in dentin. This could probably be related to the high turnover rate in alveolar bone, as compared to dentin which is not remodeled. Indeed, T is known to increase with time, once the mineralized tissue is laid down, so that younger bone packets have generally smaller T-values. In conclusion we find that mineral characteristics vary strongly between bone sites in both KKAy mice and controls, with a tendency for less well aligned tissue in the cortices of the KKAy mouse bones.

***Disclosures: Silvia Pabisch**, LION Corporation, 6*
This study received funding from: Life Science Research Laboratories, LION Corporation, Japan

SA0055

Studying bone as a complex adaptive system may help identify QTLs that regulate strength. Lauren M Smith*[1], Erin M.R. Bigelow[1], Bonnie T Nolan[1], Meghan Faillace[2], Joseph H Nadeau[3], Karl Jepsen[1]. [1]University of Michigan, USA, [2]GE Inspection Technologies, USA, [3]Pacific Northwest Diabetes Reasearch Institute, USA

Identifying fracture susceptibility genes is important for the early diagnosis of at-risk individuals and for identifying novel treatment pathways. The complex adaptive nature of bone poses a significant challenge to identifying QTLs regulating bone strength, because genetic perturbations affecting one trait often lead to coordinated changes in other traits. If the coordination is adequate then strength is maintained despite altered bone traits. In contrast, QTLs or genetic perturbations that alter the system's ability to compensate are postulated to lead to reduced bone strength. Our goal is to identify these QTLs that impact bone strength by acting through the functional adaptation process. We phenotyped 16 week old male C57BL6/J – $Chr^{A/J}$ / NaJ, chromosome substitution strains (CSS), which is a panel of inbred strains where each B6 chromosome was replaced by an intact A/J chromosome. We examined 20 strains; 19 autosomal and the X substitutions (n>10/strain). Our prior work established a predictable pattern in the way cortical area (Ct.Ar) and tissue-mineral density (TMD) functionally covary relative to the natural variation in bone robustness (total area/bone length). Total area (Tt.Ar), Ct.Ar and TMD were analyzed for each strain using nanoCT (8μm). Whole bone stiffness, max load and post-yield deflection were assessed from 4-point bending tests. We identified 7 strains that showed no effect on strength, morphology or TMD (CSS-7, 9, 11, 13, 14, 16 and X); 6 strains with significantly ($p<0.05$ per GLM ANOVA, body size as a covariate) altered morphology and/or TMD but not altered strength (CSS-4, 5, 8, 17, 18 and 19); 5 strains with significantly altered morphology and/or TMD but with decreased strength (CSS-1, 2, 10, 12 and 15); and 2 stains with decreased strength but not altered morphology or TMD (CSS-3 and 6). The magnitude of the CSS with functional changes was significant, showing decreases in stiffness ranging from 14.1-26.6% and decreases in max load ranging from 9.9-16.9% compared to the B6 control. This systems analysis identified multiple biomechanical pathways linking genetic perturbations with altered bone strength. Thus, knowledge of how bone traits functionally interact may improve our ability to identify fracture susceptibility genes. These results caution against the indiscriminate use of single traits in GWAS, as genetic perturbations affecting one trait are often associated with coordinated changes in other traits to maintain strength.

***Disclosures: Lauren M Smith**, None.*

SA0056

The Effects of Age, Weight and Femoral Shape on Cortical Thickness and Mass of the Hip. Graham Treece*, Andrew Gee, Tom Turmezei, Kenneth Poole. University of Cambridge, United Kingdom

Several studies have linked local properties of the cortex, particularly thickness, to fracture risk (Johannesdottir, Bone 2011; Yang, JBMR 2012). It is also clear that bone strengthening drugs have localised effects on the femur (Poole, PLoS1 2011). Recent developments in image processing allow accurate estimates of cortical thickness down to 0.3mm (Treece, Med Image Anal 2010, 2012). However, interpretation of the resulting data requires an improved understanding of the effects of other covariates on such data.

In this study, we determine how a priori selected covariates are predictive of cortical thickness and mass. We have previously investigated the effect of age, weight and osteophytes (Turmezei, Insights Imaging 2013): here, the explanatory variables we examine are subject age and weight, and femur size and shape. We analysed QCT data from 268 women, aged 53 to 98 years and weight 40 to 103 kg, from two studies conducted at two sites. Combining studies in this manner increases the significance of the results, provided we allow for site as a confounding variable. After spatially aligning the cortical data onto a canonical model, we use statistical parametric mapping as implemented in the SurfStat package (Worsley, NeuroImage 2009) to analyse the results. The generalized linear model for cortical thickness or mass is 1 + age + weight + site + s1 + s2 + s3 + s4 + s5, where s1-s5 are the first five modes of shape variation derived from a statistical analysis of a much larger population. The results for age, weight and shape modes 1 (size) and 3 (head-neck angle) are shown in Figure 1.

Age (approx -1% per year) and weight (approx +0.5% per kg) are predictive of cortical properties over significant areas of the femur. There are also more localised effects associated with the shape modes. Observe how larger bones (mode 1) have thinner and lighter cortices: this might explain some of the process of causation by which taller people with larger femurs are more likely to fracture (Carballido-Gamio, JBMR 2013; Whitmarsh, Bone 2012). The results for modes 2–5 (not all shown) need interpreting with greater caution: they might not be caused by thickness and mass differences, but by misregistration in the spatial alignment, since such errors depend systematically on the individual's shape. The effects for mode 3 (head-neck angle) are more widespread and perhaps indicate a genuine reduction in the cortex with increasing head-neck angle.

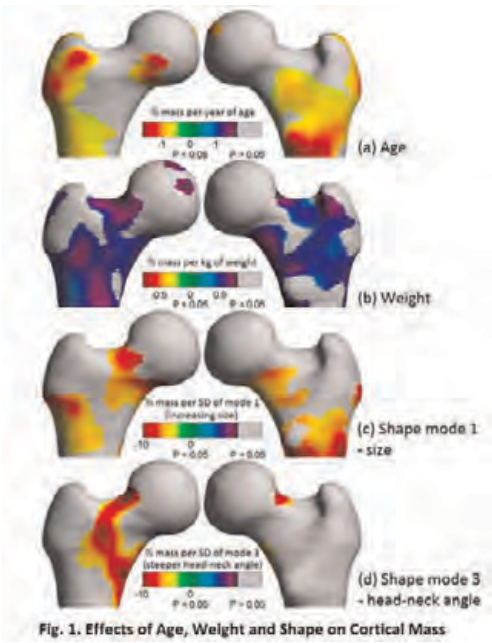

Figure 1

***Disclosures: Graham Treece**, None.*

SA0057

The Effects of Disuse and Low Steroid Hormone Level due to Hindlimb Unloading on Mouse Femora and Muscle Quality. Young Jeong*[1], Andries Ferreira[2], Marybeth Brown[2], Charlotte Phillips[3]. [1]University of Missouri, USA, [2]Biomedical Sciences & Physical Therapy Program, USA, [3]University of Missouri-Columbia, USA

Low sex hormone levels due to trauma are hypothesized to contribute to the loss of muscle and bone mass and strength, which is further exacerbated by loss of activity with bed rest. Bone is inherently mechanosensitive, and muscles typically exert the largest physiological loads that bones experience; with bone strength being directly proportional to muscle mass and load. Recent meta-analyses demonstrated significant differences in muscle mass and strength between intact mice and mice that were ovarectomized (Ovx). To investigate the role of simulated bed rest [hindlimb unloading (HLU)] on bone and muscle strength, and sex hormone levels, we analyzed the impact of 4 weeks of HLU and 3 days re-ambulation on hindlimb muscle masses and strength, uterine weight, and bone geometry and strength in intact and Ovx+HLU mice and in Ovx mice with normal cage activity. Female mice were assigned randomly to 6 groups: age-matched normal cage activity (control), HLU, HLU+3days of re-ambulation, Ovx, Ovx+HLU, and Ovx+HLU+3days of re-ambulation. For each group, the mice were anesthetized and peak tetanic contraction of the hindlimb muscles (gastrocnemius, soleus, plantaris, and tibialis anterior) was determined prior to sacrifice, and the muscles were then excised and weighed. Right femora were then excised, cleaned of the remaining soft tissue, and femoral geometry analyzed by μCT prior to the evaluation of bone biomechanical and material properties by torsional loading to failure testing. In contrast to the Sham Ovx mice, the gastrocnemius, tibialis anterior, plantaris, and soleus muscles in Ovx mice exhibited atrophy and failed to recover after 3 days of re-ambulation following HLU. By μCT analyses the femora from HLU mice demonstrated decreased cortical bone width, and biomechanically they exhibited reduced whole bone ultimate breaking strength and energy to failure as compared to control mice. Ovx+HLU femurs exhibit similar femoral geometry as HLU alone with the further diminishment of bone biomechanical properties. In addition, HLU mice had decreased uterine weights suggesting decreased estrogen levels. Our findings suggest that 4 weeks of HLU causes loss of muscle mass, bone material and biomechanical integrity, due to inactivity and disuse, as well as the result of decreased estrogen (E2) levels. Decreased E2 levels negatively impacts bone quality and when combined with inactivity the loss of bone material and strength is further exasperated.

***Disclosures: Young Jeong**, None.*

SA0058

Towards Standardized Protocols for the Reference Point Indentation Method. Alexander Setters*[1], Iwona Jasiuk[2]. [1]University of Illinois, USA, [2]University of Illinois at Urbana-Champaign, USA

Reliable bone strength prediction is still an outstanding medical challenge. The novel reference point indentation (RPI) technique has a potential to directly measure bone properties in patients. In this work, we address several issues regarding sample preparation and testing parameters using 6 month swine femurs. We investigated the effect of radiation, polishing and force magnitude on indentation distance increase (IDI) and average energy dissipated (AED). To determine radiation's effect, we tested bone samples using a 6N force before and after being exposed to Micro-CT radiation. Eighteen indents were done for each quadrant with 10 of these on the transverse surface and 8 on the longitudinal surface. The difference between IDI and AED before and after being irradiated by Micro-CT was found to not be statistically significant ($p<0.05$). The effect of polishing was much more prevalent. The bone was indented in the same manner as for the radiation tests, but indentation was done on the longitudinal surface before and after polishing. The sample was cut in half after polishing the longitudinal surface to expose mating transverse surfaces. Measurements were also done on these surfaces and they were only tested polished, as this is the standard for nanoindentation. The effect of polishing on the longitudinal surface was found to be statistically significant ($p<0.05$). The values of IDI and AED were 2-3 times greater for the unpolished samples compared to the polished samples. The difference between the polished longitudinal surface and polished transverse surface was found to not be statistically significant ($p<0.05$). In force magnitude variation, we tested the bone with 2N, 4N, 6N, 8N and 10N forces. Ten indents were done per force on the unpolished longitudinal surface. The changes due to a linear increase of the force resulted in a linear increase in the AED. IDI showed large increases from 2N to 4N and from 8N to 10N, but was relatively constant between 4N and 8N (Figure 1). In summary, through these tests we aimed to standardize the testing procedure for this novel RPI technique. Further studies on the effects of different testing parameters and sample preparations are needed to provide a more standardized testing procedure that can be used for a wide range of bone ages, types and locations. Such analysis will facilitate basic research on this method, required before this technique's use in clinical settings.

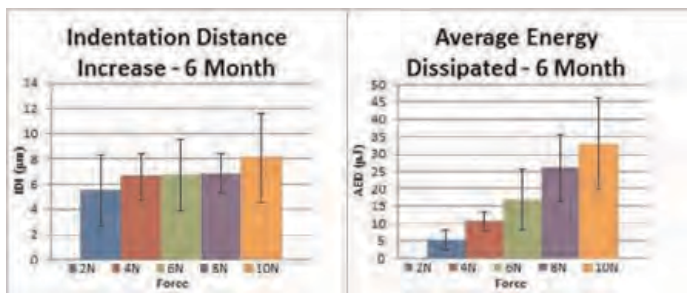

Efect of force magnitude on IDI and AED

***Disclosures: Alexander Setters**, None.*

SA0059

Trabecular bone Adaptation declined Asymmetrically with Aging: a 3D Dynamic *in vivo* Morphometry Study. Annette Birkhold*[1], Hajar Razi[1], Richard Weinkamer[2], Sara Checa[1], Georg Duda[1], Bettina Willie[3]. [1]Julius Wolff Institute, Charité Universitätsmedizin Berlin, Germany, [3]Max-Planck Institute of Colloids & Interfaces, Department of Biomaterials, Germany, [3]Charité-Universitätsmedizin Berlin, Germany

Bone adaptation to physical stimuli occurs by a balance between formation and resorption. It is known that mechanical loading shifts this balance towards increased bone formation. What is not known is how this response to loading changes with age. We hypothesized loading would increase formation and decrease resorption, but that this mechano-responsiveness would diminish with aging.

We measured structural adaptive changes of trabecular bone inside the tibia of living 10, 26, and 78 wk old female C57Bl/6J mice. Mice underwent 2 wks of in vivo cyclic loading (216 cycles/day; f = 4 Hz; εmax = 1200 με, right tibia as internal control) and *in vivo* microCT (10.5μm) at day 0, 5, 10, 15. The scan region began 50 μm below the growth plate (10% of tibia). Images were aligned using a registration algorithm. Differences between two consecutive microCT scans indicate where bone was resorbed or deposited in the time between the scans. Formation and resorption were then quantified by volume (fBV/tBV, rBV/tBV), surface area (fSA/tSA, rSA/tSA) and thickness/depth (fTh, rTh). Bone (re)modeling rates (3D-BFR, 3D-BRR, 3D-MAR, and 3D-MRR) were determined. An ANOVA assessed effects of loading, age, and interactions.

Mice of all ages had an anabolic response to loading. At day 15 the loaded limbs had (10wk: 145%, 26wk: 114%, 78wk: 67%) more fBV/tBV than control limbs and the rBV/tBV was reduced (10wk: 12%, 26wk: 21%, 78wk: 5%). Age influenced the bone formation response to loading, with differences in some parameters at day 5 (fBV/tBV, fSA/tSA, fTh; $p \leq 0.03$) and all parameters by day 15. Age influenced the bone resorption response to loading at day 5 (rBV/tBV, rSA/tSA, rTh $p < 0.007$), but no significant differences were measured at later time points, with only rBV/tBV ($p = 0.079$) and rSA/tSA ($p = 0.075$) approaching significance at day 15.Our study demonstrated that the adaptive capacity diminished with age, and that the time between loading and response became longer. While this is probably not unexpected, strikingly, adaptation was asymmetric. The bone formation response showed decreased surface area and thickness, while the bone resorptive response showed a trend of decreased surface area with aging, but a limited change in depth with aging. These structural data suggest reductions in adaptive capacity with age may be due to a lack of osteoblasts and osteoclasts and a reduced formation capacity, while resorptive capacity remains almost constant. This asymmetry further shifts the (re)modeling balance towards a net bone loss with age.

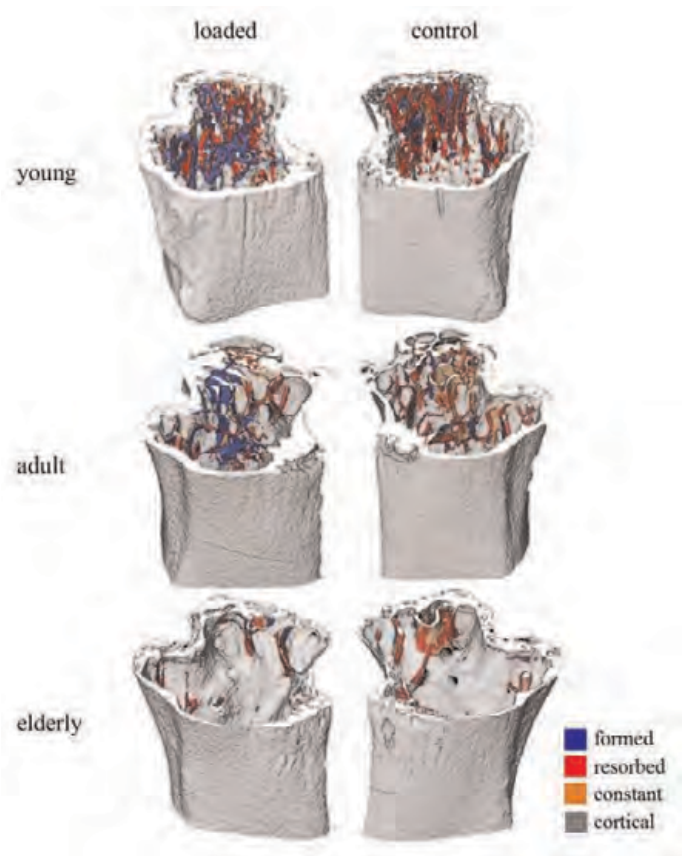

Visualization of trabecular (re)modeling in the proximal tibia

***Disclosures: Annette Birkhold**, None.*

SA0060

Validation of Mechanical Response Tissue Analysis by Quasistatic Mechanical Testing of Artificial Human Ulnas. Patricia Arnold*, Emily Ellerbrock, Lyn Bowman, Anne Loucks. Ohio University, USA

Osteoporosis is defined by NIH as a skeletal disorder characterized by compromised bone strength leading to increased risk of fracture, but no medical device measures bone strength directly *in vivo.* Bone stiffness is strongly associated with bone fracture load ($r \geqslant 0.95$), but no clinical method measures bone stiffness *in vivo,* either. Quasistatic Mechanical Testing (QMT) is the reference gold standard method for directly measuring the stiffness and strength of bones, but it can only be employed on excised bones and bone samples. Mechanical Response Tissue Analysis (MRTA) is a minimal-risk, non-invasive, radiation-free technique for directly measuring the bending stiffness of long bones *in vivo*. MRTA has been used for research purposes, but limited information about its measurement accuracy has been published. To begin to gather such information, this study quantified the precision, repeatability, and accuracy of MRTA measurements of bending stiffness in artificial human ulnas.

Standard and custom artificial human ulnas (N = 39) with -10% to +10% excess glass fill in the glass-epoxy composite emulating cortical bone were acquired from Pacific Research Laboratories/Sawbones, Vashon, WA. Ulna bending stiffness (K_b) was measured by MRTA and QMT in 3-point antero-posterior bending with proximal support by an articulating vertical Sawbones® humerus and distal support by the anterior distal radio-ulnar articular surface on a steel block. The load was applied at the mid-point of the posterior border. Precision and repeatability, respectively, were calculated without and with removal of ulnas from the humerus between repeated measures.

MRTA precision ($1.0 \pm 1.0\%$) and repeatability ($3.1 \pm 3.1\%$) were not as high as those of QMT ($0.2 \pm 0.2\%$ and $1.3 + 1.7\%$, both $p < 10^{-4}$), but regression analysis (Figure 1) found MRTA = 1.001 QMT ($R^2 = 0.999$). Bland-Altman analysis (Figure 2) showed that MRTA was unbiased (mean difference = $0.2 \pm 0.8\%$, $p = 0.67$) with respect to QMT, and individual MRTA and QMT measurements were interchangeable within limits of agreement of $\pm 5\%$.

In our hands, MRTA measurements of K_b in artificial human ulnas would be sufficiently precise, repeatable, and accurate for clinical purposes. If ongoing research finds that MRTA also achieves sufficient measurement performance in cadaveric human arms and ulnas, then MRTA may eventually prove useful for assessing, measuring bone stiffness, estimating peripheral bone strength and predicting fracture risk.

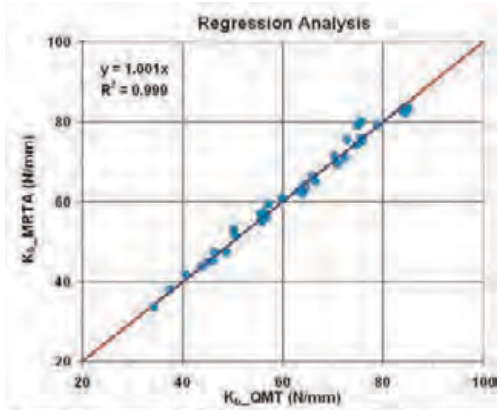

Figure 1. Regression of ulna transverse bending stiffness (K_b) measured by MRTA on paired measurements by QMT (N = 39). Red line = identity, Blue line = regression line y = 1.001x.

Figure 1– Regression Analysis

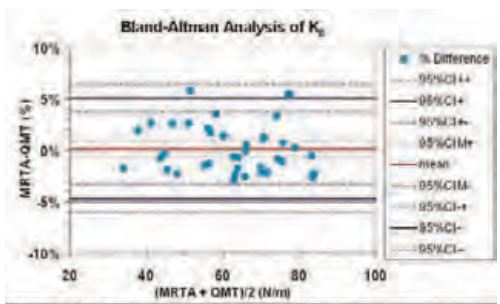

Figure 2. Bland-Altman analysis of paired measurements of K_b by MRTA and QMT in the same ulnas (N=39). CIM = confidence interval of the mean difference. CI = confidence interval of individual paired differences.

Figure 2 – Bland-Altman Analysis

***Disclosures: Patricia Arnold**, None.*

SA0061

Intermittent PTH and Mechanical Loading Increase the Quality, Quantity and Mechanical Integrity of a Porous Titanium Implant-Bone Interface. Hayden-William Courtland*[1], Matthew Grosso[1], James Sutherland[1], Kirsten Stoner[1], BIN HU[2], Joseph Nguyen[1], Anna Fahlgren[1], F. Patrick Ross[1], Timothy Bromage[2], Marjolein Van Der Meulen[3], Mathias Bostrom[1]. [1]Hospital for Special Surgery, USA, [2]New York University College of Dentistry, USA, [3]Cornell University, USA

A strong bone-implant interface is essential for successful joint replacement surgery. This study investigated the differences in bone surrounding and within a porous titanium implant after single or combined treatment with two anabolic bone therapies: intermittent parathyroid hormone (teriparatide) and mechanical loading. Porous titanium implants were inserted bilaterally on the distal lateral femurs of rabbits. The right implant was loaded daily (1 MPa, 50 cycles/day) while the left implant was not. Rabbits received daily PTH injections (20 ug/kg) or saline vehicle. Periprosthetic cancellous bone 0.5, 1.0, and 2.0 mm below the implant surface, bone at the 0.25 mm bone-implant interface and total bone within each implant were examined using tissue-level analyses (quantitative backscattered electron microscopy), cellular analyses (immunohistochemistry staining of osteoblasts with procollagen-1 and TRAP staining of osteoclasts), and shear testing (implant-bone interface). Statistical significance was determined using GEE models ($p<0.05$). For tissue located 0.5 mm below the implant, significant increases in bone area per total area (BA/TA) were observed with PTH treatment (56%) and with loading (27%). Further, an 18% increase in mineralization density with PTH treatment and a 20% increase in mineralization density with loading was found. Loading effects were not present beyond the 0.5 mm periprosthetic region, but PTH significantly increased BA/TA 2.0 mm below the implant and mineralization density 1.0 mm below the implant. Tissue-level changes were supported by increases in osteoblast activity 0.5 mm below the implant with PTH (79%) and loading (34%), as well as by minimal osteoclast changes. At the 0.25 mm implant-bone interface PTH and loading increased BA/TA (16% and 23%, respectively), but only loading increased mineralization density (7%). Further, total integrated bone area was increased 35% with PTH. Both PTH and loading enhanced the mechanical integrity of the implant-bone; shear strength increased 34% and 60%, respectively. Although combined treatment was not synergistic, both PTH and loading individually enhanced the amount and mineralization density of bone at the implant interface and immediately below the interface, thereby increasing the mechanical strength of the metal-bone interface. This research suggests that modulation of both quantity and quality of peri-implant bone may be viable options to improve implant fixation and patient outcomes.

***Disclosures: Hayden-William Courtland**, None.*

SA0062

Mechanical Loading And Big Endothelin-1 In Trabecular Bone Cores. Diane Cullen*[1], Gwendolin Alvarez[1], Luisa Meyer[2], Michael Johnson[3], Juan Vivanco[3], Robert Blank[3], Heidi-Lynn Ploeg[3], Everett Smith[3]. [1]Creighton University, USA, [2]University of Wisconsin - Madison, USA, [3]University of Wisconsin, USA

Mechanical loads are anabolic stimuli for bone, increasing formation and strength in adaptation to the stresses. Endothelin-1 (ET1), a ubiquitous autocrine/paracrine signaling molecule promotes osteogenesis associated with breast and prostate cancer. In this ex vivo study we combined both anabolic stimuli and hypothesized that bone formation would increase synergistically. Bovine sternal trabecular bone cores (5x10mm) were maintained in individual polycarbonate chambers with media changed daily over 23 days. Cores were placed into four groups blocked by stiffness and treated daily with compressive loading (-2000 με, 120 cyc, 2 Hz) and/or big ET-1 (25 ng/mL). Bone formation was labeled in culture with calcein on days 9 and 19. Bone stiffness and prostaglandin production was measured throughout the experiment. After collection cores were embedded in methylmethacrylate and sectioned for histomorphometric measurement of bone area, surface, label length, and label width. Differences among groups were analyzed by 2-way ANOVA for the effects of Load x Endothelin. There was no difference among groups in bone volume (BV/TV) of the cores. Due to the long labeling interval, single label predominated over double. Load cores had 50% more single label bone surface (sLS/BS) than NoLoad cores. Mineral apposition rate (MAR) showed a stair step pattern with a positive Load impact ($P=0.007$) and ET-1 showing a positive trend ($P=0.16$). Bone formation rate (BFR), a product of label length and MAR, was twofold greater in Load than NoLoad ($P=0.009$), but not altered by ET-1 although the same pattern was observed. There was no significant interaction between Load and ET-1. The bone formation response to Load and ET-1 correlate with the change in stiffness across the experiment. In conclusion, ex vivo mechanical loads increased bone formation and stiffness of the cores. ET-1 response in this study was less than predicted from previous work. The combined effects tended to be additive rather than synergistic.

Trt	Drug	N	BV/TV	sL/BS	MAR	BFR
NoLoad	Veh	10	17.9 (5.1)	27 (19)	0.89 (0.66)	63 (75)
	ET-1	10	16.5 (4.9)	30 (17)	1.08 (0.74)	76 (71)
Load	Veh	9	16.5 (2.4)	43 (21)	1.38 (0.67)	131 (107)
	ET-1	9	16.2 (5.4)	43 (11)	1.79 (0.41)	151 (49)
P value	Load		NS	0.01	0.007	0.009
	Drug		NS	NS	NS	NS

Table

***Disclosures: Diane Cullen**, None.*

SA0063

Mechanical Stimulation Induces the Production of Soluble RANKL to Modulate Osteogenesis of Mesenchymal Stromal Cells. Chun-Yi Chiu[1], Tsung-Lin Tsai[1], Ray Vanderby[1], Gino Bradica[2], Shyh-Liang Lou[3], Wan-Ju Li*[1]. [1]University of Wisconsin-Madison, USA, [2]Kenseynash, USA, [3]Chung-Yuan Christian University, Taiwan

Introduction: During bone formation or remodeling, mesenchymal stromal cells (MSCs) receive mechanical signals along with chemical cues to differentiate into osteoblasts and produce bone matrix. However, the biological mechanism underlying mechanically-induced osteogenesis is not clear. In addition, it has not been reported that whether sequential compressive stimulation (CS) and ultrasonic stimulation (US) can enhance MSC osteogenesis compared to CS or US alone. In this study, we aimed to compare osteogenesis of MSCs stimulated by CS and/or US, and hypothesized that soluble receptor activator of nuclear factor kappa-B ligand (RANKL) and/or osteoprotegerin (OPG) secreted from MSCs by mechanical stimulation regulate osteogenesis of MSCs.

Materials and Methods: Human MSCs (hMSCs) cultured in β-tracalcium phosphate/polylactide scaffolds were treated with optimized CS for 60 minutes and/or US for 20 minutes daily for 16 days (Fig. 1A). The mRNA expression of bone-related markers, alkaline phosphate (ALP) activity, calcium deposition of specimens were analyzed to determine osteogenic differentiation. ELISA was used to detect soluble RANKL and OPG in culture. The activity of soluble RANKL or OPG was attenuated by neutralizing antibody during mechanically-stimulated osteogenesis to determine their regulatory roles. One-way ANOVA with Holm-Sidak post hoc was performed to determine statistical significance among the experimental groups.

Results: Real-time PCR results showed that the mRNA levels of bone-related markers, including core-binding factor subunit alpha1 (CBFA1), activating transcription factor4, ALP (Fig. 1B), osteocalcium, RANKL, and OPG, of hMSCs stimulated by US were the highest among all the experimental groups. In addition, hMSCs receiving mechanical stimulation produced significantly more soluble RANKL than those in the control culture without mechanical stimulation (Fig. 1C). On the other hand, hMSCs produced comparable levels of soluble OPG in culture among the groups with and without mechanical stimulation. Attenuating the activity of soluble RANKL in the culture treated with US during osteogenesis significantly down-regulated the mRNA expression of CBFA1, osterix, ALP (Fig. 1D), and OPG, suggesting that US modulates hMSC osteogenesis through the activity of soluble RANKL.

Conclusions: US is potent mechanical stimulation for enhancing hMSC osteogenesis. Soluble RANKL induced by US modulates osteogenesis of hMSCs.

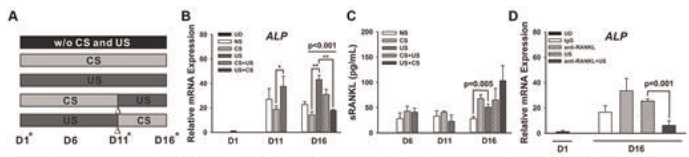

Figure 1. (A) Experimental setup of mechanical stimulations. (B) mRNA expression of ALP of hMSCs receving different mechancial stimuation during osteogenesis. (C) Production of soluble RANKL in culture treated with different mechanical stimulations. NS: no stimulation. (D) mRNA expression of ALP of hMSCs treated with or without US and with or without RANKL neturalizing antibody during osteogenesis. UD: undifferetiated.

Figure

***Disclosures: Wan-Ju Li**, None.*

SA0064

Mechanosensitivity with cyclic loading is maintained with age at a localand global level in murine caudal vertebrae. Floor Lambers*[1], Gisela Kuhn[2], Claudia Weigt[2], Kathleen Koch[2], Friederike Schulte[2], Ralph Müller[2]. [1]Cornell University, USA, [2]Institute for Biomechanics, ETH Zurich, Switzerland

Mechanosensitivity can be described as the ability of bone to respond to mechanical signals. While an increase in bone mass and bone strength with *in vivo* mechanical loading in animals has often been reported at a global level, little is known about the local bone remodeling response at the bone surface. The aim of this study was to determine the local and global mechanosensitivity of the sixth caudal vertebra after cyclic loading in mice aged 15, 52, and 82 weeks.

The sixth caudal vertebra was cyclically loaded by a force of 8N (10 Hz, 3000 cycles, three times per week for six weeks) through pins in the adjacent vertebrae for the loaded groups. Control mice were anesthetized, but no loading was applied. The bone microstructure was monitored longitudinally with *in vivo* micro-computed tomography (10.5 μm voxel size). By overlaying time-lapsed scans, three-dimensional bone remodeling rates were determined (Fig. 1a), as validated previously [1]. Scans were converted to micro-finite-element models to determine bone stiffness and the mechanical environment at surfaces where bone formation, bone resorption, or no bone remodeling followed (Fig. 1b), using strain energy density (SED) as the mechanical signal assumed to be a stimulus for bone adaptation.

Mechanical loading had beneficial effects at the global bone level in all age groups. The increase in bone volume fraction was 20% and 18% greater ($p<0.05$) in loaded than control group in 15- and 82-week-old mice, respectively. In 52-week-old mice, the greatest effect of loading on the bone microstructure was observed in the cortical bone, in which the cortical thickness decreased for the control group ($p<0.05$), but not for the loaded group. Mineralizing surface was on average 13% greater ($p<0.05$) in loaded than control groups in 15- and 82-week-old mice. Mechanical loading had a beneficial effect on bone stiffness in 52- and 82-week-old mice ($p<0.05$). SED predicted the change in bone volume fraction for loaded groups (R = 0.83-0.92), but not control groups (Fig. 2). At the local level, SED was 14%-20% greater at sites of bone formation, and 15%-20% lower at sites of bone resorption than at quiescent bone surfaces for all age groups, indicating that SED was a stimulus for bone adaptation (Fig. 3). Taken together, these results support that mechanosensitivity is maintained with age in caudal vertebrae of mice at a local and global level.

[1] Schulte *et. al.*, Bone, 2011

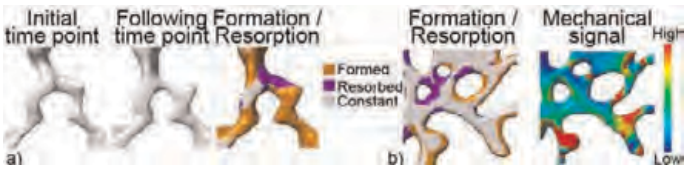

Fig1: a) Formation(yellow) and resorption(purple) from CT; b) remodeling compared to mechanical signal

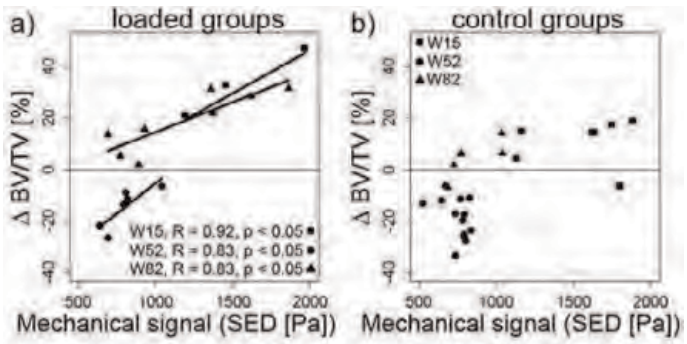

Fig2: Correlations between initial SED and resulting % change in BV/TV. W15 = 15-week-old (etc.)

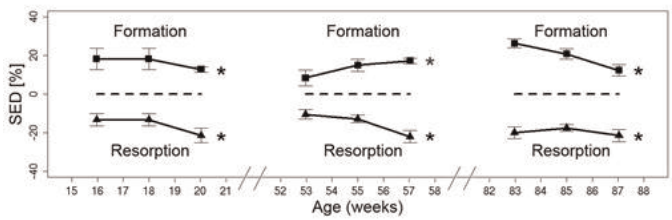

Fig3: SED at formation (square) and resorption (triangle) compared to constant surfaces, * $p<0.05$

***Disclosures: Floor Lambers**, None.*

SA0065

Wnt16 Is an Important Regulator of Bone Size and the Periosteal Bone Formation Response to Mechanical Loading. Chandrasekhar Kesavan*[1], Subburaman Mohan[1], Robert Brommage[2], Jon Wergedal[1]. [1]Jerry L. Pettis Memorial VA Medical Center, USA, [2]Lexicon Pharmaceuticals, USA

Compromised bone strength leads to increased risk of fracture with bone size and BMD key determinants of bone strength. Human GWAS studies in several populations identifying a chromosomal locus containing the Wnt16 gene contributing to BMD variations and the finding that mice with targeted Wnt16 gene disruption have reduced bone strength both suggest that Wnt16 is an important regulator of bone strength. Reduced bone strength in Wnt16 knockout (KO) mice is caused by a 30% reduction in femur cross-sectional area and 24% reduction in cortical thickness compared to littermate wild type (WT) mice. Histomorphometric studies revealed that periosteal bone formation (BFR) and mineral apposition (MAR) rates were reduced ($P<0.05$) by 55% and 32%, respectively, in Wnt16 KO vs WT mice at 12 weeks of age. In contrast, TRAP labeled surface at the periosteum was not different between the two genotypes. *In vitro* studies using periosteal cells derived from Wnt16 KO and WT mice revealed reduced proliferation potential is the cause for reduced BF and bone size in Wnt16 KO mice. To determine the mechanism for Wnt16 effects, RNA was extracted from periosteal tissue of Wnt16 KO and WT mice at 5 weeks of age for measurement of expression levels of canonical and non-canonical Wnt signaling genes by RT-PCR. Significant 30-60% reductions in the expression levels of canonical (β-catenin, Axin2, c-myc) but not non-canonical (Nfatc1, Tnnt2) signaling genes were seen in the KO mice compared to WT mice. Since mechanical strain is an important physiological regulator of periosteal BF, we next tested if mechanical loading-induced periosteal BF is compromised in Wnt16 KO mice. Application of 9N and 6N forces producing 4800 με strain to the right tibia using a four-point bending loading method for 2 weeks (6 days/week) at 2 Hz frequency, for 36 cycles per day produced significant increases ($P<0.05$, n=6) in total volume (11%), BV/TV (6%) and cortical thickness (12%) of loaded compared to externally unloaded left tibia bones in the WT but not in KO mice (<1.2% change vs unloaded tibia). Histomorphometric analyses revealed increases in periosteal BFR and MAR in the loaded bones of WT but not KO mice. In conclusion, 1) Wnt16 is a major regulator of long bone cross sectional size by affecting periosteal BF and not resorption. 2) Wnt16 acts through the canonical Wnt signaling pathway. 3) Wnt16 is critical for translating the mechanical loading signal into an anabolic response at the periosteum.

***Disclosures: Chandrasekhar Kesavan**, None.*

SA0066

Atypical Femoral Fractures were Estimated Dependent on Deterioration of Bone Quality and Curvature of Femoral Shaft. SATOSHI IKEDA*[1], Akinori Sakai[2], Hidetoshi Tanaka[1], Hideo Ohnishi[2], Yoshinori Takeuchi[2], Mitsuru Saito[3], Masako Ito[4], Toshitaka Nakamura[2]. [1]Ken-Ai Memorial Hospital, Japan, [2]University of Occupational & Environmental Health, Japan, [3]Jikei University School of Medicine, Japan, [4]Nagasaki University Hospital, Japan

Introduction: Atypical femoral fracture focused on relation of bisphosphonate use, frequently. However, the mechanism of atypical femoral fracture was not yet clarified. Atypical femoral fractures have been kept femoral shaft cortical thickness and BMD, practically. We hypothesized that atypical femoral fractures were dependent on impaired bone quality and curvature of femoral shaft.

Material & Methods: We experienced four atypical femoral fractures. One was subtrochanteric and three were shaft fracture. Two cases received bisphosphonate therapy for 3-5 years. BMD, bone metabolic markers, and bone quality markers values were obtained. Histomorphometry and collagen cross-link analysis were performed. Curvature of femoral shaft and 3-D finite element analysis in one incomplete fracture case were assessed.

RESULTS: BMD values were either maintained or not severe decreased. Deterioration of bone quality were verified that result of histomorphometry, collagen cross-link analysis, and bone quality maker. Especially, homocystine values, such as one of bone quality markers, were increased all cases. All atypical femoral shaft fractures showed outward curvature of femoral bone. One incomplete atypical femoral shaft fracture, stress was concentrated at the fracture region by 3-D finite element analysis.

CONCLUSIONS: The results of this study suggest that atypical femoral fractures were estimated dependent on deterioration of bone quality and curvature of femoral shaft.

***Disclosures: SATOSHI IKEDA**, None.*

SA0067

BMI Has a Positive Non-Linear Association with Femoral Neck BMD and Structure But a Negative Linear Association with Strength Index in a Large Canadian Cohort. Jian Shen*[1], Carrie Nielson[1], Eric Orwoll[1], Sumit Majumdar[2], William Leslie[3]. [1]Oregon Health & Science University, USA, [2]University of Alberta, Canada, [3]University of Manitoba, Canada

Emerging evidence indicates that fractures in obese individuals are of public health importance and that the relationship between obesity and fracture is complex and poorly understood. We previously reported that the relationship of BMI with hip structural and densitometric measures was non-linear in older US men. We sought to confirm these findings and extend them to women.

Using data from the Manitoba Bone Density Program, we conducted cross-sectional analyses of baseline BMI and DXA-derived measures of femoral density and structure in all women and men age ⩾ 50 y referred for DXA scan. Advanced Hip Analysis software (enCore version 13.6, GE Healthcare) was used to derive hip structural parameters including cross-sectional moment of inertia (CSMI) and cross-sectional area (CSA). Femoral strength index (SI) was calculated as the ratio of the compressive yield strength of the femoral neck to the expected compressive stress of a fall on the greater trochanter. We used both ANCOVA and generalized additive models (cubic splines with 4 df) to identify nonlinearity in the associations between BMI and hip structural parameters after adjustment for osteoporosis treatments and other relevant covariates.

Hip DXA scans were analyzed in 41,919 women (mean age: 66 y, 24.9% obese) and 4085 men (mean age: 69y, 22.4% obese). In both women and men, higher BMI was independently correlated with greater areal BMD, CSMI and CSA at the femoral neck. However, these relationships were non-linear (all P for nonlinearity <0.0001). Among individuals with BMI < 30 kg/m^2, increasing BMI was associated with progressive increases in BMD, CSMI and CSA (Table). However, the relationship appeared to reach a plateau at BMIs of 30 kg/m^2, with little additional increment in the structural parameters with further increases in BMI (all P for interaction <0.0001, obese versus non-obese). Furthermore, increasing BMI was associated with decreases in SI, and the association was linear in men and near-linear in women.

In this large Canadian cohort we confirmed that the relationships of BMI with femoral BMD and structure are nonlinear in men and we have now extended this finding to women. The positive association of BMI on hip BMD and structure is not sustained as BMI increases in the obese. Moreover, femoral strength index declines in linear fashion as BMI increases in both sexes. These results provide some mechanistic insight into fracture risk in the obese.

Table. The association between BMI and femoral neck structural measures stratified by obesity status and adjusted for relevant covariates

	BMI< 30 kg/m^2		BMI >=30 kg/m^2		Obese vs Non-obese	
	Δ per kg/m^2	P	Δ per kg/m^2	P	Slope ratio	P for interaction*
Women						
Neck BMD (g/cm^2)	0.0113	<0.0001	0.0032	<0.0001	0.28	<0.0001
CSA (mm^2)	1.9001	<0.0001	0.2959	<0.0001	0.16	<0.0001
CSMI(cm^4)	139.26	<0.0001	16.95	0.0038	0.12	<0.0001
SI	-0.0317	<0.0001	-0.0267	<0.0001	0.84	<0.0001
Men						
Neck BMD (g/cm^2)	0.0139	<0.0001	0.0047	0.0005	0.34	<0.0001
CSA (mm^2)	2.7061	<0.0001	0.5978	0.0425	0.22	<0.0001
CSMI (cm^4)	305.94	<0.0001	21.82	0.643	0.07	<0.0001
SI	-0.0259	<0.0001	-0.0231	<0.0001	0.89	0.567

*Interaction between obesity status and BMI on hip structural parameters
Abbreviations: CSA, cross-sectional area; CSMI, cross-sectional moment of inertia; SI, strength index

BMI and Hip structural measures

***Disclosures: Jian Shen**, None.*

SA0068

Bone Shock Absorbance (BSA) and Trabecular Bone Score (TBS) in Patients With Osteoporosis, With and Without Vertebral Fracture. Nelson Watts*[1], Didier Hans[2], Cyndy Cox[3], Ben House[3], Rakesh Shukla[3], Alok Dwivedi[4], Amit Bhattacharya[3]. [1]Mercy Health Osteoporosis & Bone Health Services, USA, [2]Lausanne University Hospital, Switzerland, [3]University of Cincinnati, USA, [4]Texas Tech University Health Sciences Center, USA

Purpose: To evaluate the performance of trabecular bone score (TBS) compared with bone shock absorbance (BSA) and dual-energy x-ray absorptiometry (DXA) in determining the presence of vertebral fractures in postmenopausal women with osteoporosis.

Background: Bone shock absorbance (BSA) and trabecular bone score (TBS) are noninvasive and novel tests of "bone quality." We previously showed that BSA was a better discriminator of the presence of vertebral fracture than DXA in a cohort of 67 postmenopausal women with osteoporosis (28 with vertebral fracture) (Bhattacharya et al, J Clin Densitom 2010). BSA is a dynamic, non-invasive measure of bone damping capacity using skin-mounted accelerometers at load-bearing skeletal sites. TBS is a gray-level texture measurement that is applicable to DXA.

Methods: We recruited women ages 65-86 who had T-scores of -2.5 or below in the hip or spine. Presence or absence of vertebral fracture was determined by lateral spine radiographs or Vertebral Fracture assessment using DXA. BSA was measured using previously reported methods. TBS was determined from spine DXA parameters.

Results: We studied 67 women, age 71 ± 4.2, height 162 ± 6.6 cm, weight 74 ± 16.0 kg, BMI 28 ± 5.1. Spine BMD was 0.989 ± 0.218 g/cm2 (T-score -0.5); 28 had vertebral fractures and 39 had no vertebral fractures. BSA damping value was significantly lower in patients with vertebral fractures compared with those without fracture (median -44$, range -35% to -72%). TBS was 1.281 ± 0.877. There was no significant correlation between TBS and spine BMD. Further analyses comparing TBS and BSA are ongoing and will be presented.

Conclusions: Both BSA and TBS provide additional information, over and above that obtained with DXA, to distinguish patients with vertebral fractures from those without. Further investigation is warranted to see how these measures, alone or in combination provide useful clinical information for assessment of future fracture risk.

***Disclosures: Nelson Watts**, OsteoDynamics, 7*

SA0069

Physical Activity Related to Cortical but Not Trabecular Architecture in Young Women. Joseph Kindler*[1], Hannah Goff[1], Emma Laing[1], Christopher Modlesky[2], Norman Pollock[3], Clifton Baile[1], Richard Lewis[1]. [1]The University of Georgia, USA, [2]University of Delaware, USA, [3]Georgia Regents University, USA

The purpose of this study was to determine relationships between three physical activity questionnaires and both magnetic resonance imaging (MRI)-derived measures of trabecular and cortical bone and dual energy X-ray absorptiometry (DXA)-derived areal bone mineral density (aBMD) in 18-19 year old white females (N=24). Participants completed three physical activity questionnaires at one testing visit; two bone-specific (the bone loading history questionnaire [BLHQ] and the bone-specific physical activity questionnaire [BPAQ]) and one non-bone-specific (the 7-day physical activity recall questionnaire [7-day PAR]). Bone loading scores were calculated through completion of the BLHQ and BPAQ, and energy expenditure was calculated through completion of the 7-day PAR. Trabecular and cortical bone were measured via MRI at the non-dominant tibia and radius, and aBMD of the total body, lumbar spine, femur, femoral neck, trochanter, and radius via DXA. Hip BLHQ and past BPAQ scores were positively associated with cortical volume at the mid-tibia (r=0.43 and 0.62, respectively; p<.05). Past BPAQ scores correlated positively with mid-tibia polar moment of inertia (J), section modulus (Z), and cross sectional moment of inertia (CSMI) (r=0.56; p<.02) and aBMD (r=0.45-0.63; p<.03 for all measured sites). Energy expenditure negatively correlated with mid-radius J, Z, and CSMI (r=-0.42 to -0.43; p<.05). While previous studies report positive relationships between BLHQ and BPAQ scores with calcaneal broadband ultrasound attenuation and aBMD in adults, this was the first study to observe a relationship with MRI-derived outcomes. The greater number of associations of BPAQ scores with weight-bearing bone outcomes versus BLHQ scores or energy expenditure shows that the BPAQ is a superior tool for assessing weight-bearing physical activity in bone studies involving young adult females.

Key Terms: MRI, DXA, bone loading, females

***Disclosures: Joseph Kindler**, None.*

SA0070

Presence Of Adrenal Incidentaloma induces Bone micro-architectural texture (TBS) impairment at Axial Skeleton in women. Giuseppe Guglielmi[1], Michelangelo Nasuto[2], Alfredo Scillitani*[3], Renaud Winzenrieth[4], Didier Hans[5]. [1]Department of Radiology, University of Foggia, Viale Luigi Pinto 1, 71100, Foggia, Italy; - Department of Radiology, Scientific Institute Hospital "Casa Sollievo della Sofferenza", Viale Cappuccini 1, 71013, San Giovanni Rotondo (FG), Italy, [2]Department of Radiology, University of Foggia, Viale Luigi Pinto 1, 71100, Foggia, Italy, [3]Casa Sollievo Della Sofferenza Scientific Institute, Italy, [4]Med-imaps, Hôpital X. Arnozan, PTIB, Pessac, France, [5]Lausanne University Hospital, Switzerland

RATIONAL: Adrenal Incidentaloma (AI) could induce subclinical hypercortilism (SH). This cortisol excess is associated with a bone mass alteration and a fracture risk increasing. Effects of AI and SH on bone microarchitecture in human axial skeleton have been few evaluated to date. In this study, we have evaluated the impact of AI on both bone mineral density (BMD) and bone micro-architectural texture, as assessed by TBS.

METHODS: Fourty-one caucasian italian women (mean age = 60.614.1years) with unilateral incidentaloma were recruited. Presence of hypogonadism and hypercortisolism was confirmed using at least two out of three following parameters: urinary free cortisol >70µg/die, plasma ACTH <10 pg/ml or serum cortisol >3µg/dl at 9.00 am after 1 mg dexamethasone overnight. BMD was evaluated at lumbar spine (LS) using a Hologic QDR 4500 device as well as at femur (total and neck). TBS was evaluated at lumbar spine on the same region of interest used for the LS-BMD using TBS iNsight software v1.9.2 (Med-Imaps, France).

RESULTS: Mean values of lumbar and femoral (total) T-score were -1.49 and -0.65, respectively, whereas corresponding Z-score values where normal (0.03 and 0.46, respectively). Among AI subjects, 24% were osteoporotic, 80% have hypogonadism (Hy) and 27% suffering from SH. Whatever the LS-BMD stratification, TBS is significantly lower in AI patient in comparison with Age-matched TBS reference (TBSref) values (p<0.002) while no differences were obtained for LS-BMD. Hy subjects have a significant lower LS-BMD and TBS (p<0.001). Furthermore, TBS values of these subjects was lower in comparison with TBSref values (p<.0001) whereas no differences have been obtained for LS-BMD and LS-BMD reference values (p>0.80). Finally, TBS value of SH subjects was lower in comparison with TBSref values (p<0.001).CONCLUSION: Our study showed a micro-architectural texture impairment due to AI whereas no effect has been obtained on LS-BMD. Both Hypogonadism and hypercortisolism have a negative effect on micro-architectural texture. These results suggest that the micro-architectural texture alteration at axial skeleton have to be assessed and take into account for the management of patient with adrenal incidentaloma.

***Disclosures: Alfredo Scillitani**, None.*

SA0071

Relationship between Bone Marrow Edema and Structural Parameters in Cortical and Trabecular Bone. Afrodite Zendeli*[1], Christian Muschitz[2], Lukas Fischer[3], Roland Kocijan[4], Judith Haschka[4], Wolfgang Schima[5], Fritz Lomoschitz[5], Arastoo Rahbarnia[1], Christina Marterer[1], Alexandra Kaider[6], Heinrich Resch[7]. [1]The VINFORCE Study Group - St. Vincent Hospital - Medical Department II, Austria, [2]St. Vincent's Hospital, Austria, [3]CIR LAB, Department of Radiology/Medical University Vienna Austria, Austria, [4]St. Vincent Hospital Vienna, Austria, [5]Medical Department of Radiology – St. Vincent Hospital, Vienna Austria, Austria, [6]Center for Medical Statistics, Informatics & Intelligent Systems, Section of Clinical Biometrics, Medical University of Vienna, Austria, [7]Medical University Vienna, Austria

Background:Bone marrow edema (BME) is a localised painful bone lesion, often caused by an insufficiency fracture due to moderate mechanical strain. Evidence for BME is effectively provided by MRI. We hypothesize that structural bone alterations increase the susceptibility to the development of a non-traumatic BME. The aim of this pilot study was to investigate bone micro structure, areal and volumetric bone mineral density (aBMD and vBMD), and serum BTM values in patients with non-traumatic BME of the lower limb.Methods:We consecutively investigated 26 treatment naive, otherwise healthy female and male subjects (38.4 ± 16.8 ys) with MRI diagnosed non-traumatic BME of the lower limb. We calculated structural parameters of cortical and trabecular compartments in the tibia (T) and radius (R) The data were compared to a control group consisting of 50 sex and age matched healthy individuals (HC) (39.9 ± 13.7 ys). In 3 patients BME was found in the hip, in 9 in the tibia/knee and in 14 patients in the foot/ankle region. HR-QCT and MRI showed in 6 out of 17 patients micro-fractures adjacent to the BME.HR-pQCT (Scanco Medical) analysis of the healthy contralateral distal tibia and radius as well as DXA measurements (GE Lunar iDXA) of spine and hip, and serum fasting BTM were carried out in all subjects. Results:BMD values were similar in both groups, as well as bone turnover markers, 25-OH-vit-D-levels were in all subjects above 30 ng/ml. Structural analysis by HR-pQCT revealed significant differences both for radius and tibia. BME compared to HC had decreased CtBMD [mgHA/cm^3] (R: 909.7±124.8 vs 1001.4±39.1; T: 891.9±74.7 vs 953.1±76.8) and decreased CtTMD [mgHA/cm^3] (R: 963.1±61.8 vs 1022.3±33.1; T: 975.3±46.1 vs 1014±46.1). CtPo [%] was increased in BME (R*: 4.3±0.1 vs 1.5±0.01; T: 6.7±0.04 vs 4.7±0.03), as well as CtPoV [mm^3] (R: 28.5±97.9 vs 7.1±5.7; T: 62.3±32.9 vs 40.7±22.6), EndoCtPm [mm] (R: 680.4±107.5 vs 569.5±65.5; T: 973.9±115.9 vs 836.3±85.5) and TrabArea [mm^2] (R: 277.8±92.7 vs 213.0±57.4; T: 684.3±200.7 vs 571.8±136.4) - p ≤ 0.01 for all values; * p=0.02.In the BME CtTh [mm] was significantly lower in the radius (p=0.003) and trend-wise in the tibia (p=0.06).Conclusion:Our data clearly show a ubiquitous structural alteration of cortical bone parameters and trabecular area measured by HR-pQCT. This systemic structural deficit could enhance a subject's susceptibility to suffer from a BME caused by a local insufficiency fracture due to moderate strain.

***Disclosures: Afrodite Zendeli**, None.*

SA0072

Sub-compartmental Bone Morphometry Analysis in Longitudinal HRpQCT Scans with Application to Chronic Kidney Disease. Matthew DiFranco*[1], Lukas Fischer[1], Alexander Valentinitsch[1], Franz Kainberger[1], Georg Langs[1], Janina Patsch[1], Thomas Nickolas[2]. [1]Medical University of Vienna, Austria, [2]Columbia University College of Physicians & Surgeons, USA

High resolution peripheral quantitative CT (HRpQCT, resolution 82 μm) measures true volumetric bone mineral density of the distal extremities and enables analysis of longitudinal microarchitectural changes. However, these changes may be difficult to quantify. They may be dependent on image registration and their clinical interpretation may be difficult due to disease and treatment specific effects. In order to overcome limitations of autosegmentation, we determined whether HRpQCT can detect sub-compartmental volumetric changes in mineralized bone in patients with known loss of cortical bone. We imaged 8 chronic kidney disease (CKD) patients at baseline and 1-year and applied a spatio-temporal morphometry (STM) method to longitudinal HRpQCT scans. We hypothesized that STM would detect mineralization changes specific to bone loss in CKD patients.

Baseline and follow-up scans were rigidly registered using adaptive stochastic gradient descent on a sum of squared voxel differences cost function. Optical flow was then applied to produce a deformation vector at each voxel to represent local volumetric changes of mineralized bone between the two scans. Per-voxel volume change was then quantified as the determinant, J(x), of the Jacobian matrix of a local deformation field centered on the target voxel (x). Values of $J(x) > 1$ indicate local expansion, values of $J(x) < 1$ indicate local shrinkage, and $J(x) = 1$ indicates no volume change. Using the distance of each voxel from the periosteum in conjunction with the values of J(x) at each voxel, we calculated the mean J(x) of mineralized bone within incremental and cumulative distance ranges measured from the periosteum and plotted the results against distance.

Between baseline and follow-up, mean±SD% loss in cortical density was 4.1±4.5% and thickness was 4.1±4.5%. There were no changes in trabecular density and microarchitecture. Our method detected volume loss concentrated in regions between 10% and 20% distance from the periosteum, corresponding to the endocortex. Inner trabecular results suggested negligible to slight expansion of trabecular structures.

In summary, we demonstrated a novel method for calculating sub-compartmental volumetric changes in longitudinal HRpQCT scans that may assess disease-specific mineralization changes. Larger studies are needed in patients with different disorders of bone metabolism to determine disease specific changes to sub-compartmental volume alterations.

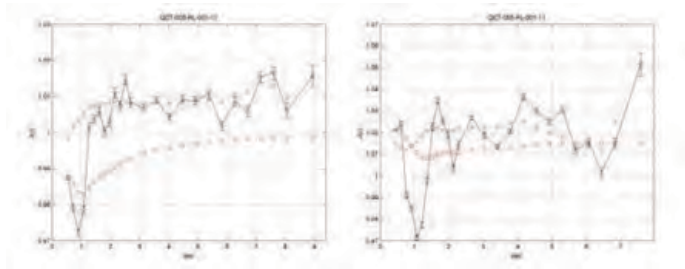

Example radius bone morphology plots for 2 CKD patients

***Disclosures: Matthew DiFranco**, None.*

SA0073

Towards Hip Fracture Prediction using Finite Element analysis and Machine Learning. Samy Missoum*[1], Peng Jiang[2], Chengcheng Hu[3], Pei-Shan Hsieh[4], Zhao Chen[5]. [1]University of Arizona Aerospace-Mechanical Engineering, USA, [2]University of Arizona Mechanical Engineering, USA, [3]University of Arizona Mel & Enid Zuckerman College of Public Health Epidemiology & Biostatistics, USA, [4]University of Arizona, USA, [5]University of Arizona College of Public Health, USA

Background: Almost 50% of US women aged 50 or older experience a hip fracture in their remaining life. Therefore, the prediction of hip fracture has become of prime importance. Different statistical models based on clinical data are currently available. However, the number of factors and the complexity of the phenomenon require further research to refine the prediction of these models.

Methods: This study proposes to use the modeling of femoral hip fractures using finite element analysis for the construction of a hip fracture model. The computational data would come as a complement to existing clinical data. The finite element model, which is fully parameterized, enables the creation of a large number of cases representative of a large cohort of patients. In order to extract a risk model from the data, a machine learning technique, known as support vector machine (SVM), is used. SVM can capture highly nonlinear relation between the factors involved in hip fracture. The risk model based on SVM is compared to the traditional logistic model. We performed the study based on computational data only, thus allowing us to obtain reference metrics since the ''true'' model is known.

Conclusions: The fully parameterized model and the use of SVM have the potential to markedly contribute to the refinement of hip fracture models. In addition, the use of a mechanically oriented model provides an essential insight into the importance of the geometric characteristics of the femur.

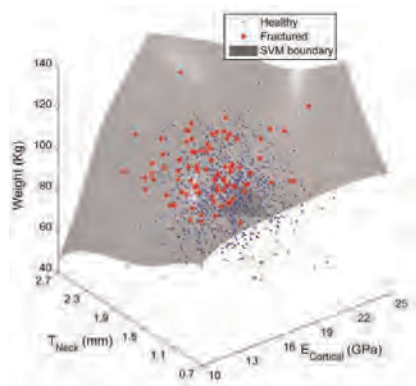

Fig. 1 Example of SVM

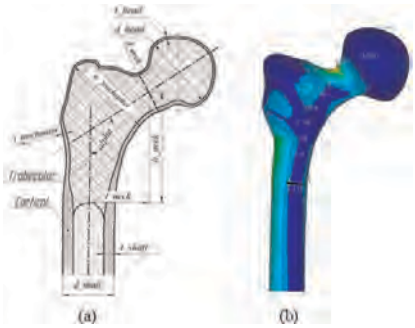

Fig. 2 Finite element model of a femur. Parameters (a) and example of strain distribution (b)

***Disclosures: Samy Missoum**, None.*

SA0074

Comparison of US and French TBS normative data. Christine Simonelli*[1], Edward Leib[2], E Mossman[3], Remy Dufour[4], Alain Heraud[5], Renaud Winzenrieth[6], Michael McClung[3], Didier Hans[7]. [1]HealthEast Osteoporosis Care, USA, [2]University of Vermont, USA, [3]Oregon Osteoporosis Center, USA, [4]Institut Sainte Catherine, France, [5]Rhumatologie, Centre hospitalier Robert Boulin, France, [6]Med-imaps, Hôpital X. Arnozan, PTIB, Pessac, France, France, [7]Lausanne University Hospital, Switzerland

Introduction: The Trabecular Bone Score (TBS, Med-Imaps, France) is an index of the trabecular bone texture, computed on antero-posterior lumbar spine DXA scans. To use TBS in clinical routine, we need to know the age-related evolution of the lumbar vertebrae trabecular texture. We have studied these trabecular texture changes at spine L1-L4 lumbar vertebrae of two cohorts of US and French Caucasian women.

Methods: Subjects were US and French white women aged 45 and older. All data have been obtained from Prodigy DXA devices (GE-Lunar, Madison, WI, USA). In US, three geographically spread off centers were used whereas two centers were used in France. Cross-calibrations between centers, for each country, were performed for both TBS and BMD. BMD and TBS were evaluated at spine L1-L4 and for others vertebrae combinations. Validation of the two cohorts was done by comparing BMD normative data of our cohorts with US or French Caucasian Lunar data provided by the manufacturer. Creation of these cohorts was done using two different approaches: a classical approach using 'healthy' subjects for the US curve and an all comers approach for the French curve.

Results: The two cohorts were composed of512 'healthy' and 5942 'all-comers' Caucasian women for the US and French curve respectively. BMD normative data obtained from these cohort were not statistically different from the US or French Caucasian Lunar normative data ($p>0.15$). In both cohorts, poor correlations have been obtained between L1-L4 TBS and BMI ($r=-0.17$) or weight ($-0.14<r<=-0.16$) while no correlation has been obtained with height. TBS values decreased significantly with age in both cohorts. There was a piecewise linear decline of -2.53 and -2.58 TBS T-score between 45 and 90 years of age (vs.-2.38 and -2.32 for BMD T-score) for the US and the French cohort respectively at L1-L4. In both cohorts, trabecular texture loss rate are exactly similar. After the age of 65 years, loss was accelerated (-0.004 to -0.006 per year) at L1-L4. Both cohorts are similar ($r^2>0.99$).

Conclusion: L1-L4 TBS, which reflects trabecular texture of the lumbar spine, decreases with age. Both the overall decline and rate per year are similar in the US and French cohorts. These results suggest that age-related changes in trabecular bone texture, as evaluated by TBS, are similar for Caucasian women, independently of the country.

***Disclosures: Christine Simonelli**, None.*

SA0075

Strontium Ranelate Treatment Improves Bone Material Level Properties and Microarchitecture of Human Transiliac Bone Biopsy Specimens. Patrick Ammann*[1], Rene Rizzoli[2]. [1]Division of Bone Diseases, Che, [2]Geneva University Hospitals & Faculty of Medicine, Switzerland

Bone strength, hence fracture risk, is dependent on bone geometry, microstructure and bone material level properties. We previously reported that microstructure and material level properties contribute independently to the increase in bone strength of rats treated with strontium ranelate for 2 years, as evaluated by μCT-based Finite Element analysis. We investigated the effects of strontium ranelate (SrRan) treatment on bone material level properties of transiliac bone biopsy and on bone microarchitecture from postmenopausal osteoporotic patients in three studies. In a longitudinal study, 84 paired biopsies were obtained at baseline, and after 6 or 12 months of treatment with 2 g/day SrRan. In SOTI/TROPOS studies 3 paired biopsies were obtained at baseline and after 36 months of treatment. Elastic Modulus, Hardness and Working Energy were blindly analyzed by nanoindentation at the level of the interstitial bone of the cortex and of trabecular nodes under humid conditions. Parameters of microarchitecture were evaluated by microCt (Scanco Medical).

Effects on bone material level properties were observed by 6, 12 and 36 months of treatment. Bone microarchitecture was significantly influenced after more than 12 months. Overall, these results detected in 90 human biopsies indicates an early improvement of bone material level properties followed by later changes on bone microarchitecture in bone specimens collected in patients treated with strontium ranelate. Both effects could contribute to increase of bone strength and to fracture risk reduction. These results suggest different kinetics of SrRan action on bone microarchitecture and bone material level properties.

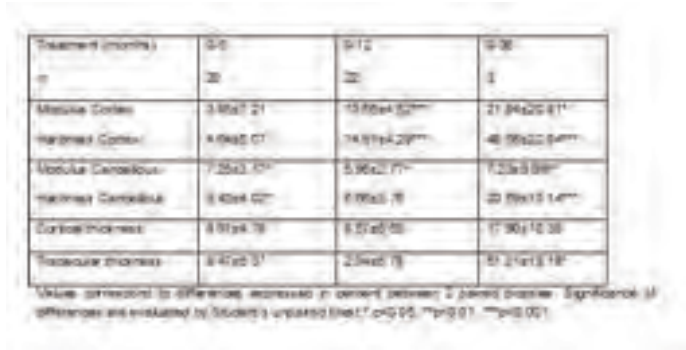

Table

***Disclosures: Patrick Ammann**, AMGEN, MSD, Nestlé, Galapagos, Institut de Recherches Internationales Servier, 6; Labatec, 2*
This study received funding from: Institut de Recherches Internationales Servier

SA0076

Bone quality in osteopenic post-menopausal women is not improved during 12 months of whole body vibration training. Anna-Maria Liphardt*[1], Michelle Kan[2], John D. Schipilow[2], Anna Steinhoff[3], Anne Bauer[4], David Hanley[2], Steven Boyd[2]. [1]German Sport University Cologne (DSHS Köln), Germany, [2]University of Calgary, Canada, [3]University Aachen, Germany, [4]German Sport University Cologne, Germany

Whole body vibration training (WBVT) has been suggested as a preventive measure against bone loss. However, results of previous studies are contradicting, which may be in part due to insufficiently sensitive outcome measures to detect relevant bone changes, as most studies have been based on areal bone mineral density (aBMD) measurements by DXA. WBVT might possibly improve bone quality through structural adaptations without increasing BMD. We hypothesized that 12 months of WBVT will improve or maintain bone micro-architecture and bone strength in osteopenic post-menopausal women between the ages of 50 – 65 yr.

A 12-month trial recruited 22 women who received supervised WBVT (Vibraflex, Galileo, Novotec, Pfortzheim, Germany; 20Hz, 3-4mm, 20 min, 2-3 sessions/wk) and 20 controls. All women had T-scores between -1.3 and -2.2 (osteopenic) and BMI between 20 and 28. Tibia bone outcomes were measured by high-resolution peripheral quantitative CT (HR-pQCT, XtremeCT, Scanco Medical) for bone macro- and microarchitecture and finite element estimated bone strength. DXA provided aBMD at LS and FN. Balance and jump performance and maximum voluntary contraction (MVC) of knee flexor and extensor muscles were recorded. All measurements were taken at baseline, 4-, 8-, and 12 months. WBVT and control group comparisons used a mixed model repeated measures ANOVA with group and time as factors. Level of significance was $p<0.05$.

31 women completed the study with approximately 90% compliance (WBVT: n=17, control N=14). No participants dropped out due to adverse affects related to WBVT. Both groups had similar characteristics and dependent variables at the onset of the study (Table 1). Tt.BMD ($p<0.001$), Ct.Ar*($p=0.004$), Ct.Th. ($p=0.011$) and Ct.Po ($p=0.024$) all significantly decreased over time in both groups; WBVT did not affect the response. Areal BMD by DXA was not affected by time or WBVT at FN (time: $p=0.332$, time*group: $p=0.843$) and LS (time: $p=0.783$, time*group: $p=0.103$). Load carried by the cortex at the distal site decreased from baseline to 4 months in the vibration group but not in the control subjects ($p=0.002$). All other bone outcomes were not affected by WBVT or time. No differences in balance, jump and MVC due to WBVT were detected.In our relatively small cohort, WBVT did not lead to improved bone quality in postmenopausal osteopenic women after 12 months of training compared to controls, and there were no detected benefits for balance and muscle strength outcomes.

Subject characteristics

Baseline	Group	N	Mean	SD	F	p
Age (yrs)	control	14	58.5	3.3	0.16	0.69
	vibration	17	59.1	4.6		
Height (m)	control	14	160.8	4.42	0.30	0.59
	vibration	17	159.7	6.20		
Weight (kg)	control	14	63.4	8.94	3.06	0.09
	vibration	17	70.5	12.9		
Lean mass (kg)	control	14	43.3	3.90	1.82	0.19
	vibration	17	45.5	4.84		
Percent body fat (%)	control	14	31.0	6.8	1.15	0.29
	vibration	17	34.2	9.3		
PASE score	control	14	167.3	91.2	0.02	0.88
	vibration	17	172.0	85.3		
Total Ca intake (mg/day)	control	14	1564.3	784.4	0.01	0.92
	vibration	17	1588.5	570.2		
Vit D Supplements (IU/day)	control	14	1252.4	712.9	1.82	0.19
	vibration	17	1959.1	1847.9		
Age at last period (yrs)	control	14	51.5	3.7	0.65	0.43
	vibration	17	50.1	5.5		
Time since last period (yrs)	control	14	6.9	2.9	1.25	0.27
	vibration	17	8.6	4.7		

Table 1: Subject characteristics

***Disclosures: Anna-Maria Liphardt**, None.*

SA0077

Variation in Bone Turnover Markers in Professional Sport Players During Training is Mediated by Changes in Sclerostin Levels. Ranuccio Nuti*[1], Daniela Merlotti[1], Michele Bisogni[2], Beatrice Franci[2], Barbara Lucani[2], Stella Campagna[2], Laura Cresti[2], Matteo Beltrami[2], Konstantinos Stolakis[2], Stefano Rotatori[2], Andrea Causarano[3], Luigi Gennari[1]. [1]University of Siena, Italy, [2]Dept. Medicine Surgery & Neurosciences University of Siena, Italy, [3]Medical Staff Siena Football Club, Italy

It is well known that bone turnover changes in response to exercise and that this effect is in part mediated by osteocytes through the release of mediators which affect osteoclast and osteoblast activity. However the variation of bone turnover and of markers of osteocyte activity following a rapid change in exercise level has not been investigated in detail. The aim of the study was to assess changes in bone turnover in 25 professional soccer players (27.8±4.3 yrs) at 3 different times: before pre-season training, at the end of the pre-season training and during the soccer season. Four different groups of males of the same age (G1, n=30), middle age (G2, n=76), elderly (G3, n=44) or long-term immobilized subjects (G4, n=20) were selected as reference. Bone alkaline phosphatase (BALP) and osteocalcin (OC) were assessed as markers of bone formation while carboxy-terminal telopeptide of type I collagen (CTX) was measured to assess bone resorption. In professional soccer players CTX levels were significantly higher before training than at the end of post training or during mid-season (1.48±0.4 vs. 0.91±0.5 vs. 1.01±0.4 ng/ml; $p<0.001$) while an opposite trend was observed for BALP (13.1±5.4 vs. 17.5±6.0 vs. 15.8±5.0 mcg/l; $p<0.01$). A parallel increase in OC was observed, which became significant at mid-season (6.1±1.7 vs. 7.1±1.5 ng/ml; $p<0.01$). Of interest, CTX levels of soccer players at the beginning of training were significantly higher than those observed in control groups of different ages but also with respect to those observed during long-term immobilization. Conversely, before exercise bone formation markers were higher than those observed in older reference groups (G3, G4) while did not significantly differ from age-matched controls (G1). After training and during soccer season either OC or BALP levels were significantly higher than correspondent levels of all the reference groups. At the beginning of pre-season, circulating sclerostin did not differ from controls of different ages but significantly decreased during pre-season training (30.6± 9 vs. 26.0±7 pmol/l; $p<0.05$). This decrease was significantly correlated with the increase in bone formation markers. These results suggest that in professional players bone adapts to the high impact exercise with an increase in bone remodeling. However, during post-season a rapid unbalance between bone resorption and bone formation occurs which appears at least in part mediated by variation in sclerostin levels.

***Disclosures: Ranuccio Nuti**, None.*

SA0078

Masticatory muscle tendon-aponeurosis hyperplasia exhibits heterotopic calcification in temporal tendon. Tsuyoshi Sato*[1], YUICHIRO ENOKI[1], Shoichiro Kokabu[2], Masahiko Okubo[1], Tetsuya Yoda[1]. [1]Saitama Medical University, Japan, [2]Harvard School of Dental Medicine, USA

Masticatory muscle tendon-aponeurosis hyperplasia (MMTAH), which was recently established in Japan, is a new disease associated with limited mouth opening. The condition of this disease advances very slowly from adolescence and both mandibular angles exhibit hyperplasia, resulting in a characteristic square mandible. MMTAH is diagnosed by a palpable dense band at the anterior border of the masseter muscle upon maximum mouth opening and square mandible configuration. A lack of recognition of this disease among general practitioners results in misdiagnosis of the temporomandibular disorders, and patients have often been treated with irreversible operations. To date, no clinical reports are available on this disease from other countries. Almost clinicians may fail to notice this disease. Previously, we have demonstrated that good long-term recovery has been reliably obtained in patients with MMTAH via resection of the hyperplastic masseter muscle aponeurosis with coronoidectomy for separation of the temporal muscle from the coronoid process. Chiba et al. mentioned that both tendon and aponeurosis in MMTAH exhibit normal tendon structure because of a lack of inflammation. These observations suggest that tendon tissues in MMTAH represent hyperplasia. In MMTAH, although tendon tissues have been analyzed light-microscopically, the microstructure of muscles and tendons remains still unclear. We thus performed microstructural analysis of muscles and tendons in MMTAH by using electron microscopic technique and energy dispersive X-ray analysis to identify the elemental composition. We assessed the structure of the muscle and tendon tissues by using both TEM and SEM. In muscle tissues, TEM showed the narrowing of vascular lumen, contraction bands and areas of myofibrillar degeneration in MMTAH compared to FD (facial deformity). In tendon tissues, the irregular particles whose diameter was between 10-100 micrometers were observed on the surface of tendon tissues under SEM. Mineralized nodules were observed in tendon tissues of MMTAH compared to FD. Element mapping of tendon tissues revealed that Ca and P were detected on the region of calcification whereas Si was detected on tendon which was not calcified around Ca and P. In summary, we have found that MMTAH exhibited heterotopic calcification of tendon tissues by using electron microscopic techniques. We would like to discuss the diseases that ectopic calcification occurs in tendon tissues.

***Disclosures: Tsuyoshi Sato**, None.*
This study received funding from: Scientific Research from the Ministry of Education, Science, Sports and Culture of Japan

SA0079

Microstructure of Narwhal Tusk Studied by Synchrotron Radiation Nano-Tomography. Mie Birkbak[1], Karl Anker Jørgensen[2], Henrik Birkedal*[3]. [1]iNANO & Department of Chemistry, Aarhus University, Denmark, [2]Department of Chemistry, Aarhus University, Denmark, [3]Aarhus University, Denmark

We investigate narwhal tusk microstructure using synchrotron radiation nano-CT to reveal a very complex hierarchical pore structure. Narwhals whose impressive tusks have inspired unicorn myth are one of the few animals that display such impressive external dentitions.

Narwhal tusk is most often a single tooth with a spiral surface composed of a central pulp chamber surrounded by primary dentine which again is surrounded by a thick layer of cementum replete with cementocytes as evidenced by very abundant cementocyte lacunae [1]. This is in opposition to normal teeth that have cementum on the interior interface between bone and tooth rather than on the outside. Narwhal dentine has roughly the same calcium content as narwhal cementum, but has a markedly higher Youngs modulus [2]. While there is some knowledge of Narwhal tusk microstructure and mechanics, the full tusk structure is far from understood. Herein we use synchrotron radiation nano-CT with 325 nm voxel size to reveal a very complex hierarchical pore structure.

The interior dentine part that dominates the tooth is dominated of mineralized bundles of about 15 µm diameter giving rise to an appearance resembling fleecy clouds in cross sectional nano-CT images. The dentine is tubular with tubule diameters of the order of 1 µm. The tubules are not perfectly straight but span long distances in a continuous manner. The tubules appear to be arranged in ribbons perpendicular to the axis of the tooth. The cementum/dentine junction is characterized by an abrupt change of microstructure. The junction itself is characterized by a microporous structure that is much less ordered than the tubular structure in the dentine layer. In the cementum layer two distinct morphologies are found. The first is replete with small pores seemingly randomly dispersed in the mineralized tissue. The other type is much more compact and only few micropores are present. However, both cementum types show cementocyte lacunae that are known to be abundant in tusk cementum [1].The biological function of the Narwhal tusk remains debated and the detailed functional implications of the present investigations will be the subject of future work

[1] Nweeia, M. T. *et al.* (2012) The Anatomical Record, 295, 1006-1016.
[2] Bread, K. *et al.* (1990) Archs Oral Biology, 35, 615-621.
Keywords: narwhal tusk, porosity, nano-CT, teeth, cementocyte lacunae

***Disclosures: Henrik Birkedal**, None.*

SA0080

Pericapillary Bone Formation by Mural Osteoblasts during Endochondral Ossification. Ichiro Takada*[1], Nobuhito Nango[2], Yoshihiro Takeda[3], Atsushi Momose[4], Yoshiaki Kubota[1], Sho Kanzaki[1], Kouji Shimoda[1], Yasunari Takada[1], Latifa Bakiri[5], Erwin Wagner[5], Koichi Matsuo[1]. [1]School of Medicine, Keio University, Japan, [2]Ratoc System Engineering Co., Ltd., Japan, [3]Rigaku Corporation, Japan, [4]Tohoku University, Japan, [5]CNIO, Spain

Blood vessel invasion of cartilage is crucial for endochondral ossification. However, spatio-temporal relationships among capillary endothelial cells, chondro/osteoclasts and osteoblasts are still under investigation. To understand potential contribution of blood vessels to cellular processes underlying replacement of cartilage by bone, we analyzed transgenic mice overexpressing the transcription factor Fra-1 (Fra-1 mice), which show enhanced bone formation. Preliminary experiments suggested that adult Fra-1 mice showed increased number and size of blood capillaries in cortical bones. Transgenic mice exhibited abundant blood capillaries even in the malleal processus brevis (mPB), a hemispherical protrusion 300 μm in diameter, from which capillaries gradually disappear during postnatal endochondral ossification in wild-type mice. The observation that capillary volume remained high until adulthood in Fra-1mice suggests persistent capillary survival within bone. Synchrotron X-ray phase-sensitive microscopy demonstrated a roughly concentric, cylindrical arrangement of osteocytic lacunae along the capillary in the wild-type mPB indicative of pericapillary bone formation. Calcein double-labeling analysis showed that osteoblasts surrounding the capillary secreted bone matrix away from the capillary, thereby reducing the circumference of the capillary lumen. We conclude that hyperactivity of "osteogenic capillaries" could underlie the previously reported enhanced bone formation seen in Fra-1 transgenic mice. These data support the view that ''osteogenic capillaries'' directly interact with and polarize mural osteoblasts, thereby determining the location and direction of bone formation within ossifying cartilage during endochondral ossification.

***Disclosures: Ichiro Takada**, None.*

SA0081

See Friday Plenary Number FR0081.

SA0082

Complete Suppression of PTHrP Signaling in Chondrocytes in the Histone Deacetylase 4 and 5 Double Knockout Mouse. Shigeki Nishimori*[1], Forest Lai[1], Marc Wein[1], Elena Kozhemyakina[2], Eric Olson[3], Andrew Lassar[2], Henry Kronenberg[1]. [1]Massachusetts General Hospital, USA, [2]Harvard Medical School, USA, [3]UT Southwestern Medical Center at Dallas, USA

Both parathyroid hormone-related protein (PTHrP) and Histone Deacetylase (HDAC) 4 suppress chondrocyte hypertrophy. We confirmed that HDAC4 is a mediator of the PTHrP signaling pathway by knocking out the HDAC4 gene in the PTHrP transgenic mouse. The similarities between the HDAC4 KO mouse and the PTHrP KO mouse also support this hypothesis. However, the delayed onset in the HDAC4 KO mouse suggests the existence of other mediators. Here we identified HDAC5 as a mediator of the PTHrP signaling pathway using mouse genetics.

The PTHrP KO mouse dies just after birth due to respiratory failure caused by ectopic chondrocyte hypertrophy and ossification in the rib cartilage (Karaplis, Genes Dev. 1994). The HDAC4 KO mouse exhibits normal rib cartilage at birth (P0), but dies around 10 days after birth (P10) with progressive chondrocyte hypertrophy and ossification in the rib cartilage (Vega, Cell. 2004). Accelerated chondrocyte hypertrophy in the PTHrP KO mouse leads to a very short proliferating region in the growth plate (30% of the wild type (WT) at P0). We found the similar short proliferating region in the HDAC4 KO mouse (60% of the WT at P0, 40% of the WT at P8).

We focused on HDAC5 as a possible mediator, because we found HDAC4 and HDAC5 show similar mRNA expression levels in the growth plate. As another Class IIa HDAC, HDAC5 might complement functions of HDAC4.

The HDAC4 KO; HDAC5 heterozygotes mouse (HET) mouse died just after birth with a rib phenotype like that of the PTHrP KO mouse, but the growth plate phenotype in the proliferating region was milder than that of the PTHrP KO mouse (50% of the WT at P0). The HDAC 4 and 5 double KO mouse died at birth with a phenotype similar to that of the PTHrP KO mouse both in the rib cartilage and the growth plates. These results suggest that HDAC5 mediates PTHrP signaling when HDAC4 is missing. HDAC5 is not essential when HDAC4 is working, judged by the normal phenotype of the HDAC5 KO mouse and the HDAC5 KO; HDAC4 HET mouse.

In the growth plate of the HDAC4 KO mouse, HDAC5 mRNA was expressed at normal level by RT-qPCR analysis. In contrast, the HDAC5 protein level was upregulated in the proliferating chondrocytes of the HDAC4 KO mouse by immunohistological analysis using confocal fluorescent microscopy. These results are consistent with the idea that HDAC5 compensates for the loss of HDAC4 as a mediator of the PTHrP signaling pathway.

Long bone phenotypes of the PTHrP KO mouse and the HDAC related KO mice

***Disclosures: Shigeki Nishimori**, None.*

SA0083

See Friday Plenary Number FR0083.

SA0084

Gene Expression Profiling Reveals Similarities between the Spatial Architectures of Articular and Growth Plate Cartilage. Michael Chau*[1], Julian Lui[1], Stephan Spath[2], Jeffrey Baron[1], Ola Nilsson[1]. [1]NICHD, USA, [2]NIH, USA

Background: In the embryo, articular cartilage is initially continuous with growth plate cartilage. Subsequently, a secondary ossification center forms within the epiphyseal cartilage, dividing it into future articular cartilage peripherally and growth plate cartilage more centrally. Articular and growth plate cartilage both consist of three distinct zones of chondrocytes.

Objective: To test the hypothesis that gene expression profiles of superficial, intermediate, and deep zones of articular cartilage are spatially similar to those of resting, proliferative, and hypertrophic zones of growth plate cartilage, respectively.

Methods: Rat articular cartilage was microdissected into superficial and intermediate/deep regions manually, mouse articular cartilage into superficial, intermediate, and deep zones by laser capture, and rat growth plate into resting, proliferative, and hypertrophic zones manually. Gene expression was analyzed by microarray (Affymetrix). A gene was considered to be spatially regulated if its expression in two adjacent zones differed by ⩾2-fold and false discovery rate <0.01.

Results: In rat, many genes that were spatially upregulated in the intermediate/deep region of articular cartilage were also upregulated in resting zone of growth plate cartilage (overlap greater than expected by chance, $P<0.001$, chi-square test). Interestingly, superficial zone of articular cartilage showed an expression profile with similarities to both proliferative and hypertrophic zones of growth plate cartilage ($P<0.001$ each). Additionally, known proliferative zone markers Gdf10, Prelp, and Olfml3 were significantly upregulated in superficial zone ($P<0.01$ each), whereas resting zone markers Sfrp5, Efemp1, and Pcp4 were upregulated in the deep/intermediate region ($P<0.01$ each). In mouse articular cartilage, we similarly found that intermediate and deep zones resembled resting zone ($P<0.001$ each), while superficial zone resembled proliferative and hypertrophic zones ($P<0.001$ each).

Conclusion: Contrary to our hypothesis, we found that intermediate-deep zones of articular cartilage were similar in gene expression profile to resting zone of growth plate cartilage and that superficial zone resembled proliferative and hypertrophic zones. Since proliferative and hypertrophic chondrocytes derive from resting zone chondrocytes, these findings raise the possibility that superficial zone chondrocytes analogously differentiate from intermediate-deep zone chondrocytes.

***Disclosures: Michael Chau**, None.*

SA0085

Histone Deacetylase 3 Controls Extracellular Matrix Degradation, Vascularization, and Secondary Ossification Formation during Endochondral Ossification. Lomeli Carpio*, Elizabeth Bradley, Meghan McGee-Lawrence, Jennifer Westendorf. Mayo Clinic, USA

Histone deacetylases (Hdacs) epigenetically regulate many cellular processes by modulating chromatin structure and repressing gene expression. Endochondral ossification is a tightly regulated and complex process and several Hdacs are involved at each stage. We previously showed that conditional deletion of Hdac3 in osterix-expressing osteo/chondroprogenitor cells resulted in severe osteopenia and growth retardation due to reduced numbers of osteoblasts and abnormal maturation of chondrocytes in the growth plate. Hdac3-deficient chondrocytes entered hypertrophy more quickly and secreted less extracellular matrix due to reduced Akt signaling than wildtype cells. In this study, we further defined the cell-autonomous role of Hdac3 in chondrocyte maturation by crossing $Hdac3^{fl/fl}$ mice with animals expressing chondrocyte-specific, tamoxifen-inducible type II collagen-Cre. Tamoxifen was

administered at postnatal day 5 and the animals were studied at 4 or 8 weeks of age by histology, microCT, and EPIC imaging. At 8 weeks of age, the Hdac3 CKO mice had increased cortical bone and trabecular bone thickness; however, trabecular number was reduced, trabecular spacing was increased and trabecular bone volume fraction was decreased. This phenotype is likely compensatory in response to disrupted growth plate development. Indeed, at 4 weeks of age, the growth plate was thicker in the Hdac3 CKO mice and associated with an expansion of hypertrophic zone chondrocytes. Secondary ossification center formation was delayed in these animals. Additionally, immunohistochemistry showed decreased expression of the angiogenic marker, platelet/epithelial cell adhesion molecule (Pecam)-1, in the secondary ossification center of the Hdac3 CKO mice compared to control animals. These data indicate Hdac3 deletion negatively impacts vascularization and chondrocyte hypertrophy. In vitro gene expression analysis of immature mouse articular chondrocyte micromass cultures demonstrated decreased expression of vascular endothelial growth factor (Vegf) and increased expression of tissue inhibitors of matrix metalloproteinase (Timps) in Hdac3-deficient chondrocytes. Together these data demonstrate Hdac3 regulates extracellular matrix degradation and subsequent vascularization in chondrocyte maturation during endochondral ossification.

***Disclosures: Lomeli Carpio**, None.*

SA0086

Identification of chondrocyte-binding peptides by phage display. Sao Fong Cheung*[1], Julian Chun Kin Lui[2], Jeffrey Baron[2]. [1]National Insitutes of Health, USA, [2]NIH, USA

Numerous genetic and environmental disorders disturb cartilage generation and maintenance in growth plate or articular cartilage, causing a wide variety of disorders. As a first step toward novel experimental and therapeutic approaches to these diseases, we sought to identify peptides that bind cartilage tissue using phage display.

An M13 phage library exhibiting random 12-amino acid peptides on the viral surface was iteratively selected for affinity to cultured murine chondrocytes by repetitive binding and amplification. From the resulting enriched phage pool, 23 clones were picked and assessed for their binding characteristics by ELISA. Of these clones, 8 showed at least a 2-fold increase in binding to cultured chondrocytes, compared to a phage lacking the inserted peptide. Phage clones C1 and C19, which display peptide sequences RLDPTSYLRTFW and HDSQLEALIKFM respectively, possessed the greatest binding to cultured chondrocytes. Using ELISA, these two phage were also demonstrated to have substantially less affinity to fibroblasts, myocytes, osteoblasts and hepatocytes, compared to chondrocytes, suggesting an interaction that was moderately tissue-specific. Immunohistochemical staining revealed that phage C1 and C19 bound to cultured chondrocytes and extracellular matrix. To determine whether the binding to chondrocytes and matrix was attributable to the affinity of the inserted peptide independent of the phage coat proteins, free peptides, conjugated with the fluorescent probe FITC, were synthesized and incubated with cultured chondrocytes. Peptides C1 and C19, but not a random peptide, bound to both cultured chondrocytes and extracellular matrix, confirming that binding involved the peptides per se. In conclusion, using phage display, we successfully identified peptide sequences that are capable of targeting chondrocytes. Further studies may be needed to determine if such cartilage-binding peptides have potential applications for treating cartilage disorders.

***Disclosures: Sao Fong Cheung**, None.*

SA0087

Identifying Sox9 regulatory programs in mammalian skeletogenesis. Xinjun He*[1], Andrew McMahon[1], Shinsuke Ohba[2]. [1]University of Southern California, USA, [2]The University of Tokyo, Japan

Sox9, an HMG-box containing transcriptional regulator, is essential for chondrocyte development. Ectopic expression of Sox9 is sufficient to reprogram several cell types to a chondrocyte state. The evidence indicates Sox9 is a key determinant of many aspects of chondrogenesis. Here, we explored the direct mechanisms of Sox9 action through a comprehensive analysis of Sox9 binding sites in mammalian, neonatal rib chondrocytes. Sox9 chromatin immunoprecipitation and next generation sequencing (ChIP-seq) identified 27,656 Sox9-associated regions in the genome. Broadly, these fall into two categories: Class I, within 500 base-pairs (bp) of a transcriptional start site (TSS) accounting for 25% of the data, and Class II where binding lies outside this local TSS domain, in some cases many hundreds of kilobases (kb) from the likely gene target. Analysis of Class I sites in conjunction with a number of measures of chromatin organization (histone acetylation and methylation) and transcriptional activity (histone methylation, RNA polymerase II and p300 association) suggest a mechanism where Sox9 associates at the TSS through protein-protein interactions rather than direct DNA-binding. Here, the level of binding reflects transcriptional activity of the target and targets encode general regulators of cell activity, not cartilage specific programs. In contrast, Class II sites correlate with active enhancer signatures, verified in transgenic studies, through direct binding of DNA target sites. Bioinformatic analysis reveals a striking chondrocyte signature with over 795 direct target genes. Motif recovery, and biochemical and transgenic studies analyzing recovered motifs, suggest that Sox9 regulates targets through sub-optimal dimeric binding sites where robust, high-level expression is achieved through the use of multiple enhancer elements. Further, these studies predict Sox9 acts in conjunction with the Ap1 family of transcriptional regulators; ChIP-seq analysis of c-Jun confirmed this prediction. These data are an important first step in identifying the gene regulatory networks regulating chondrocyte and osteoblast development.

***Disclosures: Xinjun He**, None.*

SA0088

Longitudinal Overgrowth Following Circumferential Periosteal Division of Femur of Developing Rat. Shinjiro Takata*. Tokushima National Hospital,National Hospital Organization, Japan

Circumferential periosteal division (CPD) of rat tibia produces an increase in its growth rate and in the activity of both the proliferative and hypertrophic zones (Taylor FJ et al. J Anat 151:221-231,1987). The purpose of this study was to show mechanisms of longitudinal overgrowth following CPD of femur of developing rat.Twelve male Wistar rats aged 8 weeks were used for this study. Periosteum of diaphysis of the right femur was divided circumferentially (CPD group), and the left femur was control (Control group). Rats were sacrificed 4 weeks after CPD. The longitudinal length of femur (n=6) and rate of longitudinal growth and bone turnover by bone histmorphometry were compared between CPD group and Control group 4 weeks after CPD (n=6).Longitudinal length of rat femur of CPD group and Control group were 39.4 ± 1.2 mm and 38.5 ± 0.8mm, respectively (p=0.0086), showing that CPD for 4 weeks produced an approximately 2.5% increase of rat femur compared with Control group.Bone histomorphometry shows that the rate of longitudinal growth of femur of CPD group and Control group 4 weeks after CPD was 92.3 ± 5.3 and 54.4 ± 4.6 μm/day, respectively ($p<0.0001$). Mineral apposition rate of femora of CPD group and Control group 4 weeks after CPD was 3.90 ± 0.38 and 3.07 ± 0.25 μm/day, respectively (p=0.0004). Osteoclast surface/bone surface of CPD group and Control group 4 weeks after CPD was 13.1 ± 1.0 and 9.1 ± 1.8%, respectively ($p<0.0001$).Histological analysis of distal growth plate of rat femur showed an increased number of hypertrophic chondrocytes and width of hypertrophic zone of the distal growth plate of rat femur of CPD group compared with Control group. The major finding of this study was that CPD of diaphysis of rat femur stimulates endochondral ossification to produce longitudinal overgrowth. The results suggest that periosteum of tubular bone plays an important role in endochondral ossification of growth plate.

***Disclosures: Shinjiro Takata**, None.*

SA0089

Modulating *Sost* Expression Influences the Progression and Severity of Post Traumatic Osteoarthritis in Mice. Jiun Chiun Chang*[1], Blaine A. Christiansen[2], Cynthia B. Thomas[3], Nicole M. Collette[3], Craig Blanchette[4], Gabriela Loots[5]. [1]University of California, Merced, USA, [2]UC Davis Medical Center, Department of Orthopaedic Surgery, USA, [3]Lawrence Livermore National Laboratories, Physical & Life Sciences Directorate, USA, [4]Lawrence Livermore National Laboratories, USA, [5]Lawrence Livermore National Laboratory, UC Merced, USA

Sclerostin (Sost), a Wnt antagonist known to play important roles in bone development, metabolism and fracture repair has also been implicated in regulating chondrocyte function. Recently it has been shown that Sost is expressed in articular cartilage and its levels increase in focal areas of osteoarthritis (OA) damage in surgical models of OA. Using a recently described noninvasive mouse model of post traumatic osteoarthritis (PTOA) in which the anterior cruciate ligament ruptures in response to a single tibial compression overload, we compared OA progression and cartilage damage severity in mice lacking Sost (KO) or overexpressing SOST (TG) to C57BL/6 (WT) control mice. Injured joints were examined histologically at 3, 6, 12, and 16 weeks post injury. At 6 weeks post injury WTs and TGs demonstrated minimal cartilage loss whereas the KOs showed mild OA. At 12 weeks post injury, the WTs displayed moderate OA, while the KOs had more severe cartilage loss. In contrast, TGs maintained mild OA, showing a delay in the disease progression, and a phenotype significantly less severe than the WT controls, consistent with the previous hypothesis that Sost overexpression may have a protective role in OA. We also quantified subchondral trabecular bone loss at the femoral epiphysis and ectopic bone formation by micro-computed tomography. We found significantly greater osteophyte formation in KOs than in WTs and TGs. Consistent with Sost's role in stimulating bone formation KOs sustained no significant subchondral bone loss from 10 days to 16 weeks post injury while WT femurs lost 24 ± 9%. To determine if Sost interferes with initial inflammatory response, we quantified matrix metalloproteinases (MMP) activity post injury. Fluorescent MMP-Sense substrate was administered intravenously immediately post injury, and MMP activity was quantified based on *in vivo* fluorescence levels 3 days post injury. Whereas WT and KO injured joints showed similar MMP activity levels, TG injured joints displayed 2-fold less MMP activity than WT and KO injured joints, suggesting that SOST overexpression inhibits initial inflammation and the activity of proteolytic enzymes known to degrade articular cartilage matrix. By utilizing a clinically relevant PTOA model, by 16 weeks post injury, Sost KO mice developed severe OA while Sost TG showed moderate signs of cartilage damage. Collectively, these findings support the hypothesis that Sost has a protective role in PTOA.

***Disclosures: Jiun Chiun Chang**, None.*

SA0090

Phosphate regulates signaling molecules and apoptotic proteins in hypertrophic chondrocytes. Eva Liu*[1], Francesca Gori[2], Marie Demay[3]. [1]Brigham & Women's Hospital & Massachusetts General Hospital, USA, [2]Harvard School of Dental MedicineMassachusetts General Hospital, USA, [3]Massachusetts General Hospital & Harvard Medical School, USA

Phosphate plays an essential role in growth plate maturation. Hypophosphatemia impairs hypertrophic chondrocyte apoptosis, resulting in rickets, characterized by expansion of the hypertrophic chondrocyte layer of the growth plate. Phosphate-mediated activation of the mitochondrial apoptotic pathway in hypertrophic chondrocytes requires induction of Erk1/2 phosphorylation. Phosphate induction of Erk1/2 phosphorylation in murine hypertrophic chondrocytes, is seen in response to 3mM, 5mM and 7mM phosphate with peak levels observed 15 minutes post-treatment. Phosphate has been shown to regulate levels of pro- and anti-apoptotic factors in hypertrophic ATDC5 chondrocytes treated with 20 mM phosphate. However, it is not known whether phosphate leads to acute subcellular redistribution of factors that regulate the mitochondrial apoptotic pathway. Therefore, studies were performed to determine the time course of change in signaling and apoptotic proteins following treatment of hypertrophic chondrocytes with phosphate.

Murine costal chondrocytes were cultured under conditions that promote hypertrophic differentiation. Hypertrophic chondrocytes were treated with 7 mM phosphate and subjected to subcellular fractionation. Within 15 minutes of exposure to 7 mM phosphate, C-raf and Erk1/2 phosphorylation are observed in both the cytosol and mitochondria of hypertrophic chondrocytes. After one hour exposure to 7 mM phosphate, increases in the cytosolic and mitochondrial levels of total and phosphorylated Erk1/2 are observed. Cytosolic levels of the anti-apoptotic protein Bcl-2 and of the pro-apoptotic protein Bax increased in hypertrophic chondrocytes treated with phosphate, returning to baseline by 2 hours post-treatment. Pro-apoptotic phospho- p-53 localized predominantly to the mitochondria of hypertrophic chondrocytes and did not change with phosphate treatment. Phosphate treatment of hypertrophic chondrocytes leads to changes in levels of signaling molecules and apoptotic factors in both the cytosol and mitochondria. The increase in mitochondrial pErk1/2 in response to phosphate suggests phosphate-induced pErk1/2 may play a direct role in activating the mitochondrial apoptotic pathway in hypertrophic chondrocytes.

***Disclosures: Eva Liu**, None.*

SA0091

Potential roles of neurotrophin-3 in growth plate cartilage bony repair and skeletal cell formation. Yu-Wen Su[1], Rosa Chung[1], Cristina Vincent[1], Shek Man Chim[2], Fiona Zhou[1], Alice Lee[1], Chia-Ming Fan[1], Jiake Xu[2], Xin-Fu Zhou[3], Cory Xian*[1]. [1]University of South Australia, Australia, [2]University of Western Australia, Australia, [3]University of South Australia, Azerbaijan

Injury to the growth plate cartilage often results in undesirable bony repair at the injury site causing bone growth defects in children, for which the underlying mechanisms remain unclear. Neurotrophic factors (NTs) have been shown to be involved in bone fracture healing; this study investigated potential functions of NTs in the bony repair of injured tibial growth plate in rats and during skeletal cell formation in vitro. Firstly, up-regulated expression of NGF, BDNF, NT-3, and NT-4 (with NT-3 showing the highest induction) and receptors (TrkA, TrkB and TrkC) by RT-PCR was observed at the injury site at different time points after injury. NTs were found to be immunolocalized in mesenchymal cells, chondrocytes, osteoblasts, and osteocytes at the injury site. Secondly, differentially regulated expression of NTs and receptors was detected during in vitro chondrogenesis, osteoblastogenesis, mineralization and osteoclastogenesis in rat bone marrow cells and murine progenitor cell-line cells. Thirdly, in vitro assays showed that addition of NT-3 protein decreased chondrocyte formation and expression of chondrogenesis-related genes, but enhanced expression of osteogenesis related genes (Runx2, osterix, osteocalcin and BMP-2), as well as osteoclastogenesis-related molecules (RANK and OSCAR) and osteoclast formation. Conversely, anti-NT-3 antibody treatment had the opposite effects. Neither anti-NT-3 nor NT-3 treatment affected activation of transcription factor NF-κB in osteoclast precursor RAW264.7 cells. Lastly, micro-CT and histology analyses of injured rats treated with NT3 or anti-NT-3 antibody indicated that anti-NT-3 treatment attenuated bone formation at the injury site at day 28. RT-PCR analysis with injury site samples found that anti-NT-3 treatment alleviated the injury-induced down-regulation of cartilage markers while inhibited expression of osteocalcin and osteoclast receptor gene RANK. Conversely, NT-3 treatment had a trend of suppressing levels of chondrogenesis markers (Sox9, collagen-2&10) but significantly enhanced those for both osteogenesis (Runx2, osterix and osteocalcin) and osteoclastogenesis (RANK and OSCAR). It is concluded that neurotrophic factor signaling is involved in the bony repair process at the injured growth plate and the associated skeletal cell formation; in particular, NT-3 may attenuate chondrogenesis but enhance osteogenesis and osteoclastogenesis during growth plate repair and in vitro skeletal cell formation.

***Disclosures: Cory Xian**, None.*

SA0092

RBPjκ-dependent Notch Signaling Regulates the Initiation of Chondrocyte Hypertophy via SOX9. Anat Kohn*[1], Timothy Rutkowski[2], Anthony Mirando[2], Alana Osinski[2], Yufeng Dong[1], Michael Zuscik[2], Regis O'Keefe[1], Matthew Hilton[3]. [1]UNIVERSITY OF ROCHESTER, USA, [2]University of Rochester School of Medicine & Dentistry, USA, [3]University of Rochester Medical Center, USA

We have recently identified RBPjκ-dependent Notch signaling as an important regulator of chondrogenesis and chondrocyte maturation during cartilage development. Specifically, we demonstrated that loss of RBPjκ-dependent Notch signaling results in the delayed onset of chondrocyte hypertrophy, as well as, delayed progression to terminal chondrocyte maturation *in vivo* and *in vitro*. These data have also implicated Notch signaling in the suppression of the transcription factor SOX9, indicating a possible mechanism by which Notch signaling promotes chondrocyte maturation or hypertrophy. To identify whether *Sox9* is a down-stream target of Notch signaling during chondrocyte maturation, we first analyzed RBPjκ loss-of-function (LOF) (*Prx1Cre;Rbpjκ$^{f/f}$*) and RBPjκ LOF Sox9 haploinsufficient (*Prx1Cre;Rbpjκ$^{f/f}$;Sox9$^{f/+}$*) mutant embryos at E14.5 and E18.5. Hind limbs and fore limbs from embryos at E14.5 and E18.5 were analyzed using histology, histomorphometric measurements, and *in situ* hybridization for markers of chondrocyte maturation (*Ihh, Col10a1* and *Mmp13*). At E14.5, analyses revealed that delays in the onset of chondrocyte hypertrophy seen in RBPjκ LOF embryos are rescued by Sox9 haploinsufficiency. However, analyses of E18.5 RBPjκ LOF Sox9 haploinsufficient growth plates revealed no rescue in the delayed terminal chondrocyte maturation observed in RBPjκ LOF mutant growth plates. Furthermore, our in vitro studies revealed that over-expression of the Notch Intra-Cellular Domain (NICD1 or NICD2) in chondrogenic cells leads to a significant reduction in *Sox9* expression. Similarly, over-expression of NICD1 or NICD2 suppressed luciferase expression driven by a 1kb fragment of the *Sox9* promoter. Interestingly, the 1kb fragment of the *Sox9* promoter does not contain any direct RBPjκ binding sites, but does contain N-box and E-box DNA motifs. HES/HEY factors, transcriptional repressors classically activated by RBPjκ-dependent Notch signaling, specifically bind N-box and some E-box sequences. Based on these findings we performed ChIP analyses of the *Sox9* promoter and demonstrated that several HES/HEY factors are capable of binding the N-box/E-box region of the *Sox9* promoter and may be required for Notch-mediated inhibition of *Sox9* expression. Collectively, these data suggest that RBPjκ-dependent Notch signaling promotes the initiation of hypertrophy via HES/HEY mediated suppression of *Sox9*.

***Disclosures: Anat Kohn**, None.*

SA0093

Runx1 Increased Expression in Superficial Zone Chondrocytes in Response to Mechanical Loading and in Chondrocyte Clones of Osteoarthritic Tissue: Functional Implications. Paul Fanning*[1], Kimberly LeBlanc[2], Marie Walcott[3], Tripti Guar[4], Shannon O'Connell[3], Kirti Basil[3], April Mason-Savas[3], Jason Silva[3], Andre Van Wijnen[5], Janet Stein[6], Gary Stein[7], David Ayers[8], Jane Lian[6]. [1]University of Massachusetts Medical School, USA, [2]Dept. of Cell Biology & Cancer Center, University of Massachusetts Medical School, USA, [3]Dept. of Orthopedics & Physical Rehabilitation, University of Massachusetts Medical School, USA, [4]Dept. of Cell Biology & Cancer Center, University of Massachusetts, USA, [5]Mayo Clinic, USA, [6]University of Vermont, USA, [7]University of Vermont, College of Medicine, USA, [8]UMass Memorial Medical Center, USA

Runx1 is a hematopoietic lineage transcription factor, but is present in perichondrium and chondrocytes. To address functions in supporting chondrogenesis, we determined Runx1 expression patterns in the epiphysis and articular cartilage zones in response to mechanical loading of bovine articular cartilage and during progression of osteoarthritis (OA) in a mouse model, as well as in human OA tissue. By immunohistochemistry, spared and diseased compartments in knees of OA patients were dissected for examination of Runx factors, proliferation and differentiation markers. Experimental OA in mouse was induced by surgical destabilization of the medial meniscus (DMM). We find in normal articular cartilage of normal bovine, mouse, and the lateral spared compartment of human bone, that Runx1 is enriched in superficial chondrocytes. Under loading conditions, Runx1 expression is elevated and positively correlates with increasing loading conditions. In human and mouse OA tissue, Runx1 becomes highly expressed in the superficial zone chondrocytes at the periphery of mouse OA lesions and in human OA chondrocyte 'clones'. Further characterization of these high Runx1 expressing cells identified Runx1 co-localization with VCAM-1, the mesenchymal progenitor cell marker and PRG-4, a cartilage chondroprotective protein. These OA induced cells represent a proliferative population marked by Ki-67 and PCNA staining. In complementary studies, Runx1 depletion in chondroprogenitor cells results in decreased proliferation, supporting Runx1 contribution to cell expansion. Together these data indicate that Runx1 functions in the unique phenotype of articular chondrocytes, reflected by enriched levels in superficial zone chondrocytes and upregulation under conditions of compression. We propose that co-expression of Runx1 with VCAM-1 and PRG4 in murine cell clusters and human 'clones' of OA cartilage, suggests Runx1 participates in a cooperative compensatory mechanism and anabolic function.

***Disclosures: Paul Fanning**, None.*

SA0094

See Friday Plenary Number FR0094.

SA0095

Transient,but not Sustained, NOTCH1 Signaling Promotes Articular Cartilage Maintenance. Zhaoyang Liu*[1], Anthony Mirando[2], Regis O'Keefe[3], Michael Zuscik[4], Matthew Hilton[1]. [1]University of Rochester Medical Center, USA, [2]University of Rochester Medical Center, Center for Musculoskeletal Research, USA, [3]University of Rochester Medical Center, Department of Orthopaedics & Rehabilitation, Center for Musculoskeletal Research, USA, [4]University of Rochester School of Medicine & Dentistry, USA

Recently, we have identified the Notch signaling pathway as a critical regulator of articular cartilage and joint maintenance and implicated Notch signaling in osteoarthritis (OA). Specifically, genetic ablation of Notch signaling in joint precursor cells (*Prx1Cre;Rbpjκ$^{f/f}$*) or in joint cartilages (*Col2Cre^{ERT2};Rbpjκ$^{f/f}$*) resulted in a loss of anabolic gene expression and extracellular matrix (ECM) molecules resulting in a progressive OA-like pathology in mouse. Based on these findings, we set out to determine whether Notch activation within joint cartilage could promote ECM synthesis and joint maintenance. We first developed two sustained cartilage-specific Notch gain-of-function models: *Agc1Cre^{ERT2};Rosa-NICD1* and *Col2Cre;Rosa-rtTA$^{f/+}$;tetON-NICD1* (tGOF NICD1) with high dose and frequency of doxycycline. Interestingly, both models exhibited severe joint degenerative phenotypes, including articular cartilage fibrosis, synovial tissue expansion, and growth plate collapse. IHC analyses demonstrated a significant increase in the expression of both fibrosis markers COL1A1 and COL3A1, coupled with decreases in COL2A1 in the joints of sustained Notch gain-of-function mutants. Since both loss- and sustained gain-of-function models develop OA-like phenotypes, we generated a transient Notch activation model to mimic levels and durations of physiological Notch signaling. We injected 1-month old tGOF NICD1 mutants and controls with low doses of doxycycline (1ug dox/g body weight, once/week for four weeks), and harvested knee joints at 2 and 4 months. ABH/OG staining and histomorphometric analyses of tGOF NICD1 mutant knee sections demonstrate a dramatic increase in articular cartilage area and thickness in both 2- and 4-month old mice. The mutant mice also exhibited significant increases in COL2A1 expression in all zones of the articular cartilage, with a mild enhancement of COL10A1 in the deep zone. No significant change was observed in COL1A1 or COL3A1 expression in the mutant mice. Real-time RT-PCR revealed that transient Notch signaling promoted the expression of anabolic genes such as *Sox9*, *Col2a1* and *Agc1* at both 2 and 4 months. The expression level of *Mmp13* was elevated at 2-months, although by 4-months of age was reduced by ~60%. Collectively, these data indicate that transient activation of Notch signaling enhances articular cartilage ECM synthesis, promotes joint cartilage maintenance, and implicates the Notch pathway as a novel therapeutic target for OA.

***Disclosures: Zhaoyang Liu**, None.*

SA0096

See Friday Plenary Number FR0096.

SA0097

***Mustn1* Spatiotemporal Protein Expression During Skeletal Development and Regeneration.** Michael Hadjiargyrou*[1], Amanda Zigomalis[2], Affan Haleem[3], David Komatsu[4]. [1]New York Institute of Technology, USA, [2]Stony Brook University, Department of Biomedical Engineering, USA, [3]Stony Brook University, School of Medicine, USA, [4]Stony Brook University, Dept. of Orthopaedics, USA

Since the discovery of *Mustn1*, a gene encoding a small nuclear protein, much has been learned about its mRNA expression and function in developing and regenerating musculoskeletal tissues. However, almost all studies to date have evaluated *Mustn1* expression at the transcriptional level and very little is known about the expression of *Mustn1* protein. Therefore, using a newly developed *Mustn1* antibody, we conducted a series of experiments to evaluate the spatiotemporal expression of *Mustn1* protein during embryonic skeletal development and adult skeletal regeneration. Immunostaining transverse sections from embryonic day (E) 16 and 18 mouse embryos revealed *Mustn1* protein expression in skeletal muscles, mesenchymal condensations of ribs and limb buds, and chondrocytes of the vertebrae at both time-points analyzed. Using coronal sections from post-fracture day (PFD) 1, 3, 5, 7, 10, 14, and 21 rat femoral fracture calluses, *Mustn1* expression was observed in osteocytes near the fracture line, as well as the nearby activated periosteum on PDF 1. On PFD 3 and 5 osteocytic and periosteal *Mustn1* expression progressed proximally and distally from the fracture. By PFD 7, strong *Mustn1* expression was also seen in hypertrophic chondrocytes, as well as throughout regions of fibrocartilage. This continued into days 10 and 14, when *Mustn1* expression was seen in osteoblasts lining regions of woven bone. Finally, by PFD 21, *Mustn1* expression was reduced, with moderate staining seen in osteocytes near the fracture line and osteoblasts lining regions of woven bone. These data are consistent with prior *in situ* hybridizations and additionally reveal strong expression of *Mustn1* protein in osteocytes early in bone regeneration. The expression of *Mustn1* protein in cartilage and muscle is also consistent with prior studies demonstrating the necessity of *Mustn1* expression for chondrogenesis and myogenesis. The newly detected expression of *Mustn1* in osteocytes, as well as confirmatory evidence of *Mustn1* expression in osteoblasts, suggests that *Mustn1* may also be necessary for osteogenesis. Additional experiments to test this hypothesis, as well as quantify *Mustn1* protein levels during skeletal and muscle regeneration are ongoing. Further elucidating the expression, and ultimately the function, of *Mustn1* during the development and regeneration of musculoskeletal tissues will potentially enable the discovery of new targets for treating injuries and diseases of these tissues.

***Disclosures: Michael Hadjiargyrou**, None.*

SA0098

Genome-wide alterations in polycomb-regulated epigenomic modification in embryonic osteoblasts following exposure to maternal obesity in rats. Jin-Ran Chen*[1], Jian Zhang[2], Oxana P. Lazarenko[2], Michael L. Blackburn[2], Martin J. J. Ronis[2], Thomas M. Badger[2], Kartik Shankar[2]. [1]University of Arkansas for Medical Science, Arkansas Children's Nutrition Center, USA, [2]University of Arkansas for Medical Sciences & Arkansas Children's Nutrition Center, Little Rock, AR 72202, USA

Nutritional status during intrauterine and early postnatal life impacts the risk of chronic diseases, presumably via epigenetic mechanisms. However, evidence on the impact of gestational events on regulation of bone development is sparse. Recently we showed that bone development is inhibited in gestational day 18.5 (E18.5) embryos from rat dams made obese by feeding a high-fat diet (HFD). In these studies, female Sprague-Dawley rats were fed either a low-fat AIN-93G control diet or a HFD (45% fat calories) for 10 wk starting at 6 wk of age. Fetal rat osteogenic calvarial cells (FOCCs) from HFD-fed obese dams showed impaired osteogenic potential, decreased expression of osteogenic markers and higher levels of PPARγ relative to cells from dams fed AIN-93G. More importantly, this impairment was associated with diminished mRNA/protein expression and increased promoter methylation of the osteogenic regulator HoxA10, suggesting involvement of mechanisms regulating DNA and repressive histone methylation. DNA methylation is intricately linked to histone methyltransferase (HMT) activity; especially the repressive mark H3K27me3. Since, establishment of H3K27me3 is exclusively mediated via the polycomb (PcG) HMT, Enhancer of zeste homolog 2 (Ezh2), we examined this pathway. Recent studies have also shown that suppression of Ezh2 via CDK1 promotes osteogenesis. FOCCs from obese rat dams showed significantly increased mRNA and protein expression of Ezh2. Conversely, CDK1 expression and phosphorylation of Ezh2 (an inactivation event) were significantly lower in FOCCs from obese rat dams. In line with these results, H3K27me3 abundance in FOCCs from embryos of obese dams was significantly higher compared to cells from control dams. Analysis of genome-wide localization of the repressive histone mark, H3K27me3 via ChIP-seq identified 338 genes with at least 2-fold increase in H3K27me3 in FOCCs from obese dams. Enrichment of GO terms for these genes revealed that appendage morphogenesis and bone development biological processes were signficantly enriched. Transcriptional regulation of these genes was confirmed using real-time PCR. Of these genes, H3K27me3 of IGF1 promoter was found to be increased, and H3K27me3 of BMP4 promoter was decreased, suggesting altered differentiation potential toward either osteoblasts or adipocytes. These results suggest that maternal obesity may affect fetal skeletal development through epigenetic regulation of polycomb-regulated genes, which may contribute to low bone mass in the offspring later in life. *Supported in part by ARS CRIS* #6251-51000-005-03S.

***Disclosures: Jin-Ran Chen**, None.*

SA0099

Matrix Vesicle-Bound Bone Alkaline Phosphatase for the Assessment of Peripheral Blood Admixture of Human Bone Marrow Aspirates. Evelien Nollet[1], Emeline Van Craenenbroeck[2], Wim Martinet[1], Inez Rodrigus[3], Christiaan Vrints[2], Viviane Conraads[2], Viviane Van Hoof*[4]. [1]University of Antwerp, Belgium, [2]University of Antwerp / Antwerp University Hospital, Belgium, [3]Antwerp University Hospital, Belgium, [4]University Hospital Antwerp, Belgium

Quality assessment of bone marrow (BM) aspirates is important to circumvent the problem of unreliable cytokinetic results in BM serum as a consequence of peripheral blood (PB) admixture. Quality of BM is previously determined by flow cytometric quantification of specific BM cell populations. However, since this technique is critically dependent on the presence of normal BM, its use in pathophysiological conditions in which the BM is affected, is hampered. In search for an alternative stable marker, bone alkaline phosphatase (ALP), produced by osteoblasts residing in BM, was studied as a potential marker for the assessment of PB admixture of BM aspirates.

14 patients undergoing elective cardiac surgery were included. Renal failure, abnormal bone turnover and BM disorders served as exclusion criteria. Bone marrow aspirates were taken by sternal puncture prior to sternotomy. Venous PB was sampled simultaneously. After centrifugation (15min 1500g) total ALP activity was spectrophotometrically quantified (Dimension Vista System) in BM and PB serum. Agarose gel electrophoresis allowed differentiation between ALP isoenzymes (bone, liver,

intestinal ALP). Furthermore, native PAGE experiments were performed to identify the present molecular mass (Mr) ALP isoforms.

Overall, total ALP activity was significantly higher in BM serum (130 ± 95U/L) compared to PB serum (59 ± 9U/L; p=0.002). The agarose electrophoretic pattern also showed a marked difference between both matrices: BM contained a fraction of bone origin (41 ± 17%) that was absent in PB. This fraction was retained at the origin on native PAGE, indicating its high-Mr nature. Upon butanol extraction, the high-Mr fraction was converted to tetrameric bone ALP. Based on these observations, this BM-unique fraction was identified as membrane-bound bone ALP, most likely originating from bone matrix vesicles. Future electron microscopic studies could confirm this presumption. We called this unique fraction High-Mr Bone (HMB) ALP. Based on addition experiments with different percentages of PB serum to BM serum, good quality BM aspirates were defined by a ratio of total ALP activity in PB versus BM < 0.59 and a HMB ALP fraction > 40%. Using these criteria, 5 of 14 BM samples did not meet the quality requirements.

In conclusion, total ALP activity and ALP isoenzyme patterns are different in BM as compared to PB serum and therefore could serve as markers to assess admixture of PB in BM samples.

***Disclosures: Viviane Van Hoof**, None.*

SA0100

***Prx1* and *Col1a1* promoters target distinct bone cell populations in transgenic mice.** Zhufeng Ouyang, Zhijun Chen*, Masakazu Ishikawa, Xiuzhen Yue, Edward Greenfield, Shunichi Murakami. Case Western Reserve University, USA

Background: We previously generated *Prx1CreER-GFP* transgenic mice that express CreER and GFP under the control of a 2.4 kb *Prx1* promoter. The *Prx1CreER-GFP* transgene marks osteochondro progenitor cells in the periosteum of long bones. Because a 3.2 kb *Col1a1* promoter directs transgene expression in immature osteoblasts, we hypothesized that the *Prx1*-driven transgenes and *Col1a1*-driven transgenes are expressed in distinct but overlapping domains in the bone.

Methods: To compare *Col1a1* and *Prx1*-driven transgenes, we generated *Col1a1CreER-DsRed* transgenic mice that express, in osteoblasts, CreER and DsRed under the control of a 3.2 kb *Col1a1* promoter. The expression domains of *Col1a1CreER-DsRed* and *Prx1CreER-GFP* transgenes were analyzed in *Prx1CreER-GFP; Col1a1CreER-DsRed* double transgenic mice by histological analysis. We further isolated *Col1a1CreER-DsRed* and *Prx1CreER-GFP*-expressing cells by flow cytometry, and chondrogenic and osteogenic potential was analyzed.

Results: Our histological and flow cytometric analyses demonstrated that *Col1a1CreER-DsRed* and *Prx1CreER-GFP* transgenes are expressed in distinct cell populations in the long bones and calvariae. In the periosteum of long bones, *Col1a1CreER-DsRed* is expressed in the innermost layer directly lining the bone surface, while *Prx1CreER-GFP*-expressing cells are localized immediately outside of the *Col1a1CreER-DsRed*-expressing osteoblasts. In the calvaria, *Prx1CreER-GFP*-expressing cells are also localized in the cranial suture mesenchyme, while the *Col1a1CreER-DsRed* transgene is expressed in bone lining osteoblasts. Our in vitro experiments indicated that *Col1a1CreER-DsRed*-expressing cells are committed osteoblasts lacking chondrogenic potential, while the *Prx1CreER-GFP*-expressing cells show both chondrogenic and osteogenic potential. We also showed that *Prx1CreER-GFP*-expressing cells are precursor cells for *Col1a1CreER-DsRed*-expressing osteoblasts.

Discussion: Our results demonstrate that *Prx1CreER-GFP* and *Col1a1CreER-DsRed* transgenes are expressed in distinct cell populations both in the long bones and calvariae. These transgenes will provide novel approaches for analyzing the biology of the periosteum and cranial suture mesenchyme under physiologic and pathologic conditions.

***Disclosures: Zhijun Chen**, None.*

SA0101

Advanced Glycation End Products Inhibit the Mineralization of Mouse Stromal ST2 Cells by Binding the Receptor for AGEs and Increasing TGF-β Expression and Secretion. Masakazu Notsu*[1], Toru Yamaguchi[2], Kyoko Okazaki[3], Ken-ichiro Tanaka[4], Noriko Ogawa[3], Ippei Kanazawa[2], Toshitsugu Sugimoto[4]. [1]Shimane University, Japan, [2]Shimane University Faculty of Medicine, Japan, [3]Internal Medicine 1 Shimane University Faculty of Medicine, Japan, [4]Shimane University School of Medicine, Japan

We and others have recently showed that patients with type 2 diabetes mellitus (T2DM) have a higher risk for fracture, although they have normal or slightly higher bone mineral density (BMD). These findings suggest that bone fragility in T2DM, which is not defined by BMD, may contribute to fracture risk. Hyperglycemia accelerates the formation of advanced glycation end products (AGEs) and causes diabetic complications. AGEs including pentosidine are also known to cause bone fragility due to quality deterioration in diabetic patients. We found that AGEs suppressed mineralization of mouse stromal ST2 cells by inhibiting their differentiation with reduced expressions of osteocalcin (OCN) and osterix (OSX) mRNA in the cells. Recent studies have shown that AGEs increased TGF-β expression and activated Smad signals in mesangial and nerve cells, indicating that AGEs cause diabetic complications in kidneys and nerves by activating TGF-β. It is known that TGF-β is especially abundant in bone, and that enhancement of its signals deteriorates bone quality in animal experiments. However, it is still unclear whether or not TGF-β signal is involved in the AGEs-induced suppression of osteoblastic bone formation. In this study, we made AGE3 by incubating BSA with glycolaldehyde, and examined the roles of TGF-β in the suppression of mineralization of ST2 cells induced by AGE3. Treatments of the cells with AGE3 (200μg/mL) significantly inhibited mineralization by 71.2% on experimental day 21 ($P<0.001$). Simultaneously, AGE3 significantly increased the mRNA expression and protein level of TGF-β by real-time PCR and ELISA of whole cell lysates, respectively, on days 3, 5, and 7 ($P<0.001$). Transfection of siRNA of the receptor for AGEs (RAGE) significantly inhibited the AGE3-induced increase in TGF-β protein level ($P<0.001$), and recovered mineralization in the cells ($P<0.05$). Moreover, treatments with TGF-β type I receptor kinase inhibitors (2.5uM SD208) significantly antagonized the AGE3-induced suppression of OCN and OSX mRNA expressions ($P<0.05$), and recovered mineralization completely ($P<0.001$). These findings indicate that the AGEs-RAGE pathway inhibits the mineralization of ST2 cells by increasing TGF-β expression and secretion, suggesting that TGF-β action stimulated by AGEs adversely affects not only kidney or nerve but also bone in the process of diabetic complications.

***Disclosures: Masakazu Notsu**, None.*

SA0102

Blocking β-adrenergic signaling attenuates reductions in trabecular bone mass, marrow adiposity and marrow leptin expression in high calorie diet fed but not low calorie diet fed growing mice. Kyunghwa Baek*[1], Hyo Rin Hwang[2], Hyun-Jung Park[2], Arang Kwon[2], Abdul Qadir[2], Jeong-Hwa Baek[3]. [1]Gangneung-Wonju national university, School of dentistry, South Korea, [2]Seoul National University, South Korea, [3]Seoul National University, School of Dentistry, South Korea

We sought to compare the effects of high calorie or low calorie diet on the skeletal integrity and elucidate whether β-adrenergic blockade attenuates dietary calorie alteration induced bone loss and whether such an effect is associated with leptin. Male 6-week-old C57BL/6 mice were randomly assigned into 3 groups (20 mice each): ad-lib fed control diet group (CON; 10 kcal% fat), high calorie diet group (HIGH; 60 kcal% fat), and low calorie diet group (LOW; 30% kcal restriction *vs*. CON diet). In each diet group, 10 mice were treated with vehicle (VEH) and the other 10 mice were treated with propranolol, a b-adrenergic receptor antagonist (BB; 0.5g/L in drinking water). Over 12 weeks, HIGHVEH had higher while LOWVEH had lower body weight/fat mass *vs*. CONVEH. β-blockade mitigated high calorie diet induced body weight and fat mass increase. Femoral trabecular bone mineral density (BMD) was declined in both HIGHVEH and LOWVEH but the magnitude of decline was greater in LOWVEH mice. This femoral trabecular BMD decrement was attenuated only in HIGHBB. Adipocyte number in HIGHVEH and LOWVEH was higher vs. CONVEH, but this increment was abolished in both HIGHBB and LOWBB. Reduction in marrow leptin expression was observed in HIGHVEH and LOWVEH and this decrement was abolished only in HIGHBB. In summary, the magnitude of low calorie diet induced bone loss was greater than that of high calorie diet in growing mice. β-adrenergic blockade mitigated metaphyseal bone loss and reductions in marrow adiposity and marrow leptin expression seen with high calorie diet. These data suggest an important role for β-adrenoreceptor signaling pathway in bone and marrow fat response to dietary calorie alteration.

***Disclosures: Kyunghwa Baek**, None.*

SA0103

Bmi-1 Is A Critical Molecule for Activation of the Sonic Hedgehog Signal Pathway. Jun Wu*[1], Wen Sun[2], Rong Wang[1], David Goltzman[3], Dengshun Miao[4]. [1]Nanjing Medical University, China, [2]Nanjing Medical University, The Research Center for Bone & Stem Cells, Peoples Republic of China, [3]McGill University, Canada, [4]Nunjing Medical University, Peoples Republic of China

Our previous study demonstrated that Bmi1 deficiency resulted in skeletal growth retardation and premature osteoporosis with up-regulation of p27 in bone marrow mesenchymal stem cells (BM-MSCs). In this study, we confirmed this up-regulation of p27 at both mRNA and protein levels in bone tissue from Bmi-1 deficient mice. To determine whether p27 acts downstream of Bmi1 to regulate skeletal growth and development in vivo, we generated $Bmi1^{-/-}p27^{-/-}$ double knockout mice and compared them with $p27^{-/-}$, $Bmi1^{-/-}$, and wild-type littermates. Body size, body weight, bone mineral density, trabecular bone volume, osteoblast numbers, ALP and type I collagen positive areas were increased significantly in $p27^{-/-}$ mice, but decreased significantly in $Bmi1^{-/-}$ mice compared to wild-type mice. The double mutant $Bmi1^{-/-}p27^{-/-}$ mice however closely resembled the phenotype of the $Bmi1^{-/-}$ mice, including growth retardation and premature osteoporosis. Consequently, we asked whether the signaling pathway activated by p27 deletion and leading to increased skeletal size could be blocked by the deletion of Bmi-1. To examine this question, microarray analyses of differential gene expression profiles were performed in long bone extracts from $p27^{-/-}$ mice and their wild-type littermates. Results revealed that the expression levels of molecules in the sonic hedgehog (Shh) signaling pathway, including Shh, Smoothened (Smo), Gli1/2/3 and Bmi1 were up-regulated, whereas

suppressor of fused (Sufu), a negative regulator of this pathway was down-regulated in $p27^{-/-}$ mice. Their up-regulation or down-regulation at mRNA and protein levels was confirmed by real-time RT-PCR and Western blots. We then employed Shh-N and the Shh antagonist KAAD-Cyclopamine to treat BM-MSCs derived from wild-type, $p27^{-/-}$, $Bmi1^{-/-}$ or $Bmi1^{-/-}p27^{-/-}$ mice, respectively. Results showed that cell proliferation was accelerated in a dose dependent manner in Shh-N-treated BM-MSCs derived from wild-type or $p27^{-/-}$mice, but not in those derived from $Bmi1^{-/-}$ or $Bmi1^{-/-}p27^{-/-}$ mice. In contrast, cell proliferation was inhibited in a dose dependent manner in KAAD-Cyclopamine-treated BM-MSCs derived from wild-type or $p27^{-/-}$ mice, but not in those derived from $Bmi1^{-/-}$ or $Bmi1^{-/-}p27^{-/-}$ mice. Our results demonstrated that deletion of Bmi-1 can blocks effects of p27 deficiency induced activation of Shh signal pathway. Bmi-1 therefore is a critical effective molecule for the activation of Shh signal pathway.

***Disclosures: Jun Wu**, None.*

SA0104

See Friday Plenary Number FR0104.

SA0105

Contribution of Hematopoietic Stem Cells to Dental Tissues. Amanda LaRue[1], Beneta Parthiban[2], Jasper L Cumbee IV[2], James Borke[3], Makio Ogawa[2], Meenal Mehrotra*[4]. [1]Ralph H. Johnson VAMCMedical University of South Carolina, USA, [2]MUSC, USA, [3]Western University of health Sciences, USA, [4]Medical University of South Carolina & Research Services, Ralph H Johnson VAMC, USA

While the complex structural composition of the teeth provides hardness and durability, structures like dentin and periodontal ligament (PDL) are vulnerable to damage and require constant maintenance. It is generally believed that the regeneration of both odontoblasts and PDL cells is provided by local stem cells, i.e., stem cells in the dental pulp and those residing in PDL. Recent studies have shown that bone marrow (BM) mesenchymal stem cells (MSC) can differentiate into odontoblast and regenerate the PDL and alveolar bone. BM is thought to contain two types of stem cells, MSCs and hematopoietic stem cells (HSCs). Using a single HSC transplantation model, we have previously shown that adipocytes, osteoblasts, osteocytes and fibroblasts/myofibroblasts in multiple tissues are derived from HSCs. Studies from other groups have suggested that HSCs may participate in dental tissues too. Indeed, the presence of $CD45^+$ cells has been demonstrated in reparative dentin in mice. c-kit enriched BM cells give rise to odontoblast and $CD34^+$ cells have been demonstrated in the human gingiva. Thus, we hypothesize that HSCs can differentiate into odontoblasts and cells in the PDL. Transplantation of un-manipulated BM cells harvested from enhanced green fluorescent protein (EGFP) mice into lethally irradiated recipients generated $EGFP^+$ runt-related transcription factor-2^+ ($Runx2^+$) and $EGFP^+$ Dentin Matrix Protein-1^+ ($DMP\text{-}1^+$) odontoblasts/pulp cells and $EGFP^+$ Alpha Smooth Muscle $Actin^+$ ($\alpha\text{-}SMA^+$) and $EGFP^+$ $Osteocalcin^+$ (OCN^+) cells in the PDL. Furthermore, we identified $CD45^+$ cells in the pulp and PDL, indicating their origin from the HSCs. To confirm the HSC origin of these cells, mice were lethally irradiated, transplanted with a clonal population of cells derived from a single $EGFP^+$ HSC and multilineage engraftment confirmed. Analysis of paraffin sections from the molar crown showed numerous $EGFP^+$ cells within the pulp region and the PDL attached to the tooth. Analysis of pulp showed $EGFP^+$ cells which also expressed DMP-1 and Runx-2, markers for odontoblasts/pulp cells. Immunohistochemical analysis of PDL showed $EGFP^+$ cells that expressed α-SMA and OCN, markers for fibroblasts and osteogenic cells respectively. Thus, our studies confirm that HSCs can give rise to these dental cells and may open new avenues of therapy for a number of dental diseases and injuries through the use of this novel source.

***Disclosures: Meenal Mehrotra**, None.*

SA0106

Impact of RARγ- BMP Signaling Cross-talk on Endochondral Bone Formation. Kenta Uchibe*, Jiyeon Son, Maurizio Pacifici, Masahiro Iwamoto. Children's Hospital of Philadelphia, USA

The nuclear retinoic acid receptors—RARα, β and γ—play key roles in the skeletal pattern formation and development. We previously showed that RARγ is a major regulator of chondrogenesis, which is the initial step of endochondral ossification. Pharmacological activation of RARγ effectively blocked ectopic bone formation (heterotopic ossification; HO) in several HO model mice. A series of biochemical analysis revealed that at least part of the anti-HO action of RARγ is mediated by the inhibition of the canonical BMP signaling pathway. RARγ could regulate cellular function by activating its target gene expression (genomic action) and/or indirectly modulate the function of other transcription factors by competing co-factors (trans-repression). In the present study, we further characterized the relationship between RARγ and BMP signaling pathways and evaluated its importance in endochondral ossification.

In the first experiment, we created bone defects in wild type and RARγ null mice, and compared their repair process. By day 14 after injury, mutant mice showed remarkably faster repair compared to wild type mice. Histological analysis revealed that pSmad expression is enhanced in the healing area of mutant mice. Interestingly, in mutant mice, pSmad proteins were ectopically detected at the hypertrophic zone of the growth plate where RARγ is usually expressed. To test the effect of RARγ inhibition on canonical BMP signaling, ATDC5 cells were treated with selective RARγ antagonists, and Smad phosphorylation and Id1-luc reporter activity were analyzed. Increases in pSmad1, 5 and 8 and Id1-luc reporter activity, both of which indicate BMP signaling activity, were significantly enhanced by RARγ inhibition. Lastly, to quantify the effect of RARγ inhibition on endochondral bone formation *in vivo*, we injected Matrigel/BMP-2 subcutaneously in wild type mice, treated them with RARγ antagonist or vehicle by oral administration, and examined bone formation with micro CT. We found that ectopic bone formation (BV/TV) was dramatically enhanced in RARγ antagonist-treated compared to the vehicle-treated mice.In sum, our data indicate that interference with RARγ function stimulates bone formation and does so at least in part by stimulation of the canonical BMP signaling pathway. This strategy could represent a promising new means by which the endochondral bone formation process could be stimulated in the context of various orthopaedic needs and applications.

***Disclosures: Kenta Uchibe**, None.*

SA0107

Increased Dietary Advanced Glycation End Products Induces Early Degenerative Spinal Structural Changes. Young Lu*[1], Svenja Illien-Junger[2], Sheeraz Qureshi[2], Weijing Cai[2], Helen Vlassara[2], Gary Striker[2], James Iatridis[2]. [1]Mount Sinai Medical Center, USA, [2]Icahn School of Medicine at Mount Sinai, USA

Introduction: Intervertebral disc degeneration and spinal degenerative changes are major causes of back pain and other lumbar spine pathologies in obese and diabetic individuals. The modern diet includes thermally processed foods that contain high levels of inflammatory advanced glycation end products (AGEs), known contributors to diabetes and aging complications. We previously showed that diabetes-related intervertebral disc degeneration in mice is associated with AGE accumulation. This study investigates the role of AGEs on the intervertebral discs and spine independent of hyperglycemia.

Materials and Methods: C57BL6 mice were pair-fed isocaloric diets with either high amount of AGEs, eg. methylglyoxal-derivatives (AGE/MG+: 1.8x104 nmoles/day; n = 9) or reduced AGEs (AGE/MG-: 0.65x104 nmoles/day; n = 11; $p<.01$) for 5 generations. Mice (F5) were sacrificed at 18 months. AGE/MG+, but not AGE/MG- mice, were insulin resistant but not hyperglycemic and had higher serum MG (1.59 ± 0.2 vs. 0.83 ± 0.2 nmole/ml $p<.05$), and weights (35.1 ± 1.8 vs. 29 ± 0.52g $p<.05$). Lumbar spines were analyzed using μCT and immunohistochemistry (anti-MG).

Results and Discussion: Vertebral cortical thickness and surface area were higher in AGE/MG+ compared to AGE/MG- mice ($p=0.029$ and $p=0.047$ respectively) (Table 1, Figure 1). The superior vertebral endplates of AGE/MG+ mice had significantly higher bone mineral density ($p=0.016$) but lower connectivity density ($p=0.0062$) compared to that for AGE/MG- mice (Table 1). Histological staining showed reduced proteoglycan content and an overall thinner glycosaminoglycan rich region in AGE/MG+ compared to AGE/MG- mice (Figure 2). Immunohistochemistry revealed greater MG accumulation in the vertebral endplates of AGE/MG+ mice.

Conclusions: Chronic exposure to oral AGEs promote early degenerative changes to the vertebrae, vertebral endplates, and intervertebral disc in parallel with insulin resistance, independent of hyperglycemia. Therefore, these effects were largely attributable to exogenous AGEs . Further studies are needed to mechanistically establish the role of AGEs on spinal structures relative to metabolic syndrome and diabetes.

Acknowledgement: Funded by NIH/NIAMS, R01AR051146, HL73417 and AG009453.

Figure 1

Condition	*VCT (mm)	*VCA (mm^2)	*BMD (SEP; mg/cm^3)	+BMD (IEP; mg/cm^3)	*CD (SEP; $1/mm^3$)
MG-	0.057	0.237	927.53	905.82	16284.0
	±0.019	±0.080	±61.086	±63.10	±6840.4
MG+	0.070	0.294	998.87	953.38	9210.2
	±0.018	±0.077	±46.969	±58.23	±2515.9

Abbreviations: VCT (Vertebral Cortical Thickness), VCA (Vertebral Cortical Area) BMD (Bone Mineral Density) SEP (Superior Endplate) IEP (Inferior Endplate) CD (Connectivity Density); mean±SD; *: p<0.05; +: p=0.090

Table 1

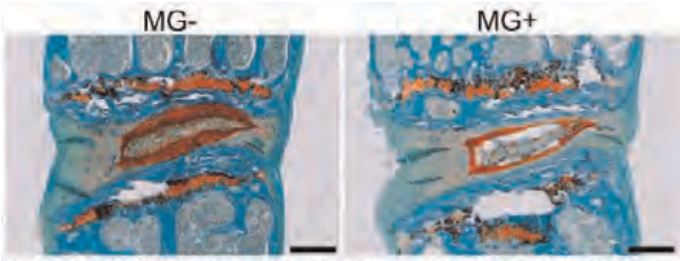

Extended FAST histology of lumbar intervertebral disc of AGE/MG+ and AGE/MG- mice (scale bar = 200 µm). The intensity of Safranin-O staining (Red-orange) is reflective of proteoglycan content, and was reduced for AGE/MG+

Figure 2

***Disclosures: Young Lu**, None.*

SA0108

Internal Ribosome Entry Site (IRES) Mediates theTranslation of Nuclear DMP1 (nuDMP1). Suzhen Wang, Chunlin Qin, Rena D'Souza, Yongbo Lu*. Texas A&M University Baylor College of Dentistry, USA

Dentin matrix protein 1 (DMP1) is highly expressed in tooth and bone. Several lines of evidence suggest that there are two forms of DMP1, a secretory form and a nuclear form (nuDMP1). The purpose of this study was to determine the nature and function of nuDMP1. Site-directed mutagenesis and PCR were employed to generate various DMP1-expressing constructs: a construct expressing full-length DMP1 with the endoplasmic reticulum (ER)-entry signal peptide deleted (SPdel-DMP1), a construct expressing a putative nuDMP1 (nuDMP1), four constructs carrying full-length DMP1 cDNA with a two-nucleotide deletion in the N-terminal 37 kDa fragment coding region and/or substitution mutations at the two putative alternative in-frame start codons and a construct in which DMP1 cDNA was fused downstream to the C-terminal end of Twist1 cDNA (Twist1-nuDMP1). Western immunoblotting and immunofluorescent staining analyses were performed to determine the expression and subcellular localization of DMP1 produced by these constructs in Cos-7 and C310T1/2 mesenchymal cells. Promoter-luciferase assays were used to analyze the effects of the various DMP1 constructs on the activity of a 5.7 kb Dspp promoter fragment. When the SPdel-DMP1 construct was transfected into Cos-7 cells, Western immunoblotting analysis showed that the SPdel-DMP1 construct produced two proteins, a full-length SPdel-DMP1 and a putative nuDMP1. Although a DMP1 construct carried a two-nucleotide deletion, which led to a premature stop codon in the N-terminal region, it still expressed the putative nuDMP1. However, the production of nuDMP1 was completely lost when the two potential downstream in-frame start codons were substituted with isoleucine. Furthermore, when the Twist1-nuDMP1 construct was transfected into Cos-7 cells, it produced both Twist1 as well as nuDMP1. In addition, when the nuDMP1 construct was transfected into C3H10T1/2 cells, immunofluorescent staining revealed the nuclear localization of the nuDMP1. Consistently, the nuDMP1 was more potent in stimulating the 5.7kb Dspp promoter activity than the full-length DMP1 with or without the ER-entry signal peptide. These data suggest that the nuDMP1 is translated from an alternative downstream in-frame start codon(s) via an internal ribosome entry site (IRES)-mediated mechanism, and that it functions as a transcription factor or co-transcription factor.

***Disclosures: Yongbo Lu**, None.*

SA0109

See Friday Plenary Number FR0109.

SA0110

Postnatal Ablation of Ext1 in Cartilage Induces Ectopic Hypertrophy of Articular Chondrocytes and Loss of Bone Volume in Primary Spongiosa. Federica Sgariglia*[1], Maria Elena Candela[2], Julianne Huegel[2], Olena Jacenko[3], Eiki Koyama[1], Yu Yamaguchi[4], Maurizio Pacifici[1], Motomi Enomoto-Iwamoto[1]. [1]Children's Hospital of Philadelphia, USA, [2]Translational Research Program in Pediatric Orthopaedics, Division of Orthopedic Surgery, Department of Surgery, Children's Hospital of Philadelphia, USA, [3]University of Pennsylvania, School of Veterinary Medicine, USA, [4]Sanford Children's Health Research Center, Sanford-Burnham Medical Research Institute, USA

EXT1 encodes a Golgi-associated glycosyltransferase primarily responsible for heparan sulfate (HS) synthesis, and genetic mutations in *Ext1* cause severe skeletal and craniofacial phenotypes in developing and postnatal mice. To determine whether long bone epiphyseal development and endochondral ossification continuously require heparan sulfate, we conditionally ablated *Ext1* in cartilage at postnatal stages in compound *Ext1flf;Col2CreER* transgenic mice by tamoxifen injection at postnatal day 5. qPCR analysis revealed that efficiency of floxed Ext1 ablation in chondrocytes was about 80%. Mutant mice displayed growth retardation, scoliosis and limb deformities starting by 2 weeks post injection. They also displayed formation of excess cartilage that extended away from the growth plate toward perichondrium and resembled exostoses seen in Hereditary Multiple Exostoses that is caused by EXT mutations. Closer histological inspection revealed that the chondrocytes were misaligned in the mutant growth plates and the typical columnar structure was disrupted. Moreover, the hypertrophic zone was reduced, as confirmed by a decrease in collagen 10-expressing chondrocytes. We also found a major decrease in bone volume in the primary spongiosa accompanied by a significant increase in osteoclast number at the chondro-osseus junction, clearly detectable at 4 weeks after tamoxifen injection. Very interestingly, a preponderance of articular chondrocytes had undergone hypertrophy in the mutants and displayed an enlarged cell size and ectopic expression of the hypertrophic markers collagen 10 and MMP13. Furthermore, immunostaining revealed that the hypertrophic articular chondrocytes had accumulated a large amount of Perlecan pericellularly, indicating that a deficiency of heparan sulfate may have affected Perlecan homeostasis or distribution. Taken together, the data indicate that Ext1 and heparan sulfate proteoglycans are essential regulators of postnatal epiphyseal cartilage development and skeletal growth. The results point to roles of Ext1 and heparan sulfate in maintaining long-term interactions between cartilage and bone and preserving chondrocyte organization and trabecular bone.

***Disclosures: Federica Sgariglia**, None.*

SA0111

Bone Shaft Revascularization after Marrow Ablation is Dramatically Accelerated in BSP-/- mice, along with Faster Haematopoietic Recolonization. Wafa Bouleftour*[1], Renata Neves Granito[1], Arnaud Vanden Bossche[1], Odile Sabido[2], Bernard Roche[1], Mireille Thomas[1], Marie-Thérèse Linossier[1], Jane Aubin[3], Marie-Helene Lafage-Proust[4], Laurence Vico[5], Luc Malaval[6]. [1]LBTO/INSERM U1059 - Université de Lyon, France, [2]Flow Cytometry Facility - Université de Lyon, France, [3]University of Toronto Faculty of Medicine, Canada, [4]INSERM Unit 890, France, [5]University of St-Etienne, France, [6]INSERM U1059-Université de Lyon-Université Jean Monnet, Saint-Etienne, France

The bone organ integrates the activity of bone tissue, bone marrow and blood vessels and the factors ensuring this coordination remain ill defined. Bone sialoprotein (BSP) is with osteopontin (OPN) a member of the Small Integrin Binding Ligand N-Linked Glycoprotein (SIBLING) family, involved in bone formation, hematopoiesis and angiogenesis. In rodents, bone marrow ablation induces a rapid formation of medullary bone which peaks by ~8 days (d8) and is blunted in BSP-/- mice (Bone, 50:1064, 2012). We investigated the coordinate hematopoietic and vascular recolonization of the bone shaft after marrow ablation of 2 month old BSP+/+ and BSP-/- mice (N=5/group).

Bone marrow was aspirated through the right femur epiphysis. Hematopoietic recolonization was analyzed by flow cytometry after labeling with specific antibodies. The bone vascular network was contrasted by barium sulfate infusion. Bone and vascular volume and density were measured on frontal sections. RT-PCR was performed on tri-reagent flushed bone marrow.

At d3, the ablated area in BSP-/- femurs showed higher vessel density (99.2 ± 4.9 vs $23.2 \pm 8.5/mm^2$, $p<0.05$, MWU) and vascular volume (x7) than BSP+/+ (Figure), along with higher VEGF (x1.95) and OPN (x1.8) expression. Interestingly, unablated BSP-/- femur marrow also contains more blood vessels than BSP+/+ (74.2 ± 8.4 vs $58.0 \pm 7.6/mm^2$, N=6, p=0.01, MWU). Vessel numbers in the shaft of ablated BSP+/+ mice reached BSP-/- values only by d8, but with a vascular volume which was twice the value in BSP-/-, reflecting smaller vessel size in mutants. At d6, a much higher number of Lin^- (x3) as well as LSK (Lin^- IL-7Rα^- Sca-1^{hi} c-Kit^{hi}, x2) and hematopoietic stem cells (HSC: $Flt3^-$ LSK, x2) were counted in BSP-/- marrow, indicating a faster recolonization. However, the proportion of LSK and HSC within the Lin^- was lower in BSP-/- and more differentiated stages were more abundant, as

also observed in unablated bone (Granito et al., submitted), suggesting that hematopoietic differentiation is favored in the absence of BSP.

In conclusion, bone marrow ablation in BSP-/- mice is followed by a faster vascular and hematopoietic recolonization, along with lower medullary bone formation. Thus, lack of BSP affects the interplay between hematopoiesis, angiogenesis and osteogenesis. The higher expression of the angiogenic SIBLING, OPN concomitant with massive revascularization in BSP-/- mice suggests a functional role, presently investigated with siRNA targeting OPN.

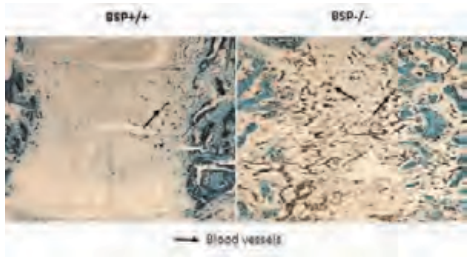

Figure

***Disclosures: Wafa Bouleftour**, None.*

SA0112

Defective Mineralization in Craniofacial Bone and Cementum in *Bsp* Null Mice. Brian Foster*[1], Yohannes Soenjaya[2], Francisco Nociti, Jr.[3], Erik Holm[4], Kamila Kantovitz[3], Helen Wimer[5], Patricia Zerfas[6], Jane Aubin[7], Graeme Hunter[8], Harvey Goldberg[9], Martha Somerman[3]. [1]National Institute of Arthritis & Musculoskeltal & Skin Diseases (NIAMS), USA, [2]Biomedical Engineering Program, Schulich School of Medicine & Dentistry, University of Western Ontario, Canada, [3]National Institute of Arthritis & Musculoskeletal & Skin Diseases (NIAMS), National Institutes of Health (NIH), USA, [4]Department of Biochemistry, Schulich School of Medicine & Dentistry, University of Western Ontario, Canada, [5]Department of Vertebrate Zoology, National Museum of Natural History, Smithsonian Institution, USA, [6]Department of Research Services, Division of Veterinary Resources, National Institutes of Health (NIH), USA, [7]University of Toronto Faculty of Medicine, Canada, [8]School of Dentistry, Schulich School of Medicine & Dentistry, University of Western Ontario, Canada, [9]The University of Western Ontario, Canada

Purpose: Bone sialoprotein (BSP) is a multifunctional extracellular matrix protein found in mineralized tissues, including bone, cartilage, tooth root cementum (both acellular and cellular types), with lesser amounts in tooth dentin. In order to understand the functional significance of BSP in biomineralization of these tissues, we analyzed intramembranous and endochondral osteogenesis, cementogenesis, and dentinogenesis, in *Bsp* null mice.

Methods: Craniofacial/dental development was analyzed in *Bsp*$^{-/-}$ and wild-type (WT) controls over a developmental time-course (1-60 days post natal; dpn) by histology, immunohistochemistry, undecalcified histochemistry, microCT, SEM, and TEM. Serum biochemistry was analyzed at 2-8 weeks.

Results: Regions of both endochondral (e.g. synchondroses) and intramembranous (e.g. calvaria, mandible, alveolar bone) ossification presented delayed mineralization, assessed by von Kossa and Goldner's trichrome stains at 1 and 14 dpn. Early osteoblast markers, osterix and alkaline phosphatase, were unchanged in *Bsp* null osteoblasts compared to WT. Cellular cementum in *Bsp* null mice featured hypomineralization parallel to that found in bone, corrected by 60 dpn. More dramatically, *Bsp* null mouse molars featured a significant reduction in acellular cementum formation (20% of WT at 60 dpn), with a lack of mineralized ultrastructure by SEM and TEM. Loss of functional acellular cementum caused periodontal breakdown, including periodontal ligament (PDL) detachment and disorganization, and extensive alveolar bone and tooth root resorption, associated with increased RANKL immunostaining and osteoclast presence. Conversely, dentin formation was unperturbed in *Bsp* null mouse molars, with no delay in mineralization, no alteration in dentin dimensions (at 1, 14, and 26 dpn), and no differences in odontoblast markers osterix, alkaline phosphatase, osteocalcin, and dentin sialoprotein. Serum calcium, phosphate, and alkaline phosphatase were undiminished in *Bsp* null mice, supporting local, tissue-specific roles for BSP that would account for different phenotypes in bone, cementum, and dentin.

Conclusions: These analyses confirm an important role for BSP in bone and cellular cementum mineralization, a critical and non-redundant function in acellular cementum formation, and lack of perceived role in molar dentin formation. Additionally, owing to its importance to cementum, BSP is essential for tooth attachment and periodontal function.

***Disclosures: Brian Foster**, None.*

SA0113

See Friday Plenary Number FR0113.

SA0114

The Calcitonin hormone regulates the Osteocye. Stephen Henry*[1], Su-Chen E Huang[2], Michael Starbuck[1], Ana Hoff[3], Gilbert Cote[4], Robert Gagel[4]. [1]University of Texas MD Anderson, USA, [2]mdanderson, USA, [3]ICESPUniversity of São Paulo, Brazil, [4]University of Texas M.D. Anderson Cancer Center, USA

Calcitonin (CT) is a peptide hormone secreted predominately by the C-cells or parafollicular cells of the thyroid gland that lowers blood calcium levels. Clinically, calcitonin is used diagnostically as a tumor marker for medullary thyroid cancer (MTC), and therapeutically to transiently lower blood calcium, treat osteoporosis (e.g., a weak antiresorptive drug), and alleviate bone pain. Calcitonin is widely known for its action upon the calcitonin receptor localized to the osteoclast, and its role in mitigating bone resorption. Recently, we have discovered that a mouse model of calcitonin deficiency exhibits not only the expected increase in osteoclastic bone resorption, but also a profound increase in bone remodeling and formation. Microcomputer tomography (micro CT) images of bones from CT-null mice and control mice, as well as other histomorphometric and kinetic parameters (double-calcein labeling) illustrate that increased bone formation occurred in the trabecular region of the calvaria and long bones in CT-null mice. Furthermore, the analysis of the differential gene expression between the RNA harvested from the bones of CT-null and control mice shows a downregulation of several osteocyte-specific genes such as SOST, Dkk1, Mepe, and DMP-1 in the CT-null mice. Interestingly, the calcitonin G-coupled receptor was upregulated 10-fold in the CT-null mice. A reciprocal experiment was performed in which exogenous, recombinant calcitonin hormone was injected subcutaneously above the calvarial bones of CT-null mice, and these same osteocyte-specific genes were upregulated, thus further substantiating that the calcitonin hormone may regulate osteocytes. We hypothesize that calcitonin regulates bone resorption positively and formation negatively; a corollary is that a calcitonin antagonist would lead to increased bone resorption and increased formation. Currently, we are intrigued with the possibility that a calcitonin antagonist may serve as a potential osteoanabolic agent that stimulates *de novo* bone formation.

***Disclosures: Stephen Henry**, None.*

SA0115

Extracellular Ca^{2+} and the calcium-sensing receptor, CaSR, are important regulators of fetal lung development. Sarah Brennan*[1], William Wilkinson[1], Hsiu-Er Tseng[1], Bethan Monk[1], Holly Dibble[1], Samantha Quilliam[1], Rebecca Wadey[1], David Warburton[2], Luis Galietta[3], Paul Kemp[1], Daniela Riccardi[1]. [1]Cardiff University, United Kingdom, [2]University of Southern California, USA, [3]University of Genoa, Italy

Immature development of the lungs continues to be one of the major complications with preterm birth. Optimal postnatal lung function depends on the co-ordinated development of lung branching morphogenesis, vasculogenesis and fluid secretion. These processes start during the *pseudoglandular* stage (weeks 9 – 17 post-conception in humans, and embryonic day (E)11.5 – 16.5 in the mouse) and our group has demonstrated that the relatively hypercalcemic environment of the fetus (~1.7 mM v ~1.2 mM for a normocalcemic adult) regulates all of these processes. Previously, we have shown that this relative hypercalcemia suppresses lung branching morphogenesis through activation of the calcium-sensing receptor (CaSR) [1].

In addition, we have also shown that fetal hypercalcemia stimulates fluid secretion in the developing mouse lung, and that this process is partly controlled by the CaSR. Fluid secretion in the developing lung lumen is driven by, and proportional to, active Cl^- transport, which results in a negative transepithelial potential difference (PD), that can be measured electrophysiologically. Using this approach, here we show that, in pseudoglandular human and mouse fetal lung explants, approximately 50% of this fluid secretion is sensitive to bumetanide, and correlates with basolateral entry of Cl^- into the lumen epithelium via the Na^+-K^+-$2Cl^-$ cotransporter, NKCC2. The remaining 50% is $Ca^{2+}{}_o$-sensitive and dependent on activation of the CaSR, since the CaSR pharmacological activator NPS-R568 could also evoke fluid secretion in the presence of lower $Ca^{2+}{}_o$ concentrations (1.05 mM $Ca^{2+}{}_o$).

Immunohistochemistry shows that a number of apical chloride channels, including bestrophin, TMEM16, and the cystic fibrosis transmembrane conductance regulator (CFTR), are expressed in human fetal lung epithelium. Inhibition of CFTR using Inhibitor-172 halved Cl^--driven fluid secretion, but only in CaSR-activating conditions (by either mimicking fetal hypercalcemia or through the use of NPS-R568), suggesting an hitherto unknown interaction between the CaSR and CFTR that is currently undergoing further investigation.

In conclusion, this study indicates that fetal hypercalcemia is an important extrinsic factor in the normal development of the human lung. Furthermore, the CaSR plays an essential role in lung development through control of lung growth and fluid secretion through activation of CFTR.

[1] Finney BA et al. (2008) J Physiol.586(24): 6007-6019.

***Disclosures: Sarah Brennan**, None.*

SA0116

Dosage Effect of a *Phex* Mutation in a Murine Model of X-linked Hypophosphatemia. Shoji Ichikawa*, Amie Gray, Emmanuel Bikorimana, Michael Econs. Indiana University School of Medicine, USA

X-linked hypophosphatemia (XLH) is caused by mutations in the *PHEX* gene, which increase circulating levels of the phosphaturic hormone, fibroblast growth factor 23 (FGF23). Since XLH is a dominant disease, one mutant allele is sufficient for manifestation of the disease. However, dosage effect of a *PHEX* mutation in XLH is not completely understood. To examine the effect of *Phex* genotypes, we compared serum biochemistries and skeletal measures between all five possible genotypes of a new murine model of XLH ($Phex^{K496X}$ or $Phex^{Jrt}$). Compared to sex-matched littermate controls, all *Phex* mutant mice had hypophosphatemia, mild hypocalcemia, and increased parathyroid hormone and alkaline phosphatase levels. Furthermore, mutant mice had markedly elevated serum Fgf23 levels due to increased *Fgf23* expression and reduced cleavage of Fgf23. Although females with a homozygous *Phex* mutation were slightly more hypocalcemic and hypophosphatemic than heterozygous females, the two groups had comparable intact Fgf23 levels. Similarly, there was no difference in intact Fgf23 or phosphorus concentrations between hemizygous males and heterozygous females. Compared to heterozygous females, homozygous counterparts were significantly smaller and had shorter femurs with reduced bone mineral density, suggesting the existence of dosage effect in the skeletal phenotype of XLH. Howevever, overall phenotypic trends in regards to mineral ion homeostasis were mostly unaffected by the presence of one or two mutant *Phex* allele(s). The lack of gene dosage effect on circulating Fgf23 (and thus, phosphorus) levels suggests that a *Phex* mutation may create the lower set point for extracellular phosphate concentrations.

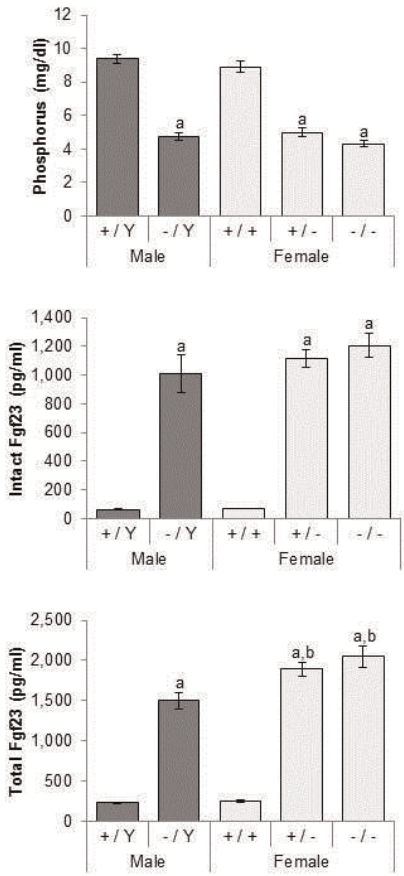

Effects of *Phex* genotypes on serum biochemistries. Total Fgf23 represents intact Fgf23 protein and C-terminal fragments of Fgf23 measured by C-terminal ELISA. Dark gray bars, males; light gray, females. Number of animals = 11-13 per group. Significant difference to same-sex littermates (+/Y vs. -/Y and +/+ vs. +/- or +/+)[a], comparable male genotypes (+/Y vs. +/+ and -/Y vs. +/- or -/-)[b], and heterozygous females (+/- vs. -/-)[c] by unpaired t-test (p-value < 0.05). All values are presented as mean ± SEM.

Figure

***Disclosures: Shoji Ichikawa**, None.*

SA0118

See Friday Plenary Number FR0118.

SA0119

Crosstalk Between Parathyroid Hormone Related Proteins And Minor Fibrillar Collagens. Minoti Hiremath*, Neda Shefa, Julia Oxford. Boise State University, USA

The aim of our study is to determine if PTHrP regulates bone growth during endochondral ossification by regulating the expression of minor fibrillar collagens. Based on abundance, collagens are classified as major collagens, including type 1 and 2, and minor collagens including type 5 and 11. Minor collagens regulate the formation of major collagen fibrils and dictate the quality of the ECM that is synthesized. In humans, heterozygous mutations in the COL11A1 gene cause chondrodysplasia with eye and ear defects designated as Stickler syndrome type II or Marshall syndrome. Collagen 11 is expressed at the periphery of the cartilage underlying the bone collar, distal to the hypertrophic zone. Based on the human diseases caused by mutations of COL11A1 and the expression profile, Collagen XI appears regulate bone growth.Parathyroid hormone related protein (PTHrP) also regulates bone growth by binding to its cognate G-protein coupled receptor, PTHR1. PTHrP maintains columns of proliferating chondrocyte and delays their differentiation into prehypertrophic chondrocytes, preventing premature ossification. Loss of PTHrP results in Bloomstrand's osteo-chondrodystrophy characterized by short bones, small ribcage and domed skulls, and is phenocopied by $PTHrP^{-/-}$ mice.

We hypothesized that one of the mechanisms by which PTHrP regulates endochondral ossification is by regulating expression of minor fibrillar collagens or their isoforms. We used C2C12 cells treated with Bmp2, as a model of osteoblasts. After 5 days of Bmp2 treatment, PTHrP was added for 24 hours and control plates were left untreated. Using semi-quantitative RT-PCR, we observed that PTHrP regulates expression of *COL11* isoforms V1b and V1bV2 in C2C12 cells. This result is intriguing because we found that V1b isoforms of *COL11* were expressed adjacent to the bony collar and distal to the hypertrophic zone. Moreover, these isoforms decrease mineralization in MC3T3-E1 and in Bmp2-treated C2C12 osteoblasts. We also tested regulation of minor collagens *COL5A1, COL5A3* and *COL11A2* by PTHrP, in C2C12 cells, using RT-PCR. Our results indicate that PTHrP reduces *COL5A1* and *COL11A2* and increases *COL5A3* expression in C2C12 cells. Thus, we demonstrate that PTHrP regulates minor collagens in myogenic and osteoblastic cell lines. We are currently examining the expression of minor collagens to determine if they are absent or mislocalized in the developing long bones $PTHrP^{-/-}$ mice.

***Disclosures: Minoti Hiremath**, None.*

SA0120

Withdrawn

SA0121

Parathyroid Hormone Agonists Linked to a Collagen Binding Domain Increase Anagen Hair Follicles and Reduce Hair Loss in Mice with Alopecia Areata. Ranjitha Katikaneni*[1], Rohan Gulati[2], Daniel Suh[1], Joshua Sakon[3], Andrew Seymour[4], Tulasi Ponnapakkam[5], Robert Gensure[6]. [1]Childrens Hospital at Montefiore/Albert Einstein College of Medicine, USA, [2]Children's Hospital at Montefiore, USA, [3]University of Arkansas, USA, [4]Pathology, Montefiore Medical Center, USA, [5]Childrens Hospital at Montefiore, New York/Albert Einstein College of Medicine, USA, [6]Children's Hospital at Montefiore, Albert Einstein College of Medicine, USA

Parathyroid hormone can stimulate the hair cycle by activating Wnt signaling and increasing production of beta-catenin and LEF-1 in keratinocytes, which causes hair follicles to transition to the anagen (growth) phase. Alopecia areata is a common form of hair loss affecting 1.7% of population, in which autoimmune-mediated destruction of anagen phase hair follicles leads to patchy hair loss; currently there is no adequate therapy. PTH-CBD is a fusion protein of PTH(1-33) linked to a bacterial collagen binding domain which targets delivery to collagen-containing tissues, including skin. We tested if PTH-CBD would promote hair growth in the mouse model of alopecia areata. 40 Female C3H/HeJ engrafted mice were obtained from Jackson Laboratories (Bar Harbor, ME). After 8 weeks (partial hair loss), mice were treated with either Vehicle, Low Dose PTH-CBD (320 mcg/kg), High Dose PTH-CBD (1000 mcg/kg), Weekly Dose PTH-CBD (1000 mcg/kg), or PTH(7-33)-CBD (antagonist - 320 mcg/kg), and monitored for 2 months. There were visible effects of treatment within the first few days, and overall improvements in hair growth pattern remained evident over the 2 month period. At the end of the study, hair regrowth or maintenance (within 40% of baseline using gray scale analysis) was observed in 17/21 (81%) total PTH-CBD treated mice vs. 3/10 (30%) vehicle control mice ($p<0.01$, Chi Square test). Animals receiving higher doses or more frequent doses of PTH-CBD appeared to have a greater response, although this was more difficult to quantify. Histological examination revealed marked increase in anagen VI follicles in PTH-CBD treated animals relative to vehicle controls (Figure 1), regardless of the dose or dose frequency. There was evidence of an ongoing immune response in most treated animals, as expected. These histological

changes were also present in the 4 treated animals with ongoing hair loss, suggesting that combined immunosuppressant treatment may result in more consistent responses. The antagonist compound appeared to have little effect on hair growth, follicle number, or immune response. Overall, PTH-CBD administration resulted in increased hair growth and a marked increase in number of growing hair follicles despite an ongoing immune reaction in C3H/HeJ engrafted mice. PTH-CBD shows promise as a therapy for alopecia areata, particularly in conjunction with a mild immune suppressant such as hydrocortisone cream.

***Disclosures: Ranjitha Katikaneni**, None.*

SA0122

Subclinical PTH resistance in a patient with a novel heterozygous GNAS mutation: Gαs haploinsufficiency as a plausible cause. Serap Turan*[1], Susanne Thiele[2], Bettina Brix[2], Zeynep Atay[3], Saygin Abali[3], Murat Bastepe[4]. [1]Marmara University Istanbul-Turkey, Turkey, [2]Division of Experimental Paediatric Endocrinology & Diabetes, University of Luebeck, Germany, [3]Pediatric Endocrinology, Marmara University, Turkey, [4]Massachusetts General Hospital, Harvard Medical School, USA

Pseudohypoparathyroidism (PHP) is characterized by hypocalcemia and hyperphosphatemia due to renal proximal tubular resistance to parathyroid hormone (PTH). PHP-Ia, which is associated with Albright's hereditary osteodystrophy (AHO) and resistance to some other hormones, results from mutations within *GNAS* that lead to loss of Gαs activity. Paternal Gαs allele is normally silenced in the renal proximal tubule, and therefore, PTH resistance develops only when these *GNAS* mutations occur on the maternal allele. The same *GNAS* mutations do not lead to PTH resistance but cause AHO alone when located on the paternal allele, i.e. pseudopseudohypoparathyroidism (PPHP). Here, we describe a patient with persistent PTH elevation without hypocalcemia (Table), who plausibly carries a paternal inactivating *GNAS* mutation. The patient is a female who presented at the age of 13.5 years with multiple AHO features, including short stature, shortening of the third and fourth metacarpals, and subcutaneous calcification. The patient was not obese (BMI=19 kg/m^2) and did not have cognitive impairment. She was born from a healthy mother, with a birth weight of 1 kg at term. There was no family history of AHO features or hormone resistance. Biochemical analysis showed no evidence for resistance to TSH or gonadotropins. Serum calcium, phosphorus, and vitamin D values were within the normal range (Table). Erythrocyte Gαs activity of the patient was reduced (46.7%). Accordingly, nucleotide analysis of leukocyte DNA revealed a novel heterozygous *GNAS* mutation (c.328 G>C; p.A109P) in the patient, which affects the C-terminal end of the Gαs alpha-helical domain. The mutation is not detected in her mother and DNA from the father was not available for genetic analyses, making it difficult to determine whether the mutation occurred de novo (maternal or paternal) or inherited from the father. However, it is possible that this mutation is located on the paternal allele, given that others and we have previously observed elevated serum PTH without hypocalcemia in mice with paternal *Gnas* disruption. Furthermore, our patient exhibited AHO features and evidence of PTH resistance but none of the PHP-Ia features associated with inactivating maternal *GNAS* mutations, such as obesity, cognitive impairment, and resistance to other hormones. We are currently performing additional investigations to determine whether this novel mutation is indeed paternal. If verified, this finding would indicate the presence of subclinical PTH resistance in PPHP and suggest the existence of Gαs haploinsufficiency in a PTH responsive tissue in which Gαs is biallelically expressed, such as bone.

Table. Serum biochemistries of the patient.

		Reference Ranges
PTH (pg/mL)	145.9-64.5-154.5-140.9	9-52
Ca (mg/dL)	9.9-10.2-9.4-10.1	8.4-10.5
Phos (mg/dL)	4.8-4.4-4.4-5	3.5-4.5
25-OH vit D (ug/L)	33-37	30-100
TSH (mIU/mL)	3.6	0.51-4.3
F-T4 (ng/dL)	1.66	0.93-1.7
FSH (mIU/mL)	8.3-6.28	3.5-10
LH (mIU/mL)	4.4-13.62	1.6-62
Estradiol (pg/mL)	38-91	12-200

Table

***Disclosures: Serap Turan**, None.*

SA0123

βAdrenergic Receptor agonist suppresses BMP-induced osteoblastic differentiation in MC3T3E-1 cells while epinephrine modulates it differently. Takayuki Yamada*[1], Tadayoshi Hayata[2], Takuya Notomi[3], Yoichi Ezura[4], Kiyoshi Harada[5], Masaki Noda[1]. [1]Tokyo Medical & Dental University, Japan, [2]Medical Reserach Institute, Tokyo Medical & Dental University, Japan, [3]GCOE, Tokyo Medical & Dental University, Japan, [4]Tokyo Medical & Dental University, Medical Research Insititute, Japan, [5]Department of Maxillofacial Surgery, Maxillofacial & Neck Reconstruction, Graduate School of Medical & Dental Sciences, Tokyo Medical & Dental University, Japan

Currently, about 10% of the total population suffers from osteoporosis and the number of patients is still increasing. Parathyroid hormone (PTH) is currently the only bone anabolic drug. However, PTH is expensive and its use is limited to less than 2 years. Therefore the first choice treatment of osteoporosis is bisphosphonate (BPs). They are efficacious in reduction of risks of pathological fractures in patients with osteoporosis, while side effect, such as bisphosphonate-related osteonecrosis of the jaw (BRONJ) have be described BRONJ could occur after surgical dental treatments such as tooth extraction. As a possible solution for this situation is to develop a drug that may enhance bone formation. The presence of ß2 adrenergic receptor (ß2AR) is essential for PTH-induced anabolic action on bone. This suggests that downstream of adrenergic pathway may modulate PTH action. Therefore, we tried to identify new ways that could increase bone formation. Specifically, we examine genes targeted by adrenergic signaling in osteoblasts. MC3T3E-1 cells were stimulated by isoproterenol or by epinephrine using cyclic treatments (every three minutes), and were then cultured for additional 3 days in the presence of low dosage of BMP. ALP activity was measured using PNPP and the obtained data were normalized against the protein. Epinephrine treatment tended to increase ALP activity in the presence of BMP, whereas, PTH did not enhance ALP activity even in the presence of BMP. We also examined ß2 adrenergic receptor agonist, isoproterenol. We found that isoproterenol inhibited ALP activity by opposing BMP action, suggesting that isoproterenol action is different from that of epinephrine. These data suggest individual effects of GPCR agonists on the expression of osteoblastic genes.

***Disclosures: Takayuki Yamada**, None.*

SA0124

Withdrawn

SA0125

See Friday Plenary Number FR0125.

SA0126

A Genetic Test to Predict Patient Response to rhBMP-2 for Lumbar Spinal Arthrodesis. Travis Burgers*[1], Jianfeng Xu[2], Martin Hoffmann[3], Debra Sietsema[4], Victoria Zismann[5], Berry Button[5], Paula Davidson[1], Sha Tao[6], Waibhav Tembe[5], Jeffrey Kiefer[5], James Mason[1], Bart Williams[7], Jeffrey Trent[8], Clifford Jones[4]. [1]Van Andel Institute, USA, [2]Translational Genomics Research Institute; Center for Cancer Genomics, USA, [3]Grand Rapids Medical Education Partners, USA, [4]Orthopaedic Associates of Michigan; Michigan State University, USA, [5]Translational Genomics Research Institute, USA, [6]Center for Cancer Genomics, USA, [7]Van Andel Research Institute, USA, [8]Translational Genomics Research Institute, USA

INTRODUCTION: The use of rhBMP-2 (Medtronic, Memphis, TN) in spinal arthrodesis remains controversial due to off-label use, cost, and reported complications despite high fusion rates. Up to 4.6% of rhBMP-2 posterolateral lumbar arthrodeses have a complication of postoperative painful seroma formation requiring secondary surgery. The biological attributes underlying these responses to rhBMP-2 have not been fully elucidated. This study aims to identify genetic variants that will predict a patient's risk of complications associated with rhBMP-2.

METHODS: Our previous analysis described the exome sequencing-based search for risk-predictive genetic markers in eight patient samples, consisting of six hyperresponders (required operative dural decompression due to seroma accumulation) and two non-hyperresponders. In the current study, we selected 200 SNPs from the exome sequencing results based on prevalence in hyperresponders and a ranking scheme using molecular associations. We then genotyped these SNPs in 108 Caucasian patients treated with rhBMP-2. Standard statistical analyses of genetic association were performed to identify SNPs that correlate with hyperresponse to rhBMP-2.

RESULTS: An allelic test comparing frequency of each SNP between hyperresponders and non-hyperresponders confirmed an association for 5 SNPs ($p<0.05$); these consisted of nonsynonymous changes or splice variants in *NID1*, *SENP7*, *FARP1*, *PRGRI*, and *CDH3*. The performance of each mutation for discriminating hyperresponders from non-hyperresponders, measured by area under the receiver

operating characteristic curves (AUC), ranged from 0.65 to 0.68. The combined AUC of these 5 variants was 0.75 (p=0.0003). Among patients with 7 or more hyperresponsive alleles, 78% were hyperresponders; in comparison, only 10% were hyperresponders among patients with 6 or fewer hyperresponsive alleles. Importantly, differentiation between the two groups is highly significant (p=0.00002).

CONCLUSION: Our results are the first to suggest that a combination of multiple genetic variants associated with pathological response to rhBMP-2 can be used to identify those at greatest risk to be hyperresponders. Studies are underway to validate the predictive power of our current panel of SNPs in independent cohorts of rhBMP-2 treated patients. This study provides the foundation to support pre-operative genetic screening to guide rhBMP-2 use in spinal arthrodesis patients.

***Disclosures: Travis Burgers**, None.*

SA0127

A Mouse Model to Study the Function of *RECQL4* on Skeletogenesis. Linchao Lu*[1], Karine Harutyunyan[2], Weidong Jin[1], Tao Yang[3], Yuqing Chen[4], Jianhong Wu[1], Brian Dawson[4], Ming-Ming Jiang[4], Kyu-Sang Joeng[1], Brendan Lee[4], Lisa Wang[1]. [1]Baylor College of Medicine, USA, [2]MD Anderson Cancer Center, USA, [3]Van Andel Research Institute, USA, [4]Baylor College of Medicine, Howard Hughes Medical Institute, USA

Background: *RECQL4* is a member of ATP-dependent DNA helicase superfamily II, and has been shown to play a role in DNA replication, homologous recombination and DNA damage repair. Deleterious mutations in *RECQL4* are responsible for several human genetic disorders, including Rothmund-Thomson syndrome (RTS), RAPADILINO syndrome, and Baller-Gerold syndrome. Skeletal abnormalities are common among these three disorders, including radial ray/thumb defects, radio-ulnar and radio-humeral synostoses, foreshortened limbs, brachymesophalangy, absent patellae, osteopenia, and craniosynostosis. Furthermore, RTS patients with *RECQL4* mutations have a significant risk of developing bone cancer (osteosarcoma). However, the molecular mechanisms underlying these findings remain to be elucidated.

Methods: To study the function of *RECQL4* on skeletogenesis *in vivo*, a mouse *Recql4* conditional allele with two loxp sites flanking exons 5 and 8 was generated by gene targeting. Transgenic mice expressing Prx1-Cre were crossed with these floxed *Recql4* mice to inactive *Recql4* in mesenchymal progenitors of developing limbs.

Results: $Recql4^{fl/fl}$;Prx1-Cre^{+} mice (Prx1-CKO) were born with a normal Mendelian ratio. However, these mice had short forelimbs and smaller hindlimbs, missing digits, and displayed severe growth retardation and increased postnatal lethality before weaning age. Dissection of different stages of embryonic development showed that Prx1-CKO embryos started to exhibit abnormal forelimb formation at E12.5. Furthermore, micro-CT analysis of skulls of 3 week old Prx1-CKO mice demonstrated bilateral synostosis of coronal and squamosal sutures. Using *Rosa26-lacZ* reporter mice, Prx1-Cre was shown to be strongly expressed in the coronal and squamosal sutures at P1 age. H&E staining of coronal suture in these Prx1-CKO mice showed that the suture was already fused at day E16.5.

Conclusions: The skeletal findings in these $Recql4^{fl/fl}$;Prx1-Cre^{+} mice recapitulate the major skeletal findings in the *RECQL4* spectrum of disorders, and suggest that *Recql4* is required for normal limb and cranial suture development. This Prx1-CKO mouse model will be used to further study the molecular mechanisms underlying the skeletal abnormalities in *RECQL4* associated diseases.

***Disclosures: Linchao Lu**, None.*

SA0128

Cinacalcet as adjunct therapy in familial hypophosphatemic rickets: 18 months experience. Uri Alon*. Children's Mercy Hospital, USA

Objective: based on preliminary findings, indicating a potential for Cinacalcet, due to its suppression of PTH (CJASN 2008;3:658), to allow the use of lower doses of oral phosphate (OP) and calcitriol in treating XLH, the objective of this study was to examine its long-term effect as adjunct treatment in children with XLH.

Methods: Eight children (F5), ages 7.8-20.9y (median 13.9), who were already treated by OP and calcitriol were enrolled in the study. Cinacalcet was added at 30mg once daily to those weighing <= 30kg and 60mg to those >30kg. Clinic visits were done every 3m; dose of medications adjusted to maintain serum P similar to baseline, PTH within its normal range and Ca^{++} >1.00 mmol/l. In case of hypercalciuria (>4mg/kg/24h) thiazide/amiloride was added. Blood was checked for creatinine, Ca^{++}, P, ALP, PTH and FGF23; urine for TP/GFR and Ca excretion. Radiographs of lower joints were done every 6 months, renal ultrasound annually.

Results: Follow-up lasted 21.2 ± 5.3m (median 18). Rickets stayed healed in all. In one child nephrocalcinosis grade 1, present at baseline did not change and in another developed after 2 years into the study. At the end of the study, 7 children were receiving Cinacalcet 30mg, and the oldest 60mg. 3 children had their growth plates closed at the beginning of the study, Height SDS improved in 2 patients, were unchanged in 2 and decreased in 1. One child was on thiazide/amiloride at baseline and in 3 it was added during the study. No side effects were observed and none of the patients discontinued the study.

Conclusions: The addition of the calcimimetic: (1) resulted in significant decreases in PTH and FGF23 and increase in TP/GFR enabling significant decreases in calcitriol and OP doses (2) requires careful attention to serum and urine calcium. Further studies are warranted exploring the beneficial effects of calcimimetics in the treatment of children with XLH.

	Start	End	p
Calcitriol dose (ng/kg/24hr)	22.0±12.0	12.5±8.9	<0.001
K-Phos dose (mg/kg/24hr)	40.4±28.4	23.3±20.7	<0.01
PTH (pg/ml)	45.0±38.8	21.9±16.3	<0.05
Ca^{++}	1.20±0.06	1.06±0.07	<0.005
P (mg/dl)	3.01±0.31	3.10±0.41	NS
Alk. Phos. (u/l)	242±160	196±120	0.06
FGF23 (RU/ml)	272±71	197±62	<0.005
TP/GFR (mg/dl)	2.24±0.33	2.49±0.41	<0.005
Urine Ca (mg/kg/24hr)	1.9±1.4	1.1±0.7	NS

Table 1

***Disclosures: Uri Alon**, None.*

SA0129

Delayed Fracture Healing in a Mouse Model for Craniometaphyseal Dysplasia. Yusuke Hagiwara, Xi Jiang, Zhifang Hao, Ernst Reichenberger, I-Ping Chen*. University of Connecticut Health Center, USA

Homozygous knock-in mice ($Ank^{KI/KI}$) carrying a Phe377del mutation in ANK replicate many features of human craniometaphyseal dysplasia (CMD), a rare genetic bone disorder characterized by hyperostosis of craniofacial bones and metaphyseal flaring of long bones with undertrabeculation of metaphyses and increased trabeculation of diaphyses. Serum TRAP5b levels are increased in $Ank^{KI/KI}$ mice whereas *in vitro* osteoclast (OC) formation and function are decreased.

We studied $Ank^{KI/KI}$ OC activity in a tibia fracture healing model where the fracture callus is actively remodeled within a 2- to 3-week period. 3-month-old male $Ank^{+/+}$ and $Ank^{KI/KI}$ mice were subjected to transverse diaphyseal fracture of the left tibia. Radiographs were taken at days 0, 7, 14 and 21 to monitor the healing progress. Mice were sacrificed at day 14 or 21 post-fracture. For the 21 day group, an intraperitoneal injection of calcein and demeclocycline was administered two weeks and one day prior to sacrifice, respectively. The fractured tibia was fixed and frozen sections were stained for TRAP using the fluorescent substrate ELF-97.

Qualitative histological analyses together with radiographs, showed significant callus remodeling in $Ank^{+/+}$ mice but less decrease in callus size in $Ank^{KI/KI}$ mice between 14 to 21 days after fracture. More calcein label was retained and larger amounts of cartilaginous callus remained in $Ank^{KI/KI}$ mice compared to $Ank^{+/+}$ mice 21 days after fracture. Trabeculae in the remodeled $Ank^{KI/KI}$ callus were reduced, both in thickness and number. Alternatively to TRAP staining, we used CD11c as a reporter to visualize OC activity during fracture healing *in vivo*. Dendritic cells (DC) were reported to be recruited to sites of inflammation to mediate bone resorption. We sorted cells positive for CD11c, a marker for DC, from bone marrow of CD11c-mCherry reporter mice. Multinucleated cells formed after treatment with M-CSF and RANKL and the majority of cells coexpressed TRAP and CD11c. Our preliminary data using the CMD mouse model expressing CD11c-driven mCherry reporter showed that CD11c-mCherry cells were located on the bone surface inside the callus and stained positive for TRAP.

Tibia fracture is a useful tool for evaluating the ability of mice to initiate bone formation followed by remodeling. Our results suggest that the decrease in new bone formation and osteoclast remodeling may account for reduced metaphyseal and increased diaphyseal trabeculation in $Ank^{KI/KI}$ mice.

***Disclosures: I-Ping Chen**, None.*

SA0130

Discoidin Receptor 2 Control of Skeletal Osteogenesis and Adipogenesis. Chunxi Ge*[1], Zhengyan Wang[2], Jinhui Liao[3], Guisheng Zhao[3], Binbin Li[3], Renny Franceschi[2]. [1]Pom Univ of Michigan School of Dentistry, USA, [2]University of Michigan, USA, [3]University of Michigan School of Dentistry, USA

Human mutations in discoidin receptor 2 (*Ddr2*) cause spondylo-meta-epiphyseal dysplasia (SMED), resulting in shortened digits and limbs and craniofacial abnormalities. DDR2, a collagen receptor tyrosine kinase, stimulates ERK1/2 and p38 MAP kinase pathways, which, in other systems, activate osteoblast differentiation and suppress adipogenesis via selective phosphorylation of RUNX2 and PPARg transcription factors. In this study, we examine effects of *Ddr2* deletion on bone structure, marrow adipogenesis and mesenchymal stem cell (MSCs) differentiation to osteoblasts or adipocytes.Bone and marrow fat was analyzed in 5 month-old *smallie* (*slie*) mice harboring a spontaneous 150 kb deletion in *Ddr2* ($Ddr2^{slie/slie}$ mice) using microCT and osmium staining. Mice were also used as a source of calvarial osteoblasts, marrow stromal cells (MSCs) or ear mesenchymal stem cells (EMSCs). Runx2 and PPARg phosphorylation was measured using antibodies specific to MAPK phosphorylation sites (RUNX2, S319; PPARg, S112). RUNX2 and PPARg transcriptional activity were measured using 6OSE2-Luc and ARE-luc reporters.

$Ddr2^{slie/slie}$ mice had multiple skeletal defects. Skulls had widened calvarial sutures and increased mandibular porosity. A progressive decrease in tibial trabecular BV/TV was observed when wild type, $Ddr2^{+/slie}$ and $Ddr2^{slie/slie}$ mice were compared. These changes were accompanied by drops in trabecular number and thickness and increased trabecular spacing in both males and females. Interestingly, cortical

thickness was not affected in males, but was lower in Ddr2$^{slie/slie}$ females. In addition, marrow fat volume was increased in Ddr2$^{slie/slie}$ mice. To examine the role of DDR2 signaling in cell differentiation, we prepared calvarial osteoblasts, BMSCs and EMSCs from the 3 genotypes and grew cells under osteogenic and adipogenic conditions. Regardless of cell source, Ddr2$^{slie/slie}$ cells exhibited defective osteoblast differentiation and accelerated adipogenesis. Furthermore, both RUNX2-S319 phosphorylation and PPARg-S112 phosphorylation were decreased in Ddr2$^{slie/slie}$ cells, resulting in decreased RUNX2 and increased PPARg transcriptional activity.

Conclusion: Ddr2 is necessary for normal bone development and MSC differentiation to osteoblasts and is able to suppress adipocyte differentiation. This regulation requires MAPK-dependent phosphorylation of RUNX2 and PPARg transcription factors.

***Disclosures: Chunxi Ge**, None.*

SA0131

ER stress response to procollagen misfolding leads to osteoblast malfunction in the Amish mouse model of OI. Lynn Mirigian, Elena Makareeva, Sergey Leikin*. National Institutes of Health, USA

Mutations that disrupt procollagen folding are responsible for most cases of severe osteogenesis imperfecta (OI). Such mutations include not only those that cause structural defects in type I procollagen but also deficiencies in proteins that chaperone procollagen folding in the Endoplasmic Reticulum (ER), e.g. deficiencies in HSP47 or in any of the P3H1/CRTAP/CYPB protein complex components. Several studies suggest that ER stress response to procollagen misfolding might disrupt differentiation and function of osteoblasts, contributing to bone pathology in OI. Yet, molecular mechanisms of this ER stress response and its role in OI pathophysiology are still poorly characterized. To address these questions, we investigated procollagen misfolding in a mouse model mimicking the α2(I)-Gly610Cys substitution in OI patients from the Old Order Amish community in Lancaster County, PA. We found at least a twofold delay in procollagen folding in osteoblasts from heterozygous animals compared to wild type littermates, resulting in excessive accumulation of misfolded molecules in the ER. At the same time, we observed no upregulation of BIP or other markers of conventional unfolded protein response, in agreement with previous studies of fibroblasts from OI patients or murine models of Gly substitutions. Consistent with this observation, inhibition of ER-associated proteosomal degradation did not cause accumulation of misfolded molecules in the cell. In contrast, increased expression of LC3B in cells from heterozygous mice and intracellular accumulation of procollagen in these cells in response to autophagy inhibitors indicated that degradation of misfolded molecules occurs via autophagy and proteolysis in lysosomes. Overall, the ER stress response was reminiscent of the ER-overload in serpinopathies. It likely underlies abnormal differentiation of osteoblasts revealed by quantitative, real-time PCR comparison of bone sialoprotein, osteocalcin and dentin matrix acidic phosphoprotein transcription in cells from heterozygous animals and their wild type littermates. Based on these observations, we are currently testing a simple dietary approach to enhancing autophagy and reducing the misfolded protein load in osteoblasts in mutant animals. However, additional studies of pathways involved in the ER response to procollagen misfolding and effects of this response on osteoblast differentiation and function are needed for identifying other treatment strategies.

***Disclosures: Sergey Leikin**, None.*

SA0132

High-Throughput DEXA and MicroCT Screening in Gene Knockout Mice Identifies Bone Mass Phenotypes. Robert Brommage*, Jeff Liu, Laura Kirkpatrick, Gwenn Hansen, David Powell, Peter Vogel. Lexicon Pharmaceuticals, USA

Screening gene function *in vivo* is a powerful approach to discover novel drug targets in the human genome (Nature Reviews Drug Discovery 2:38-51; 2003). We present data for 3779 distinct gene knockout (KO) mouse lines with viable adult homozygous mice generated using both gene-trap (1369 KOs) and homologous recombination (2410 KOs) technologies. Embryonic/neonatal/juvenile lethality or reduced viability was observed in an additional >970 KO lines. KO strategies are available for 4,077 lines at http://www.taconic.com/wmspage.cfm?parm1=2522. Bone mass was determined from PIXImus DEXA scans of male and female mice at 14 weeks of age and by microCT analyses of bones from male mice at 16 weeks of age. Wild-type (WT) littermates/cagemates were examined for each gene KO. For most lines DEXA scans were performed on 4 KO and 2 WT mice of each gender. Body BMC, aBMD, vBMD, and BMC/LBM ratio, femur BMD and spine BMD were monitored. Bone parameters were normally distributed. Volumetric BMD in KOs (N = 3632) averaged 99.5% of WT values with a SD of 3.7%. Using a Scanco Medical μCT40, trabecular bone parameters in LV5 were analyzed in 3386 lines and midfemur cortical thickness (CT) in 3350 lines (generally 4 KO and 2 WT). Specially designed plastic inserts held 48 LV5s (scanned overnight with 4 LV5s scanned simultaneously) and 18 femurs (scanned in 30 minutes with 6 femurs scanned simultaneously). LV5 trabecular BV/TV in KOs averaged 16.2% (SD = 3.9%). Femoral CT averaged 245 μm (SD = 16 μm). Since primary high-throughput screens (HTS) are susceptible to false positive findings, additional cohorts of mice from KO lines with intriguing HTS bone data were examined. Aging, ovariectomy, histomorphometry and bone strength studies were performed on lines identifying potentially novel osteoporosis drug targets, and possible non-skeletal phenotypes were explored. Together, these screens identified previously reported (Lrp5, Sost, Wnt10b, Sfrp4, myostatin, Klotho, c-Src, Ostm1, Dcstamp and Crtap) as well as novel (Wnt16 – reduced cortical bone, Lrrk1 - osteopetrosis, Fam20c – hypophosphatemic rickets, sphingosine-1P-lyase – osteopetrosis, and Cldn18 - enhanced osteoclast activity) genes regulating bone mass.

***Disclosures: Robert Brommage**, Lexicon Pharmaceuticals, 3*
This study received funding from: Lexicon Pharmaceuticals

SA0133

Neurofibromin regulates pyrophosphate homeostasis and bone matrix mineralization. Jean De La Croix Ndong*[1], Koichiro Ono[2], Alexander Makowski[3], Daniel Perrien[4], Jeffry Nyman[4], Florent Elefteriou[1]. [1]Vanderbilt University, USA, [2]Center for Bone Biology, USA, [3]Department of Veterans AffairsVanderbilt University, USA, [4]Vanderbilt University Medical Center, USA

Neurofibromatosis is caused by mutations in NF1, a gene encoding the RAS-GTPase neurofibromin. Patients with NF1 can present with a number of skeletal maladies, including tibia bowing and pseudoarthrosis (PA). Despite substantial advances in our understanding of the role of neurofibromin in bone cells, the etiology of NF1 PA remains unclear and its treatment still require multiple and invasive surgeries. Based on the existence of non-mineralized matrix in NF1 PA biopsies and the skeleton of multiple NF1 bone mouse models, we investigated whether Nf1 loss-of-function impairs the maturation and mineralization potential of Nf1-/- osteoprecursor cells. Using bone marrow stromal cells (BMSCs) isolated from Nf1col2-/- cKO mice (characterized by Nf1 deficiency in osteochondroprogenitors), we found that compared to WT BMSCs, Nf1-/- BMSCs formed a reduced number of alkaline phosphatase-positive (cfu-AP) colonies and mineralized alizarin red-positive (cfu-Ob) colonies, which was suggestive of impaired differentiation and/or mineralization. Further investigations revealed that levels of extracellular inorganic pyrophosphate (ePPi), a potent inhibitor of hydroxyapatite formation and propagation, were elevated in the conditioned medium from Nf1-/- BMSCs compared to WT BMSCs. The expression of Ank, a transporter of ePPi, Enpp1, an enzyme generating PPi, and Opn, an inhibitor of mineral nucleation was significantly increased in immature Nf1-/- BMSCs compared to WT controls, whereas the expression of Tnsalp, whose activity is to cleave PPi, was reduced. BMP2 treatment was unable to correct the differentiation and mineralization defects of Nf1-/- BMSCs, and further promoted the expression of Ank and Enpp1. These results thus indicate that the impaired bone mineralization observed in NF1 mouse models and possibly in NF1 PA is caused by accumulation of ePPI. Importantly, treatment of Nf1-/- BMSCs with a recombinant form of human TNSALP (used as a mean to catabolize ePPi) rescued their matrix mineralization defect in vitro, and daily administration of rhTNSALP in growing Nf1col2-/- mice for 18 days significantly promoted their growth, cortical thickness, mineral-to-collagen ratio and crystallinity. There results identify what we believe is an important molecular defect underlying the development of tibia bowing, fragility and PA in NF1 children, and suggest that the successful treatment of NF1 PA will require not only bone anabolic agents but also inhibitors of ePPi.

***Disclosures: Jean De La Croix Ndong**, None.*

SA0134

Osteoblast CFTR Regulates Bone Formation and Osteoprotegerin Expression in Cystic Fibrosis-Related Bone Disease. Michael Stalvey, Katrina Clines, Viktoria Havasi, W. Joon Chung, Gregory Clines*. University of Alabama at Birmingham, USA

Low bone mass and increased fracture risk are recognized complications of cystic fibrosis (CF). CF-related bone disease is characterized by uncoupled bone turnover—impaired osteoblastic bone formation and enhanced osteoclastic bone resorption. Intestinal malabsorption, vitamin D deficiency and inflammatory cytokines contribute to CF-related bone disease, but epidemiological investigations and animal models now support a direct causal link between inactivation of bone cystic fibrosis transmembrane regulator (CFTR), the gene that when mutated causes CF, and CF-related bone disease. The objective of this study was to examine the direct actions of CFTR inactivation on bone. Expression analyses revealed that CFTR mRNA and protein were expressed in osteoblasts, but not in osteoclasts. Functional studies were then performed to investigate the direct actions of CFTR on the osteoblast utilizing a CFTR knockout (Cftr-/-) mouse model. In the murine calvarial organ culture assay, Cftr-/- calvariae displayed significantly less bone formation (6430 μm2 vs. 16440 μm2, p=0.0023) and osteoblast numbers than calvariae harvested from wildtype (Cftr+/+) littermates. CFTR inactivation also reduced alkaline phosphatase expression in cultured calvarial osteoblasts. Although CFTR was not expressed in murine osteoclasts, significantly more osteoclasts formed in Cftr-/- compared to Cftr+/+ bone marrow cultures. This result suggested that other cell types in bone that regulate osteoclastogenesis are influenced by CFTR. The consequence of osteoblast CFTR inactivation on RANKL and OPG expression to indirectly control osteoclastogenesis was next examined. Although no difference in Rankl mRNA was detected, significantly less Opg was expressed in Cftr-/- compared to Cftr+/+ osteoblasts. Together, the Rankl:Opg ratio was significantly higher in Cftr-/- calvarial osteoblasts contributing to a higher osteoclastogenesis potential. The combined findings of reduced osteoblast differentiation and lower Opg expression suggested a possible

defect in canonical Wnt signaling. In fact, Wnt3a and PTH-stimulated canonical Wnt signaling was defective in Cftr-/- calvarial osteoblasts. These results support that genetic inactivation of CFTR in osteoblasts contributes to low bone mass and that targeting the osteoblast may represent an effective strategy to treat CF-related bone disease.

***Disclosures: Gregory Clines**, None.*

SA0135

Withdrawn

SA0136

Trabecular and Not Cortical Bone Is Affected in Different Forms of Osteogenesis Imperfecta. Roland Kocijan*[1], Christian Muschitz[2], Didier Hans[3], Judith Haschka[1], Janina Patsch[4], Georg Schett[5], Matthias Englbrecht[5], Afrodite Zendeli[6], Daniela Süß[6], Heinrich Resch[4]. [1]St. Vincent Hospital Vienna, Austria, [2]St. Vincent's Hospital, Austria, [3]Lausanne University Hospital, Switzerland, [4]Medical University of Vienna, Austria, [5]Friedrich-Alexander University Medical School, Germany, [6]The VINFORCE Study Group - St. Vincent Hospital - Medical Department II, Austria

Purpose: Areal bone mineral density (aBMD) by DXA as the standard measuring tool has several limitations in osteogenesis imperfecta (OI) due to partly high bone mineralization as well as vertebral fractures and scoliosis in severe cases. Therefore, the aim of this study was to evaluate alternative radiological tools at different sites in adult patients with different types of OI.

Methods: We investigated 23 patients with OI (11 female, 12 male, mean age 45.7 $\pm$ 16.4 years). OI was divided into the mild OI-I and the moderate-severe OI-III-IV group. Bone microarchitecture and volumetric BMD (vBMD) were determined by high resolution peripheral quantitative computed tomography (HR-pQCT, SCANCO Medical) at the radius and tibia. HR-pQCT data were compared to 23 healthy, age and gender matched controls (CO, mean age 42.5 $\pm$ 9.9 years). Moreover, trabecular bone score (TBS) at the lumbar spine (LS) and aBMD by DXA at the LS and hip as well as by DXL (Calscan, dual X-ray and laser) at the calcaneus were carried out in OI.

Results: At both, radius and tibia, trabecular but not cortical vBMD was significantly lower in OI-I ($p<0.05$) and OI-III-IV ($p<0.001$) compared to CO. Significantly decreased bone volume fraction (BV/TV) and trabecular number (Tb.N), as well as an increased inhomogeneity of the network and trabecular separation (Tb.Sp) were found in OI-I ($p<0.05$-0.001) and OI-III-IV ($p<0.001$ for all) compared to CO. BV/TV, Tb.N, Tb.Sp and inhomogeneity were significantly worse in OI-III-IV compared to OI-I. No differences were found regarding cortical porosity at tibia and radius.

TBS was significantly lower in moderate-severe OI-III-IV compared to mild OI-I ($p<0.05$). Correlations were found between TBS and BV/TV (r=0.460), Tb.N (r=0.518), inhomogeneity (r=-0.484), trabecular density (r=0.461) and aBMD of LS (r=0.495) and hip (r=0.720, $p<0.05$ for all). Differences in aBMD between OI-I and OI-III-IV were higher at the calcaneus ($p<0.001$), as a mainly trabecular bone, than the hip ($p<0.05$).

Conclusions: Especially trabecular and not cortical BMD and microstructure are severely affected in OI-I and even more in OI-III-IV. HR-pQCT and TBS are helpful tools to quantify microstructure in OI. Moderate correlations approve TBS for microstructure analysis. The trabecular deterioration is even reflected by simple applicable tools like TBS and DXL of the calcaneus. The latter might be optimal for BMD measurement in severe OI with vertebral fractures or scoliosis.

***Disclosures: Roland Kocijan**, None.*

SA0137

Whole Exome Sequencing is a Sensitive and Cost-Effective Means of Detecting Mutations in Patients with Marfan Syndrome and Osteogenesis Imperfecta. Emma Duncan*[1], Aideen McInerney-Leo[2], Paul Leo[2], Brooke Gardiner[2], Mhairi Marshall[2], Paul Coucke[3], Bart Loeys[4], Malcolm West[5], Jennifer west[5], Paul Wordsworth[6], Andreas Zankl[2], Matthew Brown[7], Lut van Laer[8]. [1]Royal Brisbane & Women's Hospital, Australia, [2]University of Queensland Diamantina Institute, Australia, [3]University of Ghent, Belgium, [4]Antwerp University, Belgium, [5]Prince Charles Hospital, Australia, [6]University of Oxford, United Kingdom, [7]Diamantina Institute of Cancer, Immunology & Metabolic Medicine, Australia, [8]University of Antwerp, Belgium

Marfan syndrome and Osteogenesis Imperfecta (OI) are amongst the most common Mendelian disorders. These conditions are normally diagnosed clinically without genetic testing, as the large gene sizes and diversity of mutation location and type make conventional sequencing prohibitively expensive (A$1500 for *FBN1*; $1850 for *COL1A1*/*COL1A2*). Efficient gene testing would greatly benefit at-risk family members, individuals with borderline clinical features, and genetic counselling; and allow critical differential diagnoses (e.g. non-accidental injury).Methods: We performed exome capture and massive parallel sequencing on genomic DNA from 11 patients with Marfan syndrome and 13 patients with OI in whom mutations had been previously identified conventionally. Exome capture was performed using liquid phase hybridisation and Illumina/TruSeq Exome Enrichment Kit v2.0; massive parallel sequencing was performed on Illumina HiSeq 2000 (6 multiplexed samples/flow cell lane; 100 base pair (bp) paired-end reads).CASAVA 1.8.2 was used for de-multiplexing and initial base calling. Sequence data was aligned to the current human genome build (hg19); SNPs and small indels were called using Genome Analysis Toolkit GATK (v2.4-9) and annotated using ANNOVAR. CREST and exomeCopy were used to search for large deletions. We compared our sequencing results with the previous data.

Results: We detected 13/13 mutations in OI patients and 10/11 mutations in Marfan patients, including non-synonymous SNPs and small indels (up to 10bp) in each patient group. The remaining Marfan sample was reported to carry a large deletion of both exons 1 and 2. This was not detected with either CREST or exomeCopy. CREST uses alignment discrepancy to identify mutations; as the start and stop sites of this deletion are intronic, and the sample was exome-sequenced, no such discrepancy was present. ExomeCopy relies on relative sequencing depth; however, exons 1 and 2 of *FBN1* are always poorly captured due to their high GC content. Although deletions occur in 30% of Marfan syndrome patients, most are small (<10bp); only 2% are large insertions/deletions. Our costs for exome sequencing were lower than current commercial conventional sequencing services.

Conclusions: Exome sequencing is both sensitive and cost-effective for detecting mutations in patients with either OI or Marfan syndrome, with high sensitivity (>95%) for both disorders. Providing a genetic diagnosis in these conditions provides diagnostic certainty and enables effective screening.

***Disclosures: Emma Duncan**, None.*

SA0138

A Functional Amino Acid Substitution in the Glucose-dependent Insulinotropic Polypeptide-Receptor (GIPR) Gene is Associated with Bone Mineral Density, Bone Loss, and Osteoporotic Fractures: The Danish Osteoporosis Prevention Study. Torben Harsloef*[1], Signe S Torekov[2], Torben Hansen[2], Jens J Holst[2], Oluf Pedersen[2], Lars Rejnmark[3], Bente Langdahl[3]. [1]Aarhus University Hospital, Aarhus Sygehus, Denmark, [2]Department of Biomedical sciences & Novo Nordic Center for Basic Metabolic Research, Faculty of Health Sciences, University of Copenhagen, Denmark, [3]Aarhus University Hospital, Denmark

Food ingestion decreases bone resorption. Glucose-dependent insulinotropic polypeptide (GIP) may mediate this effect. GIP is produced in the duodenum and in the presence of glucose stimulates production of insulin. A functional GIP receptor (GIPR) has been demonstrated on both osteoblasts and osteoclasts: Mice overexpressing GIP have increased osteoblast activity and are rescued from age-related bone loss. The rare allele of *GIPR* rs1800437 promotes a substitution of glutamate to glutamine. This variant decreases insulin secretion and increases 2-hour blood glucose in an oral glucose tolerance test in non-diabetic individuals. This suggests that the variant decreases the effect of GIP. We therefore investigated the relationship between the *GIPR* polymorphism rs1800437 and bone mineral density (BMD), changes therein, and risk of osteoporotic fractures in a cohort of Danish perimenopausal women.

A total of 2016 women with last menstrual bleeding within 3 months to 2 years were included. Exclusion criteria were drugs and diseases affecting BMD. Hormone therapy or placebo were initiated at baseline and continued for 10 years. DXA scans were performed at baseline and after 10 years. Incident fractures were recorded at scheduled visits during the 10 years of follow up. Vertebral fractures were documented with spinal x-rays and information on incident fractures between inclusion and June 2008 were obtained from the Danish National Patient Registry.

After 10 years women homozygous of the common G-allele of rs1800437 had significantly higher BMD at both the femoral neck (0.766 ± 0.004g/cm2 (mean $\pm$ SEM) vs. 0.747 ± 0.005 and 0.755 ± 0.015g/cm2 in women heterozygous and homozygous for the variant allele, respectively, p=0.008) and total hip (0.906 ± 0.004g/cm2 vs. 0.884 ± 0.005 and 0.881 ± 0.016 g/cm2 in women heterozygous and homozygous for the variant allele, respectively, p=0.002). Accordingly, women homozygous of the variant C-allele had a tendency towards a greater 10-year loss of BMD (p=0.07). Finally, women homozygous for the variant C-allele had an increased risk (HR 1.57 (CI: 1.0 – 2.45) p=0.05) of non-vertebral osteoporotic fractures.This is the first study associating a functional *GIPR* polymorphism (rs1800437) with BMD and fracture. Thus, it seems that the *GIPR* rs1800437, which promotes an amino acid substitution, have effects both on blood glucose regulation and on bone quality. These finding further establish GIP as involved in regulation of bone density.

***Disclosures: Torben Harsloef**, None.*

SA0139

Association of Vitamin D Binding Protein Polymorphisms, Serum 25-hydroxyvitamin D and Serum Parathyroid Hormone Concentrations in 37-47 Year Old Caucasian Women and Men in Finland. Elisa Saarnio*[1], Minna Pekkinen[2], Suvi Itkonen[1], Virpi Kemi[1], Heini Karp[1], Merja Karkkainen[1], Outi Makitie[3], Christel Lamberg-Allardt[1]. [1]University of Helsinki, Finland, [2]Folkhälsan Institute of Genetics, University of Helsinki, Finland, [3]Children's Hospital, Helsinki University Central Hospital, Finland

Vitamin D and its metabolites are bound to vitamin D binding protein (DBP) also known as group- specific component (GC) in the circulation. It is the primary protein involved in the transport of vitamin D. DBP has a high affinity to serum 25-hydroxyvitamin D (S-25OHD). DBP is a polymorphic protein and variants of it can be associated with circulating S-25OHD concentrations.

In this study we investigated the associations between the GC gene variants and S-25OHD and serum parathyroid hormone (S-PTH) concentrations in middle-aged Caucasians in Finland.

We examined 617 healthy 37-47 year old Caucasian women and men in a cross-sectional study. Fasting blood samples were collected, as well as dietary intake of vitamin D and calcium (Ca) by a validated food frequency questionnaire (FFQ). Concentrations of S-25OHD and S-PTH were determined. Background data including sunlight exposure and the amount of vitamin D and Ca supplements were collected. DNA was isolated from blood and genotyped with Taqman method. Three SNPs were genotyped based on polymorphisms in the GC gene: rs4588, rs7041 and rs705124. SNPs 4588 and 7041 combine to form six GC diplotypes.

The GC diplotype distribution was: 1S/1S (46% of the subjects), 1S/2 (25%), 1F/1F (2%), 1F/2 (6%), 1F/1S (16%) and 2/2 (4%). The distribution of the third SNP rs 705124 was: genotype 1 60%, genotype 2 34 % and genotype 3 5%. There was a difference among the GC diplotypes in S-25OHD concentrations (ANCOVA, p=0.015) when adjusted with covariates: S-PTH, vitamin D intake (including supplements), sunlight exposure and body mass index (BMI).When pairwise comparisons were made, a difference in S-25OHD concentrations was between 1S/2 (51.6 nmol/L) and 1F/1S (58.7 nmol/L) (p=0.026). Furthermore S-PTH concentrations differed between the diplotypes (ANCOVA, p=0.013) when adjusted for S-25OHD and Ca intake. No differences in S-25OHD concentrations were found among the SNP rs705124. However, there was a difference among SNP in S-PTH concentrations (p=0.018), adjusted for S-25OHD and Ca intake. When pairwise comparisons were made, there was a difference between S-PTH concentrations between the genotype 1 and 2 (p=0.016).

In conclusion, we found significant associations in S-25OHD concentrations among the GC diplotypes. In addition, there were differences in PTH concentrations among the diplotypes and among SNP 705124.

Keywords: Vitamin D binding protein (GC), S-25OHD, PTH, Single Nucleotide Polymorphism (SNP).

***Disclosures: Elisa Saarnio**, None.*

SA0140

Functional characterization of GWAS loci associated with fracture risk. Ling Oei[1], Sjur Reppe[2], Evangelia Ntzani[3], Matthew Hibbs[4], Kwangbom Choi[4], Hou-Feng Zheng[5], Karol Estrada[6], Jeroen van de Peppel[7], Carrie Nielson[8], Unnur Styrkársdóttir[9], Paul Ridker[10], Yi-Hsiang Hsu[11], Melissa Garcia[12], Aaron Aragaki[13], Emma Duncan[14], Anke Enneman[7], Terho Lehtimäki[15], Tõnu Esko[16], Stella Trompet[17], Stephen Kaptoge[18], Joel Eriksson[19], Najaf Amin[7], Annie Kung[20], Carolina Medina-Gomez[21], Konstantinos Tsilidis[3], Gudmar Thorleifsson[9], Lynda Rose[10], Joseph Zmuda[22], Ching-Ti Liu[23], Albert Vernon-Smith[24], Priya Srikanth[8], Scott Wilson[25], Graeme Clark[26], Jorma Viikari[27], Evelin Mihailov[16], Alireza Moayyeri[28], Guo Li[29], Candace Kammerer[22], Mattias Lorentzon[30], Natalia Rivera[7], Sumei Xiao[31], Jian Yang[32], Peter Visscher[32], Gregory Tranah[33], Dan Evans[33], David Karasik[34], Kristin Siggeirsdottir[35], Edwin Oei[7], Kari Stefansson[9], Ville Aalto[36], Dana Willner[26], Nicholas Wareham[37], Ryan Minster[38], Joshua Bis[29], Cornelia van Duijn[7], Alan Boyle[39], Michael Snyder[39], Lizbeth Herrera[7], L. Adrienne Cupples[23], Thor Aspelund[24], Olli Raitakari[36], Paul Leo[26], Kay-Tee Khaw[40], John Robbins[41], Yongmei Liu[42], Stephan Breda[7], Robert Luben[40], Jane Cauley[22], Alice Arnold[29], Lisette Stolk[7], Huibert Pols[1], Albert Hofman[7], Jian Shen[8], Joyce Van Meurs[1], Pak Sham[31], Maria Zillikens[7], Claes Ohlsson[43], Bruce Psaty[29], Tamara Harris[44], Jonathan Reeve[45], J. Wouter Jukema[17], Andres Metspalu[16], Mika Kahonen[15], Nathalie van der Velde[7], Matthew Brown[46], Vilmundar Gudnason[24], John Ioannidis[39], Andre Uitterlinden[47], Steven Cummings[48], Timothy Spector[28], Douglas Kiel[49], Rebecca Jackson[50], Unnur Thorsteinsdottir[9], Daniel Chasman[10], Eric Orwoll[8], Vijay Yadav[51], Johannes Van Leeuwen[1], Evangelos Evangelou[3], Elin Grundberg[5], Brent Richards[5], Kaare Gautvik[52], Fernando Rivadeneira[1], Cheryl Ackert-Bicknell*[4], the GEFOS consortium[53]. [1]Erasmus University Medical Center, The Netherlands, [2]Oslo University Hospital, Ullevaal, Norway, [3]University of Ioannina Medical School, Greece, [4]The Jackson Laboratory, USA, [5]McGill University, Canada, [6]Analytic & Translational Genetics Unit, Massachusetts General Hospital, USA, [7]Erasmus MC, Netherlands, [8]Oregon Health & Science University, USA, [9]deCODE Genetics, Iceland, [10]Brigham & Women's Hospital, USA, [11]Hebrew SeniorLife Institute for Aging Research & Harvard Medical School, USA, [12]NIA, NIH, USA, [13]Division of Public Health Sciences, Fred Hutchinson Cancer Research Center, USA, [14]Royal Brisbane & Women's Hospital, Australia, [15]University of Tampere & Tampere University Hospital, Finland, [16]University of Tartu, Estonia, [17]Leiden University Medical Center, Netherlands, [18]University of Cambridge Bone Research Group, United Kingdom, [19]Centre for Bone & Arthritis Research, Sweden, [20]Dr. Kung-Wai Chee Clinic, Hong Kong, [21]Erasmus Medical Center, The Netherlands, [22]University of Pittsburgh Graduate School of Public Health, USA, [23]Boston University School of Public Health, USA, [24]Icelandic Heart Association & University of Iceland, Iceland, [25]University of Western Australia, Australia, [26]University of Queensland Diamantina Institute, Australia, [27]University of Turku & Turku University Hospital, Finland, [28]King's College London, United Kingdom, [29]University of Washington, USA, [30]Geriatric Medicine, Center for Bone Research at the Sahlgrenska Academy, Sweden, [31]The University of Hong Kong, Peoples Republic of China, [32]Queensland Institute of Medical Research, Australia, [33]Research Institute, California Pacific Medical Center, USA, [34]Hebrew SeniorLife; Bar Ilan University, USA, [35]Icelandic Heart Association, Iceland, [36]Research Centre of Applied & Preventive Cardiovascular Medicine, University of Turku, Finland, [37]Medical Research Council (MRC) Epidemiology Unit, United Kingdom, [38]Graduate School of Public Health, University of Pittsburgh, USA, [39]Stanford University, USA, [40]University of Cambridge, United Kingdom, [41]University of California, Davis Medical Center, USA, [42]Wake Forest University School of Medicine, USA, [43]Center for Bone & Arthritis Research at the Sahlgrenska Academy, Sweden, [44]Intramural Research Program, National Institute on Aging, USA, [45]University of Oxford, United Kingdom, [46]Diamantina Institute of Cancer, Immunology & Metabolic Medicine, Australia, [47]Rm Ee 575, Genetic Laboratory, The Netherlands, [48]San Francisco Coordinating Center, USA, [49]Hebrew SeniorLife, USA, [50]The Ohio State University, USA, [51]Sanger Welcome Trust Institute, United Kingdom, [52]Institute of Basic Medical Sciences, Norway, [53]USA

We conducted a GWAS meta-analysis to search for genetic risk factors associated with fracture risk and work is now underway to determine the function of the underlying genes. We identified 3 loci at the genome-wide significant level ($P<5x10^{-8}$) and 5 loci at the highly suggestive level ($P<1x10^{-6}$). For 3 of these loci, the peak signal was either in or next to a gene with a known function in bone biology. The closest gene to the peak SNP has not been well studied in bone for the remaining loci, which included: *RNMT, SLC25A13, RASSF4*, *CPED1* and *SPTBN1*. For these, we examined gene expression patterns across osteoblastogenesis to determine if these genes function in this cell type. Specifically, RNA-seq was used to assess gene expression profiles across osteoblastogenesis in cells obtained from mouse calvaria and co-expression network analysis was used to identify clusters of genes with expression profiles across osteoblastogenesis that were similar to our signal genes. Then we applied gene-annotation enrichment analysis (DAVID, v6.7) to each cluster of correlated to genes to characterize its putative biologic function. As a follow-up we examined correlation between gene expression from whole bone tissue and BMD obtained from iliac crest biopsies in postmenopausal women. We found that genes correlated in expression with *Slc25a13* were enriched for cell cycle genes (fold enrichment=4.8, $P=6.8^{-61}$), but found no correlation between gene expression and BMD in humans. Genes with correlated expression to *Cped1* were enriched for extracellular matrix genes and increased with osteoblastogenesis (fold enrichment=2.8, $P=1.8^{-13}$). Expression was negatively correlated with hip and spine BMD T-score. Genes correlated in expression to *Sptbn1* were cell junction proteins (fold enrichment=6.5, $P=4.7^{-3}$), and expression showed a mixed association with hip and spine BMD. Expression of *RASSF4* was negatively correlated with hip and spine T-score and gene expression databases suggest that this gene is expressed in osteoclasts (biogps.org). Expression of *Rassf4* increased with osteoblastogenesis but expression correlated with too few genes to conduct meaningful annotation enrichment. Expression of *RNMT* was positively corrected with whole body BMD T-score in patient samples, but its expression in osteoblasts was very low. The work to characterize the function(s) of these genes is on going, including development of mouse models to better assess the whole organismal function of these genes.

***Disclosures: Cheryl Ackert-Bicknell**, None.*

SA0141

Haplotype Analysis Supports a "Founder" for the Balkan OPG Mutation Causing Juvenile Paget's Disease. Steven Mumm*[1], Kristin Geczi[2], Margaret Huskey[2], Dorit Naot[3], Stergios Polyzos[4], Tim Cundy[3], Wim Van Hul[5], Panagiotis Singhellakis[6], Michael Whyte[7]. [1]Washington University School of Medicine, USA, [2]Washington University, USA, [3]University of Auckland, New Zealand, [4]Aristotle University of Thessaliniki, Greece, [5]University of Antwerp, Belgium, [6]Athens University, Greece, [7]Shriners Hospital for Children, USA

Juvenile Paget's disease (JPD), a rare autosomal recessive disorder, features extremely rapid bone turnover causing skeletal pain, fracture, and deformity in early childhood. Deafness and retinopathy leading to blindness can follow. Most JPD is due to homozygous loss-of-function mutations in the *TNFRSF11B* gene encoding osteoprotegerin (OPG) – the decoy receptor that prevents RANKL binding to its cognate receptor RANK, a major stimulus element for osteoclastogenesis. A variety of mutations in *TNFRSF11B*, typically transmitted by apparent "founders" in various geographic locations worldwide, cause JPD. The severity of "OPG deficiency JPD" seems to vary depending on mutation type and how much of the OPG coding region is disrupted. In two Greek men and another Croatian man who are seemingly unrelated and manifest the mildest form of JPD, a unique homozygous deletion/insertion mutation (966_969delTGACinsCTT) has been reported. This frame-shift deletes 79 carboxy terminal amino acids from the OPG monomer, including a cysteine necessary for homodimerization. When recently referred 2 additional unrelated Greek JPD

patients homozygous for this "Balkan mutation", we studied the likelihood that all of these patients are in fact related by a distant "founder" in whom the mutation arose many generations ago. To test this hypothesis, we performed haplotype analysis of the 5 Balkan JPD patients and 2 control JPD patients from other geographic regions using SNPs within and surrounding *TNFRSF11B*. We developed primer sets for 13 informative SNPs, and then PCR-amplified and sequenced these SNPs using leukocyte-derived genomic DNA from each patient. All 5 individuals shared a homozygous common core haplotype of 4 SNPs, whereas each of the "control" JPD patients had a unique haplotype. Two of the four Greek patients shared a common haplotype of 10 homozygous SNPs, indicating closest kinship. A different Greek patient shared only 5 of these SNPs suggesting more distant relationship. The Croatian JPD patient shared only 4 common markers suggesting he is the most remotely related and consistent with his geographic distance. Hence, all Balkan JPD patients share the common OPG mutation (966_969delTGACinsCTT) and common haplotypes indicating relationship to a genetic founder. Further analysis can determine how many generations ago this founder mutation arose.

***Disclosures: Steven Mumm**, None.*

SA0142

Systematic integration of functional and computational genomics suggests that the indel rs79240969 in the *DNM3* gene influences both bone- and obesity-related traits. Melina Claussnitzer*[1], Xing Chen[2], David Karasik[3], L Adrienne Cupples[4], Douglas Kiel[5], Yi-Hsiang Hsu[6]. [1]Hebrew SeniorLife, Institute for Aging Research & Harvard Medical School, USA, [2]Harvard University, USA, [3]Hebrew SeniorLife; Bar Ilan University, USA, [4]Boston University, USA, [5]Hebrew SeniorLife, USA, [6]Hebrew SeniorLife Institute for Aging Research & Harvard Medical School, USA

Recent studies suggest shared etiologies of bone and adiposity phenotypes. Previously, we conducted a multivariate genome-wide association study (GWAS) of bone mineral density (BMD) at different skeletal sites and metabolic syndrome risk factors, and identified 31 bivariate genome-wide significant ($p<5 \times 10^{-8}$, p(bivariate) < p(univariate)/10). However, signals emerging from GWAS are merely markers for large genomic regions in linkage disequilibrium (LD), potentially harboring the disease-causing variant. Identifying the shared causal variants is central to elucidate the molecular mechanisms underlying the genetic correlation between bone and fat.

Specifically, we applied an integrative bioinformatics approach leveraging tissue-specific functional genomics and sequence data to narrow-down the potential causal variants. We identified all reported sequence variants (from the 1000 Genomes Project) within the identified bivariate GWAS loci (physical boundaries LD r2>0.7). We merged data on sequence variants with bone- and adipose-specific genome-wide epigenomic profiling data, reported from the ENCODE project, that allow for chromatin state-dependent analyses of regulatory variation. Within predicted regulatory regions, we discovered *cis*-regulatory modules (CRMs) by analyzing conserved patterns of transcription factor binding sites (TFBS) across 16 vertebrate species (923 motifs). Using our approach, we identified potential causal variants within the bivariate association loci that may be responsible for the association with BMD and obesity traits. One example is the bivariate signal at *DNM3*, 1q24.3 (GWAS SNP rs10489290, bivariate association test $p=8.4 \times 10^{-11}$ for femur neck BMD with waist-to-hip ratio). We pinpointed an intronic insertion/deletion variant rs79240969 (-/TCA, MAF=0.296, LD $r^2=1.0$), specifically mapping within predicted osteoblast and adipocyte gene regulatory regions. The cell-type specific TFBS pattern analysis revealed rs79240969 localizing within a cross-species conserved CRM relevant to bone and fat. The rs79240969 insertion allele creates a perfect binding site for the zinc-finger protein Zfp521 which has been previously shown to control bone mass.

Our bioinformatics analysis may represent a useful step toward pinpointing causal variants from potentially pleiotropic loci for direct laboratory validation and ultimately for improving therapeutic strategies addressing shared etiological mechanisms of BMD and obesity-related phenotypes.

***Disclosures: Melina Claussnitzer**, None.*

SA0143

CK2.3, a mimetic peptide of the Bone Morphogenetic Protein receptor Ia, increases endochondral bone formation *in vivo*. Kristine Olli*[1], Jeremy Bonor[1], Hemanth Akkiraju[1], Christopher Bowen[1], Beth Bragdon[2], Randall Duncan[1], Anja Nohe[1]. [1]University of Delaware, USA, [2]Boston University School of Medicine Department of Orthopaedics, USA

The goal of this study was to determine whether a novel petide CK2.3 can induce bone formation by increasing osteogenesis and decreasing osteoclastogenesis. Osteoporosis is a disease that results in a harsh loss of bone mass and affects approximately 4.5 million women and 800,000 men in America. The current treatment options are either antiresorptive or anabolic. However these options come with a myriad of negative side effects. Bone Morphogenetic Protein 2 (BMP2) is a potent inducer of bone formation. Unfortunately, it also is known to induce osteoclast activity, therefore leading to a higher rate of bone turnover in the long term. We recently developed a novel peptide, CK2.3, that acts downstream of Bone Morphogenetic Protein type Ia receptor (BMPRIa) in the BMP2 signaling pathway signaling. Systemic injection of CK2.3 into 8 week old mice led to an increase of ALP and Osteocalcin serum levels. In sharp contrast to BMP2, it decreased TRAC5b levels, a marker for bone turnover. Osteoblasts isolated from the femur of these mice showed increased mineralization ability compared to control injected mice. Additionally, bone mineral density and mineral apposition rate were enhanced. Micro CT analysis revealed increased number of trabeculi and decreased trabecular spacing. Additionally, injection of CK2.3 caused a significantly decreased number of osteoclasts and reduced osteoclast activity when compared to both the control and BMP2. Furthermore, we determined the mechanism of CK2.3 signaling in osteoclasts. Our data demonstrate that CK2.3 signals through BMPRIa in osteoclasts. Therefore CK2.3 may be the first peptide based on BMP2 signaling to reduce osteoclastogenesis and increase osteogenesis making it a potential treatment for osteoporosis.

***Disclosures: Kristine Olli**, None.*

SA0144

L51P, a BMP-2 Antagonist Inhibitor, Enhances the Osteoiduction of BMP-2 by a Negative Feedback Regulation. Hany Khattab*[1], Mitsu ONO[2], Wataru Sonoyama[3], Yasutaka OIDA[2], Shigehiko SHINKAWA[2], Kenji MAEKAWA[2], Kazushige SUGAMA[4], Walter SEBALD[5], Takuo KUBOKI[2]. [1]Okayama University Graduate School of Medicine, Japan, [2]Department of Oral Rehabilitation & Regenerative Medicine, Okayama University Graduate School of Medicine, Dentistry & Pharmaceutical Sciences, Japan, [3]Okayama University Graduate School of Medicine, Dentistry & Pharmaceutical Sci, Japan, [4]Osteopharma Inc., Japan, [5]Physiological Chemistry II, Theodor-Boveri-Institute for Biocenter of Würzburg University, Germany

Bone morphogenetic proteins (BMPs) are cytokines with promising potential for clinical bone repair. Since large amounts of BMPs are required to induce bone formation as a result of BMP antagonists, targeting these antagonists provide an attractive strategy to enhance BMP's osteogenic activity. Our group generated the BMP mutant (L51P) lacking the BMP receptor binding site. Although previous reports have shown that L51P can bind to noggin and interfere with its binding to BMP, the functions of L51P are yet not fully understood. In this study, we investigated the biological functions of L51P *in vitro* and *in vivo*. A rat critical-sized calvarial defect model was performed to examine the effect of L51P on bone formation. L51P did not possess similar osteoinductive activity like BMP-2. However, the combination of BMP-2 and L51P enhanced bone regeneration four weeks post-injury, compared to BMP-2 alone. To confirm the function of L51P *in vitro*, MC3T3E1 cells were first stimulated with BMP-2 and L51P simultaneously. While BMP-2 enhanced SMAD signaling and luciferase activity of BMP-responsive Id1 promoter, L51P did not enhance the effect of BMP-2. On the other hand, when MC3T3E1 cells were pre-treated with BMP-2 for 3 days, there was an increase in the mRNA expression levels of *noggin;* and under this condition, L51P dramatically enhanced SMAD signaling and luciferase activity. These findings support the concept of L51P as a promising down regulator of BMP negative feedback, which can be expected to renovate the future of BMP-based regenerative therapy for bone repair.

***Disclosures: Hany Khattab**, None.*

SA0145

SDF-1/CXCL12 is Critical for Bone Regeneration: SDF-1β Promotes BMP-2 Function. Samuel Herberg*[1], Manuel Pelaez[1], Nicole Howie[1], Mohammed Elsalanty[2], Mark Hamrick[2], Carlos Isales[1], Ulf Wikesjö[1], Cristiano Susin[1], William Hill[3]. [1]Georgia Regents University, USA, [2]Georgia Health Science University, USA, [3]Georgia Regents University & Charlie Norwood VAMC, USA

Purpose: Bone morphogenetic protein-2 (BMP-2) has widely been used clinically, albeit at high doses linked to adverse effects. Increasing evidence suggests that stromal cell-derived factor-1 (SDF-1/CXCL12) is involved in bone formation; however, underlying molecular mechanisms remain largely unknown. Recently, we showed that SDF-1β, the less abundant but more potent splice variant vs. SDF-1α, enhances osteogenesis through regulating BMP-2 signaling *in vitro*. Here we investigated local bone formation in a critical-size rat calvarial defect model 1) using increasing doses of BMP-2 delivered in an absorbable collagen sponge (ACS) carrier to define optimal and suboptimal BMP-2 doses, and 2) following co-delivery of suboptimal BMP-2 and SDF-1β in an ACS carrier. We tested the hypotheses that SDF-1β potentiates BMP-2 osteoinduction and that blocking SDF-1 signaling reduces the osteogenic potential of BMP-2.

Materials: Critical-size calvarial defects were created in 172 adult male Sprague-Dawley rats. Experimental defects received: 1) increasing doses of BMP-2 (0.1-20 μg), and 2) suboptimal BMP-2 (0.5 μg) ± increasing doses of SDF-1β (1-60 μg), benchmark BMP-2 (5 μg), BMP-2+AMD3100, or controls in an ACS carrier. A titanium mesh was fitted over the defects to prevent soft tissue collapse. Surgical staples were used to evert the wound margins to ensure wound closure for primary intention healing. Radiographic, μCT, and histometric analysis was performed after 4 weeks.

Results: Radiographic analysis revealed a dose-dependent increase in BMP-2 osteoinduction ($p<0.0001$) with an ED_{50} of 1.2 μg/ACS. Furthermore, radiographic

and μCT analyses showed a dose-dependent increase in SDF-1β-potentiated suboptimal BMP-2 osteoinduction ($p<0.01$), reaching comparable levels to the benchmark 10-fold greater BMP-2 dose. Co-delivery of the specific SDF-1 receptor (CXCR4) antagonist AMD3100 and BMP-2 attenuated the osteoinductive potential ($p<0.0001$), suggesting that SDF-1 signaling is pivotal for BMP-2-induced bone formation. Histometric analysis revealed a greater fraction lamellar/woven bone in SDF-1β co-delivered groups, similar to the benchmark BMP-2 dose, indicating accelerated bone maturation.

Conclusion: Our data suggest that SDF-1β provides new opportunities to broaden the clinical utility of BMP-2 by decreasing the dose, potentially reducing undesirable effects, and allowing expanded regenerative medicine approaches to treat acute/chronic bone injuries.

***Disclosures: Samuel Herberg**, None.*

SA0146

A novel oxysteol, Oxy133, promotes cranial bone regeneration through Hedgehog signaling pathway. Akishige Hokugo*[1], Andrew Li[1], Farhad Parhami[2], Reza Jarrahy[1]. [1]David Geffen School of Medicine at UCLA, USA, [2]University of California, Los Angeles, USA

Current reconstructive techniques for complex craniofacial osseous defects are associated with significant morbidity profiles. Tissue engineering solutions offer an alternative to these techniques. Bone morphogenetic protein (BMP) is an effective osteoinductive growth factor, but its clinical application is limited by exorbitant cost and undesirable side effects. Oxysterols are naturally occurring cholesterol oxidation products some of which are capable of inducing osteogenic differentiation. In this study, we investigated the effect of a novel semi-synthetic oxysterol, Oxy133, a structural analogue of the naturally occurring osteogenic oxysterol, 20(*S*)-hydroxycholesterol, in inducing in vitro osteogenesis and in vivo bone regeneration. Rabbit bone marrow stromal cells (BMSCs) were incubated with 1 μM of Oxy133 or 50 ng/ml of BMP-2. Alkaline phosphatase (ALP) activity, expression of markers of osteogenic differentiation Runx2, Collagen I and Osterix, and in vitro calcification were examined. For in vivo evaluation, Oxy133 (1 and 10 mg) or BMP-2 (45 μg) absorbed onto collagen sponge were implanted in 6 mm diameter cranial defects in 3.5-4 kg 5 months old rabbits. Six weeks after implantation, bone regeneration was assessed by microCT and histology. To determine the mechanism of action of Oxy133, rabbit BMSC were pre-treated with the Hedgehog (Hh) pathway inhibitor, cyclopamine, prior to treatment with Oxy133, and ALP activity was measured. In vivo, the role of Hh pathway was assessed by the inclusion of cyclopamine (2 mg) with Oxy133 when implanted and its effect on Oxy133-induced bone regeneration was evaluated. In vitro, ALP activity in rabbit BMSCs treated with 1 μM of Oxy133 was induced after 4 days and was significantly higher than in control cells or in cells treated with BMP-2. Expression of osteogenic markers in BMSCs treated with 1 μM of Oxy133 was significantly higher than in control group. In vivo, complete bone regeneration occurred when cranial defects were treated with Oxy133. Addition of cyclopamine inhibited the stimulatory effects of Oxy133 on ALP activity in vitro and on bone regeneration in vivo. Collectively, these results demonstrate that Oxy133 has the ability to induce osteogenic differentiation in rabbit BMSCs with an efficacy comparable to that of BMP-2, and to promote robust bone regeneration in rabbit cranial defects. Therefore Oxy133 may be a viable novel agent in bone tissue engineering.

***Disclosures: Akishige Hokugo**, None.*
This study received funding from: Annenberg Foundation

SA0147

EGF suppresses BMP-induced osteogenic differentiation through the up-regulation of Smurf1 expression. Jeong-Hwa Baek*, Hye-Lim Lee, Hyun-Mo Ryoo, Kyung Mi Woo. Seoul National University, School of Dentistry, South Korea

Although EGF has been known to inhibit osteoblast differentiation, its molecular mechanism has not been clearly elucidated. Smurf1 acts as a negative regulator of BMP signaling by inducing ubiquitination and proteasomal degradation of BMP type I receptor and R-Smads. In this study, we investigated the effect of EGF on the expression of Smurf1 and the role of Smurf1 in EGF-induced inhibition of BMP2-induced osteogenesis. EGF increased Smurf1 expression which was blocked by treatment with a specific inhibitor of EGFR tyrosine kinase, JNK or ERK. Reporter assay using the constructs containing the Smurf1 promoter sequence, demonstrated that AP-1 and Runx2 are the transcription factors activated by JNK and ERK, respectively. EGF treatment or Smurf1 overexpression suppressed BMP2-induced expression of osteogenic marker genes, whereas knockdown of Smurf1 partially rescued the expression of these genes in EGF-treated cells. Taken together, these results suggest that the JNK-c-Jun and the ERK-Runx2 signaling pathways play an important role in the regulation of Smurf1 expression by EGF and that Smurf1 partially mediates the inhibitory effect of EGF on osteogenic differentiation.

***Disclosures: Jeong-Hwa Baek**, None.*

SA0148

Enhanced Bone Regeneration Utilizing Non-Viral Nanoplex Activated Collagen Scaffolds. Satheesh Elangovan*[1], Sheetal D'Mello[2], Liu Hong[3], Ryan Ross[4], Clark Stanford[1], Georgia Johnson[3], Rick Sumner[5], Aliasger Salem[2]. [1]University of Iowa, USA, [2]University of Iowa College of Pharmacy, USA, [3]University of Iowa College of Dentistry, USA, [4]Rush University Medical Center, USA, [5]Rush University Medical College, USA

Purpose: To develop and test a non-viral gene delivery system for bone regeneration that utilizes collagen scaffold to deliver polyethylenimine (PEI) – pDNA [encoding platelet derived growth factor (PDGF)] nanoplexes.

Methods used: PEI – pDNA (PDGF) nanoplexes were synthesized and characterized for size and surface charge using Malvern Zetasizer Nano ZS and the collagen scaffold was characterized using scanning electron microscopy. The in vitro cytotoxicity and transfection efficacy of the synthesized nanoplexes were evaluated in bone marrow stem cells (BMSCs) using the MTS assay and by quantifying the amount of secreted PDGF-B in cell culture supernatants using ELISA. Heparin was used to prevent the retention of PDGF-B on the cell surface. In addition, the influence of the nanoplex-loaded scaffold on cellular proliferation was evaluated in vitro using confocal microscopy. The in vivo regenerative capacity of the gene delivery system was assessed in critical-sized calvarial defects in Fisher 344 rats with microCT.

Results: The PEI-pDNA nanoplexes were approximately 150 nm in size with a small polydispersity index (<0.3), indicating a narrow size distribution. At the concentrations used for transfection, the nanoplexes displayed low toxicity as assessed by the MTS assay. At an N/P ratio of 10, PEI-pDNA nanoplexes exhibited the maximum transfection efficiency with acceptable cytotoxicity in BMSCs. Highest PDGF protein expression levels (86.42 pg/ml) were obtained by treating the cells with 1 μg of the pDNA for 4 hours, followed by further incubation for 44 hours. Heparin, added to the cells 4 hours prior to the analysis, resulted in an increased detection in the protein levels of PDGF-B (132 pg/ml). Confocal microscopy revealed significantly higher proliferation of BMSCs on collagen scaffolds loaded with the nanoplexes, compared to empty scaffolds. In vivo studies showed a five-fold higher new bone volume in the test group after 4 weeks of implantation, compared to empty defect or the empty scaffold groups.

Conclusions: Non-viral nanoplex activated collagen scaffolds are an effective gene delivery and bone regeneration system with significant potential for clinical translation.

Keywords: Bone Regeneration, biomaterials, transfection, gene therapy

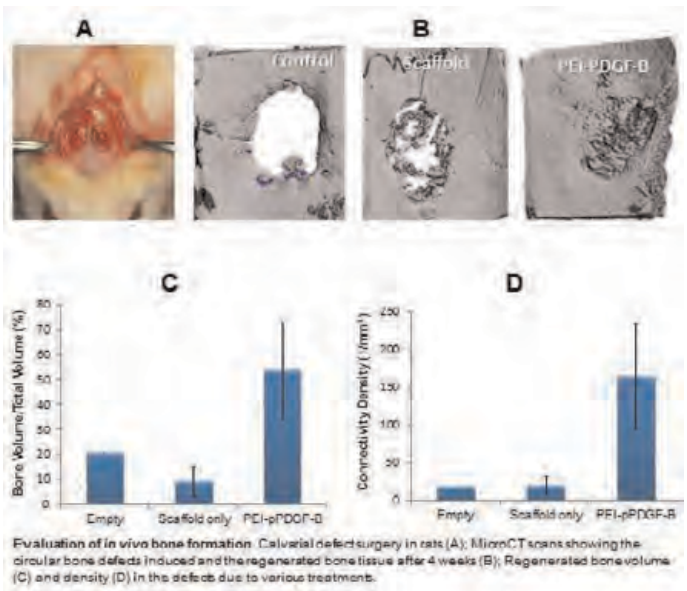

Evaluation of bone formation using calvarial defect model

***Disclosures: Satheesh Elangovan**, International Team of Implantologist Foundation, 6*
This study received funding from: International Team for Implantology Foundation

SA0149

Inhibition of Hedgehog But Not Trpv1 Signaling Sustainably Attenuates Heterotopic Ossification Induced by Midpoint Achilles Tenotomy. Ina Kramer*[1], Charles Gerard Moes[1], Annabelle Heier[1], Janet Dawson[1], Francesco Galimi[2], Mark Nash[1], Ursula Schramm[1], Michaela Kneissel[1], Sabine Guth-Gundel[1]. [1]Novartis Institutes for Biomedical Research, Switzerland, [2]Genomics Institute of the Novartis Research Foundation, USA

Heterotopic ossification (HO) of soft tissue following severe traumatic injury or complicated joint surgery represents a frequent clinical complication with unmet medical need. The heterotopic bone forms through endochondral ossification via an intermediate cartilage template and is thought to be triggered by trauma-induced release of high levels of growth factors including members of the bone morphogenetic protein (BMP) family. In addition to acting as direct osteo-inducers, BMPs can also enhance local release of neuroinflammatory molecules from peripheral nociceptive neurons. Moreover, BMP2-induced HO is suppressed in *transient receptor potential cation channel V1/Trpv1* deficient mice suggesting that neuroinflammation contributes to HO development.

Here, we tested two pharmacological principles based either on inhibition of Trpv1 activity, a key nociceptive ion channel, or chondrogenesis as an early or intermediate step of the HO process, respectively, for their therapeutic potential to prevent HO in a rat model of trauma-induced nonhereditary HO following Achilles midpoint tenotomy. 7-week-old male Sprague Dawley rats underwent unilateral Achilles tenotomy and prophylactic 10-week oral treatment with either vehicle, a selective Trpv1 antagonist or two doses of a selective Smoothened (Smo) inhibitor blocking hedgehog signaling required for normal chondrogenesis, respectively. We followed HO development by radiography at 5 and 7 weeks post-tenotomy and quantified the amount of heterotopic bone by longitudinal micro-computed tomography at 6 and 9 weeks post-injury. Neither treatment regime was able to prevent HO development, as all rats displayed heterotopic bone formation at 5 weeks post-surgery. Interestingly, at 6 weeks post-tenotomy rats treated with either pharmacologic principle had about 60% reduced heterotopic bone volume compared to vehicle-treated animals. As HO progressed, HO remained significantly lower by about 45% in rats treated with the higher dose of the Smo antagonist, whereas HO was non-significantly decreased by about 30% in rats receiving the Trpv1 inhibitor relative to vehicle-treated rats. However, in contrast to Trpv1 inhibition, at the effective dose Smo antagonism was associated with significant treatment-related side effects. Together, these findings suggest that trauma-induced HO can be reduced when interfering with critical early or intermediate steps of the heterotopic ossification process.

***Disclosures: Ina Kramer**, Novartis Institutes for BioMedical Research, 3*
This study received funding from: Novartis Institutes for BioMedical Research

SA0150

Novel Hedgehog Agonists Regulate Dental Epithelial Cell Proliferation and Differentiation. Masahiro Naruse*, Tomoko Ikeuchi, Yuta Chiba, Mariko Ono, Satoshi Fukumoto, Takashi Nakamura. Tohoku UniversityGraduate School of Dentistry, Japan

Aim: The reciprocal interactions between dental epithelium and mesenchyme preciously control tooth development to form the tooth crown and root with optimized shapes and size. Growth and differentiation of dental epithelium and mesenchyme are regulated by secreted proteins such as Sonic hedgehog (Shh). The Shh signaling pathway plays a number of roles during tooth development including the early tooth morphogenesis, cusp formation, ameloblast differentiation, and root formation.

In this study, we demonstrate that HH-Ag 1.3 and HH-Ag 1.7, novel synthetic non-peptidyl shh agonists, regulate differentiation of dental epithelium cell line and murine tooth germ.

Design: To analyze action of HH-Ag 1.3 and HH-Ag 1.7 on growth and differentiation in dental epithelial cell, we cultured the rat dental epithelial cell line HAT-7 and murine tooth germs from murine embryos at E14. We investigated cell proliferation activities and mRNA expressions of ameloblast marker genes in the presence or absence of the compounds at the different concentrations in those culture systems.

Results: Both HH-Ag 1.3 and HH-Ag 1.7 promote expression of Gli1, a hedgehog signaling target gene, in HAT-7 and cultured murine tooth germ, suggesting activation of shh signaling. Interestingly, HH-Ag 1.3 and HH-Ag 1.7 act distinct roles on cell proliferation and gene expression in HAT-7. HH-Ag 1.3 promoted cell proliferation activity, while no action was observed in cell differentiation. In contrast, HH-Ag 1.7 greatly enhanced gene expression of ameloblastin and amelogenin, ameloblast marker genes, suggesting that HH-Ag 1.7 promotes dental epithelial cell differentiation.On the other hand, HH-Ag 1.3 and HH-Ag 1.7 act positive regulators in dental epithelial cell differentiation into ameloblast in organ cultured murine tooth germ. HH-Ag 1.3 and HH-Ag 1.7 slightly enhanced expression of ameloblastin and amelogenin.

Conclusion: Our results suggest that HH-Ag 1.3 and HH-Ag 1.7 regulate cell proliferation and/or differentiation of dental epithelium. The combination of them could mimic in vivo Shh function perfectly in dental epithelial proliferation and differentiation. For therapeutics approach, small molecules are focused on the regenerative medicine due to their advantages of low biological risk. We would like to uncover the detail molecular mechanism of HH-Ag 1.3 and HH-Ag 1.7 in the regulation of proliferation and differentiation in dental epithelium cells.

***Disclosures: Masahiro Naruse**, None.*

SA0151

Oncostatin M Promotes Osteoblastic Differentiation of Human Vascular Smooth Muscle Cells. Yoshinori Kakutani*[1], Atsushi Shioi[2], Tetsuo Shoji[3], Hirokazu Okazaki[4], Hidenori Koyama[4], Masanori Emoto[1], Masaaki Inaba[1]. [1]Department of Metabolism, Endocrinology, & Molecular Medicine, Osaka City University Graduate School of Medicine, Japan, [2]Osaka City University Graduate School of Medicine, Japan, [3]Department of Geriatrics & Vascular Medicine, Osaka City University Graduate School of Medicine, Japan, [4]Department of Internal Medicine, Division of Endocrinology & Metabolism, Hyogo College of Medicine, Japan

Vascular calcification is a common feature of atherosclerotic lesions, especially in advanced stages of plaque formation and is an independent risk factor for cardiovascular disease. Macrophages may play a key role in the development of atherosclerotic calcification. By using a coculture model, we have identified oncostatin M (OSM) and tumor necrosis factor-α (TNF-α) as major cytokines derived from macrophages responsible for induction of calcifying phenotype in human vascular smooth muscle cells (HVSMC) in the presence of interferon-γ and 1α,25-dihydroxyvitamin D_3. Recently, it has been demonstrated that OSM derived from activated macrophages induces osteogenesis in bone marrow-derived mesenchymal stem cells. Therefore, OSM may also facilitate osteoblastic differentiation of HVSMC. In this study, we investigated the stimulatory effects of OSM on osteoblastic differentiation of HVSMC derived from various arteries including umbilical, aortic, and coronary arteries. Osteoblastic differentiation was induced by exposure of HVSMC to osteogenic differentiation medium (ODM) (10% fetal bovine serum, 0.1 μM dexamethasone, 10 mM β-glycerophosphate and 50 μg/ml ascorbic acid 2-phosphate in DMEM). OSM significantly increased alkaline phosphate (ALP) activity and expression of osteoblast marker genes such as Runx2 and ALP in HVSMC from all sources. Matrix mineralization was also stimulated by OSM treatment in HVSMC derived from umbilical and coronary arteries. OSM treatment induced activation of STAT3 in HVSMC from umbilical artery as evidenced by immunoblot analysis. Moreover, a JAK3 inhibitor, WHI-P154 inhibited the OSM-induced osteogenic differentiation including induction of ALP activity and its gene expression and matrix mineralization. Finally, we examined the expression of OSM in macrophages infiltrated in atherosclerotic plaque lesions of apoE-deficient mice by immunohistochemistry. OSM-positive macrophages were detected in plaque lesions. These data suggest that OSM derived from macrophages may play an important role in the development of atherosclerotic calcification by promoting osteoblastic differentiation of vascular smooth muscle cells through JAK3-STAT3 pathway.

***Disclosures: Yoshinori Kakutani**, None.*

SA0152

Remote Remodeling Does Not Contribute to Systemic Differences in Biomarkers Following Local Skeletal Insult. Ryan Ross*[1], Amarjit Virdi[1], Shou Liu[2], Kotaro Sena[3], D. Rick Sumner[1]. [1]Rush University Medical Center, USA, [2]University of Maryland, USA, [3]Kagoshima University, Japan

We recently showed that particle-induced peri-implant osteolysis in a rat model was caused by locally elevated bone resorption and suppressed bone formation. Correspondingly, CTX-1 levels increased and osteocalcin decreased in the serum. The goal of the current study was to determine if systemic remodeling contributes to changes in biomarkers levels by investigating bone remodeling at local, contiguous and remote sites following particle-induced osteolysis.

Two groups of adult male rats underwent bilateral femoral implant placement through a knee joint arthrotomy in a previously reported study. Rats received weekly intra-articular injections of vehicle or LPS-doped polyethylene (PE) particles. 12 weeks after implant surgery the animals were sacrificed and bones and blood were harvested. Bone remodeling within the femur (local), tibia (contiguous) and humerus (remote) were evaluated using dynamic and static histomorphometry. Serum concentrations of the soluble biomarkers osteocalcin, PINP, CTX-1, TRAP 5b, RANKL, OPG and SOST were measured by ELISA.

As reported previously, PE particle administration led to increased ES/BS ($p<0.001$) and decreased BFR/BS ($p=0.016$) in the peri-implant trabecular bone of the distal femur. We now show that BFR/BS was suppressed on the periosteal surface of the tibial diaphysis ($p=0.004$), but remodeling in the humerus was unaffected by PE administration in the knee joint. Following particle administration, serum osteocalcin was decreased ($p<0.001$), while PINP ($p<0.001$), CTX-1 ($p<0.001$), and OPG ($p<0.001$) were increased. Serum levels of RANKL, TRAP 5b, and SOST were not affected by particle administration. Local (peri-implant) trabecular bone BFR/BS was positively correlated with osteocalcin and negatively correlated with OPG, while ES/BS was negatively correlated with osteocalcin and positively correlated with OPG, PINP, and CTX-1. No correlations existed between humeral remodeling and the biomarker concentrations.

In addition to affecting peri-implant remodeling in the distal femur, the PE particles also affected remodeling in the tibia, presumably because the particles were administered via the knee joint. This local stimulus, however, did not alter remote remodeling as measured in the humerus. Therefore, systemic changes in the concentration of bone biomarkers were found to reflect local remodeling changes and may have potential as a means for clinical diagnosis of peri-prosthetic osteolysis and prediction of implant loosening.

***Disclosures: Ryan Ross**, None.*

SA0153

Withdrawn

SA0154

See Friday Plenary Number FR0154.

SA0155

Tissue-type Plasminogen Activator Is Involved in Bone Repair. Naoyuki Kawao*[1], Yukinori Tamura[1], Katsumi Okumoto[2], Masato Yano[1], Kiyotaka Okada[1], Osamu Matsuo[1], Hiroshi Kaji[1]. [1]Kinki University Faculty of Medicine, Japan, [2]Life Science Research Institute, Kinki University, Japan

The clarification of bone regeneration mechanism is important for the treatment of bone defects. We recently reported that plasminogen, a critical component of the tissue fibrinolytic system, plays a crucial role in bone repair through enhancement of macrophage accumulation and subsequent angiogenesis. However, the roles of plasminogen activator (PA) in the tissue fibrinolytic system in bone repair still remain unknown. We therefore investigated the role of tissue-type PA (t-PA) during bone repair using t-PA-deficient ($t\text{-}PA^{-/-}$) mice and their wild-type ($t\text{-}PA^{+/+}$) mice.

A hole was drilled in the femur of the 7-9 weeks old mice for the bone repair model. The process of bone repair was analyzed by *in vivo* quantitative computed tomography (qCT) and immunohistochemistry. The mRNA levels of osteogenic and chondrogenic markers in primary osteoblasts and chondrocytes were analyzed by real time-PCR.

The bone repair was delayed in $t\text{-}PA^{-/-}$ mice as compared with $t\text{-}PA^{+/+}$ mice, as assessed by *in vivo* qCT. Number of alkaline phosphatase-positive cells in $t\text{-}PA^{-/-}$ mice was significantly decreased as compared with $t\text{-}PA^{+/+}$ mice at the damaged site on day 7 after a femoral bone defect. The mRNA levels for Runx2, Osterix, and type I collagen in primary calvarial osteoblasts from $t\text{-}PA^{-/-}$ mice were decreased as compared with those from $t\text{-}PA^{+/+}$ mice. In alcian and toluidine blue stains, the area of cartilage matrix was comparable between $t\text{-}PA^{+/+}$ and $t\text{-}PA^{-/-}$ mice on day 7 after a femoral bone defect. In addition, the mRNA levels for type II and X collagens as well as aggrecan in primary articular chondrocytes were not significantly different between $t\text{-}PA^{+/+}$ and $t\text{-}PA^{-/-}$ mice. The accumulation of macrophages was comparable between $t\text{-}PA^{+/+}$ and $t\text{-}PA^{-/-}$ mice on day 4 at the damaged site, suggesting that the plasminogen-related macrophage accumulation during bone repair might be independent of t-PA.

In conclusion, the present study indicates that t-PA plays a key role during bone repair. Osteoblastic bone formation, but not chondrogenesis and macrophage accumulation during bone repair, seems to be involved in the process of t-PA-related bone repair. The modulation of the tissue fibrinolytic system might be a new strategy for the enhancement of bone repair and the development of bone regeneration.

***Disclosures: Naoyuki Kawao**, None.*

SA0156

See Friday Plenary Number FR0156.

SA0157

See Friday Plenary Number FR0157.

SA0158

Osteoblast-Specic Loss of IGF-1R Results in Impaired Callus Formation during Tibial Fracture Healing. Tao Wang*[1], Yongmei Wang[2], Muriel Babey[3], Frankie Fong[2], Candice GT Tahimic[4], Alicia Menendez[2], Zhiqiang Cheng[1], Daniel Bikle[4]. [1]University of California, San Francisco, USA, [2]University of California, San Francisco, California, USA, [3]UCSF, Division of Endocrinology, USA, [4]Endocrine Research Unit, Division of Endocrinology UCSF & VAMC, USA

The specific role of endogenous Insulin-like Growth Factor I (IGF-1) signaling in osteoblasts in fracture healing was investigated by generation and analysis of osteoblast-specific IGF-1 receptor (IGF-1R) conditional knockout (CKO) mice. A unilateral closed tibial fracture was induced in female IGF-IR $^{flox/flox}$ / 2.3-kb α1(I)-collagen-Cre (CKO) and IGF-IR $^{flox/flox}$ (CON) mice aged 12 weeks. Bone fracture callus samples were collected and analyzed by micro-CT, histology, and gene expression assays 10, 15, 21, and 28d after fracture. The results demonstrated that the lack of IGF-1R expression in osteoblasts leads to smaller callus size, decreased mineralization and bone formation, and delayed cartilage maturation/ossification. These findings indicate that endogenous IGF-1 signaling in osteoblasts plays an essential role in chondrocyte maturation and bone formation during fracture healing. Therefore, enhancing IGF-I signaling may provide a means to stimulate bone formation in the callus resulting in improved fracture healing.

***Disclosures: Tao Wang**, None.*
This study received funding from: National Institutes of Health

SA0159

Differential regulation of osteoblast function by toll-like receptor 2 and 4. Wareeratn Chengprapakorn*[1], Alejandro Garcia[1], Rene Chun[2], Ichiro Nishimura[1], Martin Hewison[1]. [1]University of California Los Angeles, USA, [2]UCLA/Orthopedic Hospital Research Center, USA

Toll-like receptors (TLRs) play a critical role in promoting innate immune responses to infection by recognizing pathogen associated molecular patterns (PAMPs) such as bacterial and viral particles. Osteoblasts express TLR2 and TLR4 and can therefore recognize Gram+ve and Gram-ve bacteria respectively, but the skeletal function of this response is unclear. MC3T3-E1 cells and primary mouse calvaria were used to evaluate osteoblast responses following PAMP-stimulation of TLR2 (Pam3CysK, 1 μg/ml), or TLR4 (LPS, 1 ng/ml) at different stages of differentiation (5, 14, or 21 days in osteogenic culture medium). Western blot and RT-PCR analyses confirmed expression of TLR2, TLR4 and the TLR4-specific signaling factor TRIF at all stages of osteoblast differentiation. Further RT-PCR analyses showed that Pam3CysK and LPS stimulated osteoblast expression of the inflammatory cytokine IL-6 at each differentiation time point, confirming functionality of TLR2 and TLR4. In a similar fashion, both the TLR2 and TLR4 ligands stimulated expression of osteoclastogenesis markers such as RANKL and OPG. By contrast, at day 14 and 21, LPS (TLR4) stimulated expression of the osteoblast differentiation markers alkaline phosphatase and osteocalcin, whilst Pam2CysK (TLR2) suppressed these markers. TLR2 and TLR4 share an MyD88 signaling pathway to induce inflammation and osteoclastogenesis, but only TLR4 can signal via the intracellular TRIF/TRAM pathway. Further analysis of day 14 osteoblasts showed that pro-osteoblastic differentiation effects of LPS were associated with induction of TLR4, and TRIF and TRAM. In immune cells, TLR ligands also stimulate intracrine metabolism and signaling by vitamin D. In day 14 osteoblasts LPS stimulated expression of the vitamin D receptor (VDR), the vitamin D-activating enzme CYP27B1 and the vitamin D catabolic enzyme CYP24A1, suggesting an enhanced vitamin D intracrine system. By contrast, Pam3CysK suppressed CYP27B1 and VDR, indicating decreased intracrine vitamin D activity. These data show that TLR2 and TLR4 are potent modulators of osteoblast function. However, although both Pam3CysK (TLR2) and LPS (TLR4) can promote inflammatory, pro-osteoclastogenic activity, only the TLR4 ligand LPS can promote pro-osteoblastic activity. Thus, Gram+ve (TLR2) and Gram-ve (TLR4) bacteria may exert opposing effects on bone turnover. In addition, this response may involve TLR-mediated effects on localized metabolism and function of vitamin D.

***Disclosures: Wareeratn Chengprapakorn**, None.*

SA0160

See Friday Plenary Number FR0160.

SA0161

The Molecular Mechanism of Macrophage Polarization Epigenetically Regulated by Adiponectin in Obesity. Dong Ying Xuan*, Qisheng Tu, Jake Jinkun Chen. Tufts University School of Dental Medicine, USA

The macrophage phenotype is crucial to determine wound fate, however, the molecular events in this complex system remains unknown. In particular, obesity induces a phenotypic switch in adipose tissue macrophage polarization. Adiponectin, an adipocyte-derived secreted factor that is down-regulated in the obese state, functions to switch the macrophage polarization from pro-inflammatory states to anti-inflammatory phenotypes, thereby attenuating chronic inflammation. In our experiment, the possible epigenetic mechanism of macrophage polarization was analyzed in obese mice by injection of adiponectin. The results showed that adiponectin reduced macrophage infiltration in obese adipose tissue, and abolished the up-regulation of Jmjd3, a histone 3 Lys27 (H3K27) demethylase, in peritoneal macrophages collected from diet-induced obese mice when challenged with *Porphyromonas gingivalis* lipopolysaccharide (*Pg* LPS). Jmjd3 has been implicated in the activation of macrophages, and up-regulated in the early macrophage phase *in vitro* when challenged with *Pg* LPS, however, Jmjd3 was significantly down-regulated in macrophages from obese mice. Our results showed that adiponectin regulated the Jmjd3-IRF4 axis, which regulated anti-inflammation macrophage polarization. In future studies, we will use the adiponectin knockout mouse model to explore how adiponectin affects macrophage polarization and determine the epigenetic status change. It is crucial for understanding macrophage polarization in the obese state.

***Disclosures: Dong Ying Xuan**, None.*

SA0162

See Friday Plenary Number FR0162.

SA0163

See Friday Plenary Number FR0163.

SA0164

Chronic Kidney Disease Induces a Microarchitectural Alteration at the Spine as Evaluated by TBS. Edward Leib*[1], Renaud Winzenrieth[2], Didier Hans[3]. [1]University of Vermont, USA, [2]Med-imaps, Hôpital X. Arnozan, PTIB, Pessac, France, France, [3]Lausanne University Hospital, Switzerland

Chronic kidney disease (CKD) has a negative effect on bone leading to an increased risk of fracture. It has been shown, on Iliac crest biopsy, that CKD patients have a microarchitectural impairment. HoweverCKD effects at the axial skeleton are not clear. In this study, we have evaluated microarchitectural texture impairment in patients with CKD at the lumbar spine using Trabecular Bone Score(TBS).

This mono-centric study involves US white women who underwent bone density testing. Control subjects were excluded if they had a historical fracture or past or present treatment or illness that could influence bone metabolism. Each CKD subject was matched for age ($\pm$3 years) and BMI ($\pm$2 kg/m^2) with two controls.Forty-seven women with CKD were age and BMI-matched with 94 healthy women (age=55.9$\pm$13.3 years, BMI=26.4$\pm$4.7 kg/m^2). 21% of subjects with CKD had an exposure to glucocorticoids, 3.4% had a thyroid disease and 17% had at least one low energy fracture. The majority of women were postmenopausal (73%). Correlations between spine TBS and BMD and TBS and BMI were 0.48 ($p<0.01$) and 0.08 ($p=0.4$) respectively. Spine TBS was significantly lower in subjects with CKD ($p<0.01$) whereas site-matched BMD was borderline non-significant ($p=0.054$). Of the subjects with CKD those with fracture had a significantly lower TBS ($p=0.034$) whereas no difference was seen for BMD ($p=0.46$). TBS was associated with fracture (OR = 2.5[1.02-6.15]; AUC = 0.756[0.609-0.870]) in the CKD group. In multivariate analysis, CKD was associated with TBS ($p=0.019$) and maternal history of hip fracture ($p=0.012$) whereas BMD, steroids, smoking and family history of osteoporosis were not kept in the model. After adjustment for maternal history of hip fracture, the odds ratio for fracture by TBS was 4.67[1.29-16.85].CKD has a negative effect on spine microarchitectural texture, as evaluated by TBS, whereas no such effect was seen withBMD. This is the first time that impairment of axial trabecular microarchitectural texture as measured by TBS has been observed in CKD subjects. TBS seems to be a reliable tool for CKD patient management.

***Disclosures: Edward Leib**, None.*

SA0165

See Friday Plenary Number FR0165.

SA0166

Serum Sclerostin Predicts Bone Loss more Strongly than Age in Patients with CKD-5D. Hartmut Malluche*[1], Daniel Davenport[2], Gustav Blomquist[3], Marie-Claude Faugere[1]. [1]University of Kentucky Medical Center, USA, [2]University of Kentucky, Department of Surgery, USA, [3]University of Kentucky, Department of Radiology, USA

Introduction: Virtually all patients with CKD-5D have renal osteodystrophy and low bone volume is an integral part of this disease. This prospective study was performed to identify serum markers of bone loss in CKD-5D patients.

Patients and Methods: In patients with CKD-5D, BMD was measured by QCT of the hip and spine at baseline and at one year. Biochemical markers (including intact parathyroid hormone (iPTH), bone specific alkaline phosphatase (BSAP), C-terminal telopeptides type I collagen (CTX), Dickkopf 1 (DKK1) and sclerostin) were also measured and recorded at the same time along with demographic and clinical information. Correlation and group differences were measured using Spearman's Rho and Mann-Whitney U rank tests. Significant correlates were regressed versus bone loss for their predictive value. Significance was set at $P<.05$.

Results: Sixty-four patients (mean age 56 years $\pm$ 14 SD; 46% female; 50% black, 49% white and 1% other race) completed one-year follow-up. Mean baseline body mass index was 32.6 kg/m2 $\pm$ 7.9 SD and dialysis vintage was 59 months $\pm$ 7.9 SD. Among patients: 55% were diabetic, 21% had coronary artery disease, 24% smoked within the last 2 years, 79% were treated with vitamin D analogs and 91% with phosphate binders.

At baseline, age correlated with BMD, blacks had greater BMD of both hip and spine and patients who received treatment with vitamin D analogs had lower BMD of both hip and spine (Mann-Whitney U test $p<.05$).

After one year, median change in BMD of the spine was +2.4 mg/cm^3 (interquartile range [IR] from -11.4 to +15.2 mg/cm^3) and median change in BMD of the hip was -6.6 mg/cm3 (IR from -15.6 to +3.8 mg/cm^3). iPTH, BSAP, CTX and DKK1 did not correlate with BMD changes at any site. Sclerostin and age did not correlate with BMD changes at the spine but correlated inversely with BMD changes at the hip (rho = -.464, $p<.001$ and rho = -.274, $p<.05$ respectively). In multivariable regression, sclerostin predicted bone loss after adjustment for age (Table).

Conclusion: Serum levels of sclerostin predict bone loss at the hip but not the spine. This is likely due to the predominant production of sclerostin in cortical bone, the major component of hip bone. These patient findings support the experimental findings in animals of a negative effect of sclerostin on bone formation and demonstrate a linear relationship between blood levels of sclerostin and changes in bone mass.

Table: Independent Predictors of Change in BMD at One Year.

	Multivariable Regression Results Δ QCT of the Hip at 1 Year	
	Regression Coefficient (95% CI)	Standardized Coefficient
Sclerostin, ng/mL	12.5*** (-19.5 to -5.5)	.401
Age, y	-0.435** (-0.758 to -0.111)	-.322

**P<.01, ***P<.001

Table

***Disclosures: Hartmut Malluche**, None.*

SA0167

The CKD-MBD is Established in Early CKD by Stimulation of Vascular Calcification, Modulation of Osteocyte Function and an Osteodystrophy While Ca, Pi, VitD and PTH are Normal. Keith Hruska*[1], Yifu Fang[2], Toshifumi Sugatani[1]. [1]Washington University in St. Louis School of Medicine, USA, [2]Washington University School of Medicine, USA

We tested the hypothesis that the chronic kidney disease – mineral bone disorder (CKD-MBD) causes vascular calcification (VC) in early kidney failure. We developed a model of early CKD in the background of atherosclerosis stimulated vascular calcification. The animal model was in the *ldlr-/-* mouse fed high fat diet. CKD equivalent in glomerular filtration reduction to human stage 2 CKD stimulated early VC and inhibited the expression of α-klotho in the aorta. In addition, osteoblastic transition in the aorta was stimulated by early CKD as shown by the expression of the critical transcription factor, RUNX2. The ligand associated with the α-klotho-fibroblast growth factor receptor (FGFR) complex, FGF23, was found expressed in the vascular media of sham operated mice and decreased in the early CKD mice. Increased circulating levels of osteocyte secreted proteins, FGF23, and sclerostin may have been related to circulating klotho levels. A low turnover osteodystrophy including reduction in bone formation rates, cortical porosity and decreased size was found in the skeleton. In summary, the CKD-MBD, characterized by the cardiovascular risk factor, vascular calcification, circulating klotho, FGF23 and sclerostin secretion, and a renal osteodystrophy, was established in early CKD. Early CKD caused a reduction of vascular klotho, stimulated vascular osteoblastic transition, stimulated osteocytic secreted proteins and inhibited skeletal modeling.

***Disclosures: Keith Hruska**, None.*

SA0168

Localization Of The Gene For X-linked Calvarial Hyperostosis To Xq27.3-Xqter. Vere Borra*[1], Ellen Steenackers[1], Els Van Hul[2], Ian Glass[3], Wim Van Hul[1]. [1]University of Antwerp, Belgium, [2]University & University Hospital Antwerp, Belgium, [3]University of Washington, Seattle Children's Hospital, USA

X-linked calvarial hyperostosis is a rare disorder characterized by isolated calvarial thickening. Symptoms are prominent frontoparietal bones, a flat nasal root and short upturned nose, a high forehead with ridging of the metopic and saggital sutures, and lateral frontal prominences. The mandible is normal, as are the clavicles, pelvis and long bones. The thickened bone in the skull appeared to be softer than normal bone. Despite calvarial hyperostosis, increased intracranial pressure and cranial nerve entrapment did not occur. The major disability seems to be cosmetic. The disease segregates with an X-linked recessive mode of inheritance. Female carriers do not show any clinical symptoms.To date, only one family has been described with X-linked calvarial hyperostosis including three affected individuals. In order to localize the disease causing gene, 31 polymorphic microsatellite markers spread across the X-chromosome were analyzed. Genotypes were combined in haplotypes to delineate the region. A chromosomal region spanning from Xq27.3 to Xqter cosegregates with the disorder. This region encompasses 23,53 cM or 7,92 Mb according to the DECODE map and contains 163 genes. Exome sequencing was performed on a male patient in this family. However, this did not reveal any putative mutation. CNV-analysis did not show small duplications or deletions in this region. These results indicate that a non-coding regulatory sequence might be involved in the pathogenesis of this disorder.

***Disclosures: Vere Borra**, None.*

SA0169

Denosumab Treatment of Persistent or Relapsed Hypercalcemia of Malignancy (HCM). Karl Insogna*[1], Mimi Hu[2], Ilya Glezerman[3], Sophie Leboulleux[4], Rasim Gucalp[5], Waldemar Misiorowski[6], Bennett Yu[7], Paul Zorsky[7], Diego Tosi[8], Alberto Bessudo[9], Arnaud Jaccard[10], Giuseppe Tonini[11], Wendy Ying[12], Ada Braun[12], Rajul Jain[12]. [1]Yale University School of Medicine, USA, [2]University of Texas, M. D. Anderson Cancer Center, USA, [3]Memorial Sloan-Kettering Cancer Center & Weill Cornell Medical College, USA, [4]Institut Gustave Roussy, France, [5]Montefiore Medical Center-Bronx, USA, [6]Endocrinology Department, Medical Center for Postgraduate Education, Poland, [7]Peninsula Regional Medical Center, USA, [8]Centre Val d'Aurelle Paul Lamarque, France, [9]California Cancer Associates for Research & Excellence, USA, [10]Centre Hospitalier Universitaire de Limoges - Hôpital Dupuytren, France, [11]Policlinico Universitario Campus Biomedico, Italy, [12]Amgen Inc., USA

Background. HCM, caused primarily by tumor-induced bone resorption, is commonly treated with intravenous (IV) bisphosphonates: HCM may persist or relapse despite such therapy. Denosumab binds to RANK ligand (RANKL) to inhibit osteoclast-mediated bone resorption.

Methods: In this single-arm, open-label study, patients with HCM (corrected serum calcium [CSC] >12.5 mg/dL) despite IV bisphosphonate treatment ≥7 and ≤30 days before screening received subcutaneous denosumab 120 mg on days 1, 8, 15, and 28, then every 4 weeks. The primary endpoint was the proportion of patients with CSC ≤11.5 mg/dL within 10 days of denosumab initiation.

Results: The study enrolled 33 patients; key baseline characteristics are shown in Table 1. By day 10, 21 patients (64%) reached CSC ≤11.5 mg/dL, including 7 of 13 patients (54%) with bone metastases and 14 of 20 (70%) without bone metastases. Over the course of the study, 23 patients (70%) reached CSC ≤11.5 mg/dL. A complete response (CSC ≤10.8 mg/dL) occurred in 12 patients (36%) by day 10 and in 21 patients (64%) over the course of the study. In patients who reached CSC ≤11.5 mg/dL, the estimated median duration of response was 104 days. By day 10, mean percentage reduction from baseline of urinary-n telopeptide (corrected for urinary creatinine) (uNTx/uCr) was 53% (standard deviation 36%). Of the 17 patients whose uNTx/uCr was ≥50 nmol/mmol at baseline, 14 (82%) reached CSC ≤11.5 mg/dL by day 10, including 8 of the 9 patients (89%) whose uNTx/Cr was reduced to <50 nmol/mmol. Reductions at day 10 in uNTx/uCr and CSC were associated (Spearman rank correlation coefficient 0.6216, P<0.01). The most frequently reported serious adverse events were hypercalcemia (5 patients, 15%) and dyspnea (3 patients, 9%). Two patients had isolated episodes of CSC levels ≤8.0 mg/dL; no patients had CSC <7.0 mg/dL. No osteonecrosis of the jaw was reported.

Conclusions: In this study of patients with persistent or relapsed HCM despite recent IV bisphosphonate treatment, 64% of patients responded to denosumab within 10 days. The sustained duration of response observed in this study is a clinically favorable outcome in this population. Consistent with the known mechanism of action of denosumab, reduction of bone turnover was associated with reduction of CSC from baseline. No unexpected safety findings were identified. Denosumab may offer a new treatment option for HCM.

Table 1. Baseline patient characteristics

Characteristic	Denosumab treatment group (N = 33)
Men, n (%)	21 (64)
Age, mean (SD)	60 (15)
Median (Q1, Q3) time from last bisphosphonate treatment to enrollment, days	17 (13, 22)
ECOG performance status 2-4	25 (76)
CSC, mg/dL, median (Q1, Q3),	13.7 (13.2, 14.2)
uNTx/uCr, nmol/mmol, median (Q1, Q3)	76.9 (26.0, 148.2)
Proportion of patients with uNTx/uCr ≥50 nmol/mmol, n (%)	17 (52)

SD: standard deviation

CSC: corrected serum calcium, calculated as {total serum calcium in mg/dL + [0.8 x (4–serum albumin in g/dL)]}

uNTx/uCr: urinary n-telopeptide corrected for urinary creatinine

Table 1

***Disclosures: Karl Insogna**, None.*

This study received funding from: Amgen Inc.

SA0170

A New Class of Osteoblast Ion Transport Defects Causing Delayed Mineralization. Li Liu*[1], Deborah Nelson[2], Paul Schlesinger[3], Lisa Robinson[1], Peter Friedman[4], Harry Blair[1]. [1]University of Pittsburgh, USA, [2]University of Chicago, USA, [3]Washington University, USA, [4]University of Pittsburgh School of Medicine, USA

We examined ion transport in membrane vesicles made from mineralizing nontransformed osteoblasts; using acridine orange uptake, we found H+ uptake consistent with high capacity, low gradient, acid uptake. This suggested support for mineral nucleation and phosphate deposition by facilitated removal of H+ that is evolved when phosphate salts, hydroxyapatite, precipitate in a membrane-delimited space, i.e., the osteon. Examination of H+-transport in living osteoblast cultures by monitoring intracellular pH while modifying extracellular solution composition revealed that osteoblasts have high-capacity Na+/H+ exchange polarized to the basolateral surfaces of active bone formation sites. This involves both NHE1 and NHE6; the redundant transporters likely minimize the impact of defects in either transporter. On the other hand, the Na+-H+ exchanger regulatory protein 1, which is coordinates several regulatory and transport activities in the osteoblast, when knocked out resulted in a disorder of delayed mineral deposition consistent with idiopathic osteomalacia not related to vitamin D, PTH, collagen, or phosphate defects, when a high phosphate diet was used to avoid low phosphate due to renal NHERF1 absence. If regulated Na+/H+ removal from the basolateral surface of a bone forming unit does facilitate rapid vectorial mineral deposition, then there must also be a H+ uptake mechanism at or very close to the mineralizing front. Returning to analysis of osteoblast membrane vesicle acid uptake, we eliminated active transport mechanisms, and, by varying external and internal ion composition concluded that a CLC-class cation-gradient, probably K+, driven H+/Cl- exchange mechanism might mediate H+ uptake. This would be an analog of the CLC7-dependent mechanism in the osteoclast that balances electrogenic H+ secretion by exchanging half of the H+ for Cl-. Examination of all CLC transporters expressed in murine osteoblasts showed that CLC3 and CLC5 are expressed at high levels, with 80% of CLC mRNA transcripts being CLC3. Antibody to CLC3 labeled the apical surfaces and canalicular processes of osteoblasts in mouse bone. The CLC3-/- mouse displayed delayed mineralization and reduced bone mass, in keeping with a role of this transporter in supporting vectorial H+ transport out of the osteon to allow crystal nucleation and ordered mineral deposition. This work points to a new class of cation transporters that are required to maintain normal rates of mineral deposition.

***Disclosures: Li Liu**, None.*

SA0171

The Effects of Loss of Function *PHEX*/*Phex* Mutations in X-Linked Hypophosphatemia are Mediated by Up-Regulation of the MicroRNA335 Family. Baozhi Yuan*[1], Abigail Radcliff[2], Michael Johnson[1], Robert Blank[1], Marc Drezner[1]. [1]University of Wisconsin, USA, [2]University of Wisconsin-Madison, USA

Hyp-mice manifest renal phosphate wasting, hypophosphatemia and severe rickets/osteomalacia due to a loss of function *Phex* mutation. Although our previous studies have established that mutated *Phex* results in decreased production of *Sgne1* (7B2) mRNA, the mechanism underlying PHEX effects on this pivotal biochemical alteration, which is the fulcrum for the cascade of events resulting in the *HYP* phenotype, remains unknown. However, recent studies indicate that microRNAs (miRNAs) decrease the expression level of target genes by suppressing translation or reducing mRNA abundance. Thus, in the present study, we examined the possible role of a miRNA(s) in mediating Phex effects on 7B2 gene expression. Initially, screening of a microarray with 88 known miRNAs revealed up-regulation of 7 miRNAs in bones from *hyp*-mice compared to normal mice. TargetScan software indicated that the 3' untranslated region (UTR) of the 7B2 gene has an 8mer match with miRNA335-3p and a 3' compensatory match with miRNA335-5p, suggesting that this miRNA family, with the greatest up-regulation in *hyp*-mouse bone, may target 7B2. In support of this possibility, we found a significant decrease in *Sgne1* (7B2) mRNA in h-Tert-osteoblasts, incubated with 25μM miRNA335-3p mimic (0.19 ± 0.04 vs 1.0 ± 0.04 fold; $p<0.001$) or miRNA335-5p mimic (0.23 ± 0.02 vs 1.0 ± 0.04 fold; $p<0.001$). Since miRNAs bind to the 3'UTR of a gene to regulate expression, we used a 7B2-3'UTR luciferase construct to confirm that the 7B2 gene is directly responsive to the miRNA335 family. We observed significant inhibition of 7B2-3'UTR luciferase activity in h-Tert-osteoblasts, cotransfected with the 7B2-3'UTR luciferase reporter and the miRNA335-3p mimic (0.55 ± 0.08 vs 1.0 ± 0.06 fold; $p<0.05$) or the miRNA335-5p mimic (0.69 ± 0.07 vs 1.0 ± 0.06 fold; $p<0.05$). These data indicate that the miRNA335 family directly targets the 7B2-3'UTR to regulate 7B2 gene transcription. To assure that the increment in miRNA335 is dependent upon decreased bioactive Phex, we transfected h-Tert-osteoblasts with *Phex* siRNA (5μM) and after 48 hours evaluated effects on miRNA335 expression. RT-PCR revealed a dramatic increase in the expression of miRNA335-3p (3.12 ± 0.45 vs 1.06 ± 0.20 fold; $p<0.01$) and miRNA335-5p (3.96 ± 0.51 vs 1.06 ± 0.20 fold; $p<0.01$). In concert with our previous studies, these data indicate that the *HYP* phenotype, resulting from loss of function *PHEX*/*Phex* mutations in humans and mice, is mediated by elevated miRNA335 levels.

***Disclosures: Baozhi Yuan**, None.*

SA0172

See Friday Plenary Number FR0172.

SA0173

Bone-Related Complications Reported Among Patients With Hypoparathyroidism: Patients' Attitudes and Reponses About HypoparathyroiDism TOleration EXplored (PARADOX Study). Bart Clarke*[1], James Sanders[2], Hjalmar Lagast[3]. [1]Mayo Clinic College of Medicine, USA, [2]Hypoparathyroidism Association, Inc., USA, [3]NPS Pharmaceuticals, Inc., USA

Hypoparathyroidism is a rare endocrine disorder due to absent or inappropriately low levels of parathyroid hormone. This results in low bone remodeling that leads to high bone mineral density. There are limited reports of the disease-related burden of illness. The PARADOX study assessed the clinical, personal, and social impact of hypoparathyroidism in patients (pts) aged ≥18 y and diagnosed ≥6 mo ago. Members of the Hypoparathyroidism Association, Inc., were invited to complete an institutional review board–approved, self-reported questionnaire online. This report focuses on bone-related symptoms and comorbidities experienced by pts despite being on standard symptomatic management (eg, calcium and active vitamin D).

The web-based survey received 1294 initial hits and 442 pts completed the screening portion. Of 387 pts who completed the questionnaire, 13 were excluded because they did not meet the inclusion criteria.

The study population (N=374) included mostly women (85%); with a mean age of 49 y, mean disease duration of 13 y, and moderate-severe disease condition (79%). A total of 251 pts (67%) reported symptoms of joint or bone pain in the last 12 mo, with most reporting their overall disease condition as moderate (32 mild, 129 moderate, 90 severe). Bone fractures were experienced by 7 pts in the last 12 mo (4 moderate, 3 severe) and by 41 pts in their lifetime since diagnosis (6 mild, 17 moderate, 18 severe). The reported effects on BMD were variable; 24 pts reported decreased BMD (4 mild, 10 moderate, 10 severe), and 30 pts reported elevated BMD (3 mild, 13 moderate, 14 severe) in the last 12 mo. Since diagnosis, 53 pts reported decreased BMD (13 mild, 18 moderate, 22 severe; 31 >51 y of age), and 58 pts reported elevated BMD (7 mild, 28 moderate, 23 severe; 31 >51 y of age). In the same period, 42 pts reported soft tissue calcifications (5 mild, 16 moderate, 21 severe). Other complications possibly resulting from the underlying mineral homeostasis disruption were reported: brittle nails (44%), dental problems (29%), and hypercalcemia (18%).

Pts with hypoparathyroidism have substantial burden of illness in the skeleton and joints. The unexplained large number of BMD decreases needs further study, but suggests that bone loss in postmenopausal women with hypoparathyroidism is similar to other postmenopausal women. Bone-related comorbidities afflict pts despite being on standard symptom management therapy that includes calcium and active vitamin D.

***Disclosures: Bart Clarke**, NPS Pharmaceuticals, Inc., 2*
This study received funding from: NPS Pharmaceuticals, Inc.

SA0174

See Friday Plenary Number FR0174.

SA0175

See Friday Plenary Number FR0175.

SA0176

Effects of Long Term PTH(1-84) Replacement Therapy in Hypoparathyroidism and the Consequence of Termination of Therapy. Tanja Sikjaer*[1], Lars Rolighed[2], Emil Moser[3], Leif Mosekilde[3], Lars Rejnmark[2]. [1]Department of Medicine & Endocrinology, MEA Aarhus University Hospital, Denmark, [2]Aarhus University Hospital, Denmark, [3]Department of Endocrinology & Internal Medicine, MEA, Aarhus University Hospital, Denmark

The aim of the study is to investigate the long-term effect of PTH(1-84) treatment in hypoparathyroidism (hypoPT). We have previously reported results on 62 patients with hypoPT randomized to 6 months of treatment with either PTH(1-84) 100 µg/d s.c. or similar placebo, administrated as an add-on therapy (1). We followed 42 of these patients for an extension of 2 yrs. 17 patients treated with placebo continued as a control group, 9 patients continued treatment with PTH(1-84) 100 µg/d and 15 discontinued PTH(1-84) treatment and returned to only calcium and active vitamin D analogs.

The 42 participants have had hypoPT for a mean of 12 (range: 4;32)yrs. Only 1 subject had idiopathic hypoPT whereas 41 had acquired hypoPT following surgery. Mean age of subjects was 54±12 yrs and 90% were females. There were no significant differences in plasma levels of calcium, phosphate, creatinine, eGFR or renal calcium excretion between groups.

As previously reported, 6 months of treatment with PTH(1-84) decreased BMD at the hip, spine and whole body (WB) (1). This effect was reversed during the 2 years follow up period by both discontinuation and continuously PTH(1-84) treatment. BMD increased significantly in the discontinued group at the hip by 4.7±1.5%, the lumbar spine by 7.8±2.1% and WB by 2.3±1.0 compared to the control group. In the continuously treated group, BMD increased significantly at the spine by 7.2±2.4% compared to the control group. Compared with controls, there were no differences in BMD at the hip and WB in the PTH(1-84) group. There were no differences between groups at the forearm.

Bone turnover, as assessed by levels of biochemical markers, such as bone formation: P1NP, Osteocalcin, bone-specific alkaline phosphatase and bone resorption: urinary-NTX, serum-CTX, was previously shown too increase gradually during the 6 months of treatment. After 2 years of discontinuation of PTH(1-84) the levels of bone turn over markers returned to baseline levels. Compared with the other groups, the bone markers remained significantly higher in the PTH(1-84) treated patients.

In conclusion, the previously shown reduction in BMD at the hip, spine and WB in PTH(1-84) substitution therapy is neutralized if treatment is continued for 2.5 years and even increases BMD at the spine. If the treatment is discontinued, bone turn over markers returns to baseline and BMD increases at the hip, spine and WB.

Reference: [1]Sikjaer T et al., J Bone Miner Res 2011; 26(10):2358-2370

***Disclosures: Tanja Sikjaer**, None.*

SA0177

Methylation of cytosine-guanine dinucleotide (CpG) islands of vitamin D receptor (VDR) and calcium sensing receptor (CaSR) genes in parathyroid adenomas. Sanjay Bhadada*[1], Shweta Varshney[2], Naresh Sachdeva[3], Uma Nahar Saikia[4], Ashutosh Arya[2], Arunanshu Behera[5], Sudhaker D. Rao[6]. [1]PGIMER, Chandigarh, India, [2]Department of Endocrinology, PGIMER, India, [3]Department of Endocrinology, India, [4]Department of Histopathology, PGIMER, India, [5]Department of General Surgery, India, [6]Henry Ford Hospital, USA

Aim: Exact mechanism(s) for decreased expressions of vitamin D and calcium sensing receptors (VDR & CaSR) in sporadic parathyroid adenomas is not known. However, methylation of promoter regions (so-called gene silencing) is often detected during epigenetic down regulation of gene expression. We investigated whether such epigenetic silencing is involved in the decreased expression of VDR and CaSR.

Experimental Design: Real-time PCR and immunohistochemistry were used to confirm the down regulation of VDR and CaSR genes at transcriptional and translational levels. Bisulfite-converted DNA samples from parathyroid adenomas with control samples were analyzed for methylation in the promoter region of VDR and CaSR genes.

Results: As reported by us and others, immunohistochemistry revealed significant reductions in VDR and CaSR expressions, and a significant increases in CD1 and PTH expressions in adenomatous compared to normal parathyroid tissue. Consistent with immunohistochemistry findings, both VDR and CaSR mRNAs were reduced by 0.36 and 0.45 fold change ($p<0.001$), and CD1 and PTH mRNAs were increased by 9.4 and 17.4 fold change respectively ($p<0.001$) in adenomatous parathyroid tissue. PTH mRNA correlated with plasma PTH ($r=0.864$; $p<0.001$), but not with adenoma weight, while CD1 mRNA correlated with adenoma weight ($r=0.715$; $p<0.001$). There was no relationship either between the decreases in VDR and CaSR mRNA expressions or the increases in PTH and CD1 mRNA expressions.

Most importantly, there was no significant methylation in the promoter regions of VDR or CaSR genes in the parathyroid adenomatous tissues.

Conclusions: we confirmed reductions in VDR and CaSR expressions both at the protein and mRNA levels. However, methylation-mediated silencing of VDR and CaSR promoter does not appear to be associated with these reduced expressions. This suggests involvement of other factors in the specific suppression of VDR and CaSR gene expressions in parathyroid adenomas.

***Disclosures: Sanjay Bhadada**, None.*

SA0178

Normocalcemic Primary Hyperparathyroidism: BMD gain at the individual patient level after parathyroidectomy. Eugenie Koumakis*[1], Jean-Claude Souberbielle[2], Emile Sarfati[3], Didier Borderie[4], Andre Kahan[5], Catherine Cormier[6]. [1]Hôpital Cochin, France, [2]Explorations Fonctionnelles, Hôpital Necker Enfants Malades, France, [3]Chirurgie Générale et Endocrinienne, Hôpital Saint-Louis, Paris, France, [4]Laboratoire de Biochimie Générale et Spécialisée, Hôpital Cochin, Paris, France, [5]Rheumatology Department A, Cochin Hospital, France, [6]AP-HP Groupe Hospitalier Cochin, France

In primary hyperparathyroidism (PHPT), it is unclear whether parathyroidectomy (PTX) may be beneficial in patients with a mild phenotype, in particular in normocalcemic PHPT. Our aims were to assess BMD gain after PTX at the individual level in normocalcemic PHPT patients, and to investigate the predictive factors of individual BMD gain.

Patients and Methods: longitudinal cohort study of 60 PHPT patients (aged 64.0±10.1 years) referred for low bone mass and mild abnormalities of calcium/phosphorus metabolism, and successfully treated by PTX. BMD was assessed at the spine, hip and forearm before and 1 year after PTX using QDR 4500 (Hologic). To determine the impact of PTX on BMD at the individual level, the mean difference between pre and post-PTX BMD values was calculated (g/cm^2). The least significant change (LSC) was chosen as threshold for individual BMD gain, and calculated using the ISCD recommendations: $LSC=2\sqrt{2}xSD$, with a SD of $0.01 g/cm^2$. BMD gain was considered significant if ≥ 0.030 g/cm^2 at one site or more, without any equivalent BMD loss at another site. A logistic regression analysis was performed to determine whether baseline characteristics were predictive of individual BMD gain.

Results: Two groups of patients were individualized according to baseline serum total (albumin-corrected) calcium (tCa): 39 normocalcemic patients, and 21 hypercalcemic patients. An individual gain was observed at 1 yr in 73.7% of hypercalcemic patients, and 44.4% of normocalcemic patients (p=0.05). In univariate analysis, patients with a significant BMD gain were more likely to have lower baseline eGFR (72.8±18.6 vs 79.9±13.4 ml/min/1.73m^2, p= 0.02), tended to have higher baseline serum tCa (2.56±0.14 vs 2.51±0.12 mmol/l, p=0.07) and higher ALP (79.1±30.7 vs 65.1±23.1 UI/l, p=0.06) than patients who did not. In logistic regression analysis, baseline ALP in the upper median range (67-161 UI/L) was the only variable identified as an independent predictor for BMD gain (OR=4.8, 95% CI 1.3-17.6). Similarly, baseline ALP in the upper median range was also predictive of BMD gain in the normocalcemic group (OR=8.4, 95% CI 1.4 to 56.6). No association was identified with any other baseline characteristic.

Conclusion. These results highlight that successful PTX is followed at 1 year by an increase in BMD at the individual level, in nearly 50% of patients with normocalcemic PHPT. This suggests that PTX may have a positive impact in normocalcemic PHPT patients with osteoporosis.

***Disclosures: Eugenie Koumakis**, None.*

SA0179

See Friday Plenary Number FR0179.

SA0180

Parathyroidectomy eliminates arrhythmic risk in primary hyperparathyroidism, as evaluated by exercise test. Jessica Pepe*, Mario Curione, Marisa Varrenti, Mirella Cilli, Sara Piemonte, Cristiana Cipriani, Claudio Savoriti, Orlando Raimo, Federica De Lucia, Carolina Clementelli, Elisabetta Romagnoli, Salvatore Minisola. "Sapienza", Univeristy of Rome, Italy, Italy

Objective: to investigate if parathyroidectomy (PTx) reverses risk factors for arrhythmias, related to the QT dynamic changes evaluated during bicycle ergometry exercise test (ET).

Methods: twenty four postmenopausal women with primary hyperparathyroidism (PHPT) (mean age 60.0±8.4 years) and 30, sex and age-matched, controls underwent ET, echocardiographic and biochemical evaluation. The following stages were considered during ET: rest, peak exercise, recovery (early recovery, 2 minutes, and 10 minutes after peak exercise). The patients were randomized into two groups: 12 patients underwent PTx (Group A) and 12 were followed-up conservatively (Group B). After 6 months the patients were again studied.

Results: there was no significant difference between PHPT patients (Group A and Group B) compared to controls, apart from the expected significantly mean higher levels of total, ionized calcium and PTH and significantly mean lower levels of phosphorus in PHPT patients (total calcium A:2.7±0.1, B:2.7±0.1 vs controls 2.30±0.14 mmol/l; ionized calcium A:1.45±0.16, B:1.39±0.03 vs controls 1.22±0.04 mmol/L; phosphorus A:0.89±0.11, B:0.92±0.12 vs controls 1.25±0.15 mmol/L; parathyroid hormone A:80.3±23.5, B:83.4±23.1 vs controls 34.2±10.3 ng/L, all p≤0.01). Group A and B, showed no differences in mean baseline biochemical values, echocardiographic parameters and QTc interval. PHPT patients, showed an increased occurrence of ventricular premature beats (VPBs) during ET compared with controls (37% vs 6.6%, p=0.03). Serum total calcium level was a predictor of VPBs (p=0.05). Mean value of QTc was in the normal range at baseline (A: 401.0±16.9; B: 402.25±13.5 msec), but significantly shorter than controls (417.8±25.1 msec, p<0.01); a negative correlation was found between QTc and total calcium values (p=0.03). Physiological reduction of QTc interval from rest to peak exercise was not observed in PHPT patients before surgery. After PTx, Group A had a significant reduction in VPBs compared to baseline (at baseline, 5 out of 12 vs none out of 12 patients after PTx, p=0.03) and a restored normal QT adaptation during ET. Group B showed no significant changes after a six month period.

Conclusions: PTx reduces the occurrence of VPBs and restored the QTc adaptation during ET.

Figure 1: QTc interval during exercise test in Group A and controls.

Figure 2: QTc interval during exercise test in Group B and controls.

*p≤0.01 baseline vs controls, p≤0.01 baseline vs after 6 months.

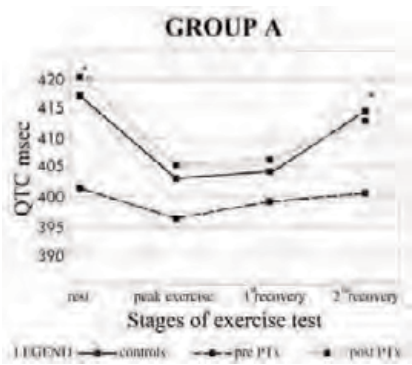

Figure 1

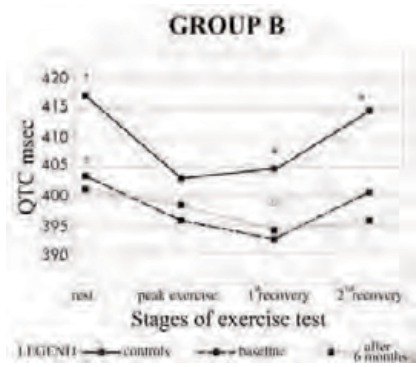

Figure 2

***Disclosures: Jessica Pepe**, None.*

SA0181

Predictors of Bone Mass Recovery Following Cure of Primary Hyperparathyroidism: 1-Year Follow-Up of 49 cases. Bruno Ferraz-de-Souza*[1], Regina M Martin[1], Manuela GM Rocha-Braz[1], Adriana M Fernandes[1], Pedro Henrique Correa[2]. [1]Univ of Sao Paulo School of Medicine (FMUSP), Brazil, [2]University of Sao Paulo School of Medicine, Brazil

Introduction: Primary hyperparathyroidism (PHPT) leads to increased bone remodeling and reduced bone mass. In PHPT patients with evident bone involvement, bone mass can be greatly recovered following surgical treatment, and hungry bone syndrome might ensue during the immediate postoperative period. Currently, most PHPT patients do not have symptoms of bone disease at diagnosis and identifiable factors predicting bone mass gain following treatment are not well established.

Objectives: To identify predictors of bone mass recovery at lumbar spine following cure of PHPT.

Methods: Retrospective analysis of PHPT cases cured by surgery followed in our center with pre- and postoperative register of: bone mineral density (BMD) and T-/Z-scores at lumbar spine (LS), total hip and forearm as determined by DXA; serum determinations of total calcium (Ca), ionized Ca, phosphorus, PTH, creatinine, 25OHD, alkaline phosphatase (ALP), P1NP, osteocalcin and CTX; 24-hour calciuria; and bone scintigraphy. Pearson's correlation coefficient and statistical significance were calculated using PAWS17.

Results: Forty-nine patients (8M, 41F) between 20 and 82 yrs of age (median 63.3) were identified. Median interval between surgery and postoperative DXA was 12.3 mo, and the adjusted 1-yr delta BMD at LS ranged from -13.4% to +47.2%. 71% of patients had delta BMD >3% and 47% had >6% gain in LS BMD in 1 yr. Delta LS BMD was significantly correlated (p<0.001) with basal serum PTH (r=0.77), ALP (r=0.72), P1NP (r=0.71) and osteocalcin (r=0.66), amongst others. No correlation was seen between delta BMD and age at surgery, basal serum Ca, CTX, 25OHD or 24-h calciuria. After the removal of delta LS BMD outliers, correlation was no longer significant for the aforementioned variables, indicating that the observed association was driven by extreme cases of PHPT with severe bone disease at diagnosis.Conclusion: Recovery of BMD in LS one year after surgical cure of PHPT was observed in a large proportion of patients, suggesting frequent bone involvement. Basal serum determinations of PTH and bone formation markers seem to best predict BMD recovery after surgery but this correlation is determined by the inclusion of severe cases. In more mild PHPT cases, routine investigation does not seem to provide predictive factors of BMD recovery. Extrapolation of these findings can have important implications for the indication of surgical treatment for asymptomatic PHPT.

***Disclosures: Bruno Ferraz-de-Souza**, None.*

SA0182

Standard Definition of Vitamin D Deficiency Does Not Identify Bone Mineral Density Differences in Mild Primary Hyperparathyroidism. Elaine Cong*[1], Marcella Walker[2], Chiyuan Zhang[2], Shonni Silverberg[2]. [1]Columbia Presbyterian Medical Center, USA, [2]Columbia University, USA

Vitamin D deficiency and primary hyperparathyroidism (PHPT) have independent skeletal effects, and vitamin D deficiency is known to exacerbate hyperparathyroidism in PHPT. In 2009, the 3rd International Workshop on the Management of Asymptomatic PHPT recommended a goal 25-hydroxyvitamin D (25OHD) level > 20 ng/dl in PHPT. However, data on PHPT patients using this cut-point for vitamin D are lacking. Although controversy remains regarding definitions of vitamin D deficiency, we sought to compare PHPT patients who are clearly vitamin D deficient (D-deficient: 25OHD < 20 ng/dl) and those who are clearly vitamin D replete (D-replete: 25OHD > 30 ng/dl). We retrospectively analyzed baseline data from our longitudinal natural history study of mild PHPT, including the 103 of 137 subjects with complete vitamin D and BMD data. Serum calcium (10.5 vs 10.6 mg/dl) and

PTH (127 vs 126 pg/ml) levels were similar to the overall cohort. D-deficiency was common (n=47, 46%; 25OHD 15±4 ng/ml) while only 18% were D-replete (25OHD 38±8 ng/ml). Deficient and replete groups did not differ by gender, menopausal status, or ethnicity. D-deficient subjects were older (57±1.6 vs 50±3.5 years, p=0.04) and had higher BMI (26±1 vs 22±1 kg/m^2, p=0.02). D-deficient subjects had higher PTH levels (148±11 vs 104±11 pg/ml, p=0.008) and tended to have lower 1,25$(OH)_2$-vitamin D levels (54±2 vs 67±6 pg/ml, p = 0.058), while serum calcium (10.6±0.1 vs 10.6±0.1 mg/dl) and alkaline phosphatase (108±7 vs 95±9 U/L, p=0.2) did not differ. D-deficient and D-replete groups also had similar and BMI adjusted BMD (lumbar spine: 0.95±0.03 vs 0.90±0.05 g/cm^2, p=0.38; femoral neck: 0.68±0.02 vs 0.67±0.02 g/cm^2, p =0.73; 1/3 radius: 0.59±0.01 vs 0.56±0.02 g/cm^2, p=0.29).

In summary, using the 25OHD cut-point of 20 ng/ml, D-deficient PHPT patients were older and heavier, as expected in any D-deficient population. With regard to PHPT disease activity, D-deficient patients had PTH levels 42% higher than those who were D-replete but other indices did not differ. Although prior analyses in this cohort demonstrated lower 1/3 radius BMD when an older definition of D-deficiency was used (25OHD < 9 ng/ml vs > 9 ng/ml: 0.48 vs 0.58 g/cm^2, p=0.05), we did not find lower BMD when stratifying subjects using the more current descriptions of vitamin D status as suggested in the 2009 Guidelines. Despite much higher PTH levels, these data do not support an important impact on BMD using a 25OHD cut-point of 20 ng/ml in mild PHPT.

***Disclosures: Elaine Cong**, None.*

SA0183

Carotid Calcification and Osteoporosis in Postmenopausal Women – OSTPRE BBA – Study. Miika Värri*[1], Tomi-Pekka Tuomainen[2], Risto Honkanen[3], Heikki Kroger[4], Marjo Tuppurainen[4]. [1]Bone & Cartilage Research Unit, University of Eastern Finland, Finland, [2]Institute of Public Health & Clinical Nutrition, University of Eastern Finland, Finland, [3]University of Eastern Finland, Finland, [4]Kuopio University Hospital, Finland

Atherosclerosis (AS) and osteoporosis (OP) are common diseases in elderly people. Several metabolic connections as well as same risk factors have been suggested for both carotid calcification and OP. The aim of this cross-sectional study was to explore the association between carotid artery intima- media thickness (IMT), carotid artery calcification and bone mineral density (BMD) in postmenopausal women. In addition, the association of postmenopausal hormone therapy (HT) with IMT and carotid calcification was studied.

Study population was drawn from the Kuopio OSTPRE- BBA (Bone-Brain and Atherosclerosis) study. In all, 346 women (mean age 73.6 years) were randomly selected for carotid IMT measurements with B-mode ultrasound; femoral neck, lumbar spine (L2-L4) and total body BMD were measured with DXA (Dual-energy X-ray absorptiometry).

In 63.6 % of cases, atherosclerotic plaques were observed at carotid arteries bifurcations. Increased right carotid maximum IMT was significantly associated with low femoral neck T-score. In the osteoporotic group (T-score < -2.5, n=20) the maximum IMT was 2.66 mm ± 1.19 SD and in non-osteoporotic group (T-score > -1, n=122) 1.95 mm ± 0.73 SD, respectively (P<0.001). The presence of carotid artery calcifications was more prevalent in the osteoporotic group than in the normal T-score group (OR = 4.6, P=0.002). IMT values were not associated with lumbar spine T-score. Maximum values of common carotid IMT were smaller in HT users (1.26 mm ± 0.16 SD) than in non-users (1.31mm ± 0.23 SD) (P=0.010). There were no associations between HT and carotid calcifications.

The results of our population-based study suggest that OP is related to AS changes in carotid arteries, and indirectly support the hypothesis of partially shared pathophysiological mechanisms in the two disorders. In addition, follow-up of carotid arteries of osteoporotic women might be useful for assessment of preventive and treatment.

***Disclosures: Miika Värri**, None.*

SA0184

Ectopic mineralization of spinal tissues in mice lacking equilibrative nucleoside transporter 1: Age-dependent alterations in the expression of genes regulating biomineralization. Hisataka Ii*[1], Sumeeta Warraich[1], Diana Quinonez[1], James R. Hammond[2], S. Jeffrey Dixon[1], Cheryle A. Séguin[1]. [1]The University of Western Ontario, Canada, [2]University of Alberta, Canada

The equilibrative nucleoside transporter 1 (ENT1) transfers adenosine across plasma membranes. We reported recently that mice lacking ENT1 (KO) exhibit progressive ectopic mineralization of spinal tissues, resembling diffuse idiopathic skeletal hyperostosis (DISH) in humans. Pathological calcification was first noted in the paraspinal ligaments of the cervical-thoracic region at 2 months of age. Lesions extended to the lumbar and caudal regions with advancing age, and eventually involved the entheses, intervertebral discs and sternocostal articulations. Moreover, plasma levels of inorganic pyrophosphate (PPi, an inhibitor of biomineralization) were greater in KO mice than in wild-type (WT) at 2 months of age. The purpose of the current study was to investigate the mechanisms underlying ectopic mineralization in KO mice. Accordingly, we quantified the expression of genes known to regulate biomineralization. Intervertebral discs (IVDs) were isolated by microdissection from KO mice and WT littermate controls at 2 months of age (when lesions were not detectable in IVDs by micro-CT) and at 6 months of age (when there was extensive involvement of the IVDs). RNA was extracted and transcripts were quantified by real-time RT-PCR. Compared to tissues from WT mice, IVDs from 2-month-old KO mice exhibited greater expression of alkaline phosphatase (*Alpl*, enzyme responsible for the hydrolysis of PPi to Pi, which promotes mineralization) and ectonucleotide pyrophosphatase/phosphodiesterase 1 (*Enpp1*, enzyme responsible for the production of PPi). On the other hand, there was no significant difference in the expression of progressive ankylosis protein (*Ank*, a putative PPi transporter). These findings are in striking contrast to the pattern of gene expression in IVDs from KO and WT mice at 6 months of age. In these older mice, expression of *Alpl*, *Enpp1* and *Ank* was significantly less in KO mice than in WT. It is possible that upregulated expression of alkaline phosphatase in the IVDs of KO mice at 2 months of age leads to the eventual mineralization of these structures seen in older mice; whereas, in older mice, there may be compensatory changes in gene expression as mineralized lesions extend into the IVDs. KO mice may be a useful model to investigate the etiology of and therapies for DISH and related disorders of mineralization in humans.

***Disclosures: Hisataka Ii**, None.*

SA0185

Effects of Irisin on Bone Metabolism and its Signal Mechanism. Jin Zhang*, Jessica Cheng, Qisheng Tu, Jake Jinkun Chen. Tufts University School of Dental Medicine, USA

Irisin, a newly discovered myokine induced in exercise, has potential effects in stimulating adipose tissue browning, and fighting obesity and diabetes. This study investigates the effects of irisin on bone metabolism and its signal mechanism.

Cultured pre-osteogenic MC3T3-E1 cells were treated with ascorbic acid (AA) and irisin. The mRNA expressions of osteogenic factors Runx2, Osterix, and Satb2 were increased several fold after irisin treatment. Bone sialoprotein (BSP), type I collagen, and osteocalcin (OCN) were considerably upregulated in the late osteogenic stage. We screened a variety of osteogenic signaling pathways and found that irisin promoted the translocation of β-catenin into the nucleus of MC3T3-E1 cells at 3, 6, and 12h. Irisin increased total b-catenin protein levels at 6h following AA induction; BMP pathway inhibitor LDN193189 further increased β-catenin protein levels. Irisin also increased phosphorylation of Smad1/5/8, which was inhibited by LDN193189, indicating that irisin affects osteoblastogenesis via the Wnt/β-catenin pathway downstream of the BMP receptor signal. Additionally, irisin increased Erk1/2, JNK, P38, AKT1, and calcineurin phosphorylation, which were all increased by β-catenin inhibitor XAV939.

We found that irisin inhibited RANKL-induced RAW264.7 cell osteoclastogenesis through NFATc1 suppression in a time and dose-dependent manner. Irisin reduced expressions of osteoclast differentiation markers TRAP and cathepsin K, and reduced numbers of TRAP+ osteoclasts. Irisin also inhibited expressions of MITF, PU1, and AKT1 and reduced AKT1 protein phosphorylation. However, expressions of p-B, p-Erk/c-Fos, p-JNK, and c-Myc, were increased. As NFATc1 was down-regulated, irisin might specifically inhibit osteoclast differentiation through calcineurin/NFATc1 and AKT1/MITF/PU1-NFATc1 pathways.

In vivo, irisin protein or FNDC5-lentivirus injections increased bone volume/total volume, trabecular thickness, and cortical thickness compared to control mice (*p<0.05), as well as BSP and OCN expressions compared to scramble-virus control. Irisin positive osteoblasts were found on the edge of the growth plate.

In conclusion, we demonstrated that irisin promoted osteoblast differentiation through the Wnt/β-catenin pathway and inhibited osteoclast differentiation by suppressing the RANKL/NFATc1 pathway. Hence, exercise-induced irisin has initially proven to be a potent factor in strengthening bone by regulating bone metabolism.

***Disclosures: Jin Zhang**, None.*

SA0186

See Friday Plenary Number FR0186.

SA0187

Interdependence of Muscle and Bone Loss Induced by Disuse and Aging. Shane Lloyd*, Yue Zhang, Emmanuel Paul, Lacee Laufenberg, Charles Lang, Henry Donahue. The Pennsylvania State University College of Medicine, USA

Mechanical unloading induces muscle atrophy and bone loss, but the relative time course and interdependence of these deleterious effects is unknown. To address this issue we subjected 4-month-old C57BL/6J mice to hindlimb suspension (HLS) or normal loading for 3 weeks. We sacrificed 12-16 mice per condition on day (d) 0, 7, 14, and 21.

^{1}H-NMR revealed a maximal 7% decrease in lean mass with HLS by d7 (Fig1A; p<0.05). The gastrocnemius (gast) was affected earliest (-8% by d7), with mass being reduced 16% by d14 (p<0.05). Quadriceps (quad) mass was unchanged at d7, but decreased 14% by d14 (p<0.05). Muscle mass did not change with age. Atrogin-1 and MuRF1 are muscle-specific ubiquitin ligases involved in protein degradation. At d7,

atrogin-1 mRNA was increased 122% and 99% in quad (Fig1B) and gast, respectively ($p<0.05$). MuRF1 mRNA was increased 88% and 44% in the quad and gast, respectively, at d7 ($p<0.05$). The mRNA content for both returned to baseline thereafter. Protein syntheses decreased by 30% in quad and gast at d7 ($p<0.05$), returning to baseline by d21 (Fig1C). The phosphorylation of S6K1 (T389) and S6 (S240/244), surrogate markers of mTOR kinase activity, was reduced in gast after 7-21 d of HLS.

Skeletal effects were not apparent until d14. There was a 4% decrease in femur cortical thickness at d14 (Fig1D; $p<0.05$) and similar response in the tibia. Distal femur trabecular parameters were not different at d7. By d14, HLS mice had a reduction in bone volume fraction (22%), trabecular thickness (15%), and tissue mineral density (16%; Fig1E; $p<0.05$); however, the effect of HLS was often eliminated by d21 due to age-related decline in trabecular microstructure in controls. Trabecular response at the proximal tibia was similar.

There was a 13% decrease in femur force to failure and bending rigidity by d14, and 17% decrease by d21 (Fig1F; $p<0.05$). Surprisingly, there was no effect of unloading on tibia strength.Our results suggest muscle atrophy, and thus reduced mechanical force, precedes bone loss during unloading and may compound unloading-induced bone loss. Countermeasures that preserve muscle may prevent or delay the deleterious skeletal effects of unloading. Furthermore, age-related trabecular bone loss in mice, similar to that which occurs in mature astronauts, is superimposed on unloading. Preservation of muscle mass, cortical structure, and bone strength with age suggests muscle may have a greater effect on cortical than trabecular bone.

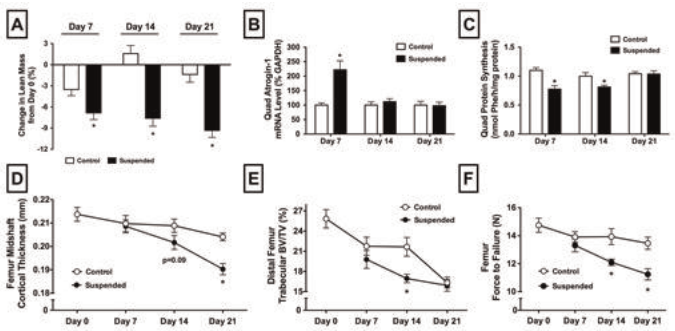

Fig1. (A) Lean Mass, (B) Atrogin-1, (C) Protein Synth, (D) Cort Thickness, (E) BV/TV, (F) Strength

***Disclosures: Shane Lloyd**, None.*

SA0188

Muscle, Physical Activity and Sedentary Time are Independent Predictors of Bone Strength in Post-Menarcheal Girls. Vina Tan*[1], Lindsay Nettlefold[2], Heather Macdonald[1], SoJung Kim[3], Douglas Race[2], Joan Wharf-Higgins[4], Patti-Jean Naylor[4], Heather McKay[1]. [1]University of British Columbia, Canada, [2]Centre for Hip Health & Mobility, Canada, [3]University of British Columbia, South Korea, [4]University of Victoria, Canada

Muscle contractions impose a dynamic force on bone during physical activity (PA). However, the interaction between PA, muscle and bone in pubertal girls is not well described. Therefore, we assessed the association between muscle, PA and sedentary time on estimated bone strength, structure and density in post-menarcheal girls.

Methods: We measured the tibia bone (left, 8% and 50% sites) using pQCT (XCT3000, Stratec) in 102 post-menarcheal girls (15.3 ± 0.4 yrs). We assessed PA by accelerometer (GT1M, ActiGraph) that girls wore for 7 consecutive days during waking hours. We included participants with at least 3 valid days (wear time $\geq$600 min/day, non-wear time defined as 60min zeros with 2min non-zero allowance block). We used age-specific cut-points to classify activity as sedentary (<1.5 metabolic equivalents (METs)), moderate-to-vigorous PA $\geq$ 4METs (MVPA) and vigorous PA $\geq$7 METs (VPA). At the distal tibia, we assessed bone strength index (BSI, mg^2/mm^4), bone area (Ar, mm^2) and density (BMD, mg/cm^3) for total (Tt) and trabecular (Tb) bone. At the midshaft, we assessed polar strength-strain index (SSI_p, mm^3), periosteal (Peri) and endosteal (Endo) circumference (mm), cortical bone area, density and thickness (Ct.Ar (mm^2), Ct.BMD (mg/cm^3), Ct.Th (mm)) and muscle cross-sectional area (MCSA, mm^2). Age at menarche was self-reported. We fit multivariable regression models to evaluate the influence of MCSA and PA levels on bone outcomes (adjusted for tibia length, ethnicity and maturity). In PA models, we also controlled for MCSA and accelerometer wear time.

Results: MCSA strongly predicted 26.5% and 31.7% of the variance in BSI and SSI_p, respectively ($p<0.001$) after controlling for covariates. MCSA explained 3.6-29.9% of variance in Tt.BMD, Tt.Ar, Tb.BMD, Tb.Ar and Ct.Ar ($p<0.05$). After additional covariates, MVPA explained 14.0% of the variance in BSI and 5.0% in SSI_p ($p<0.05$). MVPA explained 5.4-11.3% of the variance in Ct.Ar, Tt.BMD and Tb.BMD ($p<0.05$). Sedentary time was a negative predictor of SSI_p (4.8%) and Tt.BMD (5.6%) ($p<0.05$). MVPA and VPA were negative predictors of Ct.Th and Endo ($p<0.05$), accounting for 6.8-18.9% of the variance, respectively.

Conclusion: MCSA, PA levels and sedentary time have a unique influence on estimated bone strength, structure and density at the weight-bearing tibia in post-menarcheal girls. Increased PA and decreased sedentary time are modifiable factors that should be addressed to promote bone health during growth.

Table 1. Descriptive characteristics for post-menarcheal girls (n=102).

	Mean	SD
Age (years)	15.3	0.4
Height (cm)	162.8	6.4
Weight (kg)	59.0	10.0
Years post menarche	2.9	1.2
Ethnicity (Caucasian/ Others)	55/47	-
MCSA (mm^2)	3782.9	643.8
BSI (mg^2/mm^4)	8516.8	1883.2
SSI_p (mm^3)	1543.2	289.9
Accelerometer data (n=60)		
Number of valid days (3/4/5/6/7)	11/22/17/6/4	-
Total wear time (min/valid day)	791.5	57.2
Sedentary <1.5METs (min/day)	646.6	62.4
MVPA ≥4METs (min/day)	33.6	17.8
VPA ≥7METs (min/day)	4.9	4.9

Table 1

Table 2: Multivariable regression models for bone outcomes at the a) 8% tibia and b) 50% tibia ($p<0.05$), adjusted for tibia length, years post menarche and ethnicity. Models developed to predict PA outcomes also adjusted for MCSA and accelerometer wear time.

Bone outcome	MCSA		Sed		MVPA		VPA	
	R^2 diff	β	R^2 diff	β	R^2 diff	B	R^2 diff	β
a) 8% tibia								
BSI,mg^2/mm^4	26.5*	1.64	ns	-	14.0*	41.5	ns	-
Tt.Ar, mm^2	3.9	0.04	ns	-	ns	-	ns	-
Tb.Ar, mm^2	3.6	0.03	ns	-	ns	-	ns	-
Tt.BMD, mg/cm^3	8.7*	0.02	5.6	-0.17	6.9	0.71	ns	-
Tb.BMD, mg/cm^3	16.1*	0.02	ns	-	11.3	0.68	ns	-
b) 50% tibia								
SSI_p, mm^3	31.7*	0.28	4.8	-0.97	5.0	3.64	ns	-
Ct.Ar, mm^2	29.9*	0.03	ns	-	5.4	0.49	ns	-
Ct.Th, mm	ns	-	ns	-	6.8	-0.04	17.8*	-0.23
Endo, mm	ns	-	ns	-	8.2	-0.31	18.9*	-1.56

*p≤0.001; ns, not significant.

Table 2

***Disclosures: Vina Tan**, None.*

SA0189

See Friday Plenary Number FR0189.

SA0190

See Friday Plenary Number FR0190.

SA0191

17ß-Estradiol and Testosterone Exert Antiapoptotic Effects in Skeletal Muscle Cells Involving AR, ER, ERK, MnSOD and COXIV. Anabela La Colla, Lucia Pronsato, Ana Carolina Ronda, Lorena Milanesi, Andrea Vasconsuelo, Ricardo Boland*. Universidad Nacional del Sur, Argentina

17b-Estradiol (E2) and Testosterone (T) have effects in several tissues including skeletal muscle. In aged skeletal muscle both a deficit of sex hormones and prominent apoptosis are observed contributing to the pathogenesis of sarcopenia. We previously showed that E2 and T inhibit H_2O_2 - induced apoptosis in C2C12 muscle cells. Here we demonstrate that E2 has a relevant role in muscle mitochondria, up-regulating the expression and activity of manganese superoxide dismutase (MnSOD) and increasing the activity of cytochrome c oxidase IV (COXIV), through ERK signaling. Pharmacological and immunological assays employing the estrogen receptor (ER) antagonist fulvestrant indicate that ER mediates these events. In addition, MnSOD expression and COXIV activity decrease when cells are treated with H_2O_2, effects that are reversed with E2 pretreatment. Experiments with the androgen receptor (AR) antagonist flutamide involved the AR in the antiapoptotic action of T. Competitive binding assays, immunocytochemistry and Western blots supported a non-classical localization of the AR in C2C12 cells. Thus, AR was detected by immunoblots using specific antibodies after subcellular fractionation, not only in nucleus and cytosol, but also in mitochondria and microsomes. [^{3}H] T binding characteristics were established in total homogenates and subcellular fractions. Specific and saturable [^{3}H] T binding sites were detected in mitochondria and microsomes. Immunolocalization of the non-classical AR was also confirmed using confocal microscopy. Sucrose gradient fractionation demonstrated the presence of the AR in lipid rafts and caveolae. These results point to an active role of the AR during the antiapoptotic effect of T at different levels: nuclear (in the genomic response), mitochondrial (in the intrinsic pathway) and microsomal (in the response mediated by membrane proteins). Besides, coimmunoprecipitation assays indicated that the AR physically interacts with caveolin-1, association which was lost after T treatment at the same time that a decrease of AR expression was observed in the microsomal fraction, suggesting

translocation of the membrane AR to inner cellular compartments. Our studies contribute to elucidate the mechanism by which these hormones regulate signaling cascades throwing light on the molecular basis of myopathies associated with deregulation of apoptosis by sex hormone deficiency states

* *A. La Colla and L. Pronsato have equally contributed to this work*

***Disclosures: Ricardo Boland**, None.*

SA0192

See Friday Plenary Number FR0192.

SA0193

Clinical Definitions of Sarcopenia and Risk of Falls and Hip Fractures in Older Men: The Osteoporotic Fractures in Men (MrOS) Study. Peggy Cawthon*[1], Terri Blackwell[2], Jane Cauley[3], Christine Lee[4], Deborah Kado[5], Elizabeth Barrett-Connor[5], Andy Hoffman[6], Marcia Stefanick[6], Michael Nevitt[7], Nancy Lane[8], Kristine Ensrud[9], Steven Cummings[10], Eric Orwoll[4]. [1]California Pacific Medical Center Research Institute, USA, [2]CPMCRI, USA, [3]University of Pittsburgh Graduate School of Public Health, USA, [4]Oregon Health & Science University, USA, [5]University of California, San Diego, USA, [6]Stanford, USA, [7]UCSF, USA, [8]University of California, Davis Medical Center, USA, [9]Minneapolis VA Medical Center / University of Minnesota, USA, [10]San Francisco Coordinating Center, USA

We examined whether two consensus definitions of sarcopenia (and their components) were associated with incident falls and hip fractures in men aged ⩾65 yrs in MrOS (N=5934).

We assessed appendicular lean mass (ALM) by whole-body Hologic 4500 DXA; grip strength by dynamometry; and walking speed over 6 meters. Fractures were centrally adjudicated over 9.8 years. Falls were by self-report 3x/year with recurrent falls defined as ⩾2 in the year after baseline. The International Working Group (IWG) sarcopenia definition included slowness (walking speed<1.0 m/s) and low lean mass (ALM/ht^2≤7.23 kg/m^2); both must be present for ''sarcopenia''. The European Working Group on Sarcopenia in Older Persons (EWGSOP) definition included: 1) slowness (gait speed≤0.8 m/s); 2) weakness (grip strength<30 kg); and 3) low lean mass (ALM/ht^2≤7.23 kg/m^2). ''Sarcopenia'' was defined as low lean mass plus either slowness or weakness, and ''severe sarcopenia'' as all three; severe sarcopenia was rare, so ''sarcopenia/severe sarcopenia'' were analyzed together. We used logistic regression to estimate odds ratios (OR) for recurrent falls (N=694, 11.9%), and proportional hazards to estimate hazard ratios (HR) for hip fractures (N=207, 3.5%).

By the IWG, men with sarcopenia (N=277, 4.7%) were more likely have recurrent falls (OR: 2.2, 95%CI: 1.7, 3.0) and fracture a hip (HR: 2.2, 95%CI: 1.7, 3.0) than men without sarcopenia. For IWG definition components, slowness independently predicted recurrent falls and hip fractures, whereas low lean mass predicted hip fractures but not recurrent falls (Table 1).

By the EWGSOP, men with sarcopenia/severe sarcopenia were more likely have recurrent falls (OR: 2.4, 95%CI: 1.8, 3.2), and had a borderline increased risk of hip fracture than men without sarcopenia (HR: 1.7, 95%CI: 0.99, 2.7). For EWGSOP definition components, slowness predicted recurrent falls and hip fractures (Table 2), whereas weakness only predicted falls and low lean mass only predicted hip fracture.In summary, the IWG definition predicted both falls and hip fractures, whereas the EWGSOP definition was only significantly associated with falls. The component of slowness by either definition predicted falls and hip fractures, while low lean mass and weakness were not consistently associated with these outcomes. Further research with other outcomes such as disability and mortality is needed for full evaluation these consensus definitions for sarcopenia.

Table 1. Likelihood of recurrent falls & risk of hip fractures by components of IWG sarcopenia definition

Model predictors	Slowness N=1034 (17.4%)	Low lean N=1239 (20.9%)
	Falls: OR (95% CI)	
Age, slowness	2.4 (2.0, 2.9)	--
Age, low lean	--	1.1 (0.9, 1.3)
Age, slowness & low lean	2.4 (2.0, 2.9)	1.1 (0.9, 1.3)
	Hip Fractures: HR (95% CI)	
Age, slowness	1.7 (1.3, 2.4)	--
Age, low lean	--	1.5 (1.1, 2.0)
Age, slowness & low lean	1.7 (1.3, 2.4)	1.5 (1.1, 2.0)

Table 1

Table 2. Likelihood of recurrent falls & risk of hip fractures by components of EWGSOP sarcopenia definition

Model predictors	Slowness N=262 (4.4%)	Low lean N=1239 (20.9%)	Weakness N=474 (8.0%)
	Falls: OR (95% CI)		
Age, slowness	3.0 (1.9, 4.7)	--	--
Age, low lean	--	1.5 (1.1, 2.0)	--
Age, weakness	--	--	1.4 (0.9, 2.1)
Age, slowness, weakness & low lean	2.8 (1.8, 4.4)	1.4 (1.1, 1.9)	1.2 (0.8, 1.9)
	Hip Fractures: HR (95% CI)		
Age, slowness	3.6 (2.7, 4.7)	--	--
Age, low lean	--	1.1 (0.9, 1.3)	--
Age, weakness	--	--	2.0 (1.6, 2.5)
Age, slowness, weakness & low lean	3.3 (2.5, 4.4)	1.0 (0.8, 1.3)	1.8 (1.4, 2.3)

Table 2

***Disclosures: Peggy Cawthon**, None.*

SA0194

See Friday Plenary Number FR0194.

SA0195

The relationship between HRpQCT derived muscle parameters and DXA derived lean tissue mass. Marta Erlandson*[1], Eva Szabo[1], Miranda Boggild[2], Nicolas Vilayphiou[3], Robert Josse[4], Angela M. Cheung[5]. [1]University Health Network, Canada, [2]University of Toronto, Canada, [3]INSERM UMR1033, Université de Lyon & Hospices Civils de Lyon, France, [4]St. Michael's Hospital, University of Toronto, Canada, [5]University Health Network-University of Toronto, Canada

Purpose: To determine the relationship between HRpQCT-derived muscle measures obtained at the distal tibia using an experimental algorithm and DXA derived total body and lower limb lean tissue mass.

Methods: A total body DXA scan using Hologic Discovery A densitometer was performed on 67 men and women from the Toronto cohort of the Canadian Multicenter Osteoporosis Study (CaMos). Total body lean tissue mass (TBLM) and lower limb lean tissue mass (LLLM) were obtained from the scans using standard analysis protocols. Standard HRpQCT scans using Scanco Xtreme CT were acquired at the distal tibia. HRpQCT-derived muscle density (MD), muscle volume (MV) and muscle cross-sectional area (MCSA) were then calculated using a newly developed algorithm in which tight thresholding limits for muscle (34.22-194.32mgHA/cm^3) and fat (-238.6 - -84.9mgHA/cm^3) were used to identify muscle seed volumes which were then iteratively expanded. In areas where the muscle and fat volume boundaries met or overlapped after expansion iteration, a short grayscale border was added between the volumes before the next iteration. After the final iteration, any remaining grayscale areas were segmented with a threshold mid-way between the upper fat and lower muscle seeding thresholds (-25.34mgHA/cm^3). Independent sample T-tests were used to examine sex differences and Pearson correlation coefficients were calculated to assess the relationship between DXA and HRpQCT measurements.

Results: Women (n=45, mean age=68.5±9.3) had a mean TBLM (38.0±6.5kg) and LLLM (18.1±3.6kg) that was significantly lower than those of men (n=22, mean age=67.4±8.5) (55.2±7.1kg, 22.7±3.6kg; respectively) (p<0.05). However, there was no difference between men and women in HRpQCT-derived MD, MV and MCSA (13.2±3.3 vs 12.9±2.5mgHA/cm^3, 13223.8±3343.3 vs 13404.9±3497.9mm^3 and 1521.4±384.6 vs 1553.1±418.1mm^2; respectively) (p>0.05). There was no relationship between HRpQCT-derived MD, MV and MSCA and DXA TBLM and LLLM (r=-0.047 to 0.031, p=0.7-0.9).

Conclusion: These preliminarily findings suggest that MD, MV and MCSA obtained from HRpQCT may not be predictive of DXA TBLM and LLLM. There were no sex differences in HRpQCT-derived muscle parameters, perhaps because it was volumetric MD and we expect smaller absolute differences at more distal sites. Moving forward it will be important to measure muscle function and determine if functional measures are related to HRpQCT muscle parameters.

***Disclosures: Marta Erlandson**, None.*

SA0196

Apoptosis Induced by Bilirubin and Lithocholic Acid in Human Osteoblasts Is Decreased by Ursodeoxycholic Acid. Silvia Ruiz-Gaspa*[1], Marta Dubreuil[1], Andres Combalia[2], Pilar Peris[3], Ana Monegal[2], Albert Pares[4], Nuria Guanabens[5]. [1]Centro de Investigación Biomédica en Red en Enfermedades Hepáticas y Digestivas (CIBERehd), Spain, [2]Metabolic Bone Diseases Unit, Department of Rheumatology &, Spain, [3]Hospital Clínic of Barcelona, Spain, [4]Liver Unit, Digestive Diseases Institute, Hospital Clínic, IDIBAPS, University of Barcelona, Spain, [5]Universitat De Barcelona, Spain

Introduction: Low bone turnover osteoporosis is common in patients with chronic cholestasis. Ursodeoxycholic acid (UDCA) counteracts the damaging effects of bilirubin or lithocholic acid (LCA) on osteoblast viability, proliferation and mineralization. Likewise, UDCA is anti-apoptotic in a number of cell lines, but this effect has not been investigated in bone cells. Therefore, the consequences of bilirubin and LCA on apoptosis, and if UDCA has antiapoptotic effects have been assessed on osteoblastic cells. Material and Methods: The experiments were performed in primary human osteoblasts (hOB), human osteosarcoma cell line (Saos-2) and hepatocarcinoma cell line (HepG2). Cells were treated at different times and concentrations of camptothecin as proapoptotic agent, and UDCA, LCA and bilirubin. Apoptosis was determined by DNA fragmentation, flow cytometry (annexin V-FITC labeling), caspase-3 activity, and gene expression of Bcl-2–associated X protein (*BAX*) as antiapoptotic, and *BCL2* and BCL2-like 1 protein (*BCL2L*) as proapoptotic genes, respectively. Results: LCA (10 μM) and bilirubin (50 μM) significantly induced cell apoptosis as indicated by DNA fragmentation (4.7 and 3.7 fold vs control, respectively, $p<0.01$), with parallel results by flow cytometry and caspase-3 activity in Saos-2 and hOB. UDCA (100 μM) alone had no consequences on apoptosis. However, UDCA not only significantly reduced the apoptotic effects of camptothecin (0.5 μM) by 69%, ($p<0.001$), but counteracted the apoptotic effects of LCA and bilirubin as observed by DNA fragmentation (51% and 68%, respectively, $p<0.01$), cytometry and caspase-3 activity in Saos-2 cells. The counteracting effects of UDCA were lower in hOB. UDCA had no effects on *BAX* expression, but upregulated *BCL2L* gene expression (3.5 fold versus control, $p=0.002$). Moreover, UDCA neutralized the effects of LCA and bilirubin on the up-regulated *BAX* by 52% and 68%, respectively ($p<0.01$), and on the down-regulated *BCL2L* gene expression by 550% and 146%, respectively ($p<0.05$). Conclusions: Bilirubin and lithocholic acid induce apoptosis in osteoblastic cells. Ursodeoxycholic acid has clear antiapoptotic effects counteracting the consequences of these two substances increased in cholestasis. These results suggest that ursodeoxycholic acid may have further benefitial effects on neutralizing the decreased bone formation in patients with cholestasis.

***Disclosures: Silvia Ruiz-Gaspa**, None.*

SA0197

A *Gja1* Oculodentodigital Dysplasia Mutant Discloses Complex Functions of Connexin43 (Cx43) in Bone Modeling and Homeostasis. Marcus Watkins*[1], Susan Grimston[1], Jin Yi Norris[2], Roberto Civitelli[1]. [1]Washington University in St. Louis School of Medicine, USA, [2]Washington University in Saint Louis, USA

Oculodentodigital dysplasia (ODDD) is an autosomal dominant disorder linked to mutations of the Cx43 gene (*Gja1*), characterized by craniofacial and dental defects, type III syndactyly, and eye abnormalities. We have previously reported that mice in which one allele of *Gja1* is replaced by the $Gja1^{G138R}$ mutant in osteo-chondroprogenitors, using the *Dermo1 (DM1)-Cre* (DM1;cOD), have a larger cortical total tissue ($54\pm6\%$) and marrow area ($30\pm6\%$) while cortical thickness and cortical BMD is significantly decreased ($-20\pm7\%$ and $-4\pm2\%$), respectively, compared to wild type (WT) littermates. These features, linked to increased osteoclastogenic support by mutant osteoblastic cells, phenocopy mice with conditional deletion of *Gja1*, confirming that the $Gja1^{G138R}$ mutant is dominant negative for Cx43. To further determine the biologic effect of the mutant connexin, we generated mice in which gene replacement occurs later in osteoblast differentiation using the *Osterix/SP7-Cre* (Sp7;cOD), and also introduced the $Gja1^{G138R}$ allele in a *Gja1* null background ($Sp7;Gja1^{G138R/-}$). Sp7;cOD mice exhibit a similar but less pronounced phenotype relative to DM1;cOD mice, with increased total tissue ($13\pm6\%$) and marrow area ($36\pm12\%$), and decreased cortical thickness ($-23\pm12\%$) compared to WT. Cortical BMD is not altered. This phenotype is more severe in $Sp7;Gja1^{G138R/-}$ littermates, with tissue and marrow area being larger than WT littermates ($47\pm12\%$ and $108\pm20\%$, respectively). In $Sp7;Gja1^{G138R/-}$, cortical thickness and mineral density are also decreased relative to WT ($-24\pm6\%$ and $-16\pm4\%$, respectively); and endocortical osteoclast number is increased, similar to DM1;cOD mice. However, unlike other models of *Gja1* deletion/mutation, compared to WT littermates, $Sp7;Gja1^{G138R/-}$ mice have significantly reduced trabecular bone volume/tissue volume ($-49\pm16\%$), decreased trabecular number ($-31\pm9\%$) and increased trabecular separation ($39\pm18\%$), as assessed by in vivo μCT. Thus, disruption of Cx43 function by the $Gja1^{G138R}$ mutant in differentiated osteoblasts and osteocytes is sufficient to cause cortical modeling defects. Since the ODDD mutant disrupts gap junction function but not cell permeability to ATP or other large molecules, these results do not support a role of Cx43 hemichannels in cortical modeling. Finally, the more severe phenotype of $Sp7;Gja1^{G138R/-}$ mice suggests the $Gja1^{G138R}$ mutant may interfere with other connexins or with other, non-gap junction related functions of Cx43.

***Disclosures: Marcus Watkins**, None.*

SA0198

ATF4 Regulates Bone Angiogenesis by Promoting VEGF Expression And Release in the Bone Environment. Ke Zhu*[1], Hongli Jiao[2], Shuai Li[1], Huiling Cao[3], Deborah Galson[3], Zhongfang Zhao[1], Xi Zhao[1], Yumei Lai[2], Jie Fan[4], Hee-Jeong Im[5], Di Chen[6], Guozhi Xiao[6]. [1]College of Life Sciences, Nankai University, China, [2]Department of Biochemistry, Rush University Medical Center, USA, [3]University of Pittsburgh School of Medicine, USA, [4]Department of Surgery, University of Pittsburgh, USA, [5]Department of Biochemistry, Rush University Medical Center, Chicago, Illinois 60612, USA, USA, [6]Rush University Medical Center, USA

Transcription activation factor 4 (ATF4) is critical for bone remodeling during skeletal development and throughout life; however, its role in bone angiogenesis is unclear. We performed contrast-enhanced μCT imaging in Microfil-perfused femurs and showed that ATF4 deficiency strikingly reduced vessel volume and vessel number in femurs. Results from immunohistochemical staining of tibial sections using a specific antibody against CD31 revealed that both the size and density of vessels within the metaphyseal periosteum and diaphyseal endosteum from $Atf4^{-/-}$ tibiae were dramatically decreased compared to those of WT tibiae. In vitro angiogenesis assay showed that ablation of ATF4 prevented endothelial sprouting from metatarsals, which was rescued by treatment with a recombinant VEGF. Adenoviral overexpression of ATF4 increased HIF-1α and VEGF expression levels in osteoblasts in a hypoxia-dependent manner. Mechanistically, loss of ATF4 increased HIF-1α ubiquitination and decreased HIF-1α protein stability without affecting its mRNA stability and protein translation. In addition, loss of ATF4 increased the binding of HIF-1α to prolyl hydroxylases, the enzymes that hydroxylate HIF-1α protein and promote its proteasomal degradation via the pVHL pathway. Interestingly, parathyroid hormone-related protein and receptor activator of NF-κB ligand, both well-known activators of osteoclasts, increased release of VEGF from the bone matrix and promoted angiogenesis through the protein kinase C- and ATF4-dependent activation of osteoclast differentiation and bone resorption. Finally, our in vivo studies revealed that hypoxia/reoxygenation induction of HIF-1α and VEGF expression leading to bone angiogenesis, a key adaptive response to hypoxic conditions, was severely compromised in mice lacking the *Atf4* gene. Taken together, our studies demonstrate that ATF4 is a new key regulator of the HIF/VEGF axis in osteoblasts in response to hypoxia and of VEGF release from bone matrix, two critical steps for bone angiogenesis.

***Disclosures: Ke Zhu**, None.*

SA0199

c-Abl broadcasts BMP-2 function to Osterix and CSF-1 for concerted osteogenesis via PI 3 kinase/Akt. Nandini Ghosh-Choudhury*. University of Texas Health Science Center at San Antonio, USA

Receptor and non-receptor tyrosine kinases play important roles in osteoblast differentiation. c-Abl is a non-receptor tyrosine kinase, inhibition of which in experimental rat model and in human chronic myeloid leukemia patients, resulted in compromised bone remodeling due to impaired osteoblast and osteoclast activities. We have shown that BMP-2 plays a significant role in bone formation and resorption by contributing to the formation of mature osteoblasts and osteoclasts. Identification of the role of c-Abl in BMP-2-induced bone remodeling and characterization of the underlying mechanisms are the focus of this study. We used a pharmacological inhibitor (Imatinib mesylate) and a dominant negative mutant of c-Abl to block its activity in osteoblast cells. Inactivation of c-Abl significantly blocked BMP-2-induced osteoblast differentiation as evidenced by inhibition of alkaline phosphatase activity and formation of mineralized bone nodules. Formation of multinucleated osteoclasts in response to BMP-2 was severely impaired in the absence of c-Abl activation. Using primary calvarial osteoblasts prepared from c-Abl null mouse we show an absolute requirement of this tyrosine kinase in maturation of osteoblasts and osteoclasts. We have reported an essential requirement of PI 3 kinase/Akt signaling in BMP-2-induced osteoblast and osteoclast differentiation. Remarkably, inhibition of c-Abl significantly suppressed BMP-2-stimulated PI 3 kinase activity and its downstream Akt phosphorylation. We have shown that BMP-2 regulates CSF-1 expression and thus activates osteoclast differentiation. We find that c-Abl activation is critical for BMP-2-induced osteoclastogenic CSF-1 expression. Importantly, we identified requirement of c-Abl in BMP-2 gene autoregulation and osterix expression necessary for osteoblast differentiation. Smad-dependent transcription of CSF-1, osterix and BMP-2 essentially was found to require c-Abl activation. Finally, we show that c-Abl regulated Smad phosphorylation in response to BMP-2. We propose that activation of c-Abl is an important step in integrating the noncanonical PI 3 kinase and the canonical Smad signaling pathway to control BMP-2-induced osteogenesis.

***Disclosures: Nandini Ghosh-Choudhury**, None.*

SA0200

Diabetes Inhibits Bone Formation via Regulation of Histone Acetylation by HDAC2. Qianqian Han*, Liming Yu, Dong Ying Xuan, Lan Zhang, Qisheng Tu, Jake Jinkun Chen. Tufts University School of Dental Medicine, USA

Diabetes is closely related with bone disorders, and histone deacetylase, HDAC, was recently found to be involved in the renal damages caused by diabetes. Other studies demonstrated that the activity of HDAC is altered during osteogenic differentiation. HDAC2 is one of class I HDACs and has been proven to play an important role in diabetes. In this study, we hypothesized that diabetes inhibits bone regeneration via increasing the HDAC2 expression, which converts bone markers chromatin into a transcriptionally inactive conformation.

Bone marrows of wild-type mice and pre-diabetic mice were collected and RNAs were extracted. Real time PCR was used to detect the HDAC and bone marker mRNA expressions. Our results showed that HDAC2 expression was much higher while the bone marker expressions Col I, ALP, OCN, Runx2, and Satb2 were lower in bone marrow diabetic mice than in wild-type mice. These results indicated that HDAC2 might play an important role in bone disorders caused by diabetes.

MC3T3 cells, a mouse pre-osteoblast cell line and primary cultures of mouse bone marrow stem cells were cultured in a-MEM with 10% FBS, 0.1mg/ml streptomycin, and 100U/ml penicillin. After confluence, cells were treated with D-glucose at the concentrations of 5, 10, 15, or 25 mM, respectively and cells treated with 25mM mannitol were used as the negative control. After 7 days of treatment, RNAs were extracted and real time PCR was performed to detect the expression of HDAC2 and bone markers including OCN, COL I, Runx2, and OSX.When BMSCs and MC3T3-E1 cells were treated with D-glucose at the concentrations of 15 mM or 25mM for 7 days, the mRNA expression of HDAC2 was up-regulated and the expression of bone markers was down-regulated. Taken together, our results suggest, for the first time, that diabetes inhibits osteogenic differentiation via regulating the bone marker expression pattern by modulating histone acetylation states.

***Disclosures: Qianqian Han**, None.*

SA0201

Hypoxia-Inducible Factor-1α-Induced Bone Anabolism Requires Heightened Glycolysis. Jenna Regan*[1], Kyu Sang Joeng[2], Emel Esen[1], Fanxin Long[3]. [1]Washington University St. Louis, USA, [2]Baylor College of Medicine, USA, [3]Washington University School of Medicine, USA

The cancellous bone surface in contact with the bone marrow is considered among the most hypoxic regions in the bone marrow. In response to low oxygen levels, the hypoxia-inducible factor alpha (HIFα) proteins are stabilized and upregulate genes involved in a wide variety of processes, including cell metabolism and angiogenesis. We have confirmed that osteoblasts experience low-oxygen (<10 mm Hg) conditions *in vivo*. Thus the purpose of this study was to investigate how events downstream of HIF stabilization impact osteoblast-lineage cells in a cell-autonomous manner. When a stabilized form of HIF1α (HIF1-PPN) is expressed in SP7-positive cells in postnatal mice, bone volume increases nearly 6-fold within 15 days. The increased bone is a direct effect of significantly increased osteoblast numbers. In this model, the bone volume is not dependent upon an increase in cancellous vascularity, as normalization of the vascular density (through concomitant deletion of VEGF) did not impact the bone accrual. Another well-recognized set of HIF1α target genes encode components of the glycolytic metabolism pathway. Direct HIF1α targets such as PDK1 and LDHA are upregulated in SP7;HIF1-PPN bones, indicating that HIF1α stabilization is inducing a shift to glycolytic metabolism in the SP7-positive cells. To test whether glycolysis plays an important role in the increased bone mass in SP7;HIF1-PPN mice, we treated the mice with dichloroacetate (DCA) to block PDK1 activity. Strikingly, administration of DCA during the 15-day period of HIF1α stabilization completely blocked the increase in bone mass and normalized osteoblast numbers. Our results indicate that HIF1α stabilization in osteoblast-lineage cells rapidly and significantly increases osteoblast numbers and bone volume and that a shift to glycolytic metabolism is required for these effects.

***Disclosures: Jenna Regan**, None.*

SA0202

See Friday Plenary Number FR0202.

SA0203

Isolation and Characterization of Human Osteoblasts From Needle Biopsies Without *In Vitro* Culture. Koji Fujita*[1], Matthew Roforth[1], James Peterson[1], Salman Kirmani[1], Matthew Drake[2], Louise McCready[1], David Monroe[3], Sundeep Khosla[4]. [1]Mayo Clinic, USA, [2]College of Medicine, Mayo Clinic, USA, [3]Mayo Foundation, USA, [4]Mayo Clinic College of Medicine, USA

There is currently no data regarding the expression of specific genes or pathways in purified human osteoblasts that have not been subjected to extensive *in vitro* culture. Since the latter is likely to alter the RNA expression profile of these cells, we have developed methods to obtain progressively enriched human osteoblast populations within 2-4 hr of obtaining a small needle biopsy (1-2 mm x 1 cm) and coupled this to high-throughput RNA sequencing (RNAseq) and focused QPCR analyses.

Needle biopsies were obtained from the posterior iliac crest of 8 human male subjects and subjected to serial collagenase digests. Because the 1st 30 minute digest (~100 million cells) contained surface hematopoietic and loosely adherent cells, we used the 2nd 60 minute digest (~10 million cells), which contained mineralizing cells and was highly enriched for osteoblast marker genes (*col1α1*, 5-fold; osteocalcin [*ocn*], 8-fold; *bsp*, 11-fold; osteopontin [*opn*], 10-fold). The 2nd fraction was then stained with an AP antibody and the AP+ cells (~1 million cells) were rapidly isolated (within ~2 hr from biopsy) using magnetic activated cell sorting. Relative to AP- cells, the AP+ cells contained all of the mineralizing cells and were further enriched for osteoblast marker genes (*AP*, 10-fold; *col1α1*, 1000-fold; *ocn*, 300-fold; *bsp*, 300-fold; *opn*, 50-fold). We then further purified the AP+ cells by depletion of cells expressing CD45, CD34, or CD31 by FACS to obtain AP+/CD45/34/31- (AP+/—) cells (within ~4 hr from biopsy), which represented a highly enriched human osteoblast preparation devoid of hematopoietic/endothelial cells. In addition to *in vitro* mineralization, AP+/— cells expressed very low to undetectable levels of osteocyte marker genes, including *E11, dmp-1, phex, fgf23,* and *sost.*

Finally, we used high-throughput RNAseq analysis to compare the transcriptome of the AP+/— cells (n = 6) to human fibroblasts (n = 3). By Ingenuity Pathway Analysis, we identified a set of unique pathways reflecting genes expressed only in human osteoblasts (AP+/— cells) *in vivo* but not in fibroblasts, including (all $P < 0.05$) Osteoblast Related, VDR/RXR Activation, LXR/RXR Activation, NF-kB Signaling, CXCR4 Signaling, and GPCR Signaling.

In summary, we describe a novel approach to isolate and interrogate highly enriched human osteoblast populations without *in vitro* culture which should be broadly applicable to studying the pathogenesis of osteoporosis and other metabolic bone diseases.

***Disclosures: Koji Fujita**, None.*

SA0204

Microvesicles released from stromal/osteoblast facilitate ostoclast formation via RANK/RANKLOPG pathway. Lili Deng*[1], Ying Peng[1], Yu Wu[1], Yuedi Ding[1], Meilin Yang[1], Qiang Fu[2]. [1]Jiangsu Institute of Nuclear Medicine, China, [2]Institute of Nuclear Medicine, Peoples Republic of China

Microvesicles, including shedding microvesicles (100-1000nm) and exosomes (50-100nm), are membrane-bound vesicular particles that are released into the extracellular environment by almost all cell types. Microvesicles contain receptor proteins, proteolytic enzymes, miRNAs, and mRNAs, which are transferred into the target cell, in turn affect cell functions. Previous research had shown that osteocytes shed microvesicles containing bone regulatory proteins and this may represent a novel mechanism for cell-cell communication in bone. However, the detail mechanisms of microvesicles regulation in bone are not well defined. Here we demonstrated that UAMS32, the stormal/osteoblastic cell line, release microvesicles into the culture medium. Western blotting displayed that the cells with PTH treatment increase the level of RANKL, the essential cytokine for osteoclast formation, in microvesicles and decrease the level of OPG. Immune electron microscopic study revealed that the RANKL protein is located in the surface of microvesicles released from UAMS32 cells. To test the function of RANKL protein which existed in microvesicles, the microvesicles, which were collected from UAMS32 cells after treated with/without PTH for 12hrs, were co-cultured with Raw264.7 cells, the macrophage cell line that can differentiate to osteoclast after RANKL stimulation. TRAP staining has shown that osteoblast-derived microvesicles from PTH treated cells stimulate osteoclast formation, and this effect of microvesicles can be blocked by adding RANKL antibody or OPG to the culture medium. Our data demonstrated that microvesicles released from stromal/osteoblast regulate bone remodeling via RANK/RANKL/OPG pathway.

***Disclosures: Lili Deng**, None.*

SA0205

New therapeutic approach for the induction of bone formation by muramyl dipeptide. Ok-Jin Park*[1], Cheol-Heui Yun[2], Seung Hyun Han[1]. [1]School of Dentistry, Seoul National University, South Korea, [2]Department of Agricultural Biotechnology & Research Institute for Agriculture & Life Sciences, Seoul National University, South Korea

Microbiota and its molecular patterns are engaged in the regulation of immune responses and bone metabolism. Muramyl dipeptide (MDP) is the shared structural unit of peptidoglycans from both Gram-positive and Gram-negative bacteria. In the present study, we investigated the effect of MDP on the bone metabolism. When mouse osteoblast cell-line MC4 and primary osteoblasts derived from mouse calvaria were stimulated with MDP, there was a substantial increase in alkaline phosphatase (ALP) and alizaline red S staining. Moreover, MDP augmented the expression of bone sialoprotein and osteocalcin. Confocal microscopy and transient transfection followed by reporter gene assay demonstrated that MDP enhanced the nuclear translocation of Runx2 and its transcriptional activity, respectively, in MC4 cells. In addition, MDP increased the expression of nucleotide oligomerization domain 2 (NOD2), which is a MDP receptor. However, osteoblast differentiation and activation induced by MDP were not observed in the osteoblasts derived from NOD2-deficient mouse calvaria. MDP increased phosphorylation of MAP kinases (MAPK) and transcriptional activity of Runx2 and ALP staining were attenuated by inhibitors blocking MAPK. Mice intraperitoneally administrated with MDP showed an increase in the trabecular bone volume. Remarkably, not only pretreatment but also post-treatment in mice with MDP alleviated the bone loss induced by RANKL. Conclusively, these results suggest that MDP could increase the bone formation by enhancing osteoblast differentiation and activation through NOD2/MAPK/Runx2 signaling pathway and it could be potentially a new therapeutic against osteoporosis.

***Disclosures: Ok-Jin Park**, None.*

SA0206

Osteoblast GH actions promote bone mass and strength through mechanisms that are independent of local IGF-I production: Lessons from the SOCS2 knockout mouse. Ross Dobie*[1], Vicky MacRae[2], Carmen Huesa[2], Rob van't Hof[2], S. Faisal Ahmed[3], Colin Farquharson[4]. [1]Edinburgh University, United Kingdom, [2]University of Edinburgh, United Kingdom, [3]Royal Hospital for Sick Children, United Kingdom, [4]Roslin Institute, University of Edinburgh, United Kingdom

Suppressor of cytokine signalling (SOCS) -2 is an important regulator of the anabolic actions of growth hormone (GH) on bone. The SOCS2 knockout (KO) mouse has increased bone mass despite normal systemic insulin like growth factor -1 (IGF-1) and GH levels. In this study we have exploited this mouse model to unravel the anabolic mechanisms of GH on the skeleton.

In keeping with the known anabolic effects of GH, micro-CT analysis of juvenile (6 wks) and adult (17wks), male and female SOCS2 KO mice highlighted increased trabecular thickness and BV/TV compared to age and sex matched wild-type (WT) controls ($p<0.05$). Analysis of the tibial cortex revealed a sex specific difference with only male SOCS2 KO mice having increased cortical thickness (6wks, WT $246 \pm 7.96\mu m$, KO $281 \pm 11.1\mu m$; $p<0.05$; 17wks, WT $270 \pm 3.37\mu m$, KO $282 \pm 2.79\mu m$; $p<0.05$). Increased cortical parameters resulted in increased breaking strength ($p<0.05$) as determined by 3-point bending. Transcript analysis of liver samples revealed no alteration in *Igf1* levels in SOCS2 KO mice although a modest 2.21-fold increase in *Igfbp3* levels in 6wk male SOCS2 KO mice was noted ($p<0.05$). The increased bone mass of SOCS2 KO mice was not associated with increased *Igf1* or *Igfbp3* transcript levels in bone supporting a local, IGF-1 independent, mechanism for bone growth. *In vitro* mechanistic studies revealed that in WT osteoblasts, GH induced a 7.09-fold increase in *Socs2* expression levels ($p<0.001$) (but not *Socs1* or *Socs3*). This was verified at the protein level. GH also promoted enhanced STATs 1, 3 and 5 phosphorylation in SOCS2 KO calvarial osteoblasts in comparison to WT cells. This was confirmed by immunocytochemistry which revealed increased STAT5 activation within the nucleus of cultured osteoblasts. Conversely, overexpression of SOCS2 in MC3T3 osteoblast-like cells resulted in decreased STAT 5 activation following GH challenge. Furthermore, no regulatory role for SOCS2 in GH induced Akt or ERK1/2 signalling was found. As expected, GH mediated increased STAT signalling in SOCS2 KO cells resulted in elevated *Igf1* mRNA expression (1.60 fold; $P<0.05$), however the magnitude of increase was similar to that noted in WT cells (1.43 fold; $p<0.05$).

These data corroborate our in vivo observations and emphasise the critical role for SOCS2 in controlling GH anabolic bone effects. They also confirm the functional contribution to bone mass of osteoblast GH actions that are independent of local IGF-I production.

***Disclosures: Ross Dobie**, None.*
This study received funding from: IPSEN

SA0207

Osteoblastic and T Cell-derived RANKL in Bone Remodeling and Modeling. Toshio Fumoto[1], Sunao Takeshita[1], Masako Ito[2], Kyoji Ikeda*[1]. [1]National Center for Geriatrics & Gerontology, Japan, [2]Nagasaki University Hospital, Japan

RANKL is a pleiotropic cytokine and is essential for osteoclast development in bone; however, the key cellular source(s) of RANKL that generates osteoclasts under various pathophysiologic conditions remains elusive. In the present study we show that inactivation of the RANKL gene in osteoblast lineage cells (ΔOb) using osterix-cre results in typical osteopetrosis in the trabecular compartment of tibia, while the phenotype is progressively less marked in femur and vertebra in this order. In contrast to the trabecular bone, the femoral cortex of ΔOb mice was thin with suppressed bone formation in modeling process. Deletion of RANKL form T cells (ΔT) using CD4-cre resulted in a modest but significant increase in tibial trabecular bone. ΔOb, but not ΔT, mice were protected from bone loss caused by ovariectomy and partially from joint destruction associated with serum-induced arthritis. Finally, inducible deletion of RANKL preferentially in osteoblasts, with doxycycline discontinuation for 6 weeks starting at 6 weeks of age, resulted in an increased bone mass with reduced bone resorption and formation, suggesting that in addition to osteocyte-derived RANKL, RANKL produced by osteoblasts also contributes to osteoclast development in vivo.

***Disclosures: Kyoji Ikeda**, None.*

SA0208

Osteogenic Differentation and Mineralization of Adult Mesenchymal Stem Cells Isolated from Human Periodontal Ligament. Cecilia Romagnoli*[1], Niccolò Nuti[1], Roberto Zonefrati[1], Francesco Saverio Martelli[2], Marialaura Martelli[2], Elena Fanti[2], Marco Duvina[1], Paolo Tonelli[1], Luisella Cianferotti[3], Annalisa Tanini[1], Maria Luisa Brandi[1]. [1]University of Florence, Italy, [2]I.R.F. in Microdentistry, Italy, [3]University of Florence, Florence, Italy, Italy

Periodontal ligament (PDL) is a dynamic connective tissue embedded between the cementum and the alveolar bone. The role of PDL is to anchor and support the tooth root within the jaw, cushioning mechanical load that precede from mastication. Periodontal diseases are the major cause of tooth loss in adults leading to the destruction of periodontal tissues, including PDL, cementum and bone. Since mesenchymal stem cells have been isolated from PDL, this might be an ideal cell source for repairing bone defects and they are supposed to have a greatpotential in regenerative dentistry.

The aim of the present study was to isolate mesenchymal stem cells from PDL (PDLSCs) and to evaluate their osteogenic potential analyzing the expression of markers of osteoblast differentiation such as alkaline phosphatase (ALP) activity and the mineralization process.

Two primary culture of PDLSCs, LP8 and LP9, obtained from the extracted healthy third molar of patients of eighteen and twenty years old, respectively, were induced into the adipocyte lineage phenotype using the adipogenic medium (AM) composed by Ham's F12 Coon's modification medium supplemented with 10% FBS, 1 μM dexamethasone, 1 μM bovine insulin, 0.5 mM isobutylmethylxanthine and 1% antibiotics. The osteoblastic phenotype was induced using the osteogenic medium (OM) composed by Ham's F12 Coon's modification medium supplemented with 10% FBS, 10nM dexamethasone, 10mM β-glycerophosphate, 50 μg/ml L-ascorbic acid 2-phosphate and 1% antibiotics. Adipogenic and osteogenic phenotypes were assessed from 4 to 21 days in culture by appropriate cytochemical staining (Oil Red O and Fast Blue BB/naphthol AS-MX) and microscopic observations. The ALP activity and hydroxyapatite production were quantified by fluorometric assay.

Under adipogenic differentiation, accumulations of intracellular lipid-filled droplets after 21 days were observed in more than 5% of cells. Under osteogenic induction, significant increments (+86%) of ALP activity at 7 days vs not inducted control ($p<0.005$) were observed, and then ALP decreases, while mineralization increases at 14 and 21 days (+74% and +814% respectively), as demonstrated by a great deposition of hydroxyapatite vs not inducted control ($p<0.005$).

Our preliminary data suggest that PDL represents an optimal source of stem cells that can be used for bone tissue regeneration in dentistry. Studies are in progress to evaluate the effect of bioactive factors that could facilitate the process.

***Disclosures: Cecilia Romagnoli**, None.*
This study received funding from: Les Laboratoires Servier, France

SA0209

Repair of Nonunion with Percutaneous Autogenous Iliac Crest Bone Marrow Aspirate; Demineralised Bone Matrix and Bone Morphogenic Protein. Pingal Desai*, Joseph Lane, Parth Vyas. Hospital for special surgery, USA

Background: Bone is the second most common transplanted tissue after blood.[1] Bone marrow aspirated from iliac crest after concentration is more useful for healing of nonunion and concentrated cells increase the callus formation and reduce time to healing of nonunion.[2,3]Bone marrow aspirate contains osteoprogenitor cells which under the influence of bone inducing growth factors can differentiate into

osteoblasts.[4,5] The study evaluated the addition of bone marrow concentrate with BMP vs. demineralized bone matrix in nonunions and atypical femoral fractures.

Materials and methods: We did prospective age and sex matched study of concentrated autologous iliac crest bone marrow stem cells with DBM or BMPin nonunion and AFF pts. Gap in the fracture was measured with pre-operative radiograph. We hypothesized that Modified Hernigou technique is useful for the healing of fracture, useful in bones other than tibia, effective when the gap in fracture is more than 5 mm and useful in atypical fractures, and that DBM and BMP are comparable.

Results: We had total 49 patients enrolled in our study. All the patients were available for final follow up. The overall healing of fracture in our group was 79.6%. Average healing time in our study was 5.4 months.Rate of healing for fracture nonunion for femur was 73.6%, tibia was 86.9% and humerus was 71.4%. (p=0.481). The healing rate was 93% when intervention was done within 6 months while healing rate was 57.9% when intervention was done after 6 months. (p=0.008). The rate of healing in atypical fracture was 63.6% while in other fracture was 84.2% (p=0.201). The rate of healing was 80.7% when gap was less than 5 mm and 78.3% when gap was more than 5mm. (p=0.828).There was also no statistically significant difference in the rate of healing related to open fracture, communition of fracture, fixation procedure used and use of adjuvants.

Conclusion: Our modified Hernigou technique is minimally invasive procedure for treatment of fracture nonunion regardless of gap size or bone involved. The rate of healing is higher when this technique is performed within 6 months of injury. DBM is equally effective as BMP when used with concentrated autogenous iliac crest stem cells. The union rate was same for atypical fracture compared to other fractures.

Bibliography

1. Desai BM (2007)
2. Hernigou P (2005)
3. HernigouP (2006)
4. Kanakaris NK (2007)
5. Patterson TE (2008)

Table 1

Healed vs nonhealed groups

	Healed	% or SD	Non Healed	% or SD	P value
BMI	39	79.2%	10	20.8%	0.045
<25	21	90.9%	2	9.1%	
25-30	13	76.5%	4	23.5%	
30-35	3	42.9%	4	57.1%	
≥35	2	100.0%	0	0.0%	
Fracture location					0.481
Femur	14	73.7%	5	26.3%	
Tibia	20	87.0%	3	13.0%	
Humerus	5	71.4%	2	28.6%	
Atypical fracture	7	63.6%	4	36.4%	0.2
Other fracture	32	84.2%	6	15.8%	
Open vs closed fracture					0.673
Open fracture	8	72.7%	3	27.3%	
Closed fracture	31	81.6%	7	18.4%	
Communited fracture	10	76.9%	3	23.1%	
Fixation procedure					0.710
Open reduction and internal fixation	16	76.2%	5	23.8%	
Intramedullary nail	21	80.8%	5	19.2%	
Conservative	2	100%	0	0%	
Early vs late intervention					0.008
Early intervention	27	93.1%	2	6.9%	
Late intervention	11	57.9%	8	42.1%	
Atrophic/Hypertrophic nonunion					0.702
Atrophic	27	77.1%	8	22.9%	
Hypertrophic	12	85.7%	2	14.3%	
Gap					0.711
<5mm	21	80.8	5	19.2%	
≥5mm	18	78.3%	5	21.7%	
Adjuvants					0.283
DBM	19	86.4%	3	13.6%	
BMP	17	70.8%	7	29.2%	
Both DBM + BMP	3	100%	0	0%	

BMI-body mass index
DBM-demineralised bone matrix,
BMP-Bone morphogenic protein -2

Table 1

Table 2
BMP vs DBM cohorts

Variables	Total patients N=49	BMP group N=24	DBM group N=27
Age in years	53.9 (19-93)	53.8(19-84)	54.9(27-3)
Sex (% males)	67.3%	70.8%	66.2%
Early treatment (less than 6 months)	60.4%	52.2%	68.2%
Late treatment (after 6 months)	39.6%	47.8%	31.8%
Fracture characteristics			
Femur:tibia:humerus	19:23:7	12:11:1	8:11:5
Fracture gap (mm)	5.2(1-20)	5(1-16)	5.7(1-20)
Fracture gap ≥5mm	46.9%	41.7%	54.5%
Atrophic nonunion (%)	71.4%	54.2%	86.4%
Atypical fractures	22.4%	33.3%	13.6%
Fracture healing			
Rate	79.6%	70.8%	86.4%
Time (months)	4.7(2-12)	4.8(2-12)	4.5(2-12)
Healingin fracture gap ≥5mm	78.3%	80%	67%

P < 0.05 only in Atrophic nonunion(%) group
There was no statistical difference between variables in between BMP group and DBM group

Table 2

Table 3
Atypical vs other fractures

Variables	Atypical fracture	Other fracture	P value
Number	11	39	
Healed	7 (63.6%)	32(84.2%)	0.201
Not healed	4(36.4%)	7(17.9%)	
Time to healing in months	5.714±4.4	5.3±42.9	0.738
Early intervention (within 6 months)	45.5%	64.9%	0.248
Late intervention (after 6 months)	54.5%	35.1%	

Early intervention – within 6 months of original surgery
Late intervention – after 6 months of original surgery

Table 3

***Disclosures: Pingal Desai**, None.*

SA0210

See Friday Plenary Number FR0210.

SA0211

TRAPPC9 modulates osteoblast proliferation and differentiation through NIK – IKK signaling. Thomas Mbimba*[1], Kabrina Monton[2], Kevin Crowford[3], Roshanak Razmpour[3], Samir Abdelmagid[4], Safadi Fayez[5]. [1]Kent State University, USA, [2]Central State University, USA, [3]Temple University, USA, [4]Northeast Ohio Medical University, USA, [5]NEOMED, Temple University, USA

Intellectual disability (ID) is a serious disorder of the central nervous system with a prevalence of 1-3% in the general population. Recent studies identified different nonsense mutations in the trafficking protein particle complex (TRAPPC9) gene in consanguineous and non-consanguineous families of ID patients. Patients with ID also present skeletal abnormalities such as short stature, misaligned limbs and loose teeth. TRAPPC9 is one of the largest subunits of the transport protein particle II (TTRAPPII), an important membrane tethering complex for coated vesicles during intra-Golgi and early endosome to late Golgi traffic. TRAPPC9 also binds and regulates NIK and IKK signaling upstream of NF-κB, thus regulating both the canonical and non-canonical NF-κB pathways. Recent studies have identified NFkB as a major negative regulator of osteoblast proliferation and differentiation. We first examined the expression and localization of TRAPPC9 in bone. qPCR, Western blot and immunohistochemical analyses showed that TRAPPC9 is expressed in bone and the expression levels increase during osteoblast differentiation and matrix mineralization. Co-immunoprecipitation studies confirmed binding of TRAPPC9 to both NIK and IKKβ in osteoblasts. To study the role of TRAPPC9 in osteoblast differentiation and function, we performed a loss-of-function experiment using TRAPPC9 specific shRNA in MC3T3-E1 osteoblast-like cell line. TRAPPC9 shRNA-transfected cells showed decreased NIK, IKKβ and NF-κB activation, while osteoblast proliferation was increased compared to controls. Osteoblast differentiation, determined by alkaline phosphatase (ALP) staining and activity, as well as matrix mineralization, determined by Von Kossa staining revealed increased osteoblast differentiation and function in TRAPPC9 shRNA-transfected cells. qPCR analysis showed increased expression of osteoblast differentiation markers (ALP, Runx2, collagen type I, and osteocalcin) in TRAPPC9 shRNA-transfected cells. Taken together, these data suggest that TRAPPC9 is a major regulator of osteoblast proliferation, differentiation and function. These data might explain, at least in part, the increased bone mass in patients with TRAPPC9 mutations. In addition, regulation of TRAPPC9 may help to promote bone formation for the treatment of osteoporosis and other metabolic bone diseases.

***Disclosures: Thomas Mbimba**, None.*

SA0212

Aminobisphosphonates promote osteoblastic differentiation and function in association with upregulation of Cx43 in vitro. Dong Jin Chung*, Jin Ook Chung, Dong Hyeok Cho, Min Young Chung. Chonnam National University Medical School, South Korea

Aminobisphosphonates are potent antiresorptive drugs which have antifracture efficacy by reducing bone turnover rate and increasing bone mineral density. In addition to inhibiting osteoclast function, bisphosphonates have been reported to also promote survival of osteocyte and osteoblast via an anti-apoptotic effect, mediated by opening of hemi-gap junction channels formed by connexin43 (Cx43). In this study, we investigated the effect of various aminobisphosphonates such as risedronate,

alendronate, ibandronate, and zoledronate on osteoblast differentiation and Cx43 expression using the cell line C2C12. All the aminobisphosphonates increased the activity of OSE, OC and BSP-luciferase in a dose-dependent manner. They also increased ALP activity dose-dependently, and further induced enhanced alkaline phosphatase (ALP) staining in the presence of BMP-2 (5 ng/mL), indicating positive action on osteoblast differentiation. Connexin 43 promoter activity was upregulated by co-transfection of increasing concentrations of a Runx2-expressing construct. A similar effect was obtained with an Osterix and Dlx5 constructs. All the aminobisphosphonates also increased Cx43 promoter activity. As the concentration of aminobisphosphonates was increased, Cx43-promoter activity was increased by 2.5~3 fold. Furthermore, the combination of Runx2 (0.5 μg) and each aminobisphosphonate up-regulated Cx43 promoter activity to a far larger extent than did either Runx2 or each aminobisphosphonate alone, suggesting an interaction between the aminobisphosphonate and Runx2 in activating the Cx43 promoter. A similar interaction was observed between Dlx5 (0.5 μg) and each aminobisphosphonate. Western blot analysis confirmed that each aminobisphosphonate increased protein expression of Cx43, Runx2, Osterix, and Dlx5. The effective concentrations and peak responses were somewhat different among aminobisphosphonates. These results suggest that aminobisphosphonates promote osteoblastic differentiation and positively regulates Cx43 gene transcription.

***Disclosures: Dong Jin Chung**, None.*

SA0213

Epigenetic Plasticity of MSC Trans-Differentiation and Selective Distal Enhancers for Mmp13. Mark Meyer*[1], Nancy Benkusky[1], Amber Mael[1], Janet Rubin[2], J. Pike[1]. [1]University of Wisconsin-Madison, USA, [2]University of North Carolina, Chapel Hill, School of Medicine, USA

Marrow derived multipotential mesenchymal stem cells (mdMSC) have the ability to become different cell types given the appropriate chemical stimulus *in vitro*. However, trans-differentiation of the osteoblast to the adipocyte can occur even 7 days post differentiation, after substantial matrix deposition. Conversely, differentiated adipocytes (7 days) will trans-differentiate to mineralize matrix and express osteogenic genes/proteins in osteogenic media. In our studies, we demonstrate plasticity in the epigenetics of the mdMSC through ChIP-seq investigation of chromatin modifying marks H3K4me1, H3K4me2, H3K4me3, H3K9Ac, H4K5Ac, H3K36me3 and H4K20me1. Dynamic and local chromatin modifications allow trans-differentiation to occur in these cells without permanent global changes. We found the epigenetic marks are accurate in predicting gene expression by RNA-seq and identifying unique enhancers for transcription factors important to differentiation such as C/EBPβ, C/EBPα, PPARγ, RUNX2, SP7, CREB, RXR and VDR. We identified adipogenic specific enhancers unique for C/EBPα and C/EBPβ near the mouse *Pparγ* gene at +64 and +150kb. More interestingly, we found unique osteogenic enhancers within the genomic loci of many osteogenic genes, such as the mouse *Mmp13* gene. Matrix Metalloproteinase 13 (*Mmp13*, collagenase-3) has an essential role in the developing osteoblast that leads to improved bone quality and bone fracture resistance. It is known to be stimulated by compounds such as BMP-2, PTH and $1\alpha,25(OH)_2D_3$ and through transcription factors RUNX2, C/EBPβ, OSX, VDR and others. Through unbiased ChIP-seq methodology, we have discovered that there is transcriptional regulation in regions more distal to the *Mmp13* promoter. There is RUNX2 and C/EBPβ binding at -30kb upstream, C/EBPβ binding only at -20kb upstream and finally a VDR bound region at -10kb. These regions were accompanied by strong histone marks clearly denoting the enhancers. A pair of VDREs (approx. 450bp apart) that controls *Mmp13* gene expression by $1\alpha,25(OH)_2D_3$ is located at -10kb as assayed by traditional mutagenesis, large BAC luciferase reporters and even direct genome-editing using CRISPR, focused on the enhancers. Through these studies we learn that the epigenetic plasticity of mdMSC cells allows their differentiation and trans-differentiation from osteogenic and adipogenic lineages, and helps facilitate induction of many genes, including *Mmp13* stimulated by $1\alpha,25(OH)_2D_3$ from unique distal enhancers.

***Disclosures: Mark Meyer**, None.*

SA0214

Global Epigenetic Changes in Histone Post-translational Modifications Establish the Osteoblast Lineage. Jonathan Gordon*[1], Hai Wu[2], Troy Whitfield[3], Phillip Tai[4], Andre Van Wijnen[5], Janet Stein[1], Gary Stein[6], Jane Lian[2]. [1]University of Vermont, Department of Biochemistry, USA, [2]University of Vermont, USA, [3]University of Massachusetts Medical School, Department of Cellular & Developmental Biology, USA, [4]University of VermontCollege of MedicineDepartment of Biochemistry, USA, [5]Mayo Clinic, USA, [6]University of VermontCollege of Medicine, USA

Bone marrow stromal cells (BMSCs) undergo stochastic epigenetic changes initiating commitment to the osteoblast phenotype that define lineage-specific gene expression. To determine which histone modifications are indicative of osteoblast differentiation and gene expression, we generated high quality, multi-replicate data sets for histone methylations and acetylations that are markers for epigenetic regulation. These markers include H3K4me1, H3K4me3, H3K9me3, H3K9acetyl, H3K27me3, H3K27acetyl and H3K36me3). Using supervised pattern discovery models, these histone marks were segmented across the mouse genome in order to discover genomic segments associated with known and novel regulatory regions. These data sets were merged with gene expression profiles at defined stages of BMSC differentiation. These analyses have identified on a genome-wide basis have identified novel features of epigenetic regulation of differentially expressed genes. For example, we have discovered that the osteoblast-related osteocalcin (bglap2) gene locus (chr3:88181512-88182731) is not significantly associated with H3K4me3 signal, a marker generally linked to genes poised for expression. However, the bglap2 gene locus is initially enriched with H3K4me1 upon commitment and progressively accumulates H3K9acetyl and H3K27acetyl signals. This finding indicates that osteocalcin is 1) poised for expression by H3K4me1 and 2) strongly regulated by acetylation of histones within the gene body when the gene is actively expressed. These data provide a global map of epigenetic changes in genes that are classified into functional pathways during lineage commitment. The epigenetic signature generated by this study for normal events of the BMSC can be used as a platform to determine modifications in histone marks contributing to skeletal disorders.

***Disclosures: Jonathan Gordon**, None.*

SA0215

Lactoferrin activates Osx gene expression through the mitogen-activated protein kinase p38 pathway in osteoblasts. Chi Zhang*[1], Yang Li[2], Harry Kim[3]. [1]Bone Research Laboratory, Texas Scottish Rite Hospital, USA, [2]Texas Scottish Rite Hospital for Children, USA, [3]Scottish Rite Hospital for Children, USA

Lactoferrin (LF) is an iron-binding glycoprotein that belongs to the transferrin family of proteins. While diverse physiological functions have been proposed for LF, including the regulation of intestinal iron uptake, antimicrobial activity, regulation of cell growth and differentiation, anti-inflammatory activity, the precise mechanism of action of LF in many of these processes remains poorly known. LF found in human and bovine milk may have a place in osteopenia or osteoporosis remedies because it has been found to be effective in promoting bone growth. A study by Blais et al. showed that a dietary LF supplementation for 27 weeks to ovariectomized mice improved their bone mineral density. However, molecular mechanisms of LF activity on bone formation are not well understood. In this study, immunohistochemistry staining demonstrated LF expression in osteoblasts. We found that LF activated Osx expression in a dose-dependent manner and a time-dependent manner. LF also further activated expression of osteoblast marker BSP. Interestingly, a specific mitogen-activated protein kinase p38 inhibitor SP203580, but not JNK kinase inhibitor SP600125, abrogated LF activation of Osx gene expression. LF-induced increase in Osx protein level was in parallel with the phosphorylation of p38 in osteoblasts. To further investigate the effect of LF on osteoblasts in vivo, calvaria organ culture from newborn mice was performed. We showed that Osx expression level in calvaria organ increased after stimulation by LF. Taken together, we provide the first evidence to demonstrate that LF activates Osx expression through the mitogen-activated protein kinase p38 pathway in osteoblasts, suggesting a novel mechanisms by which LF promotes bone formation.

***Disclosures: Chi Zhang**, None.*

SA0216

Lysyl Oxidase is a BMP Target Gene Regulated by Smad4 and Runx2 in Osteoblasts. Valerie Salazar*[1], Gabriel Mbalaviele[2], Vicki Rosen[1], Roberto Civitelli[2]. [1]Harvard School of Dental Medicine, USA, [2]Washington University in St. Louis School of Medicine, USA

Collagen abnormalities can be an underlying cause of brittle bones and fractures in humans. Collagen biosynthesis is a complex process involving many collagen-modifying enzymes, and the signaling pathways that regulate collagen biosynthetic enzymes in the skeleton are still unknown. Whereas brittle bones and spontaneous fracture are not reported in mice with genetic manipulation of the TGF-β pathway, we previously reported these as key features in mice with genetic ablation of *BMP2* or *Smad4* in endochondral lineages of the skeleton, $Bmp2^{flox/flox}$*; Prx1-Cre* ($Bmp2^{Prx1\Delta/\Delta}$) and $Smad4^{flox/flox}$*; Osx1-Cre* ($Smad4^{Osx1\Delta/\Delta}$). We find that expression of lysyl oxidase (*Lox*), a key enzyme mediating covalent crosslinking of collagen fibrils, is reduced by >30% in $Bmp2^{Prx1\Delta/\Delta}$ and >75% in $Smad4^{Osx1\Delta/\Delta}$ bones relative to littermate controls, while mature osteoblast markers, including *Col1α1*, are expressed normally. Accordingly, picrosirius red staining and polarized light microscopy of $Bmp2^{Prx1\Delta/\Delta}$ and $Smad4^{Osx1\Delta/\Delta}$ long bones reveal reduced lamellar organization and diminished birefringence of cortical collagen. In MC3T3 cells, *Lox* mRNA is upregulated by BMP2 but not TGF-β. Upregulation of *Lox* is enhanced by Jnk inhibition, which boosts Smad-dependent transcriptional activity; and it is blocked by PI3K inhibition, *Akt* siRNA, or *Smad4* siRNA, all of which effectively prevent Smad-dependent transcriptional responses to BMP2. Interestingly however, upregulation of *Lox* is also abrogated by inhibition of p38, but this is not associated with decreased Smad-dependent transcriptional activity. These results suggest that a BMP2-responsive, p38-dependent transcription factor cooperates with Smad4 to regulate *Lox*. Indeed, ChIP analysis reveals that both Smad4 and Runx2 are recruited to the *Lox* promoter in response to BMP2; and recruitment of Runx2, but not Smad4, is fully dependent on p38. Consistently, BMP2-dependent induction of *Lox* is reduced >80% by *Runx2* siRNA and

>90% by *Runx2* siRNA plus p38 inhibition. In summary, we identify the collagen–crosslinking enzyme, *Lox*, as a novel BMP2 target gene in osteoblasts, providing initial evidence of cooperative interactions between BMP/Smad4 and p38/Runx2 signaling in regulation of *Lox* expression, and therefore in skeletal collagen processing.

***Disclosures: Valerie Salazar**, None.*

SA0217

MicroRNA-99a is a Novel Regulator of KDM6B-Mediated Osteogenic Differentiation. Yin Tang*, Lan Zhang, Qianqian Han, Dana Murray, Qisheng Tu, Jake Jinkun Chen. Tufts University School of Dental Medicine, USA

Currently little is known about the epigenetic regulation of the commitment of multipotent progenitor cells to bone tissue. One of the central epigenetic chromatin modifications is histone lysine methylation. It has been identified that histone demethylase KDM6B plays an important role in promoting osteogenic differentiation of bone marrow stem cells (BMSCs). In this study, we found that miR-99a is potentially involved in regulating the KDM6B protein level during osteogenic differentiation.

First, we selected two well-studied osteoblast cell lines, MC3T3-E1 osteoblast-like cells and MLO-A5 preosteocyte-like cells, representing two key developmental stages of the osteoblast for miRNA profiling. Both cells exhibit unique miRNA expression profiles after osteogenic induction. Statistically significant differences in the expression of 38 miRNAs between MLO-A5 and MC3T3-E1 cells also were observed. miR-99a was selected for further investigation, as its expression changed most dramatically among these 38 miRNAs, and it was significantly downregulated in MLO-A5 cells. miRNA target prediction was carried out using a combination of the following computational algorithms: targetscan, Sloan-Kettering Cancer Center Human MicroRNA Targets Data-base, and miRBase Targets. KDM6B is predicted to be a potential target of miR-99a during ostegenic differentiation.

Microarray results validated by real-time RT-PCR analysis showed that miR-99a was significantly down regulated in preosteoblast MC3T3-E1 cells compared to multipotent C3H10T-1/2 cells, and was further down regulated in preosteocyte MLO-A5 cells.

KDM6B mRNA levels decreased significantly in MC3T3-E1 cells compared to C3H10T-1/2 cells, and was further down regulated in MLO-A5 cells. However, western blot analysis revealed that KDM6B protein increased more than 2-fold in MC3T3-E1 cells compared to C3H10T-1/2 cells. We also performed experiments using primary BMSCs and similar results were obtained.These studies indicate that there is post-transcriptional regulation of KDM6B protein levels during osteogenic differentiation, and miR-99a may be involved in this regulation. Currently, we are performing luciferase assays and gain- and loss-of-function analyses to further determine the specific function of miR-99a in control of KDM6B expression in a cell- and stage-specific manner.

***Disclosures: Yin Tang**, None.*

SA0218

Oxygen-Dependent Mineralization Differences with High Intrinsic Aerobic Capacity are Associated with Osteoblast Extracellular Matrix Gene Expression. Jacqueline Cole*[1], Kristin Graf[1], Parth Patel[1], Lauren Koch[1], Steven Britton[1], Andrea Alford[1], Ronald Zernicke[1], Kenneth Kozloff[2]. [1]University of Michigan, USA, [2]University of Michigan Department of Orthopaedic Surgery, USA

Dysfunctional aerobic metabolism is associated with various age-related diseases, including cardiac arrhythmias and metabolic syndrome. We hypothesize that variation in the capacity for oxygen metabolism is a driving factor in complex disease development and that this mechanism is important for bone health. Our objective was to examine the role of aerobic capacity in the response of osteoblast lineage cells to varying oxygen tension. Female rats selected for high (HCR) and low (LCR) aerobic capacity were age- and body mass-matched (10 wk; 173 g). Aerobic capacity was 8-fold greater in HCR than LCR, measured by a run to exhaustion. For *in vitro* analyses (n=3 per group), marrow stromal cells were harvested from femora/tibiae and differentiated at 1% or 20% oxygen for 14 days using osteogenic medium. Gene expression was assessed with real-time PCR arrays. Cycle threshold data were normalized and compared across line (HCR, LCR) and oxygen level. For *in vivo* bone formation (n=15 per group), calcein and alizarin were injected at 10 and 3 days before sacrifice, respectively. Femora were fixed, embedded in PMMA, and sectioned at the mid-diaphysis and distal metaphysis for dynamic histomorphometry.

In general, differences emerged for genes regulating the osteoblast extracellular matrix (ECM). Regardless of oxygen tension, aerobic capacity affected gene expression. Compared with LCR, HCR showed a time-dependent reduction in *Col1a1* (ECM formation), *Ibsp* (ECM maturation), and *Dmp1* (ECM mineralization) (Fig. 1). Oxygen tension also impacted gene expression; cells cultured at 1% oxygen had decreased *Col1a1*, *Ibsp*, and *Dmp1* and increased *Sost* (Wnt antagonist) (Fig. 2).

At the femoral mid-diaphysis, endosteal bone formation rate and mineral apposition rate did not differ between HCR and LCR, although bone surface was 5-10% lower in HCR (Fig. 3). Analysis of dynamic cancellous bone formation is ongoing.Rats genetically divergent for aerobic capacity exhibit different osteoblast phenotypes. We previously reported that HCR mineralize less per cell than LCR, perhaps explained by the differences in ECM gene expression seen here. HCR consistently have greater tissue mineral density, likely due to greater osteoblast number. Oxygen-dependent differences in osteoblast number suggest cellular differences in oxygen utilization and metabolism, which may drive ECM regulation. Oxygen availability is important for osteoblast function, particularly in rats with high aerobic capacity.

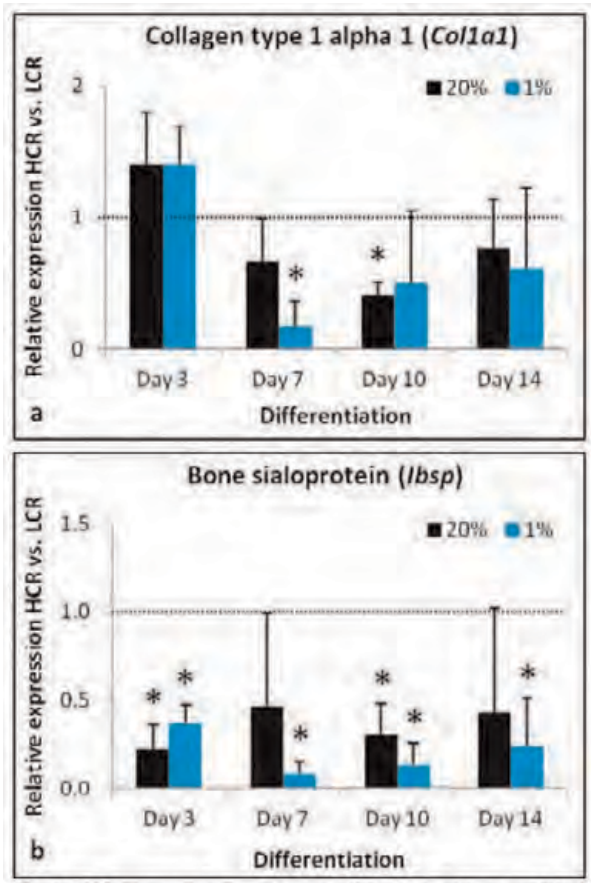

Fig. 1. HCR expressed lower levels of *Col1a1* at days 7-10 (a) and *Ibsp* at all times (b). *p<0.05 HCR vs. LCR

Fig. 1

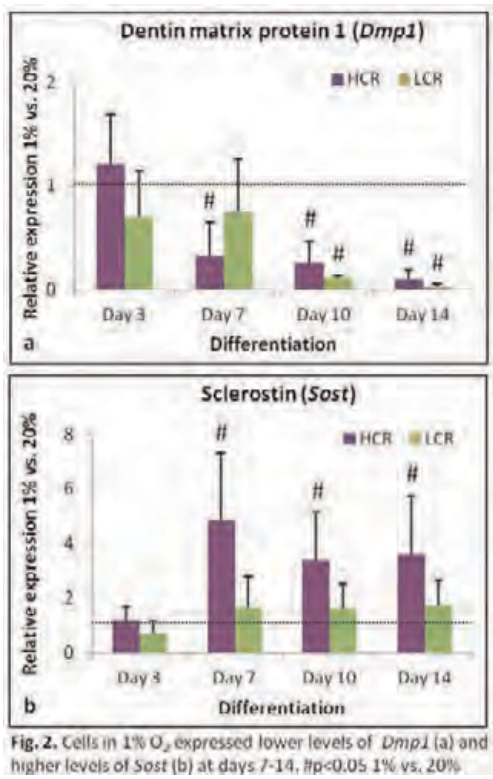

Fig. 2. Cells in 1% O_2 expressed lower levels of *Dmp1* (a) and higher levels of *Sost* (b) at days 7-14. #p<0.05 1% vs. 20%

Fig. 2

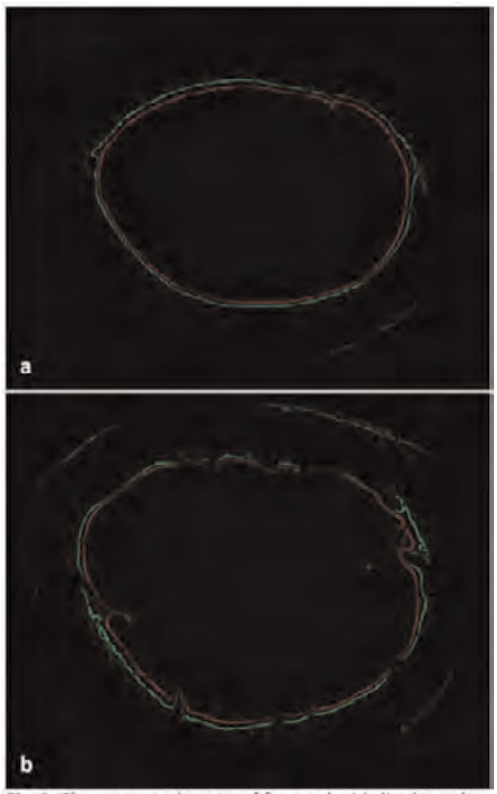

Fig. 3. Fluorescence images of femoral mid-diaphyseal sections for HCR (a) and LCR (b).

Fig. 3

***Disclosures: Jacqueline Cole**, None.*

SA0219

P2X7 Nucleotide Receptor Signaling Potentiates the Wnt/β-catenin Pathway in Osteoblasts: Implications for Mechanotransduction in Bone. Matthew Grol*, Patricia Brooks, Alexey Pereverzev, Stephen Sims, S. Jeffrey Dixon. The University of Western Ontario, Canada

Nucleotides are released from cells in response to mechanical stimuli and signal through cell-surface P2 receptors. The P2X7 and Wnt/β-catenin pathways regulate osteoblast differentiation and are critical for anabolic responses of bone to mechanical loading. However, whether these pathways interact to control bone formation is unknown. The purpose of this study was to investigate effects of P2X7 activation on Wnt/β-catenin signaling in osteoblasts. We first determined whether P2X7 couples to inhibition of GSK3β, a negative regulator of Wnt/β-catenin signaling. The phosphorylation status of GSK3β in MC3T3-E1 cells was assessed by immunoblot analysis. The P2X7 receptor agonist BzATP significantly increased inhibitory phosphorylation of GSK3β, an effect that was blocked by the P2X7 antagonist A 438079. We next monitored β-catenin nuclear localization using immunofluorescence and confocal microscopy. Canonical Wnt3a elicited a gradual increase in β-catenin nuclear localization that peaked at 3 h and slowly returned to baseline by 24 h. In contrast, BzATP caused transient nuclear localization only at 0.5 h post-treatment. Notably, Wnt3a and BzATP together elicited dramatically sustained β-catenin nuclear localization compared to Wnt3a alone. To monitor changes in β-catenin transcriptional activity, cells were transfected with a β-catenin luciferase reporter. In MC3T3-E1 cells, BzATP alone did not increase β-catenin transcriptional activity. On the other hand, Wnt3a induced a dramatic increase in β-catenin transcriptional activity that was potentiated by treatment with BzATP. Consistent with involvement of the P2X7 receptor, a high ATP concentration (1 mM, which activates many P2 receptors including P2X7) potentiated β-catenin transcriptional activity elicited by Wnt3a, whereas low concentrations of ATP, ADP or UTP (10 μM, which activate P2 receptors other than P2X7) failed to elicit a response. Moreover, BzATP-induced potentiation of Wnt3a-induced β-catenin transcriptional activity was blocked by A 438079. Finally, responses to Wnt3a in calvarial cells from *P2rx7* knockout mice were significantly less than in cells from wildtype controls. Taken together, we demonstrate for the first time that P2X7 activation prolongs and potentiates β-catenin transcriptional activity elicited by canonical Wnt signaling. Thus, crosstalk between the P2X7 and Wnt/β-catenin pathways may modulate osteoblast activity in response to mechanically-induced ATP release in bone.

***Disclosures: Matthew Grol**, None.*

SA0220

Prx-1 Coverts MAPK Regulation of Osterix Transcription from Stimulation to Inhibition. Linda Gilbert[1], Mark Nanes*[2]. [1]VA Medical Center, USA, [2]VA Medical Center & Emory University, USA

The homeobox-like protein Prx-1 (MHox, Prrx-1) is a required inducer of the limb bud during embryogenesis, normally silenced at E10. We previously showed that Prx-1 is reactivated in adult tissues by the inflammatory cytokine TNF. TNF inhibition of Osx and osteoblast differentiation is abrogated by silencing Prx-1 using shRNA and also by inhibitors of MAPK including DN-MKK1, DN-ERK1, and PD 98059, suggesting possible interaction of Prx-1 and MAPK in the regulation of Osx transcription (Lu et al J Biol Chem 281:6297 2006, Lu et al J Bone Min Res 26:209 2011). To determine how Prx-1 and MAPK regulate Osx, we used a -1269/+91 murine Osx reporter in C3H10T1/2 mesenchymal cells and tested the effects of constitutive activation of Prx-1 and/or MAPK. Surprisingly, constitutive expression of Prx-1b or activation of MAPK (CA-Prx1b or CA-MKK1) alone dose dependently stimulated, rather than inhibited, transcription of Osx. Co-expression of both CA-Prx1b and CA-MKK1 reestablished the inhibitory effect on Osx transcription in a Prx-1 dose-dependent manner. Prx-1 binds the Osx promoter at a unique TNF inhibitory response element (-512/-496) and also upstream at a homologous homeobox (HBox) consensus sequence that is contiguous with a RUNX2 binding site (-720/-705). Deletion constructs that included or excluded the TNF/Prx or HBox/Prx sites were used to localize the independent vs. interactive effects of the two stimuli. Prx-1 and MAPK stimulation of Osx transcription were mediated by upstream regions of the promoter independent of the downstream TNF or HBox binding sites, but the combined Prx-1/MAPK inhibitory effect was a function of the more proximal promoter regulatory regions containing the inhibitory TNF/Prx response element, though some combinatorial inhibitory effect was still observed upstream. CA-Prx1b and CA-MKK1 mediated independent inhibitory actions when the upstream promoter was deleted (-665/+91 or -770/+91). Our results suggest that Prx-1 converts the stimulatory effect of MAPK on Osx expression and osteoblast differentiation to an inhibitory one. This may explain the discrepancy between reports showing an overall stimulatory effect of MAPK on osteoblast differentiation with studies showing that TNF inhibition of osteoblast differentiation is mediated by MAPK. Inflammation stimulated Prx-1 may have a role in the inhibition of osteoblast differentiation.

***Disclosures: Mark Nanes**, None.*

SA0221

Role of Sirtuin 1 in the Function of PTH in Osteoblasts. Yurong Fei*, Emi Shimizu, Teruyo Nakatani, Nicola Partridge. New York University College of Dentistry, USA

Sirtuin 1 (Sirt1), an NAD-dependent deacetylase, participates in a variety of human diseases. The function of Sirt1 in bone is not well defined. More than 40 million Americans are threatened by osteoporosis. Currently, the only anabolic agent for treating osteoporosis in the US is parathyroid hormone (PTH). One downstream target of PTH in bone is collagenase 3 (MMP13). PTH significantly induces expression of MMP13 in bone. Collagenases are required for bone resorption stimulated by PTH *and* MMP13 is required for endochondral bone formation. The goal of this study is to determine the role of Sirt1 in the action of PTH in osteoblasts. Osteoblastic UMR 106-01 cells and Sirt1 knockout mice were utilized. Gene expression was analyzed by qPCR, protein interaction by immunoprecipitation, protein-DNA interaction by the chromatin immunoprecipitation assay, and promoter activity by luciferase assay. We observed that *Mmp13* mRNA expression in bone from Sirt1 knockout mice was increased significantly (five fold stimulation) compared to wild type mice. The Sirt1 activator, resveratrol, profoundly blocked *Mmp13* mRNA expression induced by PTH in UMR 106-01 cells. In contrast, the Sirt1 inhibitor, EX527, significantly enhanced *Mmp13* mRNA expression induced by PTH. Additionally, PTH after two hours of treatment enhanced Sirt1 binding to JUN, a component of the transcription factor complex, activator protein 1 (AP-1), but not to FOS. Furthermore, PTH treatment for two hours promoted Sirt1 binding to the AP-1 sites of the *Mmp13* promoter and this binding was further increased by resveratrol, implicating Sirt1 as a feedback inhibitor regulating *Mmp13* transcription. The AP-1 site of the *Mmp13* promoter is required for PTH stimulation of *Mmp13* transcription activity. When the AP-1 site was mutated, resveratrol was unable to inhibit PTH stimulated *Mmp13* promoter activity, indicating a role for the AP-1 site in Sirt1 inhibition. These data indicate that Sirt1 is a negative regulator of MMP13, Sirt1 activation inhibits PTH stimulation of *Mmp13* and this regulation is mediated by Sirt1 binding to AP-1.

***Disclosures: Yurong Fei**, None.*

SA0222

Stepwise Differentiation of Pluripotent Stem Cells into Osteoblasts with Four Small Molecules under a Serum-free Condition. Kosuke Kanke*[1], Taku Saito[2], Hironori Hojo[3], Alexander Lichtler[4], Ung-Il Chung[5], Shinsuke Ohba[1]. [1]The University of Tokyo, Japan, [2]University of Tokyo, Graduate School of Medicine, Japan, [3]The Center for Disease Biology & Integrative Medicine, USA, [4]University of Connecticut Health Center, USA, [5]University of Tokyo Schools of Engineering & Medicine, Japan

The limited number of specific cell populations obtained from animals hampers the study of protein interactions, transcriptional networks, and epigenetics in osteoblast development. Embryonic stem cell (ESC)-based osteogenic differentiation may be an attractive model for such studies, given its pluripotency and capacity for self-renewal. Here, we developed an efficient, mass-producible, and reproducible culture protocol directing mouse ESCs (mESCs) toward osteoblasts under a serum-free condition, then applying the protocol to human induced pluripotent stem cells (h-iPSCs). The protocol is composed of four phases: mESC maintenance in serum-free 2i culture (Nature 453:519, 2008), mesoderm induction (5 days), osteogenic induction (14 days), and maturation of osteoblasts (4 days). Mesoderm induction was achieved in serum-free media by inhibiting neural differentiation with the Hh signaling inhibitor cyclopamine and by inducing mesoderm differentiation with the GSK-3 inhibitor CHIR99021. Cells were then cultured with the Hh signaling activator SAG and the helioxanthin-derivative TH (Biochem Biophys Res Commun 357:854, 2007) in serum-free osteogenic media for 14 days; the cells spontaneously differentiated into mature osteoblasts without any inducers in the next maturation phase. Mesoderm markers, *T* and *Mixl1*, were transiently up-regulated by the mesoderm induction. Subsequent osteogenic induction induced GFP expression in mESCs engineered to express GFP under the control of a rat 2.3-kb *Col1a1* promoter (Col1a1-GFP). Consistent with this, osteoblast-related genes including *Runx2*, *Sp7*, *Col1a1*, *Ibsp*, and *Bglap* were strongly up-regulated by the induction ($p<0.05$ vs. control). Other lineage markers did not alter with pluripotency genes being down-regulated. Immunocytochemistry revealed that high percentages of the cells expressed Runx2 (78 $\pm$ 12%), Sp7 (66 $\pm$ 11%), and Col1a1-GFP (45 $\pm$ 6%) at the end of the osteogenic induction. When we applied our protocol to h-iPSCs, *RUNX2*, *SP7*, *COL1A1*, *IBSP* and *BGLAP* were up-regulated during the induction, and RUNX2 and SP7 proteins were highly expressed in the periphery of the cell clusters. Thus, we achieved the direct differentiation of pluripotent stem cells into osteoblasts using four small molecules under serum-free conditions. This system will be useful for in vitro mechanistic studies of osteoblast development in near in vivo settings and may be applied to stem cell-based therapies for massive bone defects.

***Disclosures: Kosuke Kanke**, None.*

SA0223

The Transcriptional Coregulator αNAC is a PKA Substrate Downstream of PTH Signaling. Martin Pellicelli*[1], Julie Miller[1], Claude Gauthier[1], Rene St-Arnaud[2]. [1]Shriners Hospitals for Children - Canada, Canada, [2]Shriners Hospital for Children & McGill University, Canada

In the nucleus of differentiated osteoblasts, the DNA-binding αNAC protein acts as a transcriptional coactivator of the *Osteocalcin* (*Ocn*) gene. The activity of αNAC is extensively modulated by post-translational modifications (PTMs). To further examine potential PTMs of αNAC, we performed *in silico* analysis which identified residue serine 99 as a potential PKA phosphoacceptor site. To evaluate if αNAC is a *bona fide* PKA substrate we performed an *in vitro* kinase assay using recombinant αNAC and PKA proteins. Our results show that wild type αNAC is phosphorylated by PKA at residue serine 99. Mutation of this amino acid to an alanine (S99A) abrogated phosphorylation. In osteoblasts, one of the main signals that lead to PKA activation is the PTH-Gsα signaling pathway. To assess whether this pathway can lead to S99 phosphorylation in living cells, we developed a specific phospho-S99-αNAC antibody. Immunoblotting revealed an accumulation of phospho-S99-αNAC in osteoblasts exposed to PTH(1-34) or 6-Bnz-cAMP, a PKA-selective activator. The same treatment also induced the nuclear translocation of αNAC. Nuclear accumulation was abrogated by the S99A mutation but enhanced when serine 99 was mutated to a phosphomimetic residue (S99D). Moreover, ChIP analysis showed that PTH(1-34) or 6-Bnz-cAMP treatment leads to accumulation of wild-type αNAC (but not S99A mutated αNAC) at the *Ocn* promoter. Finally, to validate the signaling cascade between PTH, PKA and αNAC, we have altered gene dosage for Gsα and αNAC in compound heterozygous mice. Compound Gsα;αNAC heterozygotes have a reduced bone mass phenotype and show increased numbers of osteocytes per surface area, as well as enhanced expression of osteocytic differentiation markers. Taken together, our results support that αNAC is a substrate of PKA following PTH signaling. This phosphorylation enhances αNAC translocation to the nucleus and leads to its accumulation at the *Ocn* promoter.

***Disclosures: Martin Pellicelli**, None.*

SA0224

TIEG enhances canonical Wnt signaling in the skeleton via dual mechanisms. John Hawse*[1], Kevin Pitel[1], Anne Gingery[2], Nalini Rajamannan[3], Malayannan Subramaniam[4], Thomas Spelsberg[4]. [1]Mayo Clinic College of Medicine, USA, [2]Mayo Clinic School of Medicine, USA, [3]Northwestern University Medical School, USA, [4]Mayo Clinic, USA

We have previously demonstrated that TGFβ Inducible Early Gene-1 (TIEG) plays important roles in mediating bone physiology as loss of TIEG expression *in vivo* results in a gender specific osteopenic phenotype which is observed only in female mice. Recently, TIEG has been identified in clinical studies as one of only a handful of genes whose altered expression levels or allelelic variations are associated with decreased bone mass and osteoporosis in humans. Our ongoing studies have now identified novel roles for TIEG in mediating Wnt signaling in bone. Here, we provide evidence that TIEG enhances canonical Wnt signaling in the skeleton via multiple mechanisms. Specifically, through the use of gene expression profiling studies on the cortical shells of long bones isolated from wild-type (WT) and TIEG KO mice, we determined that sclerostin mRNA levels were elevated approximately 12-fold in KO animals relative to WT controls. Serum sclerostin protein levels were also significantly elevated in KO mice. Since sclerostin is a potent inhibitor of Wnt signaling, we next utilized the TOPGAL reporter mouse to determine if loss of TIEG expression altered the activity of the canonical Wnt pathway in the skeleton. LacZ staining of the L5 vertebrae revealed a 3-fold decrease in Wnt pathway activity in TIEG KO mice relative to WT controls. In light of this observation, we next determined if TIEG could regulate Tcf/Lef enhancer elements through the use of the TopFlash reporter construct. TIEG expression was shown to increase TopFlash activity and to further enhance the Lef1 and β-catenin mediated induction of this reporter construct in osteoblasts. Co-immunoprecipitation studies revealed that TIEG also interacts with Lef1 and β-catenin. Since nuclear localization of β-catenin is essential for activation of the canonical pathway, we next sought to determine if TIEG played a role in mediating this process. Over-expression of TIEG in U2OS cells resulted in enhanced nuclear localization of β-catenin, an observation which was confirmed using wild-type and TIEG KO calvarial osteoblasts. Enhancement of β-catenin nuclear localization by TIEG appears to be mediated by TIEG's activation of AKT and subsequent inhibition of GSK3-β. Taken together, these data demonstrate that TIEG regulates canonical Wnt signaling through dual mechanisms which include the suppression of SOST expression and enhancement of β-catenin nuclear localization and transcriptional activity.

***Disclosures: John Hawse**, None.*

SA0225

Transcription factor AP2 suppresses FZD1 expression and mineralization in osteoblasts. Shibing Yu*[1], Laura Yerges-Armstrong[2], Yanxia Chu[3], Joseph Zmuda[4], Yingze Zhang[5]. [1]University of Pittsburgh Medical Center, USA, [2]University of Maryland School of Medicine, USA, [3]upmc, USA, [4]University of Pittsburgh Graduate School of Public Health, USA, [5]University of Pittsburgh, USA

FZD1 plays a role in osteoblast differentiation and mineralization. The mechanisms underlying the transcriptional regulation of FZD1 gene expression are not well understood. The aim of this study was to characterize the potential roles of transcription factor AP2 in regulating FZD1 expression and osteoblast differentiation and mineralization. Co-transfection of an AP2 expression plasmid with a full length FZD1 promoter (726bp) luciferase reporter resulted in the repression of promoter luciferase activity. Repression of FZD1 promoter by AP2 was not affected by two single nucleotide polymorphisms (rs2232157, rs2232158) that were previously associated with bone mineral density. Bioinformatic analysis of the FZD1 promoter identified multiple putative AP2 binding sites. Mutagenesis of these sites did not abolish the repression activity of AP2 on FZD1 promoter suggesting that these were not functional AP2 binding sites. In contrast, analysis of multiple truncated FZD1 promoter constructs abolished AP2 dependent repression in one of the promoter constructs suggesting AP2 binding in the full length promoter. Consistent with these results, endogenous FZD1 mRNA and protein expression in Saos2 cells were decreased by AP2 overexpression. The specificity of AP2 repression of FZD1 promoter was further confirmed using AP4, another transcription factor belonging to the Activation Protein (AP) family as it transactivated FZD1 promoter activity in Soas2 cells. Furthermore, suppression of FZD1 by AP2 overexpression led to the reduction of osteoblast differentiation and mineralization visualized by Alizarin Red staining. Taken together, our study demonstrates that AP2 is an important repressor for FZD1 gene expression and osteoblast differentiation and mineralization.

***Disclosures: Shibing Yu**, None.*

SA0226

See Friday Plenary Number FR0226.

SA0227

PTH Additively Enhances The Mechanical Stress-induced Proliferation of Calvarial Osteoblasts. Jumpei Shirakawa*[1], Yoichi Ezura[2], Makiri Kawasaki[1], Takayuki Yamada[1], Shuichi Moriya[3], Takuya Notomi[4], Tadayoshi Hayata[5], Ken Omura[1], Masaki Noda[1]. [1]Tokyo Medical & Dental University, Japan, [2]Tokyo Medical & Dental University, Medical Research Insititute, Japan, [3]Department of Orthopaedics, Juntendo University School of Medicine, Japan, [4]GCOE, Tokyo Medical & Dental University, Japan, [5]Medical Reserach Institute, Tokyo Medical & Dental University, Japan

Mechanical forces on skeletal system promote osteoblast proliferation and bone remodeling. Intermittent administration of parathyroid hormone (PTH) also stimulates osteoblast activity. Therefore, relationships between PTH and mechanical stimulation have been postulated. However, molecular links between these factors in osteoblast proliferation remains unclear. Here, we hypothesized that these factors could affect osteoblast proliferation through independent pathway at least in part, and thus could induce additive effects if both stimuli were applied. To test this hypothesis, calvaria derived osteoblastic cells (MC3T3E1) were subjected to flow-induced mechanical stress, using flow chambers with a push-pull pump or a reciprocal shaker as mechanical stress. In addition, some cells were exposed to PTH (100nM) or control buffer (PBS). BrdU incorporation after treatment indicated that mechanical stress and PTH increased osteoblast proliferation by either of the treatment. When these treatments were combined, a trend of further enhancement was observed in vitro. To examine in vivo effects, we intermittently injected PTH(1-34) daily for 7days into the mice that were subjected to mechanical stress at calvarial suture using expansion system based on application of dental coil spring. The initial force was around 1 N. PTH injection tended to increase cyclin D1 mRNA expression after the treatment in sham operated mouse calvarial suture. PTH futher enhanced cyclin D1 expression in the mice subjected to mechanical expansion. These results indicate that mechanical stress and PTH additively enhance bone formation via stimulation of osteoblasts proliferation.

***Disclosures: Jumpei Shirakawa**, None.*

SA0228

Rho GTPases control nuclear localization of beta-catenin and TCF/LEF activity in osteoblasts under flow. Qiaoqiao Wan*[1], Eunhye Cho[2], Ping Zhang[2], Hiroki Yokota[2], Sungsoo Na[2]. [1]Purdue University, USA, [2]Indiana University-Purdue University Indianapolis, USA

Mechanical loading of bone is known to influence bone growth and remodeling. Application of physiological loading to bone accelerates bone formation and fracture healing, whereas removal of loading results in bone loss. Beta-catenin dependent TCF/LEF (T-cell factor/lymphocyte enhancing factor) is known to be mechanosensitive and an important regulator for promoting bone formation. However the mechanism by which how β-catenin signaling interacts with other mechanoresponsive signaling proteins, such as Rho family GTPases, is not clearly understood. Here we show that Rac1 and Cdc42 are critical components of β-catenin signaling in shear stress-induced osteoblasts.

FRET-based GTPase biosensors were used to monitor Rac1 and Cdc42 activities. A TCF/LEF-green fluorescent protein (GFP) reporter was used to monitor the activity of β-catenin signaling. Enhanced GFP (EGFP)-β-catenin fusion proteins were used to monitor nuclear translocation of β-catenin. MC3T3-E1 osteoblasts were used for this study. The DNA plasmids were transfected into the cells using a Neon transfection system. Oscillatory (1 Hz) shear stress (10 dynes/cm2) was applied to the cells grown in the cell culture chamber. A Nikon Ti-E inverted microscope was used for imaging experiments. FRET images for GTPases activity were generated by computing an emission ratio of YFP/CFP for individual cells. The GFP images for TCF/LEF activity and β-catenin localization were background-subtracted and the fluorescence intensity was averaged over the whole cell area or over the nucleus. Images were scaled according to the color bar.

Results show that oscillatory shear stress stimulated translocation of β-catenin to the nucleus and increased TCF/LEF activity (Fig. 1A, B). Rac1 and Cdc42 displayed distinct dynamics of activation under flow (Fig. 2A, B). The shear stress-induced TCF/LEF upregulation was blocked by the inhibition of Rac1 and Cdc42 with their dominant negative mutants (Rac1-N17 and Cdc42-N17, respectively) or GTPase-specific drugs (NSC23766 and ML141, respectively) (Fig. 3). In contrast, constitutively active Rac1 and Cdc42 mutants caused a significant enhancement of TCF/LEF activity (data not shown). Our findings suggest that Rac1 and Cdc42 GTPases may play a role in regulating TCF/LEF-mediated transcription process and consequently contribute to load-induced bone repair and remodeling.

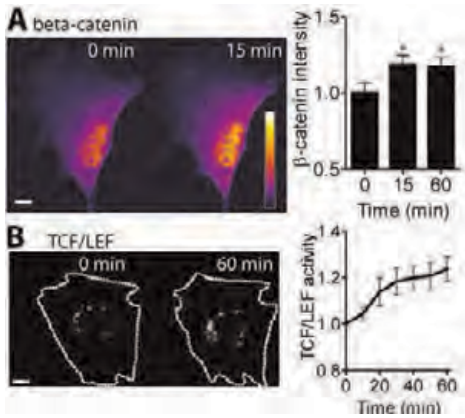

Figure 1

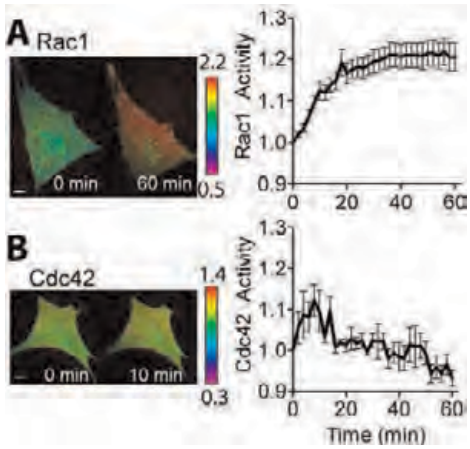

Figure 2

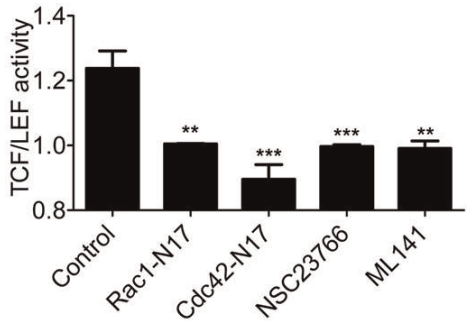

Figure 3

***Disclosures: Qiaoqiao Wan**, None.*

SA0229

Tob1, a BMP repressor, is activated by parathyroid hormone in osteoblasts in vitro and in vivo and reciprocally regulates PTH signaling. Shuichi Moriya*[1], Tadayoshi Hayata[2], Jumpei Shirakawa[3], Makiri Kawasaki[3], Takuya Notomi[4], Yoichi Ezura[5], Kazuo Kaneko[1], Masaki Noda[3]. [1]Department of Orthopaedics, Juntendo University School of Medicine, Japan, [2]Medical Reserach Institute, Tokyo Medical & Dental University, Japan, [3]Tokyo medical & dental university, Japan, [4]GCOE, Tokyo Medical & Dental University, Japan, [5]Tokyo Medical & Dental University, Medical Research Insititute, Japan

PTH receptor is expressed in bone and is involved in anabolic action of bone during intermittent administration of PTH. Tob1 (transducer of erbB2) is a member of antiproliferative family proteins and regulates bone mass as a BMP repressor (Yoshida et al. Cell 2000). However, the role of Tob1 during the action of PTH in osteoblast has not been understood. The purpose of this study was to identify the effect of PTH on Tob1 in bone. PTH directly enhanced the expression of Tob1 messenger RNA (mRNA) levels in MC3T3-E1 osteoblastic cells. This was an immediate early effect with a peak at 1 h after human PTH (1-34) treatment and the

levels returned to the baseline within 3 h. The PTH effects on the expression of Tob1 mRNA levels in vitro were dose dependent with a maximal effect at 100 nM PTH. PTH also enhanced Tob1 mRNA expression in the primary calvarial osteoblasts. PTH enhancement of Tob1 mRNA expression was suppressed by the DRB, a transcription inhibitor, while it was not inhibited by the presence of cycloheximide. These data suggested that PTH directly enhances Tob1 mRNA expression in osteoblasts at least in part via transcriptional events without requirement for new protein synthesis. In addition to the in vitro effects, PTH injection also enhanced Tob1 mRNA expression in bone in vivo. The PTH effect on Tob1 mRNA in bone was peaked at 1h after the injection and the levels returned to base line within 6 h. PTH effects were first observed at 10 μg/kg body weight and the effect was peaked at 80 μg/kg. These PTH effects on Tob1 mRNA in vivo were closely paralleling those observed in vitro on osteoblasts. Intermittent administration of PTH also elevated steady-state levels of Tob1 in bone after 7days of daily injection. To analyze the mode of PTH regulation by Tob1 gene expression, CRE (cyclic AMP response element)-Luc activity (pCRE-Luc) was used. Control cells or cells transfected with si-Tob1 or expression vector for TOB were tested for their response to 100 nM PTH or transfected constitutively active PTHR variant (His223Arg, caPPR) was performed. si-RNA for Tob1 suppressed the effects of caPPR on pCRE-luc. Conversely, Tob overexpression enhanced the caPPR-induced increase of the levels of luciferase activity. These observations indicate that Tob1 is one of the early direct target genes of PTH and Tob1 inhibits PTH signaling by interaction via transcriptional events.

***Disclosures: Shuichi Moriya**, None.*

SA0230

See Friday Plenary Number FR0230.

SA0231

A Novel hESC/iPSC Differentiation Protocol Generates a Cell Population with Endochondral Bone Formation Potential. Xiaonan Xin*, Xi Jiang, Liping Wang, Mary Louise Stover, Shuning Zhan, Jianping Huang, I-Ping Chen, Ernst Reichenberger, David Rowe, Alexander Lichtler. University of Connecticut Health Center, USA

The use of hESC and induced pluripotent stem cells (iPSC) for study and treatment of bone diseases or traumatic bone injuries requires efficient protocols to differentiate hESC/iPSC into cells with osteogenic potential, and the ability to isolate differentiated osteoblasts for analysis. Utilizing zinc finger nuclease (ZFN) technology to deliver a construct containing the Col2.3 promoter driving GFPemerald to the AAVS1 site, we successfully generated hESC and iPSC with Col2.3 promotor driven GFP or RFP (H9ZnCol2.3GFP/iPSC-ZnCol2.3RFP). We observed GFP positive osteoblasts in our mouse calvarial defect model by differentiating H9ZnCol2.3GFP into mesenchymal cells using a published protocol. With this differentiation protocol, we observed that the cells appear to undergo membranous bone formation, which may not be ideal for generating hESC/iPSC derived mesenchymal stem cells (MSC) for long bone non-union segmental defect repair. In contrast, we have developed a new differentiation protocol that may provide MSC that undergo endochondral bone formation, utilizing our H9ZnCol2.3GFP cells to facilitate evaluation of the osteogenic potential of cells produced with this protocol. The procedure involves producing embryoid bodies (EBs) with H9ZnCol2.3GFP or iPSC-ZnCol2.3RFP cells in mouse embryonic fibroblast conditioned (CM) media. After 10 days, EBs were collected and re-plated on a gelatin coated plate. MSCs were allowed to migrate out from the EBs in endothelial growth media (EGM). Cells were passaged and expanded after 10 days. The MSCs were first tested with our mouse calvarial defect model. In the defect, we observed dramatic cartilage formation after 6 weeks of implantation. Giving longer implantation time, we found increased amounts of human bone formed in the defects. Formation of hypertrophic cartilage was observed, which was replaced by bone, indicating that endochondral bone formation was taking place. We also observed human endochondral bone formation in a mouse non-union segmental long bone defect model. With these results, we believe that the newly developed differentiation protocol may provide a starting point for development of a method for producing MSC with endochondral bone formation potential that can be used clinically for repair of long bone defects in patients.

***Disclosures: Xiaonan Xin**, None.*

SA0232

Copper Coated Bone Implant Material Prevents Bacterial Growth and Stimulate Osteogenic Differentiation of Mesenchymal Stem Cells. Ines Burghardt[1], Frank Lüthen[1], Cornelia Prinz[2], Hans-Georg Neumann[2], Joachim Rychly*[1]. [1]Rostock University Medical Center, Germany, [2]DOT GmbH, Germany

To prevent infection due to bacteria, the design of anti-microbial medical implants is a great challenge in implant technology. We tested whether implant material coated with copper salts are suitable both to prevent growth of bacteria and to stimulate regeneration of bone by osteogenic differentiation of mesenchymal stem cells (MSC). Copper salts were implemented on titanium discs by galvanic deposition with an average copper load of 0.06 μg/mm^2. The anti-microbial activity of the material surface was tested with *S.aureus*. Growth of both planktonic and biofilm forming bacteria was inhibited at a Cu-concentration above 0.5 mM in the culture medium. Because of the known physiological role of copper, we studied the effect of $CuSO_4$ added to the culture medium and of Cu-ions released from the material surface on the biological responses of human MSC derived from bone marrow. We found that Cu-ions stimulated various parameters of the osteogenic differentiation of MSC. ALP activity increased due to a copper concentration of 0.1 mM in osteogenic differentiation medium after 7 days. Copper also stimulated the expression of collagen I detected by Western blot. After 28 days in Cu-containing osteogenic differentiation medium increased mineralization of MSC was detected at an optimal concentration of 0.3 mM of copper. In addition to stimulating osteogenic differentiation of MSC, proliferation of the MSC was increased at a concentration of 0.1 mM copper both in expansion and osteogenic differentiation medium.We conclude that copper containing implants are suitable to prevent bacterial infection and to promote bone regeneration by a stimulating effect on biological responses of mesenchymal stem cells. Both effects are concentration dependent. At higher concentration of Cu, i.e. immediately after implantation or directly at the implant surface, the anti-microbial action predominates, whereas in a late phase after implantation or at a greater distance from the implant surface, the implant may stimulate bone regeneration.

***Disclosures: Joachim Rychly**, None.*

SA0233

Effect of Type I Diabetes Mellitus in Circulating Osteoblastic Cells in Pheripheral Blood in Children and Young Adults. Merce Giner*[1], Ramón Pérez-Temprano[2], Mª Angeles Vázquez[3], Mª José Montoya[4], Cristina Miranda[5], Mª José Miranda[5], Ramón Pérez-Cano[2]. [1]Bone Metabolism Unit, "Virgen Macarena" University Hospital, Spain, [2]Bone Metabolism Unit, "Virgen Macarena" University Hospital & University of Seville, Spain, [3]Medicine Department, University of Seville, Spain, [4]University of Seville, Spain, [5]Bone Metabolism Unit, "Virgen Macarena" University Hospital of Seville, Spain

Introduction: Type 1 Diabetes Mellitus (DM1) has negative effects in various organs and systems, including bone tissue. In adults with DM1, there is an increased risk of osteoporotic fractures and lower BMD than the general population. This may be due to an imbalance in bone metabolism, either by accelerated bone resorption and/or less training in the growth stage.

Objectives: The purpose of our study was to determine if children and young adults with DM1 have decreased osteoblast lineage cells in peripheral blood and their association with bone mass values, the time course of the disease and metabolic control.

M & M: We studied four groups: A) 23 healthy children (5-12 years), B) 20 children with DM1 (5-12 years), C) 15 healthy young (22-38 years), D)15 young adults with DM1 (22-38 years). Mononuclear cell were isolated from whole blood by means of density gradients in Ficoll-Paque. For flow cytometry cells were incubated with antiosteocalcin antibody and a 2nd antibody marked with FITC.

Biochemical values we determined such as serum hemaglobin A 1c levels (HbA1c by HPLC), bone turnover markers (bone-specific alkaline phosphatase (BAP), procollagen type I N-terminal propeptide (P1NP), beta-crosslap, insulin growth factor 1 (IGF-1) and parathyroid hormone (PTH).

Bone mineral density (BMD) at the lumbar spine (L2-L4) and femur was measured (DXA).

Statistical analysis of the results was conducted using the T-student test and Pearson correlation coeficient (SPSS 20.0) and values were represented as means $\pm$ SD.

Results: The group of diabetic children has a significantly lower percentage of cells preosteoblasts (preOB) in peripheral blood (3.02% $\pm$ 1.8) than their control group (9.75% $\pm$ 7.4, p = 0.0001), and the same applies to the adult diabetic group, which has a smaller number of circulating pre-osteoblastic cells (2.2% $\pm$ 1.7) than their control group (5.9% $\pm$ 5.3, p = 0.013).

We observed a negative correlation between the number of pre-osteoblastic cells in blood and HbA1c (r = - 0.523, p = 0.0001) and serum glucose levels (r = -0.428 p = 0.001).

Conclusions: The enhanced bone fragility adults who have diabetes may be the result of a lower rate of bone formation in remodeling units influenced by glucose levels and metabolic control of the disease.

***Disclosures: Merce Giner**, None.*

SA0234

Epigenetic Landscaping using HDAC Inhibitors Primes Multi-Potent Human Adipose-Derived Mesenchymal Stem Cells for Osteogenic Lineage-Commitment. Amel Dudakovic*[1], Andre Van Wijnen[1], Gary Stein[2], Jennifer Westendorf[1], Sergii Kvasha[1], Xiaodong Li[1], Michael Yaszemski[3], Martin Montecino[4], Johannes Van Leeuwen[5], Eric Hesse[6], Simon Cool[7], Alan Dietz[1]. [1]Mayo Clinic, USA, [2]University of VermontCollege of Medicine, USA, [3]Mayo Clinic College of Medicine, USA, [4]Universidad de Concepcion, Chile, [5]Erasmus University Medical Center, The Netherlands, [6]University Medical Center Hamburg-Eppendorf, Germany, [7]Institute of Medical Biology, Singapore

Skeletal tissue engineering permits the restoration of damaged bone tissues that are apparent in aging orthopedic patients. Effective bone tissue engineering strategies critically depend on the ability to direct differentiation of mesenchymal stem cells into the osteogenic lineage. Epigenetic events that alter chromatin structure (e.g., histone acetylation and DNA methylation) alter the phenotype of skeletal progenitor cells through the concerted actions of histone code writers, readers and erasers. Histone acetyltransferases that mediate histone acetylation relax chromatin structure and induce gene expression, while histone deacetylases (Hdacs) that remove acetyl groups from histones reverse this effect. Histone deacetylase inhibitors (HDIs) such as vorinostat and valproate are clinically approved therapeutics (e.g., for cancer and epilepsy). HDIs have been shown to induce osteoblastic gene expression and promote terminal osteoblast maturation in mouse cells. Here, we examined whether HDIs can prime human adipose-derived mesenchymal stem cells (AMSCs) into the osteoblastic lineage using xenobiology-free conditions required for clinical bone tissue engineering. Expression of class I, II, and IV HDACs (HDACs 1-11) was measured in human AMSCs, primary fibroblasts, fetal osteoblasts (hFOB) and Saos2 osteosarcoma cells, as well as primary and immortalized TC28 chondrocytes using real-time quantitative PCR. Our data demonstrate that HDAC expression differs between these mesenchymal lineages and is altered during AMSC lineage commitment. Treatment of human AMSCs at confluence with vorinostat (1 μM for 24 hours) modestly enhances expression of representative mesenchymal lineage-specific transcription factors and bone-related extracellular matrix proteins. Strikingly, 72 hours after vorinostat removal we observed a more pronounced induction of expression for a subset of these same regulatory genes, including those encoding factors that play critical roles in AMSCs stemness (OCT4, NANOG), osteogenesis (RUNX2, SATB2, DLX5), chondrogenesis (SOX5 and SOX9), and myogenesis (MYOD). Thus, a single short-term dose of an HDI suffices to modify the epigenetic state of multipotent human stem cells to facilitate programming of transitions into alternative mesenchymal cell fates for skeletal tissue engineering.

***Disclosures: Amel Dudakovic**, None.*

SA0235

Epigenetic modification enables transdifferentiation between adipocytes and osteoblasts. YOUNG DAN CHO*[1], Won Joon Yoon[1], Kyung Mi Woo[2], Jeong-Hwa Baek[2], Hyun-Mo Ryoo[2]. [1]Seoul National University, South Korea, [2]Seoul National University School of Dentistry, South Korea

Bone marrow of a young and healthy human is filled with osteoblasts or hematopoietic cells while that of older and osteoporosis patients is filled with adipocytes indicating they have a different epigenetic landscape. DNA methylation and histone acetylation are very important epigenetic modifications that control gene expression in the promoter region, and involve latent ability to switch the cells character. We present evidence that the new possibility to rescue bone marrow adiposity through transdifferentiation from adipocytes to osteoblasts by modifying their epigenetic landscape.

We found the CpG islands in the promoter of osteogenic (ALP and Runx2) and adipogenic marker genes (PPARr and C/EBPa) with in silico analysis. The trends of these gene expression levels were correlated conversely with the methylation status of the CpG islands in the osteogenesis and adipogenesis. In the 3T3-L1 pre-adipocytic cells, hypermethylated ALP promoter legion was demethylated by treatment of 5'-aza-2'-deoxycytidine (5'-aza-2'-dC) and/or Trichostatin A (TSA), which are well characterized inhibitors of DNA methylation and histone deacetylation, respectively. Furthermore, ALP staining showed that Wnt3a treatment or overexpression of bone marker genes induced transdifferentiation from adipocytes to osteoblasts in the 5'-aza-2'-dC or TSA pretreated 3T3-L1 cells.

Taken together, these results suggest that histone acetylation and DNA demethylation at the promoter regions of osteogenic and adipogenic marker genes, and then specific signaling to drive differentiation are crucial to enable transdifferentiation between adipocytes and osteoblasts.

***Disclosures: YOUNG DAN CHO**, None.*

SA0236

Intermittent PTH administration inhibits transformation of mature osteoblasts into quiescent lining cells. Mi Gyeong Jang*[1], Seung Hye Kim[1], Jae-Yeon Yang[1], Hyojung Park[1], Jung Hee Kim[2], Sun Wook Cho[3], Jung-Eun Kim[4], Chan Soo Shin[2], Sang Wan Kim[5]. [1]Seoul National University, South Korea, [2]Seoul National University College of Medicine, South Korea, [3]National Medical Center, South Korea, [4]Kyungpook National University School of Medicine, South Korea, [5]Seoul National University Boramae Hospital, South Korea

The fates of mature osteoblasts (Obs) are either of three: buried in the bone matrix as osteocytes (Ocys) or remain on the bone surface as quiescent lining cells, or undergo apoptosis. However, whether intermittent parathyroid hormone (iPTH) could modulate the fate of mature Obs *in vivo* has been little known. We conducted a lineage tracing study using an inducible gene system to understand possible effect of of iPTH on the fate of mature Obs. *Dmp1*-CreERt2 mice were crossed with ROSA26R reporter mice to render targeted mature Obs and their descendents, lining cells or Ocys, detectable by X-gal staining. ROSA26R:*Dmp1*-Cre(+) mice were injected with 0.25 mg 4-OH-tamoxifen (4-OHTam) on postnatal day 5, 7, 9, 16 and day 23. In previous study, on 22 days after the last 4-OHTam injection, most X-gal (+) cells on the periosteal surfaces of both the calvaria and tibia were inactive lining cells. Thus, on day 25, mice were challenged with a subcutaneous injection of human PTH (1–34, 80mg/kg) or vehicle daily for 10 or 20 days. The animals were sacrificed on postnatal day 25 or 36 or 46. We evaluated the number and thickness of X-gal (+) lining Obs descendents and the number of X-gal (+) or X-gal (-) Ocys in 4-6 consecutive 100 x or 200 x microscopic fields in the calvaria of these animals. PTH increased the thickness and the number of X-gal (+) Obs descendents in the calvaria compared to the vehicle (thickness; on day 23, 5.9 $\pm$ 3.4, on day 36, PTH: 2.5 $\pm$ 1.2, vehicle: 2.3 $\pm$ 0.7, on day 46, PTH: 2.6 $\pm$ 0.8, vehicle: 1.8 $\pm$ 0.5 mm, PTH versus vehicle on day 46: $p < 0.05$, number; on day 23: 45.1 $\pm$ 35.7, on day 36, PTH:11.7 $\pm$ 11.4, vehicle: 9.3 $\pm$ 12.5, on day 46, PTH: 40.7 $\pm$ 31.4, vehicle: 5.3 $\pm$ 7.5/mm, PTH vs vehicle on day 46: $p < 0.01$, n=4~6/group). PTH also increased X-gal (+) Ocy density compared to the vehicle in the calvaria (on day 23, 11.7 $\pm$ 6.0; on day 36, PTH: 11.6 $\pm$ 4.9, vehicle: 6.9 $\pm$ 3.8, on day 46, PTH: 6.6 $\pm$ 2.7, vehicle: 4.4 $\pm$ 1.9 x $10^3/mm^2$, PTH vs vehicle on day 36 and 46: $p < 0.05$; n=4~6/group). Moreover, fraction of X-gal (+) Ocy/total Ocy per area was increased after PTH administration (on day 23, 68.0 $\pm$ 13.5; on day 36, PTH: 73.9 $\pm$ 11.9, vehicle: 64.8 $\pm$ 14.7, on day 46, PTH: 67.2 $\pm$ 15.3, vehicle: 52.0 $\pm$ 19.0 %/mm^2, PTH vs vehicle on day 46: $p < 0.01$; n=4~6/group). This data suggests that PTH could inhibit transformation of mature Obs into lining cells, and PTH could modulate differentiation of mature Obs into Ocys *in vivo*.

***Disclosures: Mi Gyeong Jang**, None.*
This study received funding from: National Research Foundation of Korea

SA0237

Normoxia vs Hypoxia: Nutrient Activation of Distinct Signaling Pathways in Bone Marrow Mesenchymal Stem Cells is Dependent on Experimental Conditions. Mona El Refaey*[1], Qing Zhong[2], Xing-Ming Shi[3], Yun Su[1], Kehong Ding[3], William Hill[4], Wendy Bollag[1], Maribeth Johnson[1], Norman Chutkan[1], Mark Hamrick[3], Carlos Isales[1]. [1]Georgia Regents University, USA, [2]Medical College of Georgia, USA, [3]Georgia Health Sciences University, USA, [4]Georgia Regents University & Charlie Norwood VAMC, USA

We have previously reported that individual amino acids were potent agonists for stimulating increases in intracellular calcium and phospho c-Raf and in promoting Bone Marrow Stromal cell (BMSCs) differentiation down the osteogenic pathway. L-type amino acids bind with high specificity to GPRC6A receptors with aromatic amino acids (Tyrosine, Phenylalanine and Tryptophan) being the most potent activators of this pathway. These experiments were done in the presence of 5% CO2 and ambient air (78% N2 and 21% O2). However, physiologic oxygen pressure inside the bone marrow environment are much lower ranging from 1-7% and as high as 10-13% in the arteries, lungs and liver. We had not previously examined the effects of different levels of oxygen tension on BMSCs. Thus, we compared a normoxic (78% N2 and 21% O2) vs. a hypoxic environment (3% O2) alone or after treatment with aromatic amino acids. Reverse phase protein arrays (which test for 171 different phospho proteins) showed that Tyrosine (100 μM), under either normoxic or hypoxic conditions, upregulated protein kinase B (Akt), Forkhead box protein M1 (FOXM1) and Ribosomal protein S6 (RPS6) signaling pathways. In contrast, Tryptophan (100 μM) while activating the Akt pathway under normoxia (2-fold), under hypoxic conditions it instead increased ribosomal protein S6 kinase, 70kDa, and polypeptide 1 (RPS6KB1). Valine (100 μM), a branched-chain amino acid, downregulated RPS6 signaling under hypoxic conditions. Thus, under normoxic conditions, pathways involved in handling reactive oxygen species and promoting BMSC differentiation were activated while under hypoxic conditions, BMSC proliferative pathways were preferentially activated. These data, suggest that oxygen tension has an impact on the signaling pathways activated in BMSCs and that results under ''hypoxic'' conditions more closely resemble the normal physiologic conditions these cells are exposed to in their niches.

***Disclosures: Mona El Refaey**, None.*

SA0238

N-Terminus Amelogenin Peptide Induces Osteoblastic Differentiation of Stem Cells through ERK1/2. Rene Olivares-Navarrete*[1], Sharon Hyzy[2], Kathryn Vesper[3], Argelia Almaguer-Flores[4], Zvi Schwartz[1], Barbara Boyan[1]. [1]Virginia Commonwealth University, USA, [2]Georgia Tech, USA, [3]Georgia Regents University, USA, [4]Universidad Nacional Autonoma de Mexico, Mexico

Porcine enamel matrix derivative (EMD), composed mostly of amelogenin, is used as a therapeutic agent in clinical applications to regenerate bone and supportive tissue around teeth. Amelogenin is produced by ameloblasts as a full length protein or splice variants. Amelogenin also can be cleaved by enzymatic activity, resulting in a broad range of peptides. It is unclear whether the therapeutic effect of EMD is due to the full-length amelogenin protein, splice variants, proteolytic peptides, or a combination. Since EMD is known to produce bone regeneration, our hypothesis is that amelogenin peptides stimulate osteogenesis of mesenchymal stem cells. The aim of this study is to demonstrate the potential of amelogenin or N-terminal amelogenin peptide (NTAP) to promote osteogenic differentiation of mesenchymal stem cells (MSCs) and to elucidate the possible signaling pathways involved in periodontal regeneration. Human MSC cultures were treated with amelogenin or NTAP. While amelogenin induced MSC osteogenesis, increasing alkaline phosphatase specific activity, osteocalcin levels, and OSX and RUNX2 gene expression, a more robust osteogenic induction was seen after NTAP treatment. A phospho-kinase proteosome array measuring phosphorylation of 35 proteins indicated that protein kinase C (PKC), ERK1/2, and β-catenin were highly phosphorylated by NTAP. This was confirmed by measuring PKC activity and levels of phospho-ERK1/2 and β-catenin. Amelogenin and NTAP increased PKC. NTAP induced higher phosho-ERK1/2 than amelogenin. Phospho-β-catenin was higher in NTAP treated cells than in amelogenin treated cells. Inhibition of ERK1/2 with chemical compounds blocked both amelogenin and NTAP induced increases in RUNX2, ALP, OCN, COL1, and BMP2 mRNA. The results demonstrate that NTAP induces osteogenic differentiation of MSCs, mediated through activation of PKC and ERK1/2 and degradation of β-catenin, indicating that NTAP is an active amelogenin peptide. Taken together, the results suggests that NTAP can be used as an extracellular matrix product for induction of ostoeblastic induction and bone regeneration.

***Disclosures: Rene Olivares-Navarrete**, None.*

SA0239

Pigment Epithelium Derived Factor Enhances Differentiation and Mineral deposition of Human Mesenchymal Stem Cells. Feng Li*[1], Na Song[1], Joyce Tombran-Tink[1], Christopher Niyibizi[2]. [1]Penn State College of Medicine, USA, [2]The Pennsylvania State University College of Medicine, USA

Pigment epithelium-derived factor (PEDF) is a potent anti-angiogenic factor found in a wide variety of fetal and adult tissues. Recent findings have shown that lack of PEDF leads to osteogenesis imperfecta (OI) type VI. The mechanisms by which PEDF leads to the development of OI type VI remain unknown. In the present report, we determined the effects of PEDF on human mesenchymal stem cells (hMSCs) differentiation and mineral deposition and signaling pathways through which PEDF displays its functions. Human MSCs incubated in maintenance medium in presence of PEDF induced expression of osteoblasts related genes. In addition, exposure of MSCs to PEDF induced expression of ALP activity and this activity was enhanced when the cells were incubated in osteogenic medium. hMSCs incubated in osteogenic medium in presence of PEDF significantly enhanced mineral deposition, as low as 50 ng/ml of PEDF enhanced mineral deposition in differentiating MSCs in comparison to the cells incubated in osteogenic medium alone. Expression of PEDF in MSCs was silenced using siRNA and the resulting cells were assessed for alkaline phosphatase activity and mineral deposition. The results revealed that MSCs deficient in PEDF expression exhibited decreased ALP activity and significant reduction in mineral deposition as assessed by Alizarin Red staining. Decreased ALP activity and reduction in mineral deposition were restored by supplementation with exogenous PEDF protein. PEDF activated ERK and AKT signaling pathways in MSCs to induce expression of osteoblast related genes and mineral deposition. Inhibition of ERK signaling pathway decreased expression of osteoblast related genes indicating that PEDF signals through this pathway to regulate osteoblasst related genes. These data demonstrate that PEDF plays a role in osteogenesis and that lack of its expression leads to reduction in mineral deposition as a result of reduced osteoblasts maturation. Thus, failure of osteoblasts maturation due to lack of PEDF may explain defects seen in type VI OI.

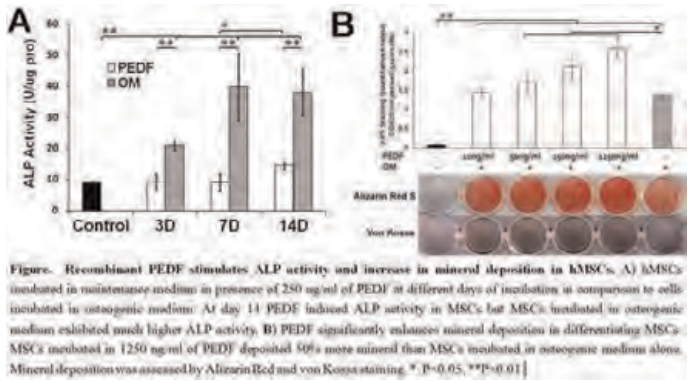

Figure. Recombinant PEDF stimulates ALP activity and increase in mineral deposition in hMSCs. A) hMSCs incubated in maintenance medium in presence of 250 ng/ml of PEDF at different days of incubation in comparison to cells incubated in osteogenic medium. At day 14 PEDF induced ALP activity in MSCs but MSCs incubated in osteogenic medium exhibited much higher ALP activity. B) PEDF significantly enhances mineral deposition in differentiating MSCs. MSCs incubated in 1250 ng/ml of PEDF deposited 50% more mineral than MSCs incubated in osteogenic medium alone. Mineral deposition was assessed by Alizarin Red and von Kossa staining. *, P<0.05, **P<0.01

Figure.1. Recombinant PEDF stimulates ALP activity and increase in mineral deposition in hMSCs

***Disclosures: Feng Li**, None.*

SA0240

Pin1 plays a critical role in Wnt3a-induced osteoblast differentiation through structural modification of β-catenin. Hea-rim SHIN*[1], Taegyung Lee[1], Young-Dan Cho[1], Won-Joon Yoon[1], Kyung Mi Woo[2], Jeong-Hwa Baek[2], Hyun-Mo Ryoo[2]. [1]Seoul National University, South Korea, [2]Seoul National University School of Dentistry, South Korea

Canonical Wnt signaling plays an important role in osteoblast differentiation, in which β-catenin is the key mediator. Pin1 (Peptidylprolyl cis/trans isomerase, NIMA-interacting 1) isomerizes only phophorylated Serine/Threonine-Proline motif. It regulates the conformational change of β-catenin, which has known to be associated with increased cancer risk, because of increased β-catenin level in nucleus. Canonical Wnt signaling also is very important in osteoblast differentiation, however, association of Pin1 in this signal transduction pathway is still unknown. The specific aim of this study was to investigate what if Pin1 is involved in the Wnt-induced osteogenesis. Inhibition of Pin1 activity by Juglone treatment repressed Wnt3a-induced osteoblast differentiation and bone marker gene expression in C2C12 cells. In contrast, overexpression of Pin1 stimulated osteoblast differentiation of C2C12 cells by Wnt3a administration. The transcriptional synergy including TOP flash and ALP promoter activity was observed with Pin1 and Wnt3a. We demonstrated that Pin1 binds to β-catenin. Its interaction was occurred by Wnt3a-induced ERK dependent phosphorylation of β-catenin and it enhanced stability of β-catenin. On the other hand, when we treated the U0126, an ERK inhibitor, the stability of β-catenin was reduced. Consequently, Pin1 increases retention of β-catenin in nucleus, which may explain the increased reporter activity. Taken together, our results reveal that Pin1 is a novel regulator that promotes osteoblast differentiation through structural modification and stabilization of β-catenin. These results provide us a great insight for the importance of Pin1 and the crosstalk between ERK MAP kinase and Wnt signaling pathway in bone development.

***Disclosures: Hea-rim SHIN**, None.*

SA0241

See Friday Plenary Number FR0241.

SA0242

See Friday Plenary Number FR0242.

SA0243

See Friday Plenary Number FR0243.

SA0244

Withdrawn

SA0245

Toll-Like Receptor 2 Modulating Lipids of *Porphyromonas Gingivalis* Inhibit Osteoblast Differentiation and Function. Yu-Hsiung Wang*, Qiang Zhu, Jin Jiang, Jianping Huang, Robert Clark, Frank Nichols. University of Connecticut Health Center, USA

Porphyromonas gingivalis (*P. gingivalis*), a Gram(-) anaerobic organism associated with chronic periodontitis, is reported to promote periodontal bone loss through engagement of Toll-like receptor 2 (TLR2). However, the virulence factors responsible for periodontal bone loss have not been identified. We have previously shown that the total lipid extract of *P. gingivalis* inhibits osteoblast-mediated bone deposition through engagement of TLR2. Recent work has shown that an unusual serine lipid, called Lipid 654, is the primary lipid class of *P. gingivalis* that engages TLR2. The purpose of the present study was to examine the effect of Lipid 654 on osteoblast differentiation, gene expression, and mineralization in cell culture. Calvarial osteoblasts were isolated from mice transgenic for pOBCol3.6GFP. This GFP reporter is activated in the early preosteoblasts and its activity intensifies as osteoblasts differentiate. Lipid 654 was highly enriched by HPLC and purity was verified by mass spectrometry. Lipid 654 was compared with the total lipid extract of *P. gingivalis* by sonicating lipids in culture medium immediately prior to addition to cell cultures. Our results showed that the expression of pOBCol3.6GFP (examined by cell fluorescence) and mineralized nodule formation (revealed by von Kossa's staining) were substantially inhibited by *P. gingivalis* total lipids. The same effects were observed in the cultures treated with Lipid 654. Gene expression using PCR showed that the expression of osteoblastic markers of bone sialoprotein, dentin matrix protein, and osteocalcin were down-regulated in cultures treated with Lipid 654 when compared with the control cultures. In contrast to the inhibition of osteoblastic markers, ELISA of culture medium from osteoblast cells treated with Lipid 654 showed a significant increase in tumor necrosis factor alpha secretion. We also examined the role of TLR2 in lipid-induced inhibition of osteoblast differentiation using cell cultures derived from mice transgenic for pOBCol3.6GFP with deleted expression of TLR2 (*TLR2*$^{-/-}$). Both *P. gingivalis* total lipids and Lipid 654 failed to inhibit the expression of pOBCol3.6GFP and the mineral nodule formation in *TLR2*$^{-/-}$ cells. These results demonstrate that a highly enriched preparation of Lipid 654 of *P. gingivalis* significantly inhibits osteoblast differentiation and function through engagement of TLR2. Future work will evaluate the effect of Lipid 654 on osteoblast cell function in vivo.

***Disclosures: Yu-Hsiung Wang**, None.*

SA0246

Abnormal Mitochondrial Energetics in Osteoblasts Derived from Aromatase Deficient Male Mice. Orhan Oz*[1], Aktar Ali[2], Jianfei Guo[2]. [1]University of Texas Southwestern Medical Center, Dallas, USA, [2]UT Southwestern Medical Center at Dallas, USA

Estrogens regulate both formation and metabolism and regulate glucose and lipid metabolism. Aromatase catalyzes the formation of estrogens from androgen precursors. Aromatase deficient (ArKO) male mice develop adiposity, have low turnover osteopenia, low lGF-I levels and increased leptin levels associated with low levels of osteocalcin, a regulator of glucose homeostasis. In vitro differentiation assays bone marrow cells from 12 week old male mice develop fewer alkaline phosphatase colonies and mineralized nodules. To determine if osteoblasts derived from ArKO mice have altered mitochondrial function we studied using the XF24 analyzer. Bone marrow cells from WT and ArKO mice were allowed to differentiate for 7- 10 days under osteogenic conditions. The differentiated cells from ArKO mice did not show a significant difference in basal respiration but showed higher maximal respiration when compared to WT cells. The maximal respiratory rate was increased by 2h treat with estradiol (10-8M) or the ERalpha agonist PPT in WT with estradiol being more potent. On the other hand the response in ArKO cells varied in different experiments from either no estradiol induced enhancement or relatively suppressed enhancement. These data show that estradiol can regulate osteoblast metabolism.

***Disclosures: Orhan Oz**, None.*

SA0247

From fibers to peptides: The mechanism of collagen degradation by cathepsin K. Dieter Bromme*. The University of British Columbia, Canada

Introduction: Cathepsin K (catK), a cysteine protease highly expressed in osteoclasts, is the only mammalian collagenase that effectively cleaves at multiple sites within triple-helical collagens. We have previously demonstrated that the collagenase activity of catK requires the presence of glycosaminoglycans (GAGs). Based on novel X-ray structures of catK-chondroitin sulfate complexes, we propose that the active collagenase forms either tetramers or dimers of catK molecules. These oligomers are responsible for the degradation of tropocollagen molecules and collagen fibers.

Methods: Various catK variants were expressed in *Pichia pastoris* and purified. The enzymatic activities of the variants as well as of wild type catK were tested using soluble and insoluble type I collagen, gelatin, and a fluorogenic peptide substrate. Atomic force microscopy (AFM) and circular dichroism (CD) were used to characterize the interactions between catK and collagens and scanning electron microscopy (SEM) was used to characterize the degradation of collagen fibers.

Results: The most effective degradation of collagen was achieved at molar ratios of 2:1 (catK : GAG). AFM studies indicated that the tetramer is active at soluble triple helical collagen whereas dimers are likely acting on insoluble collagen fibers. The tetramer forms a central pore that is sufficient to accommodate triple helical collagen. CD-analysis suggests that the tetrameric complex acts as a helicase by unwinding the collagen helix. Mutations within the pore, and at sites of the chondroitin sulfate-protein and protein-protein interactions of the complex significantly decreased the collagenase activity of the variant proteins without interfering with their non-collagenase activities. For the dimer, mutation at the protein-protein interaction sites specifically inhibited the degradation of insoluble collagen. AFM, SEM, and degradation studies suggest that catK releases triple-helical tropocollagen fragments from the fiber that are subsequently degraded into small peptides.

Conclusions: The collagenase activity of catK depends on specific dimer and tetramer forms of catK/GAG complexes. The inhibition of complex formation may represent a highly specific method to selectively inhibit the therapeutically relevant collagenase activity of this enzyme.

***Disclosures: Dieter Bromme**, None.*

SA0248

See Friday Plenary Number FR0248.

SA0249

See Friday Plenary Number FR0249.

SA0250

Effect of celecoxib on osteoclast differentiation. Kakei Ryu*[1], Hitoshi Amano[2], Haruka Emori[1], Takehiko Sambe[1], Katsuji Oguchi[1], Shinichi Iwai[3]. [1]Department of Pharmacology, School of Medical, Showa University, Japan, [2]Showa University School of Dentistry, Japan, [3]Department of Healthcare & Regulatory Sciences, School of Pharmacy, Showa University, Japan

Introduction: Prostaglandin E_2 (PGE_2) an inflammatory cytokine, produced by cyclooxygenase-2 (COX-2) acted on osteoclast formation not only bone resorption. The aim of this study was undertaken to investigate whether celecoxib, a selective COX-2 inhibitor, a direct effect on osteoclast differentiation.

Materials and Methods: Bone marrow cells from femur and tibia of five-weeks-old male ddY mice passed Sephadex G10. The cells were cultured with pH7.0 αMEM, which include CSF-1 (25 ng/ml) RANKL (100 ng/ml), with or without celecoxib (2.5 - 30 μM) and with or without PGE_2 (0.1 μM). RAW 264.7 cells for this experiment are the same as before, added only RANKL.

Result: Cells use abcam® Anti-COX2 / Cyclooxygenase 2 rabbit polyclonal antibody for primary antibody and immunostaining shows COX-2 protein was expressed in osteoclasts in the presence of CSF-1 and RANKL. After 6 days, both cells were differentiated to TRAP positive multinucleated osteoclasts. The number of osteoclast was suppressed completely with 30 μM celecoxib. Further additional PGE_2, the number of actin ring having osteoclast recovered in the presence of 2.5 μM and 5 μM celecoxib.After 8 days, pit formation assay showed bone-resorption was suppressed in a dose-dependent of celecoxib.

Discussion: These result showed that the activity of COX-2 inhibitor may directly inhibit the osteoclastogenesis and differentiation via inhibited PGE_2 synthesis.

Conclusion: COX-2 dependent signaling pathway might be involved in the process of osteoclast differentiation.

***Disclosures: Kakei Ryu**, None.*

SA0251

EphrinB2/EphB4 control of osteoclast formation is mediated by the osteoblast lineage. Stephen Tonna*[1], Farzin Takyar[2], Blessing Crimeen-Irwin[1], Patricia Ho[3], T. John Martin[3], Natalie Sims[3]. [1]St Vincent's Institute, Australia, [2]Yale University, School of Medicine, USA, [3]St Vincent's Institute of Medical Research, Australia

Osteoblasts express both the EphB4 receptor and its ligand ephrinB2, while osteoclasts express only ephrinB2. It has been reported that ephrinB2 reverse signaling in the osteoclast lineage restrains their differentiation. In addition, pharmacological inhibition of ephrinB2/EphB4 interaction within osteoblasts promoted osteoclast formation by increasing osteoblastic RANKL production (Takyar et al., JBMR 2013). To determine whether the key pathway restraining osteoclast formation is EphB4 forward signaling within the osteoblast lineage or ephrinB2 reverse signaling in the osteoclast or the osteoblast lineages, we conditionally deleted the ephrinB2-signaling domain from both lineages using Ctsk.Cre and Osx1.Cre.

Stimulation of ephrinB2 reverse signaling with exogenous clustered EphB4-Fc in osteoclast cultures (wild-type bone marrow macrophages plus RANKL/M-CSF) had

no significant effect on osteoclast numbers. In addition, the number of osteoclasts generated with RANKL/M-CSF from Ctsk.Cre.EfnB2f/f precursors was not increased compared to Ctsk.Cre.EfnB2wt/wt controls. This indicates that ephrinB2 reverse signaling within the osteoclast lineage does not restrain osteoclast formation.

In both neonate and adult Osx1.Cre.EfnB2f/f mice, osteoclast numbers were decreased compared to Osx1.Cre.EfnB2wt/wt controls. Consistent with this, Osx1.Cre.EfnB2f/f calvarial osteoblasts showed a 50% reduction in RANKL mRNA and reduced support of osteoclast formation in co-culture with wild-type bone marrow. In contrast, inhibition of ephrinB2 interaction with EphB4 by a receptor antagonist (soluble EphB4) increased RANKL expression in both Osx1.Cre.EfnB2f/f and Osx1.Cre.EfnB2wt/wt control osteoblasts. Furthermore, soluble EphB4 increased osteoclast formation to the same extent from both Ctsk.CreEfnB2f/f and Ctsk.CreEfnB2wt/wt bone marrow precursors in co-culture with wild-type osteoblasts. This demonstrates that EphB4 forward signaling in osteoblasts restrains osteoclast formation by limiting RANKL production, and that this is not modified by ephrinB2 reverse signaling in either osteoblasts or osteoclasts.

In conclusion, this data indicates that the interaction of ephrinB2 and EphB4 within the osteoblast lineage restrains osteoclast formation by limiting RANKL availability and this is mediated through EphB4 forward signalling. A role of reverse signaling through ephrinB2 inhibiting osteoclast formation in either osteoblasts or osteoclasts was not demonstrated in this work.

***Disclosures: Stephen Tonna**, None.*

SA0252

Gene Expression Profiling during RANKL-Induced Osteoclastogenesis Using RNA-Sequencing and Identification of the Novel Component of NFATc1 Transcription Complex. Tomohiko Yoshida*[1], Akitoshi Nakayama[2], Hidekazu Nagano[2], Hisashi Koide[2], Yutaka Suzuki[3], Sumio Sugano[3], Ichiro Tatsuno[4], Koutaro Yokote[2], Tomoaki Tanaka[2]. [1]Chiba University Hospital, Japan, [2]Division of Endocrinology, Diabetes & Metabolism, Chiba University Graduate School of Medicine, Japan, [3]Institute of Medical Science, University of Tokyo, Japan, [4]Center for Diabetes, Metabolism & Endocrinology, Toho University Sakura Medical Center, Japan

Background: During osteoclastogenesis, osteoclast precursors undergo dramatic changes in the morphology and function, in which mononuclear preosteoclasts proliferate in bone marrow, are fused into multinuclear osteoclasts, and are activated to resorb bone. Osteoclast differentiation is characterized by the sequential expression of specific genes in response to certain signals such as RANKL and M-CSF, and the transcription factor NFATc1 plays a pivotal role in regulating downstream gene expression. However, little is known about the constituent molecules of NFATc1 transcription complex and their role in the osteoclastogenesis. The objectives of the current study were to a) analyze the transcriptome during RANKL-induced osteoclastogenesis including non-coding RNAs using RNA-sequencing, and b) identify the key constituents of NFATc1 transcription complex and their role in the epigenetic gene regulation.

Methods: To evaluate global changes in gene expression during RANKL-induced osteoclastogenesis, gene expression profiling was performed in murine pre-osteoclastic RAW264.7 cells using Illumina® genome analyzer by comparing the difference between treatment and control groups at four different time points (2, 3, 7, 14 days after treatment with RANKL). To identify the NFATc1 binding protein(s), putative NFATc1 transcription complex was isolated from the cell lysate of HEK293 cells expressing FLAG- and HA- tagged human NFATc1 protein by tandem affinity purification, and was separated by SDS-PAGE and bands of interest are cut from the gel, and the generated peptides are sequenced by LC-MS/MS.

Results: Regarding the mRNA expression of NFATc1, calcitonin receptor, cathepsin K and β3 integrin, the highest level was observed at 3 days after treatment with RANKL. The peak gene expression of TRAP and DC-STAMP was occurred at 7 days. Moreover, several novel potential osteoclastogenic genes and non-coding RNAs (e.g., miR 146a) were found to be induced after the treatment. Polycystic kidney disease protein1 (PKD1) and other novel proteins were identified as the putative component of NFATc1 transcription complex.

Conclusions: We have identified several putative constituents of NFATc1 transcription complex, and found that each NFATc1 downstream gene has a different timing of its peak expression, suggesting stage-specific regulation of the each NFATc1 target genes.

***Disclosures: Tomohiko Yoshida**, None.*

SA0253

See Friday Plenary Number FR0253.

SA0254

Inhibitory effects of intravenous immune globulin (IVIG) on osteoclastogenesis and bone resorption. Elisha Lim, Lionel Ivashkiv, Kyung-Hyun Park-Min*. Hospital for Special Surgery, USA

Intravenous immune globulin (IVIG) is an effective therapy in a variety of autoimmune and chronic inflammatory diseases. Investigations of the therapeutic effects of IVIG have focused on the suppression of autoantibody and immune complex-mediated pathogenic mechanisms. It is increasingly appreciated that IVIG can exert its inhibitory effects through not only inhibitory Fcγ receptors but also activating Fcγ receptors. It has been shown that IVIG protects mice from developing inflammatory arthritis via a prominent contribution of activating Fcγ receptors. Here, we investigated whether IVIG directly controls osteoclast differentiation and whether this pathway represents a potential therapeutic target for osteoclast-mediated bone destruction. Using the TNF-induced supracalvarial osteolysis model, we show that IVIG administration significantly decreased serum tartrate-resistant acid phosphatase (TRAP), a marker of in vivo osteoclastogenesis and bone resorption. Consistent with this reduction, treating human blood-derived osteoclast precursor cells (OCPs) with IVIG suppressed *in vitro* osteoclastogenesis. Previously, we showed that soluble immune complexes (sICs) in the IVIG pool play an important role in its inhibitory action. In this study, we find that cross-linking Fcγ receptors with either sICs or plate-coated IVIG could efficiently block osteoclastogenesis and the expression of osteoclast-related genes such as integrin β3 and cathepsin K in a dose-dependent manner. Mechanistically, both sICs and plate-coated IVIG suppress osteoclastogenesis by downregulating RANKL-induced expression of NFATc1, the master regulator of osteoclastogenesis. Suppression of *NFATC1* expression was mediated in part by the transcriptional suppressor Bcl6. RANKL stimulation diminished levels of Fcγ receptors, and thus RANKL-pretreated cells were refractory to the inhibition of osteoclastogenesis by IVIG, further supporting the role of Fcγ receptors in IVIG-mediated inhibition of osteoclastogenesis. Taken together, our results suggest that crosslinking of Fcγ receptors directly suppresses osteoclastogenesis and regulates bone resorption.

***Disclosures: Kyung-Hyun Park-Min**, None.*

SA0255

miRNA-29 Promotes Osteoclastogenesis Through Regulation of Osteoclast Commitment and Migration. Tiziana Franceschetti*, Catherine B. Kessler, Sun-Kyeong Lee, Anne Delany. University of Connecticut Health Center, USA

Osteoclast differentiation is complex and tightly regulated at multiple levels. microRNAs (miRNAs) are key post-transcriptional factors that control gene expression, and play a critical role in osteoclastogenesis. Although disrupted miRNA processing results in osteopetrosis, the function of specific miRNAs in osteoclasts is elusive.

We analyzed the role of the miR-29 (a/b/c) family in osteoclast differentiation, using primary cultures of mouse bone marrow-derived macrophages. Retroviral-mediated miR-29a knock-down decreased osteoclast formation and size. qRT-PCR showed that expression of the miR-29 family increased during osteoclast differentiation, in concert with mRNAs for TRAP and Cathepsin K. Similar regulation was observed in the monocytic cell line RAW264.7.

To determine the function of miR-29 in osteoclastogenesis, we used as a model stably transduced RAW264.7 cells expressing a doxycycline (DOX)-inducible miR-29 competitive inhibitor, or miR-29 ''sponge'' construct. Expression of the miR-29 sponge impaired RAW264.7 differentiation into osteoclastic cells and decreased the size of cells formed. The miR-29 sponge inhibited the chemotactic migration of RAW264.7 cells toward M-CSF, and promoted macrophage lineage commitment. However, the miR-29 sponge did not affect precursor cell replication, or the actin ring formation and apoptosis of mature osteoclasts.

To better understand how miR-29 regulates osteoclast function, we validated novel miR-29 target genes using Luciferase-3'-UTR (untranslated region) reporter assays and miR-29 inhibitors. miR-29 targeted the UTR of RNAs critical for cytoskeletal organization, including Cell Division Control protein 42 (Cdc42) and SLIT-ROBO Rho GTPase activating protein 2 (srGAP2). miR-29 also targeted the UTR of RNAs associated with the macrophage lineage, including G protein-coupled receptor 85 (GPR85), Nuclear Factor I/A (NFIA), and CD93. Additional novel miR-29 targets that promote osteoclast differentiation included the proton sensor GPR68, Calcitonin receptor (CTR), and Jun Dimerization Protein 2 (JDP2).

miR-29 is a positive regulator of osteoclast formation, promoting motility and progenitor commitment. Since miR-29 also targets RNAs that are positive regulators of osteoclast differentiation, this miRNA family may control the tempo of osteoclast maturation. An expanded understanding of how miRNAs regulate osteoclast formation and activity may lead to new therapeutics for skeletal disease.

***Disclosures: Tiziana Franceschetti**, None.*

SA0256

MSK1 is a novel signaling molecule involved in RANKL-induced osteoclastogenesis. Hong-Hee Kim*[1], Hyung Joon Kim[1], Jeongim Ha[1], Hao Huang[2], Zang Hee Lee[3]. [1]Seoul National University, South Korea, [2]University of Chicago, USA, [3]Seoul National University School of Dentistry, South Korea

MSK (Mitogen- and stress-activated protein kinase) 1 is a Ser/Thr protein kinase that is activated by ERK1/2, JNK, and p38 MAPKs. This kinase has been suggested to play a role in the regulation of immune responses and mitogenic signaling. The activation of MAPK signaling pathway is one of the intracellular signaling events triggered by RANK stimulation in osteoclasts. Therefore, we explored the possibility

of MSK1 involvement in osteoclast differentiation by RANKL (receptor activator of nuclear factor kappaB lingand). We found that ERK1/2 and p38, but not JNK, could activate MSK1 upon RANKL stimulation of bone marrow-derived macrophages (BMMs) used as osteoclast progenitor cells. Inhibition of MSK1activity with a chemical reagent and suppression of MSK1 expression with a siRNA oligonucleotide resulted in a reduced formation of osteoclasts from BMMs with concomitant decrease in c-Fos and NFATc1 expression. The anti-osteoclastogenic effect of MSK1 siRNA was verified in vivo in a calvarial bone resorption model with RANKL. Our results suggest that MSK1 is an important novel signaling molecule involved in osteoclastogenesis induced by RANKL.

***Disclosures: Hong-Hee Kim**, None.*

SA0257

Mutation in SNX10 gene leads to autosomal recessive osteopetrosis and formation of osteoclasts unable to resorb bone. Petra Henning*[1], Eva-Lena Stattin[2], Per-Erik Sandström[3], Christina Stecksen-Blicks[4], Therese G. Kellgren[5], Patrik Ryden[5], Torsten Lönnerholm[6], Niklas Dahl[7], Joakim Klar[7], Ulf Lerner[8]. [1]Centre for Bone & Arthitis Research, University of Gothenburg, Sweden, [2]Department of Medical Biosciences, Medical & Clinical Genetics, Umeå University, Sweden, [3]Barnkliniken, Umeå University Hospital, Sweden, [4]Pediatric Dentistry, Department of Odontology, Faculty of Medicine, Umeå university, Sweden, [5]Department of Mathematics & Mathematical Statistics, Computational Life science Cluster (CLiC), Umeå University, Sweden, [6]Department of Radiology, Akademiska sjukhuset, Uppsala University, Sweden, [7]Department of Immunology, Genetics & Pathology, Science for Life Laboratory, Uppsala University, Sweden, [8]University of Umea, Sweden

Autosomal recessive osteopetrosis (ARO) is a rare disease having an incidence of 1 in 250,000 births. ARO can vary in severity from mild to severe and at least 10 genes leading to dysfunctional osteoclasts have been identified as causative.

We have studied eight individuals with intermediate form of ARO from the county of Västerbotten in Northern Sweden. Using Exome Sequencing, three patients were found to be homozygous for a splice site mutation in the Sorting Nexin 10 gene (SNX10) located at the donor splice site of exon 4 (c.212+1G>T). Sanger sequencing verified the mutation in all patients and their parents were found to be heterozygous. The phenotype is characterized by short stature and generalized increase in bone density with a radiological bone-within-bone appearance. All cases have experienced multiple fractures.

In vitro osteoclastogenesis using CD14+ monocytes purified from peripheral blood and cultured in M-CSF without and with RANKL was studies. There was no proliferative or morphological differences between M-CSF treated cells from controls and cells from patients. When cultured on plastic, cells from patients robustly responded to RANKL with increased formation of TRAP positive osteoclasts .

Osteoclasts formed from cells from patients were larger than osteoclasts formed from cells from controls. The increased size of osteoclasts from patients was associated with decreased number of osteoclasts. The expression of genes known to be important for osteoclastic functions such as *ACP5, CTSK, ITGB3, ITGAV*, *TCIRG1* and *DCSTAMP* were similar in cells from patients and controls. When cultured on bone, cells from patients were capable to differentiate to multinucleated TRAP positive cells. Most importantly, these cells, in contrast to osteoclasts from healthy controls, were unable to resorb bone measured as CTX release.

Splice predictor programs (SpliceSiteFinder, MaxEntScan, NNSPLICE and GeneSplicer) suggested that the SNX10 mutation would result in the absence of exon 4 in the mRNA. Using TaqMan Assays with primers spanning the exon junctions we show that exon 1-2 is expressed at similar levels in cells from patients and controls. In contrast, there was a 20-30 fold reduction of spliced exon 4-5 mRNA levels.In conclusion, we have identified a SNX10 mutation associated with ARO and showed that monocytes from the patients can be differentiated to osteoclast and that these cells are unable to resorb bone.

***Disclosures: Petra Henning**, None.*

SA0258

See Friday Plenary Number FR0258.

SA0259

See Friday Plenary Number FR0259.

SA0260

Withdrawn

SA0261

A novel role of farnesyl diphosphate synthase (FDPS) on the activity of Cl^- extrusion in osteoclasts. Hiroshi Kajiya*, Takashi Tsutsumi, Yoshiyuki Nagaoka, Kazuko Goto-T, Teruhisa Fukawa, Mina Sasaki, Fujio Okamoto, Koji Okabe. Fukuoka Dental College, Japan

Farnesyl diphosphate synthase (FDPS), an important enzyme in mevalonic acid metabolism catalyzes the production of geranyl pyrophosphate and farnesyl pyrophosphate, resulting in increase prenylation in small GTP proteins. Prenylated GTP proteins are located to the membrane and activated in migration, proliferation, and differentiation. In contrast, nitrogen-containing bisphosphonates (NBPs) have well known to inhibit FDPS, leading to disturbance of polymerization in cytoskeleton structure during bone resorption and promotion in apoptosis in mature osteoclasts.

However, little is known whether FDPS regulate directly the bone resorption activity, including in hydrochronic acid extrusion via specific transporters in mature osteoclasts. Using yeast two-hybrid screening method, we found that the FDPS were combined with cytoplasmic domain of ClC-7 Cl^- transporters. Therefore, the aim of this study was to investigate the expression and functional role of FDPS on the extrusion activity of ClC-7 Cl^- transporters in osteoclasts.

FDPS were expressed in osteoclast precursors and slightly upregulated by RANKL during osteoclastogenesis. Furthermore, FDPS was associated and colocalized with ClC-7 Cl^- transporters in mouse osteoclasts and HEK cells coexpressing FDPS and ClC-7 Cl^- transporters. Extracellular acidification induced outwardly rectifying Cl^- currents and decreased intracellular Cl^- concentration ($[Cl^-]_i$) associated with in ClC-7 Cl^- transporters in osteoclasts. Zoledronic acid and alendronate sodium, FDPS inhibitors suppressed acid-induced Cl^- currents and $[Cl^-]_i$ reduction in a dose-dependent manner. The tetracycline-induced FDPS silencing significantly suppressed the Cl^- currents and $[Cl^-]_i$ reduction. In contrast, the inhibitory action of zoledronic acid was rescued by addition of geranylgeranyl acid, a derivative of mevalonic acid metabolism. In transgenic mice overexpressing with FDPS under control of cathepsin K promoter (*ctsk* FDPS Tg-mice), bone mineral density significantly decreased with elevation of the number of osteoclasts, but not osteoblasts compared to WT mice. Furthermore, the activation of the acid-induced Cl^- currents dominantly augmented in osteoclasts derived from *ctsk* FDPS Tg-mice.

The results suggest that FDPS may contribute to regulate the bone resorption activity, especially the ClC-7 Cl^- transporter activity in mature osteoclasts because FDPS inhibitors NBPs, at least partially, suppressed the activity of Cl^- transporters.

***Disclosures: Hiroshi Kajiya**, None.*

SA0262

Dual Modulation of Activin A on Osteoclast Differentiation, Activity and Survival. Tristan Fowler*, Archana Kamalakar, Nisreen Akel, Larry Suva, Dana Gaddy. University of Arkansas for Medical Sciences, USA

The process of bone resorption is regulated at multiple levels. Current bone-active therapies primarily target bone resorption, whereas additional targets such as the formation of osteoclasts (OC), and their motility, fusion and lifespan have been largely unexplored. We and others have shown that RANKL and Activin A (ActA) are potent stimulators of murine bone marrow osteoclastogenesis. However, ActA treatment does not induce osteoclastogenesis in purified populations of murine bone marrow macrophages (BMM), but inhibits RANKL-induced OC development. We hypothesized that these factors differentially regulate the migration of both OC precursors and mature OC. We determined the effects of ActA and RANKL on BMM motility and bone resorption using time-lapse video microscopy. BMMs were plated onto culture dishes with 25 ng/ml mCSF alone for 24hr, prior to the addition of 100 ng/mL RANKL or 50 ng/mL ActA, alone or together, for up to 4d. Other BMMs were cultured on bone slices for 5d in the presence of mCSF+RANKL to stimulate OC differentiation prior to treatment with RANKL or ActA, alone or together for an additional 1-2d. Cells were imaged at 60 images/hour and the cells maintained at 37℃ and 5% CO_2/Air. The 4hr movement of ten individual motile OC precursors were tracked and analyzed with NIH ImageJ. Parameters calculated for each individual cell track included cumulative track length, migration rate, maximum instantaneous velocity, range of velocity, and percent total displacement. BMMs migrated at a constant velocity and distance from d1-4. RANKL significantly increased motility parameters on d2 and d3, an effect that was lost by d4. In contrast, ActA treatment decreased all motility parameters on d1-4. Surprisingly, when added with RANKL, ActA treatment completely blocked all RANKL stimulated OC precursor motility on plastic, as well as mature RANKL-stimulated OC motility on bone slices. ActA treatment of mature OC (d5) also suppressed RANKL-stimulated bone resorption, measured by pit formation. The suppression appeared to be associated with a decrease in OC lifespan, since ActA increased activated Caspase 3, and caused a decrease in actin ring formation in mature OC on bone slices. Collectively these data indicate a dual modulatory function of ActA on OCs. ActA indirectly stimulates murine whole bone marrow osteoclastogenesis, but it also directly inhibits RANKL-induced murine OC differentiation, motility, and resorption and enhances OC apoptosis.

***Disclosures: Tristan Fowler**, None.*

SA0263

See Friday Plenary Number FR0263.

SA0264

Loss of *Aim2* is Associated with Increased BMD and Decreased Bone Resorption. Kathryn Shultz*[1], Laura Reinholdt[1], Leah Rae Donahue[1], Katherine Fitzgerald[2], Leonard Shultz[1], Wesley Beamer[1], Cheryl Ackert-Bicknell[1]. [1]The Jackson Laboratory, USA, [2]Department of Medicine, University of Massachusetts Medical School, USA

Genetic association with bone mineral density (BMD) regulation have been demonstrated for human Chr 1q and at the distal end of mouse Chromosome 1 (Chr 1). The mouse locus, designated Bmd1, is in fact a series of smaller effect size loci. Consequently multiple genes in this region affect BMD. Using nested congenic mouse strains (C57BL/6J strain carrying small C3H/HeJ Chr 1 regions), we narrowed one of these loci to a 0.152 Mb segment containing the gene, Aim2 (Absent in melanoma2), and a predicted gene Gm4955. We found that at 16 weeks of age, female mice lacking the Aim2 gene have significantly increased whole body areal (a)BMD as compared to wildtype controls (Aim2-/-: 0.0538 ± 0.0007 vs Aim2+/+: 0.0508 ± 0.0007 g/cm2, p = 0.004). Further, femoral volumetric (v)BMD is also increased in Aim2-/- mice (Aim2-/-: 0.650 ± 0.009 vs Aim2+/+: 0.611 ± 0.012 mg/mm3, p = 0.006). Gene expression analyses suggested that Aim2 is expressed in both osteoblasts and osteoclasts. We cultured calvarial osteoblasts from neonatal Aim2-/- and Aim2+/+ mice. No differences were found in alkaline phosphatase activity between the Aim2-/- and Aim2+/+ cells at day 6 post differentiation or in mineralized nodule formation at day 14 post differentiation. Thus, Aim2 does not appear to affect bone formation or mineralization in culture. We cultured bone marrow cells from 6 week old female Aim2-/- mice in the presence of mCSF and RANK ligand. No differences in TRAP positive, multinucleated osteoclast cell number were observed between the Aim2-/- and Aim2+/+ cultures (Aim2-/-: 653 ± 59 vs Aim2+/+: 690 ± 89, p = 0.74). Thus, Aim2 did not affect either osteoclast precursor pools or osteoclast maturation. To explain the increased BMD in Aim2-/- mice, we hypothesize that the osteoclasts were deficient in activity. Urinary deoxypyridinoline (DPD, marker of bone resorption) was assayed in 8 week old female Aim2-/- and Aim2+/+ mice and found to be significantly lower in Aim2-/- vs controls (corrected for urinary creatinine, Aim2-/-: 4.67 ± 0.24 vs Aim2+/+: 6.60 ± 0.38, $p < 0.001$). The combined in vivo resorption marker and BMD data suggest that Aim2 has a regulatory role in osteoclast function. Aim2 is part of the interferon-inducible gene cluster, and its deficiency activates interferon signaling suggesting that this gene links the skeletal and immune systems. In summary, we show that loss of Aim2 impacts bone biology, supporting the hypothesis that this gene underlies one of the distal Chromosome 1 BMD loci.

***Disclosures: Kathryn Shultz**, None.*

SA0265

Molecular Mechanism of the Inhibitory Effect of Oleanolic Acid on Osteoclastogenesis. Dongfeng Zhao*[1], Xu Feng[2], Yongjun Wang[3]. [1]The University of Alabama At Birmingham, USA, [2]University of Alabama at Birmingham, USA, [3]Longhua Hospital, Shanghai University of Traditional Chinese Medicine, China

Oleanolic acid (OA) is one of the major active ingredients from Chinese medicinal herb Nvzhenzi (Fructus Ligustri Lucidi), which exerts beneficial effects on various organs including the skeleton. We have recently demonstrated that OA exerts the osteoprotective effect in part by promoting bone formation via the stimulation of osteoblast differentiation. Interestingly, a number of studies showed that OA derivatives inhibit osteoclastogenesis. The objective of this study was to investigate the effect of OA on osteoclast formation and function. Primary mouse bone marrow macrophages (BMMs) were treated with M-CSF and RANKL in the presence of different doses of OA (0, 1, 2, 4, 8, 10uM) to promote osteoclastogenesis. We found that OA inhibited osteoclastogenesis dose-dependently and 10uM OA completely blocked osteoclastogenesis. Consistently, addition of OA (10uM) led to no resorption pits in bone resorption assays. Next, we pretreated BMMs with OA (10uM) for 4 days and OA-pretreated BMMs were fully capable of forming osteoclasts with M-CSF and RANKL stimulation, ruling out that this inhibitory effect of OA resulted from cytotoxicity. Notably, while lipopolysaccharide, IL-4 and IFN-γ inhibit osteoclastogenesis from fresh BMMs, they fail to do so with RANKL-primed BMMs. To determine whether OA acts similarly, we pretreated BMMs with M-CSF and RANKL for 1, 2, or 3 days prior addition of OA (10uM). Interestingly, OA is able to inhibit osteoclast formation from BMMs pretreated by RANKL as long as 3 days. These data indicate that the effects of OA on osteoclastogenesis are not affected by RANKL-mediated lineage commitment of osteoclast precursors. To elucidate the molecular mechanism underlying the inhibitory effect of OA on osteoclastogenesis, we determined whether OA affect known RANK signaling pathways. OA exerts no effect on the activation of ERK, p38, JNK and I?B pathways. However, OA impairs RANKL-induced expression of NFATc1 and four osteoclast genes (cathepsin K, matrix metalloproteinase 9, carbonic anhydrase 2 and tartrate acid resistant phosphatase) in both fresh and RANKL-pretreated BMMs. In conclusion, we have demonstrated that OA, similar to its various derivatives, exerts an inhibitory effect on osteoclastogenesis. Moreover, unlike other anti-osteoclast factors, OA can inhibit osteoclastogenesis from both fresh and RANKL-primed BMMs. Finally, OA inhibits osteoclastogenesis by suppressing the expression of NFATc1 and osteoclast genes.

***Disclosures: Dongfeng Zhao**, None.*

SA0266

Relationship between Soluble OSCAR and Disease Activity: A 12 Month Study of Newly Diagnosed RA Patients. Anak Dharmapatni[1], Roxanne Coleman[1], Michelle Lorimer[2], Andrew Zannettino[1], Helen Weedon[3], Mihir Wechalekar[3], David Haynes[1], Malcolm Smith[3], Tania Crotti*[4]. [1]School of Medical Sciences, The University of Adelaide, Australia, [2]School of Public Health, The University of Adelaide, Australia, [3]Rheumatology, Repatriation General Hospital, Australia, [4]University of Adelaide, Australia

Rheumatoid arthritis (RA) is characterized by synovitis and an increase in osteoclast number and activity, leading to bone erosions and joint destruction. Osteoclast-associated receptor (OSCAR) is a member of the leukocyte receptor complex and is involved in co-stimulating osteoclastogenesis. Studies suggest that OSCAR may contribute to the pathogenesis and severity of RA and osteoporosis (1, 2, 3, 4,). Increased levels of membrane bound OSCAR are associated with the peripheral blood monocytes (2), and synovial tissue macrophages and the vasculature in RA synovial tissues compared to healthy controls (2, 4). Conversely soluble (s) OSCAR is lower in the serum of active RA patients compared with healthy individuals (3). OSCAR-Fc has been shown to decrease osteoclast formation in pre-osteoclast: osteoblast co-cultures (5). We propose that successful treatment of RA results in increased cleavage of cell associated OSCAR resulting in increased sOSCAR levels in the joint. Thus elevated sOSCAR suppresses osteoclastic bone resorption and its elevation may be an early marker that can predict reduced joint damage and successful treatment. This study examines the changes in serum levels of sOSCAR following individual active RA patients from initial diagnosis (before treatment) through to 12 months of combination DMARD therapy.

Methods: The levels of sOSCAR in serum were measured by enzyme-linked immunosorbent assay (ELISA) of the serum from 10 RA patients at 0, 6 and 12 months (where possible). sOSCAR levels were compared at initial diagnosis and at 12 months using a paired t-test. Associations between sOSCAR and disease activity markers C-reactive protein (CRP), as well as the erythrocyte sedimentation rate (ESR), and disease activity score (DAS28), over time were also compared.

Results: Of interest sOSCAR significantly ($p = 0.04$) increased after 12 months treatment from baseline with a mean increase of 37ng/ml. No strong associations were observed between sOSCAR levels and CRP or ESR. However, in 6 of 8 patients DAS28 decreased whilst sOSCAR increased.

Conclusion: sOSCAR increases with combination DMARD therapy and sOSCAR may be inversely correlated with DAS28 in RA.

(1) Kim et al JBMR 2005, (2) Herman et al Arth Rheum 2008 (3) Zhao et al Clin Med J Eng 2011 (4) Crotti et al ART 2012 (5) Kim et al J Exp Med 2002

***Disclosures: Tania Crotti**, None.*

SA0267

Salubrinal Inhibits Differentiation of Osteoclasts in Unloaded Mice. Ping Zhang*, Andy Chen, Hiroki Yokota. Indiana University – Purdue University Indianapolis, USA

Disuse osteoporosis is a skeletal problem induced by lack of weight bearing and imbalanced activities of osteoclasts and osteoblasts. We previously reported that salubrinal enhances healing of bone wounds. Little is known, however, about its effects on osteoclasts (OCL) in response to disuse. Herein, we addressed a question: in unloaded mice, does salubrinal suppress differentiation of OCL?

Forty C57BL/6 female mice (~14 wks) were subjected to unloading (20 for unloading controls, and 20 for salubrinal at 1 mg/kg), and 13 mice were used as age-matched controls. Changes in BMD/BMC in the lumbar spine, femur, and tibia were determined. To evaluate disuse-linked effects on OCL, bone marrow cells were harvested, and activities of OCL (formation, migration, and adhesion) as well as colony forming unit macrophage (CFU-M) were determined. Differentiation of osteoblasts was also examined using CFU assays for osteoblasts (CFU-OBL) and fibroblast-like MSCs (CFU-F).

Compared to age-matched controls, unloading induced a significant loss of BMD/BMC. Importantly, salubrinal suppressed reduction in BMD/BMC ($p<0.05$) compared to the unloading vehicle control. The cells isolated from the unloaded mice showed higher CFU-M, formation of OCL, migration of OCL progenitors, and adhesion of OCL (all $p<0.001$) compared to age-matched controls. Compared to the unloading control, salubrinal suppressed the number of CFU-M and the formation, migration and adhesion of OCL (all $p<0.001$). Salubrinal-driven reduction in the formation of OCL and CFU-M was dose-dependent. Furthermore, compared to the unloading control, salubrinal presented a significant increase in both CFU-F colonies ($p<0.01$) and CFU-OBL colonies ($p<0.001$).

This study demonstrates that unloading-reduced bone mass was significantly restored by salubrinal. The result is consistent with salubrinal's inhibitory effects on osteoclasts, as well as its stimulatory role on osteoblasts. The study provides evidence that salubrinal can be a potential therapeutic agent for preventing bone loss in disuse osteoporosis.

***Disclosures: Ping Zhang**, None.*

SA0268

The Successful Design Of A Novel Highly Potent Nitrogen-Containing Bisphosphonate With Lower Bone Affinity. Frank H. Ebetino*[1], Mark Lundy[2], Aaron A. Kwaasi[1], James Dunford[3], Xuchen Duan[1], James Triffitt[4], Adam Mazur[5], Gwyn Jeans[6], Bobby L. Barnett[7], R Graham Russell[8]. [1]University of Oxford, United Kingdom, [2]Osteoresearch LLC, USA, [3]Oxford University, Headington, United Kingdom, [4]University of Oxford Nuffield Orthopaedic Centre, United Kingdom, [5]TWI Chem LLC, USA, [6]Procter & Gamble, USA, [7]University of Cincinnati, USA, [8]University of Oxford, United Kingdom

The antiresorptive mechanism of action of the current clinically used nitrogen-containing bisphosphonates (N-BPs) appears to be due to a combination of bone affinity characteristics, which target BPs to bone, and the inhibition of the farnesyl diphosphate synthase (FPPS) enzyme within osteoclasts and their precursors. Their prolonged presence in bone may be related to their high bone affinity. Bisphosphonates with lower bone affinity may provide more even skeletal distribution, shorter residence time on bone surfaces, lesser turnover reduction, and less concern about potential skeletal side effects. We have therefore sought to improve the profile of N-BPs by optimizing their inhibition of the FPPS enzyme while reducing their bone affinity. Driven by advances in structural biology, several optimized analogs were identified. When compared with the other clinically utilized N-BPs, one of these analogs, OX-14 (1-fluoro-2-(imidazo-[1,2-a]pyridin-3-yl)-ethyl-bisphosphonic acid) has the highest inhibitory potency at the enzyme and has the lowest affinity for bone mineral. This series, led by OX-14 (IC_{50}=2.5 nM), was an even more potent inhibitor of FPPS than zoledronate (IC_{50}=4.1 nM). Urinary excretion after parenteral dosing is inversely related to skeletal retention, and was greater for Ox-14 than for other N-BPs in rats, indicative of lower bone affinity. Thus, using ibandronate as a control = 1.0, the relative 24 hour urinary excretion of Aln, Zol, Ris, OX-14 was 0.53, 0.61, 1.0, 1.24 respectively. However, adequate bone affinity and excellent in vivo efficacy was demonstrated by OX-14 in the growing rat model. Thus OX-14 (D_{20}=0.0003 mg P/kg) was a very potent antiresorptive analog in vivo relative to other N-BPs (alendronate D_{20}=0.0016 mg P/kg; ibandronate D_{20}=0.0006 mg P/kg; zoledronate D_{20}=0.0001 mg P/kg) (D_{20}= the dose needed to produce a 20% increase in bone density above vehicle control). In a model of collagen induced arthritis in rats, OX-14 demonstrated efficacy similar to other potent N-BPs. In the knee, a 0.5 mg P/kg dose of OX-14 decreased bone resorption by 100%, as did zoledronate, while no dose tested of alendronate was completely antiresorptive. Since lower bone affinity BPs, at maximally effective doses, may reduce overall skeletal turnover less, these potent new FPPS inhibitors may also offer enhanced therapeutic utility in other bone related diseases including rheumatoid arthritis, osteoarthritis and certain cancers.

***Disclosures: Frank H. Ebetino**, University of Oxford, 5; Procter & Gamble, 7*
This study received funding from: Procter & Gamble

SA0269

Periosteal Preosteoclasts Direct Cortical Bone Growth and Modeling by Secretion of PDGF. Hui Xie*[1], Zhuang Cui[2], Weizhong Chang[3], Chang-Jun Li[2], Lingling Xian[4], Bing Yu[5], Gehua Zhen[6], Janet Crane[3], Mei Wan[4], Maureen Pickarski[7], Le Thi Duong[8], Er-Yuan Liao[9], Xu Cao[3]. [1]Johns Hopkins Medical Institution, USA, [2]Department of Orthopaedic Surgery, Johns Hopkins Medical Institution, USA, [3]Johns Hopkins University, USA, [4]Johns Hopkins University School of Medicine, USA, [5]Johns Hopkins School of Medicine, USA, [6]The Johns Hopkins Hospital, USA, [7]Merck & Co., Inc., USA, [8]Merck Research Laboratories, USA, [9]Institute of Endocrinology & Metabolism, Second Xiangya Hospital of Central South University, China

Cortical bone makes up 80% of the weight of the human skeleton and provides mechanical support of the body and protection of vital organs, but little is known about factors that regulate cortical bone formation. Here we report that periosteal $Trap^+$ preosteoclasts (pOCs) secrete platelet-derived growth factor (PDGF) to induce migration of mesenchymal stem cells (MSCs) for cortical bone modeling. $Trap^+$ pOCs and osteoclasts are absent in CSF-1 knockout mice. There was a very thin cortical bone shell developed in the osteopetrotic CSF-1 knockout mice as detected by μCT and histology analysis. We hypothesized that the osteoclastic cell lineage could be essential to maintain normal cortical bone formation, and thus examined if these cells secret potential factor(s) to induce MSCs recruitment. Conditioned media from $Trap^+$ mononuclear pOCs derived from wild type (WT) mice was shown to induce migration of MSCs significantly more relative to conditioned media from $Trap^-$ monocytes. To identify the potential factor(s) secreted by pOCs, neutralizing antibodies specific for TGFβ2, TGFβ3, IGF-I, IGF-II, PDGF-AA, PDGF-BB, and noggin were evaluated with the conditioned media. The PDGF-BB antibody abolished the induced migration, though other neutralizing antibodies had no effect. Western blots confirmed that pOCs specifically secrete PDGF-BB, not PDGF-AA, and cells plated on bone slices enhanced the secretion of this growth factor. Moreover, PDGF-BB was co-localized with pOCs in the periosteum of WT mice, whereas no PDGF-BB was detectable in the periosteum of CSF-1 knockout mice. Genetic deletion of cathepsin K (CatK) in mice or pharmacological inhibition of CatK activity in ovariectomized monkeys has been shown to increase cortical thickness and periosteal bone formation. Here, the number of periosteal pOCs and the level of PDGF-BB were increased in CatK knockout mice and in WT mice treated with a CatK inhibitor. Conditioned medium of CatK-deficient pOCs or the CatK inhibitor-treated WT pOCs secreted more PDGF-BB and recruited more MSCs than conditioned medium of WT pOCs. This suggested that CatK inhibition stimulates cortical bone formation potentially via increasing pOC number and secretion of PDGF-BB. Taken together, the genetic and pharmacological evidence support the role of periosteal $Trap^+$ preosteoclasts in directing cortical bone formation by secretion of PDGF-BB.

***Disclosures: Hui Xie**, None.*
This study received funding from: Financially supported by Merck

SA0270

See Friday Plenary Number FR0270.

SA0271

See Friday Plenary Number FR0271.

SA0272

See Friday Plenary Number FR0272.

SA0273

See Friday Plenary Number FR0273.

SA0274

See Friday Plenary Number FR0274.

SA0275

See Friday Plenary Number FR0275.

SA0276

Calcium-dependent actomyosin contractility in osteocytes. Andrew Baik*[1], Ivo Kalajzic[2], Elizabeth M.C. Hillman[1], Yingxiao Wang[3], Cheng Dong[4], X Guo[1]. [1]Columbia University, USA, [2]University of Connecticut Health Center, USA, [3]University of California, San Diego, USA, [4]Penn State University, USA

Intracellular Ca^{+2} ($[Ca^{+2}]_i$) oscillations, mediated by mechanosensitive Ca^{+2} channels and the ER Ca^{+2} store, have been observed in osteocytes in response to mechanical loading *in vitro* and *ex vivo* in our laboratory (Lu XL et al., 2012, Jing D et al., 2013). While many distant downstream gene expression pathways of $[Ca^{+2}]_i$ signaling have been studied, the immediate, temporally regulated effects of these numerous $[Ca^{+2}]_i$ oscillations in osteocytes have not been elucidated. A recent study in the gene expression of primary osteocytes has suggested high levels of muscle contraction-related proteins (Paic F et al., 2009). A hallmark of muscle is its $[Ca^{+2}]_i$-dependent actomyosin contractility. We hypothesized that osteocytes utilize $[Ca^{+2}]_i$ oscillations to activate pulsing, muscle-like contractile mechanical behavior. In this study, we used a fast 3D imaging technique to simultaneously measure the contractile behavior of the actin networks *and* $[Ca^{+2}]_i$ in single osteocytes.

$[Ca^{+2}]_i$ spikes were induced using fluid flow, ATP, or ionomycin in MLO-Y4 osteocytes (Figure 1). Contraction in the actin networks was measured immediately upon onset of $[Ca^{+2}]_i$ influx in all groups, indicated by a decrease in the strain value (Figure 1 A,B,C). Microtubule networks did not display a similar contractile response (Figure 1D). Longer imaging of contractions displayed reversible, phasic contractions in the actin networks over a period of ~180 seconds (Figure 1B).

As non-muscle and smooth muscle myosin II isoforms are regulated by myosin light chain kinase (MLCK) and skeletal and cardiac myosin II isoforms by troponins, we sought to determine the myosin responsible for the observed contraction. Under ATP stimulation, MLCK inhibition by ML-7 drastically altered the kinetics of contraction (Figure 1 E,F), but skeletal and non-muscle myosin II inhibition by blebbistatin had no effect (Figure 1E). This pointed towards a smooth muscle myosin mediated contraction. Furthermore, we verified the presence of smooth muscle myosin heavy chain (SMMHC) in primary osteocytes and MLO-Y4 osteocytes by western blot.

Here, we demonstrate a novel osteocyte mechano- and transduction behavior where $[Ca^{+2}]_i$ oscillations activate dynamic actomyosin contractions. Future studies will investigate downstream behaviors of contractility in osteocytes, such as contractility-mediated vesicle exocytosis (Wollman R et al 2012).

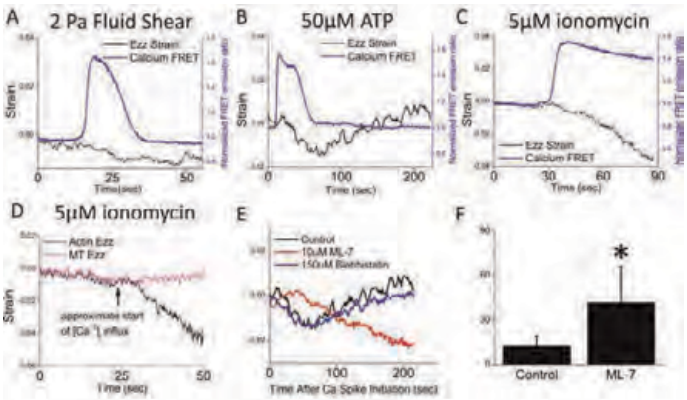

Figure 1

***Disclosures: Andrew Baik**, None.*

SA0277

See Friday Plenary Number FR0277.

SA0278

Cortical Bone Gene Expression is Altered by Post Obitum Isolation Treatment Prior to RNA Extraction in Adult Female Mouse Tibiae. Kimberly Atteberry*, Whitney Bullock, Russell Main. Purdue University, USA

Mouse cortical bone is commonly used in gene expression analyses of skeletal tissues to examine the effects of transgenic or experimental manipulations on osteocyte gene expression. Many methods are used to isolate osteocyte-enriched cortical samples prior to RNA isolation, including: (1) flushing the bone marrow with PBS and (2) flushing followed by collagenase digestion. When bone marrow is flushed with PBS, there likely remains a cellular layer lining the endosteum, which the collagenase treatment is designed to remove. To our knowledge, the effect of these different treatments on osteocyte gene expression and their ability to remove endosteal surface lining cells have not been systematically examined.

Female, 13 week old, C57Bl/6 mice were euthanized and both tibiae were extracted. The marrow was removed from all tibiae by repeated flushing with PBS. Following this, tibiae were either snap frozen in liquid nitrogen or subjected to one of two collagenase treatments (n=4-5/treatment). In Treatment 1, the tibial diaphysis was broken into fragments and subjected to a single-25 minute collagenase digestion. In Treatment 2, broken cortical tibial fragments were subjected to three-25 minute collagenase digestions. After each treatment, all samples were rinsed three times in αMEM, snap frozen in liquid nitrogen, and stored at -80˚C. RNA was subsequently isolated from all samples, quantified, and reverse transcribed to cDNA. Relative expression of DMP1 and Col1A1 were used to account for the proportion of osteocytes and osteoblasts in the sample. RPLP2 was used as an internal control gene and did not vary in expression between the Control group (PBS flush only) and Treatments 1 and 2. We hypothesized that expression of Col1A1 would decrease with the number of osteoblasts as the number of collagenase washes increased. DMP1 expression should not change across the treatments, as we expected osteocytes to be unaffected by the collagenase treatments.

Relative gene expression for Treatments 1 and 2 were calculated relative to the Control Treatment using the ΔΔCt method. Col1A1 expression did not change significantly following a single collagenase digestion in Treatment 1, but increased 240-fold in Treatment 2. DMP1 expression changed in a similar, yet less dramatic fashion. Overall, our results show that multiple collagenase treatments drastically alter cortical DMP1 and Col1A1 expression and should be avoided in future studies targeting these genes.

***Disclosures: Kimberly Atteberry**, None.*

SA0279

Osteocyte Lacuna Density Scales With Human Body Size. BIN HU*[1], Ingrid Murra[1], Yusuf Juwayeyi[2], John Chisi[3], Timothy Bromage[1]. [1]New York University College of Dentistry, USA, [2]Department of Anthropology, Long Island University, USA, [3]University of Malawi College of Medicine, Malawi

Aim: Comparative mammalian osteocyte densities are inversely relate to body mass. This relationship has never been tested among individuals that vary in body size within a single species. The goal of our research is to tally the number of osteocytes from human bone samples to evaluate the relationship between osteocyte density and body size.

Methods: Ten midshaft femurs obtained from sub-Saharan Africans of Bantu origin and known life history, and body mass index (BMI), were embedded in polymethylmethacrylate, sectioned and polished to 1μm finish. Montages of entire femur cross sections were obtained by backscattered electron microscopy in the scanning electron microscope (BSE-SEM) with a Zeiss EVO 50 SEM and SmartStich software. Monochrome 256 gray level images (0.978 μm/pixel) were converted to a binary, rendering lacunae to 0-level. Lacunae aspect ratios allowed them to be identified and automatically enumerated separately and measured in proportion to the detected bone area using Leica Quantimet 550 analysis software.

Results: The correlation between osteocyte lacuna density and body height was high, positive, and significant ($r = 0.78$, $R^2 = 0.54$, $p = 0.037$). When osteocyte lacuna density was evaluated in respect to an individual's BMI, the relationship improved further still ($r = -0.83$, $R^2 = 0.62$, $p = 0.022$), though it was negative. No relationship between osteocyte lacuna density was recovered in tests that included weight alone, nor were there any apparent associations with characteristics of an individual's social, economic, occupational, or medical history.

Conclusion: There is a relationship between human femoral osteocyte lacuna density and body height, though body weight interacts with body height to generate variability in bone cell density. In deference to comparative mammalian studies, the relationship between osteocyte lacuna density bore no relationship to body mass alone, but, instead, to a complex relationship with height and weight; i.e. BMI. Furthermore, while the comparative mammalian relationship between osteocyte lacuna density and body mass is negative, the relationship between lacuna density and height among humans is positive (though negative with BMI).

Funding: NSF awards BCS-1062680; The 2010 Max Planck Prize administered by the Max Planck Society and Alexander von Humboldt Foundation in support of Hard Tissue Research Program in Human Paleobiomics.

Key words: midshaft femur, qBSE-SEM, osteocyte lacuna density, BMI

***Disclosures: BIN HU**, None.*

SA0280

See Friday Plenary Number FR0280.

SA0281

Sclerostin expression in bone is associated with bone mass. Nathalie Bravenboer*[1], Ruben Visser[2], Angela Oostlander[3], Eveline Sohl[3], Huib Van Essen[4], Annemieke Heijboer[5], Martin Den Heijer[6], Paul Lips[1]. [1]VU University Medical Center, The Netherlands, [2]Dept Clinical Chemistry, VU Unversity Medical Center, The Netherlands, [3]dept Endocrinology, VU University Medical Center, The Netherlands, [4]VU Medical Center, The Netherlands, [5]dept Clinical chemistry, VU University Medical Center, The Netherlands, [6]VU Medical CenterPostbus 70571007 MB Amsterdam, The Netherlands

Sclerostin is a major negative regulator of osteoblastic activity. Serum sclerostin has a weak positive association with bone mineral density (BMD), but high sclerostin levels were strongly associated with increased fracture risk. These contradictions could be explained by the fact that serum sclerostin does not reflect its action in bone. The aim of this study was to investigate whether sclerostin expression in bone is related to bone mass measured as BMD or using histomorphometry.Twenty six patients with Crohn's disease and osteopenia were included. These patients were a subgroup from a large randomized clinical trial, investigating treatment with risedronate (Crohn and Bone study registered as NTR 163 Dutch Trial Register). Sclerostin expression in bone was detected on iliac crest bone biopsies, using immunohistochemistry (mouse-human antibody, R&D systems) and measured as sclerostin positive cortical area (Scl postive area) (NIS elements, Nikon). Histomorphometry was performed according to the standardized nomenclature (Dempster et al., JBMR 2013, 28, 1: 2-17). DXA was used to obtain total hip (THP-BMD) and lumbar spine bone mineral density (LS-BMD).

Scl positive area showed a positive correlation with bone mineral density: for LS-BMD and THP-BMD, respectively.R=0.38 (95%CI 0.00-0.66) and R=0.55 (95%CI 0.27-0.75). Scl postive area was only weakly correlated with trabecular bone volume (BV/TV, R= 0.07, 95%CI -0.28-0.40) but slightly positively correlated with cortical thickness (CTh, R= 0.2, 95%CI -0.05-0.58, p= 0.08) Correlations between bone formation rate and osteoclast number were weak.

In conclusion, a positive correlation was detected between sclerostin expression in bone and BMD. This correlation was previously reported for serum as well. Correlations with histomorphometric indices indicate that cortical bone is more associated to sclerostin than trabecular bone. The impact of sclerostin expression in bone on bone quality needs further study.

***Disclosures: Nathalie Bravenboer**, None.*
This study received funding from: Amgen Unrestricted Grant

SA0282

A role for cementocytes in the pathogenesis of periapical bone resorption. Andiara De Rossi*[1], Raquel Silva[2], Sandra Alves[3], Lea Assed Bezerra da Silva[2], Paulo Nelson Filho[2], Marcos Antonio Rossi[4]. [1]Faculty of Dentistry of Ribeirão Preto, University of São Paulo, Bra, [2]School of Dentistry of Ribeirao Preto - University of Sao Paulo, Brazil, [3]School of Pharmaceutical Sciences of Ribeirao Preto - University of Sao Paulo, Brazil, [4]School of Medicine of Ribeirão Preto, University of São Paulo, Brazil

Periapical bone resorption occurs as consequence of polymicrobial infection of the dental pulp and root canal system, and ultimately results in destruction of periapical tissues including periodontal ligament, cementum and bone surrounding the tooth apex. Although osteocytes has been recently suggested to play role in regulation of bone diseases, the role of cementocytes in periapical bone loss has not been suggested. The aim of the present study was to evaluate the possible role of cementocytes in the regulation of periapical bone resorption at different stages of development. Inflammatory periapical bone resorption was experimentally-induced in the lower first molars of male C57BL/6 wild-type mice, aging 6 to 8 weeks, by pulp exposure to the oral environment. Intact teeth were used as controls. At 0, 7, 21 and 42 days following pulp infection, the periapical region was evaluated under conventional microscopy (morphologic analysis), fluorescence microscopy (morphometric analysis), immunohistochemistry (neutrophils, macrophages and lymphocytes), immunofluorescence (RANK, RANKL and OPG), enzymehistochemistry (osteoclasts) and RT-PCR (RNAm expression of IL-1alpha, TNF-alpha, IFN-gamma, KC, IL-17, RANK, RANK-L, OPG and catepsin K). Our results show a progressive increase in cementum and bone resorption, inflammatory cells and osteoclasts number, accompanied by enhanced mRNA levels of IL-1alpha, IFN-gamma, IL-17, RANKL, and catepsin K. The immunofluorescence showed that RANKL was expressed on cementocytes, and its expression increased with the lesion progression. Conclusion: our findings shows that cementocytes produce RANK-L in response to endodontic infection and are involved in the pathogenesis of bone resorptive periapical lesions.

***Disclosures: Andiara De Rossi**, None.*
This study received funding from: Financial Support by FAPESP, Brazil

SA0283

See Friday Plenary Number FR0283.

SA0284

Osteocytes Produce Interferon-β to Negatively Control Osteoclastogenesis. Chiyomi Hayashida, Junta Ito, Mai Nakayachi, Mari Okayasu, Yoshiyuki Hakeda, Takuya Sato*. Meikai University School of Dentistry, Japan

Interferon (IFN)-β deficiency causes osteoporosis because of an excessive osteoclastogenesis (OC-genesis), which has been widely accepted due to an incapability of RANKL-stimulated osteoclast precursors (OC-pre) to produce IFN-β as a negative feedback factor. OC-genesis during bone remodeling is controlled by osteocytic RANKL and OPG. However, other such factors have been largely unknown. Here we searched for osteocyte-derived OC-genesis regulatory factors using osteocytic MLO-Y4 cells and a newly developed culture system of primary osteocytes. First we studied the effects of MLO-Y4 cell-conditioned medium (MLO-Y4-CM) on M-CSF-induced OC-pre generation from bone marrow (BM) cells. The cells generated by M-CSF with MLO-Y4-CM showed an increased mRNA expression of double-stranded RNA-dependent protein kinase (PKR), which is known to inhibit c-Fos translation evoked by RANKL in OC-pre. Accordingly, when treated with soluble RANKL (sRANKL), the cells induced by M-CSF with MLO-Y4-CM exhibited a reduced capability of osteoclastic differentiation concomitant with decreased c-Fos translation. The addition of neutralizing anti-IFN-β antibody (αIFN-β-Ab) to MLO-Y4-CM during M-CSF-induced OC-pre generation partially abolished the increase in *PKR* mRNA expression in the generated cells. Consequently, the decreased c-Fos production and the reduced capability of osteoclastic differentiation were partially resuced. MLO-Y4 cells expressed *IFN-β* mRNA more than 400 times higher compared to OC-pre treated with sRANKL for 3 hr, a condition for OC-pre to significantly express *IFN-β* mRNA for negative feedback regulation. Next, we developed a culture system of osteocyte-enriched bone fragments (OEBFs), that osteocytes reside in lacunae of bone matrix freed from non-osteocytic cells by sequential collagenase/EDTA treatments. OEBFs expressed osteocyte marker genes, *DMP-1* and *sost* mRNAs, but not osteoblast marker gene, *keratocan.* Importantly, OEBFs produced *IFN-β* mRNA two times higher compared to intact bone fragments. When BM cells and OEBFs were cocultured without contact during M-CSF-induced OC-pre generation, OEBFs reduced the capability of the generated cells to differentiate into OCs, which was partially recovered by the addition of αIFN-β-Ab during coculture with OEBFs. OEBFs prepared from *OPG*-knockout mice had a similar effect on OC-pre generation. These data suggest that osteocytes produce IFN-β to negatively control OC-genesis.

***Disclosures: Takuya Sato**, None.*

SA0285

See Friday Plenary Number FR0285.

SA0286

PTH/PTHrP Receptor Signaling in Osteocytes Differentially Regulates Skeletal Homeostasis during Adulthood and Aging. Vaibhav Saini*[1], Keertik Fulzele[1], Xiaolong Liu[2], Christopher Dedic[2], Hiroaki Saito[3], Eric Hesse[3], Paola Divieti Pajevic[1]. [1]Massachusetts General Hospital; Harvard Medical School, USA, [2]Endocrine Unit, Mass General Hospital, Harvard Medical School, USA, [3]University Medical Center Hamburg-Eppendorf, Germany

Parathyroid hormone (PTH) is the only FDA approved anabolic agent to treat osteoporosis. PTH modulates bone turnover by binding to the PTH/PTH- related Peptide (PTHrP) type 1 receptor (PPR), highly expressed in bone and kidneys. Osteocytes, the most abundant cells in adult bone, also express PPR. However, physiological relevance of PPR signaling in osteocytes remains to be elucidated. Osteocytes may partially mediate the anabolic effects of PTH by suppressing SOST/Sclerostin, a Wnt signaling inhibitor. To investigate the role of PPR signaling in osteocytes, we generated mice lacking PPR in osteocytes (OcyPPRKO). Littermates with floxed PPR alleles served as controls. qPCR showed significantly decreased PPR transcripts in the osteocyte-enriched tibiae of OcyPPRKO as compared with control, demonstrating successful PPR ablation. To investigate the role of PPR signaling during adulthood and aging, we compared the skeletal phenotype of 3- and 12-month-old OcyPPRKO and control. H&E and Von Kossa staining showed increased trabecular bone in OcyPPRKO at 3 months that was absent at 12 months. Dual-energy X-ray absorptiometry (DXA) analysis showed significantly increased bone mineral density (BMD) in OcyPPRKO at 4 months ($p<0.05$, $N>10$) that was absent at 12 months ($p>0.05$, $N>5$). High resolution microcomputed tomography (microCT) analysis of L5 vertebrae and femur midshafts showed significantly increased trabecular and cortical bone parameters in OcyPPRKO at 3 months ($p<0.05$, $N>10$) that was absent at 12 months ($p>0.05$, $N>5$). Histomorphometric analysis of femurs showed significantly higher bone volume (BV/TV, $p<0.05$, $N>8$) and osteoblast parameters ($p<0.05$, $N>8$), and a trend for decreased osteoclast parameters at 4 months in OcyPPRKO than control; however these parameters appeared similar between OcyPPRKO and control at 12 months ($p>0.05$, $N>5$), yet a trend for increased number of resorption lacunae was observed in OcyPPRKO at 12 months. To understand the molecular perturbation, SOST and RANKL mRNA expression was compared in osteocyte-enriched calvariae. At 3 months, there was a significant 450% increase in SOST ($p<0.05$) and 48% decrease in RANKL mRNA expression ($p<0.05$) in OcyPPRKO as compared with control, suggesting low bone turnover resulting in higher BMD. Interestingly, at 12 months, SOST mRNA expression was similar between OcyPPRKO and control ($p>0.05$); however RANKL mRNA expression was significantly increased by 378% in OcyPPRKO ($p<0.05$). These data suggest that with age OcyPPRKO and control have similar osteoblast activity, but OcyPPRKO have a significantly higher osteoclast activity than control. Our results identify a temporal regulation of osteoblasts and osteoclasts by PPR signaling in osteocytes in adult and aging skeleton.

***Disclosures: Vaibhav Saini**, None.*

SA0287

Assessment of Peri-lacunar and Peri-canalicular Tissue Mass Density Alterations in Human Jaw Bone after Bisphosphonate Treatment by 3D Synchrotron Phase NanoCT. Bernhard Hesse*[1], Peter Varga[2], Max Langer[3], Heikki Suhonen[1], Nils Maennicke[2], Susanne Schrof[2], Peter Cloetens[1], Peter Maurer[4], Françoise Peyrin[3], Kay Raum[2]. [1]European Synchrotron Radiation Facility, France, [2]Julius Wolff Institut, Charité - Universitätsmedizin Berlin, Germany, [3]Creatis, INSA-Lyon, CNRS, Université CB Lyon 1; European Synchrotron Radiation Facility, France, [4]Klinikum Bremerhaven, Germany

The interplay of osteocytes with their surrounding tissue is the subject of recent research [1]. The high connectivity of the lacunar-canalicular-network (LCN) and alterations of the mineral crystals close to the LCN has recently been demonstrated in an animal model [2].

The present study investigates alterations of mass density of the peri-canalicular and peri-lacunar matrix in human jaw bone after bisphosphonate (BP) treatment. 3D Synchrotron phase nanoCT (50 nm isotropic voxel size) enabling sufficient spatial resolution to resolve the LCN [3] in combination with a high sensitivity to the mass density was used to image bone samples. In total, 21 osteocyte lacunae and their surrounding tissue regions were investigated. The samples were obtained from BP-treated (N=3) donors and healthy (N=4) controls. The 3D analysis provided the mean mass density as functions of the shortest distances to canaliculi and lacunae.

We found significantly higher mean mineralized tissue mass densities for the BP treated samples ($F=18$, $p<0.001$). In average, 50 % of the mineralized tissue was found to be located within less than 1.4 µm and 14 µm away from the next canalicular and lacunar boundaries, respectively. Mass density was highest close to the LCN and showed a decreasing trend with increasing distance from both the canaliculi and the lacunae. Both of these mass density gradients were significantly lower for the BP treated group compared to the healthy controls (with respect to lacunae distance: $p=0.02$, canaliculi distance: $p=0.03$).

This is the first study that i) compared mass density of the peri-LCN bone matrix between healthy and BP treated samples using 3D phase nano-CT images at 50nm and ii) shows a higher mass density close to both canaliculi and lacunae in human bone. Our findings support the recent discussion on the ability of the osteocytes to interact with their surrounding matrix [1]. Furthermore, the differences found in the gradient of the mass density suggest that the osteocyte interaction with the mineralized tissue matrix does not only occur at the central lacunar boundary, but also at the canaliculi via the dendritic processes. Moreover, the reduced gradients in the treated group suggest an inhibition of cell-matrix crosstalk by BP treatment.

[1] Qing H et al. (2012), J Bone Miner Res
[2] Kerschnitzki M et al. (2013), J Bone Miner Res.
[3] Langer M et al. (2012), PLoS One

***Disclosures: Bernhard Hesse**, None.*

SA0288

See Friday Plenary Number FR0288.

SA0289

Signaling of Extracellular Inorganic Phosphate Induces the Expression of *Dmp1* in Osteoblast/Osteocyte Lineage Cells via Na^+/Pi Co-transporter and MEK/ERK Pathway. Jin Nishino*[1], Kazuaki Miyagawa[2], Masanobu Kawai[1], Miwa Yamazaki[1], Kanako Tachikawa[1], Yuko Mikuni-Takagaki[3], Mikihiko Kogo[4], Keiichi Ozono[4], Toshimi Michigami[1]. [1]Osaka Medical Center & Research Institute for Maternal & Child Health, Japan, [2]Osaka University, Japan, [3]Kanagawa Dental College & Graduate School of Dentistry, Japan, [4]Osaka University Graduate School of Dentistry, Japan

Accumulating evidence has suggested that osteocyte plays a key role in phosphate homeostasis. Several molecules responsible for hypophosphatemic rickets, including FGF23, PHEX, DMP1 and FAM20C, are expressed in osteocytes. We as well as others have previously shown that an increase in extracellular inorganic phosphate (Pi) concentration exerts signal transduction to alter gene expression in some cell types. In the current study, we examined the direct effects of Pi on the gene expression in osteocytes, using primary osteocytic cells isolated from mouse long bones by sequential digestion with collagenase and decalcification with EGTA. We treated the isolated osteocytic cells with 1 mM or 10 mM Pi for 24 h, and found that the expression of *Dmp1* was markedly increased, while that of *Fgf23*, *Phex*, and *Fam20C* was not obviously changed by 24-h treatment with 10 mM Pi. The increase in *Dmp1* expression by the elevated extracellular Pi suggests that osteocytes are responsive to the alteration in extracellular Pi concentration. Since the expression of *Dmp1* is high in osteocytes while very low in osteoblasts, we next examined whether high extracellular Pi induced the expression of *Dmp1* in osteoblasts, using the murine osteoblastic cell line MC3T3-E1. We treated the cells with various concentrations (1-10 mM) of extracellular Pi for 48 h, and found that expression of *Dmp1* and phosphorylation of ERK1/2 were induced by the increased extracellular Pi in a dose-dependent manner. Then, we examined the time course of *Dmp1* up-regulation and ERK1/2 phosphorylation by harvesting the cells at 0, 0.5, 1, 6, 12, 24 and 48 h after treatment with 10 mM Pi. The phosphorylation of ERK1/2 reached the maximum at 1 h, while the marked increase in *Dmp1* expression was observed at 12 h and thereafter. Interestingly, treatment with U0126, a MEK inhibitor, abolished the up-regulation of *Dmp1* expression by the increased Pi. Treatment with phosphonoformic acid (PFA), an inhibitor of Na^+/Pi co-transporter cancelled the increase in *Dmp1* expression by the elevated Pi, either. These results suggest that signaling by extracellular Pi leads to increased expression of *Dmp1* via Na^+/Pi co-transporter and MEK/ERK pathway.

***Disclosures: Jin Nishino**, None.*

SA0290

Assessing the balance between formation and resorption: An index of net bone formation. Albert Shieh*[1], Neil Binkley[2], Teresa Seeman[1], Gail Greendale[1], Dana Miller-Martinez[1], Carolyn Crandall[1], Arun Karlamangla[1]. [1]University of California, Los Angeles, USA, [2]University of Wisconsin, Madison, USA

Purpose: Markers of either bone formation or resorption do not individually reflect bone loss or gain, because formation and resorption are coupled. Both types of markers increase with high bone turnover, regardless of whether there is net bone gain or loss. Our objective was therefore to create and evaluate a bone balance index that quantifies excess formation relative to resorption. Methods: Data came from participants in the Midlife in the U.S. study (729 men and women, ages 25-74 years, not taking medications affecting bone metabolism). Bone formation [bone specific alkaline phosphatase (BSAP), procollagen type 1 N-terminal propeptide (P1NP)] and resorption [N-telopeptide (NTx)] markers were measured from fasting blood. On the same day, bone mineral density (BMD) was measured by dual energy x-ray absorptiometry. We regressed NTx on BSAP, P1NP, and body weight, and used the estimated regression coefficients to determine E(NTx), the expected value of the resorption marker NTx corresponding to measured levels of formation markers and weight. We created a bone balance index (BBI) as E(NTx)–NTx, to reflect excess formation relative to resorption. BBI values were compared across age categories in men and menopause transition status in women. BMD was regressed on BBI to assess the ability of BBI (assuming it has been stable for some time) to predict BMD. Results: Expected NTx was E(NTx) = 7.0 + 0.178*BSAP + 0.070*P1NP – 0.022*weight, with NTx, BSAP, and P1NP in nM BCE, μg/L, and U/L units respectively, and weight in kilograms. Accordingly, BBI = 7.0 + 0.178*BSAP + 0.070*P1NP – NTx – 0.022*weight. BBI trended downwards with increasing age in men and with progression along the menopause transition in women. But BBI was 0.25 standard deviations (SD) higher (more favorable) in postmenopausal women on hormone therapy (HT) than in late perimenopausal and postmenopausal women not on HT (p=0.04). Adjusted for age, sex, menopause transition stage, HT use, and study site, each SD increment in BBI was associated with a 0.07 SD increment in spine BMD (p=0.01), but was not associated with femoral neck BMD. Conclusions: A bone balance index that quantifies excess bone formation relative to resorption can be created from bone turnover markers and may be useful in assessing current bone metabolism and potentially in predicting future bone strength.

***Disclosures: Albert Shieh**, None.*

SA0291

Serum Levels of Procollagen type 1 Amino-terminal Propeptide (PINP) and Risk of Hip Fracture in Elderly Women. The Hordaland Health Study. Trine Elisabeth Finnes*[1], Haakon E. Meyer[2], Cathrine Marie Lofthus[3], Erik Fink Eriksen[3], Ellen Margrethe Apalset[4], Grethe S Tell[5], Kristin Holvik[6]. [1]Sykehuset Innlandet Thrust, Norway, [2]Norwegian Institute of Public Health/University of Oslo, Norway, [3]Oslo Universtiy Hospital, Norway, [4]Department of Public Health & Primary Health Care, University of Bergen. Department of Rheumatology, Haukeland University Hospital, Norway, [5]Department of Public Health & Primary Health Care, University of Bergen, Norway, [6]Division of Epidemiology, Norwegian Institute of Public Health, Oslo, Norway. Department of Global Public Health & Primary Care, University of Bergen, Bergen, Norway. Surgical Department, Diakonhjemmet Hospital, Oslo, Norway., Norway

BACKGROUND: The usefulness of bone turnover markers as determinants of fracture risk in osteoporosis needs further investigations, and IOF/IFCC recommends the bone formation marker Procollagen type 1 Amino-terminal Propeptide (P1NP) to be used in studies to clarify its utility in clinical use.

AIM: To investigate the relation between serum P1NP levels and the risk of subsequent hip fractures in elderly women with, and without bone mineral density (BMD).

MATERIALS AND METHODS: A case-cohort study was performed in a cohort of 1817 women born 1924-27 participating in a health study covering western parts of Norway from 1997-99. In a subsample of about 60% of the women, baseline total hip BMD was measured by a dual x-ray densitometer (Lunar EXPERT-XL). Information on incident hip fractures was obtained from computerized discharge diagnoses records from the hospitals serving the region. P1NP was measured in frozen serum samples obtained at baseline in all women who suffered a hip fracture, and in a randomly collected subcohort of 9% of the total cohort. P1NP was determined by Multigamma radioimmunoassay kit (Orion Diagnostica). The current analyses include women not medication known to influence on the P1NP level, and with valid BMD and P1NP measurements. The final data set included 72 women, without a hip fracture, from the subcohort, and 80 women with a hip fracture. Cox proportional hazards regression adapted for the case-cohort design was performed with penalized splines of P1NP and with tertiles of serum P1NP as explanatory variables. The lowest hazard ratio (HR) was observed in the 2nd tertile, which was used as reference. All analyses were adjusted for age by method.

RESULTS: Serum P1NP levels ranged from 13 to 124 ng/mL (median 44 ng/ mL). Unadjusted spline analysis revealed no significant relation between P1NP and the risk of hip fracture. Compared to the 2nd tertile of P1NP, HR for hip fracture in the 1st tertile was: 1.26 (95% CI: 0.60 – 2.65), and in the 3rd tertile: 1.69 (95% CI: 0.53-2.53). Adjusted for baseline BMD, a significant higher risk was seen in the 1st tertile of P1NP, compared to the 2nd tertile (HR: 3.37 (95% CI: 1.24 – 8.61), p=0.012).

CONCLUSION: A weak relation between P1NP and hip fractures was found in the unadjusted analyses. Adjusted for BMD, the current analyses revealed low P1NP to be a risk factor for hip fractures. The mechanisms causing high fracture risk among those with the lowest P1NP levels remain to be elucidated.

***Disclosures: Trine Elisabeth Finnes**, None.*

SA0292

A Low Dose 3D QCT Protocol for the Spine. Oleg Museyko[1], Axel Heinemann[2], Matthias Krause[3], Claus-C Glueer[4], Klaus Engelke*[5]. [1]University of Erlangen-Nuremberg, Germany, [2]Institute for Forensic Medicine, University of Hamburg, Germany, [3]Institute for Osteology & Biomechanics, University of Hamburg, Germany, [4]Christian Albrechts Universitaet zu Kiel, Germany, [5]University of Erlangen, Germany

Purpose: To develop a low dose 3D QCT protocol for in-vivo measurements of the spine.

Methods: QCT datasets of T6-L4 from 27 cadavers (190 vertebrae) were scanned twice on a Philips MX8000: with 120kV and 100 mAs and a lower dose protocol with 90 kV and 150 mAs. Reconstruction diameter was 15 cm, slice thickness 1.3 mm, and convolution kernel was 'B' for both scans. A BDC calibration phantom (QRM Möhrendorf, Germany) was used for conversion of HU to BMD values. MIAF-Spine was used to analyze total vertebral body volume and BMD (Figure 1). Additionally, mean and standard deviation of the HU values obtained in the three cylindrical phantom inserts (0, 100, and 200 mg/cm^3) were measured in each of the 27 dataset pairs. All parameters were compared between the two scans using matched pair t-tests (Wilcoxon signed rank test for the volume) and Pearson correlations coefficients (r). Dose reduction was estimated using ImpactDose software (CT Imaging, Erlangen).

Results: Effective dose values for the 90kV are approximately 60% lower compared to the 120kV protocol. BMD values were highly correlated but a significant offset ($p < 0.001$) indicates differences in field inhomogeneity; segmented volume was not affected by the lower kV ($p > 0.5$) (Figure 2). All correlation coefficients were significant ($p < 0.001$). Noise in the images assessed by the standard deviation of the HU values of the phantom inserts of the vertebrae were significantly higher in the 90 kV scans: 20.8 ± 4.7 HU vs. 16.2 ± 3.0 HU, 22.0 ± 4.9 HU vs. 17.1 ± 2.9 HU, and 23.3 ± 5.0 HU vs. 18.0 ± 3.1 HU in the phantom insert with 0, 100, and 200 mg/cm^3, respectively.

Conclusions: As expected, noise values were higher in the 90 kV protocol. However, increased noise had no effect on the segmentation of the periosteal surface. The difference in calibrated BMD values indicates differences in the scan field inhomogeneity at 90 and 120kV requiring different corrections. As the correlation between BMD values at 90 and 120kV was very high a linear correction approach, e.g., based on the scans of the European Spine Phantom will suffice to obtain the same BMD results at 90 and 120kV.

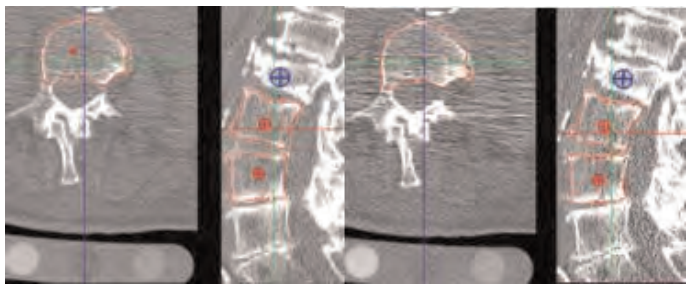

MPRs of a patient scanned with 120 kV (left) and 90 kV (right). Periosteal segmentation is shown

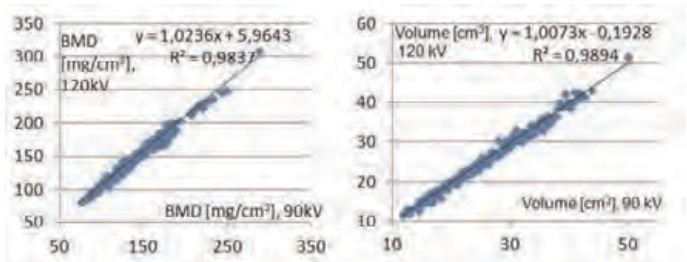

Correlation of BMD and volume of the of the 90 kV protocol against the established 120kV protocol

***Disclosures: Klaus Engelke**, None.*

SA0293

FE-based bone strength can classify femoral neck fractures in a case-control retrospective study. Enrico Schileo*[1], Cristina Falcinelli[2], Luca Balistreri[3], Fabio Baruffaldi[3], Saverio Gnudi[1], Aldo Toni[1], Ugo Albisinni[1], Francesco Ceccarelli[4], Luigi Milandri[5], Marco Viceconti[6], Fulvia Taddei[3]. [1]Istituto Ortopedico Rizzoli, Italy, [2]Laboratorio di Bioingegneria Computazionale, Istituto Ortopedico Rizzoli, Italy, [3]Laboratorio di Tecnologia Medica, Istituto Ortopedico Rizzoli, Italy, [4]Clinica Ortopedica, Università di Parma, Italy, [5]Ortopedia Programmata, Ospedale di Faenza, Italy, [6]Department of Mechanical Engineering, The University of Sheffield, United Kingdom

Introduction: Personalised Finite Element (FE) models from Computed Tomography (CT) data are superior to bone mineral density (BMD) in predicting femoral strength *in vitro* [1].

However, results similar to BMD were obtained *in vivo*, in retrospective classification of generic prevalent fractures [2] and in prospective classification of femoral fractures [3].

The aim of this work is to test, in a case-control retrospective study, the ability of a different, validated FE modelling procedure [4] to: (i) discriminate between groups of proximal femoral fractures and controls; (ii) individually classify fractures and controls.

Methods: 55 women (22 low-trauma proximal femur fractures and 33 controls) were enrolled in 3 clinical centres in Emilia Romagna region, Italy. All received CT and DXA exams (in acute conditions for fractures) with a standardised protocol.

Femoral neck aBMD was measured from DXA.

FE models were built from CT (right femur for controls, intact for fractured) [4]. Differently from existing works, FE strength was calculated for a range of 12 physiological directions of hip joint reactions [5] and 10 fall directions [6]. Bone strength (in stance and fall) was the minimum load inducing on the femoral neck surface an elastic principal strain value greater than the yield limit [7].

Fracture classification was analysed through logistic regressions and AUC of ROC curves.

Results and Discussion: Mean FE strength was significantly lower in fractured cases (Table 1). Differences were greater than those: obtained for aBMD; reported in [8].

Logistic regression on single variables

All classifiers were significant ($p<0.001$, AUC=0.88 for both stance and fall strength, slightly higher than [2,3]; $p=0.02$, AUC=0.72 for aBMD). The statistical power of the logistic regressions [9] was >0.9 for strength, 0.86 for aBMD, mildening the small sample numerosity.

Logistic regressions on multiple variables

Only strength was retained significant ($p<0.001$, AUC=0.88) when including aBMD in the regression.

Cases and controls were not age matched, but adding age to the logistic regression, FE strength and age (but not aBMD) remained significant, with AUC=0.95.

In summary, the proposed FE method may be superior to aBMD in the classification of femoral fractures.

References
1. Cody *et al,* J Biomech 1999:1013-20
2. Amin *et al,* JBMR 2011:1593-1600
3. Orwoll *et al*, JBMR 2009:475-83
4. Schileo *et al,* J Biomech 2008:356-67
5. Bergmann *et al*, J Biomech 2001:859-71
6. Grassi *et al,* J Biomech 2012:394-9
7. Bayraktar *et al*, J Biomech 2004:27-35
8. Keyak *et al,* Bone 2011:1239-45
9. Vaeth *et al*, Statist Med 2004:1781–92

	Cases(n=22)		Controls(n=33)		Diff. %	P-value
	Mean	SD	Mean	SD		
Age (years)	80	6.2	69	6.2	16%	<0.0001
Height (cm)	160	5.5	158	5.7	1%	0.3999
Weight (kg)	62	10.1	62	7.0	0%	0.9043
Femoral neck aBMD (g/cm^2)	0.608	0.152	0.693	0.086	-12%	0.01
FE Strength stance (N)	2917	926	4327	818	-33%	<0.0001
FE Strength fall (N)	1714	440	2420	396	-29%	<0.0001

Table 1

***Disclosures: Enrico Schileo**, None.*

SA0294

First Demonstration of Microdamages in the Alveolar Bone in vivo Using Computerized Magnification Radiography with Emphasis of Surface Unevenness by Changing Light's Direction to Achieve a 3D Effect.
Yoshitomo Takaishi*[1], Seizaburo Arita[2], Mitsugi Honda[3], Takeshi Sugishita[1], Aiko Kamada[4], Takashi Ikeo[4], Takami Miki[5], Takuo Fujita[6], Masahiro Nakajima[7], Katsura Ueda[8]. [1]Takaishi Dental Clinic, Japan, [2]Department of Life & Medical Sciences, Doshisha University, Japan, [3]Department of Radiology, Okayama University Hospital, Japan, [4]Osaka Dental University, Japan, [5]Osaka City University Medical School, Japan, [6]Katsuragi Hospital, Japan, [7]Second Dept. of Oral & Maxillofacial Surgery, Japan, [8]Dept.of Oral Anatomy, Osaka Dental University, Japan

Purpose: Microdamages, indicating resistance, failure and repair of the bone like material fatigue, have so far been studied only histologically in resected specimens and never in vivo by radiography. By applying surface unevenness emphasizing normal map method on computed dental micro-radiogram (Bone Right) of the alveolar bone from human first mandibular premolar, microdamages were identified and compared with those histological ground specimens from the same site after surgical resection. Correlations among the distribution density of microdamages, alveolar bone mineral density (al-BMD), lumber bone mineral density (LBMD) and fracture were calculated and possibility of predicting fracture by these parameters evaluated.

Materials and Methods: The portion of surgically removed alveolar bone containing radiologically demonstrated microdamages was subjected to dental radiography, enlarged and subjected to normal map for 3D-like emphasis of ups and downs. The specimen was then decalcified and dehydrated with 10% EDTA2 for 2 months, embedded in paraffin, deparaffinized, stained with HE and pictured, to test an agreement in the picture of microdamages with the histological specimens.

In 31 postmenopausal women (59-65 years of age), alveolar bone adjacent to the mandibular first premolar was subjected to enlargement and 3D-like silhouetting to confirm microdamages and their special distribution density, constructing a correlation diagram with fractures of spine and other sites, al-BMD, LBMD measured by Hologic 4500 divided by young adult mean, gingival depth, alveolar thickness (alveolar bucco-lingual distance 6 mm below the enamel-cement junction), BMI (body weight / height^2) and age.

Results: Excellent agreement between microdamages shown by 3D-like silhouetting of the enlarged X-ray film of the alveolar bone and those found on histological specimens.

Microdamage density distribution showed positive correlations with age and number of spine fractures and other sites at coefficients of variation of 0.462 ($p<0.01$) and 0.722 ($p<0.01$) respectively, and negative correlations with LBMD-T and al-BMD at -0.651 ($p<0.01$) and -0.637 ($p<0.01$).

Conclusion: Density distribution of microdamages in human alveolar bone showed significant positive correlations with age and fracture of the spine and other sites, negative correlations with al-BMD and LBMD(T), suggesting a usefulness in alarming bone fragility and risk of fracture.

***Disclosures: Yoshitomo Takaishi**, None.*

SA0295

In Vivo Study of Trabecular and Cortical Bone in Young Adults with Varying Trajectories of Bone Development using Multi-Row Detector CT Imaging.
Punam K. Saha, Ryan Amelon*, Yinxiao Liu, Cheng Li, Dakai Jin, Cheng Chen, Jessica Fishbaugher, Elena Letuchy, CHADI CALARGE, Kathleen Janz, Douglas Hornick, Julie Eichenberger-Gilmore, Trudy Burns, James Torner, Steven Levy. University of Iowa, USA

In contrast to DXA, multi-row detector computed tomography (MD-CT) imaging generates unique bone quality information such as volumetric bone density, isolation of trabecular from cortical bone mineral density (BMD), and characterization of micro-architecture. Using advanced image processing algorithms, MD-CT based new trabecular and cortical bone parameters were assessed in four groups of young adults with varying clinical histories likely to impact bone development.

Nine athletes (6 male/3 female), 9 participants (4 male/5 female) with cystic fibrosis (CF), and 11 participants (5 male/6 female) on continuous treatment with a selective serotonin reuptake inhibitor (SSRI) for at least one year were recruited (age: 18-23 year). Age-sex-BMI-similar healthy controls (42 male/46 female)were selected from the Iowa Bone Development Study (IBDS) cohort. MD-CT scans of the distal tibia were acquired on a 128 slice Siemens Flash scanner at 120kV, 200mAs, pitch: 1, 0.3mm slice-thickness and 10cm scan-length. A Gammex phantom was used to calibrate CT Hounsfield units into BMD (mg/cc). Cortical bone (CB) thickness (CB-Th) and porosity (CB-Poro) (over 12-16% of tibia), trabecular bone (TB) volumetric BMD (TB-vBMD), mean surface width (TB-SW), network length (TB-NL), TB thickness (TB-Th), and marrow spacing (M-Sp) (over 4-6% of tibia) were computed.

Pairwise comparisons between IBDS controls and participants from the three other groups revealed that athletes had thicker CB while participants with CF and those on SSRI therapy had reduced CB-Th, as well as compromised TB-vBMD and TB micro-architecture (Table 1). Notably, differences in bone micro-architecture measures, compared to bone density measures, most prominently distinguished the two clinical groups from the controls (Table 1). Figure 1 presents color-coded TB plate/rod classification for one BMI-matched female representative from each of the four study groups; the healthy female and the athlete have similar TB structure, while the two participants from the clinical groups have compromised TB structure.

Advanced MD-CT image processing algorithms are well-suited for *in vivo* skeletal assessment, capturing differences in volumetric and micro-architectural properties of cortical and trabecular bone. Our preliminary findings require confirmation in a larger sample, where various potential confounders are accounted for.

This study was funded by NIH grants: R01-AR054439, R01-DE012101, UL1-RR024979, and UL1-TR044206.

	CB-Th	CB-Poro	TB-vBMD	TB-SW	TB-NL	TB-Th	M-Sp
Controls from IBDS cohort	2.11mm (±0.25)	0.21 (±0.014)	1091mg/cc (±61)	1080μm (±177)	0.059 (±0.012)	188 μm (±20)	386 μm (±58)
Athletes	15.4%*** (±10.8%)	-0.1%† (±8.1%)	2.4%† (±9.2%)	4.8%† (±12.7%)	13.1%* (±18.3%)	7.7%* (±10.7%)	-4.0%† (±16.9%)
Participants with CF	-17.5%* (±17.2%)	-2.3%† (±8.3%)	-10.2%*** (±5.9%)	-19.0%** (±17.3%)	-30.9%*** (±17.7%)	-11.8%* (±12.0%)	37.1%* (±33.5%)
Participants on SSRI	-6.4%* (±7.7%)	-2.2%† (±8.2%)	-7.3%* (±8.1%)	-14.5%** (±13.0%)	-19.5%** (±17.8%)	-10.7%*** (±9.0%)	17.4%** (±24.5%)

Table 1: Row 1: Mean ± SD values of various CB and TB measures (CB-Poro and TB-NL have no unit) for healthy controls from the IBDS cohort. Row 2-4: Mean ± SD of percentage difference from controls for age-sex-BMI-similar athletes, participants with CF, and participants on SSRI. Statistical significance of pairwise t-test comparisons – †: p-value >0.5 (statistically non-significant), *: p-value < 0.05; **: p-value < 0.01; ***: p-value < 0.005.

Table 1

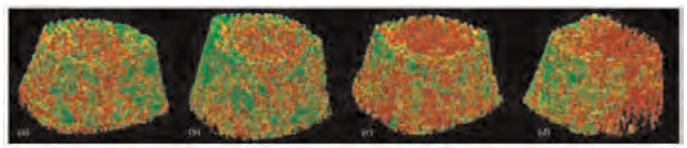

Figure 1: Color-coded illustration of trabecular bone (TB) plate/rod classification for a healthy female IBDS control (a) and sex- and BMI-matched athlete (b), a participant with confirmed diagnosis of cystic fibrosis (CF) (c), and another participant on continuous treatment with a selective serotonin reuptake inhibition (SSRI) (d). Both the healthy control and the athlete have more TB plates colored in green as compared to the two participants. No apparent difference in TB is observed between the control and the athlete; between the two participants, the CF participant has some signs of nonhomogeneous bone loss. However, this observation needs to be confirmed in a larger study and the implications further investigated.

Figure 1

***Disclosures: Ryan Amelon**, None.*

SA0296

Influence of Glucocorticoids on Trabecular Bone Score in Patients With Rheumatoid Arthritis.
Vladyslav Povoroznyuk*[1], Tetyana Karasevska[2], Berengere Aubry-rozier[3], Nataliia Dzerovych[2], Didier Hans[3]. [1]Institute of Gerontology AMS Ukraine, Ukraine, [2]Institute of Gerontology NAMS Ukraine, Ukraine, [3]Lausanne University Hospital, Switzerland

Introduction. Bone disorders are the main extra-articular complications of rheumatoid arthritis (RA). Patients with RA have a greater risk of osteoporosis and fracture than the general population. Rheumatoid arthritis (RA) is a chronic inflammatory rheumatic disease and a frequent cause of secondary osteoporosis induced by the chronic inflammatory condition and a long-term glucocorticoid therapy (GC).

The aim of this study is to evaluate the influence of GC on the trabecular bone score (TBS), bone mineral density (BMD) and TBS dynamics during one year in patients with RA.

Materials and methods. 134 examined women with RA (age 52.5±12.8 years; height 162.6±6.4 cm, weight 68.2±13.7 kg, duration of disease 9.1±7.5 years, duration of postmenopausal period 7.6±7.2 years) were divided into three groups: first group, G1, includes 37 patients who did not use GC, second group, G2 – 50 patients who used GC in a dose of more than 5 mg of prednisolone for more than 3 years, third one, G3 – 47 patients who took GC only at the exacerbated stage for less than 6 month. All the patients had been taking methotrexate as a basic treatment.

BMD of total body, PA lumbar spine, proximal femur and forearm were measured using the DXA method (Prodigy, GEHC Lunar, Madison, WI, USA) and PA spine TBS was assessed by means of TBS iNsight® software package installed on our DXA machine (Med-Imaps, Pessac, France). Evaluation of TBS dynamics in the patients of G1 & G2 groups during the year was conducted on the background of ongoing therapy which included doses of GC (for the patients of second group) and/or without any osteotropic treatment.

Results. The 3 groups did not differ as to age, basic anthropometric parameters, duration of disease and duration of postmenopausal period in these groups. TBS in G2 was significantly lower compared to G1 (TBSL1-L4: 1.147±0.168 vs 1.250±0.135; t=-3.07; p=0.003), and G3 compared to G1 (TBS L1-L4: 1.274±0.138; t=3.95; p=0.0002). However, there were no differences of BMD of PA spine and hip among groups. Only forearm BMD in the second group was significantly lower compared to the first one (0.583±0.176 g/cm2 vs 0.675±0.229 g/cm2; t=-2.18; p=0.032). Spine TBS decreased by 1.4% after one year for G1 and by 5.8% for G2.

Conclusion. For patients who are GC-users, TBS, but not BMD, reflects bone microarchitecture deterioration which is an indicator for those patients to of a higher vertebrae and non-vertebral risk of fracture. TBS is a determinant of bone state and must be monitored during the long-term treatment with GC.

***Disclosures: Vladyslav Povoroznyuk**, None.*

SA0297

Multimodality imaging and its utility to monitor marrow damage for cancer survivor bone health studies. Luke Arentsen[1], Keenan Brown[2], Susanta Hui*[1]. [1]University of Minnesota, USA, [2]Mindways Software, USA

Purpose: Cancer treatment induced bone marrow damage adversely affects bone health leading to an increased risk of osteoporotic fractures. Using the imaging procedures dual energy CT (DECT) and Water-Fat MRI (WFMRI) will provide the etiology of bone loss over time in greater detail. The goal is to develop a DECT technique to estimate marrow composition for use in women undergoing chemotherapy and radiation treatment.

Methods: Commencement of a pilot clinical study includes patients treated with radiation (5), Chemotherapy (6), and oophorectomy alone (4). A one year longitudinal study is used to compare change in marrow fat measured using WFMRI and DECT scans. WFMRI imaging was used to generate high-resolution, 3D signal fat fraction (sFF) maps extending from mid-femur to L3. This same region is scanned using dual source CT scan of 80 and 140 kVp energies within few hours of MRI scan. Identical ROIs were analyzed in WFMRI and DECT images to compare marrow composition. Attenuation properties of alcohols are accurately modeled in diagnostic x-ray energies (80 & 140kVp) using Siemens CT scanner. Water and intralipid used to as external reference for both modalities. Posterior adipose tissue and psos muscle used as internal control. Comparison of predicted and measured attenuation signals is used to assess accuracy.

Results: A 100% accuracy of rank correlation was observed between measured test solution densities and the theoretical model predictions that are based upon independent x-ray scatter calculations. A high correlation is seen between WFMRI YM assessment and DECT (r=0.813) (Figure). Individual treatment groups also showed a high correlation from baseline to 6 month and 1 year follow-up. post treatment, marrow fat increased significantly in both the L4 vertebral marrow (p=0.04) in chemotherapy patients and L5 for patients who received radiation. Chemotherapy changes were more uniform in space, whereas the radiation-induced changes were largest in marrow regions inside and close to the target radiation field.

Conclusions: The DECT may be an alternative and and effective method to estimate accurate bone marrow fat composition in cancer survivor as validated by WFMRI. DECT is routinely acquired as part of clinical care in these cancer patients, making it very practical to acquire. Pilot clinical study results indicate a significant influence of cancer treatment on marrow composition.

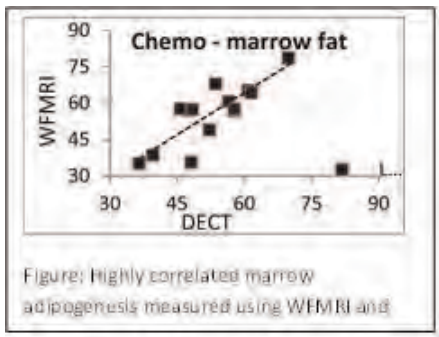

Figure

***Disclosures: Susanta Hui**, None.*

SA0298

Prediction Models for Older Women at High Risk of Unrecognized Radiographic Vertebral Fracture: Simple is Better than Complex. John Schousboe*[1], Harold Rosen[2], Tamara Vokes[3], Jane Cauley[4], Steven Cummings[5], Michael Nevitt[6], Dennis Black[6], Eric Orwoll[7], Deborah Kado[6], Kristine Ensrud[8]. [1]Park Nicollet Clinic, University of Minnesota, USA, [2]Beth Israel Deaconess Medical Center, USA, [3]University of Chicago, USA, [4]University of Pittsburgh Graduate School of Public Health, USA, [5]San Francisco Coordinating Center, USA, [6]University of California, San Francisco, USA, [7]Oregon Health & Science University, USA, [8]Minneapolis VA Medical Center / University of Minnesota, USA

Purpose: Decision rules with multiple predictors are recommended to choose who should have lateral spine imaging to detect prevalent radiographic vertebral fracture (PRVFx). It is unclear if models with many predictors discriminate those with and without PRVFx better than simpler models.

Methods: We used data from 4,894 women (mean age 75 yrs, range 68-99) who had lateral spine radiographs at the 3rd Study of Osteoporotic Fractures visit to construct 4 nested logistic models to predict PRVFx (vertebral height ratio >3SD lower than expected); model 1 (age + femoral neck bone mineral density [FNBMD]); model 2 (model 1 +height loss since age 25 yrs); model 3 (model 2 +prior non-vertebral fracture & body mass index (BMI); model 4 (model 3 + grip strength, back pain, smoking, estrogen & glucocorticoid use). We compared model discrimination for PRVFx by Receiver Operating Characteristics curve (AUC) analyses & Net Reclassification Index (NRI, Pepe method).

Results: Age, FNBMD, height loss, non-vertebral fracture, BMI, & smoking were significantly associated with PRVFx, multivariable adjusted (table 1). Model 3 discriminated those with from those without PRVFx as well as a more complex model 4 (table 2), but only minimally better than a simpler model 2.

Conclusion: A model with age, FNBMD, & height loss identifies older women at high risk of PRVFx who would benefit from lateral spine imaging nearly as well as more complex models.

Table 1

	Odds Ratio (95% CI)			
	Model 1	Model 2	Model 3	Model 4*
Age (5 year increase)	1.25 (1.17 – 1.34)	1.11 (1.03 – 1.19)	1.12 (1.04 – 1.21)	1.13 (1.05 – 1.23)
FNBMD (SD increase)	0.55 (0.50 – 0.62)	0.59 (0.53 – 0.66)	0.56 (0.50 – 0.63)	0.56 (0.50 – 0.63)
Height Loss (per SD)		1.55 (1.43 – 1.68)	1.49 (1.37 – 1.61)	1.48 (1.36 – 1.60)
Prior Non-Vert Fracture			1.34 (1.15 – 1.55)	1.34 (1.15 – 1.55)
BMI (SD increase)			1.17 (1.08 – 1.27)	1.20 (1.10 – 1.30)
Smoking				1.38 (1.06 – 1.81)
AUROC (95% CI)	0.641 (0.622-0.661)	0.676 (0.657-0.695)	0.684 (0.665-0.703)	0.684 (0.665-0.703)

*Model 4: grip strength, back pain, smoking, estrogen use, & glucocorticoid use were not associated w/ PRVFx after multivariable adjustment

Table 1

Table 2

	Model 2 vs. 1	Model 3 vs. 2	Model 4 vs. 3
AUROC chi^2, (p-value)	29.2 (<0.001)	6.1 (0.01)	0.3 (0.56)
NRI-10%^, p-value	0.038 (<0.001)	0.028 (<0.001)	0.009 (0.09)
NRI-15%^, p-value	0.052 (0.013)	-0.002 (0.58)	-0.008 (0.24)

^Incremental proportion with correct identification of PRVFx w/ complex vs. simpler model, using ≥10% or ≥15% model probability of PRVFx cut-point

Table 2

***Disclosures: John Schousboe**, None.*

SA0299

See Friday Plenary Number FR0299.

SA0300

Reasons for Referral for BMD Testing among Family Physicians. Sarah Munce*, Sonya Allin, Leslie Carlin, Gillian Hawker, Susan Jaglal. University of Toronto, Canada

Background and Purpose: Clinical practice guidelines in the United States and Canada currently recommend bone mineral density (BMD) testing in specific at-risk populations, including all men and women 65 years and older and those who experience a fragility fracture after age 40 years. In Ontario, Canada in the absence of major restrictions to BMD testing, a sharp increase in testing rates in much younger women, aged 40–44 years, for whom fracture risk is low, has been observed. In the year 2007/2008, BMD testing in women aged 40–59 years accounted for almost half of all BMD tests performed. While this high rate of testing may indicate concern about osteoporosis when approaching menopause, it also suggests unnecessary testing. At the same, there is evidence to suggest undertesting among individuals with advanced age or recent fracture (i.e., high-risk individuals). In order to understand these phenomena, the current study sought to understand the reasons for referral for BMD testing among family physicians (FPs). Analysis: A descriptive qualitative approach was used and involved telephone interviews with FPs, who make the majority of BMD test referrals in the province. Study Sample or Initiative Scope: Twenty-two FPs with practices in Ontario were recruited through an Ontario College of Family Physicians event on osteoporosis and subsequent snowball sampling. The average roster size of each physician was 1280, and the average number of BMD reports they reviewed per week was four. Findings: Overall, FPs indicated a lack of clarity on the appropriate age for referral for baseline BMD testing. This was particularly marked for older men. A tendency for baseline referral at menopause in the absence of other clinical risk factors also emerged which in some cases coincided with a patient's request for a BMD test. Family physicians also indicated uncertainty on the follow-up intervals for

BMD testing, especially for bisphosphonate monitoring. Conclusion: Findings from this qualitative study support what has been documented at the population level and suggest a tendency among FPs to refer younger women (at low risk). Emphasis on referral for high-risk groups and further education on the appropriate intervals for bisphosphonate monitoring is warranted. This may be accomplished via the development and implementation of a standardized requisition tool to assist FPs in making appropriate referrals for BMD testing.

***Disclosures: Sarah Munce**, None.*

SA0301

Shedding light on the accuracy of HR-pQCT assessment of cortical porosity through synchrotron μCT at the Canadian Light Source. Britta Jorgenson*[1], Helen Buie[2], Steven Boyd[2]. [1]Schulich School of Engineering, University of Calgary, Canada, [2]University of Calgary, Canada

Cortical porosity (CtPo) increases with age and is associated with the progression of osteoporosis and increased fracture risk. Traditionally, CtPo could only be assessed *in vitro* through analysis of harvested tissue samples. Recently, methods for *in vivo* assessment have been developed by high-resolution peripheral quantitative computed tomography (HR-pQCT); however, spatial resolution limitations (i.e. 82μm voxels) may limit measures of all pore sizes, which can be as small as 30μm. Unresolved pores are manifested as artificially lower measures of tissue mineral density (TMD) due to partial volume effects (PVE). Provided that the true TMD is relatively homogeneous throughout the bone, the apparent reduction in TMD by HR-pQCT due to PVE could be quantified to measure unresolved pores, although the presence of beam hardening artifacts may compromise that approach. This study aims to investigate the accuracy of CtPo as assessed by HR-pQCT. Cortical bone samples (N=14 cubes, 4 donors) were cut from the mid-shaft region of cadaveric tibiae. The samples were scanned by HR-pQCT (Scanco Medical) and were nominally aligned in their original orientation in order to replicate the effects of beam hardening that would be experienced in an *in vivo* scan. The samples were also scanned by synchrotron micro CT (SRμCT, Canadian Light Source, Sask.) at a voxel size of 9μm. Bone tissue was segmented by thresholding (400mg HA/cm^3 for HR-pQCT and 750mg HA/cm^3 for SRμCT). All void voxels were identified as pores and contributed to the CtPo measure. We found that HR-pQCT measurements of CtPo were consistently underestimated relative to measures by SRμCT ($p<0.01$), but there was an excellent correlation with 'ground truth' CtPo from SRμCT ($R^2=0.984$, Figure 1) indicating a strongly systematic error. When focused on larger pore sizes (> 136μm) there is a strong relationship between the two imaging methodologies ($R^2=0.992$). Analysis of pore size distributions suggests that there is a 'cut-off' pore size that can be captured accurately by threshold-based segmentation of HR-pQCT images. Beam hardening did not influence threshold-based CtPo, but the systematic error in BMC resulted in a slightly weaker correlation between BMD and CtPo ($R^2=0.964$). In conclusion, threshold-based CtPo measures do not capture small pores (<136μm), but are highly correlated with 'ground truth' CtPo from SRμCT with a consistent 5% under-estimation of CtPo.

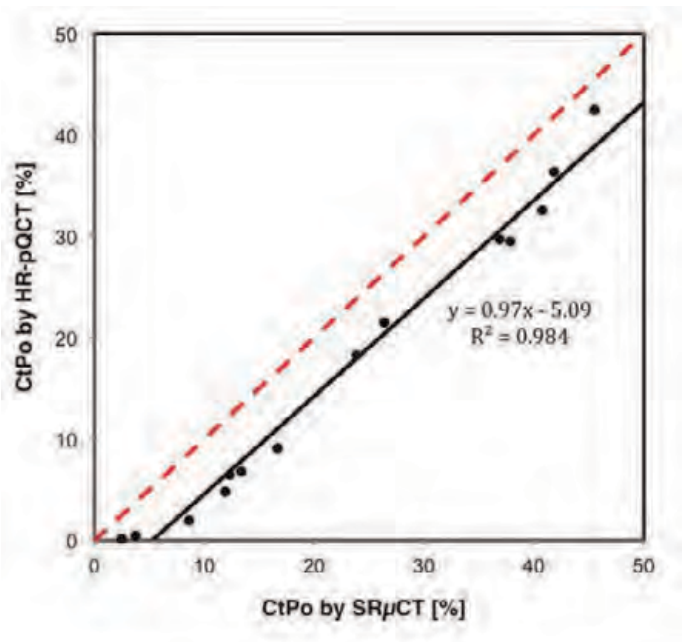

Figure 1: Cortical porosity (CtPo) as measured by threshold-based segmentation of HR-pQCT and SRμCT

***Disclosures: Britta Jorgenson**, None.*
This study received funding from: Merck Canada Inc.

SA0302

Systematic Assessment of Bone Texture by BMA-device complementary to measurement of Bone Mineral Density by DXA in Patients with Bone Gragility Fractures. Sarah Cheriet[1], Jean-François Menard[2], Olivier Vittecoq[1], Alain Daragon*[1]. [1]Department of Rheumatology, Rouen University Hospital, France, [2]Department of Biostatistics, Rouen University Hospital, France

Backbround: Bone mineral density (BMD) is a strong indicator of bone strenght but it seems to be insufficient as many fragililty fractures occur in patients without low BMD. To assess fracture risk properly, it is important to take into account other factors than BMD, such as bone microarchitecture. Bone microarchitecture measures, bone texture parameters, and parameters of bone strenght are shown to be correlated.

Methods: Enrollment included 77 patients with fragility fractures. These study patients filled in a questionnaire on clinical risk factors for osteoporosis. Their BMD was measured by dual-energy X-ray absorptiometry (DXA) at three sites (lumbar spine, femoral neck and forearm). Their bone texture parameters were measured by high resolution X-ray device (BMA^{TM} D3A Medical System) at two sites (femoral neck and forearm).

Results: We found a link between densitometry and texture parameters at the two measurement sites, with a negative correlation at the femoral neck ($p<0.05$) and a positive correlation at the forearm ($p<0.05$). We found a significant and positive correlation between parameters at the same site, but not between parameters from two different sites. The spearman correlation coefficient was positive between densitometric and morphological parameters (weight and BMI), and negative between morphological parameters and texture parameters at the femoral neck ($p<0.05$)

Conclusion: Evaluation of bone texture parameters by BMA^{TM} (D3A Medical System) at two different measurement sites can provide additionnal information to BMD, especially in obese or overweight patients in whom densitometry parameters alone often do not fully reflect risk of fracture.

***Disclosures: Alain Daragon**, None.*

SA0303

The relationship between bone architecture and density at the hip and at peripheral sites: a comparison of hip QCT and HRpQCT from the QUALYOR cohort. Jean-Baptiste Pialat*[1], Jeremy Bayet[2], Amanda Martinon[3], Pauline Azzano[2], Stephanie Boutroy[4], Anne Marie Schott[3], Eric Lespessailles[5], Roland Chapurlat[6]. [1]INSERM U1033, Team1, Université de Lyon & Hospices Civils de Lyon, France, [2]Université de Lyon, France, [3]Hospices Civils de Lyon et Université de Lyon, France, [4]INSERM U1033 & Université de Lyon, France, [5]Centre Hospitalier Regional, France, [6]E. Herriot Hospital, France

Measures of bone geometry, microarchitecture and volumetric bone mineral density (BMD) may improve the prediction of fragility fracture compared with that provided by areal BMD (aBMD). HRpQCT parameters, however, are obtained at peripheral sites that may not be representative of sites like the hip. So, we have examined the relationship between hip QCT measures and those obtained with HRpQCT.

The QUALYOR cohort is a prospective study on the value of microarchitecture to predict fracture, with 1575 postmenopausal women with a T-score < -1.0 enrolled in Lyon and Orléans (France). Data from 1075 women enrolled in Lyon were used in this analysis. Hip was assessed by QCT using QCT PRO CTXA Hip module for volumetric BMD (vBMD), and Bone Investigational Toolkit for geometric parameters (Mindways Software Inc., Austin, TX, USA). Intra and inter reader (n=2) reproducibility of the QCT analysis was tested using intraclass coefficient of correlation (ICC). Outcomes were correlated to those of hip DXA aBMD and content (BMC)) and densitometric and microarchitectural parameters obtained from radial and tibial HR-pQCT scans.

For QCT-based vBMD, inter operator reproducibility ICC was 0.97 and intra operator reproducibility was 0.82 and 0.94. Geometrical parameters had ICCs in the same range (0.79-0.97), except eccentricity (ICC=0.70). Hip vBMD assessed by QCT was well correlated with aBMD for total hip ($r=0.73$) and femoral neck ($r=0.66$); both $p<0.0001$. Comparison with HR-pQCT density parameters showed moderate correlations for total bone BMD ($r=0.53$ for tibia and $r=0.43$ for radius). Trabecular vBMD of the hip was correlated with trabecular vBMD at the tibia ($r=0.28$) and at the radius ($r=0.32$), all $p<0.0001$. Negative correlations were found between cortical density of the hip and the tibia ($r=-0.15$) or the radius ($r=-0.14$), $p<0.0001$. Most femoral neck geometrical outcomes showed significant correlations with cortical perimeter and trabecular area, with almost similar range for tibia ($0.36<r<0.57$; all $p<0.0001$) and radius ($0.31<r<0.51$; all $p<0.0001$). Femoral neck average cortical thickness was correlated with cortical thickness at the tibia ($r=0.35$) and the radius ($r=0.27$),$p<0.0001$.

In conclusion, QCT reproducibility is excellent for density analysis and good for geometry. We found a moderate correlation between hip and distal limbs density and structure.

***Disclosures: Jean-Baptiste Pialat**, None.*

SA0304

Trabecular Bone Score (TBS) Variations in Type 2 Diabetes Mellitus. Ruban Dhaliwal*, Joseph Spadaro, Chaitali Ghosh, Jennifer Kelly, Arnold Moses. State University of New York Upstate Medical University, USA

Introduction: Type 2 diabetes mellitus (T2DM) is a risk factor for osteoporotic fractures despite higher average bone mineral density (BMD) as measured by dual-emission X-ray absorptiometry (DXA). We sought explanations to this paradox by investigating variations in trabecular microarchitecture as evaluated by trabecular bone score (TBS). The aim of our study was to assess the ability of TBS to discriminate between women with and without T2DM.

Methods: We conducted a cross-sectional comparison of 37 women with T2DM and 43 controls, ages 30 to 90 years. Lumbar spine BMD was measured by DXA (GE Lunar iDXA) and TBS was calculated by examining pixel variations within the DXA images using a TBS iNsight software (Med-Imaps SA, France).

Results: The mean (SD) lumbar spine BMD (1.165 $\pm$ 0.174) was higher in T2DM women as compared to the control group (1.051 $\pm$ 0.125, p= 0.001). In contrast, mean TBS was lower in T2DM (1.218 $\pm$ 0.134 vs. 1.298 $\pm$ 0.133, p= 0.009), regardless of age. Hemoglobin A1c within the two sub-groups (defined using a cut off A1c of 7%) in T2DM showed a negative relationship with TBS, although not statistically significant (A1c $\leq$ 7%: n=14, 1.258 $\pm$ 0.153; A1c $>$ 7%: n=23, 1.193 $\pm$ 0.119, p= 0.156).

Conclusion: These data demonstrate that trabecular microarchitecture is altered in T2DM. TBS and BMD displayed opposite performance. Trabecular microarchitecture as assessed by TBS is a determinant of bone quality independent of BMD in T2DM. In addition, it seems that TBS is lower in poorly controlled T2DM. These initial data suggest that better glycemic control may improve bone quality as measured by TBS and trabecular microarchitecture assessment may also help explain the paradox of fractures at a higher BMD in T2DM.

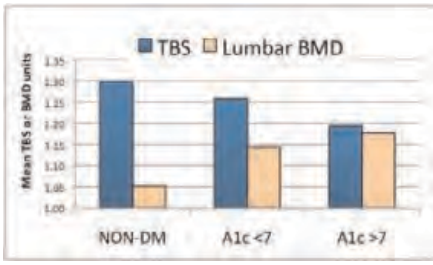

Figure 1

***Disclosures: Ruban Dhaliwal**, None.*

SA0305

See Friday Plenary Number FR0305.

SA0306

Ultrasonic Assessment of BMD at the 1/3 Radius. Emily Stein[1], Gangming Luo[2], Polly Young[3], Stanley Rosenfeld[4], Jonathan Kaufman*[2], Alfred Rosenbaum[4], Elizabeth Shane[1], Robert Siffert[5]. [1]Columbia University College of Physicians & Surgeons, USA, [2]CyberLogic, Inc., USA, [3]Columbia University, USA, [4]Computerized Diagnostic Scanning Associates, USA, [5]The Mount Sinai School of Medicine, USA

The objective of this study was to evaluate a new clinical ultrasound device (UltraScan 650, CyberLogic, Inc., New York, NY, USA) in terms of its ability to estimate BMD at the 1/3rd radius (1/3R). The device (Fig. 1) rests on a desktop and is portable, and permits real-time evaluation of the radial bone mineral density (BMD). The device measures in thru-transmission two (2) net time delay (NTD) parameters, NTD_{DW} and NTD_{CW}. NTD_{DW} is defined as the difference between the transit time of an ultrasound pulse through soft-tissue, cortex and medullary cavity, and the transit time through soft tissue only of equal overall distance. NTD_{CW} is defined as the difference between the transit time of an ultrasound pulse through soft-tissue and cortex only, and the transit time through soft tissue only again of equal overall distance. The square root of the product of these two parameters is a measure of the BMD at the 1/3R as would be measured by DXA. Two clinical IRB-approved studies were carried out; one measured 60 adults (age range 22-84, 68% female) at the 1/3R using ultrasound and DXA (range = 0.45-0.92 g/cm^2). The other study measured both arms of 3 adults at 16 locations along the radius from the 1/3 to the 10% location, using ultrasound and DXA. Linear regression between DXA (1/3R) BMD and the square root of the product NTD_{DW} * NTD_{CW} for the sixty subjects produced a linear correlation coefficient of 0.93 ($P<0.001$). Linear regression between DXA BMD and the square root of the product NTD_{DW}* NTD_{CW} for the 3 subjects (a total of 108 data points along the forearm from 1/3 to 10%) produced a linear correlation coefficient of 0.90 ($P<0.001$). We found that forearm ultrasound measurements yield results that are very closely associated with those from DXA. The results also show that the ultrasound measurements are robust with respect to radial cross-section, as changes that occur from the 1/3 to 10% locations did not significantly interfere with the ability to estimate BMD. These results are also consistent with previous computer simulation and *in vitro* studies, in terms of the ability to estimate radial bone mass. In conclusion, although x-ray methods are effective in bone mass assessment, osteoporosis remains one of the most undiagnosed diseases in the world. The research described here should enable significant expansion of the identification of bone loss as occurs in osteoporosis using an ultrasonic desktop device that can serve as a proxy for DXA BMD at the 1/3R.

UltraScan 650

***Disclosures: Jonathan Kaufman**, None.*
This study received funding from: CyberLogic, Inc.

SA0307

BMD and FRAX have Limited Ability to Identify Women with Breast Cancer who Fracture. Beatrice Edwards*[1], William Gradishar[2], Maureen Smith[2], Jennifer Pacheco[2], Jaimee Holbrook[2], June McKoy[2], Beatrice Nardone[2], Stephani Tica[2], Victoria Godinez Puig[2], Alfred Rademaker[2], Andrew Bunta[3], Paula Stern[4], Steven Rosen[2], Dennis West[2]. [1]MD Anderson Cancer Center, USA, [2]Northwestern University, USA, [3]Northwestern University Feinberg School of Medicine, USA, [4]Northwestern University Feinberg School of Medicine Department of Molecular Phar, USA

Purpose: There is a rising number of older breast cancer survivors. The CDC analyzed the SEER database between 2006 and 2007, identifying that of 11.2 million cancer survivors, 7 million are women, and 90% were women. The most common survivors were breast cancer. Our objective was to analyze whether clinical risk factors, Bone Mineral Density (BMD) or Fracture Risk Assessment Tool (FRAX) can identify women with breast cancer who fracture.

Methods: The study population consisted of breast cancer participants who participated in a genetic databank within a National Cancer Institute Comprehensive Cancer Center. Demographic, clinical and treatment characteristics were abstracted from the electronic medical record (EMR). Record abstraction was manually performed in selected cases.

Results: A total of 439 women with breast cancer were assessed; 79 women sustained fractures during the observation period (116 fractures), fractures occurred at multiple skeletal sites in 27 cases. The prevalence of fractures was 18%. Baseline characteristics revealed that women who sustained fractures were mostly Caucasian (91%, p=0.08), and had a family history of osteoporosis (36.9%, p=0.03). The time to fracture was 4.0 years (range 0-12 years) from diagnosis. Fracture cases had lower BMD at the femoral neck 0.86 $\pm$ 0.13 gm/cm^2 (T score = -1.0, p = 0.04) than non-fracture cases, although BMD was in the low normal range. Suprisingly, 90% women who fractured had a BMD Tscore>-2.5 and 55% had a T-score above -1.0. FRAX calculation was similar in both groups. Cox proportional hazard analysis failed to identify specific risk factors for fractures.

Conclusion: Fractures occur shortly after commencing cancer therapy. Occurrence of fractures in breast cancer raises the possibility of cancer-induced impairment in bone quality. BMD and FRAX calculation were not able to identify women who fractured.

***Disclosures: Beatrice Edwards**, None.*

SA0308

Gender- and skeletal site- differences of maternal and paternal inheritance for the peak bone mass in their offsprings. Kyoung Min Kim*[1], Sung Hee Choi[2], Soo Lim[2], Sang Wan Kim[3], Hak-Chul Jang[2], Chan Soo Shin[4]. [1]Seoul National University Bundang Hospitatl, South Korea, [2]Department of Internal Medicine, Seoul National University College of Medicine, South Korea, [3]Seoul National University Boramae Hospital, South Korea, [4]Seoul National University College of Medicine, South Korea

Peak bone mass is a major determinant for the risk of developing future osteoporosis. Thus, achieving optimal peak bone mass is the best measure against osteoporosis and subsequent fractures. Even though environmental components also influence bone mass accrual, peak bone mass might be largely programmed by inheritance. However, it is still not known to what extent genetic factors actually affects peak bone mass and whether the degree of genetic influences differs according to the parents-offspring pairs. The aim of this study was to investigate the degrees of maternal or paternal inheritance according to the gender and skeletal sites. This study was based on data acquired in the Fourth Korea National Health and Nutrition Examination Survey (KNHANES IV), and consisted of 510 offsprings (260 daughters and 250 sons) with an age range of 20 - 35 yrs, and 767 their parents (380 mothers and 387 fathers). The bone mineral density (BMD) was driven from dual energy x-ray absorptiometry (Discovery W, Hologic, Bedford, MA). Most of the offsprings' BMDs were strongly correlated with their parents' site-equivalent BMDs with varying degrees except for lumbar spine BMD in son-father pairs. The relationships were generally high in daughter-mother pairs but generally low in father-son pairs, and the most strong correlation was observed in lumbar spine for daughter-mother pairs ($r=0.441$, $p<0.001$). We also compared offsprings' Z score according to their parents' site-equivalent Z score groups (Z score <-1.0, $-1.0 \leq$Z score $\leq+1.0$, Z score $>+1.0$). Daughters' lumbar spine Z score increase as the mothers' Z score increase (p for trend <-0.001) with mean difference of 0.7 to 0.8 Z score. These positive trends were also observed in most other skeletal sites and most other pairs except in lumbar spine for son-father pairs and in femur neck for son-mother pairs. In comparison of influences by analyzing with AUC, maternal and paternal inheritance affects similarly on daughter's lumbar spine and femur neck BMD as body mass index (BMI) does. In sons, parental inheritance also affects lumbar spine BMD with similar level of BMI, but hereditary effects were little lower on femur neck and total hip. Genetic factors influence much on peak bone mass with variable degrees according to the skeletal site or gender. Lumber spine is more likely to be affected by heredity than femur, and even though paternal inheritance also expressed, maternal inheritance affects more strongly on bone.

***Disclosures: Kyoung Min Kim**, None.*

SA0309

Non-Osteoporotic Low-Trauma Fractures and the Burden of Re-Fracture And Mortality. Jacqueline Center*, Dana Bliuc, Nguyen Nguyen, Tuan Nguyen, John Eisman. Garvan Institute of Medical Research, Australia

Background: Approximately half of all fragility fractures occur in people with non-osteoporotic BMD. However, it is unclear whether these fractures still result in high re-fracture and mortality risk. This study aimed to determine the total burden of re-fracture and mortality according to BMD levels for all low trauma fractures.

Methods: 714 women and men 60+ from the Dubbo Osteoporosis Epidemiology Study with incident fractures were followed for re-fracture and mortality (April 1989-Dec 2012). Femoral neck BMD was measured close to initial fracture. Initial fractures were classified as: hip, vertebral and non-hip non-vertebral (NHNV). Re-fracture rates were compared to general population initial fracture rate and mortality rates were compared to age-adjusted population mortality rates.

Results: There were 528 fragility fractures in women (49% non-osteoporotic and 61% osteoporotic) and 186 in men (67% non-osteoporotic and 33% osteoporotic). Following initial fracture, 251 women and 55 men re-fractured and 249 women and 115 men died. The risk of re-fracture was highest for those with osteoporosis [women: 3.24 (95% CI, 2.72- 3.86) and men: 3.83 (95% CI, 2.81-5.21)] but was still elevated for those with osteopenia [women: 2.11 (95% CI, 1.70- 2.63) and men: 3.38 (95% CI, 2.23-5.11)] and normal BMD [women: 1.99 (95% CI, 1.19- 3.31) and men 2.11 (95% CI, 1.19- 3.76)]. Increased risk was observed in the non-osteoporotic group for all fracture types. The propensity to fall appeared to play a role in re-fracture risk in women with normal BMD [RR; 2.12 (95% CI, 1.22- 3.67)] but not in men.

In women, mortality risk was increased for all levels of BMD [normal BMD: 2.16 (1.34-3.48); osteopenia 1.32 (1.05- 1.66) and osteoporosis 1.71 (1.45- 2.02)]. Hip fractures dominated the high mortality seen in osteopenic women and NHNV fractures the high mortality in women with normal BMD. In men increased mortality rates were observed in those with osteoporosis [SMR 2.67 (95% CI, 1.98- 3.60)] and osteopenia [SMR 2.21 (95% CI, 1.67- 2.92)], but not in those with normal BMD [SMR 1.0 (95% CI, 0.6- 1.7)].

The population attributable risk of re-fracture for non-osteoporotic fractures was 69% for women and 72% for men. Population attributable risk for premature mortality was 39% for women and 22% for men.

Conclusion: Non-osteoporotic low-trauma fractures were associated with increased and substantial risk of re-fracture and mortality for both women and men.

***Disclosures: Jacqueline Center**, None.*

SA0310

Prevalence of vertebral fractures and densitometric osteoporosis in Spanish adult men. The Camargo cohort study. Jose Olmos[1], José L. Hernández[2], Josefina Martínez[2], Pilar García-Velasco[3], Daniel Nan[2], Sheila Ruiz[2], Jesús González-Macías*[2]. [1]Hospital Universitario M. Valdecilla, Spain, [2]Department of Internal Medicine, Hospital Universitario Marqués de Valdecilla-IFIMAV, Universidad de Cantabria. RETICEF, Spain, [3]Centro de Salud de Camargo, Spain

Aims: To estimate the prevalence of vertebral fracture and densitometric osteoporosis in men over 49 years from Cantabria, Spain.

Methods: A community-based population of 1062 men older than 49 yrs (range 50-98) was evaluated. Data regarding risk factors for osteoporosis and fractures were collected by means of a structured questionnaire. BMD at lumbar spine (LS), femoral neck (FN) and total hip (TH) was determined by DXA (Hologic, QDR 4500), and lateral X-rays of the thoracic and lumbar spine were taken. Osteoporosis was defined as a T-score of 2.5 or more below the young men average, and vertebral fractures were diagnosed and classified according to Genant's semiquantitative method.

Results: Te mean ($\pm$SD) age of participants was 65.9 ± 17.8 years. The prevalence of all vertebral fractures considered as whole was 17.1% (n=182), and that of moderate and severe fractures considered separately, about 5% (moderate: 4% [n=42]; severe: 1.3% [n=14]). As expected, prevalence of fractures rose with age: from 9.3% at the age of 50-54 years to 23.0% in men 75 years and older. Twelve percent (n:126) of men had densitometric osteoporosis, with marked differences between the spine and the hip (10.6% at the LS, 2.3% at the FN and 0.6% at the TH). Osteopenia was seen in 41% of men (34% in LS [n:361], 37% in FN [n:394] and 20% in TH [n:214]). Contrary to vertebral fractures prevalence, the prevalence of densitometric osteoporosis did not change very much with age (11% in the youngest group [50-54 years] and 14% in the oldest group [75 years and older]).Only 5% of the osteoporotic patients had a previous diagnosis of the disease.

Conclusions: The most striking data of our results is the huge difference between the percentage of patients with densitometric osteoporosis at the hip and that at the spine. This is a fact that must be taken into account by those considering hip BMD measurement enough for diagnosis. Besides, figures reported here are similar to those previously reported in other European countries.

Supported by a grant from the "ISCIII", Spain (PI11/01092)

***Disclosures: Jesús González-Macías**, None.*

SA0311

Trabecular Bone Score Improves Prediction Ability for Vertebral Fracture over 10 Years in Middle-aged and Elderly Women Evaluated by Reclassification Improvement Measures: The Japanese Population-based Osteoporosis (JPOS) Cohort Study. Masayuki Iki*[1], Junko Tamaki[2], Yuho Sato[3], Eiko Kadowaki[1], Namiraa Dongmei[1], RENAUD WINZENRIETH[4], Sadanobu Kagamimori[5], Yoshiko Kagawa[6], Hideo Yoneshima[7]. [1]Kinki University Faculty of Medicine, Japan, [2]Kinki University School of Medicine, Japan, [3]Jin-ai University, Japan, [4]Center of Bone diseases, Lausanne University Hospital, Lausanne, Switzerland, France, [5]University of Toyama, Japan, [6]Kagawa Nutrition University, Japan, [7]Shuuwa General Hospital, Japan

Aims: To evaluate whether trabecular bone score (TBS) improves the prediction ability achieved by bone mineral density (BMD) for vertebral fractures (VFx) over 10 years in middle-aged and elderly women.

Methods: Among 900 women aged 50 to 79 years selected randomly from 3 areas of Japan, 728 completed the baseline survey and at least one follow-up over 10 years. Each survey included spinal imaging by absorptiometry and spine BMD measurement (QDR4500A, Hologic, USA). TBS was calculated at baseline in the same vertebrae using TBS iNsight software (Med-Imaps, France). Incident vertebral fracture was determined when a vertebral height was reduced by 20% or more during follow-up and the vertebra satisfied McCloskey-Kanis criteria or Genant's grade 2 fracture. Prediction validity of BMD and TBS was evaluated by the area under receiver operating characteristic curve (AUC) and newly developed and more powerful reclassification improvement measures, integrated discrimination improvement (IDI) and net reclassification improvement (NRI).

Results: Among 685 women (mean age, 64.2 ± 8.2 years) with no conditions affecting bone metabolism, 102 suffered incident VFx (17.3/103 person-years). These women were older and had lower BMD and TBS than those with no fractures.

Participants were classified into TBS tertile groups within each stratum of BMD (normal, osteopenia and osteoporosis, defined according to WHO criteria). Lower BMD and TBS of participants were both significantly associated with higher incidence rates of VFx (both $p<0.001$). Interestingly, the lowest TBS group in osteopenic women had a higher risk of VFx than the highest TBS group in osteoporotic women (22.9 vs 15.8/1000 person-years, respectively) (Fig).

The area under receiver operating characteristic curve (AUC) of TBS and BMD combined was 0.702 for VFx prediction and only marginally greater than the AUC of BMD alone (0.669, $p=0.086$). However, the reclassification improvement measures showed significant increases in classification accuracy achieved by BMD and TBS in combination compared with BMD alone (IDI: 0.028 (95% confidence interval (CI): 0.011, 0.046); NRI: 0.234, (95% CI: 0.024, 0.443)).

Conclusions: Lower TBS was associated with a higher risk of VFx over 10 years independently of BMD in middle-aged and elderly Japanese women. TBS could effectively improve fracture prediction by BMD alone.

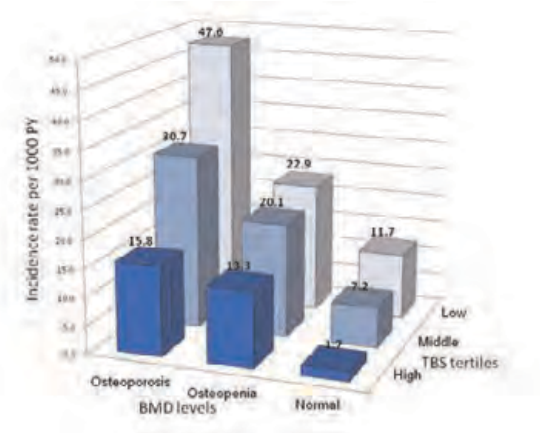

Fig. Incidence rates of vertebral fractures in TBS tertile groups within BMD strata.

***Disclosures: Masayuki Iki**, None.*

SA0312

Adherence to a Vegetable-fruit-soy Dietary Pattern or the Alternate Healthy Eating Index is Associated with Lower Hip Fracture Risk among Singapore Chinese. Zhaoli Dai*[1], Lesley Butler[2], Rob M. van Dam[3], Li-Wei Ang[4], Jian-Min Yuan[2], Woon-Puay Koh[5]. [1]Saw Swee Hock School of Public Health, National University of Singapore, Sgp, [2]Division of Cancer Control & Population Sciences, University of Pittsburgh Cancer Institute, Pittsburgh, Pennsylvania, USA; Department of Epidemiology, Graduate School of Public Health, University of Pittsburgh, Pittsburgh, Pennsylvania, USA, USA, [3]Saw Swee Hock School of Public Health, National University of Singapore, Singapore, Singapore, [4]Epidemiology & Disease Control Division, Ministry of Health, Singapore, Singapore, [5]Saw Swee Hock School of Public Health, National University of Singapore, Singapore; Duke-NUS Graduate Medical School Singapore, Singapore, Singapore

Evidence for a relationship between the overall diet and fracture risk is scarce with mixed results. We studied the diet-hip fracture association by assessing two distinct Chinese dietary patterns in Singapore, namely the vegetable-fruit-soy (VFS) and the meat dim-sum (MDS) patterns, as well as the Alternate Healthy Eating Index 2010 (AHEI 2010), which was created based on the foods and nutrients consistently predictive of chronic disease risk in the U.S.

We used prospective data from the Singapore Chinese Healthy Study, a population-based cohort of 63,257 Chinese men and women aged 45-74 years at recruitment between 1993 and 1998. Dietary patterns were identified from the baseline habitual dietary intakes, which were recorded using a validated food frequency questionnaire. We derived the VFS (23 vegetable, 4 fruit and 5 soy food items) and the MDS (18 meat, 7 rice and 5 noodle items) patterns by principal component analysis (a posteri approach). The overall dietary quality was estimated according to the AHEI 2010, which reflects adherence to healthier food choices in disease prevention (a priori method). Quintile cutpoints of each dietary score were derived based on the distribution of the whole cohort and were examined in relation to hip fracture incidence using Cox regression after adjusting for potential confounders.

A total of 1,630 incident hip fracture cases were identified via record linkage with the nationwide hospital discharge database through 2010, after excluding 103 prevalent cases at recruitment. The VFS pattern had moderate correlation with the AHEI 2010 (r=0.42). We observed strong dose-dependent inverse associations for both higher scores of the VFS pattern and the AHEI 2010 with hip fracture risk (p for trend<0.0001) (Figure 1). Compared with the lowest quintile, subjects in the highest quintile had a 34% lower hip fracture risk (95% CI: 22% to 45%) for the VFS pattern and a 27% lower risk (95% CI: 15% to 38%) for the AHEI 2010. Results were similar in both genders. The MDS pattern was not associated with hip fracture risk.

This is the first study demonstrating that the risk of hip fracture may be reduced by a healthy dietary pattern defined either as a typical Chinese diet rich in fruits, vegetables and soy, or as a pattern with greater adherence to healthier food choices recommended for chronic disease prevention. Our findings support the importance of promoting an overall healthy diet to protect against osteoporotic fractures.

Figure 1. Hazard ratio (HR) of hip fracture according to quintile of the VFS pattern score and the AHEI 2010 score for overall (n=63,154), the Singapore Chinese Health Study

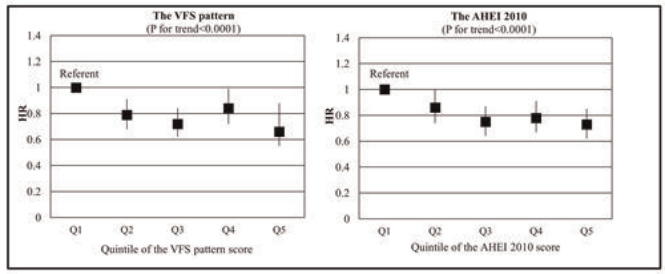

Figure 1

***Disclosures: Zhaoli Dai**, None.*

SA0313

See Friday Plenary Number FR0313.

SA0314

Impact of a Theory-Based Osteoporosis Education Intervention and BMD Screening on Calcium and Vitamin D Intake in Older Men and Women. Katherine McLeod*[1], Shanthi Johnson[2], Drona Rasali[3]. [1]Faculty of Kinesiology & Health StudiesUniversity of Regina, Canada, [2]Saskatchewan Population Health & Evaluation Research Unit, University of Regina, Canada, [3]University of Regina, Canada

Purpose: Adequate calcium and vitamin D intake play an important role in prevention and management of osteoporosis and related fracture. However, the majority of at-risk men and women are not engaging in these health behaviours. We determined the impact of a theory-based osteoporosis education intervention and BMD screening on older men and women's decisions to start or increase total calcium and vitamin D intake (food and supplement). Methods: A 6-month randomized controlled trial was carried out in Saskatchewan, Canada. Eligible subjects were recruited from a local hospital and included men and women 50 years of age and older, referred by their physician for BMD screening for the first time. Subjects (N = 203, mean age = 59.7 years, SD 7.1) were randomly assigned to an intervention group (n = 102) or usual care group (screening alone) (n = 101). After screening, and prior to discussing results with a physician, subjects completed a 3-day food diary, health history questionnaire and reported use of all supplements. The intervention group also received theory-based osteoporosis education using constructs of the Revised Health Belief Model as a guiding framework. The intervention included a package of print material and calcium/vitamin D magnets, short video, and one-on-one discussion. Six months post-baseline, subjects completed a series of follow-up questionnaires and 3-day food diary. Results: At baseline, intervention and usual care groups had mean total calcium intake (1,152.0 mg/day and 1,173.1 mg/day, respectively) and vitamin D intakes (778.4 IU/day and 773.3 IU/day, respectively) below recommendations. At 6-month follow-up total calcium and vitamin D intake increased in both groups; however, there was a significant mean difference in calcium (250.4 mg/day) and vitamin D (242.5 IU/day) intake in the intervention group compared to usual care (p = .03). Overall, 58.6% and 69.7% started or increased calcium and vitamin D intake, respectively. In multivariate adjusted models, receiving osteoporosis education intervention, low total calcium intake and not taking vitamin D supplements at baseline were associated with change in intake. Conclusions: Theory-based osteoporosis education intervention improved calcium and vitamin D intake in newly screened older men and women. Taking health beliefs into consideration when developing and implementing education interventions may be useful in both research and practice for osteoporosis prevention and management.

***Disclosures: Katherine McLeod**, None.*

SA0315

See Friday Plenary Number FR0315.

SA0316

Withdrawn

SA0317

Can Changes in FRAX Probability Be Used to "Treat-to-Target"? A Clinical Feasibility Study. William Leslie*[1], Lisa Lix[1], Suzanne Morin[2], Sumit Majumdar[3], Helena Johansson[4], Eugene McCloskey[5], Anders Oden[6], John Kanis[7]. [1]University of Manitoba, Canada, [2]McGill University, Canada, [3]University of Alberta, Canada, [4]Swedish University of Agricultural Sciences, The Biomedical Center, Sweden, [5]University of Sheffield, United Kingdom, [6]Consulting statistician, Sweden, [7]University of Sheffield, Belgium

Background: FRAX is intended to select individuals for treatment based upon fracture risk. It is unknown how responsive FRAX is to treatment or whether it can serve as a target for guiding duration of therapy

Objective: To describe predictors of change in FRAX probability in older women.

Methods: We identified 11,049 untreated women age >50 years undergoing baseline and subsequent DXA examinations (1998-2011) in a large clinical database for the Province of Manitoba, Canada. By linking to a population-based data repository, we identified relevant risk factors, any intervening osteoporosis treatment (OTX), and incident fractures to March 2011. FRAX probabilities for major osteoporotic fracture (MOF) and hip fracture (HF) were computed for each DXA scan using the subject's most current (updated) FRAX input variables. Changes in FRAX probabilities from baseline were stratified by testing interval (1-3y, 3-5y and >5y) and OTX expressed as medication possession ratios (MPR=0 [reference], <0.50 [low], 0.50-0.79 [moderate], 0.80+ [high]). Odds ratios (OR) for predictors of change in FRAX probability and hazard ratios for incident fractures were adjusted for baseline risk.

Results: Over time, median FRAX probabilities increased in all MPR categories, including high MPR women despite increased BMD (Table). Although OTX attenuated increases in FRAX score (p-for-trend <.001), differences were small (<1%) and within the range of rounding error. Only 1.6% of high MPR women had a decrease in MOF probability over 5%, while 9.0% had a decrease in HF probability over 1%. Compared with MPR=0, OTX was associated with smaller increases in MOF FRAX probability (lowest versus highest change quartile): OR 2.3 (95%CI 1.8-2.9) for MPR <0.50, 7.3 (95%CI 5.6-9.6) for MPR 0.50-0.79, 12.0 (95%CI 9.5-15.2) for MPR 0.80+. Changed FRAX inputs associated with change in MOF probabilities in decreasing order of importance were: BMD, age, glucocorticoids, prior fracture, alcohol, rheumatoid arthritis, smoking, and BMI. Similar findings were seen for changes in HF probability. Overall and stratified by treatment, changes in FRAX probability did not contribute to prediction of future MOF or HF.

Conclusions: FRAX probabilities generally increase over time, and are only weakly affected by treatment. This finding was true even among the most highly adherent women. Few women had clinically important reductions in FRAX probabilities, nor did change in FRAX probabilities enhance fracture prediction.

Interval	Treatment	N	Δ MOF with BMD	Δ HF with BMD	Δ BMD Lumbar spine	Δ BMD Femoral neck
1-3 years	None (MPR=0)	1277	0.7 (0.3:1.3)	0.2 (0.0:0.5)	-1.2% (-3.9:1.7)	-1.3% (-4.2:1.3)
	MPR <0.50	528	0.7 (0.1:1.5)	0.2 (-0.1:0.6)	0.8% (-2.3:5.3)	0.2% (-3.1:3.3)
	MPR 0.50-0.79	384	0.5 (-0.3:1.2)	0.0 (-0.2:0.4)	3.7% (1.3:7.3)	2.0% (-0.9:5.1)
	MPR 0.80+	845	0.3 (-0.5:0.9)	0.0 (-0.4:0.3)	5.6% (2.4:9.1)	2.9% (0.1:5.9)
3-5 years	None (MPR=0)	1866	1.2 (0.7:2.1)	0.3 (0.1:0.8)	-1.1% (-4.2:1.9)	-2.2% (-5.2:0.7)
	MPR <0.50	1000	1.2 (0.6:2.2)	0.3 (0.1:0.8)	0.8% (-3.3:4.9)	-0.5% (-3.8:2.6)
	MPR 0.50-0.79	709	0.8 (0.0:1.6)	0.1 (-0.1:0.6)	5.0% (1.6:8.5)	2.2% (-0.8:5.4)
	MPR 0.80+	1259	0.6 (-0.2:1.4)	0.1 (-0.2:0.5)	6.6% (3.1:10.4)	3.0% (0.3:5.9)
>5 years	None (MPR=0)	1372	2.2 (1.4:3.5)	0.6 (0.2:1.2)	-1.6% (-5.7:2.2)	-3.5% (-7.3:0.0)
	MPR <0.50	923	2.4 (1.4:4.4)	0.7 (0.2:1.7)	-0.1% (-4.6:5.1)	-2.2% (-5.8:2.0)
	MPR 0.50-0.79	369	1.8 (0.9:3.4)	0.5 (0.1:1.4)	5.2% (0.4:10.9)	1.6% (-2.9:5.1)
	MPR 0.80+	517	1.5 (0.4:3.0)	0.4 (0.0:1.3)	7.8% (3.1:12.6)	2.8% (-0.4:7.3)
Overall		11049	1.1 (0.4:2.3)	0.3 (0.0:0.8)	1.6% (-2.6:6.3)	-0.1% (-3.8:3.4)

Median (IQR) change in FRAX MOF probability, HF probability and BMD by treatment and interval

***Disclosures: William Leslie**, None.*

SA0318

Lumbar Spine Trabecular Bone Score (TBS) combined with FRAX improves fracture prediction: The Manitoba BMD Cohort. William Leslie*[1], John Kanis[2], Olivier Lamy[3], Helena Johansson[4], anders oden[5], Eugene McCloskey[5], Didier Hans[6]. [1]University of Manitoba, Canada, [2]University of Sheffield, Belgium, [3]University Hospital, Switzerland, [4]Swedish University of Agricultural Sciences, The Biomedical Center, Sweden, [5]University of Sheffield, United Kingdom, [6]Lausanne University Hospital, Switzerland

TBS, a novel gray-level measurement derived from lumbar spine DXA image texture, is related to microarchitecture and fracture risk independently of BMD. FRAX estimates the 10-year probability of hip and major osteoporotic fracture (MOF) using risk factors that act independently of femoral neck BMD. We assessed the value of combining FRAX probability with lumbar spine TBS.

42,170 women age >50 years at the time of baseline DXA were identified in a database of all clinical results for Manitoba, Canada. Lumbar spine TBS was calculated blinded to clinical parameters and outcomes. Health service records were assessed for FRAX covariates at the time of DXA and for incident non traumatic MOF and hip fracture codes to March 31st 2011. FRAX probabilities were calculated with BMD. Cox proportional hazards models including competing mortality were developed for time to first fracture based upon TBS (continuous or tertiles), osteoporosis medication use, and FRAX probability. Two-way interactions between TBS and FRAX risk factors were tested. Additional models included lumbar spine BMD and the spine-hip T-score "offset".

The mean age of the population was 65.7 ± 9.5 y. During mean 5.6 y, incident MOFs were identified in 2661 women (674 hip fractures). Lower lumbar spine TBS and higher FRAX probabilities were found in fracture vs non fracture women (all P<0.001). TBS modulated fracture risk after adjustment for treatment and individual FRAX risk factors (hazard ratio [HR] per SD reduction in TBS: MOF 1.21 [95% CI 1.16-1.250, P<0.001; hip fracture 1.14 [95% CI 1.05-1.23), P=0.001). Results were largely unaffected by including lumbar spine BMD or spine-hip T-score "offset" in the model. A preliminary method to adjust FRAX probability based upon lumbar spine TBS tertile is shown in the Table. When used to reclassify fracture risk, this gave a significant increase in integrated discrimination index for MOF (+1.3%, P<0.001) and hip fracture (+1.3%, P<0.001), with net reclassification improvement +4.6% for MOF (P<0.001). There was an age interaction with larger TBS effects in younger than older women age for MOF (P<0.001) and hip fracture (P=0.002).

In summary, an incremental improvement in fracture prediction was seen by using lumbar spine TBS in combination with FRAX. An approach that addresses the age-TBS interaction may be required. If validated in other prospective cohorts, lumbar spine TBS may become clinically useful for enhancing fracture prediction from FRAX.

	Change to Major Osteoporotic Fracture probability	Change to Hip Fracture probability
If L1L4TBS is in the lowest tertile:	Increase 25%*	Increase 30%*
If L1L4TBS is in the middle tertile (referent):	No change	No change
If L1L4TBS is in the highest tertile:	Decrease 21%*	No change
*P<0.001		

Table

***Disclosures: William Leslie**, None.*

SA0319

Correlation between early Micro-Architectural Changes and Patient-Rated Wrist Pain and Disability 12 weeks after a Distal Radius Fracture. Joost De Jong*[1], Ursina Meyer[2], Sandrine Bours[3], Paul Willems[4], J. J. Chris Arts[4], Peter Brink[5], Tineke Van Geel[6], Bert Rietbergen[7], Joop Van Den Bergh[8], Piet Geusens[9]. [1]Maastricht University Medical Center, The Netherlands, [2]Department of Human Movement Sciences, Maastricht University, Netherlands, [3]Maastricht University Medical Centre, The Netherlands, [4]Department of Orthopaedic surgery, Maastricht University Medical Centre, Netherlands, [5]Department of Trauma Surgery, Maastricht University Medical Centre, Netherlands, [6]Maastricht University, The Netherlands, [7]Eindhoven University of Technology, The Netherlands, [8]VieCuri MC Noord-Limburg & Maastricht UMC, The Netherlands, [9]University Hasselt, Belgium

Factors affecting patient-reported pain and disability after distal radius fractures are essential elements in understanding the process of fracture healing. High resolution peripheral quantitative computed tomography (HR-pQCT) combined with micro finite element analysis (μFEA) allows to assess changes in bone mineral density (BMD), micro-architecture and calculated biomechanical competence during fracture healing. We assessed the association between these early changes and wrist-specific pain and disability at 12 wk post-fracture in postmenopausal women with a stable distal radius fracture.

Eighteen women (aged 68±8 yr) with a stable, conservatively treated distal radius fracture were recruted. At four visits (1-2, 3-4, 6-8, 12 wk post-fracture), patients rated their pain and disability using Patient Rated Wrist Evaluation (PRWE; range 0-100) and

Quick Disabilities of the Arm Shoulder and Hand (QuickDASH; 0-100) questionnaires, and a visual analogue scale (VAS; 0-100) with higher values indicating worse status. At each visit, BMD, micro-architecture and mechanical parameters of the fracture region were assessed by HR-pQCT and μFEA, and serum bone markers [procollagen type-I N-terminal propeptide (P1NP) and carboxy-terminal telopeptide of type I collagen (ICTP)] were measured. Pain and disability at visit 4 were linearly regressed on changes in bone parameters from visit 1 to 2, adjusted for number of days post-fracture.

PRWE at 12 wk (mean 42±29) correlated negatively with the increase in trabecular BMD [β=-0.95 (95%CI: -1.75 to -0.16) mgHA·cm^{-3}, p=0.02], positively with the change in trabecular separation [208 (14.6 to 401) mm, p=0.04], and negatively with the change in torsional stiffness [-0.14 (-0.28 to -0.004) kN·mm·rad^{-1}; p=0.04]. Further, PRWE at 12 wk correlated positively to the change in ICTP [12.0 (-0.032 to 24.0) μg/l; p=0.051]. Comparable results were found for QuickDASH, but not for the VAS-score. Adjusting for DXA T-score, fracture type, fracture at dominant side or serum vitamin D levels did not affect the results.

Changes in the trabecular density, torsional stiffness and bone resorption during the first weeks after radius fracture were correlated with the pain and disability at 12 wk post-fracture. These results suggest that assessment of changes in micro-architectural parameters during early stages of fracture healing could provide valuable information for predicting the clinical outcome of distal radius fractures.

***Disclosures: Joost De Jong**, None.*
This study received funding from: Weijerhorst foundation

SA0320

Efficacy of a Hospital-Based Fracture Liaison Service in the Secondary Prevention of Osteoporotic Fractures. Elizabeth McAninch*[1], Violet Lagari[2], Sanford Baim[3]. [1]University of Miami/Jackson Memorial Hospital, USA, [2]University of Miami, USA, [3]Miller School of Medicine, University of Miami, USA

Despite the high prevalence of osteopenia and osteoporosis, these conditions remain underdiagnosed and -treated, resulting in undue morbidity and economic burden. The ASBMR advocates for secondary fracture prevention by formal implementation of Fracture Liaison Services [Eisman, et al. Making the First Fracture the Last Fracture: ASBMR Task Force Report on Secondary Fracture Prevention. JBMR. 2012;27(10):2039-46]. The University of Miami Hospital offers a unique setting for implementation of such a service as it exemplifies an "open" healthcare system. Here we propose our plan to create the University of Miami Hospital Fracture Liaison Service (UMH FLS).

The UMH FLS is an in-hospital consult service staffed by osteoporosis experts that will identify patients aged 50 and over admitted with acute fractures. The UMH FLS provides comprehensive osteoporosis assessments and direct physician-to-patient education about the diagnosis and implications of having osteoporosis. During the patient encounter we will perform a thorough history and physical exam to determine the etiology of the fracture, provide verbal/written osteoporosis patient education, refer the patient for outpatient follow up for initiation of FDA-approved osteoporosis treatment when medically appropriate, and refer to specialized physical/occupational osteoporosis therapy inclusive of a home falls prevention program. Informed consent will be obtained during the inpatient encounter that will allow the UMH FLS to send questionnaires and directly contact participants at 3 months and annually for a total of five years post-discharge through an IRB-approved protocol. The questionnaire will ascertain participant osteoporosis outcome measures such as information regarding health status (specifically incident fractures) and compliance with physician follow up, medical therapies, DXA tests, and physical/occupational therapy. To assess for benefit of the UMH FLS, we will perform a three-year retrospective analysis of incident fractures through chart review.

We hypothesize that implementation of the hospital-based UMH FLS will improve care for patients with osteoporotic fractures in a cost-effective manner resulting in subsequent prevention of secondary fractures. If evidence confirms reduced morbidity, mortality and economic burden as a result of the UMH FLS, this would further support the adoption of our methodology as a standard of care in the treatment of inpatients with acute osteoporotic fracture.

***Disclosures: Elizabeth McAninch**, None.*

SA0321

Fracture Burden For Men, In Relation To Osteopenia And Osteoporosis Defined By Male And Female Reference Data For Areal Bone Mineral Density. Julie Pasco*[1], Stephen Lane[1], Sharon Brennan[2], Elizabeth Timney[1], Gosia Bucki-Smith[1], Amelia Dobbins[1], Mark Kotowicz[3]. [1]Deakin University, Australia, [2]The University of Melbourne, Australia, [3]Deakin University School of Medicine, Australia

Purpose: The purpose of this study was to quantify fracture risk associated with osteopenia and osteoporosis in older men, defined by areal bone mineral density (BMD) and using cut-points derived from male and female reference data.

Methods: In this prospective analysis we followed 619 men aged 60-93 years (median 74.4yr) for a median 6.4yr, after baseline BMD assessments (performed 2001-6) as part of the Geelong Osteoporosis Study. Based on WHO criteria, and using male reference data, 207 men had normal BMD at the femoral neck, 357 were osteopenic and 55 osteoporotic. Using female reference data, corresponding numbers were 361, 227 and 31, respectively. Participants were followed until the end of 2010, or until sustaining a fracture, death, or emigration. Post-baseline fractures were ascertained radiologically.

Results: During the study 130 men died, 15 left the region, 63 sustained at least one fracture. Using male reference data, most (86.6%) of the fractures occurred in men without osteoporosis on BMD criteria (17.9% with normal BMD, 68.7% with osteopenia) whereas 13.5% of the fractures occurred in men with osteoporosis. The pattern differed when female reference data were used; while most fractures arose from men without osteoporosis (88.2%), the burden shifted from those with osteopenia (35.0%) to those with normal BMD (53.2%).

Conclusions: Categories of decreasing BMD defined increasing risk of fracture. Although men with osteoporotic BMD were at greatest risk, they made a relatively small contribution to the total burden of fractures. Using male reference data, two-thirds of the fractures arose from men with osteopenic BMD. However, using female reference data, approximately half of the fractures arose from those with normal BMD.

***Disclosures: Julie Pasco**, None.*

SA0322

FRAX in combination with Lumbar Spine Trabecular Bone Score (TBS) better discriminates vertebral fracture than BMD, TBS or FRAX alone: The OsteoLaus Study. Olivier Lamy*[1], Marc-Antoine Krieg[2], Delphine Stoll[3], Berengere Aubry-rozier[4], Marie Metzger[5], Didier Hans[4]. [1]Chief of the Bone Unit, Switzerland, [2]University Hospital, Switzerland, [3]MD, Bone Unit, University hospital, Switzerland, [4]Lausanne University Hospital, Switzerland, [5]Bone Unit, University hospital, Switzerland

Osteoporosis (OP) is a systemic skeletal disease characterized by a low bone mineral density (BMD) and a micro-architectural (MA) deterioration. TBS, a novel gray-level measurement derived from lumbar spine DXA image texture, is related to microarchitecture and fracture risk independently of BMD. FRAX estimates the 10-year probability of hip and major osteoporotic fracture (MOF) using risk factors that act independently of femoral neck BMD. We assessed the value of combining FRAX probability with lumbar spine TBS versus each parameter alone in discriminate vertebral fracture from controls. The OsteoLaus cohort (1500 women 50 to 80 years living in Lausanne, Switzerland) started in 2010. Clinical risk factors for osteoporosis / fracture, FRAX, lumbar spine and hip BMD, VFA by DXA and microarchitecture evaluation by TBS are recorded in OsteoLaus. Preliminary results are reported. Sensitivity and specificity in regard to vertebral fracture grade 2/3 has been calculated for all Bone modalities as stand-alone or combined approaches. A first approach to adjust FRAX by TBS has been applied. Integrated discrimination index and net reclassification improvement have also been investigated. We included 911 women: mean age 65.2+/-7.9 y, BMI 25.7+/-4.4, mean lumbar spine BMD 0.931+/-0.16(T-score -1.04 SD), TBS 1.289+/-0.100. As expected, correlation between BMD and site matched TBS is low (r2=0.16). Prevalence of VFx grade 2/3 and MOF are 7.5% and 15.0% respectively. Sensitivity and specificity for different combination can be found in the table. When used to reclassify fracture risk, this gave a significant increase in integrated discrimination index for VFx (+2.5%, P<0.001), with net reclassification improvement +7.6% for VFx (P<0.001).

While the optimal threshold for TBS should be investigated, an incremental improvement in fracture identification was seen by using lumbar spine TBS in combination with FRAX. If validated in prospective cohorts, lumbar spine TBS may become clinically useful for enhancing fracture prediction from FRAX. Such simple way to take TBS into account would allow the use of current medical society recommendation regarding osteoporosis management with only minor adaptation.

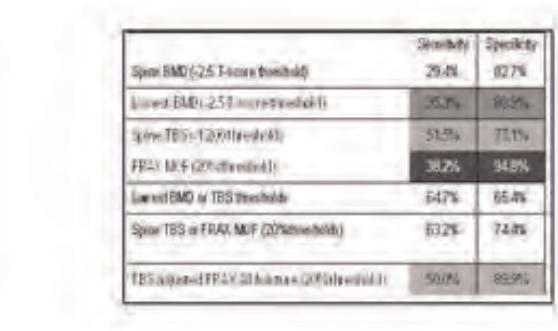

table

***Disclosures: Olivier Lamy**, None.*

SA0323

Hip Fracture Trends in Denmark 1980-2010 with Age-Period-Cohort-effects.
Bjorn Rosengren*[1], Jonas Björk[2], Cyrus Cooper[3], Bo Abrahamsen[4]. [1]Skåne University Hospital Malmö, Lund University, Sweden, [2]Unit for Medical Statistics & Epidemiology at R&D Centre Skåne, Skåne University Hospital, Sweden, [3]University of Southampton, United Kingdom, [4]University of Southern Denmark, Denmark

Background: The origin of the recent levelling-off in hip-fracture incidence in several settings is unknown.

Methods: Using Danish national inpatient data for individuals aged ⩾50 years during 1980-2010, we examined annual number and incidence of hip fractures and age, period, and cohort effects by log-likelihood estimates in Poisson regression models. Age adjustment was done by direct standardization, time-trend analysis by linear regression, and identification of breakpoints in linear trends by join-point analyses.

Results: There were 240 121 hip fractures, 74% in women. Before 1993, the annual age-standardized hip fracture incidence increased (2.8% per year [95% confidence interval 2.3% to 3.3%]), and the annual number of hip fractures increased (4.4% per year [3.8% to 5.0%]). After 1993, the age-standardized hip fracture incidence decreased (-1.2% per year [-1.5% to -0.9%]) and the number of hip fractures was stable (-0.3% per year [-0.7% to -0.0%]).

The combined period+cohort effects were more marked in men, with an incidence rate ratio (IRR) ranging from 0.4 to 1.2 depending on 6-year birth cohort and 0.7 to 1.1 depending on 3-year period. In women the corresponding results were IRR 0.8 to 1.4 and 0.9 to 1.2.

Analyses of specific cohort effects (estimated by deviations from underlying linear trends in cohort) in the full APC-model showed higher risk in men born 1900-1926 and in women born 1897-1938. The corresponding specific period analyses revealed increasing risk for men with later period while a higher risk was evident in the middle of the examination period for women.Conclusion

The annual age-standardized hip fracture incidence has decreased in Denmark since 1993, resulting in a stable annual number of hip fractures. The magnitude of the period+cohort effects suggests a risk modulation in parity with other established risk factors for hip fracture. Gender-specific differences may partly result from changes in hormone-replacement or anti-osteoporosis therapy.

***Disclosures: Bjorn Rosengren**, None.*

SA0324

How to Adjust the Overestimate of the Incidence of Major Osteporotic Fracture When Using Summary Data.
Thor Aspelund*[1], Kristin Siggeirsdottir[1], Elias Gudmundsson[1], Brynjolfur Y Jonsson[2], Brynjolfur Mogensen[3], Vilmundur Gudnason[4], Gunnar Sigurdsson[3]. [1]Icelandic Heart Association, Iceland, [2]Skane University Hospital, Sweden, [3]Landspitalinn University Hospital, Iceland, [4]Icelandic Heart Association Research Institute, Iceland

Major osteporotic site (MOS) fracture is a fracture of any of hip, vertebral, distal forearm or proximal humerus. This event is common and the risk increases with age. It is important to have a reliable estimate of the incidence for better management of resources and to recognize who is at risk. When individual data is not available an estimate can be constructed by adding up the incidence of the individual fracture types which may be easier to obtain. This results in an overestimate because individuals can sustain fractures of different types. Knowledge about the overlap can be used to calibrate the MOS fracture incidence estimate.

The Icelandic Reykjavik Study is a population based cohort study of men and women with almost 19000 participants recruited between 1967 and 1992. We used the fracture registration associated with the Reykjavik Study to estimate the MOS fracture incidence (any-of-4), the incidence of the 4 fracture types and their sum (sum-of-4). The incidence was estimated for men and women from age 45 to 90. The ratio between the sum-of-4 to any-of-4 was computed to estimate the magnitude of the overestimate due to overlap by sex and age.

The overestimate was about 3% for the age group 45-49, 10% for the age group 65-69, and increased linearly up about 22% for the age 85-89. These results about the overlap were in strong agreement with results from the Malmö study in Sweden. This means that the overlap adjustments from the Malmö study could be applied to the sum-of-4 from the Reykjavik Study to provide almost identical MOS fracture incidence estimates (any-of-4) as directly estimated from the Reykjavik Study. This supports the methodology of adding incidence of individual fracture types and then apply overlap adjustments from the Malmö study to construct MOS fracture incidence, which has been used as a calibration for FRAX when individual data is not available.

***Disclosures: Thor Aspelund**, None.*

SA0325

Impact of a Fragility Fracture on Quality of Life 6 and 18 Months Post Fracture.
Claudia Beaudoin*[1], Sonia Jean[2], Louis Bessette[3], Louis-Georges Ste-Marie[4], Jacques P. Brown[3]. [1]Centre de recherche du CHU de Québec, Canada, [2]INSTITUT NATIONAL DE SANTÉ PUBLIQUE DU QUÉBEC, Canada, [3]CHU de Quebec Research Centre, Canada, [4]CHUM, Canada

Purpose: To assess the health-related quality of life (HRQoL), over time, in women (⩾ 50 years) after a fragility fracture (FF). Methods: In the Recognizing Osteoporosis and its Consequences in Quebec programme, a cohort of women who recently suffered from a FF were recruited from hospitals and an administrative database-generated list. The HRQoL was assessed with the EQ-5D health questionnaire which was mailed to women 6 and 18 months post fracture. In the EQ-5D questionnaire, 5 dimensions of health were covered (mobility, self-care, usual activities, pain/discomfort and anxiety/depression) and the perception of general health was evaluated using a visual analogue scale where 0 represents the worst health and 100, perfect health. As a comparison group, data from a general population cohort of 262 women from Alberta aged ⩾ 50 years were used (Johnson et al, 2000). In women suffering each fracture type, the mean health perception score and the proportion of women reporting problems were compared with the reference population using age-weighted chi-square and student tests. Results: 1979 and 1927 women completed the EQ-5D questionnaire at 6 and 18 months, respectively. Six months following a hip/femur fracture, the proportions of women reporting problems with self-care (18%), usual activities (52%), pain/discomfort (83%) and anxiety/depression (45%) were significantly greater than in women from the general population (Figure 1). Problems with usual activities (51%), pain/discomfort (79%) and anxiety/depression (41%) remained significantly greater 18 months after a hip/femur fracture (Figure 2). For women who suffered a humerus fracture, the proportion reporting problems was also significantly greater for self-care (17%) and pain/discomfort (79%) at 6 months, and for pain/discomfort (70%) at 18 months when compared to the general population. Having suffered an ankle/tibia/fibula/foot or a forearm/elbow/wrist fracture did not result in a significant impact on the EQ-5D. At 6 and 18 months, the general health perception for women with a hip/femur fracture (mean scores of 69 and 70, respectively) was significantly lower than that in the general population (mean score of 75). Conclusions: This study shows that the HRQoL of women who suffered a hip/femur or humerus fracture remains lower than in the general population even 6 months post FF. After 18 months, some dimensions of quality of life in women with a previous FF at some fracture sites are still compromised.

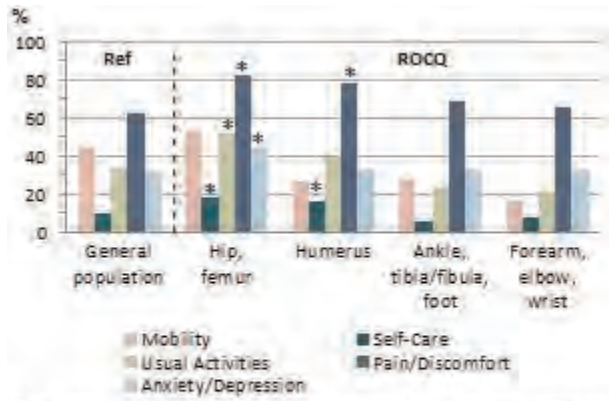

Figure 1: Percentage (%) of women reporting health-related problems 6 months following fracture

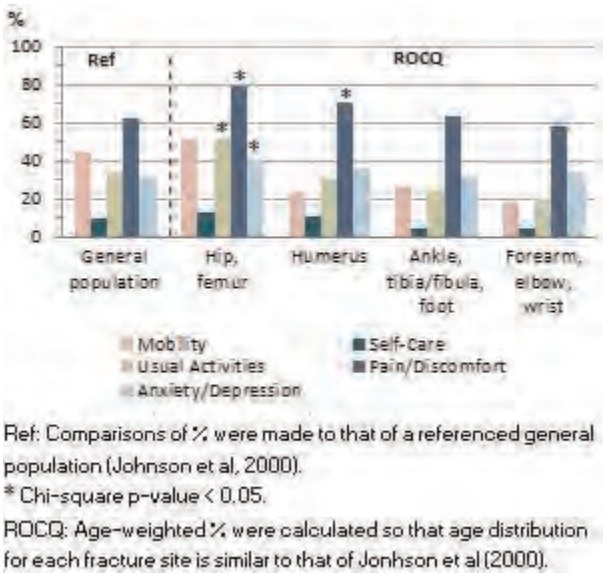

Figure 2: Percentage (%) of women reporting health-related problems 18 months following fracture

***Disclosures: Claudia Beaudoin**, None.*
This study received funding from: Merck, sanofi-aventis,Warner Chilcott, Amgen, Eli Lilly, Novartis

SA0326

Clinical and Economic Characteristics of Hip Fracture Patients in the United States with Poor Health Outcomes. Zhanglin Cui*[1], Yang Zhao[2], Lei Chen[3], Yi Chen[4], Russel Burge[1]. [1]Eli Lilly & Company, USA, [2]Novartis Pharmaceuticals Corporation, USA, [3]Eli Lilly, USA, [4]inVentiv Health Clinical, USA

Purpose: To identify characteristics of hip fracture patients with or without muscle disuse atrophy/weakness (MAW, identified by ICD-9 code); predictors of poor post-fracture outcomes (high costs, high healthcare utilization, long hospitalization); and subgroups at increased risk for poor outcomes.

Methods: Thomson Reuters MarketScan® data were used to identify United States (US) patients aged ⩾50 years, with inpatient hospital stays for hip fracture Jan 2006 - Sep 2010. Patients had ⩾12 months of continuous enrollment, prior to the index hospitalization, and 12 months following the discharge date, with no hip fracture diagnoses 7 days - 1 year prior to the index date. Predictive characteristics of patients with poor outcomes were identified via multiple logistic regression analyses. Poor outcomes subgroups were identified by classification and regression tree (CART) analyses.

Results: Commercial (n=5,350) and Medicare (n=29,643) patients with hip fracture were identified (mean age: 57.9 and 81.8 years, respectively). More than 10% of each cohort had osteoarthritis, osteoporosis, diabetes, chronic pulmonary disease, or tumors. Prior hospital stays, outpatient visits, and emergency room visits were common (⩾25%) among patients. The mean index hospitalization costs were $31,051 (commercial patients) and $19,331 (Medicare patients). Index stay durations were about 6 days in both cohorts. On average, post-fracture, 1-year, all-cause healthcare costs ($41,718) were higher than costs for the previous 1 year ($28,852; $p<0.05$). Compared to patients without MAW, patients with MAW had greater 1-year healthcare utilization and costs ($p<0.05$). In multiple logistic regression analyses, greater post-fracture costs were associated with higher prior hospitalization counts, prior emergency room visit counts, length of index hospital stay, and Charlson Comorbidity Index (CCI), as well as with discharge status,; diagnosis of rheumatoid arthritis or osteoporosis; and prior use of antidepressants, anticonvulsants, muscle relaxants, opioids, and oral corticosteroids (all $p<0.05$). From CART analysis, subgroups of high-cost patients included those with MAW, longer prior hospitalizations, and high CCI score. Subgroups of patients with longer hospital stays included those with MAW and longer prior hospitalizations.

Conclusions: Among US patients with hip fractures, poor post-fracture outcomes were associated with MAW, prior hospitalizations, comorbidities, and medications.

***Disclosures: Zhanglin Cui**, Eli Lilly and Company, 3*
This study received funding from: Eli Lilly and Company

SA0327

See Friday Plenary Number FR0327.

SA0328

Osteoporosis Treatment after Vertebral and Hip Fractures: Analysis of a Managed Care Population in the US. Ankita Modi[1], Amber Wilk[2], Chun-Po Steve Fan[3], Shiva Sajjan*[1], Panagiotis Mavros[1]. [1]Merck & Co., Inc., USA, [2]Virginia Commonwealth University, USA, [3]AsclepiusJT LLC, USA

Purpose: It is recommended that fractures patients be treated with pharmacological treatment for osteoporosis to mitigate subsequent fracture risk. This study examined osteoporosis treatment use after vertebral or hip fractures in a US managed care population. Methods: A retrospective analysis using i3 Invision Datamart, a large claims database, from January 2003 to June 2012 (study period) was conducted. Women ⩾ 50 years of age with vertebral and/or hip fracture during the study period with continuous enrollment 24 months before (pre-index) and 12 months after (post-index) the first fracture (index date) were included. Women with Paget's disease or malignant neoplasms were excluded. Fractures were identified using ICD-9 diagnosis codes. Osteoporosis treatment included bisphosphonates (alendronate, ibandronate, risedronate, zoledronic acid) and non-bisphosphonates (calcitonin, raloxifene, teriparatide, denosumab), which were identified by NDC and HCPCS codes. Charlson comorbidity index (CCI) was used to quantify a patient's overall comorbid conditions. Pre- and post-index osteoporosis treatment use was assessed by fracture site. Results: 11,433 women ⩾ 50 years of age (7,834 vertebral; 3,599 hip fracture) were included in the study. Hip fracture patients were on average older than the ones with vertebral fracture patients (71.3 *vs*. 66.8 years, $p<.001$). Hip fracture patients had a significantly higher average CCI than vertebral fracture patients (1.5 *vs*. 1.3, $p<.001$). Despite occurrence of fracture, 82.1% of patients did not receive treatment within the 3-month post-index period, and 77% remained untreated at 1-year post-index. The number of hip fracture patients not receiving treatment within 3-month and 1-year post-index periods was significantly higher than that of the vertebral fracture patients (3-month untreated rate: 81.6% *vs*. 69.4%, $p< .001$; 1-year untreated rate: 75.0% *vs*. 62.5%, $p<.001$). Among those treated within 3-month (1-year) post-index, the average time between fracture and treatment were 13.8 (46.5) and 20.7 (65.4) days for vertebral and hip fracture patients, respectively. Conclusions: This study shows a high rate of undertreatment of osteoporosis with medications after patients experienced vertebral and hip fractures despite treatment recommendations for these high-risk patients. This warrants a need for further education regarding osteoporosis management for patients with prior fractures.

***Disclosures: Shiva Sajjan**, Merck & Co., Inc, 3*
This study received funding from: Merck & Co., Inc.

SA0329

Prevalence and Predictive Capacities of Different Definitions of Severe Osteoporosis. Claudie Berger*[1], Lisa Langsetmo[2], David Goltzman[3], George Ioannidis[4], Jerilynn Prior[5], Youb Chalabi[6], Robert Josse[7], Stephanie Kaiser[8]. [1]CaMos, McGill University, Canada, [2]Canandian Multicenter Osteoporosis Study, Canada, [3]McGill University, Canada, [4]McMaster University, Canada, [5]University of British Columbia, Canada, [6]Eli Lilly, Canada, [7]St. Michael's Hospital, University of Toronto, Canada, [8]Dalhousie University, Canada

Severe osteoporosis is variously defined. We assessed the prevalence, risk factors, use of antiresorptive therapy, and risk of subsequent fragility fracture (ffx) associated with different definitions of severe osteoporosis.

We examined 2187 men and 5566 women aged 50 years (y) and older from the Canadian Multicentre Osteoporosis Study (CaMos). Participants had a questionnaire and bone mineral density (BMD) measurements at baseline (1995-7) and were contacted annually for 14 y about incident ffx. We defined 6 groups of severe osteoporosis: (1) BMD T-score (L14 or total hip or neck) <-2.5; (2) definition 1 and prior 4-ffx (hip, back, forearm/wrist, shoulder); (3) at least 2 ffx (any site excluding hands, feet, skull); (4) BMD T-score (L14 or total hip or neck) <-3; (5) FRAX 4-ffx risk >20%; and (6) FRAX 4-ffx risk >20% and a prior 4-ffx. Logistic regressions were used to assess the odds ratios (OR) of 14-y incident ffx for severe osteoporosis compared to normal participants (T-score [L14 and total hip and femoral neck] >-1 and no prior ffx).

The Canadian prevalence of severe osteoporosis varies by definition (Table 1); it is higher with T-scores versus prior ffx or FRAX scores. At baseline, the antiresorptive use in Canadian women with severe osteoporosis was 16-25% and near zero in men. After 5-y (2000-2), antiresorptive use more than doubled in women with severe osteoporosis (by definitions 1-4) and varied from 4-15% in men. In women, older age, lower body mass index (BMI), shorter height, non use of hormone therapy, family history of osteoporosis and lower SF-36 physical health component score were associated with severe osteoporosis irrespective of definition. Current use of cigarettes, less alcohol intake, more sedentary hours/day, lower dietary calcium intake and no use of calcium and vitamin D supplements were related to one or more of the definitions. In men, older age and lower BMI were related to all severe osteoporosis definitions. The ORs for 14-y incident ffx for severe osteoporosis versus controls are shown in Figure 1. FRAX scores gave the highest ORs for 14-y incident ffx but also showed the widest confidence intervals.

Elevated ffx risk was observed in those with severe osteoporosis by all definitions, but was highest among those with a history of ffx, thus establishing priority for those with prior ffx. Those without previous ffx are a much more prevalent subgroup but are still at substantial risk of future ffx.

Table 1: Canadian prevalence of severe osteoporosis at baseline by six definitions in women and men aged 50 and older.

Definition of severe osteoporosis	Women	Men
T[1] <-2.5	35.1	16.7
T[1] <-2.5 & ≥ 1 prior 4-ffx[2]	6.1	1.5
≥ 2 prior ffx (any site[3])	4.7	3.0
T[1] < -3	25.0	13.1
FRAX 4-ffx risk > 20%	9.4	0.4
FRAX 4-ffx risk > 20% & ≥ 1 prior 4-ffx[2]	3.2	0.2

[1] T-score is L14 or total hip or femoral neck
[2] 4-ffx = fragility fracture of the hip, back, forearm/wrist, or shoulder
[3] Excluding head, hand, foot

Table 1: Canadian prevalence of severe osteoporosis at baseline

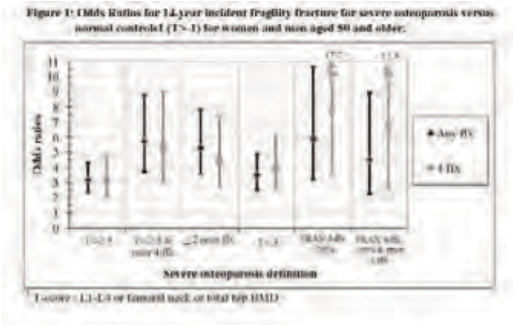

Figure 1: Odds ratios for 14-year incident fragility fracture

***Disclosures: Claudie Berger**, None.*

SA0330

Secular Trends in the Incidence of First Hip, Clinical Vertebral, Distal forearm and Proximal Humerus Fractures in Icelandic Men and Women in 1989-2008. Gunnar Sigurdsson*[1], Kristin Siggeirsdottir[2], Elias Gudmundsson[2], Brynjolfur Y Jonsson[3], Brynjolfur Mogensen[4], Thor Aspelund[2], Vilmundur Gudnason[5]. [1]Landspitali, Iceland, [2]Icelandic Heart Association, Iceland, [3]Skane University Hospital, Sweden, [4]Landspitalinn University Hospital, Iceland, [5]Icelandic Heart Association Research Institute, Iceland

Incidence estimate for first fracture of hip, vertebra, distal forearm and proximal humerus is available in Iceland for the age group 70-85 between the years 1989 and 2008. This allows examination of secular change in the incidence of these major osteoporotic sites (MOS) fractures. It is important to quantify the trend of this public health problem in an ageing population, with 7.1% over the age of 70 in 1989, 8.4% in 2009 and projected to be 10% in 2020.

The Reykjavik Study is a population based cohort study of men and women with almost 19000 participants recruited between 1967 and 1992. We used the fracture registration associated with the study to estimate the incidence of the MOS fractures. In 1967 the participants were of age 33-64 and in 1989 enough participants had reached the age of 70. The follow-up period was divided into 5 time periods: 1989-1992,1993-1996,1997-2000,2001-2004 and 2005-2008. The incidence of first fracture was estimated for the age group 70-85 in each period using life table methods: the number of new fractures was counted and the total person time computed for those without previous fracture. The incidence was then reported per 100000 person years. The estimate for each period was analyzed using a generalized linear model, assuming a Poisson distribution for the number of fractures with person years as offset to estimate the rates. The estimates were age standardized using the population of Iceland in 2008. A linear and quadratic change in the incidence rate was tested using polynomial contrasts.

The hip fracture rate increased for women between the period 1989-1992 and 1997-2000. After that the rate decreased, ending with a 20% lower rate in the period 2005-2008 compared to 1997-2000 (p=0.039), and ending in 7% lower rate than in 1989-1992. The age standardized rate in 2005-2008 was 500 events per 100000 person years. In contrast, the rates for men have been increasing (p=0.0078) until 2001 when it leveled off. The rate in 2005-2008 was 40% higher than the rate in 1989-1992, ending in 326 events per 100000 person years. Female/male ratio changed from 2.6 to 1.7 during the 20 year period.

In comparison the incidence for the other MOS fractures increased until year 2001 for men and women and showed similar decline for both sexes during the last decade. In contrast the hip fracture incidence in men remains unchanged during the last decade, possibly indicating different underlying contributors to these secular changes.

***Disclosures: Gunnar Sigurdsson**, None.*

SA0331

Site-specific Associations between Fracture and Height, Weight and Body Mass Index in Postmenopausal Women: GLOW Registry. Juliet Compston*[1], Julie Flahive[2], Jonathan Adachi[3], Silvano Adami[4], Steven Boonen[5], Roland Chapurlat[6], Cyrus Cooper[7], Adolfo Diez-Perez[8], Stephen Gehlbach[9], Susan Greenspan[10], Andrea Lacroix[11], Robert Lindsay[12], Lyn March[13], Coen Netelenbos[14], Johannes Pfeilschifter[15], Maurizio Rossini[4], Christian Roux[16], Kenneth Saag[17], Ethel Siris[18], Stuart Silverman[19], Nelson Watts[20]. [1]University of Cambridge School of Clinical Medicine, United Kingdom, [2]Center for Outcomes Research, UMASS Medical School, USA, [3]St. Joseph's Hospital, Canada, [4]University of Verona, Italy, [5]Center for Metabolic Bone Disease & Division of Geriatric Medicine, Bel, [6]E. Herriot Hospital, France, [7]University of Southampton, United Kingdom, [8]Autonomous University of Barcelona, Spain, [9]University of Massachusetts, USA, [10]University of Pittsburgh, USA, [11]Fred Hutchinson Cancer Research Center, USA, [12]Helen Hayes Hospital, USA, [13]Royal North Shore Hospital, Australia, [14]VU Medical Center, The Netherlands, [15]Alfried Krupp Krankenhaus Steele, Germany, [16]Hospital Cochin, France, [17]University of Alabama at Birmingham, USA, [18]Columbia University College of Physicians & Surgeons, USA, [19]Cedars-Sinai/ UCLA, USA, [20]Mercy Health Osteoporosis & Bone Health Services, USA

Introduction: Low body mass index (BMI) is a well-established risk factor for fracture in postmenopausal women. However, recent data indicate that high BMI, whilst protective for some fractures, is associated with increased risk of others. The aim of this study was to investigate the relationships of weight, BMI and height with incident clinical fracture at multiple sites in postmenopausal women.

Methods: GLOW is an observational longitudinal study of non-institutionalized women aged ⩾55 years recruited from 723 primary physician practices in 10 countries. Self-administered questionnaires were mailed, and data collected included demographics, co-morbidities, and previous and incident fractures. For each of 10 fracture sites (hip, spine, wrist, pelvis, rib, upper arm/shoulder, clavicle, ankle, lower leg, upper leg) we modelled the time to incident fracture over a 3-year period using the Cox proportional hazards model and fitted the best linear or non-linear models containing height, weight and BMI.

Results: 3,628 of 52,939 women (6.9%) sustained an incident clinical fracture during the 3-year follow-up period. As expected, adjusted hazard ratio (HR) per increase of 5 kg/m2: 0.80 (95% CI 0.71, 0.90), p=0.0002; 0.83 (0.76, 0.92), p=0.0001; 0.88 (0.83, 0.94), p<0.0001; respectively, whereas for ankle fractures linear weight showed the strongest association: adjusted HR 1.05 (95% CI 1.02, 1.07) per 5-kg increase (p<0.001). For upper arm and clavicle fractures, only linear height was significantly associated: adjusted HR per 10-cm increase 0.85 (95% CI 0.75, 0.97), p=0.02; and 0.73 (95% CI 0.57, 0.92), p=0.009; respectively. For pelvic and rib fractures, the best model was for non-linear BMI or weight (p=0.05 and p=0.03, respectively), with inverse associations at low BMI/body weight and positive associations at high values.

Conclusions: The relationships between fracture and weight, BMI and height are site-specific. BMI and weight show the strongest associations, with the exception of clavicle and upper arm fractures. The direction of effect of BMI and weight on fracture risk and the linearity of the relationship varies according to fracture site. These different associations may reflect, at least in part, effects of weight and BMI on bone mineral density, bone geometry, and the patterns of and protective response against falling.

***Disclosures: Juliet Compston**, Warner Chilcott Company and sanofi-aventis, 6*
This study received funding from: Warner Chilcott Company, LLC, sanofi-aventis

SA0332

The Burden of Osteoporotic Fracture: Epidemiology and Health-care Utilisation in Older Adults, 1997-2010. Sonia Jean*[1], Philippe Gamache[2], Louis Bessette[3], Étienne Belzile[4], Suzanne Morin[5], Mathieu Gagné[2], Jacques P. Brown[3]. [1]INSTITUT NATIONAL DE SANTÉ PUBLIQUE DU QUÉBEC, Canada, [2]Institut national de santé publique du Québec, Canada, [3]CHU de Quebec Research Centre, Canada, [4]Centre du recherche du CHUQ-CHUL, Canada, [5]McGill University, Canada

Purpose: Information on health-care utilization related to osteoporotic fractures is essential for allocation budget and resources planning. The purpose of this population-based study was to examine trends in incidence rates, utilisation of hospital and surgical care of non-vertebral osteoporotic fractures in women and men 50 years and older.

Methods: Using a validated algorithm based on physicians' cliams databases, 390,298 patients (69.5% women) were identified with an incident fractures at non vertebral osteoporotic sites between 1997 and 2010 in the province of Quebec, Canada. Fractures were grouped by anatomical sites as occuring at the hip/femur,

pelvis, forearm/wrist, shoulder/humerus, tibia/fibula, or ankle/foot. Administrative databases of health services available to all residents in Quebec were used to establish fracture-related hospitalisations and surgical care. Data were linked by a unique personal identifier, creating a longitudinal cohort of health resource utilization. According to fracture site, we examined trends in incidence rates, utilization of hospital and surgical care over the study period. Joinpoint regression and linear regression analysis were use to test for linear change in trends.

Results: During the study period, the age-standardized incidence rates fell for the majority of osteoporotic fracture sites in both sexes (Figure 1). The mean annual linear percent change (APC) varied between -1.6 and -3.3 percent for hip/femur and foot/ankle fractures, respectively (Table1). Only pelvic fractures did not show a significant decline. Although hip/femur fractures continue to represent the highest rates of health resources utilization, the proportion of surgery (90%) and hospital (90%) care remained constant over time (Table 2 and 3). For pelvic fractures, surgery care increased slightly during the study period and hospitalisation remained constant but high. For all other fracture sites, surgery and hospital care related to fracture treatment became more common during the study thus imposing heavy pressure on health care resources.

Conclusions: Because of changes in surgical procedure rates related to osteoporotic fracture, the burden of these fracture on health care resources utilization increased over time. With an aging population and an increased prevalence of these fractures, strategies to improve osteoporosis management need to be introduced to reduce the burden on health care resources.

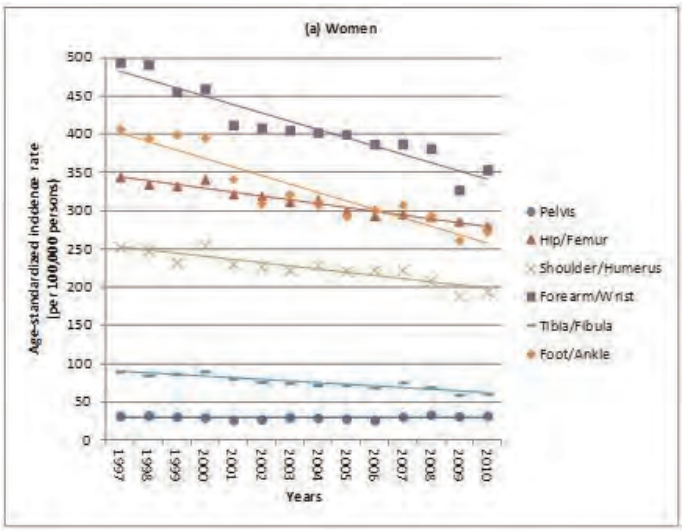

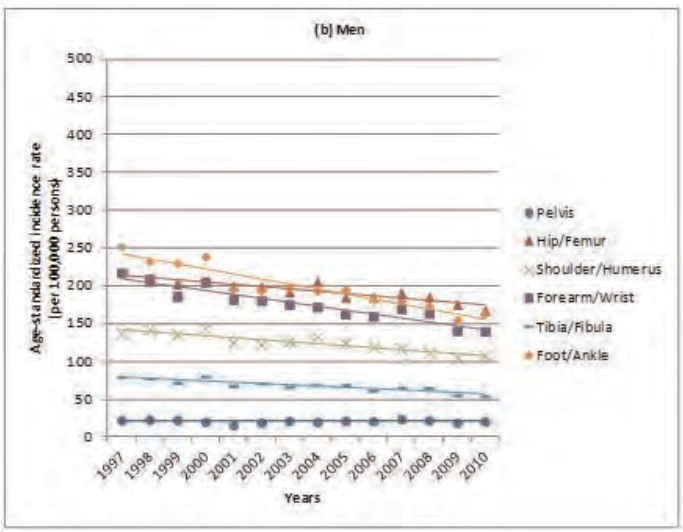

Figure 1: Age-standardized incidence rates in (a) women and (b) men, 1997-2010

Fracture site	1997	1999	2001	2003	2005	2007	2009	APC[a] (CI 95%)
	Incidence rates (per 100,000 persons)							
Women								
Pelvis	31.6	30.4	25.9	29.6	27.7	30.2	30.9	0.3 (-0.9;1.5)
Hip/Femur	344.2	332.1	321.8	311.5	299.2	295.5	285.9	-1.6 (-1.8;-1.4)
Shoulder/Humerus	252.5	232.0	230.2	222.1	220.8	222.5	188.3	-1.9 (-2.4;-1.3)
Forearm/wrist	493.6	455.1	412.3	405.0	399.9	387.3	327.1	-2.6 (-3.1;-2.0)
Tibia/Fibula	89.8	86.5	80.4	74.9	72.4	75.4	59.1	-2.9 (-3.6;-2.1)
Foot/Ankle	407.0	399.7	341.5	321.5	292.9	307.8	261.3	-3.3 (-4.0;-2.5)
Men								
Pelvis	22.1	22.3	15.5	21.1	21.1	23.8	18.8	-0.1 (-1.5;1.4)
Hip/Femur	218.4	202.6	199.3	191.3	184.2	190.1	175.1	-1.6 (-2.0;-1.1)
Shoulder/Humerus	137.2	135.4	125.2	126.6	124.3	117.0	104.1	-2.2 (-2.8;-1.6)
Forearm/wrist	217.0	186.1	181.9	175.2	162.6	169.3	140.2	-2.9 (-3.6;-2.3)
Tibia/Fibula	78.7	71.8	67.8	66.1	68.6	65.2	54.9	-2.5 (-3.3;-1.7)
Foot/Ankle	252.1	230.0	196.3	197.4	198.4	179.6	155.0	-3.3 (-3.9;-2.6)

Table 1: Age-standardized fracture rates in men and women and mean annual percent change

Fracture site	1997	1999	2001	2003	2005	2007	2009	APC[a] (CI 95%)
	Proportion of fracture with hospitalisation							
Women								
Pelvis	59.7	64.0	63.4	65.6	74.1	68.5	60.2	0.0 (0.7;0.7)
Hip/Femur	92.1	91.9	91.2	91.2	90.6	92.0	92.3	0.0 (0.0;0.0)
Shoulder/Humerus	28.8	30.6	31.0	31.1	30.6	33.9	36.1	0.6 (0.4;0.9)
Forearm/wrist	22.3	25.0	27.5	29.9	32.7	35.0	41.1	1.5 (1.3;1.7)
Tibia/Fibula	46.3	44.6	51.2	49.6	53.4	55.1	56.0	0.9 (0.7-1.1)
Foot/Ankle	21.1	20.3	22.4	25.1	26.7	30.6	30.3	1.0 (0.8;1.1)
Men								
Pelvis	65.5	68.1	68.0	66.8	76.5	71.9	55.9	-0.6 (-1.3;0.2)
Hip/Femur	88.5	89.6	89.5	87.3	86.8	89.7	89.1	0.0 (0.0;0.0)
Shoulder/Humerus	27.3	29.0	28.6	28.1	28.1	28.9	32.0	0.3 (0.1;0.5)
Forearm/wrist	22.8	23.5	26.3	28.7	30.6	33.8	38.6	1.3 (1.2;1.5)
Tibia/Fibula	51.3	54.0	56.6	58.9	57.2	57.7	62.0	0.8 (0.6;1.0)
Foot/Ankle	22.6	22.0	25.7	29.9	28.6	32.6	31.6	1.0 (0.8;1.2)

Table 2: Proportion hospital care for osteoporotic fractures and mean annual percent change

Fracture site	1997	1999	2001	2003	2005	2007	2009	APC[a] (CI 95%)
	Proportion of fracture with operative care							
Women								
Pelvis	2.82	3.50	2.77	4.59	7.34	5.01	7.81	0.4 (0.2;0.5)
Hip/Femur	88.4	89.0	88.5	88.1	89.5	89.5	88.8	0.1 (-0.1;0.2)
Shoulder/Humerus	14.9	13.9	15.4	16.4	16.8	20.9	18.6	0.9 (0.6;1.2)
Forearm/wrist	7.6	10.1	10.7	11.6	11.8	12.9	18.6	0.8 (0.5;1.0)
Tibia/Fibula	30.2	31.1	37.5	36.4	41.2	44.4	46.9	1.5 (1.3;1.7)
Foot/Ankle	15.7	15.5	18.0	20.5	21.9	25.1	24.6	0.9 (0.8;1.1)
Men								
Pelvis	5.20	8.09	6.77	10.6	11.8	12.5	8.5	0.3 (0.1;0.6)
Hip/Femur	85.4	86.3	85.6	85.1	86.1	85.4	86.0	0.0 (-0.1;0.1)
Shoulder/Humerus	14.6	14.7	15.0	16.9	15.5	18.6	22.9	0.8 (0.5;1.0)
Forearm/wrist	13.0	13.5	15.6	17.3	17.5	19.8	25.8	1.1 (0.8;1.3)
Tibia/Fibula	40.3	45.0	48.0	51.0	50.6	53.0	56.8	1.2 (0.9;1.4)
Foot/Ankle	17.2	17.1	20.7	25.5	23.9	27.1	26.6	1.0 (0.8;1.2)

Proportion of surgical care for osteoporotic fractures and mean annual percent change

***Disclosures: Sonia Jean**, None.*

SA0333

Association of Genetic Variants Detected by Whole Genome Sequencing with Fracture Risk. Scott Wilson*[1], David Evans[2], Brent Richards[3], Josine Min[2], Klaudia Walter[4], Nicole Soranzo[4], Richard Durbin[4], Nicholas Timpson[2], on behalf of the UK10K Consortium .[4]. [1]University of Western Australia, Australia, [2]University of Bristol, United Kingdom, [3]McGill University, Canada, [4]Wellcome Trust Sanger Institute, United Kingdom

Fracture risk is heritable, but the genes involved remain largely unknown. A recent meta analysis of GWAS for fracture identified fourteen BMD-associated loci that were also associated with fracture risk however a substantial proportion of the heritability of fracture risk remains to be explained. We undertook a GWAS of fracture using whole genome sequence data available on the ALSPAC cohort to detect additional loci relevant to fracture risk.

Whole genome sequencing (WGS) to an average 6.5x coverage using next-generation sequencing technology was performed on the Avon Longitudinal Study of Parents and Children (ALSPAC) discovery cohort (n = 2000) as part of the UK10K project. Imputation was performed on existing data from high density SNP arrays using 1000genomes and UK10K reference panels in 3450 individuals in the replication cohort. All fractures recorded by age 11 years were included in the association analysis which was performed with SNPTEST. GWAS meta-analysis of discovery and replication studies was conducted using GWAMA.

We aim to report on the results of this genome-wide association study assessing a comprehensive collection of genetic variants down to and below 1% minor allele frequency (MAF). In preliminary analyses, among fifty loci that were identified with $P < 1E-5$, seventeen loci were in the vicinity of a gene with a credible role in bone. Odds ratios ranged 0.58 - 4.57 and 58% of these loci had MAFs less than 0.05. Four of the loci that showed suggestive association had not been previously identified in dbSNP or 1000genomes and 16% of loci were multi-nucleotide variants.

Although the pathophysiology of fracture in children may differ from that of fragility fracture in adults with osteoporosis, these data should aid researchers in prioritising loci for focused genotyping studies relevant to fracture.

***Disclosures: Scott Wilson**, None.*
This study received funding from: Wellcome Trust Sanger Institute

SA0334

Attenuated Monocyte Apoptosis, A New Mechanism For Osteoporosis Suggested By A Transcriptome-Wide Study Of Monocytes. Yaozhong Liu, Yu Zhou, Yongjun Liu, Lei Zhang, Jian Li, Qing Tian, Jigang Zhang, Hong-Wen Deng*. Tulane University, USA

Background: Osteoporosis is caused by excessive bone resorption (by osteoclasts) over bone formation (by osteoblasts). Monocytes are important to osteoporosis by serving as progenitors of osteoclasts and produce cytokines for osteoclastogenesis.

Objective: To identify osteoporosis genes by microarray analyses of monocytes in high vs. low hip BMD (bone mineral density) subjects.

Method: Microarray analyses of monocytes were performed using Affymetrix 1.0 ST arrays in 73 Caucasian females (age: 47-56) with extremely high (mean ZBMD =1.38, n=42, 16 pre- and 26 postmenopausal subjects) or low hip BMD (mean ZBMD=-1.05, n=31, 15 pre- and 16 postmenopausal subjects). Differential gene expression analysis in high vs. low BMD subjects was conducted in the total cohort as well as pre- and post-menopausal subjects. Focusing on the top differentially expressed genes identified in the total, the pre- and the postmenopausal subjects (with a p <5E-03), we performed replication of the findings in 3 independent datasets of microarray analyses of monocytes in: 1) 80 Caucasian females (40 high vs. 40 low BMD subjects); 2) 19 Caucasian females (10 high vs. 9 low BMD subjects); and 3) 26 Chinese females (14 high vs. 12 low BMD subjects).

Result: We identified (in the 73 subjects) and successfully replicated in all the 3 independent datasets 2 genes, DAXX and PLK3. Interestingly, both genes are apoptosis induction genes and both down-regulated in the low BMD subjects. In addition, among the list of genes (n = 102) that are replicated in the largest replication cohort containing the 80 subjects, 2 other genes (PDCD5 and VDAC1) that are ranked at the top (7th and 17th, respectively, based on meta-analysis p values) are also apoptosis induction genes and down-regulated in the low BMD subjects. Overall, our result may suggest that there might be a lower apoptosis activity of monocytes in the low BMD subjects.

Conclusion: Our study for the first time suggested a lower apoptosis rate (hence an increased survival) of monocytes, an important osteoclastogenic cell, as a novel mechanism for osteoporosis.

***Disclosures: Hong-Wen Deng**, None.*

SA0335

Copy Number Variations are associated with Bone Mineral Density: A large-scale genome-wide analysis in the Framingham Study. Wen-Chi Chou*[1], Kannabiran Nandakumar[2], David Karasik[3], Ching-Ti Liu[4], Adrienne Cupples[4], Douglas Kiel[1], Yi-Hsiang Hsu[5]. [1]Hebrew SeniorLife, USA, [2]Hebrew Senior Life Harvard Medical School, USA, [3]Hebrew SeniorLife; Bar Ilan University, USA, [4]Boston University School of Public Health, USA, [5]Hebrew SeniorLife Institute for Aging Research & Harvard Medical School, USA

Bone mineral density (BMD) is a complex phenotype with high heritability. Our previous genome-wide SNP association study identified more than 56 BMD loci in Caucasian populations, explaining < 6% of BMD variation. Copy number variation (CNV), a type of genomic structural variation, accounts for > 20% variation of the human genomic structure between individuals. CNVs may explain the missing heritability of BMD. Thus, we conducted a genome-wide CNV association analysis with BMD in Framingham Study participants.

This study included 7,451 adult Caucasians (4,126 men and 3,325 women) with mean age of 55 years. BMD at lumbar spine (LS) and femur neck (FN) was measured by dual energy X-ray absorptiometry. CNVs were estimated using Affymetrix 500K genotyping array and PennCNV package. A CNV was defined as a DNA segment longer than 1 kbp and composed of at least three consecutive genotyping probes. Under an additive genetic model, we employed a linear mixed effects model to account for family relatedness, and also adjusted for age, sex, estrogen usage, menopause status, cohorts within the Framingham Study and principal components for population stratification. To correct for multiple-testing, a genome-wide significant cutoff ($p < 4 \times 10^{-6}$) was defined by a false-discovery rate as less than one false-positive result among the genome-wide significant findings. Up to 6,398 individuals had valid CNV calls and information on covariates.

Two CNVs (at chrom 2q14.2 and 6q25.3) and four (at chrom 5q23.1, 15q22.31, 17p13.1 and 17q21.2) were significantly associated with LS BMD and FN BMD, respectively. The length of the CNVs ranged from 133 kbp to 1,025 kbp. The most significantly associated CNV with $p = 1.9 \times 10^{-20}$ was located at chromosome 15q22.31 (*SMAD6*). The Smad6 protein inhibits signaling of bone morphogenetic proteins. Among 6,398 individuals included in the association analysis of the CNV, 5 had this CNV. Individuals with deleted CNVs had lower FN BMD. In addition, we identified three genome-wide suggestive CNVs associated with BMD at $p < 2.7 \times 10^{-6}$.

In summary, we identified six genome-wide significant CNVs and three genome-wide suggestive CNVs associated with FN BMD or LS BMD in the Framingham Study. To replicate the CNV-BMD associations, we are performing analyses in independent samples. The newly identified CNVs in this study may provide additional biological information regarding the genetic determinants of BMD and may explain some of the missing heritability.

***Disclosures: Wen-Chi Chou**, None.*

SA0336

Family-based genome wide association reveals genetic determinants of total body bone mineral density and fat content in adults of Northern European descent. Yi Zhang*[1], Jack Kent[2], Bradford Towne[3], Stefan Czerwinski[4], Tom Dyer[2], Michael Olivier[5], Ulrich Broeckel[5], Omar Ali[5], Diana Cerjak[5], Roland James[5], Ahmed Kissebah[5], John Blangero[2], Robert Blank[6]. [1]Medical College of Wisconsin, USA, [2]Texas Biomedical Research Institute, USA, [3]Wright State University, USA, [4]Wright State University Boonshoft School of Medicine, USA, [5]Medical College of Wisconsin, USA, [6]University of Wisconsin, USA

Background Bone mineral density (BMD) is correlated with total body mass and muscle mass but its relationship to fat mass has not been well characterized. We study the genetic basis of obesity and the metabolic syndrome in a family-based cohort of Northern European descent. The purpose of this study is to examine the correlation between BMD and % body fat (BF%) and to identify shared genetic determinants for both.

Methods We studied 401 subjects (18-84ya) from 39 extended families. Each family was recruited through an obese proband (BMI≥30) with at least one obese sibling and one never-obese (BMI≤27) and at least one parent willing to participate. We measured total body BMD and body composition by dual-energy X-ray absorbtiometry (DXA) and evaluated the heritability and genetic correlation of BMD and BF% with the genetic software SOLAR. We adjusted BMD for age, sex, and weight and BF% for age, age^2 and sex following stepwise regression. We conducted genome-wide association (GWA) analysis in SOLAR using ~2.5×10^6 empirical and imputed SNPs.

Results Heritability of whole body BMD was 0.54 ± 0.09 and BMD was negatively genetically correlated with BF% (ρ_G=-0.24 ± 0.13; p=0.085). In sex-specific and combined-sex GWAs, the most significant associations with BMD included: in men

only, rs9386528 ($p=1.6\times10^{-7}$) located 100kb upstream of the first exon of UFL1, a negative regulator of NF-kappaB activity; and SNPs in the microRNA gene MIR548A3 ($p=7.87\times10^{-6}$ in women, $p=5.32\times10^{-6}$ in both sexes). In both sexes, strong associations near the inositol 1,4,5-trisphosphate receptor 1 gene ITPR1 are shared by both BMD and BF% ($p=7\times10^{-8}$). In mice, spontaneous ITPR1 mutations are known to cause decreased body size, muscle abnormalities and early aging. Several of our top associations map to genes or gene families, including ITPR1, identified by other human GWA studies for obesity-related or regional BMD traits.

Conclusion In a family cohort recruited through obese probands, we identified shared and specific genetic factors underlying total body BMD and fat content. We are now replicating the most significant associations in an independent family cohort (n=1,286) of similar ancestry.

***Disclosures: Yi Zhang**, None.*

SA0337

GWAS meta-analysis of vertebral trabecular volumetric BMD by QCT. Carrie Nielson*[1], Ching-Ti Liu[2], Johanna Jakobsdottir[3], Jeanne Latourelle[4], Albert Smith[5], Melissa Garcia[6], Michael Nalls[7], Christina Wassel[8], Priya Srikanth[9], Matthew Budoff[10], Jeffrey Carr[11], Richard Myers[4], Elizabeth Samelson[12], Kristin Siggeirsdottir[3], Joseph Zmuda[13], L Adrienne Cupples[2], Eric Orwoll[1], David Karasik[14], Mary Bouxsein[15], Thomas Lang[16], Vilmundur Gudnason[17], Tamara Harris[18], Douglas Kiel[19], Yi-Hsiang Hsu[20]. [1]Oregon Health & Science University, USA, [2]Department of Biostatistics, Boston University School of Public Health, USA, [3]Icelandic Heart Association, Iceland, [4]Department of Neurology, Boston University School of Medicine, USA, [5]Icelandic Heart Association, Kopavogur, Iceland; Faculty of Medicine, University of Iceland, Reykjavik, Iceland, Iceland, [6]Laboratory of Epidemiology, Demography, & Biometry, National Institute on Aging, USA, [7]Laboratory of Neurogenetics, National Institute on Aging, National Institutes of Health, USA, [8]Department of Epidemiology, University of Pittsburgh, USA, [9]Department of Public Health & Preventive Medicine, Oregon Health & Science University, USA, [10]Los Angeles Biomedical Research Institute, USA, [11]Wake Forest School of Medicine, USA, [12]Hebrew SeniorLife, Harvard Medical School, USA, [13]University of Pittsburgh Graduate School of Public Health, USA, [14]Hebrew SeniorLife; Bar Ilan University, USA, [15]Beth Israel Deaconess Medical Center, USA, [16]University of California, San Francisco, USA, [17]Icelandic Heart Association Research Institute, Iceland, [18]Intramural Research Program, National Institute on Aging, USA, [19]Hebrew SeniorLife, USA, [20]Hebrew SeniorLife Institute for Aging Research & Harvard Medical School, USA

Background: Low lumbar vertebral BMD is heritable and associated with vertebral fracture, pain, height loss, and mobility restriction in older adults. Areal BMD is confounded by bone size and common degenerative conditions and cannot distinguish between trabecular and cortical compartments. Genetic association studies using volumetric QCT may identify genes that affect vertebral trabecular BMD.

Methods: We performed inverse-variance fixed-effects meta-analysis using ~2.7 million imputed SNPs from six genome-wide association studies for trabecular vBMD of the lumbar spine (L2 or L3 vertebra). Cohorts included Age Gene/Environment Susceptibility Study (AGES), Framingham Study, Family Heart Study, Healthy Aging and Body Composition (Health ABC), Multi-Ethnic Study of Osteoporosis (MESA), and Osteoporotic Fractures in Men (MrOS), for a total of 12,287 adult participants. Additive genetic models were tested using HapMap II imputed datasets, with adjustment for age, weight, clinic site and population stratification principal components. In familial studies, linear mixed effects models were used to account for relatedness. Genome-wide significance level was 5×10^{-8}, and suggestive level was $p < 5 \times 10^{-6}$ after overall genomic control correction and considering consistent effect sizes across all cohorts ($I^2 < 50$ and p for heterogeneity c^2 test $> 5 \times 10^{-5}$).

Results: Genome-wide significant SNPs for trabecular vBMD were found in loci previously reported for LS BMD, on 1p36.12 (near *WNT4* and *ZBTB40*), 1q43 (near *FMN2* and *GREM2*), and 13q14 (*TNFSF11*); and one new locus, 5p13 (*SLC1A3*). We also identified 6 loci as genome-wide suggestive SNPs that have previously been reported for LS BMD (Table). Five additional suggestive loci were newly identified and include 3p21.31 (*PLXNB1*), 3q26.1 (*BCHE*/*ZBBX*), 10q25 (*DUSP5*), 12p13.3 (*CACNA1C*), and 12q21.3 (*ATP2B1*).

Conclusion: GWAS of trabecular vBMD by QCT confirm previous findings from meta-analyses of lumbar spine BMD by DXA. In addition, several new loci were identified that may also explain some heritability in vertebral vBMD specific to the trabecular compartment. For example, *SLC1A3* (aka *GLAST*) is involved in glutamate signaling necessary for osteogenic mechanical loading. *PLXNB1,* which encodes receptors on osteoblasts for semaphorin 4D, is involved in IGF-1 signaling and osteoblast mobility. Variants in these newly discovered genes deserve further evaluation for their roles in vertebral osteoporosis and fracture risk if replicated in other studies.

Table. GWAS meta-analysis of lumbar spine trabecular vBMD in 6 cohorts (N=12,287)

Locus	SNP	A1/A2	A1 frequency	Nearest gene(s)	Beta	SE	P value	Heterogeneity I^2	Locus previously reported for LS BMD
Genome-Wide Significant									
1p36.12	rs932371	C/T	0.27	WNT4	-0.082	0.013	3.74×10^{-10}	0	Yes
1p36.12	rs12742784	C/T	0.21	ZBTB40	0.094	0.015	1.16×10^{-10}	0	Yes
1q43	rs9661787	C/G	0.81	FMN2/GREM2	-0.098	0.015	1.24×10^{-10}	0	Yes
5p13	rs2468531	C/G	0.97	SLC1A3	-0.221	0.037	1.45×10^{-9}	0	No
13q14	rs17457561	A/G	0.25	AKAP11/TNFSF11	-0.095	0.014	1.95×10^{-12}	0	Yes
Suggestive									
2p21	rs2941584	C/T	0.32	SPTBN1	-0.060	0.012	1.24×10^{-6}	33.5	Yes
3p21.31	rs9883759	A/T	0.47	PLXNB1	-0.067	0.013	2.36×10^{-7}	0	No
3q26.1	rs13082929	A/G	0.30	BCHE/ZBBX	0.059	0.013	3.31×10^{-6}	0	No
4q21	rs2869695	T/C	0.83	DMP1/IBSP/MEPE	-0.078	0.017	3.88×10^{-6}	17	Yes
6q25	rs10872673	G/T	0.60	C6orf97/ESR1	0.065	0.012	5.86×10^{-8}	0	Yes
8q24	rs1485303	A/G	0.44	TNFRSF11B	-0.057	0.012	7.35×10^{-7}	14.7	Yes
10q25	rs4918534	A/G	0.75	DUSP5	-0.063	0.014	3.46×10^{-6}	0	No
12p13.3	rs7301013	A/G	0.83	CACNA1C	-0.076	0.016	1.45×10^{-6}	39.5	No
12p12.1	rs12813778	A/G	0.23	PTHLH/CCDC91	-0.068	0.014	1.16×10^{-6}	32.9	Yes
12q21.3	rs4842697	G/T	0.57	ATP2B1	-0.057	0.012	9.09×10^{-7}	22.4	No
16p13.3	rs9921222	C/T	0.47	AXIN1	-0.059	0.012	6.03×10^{-7}	0	Yes

Beta corresponds to the additive effect of the A2 allele.

Table. GWAS meta-analysis of lumbar spine travecular vBMD

***Disclosures: Carrie Nielson**, None.*

SA0338

Identification of Novel Genes and Regulatory Network Modules for Bone Mineral Density by Integrated Analyses of Transcriptome, miRNAome and Methylome Data. Li-Jun Tan[1], Tianhua Niu*[2], Jigang Zhang[2], Chuan Qiu[2], Yu Zhou[2], Hui Shen[3], Jian Li[2], Shu-Feng Lei[1], Xiang-Ding Chen[1], Hong-Wen Deng[3]. [1]College of Life Sciences, Hunan Normal University, China, [2]Center for Bioinformatics & Genomics, Dept of Biostat & Bioinformatics, Tulane University SPHTM, USA, [3]Tulane University, USA

Aim: MicroRNA expression (ME), DNA methylation (DM), and mRNA gene expression (GE) may work interactively to form essential gene regulatory networks. An integrated analysis of these multi-level functional genomic/epigenomic data may provide higher power to identify novel genes and network modules that would be otherwise miassed at individual-omic level analysis.

Methods: We performed a pilot multi-omics study at ME, DM and GE levels for a sample of 5 extremely low (bottom 15 percentile) hip bone mineral density (BMD) (Age: 24.41 ± 1.23 Yr) and 5 extremely high (top 15 percentile) hip BMD (Age: 23.76 ± 1.59 Yr) women in Hunan, CHina. ME, DM, and GE levels were measured from the same peripheral blood monocytes (PBMs) by Affymetrix miRNA 2.0 Array, Methylated DNA ImmunoPrecipitation-sequencing (MeDIP-seq), and Human Exon 1.0 ST Array, respectively. Traditional (correlation, clustering) methods and advanced MAGIA[2] tool were applied in integrated analysis.

Results: In ME-GE correlation analysis, *hsa-mir-34a* (High BMD vs Low BMD, $P = 9.76\times10^{-4}$), which is critical for bone development, is top miRNA negatively correlated with *FLOT2* mRNA expression (ρ = -0.82). In DM-GE correlation analysis, *ADAMTS5*, which as associated with cartilage growth, is the top known gene negatively correlated with its promoter methylation (ρ = -0.85). In MAGIA[2] analysis, total 38 network modules were revealed for ME-GE joint analysis for entire data (n=10). Of 9 modules with $\geqslant$ 5 nodes, hub genes *GATA3*, *ATF2*, *FOXC1*, *hsa-mir-17*, and *hsa-mir-let7c* have been previously associated with osteoporosis-related phenotypes. *SMOC1* gene was also detected.

Conclusion: Integrated approach may uncover novel genes and combinatorial network patterns in multi-dimensional omic data for complex phenotypes such as osteoporosis, which could have significant implications for clinical applications and fundamental basic research.

(L Tan and T Niu have equal contributions)

***Disclosures: Tianhua Niu**, None.*

SA0339

Effects of vitamin D and Exercise on Bone Health and Physical Performance in Elderly Women: Preliminary Results. Kirsti Uusi-Rasi*[1], Saija Karinkanta[1], Pekka Kannus[1], Kari Tokola[1], Christel Lamberg-Allardt[2], Harri Sievänen[1]. [1]UKK Institute for Health Promotion Research, Finland, [2]University of Helsinki, Finland

This two-year randomized (double blind for vitamin D) placebo-controlled intervention trial assessed the effects of exercise and vitamin D on bone traits and physical performance in elderly Finnish women. 409 women aged 70 to 80 years were randomly assigned into four groups: 1) 20 µg of vitamin D + exercise (D+Ex+), 2) 20 µg vitamin D + no exercise (D+Ex-), 3) placebo + exercise (D-Ex+), and 4) placebo + no exercise (D-Ex-). The inclusion criteria were no regular exercise more than twice a week at baseline, at least one fall during the previous year, and no contraindication to exercise. Measurements were done at baseline and at 24 months. The final data were obtained from 360 women. Supervised exercise training was given twice a week for 12 months, and once a week for the subsequent 12 months.

In addition to DXA-measured femoral neck BMD and pQCT-measured distal tibia trabecular density (TrD), maximal isometric lower limb extension force, timed-up and-go (TUG) time, and normal walking speed were assessed. Generalized linear models with log link function were used in estimating between-group differences using age, height, weight, and baseline value as covariates. Femoral neck BMD declined significantly more in D-Ex- group ($p=0.04$) than in the other groups, while tibial TrD showed no significant change in any group. The lower limb extension force improved in exercisers ($p<0.001$) more than in non-exercisers, while vitamin D had no effect on this variable. Neither exercise nor vitamin D affected walking speed, but exercise slightly improved the TUG time ($p=0.07$). Lack of vitamin D supplementation and exercise suggested negative interaction on TUG time ($p=0.069$).

Neither exercise nor vitamin D improved femoral neck BMD or tibial TrD among elderly women, but both of these factors were needed to prevent femoral bone loss. Exercise improved force and slightly the TUG time, whereas vitamin D had no effect on these variables.

***Disclosures: Kirsti Uusi-Rasi**, None.*

SA0340

Health beliefs and educational needs among patients with osteoporosis : a qualitative study according to gender and types of osteoporosis from the workgroup SOLID'OS. Catherine Beauvais[1], Eric Lespessailles*[2], Yves Magar[3], Corinne Thevenot[4], Liana Euller Ziegler[5], Edith Filaire[6], Sylvie Gendarme[7], Karine Legrand[7], Florence Levy-Weil[8], Dominique Aubraye[9], Bernard Cortet[10], Didier Poivret[11], Mickael Rousiere[12], Anne Christine Rat[7]. [1]Service de Rhumatologie, C.H.U Saint-Antoine, France, [2]Centre Hospitalier Regional, France, [3]Edusanté, France, [4]Médecine Interne et Spécialité, C.H., France, [5]Service de Rhumatologie, C.H.U. L'Archet, France, [6]CIAMS EA4532, Université Orleans, Université Paris-Sud, France, [7]Epidémiologie et Evaluation Cliniques et Cic-Ec Cie6, C.H.U. Nancy-Brabois, France, [8]Centre Hospitalier Victor Dupouy, France, [9]Service de Rhumatologie, C.H. Victor Dupouy, France, [10]Service de Rhumatologie, France, [11]Unité ETP Rhumatologie, Centre Hospitalier régional Metz-Thionville, France, [12]Hôpital Saint Antoine, France

Background and objective: Real life experience and health beliefs impact quality of life and adherence to medication.

The objective was to understand perceptions and educational needs of patients with different types of osteoporosis. The aim was to target patients perspective to help the construction of educational programs.

Methods: Focus group were conducted among 18 post-menopausal women with osteoporotic fractures (2 groups), 10 post-menopausal women without osteoporotic fractures (2 groups), 14 men with osteoporosis (2 groups) and 10 patients with corticosteroid (CS) -induced osteoporosis (2 groups). Each group included 4 to 10 patients in 7 different cities. A semi directive interview guide was used, developed by the multidisciplinary workgroup SOLID'OS including rheumatologists, health care professionals, members of a patient association. Thematic analysis was performed.

Results: A wide range of health beliefs was found: OP is considered as a natural consequence of aging or on the contrary leads to dramatic feelings and self-depreciation. Patients are in fear of new fractures and consequently limit their daily life activities. Patients with CS-induced osteoporosis take better care of the causal disease than of OP. Men have negative perceptions and have difficulties coping with the loss of their functional abilities.

Patients have a rather good knowledge of treatment except for CS treated patients whose knowledge is lower. Some patients are confident in health care providers and medication efficacy whereas others focus on adverse effects and doubt of the benefit of treatments. All patients need support and look for evidence of treatments efficacy. Patients show a great interest for non-pharmacologic management such as calcium intake and physical activity. Errors are frequent about calcium and milk.

Patients are looking for follow up by health professionals to enhance their motivation. They show preferences for group education close to their place of residence. Men often go on the Internet for brief information and like booklets. Education should include physical activity, fall prevention and dietetics.

Conclusion: This qualitative study showed that patients' perspective differ according to gender and type of osteoporosis. A personalized assessment of patients' needs and objectives should be performed before inclusion in educational programs. Patients are interested by non-pharmacological treatments and prefer group education.

***Disclosures: Eric Lespessailles**, None.*

SA0341

Adding VFA to DXA Changes Clinical Classification and Improves Detection of Fracture Risk. Jay Ginther*, Dixie Burk. Cedar Valley Bone Health Institute of Iowa, USA

Problem:

Even patients with known vertebral fractures and vertebroplasties can have "osteopenia" or "normal BMD" by DXA. Doing VFA on those patients I judged to need it, I was always correct. That meant I was missing some vertebral fracture deformities. How many?

Methods:

We performed VFA on every DXA patient from February 2010 through September 2012. 941 patients were evaluated with VFA for the first time. We had 792 women and 149 men with a mean age of 65 years. All DXA and VFA were read by the same ISCD Certified clinician.

Results:

By DXA alone 44.6% were Osteoporosis, 40.3% Low BMD, and 15.1% Normal BMD. Adding VFA, 76.6% were Osteoporosis, 18.1% Low BMD, and 5.1% Normal BMD. 32.0% of the time, adding VFA changed the clinical diagnosis. Further analysis by grades and numbers of vertebral deformities are presented.

Conclusions:

1. This study presents less than 1000 patients from a small referral practice, and may not be typical of the general population.

2. Many patients were sent to us because their primary physicians could not confirm osteoporosis by DXA alone. Many patients had "mush for bone" at the time of orthopedic surgery.

3. 48 patients had Normal Bone Mineral Density combined with grade 2 vertebral deformities. Most of those morphometric fractures were not apparent clinically.

4. 25% of our patient population were improperly classified Normal or Low Bone Mineral Density, despite grade 3 or grade 2 vertebral deformities, when studied by DXA alone.

5. These numbers are of sufficient magnitude that a much larger, multi-center study should be organized.

***Disclosures: Jay Ginther**, Amgen - Prolia Orthopedic Surgeon Advisory Board, 2; Lilly,; www.BoneDocBlog.com, 8*

SA0342

See Friday Plenary Number FR0342.

SA0343

Comorbidity in Subjects with Osteoporosis or Fractures: a Cross Sectional Survey (A.M.I.C.O.Study, Italian Multicentric Analysis on Comorbidities in Osteoporosis). Luigi Gennari*[1], Stefano Gonnelli[1], Giovanni D'Avola[2], Emilio D'Erasmo[3], Luigi Di Matteo[4], Ombretta Di Munno[5], Carmelo Fiore[6], Giovanni Gandolini[7], Salvatore Gatto[8], Giovanni Iolascon[9], Giancarlo Isaia[10], Nazzarena Malavolta[11], Giuseppe Martini[1], Giovanni Minisola[12], Maurizio Muratore[13], Daniela Merlotti[1], Stefano Rotatori[14], Chiara Alessi[14], Ranuccio Nuti[1]. [1]University of Siena, Italy, [2]Reumatology Unit AUSL3 Catania, Italy, [3]Internal Medicine II Policlinic Rome, Italy, [4]Reumatology Unit, Ospedale S.Spirito, Pescara, Italy, [5]Reumatology Unit, Azienda Ospedaliera Univerasitaria Pisana Ospedale "S.Chiara", Pisa, Italy, [6]University of Catania Clinica Medica OVE, Italy, [7]Fondazione Don C.Gnocchi Onlus IRCCS "S.Maria Nascente" Milan, Italy, [8]A.O.U. OO.RR. San Giovanni di Dio e Ruggi D'Aragona, Salerno, Italy, [9]Department of Ortopedic & Rehabilitation University of Naples, Italy, [10]University of Torino, Italy, [11]Azienda Ospedaliera Universitaria Di Bologna, Italy, [12]Reumatology Unit Ospedale San Camillo, Rome, Italy, [13]Reumatology Unit, Presidio Ospedaliero A. Galateo, Lecce, Italy, [14]Department of Medicine, Surgery & Neurosciences, University of Siena, Italy

Osteoporosis and fractures often coexist with other diseases and may be also associated with the use of different drugs. In order to improve our knowledge about major disorders associated with bone fragility and the skeletal effects of related treatments we performed a multicentric national survey in 1710 consecutive women (mean age 67.9 ± 10 yrs). To this aim a detailed questionnaire including general characteristics and risk factors, medication use, fracture history and medical diagnoses was performed during outpatient service for skeletal disorders in postmenopausal women. For all subjects the presence of osteoporosis was assessed by DXA analysis. Based on WHO criteria, osteoporosis was observed in 55% of women, while prevalent fractures were described in 50% of cases (of which 68%, 27%, and 5% occurred in osteoporotics, osteopenics or normal women, respectively). The high prevalence of osteoporosis and fractures in this population (likely due to the clinical setting of recruitment) allowed us to separately assess the effect of comorbidity on bone density (BMD) and bone fragility. When DXA criteria for osteoporosis were used (and after adjusting for age) depression, rheumatoid arthritis, gastrointestinal disorders, chronic renal failure and chronic obstructive pulmonary disease (COPD) were more prevalent in osteoporotic and osteopenic women than in normal women. A similar but not significant trend was observed for hypertension and Parkinson disease. Conversely, a slight but not significant prevalence of normal BMD levels was observed in patients with type 2 but not type 1 diabetes. Of interest and consistent with the observations using DXA criteria, when women with or without fractures were compared, we evidenced a significant association between fracture prevalence and depression, rheumatoid arthritis, gastrointestinal disorders and COPD. However we also evidenced a BMD-independent association between fractures and other disorders such as type 1 and 2 diabetes and ischemic heart disease. The latter association was less evident in subjects treated with beta blockers. Moreover, despite mean BMD levels were increased and the prevalence of osteoporosis was lower in patients with

osteoarthritis (OA), fractures were more prevalent in patients with either generalized OA or OA of the hip and spine. Among the different medications, corticosteroids, ACE inhibitors, proton pump inhibitors, and SSRI were significantly associated with fracture prevalence.

***Disclosures: Luigi Gennari**, None.*

SA0344

Fall Risk in Relation to Bioavailable Vitamin D: The Osteoporotic Fractures in Men (MrOS) Study. J Cai Gillis*[1], Lynn Marshall[1], Jodi Lapidus[1], Iva Miljkovic[2], Amy Warriner[3], Jeffrey Curtis[3], Tien Dam[4], James Shikany[5], Peggy Cawthon[6], Rene Chun[7], Martin Hewison[8], Michael Nevitt[9], Eric Orwoll[1], Carrie Nielson[1]. [1]Oregon Health & Science University, USA, [2]Department of Epidemiology, University of Pittsburgh, USA, [3]University of Alabama At Birmingham, USA, [4]Columbia University Medical Center, USA, [5]University of Alabama at Birmingham School of Medicine, USA, [6]California Pacific Medical Center Research Institute, USA, [7]UCLA/ Orthopedic Hospital Research Center, USA, [8]University of California, Los Angeles, USA, [9]University of California, San Francisco, USA

Purpose: Bioavailable 25-hydroxyvitamin D (bio25(OH)D) is that fraction of total 25(OH)D not bound to vitamin D binding protein (DBP). However, little is known about effects of bio25(OH)D on health outcomes. Vitamin D effects on neurological and muscular outcomes might manifest in a higher fall risk among those with lower levels of bio25(OH)D. In this study, we evaluated associations of bio25(OH)D and total 25(OH)D with risk of falls in elderly men.

Methods and Results: The MrOS study enrolled 5,994 ambulatory men ⩾65 years old from March 2000 to April 2002 at 6 sites in the US. Total 25(OH)D assays were performed in serum obtained at enrollment from 1,608 randomly chosen participants. Of these, a random sample of 678 was selected for additional assays to estimate free and bio25(OH)D.

Bio25(OH)D levels were estimated using validated mathematical models that account for DBP concentration and genotypically determined binding affinity. Falls were self-reported every 4 months by mailed questionnaires during 12 months of follow-up. We used log-binomial regression models to obtain relative risk (RR) estimates for any fall in relation to bio25(OH)D quartile. All models were adjusted for age, BMI, race, season of blood draw and clinic site. Potential confounders included medications, self-reported comorbidities and physical activity; confounding was assessed by a change in the RR of ⩾10%. Four participants were missing fall information.

In the sample of 674, the mean (±sd) for bio25(OH)D was 12.98 (±5.65) nmol/L and for total 25(OH)D was 62.2 (±19.9) nmol/L. A fall was reported by 195 men (29%). Bio25(OH)D was correlated with total 25(OH)D (r=0.55) and fall risk did not significantly vary according to total 25(OH)D quartile.

Regression analysis showed a 0.66 (RR) for the 3rd quartile of bio25(OH)D compared to the highest (95% CI: 0.45-0.96). No significant association was observed for the two lowest quartiles of bio25(OH)D compared to the highest quartile.

Conclusions: Bio25(OH)D was more strongly associated with falls than total serum 25(OH)D The 3rd quartile of bio25(OH)D had a significantly lower risk than the 4th quartile. Those in the highest quartile for bio25(OH)D did not have a significantly lower proportion of falls compared to the other quartiles. Future research should examine the possibility of nonlinear associations for bio25(OH)D levels.

Tables. Bioavailable and Total 25(OH)D with any fall in the first year of follow-up, MrOS cohort (N=674)

Bioavailable 25(OH)D Quartile	Range (nmol/L)	Any Falls, n (%)	RR* (95% CI)	Total 25(OH)D Quartile	Any Falls, n (%)	RR* (95% CI)
1	1.87-9.17	59 (35%)	**1.11 (0.81 to 1.53)**	1	58 (34%)	**1.12 (0.81 to 1.56)**
2	9.21-12.07	51 (30%)	**0.97 (0.70 to 1.34)**	2	40 (23%)	**0.79 (0.56 to 1.13)**
3	12.08-15.67	34 (20%)	**0.66 (0.45 to 0.96)**	3	47 (28%)	**0.96 (0.69 to 1.33)**
4	15.75-43.19	51 (30%)	Ref	4	50 (30%)	Ref

*Adjusted for age, BMI, race, season of blood draw and site

Tables. Bioavailable and total 25(OH)D with any fall

***Disclosures: J Cai Gillis**, None.*

SA0345

Femoral Cortical Index: Is the Really Strength of Femur?. Cecilia Rao*[1], Monica Celi[1], Maurizio Feola[1], Valerio Tempesta[1], Elena Gasbarra[1], Umberto Tarantino[2]. [1]University of Rome Tor Vergata, Italy, [2]Università degli Studi di Roma Tor Vergata, Italy

The femoral cortical index (FCI) assesses bone stock using the ratio between the diameter of the femoral shaft and the thickness of the cortical bone calculated 10 cm distal to the center of the small trochanter in an AP view X-Ray of the femur. It's not clear if low values ??of FCI may be associated with a condition of altered bone metabolism and bone fragility in fractured patients. Aim of our study is to evaluate a possible association among low values ??of FCI, risk factors, comorbidities and serum 25 hydroxyvitamin D levels and to establish the importance of FCI as a potential predictor of a new fracture.

Materials and Methods. We conducted a retrospective study on 160 consecutive patients (44 men and 116 women) (range 60 to 103 ya) surgically treated for hip fractures in 2012,after informed consent in our Orthopaedic Department and that never received any medical treatment for osteoporosis. FCI has been calculated by routine clinical radiographs of the pelvis both on fractured femur and on the opposite side. For each patient, we analyzed the presence of comorbidities (such as diabetes, hypertension, IRC, rheumatoid arthritis),osteoporosis risk factors and blood levels of vitamin D, usually evaluated in our patients with fragility fractures.

Results. Average values ??of FCI were 0.42 (range 0.18 to 0.58) at the fractured femur and 0.48 at the opposite side (range 0.25 to 0.66) with a statistically significant difference ($p = 0.002$). At the fractured side an average value of 0.45 was found in men, and of 0.40 in women. Patients with severe hypovitaminosis D (serum concentration <12 ng / ml) had a minor FCI compared to those with a moderate deficiency (0.41 vs. 0.46, $P < 0.01$). The presence of comorbidities or osteoporosis risk factors had a different influence on the values of FCI.

Conclusion. In our study, we found a correlation among low values of FCI, clinical factors related to bone fragility and severe hypovitaminosis D in elderly patients with hip fractures. Comorbidities and risk factors have a different weight in FCI variations, while the severe hypovitaminosis has a major impact on it. As described in the literature regard the DXA limitations in elderly FCI could be an useful tool in terms of bone fragility evaluation and fracture risk prediction. As osteoporosis causes a cortical bone trabecolarization that leads to fracture, this index can therefore give a measure of specific cortical bone at low cost using a X-ray standard examination.

***Disclosures: Cecilia Rao**, None.*

SA0346

FRAX® Predicts Future Falls in Elderly Men. MrOs Sweden. Helena Johansson*[1], Anders Odén[2], Magnus Karlsson[3], Bjorn Rosengren[3], Osten Ljunggren[4], Eugene McCloskey[5], John Kanis[6], Claes Ohlsson[7], Dan Mellström[8]. [1]Swedish University of Agricultural Sciences, The Biomedical Center, Sweden, [2]WHO Collaborating Centre for Metabolic Bone Diseases, University of Sheffield, Sheffield, UK, United Kingdom, [3]Skåne University Hospital Malmö, Lund University, Sweden, [4]Uppsala University Hospital, Sweden, [5]University of Sheffield, United Kingdom, [6]University of Sheffield, Belgium, [7]Center for Bone & Arthritis Research at the Sahlgrenska Academy, Sweden, [8]Centre for Bone & Arthritis Research (CBAR), Sahlgrenska Academy, University of Gothenburg, Gothenburg, Sweden, Sweden

FRAX® calculates 10-year fracture probability from readily obtainable clinical risk factors (CRFs) in men and women with or without BMD. Falls is an established risk factor for future fracture risk but is not included in FRAX as a separate input variable. The aim of the present study was to determine whether FRAX without information on falls risk was associated with future falls risk in elderly men, since some of the risk factors used by FRAX may be related to future fall risk.

We studied the relationship between FRAX and the risk of falls in 1990 elderly men recruited to the MrOS study from the general population in Sweden. Baseline data included clinical risk factors used by FRAX, age, BMI, BMD at femoral neck and FRAX probabilities. Incident falls were captured during an average of 1.8 years follow up (maximum 3.0 years). An extension of Poisson regression was used to investigate the relationship between FRAX, other risk variables and the time-to-event hazard function of falls. All associations were adjusted for age and time since baseline.

At baseline 15% of the men had fallen during the preceding 12 months (past falls) and 34% experienced one or more falls during follow up (incident falls). Past falls were a significant risk factor for incident falls (HR 2.90; 95% CI 2.44-3.44). The risk of incident falls increased with increasing FRAX probabilities at baseline (HR per SD=1.23; 95% CI=1.14-1.33). The association between incident falls and FRAX remained after adjustment for past falls (HR per SD=1.19; 95% CI = 1.11-1.29). In men with high fracture probabilities (>18%) FRAX was a predictor of falls (HR 1.40; 95% 1.15-1.72). The prevalence of past falls increased with increasing fracture probability (r=0.10; 95% CI 0.06-0.15).Although falls are not included as an input variable in FRAX, FRAX significantly captures a component of the fracture risk associated with falls.

***Disclosures: Helena Johansson**, None.*

SA0347

Hip Fracture In Early Stages of Type 2 Diabetes: A Population-Based Cohort Study. Daniel Prieto-alhambra*[1], Daniel Martinez-Laguna[2], Cristian Tebé[3], Xavier Nogues[4], Adolfo Diez-Perez[5]. [1]University of Oxford, United Kingdom, [2]GREMPAL Research Group, IDIAP Jordi Gol Primary Care Research Institute; Primary Care Department, Institut Català de la Salut, Spain, [3]Agencia de Qualitat i Avaluació Sanitàries de Catalunya, Spain, [4]Institut Municipal D'Investigació Mèdica, Spain, [5]Autonomous University of Barcelona, Spain

PURPOSE

We study the association between recently diagnosed type 2 diabetes mellitus (T2DM) and hip fracture risk. Secondly, we assess the key predictors of hip fracture among newly diagnosed T2DM patients, and provide a clinical tool to assess their risk based on these.

METHODS

We conducted a population-based cohort study using data from the SIDIAP Database (www.sidiap.org). SIDIAP contains clinical information from primary care electronic medical records, hospital admissions, and pharmacy invoice data for >5 million patients (80% of the population) in Catalonia, Spain.

Participants were all newly diagnosed T2DM patients registered in SIDIAP in 2006-2010 (T2DM cohort). Up to 3 diabetes-free controls were matched to each T2DM participant on age, gender, and primary care practice.

Main outcome was incident hip fracture, ascertained using ICD10 codes. Main exposure was T2DM status.

We used Fine and Gray survival modelling to estimate risk of hip fracture according to T2DM status accounting for competing risk with death, and adjusted for body mass index, previous fracture and use of oral glucocorticoids.

Secondly, backwards stepwise Fine and Gray regression was used to identify key predictors of hip fracture in the T2DM cohort, among a list of a priori defined potential risk factors: history of cataracts, stroke, IHD, T2DM complications (polineuropathy, nephropathy), anti-osteoporosis medications, body mass index, smoking, alcohol drinking, and history of falls and fractures. The estimated coefficients were used to create a clinical predictive tool, which was tested for discrimination and calibration using ROC curves, and predicted/observed rates for each risk decile respectively.

RESULTS

444/55,275 diabetic patients sustained a hip fracture (Incidence Rate 2.7/1,000 person-years) compared to 776/113,448 matched controls (2.4/1,000): unadjusted SHR 1.11 [0.99-1.24], adjusted SHR 1.20 [1.06-1.35].

Key predictors of hip fractures in T2DM patients are shown in the enclosed Table. The proposed predictive tool had an area under the ROC curve of 0.74 [95%CI 0.72-0.77], and discrepancies between predicted and observed risk were seen only for extreme risk deciles [see Figure].

*CONCLUSIONS*Newly diagnosed T2DM patients are at a 20% increased risk of hip fracture even in the early stages of disease. We propose a simple predictive tool, which can be used to identify diabetic patients at high risk of hip fracture at the time of T2DM diagnosis.

TABLE. Key predictors of hip fracture in T2DM patients.

Predictors	Beta	Score
Male Gender	-0,649	-6
Age (per 1 year above 75)	0,117	1
BMI (per 1 kg/m2 above 30)	-0,037	0
Previous fracture	1,252	13
Previous IHD	0,341	3
Previous nephropathy	0,579	6
Oral glucocorticoids	0,03	0
Age x Nephropathy	0,057	-1
Male Gender x Oral glucocorticoids	0,681	7

FIGURE. Calibration of the provided predictive tool: observed (red) versus predicted (blue) risk in each risk decile.

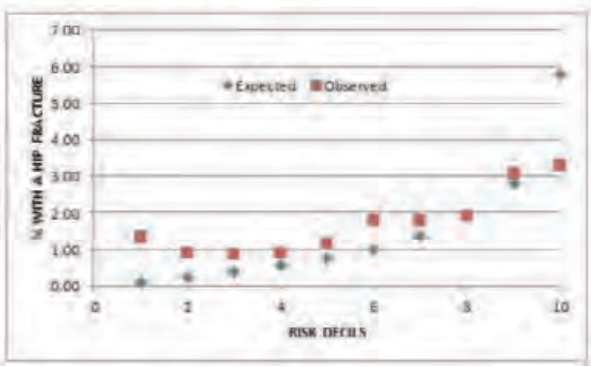

Table and Figure

***Disclosures: Daniel Prieto-alhambra**, AMGEN, 6; BIOIBERICA SA, 6*

SA0348

Identifying Barriers and Facilitators of Informed Consent for an Osteoporosis Pragmatic Clinical Trial. Rachael Moloney[1], Donna Messner[1], Kenneth Saag[2], Jeffrey Curtis[2], Amy Warriner[2], Nicole Wright*[2], Phillip Jeffrey Foster[2]. [1]Center for Medical Technology Policy, USA, [2]University of Alabama at Birmingham, USA

Purpose: Community practice-based osteoporosis research is critical for assessing the effectiveness of osteoporosis therapies, yet obtaining informed consent (IC) is a major barrier to conducting randomized trials in these practice settings. Our goal was to identify deficiencies and develop approaches to improve the IC process for osteoporosis pragmatic clinical trials (PCTs) by collecting perspectives on barriers and facilitators to conducting PCTs. We also explored streamlining consent through the use of an innovative iPad-based tool. Methods: We interviewed physicians and practice staff key informants (KIs), from two practice-based research networks having a range of experiences with IC and PCTs in practice, to understand challenges they face when conducting PCTs with daily clinical practice, and whether an iPad-based tool might streamline screening and IC procedures. Results: We completed 18 physician interviews and 3 staff interviews. Practices sizes varied: solo practice (1 attending physician; n=4), small practices (2-4 attending physicians; n=6), medium (5-6 attending physicians; n=10), and a large multi-group practice (n=1). Seven KIs were from rural practices, 7 from suburban and 7 from urban practices. We found heterogeneity in the types of barriers encountered and preferences for incorporating informed consent in their workflow. KIs differed on how best to introduce the iPad, where to do so, who should do it, how long IC should take, whether IC is a "workable" process, and other questions. Physicians and staff having experience doing clinical trials tended to suggest more modifications for iPad programming and have more expectations for flexibility in iPad use in practice. KIs from rural practices were more likely to be concerned about low verbal and technological literacy of their patient populations. However, most KIs were optimistic about the use of iPad technology for reducing administrative burden. Conclusion: KI interviews revealed heterogeneity in composition and staffing of practices, procedures used (or thought likely to be used) for screening and informed consent, and attitudes on which patients might benefit most from using the iPad tool for learning about a clinical trial and giving consent. Protocols that incorporate practice preferences and allow for some controlled flexibility in screening and consent procedures may improve in feasibility and reduce some of the barriers to practice participation and successful recruitment.

***Disclosures: Nicole Wright**, None.*

SA0349

Increased Serum Low-Density Lipoprotein and Triglycerides Negatively Affect Cortical Bone in Women with a High Body Mass Index. Peter Dellatore*[1], Deeptha Sukumar[1], Yvette Schlussel[1], Xiangbing Wang[2], Claudia Pop[1], Sue Shapses[1]. [1]Rutgers University, USA, [2]Robert Wood Johnson Medical School, USA

Hyperlipidemia, associated with a high fat diet, has been shown to negatively affect bone. In addition, high levels of oxidized low density lipoprotein (LDL) may attenuate the anabolic effect of intermittent parathyroid hormone on bone. In this cross-sectional study, we examined the effect of lipids on bone mineral density (BMD), bone geometry, and strength parameters, and the interaction with serum parathyroid hormone (PTH) in 248 obese and overweight women (ages 24-73 years of age, body mass index (BMI) of 29.4 $\pm$ 3.9 kg/m^2). Areal BMD was measured by dual energy x-ray absorptiometry and a subset were measured for volumetric BMD (vBMD), bone geometry, and strength parameters using peripheral quantitative computed tomography at the tibia. Serum 25-hydroxyvitamin D, PTH, calcium, total cholesterol, triglycerides (TAG), LDL, and high-density lipoproteins were measured. Multiple linear regression analysis was used to determine the effects of serum hormones, lipids and calcium on bone. Overall, there was no detrimental effect of any lipid fraction on trabecular (Tb) bone and the effect was positive on some bone variables. However, most cortical (Crt) bone parameters were negatively affected by serum lipids. The inverse relationship between LDL and Crt vBMD ($r = -0.42$; $p < 0.02$) accounted for 18% of the variance in premenopausal women that was still present when controlling for body weight. To estimate how LDL affects bone without oxidized particles, we examined the LDL/HDL ratio on bone and found no negative correlation with bone. In contrast, LDL and LDL/HDL were both positively correlated with Tb vBMD. This may suggest that oxidized LDL is causing the negative effect on Crt vBMD, but has no effect on Tb vBMD. In postmenopausal women, TAG either showed a significant or inverse trend with Crt BMC, area, periosteal circumference and the stress strain index. In addition, a multiple regression model to examine the interaction between serum PTH and lipid fractions on bone showed a negative association between TAG and areal BMD at the spine and hip. Serum PTH also strengthened the negative association between TAG and Crt bone parameters. In conclusion, these data show that there is a detrimental effect of serum lipids on cortical bone parameters. This could partially explain poor bone quality found previously in obese subjects that may be worse for those with high serum lipid levels.

***Disclosures: Peter Dellatore**, None.*

SA0350

See Friday Plenary Number FR0350.

SA0351

Withdrawn

SA0352

Racial/ethnic Differences in Bone Loss among Aging Men are Attributable to Variation in Socioeconomic Status, Morbidity and Health Behaviors. Andre Araujo*[1], Gretchen Chiu[1], Benedetta Bartali[1], Thomas Travison[2], Mary Bouxsein[3], Joseph Zmuda[4]. [1]New England Research Institutes, USA, [2]Brigham & Women's Hospital, USA, [3]Beth Israel Deaconess Medical Center, USA, [4]University of Pittsburgh Graduate School of Public Health, USA

Rates of osteoporotic fractures are lower in some racial/ethnic groups, due in part to higher peak bone mass. However, racial/ethnic variation in rates of bone loss is poorly understood, particularly among men. We used data from the BACH/Bone Survey, a longitudinal population-based cohort study of racially diverse (Black, Hispanic, and White) men to examine the impact of race/ethnicity on rates of bone loss. A total of 692 (70% of eligible) men with average age 51 ± 12y at baseline completed follow-up 7.0 ± 0.6y later. Femoral neck bone mineral density (fnBMD) was assessed by DXA. Race/ethnicity was self-identified. Multivariable linear regression was used to examine the association of race/ethnicity with annualized percent (%) change in fnBMD, controlled for baseline fnBMD, age, household income, smoking, diabetes, self-rated health, physical activity, and BMI. Mean total bone loss was 0.04 g/cm^2, for an annualized decline of -0.006 g/cm^2/y. Mean (relative standard error (RSE)) % decline in fnBMD was -0.67(0.30)%/y, with steeper declines in men ⩾70y (1.01(0.12)%). Bone loss rates were greater in Black (0.75(1.1)%) and Hispanic (0.73(0.06)%) vs. White (0.58(0.05)%) men, differences which were reduced with adjustment for baseline age and fnBMD, and eliminated with multivariable adjustment (Table). Baseline covariates contributing most to between-subject variations in bone loss were age (32%), income (20%), fnBMD (13%), and smoking (11%). Income was strongly and consistently associated with bone loss, even after adjustment for covariates, including race/ethnicity. The estimated mean differences in bone loss between lower vs. higher income groups were reduced by approximately 50% with adjustments for income, lifestyle factors, and health status (Table). In summary, rates of hip bone loss in this cohort are consistent with previous studies in men, and are about half the rate of similar-aged women. Self-identified minority men experienced greater bone loss, due apparently to disproportionate exposure to lower income, illness, smoking, and other factors. While race/ethnicity may embed genetic/biological/social factors that are strongly associated with bone mass cross-sectionally, the contributions of income and other potentially modifiable factors appear to overpower the role of race/ethnicity in explaining variations in rates of bone loss with aging in men.

Table. Femoral neck bone loss by race/ethnicity and HH income

Model	Category	Mean % bone loss/y (95% CI)	% difference vs. ref	p-value vs. ref
Race, Unadjusted	Black	-0.75(-0.86,-0.64)%	29%	0.0273
	Hispanic	-0.73(-0.84-0.62)%	26%	0.0572
	White	-0.58(-0.68,-0.49)%	-	-
Race, Multivariable -adjusted	Black	-0.67(-1.25,-0.08)%	-1%	0.8842
	Hispanic	-0.71(-1.26,-0.14)%	4%	0.7399
	White	-0.68(-1.23,-0.12)%	-	-
HH Income, Unadjusted	<$10k	-1.02(-1.61,-0.44)%	80%	0.0002
	$10k-<$30k	-0.85(-1.43,-0.26)%	38%	0.0356
	$30k-<$60k	-0.76(-1.34,-0.17)%	14%	0.5086
	>$60k	-0.72(-1.31,-0.12)%	-	-
HH Income, Multivariable -adjusted	<$10k	-0.90(-1.02,-0.76)%	43%	0.0147
	$10k-<$30k	-0.69(-0.79,-0.60)%	18%	0.2002
	$30k-<$60k	-0.57(-0.72,-0.42)%	6%	0.7683
	>$60k	-0.50(-0.65,-0.34)%	-	-

Table

***Disclosures: Andre Araujo**, None.*
This study received funding from: NIH

SA0353

Relationship between specific antidepressants use and bone mineral density – A longitudinal study on postmenopausal women. Päivi Rauma[1], Risto Honkanen*[1], Heikki Kroger[2], Marjo Tuppurainen[2], Lana Williams[3], Heli Koivumaa-Honkanen[4]. [1]University of Eastern Finland, Finland, [2]Kuopio University Hospital, Finland, [3]The University of Melbourne, Australia, [4]University of Oulu, University of Eastern Finland, Lapland Hospital District, Finland

The relationship between antidepressants and lower bone mineral density (BMD) has been suggested mainly in cross-sectional studies. The purpose was to study this relationship longitudinally by taking into account possible differences between subgroups of antidepressants.

The study population consisted of the 1988 women (born in 1932-41) of the Kuopio Osteoporosis Risk Factor and Prevention (OSTPRE) Study cohort. Subjects responded to postal enquiries in 1999 and 2004 and underwent femoral BMD densitometry after enquiries. Information on antidepressants (ATC-codes: N06A, N06CA) purchased from pharmacies in 1999-2004 was obtained from the National prescription register of Finland. Tricyclic antidepressants (TCA; N06AA, N06CA01), selective serotonin reuptake inhibitors (SSRI; N06AB), other (N06AX) and multiple use were used as subgroups. The association between use of antidepressants and femoral BMD change over 5 years was studied with multivariate linear regression including age, body mass index, weight change, dietary calcium, smoking, alcohol use, grip strength, suffering from depression and use of bisphosphonates, hormone replacement therapy and corticosteroids as covariates.

A total of 319 women had purchased antidepressants in 1999-2004. Out of them, 86 had used only TCA, 106 SSRI, 53 other antidepressant and 74 women two or more kinds of antidepressants. Mean femoral BMD was 0.881g/cm2 (SD 0.123) at baseline and bone loss in 1999-2004 was -0.006g/cm2 (SD 0.047). Bone loss was 80% greater (p=0.130) in antidepressant users than non-users. In TCA users it was 200% (p=0.032), in SSRI users 50% (p=0.555) and in multiple antidepressants users 111% (p=0.254) greater. On the contrary, mean BMD did not decrease during the study period in the group of other antidepressant users and bone loss was 104% less than in non-users (p=0.419). In multivariate analyses, higher number of purchased antidepressant packages demonstrated higher annual bone loss (%) in TCA's (B=-0.018, p=0.098), SSRI's (B=-0.031, p=0.006) and multiple use (B=-0.006, p=0.248), while increasing number of packages decreased bone loss (B=0.025, p=0.012) in the users of other antidepressants.

In conclusion, use of TCA or SSRI antidepressants seems to be associated with higher but use of other antidepressants with lower postmenopausal bone loss.

***Disclosures: Risto Honkanen**, None.*

SA0354

Serotonin Transporters in Bone: A Longitudinal Study of Bone Turnover After Initiation of Selective Serotonin Reuptake Inhibitors in Older Adults. Elizabeth Haney*[1], Melanie Abrahamson[1], Zunqiu Chen[1], Yiyi Chen[1], Amy Eshleman[1], Kimberly Vesco[2], Elizabeth Eckstrom[1], Martha Gerrity[1], Eric Orwoll[1], Jodi Lapidus[1], Michael Bliziotes[3]. [1]Oregon Health & Science University, USA, [2]Kaiser Permanente Center for Health Research, USA, [3]OHSU/Portland VA Medical Research Center, USA

Identification of a functional serotonin signaling system in osteoclasts, osteocytes and osteoblasts has led to theories about the role of serotonin in bone metabolism. Selective serotonin reuptake inhibitors, or SSRIs, are commonly prescribed antidepressant medications that potently and specifically block the serotonin transporter. We undertook a prospective cohort study of SSRI users and non-users to evaluate markers of bone turnover in patients starting SSRIs (users) compared to those not on SSRIs (non-users).

Men and women over age 50 starting SSRIs were recruited for prospective measurements of n-telopeptide (NTX, Osteomark, adjusted for creatinine), osteocalcin (OC, Immulite), and bone mineral density (BMD); controls (non-users) were recruited on the basis of gender, age and clinic site. To compare differences between groups we conducted t-tests/rank sum and created linear regression models accounting for potential confounders.

Overall the SSRI users (n=92) were more likely than SSRI non-users (n=105) to report history of anxiety (67.4% vs 13.3%, p<0.0001) and depression (33.7% vs. 5.8%, p<0.0001). SSRI users had higher scores on objective measures of anxiety and

depression, and were less likely than non-users to have a parental history of hip fracture (3.3% vs 11.4%, p=0.03). Baseline OC levels were 9.3 (SD 5.3) for the SSRI users and 8.6 (SD 4.0) for the SSRI non-users group (p=0.7); baseline NTX were 45.0 (SD 29.1) for the SSRI users and 39.0 (SD 18.) for the non-users (p=0.42) respectively. There was no difference in the change in OC and NTX between SSRI users and non-users at 3 months (OC: -0.15, 95% CI -1.12, 0.83 vs -0.13, 95% CI -0.81, 0.56; NTX: -1.62, 95% CI -6.7, 3.5 vs 1.4, 95% CI -2.2, 5.0). There were no significant differences in biomarkers or BMD change at 12 months. Limiting our analysis to the 50 SSRI users who were taking their SSRI for a full 12 months did not change these results; nor did adjusting for BMI, depression and season.

This prospective study showed no difference between SSRI users and non-users in the change in bone turnover or BMD after initiation of SSRIs. Despite potential limitations (non-randomized study, small size, potential for varied time on SSRI prior to baseline assessment), these results do not support a direct negative effect of SSRIs on bone metabolism as measured by OC and NTX. Further studies to understand serotonin-bone interactions, and to confirm the effect of SSRIs on bone are warranted.

***Disclosures: Elizabeth Haney**, None.*

SA0355

Using FRAX® to Evaluate Incidental Osteoporotic Vertebral Fractures in Patients Treated with Bisphosphonate. Yuji Kasukawa*[1], Naohisa Miyakoshi[1], Toshihito Ebina[2], Michio Hongo[1], Koji Nozaka[1], Yoshinori Isikawa[1], Toshiaki Aizawa[3], Yoichi Shimada[1]. [1]Akita University Graduate School of Medicine, Japan, [2]Kakunodate General Hospital, Japan, [3]Kitaakita General Hospital, Japan

Introduction: According to Japanese guidelines, the FRAX®-determined cut-off value (15%) of a 10-year probability of experiencing major osteoporotic fractures with low bone mass and younger than 75 years old is recommended to start the treatment for osteoporosis. However, the cut-off value for when to initiate pharmacological treatment to effectively prevent osteoporotic fracture is still unclear. The purpose of this study was to first determine the risk of major osteoporotic fractures by FRAX® before treatment for osteoporosis. Then, we evaluated the effects of cut-off value on incidental osteoporotic vertebral fracture in the patients with bisphosphonate treatment.

Patients and Methods: We enrolled 74 osteoporotic women older than 60 years of age in this study. We used FRAX® to evaluate the risk of major osteoporotic vertebral fractures in patients younger (n=31) or equal to or older (n=43) than 75 years old before treatment with risedronate (17.5 mg/week). The prevalent and incidental vertebral fractures were evaluated radiographically at the beginning of treatment and at the final follow-up. We measured bone metabolic markers including serum cross-linked N-telopeptide of type 1 collagen (NTX) and bone alkaline phosphatase (BAP) at the beginning of treatment. We also determined the bone mineral density (BMD) by dual-energy X-ray absorptiometry from the distal third of the forearm.

Results: The risk of major osteoporotic vertebral fractures in patients ⩾ 75 years (27.1%) was significantly higher than that of patients < 75 years (16%) ($p<0.001$). Prevalent vertebral fractures were observed in 12 patients < 75 years (38.7%) and in 21 patients ⩾ 75 years (48.8%) at the beginning of treatment. The BMD of patients < 75 years was significantly higher than that of patients ⩾ 75 years (p=0.0001). Twenty-seven patients < 75 years (87.1%) and 40 patients ⩾ 75 years (93.0%) continued treatment. Incidental osteoporotic vertebral fractures were observed in 2 patients < 75 years (7.4%) and 7 patients ⩾ 75 years (17.5%). Within their age groups, there were no significant differences in the risk of major osteoporotic vertebral fractures at the beginning of treatment between patients with or without incidental osteoporotic vertebral fractures (< 75 years, 20.5% and 16.2%, respectively ; ⩾ 75 years 30.9% and 27.6%, respectively). There were also no significant differences in the changes of bone metabolic markers and BMD between patients with and without incidental osteoporotic vertebral fractures.

ConclusionsUsing FRAX® to evaluate the risk of major osteoporotic vertebral fractures at the beginning of treatment, we found no significant differences between patients with and without incidental osteoporotic vertebral fractures during risedronate treatment.

***Disclosures: Yuji Kasukawa**, None.*

SA0356

See Friday Plenary Number FR0356.

SA0357

When, Where and How Osteoporosis-Associated Fractures Occur: An Analysis from the Global Longitudinal Study of Osteoporosis in Women (GLOW). Aline Costa*[1], Allison Wyman[2], Ethel Siris[3], Nelson Watts[4], Stuart Silverman[5], Kenneth Saag[6], Christian Roux[7], Maurizio Rossini[8], Johannes Pfeilschifter[9], Jeri Nieves[10], Coen Netelenbos[11], Lyn March[12], Andrea Lacroix[13], Frederick Hooven[14], Susan Greenspan[15], Stephen Gehlbach[16], Adolfo Diez-Perez[17], Cyrus Cooper[18], Juliet Compston[19], Roland Chapurlat[20], Steven Boonen[21], Fred Anderson[16], Jonathan Adachi[22], Silvano Adami[23]. [1]Columbia University, USA, [2]UMASS Medical School, USA, [3]Columbia University College of Physicians & Surgeons, USA, [4]Mercy Health Osteoporosis & Bone Health Services, USA, [5]Cedars-Sinai/UCLA, USA, [6]University of Alabama at Birmingham, USA, [7]Hospital Cochin, France, [8]University of Verona, Italy, [9]Alfried Krupp Krankenhaus Steele, Germany, [10]Columbia University & Helen Hayes Hospital, USA, [11]VU Medical Center, The Netherlands, [12]Royal North Shore Hospital, Australia, [13]Fred Hutchinson Cancer Research Center, USA, [14]University of Massachusetts Medical School, USA, [15]University of Pittsburgh, USA, [16]University of Massachusetts, USA, [17]Autonomous University of Barcelona, Spain, [18]University of Southampton, United Kingdom, [19]University of Cambridge School of Clinical Medicine, United Kingdom, [20]E. Herriot Hospital, France, [21]Center for Metabolic Bone Disease & Division of Geriatric Medicine, Bel, [22]St. Joseph's Hospital, Canada, [23]University of Verona, Italy

AIM: To examine when, where and how fractures occur in postmenopausal women.

PATIENTS AND METHODS: We analyzed data from the Global Longitudinal Study of Osteoporosis in Women (GLOW), including women age ⩾55 from Australia, Belgium, Canada, France, Germany, Italy, The Netherlands, Spain, US and UK. Women completed questionnaires including fracture data at baseline and years 1, 2 and 3.

RESULTS: Among 60,393 postmenopausal women, 4122 incident fractures were reported (86% non-hip, non-vertebral [NHNV], 8% vertebral, 6% hip). Hip fractures were more likely to occur in spring, with little seasonal variation for NHNV or clinical spine fractures. Hip fractures occurred equally inside or outside the home, whereas 65% of NHNV fractures occurred outside and 61% of vertebral fractures occurred inside the home. Falls preceded 68-86% of NHNV and 68-83% of hip fractures among women aged ≤64 to ⩾85 years, increasing with age. Between 40% and 50% of vertebral fractures were associated with falls in all age groups except those >85, when only 24% occurred after falling (Fig1).

CONCLUSION: Only hip fracture had a seasonal variation, with a higher proportion in spring. Hip fractures occurred equally within and outside the home, spine fractures more often in the home and NHNV fractures outside the home. Falls were a proximate cause of most hip and NHNV fractures.

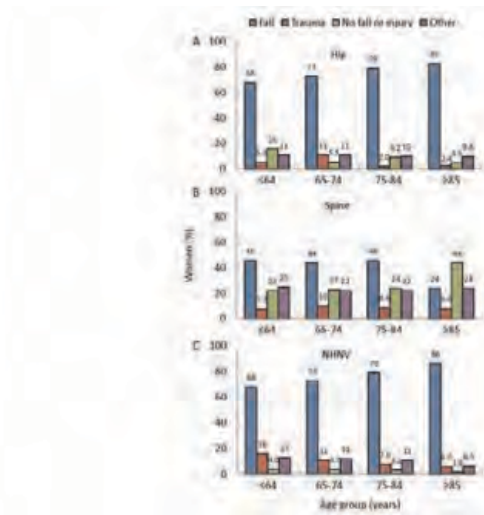

Figure

***Disclosures: Aline Costa**, Warner Chilcott Company, 6; sanofi-aventis , 6*
This study received funding from: Warner Chilcott Company, LLC, sanofi-aventis

SA0358

Association of Bone Marrow Sphingosine 1-Phosphate Levels with Osteoporotic Hip Fractures. Seong Hee Ahn*[1], Jung-Min Koh[2], Sun-Young Lee[3], Seongeun Byun[4], Beom-Jun Kim[2], Seung Hun Lee[1], Jae Suk Chang[4], Ghi Su Kim[1]. [1]Asan Medical Center, University of Ulsan College of Medicine, South Korea, [2]Asan Medical Center, South Korea, [3]Asan Institute for Life Sciences, South Korea, [4]Division of Orthopedic Surgery, Asan Medical Center, University of Ulsan College of Medicine, South Korea

Objective: Sphingosine 1-phophate (S1P) has been discovered to be a critical regulator of bone metabolism. Very recently, we found that higher circulating S1P levels were associated with higher rate of prevalent osteoporotic fracture in human.

Methods: This was a cross-sectional study of 16 patients who underwent hip replacement surgeries. Bone marrow fluids were obtained during hip surgeries, and the S1P levels were measured using a competitive ELISA assay. Bone mineral densities (BMDs) at various skeletal sites were obtained using dual energy x-ray absorptiometry.

Results: Among 16 patients, 4 patients were undergone operations due to hip fractures, and the others were done by any other causes. Bone marrow S1P levels were significantly lower in patients with hip fractures than in those without, before and after adjusting for confounding factors (P = 0.047 and 0.025, respectively). We failed to demonstrate significant associations between bone marrow S1P levels and any BMD values (γ = 0.026 - 0.482, P = 0.171 - 0.944).

Conclusions: In conjunction with our previous findings, these suggest that the effects of gradient between peripheral blood and bone marrow, but not S1P itself, may be the most critical on bone metabolism.

Keywords: Sphingosine 1-phosphate, osteoporotic fracture, bone density

Disclosures: Seong Hee Ahn, *None.*

SA0359

The 3 Chinese Herbs extracts Mixture Reverse Glucocorticoid-Induced Osteoporosis in Rat. Jian Wang*[1], Hongxin Zheng[2], Fang Yang[2], Dezhi Tang[3], Tianfang Li[4], Hui Zhu[2], zhangguo Zhang[2]. [1]Liaoning University of Traditional Chinese Medicine, USA, [2]Liaoning University of Traditional Chinese Medicine, China, [3]Shanghai University of Traditional Chinese Medicine, , [4]Rush University Medical Center, USA

Objective – To investigate the effect of the mixture of extracts from 3 Chinese Herbs, namely, pilose antler, epimedium, and oyster, (PEO), on glucocorticoid-induced osteoporosis (GIO) in rats.

Methods – A Rat GIO model was established by intramuscular injection of dexamethasone (2.5mg/kg, twice per week, for 9 weeks). The GIO rats were treated with intragastric administration of PEO for 9 weeks, and then were sacrificed. Bone mineral density (BMD) and histological changes of femoral heads were evaluated. Femoral head samples were harvested and the mRNA and protein expression of Runx2, Osterix, Msx2 and Dlx5 in bone tissues. Normal bone tissue and the samples from the GIO rats without PEO were used as controls.

Results – PEO treatment increased BMD in the GIO rats. Histological examination demonstrated that PEO treatment improved the structural integrity of bone in GIO rats. Morphological analysis demonstrated better bone trabecular condition, more compact structure, less remaining bone remodeling space, and reduced bone marrow cavities, in the PEO treated rats. PEO treatment increased the mRNA and protein expression of Runx2, Osterix, and Dlx5 and decreased the mRNA and protein expression of Msx2 in bone tissues.Conclusion – (1) The rat GIO model can be established successfully by intramuscular injection with dexamethasone. (2) In the GIO rats, Msx2 expression was significantly up-regulated, while the expression of Runx2Dlx5 and Osterix was dramatically decreased. (3) The PEO, traditional Chinese medicine compounds, prevent and decelerate bone loss in GIO rat by down-regulating Msx2 expression and up-regulating expression of Dlx5, Runx2 and Osterix in bone tissue.

Group	n	Femur BMD (g/cm²)
normal control	22	0.1080±0.0072△△
OP control	21	0.0993±0.0059**
OP PEO treated	18	0.1062±0.0061△△

**:compared with normal control,$P<0.01$;
△△: compared with OP control ,$P<0.01$

PEO prevents dexamethasone mediated bone loss in rat

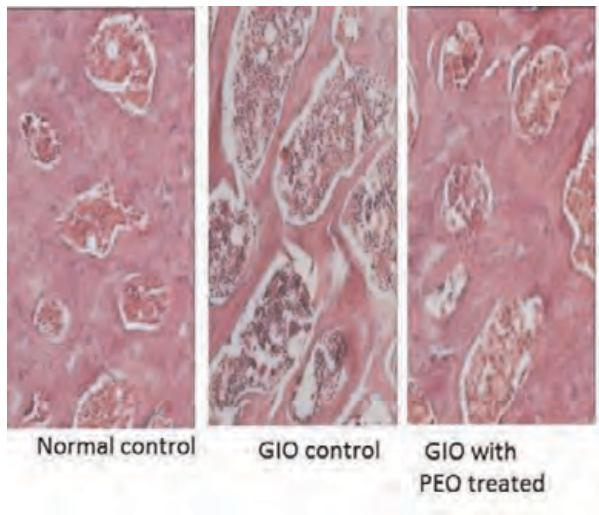

PEO reverses trabecular bone condition of GIO rat

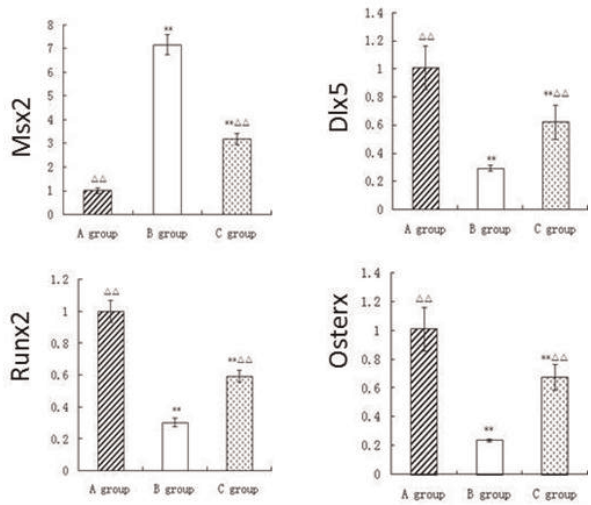

PEO down-regulate mRNA expression of Msx2 and up-regulate mRNA expression of Dlx5 Runx2 and Osterix

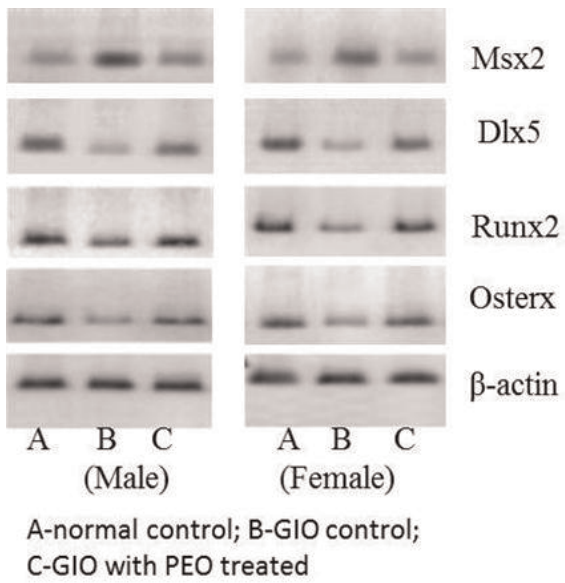

PEO decreases Msx2 and increases Dlx5 Runx2 and Osterix protein level in bone tissues

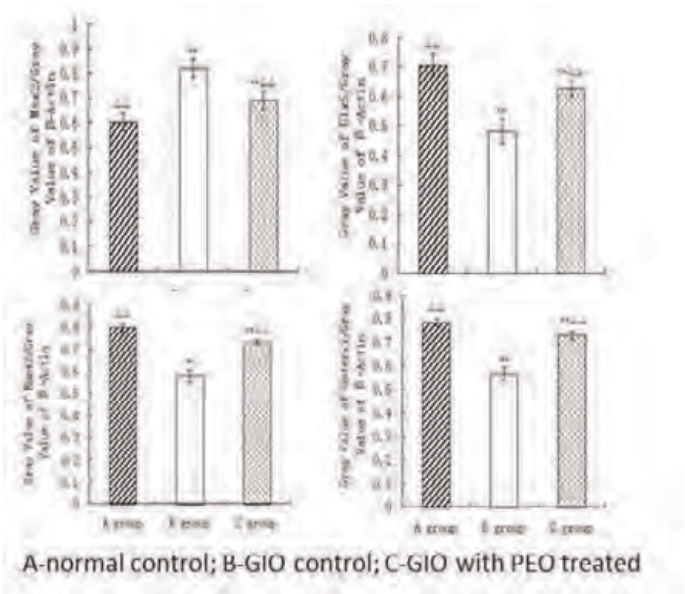

Relative protein level of Msx2 Dlx5 Runx2 and Osterix in bone tissue

***Disclosures: Jian Wang**, None.*
This study received funding from: National Basic Research Program of China (973 Program, 2010CB530401)

SA0360

Analysis of 48-hr Profiles of Melatonin and the Bone Resorption Marker Crosslinked N-terminal Telopeptide of Collagen I (NTx) in Blind Women With and Without Light Perception. Melissa St. Hilaire[1], Erin Flynn-Evans[1], Suzanne Higginbotham[2], Paula Witt-Enderby*[3], Steven Lockley[1]. [1]Division of Sleep Medicine, Department of Medicine, Harvard Medical School, Brigham & Women's Hospital, USA, [2]Division of Clinical, Social & Administrative Sciences, School of Pharmacy, USA, [3]Duquesne University, School of Pharmacy, USA

There is some evidence that bone metabolism displays a diurnal rhythm in humans that may be influenced by melatonin production, the light/dark cycle, or both. We took advantage of a natural model of altered melatonin timing in blind individuals both with (LP) and without light perception (NLP) to assess these relationships across 24 hours. The current analysis included urine samples from 35 blind female participants (17 LP, 18 NLP). Menopause stage was reported by all participants; 13 were pre-menopausal (6 NLP), 8 were peri-menopausal (5 NLP) and 14 were post-menopausal (7 NLP). Urine was collected across a 48-hr period at 4-hr intervals during wake and at 8-hr intervals overnight. Levels of 6-sulfatoxymelatonin (aMT6; ng/hr) and NTx (BCE nM/hr), corrected for both the urine volume and sampling interval, were analyzed. Both aMT6 and NTx were fit by a cosinor model to determine significant 24-hr rhythms. The results from this analysis reveal that (1) aMT6 had a significant fit 24-hr rhythm for all but 7 participants; (2) NTx did not have a significant 24-hr rhythm except in 3 participants; (3) significant day-to-day variability was observed in the 24-hr NTx outputs; (4) no relationships were found between NTx levels and light perception status or menopause stage with aMT6 acrophase timing (Night vs. Day); (5) 24-hr NTx output of the participants with aMT6 acrophases occurring during the biological night was not significantly different from the 24-hr NTx output of the participants with aMT6 acrophases occurring during the biological day; (6) the 24-hr NTx output was not significantly different between participants with or without light perception; (7) trends towards increases in NTx levels were observed in postmenopausal (combined LP and NLP) vs. premenopausal women (combined LP and NLP; p=0.08) and between perimenopausal women with LP vs. NLP (p=0.07). Future studies should continue to examine the relationship between bone metabolism rhythms in blind individuals with NLP to determine the influence of the melatonin rhythm independent from the influence of the light-dark cycle and should also assess the influence of menopausal status.

***Disclosures: Paula Witt-Enderby**, None.*

SA0361

B Cell Dysregulation Promotes HIV-induced Bone Loss. Kehmia Titanji*, Ashwani Vunnava, Anandi Sheth, Jeffrey Lennox, Ighovwerha Ofotokun, M. Neale Weitzmann. Emory University School of Medicine, USA

Background: Adaptive immune responses potently impact the skeleton as a consequence of the immuno-skeletal interface, a convergence of cells and cytokine effectors mediating critical albeit different functions in both organ systems. HIV infection assaults adaptive immunity and is associated with high rates of osteoporosis and bone fractures, but the mechanisms remain obscure. Bone-degrading osteoclasts are regulated primarily by the ratio of Receptor-Activator of NF-kappaB (RANKL), the key osteoclastogenic cytokine, to that of its decoy receptor and physiological inhibitor, osteoprotegerin (OPG). Using the HIV-1 transgenic rat model, we recently reported severe skeletal destruction due to increased B cell RANKL expression, compounded by reduced B cell OPG expression, favoring enhanced osteoclastogenesis. These findings suggested that HIV-induced bone loss is aligned with dysregulation of B cell function. In the current study we have attempted to ratify this putative mechanism by translating our basic research findings back into the human system.

Methods: In a prospective cross-sectional comparative study, we characterized the immunoskeletal profile of 45 HIV- and 45 ARV-naïve HIV^+ volunteers. We studied the distribution of B and T cell subsets, cellular activation profile, and production of OPG and RANKL by flow cytometry. We also measured plasma levels of bone turnover markers, C-terminal telopeptide of collagen (CTX-bone resorption) and osteocalcin (OCN–bone formation) by ELISA.

Results: Our data revealed a profound immune activation signature characteristic of HIV/AIDS, as well as a 50% elevation in bone resorption (CTX) in the HIV^+ compared to the HIV^- population ($p = 0.001$). Importantly, similar to our animal studies, we observed a 30% down-regulation of B cell expression of OPG ($p < 0.5$), concurrent with significant up-regulation of RANKL production (60%, $p = 0.001$), reflecting an imbalance in the RANKL/OPG ratio in a direction that favors enhanced bone degradation. Interestingly, this imbalance was age-associated and even more pronounced in individuals >40 years, consistent with higher stress fracture rates in this group.

Conclusions: These data validate our basic research findings, and suggest that dysregulation in B cell function leading to a switch from bone protecting OPG to bone degrading RANKL expression during HIV-infection contributes to viral-induced bone loss in ARV-naïve HIV^+ individuals.

***Disclosures: Kehmia Titanji**, None.*

SA0362

Circulating Sclerostin, Bone Turnover Markers and BMD In Type-2 Diabetic Women Treated With Metformin or Pioglitazone. Mohammed-Salleh Ardawi*[1], Daad Akbar[2], Abdulrahman Al-Shaik[2], Maimoona Ahmed[2], Mohammed Qari[3], Abdulrahim Rouzi[1], Rajaa Raddadi[4]. [1]Center of Excellence for Osteoporosis Research & Faculty of Medicine, Saudi Arabia, [2]Center of Excellence for Osteoporosis Research & Department of Internal Medicine & KAU Hospital,Faculty of Medicine, King Abdulaziz University, Saudi Arabia, [3]Center of Excellence for Osteoporosis Research & Department of Haematology, Faculty of Medicine & KAU Hospital, King Abdulaziz University, Saudi Arabia, [4]Center of Excellence for Osteoporosis Research, King Abdulaziz University, Saudi Arabia

Background: Sclerostin is involved in the regulation of bone formation through the inhibition of the Wnt/β-catenin signaling pathway. Type 2 diabetes mellitus (T2DM) have an increased risk of fractures that is increased by thiazolidinediones (TZDs) therapy. We hypothized that abnormal sclerostin production contributes to the pathogenesis of increased osteofragility in T2DM treated with TZDs.

Methods: We examined the association between circulating sclerostin levels and the changes in bone turnover markers (BTMs) [including: s-P1NP, s-bone ALP, p-CTX, and u-NTX], and bone mineral density (BMD) [lumbar spine (L_1-L_4); neck femur] [measured by DXA] among 280 women diagnosed with T2DM and treated with either metformin (MET) (850mg twice daily) (n=140) or pioglitazone (PIO) (30mg once daily) (n=140). Baseline values of serum sclerostin, BTMs and BMD were compared with age- and body mass index (BMI)- matched healthy controls (n=280).

Results: Compared with controls, T2DM women had significantly higher serum sclerostin levels (56.78 ± 11.66 vs 41.22 ± 9.35 pmol/L, $P<0.001$), and lower p-CTX ($P<0.001$) and u-NTX ($P<0.001$); but similar s-P1NP and s-bone-ALP levels, respectively. After 12 months of treatment, serum sclerostin levels increased by 48% in PIO-treated and decreased by 27.3% in MET-treated women ($P<0.0001$); whereas BMD [lumbar spine (L_1-L_4) and neck femur] significantly decreased ($P<0.05$) in PIO-treated (% change, -4.46 ± 3.22%) with no marked changes in MET-treated ($P=0.351$) women following therapy.

Conclusions: Women with T2DM had higher serum sclerostin levels than age- and BMI-matched healthy controls, and such levels further increased following therapy with PIO, which is also associated with increased p-CTX and u-NTX and decreased BMD values. Such observations suggest that higher sclerostin levels may be involved in the pathogenesis of increased osteofragility in women with T2DM in general which maybe aggravated by TZDs therapy.

***Disclosures: Mohammed-Salleh Ardawi**, None.*

SA0363

See Friday Plenary Number FR0363.

SA0364

See Friday Plenary Number FR0364.

SA0365

See Friday Plenary Number FR0365.

SA0366

Premenopausal women with idiopathic osteoporosis and those with anorexia nervosa have similar bone structural defects but differ in terms of marrow fat. Anna Kepley[1], Wei Shen[2], Laurel Mayer[2], Elizabeth Shane[3], Julia Weigel[2], Lindsay Kenney[2], Polly Young[2], Chiyuan Zhang[2], Robert Recker[2], Joan Lappe[4], Adi Cohen*[1]. [1]Columbia University Medical Center, USA, [2]Columbia University, USA, [3]Columbia University College of Physicians & Surgeons, USA, [4]Creighton University Osteoporosis Research Center, USA

Bone marrow adipocytes and osteoblasts share a common mesenchymal precursor. Reciprocal relationships between these cells have been implicated in several forms of osteoporosis, including anorexia nervosa (AN). However, animal studies also suggest that the adipocytes and osteoblasts can be regulated independently.

In a transiliac bone biopsy study, we reported that premenopausal women with idiopathic osteoporosis (IOP) have substantially lower trabecular bone volume fraction, and abnormal trabecular and cortical microarchitecture compared to healthy premenopausal controls. Marrow fat (MF) was significantly higher in IOPs than controls, even after controlling for their lower bone volume fraction. Because IOP women had lower BMI than controls, we hypothesized that IOPs would have a bone phenotype similar to women with AN, who also have both bone structure defects and increased MF. We recruited 11 women with IOP (spine or hip Z score ≤ -2.0 and/or low trauma fracture, normal menses, no eating disorder, no secondary cause of osteoporosis), 12 women with AN studied within 3 wks of inpatient admission (% ideal body wt 73±5; yrs amenorrheic 7±5; 7/12 with history of fracture) and 28 premenopausal Controls (C; normal BMD and menses, no fractures). Areal BMD and body composition were measured by DXA, volumetric BMD/microarchitecture by HR-pQCT (Scanco AG), and MF fraction of the L3 vertebra and the femoral neck by 1H-magnetic resonance spectroscopy (MRS). Age was similar and body composition differed as expected (Table). While BMD and bone structure defects were remarkably similar between AN and IOPs, those with AN had higher MF, particularly at the spine. Spine MF correlated with age (r=0.45,p=0.02) and femoral MF with whole body fat (r=0.41,p=0.03) in C, but neither age nor body fat correlated with MF in IOP or AN. While radial vBMD and cortical thickness correlated directly with MF at the spine (both r=0.42,p=0.02) and femur (r=0.37-0.41,p=0.03-0.049) in C, inverse relationships were seen between spine MF and tibial cortical thickness (r=-0.78,p=0.003) and femur MF and total hip BMD (r=-0.65,p=0.02) in IOPs. MF did not correlate with amenorrhea or BMD variables in this AN cohort. We conclude that despite quite similar deficits in BMD and microarchitecture, IOPs have significantly less marrow adiposity than women with AN. Further research is required to investigate potential mechanisms for the differences in relationships between fat and bone in IOP and AN.

Median (IQR)	Control (n=28)	IOP (n=11)	AN (n=12)
Age (yrs)	28 (24, 36)	30 (26, 35)	28 (21, 34)
Height (cm)	167 (163, 170)* °	161 (158, 164)	161 (151, 168)
Weight (kg)	65.8 (62.4, 69.2)* °°	55.6 (53.1, 66.7)	43.8 (40.6, 50.8)**
BMI (kg/m²)	23.4 (22.3, 25.7)***	20.9 (20.1, 24.0)	16.3 (16.0, 18.1)**
DXA Whole Body Fat (%)	35.6 (29.8, 38.3)***	30.8 (27.0, 36.2)	16.2 (13.4, 19.3)**
DXA Trunk Fat (%)	28.7 (25.0,35.3)***	25.2 (19.8, 33.0)	16.0 (12.0, 17.8)**
MRS			
L3 Fat Fraction	0.306 (0.234, 0.332)* °°	0.370 (0.316, 0.469)	0.492 (0.426, 0.553)*
Femoral Fat Fraction	0.627 (0.550, 0.747)°°	0.686 (0.636, 0.864)	0.826 (0.749, 0.884)
BMD by DXA (g/cm²)			
Lumbar Spine	1.05 (0.99, 1.15)*** °°°	0.76 (0.70, 0.81)	0.84 (0.71, 0.98)
Total Hip	1.00 (0.97, 1.06)***,°°°	0.76 (0.66, 0.92)	0.78 (0.60, 0.84)
Femoral Neck	0.89 (0.82, 0.94)***,°°°	0.68 (0.55, 0.74)	0.68 (0.58, 0.77)
Distal Radius	0.72 (0.70, 0.74)**	0.63 (0.62, 0.69)	0.70 (0.68, 0.76)
HR-pQCT: Radius			
Total Density (mgHA/cm³)	337.1 (306.4, 379.0)***,°°	241.5 (204.1, 300.8)	241.1 (216.9, 330.8)
Cortical Density (mgHA/cm³)	908.9 (858.9, 943.2)*	872.0 (816.4, 890.2)	828.4 (779.7, 921.6)
Cortical Thickness (mm)	0.82 (0.73, 1.00)***,°	0.64 (0.51, 0.72)	0.57 (0.48, 0.84)
Trabecular Density (mgHA/cm³)	157.1 (141.6, 192.5)***,°°	98.6 (81.1, 127.6)	119.9 (81.6, 132.6)
Trabecular Number (1/mm)	2.00 (1.88, 2.26)**,°°	1.61 (1.56, 1.86)	1.65 (1.40, 1.87)
Trabecular Thickness (mm)	0.067 (0.060, 0.074)**	0.049 (0.044, 0.061)	0.057 (0.048, 0.076)
HR-pQCT: Tibia			
Total Density (mgHA/cm³)	315.4 (294.0, 335.7)***,°°	237.1 (216.9, 285.2)	263.8 (218.3, 299.8)
Cortical Density (mgHA/cm³)	902.1 (878.2, 923.8)	863.4 (817.1, 916.3)	898.6 (814.1, 955.8)
Cortical Thickness (mm)	1.23 (1.07, 1.32)**,°	0.95 (0.78, 1.11)	0.99 (0.67, 1.21)
Trabecular Density (mgHA/cm³)	179.2 (161.4, 202.2)***,°°	128.1 (111.7, 154.7)	137.2 (106.6, 161.5)
Trabecular Number (1/mm)	2.00 (1.84, 2.16)**,°°	1.62 (1.46, 1.86)	1.64 (1.06, 1.82)
Trabecular Thickness (mm)	0.073 (0.067, 0.090)	0.065 (0.056, 0.079)	0.074 (0.068, 0.084)

Nonparametric (Wilcoxan): *p < 0.05, **p<0.01, ***p<0.001 vs IOP; °p<0.05, °°p<0.01, °°°p<0.001 vs AN

Table

***Disclosures: Adi Cohen**, None.*

SA0367

Vitamin D status and response to treatment of vitamin D in Korean women initially diagnosed as osteoporosis. Sung Soo Kim*[1], Jin Ju Kim[2]. [1]Chungnam National University School of Medicine, South Korea, [2]Chungnam National University Hospital, South Korea

Background: The aim of this study is to evaluate whether the recommended dose is appropriate in vitamin D deficient patients.

Methods: This was a prospective study. Women (n = 30) first diagnosed with osteoporosis were recruited in outpatient clinic. They were recommended to be exposed to sun light for more than 30 minutes a day. Subjects were divided into 3 groups according to serum 25-hydroxyvitamin D_3 (25OHD) status: deficiency (less than 20 ng/mL), insufficiency (20 to 30 ng/mL) and sufficiency (30 ng/mL or more). Insufficient and sufficient patients received the recommended dose (1000 IU/day) but deficient patients received recommended or double dose (1800 to 2000 IU/day). We compared 25OHD levels at baseline and after vitamin D supplementation for 12 months.

Results: Mean (SD) serum 25OHD concentration at baseline was 17.60 (8.44) ng/mL and the proportion of deficient, insufficient and sufficient groups were 66.7% (20/30), 20.0% (6/30) and 13.3% (4/30) respectively. All insufficient patients achieved optimal level (30 ng/mL or more) with the recommended dose. However, 63.6% (7/11) of the deficient patient with recommended dose achieved optimal level and 88.9% (8/9) of those with double dose did (P = 0.016).

Conclusions: One third of osteoporotic women treated with recommended dose of vitamin D may not achieved optimal level of 25OHD if they have deficient level of 25OHD. They may require double dose of vitamin D in case of deficient level of 25OHD.

***Disclosures: Sung Soo Kim**, None.*

SA0368

Identification of proteins important for male osteoporosis from human peripheral blood monocytes. Yingchun Zhao*, Lan Zhang, Hualin Huang, Yao-Zhong Liu, Yong-Jun Liu, Fei-Yan Deng, Hong-Wen Deng. Tulane University, USA

Introduction: Osteoporosis is a major public health problem, mainly characterized by low bone mineral density (BMD), which is largely genetically determined with gender-specificity. Although women generally have lower BMD than men, men suffer significantly higher mortality rate upon osteoporotic fractures. However, current studies have been largely focused on female osteoporosis. Low BMD may result from bone resorption (by osteoclasts) exceeding bone formation (by osteoblasts). Peripheral blood monocytes (PBMs) are precursor cells for osteoclasts. We are utilizing PBMs, which are directly isolated from male subjects with high or low BMD, for protein profiling with subcellular extraction and 2D-nanoLC-ESI-MS/MS^E for the purpose of identifying proteins important for male osteoporosis.Method: PBMs are isolated from the whole blood with the negative immunomagnetic separation method. We used ProteoExtract Subcellular Proteome Extraction kit to isolate proteins of membrane, cytosolic, nuclear, and cytoskeletal fractions. After trypsin digestion, the peptide mixture is separated with 2-dimensional NanoAquity System. The five fractions generated from the high pH first dimension LC are further separated with the reverse phase second dimension LC. The separated peptides were analyzed with Synapt G2 MS^E system. Data collection was controlled by Masslynx 4.1. Protein identification and quantification were performed in PLGS 2.4. Data analysis was performed in SPSS and Excel.Results: We have recruited and phenotyped 120 males at peak bone mass ages of 25-50 based on low and high hip BMD values. We are using half of the sample (30 low vs. 30 high BMD subjects) for protein profiling. After searching against IPI database (v3.83), a typical profiling generated 3275 proteins for cytoplasm fraction, 3203 proteins for membrane fraction, 1037 proteins for nuclear fraction, and 967 proteins for cytoskeletal fraction with a total of 8483 proteins. We identified 33 upregulated and 3 downregulated proteins (low BMD vs high BMD) in cytosolic component; 87 upregulated and 17 downregualted proteins in membrane component; 4 upregulated and 3 downregualted proteins in nuclear component; and 39 upregulated and 30 downregulated proteins in cytoskeletal component. Western blot validation of selected significant proteins is being carried out. Functional study wil be pursued for those validated significant proteins.

***Disclosures: Yingchun Zhao**, None.*

SA0369

Serum Dickkopf1 (DKK1): Relationship With Bone Metabolism And Atherosclerotic Disease In Type 2 Diabetes Mellitus. Rebeca Reyes-García*[1], Pedro Rozas-Moreno[2], Antonia Garcia-Martin[3], Beatriz Garcia-Fontana[4], Sonia Morales-Santana[4], Manuel Munoz-Torres[5]. [1]Hospital Rafael Méndez, Spain, [2]Endocrinology Division. Hospital General de Ciudad Real. Ciudad Real, Spain., Spain, [3]Hospital Comarcal del Noroeste, Spain, [4]Hospital Clínico San Cecilio, Spain, [5]Hospital Universitario San Cecilio, Spain

Type 2 diabetes (T2DM) is a risk factor for osteoporotic fractures and cardiovascular disease. The Wnt signaling pathways are involved in diverse develop mental and physiological processes, including anabolic effects on bone and

atheroesclerotic disease (AD). Dickkopf-1 (DKK1) is a potent inhibitor of Wnt signaling. The aims of our study were to evaluate serum DKK1 levels in a cohort of T2DM patients and to analyze its relationships with bone metabolism and AD. We studied 122 subjects: T2DM patients (n: 72, mean age 58,2 ± 6 years) and non-diabetic subjects (n:54, mean age 55,4 ± 7 years). BMD was measured by DXA. The presence of AD (cerebrovascular disease, peripheral arterial disease, ischemic heart disease) was recorded. Intima-media thickness (IMT) was determined by Doppler ultrasonography and aortic calcification by evaluation of lateral view conventional X-rays. We no found significant differences in DKK1 between groups. Serum DKK1 concentrations were significantly higher in females in total sample (24,3 ± 15,2 vs 19,6 ± 10,2 pmol/L, p = 0,046) and in T2DM group (27,5 ± 17,2 vs 19,8 ± 8,9 pmol/L, p = 0,025). There was a positive correlation between serum DKK1 and LS BMD in total sample (r = 0,183, p = 0,048). However, we no found a significant relationship with osteoporosis diagnosis or morphometric vertebral fractures. Serum DKK1 was significantly higher in T2DM patients with AD (26,4 ±14,5 pmol/L vs 19,1 ± 11,6 pmol/L, p = 0,026) and also in patients with abnormal IMT (26,4 ± 15,1 pmol/L vs 19,8 ± 11,3 pmol/L, p = 0,038). DKK1 levels were independent predictors of the presence of AD in T2DM independently others atherosclerotic risk factors (odds ratio: 1,064, 95% confidence interval: 1,107–1,125; p = 0,028). In the ROC curve analysis, In the ROC curve analysis to evaluate the usefulness of sclerostin as a marker for high risk of AD, the area under the curve was 0,667 (95% confidence interval: 0,538-0,795; p = 0,016). A concentration of 17,3 pmol/L or higher showed a sensitivity of 71,4 % and a specificity of 60 % to identify an increased risk of AD. In conclusion, we no found sigificant differences in DKK1 between T2DM and circulating DKK1 levels are higher in T2DM with AD.

***Disclosures: Rebeca Reyes-García**, None.*

SA0370

Second generation antipsychotic drugs have direct effects on the skeleton via G-protein coupled neural receptors: Implications for bone and energy metabolism. Karen Houseknecht[1], Katherine Motyl*[2], Rachel Mayer[3], Shail Patel[3], Deborah Barlow[3], John Streicher[3], Daniel Brazeau[3], Clifford Rosen[4]. [1]University of New EnglandCollege of Pharmacy, USA, [2]1Maine Medical Center Research Institute, USA, [3]University of New England, USA, [4]Maine Medical Center, USA

Second generation antipsychotics (SGAs) are widely prescribed to treat psychiatric disorders in adults and children. The pharmacology of SGAs is complex: they potently antagonize multiple G protein coupled receptors (GPCRs) including dopamine (D2), serotonin (5-HT), α2 and H1. Side effects of SGAs include obesity and type 2 diabetes. Recent evidence indicate SGAs such as risperidone (RIS) increase fracture risk and reduce bone mineral density in humans; the underlying pharmacological mechanisms are unknown. Our hypothesis is that SGA therapy is associated with significant bone loss, and this adverse side effect occurs via multiple mechanisms including directly binding to, and antagonizing receptors on bone cells. The specific aims of this study were 1) determine if GPCR targets of SGA action in the CNS are expressed in bone cells, 2) determine if RIS accumulates in bone marrow following oral dosing and 3) determine if RIS has direct effects on osteoblast gene expression and function. GPCR gene expression was determined by qPCR analysis using MC3T3 cells during proliferation and following exposure to osteoblast differentiation media. D2, 5HT-2A & 5HT-2C receptor mRNA was expressed in MC3T3 cells (comparable to brain control), and expression was induced upon differentiation. Interestingly, expression was highest at day 7 of differentiation, and then returned to levels comparable to proliferating osteoblasts by day 21, suggesting these receptors are important for osteoblast differentiation and/or function. Drug exposure in plasma and bone marrow was determined in mice dosed orally with RIS (1.0 mg/kg) by LC/MS/MS detection. RIS and the active metabolite, 9-OH-RIS were present in bone marrow, consistent with plasma exposure. Finally, MC3T3 cells were differentiated in the presence of vehicle, 6, 30 or 150 nM RIS, representing sub-clinical, clinical and supra-clinical exposure, respectively. Alkaline phosphatase and Von Kossa mineral stain were not changed by RIS, despite the previously known reduction in osteoblast function in vivo. However, RIS did suppress expression of osteoprotegerin (OPG), the soluble decoy receptor for RANKL. This finding is consistent with low OPG expression and high osteoclast activity that we have previously demonstrated in mice and increased osteoclast number that we have shown in primary osteoclasts treated with RIS. Furthermore, RIS had dose-dependent effects on ATF4 and osteocalcin expression, including suppression of these factors at clinical and supra-clinical levels, which could negatively affect glucose homeostasis in vivo. These data support the notion that adverse SGA effects on bone and metabolism may be mediated, at least in part, by direct effects on bone cells in vivo.

***Disclosures: Katherine Motyl**, None.*

SA0371

See Friday Plenary Number FR0371.

SA0372

See Friday Plenary Number FR0372.

SA0373

Comparison of Analgesic Action of and Vertebral Collapse Prevention by Teriparatide and Risedronate Administration for Fresh Osteoporotic Vertebral Fracture. Hiroyuki Tsuchie*[1], Naohisa Miyakoshi[2], Yuji Kasukawa[2], Tomio Nishi[1], Hidekazu Abe[1], Masaaki Takeshima[1], Toyohito Segawa[2], Yoichi Shimada[2]. [1]Ugo Municipal Hospital, Japan, [2]Akita University Graduate School of Medicine, Japan

Purpose: Vertebral fracture is often seen in aged osteoporotic patients, and it causes a decline in activities of daily living. Because teriparatide has a potent osteogenic effect, it is expected to promote bone union after fracture and reduce fracture-related pain. Therefore, we evaluated the analgesic action of and vertebral collapse prevention by administering teriparatide to fresh vertebral fracture patients, comparing the effects with those of risedronate administration.

Methods: Seventeen patients with fresh osteoporotic vertebral fracture (24 vertebrae) hospitalized for treatment (male/female: 2/15, mean age: 80 years) participated in the present study. They were administered either teriparatide or risedronate for osteoporosis treatment based on their choice, and 8 patients (14 vertebrae) were administered teriparatide (PTH group, male/female: 1/7, mean age: 82 years), and 9 patients (10 vertebrae) were administered risedronate (RIS group, male/female: 1/8, mean age: 80 years). We compared serum cross-linked N-telopeptide of type I collagen (NTX), bone-specific alkaline phosphatase (BAP), calcium (Ca), inorganic phosphorus (IP), the visual analogue scale (VAS), hospitalization period, vertebral collapse rate compared to that at the initial visit, and local kyphotic angle of fractured vertebrae compared to the initial visit.

Results: At the start of treatment, there was no significant difference in the age, laboratory examinations, bone mineral density, VAS, vertebral collapse rate, and local kyphotic angle between the 2 groups. At 8 weeks after the initial visit, VAS in the PTH group was significantly lower than in the RIS group ($P<0.05$).At 4 and 8 weeks after the initial visit, the differences in the vertebral collapse rate and local kyphotic angle in the PTH group were significantly lower than in the RIS group ($P<0.01$, respectively). There was no significant difference in the hospitalization period.

Conclusions: Teriparatide is more promising for analgesia and the prevention of vertebral collapse progression after osteoporotic fresh vertebral compression fracture than risedronate.

***Disclosures: Hiroyuki Tsuchie**, None.*

SA0374

See Friday Plenary Number FR0374.

SA0375

Early Bone Resorptive Response to Teriparatide Predicts Bone Density Outcome at 2 Years. Richard Bockman*[1], Erik Nielsen[2], Wei-Ti Huang[2]. [1]Hospital for Special Surgery, Weill Cornell Medical College, USA, [2]Hospital for Special Surgery, USA

Not all patients show improved bone mineral density (BMD) with Teriparatide (TPTD), an expensive and prolonged osteoanabolic therapy for osteoporosis (OP). As an approach to improving and predicting BMD outcome, we analyzed early metabolic bone parameters and BMD changes in OP patients newly treated with TPTD. The clinical course of 78 patients with severe OP (mean T score at lumbar spine -2.7) who were prescribed TPTD was monitored by measuring bone specific alkaline phosphatase (BSAP) and N-terminal bone collagen protein (NtX) markers every 4 months and Lumbar Spine (LS)-BMD measured at 2 years. Responders were defined as showing greater than 3.5% increase in LS-BMD at 2 years. Sixty percent (59/78) of TPTD-treated patients were ''Responders'' at the end of two years of study. There were no significant differences in BMD, BMI, mean 25 OH Vit D, serum calcium, creatinine, age, gender, or history of prior fractures at baseline between Responders and Non-responders. The peak BSAP and NtX response was seen at 4 months, Fig 1. There were no differences in the BSAP response for Responders and Non-responders. A significant difference in the magnitude and duration of the NtX elevation was seen in the Non-responder population. This difference is more evident in the plot of the ratio of NtX to BSAP, Fig 2. Using a Generalized Estimating Equations (GEE) analysis, the Responders had an 11.6 unit lower NtX value compared to Non-responders across the 2 years with a p-value=0.0014. This result remained significant after adjusting for potential confounders or effect modifiers such as 25 OH Vit D, calcium, creatinine levels, or BMI, age, gender, prior fracture history, or prior bisphosphonate use. No significant difference in the mean BMD increase was seen in the patients who were naïve or those previously treated with bisphosphonates (9.11 vs 8.44%). In summary, no difference in the BSAP response was seen between the Responders and Non-responders. The Non-responding patients showed a greater and more prolonged increase in NtX across the 2 years of study, even after adjustment for gender, age and history of prior fracture. Baseline parameters and prior bisphosphonate therapy had no significant effect on final BMD outcome. In conclusion, an

early robust increase in the resorptive response predicted an attenuated response to TPTD therapy. Initiation of antiresorptive therapy after 4 months of starting TPTD therapy may abrogate non-response thereby improve overall BMD outcomes.

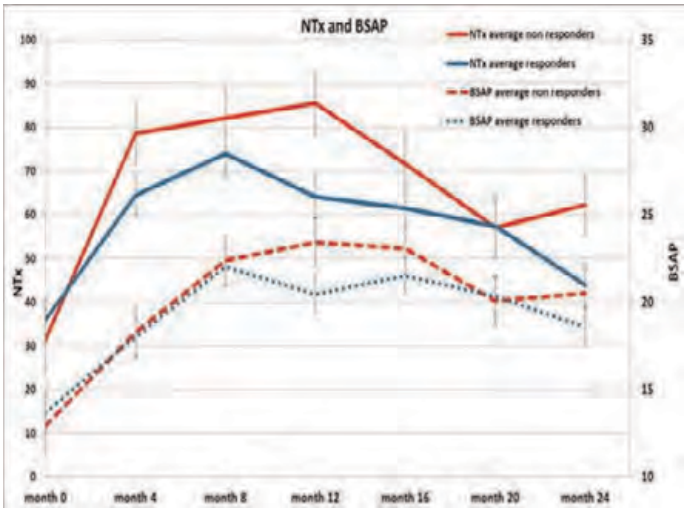

Fig 1

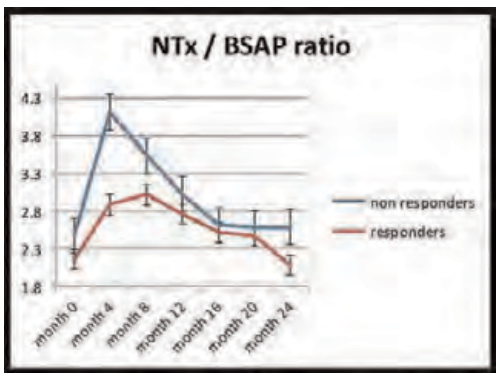

Fig 2

***Disclosures: Richard Bockman**, None.*

SA0376

See Friday Plenary Number FR0376.

SA0377

Overlapping and Follow-up of Alendronate to Teriparatide Results in Continuing Volumetric Bone Mass Increase Measured by Quantitative Computed Tomography. Christian Muschitz*[1], Roland Kocijan[2], Wolfgang Schima[3], Judith Haschka[2], Afrodite Zendeli[4], Astrid Fahrleitner-Pammer[5], Heinrich Resch[6]. [1]St. Vincent's Hospital, Austria, [2]St. Vincent Hospital Vienna, Austria, [3]Department of Radiology - St. Vincent Hospital, Austria, [4]The VINFORCE Study Group - St. Vincent Hospital - Medical Department II, Austria, [5]Medical University Graz, Austria, [6]Medical University Vienna, Austria

Purpose: After 9 months of teriparatide (TPTD) treatment the combination of alendronate (ALN) and TPTD for the consecutive 9 months results in enhanced bone mineral density (BMD) gain when compared with 18 months of TPTD monotherapy. Use of raloxifene (RAL) instead of ALN was less advantageous. During a subsequent 12 months maintenance therapy, hip BMD only increased in the ALN group. Our aim was to investigate changes of cortical and trabecular bone by quantitative computed tomography (QCT).

Methods: 125 postmenopausal women (mean age 71.7±8.5 ys, 91.5% fracture prevalence, 95.7% prior antiresorptive treatment > 2 ys) were randomized after 9 months of TPTD treatment into three open-label groups for another 9 months: ALN (70 mg/week, 41 pts) or RAL (60 mg/day, 37 pts) added to TPTD treatment or TPTD monotherapy/Ca+Vit D group (47 pts). After TPTD termination, patients were maintained on their respective treatment regime for another 12 months. All subjects received 1g calcium/800 IU vitamin D daily. Trabecular bone in 2nd lumbar vertebra (L2), cortical and trabecular bone in total hip and femoral neck were measured at randomization, end of TPTD and of the maintenance by QCT (Siemens Somatom Definition AS+).

Results: L2 bone volume changed by (mean %±SD) 12.1±4.5, 14.6±8.9 and 7.2±7 during combination and 21.9±8.3, 23.6±10 and -3.9±5.7 % ($p < 0.001$ for all) at the end of maintenance treatment for the ALN, RAL and Ca+Vit D groups, respectively. Ca+Vit D group was inferior to the other groups at both time points ($p<0.01$). The corresponding changes of trabecular bone in the total hip were 10.7±4.4, 5.1±2.3 and 4.8±2.6 as well as 16.7±4.4, 8±3.2 ($p < 0.001$ for all) and -0.4±4% (n.s.), respectively. Changes in both time points were superior in the ALN group. The increase of the RAL was greater than of the Ca+Vit D group at the end of the maintenance ($p=0.02$). In contrast, cortical bone in the total hip changed by 6.6±2.2 ($p < 0.001$), -1.7±5.8 ($p=0.01$) and 2.8±3.1 ($p=0.002$) and 13.8±2.9, -3.9±6 ($p<0.001$ both) and 0.7±3.3% (n.s.), respectively. In both intervals, cortical bone increased in the ALN group significantly more than in the other groups ($p<0.001$). The decrease observed in the RAL group was significantly different from changes in the Ca+Vit D group.

Conclusion: Continuation of ALN after its addition to the second 9 months of an 18-month TPTD treatment cycle resulted in a robust increase especially in cortical bone of the hip in severe postmenopausal osteoporosis.

***Disclosures: Christian Muschitz**, None.*

SA0378

See Friday Plenary Number FR0378.

SA0379

Alendronate Sodium/Vitamin D_3 Combination Tablet versus Calcitriol for Osteoporosis in Chinese Postmenopausal Women: A 6-Month, Randomized, Open-Label, Active-Comparator Controlled Study with a 6-Month Extension Phase. Zhenlin Zhang*[1], Er Yuan Liao[2], Bo Xia Wei[3], Hua Lin[4], Li Wang[5], De Cai Chen[6], Hai Tang[7], Wei Hong[8], Yong Qiang Hao[9], Yong De Peng[10], Liang He[11], Zhao Heng Hu[12], Fang Wei[13], Jue Wang[13], Arthur Santora[14]. [1]Shanghai Sixth People's Hospital, Shanghai Jiaotong University School of Medicine, China, [2]The Second Xiangya Hospital of Central South University, China, [3]Peking Union Medical College Hospital, China, [4]Nanjing Drum Tower Hospital, China, [5]TianJin Hospital, China, [6]West China School Of Medicine, West China Hospital, Sichuan University, China, [7]Beijing Friendship Hospital, Capital Medical University, China, [8]Huadong Hospital Affiliated to Fudan University, China, [9]Shanghai Ninth People's Hospital, China, [10]Shanghai First People's Hospital, China, [11]Beijing Jishuitan Hospital, China, [12]Peking University People's Hospital, China, [13]Merck Sharp & Dohme Corp., China, [14]Merck Sharp & Dohme Corp, USA

Purpose: Postmenopausal osteoporosis is a major health concern in China; however, the prevalence of vitamin D insufficiency in treated patients is not fully recognized in the clinical setting. Alendronate/Vitamin D3 may offer therapeutic benefits by modifying bone resorption and mineralization. Our objective was to investigate the efficacy and safety of alendronate 70 mg/vitamin D_3 5600 IU (ALN/D5600) as compared with calcitriol in Chinese postmenopausal women.

Methods: Postmenopausal women over 55 years of age with osteoporosis (low BMD with or without prior non-pathological fracture) were eligible. A total of 219 patients were randomized to receive 70 mg ALN/D5600 once weekly (n=111) or calcitriol 0.25 mcg once daily (n=108) for 12 months. The primary efficacy endpoint was percent change from baseline in the lumbar spine BMD at month 6. BMD was measured by a Hologic or Lunar DXA machine at baseline, month 6 and 12. Hypercalciuria was prespecified as an event of interest for safety evaluation.

Results: Baseline characteristics were similar, and 30.7% of patients had a baseline 25(OH) D level <15ng/mL. Women who received ALN/D5600 had significantly greater increases in BMD compared with those receiving calcitriol. At month 6, percent changes from baseline of lumbar spine BMD were 3.54%, 1.59% in ALN/D5600 and calcitriol treated groups. Mean treatment difference (±SE) was 1.95±0.56% between groups ($p<0.001$). Results of key secondary and exploratory analyses favored ALN/D5600. At month 12, mean differences in BMD percent changes from baseline were 2.92±0.59% at the lumbar spine, 2.53±0.65% at the total hip, 2.89±0.96% at the femoral neck, and 2.28±1.01% at the trochanter ($p<0.05$ for all comparisons). Mean differences at month 6 in P1NP and s-CTx percent changes from baseline were -41.35%, -50.49%, respectively ($p< 0.001$ for both comparisons). ALN/D5600 treatment was associated with a 96% reduction in the proportion of patients with serum 25(OH) D <15 ng/mL at Month 12 (1.0% vs. 25.5% with calcitriol, $p<0.001$). Hypercalciuria was less frequent in the ALN/D5600 group (0.9% vs. 2.8%, p=NS). The overall safety profile was similar between groups. The proportion of patients with fracture was lower in the ALN/D5600 group (0.9% vs. 3.7%).

Conclusions: ALN/D5600 once weekly is superior to calcitriol in BMD increase at the lumbar spine, bone turnover marker decrease, and vitamin D insufficiency correction in Chinese women with osteoporosis. ALN/D5600 is well tolerated.

***Disclosures: Zhenlin Zhang**, Merck, 6*
This study received funding from: Study was funded by Merck

SA0380

See Friday Plenary Number FR0380.

SA0381

Bone Mineral Density Increases with Monthly i.v. Ibandronate Injections Contribute to its Fracture Risk Reduction in Primary Osteoporosis: 3-Year Analysis of the Phase III MOVER Study. Hiroshi Hagino*[1], Toshitaka Nakamura[2], Masako Ito[3], Tetsuo Nakano[4], Junko Hashimoto[5], Masato Tobinai[6], Hideki Mizunuma[7]. [1]Tottori University, Japan, [2]National Center for Global Health & Medicine, Japan, [3]Nagasaki University Hospital, Japan, [4]Tamana Central Hospital, Japan, [5]Chugai Pharmaceutical Corporation Limited, Japan, [6]Chugai Pharmaceutical Co. Ltd., Japan, [7]Hirosaki University, Japan

Purpose: The MOVER (MOnthly intraVenous ibandronatE versus daily oral Risedronate) study compared the efficacy and safety of monthly i.v. ibandronate (IBN) with oral risedronate (RIS) in patients (pts) with primary osteoporosis. The aim of the study was to show non-inferiority of IBN versus RIS in the incidence of non-traumatic vertebral fractures. We present 3-year efficacy data and examine the relationship between bone mineral density (BMD) increases and vertebral fracture risk reduction.

Methods: MOVER was a randomized, double-blind study in ambulatory pts aged ⩾60 years with fragile bone fracture, BMD of the lumbar spine L2–L4 or proximal femur (hip and femoral neck) <80% of the young adult mean (T-score: –1.7, –1.6, and –1.4), and 1–5 vertebral fractures in the thoracic and lumbar spine. 1265 pts were randomized to receive i.v. IBN 0.5 or 1 mg/month + oral daily placebo, or oral RIS 2.5 mg/day (licensed Japanese dose) + monthly i.v. placebo.

Results: The per-protocol set comprised 1134 pts (IBN 0.5 mg n=376, IBN 1 mg n=382, RIS n=376). Baseline patient characteristics were balanced across the groups. Over 3 years, cumulative incidences of new/worsening vertebral fractures were 19.9% (95% CI 15.6–24.1) for IBN 0.5 mg, 16.1% (95% CI 12.2–19.9) for IBN 1 mg, and 17.6% (95% CI 13.6–21.6) for RIS. Both IBN doses were non-inferior to RIS (non-inferiority limit 1.55): 0.5 mg, hazard ratio (HR) 1.09 (95% CI 0.77–1.54); 1 mg, HR 0.88 (95% CI 0.61–1.27). The 1 mg IBN group showed a 27% relative risk reduction in the incidence of the major six non-vertebral fractures, and a 15% reduction in total clinical fractures versus RIS. BMD gains were substantial at all sites and significantly improved from baseline with all treatments after 6 months. Fracture-free pts achieved greater hip BMD gains with 1 mg IBN (3.4%) than with RIS (2.1%). Hip BMD gains after 6 months predicted the future risk reduction of vertebral fractures. Reductions in bone turnover markers were substantial with all treatments after 3 months.Conclusions: These data show non-inferiority of monthly i.v. IBN to the licensed Japanese daily oral dose of RIS in reducing the incidence of vertebral fractures in Japanese pts with osteoporosis. The results suggest that BMD gains after 6 months of treatment with 1 mg i.v. monthly IBN could lead to vertebral fracture risk reduction. Monthly 1 mg IBN injections could be an alternative option for the long-term treatment of osteoporosis in Japanese pts.

***Disclosures: Hiroshi Hagino**, Asahi Kasei Pharma, Astellas Pharma, Banyu Pharmaceutical Co, Chugai Pharmaceutical Co Ltd, Eisai Co Ltd, Eli Lilly Japan KK, Mitsubishi Tanabe Pharma Corp, Ono Pharmaceutical Co Ltd, Pfizer Inc, Takeda Pharmaceutical Co Ltd, and Teijin Pharma Ltd, 2*
This study received funding from: Chugai Pharmaceutical Co. Ltd, Japan

SA0382

Differential Effects of Intravenous Bisphosphonates on First-dose Acute-phase Reactions in a Clinical Setting. Albrecht Popp*, Renate Senn, Helene Buffat, Christoph Senn, Philipp Popp, Ivanka Curkovic, Kurt Lippuner. Department of Osteoporosis, University Hospital & University of Berne, Switzerland

Introduction: Intravenously administered aminobisphosphonates (BP) such as zoledronate 5 mg once yearly (ZOL) and ibandronate 3 mg every three months (IBN) are first line therapies of postmenopausal osteoporosis. First-dose acute-phase reactions (APR) are common side-effects occurring within 24 to 72 hours after IV BP administration. In the randomized controlled pivotal trials (RCTs) with ZOL and IBN, reported APR rates were 31.6% after a BP washout period dependent on previous use (HORIZON study)[1] and 4.9% after exclusion of women with oral BP use in the previous 6 months or any previous use of IV BP (DIVA study)[2], respectively. The aim of the present study was to determine the APR rate after the first IV infusion of ZOL or IBN under conditions of daily practice.

Methods: Consecutive postmenopausal women with osteoporosis treated with either IV ZOL or IBN at the Department of Osteoporosis of the University Hospital of Berne, Switzerland, were included. All patients completed a standardized recall questionnaire administered by a trained physician three months after the first IV infusion. Recorded signs and symptoms during the first 3 days after IV infusion were: myalgia, arthralgia, pyrexia, tiredness, nausea, chills, and vertigo, with the presence of one or more items being regarded as an APR. The prevalence of first-dose APR was compared between ZOL and IBN, overall as well as in BP-naïve and BP-pretreated patients.

Results: First-dose IV BP was administered to 725 women (314 IBN and 411 ZOL). Groups did not significantly differ with regard to mean age, BMI, BMD, and prevalent vertebral fractures. APR were reported by 302 women (42%), significantly more frequently with ZOL (N=197, 48%) than with IBN (N=105, 33%), $p < 0.001$. Women in the IBN group were significantly more likely to have received prior HRT (10 vs. 5%, p=0.011) or prior BP therapy (72 vs. 62%, p=0.006). However, among BP-naïve patients, APR remained significantly more frequent in women after ZOL than IBN (69% vs. 38%, $p < 0.001$). When comparing BP-pretreated with BP-naïve patients, the APR rate was significantly lower with ZOL ($p < 0.001$) but not with IBN (p=0.289).

Conclusion: After first-dose IV BP administration, APR were consistently more frequent than reported in pivotal RCTs and more frequent with ZOL than with IBN. Pretreatment with a BP reduced the rate of first-dose APR in patients treated with ZOL only.

References:

1. Black DM, Delmas PD, Eastell R, et al. Once-yearly zoledronic acid for treatment of postmenopausal osteoporosis. The New England journal of medicine 2007;356:1809-22.

2. Delmas PD, Adami S, Strugala C, et al. Intravenous ibandronate injections in postmenopausal women with osteoporosis: one-year results from the dosing intravenous administration study. Arthritis and rheumatism 2006;54:1838-46.

***Disclosures: Albrecht Popp**, None.*

SA0383

Effect of Denosumab Two Years Therapy in Women with Osteoporosis and Contraindications to Oral Bisphosphonates on Bone Mineral Density – One Centre Open Study Results. Andrzej Sawicki*. Synexus Poland, Poland

Andrzej Sawicki

Medical Centre Synexus, Warsaw, Poland

Objectives: In FREEDOM trial denosumab treatment was well-tolerated and significantly increased BMD. The aim was to evaluate whether osteoporotic women with contraindication to oral bisphosphonates treatment (e.g. GERD) or intolerance or resistance, have positive effect on bone mass after denosumab as in FREEDOM study patients, in open study in one out-patients clinic. We report observational BMD results from the first 2 years of treatment.

Materials/Method: The study was performed in 85 women with osteoporosis aged 29 to 87 with contraindication to oral bisphosphonates treatment or intolerance or resistance. Bone Mineral Densitometry (BMD) was assessed by Hologic 4500 before and after 6, 12, 18 and 24 months denosumab treatment and calcium and vitamin D daily.

Results:

Table1 : Percentage change in BMD from baseline and after 6, 12, 18 , 24 months denosumab

Note: number of patients in 6, 12, 18, 24 months groups is not the same.

Denosumab treatment was well accepted and tolerated.

Conclusions: These data demonstrated that denosumab treatment for up to 2 years in patients with contraindication to oral bisphosphonates treatment or intolerance or resistance was associated with continued gains in BMD in patients and have similar positive effect on bone mass as in FREEDOM study patients.

Acknowledgement: This study was supported by Synexus.

Disclosure of Interest: Andrzej Sawicki is Senior Medical Adviser for Synexus. Research grants from Amgen, Aventis, Astra Zeneca, Danone, Eli Lilly, Servier, Novartis, Pfizer, MSD, and Roche

Months / Region	6 m	12m	18 m	24 m
L1-L4	+ 4,45	+5,58	+8,97	+ 6, 14
F Neck	+3,98	+3,73	+ 3,98	+5,01
Total Hip	+2,47	+2,55	+3,46	+2,66

Table 1

***Disclosures: Andrzej Sawicki**, None.*

SA0384

Effect of odanacatib on BMD and fractures: Results from Bayesian univariate and bivariate meta-analyses. Olga Gajic-Veljanoski*[1], George Tomlinson[2], Jeevitha Srighanthan[3], Jonathan Adachi[4], Robert Josse[5], Jacques P. Brown[6], Angela M. Cheung[7]. [1]University Health Network, Canada, [2]Dalla Lana School of Public Health, University of Toronto, Canada, [3]Osteoporosis Program, University Health Network, Toronto, Canada, [4]St. Joseph's Hospital, Canada, [5]St. Michael's Hospital, University of Toronto, Canada, [6]CHU de Québec Research Centre, Canada, [7]University Health Network-University of Toronto, Canada

Odanacatib (ODN) is a selective cathepsin K inhibitor that increases BMD and is currently in Phase 3 development for fracture prevention.

We systematically reviewed Medline, EMBASE, Cochrane library, conference proceedings and bibliographies, and included RCTs that compared ODN 50mg/week

to placebo for at least 12 months and reported BMD and / or fractures as adverse events. We used Bayesian univariate and bivariate meta-analyses to estimate the efficacy of ODN on BMD and fractures in current trials and to predict these in a future trial. Bayesian bivariate meta-analysis accounts for all available data and within- and between-study correlations between the treatment effects on BMD and fractures.

Of 31 potentially eligible articles, 6 articles describing 4 RCTs (788 patients, duration 1-5 years) were included. Table shows the effect of ODN on BMD based on Bayesian univariate meta-analysis. Bayesian bivariate meta-analysis resulted in similar results with narrower credible intervals. Greater duration of ODN use was associated with greater percent increase in BMD: LS BMD by 1.3%/year (95%CrI [Credible Interval]: 0.1, 2.2), TH BMD by 1.1%/year (95%CrI: 0.5, 1.7) and FN BMD by 1.1%/year (95%CrI: 0.4, 1.8). The predicted mean increase in BMD over 1-3 years, adjusted for the effect on fractures, in a future trial ranged between 2.3% and 7.5% for LS, 1.4% and 5.1% for TH, and 1.5% and 5.2% for FN. ODN for 2-3 years decreased odds of all fractures (population OR=0.3, 95%CrI: 0.1, 0.8). After accounting for the effect on BMD, ODN over 1-3 years decreased future odds of all fractures by 50% (future OR=0.5, 95%CrI: 0.1, 1.6). Evidence weighted odds of any benefit on both bone outcomes were 9:1 in current and future trials. Our estimates remained robust in sensitivity analyses.

In conclusion, we predict that ODN will increase BMD and decrease all fractures in the Phase 3 fracture outcome trial. Whether our prediction of benefit is in a similar range to that observed remains to be seen.

Table. Effect of ODN on BMD: Bayesian univariate meta-analysis

Duration of Treatment Years	Lumbar Spine (LS) Mean Difference, % (95% CrI)	Total Hip (TH) Mean Difference, % (95% CrI)	Femoral Neck (FN) Mean Difference, % (95% CrI)
1 year	4.0 (1.6, 6.5)	2.1 (-0.1, 4.3)	2.2 (0.0, 4.4)
2 Years	4.6 (1.9, 7.3)	3.4 (1.1, 5.7)	3.8 (1.4, 6.2)
1-3 Years	5.0 (2.6, 7.4)	3.4 (1.3, 5.6)	3.4 (1.3, 5.8)
1-5 Years	5.2 (2.8, 7.7)	3.4 (1.3, 5.7)	3.7 (1.4, 5.9)

Table. Effect of ODN on BMD: Bayesian univariate meta-analysis

***Disclosures: Olga Gajic-Veljanoski**, None.*

SA0385

Efficacy and Safety of Zoledronic Acid in Postmenopausal Osteoporosis Patients Between 50-65 Years Old. NURTEN ESKIYURT*[1], Rezzan Gunaydin[2], Belgin Erhan[3], Hatice Bodur[4], Mehmet Kırnap[5], Vesile Sepici[6], Banu Kuran[7], Gulay Dincer[8], Hatice Ugurlu[9], Bulent Butun[10], Serhan Sevgi[11], Merih Sarıdogan[12]. [1]Istanbul University, Turkey, [2]Izmir Training & Research Hospital, Turkey, [3]Istanbul Physical Treatment & Rehab. Training & Research Hospital, Turkey, [4]Ankara Numune Trainig & Research Hospital, Turkey, [5]Erciyes University Faculty of Medicine, Turkey, [6]Gazi University Faculty of Medicine, Turkey, [7]Sisli Etfal Training & Research Hospital, Turkey, [8]Ankara University Faculty of Medicine, Turkey, [9]Necmettin Erbakan University Faculty of Medicine, Turkey, [10]Akdeniz University Faculty of Medicine, Turkey, [11]Novatis Pharma, Turkey, [12]Istanbul University Cerrahpasa Faculty of Medicine, Turkey

Purpose : Although many osteoporosis patients are under 65 years old, studies evaluating the response to bisphosphonates (BP) have usually focused on older (>65 years) postmenopausal patients . In this study, the efficacy and safety of single IV infusion of zoledronic acid 5 mg on both bone mineral density (BMD) and serum bone turnover markers were assessed in ''relatively younger'' (50-65 years old) population of postmenopausal osteoporosis (PMO) patients.

Methods: 112 PMO patients 55-65 years of age (mean age 58.4) were enrolled in this open label, prospective, 1 year, multicenter (12 centers) study. 101 patients (90.2%) of them completed the trial The change in BMD in lumbar spine (L1-L4) and femoral neck assessed by DEXA at 12 months were the primary endpoints. The serum bone turnover markers (procollagen 1N-terminal peptide (P1NP) and C-telopeptide (CTX)) were evaluated at 6 and 12 months as secondary endpoints. Safety evaluation was based on adverse event (AE) reporting. The study was approved by institutional and central ethics committees.

Results: Zoledronic acid increased BMD in femoral neck and lumbar spine at 1 year versus baseline by 5.2% and 13.1%, respectively. ($p<0.001$ for both in per protocol population). Serum P1NP and CTX levels decreased significantly versus pretreatment values at 6 and 12 months. The mean P1NP level was 51.3 ± 22 ng/ml at baseline and decreased to 18.5 ± 10.5 ng/ml and 21.9 ± 10.5 ng/ml at 6 and 12 months respectively ($p<0.001$ for both). The mean serum CTX level which was 345.6 ± 161.7pg/ml at baseline decreased to $125,4 \pm 78.8$ pg/ml and 164.6 ± 9.7 pg/ml at 6 and 12 months, respectively ($p<0.001$ for both). 42 patients (37.5%) experienced 88 AEs which were mostly (77.3%) mild and moderate in severity. Myalgia (n=29) and arthralgia (n=10) were the most common adverse events. 7 serious AEs were observed in 2 (1.8%) patients: concurrent coronary artery disease and acute myocardial infarction in one patient and concurrent nausea, vomiting, hypotension, cholelithiasis and cholecystectomy in the other patient. No cases of deterioration of renal function, atrial fibrillation or osteonecrosis of the jaw were observed. Deterioration of renal functions, atrial fibrillation and osteonecrosis of jaw attributed to BFs were not observed. No patient was withdrawn from the study due to AEs.

Conclusion: Single infusion of zoledronic acid 5mg was associated with significant improvements in BMD and serum bone turnover markers in 50-65 years old PMO patients and favorable overall tolerability profile. The efficacy and safety profile of zoledronic acid infusion observed in this study conforms to the results of previous studies conducted in elderly (>65 years) patients.

***Disclosures: NURTEN ESKIYURT**, None.*
This study received funding from: Novartis Pharma

SA0386

Efficacy and Safety Results from a Six Month Double-Blind Study Comparing 60 mg Denosumab (DMAb) and Placebo in Korean Postmenopausal Women with Osteoporosis. Jung-Min Koh*[1], Han-Jin Oh[2], Il Hyung Park[3], In-Ju Kim[4], Moo-Il Kang[5], Sung-Kil Lim[6], Yong-Ki Min[7], Yoon-Sok Chung[8], Yil-Seob Lee[9], Barbara Kravitz[10], Brian Waterhouse[10], Antonio Nino[10], Lorraine Fitzpatrick[10]. [1]Asan Medical Center, South Korea, [2]Cheil General Hospital, Kwandong University, South Korea, [3]Kyungpook National University Hospital, South Korea, [4]Pusan National University Hospital, South Korea, [5]Seoul St. Mary's Hospital, South Korea, [6]Yonsei University College of Medicine, South Korea, [7]Samsung Medical Center, South Korea, [8]Ajou University School of Medicine, South Korea, [9]GlaxoSmithKline Pharmaceuticals, South Korea, [10]GlaxosmithKline Pharmaceuticals, USA

Purpose: To determine the efficacy and safety of denosumab compared with placebo in Korean postmenopausal women with osteoporosis.

Methods: This randomized, double-blind, placebo-controlled multicenter study in Korea enrolled 135 postmenopausal women with osteoporosis, aged 60-90 years, with serum 25(OH) vitamin D $\geq$50 nmol/L. Other inclusion criteria included a screening DXA BMD equivalent to a T-Score <-2.5 and $\geq$ -4.0 at either the lumbar spine or total hip. Changes in BMD at the lumbar spine, total hip, femoral neck, and trochanter, serum bone turnover markers, (s-CTx and s-PINP), and safety were evaluated. All subjects received daily supplements of oral calcium (at least 1000 mg) and vitamin D (at least 400 IU). All sites obtained approval from their Ethics Committees and all subjects signed informed consent.

Results: Treatment groups were comparable at baseline and mean age was 66.5 years (SD 4.83). After 6 months of treatment the difference in mean % changes from baseline between DMAb and placebo was statistically significant at the lumbar spine (primary endpoint), total hip, femoral neck and trochanter (Table 1). After 6 months of treatment the difference in median % changes from baseline between DMAb and placebo was statistically significant for s-CTx and s-PINP (Table 2). No new safety signals were detected with 55% DMAb and 48% placebo subjects experiencing adverse events. Six subjects (DMAb) and two (placebo) experienced serious adverse events; none attributed to study drug by investigators.

Conclusions: After 6 months of treatment, DMAb statistically significantly increased BMD at the lumbar spine, total hip, femoral neck and trochanter and significantly decreased serum bone turnover markers, s-CTx and s-PINP compared to placebo. No new or unexpected safety signals were detected.

This study was sponsored by GlaxoSmithKline Pharmaceuticals.

Table 1 BMD Results by Anatomical Site

6 Month Difference between DMAb and Placebo in % change from baseline in BMD	Model Adjusted Mean	95% CI	p-value
Lumbar spine	3.2%	(2.1%, 4.4%)	<0.0001
Total hip	1.7%	(1.0%, 2.4%)	<0.0001
Femoral neck	1.4%	(0.4%, 2.3%)	0.0042
Trochanter	2.0%	(0.8%, 3.2%)	0.0012

Table 2 Serum Bone Turnover Markers

6 Month Difference between DMAb and Placebo in % change from baseline	Median	95% CI	p-value
s-CTx	-52%	(-61%, -43%)	<0.0001
s-PINP	-48%	(-57%, -39%)	<0.0001

Efficacy Results:Comparing Denosumab and Placebo

***Disclosures: Jung-Min Koh**, None.*
This study received funding from: GlaxoSmithKline Pharmaceuticals

SA0387

Factors associated with negative BMD response to Risedronate. Ryoichi Muraoka[1], Ryo Okazaki*[2]. [1]Ajinomoto Phamaceuticals Co, Ltd., Japan, [2]Teikyo University Chiba Medical Center, Japan

Objectives: Risedronate (RIS) has been shown to inhibit osteoporotic fractures and widely used in the world. However, there are some non-responders in terms of BMD increase. We performed post-hoc analyses of two RIS Phase III trials (including the Phase III trial of once-a-month 75 mg tablet) conducted in Japan to explore factors associated with negative BMD response to RIS.

Subjects and methods: 1261 subjects whose serum 25(OH)D were measured prior to RIS administration and lumber spine BMD data were available both at the baseline and at least once after RIS treatment were analyzed (once-a-day 2.5mg: 641 patients, once-a-week 17.5mg: 228 patients, once-a-month 75mg: 392 patients). In those trials vitamin D supplementation was not given. Subjects were classified into non-responders (NR)(n=118) whose BMD change was equal to or less than 0% and responders (R) (n=1143). We conducted logistic regression analyses in which NR was a response variable. Baseline serum(s) 25(OH)D, sBAP, urinary(u) NTX, and uCTX levels were transformed into dichotomous variables with cut-off values at 16 ng/mL (the 1st quartile of the study population), 21.1 U/L, 35.3 nmolBCE/mmol-Cr, 184.1 ug/mmol-Cr (mean+1.0 SD for Japanese premenopausal women), respectively. Comorbid diseases, demographic profiles, drug adherence (actual number of tablets taken/ prescribed number by the protocol * 100), existing vertebral fracture, and baseline BMI, Ca and P were also added as independent variables.

Results: Among those variables, 4 factors were significantly associated with NR: low 25(OH)D [OR (odds ratio) 1.978, P= 0.018], low BAP (OR 1.959, P= 0.0028), presence of hypertension (OR 0.610, P = 0.0409), and poor drug adherence (1% decrease OR 1.026, P= 0.0490). In subjects with low 25(OH)D, 14.0% were NR, whereas 8.1% in higher 25(OH)D group (P= 0.0032). Those results were not different among once-a-day, once-a-week, once-a-month treatment groups.

Conclusions: These results confirm that vitamin D deficiency is an easily correctable condition associated with a poor response to RIS. Serum 25(OH)D level should be adequately increased prior to RIS treatment to ensure positive BMD response to RIS.

***Disclosures: Ryo Okazaki**, None.*

SA0388

See Friday Plenary Number FR0388.

SA0389

The Effect of 6 versus 9 Years of Zoledronic Acid Treatment in Osteoporosis: A Randomized Extension to the HORIZON-Pivotal Fracture Trial (PFT). Dennis Black*[1], Ian Reid[2], Jane Cauley[3], Steven Boonen[4], Felicia Cosman[5], Ping Leung[6], Peter Lakatos[7], Zulema Man[8], Steven Cummings[9], Trisha Hue[1], Guoqin Su[10], Christina Bucci-Rechtweg[11], Monique Tan[10], Paul Aftring[10], Richard Eastell[12]. [1]University of California, San Francisco, USA, [2]University of Auckland, New Zealand, [3]University of Pittsburgh Graduate School of Public Health, USA, [4]Center for Metabolic Bone Disease & Division of Geriatric Medicine, Bel, [5]Helen Hayes Hospital, USA, [6]Chinese University of Hong Kong, China, [7]Semmelweis University Medical School, Hungary, [8]Centro Médico TIEMPO, Argentina, [9]San Francisco Coordinating Center, USA, [10]Novartis pharmaceuticals, USA, [11]Novartis Pharmaceuticals Corporation, USA, [12]University of Sheffield, United Kingdom

Purpose: Zoledronic acid 5 mg (ZOL) used annually for 3 years is effective in increasing bone mineral density (BMD) and decreasing fractures. BMD and fracture results from the extension to 6 years suggested that patients at high risk of fracture may benefit from maintenance of BMD and reduced risk of new vertebral fracture with continued annual ZOL therapy up to 6 years. This subsequent extension will assess efficacy and long term safety of ZOL in post-menopausal women with osteoporosis after 9 consecutive annual doses.

Methods: 190 women who had received ZOL for 6 years in both the core and extension-1 studies were randomized to 3 additional years of ZOL (Z9) or placebo (Z6P3). The primary endpoint for comparison of Z9 with Z6P3 is percentage change in total hip (TH) BMD at Year (Y) 9 vs. Y6. Secondary endpoints include TH and femoral neck (FN) BMD at Y7, Y8, and Y9 vs. Y0, at Y7 and Y8 vs Y6, and FN at Y9 vs Y6; biochemical markers (β-C-terminal telopeptides of type 1 collagen [β-CTx], procollagen type 1 amino-terminal propeptide [P1NP] and bone-specific alkaline phosphatase [BSAP]) at Y7, 8 and 9 vs Y6; exploratory endpoints include incidence of clinical and vertebral fractures after Y6 and safety.

Results: Among the women randomized, the mean age was 78 years with 28% over age 80. 63% were from Europe, 32% from N/S America and 6% from Asia. The last patient was seen in April 2013. As of the time of this submission, the study remains blinded. However, the data will be unblinded and analyses completed by August 2013, so results may be presented during the meeting.

Conclusion: This extension will provide unique data on the effect of 9 annual injections of ZOL on BMD.

***Disclosures: Dennis Black**, Amgen, Lilly, 2; Merck, Novartis, 6*
This study received funding from: Novartis AG

SA0390

The Pharmacokinetics of Odanacatib 50 mg Are Not Affected by Severe Renal Insufficiency. Aubrey Stoch*[1], Chengcheng Liu[2], Stefan Zajic[3], Rose Witter[2], Julie Stone[2], Anish Mehta[2], Patrice Auger[4], Daria Stypinski[4], Nancy Wang[4], Anne Hohnstein[4], William Smith[5], Harry Alcorn[6], Thomas Marbury[7]. [1]Merck Sharp & Dohme, USA, [2]Merck Sharp & Dohme Corp., USA, [3]Merck Research Laboratories, USA, [4]Celerion, USA, [5]Volunteer Research Group/ Graduate School of Medicine, University of Tennessee, USA, [6]DaVita Clinical Research, USA, [7]Orlando Clinical Research Center, USA

Objectives: Odanacatib, a selective cathepsin-K (CatK) inhibitor, is in development for the treatment of osteoporosis. Approximately 10% of the clearance of odanacatib is believed to be due to renal elimination. This study was done to determine the effect of severe renal insufficiency on odanacatib pharmacokinetics, pharmacodynamics, and tolerability.

Methods: In this open-label, single-dose study, odanacatib was orally administered to subjects (age: 40-79 years) with severe renal insufficiency (defined as a creatinine clearance of <30 mL/min) and healthy control subjects (creatinine clearance $\geqslant 90$ mL/min), matched for age, gender, and body mass index (BMI). Plasma and urine samples were collected for the analysis of odanacatib concentrations and biomarkers at predose and at specified time points over 15 days postdose. An analysis of covariance (ANCOVA) model was used to analyze odanacatib $AUC_{0-\infty}$ on log scale. The $AUC_{0-\infty}$ geometric mean ratio (GMR) was determined to evaluate the similarity of pharmacokinetics between the two groups based on the 90% CI for the GMR contained within the comparability bounds of (0.40, 2.50). C_{max} was analyzed in a similar fashion. Summary statistics were computed for T_{max} and apparent terminal $t_{1/2}$. Bone biochemical markers (serum NTx and urine NTx/Creatinine) were also assessed to evaluate pharmacodynamics; a linear mixed effect model was used for the analysis of these parameters. Adverse events (AEs) were monitored throughout the study and evaluated for severity and relation to study medication at study visits.

Results: The GMRs (90% CI) for $AUC_{0-\infty}$ and C_{max} were 1.62 (1.17, 2.24) and 1.47 (1.19, 1.80), respectively. The geometric mean half-life for odanacatib 50 mg was 74.2 hours subjects with renal impairment and 80 hours in the healthy matched controls. At 168 hours postdose, Least Square (LS) Mean (95% CI) serum NTx values were -36.5 (-47.30,-23.38) [renal impairment] and -43.2 (-53.39, -30.76) [healthy]; LS Mean (95% CI) urine NTx/Cr values were -59.3 (-65.81, -51.51) [renal impairment] and -43.4 (-52.83, -32.08) [healthy]. There were no serious AEs or discontinuations due to AEs. Mild headache was the most common drug-related AE and was reported in 1 patient in the renal impairment group and 1 patient in the healthy control group.

Conclusions: There were no meaningful differences between subjects with severe renal impairment compared with healthy-matched controls in odanacatib 50 mg pharmacokinetics, as assessed by comparison of $AUC_{0-\infty}$ values, or its pharmacodynamics, as assessed by change from baseline in serum NTx and urine NTx/Cr. Odanacatib 50 mg was generally well tolerated in patients with severe renal impairment.

***Disclosures: Aubrey Stoch**, Merck , 3*
This study received funding from: Merck Sharp & Dohme Corp. sponsored this study

SA0391

See Friday Plenary Number FR0391.

SA0392

Baseline characteristics of a prospective observational study in Germany, Austria, Greece and Belgium to evaluate medication-taking behavior of women with postmenopausal osteoporosis (PMO) receiving denosumab (DMab) in clinical practice. Nikolaos Papaioannou*[1], Astrid Fahrleitner-Pammer[2], Maurille Feudjo Tepie[3], Gerd Moeller[4], Eddie Zhang[3], Peyman Hadji[5]. [1]University of Athens, KAT Hospital, Greece, [2]Medical University Graz, Austria, [3]Amgen Ltd, United Kingdom, [4]Amgen (Europe) GmbH, Switzerland, [5]Philipps-University of Marburg, Germany

Purpose: Persistence to osteoporosis therapy is important for optimal outcomes, particularly reduced fracture risk. Therapies with frequent administration schedules are associated with poor adherence and persistence which may negatively affect their fracture risk reduction. A large observational study is being conducted to evaluate

persistence and adherence to 6-monthly subcutaneous DMAb injections. We report baseline data from this study.

Methods: This ongoing, non-interventional study plans to enroll 1500 women with PMO receiving DMab in clinical practice in Germany, Austria, Greece and Belgium. Data recorded as per clinical practice is collected for 2 years after enrolment, with pts expected to return every 6 months as part of their routine care and no additional procedures required. Study outcomes include pt characteristics, and persistence and adherence to DMab at 12 and 24 months. Centers in Belgium started enrolment later than other countries, and did not have baseline data at the time of this analysis. Hence we report data from pts enrolled at 101 centers in Germany, Austria and Greece.

Results: As of February 2013, 1200 pts had enrolled and were included in the analysis; with half (n=600) enrolled at sites in Germany, and one-quarter (300) each at sites in Austria and Greece. Pts had multiple co-morbidities, with PMO diagnosed, on average, 6 years prior to enrolment (Table 1). Approximately half of all pts had prior osteoporotic fracture (Table 1); over 80% had received PMO therapy prior to enrolment with the majority receiving oral bisphosphonates (Table 2). Baseline DXA assessments were not mandatory, and were available (at the physician' discretion) for 83% (n=991) of pts. Mean (SD) baseline BMD T-scores at total hip (n=674) and lumbar spine (n=948) were -2.0 (0.84) and -2.7 (0.98), respectively.

Conclusions:

These baseline data provide valuable information regarding pts being prescribed DMab in routine clinical practice in Germany, Austria and Greece. The pts enrolled in the current study have baseline characteristics typical of the general PMO population, i.e. multiple co-morbidities, history of osteoporotic fracture. Moreover, the majority of pts had received PMO therapies prior to initiating Dmab yet baseline BMD remained low. Future data from this study will provide additional insights regarding persistence with DMab in women with PMO.

Table 1. Baseline age and disease characteristics

	All patients (N=1200)
Age, mean (SD), years	70.6 (9.3)
Aged ≥75 years, n (%)	417 (35)
Years since PMO diagnosis*, mean (SD)	6.2 (6.0)
Historical osteoporotic fracture†, n (%)	586 (49)
Vertebral, n (%)	244 (20)
Non-vertebral, n (%)	426 (36)
At least one co-morbidity, n (%)	1098 (92)
Number of co-morbidities, mean (SD)	3.2 (2.3)
Number of baseline prescription medications, mean (SD)	2.4 (2.7)
Prior glucocorticoid use, n (%)	126 (11)
Prior secondary osteoporosis, n (%)	137 (11)
Prior hospitalization for osteoporotic fracture, n (%)	177 (15)
At least one fall in the 12 months prior to enrolment, n (%)	209 (17)
Height loss greater than 2cm, n (%)	607 (51)

n, number of patients; PMO, post menopausal osteoporosis

*Time since diagnosis to first DMab injection; †Excludes fractures of the skull, facial bones, fingers and toes, fractures associated with known high trauma severity, and pathological fractures.

Table 1

Table 2. PMO treatment history

	All patients (N=1200)
Prior PMO therapy, n (%)	1028 (86)
Calcium supplements	555 (46)
Vitamin D supplements	555 (46)
Oral bisphosphonate	712 (59)
Oral strontium ranelate	138 (12)
IV ibandronate	131 (11)
PTH/Teriparatide	98 (8)
IV zoledronate	90 (8)
Number of prior PMO medications excluding vitamin D, calcium and HRT, mean (SD)	1.3 (1.2)
PMO therapy in the 12 months prior to enrolment, n (%)	914 (76)

HRT, hormone replacement therapy; IV, intravenous; n, number of patients; PMO, post menopausal osteoporosis

Table 2

***Disclosures: Nikolaos Papaioannou**, Amgen, Eli Lilly, 6; Amgen and Servier,; Amgen, 2 This study received funding from: Amgen and GlaxoSmithKline*

SA0393

Healthcare Consequences Associated With Non-Compliance in a Managed Care Population. Ankita Modi*[1], Jackson Tang[2], Ethel Siris[3], Shuvayu Sen[1]. [1]Merck & Co., Inc., USA, [2]AsclepiusJT LLC, USA, [3]Columbia University College of Physicians & Surgeons, USA

OBJECTIVE: To examine consequences associated with non-compliance to osteoporosis (OP) medication in terms of fracture rates and healthcare resource utilization

METHODS: A retrospective analysis using i3 Invision Datamart (Ingenix, Eden Prairie, MN) from January 1, 2001 to December 31, 2010 (study period) was conducted. Women ⩾55 years of age who initiated an OP medication (alendronate, ibandronate, risedronate, zoledronate, raloxifene, calcitonin, teriparatide) during the study period and had enrolled in the database for 3 consecutive years: 1 year before the index prescription (baseline), a compliance year (year 1), and a follow-up year (year 2) were included in the study. Subjects were excluded if they had Paget's disease or diagnosis of malignant neoplasm. Non-compliance to OP medication was defined as medication possession ratio (MPR) <0.8 during year 1 (MPR = total number of days' supply/365 days). Occurrence of OP-related hip, vertebral, and non-vertebral fracture and healthcare resource use were assessed during year 2. Logistic regression was conducted to assess the association of non-compliance on occurrence of fractures and healthcare resources and Poisson regression was conducted to assess the association with number of healthcare events.

RESULTS: Among 57,913 women who met eligibility criteria, 34,483 (59.5%) were non-compliant to OP therapy during year 1 (mean [SD] age, 64.2 [8.9] years). Compared to compliant patients (N=23,430 (40.5%)), a significantly higher proportion of non-compliant patients developed vertebral (0.79% vs. 0.48%), hip (0.42% vs. 0.25%) and non-vertebral (1.93% vs.1.52%) fractures during year 2 (all p<0.01). Logistic regression showed that non-compliance was associated with a higher likelihood of fractures (Odds ratio (OR): 1.19, 95%CI: [1.06,1.30]) and hospitalization occurrence (OR: 1.16, 95%CI: [1.10,1.23]). Poisson regression showed that non-compliance was associated with more hospitalization stays (incidence rate ratio: 1.27, 95%CI: [1.19,1.33]).

CONCLUSION: Rate of non-compliance was found to be high in a managed care population with osteoporosis. Non-compliance was associated with a higher rate of osteoporotic fractures and healthcare utilization. The results emphasize the importance of good treatment compliance in order to achieve optimal treatment benefit and thereby reduce the burden that osteoporosis and its associated fractures place on individuals and healthcare systems.

***Disclosures: Ankita Modi**, Merck, 7; Merck, 3*

SA0394

Non-pharmacological Strategies used by Patients at High Risk for Future Fracture to Manage Fracture Risk - A Qualitative Study. Joanna Sale*[1], Monique Gignac[2], Gillian Hawker[3], Dorcas Beaton[4], Earl Bogoch[1], Fiona Webster[3], Lucy Frankel[1], Victoria Elliot-Gibson[1]. [1]St. Michael's Hospital, Canada, [2]University Health Network, Canada, [3]University of Toronto, Canada, [4]Keenan Research Centre, St Michael's Hospital, Canada

Purpose: We examined patients' understanding of bone health and self-management decisions regarding bone health and fracture risk, particularly behaviours other than medication use and seeking diagnostic testing.

Methods: A phenomenological (qualitative) study was conducted. English speaking patients 65+ years old, who were ''high risk'' for future fracture and prescribed pharmacotherapy after being screened through a post-fracture osteoporosis initiative were eligible. Patients were interviewed for 1-2 hours and were asked to discuss perceptions of bone health status (bone densitometry results, perceived fracture risk), recommendations received for bone health, and lifestyle changes since their most recent fracture. We analyzed the data guided by Giorgi's methodology.

Results: We interviewed 21 fracture patients (6 males, 15 females), aged 65 to 88 years old. With the exception of one participant, all participants appeared to understand that they had low bone mass and were at risk of sustaining another fracture. Most participants (n=20) were predominantly concerned about being careful and they focused their responses on personal and environmental factors that they perceived to be modifiable. Participants also spoke about strategies to manage their bone health such as exercise, having a healthy diet and taking supplements, and using aids and devices. Non-pharmacological strategies used by patients appeared to be independent of current use of pharmacotherapy.

Conclusions: Awareness of fracture risk was accompanied by a number of positive lifestyle changes in participants' lives such as being careful and engaging in exercise. Future research needs to evaluate how lifestyle changes such as being careful mitigate fracture risk.

***Disclosures: Joanna Sale**, None.*

SA0395

Patterns and Predictors of Osteoporosis Medication Switching in Low-Income Elderly Patients. Daniel Solomon*[1], David Chandler[2], Erika Brown[3], Helen Mogun[3], Jessica Myers Franklin[3]. [1]Harvard Medical School, USA, [2]Amgen, USA, [3]Brigham & Women's Hospital, USA

Background: Patterns and predictors of osteoporosis (OP) medication switching have not been well described.

Methods: An analysis of health and pharmacy insurance claims for a large cohort of low-income Medicare beneficiaries qualifying for state drug benefits (Pennsylvania PACE and New Jersey PAAD programs) for the years 1998-2008 was undertaken. Inclusion criteria for subjects were documented Medicare claims for 180 days (baseline) and no receipt of OP medications during the baseline (i.e., bisphosphonate, raloxifene, calcitonin, teriparatide, or hormononal therapy). All subjects were required to start an OP medication, and this was considered the start of follow-up. Baseline patient and prescriber characteristics were assessed in multivariable Cox regression models to identify correlates of adding or switching an OP medication. Clinical events after baseline (fractures, bone mineral density (BMD) testing, and visits with endocrinologists or rheumatologists) were also examined as correlates.

Results: Of 125,954 new users of OP medications, the mean age was 78 years, with 97% being female, and 92% of subjects were white. OP medication prescribers included endocrinologists/rheumatologists (6.2%), orthopedic surgeons (1.0%), PCPs (internists/FPs/GPs/OB-GYN) (64.9%), others (3.7%), and missing (24.1%). Of these subjects, 23% added or switched OP medications during follow-up, with the first addition or switch occurring a mean of 739 days after baseline; 4% added or switched more than once. In adjusted models, baseline variables that correlated with switching or adding and OP medication included: older age; female gender; the use of calcitonin, raloxifene, or teriparatide (compared with bisphosphonate); prescription from an endocrinologist/ rheumatologist or an orthopedic surgeon (versus PCPs); prior fracture; the use of steroids; prior malignancy; more prescription drugs or MD visits; and a prior osteoporosis diagnosis. Black race, prior BMD, increased comorbid conditions, and more acute care hospitalizations correlated with a reduced likelihood of switching or adding. However, the strongest predictors of switching or adding were post-baseline events: fractures, BMD testing and specialist visits.

Conclusion: Adding or switching OP medications is not uncommon and correlated with specific patient or prescriber characteristics. The frequency of adding and switching OP medications suggests the value of long-term sequential treatment strategy trials.

***Disclosures: Daniel Solomon**, Lilly, 6; Amgen, 6*
This study received funding from: Amgen

SA0396

Active Vitamin D3 Analog (eldecalcitol) Improves Muscle Strength and Dynamic Balance in Postmenopausal Osteoporotic Women. Kimio Saito*[1], Naohisa Miyakoshi[2], Michio Hongo[2], Yuji Kasukawa[2], Yoichi Shimada[3]. [1]Akita University, Japan, [2]Akita University Graduate School of Medicine, Japan, [3]Department of Orthopedic Surgery, Akita University Graduate School of Medicine, Japan

INTRODUCTION: Eldecalcitol, an active vitamin D3 analog, increases bone mass in osteoporotic patients. Additionally, it may reduce the incidence of falls, as has been reported with vitamin D. It is speculated that improvement of muscle strength or balance ability by eldecalcitol is one of the mechanisms by which it reduces the incidence of falls. However, details about the effects of eldecalcitol on trunk muscle strength and balance control remain unclear. The purpose of this study was to quantitatively evaluate whether eldecalcitol improves trunk muscle strength and balance control in postmenopausal osteoporotic women.

METHODS: Thirty-one postmenopausal women (mean age, 74 years) diagnosed with osteoporosis were enrolled in this prospective study and randomly divided into the following two groups: 1) the eldecalcitol group (n=17), which was prescribed eldecalcitol (0.75 μg/day) and alendronate (35 mg/week); and 2) the alendronate group (n=14), which was prescribed alendronate alone, serving as a control for eldecalcitol. Trunk muscle strength, including back extensor strength and iliopsoas strength, was measured. Static standing balance with a stabilometer was performed for static balance evaluation. Dynamic sitting balance with a dynamic stabilometer and the Timed Up and Go Test were performed for dynamic balance evaluation. These evaluations were recorded at the beginning of treatment and six months after the treatment.

RESULTS: No significant difference was observed in static standing balance before and after the treatment in both groups.Eldecalcitol significantly increased back extensor strength ($p=0.0011$) and iliopsoas strength ($p=0.0343$), and improved both dynamic sitting balance ($p=0.0496$) and the results of the Timed Up and Go Test ($p=0.0016$) after six months of treatment compared with their values at the start of treatment. However, alendronate alone treatment did not result in significant changes in these parameters.

CONCLUSIONS: The results of the present study demonstrate that eldecalcitol increases trunk muscles strength, including back extensor strength and iliopsoas strength, and improves dynamic balance within six months of treatment. Improvement in trunk muscle strength and dynamic balance by eldecalcitol may reduce the risk of falls in osteoporotic women.

***Disclosures: Kimio Saito**, None.*

SA0397

Fracture?, Think Osteoporosis: Rehabilitation of Patients Post Hip Fracture. George Ioannidis*[1], Naomi Dore[1], Pauline Fisher[2], Courtney Kennedy[1], Lisa Dolovich[1], Jonathan Adachi[3], Leo Farrauto[1], Alexandra Papaioannou[2]. [1]McMaster University, Canada, [2]Hamilton Health Sciences, Canada, [3]St. Joseph's Hospital, Canada

Background: Hip fracture patients are at high risk for recurrence. Appropriate pharmacotherapy reduces this risk and is associated with reduced mortality after hip fracture, but a care gap exists for fracture prevention in these patients. This evaluation determined rates of osteoporosis treatment and bone mineral density (BMD) testing in hip fracture patients following discharge from a rehabilitation unit. Methods: A prospective cohort study of hip fracture patients aged > 50 on an inpatient rehabilitation unit in 2008 and 2011. Patients were seen by a nurse specialist, and encouraged to see their family physician for further assessment and treatment. Physicians were sent a letter indicating the need to follow up with their patient. Patients were contacted following discharge from hospital to determine treatment rates.Results: Of 310 eligible hip fracture patients admitted to the rehabilitation unit in the years studied, 207 patients were reached post-discharge and provided data. For the entire cohort of n=207, the mean age was 81.4 (SD 9.14) years, and 57/207 (27.5%) were male. Of patients who were not previously taking osteoporosis medication, 50% of patients had osteoporosis treatment initiated by six months following discharge. By 2 months following discharge, 46% of patients in the 2008 cohort had a new BMD performed or scheduled, while this was true for 14% of patients from the 2011 cohort. In 2011, approximately 75% of patients had seen their family physician by 6 months following discharge. Discussion: Rates for osteoporosis treatment and BMD were higher than those reported in the literature for patients not enrolled in case manager programs. BMD testing declined from 2008 to 2011. Lower treatment rates may be due to concerns regarding bisphosphonates. There remains room for improvement for follow up with family physicians.

***Disclosures: George Ioannidis**, None.*
This study received funding from: Merck Frosst grant in aid

SA0398

VitaminD Supplementation Protocol in Osteoporosis: Chart Review. Vithika Sivabalasundaram*[1], Sandra Kim[2], Ina Radziunas[3], Sophie Jamal[1]. [1]The University of Toronto, Canada, [2]Women's College Hospital, University of Toronto, Canada, [3]Women's College Hospital, Canada

Introduction: There is strong evidence that vitamin D supplementation prevents against fractures, and many treatment options for osteoporosis require adequate vitamin D stores for improved efficacy. Current guidelines recommend supplementation to a target 25-OH vitamin D level of 75 nmol/L (30 ng/ml) or greater. The ideal dosing strategy to achieve this target however remains undetermined. In addition, given the high cost of vitamin D serum testing, a cost effective method of restoring and monitoring vitamin D levels is required. The purpose of this study is to evaluate the efficacy of a newly developed dosing protocol to guide vitamin D supplementation and testing.

Methods: This chart review gathered clinical information from 376 subjects seen in the Osteoporosis Program at Women's College Hospital who were found to be 25-OH vitamin D deficient (<50 nmol/L) or insufficient (50-74 nmol/L) and underwent treatment with the Vitamin D Protocol. This protocol outlined a specific algorithm for physicians to replace vitamin D. Patients were instructed to repeat blood work in 6 months. Patients with the following medical co-morbidities were excluded: renal failure, hypercalcemia, hypercalciuria, renal calculi and teriparatide therapy.

Results: 376 charts were reviewed and of the 325 eligible subjects, 169 (52%) completed post-protocol blood work. The mean increase in 25-OH vitamin D after treatment was 23.0 +/- 31.1 nmol/L. 56% of subjects achieved the target 25-OH Vitamin D level of 75 nmol/L or greater following the protocol. Patients with a post-protocol 25-OH vitamin D level <75 nmol/L were more likely to have a malabsoprtion syndrome (18.9% vs 7.4%, $p=0.02$) and took longer to complete their post protocol blood work (9.3 vs 7.9 months, $p=0.002$). Other demographic and clinical factors such as gender, age, BMI, baseline BMD and history of fragility fracture were similar in both groups.

Conclusion: This is the first protocol for vitamin D supplementation to be studied and demonstrates a significant improvement in vitamin D levels by nearly 50%. Compliance in our study was low with 52% of patients completing blood work. Among patients who completed their blood work within 6 to 6.9 months, 77% achieved target 25-OH vitamin D level of > 75 nmol/L, while only 45% of those who did blood work after 9 months reached target. Overall, this protocol was found to be safe and effective in those who demonstrated adequate compliance through timely blood work.

***Disclosures: Vithika Sivabalasundaram**, None.*

SA0399

Changes in Lumbar Spine QCT, DXA, and TBS in Postmenopausal Women With Low Bone Mass Treated With Denosumab, Alendronate, or Placebo. Thierry Thomas*[1], Angela M Cheung[2], Elizabeth Shane[3], Jose R Zanchetta[4], Ann Kearns[5], Didier Hans[6], Celia JF Lin[7], Matthew Austin[7], Cesar Libanati[7]. [1]INSERM U1059, University Hospital of St Etienne, France, [2]University of Toronto, Canada, [3]Columbia University, USA, [4]Instituto de Investigaciones Metabólicas, Argentina, [5]Mayo Clinic, USA, [6]Lausanne University Hospital, Center of Bone Diseases, Switzerland, [7]Amgen Inc., USA

Patients who suffer from osteoporosis require treatment with therapies aimed at reducing the risk of fracture. Fracture risk at the spine is significantly influenced by trabecular bone. Quantitative computed tomography (QCT) and dual x-ray absorptiometry (DXA) allow for bone mineral density (BMD) measurement at the spine, and BMD is a robust indicator of fracture risk. Trabecular bone score (TBS), a novel gray-level measurement derived from spine DXA image texture, is related to microarchitecture and fracture risk independently of BMD. Denosumab (DMAb) is associated with greater gains in BMD compared with oral bisphosphonates. In a recent Japanese study, this larger improvement in BMD was associated with a larger reduction in vertebral fracture with DMAb compared with alendronate (ALN; Nakamura, ASBMR 2012). To further characterize the trabecular response with

DMAb and ALN, we compared QCT vBMD, DXA aBMD, and TBS from spine scans obtained in postmenopausal women with low BMD.

Postmenopausal women aged 50 to 70 years with low BMD at the spine or total hip were randomized in a double-blind, double-dummy fashion to DMAb (60 mg SC every 6 months), branded ALN (70 mg orally every week), or placebo (pbo) for 12 months (Seeman, *JBMR* 2010). Lumbar spine QCT vBMD, DXA aBMD, and TBS were measured from scans obtained at baseline and month 12.

There were 215 women (73 DMAb, 68 ALN, 74 pbo) who had TBS values at baseline and month 12. Mean age was 60 and at the lumbar spine, mean QCT vBMD was 90.4 mg/cm^3, mean DXA aBMD T-score was –2.4, and mean TBS was 1.234. Overall, QCT vBMD, DXA aBMD, and TBS decreased with pbo; increased or were maintained with ALN; and improved, compared with both pbo and ALN, with DMAb (Figure). At baseline, TBS was better correlated with QCT vBMD (r = 0.42, $P < 0.001$) than with DXA aBMD T-score (r = 0.13, $P = 0.051$). TBS percentage changes did not positively correlate with those in QCT vBMD or DXA aBMD in any of the treatment groups (Table). In postmenopausal women with low BMD, DMAb increased QCT vBMD, DXA aBMD, and TBS compared with ALN and pbo over 12 months. QCT trabecular vBMD correlated moderately with TBS but changes with therapy did not, suggesting that TBS changes are not biased by BMD changes. These data support the concept that TBS acquires information not captured by standard bone density and warrant further investigation of the clinical significance of the changes in TBS in response to therapies.

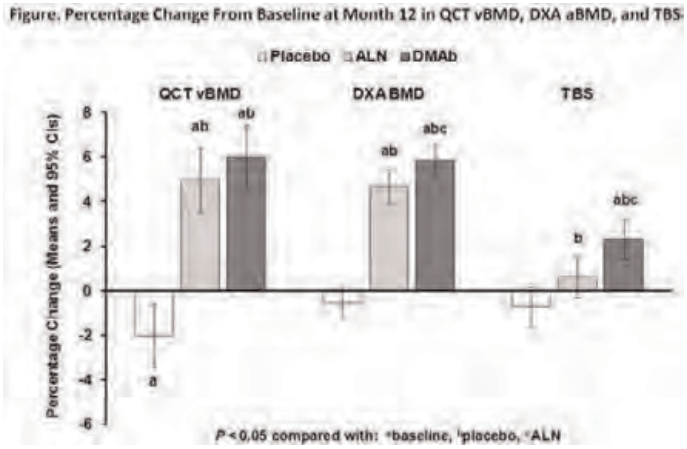

Figure

Table. Correlation Between Percentage Change From Baseline to Month 12 in DXA aBMD and TBS and QCT vBMD and TBS by Treatment

	Placebo	ALN	DMAb
DXA aBMD and TBS	n = 74 r = –0.31 *P* = 0.007	n = 68 r = 0.20 *P* = 0.110	n = 73 r = 0.08 *P* = 0.497
QCT vBMD and TBS	n = 68 r = 0.06 *P* = 0.646	n = 63 r = 0.10 *P* = 0.439	n = 69 r = 0.14 *P* = 0.241

Table

***Disclosures: Thierry Thomas**, Amgen, UCB, Novartis,; Abbvie, Novartis, Rochel Chugaï, 6; Gibaud, GSK, Ipsen, Eli Lilly, MSD, 2*
This study received funding from: Amgen Inc.

SA0400

Cortical Bone Parameters at the Hip in Response to Denosumab vs Placebo and the Clinical Relevance of These Changes in Postmenopausal Women With Osteoporosis <75 and ⩾75 Years Old. Harry K. Genant*[1], Tony M. Keaveny[2], Carol Zapalowski[3], Klaus Engelke[4], Thomas Fuerst[4], David L. Kendler[5], Christopher Recknor[6], Steven Boonen[7], Andrea Wang[3], Paula Dakin[3], Cesar Libanati[3], Michael R. McClung[8]. [1]UCSF & Synarc Inc., USA, [2]UC Berkeley & O.N. Diagnostics, USA, [3]Amgen Inc., USA, [4]Synarc Inc., USA, [5]University of British Columbia, Canada, [6]United Osteoporosis Centers, USA, [7]Leuven University, Belgium, [8]Oregon Osteoporosis Center, USA

Purpose: Cortical bone deterioration is now recognized as an important contributor to the exponential increase in fracture risk seen in women around the 8th decade of life. Treatment efficacy data in this group of women at higher risk for fracture are lacking with existing therapies. In FREEDOM, denosumab (DMAb) treatment resulted in improvements in both the cortical and trabecular bone compartments, with significant gains in hip volumetric BMD (vBMD), hip cortical thickness and mass, as well as hip strength. In addition, DMAb significantly reduced the risk of hip fracture in postmenopausal women with osteoporosis at higher risk for fracture. To further explore these associations, we evaluated the effects of DMAb on cortical bone parameters in women <75 and ⩾75 years of age.

Methods: In FREEDOM, women received DMAb 60mg or placebo Q6M for 36 months and daily calcium and vitamin D. Hip QCT scans were obtained at baseline and at months 12, 24, and 36, in a subset of women (51 DMAb; 48 placebo). These scans were analyzed in a blinded-to-treatment manner at 36 months to measure hip vBMD using MIAF; hip cortical thickness and mass using bone mapping; and hip strength using FEA. The analyses included subjects with observed data at baseline and month 36.

Results: In women <75 (n=57) and ⩾75 (n=42), DMAb resulted in similar and significant increases in hip vBMD and cortical thickness and mass compared with baseline and placebo at 36 months ($p<0.02$; Fig. 1). These improvements were associated with significant increases in hip integral and cortical strength compared with baseline in both age groups ($p<0.02$; Fig. 2). In general, for placebo-treated subjects, a significant decay in measured parameters of cortical bone at the hip was observed in women ⩾75 but not in those <75.

Conclusion: With DMAb treatment, increases in hip vBMD, cortical thickness and mass, and resulting strength, were observed regardless of age (<75 and ⩾75). Consistent with available literature, decreases in measured cortical parameters were observed in women ⩾75 in the placebo group. The observed significant improvements in cortical bone parameters in women ⩾75 with DMAb compared with placebo, and perhaps more importantly compared with baseline, may be particularly relevant as they are occurring at a time when cortical bone is deteriorating and fracture risk is exponentially increasing. DMAb may be addressing the mechanism of decay responsible for this increased nonvertebral fracture risk.

Fig. 1. Effects of DMAb Treatment on Hip Integral and Cortical BMD and Hip Cortical Thickness and Mass at 36 Months

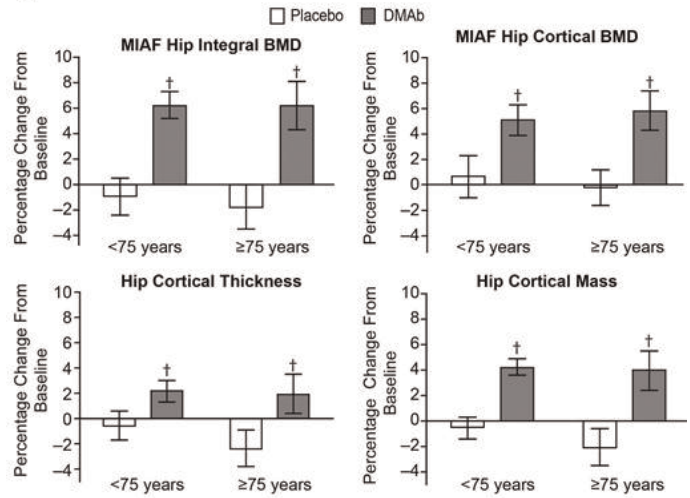

Data are least-squares means and 95% confidence intervals estimated from an analysis of covariance model including treatment and baseline value. †$p<0.02$ for DMAb compared with baseline and placebo.

Fig. 1

Fig. 2. Effects of DMAb Treatment on Hip Integral and Cortical Strength at 36 Months

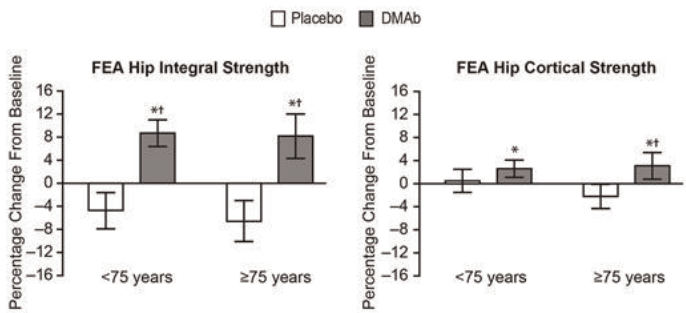

Data are least-squares means and 95% confidence intervals estimated from an analysis of covariance model including treatment and baseline value. *$p<0.02$ for DMAb compared with baseline. †$p<0.02$ for DMAb compared with placebo.

Fig. 2

***Disclosures: Harry K. Genant**, Amgen, Merck, Lilly, Pfizer, Janssen, Servier, Novartis, Radius,; Synarc, 8; Novartis, Merck, 9; Synarc, 2; Synarc, 7*
This study received funding from: Amgen Inc.

SA0401

See Friday Plenary Number FR0401.

SA0402

Treatment Criteria of Osteoporotic Vertebral Compression Fractures(VCFS). Mashood Siddiqi*[1], Giovanni Anselmetti[2], Jason Bernard[3], Christian Kasperk[4], Thomas Blattert[5], Charles Court[6], Daniel Fagan[7], Hendrik Fransen[8], Patrick Fransen[9], Tarun Sabharwal[10], Frederic Schils[9], Rupert Schupfner[5]. [1]University Hospital AintreeLiverpool, United Kingdom, [2]Interventional Radiologist, Italy, [3]Orthopaedic Surgeon, United Kingdom, [4]University of Heidelberg, Germany, [5]Trauma Surgeon, Germany, [6]Orthopaedic surgeon, France, [7]Spinal Surgeon, United Kingdom, [8]Interventional Radiologist, Belgium, [9]Neurosurgeon, Belgium, [10]Interventional Radiologist, United Kingdom

Objective To establish / refine criteria for the appropriate treatment of VCF at the patient-specific level and to translate these criteria into clinically useful recommendations.

Material and Methods Using the RAND/UCLA Appropriateness Method (RAM)[1], a European multidisciplinary panel of 12 experts (Interventional radiologists, Orthopaedic, Spinal, Trauma and Neuro Surgeons and Internists) assessed the appropriateness of non-surgical management (NSM), vertebroplasty (VP), and balloon kyphoplasty (BKP) for 128 hypothetical patient profiles. These were combinations of clinical factors considered relevant to treatment choice (time since fracture, MRI findings, impact and evolution of symptoms, spinal deformity, ongoing fracture process, and pulmonary dysfunction). After two individual rating rounds and meetings, appropriateness statements were calculated for all clinical scenarios.

Results Appropriateness outcomes showed specific patterns for the three treatments. For three-quarters of the profiles, only one treatment was considered appropriate: NSM 25%, VP 6%, and BKP 45%.A detailed decision-tree analysis showed pronounced patterns of appropriateness in relation to combination of clinical conditions. Based on these figures, the panel formulated a set of summary recommendations.(Table 1)

Conclusions ThisRAND-UCLA study provides recommendations for treatment of osteoporotic VCFs at the level of individual patients which are more specific than currently available guidelines.

	Usually appropriate	Usually inappropriate
NSM	• Negative MRI • Positive MRI and no other unfavourable conditions	• Proof of ongoing fracture process • ≥2 other unfavourable factors
VP	• Positive MRI, time since fracture ≥ 6 weeks and no spinal deformity	• Negative MRI and presence of spinal deformity
BKP	• Ongoing fracture process • Positive MRI and ≥1 other unfavourable factors	• Negative MRI and time since fracture ≥ 3 months • Negative MRI, time since fracture 6 weeks – 3 months and moderate impact of symptoms

Table-1

***Disclosures: Mashood Siddiqi**, None.*
This study received funding from: Medtronic Spinal & Biologics Europe

SA0403

Variations in Patients Receiving DXA Across Three Health Care Systems. Mollie Giller[1], Nicole Wright[2], Fredric Wolinsky[1], Thuy Nguyen[1], Douglas Roblin[3], Kenneth Saag[2], Peter Cram*[4]. [1]University of Iowa Hosptials & Clinics, USA, [2]University of Alabama at Birmingham, USA, [3]Kaiser Permanante of Georgia, USA, [4]University of Iowa, USA

Purpose: Currently, in the United States (US) DXA screening is recommended for men and women meeting certain specified criteria. Clinical practice guidelines exist for DXA and are designed, in part, with the purpose of reducing variations in care. However, little is known about variations in geographic or center-specific differences in patients receiving DXA. We used a detailed clinical registry from a large multicenter trial to examine variation in patients receiving DXA across three diverse healthcare systems.

Methods: We identified 3,454 patients enrolled in the Patient Activation After DXA Receipt Notification (PAADRN) Study (Clinical Trials # NCT01507662) who received DXAs at three sites between February 1, 2012 and February 28, 2013: 1) The University of Iowa (UI) (N=765); 2) University of Alabama Birmingham (UAB)(N=1369); and Kaiser Permanente Georgia (KP)(N=1320). We compared demographics (age, sex), prior receipt of DXA, and osteoporosis specific knowledge of patients across the three sites.

Results: Mean ages of patients receiving DXA at the three sites were 63.8 at UI, 67.3 at UAB, and 68.4 and KP (P<.001). The percentage of DXA recipients who were men was 29.2% at KP, 16.2% at UI, and 6.6% at UAB (P<.0001). The proportion of patients who had not received a prior DXA varied from 50.6% at KP to 27.7% at UI and 17.5% at UAB (P<.0001). The mean score on osteoporosis knowledge scale (the 'Osteoporosis and You' instrument) was 8.0 at UI, 7.4 at UAB, and 7.5 at KP (P=<.0001).

Conclusion: There were significant differences in the characteristics of patients receiving DXA across three large healthcare systems as well as the osteoporosis knowledge of these patients. These results highlight variability in clinical practice surrounding osteoporosis even in an era of practice guidelines.

***Disclosures: Peter Cram**, None.*
This study received funding from: US Department of Health & Human Services, National Institutes of Health

SA0404

See Friday Plenary Number FR0404.

SA0405

Bone Anabolic Effect of Sclerostin Antibody is Maintained with Antiresorptive Agents in Osteopenic, Ovariectomized Rats. Yanfei Ma*[1], Qianqiang Zeng[1], Rick Cain[1], Mary D Adrian[1], Guilherme V Rocha[1], Anita Harvey[1], Matthew J Hamang[1], Jonathan D Lucchesi[1], Henry Bryant[1], Venkatesh Krishnan[1], Victor Obungu[1], Stuart Kuhstoss[1], Masahiko Sato[2]. [1]Eli Lilly & Company, USA, [2]Lilly Research Labs, USA

Sclerostin is a protein known to be a negative regulator of bone formation. Sclerostin inhibition with selective monoclonal antibodies has been shown to stimulate bone formation and robustly enhance bone mass and strength in ovariectomized (OVX) rats. We examined maintenance of the bone gains stimulated by sclerostin antibody (ab) treatment followed by treatment with antiresorptive agents raloxifene (Ral), alendronate (ALN) or a reduced frequency of sclerostin-ab treatment. Eight month old rats were ovariectomized and allowed to lose bone for 2 months. Animals were treated with a chimeric sclerostin ab, 10mg/kg/week sc for 6 weeks, followed by different maintenance treatments for an additional 8 weeks. Treatment groups (n=8-10/group) included : a) vehicle, b) raloxifene (Ral) 3mg/kg/d sc, c) alendronate (ALN) 28μg/kg/twice per week sc, d) sclerostin ab one injection at week 10. Sclerostin ab weekly treatment for 6 weeks completely restored OVX induced bone mineral content and bone mineral density (BMD) loss in lumbar vertebrae (LV) and BMD in femoral neck (FN) to sham levels. The increased bone mass was accompanied by significantly improved bone strength compared to OVX control in LV, mid-femur (MF) and FN. Switching to vehicle or a single sclerostin ab injection resulted in gradually declining BMD in LV, distal femur (DF), FN and MF, with the BMD loss reaching statistical significance in LV. Bone strength of LV, MF and FN also tended to decline when animals were switched to vehicle or sclerostin ab single injection groups. BMD and bone strength gains were largely maintained or slightly increased with Ral or ALN at all sites. By the end of the 8-week maintenance period, BMD and bone strength in all groups previously treated with weekly sclerostin ab were still significantly higher than those in the OVX controls, with the exception of the sclerostin ab single injection group, where the bone strength of the FN declined to a level not significantly different from OVX control. Histomorphometric analyses are ongoing. Our data confirm the robust bone anabolic effects with a sclerostin monoclonal antibody, but BMD and strength declined when treatment was discontinued. Our data also suggest antiresorptive agents such as alendronate or raloxifene treatment can maintain the bone mass and strength stimulated by sclerostin ab treatment in osteopenic, OVX rats.

***Disclosures: Yanfei Ma**, Eli Lilly Company, 3*
This study received funding from: Eli Lilly Company

SA0406

Bone Formation Response in Mice During Administration and Following Rechallenge With an Antibody to Sclerostin. Martyn Robinson*[1], Kevin Greenslade[2], Jose Joby[2], Zofia Stencel[2], Hishani Kirby[2], Gill Holdsworth[2], Adrian Moore[2]. [1]UCB-Celltech, United Kingdom, [2]UCB Pharma, United Kingdom

Dosing with antibodies to sclerostin (Scl-Ab) has been shown to lead to a rapid increase in bone formation in animal models and in human clinical trials. However, the initial rapid rate of bone formation often attenuates during longer administration of the antibody (1, 2).In the current study, 8-10 week old BALB/c mice dosed with Scl-AbI exhibit a marked increase in circulating levels of the bone formation marker P1NP that peaks 4 days after dosing and returns to baseline after 7 days. After five doses of Scl-AbI (weekly, 10mg/kg sc) the peak serum PINP level (64ng/ml) was significantly lower than in age-matched animals dosed with Scl-AbI for the first time (101ng/ml). An increase in P1NP was observed after each administration of Scl-Ab, but the fifth dose only resulted in a 24% increase in P1NP levels (% increase from predose to peak levels measure 4 days later) whilst age-matched animals dosed for the first time showed a 130% increase. The difference in P1NP response between the two groups was not due to differences in antibody exposure or to changes in the kinetics of the P1NP response. Mice that had received five doses of Scl-AbI (showing an attenuated P1NP response) were allowed an 8 week interval with no further doses of

Scl-AbI. After 8 weeks these animals were again dosed with Scl-AbI and produced a P1NP response that was similar to that seen in age-matched animals dosed with Scl-AbI for the first time (increases in P1NP of 111% versus 109% after first Scl-AbI exposure). This suggests that re-challenge with Scl-AbI can be timed to overcome the attenuated response to Scl-AbI seen after multiple doses. A further 6 doses with Scl-AbI (weekly) again resulted in an attenuated response to Scl-AbI, which was again reversed after a second 8 week period without dosing. Each dosing interval was associated with significant increases in whole body areal BMD and each dosing interruption resulted in a decline in areal BMD

In conclusion, we have demonstrated that i) bone formation, as assessed by a serum biomarker, rapidly and significantly increased after Scl-AbI administration, ii) that while this increase in bone formation was observed with continued dosing, its magnitude was markedly attenuated compared to the first exposure; and iii) that a first-dose level increase in bone formation can be achieved after a period of Scl-AbI discontinuation.

1) Paszty et al. JBMR. 2010;25:1897
2) JBMR 27 (Suppl 1)2012; abst. 1025.

***Disclosures: Martyn Robinson**, UCB Pharma, 7; UCB Pharma, 3*
This study received funding from: UCB Pharma

SA0407

See Friday Plenary Number FR0407.

SA0408

Combined Effects of Treadmill Exercise and Sclerostin Antibody in Ovariectomized Rats. Hechmi Toumi[1], Delphine Benaitreau*[1], Michael Ominsky[2], Claude Laurent Benhamou[3], Eric Lespessailles[4], Stephane Pallu[5]. [1]EA4708 I3MTO University of Orleans, France, [2]Amgen Inc., USA, [3]CHR ORLEANS, France, [4]Centre Hospitalier Regional, France, [5]EA 4708 - I3MTO Orléans, France

Bone formation and bone mineral density (BMD) have been shown to be enhanced by physical activity (Maurel *et al.*, J Bone Spine. 2013) as well as by administration of sclerostin antibody (Scl-Ab; Li *et al.*, J Bone Miner Res, 2010). Purpose: The current study investigated whether a combination of both could provide a further improvement by comparing the effect of a modest dose of sclerostin antibody, physical exercise, and the combination of both on bone formation and strength in a rat osteopenia model. Method: Sixty Wistar female 9 month old rats (mass 341 $\pm$ 24 g) were divided into five groups that received subcutaneous injections twice weekly: (1) Sham: saline + no exercise, (2) OVX: ovariectomized + saline + no exercise, (3) OVX+E: OVX + saline + exercise, (4) OVX+S: OVX + Scl-Ab (Scl-AbVI, 5 mg/kg) + no exercise, and (5) OVX+S+E: OVX + Scl-Ab + exercise. The exercise protocol consisted of 1 hour intermittent running, 5 days a week for a 14 week period. BMD was measured by DXA before training and after. Morphological properties of the trabecular bone from femurs were analyzed by micro-CT and mechanical properties were generated by 3 point bending at the femur midshaft. Serum osteocalcin (OCN) and N-telopeptide of type I collagen (NTX) were evaluated at termination. Results: Exercise attenuated the increase in fat mass after OVX, without an effect on lean mass. Scl-Ab treatment had no effect on lean or fat mass, independent of exercise status. Bone mass was greater in the Scl-Ab groups, with significant increases in whole body BMD, distal femur trabecular BV/TV, and femur cortical volume compared to OVX controls. Cortical bone volume was significantly higher in the Scl-Ab groups compared to the other groups. Exercise alone or in combination with Scl-Ab had no effect on these parameters. Exercise resulted in an increase in cortical porosity compared to OVX controls, an effect that was abrogated by Scl-Ab treatment. Ultimate load, Young's modulus and stiffness were significantly lower in OVX and OVX+E, and were significantly increased by Scl-Ab treatment compared to Sham. Exercise significantly decreased NTX but did not affect OCN, while Scl-Ab increased OCN with a non-significant decline in NTX. Conclusions: Low dose Scl-Ab was effective at increasing bone formation, bone mass, and strength in OVX rats. The current intermittent treadmill training produced no notable effect in OVX rats alone nor when combined with sclerostin antibody, other than a decrease in serum NTX.

***Disclosures: Delphine Benaitreau**, None.*

SA0409

See Friday Plenary Number FR0409.

SA0410

See Friday Plenary Number FR0410.

SA0411

Therapeutic Potential of Sclerostin Antibody in Extreme Disuse-induced Bone Loss after Spinal Cord Injury: a Preclinical Study. Weiping Qin*[1], Xiaodong Li[2], Jay Cao[3], Lauren Collier[4], Yuanzhen Peng[5], Jiliang Li[6], Hua Zhu (David) Ke[2], William A. Bauman[4], Christopher Cardozo[4]. [1]Bronx Veterans Affairs Medical Center, USA, [2]Amgen, Inc., USA, [3]USDA ARS, USA, [4]James J. Peters Veteran Affairs Medical Center, USA, [5]The Mount Sinai School of Medicine, USA, [6]Indiana University Purdue University Indianapolis, USA

The rapid and extensive sublesional bone loss after spinal cord injury (SCI) is a difficult medical problem that has been refractory to available interventions tested to date (1-3). Inhibition of sclerostin by sclerostin monoclonal antibody (Scl-Ab) has been shown to increase bone formation and improve bone mass and strength in animal models of bone loss due to estrogen deficiency and immobilization (4). Scl-Ab also increased bone mineral density (BMD) in healthy men and postmenopausal women (4). In addition, sclerostin has been proposed as a potential mediator of mechanotransduction (5). Therefore, we hypothesized that sclerostin could be responsible for the bone loss due to SCI and, if so, that sclerostin inhibition with Scl-Ab could provide a hopeful solution for this challenging medical problem. To test our hypotheses, we first performed complete spinal cord transection in sclerostin knockout (SOST $^{-/-}$) mice and wild type (WT) controls. Eight weeks after SCI, significant bone loss was observed at the distal femur and proximal tibia in WT mice. However, no bone loss was observed in SOST $^{-/-}$ mice. These findings suggest that sclerostin mediates sublesional bone loss after SCI. To explore the therapeutic potential of sclerostin inhibition in SCI, male Wistar rats underwent complete spinal cord transection; 7 days after SCI, the rats were treated with Scl-Ab at 25 mg/kg/week or vehicle for 7 weeks. SCI resulted in significant decreases in BMD (-25%) and trabecular bone volume (-66%) at the distal femur. Scl-Ab completely prevented the loss of BMD and trabecular bone volume. Additionally, in SCI rats administered Scl-Ab, Tb.Th was increased to levels above values for non-SCI controls, and Tb.N tended to be higher than SCI controls. Preliminary histomorphometric analysis demonstrated that Scl-Ab increased trabecular bone formation. In cultures of bone marrow cells, SCI increased the number of $TRAP^{+}$ multinucleated cells as well as mRNA levels of osteoclast differentiation markers, and reduced the number of osteoblasts and mRNA levels of the osteoblast differentiation markers. None of these deleterious changes were observed in the Scl-Ab-treated group. In summary, our findings indicate that Scl-Ab fully prevented sublesional loss of BMD and metaphysis trabecular bone volume by increasing bone formation and decreasing bone resorption, strongly suggesting that Scl-Ab may represent a promising novel approach to mitigate the striking bone loss after SCI.

***Disclosures: Weiping Qin**, None.*
This study received funding from: Amgen Inc. and UCB Pharmap provided Scl-Ab

SA0412

ALX-0141, An Anti-RANK-L Targeting Nanobody®, Increases Bone Mass in Cynomolgus Monkeys. Rana Samadfam*[1], Sandy Jacobs[2], Maarten Van Roy[2], Aidan McGuire[3], Pieter Schoen[2], Judith Baumeister[2], Susan Y. Smith[1], Josefin-Beate Holz[2]. [1]Charles River Laboratories, Canada, [2]Ablynx NV, Belgium, [3]Charles River Laboratories, United Kingdom

Nanobodies are therapeutic proteins based on the smallest functional fragments of naturally occurring heavy chain only antibodies. The trivalent Nanobody ALX-0141 targets RANK-L with high specificity and inhibits osteoclast differentiation, activation and survival. The pharmacological effect of long-term treatment with ALX-0141 on bone was evaluated. Cynomolgus monkeys (3-3.5 years old) received ALX-0141 at 5, 50 or 100 mg/kg or the vehicle control (formulation buffer) by repeated subcutaneous administration using a single dose every 2 weeks during 26 weeks. For each gender, 4 animals/group were sacrificed at the end of treatment and 2 animals/group (in the control and the high dose group) were sacrificed after an additional 26-week recovery period. Blood was collected for analysis of serum biochemistry and bone turnover markers (CTx-1, P1NP, and TRAPC5b) at pre-treatment and during the treatment and recovery period. At necropsy, whole femur and lumbar vertebrae were collected for bone densitometry evaluation by DXA and pQCT.

Treatment of cynomolgus monkeys with ALX-0141 resulted in marked suppression of bone turnover markers in all dose groups. Positive effects on bone mass were noted at the lumbar spine and femur, most markedly for the males. A higher magnitude of response was noted for trabecular bone (up to 140% increase) compared to cortical/subcortical compartment (up to 30% increase) at the lumbar spine and distal femur metaphysis. Overall the greatest effects were seen at the highest dose level. The effects on bone densitometry persisted through the 26-week treatment-free period for male animals, but not for females.

In conclusion, treatment of cynomolgus monkeys (males and females) with ALX-0141 for 26 weeks resulted in marked suppression of bone turnover markers and positive effects on bone mass with increases in BMC and BMD at the lumbar spine and femur, most notably in males. Results were consistent with the expected pharmacology of ALX-0141 and support the further development of ALX-0141 in bone-related disorders.

***Disclosures: Rana Samadfam**, None.*
This study received funding from: Ablynx

SA0413

Effect of Dosing Interval Duration of Intermittent Ibandronate Treatment on the Healing Process of Femoral Osteotomy in a Rat Fracture Model. Tasuku Mashiba*[1], Takeshi Manabe[2], Ken Iwata[3], Tetsuji Yamamoto[3]. [1]Kagawa University Faculty of Medicine, Japan, [2]Kinashi Obayashi Hospital, Japan, [3]Kagawa University, Japan

Purpose

The effects of bisphosphonate treatment schedule on fracture healing have not previously been tested. We evaluated the effect of ibandronate dosing interval duration on the healing process following surgical 'fracture' (osteotomy), especially callus remodeling, geometrical changes and mechanical properties of fractured bone using a rat femoral fracture model.

Materials and methods

6-week-old rats (n = 160) underwent transverse osteotomy at the midshaft of the left femur, and were then allocated into vehicle control (CNT) or an ibandronate treatment group: 5 μg/kg/day (DAY; 5 days/week), 75 μg/kg once every 3 weeks (I-3), 150 μg/kg once every 6 weeks (I-6), resulting in the same total ibandronate dose over the study. Rats were sacrificed after 6 or 18 weeks. Fractured femur was evaluated by radiograph, pQCT, histomorphometry and mechanical testing.

Results

At 18 weeks, all fracture lines had disappeared in the CNT and I-6 groups; approximately 10% of fracture lines remained in the DAY and I-3 groups (Fig.1). Ibandronate-treated groups showed large callus areas around the fractures, which shrank between 6 and 18 weeks after surgery; the extent of shrinkage decreased with shorter dosing interval (Fig.2). In histomorphometry, callus remodeling was suppressed by ibandronate; this became more apparent at shorter dose intervals. The structural properties of osteotomized femora were increased in the DAY group compared with CNT, but intrinsic material properties reduced inversely and became closer to those of the CNT in response to increased dosing interval.

Conclusion

Ibandronate induced formation of large calluses around osteotomies but delayed woven bone remodeling into lamellar bone and reduced intrinsic material properties in a rat fracture model. Extending the dosing interval of intermittent ibandronate treatment appeared to reduce the suppression of callus remodeling caused by ibandronate that would have delayed healing after osteotomy.

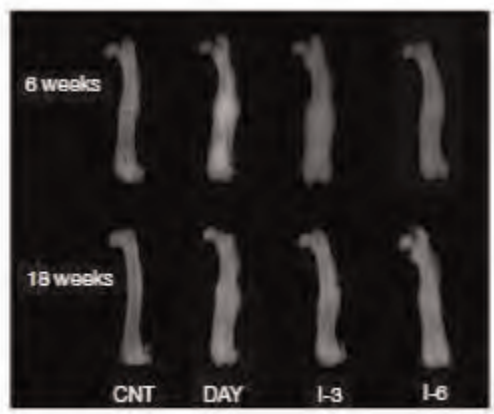

Fig.1. Soft X-ray photography of fractured femora

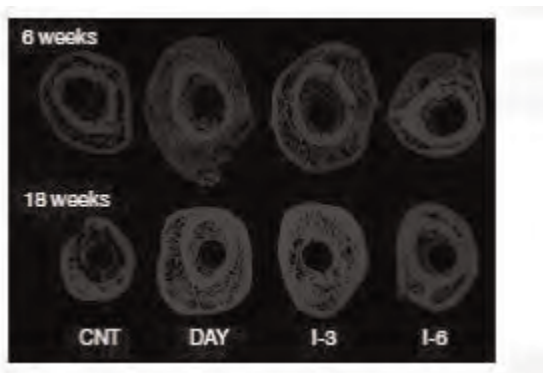

Fig.2. Contact microradiographs of cross-sectional specimens

***Disclosures: Tasuku Mashiba**, None.*
This study received funding from: Chugai Pharmaceutical Co. Ltd.

SA0414

See Friday Plenary Number FR0414.

SA0415

Efficacy of odanacatib versus alendronate in the treatment of bone loss in orchidectomized male rabbits. Charles Chen*[1], Brenda Pennypacker[2], Mary Belfast[3], Le Thi Duong[2]. [1]Merck & Co., Inc., USA, [2]Merck Research Laboratories, USA, [3]Merck & Company, USA

Odanacatib (ODN) is a selective cathepsin K inhibitor demonstrated to increase bone mass in postmenopausal women with osteoporosis. The aim of this study was to compare the effects of ODN vs. alendronate (ALN) on bone mass and remodeling in orchidectomized (ORX) male rabbits, a preclinical model of male osteoporosis. Skeletally mature (11-mo.old) male rabbits were either sham-operated (n=20) or ORX (n=24/group). After 7.5 mo., ORX-animals exhibited decreased levels of testosterone and estradiol by 89% and 46%, respectively, and reduced lumbar vertebral areal bone mineral density (LV aBMD) by 5% vs Sham. ORX rabbits were randomized to either vehicle (Veh), ALN (300μg/kg/wk, sc) or ODN (1.5 and 6mg/kg, daily in food, providing ~1- and ~7-fold of clinical exposure, respectively) treatments for 14 mo. LV5-6DXA, urine and serum were collected at 0, 3, 6, 9, 12 and 14 mo. Calcein labeling (15-d) was administered prior to necropsies. Longitudinal LV.BMD was significantly increased in ORX-rabbits treated with ODN 1.5mg/kg by 9-19% and 6mg/kg by 6-27% vs Veh, and compared to an increase by 9% in the ALN group at study end. Persistent and significant reductions of the bone resorption marker helical peptide of collagen type I (HP) were observed in animals treated with both ODN doses (43-71% and 47-62%), compared to ALN (24-50%) vs Veh throughout the study. Levels of the bone formation marker bone specific alkaline phosphatase (BSAP) were significantly reduced (16-34%) in the ALN group, maintained with ODN 1.5mg/kg and trended up (16-30%) with ODN 6mg/kg compared to Veh. Terminal histomorphometry of LV3 showed that Veh-treated ORX-rabbits had decreased BV/TV by 19% ($p<0.05$) vs Sham. ALN tended to increase BV/TV by 13% (p=0.124) vs Veh. ODN at both doses significantly increased BV/TV by 55-57% ($p<0.001$) vs Veh, and 37-39% ($p<0.001$) above ALN. Interestingly, ODN treatment for 14 mo. reduced lumbar spine formation parameters, including MS/BS by 41-44%, BFR/BS by 51-52% and MAR by10-15%. Compared to ALN and Veh, trabecular osteoclast surface and number were higher ($p<0.001$) in both ODN groups. Taken together, this study demonstrated proof of concept for the cathepsin K inhibitor ODN dosed in treatment mode was highly efficacious in restoring lumbar spine bone mass in ORX male rabbits, supporting the clinical evaluation of ODN for the treatment of osteoporosis in men.

***Disclosures: Charles Chen**, Merck, 3*
This study received funding from: Merck & Co.

SA0416

Short-Term Effects of Zoledronic Acid and Teriparatide on Microcrack Density in Ewes: Comparison between Iliac Crest and Lumbar Vertebra. Nathalie Portero-Muzy*[1], Pascale Chavassieux[2], Evelyne Gineyts[1], Marlène Pierre[1], Roland Chapurlat[1]. [1]INSERM UMR 1033 et Université de Lyon, France, [2]INSERM UMR1033, Université De Lyon, France

Iliac crest bone biopsies are used to assess the mechanism of action of therapeutic agents, yet there is little data comparing this site to sites prone to fracture. We have previously shown in ewes that zoledronic acid (ZOL) markedly depressed the bone turnover, by a different magnitude at the 1st lumbar vertebra and iliac crest. Teriparatide (TPTD) induced an augmentation of the static parameters of bone formation and resorption only in LV1 ($p<0.05$) (1). Bisphophonates have been suggested to trigger the formation of microcracks, in contrast to TPTD.

The purpose of this study performed in ewes was to compare the microcrack density (Cr.Dn) at the iliac crest and lumbar vertebra, 3 months after either vehicle (CTRL) or one single dose of 10 mg ZOL or 20 μg/day TPTD. The microcrack analysis was performed after bulk-staining of the specimens with 5 mM xylenol orange in 70% ethanol. In CTRL, microcracks were mainly observed in cortical bone at LV1 and IC with Cr.Dn twice as great at IC as at LV1. After ZOL, Cr.Dn significantly increased in cortical bone both at LV1 and IC ($p < 0.01$), with a same magnitude (x 2.75). In trabecular bone, the augmentation in Cr.Dn was similar at IC and LV1, but the mean Cr.Dn was greater at LV1 than at IC. This increased Cr.Dn was associated with a marked diminution of the bone turnover and DPD content. Cr.Dn and MS/BS were negatively and significantly correlated, regardless of type of treatment, at IC and LV1 ($0.003<p<0.03$). In all three treatment groups, DPD content in cortical bone was significantly and negatively correlated with Cr.Dn at LV1 ($p\leq0.04$). After TPTD, no significant change of Cr.Dn was observed at both sites.

In conclusion, this study performed in ewes shows that the early effects of ZOL and TPTD on bone turnover, collagen crosslinks content and microcrack density are observed both at IC and LV1, but with a different magnitude according to the skeletal site. To fully understand the mechanisms underlying the anti-fracture efficacy of osteoporosis therapies, the distinction of bone sites appears meaningful.

1 - Portero-Muzy N.R. *et al.*, Bone 51:714-719, 2012.

***Disclosures: Nathalie Portero-Muzy**, None.*

SA0417

Dietary Dried Grape Improves Bone Calcium Retention in Ovariectomzied Rats. Emily Hohman*[1], Connie Weaver[2]. [1]Purdue University, USA, [2]Purdue University, Dept of Nutrition Science, USA

Grapes and their associated phytochemicals have been extensively investigated for beneficial effects on cardiovascular health, cancer prevention, and other chronic diseases, but the effect of grape consumption on bone health has not been determined. We previously found short term benefits of dietary grape products on reducing bone turnover in ovariectomized (OVX) rats. To determine long term benefits to bone and to further investigate mechanisms, we conducted an 8-week feeding study in 5-month-old OVX rats. Sprague Dawley rats were ovariectomized at 3 months of age and then were given a single dose of ^{45}Ca to pre-label bones at 4 months of age. Following a one month equilibration period, baseline ^{45}Ca excretion was determined as a measure of baseline net bone turnover. Rats (n=22/group) were then randomized to a modified AIN93M diet containing 25% freeze dried grape powder or control diet for 8 weeks. Urinary ^{45}Ca excretion was monitored throughout the study to determine changes in net bone turnover. Calcium balance was assessed after 1 week and 8 weeks on the experimental diets, and calcium kinetics were measured after 8 weeks. At sacrifice, femurs, tibias, and vertebrae were collected for microCT imaging, 3-pt bending, and reference point indentation. Rats consuming the grape powder diet had improved net bone calcium retention compared to rats fed the control diet. We conclude that consumption of grape products may improve bone health in the postmenopausal state.

***Disclosures: Emily Hohman**, None.*
This study received funding from: California Table Grape Commission

SA0418

Effects of Vitamin C and Minodronate on Bonemineral Density, Quality, and Strength in Vitamin C-deficient Rats. Toyohito Segawa*[1], Naohisa Miyakoshi[1], Yuji Kasukawa[1], Hiroshi Aonuma[1], Hiroyuki Tsuchie[2], Yoichi Shimada[1]. [1]Akita University Graduate School of Medicine, Japan, [2]Ugo Municipal Hospital, Jpn

[Introduction] Minodronate inhibits bone resorption and increases bone mineral density (BMD), helping to prevent osteoporotic fractures. Preventive effects on fractures are reduced in the elderly. Deficiency of vitamin C (ascorbic acid, AA) in aged people, which is related to bone quality, may be one reason for reduced bone quality and reduction of bone strength. However, the efficacy of AA supplementation and minodronate on BMD, bone quality, and strength in AA deficiency is unclear. This study evaluated the efficacy of AA supplementation and minodronate administration on BMD, bone quality, and strength in AA-deficient rats.[Materials and Methods] AA-deficient rats (Osteogenic Disorder Shionogi Rats) were bred with normal concentration AA water (2 mg/mL) until 4 months of age and with low concentration AA water (0.5 mg/mL) thereafter until 8 weeks to develop vitamin C deficiency (n=40). Thereafter, rats were assigned to one of the following groups: 1) AA-deficient (AA-) group receiving low concentrations of AA water, 2) AA supplementation (AA+) group receiving normal concentrations of AA water, 3) AA-deficient and minodronate (0.15 mg/kg body weight, once a week subcutaneous injection) administration (AA-M) group, and 4) AA supplementation and minodronate administration (AA+M) group (n=10 in each group). After 4 weeks, the bilateral femora and right tibia were harvested. Right proximal femur was used for BMD measurement, and left femur was evaluated for bone strength by femoral neck compression test and three-point bending test of diaphysis. Right proximal tibia was used to measure collagen maturity by Fourier transform infrared spectroscopy (FTIR) for bone quality evaluation.[Results] BMD in the AA+M group was significantly higher than in the other groups ($p<0.05$). Bone strength indices including maximum load, bone breaking force, and breaking energy in the femoral neck compression test and three-point bending test of diaphysis in the AA+ and AA+M groups were significantly higher ($p<0.05$) than in the AA- group. Collagen maturity evaluated by FTIR showed no significant differences among groups; however, the AA+ group showed higher values ($p=0.09$) than the AA- group regardless of minodronate administration. [Discussion and Conclusion] AA deficiency resulted in reduced bone strength. The combination of AA supplementation and minodronate increased BMD and bone strength in AA-deficient rats, suggesting that AA supplementation may improve bone quality.

***Disclosures: Toyohito Segawa**, None.*

SA0419

Eldecalcitol Improves Endothelial Function Deteriorated by the Oxidative Stress in the Femoral Artery and Prevents Bone Loss in Ovariectomized Rats. Koichi Endo[1], Ken-ichi Serizawa*[2], Satoshi Takeda[2], Yoshihito Tashiro[2], Kenji Yogo[2]. [1]Chugai Pharmaceutical Co., Ltd., Japan, [2]Product Research Department, Chugai Pharmaceutical Co., Ltd., Japan

Eldecalcitol (ED-71; ELD), a 2β-hydroxypropyloxy derivative of 1a,25(OH)2D3, is an active vitamin D3 analog and used for the treatment of osteoporosis in Japan since 2011. Although native vitamin D is reported to exert a protective effect on endothelial dysfunction in diabetes or renal disease, the protective effects of vitamin D3 in osteoporosis remain unclear. This study evaluated the endothelial protective effect of the pharmacological dosage of ELD in osteoporosis of ovariectomized (OVX) rats. Female Sprague-Dawley rats (12-weeks old) were ovariectomized. ELD (20 ng/kg) was orally administered 5 times a week for 4 weeks from one day after surgery. Four weeks after the surgery, flow-mediated dilation (FMD) as an indicator of endothelial function was measured by high-resolution ultrasound in the femoral artery of living rats. After vertebrae had been harvested, the BMD of the L2-L4 vertebrae was measured by DXA. FMD was significantly reduced in the OVX + vehicle group (OVX+v) compared with the sham group (Sham). ELD restored the reduction of FMD in OVX (Sham: 14.3 ± 2.5, OVX+v: 8.2 ± 1.5, OVX+ELD: 15.0 ± 1.1%, mean$\pm$SD, n=7-8). Nox4 expression (a NADPH oxidase component) and nitrotyrosine content (a marker of peroxynitrite) increased and eNOS dimer/monomer ratio was decreased in OVX rat femoral arteries, indicating eNOS dysfunction in OVX rat femoral arteries. In femoral arteries of OVX rats, PPARγ expression decreased and NF-κB p65 expression increased. ELD reduced Nox4 expression and nitrotyrosine content in OVX rat femoral arteries and improved the eNOS coupling state. In addition, ELD increased PPARγ expression and decreased NF-κB p65 expression in femoral arteries of OVX rat. The BMD of the L2-L4 vertebrae in OVX+v was significantly lower than that of Sham. The treatment with ELD prevented OVX-induced reduction of BMD of the vertebrae (Sham: 145.4 ± 7.4, OVX+v: 133.9 ± 6.6, OVX+ELD: 152.9 ± 7.3 mg/cm2). ELD slightly increased plasma Ca concentration (Sham: 8.8 ± 0.1, OVX+v: 8.5 ± 0.1, OVX+ELD: 9.1 ± 0.2 mg/dL). These results suggested that ELD ameliorated endothelial dysfunction in OVX rats. An antioxidative effect of ELD was thought to improve eNOS coupling state at the pharmacological dosage in osteoporosis model. ELD would be expected to exert as an osteoporotic therapeutic agent with additional value, improving endothelial function, for osteoporosis patients.

***Disclosures: Ken-ichi Serizawa**, None.*

SA0420

Effects of AB-25E9, a Monoclonal Antibody Targeting Siglec-15, on Biomarkers of Bone Remodeling in Estrogen-Deficient Cynomolgus Monkeys. Julie Laurin*, Mauricio Lemus, Elisabeth Viau, Anna Moraitis, Martine Pagé, Gilles Tremblay, Mario Filion. Alethia Biotherapeutics, Canada

Siglec-15, an immunoglobulin-like sialic acid-binding receptor, is expressed specifically on the surface of osteoclasts and plays a role in their normal differentiation and function. In rodent models, administration of a Siglec-15 antibody resulted in increased bone mineral density and decreased serum TRAP5b levels, indicating a direct effect on osteoclasts in vivo. Interestingly, the results from these studies suggested that inhibiting Siglec-15 also stimulated bone formation. To explore the effects of Siglec-15 inhibition on bone biomarkers in primates, we administered the humanized monoclonal antibody targeting Siglec-15, AB-25E9, to estrogen-deficient female cynomolgus monkeys.

Two intravenous injections of vehicle (PBS) or AB-25E9 at 10 mg/kg were administered to two groups at an 8-week interval with a follow-up period of 6 months. Estrogen deficiency was induced by the repeated subcutaneous administration of a gonadotropin-releasing hormone agonist every 4 weeks starting 3 months prior to administering AB-25E9 and throughout the follow-up period. Serum and urine samples were collected weekly to evaluate the bone resorption and formation biomarkers, determine the PK profile of AB-25E9 and monitor for the presence of antibody-drug antibodies (ADA).

Treatment with AB-25E9 rapidly decreased bone resorption biomarkers (urinary NTx, serum CTx and TRAP5b) by 30% to 45% demonstrating the anti-resorptive properties of AB-25E9. Strikingly, the bone formation biomarkers (osteocalcin and BSAP) did not rapidly decrease and were minimally affected. The decrease in the levels of bone resorption biomarkers began to attenuate at approximately Week 6, which coincided with the appearance of ADAs. Interestingly, this attenuation was not observed before Week 20 in animals where little or no ADAs were detected. In agreement with these findings, the decline in AB-25E9 serum concentrations was faster in animals in which ADAs were detected. In monkeys that were negative for ADAs, the terminal elimination half-life of AB-25E9 ranged between 5 – 12 days.Taken together, the biomarker profiles presented here show that AB-25E9 has anti-resorptive activity and maintains bone formation estrogen-deficient cynomolgus monkeys. These results underscore the novel mechanism of action of AB-25E9 and highlight its potential for osteoclast-targeted therapy of bone-related diseases.

***Disclosures: Julie Laurin**, Alethia Biotherapeutics, 3*
This study received funding from: Alethia Biotherapeutics

SA0421

Effects of alfacalcidol and ED-71/eldecalcitol alone or in combination with risedronate in ovariectomized rats: histomorphometric analysis. Tetsuo Yano*[1], Mei Yamada[1], Makoto Shiozaki[2], Daisuke Inoue[3]. [1]Ajinomoto Pharmaceuticals Co., LTD, Japan, [2]Ajinomoto Pharmaceuticals, Japan, [3]Teikyo University Chiba Medical Center, Japan

Background/Aim: We previously demonstrated efficacy of eldecalcitol (ED-71), a new 1a,25(OH)2D3-derivative, on ovariectomy-induced osteoporosis in rats. ED-71 improved both trabecular and cortical bone architecture in micro-CT analysis at least to a similar extent that alfacalcidol (ALF) did, when combined with risedronate (RIS).

We report here results of histomorphometric analysis in ovariectomized rats treated with ED-71 and ALF, each alone or in combination with RIS

Methods: Female Sprague Dawley rats at 24 weeks of age were divided into one sham-operated and five ovariectomized groups (1: vehicle, 2: ED-71, 3: ALF, 4: RIS, 5: RIS + ED-71, and 6: RIS + ALF). RIS (3.5 μg/kg, s.c.) and ED-71 (0.2 μg/kg, p.o.) were given twice per week for 16 weeks. ALF (0.4 μg/kg, p.o.) was given three times per week for 16 weeks. Bone strength and histomorphometry were measured at 16 weeks treatment. BMD and bone architecture were evaluated every 4 weeks by micro CT.

Results: At 16 weeks, cortical thickness and area in RIS, ED-71, RIS + ALF and RIS + ED-71 was significantly increased, compared with vehicle. And maximum load of ED-71, RIS, RIS + ED-71, and RIS + ALF groups was significantly increased, compared with vehicle. In histomorphometric analysis, structural indices of trabecular bone in vehicle deteriorated, compared with sham. These parameters in ED-71 + RIS and ALF + RIS showed a greater improvement than that in monotherapy. Mineralizing surface and bone formation rate were significantly decreased by combination therapy. The number of mini-modeling in ED-71 + RIS and ALF + RIS was also significantly decreased, compared with vehicle. The change of the number of mini-modeling in RIS and ED-71 + RIS was significantly greater than that in the ED-71 monotherapy group.

Conclusions: Combination therapy with RIS and active vitamin D3 derivatives significantly improved bone histomorphometry greater than each alone. RIS + ED-71 was at least as efficacious as RIS+ALF in improving bone histomorphometry, validating the combination of risedronate and ED-71 as a treatment option for osteoporosis caused by estrogen withdrawal.

***Disclosures: Tetsuo Yano**, Ajinomoto Pharmaceuticals, 3*

SA0422

Green tea polyphenols improve bone matrix in alcohol-induced bone loss of young male rats. Chwan-Li Shen*[1], Susan Bergeson[1], Peter Syapin[1], Raul Dagda[1], Jia Jia Chen[1], Jennifer Graef[2], Gordon Brackee[1], Brenda Smith[2]. [1]Texas Tech University Health Sciences Center, USA, [2]Oklahoma State University, USA

Our previous studies have shown that the osteo-protective effects of green tea polyphenols (GTP, green tea extract) in various bone loss models. In this study, we used the same approach of green tea supplementation in drinking water to evaluate GTP's impacts on bone health along with safety in a binge drinking-induced bone loss model. Forty-eight 30-day-old SD male rats were assigned to a 2 (placebo vs. alcohol i.p. at 3 g/kg body weight on 3 consecutive days/week) × 3 (0, 0.1%, and 0.5% (w/v) GTP in drinking water) factorial design for 6 weeks. Bone parameters [femoral and lumbar vertebrae-4 (LV-4) area (BMA), bone mineral content (BMC), and bone mineral density (BMD)] were measured by dual-energy absorptiometry. Bone turnover biomarkers [serum osteocalcein (OC) and tartrate-resistant acid phosphatase-5b (TRAP-5b)] were measured using respective ELISAs. Blood chemistry panels were determined by an automatic chemical analyzer. Data were analyzed by two-way ANOVA followed by Fisher's LSD test. Throughout the study period, alcohol administration reduced body weight and food consumption, while GTP supplementation reduced water consumption. The blood chemistry results show that alcohol administration significantly decreased albumin, glucose, alkaline phosphatase, and amylase levels; increased globulin, phosphorus, creatine kinase, cholesterol, and potassium levels; and had no effect on protein, calcium, blood urea nitrogen, creatinine, aspartate aminotransferase, alanine aminotransferase, sodium, and chloride. GTP supplementation significantly suppressed alkaline phosphatase levels and had no impact on other blood chemistry parameters. Regarding bone aspects, 6-week alcohol administration lowered BMA, BMC, and BMD of the femur and LV-4, as well as serum TRAP-5b, but had no impact on serum OC. Supplementation of GTP into the drinking water for 6 weeks increased BMC of the femur (P=0.091) and LV-4 (P=0.016) as well as BMD of the femur (P=0.030) and LV-4 (P=0.068). GTP had no effect on scanned BMA and serum OC, and tended to increase serum TRAP-5b concentration (P=0.092). There was an interaction between the alcohol administration and GTP dosage in serum TRAP-5b. This study demonstrates that GTP supplementation in drinking water can increase bone matrix through suppressing bone turnover rate in young male rats administered with alcohol, an animal model of binge drinking.

***Disclosures: Chwan-Li Shen**, None.*

SA0423

Icariin exerts an osteogenic effect in OVX-mice via suppression of ERK and stimulation of p38 MAPK. Qin Bian*[1], Zhu Yang[2], Yongjian Zhao[2], Xiangyin Mao[3], Shufen Liu[2], Jianhua Huang[4], Zinyin Shen[4], Yongjun Wang[2]. , [2]Department of Orthopaedics & Traumatology, Longhua Hospital, Shanghai University of Traditional Chinese Medicine, China, [3]Institute of Life Science, Fudan University, China, [4]Institute of integrated Traditional Chinese Medicine & Western Medicine, Huashan Hospital, Fudan University, China

Objective—Icariin (ICA), an extract from epimedium, has been reported to be effective in promoting bone formation. The objective of the study is to search for the molecular targets of Icariin (ICA) in bone mesenchymal stem cells (bMSCs) from the mice with ovariectomy (OVX)-induced osteoporosis.

Methods—Six-month-old Imprinting Control Region (ICR) mice that underwent OVX were treated with ICA. After 3 months, bone mass was evaluated by microcomputed tomography, morphometry and immunohistochemical detection. BMSCs were isolated from the femur and tibia to observe the self-renewal and differentiation capacity using Colony. forming unifibroblastic (CFU-F), Colony. forming adipocyte (CFU-Adipo) and alkaline phosphatase (ALP) staining. Real time RT-PCR and ALP detection were performed to observe the osteogenetic effects of ICA on bMSCs *in vitro*. In addition, the expression of 26991 genes of bMSCs *ex vivo* at 2 weeks after ICA-treatment was measured and analyzed using microarray and pathway analysis. The signaling pathway was further explored by western blot assay and inhibitors of p38 and ERK: SB203508 and PD98059.

Results—Micro-CT displayed a decrease in bone mass at 3 month after OVX. ICA treatment increased the trabecular thickness (Tb.Th), osteoblast while decreased osteoclast number, elevating osteocalcin (OC) protein levels *in vivo* and facilitating the self-renewal and osteoblastic differentiation of bMSCs *ex vivo*. The osteogenic related genes ALP, BSP and Runx2 expressions were upregulated by ICA treatment and 10-5M showed the strongest effect in ALP assay in vitro. Pathway analysis from *in vivo* data revealed that the core genes acted by ICA were highly involved in MAPK signaling pathway. Further study demonstrated ICA suppressed ERK1/2 while stimulated p38 MAPK phosphorylation to promote osteoblastic differentiation *in vitro*.

Conclusion— Icariin promotes bone formation in OVX-mice. The suppression of ERK and stimulation of p38 might be involved in the process.

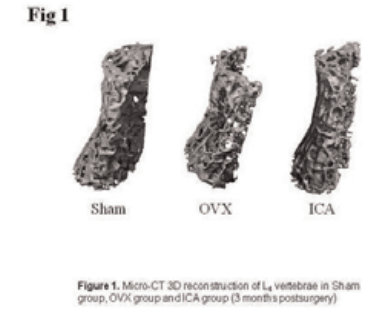

figure 1

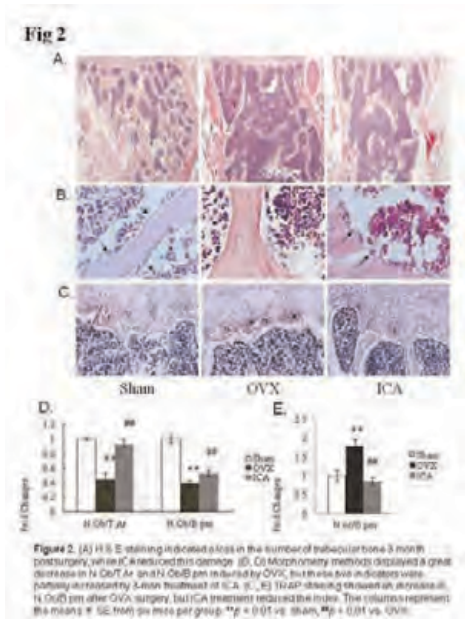

figure 2

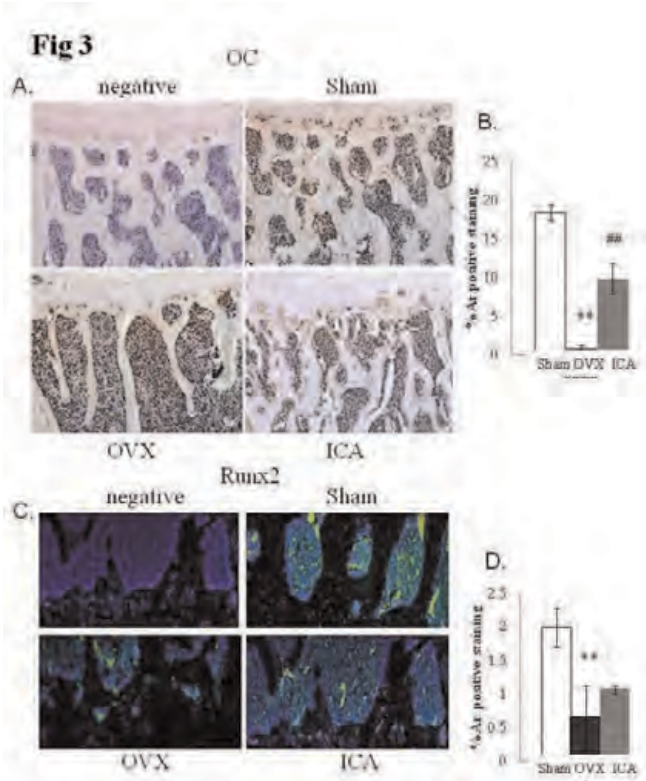

Figure 3. Reduced positive staining for OC (brown) and Runx2 (green) was observed, especially on the surface of bone lacuna in the OVX group. In the ICA group, OC protein was increased but Runx2 protein had little changes. The columns represent the means ± SE from six mice per group. $^{**}p < 0.01$ vs. sham, $^{\#\#}p < 0.01$ vs. OVX.

figure 3

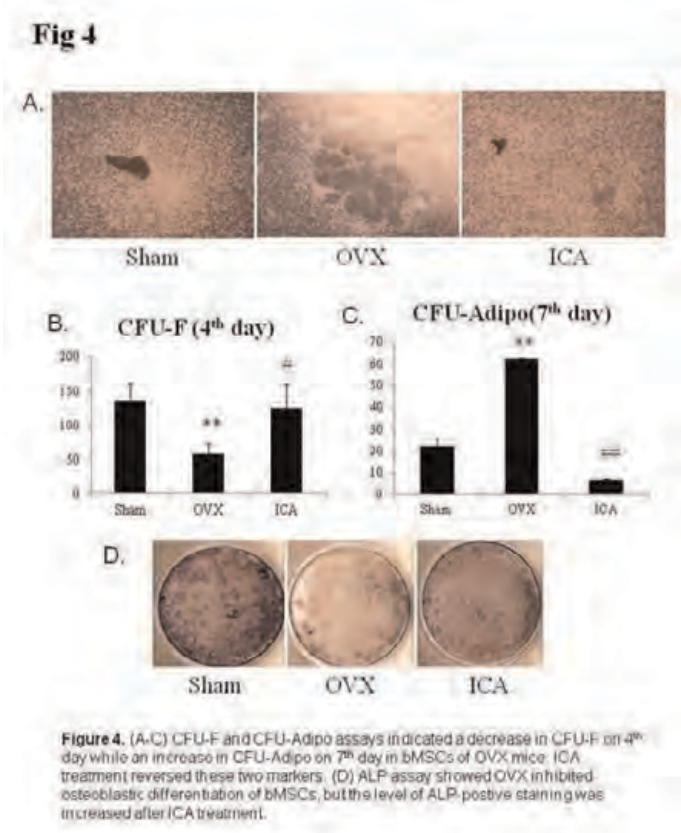

Figure 4. (A-C) CFU-F and CFU-Adipo assays indicated a decrease in CFU-F on 4th day while an increase in CFU-Adipo on 7th day in bMSCs of OVX mice. ICA treatment reversed these two markers. (D) ALP assay showed OVX inhibited osteoblastic differentiation of bMSCs, but the level of ALP-postive staining was increased after ICA treatment.

figure 4

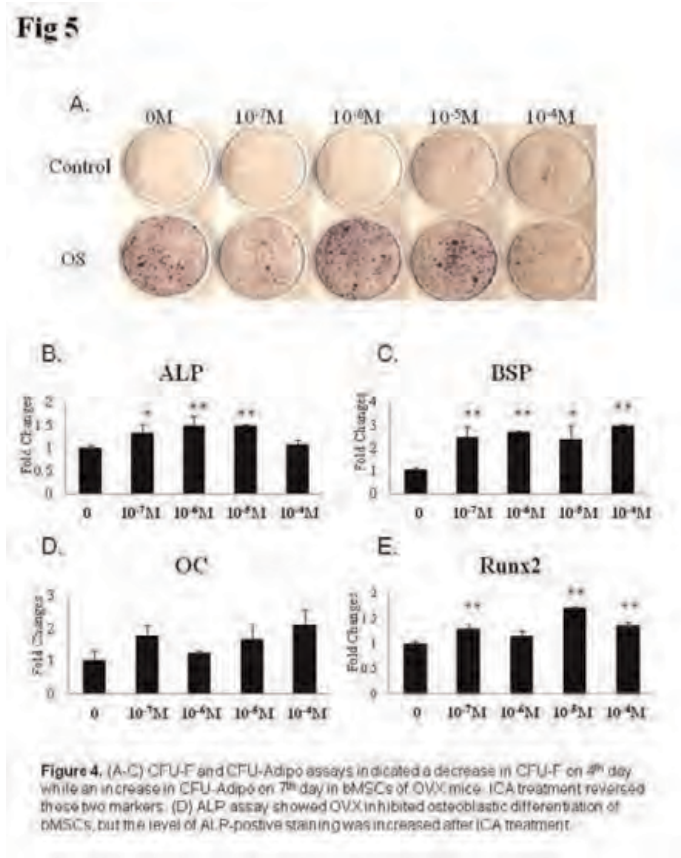

Figure 4. (A-C) CFU-F and CFU-Adipo assays indicated a decrease in CFU-F on 4th day while an increase in CFU-Adipo on 7th day in bMSCs of OVX mice. ICA treatment reversed these two markers. (D) ALP assay showed OVX inhibited osteoblastic differentiation of bMSCs, but the level of ALP-postive staining was increased after ICA treatment.

figure 5

***Disclosures: Qin Bian**, None.*

SA0424

Improved Bone Quality in Diet-Induced Obesity by Low Intensity Vibrations is Paralleled by Suppressed Bone Marrow Adiposity and Reduced Pro-Inflammatory State of Mesenchymal Stem Cells. M. Ete Chan*[1], Benjamin Adler[1], Danielle Green[1], Gabriel Pagnotti[1], Vihitaben Patel[2], Denis Nguyen[2], Clinton Rubin[3]. [1]Stony Brook University, USA, [2]Biomedical Engineering Department, Stony Brook University, USA, [3]State University of New York at Stony Brook, USA

Obesity-induced chronic inflammation has recently been recognized to increase the risk of both type 2 diabetes and bone fracture in part due to disruptions to the bone marrow niche. Mechanical signals delivered via low intensity vibrations (LIV) have been shown to improve obesity-induced deterioration of bone via influencing the bone marrow niche and promoting the osteogenic potential of mesenchymal stem cells (MSCs). In addition to being the progenitor of bone-forming osteoblasts, MSCs possess an immunomodulatory property which could alter the inflammatory status of the bone marrow niche. To explore how LIV influences the bone marrow environment and, more particularly, the skeletal-immune system interplay during obesity, a murine model of diet-induced obesity was adopted in this study. In an 8-week study, thirty 5w old male C57BL/6J mice were divided into 3 groups (n=10): regular diet (RD; 10 kcal% fat), high fat diet (HF; 45 kcal% fat) and high fat diet with LIV (HFv). LIV was delivered via a vertically oscillating plate (30min/day, 5 day/wk at 90Hz and 0.2g) to HFv, while HF and RD were sham-handled. The obese phenotype was evident in HF and HFv with a +12% higher body mass relative to RD ($p=0.01$). Biomechanical testing showed that the tibiae of HF had lower stiffness (-22%) and elastic modulus (-45%) than RD ($p=0.03$), indicating an increased fracture risk in obesity (Fig. A). The compromised bone quality in HF was paralleled by the disturbance of bone marrow niche as indicated by an increased bone marrow adiposity (Fig. B) and increased pro-inflammatory marker toll like receptor 4 (TLR4) of MSCs ($p<0.05$) (Fig. C). Interestingly, LIV increased the stiffness and elastic modulus of tibia in HFv by +27% and +108% compared to HF ($p=0.02$), respectively. Accompanying these improvements are the reduction of bone marrow adiposity (Fig. B), the increase of bone marrow MSC populations (+53%) and the reduced expression of TLR4 (-25%) in HFv relative to HF ($p<0.05$) (Figs. B and C). This study shows that obesity disrupts the bone marrow niche by increasing bone marrow adiposity and by promoting inflammation. LIV improves the bone marrow composition via lowering the adipose burden and regulating the number and immunomodulatory properties of MSCs in the bone marrow, which improves the bone quality and decreases fracture risk.

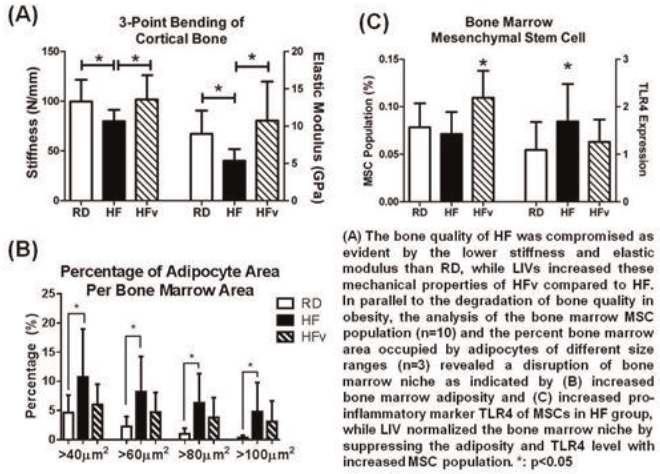

(A) The bone quality of HF was compromised as evident by the lower stiffness and elastic modulus than RD, while LIVs increased these mechanical properties of HFv compared to HF. In parallel to the degradation of bone quality in obesity, the analysis of the bone marrow MSC population (n=10) and the percent bone marrow area occupied by adipocytes of different size ranges (n=3) revealed a disruption of bone marrow niche as indicated by (B) increased bone marrow adiposity and (C) increased pro-inflammatory marker TLR4 of MSCs in HF group, while LIV normalized the bone marrow niche by suppressing the adiposity and TLR4 level with increased MSC population. *: p<0.05

Figures A-C

***Disclosures: M. Ete Chan**, None.*

SA0425

See Friday Plenary Number FR0425.

SA0426

Small Bone Size and Compromised Bone Strength Characterize the Tibia in Young Amenorrheic Exercising Women. Rebecca Mallinson*[1], Nancy Williams[2], Daniel Schiferl[3], Emily Southmayd[1], Mary Jane De Souza[1]. [1]Pennsylvania State University, USA, [2]The Pennsylvania State University College of Medicine, USA, [3]Bone Diagnostic, Inc., USA

An energy- and estrogen-deficient environment contributes to low bone mineral density (BMD) in amenorrheic athletes; however, habitual exercise is beneficial for bone strength. To determine the opposing effects of menstrual dysfunction and exercise on bone health in amenorrheic athletes, it is essential to assess both bone mass and geometry. The purpose of this study is to determine if exercising amenorrheic (ExAm) and eumenorrheic (ExEu) women differ with respect to volumetric BMD (vBMD), bone geometry, and estimated bone strength at the tibia. Exercising women were categorized as ExAm if they reported no menses for the past 3 months or ExEu if they reported ⩾10 menstrual cycles in the past 12 months. Body composition and areal BMD were assessed by dual-energy x-ray absorptiometry. vBMD, bone geometry, and muscle area at the tibia were measured by peripheral quantitative computed tomography, and the bone strength index (BSI) and strength strain index (SSI) were calculated at the distal and proximal tibia, respectively. ExAm (n=13) and ExEu (n=12) women aged 20.6 years did not differ in height, body mass index (BMI), age of menarche, or hours of habitual physical activity. Body mass (p=0.023) and lean mass (p=0.014) were lower in ExAm women compared to ExEu women, but fat mass was similar between groups. Duration of amenorrhea in ExAm women was 343 days; 69% and 33% of ExAm and ExEu women, respectively, reported prior episodes of amenorrhea. No differences in vBMD, bone area, or BSI were observed between groups at the distal tibia. At the proximal tibia, ExAm women had smaller total bone area (ToA, p=0.005), periosteal circumference (PCircum, p=0.005), SSI (p=0.010) and muscle area (p=0.016) compared to ExEu women but greater cortical vBMD (p=0.048). Lean mass ($p<0.001$) and habitual physical activity ($p<0.03$) were positively correlated with ToA, PCircum, and SSI at the proximal tibia; whereas, fat mass and BMI were positively correlated with vBMD and BSI at the distal tibia ($p<0.05$). Compromised bone size and strength at the proximal tibia of ExAm women may indicate that the normal response of bone to mechanical loading is attenuated in an energy- and estrogen-deficient environment that persists into adulthood; however, lean mass may also play a role in the differences in bone size and strength between groups. Lean mass may strongly influence bone strength at proximal sites; whereas, nutritionally-related factors may be more influential at distal sites.

***Disclosures: Rebecca Mallinson**, None.*

SA0427

A Dual Isotope Hybrid μCT-PET System Reveals Functional Heterogeneity of Bone Lining Cells and Longitudinal Changes in Marrow from Local Radiation and Chemotherapy. Masashi Yagi*[1], Luke Arentsen[1], Yutaka Takahashi[1], Leslie Sharkey[1], Masahiko Koizumi[2], Cory Xian[3], Clifford Rosen[4], Douglas Yee[1], Susanta Hui[1]. [1]University of Minnesota, USA, [2]Osaka University, Japan, [3]University of South Australia, Australia, [4]Maine Medical Center, USA

Despite the increase of long-term cancer survivors, the impact and mechanism of radiation and/or chemotherapy on normal bone and bone marrow are not well characterized. μCT-PET in a mice model allows investigation of the entire skeleton and monitoring of functional changes by imaging radiotracer behavior in vivo. We report the skeletal and marrow response to clinically relevant local radiation and chemotherapy using μCT-PET and reveal a potentially important role for bone lining cells in mediating the skeletal response to local and systemic injury.

Mice were given systemic methotrexate (MTX, 2.5mg/kg, 3 days) or 16Gy local radiation to legs. Longitudinal FDG (days -4, 2) and NaF (days -3, 3, 7, 14, 29) μCT-PET scans were performed (Fig. 1). Eight skeletal regions were monitored. Distal femora were harvested for cellular histology.

We observed significant functional heterogeneity throughout the skeleton for bone mineral remodeling as measured by NaF (<0.0001, Fig. 2) and marrow metabolic function (FDG) (<0.0001, Fig. 3). Radiation caused an early decrease in marrow metabolic function, consistent with histologic studies, in which marrow cellularity was drastically reduced in day 3 post radiation (Table). We found a high correlation (R=0.90) between pre- and post-radiation FDG uptake. This supports the idea of an initial physiological status that predicts the response to treatment. It also suggests that marrow cells post treatment (day 30) are as metabolically active as pre-treatment. The early increase in NaF uptake (<0.05, Fig. 4) post-radiation (day3) was associated with an increase in sinusoid and lining cells in endosteal regions of the skeleton (Table). There were also significant distant effects (outside radiation sites) measured by both tracers that may be due to increased cytokines and vascular permeability. Acute MTX induced inflammation also causes an early increase in NaF uptake, and both local radiation and chemotherapy shows similar patterns of NaF changes over time (Fig. 5). Reduction in NaF uptake over time is a result of diminished mineralization due to a change in bone remodeling.

Dual isotope μCT-PET revealed functional heterogeneity of the skeleton in response to local radiation or chemotherapy. These studies demonstrate an important role for bone lining cells in mediating the skeletal and possibly the marrow response to injury. This methodology also establishes a translational model for studying the skeletal health of cancer survivors.

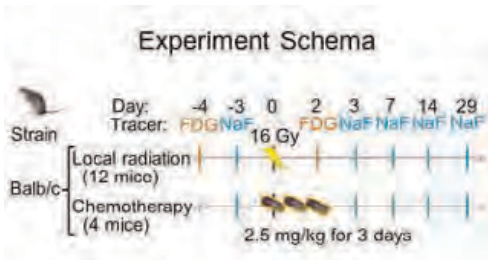

Figure 1. Schema of this experiment

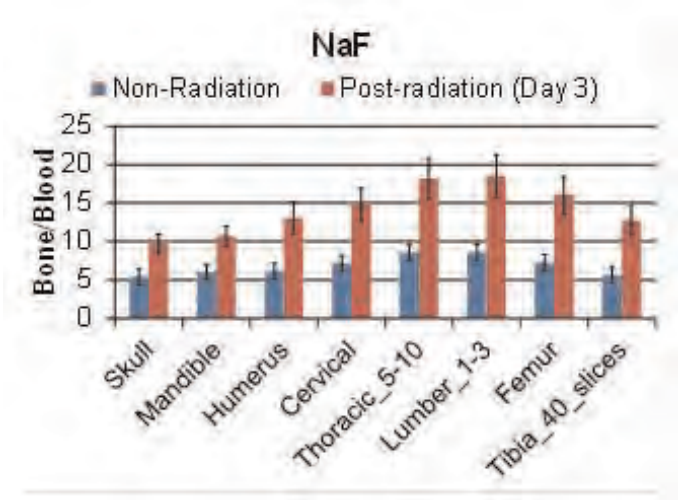

Figure 2. NaF uptake of all skeletal regions before and after local radiation

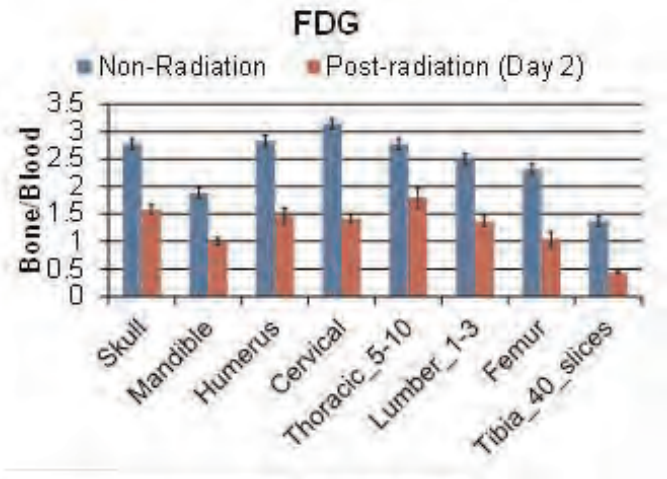

Figure 3. FDG uptake of all skeletal regions before and after local radiation

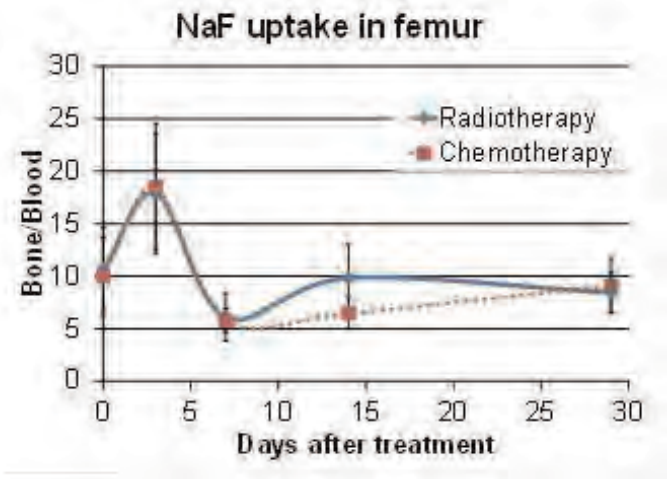

Figure 4. Comparison of time course change of NaF uptake between local radiation and chemotherapy

Status	number	Day	% cellularity	sinusoidal dilation	edema	congestion	inflammation	necrosis	Osteoblasts /clasts lining cortical bone
Control	5	5	95%	0	0	0	0	0	Flat lining cells
Radiation	5	5	5%	2+	0	2+	0	0	Focally pump lining cells
Control	5	5	95%	0	0	0	0	0	Flat lining cells
Radiation	5	5	15%	2+	2+	2+	0	0	Flat lining cells
Control	5	30	96%	0	0	0	0	0	Flat lining cells
Radiation	5	30	72%	0	0	1+	0	0	Flat lining cells

Figure 5. H&E stained histology analysis data

***Disclosures: Masashi Yagi**, None.*

SA0428

See Friday Plenary Number FR0428.

SA0429

Bone Density in Apheresis Donors compared to Whole Blood donors. Carolien Boot[1], Jessie Luken[2], Peter van den Burg[2], Wim de Kort[2], Rianne Koopman[2], Hans Vrielink[2], Natasja van Schoor[1], Martin Den Heijer[3], Paul Lips*[1]. [1]VU University Medical Center, The Netherlands, [2]Sanquin Blood Supply, Netherlands, [3]VU Medical CenterPostbus 70571007 MB Amsterdam, The Netherlands

Apheresis donation is a procedure in which blood components, such as platelets or plasma, are separated and collected from whole blood. During the procedure the processed blood is returned to the donor. Trisodium citrate complexing calcium is used as an anticoagulant. This complexing can cause symptomatic hypocalcemia and hypomagnesemia. In the first 24 hours after donation an increase of serum parathyroid hormone (PTH) is seen. The potential long-term consequences are not known, such as decrease of bone mineral density, or occurrence of osteoporosis. The aim of the study was to compare bone mineral density of postmenopausal apheresis donors with postmenopausal whole blood donors.

This pilot study was done in 20 female postmenopausal apheresis donors (mean age 62.7 years old, SD 3.9) who underwent plasma apheresis donation more than 100 times in the last 15 years. Controls were 20 female whole blood donors (mean age 62.7 years, SD 3.9). Both groups underwent a DXA scan, and blood samples were collected (including 25-hydroxyvitamin D, PTH, serum C-terminal telopeptide (CTx) and procollagen type 1 N-terminal propeptide(P1NP)). Potential risk factors for osteoporosis were assessed by a questionnaire. Absolute bone mineral density of the lumbar spine was 1.00 (SD 0.18) in apheresis donors and 0.92 (SD 0.12) in whole blood donors ($p = 0.09$). T-scores of the lumbar spine were -0.45 (SD 1.57) in apheresis donors and – 1.18 (SD 1.10) in whole blood donors (p 0.099). Absolute bone mineral density of the hip was 0.86 (SD 0.12) and 0.88 (SD 0.14) in apheresis donors and whole blood donors respectively ($p=0.88$). T-scores of the hip were -0.71 (SD 0.90) in apheresis donors and -0.63 (SD 1.15) in whole blood donors ($p=0.83$) 25-hydroxyvitamin D was in apheresis donors 58.6 nmol/L (SD 17.6), in whole blood donors 52.4 nmol/L (SD 18.5), PTH was respectively 6.4 pmol/L (SD 1.8) and 6.7 pmol/L (SD 1.9). 25-hydroxy vitamin D and PTH levels were not different between the groups.

With regard to bone mineral density no significant difference between apheresis donors and whole blood donors was found. However, in the apheresis group a trend towards a higher bone mineral density was suggested. This could possibly be caused by a short PTH elevation resulting in an anabolic response. On the basis of our pilot study apheresis donation appears to be safe. To gain more knowledge further investigation with larger study groups has to be done

***Disclosures: Paul Lips**, None.*
This study received funding from: Sanquin Blood Supply

SA0430

See Friday Plenary Number FR0430.

SA0431

See Friday Plenary Number FR0431.

SA0432

See Friday Plenary Number FR0432.

SA0433

Early Dental Implant Stability Correlates with Bone Turnover in Bisphosphonate Exposed Patients. Pamela Taxel MD*, Denise Ortiz MPH, David Shafer DMD, David Pendrys DDS PhD, Susan Reisine PhD, Kandasamy Rengasamy, D.D.S., Martin Freilich DDS. University of Connecticut Health Center, USA

Purpose: To assess the relationship between dental implant stability and bone turnover in patients with or without bisphosphonate (BP) exposure for the treatment of osteopenia or osteoporosis.

Methods: One dental implant site was evaluated in 72 postmenopausal women with a spectrum of bone health enrolled in a descriptive ''best practice'' prospective cohort study. BP exposure at enrollment was categorized as ''never'' or ''past/current'' exposure. Per dental guidelines, participants were asked to discontinue BPs around dental implant placement. Implant stability was assessed by resonance frequency analysis (RFA ISQ value) at surgery and eight weeks following implant placement.

Measurement of sCTX, a marker of bone turnover, was obtained pre-treatment, one and eight weeks following implant surgery.

Results: The patients' mean age was 61.6 ± 5.2 years and 68% were osteopenic or osteoporotic; 25 of 72 participants (35%) were "past/current" BP users. At implant placement the average RFA ISQ value for the entire sample was 65.6 ± 10.9 (values > 50 considered adequate), and increased 8 weeks post-surgery to 75.2 ± 8.3 ($p<0.01$). The "never" and "past/current" groups each had RFA ISQ increases from implant placement to 8 weeks ($p<.01$, respectively). Among "past/current" BP users there was a significant negative correlation between RFA ISQ and sCTX values at one week ($r_s=-.56$, $p<0.01$) and eight weeks ($r_s=-.47$, $p<0.05$). A similar relationship was not seen in "never" users.

Conclusion: Dental implant stability as measured by RFA ISQ increased equally in "never" or "past/current" BP users between implant placement and eight weeks post-surgery consistent with successful osseointegration. However, in "past/current" BP users lower bone turnover was associated with higher short-term implant stability, as measured by RFA ISQ. The relevance of this finding to long-term dental implant stability is unclear at the present time. Thus, these interim findings require further long-term follow-up and investigation in a larger population with and without BP exposure to determine if implant stability is improved by exposure to antiresorptive medications.

***Disclosures: Pamela Taxel MD**, None.*

SA0434

Factors Associated with Nonunion in 97 Consecutive Type 2 and Type 3 Odontoid Fractures in Elderly Patients. Debra Sietsema*[1], Michael Merrick[2], Casey Smith[2], Tan Chen[3], Scott Russo[4], Clifford Jones[1], James Stubbart[4]. [1]Orthopaedic Associates of Michigan; Michigan State University, USA, [2]Grand Rapids Medical Education Partners, USA, [3]Michigan State University, USA, [4]Orthopaedic associates of Michigan, USA

Purpose: Odontoid fractures are the most common cervical spine injury in older adults and have high rates of morbidity and mortality. The purpose of this study was to determine factors that were associated with nonunion in odontoid fractures. Methods: Between 2002 and 2011, 97 consecutive patients, age 65 years and over, with type 2 and type 3 odontoid fractures were treated at a single Level I trauma center, were followed in a single private practice, and retrospectively evaluated. Radiographs were reviewed and fusion was determined by flexion/extension x-rays, CT scan, or both. Twenty-three mortalities occurred prior to six months post-injury, and they were excluded from the fusion analysis. One patient was lost to follow-up prior to evaluation for fusion. Results: There were 31 (42%) males and 42 (58%) females with a mean age of 80 (range 65-93) who were evaluated for fusion of their type 2 (55, 75%) or 3 (18, 25%) odontoid fracture. Mean body mass index was 26.9 (range 17.1-37.5). The overall fusion rate in the 73 patients who were living at the time of fusion analysis was 71.2%. Patients treated with non-operative management had a lower rate of fusion (31/51, 60.8%) compared to patients who were treated with surgery (21/22, 95.5%), ($x^2=0.003$). Males had a lower fusion rate (18 of 31, 58.1%) than females (34 of 42, 81%), ($x^2=0.033$). Fusion was affected by comorbidities. Those with fusion had a lower Charlson score (1.65) than those who did not fuse (2.67) (t=-2.045, sig =0.045). Additionally, congestive heart failure (CHF) was a significant independent medical comorbidity associated with nonunion. Out of the 21 patients who were found to have nonunion, 8 had a diagnosis of CHF at the time of admission (38.1%). 52 patients were found to have a fusion of their odontoid fracture, and only 4 of those patients had congestive heart failure (7.7%), ($x^2=0.002$). Factors without statistical significance included age, BMI, tobacco use, sagittal fracture displacement, direction of displacement, type of odontoid fracture, odontoid angle, time to surgery, method of non-operative management, time to discontinuation of rigid collar, and operative technique. Conclusion: Factors associated with nonunion in older patients with odontoid fractures include: non-operative treatment, males, higher numbers of medical comorbidities, and congestive heart failure.

***Disclosures: Debra Sietsema**, Lilly USA,*

SA0435

DXA vs QCT Imaging of the Knee in People with Spinal Cord Injury. Apoorv Prasad[1], William Edwards[2], Kristine Herrmann[1], Danielle Barkema[1], Narina Simonian[1], Renita Yeasted[1], Karen Troy[2], Thomas Schnitzer*[1]. [1]Northwestern University, USA, [2]University of Illinois at Chicago, USA

Purpose: Bone loss is a common consequence of spinal cord injury (SCI) and is associated with a marked increase in fractures, particularly at sites around the knee. DXA measurement of the distal femur has been advocated to assess bone status though comparison with QCT has not been reported. This study was undertaken to compare DXA measurement to QCT imaging at the distal femur and proximal tibia.

Methods: A convenience sample of 31 individuals with SCI was studied; 11 were evaluated within 4 months of acute injury and the remainder had their injury for > 2yrs. Imaging of the knee by both QCT and DXA (Hologic QDR4500A) was accomplished within a 2 week timeframe in each individual. DXA of the knee was performed in duplicate. QCT data were analyzed to evaluate integral, trabecular and cortical BMD of three regions of the knees–distal femoral epiphysis, distal femoral metaphysis and proximal tibial epiphysis—per Drillis and Contini anthropometric proportionality constants (1966). DXA analysis utilized forearm software and a similar anatomic approach as the QCT analysis, with duplicate values for each region averaged. Correlation coefficients (Pearsons' r) were calculated using SPSS to evaluate correlations between site-specific DXA and QCT values.

Results: The study population was 67.7% male, average age 36.4 ± 13.6 yr, duration of SCI 11.4 ± 12.6 yr. There was excellent correlation between DXA and QCT trabecular and integral BMD measurements at the femoral epiphysis, femoral metaphysis and tibial epiphysis ($r>0.9$, $p<0.001$ for all), but weaker correlation between DXA and QCT cortical BMD values (Table 1).

Conclusions: A strong correlation exists between the DXA BMD and the integral and trabecular, but not the cortical, QCT values of the knee in all regions. QCT alone provides information regarding cortical bone status, important in assessing bone strength and fracture risk in SCI populations.

Table 1. Pearson's r for Regions of the Knee: DXA vs QCT

	Integral	Trabecular	Cortical
Femoral epiphysis	0.96	0.96	0.39
Femoral metaphysis	0.93	0.92	0.53
Tibial epiphysis	0.94	0.94	0.73

Table 1

***Disclosures: Thomas Schnitzer**, None.*

SA0436

Postpartum Osteoporosis and 1,25-Dihydroxyvitamin D-Mediated Hypercalcemia. Stephanie Stein*[1], Elizabeth Streeten[2]. [1]University of Maryland Medical Center, USA, [2]University of Maryland School of Medicine, USA

Background: During pregnancy and lactation, PTHrP secretion increases and serum levels correlate with postpartum bone loss but eucalcemia is maintained. In both postpartum osteoporosis and hypercalcemia, excessive PTHrP is usually the mediator. We report a case of postpartum osteoporosis with apparent 1,25(OH)2D-mediated hypercalcemia.

Clinical Case: A healthy 29 y.o. female presented 2 months postpartum with acute back pain and multiple atraumatic vertebral fractures. Her pregnancy was uncomplicated, and she had breastfed since delivery. MRI showed compression fractures of T8-12 and L1-5. She had no prior fracture and no family history of osteoporosis. Labs showed: serum Cr 0.6 mg/dL, hematocrit 37.5%, Ca 9.6 mg/dL, P 4.5 mg/dL, Mg 2.0 mg/dL, 25(OH)D 43 ng/ml, 1,25(OH)2D 41 pg/mL (nl 18-72), PTH 8 pg/mL (nl 12-68), TSH 1.8 uIU/mL, alkaline phosphatase (AP) 202 units/L (nl 38-126), SPEP/UPEP normal. Repeat labs 2 weeks later showed: Ca 12.5 mg/dL, 1,25(OH)2D 25 pg/mL, PTH <4 pg/mL, PTHrP 5 pg/mL (nl 14-27), AP 189 units/L, C-telopeptide 1185 (nl 64-640), prolactin 15.5 ng/mL. Serum Ca prior to pregnancy was normal. DXA Z-scores: L2-4 -2.5, total hip -1.9, femoral neck -1.8. Given her suppressed PTH and PTHrP with inappropriately normal 1,25(OH)2D, lymphoma and granulomatous diseases were considered. PET/CT was negative. She stopped breastfeeding and was given IV zoledronic acid 4 mg. Her back pain improved and 3 weeks later Ca was 9.0 mg/dL.

Discussion: We present a case of postpartum osteoporosis with hypercalcemia, high bone turnover, suppressed PTH and PTHrP and inappropriately normal 1,25(OH)2D consistent with upregulation of 1α-hydroxylation independent of PTH and PTHrP.

***Disclosures: Stephanie Stein**, None.*

SA0437

See Friday Plenary Number FR0437.

SA0438

Treatment with intravenous ibandronate does not affect renal function - a 24 months prospective controlled trial on renal function. Doris Wagner*[1], Georg Werkgartner[2], Hans Jörg Mischinger[2], Alexander R Rosenkranz[3], Karl Fenzl[4], Astrid Fahrleitner-Pammer[1]. [1]Medical University of Graz, Austria, [2]Department of Surgery, Divison of General Surgery, Medical University of Graz, Austria, [3]Department of Internal Medicine, Division for Nephrology, Medical University of Graz, Austria, [4]Roche Austria GMBH, Austria

Introduction: Renal safety of intravenous qualterly ibandronate (IBN) treatment has been questioned. Only measured glomerular filtration rates depict renal function accurately. This study aimed to investigate a potential effect of IBN on the measured GFR.

Patients and Methods: 79 patients who all suffered from osteoporosis (OPO) related to a past liver transplantation - were divided into two groups and enrolled into the study at the timepoint of IBN administration. The TRT group (patients with OPO) received 3 mg IBN, calcium and Vitamin D supplementation CTR group (patients without OPO) calcium and Vitamin D supplementation. The GFR was measured using the Inulin clearance (IC) at the start of IBN as well as 12 and 24 months thereafter. Spine X rays, BMD measurement at the distal radius and the femoral neck and serum markers were performed for group assignment and 12 and 24 months thereafter.

Results: The median IC was 65.4 mL/min1.73m2 in TRT and 66.7 mL/min1.73m2 in CTR patients at baseline. The IC decreased throughout the study period (CTR patients 12 months: -4.2 mL/min1.73m2, TRT patients 24 months: -6.7 mL/min1.73m2; CTR patients 12 months: -5.3 mL/min1.73m2, TRT patients 24 months: -7.5 mL/min1.73m2) in both groups but did not differ in between. Serum cross laps as well as TRAP 5b decreased significantly in TRT patients (-51% sCTX, -34% TRAP 5b, p vs baseline: 0.0001) but increased in CTR patients (+11% sCTX, + 15% TRAP 5b, p vs baseline: 0.05). T scores at the femoral neck and the distal radius increased in TRT patients (overall increase: + 16% femoral neck, + 27% distal radius, p vs baseline both : 0.001).

Conclusion: Renal function did not differ significantly between patients with and without IBN throughout the study so IBN treatment seems to be safe for OLT patients.

***Disclosures: Doris Wagner**, None.*

SA0439

See Friday Plenary Number FR0439.

SA0440

See Friday Plenary Number FR0440.

SA0441

Pharmacogenomics Of Bisphosphonate Treatment In Paget's Disease Of Bone: Retrospective And Prospective Analysis. Daniela Merlotti*[1], Fernando Gianfrancesco[2], Domenico Rendina[3], Riccardo Muscariello[3], Teresa Esposito[2], Beatrice Franci[4], Barbara Lucani[4], Stella Campagna[4], Laura Cresti[4], Pasquale Strazzullo[3], Ranuccio Nuti[1], Luigi Gennari[1]. [1]University of Siena, Italy, [2]Institute of Genetics & Biophysics - National Research Council of Italy, Italy, [3]Department.of Clinical & Experimental Medicine, University of Naples Federico II, Italy, [4]Dept. Medicine Surgery & Neurosciences University of Siena, Italy

Mutations in *SQSTM1* gene have been identified in up to 15-20% of patients with Paget's disease of bone (PDB). In a preliminary analysis we evidenced a reduced response to iv pamidronate in *SQSTM1* mutation carriers (*SQSTM1*+). In order to confirm and extend this observation, we investigated the effect of *SQSTM1* mutation and polymorphisms in 3 genes associated with PDB (*TNFRSF11A* rs1805034; *OPTN* rs1561570; *TNFRSF11B* rs2073617) on the response to the treatment with different bisphosphonates. As first, genetic analysis was performed retrospectively in 335 patients involved in previous studies with clodronate (CLN) 1500 mg every 6 months (n=84), pamidronate (PAM) 60mg iv every 6 months (n=75), risedronate (RIS) 30 mg/day for 2 months (n=57), neridronate (NER) 200mg im o iv (n=61) and zoledronic acid (ZOL) 4mg or 5 mg iv (n=48). Overall, *SQSTM1*+ patients had an increased disease severity and showed a reduced response to CLN or PAM than *SQSTM1*- patients (biochemical response at 6 months 37% vs 82% with CLN and 31% vs 60% with PAM, $p<0.001$, respectively in *SQSTM1*+ vs *SQSTM1*-). Despite carriers of *TNFRSF11A* rs1805034 CC genotype had increased PDB severity, there was no association between this genotype and the response to any treatment. Conversely, there was an increased prevalence of TT carriers of rs1561570 (*OPTN*) in nonresponders than responders to CLN. Normalization after the first CLN course was achieved in 69% of CC vs 42% of TT carriers despite no significant differences in disease extension or activity, and this effect increased when *SQSTM1*- patients were considered. A similar but not significant trend was observed for PAM. Conversely, RIS, ZOL and NER were effective in most patients without any association with *SQSTM1* or other gene polymorphisms. We then designed a prospective analysis in patients treated with iv ZOL 5mg (n=130) or NER 200mg (n=70) and followed-up for more than 3 years (range 3-6 yrs). After the infusion no treatment was given except in case of relapse. Even though most patients achieved biochemical remission after the first NER course for more than 12 months, there was a trend for an earlier relapse in *SQSTM1*+ vs *SQSTM1*-patients (22 ± 11 vs 36 ± 15 months, $p=0.07$). Conversely most ZOL treated patients achieved biochemical remission independent of *SQSTM1* mutation and did not need retreatment. These results suggest that PDB patients with *SQSTM1* mutation may require a more aggressive treatment regimen for long-term disease remission.

***Disclosures: Daniela Merlotti**, None.*

SA0442

Glucocorticoid Receptor in Inflammatory Bone Disease and Osteoporosis: New Mechanisms of Action and new functional relevant Target Genes identified. Ulrike Baschant[1], Stephanie Wittig-Blaich[1], Mubashir Ahmad[1], Jeanette Knoll[2], Torsten Kroll[2], Stephan Culemann[2], Alexander Rauch[2], Gerhard Krönke[3], Markus Seibel[4], Hong Zhou[4], Aspasia Ploubidou[2], Jan Tuckermann*[5]. [1]Institute for General Zoology & Endocrinology, University of Ulm, Germany, [2]FLI, Leibniz Institute for Age Research, Jena, Germany, [3]Med. Clinic III, University of Erlangen, Germany, [4]Bone Research Program, ANZAC Research Institute, University of Sydney, Australia, [5]University of Ulm, Germany

Glucocorticoids (GCs) belong to the standard therapy of rheumatoid arthritis (RA), a severe auto-immune inflammatory bone disease. One major side effect of GCs affects the bone itself leading to GC induced osteoporosis (GIO), the most prevalent form of secondary osteoporosis.

GCs act via the glucocorticoid receptor (GR) that can alter gene expression by binding as a dimer to GC response elements in the promoter region of target genes or by interacting with and thus interfering with other transcription factors as a monomer. Using conditional and functional selective targeted mutations of the GR in mice, we previously established that dimerization of the GR in IL-17 producing T cells is indispensable for the anti-inflammatory effect in antigen-induced arthritis (PNAS 2011 108:19317). Now, we demonstrate that, surprisingly, in the K/BxN serum induced arthritis model GR dimer dependent gene regulation in non-hematopoietic cells (presumably in mesenchymal cells) is critical for the anti-inflammatory effects of GCs. Thus, for immunosuppression of arthritis GR dimerization is required in distinct cell types, which are of hematopoietic and mesenchymal origin.

In a model of GIO we previously showed that unexpectedly interaction of the GR monomer with AP-1, but not NF-kB in osteoblasts is decisive for bone loss (Cell Metabolism 2010 11:517).

Here, we report the identification of novel GR monomer-regulated target genes, employing a micro-array and functional genomics combined approach. In addition we describe a screening platform for the search for new GR agonist-derivatives not affecting osteoblast function.

Taken together, our approach gives new insights into GC action on arthritis and bone integrity that can be translated into new concepts for anti-inflammatory therapies preventing GIO.

***Disclosures: Jan Tuckermann**, None.*

SA0443

See Friday Plenary Number FR0443.

SA0444

See Friday Plenary Number FR0444.

SA0445

See Friday Plenary Number FR0445.

SA0446

See Friday Plenary Number FR0446.

SA0447

See Friday Plenary Number FR0447.

SA0448

See Friday Plenary Number FR0448.

SA0449

Calmodulin Mediates 1α,25(OH)$_2$D$_3$-Induced Activation of CaMKII in Osteoblasts. Sharon Hyzy[1], Maryam Doroudi*[2], Barbara Boyan[3], Zvi Schwartz[2]. [1]Georgia Tech, USA, [2]Georgia Institute of Technology, USA, [3]Virginia Commonwealth University, USA

Objective: Vitamin D plays an important role in maintaining bone and mineral homeostasis. 1α,25-dihydroxyvitamin D3 [1,25D3], an active metabolite of vitamin D3, is known to exert its rapid membrane-mediated effects via receptor (Pdia3) in caveolae, activating phospholipase-A2 (PLA2)-activating protein (PLAA) and Ca2+/calmodulin-dependent protein kinase II (CaMKII) and stimulating PLA2, resulting in prostaglandin-E2 (PGE2) release and PKC activation. We previously reported that PLAA is required for mediating the signal from Pdia3 receptor to cytosolic PLA2 (cPLA2). Further investigations confirmed the binding of PLAA to Pdia3 within 9 minutes after 1,25D3 treatment indicating that PLAA mediates the signal from Pdia3 receptor complex via a direct protein interaction. However, it is not clear how PLAA mediates the signal from caveolae to CaMKII, and signaling molecules linking PLAA to CaMKII remain to be identified. Previous reports suggested melittin, which has a region of homology with PLAA, binds tightly to calmodulin (CaM) in the presence of calcium. CaM is also a known regulator of CaMKII activation. The aim of this study was to evaluate if and how calmodulin mediates 1,25D3-activated CaMKII. Method: MC3T3-E1 osteoblasts were treated with 1,25D3 for 9 minutes. Whole cell lysates (WCL) were collected for plasma membrane fractionation and immunoprecipitation experiments. To investigate the effects of CaM inhibition on 1,25D3 membrane-mediated pathway, cells were pretreated with W-7, a CaM-specific inhibitor, for 30 minutes and next treated with 1,25D3 for 9 minutes. Activities of PKC, CaMKII and PGE2 release were measured. Results: Western blots of the plasma membrane fractions indicated that CaM was present in the plasma membranes with its greatest concentration in fraction 3, which represents caveolae microdomains. Intensity analysis of CaM bands indicated that 1,25D3 treatment reduced the abundance of CaM in caveolae. CaM was immunoprecipitated with PLAA protein complex from WCL treated with 1,25D3. No protein interactions between Pdia3/CaM and Cav-1/CaM were detected. CaM-specific inhibitors reduced CaMKII and PKC activities and PGE2 release in response to 1,25D3 treatment in a dose-dependent manner. Conclusion: Taken together, the results suggest that CaM plays a crucial role in mediating 1,25D3 rapid actions. CaM serves as a linking protein mediating the signal from PLAA protein complex to CaMKII. Supported by the Price Gilbert, Jr. Foundation.

***Disclosures: Maryam Doroudi**, None.*

SA0450

See Friday Plenary Number FR0450.

SA0451

Effect of Combined Calcium and Vitamin D Supplementation on Insulin Secretion and Insulin Sensitivity in Vitamin D-deficient Adults at High Risk of Type 2 Diabetes. Claudia Gagnon*[1], Robin Daly[2], André Carpentier[3], Zhong X. Lu[4], Catherine Shore-Lorenti[5], Ken Sikaris[4], Sonia Jean[6], Peter Ebeling[7]. [1]Centre hospitalier universitaire de Québec, Université Laval, Canada, [2]Centre for Physical Activity & Nutrition Research, Deakin University, Australia, [3]Department of Medicine, University of Sherbrooke, Canada, [4]Melbourne Pathology, Australia, [5]Department of Medicine, NorthWest Academic Centre, The University of Melbourne, Western Health, Australia, [6]INSTITUT NATIONAL DE SANTÉ PUBLIQUE DU QUÉBEC, Canada, [7]The University of Melbourne, Australia

Epidemiological data indicate that low serum 25-hydroxyvitamin D (25OHD) levels and calcium intake increase the risk of developing type 2 diabetes (T2D). This 6-month double-blinded placebo-controlled trial examined whether vitamin D and calcium supplementation improves insulin sensitivity and secretion as well as cytokines, adiponectin, osteocalcin, lipids and blood pressure in adults with low vitamin D status (serum 25OHD ≤22 ng/mL) who were at high risk of T2D (with prediabetes or an AUSDRISK score ⩾15). Ninety-five adults were randomized to receive combined calcium carbonate (1,200 mg) and cholecalciferol (2,000-6,000 IU to target 25OHD >30 ng/mL) daily or matching placebo pills. A 75g 2-h OGTT with repeated measures of glucose, insulin and C-peptide was performed at 0 and 6 months. Indices of insulin sensitivity (HOMA2%S; Matsuda index) and insulin secretion (insulinogenic index using C-peptide) were calculated. The lipid profile, CRP, TNF-α, IL-6, adiponectin, total and uncarboxylated osteocalcin were also assessed at 0 and 6 months. Analyses were performed on the 80 participants who completed the baseline and final visits (treatment n=35; placebo n=45). Participants were middle-aged adults (mean age 55 years; 69% women; 69% European background) at high risk of T2D (mean BMI 31 kg/m^2; 60% with impaired glucose tolerance). Supplement compliance was similar between the groups for calcium (treatment=81%; placebo=77%) and vitamin D (treatment=88%; placebo=86%). Mean baseline 25OHD was 18 ng/mL and increased to 36 ng/mL in the treatment group but remained unchanged in controls (16 ng/mL). Overall, 91% of participants in the treatment group achieved a 25OHD >30 ng/mL at 6 months. There were no significant changes in insulin sensitivity assessed by HOMA2%S or by Matsuda index, or insulin secretion, in either the treatment and placebo groups (Table 1). Moreover, treatment did not affect blood pressure, lipids, cytokines, adiponectin, total or uncarboxylated osteocalcin levels. These results remained unchanged after adjustment for potential confounders. No participant developed hypercalcemia but 6 participants in the treatment and 3 in the placebo group developed hypercalciuria (>300 mg/d). In conclusion, high-dose vitamin D and calcium supplementation to a target 25OHD level of >30 ng/mL for 6 months did not change OGTT-derived measures of insulin secretion and sensitivity in adults with low serum 25OHD at high risk of T2D.

Table 1. Change in insulin sensitivity and insulin secretion after 6 months of calcium and vitamin D supplementation or placebo.

	Treatment (n=35)	Placebo (n=45)	P value*	Adj. P value**
HOMA2%S				
Baseline	54 (43, 83)	44 (30, 82)	0.07	
6 months	56 (40, 74)	43 (30, 74)	0.09	
Change	-2 (-12, 8)	-3 (-10, 5)	0.75	0.61
Matsuda Index				
Baseline	44 (33, 68)	36 (23, 57)		
6 months	40 (30, 66)	35 (24, 46)		
Change	1 (-8, 9)	-1 (-8, 6)	0.72	0.34
Insulinogenic Index				
Baseline	0.5 (0.3, 0.6)	0.5 (0.4, 0.7)	0.25	
6 months	0.5 (0.3, 0.7)	0.4 (0.3, 0.7)	0.76	
Change	0 (-0.1, 0.1)	0 (-0.1, 0.1)	0.86	0.79

Data are presented as median (25th, 75th percentile).
* Wilcoxon test.
** ANOVA on rank with adjustment for variables that were different between treatment groups at baseline (fasting glucose, fasting insulin, season of blood sampling, systolic blood pressure, IL-6 and current smoking).

Table 1

***Disclosures: Claudia Gagnon**, None.*

SA0452

The Metabolite 24R,25-dihydroxyvitamin D Plays a Role in Primary Human Bone Cell Differentiation. Karen Van Der Meijden*, Paul Lips, Nathalie Bravenboer. VU University Medical Center, The Netherlands

Vitamin D plays an essential role in human skeletal health and mineral homeostasis. Human bone cells are able to synthesize the active metabolite 1,25-dihydroxyvitamin D (1,25(OH)$_2$D) from its precursor 25-hydroxyvitamin D (25(OH)D) by the enzyme 1α-hydroxylase (CYP27B1). Locally synthesized 1,25(OH)$_2$D might affect bone cell differentiation in an autocrine or paracrine way. In vitro, both 1,25(OH)$_2$D and 25(OH)D can stimulate bone cell differentiation, although the actions of 25(OH)D probably occur through hydroxylation into 1,25(OH)$_2$D. On the other hand, human bone cells may also convert 25(OH)D to 24R,25(OH)$_2$D as bone cells express CYP24. Therefore the aim of this study was to examine whether the actions of 25(OH)D occur via hydroxylation into 1,25(OH)$_2$D and to investigate whether 24R,25(OH)$_2$D can affect bone cell differentiation as well.

Primary human bone cells, obtained as outgrowth of bone trabeculae from the iliac crest, were electroporated with either CYP27B1-silencing RNA or non-targeting RNA. The reduction of CYP27B1 mRNA was determined after 48 hours using RT-qPCR. The electroporated cells were cultured in the presence of 0 or 400 nM 25(OH)D for 3 days and mRNA expression of alkaline phosphatase and osteocalcin was determined as markers for osteoblast differentiation. Primary human bone cells were also cultured in the presence of 0, 100, 200 or 400 nM 24R,25(OH)$_2$D for 3 days and mRNA expression of alkaline phosphatase, collagen type 1, osteocalcin, osteopontin, as well as CYP27B1, VDR and CYP24 was determined.

CYP27B1-silencing RNA reduced the mRNA expression for 60% compared to the non-targeting cells. The alkaline phosphatase and osteocalcin mRNA expression was increased in response to 25(OH)D both in the CYP27B1-silenced cells as in the non-targeting cells. The metabolite 24R,25(OH)$_2$D stimulated the mRNA expression of alkaline phosphatase, osteocalcin and osteopontin significantly, although collagen type 1 mRNA did not respond to 24R,25(OH)$_2$D. Furthermore, 24R,25(OH)$_2$D significantly increased CYP24 mRNA expression. CYP27B1 and VDR mRNA expression were not affected by 24R,25(OH)$_2$D.

These results suggest that the actions of 25(OH)D on osteoblast differentiation not only occur via hydroxylation into 1,25(OH)$_2$D. The metabolite 24R,25(OH)$_2$D may play a role in bone cell differentiation as well by regulating gene expression. In addition, this metabolite is also able to stimulate its own synthesis leading to higher local availability of 24R,25(OH)$_2$D.

***Disclosures: Karen Van Der Meijden**, None.*

SA0453

See Friday Plenary Number FR0453.

SA0454

Thyroid hormones decrease plasma 1α,25-dihydroxyvitamin D levels through directly and indirectly transrepression of the renal 25-hydroxyvitamin D_3 1α-hydroxylase gene (CYP27B1). Hironori Yamamoto*[1], Mina Kozai[2], Tomohiro Kagawa[2], Nagakatsu Harada[2], Shoko Ikeda[2], Otoki Nakahashi[2], Yutaka Taketani[2], Ken-ichi Takeyama[3], Shigeaki Kato[4], Eiji Takeda[5]. [1]University of Jin-ai, Japan, [2]University of Tokushima, Japan, [3]University of Harvard, USA, [4]Fukushima Medical University, Japan, [5]University of Tokushima School of Medicine, Japan

Hyperthyroid patients have been reported to have low levels of plasma 1α,25-dihydroxyvitamin D ($1,25(OH)_2D$), however, its detailed mechanism is still poorly understood. The present study determined whether renal 25-hydroxyvitamin D-1α-hydroxylase (CYP27B1) gene expression was negatively regulated by thyroid hormones. 3,3',5-tri-iodothyronine (T_3)-induced hyperthyroid mice showed marked decreases in plasma $1,25(OH)_2D$ levels and in renal expression of CYP27B1 mRNA. In addition, we observed that T_3 administration significantly decreased plasma $1,25(OH)_2D$ and renal CYP27B1 mRNA levels that were increased by low calcium diet, and induced hypocalcemia in mice fed a low calcium diet. Promoter analysis revealed that T_3 decreases the basal transcriptional activity of the CYP27B1 gene through thyroid hormone receptors (TRα, TRβ1) and the retinoid X receptor α (RXRα) in renal proximal tubular cells. Interestingly, we identified an everted repeat negative thyroid hormone response element (1α-nTRE) overlapping the sterol response element (SRE) and the TATA-box -50 to -20 bp from the human CYP27B1 gene transcription start site. We also established that CYP27B1 gene transcription is positively and negatively regulated by SRE-binding proteins (SREBPs) and T_3-bound TRβ1/RXRα via the 1α-nTRE. Furthermore, the renal SREBP-1c mRNA expression was down-regulated by T_3. These results suggest that transcriptional repression of the CYP27B1 gene by T_3-bound TRs/RXRα and SREBPs, acting through the 1α-nTRE, results in decreased renal CYP27B1 expression and plasma 1,25(OH)2D) levels.

***Disclosures: Hironori Yamamoto**, None.*

SA0455

See Friday Plenary Number FR0455.

SA0456

See Friday Plenary Number FR0456.

SA0457

See Friday Plenary Number FR0457.

SA0458

See Friday Plenary Number FR0458.

SA0459

See Friday Plenary Number FR0459.

SA0460

See Friday Plenary Number FR0460.

SA0461

Role of the stathmin gene in development of prostate cancer bone metastasis. Rongrong Zhang*[1], Asim Abdel-Mageed[1], Babatunde Oyajobi[2], Hong-Wen Deng[1], Ming Zhao[1]. [1]Tulane University, USA, [2]University of Texas Health Science Center at San Antonio, USA

Prostate cancer (PCa) has a propensity to metastasize to the skeleton and causes osteosclerotic and osteolytic lesions. In the bone microenvironment, PCa cells which possess osteoblast and osteoclast properties interact with bone remodeling cells. However, the molecular mechanisms responsible for the role of bone microenvironment in development of PCa metastasis are yet to be elucidated. Recently, we have identified stathmin, a microtubule targeting protein, as a powerful regulator of bone remodeling. Null for stathmin in mice resulted in a skeletal phenotype attributed to dysfunction of both osteoblasts and osteoclasts. The stathmin gene (oncoprotein 18) is associated with a number of malignancies, including PCa. Therefore, we hypothesize that deficiency of stathmin will diminish PCa metastatic bone lesions by altering osteoblastic and osteoclastic bone remodeling in the bone microenvironment. To test the hypothesis, first, we generated immunodeficient stathmin knockout (KO) mice by crossbreeding the stathmin KO mice with immunodeficient Rag2 null mice in which both T and B cell functions are depleted. Then, we performed tumor inoculation studies on these mice. PCa C4-2B cells, which are capable of causing both osteolyitc and osteoslerotic metastasis, were inoculated by intra-cardiac injection into stathmin/Rag2 double knockout (dKO) mice ($STMN^{-/-};Rag2^{-/-}$), control mice ($STMN^{+/+};Rag2^{-/-}$), and non-immunodeficient wild-type mice ($STMN^{+/+};Rag2^{+/+}$). X-ray and micro-computed tomography (μCT) scanning 6 weeks after tumor inoculation showed that while all wild-type $STMN^{+/+};Rag2^{+/+}$ mice did not develop any bone metastasis, all $STMN^{-/-};Rag2^{-/-}$ and $STMN^{+/+};Rag2^{-/-}$ mice developed bone metastasis as evidenced by both osteolyitc lesions in metaphyseal regions of both the tibia and femur and osteoslerotic lesions on cortical bone of tibia. However, compared to $STMN^{+/+};Rag2^{-/-}$ control mice, stathmin deficiency in $STMN^{-/-};Rag2^{-/-}$ dKO mice substantially reduced both osteolyitc and osteoslerotic metastases. Histology provides further evidence for bone metastasis in these mice. These results demonstrate that stathmin plays a critical role in development and progression of PCa bone metastasis, suggesting that targeting the stathmin gene, which not only inhibits tumor growth but also alters the bone microenvironment, could be a promising therapeutic approach for PCa bone metastasis.

***Disclosures: Rongrong Zhang**, None.*

SA0462

See Friday Plenary Number FR0462.

SA0463

See Friday Plenary Number FR0463.

SA0464

Osteosarcoma Cells modulate Bone Microenvironment via Extracellular Membrane Vesicle Biogenesis and Calcium Signaling Pathways. Rama Garimella*[1], Laurie Washington[2], Janalee Isaacson[3], Ossama Tawfik[4], Raymond Perez[5], Peter Rowe[1], Julian Vallejo[3], Madoka Spence[3], Marco Brotto[6]. [1]University of Kansas Medical Center, USA, [2]Division of Medical Clinical Oncology, Department of Internal Medicine, The University of Kansas Medical Center, USA, [3]Muscle Biology Research Group, School of Nursing & Health Studies, University of Missouri-Kansas City, USA, [4]Department of Pathology, The University of Kansas Medical Center, USA, [5]Division of Medical Clinical Oncology, Department of Internal Medicine, The University of Kansas Cancer Center, The University of Kansas, USA, [6]University of Missouri - Kansas City, USA

In recent years, the role of exosomes or nano-sized extra-cellular membrane vesicles (EMVs) as modulators of tumor microenvironment is a topic of emerging interest in cancer-bone interaction. The role of EMVs in osteosarcoma (OS), a highly aggressive bone tumor is not known. It is our hypothesis that calcium signaling in the OS bone microenvironment induces cytoskeleton rearrangements in tumor cells, stimulates Ca-dependent EMV biogenesis, and modulates OS invasion via secretion of EMV-derived growth factors and enzymes. The long term goal of the study is to investigate the role of exosomes or EMVs in OS pathobiology. We had previously demonstrated the presence of EMVs in the preclinical bioluminescent osteosarcoma orthotopic mouse (BOOM) model. In the current study, we have successfully isolated EMVs from the conditioned media of 143B human osteosarcoma cell cultures using differential ultracentrifugation, demonstrating that OS cells shed extra-cellular membrane vesicles. Nano-particle tracking analysis of 143B-EMVs indicated their size range to be 50-200 nm. Transmission electron microscopy confirmed the ultra-structure of 143B-EMVs, and detected the presence of both vesicular and perivesicular hydroxyapatite like-mineral, and multivesicular bodies (MVBs). Detection of MVBs and presence of exosome-specific biomarker CD-9 suggest that 143B-derived EMV preparations include exosomes. Biochemical characterization of 143B-EMV cargo demonstrated the presence of MMP1 and MMP13. To our best knowledge, the expression of MMP1 and MMP13 in 143B-derived EMVs is a novel finding. The role of calcium influx in vesicle biogenesis and cancer progression is a subject of immense interest. In this study, we observed that 143B cells actively mobilize calcium in the presence of ionomycin in a dose dependent manner, and cause cytoskeleton rearrangement as detected by calcium fluorescent imaging. Pre-treatment with 10μM forskolin, an adenylate cyclase activator increased calcium mobilization of 143B OS cells and induced cytoskeleton rearrangements leading to vesicular biogenesis. These findings suggest that the calcium response of osteosarcoma cells is sensitized by forskolin, and EMVs are modulated by adenylate cyclase activation. In conclusion, our results suggest a novel role for cAMP/calcium dependent pathway as a candidate mechanism for EMV biogenesis in the OS bone microenvironment.

***Disclosures: Rama Garimella**, None.*

SA0465

See Friday Plenary Number FR0465.

SA0466

The Potential Role of JAB1 in Osteosarcoma Pathogenesis. Lindsay Bashur*, Guang Zhou. Case Western Reserve University, USA

Osteosarcoma is the most common malignant primary bone tumor. Osteosarcoma patients with metastases have a survival rate of only 25%. Therefore, a greater understanding of the pathogenesis of osteosarcoma is needed for better diagnosis and treatment. A novel player in tumorigenesis that has emerged is the transcriptional cofactor JAB1 (also named CSN5), through its effects on cell proliferation, differentiation, survival, and cell cycle progression. Our laboratory has recently shown that JAB1 plays critical roles in the successive steps of skeletogenesis *in vivo*. JAB1 has been shown to be over-expressed in different types of cancers, including breast and lung, but has not been studied in bone cancer. Thus, the goal of this study is to determine the potential role of JAB1 in the pathogenesis of osteosarcoma. We first showed, by immunohistochemistry, that JAB1 was highly expressed in twelve osteosarcoma patients' biopsy samples. Next, to determine whether down-regulating JAB1 expression in osteosarcoma reduces tumorigenesis, we knocked down JAB1 expression in the 143B highly metastatic osteosarcoma cell line, using shRNA lentiviral vectors. The *JAB1* knockdown cells exhibited significantly reduced cell proliferation, colony formation, and motility compared with the control cells. In addition, a real-time RT-PCR array of the tumorigenesis pathway suggests that *JAB1* knockdown cells have increased differentiation with elevated *RUNX2* expression. Therefore, these results suggest that down-regulating JAB1 expression in osteosarcoma might reduce tumorigenesis. We will determine whether the down-regulation of JAB1 in 143B cells reduces tumorigenesis *in vivo* in xenograft experiments. On the other hand, to study the consequence of JAB1 over-expression *in vivo*, we have generated *Col1a1-JAB1* transgenic mouse lines using a well-characterized 2.3kb *Col1a1* promoter to over-express JAB1 in osteoblasts specifically. Previous mouse genetic studies have shown that p53 is a critical factor in the development of osteosarcoma, and that JAB1 is a negative regulator of p53 activity in other cancers. Therefore, we will determine whether increased *JAB1* expression promotes bone tumorigenesis *in vivo* in a p53-dependent manner using this novel *Col1a1-JAB1* transgenic mouse model. Ultimately, new therapies based on controlling the JAB1-mediated tumorigenesis will open new avenues for treating osteosarcoma and other skeletal malignancies.

***Disclosures: Lindsay Bashur**, None.*

SA0467

Tumor Suppressive Function of MicroRNA34c in Osteosarcoma. Yangjin Bae*[1], Huan-Chang Zeng[1], Jianning Tao[1], Lisa Wang[1], Jason Yustein[1], Brendan Lee[2]. [1]Baylor College of Medicine, USA, [2]Baylor College of Medicine & Howard Hughes Medical Institute, USA

MicroRNAs (miRNAs) have been implicated in diverse biological roles including development, cell proliferation, apoptosis, metabolic stress and tumorogenesis.The miR-34 family, tumor suppressive miRNA, is evolutionally conserved and directly regulated by p53 in response to DNA damage and oncogenic stress, inducing apoptosis and cell-cycle arrest. Our recent study of osteoblast-specific gain of function *miR-34c* mice (*Col1a1 2.3 kb-miR34c*) demonstrated a critical role for *miR-34c* during bone development and homeostasis by targeting multiple components of the Notch signaling pathway. We and others have shown that an osteoblast-specific Notch gain of function mouse model can stimulate proliferation of immature osteoblasts while inhibiting their differentiation into mature osteoblasts. Furthermore, this gain of function phenotype leads to the development of osteoblastic tumors and indeed, Notch signaling was also up-regulated in human osteosarcoma (OS) samples. Consistent with this observation, our transcriptional profiling of OS from p53 +/- mice exhibited elevated expression of Notch signaling, which leads to the proliferative and metastatic potential of OS. The genetic and epigenetic alterations in OS lead to a decreased miR-34 expression levels. *Here, we hypothesize that the miR-34 family plays a critical role as a negative regulatior of Notch signaling in osteoblasts and exhibits a potential mechanism to modulate the proliferative effect of Notch in the committed osteoblast progenitors. Hence, perturbation of the crosstalk between miR-34s, p53, and Notch may contribute to the pathogenesis of OS.* To examine whether GOF *miR-34c* can affect OS formation and progression, *Col1a1 2.3kb-miR34c* was crossed with *Col1a1 2.3kb Cre/+; p53 $^{f/f}$* (osteoblast-specific loss of *p53*). We assessed survival, hind limb paralysis, tumor progression and metastases of these mice. Also xenografts was performed using the hOS cell line 143b (p53-/-) stably expressing *miR-34c* (143b-34c) with proper controls to examin OS progression *in vivo*. In our genetic mouse model, we found that *Col1a1 2.3kb-miR34c*; *Col1a1 2.3kb Cre/+; p53 $^{f/f}$* mice significantly increased survival compared to *Col1a1 2.3kb Cre/+; p53 $^{f/f}$* mice. Furthermore, xenograft study showed regression of tumor growth in 143b-34c compared to 143b-controls. Overall, these results suggest that miR-34c acts as a tumor suppressor in osteosarcoma. The underlying molecular mechanism of miR-34c in OS is currently being pursued.

***Disclosures: Yangjin Bae**, None.*

SU0001

Aged related Gait Disturbance in Fibroblast Growth Factor 2 knockout mice. Toru Nishikawa*[1], Collin Homer-Bouthiette[2], Liping Xiao[2], Morgan Carlson[2], Marja Marie Hurley[3]. [1]Aichi Gakuin University, Japan, [2]University of Connecticut Health Center, USA, [3]University of Connecticut Health Center School of Medicine, USA

Sarcopenia is associated with a progressive degenerative loss of skeletal muscle mass, quality and strength. These symptoms are particularly exacerbated in frail elderly patients where sarcopenia becomes rapidly accelerated for causes still unknown. Fibroblast growth factor 2 (FGF2) plays a critical role in the recruitment of muscle stem cells (satellite cells) for adult regenerative myogenesis. Disruption of the Fgf2 gene in mice results in accelerated age-related bone loss however, the impact of Fgf2 knockout on age-related muscle function has not been reported. We examined whether aging is associated with changes in Fgf2 expression in muscle, and whether disruption of the Fgf2 gene in mice results in phenotypic differences between "resting" and ''exercised'' muscle with age. *Approach:* Fgf2 mRNA and protein levels were determined from tibialis anterior and gastrocnemius hindlimb skeletal muscles harvested from young (2 months) and aged (18 months) wild-type mice. Since previous studies reported that FGF2 and FGF6 have some common properties to support myogenesis, Fgf6 mRNA expression was also determined in muscles from young and aged WT and Fgf2KO mice. To assess whether knockout of the Fgf2 gene resulted in gait disturbances, ventral plate videography (DigiGait) analysis was performed whereby young and aged WT and Fgf2KO mice walked on a transparent treadmill belt. *Results:* A significant decrease in Fgf2 mRNA and protein was evident in muscles from aged WT mice compared with young. Interestingly there was a significant increase in Fgf6 mRNA expression in young Fgf2KO compared with young WT. Gait analysis revealed that hind limb propulsion duration (an indicator of muscle strength) was similar in young WT and Fgf2KO mice, but significantly shorter in aged KO mice (105.6 $\pm$ 57.9 ms) compared with WT littermates (189.6$\pm$65.5 ms $p<0.05$). Additionally, hindpaw eversion (an indicator of muscle weakness) was similar in young WT and Fgf2KO mice, but significantly greater in aged KO mice (12.6$\pm$3.0 ms) compared with WT (9.3$\pm$4.5 ms $p<0.05$). Braking duration (an indicator of ground reaction forces) was similar between young and old WT and KO mice. Since no gait dysfunction was observed between young WT and young Fgf2KO mice, we hypothesize that FGF6 may be able to compensate for FGF2 loss in young, but not aged mice. We conclude that knockout of Fgf2 or age-associated decreases likely contribute to impaired muscle function and the onset of sarcopenia phenotypes.

***Disclosures: Toru Nishikawa**, None.*

SU0002

Age-related switch of bone mass in p47^{phox} deficient mice through increased inflammatory milieu in bone. Jin-Ran Chen*[1], Oxana P. Lazarenko[2], Jian Zhang[2], Kelly Mercer[2], Michael L. Blackburn[2], Thomas M. Badger[2], Martin J. J. Ronis[2]. [1]University of Arkansas for Medical Science, Arkansas Children's Nutrition Center, USA, [2]University of Arkansas for Medical Sciences & Arkansas Children's Nutrition Center, Little Rock, AR 72202, USA

Bone remodeling is age-dependently regulated and changes dramatically during the course of development. Excessive accumulation of reactive oxygen species (ROS), including superoxide, hydrogen peroxide, and hydroxyl radicals, has been suggested to be the leading cause of many inflammatory and degenerative diseases and underlie the effects of ageing. In contrast, how physiological levels of ROS regulate bone remodeling at each life stage remains unknown. In addition to the mitochondrial electron transport chain, the NADPH oxidase (NOX) complex produces a large amount of ROS in the plasma membrane and cytosol. Here, we utilized a p47phox knockout mouse model in which NOX2 activity is lost as the result of loss of an essential cytosolic co-activator to characterize the bone phenotype at both 6 weeks and 24 months of age in male mice. Using peripheral quantitative CT (pQCT), μCT and femur three point bending analyses, in p47phox -/- mice at 6 weeks of age, we found that bone mass (including both trabecular and cortical bone mineral density and bone mineral content), bone volume, trabecular number, and bone strength were all significantly higher compared to wild type mice ($p< 0.05$). On the other hand, in p47phox -/- mice at 24 months of age, bone mass, bone volume and trabecular number were all significantly lower ($p<0.05$), while bone trabecular separation was higher compared to their age-matched wild type controls. Flow cytometric assay showed decreased ROS generation in bone marrow cells from both young and aged p47phox -/- mice compared with their respective controls. Serum bone formation marker alkaline phosphatase was higher in 6-week-old p47phox -/- mice compared to their wild type controls. Serum bone resorption marker TRAP 5b is higher in 24-month-old p47phox -/- mice compared to their wild type controls. While we did not observe any differences in proinflammatory cytokines such as IL6, TNFalpha, RANKL and MMP9 expression in 6-week-old p47phox -/- mice compared to wild type mice, these cytokines were all significantly higher in 24-month-old p47phox -/- mice compared to their wild type controls. These data indicate that the observed age-related switch of bone mass in p47phox deficient mice occurs through an increased inflammatory milieu in bone and that NOX2-dependent physiological ROS signaling suppresses inflammation in ageing. Supported in part by ARS CRIS #6251-51000-005-03S and R01 AA18282 (MJJR).

***Disclosures: Jin-Ran Chen**, None.*

SU0003

Bmi1 Plays A Critical Role in Preventing Bone Aging by Inhibiting Oxidative Stress. Qian Wang*[1], Rong Wang[1], Jianliang Jin[2], David Goltzman[3], Dengshun Miao[4]. [1]Nanjing Medical University, China, [2]Nanjing Medical University, Peoples Republic of China, [3]McGill University, Canada, [4]Nunjing Medical University, Peoples Republic of China

We previously demonstrated that Bmi1 deficiency results in premature osteoporosis. In the present study we examined whether the premature osteoporosis caused by Bmi1 deficiency was associated with oxidative stress-induced bone aging. We found that hydrogen peroxide concentration and the content of the lipid peroxidation product malondialdehyde (MDA) were both increased significantly in the bone tissue of 5-week-old Bmi1$^{-/-}$ mice compared with that of WT mice. We next treated 3-week-old Bmi1$^{-/-}$ mice with the antioxidant N-acetylcysteine (NAC, 1mg/ml) in their drinking water, and compared their phenotype with the phenotype of untreated Bmi1$^{-/-}$ and WT mice. NAC supplementation of Bmi1$^{-/-}$ mice resulted in a longer lifespan and increased body weight, although Bmi1$^{-/-}$ mice were not normalized. After 2 weeks, NAC-treated Bmi1$^{-/-}$ mice, when compared to untreated Bmi1$^{-/-}$ mice, displayed significantly increased bone mineral density, cortical and trabecular bone volume, osteoblast numbers, ALP and type I collagen positive areas and mineral apposition rate. The number of bone marrow adipocytes, the percentages of 8-hydroxy-2-deoxyguanosine positive or β-galactosidase positive osteocytes and the protein expression levels of PPARγ, γ-H2AX and p16^{INK4a} were reduced significantly in NAC-treated Bmi1$^{-/-}$ mice compared to untreated Bmi1$^{-/-}$ mice. Simultaneously, hydrogen peroxide concentration and MDA content were reduced significantly, whereas total antioxidant capacity, glutathione concentration, and superoxide dismutase protein and activity levels were increased significantly in NAC-treated Bmi1$^{-/-}$ mice compared to untreated Bmi1$^{-/-}$ mice. The number of total CFU-f and ALP^{+} CFU-f, the expression levels of Runx2 and cell proliferation were increased significantly, while oil Red positive cells and the percentage of apoptotic cells and the expression levels of PPARγ and p16INK4a were reduced significantly. Reactive oxygen species levels were reduced significantly, whereas the gene expression levels of glutathione reductase, glutathione peroxidase 1 and 4, and thioredoxin were up-regulated in bone marrow mesenchymal stem cell ex vivo cultures from NAC-treated Bmi1$^{-/-}$ mice compared to these from untreated Bmi1$^{-/-}$ mice. Nevertheless, all of the above parameters did not reach the normal levels of WT mice. These studies therefore indicate that Bmi1 plays a critical role in preventing bone aging by inhibiting oxidative stress.

***Disclosures: Qian Wang**, None.*

SU0004

Bone Breaks and Heart Aches- the Association between Bone Mass and Vascular Function. Lynae Hanks*[1], Ambika Ashraf[1], Barbara Gower[1], Jessica Alvarez[2], Krista Casazza[3]. [1]University of Alabama at Birmingham, USA, [2]Emory University, USA, [3]UAB, USA

An association between osteoporosis and cardiovascular disease has become apparent, indicating a relationship between bone degeneration and vascular dysfunction– particularly among the elderly and individuals with cardiometabolic abnormalities (i.e., hypertension). Little is known about early coincidental changes in bone and arterial properties, particularly in the context of bone anabolism (as in puberty) and state of relative equilibrium (early adulthood). The objective of this study was to determine if intermediate endpoints of vascular function (i.e. endothelial function, arterial stiffness) are associated with bone mineral content (BMC) in healthy females ages 14-42 years, and if there was a developmental effect in the relationship. In order to more comprehensively understand disease progression, this study also evaluated contribution of factors previously identified to play a role in bone and vascular integrity (i.e., insulin; vitamin D status, 25OHD; markers of inflammation). Endothelial function was assessed by flow mediated dilatation (FMD), arterial stiffness by pulse wave velocity (PWV) and augmentation index (AIx), systolic blood pressure (SBP) using average of three seated sphyngomamometer readings, BMC by DXA, and systemic factors assessed during fasting blood draw. We observed a positive association between SBP and BMC when all subjects were included which was independent of 25OHD, insulin or markers of inflammation. When stratified by age using 19 years as a cut-point, there was an inverse relationship between AIx in adolescent females when insulin ($p<0.10$) or markers of inflammation ($p<0.10$) were included as covariates. Conversely, there was a positive relationship between PWV and AIx in young adult females ($p<0.05$) independent of 25OHD, insulin or markers of inflammation. The link between bone and vascular linkage may be lifestage-dependent. Compromised vessel flow and deficits in bone mineralization early in life when the strength-structure of bone and vasculature are arguably most vulnerable could have profound effects on long-term bone and vascular health. Moreover, in the context of a less dynamic bone remodeling microenvironment, metabolic factors appear to moderate less of an effect than hemodynamics on structural properties centering the bone-vessel relationship.

***Disclosures: Lynae Hanks**, None.*

SU0005

CK2.1 a novel mimetic peptide, induces cartilage formation in vivo. Hemanth Akkiraju*, Anja Nohe. University of Delaware, USA

The goal of this study was to determine the mechanism of CK2.1, a mimetic peptide of Bone Morphogenetic Protein Receptor type Ia (BMPRIa), on cartilage formation. Osteoarthritis (OA) is a degenerative idiopathic disease characterized by calcification and degeneration of the articular cartilage. Only limited treatment options exist that focus on pain relief. New Treatments that can reverse the process of cartilage deterioration are desperately needed. Growth factors, like Bone Morphogenetic Protein 2 (BMP2), induce chondrogenesis and enhance extracellular matrix (ECM) production of pre-chondrocytes and chondrocytes. However the anabolic effects of chondrocytes, such as production of Collagen type II and Collagen type IX are short lived and result in cartilage hypertrophy in the long term. Chondrocyte hypertrophy leads to production of Collagen type X followed by degeneration of the ECM mediated by upregulation of MMP-13. Recently we identified a new BMP2 receptor interacting protein, Casein Kinase 2 (CK2). We designed novel peptides CK2.1 that release CK2 from the BMPRIa isoform activating the downstream BMP signaling pathways in the absence of BMP2. Treatment of CK2.1 on mesenchymal cells led to the increase of Collagen type II, while articular chondrocytes stimulated with CK2.1 led to the expression of Collagen type II and Collagen type IX. Contrary to BMP2, CK2.1 did not induce Collagen type X and MMP-13 protein expression. Additionally, CK2.1 increased *COMP, CREB, SOX9* mRNA levels in cultured mature articular chondrocytes. To verify the potential of CK2.1 in cartilage formation CK2.1 was injected into the tail vein of C57BL/6J mice. This injection resulted in an increased cartilage production compared to control. Additionally, the hypertrophic region in the growth plate was decreased in comparison to both control and BMP2 injected. Based on these findings we propose that peptide CK2.1 can be used for cartilage growth and repair.

***Disclosures: Hemanth Akkiraju**, None.*

SU0006

Decreased *Nfat1* Expression Contributes to Dysfunction of Articular Cartilage in Aging Mice. Mingcai Zhang*[1], Qinghua Lu[1], Kenneth Caldwell[1], Jamie Crist[1], Clayton Theleman[1], Jinxi Wang[2]. [1]Department of Orthopedic Surgery, University of Kansas Medical Center, USA, [2]University of Kansas Medical Center, USA

Purpose:NFAT1 (*Nfat1*) is a member of NFAT (nuclear factor of activated T cells) transcription factors.Mice lacking *Nfat1* exhibit normal skeletal development but begin to show articular cartilage degradation and early osteoarthritis (OA)-like changes in young adults, suggesting that *Nfat1* is not required for joint development but is essential for articular cartilage function in young adult mice. However, the effect of *Nfat1* on aging cartilage remains unknown. This study aimed to investigate the role of *Nfat1* in regulation of articular chondrocyte function in aging mice.

Methods:The hip, knee, and shoulder joints were harvested from wild-type BALB/c mice at 5, 12, 15, and 18 months of age for histochemistry, immunohistochemistry, and isolation of RNA, genomic DNA, chromatins, and articular chondrocytes. Total RNA isolated from femoral head cartilage was used for gene expression analysis by quantitative real-time PCR (qPCR).Genomic DNA and chromatins obtained from femoral and humeral head cartilage were used for Methylated DNA immune-precipitation assay and ChIP assay, respectively. *Nfat1* overexpression experiments were performed in cultured articular chondrocytes.

Results:Loss of proteoglycan staining was seen in aging (12 and 18 months) articular cartilage. qPCR revealed a significant decrease in mRNA for *Acan*, *Col2a1*, *Col9a1*, *Col11a1* and a significant increase in *Il1b* expression in aging articular cartilage (Figure 1). *Nfat1* mRNA and protein expression in articular cartilage was significantly decreased after 12 months of age. Forced *Nfat1* expression in the cultured articular chondrocytes of aging mice partially rescued the abnormal metabolic activities. DNA methylation of the *Nfat1* promoter region was low and there was no significant difference between the age groups. In contrast, the levels of histone methylation (H3K4me2, a histone code for transcriptional activation) were significantly decreased in aging articular chondrocytes (Figure 2).

Conclusions:These findings suggest that reduction of *Nfat1* expression causes dysfunction of aging articular chondrocytes which explains, at least in part, the high incidence of joint degeneration or OA in aging individuals. The decrease in *Nfat1* expression in aging articular cartilage is primarily mediated by epigenetic histone methylation.

Key words: *Nfat1*, epigenetics, aging, osteoarthritis, cartilage

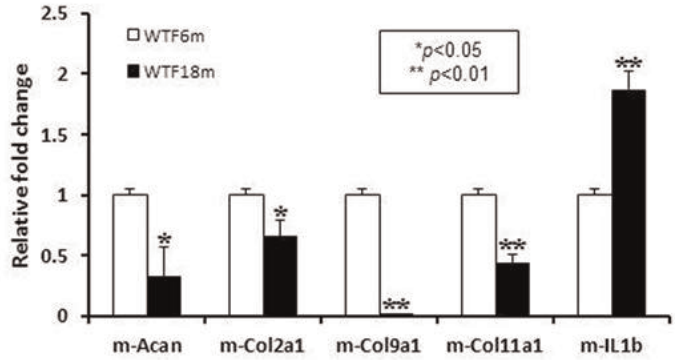

Figure 1. Dysfunction of aging articular cartilage confirmed at the mRNA level

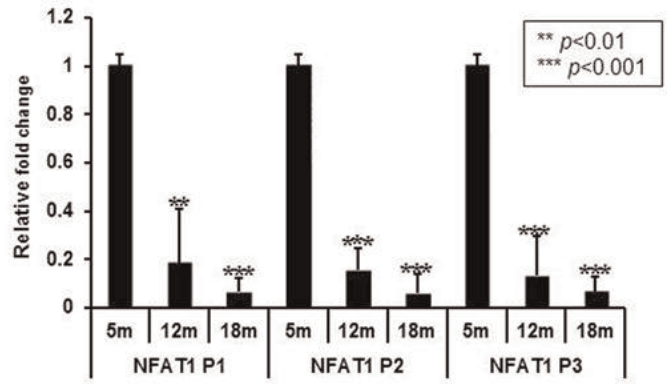

Figure 2. Epigenetic modification of Nfat1 promoter region. H3K4me2 ChIP followed by qPCR.

***Disclosures: Mingcai Zhang**, None.*

SU0007

microRNAs in the Regulation of Resorption and Healing of Bone Erosions in Rheumatoid Arthritis. Yukiko Maeda*[1], Paul Fanning[1], Jane Lian[2], Ellen Gravallese[1], Melissa Matzelle[1], David Ayers[3]. [1]University of Massachusetts Medical School, USA, [2]University of Vermont, USA, [3]UMass Memorial Medical Center, USA

MicroRNAs (miRNAs) are important regulators of skeletal remodeling and expression of several miRNAs, including miR-23b and miR-132 is modulated in synovial tissues in rheumatoid arthritis (RA). RA is characterized by inflammation of the synovial joint lining that results in the destruction of bone. Focal articular bone loss (erosion) is mediated by osteoclasts, and begins early in the course of disease. Repair of bone erosion is rare despite the use of potent anti-inflammatory therapies, and mechanisms inhibiting bone formation and repair are poorly understood. Since miRNAs have been demonstrated to regulate both inflammation and bone remodeling, we hypothesized that miRNAs might play a regulatory role in the development and repair of bone erosions in RA. Using a modification of the serum transfer model for the study of bone erosion in RA, we have previously demonstrated that in the setting of resolving inflammation, repair of articular bone erosion does occur, accompanied by alterations in the expression of components of the Wnt signaling pathway. Moreover, treatment with TNF suppresses Wnt signaling activity in primary calvarial osteoblasts collected from Wnt reporter (Top-gal) mice. To begin to address the role of miRNAs in these pathogenic events, we performed Fluidigm high-throughput expression profiling of 760 mouse miRNAs in pooled synovial samples from non-arthritic and arthritic (day 10) mice and mice with resolving inflammation (day 21). We also performed gene array (Affymetrix) analysis in the same samples used for miRNA array studies, and compared gene and miRNA array results, followed by gene ontology analysis. We found 136 genes to be down-regulated that are predicted targets of miRNAs that were up-regulated (2 fold) in arthritic compared with non-arthritic synovium. Gene ontology analysis showed enrichment of genes in the Wnt pathway and pathways involved in bone development. We also identified 199 genes to be up-regulated that are predicted targets of down-regulated miRNAs (2 fold) in arthritic compared with non-arthritic synovium. Pathways involved extracellular matrix organization, cell cycle, inflammation, blood vessel and bone development. In conclusion, we identified stage-specific miRNAs in this murine model of RA, including two miRNAs previously reported to play a role in RA, miR-23b and miR-132. Further analysis of miRNAs in these pathways may prove fruitful for developing therapeutic strategies for bone erosion.

***Disclosures: Yukiko Maeda**, None.*

SU0008

Associations between Sarcopenia and Osteopenia/Osteoporosis in 2400 Japanese Women. Naohisa Miyakoshi*[1], Michio Hongo[1], Yoichi Mizutani[2], Yoichi Shimada[1]. [1]Akita University Graduate School of Medicine, Japan, [2]Joto Orthopedic Clinic, Japan

Introduction: Sarcopenia and osteoporosis are both significant health burdens among postmenopausal women. This study examined associations between sarcopenia and osteopenia/osteoporosis in Japanese women and evaluated the prevalence of sarcopenia in women with osteopenia and osteoporosis.

Methods: A total of 2400 Japanese women aged 40-88 years who visited orthopedic clinics and underwent whole-body and regional (lumbar spine and total hip) dual-energy X-ray absorptiometry (DXA) were enrolled in this study. All subjects were orthopedic patients who had minor symptoms (i.e., sprain, contusion, transient joint pain, etc.) and requested examination for osteoporosis, or were examinees in a regional screening program for osteoporosis who were referred to our clinics for confirmation of whether osteoporosis was present. Osteopenia and osteoporosis were defined according to World Health Organization criteria using bone mineral density (BMD) of the lumbar spine or hip. Sarcopenia was defined as a relative skeletal muscle index (RSMI) more than 2 standard deviations below the mean for a young adult reference population, calculated as the appendicular skeletal muscle mass obtained from whole-body DXA divided by height in meters squared.

Results: Significant and marginal/moderate positive correlations were observed between RSMI and lumbar spine/total hip BMDs ($r=0.197$ and $r=0.274$, respectively; $p<0.0001$ each). BMDs of the lumbar spine and total hip showed significant moderate negative correlations with age ($r=-0.270$ and $r=-0.375$, respectively; $p<0.0001$ each), but RSMI showed no association with age in this population ($r=0.056$). When osteopenia/osteoporosis was defined using lumbar spine BMD, prevalences of sarcopenia in subjects with normal BMD, osteopenia and osteoporosis were 10.4%, 16.8%, and 20.4%, respectively. When osteopenia/osteoporosis was defined using total hip BMD, prevalences of sarcopenia in these subjects were 9.0%, 17.8%, and 29.7%, respectively. A chi-square test for independence showed a significant association between sarcopenia and osteopenia/osteoporosis ($p<0.0001$).

Conclusions: These results indicate that sarcopenia is significantly associated with osteopenia and osteoporosis in Japanese women. However, the results should be interpreted with care, as the subject cohort may have suffered selection bias in that all subjects had visited orthopedic clinics.

***Disclosures: Naohisa Miyakoshi**, None.*
This study received funding from: Japan Osteoporosis Society

SU0009

Differential effects of age and menopause on proximal femur structure: a cross-sectional study of 719 Caucasian females aged 20 to 89 years. Richard Prince*[1], Ben Khoo[2], Joshua Lewis[3], Keenan Brown[4], Christopher Cann[5]. [1]Sir Charles Gairdner Hospital, Australia, [2]Medical Technology & Physics, Sir Charles Gairdner Hospital, Perth, Western Australia, Australia, [3]University of Western Australia, Sir Charles Gairdner Hospital, Australia, [4]Mindways Software, USA, [5]University of California, San Francisco, USA

Areal bone mineral density (aBMD), although useful for fracture prediction, obscures changes in cancellous and cortical mass and volume by integrating mass over a planar area of interest. We have previously reported the changes in proximal hip structure over the female life span using DXA (Price R et al., J Clin Densitom 2003; 6: 51). We now analyse the changes in the cancellous and cortical compartments assessed by three dimensional quantitative computed tomography (QCT) techniques to define the cancellous and cortical compartments.

Proximal femur structure was measured in 719 female Caucasians aged 20 to 89 years using QCT (Khoo et al., Osteoporos Int 2009: 20: 1539). CT scanner performance and protocols were characterized using a Mindways QA phantom and QA scans and mineral mass estimates normalized by CT-scanner specific field-uniformity correction using Mindways BIT software (Mindways Software Inc., Austin, Texas USA). Three regions of interest were defined using an algorithm derived from the DXA approach, the femoral neck (FN), trochanter (TR) and intertrochanter (IT). Voxels with a density threshold of greater than 350 mg/cm^3 were classified as cortical. The mineral mass and volume were computed for the integral, cancellous and cortical segments of the regions analysed and modelled using linear or bilinear (split plot) models using goodness of fit criteria without specification of the crossing point.

Integral volume at the femoral neck (FN), trochanter (TR) and intertrochanter (IT) sites expanded linearly from 20 to 89yrs by between 18 and 37% (27 to 175 µl/yr). Cancellous volume increased by between 65 and 79% (58 to 244 µl/yr). Between 20 and 89yrs FN cortical volume decreased linearly by 45% (30 µl/yr) and mass by 43% (18mg/yr) but at both the TR and IT sites cortical volume and mass were constant until menopause and decreased linearly thereafter: volume 42 and 25% (66 and 103 µl/yr): mass 46 and 30% (39 and 97 mg/yr).

At all sites periosteal and endosteal expansion is large and linear from age 20. FN cortical bone mass and volume shows linear contraction with age as previously described. However at the TR and IT sites, before menopause periosteal and endosteal expansion is balanced preserving cortical bone mass and volume, after menopause contraction of the cortical compartments is linear with age. The biomechanical effects of these large changes require further analysis.

***Disclosures: Richard Prince**, None.*

SU0010

Fall risk assessment using muscle mass, muscle strength and timed up and go test in hospitalized adults. Hideki Tsuboi*[1], Jun Hashimoto[2]. [1]Osaka Minami Medical Center, Japan, [2]National Hospital Organization, Osaka Minami Medical Center, Japan

Introduction; Falls in elderly are problems associated with increased morbidity and disability. Falls are also severe problem in hospitalized patients. In many hospitals, the fall risk is assessed by questionnaires provided by their medical safety committees. Therefore, the purpose of this study is to investigate the possibility to assess fall risks by muscle mass in lower extremity, muscle strength and physical performance.

Materials and Methods; 67 patients (44 male, 23 female) were enrolled in this study. The patients had a mean age of 68.8 (39-88) years. 44 patients had gastrointestinal disease, 20 patients lung disease and 3 patients others. All patients were classified in three groups at the time of admission using fall risk assessment questionnaire provided by medical safety committee in our hospital, A; high risk group, B; moderate risk group, C; low risk group. In addition, the muscle mass in lower extremity was measured using by BIA (Bioelectrical Impedance Analysis; MC190,Tanita, Tokyo, Japan) method and Muscle strength was assessed by hand grip strength. Moreover, physical performance assessment was evaluated measuring timed up and go test (TUG).

Results; 4 patients were excluded because of their gait disturbance, therefore, 63 patients were assessed finally. 9 patients (4 male, 5 female) were assessed in Group A, 30 patients (22, 8) were assessed in Group B and 24 (15, 9) were group C. In Group A, muscle mass of lower extremities were 12.9 ± 2.7 kg in male and 10.8 ± 2.0 kg in female respectively. In Group B, 16.1 ± 2.2 and 11.3 ± 1.8 respectively, and in Group C, 16.4 ± 2.7 and 11.4 ± 1.8 respectively. Hand grip strength in Group A were 25.8 ± 2.5 kg in male and 12.3 ± 4.5 kg in female respectively, in Group B; 25.6 ± 8.3 and 14.1 ± 5.0 respectively, and in Group C; 30.3 ± 9.1 and 17.5 ± 7.6 respectively. TUG in Group A were 9.3 ± 2.0 sec. in male and 13.7 ± 0.6 sec. in female respectively, in Group B; 8.2 ± 2.6 and 10.7 ± 2.1 respectively, and in Group C; 7.9 ± 1.9 and 6.8 ± 1.8 respectively.

Discussions and Conclusion; This study shows that results of muscle mass in lower extremities, hand grip strength and TUG were tend to decrease as the assessment for fall risks was worse. In male, muscle mass were reflected more clearly in fall risks, on the other hand, TUG were reflected more clearly in fall risks in female. Therefore, these examinations may be useful as a screening test for assessment for fall risk in hospitalized patients.

***Disclosures: Hideki Tsuboi**, None.*

SU0011

Investigating the predictive ability of gait speed and quadriceps strength for incident falls in community-dwelling older women at high risk of fracture. David Scott*[1], Geoffrey Nicholson[2], Amanda Stuart[3], Peter Ebeling[1], Kerrie Sanders[4]. [1]The University of Melbourne, Australia, [2]The University of Queensland, Australia, [3]Department of Clinical & Biomedical Sciences, The University of Melbourne, Barwon Health, Australia, [4]NorthWest Academic CentreThe University of MelbourneWestern Health, Australia

Purpose: Sarcopenia, the age-related decline in skeletal muscle mass and function, is an independent predictor of falls in older adults. Recent consensus operational definitions of sarcopenia call for assessment of gait speed (GS), but this may not always be clinically practical. We aimed to determine whether quadriceps strength (QS) has similar predictive ability to GS for assessing falls risk in community-dwelling women at high risk of fracture.

Methods: 135 female participants (mean $\pm$ SD age 76.7 ± 5.0 years; range 70–92) of the Vital D study were randomly selected to participate in a sub-study. At baseline, QS was measured using a handheld dynamometer and self-selected GS was assessed using the GaitRITE system. Low QS and GS were defined as <7.0kg (based on lowest tertile) and <1.0m/s (based on International Working Group on Sarcopenia criteria), respectively. Incident falls were reported monthly by participants for mean $\pm$ SD 3.7 ± 1.2 years. Receiver operating characteristic (ROC) curves, adjusted Cox proportional hazards regression models, and Kaplan-Meier survival curves were obtained to determine the ability of QS and GS to predict incident falls.

Results: N = 99 (73%) participants fell a total of 355 times during the follow-up period (mean fall rate 83 per 100 person years). 32 and 36% of participants were classified as having low QS and GS, respectively, and 15% had combined low QS and GS. There was a moderate positive correlation between QS and GS ($r = 0.39$; $P < 0.001$). The accuracy of both measures for predicting incident falls was poor but ROC curves revealed a larger area under the curve for QS than GS (0.69 vs 0.61; $P = 0.198$). Adjusted Cox proportional hazards regression models demonstrated that the relative hazard for incident falls decreased by around 10% per additional kg of baseline QS (Hazard ratio [95% CI]: 0.90 [0.83, 0.98]), but there was no change in risk according to GS. There was a significant difference for time to first fall for those with low compared to those with normal QS (Figure 1), with estimated mean survival times of 1.54 [1.02, 2.06] vs 2.23 [1.82, 2.64] years, respectively. No significant differences in time to first fall were observed between those with low vs normal GS ($P = 0.161$).

Conclusions: In older women, QS may be a better predictor of incident falls than GS. The easily-performed QS test may be preferable to a GS test for sarcopenia assessment in clinical settings.

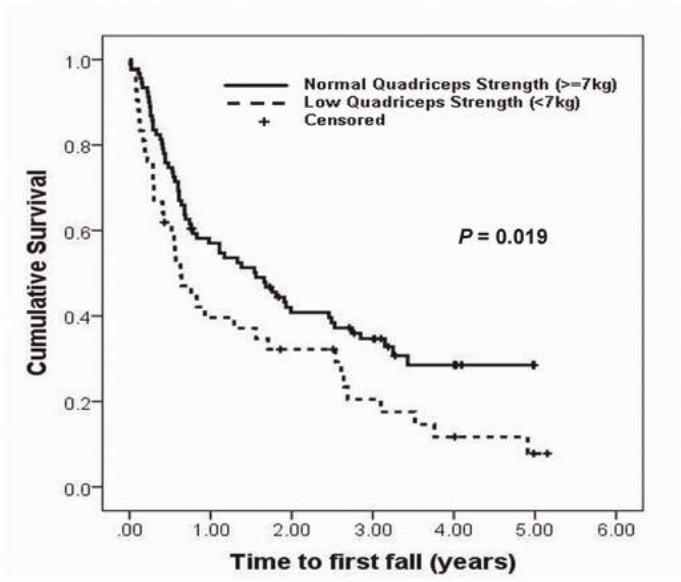

Figure 1. Kaplan-Meier survival curves for incident falls according to quadriceps strength

***Disclosures: David Scott**, None.*

SU0012

Physical Ability Tests Predict Incident Falls – A Prospective Study of 3014 Men in MrOs Sweden. Bjorn Rosengren*[1], Jan-Ake Nilsson[2], Osten Ljunggren[3], Eva Ribom[4], Dan Mellstrom[5], Mattias Lorentzon[6], Claes Ohlsson[7], Magnus Karlsson[1]. [1]Skåne University Hospital Malmö, Lund University, Sweden, [2]Clinical & Molecular Osteoporosis Unit, Dep of Orthopedics & Clinical Sciences, Skåne University Hospital, Lund University, Sweden, [3]Uppsala University Hospital, Sweden, [4]Department of Surgical Sciences, University Hospital, Sweden, [5]Sahlgrenska University Hospital, Sweden, [6]Geriatric Medicine, Center for Bone Research at the Sahlgrenska Academy, Sweden, [7]Center for Bone & Arthritis Research at the Sahlgrenska Academy, Sweden

Background: Propensity to fall is a major risk factor for fracture and interventions that reduce fall risk have been identified in RCTs. It is however clinically demanding to identify high risk individuals suitable for intervention. As low physical ability is associated with falls we investigated the predictive ability of simple physical test.

Methods: 3014 ambulatory men aged 69-81 years in the MrOs Sweden population based study performed simple physical ability tests at baseline (Right and left hand grip strength (RGS and LGS ; kg/cm^2), timed stands test (TST; s), 6 m walking test (6WT; s and 6WS; number of steps) and narrow walking test (NWT; s). Incident falls were recorded tri-annually by a mailed questionnaire.

Due to the repeated assessment of falls, where some participants did not answer all questionnaires (86% completed all three questionnaires, 11% two, 2% one and 1% none) the probability of falling within a 4-month tri-annual evaluation cycle of one year was estimated by generalized estimating equations. We utilized Odds Ratio to estimate the relative risk (RR) with 95% CI.

The men were stratified into quartiles for each test where after we estimated the age-adjusted RR for falls between those in the worst quartile and others. We also evaluated the effect on fall risk of each 1 SD deterioration in the tests.

Results: During the first year 595 men (22%) reported at least one fall (in ages 69-72 years 22%, in ages 73-76 years 20% and in ages 77-81 years 26% (p<.001)).

Each 1 SD lower performance in a test was depending on the particular test associated to a 10-20% higher incident fall risk (RR RGS 1.2 (1.1, 1.3), LGS 1.2 (1.1, 1.3), TST 1.2 (1.2, 1.3), 6WT 1.1 (1.1, 1.2), 6WS 1.2 (1.1, 1.3) and NWT 1.2 (1.1, 1.2)).

Men in the lowest quartile of a test had depending on the particular test a 30-60% higher incident fall risk compared to other men (RR RGS 1.3 (1.1, 1.6), LGS 1.5 (1.2, 1.8), TST 1.4 (1.2, 1.7), 6WT 1.6 (1.4, 1.9), 6WS 1.5 (1.3, 1.8) and NWT 1.4 (1.2, 1.7)).

Men in the worst quartile of all of the three tests LGS, TST and 6WT (n=139) had a 70% higher fall risk compared to other men (RR 1.7 (1.2, 2.3) while men in the worst quartile of all 6 tests (n=68) had a 60% higher risk (RR 1.6 (1.0, 2.6).

ConclusionSimple physical ability tests predict incident falls. One test seems as effective as combinations of tests. The use of a single simple test to facilitate identification of high fall risk individuals is advocated.

***Disclosures: Bjorn Rosengren**, None.*

SU0013

Possible Pathways for the Association of Appendicular Skeletal Muscle Mass with Leptin, Insulin, Myoglobin and Inflammatory Markers. Zhao Chen*[1], Andriene Grant[1], Walter Klimecki[2], Nicole Wright[3], Chengcheng Hu[4], Jennifer Wright[1], Scott Going[1], J. Skye Nicholas[5], Patricia Thompson[1]. [1]The University of Arizona, USA, [2]University of Arizona Pharmacology & Toxicology, USA, [3]University of Alabama at Birmingham, USA, [4]University of Arizona College of Public Health, USA, [5]University of Arizona Mel & Enid Zuckerman College of Public Health, USA

Background: Age-related skeletal muscle loss is common and may be associated with changes in quality of life and disability. Understanding the biological mechanisms regulating loss of skeletal muscle mass (SMM) in the aging population is critical for implementing prevention and intervention strategies. Previously we have reported associations between total SMM and selected biomarkers, including leptin, insulin and inflammatory factors in postmenopausal women from the Women's Health Initiative (WHI). The overall goal of this study was to investigate potential pathways for these observed associations with appendicular SMM (ASMM). Methods: Appendicular lean mass from Dual-energy X-ray Absorptiometry (DXA) was used to estimate ASMM. Serum biomarkers were analyzed using a multiplex immunoassay that measures 89 biomarkers in parallel. A total of 1,001 women from WHI were included in the analysis. Simple and multiple linear regression analysis, random forest analysis as well as path analysis was used to explore biological mechanisms for the association between ASMM and biomarkers. Age, weight, height, race/ethnicity and percent body fat were covariates in the multiple linear regression analysis and random forest analysis. Results: Loss of ASMM with aging was greater than loss in total body SMM. Further, leptin, insulin and myoglobin levels were more consistently correlated with ASMM in the simple and multiple linear regression analysis, even after the adjustment for multiple comparisons. For predicting ASMM, leptin and insulin were the most important measured biomarkers. In addition, factor-VII (β = -0.023, p<0.001), MIP-1 beta (β = -0.016, p= 0.0017), EN-RAGE (β = 0.008, p= 0.007) and IgM (β = -0.010, p =0.0367), were significantly associated with ASMM even after adjusting for leptin, insulin and myoglobin. Conclusion: We observed a significant association between inflammation and ASMM, but inflammatory factors were not strong predictors of ASMM. Relative to inflammation, leptin and insulin were stronger predictors of ASMM. Age, race/ethnicity and body size only partially attenuated the association between ASMM, leptin and insulin, suggesting that leptin and insulin affect ASMM through pathways other than body size.

***Disclosures: Zhao Chen**, None.*

SU0014

Precision and Monitoring Time Intervals for pQCT-Derived Muscle Area and Density in Community-Dwelling Older Adults. Andrew Frank*[1], W.P. Olszynski[2], Saija Kontulainen[1]. [1]University of Saskatchewan, Canada, [2]Midtown Professional Center (#103), Canada

Peripheral quantitative computed tomography (pQCT) is an imaging tool designed for the estimation of bone properties. Musculoskeletal research has also applied pQCT to measure muscle area and muscle density (a surrogate of inter- and intramuscular adipose infiltration). Despite the growing use of pQCT-derived muscle measures, precision values for older adults have not yet been reported. Measurement precision and follow-up data can be used to calculate the monitoring time interval (MTI); an estimate of the time required between measurements where 50% of population will demonstrate a significant age-related change. MTI's are needed to inform and optimize pQCT-based study designs in aging populations. Our objective was to determine the precision error, as well as overall and age-specific MTIs for pQCT-derived muscle area and density in a cohort of older women.

Women (N=115) age 60 to 90 (mean 73.9, SD 7.9y) were recruited from the Saskatoon Cohort of the Canadian Multicentre Osteoporosis Study.Repeated pQCT scans were acquired an average of 347 (SD 15) days apart at 65% of radius and 66% of tibia length to determine forearm and lower leg muscle area and density. A subsample of these participants (n=35), mean age 73.7 (SD 7.7) years were randomly selected for the calculation of short-term precision error by repeated scans 9.7 (SD 3.6) days apart. Precision error was calculated as a percentage using a root mean square coefficient of variation (CV_{rms}%). MTI was calculated as the least significant change (2.77*CV_{rms}%) divided by the median annual percent change. MTIs were calculated for the entire cohort and age decades (60-69, 70-79, 80+).

The precision error for pQCT muscle measures were 2.2% and 3.6% for muscle area and 1.4% and 1.9% for density in the forearm and lower leg respectively. For the entire cohort, MTIs were 3 and 19 years for muscle area, and 18 and 6 years for density, in the forearm and lower leg respectively. From the youngest to oldest decades, forearm MTIs were 4, 2, & 3 years for muscle area, and 13, 35 & 19 years for density. In the lower leg MTIs were 91, 62, & 4 years for muscle area, and 8, 7, & 5 years for density.

The most practical monitoring time intervals for muscle properties in community-dwelling older women is forearm muscle area at 2-4 years, and lower leg muscle density with 5-8 years. The MTIs vary with baseline age. These results will inform and streamline longitudinal study design in musculoskeletal health & aging.

***Disclosures: Andrew Frank**, None.*

SU0015

Severity of Thoracic Curvature Increases Lung Function Decline: The Framingham Study. Elizabeth Samelson*[1], George O'Connor[2], L Adrienne Cupples[3], Yanhua Zhou[3], Elana Brochin[4], Douglas Kiel[5], Harold Rosen[6]. [1]Hebrew SeniorLife, Harvard Medical School, USA, [2]Boston Medical Center, USA, [3]Boston University, USA, [4]Institute for Aging Research, USA, [5]Hebrew SeniorLife, USA, [6]Beth Israel Deaconess Medical Center, USA

Older adults with hyperkyphosis, or excessive forward curvature of the thoracic spine, suffer greatly from this common condition and its associated reduction in quality of life. Impaired pulmonary function, as measured by spirometry, predicts both mortality and functional limitation. Although hyperkyphosis is clinically recognized to restrict lung expansion, there are no prospective studies that have quantified its impact on pulmonary function impairment. We conducted a prospective study to evaluate severity of kyphosis and subsequent declines in pulmonary function in older women.

Participants included a convenience sample of 193 women in the Framingham Original Cohort (mean age, 63 years; range, 50-79) who had thoracic spine x-rays in 1975-76. We measured baseline kyphosis angle (KA), in degrees, from T4 to T12. Pulmonary function testing was used to measure the volume of air exhaled in 1 second (forced expiratory volume, FEV1) at 4 clinical examinations over 13-years of follow-up. Linear mixed effects regression was used for longitudinal analysis to estimate the association between baseline KA and decline in lung function, adjusted for baseline age, height, weight, vertebral fracture, smoking, and physical activity.

Mean KA at baseline was 40♂ in women and ranged from 4-76♂ (median=40♂, IQR=18♂). During 13 years of follow-up, FEV1 declined a mean of 234 ml (18 ml/yr) and ranged from a decrease of 810 ml (62 ml/yr) to an increase of 880.0 (68 ml/yr). Women with the greatest severity of baseline KA had the greatest decline in FEV1 (TABLE). Mean decline in FEV1 over 13 years was 368 ml, 453 ml, and 532 ml in women in the lowest, middle, and highest (most severe) tertile of KA, respectively (trend, p=0.03).

We found that older women with more severe kyphosis experienced greater declines in pulmonary function over 13 years than women with less severe kyphosis, independently of smoking, vertebral fracture, and other confounding factors. The 164 ml excess decline for women in the highest compared to the lowest tertile is more than half the impact of smoking on FEV1 (estimated at 312 ml/13 yr). Efforts to prevent or slow progression of kyphosis may reduce the burden of pulmonary function impairment, an important cause of morbidity and mortality in older adults.

Decline in Forced Expiratory Volume in 1 Second (FEV1, ml) over 13 Years of Follow-Up, According to Severity of Baseline Kyphosis Angle (KA°), Framingham Original Cohort

Kyphosis Angle (KA°) Tertile	Range	Decline in FEV1 (ml) over 13 Years Mean (95% Confidence Interval)*
Low	4-33°	368 ml (262-473)
Medium	34-46°	453 ml (381-525)
High**	47-76°	532 ml (427-638)
		Trend, p=0.02

*Adjusted for age, height, weight, vertebral fracture, smoking, and physical activity
** High=most severe kyphosis

Severity of Thoracic Curvature and Lung Function Decline: The Framingham Study

***Disclosures: Elizabeth Samelson**, None.*

SU0016

Skeletal Muscle Function Deficit. Rosaly Correa-de-Araujo*. National Institute on Aging, National Institutes of Health, USA

Considerable efforts have been taken to better characterize and define sarcopenia in an attempt to help identify patients who might benefit from available therapeutic or preventive interventions, and to support the development of new therapeutic approaches. Throughout the years, the work of numerous international groups resulted in the addition of performance criteria to muscle mass alone or inclusion of both lean mass and gait speed as diagnostic criteria for sarcopenia. More recently, the Foundation for the National Institutes of Health (FNIH) Sarcopenia Project established criteria for clinically relevant low muscle mass and low muscle strength through the identification of strength and muscle mass cutpoints and the demonstration of the relationship between mobility impairment and these cutpoints. With the evolving concepts of sarcopenia, a better terminology is needed to reflect not only sarcopenia's original definition (loss of muscle mass), but also to embrace the alterations in muscle strength and function that ultimately may lead to mobility disability. The author proposes Skeletal Muscle Function Deficit (SMFD) as such terminology and will discuss the rationale of how it can provide a framework for the diagnosis and potential therapeutic approaches to sarcopenia and age-related muscular dysfunctions.

***Disclosures: Rosaly Correa-de-Araujo**, None.*

SU0017

Strength-to-weight ratio in population studies: toward a definition of sarcopenic-obesity that is relevant for mobility limitation. Robert McLean*[1], Marian Hannan[1], Joanne Murabito[2], Alyssa Dufour[1], Douglas Kiel[1]. [1]Hebrew SeniorLife Institute for Aging Research & Harvard Medical School, USA, [2]Framingham Heart Study & Boston University School of Medicine, USA

Both sarcopenia and obesity are associated with mobility limitations in older adults, and risk may be highest when both co-exist as sarcopenic-obesity. Thus identification of sarcopenic-obesity is essential for prevention and treatment, yet no consensus definition exists. Current definitions classify sarcopenia as low absolute strength. We propose that low strength-to-weight ratio (SWR) is more relevant because insufficient strength relative to body weight is a main cause of physical limitations. Our objective was to compare a sarcopenic-obesity definition that classifies sarcopenia based on low absolute strength with one based on SWR, and determine their associations with mobility limitations. Participants were 557 older adults (age 72-98 years, 62% women) from the Framingham Original Cohort (1992-93). Maximum grip strength was measured (kg), and sarcopenia was defined as the lowest sex-specific tertiles of 1) absolute grip strength and 2) grip SWR (grip strength/body weight). Obesity was defined as BMI ⩾30 kg/m^2. Sarcopenic-obesity categories (sarcopenic-obesity, sarcopenia only, obesity only, neither) were defined 2 ways: based on absolute grip strength and grip SWR. For each sarcopenic-obesity definition, logistic regression was used to calculate prevalence odds ratios (OR) for mobility limitations (self-reported inability to walk ½ mile or up and down 1 flight of stairs) for the sarcopenia only, obesity only and sarcopenic-obesity groups relative to neither. Models were adjusted for sex, age, high school education, current smoking, >3 alcoholic drinks/week, and number of comorbidities. The SWR-based definition reclassified 54% of obesity only to sarcopenic-obesity, and 34% of sarcopenia only to neither (Table 1). For the low strength definition, odds of mobility limitation was similar (OR=4.2) for the obesity alone and sarcopenic-obesity groups (Table 2). For the SWR definition, sarcopenic-obesity was most strongly associated with mobility limitation (OR=5.0), but obesity alone was not (OR=1.0). Associations for sarcopenia alone were similar for both definitions (OR=2.3). Our results show that a sarcopenic-obesity definition based on low SWR may better describe the synergistic relation between sarcopenia and obesity since obesity may not be associated with mobility limitation when strength is sufficient for body weight. Further refinements of sarcopenia and obesity criteria are needed before a consensus definition is established.

Table 1. Classification for 2 sarcopenic-obesity definitions among 557 elderly men and women in the Framingham Original Cohort.

Absolute grip strength, BMI	Grip strength-to-weight ratio, BMI: Neither	Sarcopenia only	Obesity only	Sarcopenic-obesity	Total
Neither	281	10	0	0	291
Sarcopenia only	54	98	0	0	152
Obesity only	0	0	37	44	81
Sarcopenic-obesity	0	0	0	33	33
Total	335	108	37	77	557

Table 1

Table 2. Prevalence odds ratios* (95% CI) for mobility limitation for 2 sarcopenic-obesity definitions among 557 elderly men and women in the Framingham Original Cohort.

	Absolute grip strength, BMI	Grip strength-to-weight ratio, BMI
Neither	1.0	1.0
Sarcopenia only	2.3 (0.9, 5.8)	2.3 (0.9, 5.8)
Obesity only	4.2 (1.5, 11.7)	1.0 (0.1, 8.5)
Sarcopenic-obesity	4.2 (1.1, 15.6)	5.0 (2.0, 12.3)

*Adjusted for sex, age, education, smoking, alcohol, comorbidities

Table 2

***Disclosures: Robert McLean**, None.*

SU0018

Bisphosphonate Rescues Cartilage from Trauma Damage by Promoting the Spontaneous Calcium Signaling in Chondrocytes. Yilu Zhou*, Lauren Resutek, Christopher Price, Liyun Wang, X. Lucas Lu. University of Delaware, USA

Our previous study found that systemic injection of zoledronic acid (ZA), a bisphosphonate for bone loss treatment, could suppress the development of post-traumatic osteoarthritis in the DMM (destabilization of medial meniscus) mouse model. We hypothesized that the presence of bisphosphonate could recover the

cartilage from traumatic damage under *in vitro* culture, and that the chondro-protective function of ZA is related to the calcium signaling of chondrocytes.

Cartilage allografts from calf knee joints were cultured in medium with serum (10% FBS) or without serum for four weeks to evaluate the adverse effects of serum on cartilage. Another two groups of allografts were exposed to serum medium for 1 week to simulate joint bleeding, followed by a 4-week serum-free culture with or without the presence of 1 mM zoledronic acid. Longitudinal mechanical properties of allografts were measured weekly. In order to record the spontaneous calcium responses of *in situ* chondrocytes, the allografts were dyed with Fluo-8 and imaged on a confocal microscope.

The adverse effects of serum on mechanical integrity of cartilage were correlated with the spontaneous calcium responses of *in situ* chondrocytes. At day 28, the Young's modulus was 0.17 MPa in serum group and 0.9 MPa in the non-serum group. The responsive rate of chondrocytes dropped constantly from 18% (day 1) to 7% (day 29) in the serum group, while the non-serum group remained at 20%. For damaged cartilage with 1-week serum exposure, the Young's modulus of allografts increased more than 200% after 4-week rescuing culture in medium contained ZA, while non-ZA group showed a 56% increase (Fig A). In the non-ZA group, 19% of chondrocytes showed spontaneous calcium responses in 15 minutes of imaging, and this value remained constant for 4 weeks. Interestingly, the responsive percentage of cells in ZA treated group increased simultaneously with culture time (Fig B). Linear regression proved that the responsive rate is also positively correlated with the tissue stiffness. Further image processing showed that presence of ZA promoted the calcium signaling of chondrocytes residing in the explants.

We conclude that zoledronic acid directly regulates the metabolic activities of chondrocytes in cartilage. Treatment with ZA can rescue the mechanical integrity of cartilage after trauma damage induced by serum exposure. The chondro-protective effect of ZA is correlated with the intracellular calcium signaling in chondrocytes.

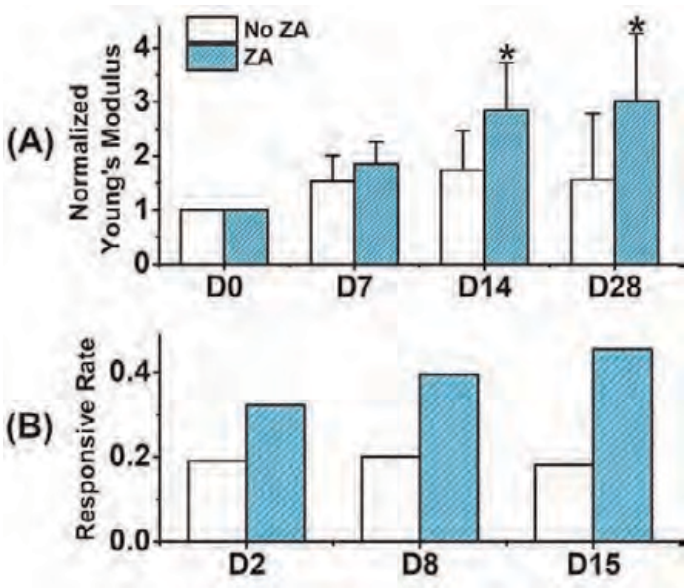

Figure: (A) Young's modulus normalized to day 1; (B) Calcium responsive percentage of chondrocytes

***Disclosures: Yilu Zhou**, None.*

SU0019

In Very Early Rheumatoid Arthritis Bone Changes can be Detected by Peripheral Quantitative Computed Tomography but not Dual-Energy X-ray Absorptiometry. Mart Kull*[1], Raili Müller[2], Annika Aart[2], Riina Kallikorm[2], Margus Lember[2]. [1]University of Tartu, Estonia, [2]University of Tartu, Department of Internal Medicine, Estonia

Background: Rheumatoid arthritis (RA) is a chronic debilitating autoimmune disease resulting in progressive joint damage. The presence of bone changes is known to be a prognostic factor of the disease and predicts later morbidity.

We aimed to compare peripheral computed tomography (pQCT) with dual energy x-ray absoptiometry (DXA) in detecting the effect of rheumatoid arthritis on bone parameters in very early rheumatoid arthritis.

Methods: Our study recruited 46 consecutive early RA patients (mean age 51.8 years and average time from diagnosis 33 days). All patients underwent a laboratory panel and thorough physical examination and tender/swollen joint counts. Bone mineral changes were assessed by pQCT (Stratec XCT2000, Germany) and DXA (GE Lunar, US) measurements of the forearm.

Association of bone parameters with disease indices were studied using multivariate linear regression method. Models for radius trabecular bone mineral density and area (pQCT), cortical bone mineral density and area (pQCT), ultradistal radius BMD (DXA) and radius distal third BMD (DXA) were generated using age, time from diagnosis, DAS28 score, CRP level, rheumatoid factor and aCCP positivity, 25(OH) vitamin D, parathyroid hormone level, usage of glucocorticoid treatment and the HAQ score as independent variables.

Results: In early RA patients the DAS28 disease score was independently associated with radial bone cortical density (p=0.04), trabecular density (p=0.01) and trabecular area (p=0.008; Table) when measured by pQCT. DXA measured bone mineral density and bone area in the trabecular (radius ultradistal region) and cortical (distal third of radius) regions did not show a significant association with disease parameters (p>0.05) in this patient cohort.

Conclusion: In this very early stage of RA (~1 month from diagnosis) independent associations of bone mineral density with disease indicators are already seen with pQCT but not with DXA. This suggests that pQCT is a more sensitive method for the detection of early RA associated bone changes in the forearm.

p-value		Independent variable	Model r^2	Age	CRP	DAS28 score	GCS treatment	25(OH)D	RF positive	aCCP positivity	HAQ score	PTH	Time from diagnosis
Forearm paramater	Method	unit		years	mg/L	score	Yes/No	nmol/L	neg/pos	neg/pos	score	umol/L	# in days
Cortical area	pQCT	mm2	0.14	NS	NS	NS	NS	NS	NS	NS	NS	NS	NS
Cortical density	pQCT	mg/mm3	0.48	**0.02**	NS	**0.04**	0.06	NS	NS	NS	NS	NS	NS
Trabecular area	pQCT	mm2	0.14	NS	NS	**0.008**	NS	NS	NS	NS	NS	0.1	NS
Trabecular density	pQCT	mg/mm3	0.46	0.09	0.07	**0.01**	0.07	NS	NS	NS	NS	NS	NS
Ultra distal BMD	DXA	g/cm2	0.13	NS	NS	NS	NS	NS	NS	NS	NS	NS	NS
Ultra distal area	DXA	cm2	0.12	NS	NS	NS	NS	NS	NS	NS	NS	NS	NS
33% radius BMD	DXA	g/cm2	0.20	NS	NS	NS	NS	NS	NS	NS	NS	NS	NS
33% radius area	DXA	cm2	0.16	NS	NS	NS	NS	NS	NS	NS	NS	NS	NS

Table. Multivariate modeling results (p-values) and model coefficients

***Disclosures: Mart Kull**, None.*

SU0020

MicroRNAs Are Related to Progression of Osteoarthritis (OA) in the DMM (destablization of medial meniscus) Mouse Model. Paul Fanning*[1], Christopher Raskett[2], Eric Mick[3], Yukiko Maeda[1], Nicholas Farina[4], Ellen Gravallese[1], Gary Stein[5], David Ayers[6], Jane Lian[7]. [1]University of Massachusetts Medical School, USA, [2]Dept. of Orthopedics & Rehabilitation, University of Massachusetts Medical School, USA, [3]Dept. of Quantitative Health Sciences, University of Massachusetts Medical School, USA, [4]Dept. of Biochemistry, University of Vermont Medical School, USA, [5]University of VermontCollege of Medicine, USA, [6]UMass Memorial Medical Center, USA, [7]University of Vermont, USA

MicroRNAs (miRNAs)have emerged as key regulators of normal cellular processes and metabolic pathways in the skeleton and are associated with disease. Studies of OA tissue have identified gain and loss of miRNAs that reflect loss of the articular surface, tissue degradation, pain and inflammation. Here we addressed the temporal and spatial changes in miRNA expression from the onset and during progression to late stage of degeneration of the joint surface, not represented in samples from the terminal stage of total joint replacement. The DMM model mimics the events that occur in human disease including initial fibrillation of articular cartilage (day 10 after surgery), erosion of the cartilage matrix, active chondrocytes at the margins of degenerated tissue (days 12 – 21) and finally the beginning of sclerotic bone lesions by day 10 increasing through day 28. In n=5 mice per group (5 time points and controls), we compared expression of miRNAs using a Q-PCR array of 678 miRNAs (Fluidigm, UMASS High Throughput Gene Expression Core). Samples microdissected from the medial and lateral compartments of the operated knee were examined to better asses miRNAs of the OA disease state compared to the spared control tissue in the same mouse. Raw data was analyzed after applying the modified global means normalization to the raw data prior to miRNA expression analyses. A total of 243 miRNA were expressed with ~100miRNAs with 3 fold or at any one time point in the OA tissue and were clustered into several different expression patterns during the time course. Subgroups of these RNAs were linked to functional activities through analyses of their targets that formed networks related to angiogenesis, growth factor signaling ((TGFB, IGF, PDGF, FGF, Wnt), inflammation (cytokines and chemokines), apoptosis and kinase pathways. The functional activities of miRNAs with the highest fold changes that have not been previously reported in OA, are being further examined for their biological effects in chondrocytes. Many miRNAs we find exhibiting stage –dependent expression in the DMM mouse model, had been reported in human OA tissue (e.g miR -155, miR 34a, , miR 140, miR 27). Hence, these miRNAs have the potential for diagnostic value and intervention of OA.

***Disclosures: Paul Fanning**, None.*

SU0021

Notch Inhibition Prevents Inflammatory Bone Loss by Targeting Mesenchymal Stem Cells. Hengwei Zhang*[1], Matthew Hilton[2], Jennifer Anolik[1], Zhenqiang Yao[1], Brendan Boyce[2], Lianping Xing[1]. [1]Univeristy of Rochester, USA, [2]University of Rochester Medical Center, USA

Notch plays critical roles in maintaining bone homeostasis by regulating the functions of osteoblasts and osteoclasts. However, its role in common bone disorders is less clear. We reported that Notch is activated in mesenchymal stem cells(MSCs) from TNF transgenic(TNF-Tg) mice, a model of inflammatory osteoporosis and rheumatoid arthritis(RA) and the Notch inhibitor DAPT prevents bone loss in TNF-Tg mice. To determine if this effect of DAPT in TNF-Tg mice is directly mediated by MSCs, we used a SCID mouse tibial defect model in which we filled the defects with a scaffold of decalcified bone matrix into which we injected CFU cells from DAPT or vehicle treated TNF-Tg mice and assessed new bone formation using uCT and histomorphometry. Cells from DAPT treated mice formed significantly more new bone in defects compared with cells from vehicle treated mice(BV/TV: 21 ± 3 vs $14\pm2\%$; new bone area: 0.027 ± 0.002 vs $0.017\pm0.003mm^2$). To determine if TNF activates Notch in MSCs *in vivo,* we used Hes1-GFP mice, which have been used to visualize Hes1-expressing neural stem cells. $CD45^-GFP^+$ cells from Hes1-GFP mice express MSC markers(61% $Scal1^+$, 68% $CD105^+$ and 99% $CD31^-$), formed CFU-ALP^+ colonies and expressed low levels of Runx2. TNF injection (0.5mg/d/inj x 5d) significantly increased the #s of $CD45^-Hes1^+$ cells in bone marrow of Hes1-GFP mice compared to PBS treated mice(2.5 ± 0.8 vs 0.3 ± 0.1 x10^5 cells). $CD45^-Hes1^+$ cells from TNF treated mice expressed high levels of *Hes1* and formed fewer CFU-ALP^+ colonies. We observed no change in OC formation or $CD45^+Hes1^+CD11b^+/Gr\text{-}1^{-/low}$ OC precursor numbers. Scattered Hes1-GFP^+ cells were observed in bone marrow sections and some of them are adjacent to the endosteal surfaces of trabecular bones. TNF significantly increased the #s of Hes1-GFP^+ cells adjacent to the endosteal surface(#s/femur: 115 ± 15 vs 43 ± 8 in PBS treated mice). To determine if elevated Notch and reduced obl differentiation occur in human RA, we examined expression levels of Notch target genes and Runx2 in $CD45^-$ cells from peripheral blood of 12 patients with active RA who were not on biologics and 15 healthy controls(HCs). Similar to findings in TNF-Tg RA mice, increased Notch(*Hes1*: 3.85 ± 1.4; *Hey1*:2 ± 0.5 fold) and decreased Runx2(*Runx2*: 0.5 ± 0.1 fold) expression was detected in RA patients compared to HCs. Our data suggest that chronic inflammation leads to abnormal Notch activation in MSCs. Notch inhibition is a potential therapeutic approach for inflammatory bone loss.

***Disclosures: Hengwei Zhang**, None.*

SU0022

Prevention of Osteoarthritis by Combination of Proteoglycan 4 and Interleukin 1 Receptor Antagonist Expression. Zhechao (Merry) Ruan*[1], Kilian Guse[1], Ayelet Erez[1], Vincenzo Cerullo[1], Brian Dawson[1], Michael Heggeness[1], Francis Gannon[1], Brendan Lee[2]. [1]Baylor College of Medicine, USA, [2]Baylor College of Medicine & Howard Hughes Medical Institute, USA

Purpose: Osteoarthritis (OA) is characterized by degeneration of articular cartilage, and is the top three cause of chronic disability. Although its prevalence is rising globally with aging of the population, current therapy is limited to symptomatic relief and in severe cases, joint replacement surgery. We aim to develop novel therapeutic modalities by intra-articular over-expression of proteoglycan 4 (Prg4) and interleukin 1 receptor antagonist (Il1ra). In addition, we aim to investigate the related mechanism in the pathogenesis of OA.

Methods: To study the effects of long-term expression of Prg4 on OA, we over-expressed Prg4 in intra-articular space by generating transgenic mice and intra-articular injection of helper-dependent adenoviral vectors (HDV) in wild type mice. To enhance the therapeutic index of HDV based treatment, we modified HDV to retarget chondrocytes and delivered Prg4 in combination of Il1ra. To investigate the related mechanism of OA pathogenesis, we performed gene expression profiling of mouse articular cartilage obtained by laser capture micro-dissection (LCM), in vitro cell studies and analysis of human OA gene profiling.

Results: Long-term Prg4 expression under the type II collagen promoter (Col2a1) does not adversely affect skeletal development but protects from developing signs of age-related and post-traumatic osteoarthritis. Moreover, intra-articular injection of HDV expressing Prg4 protects against the development of post-traumatic osteoarthritis. The therapeutic index increases by 10 fold when we either inject HDV modified to retarget chondrocytes or perform combinatorial injection of Prg4 and Il1ra. Gene expression profiling of mouse articular cartilage obtained by LCM shows that Prg4 expression inhibits the transcriptional programs that promote cartilage catabolism and hypertrophy. Results from in vitro cell studies and analyses of available human OA datasets are consistent with the predictions of this model.

Conclusions: Our data offer long-term intra-articular expression of Prg4 and Il1ra by HDV delivery as a potential chondro-protective approach to OA treatment and provide insight into the mechanisms for OA development.

***Disclosures: Zhechao (Merry) Ruan**, None.*

SU0023

Gender Different Pleotropic Bone-Muscle Relationship in The Elderly: From A Nationwide Survey (KNHANES IV). Ji Hye Huh*[1], Kwang Joon Kim[2], Kyeong Hye Park[3], Jo Eun Kim[4], Kyoung Min Kim[5], Yumie Rhee[6], Sung-Kil Lim[7]. [1]Division of Endocrinology & Metabolism, South Korea, [2]Severance Hospital, South Korea, [3]Executive Healthcare Clinic , Severance Hospital, South Korea, [4]Division of Endocrinology & Metabolism,Department of Internal, South Korea, [5]Department of Internal Medicine, Bundang Seoul National University Hospital, South Korea, [6]Department of Internal Medicine, College of Medicine, Yonsei University, South Korea, [7]Yonsei University College of Medicine, South Korea

Context: There is a clear evidence of genetic pleiotropy between the muscle and the bone. However, there are few studies concerning gender differences in the effect of low muscle mass on bone and glucose and lipid metabolism in elderly subjects.

Objective: To assess the gender-specific influence of muscle mass on the bone and metabolic parameters.

Design and Setting: A population-based, cross-sectional study from the Fourth Korea National Health and Nutrition Examination Surveys (2008-2009).

Participants: A total of 5,003 men and 6,500 women aged 10 and older who completed the body composition examination using a dual-energy X-ray absorptiometry (DXA) were recruited. A total of 2,264 participants (940 men and 1,324 women) whose age ranged from 65 to 92 years were further analyzed.

Main outcome measurements: Those whose muscle mass was lower by one standard deviation or greater from the mean of young healthy subjects were allocated into sarcopenia group, and the others were classified as the control group. BMD at the spine and the hip was measured using DXA.

Results: The peak muscle mass accrual was obtained at age of 20-39 years in men and 40-59 years in women. The age-related trend in bone and muscle coincided in men but not in women. Femoral neck (FN) and total hip (TH) BMD were highly correlated with muscle mass in both genders. However, in women, this correlation was not significant in lumbar spine(LS). In addition, this positive correlation was stronger in cortical bone-rich FN or TH than in trabecular bone-rich LS, and it was stronger in men than in women. There was a strong correlation between muscle mass and femoral cortical thickness in both genders. Subjects with sarcopenia were at a higher risk for osteoporosis at FN, TH and LS in men, and in TH and FN in women. Muscle mass and metabolic profiles did not show any remarkable association.

Conclusion: Our largest population based study showed that subjects with low muscle mass were more prone to deterioration of the bone, especially cortical bone, than to altered glucose and lipid metabolism in elderly populations. This muscle-bone relationship was more prominent in men than in women. The gender differences in acquisition and age-related loss in bone and muscle tissues may be important and helpful for development of gender-specific preventive strategies and treatment options for sarcopenia and osteoporosis in the elderly.

***Disclosures: Ji Hye Huh**, None.*

SU0024

Larger Bone Size is Associated With Increased Risk of Forearm Fracture in Young Girls. Mikko Maatta*[1], Christa Hoy[1], Douglas Race[1], Lindsay Nettlefold[1], Leigh Gabel[1], Kishore Mulpuri[2], Heather Macdonald[1], Heather McKay[1]. [1]University of British Columbia, Canada, [2]Child & Family Research Institute, Canada

The incidence of distal forearm fractures in children and adolescents has risen in recent decades. However, the relationship between bone microstructure, bone strength and fracture risk during growth is not clear. Thus, we aimed to compare distal radius bone microstructure and strength between girls and boys without a history of forearm fracture (NF group) with those who sustained a low to moderate energy forearm fracture (Fx group). We assessed bone microstructure of the non-dominant (NF) and non-fractured (Fx) distal radius (7% site) using high-resolution pQCT (Scanco Medical) in 57 pre- and early pubertal girls (10.7 y $\pm$ 1.5, 30 NF, 27 Fx) and 62 boys (12.0 y $\pm$ 1.6, 20 NF, 42 Fx). Standard morphological outcomes included total bone mineral density (Tt.BMD), trabecular bone volume ratio (BV/TV), trabecular thickness (Tb.Th) and number (Tb.N). We used a customized auto-segmentation algorithm to determine total bone area (Tt.Ar), cortical BMD (Ct.BMD), thickness (Ct.Th) and porosity (Ct.Po), and applied finite element analysis to estimate bone strength (failure load, FLoad). We used ANOVA to compare bone outcomes across Tanner stages I, II and III in girls and boys. To determine whether bone outcomes were predictive of fracture, we fit sex-specific logistic regression models for each bone outcome, and adjusted for forearm length, maturity (Tanner stage) and percent body fat (DXA, Hologic QDR 4500W). Girls in the Fx group had significantly higher percent body fat compared with NF girls (15%, p=0.03). Girls in NF group had significantly higher Ct.BMD at Tanner stage III compared with Tanner stage I (11%, p=0.04). This maturity difference in Ct.BMD was absent in the Fx group. Ct.Th was significantly lower in Fx girls compared with their NF peers at Tanner stage II (11%, p=0.04). The FX girls also had significantly larger Tt.Ar than NF girls at Tanner stage II (14%, p=0.04). The higher Tt.Ar in Fx girls was associated with a significantly

higher fracture risk (OR=1.03 per 1 unit increase, p=0.03). Trabecular microstructure, Ct.Po and FLoad were not associated with fracture in girls or boys. With growth-related increases in bone size a concomitant increase in cortical thickness and BMD may be necessary to prevent fracture in girls. Factors that underpin fracture during growth are sex-specific. In girls, the influence of excess adiposity on fracture risk requires further study.

***Disclosures: Mikko Maatta**, None.*

SU0025

Withdrawn

SU0026

Age effect on pediatric longitudinal BMD by multiple loci uncovered in adult BMD-related GWAS meta-analyses. Babette Zemel*[1], Heidi Kalkwarf[2], Mingyao Li[3], Sandra Deliard[4], Cecilia Kim[4], Liming Qu[3], Rosetta Chiavacci[4], Donna Paulhamus[4], Joan Lappe[5], Vicente Gilsanz[6], Hakon Hakonarson[4], Sharon Oberfield[7], John Shepherd[8], Benjamin Voight[3], Andrea Kelly[4], Struan Grant[1]. [1]Children's Hospital of Philadelphia, USA, [2]Cincinnati Children's Hospital Medical Center, USA, [3]University of Pennsylvania, USA, [4]The Children's Hospital of Philadelphia, USA, [5]Creighton University Osteoporosis Research Center, USA, [6]Children's Hospital Los Angeles, USA, [7]Columbia University Medical Center, USA, [8]University of California, San Francisco, USA

Objective: Genome wide association studies (GWAS) have identified over 70 loci associated with adult bone density and/or osteoporosis. Discerning which of these loci impact bone development early in life has not been systematically investigated. We tested the associations of these single nucleotide polymorphisms (SNPs) with areal bone mineral density (aBMD) of the spine, total hip, femoral neck, distal 1/3 radius and bone mineral content (BMC) of total body less head (TBLH) in a well-characterized cohort of European American children.

Methods: The Bone Mineral Density in Childhood Study was a multi-center, longitudinal study of children ages 5 to 19. aBMD/BMC was measured annually (up to 7y) using Hologic DXA devices. Growth, puberty stage, dietary intake and physical activity were also measured. Biospecimens were genotyped on the Illumina OmniExpress BeadChip (>700,000 SNPs). Principal component analysis confirmed self-reported European ancestry. Longitudinal mixed effects models tested associations between aBMD/BMC Z-scores and 77 SNPs previously identified in adulthood, accounting for sibships and multiple observations per subject. Models were adjusted for height and BMI Z-score, age, sex, puberty, calcium intake and physical activity. A SNP x age interaction term was tested to determine if associations were age dependent. A P-value of 0.05 was considered statistically significant, as these are previously identified SNPs.

Results: Over 4,000 observations on ~690 subjects were evaluated. Numerous GWAS-established adult bone density loci were associated with aBMD/BMC independent of known covariates such as growth and physical activity, especially when a SNP x age interaction term was included (see Table). Interestingly, this interaction was consistently observed for *ARHGAP1, FOXL1, SMG6, WNT16, LRP4 and TNFRSF11B* at all skeletal sites.

Conclusions: These findings suggest that multiple variants originally associated with adult bone density exert effects earlier in life. Most notably, these longitudinal models revealed age-dependent effects during childhood that would otherwise have gone undetected.

Table. SNPs assocoated wtih aBMD/BMC in children in models with and without an age interaction

Skeletal Site	Model type*	Associated SNPs
Spine aBMD	SNP	*LACTB2/XKR9, GPATCH1, DHH, WLS, IDUA, LRP5, SPTBN1, STARD3NL*
	SNP x Age	*C12orf23, ARHGAP1, SP7, GPATCH1, JAG1, MEF2C, FOXL1, PKDCC, SMG6, SPTBN1, C17orf53/HDAC5, C16orf38/CLCN7, CYLD, INSIG2, WNT16, CTNNB1, NTAN1, FAM9B, LRP4, TNFRSF11B, FUBP3, KCNMA1, SOX9, KLHDC5/PTHLH, ESR1, RANKL/AKAP11*
Total hip aBMD	SNP	*C12orf23, GPATCH1, WLS, KCNMA1*
	SNP x Age	*ARHGAP1, GALNT3, LACTB2/XKR9, DNM3, RANK, LEKR1, ERC1, AXIN1, MEF2C, FOXL1, CPN1, SMG6, C17orf53/HDAC5, TNFRSF11B, C16orf38/CLCN7, WNT16, LRP4, ABCF2, KCNMA1, KLHDC5/PTHLH*
Hip Neck aBMD	SNP	*C12orf23, AXIN1, CPN1, WLS, FUBP3, KCNMA1, LIN7C*
	SNP x Age	*ARHGAP1, GALNT3, AXIN1, MEF2C, FOXL1, CPN1, SMG6, WNT4, C17orf53/HDAC5, TNFRSF11B, SOST, CYLD, IDUA, WNT16, CTNNB1, LRP4,*
Distal 1/3 radius aBMD	SNP	*SP7, GPATCH1, DNM3, AXIN1, C7orf58, WNT16, TNFRSF11B*
	SNP x Age	*ARHGAP1, GPATCH1, DNM3, LEKR1, ERC1, FOXL1, ESR1, SMG6, WNT4, MARK3, MHC, WNT16, CTNNB1, LRP4, TNFRSF11B, TNFRSF11A, RANKL/AKAP11*
TBLH BMC	SNP	*GPATCH1, DNM3, IDUA, WNT16*
	SNP x Age	*ARHGAP1, GALNT3, SP7, DNM3, LEKR1, MBL2, MEF2C, FOXL1, SMG6, TNFRSF11B, C16orf38/CLCN7, MARK3, MARK3, WNT16, CTNNB1, MPP7, LRP4, SOX9, KLHDC5/PTHLH*

*All models adjusted for age, sex, puberty, Height Z, BMI Z, calcium intake and physical activity

table

***Disclosures: Babette Zemel**, None.*

SU0027

Association Between Lower Extremity Muscle Mass and Bone Structure in Individuals With Unilateral Cerebral Palsy. Harshvardhan Singh*[1], Christopher Modlesky[1], Freeman Miller[2], Brianne Mulrooney[1], Jacques Riad[3]. [1]University of Delaware, USA, [2]AIduPont Hospital for Children, USA, [3]Astrid Lindgrens Children's Hospital, Sweden

Cerebral palsy (CP) is associated with underdeveloped bone structure which results in low bone strength. This may be ascribed to underdeveloped musculature; however, no studies have investigated the relationship between muscle mass and bone structure in individuals with CP. The objective of this study was to examine the relationship between interlimb differences in muscle mass and structure and strength of the midtibia in individuals with spastic unilateral CP. Ambulatory individuals with unilateral CP (n = 30; 13 to 24 years) and a Gross Motor Function Classification of 1 or 2 were studied. All participants were classified as type 0 or 1 using the Winters classification based on sagittal plane gait analysis. Magnetic resonance images of the tibia (0.5 cm thick and 1.0 cm apart) were collected from both lower limbs. Mass of the hip adductors, quadriceps, hamstrings, plantarflexors, and dorsiflexors, and cortical volume, medullary volume, total volume, and estimates of bone strength [section modulus (Z) and polar moment of inertia (J)] for images at the level of the middle-third of the tibia were analyzed using custom software (Interactive Data Language, Boulder, CO). Regression analyses showed that interlimb differences in quadriceps mass was positively related to interlimb differences in cortical volume ($r = 0.577$, $p = 0.001$), total volume ($r = 0.636$, $p = 0.0004$), Z ($r = 0.662$, $p = 0.0002$) and J ($r = 0.648$, $p = 0.0003$) at the midtibia. An inverse relationship between hamstrings mass and cortical volume ($r = -0.446$, $p = 0.022$), Z ($r = -0.459$, $p = 0.018$), and J ($r = -0.443$, $p = 0.023$) at the midtibia was found but the relationships were weaker. None of the other muscle groups were related to any bone measures. Compared to the unaffected limb, lower muscle mass may be a significant contributor to the poor structural development of the midtibia in individuals with unilateral CP. Future studies should investigate if specific strengthening of the quadriceps could lead to increased bone strength at the tibia.

***Disclosures: Harshvardhan Singh**, None.*
This study received funding from: oU Kärnsjukhuset Skövde Sweden

SU0028

Bone mass, Bone microarchitecture (TBS) and anthropometric measurements during childhood growth in Spanish girls. Luis Del Rio[1], Renaud Winzenrieth*[2], Catherine Cormier[3], Silvana Di Gregorio[4]. [1]Cetir Centre Medical, Spain, [2]Med-imaps, Hôpital X. Arnozan, PTIB, Pessac, France, France, [3]AP-HP Groupe Hospitalier Cochin, France, [4]CETIR Centre Mèdic, Spain

The aim of the present study was to evaluate bone mass and bone micro-architectural texture as assessed by TBS (Trabecular Bone Score) modification at spine during childhood growth in girls.

The study group was composed of 415 healthy girls aged between 2 and 17 years old. Height, weight and BMI Z-scores were evaluated and compared to The WHO Child Growth Standards. Pubertal stage was evaluated using Tanner score. The areal BMD (aBMD) was assessed at spine L1-L4 using a prodigy densitometer (GE-LUNAR, USA). Pseudo 3D BMD (vBMD) was calculated based on cylindrical model proposed by Kroeger et al. (Bone Mineral, 1992). TBS was evaluated using TBS iNsight v2.0 (Medimaps, France). The LMS statistical method proposed by Cole and Green (Stat Med, 1992) was used to construct aBMD, vBMD and TBS age-related curves using R software (v2.15.3).

Mean age, Weight, Height and BMI Z-scores were respectively 10.9 ± 4.4 years, -0.22 ± 1.3, -0.44 ± 1.3 and 0.02 ± 1.2 SD respectively. Positive significant correlations ($p<.05$) exists between TBS and age, BMI, aBMD and vBMD ($r= 0.39, 0.27, 0.47$ and 0.43 respectively). Height, weight and BMI followed normal pattern with age (data not show).aBMD increases with the growth with an acceleration at the puberty (as presented figure 1 a). This finding is consistent with the data of Kalkwarf et al (JCEM 2007). When normalized by the 3D volume, effect of puberty on vBMD is more visible (see figure 1b). Before the puberty, vBMD trend seems to be flat. Concerning TBS, we observed first a decreasing phase until the puberty follow by an increasing phase until 17 (fig 1c).

DXA can be used to assess trabecular bone microarchitectural texture, as assessed by TBS, in children with a high degree of reliability. Age-related TBS curve can be useful, in complement to the BMD curve, to help clinician to identify children with bone microarchitectural modifications induced by chronic diseases or drug therapies.

***Disclosures: Renaud Winzenrieth**, None.*

SU0029

Cortical Bone Fragility Contributes to Fractures in Children. Sandra Iuliano-Burns*[1], Qingju Wang[1], Xiaofang Wang[2], Ali Ghasem-Zadeh[2], Roger Zebaze[1], Yohann Bala[3], Ego Seeman[1]. [1]Austin Health, University of Melbourne, Australia, [2]University of Melbourne, Australia, [3]University of Melbourne, Dept. of Medicine, Australia

Fractures are common in children, with up to 50% of boys and 40% of girls fracturing by the age of 18 years, and with reduced bone mineral density (BMD) observed in fracture cases. The highest incidence coincides with the pubertal growth spurt, when there is a transient reduction in volumetric vBMD and cortical thickness. We hypothesize that deficits in cortical thickness and increased cortical porosity are present in children with fractures.

We recruited 54 children (28 males, 26 females) with low trauma fractures and imaged their distal metaphyses of the contralateral radius and tibia using high-resolution peripheral quantitative computed tomography (Xtreme CT, Scanco, Switzerland). Cortical porosity, degree of mineralization (tissue mineralization density), and dimensions of the transitional zone (area between the hard cortex and trabecular bone) were determined using StrAx 1.0 software. Fracture case was compared to 54 age (11.9 $\pm$ 2.9 vs 11.7 $\pm$ 2.8 yrs), height (152.4 $\pm$ 16.7 vs 150.7 $\pm$ 15.2 cm) weight (46.6 $\pm$ 15.6 vs 45.8 $\pm$ 15.3 kg) and maturity matched controls.

Bone total cross sectional area was similar in cases and controls (total area; 224 $\pm$ 66 v 208 $\pm$ 59 mm2) however, compared to controls, distal radius cortical vBMD was 5% lower in cases (773 $\pm$ 114 vs. 819 $\pm$ 135 mg HA/cm3, $p < 0.05$) due to their 6% higher porosity (53 $\pm$ 8 vs. 50 $\pm$ 9%, $p < 0.05$) and 3% lower tissue mineralization density (61 $\pm$ 3 vs. 63 $\pm$ 3%, $p < 0.0001$). These differences were most evident in pre-pubertal boys ($n = 26$) in whom those with low trauma fractures had 26% thinner cortices (0.30 $\pm$ 0.07 vs 0.41 $\pm$ 0.12mm, $p < 0.01$), and a 9% wider transitional zone (2.77 $\pm$ 0.19 vs 2.55 $\pm$ 0.30 μm, $p < 0.05$) than controls. Fracture cases had greater trabecular area (107 $\pm$ 27 vs 84 $\pm$ 28 mm2, $p < 0.05$) with thicker (0.08 $\pm$ 0.01 vs 0.07 $\pm$ 0.0 mm, $p < 0.01$), fewer (1.8 $\pm$ 0.2 vs 2.1 $\pm$ 0.3 1/mm, $p < 0.01$) and more separated trabeculae (0.49 $\pm$ 0.08 vs. 0.41 $\pm$ 0.06 mm, $p < 0.01$) than controls. Similar deficits in bone structure were observed at the tibia with 6% lower cortical vBMD ($p < 0.05$), 2% lower tissue mineralization density ($p < 0.001$), and 9% higher porosity ($p < 0.05$) observed in all cases relative to controls.

We infer that material and structural abnormalities in the cortex contribute to bone fragility during accelerated growth in children and predispose to fractures should a fall occur.

***Disclosures: Sandra Iuliano-Burns**, None.*

SU0030

Development of a New Tool for Evaluating Bone Mineralization as a Function of Age in Pediatric Patients. Joyce Keyak*[1], Liliane Gibbs[2], Sandra Murray[3], Antoine Hamedi-Sangsari[4], Diana Lubyanaya[5], AiChun Chen[5]. [1]Department of Radiological Sciences, University of California, Irvine, USA, [2]Pediatric Radiology, RADNET; & Department of Radiological Sciences, University of California, Irvine, USA, [3]University of California, Irvine & Miller Children's Hospital, Long Beach, USA, [4]School of Biological Sciences, University of California, Irvine, USA, [5]Department of Mathematics, University of California, Irvine, USA

Evaluating the underlying etiology of bone fractures in pediatric patients is an essential part of good medical practice but can be challenging because bone mineralization and size change with age. Knowledge of bone mineralization and size as a function of age is essential for differentiating fractures of healthy bones from fractures of diseased bones. Dual-energy x-ray absorptiometry, the most common method for evaluating bone mineral, provides areal measures of bone size and density that cannot distinguish thinner bones from lower density bones. In contrast, quantitative CT (QCT) scans provide true volumetric measures of bone size and density. CT scans are ordered routinely in pediatrics to diagnose injury or disease and could be used concurrently to evaluate bone mineralization. Thus, we are developing a CT scan-based tool and normative database to evaluate bone mineralization in pediatric patients.

We performed a pilot study using anonymized QCT scans of 9 male patients, age 3-17y, who were imaged for reasons unrelated to this study. Volume (V), bone mineral content (BMC) and bone mineral density (BMD) in one slice through the middle of each vertebral body were determined in the mineralized portions of T9 through L5. V and BMC were normalized to a 3mm-thickness. Linear regression was performed to quantify V, BMC and BMD at each level of the spine as a function of age.

Age predicted V ($p \leq 0.005$) and BMC ($p \leq 0.02$) at all spinal levels, but only predicted BMD at T10 ($p=0.04$) (Fig. 1). Standard errors of the estimates (SEE), which quantify scatter about the regression lines, were 11-19% of the mean V and 16-35% of the mean BMC. SEE was 6% of the mean BMD at T10, but the standard deviation (SD) was 8-17% of the mean BMD at each level, without the need to control for age.

This pilot study showed that V and BMD in 9 male patients age 3-17y were measured with a promising level of precision (SEE and SD=6-19%), despite substantial age-related anatomical variation. Developing this method for differentiating between healthy and diseased bone will require study of additional subjects, including girls of all ages, children under age 12 (who were underrepresented here), and patients with bone disease (to be evaluated as positive controls). Confidence limits for V, BMC and BMD of healthy bone as a function of age will then be established. Patients whose bone falls outside these limits would be considered abnormal and would be subject to further diagnostic testing.

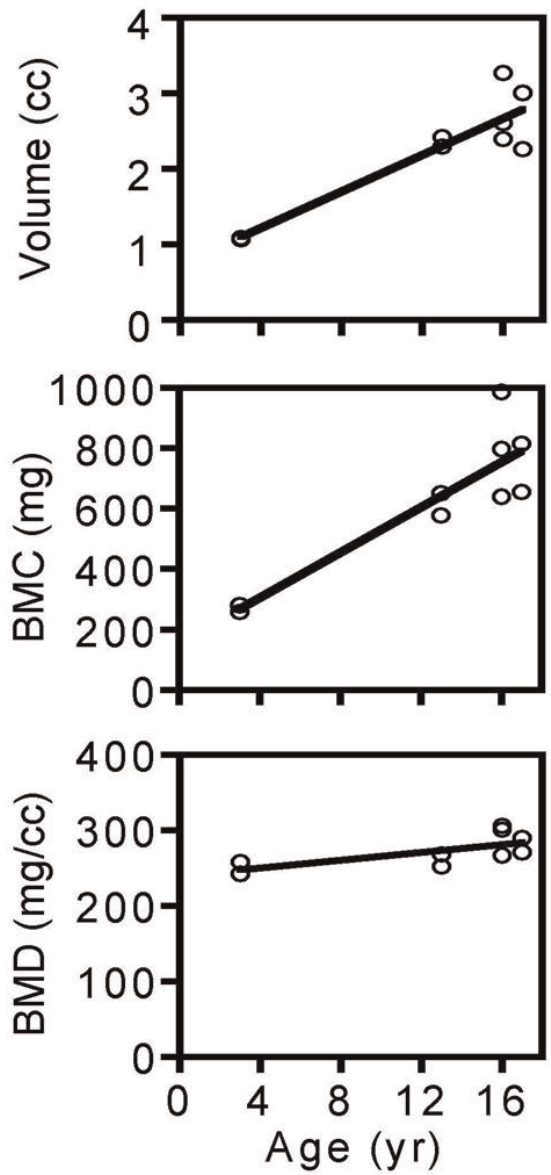

Fig. 1. T10 vertebral body volume, BMC and BMD versus age

***Disclosures: Joyce Keyak**, None.*

SU0031

Maternal Pregnancy Vitamin D Status and Offspring Bone Health: A Systematic Review and Meta-analysis. Nicholas Harvey*[1], Christopher Holroyd[1], Georgia Ntani[1], Kassim Javaid[2], Philip Cooper[1], Rebecca Moon[1], Zoe Cole[1], Tannaze Tinati[1], Nicholas Bishop[3], Keith Godfrey[4], Elaine Dennison[1], Janis Baird[1], Cyrus Cooper[1], UK Vitamin D in Pregnancy Working Group[1]. [1]MRC Lifecourse Epidemiology Unit, University of Southampton, United Kingdom, [2]NIHR Musculoskeletal Biomedical Research Unit, University of Oxford, United Kingdom, [3]Academic Unit of Child Health, University of Sheffield, United Kingdom, [4]MRC Lifecourse Epidemiology Unit, University of Southampton, & NIHR Southampton Biomedical Research Centre, University of Southampton & University Hospital Southampton NHS Foundation Trust, United Kingdom

We aimed to elucidate whether 1) maternal circulating 25(OH)-vitamin D [25(OH)D] during pregnancy is associated with maternal and neonatal bone health; and 2) maternal supplementation with vitamin D in pregnancy leads to an improvement in these outcomes. Other health outcomes were also assessed.

Major electronic databases were searched from inception till June 2012, together with hand-searching of bibliographies and author contact. Primary outcomes: Maternal osteomalacia; Neonatal hypocalcaemia, rickets and bone mass. Secondary outcomes: Maternal quality of life; Neonatal body composition and bone mass, later offspring health (including asthma, diabetes, immune disease). We performed systematic review and where possible meta-analysis. All assessments were performed by two reviewers and according to UK CRD guidance.

After screening of 16,841 citations, 172 remained, with 73 finally included (including 10 clinical trials). There was considerable heterogeneity between the studies and for most outcomes there was conflicting evidence; however modest positive relationships were found between maternal serum 25(OH)D and 1) offspring birth weight in meta-analysis of 3 observational studies using log-transformed 25(OH)D concentrations; 2) offspring cord blood or postnatal calcium concentrations in a meta-analysis of 6 intervention studies (all found to be at high risk of bias); and 3) offspring bone mass in 5 observational studies judged to be of good quality, but which did not permit meta-analysis.

Although there was weak evidence to support a relationship between maternal 25(OH)-vitamin D status and offspring birth weight, bone mass and serum calcium concentrations, these findings were limited by their observational nature or low quality and risk of bias. High-quality intervention studies to investigate these outcomes would be appropriate, but the current evidence base is insufficient to directly inform clinical practice.

Acknowledgements:

The UK Vitamin D in Pregnancy Working Group

***Disclosures: Nicholas Harvey**, None.*

SU0032

Pre- and Early Post-Natal Methylphenidate Exposure and Rat Skeletal Development. David Komatsu*[1], David Fealey[2], Alexandra Filippi[2], Lacey Schwab[3], Jordan Fakhoury[4], Panayotis Thanos[5], Sherry A Ferguson[6]. [1]Stony Brook University, Dept. of Orthopaedics, USA, [2]School of Medicine, Stony Brook University, USA, [3]Department of Materials Science & Engineering, Stony Brook University, USA, [4]Department of Biology, Stony Brook University, USA, [5]Behavior Neuropharmacology & Neuroimaging Lab, Medical Department, Brookhaven National Laboratory, USA, [6]Division of Neurotoxicology, National Center for Toxicological Research/FDA, USA

The psychostimulant methylphenidate (MP) is widely prescribed to treat Attention Deficit Hyperactivity Disorder (ADHD). Although MP effectively attenuates ADHD symptoms, chronic treatment has been associated with significant growth impairment in children and adolescents. Moreover, our recent results have shown that chronic exposure of adolescent rats to MP not only impairs skeletal growth, but is also associated with less mineralized and biomechanically inferior bones. Approximately 4.4% of adults are diagnosed with ADHD and many of these are women of reproductive age. However, insufficient data exist regarding the use of MP during pregnancy. Our recent data in adolescent rats suggest that pre- and early post-natal MP treatment might produce similar alterations in skeletal development. To test this, Sprague Dawley dams were orally treated 3x/day with vehicle, MP-Low (2 mg/kg), MP-Medium (6 mg/kg), or MP-High (14 mg/kg) from gestational days 6-21. The pups were orally treated 2x/day with the same total daily dose (i.e., 0, 6, 18, or 42 mg/kg/day) as their dam on postnatal days 1-21, at which time bone samples were obtained. Samples (N=5-11/sex/treatment group) were analyzed and compared by 2-way ANOVA (sex, treatment, and interaction) with alpha=0.05. Length and diameter of left tibiae were measured with calipers but there were no significant treatment or sex differences. MicroCT was used to quantify cortical parameters at the mid-diaphysis and trabecular parameters at the distal metaphysis of left femora. Mid-diaphyseal periosteal volume was the sole parameter to show a significant treatment effect, with comparisons indicating that the MP-Low group was increased relative to vehicle. Comparisons of mid-diaphyseal periosteal and endosteal volume, trabecular spacing, and distal endosteal volume identified significant sex effects, with male values higher in all instances. There were no significant treatment by sex interactions. Overall, these data suggest that pre-natal and early post-natal exposure to MP may not adversely affect rat skeletal development. However, definitive conclusions cannot be reached until our analyses, in terms of both outcomes and full statistical power, have been completed. These studies are ongoing and their completion should allow determination of the extent to which developmental exposure to MP adversely affects rat skeletal development. Such data will provide much needed guidance to clinicians treating pregnant ADHD patients.

***Disclosures: David Komatsu**, None.*

SU0033

Relationships between Muscle Power, Force, Density and Bone Quality in Children, Adolescents and Young Adults. Leigh Gabel*, Heather McKay, Danmei Liu, Heather Macdonald. University of British Columbia, Canada

Purpose: The growing skeleton continually adapts to mechanical forces imposed by muscular contractions. Thus, we aimed to determine the influence of direct and surrogate measures of muscle power, force and density on bone quality.

Methods: We used high-resolution pQCT (HR-pQCT, Scanco Medical) to measure bone quality (bone macro-, microstructure, BMD and bone strength) at the distal tibia (8% site) in 173 females (14.5 y $\pm$ 3.9) and 146 males (15.5 y $\pm$ 3.4) who were participants in the UBC Healthy Bones III Study. Bone outcomes included total area (Tt.Ar, mm2) and bone mineral density (Tt.BMD, mg HA/cm3), trabecular bone volume ratio (BV/TV), thickness (Tb.Th, mm), number (Tb.N, 1/mm) and cortical density (Ct.BMD, mg HA/cm3), porosity (Ct.Po, %) and thickness (Ct.Th, mm). We applied finite element analysis to estimate bone strength (ultimate stress, UStress, MPa). We directly measured maximum muscle power from a single two-legged jump using a force plate (Watts, Novotec/Stratec Leonardo) and estimated muscle power from vertical jump height (VJH, cm) obtained with a Vertec device (Fitness Source). We used pQCT-derived muscle cross-sectional area (MCSA, mm2) at the tibial midshaft (50% site) as an estimate of muscle force and measured muscle density (mg/cm3) at the midshaft with pQCT (Novotec/Stratec XCT3000). We fit sex-specific multivariable regression models adjusting for maturity (menarcheal status in females, Tanner stage in males) and tibia length (surrogate for moment arm).

Results: All measures of muscle power and force were positively related (r=0.41-0.86; $p<0.001$). Muscle power explained 2-9% of the variance in all bone quality outcomes with the exception of Tb.Th and Ct.BMD in females and Tb.Th, Ct.Po and UStress in males. VJH explained 1-3% of the variance in Tb.Th, BV/TV, Tt.BMD and UStress in females and Tb.Th and Ct.Th in males. MCSA explained 2-15% of the variance in all bone quality outcomes with the exception of Tb.Th, Ct.BMD, and Ustress in females and Ct.Po and UStress in males. Muscle density was not an independent predictor of bone outcomes in females or males.

Discussion: Direct measures of muscle power and MCSA were significant predictors of bone quality and explained a similar amount of variance. Thus, either measure can be used to characterize the relationship between muscle and bone quality. In addition, our results indicate that muscle density is not a key determinant of bone quality in healthy children, adolescents and young adults.

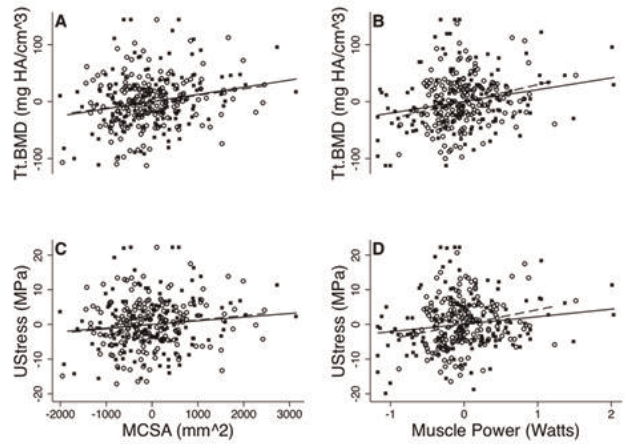

Figure 1. Relationships between residuals of MCSA, muscle power and bone quality (adjusted for maturity and moment arm) in females (open circles and dashed line) and males (solid squares and line).

Relationships between residuals of MCSA, muscle power and bone quality

***Disclosures: Leigh Gabel**, None.*

SU0034

Cessation of Ambulation Not Corticosteroid Exposure Results in a Dramatic loss of Trabecular Bone Density in Boys with Duchenne Muscular Dystrophy (DMD). Nicola Crabtree*[1], Natalie Bebbington[1], Heather McMurchie[2], Helen Roper[2], Nicholas Shaw[1]. [1]Birmingham Children's Hospital, United Kingdom, [2]Heart of England Hospital, United Kingdom

Fifty children were studied, 14 healthy boys (HB), 13 boys with DMD who remained ambulant (DMD-RA) and 23 boys with DMD who lost ambulation (DMD-LA). All boys with DMD were taking oral steroids. Peripheral quantitative computed tomography was used to measure bone geometry, density, strength and muscle mass of the non-dominant tibia. Measurements were made at baseline, 12 and 24 months at the distal metaphysis and mid diaphysis sites. Differences between the three groups were evaluated using ANOVA and a repeated measures model. There were no significant differences in age between the groups, mean age was 9.4(2.7), 8.7(1.9), 8.8(1.8) years for HB, DMD-RA and DMD-LA, respectively. There was no significant difference in steroid exposure between DMD groups. However, boys who lost ambulation had significantly lower muscle function. Healthy boys had significantly greater trabecular bone density (26%) than boys with DMD ($p<0.001$). However, the rate of change of trabecular bone density was only significant for boys who lost ambulation. By 2 years non-ambulant boys had 51% less trabecular bone than their healthy age matched peers (See Figure 1). Previous work has suggested that loss of ambulation can be predicted by assessment of muscle function.

Since this study highlights the dramatic loss of bone density with loss of ambulation it is likely that functional assessment can help identify the point at which medical intervention to strengthen bones should be considered.

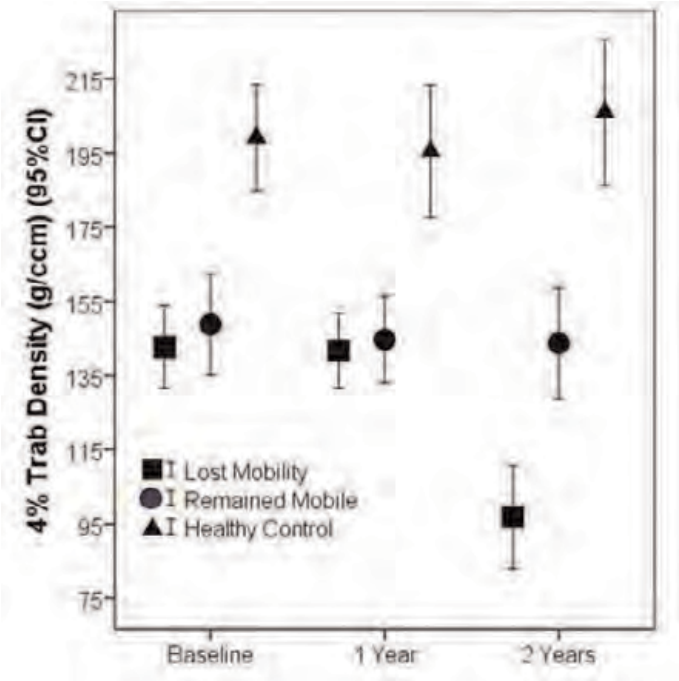

Figure 1

***Disclosures: Nicola Crabtree**, None.*

SU0035

Trabecular Bone Microarchitecture Impairment in Juvenile Systemic Lupus Erythematous (JSLE) with Low BMD for Chronological Age. Rosa Pereira*, Juliane Paupitz, Glauce Lima, Liliam Takayama, Jackeline Alvarenga, Luciana Seguro, Eloisa Bonfa. Faculdade de Medicina da Universidade de São Paulo, Brazil

Introduction: Young women with Lupus (SLE) are at high risk of low bone mass and fractures. Besides the effects of bone density, changes in microarchitecture also play an important role in bone disease in these patients. The objective of this study was to analyze bone microarchitecture in juvenile SLE (JSLE) patients with low and normal bone mineral density (BMD) for chronological age and clinical risk factors, glucocorticoid (GC) use and vitamin D status.Patients and Methods: Fifty-two JSLE female patients were evaluated. Demographic, anthropometric and clinical data including disease duration, disease activity score (SLEDAI) and GC use were recorded by interview and chart review. BMD and Vertebral Fracture Assessment (VFA) were analyzed by Dual-energy X-ray absorptiometry (DXA). Bone microarchitecture was measured using High-Resolution peripheral Quantitative Computed Tomography (HR-pQCT) at the distal radius and tibia. 25-hydroxyvitamin D levels were measured by radioimmunoassay. The patients were divided according BMD: low BMD for chronological age (Z-score of lumbar spine/or whole body ≤-2.0) n=20 and normal BMD for chronological age (Z-score of lumbar spine/or whole body >-2.0) n=32.Results: No difference was found between the 2 groups regarding age, body mass index, disease duration, SLEDAI. Patients with low BMD used higher GC maximum dose (48.75±20.12 vs. 30.54± 24.11 mg; p=0.006) and GC cumulative dose (92.84±72.32 vs. 46.76±58.71 g; p=0.02). Patients with low BMD also presented lower vitamin D levels (20±4.53 vs. 25.07± 8.92ng/mL;p=0.041), higher percentage of patients with fractures (25 vs. 6%;p=0.05) and higher number of total fractures (6 vs. 1.5%;p=0.002). Regarding HR-pQCT, patients with low BMD had lower values of bone microarchitecture parameters in distal radius (Table 1) and tibia (Table 2) as described below. Conclusion: The trabecular bone microarchitecture was significantly impaired in JSLE with low BMD for chronological age. GC use, lower vitamin D concentrations were also parameters related to low BMD. Further studies are necessary to assess the contribution of bone microarchitecture in the risk of fractures in JSLE patients.

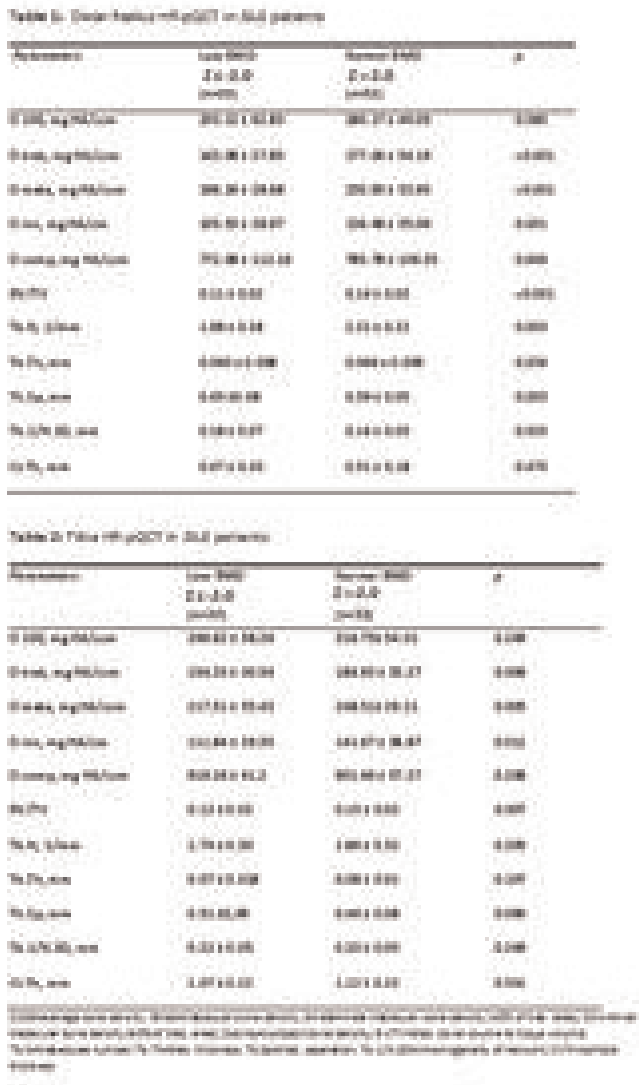

Table 1 and Table 2

***Disclosures: Rosa Pereira**, None.*

SU0036

Gnathodiaphyseal Dysplasia due to Mutations in the Cleavage Site of the C-propetide region of *COL1A1*: a Form of Osteogenesis Imperfecta with Bone Fragility, Increased Bone Mineral Density and Fibro-osseus Lesions of the Skull and Jaw. Emma Duncan*[1], Aideen McInerney-Leo[2], Andreas Zankl[2], Matthew Brown[3]. [1]Royal Brisbane & Women's Hospital, Australia, [2]University of Queensland Diamantina Institute, Australia, [3]Diamantina Institute of Cancer, Immunology & Metabolic Medicine, Australia

We report a mother and son with increased bone fragility, irregular bone density and fibro-osseus lesions in the skull and jaw, suggestive of the disorder gnathodiaphyseal dysplasia, but in whom sequencing revealed no mutation in Anoctamin-5 (*ANO5*), previously described as a causative gene for this condition. Whole exome sequencing revealed a de novo mutation A1218T in *COL1A1* in the mother, also inherited by her affected son. The mutation alters an amino acid within the C-propeptide region which is required for cleavage of the C-propeptide from the fibrillar collagen component during collagen maturation. Similar mutations have been reported in patients with a clinical picture of osteogenesis imperfecta but with normal or increased bone density. We conclude that C-propeptide mutations in *COL1A1* not only cause an unusual form of osteogenesis imperfecta with paradoxically increased bone mass, but also manifest other abnormalities including irregular bone density and fibro-osseus lesions in the skull and jaw. Further, we suggest that cases of gnathodiaphyseal dysplasia that are negative for *ANO5* be evaluated for mutations in the C-propeptide cleavage region of procollagen type 1.

***Disclosures: Emma Duncan**, None.*

SU0037

Etanercept Administration to Neonatal SH3BP2 Knock-In Cherubism Mice Prevents TNF-α-induced Inflammation and Bone Loss. Teruhito Yoshitaka[1], Shu Ishida[2], Tomoyuki Mukai[2], Ernst Reichenberger[3], Yasuyoshi Ueki*[1]. [1]University of Missouri-Kansas City, School of Dentistry, USA, [2]University of Missouri-Kansas City, USA, [3]University of Connecticut Health Center, USA

Cherubism is a craniofacial disorder caused by gain-of-function mutations in the signaling adaptor protein, SH3BP2. In a mouse knock-in model for cherubism, we previously demonstrated that homozygous mutant mice develop T/B cell-independent systemic macrophage inflammation leading to bone erosion and joint destruction, while cherubism lesions in humans appear to be primarily limited to jaw bones. Previously we identified a critical role of TNF-α in this disease as inflammation and bone destruction were rescued in TNF-α-deficient cherubism mice. In the current study, we examined whether postnatal administration of etanercept, an anti-TNF-α antagonist, can prevent or ameliorate disease progression in cherubism mice. Neonatal (1 week old) homozygous mutants, where active inflammation has not yet developed, were treated twice/week for 7 weeks with a high dose (25mg/kg) or low dose (0.5mg/kg) etanercept. High dose treatment effectively rescued facial swelling in all mutants (n=7), as well as bone loss in the jaws and calvariae (n=7, $p<0.05$). Destruction of joints was fully rescued in all high dose-treated mutants. Moreover, the high dose treatment group showed a significant decrease in lung ($2.7\pm2.3\%$ vs. $9.1\pm4.0\%$) and liver ($0.1\pm0.1\%$ vs. $10.6\pm5.0\%$) inflammatory lesions ($p<0.05$). No significant effect was observed in low dose and vehicle (PBS)-treated groups; low-dose group ($9.6\pm5.6\%$ in lung, $9.9\pm7.2\%$ in liver, n=6) and vehicle group ($9.1\pm4.0\%$ in lung, $10.6\pm5.0\%$ in liver, n=6). However, when 10-week-old adult cherubism mice with fully active inflammation were treated with etanercept for 7 weeks (n=7), while high dose treatment effectively reduced liver inflammation ($4.1\pm3.5\%$ in etanercept group vs. $10.6\pm6.1\%$ in PBS group), the high dose administration did not rescue facial swelling and did not decrease bone loss and lung inflammation ($7.4\pm4.3\%$ vs. $5.2\pm2.7\%$). Mutant macrophages express more IL-1β in response to TNF-α and in turn IL-1β induces more TNF-α production in mutant macrophages, suggesting that IL-1β-driven inflammation may be responsible for the reduced effectiveness of etanercept treatment in the adult. Taken together, our study suggests that anti-TNF-α therapy may be an effective prophylactic treatment in young cherubism patients, if treated before establishment of inflammation or bone resorption. Therefore, early genetic diagnosis and early treatment with anti-TNF-α antagonists may be important to prevent or ameliorate cherubism lesions in humans.

***Disclosures: Yasuyoshi Ueki**, None.*

SU0038

Sclerostin Antibody Increases Cortical Bone Thickness in a Rapidly Growing Brtl/+ Model of OI by Inducing Bone Formation on Quiescent or Resorbing Surfaces. Benjamin Sinder*[1], Joseph Salemi[1], Michael Ominsky[2], Michelle Caird[1], Joan Marini[3], Kenneth Kozloff[4]. [1]University of Michigan, USA, [2]Amgen Inc., USA, [3]National Institute of Child Health & Human Development, USA, [4]University of Michigan Department of Orthopaedic Surgery, USA

Osteogenesis imperfecta (OI) is a genetic collagen-related disorder characterized by brittle bones, which presents most severely in children. Treatment with sclerostin antibody (Scl-Ab) has been shown to increase bone formation and bone strength with modest reductions in bone resorption in murine models of OI (Sinder et al JBMR 2013). Using 3 week-old male Brtl/+ mice with dominant OI, that carry a G349C substitution on one col1a1 allele, we previously showed that 5 weeks of Scl-Ab (25mg/kg, 2x week) increased femoral cortical bone mass and strength (Sinder et al, ASBMR 2012). Here, we performed dynamic histomorphometry to examine Scl-Ab effects on the spatial pattern of bone formation in these rapidly growing mice.

Mineralizing surface (MS/BS) and mineral apposition rate (MAR) were quantified from WT and Brtl/+ femurs contralateral to those previously tested (n=5-7/group). Fluorescent labels given 1 week and 1 day before sac were analyzed on a cortical section immediately distal to the third trochanter. To assess spatial variation across the cortex, MS/BS and MAR were quantified separately on periosteal and endosteal surfaces in the posterior and anterior quadrants using a method similar to Bivi et al (JBMR 2012).

We confirmed a strong posterior-shifting cortical drift in untreated WT and Brtl/+, with MS/BS near 100% on the posterior periosteal surface and anterior endosteal surface (Figure). On the opposing surfaces (posterior endosteal and anterior periosteal) where resorption would be expected to occur consistent with drift direction, MS/BS was much lower (0-38%). Scl-Ab increased MS/BS on these low bone-forming surfaces in both WT and Brtl/+ mice (Table). On high bone-forming surfaces, MAR was marginally elevated (posterior periosteal) or slightly reduced (anterior endosteal). This slight decrease in anterior endosteal MAR may be compensatory to the robust increase in anterior periosteal bone formation. Regardless of the mechanism, Scl-Ab increased cortical thickness in both the anterior and posterior compartment of Brtl/+.

In this study, Scl-Ab increased cortical thickness in Brtl/+ and WT mice by activating bone formation on regions of the cortex that typically undergo resorption as part of a modeling drift. These results highlight the ability of Scl-Ab to activate new bone formation on quiescent or resorptive surfaces, while maintaining the modeling based bone formation that occurs in rapidly growing animals.

	WT Veh	WT Scl-Ab	Brtl Veh	Brtl Scl-Ab
Anterior				
Cort. Thick. (μm)	187 ± 17	220 ± 27	157 ± 24	199 ± 19*
Periosteal MS/BS	0.00 ± .00	0.42 ± .52	0.38 ± .25	0.79 ± .14*
Periosteal MAR	0.00 ± .00	0.56 ± .77	0.56 ± .39	1.14 ± .48
Endosteal MS/BS	0.99 ± .02	0.97 ± .04	0.95 ± .09	0.81 ± .08
Endosteal MAR	2.06 ± .28	1.63 ± .66	1.28 ± .52	0.86 ± .27*
Posterior				
Cort. Thick (μm)	213 ± 16	277 ± 42*	167 ± 20	234 ± 14*
Periosteal MS/BS	0.97 ± .07	0.99 ± .02	0.99 ± .02	0.99 ± .02
Periosteal MAR	1.96 ± .57	2.48 ± .78	2.00 ± .45	2.44 ± .62
Endosteal MS/BS	0.08 ± .08	0.74 ± .15*	0.32 ± .19	0.94 ± .06*
Endosteal MAR	0.55 ± 1.1	0.91 ± .31	0.48 ± .32	1.02 ± .43

Data is mean±S.D. MAR is μm/day. *p<0.05 Scl-Ab effect within genotype.

Table: Cortical Thickness and Dynamic Histomorphometry

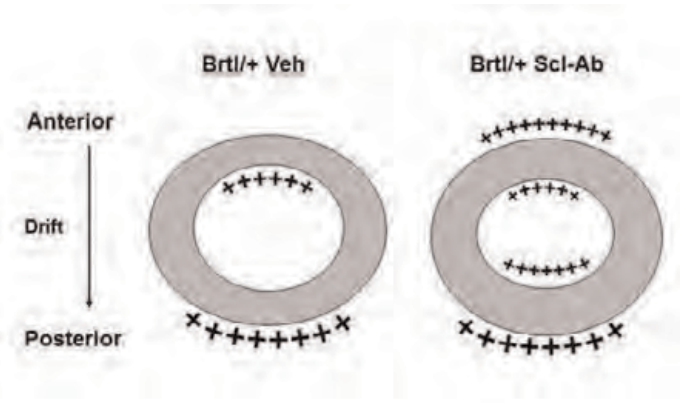

Figure: Summary of Bone Formation Changes in Brtl/+

***Disclosures: Benjamin Sinder**, None.*

SU0039

3D Visualization of Reference-Point Indentation in Human and Murine Bone. John Jameson*[1], Alexander Proctor[2], Carolyne Albert[3], Gerald Harris[3]. [1]Lawrence Berkeley National Lab, USA, [2]Active Life Scientific, USA, [3]Orthopaedic & Rehabilitation Engineering Center, Department of Biomedical Engineering, Marquette University, USA

Traditional techniques for assessing bone strength and fracture resistance such as 3 or 4-point bending of whole bones or machined beams are well-developed but destructive. Recently, Reference-Point Indentation (RPI) has been introduced as a minimally destructive method of determining bone tissue properties at physiologically relevant length scales [1-2]. However, to date there is no data showing the 3D damage mechanisms associated with RPI. The purpose of this study was to use high-resolution imaging to visualize RPI tests of human and murine bone, as well as to compare indents from healthy and pathological tissue.

Femora from healthy mice and a mouse model for severe osteogenesis imperfecta (oim; $N_{control}=N_{oim}=3$, Age=12wks) were extracted and tested with repeated RPI measurements (BioDent Hfc, Active Life Scientific, Inc.) along the long axis of the bone using a maximum force of 5 N at 2 Hz for 7 cycles. Each indent was imaged by synchrotron radiation on the X-ray microtomography (SRμCT) beamline at the Advanced Light Source (ALS, Berkeley, CA) with a nominal pixel size of 1.33 μm. Similar imaging was performed on indents from a healthy human tibia donated from an unrelated cadaver study.

Oim femora showed inferior material behavior as assessed by RPI measures (Table 1). On average, first cycle indentation distance (ID), ID increase (IDI), total ID (TID), and creep ID (CID) were higher in oim bones compared to controls, while the slope of the unloading portion of the first cycle (US) was reduced. SRμCT images of representative damage regions revealed an increase in the degree of micro-cracking in oim bone compared to controls (Fig 1-2). Healthy human bone also appeared to display evidence of crack bridging, a common extrinsic toughening mechanism (Fig 3).

The results of this preliminary study suggest that RPI is an effective method for evaluating differences in the material behavior of healthy versus oim mouse bone. Similar trends in RPI parameters have been reported in control versus diabetic rat bone, which is known to exhibit increased fragility [2]. For the first time, we also show how SRμCT can be used to complement RPI testing by providing valuable 3D information on sub-surface fracture behavior. In oim bone, increased micro-cracking is likely a toughening mechanism required to mitigate the reduced initiation toughness.

[1] Diez-Perez et al, J Bone Miner Res, 2010.
[2] Gallant et al, Bone, 2013.

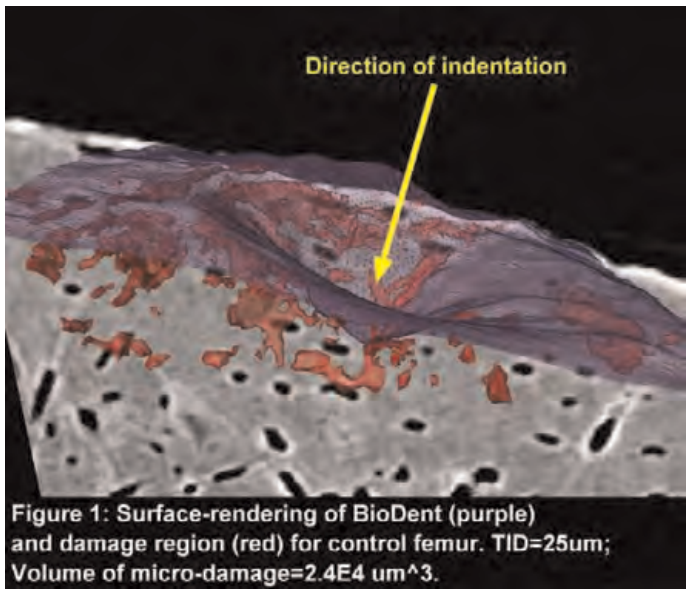

Figure 1: BioDent of control mouse bone

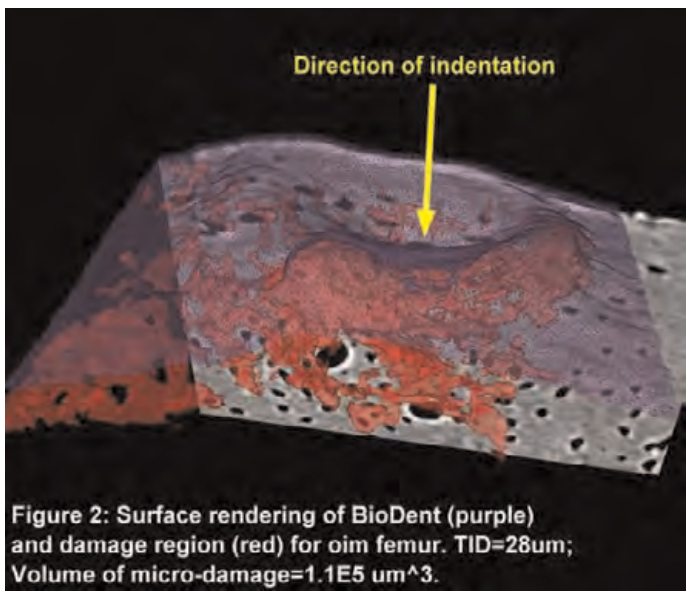

Figure 2: BioDent of oim (brittle) mouse bone

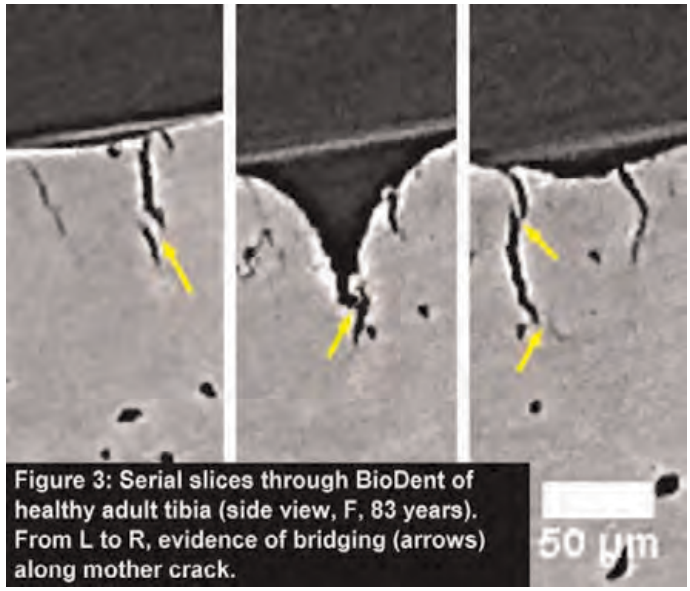

Figure 3: BioDent of healthy human bone

	Control	Oim
Number of indents	32	14
ID (μm)	28.7 ± 5.2	31.3 ± 9.6
IDI (μm)	4.1 ± 1.3	6.6 ± 4.6
TID (μm)	30.5 ± 5.2	34.9 ± 10.8
CID (μm)	3.0 ± 1.0	3.9 ± 2.6
US (N/μm)	0.74 ± 0.12	0.66 ± 0.10

Table 1: Summary of BioDent mouse data

***Disclosures: John Jameson**, None.*

SU0040

A New Viewpoint on Using Glycine to Prevent and Treat Rats' Osteoporosis.

Jingkun Zhang*. Nankai University, Peoples Republic of China

Abstrat: This study will show a new viewpoint about osteoporosis(OP), which proposes that the lack of glycine is the main cause for OP. Glycine determines the structure and properties of bone matrix.Scientifically added glycine and let it participate in the transform of bone trabeculae, in which process to optimize and strengthen the structure of bone trabeculae and further to repair the damaged bone matrix, is the biological route to prevent and treat osteoporosis. The SD rat osteoporosis model was made by removing SD female rat's two ovaries. In order to overcome the barriers of the small intestine, the glycine was replaced by glycine chelated calcium(GCC) in this experiment. In addition to the GCC group, three control groups (ovariectomized group, bisphosphate group, sham operated group) were all fed for 100 days, then were executed and the microstructure of their femur trabeculae were detected. The trabeculae of the GCC group is orderly, grossus and presents prominent mechanical properties, while the group of bisphosphate is disorderly and with serious obstacles of metabolism. All 12 parameters of dynamic and static morphometry in GCC group rats' bone structure are significantly better than the corresponding bisphosphate group. Some important physical parameters in the GCC group's bone structure, e.g. BMD?strength and deflection of femur, are remarkable higher than the sham operated group, which indicated that some important physical properties of rats' femur are notable improved. Effectively added glycine and let it participate in the bone metabolism, not only can treat osteoporosis, but also can conspicuously prevent osteoporosis.

Key words:glycine, osteoporosis, treat, prevent

***Disclosures: Jingkun Zhang**, None.*

SU0041

A Proteome Profile of Fragile Human Bones. Corinne Thomas*, Dmitri Zagorevski, Grazyna Sroga, Pankaj Karande, Deepak Vashishth. Rensselaer Polytechnic Institute, USA

Introduction: Bone fragility fractures are a leading health concern in many countries, including the United States. Currently, the susceptibility of bone to fragility fracture is assessed through a dual-energy X-ray absorptiometry (DXA) scan which measures bone mineral density (BMD), or by peripheral quantitative computed tomography (pQCT) which is expensive and inaccessible to many patients[1]. None of the assessment techniques account for the chemical modifications in bone that occur with age and health. BMD may not be enough to accurately predict bone fragility and a recent study by our group[2] demonstrated that the levels of the proteins osteopontin, osteocalcin, and the advance glycation end products (AGEs) of collagen are better predictors of bone fracture than BMD. The objective of this study was to develop a mass spectrometry protocol that will allow for a comparison of the proteome of healthy bone to fragile bone, and identify any other potential targets that may characterize bone quality.

Methods: The mass spectrometry protocol was developed and optimized using in vitro glycation of synthesized peptide fragments mimicking those of osteocalcin. Bone samples from donors aged 29 - 89 years old were selected to provide a wide range of bone quality for comparison. These samples were powdered and the proteins extracted for proteomic analysis. The separated proteins were subjected to proteolytic digestion from a variety of proteases. The digests were then analyzed using MALDI-TOF mass spectrometry as well as LCMS.

Results: Glycation of peptide samples caused a peak shift in the MALDI spectrum. Depending on the protease treatment and age of the donor, select peaks were lost or demonstrated a shift in bone samples. Peak shift occurred in areas where the mass of a peptide fragment changed due to a modification such as glycation, and the loss of peak was associated with the loss of a polypeptide fragment was not formed due to the cleavage site being blocked. The differing fragments shown with each enzyme (Figure 1) allowed for specific proteins and their modifications to be identified.

Acknowledgements: RPI Seed Grant

[1] Melton LJ, III, et al. JBMR 22:1885-1892, 2007

[2] Karim et al. Proceedings of the 58th Annual Meeting of the ORS. Vol. 37, p. 0116, 2012

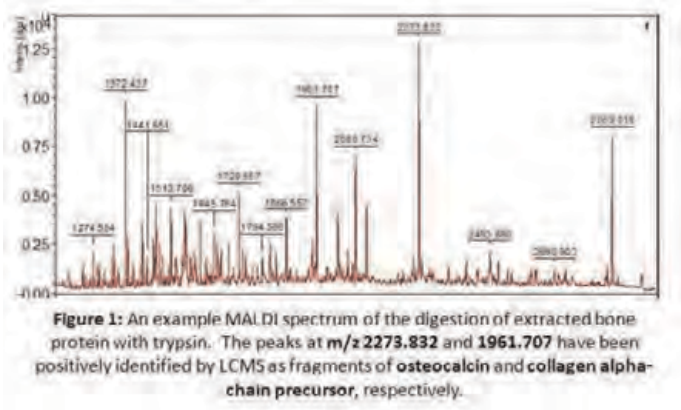

Figure 1: Sample MALDI spectrum

***Disclosures: Corinne Thomas**, None.*

SU0042

Altered Chemokine Signaling in Fracture Callus in Response to Binge Alcohol Exposure. Roman Natoli*[1], Rachel Nauer[1], John Callaci[2]. [1]Loyola University Medical Center Chicago, USA, [2]Loyola University of Chicago, USA

Alcohol use increases the risk of impaired fracture healing, however the underlying mechanisms are not well understood. Using a clinically relevant paradigm, our laboratory has shown that binge alcohol exposure prior to creation of a stabilized fracture in rodents impairs fracture healing, leading to defects in callus size, tissue composition, and strength, and suggesting possible impairment in mesenchymal stem cell (MSC) homing to or activity at the injury site. It is known that MSCs are recruited to healing fractures through chemokine interactions such as stromal cell-derived factor-1 (SDF-1)/CXCR4 and osteopontin (OPN)/CD44. Therefore, we hypothesized that alcohol exposure may deregulate SDF-1 and/or OPN signaling in the fracture callus during early stages of healing.

Adolescent male C57BL/6 mice were exposed to a binge alcohol (EtOH) paradigm. Exposure consisted of a 20% EtOH in saline solution administered via intraperitoneal (IP) injection at a dose of 2g/kg for 3 days 1 week prior to injury and then 3 consecutive days leading up to fracture. Control mice were given equal volume of saline IP. On the day of injury the tibia was stabilized with a stainless steel pin with subsequent surgical creation of a fracture. Saline or EtOH exposure was continued daily after injury. Mice were euthanized at 3 and 7 days post-fracture, and protein was isolated from intact contralateral tibiae and the calluses of fractured limbs. OPN levels were assessed via Western blotting and SDF-1 via ELISA. Data were analyzed using a 2-way ANOVA with Tukey's post-hoc testing.

Histologic examination revealed diminished external callus in the EtOH group consisting of undifferentiated mesenchymal tissue. Protein analysis showed decreased SDF-1 and OPN levels at 3 days post-fracture in control and EtOH fracture calluses compared with contralateral tibiae. At 7 days post-injury, calluses from control mice showed a significant increase in OPN expression compared to contralateral tibiae; this change was not observed in mice exposed to EtOH (Fig. 1). In contrast, SDF-1 levels remained decreased in the fracture callus in both control and EtOH exposed mice at 7 days. These results suggest impaired fracture healing following binge alcohol exposure may be related to changes in OPN/CD44 signaling at the fracture site. This finding has implications for understanding the mechanisms underlying alcohol-deficient fracture repair and the possible clinical use of MSCs as a cell based therapy.

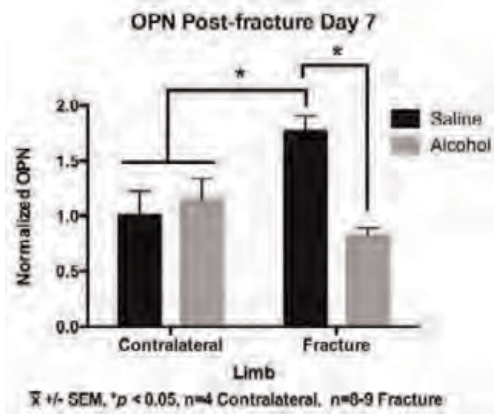

Figure 1

***Disclosures: Roman Natoli**, None.*

SU0043

Bone Material Properties Are Impaired in Fractured-patients with Type 1 Diabetes Mellitus. Delphine Farlay*[1], Laura Armas[2], Anne-sophie Bravo Martin[1], Robert Recker[2], Georges Boivin[1]. [1]INSERM, UMR1033; Université De Lyon, France, [2]Creighton University, USA

Patients with Type 1 diabetes (T1D) have more fractures than non-diabetic controls[1-2]. As no difference in BMD was observed between T1D and controls, it was hypothesized that abnormalities in bone material properties occurred in T1D patients[3]. The aim of present study was to analyze such modifications in intrinsic material properties in bone of T1D patients versus corresponding controls. Five iliac bone samples from fractured patients (35+/-12 year-old) with T1D (treated with insulin) and 5 iliac samples from non-diabetic controls (CTR, age and sex matched) were used[3]. Microradiography was performed on 100 µm-thick sections to measure the mean degree of mineralization (DMB, g/cm^3) and the mean heterogeneity index of mineralization (HI, g/cm^3)[4]. Vickers microhardness was calculated on 100 µm-thick sections (20 indents in each cortical and 20 in trabecular bone)[4]. Finally, Fourier Transform Infrared Microspectroscopy[5-6] was performed in the vicinity of indents. Results showed that in T1D versus CTR, DMB increased in both cortical and trabecular bone but HI was not different. Microhardness tended to increase in T1D, but not significantly. Relationships between microhardness and mineral and organic characteristics have then been performed. Significant correlations between micro-hardness and mineralization index was always found, in CTR (r'=0.29, p=0.0018) and T1D (r'=0.180, p=0.0178). Moreover, in T1D, correlations were found close to indents, especially between microhardness and either crystallinity index (r'=0.28, p=0.0002), or collagen maturity (r'=0.16, p=0.037). These correlations were not found in CTR. This preliminary study suggests that alterations in bone materials properties of T1D patients could explain in part their bone fragility.

1 - Melton III et al. J Clin Endocrinol Metab 2008, 93:4804.
2 - Vestergaard Osteoporos Int 2007, 18:427.
3 - Armas et al. Bone 2012, 50(1):91.
4 - Boivin et al. Bone 2008, 43:532.
5 - Farlay et al. J Bone Miner Metab 2010, 28:433.
6 - Farlay et al. PLoS One 2011, 6(12):e28736.

***Disclosures: Delphine Farlay**, None.*

SU0044

Bone quality adaptations to running in a murine model of impaired reactive oxygen species (ROS) scavenging. Vanessa Sherk*[1], Lillian Chatham[1], Kathryn Pate[2], Elizabeth Regan[2], Wendy Kohrt[1], Dana Carpenter[1]. [1]University of Colorado Denver, USA, [2]National Jewish Health, USA

A polymorphism (R213G) in the extracellular superoxide dismutase (EcSOD) gene decreases EcSOD protein in tissue extracellular matrix, leaving tissues that normally have high levels of EcSOD (i.e. bone and cartilage) susceptible to oxidative damage. It is unclear whether increased oxidative stress has a negative effect on bone quality. The purpose was to determine whether reduced ROS scavenging ability alters the skeletal adaptations to exercise training. Methods: Heterozygous EcSOD-deficient (Het; n=12) and C57BL/6 wild-type (WT; n=12) adult mice were randomized to treadmill running (Run: 5 d/wk, 45 min/d, 15 m/min) or sedentary (Sed) controls for 8 weeks. Tibias were harvested after sacrifice. Cross-sectional area (CSA) and estimates of bone strength (I_{max}, Z_{max}) were determined with microcomputed tomography. Stress at a standard (100N) compressive load ($Stress_{Std}$) was estimated by finite element analysis. Failure load (F_{max}) was measured in compression. Results: Increased protein nitration and DNA oxidation in knee articular cartilage of Het runners suggested increased oxidative stress. Exercise increased ($p<0.05$) CSA, I_{max}, and Z_{max} in Het mice only. $Stress_{Std}$ was reduced by exercise ($p<0.05$) and was lower in WT than Het ($p<0.001$) (Table 1). F_{max} did not differ among groups. Conclusion: EcSOD-deficient mice had more favorable bone architectural (CSA, I_{max}, Z_{max}) adaptations to running at the tibial mid-diaphysis than WT mice, but the 3D structures of the tibia resulted in lower estimated stress levels at the tibial mid-diaphysis in WT than in Het mice. Oxidative stress may be detrimental to skeletal health when sedentary, but may trigger more robust skeletal adaptations to exercise.

Table 1. CSA, strength and stress (Mean ± SD)

*$p<0.05$ Strain x exercise interaction; #$p<0.05$ Main effect for exercise; †$p<0.001$ Main effect for strain; [a]$p<0.05$ vs. WT-Sed; [b]$p\leq0.05$ vs. Het-Run

	Het-Run	Het-Sed	WT-Run	WT-Sed
Weight (g)	32.0±5.3	37.5±5.6	32.3±4.8	33.5±5.5
CSA (mm^2)*	0.88±0.13	0.73±0.04[b]	0.78±0.04	0.79±0.08
I_{max} (mm^4)*	0.141±0.047	0.086±0.006[ab]	0.110±0.019	0.114±0.024
Z_{max} (mm^3)*	0.176±0.045	0.129±0.009[ab]	0.152±0.012	0.159±0.023
F_{max} (N)	78.8±32.7	62.8±19.5	68.3±15.1	73.7±19.9
$Stress_{Std}$ (MPa)*†	102.1±11.4	117.6±17.6	86.5±7.0	92.1±9.4

Table 1

***Disclosures: Vanessa Sherk**, None.*

SU0045

Bone Regeneration Varies in Four Different Mouse Strains after Marrow Ablation. Meghan Moran*[1], Amarjit S Virdi[1], Kotaro Sena[2], Margaret A McNulty[3], D.R. Sumner[1]. [1]Rush Medical College, USA, [2]Kagoshima University, Japan, [3]Louisiana State University, USA

It is well-established that mouse strains exhibit different bone phenotypes, including bone mass, bone mineral density and mechanical properties. Various mouse strains and genetic models also exhibit different responses to injury challenges such as ear punches and fracture healing. One such fracture healing study showed more bone was present in the femoral fracture callus and healing proceeded more quickly in C57Bl/6 mice than C3H/He mice, supporting the idea that genetic variability contributes to bone repair (Manigrasso and O'Connor, 2008). There is very limited data on intramembranous bone regeneration, which is a part of fracture healing, after an injury challenge in different mouse strains. We sought to determine if intramembranous bone regeneration differs in four wild-type inbred mouse strains (BALB/C, C3H/He, C57Bl/6, FVB/N) in response marrow ablation.

Mechanical ablation of the marrow space was performed in 27 to 33 week old females of the four selected strains. Animals were euthanized 3 weeks post-surgery. All bone within the medullary canal of the operated and contra-lateral femurs was analyzed in the region between 30% and 60% of the total femur length by microCT (6 μm voxels). This region is normally lacking bone in intact animals. The sample size was 4 animals per strain.

Mean BV/TV varied between 4.3% and 19.5% in the operated femurs (Table 1, one-way ANOVA p=.004). Specifically, compared to BALB/C mice, FVB/N mice had approximately 4.5-fold more BV/TV (p=.007) and C3H/He mice had 4.1-fold more BV/TV (p=.017). C57Bl/6 mice were not different than any of the other three strains. The differences in BV/TV were due to various combinations of differences in trabecular number, trabecular thickness and trabecular spacing. As expected, the non-operated contra-lateral femurs had much lower mean BV/TVs (0-1.8%).These findings show that there was a large variation in the response to the marrow ablation challenge in these strains. These differences may be due to direct genetic effects on bone healing or possibly to indirect effects because these mouse strains also have inherent differences in bone geometry.

***Disclosures: Meghan Moran**, None.*

SU0046

Compressive Loading Reveals Local Changes in Bone Maturation Levels. Ingrid Bergstrom*[1], Jemma kerns[2], Allen Goodship[2], Sara Windahl[3]. [1]Karolinska Institutet, Sweden, [2]UCL Institute of Orthopaedics & Musculoskeletal Science, Royal National Orthopaedic Hospital, United Kingdom, [3]Center for Bone & Arthritis Research, Sahlgrenska Academy, Sweden

Introduction: Bone maturation and metabolism are optimised to accommodate specific physical activity. The role of increased mineral content is to stiffen the material and structure. The strength of bone, however, is dependent on both the mineral and the organic collagen matrix.

Aim: To explore the hypothesis that structural and material properties (bone matrix chemistry) change in adaptation to a specific loading regimen.

Methods: At three months of age, the right tibia of 7 mice were subjected to short periods of cyclic compressive loading three times a week for two weeks (40 cycles, peak strain 3097με). Following dissection, Raman spectra (830nm laser, Renishaw, UK) were acquired directly from 4 positions (cranial, medial [tensile area], caudal/medial and caudal/lateral [compression area]) at the mid-diaphysis of each bone. Raman spectra were analysed to determine mineralisation levels, crystallinity and collagen characteristics. Further, multivariate analysis was employed to determine the variance across each position for loaded vs. non-loaded data, at each position. Reference point indentation (RPI) measurements were acquired along the medial side of each bone, from proximal to distal, at 2N for 10 cycles (Active Life Scientific, USA).

Results: Analysing the spectra by anatomical position revealed that there was a significant difference between the non-loaded and loaded bones. Specifically the medial position showed that non-loaded bones had a significantly higher proportion ($p=0.01$) of mineral to collagen. Compared with the non-loaded bone, the loaded bone crystal maturity was lower for the caudal/lateral, but elevated for the medial position. Indentation results along the medial position of the bones revealed that both the non-loaded and loaded bones were more resistant to indentation in the mid-diaphysis than at either metaphysis.

Conclusions: Overall the loaded bones are less mineralised than the non-loaded bones, indicating new bone that is not fully mineralised. This supports the hypothesis that the bone matrix chemistry changes in response to loading. The pattern of bone matrix chemistry at different anatomical positions of the non-loaded and loaded bone is also different, suggesting that as bone remodels it responds locally to the loading conditions of the prevailing environment. Our data support the hypothesis that local and specific changes occur in both material and structural adaptation of bone to new loading conditions.

***Disclosures: Ingrid Bergstrom**, None.*

SU0047

Cortical bone Adaptation is greater at the Metaphysis than Diaphysis. Annette Birkhold*[1], Hajar Razi[1], Georg Duda[1], Sara Checa[1], Bettina Willie[2]. [1]Julius Wolff Institute, Charité Universitätsmedizin Berlin, Germany, [2]Charité- Universitätsmedizin Berlin, Germany

Age-related bone loss is a major clinical problem that occurs already during adulthood, at which time it mainly affects trabecular bone. It is unclear whether cortical bone at the metaphysis compensates for the loss of trabecular bone to maintain the bone's ability to withstand external loading. We hypothesized that metaphyseal cortical bone has a greater adaptive capacity than diaphyseal cortical bone, load-induced bone formation would be higher and resorption lower.

Six female 26wk old C57Bl/6J mice underwent 2 weeks of in vivo cyclic tibia loading (*216 cycles/day; f = 4 Hz; Fmax = -11 N; εmax = 1200 μstrain*, right tibia internal control). In vivo microCT (10.5μm) was performed at day 0, 5, 10, and 15. The metaphyseal region began below the growth plate and the diaphyseal region was centered at the midshaft, both extended 5% of tibia length. Images were aligned using rigid registration, binarized and separated into trabecular and cortical regions. Static measure included: cortical volume (ctBV) and mean cortical thickness (ctTh). Dynamic measures of bone formation/resorption included: volume (fBV/tBV, rBV/tBV), surface area (fSA/tSA, rSA/tSA) and thickness/depth (fTh, rTh). Local strains were determined using a FE model, validated by strain gauge data (day 0, n=7 mice). An ANOVA assessed effects of loading, region, and interactions.

In the nonloaded control tibia, (re)modeling at all time points (fBV/tBV, fSA/tSA, rBV/tBV, rSA/tSA) was greater at the metaphysis than at diaphysis. Loading increased metaphyseal cortical bone formation (ctBV, all time points, fBV/tBV and fSA/tSA at 5, 10d) and fTh at 10, 15d), but did not alter resorption. Loading increased diaphyseal cortical bone formation (ctTh and ctBV at 10, 15d, fBV/tBV and fSA/tSA at 5, 10, 15d) and reduced resorption (rBV/tBV at 10, 15d).The cortical bone location affected the response to loading: formation increased more with loading in metaphysis compared to diaphysis (fBV/tBV, fSA/tSA, fTh); rSA/tSA decreased more in diaphysis. Local maximal strain was similar in both regions: 1400 ± 950 με at diaphysis and 1100 ± 740 με at metaphysis.

These data indicate that metaphyseal cortical bone has a greater mechano-reponsiveness than diaphyseal cortical bone. The resulting increased formation in metaphysis may compensate for the loss of trabecular bone and maintain the ability of the metaphyseal region to withstand external loading with diminishing trabeculae with increasing age.

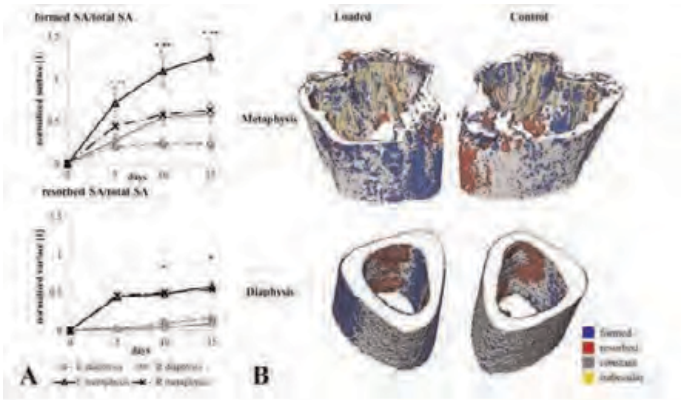

Fig: A. Surface areas of formation and resorption. B. Visualization of (re)modeling

***Disclosures: Annette Birkhold**, None.*

SU0048

Distinguished Density and Structure Analysis of the Distal Radius under the Aspects of Trauma Surgery. Volker Kuhn*[1], Gerald Degenhart[1], Thomas Müller[2], Felix Eckstein[3], Martin Lutz[1]. [1]Medical University Innsbruck, Austria, [2]ETH Zürich, Switzerland, [3]PMU Salzburg, Austria

Knowledge of the mechanical competence of osteoporotic bone is a big challenge in the surgical treatment of fragility fractures in the distal radius. Due to the thin cortical bone fracture fixation occurs predominantly in the trabecular compartment.

Purpose of this study was to compare DXA, HR-pQCT and loads from a biomechanical fall simulation upon the outstrechted forearm.

156 forearm specimens were harvested from formalin-fixed cadavers (mean age: 79.5+/-10.3; ranging 52-100; 82 male; 44 female). 21 were excluded due to former fractures.

DXA scans (pDEXA; Norland/Stratec) were analyzed within the clinically typical ROIs, and trabecular analyses from HR-pQCT data (Scanco) were performed for different distal and ultradistal slices. Under the aspect of usual surgical approaches, there was an additional division in dorso-palmar aligned halves and thirds for the slices, respectively.

According T-score 33% of the specimens presented normal bone quality, 37% were osteopenic, and 30% osteoporotic. Failure loads ranged from 250N to 5038N and were 43% higher in males (2645+/-1097N) compared with females (1512+/-711N). Fractures were comparable with types seen clinically.

DXA vs. failure loads provided the highest correlations (BMC: r = 0.806; BMD: r = 0.781). Structure parameters (Tb.N., Th.Th., Tb.Sp.) of the variably placed trabecular slices correlated only slightly smaller (r = 0.65 to 0.70) with the failure loads, especially for the density related parameters (BV/TV and app. density) (r = 0.75 to 0.77). Highest values were found close-by the subchondral plate. A central placed cylindric ROI presented only moderate correlations (r = 0.54 to 0.66).

Comparing palmar and dorsal subregions of the trabecular bone in the distal radius, the palmar compartment provided 6 to 10% higher values for density based parameters. Under this aspect it might make sense to favour the palmar side in the case of surgical treatment of fragility fractures. On the other hand, the surgeon has always to consider the individual fracture type concerning his approach.

***Disclosures: Volker Kuhn**, None.*

SU0049

Evaluation of Bone Mineral Density and Bone Strength in Autochthonous Transgenic Mice for Diabetes Mellitus (Akita mice). Kentaro Ohuchi*, Naohisa Miyakoshi, Yuji Kasukawa, Koji Nozaka, Toyohito Segawa, Hayato Kinoshita, Yoichi Shimada. Akita University Graduate School of Medicine, Japan

Introduction: It is widely known that diabetes mellitus (DM) causes osteoporosis or bone fragility. However, detailed analyses of bone mineral density (BMD) or bone strength changes in type II DM have not been done to date. Akita mice (AM) spontaneously present severe diabetes and are a model of non-obese type II DM in humans. These mice are used to investigate mechanisms of type II DM complications, and to evaluate the effects of medication. However, the evaluation of bone in Akita mice has yet to be performed. The objective of this study was to evaluate the effects of type II DM on BMD and bone strength in Akita mice.

Materials and Methods: Akita mice and control mice (C57/BL/6NCrSlc: CM) were used in this study. Left tibias and right femurs were harvested from both genders (AM-male: n=7, AM-female: n=10, CM-male: n=7, CM-female: n=10) at the age of 14 weeks. BMD with dual energy X-ray absorptiometry was measured in the left tibia, and the right femur was evaluated for bone strength by three-point bending tests at the midshaft.

Results: The BMD of the AM-group was significantly lower than that of the CM-group (male: p=0.0088, female: p=0.0006). Moreover, in the AM-group, the BMD of the female mice was significantly lower than that of the male mice (p=0.0226). The breaking force of the AM-group for the three-point bending tests was significantly lower than that of the CM-group (p=0.041) in females, but not in males. On the other hand, the maximum load of the AM-group was significantly lower than that of the CM-group (p=0.0168), but only in males. Breaking deformation and breaking time in the AM-group were higher than in the CM-group, but the differences were not statistically significant (p=0.0719-0.0789).

Conclusion: BMD and bone strength in the AM-group were significantly lower than in the CM-group in the present study. Thus, prolonged hyperglycemia in type II DM might lower BMD and bone strength. Akita mice may be a useful model to evaluate bone metabolism in type II DM.

***Disclosures: Kentaro Ohuchi**, None.*

SU0050

Genetic Regulation of Bone Morphology is Strongly Non-Uniform within a Single Bone. Jeyantt Srinivas Sankaran*[1], Svetlana Lublinsky[1], Weidong Zhang[2], Leah Rae Donahue[2], Stefan Judex[1]. [1]Stony Brook University, USA, [2]Jackson Laboratory, USA

Genetic variations are the primary determinant of differences in bone morphology across individuals. These relationships have typically been established for a specific skeletal site. While the genetic influence on one bone can, at least in part, transfer to other sites within the skeleton, little is known about the uniformity of the genetic influence within a single bone. To this end, we tested whether the degree of the genetic contribution is similar across functionally similar, as well as contiguous regions within the mouse femur. Two inbred strains with distinct bone morphology, BALB/cByJ and C3H/HeJ, were double-crossed to produce genetically heterogeneous offspring. Six different anatomical sites within the femur of each of the F2 male mice were analyzed via μCT and variables indicative of bone quantity, architecture, and tissue density were correlated across six regions containing trabecular and cortical bone (head, neck, proximal and distal metaphysis, diaphysis, distal epiphysis). When limiting correlations across all mice to the two regions that are functionally the most similar, the proximal and distal metaphysis, R2 values for trabecular indices ranged from 0.06 for Tb.N to 0.32 for BV/TV. Reflecting these low correlations, mice that were at the 95th and the 90th percentile for trabecular number and connectivity density in the proximal metaphysis were as low as the 50th and 25th percentile in the distal metaphysis for the same variables. Correlations of cortical indices between these two regions were similarly low (R2=0.06-0.37 for Ct.Th-Ct.Ar). Mice at the 95th percentile for cortical area and cortical thickness at the distal metaphysis were as low as the 5th percentile at the proximal metaphysis. Focusing the correlations on two regions that are spatially separated by less than 1mm, the distal metaphysis and epiphysis, R2 values remained low for both trabecular (0.11-0.28) and cortical (0.06-0.28) variables. Expanding the correlations across all anatomical sites considered here did not significantly improve the coefficients of determination for either trabecular or cortical bone. Correlations between trabecular BV/TV and cortical area at any given site were low, indicating a low level of co-regulation. Even when considering environment-gene interactions, these data suggest a strongly non-uniform genetic regulation of trabecular and cortical bone morphology with potential implications for the detection and treatment of osteoporosis.

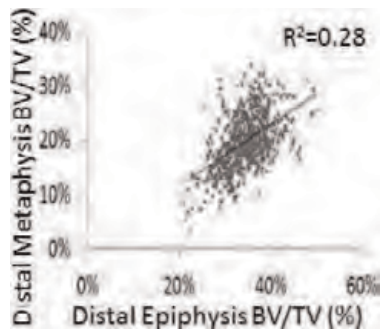

Correlation of BV/TV between the distal epiphysis and metaphysis

***Disclosures: Jeyantt Srinivas Sankaran**, None.*

SU0051

In silico simulations of bone remodeling with improved parameter estimation from local strains and dynamic morphometry in vivo. Alina Levchuk*[1], Remo Sommer[2], Sandro D. Badilatti[2], Friederike A. Schulte[2], Davide Ruffoni[2], Claudia Weigt[3], Gisela Kuhn[2], Ralph Müller[2]. [1]ETH Zurich, Switzerland, [2]ETH Zurich, Insitute for Biomechanics, Switzerland, [3]ETH Zurich, ETH Phenomics Center, Switzerland

Today, in silico simulations allow prediction of bone remodeling over time. A recent study on the algorithm validation using a mouse model of bone adaptation showed good agreement between in vivo and in silico outcomes. Yet, such simulations typically have a number of input parameters that must be defined, and thus cannot account for physiological differences in animals. We hypothesized that estimation of these parameters directly from in vivo measurements at the onset of the study would improve the simulations. For the study, C57Bl/6 mice were ovariectomized or sham operated at week 15 (OVX, SHM). At week 26, the 6th caudal vertebra was loaded (8N, 3000 cycles, 10 Hz, 3/wk, 4 wks). In vivo micro-CT scans were taken at weeks 26, 28 and 30. Formed, quiescent, and resorbed areas of bone were identified from in vivo scans. In silico parameters for formation and resorption set points were derived from strain energy density (SED) distributions calculated using micro-finite element analysis. Maximum remodeling rates were set directly from the in vivo dynamic morphometry. Finally, parameters controlling remodeling sensitivities to SED were selected iteratively within the algorithm. Condition-specific mechanostat curves were based on the selected parameters. Simulations were compared to in vivo data using local surface evaluation as well as static and dynamic morphometry, followed by repeated measures ANOVA. Results showed that cyclic loading decreased remodeling sensitivity more than twofold, while increasing remodeling set points. This led to the emergence of an SED range at which bone remained quiescent, corresponding to a "lazy zone". Ovariectomy also lowered remodeling sensitivity and increased thresholds. Deriving in silico input parameters directly from these calculations reduced prediction errors in the simulations. Static morphometry was not significantly different between experiment and simulations, except for trabecular thickness in the loaded OVX group. For dynamic morphometry, only bone resorption rate showed significant differences ($p<0.05$). Neighborhood comparison of local remodeling sites produced matches greater than 50%. These results indicate that accurate simulation of bone remodeling can be achieved through incorporation of in vivo derived parameters measured at the onset of the study. Modified mechanostat curves translate physiological differences in animals into computational terms, thus allowing improved prediction of biological processes.

***Disclosures: Alina Levchuk**, None.*

SU0052

Inequivalence in Functional Morphology among Individuals: An Intraskeletal Investigation into Covarying Traits. Stephen Schlecht*, Karl Jepsen. University of Michigan, USA

Previous investigations found tibial robustness (i.e. total bone area relative to length) to significantly covary with cortical tissue mineral density (Ct.TMD) and cortical area (Ct.Ar). Moreover, varying tibial robustness and strength was found to be inadequately compensated for via the adjustment of Ct.TMD and Ct.Ar, resulting in a variable degree of functional inequivalence. How these traits covary across bones and whether the degree of functional inequivalence in these traits is consistent throughout the appendicular skeleton is unknown.

Using pQCT, the level of covariance among robustness, Ct.Ar, and Ct.TMD was assessed in the femoral, tibial, humeral, radial, and 2nd and 3rd metacarpal diaphyses of 115 male and female young adult cadavers. Significant covariance between traits within all bones was observed, finding that slender bones are predictably 5-8% higher in Ct.TMD and 25-50% lower in Ct.Ar compared to robust bones. The attainment of similar trait sets was consistent throughout the skeleton irrespective of body size and the weight-bearing status of the bone (Fig 1A). Thus, individuals with more/less Ct.Ar or higher/lower Ct.TMD in one long bone, relative to robustness and body size, demonstrated the same impairment throughout their skeleton, except within the metacarpi. Additionally, Ct.TMD ($r = 0.79$-0.66, $p < 0.0001$) and Ct.Ar ($r = 0.71$-0.29, $p < 0.05$), in all bones except the metacarpi, significantly varied in a predictable manner across skeletal elements, regardless of body size and robustness (Fig 1B and C). Bones that were slender were as much as 2x less stiff for body size compared to those that were more robust ($R^2 = 0.52$-0.79, $p < 0.0001$). This functional inequivalence was relatively consistent and significantly predictable throughout the skeleton, suggesting that there are intrinsic (biological) limitations to the functional adaptation process that are responsible for naturally varying strength among individuals. How this limitation can be dealt with clinically remains unknown.

These findings indicate that robustness trait sets naturally vary among individuals in a systemic fashion. This variation is of a significant magnitude, warranting consideration of functional inequivalence between traits when clinically assessing an individual's susceptibility to fracture. Better understanding of how these traits covary will help to identify genetic and environmental perturbations contributing to diminished bone accrual.

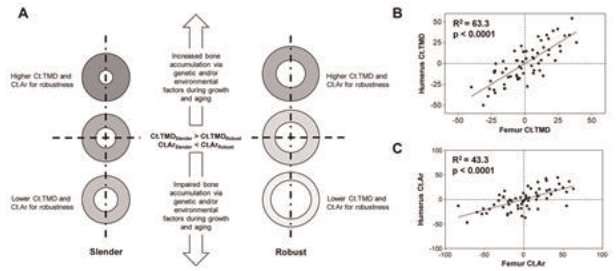

Figure 1. Trait covariance of slender and robust phenotypes. A) schematic diagram demonstrating the variation in robustness, Ct.TMD, and Ct.Ar between males and females within the study population; B) linear regression of Ct.TMD values adjusted for body size and robustness between male femora and humeri; C) linear regression of Ct.Ar values adjusted for body size and robustness between male femora and humeri.

Figure 1

***Disclosures: Stephen Schlecht**, None.*
This study received funding from: U.S. Department of Defense

SU0053

Measuring Bone Heterogeneity with Raman Spectroscopy to Explain Aging Differences in Human Fracture Toughness. Alexander Makowski*[1], Sasidhar Uppuganti[2], Ahbid Zein-Sabatto[2], Jack Whitehead[2], Mathilde Granke[3], Anita Mahadevan-Jansen[2], Jeffry Nyman[3]. [1]Department of Veterans Affairs, Vanderbilt University, USA, [2]Vanderbilt University, USA, [3]Vanderbilt University Medical Center, USA

Heterogeneity is thought to be an important determinant of bone quality, but how compositional or organizational heterogeneity influences the age-related decrease in fracture resistance is unclear. Because Raman spectroscopy (RS) is sensitive to the orientation and composition of both mineral and collagen, it was used to assess these relationships between tissue heterogeneity and age-related decreases in fracture resistance.

Bone samples were cut from the distal lateral midshaft of 9 cadaveric femurs (males age 24yo to 91yo) and polished to create 3pt bend notched beam specimens. Following ASTM standards for fracture toughness testing, stress intensity factor K_{Ic} and J-integral were calculated from force-displacement curves where the crack was propagated against the osteonal axis.

For each sample, RS maps (32x32 samples) were obtained on the polished surface normal to crack propagation at an osteonal-interstitial border for 0 and 90° rotations. RS peak ratio intensity was analyzed for mineralization, crystallinity, and carbonate substitution. Peak ratio heterogeneity was quantified as image contrast (histograms), mean intensity value, and the coefficient of variation (COV). Linear regressions of ratio intensity mean and COV were used to explain fracture toughness.

RS peak ratio maps of composition (polarization insensitive) –mineralization (v1 Phosphate/Proline, v2 Phosphate/AmideIII), carbonate substitution (Carbonate/ v1 Phosphate) and crystallinity ($FWHM^{-1}$ v1Phosphate)– illustrate contrast between the osteon and interstitial space only at high J-integral values. This suggests that compositional heterogeneity between osteonal and interstitial space fades with the age-related decrease in fracture toughness. Mapping a peak ratio that is influenced by tissue organization (v1 Phosphate/Amide I) further reveals lamellar contrast, but only in specimens with high fracture toughness.

High J and high K_{Ic} correspond to bivariate and platykurtic histograms, respectively; regardless of histogram shape, lack of heterogeneity corresponds to low fracture toughness. Multivariate regressions using the mean and COV of mineralization or carbonate substitution each significantly (F test; $p<0.05$) explain K_{Ic}. Regressions of COV only for v1 Phosphate/Amide I or crystallinity ($FWHM^{-1}$ v1 Phosphate) each significantly explain J integral. Increases in both compositional and organizational heterogeneity of bone separately correspond to increases in fracture toughness.

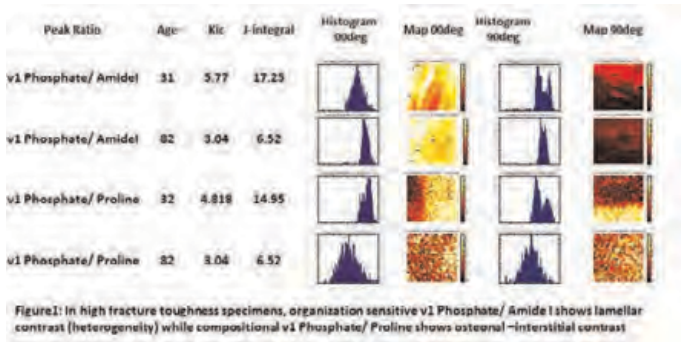

Figure1: RS Maps Explain Fracture Toughness

***Disclosures: Alexander Makowski**, None.*

SU0054

Non-Collagenous Proteins in Genetically Modified Mice Exercise a Control on Bone Size and Shape. Stacyann Morgan*[1], Atharva Poundarik[2], Caren Gundberg[3], Deepak Vashishth[1]. [1]Rensselaer Polytechnic Institute, USA, [2]Rensselaer Polytechnic University, USA, [3]Yale University School of Medicine, USA

Osteocalcin (OC) is the most abundant non-collagenous protein (NCP) in bone. It is produced during bone formation, late after mineralization by osteoblasts and forms a complex with Osteopontin (OPN) and other molecules in the extra-cellular matrix. Both OC and OPN controls mineral size and orientation. Recent studies in our laboratory showed that the OC-OPN complex regulates bone toughness through its control over matrix quality. Such control may also help in determining bone size. Therefore, we investigated whether these proteins play a role in regulating bone size and shape.

Radii from male 6 month old $OC^{-/-}$, $OPN^{-/-}$, $OC\text{-}OPN^{-/-;-/-}$ and Wild Type mice (n=12 per group) were separated from the ulna and stored in saline soaked gauze at -80 C until use. Samples were scanned using μCT with a 10.5 μm voxel size (μCT 40; Scanco Medical) in saline eppendorf tubes. Bone geometry was determined from the mid-shaft of each sample and the parameters measured were: length, moment of inertia, cross-sectional area (CSA), cortical thickness and bone mineral density (BMD). Differences between the groups were tested for significance using one-way ANOVA ($p<0.05$) with post-hoc Tukey multiple comparison test (SigmaPlot11.0).

The ANOVA results showed that double knockouts were shorter (10.08 mm, $p=0.005$) with thicker cortices (0.160 mm, $p=0.017$) and larger CSA(0.270 mm^2, $p=0.005$) compared to WTs. There was no statistically significant difference between single and double knockouts or single knockouts and WTs for the above traits. ANOVA showed lack of significant difference between the groups ($p=0.095$) for BMD. Individual groups were therefore compared using t-tests. BMD values of double knockouts (1185.20 mgHA/ccm) and $OC^{-/-}$ (1177.80 mgHA/ccm) were both significantly higher than WT (1160.30 mgHA/ccm) with $p<0.05$, but there were no differences between the other groups.

Taken together, this study demonstrates for the first time that Osteocalcin and Osteopontin play a redundant role in regulating bone size (length, cortical thickness and cross-section area) where the absence of OC is compensated by OPN and vice versa. BMD, in contrast, is regulated only by Osteocalcin.Acknowledgements: NIH RO1 AR38460 and AR 49635

***Disclosures: Stacyann Morgan**, None.*

SU0055

Physical Activity Producing Loads from Diverse Orientations Enhances Growing Bones. Ian Wallace*[1], Brigitte Demes[1], Stefan Judex[1], Andrea Kwaczala[1], Kristian Carlson[2]. [1]Stony Brook University, USA, [2]University of the Witwatersrand, South Africa

Objective: An experiment was conducted to determine if emphasizing habitual activities that produce loads from diverse directions can augment the growing skeleton. Methods: At 4 weeks postnatal, female C57BL/6J mice were housed individually for 3 months in custom-built cages with tunnel apparatuses that accentuated either non-linear locomotion (diverse-orientation loading) or linear locomotion (stereotypic-orientation loading) (n=10 animals per cage type). Daily behavioral assessments were performed throughout the experimental period to quantify home-cage activity level and profile. At the end of the experiment, trabecular bone morphology in the humeral head and distal femoral metaphysis were assessed with micro-CT. Results: Throughout the experiment, groups did not differ in cage activity level or profile. Yet, at the end of the experiment, animals that experienced more diverse-orientation loading had 12% greater bone volume fraction in the proximal humerus (p=0.004) and 24% greater bone volume fraction in the distal femur (p=0.04). In both skeletal regions, group differences in bone volume fraction were primarily the result of differences in trabecular thickness. Conclusions: Diverting habitual physical activities to involve loading from more diverse directions can enhance the growing mouse skeleton. This study suggests that low-intensity physical activities that engender loads from diverse directions may be a viable alternative to vigorous, high-impact activities as a way to improve skeletal health during the growing years. Our results may also be pertinent to the designs of physical activity regimens aimed at stemming bone loss in adults, particularly frail individuals for whom intense exercise imposes a high risk of injury.

***Disclosures: Ian Wallace**, None.*

SU0056

RANKL and OPG Administration Influence the Pattern and Location of Fractures Created During Biomechanical Testing of Intact and Fatigued Mouse Tibia. Nicolas Bonnet*[1], Paul Kostenuik[2], Mike Ominsky[3], Serge Ferrari[4]. [1]University Geneva Hospital-Department of Internal Medecine Specialities, Switzerland, [2]Amgen Inc., USA, [3]Metabolic disorders, Amgen Inc., USA, [4]Geneva University Hospital & Faculty of Medicine, Switzerland

The pattern and anatomical location of long bone fractures can depend on the loading type, bone mass, structure, and potentially accumulation of prior damage. We sought to discern how these factors might influence fracture patterns by inducing fatigue damage in low- and high bone mass states caused by osteoclast activation or inhibition, respectively.

Adult male mice were treated with RANKL (2mg/kg/day), OPG-Fc (5mg/kg 2x/week) or PBS (Veh) for 28 days prior to fatigue loading of one tibia for 20 minutes by in vivo axial compression (14N, 4 Hz). Treatments continued for 1 week, and fatigued and non-fatigued (NF) tibiae were collected for microCT and destructive axial compression testing. The resulting test-induced fracture was evaluated by caliper measures of the greatest (Dmax) and lowest (Dmin) distances from the proximal tibial plateau to the fracture site. Fracture location was assessed by Dmean (average of Dmax and Dmin), and fracture pattern (obliqueness) by Dmax-Dmin (Delta). Crack number per cortical bone area (CrN/BA) was investigated by fuchsin staining of proximal and distal transverse sections located 2 and 8mm from the plateau, respectively.

In the NF tibia, RANKL decreased Tb.BV/TV, CtTh and Dmean (-94.9%, -32.3%, -47.5%, $p<0.001$) and increased Delta (+152%, $p<0.01$) compared to Veh, indicating that with high bone remodelling and low bone volume the fracture was more proximal and oblique. OPG-Fc treatment of NF tibia increased BV/TV and CtTh vs Veh (+58.5% and +3.4%, $p<0.01$) without modifying Dmean or Delta. Fatigue increased CrN/BA, with RANKL>Veh>OPG in the proximal section and RANKL>Veh=OPG distally. In Veh controls, fatigued tibiae exhibited test-induced fractures that were more proximal (Dmean -18%, $p<0.05$) and oblique (Delta +376%, $p<0.05$) compared to NF tibia. In contrast, with OPG-Fc, Dmean and Delta did not differ between fatigued and NF tibia, with fractures in both states occurring more distally and more transversely vs Veh controls. Similar to their NF tibia, fatigued tibia from RANKL animals fractured more proximally (Dmean -31.9%, $p<0.05$) and obliquely compared to the fatigued Veh. Across groups, linear regression analysis demonstrated that fracture location was better associated with proximal aBMD($R=0.75$) than with diaphyseal damage (CrN/BA, $R=0.55$).

These observations suggest that the location and obliqueness of a test-induced fracture can be modulated by fatigue damage, and by changes in bone remodelling rate and/or bone mass.

***Disclosures: Nicolas Bonnet**, Amgen , 6*
This study received funding from: Amgen

SU0057

The involvement of tumor necrosis factor-α in osteoclast differentiation induced by mechanical stress in a murine maxilla loading model. Kengo Fujiki*[1], Noriyuki Wakabayashi[2], Natsuki Suzuki[2], Libor Borák[3], Keiichi Ohya[1], Kazuhiro Aoki[1]. [1]Tokyo medical & dental university, Japan, [2]Department of Removable Partial Prosthodontics, Graduate School, Tokyo Medical & Dental University, Tokyo, Japan, [3]Institute of Solid Mechanics, Mechatronics & Biomechanics, Brno University of Technology, Czech Republic

Introduction: Mechanical loading at the residual ridge by denture is known to induce bone resorption in the jaw bone of edentulous patients. Although animal studies show that inflammatory cell infiltration appears near the site of mechanical loading in the jaw bone, it is not still clear whether the denture-bearing-bone-resorption promotes by loading-induced inflammation or not. The aim of this study is to clarify the involvement of tumor necrosis factor-α in osteoclast differentiation appeared at the site of mechanical loading.

Materials and Methods: The thirteen-week-old male TNF-α-deficient mice (n=8) and C57BL/6 mice as a wild type (WT) mice (n=8) were used in this study. Both kinds of mice were divided into two experimental groups, 1) mice with loading stimulation (n=4) and 2) without loading stimulation (n=4) to the maxilla. Each mouse was fixed on the loading device and was subjected to continuous pressure on the hard palate region of 2kPa or 0 kPa for 30min/day for 7 consecutive days (See figure). Mice were sacrificed on 16 hours after the last loading and bone histomorphometric analyses were performed by using the cross sections of maxilla.Two measuring regions for bone histomorphometry were set as ROI1 and ROI2 (See figure). ROI1 was set close to the loading site and ROI2 was set far from the loading site. Both ROI1 and ROI2 were proven to bear a similar mechanical stress by using finite element analyses.

Results: A significant increase of inflammatory cell infiltration was appeared in the ROI1 of WT mice, whereas ROI2 of WT mice and ROI1 and 2 of TNF-α-deficient mice showed no significant increase of those cells. Bone histomorphometric analyses revealed that the number of osteoclasts(N.Oc/BS) was increased 6.8 times higher by the mechanical loading than that of no loaded group in ROI1 of WT mice, whereas it was just 2-3times increase by the same loading schedule in ROI2 of WT mice and in ROI1 and ROI2 of TNF-α-deficient mice. The increasing rate of eroded surface (ES/BS) by the mechanical loading also showed the same tendency as that of N.Oc/BS.

Discussion and conclusion: These results suggest that the bone resorption in jaw bone induced by mechanical loading could be accelerated by inflammation, possibly via the TNF-α-related mechanism, hopefully leading to the future development of therapeutic interventions against unexpected bone resorption of jaw bone induced by mechanical loading by use of denture in edentulous patients.

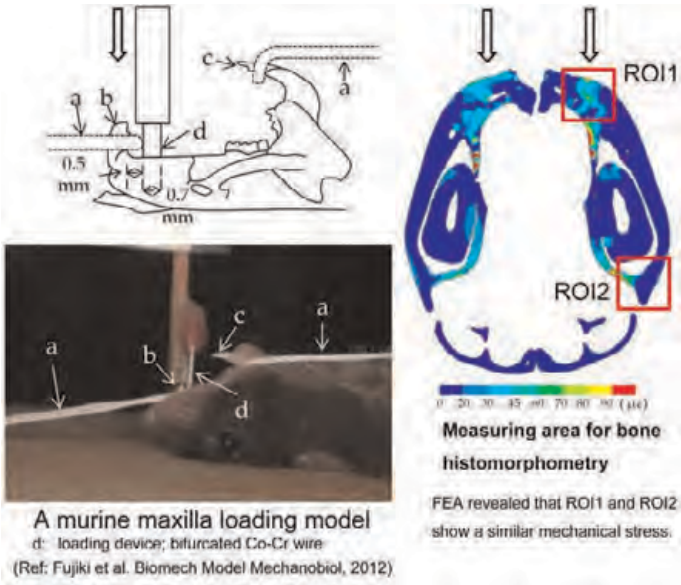

Schematic view of the loading conditions and region of interest (ROI) setting

***Disclosures: Kengo Fujiki**, None.*

SU0058

The Relationship Between Microscopic Damage Accumulation and Impaired Biomechanical Performance in Cancellous Bone Under Fatigue Loading. Floor Lambers*[1], Amanda Bouman[1], Kristin Regan[1], Clare Rimnac[2], Christopher Hernandez[1]. [1]Cornell University, USA, [2]Case Western Reserve University, USA

Stress fractures associated with osteoporosis are believed to develop over time as a result of the accumulation of microscopic tissue damage during cyclic loading. While an increase in the number of microcracks has been associated with stiffness loss in cortical bone, few studies have investigated the effects of microscopically observed microdamage on biomechanical performance in cancellous bone. The aim of the current study was to determine the relationship between the amount of fatigue loading, the accumulation of microdamage, and reductions in specimen stiffness during cyclic loading of human cancellous bone.

Cancellous bone cores (n=34, 8 mm diameter) from the third lumbar vertebra of 16 donors (10 m, 6 f, age 76±8.8) were subjected to compressive fatigue loading, using a sinusoidal waveform between 0 N and a normalized load (σ/E_0 of 0.0035 mm/mm, where E_0 is the initial Young's modulus determined from preconditioning). Fatigue loading was stopped before failure based on the slope of the fatigue curve at 1 of 7 different predetermined regions (Fig. 1). The relation between mechanical parameters and fatigue life was estimated from the average fatigue curve to failure. After cyclic loading, specimens were stained for microdamage using lead-uranyl acetate and scanned with μCT at a voxel size of 10 μm to determine damage volume per bone volume fraction (DV/BV).

DV/BV varied from 0.9±0.5% (mean±SD) in the group with no loading to 3.4±2.1% in the group loaded to complete failure. DV/BV waslinearly related to the reductions in Young's modulus caused by fatigue loading (Fig. 2). Creep strain, cyclic strain, and energy dissipation increased almost linearly in the secondary phase and exponentially in the tertiary phase.

Our data express the biomechanical meaning of previously reported measures of naturally occurring microscopic damage in human cancellous bone. Our results suggest that an observed DV/BV of 2% caused by fatigue loading is on average associated with a 40% reduction in Young's modulus and a 10-fold reduction in fatigue life. In addition to impairing fatigue life and contributing to stress fractures, microdamage accumulation may reduce the ability to resist overloads due to falls or heavy lifting.

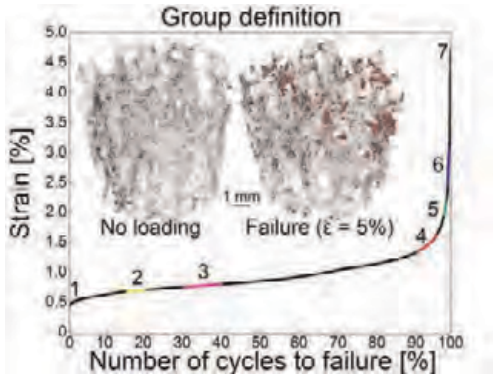

Fig1: Fatigue curve with regions where loading was stopped for the 7 groups. Damage (red) in bone

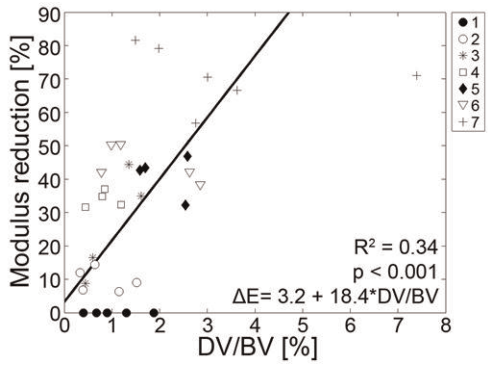

Fig2: Linear association between DV/BV and reduction in Young's modulus. Symbols indicate groups.

***Disclosures: Floor Lambers**, None.*

SU0059

Tissue-scale Bone Mechanical Behavior Varies between Measurement Sites and Mouse Strains. Pinaki Bhattacharya*[1], An-Katrien Braeken[1], Michael Laurent[2], Dirk Vanderschueren[3], Steven Boonen[4], Harry Van Lenthe[5]. [1]Biomechanics Section, KU Leuven, Belgium, [2]Laboratory of Molecular Endocrinology & Gerontology & Geriatrics, KU Leuven, Belgium, [3]Catholic University of Leuven, Belgium, [4]Center for Metabolic Bone Disease & Division of Geriatric Medicine, Bel, [5]Katholieke Universiteit Leuven, Belgium

Reference-point indentation (RPI) is a novel technique for in vivo assessment of bone tissue mechanical properties. Similar to nanoindentation, the elastic response of bone tissue is related to the average unloading slope (US) of an RPI measurement, while the total indentation distance (TID) is a measure of the tissue inelastic behavior combining elasticity, plasticity, viscoelasticity and damage. Yet, the significance of RPI parameters in determining fracture risk is unclear; furthermore, potential site-specific variations have not received attention. Therefore, the aim of this study was to quantify US and TID at multiple locations within a specific bone in two inbred mouse strains with known bone morphological differences.

Left tibiae from 7 C57BL/6 (B6) mice and left and right tibiae from 7 C3H/He (C3H) mice were excised. All mice were male and 12 weeks of age. RPI tests were performed at three anatomical regions labeled R1, R2 and R3 (Fig. 1) using the BioDent (Active Life Scientific, Santa Barbara, CA) using a maximum force of 2 N and 10 indentation cycles/measurement. Three measurements were made at R1, two at R2, and two at R3. The measurements were calibrated against those on PMMA. Wilcoxon rank-sum test was used to test for significant differences in US and TID between strains and between anatomical sites.

Site-specific variation in US and TID was found in B6 and C3H (Fig. 2). For left tibiae in each strain, US at R2 was lower than US at R1 and R3 ($p < 0.05$). In left tibiae of B6, TID at R1 was lower than TID at R2; in right tibiae of C3H, TID at R1 was lower than TID at both R2 and R3. Furthermore, inbred strain-specific variation in US was found comparing only the left tibiae; for each of the three sites, US in C3H was higher than US in B6 ($p < 0.01$). In C3H, no left–right differences in US were found ($p > 0.40$). However, TID at sites R2 and R3 were higher on the right tibiae than TID at R2 and R3 respectively on the left tibiae ($p < 0.05$).

We conclude that RPI could detect differences in US between B6 and C3H mice. The higher US in C3H agrees with the higher modulus in C3H as measured in tensile testing tests[1]. The different response of the left and right tibiae needs confirmation. The site-specific variation may relate to growth patterns in these bones and could be helpful in evaluating fracture behavior of these bones.

References
1. Courtland et al. (2008). Calcif Tissue Int; 83: 342–353.

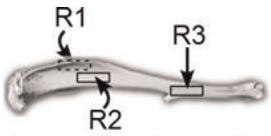

Figure 1. Boxes show anatomical regions on mouse tibia where RPI measurements were performed: R1 on the medial surface (behind the plane of the picture), R2 on the lateral surface and R3 near the tibia-fibula junction.

Figure 1

Figure 2. Mean (± SEM) values of unloading slope (US) and total indentation distance (TID). **(A)** Significant differences in US were found between left tibiae of B6 and C3H at each anatomical site. **(B)** In the right tibiae of C3H, TID at R2 and R3 were significantly higher than TID at R1. At R2 and R3, TID on the right tibiae of C3H were significantly higher than corresponding sites on the left tibiae.

Figure 2

***Disclosures: Pinaki Bhattacharya**, None.*

SU0060

Trabecular Bone Matrix Composition in Cynomolgus Monkeys Treated with Sclerostin Antibody. Ryan Ross*[1], Michael Ominsky[2], Alvin Acerbo[3], Lisa Miller[3], D. Rick Sumner[1]. [1]Rush University Medical Center, USA, [2]Amgen Inc., USA, [3]Brookhaven National Laboratory, USA

Sclerostin antibody (Scl Ab) leads to increased bone formation, but the effect of Scl Ab treatment on bone matrix mineralization is largely unknown. We sought to determine if Scl Ab treatment affected global mineralization or the rate of matrix maturation in a primate model.

Lumbar vertebrae (L2) from a previous fibular osteotomy study in which 4-5 year old male cynomolgus monkeys were treated with vehicle or 30 mg/kg Scl Ab (romosozumab) once every 2 weeks for 10 weeks (n=10 per group) were used. Global bone mineral density distributions (BMDD) were assessed using backscattered SEM. Mineralization kinetics were assessed by examining tissue between fluorochrome labels which had been given 0.5, 2, 6.5 and 8 weeks prior to sacrifice with Fourier-transform infrared microspectroscopy.

Scl Ab treatment led to 42% more trabecular bone volume (p=0.001). The mean global mineralization was 0.8% lower in the Scl Ab group, although not significant (p=0.097). The standard deviation of the BMDD was 9% lower in the treated animals (p=0.012) without affecting skewness. The number of highly mineralized bone pixels was reduced (p=0.035) with only a marginal increase in low density pixels (p=0.092). Scl Ab caused a 2-fold increase in BFR/BS (p=0.009), and a 46% reduction in the eroded surface (p=0.014). Local analysis of tissue mineralization (mineral-matrix ratio) for tissue of known age showed a significant tissue age effect ($p<0.001$) with no difference between groups. Specifically, the tissue between 0.5 and 2 weeks old was ~80% mineralized, and the tissue between 2 and 8 weeks old was >90% mineralized compared to the oldest tissue (>8 weeks).

BMDD is related to both the average tissue age and the rate of matrix mineralization. Even though a larger fraction of the tissue in the Scl Ab group was young compared to the control group, there was only a small non-significant lowering of mean global mineralization, which would seem to imply that the rate of mineralization must have been accelerated. However, direct examination of tissue of known age showed that Scl Ab treatment did not affect mineralization kinetics despite the elevated bone formation rate. The finding that newly formed bone in the control animals had already reached 80% of its mineralization potential within 0.5 to 2 weeks suggests rapid inherent mineralization within the trabecular bone of cynomolgus monkeys, but ultimately the mineralization process was unaffected by Scl Ab treatment.

***Disclosures: Ryan Ross**, None.*
This study received funding from: Amgen, Inc

SU0061

Alterations of Gene Expressions of Osteogenic Growth Factors and Transcription Factors in Response to Dynamic Fluid Flow Stimulation. Minyi Hu*[1], Yi-Xian Qin[2]. [1]Stony Brook University, USA, [2]State University of New York at Stony Brook, USA

Non-pharmaceutical interventions with mechanotransduction approaches are promising in promoting bone formation. We have shown that a dynamic hydraulic stimulation (DHS) is capable to induce osteogenic responses. Subsequent research points to the functional process of how DHS-derived mechanical signals act on bone cells to regulate bone metabolism. The objective of this study was to evaluate the alterations of the gene expressions of osteogenic growth factors and transcription factors in response to DHS over time. Using hindlimb suspended (HLS) female SD rats, DHS was applied to the right tibiae with a loading frequency of 2Hz and a magnitude of 30mmHg static pressure+30mmHg (p-p) dynamic pressure. The daily loading regime was "10 min on–5 min off–10 min on" over a time course of 3, 7, 14, and 21 days. Rats in the 3-day group were stimulated for 2 days; and the rats in the other groups were stimulated for 5 days/week. According to the time points, animals were sacrificed and the total RNA was isolated from the tibiae for quantitative real-time PCR analysis of the selected osteogenic genes (RUNX2, β-catenin, osteopontin, VEGF, BMP2, IGF-1, and TGF-β). Interesting data indicated a time-dependent fashion of gradual changes in mRNA levels in response to DHS. Great reductions of the overall mRNA levels of the selected genes were observed in the HLS rats compared to the age-matched. On the other hand, while DHS-driven fold changes of the mRNA levels remained low before day 7, the fold changes started to elevate by day 14 (3.0 (RUNX2), 4.5 (β-catenin), 3.5 (osteopontin), 3.5 (VEGF), 3.7 (BMP2), 4.6 (IGF-1), and 3.2 (TGF-β)) and then became less pronounced by day 21 (Figure 1). This study indicated that the gene expressions of the selected osteogenic growth factors and transcription factors were altered in response to DHS. However, it was highly time-dependent. This study gave insights into the molecular mechanism of DHS-derived mechanical signals. Augmented external biomechanical stimulation, such as DHS in the present study, may trigger the recognition of mechanical signals by osteoblasts. The received signals then ultimately induce secretion of growth factors that act as local regulators for osteogenesis. Potent growth factors, including IGF, TGF-β, BMP and VEGF, strongly modulate the osteoblastic activities as well as other bone growth regulators. These genes play critical roles in the fate of osteoblastogenesis, which is crucial for bone formation.

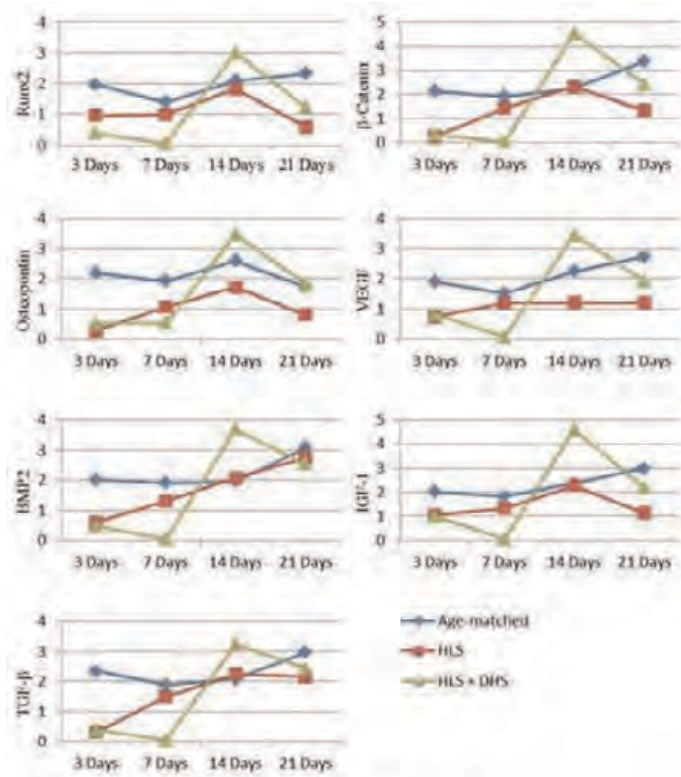

Figure 1. Summary of mRNA fold changes of the selected osteogenesis related genes over the 21-day time course. In general, the mRNA levels of the selected genes in the HLS groups attempted to catch up to the according age-matched levels. However, the mRNA levels of these genes in the HLS+DHS groups did not elevate until day 14.

Figure 1

***Disclosures: Minyi Hu**, None.*

SU0062

Enhancement of Nucleo-Cytoskeletal Connectivity by Low Intensity Vibration Augments Mechanosensitivity in Mesenchymal Stem Cells. Gunes Uzer*[1], Buer Sen[2], Zhihui Xie[1], William Thompson[1], Maya Styner[3], Clinton Rubin[4], Stefan Judex[5], Janet Rubin[3]. [1]University of North Carolina, USA, [2]University of North Carolina At Chapel Hill, USA, [3]University of North Carolina, Chapel Hill, School of Medicine, USA, [4]State University of New York at Stony Brook, USA, [5]Stony Brook University, USA

Mechanical loading, including low intensity, high frequency vibration (LIV), improves bone strength through biasing of mesenchymal stem cell (MSC) lineage. *In vitro* application of both LIV (<0.001% substrate strain) and high-magnitude strain (1-2%; HMS) limits MSC adipogenesis via mTORC2/Akt/GSK3β induced increases in β-catenin. This signaling pathway is amplified at a second mechanical treatment; the amplification after HMS is dependent on increased cytoskeletal elements connected at cell attachments. Although virtually absent of strain, LIV is also amplified at a repeated bout. We hypothesized that signal amplification after LIV would be dependent on cytoskeletal changes distinct from those induced by HMS. To test this hypothesis, we applied 90Hz 0.7g LIV to marrow derived MSCs. A single bout of LIV showed insignificant induction of pAkt (Tyr-473) but a 2nd LIV bout increased pAkt to 169 ±37%. To test whether the 2nd LIV response was sensitive to the actin cytoskeleton, we replaced the 1st LIV bout with lysophosphatidic acid (LPA, 62.5 uM) to activate RhoA and actin connectivity. LPA increased both basal (194 ±40%) and LIV induced (383 ±110%) pAKT. Similarly, FAK activation (pFAK, Tyr-397), also induced by LIV, was increased to 266 ±130% after a 2nd LIV tx, and to 671 ±34% when LIV followed an LPA pretreatment, adding evidence for a cytoskeletal role in signal enhancement. As well, disrupting the cytoskeleton with cytochalasin-D reduced basal (10-fold) and LIV-induced (62%) pFAK. In contrast, preventing microtubule polymerization with colchicine did not prevent LIV responses. Importantly, actin and vinculin staining showed that, in contrast to the stress fibers forming following HMS that arc between peripheral focal adhesions (FAs), LIV induced formation of short actin fibers which spanned from the nucleus to peripheral FAs. These results suggest that LIV induces a cytoskeletal reorganization typified by nucleo-cytoskeletal connections, and that this adaptive reorganization serves to amplify a response to a 2nd LIV treatment. As both Akt and FAK are found in FAs, this might indicate that nuclear motion driven by LIV activates signaling molecules at FAs by pulling nuclear-actin tethers, a force distinct from that of substrate strain. As such, LIV induced nuclear motion might represent a novel form of "inside-inside" signaling, in contrast to the "outside-in" signaling generated when HMS pulls on the cytoskeleton via integrins.

***Disclosures: Gunes Uzer**, None.*

SU0063

Enhancement of Osteogenic Ingrowth and Proliferation in 3-D Scaffolds with Low-Intensity Pulsed Ultrasound. Lin Wu*, Liangjun Lin, Yong Gao, Yi-Xian Qin. State University of New York at Stony Brook, USA

Bone tissue engineering approaches represent a great potential for improved regeneration of damaged bone in comparison with conventional therapies [1]. It is hypothesized that mechanotransduction may enhance cell dynamics and proliferation. The low-intensity pulsed ultrasound in vivo studies have shown to enhance osteoconduction into porous implants made of hydroxyapatite (HA), titanium, tantalum, and bioglass [2]. However, the mechanism of ultrasound on the osteoblast behavior inside the porous scaffold are still unknown. The aim of this study is to evaluate the effects of ultrasound induced mechanotransduction in promoting osteoblastogenic ingrowth and proliferation through 3D porous scaffolds. Porosity of two kinds of ceramic scaffolds, SiC and HA/TCP scaffolds, were measured using μCT. Quantitative ultrasound (QUS) measurement was performed to evaluate the ultrasound attenuation in the scaffolds. Seeded MC3T3-E1 mouse pre-osteoblasts on the scaffolds were cultured for 4 and 7 days with daily 20min ultrasound treatment, and were evaluated for Cell viability, in depth ingrowth, and volumetric proliferation. The porosities of SiC and HA/TCP were observed as 75% and 52%, 0.36mm and 0.19mm of pore size, respectively. The simulated ultrasound attenuation was significantly different (16%, $p<0.05$) between SiC (20.87±1.28dB) and HA/TCP (17.91±3.31dB) ($p<0.05$). After 4 and 7 days of culture and ultrasound exposure, cell density was higher in the ultrasound group compared with the sham group on both SiC and HA/TCP scaffolds. Cell ingrowth depths of SiC scaffolds significantly increased in the scaffolds with ultrasound radiation compared with those with sham radiation after both 4 and 7 days post-seeding. Whereas HA/TCP scaffold was only remarkable at 7 days post-seeding (Fig 1). There were significant differences in the dsDNA content between the ultrasound group and the sham group both on SiC scaffolds and HA/TCP scaffolds. Ultrasound group of SiC construct showed 9% ($p<0.05$) and 27% ($p<0.05$) increase in the average dsDNA content at 4 days and 7 days over the sham control group, And as to HA/TCP construct, 28 % and 24 % increase, respectively (Fig 2). ANOVA test showed significant difference ($p<0.05$) between ultrasound and sham groups and between SiC and HA/TCP scaffolds, at both 4 and 7 days. These results suggested that ultrasound facilitated ingrowth and enhance the proliferation of osteoblast in both SiC and HA/TCP scaffolds, but with different kinematics.

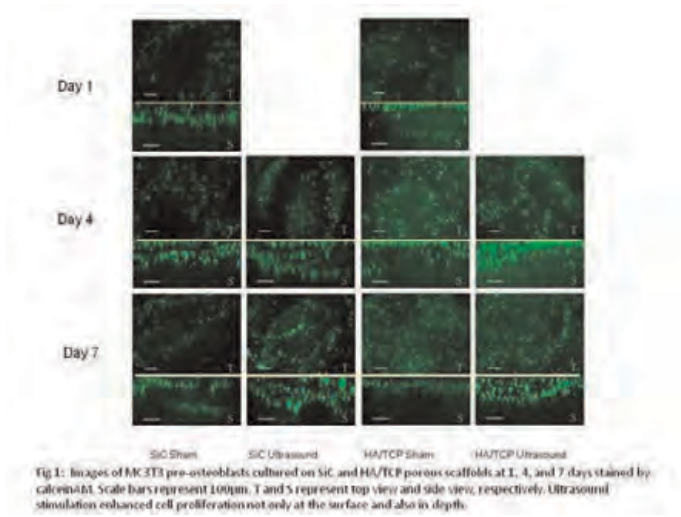

Fig 1: Images of MC3T3 pre-osteoblasts cultured on SiC and HA/TCP porous scaffolds at 1, 4, and 7 days stained by calcein-AM. Scale bars represent 100μm. T and S represent top view and side view, respectively. Ultrasound stimulation enhanced cell proliferation not only at the surface and also in depth.

Fig 1

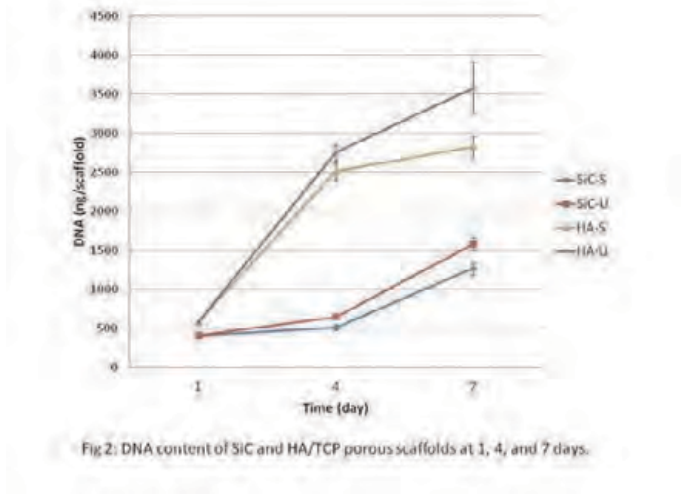

Fig 2: DNA content of SiC and HA/TCP porous scaffolds at 1, 4, and 7 days.

Fig 2

***Disclosures: Lin Wu**, None.*
This study received funding from: NIH

SU0064

Mechanically Activated Fyn Modulates Adipogenic Commitment through mTORC2/Akt/RhoA Effects on Mesenchymal Stem Cell Cytoskeleton. William Thompson*[1], Sherwin Yen[2], Buer Sen[3], Zhihui Xie[2], Natasha Case[4], Gunes Uzer[1], Maya Styner[4], Janet Rubin[4]. [1]University of North Carolina, USA, [2]University of North Carolina Department of Medicine, USA, [3]University of North Carolina At Chapel Hill, USA, [4]University of North Carolina, Chapel Hill, School of Medicine, USA

Bone density is dependent on mesenchymal stem cell (MSC) lineage allocation where adipogenic commitment depletes the pool available for osteogenesis. Cell architecture influences lineage decisions, as the cytoskeleton provides critical elements allowing response to the mechanical and physical environment. We have shown that mTORC2 is proximal to activation of Akt and inhibition of GSK3β that leads to downstream β-catenin preservation. We recently demonstrated that the Src-like kinase Fyn is proximate to mechanical activation of mTORC2, a kinase involved in downstream RhoA activation. RhoA is critical for cytoskeletal reorganization, as it directs actin stress fiber formation. As such, we asked if Fyn might modulate cellular architecture and lineage allocation of mdMSCs. First we showed that Fyn was recruited to FA sites following substrate strain. Strain (2%, 100 cycles) enhanced Fyn association with the FA protein vinculin. Further, pharmacological inhibition of Fyn prevented the actin stress fiber formation observed following mechanical strain, and specific disruption of Fyn function, using siRNA, prevented mechanical activation of RhoA. As it is known that inhibition of RhoA suppresses osteogenesis and enhances adipogenesis, our data showing that Fyn played a critical role in actin stress fiber formation and RhoA activation suggested that Fyn might regulate basal MSC cytoskeletal control of mdMSC lineage. Indeed, siRNA knockdown of Fyn led to an enhancement of mdMSC adipogenic lineage commitment. Protein levels of the adipogenic markers adipocyte protein 2 (aP2), adiponectin (APN),

peroxisome proliferator-activated receptor gamma (PPARγ), and perilipin were all significantly increased when Fyn expression was suppressed. Protein quantities for adipogenic markers were normalized to β-actin expression and fold increases over treatment with a control siRNA were 2±0.3, 35±3.4, 6±0.9, and 89±11.3 respectively. Adaptation of the structural framework of the cell reinforces essential mechanical signals that guide lineage decisions, biasing MSC commitment away from adipogenesis and towards osteogenesis. As such, Fyn expression in mdMSCs regulates basal cytoskeletal architecture and, associated with FAs, functions as a proximate mechanical effector transmitting environmental signals that influence MSC lineage allocation.

***Disclosures: William Thompson**, None.*

SU0065

Novel Silorane Bone Cements Exhibit Similar Mechanical Properties but None of the *in vivo* Inflammatory Effects of Commercial Bone Cement. Lianxiang Bi*[1], David Eick[1], Kathleen Kilway[1], Rachel Weiler[1], Bradley Miller[1], Thomas Schuman[2], Lynda Bonewald[1]. [1]University of Missouri Kansas City, USA, [2]Missouri University of Science & Technology, USA

Bone cement is typically used for the more than 1 million total joint replacements performed annually in United States. However, the typical bone cement can be toxic, have high heat generation and shrinkage and can potentially have negative effects such as cardiopulmonary complications mainly due to a major component, polymethylmethacrylate. We have developed novel bone cements using silorane resin which have no heat generation, low shrinkage, improved biocompatibility and excellent biomechanical properties in dry (DY5-ECHE, 5.853±0.519; DY5-1TOSU, 5.249±0.256; M12-ECHE, 5.327±0.762; M12-1TOSU, 5.327±0.762; Simplex 5.393±0.202 MPa) and wet environment (M12-1TOSU, 2.288±0.466; M12-ECHE, 1.960±0.259; DY5-1TOSU, 1.896±0.396; Simplex P, 3.067±0.193 MPa). Using MLO-A5 osteoblast cells to examine toxicity, not only were the silorane bone cements non-toxic as compared to the toxicity of commercial bone cement, but bone cells plated on silorane bone cement discs showed increased alkaline phosphatase enzyme activity (DY5-U,2.981±0.135; DY5-ECHE, 2.574±0.276; control, 1.352±0.069; Simplex P, 1.082±0.141) and increased mineralization (DY5-U, 0.032±0.003; DY5-ECHE, 0.033±0.001; control, 0.016±0.003; Simplex P, 0.013±0.001, using the alizarin red assay O.D/ug protein) suggesting osteogenic potential. To examine the properties of the silorane bone cement *in vivo*, rat femora were implanted with a titanium rod in the bone cements. Periosteal inflammation was monitored by radiography at week 1, 4 and 8, and the body weight of rats was measured at week 1, 2, 4, 6 and 8 post surgery. The body weight of rats implanted with commercial bone cement were significantly decreased by 8% at week one post surgery compared to the silorane cement groups ($p<0.01$). A periosteal reaction in the commercial bone cement was observed at weeks 4 and 8 post surgery (76% of animals), in contrast to no reaction in the silorane cement groups. Pull-out and histological evaluation are underway. In summary, the silorane-based bone cements enhance bone cell differentiation and mineralization *in vitro* and do not have inflammatory effects *in vivo.* The silorane cements are promising materials for bone repair and joint replacements.

***Disclosures: Lianxiang Bi**, None.*

SU0066

Elevated Serum Sclerostin Levels Point Towards Compromised Mechanotransduction in Type 2 Diabetic Postmenopausal Women with Fragility Fractures and Have Potential as Biomarker for Fracture Risk Assessment in Type 2 Diabetics. Ursula Heilmeier*[1], Janina Patsch[2], Dana Carpenter[3], Roy Harnish[1], Joyce Keyak[4], Thomas Baum[5], Gabby B. Joseph[1], Andrew J Burghardt[6], Ann Schwartz[1], Thomas Lang[1], Thomas Link[1]. [1]University of California San Francisco, USA, [2]Medical University of Vienna, Austria, [3]University of Colorado Denver, USA, [4]Department of Radiological Sciences, University of California, Irvine, USA, [5]Klinikum rechts der Isar, TU Muenchen, Germany, [6]Department of Radiology & Biomedical Imaging, University of California San Francisco, USA

The osteocyte-specific Wnt-inhibitor sclerostin is a key regulator of mechanotransduction and increasingly recognized as a protein of potential clinical relevance. Diabetic bone disease is a complication of type 2 diabetes mellitus (T2DM) with paradoxically increased fracture risk despite relatively high bone mineral density (BMD). The purpose of this study was to assess bone fragility properties (fracture load, BMD) and sclerostin serum levels in diabetic patients with a history of fragility fractures, compared to fracture-free diabetics and normal postmenopausal controls with and without fragility fractures. All subjects (controls [Co] n=20; controls with fragility fractures [Fx] n=20; diabetics without fractures [DM] n=20; diabetics with fractures [DMFx] n=20) were mobile, free of bone affecting diseases or medications and underwent quantitative computed tomography (QCT) of the left proximal femur, DXA (hip, spine), and blood draw for sclerostin, Vitamin D, PTH, HbA1c and eGFR measures. QCT scans were used to compute femoral neck BMD and femoral fracture load for fall and stance loading via finite element modeling. Using multiple linear regressions adjusted for age, race and BMI we found that sclerostin levels were significantly elevated in DMFx women compared to DM (p=0.013), Fx (p=0.033) and controls subjects (p=0.028) (Fig.1) while all groups did not differ significantly in height, weight, BMI, PTH, Vitamin D, eGFR or stance fracture load. DMFx and DM subjects had comparable HbA1c levels (7.9 ± 0.6 vs. 7.9 ± 0.3). All fragility fractures were at least 5 months old. Average fracture age was 3.5 ± 0.6 years for DMFx and 3.7± 0.8 years for Fx subjects. Areal BMD was particularly high in DM subjects, whereas it was normal to osteopenic in all other groups. DM subjects had significantly higher volumetric BMD than controls (p=0.033) or DMFx subjects (p=0.041), but not higher bone strength under fall conditions. In contrast, DMFx subjects showed normal vBMD, similar to controls, but significantly reduced fall failure loads (p=0.042). We conclude that elevated sclerostin levels in DMFx women suggest that mechanotransduction in diabetic patients with fragility fractures could be compromised. Sclerostin might also serve as a novel biomarker to assess fracture risk in diabetics and be a potential therapeutic target for diabetic bone disease. However, the pathophysiology leading to elevated sclerostin levels in diabetics with fractures remains to be elucidated.

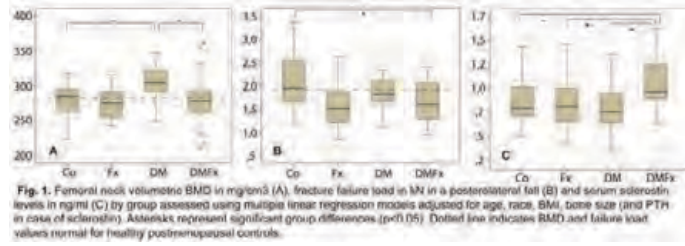

Fig. 1. Femoral neck volumetric BMD in mg/cm3 (A), fracture failure load in kN in a posterolateral fall (B) and serum sclerostin levels in ng/ml (C) by group assessed using multiple linear regression models adjusted for age, race, BMI, bone size (and PTH in case of sclerostin). Asterisks represent significant group differences ($p\leq0.05$). Dotted line indicates BMD and failure load values normal for healthy postmenopausal controls.

Figure 1

***Disclosures: Ursula Heilmeier**, None.*

SU0067

Femoral strength computed from QCT-based finite element analyses is not influenced by voxel or smooth mesh type. Dieter Pahr*[1], Michael Kinzl[1], Enrico Dall'Ara[1], Oleg Museyko[2], Klaus Engelke[2], Jarunan Panyasantisuk[3], Philippe Zysset[3]. [1]Vienna University of Technology, Austria, [2]University of Erlangen, Germany, [3]University of Bern, Switzerland

Femoral fractures represent an important endpoint in clinical trials in osteoporosis. Areal bone mineral density (aBMD) measured by DXA is still the current gold standard to evaluate fracture risk in vivo. Although quantitative computed tomography (QCT)-based homogenized finite element (FE) models are more accurate predictors of femoral strength than aBMD. The aim of this study was to evaluate the influence of the model's mesh type – homogenized voxel (hvFE) or smooth (hsFE) finite element meshes - with respect to prediction of strength in vitro.

Thirty-six pairs of femora were scanned with QCT and total femur BMC was evaluated. For each pair, one femur was positioned in one-legged stance configuration (STANCE) and the other in a sideways impact configuration (SIDE). Non-linear hvFE models were directly generated from the QCT images (linear hexahedral elements, 3mm edge length), whereas in case of smooth hsFE models the cortical and trabecular compartments were segmented using MIAF and meshed with quadratic tetrahedral elements (~4.5mm edge length). The same isotropic, density dependent, non-linear material law was used for all elements and bone compartments in order to change only the parameter ''mesh type''. Loading configurations were imposed from the biomechanical tests. All models were generated with MEDTOOL and analysed with ABAQUS. The ultimate loads were computed from the models and compared to those measured in the experiments.

In both configurations, hvFE/hsFE show similar predictability of femoral ultimate load ($adjR^2$=0.794/0.785 for STANCE and $adjR^2$=0.849/0.852 SIDE with $p>0.49$). The relative root mean square errors (RMSE) were comparable (17.9%/17.7% for STANCE and 18.0%/16.3% for SIDE) and slightly lower for smooth models. The hvFE/hsFE slopes (0.649/0.569 for STANCE and 0.902/0.735 SIDE) were different but not significantly ($p>0.08$ for STANCE/SIDE). For both mesh types, FE predicted femoral ultimate load better than BMC ($adjR^2$=0.678 for STANCE or $adjR^2$=0.696 for SIDE).

This study shows that the mesh type (voxel or smooth) has no influence on the quality of the strength predictions. Only the slopes changed, but not significantly. Smooth models included modelling of the cortex but with the same material behaviour as trabecular bone. Thus, smooth models offer space for improvements with respect to the geometrical definition and material behaviour of the cortex, but to the cost of increased complexity and effort for mesh generation.

***Disclosures: Dieter Pahr**, None.*

SU0068

Highly efficient HRpQCT-based plate and rod (PR) finite element models of whole bone distinguish postmenopausal women with vertebral fractures. Ji Wang*[1], Bin Zhou[1], Emily Stein[2], Elizabeth Shane[2], X Guo[1]. [1]Columbia University, USA, [2]Columbia University College of Physicians & Surgeons, USA

In postmenopausal women, risk of fragility fractures is associated with impaired whole bone strength. *In vivo* assessment of whole bone strength at distal tibia and radius has been possible through micro finite element (μFE) analyses based on high-resolution peripheral quantitative computed tomography (HRpQCT) images, but

demands high computational efforts. We have recently developed a highly efficient HRpQCT-based plate-rod (PR) model that allows fast and accurate prediction of elastic modulus and yield strength of trabecular bone, and found that vertebral fracture is associated with a remarkable decrease in elastic modulus and yield strength of the trabecular bone at both distal radius and tibia. In this study, we extended the PR modeling technique to include the cortical bone and created a patient-specific whole bone PR model, in which cortical bone was modeled with triangular shell elements enclosing the trabecular compartment composed of beam and shell elements, representing rod-and plate-like trabeculae, respectively. To evaluate the technique, we applied a whole bone PR FE model to HRpQCT images at the distal radius in 50 postmenopausal women with (n=25, age 69±1, 86% Caucasian, 28% Hispanic) and without (n=25, age 69±1, 93% Caucasian, 5% Hispanic) a history of vertebral fracture, and compared predictions by PR models with those of voxel models (Fig 1). Both PR and voxel μFE model analyses showed that whole bone stiffness at the radius was 10% lower in fracture patients than controls. Whole bone stiffness estimated by the PR model was significantly correlated with that of the voxel model (r=0.80, Fig 2). Furthermore, the whole bone PR model reduced the number of elements by 76-fold, leading to an over 1,300-fold reduction in μFE computation time (Table 1). PR models of the fracture patients had fewer elements, given the lower bone volume fraction and trabecular number. Overall, we evaluated a HRpQCT-based whole bone PR model with respect to a voxel model in estimating whole bone stiffness of distal radius, demonstrating the interesting potential of this highly efficient PR approach. Both models revealed weakened whole bone stiffness in vertebral fracture patients. However, mechanical properties of whole bone in individual patients can be assessed in about 5 seconds on a laptop PC. Due to its efficacy and efficiency, the HRpQCT whole bone PR model has great promise to assist in biomechanical functionality-based assessment of vertebral fracture risk.

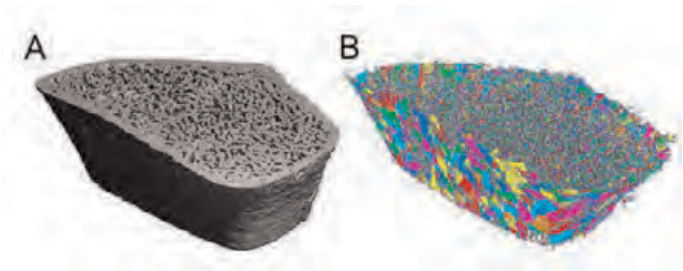

Figure 1. A) HRpQCT image of distal radius. B) Whole bone plate-rod μFE model.

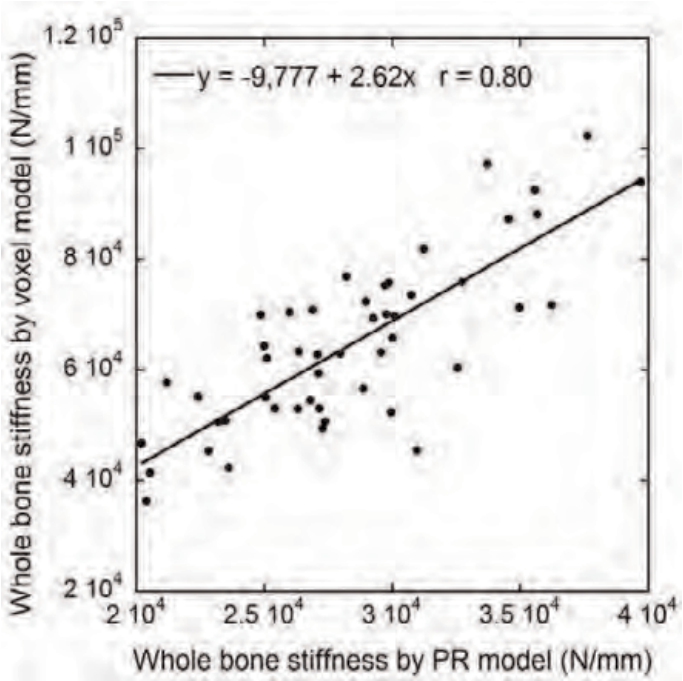

Figure 2. Linear regression of whole bone stiffness estimated by the PR and voxel μFE model

Table 1. Comparison of whole bone stiffness, model parameters between subjects with and without vertebral fractures. SEM, standard error of mean. * p<0.05.

	Fracture n=25 (mean ± SEM)	Nonfracture n=25 (mean ± SEM)	p value
Voxel model (N/mm)	59,853.8 ± 3,024.2	68,907.2 ± 2,826.9	**0.034***
PR model (N/mm)	26,662.4 ± 906.6	29,899.4 ± 844.2	**0.012***
Voxel computation time (min)	102.5 ± 10.2	115.1 ± 6.2	0.296
PR computation time (sec)	4.29 ± 0.56	5.65 ± 0.60	0.105
Voxel model size	1,391,052 ± 49,037	1,476,101 ± 44,143	0.206
PR model size	18,469 ± 1,100	19,596 ± 894	0.430

Table 1. Comparison of whole bone stiffness, model parameters between fracture and control subjects

***Disclosures: Ji Wang**, None.*

SU0069

HIV Infected Patients have Deteriorated Bone Material Properties at a Tissue Level Measured by "in vivo" Microindentation. Robert Guerri Fernandez*[1], María Rodríguez Sanz[2], Judit Villar-Garcia[2], Natalia Garcia-Giralt[3], Elisa Torres del Pliego[4], Laia Vilaplana Marz[4], Ana Guelar-Grinberg[2], Xavier Nogues[5], Leonardo Mellibovsky[2], Daniel Prieto-alhambra[6], Hernando Knobel[2], Adolfo Diez-Perez[7]. [1]Fundacio IMIM, Spain, [2]Internal Medicine-Infectious Diseases. Hospital del Mar, Spain, [3]IMIM, Spain, [4]Internal Medicine-Infectious Diseases, Spain, [5]Institut Municipal D'Investigació Mèdica, Spain, [6]University of Oxford, United Kingdom, [7]Autonomous University of Barcelona, Spain

Background: HIV infection and anti-retroviral therapies have detrimental effects on bone metabolism, high prevalence of osteopenia and osteoporosis was described in HIV-infected patients, and there is a growing evidence of the association between HIV infection and fracture risk. The etiology is not well understood, but bone material properties might be deteriorated.

Patients and Methods: In a HIV group of patients, we analyzed the bone material properties at a tissue level by microindentation. Two groups of patients were included: HIV + (with and without Antiretroviral Treatment (ART)), and controls, without HIV infection and no bone disease. A general laboratory workup, bone densitometry by DXA, and bone microindentation were carried out. Bone Material Strength (BMS) was measured with Osteoprobe® applying a 20N force on the anterior mid tibia normalized on a PMMA phantom. Age and gender-adjusted ANOVA was used for comparisons.

Results: 23 HIV patients (9 on ART) and 43 controls were included. Age (42+9.9 vs 69+13.4) and gender (14 men, 9 women vs. 4 men and 39 women) for HIV+ and controls respectively. After adjusting by age and gender, HIV+ patients showed worse (lower) BMS (79.6+12.7) (mean±SD) than controls (84.9±6.2, p=0.013). The BMS is lower in HIV+ treated patients (76±8)) with regard controls (p<0.001) and with regard to HIV+ untreated (BMS 81±14), nevertheless the difference was not significant between HIV-infected patients. T-scores in lumbar spine (-1.5+1.7) and total hip (-1.2+1.7) were, on average, in the range of osteopenia in the HIV+ patients. No differences in BMD were observed between HIV+ and controls. There was no correlation between BMS and lumbar spine BMD (R2=0.002, p=0.80) or total hip BMD (R2=0.002, p=0.81).

Conclusions: HIV-infected patients have deteriorated bone material properties at a tissue level measured by microindentation and this effect seems more pronounced in those receiving ART. BMD values do not reflect this bone deterioration. BMS does not correlate with bone density reinforcing the concept that measures a different bone dimension.

***Disclosures: Robert Guerri Fernandez**, None.*

SU0070

Microstructural and Biomechanical Properties, Bone Mineral Density and Bone Turnover in Patients with Hip Osteoporotic Fracture vs. Osteoarthritis.

Mª José Montoya*[1], Merce Giner[2], Cristina Miranda[3], Mª Angeles Vazquez[1], Ramón Pérez-Temprano[4], David Guede[5], José Ramón Caeiro[6], Ramon Perez-Cano[1]. [1]University of Seville, Spain, [2]Bone Metabolism Unit, "Virgen Macarena" University Hospital, Spain, [3]Bone Metabolism Unit, "Virgen Macarena" University Hospital of Seville, Spain, [4]Bone Metabolism Unit, "Virgen Macarena" University Hospital & University of Seville, Spain, [5]Parque Tecnolóxico de Galicia, Spain, [6]Department of Orthopaedic Surgery, Complexo Hospitalario Universitario de Santiago de Compostela, A Coruña, Spain

Introduction: Osteoporosis (OP) and osteoarthritis (OA) are the most prevalent musculoskeletal disorders in the elderly but the relationship between them is unclear.

Clinical and epidemiological studies have showed an inverse relationship between these diseases. However other studies, from different points of view, have reported the opposite hypothesis.Objectives: The purposes of this study are to analyze the bone turnover markers (BTM), bone mineral density (BMD) and the structural and mechanical properties of trabecular bone in patients with OP and OA, and to explore the level of relation among them.Materials and Methods: We studied 25 patients: 12 patients with hip osteoporotic fracture undergoing prosthetic hip replacement (OP group) and 13 patients with hip osteoarthritis undergoing total hip arthroplasty (OA group) (age range: 65-80). We analyzed bone parameters (PTH, Vitamin D, β-Crosslaps and PINP), BMD (DXA) and microstructural and biomechanical parameters (micro-CT).Statistical analysis of the results was conducted using the T-student test. Correlations between variables were assessed with the Pearson correlation coefficient. Statistical package SPSS 20.0 for Windows (IBM Corp., Armonk, NY, USA) was used and results with a $p<0.05$ were considered statistically significant.Results: OA group has lower levels of β- Crosslaps and higher BMD at femoral neck. Also, OA patients have an increased volume of trabecular bone and trabecular number, with architecture showing prevalence of plate-like trabeculae and with better connectivity than OP patients. The biomechanical parameters were better in OA group.

BMD was correlated with almost structural and biomechanical parameters, the best correlation was with volume of trabecular bone. β-Crosslaps was negatively correlated with hip BMD and with bone surface density and positively with trabecular separation.Conclusions: BTM, BMD and bone microstructural changes in osteoarthritis are opposite to those of OP. These findings mostly justified a more resistant bone with less risk of fragility fractures in OA respect to OP patients, as clinical and epidemiological studies have pointed out for decades.

***Disclosures: Ma José Montoya**, None.*

SU0071

Regional Heterogeneity of Trabecular Bone Microcrack Density in Association with Trabecular Microarchitecture and Bone Resorption in Whole Human Lumbar Vertebrae.

Vincent Carpentier[1], Helen Tsangari[2], Nicola Fazzalari[3], Julia Kuliwaba*[2]. [1]Harvard School of Dental Medicine, USA, [2]SA Pathology, Australia, [3]The University of Adelaide, Australia

Purpose: Vertebral deformity, intervertebral disc disorganisation, and changes to vertebral bone architecture are morphological features associated with degeneration of the spine and with back pain. Vertebral strength is determined by bone size, shape, bone mineral density, microarchitecture, and bone material properties (eg. collagen characteristics, mineralisation, microdamage). Despite its importance to vertebral biomechanics, no studies have reported on the variation of bone microdamage present in the human vertebra. Thus, the purpose of this study was to assess regional changes in trabecular bone microdamage in association with bone microarchitecture and resorption in whole human lumbar vertebrae.

Methods: L2 vertebrae were obtained from twelve human cadaveric spines (six males, aged 53-82 years; six females, aged 56-87 years), with no history of spinal surgery, vertebral fracture, or disease/medication that may have affected bone turnover. Parasagittal slices, low speed diamond wheel saw cut from each vertebral body, were *en bloc*-stained in basic fuchsin, cut into 9 sectors, and resin embedded. Histomorphometric assessment of trabecular bone microarchitecture, *in vivo* bone microdamage, and extent of bone resorption was undertaken.

Results: Data analysis revealed few differences for the 9 sectors and no differences for the antero-posterior axis were observed. For the cranio-caudal axis, the mid-vertebral region had the lowest bone volume fraction ($p<0.03$), trabecular number ($p<0.02$), and highest trabecular separation ($p<0.03$). Microcrack density parameters were highest in the mid-vertebral region ($p<0.04$); with the shortest crack lengths observed in the caudal region ($p<0.04$). Diffuse microdamage was minimal or absent. Bone resorption was highest in the cranial region (eroded bone surface, $p<0.04$).

Conclusions: For the cranio-caudal axis of the L2 human vertebra, the mid-vertebral region may be biomechanically compromised due to reduced bone volume and microarchitectural changes being accompanied by an increased microcrack burden. The increased bone resorption found in the cranial region may be an adaptive response to intervertebral disc degeneration. This is the first study to report on the regional variation of *in vivo* bone microdamage in whole human vertebrae. The implications of these observations are being further investigated with comparison to available biomechanical and intervertebral disc grading data.

***Disclosures: Julia Kuliwaba**, None.*

SU0072

Substitutability of Cortical Parameters of Bone Strength Assessed by DXA and HR-pQCT in Premenopausal Women at the Distal Tibia.

Albrecht Popp*[1], Helene Buffat[1], Kurt Lippuner[1], Ursula Eberli[2], Manuela Ernst[2], R Geoff Richards[2], Vincent Stadelmann[2], Markus Windolf[2]. [1]Department of Osteoporosis, University Hospital & University of Berne, Switzerland, [2]AO Research Institute Davos, Switzerland

Introduction: With regard to bone strength, structural elements of bone add information to Bone Mineral Density (BMD). A novel index, which combines areal BMD (aBMD) and the polar moment of inertia (pMOI) calculated directly from a single dual X-Ray absorptiometry (DXA) measurement, was shown ex vivo to be a good predictor of bone strength and stiffness assessed by high resolution peripheral quantitative computed tomography (HR-pQCT) at the distal tibia diaphysis (T-DIA), with a high correlation coefficient of $R^2=0.88$ (Popp AW Bone 2012). Whether this also applies in vivo is unknown.

Methods: A random cohort of healthy, community-dwelling, non-pregnant, 20 to 40-year old women living in the region of Davos, Switzerland, was generated by using a commercial nationwide address database. Women were contacted by regular mail (N=485). After given informed consent, 72 participants underwent volumetric BMD (vBMD) measurement at T-DIA by HR-pQCT (XtremeCT™, Scanco Medical AG, Brüttisellen, Switzerland) and aBMD measurement at T-DIA and femoral neck (FN) by DXA (Hologic Discovery C™, Hologic, Bedford, MA, USA). Cortical thickness (CTh) at T-DIA was either directly assessed by HR-pQCT or calculated from T-DIA DXA scans by using DICOM images, analyzed with a Canny threshold-based tool implemented in MATLAB™ (MathWorks™, Natick, MA, USA). Corresponding pMOIs were either directly determined (HR-pQCT) or derived from CTh values (DXA), following a methodology described earlier (Popp AW Bone 2012).

Results: In total, 72 healthy premenopausal women were included. Mean (±SD) age was 33.8 (±5.2) years, with 167.6 (±6.2) cm for height, and 23.2 (±4.1) kg/m^2 for BMI. Mean FN BMD was 0.853 (±0.119) g/cm^2 corresponding to a mean Z-score of 0.0 (±1.1). At T-DIA, a high correlation ($R^2 = 0.74$) was found between the cortical bone strength indexes assessed by DXA (aBMD × pMOI) and HR-pQCT (vBMD × pMOI), indicating that bone strength assessed by DXA and HR-pQCT are predictive of each other.

Conclusion: In a cohort of randomly selected premenopausal women, bone strength assessed by combining structural and densitometric parameters of bone determined by either DXA or HR-pQCT were highly correlated.

***Disclosures: Albrecht Popp**, None.*
This study received funding from: AO Research Institute Davos

SU0073

The Trabecular Bone Score is Associated with Volumetric Bone Density and Microarchitecture as Assessed by cQCT and HRpQCT in Chinese-American and Caucasian Women.

Alice Abraham*[1], Barbara Silva[2], Marcella Walker[1], Stephanie Boutroy[3], Chiyuan Zhang[1], Donald McMahon[4], George Liu[5], Didier Hans[6], John Bilezikian[4]. [1]Columbia University, USA, [2]Columbia University Medical Center, USA, [3]INSERM U1033 & Université de Lyon, France, [4]Columbia University College of Physicians & Surgeons, USA, [5]New York Downtown Hospital, USA, [6]Lausanne University Hospital, Switzerland

High resolution peripheral quantitative computed tomography (HRpQCT) indicates that Chinese-American (CH) women have smaller bone size but denser and thicker cortices and more plate-like trabeculae at the radius and tibia than Caucasian (CA) women. Central quantitative computed tomography (cQCT) also demonstrates cortical advantages at the hip among CH women but similar trabecular (Tb) volumetric bone mineral density (vBMD) at the central skeleton between races. While high resolution imaging has advanced the assessment of bone microarchitecture, it is not readily available in the clinical setting. The trabecular bone score (TBS) provides an estimate of Tb microarchitecture from DXA spine images and predicts fracture risk independent of areal BMD (aBMD). In this analysis, we assessed if TBS reflects vBMD and microarchitecture measured by cQCT and HRpQCT in pre- (PreM; n=71) and postmenopausal (PostM; n=44) CH and CA women. Age was comparable between races. Height and weight were higher in CA vs. CH women. TBS did not differ by race (PreM: 1.465±0.091 vs. 1.467±0.064, p=0.92; PostM: 1.336±0.097 vs. 1.318±0.089, p=0.52) before or after adjusting for weight. In the entire cohort, TBS correlated with lumbar spine (LS) Tb vBMD ($r=0.664$; $p<0.001$); femoral neck (FN) integral ($r=0.651$, $p<0.001$), Tb ($r=0.641$, $p<0.001$) and cortical (Ct) vBMD ($r=0.346$, $p<0.001$) and Ct thickness (C/I; $r=0.540$, $p<0.001$) by cQCT.

TBS also correlated with integral (r=0.643, p<0.001), Tb (r=0.574, p<0.001) and Ct vBMD (r=0.491, p<0.001) and C/I (r=0.541, p<0.001) at the total hip (TH). LS aBMD correlated with all cQCT indices at all sites except FN cortical vBMD. Together, TBS and LS aBMD explained more of the variance in cQCT measures vs. aBMD alone (LS Tb vBMD R^2 0.605 vs. 0.474, p=0.005; FN: integral vBMD R^2 0.467 vs. 0.258, Tb vBMD R^2 0.540 vs. 0.401, C/I R^2 0.338 vs. 0.210, all p<0.01; TH: integral vBMD R^2 0.510 vs. 0.352, C/I R^2 0.301 vs. 0.126, all p<0.05). TBS was associated with all HRpQCT indices (r=0.20-0.52) except radial cortical thickness and tibial Tb thickness. Similar to our prior LS cQCT results, Tb indices by TBS did not differ by race in this cohort. TBS was associated with most HRpQCT and cQCT indices except for bone size. In conclusion, TBS reflects vBMD and bone microarchitecture derived from higher resolution imaging and may be a useful adjunct to aBMD for assessing central Tb microstructure between races or other groups with differences in bone size.

***Disclosures: Alice Abraham**, None.*

SU0074

Bone geometry and strength are negatively affected even by low-normal or subclinical thyrotoxic range of TSH level in the elderly. Su Jin Lee*[1], Kyoung Min Kim[2], JO EUN KIM[1], Sung-Kil Lim[3], Yumie Rhee[4]. [1]Yonsei University Health System, South Korea, [2]Seoul National University Bundang Hospitatl, South Korea, [3]Yonsei University College of Medicine, South Korea, [4]Department of Internal Medicine, College of Medicine, Yonsei University, South Korea

Overt hyperthyroidism has been recognized by a secondary cause of osteoporosis. More studies have suggested that subclinical hyperthyroidism may also result in decreased bone mineral density (BMD). We analyzed bone geometry and BMD to investigate whether bone strength properties could be different according to the level of thyrotropin (TSH) in the elderly.

Inclusion criteria were patients older than 65-year-old and who had the level of TSH lower than 5.0 mIU/mL without any histories of functional thyroid diseases. Bone mineral density (BMD) was measured by dual energy X-ray absorptiometry (DXA) and further analyzed for hip geometry properties with APEX program. A total of 286 men and 588 women were included and stratified into 3 groups according to the level of TSH ; lower group with lower than 1.0 mIU/mL, middle group with 1.0 to 3.0 mIU/mL, and upper group with higher than 3.0 mIU/mL.

TSH level showed positive correlations with femur neck cortical thickness in both men and women (r=0.184, p<0.05 for men; r=0.096, p<0.05 for women). The lumbar spine BMD was not different according to the group of TSH levels. However, BMD and cortical thickness of the femur neck vary positively with the TSH groups in both men and women (p for trends <0.05, respectively). In addition, the buckling ratio of the femur neck in the lower TSH group was significantly higher in women (p<0.05) and showed higher tendency in men (p=0.09). These associations were consistently observed even after adjusting for age, BMI and PTH levels.

In conclusion, low-normal or subclinical thyrotoxic range of TSH level negatively affects bone strength in the hip via thinning of the cortex and increased buckling ratio in the older population who have the highest risk of hip fracture.

***Disclosures: Su Jin Lee**, None.*

SU0075

Changes in Fracture Strength as a Function of Time since Spinal Cord Injury. William Edwards*[1], Thomas Schnitzer[2], Karen Troy[1]. [1]University of Illinois at Chicago, USA, [2]Northwestern University, USA

Spinal cord injury (SCI) is characterized by marked bone loss at regions below the neurological lesion. The clinical consequence of this bone loss is a rate of low-energy fracture similar to that of post-menopausal osteoporotic women. The greatest reductions in bone are observed around regions of the knee. Within the first 2 to 3 years of SCI, some 50% of the bone mineral at the distal femur and proximal tibia is resorbed. Unfortunately, the mechanical consequence of this bone loss remains unclear. Therefore, our purpose was to quantify changes in fracture strength at the proximal tibia as a function of time since SCI. Fifty one adults with SCI and a reference group of 5 able-bodied adults participated in this study. Computed tomography (CT) data were acquired for the proximal most 15cm of the non-dominant tibia. All CT images included a calibration phantom to convert CT attenuation to bone equivalent density. Bone mineral content (BMC) and volumetric bone mineral density (vBMD) were determined. Fracture strength of the proximal tibia loaded in torsion was quantified using validated patient-specific finite element modeling procedures. Exponential decay curves were used to describe changes in bone parameters and fracture strength as a function of time since SCI: y = Aexp(-bt)+C, where A is the loss amplitude; b, the loss rate; C, the new steady state; and t the time in years. Reductions in BMC (r^2 = 0.60), vBMD (r^2=0.71), and fracture strength (r^2=0.63) with time since SCI were well described using exponential relationships. New steady state values in bone mineral and fracture strength were met within 2.0 – 2.4 years after SCI, depending on the parameter (Figure 1). Whereas, new steady state values for bone parameters were approximately 47% lower than the reference group, the new steady state value for fracture strength was approximately 63% lower than the reference group. In summary, fracture strength of the proximal tibia decreased exponentially and reached a new steady state following SCI. Although the time to reach steady state was similar amongst bone parameters and fracture strength, steady state values for fracture strength were considerably lower than bone parameters when expressed relative to an able-bodied reference group. These data provide a more in-depth understanding of the mechanical consequence of bone loss after SCI, which ultimately may help in the prevention of SCI-related fragility fracture.

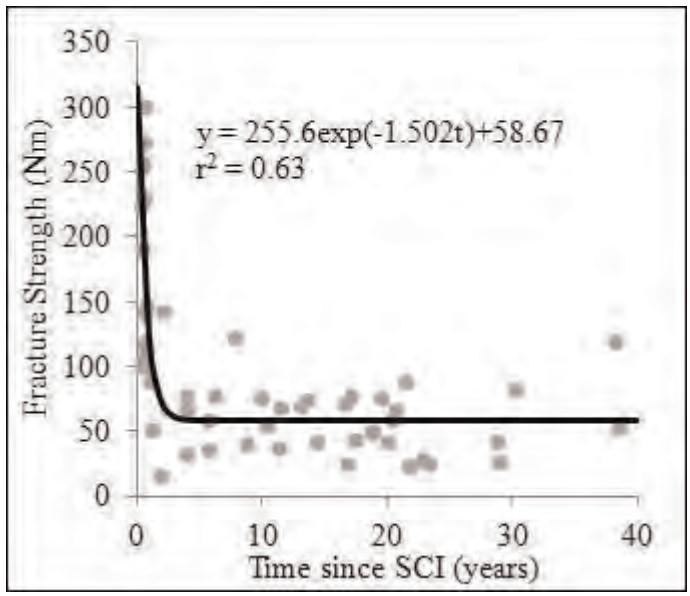

Figure 1. Fracture strength vs. time since SCI

***Disclosures: William Edwards**, None.*

SU0076

Influence of Physical Activity on the Distribution of Human Cortical Tissue as a Function of its Mass and its Mechanical Quality. Paola Reina[1], Gustavo Roberto Cointry[1], Laura Nocciolino[1], Sara Feldman[1], Jose Ferretti*[2], Joern Rittweger[1], Ricardo Francisco Capozza[1]. [1]Center for Phosphocalcic Metabolism, Argentina, [2]National University of Rosario, Argentina

Increasing evidence shows that bone *mechanostat* would optimize bone structural stiffness as a function of the usage-derived peak strains sensed by osteocytes. One mechanism proposed to achieve this homeostatic control of bone structure is the spatial orientation of modeling drifts as a function of the maximal loads determined by customary mechanical usage of the skeleton.

To test that hypothesis, we analyzed the correlations between pQCT indicators of the mass (BMC), the mechanical "quality" (vDMO, a variable known to vary linearly with bone tissue stiffness), and the efficiency of the spatial distribution of cortical tissue to resist deformation in bending or torsion (cross-sectional moments of inertia, MIs) in slices taken at every 5% of the tibia length, as well as the maximal cross-sectional muscle area (MA) of the calf, in 22 males and 20 females aged 25-35 years who either had sedentary habits or were trained in long-distance running during more than 8 years.

All MIs (y) correlated with cortical CMO following positive, exponential relationships ("distribution/mass" curves, d/m) and with cortical vDMO following negative, hyperbole-like relationships ("distribution/quality" curves, d/c) in all bone sites. The distribution of correlation coefficients of both d/m and d/c curves along the bone were described by bell-shaped curves, with maximum values toward the central region of the diaphyses, reflecting the predominance of the usual bending and torsion stresses over that of compression stress. The residual values of both the d/m and d/c curves correlated linearly with MA (p<0.001) in every group and also in all the individuals analyzed as a whole ("bone/muscle" relationships, b/m).

Results verify no less than 3 correlative hypotheses: 1: That the preferential distribution of the available bone cortical tissue in specific sites across the diaphyseal section results from the directional optimization of local modeling drifts (d/m curves), 2. That that geometrical adaptation is more evident in sites where the bone tissue is less stiff (d/c curves), and 3. That local muscle strength and/or usage is synergic with those two manifestations (b/m curves). In addition, the collected evidence a. supports the proposed role of bone *mechanostat* with inedit arguments for the human skeleton, and b. offers a basis for developing reference graphs suitable for a comparative diagnosis of the *mechanostat* condition in individual cases.

***Disclosures: Jose Ferretti**, None.*

SU0077

Muscle Force and Bone Strength in Osteogenesis Imperfecta Type I. Louis-Nicolas Veilleux*, Frank Rauch. McGill University/Shriners Hospital for Children, Canada

Context: Osteogenesis imperfecta (OI) type I is a heritable bone fragility disorder that most often is caused by mutations affecting collagen type I. We have recently shown that patients with OI type I often have muscle weakness. In healthy individuals muscle force is closely related to bone strength. If this relationship is maintained in OI, this would suggest that muscle weakness contributes to the disease-related bone fragility.

Objective: The objective of the current study was to investigate the functional muscle-bone unit of the lower leg in patients with OI type I and healthy age- and gender-matched controls.

Patients and Other Participants: Thirty children and adolescents with OI type I (20 females; mean age [SD]: 11.2 years [3.9]) who had never received bisphosphonate treatment were compared to 30 healthy age- and gender-matched controls (mean age [SD]: 11.1 years [4.5]).

Main Outcome Measures: In order to estimate bone strength, tibia bone mineral content (BMC; mg/mm) was measured by peripheral quantitative computed tomography. Lower extremity peak force (kN) was measured by jumping mechanography through the multiple two-legged hopping test.

Results: Compared to age- and gender-matched controls, patients with OI type I had 17% lower peak force (1.3 kN vs. 1.7 kN; $p = 0.002$) as well as a 22% lower BMC (128 mg/mm vs. 165 mg/mm; $p < 0.001$). Multiple regression analysis showed that muscle force and tibia length were positively related to BMC ($r^2 = 0.90$, $p < 0.001$). On the contrary disease status was negatively related to bone strength indicating that patients with OI type I have a 20 mg/mm disadvantage on BMC as compared to age- and gender matched controls.

Conclusions: These results suggest that the muscle-bone relationship differs in OI type I as compared to healthy age- and gender-matched controls. More specifically, the regression analyses indicate that at a specific peak muscle force and tibia length, patients with OI type I will have a 12% lower BMC relative to the average control results. Therefore, our results suggest that both muscle weakness and the disease status effect on the muscle-bone relationship contribute to decreased bone strength in patients with OI type I.

***Disclosures: Louis-Nicolas Veilleux**, None.*

SU0078

Association Between Lumbar Bone Density (BMD) and Lumbar Disc Degeneration (LDD). Sami Salo*[1], Ville Leinonen[2], Toni Rikkonen[3], Pauli Vainio[2], Risto Honkanen[1], Heikki Kroger[2], Joonas Sirola[4]. [1]University of Eastern Finland, Finland, [2]Kuopio University Hospital, Finland, [3]University of Eastern Finland, Bone & Cartilage research unit, Finland, [4]University of Eastern Finland / Kuopio, Finland

Introduction: Osteoporosis and lumbar disc degeneration (LDD) are common among the elderly. Higher vertebral BMD has been found to be related with LDD. On the other hand in a couple of studies it has been reported that many patients with osteoporosis have severe disc degeneration. The aim of our research was to study relationship between LDD and BMD in lumbar spine.

Materials and methods: The study population consisted of 168 postmenopausal women (aged 63,3 - 75,0 years, mean 68,6 years) belonging in the prospective OSTPRE and OSTPRE-FPS study cohorts. Out of all study subjects with valid lumbar DXA-measurements 168 had a history of lumbar MRI-scan (1,5 T unit). The severity of LDD was graded from T2-weighted images using 5-grade Pfirrmann classification. Four vertebral levels (L1-L4) were studied (altogether 672 discs). The association between lumbar BMD and severity of LDD was studied separately for each vertebra level with UNIANOVA test with controlling for the effect of confounding factors, including age, body mass index (BMI) and the time between DXA-measurements and MRI-scan.

Results: Higher lumbar BMD was associated with more severe LDD in all levels (L1-L4): between L4-L5 disc and L4 BMD ($p=0.044$), between L2-L3 disc and L3 BMD ($p=0.001$), in all other levels ($p<0.001$). All results remained statistically significant after controlling for the confounding factors.

Conclusions: Higher lumbar BMD seems to be associated with more severe LDD. Higher lumbar BMD seems to be associated with more severe LDD. This might be related to dehydration of nucleus and shift of load to the annulus and endplate. However, the causality should be more closely studied in further studies.

keywords: bone mineral density, intervertebral disc degeneration, postmenopausal women, lumbar spine, osteoporosis

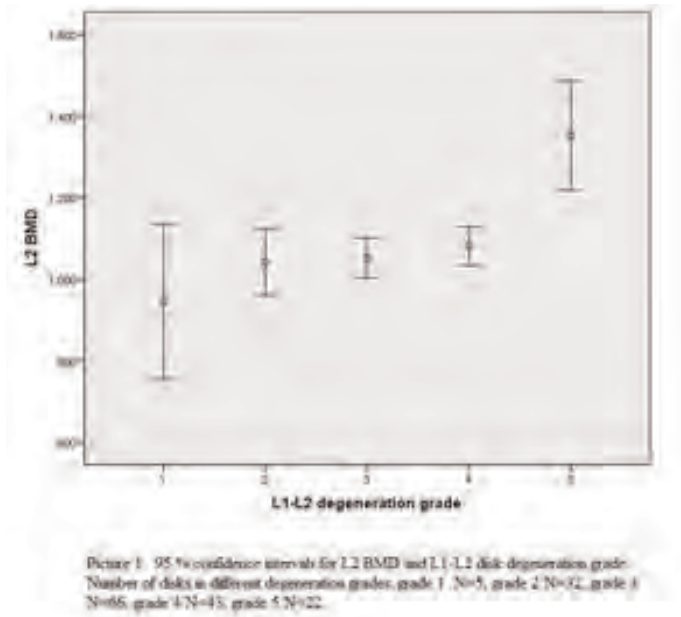

Picture 1. 95 % confidence intervals for L2 BMD and L1-L2 disk degeneration grade. Number of disks in different degeneration grades: grade 1 N=5, grade 2 N=42, grade 3 N=66, grade 4 N=43, grade 5 N=22.

Results, L1-L2 disc vs. L2 BMD

***Disclosures: Sami Salo**, None.*

SU0079

Plasma Concentration and Expression of Matrix Gla Protein (MGP) in Ectopic Calcification Model Rats. Naoko Tsugawa*, Haruna Sakurai, Tetsushi Kasuga, Toshio Okano. Kobe Pharmaceutical University, Japan

OBJECTIVE: Matrix Gla protein (MGP) is known as a potent vascular calcification inhibitor. MGP is a vitamin K dependent protein (VKDP) which is activated by gamma-carboxylation of Glu residues (Gla) in the presence of vitamin K. Previous *in vitro* study has shown that MGP expression was induced in vascular smooth muscle cells by stimulation of calcification. However, it is unclear whether gene expression of MGP is stimulated in ectopic calcified tissues *in vivo*. The aim of our study was to investigate the changes of the plasma concentration of inactive form of MGP (uncarboxylated MGP: ucMGP), and the gene expression of MGP in ectopic calcification model rats induced by administration of excess vitamin D or adenine-containing diets.

METHODS: Ectopic calcification model rats were generated by two methods. Wistar male rats (10 weeks of age) were fed 0.75% adenine-containing diet for 3 week (Ad group). In another group, vitamin D_3 (25 mg/kg/d) were administered to Wistar male rats (9 weeks of age) for 7 days (VD group). Calcium and phosphorus concentrations in plasma and soft tissues (aorta, heart, kidney, lung and trachea) were measured. The expression of MGP mRNA in soft tissues was measured by real-time RT-PCR. Plasma concentration of ucMGP was measured by ELISA.

RESULTS: Plasma calcium concentrations in VD group and phosphorus concentration in the Ad group were elevated significantly. Ectopic calcification in soft tissues was observed in the VD and Ad group, and the VD group showed more severe calcification than did the Ad group. Gene expression of MGP was up-regulated in ectopic calcified tissues, but not in cartilage. Plasma ucMGP concentration was remarkably elevated in the Ad group, but its elevation in the VD group was not significantly.

CONCLUSION: The mRNA expression of MGP was prominent in aorta, heart, kidney, lung and trachea of both ectopic calcification model rats. However, the two model rats displayed different profiles in plasma ucMGP concentrations. These results suggest that plasma ucMGP concentration does not necessarily correlate with expression of MGP in ectopic calcified tissues.

***Disclosures: Naoko Tsugawa**, None.*

SU0080

Post-Union Response to External Fixation versus Intramedullary Pinning in Mouse Tibia Fracture Healing. Yusuke Hagiwara*, Douglas Adams, Nathaniel Dyment, Xi Jiang, David Rowe. University of Connecticut Health Center, USA

Progression of long bone fracture healing to union, and subsequent remodeling of callus and original cortex toward restoration of anatomy, are modulated by the stability and compliance afforded by fixation. Our previous work compared intramedullary pinning (IMP) to external fixation (EF) in the mouse tibia fracture model, reporting a larger cartilaginous callus for IMP at 2 weeks. IMP allowed

deformities such as angulation, rotation, or shortening which were greatly reduced with EF. The relatively simple, cost-effective method of EF (3×25G proximal and 3×28G distal percutaneous needles held laterally with a tuberculin syringe barrel) holds the potential for further modulating repair by removing structural components to increase load transfer. This study extended the comparison of IMP vs EF through 5 weeks of healing to elucidate the effects of internal vs external fixation and associated compliances on post-union remodeling at 2 and 5 weeks post-fracture (32 animals, 8/group, 4 mo old). Fixation was placed prior to creating a single, transverse fracture located proximal of the tibia-fibula junction, using a standard drop-weight method. IMP employed the Ender nailing technique, whereby IM pin diameter was maximized to the canal and inserted with slight pre-bent angulations at the tip and midspan, using a twisting motion to navigate tibia curvature. EF was achieved by placing all components, removing the syringe barrel to create the fracture, and replacing it to achieve anatomical reduction. Healing and measurement of deformity were followed longitudinally using digital radiographs, and with μCT imaging of excised specimens. EF achieved union without substantial callus formation (Figure) and maintained rotational alignment ($<10^{\circ}$ deformity). IMP demonstrated persistent callus with a substantial and variable rotational deformity (20-40°) by radiographic and gait analysis (DigiGait). Incidence of spontaneous fibula fracture was higher for IMP (80 & 89% at 2 & 5 wks) than for EF (12 & 40%). Mechanical integrity was measured at 5 wks via torsion tests, suggesting lower strength for EF vs IMP. At 2 weeks, EF specimens (and IMP specimens lacking significant callus) demonstrated a propensity to break at the fracture site during manual manipulation of soft tissue dissection. These findings suggest a trade-off between establishing anatomical reduction and mechanical integrity of repair that might be accomplished by progressively increasing the compliance of EF.

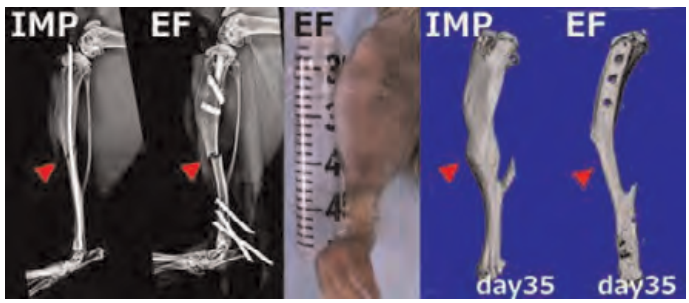

Fixation with IMP resulted in persistent callus that was not present for EF

***Disclosures: Yusuke Hagiwara**, None.*

SU0081

Tissue-specific Extracellular Matrix Controls the Fate of Bone Marrow-derived Mesenchymal Stem Cell Differentiation. Rubie Rakian[1], Zhi-Liang Zhang[2], Travis Block[1], Qiuxia Dai[1], Zhongding Lu[1], Xiao-Dong Chen*[1]. [1]University of Texas Health Science Center at San Antonio, USA, [2]Ren-Ji Hospital, Shanghai Jiao-Tong University School of Medicine, China

Mesenchymal stem cells (MSCs) differentiate into many distinct cell lineages depending upon the local microenvironment that is mainly constituted by extracellular matrix (ECM) proteins and associated growth factors. However, it has been challenging to dissect the key components that direct the differentiation of MSCs because of the limited availability of in vitro models. Previously, we reported that in both mice and humans, cell-free ECM prepared from marrow stromal cells (BM-ECM) significantly promoted proliferation of MSCs and preserved their stem cell properties. Here, we wanted to investigate whether the BM-ECM was unique in its ability to preserve MSC properties by comparing to ECM made by fibroblasts derived from different tissues such as skin and fat. Cell-free bone marrow-, skin-, and adipose-derived ECMs were prepared by cultured bone marrow cells, skin fibroblasts and adipose stem cells (ASCs), respectively. Human marrow stromal cells (hMSCs, passage 1 to 3) were cultured on the various ECMs, or tissue culture plastic (TCP) in expansion medium until confluence (~7 days), then maintained under conditions known to induce commitment to a specific cell lineage including osteoblasts and adipocytes. The lineage specific transcripts were measured by TaqMan PCR at day 7, 14, 21 and 28 post-confluence. We found that hMSCs maintained on BM-ECM expressed much higher levels of alkaline phosphatases (ALP), type I collagen and bone sialoprotein than cells maintained on adipose-ECM and skin-ECM after treatment with osteoblast differentiation medium. The cells maintained on skin-ECM did not respond to the treatment of osteoblast differentiation medium, showing no increased expression of these osteoblast markers compared to the untreated cells. In contrast, hMSCs maintained on adipose-derived ECM in both the expansion and adipose differentiation media expressed significantly higher levels of PPARγ2, and C/EBPα (a key regulator of adipogenesis) than the cells maintained on TCP, BM-ECM or skin-ECM. Interestingly, only hMSCs cultured on skin-ECM in the expansion medium expressed a considerable high level of keratin 6A (an early differentiation marker of epithelial cells). We conclude that the differentiation of hMSCs can be directed by exposure to tissue-specific ECM. The unique protein profiles for these ECMs will be further determined using proteomic analysis.

***Disclosures: Xiao-Dong Chen**, None.*

SU0082

An Essential Role of Bmp Receptor1A (ALK3) in Postnatal Skeleton Formation. Junjun Jing*[1], Zhaowen Zhong[2], Chuanju Liu[3], Nobby Kamiya[4], Ying Liu[5], xuedong zhou[6], Jian Feng[7]. [1]Baylor college of dentistry,TA&M Health Science Center, USA, [2]TX A&M Baylor College of Dentistry, USA, [3]New York University, USA, [4]Texas Scottish Rite Hospital for Children, USA, [5]baylor college of dentistry, USA, [6]State Key Laboratory of Oral Diseases, West China Stomatology Hospital, China, [7]Texas A&M Health Science Center, USA

ALK3 plays a critical role in both chondrogenesis and osteogenesis during embryonic development. To test the postnatal role of ALK3 in skeletal tissues, we initially studied the skeletal phenotype in 2-wk, 4-wk and 8-wk in *Alk3 c*onditional knockout (cKO) mice, which were crossed between $Alk3^{fl}$ and aggrecan-Cre^{ER} (specific for cartilage tissues) and induced by tamoxifen at postnatal day 7. The X-ray and mCT images displayed a reduced bone length in null femora and vertebrae, 40% and 30% reduction, respectively. There was no apparent change in the cortical bone quantity as well as other flat bones such as calvarial and alveolar bones as assessed by bone volume/total volume. H&E and Toluidine Blue stains showed no evidence of chondrocytes in the null epiphysis and metaphysis, suggesting a complete block of endochondral bone formation in Alk3-cKO mice. Moreover, sulfated proteoglycan and Sox9 (an essential early transcription factor for chondrogenesis) were undetectable in the cKO epiphyseal and growth plate cartilage. Interestingly, mice lacking Alk3 in the late chondrocyte obtained from the offspring of mice crossing between *Col X-Cre & Alk3fl* showed no apparent change in the cartilage, suggesting an essential early (but not late) role of ALK3 in controlling postnatal chondrogenesis, likely via regulation of SOX9. Of note is that the ribs are composed of true (bonny) and false (cartilage) components, whereas ribs are known to undergo intramembranous ossification. Surprisingly, the inactivation of Alk3 in early cartilage led to a sharp cortical bone volume increase in the boney ribs, indicating that rib ossification is cartilage-dependent and regulated by ALK3. Finally, we showed that inactivation of *Alk3* in cartilage led to a switch from the epiphysial perichondrium to a periosteum-like structures such as the lack of cartilage and great expansions of the bone bark (>10-fold increase) as evidenced by X-rays, uCT, immunostain, Safranin O and Toluidine Blue stains. In summary, our data support the vital role of ALK3 in postnatal endochondrogenesis via regulation of Sox9. The finding that severe defects in rib ossification but not in other flat bones suggest that rib bone formation is chondrocyte-dependent, in which ALK3 plays an essential role.

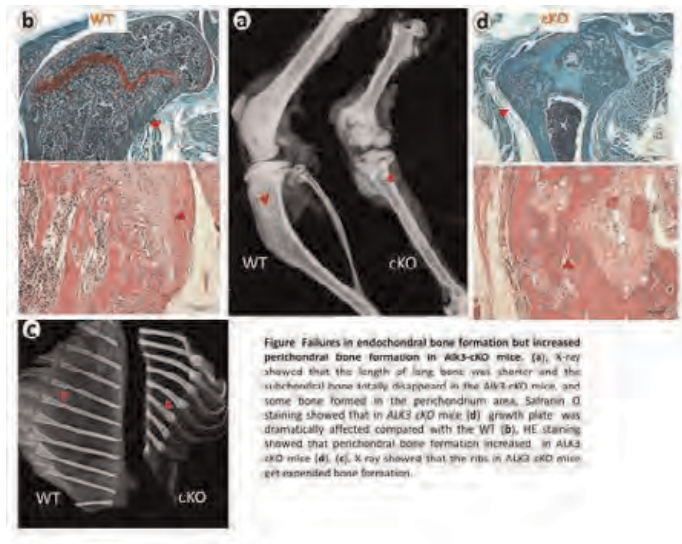

Fig-1

***Disclosures: Junjun Jing**, None.*

SU0083

C-raf is Required for Normal Postnatal Growth Plate Maturation. Eva Liu*[1], Adalbert Raimann[2], Eric Zhu[3], Marie Demay[4]. [1]Brigham & Women's Hospital & Massachusetts General Hospital, USA, [2]Medical University Vienna & Massachusetts General Hospital, Austria, [3]Massachusetts General Hospital, USA, [4]Massachusetts General Hospital & Harvard Medical School, USA

Growth plate maturation is dependent upon differentiation of proliferative chondrocytes expressing type II collagen into type X collagen(Col X)-expressing hypertrophic chondrocytes. Hypertrophic chondrocyte apoptosis and signaling of vascular invasion are critical for replacement of cartilage by bone during endochondral bone development. Hypophosphatemia leads to rickets by impairing

hypertrophic chondrocyte apoptosis. Inhibiton of MEK1/2 blocks phosphate-induced Erk1/2 phosphorylation and hypertrophic chondrocyte apoptosis. However, it is unclear what signaling molecules upstream of MEK1/2 lead to phosphate-induced hypertrophic chondrocyte apoptosis. Lack of A-Raf and B-Raf in chondrocytes does not lead to a growth plate phenotype. However, C-raf is the predominant Raf isoform in hypertrophic chondrocytes and the role of C-Raf in the postnatal growth plate has not been examined.

Chondrocyte specific C-raf knockout (*C-raf$^{fl/fl}$*/Cre+) mice were generated by mating *Col2a1*- Cre transgenic mice to mice with floxed *C-raf* alleles. *C-raf$^{fl/fl}$*/Cre+ mice are born at normal mendelian ratios and are phenotypically indistinguishable from normal littermates at birth. Studies of the tibial growth plates of day 18 *C-raf$^{fl/fl}$*/Cre+ mice demonstrated a 2.5 fold increase in the number of hypertrophic chondrocytes per column compared to those of the *C-raf$^{fl/fl}$*/Cre- mice. *In situ* hybridization analyses for Col X confirm that the growth plate phenotype is secondary to an expansion of the hypertrophic chondrocyte layer and TUNEL labeling demonstrates a decrease in hypertrophic chondrocyte apoptosis, supporting the important role of C-raf in growth plate maturation. Immunohistochemical analyses show impaired Erk1/2 phosphorylation in hypertrophic chondrocytes on day 18. The growth plate phenotype of the C-*raf$^{fl/fl}$*/Cre+ mice persists but is milder at day 35.

Hypertrophic chondrocytes isolated from C-*raf$^{fl/fl}$*/Cre+ mice exhibit impaired Erk1/2 phosphorylation in response to 3 mM sodium phosphate, but not 7 mM sodium phosphate. These studies place C-raf upstream of MEK1/2 and Erk1/2 phosphorylation in the pathway of phosphate-induced hypertrophic chondrocyte apoptosis. They also suggest that high doses of phosphate may activate alternative signaling pathways that compensate for the lack of C-raf in the postnatal growth plate.

***Disclosures: Eva Liu**, None.*

SU0084

Dullard/Ctdnep1 regulates endochondral bone formation through limiting TGF-ß signaling. Tadayoshi Hayata*[1], Yoichi Ezura[2], Makoto Asashima[3], Ryuichi Nishinakamura[4], Masaki Noda[5]. [1]Medical Reserach Institute, Tokyo Medical & Dental University, Japan, [2]Tokyo Medical & Dental University, Medical Research Insititute, Japan, [3]Research Center of Stem Cell Engineering, National Institute of Advanced Industrial Science & Technology (AIST), Japan, [4]Department of Kidney Development, Institute of Molecular Embryology & Genetics, Kumamoto University, Japan, [5]Tokyo Medical & Dental University, Japan

TGF-ß signaling plays critical roles during skeletal development and homeostasis. Although excessive TGF-ß signaling is involved in pathogenesis of connective tissue genetic disease, little is known about maintenance of TGF-ß signaling at proper level during normal skeletal development. Unexpectedly, we found that Dullard/Ctdnep1, a phosphatase that negatively regulates BMP signaling and is required for kidney maintenance after birth, controls endochondral bone formation by suppressing TGF-ß signaling. Genetic inactivation of Dullard gene in limb bud and sternum by Prx1-Cre displays impairment of growth and ossification of skeletal elements and sternum leading to postnatal lethality. Ossification of sternum was severely impaired. There was no bone marrow space in sternebra, which was occupied with hypertrophic chondrocytes. To investigate how endochondral bone formation is affected by Dullard deficiency, we performed micromass culture experiment using early limb bud mesenchymal cells. Dullard-deficient limb bud mesenchymal cells show enhanced condensation and cartilage differentiation, which resembles TGF-ß-treated cells rather than those with treated with BMP. Moreover, LY-364947, a TGF-ß receptor I inhibitor, partially restored this phenotype in a dose-dependent fashion. Immunostaining experiment showed that levels of phospho-Smad2 are increased in Dullard-deficient micromass culture, while levels of phospho-Smad1/5/8 are comparable. When cultured in mineralizing condition, Dullard-deficient cartilage nodules did not show mineralization even without treatment with TGF-ß that can suppress mineralization. Although expression of hypertrophic chondrocyte marker genes including Col10a1, CTGF, Vegfa was upregulated, expression of genes related to mineralization including Alpl was suppressed, suggesting that terminal differentiation of hypertrophic chondrocyte was impaired by Dullard deficiency. Thus, we identified Dullard as a novel suppressor of TGF-ß signaling to regulate endochondral bone formation during skeletal development.

***Disclosures: Tadayoshi Hayata**, None.*

SU0085

Endogenous BMP7 activity maintains articular cartilage integrity by modulating inflammatory and catabolic factors. Kahaer Abula*[1], Takeshi Muneta[1], Kazumasa Miyatake[1], Jun Yamada[1], Yu Matsukura[1], Makiko Inoue[1], Ichiro Sekiya[1], Daniel Graf[2], Aris Economides[3], Vicki Rosen[4], Kunikazu Tsuji[1]. [1]Tokyo Medical & Dental University, Japan, [2]University of Zurich, Switzerland, [3]Regeneron Pharmaceuticals, Inc., USA, [4]Harvard School of Dental Medicine, USA

While the chondro-inductive activities of recombinant bone morphogenetic protein 7 (BMP7) are well established, evaluation of the role of endogenous BMP7 in articular cartilage homeostasis has been hampered by perinatal lethality in BMP7 knockout mice. To overcome these problems, we employed conditional deletion of BMP7 from the embryonic limb prior to the onset of skeletogenesis to create limb skeletons lacking BMP7. We have reported that the absence of locally produced BMP7 reduced proteoglycan contents in articular cartilage in the adult mice (at 8 and 24 weeks of age) and this was not due to the defect in cartilage formation since there was no significant alteration in both articular structure and proteoglycan contents in the juvenile BMP7 knockout mice (at 4 weeks of age).

To further analyze the physiological roles of BMP7 in the maintenance of articular cartilage, we investigated the chondrocyte survival, severity of synovial inflammation, and expression of matrix-degrading enzymes, such as hyaluronidase and MMP-13, in the BMP7 knockout mice. TUNEL staining of articular cartilage revealed that BMP7 did not affect chondrocyte survival at 8 weeks of age. Histological evaluation revealed that extensive synovial hyperplasia was observed in 8-week old BMP7 knockout mice. It seemed that severe synovitis occurred in the knockout mice since significant numbers of the cells in synovial membrane were positive for F4/80, a surface marker for mice macrophages. In contrast, appearance of synovial membrane was quite similar between control and BMP7 knockout mice at 4 weeks of age. Gene expression analysis of joint tissue from BMP7 knockout mice revealed that the expression of MMP-13 but not hyaluronidase was increased at 24 weeks of age. These data suggest that BMP7 maintains articular cartilage by negatively regulating synovial inflammation and MMP expression in the adult mice.

***Disclosures: Kahaer Abula**, None.*

SU0086

Essential roles of Cdc42 during endochondralossification. Wataru Suzuki*[1], Atsushi Yamada[1], Ryo Aizawa[2], Dai Suzuki[2], Mutsuko Nakayama[2], Shu Takeda[3], Koutaro Maki[2], Matsuo Yamamoto[4], Atsu Aiba[5], Kazuyoshi Baba[2], Ryutaro Kamijo[4]. [1]Showa University School of Dentistry, Japan, [2]Showa University, Japan, [3]Keio University, Dept. of Nephrology, Endocrinology & Metabolism, Japan, [4]Showa University School of Dentistry, Japan, [5]Tokyo University, Japan

Rho GTPases are regulators of multiple cellular functions, including cytoskeletal organization, cell migration, proliferation, and apoptosis. We previously reported that Cdc42, one of a Rho GTPases, is essential for limb development and limb bud interdigital programmed cell death using limb bud mesenchyme-specific inactivated Cdc42 mice (*Cdc42$^{fl/fl}$; Prx1-Cre*) (Aizawa R. *et al.* 2012 ASBMR Annual Meeting; Aizawa R. *et al. Mech. Dev.* 129; 38-50, 2012). In the present study, to investigate the physiological functions of Cdc42 during cartilage development, we generated chondrocyte-specific inactivated Cdc42 mutant mice (*Cdc42$^{fl/fl}$*; *Col2-Cre*), since conventional *Cdc42* null-embryos (*Cdc42$^{-/-}$*) die before embryonic day 7.5. The gross morphology of mutant neonates showed shorter limbs and body as compared to the control mice (*Cdc42$^{fl/fl}$*). Skeletal preparations stained with alcian blue and alizarin red also revealed that the body and long bone length of the mutants were shorter. Furthermore, severe defects were found in growth plate chondrocytes of the femur sections of mutant mice, characterized by a reduced height of proliferating zone, wider hypertrophic zone, and loss of columnar organization in proliferating chondrocytes. We speculated that this growth plate disorganization in the mutant mice was caused by abnormal differentiation of chondrocytes. *In situ* hybridization analyses were performed to investigate the expressions of cartilage differentiation marker genes, such as *type II collagen*, *type X collagen* and *Matrix metalloproteinase 13*, in growth plates of femur sections. The expression levels of those marker genes in mutant mice were decreased as compared to the control mice. Finally, Villanueva bone staining performed to detect mineralization of trabecular bones in femur sections showed it is decreased in mutants as compared to control mice, whereas osteoid volume was increased. Together, these results suggested that chondrocyte proliferation and differentiation in growth plates of the present mutant mice were not normally organized, which contributed to abnormal bone formation. We concluded that Cdc42 is essential for cartilage development during endochondral ossification.

***Disclosures: Wataru Suzuki**, None.*

SU0087

Estrogen Via Estrogen Recptor Beta Inhibits Growth Of The Mandibular Condylar Cartilage. Sunil Wadhwa*[1], Manshan Xu[2], Jing Chen[1], Yoskue Kamiya[1]. [1]Columbia University, USA, [2]University of Connecticut Health Center, USA

Objective- Approximately 10 % of the United State population has suffered from temporomandibular joint disorders (TMD). 70% of the patients who present for TMD treatment are women of childbearing ages (16-35 years of age), suggesting that estrogen plays a role in TMD. However, the biological mechanism is largely unknown. It has been previously shown that ovariectomized female Willdtype (WT) mice have increased thickness and number of cells in their mandibular condylar cartilage compared to sham operated controls. In this study, we wanted to examine the role of estrogen receptor beta (ER Beta) in mediating the response.

Material and Methods- 21 day-old female WT and ER Beta Knock Out (KO) were divided into 3 groups- 1) Sham, 2) ovariectomy + vehicle and 3) ovariectomy + estrogen (0.01 mg/60 days), with an n=6-8 for each of the groups. The mice were sacrificed when they were 49 days of age. Histomorphometry of the mandibular condyle was performed. Measurements included cartilage thickness and cell counts for

the total mandibular condylar cartilage and for each of its 4 zones (articular, polymorphic, flattened and hypertrophic)

Results- *Intragroup*-We found that ovariectomy in female WT mice caused a significant increase in cell counts and thickness for the whole mandibular condylar cartilage and in the articular, polymorphic and flattened zone compared to sham operated WT mice. Further, this effect was reversed by exogenous estrogen treatment. In contrast, ovariectomy in female ER beta KO mice caused only a significant increase in cell counts and thickness in the hypertrophic zone compared to sham operated ER Beta KO controls. *Intergroup*- There was a significant increase in mandibular condylar cartilage thickness between Ovariectomized WT, Sham operated ER beta KO and Ovariectomized ER beta KO compared to sham operated WT controls and ovariectomized WT mice treated with estrogen supplementation.

Conclusion-The increase in mandibular condylar cartilage thickness by ovariectomy is mainly due to decreased estrogen - estrogen receptor beta signaling.

***Disclosures: Sunil Wadhwa**, None.*

SU0088

Expression of PPARα, β, γ, and H- and L-PGDS During Osteoarthritis in the Spontaneous Hartley Guinea Pig and the Experimental Dog Models. Sarah Salwa Nebbaki*, Fatim Ezzahra El Mansouri, Hassan Fahmi. Osteoarthritis Research Unit, Research Center- Hospital Center of Montreal University, Canada

Purpose: To investigate the expression of peroxisome proliferator-activated receptor (PPAR) α, β, γ, and hematopoietic and lipocaline-type prostaglandin D synthase (H- and L-PGDS) over the course of osteoarthritis (OA) in the spontaneous Hartely guinea pig and the anterior cruciate ligament transection dog models.

Methods: Guinea pigs were sacrificed at 2 (control group), 4, 8, and 12 (n = 5 per group) months of age. Non-operated (control) and operated dogs were sacrified at 4, 8 and 12 weeks post-surgery. Cartilage was evaluated histologically using the Osteoarthritis Research Society International (OARSI) guidelines. The expression of PPARα, β, γ, and H- and L-PGDS were evaluated by real-time PCR and immunohistochemistry. The non-parametric Spearman test was used for correlation analysis.

Results: PPARα, β and γ were detected in medial tibial plateau from control animals in both the spontaneous and surgical models. The levels of PPARα and β did not change over the course of OA, whereas PPARγ levels decreased during the progression of the disease. We also showed that the expression of H-PGDS remained unchanged, whereas that of L-PGDS increased over the course of OA. PPARγ levels correlated negatively, whereas L-PGDS levels correlated positively, with the histological score of OA.

Conclusion: The level of PPARγ decreased, whereas that of L-PGDS increased during the progression of OA. These data suggest that reduced expression of PPARγ may contribute to the pathogenesis of OA, whereas enhanced expression of L-PGDS may be part of a reparative process.

***Disclosures: Sarah Salwa Nebbaki**, None.*

SU0089

H3K9 Demethylation by LSD1 Contributes to IL-1-Induced mPGES-1 Expression in OA Chondrocytes. Fatima Ezzahra El Mansouri*[1], Hassan Fahmi[2]. [1]Research Center-CHUM, Canada, [2]Osteoarthritis research Unit, Research Center- Hospital Center of Montreal University, Canada

Introduction: Microsomal prostaglandin E synthase-1 catalyzes the terminal step in the biosynthesis of PGE_2, which plays a critical role in the pathophysiology of osteoarthritis.

Purpose: To investigate the role of histone H3 (H3K9) methylation in interleukin-1b (IL-1)-induced microsomal prostaglandin E synthase-1 (mPGES-1) expression in human osteoarthritic (OA) chondrocytes.

Methods: Chondrocytes were stimulated with IL-1 and the expression of mPGES-1mRNA was analyzed using real-time reverse transcriptase-polymerase chain reaction. H3K9 methylation and the recruitment of the histone demethylase LSD1 to the mPGES-1 promoter were evaluated using chromatin immunoprecipitation assays. The role of LSD1 was further evaluated using the the amino oxidase inhibitor tranylcypromine (a potent inhibitor of LSD1 activity).

Results: Treatment with IL-1 induced mPGES-1 expression in a time dependent manner. The induction of mPGES-1 expression by IL-1 was associated with H3K9 demethylation at the mPGES-1 promoter. These changes were concomitant with the recruitment of the histone demethylase LSD1. Treatment with tranylcypromine inhibited IL-1-induced H3K9 demethylation as well as IL-1-induced mPGES-1 expression.

Conclusion: These results indicate that H3K9 demethylation by LSD1 contributes to IL-1-induced mPGES-1 expression and suggest that this pathway could be a potential target for pharmacological intervention in the treatment of OA and possibly other arthritic diseases.

***Disclosures: Fatima Ezzahra El Mansouri**, None.*

SU0090

Hdac3 Promotes Chondrocyte Proliferation and β-Catenin Stability. Elizabeth Bradley*, Lomeli R. Carpio, Jennifer Westendorf. Mayo Clinic, USA

Histone deacetylases (Hdacs) modify histones and other proteins posttranslationally to influence gene expression and other cellular processes. We recently reported that conditional deletion of Hdac3 in osterix-expressing osteo-chondroprogenitor cells disrupts the maturation of growth plate chondrocytes and causes severe osteopenia and decreased bone length. Hdac3-deficient chondrocytes are smaller, have decreased expression of matrix genes and Vegf, and secrete less extracellular matrix. The decrease in matrix production is due to increased expression of the protein phosphatase Phlpp1, which dephosphorylates and inactivates the intracellular kinase, Akt. Here we report that β-catenin levels are also repressed by Hdac3 deficiency, as well as by Hdac inhibitors. Since β-catenin promotes chondrocyte division, we measured chondrocyte proliferation in Hdac3-deficient animals. Conditional deletion of Hdac3 decreased the number of proliferating, Ki67-positive chondrocytes in newborn mice. Wnt3a, an activator of β-catenin, did not alleviate the effects of Hdac3-deficiency on matrix production, suggesting that the effects of Hdac3 deficiency are due to defects in downstream signaling. Gsk3β, a kinase that triggers β-catenin degradation and is subject to negative regulation by Akt, is more active in Hdac3-deficient and Hdac-inhibitor treated cells. Inhibiting Gsk3β activity with lithium chloride partially rescued β-catenin levels, matrix deposition, and expression of Vegf. Constitutively active Akt also partially restored matrix production, Gsk3β inactivation and β-catenin levels caused by Hdac inhibition. However, proteasome inhibition completely restored β-catenin levels. Thus, Hdac3-deficiency reduces chondrocyte proliferation by promoting β-catenin phosphorylation and ubiquitination. These data demonstrate that Hdac3 represses both Gsk3β-dependent and -independent mechanisms to control β-catenin levels in chondrocytes.

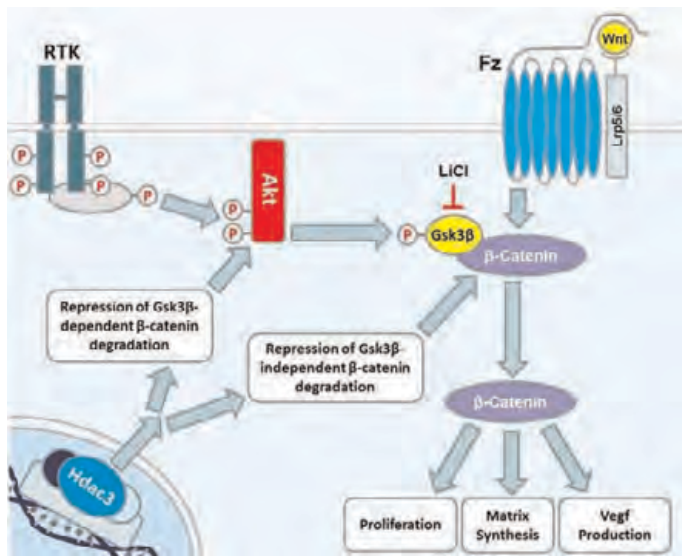

Figure

***Disclosures: Elizabeth Bradley**, None.*

SU0091

Hif-2α inhibits chondrocyte differentiation through Runx2 degradation. Xiangguo Che*[1], Na-Rae Park[1], Gyoung-Ho Cho[1], Min-Su Han[1], Kyung-Eun Lim[1], Eui Kyun Park[1], Seungwoo Han[2], Youn-Kwan Jung[2], Gun-Woo Kim[2], Jae-Hwan Jeong[3], Je-Yong Choi[3]. [1]Kyungpook National University, South Korea, [2]Daegu Fatima Hospital, South Korea, [3]Kyungpook National University, School of Medicine, South Korea

Skeletogenesis is controlled by the cooperative activity of transcription factors. Runx2 is a critical regulator for both osteogenesis and chondrogenesis. Hypoxia inducible factor-2α (Hif-2α) has been known as an upstream regulator of Runx2 in osteoblasts. However, Hif-2α regulation of Runx2 in chondrocytes has not been determined. We found that forced expression of Hif-2α degraded Runx2 with no change of Runx2 mRNA expression in chondrocytes. Hif-2α-mediated Runx2 degradation was dependent on polyubiquitination-proteosome pathway. Interestingly, Hif-2α-mediated Runx2 degradation was blocked by overexpression of Cbfβ, suggesting the protective role of Cbfβ in Runx2 degradation. With respect to the effects of Hif-2α on Cbfβ function, Hif-2α inhibited nuclear localization of Cbfβ while its expression was not changed in chondrocytes. Diminished nuclear localization of Cbfβ by Hif-2α was due partly to the upregulation of Hdac4. Indeed, Hif-2α increased Hdac4 expression, and Hif-2α shRNA decreased Hdac4 expression in chondrocytes. Overexpression of Hdac4 decreased Runx2 and Runx2/Cbfβ complex formation in

chondrocytes. Both knockdown of Hif-2α in chondrocytes and micromass culture of mesenchymal cells derived from Hif-2α heterozygous mice accelerated chondrocyte differentiation. Collectively, these findings indicate that Hif-2α accelerates Runx2 degradation through upregulation of Hdac4, which inhibits chondrocyte differentiation.

***Disclosures: Xiangguo Che**, None.*

SU0092

NELL-1 Exerts Stage Specific Chondrogenic Effects During Chondrogenesis. Chenshuang Li*[1], Jie Jiang[1], Varsha Gupta[1], Michelle Ruano[1], Steven Shen[1], Chelsea Fan[1], Xinli Zhang[1], Chia Soo[1], Yanheng Zhou[2], Kang Ting[1]. [1]University of California, Los Angeles, USA, [2]Peking University, School & Hospital of Stomatology, China

Chondrogenesis is a complex process that leads to the establishment of cartilage and bone. Recently, our lab and others have shown NELL-1, a secreted growth factor, plays a significant role in this process. We found NELL-1 to be normally expressed in resting chondrocytes in the developing limb (P1) and in adult articular cartilage. Previous reports have shown Nell-1 deficiency results in abnormal skeletal development. Here we show that lack of Nell-1 results in the reduction of cartilaginous matrix deposition in both the vertebral body and the rib cage. In addition, we observed dis-regulation of the hypertrophic region in the vertebra and developing limbs. To further examine the role of NELL-1 during chondrogenesis we tested its chondrogenic effect on embryonic mesenchyme cell line, C3H10T1/2, as well as primary murine limb bud mesenchymal stem cells (E11.5). C3H10T1/2 cells were seeded in high density micromass culture. NELL-1 alone suppressed chondrogenic differentiation while combination of NELL-1 and BMP-2 enhanced the chondrogenic effect of BMP2 treatment after 6 days. Primary embryonic mesenchymal progenitor cells underwent chondrogenesis in pellet culture. NELL-1 treatment suppressed the expression of several chondrogenic differentiation markers including Sox9, Col2a1 and Agg. By Day 21, extensive cellular hypertrophy was seen histologically and a significant increase in hypertrophic markers was evident through qPCR. NELL-1 treated groups showed significant suppression of both hypertrophic (Adamts4, Mmp13, Col10, Ihh) and calcification markers (Alp, Ocn). Unlike Day 7, NELL-1 treatment also resulted in the up-regulation of anabolic cartilage markers (Col2a1, Agg) at Day 21.Our data demonstrates that NELL-1 plays an important role in skeletal development and chondrogenesis. We show here that NELL-1 exerts stage specific chondrogenic effect during chondrogenesis. It inhibits initial chondrogenic differentiation of progenitor cells, but promotes cartilage matrix deposition and inhibits hypertrophy and calcification in differentiated chondrocytes.

***Disclosures: Chenshuang Li**, None.*

SU0093

Neutral Sphingomyelinase 2 Is Increased During BMP-induced Differentiation of ATDC5 Chondrocytes to Suppress the Maturation as a Negative Feedback Mechanism. Shingo Maeda*[1], Hironori Kakoi[2], Kanehiro Matsuyama[2], Katsuyuki Imamura[2], Ichiro Kawamura[2], Naohiro Shinohara[2], Masahiro Yokouchi[2], Yasuhiro Ishidou[2], Setsuro Komiya[2]. [1]Graduate School of Medical & Dental Sciences, Kagoshima University, Japan, [2]Department of Orthopaedic Surgery, Graduate School of Medical & Dental Sciences, Kagoshima University, Japan

Neutral sphingomyelinase 2 (nSMase2) is encoded by Sphingomyelin phosphodiesterase 3 gene (*Smpd3*). nSMase2 generates a lipid second messenger ceramide from a cell membrane component sphingomyelin. *Smpd3* knockout mice, or mice with a chemically induced loss-of-function genetic mutation called *fragilias ossium* (*fro*), show adult bone loss accompanied by impaired bone matrix mineralization. Interestingly, these mice displayed chondrodysplasia with increased chondrocyte maturation and decreased apoptosis of hypertrophic chondrocytes in developing bone growth plates. In fibroblasts, *Smpd3*/nSMase2-ceramide axis was shown to block Akt signaling and subsequent expression of hyaluronan synthase 2 (*Has2*), which enzyme is known to be crucial for hyaluronan synthesis in chondrocytes. However, the cell-autonomous roles of *Smpd3*/nSMase2 in chondrocytes remain largely unclear. Here, in ATDC5 chondrocytes, *Smpd3* was gradually up-regulated upon BMP-2 treatment. siRNA-mediated loss of *Smpd3*, or application of nSMase inhibitor GW4869, enhanced the expression of BMP-2-induced *Col2a1*, whereas overexpression of *Smpd3* by adenovirus, or addition of membrane permeable C2-ceramide, suppressed it. Knockdown of *Smpd3* specifically enhanced the phosphorylation of Akt and down stream ribosomal protein S6, assessed by examinations of receptor tyrosine kinase antibody arrays and immunoblotting. Expression of *Has2* was suppressed or elevated by gain or loss of function of nSMase2, respectively. By immunofluorescence of E17.5 mouse humerus growth plate, nSMase2 protein was detected not only in bone matrix, but also in maturating proliferating chondrocytes, prehypertrophic and hypertrophic chondrocytes. In contrast, Has2, as well as hyaluronan-binding protein (HABP), was detected in proliferating and prehypertrophic chondrocytes, but excluded from hypertrophic chondrocytes. Importantly, siSmpd3-mediated up-regulation of *Col2a1* and *Has2* in ATDC5 cells was cancelled by application of inhibitors for PI3K, Akt, or mTOR. Finally, by TUNEL staining, we found that knockdown of *Smpd3* decreased the rate of apoptosis in BMP-induced maturating ATDC5 chondrocytes. In conclusion, Smpd3/nSMase2-ceramide pathway is activated during BMP-induced chondrocyte maturation to inhibit PI3K-Akt-mTOR pathway, thereby keeping chondrocyte in immature state producing hyaluronate, as a negative feedback. In addition, nSMase2-produced ceramide seemed to prevent ATDC5 chondorcytes from apoptosis.

***Disclosures: Shingo Maeda**, None.*

SU0094

The distinct role of the infrapatellar fat pad in a murine high-fat diet-induced osteoarthritis model. Munetaka Iwata*[1], Hiroki Ochi[2], Yasushi Hara[3], Masahiro Tagawa[3], Daisuke Koga[4], Atsushi Okawa[4], Yoshinori Asou[5]. [1]Nippon Veterinary & Life Science University, Japan, [2]Laboratory of Veterinary Microbiology, Nippon Veterinary & Life Science University, Japan, [3]Division of Veterinary Surgery, Department of Veterinary Science, Faculty of Veterinary Medicine, Nippon Veterinary & Life Science University, Japan, [4]Department of Orthopaedic Surgery, Tokyo Medical & Dental University, Japan, [5]Tokyo Medical & Dental University, Japan

Obesity and high body mass index are associated with a higher incidence of osteoarthritis (OA). As the infrapatellar fat pad (IPFP) from OA patients contains inflammatory cytokines, the IPFP could play an important role in the initiation and progression of knee-OA. However, the precise roles of the IPFP at the initiation of OA have not been elucidated. The aim of this study is to investigate the involvement of the IPFP in the sub-acute effect of a high fat diet (HFD) on the development of knee-OA. C57BL/6J male mice were fed either a HFD or a normal diet beginning at seven weeks of age. As excess weight caused by obesity introduces increased weight bearing on the knee joints, a tail suspension model (HFD+TS) was employed for HFD mice to clarify the involvement of mechanical stress in the histological alteration in the knee joints of the HFD mice. Tissue sections were evaluated with immunohistological analysis. The IPFP tissue was excised using a surgical microscope and microsurgical technique at sacrifice, and mRNA expression profiles were compared using real-time RT-PCR analysis. As results, osteoarthritic changes were initiated in the HFD and the HFD+TS group after 8 weeks of diet. Increased synovial cell number and angiogenesis at the anterior edge of the tibial plateau were exhibited prior to osteophyte formation. Quantitative histological analysis indicated that osteophyte volume was significantly increased both in the HFD and the HFD+TS group after 8 weeks, along with an increase in the IPFP volume, the size of individual adipocytes and the number of vessels in the IPFP. Histomorphometrical analysis revealed osteophyte area was significantly associated with IPFP area, individual adipocyte area and vascular area. Real-time RT-PCR analysis demonstrated elevated mRNA expression of inflammatory cytokines, growth factors, and adipokines, such as Nampt, Leptin, Chemerin and Lipocalin2, in the IPFP after eight weeks of the HFD regardless of TS. These findings were in parallel with increased expression of the CD68 in the IPFP. Moreover, expression levels of the adipokines were significantly correlated with the expression of TNF-α, VEGF and TGF-β. TUNEL-positive cells were abundantly observed in the superficial layer of the articular cartilage and at the site of osteophyte formation in the HFD and the HFD+TS mice. These observations suggest the IPFP plays a pivotal role in the formation of osteophytes and functions as a secretory organ in response to a HFD.

***Disclosures: Munetaka Iwata**, None.*

SU0095

A ChIP-seq Defined Genome-wide Map of MEF2C Binding Reveals Pathways Associated with Bone Disease. Matthew Johnson*[1], Sandra Deliard[1], Fengchang Zhu[2], Andrew Wells[1], Kurt Hankenson[2], Struan Grant[1]. [1]Children's Hospital of Philadelphia, USA, [2]University of Pennsylvania, USA

Genome-wide association studies (GWAS) have demonstrated that genetic variation at the *MEF2C* (MADS box transcription enhancer factor 2, polypeptide C) locus is robustly associated with bone mineral density (BMD), primarily at the femoral neck (Estrada *et al*, Nat Genet 2012). MEF2C is a transcription factor known to operate via the Wnt signaling pathway. Our hypothesis is that MEF2C regulates the expression of a set of molecular pathways critical to skeletal function. Drawing on our laboratory and bioinformatic experience with ChIP-seq with another GWAS-implicated member of the Wnt signaling family, namely TCF7L2 [the most strongly associated locus for type 2 diabetes reported to date (Grant *et al*, Nat Genet 2006)], we analyzed ChIP-seq data for MEF2C available via the ENCODE project to similarly gain insight in to its global genomic binding pattern.

We aligned the ChIP-seq data generated for GM12878 (an established lymphoblastoid cell line). A total of 17,611 binding sites were observed using HOMER set at a false discovery rate of 1%, corresponding to 8,118 known genes.

We then performed a pathway analysis of the gene list using Ingenuity. Interestingly, the category entitled 'Cell Morphology, Skeletal & Muscular Disorders, Skeletal & Muscular System Development and Function' was ranked the most significantly enriched for 'Associated Network Functions'. Furthermore, when considering 'Ingenuity Canonical Pathways', ''RANK Signaling in Osteoclasts'' was among the top 10 most significant categories (P=9.3x10^{-10}; corrected P=6.85x10^{-8}), while ''Increased activation of Alkaline Phosphatase'' was significantly enriched in 'Top Tox Functions'. We also observed that MEF2C binding sites were significantly enriched near both inflammation and cardiovascular associated genes identified from GWAS; indeed, a similar enrichment for inflammation genes has been reported

previously using a similar approach for the vitamin D receptor, an established key regulator of bone turnover (Ramagopalan *et al*, Genome Res 2010).

These results represent the first ever reported ChIP-seq derived genome wide map of MEF2C binding. Our analyses point to known connective tissue and skeletal processes but also provide novel insights in to networks involved in skeletal regulation. The fact that specific GWAS categories are significantly enriched among genes bound by MEF2C not only speaks to its known cardiac role but also points to a possible role of inflammation through which it impacts BMD.

***Disclosures: Matthew Johnson**, None.*

SU0096

Altered collagen pro-peptide endopeptidases, bone morphogenetic protein-1 and a disintegrin and metalloproteinase with thrombospondin motifs-2, in thrombospondin-2 deficient osteoblasts. Eugene Manley, Jr.*, Andrea Alford. University of Michigan, USA

Our recent data suggest that thrombospondin-2 (TSP2) deficiency is associated with decreased collagen levels in the extracellular matrix (ECM) assembled by mesenchymal stem cells (MSC) undergoing osteoblastic differentiation in culture. Western blot analysis implicates deficient type I collagen pro-peptide removal. Here, our objective was to investigate factors associated with collagen processing and matrix stabilization in the context of TSP-2 deficiency.

Bone marrow-derived MSC were obtained from 6-week old male wild-type and TSP-2 null C57/B6 mice. Adherent cells were passaged and cultured in osteoblastic medium. After 4 days, RNA was harvested and reverse transcribed to cDNA, which was then used in quantitative RT-PCR reactions. Relative expression values, normalized to β-actin, were determined using the ΔΔCt method. Gene expression data are from MSC pooled from 2 animals per genotype and are presented as mean fold change. In two additional cell harvests, conditioned medium was collected for ELISA after day 4 and day 10. Protein data are mean and SD from two independent cell harvests totaling 6-9 wells per genotype.

At day 4, relative expression of the C-terminal pro-peptidase, bone morphogenic protein -1 (BMP-1) was decreased 1.75 fold in TSP2-null vs. wild-type cells. Conversely, at this time point, total BMP-1 protein levels were significantly increased in TSP2-null MSC-conditioned medium (153.9 $\pm$ 17.3 vs. 100.6 $\pm$ 30.5 ng/mL in TSP2-null and wild-type cultures, respectively, $p<0.001$). BMP-1 protein levels were similar after 10 days (147 $\pm$ 23.3 vs. 149.4 $\pm$ 12.3 ng/mL in TSP2-null and wild-type cultures, respectively). Compared to wild-type cells, expression of the N-terminal pro-peptidase, ADAMTS-2 was decreased 2.27 fold in TSP2-null cultures. We observed no differences in gene expression levels for procollagen C-endopeptidase enhancer 1 (PCPE1). We were unable to detect PCPE2. Lysyl oxidase (LOX), as well as lysyl oxidase-like 1-4 (LOXL1-4) catalyze intermolecular lysine-lysine bonds in the collagen ECM and these genes were not affected by TSP2-deficiency. Our preliminary data suggest that alterations in expression, bioavailability at the cell surface or activity of collagen pro-peptide endopeptidases may be responsible for impaired collagen matrix formation observed in TSP2-null osteoblasts.

***Disclosures: Eugene Manley, Jr.**, None.*

SU0097

Differentiation Potential and Molecular Characterization of Mesenchymal Stem Cells During Long-Term Monolayer Culture. Ali Mirsaidi[1], Reto Luginbuehl[2], Willy Hofstetter[3], Rainer Egli*[2]. [1]Bone & Stem Cell Research Group, CABMM, University of Zürich, Switzerland, [2]RMS Foundation, Switzerland, [3]University of Bern, Switzerland

Mesenchymal stem cells (MSC) are promising for regenerative approaches of musculoskeletal tissues. Due to their scarce occurrence, an *in vitro* culture expansion phase is necessary where the MSC lose their differentiation potential, which limits their clinical application. In this study we characterized the molecular changes in monolayer cultures of MSC and correlated those with the cells' differentiation potential. Human bone marrow derived MSC were obtained from a commercial supplier at passage 2 (P2) and were further expanded to P11 (= 16 population doublings (PD) from P2 - P11). Cells from all passages could be differentiated towards the adipogenic and osteogenic lineages in monolayer cultures with appropriate supplements. Chondrogenic differentiation and formation of a cartilaginous matrix in the presence of $TGF\beta_1$ was successful until P8 (= 13 PD) in micromass cultures. However, from P6 - P8 a gradual decrease was observed in levels of transcripts encoding collagen type II and aggrecan and in the staining intensity for glycosaminoglycans within the micromasses. The expression of MSC specific markers (CD44, CD105, CD166, CD271) did not change in monolayer cultures from P4 - P11, as assessed by flow cytometry. Transcript levels of 182 genes (MSC markers and molecules governing lineage specific differentiation) were measured in monolayers from P5 - P11. 48 genes were found with higher (up to 11-fold compared to P5) or lower (up to 4-fold) transcript levels with increasing passage numbers. We further selected for genes whose transcript levels are altered in parallel with the reduction of the chondrogenic potential to identify factors regulating chondrogenesis. Interestingly, whereas levels of transcripts encoding 2 TGFβ signaling inhibitors (BAMBI and BMPER) were found to be elevated (2-3-fold) in cells which lost their chondrogenic potential, no changes were observed in the transcript levels of TGFβ receptors. Thus, increased expression of these inhibitors may reduce the efficiency of exogenously added $TGF\beta_1$ to induce a signal cascade and as a consequence inhibit chondrogenic differentiation. Other genes that exhibit a change of transcript levels at least by a factor of 2 at P11 as compared to P5 and paralleling the loss of chondrogenic potential were ICAM1, PDE1A, SLC40A1, CREB3, IGFBP1 and IGF1. How the different transcript levels translate into protein levels and whether these are relevant in chondrogenesis of MSC requires further elucidation.

***Disclosures: Rainer Egli**, None.*

SU0098

Second Generation Sequencing Reveals the micro-RNA Expression Patterns in Primary Human Bone Cells treated with Parathyroid Hormone or Dexamethasone. Navya Laxman*[1], Carl-Johan Rubin[1], Hans Mallmin[2], Olle Nilsson[1], Christian Tellgren-Roth[1], Andreas Kindmark[2]. [1]uppsala University, Sweden, [2]Uppsala University Hospital, Sweden

Objective: Parathyroid hormone (PTH) has a positive effect and Dexamethasone (DEXA) has a negative effect on bone formation. In the present project, we have investigated the impact of treatment of parathyroid hormone (PTH) and dexamethasone (DEXA) on global miRNA expression in primary human bone (HOB) cells by second generation sequencing of small RNA. Micro-RNAs (miRNAs), small non-coding RNAs, identified as regulators in various biological processes, have been shown to be involved in human development and disease. By binding to complementary RNA strands, they efficiently affect mRNA levels and/or mRNA translation.

Method: HOB cells were isolated from human trabecular bone collected from donors undergoing total hip replacement, and treated with either PTH or DEXA or left untreated for 2 and 24 hours. Small RNA was isolated from these cells and cDNA synthesized using SOLiD library reagents. Second generation sequencing was performed using SOLiD4 on barcoded library constructs of small RNA 50bp plus barcode, at the Uppsala Genome Center. Sequence reads were aligned to a scaffold consisting of all known miRNA sequences, and number of sequence reads mapping uniquely to each miRNA were counted. The value used for each miRNA was the number of reads per miRNA normalized to per million total reads.

Results: A total of 207 million reads from the small RNA library constructs was obtained, and normalized absolute expression was retrieved for the 500 most abundant miRNAs. The 75 miRNAs that exhibited the highest mean expression across the four experiments per individual were taken forward for downstream analyses. Expression levels were set to percent of each samples respective untreated control, and results show a significant effect of treatment with PTH vs treatment with DEXA at 2 hours and even more pronounced at 24 hours on miRNA expression. Interestingly, several miRNAs exhibiting significant differences in expression have predicted mRNA targets involved in bone metabolism, e.g. miR-197 targeting IGF and Wnt pathway members. Also, miR-31 showed differential expression, and we have previously shown that miR-31 expression in bone cells is correlated with mRNA expression for WNT, WNT3A, b-Catenin and GSK3b.

Conclusion: miRNA absolute expression data from second generation sequencing show that PTH and DEXA affect miRNA expression in primary human bone cells, and that these miRNAs in turn are correlated to expression levels of mRNAs known to affect bone metabolism.

***Disclosures: Navya Laxman**, None.*

SU0099

Comparison of a Novel Osteogenic Oxysterol Molecule and rhBMP2 Fusion Rates in a Rabbit Posterolateral Lumbar Spine Model. Trevor Scott*[1], Kevin Phan[1], Scott Montgomery[1], Akinobuh Suzuki[1], Haijun Tian[1], Michael Daubs[1], Sotirios Tetradis[2], Elisa Atti[1], Theodore Hahn[3], Jeffrey Wang[1], Farhad Parhami[2]. [1]UCLA, USA, [2]University of California, Los Angeles, USA, [3]VA Greater Los Angeles/ UCLA Medical Center, USA

The non-union rate following lumbar spinal fusion is potentially as high as 35%. This can be a significant clinical problem. Traditionally iliac crest autograft was used as a fusion adjunct, but its use is limited by donor site morbidity and lack of available graft volume required for large fusion surgeries. Over the past 10 years recombinant human bone morphogenic protein 2 (rhBMP2) has been used as a biological adjunct to promote bony fusion. However, recently there have been increasing concerns about rhBMP2 relating to increased inflammatory response, and potential problems with bone fusion quality. The small molecule osteogenic oxysterol 133 (Oxy133) has been shown to promote excellent fusion rates in rodent lumbar spine models and offers a potential alternative to rhBMP2. The purpose of this study, a randomized control trial in an animal model, was to compare the fusion rate of rhBMP2 and Oxy133 in a posterolateral lumbar rabbit spinal fusion model.

24 male adult white New Zealand rabbits (3-3.5kg) underwent bilateral posterolateral lumbar spinal fusion at L4-L5. Rabbits were divided into 4 groups: control (A), 30 ug rhBMP2 (B), 20 ug oxy (C), and 60 ug oxy (D). A mineral collagen matrix infused with saline for control or one of the above compounds was implanted at the

fusion site. At 4 weeks fusion was evaluated by fluoroscopy. At 8 weeks the rabbits were sacrificed and fusion was evaluated radiographically and by manual palpation of excised spines. At 4 weeks fusion rates were as follows: group A 25%, group B 67.7%, group C 91.7%, group D 90.0%. At 8 weeks fusion rates by radiographic analysis were: group A 40.0%, group B 91.7%, group C 91.7%, and group D 100%. Groups C and D had a significantly higher fusion rate than group A at 4 weeks (P= 0.003 A vs. C, P=0.004 A vs. D). At 8 weeks group D had a significantly higher fusion rate than group A (P= 0.011). When the fusion masses were evaluated by manual palpation group A was 40% fused, group B was 67.7% fused, group C was 67.7% fused, and group D was 100% fused. Based on these results, in a rabbit model low dose Oxy133 appears to promote earlier fusion than rhBMP2 and our high dose oxysterol group seemed to have both earlier fusion and a greater ultimate fusion rate than rhBMP2 (100% vs. 67.7%, respectively). Given its osteogenic potency, anticipated lack of immunogenicity, and low cost of production, Oxy133 may be an excellent alternative to rhBMP2 for spinal fusion procedures.

***Disclosures: Trevor Scott**, None.*
This study received funding from: MAX BioPharma

SU0100

Dose dependent effect of low intensity pulsed ultrasound on the condylar growth during functional appliance treatment. Harmanpreet Kaur*, Hasan uludag, Douglas Dederich, Tarek El-Bialy. University of Alberta, Canada

Objective: One of the common anomalies of oro-facial region is underdeveloped lower jaw, also known as Class ll malocclusion. Underdeveloped lower jaw can compromise airway and may lead to sleep apnea. Treating malocclusions in growing patients by using functional appliance is believed to produce satisfactory improvement in esthetics and minimize the need for the surgical intervention. However, the effectiveness of these functional appliances is controversial. Previous studies have found that therapeutic ultrasound (low intensity pulsed ultrasound LIPUS)can stimulate cartilage and bone growth, but optimum LIPUS treatment to maximize lower jaw growth is not known. The objective of this study is to evaluate the synergetic effect of functional appliance combined with daily 20 min or 40 min LIPUS on the mandibular condyle growth.

Materials & Method: 54 Sprague Dawley rats were divided into 6 groups (n=9) namely; 1 conrol- no functional appliance or LIPUS application, 2 Functional Appliance group, 3 LIPUS 20 min application, 4 LIPUS 40 min application, 5 Functional Appliance + LIPUS 20 min, 6 Functional Appliance + LIPUS 40 min. The appliance was custom made for each rat and was placed on upper anterior teeth when the rats were 28 days old. LIPUS was applied for 20 min or 40 min per day for 4 weeks. After euthanasia, mandibles were dissected and were fixed in 10% formalin for the anthropometric measurements and the condyles were decalcified and processed for histological examination.

Results: Anthropometric measurements showed increase in mandible length, height and condyle length which was statistically significant in both LIPUS treated functional appliance groups ($p<0.05$). Similarly, histological studies showed increase in proliferative and hypertrophic cell counts in both LIPUS treated functional appliance groups ($p<0.05$). LIPUS treated functional appliance groups showed increase in the thickness of proliferative and hypertrophic cell layers. However, no significant difference was found between 20 min and 40 min LIPUS application in functional appliance groups.

Conclusion: LIPUS enhances the condylar growth when combined with the functional appliance. The effect of LIPUS and functional appliance on the growing condyle is expressed through the increase in anthropometric measurements (length, height of mandible and condyle length) and increase in the cell numbers. However no significant difference was found between 20 min and 40 min LIPUS appcation.

***Disclosures: Harmanpreet Kaur**, None.*

SU0101

Effects of Selective Serotonin Reuptake Inhibitor Exposure on Markers of Osteogenesis. James Cray*[1], Kameron Khaksarfard[1], Seth Weinberg[2], Mohammed Elsalanty[3], Jack Yu[1]. [1]Georgia Regents University, USA, [2]University of Pittsburgh, USA, [3]Georgia Health Science University, USA

Recently, serotonin has been shown to have an effect on the development and maintenance of bone. Selective Serotonin Reuptake Inhibitor (SSRI) drugs have been implicated in both birth defects of the craniofacial skeleton, e.g. craniosynostosis, and long term disruption of bone health, e.g. osteoporosis. Here we provide a preliminary report of the effects of exogenous SSRI exposure on cells derived from murine calvaria. Murine derived calvaria cells were exposed to the SSRI, escitalopram oxalate at critical doses for 3 or 7 days in culture. Endpoint assays were designed to determine the effects of the drug exposure on markers of osteogenesis and included, MTS proliferation, quantitative ALP activity, quantitative PCR (qPCR) for osteogenic markers (*Runx2, Alp, Ocn*), and target receptors of the drug (*Slc6a2, Slc6a3, Slc6a4*), and genome-wide arrays with qPCR confirmation of dysregulated targets. There appeared to be little effect on proliferation after drug treatment. However, exogenous exposure to SSRI appears to stimulate cells to express ALP in a dose dependent manner. *Alp* and *Ocn* were confirmed to be significantly upregulated (>2 fold) after 7 days in culture treated with SSRI. In addition, *Slc6a4*, the serotonin transporter, was the only monoamine transporter target that was significantly downregulated after treatment. The genome wide microarray identified 35 genes that were significantly dysregulated (>2 or <-2 fold change in regulation of mRNA). 17 targets were chosen due to identification in bone or craniofacial development pathways. 3 genes were confirmed as upregulated (*Msx1,Notch1, Fgf2*) and 6 genes (*Aspn, Col2a1, Fgfr2, Gdf6,Igf1, Tgfβ2*) were confirmed as downregulated after treatment. These data appear to suggest multiple influences of SSRI drugs on bone likely through its effects on serotonin. The dysregulation of *Aspn* and the *Fgf*s are likely candidates for mechanism of action in craniosynostosis, while the downregulation of *Igf1, Gdf6*, and *Tgfβ* after drug treatment make likely candidates in the cascade of events influencing osteoporosis.

***Disclosures: James Cray**, None.*

SU0102

Withdrawn

SU0103

Human Dental Pulp Cells as Sources for iPS Cell Banking. Ken-Ichi Tezuka*[1], Tomoko Kawaguchi[2], Naritaka Tamaoki[2], Kazuki Iida[2]. [1]Gifu University Graduate School of Medicine, Japan, [2]Gifu University, Japan

Human dental pulp cells (DPCs) are present in the cell population isolated from dental pulp tissues. We reported that viral introduction of four transcription factors (*OCT3/4*, *SOX2*, *KLF4*, and *c-MYC*) can reprogram DPCs into induced pluripotent stem (iPS) cells. However, we also found that establishing validated iPS cell lines from a number of patients require considerable time and cost. Human leukocyte antigen (HLA) plays a major role in rejection of tissues and cells transplanted from allogenic donors. Because of shortage of the donors, immnosuppressants are frequently used to suppress rejection; however, when the immune system function is suppressed, there is an increased susceptibility to infectious diseases and cancers.

To solve this problem, usage of HLA haplotype-homo donors has been considered in iPS cell therapy. HLA haplotype-homo donors have a couple of identical HLA gene sets. Therefore, iPS cells derived from HLA haplotype-homo donors are expected to be successfully transplanted to many patients with less possibility of rejection. We screened 171 DPC lines to find three patients having only one genotype in each of three HLA loci, A, B, DRB1. If iPS cells will be established from these three patients, they are expected to show complete match with approximately 20% of the Japanese population.DPCs are medical wastes collected from a large number of healthy donors without large ethical problems. Therefore, DPCs will be considered as one of the somatic cell sources for future iPS cell banking and regenerative medicine.

***Disclosures: Ken-Ichi Tezuka**, None.*

SU0104

IDG-SW3 osteocyte-like cell line expresses insulin receptor as well as GLUT1 and GLUT3. Donna Pacicca*[1], Tammy Brown[1], Karen Kover[1], Lynda Bonewald[2]. [1]Children's Mercy Hospital, USA, [2]University of Missouri - Kansas City, USA

As diabetes can affect bone quality and the osteocyte product sclerostin has been shown to be elevated in diabetes, we sought to determine if high or low concentrations of glucose will have an effect on osteocyte products. The IDG-SW3 cell line was used as this cell differentiates in culture from a late osteoblast to early osteocyte to late osteocyte. IDG-SW3 cells were cultured under four different glucose concentrations: low (2.5 mM), normal (10mM), high (25mM) and mannitol control for high osmolarity (glucose 10mM with mannitol 15mM). Media was changed daily and cells were harvested at 7, 14 and 21 days. Assays were performed for LDH, lactate, glucose and gene expression. PCR array was performed to evaluate for gene expression versus normal mouse tissues, and qPCR was performed on samples from the four groups. Glucose utilization and lactate production increased over time, with similar rates across. PCR demonstrated expression of insulin receptor, and glucose transport proteins 1 and 3 at levels similar to those previously reported. GLUT1 was significantly decreased in high glucose, with no significant changes in osteocalcin, E11/gp38, sclerostin and FGF23. IDG-SW3 cells demonstrate primarily glycolytic use of glucose, similar to findings using whole bone. They also express GLUT1, responsible for basal cell uptake of glucose, as well as GLUT3 similar to neurons. Hypo- and hyperglycemic conditions did not appear to have an adverse effect on osteocyte gene expression, however the osteoblast marker keratocan was elevated with high and decreased with low glucose. We also show that osteocytes express InsR which has not previously been seen in vivo in osteocytes. Our data suggest that osteocytic cells may be able to tolerate changes in glucose concentration without affecting their function in bone.

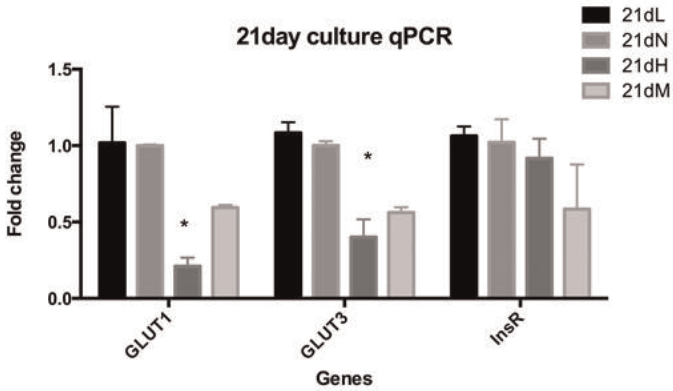

qPCR 21d metabolic

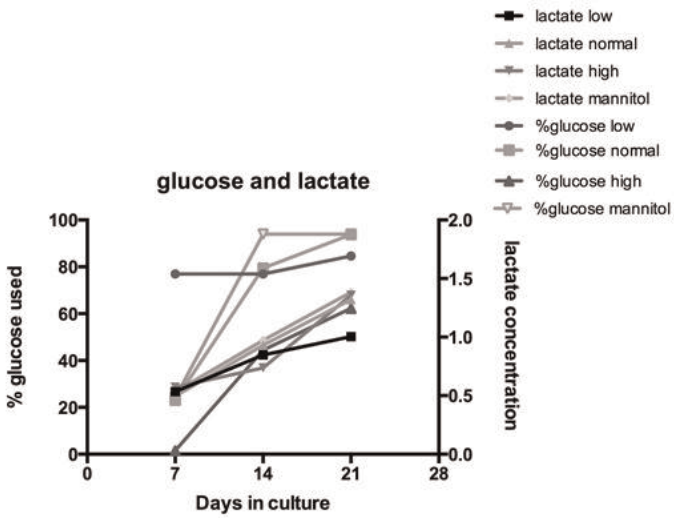

lactate vs glucose over time

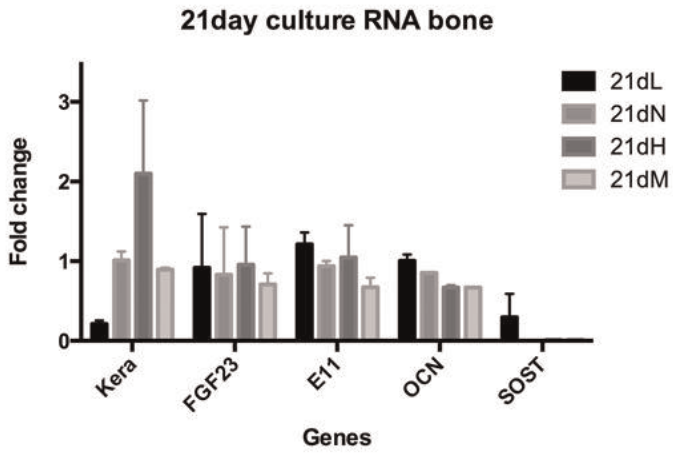

qPCR 21d bone

***Disclosures: Donna Pacicca**, None.*

SU0105

MLB13 Cells Recapitulate In Vitro Endochondral Bone Formation with Distinct Responses to Various Skeletal Growth Factors. Valerie Salazar*, Vicki Rosen. Harvard School of Dental Medicine, USA

Immortalized mouse limb bud cells from E13 embryos, or MLB13 cells, were originally used to demonstrate sequential induction of chondrocyte and osteoblast markers by bone morphogenetic protein 2 (BMP2). To understand how these clonal endochondral progenitors respond to other growth factors that regulate bone mass, we conducted a timecourse study to monitor the effects of Noggin, BMP2, TGF-β, Wnt3a, or PTH_{1-34} on osteoblast and chondrocyte lineage markers, and performed endpoint biochemical stains to identify the type of mature matrix produced. Consistent with our previous study, MLB13 cells (clone 14) respond vigorously to exogenous BMP2, exhibiting robust collagen deposition and alkaline phosphatase (ALP) activity coupled with matrix calcification and cartilage formation. Osteogenic markers such as *Alp1*, *Osx*, *Ocn*, and *Opn* are induced at the mRNA level, in addition to the chondrocyte markers *Ihh* and *Col10*. Noggin has reciprocal effects, with dramatically diminished collagen deposition and ALP activity, and undetectable amounts of mineralized or cartilage matrix, thus revealing that endogenously produced BMPs drive basal levels of osteochondral activity in these cells. Wnt3a mildly increases collagen production but has little impact on expression of osteoblast markers, ALP activity or matrix calcification. Consistent however with reports that Wnts antagonize chondrogenesis, MLB13s downregulate *Ihh* and *Col10* mRNAs and do not deposit cartilage in the presence of Wnt3a. PTH_{1-34} has similar effects, resulting in a strong suppression chondrogenesis without a compensatory increase in osteoblast formation. In fact, ALP activity was mildly diminished by PTH_{1-34} relative to control cultures. TGF-β has a striking inhibitory effect, completely blocking ALP activity, matrix calcification, and cartilage deposition, in correlation with strong downregulation of *Osx*, *Alp1*, *Ocn*, and *Ihh*. TGF-β has minimal effects on *Col1α1*, *Col2* and *Col10*. Meanwhile, *Col2* and *Col10*, but not *Col1α1*, are reciprocally regulated by Noggin and BMP2. Interestingly, total collagen deposition is not predicted by collagen mRNA expression alone, suggesting additional mechanisms contribute to collagen biosynthesis. Furthermore, collagen deposition plus ALP activity does not predict production of mineralized or cartilage matrix. In summary, our study presents MLB13 cells as a robust *in vitro* model of osteochondrogenesis, with particular suitabililty for studies on BMP/TGF-β signaling.

***Disclosures: Valerie Salazar**, None.*

SU0106

Nutritionally Induced Delayed Union Model of Femur Fractures In Mice. Anthony De Giacomo*[1], Joshua Teich[1], Marie Demay[2], Elise Morgan[3], Louis Gerstenfeld[1], Thomas Einhorn[4]. [1]Boston University School of Medicine, USA, [2]Massachusetts General Hospital & Harvard Medical School, USA, [3]Boston University, USA, [4]Boston Medical Center, USA

Introduction: Fracture healing, a complex biologic process, requires the synchronization of several cell types to regain mechanical competence and allow weight bearing. Failure in coordinating, or completing, this biologic process results in a non-union of the fractured bone. Inorganic phosphate, an essential mineral for maintaining healthy bones, is believed to be a critical component for bone healing. The goal of this study was to generate a nutritionally induced murine non-union model of fracture healing.

Methods: A standard diet and one deficient in phosphate, was administered to C57/B6 mice two days prior to closed fracture of the femur. Mice were maintained on the phosphate deficient diet for 5, 10, 15, and 20 days prior to being returned to the normal diet. RNA was isolated from the callus at various time points (3-35days). Plain film and MicroCT radiography was used to assess the progression of fracture healing. The biologic process of bone healing was assessed by histology and qRT-PCR was used to evaluate mRNA expression for multiple marker genes of chondrogenesis (Aggrecan, Collagen 2a1, Collagen10a1) and osteogenesis (Osterix, RUNX2, ID1).

Results: Delayed bone healing was induced by a phosphate restricted diet. The phosphate restricted diet led to a time dependent impairment of healing where mice maintained on longer periods of phosphate restriction (i.e. 15 & 20 days) showed a more prolonged period of impaired healing. Phosphate restriction did not inhibit chondrogenesis, but rather led to a delayed and enhanced expression of chondrogenic markers, indicating that the callus remained primarily cartilage. Conversely, compared to controls, osteogenic gene expression was blunted and a progressive delay in initiation of osteogenic gene expression was observed with progressively longer periods of dietary phosphate restriction. When phosphate was re-introduced to the diet, the process of fracture healing reinitiated; however, progressively longer periods of time were required to achieve union based on the initial period of phosphate restriction.

Discussion: Phosphate restriction demonstrated an inhibitory affect on bone healing by impairing osteogenesis, but not necessarily chondrogenesis. The data suggest that dietary restriction of phosphate can be used as a model of nutritionally induced delayed union of femur fracture, while allowing identification of, the molecular events that promote cartilage mineralization and initiation of osteogenesis.

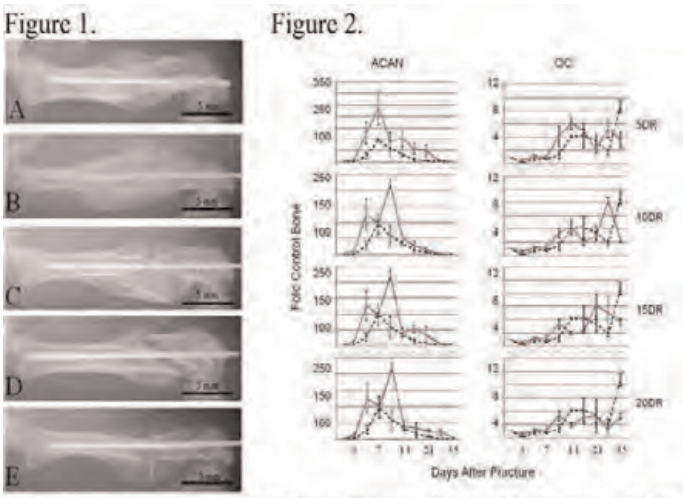

Figure 1. Day 18 Post Fracture Radiographs. A: Control B: 5 Day Diet Restriction C: 10 Day Diet Restriction D: 15 Day Diet Restriction E: 20 Day Diet Restriction

Figure 2. Gene expression data of a selected gene for chondrogenesis (ACAN) and osteogenesis (OC). Solid red line represents the diet restrictive groups and dotted black line is the control group

Figure 1 and 2

Disclosures: ***Anthony De Giacomo****, None.*
This study received funding from: National Institutes of Health (NIH)

SU0107

PLGA/TCP Scaffolds Incorporating Phytoestrogenic Molecule Icaritin Developed for Bone Defect Repair. Shihui Chen*[1], Lizhen Zheng[2], Xinhui Xie[2], Xinluan Wang[2], Ling Qin[3]. [1]Prince of Wales Hospital, Hong Kong, [2]The Chinese University of Hong Kong, Hong Kong, [3]Chinese University of Hong Kong, Hong Kong

Introduction: The concept of bone loss therapy focuses on the conductive scaffold for tissue regeneration. In this project, growth factor BMP2 or phytoestrogenic small molecule icaritin (ICT) was combined respectively with PLGA/TCP scaffolds served as a delivery system for bone regeneration, namely PLGA/TCP/icaritin with three different doses and PLGA/TCP/BMP2 by low temperature pro-typing technology. The hypothesis is that the technology can maintain the original bioactivity of BMP2 and icaritin, which will lead to ready to use production for efficient orthopaedics application.

Methods: Fabricated scaffolds: P/T (A), P/T/LICT (B), P/T/MICT (C), P/T/HICT (D), P/T/BMP2 (E). Our previous *in vitro* results demonstrated the increasing ALP activity and calcium deposition of BMSCs onto scaffolds of group B, C, D compared to group A and E, we further detected the mRNA expression of osteogenic genes. We established an ulnar bone defect model in rabbits and measured X-ray, Xtreme CT and histology at weeks 2, 4 and 8. One-way ANOVA was used for statistical analysis.

Results: The scaffolds were fabricated with $78 \pm 3.63\%$ porosity and 300-450 μm pore diameter (Figure 1). mRNA expression of Collagen type I and Osteopontin were up-regulated in P/T/ICT compared with P/T and P/T/BMP2 scaffolds. At weeks 2, 4 and 8, the radiographic results showed that there were more bone regeneration in the pores of scaffolds in group B, C, D compared with group A and E (Figure 2). CT analysis showed the better bone formation in group B, C, D in comparison with those in group A and E (Figure 3). H&E staining in decalcified histology of the rabbit ulna segmental bone defect at week 2, 4 and 8 post surgery also indicated the same results.

Discussion: *In vitro* study, the results demonstrated that P/T/ICT could enhance significantly osteogenic differentiation of cultured BMSCs, as ICT was able to keep its normal activity during fabrication procedure. However, P/T/BMP2 did not show initially osteogenic effects, which might be explained by that BMP-2 exerted unstable bioactivity during preparation of scaffolds, which however did not occur using immersion protocol. In bone defect model, P/T/ICT treatment showed enhanced bone regeneration than P/T and P/T/BMP2 treatments. However, the osteogenesis mechanism of composite scaffolds still need to be deteced in the next step. P/T/ICT as innovative composite scaffolds possess osteogenic differentiation potential *in vitro* or *in vivo* data.

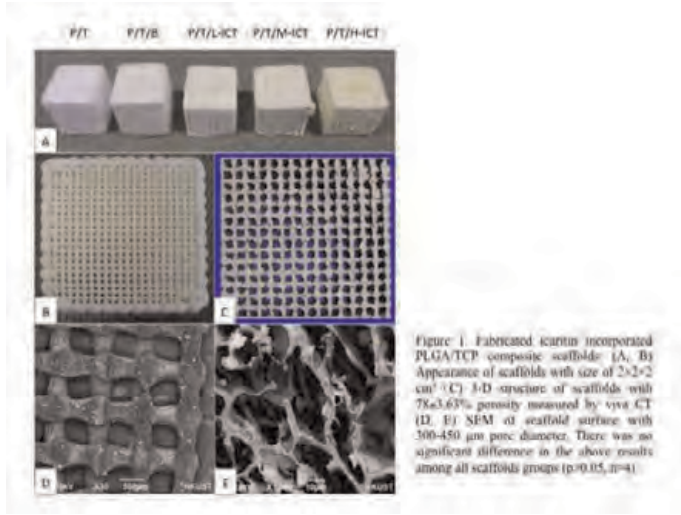

Figure 1. Fabricated icaritin incorporated PLGA/TCP composite scaffolds (A, B) Appearance of scaffolds with size of 2×2×2 cm^3 (C) 3-D structure of scaffolds with 78±3.63% porosity measured by vivo CT (D, E) SEM of scaffold surface with 300-450 μm pore diameter. There was no significant difference in the above results among all scaffolds groups (p>0.05, n=4)

Figure 1

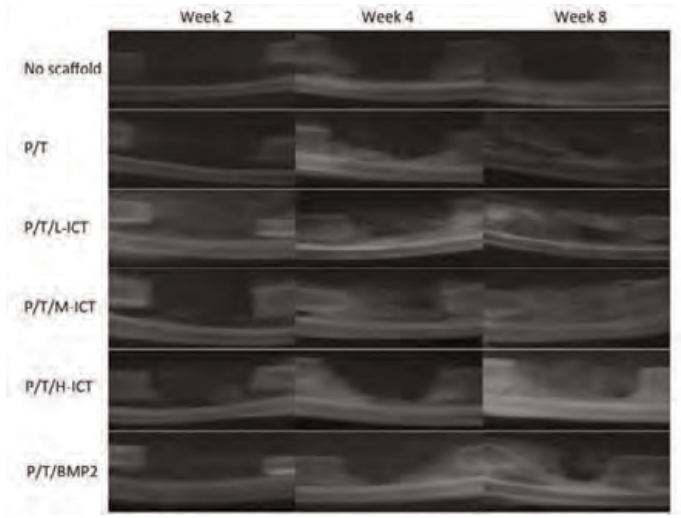

Figure 2a

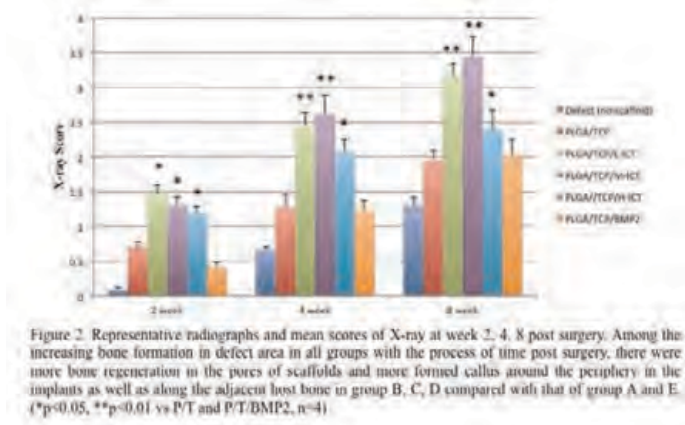

Figure 2. Representative radiographs and mean scores of X-ray at week 2, 4, 8 post surgery. Among the increasing bone formation in defect area in all groups with the process of time post surgery, there were more bone regeneration in the pores of scaffolds and more formed callus around the periphery in the implants as well as along the adjacent host bone in group B, C, D compared with that of group A and E. (*p<0.05, **p<0.01 vs P/T and P/T/BMP2, n=4)

Figure 2b

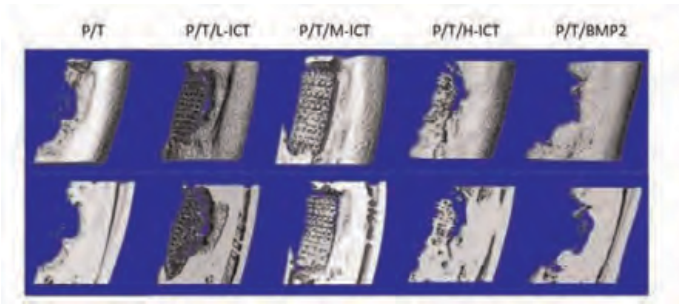

Figure 3a

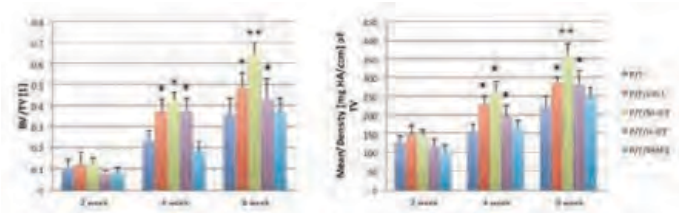

Figure 3 Representative XtremeCT analysis images and evaluated data at week 4,8 post surgery. Images showed the better bone formation in defects of group B, C and D compared to that in group A and E, and bone density and relative bone volume in defect area demonstrated the significant increasing in group B, C, D in comparison with those in group A and E. (*p<0.05, ** p<0.01 vs P/T and P/T/BMP2, n=4)

Figure 3b

***Disclosures: Shihui Chen**, None.*

SU0108

Serum Undercarboxylated Osteocalcin correlates with aging related hearing loss. SANG HYEON JE[1], Duck Joo Lee*[2]. [1]Ajou University Hospital, Department of Family Medicine, South Korea, [2]Ajou University School of Medicine, South Korea

Background: Recent studies have revealed that elevated levels of serum UCOC (undercarboxylated osteocalcin) are associated with low bone mineral density. Further studies have proved bone mineral density in lumbar vertebra increases after taking vitamin K, which is a strong factor in decreasing serum UCOC. Because bone metabolism also affects ear bones, the serum UCOC may affect ear bone mineral density. The aim of this study is to understand the relationship between levels of serum UCOC and hearing loss.

Materials and methods: The study comprised of 2,316 patients who had visited Geoje Health Promotion center, Daewoo Hospital for general health checkups. The levels of serum UCOC, PTA, Fasting blood glucose, GOT, GPT, Uric acid, insulin, ESR, CRP were measured. PTA (pure tone audiogram) was used to measure hearing loss. We used statistical software SPSS 11.0 for data analysis.

Results:The serum UCOC levels were significantly correlated with decibels in all frequency levels of PTA (0.280 in 1000 Hz and 0.184 in 4000 Hz, $P<0.05$). The higher the decibels in PTA are, the lower the hearing ability is. Both men and women groups showed a similar result in hearing ability by each PTA frequency and in UCOC levels.The 30s age group showed a significant decrease in serum UCOC levels (1.27 ± 0.81ng/mL) as compared with 40s or 50s age group. The decibel in PTA was significantly higher in the high serum UCOC group (15.21 ± 13.39 DB in 1000 Hz) than in the low serum UCOC group (13.74 ± 11.50 in 1000 Hz, $P < 0.05$) and nonsignificantly higher in other frequency groups.

Conclusion: Serum UCOC's effects on hearing bones may point toward their possible application of vitamin K supplements in improving hearing, especially for the aging related hearing loss. However, as we used PTA, we don't know whether the loss is caused by a sensory problem or a mechanical problem. Further studies should be followed.

***Disclosures: Duck Joo Lee**, None.*

SU0109

Characterization of an Fkbp10$^{-/-}$ mouse model of recessive Osteogenesis Imperfecta. Caressa Lietman*[1], Erica Homan[1], Tao Yang[2], Elda Munivez[1], Ming-Ming Jiang[1], Terry Bertin[1], Yuqing Chen[1], Deborah Krakow[3], Brendan Lee[4]. [1]Baylor College of Medicine, USA, [2]Van Andel Research Institute, USA, [3]UCLA, USA, [4]Baylor College of Medicine & Howard Hughes Medical Institute, USA

Osteogenesis Imperfecta (OI) is the most commonly inherited form of brittle bone disease and displays a spectrum of severity from mild phenotypes to severe early lethality. Key clinical features of OI are bone fragility and low bone mass, whereas patients may also display blue sclera, dentinogenesis imperfecta, joint and skin laxity, hearing impairment and/or wormian bones on the skull. Mutations in FK506 Binding Protein 10 (*FKBP10*) that encode the FKBP65 protein result in recessive OI as well as Bruck Syndrome. FKBP65 is thought to act as a collagen chaperone and possesses PPIase activity for proper trimer formation. Currently, we do not understand the consequences of *FKBP10* loss and its role in collagen and ECM formation. Therefore our goal is to elucidate the role of *FKBP10* in the skeleton and how null mutations lead to progressively deforming OI and Bruck syndrome. We generated a mouse model using the EUCOMM allele to further elucidate the effects of FKBP65 in bone development. We have utilized the LacZ knockin allele to assess expression during development as well as the knockout first allele to discern the phenotypic outcomes of FKBP65 loss in the mouse. Furthermore, mouse embryonic fibroblasts (MEFs) have been used for comparison to human cells and for collagen studies and analysis. We found that *Fkbp10* is expressed at low levels at E13.5 particularly in skeletal tissues and increasing through E17.5 with expression in not only skeletal tissues, but also other mesothelial lined tissues, vessels and villi of intestine. Postnatally, expression is limited to developing bone and ligaments, suggesting a more restricted role at this timepoint. Null mice display neonatal lethality with viable embryos isolated up to E18.5 but not after birth, growth delay and generalized tissue fragility. *Fkbp10*$^{-/-}$ mouse embryonic fibroblasts show retention of procollagen in the cell layer after ascorbic acid stimulation, similar to what is seen in patient fibroblasts. These data suggest a requirement for *Fkbp10* function during embryonic connective tissue development in mice but restricted expression postnatally in bone, ligaments, and tendons correlating with the bone fragility and contracture phenotype in humans.

***Disclosures: Caressa Lietman**, None.*

SU0110

Expression of both Bone Sialoprotein and Osteopontin Is Necessary to the Anabolic Action of PTH on Mouse Calvaria Bone. Wafa Bouleftour*[1], Guénaëlle Bouët[2], Renata Neves Granito[1], Mireille Thomas[1], Marie-Thérèse Linossier[1], Arnaud Vanden Bossche[1], Jane Aubin[3], Marie-Helene Lafage-Proust[4], Laurence Vico[5], Luc Malaval[6]. [1]LBTO/INSERM U1059 - Université de Lyon, France, [2]LBTO/INSERM U1059 - F42023 Université de Lyon, France, [3]University of Toronto Faculty of Medicine, Canada, [4]INSERM Unit 890, France, [5]University of St-Etienne, France, [6]INSERM U1059-Université de Lyon-Université Jean Monnet, Saint-Etienne, France

Bone remodeling is tightly regulated by central, systemic, and local factors, including extra-cellular matrix proteins. Among these, osteopontin (OPN) and bone sialoprotein (BSP), both members of the "small integrin-binding ligand, N-linked glycoprotein" (SIBLING) family, are coexpressed in both osteoblasts and osteoclasts and involved in primary and secondary ossification. Previous work suggested that some functions of BSP and OPN are redundant while others are not. Here, we investigated their degree of specificity and redundancy in a local (calvaria) model of PTH-induced remodeling.

Comparison of calvaria cell cultures from BSP+/+ and BSP-/- mice revealed few osteoblast colonies (bone nodules) and no mineralization in mutant dishes, along with little/no expression of osteocalcin (OCN) nor SIBLING proteins MEPE or DMP1. In contrast, OPN levels showed a 5x increased in BSP-/- vs BSP+/+ cultures. Treatment of the cultures with 50 ng/ml hPTH1-34 induced an increase in alkaline phosphatase (ALP) activity at day 6 in BSP +/+ and BSP-/- cultures, with the appearance of OCN expression in BSP-/- dishes, and their mineralization (at day 17). In a model of intermittent injection of hPTH1-84 (8µg daily, 14 days, 5 mice/group) over the periosteum of the right mouse hemicalvaria, µCT and histomorphometry analysis showed that PTH stimulates bone formation in the injected side in both genotypes, increasing to the same degree the thickness and vascularity of the periosteum, osteoid thickness, total bone volume (BV, BSP+/+:427 ± 65 vs $254 \pm 48 \mu m^3$ in NaCl injected controls, BSP-/-: 420 ± 64 vs $270 \pm 34 \mu m^3$, $p<0.001$ for both genotypes, N=5, MWU), bone thickness and porosity, BFR/BS as well as the expression of bone formation and mineralization markers (OPN, osterix, OCN, DMP1 and the endopeptidase PHEX). SiRNA blocking of OPN expression concomitant to PTH treatment did not affect the anabolic action of PTH in BSP+/+ calvaria (BV:450 ± 84 vs $432 \pm 73 \mu m^3$ in PTH+scrambled RNA controls, NS). In contrast, the reduction in OPN production blunted the increase in bone thickness and volume induced by PTH in the BSP-/- (BV: 344 ± 24 vs $482 \pm 31 \mu m^3$, $p<0.01$).

In conclusion, full expression of both OPN and BSP is necessary for the anabolic effect of PTH at least in the calvaria injection model. This suggests that OPN may functionally compensate the lack of BSP in the response to this hormonal challenge, and provides evidence of functional overlap between these two cognate proteins.

***Disclosures: Wafa Bouleftour**, None.*

SU0111

Two Fibronectin Isoforms Exert Opposite Effects on Osteoblast Differentiation and Affect the Interaction of the Integrin–Wnt Signaling Cascades. Carla Sens, Carina Wuerfel, Anja von Au, Inaam Nakchbandi*. Max-Planck Institute of Biochemistry & University of Heidelberg, Germany

Fibronectin is an extracellular matrix protein involved in cell differentiation. It is secreted in various isoforms, the role of which remains to be clarified. In earlier work we have shown that the oncofetal isoform of fibronectin (oFN) inhibited osteoblast

differentiation *in vitro* and *in vivo* (>80%). The aim of this study was to evaluate how this isoform inhibits osteoblast differentiation and whether other isoforms exert any effects on osteoblasts.

oFN is defined by an O-glycosylation at threonine 33 in the variable region. Enzymatic O-deglycosylation and site-directed mutagenesis revealed that the O-glycosylation was responsible for inhibiting osteoblast differentiation in vitro. Another isoform containing the extra-domain-A (EDA) is produced by osteoblasts during differentiation. Indeed, osteoblast transfections with EDA showed a significant increase in their differentiation *in vitro* (2-fold). Since both the variable region and EDA bind to α4β1 and α4β7 integrins, and EDA to α9β1 we evaluated their expression during differentiation. α4 protein expression increased 4-fold, α9 3-fold, while β1 decreased 10% and β7 protein was not expressed. In line with this, oFN addition resulted in significant decrease in α4 protein (50%), while EDA transfection was associated with a significant increase in α4 mRNA (40%). α9 did not change. To test this further, β1 integrin deletion in osteoblasts using the collagen-α1(I) promoter in floxed β1 integrin mice results in significant delay in mineralization (37%). Normal osteoblasts were then cultured onto a VCAM-matrix which binds α4. This resulted in increased a4 expression and differentiation (1.5-2 Fold). These data suggest that α4β1 integrin, at least in part, mediates fibronectin effects on osteoblast differentiation.

Because of the possibility of interaction between α4 integrin and wnt signaling, we asked whether fibronectin affected wnt signaling. EDA significantly increased rac1 expression, which is downstream of integrin signaling (2-fold). In addition, b-catenin protein increased 2-fold and wisp-1 mRNA 30%, suggesting increased wnt signaling. Thus, the pro differentiation effects of fibronectin seem to be mediated by an interaction between α4β1 integrin and the wnt signaling pathway.

In summary, we identified a new mechanism for fibronectin-mediated osteoblast differentiation mediated by EDA and α4β1 integrin, and some of this effect is mediated by potentiation of wnt signaling in the osteoblasts.

***Disclosures: Inaam Nakchbandi**, None.*

SU0112

WISP3 Affects Cell Survival in Human Chondrocytes and Mesenchymal Stem Cells. Sylvia Hondke*[1], Viola Zehe[2], Katrin Schlegelmilch[2], Susanne Wiesner[2], Alexander Keller[3], Norbert Schütze[2]. [1]University of Wuerzburg, Germany, [2]University of Wuerzburg - Orthopedic Center for Musculoskeletal Research, Germany, [3]University of Wuerzburg - Biocenter - DNA Analytics, Germany

Introduction: WISP3 (wnt1 inducible signaling pathway protein3) is known as an important signal modulator connected to the extra cellular matrix. It is essential for musculoskeletal development, induces the expression of chondrogenic markers and regulates chondrocyte homeostasis. Mutations in WISP3 are associated with progressive pseudorheumatoid dysplasia (PPD), a disease characterized by joint swelling and stiffness leading to cartilage degeneration. In this study, we examined consequences of WISP3 signaling through an enforced loss or treatment of the protein in human mesenchymal stem cells (hMSC) and chondrocytes.

Materials&Methods: Gene silencing was performed with specific lentiviral shRNA constructs affecting endogenous WISP3 expression in different cell types in vitro. Microarray analysis of WISP3 deficient hMSC (n=3, knock down vs. scrambled) was performed and validated by RT-PCRs of selected differentially expressed genes. WISP3 treatment of chondrocytes was performed with recombinant WISP3-Fc produced in Sf21 cells using a baculovirus expression system.

Results: Successful down-regulation of WISP3 considerably affected viability of several cell types of the musculoskeletal system. Apoptosis was shown by annexin V staining. Array analysis confirmed this observation by uncovering distinct clusters of differentially expressed genes connected to apoptosis or cell survival. For example, loss of WISP3 significantly influences pathways like TGFβ and p53. Results of the array analysis could be validated by RT-PCR. Treatment of WISP3 deficient chondrocytes with rWISP3 could not rescue the phenotype, but led to a positive feedback loop with the up-regulation of endogenous WISP3.

Discussion: Hereby, we present for the first time that a loss of WISP3 leads to cell death in distinct cell types. Global gene expression patterns provide new insights into gene expression changes, which indicate signaling of different apoptotic pathways. Thus, these findings generated an essential fundament for further examinations to clarify the role of WISP proteins on cell survival.

***Disclosures: Sylvia Hondke**, None.*

SU0113

Visualization of Chondrocyte Mechanotransduction in 3D. Qiaoqiao Wan*[1], Eunhye Cho[2], Seungman Park[1], Bumsoo Han[1], Hiroki Yokota[2], Sungsoo Na[2]. [1]Purdue University, USA, [2]Indiana University-Purdue University Indianapolis, USA

Articular cartilage is subjected to dynamic mechanical loading during normal daily activities. This complex mechanical loading, including cell compression and interstitial fluid flow, affects chondrocyte mechano-chemical signaling and subsequent cartilage homeostasis and remodeling. FAK and Src are known to be main mechanotransduction proteins, but little is known about the effect of mechanical loading on FAK and Src under its varying magnitudes and types.

In this study, C28/I2 chondrocytes were used for this study. Type II collagen-conjugated 3D agarose gels were used to mimic the physiologically relevant cell environment. During imaging, pulsed (0.2 Hz) fluid flow (2, 5, 10, 20 μl/min) was applied to the cells/gel construct in the chamber. Two different types of mechanical loading were subjected to the cells: interstitial fluid flow (IFF) only and combined cell compression/IFF. Cell compression was measured by computing the ratio of changes in cell diameter to the original cell diameter in the direction of fluid flow. FRET-based biosensors for monitoring FAK and Src activities were used. The DNA plasmids were transfected into the cells using a Neon transfection system. A Nikon Ti-E inverted microscope was used for imaging experiments. FRET images for FAK and Src activity was generated by computing the emission ratio of CFP/YFP for individual cells using NIS Elements software.

Results show that the cell compression was negligible under IFF only (Fig. 1A), whereas under combined loading (i.e. cell compression + IFF), it was dependent on the magnitude of the loading (Fig. 1B). Under 10 μl/min IFF, we observed a transient increase in Src activity, followed by a decrease at 20 min (Fig. 2A). However, under combined loading (4.4% cell compression + 10 μl/min IFF), Src activity decreased rapidly within 2 min and gradually increased until 60 min (Fig. 2B). These results suggest that Src activity is loading type dependent. In contrast, FAK activity is not dependent on the types of loading (data not shown). Both FAK and Src were similarly increased or decreased depending on the fluid flow magnitude under IFF (Fig. 3A). However, they behaved differently under combined loading (Fig. 3B), possibly due to the additive effects of the two different types of loading on Src activity (Fig. 2). Collectively, the data suggest that the intensities and types of mechanical loading are critical in regulating FAK and Src activities in chondrocytes.

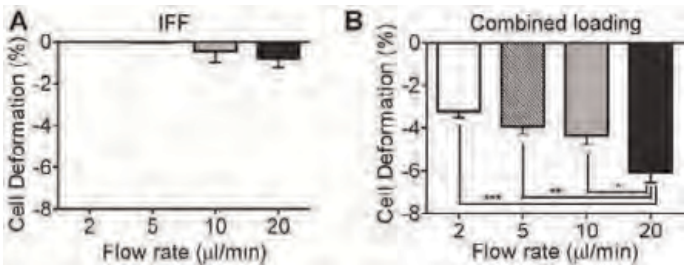

Figure 1

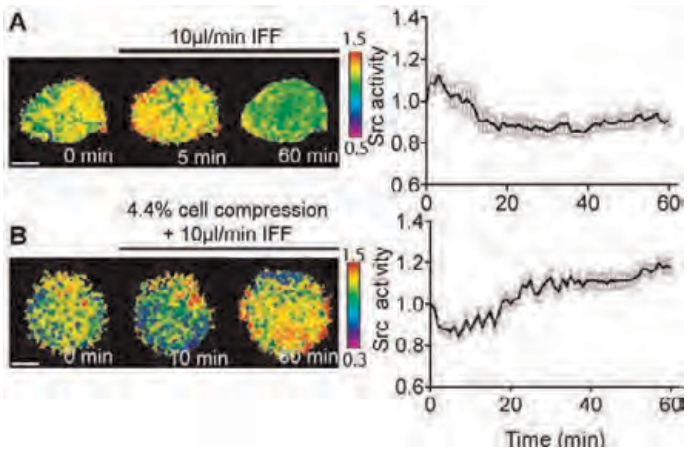

Figure 2

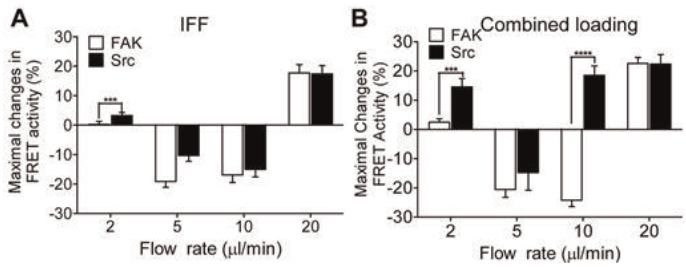

Figure 3

***Disclosures: Qiaoqiao Wan**, None.*

SU0114

Association of 25-hydroxyvitamin D, Parathyroid Hormone Levels with Blood Pressure in Elderly Populations. HyeonMok Kim*[1], Beom Kim[2], Jung-Min Koh[3]. [1]South Korea, [2]Departments of Internal medicine, Seoul Veterans Health service medical center, Seoul, Korea, South Korea, [3]Asan Medical Center, South Korea

Background: Although lower vitamin D status or higher parathyroid hormone(PTH) status have been associated with higher blood pressure(BP), there are few studies in the general population.

Objective: The purpose of this study is to investigate the association between serum vitamin D, PTH level and blood pressure, in population with or without antihypertensive medication.

Methods: A population-based, cross-sectional study from the Korea National Health and Nutrition Examination Surveys. Participants included 2,019 men and 2,494 women aged over 50yrs or older. Serum 25-hydroxyvitaminD3 and PTH were measured by radioimmunoassay and BP was determined with a sphygmomanometer. We performed univariate linear regression analysis and analysis of covariance(ANCOVA) to examine the influence of serum 25(OH)D3 and PTH on blood pressure with adjustments for age, weight, height, antihypertensive medication, waist circumference, estimated glomerular filtration rate, Diabetes mellitus prevalence, smoking status, exercise status.

Results: In general population, serum 25(OH)D3 showed negative correlation with BP in women, but not in men. Serum PTH was positively associated with BP in both genders. In the group without antihypertensive medication, both 25(OH)D3 and PTH showed significant correlation with blood pressure. Also consider the interaction between 25(OH)D3 and PTH to Blood pressure, adjustment for PTH resulted in an inverse correlation of serum 25(OH)D3 with blood pressure in non BP med users, and PTH is independently positive correlation with blood pressure, when adjusted for 25(OH)D3

Conclusion: Participants who did not take BP medication, 25(OH)D3 can be a negative predictor of BP, independent of PTH and other confounders. Also PTH can be a positive predictor of BP.

***Disclosures: HyeonMok Kim**, None.*

SU0115

Gain-of-Function Mutations in Gα11 Cause a Novel Form of Autosomal-Dominant Hypoparathyroidism. Michael Mannstadt*[1], M. Andrew Nesbit[2], Sarah Howles[2], Angela Rogers[2], Rajesh Thakker[2], Harald Jueppner[3]. [1]Massachusetts General Hospital Harvard Medical School, USA, [2]Nuffield Department of Clinical Medicine, University of Oxford, United Kingdom, [3]Massachusetts General Hospital, USA

Purpose: Heterotrimeric G-proteins play pivotal roles in the transmission of signals from ligand-activated seven transmembrane receptors such as the PTH/PTHrP receptor or the calcium-sensing receptor (CASR) to intracellular effector molecules such as cAMP and intracellular free calcium ($[Ca^{2+}]_i$), respectively. Post-zygotic or somatic mutations in G proteins resulting in gain-of-function contribute to the development fibrous dysplasia or tumors such as uveal melanoma. By contrast, germline gain-of-function mutations are extremely rare. Here, we provide initial functional characterization of two heterozygous mutations in *GNA11,* encoding the a-subunit of G11 (Gα11), recently identified in patients with autosomal dominant isolated hypoparathyroidism (AD-IHP).

Methods: The underlying genetic defect in two large unrelated families with AD-IHP had been identified through genome-wide linkage analysis and exome sequencing. Functional consequences of the mutations were now studied using HEK293 cells stably expressing the CASR (HEK-CASR). $[Ca^{2+}]_i$ responses to different extracellular calcium concentrations $[Ca^{2+}]_o$ were measured after transfecting HEK-CASR cells with wildtype or mutant Gα11, and the EC_{50} values determined.

Results: Genome-wide linkage analysis combined with exome sequencing had revealed two distinct heterozygous missense Gα11 mutations, leading to the alterations R60C and S211W. Both affect highly conserved residues, are present in all affected family members, and absent in available unaffected members and databases. *In silico* modeling based on the crystal structure of the closely related Gαq had suggested that both mutations lead to a gain-of-function. Consistent with this prediction, functional *in vitro* assays revealed a leftward shift in the calcium concentration-response curves with significantly lower EC_{50} values when the HEK-CASR cells were transfected with the R60C or S211W mutant, compared to transfection with the wildtype Gα11.

Conclusions: In two different families, heterozygous germline Gα11 mutations were identified as a novel cause of AD-IHP. *In vitro* studies using HEK293-CASR cells transiently transfected with wildtype or mutant Gα11 suggest that both mutations lead to a gain-of-function.

***Disclosures: Michael Mannstadt**, None.*

SU0116

Chronically Elevated Circulating Fgf23 Modulates Renal Sodium Handling in *Hyp* Mice. OLENA ANDRUKHOVA*[1], Ute Zeitz[2], Sathish Kumar Murali[2], Reinhold Erben[3]. [1]INST. OF PHYSIOLOGY, PATHOPHYSIOLOGY & BIOPHYSICS, Austria, [2]Department of Biomedical Research University of Veterinary Medicine, Austria, [3]University of Veterinary Medicine, Austria

Patients with X-linked hypophosphatemia (XLH) and hypophosphatemic (*Hyp*) mice, a mouse model of XLH, show profoundly increased serum concentrations of fibroblast growth factor 23 (FGF23). FGF23 is a hormone originating from bone, regulating renal phosphate reabsorption and vitamin D synthesis. We previously reported that FGF23 also directly regulates the sodium (Na)-chloride cotransporter NCC in distal renal tubules through a pathway involving extracellular signal-regulated kinase 1/2 (ERK1/2), serum/glucocorticoid-regulated kinase 1 (SGK1), and with-no lysine kinase-4 (WNK4). NCC and the epithelial Na channel (ENaC) are the principal ion channels regulating Na reabsorption in the distal nephron. To determine the role of chronically elevated Fgf23 levels in renal Na reabsorption we examined 3-month-old male *Hyp* mice. Analysis of Na homeostasis in *Hyp* mice revealed unchanged urinary but increased serum Na levels as compared to wild-type controls. Serum aldosterone as well as heart-to-body weight ratio were increased in *Hyp* mice. Immunoblotting of renal membrane preparations revealed increased expression of NCC and increased NCC phosphorylation at Thr53, Thr58 and Ser71 in *Hyp* mice. In addition, phosphorylated ERK1/2 and SGK1 as well as total WNK4 protein expression were markedly elevated in kidney homogenates of *Hyp* mice. Interestingly, *Hyp* mice showed 2.2-fold increased renal membrane expression of the alpha ENaC subunit essential for the channel activity, but 5-fold increased expression of beta and gamma ENaC subunits involved in ERK1/2-induced channel internalization and degradation. This finding may imply that the aldosterone-driven upregulation of alpha ENaC is possibly counteracted in *Hyp* mice by an Fgf23-ERK1/2-mediated upregulation of beta and gamma ENaC subunits. Therefore, increased renal membrane expression and phosphorylation of NCC, mediated through the Fgf23/ERK1/2/SGK1/WNK4 signaling axis, may partially be counterbalanced by increased ENaC degradation in *Hyp* mice. Taken together, our study showed that chronically elevated serum Fgf23 results in hypernatremia, increased serum aldosterone, and heart hypertrophic changes under steady state conditions in *Hyp* mice. Thus, our findings may have important implications for the pathophysiological mechanisms underlying the association between serum FGF23 levels and cardiovascular risk in chronic kidney disease patients.

***Disclosures: OLENA ANDRUKHOVA**, None.*

SU0117

Deletion of *Fgf23* does not Perturb Fetal Mineral Homeostasis, Skeletal Mineral Content, Placental Phosphorus Transport, or Placental Expression of FGF23 Target Genes. M. Manoharee Samaraweera*[1], Yue Ma[1], Beth J. Kirby[1], S. Teja Vatturi[1], Beate Lanske[2], Christopher Kovacs[1]. [1]Memorial University of Newfoundland, Canada, [2]Harvard School of Dental Medicine, USA

FGF23 is a key regulator of phosphorus (P) homeostasis in the adult; its absence causes severe hyperphosphatemia and early mortality. Its role during fetal development is unknown.

We mated $Fgf23^{+/-}$ males and females together and studied their WT, $Fgf23^{+/-}$, and *Fgf23* null fetuses. On embryonic day (ED) 17.5, amniotic fluid (largely urine) was collected, while placental ^{32}P transport was determined by administering ^{32}P and ^{51}Cr-EDTA by intracardiac injection to the mother, and measuring isotopes in the fetuses after 5 min. Serum was collected from ED17.5 and 18.5 fetuses. Whole bodies at ED17.5 and 18.5 were reduced to ash and the mineral content was assayed. qPCR was done on ED18.5 placentas and kidneys. Intact FGF23 was measured by EIA (Kainos).

Serum FGF23 was undetectable (<3.0 pg/ml) in *Fgf23* nulls as compared to 23.8 ± 2.9 in $Fgf23^{+/-}$ and 53.8 ± 4.9 in WT ($p<0.001$), and much lower than the maternal value (236 ± 32.9) ($p<<0.001$). Serum P did not differ between genotypes (3.93 ± 0.24 mM in null vs. 3.91 ± 0.15 mM in WT), and there was also no difference in excretion of P or Ca into amniotic fluid. Fetal ash weight, and P, Ca, or Mg ash content did not differ between genotypes at ED 17.5 or 18.5. Placental ^{32}P transport, normalized to the value of $Fgf23^{+/-}$ fetuses, also did not differ ($97.5 \pm 3.3\%$ in null, $100.5 \pm 1.7\%$ in $Fgf23^{+/-}$, and $103.3 \pm 5.5\%$ in WT).

qPCR revealed low level expression of *Fgf23* in WT placentas which was absent in the *Fgf23* null ($p<0.02$). Placentas of *Fgf23* null and WT expressed all three sodium-phosphate cotransporters (*NaPi2abc*), all four FGF23 receptors (*Fgfr1-4*), FGF23's co-receptor *Klotho,* and *Cyp27b1* and *Cyp24a1*. However, there were no differences in relative expression of these target genes between WT and *Fgf23* null placentas. *Fgf23* null kidneys showed ~1.5 to 2-fold increased expression of *Klotho* and *NaPi2abc*, but no change in *Fgfr1-4*.

In summary, intact FGF23 does not cross the placenta from mother to fetus. Deletion of *Fgf23* did not disturb any measured parameter of fetal mineral homeostasis, including serum and amniotic fluid P, skeletal mineral content, and placental ^{32}P transport. Placentas and kidneys abundantly express FGF23 target genes but only kidneys showed altered gene expression in *Fgf23* null.

In conclusion, despite FGF23's presence in the fetal circulation and expression of its target genes in placenta and kidneys, FGF23 is not an important regulator of fetal P. Placental P delivery may override effects of FGF23's absence.

***Disclosures: M. Manoharee Samaraweera**, None.*
This study received funding from: Research and Development Corporation of Newfoundland and Labrador

SU0118

Metabolic Acidosis Stimulates Fibroblast Growth Factor 23 in Osteoblasts by a Calcium- and Prostaglandin-Mediated Mechanism. Nancy Krieger*[1], Christopher Culbertson[2], Kelly Kyker-Snowman[2], David Bushinsky[1]. [1]University of Rochester, USA, [2]University of Rochester School of Medicine, USA

Serum fibroblast growth factor 23 (FGF23) increases significantly with progressive chronic kidney disease (CKD), leading to reduced renal tubular phosphate (Pi) reabsorption, decreased serum $1,25(OH)_2D_3$ and is associated with increased mortality. FGF23 is synthesized in osteoblasts and osteocytes; however, the primary factors regulating its production are not clear. Patients with CKD have decreased renal net acid excretion leading to metabolic acidosis (MET). During MET, acid is buffered by bone with release of mineral calcium (Ca) and Pi. MET increases intracellular Ca signaling and cyclooxygenase 2 (COX2)-induced prostaglandin production in the osteoblast leading to decreased osteoblastic bone formation and increased osteoclastic bone resorption. We recently found that MET directly stimulates FGF23 in mouse bone and primary osteoblastic cells. We hypothesized that MET would increase FGF23 through similar pathways that lead to bone resorption. Neonatal mouse calvariae were incubated in neutral (NTL, pH=7.44, Pco_2=38 mmHg, $[HCO_3^-]$=27 mM) or acid (MET, pH=7.18, Pco_2=37 mmHg, $[HCO_3^-]$=13 mM) medium in the absence or presence of 2-APB (50 μM), a pharmacologic inhibitor of intracellular Ca signaling. 2-APB significantly inhibited the MET-induced increased medium FGF23 protein and calvarial FGF23 RNA as well as bone resorption at 48h (Table 1). To exclude the potential contribution of MET induced bone Pi release to the increase in FGF23, we utilized primary osteoblastic cells isolated from mouse calvariae. In these cells 2-APB inhibited the MET-induced increase in FGF23 RNA expression at 6h. Similarly, NS398 (1 μM), which is a specific inhibitor of COX2, also inhibited the MET-induced increase in FGF23 RNA at 6h. Thus, the stimulation of FGF23 by MET in mouse osteoblasts appears to utilize the same initial signaling pathways as MET-induced bone resorption. Therapeutic interventions directed toward correction of MET, especially in CKD, have the potential to not only prevent bone resorption but also lower FGF23 and perhaps decrease mortality.

Calvariae at 48h:	NTL	MET	NTL+2-APB	MET+2-APB
FGF23 protein (pg/ml)	156±36	295±50*	26±9*#	50±6*#
FGF23 RNA (rel. exp.)	1.1±0.2	2.7±0.2*	2.3±0.3*	2.0±0.5
Ca release (nmol)	356±97	791±96*	12±43*#	384±111*#
Osteoblasts at 6h				
FGF23 RNA (rel. exp.)	0.9±0.2	1.6±0.3*	1.1±0.3	1.1±0.2
			NTL+NS398	MET+NS398
FGF23 RNA (rel. exp.)	1.5±0.4	3.2±0.6*	1.8±0.3	0.9±0.2

*p<0.05 vs NTL; #p<0.05 vs MET; # p<0.05 vs NTL+APB or NS

Table 1

***Disclosures: Nancy Krieger**, None.*

SU0119

Disruption of LRP6 in Osteoblasts Blunts the Bone Anabolic Activity of PTH. Changjun Li*[1], Qiujuan Xing[1], Bing Yu[2], Hui Xie[1], Janet Crane[3], Xu Cao[3], Mei Wan[1]. [1]Johns Hopkins University School of Medicine, USA, [2]Johns Hopkins School of Medicine, USA, [3]Johns Hopkins University, USA

Mutations in Low-density lipoprotein receptor-related protein 6 (LRP6) are associated with human bone disorders. We previously revealed that LRP6 is a key element in PTH-activated both β-catenin and cAMP/PKA signaling in osteoblasts. Here we investigated whether LRP6 directly regulates bone remodeling and mediates PTH bone anabolic effects by analysis of the bone phenotype in mice lacking *Lrp6* specifically in mature osteoblasts (Oc-Cre; *Lrp6$^{f/f}$*, named "KO" hereafter).

Three month-old LRP6 KO mice had a significant reduction in bone mass in the femura secondary spongiosa relative to their WT littermates, whereas marginal changes were seen in femura of 1 month-old KO mice, indicating that LRP6 deficiency in osteoblasts primarily affected trabecular bone remodeling in adults. The remodeling area of the 3 month-old LRP6 KO mice showed a decreased bone formation rate as detected by Goldner's Trichrome staining and calcein double labeling. Bone histomorphometric and immumohistochemical analysis revealed a reduction in bone surface osteoblasts but little change in the numbers of osteoclasts in LRP6 KO mice. Consistently, mRNA levels of bone matrix proteins produced by osteoblasts and osteocytes were decreased in bone tissue from 3 month-old KO mice. In addition, the percentage of the apoptotic osteoblasts on bone surface was higher in KO mice as detected by TUNEL assays. Thus, LRP6 deficiency increased the apoptosis and decreased the differentiation of osteoblasts, leading to the reduction in the number of bone surface osteoblasts and bone formation.

We then examined whether LRP6 in osteoblasts is required for PTH anabolic effects on bone. Two month-old KO mice and WT littermates were injected with PTH1-34 daily for 4 weeks. PTH had no effect on bone mass nor osteoblastic bone formation in either trabecular and cortical bone in KO mice, whereas all were enhanced in WT littermates. Consistently, serum osteocalcin level was not stimulated in PTH-treated KO mice as significantly as in PTH-treated WT mice, whereas the PTH-stimulated increase in serum CTX-I level was similar in KO and WT mice. The anti-apoptotic effect of PTH on osteoblasts in LRP6 KO mice was less significant compared to WT mice, indicating that LRP6 is required for osteoblast survival in PTH-stimulated bone remodeling. Collectively, our findings demonstrate that LRP6 in osteoblasts is essential for osteoblastic differentiation during bone remodeling and the anabolic effects of PTH.

***Disclosures: Changjun Li**, None.*
This study received funding from: NIH

SU0120

Hospital Care for Primary Hyperparathyroidism in Italy: a Six-Year Register-Based Study. Cristiana Cipriani*[1], Vincenzo Carnevale[2], Elisabetta Romagnoli[1], Rina Fratelloreto[1], Jessica Pepe[1], Sara Piemonte[1], Alfredo Scillitani[3], Salvatore Minisola[1]. [1]"Sapienza", University of Rome, Italy, [2]IRCCS "Casa Sollievo della Sofferenza" Hospital, Italy, [3]Casa Sollievo Della Sofferenza Scientific Institute, Italy

Purpose: Primary hyperparathyroidism (PHPT) is one of the most frequently diagnosed endocrine disorders, but few studies focused on hospital management of the disease in Europe. We investigated the frequency of hospital admission for the diagnosis and surgical treatment for PHPT in Italy.

Methods: We performed a retrospective study on data from the Archive of the forms of Hospital Discharge (SDO) of the Italian Health Ministry, from the year 2006 to 2011, when the Italian version of the ICD-9 CM classification system with two decimals was utilized. We analyzed the codes corresponding to the following medical diagnoses: "PHPT", "not specified hyperparathyroidism", "multiple endocrine neoplasia", "benign parathyroid neoplasia", "malignant parathyroid neoplasia", non tumor-related "hypercalcemia", as well as the following surgical diagnoses: "complete parathyroidectomy", "other parathyroidectomy", "other parathyroid procedures".

Results: Overall, 46,275 hospitalization episodes for PHPT were identified during the entire period, among which 69% in women and 31% in men, (female/male ratio 2.23:1; mean age 63.3 ± 39.8 years). The total admissions were 7,715 in the year 2006, 7,454 in 2007, 7,809 in 2008, 7,876 in 2009, 7,899 in 2010, and 7522 in 2011. Patients' mean age significantly increased during the six years (from 62.7 ± 37.5 in 2006 to 65.8 ± 18.6 in 2011; $p<0.001$). The mean length of stay was 8.2 ± 10.5 days (28% of the episodes requiring less than 3 days of stay). The overall number of admissions for surgical procedures was 11,196, that is the 24.4% of the total hospitalization rate over the six investigated years. There was a trend to a significant increase in the percentage of surgery during the entire period (25.7% in 2006, 26.6% in 2007, 26.8% in 2008, 27.8% in 2009, 26.9% in 2010 and 27.6% in 2011; $p<0.05$). In the year 2011 only, the overall hospitalization rate was 11,426/100,000 for any disease, 11.9/100,000 for PHPT and 19.8/100,000 for uncontrolled diabetes, the most prevalent endocrine disorder.

Conclusions: PHPT considerably impacts the Italian Hospital healthcare system. We observed a tendency to a decrease in the frequency of hospitalization during the period 2006-2011, most probably because of economic issues. Furthermore, there was a concomitant increased age of the patients hospitalized for the disease, and, interestingly, also a progressive increase in the percentage of surgical treatment among patients admitted for PHPT.

***Disclosures: Cristiana Cipriani**, None.*

SU0121

SILAC-Based Quantitative Analysis of Phosphorylation Dynamics in Osteoblasts Simulated with Parathyroid Hormone (PTH 1-34). Lauren Ball, Grace Williams*, Louis Luttrell, Mary Berkaw. The Medical University of South Carolina, USA

Recombinant human PTH, residues 1-34, is used for treatment of osteoporosis. In an unbiased approach to identify proteins that undergo a change in phosphorylation status with acute stimulation of the PTH receptor with PTH 1-34, a quantitative phosphoproteomic strategy was applied to differentiating osteoblasts. MC3T3-E1 pre-osteoblasts were grown in the presence of stable, isotopically labeled "light", "medium", or "heavy" lysine and arginine (SILAC) for 6 passages. Cells grown to confluence were induced to differentiate in osteogenic media supplemented with ascorbic acid, beta glycerol phosphate, 10% dialyzed FCS, and isotopically labeled amino acids for 9 days. On day 9, FCS was reduced to 1% for 18 hr prior to receptor stimulation with rhPTH 1-34 for 0, 1, or 5 min. Cells were lysed in urea and 5 mg protein from each treatment condition was combined and digested with trypsin. Peptides were fractionated by SCX chromatography and phosphopeptides were enriched from each fraction by TiO2. Resulting peptides were separated by C18RP-nLC and analyzed by tandem mass spectrometry (Orbitrap Elite) using CID MS/MS

and ETD MS/MS with a decision tree approach. Phosphopeptides were identified, the sites of phosphorylation localized, and changes in the extent of phosphorylation quantified using Proteome Discoverer (Thermo) and Maxquant software packages. Initial analyses yielded 357 peptides that changed in the extent of phosphorylation by 2 fold or greater following stimulation with PTH 1-34. Elevated phosphorylation was observed within the C-terminus of PTH R1 at sites known to be responsive to receptor stimulation indicating effective stimulation. Motif analysis of peptides that were phosphorylated in response to PTH 1-34 suggests activation of cAMP-dependent PKA and CamKII as anticipated based on canonical PTHR signaling via Gs and Gq/11 coupling. Changes in phosphorylation were also observed in regulatory subunits of phosphatases PP1 and PP2a. Interestingly, changes in IRS1 phosphorylation were observed which may represent a node of interaction between PTHR and IGF1/insulin receptor signaling. The goals of these studies are to provide novel information regarding PTH receptor signaling in osteoblasts and to serve as a control for future studies aimed at identifying signaling components employed by functionally selective (biased) agonists of the PTH receptor. This work is supported by RO1 DE020925 (LEB), S10 D010731(LEB), and R01 DK055524 (LML).

***Disclosures: Grace Williams**, None.*

SU0122

Three Dimentional Structure of Human PTH (1-84). Abdulhafez Selim*. Center for Chronic Disorders of Aging, PCOM, USA

Parathyroid hormone (PTH), is secreted by the chief cells of the parathyroid glands as a polypeptide containing 84 amino acids. It acts to increase the concentration of calcium (Ca2+) in the blood. PTH is acting upon the parathyroid hormone 1 receptor (high levels in bone and kidney) and the parathyroid hormone 2 receptor (high levels in the central nervous system, pancreas, testis, and placenta).

Parathyroid hormone plays a very important role in calcium phosphate homeostasis and in regulating bone metabolism. It has been reported that full length PTH (1-84) and the C-terminal fragments play distinct biological roles when compared to the N-terminus PTH (1-34).The N-terminal fragment 1-34 of parathyroid hormone (PTH) has been successfully crystallized and the structure has been refined to 0.9 Å resolutions. Due to technical difficulties, no previous studies succeeded in crystallizing the full length PTH (1-84) or its carboxyl-terminal fragments.

It is of great importance to identify the secondary and tertiary structures of PTH (1-84) as well as the C-terminal fragments (34-84, and 53 to 84).

To achieve this object, we used validated bioinformatics tools to create three dimensional models and to screen the models for potential targets (matrix proteins or cell surface receptors). Validated bioinformatics tools can produce high quality models that could be comparable to actual crystallization. It is important to mention that our methods were not based on homology modeling that could be misleading if there is no enough homology with database models. Instead, we used a validated Monte Carlo simulation tools. We used PTH (1-34) three dimensional models (based on crystallization data; PDB ID# 1ET1) as a positive control and we used scrambled peptide as a negative control. Positive control (PTH 1-34) modeling demonstrated valid modeling outcomes that were 100% comparable to the crystallized model of PTH (1-34) [1ET1].

PTH (1-84) model was formed of two alpha helices and one loop; one helix was toward the N-terminus (1-37) and the other helix toward the C-terminus (71-84). The two helices were connected by a large loop (38-70). The three dimensional model of the C-terminal fragment (39-84) was similar not identical to the same region in the full length model (1-84); alpha helix (71-84) was maintained, but the region between 30 and 69 changed from loop (in the 1-84 model) to form a smaller loop (63-89) and two small beta sheets (49-62). The alpha helix domain (71-84) was also maintained in the three dimensional model of PTH (53-84).

The generated PDB files (three dimensional models) were used to identify interacting residues, determine accessibility, search for potential cell surface receptors and interacting extracellular matrix proteins. The data presented in this study will be of great value determining the active sites of the full length (1-84) and designing of agonists and antagonists to modulate the functions of CPTH receptor(s).

Figure 1: Three dimensional structure of Human PTH 1-84

Figure 2: Three dimensional structure of CPTH 39-84

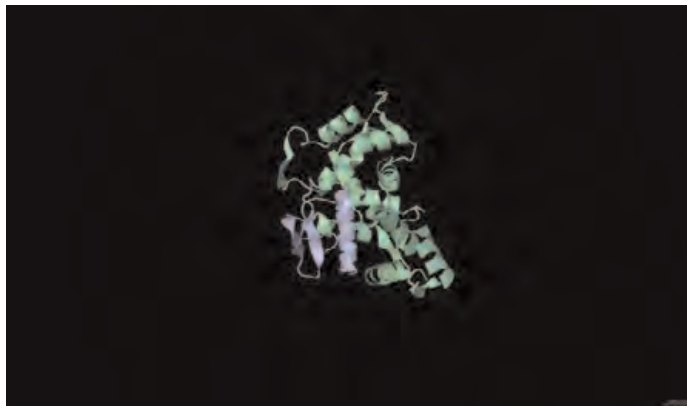

Figure 3: Ligand receptor complex of CPTH 39-84 (blue) and one of the potential CPTHRs (green).

***Disclosures: Abdulhafez Selim**, None.*

SU0123

Vitamin D Supplementation Increases Calcium Absorption without a Threshold Effect. Mageda Mikhail*[1], John Aloia[1], Steven Abrams[2], ruban dhaliwal[1], Albert Shieh[3], melissa fazzari[1], louis ragolia[1]. [1]Winthrop University Hospital, USA, [2]Baylor College of Medicine, USA, [3]University of California, Los Angeles, USA

BACKGROUND: The maximal calcium absorption in response to vitamin D has been proposed as a biomarker for vitamin D sufficiency.

OBJECTIVES: To determine if there is a threshold beyond which increasing doses of vitamin D (or level of serum 25OHD) no longer increase calcium absorption.

DESIGN: This was a placebo-controlled, dose-response, randomized double blinded study of the effect of vitamin D on calcium absorption in healthy, postmenopausal women. The gold standard technique of dual isotopes of stable calcium was used with physiologic calcium carrier.

RESULTS: 76 healthy, postmenopausal women were randomly assigned to placebo, 20 mcg, 50 mcg, or 100 mcg of vitamin D3 for 8 weeks. Mean age was 58.8 years. Mean calcium intake was 1142 + 509 mg/day and mean serum 25OHD level was 63 + 14 nmol/L. There was a statistically significant linear trend of increase in calcium absorption adjusted for age and BMI with increasing vitamin D3 dose or serum 25OHD concentration (ANOVA). The absolute increase in the highest vitamin D group (100 mcg) was 6.7%. There was no evidence for non-linearity in the dose-response curve. As serum 25OHD level increased by 10 nmol/L, calcium absorption increased by 1.3%.

CONCLUSION: There is no evidence for a threshold of calcium absorption with a serum 25OHD level range from 40 - 130 nmol/L. Calcium absorption in this range is not a useful biomarker to determine nutritional recommendations for vitamin D.

***Disclosures: Mageda Mikhail**, None.*
This study received funding from: Merck

SU0124

MAGI-3 Regulates PTH Receptor Signaling in Osteoblasts. Bin Wang*, Harry Blair. University of Pittsburgh, USA

Parathyroid hormone receptor (PTHR), a G-protein coupled receptor (GPCR), mediates PTH actions to maintain mineral homeostasis and bone remodeling. However, the regulation of PTHR signaling has not been fully elucidated. Postsynaptic density 95/discs large/zona occludens (PDZ) scaffolding proteins comprise a key class of GPCR-interacting proteins and influence the signaling of GPCRs like the PTHR that possess a PDZ ligand. In the present study, a GST-tagged carboxyl-terminal 22 amino acid fragment of the wild-type PTHR (PTHR-ctM) and a construct harboring a mutation of the terminal methionine residue to alanine (PTHR-ctA) were generated. PTH1R-ctM and PTH1R-ctA were screened against a newly developed proteomic array of 96 PDZ domains. One novel PTH1R-interacting protein, membrane-associated guanylate kinase with inverted orientation 3 (MAGI-3), was identified. The coimmunoprecipitation data demonstrated that full-length PTHR interacts with MAGI-3, and this association is abolished by mutation of the PTHR terminal methionine residue to alanine, consistent with the overlay results. PTH(1-34)-induced receptor desensitization was measured after 48 hours transfection with vector or MAGI-3 by determining adenylyl cyclase activity following a second exposure to PTH. The results show that MAGI-3 significantly inhibited PTHR desensitization. MC3T3-E1 cells and ROS17/2.8 cells endogenously express MAGI-3. Finally, we examined whether MAGI-3 affected PTHR signaling in osteoblasts. Our data show that overexpression of MAGI-3 in ROS17/2.8 cells does not affect adenylate cyclase activity. However, cAMP formation induced by PTH(1-34) in osteoblasts significantly increased. We conclude that MAGI-3 is a novel PTHR-interacting protein that regulates PTH receptor signaling in osteoblasts.

***Disclosures: Bin Wang**, None.*
This study received funding from: NIH

SU0125

Osteocytic PTH Receptor is Required for Bone Anabolism Induced by Intermittent PTH Administration, but is Dispensable for Bone Resorption and the Loss of Bone Induced by Chronic PTH Elevation. Xiaolin Tu*[1], Kevin McAndrews[1], Jesus Delgado-Calle[1], Naomie Olivos[2], Abdulah Ben-Awadh[1], Wonjin Kim[3], Rafael Pacheco da Costa[1], Danielle Richardson[1], Munro Peacock[4], Lilian Plotkin[1], Teresita Bellido[1]. [1]Indiana University School of Medicine, USA, [2]IUPUI, USA, [3]Department of Internal Medicine, College of Medicine, Yonsei University, Korea, democratic people's republic of, [4]Indiana University Medical Center, USA

Some skeletal actions of PTH might be mediated by direct effects of the hormone on osteocytes. To explore the role of the osteocytic PTH receptor (PTHR1) in the skeletal response to PTH, we used conditional knockout mice (cKO) generated by mating $PTHR1^{flox/flox}$ mice with DMP1-8kb-Cre mice. 4-month old cKO and $PTHR1^{flox/flox}$ littermate controls received daily injections of human PTH (1-34, 100 ng/g/day) or vehicle, for 28 days (iPTH); and 1 month old cKO and $PTHR1^{flox/flox}$ littermate controls were fed low (0.01%) or normal (0.4%) Ca diets for 14 days to increase continuously endogenous PTH (cPTH). Eight to 10 female and 8 to 10 male mice per group were used. PTHR1 mRNA expression was decreased approximately 70% or 60% in long bone diaphyses enriched in osteocytes of 4 month old or 1 month old cKO mice, respectively. We found that iPTH increased total, spinal and femoral BMD in control male mice (7.9, 11.6, and 8.7% change compared to initial BMD); whereas vehicle induced minimal changes in BMD (0.5, 2.6, and -1.8%). iPTH induced similar increases in BMD in female control mice. In contrast, male and female cKO mice failed to respond to iPTH. Thus, iPTH induced only 1, 2.7, and 0.6% change in total, spinal, and femoral BMD in male mice. In addition, female mice treated with iPTH lost bone in the spine (-7.9% change). uCT analyses revealed a 2-fold increase in cancellous bone volume (BV/TV) of the distal femur in iPTH-treated control mice; whereas no increase was found in cKO mice. Further, whereas iPTH increased circulating AP activity in control mice, it failed to do so in cKO mice. iPTH did not change CTX levels in either group. Sost expression was not changed by iPTH in either group. In contrast, cKO mice responded similarly to controls to endogenous cPTH elevation. Thus, control or cKO mice fed a normal calcium diet gained ~ 30% BMD; whereas control or cKO mice fed the calcium deficient diet exhibited a similar loss of BMD (~ -2 to -3%). Moreover, cPTH increased circulating levels of CTX and AP similarly in control and cKO mice. Further, the expression of Sost was decreased in both control and cKO mice. We conclude that osteocytic PTH receptor is required for bone anabolism induced by intermittent PTH administration, but is dispensable for bone resorption and the loss of bone induced by chronic PTH elevation.

***Disclosures: Xiaolin Tu**, None.*

SU0126

Lentiviral transduction of TCIRG1 into CD34+ IMO cells rescues osteoclast function in a cell stage dependent but promoter independent manner. Christian Thudium*[1], Ilana Moscatelli[2], Carmen Flores[2], Karoline Natasja Stæhr Gudmann[1], Morten Karsdal[1], Johan Richter[2], Kim Henriksen[1]. [1]Nordic Bioscience A/S, Denmark, [2]Lund University, Sweden

The a3 subunit of the V-ATPase is almost exclusively expressed in osteoclasts, and its function is indispensable for osteoclast functionality, as illustrated by the lethal phenotype observed in infantile malignant osteopetrosis caused by mutations in *TCIRG1*, the gene encoding the a3 subunit. Treatments of malignant osteopetrosis are limited to bone marrow transplantations, and hence approaches to rescue the dysfunctional osteoclasts as well as insight into the molecular regulation of TCIRG1 are of great interest. With these things in mind we aimed at developing a lentiviral rescue system for expression of TCIRG1, both as a proof-of-concept and as a means to investigating the threshold of TCIRG1 expression needed for functionality in osteoclasts.

$CD34^+$ cells from peripheral blood of 5 IMO patients and from normal cord blood were transduced with SIN lentiviral vectors expressing endogenous *TCIRG1* and *GFP* under a SFFV promoter. The cells were expanded for 2 weeks, During which they were transduced. Cells were then differentiated for 10 days on bone slices with M-CSF and RANKL to mature osteoclasts, and osteoclastogenesis, activity and expression of TCIRG1 investigated.

qPCR analysis and western blot revealed increased mRNA and protein levels of TCIRG1 compared to GFP transduced controls. TCIRG1 protein was, however, only expressed at late stages of osteoclast differentiation, but not late stages of macrophages not incubated with RANKL, whereas GFP was seen throughout both the expansion and osteoclast differentiation period. Furthermore, this regulation seemed isolated to the hematopoietic lineage as TCIRG1 was readily expressed in HT1080, a non-hematopoietic control cell line. Vector corrected IMO osteoclasts generated increased Ca^{2+} release and CTX-1 into the media and showed clearly visible resorption pits, while non-corrected IMO osteoclasts developed normally but failed to resorb bone. Osteoclast functionality largely relied on TCIRG1 expression in a dose dependent manner, partly restoring bone resorption at rescue percentages as low as 5%.In conclusion, we show that lentiviral-mediated correction of osteoclasts can restore resorptive function, in a TCIRG1 dose dependent manner. In addition, we observed a differentiation dependent regulation of TCIRG1 using a viral promoter, a phenomenon which will is clearly beneficial for future studies working on the rescue of TCIRG1 functionality in vivo.

***Disclosures: Christian Thudium**, None.*

SU0127

Adipose Tissues are Reduced in Transgenic Mice with Induced $G_s\alpha$ Signaling in Osteoblasts. Corey Cain*, Edward Hsiao. University of California, San Francisco, USA

Purpose: Osteoporosis and obesity are significant medical conditions that contribute to morbidity and mortality. Although these diseases are often considered separate entities, studies suggest that obese people may be protected from osteoporosis and weight loss can result in bone loss. This clinical link is controversial since other studies show bone mass is inversely correlated with bone marrow adiposity. Bone and adipose tissue have distinct developmental pathways; however, disease states that increase bone tissue may occur because of direct conversion of adipose tissue to bone tissue and lead to systemic metabolic effects.

Methods: In this study, we used the ColI(2.3)+/Rs1+ transgenic mouse model which uses the engineered G-protein coupled receptor Rs1 to activate Gsα G-protein coupled receptor signaling in osteoblastic cells. These mice showed dramatically increased trabecular bone formation resembling fibrous dysplasia of the bone. Mice were subjected to Comprehensive Lab Animal Monitoring System (CLAMS) studies for 48 hours to measure O2 consumption, CO2 production, movement, food, and water consumption. Additionally, Echo MRI was used to determine total and bone marrow fat content in the mice. Blood and sera were collected from control and mutant mice and analyzed for glucose levels after fasting.

Results: EchoMRI showed whole body adipose tissue (Control: 13.85% +/- 2.01%, Transgenic: 7.71% +/- 1.42%) and bone marrow fat content (Control: 3.59%, Transgenic: 0.47%) were both reduced in the mutant mice. ColI(2.3)+/Rs1+ mice showed increased food, water, O2 consumption, and CO2 production despite reduced activity. Preliminary data indicate a sex specific differences in glucose levels, with males having reduced blood glucose and females having increased blood glucose levels (Male: Control: 124 mg/dl Transgenic: 44 mg/dl, Female: Control: 107.3 mg/dl +/- 22.3 mg/dl, Transgenic: 156.3 mg/dl +/- 9.5 mg/dl).

Conclusions: ColI(2.3)+/Rs1+ mice showed significant changes in whole-animal metabolic parameters consistent with recently described endocrine functions of bone. In addition, the ColI(2.3)+/Rs1+ mice showed significant local decreases in the bone marrow fat content, suggesting that activation of Gs-GPCR signaling in osteoblasts may also have a direct effect on local adipocytes. Our findings suggest that adipocytes contribute not only to metabolic homeostasis but may have important roles in the pathophysiology of bone overgrowth diseases.

***Disclosures: Corey Cain**, None.*

SU0128

Alveolar Bone-Associated Dental Anomalies in Craniometaphyseal Dysplasia Patients and Mouse Model. I-Ping Chen*, Aditya Tadinada, Eliane Dutra, Achint Utreja, Flavio Uribe, Ernst Reichenberger. University of Connecticut Health Center, USA

Craniometaphyseal Dysplasia is a rare genetic bone disorder involving hyperostosis of craniofacial bones, metaphyseal widening of tubular bones and dental abnormalities. A knock-in (KI) mouse model ($Ank^{KI/KI}$) carrying a Phe377del in ANK develops many skeletal features of CMD including dental anomalies such as excessive cementum. We examined CMD patients by cone beam computed tomography (CBCT) and by orthodontic indices. We also applied orthodontic force in mice to further evaluate consequences of tooth movement in $Ank^{KI/KI}$ mice.

All work involving human subjects was approved by the UCHC Institutional Review Board. We recruited 7 CMD patients carrying Phe377del or Ser375del mutations in ANKH. Each patient was subjected to dental examination, intraoral photographs and 12-inch field of view CBCT images. 10-week-old male $Ank^{+/+}$ and $Ank^{KI/KI}$ mice received orthodontic tooth movement using a NiTi closed-coil spring between the upper incisors and the left first molars for 14 days. The teeth and maxillae were fixed, subjected to micro-CT analyses, decalcified, embedded in paraffin, sectioned and stained with TRAP.

All patients had a history of delayed eruption of permanent teeth. Intraoral examination revealed normal soft tissue. CBCT data showed significant bucco-lingual expansion of jawbones, with expansion in maxillae more pronounced than in mandibles, however, there was no measurable increase in bone density. The majority of CMD patients had narrowed foramina and multiple impacted teeth. Orthodontic analyses showed all CMD patients had short anterior cranial base, short upper facial height and short maxillary length whereas the relationship between maxillae and mandibles in the anterior-posterior axis was inconsistent. Micro-CT analyses after orthodontic tooth movement in mice showed that $Ank^{KI/KI}$ molars can be moved without ankylosis but at a slower rate. As a result the spacing between first and second molars in $Ank^{+/+}$ mice was wider compared to $Ank^{KI/KI}$ mice ($p<0.05$). Qualitative histologic analyses showed TRAP staining on bone surfaces of the compression sites in both $Ank^{+/+}$ and $Ank^{KI/KI}$ molars, however, the size and numbers of $TRAP^+$ cells were decreased in $Ank^{KI/KI}$ mice. Root resorption was only observed in the $Ank^{KI/KI}$ molars suggesting that excessive cementum formation is more susceptible to OC resorption. Alveolar bone and dental anomalies should be considered when treating CMD patients orthodontically.

***Disclosures: I-Ping Chen**, None.*
This study received funding from: NIH

SU0129

Bone Deficits Resulting from MeCP2 Deficiency in a Mouse Model of Rett Syndrome are Partially Restored by Treatment with Teriparatide or Zoledronic Acid. Jay Shapiro*. Kennedy Krieger Institute, Johns Hopkins, USA

Introduction: While 50% of children and young adults with Rett Syndrome (RTT) have osteoporosis, the effect of MECP2 mutations on bone cell function is unknown, and there is no recognized treatment for osteoporosis in RTT. Purpose: To determine the effects of MeCP2 deficiency on osteoblast, osteoclast and osteocyte function in vitro and in vivo and to assess the effectiveness of treatment with teriparatide (anabolic, TPH) or zoledronic acid (antiresorptive, ZA). Methods: We conducted bone micro-CT, histomorphometry analyses and established osteoblast cell cultures from WT male and female Mecp2-null and Mecp2-HET mice using the Bird model of MeCP2 deficiency. For baseline data, untreated mice were sacrificed at 5 weeks (Mecp2-null and WT males) or 8 weeks of age (HET and WT females) and their tibias and femurs were retrieved. Starting at 3 (WT and Mecp2-null M mice) or 8 weeks (WT and HET F mice), teriparatide (TP, 40 mg/kg/day) zoledronic acid (ZA, 20 mg/kg/week) or vehicle (saline), was injected for 6 weeks. Results: On MicroCT, trabecular and cortical bone parameters were significantly decreased in Mecp2-null mice, while trabecular bone thickness was increased in HET compared to WT mice. Osteoblast cells from Mecp2-null mice did not express MeCP2 and had accelerated logrithmic growth rates and increased cell density compared to WT osteoblasts. Alkaline phosphatase activity (by immunostaining) in femur metaphysis showed that the secondary trabeculae (further from the growth plate) and along the endosteal surface, the Mecp2-null osteoblasts appear very thin and small, similar in shape to ''resting cells''. Trabecular bone from HET mice had less alkaline phosphatase activity than in WT, suggestive of deficient osteoblast activity and reduced bone formation in HET mice. Tartrate resistance acid phosphatase (TRAP) staining of osteoclasts showed that Mecp2-null mice had less bone and fewer osteoclasts than WT or HET mice. In WT and Mecp2-null male mice, ZA treatment increased bone volume fraction and tissue mineral density in trabecular and cortical bone, increased trabecular number and decreased trabecular bone separation to a greater amount than did TP. For cortical bone, polar moment of inertia was not significantly different in vehicle, ZA or TP treated null mice. Conclusions: Our preliminary results indicate a defect in osteoblast morphology and function, that osteoblast growth is altered by MeCP2 deficiency, and suggest that ZA may be more effective than TP in promoting increased bone growth and preventing bone loss in this RTT mouse model. Support: International Rett Syndrome Foundation and Rett Research Trust.

***Disclosures: Jay Shapiro**, None.*

SU0130

Calcific periarthritis as the only complication of adult hypophosphatasia in three middle-aged sisters. Nuria Guanabens*[1], Steven Mumm[2], Ingrid Möller[3], Eva Gonzalez-Roca[4], Pilar Peris[5], Jennifer Demertzis[6], Michael Whyte[7]. [1]Universitat De Barcelona, Spain, [2]Washington University School of Medicine, USA, [3]Institute Poal of Rheumatology, Spain, [4]Immunology Department, Hospital Clinic, Spain, [5]Hospital Clínic of Barcelona, Spain, [6]Musculoskeletal Disease Section, Mallinckrodt Institute of Radiology at Barnes-Jewish Hospital, USA, [7]Shriners Hospital for Children-Saint Louis, USA

Hypophosphatasia (HPP) is the inborn-error-of-metabolism characterized by low serum alkaline phosphatase (ALP) activity due to loss-of-function mutation(s) within the gene that encodes the tissue nonspecific isoenzyme of ALP (TNSALP). In HPP, extracellular accumulation of inorganic pyrophosphate (PPi), a TNSALP substrate and inhibitor of mineralization, leads frequently to premature tooth loss and often to rickets or osteomalacia. In affected adults, the PPi accumulation sometimes also manifests as calcium pyrophosphate dihydrate (CPPD) deposition, PPi arthropathy, or as seemingly paradoxical deposition of hydroxyapatite crystals in ligaments and around joints called calcific periarthritis (CP).

We report three middle-aged sisters with CP as the only clinical complication of HPP. Each presented during early adult life with recurrent episodes of pain principally around the shoulders, elbows, wrists, hips, or Achilles tendon. They were otherwise in good health including no history of unusual dental disease, fractures, or pseudofractures. Calcific deposits were identified in symptomatic areas (Figure) of each sister principally by ultrasonographic assessment compared to radiographic studies. All three sisters had low serum levels of total and bone-specific ALP, hyperphosphatemia, and increased serum concentrations of the TNSALP substrate pyridoxal 5′-phosphate together characteristic of HPP. Mutation analysis revealed a single unique 18-bp duplication within *TNSALP* (c.188_205dup18, p.Gly63_Thr68dup) carried by the sisters, their mother with knee osteoarthritis and no CP or CPPD deposition, and two healthy sons. CP has been reported in a few adult patients with HPP. We find that CP can be the only manifestation of the adult form of HPP. Thus, CP with multiple juxta-articular deposits of hydroxyapatite may be a useful sign of HPP, especially when CP is familial.

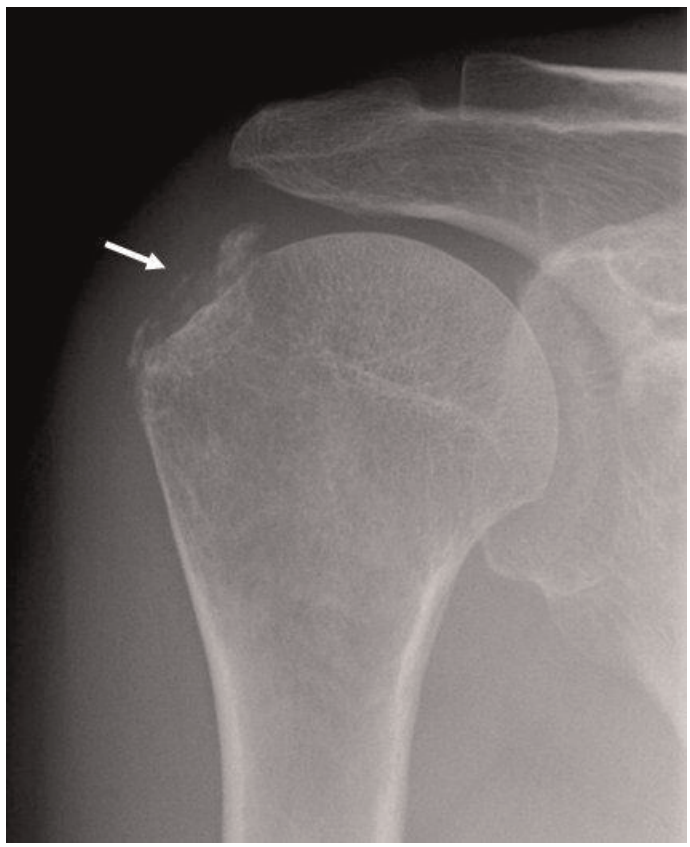

Figure

***Disclosures: Nuria Guanabens**, None.*

SU0131

Cyclophilin B KO Mouse Model of Type IX OI has Diminished Hydroxylation of Specific Collagen Helical Lysines Causing Altered Bone Crosslink Patterns. Wayne Cabral*[1], Irina Perdivara[2], MaryAnn Weis[3], Masahiko Terajima[4], Angela Blissett[1], Weizhong Chang[1], Elena Makareeva[5], Edward Mertz[5], Sergey Leikin[5], Kenneth Tomer[2], David Eyre[3], Mitsuo Yamauchi[4], Joan Marini[1]. [1]Bone & Extracellular Matrix Branch, NICHD, NIH, USA, [2]Laboratory of Structural Biology, NIEHS, NIH, USA, [3]Orthopaedic Research Laboratories, University of Washington, USA, [4]North Carolina Oral Health Institute, University of North Carolina, USA, [5]Section on Physical Biochemistry, NICHD, NIH, USA

Osteogenesis Imperfecta (OI) is a collagen-related bone dysplasia with bone fragility and short stature. Absence of proteins involved in collagen post-translational interactions results in recessive forms of OI, most of which involve components of the collagen prolyl 3-hydroxylation complex, CRTAP, P3H1 and PPIB/CyPB (OI types VII-IX, respectively). To investigate the role of CyPB in collagen folding and modification, *Ppib* knockout (KO) mice were generated using a gene-trap ES cell clone. KO mice are small, with reduced femoral aBMD, Tb & Ct BV/TV, and MOI. KO mice completely lack *Ppib* transcripts in skin, fibroblasts (FB), femora and calvarial osteoblasts (OB). CyPB was absent on immunoblots of KO cultured FB and OB lysates. The α1(I)P986 3-hydroxylation of cell culture- and tissue-derived collagen was severely reduced (2-11% of WT). Delayed intracellular folding and reduced electrophoretic migration of steady-state collagen from KO cells support the rate-limiting role of CyPB in collagen folding. In contrast, total hydroxylysine and 4-hydroxyproline content was normal in KO cell collagen, suggesting increased glycosylation caused the electrophoretic delay. In skin tissue collagen, total Hyl is reduced, consistent with more rapid gel migration of collagen alpha chains. However, total collagen Hyl is normal in KO bone, with near-normal gel migration and glycosylation. Detailed analysis of bone and OB type I collagen by mass spectrometry revealed site-specific alterations in post-translational modifications. There is dramatic underhydroxylation of helical crosslink residue Lys87 in both α1 (↓20% in OB, ↓40% in bone) and α2 (↓15% in OB, ↓20% in bone) chains, with consequent underglycosylation. The altered Lys modification changes the type and quantity of collagen crosslinks in KO bone. There is a 4-fold increase in trivalent LP crosslinks ($p=0.001$) and a corresponding decrease in the HP/LP ratio detected in bone tissue. Although total bone collagen crosslinks (HP+LP) in KO were double WT ($p=0.003$), abnormal collagen modification and crosslinking is associated with a 70-80% reduction of collagen deposited into KO matrix in culture. These findings suggest a novel role for CyPB in supporting the activity of tissue-specific collagen lysyl hydroxylase(s), thus indirectly regulating collagen glycosylation, crosslinking and fibrillogenesis, and promoting normal bone mineralization and strength. Abnormal crosslinks may be a common pathological feature of OI bone.

***Disclosures: Wayne Cabral**, None.*

SU0132

Genetic Variation In The Obesity Related GeneMC4R Is Associated With Bone Quality In Elderly Women. Gaurav Garg*[1], Jitender Kumar[2], Fiona McGuigan[3], Mattias Callréus[4], Paul Gerdhem[5], Kristina Akesson[6]. [1]Clinical Research Center, Lund University, Sweden, [2]Upsala University, Sweden, [3]University of Lund, Malmö, Skane University Hospital, Malmö, Sweden, [4]Skåne University Hospital, Sweden, [5]Karolinska Institutet, Sweden, [6]Skåne University Hospital, Malmö, Sweden

Introduction: Osteoporosis is characterized by reduced bone mineral density (BMD) and increased fracture risk. Fat and lean mass are established determinants of bone strength with a strong genetic component. The relationship between obesity and BMD or bone quality are still unclear. In this study we examined the association between three obesity related genes with bone properties and fracture.

Methodology: We studied 2 cohorts of Swedish women at different ages: PEAK25 (all 25 years, n=1061) and OPRA (all 75 years, n=1044). Five common variants from 3 genes identified through GWAS were analysed to determine age related effects on body composition and bone phenotypes: rs17782313 and rs1770633 (MC4R: Melanocortin 4 receptor); rs7566605 (INSIG2: Insulin induced gene 2) and rs9939609 and rs1121980 (FTO- Fat mass and obesity associated).

Results: BMI, total body fat and lean mass were strongly and positively correlated with total body BMD, femoral neck BMD and ultrasound parameters in both cohorts ($r^2=0.2$-0.6). MC4R gene polymorphism rs17782313 was significantly associated with ultrasound, but only in the elderly cohort. Individuals with the rare CC genotype had higher values for all QUS parameters (BUA: $p=0.007$; 0.002); (SoS: 0.02; 0.007); (Stiffness: 0.001; <0.0001) under co-dominant and dominant models respectively. Interestingly, rs17782313 'C' carriers also had lower folate and vitamin D levels ($p=0.03$) and high homocysteine levels ($p=0.06$). MC4R SNPs rs17782313 and rs1770633 were not significantly associated with BMD or body composition in either OPRA or PEAK25. Fracture incidence in the elderly women did not differ with MC4R genotype. The FTO gene was associated with body composition in the young women ($p<0.006$) but FTO and INSIG2 polymorphisms were not associated with bone parameters in either cohort. However vertebral fracture incidence between baseline and 5-year follow-up was lower in elderly women with the rare INSIG2 rs7566605 genotype ($p=0.01$).

Conclusion: Body composition is one of the strongest determinants of bone strength. Genetic variation in theobesityassociatedgeneMC4R contributes to improved bone quality directly and through a trend towards increased BMI among carriers of the rare rs17782313 'C' allele. Our results are supported by other studies in an animal model showing decreased bone resorption with this polymorphism. Further studies are warranted to reveal the mechanism underlying the role of these genes on bone metabolism.

***Disclosures: Gaurav Garg**, None.*

SU0133

IFITM5 c.−14C>T Mutation Causing Type V Osteogenesis Imperfecta Decreases COL1A1 Expression and Increases Mineralization by Cultured Proband Osteoblasts. ADI REICH*[1], Alison S Bae[2], Aileen M Barnes[2], Wayne A Cabral[2], David Chitayat[3], Joan Marini[1]. [1]National Institute of Child Health & Human Development, USA, [2]NIH/NICHD/BEMB, USA, [3]The Hospital for Sick Children, & the Department of Obstetrics & Gynecology, The Prenatal Diagnosis & Medical Genetics Program, Canada

Osteogenesis imperfecta (OI) is a genetically heterogeneous disorder characterized by bone fragility. Most cases have dominant mutations of type I collagen, while recessive OI is caused by defects in genes whose products interact with type I collagen. Type V OI probands have dominant inheritance; characteristic skeletal findings include ossification of the forearm interosseus membrane, radiodense metaphyseal bands, propensity for hyperplastic callus formation, and mesh-like lamellation on bone histology. Type V OI probands are reported to have white sclerae. The cause of type V OI was recently shown to be a unique heterozygous mutation in *IFITM5* (c.-14C>T), which encodes Bril, a transmembrane protein expressed in osteoblasts. The mutation generates a start codon in the 5'-UTR, adding five residues to the Bril N-terminus. However, the mechanism that leads to the type V OI phenotype and its relationship with type I collagen is unknown. We identified 5 patients with the *IFITM5* (c.-14C>T) mutation : 3 patients with typical type V OI histology and radiographic findings, and 2 patients not previously classified as type V OI. The latter two patients have an atypical phenotype, including a child with strongly blue sclerae and no dense metaphyseal bands and an adult with progressive deforming OI. Using cultured osteoblasts (OB) from patients with characteristic type V OI, we verified expression of mutant *IFITM5* transcripts. Next, type V OI and control OB were cultured in osteogenic differentiation media. During D10-15 of the differentiation timecourse, type V OI OB had less than half the *COL1A1* expression of control, while osteocalcin (*BGLAP)* expression was increased during this timeframe, ranging from 2-8x control. Type V OI differentiated OB also had increased mineralization by alizarin-red assay. Comparison of type V OI and control OB transcripts on osteogenic arrays revealed other significantly altered transcripts, currently being validated. Electrophoretic migration of steady-state type I collagen was normal from proband OB with typical type V OI. We conclude that OI patients without the well-described type V OI phenotype may also have the same *IFITM5* mutation. The collagen-related defect and increased mineralization demonstrated in type V OI OB during differentiation may underlie the overactive tissue calcification and hypertrophic callus formation seen in affected individuals.

***Disclosures: ADI REICH**, None.*

SU0134

Sclerostin antibody treatment improves bone mass and microarchitectural parameters in young Crtap-/- mice, a model of pediatric recessive Osteogenesis Imperfecta. Ingo Grafe*[1], Tao Yang[2], Caressa Lietman[3], Erica Homan[3], Elda Munivez[3], Yuqing Chen[3], Ming-Ming Jiang[3], Terry Bertin[3], Brian Dawson[3], Franklin Asuncion[4], Hua Zhu (David) Ke[4], Michael Ominsky[4], Brendan Lee[5]. [1]Department of Molecular & Human Genetics, Baylor College of Medicine, USA, [2]Van Andel Research Institute, USA, [3]Baylor College of Medicine, USA, [4]Amgen Inc., USA, [5]Baylor College of Medicine & Howard Hughes Medical Institute, USA

Recently, we demonstrated efficacy of sclerostin antibody (Scl-Ab) treatment in adult Crtap-/- mice, a model of recessive Osteogenesis Imperfecta (OI) with defects in posttranslational modifications of type I collagen (Grafe et al ASBMR 2012). Scl-Ab treatment resulted in improved bone mass, bone microarchitecture and increased bone strength. However, whether Scl-Ab treatment is also effective on the growing skeleton in young Crtap-/- mice is still unknown. Consequently, in this study we tested the effects of Scl-Ab treatment in growing Crtap-/- mice as a potential model of pediatric treatment.

One week old female Crtap-/- mice were treated with Scl-Ab for 6 weeks (Scl-AbVI, 25 mg/kg, s.c., twice per week), PBS treated Crtap-/- and wildtype (WT) mice served as controls (n=6/group). After treatment, spines and femurs were analyzed by MicroCT.

At vertebral body L4, Scl-Ab treatment of Crtap-/- mice significantly improved BV/TV (+141%), Tb.N (+61%) and Tb.Sp (-45%) compared to PBS-treated Crtap-/- mice. Tb.Th was increased by 49% and not statistically different from WT mice. Cortical thickness at the femur midshaft was significantly increased by 14%, and at the femur metaphysis, Scl-Ab significantly increased Tb.N (+53%) and BV/TV (+63%), while Tb.Th remained unchanged. Interestingly, the findings in the trabecular bone of femurs differed from a previous report of the effects of the same Scl-Ab in young Brtl/+ mice (a model of dominant OI due to a mutation in the Col1a1 gene), where treatment resulted in improved Tb.Th, but had no significant effects on BV/TV and Tb.N (Sinder et al

ASBMR 2012). These distinctions in treatment outcomes may be due to different genders, treatment duration or genetic background of the mice in these studies. However, it is also possible that the beneficial effects of stimulating the Wnt signaling pathway with Scl-Ab on trabecular bone in the growing skeleton may be different in OI due to mutations in genes involved in post-translational collagen modifications compared to those with OI caused by mutations in the genes encoding type I collagen.

In summary, our results indicate that Scl-Ab treatment improves bone mass and bone microarchitecture in young Crtap-/- mice. These findings suggest that Scl-Ab treatment may be beneficial in pediatric patients with OI, in particular with recessive forms of the disease.

***Disclosures: Ingo Grafe**, None.*

SU0135

Sexual Dimorphism of Trabecular Bone Is Epigenetically Imprinted. Beth Bragdon*[1], Robert Burns[2], Amelia Baker[2], Anna Belkina[2], Gerald Denis[2], Elise Morgan[3], Louis Gerstenfeld[2], Jennifer Schlezinger[4]. [1]Boston University School of Medicine Department of Orthopaedics, USA, [2]Boston University School of Medicine, USA, [3]Boston University, USA, [4]Boston University, School of Public Health, USA

Introduction: It is well established that females have reduced bone mineral density compared to males and that levels of marrow fat affect bone health. A study of sex linked differences in the anabolic potential of osteoblast and adipocyte differentiation was carried out in mice.

Methods: Male and female C57BL6 (B6) mice (N=4-7) were assessed at 3, 6, and 9 months. Micro-computed tomography (MicroCT) was used to asses the structure of the right tibia. Immunohistological analysis for perilipin was used to assess marrow adipocyte content. RNA was isolated from the whole humeri, and expression of cassettes of mRNAs for osteoblasts/osteocytes (RUNX2, osteocalcin, DMP1, SOST) and adipocytes (PPARγ, FABP4, adipsin, perilipin) was assessed by qRT-PCR. Primary bone marrow stromal cells (BMSC) were cultured from the remaining hind limb long bones to assess their osteogenic and adipogenic potential. Osteogenesis was stimulated with ascrobate and β-glycerolphosphate. Adipogenic potential was based on responsiveness to rosiglitazone (ROSI). Estrogen effects were assessed by comparing BMSCs from mice ovariectomized (OVX) at 4 weeks of age to those from intact females or by culturing female BMSCs in estrogen-stripped or estrogen-supplemented media.

Results: MicroCT showed female mice at all ages had lower trabecular bone compared to age matched males. Immunohistology showed that females always had greater adipocyte content in their marrow than males. Similar expression of bone- and adipocyte-related genes was seen in males and females at 3 and 9 months, while at 6 months, females exhibited ~2X greater expression of both bone- and adipocyte-related genes than males. BMSC cultures retained these sex-linked differences. Female BMSC cultures consistently showed 1.5-2.0X higher expression of bone-associated genes, and female cultures were ~2-3X more responsive to ROSI-induced adipogenesis. BMSCs prepared from OXV mice showed similar results compared to BMSC from intact females. Estrogen-stripped media increased the adipogenic response to ROSI while decreasing the response to osteogenic signals.Conclusions: Even though females have decreased BV/TV compared to males, their bone metabolism is increased. These results suggest that the increased metabolic activity in females renders them more susceptible to adipogenesis resulting in greater adipocyte accumulation. Together, these results suggest an epigenetic component to the sexual dimorphic differences in skeletal tissue.

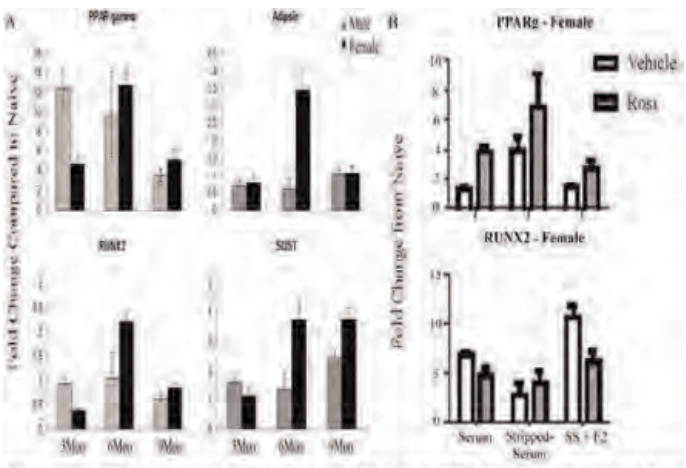

Messenger RNA expression for whole bone (A) and BMSCs (B). A. RNA isolated from humuri of male (gray bars) and female (black bars) B6 mice. B. BMSCs from B6 females cultured in media containing unmodified serum, charcoal-stripped serum, or estradiol (10^{-8}M) supplemented stripped serum (SS+E2) were stimulated to undergo osteogenesis and treated with vehicle (white bars) or ROSI (gray bars).

Figure 1

***Disclosures: Beth Bragdon**, None.*
This study received funding from: Ellison Foundation Grant

SU0136

The G60S Connexin 43 Mutation Activates the Osteoblast Lineage and Results in a Resorption-Stimulating Bone Matrix and Abrogation of old Age-Related Bone Loss. Tanya Zappitelli*[1], Frieda Chen[1], Luisa Moreno[1], Ralph Zirngibl[1], Marc Grynpas[2], Janet Henderson[3], Jane Aubin[4]. [1]University of Toronto, Canada, [2]Samuel Lunenfeld Research Instituteof Mount Sinai Hospital, Canada, [3]Division of Orthopedics, Montreal General Hospital, Canada, [4]University of Toronto Faculty of Medicine, Canada

Gja1^{Jrt}/+ mice carry a mutation in the gap junction protein, alpha 1 gene (*Gja1*), encoding for a dominant G60S Connexin 43 (Cx43) mutant protein, resulting in production of less than 50% wild type (WT) levels of Cx43 protein and significantly reduced gap junction formation and function in Cx43-expressing cells. Similarly to other Cx43 mutants with loss or reduction in Cx43 gap junction formation and or function, including a global Cx43 deletion, four skeletal cell conditional-deletion mutants and a Cx43 missense mutant (G138R/+), the *Gja1*^{Jrt}/+ mice exhibit early onset osteopenia and changes in the structural (reduced cortical thickness, increased marrow space) and biomechanical properties (reduced material and structural properties) of femoral bones. In contrast to other Cx43 mutants, however, we found that the early osteopenic phenotype results from increased appendicular skeleton osteoblast activity leading to cell autonomous upregulation of both matrix bone sialoprotein (BSP) and membrane-bound receptor activator of nuclear factor kappa-B ligand (mbRANKL). In younger *Gja1*^{Jrt}/+ mice, these contribute to increased osteoclast number and activity on trabecular and endosteal bone surfaces, resulting in early onset high turnover osteopenia. Additionally, *Gja1*^{Jrt}/+ is the only Cx43 mutant mouse model reported to display a protection from old-age related diminution in BMD and exhibit age-related improvement in femoral bone structural and material properties. This is manifested by elimination or abrogation of the reduced trabecular BV/TV, cortical thickness, increased marrow space and reduced material properties in older compared to younger *Gja1*^{Jrt}/+ mice versus WT mice. The age-related protection and improvement in *Gja1*^{Jrt}/+ bone parameters appears to result from increased serum alkaline phosphatase (ALP), osteoprogenitor numbers, and serum osteoprotegerin (OPG) levels, which increase mineral deposition, contribute to the generation of active osteoblasts, and reduce bone resorption, respectively, allowing cortical and trabecular bone thickness to increase over time. Our study is the first to describe a Cx43 mutation in which osteopenia is caused by increased rather than decreased osteoblast function, where production of an abnormal bone matrix activates osteoclastogenesis and bone resorption, and where mice are protected from old-age related bone loss with improvement in structural and material parameters over time.

***Disclosures: Tanya Zappitelli**, None.*

SU0137

The Osteogenesis Imperfecta Adult Natural History Initiative: a web-based survey. Laura Tosi*[1], Matthew Oetgen[1], Melanie Rak[2], Marianne Floor[1], Carole Tucker[3], Tracy Hart[4], Mary Beth Huber[4], Fergus McKiernan[5]. [1]Children's National Medical Center, USA, [2]Rehabilitation Institute of Chicago, USA, [3]Temple University, USA, [4]Osteogenisis Imperfecta Foundation, USA, [5]Marshfield Clinic, USA

Introduction: Osteogenesis imperfecta (OI), is a heterogeneous, rare disorder most commonly affecting Type I collagen. Patients with OI face the possibility of complications in nearly every organ system in the body. There is little information about the natural history of OI beyond childhood.The OI Adult Natural History Initiative (OI ANHI) was developed in collaboration with adults with OI, the Osteogenesis Imperfecta Foundation (OIF), and members of the medical community in order to address this data and care gap. The team established a web-based portal within the existing OIF website to create a cost-effective outreach and data management clearinghouse with which to survey the OI community and capture a first-ever ''snapshot'' of the health status, needs, and priorities of adults with OI.

Methods: The ANHI web-based survey was created using the National Institutes of Health (NIH)-sponsored tool PROMIS® (Patient-Reported Outcomes Measurement Information System) and was conducted over 3-months. The survey included questions on general health concerns and health behaviors plus a review of systems, with scale-based rankings of respondents' priorities, concerns, and the impact of common impairments and conditions within each medical system. Respondents were recruited through letters to individuals on the OIF mailing list, as well as through social networking sites.

Results: A total of 959 surveys were fully completed. Over 93% of respondents completed the survey on the web. 70% of respondents were women and 89% were white. 31% of respondents reported they did not know their OI type. Survey analyses suggest that adults with OI have more pulmonary and cardiovascular issues than the general US population. There was limited correlation with respondents' description of themselves as having mild, moderate or severe disease (or OI type) and patient-reported measures of health status

Conclusions: The OI ANHI survey underscored numerous health concerns faced by the adult OI community and identified numerous opportunities for future research. The marked heterogeneity of OI also demands a clearer methodology for stratifying patients; therefore we plan to use survey measures to explore the development of a

new classification/stratification system for OI that might allow both patients and clinicians to assign risk for both skeletal and non-skeletal complications with greater confidence. It will be essential to recruit more men and minorities in future surveys.

***Disclosures: Laura Tosi**, None.*

SU0138

Yunis-Varón syndrome is caused by mutations in *FIG4* encoding a phosphoinositide phosphatase. Philippe Campeau*[1], Guy Lenk[2], James Lu[3], Yangjin Bae[4], Lindsay Burrage[4], Peter Turnpenny[5], Jorge Román Corona-Rivera[6], Lucia Morandi[7], Marina Mora[7], Heiko Reutter[8], Anneke Vulto-van Silfhout[9], Laurence Faivre[10], Eric Haan[11], Richard Gibbs[12], Miriam Meisler[13], Brendan Lee[14]. [1]Baylor College of Medicine, USA, [2]Department of Human Genetics, University of Michigan, MI, 48109-0618, USA, [3]Human Genome Sequencing Center, Baylor College of Medicine, USA, [4]Department of Molecular & Human Genetics, Baylor College of Medicine, USA, [5]Clinical Genetics Department, Royal Devon & Exeter Hospital, United Kingdom, [6]Genetics service, Division of Pediatrics, ''Dr. Juan I. Menchaca'' New Civil Hospital of Guadalajara, Mexico, [7]Neuromuscular Diseases & Neuroimmunology Unit, Foundation IRCCS Neurological Institute ''Carlo Besta'', Italy, [8]Department of Neonatology & Institute of Human Genetics, Children's Hospital, University of Bonn, Germany, [9]Department of Human Genetics, Radboud University Nijmegen Medical Centre, Netherlands, [10]Centre de Génétique, Centre de Référence Maladies Rares "Anomalies du Développement et Syndromes Malformatifs", Hôpital d'Enfants, France, [11]South Australian Clinical Genetics Service, SA Pathology at Women's & Children's Hospital, & Discipline of Paediatrics, The University of Adelaide, Australia, [12]Human Genome Sequencing Center & Department of Molecular & Human Genetics, Baylor College of Medicine, USA, [13]Department of Human Genetics, University of Michigan, USA, [14]Baylor College of Medicine & Howard Hughes Medical Institute, USA

Yunis-Varón syndrome (YVS) is an autosomal recessive disorder with cleidocranial dysplasia, digital anomalies and severe neurological involvement. Enlarged vacuoles are found in neurons, muscle, and cartilage. By whole exome sequencing, we identified frameshift and missense mutations of *FIG4* in affected individuals from three unrelated families. *FIG4* encodes a phosphoinositide phosphatase required for regulation of $PI(3,5)P_2$ levels, and thus endosomal trafficking and autophagy. In a functional assay, both missense substitutions failed to correct the vacuolar phenotype of *Fig4* null mouse fibroblasts. Homozygous *Fig4* null mice exhibit features of YVS, including neurodegeneration and enlarged vacuoles in neurons. We demonstrate that *Fig4* null mice also have small skeletons with reduced trabecular bone volume and cortical thickness, and that cultured osteoblasts accumulate large vacuoles. Our findings demonstrate that homozygosity or compound heterozygosity for null mutations of *FIG4* is responsible for YVS, the most severe known human phenotype caused by defective phosphoinositide metabolism. In contrast, in Charcot-Marie-Tooth disease type 4J also caused by *FIG4* mutations, one of the *FIG4* alleles is hypomorphic and disease is limited to the peripheral nervous system. This genotype-phenotype correlation demonstrates that absence of FIG4 activity leads to central nervous system dysfunction and extensive skeletal anomalies. Our results describe a previously unrecognized role for $PI(3,5)P_2$ signaling in skeletal development and maintenance.

***Disclosures: Philippe Campeau**, None.*

SU0139

Association between Polymorphisms in Leptin, its Receptor and Beta Adrenergic Receptor Genes and Bone Response to Hormone Therapy in Postmenopausal Korean Women. Jung-Gu Kim*[1], Hoon Kim[2], Seung-Yup Ku[2], Seok Hyun Kim[2], Young Min Choi[2], Jong Hak Kim[3]. [1]Seoul National University Hospital, South Korea, [2]Department of Obstetrics & Gynecology, Seoul National University College of Medicine, South Korea, [3]Ewha Womans University Mokdong Hospital, South Korea

Objective: The purpose of this study was to investigate the association between polymorphisms in leptin (LEP), its receptor (LEPR) and beta adrenergic receptor (ADRB) genes and bone response to hormone therapy (HT) in postmenopausal Korean women.

Methods: The LEP c.280G>A, LEPR c.326A>G, c.668A>G, c.1968G>C, c.2096C>T, ADRB2 c.46A>G, c.79C>G, c.718T>C, c.741G>T, c.769G>A, and ADRB3 c.190T>C polymorphisms were analyzed by polymerase chain reaction-restriction fragment length polymorphsim (PCR-REFLP), Taqman assay or direct DNA sequencing in 512 postmenopausal Korean women receiving sequential HT for 1 year. BMD at the lumbar spine (LS) and femoral neck (FN) was determined by dual energy X-ray absorptiometry.

Results: Among SNPs measured, ADRB2 c.46A>G polymorphism only was associated with annual percent changes in BMD at the femoral neck after 1 year of HT (P=0.01), and BMD at the femoral neck in the AA genotype of ADRB2 c.46A>G polymorphism decreased significantly compared to those in other genotypes. When a non-responder was defined as a woman who had lost more than 3% of BMD per year after HT, ADRB2 c.46A>G and ADRB3 c.190T>C polymorphisms among genetic polymorphisms studied were associated with the risk of non-response of HT. The AA genotype of ADRB2 c.46A>G showed a 1.82-times higher risk of non-response at FN (P=0.01) and 1.63-times higher risk of non-response at LS and/or FN (P=0.02), as compared with non-AA genotype. In the analysis of ADRB3 c.190T>C polymorphism, women with the TT genotype demonstrated a 1.51-times higher risk of non-response at LS and/or FN (P=0.03) compared with non-TT genotype.

Conclusions: The ADRB2 c.46A>G and ADRB3 c.190T>C polymorphisms may be associated with risk of non-response to HT in postmenopausal Korean women.

Funding Support: This research was supported by Basic Science Research Program through the National Research Foundation of Korea (NRF) funded by the Ministry of Education, Science and Technology (2011-0022334).

***Disclosures: Jung-Gu Kim**, None.*

SU0140

Identification and characterization of novel FGFR2 mutation causing craniosynostosis. Han-sol Bae*[1], Hyun-Mo Ryoo[2], Ye-jin Seo[1], Seung-Hak Baek[3]. [1]Seoul National University, South Korea, [2]Seoul National University School of Dentistry, South Korea, [3]A professor responsible for management, South Korea

Craniosynostosis(CS) is characterized by the premature obliteration of cranial sutures. Fibroblast growth factor receptor2 (FGFR2) mutations have been reported as the most common genetic cause of CS. Our previous studies indicate that activated FGFR2 stimulates an osteogenic master transcription factor, Runx2, through the MAP kinase. Here we identified novel mutation of FGFR2 gene obtained from sequence analyses of 30 Korean CS patients, FGFR2L617F. Features of this newly identified clinical disorder exhibited exorbitism and midface hypoplasia. This mutation occurs in the 2nd tyrosine kinase domain in the C-terminal cytoplasmic region of the molecule. It was verified by Restriction Fragment Length Polymorphism (RFLP). The amino acid sequence alignment revealed that eight species of vertebrates showed high homology around the position of the novel mutation. The high conservation of that domain in many kinds of organism means, the relevant position of L617 is functionally important and the mutation on that site is pathogenic. The mutation displayed high expression of several bone marker genes and enhanced Runx2 transacting activity. Moreover, it also showed strong activation of the ERK-MAPK signaling pathway and FGF signaling through increased phosphorylation of signaling factors and FGFR. These findings would support that L617F mutation may induce aberrant gain of function such as constitutive activation which is leading to early closure of cranial suture. This work identifies FGFR2L617F as a unique mutation causing CS and provides a pathway-based phenotypic link of FGFR2 mutation with the human disease.

***Disclosures: Han-sol Bae**, None.*

SU0141

On Genome-wide Association Studies and their Meta-analyses – Lessons Learned from Osteoporosis Studies. Yongjun Liu*[1], Lei Zhang[1], Yufang Pei[2], Christopher Papasian[3], Hong-Wen Deng[1]. [1]Tulane University, USA, [2]Tulane, USA, [3]UMKC, USA

Osteoporosis, the most common metabolic skeletal disorder in humans, has strong genetic determination; however, the majority of genetic variants contributing to risk of osteoporosis remain undiscovered. In the past 4 years, the bone field has witnessed great advances in genome-wide association studies (GWASs) of osteoporosis, with a number of promising genes identified. In particular, meta-analysis of GWASs, aimed at increasing the power of studies by combining the results from different study populations, have led to the identification of novel associations that would not otherwise have been identified in individual GWASs. However, it is important to note that inconsistent findings are seen among and between GWASs and meta-analyses, and inconsistencies have even been observed between meta-analyses whose samples overlapped to a large extent. Consequently, the limitations of GWASs and their meta-analyses must be carefully evaluated, with an emphasis on understanding the reasons for inconsistent results between different meta-analyses, before we can correctly interpret the extensive results generated from these meta-analyses. Here we reviewed prominent empirical findings and problems in GWASs and meta-analysis of GWASs on osteoporosis, and then performed computer simulation analyses to help understand these findings and problems. We show that discordant findings in GWASs and meta-analyses are not unexpected, even for true susceptible genes. Importantly, contrary to the general belief, meta-analyses should not be used as a gold standard to evaluate the results of individual GWASs. In particular, individual GWASs in homogeneous populations can detect true disease genes that meta-analyses may have low power to replicate.

***Disclosures: Yongjun Liu**, None.*

SU0142

SIBLING Family Genes and Bone Mineral Density: Association and Allele-specific Expression in Human. Imranul Alam*[1], Leah Padgett[2], Shoji Ichikawa[1], Mohammed Alkhouli[2], Daniel Koller[1], Dongbing Lai[3], Munro Peacock[4], Xiaoling Xuei[5], Tatiana Foroud[3], Howard Edenberg[6], Michael Econs[1]. [1]Indiana University School of Medicine, USA, [2]Medicine, IUPUI, USA, [3]Medical & Molecular Genetics, IUPUI, USA, [4]Indiana University Medical Center, USA, [5]Biochemistry & Molecular Biology, USA, [6]Biochemistry & Molecular Biology, Medicine, IUPUI, USA

Osteoporosis is a common complex disorder with reduced bone mineral density (BMD) and increased susceptibility to fracture at multiple skeletal sites. Peak BMD is one of the primary skeletal determinants of osteoporotic fracture risk and is under substantial genetic control. Extracellular matrix (ECM), a major component of bone and a highly dynamic structure, influences BMD as it regulates mineral deposition and maintains cellular activity. ECM of bone contains several SIBLING family proteins, null mutations of which cause mineralization defects in humans. In this study, we tested 9 single-nucleotide polymorphisms (SNPs) located in the 5 SIBLING family genes (*DSPP*, *IBSP*, *DMP1*, *SPP1* and *MEPE*) for association with normal variation in peak BMD in healthy men and women. We measured femoral neck (FN) and lumbar spine (LS) aBMD by DXA in 1,692 premenopausal white women, 512 premenopausal black women and 715 white men. SNPs genotyping determined using the Sequenom MassARRAY system was tested for association with the 2 key BMD phenotypes in the 3 study subsamples. In the white women, we observed association ($p<0.005$) with FN-BMD for SNPs in *IBSP* and *DMP1*, and for LS-BMD with SNPs in *DSPP*, *IBSP* and *MEPE*. One SNP in *SPP1* was associated ($p<0.05$) in black women for FN-BMD. Three SNPs, one in each of *DSPP*, *DMP1* and *SPP1* were associated ($p<0.05$) with FN-BMD and one SNP in *DMP1* was associated ($p<0.05$) with LS-BMD in white men. To identify whether there was preferential allelic expression of these genes at these SNPs we measured the allele-specific expression (ASE) by the MassARRAY system using 52 human bone samples obtained from femoral neck during surgical hip replacement (27 female, 25 male, 44 Caucasian and 8 African-American). This approach tests for differences in expression between 2 alleles within the same heterozygous individual. We observed an allelic imbalance in mRNA expression (higher or lower expression of one allele compared to the other) for the SIBLING genes: higher expression of G allele for SNP rs2615497 in *DMP1*, A for SNP rs6812524 in *SPP1* and T for SNP rs1054629 in *IBSP*; lower expression of A for SNP rs2736982 in *DSPP*, G for SNP rs17013182 in *IBSP*, G for SNP rs17013285 in *MEPE* and T for SNP rs1126616 in *SPP1*. Our data shows that SIBLING genes are associated with BMD in healthy subjects and SNPs within the mRNA are associated with variation in allelic specific mRNA expression. ASE of SIBLING genes may contribute to normal variation of peak BMD.

***Disclosures: Imranul Alam**, None.*

SU0143

BMP-2 Delivery using Electrospun PLLA/Collagen I Scaffolds with Surface Adsorbed plasmid DNA/Transfection Complexes. Xia Zhao[1], David Komatsu[2], Michael Hadjiargyrou*[3]. [1]Stony Brook University, USA, [2]Stony Brook University, Dept. of Orthopaedics, USA, [3]New York Institute of Technology, USA

Delivery of BMP-2 protein is a wildly used strategy to engineer new bone. However, BMP-2 protein has a very short half-life in vivo which necessitates the delivery of doses ranging from hundreds of micrograms to low milligram levels to ensure significant bioactivity. As an alternative, we hypothesized that BMP-2 plasmid DNA delivery can serve as a lower cost and biologically effective approach. Our laboratory previously fabricated PLLA/Collagen I electrospun scaffolds which supported robust osteoblast cell attachment, proliferation, migration and differentiation. As such, we utilized these scaffolds to test whether the delivery of surface adsorbed BMP-2 plasmid DNA complexed with commercial transfection reagents is able to induce ectopic bone formation. We initially prepared scaffolds with surface adsorbed β-gal plasmid DNA complexes and evaluated their ability to transfect Hela cells *in vitro.* Visual analysis of the treated cells showed the scaffolds to have a ~40% transfection efficiency. Similar studies conducted using MC3T3 preosteoblastic cells revealed that exposure to the scaffolds with adsorbed BMP-2 plasmid DNA/transfection complexes resulted in a robust increase in BMP-2 mRNA levels, verifying the successful delivery and expression of the BMP-2 gene. An *in vivo* study was then performed using the mouse quadriceps muscle pouch model of ectopic bone formation. PLLA/Collagen I scaffold discs (5mm in diameter) with or without surface adsorbed BMP-2 plasmid DNA/transfection complexes were implanted into each muscle pouch. Gene expression analyses of day 7 samples showed a 3-fold increase in BMP-2 mRNA. Similarly, immunohistochemistry of day 7 samples revealed strong expression of BMP-2 protein. Further, ongoing microCT analyses of day 14 and day 28 samples show evidence of ectopic bone formation. Overall, these data demonstrate that electrospun PLLA/Collagen scaffolds with surface adsorbed BMP-2 plasmid DNA/transfection complexes can safely and effectively drive transgene expression both *in vitro* and *in vivo* and suggest that these scaffolds have the potential to advance skeletal tissue engineering.

***Disclosures: Michael Hadjiargyrou**, None.*

SU0144

PERK-ATF4-CHOP Signaling Contributes to TNFα-induced Vascular Calcification. MASASHI MASUDA*, Shinobu Miyazaki, Makoto Miyazaki. University of Colorado-Denver, USA

Purpose: TNFα is a critical regulator of vascular calcification. The purpose of the present study was to investigate whether the PERK-ATF4-CHOP axis of the endoplasmic stress contributes to TNFα induced vascular calcification in chronic kidney disease (CKD).

Methods and Results: We examined the effects of TNFα in the endoplasmic reticulum stress of vascular smooth muscle cells (VSMCs). TNFα treatment drastically induced the PERK-eIF2α-ATF4-CHOP axis of the endoplasmic reticulum (ER) stress response in VSMCs. PERK, ATF4 and CHOP shRNA knockdowns inhibited mineralization and osteogenesis of VSMCs induced by TNFα. CKD induced by 5/6 nephrectomies induced PERK-eIF2α-ATF4-CHOP axis of the ER stress response in the aortas of ApoE-/- mice with increased aortic TNFα expression and vascular calcification. Treatment 5/6 nx ApoE-/- mice with the TNFα neutralizing antibody reduced aortic PERK-eIF2α-ATF4-CHOP signaling increased by CKD, resulting in the inhibition of CKD-dependent vascular calcification.

Conclusions: These results suggest that the PERK-eIF2α-ATF4-CHOP axis of the ER stress mediates TNFα-induced vascular calcification.

Key words: vascular calcification, TNFα, endoplasmic reticulum stress, ATF4, CHOP

***Disclosures: MASASHI MASUDA**, None.*
This study received funding from: American Heart Association

SU0145

Rescuing Impaired Bone Healing in Type 1 Diabetes BBDP/Wor Rats. Tera Filion*[1], David Ayers[2], Jie Song[3]. [1]UMASS Medical School, USA, [2]UMass Memorial Medical Center, USA, [3]University of Massachusetts Medical School, USA

Bone healing in diabetic patients following orthopedic trauma is a significant clinical challenge. We developed an osteoconductive hydrogel-mineral composite containing 50% nanocrystalline HA (nHA) as a synthetic bone graft substitute. When pre-absorbed with a single dose of 400-ng rhBMP-2/7 and press-fit in 5-mm rat femoral segmental defects, the functional repair of the defect in normal rats was enabled by 12 weeks[1]. In this study, the same treatment failed to repair the critical-size defect in BBDP/Wor rats exhibiting diabetes. Delivery of a higher dose of rhBMP-2/7 (3-μg) or rhBMP-2 (6-μg) via the synthetic scaffold was required to induce the formation of a bony callus fully bridging the defect. Taking advantage of the ability of the nHA component of the synthetic scaffold to absorb endogenous proteins, we addressed the mechanism by which diabetic bone microenvironment prevents bone healing. The hydrogel-nHA scaffold alone was fit in the femoral defects in diabetic vs. normal rats and retrieved at 1, 2, 4, and 7 days for immunohistochemical detection of TGFβ, IL-1β, TNFα, VEGF, RANKL, BMP-2, -7, IGF-1 and SDF-1 retained on the scaffold. Absorption of these endogenous factors associated with the initiation of the inflammation/graft healing cascade or stem cell recruitment by the synthetic scaffold was significantly delayed/mitigated in diabetic rats, revealing an impaired biochemical microenvironment underlying the retarded healing. Meanwhile, bone marrow derived stromal cells (MSCs) and periosteal derived cells (PDCs) isolated from the long bones of diabetic rats (n=4) exhibited significant functional impairment in culture compared to normal skeletal progenitor cells. The diabetic MSCs and PDCs contained a significant senescent population, proliferated much slower and underwent highly impaired osteogenic differentiation upon culture induction compared to the normal controls. These findings suggest that co-delivery of multiple therapeutic agents that more effectively rescue the function of impaired skeletal progenitor cells in diabetic rats may be necessary for effective bone healing. Indeed, when IGF-1 and BMP-2 was co-delivered via the synthetic scaffold, a more robust bony callus bridged over the defect by 12 weeks. On-going investigations aim to identify more effective synergistic combinations of therapeutic agents and delivery scaffolds to reduce minimal loading doses of exogenous factors.

Ref:

1. Filion, T. M., Li, X. N., Mason-Savas, A., Kreider, J. M., Goldstein, S. A., Ayers, D. C., Song, J. (2011) *Tissue Eng Pt A* 17, 503-511.

***Disclosures: Tera Filion**, None.*

SU0146

Robust and Distinct Patterns of Transcriptional Activity of *Bmp2*, *Bmp4*, and *Noggin* in the Postnatal Skeleton. Steven Pregizer*, Douglas Mortlock. Vanderbilt University Medical Center, USA

BMP signaling plays an important role in the development, maintenance, and repair of skeletal tissues, including bone and cartilage. Nevertheless, the precise etiology of BMP signaling in the skeleton beyond embryogenesis is unclear. In this study, we used a collection of transgenic reporters to highlight the transcriptional activity of two BMP ligands (*Bmp2* and *Bmp4*) and their antagonist (*Noggin*) in the postnatal skeleton during normal development and aging. All three genes are robustly transcribed in distinct patterns one month after birth, a point of peak skeletal growth. Transcription of *Noggin* and *Bmp4* is lineage-dependent, with *Noggin* transcribed

exclusively in cells of the chondrogenic lineage, and *Bmp4* transcribed exclusively in cells of the osteogenic lineage. In contrast, *Bmp2* transcription is tightly linked to maturational status, with cells of both lineages exhibiting robust reporter activity as they progress towards terminal differentiation. At one year of age, when skeletal growth has ceased and the tissues are in a state of maintenance, only *Bmp2* retains transcriptional activity in the skeleton. Interestingly, it is restricted to chondrocytes found at the articular cartilage surface, with no appreciable activity in osteogenic cells. Taken together, these results illuminate the dynamics and cellular localization of *Bmp2*, *Bmp4*, and *Noggin* transcriptional activity in the postnatal skeleton. A fuller appreciation of these nuances will facilitate a better understanding of how BMP signaling orchestrates the development and maintenance of skeletal tissues.

***Disclosures: Steven Pregizer**, None.*

SU0147

FGF2 Primes Periosteal Cells for Endochondral Ossification via Maintenance of Skeletal Precursors and Modulation of BMP Signaling. Nick Van Gastel*[1], Steve Stegen[1], Riet Van Looveren[1], Ingrid Stockmans[1], Jan Schrooten[2], Daniel Graf[3], Frank Luyten[4], Geert Carmeliet[5]. [1]Laboratory of Clinical & Experimental Endocrinology, KU Leuven, Belgium, [2]Department of Metallurgy & Materials Engineering, KU Leuven, Belgium, [3]Orofacial Development & Regeneration, Institute of Oral Biology, Center for Dental Medicine, University of Zurich, Switzerland, [4]University Hospitals KU Leuven, Belgium, [5]Katholieke Universiteit Leuven, Belgium

Cell-based tissue engineering may be a promising approach for the repair of large bone defects. The bone marrow has traditionally been the preferred cell source, but evidence suggests that periosteum represents a valuable alternative. Given the beneficial effects of fibroblast growth factor 2 (FGF2) on bone formation by bone marrow stromal cells and the potential of this factor to promote fracture healing, a periosteum-driven process, we hypothesized that FGF2 addition during culture expansion could enhance the bone-forming potential of murine periosteum-derived cells (mPDC).

The addition of FGF2 promoted mPDC proliferation and inhibited culture-induced senescence, confirming known effects of FGF2 on mesenchymal stem cells (MSC). When FGF2-pretreated mPDC ($mPDC^{FGF2}$) were implanted on a calcium phosphate-collagen carrier at an ectopic or orthotopic site in mice, a remarkable increase in newly formed bone, associated with large amounts of bone marrow, was observed after 8 weeks compared to control cells. Unexpectedly, $mPDC^{FGF2}$ also formed small islands of mature cartilage at both locations. To further investigate this aspect, we subcutaneously injected cells in collagen gels, which already after 1 week resulted in robust cartilage formation by $mPDC^{FGF2}$, but not by control mPDC. By 2 weeks this cartilage template underwent endochondral ossification, evidenced by the presence of invading blood vessels, chondroclasts and osteoblasts as well as mineralized matrix.

To elucidate the underlying mechanisms we assessed the number of skeletal precursors in the cultures. The $mPDC^{FGF2}$ populations contain significantly more $Nestin^{+}$ mesenchymal stem cells (MSC) as well as osteoprogenitor cells, shown by increased *Runx2* expression and a higher number of osteogenic colony-forming units. Surprisingly, the expression of chondrogenic lineage markers was reduced, indicating that the enhanced *in vivo* chondrogenesis of $mPDC^{FGF2}$ is associated with the higher number of MSC. As we also detected a striking increase in *Bmp2* expression in $mPDC^{FGF2}$, a factor with known osteochondrogenic potential, we genetically knocked down *Bmp2* levels, which resulted in a reduction of the endochondral bone-forming potential of the $mPDC^{FGF2}$.Taken together, our results show that FGF2 markedly enhances the *in vivo* bone-forming potential of PDC, providing new insights in the regulation of periosteal cells and an attractive therapeutic approach for non-healing bone defects.

***Disclosures: Nick Van Gastel**, None.*

SU0148

Molecular Characterization of FGF-18 and FGF Receptors 1, 2 and 3. Abdulhafez Selim[1], Sherry Wang*[2]. [1]Center for Chronic Disorders of Aging, PCOM, USA, [2]Medical Device & Biomedical Technologies Labratory, Industrial Technology Research Institute, Taiwan

Osteoarthritis (OA) and degenerative disc disease (DDD) are prevalent diseases in the United States with staggering socioeconomic effects on today's society and together OA and DDD constitute a major source of health care costs. One particular family of growth factors, the fibroblast growth factor (FGF) family, has been implicated in the regulation of both articular cartilage and intervertebral disc (IVD) homeostasis. This large family of structurally-related proteins binds heparin and heparan sulfate modulates the growth, differentiation, migration and survival of a wide variety of cell types. Specifically, two particular members of the FGF family, basic fibroblast growth factor (bFGF; also known as FGF-2) and fibroblast growth factor-18 (FGF-18), have been found to play prominent regulatory roles in cartilage matrix homeostasis.

There are no previous studies that describe the three dimensional structure of FGF 18 or its interaction with FGF Receptors 1, 2, or 3. Our study is the first one that approaches the molecular characterization FGF18/FGFR complexes. For this purpose, we used validated bioinformatics tools to build three dimensional models for FGF 18, FGF 18/FGFR1 complex, FGF 18/FGFR2 complex and FGF 18/FGFR3 complex. We further analyzed the interface between FGF 18 and FGF receptors (1, 2 and 3).

Study results demonstrated high similarity between FGF 18 and FGF family members. FGF 18 has ten blades of beta sheets and one alpha helix domain. Study results demonstrated that FGF 18 has high affinity to interact with FGFR 3 and least affinity to interact with FGFR 2. FGF 18 has the same interfacing regions to interact with FGFR 1, 2 and 3. There was medium affinity to interact with FGFR 1. FGF 18 interaction with FGFR 3 was mediated by 9 hydrogen bonds and one salt bridge bond. Fewer bonds were involved in FGF 18 interaction with FGFR 1(7 hydrogen bonds and zero salt bridges) and FGF 18 interaction with FGFR 2 (Three hydrogen bonds and zero salt bridges).This affinity profile is very unique to FGF 18 and might explain its unique biological functions compared to other FGFs.

This study will help design therapeutic agonists and antagonists to modulate the functions of FGF 18. The resultant molecules may be of great role in treating cartilage and bone diseases.

Figure 1: FGF-18/FGFR1 Complex. FGF-18 is blue, FGFR1 is pink

Figure 2: FGF-18/FGFR2 Complex. FGF-18 is blue, FGFR2 is pink

Figure 3: FGF-18/FGFR3 Complex. FGF-18 is blue, FGFR3 is green

Complex	Receptor Interfacing Residues	Ligand Interfacing Residues	Interfacing Area A²	Energy kcal/mol	Hydrogen bonds	Salt Bridges	Disulfide Bridges	AIG P-value
FGF-18/FGFR1	38	28	829	-10.8	9	1	0	0.351
FGF-18/FGFR1	31	25	952	-11.1	7	0	0	0.195
FGF-18/FGFR2	32	28	856	-11.8	1	0	0	0.118

Figure 4: FGF-18/FGFRs Interface Comparisons

***Disclosures: Sherry Wang**, None.*

SU0149

Adiponectin Modulates Bone Metabolism Via a Hypothalamic Relay Through the Epigenetic Regulation of CB1 Signaling Pathway. Hua Jiang*[1], Yuwei Wu[2], Qisheng Tu[1], Dana Murray[1], Jin Tang[1], Qianqian Han[1], Jake Jinkun Chen[1]. [1]Tufts University School of Dental Medicine, USA, [2]Tufts University, USA

Objective: Adiponectin is an adipose tissue derived hormone. Our previous studies have shown that adiponectin inhibits osteoclastogenesis and bone resorption. Adiponectin increases bone mass via a hypothalamic relay and exerts its effect through the APPL1 (Adaptor protein containing pleckstrin homology domain, phosphotyrosine domain, and leucine zipper motif) signaling pathway. The cannabinoid system is known for its involvement in regulating bone mass *in vivo*. The cannabinoid type 1 (CB1) receptor is expressed in the hypothalamus and regulates bone metabolism via the hypothalamus. However, whether adiponectin mediates bone metabolism through CB1 receptor remains to be determined. We explored the signaling pathways in which adiponectin modulates bone metabolism via a hypothalamic relay through epigenetic regulation of CB1 receptor.

Methods: Embryonic Mouse Hypothalamic Cell Line N-1 (mHypoE-N1, CELLutions Biosystems INC., Canada) were maintained in DMEM culture medium containing 10% fetal bovine serum (FBS) at 37°C in 5% CO_2/95% air. mHypoE-N1 cells were subjected to serum starvation overnight with or without 10^{-10} M globular adiponectin. Specific APPL1 small hairpin RNA (shRNA) and scramble control non-specific lentiviral-shRNA were transduced into N1 cells to generate stable cell lines.

Cell extracts were used for western blot, real-time PCR and chromatin immunoprecipitation (ChIP) assays.

Results: Real-time PCR and western blot analyses showed that adiponectin stimulation dramatically decreased CB1 expression ($p < 0.01$) and significantly enhanced histone deacetylase 5 (HDAC5) expression ($p < 0.01$) in mHypoE-N1 cells. However, specific APPL1 shRNA pretreatment showed no effects on CB1 and HDAC5 expression. In the mHypoE-N1 cells, the ChIP assay demonstrated HDAC5 occupancy in the CB1 promoter region upon adiponectin stimulation.Conclusions: Adiponectin decreased CB1 expression by regulating HDAC5, which was independent of APPL1 signaling pathway. These results indicate a novel signaling pathway for adiponectin modulating bone metabolism via a hypothalamic relay through epigenetic regulation of CB1.

***Disclosures: Hua Jiang**, None.*

SU0150

Disulfide Bond Requirements for Active Wnt Morphogens. Bryan MacDonald*[1], Annie Hien[2], Xinjun Zhang[2], Xi He[2]. [1]Children's Hospital Harvard Medical School, USA, [2]The F. M. Kirby Neurobiology Center, Boston Children's Hospital, Harvard Medical School, USA

Secreted Wnt glycoproteins are cysteine-rich, lipid modified morphogens that bind to the Frizzled (FZD) receptor to initiate Wnt signaling. The structure of Wnt proteins proved elusive until recently with the reported co-crystallization of Xwnt8 with a FZD extracellular cysteine rich domain (CRD). Wnt engages FZD through two protruding finger like domains, each assembled from paired beta strands secured by several disulfide bonds, which grasp both ends of the CRD. However with this new structural information, questions remain regarding the importance of each disulfide bond for Wnt function and their impact on Wnt solubility and receptor binding.

To address these questions we have performed a thorough analysis of the Wnt3a disulfide bonds by cysteine mutagenesis and examined their effect on Wnt biogenesis and activity. Our data show that removal of any one cysteine of Wnt3a results in large aggregations via ectopic, and presumably intermolecular, disulfide bonds which prevent receptor binding. Residual activity from the cysteine mutants shows a tolerance for alterations in the amino saposin-like domain of Wnt while mutations in the cysteine-knot of the cytokine-like domain are not compatible with monomeric solubility.

With solubility and activity affected in most of the single cysteine Wnt3a mutants, we examined a few select double cysteine mutants based on the normal disulfide bond pattern in an attempt to restore Wnt solubility and analyze binding to the FZD CRD. We find that paired mutation of the distal index finger cysteines results in a secreted monomeric ligand with greatly diminished FZD binding and dominant negative signaling properties. Additionally our studies of the amino terminal cysteines of Wnt3a, which are not represented in the shorter crystallized Xwnt8 protein, support a disulfide bond between the first two cysteines found in most Wnt ligands.

Recently loss of function WNT1 mutations have been reported in patients with osteogenesis imperfecta. Of the five reported missense mutations (C143F, G177C, R235W, F298C and V355F) several result in the addition or subtraction of cysteine residues. We have independently tested the five published OI missense mutations and compared their signaling ability with our Wnt3a study and find correlations based on the location of the cysteine mutants. The results of our study will provide a predictive level of severity for future WNT1 cysteine mutations.

***Disclosures: Bryan MacDonald**, None.*

SU0151

EGFR Signaling Promotes Proliferation and Survival in Osteoprogenitors by Increasing Egr2 Expression. Abhishek Chandra*[1], Shenghui Lan[1], Ji Zhu[2], Valerie Siclari[1], Ling Qin[1]. [1]University of Pennsylvania, USA, [2]University of Pennsylvania, School of Medicine, USA

Deficiency in mesenchymal stem cells and osteoprogenitors leads to insufficient number of osteoblasts and low bone formation. Mice with conditional inactivation of epidermal growth factor receptor (EGFR) in osteoprogenitor/osteoblasts (3.6kb collagen1a1-Cre $Egfr^{Wa5/flox}$, Col-CKO) displayed an osteopenia bone phenotype caused by a decreased bone formation and reduced number of bone marrow mesenchymal progenitors, indicating a critical role of EGFR signaling in maintaining the osteoprogenitor pool. EGFR ligands, such as EGF, are known mitogens for osteoprogenitors but the underlying transcriptional machinery remains elusive. Moreover, whether activation of EGFR in these cells stimulates cell survival has not been investigated. EGF treatment significantly increased the proliferation of MC3T3, an osteoprogenitor cell line, and primary calvarial osteoprogenitors through both MAPK/Erk and PI3K/Akt-dependent pathways, and it potently suppressed the serum depletion- and TNFalpha-induced apoptosis of these cells by MAPK/Erk pathway. Furthermore, mouse calvarial organ culture revealed that EGF elevated the number of proliferative cells and decreased the number of apoptotic cells, which led to an increase in calvarial osteoblasts. Microarray analysis revealed that EGFR signaling stimulates the expression of Mcl1, an anti-apoptotic protein, and a family of early growth response protein (Egr) transcription factors (Egr1, 2, and 3) in MC3T3 cells. This up-regulation, mainly through MAPK/Erk pathway, was further confirmed in MC3T3 cells at both RNA and protein levels and in wild-type calvarial osteoprogenitors but not in those from Col-CKO mice. Overexpression of Nab2, a co-repressor for Egrs, abrogated the EGF-induced increase in osteoprogenitor number. Interestingly, knocking down the expression of Egr2, but not Egr1 or 3, not only attenuated the EGF-induced increase of Mcl1 protein expression but also abolished the EGF-induced survival and proliferation. In contrast, overexpression of Egr2 protein resulted in an increased expression of Mcl1 protein, a decrease in apoptosis, and an increase in cell proliferation of MC3T3 cells. Taken together, our data demonstrate that EGFR signaling activates MAPK/Erk pathway to stimulate the expression of Egr2, which in turn leads to cell growth and Mcl1-mediated cell survival. This study reveals a critical role of Egr2 transcription factor in regulating osteoprogenitor population and new bone formation by EGFR signaling.

***Disclosures: Abhishek Chandra**, None.*

SU0152

Erythropoietin (EPO) excess results in Bone Loss in a Transgenic mouse model that overexpresses EPO. Paraskevi-Rea Oikonomidou*[1], Stefano Rivella[2], Jae Hyuck Shim[2], Stephen Doty[3], Sara Gardenghi[2], Zhiwei Yang[2], Carla Casu[2], Maria Vogiatzi[4]. [1]Cornell University, USA, [2]Weill Cornell Medical College, USA, [3]Hospital for Special Surgery, USA, [4]New York Presbyterian Hospital, Weill Cornell Medical College, USA

Erythropoietin (EPO) is a member of the type I cytokine superfamily known for its function to stimulate and support erythropoiesis. However, recent studies suggest that EPO exhibits additional diverse cellular functions in non-hematopoietic tissues such as tissue protection against injury, immune response and cancer. The effect of EPO on bone metabolism has been debatable. EPO administration in wild type (wt) mice resulted in changes in bone mass, albeit the results were contradictory. The tg6 transgenic mice (tg6) that overexpress human EPO driven by the human platelet-derived growth factor B-chain promoter show a 12-fold elevation of serum EPO concentrations and polycythemia vera (hematocrit levels at 80-90%). To gain further insight on the role of EPO on bone remodeling in vivo, we analyzed bone mass in these tg6 mice and wild type littermate controls using micro-CT (n=6/group, age 3mo, all males; Table). Our preliminary findings showed cortical and trabecular bone loss in tg6 mice, suggesting that EPO has an effect on bone mass. Histology, dynamic histomorphometry and measurement of markers of bone turnover are under way to help us determine the specific changes in bone remodeling that are induced by EPO.

Keywords:erythropoietin, bone loss, tg6 mouse

TABLE. micro-CT analysis of tg6 mice compared to their wt controls at age 3 months

	wt	tg6
Trabecular bone		
BV/TV (1)	0.14 ± 0.03 **	0.07 ± 0.03
Trabecular Number (1/mm)	3.11 ± 0.4 **	3.43 ± 0.6
Trabecular thickness (mm)	0.04 ± 0.002	0.03 ± 0.006
Trabecular Spacing (mm)	0.19 ± 0.02 **	0.30 ± 0.05
Cortical bone		
BV/TV (1)	0.42 ± 0.02 **	0.36 ± 0.02
Cortical thickness (mm)	0.18 ± 0.01 **	0.15 ± 0.01

*p<0.05

**p<0.01

Values are expressed as mean ± SD

Table

***Disclosures: Paraskevi-Rea Oikonomidou**, None.*

SU0153

Induction of CXC Chemokines in Human Mesenchymal Stem Cells (hMSCs) by Stimulation with Secreted Frizzled-Related Proteins (sFRPs). David Bischoff*, Jian-hua Zhu, Nalini Makhijani, Dean Yamaguchi. VA Greater Los Angeles Healthcare System, USA

CXC chemokines such as CXCL1 and CXCL8 are elaborated from hMSCs during osteogenesis and may be involved in angiogenic stimulation during bone repair. Differentiation of hMSCs with osteogenic differentiation medium (OGM) and dexamethasone (DEX), an OGM component, stimulated the production of the CXC chemokine CXCL5, with an 8- and 5-fold increase in mRNA expression, respectively, compared to control, non-differentiation growth medium (HMSCGM). In addition, non-canonical Wnt signaling is involved in the stimulation of CXCL5 by OGM. Conditioned medium (CM) from L-cells expressing non-canonical Wnt5a, stimulated an increase in CXCL5 mRNA expression and protein secretion in comparison to control L-cell CM. Dikkopf-1 (Dkk-1), an inhibitor of canonical Wnt signaling inhibited basal levels of CXC5 expression at 7 days of culture of hMSCs in OGM but not at 10 days of culture. RoR2, a co-receptor for non-canonical Wnt signaling was also significantly up-regulated by OGM and DEX by approximately 12-fold

compared to control HMSCGM medium. Ru486, a glucocorticoid receptor (GR) antagonist inhibited the OGM- and DEX-stimulated increases in RoR2. Secreted frizzled-related protein1 (sFRP1), which should inhibit both canonical and non-canonical Wnt signaling, enhanced the expression of CXCL5 in hMSCs at 7 and 10 days in culture. We have now tested all four sFRPs and show that all sFRPs induce CXCL8 expression in a dose- and time-dependent manner with maximum expression at 150 nM at 7 days post-treatment. Previously, we demonstrated that sFRP1 stimulated phosphorylation of the extracellular signal regulated kinase (ERK) in hMSCs with maximum stimulation at 5 minutes after sFRP1 addition. We have extended our analysis using specific inhibitors of ERK (PD98059, U0126), p38 mitogen-activated protein kinase (MAPK) (p38 inhibitors SB203589, SB202190), and c-Jun NH2-terminal kinase (JNKII inhibitor) to test for the inhibition of sFRP1-stimulated CXCL8 expression. Initial results indicate that these ERK and p38 inhibitors prevent sFRP1-stimulated CXCL8 up-regulation whereas JNK inhibition had no effect on CXCL8 stimulation. Conclusions: 1) expression of CXC chemokines, CXCL8 and CXCL5, is enhanced in hMSCs undergoing osteoblastogenesis; 2) the non-canonical Wnt pathway appears to be invovled in CXC chemokine expression during osteogenic differentiation; 3) sFRPs which further stimulated CXCL5 and CXCL8 expression in OGM may do so in part via ERK and p38 MAPK signaling pathways.

***Disclosures: David Bischoff**, None.*

SU0154

Myeloid-derived suppressor cells as key immune regulators of nonunion fractures. Seth Levy*[1], Anandi sawant[2], Shawn Gilbert[1], Selvarangan Ponnazhagan[2]. [1]The University of Alabama At Birmingham, USA, [2]UAB, USA

Every year there are more than 6 million fractures in the United States alone and approximately 10% of them result in delayed healing or develop into nonunion fractures. Normally, fractures heal with overlapping phases of inflammation, cell proliferation, and bone remodeling. Osteogenesis and angiogenesis are known to work in concert to control many stages of this process, and when one is impaired it leads to failure of bone healing, termed a nonunion fracture. During fracture, there is an abundant infiltration of immune cells at the fracture site that not only mediate the inflammatory responses but also exert influence on neovasculature. Thus, further understanding the effects of immune cell participation at the fracture site throughout fracture healing may not only lead to additional knowledge as to why some fractures heal while others remain nonunions, but also to the development of novel therapeutics modulating immune cells to increase fracture healing and prevent nonunions. The present study demonstrates the impact of immune cells on angiogenesis in the early stages of fracture healing suggesting key immune modulatory mechanisms may exert an effect on angiogenesis required for proper bone healing.

Results indicate that among infiltrating immune cells, there was a significant increase only in myeloid-derived suppressor cells (MDSC). MDSC, a heterogeneous population of progenitor cells, suppress lymphocytes through cytokines or the release of nitric oxide. MDSC are not only pro-angiogenic through molecules independent of VEGF, but we have demonstrated that MDSC in the presence of breast cancer can differentiate into osteoclasts and aid in bone degradation (Sawant et al. 2013). Thus, in order to further understand the role of immune cells on angiogenesis and osteogenesis we plan to elucidate if MDSC act as immune regulators throughout fracture healing.

During the initial phase of fracture healing there is a dramatic increase in the number and percentage of MDSC in the fracture area followed by a decrease in the number and percentage of MDSC as the fracture heals. Using gemcitabine to specifically decrease the levels of MDSC, we observe delayed healing in the absence of MDSC, further signifying the role of MDSC in fracture healing. Based on this data we predict that MDSC may play a significant role in nonunion fractures and therapeutic targeting of MDSCs after fracture would minimize the chances of eventual nonunion pathology.

***Disclosures: Seth Levy**, None.*

SU0155

The Metabolic Nature of Marrow Fat: insulin signaling, CREB phosphorylation and the 'adiponectin paradox'. Erica Scheller*[1], William Cawthorn[2], Brian Learman[2], Hiroyuki Mori[2], Becky Simon[2], Sebastian Parlee[2], Xiaomin Ning[2], Joshua Miller[3], Katherine Gallagher[4], Pouneh Fazeli[5], Clifford Rosen[6], Mark Horowitz[7], Anne Klibanski[8], Ormond MacDougald[2]. [1]University of Michigan, USA, [2]Department of Molecular & Integrative Physiology, University of Michigan, USA, [3]Department of Orthopedics, University of Michigan, USA, [4]Medical School, University of Michigan, USA, [5]Massachusetts General Hospital & Harvard Medical School, USA, [6]Maine Medical Center, USA, [7]Yale University School of Medicine, USA, [8]Massachusetts General HospitalHarvard Medical School, USA

Marrow adipose tissue (MAT) fills 70% of the skeleton, weighs ~2.6 kg in an average adult and contains ~23,000 kcal of stored energy. Unlike peripheral white adipose tissue, MAT increases in rodents and humans during states of calorie restriction. This implies that MAT is differentially regulated by nutritional status. It also suggests that preservation of MAT may be advantageous to metabolic function. However, the ability of MAT to both contribute to and respond to systemic change is poorly understood.

To address this we profiled adipose tissue mRNAs and observed >300 adipocyte-related gene expression differences in MAT compared to white adipose tissues. Ingenuity pathway analysis predicted that MAT has impaired fatty acid metabolism and insulin sensitivity. *In vivo* injections of insulin and isoproterenol pinpointed differences in signaling intermediates, including altered phosphorylation of Akt in response to insulin and a lack of CREB phosphorylation in response to lipolytic β-adrenergic stimulation. These findings begin to explain fundamental differences in the metabolic response of the bone marrow adipocyte.

MAT also has the potential to secrete regulators of systemic metabolism such as adiponectin. Despite being predominantly an adipocyte-derived protein, the circulating concentration of adiponectin is inversely correlated with % body fat. Although first reported in 1999, this 'adiponectin paradox' remains only partially explained. Like adiponectin, MAT is increased in states of low body fat including anorexia and type I diabetes. Thus, we hypothesized that increases in MAT are the source of elevated serum adiponectin. We found that expression of adiponectin protein is disproportionately conserved in MAT when compared to white adipose tissues. We then examined whether inhibition of MAT accumulation reduces circulating adiponectin. Ocn-Wnt10b transgenic mice overexpress Wnt10b, a secreted inhibitor of adipogenesis, under control of the osteoblast-specific osteocalcin promoter. Calorie restricted Ocn-Wnt10b mice resisted increases in both marrow fat and serum adiponectin (Fig.1). This supports the concept that expansion of MAT is necessary to increase serum adiponectin in states of calorie restriction and explains, at least in part, the 'adiponectin paradox'. Though there is much left to discover, these findings solidify the notion that MAT is a unique adipose depot that can both respond to and contribute to systemic metabolic change.

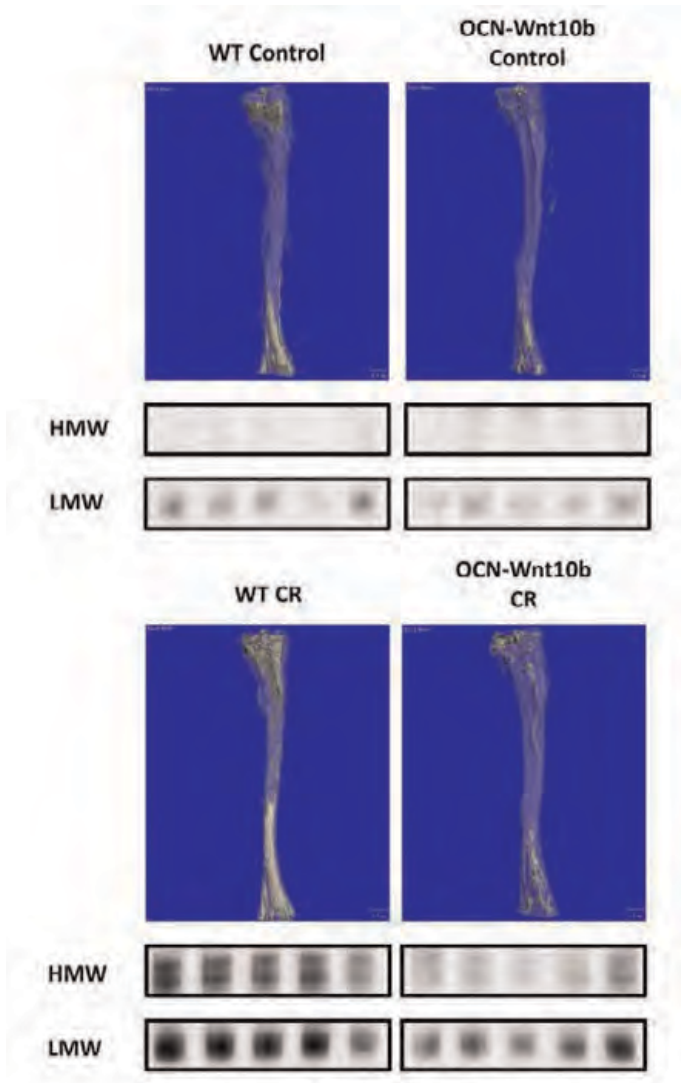

Figure 1. Ocn-Wnt10b mice resist increases in MAT and serum adiponectin with calorie restriction

***Disclosures: Erica Scheller**, None.*

SU0156

TLR-2 Serum Level is Higher in Prosthetic Joint Infection Patients: A New Potential Diagnostic Marker of Implant Infection?. Lorenzo Drago[1], Christian Vassena[2], Monica Gioia Marazzi[3], Lucia Salcito[3], Massimiliano Marco Corsi Romanelli[4], Emanuela Galliera*[5]. [1]Department of Bioemdical Science for health, Università degli Studi di Milano, Milan , Italyand IRCCS Galeazzi Orthopaedic Institute, Milan, Italy, [2]IRCCS Galeazzi Orthopaedic Institute, Italy, [3]Department of Biomedical Science for health, Università degli Studi di Milano, Milan, Italy, [4]Department of Biomedical Science for health, Università degli Studi di Milano, Milan , Italy & IRCCS Policlinico San Donato, San Donato, Italy, [5]Department of biomedical, Surgical & Oral Science , Università degli Studi di Milano, Milan , Italy & IRCCS Galeazzi Orthopaedic Institute, Milan, Italy

The interplay between the immune system and bone metabolism has been recognized as important for both of these systems. Toll-like receptors (TLRs) sense pathogen-derived molecules and initiate the inflammatory reactions of innate immune cells.TLR2 and TLR4 are also expressed in bone cells, and their activation affects osteoclasts differentiation and activity: TLRs block the differentiation of early osteoclasts precursors, while they stimulate differentiation survival of differentiating, mature osteoclasts. Moreover, in osteoblasts TLRs induce the production of osteoclastogenic cytokines, thereby contributing to TLR ligand-induced osteoclastogenesis. These processes are the reason for the bone loss observed in variety of infectious diseases. Various factors produced and released during immune responses markedly affect bone cells and bone metabolism, for example in bone osteolysis, the local bone loss due to inflammation in response to pathogen infection. In particular implant infection is a severe complication requiring implant replacement. Prosthetic joint infection (PJI) is a major problem in patients undergoing athroplasty, but since the clinical presentations and the efficacy of diagnostic approaches are different; there is still a continuous need to improve diagnostic methods. PJI is mainly due to Staphylococcus Aureus, a Gram positive bacterium recognized by TLR2, and more rarely by Gram negative bacteria such as Pseudomonas, recognized by TLR4.

In this study TLR2 and TLR4 serum levels, as well as inflammatory marker (IL-6, TNF alpha ,IL-1 , C-Reactive Protein) were evaluated in 30 post-operative PJI patients and in 27 not septic patient, in order to evaluate the potential diagnostic role of TLR2 and TLR4 in PJI. While TLR4 displayed no significative differences, TLR2 level was higher in septic patients , in accordance with IL-6 and C-Reactive Protein increased levels. Accordingly, IL-1, the main TLR2 co-player of the inflammatory response to S.Aureus, resulted higher in septic patients.

These results indicated that TLR2 plays an important role in the inflammatory response to prosthetic join infection. Therefore, the measure of TLR2 serum level could be considered a potential diagnostic tool that could be used in association with canonical inflammatory parameters for the early detection and diagnosis of prosthetic join infection.

***Disclosures: Emanuela Galliera**, None.*

SU0157

Crosstalk of IGF-1 Signaling with the Mechanosensing Machinery of Osteogenic Cells. Candice GT Tahimic*[1], Roger Long[2], Takuo Kubota[3], Alicia T Menendez[1], Chak Fong[1], Jean-Pierre Vilardaga[4], Yongmei Wang[5], Daniel Bikle[1]. [1]Endocrine Research Unit, Division of Endocrinology UCSF & VAMC, USA, [2]University of California, San Francisco, USA, [3]Osaka University Graduate School of Medicine & Dentistry, Japan, [4]University of Pittsburgh, School of Medicine, USA, [5]Endocrine Unit, University of California, San Francisco/VA Medical Center, USA

Physical activity promotes bone formation as observed in long-term tennis players whose playing arms have a higher bone mass compared to their contralateral arms. On the other hand, skeletal unloading in rodents results in bone loss. Our long-term research interest is to determine how the skeleton senses mechanical forces and translates these stimuli into signals regulating osteogenic proliferation and differentiation to ultimately result in bone formation. We have found that one mechanism by which this occurs is via crosstalk between IGF-1 and Integrin signaling. Integrins are membrane-bound proteins that bind to ECM molecules and function in cell adhesion and mechanosensing. In this study, we aim to determine the mechanisms of this crosstalk as examined at three levels: (a) membrane protein-protein interactions between IGF-1R and Integrins, (b) adaptor molecules such as FAK and filamins, and (c) effectors represented by Akt, Erk1/2 and non-receptor tyrosine kinase Src. Our methods for studying protein-protein interactions between IGF-1R and Integrin signaling pathways include a combination of biochemical and pharmacologic approaches and bimolecular fluorescence complementation (BiFC). Our findings indicate that this crosstalk occurs firstly, at the level of the membrane receptors, as indicated by co-imunoprecipitation (co-IP) of Integrin β3 and IGF-1R. The interaction between these two proteins is enhanced by IGF-1 treatment, as determined through BiFC. Moreover, inhibition studies using small molecules show that IGF-1-induced activation of its downstream effectors Akt and Erk1/2 is dependent on FAK and Src, both members of the Integrin signaling pathway. FAK inhibition also abrogates ligand-induced phosphorylation of IGF-1R, suggesting that modulation of IGF-1R activity can be achieved not only through ligand binding but also through internal signals, reminiscient of the outside-in and inside-out components of Integrin signaling. On the other hand in HOS cells subjected to shear stress by pulsatile fluid flow, inhibition of IGF-1 signaling via neutralizing antibodies against its receptor or ligand blunts Akt and Erk1/2 activation, suggesting the role of IGF-1 signaling in modulating the response to mechanical stimulation in osteogenic cells. Taken together, these results highlight the role of integrin signaling in modulating the response of osteogenic cells to IGF-1, and IGF-1 signaling in modulating the response of osteogenic cells to mechanical load.

***Disclosures: Candice GT Tahimic**, None.*

SU0158

GH induced linear bone growth in SOCS2 knockout mice is IGF-1 independent. Ross Dobie*[1], S. Faisal Ahmed[2], Katherine Staines[3], Chloe Pass[4], Seema Jasim[4], Vicky MacRae[4], Colin Farquharson[5]. [1]Edinburgh University, United Kingdom, [2]Royal Hospital for Sick Children, United Kingdom, [3]Royal Veterinary College, United Kingdom, [4]University of Edinburgh, United Kingdom, [5]Roslin Institute, University of Edinburgh, United Kingdom

Growth hormone (GH) signalling is essential for post-natal linear bone growth. However, determining the contribution of systemic versus local mechanisms responsible for GH action has proven difficult. The importance of systemic insulin like growth factor-1 (IGF-1) has recently been called into question. To unravel the mechanisms of local GH action we exploited the Suppressor of Cytokine Signalling (SOCS2) -2 KO mice which have enhanced growth despite normal systemic IGF-1 and GH levels.

To determine the mechanisms involved in local GH action embryonic day 17 metatarsals were cultured from wild-type (WT) and SOCS2 KO mice in the presence of GH for a 12 day period to assess downstream signalling and gene expression.

In response to GH, WT bones showed a 17-fold increase in *Socs2* expression ($p<0.01$) with no increase in linear growth. Expression of *Socs1* and *Socs3* were not altered. Conversely, SOCS2 KO metatarsals showed increased linear growth and increased STAT5 phosphorylation in response to GH compared to untreated (Ut) bones ($p<0.01$). Transcript (RT-qPCR) and conditioned medium analysis (ELISA) of SOCS2 KO metatarsals revealed no increase in *Igf1* mRNA (1.01 fold; p=0.9) or protein levels (Ut 3.31 ± 0.39ng/ml, GH 2.76 ± 0.27ng/ml; p=0.29). These data confirm in vivo transcript analysis of micro-dissected growth plates from 7 week-old WT and SOCS2 KO mice, which disclosed similar *Igf1* mRNA levels. Analysis of IGFBP3 levels revealed a modest 1.62-fold increase in transcript expression (p=0.08) and protein levels (Ut 24.99 ± 5.09ng/ml, GH 39.81 ± 3.69; $p<0.05$) in GH treated WT metatarsals. Conversely, in response to GH, SOCS2 KO metatarsals showed a 3.47-fold increase in *Igfbp3* transcript levels ($p<0.01$) and a 124% increase in protein levels within the conditioned medium ($p<0.001$). To further assess the potential of an IGF-1 independent action of GH on linear bone growth we next cultured SOCS2 KO metatarsals in the presence of an IGF-1R inhibitor (NVP-AEW541). Inhibition of endogenous IGF-1 signalling caused, as expected, a decrease in metatarsal growth, however GH was still able to stimulate linear growth (inhibitor 43.92 ± 1.69%, inhibitor + GH 52.06 ± 1.27%; $p<0.01$) .

These studies emphasise the critical importance of SOCS2 in the regulation of GH stimulation of linear bone growth and indicate that GH can enhance linear growth by initiating molecular pathways intrinsic to the growth plate that are independent of local IGF-I production.

***Disclosures: Ross Dobie**, None.*
This study received funding from: IPSEN

SU0159

IGF-1 Signaling Is Essential for Differentiation of Mesenchymal Stem Cells for Peak Bone Mass. Janet Crane*[1], Luo Zhao[2], Joseph Frye[3], Lingling Xian[4], Tao Qiu[4], Xu Cao[1]. [1]Johns Hopkins University, USA, [2]Peking Union Medical College, China, [3]University of Missouri School of Medicine, USA, [4]Johns Hopkins University School of Medicine, USA

Survival of children with chronic medical illnesses is leading to an increase in secondary osteoporosis due to impaired peak bone mass (PBM). Insulin-like growth factor type 1 (IGF-1) levels correlate with the pattern of bone mass accrual and many chronic illnesses are associated with low IGF-1 levels. Reduced serum levels of IGF-1 minimally affect the integrity of the skeleton, whereas recent studies suggest that skeletal IGF-I regulates PBM. To determine the role of local IGF-1 in postnatal bone mass accrual, we established an inducible type 1 Igf receptor *Crellox* knockout mouse model, in which the type 1 Igf receptor was deleted inducibely in the mesenchymal stem cells (MSCs) from 3-7 weeks of age. The size of the mouse was not affected as knockout and wild type mice had similar body weights and nasoanal and femoral lengths. However, bone volume and trabecular bone thickness were decreased in the secondary spongiosa of female knockout mice relative to wild type controls, indicating that local IGF-1 is critical for maintenance of bone mass. IGF-1 signaling in MSCs in vitro has been implicated to be involved in both migration to the bone surface and differentiation into bone forming osteoblasts. To clarify the exact role of IGF-1 in bone, we found by immunohistochemical analysis that a similar number of Osterix–positive osteoprogenitors were on the bone perimeter, indicating migration of MSCs was not affected. Most importantly, 56% fewer osteocalcin-positive mature osteoblasts were present on the bone perimeter in the secondary spongiosa in knockout mice versus wild type controls. These in vivo data demonstrate that the primary role of skeletal IGF-1 is for the terminal

differentiation of osteoprogenitors, but refute the role of IGF-1 in MSC migration in vivo. Additionally, these findings confirm that impaired IGF-1 signaling in bone MSCs is sufficient to impair bone mass acquisition.

***Disclosures: Janet Crane**, None.*

SU0160

Depletion of TLR4 in Macrophage Involved in Accelerated Bone Healing. Dan Wang*, James R. Gilbert, Melissa A. Shaw, Adam A. Kubala, Sameer Shakir, Joseph E. Losee, Timothy R. Billiar, Gregory Cooper. University of Pittsburgh, USA

OBJECTIVE: Macrophage-mediated inflammation is an essential component during musculoskeletal repair and reconstruction following injury. Expression of the toll-like receptors (TLRs) is found within macrophage, neutrophil, dendritic cell, and bone cell lineages. In previous studies, TLR4-mutant mice ($TLR4^{-/-}$) showed accelerated calvarial bone healing with earlier and higher expression of genes associated with osteoclast differentiation. Here we tested the hypothesis that specific depletion of TLR4 expression in macrophages would demonstrate accelerated bone healing, similar to that seen in global $TLR4^{-/-}$ mice.

METHODS: Circular bone defects were made in the parietal bones using a 1.8mm outer diameter trephine in wild-type (WT) mice, $TLR4^{-/-}$ mice and Lyz cre $TLR4^{-/-}$ (specific depletion of TLR4 in macrophages) mice. Calvarial healing was assessed at different time points using live μCT and histological analyses.

RESULTS: μCT analyses demonstrated accelerated calvarial healing in $TLR4^{-/-}$ and Lyz cre $TLR4^{-/-}$ mice compared to WT mice on postoperative day7, while a similar amount of bone formation was observed by day 28 among all groups. On day7, histomorphometric measurement showed significantly larger new bone area and more surface lining osteoclasts in $TLR4^{-/-}$ and Lyz cre $TLR4^{-/-}$ mice compared to WT. No significant difference was shown on day28. More intense and prolonged macrophage infiltration was also observed in $TLR4^{-/-}$ and Lyz cre $TLR4^{-/-}$ mice compared to WT mice.

CONCLUSIONS: These data suggest that depletion of TLR4 signaling in macrophages cells is responsible for the accelerated healing in global $TLR4^{-/-}$ mice. Further work is required to determine the effect of TLR4 signaling on the inflammatory phenotype of macrophages and how that, in turn, alters calvarial bone healing.

***Disclosures: Dan Wang**, None.*

SU0161

HMGB1 is Essential for Autologous Bone Graft Induced Calvarial Bone Healing. Dan Wang*, James R Gilbert, Adam A Kubala, Melissa A. Shaw, Sameer Shakir, Joseph E Losee, Timothy R Billiar, Gregory Cooper. University of Pittsburgh, USA

Background and Purpose: The synthesis and deposition of extracellular bone matrix and the osteogenic potential of cellular components have been observed to play a role in bone repair. It has only been appreciated recently that extracellular matrix (ECM) and necrotic cells can induce an inflammatory response, which is also involved in tissue regeneration. Previous studies revealed that the release of High-mobility group protein B1 (HMGB1) is important for the survival of ECM scaffolds in vitro. Here we tested the hypothesis that inhibition of HMGB1 signaling released from autologous bone graft will decrease the calvarial healing.

Methods: Suspensions of grounded bone grafts were obtained from femurs and tibias of wild-type (WT) mice. Bone graft suspension was mixed with and without anti-HMGB1 peptide (anti-HMGB1 group and "Bone graft" group). 1 ml PBS was prepared as "control group". All suspension was mixed with fibrinogen and thrombin before surgery. Circular bone defects were made in the parietal bones using a 1.8mm outer diameter trephine in WT mice (n=20). All three groups (Control, anti-HMGB1, bone graft) were implanted into the calvarial defects during the surgeries. Calvarial bone healing was assessed at designed time points using μCT and histologic analyses.

Results: μCT analysis showed that significantly less bone healing was observed in "anti-HMGB1 group" than "bone graft group" on postoperative day28. No significant difference was obtained between "anti-HMGB1 group" and control group. Similar histological healing patterns were shown in all groups on postoperative day28.

Conclusions: These data are consistent with our hypothesis that HMGB1 signaling from implanted autologous bone graft is essential for the calvarial bone healing result. Further work is required to determine if the decreased bone healing is a result of affected host local inflammation due to the inhibition of HMGB1 signaling.

***Disclosures: Dan Wang**, None.*

SU0162

Multiplex Magnetic Bead Assay Panels for Human, Rat and Mouse Bone Metabolism Related Biomarkers Using Luminex xMAP Technology. Munmun Banerjee*[1], Wen-rong Lie[1], Jehangir Mistry[2], Qiang Xiao[1]. [1]EMD Millipore, USA, [2]EMD Millipore.com, USA

Bone metabolism is the dynamic process of ongoing bone deposition and resorption, controlled by osteoblasts, osteocytes, and osteoclasts. The disruption of bone metabolism results in various diseases such as osteoporosis, osteoarthritis, rheumatoid arthritis, chronic kidney disease, and cancer bone metastases. To facilitate basic researches and clinical studies in bone metabolism, we have developed multiplex immunoassay magnetic bead panels using the Luminex® xMAP® technology to measure bone related biomarkers in human, rat and mouse samples including serum/plasma and cell culture media. The Human Bone Panel includes 13 analytes (ACTH, DKK1, IL-6, Insulin, Leptin, TNFa, OPG, OC, OPN, SOST, IL-1b, PTH and FGF23), while both Rat Bone Panel and Mouse Bone Panel include 10 analytes (Rat : ACTH, OPG, Insulin, Leptin, PTH, DKK1, SOST, OPN, FGF23, and OC; Mouse: ACTH, IL-6, OPG, OC, Insulin, Leptin, DKK1, SOST, TNFa and FGF23). The human, rat, and mouse bone multiplex immunoassay panels were fully validated and the validation data demonstrated the robustness of these assays in assay specificity (no cross-reactivity among analytes within each panel), accuracy (recovery within 80-120%), low intra-/inter- assay variability (intra CV <10%, inter CV <15%), and good dynamic range. These human and rodent multiplex magnetic bead assays are useful tools for studying bone metabolism and biomarker analysis in bone-related diseases.

***Disclosures: Munmun Banerjee**, None.*

SU0163

Chronic kidney disease differentially influences bone across two mouse strains. Andrew Cureton[1], Alicia Ortega*[2], Ryan Clark[3], Laura Shum[3], Eric Livingston[4], Xiaoxin Wang[3], Ted Bateman[4], Moshe Levi[3], Karen King[5], Virginia Ferguson[2]. [1]Mechanical Engineering, University of Colorado, USA, [2]University of Colorado, USA, [3]University of Colorado Denver, USA, [4]University of North Carolina, USA, [5]University of Colorado School of Medicine, USA

How bone quality is affected by 5/6 nephrectomy (5/6Nx), an established model of moderate chronic kidney disease (CKD), was examined in two strains of mice previously noted to possess low bone mass. 5/6Nx or sham surgery was performed on 10-week old male FVB and C57Bl/6 mice (n=12/group). Ten weeks post-surgery, mice were euthanized. Serum was collected and bone tissues harvested for: tibia gene expression (SYBR green real time RT-PCR method), femur three-point bending, and proximal tibia and femur diaphysis μCT assessment. All animal work was approved by the institutional IACUC. Data were analyzed using two-way ANOVA with Tukey's HSD post-hoc analysis (α=0.05). Results: Among the sham groups, the FVB strain showed impaired trabecular microstructure as compared to the C57 strain, via metrics including significantly lower BV/TV (-38.1%), Tb.N (-23.8%), Conn.D (-48.6%), and higher Tb.Sp (+37.3%) and SMI (+18.1%). The FVB femur yield strength was also -26.1% less than in C57 mice, possibly due in part to a -22.0% lower polar moment of inertia; however, the TMD at the FVB femur diaphysis was +2.5% greater than in C57 mice. 10 weeks after 5/6Nx, impaired kidney function was indicated in both FVB and C57 strains by significantly increased serum blood urea nitrogen (BUN; +690% and +502%, respectively) and creatinine (+57.5%, +35.3%) levels. Bone quality is noted to diminish with CKD. While proximal tibia trabecular microarchitecture was not significantly altered by 5/6Nx, femur diaphysis cortical bone showed reduced Ct.Th (-10.4%, -4.0% NS) and TMD (-1.9%, -1.9%). Also with 5/6Nx, gene expression profiles in the two strains were opposite. In the FVB mice, RANKL and OPG showed 2.13 and 3.22 fold decreases in expression, respectively, after 5/6Nx, while the C57 mice showed a 1.39 and 1.52 fold increase in expression. Both strains showed a decrease in FGF23 expression with the FVB expression (4.51 fold) and the C57 expression (2.10 fold) after 5/6Nx. Discussion: The trabecular microstructure in sham FVB mice was of lower quality than the C57 mice. However, 5/6Nx may have exerted a greater influence on cortical bone than trabecular bone. While kidney disease was clearly detected in both strains, its etiology and influence on bone and mineral metabolism differed across strains. Moreover, the varied changes observed with 5/6Nx suggest that mineral regulation is complex in CKD. In this study, moderate CKD exists where extensive metabolic changes have yet to occur.

	C57BL/6 Strain		FVB Strain	
	Sham	5/6 Nx	Sham	5/6 Nx
Proximal Tibia				
BV/TV (%)	15.41 ± 2.68 *	15.35 ± 1.71	9.53 ± 2.94	9.89 ± 2.75
Tb.N (1/mm)	4.81 ± 0.28 *	4.53 ± 0.28	3.66 ± 0.44	3.85 ± 0.28
Tb.Sp (mm)	0.20 ± 0.01 *	0.22 ± 0.01	0.28 ± 0.04	0.26 ± 0.02
SMI	1.73 ± 0.30 *	1.61 ± 0.24	2.04 ± 0.22	1.90 ± 0.22
Conn.D (1/mm³)	126.3 ± 27.3 *	136.5 ± 29.6	64.9 ± 29.2	91.8 ± 18.8
Femur Diaphysis				
Yield Strength (N)	16.1 ± 3.3 *	16.4 ± 3.0	11.9 ± 1.7	11.8 ± 2.5
TMD (mg/cm³)	1043.7 ± 12.4 *†	1024.0 ± 12.1	1070.1 ± 17.1 ‡	1049.5 ± 20.3
pMOI (mm⁴)	0.422 ± 0.086 *	0.379 ± 0.062	0.329 ± 0.052	0.315 ± 0.043
Ct.Th (mm)	0.167 ± 0.012	0.160 ± 0.009	0.172 ± 0.012 ‡	0.154 ± 0.011
Serum Chemistry				
BUN (mg/dL)	7.42 ± 5.68	44.68 ± 8.68	8.93 ± 5.31	70.63 ± 14.03
Creatinine (mg/dL)	0.37 ± 0.15 †	0.50 ± 0.06	0.31 ± 0.04 ‡	0.48 ± 0.13

* P < 0.05 for C57BL/6 Sham vs. FVB Sham, † P < 0.05 for C57BL/6 Sham vs. 5/6Nx,
‡ P < 0.05 for FVB Sham vs. 5/6 Nx

Table Showing Key Outcomes: Mouse Strain and 5/6Nx

***Disclosures: Alicia Ortega**, None.*

SU0164

Nutritional Status and Bone Turnover Markers in Adult Post-kidney Transplantation Recipients. Atsushi Suzuki*[1], Hitomi Sasaki[2], Midori Hasegawa[3], Hiroyuki Hirai[1], Yoshiteru Maeda[4], Sahoko Sekiguchi-Ueda[1], Megumi Shibata[1], Yukio Yuzawa[3], Kiyotaka Hoshinaga[2], Kazuhiro Uenishi[5], Mitsuyasu Itoh[4]. [1]Fujita Health University, Division of Endocrinology, Japan, [2]Department of Urology, Fujita Health University, Japan, [3]Division of Nephrology, Fujita Health University, Japan, [4]Division of Endocrinology & Metabolism, Fujita Health University, Japan, [5]Kagawa Nutrition University, Japan

Background: Despite Kidney transplantation (KTx) could restore many disorders in end-stage renal diseases (ESRD) patients, pre-existing chronic kidney disease-mineral and bone disease (CKD-MBD) and other clinical risk factors such as hyperparathyroidism and glucocorticoid therapy would make osteoporosis as a serious problem in post-KTx patients. Because of glucocorticoid therapy and co-existence of diabetes mellitus, KTx recipients often need to restrict their calorie intake. We have previously reported that post-KTx patients in Japan seemed to restrict their calorie intake for the prevention of their overweight and metabolic disorder. The aim of this study is to estimate the association of nutritional status of Ca and other nutrients and bone turn over markers in post-KTx recipients.

Subjects and Methods: Post-KTx recipients in outpatient clinic of Fujita Health University Hospital were recruited (n=81, M/F=48/33, age, 52.8 ± 12.6 years old, mean duration from KTx, 108 ± 77months). Methylprednisolone was prescribed to 78 cases out of 81 patients, and more than a half of them (42/82) took oral bisphosphonate (BP). Median serum albumin and creatinine levels were 4.3 g/dL(3.4-5.0) and 1.14 mg/dL (0.54-3.17). We estimate intake of nutrients including Ca, vitamin D (VD) and other nutrients by simple food frequency questionnaire by Uenishi et al (J Nutr Sci Vitaminol 2008; 54:25-29). Data are median (25^{th}–75^{th}) and 95% cut-off index (CI).

Results: Median body mass index of KTx recipients was 20.4 kg/m^2(15.9-32.5). Median total energy in KTx recipients was 1544 kcal/day (7769-2383). Their daily intake of Ca, VD and vitamin K were 380 mg (139-766), 10 mg (6.5-16.0), and 140 mg (35-553), respectively. Median intact parathyroid hormone (iPTH), Bone ALP (BAP), osteocalcin (OC) and TRAP5b were 129 pg/mL (54-956), 12.5 mg/L(6.1-31.4), 4.8 ng/mL (1.5-22.0) and 287 mU/dL (79-767) respectively.In non-BP user, total calorie intake, Ca intake, VD or VK did not affect bone turnover markers. However, in BP users, VD intake was positively associated with BAP level.

Conclusion: Our findings suggest that sufficient VD intake might contribute to maintain bone formation in BP users after KTx.

Disclosures: ***Atsushi Suzuki****, None.*

SU0165

Parathyroidectomy and Heart Rate Variability in Patients with Stage 5 Chronic Kidney Disease. Ningning Wang*[1], Jing Zhang[2], Bin Sun[2], Jianling Bai[3], Yongyue Wei[3], Xiaoming Zha[2], Yiyao Cui[2], Ming Zeng[2], Jingjing Zhang[2], Jia Liu[2], Huijuan Mao[2], Bo Zhang[2], Haibin Ren[2], Yifei Ge[2], Xueqiang Xu[2], Zhixiang Shen[4], Changying Xing[2], Kejiang Cao[2], Xiangbao Yu[2]. [1]Nanjing Medical University, Peoples Republic of China, [2]First Affiliated Hospital of Nanjing Medical University, China, [3]Nanjing Medical University, China, [4]Jiangsu Province Geriatric Hospital, China

Objective: Lower heart rate variability (HRV) implies increased risk of cardiovascular disease (CVD). This study aimed to evaluate the relationship between mineral metabolism and HRV and longitudinal changes of HRV after parathyroidectomy (PTX) in stage 5 chronic kidney disease (CKD) patients.

Methods: We conducted a cross-sectional study including 118 stage 5 CKD patients, 87 controls and a prospective study in two subgroups classified as successful (n=17), unsuccessful (n=4) PTX follow-up enrolled from March 2011 through December 2012. Blood examination and 24 hour Holter for HRV were measured.

Results: Clinical characteristics and laboratory results of all participants were shown in Table 1. Prevalent disorders in mineral metabolism, especially serum P, alkaline phosphatase (ALP) and intact parathyroid hormone (iPTH) abnormality was observed in stage 5 CKD patients. Baseline HRV indices were lower in stage 5 CKD patients than controls except for high-frequency (HF) (Table 2). In multivariate stepwise regression models (Table 3), serum iPTH was correlated with mean normal-to-normal R-R intervals (mean NN) (P=0.007), mean HR (P=0.004) and very-low frequency (VLF) (P=0.04), serum calcium was correlated with standard deviation of 5-min average of normal R-R intervals (SDANN) (P=0.004) and serum phosphorus was correlated with VLF (P=0.02) and LF/HF (P=0.002). Serum indices of mineral metabolism were corrected in successful PTX group (Figure 1). Serum iPTH levels were lower from 1717.8(1350.8-3209.7)pg/ml to 72.4(42.7-242.5)pg/ml (P<0.001) and serum P levels were decreased from 6.9 ± 1.8mg/dl to 2.9 ± 1.5mg/dl (P<0.001). There was also significant downregulation of serum Ca levels (10.5 ± 0.6mg/dl vs 8.9 ± 1.0mg/dl, P<0.001) and serum ALP levels {527.3(228.3-1006.8)μ/l vs 169.9(111.0-244.8)μ/l, P<0.001}. A significant increase in serum albumin levels (38.8 ± 4.8g/l vs 41.9 ± 3.7g/l, P<0.05) was also observed. Compared with baseline, successful PTX subgroup had significant improvements (Table 4) in mean NN, mean HR, SDNN, SDANN, VLF, HF and LF/HF. There were no significant changes of HRV in patients after unsuccessful PTX (Table 4).

Conclusions: Disorders of mineral metabolism are associated with decreased HRV in stage 5 CKD. Successful PTX may contribute to reverse this CVD risk in severe secondary hyperparathyroidism patients.

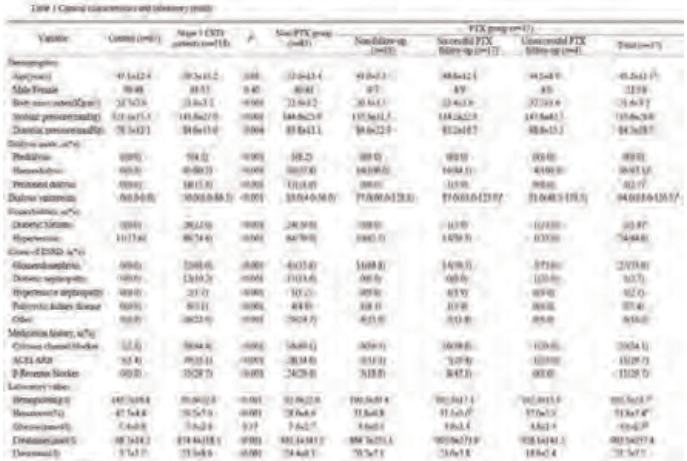

Table 1

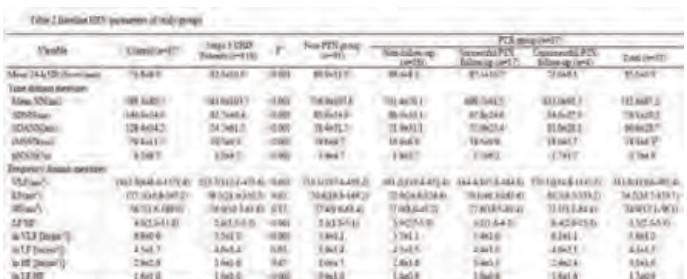

Table 2

Table 3 Multiple stepwise regression models predicting 24-h HRV parameters (n=118)

Dependent variable	Independent variable	Correlation coefficient	Regression coefficient (95% CI)	P
Mean NN	iPTH	-0.25	-0.03 (-0.03,-0.01)	0.007
SDNN	DBP	-0.21	-0.68 (-1.26,-0.10)	0.02
SDANN	Hemoglobin	0.22	0.58 (0.10,1.07)	0.02
	Calcium	-0.10	-8.66 (-18.96,-0.31)	0.04
rMSSD	Hemoglobin	0.31	0.13 (0.06,0.20)	0.001
	Triglyceride	-0.18	-1.05 (-2.26,-0.09)	0.02
pNN50	SBP	-0.27	-0.05 (-0.08,-0.07)	0.004
	Glucose	0.19	0.33 (0.01,0.65)	0.04
Mean HR	iPTH	0.26	0.09 (0.00,0.01)	0.004
ln VLF	Albumin	0.22	0.04 (0.01,0.07)	0.02
	Hemoglobin	0.33	0.01 (0.01,0.02)	0.001
	Phosphorus	0.22	0.13 (0.02,0.21)	0.02
	Triglyceride	-0.29	-0.26 (-0.42,-0.10)	0.002
	Age	-0.26	-0.02 (-0.03,-0.01)	0.005
	iPTH	-0.20	0.00 (0.00,0.00)	0.04
ln LF	Age	-0.35	-0.04 (-0.05,-0.02)	<0.001
	Hemoglobin	0.30	0.02 (0.01,0.03)	0.001
	Triglyceride	-0.25	-0.27 (-0.50,-0.04)	0.02
ln HF	BMI	-0.23	-0.12 (-0.21,-0.03)	0.01
ln LF/HF	Albumin	0.32	0.05 (0.02,0.08)	0.001
	Phosphorus	0.22	0.12 (0.02,0.21)	0.02

HRV, heart rate variability; iPTH, intact parathyroid hormone; DBP, diastolic blood pressure; SBP, systolic blood pressure; BMI, body mass index; HR, heart rate; Mean NN, the mean normal-to-normal R-R intervals; SDNN, standard deviation of the normal-to-normal R-R intervals; SDANN, standard deviation of 5-min average of normal RR intervals; rMSSD, root-mean square of differences between adjacent normal RR intervals; pNN50%, proportion of adjacent RR intervals differing by >50ms over 24 h; VLF, very-low frequency; LF, low-frequency; HF, high-frequency.

Table 4.HRV at severe SHPT patients before and after PTX

	Baseline	After PTX	Mean difference	P
Successful PTX follow-up (n=17)†				
Mean 24-h HR (beats/min)	87.1±10.7	76.8±8.1	-10.4±8.2	<0.001
Time domain measures				
Mean NN(ms)	690.7±91.5	790.9±83.6	91.2±74.1	0.001
SDNN(ms)	97.8±24.6	84.2±28.6	-16.4±19.0	0.003
SDANN(ms)	57.9±25.4	73.3±29.7	15.4±15.6	0.004
rMSSD (ms)	19.5±9.9	23.5±9.2	3.9±10.9	0.16
pNN50(%)	3.7±6.5	5.8±7.9	2.1±8.7	0.40
Frequency domain measures				
lnVLF [ln(ms^2)]	5.4±0.5	5.8±0.7	0.5±0.7	0.008
lnLF [ln(ms^2)]	4.4±1.0	3.7±1.7	-0.7±1.7	0.09
lnHF [ln(ms^2)]	3.4±1.1	1.1±2.8	-1.8±2.9	0.03
lnLF/HF	1.0±0.8	3.0±1.4	1.0±1.4	0.008
Unsuccessful PTX follow-up (n=6)‡				
Mean 24-h HR (beats/min)	75.0±8.1	74.3±12.4	0.5±5.8	0.87
Time domain measures				
Mean NN(ms)	835.0±91.3	844.3±138.7	11.3±60.3	0.73
SDNN(ms)	94.0±77.0	91.3±11.8	-0.8±19.1	0.94
SDANN(ms)	81.0±28.1	82.5±7.5	1.5±21.1	0.90
rMSSD (ms)	18.0±5.7	17.8±5.0	-0.3±4.4	0.92
pNN50(%)	1.7±1.7	2.3±2.4	0.8±2.0	0.51
Frequency domain measures				
lnVLF [ln(ms^2)]	6.1±1.1	5.7±1.0	-0.3±0.4	0.17
lnLF [ln(ms^2)]	4.0±2.1	3.4±1.5	-0.6±3.1	0.75
lnHF [ln(ms^2)]	2.4±2.4	2.3±2.6	-0.2±4.3	0.93
lnLF/HF	1.6±1.5	1.1±1.9	-0.5±1.2	0.51

Data are mean ± standard deviation (SD)
†Patients were followed up in a median period of 5.0 months
‡Patients were followed up in a median period of 2.3 months

Table 4

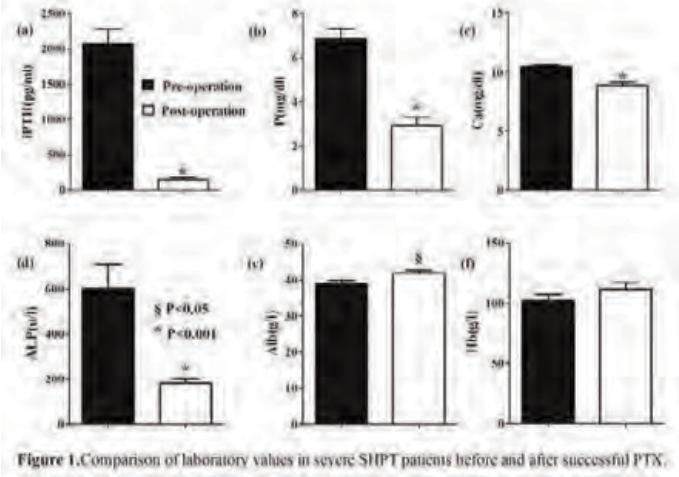

Figure 1. Comparison of laboratory values in severe SHPT patients before and after successful PTX.

Fig 1

***Disclosures: Ningning Wang**, None.*

SU0166

Sclerostin Levels Increase as Kidney Function Declines and Associate Directly with FGF23 Levels in Chronic Kidney Disease (CKD). Tamara Isakova*[1], Katherine Wesseling-Perry[2], Ina Kramer[3], Michaela Kneissel[3]. [1]University of Miami, USA, [2]UCLA Medical Center, USA, [3]Novartis Institutes for Biomedical Research, Switzerland

Sclerostin encoded by the *Sost* gene is secreted by osteocytes and inhibits the canonical Wnt/beta-catenin pathway, which is critical for normal bone homeostasis. *Sost*/sclerostin expression is suppressed by parathyroid hormone (PTH) signaling. A recent study reported that early in the course of CKD in mice *Sost*/sclerostin expression is increased in a PTH-independent manner, suggesting that primary osteocyte dysfunction in CKD may initiate progressive mineral metabolism abnormalities, including excess production of fibroblast growth factor 23 (FGF23).

To examine the association of sclerostin levels with kidney function and FGF23 levels in CKD, we measured sclerostin levels in 37 human subjects (control, n=15; CKD stage 3-4, n=12; and dialysis, n=10, Figure) using the Biomedica ELISA assay. We found that sclerostin levels rise with declining kidney function, and that there is a direct correlation between FGF23 and sclerostin levels (Figure). Further support for a link between sclerostin and FGF23 emanates from the observation that *Sost*/sclerostin deficient mice show decreased FGF23 expression. In 6-month-old *Sost* deficient female mice, *Fgf23* expression was strongly and significantly decreased by 63% relative to wild-type. Concurrently, intact serum FGF23 levels, as determined by ELISA (Kainos Laboratories), were also significantly reduced by 24% in aged *Sost* KO females, and by 37% in aged *Sost* KO male mice.

Taken together, these data suggest that sclerostin may be an important factor in the pathogenesis of disordered mineral metabolism in CKD.

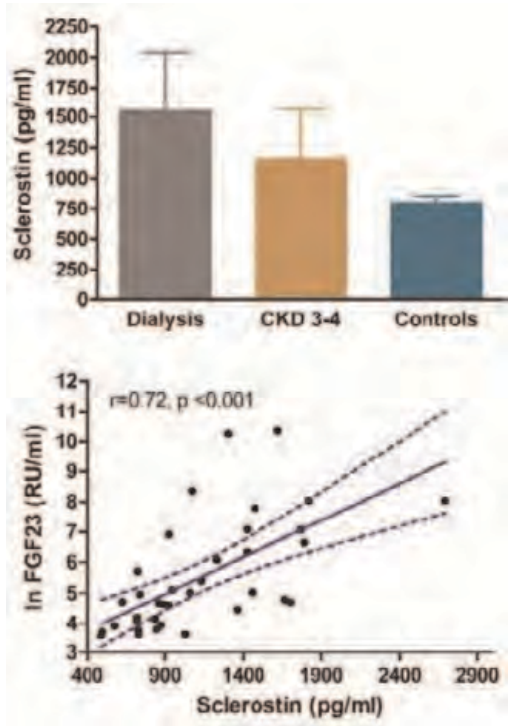

Figure

***Disclosures: Tamara Isakova**, None.*
This study received funding from: Novartis

SU0167

Fibrous Dysplasia with Normal Bone Resorption Markers: An Unexplained Phenomenon. Ruban Dhaliwal*[1], Arnold Moses[2]. [1]SUNY Upstate Medical University, USA, [2]State University of New York Upstate Medical University, USA

Background: Fibrous dysplasia (FD) is a rare skeletal disease characterized by enhanced osteoclastogenesis, marrow fibrosis and osteomalacia. Postzygotic missense mutations of Gsα are correlated with the disease. Bone turnover markers (BTMs) are elevated in parallel, relative to disease activity. We describe a unique case of FD with an isolated elevation of bone specific alkaline phosphatase (BSAP).

Case: A 21-year-old Caucasian female with a history of transient hepatitis following an episode of mononucleosis had persistently elevated alkaline phosphatase 680 IU/L (nl:25-150). Physical examination revealed a protuberance over the left parietal bone. No associated dysmorphic facial features or skeletal deformities were noted. She had no family history of metabolic bone disease.

Further investigation showed markedly elevated serum BSAP 262 ug/L (nl:<21.3) and normal urine NTx 43 nM BCE/mM Cr (nl:5-65). Radiograph of skull showed increased bone formation at left skull base, but not particularly exuberant. Radiographs of extremities were normal. Bone scintigraphy was in keeping with FD, and showed a large area of intensely increased uptake in the left skull base. Computed tomography of head showed pagetoid type lesion of FD (5.6x4.5x4.5cm) involving the left temporal and occipital bones, displacing the left cerebellar hemisphere. Magnetic resonance imaging confirmed the lesion representative of FD with mass effect on the left cerebellum and minimal effacement of the 4th ventricle. Gsα mutation was undetectable in blood. Notably, despite this clinical presentation and persistent elevation of BSAP, all other BTMs were unremarkable (Table 1).

Conclusion: FD is usually an incidental finding. Mosaic nature of the Gsα mutation presents a diagnostic challenge as demonstrated in this case. Clinical sensitivity of mutational analysis is 50% in blood and 90% in the affected tissue. Location of the lesion may render biopsy less feasible. Nevertheless, bone formation and resorption markers have always been reported to be elevated in parallel and indeed a decline in BTMs is considered an indicator of effectiveness of treatment. In this case, an elevation of BSAP in the presence of normal resorption markers is inconsistent with the known pathophysiology of FD. Normal osteocalcin and P1NP further add to the complexity. Therefore, yet unknown mechanisms may contribute to the pathogenesis of FD and further studies are needed to explain this observation.

Table 1: Serum Laboratory Parameters					
Variable (normal range)	Oct. 2011	July 2012	Nov 2012	Jan 2013	Feb 2013
BSAP (4.5-16.9 ug/L)	–	262.8	276.6	–	212.8
P1NP (22-104 mcg/L)	–	–	–	90	–
Osteocalcin (8-32 ng/ml)	–	–	–	–	13
NTX (6.2-19.0 nM BCE)	–	–	13.3	–	–
CTX (64-640 pg/ml)	–	–	–	197	177
PTH (15-65 pg/ml)	12	–	24	–	36
Phosphorus (2.5-4.9 mg/dL)	–	2.7	2.7	–	–
Calcium and 25-hydroxy vitamin D were normal					

Serum Laboratory Parameters

***Disclosures: Ruban Dhaliwal**, None.*

SU0168

Mutation in the Ligand-Binding Domain of the Vitamin D Receptor (VDR) in a Patient with Spontaneous Recovery of Hereditary Vitamin D-Resistant Rickets (HVDRR). Flavia M Damiani*[1], Regina M Martin[1], Ana Claudia Latronico[1], Pedro Henrique Correa[2], Bruno Ferraz-de-Souza[1]. [1]Univ of Sao Paulo School of Medicine (FMUSP), Brazil, [2]University of Sao Paulo School of Medicine, Brazil

Introduction: Mutations in the vitamin D receptor (VDR) cause hereditary vitamin D-resistant rickets (HVDRR), an autosomal recessive disorder characterized by resistance to calcitriol, severe hypocalcemia and early-onset rickets. Approximately 50 inactivating VDR mutations have been described in HVDRR so far, but relatively little is known about the long-term evolution of these patients.

Objective: To establish the molecular diagnosis in an adult female patient with HVDRR.

Methods: Peripheral blood leukocyte DNA samples were obtained from patient, relatives and controls after informed consent, with IRB approval. The full coding region of VDR was PCR-amplified and directly sequenced. RFLP was used to confirm sequence variants and to screen controls.

Results: A 35 yo female patient with HVDRR has been followed in our institution since infancy. Born to distantly consanguineous parents, she developed diffuse alopecia at 6 mo of life accompanied by progressive muscle weakness and inability to walk. She was first evaluated at 2 y 5 mo, showing low serum calcium and high alkaline phosphatase levels. Treatment was initiated with calcitriol and 200,000 IU of oral ergocalciferol per day, with improvement of symptoms. From 3 yrs of age, she maintained normocalcemia with 600,000 IU ergocalciferol monthly, but evolved to total alopecia. Around puberty, hypercalciuria and nephrolithiasis were detected, resulting in full suspension of treatment by the age of 20. At 32 yrs, she got pregnant and did not have hypocalcemia during gestation or lactation, without any supplementation. Mutational analysis reveals a homozygous p.Gly319Val mutation in the ligand-binding domain of VDR, confirmed by RFLP. Her asymptomatic parents and child are heterozygous for this change, which was not found in 380 Brazilian control alleles. This mutation has been previously reported in association with HVDRR and *in silico* analysis indicates high-probability of disease causation.

Conclusion: We report the long-term follow-up of a female HVDRR patient harboring a homozygous p.Gly319Val mutation in VDR. In accordance with previous reports, mutations in the ligand-binding domain of VDR tend to result in milder forms of rickets with better response to treatment, as seen here. Importantly, despite the permanent molecular defect and maintenance of alopecia, she spontaneously recovered from rickets and hypocalcemia around puberty, as observed by ourselves and others in patients with HVDRR.

***Disclosures: Flavia M Damiani**, None.*

SU0169

Pharmacokinetics and Pharmacodynamics of a Human Monoclonal Anti-FGF23 Antibody (KRN23) after Single-Dose Administration to Patients with X-linked Hypophosphatemia. Xiaoping Zhang*[1], Thomas Carpenter[2], Erik Imel[3], Mary Ruppe[4], Thomas Weber[5], Mark Klausner[1], Tetsuyoshi Kawakami[1], Takahiro Ito[1], Jeffery Humphrey[1], Karl Insogna[2], Munro Peacock[6]. [1]Kyowa Hakko Kirin Pharma Inc, USA, [2]Yale University School of Medicine, USA, [3]Indiana University School of Medicine, USA, [4]The Methodist Hospital, USA, [5]Duke University Medical Center, USA, [6]Indiana University Medical Center, USA

Purpose: In X-linked hypophosphatemia (XLH), elevated serum FGF23 causes low serum phosphorus (P) and inappropriately normal 1,25-dihydroxyvitamin D ($1,25(OH)_2D$) levels. KRN23, a human monoclonal antibody blocking FGF23 activity, is a promising novel treatment for XLH. We report pharmacokinetics (PK) and pharmacodynamics (PD) of KRN23 following single ascending dose administration in adults with XLH.

Methods: 38 subjects were randomized to receive a single dose of KRN23 or placebo either intravenously (IV) (0.003-0.3 mg/kg) or subcutaneously (SC) (0.1-1.0 mg/kg). PK and PD samples were obtained from baseline through Day 50. PD samples were analyzed using commercial assay kits. PK samples were assayed using a validated ELISA method. PK and PD parameters were estimated using non-compartmental analysis method with WinNonlin software (Versions 5 and 6, Pharsight Co. CA).

Results: 22 subjects participated in the IV treatment arm (17 KRN23, 5 placebo), and 16 in the SC treatment arm (12 KRN23, 4 placebo). Age, sex, weight, and height of all groups were comparable. Serum P and intact FGF23 levels at baseline were not correlated (Spearman's correlation coefficient = -0.029). Mean KRN23 terminal half-life was shorter for IV (11-12 days) than for SC (13-19 days) administration. Absolute bioavailability was approximately 100% with SC dosing. There was a dose-proportional increase in circulating KRN23 levels in both IV and SC groups. With SC administration peak serum KRN23 concentration and peak serum P occurred at the same time. Area under the curve (AUC_{last}) for changes from baseline in serum P, $1,25(OH)_2D$, and TmP/GFR were linearly correlated with AUC_{inf} for serum KRN23 concentration. At the same dose level, AUC_{last} for P appears to be similar for IV vs. SC treatment. However, SC dosing exhibited a slow absorption profile (peak time: 8-11 days) and a more sustained effect than IV dosing as indicated by the delayed time to reach maximum mean serum P level (peak time: 8 -15 vs 4 days) and longer time to return to baseline (50 vs 29 days). Dose-normalized serum P AUC_{last} was independent of baseline intact FGF23 levels (r = 0.011).

Conclusions: KRN23 is a promising treatment for XLH patients. Complete absorption, sustained effect on serum P beyond 4 weeks, and a direct linear relationship between PK and PD effects support an SC treatment regimen of once every 4 weeks for KRN23 in XLH patients.

***Disclosures: Xiaoping Zhang**, Kyowa Hakko Kirin Pharma Inc, 3*
This study received funding from: Kyowa Hakko Kirin Pharma Inc

SU0170

Spondyloepimetaphyseal Dysplasia: A Distinctive Phenotype In A Three-Generation Family. Gary S Gottesman*[1], William McAlister[2], Michael P Whyte[1]. [1]Shriners Hospital for Children-Saint Louis, USA, [2]Washington University School of Medicine, USA

Skeletal dysplasias are developmental disorders of chondroosseous tissue. Over 450 distinct entities have been identified. Most are classified based on the location of abnormal skeletal features on radiographs. Spondyloepimetaphyseal dysplasia (SEMD) refers to developmental shaping abnormalities of the spine together with distortions at long bone ends (epiphyses and metaphyses). Current nosology lists approximately 15 SEMDs. Only 6 are autosomal dominant disorders and the genetic basis is known for each [Missouri type (MMP-13 mutation), 4 entities resulting from mutations in TRPV4, and short limb-abnormal calcification type (DDR2 mutation)].

We report a 3-generation kindred with SEMD that mimics the findings reported in a single unclassified family identified with a new autosomal dominant SEMD.[(1)] A 16-year-old woman with normal facial features presented for a skeletal disorder, previously considered Morquio syndrome versus spondyloepiphyseal dysplasia. She was short (-4.0 SD) with chronic knee pain. Her mother, maternal grandmother, and older brother had similar findings. Each had been evaluated during childhood at Shriners Hospital for Children-St. Louis. Radiographs for each individual permitted assessment of epiphyseal, physeal, metaphyseal, and vertebral development. Remarkable delay in the appearance of mal-shaped epiphyses occurred at the proximal femur. Epiphyseal contours were flattened and irregular along with mild widening and beaking of metaphyses (Figure). In the spine, each had mild-moderate platyspondyly with endplate irregularities (Figure) with prominent lordosis. Family members underwent physeal stapling and osteotomies for genu valgum during childhood, and hip replacements as adults. Notably, male-to-male transmission was absent in this kindred and in the previous family report. Thus, X-linked dominant or autosomal dominant inheritance remains possible.

Reference:

[(1)]De Ravel TJL, De Smet L, Fryns JP. Apparently new autosomal dominant spondyloepimetaphyseal dysplasia: gonadal mosaicism onset. Clinical Dysmorphology 2002, 11:261–266.

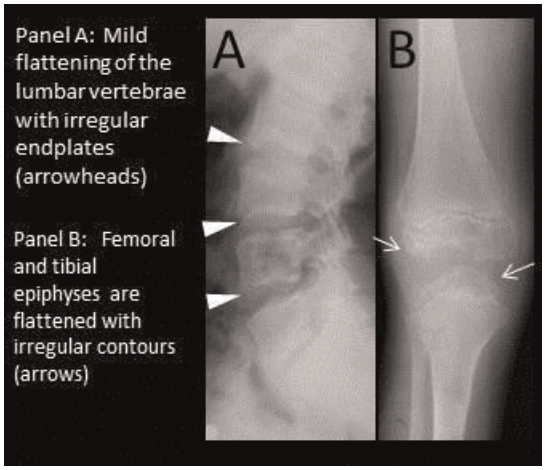

Figure

***Disclosures: Gary S Gottesman**, None.*

SU0171

Whole Body Muscle Mass Is Low and Fat Mass Is High in Osteoporosis Pseudoglioma Syndrome. Sarada Jaimungal*[1], Jin Long[2], Mary Leonard[2], Elizabeth Streeten[3]. [1]University of Maryland Medical Center, USA, [2]Children's Hospital of Philadelphia, USA, [3]University of Maryland School of Medicine, USA

Introduction: Osteoporosis - pseudoglioma syndrome (OPPG) is a rare, autosomal recessive disorder characterized by severe juvenile osteoporosis and congenital blindness due to inactivating mutations in the LDL receptor-related protein 5 (LRP5). We previously found by pQCT low muscle mass and high fat mass in OPPG at the tibia. We hypothesized that similarly abnormal body composition would be present in the whole body in OPPG and would be associated with adverse metabolic consequences.

Methods: Four patients with OPPG underwent whole body DXA at the UM Amish Research Clinic. Sex and race specific Z scores were generated for whole body minus head for lean body mass and fat mass using reference data from the Children's Hospital of Philadelphia in over 900 healthy children and adolescents. Fasting serum lipids and HbA1c were measured.

Results: In spite of normal BMI, fat mass was high and muscle mass low in the 4 patients with OPPG- See Table 1. Lipid profiles and hemoglobin A1c levels were normal in all.

Discussion: To our knowledge, this is the first report of body composition by whole body DXA in patients with OPPG. The 4 patients studied had dramatic lean body mass deficits and fat mass excess which were too severe to attribute to their low levels of activity. In high bone mass due to activating mutations of LRP5, adipogenesis was inhibited both in vivo and in vitro. The opposite effect was found in inactivating LRP5 mutations in vitro in human mesenchymal stem cells. The WNT/LRP5 pathway appears to be important for adipocyte differentiation of marrow stromal cells.

The LRP5 -/- mouse develops hypercholesterolemia when fed a high fat diet and has impaired glucose tolerance on a normal diet. Impaired glucose metabolism was also found in seven adult patients with either homozygous or heterozygous LRP5 mutations. Our patients had no demonstrable abnormalities in glucose or lipid metabolism despite having high fat and low muscle mass. We speculate that metabolic consequences of the abnormal body composition in OPPG may become apparent with age.

In conclusion, we found reduced muscle and high fat mass on whole body DXA in 4 children with OPPG with normal lipids and HbA1c. These body composition abnormalities appear to be intrinsic to the OPPG phenotype.

Table 1 - Body composition in 4 OPPG patients
*Subtotal = whole body minus head

Age/ years	Sex	Z score - Height	BMI	Z score - BMD	Z score - Subtotal Fat mass	Z score – Subtotal muscle mass	% Body fat
5.1	M	-2.41	15.1	-3.4	2.12	-1.57	26.8
8.5	M	-1.85	15.6	-3.1	1.16	-1.33	25.3
9.75	F	-1.04	21.4	-0.8	2.08	-1.56	45.9
15.7	M	-2.4	20.7	-2.5	1.27	-0.97	26.5

Table 1 - Body composition in 4 OPPG patients

***Disclosures: Sarada Jaimungal**, None.*

SU0172

Occult Hyperosteoidosis in Subjects Undergoing Orthopedic Surgery. Julie Glowacki*, Sherwin Erfani, Laurence Higgins, Shuanhu Zhou, Thomas Thornhill, Lisa Gao, Meryl LeBoff. Brigham & Women's Hospital, USA

Although there is growing awareness of vitamin D-deficiency in the USA, there is little information about prevalence of bone mineralization defects. Bone that is discarded during orthopedic surgery provides an opportunity to assess the prevalence of hyperosteoidosis. Subjects were eligible if they required a joint prosthesis for non-inflammatory disorders; we excluded subjects taking medications or with co-morbid conditions that could affect skeletal metabolism. Bone specimens were obtained with IRB approval either from enrolled subjects consenting for additional research tests or as de-identified material. There were 38 subjects with hip osteoarthritis (OA), 73 with shoulder OA, and 48 with rotator cuff arthropathy (RCA), a disorder associated with rotator cuff tear, "soft" quality of the humeral bone noted at the time of arthroplasty, fatty infiltration of shoulder muscles, and radiographic osteopenia. We tested the hypothesis that osteoid is increased in subjects with RCA, compared with shoulder OA. Portions of trabecular bone from the discarded femoral or humeral head were prepared for non-decalcified histology; they were graded for osteoid relative to bone surfaces on an Osteoid Index (OI) scale of 0-3, without knowledge of diagnoses. For subjects with available serum levels, there was the expected inverse correlation between 25(OH)D and PTH ($p=0.0036$). For hip OA subjects, there was a significant inverse correlation between OI and serum 25(OH)D (Spearman $r=-0.35$, $p=0.033$). The hip OI was 2.6-fold higher in vitamin D-deficient (<20 ng/ml 25OHD) subjects (1.3 ± 0.2) than in non-deficient subjects (0.5 ± 0.1, $p=0.007$). With the shoulder cohorts, there was a significant 1.6-fold higher OI for subjects with RCA (1.1 ± 0.1, $n=48$) than for subjects with shoulder OA (0.7 ± 0.1, $p=0.007$, $n=73$). Likewise, for a subgroup of shoulder subjects for whom serum 25(OH)D levels were available, there was a significant 2.2-fold higher OI for RCA (1.1 ± 0.2, $n=19$) than for shoulder OA (0.5 ± 0.1, $n=21$, $p=0.029$), despite no difference in current serum 25(OH)D levels or other evidence of vitamin D-deficiency. In sum, hyperosteoidosis was evident in RCA and in hip OA subjects with vitamin D-deficiency. Although current D-deficiency can account for hyperosteoidosis in hip OA subjects, it does not explain RCA.

***Disclosures: Julie Glowacki**, None.*

SU0173

Preadipocyte Cell Lines to Evaluate the Role of PHEX on Osteoblast Differentation and Mineralization *in Vitro*. Cecilia Romagnoli*, Roberto Zonefrati, Gianna Galli, Caterina Fossi, Valeria Nardone, Gaia Palmini, Alessia Gozzini, Luisella Cianferotti, Laura Masi, Annalisa Tanini, Maria Luisa Brandi. University of Florence, Italy

Purpose: X-linked hypophosphatemia (XLH), the most common inherited form of rickets, is a dominant disorder characterized by defective calcification of cartilage and bone, growth retardation, impaired renal tubular resorption of inorganic phosphate (Pi) and abnormal vitamin D metabolism. The PHEX gene (locus Xp22.11), a phosphate regulating gene with homologies to endopeptidases in the X chromosome, was identified as the candidate gene for XLH. It codifies a 749 amino acid protein and it is expressed in particular in cartilage, bone and teeth. PHEX is a member of the M13 family of type II cell-surface membrane zinc-dependent peptidases and, although its precise physiological role is still unknown, it might have a role in regulating the activity of extracellular peptides that act controlling the renal Pi resorption and the skeletal mineralization.

The aim of the present study was to elucidate the effect of this mutation on osteogenic differentiation of human adipose tissue derived mesenchymal stem cells (hADSCs), or preadipocytes, obtained from the patient.

Methods: Two primary culture of hADSCs, PA4 e PA9, were obtained from a patient of three years old and from a healthy child of the same age, respectively, and induced into the osteoblastic phenotype using the osteogenic medium (OM) composed by Ham's F12 Coon's modification medium supplemented with 10% FBS, dexamethasone 10nM, β-glycerophosphate 10mM, L-ascorbic acid 2-phosphate 50 µg/ml and 1% antibiotics. The role of PHEX was evaluated from 4 to 35 days of osteinduction, monitoring the alkaline phosphatase (ALP) activity and the hydroxyapatite production by quantitative analysis with fluorometric methods and by microscopic observations (brightfield, epifluorescence, confocal laser scanning microscopy (LSCM)).

Results: During the PA4 and PA9 induction with OM, we observed significant increments in ALP activity and hydroxyapatite production, respect to the control groups cultivated in GM. In particular, both ALP activity and mineralization analysis of PA4 have shown a trend similar to PA9, although the ALP activity decreases faster in PA4 (after 21 days) respect to PA9 (after 35 days) and the beginning of the mineralization process is delayed in PA4 (after 21 days) respect to PA9 (after 14 days).

Conclusions: The data presented suggest that PHEX activity is required for proper bone formation and controls bone matrix mineralization both through regulation of ALP activation and hydroxyapatite deposition.

***Disclosures: Cecilia Romagnoli**, None.*

SU0174

Tenofovir-Induced Osteomalacia. Catherine Anastasopoulou[1], Patamaporn Lekprasert*[2], Nissa Blocher[2]. [1]Albert Einstein Medical Center Endocrine Associates, USA, [2]Albert Einstein Medical Center, USA

Tenofovir is widely used as an effective treatment for HIV and HBV infection. Tenofovir-induced osteomalacia is rare and mainly caused by renal phosphate wasting from proximal tubular dysfunction. We report a case of tenofovir toxicity with severe osteomalacia due to complete Fanconi syndrome.

A 54 year-old Caucasian male with HIV/AIDS infection presented with bone pain and multiple fractures: legs, pelvis, scapula and ribs after a simple fall. He had been on tenofovir-based antiretroviral regimen for 10 years. His HIV was controlled with recent CD4 counts of 510 cells/ml3, and undetectable viral load.

In addition to severe diffused osteopenia and multiple fractures on radiographs, further evaluations are shown in table 1. All findings indicated severe proximal tubular dysfunction or Fanconi syndrome. Intact parathyroid hormone was normal (79 pg/ml), with 25-hydroxy vitamin D of 28.1 (30-100) ng/mL, and 1,25-hydroxy vitamin D of 17.5 (10-75) pg/mL.

The patient was given high-dose phosphate and potassium replacement, calcitriol, and sodium citrate for metabolic acidosis. Antiretroviral regimen was switched to zidovudine, lamivudine, and raltegravir. After 10 weeks, the patient still had persistent hypophosphatemia with hyperphosphaturia, reflecting incomplete recovery of tubular function.

Long-term exposure to tenofovir may lead to severe proximal tubular dysfunction and osteomalacia. Incomplete recovery has been reported after discontinuing tenovofir for 6-20 months. Screening and close monitoring of tubular function is required in those patients.

Laboratory data	Baseline	10 weeks after admission
Phosphorus (mg/dL)	0.7	2.5
Fraction excretion of phosphorus (%)	82%	74%
Creatinine (mg/dL)	0.5	0.5
Potassium (mmol/L)	3.3	3.4
Corrected calcium (mg/dL)	9.5	8.54
Alkaline phosphatase (U/L)	355	488
Hyperchloremic metabolic acidosis	present	present
Normoglycemic glucosuria (mg/dL)	>1,000 mg/dL	Not available
Proteinuria (mg/dL) and aminoaciduria	148 mg/dL	100 mg/dL

Table 1

***Disclosures: Patamaporn Lekprasert**, None.*

SU0175

After parathyroidectomy in primary hyperparathyroidism, sclerostin, osteocalcin, and undercarboxylated osteocalcin change rapidly. Aline Costa*[1], Zachary Lenane[1], Chiyuan Zhang[1], Elzbieta Dworakowski[1], Serge Cremers[1], James Lee[1], John Bilezikian[2]. [1]Columbia University, USA, [2]Columbia University College of Physicians & Surgeons, USA

Primary hyperparathyroidism (PHPT) can be cured by surgical removal of the abnormal parathyroid gland(s). With removal of the offending abnormal parathyroid tissue by parathyroidectomy (PTX), parathyroid hormone (PTH) levels fall immediately with slower changes in standard bone turnover markers. No studies have yet been conducted to track rapid changes in newer markers of bone metabolism such as sclerostin and undercarboxylated osteocalcin after PTX. To this end, we conducted a proof-of-concept study to investigate the rapidity and extent to which rapid reductions in sclerostin, osteocalcin and undercarboxylated-osteocalcin follow PTX. We studied four subjects (1 man, 3 postmenopausal women) with PHPT (mean age 59.5$\pm$16yrs) who underwent successful minimally invasive PTX. Acute changes in PTH [RIA(Scantibodies)], sclerostin [ELISA (TECOmedical)], osteocalcin [ELISA (IDS)], and undercarboxylated osteocalcin [ELISA (Takara)] were measured in serum samples obtained at the time of surgery immediately before parathyroid gland(s) removal (baseline) and thereafter at 5, 30, 60 and 120 minutes. After PTX, PTH levels fell quickly (-45% at 5 min, $p<0.0001$) and reached a nadir of 80% reduction ($p<0.0001$) by 60 min. Sclerostin levels tended to increase quickly ($p=0.07$) while osteocalcin and undercaboxylated osteocalcin levels showed a tendency to decline (Fig. 1). These results indicate that PTX is associated with acute changes in markers of bone metabolism that could signify rapid correction of abnormal bone metabolism in PHPT. This is the first study to access acute perturbations on newer markers of bone metabolism after PTX. Additional prospective studies with larger numbers are likely to identify further the utility of these markers in the context of PTX and as forecasters of improvements in bone mineral density and microarchitecture.

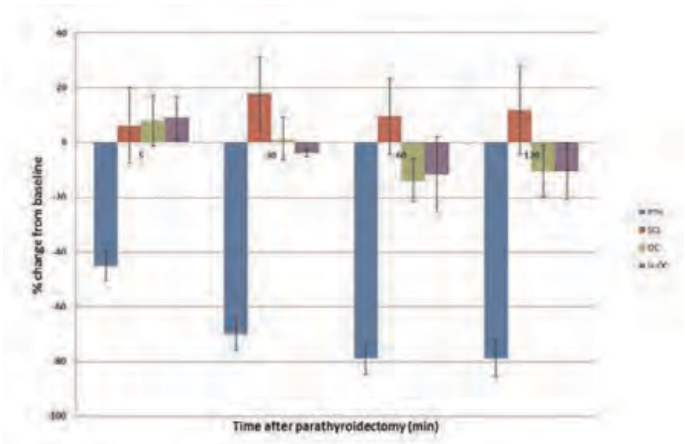

Changes in sclerostin, osteocalcin and undercarboxilated osteocalcin after parathyroidectomy in PHPT

***Disclosures: Aline Costa**, None.*

SU0176

Long-term Outcome of Bisphosphonate Therapy in Patients with Mild Primary Hyperparathyroidism. D Segula[1], V Mishra*[2], E MARKS[2], LR RANGANATHAN[2], S NIKOLOVA[2]. [1]University of liverpool, United Kingdom, [2]Royal Liverpool & Broadgreen University Hospital NHS Trust, United Kingdom

Background: Bisphosphonates therapy has been used in patients with primary hyperparathyroidism (PHPT) with the aim of increasing bone mineral density and reducing fragility fractures. We evaluated the effect of bisphosphonate treatment on bone mineral density, rate of fragility fracture and biochemical markers in 50 patients with PHPT who were not suitable for parathyroidectomy.

Results: The mean age of PHPT patients was 74 years, 94% females. Baseline mean serum adjusted calcium (2.74mmol/L, reference range 2.20-2.60mmol/L), mean serum creatinine 99.5µmol/L (reference range, 25-125µmol/L), bone mineral density for lumbar spine (L2-L4, mean T-score -2.5), and left femoral neck (mean T-score -2.1). 14 patients (28%) had bone fragility fractures at baseline. The duration of bisphosphonate therapy was 4.8$\pm$3(mean$\pm$ standard deviation)years.50% patients received either intravenous pamidronate or oral alendronic acid. 36% were treated with more than one bisphosphonate therapy. After a mean 4.8 years of bisphosphonate treatment, there was a significant decrease in serum adjusted calcium to 2.60mmol/L ($p<0.001$), urine calcium to creatinine ratio (0.70 and 0.55 before and after treatment, respectively, $p<0.0001$, reference range 0.3-0.7) and no significant change in renal functions (mean serum creatinine 96.4µmol/L) were seen. There was a significant increase in lumbar spinal bone density (T score L2-L4, -2.1) ($p=0.013$) with no significant change in left femoral neck bone density (T score -2.2). There was no change in rate of bone fragility fracture ($p= 0.167$). Out of the 14 patients who had fragility fractures at baseline, only one patient had a recurrent fracture after 4 years of therapy. A total of 7 patients (including the recurrent fracture) had new fragility fractures after duration of 6$\pm$2.5(mean $\pm$ standard deviation) years of bisphosphonate treatment. 21 PHPT patients received vitamin D supplementation while they were on bisphosphonate therapy. This group showed a significant reduction in serum adjusted calcium ($p<0.0001$) but had no effect on bone mineral density or fragility fractures.

Conclusion: Bisphosphonate therapy in PHPT patients significantly improved the lumbar spine bone mineral density and prevented further increase in rate of fragility fracture. Additionally, the therapy significantly reduced serum adjusted calcium, urinary calcium excretion and prevented deterioration in renal functions.

Table 1: Comparison of Pre- and Post-Bisphosphonate treatment on biochemical markers

Characteristic	Baseline	Post-treatment	p-value
Serum adjusted calcium (mmol/L)			
Mean (SD)	2.74 (0.13)	2.60 (0.12)	<0.0001
Urine calcium (mmol/ 24hours)			
Median (IQR)	4.2 (1.9 – 6.6)	3.8 (1.4-5.5)	0.064
Serum calcium: creatinine ratio			
Median (IQR)	0.70 (0.40 – 0.93)	0.55 (0.30– 1.0)	<0.0001
Serum creatinine (µmol/L)			
Mean (SD)	99.5 (36.9)	96.4 (31.7)	0.930
Serum PTH (pmol/L)			
Mean (SD)	10.6 (5.7)	10.3 (5.1)	0.862
Serum CTx (ug/L)			
Median (IQR)	0.3 (0.14-0.45)	0.28 (0.14 – 0.39)	0.140

IQR: Interquartile range; SD: Standard deviation; PTH: Parathyroid hormone; Cto: C-terminal telopeptide

Table 1

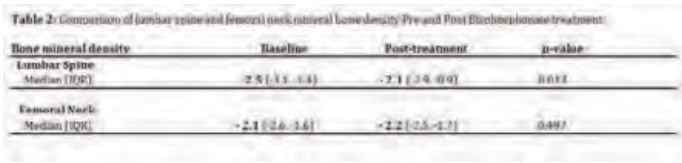

Table 2

Table 3

***Disclosures: V Mishra**, None.*

SU0177

Low Vitamin D Levels in Primary Hyperparathyroidism Are Associated with Low Cortical Bone Density at the Radius Independent of PTH. Marcella Walker*[1], Elaine Cong[2], Polly Young[1], Nicole Weber[1], Anna Kepley[3], Chiyuan Zhang[1], Donald McMahon[4], James Lee[1], Shonni Silverberg[1]. [1]Columbia University, USA, [2]Columbia Presbyterian Medical Center, USA, [3]Columbia University Medical Center, USA, [4]Columbia University College of Physicians & Surgeons, USA

Low levels of vitamin D (25OHD) are common in primary hyperparathyroidism (PHPT) but data regarding the skeletal effects of low vitamin D in PHPT are limited. Patients with mild PHPT (n=79; 80% female, age±SEM 62±1yrs, calcium 10.7±0.1mg/dl, PTH 84±5pg/ml; 25OHD 29±1ng/ml) were studied with bone markers, dual x-ray absorptiometry (DXA) and high-resolution peripheral quantitative computed tomography (HRpQCT). 25OHD levels in the deficient and insufficient range were common (21%≤20ng/ml, mean 13±1ng/ml; 53%<30ng/ml, mean 21±1ng/ml). 25OHD correlated positively with age (r=0.35, p=0.002), serum phosphate (PO_4; r=0.31, p=0.006) and FGF-23 (r=0.27, p=0.02), and inversely with GFR (r=-0.35, p=0.001) and BMI (r=-0.29, p=0.01). With regard to PHPT disease activity, 25OHD levels were associated with PTH (r=-0.43, p<0.0001), but not serum calcium, CTX or BSAP, DXA BMD or HRpQCT indices. Those with 25OHD<30 vs. ⩾30ng/ml (mean 38±1ng/ml) did not differ by PHPT duration, nephrolithiasis, fractures, meeting surgical guidelines or race, but they were younger (57±2 vs. 67 ± 2yrs, p=0.0005), more likely to be male (31% vs. 8%; p=0.01) and had higher BMI (29.4±0.9 vs. 26.4±1.0kg/m^2, p=0.03). Before and after adjusting for age and BMI, those with 25OHD<30ng/ml had higher PTH (97±7 vs. 69±7pg/ml; p=0.008), and lower PO_4 (2.9±0.1 vs. 3.3±0.1mg/dl, p=0.003) and FGF-23 (86±20 vs. 143±20 RU/ml, p=0.056) levels but did not differ in serum calcium, CTX or BSAP. They also had lower BMD by DXA at the 1/3 rad (0.633±0.01 vs. 0.669±0.01g/cm^2, p=0.07; T-Score -1.6±0.2 vs. -0.7±0.2; p=0.005) and lower radial cortical density on HRpQCT. Cortical differences by DXA (1/3 rad) and HRpQCT (rDcort 794±14 vs. 842±14 mgHA/cm^3; p=0.03) persisted after adjusting for PTH. Radial trabecular indices and tibial measures did not differ. The small group with 25OHD≤20ng/ml had higher PTH levels (≤ 20 vs. ⩾30ng/ml: 120±9 vs. 72±7pg/ml, p=0.0001; vs. >20ng/ml: 75±5pg/ml, p=0.001), but did not differ by DXA or HRpQCT. Similar findings were seen in women only. In summary, in mild PHPT as in non-PHPT subjects, 25OHD is associated with age, BMI, GFR and FGF23. 25OHD < 30ng/ml is common and associated with higher PTH levels and modestly lower cortical BMD (1/3 radius by DXA and rDcort by HRpQCT) that is not solely mediated by the higher PTH. Although we had few patients with 25OHD < 20ng/ml, these findings suggest that current cut-points for low vitamin D do not have a major impact on the skeleton in mild PHPT.

***Disclosures: Marcella Walker**, None.*

SU0178

Major changes in the clinical phenotypes of primary hyperparathyroidism in the United States and China over the past 20 years: a tale of two countries. Jian-min Liu*[1], Barbara C Silver[2], Lin Zhao[3], Xiao-yan He[3], Bei Tao[3], Li-hao Sun[3], Hong-yan Zhao[3], Natalie Cusano[4], Wen-wei Fan[2], Megan E. Romano[2], Guang Ning[3], John Bilezikian[4]. [1]Rui-jin Hospital, Shanghai Jiao-tong University School of Medicine, Peoples Republic of China, [2]Department of Medicine, Division of Endocrinology, College of Physicians & Surgeons, Columbia University, USA, [3]Department of Endocrine & Metabolic Diseases, Rui-jin Hospital, Shanghai Jiao-tong University School of Medicine, China, [4]Columbia University College of Physicians & Surgeons, USA

Twenty years ago, primary hyperparathyroidism (PHPT) presented with two distinctly different clinical profiles: in the United States as primarily an asymptomatic disease and in China as primarily a symptomatic disease. With changing clinical standards of care, greater routine availability of serum calcium determinations in China and PTH assays in the United States, we hypothesized that the clinical evolution of PHPT over the past 20 yrs will reflect further major changes in recognition patterns in these two countries. To this end, we compared subjects with PHPT in Shanghai, China (n=249) and in New York, USA (n=77), encompassing a recent experience over the past 10 yrs.

In contrast to virtually 100% symptomatic PHPT in China 20 yrs ago, about 40% of PHPT seen in China is of the asymptomatic variant in the past 10 yrs with the percentage rising even further to 50% in the past 5 yrs. In the USA, asymptomatic PHPT still predominates with over 80% in this category. Normocalcemic PHPT, not seen in Shangeai cohort, has become evident in USA, but constituting a small percentage of subjects (<10%).

Compared to American PHPT, subjects in China were younger (51.3±16 vs 66.4±12 yr, p<0.001), and less likely to be women (68% vs 82%, p=0.015). Chinese had a shorter duration of the disease than American subjects [1 (0-15) vs 5 (1-11) yr, (p<0.001)].

PHPT was more advanced in Shanghai than in New York with higher serum calcium (11.7±1.4 vs 10.6±0.6 mg/dL, p<0.001), PTH [402 (103-2700) vs 67.5 (47.9-94.9) pg/mL, p<0.001], alkaline phosphatase [112 (50-1419) vs 75 (62-92) IU/L, p<0.001], creatinine [1.03(0.55-2.75) vs 0.79 (0.59-1.23) mg/dL, p<0.001] levels, and lower serum 25(OH)D [13.0 (5.2-30) vs 35.3 (24.8-43.0) ng/mL, p<0.001] levels. Nephrolithiasis was more prevalent in Shanghai (48.2%) than in New York (14.3%), p<0.001. While not detected in New York, parathyroid cancer was present in 6% of the subjects in Shanghai (p=0.028). BMD at lumbar-spine was significantly reduced in Shanghai cohort as compared with New York cohort (T-score,-1.905±1.71 vs -1.118±1.68, p=0.002) . The two cohorts did not differ in BMD at femoral neck (T-score: -1.608±1.41 vs -1.705±1.09, p=0.613), fracture rate (17.2 % vs 14.3%, p= 0.596), or eGFR (76.8±42 vs 80.0±19 ml/min, p=0.662).

Although the phenotypes of PHPT in both countries are evolving, towards less evident disease, sharp clinical and biochemical differences are still apparent in PHPT as expressed in China and the United States.

***Disclosures: Jian-min Liu**, None.*

SU0179

Major Differences in Trabecular Bone Score Between Primary Hyperparathyroidism and Hypoparathyroidism Remain 1 Year After Reversal of the Abnormal Parathyroid State. Barbara Silva*[1], Natalie Cusano[2], Wen-Wei Fan[1], Megan Romano[1], Jim Sliney Jr[1], Zachary Lenane[3], Laura Beth Anderson[3], Didier Hans[4], Mishaela Rubin[3], John Bilezikian[2]. [1]Columbia University Medical Center, USA, [2]Columbia University College of Physicians & Surgeons, USA, [3]Columbia University, USA, [4]Lausanne University Hospital, Switzerland

We have shown that bone microstructure assessed by HRpQCT is markedly different in primary hyperparathyroidism (PHPT) and hypoparathyroidism (HypoPT). Compared to PHPT, HypoPT subjects have denser and thicker cortices, along with denser, thicker, more numerous, and less widely distributed trabeculae. Yet, it is not known if the return of PTH to normal by parathyroidectomy (PTX) in PHPT, or replacement of PTH in HypoPT can reverse the differences in bone structure observed between them. Trabecular bone score (TBS) is a quantitative estimate of trabecular microarchitecture that correlates with measures of bone microstructure by μCT and HRpQCT. In this study, we examined the differences in TBS between PHPT and HypoPT at baseline, and 1yr after PTX in PHPT and PTH(1-84) replacement in HypoPT.

The study group consisted of 12 subjects with PHPT followed for 1yr after successful PTX, and 12 sex-, age-, and BMI-matched HypoPT individuals treated with PTH(1-84) for 1 year. Site-matched spine TBS data were extracted from the DXA image (Hologic) using TBS iNsight software. Differences in continuous variables between PHPT and HypoPT were assessed by Student's t-test.

Each group constituted 8 postmenopausal women and 4 men. PHPT and HypoPT subjects were well matched in age (64±4 vs 57±3 yrs; p=0.2) and BMI (28.8±2.0 vs 27.2±1.2 kg/m2; p=0.5). Serum calcium was higher in PHPT than in HypoPT subjects (10.8±0.2 vs 8.8±0.2 mg/dl; p<0.001). Compared to PHPT, mean duration of disease was longer in HypoPT (23±3 vs 7±5 yrs; p=0.02). At baseline, mean TBS

was lower in PHPT than in HypoPT individuals (1.216±0.054 vs 1.388±0.034; p=0.01). TBS improved by +3.3±2.4% at 12 months post PTX in PHPT, and remained unchanged after 1 yr of PTH treatment in HypoPT (0.8±0.9%). At 1 yr, TBS was still lower in PHPT than in HypoPT subjects (1.247±0.042 vs 1.398±0.029; p=0.01).

We have shown, in agreement with previous studies by HRpQCT, that trabecular microarchitectural texture by TBS is greater in HypoPT than in PHPT subjects. TBS measures remain higher in HypoPT as compared to PHPT at 1 year after reversal of the abnormal parathyroid state. Further follow-up in both groups is required to determine if the correction of PTH excess or deficiency will eventually eliminate the differences in TBS that are evident before therapeutic intervention in PHPT and HypoPT.

***Disclosures: Barbara Silva**, None.*

SU0180

PTH(1-84) Administration Improves Three Dimensional Cancellous Bone Structure in Hypoparathyroidism Early in Treatment. Mishaela Rubin*[1], Alexander Zwahlen[2], David Dempster[1], Hua Zhou[3], Natalie Cusano[4], James Sliney[1], maryann dellabadia[1], Donald McMahon[4], Ralph Muller[2], John Bilezikian[4]. [1]Columbia University, USA, [2]Institute for Biomechanics ETH Zurich, Switzerland, [3]Regional Bone Center, Helen Hayes Hospital, USA, [4]Columbia University College of Physicians & Surgeons, USA

Hypoparathyroidism (HypoPT) is characterized by altered trabecular microarchitecture, with increased trabecular bone volume (BV/TV) and thickness (Tb.Th). We previously found, using conventional 2-D histomorphometric analysis of the iliac crest bone biopsy, that PTH(1-84) treatment in HypoPT was associated with an increase in trabecular number (Tb.N) at 1 and 2 yrs and a decrease in Tb.Th at 1 yr. We now investigated whether such changes are also detectable by direct 3-D analysis and how they may relate to bone strength. Fifty-seven HypoPT (26 premenopausal, 15 postmenopausal, 16 men; age, 18-72 years) were treated with PTH(1-84) for 2 yrs. All underwent iliac crest bone biopsies which were analyzed by high-resolution μCT with assessment of bone strength by μFE. Biopsies were performed at baseline (n=44) and at 1 (n=13) or 2 (n=16) yrs; 13 other subjects had one biopsy at 3 months. When compared to the untreated HypoPT biopsies (n=44), the 13 biopsies obtained after only 3 months of PTH had decreased bone surface density (15.69 ± 4.2 vs. 14.28 ± 2.1 mm^2/mm^3; p=0.01), trabecular separation (0.64 ± 0.1 vs 0.56 ± 0.1 mm; p=0.01) and trabecular heterogeneity (0.19 ± 0.03 vs 0.17 ± 0.03 mm; p=0.03), but increased Tb.N (1.84 ± 0.54 vs 2.36 ± 1.31 mm^{-1}; p=0.02). After 1 yr of PTH (n=13), the comparison within only 13 pairs from baseline to 1 yr showed that Tb.Th decreased (0.205 ± 0.04 vs 0.182 ± 0.03 mm; p=0.07) while connectivity density increased (14.10 ± 15 vs 30.70 ± 40 /mm^3; p=0.05). When using the same baseline biopsies as comparators (n=44), treated subjects at 1 yr tended to have an increase in apparent Young's modulus (649.4 ± 460 vs 1050.8 ± 824 N/m^2, p=0.09). The biopsies obtained after 2 yrs of PTH (n=16) showed that within the corresponding baseline 16 pairs, there was a decrease in Tb.Th, although it was not significant (0.194 ± 0.04 vs 0.184 ± 0.03 mm; p=0.3), while there was no difference from the overall baseline group (n=44). These data suggest that administration of PTH(1-84) in HypoPT is associated with early changes in microstructure as determined by direct 3-D histomorphometric analysis. Structural changes at 1 yr are consistent with trabecular tunneling, as indicated by thinner trabeculae and improved trabecular connectivity. The changes at 2 years were not as pronounced, which is similar to our previous observations by 2D analysis. We conclude that PTH(1-84) improves abnormal skeletal quality in hypoparathyroidism early in treatment.

***Disclosures: Mishaela Rubin**, NPS Pharmaceuticals, 6*
This study received funding from: NPS Pharmaceuticals

SU0181

Skeletal Microstructure Improves Markedly After Parathyroidectomy in Primary Hyperparathyroidism: Site- and Gender-specific Differences. Natalie Cusano*[1], Barbara Silva[2], Chiyuan Zhang[3], Kyle Nishiyama[3], Wen-Wei Fan[1], Megan Romano[1], John Bilezikian[1]. [1]Columbia University College of Physicians & Surgeons, USA, [2]Columbia University Medical Center, USA, [3]Columbia University, USA

It is well known that BMD improves after parathyroidectomy (PTX) in primary hyperparathyroidism (PHPT) but little is known about post-PTX changes in skeletal microstructure. Sex-specific differences after PTX have also not been explored. We report post-PTX results in 17 subjects (Age: 65 ± 13 yrs, 96% Caucasian) studied at baseline and at 6 months. Of these participants, 11 were also assessed at 1 yr and 6 at 1.5 yrs. We scanned 12 women (11 postmenopausal) and 5 men at the distal radius and tibia using high resolution peripheral quantitative computed tomography (HRpQCT, Scanco Medical AG) to assess volumetric BMD and bone microstructure. To evaluate changes 18 months after PTX, we used a linear mixed model for repeated measures. At the radius, there were significant increases in cortical area (Ct.Ar; p=0.04) and thickness (Ct.Th; p=0.02) (Table). At the tibia, there were significant changes in total (p=0.002), cortical (p=0.001), and trabecular area (Tb.Ar; p=0.001), total volumetric density (vBMD; p=0.02), Ct.Th (p=0.001), and trabecular thickness (p=0.02).

We investigated sex-specific differences using sex as a covariate in the model. Age was similar (Men: 61 ± 21 vs Women: 67 ± 10 yrs; p=0.6). Men demonstrated shorter duration of disease (0.8 ± 0.3 vs 11 ± 10 yrs; p=0.006) and higher alkaline phosphatase activity (86 ± 11 vs 70 ± 16 U/L; p=0.04). There were no differences in height, weight, BMI, or serum calcium at baseline. We found gender-specific differences at the radius between baseline and 12 months in cortical vBMD (p=0.047) and at the tibia for the following parameters: Tb.Ar (p=0.001), total vBMD (p=0.004), trabecular vBMD (p<0.0001), inner (p=0.001) and outer trabecular density (p=0.001), and bone volume fraction (p<0.0001).

In one of the first reports to describe PTX-associated changes in skeletal microstructural indices by HRpQCT, we also report site-specific, and for the first time, gender-specific differences in cortical and trabecular geometry and microstructure. The changes are mostly present at the weight-bearing site of the tibia. The etiology for sex-specific differences in response to PTX is unclear; others have shown sex-specific differences in HRpQCT parameters with aging. This report also provides the longest post-PTX results for HRpQCT to date. The results help to establish that bone quality improves after PTX and that there are striking differences between men and women.

Table. Percentage change in cortical (Ct) and trabecular (Tb) HRpQCT parameters 18 months after PTX in all subjects with PHPT. Men and postmenopausal women analyzed separately 12 months after PTX.

Radius	**All (%)**	**Men (%)**	**Women (%)**
Ct Area	5.2 ± 16[a]	5.1 ± 19	-0.1 ± 13
Ct Thickness	5.9 ± 17[a]	4.7 ± 19	0.7 ± 14
Ct vBMD	0.3 ± 5%	1.0 ± 6[b]	-1.1 ± 4
Tibia	**All (%)**	**Men (%)**	**Women (%)**
Total area	0.3 ± 0.5[a]	0.08 ± 0.6	0.2 ± 0.5
Ct Area	9.1 ± 17[a]	9.6 ± 17	4.5 ± 12
Ct Thickness	9.6 ± 18[a]	9.6 ± 19	5.1 ± 14
Tb Area	-0.6 ± 1[a]	-0.7 ± 0.8[b]	-0.3 ± 0.6
Total vBMD	1.9 ± 5[a]	3.6 ± 6[b]	0.7 ± 4
Tb vBMD	0.8 ± 6	3.8 ± 6[b]	-0.2 ± 4
Inner Tb vBMD	1.4 ± 8	5.2 ± 9[b]	1.0 ± 6
Meta Tb vBMD	0.7 ± 5	2.7 ± 6[b]	-0.6 ± 4
BV/TV	0.7 ± 6	3.7 ± 6[b]	-0.4 ± 4
Tb Thickness	5.8 ± 15[a]	3.4 ± 21	3.9 ± 15

Mean ± SD; vBMD, volumetric bone mineral density; BV/TV, Tb bone volume fraction; [a]p<0.05 entire cohort from baseline, [b]p<0.05 men vs women

Table

***Disclosures: Natalie Cusano**, None.*

SU0182

Vitamin D Treatment in Primary Hyperparathyroidism: a Randomized Placebo Controlled Trial. Lars Rolighed*[1], Lars Rejnmark[1], Tanja Sikjaer[2], Lene Heickendorff[3], Peter Vestergaard[4], Leif Mosekilde[1], Peer Christiansen[5]. [1]Aarhus University Hospital, Denmark, [2]Department of Medicine & Endocrinology, MEA Aarhus University Hospital, Denmark, [3]Dept. of Clinical Biochemistry, Denmark, [4]Aalborg University Hospital, Denmark, [5]Dept. of Surgery P, Denmark

Low levels of 25-hydroxy vitamin D (25OHD) are common in patients with primary hyperparathyroidism (PHPT) and associated with higher PTH levels and hungry bone syndrome following surgery. However, concerns have been raised on the safety of vitamin D supplementation in terms of aggravated hypercalcemia and hypercalciuria and subsequent impairment of renal function.

We aimed to assess effects of supplementation with high doses of vitamin D in patients with PHPT.

Using a double-blinded design, we randomized 46 patients with PHPT and 25OHD-levels < 80 nmol/l to a daily supplement with 70 microgram (2800 IU) of cholecalciferol or identical placebo for 52 weeks. Accordingly, treatment was administered for 26 weeks prior to parathyroidectomy and continued for 26 weeks following surgical cure.

Patients had a mean age of 58 (range 29-77) years and 76% were women. Preoperatively, 25OHD increased from 50 to 94 nmol/l in the treatment group, whereas levels decreased slightly by 9% in the placebo group (p<0.001 for between group difference). Compared with placebo, cholecalciferol treatment decreased PTH significantly by 17% prior to parathyroidectomy (p=0.01). Postoperatively, PTH levels remained lower in the cholecalciferol- compared with the placebo group (p=0.04). Creatinine, plasma and urinary calcium did not change in response to treatment. Compared with placebo, BMD at the lumbar spine increased in the cholecalciferol group by 2.4% prior to surgery (p=0.01). There were no differences

between groups in the pre- and post-operative BMD changes in the hip or forearm.In conclusion, optimization of vitamin D status in patients with PHPT by supplementation with a daily dose of 70 microgram of cholecalciferol does not seem to possess safety concerns, but may lower plasma PTH and improve BMD.

***Disclosures: Lars Rolighed**, None.*

SU0183

Bone micro-architectural anomalies and vascular calcification in uremic rats. Fabrice Mac-Way*[1], Alexandra Gauthier-Bastien[2], Ioan-Andrei Iliuta[2], Roth-Visal Ung[2], Richard Lariviere[2], Mohsen Agharazii[2]. [1]L'Hôtel-Dieu de Québec, Canada, [2]CHU de Quebec Research Center, Canada

Background: The relationships between development of vascular calcification and bone micro-architectural disorders, in chronic kidney disease (CKD), are poorly understood. We aimed to evaluate the anomalies of bone micro-architecture and mineralisation in uremic rats with vascular calcification as compared to non CKD rats.

Methods: CKD was induced by 5/6 nephrectomy in male Wistar rats. Vascular calcification was induced by high Ca/P diet and 1.25 $(OH)_2D$ (Ca/P/Vit D). Four groups were studied: (1) CTL + standard diet; 2) CTL + Ca/P/Vit D; 3) CKD + standard diet; 4) CKD + Ca/P/Vit D. After 4-6 weeks, the animals were sacrificed for blood biochemistry, bone specimens and thoracic aorta analysis. Von Kossa quantification was used for aorta calcification and left tibiae of each rats were imaged with high resolution Micro-CT for architectural analysis and further bone histomorphometry analysis.

Results: Von Kossa analysis showed a significantly higher thoracic aorta calcification in CKD + Ca/P/Vit D as compared to CKD + standard diet and CTL group (Figure 1). Bone micro-architectural analysis by Micro-CT showed a significantly lower cortical BMD in CKD vs CTL and a lower cortical thickness in CKD + Ca/P/Vit D vs CTL due to a decreased outer perimeter. Cortical thickness is also significantly lower in CKD + Ca/P/Vit D vs CKD + standard diet (Figure 2) while trabecular bone volume fraction was higher, although non significantly. The thoracic calcification was inversely correlated to the cortical bone thickness (Figure 3).

Conclusions: CKD has a negative effect on bone micro-architecture as shown by decreasing bone cortical thickness and mineral density. Vascular calcification is linked to bone micro-architectural disturbance as bone cortical thickness is even lower in CKD rats with vascular calcification, and that the extent of aortic calcification is negatively correlated to cortical bone thickness of tibiae. This study underlines the interrelationship between vascular calcification and bone micro-architecture in uremic state.

Figure 1. Von Kossa vascular calcification in CKD rats fed with high Ca/P/Vit D diet

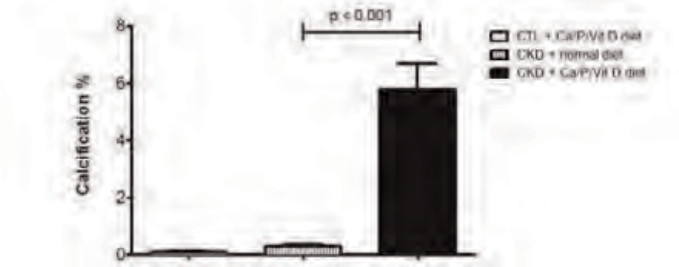

Von Kossa vascular calcification in CKD rats fed with high Ca/P/Vit D diet

Figure 2. Rats with vascular calcification had lesser bone cortical thickness

Rats with vascular calcification had lesser bone cortical thickness

Figure 3. Aortic calcification and bone cortical thickness in CKD rats

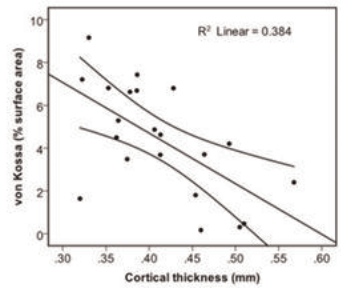

Aortic calcification and bone cortical thickness in CKD rats

***Disclosures: Fabrice Mac-Way**, None.*

SU0184

Reduced Nedd4 Function Promotes Vascular Calcification through Stabilizing a Smad1. Ji-Hyun Lee*[1], Michiko Takeda[2], Jae-Jin Cho[3], Je-Yong Choi[4], Hiroshi Kawabe[2], Nils Brose[2], Je-Yoel Cho[5]. [1]Veterinary Medicine, Seoul National University, South Korea, [2]Max Planck Institute of Experimental Medicine, Germany, [3]Seoul National University, South Korea, [4]Kyungpook National University, School of Medicine, South Korea, [5]College of Veterinary Medicine, Seoul National University, South Korea

Vascular calcification is associated with atherosclerosis, diabetes and chronic kidney disease, and it has been suggested that this process is similar to bone mineralization. However, the mechanisms underlying vascular calcification are poorly understood. Neural precursor cell-expressed, developmentally down-regulated protein 4 (NEDD4) is an ubiquitin-protein ligase that contains a calcium/lipid-binding domain, multiple WW domains and a C-terminal HECT domain. We previously reported that Nedd4 may be a modulator of Smad1 in BMP2/TGFβ1 signaling. In the current study, we assessed the effect of Nedd4 in vascular calcification using in vivo and in vitro. The in vivo model of vitamin D_3-induced vascular calcification was significantly promoted in the *Nedd4$^{fl/fl}$;SM22α-cre* mice in compare with their control littermates. In a calcified aortas region associated with increased expression of not only p-Smad1 but also bone related markers. Nedd4 protein level was prominently reduced in both calcified VSMCs and aortas. Moreover, the knockdown of Nedd4 increased bone-related gene expression levels and the formation of mineralized nodules by VSMCs in presence of calcifying medium. These results demonstrated that Nedd4 knockdown repressed its inhibitory effect on osteoblastic differentiation, thereby leading to the calcification of aortas through a process that is mediated by the Nedd4/Smad1 signaling pathway. These results provide evidence for the hypothesis that Nedd4 plays a protective role against vascular calcification.

***Disclosures: Ji-Hyun Lee**, None.*

SU0185

Delayed Bone Regeneration Is Linked To Chronic Inflammation In Murine Muscular Dystrophy. Rana Abou-Khalil*[1], Frank Yang[2], Marie Mortreux[2], Shirley Lieu[2], Yan Yiu Yu[3], Maud Wurmser[2], Catia Pereira[1], Frederic Relaix[4], Theodore Miclau[2], Ralph Marcucio[3], Celine Colnot[1]. [1]INSERM U781, Université Paris Descartes-Sorbonne Paris Cité, Institut Imagine, Hôpital Necker Enfants Malades, France, [2]Department of Orthopaedic Surgery, University of California at San Francisco, USA, [3]University of California, San Francisco, USA, [4]INSERM, UMR-S 787, UPMC Paris VI, Institut de Myologie, Faculté de Médecine Pitié-Salpétrière, France

Duchenne muscular dystrophy (DMD) patients exhibit skeletal muscle weakness with continuous cycles of muscle fiber degeneration/regeneration, chronic inflammation, as well as low bone mineral density and increased risks of fracture. Fragility fractures and associated complications are thus considered as a consequence of the osteoporotic condition in these patients. Here, we aimed to establish the relationship between muscular dystrophy and fracture healing by assessing bone regeneration in mdx mice, a model of DMD with absence of osteoporosis. Our results illustrate that muscle defects in mdx mice impact the process of bone regeneration at various levels in a non-stabilized tibial fracture model. In mdx fracture callus, histomorphometric analyses showed that both cartilage and bone deposition were delayed followed by a delay in cartilage and bone remodeling. As indicated by PECAM staining and quantification of blood vessels via stereology, vascularization of mdx fracture calluses

was also compromised during the early stages of repair. Dystrophic muscles are known to contain elevated numbers of macrophages contributing to muscle degeneration. Accordingly, using stereological quantification of F4/80 staining, we observed increased macrophage recruitment in the mdx fracture calluses and abnormal accumulation of macrophages throughout the process of bone regeneration. These changes in the inflammatory environment subsequently had an impact on the recruitment of TRAP-positive osteoclasts and the remodeling phase of repair. Further damage to the mdx muscle, using a novel model of muscle trauma, amplified both the chronic inflammatory response and the delay in bone regeneration. In addition, PLX3397 treatment of mdx mice, a cFMS inhibitor in monocytes, partially rescued the bone repair defect through increasing cartilage deposition and decreasing macrophage number. In conclusion, impaired inflammatory response in mdx mice is responsible for the fracture healing delay and is associated with defects in angiogenesis and osteoclastogenesis. By revealing the role of dystrophic muscle in regulating the inflammatory response during bone repair, our results emphasize the implication of muscle in the normal bone repair process and may lead to improved treatment of fragility fractures in DMD patients.

***Disclosures: Rana Abou-Khalil**, None.*

SU0186

Muscle-derived Cytokines and Chemokines Inhibit Osteoblast Function. Rachelle Johnson*[1], Jason White[2], Emma Walker[1], T John Martin[1], Natalie Sims[1]. [1]St. Vincent's Institute of Medical Research, Australia, [2]Murdoch Childrens Research Institute, Royal Childrens Hospital; School of Veterinary Medicine, University of Melbourne, Australia

The proximity of muscle to the periosteum suggests an inter-tissue pathway of communication controlling cortical bone's response to mechanical and adjacent paracrine stimuli, but the key muscle-secreted factors that might regulate periosteal osteoblast activity are not yet known. Since osteocyte-specific deletion of the glycoprotein130 (gp130) co-receptor and global deletion of the gp130-binding cytokine CNTF both increase periosteal circumference, we hypothesized that 1) muscle-derived cytokines (myokines) inhibit cortical bone formation, and 2) this is dependent on CNTF/gp130 signalling.

To assess whether myokines inhibit osteoblast function, calvarial osteoblasts were harvested from C57BL/6 neonates and cultured for 24 hours in conditioned media (CM) from differentiated myogenic C2C12 myotubes grown for 1, 2 and 3 days in fusion media. These osteoblasts produced dramatically less alkaline phosphatase (ALP) mRNA and protein in the presence of C2C12 CM compared to osteoblasts in non-conditioned media ($p<0.0001$). This inhibition increased with myotube culture length (1day=58-70%, 2days=69-76%, 3days=80-87% mRNA inhibition). Similar effects were observed in primary osteoblasts differentiated in osteogenic media for 23 days until osteocytic genes were expressed, where C2C12 CM treatment dramatically reduced OSX, ALP, PTHR1, osteocalcin and sclerostin mRNA (>7-50-fold, $p<0.01$), and increased RANKL expression >8-fold ($p<0.01$).

To determine whether the inhibitory effect of muscle on periosteal osteoblasts may be gp130-dependent, skeletal muscle was collected from wildtype C57BL/6 mice ($n\geqslant6$) and analysed for gp130 cytokine mRNAs by qPCR. CNTF mRNA levels were 10-fold greater than levels of OSM, IL-11, LIF and IL-6, suggesting it as a candidate inhibitory myokine; however, neutralising antibodies to CNTF or CNTF receptor (10μg/ml) did not block the reduction in ALP mRNA when added to C57BL/6 osteoblasts+C2C12 CM cultures, indicating that a myokine other than CNTF inhibits osteoblasts. Cytokine array analysis of the C2C12 CM revealed TIMP-1, MCP-1, and CXCL10 were the most abundantly secreted proteins, followed by CXCL1, M-CSF, and CCL5. Many of these factors stimulate monocyte migration, but the abundance of these chemokines in the muscle CM suggests that TIMP-1 and MCP-1 are myokines that directly stimulate osteoclastogenesis by promoting osteoblastic RANKL expression, and inhibit osteoblast differentiation on the periosteal surface via paracrine signalling.

***Disclosures: Rachelle Johnson**, None.*

SU0187

Role of the osteoinductive factors, Tmem119, BMP-2 and the ER stress response PERK-eIF2α-ATF4 pathway in the commitment of myoblastic into osteoblastic cells. Ken-ichiro Tanaka*[1], Hiroshi Kaji[2], Ippei Kanazawa[3], Lucie Canaff[4], Geoffrey Hendy[5], Toshitsugu Sugimoto[1]. [1]Shimane University School of Medicine, Japan, [2]Kinki University Faculty of Medicine, Japan, [3]Shimane University Faculty of Medicine, Japan, [4]McGill University, Canada, [5]McGill University, Royal Victoria Hospital, Canada

The endoplasmic reticulum (ER) is crucial for biosynthesis, folding and modification of secreted proteins. Differentiating osteoblasts synthesize and secrete large amounts of bone matrix proteins and ER stress response pathways monitor this process. Fibrodysplasia ossificans progressiva (FOP) is a genetic disease in which heterotopic ossification occurs in muscle. Constitutively activating BMP type 1 receptor mutations underlie the molecular pathogenesis of FOP. We demonstrated that Tmem119, a PTH-responsive Smad3-related osteoinductive factor, is increased by overexpressing an FOP mutant BMP type 1 receptor and promotes the differentiation of myoblasts into osteoblasts by the induction of BMP-2 and the interaction with the BMP signaling pathway (J Biol Chem 2011, BONE 2012). Although both BMP-2 and Tmem119 promote the differentiation of myoblasts into osteoblasts and each increase the levels of the other, the relative contributions of BMP-2 and Tmem119 to the osteogenic differentiation and the mechanisms involved are incompletely understood. In this study, we examined the relationships among BMP-2, Tmem119 and the PERK-eIF2α-ATF4 ER stress response pathway in the osteoblastic differentiation of myoblastic C2C12 cells. Both BMP-2 and Tmem119 induced levels of Runx2, Osterix, Col1a1, ALP and osteocalcin, as well as mineralization. BMP-2 activation of the ER stress sensor PERK stimulated phosphorylation of eIF2α and led to increased biosynthesis of the osteoblast differentiation factor ATF4. When dephosphorylation of eIF2α was blocked by the selective inhibitor salubrinal, the osteogenic effects of BMP-2 and Tmem119 were enhanced further. While BMP-2 stimulated both P-eIF2α and ATF4 levels, Tmem119 had no effect on P-eIF2α but stimulated ATF4 only. Tmem119 siRNA reduced both baseline and BMP-2-stimulated levels of the ATF4 protein. In conclusion, BMP-2 stimulates differentiation of myoblasts into osteoblasts via the PERK-eIF2α-ATF4 pathway but in addition stimulates Tmem119 that itself increases ATF4. Hence, BMP-2 stimulates ATF4 both dependently and independently of the PERK-eIF2α ER stress response pathway. Abbreviations: PERK, protein kinase RNA-like endoplasmic reticulum kinase; eIF2α, eukaryotic translation initiation factor 2 subunit alpha; ATF, activating transcription factor.

***Disclosures: Ken-ichiro Tanaka**, None.*

SU0188

Imaging and Quantifying Muscle-Bone Crosstalk via Intact Periosteum. Xiaohan Lai*, Christopher Price, Liyun Wang. University of Delaware, USA

During skeletal growth, strong functional relationships exist between muscle and bone. Recent evidence suggests that soluble factors produced by the muscle could regulate bone cell activity. The periosteum, a fibrous membrane that tightly covers bone's outer surface, lies adjacent to muscle, and contains osteoprogenitor cells crucial for bone modeling, may be a target of these muscle-derived factors. Furthermore, as an interface, the periosteum may act as a molecular sieve, controlling the penetration and transport rates of these factors into the bone tissue. However, few data are available on the permeability of the periosteum.

In this study we aimed to image and quantify the permeability of intact periosteum. Confocal xz imaging was first used to identify the periosteum on the mouse tibial mid-shaft. Using the reflected-light imaging, periosteum's dense irregular connective tissue allowed identification of the periosteum, which was further confirmed by staining the bone using Texas red C2-dichlorotriazine, an amine reactive dye (red channel, Fig. 1). For a 5-month old C57BL/6J mouse the thickness of periosteum was found to be ~ 40 μm. After the periosteum was identified, the PBS solution in the imaging chamber was replaced with a well-mixed solution of sodium fluorescein (376 Da). A time series of x-z line scan was then collected to track tracer penetration into the periosteum. Sodium fluorescein could penetrate into the periosteum within 30 seconds (Fig 2).

To obtain the dynamic transport characteristics, the time series were analyzed using MatLab. From the reflected light intensity profile, the periosteum's boundaries were defined at the half maximal intensity in the profile (Fig. 3). The spatiotemporal profiles agreed qualitatively with the predicted diffusion profiles, where the concentration increased inside the periosteum with time (Fig. 4). The time lag between two adjacent profiles was 6 sec and sodium fluorescein could penetrate (reaching 50% of bath concentration) into the mid-plane of the periosteum within 12 sec. The effective tracer diffusivity can thus be derived. The dependency of the diffusivity on tracer size, animal age and bone site is currently under investigation. The results are expected to identify the rate-limiting factors during this muscle-bone interaction process.

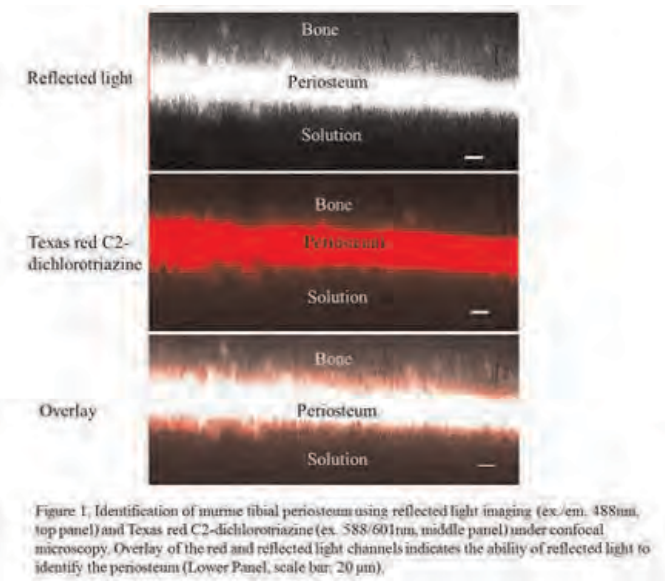

Figure 1. Identification of murine tibial periosteum

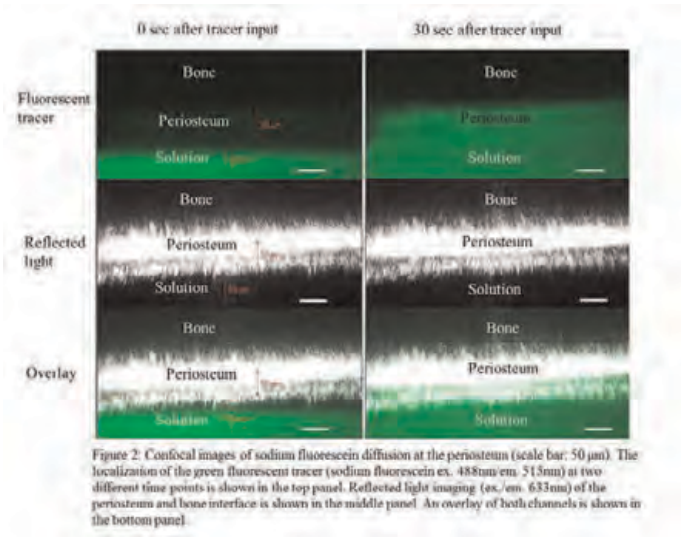

Figure 2: Confocal images of sodium fluorescein diffusion at the periosteum (scale bar: 50 μm). The localization of the green fluorescent tracer (sodium fluorescein ex. 488nm/em. 515nm) at two different time points is shown in the top panel. Reflected light imaging (ex./em. 633nm) of the periosteum and bone interface is shown in the middle panel. An overlay of both channels is shown in the bottom panel.

Figure 2: Confocal images of sodium fluorescein diffusion at the periosteum

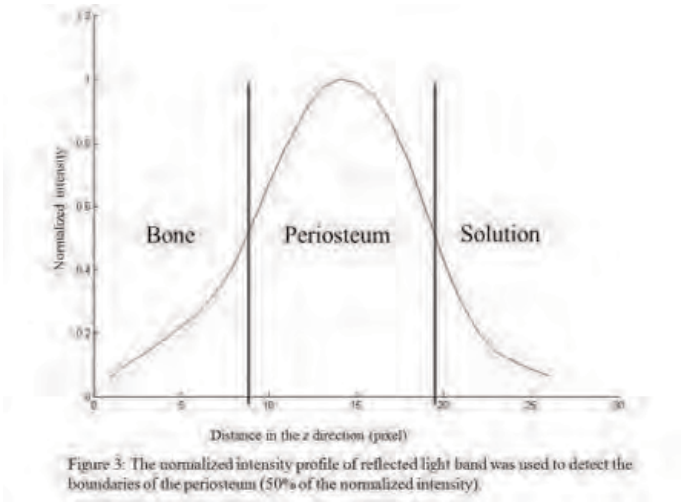

Figure 3: The normalized intensity profile of reflected light band was used to detect the boundaries of the periosteum (50% of the normalized intensity).

Figure 3: The normalized intensity profile of reflected light

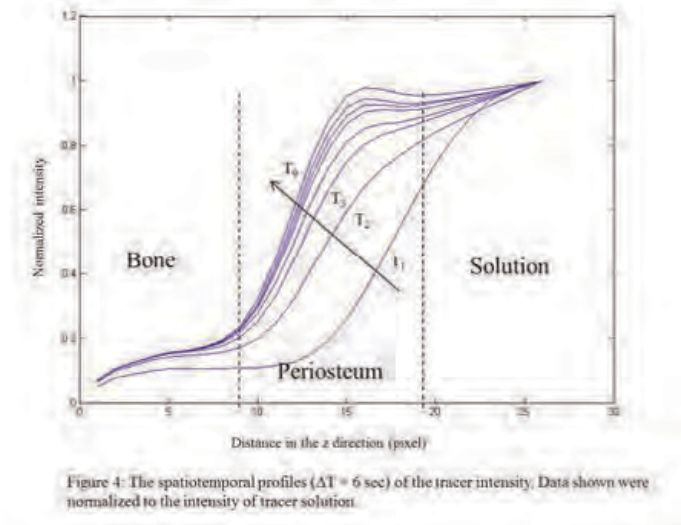

Figure 4: The spatiotemporal profiles (ΔT = 6 sec) of the tracer intensity. Data shown were normalized to the intensity of tracer solution.

Figure 4: The spatiotemporal profiles of the tracer intensity.

***Disclosures: Xiaohan Lai**, None.*

SU0189

Recombinant Osteocalcin Improves Insulin-stimulated Glucose Uptake Following Muscle Contraction. Itamar Levinger*[1], xuzhu lin[1], Xinmei Zhang[1], Alan Hayes[1], George Jerums[2], Mathieu Ferron[3], Gerard Karsenty[3], Ego Seeman[4], Glenn McConell[1]. [1]Victoria University, Australia, [2]University of Melbourne & the Department of Endocrinology, Austin Health, Australia, [3]Columbia University, USA, [4]Austin Health, University of Melbourne, Australia

Background: Studies in mice suggest that osteocalcin (OC), an osteoblast-specific secreted hormone, in its undercarboxylated form (ucOC), increases insulin secretion and insulin sensitivity. Acute exercise increases skeletal muscle insulin sensitivity as well as circulating levels of ucOC post- exercise by mechanisms that are incompletely understood. We tested the hypothesis that OC plays a direct role in the increase in muscle glucose uptake post contraction in C57BL/6J wild-type mice.

Methods: We used an *ex-vivo* muscle contraction model to assess whether recombinant OC can improve insulin-stimulated glucose uptake post contraction. We have compared the differences in EDL muscle glucose uptake from C57BL/6J mice between rest and 3 treatments including (a) contraction alone, (b) contraction plus insulin and (c) contraction plus insulin plus recombinant OC. Data reported as mean ± SEM.

Results: There was a linear increase in muscle glucose uptake across treatments (rest: 1.4 ± 0.2, contraction alone: 1.7 ± 0.2, contraction plus insulin: 2.3 ± 0.1 and contraction plus insulin plus OC: 2.6 ± 0.1 μmol/g/h, p=0.006). Muscle glucose uptake with OC treatment (contraction plus OC plus insulin) post ex-vivo muscle contraction was higher by ~ 14% (p=0.04) compared to contraction plus insulin alone.Conclusion: Our data suggest the OC treatment improves insulin-stimulated muscle glucose uptake following an *ex vivo* muscle contraction. In addition, exercise increases circulating ucOC (from our previous study) and this elevation may account, at least in part, for the insulin sensitizing effect of exercise.

***Disclosures: Itamar Levinger**, None.*

SU0190

Wnt3a Potentiates Myogenesis in C2C12 Myoblasts by Orchestrated Changes in IP3-mediated Calcium Signaling and β-catenin Activation. Jian Huang*, Chenglin Mo, Sandra Romero-Suarez, Lynda Bonewald, Marco Brotto. University of missouri kansas city, USA

Wnts have a significant potential to directly influence muscle function. We previously found the expression of Wnts, especially Wnt3a significantly increased in MLO-Y4 osteocytes exposed to fluid flow shear stress. To test Wnt3a roles in skeletal muscle myogenesis, C2C12 myoblasts were exposed to 10ng/ml Wnt3a which led to increased number and size of myotubes (4,319 ± 642 μm^2 untreated, vs. 9,833 ± 1,013 μm^2 for Wnt3a treated C2C12, $p < 0.001$). Considering that the concentration of 10ng/ml Wnt3a might be supra-physiological, we have conducted pilot studies with concentrations of Wnt3a ranging from 0.1 to 10ng/ml. A concentration as low as 0.5ng can consistently increase both the number and the size of myotubes during differentiation, a finding that was confirmed morphologically (4,299 ± 594 μm^2 untreated, vs.7,957 ± 1,269 μm^2 for Wnt3a treated myotubes, $p < 0.001$) and also with the concomitant double staining of myosin heavy chain (MHC) and nuclei. Furthermore, when Wnt3a was added to differentiation media, translocation of β-catenin to the nucleus increased by 2-fold compared to control suggesting that Wnt3a might stimulate β-catenin translocation leading to the downstream activation of muscle regulatory factors. Intriguingly, the potent effect of Wnt3a on stimulating the activation of the β-catenin signaling pathway in C2C12 cells strongly correlated with the appearance of intracellular calcium oscillations (ranging from 150-500nM free calcium) in myotubes measured with Fura-2. In a search for the molecular machinery responsible for this enhanced calcium oscillation activity we used several pharmacological agents to specifically block calcium regulatory mechanisms related to store-operated calcium entry, ryanodine receptor mediated calcium release, and IP3 receptor mediated calcium. Only by treating the cells with both gentamycin and 2-APB, which effectively blocks the production of IP3 and inhibits the IP3R, were calcium oscillations abolished, suggesting that the IP3-calcium signaling pathway is involved in this enhanced calcium oscillation activity induced by Wnt3a. In agreement, focused qRT-PCR arrays revealed a 6-fold increase in IP3-R1, and IP3R3, and a 2-fold increase in MyoD expression. We propose that Wnt3a acts through the modulation of intracellular calcium homeostasis, resulting in translocation of β-catenin that enhances expression of MyoD, IP3-1 and IP3-3, which together act in concert to enhance myogenesis.

***Disclosures: Jian Huang**, None.*

SU0191

Effects of Sex Steroid Deprivation on Skeletal Muscle Function and Ryanodine Receptor (RyR1) Modulation. Laura Wright*[1], Dennis Joseph[1], Ahmed Harhash[1], David Waning[2], Sutha John[1], Khalid Mohammad[1], Andrew Marks[3], Theresa Guise[1]. [1]Indiana University, USA, [2]Indiana University School of Medicine, USA, [3]Columbia University, USA

Adjuvant androgen- or estrogen (E_2)-deprivation therapy commonly causes musculoskeletal complications in cancer patients. The mechanism(s) of androgen- and E_2-deprivation-induced muscle dysfunction has not been identified, although both have been associated with increased oxidative stress. The ryanodine receptor (RyR1)/calcium release channel on the sarcoplasmic reticulum (SR) is required for muscle excitation-contraction coupling where the force of contraction is determined by the amount of calcium released via RyR1. Pathological oxidation-dependent depletion of the stabilizing subunit calstabin from RyR1 results in leaky channels and impaired muscle function in other diseases. To determine the role of sex steroid deficiency in skeletal muscle function, young male and female C57BL/6 mice underwent orchiectomy (ORX; n=10) or ovariectomy (OVX; n=5) and were assessed for changes in body composition and bone by dual energy X-ray absorptiometry (DXA) and μCT (SCANCO vivaCT40). Skeletal muscle function was assessed by measurement of maximum contractile force, corrected for muscle size, of the extensor digitorum longus (EDL). The amount of calstabin bound to RyR1 was determined by immunoprecipitation of RyR1 followed by immunoblotting for RyR1 and calstabin. In male ORX mice, percent fat mass increased ($p<0.0001$), bone mineral density (BMD) decreased ($p<0.0001$) and grip strength declined ($p=0.006$) 20 weeks after surgery. Muscle mass was reduced ($p<0.0001$) yet muscle-specific force production of the EDL was greater in ORX mice relative to controls. Expression of calstabin:RyR1 was not different. Female OVX mice similarly had increased percent fat mass ($p=0.037$), decreased BMD and bone volume fraction ($p<0.05$), with associated reduction in grip strength relative to controls. EDL mass was increased ($p<0.05$) yet muscle-specific force production of the EDL was lower in OVX mice and fatiguability was increased ($p<0.0001$). Consistent with the observed muscle dysfunction in OVX mice there was remodeling of RyR1 (i.e. decreased bound calstabin) indicating leaky channels. Thus, sex-steroid deficiency results in muscle weakness, but the mechanisms may differ between androgen and E_2-deprivation, with the former resulting in decreased muscle mass and the latter decreased function. Further studies are needed to determine the mechanism by which E_2-deprivation causes remodeling of RyR1 and whether pharmacological stabilization of RyR1-calstabin might ameliorate muscle weakness.

***Disclosures: Laura Wright**, None.*

SU0192

Uniaxial Cyclic Stretch Enhance Adipose-Derived Stem Cell Myogenesis. Pinar Yilgor Huri*[1], Colin Cook[1], Daphne Hutton[1], Brian Goh[2], Douglas Digirolamo[1], Warren Grayson[1]. [1]Johns Hopkins University, USA, [2]Johns Hopkins University School of Medicine, USA

Purpose: The regeneration capacity of skeletal muscle is limited in cases of large volumetric loss and autograft therapies are limited by the availability of suitable donor tissues [1]. Adipose-derived stem cell (ASC)-based tissue engineered muscle grafts could provide an effective alternative therapy. However, their therapeutic potential is limited by their low differentiation efficiency into myoblasts (0.5-5%) [2]. The aim of this study was to increase the efficiency of ASC myogenesis through the application of uniaxial cyclic stretch which mimics the native biophysical cues.

Methods: Human ASCs were seeded in specialized well plates with flexible membrane substrates. After 24 h, myogenic induction medium (MIM) was added to the *Induced* group for one day (biochemical induction) then replaced with expansion medium. *Un-induced* cells were retained in expansion medium. ASCs in these groups were grown in *Static* or *Dynamic* conditions. From Days 3 – 14 of culture, *Dynamic* cultures were exposed to uniaxial cyclic (11% strain, 0.5 Hz, 1h/day) stretch (biophysical induction). *Static* cells were not subjected to strain. We assessed cell morphology via phase contrast microscopy and actin filament staining and myogenesis was evaluated using immunocytochemistry and RT-PCR for muscle-specific markers. Images were quantified with Image J software.

Results: ASCs align and fuse upon induction where uninduced controls proliferated randomly on Static (Fig.1; day 14 (40x), red: Phalloidin-TRITC, blue: DAPI, FI: Fusion index and quantification of alignment). Although uninduced cells have a tendency to align on Dynamic, they do not specifically fuse in the absence of biochemical induction. Alignment and multinucleation became most pronounced with the application of both biochemical and biophysical induction; the fusion index increased almost 3 times in Induced-Dynamic compared to Induced-Static (2.6 ± 1.3 vs. 7.6 ± 4.8). ASCs in Dynamic conditions exhibited significantly higher Desmin and MyoD protein expression compared to Static (Fig.2) on days 3, 7 and 14. mRNA levels of Desmin, MYF5, Myog and Myosin heavy chain were significantly enhanced under Dynamic conditions (not shown).

Conclusion: ASC differentiation along the myogenic lineage could be significantly enhanced by mimicking the biophysical cues present within the native muscle microenvironment.

References: [1] Turner N.J.[+], Cell Tiss Res (2012) 347: 759-774. [2] Choi Y.S. [+], Biomaterials (2012) 33: 6943-6951.

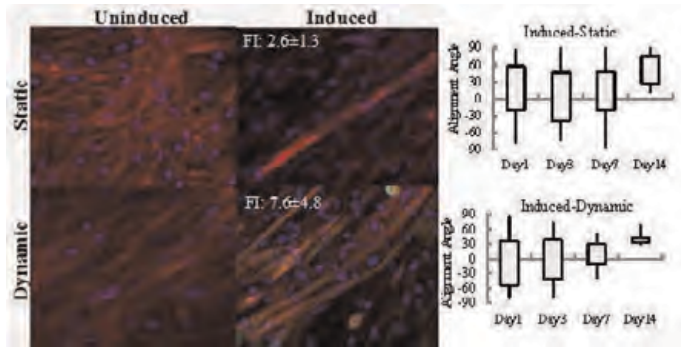

Fig1. Effect of biochemical and biophysical induction on ASC morphology and multinucleation

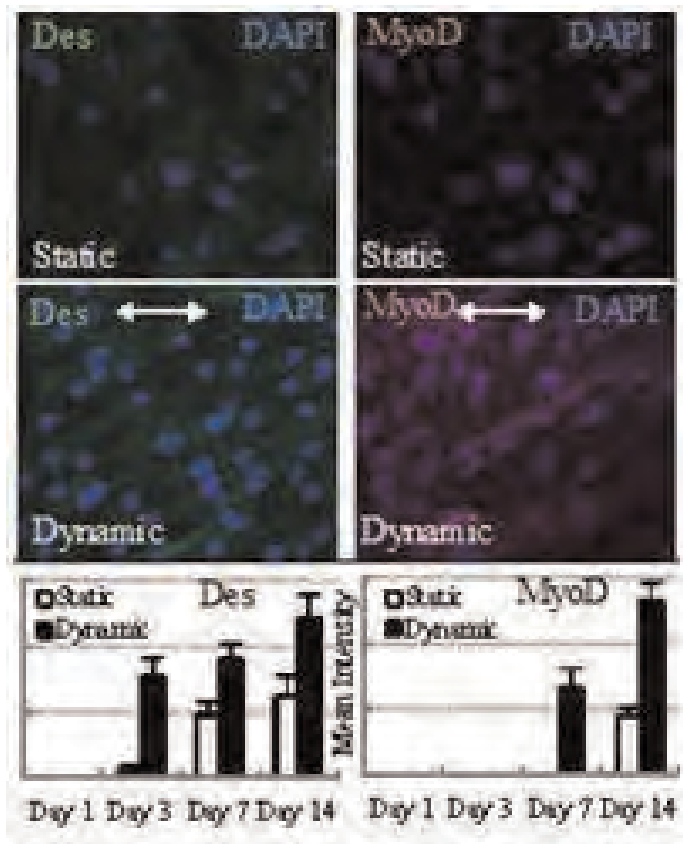

Fig2. Desmin and MyoD expression evaluated by ICC and quantification of their intensity

***Disclosures: Pinar Yilgor Huri**, None.*

SU0193

Muscle Strength and the Functional Muscle-Bone Unit in Children and Adolescents with Chronic Disease. Dale Lee*, Rachel Wetzsteon, Babette Zemel, Justine Shults, Mary Leonard. Children's Hospital of Philadelphia, USA

Measures of muscle size are often used as surrogates of muscle forces acting on bone. However, chronic diseases may be associated with low muscle strength relative to muscle size, further contributing to bone deficits in these disorders. The relations between muscle and bone were examined in 54 children with chronic kidney disease (CKD), and in 64 children at the time of Crohn disease (CD) diagnosis, and compared with 264 healthy controls. Muscle torque was assessed by isometric dynamometry in ankle dorsiflexion, and lower leg muscle cross-sectional area and tibia cortical section modulus by quantitative CT. Log linear regression was used to determine relations between muscle and bone parameters, adjusted for tibia length, age, Tanner stage, sex, and race.

Compared to controls, muscle area was significantly lower in severe CKD (Stage 4-5) and in mild to severe CD (Table). Muscle Torque relative to muscle area was markedly reduced in all stages of CKD and marginally reduced in severe CD. Cortical section modulus was significantly reduced in CKD, but preserved in CD. In multivariate models in CKD and in CD, greater muscle area and muscle force were

independently associated with greater section modulus (all $p<0.01$; model $R^2 = 0.92$ in CD and CKD). In severe CKD, adjustment for muscle area attenuated the section modulus deficit from 11.5 to 6.7% (p=0.05 compared with controls). With further adjustment for muscle torque, section modulus was no longer significantly lower in CKD (-4.5%;,p=0.19). Section modulus in severe CD was 7.4% greater than predicted (p=0.01) given the muscle area and force deficits, compared with controls.

In conclusion, advanced CKD was associated with significant deficits in muscle area, muscle strength relative to muscle area, and cortical structure. The lower muscle strength may be due to edema or abnormal protein catabolism. These data suggest that muscle area is not an adequate surrogate for muscle loading in CKD and studies should consider the independent effects of muscle strength. In contrast, CD was associated with significant deficits in muscle area due to malnutrition and inflammation, but muscle strength relative to muscle area was largely preserved. The greater section modulus in newly diagnosed CD, relative to the substantial muscle area deficits, may have been due to acute muscle loss preceding diagnosis. It is possible that bone loss from decreased mechanical loading lags behind rapid loss of muscle.

Percent Deficits in Chronic Disease compared with Healthy Controls

	Muscle Area	Muscle Torque Relative to Muscle Area	Cortical Section Modulus
Chronic Kidney Disease			
Mild to Moderate	-2.9 (p=0.35)	-14.3 (p<0.001)	-7.0 (p<0.05)
Severe	-6.7 (p=0.01)	-22.9 (p<0.001)	-11.5 (p=0.005)
Crohn's Disease			
Mild	-9.5 (p=0.002)	-1.7 (p=0.72)	-2.7 (p=0.47)
Moderate to Severe	-14.1 (p<0.001)	-7.6 (p=0.05)	-4.7 (p=0.15)

Models adjusted for age, sex, race, tibia length and sex-Tanner interactions if significant.

Table

***Disclosures: Dale Lee**, None.*

SU0194

Magnetic Resonance Imaging (MRI)-Based Measures of Muscle Structure and Fat Infiltration in the Lower Leg of Postmenopausal Women with Osteopenia and Osteoporosis. Amanda Lorbergs*, Mike Noseworthy, Norma MacIntyre. McMaster University, Canada

Background: Age-related muscle loss and increased fat content between and within skeletal muscles may contribute to bone loss if the critical threshold for bone strain is not achieved. Advanced MRI techniques like diffusion tensor (DT)-MRI and proton MR spectroscopy (^{1}H-MRS) have been recently applied to assess skeletal muscle. While DT-MRI evaluates the shape and orientation of skeletal muscle fibres,^{1}H-MRS can noninvasively discriminate fat deposits within the muscle fibre (intramyocellular lipid, IMCL) from fat deposits external to the muscle fibre (extramyocellular lipid, EMCL).

Purpose: To compare muscle structure and fat deposits in the lower leg of postmenopausal women with osteopenia (OPN) or osteoporosis (OP) using axial MRI, DT-MRI, and ^{1}H-MRS.

Methods: Lower leg images were acquired (GE Signa750 3T MRI scanner) in 8 postmenopausal women (mean age$\pm$SD=71.6$\pm$3.9y; 4 OPN, 4 OP matched for physical activity level). Using custom and commercial software, total muscle cross-sectional area (MCSA) and intermuscular adipose tissue (IMAT), and DT-MRI derived eigenvalues (λ_1, λ_2, λ_3), fractional anisotropy (FA) and apparent diffusion coefficient (ADC) were quantified for medial and lateral gastrocnemius heads, soleus, tibialis posterior, and tibialis anterior (TA) muscles. TA IMCL and EMCL content were measured using ^{1}H-MRS spectra. One-way ANOVAs were performed to compare group means for each muscle outcome.

Results: OPN and OP groups were similar in age, height, and weight ($p>0.05$). No group differences were observed in MCSA ($p=0.68$) or IMAT ($p=0.83$). Compared to the OPN group, TA in the OP group had significantly greater λ_1 (OPN: 2.07 ± 0.03 x10^{-3}mm^2/s, OP: 2.25 ± 0.12 x10^{-3}mm^2/s, $p<0.05$), λ_2 (OPN: 1.42 ± 0.05 x10^{-3}mm^2/s, OP: 1.72 ± 0.08 x10^{-3}mm^2/s, $p<0.01$) and λ_3 (OPN: 1.32 ± 0.04 x10^{-3}mm^2/s, OP: 1.50 ± 0.10 x10^{-3}mm^2/s, $p<0.05$), and reduced FA (OPN: 0.25 ± 0.02, OP: 0.21 ± 0.01, $p<0.05$) and ADC (OPN: 1.61 ± 0.04 x10^{-3}mm^2/s, OP: 1.82 ± 0.10 x10^{-3}mm^2/s, $p<0.01$). No other DT-MRI metrics differed between groups. Similarly, groups did not differ in IMCL ($p=0.73$) or EMCL ($p=0.41$).

Conclusion: Muscle size and IMAT content are similar in OPN and OP women; however, differences in DT-MRI metrics suggest that OP is associated with structural changes in the predominantly slow twitch TA muscle. Future studies should evaluate whether this difference in TA muscle structure is observed in men, other predominantly slow twitch muscles, and is predictive of physical function and fracture risk.

***Disclosures: Amanda Lorbergs**, None.*

SU0195

Thigh muscle attenuation measured by computed tomography was associated with the risk of low bone density in community-dwelling elderly population. Jung Hee Kim*[1], Sung Hee Choi[2], Soo Lim[2], Jae Young Lim[3], Ki Woong Kim[2], Hak Chul Jang[2], Chan Soo Shin[1]. [1]Seoul National University College of Medicine, South Korea, [2]Department of Internal Medicine, Seoul National University Bundang Hospital, South Korea, [3]Department of Rehabilitation Medicine, Seoul National University Bundang Hospital, South Korea

Although muscle mass has been shown to be positively related with bone mineral density (BMD), there are only a few studies that investigated the association between muscle strength or muscle quality and BMD. We investigated the effects of muscle strength and muscle fat infiltration, as a measure of muscle quality, adjusted for muscle mass on femoral neck BMD in Korean elderly cohort.

We recruited 242 men and 231 women aged over 65 years who participated in the Korean Longitudinal Study on Health and Aging (KLoSHA). Leg muscle mass and femoral neck BMD were measured by dual-energy X-ray absorptiometry (DXA). Isokinetic strength of knee extensors was measured as a peak torque value by an isokinetic device. Computed tomography scan of the mid-thigh measured the mean Hounsfield unit (HU) of the lean tissue. Low bone density was defined as femoral neck T-score $\leq$ -2.0.

Leg muscle mass, knee extensor strength and thigh muscle HU values were significantly positively correlated with femoral neck BMD in both men and women. However, muscle strength was not a significant determinant for the presence of low bone mass after adjusting for muscle mass in multiple logistic regression analyses. Notably thigh muscle HU values were strong and independent determinant for the risk of low bone density.

Decreased thigh muscle HU values, a measure of fatty infiltration of muscle, were independently associated with increased risk of low bone density in the elderly population.

***Disclosures: Jung Hee Kim**, None.*

SU0196

Prevention of Palmitate-induced Lipotoxicity in Human Osteoblasts. Krishanthi Gunaratnam*[1], Christopher Vidal[2], Chris Brooks[3], Ross Boadle[4], Gustavo Duque[5]. [1]Sydney Medical School-NepeanLevel 5 South Block, Australia, [2]University of Sydney, Australia, [3]Ageing Bone Research Program, Sydney Medical School Nepean, The University of Sydney, Australia, [4]Electron Microscope Laboratory, ICPMR, Westmead, Australia, [5]Ageing Bone Research Program, University of Sydney, Australia

Lipotoxicity is an overload of lipids in non-adipose tissues that affects function and induces cell death. Fatty acids, predominantly palmitic acid (PA), exert a lipotoxic effect on human osteoblasts (Ob) by inducing apoptosis (known as lipoapoptosis) and autophagy. We have previously reported that lipoapoptosis in Ob has a mitochondrial mechanism that could be prevented by inhibiting JNK phosphorylation. However, the role of autophagy in lipotoxicity and the therapeutic approach to prevent lipotoxicity in Ob remain unexplored. Autophagy was identified in PA-treated Ob (Lonza, Switzerland) using western blot (WB), immunofluorescence and electron microscopy (EM). PA induced early autophagy in cultured Ob, which was preceded by the activation of autophagosomes surrounding PA droplets. WB showed an increase in LC3-II/LC3-I protein ratio in PA-treated Ob, indicative of autophagy, in a dose and time dependent manner ($p<0.01$). These observations were confirmed by immunofluorescence of LC3-II punctate expression, which was significantly increased in a dose- and time-dependent manner ($p<0.01$). EM showed increased number of double-membrane and larger diameter autophagosomes at higher concentrations of PA. To evaluate whether autophagic activity could be inhibited, we treated Ob with PA in the presence or absence of 5mM 3-methyladenine (3MA), which has been reported to have a strong inhibitory effect on autophagy. We found a significant reduction in autophagosome formation in 3MA-treated Ob with a concomitant reduction in PA-induced apoptosis ($p<0.01$). Furthermore, to test the potential effect of vitamin D on lipotoxicity, we treated Ob with vitamin D using a well-known anti-apoptotic dose (10^{-8} M). WB showed a significant decrease in the pro-apoptotic proteins cytochrome C and Bax with an increase in BCl-2 in PA+vitamin D-treated Ob as compared with vehicle-treated controls. No changes in LC3 II/LC3-I ratio were observed in PA+vitamin D-treated Ob, thus suggesting that vitamin D has an effect on lipoapoptosis but not on PA-induced autophagy. In summary, we have identified that lipoapoptosis in Ob is induced through the activation of early autophagy followed by activation of mitochondrial apoptotic pathways. Vitamin D prevented lipoapoptosis whereas both autophagy and lipoapoptosis were inhibited by 3MA. The inhibition of lipoapoptosis and autophagy would protect Ob against marrow fat and could become a potential therapeutic target for osteoporosis in the future.

***Disclosures: Krishanthi Gunaratnam**, None.*

SU0197

***In Vitro* Cultures of Human Adipose Tissue Mesenchymal Stem Cells and Human Bone Marrow Mesenchymal Stem Cells: Effects of Strontium on Proliferation and Osteoinduction.** Valeria Nardone*, Roberto Zonefrati, Carmelo Mavilia, Gaia Palmini, Cecilia Romagnoli, Gianna Galli, Annamaria Carossino, Laura Masi, Annalisa Tanini, Maria Luisa Brandi. University of Florence, Italy

Introduction: Human adipose tissue mesenchymal stem cells (hAMSCs) are able to differentiate into osteoblasts with analogous characteristics to human bone marrow mesenchymal stem cells (hBMMSCs) producing alkaline phosphatase (ALP) and calcified nodules composed by hydroxyapatite (HA). These characteristics make hAMSCs a good cellular model for *in vitro* studies on the pharmacological responses to the treatment of metabolic bone diseases, such as osteoporosis. Strontium ranelate (SR) is an approved drug for the treatment of postmenopausal osteoporosis. Unlike other drugs, it has a dual effect on bone remodelling. The aim of our study is to evaluate the effects of Strontium (Sr^{2+}) on proliferation and osteoinduction in both hAMSCs and hBMMSCs.

Materials and Methods: Cell cultures of hAMSCs and hBMMSCs were isolated respectively from subcutaneous adipose tissue biopsy and bone marrow aspirate from healthy donors. The cells were cultured in growth medium (GM) and characterizated, to verify their multi-potency, by studying both the adipogenic (AM) and the osteogenic differentiation (OM), utilizing specific media. The cells were cultured in OM in presence of scalar concentrations of Sr^{2+} from 0,5 to 100 μg/ml. Osteoinduction was evaluated quantitatively by fluorometric assays for ALP and HA production during 4-35 days of induction. Cell proliferation was evaluated in presence of scalar concentrations of Sr^{2+} from 1 to 1000 μg/ml in GM containing 1.5% FBS each 3 days from 0 at 12^{th} day.

Results: The highest concentrations of Sr^{2+} tested significantly stimulated the ALP production, with increase in the time of the enzymatic activity; while the lower concentrations of Sr^{2+} tested significantly stimulated the HA deposits formation after 21 days of induction. Cell proliferation analysis has shown that concentrations of Sr^{2+} from 50 to 1000 μg/ml enhance proliferation activity of both hAMSCs and hBMMSCs compared to control, with a maximum response at concentration of Sr^{2+} 500 μg/ml.

Conclusions: Our data confirm that the adipose tissue is an abundant reserve of mesenchymal stem cells and that these cells can be used as a cell model for *in vitro* studies in the field of cell therapies. Finally, these preliminary results suggest that SR has the capacity to stimulate cell growth and to enhance osteoinduction of both hAMSCs and hBMMSCs opening future applications in the bone repair.

***Disclosures: Valeria Nardone**, None.*
This study received funding from: Les Laboratories Servier, France

SU0198

Withdrawn

SU0199

Acute Cold-Induced Thermogenesis Uncouples Bone Remodeling by Activation of TRPM8 in a Non-Cell Autonomous Manner. Katherine Motyl*[1], Casey Doucette[1], Daniel Brooks[2], Mary Bouxsein[2], Clifford Rosen[3]. [1]Maine Medical Center Research Institute, USA, [2]Beth Israel Deaconess Medical Center, USA, [3]Maine Medical Center, USA

Recent clinical evidence has uncovered a role for brown-like adipose tissue in cold-induced thermogenesis (CIT) and has led to the development of new pharmacologic approaches to treat obesity. Thermogenesis is controlled by the sympathetic nervous system (SNS), which uncouples bone remodeling by suppressing formation and increasing resorption. We recently demonstrated that SNS activation to compensate for impaired preformed brown adipose tissue function caused accelerated trabecular bone loss in *Misty* mice. To understand the mechanism of thermogenic regulation of bone turnover, we exposed 8-wk-old female C57BL/6 mice to 4℃ for 6 hrs. Although changes in bone microarchitecture are not detectable during this short period, we found that cold suppressed *Runx2* mRNA expression in whole bone. Furthermore, cold significantly increased *Rankl* and suppressed *Opg* expression, resulting in a *Rankl/Opg* ratio that was 1.8-fold higher in 4℃-treated vs 22℃-treated mice (p=0.006). To test whether effects of cold were mediated in a non-bone cell autonomous manner through the SNS, we performed the same experiment in B6 mice with a deletion in the cold-sensing receptor TRPM8, which have suppressed sensitivity to cold. In contrast to wildtype, *Rankl/Opg* ratio was unchanged in *Trpm8*$^{-/-}$ mice at 4℃ compared to mice at 22℃. Furthermore, *Runx2* expression was not suppressed in response to cold in -/- mice. Two-way ANOVA demonstrated a significant genotypeXtemperature effect with both *Rankl/Opg* ratio ($p<0.01$) and *Runx2* expression (p=0.04). Next, to determine if deletion of TRPM8 had an effect on bone mass in mice maintained at 22℃ (below thermoneutrality), we examined total BMD by DXA and trabecular microarchitecture by mCT. Although no changes were visible by DXA, femoral trabecular thickness was significantly higher in -/- mice at 16 wks, but not at 8 wks, suggesting age-related trabecular bone loss was attenuated (ageXgenotype p=0.01). Consistent with a neuron-specific role of TRPM8, primary osteoblast and osteoclast differentiation *in vitro* were not affected by deletion of TRPM8. In conclusion, TRPM8 mediates acute cold-induced changes in osteoblastic gene expression in a non-cell autonomous manner. Studies on the effects of long-term cold exposure on BMD and bone cell function are underway to understand how CIT affects bone remodeling. Our findings suggest that pharmacologic agents that enhance brown-like thermogenesis for weight loss may have deleterious effects on bone.

***Disclosures: Katherine Motyl**, None.*

SU0200

Biglycan Modulates Angiogenesis and Bone Formation During Fracture Healing. Aaron Brown, Emily Pinnow, Agnes Berendsen, Nancy McCartney-Francis, Vardit Kram, Azusa Maeda, Tina Kilts, Marian Young*. National Institutes of Health, USA

Fracture healing involves a sequence of physiological events, including hematoma formation, inflammation, callus formation, neovascularization, osteoblastic callus mineralization, and osteoclastic remodeling of bone. This process results in the formation of new lamellar bone in the fracture area. Biglycan (Bgn) is a member of the small leucine-rich proteoglycan (SLRP) family that is highly present in bone. Bgn-deficient mice have a reduced growth rate and decreased bone mass due to lower levels of bone formation. To further understand the role Bgn plays in bone formation we created fractures in femurs of 6-week-old male wild type (WT) and Bgn-deficient mice using a custom-made standardized fracture device and analyzed the process of healing over time. The formation of a callus around the fracture site was observed at both 7 and 14 days post-fracture in WT and Bgn-deficient mice and immunohistochemistry revealed that Bgn was expressed in the fracture callus of WT mice localizing around woven bone and cartilage. Micro computed tomography (Micro-CT) analysis of the region surrounding the fracture line showed that the Bgn-deficient mice had a smaller callus with a bone volume and total mineral density (TMD) almost half of that of the WT mice. Histology of the same region also showed the presence of less cartilage and woven bone in the Bgn-deficient mice compared to WT mice. Picrosirus staining of the callus visualized under polarized light showed there was less fibrillar collagen in the Bgn-deficient mice, a finding confirmed by immunohistochemistry using antibodies to type I collagen. The reduction in collagen content could be one basis for the reduced TMD observed in the Bgn-deficient mice. Micro-CT imaging of vessel casting using the radiopaque silicon injection compound Microfil suggested decreased vessel formation in the callus of Bgn-deficient mice. In addition, real time RT-PCR at 7 days post-fracture showed a significant decrease in relative vascular endothelial growth factor (VEGF) gene expression by Bgn-deficient mice as compared to WT. Moreover, VEGF was shown to bind directly to Bgn through a solid-phase binding assay. These results suggest that Bgn plays an important role in the process of bone formation during fracture healing, and further that reduced angiogenesis could be the molecular basis for this deficiency.

***Disclosures: Marian Young**, None.*

SU0201

Inhibition of GSK3-β Rescues the Impairments in Bone Formation and Mechanical Properties Associated with Fracture Healing in Osteoblast/Osteocyte-Selective Connexin 43 Deficient Mice. Alayna Loiselle*[1], Shane Lloyd[2], Emmanuel Paul[2], Gregory Lewis[2], Henry Donahue[2]. [1]Penn State Hershey, USA, [2]The Pennsylvania State University College of Medicine, USA

Connexin 43 (Cx43) is the main gap junction protein in bone and is required for osteoblastic differentiation and bone homeostasis. We generated mice with osteoblast/osteocyte-selective deficiency of Cx43 using Col1-Cre (2.3Kb) to test the hypothesis that Cx43 deficiency results in impaired bone formation during fracture healing as a result in increased GSK3-β activity and decreased β-catenin expression. Peak expression of Cx43, as measured by qPCR of tissue from the fracture callus, occurred at 28 days in wild type (WT) fractures, and was significantly decreased in Cx43 deficient (cK0) fractures relative to WT during healing. Callus bone volume/ total volume (BV/TV) was significantly decreased in cKO fractures relative to WT at 28 days (WT: 0.3 ± 0.01; cKO: 0.24 ± 0.02, p=0.03). Functionally, cKO fractures displayed a significant decrease in ultimate torque at failure (T_{ult}) at 28 days relative to WT (WT: 21.6 ± 4.9N*mm; cKO: 12.7 ± 1.5, p=0.009). Expression of β-catenin, which plays an important role in bone formation during fracture healing, was significantly attenuated in cKO fractures at 14 (-60%, $p<0.001$) and 21 days (-30%, $p<0.05$) relative to WT. Additionally, expression of GSK3-β, a key component of the β-catenin proteasomal degradation complex was significantly increased at 21 days post-fracture in cKO mice (+45 %, $p<0.001$) relative to WT. To determine if Cx43 may regulate bone formation during fracture healing by modulating GSK3-β levels and thus β-catenin, GSK3-β activity was inhibited during fracture healing with Lithium Chloride (LiCl). LiCl increased BV/TV in WT and cKO fractures relative to untreated genotype controls at 21 and 28 days. Indicative of restoration of normal bone volume fraction in cKO fractures, BV/TV was not significantly different between WT and cKO fractures treated with LiCl at 21 (p=0.69) and 28 days (p=0.72). Biomechanically, LiCl resulted in a significant increase in T_{ult} in both genotypes relative to their respective untreated controls at 28 days, while T_{ult} was no longer significantly decreased in cKO fractures (36.41 ± 5.11N*mm) relative to WT (31.34 ± 4.87N*mm, p=0.61) following LiCl treatment at 28 days (Figure 1). Taken together these data identify a previously unknown role for Cx43 in modulating bone formation during fracture healing through the regulation of β-catenin via GSK3-β, and suggest Cx43 as a potential therapeutic target to enhance fracture healing.

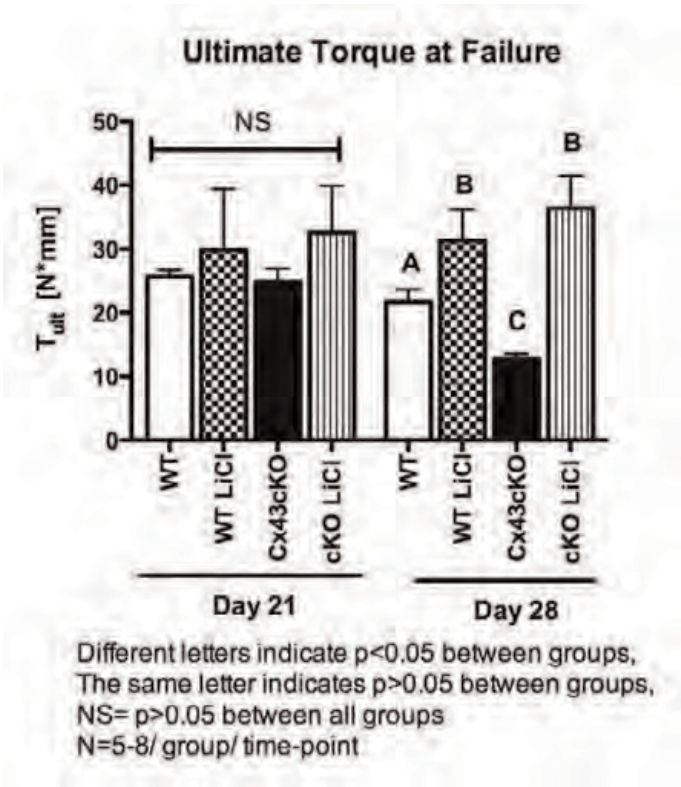

Figure 1.

***Disclosures: Alayna Loiselle**, None.*

SU0202

MiR-142-5p Promotes Osteoblast Activity and Bone Repair by Targeting WWP1. Chao Chen*[1], Peng Chen[2], Jiaji Gong[2], Eryuan Liao[2], Xianghang Luo[2]. [1]The Second Xiangya Hospital of Central South University, Peoples Republic of China, [2]Institute of Endocrinology & Metabolism, China

MicroRNAs (miRNAs) play important roles in regulating bone regeneration and remodeling. However, no study has established the pathophysiological role for miRNAs in bone repair. Here we identify a significant up-regulation of miR-142-5p during the bone healing process. Mice with osteoblast-specific over-expression of miR-142-5p showed increased bone formation and accelerated fracture healing than wild-type mice. Mice with osteoblast-specific deficiency of miR-142-5p by miRNA sponge revealed delayed fracture repair, decreased bone formation and age-related bone loss. In vitro miR-142-5p promoted osteoblast activity and matrix mineralization by targeting WWP1 (WW domain containing E3 ubiquitin protein ligase 1). We also found that the expression of miR-142-5p in the callus of aged mice were lower than in those of young mice and directly correlated with the age-related delay in bone healing. Furthermore, in patients with age-related delayed healing of bone fracture, we found that miR-142-5p expression in callus was markedly lower. Notably, osteoblast-specific delivery of miR-142-5p in mice using our aptamer delivery system stimulated osteoblast activity and fracture repair in aged mice. Thus, our study revealed that miR-142-5p play a crucial role in maintaining osteoblast activity, and providing a new molecular target therapeutic strategy for bone healing.

***Disclosures: Chao Chen**, None.*

SU0203

P2X7 Receptor Polymorphisms Modulate Osteoblast Cell Functions. Qi Guang Wang*[1], Elena Adinolfi[2], Alison Gartland[3]. [1]Mellanby Centre for Bone Research, United Kingdom, [2]University of Ferrara, Italy, [3]The Mellanby Centre for Bone Research, The University of Sheffield, United Kingdom

The P2X7 receptor (P2X7R) gene is highly polymorphic with at least six non-synonymous single-nucleotide polymorphisms (SNPs) being previously described as having either loss-of-function (LOF) or gain-of-function (GOF) effects. We have previously demonstrated expression of functional P2X7R on both osteoblasts and osteoclasts and found an association of LOF *P2RX7* polymorphisms and LS-BMD. The exact mechanism behind this observed association is currently unknown. We provide evidence here that it is the effects of *P2XR7* SNPs on osteoblast cells that may be driving the observed association with lower BMD in individuals with *P2XR7* SNPs.

To determine the effect of *P2XR7* SNPs on osteoblast cell function, Te85 cells were transfected with P2XR7 wild type (WT) or SNPs cDNA. P2X7R activation, intracellular calcium levels, cell proliferation, alkaline phosphatase (ALP) activity and in-vitro mineralisation were measured.

Transfected WT or *P2XR7* SNPs did not function in Te85 cells unless co-transfected with a naturally occurring truncated isoform, splice variant B (P2X7B). Upon ATP stimulation, pore formation was observed in the WT and GOF SNP, 155Y; but not in any of the three LOF SNPs; 496A, 568N, or 307Q. Increased intracellular calcium levels were found in all co-transfected Te85 cells, compared to the naïve or single P2X7B transfected cells. As expected, cell proliferation increased in Te85 cells transfected with the trophic P2X7B isoform, but co-transfection of WT or *P2XR7* SNPs reduced cell proliferation. Transfection of P2X7B alone significantly decreased ALP activity by 23% compared to naïve cells, whilst co-transfection of P2X7B and WT significantly increased ALP activity by 36%. Co-transfection with the LOF 496A and 568N *P2XR7* SNPs gave significant decreases in ALP of 15% and 13% respectively. In-vitro mineralisation was also significantly increased with co-transfection of P2X7B and WT or 307Q SNP compared to naïve cells, but this increased mineralisation was not detected with other *P2XR7* SNPs.

The results of this study demonstrate that the P2X7B isoform is necessary for P2X7R-mediated osteogenesis in Te85 osteoblasts cells and that *P2XR7* SNPs significantly alter osteoblast cell function which may account for the reduced BMD previously observed in women with P2X7R polymorphisms. The results of this study extend our knowledge into the role of the P2X7R in maintaining bone homeostasis, and may help identify people at risk of developing osteoporosis.

***Disclosures: Qi Guang Wang**, None.*

SU0204

Real time monitoring for differentiation of primary osteoblast culture by using Raman microscopy. Yusuke Oshima*[1], Atsuhiko Hikita[1], Takeshi Imamura[2]. [1]Ehime University, Japan, [2]Ehime University Graduate School of Medicine, Japan

Osteoblasts are derived from mesenchymal stem cells that play a pivotal role during bone growth and mineralization. Understanding the molecular and cellular details of the mechanism that control bone formation and remodeling is essential for the drug discovery of bone metabolic diseases. Osteogenic differentiation of mesenchymal stem cells is induced by osteoblast-specific transcription factors such as Runx2 and Osterix, and numerous secreted factors of paracrine, autocrine, and endocrine origin. However, the mechanisms of osteoblast-specific gene expression and bone matrix formation are still poorly understood.

Raman spectroscopy is a label-free analytical tool for live cells and provides us detailed information of intracellular molecular composition based on the molecular vibrational mode. Raman spectroscopic studies for osteogenic differentiation have been reported in the last decade. The sensitivity of vibrational spectroscopy to both the mineral and organic elements of bone facilitates the study of both components and their interactions with each other.

To clarify the molecular mechanisms of the differentiation of osteoblasts, we performed Raman spectroscopic observation of mouse primary osteoblasts that were induced osteogenesis by bone morphogenetic protein 2 (BMP2). The primary osteoblasts were isolated from calvaria of neofetal mice (P0-P3, C57BL6) by collagenase digestion. Raman spectra were obtained by focusing a laser beam onto osteoblasts cultured with and without BMP2 treatment, respectively. The degree of osteogenesis was assessed by alizarin red staining.In the result, the Raman band at 960 cm^{-1} assigned to phosphate moiety (PO_4^{3-}) of osteoblasts with BMP2 treatment was significantly larger than that without BMP2 treatment. Increase of the phosphate Raman band may reflect accumulation of mineral component such as hydroxyapatite. The results suggest that the Raman spectrum captures the process of extracellular matrix formation. We will perform further study to reveal the function of vesicular secretion by using the high-sensitive custom-made Raman microscopy system.

***Disclosures: Yusuke Oshima**, None.*
This study received funding from: KAKENHI

SU0205

Supplementation of Bone Substitutes with Prolyl Hydroxylase Inhibitors: Insights in the Cellular Responses and the Effect on Craniofacial Bone Regeneration. Hermann Agis*[1], Heinz-Dieter Müller[2], Ulrike Kuchler[2], Barbara Cvikl[3], Reinhard Gruber[4]. [1]Medical University of Vienna, Austria, [2]Department of Oral Surgery, Medical University of Vienna & Austrian Cluster for Tissue Regeneration, Austria, [3]Department of Conservative Dentistry & Periodontology, Medical University of Vienna & Austrian Cluster for Tissue Regeneration, Austria, [4]Laboratory of Oral Cell Biology, School of Dental Medicine, University of Bern, Switzerland

Prolyl hydroxylase (PHD) inhibitors stimulate regeneration of hard and soft tissue by stabilizing the labile hypoxia-inducible factor (HIF)-1alpha, a central mediator of angiogenesis. Whether PHD inhibitors can also support craniofacial tissue regeneration is unclear. Here, we followed an innovative approach where bone substitutes and collagen barrier membranes were supplemented with the PHD inhibitors. We assessed

the release kinetic of PHD inhibitors by functional assays and tested the effect on bone regeneration in a calvaria defect model in diabetic rats.

PHD inhibitors released from bone substitutes and collagen barrier membranes maintained their capacity to stimulate HIF-1alpha levels and the production of vascular endothelial growth factor in periodontal fibroblasts. Moreover, PHD inhibitors reduced plasminogen activation in fibroblasts, and decreased osteoclastogenesis and resorption in murine bone marrow cultures. However, supplementation of bone substitutes with PHD inhibitors did not support bone regeneration.

In summary, our results suggest that even though the PHD inhibitors provoke a strong cellular response in vitro, further research is required to optimize the release kinetic of PHD inhibitors to support craniofacial tissue regeneration.

Acknowledgment: This study was supported by the International Team for Implantology (Grant RCL 653), the Osteology Foundation (Grant 10-063), and the Austrian Science Fund (Erwin Schrödinger Fellowship J 3379-B19).

***Disclosures: Hermann Agis**, None.*

SU0206

The Phosphorylation and GTPase activity of Dynamin are Critical for Osteoblast Function. Pierre Eleniste*, Su Huang, Heather Largura, Kornchanok Wayakanon, Angela Bruzzaniti. Indiana University School of Dentistry, USA

Osteoblasts (OB) migrate to eroded bone surfaces to form new bone. Dynamin has been shown to be important for cytoskeletal remodeling, focal adhesion turnover and endocytosis, but its function in bone cells is largely unknown. Dynamin GTPase activity is stimulated in part by tyrosine phosphorylation, but the mechanism that leads to its dephosphorylation by phosphatases and subsequent GTPase inactivation remains to be determined. We previously reported that inhibition of dynamin inhibits osteoclast bone resorbing activity and migration. In the current study, we examined the novel role of dynamin in OBs. We found that chemical inhibition of dynamin or over-expression of a dynK44A, a GTPase-defective mutant, increased alkaline phosphatase (ALP) activity in calvarial OBs, but led to inhibition of OB migration (-45%, $p<0.05$) in vitro. Next, to examine the mechanism of dynamin activation, we examined whether tyrosine dephosphorylation of dynamin by the protein tyrosine phosphatase PTP-PEST affected dynamin GTPase activity and OB function. For these studies dynamin was co-expressed with or without PTP-PEST, and dynamin phosphorylation and GTP-hydrolyzing activity were then quantified by immunoprecipitation and chemical GTPase activity assays, respectively. PTP-PEST decreased dynamin phosphorylation and activity in a dose-dependent manner. Further, we found that the dynamin tyrosine mutants Y231F, Y597F and Y231F/Y597F exhibited reduced tyrosine phosphorylation (~70% reduction for all mutants) and were resistant to dephosphorylation by PTP-PEST, suggesting they were PTP-PEST target sites. In addition, these mutants exhibited reduced dynamin GTPase activity (~70% reduction for all mutants). In contrast to dynK44A, we found that dynY231F/Y597F had no effect on ALP expression in MC3T3-E1 cells, but inhibited OB migration by 80%. These studies suggest that PTP-PEST regulates dynamin phosphorylation and consequently its GTPase activity. Furthermore, dynamin phosphorylation and GTPase activity have distinct, but overlapping effects in OBs, which are mechanistically linked with OB differentiation and migration. Finally, our findings suggest that inhibitors that target dynamin GTPase activity may be useful for the treatment of bone loss through their ability to inhibit osteoclast activity and promote osteoblast differentiation.

***Disclosures: Pierre Eleniste**, None.*

SU0207

The Role of Donor and Host Age on Human Muscle Derived Stem Cells Mediated Bone Regeneration. Xueqin Gao*[1], Johannes Schneppendahl[1], Ying Tang[1], Aiping Lu[1], Bing Wang[1], Johnny Huard[2]. [1]University of Pittsburgh, USA, [2]Orthopaedic Surgery, USA

Introduction: Human muscle derived stem cells (hMDSCs) have been shown to efficiently repair a critical sized bone defect when transduced with lenti-BMP2; however, the role that the age of the donor hMDSCs and host have on the cells capacity to regenerate bone have not been evaluated. In order to address this question, we tested the bone repair capacity of young and old donor hMDSCs in both young and old host ICRSCID mice using a critical size calvarial bone defect model. Material and Methods: hMDSCs were isolated from young (23yo) and old (76yo) muscle biopsies. hMDSCs were transduced with lenti-BMP2/GFP and sorted for GFP. BMP2 secretion was measured with ELISA. Ten 1 year old and 10 six weeks old male ICRSCID mice were divided into 4 groups(N=5):(1)Young cells+young mice;(2)young cells+old mice;(3)old cells+young mice;(4) old cells+old mice. After creating a 5mm defect in the right parietal bone, 1.5 million hMDSCs were implanted into the defect using fibrin sealant as a scaffold. Bone formation was monitored using microCT biweekly. At 6 weeks, mice were sacrificed and skull tissues were harvested, fixed and decalcified. GFP immunostaining was performed to identify the donor cells. Herovici's staining was used to determine collagen I formation. TRAP staining was used to identify osteoclasts.

Results: At 2 weeks, microCT scanning showed that there were no differences in new bone volume between the young and old host using either young or old donor cells; however, bone density was significantly higher in the old host animals with both cell types. At 4 and 6 weeks, there was significantly less new bone volume in the defect area of the old mice than in the young mice using either the young or old cells. By 6 weeks there was no difference in the bone density between the young and the old host mice. A higher bone volume was generated by the old donor cells in both the young and old host mice and also covered the defect area significantly greater than the young cells in the old host mice. The young host mice had a greater number of GFP+ donor cells, both young and old, than the old host mice. TRAP staining indicated more osteoclasts in the new bone area of old mice than that in young mice. Herovici's staining identified collagen I matrix in all the groups. Conclusion: Our study revealed that old donor hMDSCs are as efficient as young donor hMDSCs for regenerating bone in young and old mice; however, the new bone in the old hosts was resorbed more quickly.

***Disclosures: Xueqin Gao**, None.*

SU0208

The role of intracellular calcium phosphate in monoosteophil-mediated bone apatite formation. Zhifang Zhang*[1], Keith Le[2], Frances Chang[2], John Shively[2]. [1]City of hope, USA, [2]Department of Immunology, City of Hope, USA

ABSTRACT

BACKGROUND: Monoosteophils, derived from LL-37-treated monocytes, are a novel type of calcifying/bone forming cells. We have shown that monoosteophils have the ability to form bone-like nodules in vitro and ectopic bone in vivo and accelerate bone repair in a drilled bone model. Since monoosteophils do not express alkaline phosphatase, it suggests that monoosteophils may use a different mechanism to form bone nodules in comparison with well-known osteoblasts which predominantly express alkaline phosphatase.RESULTS: Here we show that monoosteophils release 1-2 μm bone-like nodules on osteologic disc in low Ca^{2+} concentration 10% FBS RPMI1640 medium after 3 weeks by using scanning electronic microscopy. Furthermore, transmission electron microscopy showed that monoosteophils, harvested from osteologic discs, express intracellular vesicles of calcium phosphate. Even in the absence of osteologic discs, our results from transmission electronic microscopy showed that monoosteophils still form intracellular bone-like nodule granule in RPMI1640 medium after cultured for 6 weeks. When monoostophils were cultured in the 10% FBS αMEM medium with 2.5mM $CaCl_2$ for 3 weeks, significant intracellular calcium phosphate formations were observed by phase contrast microscopy and scanning electron microscopy and monoosteophils were positive using alizarin Red S staining in comparison with control monocytes.CONCLUDION: Our observations highlight the unique mechanism of bone formation of monoosteophils. These observations may have important implications in deciphering both how normal bone forms and in understanding pathological mineralization.

***Disclosures: Zhifang Zhang**, None.*

SU0209

Thrombin receptor deficiency leads to osteopetrosis by decreasing the RANKL/OPG ratio. Bram Van Der Eerden*[1], Kukiat Tudpor[2], Prapaporn Jongwattapapisan[2], Marijke Schreuders-Koedam[3], Cindy van der Leije[3], Titia E Woudenberg-Vrenken[2], Rene JM Bindels[2], Joost GJ Hoenderop[2], Johannes PTM van Leeuwen[3]. [1]Erasmus MC, The Netherlands, [2]Cell Physiology, Radboud University Nijmegen Medical Centre, Netherlands, [3]Internal Medicine, Erasmus MC, Netherlands

Communication between osteoblasts and osteoclasts is crucial for bone remodeling. Thrombin and its thrombin receptor (TR; PAR-1) are expressed in osteoclasts and osteoblasts, respectively. However, the physiological roles of thrombin and TR in bone metabolism have been poorly studied. Therefore, we characterized the bone phenotype of mice lacking the thrombin receptor.

We performed bone microarchitectural analyses of the femurs of 10-12 week old wild type (WT) and TR knockout (TRKO) mice, using micro-computed tomography (μCT) and histomorphometry. We found an increased trabecular bone volume fraction (20.9 ± 1.2 vs 15.1 ± 0.2 %; $p=0.002$) and cortical bone volume (0.42 ± 0.004 vs 0.35 ± 0.004 mm^3; $p<0.001$) in TRKO mouse femurs compared to WT littermates. Trabecular bone thickness (8%) and connectivity (33%) were also significantly enhanced. In addition, the TRKO mice showed increased bone mineral density (BMD; 1.25 ± 0.006 vs 1.21 ± 0.004 g/cm^3; $p=0.003$) and decreased urinary deoxypyridinoline crosslinks (DPD) concentration (114 ± 9 vs 79 ± 4 nM; $p=0.007$), indicating reduced bone resorption. TRKO cortical bones had a larger diaphyseal perimeter (12.9 ± 0.23 vs 10.4 ± 0.02 mm; $p<0.001$) and a higher moment of inertia (0.60 ± 0.01 vs 0.42 ± 0.01 mm^4; $p<0.001$), implying stronger bones. Besides thicker trabeculae, histological examination did not reveal any abnormalities in the morphology of the TRKO femurs. Osteoblast and osteoclast surface and number corrected for bone surface were all similar between WT and TRKO mice. Compared to WT, the serum RANKL/OPG ratio in the TRKO mice was 80% reduced, which was primarily explained by inhibition of RANKL. In line with this, conditioned medium from thrombin-treated MC-3T3 osteoblasts contained a higher RANKL/OPG ratio (+135%) compared to non-treated cells, predominantly by stimulation of RANKL production. The thrombin-induced RANKL/OPG ratio was completely normalized to non-treated cells both by a TR antagonist (SCH79797) and by the p42/p44-ERK inhibitor U0126.

We conclude that the thrombin/TR system maintains normal bone remodeling through activating RANKL and limiting OPG synthesis by osteoblasts through the p42/44-ERK signaling pathway. Although the precise mechanism behind the thrombin effect on osteoclasts remains to be determined, TR deficiency leads to reduced osteoclast activity and osteopetrosis, making this receptor an interesting drug target candidate.

***Disclosures: Bram Van Der Eerden**, None.*

SU0210

Wnt5a Enhances Wnt/β-catenin Signaling Through the Up-regulation of Lrp5/6 During Osteogenesis. Masanori Okamoto*[1], Nobuyuki Udagawa[2], Teruhito Yamashita[2], Shunsuke Uehara[2], Hiroyuki Kato[1], Naoto Saito[3], Yasuhiro Minami[4], Naoyuki Takahashi[2], Yasuhiro Kobayashi[2]. [1]Department of Orthopaedic Surgery, Shinshu University School of Medicine, Japan, [2]Matsumoto Dental University, Japan, [3]Department of Applied Physical Therapy, Shinshu University School of Health Sciences, Japan, [4]Department of Physiology & Cell Biology, Kobe University Graduate School of Medicine, Japan

Wnt proteins regulate bone formation through β-catenin-dependent canonical and –independent noncanonical Wnt pathways. Human and mouse genetic studies have revealed that LRP5/6, co-receptors for the canonical Wnt pathway, are critical for osteogenesis. Canonical Wnt10b suppresses Ppar-γ expression and inhibits adipogenesis. Noncanonical Wnt5a also suppresses adipogenesis and promotes osteogenesis. We and others have reported that *Wnt5a*$^{+/-}$ mice exhibit impaired bone formation. These findings indicate that the canonical and non-canonical Wnt pathways cooperate with each other during osteogenesis and adipogenesis, although Wnt5a antagonizes the canonical Wnt pathway in various types of cells. Here, we show that Wnt5a up-regulates *Lrp5/6* expression, thereby enhancing osteogenesis and suppressing adipogenesis. 1) The expression of *Wnt5a, Wnt10b* and *Lrp5/6* but not *Ror2*, a co-receptor of Wnt5a, was increased in calvaria-derived osteoblastic cells (calvarial cells) under osteogenic culture conditions. 2) Treatment of calvarial cells with Dkk-1, which disrupts Lrp5/Wnt interactions, failed to suppress the up-regulation of *Lrp5/6*, suggesting that the canonical pathway is not involved in the up-regulation of *Lrp5/6*. 3) Short hairpin RNA-mediated knockdown of Wnt5a in calvarial cells reduced expressions of *Lrp5/6*. 4) Calvarial cells obtained from *Wnt5a*$^{-/-}$ mice exhibited impaired mineralization in culture. The expression level of *Lrp5/6* in *Wnt5a*$^{-/-}$ calvarial cells was lower than that in wild-type cells. This finding was further confirmed by reduced expression of *Axin2*, a target gene of the canonical Wnt pathway, in *Wnt5a*$^{-/-}$ cells. 5) Treatment with recombinant Wnt5a up-regulated *Lrp5/6* expression, which in turn rescued the impaired mineralization in *Wnt5a*$^{-/-}$ calvarial cells. 6) Adenovirus-mediated gene transfer of *Lrp5* to *Wnt5a*$^{-/-}$ calvarial cells rescued impaired mineralization, and suppressed adipogenesis. 7) μCT analysis showed that osteoblast-lineage-specific *Wnt5a*-deficient mice (*Osterix*-Cre: *Wnt5a*-floxed mice) exhibited low bone mass, but osteoblast-lineage-specific *Ror2*-deficient mice (*Osterix*-Cre: *Ror2*-floxed mice) did not. These results suggest that Wnt5a-induced noncanonical signals enhance the canonical Wnt pathway through up-regulation of Lrp5/6 to achieve proper bone formation, and that the stimulatory effect of Wnt5a on the canonical Wnt pathway is independent of Ror2-mediated signals.

***Disclosures: Masanori Okamoto**, None.*

SU0211

Both the Connexin43-specific Channel and C-terminus Are Required for the Regulation of Runx2 Activity and Osteoblast Gene Expression. Carla Hebert*[1], Joseph Stains[2]. [1]University of Maryland, USA, [2]University of Maryland School of Medicine, USA

Connexin43 (Cx43) plays an important role in regulating osteoblastogenesis, bone formation and turnover and the acquisition of peak bone mass. In this study, we examined the structure-function relationship between Cx43 and the regulation of Runx2 activity, downstream signaling and the expression of osteoblast genes. We hypothesized that the function of Cx43 in osteoblasts requires not only the ability to exchange small molecules (channel function), but also the ability to locally recruit signaling complexes (signal docking function) to the C-terminus of Cx43. Accordingly, we show in MC3T3 cells that overexpression of a truncated Cx43 construct lacking the C-terminus (Cx43 S244Stop) is less effective than full length Cx43 at activating Runx2 activity when stimulated with fibroblast growth factor 2. Similarly, we show that overexpression of Cx43, but not Cx43 S244Stop, stimulates the expression of *Bglap* (osteocalcin), *Col1a1*, *Sp7* (osterix) and *Tnfrsf11b* (osteoprotegerin) in cultured MC3T3 cells. In contrast to full length Cx43, overexpression of just the Cx43 C-terminus (amino acids 236 to 382) inhibited both transcription from a Runx2 reporter and signaling via PKCδ and ERK, indicating that the C-terminus is necessary but not sufficient to effect osteoblast function. To further explore the mechanism of Cx43 regulation of osteoblasts, we examined the ability of chimeric connexin constructs to affect Runx2 activity. In contrast to Cx43, overexpression of Cx45, a connexin that forms a channel with reduced permeability and an unconserved C-terminus, inhibited Runx2 activity. Similarly, a construct that possess the Cx43 channel but the Cx45 C-terminus (Cx43/45) and a construct that possess the Cx45 channel but the Cx43 C-terminus (Cx45/43) were unable to stimulate Runx2 activity. Using a series of pathway specific luciferase reporters, we demonstrate that the full-length Cx43 construct is most effective among the chimeras and truncation mutants to stimulate, not only Runx2 activity, but also signal transduction via the PKA, MAPK, β-catenin and NFκB pathways. In total, the data support our hypothesis in which an intact Cx43 is required for both signal propagation/permeability (channel function) and local recruitment of signaling complexes to the C-terminus (signal docking function) in order to mediate its cellular effects and highlights potential new modes of activation of osteoblast function.

***Disclosures: Carla Hebert**, None.*

SU0212

Decipering the Role of Parafibromin in Wnt Transcription During Osteoblast Differentiation. Casey Droscha*[1], Cassandra R. Zylstra-Diegel[2], Travis Burgers[1], Jake Baker[3], Bart Williams[2]. [1]Van Andel Institute, USA, [2]Van Andel Research Institute, USA, [3]VAI, USA

Hyper-parathyroidism-jaw tumor (HPT-JT) syndrome is an autosomal dominant disorder in which patients present with fibro-osseous tumors of the maxilla or mandible. HPT-JT is caused by loss of heterozygosity or inactivating mutations within the hyperparathyroidism 2, (*HRPT2*) gene that encodes the protein product parafibromin. As a core member of the Polymerase Associated Factors (PAF complex), parafibromin binds to nuclear β-catenin and is known to associate with RNA Polymerase II to facilitate transcriptional initiation and elongation. Recently, the ability of parafibromin to associate with β-catenin and drive Wnt target gene transcription was found to be dependent on dephosphorylation by protein tyrosine phosphatase 2 (Shp2). Additionally, Bruton's Tyrosine Kinase (BTK) has been identified as a negative regulator of Wnt target gene transcription through interaction with parafibromin. Together, these findings suggest that the phosphorylation status of parafibromin may define its role as a transcriptional repressor or activator. It is our objective to determine how the phosphorylation status of parafibromin regulates Wnt target gene transcription. As Wnt is well known as a positive regulator of osteogenesis, it is also important to decipher the role parafibromin plays within osteoblast differentiation. Conditional deletion of *Hrpt2* within mature osteoblasts using osteocalcin (OC) Cre results in increased bone mineral density, cortical thickness, and overall stiffness of 3- and 6-month-old murine femurs. In addition, loss of *Hrpt2* within mesenchymal progenitors using Dermo1-Cre results in embryonic lethality at approximately E12.5. However, initial *in vitro* investigations assessing rates of mineralization and calcium deposition within Hrpt2-null osteoblasts show no significant changes as compared to wildtype controls. From these results, it is clear that parafibromin is essential for embryonic development and is a potential inhibitor of bone mass accrual, yet further investigation as to what genes are being occupied and regulated by parafibromin is needed. These findings will help to further elucidate the genetic mechanisms that govern bone development and homeostasis.

***Disclosures: Casey Droscha**, None.*

SU0213

DICER is Specifically Regulated by RUNX2 During Osteogenesis and Enhances Osteogenic MicroRNA Expressions. Leilei Zheng*, Shu Meng, Liming Yu, Lan Zhang, Qisheng Tu, Jake Jinkun Chen. Tufts University School of Dental Medicine, USA

DICER, an RNase III endonuclease, is the central enzyme that cleaves precursor microRNAs (miRNAs) into 21-25 nucleotide duplex in cell lineage differentiation, identity, and survival. However, the mechanism regulating DICER expression in bone development or disease is unknown. In this study, we demonstrated that DICER played an important role in osteogenesis by enhancing "osteogenic" miRNAs expression, and was specifically regulated by the osteogenic master gene, runt-related transcription factor 2 (RUNX2), which specifically binds DICER promoter.

Cultured C3H10T-1/2, MC3T3-E1, MLO-Y4, and MLO-A5 cells were induced with 50 mg/mL of ascorbic acid for 1, 4, 7, and 10 days. Expression of bone metabolism genes and osteogenic-related miRNAs was determined by real-time PCR and western blot analyses. MC3T3-E1 cells were cotransfected with the DICER luciferase promoter reporter, pMIR-beta-gal and transcriptional factor cDNA plasmids to detect luciferase level. C3H10T1/2 and MC3T3 cells were transiently transfected with a RUNX2 overexpression or empty vector. Furthermore, calvarial cells from RUNX2-/- mice embryos were cultured *in vitro*, and were transiently transfected with a DICER overexpression or empty vector. Expression of bone metabolism genes and osteogenic-related miRNAs were determined.

miR-335-5p mRNA levels initially decreased when osteogenic differentiation was initiated, and the target gene DKK1 expression increased. miR-17~92 cluster increased during osteogenesis while the target gene, BIM expression decreased. DICER and RUNX2 mRNA and protein expressions increased simultaneously, while DKK1 expression was down-regulated. The DICER luciferase activity dramatically increased after co-transfection with RUNX2 when compared with the empty vector control. DICER expression increased 3-5 folds in C3H10T-1/2 and MC3T3-E1 cells overexpressed with RUNX2. Dicer overexpression in RUNX2-/- embryo calvarial cells increased 4-5 folds in miR-17~92 and decreased 2-3 folds in BIM.

These results suggest that DICER is specifically regulated by the osteogenic master gene RUNX2, which can bind the DICER promoter. Consequently, DICER cleaves pre-miR-335-5p and miR-17~92 cluster to form mature miRNAs, which target and decrease the DKK1 and BIM levels, and therefore promote bone formation. These observations first reveal a central mechanism underlying lineage-specific regulation by miRNAs during osteogenic differentiation and bone development.

***Disclosures: Leilei Zheng**, None.*

SU0214

Ebf1 Promotes Early But Suppresses Late Osteoblast Differentiation. Vappu Nieminen-Pihala[1], Kati Tarkkonen[2], Julius Laine[2], Kei Yamana[3], James R. Hagman[4], Roland Baron[5], Riku Kiviranta*[2]. [1]Department of Medical Biochemistry & Genetics & Department of Medicine, Finland, [2]Department of Medical Biochemistry & Genetics & Department of Medicine, University of Turku, Finland, [3]Teijin Institute for Biomedical Research, Japan, [4]University of Colorado, National Jewish Medical Research Center, USA, [5]Harvard School of Medicine & of Dental Medicine, USA

Early B cell factor 1 (Ebf1) is a zincknuckle containing transcription factor that regulates differentiation of multiple cell types including B- and neuronal cells. We and others have shown that Ebf1 is expressed in osteoblasts (OBs) and that deletion of Ebf1 results in increased bone formation. Conversely, overexpression of Ebf1 in osteoblasts with type I collagen 2.3 kb promoter resulted in impaired bone formation implicating Ebf1 as a negative regulator of osteoblast function. Despite these data, it has remained unclear which of the effects of Ebf1 are autonomous for bone cells. We aimed to determine, whether Ebf1 had a cell autonomous role in OBs to regulate their differentiation and function.

We first overexpressed Ebf1 in mesenchymal cell line C3H10T1/2 cells. Elevated levels of Ebf1 led to enhanced OB differentiation showed by increased alkaline phosphatase (ALP) activity and expression of Osterix (Osx) mRNA. Conversely, $Ebf1^{-/-}$ calvarial cells had severely impaired differentiation capacity seen as low ALP activity and impaired formation of mineralized bone nodules. To reconcile these data with our previous in vivo findings, we hypothesized that Ebf1 could have a dual role in OB differentiation promoting early but inhibiting late stages, as has been suggested for Runx2. To allow for some Ebf1 activity to overcome the early defect in differentiation we used haploinsufficient $Ebf1^{+/-}$ calvarial cells. $Ebf1^{+/-}$ cells showed reduced expression of Osx and ALP at early stages of the culture (days 0-14), although the phenotype was milder than in $Ebf1^{-/-}$ cells. Interestingly, on day 21 $Ebf1^{+/-}$ cells had caught up or even passed the control cells showing significantly higher expression of Osx and ALP compared to controls suggesting indeed a dual function for Ebf1 in OBs.

To test whether these findings would be true in vivo, we generated conditional Ebf1 knockout mice in which Ebf1 deletion was targeted to early or late OBs by crossing with Osx- or hOC-Cre mouse lines, respectively. Deletion of Ebf1 in early OBs with Osx-Cre resulted in significantly increased bone volume (BV/TV) and trabecular number (Tb.N) in the tibia at the age of 12 weeks by mCT analysis. However, $Ebf1_{hOC}^{-/-}$ mice tibia had no changes compared to controls. These data are being confirmed by histomorphometry.

Taken together our data suggests that Ebf1 has a cell autonomous role in OBs promoting mesenchymal stem cell commitment to the OB lineage but suppressing the function of mature cells.

***Disclosures: Riku Kiviranta**, None.*

SU0215

Epigenetic control of osteoblast differentiation by Osterix and NO66 histone demethylase. Krishna Sinha*[1], Xin Zhou[2], Hideyo Yasuda[1], Benoit DeCrombrugghe[1]. [1]U.T.M.D. Anderson Cancer Center, USA, [2]MD Anderson Cancer Center, USA

Osterix (Osx) triggers the *Runx2*-expressing precursor osteoblasts to differentiate into functional osteoblasts and then osteocytes, through activation of a large repertoire of genes essential for bone formation. In *Osx*-null embryos, *Runx2*-positive *Osx*-null cells are arrested in their differentiation and expression of Osx-target osteoblast genes is absent. It is not yet known whether Osx has a role in remodeling the chromatin architecture of its target genes during transition of preosteoblast to osteoblast. In testing the hypothesis that Osx is indispensible for active chromatin architecture, we first showed that in *Osx*-null calvarial cells, occupancy of the transcriptional activators Runx2, c-Myc and Wdr5 at the Osx target gene *Bsp* was very markedly decreased. The levels of methylation of lysine 4 and 36 and acetylation of histone H3, markers for active chromatin, were also reduced at the *Bsp* gene in these cells. In contrast, occupancy of the transcriptional repressors HP1 and the NO66 histone demethylase previously identified as an Osx-interacting protein was increased at the *Bsp* gene in *Osx*-null calvarial cells. Further, the *Bsp* promoter was hypermethylated in ES cells and in E9.5 embryos, but was markedly hypomethylated in calvaria of E18.5 embryos, coinciding with robust *Bsp* expression. In contrast, CpG methylation in the *Bsp* promoter remained high in *Osx*-null calvaria compared to *Osx*-wt calvaria. Our data also revealed that NO66 interacted with DNMT1A and HDAC1A as well as HP1 which are known to control the histone and DNA methylation. In addition, HP1 stimulated the demethylase activity of NO66 for its substrates H3K4me3 and H3K36me3, suggesting that the interaction of NO66 with the chromatin of the *Bsp* and *Oc* genes during repression of these genes in *Osx*-null cells might regulate histone methylation levels at the chromatin through its demethylase activity. Our findings strongly suggest that in the absence of Osx, the chromatin of Osx target genes is transcriptionally inactive. We propose that Osx is a molecular switch for the formation of an active chromatin state during osteoblast differentiation, whereas NO66 helps gene repression through histone demethylation and/or by participating in formation of a repressor-complex resulting in a multi-layer control of the chromatin architecture of specific osteoblast genes.

***Disclosures: Krishna Sinha**, None.*

SU0216

Hepatic Lipase Is Expressed by Osteoblast and Affects Bone Mass in Diet-induced Obesity in Mice. Alexander Bartelt[1], Timo Beil[1], Brigitte Müller[1], Till Koehne[1], Markus Heine[1], Tayfun Yilmaz[1], Jörg Heeren[1], Thorsten Schinke[2], Andreas Niemeier*[1]. [1]University Medical Center Hamburg-Eppendorf, Germany, [2]Department of Osteology & Biomechanics, University Medical Center Hamburg Eppe, Germany

Purpose: A number of unexpected molecules were recently identified that link bone homeostasis to systemic energy metabolism. Here we identify the lipolytic enzyme hepatic lipase (HL, encoded by *Lipc*) as a novel cell-autonomous regulator of osteoblast function.Methods and Results: In an unbiased genome-wide expression analysis, *Lipc* was found to be highly induced upon osteoblast differentiation, as verified by quantitative Taqman analyses of primary osteoblasts *in vitro* and of bone samples *in vivo*. Functionally, loss of HL in vitro led to increased expression and secretion of osteoprotegerin (OPG), while osteoblast differentiation was mildly impaired. Challenged with diet-induced obesity (DIO), lack of HL led to a significant increase in bone formation markers and a decrease in bone resorption markers. Accordingly, in the DIO setting, we observed in *Lipc*-/- animals but not in wild-type controls a significant increase in lumbar vertebral trabecular bone mass and an increase in bone formation rate as determiend by histomorphometry. Taken together, here we demonstrate that HL expressed by osteoblasts has an impact on osteoblast OPG expression and that lack of HL leads to increased bone formation in DIO. Conclusions: These data represent a novel and completely unexpected molecular link between osteoblasts and systemic lipid metabolism. HL may ultimately evolve as a drug target for disorders associated with low bone mass in obese individuals.

***Disclosures: Andreas Niemeier**, None.*

SU0217

Identification of Slc9a9 as a candidate gene for a bone mineral density locus on mouse Chromosome 9. Kwangbom Choi[1], Kathryn Shultz[1], Dana Godfrey[1], Rong Yuan[2], Matthew Hibbs[3], Daniel Gatti[1], Gary Churchill[1], Beverly Paigen[1], Wesley Beamer[1], Cheryl Ackert-Bicknell*[1]. [1]The Jackson Laboratory, USA, [2]Southern Illinois University School of Medicine, USA, [3]Department of Computer Science, Trinity University, USA

Over 80% of the variance in peak bone mass is due to heritable factors. We have previously published a vertebral bone mineral density (BMD) locus on mouse Chromosome (Chr) 9 at 44.24 cM. We have since confirmed that this locus affects both vertebral BMD and whole body areal BMD by generating and phenotyping congenic mice wherein c3h alleles were introgressed onto an otherwise C57BL/6J genetic background. Specifically, c3h/c3h congenic female mice have lower whole body areal BMD (b6/b6 = 0.0533 vs. c3h/c3h = 0.0507 mg/cm2, P = 0.008) and lower lumbar spine BMD (b6/b6 = 0.0894 vs. c3h/c3h = 0.0727 mg/cm2, P = 0.004), however no difference was observed in males. This BMD locus has previously been identified in other genetic crosses: MRLxSJL (42.3 cM), NZBxSM (46.08 cM) and in a new cross of: PL/J x KK/HIJ(45.3 cM). The confidence intervals for these overlapping loci, along with the known boundaries of the c3h-like interval for our congenic were used to define the genomic interval most likely to contain the underlying gene(s). The single nucleotide polymorphisms (SNP) allele pattern in this interval was examined to identify genes wherein all strains contributing the high BMD allele for the locus shared the same SNP allele and vice versa. Only three SNP within the interval possessed this allele distribution pattern and all were found within the Slc9a9 gene. This gene codes for one of the many solute transporter transmembrane proteins, but little is known about the function of this gene in particular. Using next generation RNA-seq we examined the expression profile of genes during osteoblastogenesis in primary calvarial osteoblasts. From this data, we determined that expression of Slc9a9 is low early in osteoblastogenesis, but expression increased with maturation. We identified 537 genes with expression profiles that were highly positively correlated (R2 $>$ 0.9) with that of Slc9a9 by using co-expression network analysis. These genes included Bmpr1a, Lrp6 and Mmp2. Gene-annotation enrichment analysis showed that this list of 537 genes is highly enriched for proteinaceous extracellular matrix genes (fold enrichment = 4.4, Bonferroni corrected P = 9 x 10-12). This list was also enriched for genes annotated as being involved with ossification (fold enrichment = 5.1, Bonferroni corrected P = 6 x 10-3). In summary, Slc9a9 is a strong candidate for a BMD locus on mouse Chr 9 and may be associated with osteoblast function.

***Disclosures: Cheryl Ackert-Bicknell**, None.*

SU0218

Novel Compounds Mimic Hedgehog Activity and Promote Osteoblast Differentiation in C3H10T1/2 Cells and Osteoblastic Cells from Runx2-Deficient Mice. Takashi Nakamura*[1], Masahiro Naruse[1], Tomoko Ikeuchi[1], Toshihisa Komori[2], Aya Yamada[1], Masahiro Iwamoto[3], Satoshi Fukumoto[1]. [1]Tohoku University Graduate School of Dentistry, Japan, [2]Nagasaki University Graduate School of Biomedical Sciences, Japan, [3]Children's Hospital of Philadelphia, USA

Hedgehog proteins are involved in multiple cellular actions including cell proliferation, migration, differentiation, and cell fate determination. Recently, HH-Ag 1.3 and HH-Ag 1.7 have been discovered by the high throughout screening of small molecule compounds that activate the expression of Gli1, a target gene of hedgehog signaling. Hedgehog signaling exerts important roles in hard tissue development such as bone, cartilage, and tooth. In this study, we demonstrate that HH-Ag 1.3 and HH-Ag 1.7 strongly activated the expression of endogenous Gli1 and promoted osteoblastic differentiation in pluripotent mesenchymal cell line C3H10T1/2.

Both HH-Ag compounds stimulate alkaline phosphatase (ALP) activities in dose dependent manners and were induced osteoblast marker expressions in C3H10T1/2 cells. These results suggest that both those compounds promote osteoblast differentiation in C3H10T1/2 cells. Interestingly HH-Ag 1.7 exerts synergistic promotion on ALP activities in C3H10T1/2 cells with BMP-2. We hypothesize that those compounds induced an intra-cellular signaling crosstalk between hedgehog and BMP. Because both compounds promotes osteoblastic differentiation in C3H10T1/2 cells, we screened several osteoblastic marker genes including Runx2 and Sp7. HH-Ag 1.7 strong induced Sp7 expression, while no significant upregulation was observed for Runx2 expression in C3H10T1/2 cells. This result suggests that HH-Ag 1.7 activates the downstream target molecules of Runx2 in osteoblast differentiation. To confirm this result, we used osteoblastic cells derived from Runx2 KO mice. Interestingly, Runx2 KO cells gain the ALP activity by HH-Ag 1.7, while no ALP activity was observed in control. It has been reported that the SNP alleles of Runx2 gene are associated with the reduction of bone mineral density as well as femoral neck fracture in osteoporosis patients. Thus, our research will contribute to develop novel therapies for fracture and bone defect, and especially osteoporosis patients.

***Disclosures: Takashi Nakamura**, None.*

SU0219

Odd-skipped related 2 regulates Wnt signaling pathway through Dkk1. Shinji Kawai*[1], Atsuo Amano[2]. [1]Osaka University Graduate School of Dentistry, Japan, [2]Osaka University, Japan

Zinc finger transcription factor Odd-skipped related 2 (Osr2) is one of the factors which functions in bone formation. We previously used the transgenic mice of dominant negative type Osr2, and reported the function as a factor which controls proliferation of osteoblast cells and bone formation. Moreover, joint fusion, supernumerary teeth, and cleft palate have been reported on the Osr2 knockout mice. On another front, Wnt family is secreted protein and related with embryogenesis and oncogenesis, and also plays the important role in bone formation and cartilage formation. In this study, we aim to clarify the relationship between Osr2 and Wnt signal pathway. We reported last year that the expression profile of signal pathway genes was analyzed on Osr2 over-expressed cells by DNA microarray. As a result of clustering analysis, Wnt signal pathway was most controlled among various kinds of signal pathways. Osr2 regulated TopFlash activity. In this study, we found that Osr2 negatively regulated the expression of Wnt target genes (cyclin D and Ror2), Wnt signaling factors (beta-catenin, LEF, and TCF), and several Wnt genes. Conversely, Osr2 positively regulated the expression of Wnt signaling inhibitors (Dkk1 and Sost). From reporter assay of Dkk1 promoter and luciferase, Dkk1 promoter contained Osr2 binding site between -500 and -120 region. Consequently, it is suggested that Osr2 negatively regulates Wnt signal pathway and participates in bone formation or joint formation.

***Disclosures: Shinji Kawai**, None.*

SU0220

Persistent low level of Osterix accelerates interleukin-6 production and impairs regeneration after tissue injury. Wook-Young Baek*[1], Seung-Yoon Park[2], Yeo Hyang Kim[3], Yeon-Ju Lee[1], Tae-Hwan Kwon[1], Kwon-Moo Park[1], Benoit de Crombrugghe[4], Jung-Eun Kim[1]. [1]Kyungpook National University School of Medicine, South Korea, [2]Department of Biochemistry, School of Medicine, Dongguk University, South Korea, [3]Department of Pediatrics, Keimyung University School of Medicine, South Korea, [4]University of Texas M. D. Anderson Cancer Center, USA

Osterix (Osx) is an essential transcription factor for osteoblast differentiation and bone formation. Osx knockout show a complete absence of bone formation, whereas Osx conditional knockout in osteoblasts produce an osteopenic phenotype after birth. Here, we questioned whether Osx has a potential role in regulating physiological homeostasis. In Osx heterozygotes expressing low levels of Osx in bones, the expression levels of pro-inflammatory cytokines were significantly elevated, indicating that reduced Osx expression may reflect an inflammatory-prone state. In particular, the expression of interleukin-6, a key mediator of chronic inflammation, was increased in Osx heterozygotes and decreased in Osx overexpressing osteoblasts, and transcriptionally down-regulated by Osx. Although no significant differences were revealed in renal morphology and function between Osx heterozygotes and wild-type under normoxic conditions, recovery of kidneys after ischemic damage was remarkably delayed in Osx heterozygotes, as indicated by elevated blood urea nitrogen and creatinine levels, and by morphological alterations consistent with acute tubular necrosis. Eventually, protracted low Osx expression level caused an inflammatory-prone state in the body, resulting in the enhanced susceptibility to renal injury and the delayed renal repair after ischemia/reperfusion. This study suggests that the maintenance of Osx expression in bone is important in terms of preventing the onset of an inflammatory-prone state.

***Disclosures: Wook-Young Baek**, None.*

SU0221

Primary osteoblasts from CKD patients retain abnormal gene expression ex vivo. Renata Pereira*[1], Barbara Gales[1], Navdeep Tumber[1], Harald Jueppner[2], Isidro Salusky[3], Katherine Wesseling-Perry[4]. [1]UCLA, USA, [2]Massachusetts General Hospital, USA, [3]University of California, Los Angeles School of Medicine, USA, [4]UCLA Medical Center, USA

Over the past decade, osteocytes have been identified as key regulators of mineral metabolism and skeletal mineralization and expression of osteocytic proteins are markedly altered by CKD. Evaluation of human osteocytes is limited by the lack of stable human osteocyte cells lines; morever, whether abnormalities in cells of osteoblast/osteocyte lineage are intrinsic to bone or are mediated solely by changes in circulating mineral metabolism is unknown. Thus, primary osteoblasts were cultured from bone biopsies from 24 pediatric PD patients (14M, 10F), age 17.1 + 0.7 years who had varying types of renal osteodystrophy. 8 subjects received active vitamin D sterols at the time of biopsy; 16 subjects were not on vitamin D sterols for at least 4 weeks prior to the biopsy. Biochemical values were: Ca: 8.9+0.2 mg/dl, P: 6.5+0.4 mg/dl, PTH: 589+79 pg/ml, FGF23: 1826(425, 4825) RU/ml. Histomorphometric analysis was performed on all biopsies and RNA was isolated in TRIzol from bone cores. Trabecular bone fragments were washed in DMEM with antibiotics, minced into small pieces, and incubated in fetal bovine serum for 2 hours in 5% CO_2 at 37°C until adherent to plates. 7 cc of DMEM supplemented with 20% FBS and ascorbic acid was added to each plate and incubated at 37°C. Media was changed twice weekly until formation of 7-20 cell colonies per plate (1 to 4 weeks). Colonies were split and grown until semi confluent. Cells were collected and frozen for later experiments; one plate was kept at confluence for RNA extraction. Expression of osteoblastic and osteocytic gene expression was evaluated at passage 0 by qPCR and normalized by GAPDH expression in each sample. Expression in dialysis patients was then normalized by RNA from normal control primary osteoblasts. RNA was of high quality and was non-degraded. (Table 1)

As evidenced by the increased expression of multiple markers of osteoblast maturation and function and by correlations with osteoblastic genes involved in cell-signaling from bone cores, osteoblast function is dysregulated in CKD and primary osteoblasts retain these characteristics ex vivo. Whether these factors differ in different subtypes of ROD and whether they translate into alterations apparent in mature osteocytes remain to be evaluated.

	Core	Cells	Correlation
Early osteoblast markers			
Osterix	10.23 ± 1.58 8.84 (4.74, 13.84)	3.25 ± 0.51 2.93 (1.01, 5.20)	R=0.30, p=0.18
Cbfa1/Runx2	3.90 ± 0.42 3.36 (2.53, 5.49)	2.76 ± 0.24 2.61 (1.79, 3.40)	R=0.30, p=0.18
Mature osteoblast markers			
Collagen Type 1	3.78 ± 0.20 3.83 (3.28, 4.37)	1.40 ± 0.08 1.37 (1.10, 1.70)	R=0.34, p=0.12
Osteocalcin	8.28 ± 0.95 7.91 (3.92, 10.44)	1.55 ± 0.26 1.13 (0.56, 2.03)	R=0.19, p=0.39
Osteoprotegerin	7.87 ± 2.93 4.23 (3.11, 7.08)	1.32 ± 0.14 1.36 (0.64, 1.92)	R=0.44, p=0.04
Alkaline phosphatase	5.92 ± 0.92 5.15 (3.21, 6.41)	3.83 ± 0.67 2.96 (1.79, 5.59)	R=0.03, p=0.90
Matrix gla protein	3.39 ± 0.48 3.23 (1.69, 4.07)	2.98 ± 0.52 2.35 (1.24, 3.65)	R=0.18, p=0.43
Bone morphogenic protein 2	4.01 ± 0.59 2.93 (1.81, 5.14)	4.32 ± 0.99 2.46 (1.74, 4.22)	R= - 0.06, p=0.80
Cell signaling			
Cyp24	0.21 ± 0.06 0.04 (0.01, 0.43)	2.36 ± 0.54 1.29 (0.45, 3.69)	R=0.42, p=0.05
Cyp27	3.13 ± 0.42 2.45 (1.66, 4.13)	1.22 ± 0.12 0.96 (0.77, 1.75)	R=0.73, p=0.0001
Vitamin D receptor	3.06 ± 0.29 2.49 (2.07, 3.88)	3.00 ± 0.25 2.79 (1.98, 3.97)	R=0.45, p=0.04
FGF receptor 1	4.63 ± 0.54 4.33 (2.52, 6.05)	1.71 ± 0.13 1.68 (1.13, 2.09)	R=0.49, p=0.02
PHEX	8.87 ± 1.46 6.46 (4.42, 12.48)	1.26 ± 0.15 0.99 (0.70, 1.60)	R=0.36, p=0.10
Receptor activator of nuclear factor kappa-B ligand	10.42 ± 2.55 6.50 (4.46, 12.08)	4.40 ± 1.87 1.63 (0.24, 2.98)	R= - 0.07, p=0.75
Na(+)/H(+)-exchanger regulatory factor1	1.23 ± 0.13 1.04 (0.82, 1.66)	2.80 ± 0.29 2.42 (1.83, 3.19)	R=0.64, p=0.001
Parathyroid hormone receptor 1	9.21 ± 1.29 8.25 (4.91, 11.08)	5.50 ± 0.97 4.77 (1.83, 6.73)	R= - 0.18, p=0.43
Insulin growth factor 1	1.92 ± 0.22 1.60 (1.19, 2.51)	6.43 ± 1.15 4.14 (1.96, 9.15)	R=0.47, p=0.03
Osteocyte markers			
Dentin matrix protein 1	12.75 ± 2.71 10.06 (5.21, 16.32)	0.77 ± 0.09 0.96 (0.53, 1.04)	R=0.17, p=0.46
Fibroblast growth factor 23	7.09 ± 1.82 3.88 (1.55, 8.95)	1.04 ± 0.04 1.10 (0.89, 1.22)	R= - 0.06, p=0.80
Matrix extracellular phosphoglycoprotein	9.94 ± 2.12 6.29 (4.38, 11.62)	7.39 ± 1.74 3.82 (2.22, 9.86)	R=0.04, p=0.85

Gene expression (relative to normal control)

***Disclosures: Renata Pereira**, None.*

SU0222

Reciprocal Control of Adipogenesis and Osteogensis by ERK/MAP Kinase Phosphorylation of PPARg In Vitro and In Vivo. Chunxi Ge*[1], Guisheng Zhao[2], Hui Li[2], Binbin Li[2], Renny Franceschi[3]. [1]Pom Univ of Michigan School of Dentistry, USA, [2]University of Michigan School of Dentistry, USA, [3]University of Michigan, USA

Osteoblasts and adipocytes differentiate from a common mesenchymal stem cell (MSC). Accumulating evidence suggests a reciprocal relationship between osteogenesis and adipogenesis mediated by the relative activity of PPARg and RUNX2. Increased PPARg activity stimulates adipogenesis and suppresses osteogenesis while excess RUNX2 has the opposite effect. The ERK/MAPK pathway stimulates MSC commitment to osteoblasts and inhibits adipogenesis. This effect is explained by phosphorylation of RUNX2 and PPARg at specific serine residues (S301/S319 for RUNX2, S112 for PPARg) leading to stimulation of RUNX2 transcriptional activity and inhibition of PPARg (Ge et al. JBMR 27:S23, 2012).

To examine the importance of PPARg phosphorylation in the reciprocal control of MSCs, knock-in mice harboring a S112A mutation in PPARg rendering it resistant to ERK/MAPK inhibition (Ragwala et al, Dev Cell 5:657,2003) were examined for in vitro and in vivo adipogenesis and osteogenesis. Calvarial osteoblasts, marrow stromal cells (MSCs) or ear mesenchymal stem cells (EMSCs) isolated from wild type, heterozygous and homozygous PPARg S112A mice were grown under osteogenic or adipogenic conditions and differentiation was assessed by Alizarin Red or Oil Red O staining and measurement of marker gene expression. Bone density from new born and 3 month old mice was assessed by microCT.

Overall BMD of new-born mice was dramatically decreased in homozygous PPARg S112A mice compared to wild type litter mates. Wider calvarial sutures and delayed maturation of multiple bones was also observed. Analysis of 3 month old S112A mice revealed a decrease in BV/TV in tibia accompanied by decreased trabecular thickness and increased trabecular spacing with no apparent change in cortical bone. Cell culture studies using primary calvarial osteoblasts, MSCs and EMSCs from wild type and mutant mice revealed that the PPARg S112A mutation increased adipocyte differentiation (increased Oil Red O staining and induction of PPARg, C/EBP, Adiponectin and AP2 mRNA) and suppressed osteoblast differentiation (decreased Alizarin Red staining and Runx2, OCN and BSP mRNA). Interestingly, even under osteogenic conditions, calvaria osteoblasts from homozygous S112A mice spontaneously differentiated to adipocytes.

These studies indicate that ERK/MAP dependent phosphorylation of PPARg affects bone as well as fat development.

***Disclosures: Chunxi Ge**, None.*

SU0223

Small Interfering RNA Targeting Smad1 suppresses osteoclast differentiation. Yoshihiro Yoshikawa*, Eisuke Domae, Seiji Goda, Isao Tamura, Aiko Kamada, Takashi Ikeo. Osaka Dental University, Japan

Bone morphogenetic protein 2 (BMP-2) plays a critical function in the differentiation of bone cells. It has also been suggested that BMP-2 promotes osteoclast differentiation. BMP-2 phosphorylates Smads (R-Smads), including Smad1. Smads play central roles in the downstream signaling effectors of BMP receptors. However, it is unclear whether Smad1 is involved in osteoclast differentiation.

To examine the effects of Smad1 on osteoclast differentiation, we cocultured bone marrow (BM) cells isolated from mouse tibia and primary osteoblasts (POB) isolated from calvaria of newborn mice and performed tartrate-resistant acid phosphatase (TRAP) staining. We evaluated expression of genes by real-time PCR and proteins by Western Blot and immunofluorescence in the presence of 10^{-8} M $1,25(OH)_2D_3$ and 100 ng/ml BMP-2 in POB. In addition, mouse osteoblast-like cells (MC3T3-E1) were transfected with vitamin D receptor element (VDRE)-Luc reporter construct and POB were transfected with siRNA (Smad1) using siRNA transfection reagents. Subcellular localization of Smad1 and vitamin D receptor (VDR) was detected by a fluorescence-based assay in MC3T3-E1.

Results showed that BMP-2 alone had no effect, but BMP-2 upregulated numerous TRAP-positive multinucleated osteoclasts formation when combined with $1,25(OH)_2D_3$. The differentiation of BM cells into osteoclasts was significantly suppressed by Smad1 siRNA. In addition, BMP-2 upregulated the mRNA expression of the VDR target gene receptor activator of nuclear factor-κB ligand (RANKL) in POB. It also upregulated transcription of a reporter gene in a VDRE-dependent manner in MC3T3-E1.Similarly, mRNA expression of RANKL was significantly suppressed by Smad1 siRNA. Next, we examined whether BMP-2 affected nuclear translocation of VDR. VDR acts as a transcription factor, which requires nuclear translocation. BMP-2 increased the expression of VDR protein and promoted nuclear translocation of VDR in MC3T3-E1.

We suggest that Smad1 not only promotes osteoblast differentiation, but also promotes osteoclast differentiation by interacting with VDR.

***Disclosures: Yoshihiro Yoshikawa**, None.*

SU0224

The Osteoblast Negative Regulator, BRM-SWI/SNF, is a Positive Regulator of Adipocyte Differentiation. KEVIN HONG NGUYEN*[1], FUHUA XU[2], Stephen Flowers[3], Shruti Goel[1], Elizabeth Moran[4]. [1]Department of Orthopaedics & NJMS-UH Cancer Center, UMDNJ, USA, [2]New Jersey Medical School, UMDNJ, USA, [3]NJMS-UH Cancer Center, University of Medicine of Dentistry of New Jersey, USA, [4]University of Medicine & Dentistry of New Jersey, Cancer Center, USA

The chromatin remodeling complex SWI/SNF, with its core ATPase BRG1, is required for tissue-specific gene expression. A subset of SWI/SNF, powered by the alternative ATPase BRM, generally has auxiliary effects. In osteoblast precursors, BRM-SWI/SNF represses tissue-specific gene expression, preventing premature induction of osteogenic genes whose activation is BRG1-dependent and BRM-independent. The role of BRM in other lineages derived from bone marrow stromal cells (BMSCs) is largely unknown, but its role in adipocyte differentiation is of particular interest because an improper balance of adipocyte *versus* osteoblast differentiation underlies certain skeletal pathologies. To address this question, stable knockdown lines targeting BRM or BRG1 were generated in 3T3-L1 preadipocytes. In contrast to their opposing roles in osteoblasts, BRM and BRG1 are both required for adipogenesis. Depletion of either BRM or BRG1 has a similar effect in inhibiting adipogenesis and expression of key early and late adipocyte markers, whose promoters they co-target. The finding of opposing roles for BRM in osteoblast *versus* adipocyte differentiation suggests a future possibility of targeting BRM to perturb the fate of BMSCs so as to increase bone formation and reduce bone marrow adiposity *in vivo*.

***Disclosures: KEVIN HONG NGUYEN**, None.*

SU0225

Accumulation of Menaqunone-4 in the Bones of Mice Orally Given K Vitamers and Its Biological Activity in Osteoblasts. Kimie Nakagawa*[1], Yoshitomo Suhara[2], Toshio Okano[1]. [1]Kobe Pharmaceutical University, Japan, [2]Shibaura Institute of Technology, Japan

Aims: Vitamin K serves as a cofactor for gamma-glutamyl carboxylase (GGCX) that converts glutamate residues to gamma-carboxyglutamate residues in vitamin K-dependent proteins. Thus, vitamin K may exert beneficial effects on bone formation and remodeling. There are two forms of naturally occurring vitamin K, phylloquinone (PK) and menaquinones (MK-n). Moreover, menadione (MD) is a synthetic compound lacking a side chain. Clinically, menaquinone-4 (MK-4) has been shown to prevent bone fractures in osteoporotic patients although the mechanism underlying the suppression of bone fractures by MK-4 remains unclear. Recently, we identified a novel enzyme, UbiA prenyltransferase domain containing 1 (UBIAD1) that is responsible for the conversion of PK to MK-4 in mammals [*Nature* (2010), 468:117]. In the present study, we examined whether orally given K vitamers are converted to MK-4 and accumulate in the bones of mice. We also examined the biological activities of K vitamers in terms of the steroid and xenobiotic receptor (SXR)-mediated transcriptional activity and GGCX activity in human osteoblast like MG-63 cells.

Methods: Female mice, 8 weeks of age, were given orally deuterium (D)-labeled–K vitamers at the single dose of 10 μmol/kg body weight. After 24 h, the mice were sacrificed, and femur were collected and the concentrations of MK-4-d_7 were measured by LC-APCI-MS/MS. MG-63 cells were treated with PK-d_7 and MD-d_8 at the concentration of 10^{-6} M for 24 h, and the concentrations of MK-4-d_7 were measured by LC-APCI-MS/MS. SXR-mediated transcriptional activity and GGCX activity were measured by a SXR-GAL4 hybrid luciferase assay and an enzyme assay using mouse liver microsomes, respectively. Regulatory activities of K vitamers on proliferation and differentiation of MG-63 cells were examined by WST-1 assay and von Kossa staining, respectively. Results and Discussion: Accumulation of MK-4-d_7 in the bones of mice orally given D-labeled K vitamers was consistently observed in all mice tested and the amounts of MK-4-d_7 were almost similar among the animals. This finding suggest that MK-4 is a common metabolite of K vitamers in mice. Among the K vitamers, MK-4 exhibited the highest biological activity not only in the transcriptional activity and GGCX activity but also regulation of proliferation and differentiation of MG-63 cells. This finding strongly suggests that MK-4 may be an active metabolite of vitamin K and play an important role in osteoblast function.

***Disclosures: Kimie Nakagawa**, None.*

SU0226

Both SOST and SOSTDC1 Bind to E1 Domain of LRP5 and Inhibit Wnt/b-catenin Signaling in MC3T3E1 Cells and INS-1 Cells. Mi Jeong Lee*[1], Sung Kil Lim[2], Eun Jin Kim[2], Myung Jin Lee[2], Han Seok Choi[3], Si Hoon Lee[4]. [1]Yonsei University Health System, South Korea, [2]Yonsei University, South Korea, [3]Dongguk university, South Korea, [4]Gachon university, South Korea

Wnt/ b-catenin signaling is important for bone development and osteoblast differentiation and it is also involved in pancreas development, islet function, and insulin production and secretion. SOSTDC1 is expressed in pancreas as well as bone during early embryonic period. SOSTDC1 has moderate homology with Sclerostin, and both SOSTDC1 and Sclerostin inhibit Wnt/b-cateninsignaling in in-vitro assays by binding to YWTD propeller 1 and 2 of LRP5 or LRP6. Recently, Sclerostin-neutralizing monoclonal antibodies have been developed to inhibit binding of Sclerostin to bind the LRP5,6 receptors, resulting in activation of Wnt/b-catenin signaling pathway. To study the inhibitory potency of SOSTDC1 and abrogation capacity of Sclerostin inhibitors on Wnt//b-cateninsignaling and insulin secretion, we expressed Sclerostin and SOSTDC1 in E-coli as a fusion protein and insect cells, and E1 domain of LRP5 was also expressed as a fusion protein in E-coli, and tested the effects of known oligopeptide-DKK1 or SOST inhibitors in MC3T3E1-Top flash reporter cells and INS-1 cells transfected with LEF-TCF reporter DNA. In XPR-36 analysis, Sclerostin and SOSTDC1 revealed a comparable binding activity to E1 domain of LRP5. Wnt3a and Wnt7a stimulate Wnt/b-catenin signaling in both MC3T3E1 and INS1 cells. Furthermore both Sclerostin and SOSTDC1 could inhibit Wnt3a induced Wnt//b-catenin signaling in MC3T3E1-Top flash reporter cells and INS-1 cells with comparable potency. Interestingly, a lineal oligopeptide did not show any abrogating activity at all, meanwhile a cyclized oligopeptide abrogated Wnt/ b-cateninsignaling inhibited by Sclerostin but not by SOSTDC1, which indicated that the binding site of SOSTDC1 on E1 domain of LRP5 might be little different from that of Sclerostin. We are now studying the effects of Sclerostin, SOSTDC1, and Dkk1 or SOST inhibitors on insulin secretion in INS-1 cells.Key words: Sclerostin, SOSTDC1, Wnt signaling, insulin

***Disclosures: Mi Jeong Lee**, None.*

SU0227

Dock7 plays an Integral role in the Adhesion, Migration and Morphology of Osteoblasts. Kathleen Bishop*[1], David Maridas[1], Katherine Motyl[1], Clifford Rosen[2]. [1]Maine Medical Center Research Institute, USA, [2]Maine Medical Center, USA

Dock7 is a guanine nucleotide exchange factor (GEF) important in neuronal cell function and axon tracking; however, little is known about the role of Dock 7 in bone remodeling. Mice with an insertion in the Dock7 locus, the Misty mouse, have undetectable Dock7 protein levels. Loss of Dock7 expression in the Misty model resulted in a low bone mass phenotype and accelerated age related bone loss, possibly related to both non-cell autonomous factors (i.e. increased sympathetic tone) and cell autonomous defects. In support of the latter, Misty mice have decreased osteoblast and bone lining cell numbers, but increased osteoclast and marrow adipocyte numbers by histomorphometry. In order to further elucidate the role of Dock7 in bone, primary bone marrow stromal cells (BMSCs) were isolated from 6-8 wk old mice and expanded *ex vivo* in culture. Osteogenic differentiation was impaired in cells from the Misty mouse as shown by decreased Von Kossa and alkaline phosphatase staining while osteoclast differentiation was accelerated. Cell migration was evaluated using Collagen I coated Boyden chambers in serum free media. Misty BMSCs showed decreased cell migration onto the Collagen I matrix compared to cells isolated from control mice. As cell mobility is heavily dependent on the strength of cell attachment, cell adhesion was assessed. Both control and Misty BMSCs were incubated on Collagen I or Fibronectin coated plates and non-adherent cells were removed once cells began to attach and adherent cells counted. BMSCs from Misty mice had increased adhesion on both matrices when compared to cells from control mice suggesting a differential expression and/or function of adhesion complex proteins and likely an increased expression of both Collagen- and Fibronectin-binding integrins. In support of these data, analysis of the F-actin cytoskeleton in Misty BMSCs by immunocytochemistry suggests decreased cell spreading and a more cuboidal morphology. The delay in cell migration associated with increased cell adhesion and changes in cell morphology in Misty BMSCs points to a novel cell autonomous role for Dock7 in mesenchymally derived bone cells and may contribute to the skeletal changes observed in the Misty mouse. Alterations in cell adhesion may be the principal mechanism of decreased migration observed with Dock7 deficiency and could play a role in the osteoclastic recruitment of osteoblasts to sites of bone remodeling within the bone microenvironment.

***Disclosures: Kathleen Bishop**, None.*

SU0228

Macrophage Stimulating Protein Stimulates Osteoblast Differentiation via ERK Signaling Pathway. Byung-Chul Jeong*[1], Hyuck Choi[2], Jeong-Tae Koh[3]. [1]Chonnam National University School of Dentistry, South Korea, [2]Post-doctoal fellowship, South Korea, [3]Chonnam National University, South Korea

Macrophage-stimulating protein (MSP) plasys an important role in calcium homeostasis and skeletal mineralization in zebrafish. However, the precise role of MSP in osteoblast differentiation is not fully understood. In this study, we examined the effects of MSP on osteoblast differentiation using mesenchymal C3H10T1/2 and pre-osteoblast MC3T3-E1 cells. Expression of Ron receptor for MSP is significantly increased during osteoblast differentiation. Introduction MSP peptide increases the gene exprssion of osteogenic markers including alkaline phosphatase (ALP), osteocalcin (Ocn), Type I collagen (Col 1a), osterix (Osx) and Runx2, and ALP staining was enhanced as well. Consequently, mineralized nodules formations were remarkably stimulated by MSP in a dose-dependent manner. Furthermore, treatment of MSP significantly enhanced ERK1/2 phosphorylation, and pre-treatment of ERK inhibitor PD98059 attenuated the osteoblast differentiation by MSP. Taken together, these data demonstrate that MSP is an regulator for promoting osteoblast differentiation via ERK1/2 MAPK signaling pathway.

***Disclosures: Byung-Chul Jeong**, None.*
This study received funding from: Basic Science Research Program through the National Research Foundation of Korea (NRF) funded by the Ministry of Education, Science and Technology (2012R1A1A2041418)

SU0229

Mechanism of Action for Cell Cycle and Apoptosis Regulatory Protein (CARP)-1 expression and Cytoplasmic Translocation by PTH in Differentiated Osteoblasts. Sonali Sharma, Varsha Das, Chandrika Mahalingam, Nabanita Datta*. Wayne State University School of Medicine, USA

The mechanisms underlying the actions of Parathyroid hormone (PTH) in osteoblast proliferation, differentiation, apoptosis and bone mass are complex and incompletely understood. PTH controls osteoblast cell cycle regulatory proteins and suppresses mature osteoblasts apoptosis. Cell Cycle and Apoptosis Regulatory Protein (CARP)-1 (aka CCAR1) is a novel regulator of apoptosis signaling by diverse agents including cell growth and differentiation factors. Our previous report identified significant presence of CARP-1 protein for the first time in osteocytes, osteoblasts (mice femora and calvariae), and MC-4 (MC3T3-E1 clone-4) osteoblastic cells. In this study Western blot analysis with anti-CARP-1 polyclonal antibody reveals that PTH down-regulates CARP-1 protein 2-3 fold in 7-day differentiated MC-4 cells or primary calvarial osteoblasts in a dose- and time-dependent manner compared to vehicle treated control cells. PMA, a protein kinase C (PKC) agonist, mimics PTH action, and the PKC inhibitor, GF109203X, partially blocks down-regulation of CARP-1, implying involvement of PKC. H-89, a protein kinase A (PKA) inhibitor, partially antagonizes PTH action suggesting PKA pathway to be a mediator of PTH inhibition of CARP-1 protein expression in differentiated osteoblasts. U0126, a MEK inhibitor, does not alter the effect of PTH, and SB208530, P-p38 inhibitor, attenuates PTH down-regulation of CARP-1 protein expression implying a P-p38 dependent and P-ERK independent mechanism. Immunofluorescence staining reveals nuclear to cytoplasmic translocation of CARP-1 protein in differentiated osteoblasts following PTH induction. The significance of CARP-1 protein translocation and its role in PTH regulation of apoptosis and bone anabolic action remains to be investigated. These findings highlight CARP-1 protein as a potential candidate in PTH signal transduction pathways in osteoblasts.

***Disclosures: Nabanita Datta**, None.*

SU0230

Osteoblast Differentiating Activities of Thyroxine (T4), 3,5,3'-triiodo-L-thyronine (T3) and Their Metabolites. Shaohong Cheng*[1], Weirong Xing[2], Sheila Pourteymoor[3], Subburaman Mohan[4]. [1]VA Loma Linda Health Care Systems, USA, [2]Musculoskeletal Disease Center, Jerry L. Pettis Memorial Veteran's Admin., USA, [3]Jerry L Pettis VA Medical Center, USA, [4]Jerry L. Pettis Memorial VA Medical Center, USA

Studies involving human genetic mutations and mutant mouse models involving production and actions of thyroid hormone (TH) have provided irrevocable evidence for a key role for TH in the regulation of skeletal growth. Thyroid glands predominantly secrete the pro-hormone, T4, which is deiodinated by iodothyronine deiodinase enzymes to generate active T3 and their inactive metabolites, 3,3',5'-T3 (reverse T3) and 3,3'-diodothyronine (T2). While T3 binds to TH receptors with higher affinity than T4, T4 occupied TH receptors has also been reported in the nucleus under euthyroid conditions raising the possibility that T4 bound nuclear receptors may be biologically relevant in thyroid syndromes with elevated free T4 and reduced T3 levels. We, therefore, evaluated the direct effects of T4, T3 and their metabolites (rT3 and T2) in stimulating osteoblast differentiation using MC3T3-E1 osteoblasts which do not produce detectable levels of deiodinases, thereby eliminating

the confounding effects caused by local conversion of T4 to T3. Under serum-free conditions, 24 hour treatment of MC3T3-E1 cells with TH caused a dose-dependent increase in osteocalcin (OC) mRNA levels with 1125 and 1050-fold increases at 100 and 1000 ng/ml T3 and T4, respectively. T2 and rT3 were less active with the potency of T3>T4>T2 >rT3. At circulating concentrations, T3 and T4 caused a similar increase in OC expression (approximately 100-fold) while T2 and rT3 had no significant effect. Treatment with T4, T3 and its metabolites also increased osterix expression (12-fold maximum, $P<0.01$) with dose effects comparable to that of OC expression. Besides the classical genomic mechanism of action of TH, there is evidence for non-genomic action of T4 involving integrin, $\alpha v\beta 3$. To determine if T4 and T3 effects on OC expression is mediated via activation of integrin signaling, we pretreated MC3T3-E1 cultures with inhibitors of integrin signaling, cycloRGDfv peptide (5 μM) or echistatin (20nM) prior to TH treatment. Surprisingly, inhibition of integrin signaling with both cycloRGDfv and echistatin increased the T3 and T4 effect on OC expression by 50-200% ($P<0.01$). Based on these data, we conclude that elevated T4 levels in the absence of T3 may exert stimulatory effects on osteoblast differentiation. The establishment of cell-specific effects of T4 on osteoblasts may provide a strategy to generate T4 mimics that exert skeletal specific effects without the confounding T3 effects on other tissues.

***Disclosures: Shaohong Cheng**, None.*

SU0231

Utilizing hTERT-immortalized Primary Mouse Osteoblasts to Assess the Role of Cx43 in Osteoblast Signaling Pathways. Atum Buo*, Joseph Stains. University of Maryland, School of Medicine, USA

The coupling of osteoblasts by connexin43 (Cx43)-comprised gap junctions is critical for osteoblastogenesis and optimal bone formation. We have begun to define the molecular details that enable Cx43 to regulate osteoblast differentiation and function. Previously, using MC3T3-E1 osteoblast-like cells, we identified several signaling cascades that are affected by overexpression or knockdown of Cx43. Further, alterations of these signaling cascades modulate the activity of the essential osteogenic transcription factors Runx2 and Osterix. In this preliminary study, we used a recently reported human telomerase reverse transcriptase (hTERT)-immortalized primary mouse osteoblast cell line isolated from Cx43-null mice (MOB-Cx43KO) and a paired wild type control cell line (MOB-WT) (M. Thi *et al.*, *Am J Phys Cell Phys.* 2010) to determine if the effects observed in MC3T3-E1 cells translated into this more sophisticated cell system. We examined the hypothesis that the osteogenic defects characterized in Cx43-deficient cells are due to reduced signaling resulting in impaired Runx2 and Osterix activation. Confluent cultures of MOB-Cx43KO and MOB-WT cells were examined by western blotting for levels of Cx43, Runx2, Osterix, and key signaling molecules. To test the effects of growth factor signaling, cells were serum starved overnight and then treated with FGF2 for 0, 5, or 30 minutes and analyzed for phospho-extracellular signal-regulated kinase (pERK) and phospho-protein kinase C delta (pPKCδ) levels. Under standard culture conditions, we found that MOB-Cx43KO cells had reduced pERK and pPKCδ levels compared to MOB-WT cells. Runx2 abundance was unaffected by loss of Cx43. Conversely, Osterix expression was diminished in MOB-Cx43KO compared to MOB-WT cells. Additionally, MOB-Cx43KO cells displayed reduced pERK and pPKCδ levels relative to MOB-WT cells when treated with FGF2. These findings are consistent with our results in mouse MC3T3-E1 osteoblasts that implicate ERK and PKCδ as downstream mediators of the Cx43-dependent effects on Runx2 and Osterix activity. Future studies will examine Runx2 and Osterix recruitment to target osteoblast promoters by chromatin immunoprecipitation assays. In summary, our data support the hypothesis that the presence of Cx43 is needed for efficient basal and growth factor induced activation of ERK and PKCδ and highlight that this model (MOB-Cx43KO cells) is appropriate for more detailed mechanistic studies of Cx43 function in osteoblasts.

***Disclosures: Atum Buo**, None.*

SU0232

Active DNA demethylation controls osteoblastic and adipocytic differentiation. Roman Thaler*[1], Monika Rumpler[1], Ines Sturmlechner[1], Silvia Spitzer[1], Klaus Klaushofer[2], Franz Varga[1]. [1]Ludwig Boltzmann Institute of Osteology, Austria, [2]Hanusch HospitalLudwig Boftzmann Institute of Osteology, Austria

Osteoporosis is associated with reduced bone mass and increased bone marrow fat. Osteoblasts (OBs) and adipocytes differentiate both from mesenchymal stem cells and aberrantly increased adipocyte differentiation may trigger osteoporosis development.

Expression of several osteoblastic genes like osteocalcin (*Bglap2*), Msh homeobox 2 (*Msx2*), distal-less homeobox 5 (*Dlx5*) or alkaline phosphatase (*Alpl*) can be silenced by epigenetic DNA methylation of their promoters by DNA (cytosine-5-)-methyltransferases (DNMTs). The inverse process, namely active DNA demethylation by proteins of the Tet-methylcytosine-dioxygenase (TET) gene family emerges as a new and essential molecular mechanism controlling tissue development and cellular differentiation. We have recently demonstrated that activation of *Dlx5* expression via active DNA demethylation stimulates osteoblastic differentiation. Here we tested if active DNA demethylation modulates osteoblastic and adipocytic differentiation.

Pre- and differentiated OBs form calvaria of newborn mice were transfected with *Tet1* or *Tet2* siRNA and cultured in osteogenic medium for 2-3 weeks for mRNA and protein expression analysis and for mineralization assessment. 3T3-L1 pre-adipocytes were transfected with *Tet1* and *Tet2* siRNA and induced to adipocytic differentiation for 10 days. Thereafter, mRNA isolation and red oil O staining (fat droplet formation) were performed. Expression patterns of genes involved in DNA methylation and of genes implicated in active DNA demethylation were very similar between OBs and adipocytes during differentiation. Thus, expression of *Dnmt1* and TET1 was down regulated whereby *Dnmt3a* and *Tet2* were up-regulated during differentiation. Although cultured in osteogenic medium, knock down of both, *Tet1* and *Tet2* strongly induced fat droplet formation in pre- and in differentiated OBs. Moreover, *Tet2* knockdown significantly decreased expression of *Runx2*, *Lox*, *Col1a2* or *Bglap2* and strongly enhanced *Plin1* expression, a marker for mature adipocytes. In adipocytes, although cultured in adipocytic medium, knock down of both *Tet1* and *Tet2* dramatically decreased fat droplet formation and *Plin1* gene expression. Furthermore, expression of osteoblastic genes like *Runx2*, *Lox*, *Col1a2* or *Bglap2* was significantly increased. In summary, we found that expression of *Tet1* and *Tet2* maintains the osteoblastic and adipocytic phenotype, while knocking down these gene results in inversion of their differentiation status.

The involvement of genes responsible for active DNA demethylation in maintenance of the osteoblastic and adipocytic phenotype suggests active DNA demethylation as a central regulator for OB and adipocytic differentiation.

***Disclosures: Roman Thaler**, None.*

SU0233

Constitutive Activation of NF-κB Impairs Osteogenesis and Skeletal Development. Yousef Abu-Amer[1], Gaurav Swarnkar*[2], Kaihua Zhang[3], Fanxin Long[4]. [1]Washington University in St. Louis School of Medicine, USA, [2]Washington University SOM, USA, [3]Washington University, USA, [4]Washington University School of Medicine, USA

Pathologic conditions impair bone homeostasis. The transcription factor NF-κB regulates bone homeostasis and is central to bone pathologies. Whereas contribution of NF-κB to heightened osteoclast activity is well-documented, the mechanisms underlying NF-κB impact on chondrocytes and osteoblasts are not well defined. In this study, we examined the effect of constitutively active IKK2 (IKK2ca) on chondrogenic and osteogenic differentiation. We show that retroviral IKK2ca but not GFP, IKK2WT, or the inactive IKK2 forms IKK2KM and IKK2SSAA, strongly suppressed differentiation of ST2 and ATDC5 cells. In order to explore the effect of constitutive NF-κB activation on bone formation in vivo, we activated this pathway in a conditional fashion. We crossed the R26StopIKK2ca mice with mice carrying the Col2-cre in order to express IKK2ca in osteoblasts (OB) and chondrocytes (CHC). Both CHCs and OBs derived from Col2Cre/IKK2ca expressed Flag-tagged IKK2ca as detected by western blot. Mice were born alive yet died shortly thereafter. Histologically, newborn Col2Cre+/RosaIKK2ca hets (Cre+/fw) and homozygotes (Cre+/ff) showed smaller skeleton, deformed vertebrate and reduced or missing digit ossification. The width of neural arches as well as ossification in vertebral bodies of Cre+/fw and Cre+/ff were reduced or diminished. H&E staining of proximal tibia from new born pups showed that Cre+/fw displayed disorganized hypertrophic zones within the smaller epiphysis. X-ray analysis of 4-wk old Cre+/fw and WT littermate showed that Cre+/fw mice have deformed and thinner vertebrate compared to WT littermates. Micro-CT analysis showed that 4-wk old Cre+/fw has abnormal trabecular bone in proximal tibia compared to WT littermate. Mechanistically, ex-vivo experiments show that expression of the differentiation marker alk phos in calvaria derived from newborn IKK2ca knock-in mice cultured in vitro under osteogenic conditions was diminished compared to WT-derived cells. Further, IKK2ca, but not GFP, inhibited cellular levels of b-catenin concomitantly with increased expression of RBPjk (mediator of Notch signaling). ISH studies showed that the hypertrophic chondrocyte marker type-X collagen (Col X), the pre-hypertrophic chondrocyte markers IHH and AP, and the early markers Aggrecan and type-II collagen (Col II) were reduced in Cre+/fw mice. Altogether, the in-vitro, in vivo and ex-vivo evidence suggest that IKK2ca perturbs osteoblast and chondrocyte maturation and impairs skeletal development.

***Disclosures: Gaurav Swarnkar**, None.*

SU0234

Human Serine Protease HTRA1 is A Novel Mediator of Human Bone Marrow-Derived Stromal Cell Osteogenesis. Andre Tiaden*[1], Maike Breiden[2], Ali Mirsaidi[1], Fabienne Weber[1], Gregor Bahrenberg[1], Stephan Glanz[1], Paolo Cinelli[1], Michael Ehrmann[2], Peter Richards[3]. [1]University of Zürich, Switzerland, [2]University Duisburg-Essen, Germany, [3]CABMM, Zurich University, Switzerland

Human high-temperature requirement serine protease A (HTRA1) is a secreted member of the broadly conserved HTRA family of trypsin-like serine proteases. A prominent feature of this protein is its ability to degrade and modify a variety of extracellular matrix (ECM) proteins. As such, HTRA1 is now regarded as being an important mediator of musculoskeletal development and disease. In the current study, we aimed to establish a role for HTRA1 in bone formation by examining the effects of HTRA1 loss- or gain-of-function on human bone marrow-derived stromal cell (hBMSC) osteogenesis and subsequent mineral formation. Extracellular addition of recombinant HTRA1 enhanced osteogenesis of hBMSCs as evidenced by significant alterations in several osteogenic markers including integrin-binding sialoprotein (IBSP), bone morphogenetic protein 5 and sclerostin. HTRA1 also enhanced mineral formation in differentiating osteoblasts as shown by increased Alizarin red staining

and was dependent on its proteolytic activity. Conversely, matrix mineralization was completely abolished in these cultures following treatment with small interfering RNA (siRNA) specific for HTRA1. Immunofluorescence studies identified high levels of HTRA1 protein in association with IBSP at sites of newly formed bone mineral both in vitro and in vivo. Indeed, proteolytic enzyme assays confirmed IBSP as being a novel HTRA1 substrate. In contrast to its positive role in osteogenesis, HTRA1 imparted a negative effect on adipogenesis as demonstrated by its ability to significantly reduce lipid droplet formation in BMSCs undergoing adipogenic differentiation. This was confirmed by loss-of-function studies, where HTRA1 silencing resulted in a significant increase in the adipogenic potential of hBMSCs as demonstrated by increases in the expression levels of specific adipogenic markers including peroxisome proliferator-activated receptor gamma and fatty acid binding protein 4. This differential effect of HTRA1 on BMSC differentiation was further emphasized by its secretion profile, where increases in the levels of endogenous HTRA1 protein were observed during osteogenic differentiation only. In summary, our data reveals HTRA1 as being an essential requirement for osteogenesis. Its dual role as both an osteogenic promoter and an adipogenic inhibitor may have significant implications in terms of its functional involvement in diseases such as osteoporosis, where deficiencies in BMSC lineage commitment are evident.

***Disclosures: Andre Tiaden**, None.*

SU0235

LIF: A Mediator of Reciprocal Regulation by *Pkig* of Osteoblast and Adipocyte Differentiation. Xin Chen*[1], Bryan Hausman[1], Guangbin Luo[1], Guang Zhou[1], Shunichi Murakami[1], Janet Rubin[2], Edward Greenfield[1]. [1]Case Western Reserve University, USA, [2]University of North Carolina, Chapel Hill, School of Medicine, USA

The Protein Kinase Inhibitor (*Pki*) gene family inactivates nuclear PKA and thereby terminates PKA-induced gene expression. We previously showed that *Pkig* is the primary *Pki* expressed in osteoblasts. We also showed that *Pkig* knockdown significantly increases the effects of parathyroid hormone on PKA activation, rapid gene expression, and inhibition of apoptosis. More recently, we showed that PKA activation by *Pkig* knockout (KO) or knockdown reciprocally increases osteogenesis and inhibits adipogenesis. Leukemia Inhibitory Factor (LIF) is a PKA-regulated cytokine that can stimulate osteogenesis and inhibit adipogenesis. The goal of this study was therefore to determine whether LIF mediates the reciprocal regulation of osteogenesis and adipogenesis by *Pkig*. Murine Embryonic Fibroblasts (MEFs) from *Pkig* KO mice generated in our lab were compared with wild type MEFs. *Pkig* KO significantly increases nuclear PKA activation induced by forskolin and thereby significantly increases expression of *Lif* mRNA and LIF protein. An antibody that neutralizes mouse LIF significantly reduces the effects of *Pkig* KO on osteogenesis as determined by Alkaline Phosphatase (ALP) activity and staining, and Alizarin Red S staining of mineralization. The LIF antibody also significantly reduces the effects of *Pkig* KO on adipogenesis as determined by Oil Red O staining of lipid accumulation. Similar results were also obtained in mesenchymal stem cells (MSCs) following siRNA-mediated *Pkig* knockdown. Thus, real time RT-PCR for mRNA markers of osteogenesis (ALP and osteocalcin) and adipogenesis (PPARγ, C/EBPα, Adiponectin, and Leptin) showed that the LIF antibody significantly reduces the effects of *Pkig* knockdown on both osteogenesis and adipogenesis in murine marrow-derived MSCs. Moreover, an antibody that neutralizes human LIF significantly reduces the effects of *PKIG* knockdown on expression of ALP and osteocalcin mRNAs by human MSCs. In conclusion, our results show that the reciprocal regulation of osteogenesis and adipogenesis by *Pkig* is mediated, at least partially, by LIF.

***Disclosures: Xin Chen**, None.*

SU0236

Metformin stimulates compact bone mesenchymal stem cells and accelerates wound healing in a Type 2 Diabetes mouse model. Xin Li*[1], Satoko Matsumura[2], Yuqi Guo[2], Huawei Yuan[2], Wenbo Yan[3]. [1]New York University, USA, [2]New York University College of Dentistry, USA, [3]Nyack College, USA

Background: Type 2 diabetes (T2D) is associated with increased fracture in spite of having a normal or even higher bone mineral density. Multipotent mesenchymal stem cells (MSCs) in bone are critical in bone health and regeneration. It is possible that MSCs are impaired in T2D patients which leads to bone fracture. However, it is unclear whether and how hyperglycemia affect MSCs. Metformin, an anti-T2D medicine stimulates osteoblasts while inhibites osteoclasts. It has been suggested that metformin stimulates MSCs in bone marrow. Compact bone MSCs are more abundant and metabolically more active compared to bone marrow MSCs. However, effects of metformin on compact bone MSCs are unknown. We hypothesize that metformin helps to enhance population and function of MSCs residing in compact bone and improve bone metabolism and regeneration under T2D condition.

Methods: We evaluate the effects of metformin on compact bone MSCs *in vivo* and *in vitro* using male T2D MKR mice. MSCs derived from bone marrow flush or compact bone digestion were analyzed by flow cytometry with markers: $CD45^{low}$-$Ter119^{low}Sca1^{+}CD105^{+}CD29^{+}$. MSCs digested from compact bones were cultured with and without metformin *in vitro* for CFU-F, osteogenesis and adipogenesis assays. To study the effects of metformin on MSCs in T2D MKR mice *in vivo,* ten-weeks-old MKR mice were daily treated with vehicle or metformin for 14 days. The percentages of compact bone MSCs were determined and CFU-F, osteogenesis and adipogenesis were analyzed. To evaluate metformin effects on bone regeneration in 10-week-old MKR mice, we applied a drill-hole model in which an 8-μm hole was drilled in the left femur mid-diaphysis. After surgery, mice were randomly divided into two groups for a 14-day vehicle or metformin treatment. Femurs were analyzed by microCT and histomorphometry. Body weight and length, fat tissue weight, blood glucose, insulin levels in metformin treated mice were determined and compared with vehicle group. RNAs were isolated from MSC cultures, bone marrow flush and cortical bones for gene expression.

Results: In male MKR mice: (1) Compact bone digestion method yielded 10-fold higher MSCs population compare to bone marrow flush; (2) direct treated MSCs culture with metformin in vitro stimulates ALP and Runx2 expression; (3) Compact bone MSCs were stimulated in metformin treated mice: the population increased by 20%, proliferation increased by 3-fold and osteogenesis increased by 35% compare to vehicle treated mice; (4) Metformin facilitated wound healing process in hyperglycemic mice (Attached Fig); (5) Metformin regulated a panel of bone metabolism related genes including DMP-1, Runx2, PPARγ and ALP *in vivo*.

Conclusion: Our study suggests that by promoting compact bone MSCs proliferation and differentiation, metformin is a promising agent to maintain bone health and facilitate bone regeneration under T2D condition.

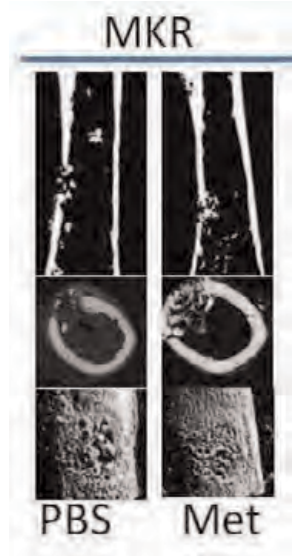

Fig

***Disclosures: Xin Li**, None.*

SU0237

NF-κB RelB-/- Mice Have Enhanced Mesenchymal Progenitor Cell Differentiation and Fracture Repair. Zhenqiang Yao*[1], Yanyun Li[2], Lianping Xing[1], Brendan Boyce[2]. [1]University of Rochester, USA, [2]University of Rochester Medical Center, USA

Fracture repair recapitulates aspects of endochondral ossification with mesenchymal progenitor cell (MPC) differentiation into chondroblasts and osteoblasts (OBs) to bridge fracture gaps followed by callus remodeling by osteoclasts (OCs) to complete fracture repair. NF-κB RelA promotes MPC proliferation and inhibits differentiation of mature OBs, but the role of RelB in MPC differentiation or bone repair is unknown. We derived CD45-Sca-1+ MPCs from WT and RelB-/- mouse long bones (bMPCs). WT and -/- bMPCs express MPC marker, CD105 (51% and 61%, respectively). RelB-/- bMPCs have enhanced differentiation into ALP+ OBs (32 ± 4 vs 15 ± 1/mm2, $p<0.05$) and chondrocytes (42 ± 5 vs 9 ± 3 cells per pellet), the latter associated with early increased Sox9 mRNA expression and larger chondrocyte pellets than WT cells. We performed closed femoral fractures in 2-month-old WT and RelB-/- mice and found significantly increased bone volume in the callus evaluated by μ-CT in RelB-/- mice at day 14 (BV/TV 12 ± 3 vs 8 ± 3% vs WT, $p<0.05$), but not at day 21. Histomorphometry showed that the area of total callus, cartilage and woven bone were also significantly increased in RelB-/- mice at day 14 (2.7 ± 0.8 vs 1.5 ± 0.7 mm2, 0.9 ± 0.4 vs 0.3 ± 0.2 mm2 and 0.8 ± 0.1 vs 0.56 ± 0.14 mm2 vs WT mice, respectively). By 21 day, cartilage had been resorbed in both mice, but there was more woven bone in sections from RelB-/- than WT mice. Fracture callus in RelB-/- mice had significantly more OCs at day 21 (170 ± 54 vs 79 ± 49/mm2,$p<0.05$) when the woven bone is being actively remodeled, and spleen cells from RelB-/- formed more OCs and resorption pits in vitro. Quantitative RT-PCR mRNA expression levels of Sox9, Osx and Runx2 were significantly higher in fracture callus at day12 in RelB-/- than in WT mice. RelA directly targets Sox9 to stimulate chondrocyte proliferation and differentiation and also promotes Osx activation. We found that RelA protein levels and nuclear translocation were significantly increased in RelB-/- MPCs. Importantly, RelB formed a complex with RelA in WT MPCs and dose-dependently inhibited RelA-induced Sox9 and Osx luciferase activity in ADTC and C2C12 cells. In

summary, RelB-/- MPCs have enhanced chondro- and osteoblast differentiation and RelB-/- mice have accelerated fracture callus formation and remodeling. Inhibition of RelB in MPCs could be novel strategy to enhance fracture repair.

***Disclosures: Zhenqiang Yao**, None.*

SU0238

No correlation between in vitro osteogenic differentiation of MSCs and hip implant healing. Jessica Alm*, Niko Moritz, Hannu Aro. University of Turku, Finland

Mesenchymal stem cells (MSCs) are involved in the osseointegration of cementless total hip arthroplasty (THA). A recent study showed that aging, low BMD and geometric changes of the proximal femur are risk factors for early migration and delayed osseointegration of femoral stems in postmenopausal female THA patients. Individual variations in MSCs reservoirs and functional capacity may also influence the speed of osseointegration. We asked how the in vitro proliferative and osteogenic capacities of MSCs reflect in the magnitude of initial stem migration and time point for osseointegration.

A cohort of 19 women with primary hip osteoarthritis (mean age 64 years, range 41-78) underwent successful preoperative analysis of bone marrow-derived plastic adherent MSCs as well as a two-year radiostereometric analysis (RSA) of stem migration after cementless THA. Stem migration was defined as micromotions exceeding the precision values of RSA measurements (0.40 mm for translation vector and 1.32 degrees for rotation vector). The growth kinetics of MSCs was evaluated by calculating population doublings (PD). Osteogenic capacity was evaluated by analyses of alkaline phosphatase (ALP) expression and mineralization after culturing in osteogenic medium. Associations between MSC parameters and the magnitude of RSA stem migration were analyzed with linear correlations and with partial correlation controlling for confounding factors (age and canal flare index). MSCs of younger fracture patients (F/M 8/5, mean age 37 years, range 19-60) served as the reference for the MSC capacities of the THA patients and the comparisons were made using Student's t-test and ANCOVA with adjustment for age.

As an indicator of age-related decline in MSC capacities of THA patients, PD-rate, average ALP and von Kossa stained areas were around 50% of the reference values. There were no significant correlations between the in vitro assayed osteogenic or proliferative capacity of the patients' MSCs and the magnitude of stem migration or time point for osseointegration.

This study represents a first attempt of comparing in vitro osteogenic properties of MSCs with clinical implant healing in vivo. Against our hypothesis, decreased osteogenic capacity of MSCs did not reflect in stem migration or delayed osseointegration in this female cohort. These findings support the concept that non-biological factors such as physiological loading predominate in dictating the progress of femoral stem osseointegration.

***Disclosures: Jessica Alm**, None.*

SU0239

Novel Potent Lactam Acetylene EP_4 Agonists Stimulate Alkaline Phosphatase Production and Differentiation in Bone Marrow Cells. Stephen Barrett*[1], Gregory Endres[1], Thomas Owen[2], Adam Uzieblo[1], Bradlee Germain[1], Andrei Kornilov[1], Joseph Colombo[1], James Kramer[1], Liyue Huang[1], Jeffrey Johnson[1], Jim O'Malley[2]. [1]Cayman Chemical Company, Inc., USA, [2]Myometrics, LLC, USA

The prostaglandin E G-protein coupled receptors (GPCR) subtypes 2 and 4 (EP_2 and EP_4 receptors, respectively) are stimulated by interaction with two eicosanoid products of the cyclooxygenase-catalyzed pathway, prostaglandin E_1 (PGE_1) and prostaglandin E_2 (PGE_2), and signal by increasing intracellular cAMP levels. Expression of EP_2 and EP_4 receptors in human bone and their roles in differentiation, growth, and remodeling have been previously investigated. Although the presence and function of the EP_2 receptor remains ambiguous, the clear significance of the EP_4 receptor in bone anabolism has been demonstrated through the extensive drug discovery work prosecuted on the target in the form of both systemic and locally-administered selective EP_4 agonists. Most initial osteoporosis programs focused on generating agonists with high systemic exposure and selectivity for EP_2/EP_4 versus EP_1 and EP_3. Substituted g-lactam (pyrrolidinone) derivatives that structurally mimic the carbocyclic prostaglandin scaffold were found to possess notable selectivity for EP_4 over the other EP receptor subtypes, especially EP_1. As the osteoporosis development programs were failing for safety reasons associated with their systemic exposures, attention shifted to localized delivery of anabolic agents to bone, resulting in the approval of the costly recombinant human bone morphogenetic protein 2 (BMP-2) for orthopedic indications. We have prepared and screened a novel potent series of g-lactam derivatives designed to maximize selectivity for EP_4 versus EP_1, EP_3, and other prostanoid receptors and to minimize systemic exposure through localized administration to bone in suitable delivery matrices and rapid metabolic elimination. These compounds were first tested for cellular activity by measuring cAMP formation following treatment of EP_4 transfected cells and by measuring SEAP formation following treatment of EP_2 transfected cells. Compounds of interest were then tested for their ability to stimulate osteoblastic differentiation of primary rat bone marrow cells.

***Disclosures: Stephen Barrett**, None.*
This study received funding from: Cayman Chemical Company, Inc.

SU0240

Osteoanabolic Effect of Alendronate and Zoledronate on Bone Marrow Stromal Cells (BMSCs) Isolated from Senile Osteoporotic Patients and its Implications for their Mode of Action in the Treatment of Age-related Bone Loss. Richard Lindtner[1], André Tiaden[2], Konstantin Genelin[1], Hannes Ebner[1], Claudia Manzl[1], Marina Klawitter[2], Ingrid Sitte[1], Brigitte von Rechenberg[2], Michael Blauth[1], Peter Richards*[3]. [1]Innsbruck Medical University, Austria, [2]Zurich University, Switzerland, [3]CABMM, Zurich University, Switzerland

The primary purpose of this study was to evaluate the osteogenic potential of human bone marrow stromal cells (hBMSCs) isolated from aged osteoporotic patients following *in vitro* and/or *in vivo* exposure to aminobisphosphonates.

The influence of aminobisphosphonate treatment on hBMSC osteogenesis was assessed by the quantitative measurement of alkaline phosphatase (ALP) activity and qRT-PCR analysis of known osteogenic markers. Mineralized matrix formation by hBMSC-derived osteoblasts was visualized and quantified using Alizarin red staining.

No significant changes in cell viability or proliferation were observed in hBMSC cultures treated for up to 72 hours with zoledronate (10 and 100 nM) as assessed by the Annexin V and WST-1 assays respectively. Human BMSC cultures treated with osteogenic medium supplemented with zoledronate demonstrated a significant increase in Alizarin red staining after 3 weeks as compared to cells cultured in osteogenic medium alone. Similarly, cultures of differentiating hBMSCs isolated from patients receiving alendronate treatment also demonstrated an increased propensity for osteoblastogenesis, even in the absence of further *in vitro* stimulation by zoledronate. The stimulatory effects of aminobisphosphonate treatment on hBMSC osteogenic potential were independent of any alterations in ALP activity, although significant changes in the mRNA expression levels of osteocalcin and osteopontin were evident in hBMSCs following either *in vitro* or *in vivo* exposure to aminobisphosphonates.

The results presented here demonstrate for the first time that aminobisphosphonate treatment of osteoporotic hBMSCs *in vitro* or *in vivo* enhances their capacity for osteoblast formation and subsequent mineral deposition, thus supporting the concept of aminobisphosphonates as having an osteoanabolic effect in senile osteoporosis.

Keywords: Osteoporosis, Aminobisphosphonate, Bone marrow stromal cell, Osteogenic differentiation, mineralization.

***Disclosures: Peter Richards**, None.*

SU0241

P2X7 receptors – do they have a role in commitment of mesenchymal stem cells?. Solveig Petersen*[1], Susanne Syberg[2], Peter Schwarz[2], Niklas Jorgensen[3]. [1]Research Center for Ageing & Osteoporosis, Departments of Diagnostics & Medicine, Glostrup Hospital, Denmark, [2]Glostrup Hospital, Denmark, [3]Copenhagen University Hospital Glostrup, Denmark

The purinergic P2X7 receptor is an ATP-gated ion-channel that is primarily expressed in cells of hematopoietic origin such as osteoclasts and macrophages. It is also expressed in mature osteoblasts and is involved in the regulation of bone metabolism. We have previously reported that P2X7 null mice have increased body weight and that expression of markers of bone- and fat metabolism are altered in bone marrow isolated from P2X7-null mice compared to wild type mice. However, no reports have demonstrated the role of the P2X7 receptor in the determination of phenotype of adult mesenchymal stem cells, nor the role of the receptor in regulation of fat metabolism. The aim of this study was therefore to demonstrate the expression of P2X7 receptors in fat cells and to determine the role of the receptor in the differentiation of adipocytes versus osteoblasts.

White and brown fat tissue was isolated from wild type BALB/cJ mice. Expression of RNA coding for the P2X7 receptor was determined using reverse-transcriptase polymerase chain reaction (RT-PCR). P2X7 receptor protein expression was determined by Western Blotting and immune-staining. Mesenchymal stem cell differentiation into osteoblasts and adipocytes was determined using real-time PCR determination of expression of RUNX-2 and PPAR-gamma genes and by staining with and Oil-Red O and Alizarin Red , respectively.

RT-PCR made on RNA isolated from white and brown fat tissue from the mice showed expression of P2X7 receptors in white fat tissue from both intestinal and subcutaneous fat, while brown fat only expressed low levels of P2X7 receptors. When determining expression of the P2X7 receptor protein a similar picture was found. – white fat from both the intestinal and subsutaneous compartments expressed high levels of P2X7 receptor protein while brown fat only expressed very small amounts of receptor protein. Experiments determining the role of P2X7 receptors in commitment of bone marrow-derived mesenchymal cells into either adipoctyes or osteoblasts are currently ongoing.

In conclusion, P2X7 receptors are expressed in high amounts in white fat tissue while only small amounts are expressed in brown fat. P2X7 receptors might play an important role in determining the fate of mesenchymal stem cells and in the regulation of fat and energy metabolism.

***Disclosures: Solveig Petersen**, None.*

SU0242

Pulsed Electromagnetic Field Stimulates Human Osteoblastic Cells and Inhibits Human Osteoclastic Cells. Nicola Partridge*, Zhiming He. New York University College of Dentistry, USA

The beneficial therapeutic effects of low energy, time varying pulsed electromagnetic fields (PEMFs) have been widely documented to treat therapeutically resistant problems of the musculoskeletal system, though its mechanisms remain unclear. Our previous work has shown the PEMF (by Orthofix, Inc.) effects on stimulating both cell proliferation and early differentiation in rat calvarial osteoblastic (OB) cells. Here we have studied the effects of PEMF (by Orthofix, Inc.) on human bone marrow stromal cells (hBMSCs) differentiated to OB cells and human bone marrow monocytic cells (hBMMs) differentiated to osteoclasts (OCs) as well as some of the mechanisms of action of PEMF. Fresh hBM samples were obtained from the iliac crest of females (27-65 years old). Purified mononuclear cells were used to acquire stromal and non-adherent monocytic cells. Both types of cells were treated with/without 4h daily PEMF exposure. PEMF significantly stimulated proliferation of pre-OBs from young women. ERK/MAPK activation was seen after 30-60 min of PEMF exposure on day 5 of culture (paralleled by stimulation of cyclin A). PEMF stimulated early gene expression and mineralization of BMSCs from young women, but less so for a postmenopausal woman. Gene expression analysis of PEMF vs. control with hBMSCs of the 27 year old woman using Affymetrix GeneChip Arrays (HG-U133 P2) showed 37 and 173 known genes with at least 1.5 fold changes were regulated by PEMF in the differentiation and mineralization stages, respectively. Gene ontology analysis showed that differentially expressed genes were mainly involved in transcription, cell cycle, transport, signal transduction, metabolic processes, growth factors, etc. In contrast, PEMF had striking inhibitory effects on OCs from cells of older women (50-65%) which were greater than the inhibitory effects seen with cells from a younger woman (22%). In all cases, there was a significant inhibition of OCs formed. This was paralleled by OC gene marker results. In conclusion, PEMF stimulates proliferation, ERK activation and early gene expression and mineralization of human pre-OBs from BMSCs of young women and microarray analysis shows a pattern of PEMF-regulated gene expression. PEMF inhibits human female OC formation at all ages, with greatest effects on cells from older subjects. Thus, PEMF may be very effective for bone mass maintenance for potential reduction in adjacent vertebral compression fractures in spinal fusions.

***Disclosures: Nicola Partridge**, Orthofix, Inc., 2; Orthofix, Inc., 6*
This study received funding from: Orthofix, Inc.

SU0243

The Nuclear Envelope Protein Emerin Regulates Mesenchymal Stem Cell Differentiation. Sandra Bermeo*[1], Christopher Vidal[1], Wei Li[2], Gustavo Duque[3]. [1]University of Sydney, Australia, [2]University of Sydney, Nepean Clinical School, Australia, [3]Ageing Bone Research Program, University of Sydney, Australia

Emerin is a nuclear envelope protein required for the regulation of diverse nuclear functions including cell differentiation and protein translocation. We have previously reported that other proteins of the nuclear envelope, such as lamin A and MAN1, play an essential role in mesenchymal stem cell (MSC) differentiation and thus in the pathophysiology of age-related bone loss and osteoporosis. However, the role of emerin in MSC differentiation remains unknown. Since the proteins of the nuclear envelope are in constant interaction, and since emerin has shown to be an important regulator of β-catenin trafficking in other cell models, we therefore hypothesized that emerin is also required in MSC differentiation. Human MSC (Lonza, Switzerland) were induced to differentiate into either osteoblasts or adipocytes. Emerin gene was knocked down using 20nM of siRNA Emerin (Santacruz), with transfections performed at day 1, 3 and 6 of differentiation. Transfection efficiency showed an emerin gene expression of 20% at days 3, 6 and 9 of differentiation. Osteogenesis was decreased as demonstrated by significantly reduced alkaline phosphatase and alizarin red staining and quantification when compared with control siRNA-transfected cells ($p<0.01$). Additionally, osteogenic markers evaluated by RT-PCR showed down regulation of alkaline phosphatase and osteoprotegerin gene expression. In addition, confocal microscopy identified alterations in the expression and localization of lamin A, MAN1 and β-catenin together with changes in the nuclear shape and actin fibers disposition in emerin siRNA-transfected MSC. On the other hand, adipogenesis was significantly increased as a result of the lack of emerin expression as demonstrated by a significantly higher number of adipocytes ($p<0.01$), oil red O staining ($p<0.01$), and significantly lower expression of adipogenic genes ($p<0.01$) in emerin siRNA-treated cells. In summary, emerin is essential in MSC differentiation. Low levels of emerin expression affect the proper differentiation of MSC towards the osteogenic lineage, alter the interaction between the proteins of the nuclear envelope involved in osteogenesis, block osteogenic signals, and favor adipogenesis. We therefore conclude that emerin plays an important role in the pathophysiology of age-related bone loss and osteoporosis that deserves further investigation.

***Disclosures: Sandra Bermeo**, None.*

SU0244

Transcriptional control of bone and fat lineage determination by Zinc finger protein 521 (Zfp521). William Addison*[1], Martin Fu[1], Helen Yang[1], Zhao Lin[1], Francesca Gori[2], Roland Baron[3]. [1]Harvard Medical School & Harvard School of Dental Medicine, USA, [2]Harvard School of Dental Medicine, Massachusetts General Hospital, USA, [3]Harvard School of Medicine & of Dental Medicine, USA

Osteoblasts and adipocytes arise from a common mesenchymal precursor cell. The cell-fate decision of a mesenchymal precursor cell is under the influence of multiple molecular cues and signaling pathways that are integrated into the activation or repression of lineage-specific transcription factor expression and/or activity. Epigenetic events, characterized by histone modifications on chromatin, determine the transcriptional status of these lineage-specific master transcription factors. Little is known about the epigenetic regulatory mechanisms that repress transcription factors of alternate lineages during differentiation. In this study, we examined the role of Zfp521, a regulator of lineage progression in multiple immature cell populations and a key promoter of osteoblastogenesis (Hesse et al., 2010; Kiviranta et al., 2013), on lineage specification in mesenchymal progenitor cells during BMP-induced differentiation. Knockdown of Zfp521 in stromal cells resulted in increased expression of the master adipocyte commitment and transcription factors, Zfp423 and PPARγ. This was associated with reduced Histone H3K9 methylation and increased H3K9 acetylation at their promoter regions, an epigenetic signature typical of transcriptionally active chromatin. This demonstrates that Zfp521 deletion led to derepression of transcriptional activity of these factors. Indeed, we found that Zfp521 occupies the promoter regions of both Zfp423 and PPARγ. Accordingly, conditional deletion of Zfp521 in mesenchymal precursors inhibited heterotopic bone formation in response to calvarial injection of BMP2 *in vivo*. Interestingly, marrow adiposity, Zfp423 and PPARγ expression within BMP2-induced bone was markedly increased in Zfp521 deficient mice suggesting that precursor cells lacking Zfp521 differentiate preferentially into adipocytes instead of osteoblasts. Consistent with a cell-autonomous role of Zfp521 in mesenchymal precursors, deletion of Zfp521 in stromal cells prevented BMP2-induced osteoblast-marker expression and simultaneously enhanced the expression of adipocyte-related genes and lipid droplet accumulation. Taken together, the data suggests that Zfp521 is a critical cell-fate switch that favors osteoblast differentiation and inhibits adipocyte commitment. We propose that Zfp521 is important for the epigenetic maintenance of transcriptional silencing of adipocyte lineage factors in mesenchymal precursors in an undifferentiated state or during osteoblastogenesis.

***Disclosures: William Addison**, None.*

SU0245

Up-regulation of Inhibitors of DNA Binding/differentiation Gene During Alendronate-Induced Osteoblast Differentiation. Min Hyung Jung[1], Hoon Choi*[2], Heung Yeol Kim[3]. [1]School of Medicine, Kyung Hee University, Kyung Hee Medical Center, South Korea, [2]Inje University Sanggyepaik Hospital, South Korea, [3]Department of Obstetrics & Gynecology, College of Medicine, Kosin University, South Korea

Purpose: To investigate the effect of alendronate on the expression of Id genes in osteoblast differentiation.

Methods: C2C12 cells were treated with alendronate for various concentrations and time periods. For evaluation of alendronate-induced osteoblast differentiation in C2C12 cells, alkaline phosphatase (ALP) activity was measured. The expression of osteoblast differentiation markers such as ALP, type-1 collagen (Col 1), and osteocalcin (OCN), and the expression of Id-1 and Id-2 were measured by RT-PCR. In order to understand the mechanism underlying the regulation of Id genes, the promoter region of the Id-1 gene was identified. Database analysis of the promoter region for Id-1 using known consensus sequences identified several putative response elements, including CCAAT/enhancer-binding protein beta (C/EBPβ).

Results: Alendronate treatment significantly increased not only ALP activity but also the expression of ALP, Col 1, and OCN, Id-1 and Id-2. C/EBPβ and alendronate cooperatively increased the promoter activity and expression of Id-1.

CONCLUSIONS: These results suggest that C/EBPβ-mediated Id-1 transcriptional activation may regulate alendronate-induced osteoblast differentiation of C2C12 cells.

***Disclosures: Hoon Choi**, None.*

SU0246

Using mouse embryonic and human induced pluripotent cells, differentiated into osteoblasts, to identify genes critical for osteoblastogenesis to pave ways for future genetic engineering. Pablo Roman-Garcia*, Linda Raphel, Vijay Yadav. Systems Biology of Bone, Wellcome Trust Sanger Institute, United Kingdom

With the advancements in gene targeting in mouse embryonic and human induced pluripotent stem cells (ES and HiPS), gene-deficient cells can be generated and the potential of stem cells lacking a specific gene to form osteoblasts can be investigated. However, protocols for differentiation of ES and HiPS cells into osteoblasts and the

underlying mechanisms remain unclear. The aim of this study was to set up a reliable osteogenic differentiation protocol and investigate gene expression changes through RNA sequencing during the differentiation of pluripotent stem cells into mature osteoblasts. It is well established that retinoic acid reduces mesodermal differentiation but enhances expression of markers of neural crest. Substitution, in the differentiation protocol, of the adipogenic factors with BMP4 results in the development of a mature osteogenic phenotype.

To achieve differentiation of ES or HiPS into osteoblasts cells were cultured in a non-differentiating medium to form embryoid bodies (EBs) and treated with retinoic acid for 48hrs and then plated on to gelatin and supplemented with BMP4 and TGFβ to form osteogenic media. The EBs were harvested at different days post addition of osteogenic media and qRT-PCR, alkaline phosphatase (ALP) activity and alizarin red staining were used to test their differentiation status compared to primary osteoblasts

Gene expression analysis of osteoblastic markers such as *Runx2 and Osteocalcin*, showed that the stem cells were successfully differentiated into mature osteoblasts, and were able to mineralize the matrix; on the other hand the stem cell markers were undetectable. In addition, ALP activity assay showed a 3.5-fold increase during differentiation from day 0 to day 20. Analysis of transcriptome trough Illumina RNA-sequencing revealed 765 differentially expressed genes; of them, 520 were up-regulated, and 245 were down-regulated. Gene interaction network analysis and gene set enrichment analysis on the differentiated cells' transcriptome showed that the secretory pathway(s) were amongst the most highly perturbed pathways.

Together, we have established a reproducible protocol to differentiate ES and HiPS cells into mature osteoblasts, and identified genome wide expression changes that define mouse and human osteoblasts. Currently efforts are underway to genetically target HiPS cells to pave a way in future for patient-specific generation of osteoblasts to investigate the underlying pathophysiological changes.

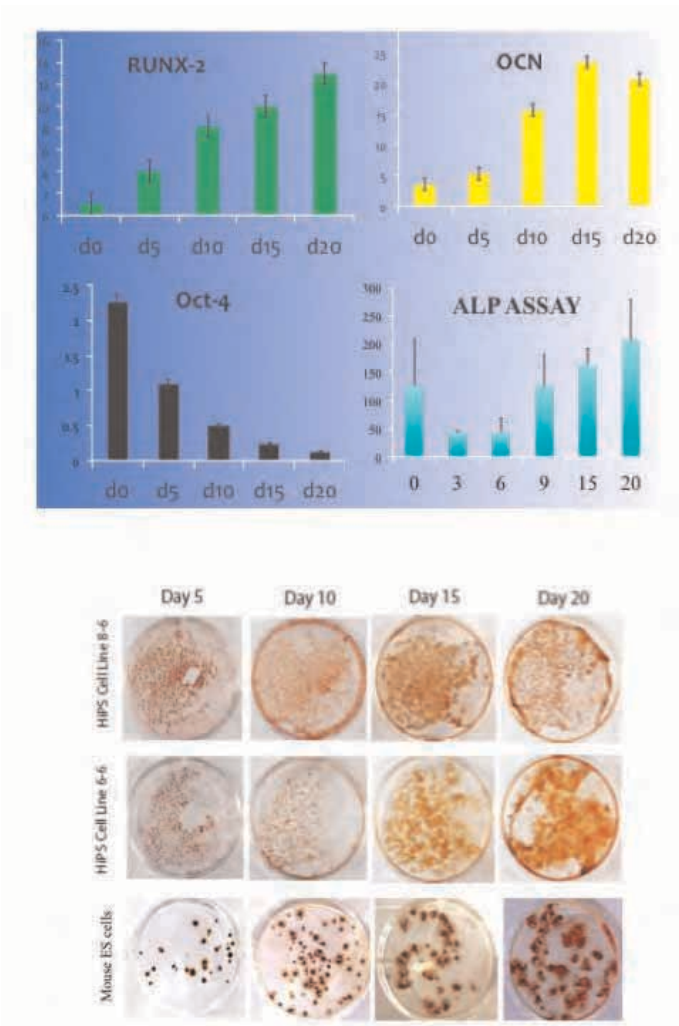

Gene expression, ALP activty and alizarin red staining

***Disclosures: Pablo Roman-Garcia**, None.*

SU0247

Consequences of calcification, ageing and deglycosylation on collagen fiber degradation by cathepsin cysteine proteases. PREETY PANWAR*. University of British Columbia, Canada

Introduction: Collagens are the crucial elements of the extra cellular matrix and provide anchorage, support, and structure to tissues. Abnormal degradation of collagens by proteolytic enzymes contributes to a variety of processes, including osteoporosis and atherosclerosis. Cathepsin K (catK), a cysteine protease is of particular interest as this enzyme is critically involved in bone degradation and at the same time responsible for weakening of arteries. Interestingly, there is a strong correlation between osteoporosis, the loss of bone, and the formation of mineral deposits in arteries. The present study is aimed to explore the effect of calcification, ageing and deglycosylation of collagen fibers and their degradation by cathepsin cysteine proteases.

Methods: Different categories of collagen fibers (calcified, uncalcified, age-modified and deglycosylated) were incubated with cathepsins and the consequences on their structural integrity and mechanical functionality were analyzed by different biochemical methods, scanning electron microscopy and tensile strength measurements.Results: Our data revealed that calcification and deglycosylation of collagen fibers decrease their hydrolysis by catK as indicated by reduced levels of collagen a-chain fragments. However, age modification elevated collagen degradation. Deglycosylated fibers showed minimum degradation as GAGs are required for the generation of collagenolytically active catK/GAG complexes for the complete degradation of collagen fibers. Structural analysis showed that the shape of calcified collagen fibers remains intact for longer time during degradation. However, non-calcified and age-modified fibers were completely destroyed by cathepsin K before calcified and deglycosylated fibers. Besides their structural disintegration, a strong reduction in the tensile properties of calcified, deglycosylated and age-modified fibers was observed when compared with control fibers before and after catK treatment. In contrast to catK, other cysteine proteases such as cathepsins S, B, L, and V had little or no effect on non-calcified, calcified, deglycosylated and age-modified collagen fibers.

Conclusion: Calcification leads to a partial protection against catK activity but leads to an overall loss of mechanical stability. Age-associated modifications of collagen fibers result into an increased susceptibility towards catK mediated hydrolysis. Our data provide new insights in matrix degradation which participate in various (patho) physiological processes.

***Disclosures: PREETY PANWAR**, None.*

SU0248

Exosite inhibitors targeting the collagenase activity of cathepsin K . Dieter Bromme*. The University of British Columbia, Canada

Introduction: Cathepsin K (catK) is the major collagen-degrading protease in osteoclasts. Several catK inhibitors are presently in clinical trials for osteoporosis. However, some drug candidates failed due to adverse effects. This may be caused less by off-target effects but rather by the inhibition of non-skeletal functions of the protease. Thus, the selective inhibition of the collagenolytic activity of catK without blocking its non-collagenolytic activities would be a desirable feature of novel inhibitors. The collagenase activity of cathepsin K depends on the formation of oligomeric complexes with glycosaminoglycans and the inhibition of this complex formation by exosite inhibitors would lead to the selective inhibition of the collagenase activity. Using specific assays discriminating between the inhibition of catK complex formation and the inhibition of its active site allowed us to identify selective anti-collagenase inhibitors of catK.

*Methods:*A flurorometric polarization assay was developed to screen for anti-complex formation inhibitors of catK. Fluorogenic peptide substrate assays were used to exclude inhibitors affecting the active site of the protease and a collagen-degradation assay to demonstrate the anti-collagenase activities of these inhibitors. AFM and SEM were used to demonstrate the interference of these inhibitors with complex formation and the selective inhibition of collagen fiber degradation.

Results: We have screened a 1700-member drug library and have identified several selective anti-collagenolytic compounds. Of particular interest are polyaromatic compounds, which included flavonoid, terpenoid, and SERM-like molecules. IC50 values for complex formation inhibitors were between 0.7-80 μM in the collagenase assay. For comparison, the active site inhibitor, odanacatib, revealed an IC50 of 0.4μM. Molecular docking suggests the binding of these inhibitors either at protein-protein or protein-glycosaminoglycan interaction sites. AFM studies revealed the prevention of ring-like catK complexes associated with its collagenase activity by these inhibitors and the inhibition of fibrillar collagen fiber degradation. These compounds were also effective in bone resorption assays.

Conclusion: We identified a novel class of catK inhibitors that specifically targets the collagenase activity of the protease. These inhibitors may overcome intrinsic off-substrate effects of active site-directed inhibitors presently in development.

***Disclosures: Dieter Bromme**, None.*

SU0249

Subcellular calcium-calpain signaling regulates uropod retraction, but not lamellipod outgrowth in migrating osteoclasts. Benjamin Wheal*[1], Natsuko Tanabe[2], S. Jeffrey Dixon[1], Stephen Sims[1]. [1]The University of Western Ontario, Canada, [2]Nihon University School of Dentistry, Japan

Osteoclasts are large multinucleated cells responsible for the resorption of bone and other mineralized tissues during development, physiological remodeling and pathological bone loss. Osteoclasts have the unique ability to resorb substrate while concurrently migrating. However the subcellular processes underlying osteoclast migration are not well understood. It has been proposed that, in other cell types, cytosolic free Ca^{2+} concentration ($[Ca^{2+}]_i$) regulates cell protrusion as well as retraction. Integration of these distinct events would require precise spatiotemporal patterning of subcellular Ca^{2+}. The large size of osteoclasts offers a unique opportunity to monitor patterns of Ca^{2+} during migration. Our purpose was to characterize spatiotemporal changes in cytosolic calcium of osteoclasts and examine the role for calcium in regulating cell motility. We used ratiometric imaging to map $[Ca^{2+}]_i$ within authentic rat osteoclasts. Migration was characterized by lamellipodial outgrowth at the leading edge along with intermittent retraction of the uropod at the rear. Migrating osteoclasts displayed elevation of $[Ca^{2+}]_i$ in the uropod, preceding retraction. Dissipation of this $[Ca^{2+}]_i$ gradient by loading osteoclasts with the Ca^{2+} chelator BAPTA abolished uropod retraction. In contrast, elevation of $[Ca^{2+}]_i$ using the Ca^{2+} ionophore, ionomycin, initiated prompt uropod retraction. To investigate downstream effectors, we treated cells with calpain inhibitor-1, which impaired uropod retraction. Furthermore, direct application of ionomycin to calpain inhibitor-1-treated cells failed to induce prompt uropod retraction, implicating calpain acts downstream of Ca^{2+}. However, lamellipodial outgrowth at the leading edge of osteoclasts was unaffected by any of these interventions, indicating that the signals regulating outgrowth are distinct from those triggering retraction. The large size of mature, multinucleated osteoclasts allowed us to discern a novel spatiotemporal pattern of Ca^{2+} involved in cell migration. Whereas localized elevation of Ca^{2+} is necessary for uropod retraction, lamellipod outgrowth is independent of Ca^{2+} – a heretofore unrecognized degree of specificity underlying the regulation of osteoclast migration.

***Disclosures: Benjamin Wheal**, None.*

SU0250

Downstream Effects of BMP Signaling in Osteoclasts: BMPs Induce MKP1 Activity and NFATc1 Nuclear Localization. Broege Aaron*, Raphael Huntley, Zainah Shaker, Eric Jensen, Kim Mansky, Raj Gopalakrishnan. University of Minnesota, USA

Osteoclasts are multinucleated cells responsible for resorbing damaged bone during the process of bone remodeling. Receptor activator of NF-kB ligand (RANKL) is the primary cytokine responsible for differentiating cells of the monocyte-macrophage lineage into mature, multinucleated osteoclasts. Numerous other factors can also modulate osteoclast differentiation. Our lab has previously shown BMPs to enhance RANKL-mediated osteoclast differentiation. Furthermore, we have shown that the intracellular signaling events during osteoclastogenesis in response to BMPs are complex – BMPs signal through MAPKs in pre-fusion osteoclasts and switch to canonical signaling around fusion. Our focus is now to elucidate the mechanism by which BMPs direct osteoclast differentiation as well as how BMP signaling shifts from non-canonical to canonical signaling during differentiation. In this study we explore two downstream intracellular effects of BMPs: 1) modulation of MAPK signaling; and 2) regulation of NFATc1 localization. By quantitative RT-PCR analysis we show that BMP2 represses the expression of MAPK Phosphatase-1 (MKP1) early in differentiation. In addition, we have found that in osteoclasts that have been starved for 4 hours, stimulation with BMP2 induces phosphorylation of MKP-1, suggesting that BMPs are also able to affect activation of MKP-1 in osteoclasts. Regulating MKP expression at the transcriptional and protein activity level are two ways through which BMP may modulate MAPK signaling within the cell. We also explored regulation of NFATc1, a transcription factor required for osteoclast differentiation, by BMP2 treatment in osteoclasts. Treatment with BMP2 throughout differentiation leads to an increase in nuclear localization of NFATc1 as assessed by western blot. We are currently investigating the mechanism by which BMP signaling affects NFATc1 localization in osteoclasts. This study expands our understanding of how BMP signals affect osteoclast differentiation.

***Disclosures: Broege Aaron**, None.*

SU0251

Leptin increases polyethylene particle-induced osteolysis in *oblob* mice. Kenneth Philbrick*, Carmen Wong, Russell Turner, Urszula Iwaniec. Oregon State University, USA

Particles generated from wear of prosthesis joint bearing surfaces induce inflammation and promote pathological periprosthetic osteoclast-mediated bone resorption (osteolysis). Obesity increases the risk of prosthesis failure. However, despite being morbidly obese, leptin-deficient *oblob* mice are resistant to osteolysis. We therefore investigated if leptin treatment increases osteolysis in *oblob* mice. 6-week-old *oblob* mice were randomized into 3 treatment groups: 1) no-treatment (N=8), 2) particles (N=8), and 3) particles+leptin (N=6). 2.5 mg of polyethylene particles were suspended in 95% ethanol and implanted over the calvarial periosteum to induce osteolysis. An additional control consisted of wild type (WT) mice treated with particles (N=8). Osmotic pumps delivering leptin (6 µg/d) were implanted subcutaneously in the leptin-treated mice. All mice were sacrificed 2 weeks after surgery. Body composition was assessed by DXA. Calvarial bone volume was quantified by µCT and osteolysis scored blinded from 0 (no osteolysis) to 4 (severe osteolysis). Leptin-treated *oblob* mice weighted slightly less at sacrifice than particle-treated *oblob* mice (P=0.011, Table). Blood leptin at sacrifice in leptin-treated *oblob* mice was only slightly less than in particle-treated WT mice (P=0.032, Table). As expected, calvaria from WT mice treated with particles had a greater osteolytic score (P=0.044) and lower bone volume (P=0.004) than *oblob* mice treated with particles (Table & Figure). Calvaria from *oblob* mice treated with particles+leptin exhibited a greater osteolytic score (P=0.033) and lower bone volume (P=0.035) than particle-treated *oblob* mice (Table & Figure). These findings provide evidence that leptin acts to increase particle-induced osteolysis in *oblob* mice. Ongoing studies are directed toward determining the respective role of leptin in promoting osteoclast recruitment, differentiation, and function during particle-induced osteolysis.

Table: Body weight, blood leptin, osteolysis score, and calvarial bone volume (BV) from ob/ob mice, particle-treated ob/ob mice, particle+leptin treated ob/ob mice, and particle-treated WT mice. Data ± SE.

	ob/ob	ob/ob (particles)	ob/ob (particles+leptin)	WT (particles)
N	8	8	6	8
Body Weight (g)	28 ± 1	27 ± 1	25 ± 0	18 ± 1
Blood Leptin (ng/mL)	0.0 ± 0.0	0.0 ± 0.0	10.0 ± 1.5	14.5 ± 1.0
Osteolysis Score (0 – 4)	0.0 ± 0.0	1.2 ± 0.2	2.2 ± 0.4	2.0 ± 0.5
Calvarial BV (mm³)	2.9 ± 0.1	2.9 ± 0.1	2.8 ± 0.1	2.4 ± 0.2

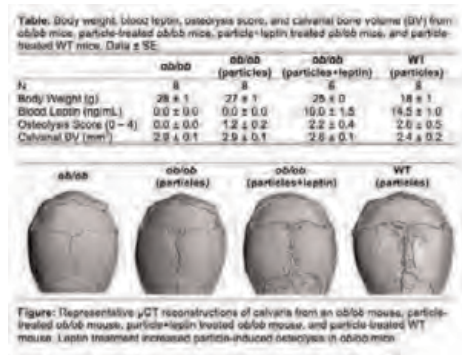

Figure: Representative µCT reconstructions of calvaria from an ob/ob mouse, particle-treated ob/ob mouse, particle+leptin treated ob/ob mouse, and particle treated WT mouse. Leptin treatment increased particle-induced osteolysis in ob/ob mice.

Table and Figure

***Disclosures: Kenneth Philbrick**, None.*

SU0252

BMP-Binding is Essential for Inhibitory Effect of Twisted Gastrulation on Osteoclast Differentiation. Raphael Huntley*, Raj Gopalakrishnan, Charles Billington, Lan Pham, Eric Jensen, Aaron Broege, Anna Petryk, Kim Mansky. University of Minnesota, USA

Twisted gastrulation (TWSG1), a secreted glycoprotein, is an extracellular regulator of bone morphogenetic protein (BMP) signaling. We have previously shown that *Twsg1-/-* mice are osteopenic because of enhanced osteoclastogenesis and bone resorption mediated through increased BMP signaling. We also showed that BMP2 can directly enhance RANKL-mediated differentiation and increase phosphorylated Smad1/5/8 (P-SMAD) levels in wildtype osteoclast cultures. In this study we investigated the functional significance of three previously identified sites that mediate BMP binding (two glycosylation sites within exon 4 [QQ], and a conserved tryptophan residue in the N-terminus [W66]) in the inhibition of BMP signaling and osteoclastogenesis. Adenoviral vectors overexpressing wildtype or mutant TWSG1 ($TWSG1^{QQ}$ and $TWSG^{W66}$) were generated. Overexpressing WT TWSG1 in bone marrow derived osteoclasts decreased their size and number compared to cultures infected with control adenoviral vector. On the other hand, differentiation of cultures overexpressing either $TWSG1^{QQ}$ or $TWSG1^{W66}$ mutants was not inhibited. WT TWSG1 decreased the level of P-SMAD whereas $TWSG1^{QQ}$ and $TWSG1^{W66}$ mutants did not. Interestingly, unlike WT TWSG1, which reversed the enlarged osteoclast phenotype of *Twsg1*$^{-/-}$ osteoclasts, *Twsg1*$^{-/-}$ cultures expressing $TWSG1^{QQ}$ and $TWSG1^{W66}$ mutants were further increased in size compared to control adenovirus-infected cultures. In conclusion, our studies demonstrate that the ability of TWSG1 mutant proteins to inhibit osteoclast differentiation correlates with their ability to bind BMPs.

***Disclosures: Raphael Huntley**, None.*

SU0253

Caspase-2 as a Mediator of Osteoclast Apoptosis and Differentiation. Danielle Victor*[1], Brian Herman[2], Jean Jiang[3]. [1]University of Texas, USA, [2]UT HSC San Antonio, USA, [3]University of Texas Health Science Center at San Antonio, USA

Caspase-2 is a cysteine protease that is well known for its role as an upstream initiator of apoptosis. Loss of caspase-2 has been shown to have deleterious effects on bone of old mice (>24 mos). Namely, mice lacking caspase-2 (*Casp2*$^{-/-}$) exhibit decreased trabecular bone volume, increased levels of urinary deoxypyridinoline (a clinical marker for bone resorption), and, interestingly, increased numbers of osteoclasts compared to wild-type (WT) animals. Evidence points towards an osteoclast-based defect underlying the decreased bone density in *Casp2*$^{-/-}$ animals; however, the role of caspase-2 in osteoclasts has not yet been described. Here, we

show that caspase-2 is involved in both osteoclast apoptosis and differentiation. An immunoblot for osteoclasts treated with H_2O_2 (≥300 μM) for 6 hours shows an increase in cleaved caspase-2 relative to total caspase-2, indicating apoptosis initiation. Additionally, osteoclasts derived from *Casp2*$^{-/-}$ mice exhibit protection from apoptosis compared to cells from WT mice when treated with rotenone (≥1μM) and H_2O_2 (≥700μM). Furthermore, primary osteoclasts treated with the chemical inhibitor of caspase-2, zVDVAD, showed a decrease in spontaneous apoptosis after 24 hours compared to untreated controls, suggesting that loss of caspase-2 confers protection against apoptosis not only under conditions of oxidative stress, but also in natural cell death.Osteoclast differentiation is reliant on reactive oxygen species (ROS) in order to activate signaling pathways to promote osteoclast gene transcription. Because caspase-2, also, has a close relationship with ROS, it is possible that caspase-2 may be involved in osteoclast differentiation. In both RAW 264.7 and primary macrophages induced to differentiate into osteoclasts with sRANKL, caspase-2 protein levels decreased steadily during the differentiation process. Strikingly, caspase-2 levels were reduced more than 10-fold during late stage differentiation when mature osteoclasts appear in culture. Furthermore, primary cultures from *Casp2*$^{-/-}$ animals yielded more TRAP^{+} multi-nuclear cells then that of the WT, suggesting that loss of caspase-2 promotes increased osteoclastogenesis in accordance to what was seen in the bone phenotype of these animals. Together, these data suggest the involvement of caspase-2 in osteoclast apoptosis and a novel role as a mediator of osteoclastogenesis.

***Disclosures: Danielle Victor**, None.*

SU0254

Epigenetic regulation of osteoclastogenesis. Naohiro Izawa*[1], Takanori Fujita[2], Seitaro Nomura[2], Hiroyuki Aburatani[2], Sakae Tanaka[1]. [1]The University of Tokyo, Japan, [2]Genome Science Division, Research Center for Advanced Science & Technology, The University of Tokyo, Japan

Recent studies have uncovered that the epigenetic regulation, such as histone methylation and acetylation, plays a critical role in determining cell fate. Osteoclasts are terminally differentiated cells derived from monocyte/macrophage-lineage precursor cells, and receptor activator of nuclear factor kappa B ligand (RANKL) plays an essential role. Although several genes essential for osteoclast differentiation have been identified, its epigenetic regulatory process is barely understood. Using chromatin immunoprecipitation sequencing (ChIP-seq) analysis, we generated a genome-wide map of acetylated histone H3 Lysine 27 (H3K27ac) marks, which distinguish active enhancer regions, in murine bone marrow-derived macrophages treated with RANKL. We also performed formaldehyde-assisted isolation of regulatory elements sequencing (FAIRE-seq) analysis, which detects open chromatin conformations. In the enhancer regions of many osteoclast-specific genes, such as Acp5 (expressing TRAP) and Calcr (Calcitonin receptor), RANKL treatment markedly increased H3K27ac marks as the differentiation proceeded. On the other hand, H3K27ac marks were abundantly found in many genes associated with inflammatory/immune responses such as Cd28, Tlr8 (Toll-like receptor 8) and Ccr2 (C-C chemokine receptor type 2) before RANKL treatment, which rapidly decreased in response to RANKL. Peaks of H3K27ac and FAIRE were largely overlapped, confirming that enhancer binding regions exhibited an open chromatin conformation. Motif analysis of these regions identified some transcription factors such as PU.1, STAT and FOX, which are considered to play important roles in osteoclastogenesis. These results suggest that RANKL treatment dramatically changed the epigenetic landscapes in osteoclast precursors, particularly in genes implicated in inflammatory/immune responses and osteoclast differentiation.

***Disclosures: Naohiro Izawa**, None.*

SU0255

Metabolic Adaptation during Osteoclastogenesis. Yoriko Indo[1], Sunao Takeshita*[1], Hiroyuki Aburatani[2], Kyoji Ikeda[1]. [1]National Center for Geriatrics & Gerontology, Japan, [2]RCAST, Univ of Tokyo, Japan

The osteoclast is a giant cell that resorbs calcified matrix by secreting acids and collagenolytic enzymes. The molecular mechanisms underlying metabolic adaptation to the increased biomass and energetic demands of osteoclastic bone resorption remain elusive. In the present study we show that during osteoclastogenesis the expression of both Glut1 and glycolytic genes is increased, along with increases in lactate production and glucose consumption. The knockdown of HIF1α, as well as glucose deprivation, inhibits the bone-resorbing function of osteoclasts, with no inhibition on differentiation, and the suppression of resorbing function was associated with down-regulation of Glut1 and glycolytic gene expression. Furthermore, the expression of the glutamine transporter Slc1a5 and glutaminase 1 was increased early in differentiation, and a depletion of L-glutamine or pharmacological inhibition of the Slc1a5 transporter suppressed osteoclast differentiation and function. Inhibition of c-Myc function with a small molecule inhibitor JQ1 abrogated osteoclast differentiation and function, along with a suppression of Slc1a5 and glutaminase 1 gene expression. Thus, the uptake of glucose and glutamine and utilization of the carbon sources derived from them, coordinated by HIF1α and c-Myc, is essential for osteoclast development and bone-resorbing activity.

***Disclosures: Sunao Takeshita**, None.*

SU0256

Withdrawn

SU0257

Withdrawn

SU0258

The *rankl* knock-out medaka exhibits a defective phenotype of bone resorption following abnormal organogenesis together with a small number of osteoclasts regulated by RANKL-independent osteoclastogenesis. Masahiro Chatani*[1], Tomoko Ishikawa[2], Takeshi Todo[2], Akira Kudo[1]. [1]Tokyo Institute of Technology, Japan, [2]Graduate School of Medicine, Osaka University, Japan

Bones have a variety of shapes in the body for supporting various organs, mainly nerves and blood vessels. The bone shapes are regulated by osteoclasts that are bone resorptive cells. RANKL (Receptor Activator of Nuclear Factor Kappa-B Ligand) binds to RANK, the osteoclast cell-surface receptor, and functions as a key factor for osteoclast differentiation. The *rankl* knock-out mouse exhibits severe osteopetrosis, however, bone resorption may occur during endochondral ossification. Therefore, it is unclear how RANKL is involved in bone resorption in the early bone development.

We previously reported that osteoclasts are important for bone modeling including organogenesis in medaka and zebrafish (Chatani et al., 2011). Here, to study the function of RANKL, we established the *rankl* knock-out medaka by using the Tilling (Targeting Induced Local Lesions In Genomes) method. The mutant survives to adulthood and generates offspring. To study bone phenotypes, we performed the Alizarin Red staining. The pharyngeal bone that forms a spongy structure like trabecular bone to support teeth was disordered, which was caused by abnormal bone remodeling. In the vertebral bone, the diameters of neural and hemal canals became narrower. To investigate the resorptive cells, we generated a hybrid line showing an osteoclast-specific mutant (*TRAP*-GFP/*rankl* -/-). Interestingly, fewer osteoclasts were emerged in the developmental stages of spinal cord and blood vessels, followed by the abnormal organogenesis in the mutant. These results suggested that the disorder of bone resorption in the mutant is associated with osteoclasts generated from the RANKL-independent signaling.

***Disclosures: Masahiro Chatani**, None.*

SU0259

***Nrp2* Deficiency Leads to Trabecular Bone Loss and Is Accompanied by Enhanced Osteoclast and Reduced Osteoblast Numbers.** Lieve Verlinden*[1], Carsten Kriebitzsch[2], Ine Beullens[2], Geert Carmeliet[3], Annemieke Verstuyf[3]. [1]KULeuven, Belgium, [2]KU Leuven, Clinical & Experimental Endocrinology, Belgium, [3]Katholieke Universiteit Leuven, Belgium

Neuropilin 1 (Nrp1) and Nrp2 are transmembrane receptors that can bind class 3 semaphorins (Sema3A-G) in addition to VEGF family members to play important roles in axonal guidance, angiogenesis and immune responses. Moreover, recent evidence implicates Sema3A/Nrp1-mediated signaling in bone metabolism. However, to date the expression of Nrp2 in bone has not been investigated and a possible role for Nrp2 in bone homeostasis *in vivo* remains unexplored. Here we show that *Nrp2*, together with its possible coreceptors (Plexin A family members and Plexin D1) and class 3 semaphorin ligands, were expressed during *in vitro* osteogenic differentiation of bone marrow stromal cells. Moreover, Nrp2 transcript and protein levels were highly induced in hematopoietic bone marrow cell-derived osteoclast cultures. Osteoblastic as well as osteoclastic Nrp2 expression was confirmed by immunohistochemistry of the long bones of mice. Interestingly, *Nrp2* knockout mice displayed a low bone mass phenotype which was accompanied by a decreased osteoblast count and an increased number of osteoclasts. In accordance, coculture experiments of calvarial osteoblasts and hematopoietic cells derived from either *Nrp2* wildtype or knockout mice revealed an increased support of osteoclastogenesis by *Nrp2* deficient osteoblasts as well as an improved ability of *Nrp2* deficient hematopoietic cells to differentiate towards osteoclasts. Collectively, these data point to a physiological role for Nrp2 in bone homeostasis.

***Disclosures: Lieve Verlinden**, None.*

SU0260

An antibody targeting Siglec-15 decreases bone loss in OVX rats by reducing osteoclast activity and increasing bone formation. Anna Moraitis*, Émilie Turcotte, Dominique Bédard, Martine Pagé, Elisabeth Viau, Mauricio Lemus, Julie Laurin, Matthew Stuible, Mario Filion, Gilles Tremblay. Alethia Biotherapeutics, Canada

Siglec-15 has recently emerged as an osteoclast-specific receptor that could potentially be targeted therapeutically for treatment of bone loss. Antibodies targeting this receptor impair osteoclast differentiation, reduce secretion of TRAP5b and block osteoclast resorptive activity. The objective of this study was to determine the effect of an antibody targeting Siglec-15 in the rat ovariectomy (OVX) model.

Forty Sprague-Dawley rats were sham operated or ovariectomized and treated 12 weeks later with PBS (q28d), Siglec-15 antibody (25B2, 10 mg/kg, q28d) or zoledronic acid (ZOL, 0.1 mg/kg, single injection). After a twelve-week treatment, bones were analyzed by densitometry, microCT, histomorphometry, 3-point bending (femur) and axial compression (LV4) and serum was analyzed for TRAP5b and ALP levels.

As expected, bone mineral density (BMD) was reduced dramatically in the OVX-PBS group compared to the sham operated animals, while ZOL treatment increased BMD. Administration of 25B2 caused a significant increase in BMD at all sites. These changes were confirmed by microCT analyses, which showed significant increases in bone volume, trabecular (Tb) number and corresponding decreases in Tb separation compared to the control group. Correspondingly, improvements in bone strength in animals treated with the 25B2 antibody were observed by biomechanical analysis: maximum load, stiffness and energy-to-failure parameters were all increased. Examination of tibial sections showed that the number of osteoclasts was significantly increased by 25B2 treatment, but the TRAP-positive cells were smaller and more intensely stained. Serum TRAP5b was decreased in the 25B2 group consistent with a decrease in secretion of this enzyme by osteoclasts. Interestingly, the serum level and the histological staining of ALP were unchanged in the 25B2-treated animals. This contrasts with the effect of ZOL treatment, which caused a significant decrease in ALP staining. Dynamic histomorphometry analysis using dual-calcein labeling indicated that the endosteal mineral apposition rate was greater in the 25B2-treated group compared to both the vehicle and ZOL treated groups, suggesting stimulation of new bone formation by 25B2.

Taken together, our results reveal that targeting Siglec-15 with a monoclonal antibody in a pathologic bone loss model improves bone quality and strength, likely due to combined inhibition of osteoclast function and maintenance of osteoblast activity.

***Disclosures: Anna Moraitis**, Alethia Biotherapeutics, 3*
This study received funding from: Alethia Biotherapeutics

SU0261

Dual functions the role of Pax6 in the regulation of bone and glucose metabolism. Masahito Matsumoto*[1], Masakazu Kogawa[2], Koji Hisatake[3], Gerald Atkins[4], David Findlay[4], YUICHIRO ENOKI[5], Tsuyoshi Sato[5], Seiki Wada[6], Aya Fukuda[3], Shigehiro Katayama[7], Tetsuya Yoda[8], Tatsuo Suda[9], Yasushi Okazaki[10]. [1]Saitama Medical University, Japan, [2]Discipline of Orthopaedics & Trauma, The University of Adelaide, Australia, [3]Laboratory of Gene Regulation, Faculty of Medicine, University of Tsukuba, Japan, [4]University of Adelaide, Australia, [5]Saitama Medical University, Japan, [6]Musashifujisawa Central Clinic, Japan, [7]Department of Endocrinology & Diabetic Internal Medicine, Saitama Medical University, Japan, [8]Department of Oral & Maxillofacial Surgery, Saitama Medical University, Japan, [9]Research Center for Genomic Medicine Saitama Medical School, Japan, [10]Division of Functional Genomics & Systems Medicine, Research Center for Genomic Medicine, Saitama Medical University, Japan

Paired-box homeodomain transcription factor Pax6 is essential for normal development of eye and pancreatic endocrine cells producing hormones that affect muscle and liver, resulting in the maintenance of glucose homeostasis. However, little is known about the role of Pax6 in bone metabolism. Herein we show the Pax6 acts as an intrinsic negative regulator of RANKL-mediated osteoclast differentiation. Electrophoretic mobility shift and reporter assays found that Pax6 binds endogenously the proximal region of the *tartrate-acid phosphatase (TRAP)* gene promoter and suppresses NFATc1-induced *TRAP* gene expression. Introduction of Pax6 retrovirally into bone marrow macrophages (BMM) attenuates RANKL-induced osteoclast formation. Moreover, we found that the Groucho family member co-repressor Grg6 contributes to Pax6-mediated suppression of the *TRAP* gene expression induced by NFATc1. These results suggest that Pax6 interferes with RANKL-mediated osteoclast differentiation together with Grg6. Our results demonstrate that the Pax6 pathway constitutes a new aspect of the negative regulatory circuit of RANKL-RANK signaling in osteoclastogenesis and that the augmentation of Pax6 might therefore represent not only for a novel target to block pathological bone resorption but also for glucose metabolism by appropriate cell fate specification (Kanzawa Medical Research, the Kowa Life Science Foundation, the Life Science Foundations, Saitama Medical University internal research grant and Kawano Masanori Memorial Foundation for promotion of Pediatrics.)

***Disclosures: Masahito Matsumoto**, None.*

SU0262

Ectopic Expression of Human Leucine Rich Repeat Kinase 1 (hLRRK1) in *Lrrk1* Knockout Osteoclast Precursors Rescues the Bone Resorption Defect *in vitro* by Modulating C-Terminal Src Kinase (Csk) Activity. Weirong Xing*[1], Shaohong Cheng[2], Subburaman Mohan[3]. [1]Musculoskeletal Disease Center, Jerry L. Pettis Memorial Veteran's Admin., USA, [2]VA Loma Linda Health Care Systems, USA, [3]Jerry L. Pettis Memorial VA Medical Center, USA

We have recently shown knockout (KO) of *Lrrk1* in mice resulted in the highest observed body aBMD by DXA high-throughput screening (Z-score of 9.0 above the mean) of 3629 distinct gene KO lines. The osteopetrosis phenotype is much more severe in the *Lrrk1* KO mice than *Sost* or *c-Src* KO mice. Precursors derived from *Lrrk1* KO mice differentiate into multinucleated osteoclasts (OCs) in response to M-CSF/RANKL treatment, but fail to resorb bone due to defects in the formation of peripheral sealing zones and ruffled borders. The phosphorylation of c-Src at Tyr-527 is significantly elevated whereas at Tyr-416 is decreased in LRRK1 deficient OCs in response to MCSF/RANKL treatment. To determine if *hLrrk1* functions similar to mouse *Lrrk1* (*mLrrk1*), precursors-derived from *Lrrk1* KO mice were transduced with lentivirus containing either *hLrrk1* or GFP control and the transduced cells were then differentiated in the presence of MCSF/RANKL. Ectopic expression of full length hLRRK1 in *Lrrk1* null cells completely rescued OC resorptive functions *in vitro*. Although *Lrrk2*, a structural homolog of *Lrrk1*, is also expressed in macrophage lineage cells, there was no obvious skeletal phenotype in *Lrrk2* KO mice, suggesting that *Lrrk1* has a unique function in bone, and the distinguishing ankyrin (ANK) structure present in *Lrrk1* but not *Lrrk2* may determine its specific function. Sequence analyses found that hLRRK1 and mLRRK1 contain ANK repeats that are 34% identical to the ANK repeat consensus sequence. Because the predicted 3-D structure of hLRRK1 ANK contains functional motifs that have been implicated in protein-protein interactions and overexpression of ANK repeats containing protein ASPP2 in choriocarcinoma cells decreased pY416 c-Src activation, and this c-Src inactivation can be abolished by knocking down Csk expression, we hypothesize that the hLRRK1 ANK repeats may mediate hLRRK1 specific function through interacting with Csk in OCs. Accordingly, our computer-based analyses predict the residues of the inner helices andturns of ANK repeats 1-3 of hLRRK1 contact the SH2 domain (93-116) and the N-terminal of the Csk kinase domain (268-279). Immunoprecipitation studies using RANKL treated RAW264.7 cells that were transfected with pcDNA-Flag/hLrrk1 revealed that hLRRK1 interacted with Csk in OCs. In conclusion, our data indicate that hLRRK1 plays a critical role in regulating OC activity by suppressing Csk kinase activity, and could be a novel anti-resorptive drug target.

***Disclosures: Weirong Xing**, None.*

SU0263

Inhibition of osteoclastogenesis and inflammatory bone resorption by targeting bromodomain-containing chromatin regulators. Kyung-Hyun Park-Min*[1], Elisha Lim[1], Rab Prinjha[2], Lionel Ivashkiv[1]. [1]Hospital for Special Surgery, USA, [2]GlaxoSmithKline, United Kingdom

Although it was recently appreciated that RANKL-induced changes in the chromatin state of osteoclast precursor cells (OCPs) are important for osteoclast differentiation, the epigenetic mechanisms that regulate osteoclast function are not clear. In addition to enzymes that deposit and remove chromatin modifications, so-called "readers" directly bind to modified histones and recruit regulatory complexes to control gene expression. Among such readers, bromodomain (BRD)-containing proteins recognize acetylated lysine residues. Recently, small molecule inhibitors, named I-BET and JQ1, that suppress binding of the BET subfamily of BRD proteins to acetylated histones were described. BET inhibitors effectively suppress cancer growth in mouse models, but their effects on osteoclastogenesis and bone resorption have not been described. Here, we investigated the effects of the BET inhibitor I-BET on osteoclastogenesis, and on pathological bone resorption in vivo. Treatment of human blood-derived OCPs or mouse bone marrow-derived OCPs with I-BET strongly inhibited RANKL-induced osteoclastogenesis in a dose-dependent manner. These suppressive effects were mediated by inhibition of RANKL-induced expression of NFATc1, a master regulator of osteoclastogenesis. Furthermore, I-BET administration suppressed inflammatory arthritis and TNF-induced inflammatory osteoclastogenesis and bone resorption in vivo, demonstrating for the first time therapeutic efficacy of epigenetic drugs in suppressing pathological bone resorption. The mechanism of I-BET action was suppression of the expression and binding of MYC to the NFATc1 promoter, which resulted in decreased histone acetylation and expression of *NFATC1*. Experiments targeting MYC using pharmacological inhibitors or RNA interference (RNAi) established a role for RANKL-induced MYC in osteoclast differentiation. These data implicate MYC as an important factor in osteoclastogenesis and suggest targeting MYC as another therapeutic strategy to control bone resorption. Taken together, our findings provide insights into new transcriptional and epigenetic mechanisms that control osteoclastogenesis, and suggest that targeting of chromatin regulators such as BET proteins represents a promising new approach to treat pathological bone resorption.

***Disclosures: Kyung-Hyun Park-Min**, None.*

SU0264

Jaw Bone Marrow-Derived Osteoclast Precursors Internalize More Bisphosphonate than Long-Bone Marrow Precursors. Jenny Vermeer*[1], Ineke Jansen[2], Matangi Marthi[1], Fraser Coxon[3], Charles McKenna[4], Shuting Sun[4], Teun De Vries[5], Vincent Everts[6]. [1]Department of Oral Cell Biology & Functional Anatomy, Academic Centre for Dentistry Amsterdam (ACTA), University of Amsterdam & VU University Amsterdam, MOVE Research Institute Amsterdam, Netherlands, [2]Department of Periodontology, Academic Centre for Dentistry Amsterdam (ACTA), University of Amsterdam & VU University Amsterdam, MOVE Research Institute Amsterdam, Netherlands, [3]Musculoskeletal Programme, Division of Applied Medicine, Institute of Medical Sciences, University of Aberdeen, Foresterhill, Aberdeen, United Kingdom, [4]Department of Chemistry, University of Southern California, Los Angeles, CA, USA, [5]ACTA, University of Amsterdam & VU University, The Netherlands, [6]Department of Oral Cell BiologyAcademic Centre of Dentistry Amsterdam (ACTA), The Netherlands

Bisphosphonates (BPs) are widely used to treat several bone diseases, such as osteoporosis and cancers that have metastasized to bone. Due to their ability to potently inhibit osteoclastic bone resorption, they improve bone quality and reduce fracture risk. Osteonecrosis of the jaw (ONJ) has been reported in some patients receiving a high intravenous dose of certain BPs, but it is not clear why in particular jaw bone is affected. We hypothesized that BPs could have distinct effects on jaw and long-bone-marrow-derived osteoclasts and their precursors, for example as a result of differences in the ability to endocytose the drugs. To investigate this, jaw and long-bone marrow cells were isolated from mice and the cells were primed to differentiate into osteoclasts with the cytokines M-CSF and RANKL. Before fusion occurred, cells were incubated with fluorescein-risedronate (FAM-RIS) for 4 or 24 hours and uptake was determined by flow cytometry. We found that cultures obtained from the jaw internalized 1.7 to 2.5 times more FAM-RIS than long-bone cultures, both after 4 and 24 hours. Accordingly, more unprenylated Rap1a accumulated in jaw osteoclasts after treatment with BPs for 24 hours. Surprisingly, differences in BP uptake did not differentially affect osteoclastogenesis on plastic. On bone, however, 1 μM of BP significantly stimulated osteoclastogenesis of long-bone marrow precursors, but not of jaw bone marrow precursors. In conclusion, our findings are the first to demonstrate different responses of bone-site-specific osteoclast precursors to bisphosphonates. This study may help to improve the understanding of the association between BPs and osteonecrosis of the jaw.

***Disclosures: Jenny Vermeer**, None.*

SU0265

Long-chain Fatty Acid Analogues Inhibit Osteoclastogenesis. Jillian Cornish*, Jian-ming Lin, Karen Callon, Andrew Marshall, William Denny, Ian Reid, Andrew Grey. University of Auckland, New Zealand

Body weight, particularly fat mass, is positively correlated to bone mass. The relationship between fat and bone is mediated through skeletal loading, hormonal and neuronal pathways. Experiments showing that feeding acutely influences bone turnover, raising the possibility that ingested nutrients have direct bone effects and could function as an additional link between fat and bone. We recently reported long-chain, saturated fatty acids such as. palmitic acid (C18) inhibit osteoclastogenesis *in vitro* and G-protein coupled receptors (GPR) for fatty acids are expressed in bone cells.. It is likely this effect is mediated by binding of fatty acids to the cell surface receptor GPR120, with known GPR120 receptor agonist GW9508 also inhibiting osteoclastogenesis. We have also shown that the marrow stromal cell (Kusa4b 10) is a novel target of palmitic acid, possibly by signalling through GPR120 and GPR40/41. Therapeutic exploitation of these observations is complicated by the modest potency, rapid metabolism and relative insolubility of the natural long-chain fatty acids, which likely limit them reaching the bone environment in sufficient concentration for long enough to exert a substantial therapeutic effect *in vivo*. Thus in this study we explored two new classes of analogues and evaluated their activity in an *in vitro* osteoclastogenesis assay.

Two novel classes of palmitic acid analogues: 8 compounds modified by ether or 6 compounds by triazole units were constructed. They were prepared by condensation of alkyl halides and diols, followed by Jones oxidation; triazolyl acids by copper-catalysed click chemistry between the appropriately-protected azides and alkynes, followed by deprotection and oxidation. The analogue activity was assessed in primary murine bone marrow cultures and the most potent were compared in efficacy to palmitic acid, the GPR120 agonist GW9508, and OPG.

The findings of this study indicate the anti-osteoclastogenic activity of natural long-chain saturated fatty acids is changed very little by introduction of an ether moiety anywhere in the chain, but is improved markedly by the introduction of a more rigid triazole group, placed distant from the acid unit (most potent reduced osteoclastogenesis by 88% at 10 ug/mL).

In clinical practice, agents that decrease bone resorption by 50-80% are effective in reducing the risk of fragility fractures. Further characterization of the skeletal effects of these compounds is therefore justified.

***Disclosures: Jillian Cornish**, None.*

SU0266

Novel Human RANKL Inhibitors Targeting Its Trimerization. Vagelis Rinotas[1], Fotini Violitzi[1], Polyxeni Alexiou[2], Fotini Liepouri[3], Anna Maranti[3], Katerina Tsiliouka[3], Alexandros Strongilos[3], Thanos Papakyriakou[2], Christos Papaneophytou[4], George Kontopidis[4], Elias Couladouros[2], Elias Eliopoulos[2], Eleni Douni*[5]. [1]BSRC Alexander Fleming, Greece, [2]Agricultural University of Athens, Greece, [3]pro-ACTINA SA, Koropi Attikis, Greece, [4]Centre for Research & Technology-Thessaly, Greece, [5]Agricultural University of Athens/ BSRC Al. Fleming, Greece

Receptor activator of nuclear factor-κB ligand (RANKL), a trimeric tumor necrosis factor (TNF) superfamily member, is the central mediator of osteoclast formation and bone resorption. Functional mutations in RANKL lead to human autosomal recessive osteopetrosis (ARO), whereas RANKL overexpression has been implicated in the pathogenesis of bone degenerative diseases such as osteoporosis. Following a forward genetics approach using chemical random mutagenesis, we have recently shown that a novel loss-of-function allele of Rankl with a glycine-to-arginine mutation at codon 278 (G278R) at the extracellular inner hydrophobic F beta-strand of RANKL, causes severe recessive osteopetrosis in mice. RANKLG278R monomers fail to assemble into homotrimers, are unable to bind and activate the RANK receptor but interact with wild-type RANKL exerting a dominant-negative effect on its trimerization and function in vitro. Furthermore, as G278 is highly conserved within the TNF superfamily, we identified that similar substitutions in TNF and B-cell activating factor (BAFF) also impaired trimerization and binding to cognate receptors, resulting in loss of biological activity. Notably, SPD304, a small molecule inhibitor of TNF trimerization, also binds and inhibits RANKL, suggesting similar inhibitory mechanisms. Based on the trimeric structure of RANKL and its interaction with SPD304, novel small molecules were designed to abrogate trimer formation and biological function displaying higher specificity and less toxicity compared to SDP304. Of the 72 SPD304-like derivatives synthesized and tested, 13 displayed complete inhibition of human RANKL function in osteoclastogenesis assays with less cytotoxicity compared to SPD304 using MTT assays. Our results identified potent small molecule inhibitors of human RANKL designed to target and block its trimerization. The more effective inhibitors will be further evaluated in vivo using our unique human RANKL-expressing transgenic mouse models of osteoporosis.

***Disclosures: Eleni Douni**, None.*

SU0267

S1P-mediated Osteoclast Precursor Monocyte Migration Is a Critical Point of Control in Antibone-resorptive Action of Active Vitamin D. Junichi Kikuta*[1], Fumie Okiji[1], Mai Shirazaki[1], Sadaoki Sakai[2], Hitoshi Saito[2], Masaru Ishii[1]. [1]Department of Immunology & Cell Biology, Graduate School of Medicine & Frontier Biosciences, Osaka University, Japan, [2]Medical Affairs Division, Chugai Pharmaceutical Co., Ltd., Japan

Osteoclasts are bone-resorbing giant polykaryons that differentiate from mononuclear macrophage/monocyte-lineage hematopoietic precursors. The migratory mechanisms of osteoclast precursor monocytes in systemic circulation and homing into bone spaces are controlled by the blood-enriched lipid mediator sphingosine-1-phosphate (S1P) and have recently been shown to be critical points of control in osteoclastogenesis and bone homeostasis.

Active vitamin D analogs have been clinically used for bone and mineral disorders, although the actual pharmacological action in bone has remained elusive. Here, we showed the potential role of vitamin D signaling in the control of osteoclast precursor migration.

First, we examined the effects of the active form of vitamin D, calcitriol (1,25-D), and its clinically used active vitamin D analog,eldecalcitol (ELD), on the expression of several chemokine receptors in a monocytoid cell line, RAW264.7. Both 1,25-D and ELD significantly suppressed the expression of S1PR2, a chemo-repulsive receptor for blood S1P, in a dose-dependent manner, whereas the expression levels of other chemokine receptors were essentially unaltered. By using an *in vitro* chemotaxis assay, we also found that active vitamin D-treated RAW264.7 cells could more readily migrate to a high concentration of S1P, such as in the blood.

Next, we examined the *in vivo* effects of active vitamin D on mice. Oral treatment both with 1,25-D and ELD prevented ovariectomy-induced bone loss. Under this condition, the $CD11b^+$-circulating osteoclast precursor monocytes in mice treated with active vitamin D expressed lower levels of S1PR2 than cells that were subjected to the control conditions.

Finally, we examined the *in vivo* mobility of $CX_3CR1\text{-}EGFP^+$ osteoclast precursor monocytes in living bone tissues by using an intravital multiphoton microscopy. The mobility of the $CX_3CR1\text{-}EGFP^+$ monocytoid cells was significantly increased in mice treated with active vitamin D drugs such as 1,25-D and ELD, suggesting that *in vivo* treatment with active vitamin D action suppresses S1PR2 expression and the mobilization of osteoclast precursor monocytes from the bone to the blood circulation.

These findings demonstrate a novel mechanism of active vitamin D for controlling the migratory behavior of circulating osteoclast precursors, and this action should be conducive to limiting osteoclastic bone resorption in vivo, which is the main therapeutic effect of active vitamin D.

***Disclosures: Junichi Kikuta**, None.*

SU0268

An Osteoclast Transmembrane Protein-tyrosine Phosphatase, PTP-oc, Enhances Osteoclast Activity In Part Through Dephosphorylation of the EphA4 Receptor in Osteoclasts. Kin-Hing William Lau*[1], Virginia Stiffel[1], Matilda Sheng[2], Shin-Tai Chen[1], Mehran Amoui[1]. [1]Jerry L. Pettis Memorial VA Medical Center, USA, [2]Loma Linda University, USA

We have previously shown that an osteoclast (OCL)-specific protein-tyrosine phosphatase (PTP-oc) is a positive regulator of OCL activity, and its action is in part mediated via dephosphorylation of phosphotyrosine (pY)527 of Src and Src-dependent activation of several downstream pathways. However, our PTP-oc trapping mutant pull-down assay showed that EphA4 may also be a potential cellular substrate of PTP-oc. We have previously presented preliminary evidence that EphA4 is a negative regulator of OCL activity. In this study, we also showed that reintroduction of EphA4 in EphA4 KO OCLs with lenti-Epha4 led to formation of ~40% smaller resorption pits than those of control OCLs (0.29 ± 0.01 vs. 0.49 ± 0.1 cm^2, $p<0.05$). Thus, we sought to test the hypothesis that PTP-oc enhances OCL activity also through PTP-oc-mediated dephosphorylation and inactivation of EphA4. OCLs derived from PTP-oc transgenic mice reduced the overall pY-EphA4 level in OCL to <5% ($p<0.05$) compared with WT OCLs. There are 4 important pY residues (pY596, pY602, pY779, and pY928) in EphA4. Overexpression of PTP-oc in OCLs also reduced the pY602-EphA4 and the pY779-EphA4 level (normalized against total EphA4) to <5% ($p<0.05$ for each) of that in WT OCLs. Transduction of EphA4 KO OCLs with lenti-Y779F-Epha4 led to $318 \pm 14\%$ ($p<0.01$) increase in pY174-Vav3 (normalized against Vav3) (used as a surrogate indicator of OCL activity), whereas transduction with lenti-WT-Epha4 reduced the pY173-Vav3 by $48 \pm 11\%$ ($p<0.05$). Transduction with lenti-Y602F-Epha4 resulted in only a marginal increase ($158.1 \pm 10\%$, p=N.S.). Epha4 expression in OCLs yielded contrasting effects on the activation status of Rho vs. Rac, as deficient EphA4 expression in OCLs increased GTP-Rac (by ~2.5-fold, $p<0.05$) but reduced GTP-Rho (by~60%, $p<0.05$) without affecting total Rho or Rac levels. Overexpression of PTP-oc also resulted in higher levels of GTP-Rac (~300% of WT, $p<0.05$) but reduced levels of GTP-Rho (~50% of WT, $p<0.05$). The total Rho and Rac levels were also not different. The similarity between EphA4 KO and PTP-oc overexpression on the differential actions on Rho vs. Rac provides further support for the premise that PTP-oc enhances OCL activity may in part involve the relief of the suppressive action of EphA4 on OCL activity. In conclusion, PTP-oc acts not only through Src-dependent activation of the various stimulatory pathways of OCL activity but also via Src-independent mechanism to reduce the suppression action of EphA4.

***Disclosures: Kin-Hing William Lau**, None.*

SU0269

DOK3 negatively regulates RANKL-induced osteoclastogenesis. Mary Beth Humphrey*, Courtney Long. University of Oklahoma Health Sciences Center, USA

Osteoclasts are giant, multinucleated cells of myeloid lineage activated to resorb bone. Receptor activator of NF-kB ligand (RANKL) promotes osteoclast differentiation and function but requires costimulation of immunoreceptor tyrosine-based activation motif (ITAM)-coupled immunoreceptors. One such receptor is triggering receptor expressed on myeloid cells (TREM)-2 which is coupled to ITAM-adaptor protein DAP12 and mediates PI3K production and intracellular calcium release during osteoclastogenesis. We have recently shown that downstream of kinase-3 (DOK3) negatively regulates TREM2-DAP12 signaling and inflammatory cytokine production in response to TLR stimulation of macrophages. To test the hypothesis that DOK3 negatively regulates TREM2-DAP12 ITAM signaling in osteoclasts, we evaluated bone micro-architecture and histology of sex matched 16 week old control and DOK3-deficient (DOK3ko) mice. DOK3ko mice have significantly reduced trabecular bone mass at the tibia and femur whereas cortical bone is unchanged. Bone formation rates are similar between the groups. Pre-osteoclasts derived from DOK3ko mice exhibit increased sensitivity to 5-35ng/ml RANKL with significantly increased osteoclast numbers compared to control. DOK3ko osteoclasts have significantly increased resorption compared to controls. In response to TREM2 crosslinking but not RANKL stimulation, DOK3 becomes phosphorylated and associates with SHIP1. Further studies are underway to determine the effect of DOK3 on ITAM signaling in osteoclasts. In conclusion, our data supports an important role for DOK3 in the regulation of osteoclastogenesis in vivo and in vitro.

***Disclosures: Mary Beth Humphrey**, None.*

SU0270

Mice deficient in CD44 display reduced pro-MMP9 activation and membrane localization of MT1-MMP in osteoclasts. Meenakshi Chellaiah*. University of MarylandDental School, USA

CD44, MT1-MMP and MMP9 are implicated in osteoclast migration and bone resorption. This study was designed to determine the functional relationship between CD44 and MT1-MMP in the activation of pro-MMP9. We used osteoclasts isolated from wild-type and CD44-null mice. Results showed that MT1-MMP is present in multiple forms with a relative molecular mass of 63, 55, and 45kDa in the membrane of wild-type osteoclasts. CD44-null osteoclasts demonstrated a 55kDa-active MT1-MMP form in the membrane and conditioned medium. It failed to activate pro-MMP9 because TIMP2 binds and inhibits this MT1-MMP (~55kDa) in CD44-null osteoclasts. The role of MT1-MMP in the activation of pro-MMP9, CD44 expression and migration was confirmed in wild-type osteoclasts knockdown of MT1-MMP. Although, MMP9 knockdown suppressed osteoclast migration, it had no effects on MT1-MMP activity or CD44 expression. These results suggest that CD44 and MT1-MMP are directly or indirectly involved in the regulation of pro-MMP9 activation. Surface expression of CD44, membrane localization of MT1-MMP and activation of pro-MMP9 are the necessary sequence of events in osteoclast migration.

***Disclosures: Meenakshi Chellaiah**, None.*

SU0271

Myo9B, a Rho-GAP Protein Associated with Inflammatory Bowel Disease, is Critical for Osteoclast Function. Beth Lee*[1], Brooke McMichael[2]. [1]Department of Physiology & Cell Biology, Ohio State University, USA, [2]Ohio State University, USA

Inflammatory disorders of the gut, including the inflammatory bowel diseases (Crohn's disease and ulcerative colitis) and celiac disease are associated with high rates of osteoporosis and with growth retardation in juvenile patients. Nutritional deficit and inflammation, especially as mediated by TNFα, contribute to these conditions. Here we demonstrate that a recently described gene associated with these diseases, Myo9b, is highly expressed in osteoclasts and may contribute directly to intrinsic bone defects associated with these intestinal diseases. Myo9b is a myosin that contains a Rho inhibitory (Rho-GAP) domain and is highly expressed in hematopoietic cells of the monocyte lineage and in gut epithelia. Loss of Myo9b function in gut epithelia results in loss of tight junction integrity, a known contributor to inflammatory bowel disorders. In this study, the consequences of loss of Myo9b on osteoclast function were examined. Because of the well-established importance of Rho signaling to osteoclast cytoskeletal organization, it was predicted that loss of Myo9b, a Rho inhibitor, would enhance osteoclast function. Unexpectedly, knockdown of Myo9b resulted in a loss of osteoclast activity, including cell spreading, motility, and bone resorptive capacity. A dramatic loss of bone resorptive capacity was noted even though sealing zones appeared normal. These losses in function were reversible with addition of a Rho inhibitor. Further experimentation demonstrated that lack of resorptive function in cells with diminished Myo9b levels might be explained by poor stabilization of microtubules or by mislocalization of c-Src, a tyrosine kinase with critical effects on osteoclast actin cytoskeletal rearrangement and function. Importantly, treatment of Myo9b-suppressed osteoclasts with TNFα strongly reversed the osteoclast dysfunction, demonstrating the potential of this factor to activate what are otherwise defective osteoclasts. These results indicate that the RhoGAP activity of Myo9b plays a key role in regulating the actin-based structures necessary for osteoclast motility and resorption, and is suggestive that variants of Myo9b associated with inflammatory gut diseases may also play key roles in bone metabolism.

***Disclosures: Beth Lee**, None.*

SU0272

PDK1/Akt pathway in osteoclast signaling in Paget's disease of bone. Stephen McManus*, Gino Laberge, Martine Bisson, Sophie Roux. University of Sherbrooke, Canada

Introduction: In Paget's Disease of Bone (PDB), osteoclasts (Ocs) are increased in size and number, overactive, and resistant to apoptosis. All of the mutations identified to date in PDB are clustered either within or near the UBA domain of the signaling protein p62, indicating a critical importance of p62 in bone pathophysiology. In rodent and human osteoclasts, p62 is a major scaffold involved in the RANKL-induced signaling complex that includes TRAF6 and atypical PKCζ. We have previously shown that PDK1 also associates to p62 in response to RANKL, and may play an important role in p62-driven Oc activation. The PI3K/Akt pathway, a major target of PDK1, is involved in osteoclast formation and survival, and through mTORC1 activation, inhibits autophagy. Our aim was to investigate the activation of the Akt pathway in Pagetic osteoclasts.

Methods: We used an *in vitro* human osteoclast model from peripheral blood monocytes (PBMCs) obtained from patients with PDB (n=8) and healthy donors (n=8), and HEK293T cells transfected to express RANK. Akt is known to be activated/phosphorylated at two unique sites, stimulated by RANKL-induced signals at Ser473, and at Thr308 through PDK1. We used Western blot analysis to study the phosphorylation of Akt at both sites, and LC3 expression.

Results: In HEK293T cultures, the presence of an inhibitor specific to PDK1 (3-hydroxy-anthranilic acid) inhibited the RANKL-induced Thr308 phosphorylation, but Ser473 activation appeared unimpaired, consistent with expectations. In Oc cultures, p-Akt/Akt significantly increased after RANKL stimulation at Ser473, and the basal phosphorylation of Akt was significantly increased in the PDB cohort compared to controls, at both phosphorylation sites, particularly Thr308, suggesting that PDK1 may have a role in the overactivation of Akt in Pagetic Ocs. The autophagy flux was assessed in Oc cultures. We found that the basal LC3-II/LC3-I ratio, a reliable marker for autophagy, was higher in Pagetic osteoclasts than in controls.Conclusion: Our results show that PDK1 and Akt pathway are involved in RANKL-induced Oc signaling, and provide an additional potential contributor to the

pathology of PDB. These new insights to the events following RANKL stimulation may help further explain the increased signaling as well as the potential autophagy impairment in Pagetic osteoclasts.

***Disclosures: Stephen McManus**, None.*

SU0273

Regulator of Calcineurin 1 (Rcan1) is Highly Induced in Mouse Osteoclasts Generated on Bone and Regulates RANKL-induced Calcineurin Activity and Osteoclast Formation. Diana Metz-Estrella*[1], Kofi Mensah[1], Bryant Darnay[2], Betty Lamothe[3], Ed Purdue[1], Allison Shaber[1], Song Xue[4], Steven Goldring[1], Kevin McHugh[4], F. Patrick Ross[1]. [1]Hospital for Special Surgery, USA, [2]University of Texas M.D. Anderson Cancer Center, USA, [3]MD Anderson Cancer Center, USA, [4]University of Florida, USA

Microarray profiling of mouse osteoclast (OC) precursors differentiated on bone or plastic identified molecules involved in OC terminal differentiation. We focused on regulator of calcineurin *(Rcan)1,* a gene highly enriched on bone and expressed as two isoforms, 1.1 and 1.4. Human *RCAN1* was identified as Down syndrome (DS) critical region 1 gene (DSCR1) based on its presence within the locus duplicated in the partial trisomy 21 associated with DS. In cardiomyocytes Rcan1.4 controls calcineurin (CN) phosphatase function and thus NFATc1 nuclear translocation by a mechanism involving phosphorylation by TGFβ activated kinase (TAK1), leading to its dissociation from CN and and augmented activity of the phosphatase. We find that Rcan1.4, but not Rcan1.1 mRNA increases markedly during osteoclastogenesis (OCg). This result, combined with its cardiac role, suggests Rcan1.4 regulates OCg and may contribute to DS bone disease. Relevantly, TAK1 and NFATc1 are key regulators of OC formation. Given all these facts we focused on the role of Rcan1 in bone homeostasis, using WT mice or those lacking the gene. OCg is induced more rapidly and robustly in Rcan1 null versus WT BMMs suggesting Rcan1 is inhibiting the canonical calcium ion flux pathway. CN levels are unchanged during OCg of Rcan1 bone marrow macrophages (BMMs), but its phosphatase activity increases significantly in Rcan1$^{-/-}$ OCs but not BMMs; thus, Rcan1 mediates RANKL-induced CN function. Consistent with this hypothesis, NFATc1 nuclear translocation is much higher in OCs lacking Rcan1 and mRNA levels of NFATc1, TRAP, cath K and beta3 integrin subunit increase more rapidly and to higher levels during OCg of Rcan1 null BMMs versus WT cells. Turning to mechanism, both M-CSF and RANKL stimulate phosphorylation of TAK1 in WT BMMs. Pharmacological inhibition of TAK1 activity decreases significantly OCg of WT BMMs, while affecting Rcan1 null precursors to a lesser degree, suggesting that TAK1 and Rcan1 have an epistatic relationship. Since Rcan2 null mice have only an osteoblastic phenotype it is not surprising that the high expression of Rcan2.4 in Rcan1 null OCs, fails to suppress the enhanced OCg of Rcan1 null BMMs. In summary, we find that Rcan1 is an inhibitor of CN activity, and hence its deletion results in increased osteoclastogenesis.

***Disclosures: Diana Metz-Estrella**, None.*

SU0274

The Transcription Factor Sox4 Regulates TRAF6 Activity and Subcellular Localization. Philip Auron[1], Deborah Galson[2], Juraj Adamik[2], An-Jey Su*[1]. [1]Duquesne University, USA, [2]University of Pittsburgh School of Medicine, USA

Pathologies associated with the skeletal diseases osteoporosis, multiple myeloma and rheumatoid arthritis result from misregulated osteoclast differentiation and activity. The E3 ubiquitin ligase, Tumor necrosis factor receptor-associated factor 6 (TRAF6) is an indispensible cytoplasmic signal transducer for the RANKL/RANK/NF-kB axis of osteoclastogenesis. Understanding the molecular and mechanistic details of TRAF6 and its interacting proteins is necessary to develop effective skeletal disease therapies. Many studies use overexpression of TRAF6 as a dominant positive for NF-kB activity in HEK293. We report that overexpression of TRAF6 in two distinct murine osteoclast precursor cell lines (calvaria derived 4B12 and monocyte/macrophage RAW246.7) cannot activate NF-kB. 4B12 cells only differentiate into functional osteoclasts in the presence of both M-CSF and RANKL, physiologically akin to primary cell differentiation. TRAF6 interacts with signaling partners bearing TIMs: TRAF Interaction Motif(s). We report novel TIM sequences within the linker region (194-200) between the two scaffolding PDZ domains of Syntenin (Syn-1) and two TIMs in the GRR: lysine rich region of Sox4 (151-155; 193-197). Our experiments using both endogenous and various ectopically expressed muteins and tagged proteins indicate both Syn-1 and Sox4 can attenuate TRAF6 dependent signaling but Syn-1 interacts with TRAF6 in a Ubiquitin dependent manner. Further we observed intranuclear translocation of all three molecules (TRAF6, Syn-1, Sox4) of the protein-complex upon stimulation. The endogenous proteins of the triad were observed to rapidly translocate to the nucleus when the murine cells were stimulated with RANKL or LPS. These results provide a direct mechanism for the normally cytoplasmic TRAF6 to enter the nucleus as well as novel targets for treating bone disease.

***Disclosures: An-Jey Su**, None.*

SU0275

Functional Interplay between Connexin Hemichannels, Integrins, and PI3K-AKt Signaling in Mechanotransduction of Osteocytes. Jean Jiang*. University of Texas Health Science Center at San Antonio, USA

Mechanical loading induces the release of small factors, such as prostaglandins, from osteocytes and this release is mediated by opening of connexin 43 (Cx43) hemichannels at the cell surface. However, the mechanism for mechanotransduction that leads to the opening of these hemichannels is unknown. Integrinsexpressed on the cell surface are thought to be mechanical sensors in the osteocytes. Our recent study showed that activation of PI3K/AKT induced the conformational activation of integrin α5 upon mechanical stimulation in the form of fluid flow shear stress (FFSS), and led to the opening of Cx43 hemichannels in osteocytic MLO-Y4 cells. Here, we show that integrin αvβ3 located in the dendritic processes is the primary mechanosensor that activates PI3K/AKT signaling. Activated AKT further phosphorylates both Cx43 and integrin α5, enhances their interaction and increases Cx43 hemichannel activity in the cell body. Integrin αv colocalized with integrin β3 but not Cx43 on the dendritic side of the cells. Inhibition of integrin αv activation upon FFSS attenuated the activation of PI3K/AKT and blocked hemichannel opening on the cell body. Interestingly, integrin αvβ3 present on the dendritic processes activated PI3K, which was required for the activation of integrin α5β1 and opening of Cx43 hemichannels on the cell body. FFSS activated AKT and facilitated hemichannel opening. Cx43 and integrin α5 were both directly phosphorylated by AKT and FFSS increased their phosphorylation due to activation of AKT. AKTi, an inhibitor specific to AKT, disrupted the interaction between Cx43 and integrin α5, preventing the hemichannel from opening. These results show that the interaction is essential for Cx43 hemichannels to open. Taken together, these results suggest that integrin αvβ3 is the mechanical sensor that activates PI3K/AKT leading to the increased phosphorylation of integrin α5 and Cx43, and enhanced their interaction, thereby inducing the Cx43 hemichannels to open and release important bone modulating factors.

***Disclosures: Jean Jiang**, None.*

SU0276

Integrin αv in the Mechanical Response of Osteoblast Lineage Cells. Keiko Kaneko*[1], Masako Ito[2], Adam Lacy-Hulbert[3], Kyoji Ikeda[4]. [1]NCGG, Japan, [2]Nagasaki University Hospital, Japan, [3]MGH, USA, [4]National Center for Geriatrics & Gerontology, Japan

Osteocytes, terminally differentiated from osteoblasts, are thought to be a primary mechanosensory cell in bone; however the identity of the mechanosensing machinery and downstream signaling pathways remain largely unknown. To investigate the role of integrin αv in mechanotransduction in bone, we first generated mice lacking αv in osteoblast lineage using Osx-Cre (ΔOB). The ΔOB mice exhibited a lower BV/TV at baseline by microCT, along with reductions in serum CTX and OCN concentrations, compared with control, pointing to a lower turnover osteopenic state. When we subjected the ΔOB mice to tail suspension, a decrease in hindlimb BV/TV was attenuated. Histomorphometric analysis at the proximal tibia revealed that OS/BS, Ob.S/BS and BFR/BS were suppressed during tail suspension in the control group, whereas a significant suppression was not observed in the ΔOB mice.

We also generated mice lacking αv in osteocytes using Dmp1-Cre (ΔOCy). Similar to the ΔOB mice, the ΔOCy mice displayed a tendency of lower bone mass with lower turnover at baseline than the control group. Again, bone loss during tail suspension of the ΔOCy mice was less than that of control, suggesting the role of osteocytic αv integrin in mechanotransduction.

Finally, we examined a signaling pathway downstream of αv integrin in vitro using αv flox/flox primary osteoblastic cells, with or without adeno-Cre infection, mechanically stimulated with fluid shear stress (FSS). FSS increased phosphorylation of a Src substrate p130Cas and JNK, along with nuclear translocation of YAP/TAZ and subsequent transcriptional activation of target genes, ANKRD1 and CTGF. In the absence of αv integrin, phosphorylation of p130Cas and JNK in response to FSS was impaired, along with attenuation of YAP/TAZ nuclear translocation and ANKRD1 and CTGF gene expression. Thus, αv integrin may constitute the mechanosensing machinery in osteoblasts/osteocytes and transduce a mechanical signal through a Src-JNK-YAP/TAZ pathway.

***Disclosures: Keiko Kaneko**, None.*

SU0277

Lower Bone Volume Fraction and Bone Formation Rate in Premenopausal Women with Abdominal Obesity Are Associated with Less Physical Activity and Higher Serum Sclerostin. Adi Cohen*[1], Aline Costa[2], Robert Recker[3], Joan Lappe[4], Serge Cremers[2], David Dempster[2], Hua Zhou[5], Alexander Zwahlen[6], Ralph Müller[7], Emily Stein[8], Thomas Nickolas[8], Clifford Rosen[9], Elizabeth Shane[8]. [1]Columbia University Medical Center, USA, [2]Columbia University, USA, [3]Creighton University, USA, [4]Creighton University Osteoporosis Research Center, USA, [5]Helen Hayes Hospital, USA, [6]ETH Zurich, Switzerland, [7]ETH Zurich, Institute for Biomechanics, Switzerland, [8]Columbia University College of Physicians & Surgeons, USA, [9]Maine Medical Center, USA

Recent studies have linked abdominal obesity to low bone mass and decreased bone formation. Additionally, abdominal obesity is associated with a sedentary lifestyle that may lead to less mechanical stimulation of bone. Sclerostin is an inhibitor of Wnt signaling, secreted by osteocytes, and mechanical stimulation has been shown to down-regulate sclerostin levels. Because sclerostin is a negative regulator of bone formation, we hypothesized that young women with more abdominal fat would have higher circulating sclerostin levels, and that sclerostin would be inversely associated with bone volume fraction and bone formation at the tissue level. We divided 40 healthy premenopausal women (age 37 ± 8 yrs; BMI 25.8 ± 4.7 kg/m^2) into tertiles based on DXA % trunk fat, a surrogate for visceral adiposity (Table). All were normally menstruating, had normal areal BMD by DXA, no history of fragility fracture and no known cause of bone loss. As previously reported, those with the most abdominal fat had substantially lower bone formation rates and lower bone volume fraction in iliac crest biopsies compared to those with the least abdominal fat. In addition, those with more abdominal fat reported significantly less physical activity (modified Baecke questionnaire), suggesting a state of low mechanical stimulation. Circulating sclerostin concentrations (ELISA, Tecomedical, Sissach, Switzerland) were highest in those with the most abdominal fat. Circulating sclerostin was significantly and directly related to age and abdominal adiposity and was inversely related to bone volume fraction, mineralizing perimeter, bone formation rate, exercise level, serum PINP and IGF-1. We conclude that lower mechanical stimulation and higher sclerostin levels may contribute to the lower bone formation and inferior microarchitecture seen among healthy premenopausal women with abdominal obesity.

Tertiles Based upon DXA Trunk Fat and Correlations with Sclerostin	Tertile 1 N=13	Tertile 2 N=14	Tertile 3 N=13	p Tertile 1 vs Tertile 3	Correlation with Sclerostin (Spearman Correl coeffic, p)
Age (yrs)	33.3 ± 7.6	38.9 ± 8.8	39.5 ± 7.1	**0.04**	**0.38, 0.01**
BMI (kg/m^2)	21.6 ± 1.3	26.0 ± 3.1	29.8 ± 4.6	**<0.0001**	0.27, 0.09
DXA Trunk fat (%)	22.3 ± 3.5	32.9 ± 3.2	42.4 ± 3.7	**<0.0001**	**0.36, 0.02**
BMD by DXA (g/cm^2)					
Lumbar Spine	1.11 ± 0.12	1.09 ± 0.06	1.09 ± 0.10	0.5	0.08, 0.6
Total Hip	1.01 ± 0.09	0.96 ± 0.06	0.98 ± 0.08	0.7	-0.14, 0.4
Femoral Neck	0.88 ± 0.08	0.86 ± 0.07	0.87 ± 0.08	0.5	0.01, 0.9
Bone Biopsy: Cancellous bone					
Bone volume fraction by µCT (%)	29.1 ± 6.1	21.6 ± 8.1	20.4 ± 5.8	**0.001**	**-0.32, 0.046**
Bone formation rate (mm^3/mm/yr)	0.011 ± 0.008	0.009 ± 0.007	0.004 ± 0.002	**0.006**	**-0.34, 0.04**
Mineralizing Perimeter (%)	4.45 ± 2.75	3.59 ± 2.83	1.69 ± 0.87	**0.004**	**-0.57, 0.0001**
Serum Hormones & Biochemistries					
PINP (µg/L)	58.9 ± 22.7	43.0 ± 14.1	38.0 ± 7.7	**0.007**	**-0.34, 0.03**
CTX (ng/mL)	0.412 ± 0.275	0.231 ± 0.091	0.224 ± 0.057	**0.03**	-0.27, 0.09
IGF-1 (ng/mL)	203 ± 74	187 ± 46	163 ± 34	0.1	**-0.41, 0.008**
PTH (pg/mL)	23.0 ± 8.8	20.6 ± 9.7	23.7 ± 9.2	1.0	0.02, 0.9
25-OH Vitamin D (ng/mL)	35.5 ± 17.5	26.4 ± 10.9	29.2 ± 9.8	0.1	-0.07, 0.7
Current exercise (min/wk)	150 ± 46	171 ± 46	98 ± 46	**0.01**	**-0.45, 0.005**
Circulating Sclerostin (ng/mL)	0.637 ± 0.182	0.661 ± 0.295	1.140 ± 0.561	**0.008**	----------

Table

***Disclosures: Adi Cohen**, None.*

SU0278

Post-Natal Deletion of the Connexin43 Gene (*Gja1*) in Osteoblasts/Osteocytes: Model Development. Susan Grimston*[1], Marcus Watkins[1], Michael Brodt[2], Matthew Silva[1], Roberto Civitelli[1]. [1]Washington University in St. Louis School of Medicine, USA, [2]Washington University in St. Louis, USA

Mice with a conditional *Gja1* deletion develop a cortical (Ct) phenotype reminiscent of bone subject to disuse, and have reduced resistance to bending despite an increased moment of inertia (MOI). Earlier gene deletion reduces BMD and results in collagen matrix disorganization. Cx43 deficient bones require greater force to generate similar periosteal (Ps) strains compared to WT, while the Ps bone formation response to in vivo mechanical loading is enhanced. To gain insights regarding development of the structural abnormalities in Cx43 deficient bones, we used two approaches to achieve post-natal *Gja1* ablation. First, we treated *Osx-Cre;Gja1^{flxl}*-(*Osx-Cre;*cKO) mice with doxycycline (Doxy), to suppress the tetracycline repressible *Osx* promoter. Although Doxy dose-dependently attenuated the development of the Ct phenotype, even at the highest dose (200 mg/ml) we found expansion of Ma.Ar (+50.1±18.1%*) and Tt.Ar (+34.4±22.8%*), with Ct thinning (-12.7±7.9%*) and increased pMOI (+25.2±13.9%*) in *Osx-Cre*;cKO mice vs WT. Since *Gja1$^{+/-}$* are normal, development of Ct expansion despite Doxy suppression in *Osx-Cre;*cKO mice may reflect submaximal Cre repression by Doxy, resulting in >50% reduction in Cx43 relative to WT leading to the Ct phenotype. Secondly, we utilized the Tamoxifen (Tmx) inducible *Osx-CreER^{T2}* system were Cre expression is induced by 5 daily Tmx injections (100 mg/kg). In vivo µCT scanning revealed no differences in Ct parameters pre vs post Tmx treatment. Accordingly, and in contrast to other *Gja1* deletion models, strain gauge testing revealed similar force-strain relationships in Tmx-treated WT and *Osx-CreER^{T2};*cKO mice, suggesting that acute loss of Cx43 does not alter this relationship. In whole bone extracts, Cre mRNA was strongly induced by Tmx. However, total *Gja1* mRNA was only slightly reduced vs WT (0.7±0.4 vs 1.1±0.3), probably reflecting persistent *Gja1* expression in osteocytes (OCY). Indeed, immunohistochemistry revealed decreased but not complete loss of punctate Cx43-specific staining within the Ct OCY network of *Osx-CreER^{T2};*cKO 1 wk after Tmx treatment. Conversely, Cx43-specific stain was completely absent in Ps cells of Tmx-treated mutant mice. These data support the notion that Ct expansion and bone matrix abnormalities in Cx43 deficient bones are the result of a post-natal modeling defect. Tmx inducible *Gja1* deletion represents a good strategy for defining the role of Cx43 in mechanotransduction in adult animals.*p<0.05

***Disclosures: Susan Grimston**, None.*

SU0279

New Tool to Study Human Sclerostin Gene Expression In Vitro. Jesus Delgado-Calle*[1], Carolina Sañudo[2], Marta Morante[3], Jose Riancho[4]. [1]Indiana University School of Medicine, USA, [2]IFIMAV, Spain, [3]Univ Francisco de Vitoria, Spain, [4]University of Cantabria, Spain

The osteocyte product sclerostin is emerging as a critical factor in bone remodeling and, consequently, in determining bone mass. However, the study of the factors involved in the regulation of sclerostin expression and activity is compromised by the absence of human osteocytic cell lines and protocols suitable to isolate human osteocytes. In an attempt to circumvent these problems, we aimed to establish a cell line that expressed high levels of sclerostin in vitro.

The human osteoblast-like cell line SaOs was cultured under standard conditions and the expression of SOST (the gene encoding sclerostin) and other genes was determined by real time PCR with Taqman assays and normalized to the housekeeping gene TBP. The methylation level of CpG islands located in gene promoters was determined by methylation-specific quantitative real time PCR (qMSP).

We confirmed that SaOs expressed low levels of sclerostin (SOST:TBP, 0.01 relative units). Then, they were subjected to limiting dilution in 96-well plates attempting to seed one cell per well and several clones were tested for sclerostin expression. Four clones with opposite expression levels were eventually selected and grown in culture.

In cultures of the two negative clones, sclerostin expression was very low (0.0006-0.06 r.u.), whereas the two positive clones expressed high levels of sclerostin (0.7-8.5 r.u.), similar to the level found in whole bone tissue and about 300-fold higher than the expression level in the original SaOs cultures. Those differences persisted through cell passages for several months, but sclerostin decreased in cultures reaching confluence. Sequencing the 5' region (1400 bp) of the SOST gene that includes its promoter revealed no differences across the clones. However, the differences in gene expression were inversely correlated with the methylation level of a CpG island in the sclerostin gene promoter, which was >90% methylated in the negative clones and only 27±11% in the positive clones. However, there were no consistent differences across sclerostin-positive and sclerostin-negative clones regarding the expression or the methylation of other genes, such as alkaline phosphatase and RANKL. In line with these results, the demethylating agent AzadC induced a 6-fold increase in SOST expression by the parental cell line.

In conclusion, these SaOs-derived clones may be a useful tool to study the mechanisms and factors regulating sclerostin expression. Additionally, these results confirm the influence of DNA methylation on sclerostin expression.

***Disclosures: Jesus Delgado-Calle**, None.*

SU0280

Novel immortalized cell lines expressing a membrane targeted GFP variant in osteocytes – identification of a "mini-bone" forming clone. Lisa Le*, Patricia Veno, Sarah Dallas. University of Missouri - Kansas City, USA

We have previously shown that osteocytes show dynamic properties by the extension and retraction of dendrites and that they shed membrane-bound microvesicles which may provide a novel mechanism for intercellular communication. To facilitate further studies of osteocyte dynamic properties and the function of osteocyte-derived microvesicles, immortalized cell lines were generated from transgenic mice expressing a membrane-targeted green fluorescent protein(GFP) variant driven by the 10kb dentin-matrix-protein-1 promoter (Dmp1-memGFP-mouse). Calvarial cells from these mice were transfected with SV40T antigen using the pSV3neo immortalizing vector and stable clones were generated. Two clones, OmGFP-10 and OmGFP-66, were selected for further characterization of their osteocytic properties over a 4 week culture period. Both cell lines initially showed strong alkaline phosphatase activity, a marker of the late osteoblast. Expression of the early osteocyte marker, Dmp1-memGFP, was induced in the presence of ascorbate and β-glycerophosphate. Mineralized foci were formed in association with GFP+ve cells that had a stellate osteocyte-like morphology. Western blotting in OmGFP-10 showed that the early osteocyte marker, E11/gp38 was expressed by day 3, with

expression peaking on days 14-21. Sclerostin was faintly detectable by day 21, with robust expression by day 28, consistent with progression from an early to a late osteocyte-like phenotype. Clone OmGFP-66 had the unique property of producing highly structured trabecular bone-like spicules, which we have termed "mini-bones". These mini-bones formed well organized lacunae containing embedded GFP-positive cells with an interconnected dendritic morphology and an inter-cell spacing closely mimicking osteocytes in bone tissues. Both cell lines released microvesicle-like structures into the matrix and culture media. Culturing OmGFP-66 on a collagen gel containing hydroxyapatite strongly induced expression of Dmp1-mem-GFP, suggesting that collagen-HA gels may provide a culture system in which acquisition of the osteocyte-like phenotype can be accelerated. These two new osteocyte-like cell lines will provide novel tools with which to study osteocytes and their dynamic properties and the composition and function of microvesicles

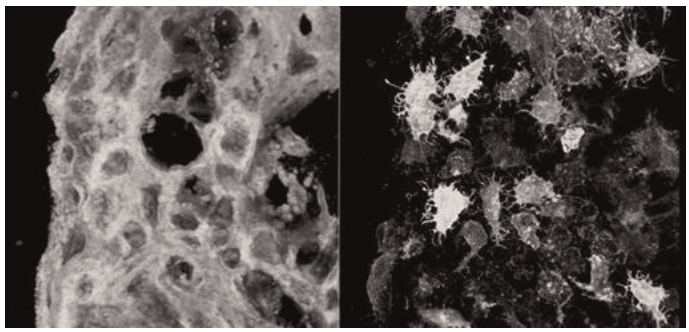

Clone OmGFP66 alizarin red (left) and GFP (right) immunofluorescence

***Disclosures: Lisa Le**, None.*

SU0281

Osteocyte-derived Notch is a Determinant of Bone Mass and has Sexually Dimorphic Effects on Skeletal Remodeling. Ernesto Canalis, Stefano Zanotti*. St. Francis Hospital & Medical Center, USA

Notch are transmembrane receptors that play a critical role in cell fate decisions. Notch regulates skeletal development, chondrogenesis and osteoblastic cell differentiation, but its function in osteocytes remains poorly understood. In the present study, we define the function of Notch in osteocytes by studying the dual conditional *Notch1* and *2* inactivation in these cells. Mice where the *Notch1* and *2* alleles were targeted with *loxP* sequences were crossed with transgenics expressing the Cre recombinase under the control of the Dentin matrix protein 1 promoter (*Dmp1-Cre*) to create *Dmp1-Cre;Notch1/2$^{\Delta/\Delta}$* conditional null mice. Since Osterix (Osx)-expressing cells differentiate into osteocytes, *Notch1* and *2* conditional mice also were crossed with *Osx-Cre* transgenics to create *Osx-Cre;Notch1/2$^{\Delta/\Delta}$* null mice. Microcomputed tomography and histomorphometry demonstrated that male and female *Dmp1-Cre;Notch1/2$^{\Delta/\Delta}$* conditional null mice had increased trabecular bone volume and connectivity at 3 months of age due to an increase in trabecular number. The phenotype was transient in male and sustained and more pronounced in female *Notch1/2* null mice, which exhibited a sustained increase in cancellous bone for up to 6 months of life. Cortical bone was not affected in either sex. Male and female *Dmp1-Cre;Notch1/2$^{\Delta/\Delta}$* null mice displayed an early increase in osteoblast and a decrease in osteoclast number, explaining the increase in trabecular bone. The cellular phenotype evolved, and male, but not female, mice exhibited a 1.5 fold increase in osteoclast number and eroded surface at 3 months of age, explaining why the sustained increase in bone volume was observed in female, but not in male, *Notch1/2$^{\Delta/\Delta}$* conditional null mice. The skeletal phenotype of *Osx-Cre;Notch1/2$^{\Delta/\Delta}$* mice was similar, and male mice exhibited a transient increase in trabecular bone volume at 3 months of age due to an increase in trabecular number caused by an increase in osteoblast and a decrease in osteoclast number and bone resorption. Female *Osx-Cre;Notch1/2$^{\Delta/\Delta}$* mice exhibited a pronounced (2.5 – 2.75 fold) and sustained increase in cancellous bone for up to 6 months of life. In contrast, cortical bone was thinner and porous in *Osx-Cre;Notch1/2$^{\Delta/\Delta}$* mice, suggesting sex and compartment specific effects of Notch in the skeleton. In conclusion, osteocyte-derived Notch regulates the osteoblast and osteoclast cell pool and as a consequence it is a determinant of bone mass.

***Disclosures: Stefano Zanotti**, None.*

SU0282

Rapid, Automated Counting of Osteocytes from Histological Sections Using Matlab Based Software. Ganesh Thiagarajan[1], Nuria Lara[1], Bhavani Ramneedi[2], Mark Johnson*[3]. [1]University of Missouri - Kansas City, USA, [2]UMKC School of Computing & Engineering, USA, [3]University of Missouri, Kansas City Dental School, USA

We have previously shown using the TOPGAL mouse that there is a rapid activation of the β-catenin signaling pathway in osteocytes and eventually to cells on the bone surfaces following in vivo forearm loading. These data were quantitated using a manual counting method that has proven to be labor intensive, time consuming and subject to potential bias. Therefore we have developed an automated counting program using the Matlab software platform that greatly expedites and improves data quantitation. Following in vivo loading of the right forearm, both forearms were harvested and stained for β-galactosidase activity, followed by sectioning and immunostaining using fluorescent antibodies against proteins of interest and finally bright field and fluorescence photography. Manual counting of these images for β–gal positive, immuno-positive and total osteocytes requires ~30 minutes/section and does not take into consideration color intensity. To reduce potential bias and insure accuracy, data generated by two individuals blinded to each other's results were compared. The advantages of the automated software are a significant reduction in time required for analysis, a reduction in individual bias and greater accuracy with regards to quantitative staining intensity. The automated method first quantitates a nonimmune IgG image to set a lower threshold for the immunostained images, counts the DAPI image to obtain the total number of osteocytes in the section, then obtains stained areas, various distance and size information, and finally analyzes the β-galactosidase and immunostained images. The program operator has the ability to select any area of the image to be analyzed at multiple points while the program is being executed, guided by user interface prompts. Specific sized areas can be excluded to remove blood vessels and filter out sectioning artifacts. The entire image capture and analysis is ~2 minutes/section. We have performed a number of correlation studies to compare manual versus automated counting and obtained correlation coefficient (r^2) values of 0.98 for total and β–galactosidase positive cells, 0.92 for DAPI counts and 0.97 for sclerostin positive cells. This automated method is a major advance in terms of manual counting of osteocytes from histological sections and the procedure is easily adaptable to any staining method and color combinations. Further development of this program is underway to enable counting of bone surface cells.

***Disclosures: Mark Johnson**, None.*

SU0283

Altered Osteocyte Mechanosensitivity in Response to Elevated Extracellular Glucose Levels. Chao Liu*[1], Hashem Al-Dujaili[2], Christian Fischer[3], Liyun Wang[4], Lidan You[5]. [1]University of Toronto, Canada, [2]University of Western Ontario, Canada, [3]University of Würzburg, Germany, [4]University of Delaware, USA, [5]Mechanical & Industrial Engineering, University of Toronto, Canada

Introduction: Hyperglycemia contributes to resulting in bone loss, and an elevated risk of bone fracture in diabetic patients. The effects of hyperglycemia on osteocyte mechanosensitivity are unknown. Osteocytes are bone cells that detect mechanical stimulation, and regulate osteoblasts and osteoclasts via paracrine pathways. This study tests the hypothesis that hyperglycaemia suppress the effects of mechanical loading (fluid shear) on osteocytes. We will examine secretion of anabolic cytokine, PGE2, catabolic cytokine RANKL and osteocyte apoptosis, which play a role in initiation of bone remodeling.

Methods: MLO-Y4 cells were seeded on rat tail type I collagen coated slides at a density of 3000 cells/cm2 and incubated for 72 hours in one of three media: i) Normglycemic control medium, ii) osmotic control medium with 20 mM of D-mannitol; and iii) hyperglycaemic medium with 20 mM D-glucose.

Parallel plate flow chambers were used to apply 10 dynes/cm2 of oscillating shear stress at 1Hz for 2 hours. Then, they are incubated at 37C with fresh media. Media were collected after 24 hours of incubation.

Protein Quantification: ELISA was used to quantify RANKL in media. PGE2 levels were quantified using EIA assay. Total protein was determined using a colorimetric kit and lysis buffer

Apoptosis Measurement: Caspase 3/7 level was measured with fluorescent kit.

Results: Osteocytes in the normglycemic or mannitol-supplemented media showed decreased apoptosis induced by fluid flow (Fig 1), which was abolished in hyperglycaemic medium. In normglycemic and osmotic control media, fluid flow resulted in decreased secretion of RANKL by osteocytes, which was inhibited in hyperglycaemic medium (Fig 2). PGE2 production increased in fluid flow conditions in normglycemic and osmotic control media was suppressed in hyperglycemia media (Fig 3).

Discussion: This study investigated how hyperglycaemia affected protein expression of markers involved in bone remodeling in osteocytes under mechanical loading. Hyperglycemia abolished mechanical loading induced changes in RANKL and PGE2 levels released by MLO-Y4 cells. Osmotic controls did not exhibit the same effect on osteocytes, suggesting hyperglycaemic condition may have direct effects on osteocytes, adversely influencing osteocyte's ability to respond to mechanical loading. This effect may be responsible for the impaired bone structure and properties seen in diabetic patients.

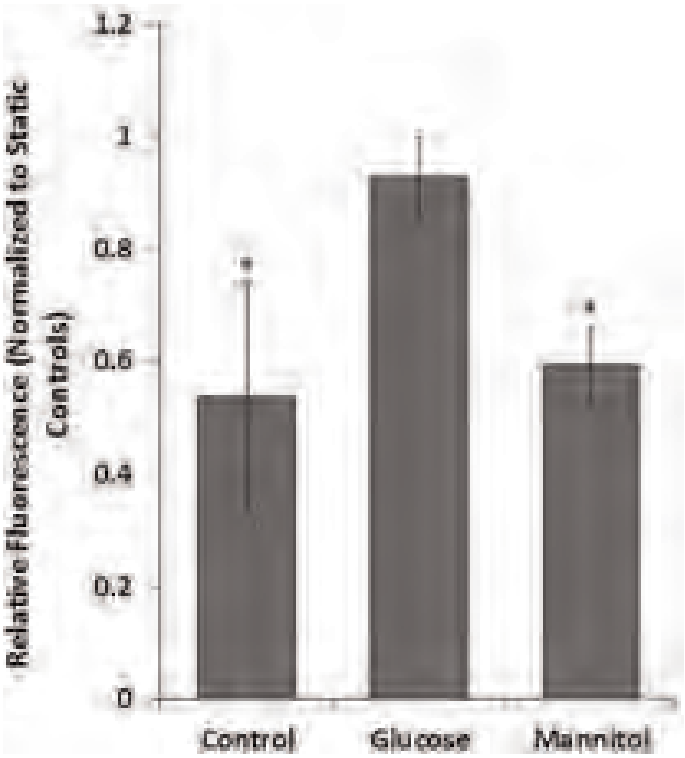

Fig 1. Caspase 3/7 expression in osteocytes under fluid flow * P < 0.05 vs. hyperglycemia n = 4

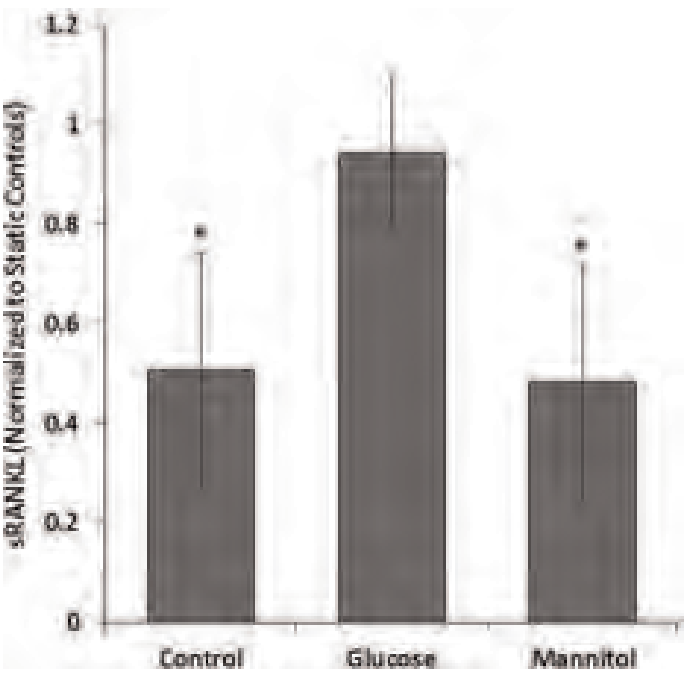

Fig 2. Soluble RANKL concentration under fluid flow * P < 0.05 vs. hyperglycemia n = 4

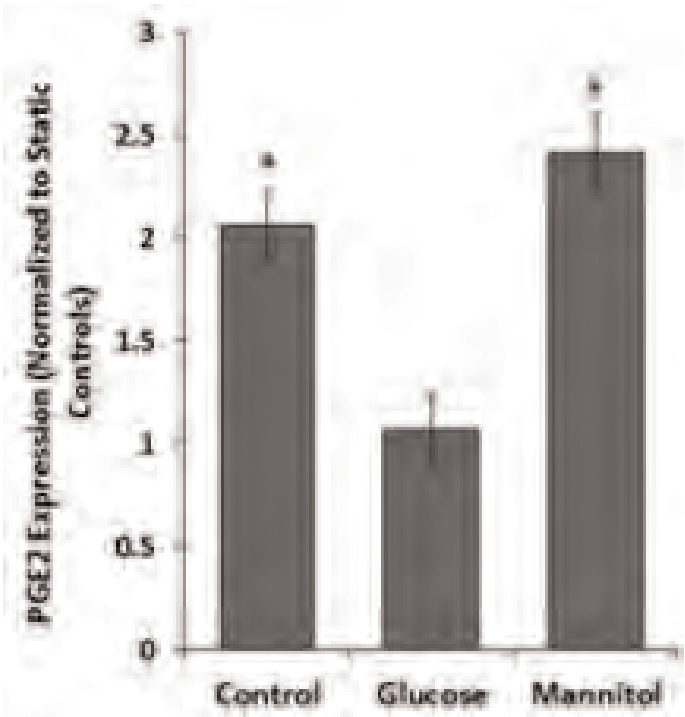

Fig 3. PGE2 production under fluid flow * P < 0.05 vs. hyperglycemia n = 4

***Disclosures: Chao Liu**, None.*

SU0284

Osteocyte Specific Deletion of Superoxide Dismutase2 Induces Osteocyte Loss Resulting in Bone Loss Associated with Impairment of Bone Remodeling. Keiji Kobayashi*[1], Hidetoshi Nojiri[2], Yoshitomo Saita[3], Daichi Morikawa[4], Masato Koike[5], Yusuke Ozawa[6], Yoshinori Asou[7], Kazuo Kaneko[8], Takahiko Shimizu[9]. [1]Chiba university, Graduate school of medicine, Japan, [2]Juntendo University, School of Medicine, Japan, [3]Department of Orthopaedics, Juntendo University School of Medicine, Japan, [4]Juntendo Univerisity, Japan, [5]Juntendo University, Japan, [6]Chiba university, Graduate school of medicine, Japan, [7]Tokyo Medical & Dental University, Japan, [8]Juntendo university, Japan, [9]Chiba University Graduate School of Medicine, Japan

Superoxide dismutase 2 (*Sod2*) is a mitochondrial antioxidant enzyme that plays a pivotal role in the maintenance of mitochondrial redox balance. However, the physiological function of *Sod2* in bone metabolism has not been fully elucidated. To address this question, mice lacking *Sod2* in osteocytes were generated by cross-breeding mice harboring a *Sod2* conditional allele with *Dmp1*-Cre transgenic mice (*Sod2* cKO). pQCT and micro-CT analyses revealed that BMD (-20%), BV/TV (-29%), Tb.N (-25%), and cortical thickness (-12%) were significantly reduced in *Sod2* cKO femora, while Tb.Sp was increased (+63%) in *Sod2* cKO. In the three-point bending test, bone stiffness was significantly weakened in *Sod2* cKO (-23%). Furthermore, *Sod2* deficiency significantly suppressed bone formation parameters such as MS/BS (-24%), MAR (-32%), and BFR/BS (-41%) in *Sod2* cKO. *Sod2* loss also significantly increased osteoclast number (+35%) and osteoclast surface (+37%) in *Sod2* cKO. These data indicated that *Sod2* deficiency in *Dmp-1* positive cells exhibited bone loss and fragility due to impaired bone remodeling. In addition, histomorphometric analyses revealed that *Sod2* loss significantly increased number of empty lacunae and markedly disorganized bone canaliculi in the cortical bones, indicating osteocyte loss and dysfunction. Since osteocyte dysfunction up-regulates *Rankl* expression in osteocytes, we investigated the expression levels of *Rankl* and *Opg* in bone. Quantitative PCR analysis revealed that *Rankl*/*Opg* ratio was significantly increased by four-fold in bones of *Sod2* cKO, supporting the increase of osteoclast number and activity. In culture experiments, mineralized nodule formation was markedly suppressed in both calvaria- and bone marrow-derived cells in *Sod2* cKO mice, suggesting the impairment of bone forming ability. These findings demonstrated that *Sod2* deficiency in osteocytes induced osteocyte cell death resulting in bone loss associated with *Rankl*-mediated bone resorption and impaired bone forming ability.

***Disclosures: Keiji Kobayashi**, None.*

SU0285

Osteocytes Reveal NADH Fluorescence Heterogeneity *in Situ* in Response to Ischemia. Dorra Frikha-Benayed*[1], Jelena Basta-Plajkic[2], Robert Majeska[3], Mitchell Schaffler[4]. [1]The City University of New York, USA, [2]City college of NY, USA, [3]City College of New York, USA, [4]City College of New York, USA

Osteocyte apoptosis (OtAp) is a key signaling step in bone remodeling. Hypoxia is thought to be a major cause of OtAp and subsequent signaling. NADH levels rise in hypoxia as mitochondria stop producing ATP by oxidative phosphorylation. Since NADH autofluorescence can be monitored in situ, we therefore tested if this could serve to assess Ot cell stress in intact bones subjected to ischemia. To image osteocytes, dorsal surfaces of adult C57BL/6J mouse metatarsals were exposed under anesthesia, preserving periosteum and blood supply (IACUC approved). In situ Ot NADH was visualized by multiphoton microscopy (40X Obj; Ex: 833 nm, Em: 460 nm) at baseline, and following euthanasia to induce ischemia. Ots were imaged over time at depths to 100μm below the periosteum and fluorescence intensity values for individual cells were measured. NADH fluorescence was not detected in Ot at baseline in vivo, but began to accumulate within 20 min after onset of ischemia (Fig 1). NADH accumulation in osteocytes was not uniform throughout the cortex. In cells < 40 μm below periosteum, NADH accumulation peaked at 84 ± 10 min after ischemia (Fig 2). Ot deeper in bone reached peak NADH levels at 145 ± 10 min after ischemia (Fig 2). In both regions, NADH fluorescence declined thereafter (not shown). These results show that NADH autofluorescence can be used to monitor changes in Ot redox state in situ. Changes in Ot NADH fluorescence after ischemia resembled those seen in other aerobic tissues. Absence of NADH signal under basal conditions indicates that Ot reside in a normoxic environment, while increases in NADH levels following hypoxic stress indicate mitochondrial dysfunction from lack of O2. Later declines in NADH levels likely reflect ATP depletion and onset of cell death. Most interesting were the spatial differences in Ot NADH accumulation with cortical depth. These may result from differing proximity to blood supply, but could also indicate intrinsic differences in Ot metabolism at different cortical depths. Regardless of the cause, our results are the first to show that Ot in situ are clearly a heterogeneous cell population with regard to metabolic state. Since metabolic stress is considered an essential step for initiation of Ot signaling in response to many stimuli, we posit that NADH monitoring in vivo will be an important new approach for identifying Ot that are ''at risk'' to undergo apoptosis following mechanical or metabolic insult.

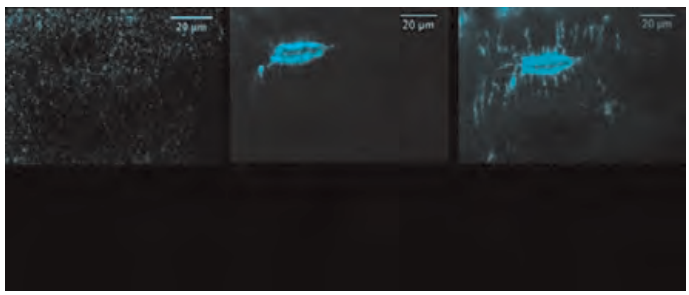

Fig1

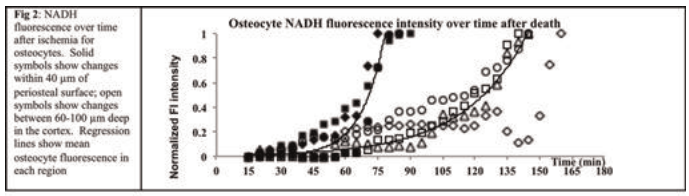

Fig2

***Disclosures: Dorra Frikha-Benayed**, None.*

SU0286

Osteocytic Osteolysis Induced by Immobilization in Rats. Fiona Bach-Gansmo*[1], Jesper Thomsen[1], Annemarie Brüel[2], Henrik Birkedal[1]. [1]Aarhus University, Denmark, [2]University of Aarhus, Denmark

We measured osteocyte lacunar volumes to show that disuse osteoporosis induces osteocytic osteolysis. The ability of osteocytes to demineralize the perilacunar matrix, osteocytic osteolysis, has been heavily debated for more than a century [1]. Osteocytes are housed in lacunae, and form a vast interconnected 3D lacuno-canalicular network (LCN) with a large surface area. Osteocytic osteolysis is expected to manifest itself through increased lacunar (and/or canalicular) volumes, as the LCN is the negative imprint of the cellular/dendritic network and its activities. The mechanism for such a resorptive capability remains unclear. Much effort is currently being put into characterizing and understanding the activity of the LCN. Previous studies have reported that while lactation induces osteocytic osteolysis, immobilization does not [2], or even result in reduced lacunar volumes [3]. Here we show that osteocytic osteolysis does occur upon immobilization.

The right hind limbs of female 3-months-old Wistar rats (N=5) were immobilized using injections of botolinum toxin A (Botox), with the contralateral leg serving as a biologically matched control [4]. A second group of animals (N=5) were injected with saline, and their right hind limbs used as an external control. Samples of mid-femoral cortical bone were obtained from animals put down 4 weeks post treatment. The lacunar volumes of more than 530000 osteocytes were determined using high resolution (0.37 μm voxel size) synchrotron radiation nano-tomography.

Osteocyte lacunar volumes were signifcantly larger in immobilized (median 226 μm^3) than contralateral (199 μm^3) and control samples (202 μm^3), see the figure. A model was developed to obtain quantitative understanding of the change in lacunar volume distributions between the Botox treated and contralateral legs (orange curve in figure).

The present results reveal that osteocytic osteolysis can be induced by immobilization in rat cortical bone in contrast to previous reports [2,3]. These prior studies were based on measurements of fewer lacunae and/or with poorer spatial resolution than in the present work.

1 A. Teti *et al.*, *Bone*, 44: 11-16 (2009).
2 H. Qing *et al.*, *J Bone Miner Res*, 27:1018-1029 (2012).
3 H. M. Britz *et al.*, *Bone*, 51, 913-919 (2012).
4 J. S. Thomsen *et al.*, *Calcif Tissue Int*, 90:294-306 (2012).

Key words: Osteocytes, Osteocytic Osteolysis, Immobilization, Disuse Osteoporosis, Nano-tomography, Cortical Bone, Rat

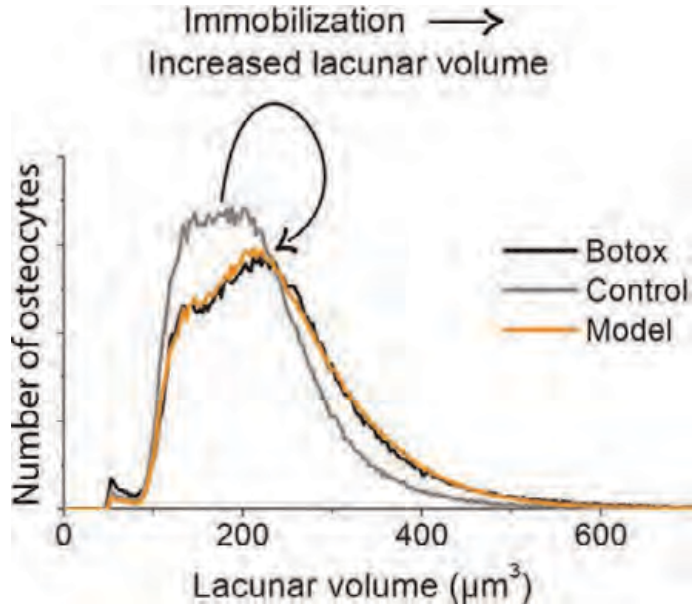

Distributions of lacunar volumes for immobilized and contralateral legs, pooled for all animals

***Disclosures: Fiona Bach-Gansmo**, None.*

SU0287

TNF-α upregulates sclerostin expression through NF-κB signaling pathway in high fat diet fed obese mice. Kyunghwa Baek*[1], Hyo Rin Hwang[2], Hyun-Jung Park[2], Arang Kwon[2], Abdul Qadir[2], Seong-Hee Ko[3], Jeong-Hwa Baek[4]. [1]Gangneung-Wonju national university, School of dentistry, South Korea, [2]Seoul National University, South Korea, [3]Gangneung-Wonju National University, South Korea, [4]Seoul National University, School of Dentistry, South Korea

Sclerostin, the osteocyte-specific glycoprotein, is known to lower bone mass by antagonizing Wnt signaling pathway. We examined whether obesity-induced bone loss is associated with Sclerostin expression and whether obesity-related inflammatory cytokine tumor necrosis factor-α (TNF-α) directly upregulates Sclerostin expression. Five weeks old male mice were assigned into two groups (n=10 each): control diet (10% kcal from fat) fed mice (CON) and high fat diet (60% kcal from fat) fed mice (HF) during 12 weeks. After the 12-week experimental period, final body weight and whole body fat mass of HF mice were higher than those of CON mice. Distal femur cancellous bone mineral density and bone formation rate was lower in HF mice *vs* CON mice (by 17% and by 73%, respectively). Percent resorbing surface was higher by 7-fold in HF *vs* CON mice. The expression level of Osteocalcin in femur was lower in HF mice *vs* CON mice while the ratio of receptor activator of NF-kB and Osteoprotegerin was higher in HF mice *vs* CON mice. Serum level and femoral osteocytic protein expression level of TNF- α was significantly higher in HF mice *vs* CON mice. Sclerostin expression in mRNA level and osteocytic protein level in femoral cortex was also higher in HF mice *vs* CON mice. Sclerostin expression in

MLO-Y4 osteocytes increased with TNF-α treatment and TNF-α-induced Sclerostin expression was blocked by the inhibition of NF-kB activation. Chromatin immunoprecipitation and luciferase reporter assay demonstrated that NF-kB directly binds to the NF-kB binding elements on the mouse *sost* promoter, stimulating Sclerostin expression. These results support an idea that, in the context of obesity or other inflammatory diseases increasing production of TNF-α, TNF-α upregulates the expression of Sclerostin through NF-kB signaling pathway, contributing to bone loss.

This work was supported by the National Research Foundation of Korea (NRF) grant funded by the Korean government (MEST) (2011-0016548 and 2010-0005836).

***Disclosures: Kyunghwa Baek**, None.*

SU0288

Imaging Mass Spectrometry-based Molecular Histology of Bone Shows the Implication of MEPE-ASARM for the Klotho-Deficient Phenotype. Yoko Fujino*[1], Tomoko Minamizaki[2], Kaoru Sakurai[1], Yasumasa Irie[3], Hirotaka Yoshioka[2], Yuichiro Takei[2], Katsuyuki Kozai[2], Mitsugi Okada[2], Yuji Yoshiko[2]. [1]Hiroshima University Graduate School of Biomedical & Health Sciences, Japan, [2]Hiroshima University Institute of Biomedical & Health Sciences, Japan, [3]Hiroshima University Faculty of Dentistry, Japan

Recent growing evidence suggests that osteocytes play a significant role in bone, while their functions remain largely unknown. We searched biomolecules linked to osteocyte functions not only in normal mice but also in Klotho-deficient (*kl/kl*) mice. Klotho, originally identified as a putative aging-suppressor, exhibits diverse functions in mice depending on its binding partners, causing a limited understanding of skeletal anomalies in Klotho deficiency. We initially analyzed bone samples by using a combination of two-dimensional-liquid chromatography-tandem mass spectrometry (2DLC-MS/MS) and plant proteomic techniques (Proteomics, 12: 1870, 2012). Moreover, osteocytes were fractionated and subjected to microarray analysis. To define osteocyte origin, we focused on small proteins/peptides detectable by high-resolution matrix-associated laser desorption ionization (MALDI)-imaging mass spectrometry (IMS) which provide label-free localization of molecules in tissue samples. To do this, we prepared fresh frozen bone sections with or without decalcification. 2DLC-MS/MS and microarray revealed a variety of proteins/genes including multiple cell origins. MALDI-IMS could identify molecules less than 20-kD including proteins/peptides localized in osteocytes. Amongst these molecules, we concluded that one of peaks corresponding to Klotho-deficient mouse osteocytes was matched to that of matrix extracellular phosphoglycoprotein-derived acidic serine and aspartic acid-rich motif peptide (MEPE-ASARM). To confirm whether MEPE-ASARM accumulation in *kl/kl* osteocytes is dependent on *Mepe* gene expression, we examined mRNA and/or protein levels of MEPE, together with other SIBLING family members such as osteopontin, bone sialoprotein and dentin matrix protein 1. Cathepsin B involved in MEPE degradation was also examined. In comparison to wild-type mice, expression levels of these molecules were not apparently changed in *kl/kl* mice. However, in parallel with MALDI-IMS, immunohistochemistry revealed that MEPE-ASARM was abundantly accumulated in *kl/kl* osteocytes. Because MEPE-ASARM was detectable in circulation and inhibited mineralization not only in osteoblast cultures but also in vascular smooth muscle cell cultures, MEPE-ASARM from osteocytes may be involved in biological mineralization processes. Thus, molecular histology using MALDI-IMS may provide new insight into osteocyte and bone biology.

***Disclosures: Yoko Fujino**, None.*

SU0289

Selective Deletion of c-fms in Osteocytes Increases Cortical and Trabecular Tissue Mineral Density. Meiling Zhu*[1], Benhua Sun[2], Joshua VanHouten[2], Christine Simpson[2], Karl Insogna[2]. [1]Yale University, USA, [2]Yale University School of Medicine, USA

Background: How osteocytes remodel their lacunae is poorly understood. Recent evidence suggests that this process is dynamic and may contribute to systemic mineral homeostasis. Osteocytes also express biochemical features of mature osteoclasts in certain physiologic states such as lactation. Since osteocytes express the CSF1 receptor, c-fms and since CSF1 plays a key role in osteoclast differentiation and survival as well as in mature osteoclast function, the role of c-fms in osteocytes was examined.

Methods: Mice with two floxed c-fms alleles were crossed with transgenic animals expressing cre recombinase under the control of an 8 kb DMP1 promoter and then appropriately backcrossed to yield animals with either a $cre^{+/}$ -c-$fms^{flox/flox}$ genotype (k/o) or a $cre^{-/}$ -c-$fms^{flox/flox}$ genotype (control). Bone density was analyzed by DXA and by microCT using a Scanco 35 instrument at 6 micron nominal resolution. Serum CTX, FGF23 and sclerostin were measured using commercially available kits. Serum phosphorus was measured with a Roche autoanalyzer. .

Results: The k/o mice exhibited normal growth. BMD measured by DXA adjusted for body weight was not different in these animals compared to controls (28.9 ± 1.2 vs. 28.0 ± 1.2, 33.8 ± 1.2 vs. 32.7 ± 0.9 and 24.0 ± 0.8 vs. 23.8 ± 1.0, gms/cm2x10,000/g-bw; spine, femur and total body; knock out vs. controls respectively). However, when analyzed by microCT, cortical BV/TV was significantly higher in the k/o animals(0.915 ± 0.003 vs. 0.907 ± 0.002 g/cm3, p=0.02). Tissue mineral density (TMD) was also significantly higher in cortical bone (1045.5 ± 5.3 vs.973.1 ± 7.9 g/cm3, p<0.0001). In addition there was a significant increase in TMD in trabecular bone (885.1 ± 4.1 vs. 834.6 ± 6.9 g/cm3, p<0.001). Mean serum CTX was 19.6 ± 2.3 ng/ml in k/o animals and 18.9 ± 2.6 pg/ml in controls. Serum sclerostin values were slightly higher in the k/o animals but the difference was not significant (538 ± 50 vs. 509 ± 48 pg/ml). Serum FGF23 levels were also slightly higher in the k/o animals (313.3 ± 23.6 vs. 300.0 ± 28.8 pg/ml) but again the difference was not significant. Mean serum phosphorus was 8.1 ± 0.9 mg/dl in k/o animals and 7.2 ± 0.8 mg/dl in controls.

Conclusions: TMD is influenced by the composition of the extracellular matrix and by osteocyte lacunar frequency and size. Deleting c-fms in these cells changes one or both of these parameters.

***Disclosures: Meiling Zhu**, None.*

SU0290

Distributions of serum total osteocalcin, undercarboxylated osteocalcin, N-propeptide of Type 1 collagen and C-telopeptide of Type 1 collagen in older men. The Health In Men Study. Peter Ebeling*[1], SA Paul Chubb[2], Elizabeth Byrnes[2], John Beilby[2], Kieran A McCaul[3], Samuel Vasikaran[2], Paul E Norman[4], Leon Flicker[5], Bu B Yeap[6]. [1]The University of Melbourne, Australia, [2]PathWest Laboratory Medicine, Australia, [3]Western Australian Centre for Health & Ageing, Centre for Medical Research, University of Western Australia, Australia, [4]School of Surgery, University of Western Australia, Australia, [5]University of Western Australia, Australia, [6]School of Medicine & Pharmacology, University of Western Australia, 6Department of Endocrinology & Diabetes, Fremantle Hospital, Australia

Bone turnover markers (BTMS) have been advocated as a means of stratifying fracture risk in conjunction with assessment of bone mineral density, and for monitoring responses to anti-osteoporosis therapy. We aimed to characterise the distribution of bone turnover markers in older men, and to describe analyte reference ranges based on levels found in healthy older men.

We assayed early morning serum aliquots from 4,020 community-dwelling men aged 70-89 years resident in Perth, Western Australia. Total osteocalcin (TOC), N-propeptide of Type 1 collagen (P1NP) and C-terminal cross-linking telopeptides of Type 1 collagen (CTX) were assayed using an automated analyser (Roche E170, Roche Diagnostics, Australia). Undercarboxylated osteocalcin (ucOC) was assayed before and after hydroxyapatite binding (Roche E170, Roche Diagnostics, Australia).

Distributions of TOC, ucOC, P1NP and CTX were skewed to the right. Correlations between bone turnover markers (Spearman's rho) were: TOC and ucOC 0.87, TOC and P1NP 0.77, TOC and CTX 0.75, P1NP and CTX 0.75. After excluding men with Paget's disease, osteoporosis, recent bone fracture, or receiving warfarin, glucocorticoids or bisphosphonates, median (interquartile range) for bone turnover markers in 3,442 men were: TOC 18.7 (14.7-24.1) ng/ml, ucOC 10.1 (8.0-12.9) ng/ml, P1NP 36.8 (28.1-49.2) ng/ml and CTX 0.282 (0.201-0.390) ng/ml/. All BTMs were positively correlated (Spearman's rho) with age TOC 0.22, ucOC 0.17, CTX 0.14, and P1NP 0.09 - all p<0.0001.

In a reference group of 366 very healthy older men, the 2.5^{th} to 97.5^{th} percentiles were: TOC 10.0-40.8 ng/ml, ucOC 5.1-20.1 ng/ml, P1NP 17.8-117.0 ng/ml and CTX 0.105-0.683 ng/ml.

In older men, BTMs are distributed in similar fashion with moderately strong correlations between markers of bone formation and resorption and all show age-related increases. This supports prior data showing that bone remodeling increases with age in elderly men. However, additional research is needed to clarify the value of individual bone turnover markers to predict fracture risk, and to ascertain the value of biochemical reference ranges for BTMs in the assessment of responses to anti-osteoporotic therapy in older men.

***Disclosures: Peter Ebeling**, None.*

SU0291

Serum Levels of Sclerostin and dickkopf-1 in Geriatric Patients with Osteoporotic Hip Fractures. Sonja Dorfer[1], Andrea Kapfenberger[1], Ursula Föger-Samwald[1], Stefan Kudlacek[2], Peter Dovjak[3], Peter Pietschmann*[1]. [1]Department of Pathophysiology & Allergy Research, Medical University Vienna, Austria, [2]Department of Medicine, Hospital Barmherzige Brüder, Austria, [3]Department of Geriatric Acute Care, Hospital Gmunden, Austria

Sclerostin and dickkopf-1 are inhibitors of the canonical wnt signaling pathway and consequently decrease bone formation. Since osteoblast dysfunction is an important aspect of age related osteoporosis, we studied serum levels of the afore mentioned wnt inhibitors in 164 patients with osteoporotic hip fractures (mean age: 81 ± 8 years), 119 geriatric control subjects and in 68 young control subjects (mean age: 23 ± 5 years). Serum concentrations of sclerostin and dickkopf-1 were measured by ELISA (Biomedica Medizinprodukte GmbH & Co KG, Vienna, Austria).

In men (but not in women) a significant increase of serum sclerostin levels with age was seen. Sclerostin levels were consistently higher in men than in women. In women with hip fractures, serum sclerostin was significantly lower than in young control women. Serum dickkopf-1 levels increased significantly with age in women and in

men. Dickkopf-1 levels were significantly higher in hip fracture patients than in geriatric or young controls.

We conclude that the determination of sclerostin and dickkopf-1 is useful for the study of age related bone fragility. Nevertheless, sclerostin and dickkopf-1 levels in the peripheral circulation appear to reflect different biologic events.

***Disclosures: Peter Pietschmann**, None.*
This study received funding from: Biomedica Medizinprodukte GmbH & Co KG, Vienna, Austria

SU0292

A novel image analysis method for longitudinal assessment of trabecular volumetric bone mineral density (vBMD) in rabbit lumbar vertebrae using Quantitative Computed Tomography (QCT). Randolph Crawford*[1], Sangeetha Somayajula[1], Brenda Pennypacker[2], Dahai Xue[1], Christopher Winkelmann[3]. [1]Merck & Co., USA, [2]Merck Research Laboratories, USA, [3]Merck, USA

Ovariectomized (OVX) rabbits are a model for post-menopausal osteoporosis. We employed longitudinal QCT imaging to evaluate the impact of novel therapies on trabecular vBMD (Tb.vBMD) of the rabbit vertebrae. An automated tool was developed to provide efficient evaluation of Tb.vBMD. This novel tool was applied to an efficacy study where OVX rabbits (n=12-19/group) were treated with vehicle, alendronate (ALN), and/or parathyroid hormone (PTH) over the course of 10 months. Rabbits were scanned on the GMI eXplore Locus Ultra at baseline, 3, 6, and 10 mo. The caudal $5^{th}/6^{th}$ region of the 6^{th} lumbar vertebra was chosen as the region of interest (ROI) because it contains the largest amount of trabecular bone and avoids both the caudal physis and the region of absent trabecular bone in the middle of the vertebra. We developed custom programs that performed the following steps: (1) convert the CT images from Hounsfield units (HU) to mg/cc of hydroxyapatite (HA) using a density phantom, (2) isolate the 6^{th} lumbar (L6) vertebra from the QCT images, (3) rigidly co-register (no scaling) all later time point L6 images of each rabbit to its own baseline , (4) create a mask of trabecular bone from the caudal $5^{th}/6^{th}$ region of the L6 baseline image (average volume of 94.9 mm^3), (5) apply this mask to the registered longitudinal images for each rabbit, and (6) output the average Tb.vBMD (mg/cc HA) of this region. The co-registration of the later time points to baseline of each rabbit ensures longitudinal consistency of measurement ROI . Total automated image processing run time for ~500 image data sets was ~8 hours. The manual component was reduced to visual inspection and/or correction as needed for <10% of the images. The manual correction rate could be further reduced by standardization of animal positioning and imaging field of view. Longitudinal analysis of QCT images showed robust increases in Tb.vBMD in the ALN (9.0%) and PTH (13.3%) treated groups at 10 months compared to vehicle. QCT analysis resulted in significance between groups at 3 mo. compared to 6 mo. for DXA results. With slight modification of the tool, additional analyses could be performed including evaluating L6 cortical and sub-cortical bone regions, and voxel by voxel analysis of BMD changes to evaluate longitudinal BMD difference "maps" of L6. In summary, this tool allowed for robust, efficient evaluation of Tb.vBMD of large, longitudinal rabbit L6 QCT data sets.

***Disclosures: Randolph Crawford**, Merck and Co., 3*
This study received funding from: Merck and Co.

SU0293

Agreement Between Forearm Measurements Performed on the Norland pDEXA and the Norland XR-800 Table Scanner. Jingmei Wang*[1], Felix Rajan[2], Chad Dudzek[3], Terry Schwalenberg[3], Tom Sanchez[4]. [1]Norland–a CooperSurgical Company, China, [2]Siemens Healthcare, USA, [3]Norland–a CooperSurgical Company, USA, [4]Norland - A Cooper Surgical Company, USA

Differences have often been reported between measurements made using different models of DXA equipment. These differences result from differences in beam geometry, calibration and analysis routines. While the Norland pDEXA and table scanners are calibrated against the same chemical standards and have similar analysis routines we wanted to directly examine the relationship between forearm measurements performed on these two significantly different Norland DXA systems to establish if studies done on the two systems may be comparable.

Five repeated scans of seventeen forearm phantoms were performed, using standard scan settings, on the Norland pDEXA System (scan speed of 16mm/s and resolution of 1.0 mm x 1.0 mm) and Norland XR-800 System (scan speed of 8mm/s and resolution of 1.0mm x 1.0mm). Agreement between the two systems for the Distal Radius + Ulna, Proximal Radius + Ulna and Proximal Radius Bone Mineral Density, Bone Mineral Content and Bone Area measurements was evaluated by Regression Analysis and a Bland-Altman Analysis.

Regression analysis and a Bland-Altman Analysis showed a very strong positive agreement between measurements of Bone Mineral Density for the Distal Radius + Ulna (difference 0.2%, r=0.9977), Proximal Radius + Ulna (difference 0.9%, r=0.9863) and Proximal Radius (difference 0.9%, r=0.9801). Measurements of Bone Mineral Content—where calibration differences might cause a greater effect—showed the XR-800 had a slightly higher value but a very positive relationship in regression analysis for the Distal Radius + Ulna (0.6% difference, r=0.9983), Proximal Radius + Ulna (1.8% difference, r=0.9944) and Proximal Radius (1.9% difference, r=0.9943). Finally, measurements of Bone Area—where differences in beam geometry might cause an effect—also showed the XR-800 had a slightly larger area with a very strong positive relationship in regression analysis for the Distal Radius + Ulna (0.5% difference, r=0.9701), Proximal Radius + Ulna (1.0% difference, r=0.9831) and Proximal Radius (1.0% difference, r=0.9866).

In conclusion, evaluation of forearm phantom studies done on the Norland Table Scanner and the pDEXA showed equality in results for Bone Density, Bone Mineral Content and Bone Area for the three regions of interest evaluated by the systems in default settings. This supports a conclusion that results on the two systems are directly comparable.

***Disclosures: Jingmei Wang**, None.*

SU0294

Bone Micro-Architecture Assessed by Spine TBS Predicts Osteoporotic Fractures in Men: The Manitoba Study. William Leslie*[1], Berengere Aubry-rozier[2], Didier Hans[2]. [1]University of Manitoba, Canada, [2]Lausanne University Hospital, Switzerland

One quarter of hip fractures and a similar proportion of other osteoporotic fractures occur in men. TBS, a novel gray-level measurement derived from lumbar spine DXA image texture, is related to microarchitecture and fracture risk independently of BMD. Previous studies have reported the ability of spine TBS to discriminate and predict osteoporotic fracture in women. Our aim was to evaluate the ability of lumbar spine TBS to predict clinical osteoporotic fractures in men.

3,620 men age ⩾50 years at the time of baseline hip (femoral neck) and spine (L1-4) DXA were identified from a database containing all clinical results for the Province of Manitoba, Canada. Health service records were assessed for the presence of non-traumatic osteoporotic fracture codes after BMD testing. Lumbar spine TBS (TBS iNsight®) was derived from each spine DXA examination blinded to clinical parameters and outcomes. We used Cox proportional hazard regression to analyze time to first fracture with adjustment for clinical risk factors (FRAX score derived without BMD), recent osteoporosis treatment (OTX) and BMD (hip and spine).

Mean age of the men was 67.6 ± 9.8 y. During mean 4.5 y of follow up there were 183 (5.1%) men with major osteoporotic fractures (MOF), 91 (2.5%) clinical vertebral fractures (CVF), and 46 (1.3%) with hip fractures (HF). Correlation between spine BMD and spine TBS (adjusted for BMI) was modest (r=.31) and less than the correlation between spine and hip BMD (r=.63), consistent with a skeletal parameter largely unrelated to BMD. Significantly lower spine TBS parameters were found in fracture versus non-fracture men for MOF (p<.001), HF (p<.001) and CVF (p=.003). ROC analysis for incident fracture discrimination was significantly better than chance (MOF AUC=0.59, p<.001; HF AUC=0.67, p<.001; CVF AUC=0.57, p=.032). TBS predicted MOF and HF (but not CVF) in models adjusted for cliniucal risk factors (FRAX without BMD) and OTX. TBS remained a predictor of HF (but not MOF) after further adjustment for hip BMD or spine BMD.

In conclusion, despite the relatively small number of incident fractures, we observed that spine TBS predicted MOF and HF independently of the clinical FRAX score. Furthermore, TBS predicted HF independent of FRAX and BMD. TBS may be able to improve fracture risk assessment in men, but studies with larger numbers of incident fractures are needed to confirm these findings.

	HR per SD decrease in spine TBS (95% CI)		
Covariate adjustments	MOF	HF	CVF
FRAX, OTX*	1.22 (1.06 – 1.41)	1.60 (1.21 – 2.11)	1.12 (0.91 – 1.38)
FRAX, hip BMD, OTX*	1.12 (0.96 – 1.30)	1.36 (1.01 – 1.83)	1.14 (0.97 – 1.34)
FRAX, spine BMD, OTX*	1.08 (0.93 – 1.26)	1.57 (1.19 – 2.07)	1.02 (0.81 – 1.27)

* FRAX score computed without BMD (Canadian tool), OTX=recent osteoporosis treatment

Adjusted hazard ratios for major osteoporotic fx (MOF), hip fx (HF) and clinical vertebral fx (CVF)

***Disclosures: William Leslie**, None.*

SU0295

Bone Strength Differences in Older Women With and Without a Recent Distal Radius Fracture. Katie Crockett*, Cathy Arnold, Jonathan Farthing, Phil Chilibeck, Adam Baxter-Jones, Saija Kontulainen. University of Saskatchewan, Canada

Introduction: Distal radius fracture (DRF) in women over age 50 is one of the first signs of bone fragility and a strong predictor of fracture risk. Dual-energy X-ray absorptiometry (DXA) measured areal bone mineral density (aBMD) derived t-score of the femoral neck is the primary clinical tool to diagnose osteoporosis and assess fracture risk; however, most fractures occur in women who are not diagnosed as osteoporotic possibly due to the deterioration in bone structure and strength, which planar DXA measures cannot detect. The aim of this study was to compare bone properties at the forearm measured with peripheral quantitative computed tomography (pQCT) and DXA in postmenopausal women with and without a recent DRF. Methods: 77 postmenopausal women age 50-78 with (Fx) and without (Ctl) a recent DRF (6-24 months post-fracture) were recruited from local clinics and through advertisement. Participants (N=35) were excluded for: corticosteroid, bisphosphonates or hormone replacement therapy in the past year, medical conditions that

severely affected daily living or the upper extremity. We compared bone properties between age matched Fx (n=21) and Ctl (n=21). All bone measures were from the non-dominant (Ctl) or non-fractured limb (Fx). We used pQCT to measure total (To), trabecular (Tr), and cortical (Co) density (D), area (A), content (C) and estimate bone strength in compression (BSIc) at the distal radius and stress strain index in torsion (SSIp) at the shaft. DXA was used to measure aBMD and BMC at the ultradistal forearm, spine and femoral neck. Differences in aBMD at the hip and spine were assessed using independent t-tests and differences for TrD and BSIc at the distal radius, SSIp at the radial shaft, and aBMD and BMC at the ultradistal forearm with MANCOVA using $p < 0.05$. Results: There were no significant differences in aBMD at the femoral neck or lumbar spine. After controlling for forearm muscle cross sectional area and height, there was a significant MANCOVA group difference Pillai's Trace, $p < 0.001$, with the Fx group demonstrating lower TrD, TrC, ToC, BSIc at the distal radius, lower CoD and CoC at the radius shaft, and lower aBMD and BMC of the ultradistal forearm (Table 1). Conclusions: Women with a recent DRF have lower pQCT derived TrD, estimated bone strength, DXA derived aBMD and BMC at the distal radius/forearm. Site specific measurement of bone may improve the assessment of distal radius fracture risk in postmenopausal women.

Table 1. DXA: Derived t-score classification and MANCOVA results

DXA**		Control (n=21)	Fracture (n=19)		
Femoral neck derived t-score classification	Normal	11 (52.4%)	5 (23.8%)		
	Osteopenic	10 (47.6%)	13 (61.9)		
	Osteoporotic	0	1 (5.3%)		
		Control (n=21)	**Fracture (n=19)**	**% Difference**	**Significance**
DXA**					
Ultradistal forearm	aBMD (g/cm²)	0.62	0.49	20%	p = 0.035*
	BMC (g)	3.05	1.68	45%	p = 0.000*
pQCT		**(n=21)**	**(n=21)**		
Distal radius	ToA (mm²)	398.45	387.31	3%	p = 0.453
	ToD (mm/cm³)	260.63	248.04	5%	p = 0.457
	ToC (mg/mm)	102.94	92.59	10%	p = 0.003*
	TrA (mm²)	363.46	355.51	2%	p = 0.592
	TrD (mg/cm³)	217.21	199.24	8%	p = 0001*
	TrC (mg/mm)	78.84	70.34	11%	p = 0.031*
	BSI_c (mg²/mm⁴)	26.95	23.12	14%	p = 0.042*
Radius shaft	ToA (mm²)	132.79	131.27	1%	p = 0.852
	CoA (mm²)	84.58	81.6	4%	p = 0.300
	CoD (mm/cm³)	1050.71	1019.80	3%	p = 0.064
	CoC (mg/mm)	88.67	83.20	6%	p = 0.048*
	SSI_p (mm³)	272.57	246.46	10%	p =0.066

*Indicates significant between subject differences, $p < 0.05$.
** Data for 2 subjects were not available for DXA measurements

Table 1

***Disclosures: Katie Crockett**, None.*

SU0296

Cortical Thickness Mapping from Multi-view DXA. Nikolaos Tsaousis*[1], Andrew Gee[2], Graham Treece[3], Kenneth Poole[3]. [1]Cambridge University, United Kingdom, [2]University of Cambridge Engineering Department, United Kingdom, [3]University of Cambridge, United Kingdom

Cortical thickness maps, which show the precise distribution of cortical bone around the proximal femur, have recently opened up new areas of understanding in fracture mechanisms (Poole et al., 2012) and therapy monitoring (Poole et al, 2011). Currently, localised cortical thickness can be estimated accurately down to 0.3mm from CT data of the hip (Treece et al., 2010, 2012). While CT remains the gold standard for scientific investigation, low dose DXA imaging is the leading tool for clinical fracture risk estimation, so applying cortical mapping technology to the DXA platform is highly desirable. In this study, we constructed a statistical model of the proximal femur, encoding both its shape and the cortical thickness distribution. The model was generated from CT scans of 642 femurs from 642 individuals. Each femur was segmented manually and then the cortical thickness was estimated at all points around the surface. Next, each femur was spatially registered to a canonical femur shape, using a similarity transformation followed by a B-spline free-form deformation. The cortical thicknesses were then projected onto the canonical femur. We thus obtained 642 cortical thickness maps, all expressed on the canonical morphology, and 642 deformation fields describing the femoral shapes. Principal compoment analysis identified the dominant modes of shape and thickness variation. We retained 12 shape and 12 thickness modes, accounting for 69% and 59% of the population variance respectively.The resulting 24-parameter model was subsequently fitted to multi-view DXA scans of 48 test subjects. The DXA images were actually digitally-reconstructed radiographs (DRRs) generated from CT data: in this manner, we could also calculate cortical thickness from the gold-standard CT data, and compare the two sets of results. To fit the model, we synthesised DXA views by ray-casting through the model, and then optimized for the model parameters that caused the synthetic views to best match the DRRs. The results for 20 DRRs in the range 0-171 degrees (validation), and 4 DRRs in the range 0-51 degrees (clinically viable) are shown in Figure 1. Compared with CT, DXA thickness estimation errors are -0.07+/-0.56mm for 20 views, and 0.11+/-0.61mm for 4 views. It remains to be seen whether this performance meets clinical requirements: this will depend on the location and size of fracture-predicting regions of interest that are only now beginning to emerge from cohort studies.

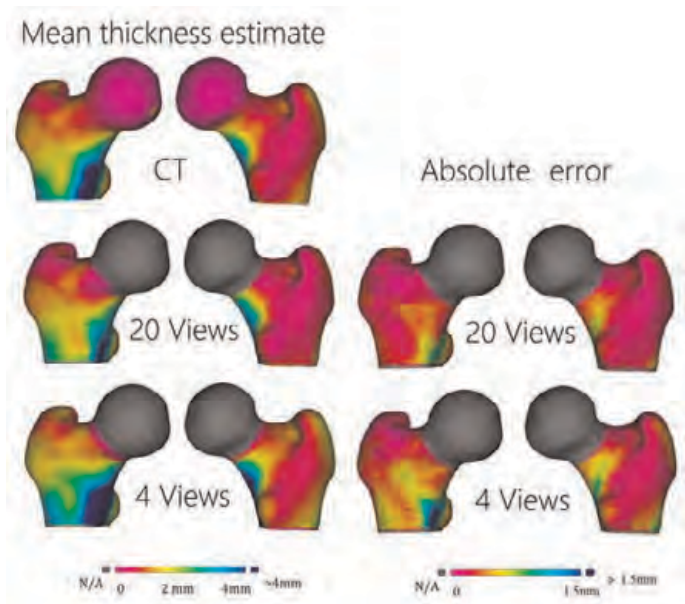

Cortical thickness maps

***Disclosures: Nikolaos Tsaousis**, None.*

SU0297

Interpreting Bone Mineral Density Results: Whose Job Is It, Anyway?. Sonya Allin*, Sarah Munce, Leslie Carlin, Gillian Hawker, Susan Jaglal. University of Toronto, Canada

Background and Purpose: Current Osteoporosis Canada guidelines promote fracture risk assessment as the basis for osteoporosis treatment recommendations. However, risk assessments as they appear on bone mineral density (BMD) reports have a tendency to omit modifying risk factors, like fracture history. In a 2008 sample of BMD reports for Ontarians with verified recent fragility fractures, over 50% did not include fracture history; risk was under-estimated on these reports as a result. The research presented here sought to determine referring physicians' understanding of potential errors on BMD reports, and the tools they use to detect and compensate for these. In addition, the research explored referring physicians' use of treatment recommendations that accompany risk assessments on BMD reports. Methods and Analysis: A descriptive qualitative approach was used and involved telephone interviews with family physicians (FPs), who make the majority of BMD test referrals in the province. Study Sample or Initiative Scope: Twenty-two FPs with practices in Ontario were recruited through an Ontario College of Family Physicians event on osteoporosis and subsequent snowball sampling. The average roster size of each physician was 1280 patients, and the average number of BMD reports they reviewed per week was four. Findings: 18 of the 22 physicians (82%) acknowledged the possibility of error related to risk assessment on BMD reports, including inaccurate patient self-reports, machine error, inconsistencies between competing assessment heuristics and inaccurate definitions of fragility fracture. 10 physicians (45%) reported that they regularly double-checked or re-computed risk assessments themselves; several others indicated desire, but inability to perform such checks due to time constraints. Physicians were divided as to whether treatment recommendations should be included on reports or left to the referring physician to determine. Conclusion: While risk assessments are the basis for treatment decisions, FPs are divided as to the role of the BMD report in determining risk. Referring physicians have assumed at least partial responsibility for risk assessment despite practical constraints and potential duplication of work. Efforts to improve assessments on BMD reports and to expedite assessments made by FPs may ameliorate inefficiencies caused by ambiguity in fracture risk assessment responsibility.

***Disclosures: Sonya Allin**, None.*

SU0298

Investigation of the Local Relationship Between Bone Marrow Fat Content and Bone Mineral Density in the Proximal Femur of Subjects With and Without Fragility Fractures. Julio Carballido-Gamio*[1], Dimitrios C. Karampinos[2], Andrew Lai[3], Sonia Lee[3], Roland Krug[3]. [1]University of California, San Francisco, USA, [2]Musculoskeletal & Quantitative Imaging Research Group, Department of Radiology & Biomedical Imaging, University of California, San Francisco, USA; Department of Diagnostic & Interventional Radiology, Technische Universität München, Germany, [3]Musculoskeletal & Quantitative Imaging Research Group, Department of Radiology & Biomedical Imaging, University of California, San Francisco, USA

Marrow fat content partly explains bone strength independently of BMD. Here we assess the local relationship of marrow fat content measured by MRI, and BMD measured by QCT, in the proximal femur of postmenopausal women; and determine the spatial variation of fat content and BMD in postmenopausal women with fragility fractures and healthy controls using Computational Anatomy.

Fifteen postmenopausal women, 6 without fracture (Controls; age=62.4±8years), and 9 with fragility fractures (Cases; age=62.8±9 years) were included in this study. Coronal-oblique images of the proximal femur were acquired at 3 Tesla with a novel fat quantification technique based on chemical shift MRI-—a 3D spoiled gradient echo pulse sequence with 6 echoes and a very accurate multi-frequency model of fat using IDEAL (Reeder 2005)—to generate Fat-Fraction (FF) maps. QCT scans of both hip joints were obtained and calibrated to generate BMD maps. FF and BMD maps were spatially normalized to an atlas (Carballido-Gamio 2011), and FF- and BMD-difference maps (Cases minus Controls), and FF-BMD Pearson correlation coefficient maps (Controls vs Controls, and Cases vs Cases) were generated. Due to the small sample size, and that small BMD and FF differences were expected between Controls and Cases, significance of the difference maps was not evaluated. Significance of the correlation coefficient maps was evaluated based on paired t-tests, and false-discovery rate (FDR) correction was used to correct for multiple comparisons.

Figure 1 summarizes the results of this study. Results showed positive and negative BMD differences between Cases and Controls, and higher FF values in the neck and intertrochanteric regions in Cases. As it was expected based on previous studies, BMD and FF were mostly negatively correlated, however, small regions with positive correlations were also observed. Although regions with significant correlations between BMD and FF were similar between Controls and Cases, Cases showed a distinct pattern.

Unfortunately, the main limitation of this study is the small sample size, which is a potential explanation of the variability of the BMD difference maps, and a reason to avoid any strong conclusions. We are currently recruiting more subjects to investigate if the observed patterns in the correlation map of Cases are due to changes in BMD alone, FF alone, or both, and to apply techniques such as voxel-based morphometry (Carballido-Gamio 2013) for further analysis.

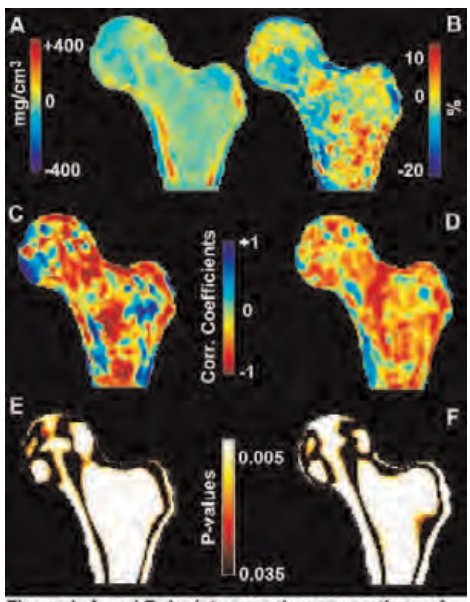

Figure 1. A and B depict coronal cross-sections of the BMD and FF difference maps (Cases minus Controls), respectively. C and D show the correlation coefficient maps of BMD and FF values for Controls and Cases, respectively. E (Controls) and F (Cases) indicate regions where correlations were significant after FDR correction.

Figure 1

***Disclosures: Julio Carballido-Gamio**, None.*

SU0299

No More annual BMD exam in Rheumatoid Arthritis Patients with Osteoporosis. Mie Jin Lim*[1], Won Park[2], Seong Ryul Kwon[2], Kyung Hee Jung[2], Kowoon Joo[2], Hoyeon Joo[3]. [1]Inha University Hospital, Republic of Korea, [2]Inha University Hospital, South Korea

Introduction: There are controversies regarding how often patients with osteoporosis should take bone mineral density (BMD) exam. Rheumatoid arthritis (RA) and glucocorticoid are classified as risk factors for osteoporosis. In order to evaluate the progression of osteoporosis, BMD exams were performed annually in RA patients with osteoporosis.

Goal: We aimed to find out that annual BMD exams in high risk patients such as RA patients with osteoporosis are clinically useful.

Methods: RA patients (n=139, age of 64.6 ± 9, 124 women and 15 men) who visited Inha university hospital in Incheon, Korea during January, 2012 ~ June, 2012 were recruited. All of them were previously diagnosed as osteoporosis and were on anti-osteoporotic medication. BMD results of past 5 years were retrospectively reviewed. We compared results of total L spine, femur neck and total hip at baseline to sequential follow-ups.Results: Nineteen percent of patients (n=26, 66.6 ± 9.7 years old, 22 women and 4 men) quitted anti-osteoporotic medication as follow-up BMD result improved. Over past 5 years, 339 follow-up BMD exams were performed and 26 follow-up BMD (8% of total exams) were shown to be T score > -2.5. As shown in Table 1, BMD results significantly improved after 2 years, except density of femur neck. In case of femur neck, T-score failed to show clinical improved after a year.

Conclusion: Most RA patients (81%) continued on anti-osteoporotic medication over 5 years and only a small fraction of follow-up BMD exams showed recovery from osteoporosis. BMD results of RA patients with osteoporosis did not change much over 2 years. Thus, we recommend performing BMD in RA patients with osteoporosis at intervals of least 2 years.

	Mean of Total L spine		Mean of Femur Neck		Mean of Total Hip	
	T score	Density (g/m²)	T score	Density (g/m²)	T score	Density (g/m²)
Baseline	-2.75	0.72	-2.54	0.56	-2.25	0.63
Post 1 year	-2.73	0.75	-2.53	0.58***	-2.32	0.64
Post 2 years	-2.53**	0.8*	-2.44**	0.67*	-2.54	0.67*
Post 3 years	-2.5**	0.84*	-2.38*	0.65*	-2.31	0.68*
Post 4 years	-2.45**	0.85*	-2.58**	0.63*	-2.64	0.65*

* $p < 0.001$, ** $p < 0.01$, *** $p < 0.05$, Baseline vs. follow-up

Table 1. BMD results for past 5 years in RA patients with osteoporosis

***Disclosures: Mie Jin Lim**, None.*

SU0300

Potential Sources of Quantification Error When Retrospectively Assessing Metacarpal Bone Loss from Historical Radiographs by Using Digital X-ray Radiogrammetry. Johan Kälvesten*[1], Torkel Brismar[2], Anders Persson[3]. [1]Linköping UniversitySectra, Sweden, [2]Karolinska Institutet, Sweden, [3]Linköping University, Sweden

Introduction: During the past decade, digital X-ray radiogrammetry (DXR) has been used to measure metacarpal bone mineral density (BMD). DXR is often used to measure BMD in existing cohorts where X-ray images are available but were not acquired in accordance with the DXR imaging protocol (DIP). The purpose of the current study was to investigate how deviations from DIP in historical cohorts may affect the reproducibility of DXR-BMD measurements.

Method: Five anthropomorphic cadaver hand phantoms (The Phantom Laboratory, Salem, NY, USA) were used to perform repeat measurements of deviations from DIP with respect to voltage, exposure, lateral displacement, supination, combination of lateral displacement and supination or rotation, extension of the wrist, and edge enhancement. The phantoms ranged in DXR-BMD from 0.35 to 0.60 g/cm^2, corresponding to T-score values of -4.9 to 0.5. Direct digital radiography (Aristos; Siemens Healthcare, Erlangen, Germany) was used for image acquisition, and dxr-online (Sectra, Linköping, Sweden) for DXR-BMD measurements.

Results: The impact of the tested deviations from DIP ranged from 0 mg/cm^2 to 32.5 mg/cm^2 (0–6.8%). Influence from specific deviations are listed in Table 1. On repetition with the same phantom specimen, none of the deviations resulted in a within-specimen reproducibility error greater than 2 mg/cm^2 (0.4%, equivalent to a T-score of 0.042) (Table 1).

Conclusions: All the tested deviations except tube voltage had a magnitude greater than the normal measurement noise for the technique but moderate relative to absolute BMD. When performing a retrospective study based on absolute BMD, e.g. for fracture risk, impact from the tested deviations is limited. When performing a retrospective study based on change of BMD, e.g. for rheumatoid arthritis, impact from the tested deviations can be significant. When designing and planning a study with DXR-BMD change measurements made on historical radiographs, an analysis should be made on which image deviations are acceptable for the study setup. The data in this current study may be used for such calculations. This study is valid only

for retrospective off-label use of DXR-BMD and does not consider its prospective on-label use.

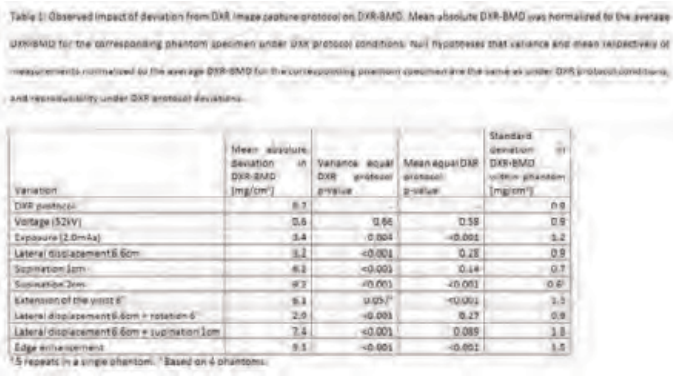

Table 1: Observed impact of deviation from DXR image capture protocol

***Disclosures: Johan Kälvesten**, Sectra AB, 3*
This study received funding from: Sectra AB

SU0301

Prevalent Osteoporotic Fracture and Past Use of Glucocorticoids Induce a Microarchitectural Impairment in Subjects Treated with Glucocorticoids. Edward Leib*[1], Renaud Winzenrieth[2], Didier Hans[3]. [1]University of Vermont, USA, [2]Med-imaps, Hôpital X. Arnozan, PTIB, Pessac, France, France, [3]Lausanne University Hospital, Switzerland

Aim: The aim of the study was to evaluate whether microarchitectural changes as measured by Trabecular Bone Score (TBS) can identify those patients who are more likely to fracture and are on glucocorticoid (GC) therapy either presently or in the past.*Materiel and Methods:* The study group was composed of women aged 40 and older receiving GCs (⩾ 5mg/day for ⩾3months). BMD was assessed at the lumbar spine (L1-L4) using a Prodigy densitometer (GE-Lunar, Madison, USA). TBS was calculated at L1-L4 using the TBS iNsight® (Medimaps, France). Clinical data, presence of osteoporotic fracture (OPF), GC treatment and common clinical risk factors (CRFs) were documented. Logistic regressions (backward) were used to investigate possible relationships between independent variables and the presence of fracture for subjects presently on or with past use (p_GC) of GC. Odds ratio per standard deviation decrease (OR) was calculated.

Results: The cohort consisted of 362 women treated with GCs who had TBS testing. Mean age and BMI were 62.0±11.2 yrs and 25.5±4.1 Kg/m^2. 92% were postmenopausal, 31% had a family history of osteoporosis, 10% had a maternal history of OPF. In addition, 13% had sustained a prevalent OPF (all types) and 9% had p_GC. Correlation between TBS and BMD was, as expected, low (r=0.32) and there was no correlation between TBS and BMI (r = -0.09). There were no differences in terms of age, BMI, weight and height between subjects with or without fracture (p>0.2). GC-treated patients who had sustained an OPF compared to those without OPF were characterized by a lower TBS (p=0.004) while no difference in BMD was observed (p=0.36).TBS was associated with the presence of OPF (OR=1.63[1.22-2.17]). TBS was significantly lower in all subjects with p_GC use than in subjects on GCs only presently (p=0.025) whereas BMD was not significantly different (p=0.19). Finally, in only those subjects without fracture, p_GC users had a lower TBS compared with current GC users (p<0.03) while no difference was observed for subjects with fracture (p=0.76).*Conclusion:* GCs induced a microarchitectural texture impairment whereas no change was observed with BMD measurement. These results are consistent with previous TBS studies on GCs. We have also observed that past use of GCs has a negative effect on microarchitectural texture which is similar to the presence of an OPF. TBS is a reliable tool for management of patients with present or past GC treatment, and outperforms BMD measurement in its ability to identify a population on glucocorticoids at greater risk for fracture.

***Disclosures: Edward Leib**, None.*

SU0302

Relationships Between Age, Sex and Bone Microarchitecture at the Distal Radius and Tibia in Late Adulthood. Mark Edwards*[1], Camille Parsons[1], Jennifer Thompson[2], Ann Prentice[2], Cyrus Cooper[1], Elaine Dennison[1], Kate Ward[2]. [1]MRC Lifecourse Epidemiology Unit, University of Southampton., United Kingdom, [2]MRC Human Nutrition Research, United Kingdom

Bone health is known to deteriorate with age but exact relationships are thought to vary between men and women. The advent of high resolution peripheral quantitative computed tomography (HRpQCT) scanners has permitted the direct and indirect non-invasive assessment of bone macro- and micro-architecture, including detailed delineation of cortical and trabecular structure. We used this new technique to explore differences in bone according to age and sex in a large, well characterised, cohort of older adults. 198 men and 178 women from the Hertfordshire Cohort Study born between 1931 and 1939 were studied. HRpQCT (Xtreme CT, Scanco Medical) images (voxel size 82μm) of the non-dominant distal radius and tibia were acquired. Standard morphological analysis was performed for assessment of macrostructure, density, cortical porosity and trabecular microarchitecture. The mean(SD) age of participants was 76.1(2.5) and 76.5(2.6) years in men and women respectively (range 72.1 to 81.4 years). At both radius and tibia, men had greater bone area (cortical, trabecular, total); trabecular volumetric density; and trabecular number than women (all p<0.001). Trabecular thickness was greater in men than women at the radius (p<0.001) but not the tibia (p=0.2). Conversely, cortical volumetric density was greater in men in the tibia (p<0.001) but did not differ at the radius (p=0.8). Radial cortical porosity was higher in men whereas tibial cortical porosity was greater in women. In the radius and tibia of women, there was a negative association between age and both cortical area and thickness, and a positive association with trabecular area. In this group we also observed an inverse association between age and both cortical and trabecular density at both sites (p<0.05). Furthermore, trabecular number and thickness were lower in older women, particularly in the radius. These relationships were not seen in men. In summary, using HRpQCT techniques to ascertain bone macro- and microarchitecture, we have confirmed consistently greater bone areas in men than women. Conversely, sex differences in trabecular microarchitecture and cortical density and porosity appear to be site specific. In this cross-sectional study, we noted an age-difference in cortical and trabecular density, trabecular microarchitecture, and bone geometry at both sites in the eighth decade among women; no such difference was observed in men.

***Disclosures: Mark Edwards**, None.*

SU0303

Screening for Osteoporosis Using Digital X-ray Radiogrammetry (DXR) in Conjunction with a National Mammography Screening Program. Michael Wilczek*[1], Christel Nielsen[2], Johan Kälvesten[3], Jakob Algulin[4], Torkel Brismar[5]. [1]Karolinska Institutet, Sweden, [2]Region Skåne, Sweden, [3]Linköping UniversitySectra, Sweden, [4]Sectra, Sweden, [5]Karolinska Institutet, Sweden

PurposeIn this first report from the Stockholm Osteoporosis Project (STOP) we assess the feasibility of mass screening using digital X-ray radiogrammetry (DXR) in conjunction with the Swedish national mammography screening program (women aged 40-74 years). The association between DXR T-score and clinical risk factors for hip fracture is also studied.Method and Materials

This study was conducted two days per week at a single mammography screening center (Unilabs AB, Tumba, Sweden) between March 2010 and June 2012. The local participation in the mammography screeningprogram was approximately 70%. Women who chose to participate in our study (n =8,810) answered a questionnaire about clinical risk factors and a radiograph of the non-dominant hand was taken. DXR-T-score was obtained by analyzing metacarpals II-IV.

Univariate associations between bone density, analyzed as T-score, and potential risk factors for osteoporosis were examined. A generalized linear regression model was fitted to independent variables with univariate associations at P<0.05. The model was reduced through manual backward elimination, with P>0.1 as the exclusion criterion. Observations with non-missing values for the identified independent variables (n =7,384) were used in the multivariate analysis.Results

76% of the patients chose to participate in our study. The difference in number of daily mammograms performed on days with or without DXR was not significant. All univariate associations between DXR-T-score and potential risk factors were highly significant. In a multivariate setting heredity was no longer significant, and was thus excluded from the multivariate model. Smoking status was not significant as a main effect, but an interaction term between smoking status and age was fitted together and found to be significant (P=0.009). The multivariate model included height, weight, age, right-handedness, menopause, alcohol consumption, cortisone treatment, rheumatic disorder, age × smoking status. The coefficient of determination of the model was 0.37.Conclusion

It is possible to combine DXR with mammography screening. The acceptance rate of patients was high and no impact on clinical workflow was observed. Clinical risk factors partially predicted DXR-T-score, indicating an additive value of combining clinical risk factors and DXR in fracture risk estimation.

***Disclosures: Michael Wilczek**, None.*

SU0304

Systematic Bias between Results Measured on Cross-calibrated DXA Scanners in Pediatric and Young Adult Females. Jodi Dowthwaite*[1], Paula Rosenbaum[2], Tamara Scerpella[3]. [1]SUNY Upstate Medical University;Syracuse University, USA, [2]SUNY Upstate Medical University, USA, [3]University of Wisconsin, USA

Purpose: Consistency of DXA scan results is critical for data integrity. For pediatric subjects, the extent to which cross-calibration of DXA scanners alleviates model to model scanner differences is unclear. In the current study, DXA bone outcomes were compared for same-day measurements performed using different scanner models that had been cross-calibrated to alleviate discrepancies.

Methods: Differences between results for the two scanners were evaluated in approximately 130 females aged 8 to 24 years. Whole body, forearm, hip and lumbar spine scans were performed in a single session on both a Hologic QDR4500W scanner

(QDR) and a cross-calibrated Discovery A scanner (Disco). Results were compared for standard projected Area, bone mineral content (BMC), and areal bone mineral density (BMD) for Whole body (total and sub-regions), radius (1/3 and ultradistal regions), lumbar spine (Vertebra L3) and femoral neck output. Wilcoxon Signed Rank tests evaluated differences between results for the two scanners.

Results: Although inter-scanner correlations were high for all outcomes (rho> 0.93, p<0.001; except Head Area rho= 0.76 p<0.05), significant differences were found between scanner results. In most cases, QDR values were significantly lower than Discovery values (p< 0.05). Exceptions where QDR results were significantly higher included: Head Area, Head BMC, Head BMD. Significant differences were not detected for Ultradistal Radius BMD, Femoral Neck BMD or Lumbar Spine Area.

Conclusion: In pediatric and young adult subjects, systematic differences were noted between scans obtained on Hologic Discovery A and QDR 4500W model scanners, despite cross-calibration. Values appear to be systematically higher for Discovery A results. These findings have important implications for both clinical and research purposes. In the event that substitution of scanners is required, it would be advisable to repeat measurements on each scanner within the same session to evaluate and address any systematic bias.

***Disclosures: Jodi Dowthwaite**, None.*

SU0305

Trabecular bone score (TBS) marginally improves the prediction of prevalent vertebral fractures with bone densitometry in primary care. Petra Elders*[1], Thomas Merlijn[2], Martin Den Heijer[3], Coen Netelenbos[4]. [1]Free University Medical Centre, The Netherlands, [2]dpt General Practice & Elderly Care, VU Medical Centre, Netherlands, [3]VU Medical CenterPostbus 70571007 MB Amsterdam, The Netherlands, [4]VU Medical Center, The Netherlands

Introduction: The trabecular bone score TBS is a quantification technique of local variations in gray level that can be applied to an existing DEXA exam. In case control studies TBS has been shown to give an incremental increase in the odds ratio for spine fracture when combined with lumbar BMD [1]. Also it has been shown to predict clinical fractures independently from and equally well as spinal BMD [2].

Research question

We studied whether the TBS of the lumbar spine (TBS) improves the prediction of prevalent vertebral fractures with FRAX and bone densitometry measurements in the prediction of vertebral fractures in primary care.

Design: N=3601 women who were referred for bone densitometry in a primary care laboratory by there GP's filled in a fracture risk questionnaire, received bone densitometry and instant vertebral assessment (IVA) and had their height and weight measured. Single component and multiple component prediction models consisting of FRAX (estimated absolute risk of major osteoporotic fractures without BMD, UK reference data), BMD measurements and TBS were compared with both univariate and multivariate regression analysis and receiver operator curve (ROC) analysis.

Results: Mean age ± SD of the women was 64.4 ± 11.4 years. Mean BMI ± SD was 26.5± 4.8 kg/m^2. Of the women 42% had previous fracture(s) and 16% had apparent vertebral fractures on IVA (thoracic spine: ⩾ Genant grade 2, lumbar spine; ⩾ Genant grade 1). Odds ratio's and AUC of the univariate, bivariate and multivariate logistic regression models are shown in table 1.

Condusion: TBS predicted vertebral fractures independently from BMD and FRAX and improved the prediction with both BMD measurements. However, the differences were small. FRAX was the best single predictor of prevalent vertebral fractures and performed equally well as the model in which BMD and TBS were also included.

References

1. Boutroy S, Hans D, Sornay-Rendu E et al. Osteoporos Int (2013) 24: 77-85
2. Hans D, Goertzen AL, Krieg M-A et al. J Bone Min Res (2011) 26: 2762-2769

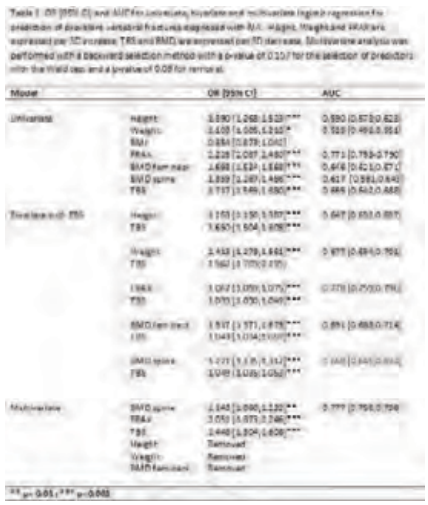

Table1

***Disclosures: Petra Elders**, None.*

SU0306

Trabecular Bone Score: Evaluation of Precision and Comparison of Values Between GE Lunar Prodigy and Lunar iDXA Densitometers. Diane Krueger*, Jessie Libber, Neil Binkley. University of Wisconsin, Madison, USA

Trabecular bone score (TBS), a novel gray-level measurement derived from lumbar L-spine DXA image texture, is related to microarchitecture and fracture risk independently of BMD and clinical risk factors. Widespread clinical TBS use will require stability over time and ideally comparability across scanners. This study explored short-term TBS reproducibility and evaluated whether TBS differs between GE Lunar Prodigy and iDXA densitometers.

Reproducibility was assessed from replicate scans in 30 women participating in a comparative Prodigy/iDXA precision assessment and 180 men and women evaluated to compare BMD precision between sex and technologist on an iDXA. Comparability between instruments was evaluated in 3 groups; 72 participants in a Prodigy/iDXA comparison, 30 women participating in the precision assessment noted above and 30 men and women in a clinical cross calibration exercise using 3 instruments (2 Prodigy, 1 iDXA). All scans were obtained on each instrument the same day, except for the cross-calibration exercise, which was performed over 2 weeks. Prodigy and iDXA TBS values were compared using linear regression and Bland-Altman analyses. Precision was assessed with the ISCD Precision Calculator and compared by F-test or factorial ANOVA. All analyses were performed on raw TBS values without TBS phantom cross-calibration.

Short-term L1-L4 BMD and TBS precision was similar on iDXA and Prodigy; L1-4 BMD %CV = 1.9% and 1.5% respectively. TBS %CV = 1.6% on Prodigy and 1.4% on iDXA. iDXA precision in 3 technologists ranged from a %CV of 0.96 - 1.59 for BMD and 1.46 - 2.72 for TBS. Between technologist differences ($p < 0.05$) of similar magnitude were observed for both BMD and TBS. No sex difference was observed with either method.

Prodigy to Prodigy TBS values were highly correlated; $R^2 = 0.90$ with bias of -0.013 TBS units (~ 0.14 SD). Agreement was less robust comparing multiple Prodigy and iDXA instruments; TBS $R^2 = 0.63 – 0.85$ with biases of -0.008 to -0.035 TBS units (up to ~ 0.3 SD).In conclusion, TBS precision is comparable to that of BMD and does not differ between men and women. Additionally, in these small samples, slight TBS differences were observed between iDXA and Prodigy scans. These data suggest a potential difference between instruments, perhaps due to higher iDXA image resolution. Further study to clarify potential between-instrument TBS differences, and whether such differences have clinical significance, is indicated.

***Disclosures: Diane Krueger**, None.*

SU0307

A novel method for obtaining bone mineral densities from a dataset of radiology reports and clinic notes: Natural language processing in a national cohort of postmenopausal veterans. Joanne LaFleur*[1], Thomas Ginter[2], Jeffrey Curtis[3], Robert Adler[4], Irene Agodoa[5], Brad Stolshek[5], Richard Nelson[2], Scott DuVall[2]. [1]University of Utah, USA, [2]University of Utah Division of Epidemiology, USA, [3]University of Alabama at Birmingham, USA, [4]McGuire VA Medical Center, USA, [5]Amgen Inc, USA

BACKGROUND Large epidemiology studies of osteoporosis are often limited to structured data such as claims (medical diagnosis, procedure codes, and pharmacy records) and electronic medical records (problem lists, medication lists, and laboratory findings). It is difficult to assess patient bone mineral density (BMD) T-scores in such studies without human chart review because these data are rarely recorded in discrete fields.

OBJECTIVE We developed a natural language processing (NLP) tool that could extract these data from narrative clinic notes and radiology reports.

METHODS We identified female veterans ⩾50 years of age who filled a bisphosphonate (BP) prescription in 2003-11. Of those, incident and prevalent BP users were included if they received care at least 6 months prior to the first BP fill. Narrative records for all patients including radiology reports and clinic notes were mined using NLP techniques for mentions of T-score observations at the femoral neck, total hip, lumbar spine, or 1/3 radius. A random sample of these records was reviewed by trained human annotators to assess the accuracy of the tool for extracting anatomy, T-score, and the relationship between anatomy and T-score. These findings were compared to the proportion of women who had a procedure code for a BMD scan in the structured data.

RESULTS Out of 1.6 million female veterans, 43,543 (2.6%) received a BP during the study period, of which 36,280 (83.3%) had ⩾6 months pre-index observation and were included in the cohort. The mean (SD) age was 65.7 (12.5). The NLP tool identified 22,964 (63.3%) with at least one BMD T-score at within 6 months before and 3 months after the index BP. Validation showed that overall accuracy was 92.6% for anatomic site, 82.8% for T-score value, and 82.8% for the relationship between the two. Accuracy was much higher for radiology reports than for clinic notes: 92.8%, 92.8%, and 90.4% (anatomic site, T-score, and relationship, respectively) in radiology reports versus 94.4%, 72.8%, and 75.2% in clinic notes. The figure shows the proportions with results versus procedure codes. Of those with at least one T-score observation, the mean (SD) was -1.58 (1.75); 11,105 (48.3%) had osteopenia and 7,139 (31.1%) had osteoporosis.CONCLUSIONS NLP was effective at extracting BMD T-score results from narrative records, particularly radiology reports. This new tool makes available clinical data previously unavailable in large secondary datasets.

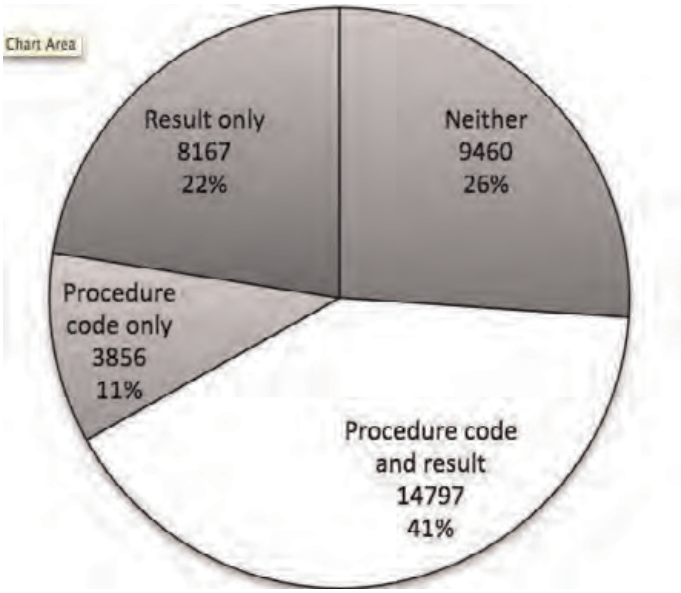

Figure. Proportions of patients with bone mineral density test results and/or procedure codes

***Disclosures: Joanne LaFleur**, Amgen Inc, 6; Merck, 6; Amgen Inc, 2*
This study received funding from: Amgen Inc

SU0308

Bone Mineral Density in Korean Women with Uterine Leiomyoma. Tae-Hee Kim*[1], Hae-Hyeog Lee[2], Junsik Park[2], Soo-Ho Chung[2], Dong-Won Byun[3]. [1]Soonchunhyang University College of Medicine, South Korea, [2]Department of Obstetrics & Gynecology, Soonchunhyang University College of Medicine, South Korea, [3]Internal Medicine, Soonchunhyang University College of Medicine, South Korea

Objective: Uterine leiomyomas, benign pelvic tumors, are prevalent and main cause of hysterectomy. As leiomyomas' growth has been reported to be linked with estrogen hormones, the question of whether there is any association between leiomyomas and bone health arises. The objective of the present study was to examine the relationship between leiomyomas and bone health in Korean women. Design: Retrospective observational study. Material & methods: We collected past data of 426 Korean women who underwent bone densitometry from January, 2010 to December, 2012. BMD and T-score of lumbar spine and femur neck were measured using DXA machine (GE Lunar Prodigy, GE Lunar Corp., Madison, WI, USA). Data are presented as mean ± SEM. Results: For the entire study population, the mean age (years) was 56.66. Uterine leiomyoma group was 158 and control group was 304. There was a significant difference in the mean BMD (g/cm^2) in the uterine leiomyoma group (spine :1.04 ± 0.01, femur neck : 0.85 ± 0.01), compared with control group (spine : 0.98 ± 0.01, p=0.003, femur neck: 0.81 ± 0.01, p=0.001). The T–score of spine for uterine leiomyoma group was significantly higher, compared with the control group (spine: -0.79 ± 0.01 and -1.25 ± 0.08 with p=0.001, femur neck: -0.62 ± 0.08 and -1.01 ± 0.06 with p=0.000). Conclusion: Consistent with previously reported data, our data showed a significantly higher BMD in Korean women with uterine leiomyoma. The implications of these findings need to be confirmed in future longitudinal studies. For comparison not only with BMD, but also with actual fracture risk in both groups, further studies are suggested.

***Disclosures: Tae-Hee Kim**, None.*

SU0309

Differences in bone geometry, mass and microarchitecture between Caribbean-Hispanic and Caucasian young men. Anna Kepley*[1], Chiyuan Zhang[2], Donald McMahon[3], Elizabeth Shane[3], Thomas Nickolas[3]. [1]Columbia University Medical Center, USA, [2]Columbia University, USA, [3]Columbia University College of Physicians & Surgeons, USA

United States epidemiologic data on bone mass in Hispanics are currently based upon Mexican-Americans and may not be generalizable to Caribbean-Hispanics who may have more African racial admixture than Mexican-Americans. In addition, it is not known whether bone geometry, mass and microarchitecture differ between Caribbean-Hispanic and Caucasian men at peak bone mass. Therefore, we enrolled 60 healthy young men between the ages of 25 and 35, 22 Caribbean Hispanic and 38 Caucasian (n=38) men in a cross-sectional study. We measured areal bone mineral density (BMD) by dual energy X-ray absorptiometry (DXA) of the lumbar spine (LS), total hip (TH), femoral neck (FN), 1/3- and ultra- distal radius (1/3R and UDR, respectively). High-resolution peripheral quantitative tomography (HRpQCT, Scanco Medical) was used to assess bone geometry, mass and microarchitecture at the distal radius and tibia. Results are expressed as Means ± SD. Univariate comparisons were made with Students T-Test; multivariate comparisons were made with generalized linear models adjusted for age and anthropometric differences. Hispanics were slightly but significantly older and considerably heavier with higher BMI than Caucasians. By DXA, univariate models demonstrated that Hispanics had greater UDR BMD ($p<0.05$). In multivariate models, differences in areal BMD were no longer significant. By HRpQCT at the radius, univariate models demonstrated that Hispanics had smaller trabecular area ($p<0.05$), but greater cortical area ($p<0.01$), thickness ($p<0.01$) and density ($p<0.01$); these relationships persisted in multivariate models, which also revealed that Hispanics had thicker trabeculae than Caucasians ($p<0.05$). At the tibia, Caribbean-Hispanics had greater cortical area ($p<0.001$), thickness ($p<0.001$) and density ($p<0.001$); these relationships persisted in multivariate models, which also revealed greater total density ($p<0.05$) than Caucasians. In conclusion, after adjustment for differences in anthropometric measures, Caribbean-Hispanic men had equivalent areal BMD to Caucasian men. However, by HRpQCT Caribbean-Hispanic men had smaller bones with thicker and denser cortices, differences that could lead to greater bone strength. Further studies are needed to elucidate genetic, biochemical and metabolic factors that could lead to differences in skeletal structure between Caribbean-Hispanics and Caucasians, and to assess skeletal differences between Hispanics of Caribbean and non-Caribbean origin.

Table. Univariate comparisons using Students T-Test. Multivariate comparisons using a generalized linear model adjusted for age, weight, height and height-weight interactions.

	Hispanic (n=22)	Caucasian (n=38)	Univariate p-value	Adjusted p-value
Age (years)	31.3±3.3	28.4±2.6	<0.01	-
Height (cm)	178.3±6.7	181.6±7.4	NS	-
Weight (kg)	95.1±18.2	81.2±10.4	<0.01	-
BMI (kg/m^2)	29.8±5.0	24.6±2.5	<0.0001	-
BMD by DXA				
Lumbar Spine (g/cm^2)	1.112±0.122	1.076±0.106	NS	NS
Total Hip (g/cm^2)	1.152±0.109	1.094±0.117	NS	NS
Femoral Neck (g/cm^2)	1.035±0.132	0.971±0.131	NS	NS
1/3R (g/cm^2)	0.827±0.065	0.816±0.055	NS	NS
Ultradistal Radius (g/cm^2)	0.570±0.055	0.534±0.047	<0.05	NS
HR-pQCT: Radius				
Total Area (mm^2)	335±71	371±65	NS	NS
Cortical Area (mm^2)	80±15	68±12	<0.01	<0.01
Trabecular Area (mm^2)	256±72	303±71	<0.05	<0.05
Total Density (mg HA/cm^3)	387±63	340±55	<0.01	<0.01
Cortical Density (mg HA/cm^3)	884±50	851±51	<0.05	<0.05
Trabecular Density (mg HA/cm^3)	214±38	205±31	NS	NS
Cortical Thickness (mm)	1.003±0.199	0.821±0.190	0.001	<0.01
Trabecular Thickness (mm)	0.082±0.015	0.079±0.011	NS	<0.05
Trabecular Number (1/mm)	2.2±0.3	2.2±0.3	NS	NS
Network Heterogeneity (mm)	0.156±0.030	0.155±0.027	NS	NS
HR-pQCT: Tibia				
Total Area (mm^2)	919±179	974±136	NS	NS
Cortical Area (mm^2)	169±23	143±28	<0.001	<0.05
Trabecular Area (mm^2)	750±183	831±148	NS	NS
Total Density (mg HA/cm^3)	338±50	314±50	NS	<0.05
Cortical Density (mg HA/cm^3)	884±41	845±37	<0.001	<0.001
Trabecular Density (mg HA/cm^3)	205±30	217±31	NS	NS
Cortical Thickness (mm)	1.440±0.261	1.165±0.285	<0.001	<0.05
Trabecular Thickness (mm)	0.074±0.010	0.080±0.009	NS	NS
Trabecular Number (1/mm)	2.3±0.3	2.3±0.3	NS	NS
Network Heterogeneity (mm)	0.158±0.039	0.159±0.033	NS	NS

Table

***Disclosures: Anna Kepley**, None.*

SU0310

Impact of a Patient Self-Referral of DXA Intervention on Patient-Provider Communication about Osteoporosis Testing and Treatment: A Randomized Trial in Two Large Regional Healthcare Systems. Amy Warriner*[1], Ryan Outman[1], Jeffrey Curtis[1], Adrianne Feldstein[2], David Redden[1], Junling Ren[3], Brandi Robinson[3], Douglas Roblin[3], Ana Rosales[4], Monika Safford[1], Kenneth Saag[1]. [1]University of Alabama At Birmingham, USA, [2]Kaiser Permanente Center for Health Research, USA, [3]Kaiser Permanente Georgia, USA, [4]Kaiser Permanente Northwest, USA

Purpose: Patient-provider communication around osteoporosis testing and treatment is suboptimal and methods to improve it are incompletely understood. Using traditional care approaches, treatment is often not initiated following abnormal DXAs due to inadequate provider-patient communication. We hypothesized that a DXA self-referral intervention would lead to greater patient-provider communication about osteoporosis testing and treatment than the usual practice of physician referral.

Methods: We conducted a group randomized controlled trial involving 14 Kaiser Permanente Northwest (KPNW) primary care clinics and 15 Kaiser Permanente Georgia (KPG) primary care clinics. Women 65 years or older with no identifiable

DXA scan in the past 5 years and no osteoporosis treatment in the past year were eligible. Clinics were randomized into 1 of 3 groups: A self-referral intervention (SELF) (invitation by mail to self-schedule a DXA); SELF+DVD (consisting of SELF, plus an educational brochure and DVD promoting patient-provider communication about osteoporosis); and, Usual Care (UC) (No DVD or self-referral). Providers in all groups were directed to web-based CME training on osteoporosis screening and treatment. Nine months after randomization, patients were mailed a survey to assess whether they had talked with a provider about osteoporosis testing and treatment.

Results: In KPNW, 3191 women were randomized to SELF, 3720 to SELF+DVD, and 1889 to UC of which 1659 (52%), 1438 (39%) and 989 (52%), respectively, completed the survey. In KPG, 1064 women were randomized to SELF, 1005 to SELF+DVD, and 1170 to UC of which 327 (31%), 278 (27.7%) and 406 (34.7%), respectively, completed the survey. The table shows the rates and odds of communication with providers about osteoporosis testing and treatment by study arm and region.

Conclusions: In both regions, patients receiving a DXA self-referral intervention reported significantly higher rates of communication with a provider about osteoporosis testing. In KPNW, intervention patients also reported significantly higher rates of communication about osteoporosis treatment. The addition of an educational DVD promoting patient-provider communication did not result in significantly higher rates of communication over the self-referral intervention alone. Allowing eligible women to self-schedule DXA scans may be an effective low cost strategy to increase patient-provider communication about osteoporosis related behaviors.

Table. Rates and odds of patient-provider communication related to osteoporosis testing and treatment by study arm and region.

Region	Study Arm	Total Survey Respondents n	Communication about Osteoporosis Testing n (%)	Odds Ratio (95% CI)	Communication about Osteoporosis Treatment n (%)	Odds Ratio (95% CI)
KPNW	Self	1659	481 (29.0%)	1.8 (1.5-2.2)*	209 (12.6%)	1.9 (1.4-2.6)*
	Self +DVD	1438	455 (31.6%)	2.0 (1.7-2.5)*	180 (12.5%)	1.9 (1.4-2.6)*
	UC	989	184 (18.6%)	REF	69 (7.0%)	REF
KPG	Self	327	118 (36.1%)	1.4 (1.0-1.9)†	53 (16.2%)	1.2 (0.8-1.9)
	Self +DVD	278	107 (38.5%)	1.5 (1.1-2.2)‡	51 (18.4%)	1.4 (0.95-2.2)
	UC	406	116 (28.6%)	REF	55 (13.6%)	REF

* p <.0001, † p = 0.03, ‡ p = 0.006
CI = Confidence Interval

Table

***Disclosures: Amy Warriner**, None.*

SU0311

National osteoporosis risk factor's and BMD measurements study of postmenopausal women population in Latvia. Inese Pavlina*[1], Ingvars Rasa[1], Inara Adamsone[2], Ilze Daukste[3], Sandra Jaundzeikare[1], Dainis Kaneps[4], Ingrida Kaze[1], Agita Medne[5], Signe Zelca[1]. [1]Riga East Clinical University Hospital, Latvia, [2]Pauls Stradins Clinical University Hospital, Latvia, [3]Riga 2nd Hospital, Latvia, [4]Latvian Maritime Medicine Cente, Latvia, [5]Health Centre 4, Latvia

Objective(s): We aimed to assess the prevalence of osteoporosis (OP) risk factors, OP preventive and therapeutic measures among postmenopausal women in Latvia. We also aimed to correlate bone mineral density (BMD) with those OP risk factors in the population.

Material & Methods: 1,598 women took part in a national cross-sectional study conducted during May-October 2012. All women filled out a questionnaire with 25 multiple choice questions regarding to OP risk factors, i.e. fragility fractures, family history of fractures, physical exercises.Previous DXA, calcium, vitamin D usage and antiosteoporosis medication were recorded. BMD was subsequently measured in all participants by DXA in lumbar the spine (L1-L4) and total hip.

Results: The mean age of patients (pts) was 65.6 ±9.0 years. The mean body weight was 71.9 ±13.7 kg. The mean height was 159 ±6.3 cm, the mean time since menopause was 16.3 ± 4.6 years. Progressively reduced height was recorded in 79.2% of the patients. Previous fragility fractures were recorded in 38.6% patients, 26.8% had a family history of fractures. 59.5% had no physical activities. 63% of pts underwent DXA scan before, in 41.9% of them OP was previously diagnosed. 40.3% of pts measured 25 (OH) vitamin D before. 66.1% of them had reduced 25 (OH) vitamin D level. 60.7% of the pts used supplemental calcium and 36.2% - vitamin D. 31.3% received specific osteoporosis treatment. By over all DXA scan 14.3% of pts were identified as having osteoporosis, 56.4% were osteopenic values, and 29.3% had normal BMD. BMD measurements in the lumbar spine revealed that 30.8% of pts had normal BMD, 46.4% - were osteopenic, and 22.8% had osteoporosis. Different situation were in the hip measurments. Left hip measurements showed normal BMD in 27.7% pts, osteopenic values – in 62.7% patients, osteoporosis – in 9.6% pts. Right hip - BMD was found normal in 29.6%, but osteopenic values were found in 62.7% and osteoporosis in 7.8% of pts. BMD measurements in the lumbar spine, left and right hip negatively correlated with age ($p< 0.001$, $p< 0.001$ and $p< 0.001$ respectively), positively correlated with body weight ($p< 0.001$, $p< 0.001$ and $p< 0.001$ respectively).

Conclusion(s): This survey suggests that OP is suboptimally diagnosed, in Latvia, and insufficient attention is paid to OP risk factors. The results of this study also suggest that advancing age and lower weight are significant risk factors for low BMD in postmenopausal women in Latvia.

***Disclosures: Inese Pavlina**, None.*

SU0312

Reliable Osteoporosis Diagnostics with Pocket Size Ultrasound Instrument. Janne Karjalainen*[1], Ossi Riekkinen[1], Juha Töyräs[2], Jukka Jurvelin[2], Heikki Kroger[3]. [1]Bone Index Finland Ltd., Finland, [2]University of Eastern Finland, Finland, [3]Kuopio University Hospital, Finland

As we lack effective diagnostic devices at primary healthcare, over 75% of osteoporotic patients are not diagnosed nor receive treatment for their pathological condition[1]. In this study, a pocket size ultrasound (US) device was validated by using International Society for Clinical Densitometry (ISCD) and National Osteoporosis Society (NOS) guidelines for osteoporosis (OP) diagnostics[2,5]. The guidelines suggest a triage approach for reliable use of peripheral densitometry techniques. This approach requires determination of 90% sensitivity and specificity thresholds for osteoporosis as measured with axial DXA[2,3].

Elderly Caucasian women (n = 445, age = 68.8 ± 8.5 years) under OP suspicion were examined using pulse-echo US measurements (2.5MHz) of cortical bone thickness in proximal tibia (Bindex® prototype, Bone Index Finland Ltd., Kuopio, Finland). The device provides a diagnostic parameter, Density index, DI[4] (patent pending), based on the US measurements and subject characteristics. Further, bone mineral density of the femoral neck (BMD_{neck}) and total hip (BMD_{total}) was determined by using axial DXA. Osteoporosis was diagnosed in individuals with T-Score lower than -2.5 in total hip or femoral neck. The 90% sensitivity and specificity thresholds for DI were determined according to the ISCD guidelines. In addition, the reproducibility (root mean square coefficient of variation (CV_{rms} %)) of DI measurement was analyzed as average of two operators CV_{rms}, who measured 16 subjects three times.

In total 16.9% of the patients were diagnosed with OP osteoporotic by DXA. By using triage approach for DI, 50.3% of patients were over the healthy threshold , 17.1% was under the osteoporotic threshold and only 32.6% of the patients were found to require additional DXA measurement to verify osteoporosis diagnosis. The mean reproducibility of DI measurement was 2.5%.The results demonstrate that the ultrasound instrument provides a fast (~ 1 minute) and reliable method for osteoporosis diagnostics, feasible at primary healthcare. According to the NOS guidelines, treatment is recommended for patients with peripheral densitometry value under the osteoporotic threshold (90% specificity threshold)[5]. By using the triage approach and the US technology the treatment of osteoporosis would significantly increase.

References

[1]Nguyen,Med J Aust.,2004, [2]Hans,J Clin Densitom.,2008, [3]Blake,Osteoporos Int.,2005, [4]Karjalainen,Osteoporos Int.,2012, [5] Patel,NOS practical guide,2011.

***Disclosures: Janne Karjalainen**, Bone Index Finland Ltd., 3*
This study received funding from: Bone Index Finland Ltd.

SU0313

The relationship between sarcopenia and bone mineral density over the year post hip fracture. Denise Orwig*[1], Marc Hochberg[2], Emma G. Shledon[1], William G. Hawkes[2]. [1]University of Maryland, Baltimore, USA, [2]University of Maryland School of Medicine, USA

The relationship between muscle mass and bone mineral density (BMD) is complex and understanding these interactions is critical among older adults who are at risk for declines in both. There is growing evidence linking low muscle mass (sarcopenia) to functional disability, falls, and decreased BMD. Studies have reported high levels of sarcopenia following hip fracture and hip fracture patients can lose up to 6% additional BMD in the year post fracture. However, little is known about the relationship between sarcopenia and loss of BMD following a hip fracture. We performed a post-hoc analysis of data from the Baltimore Hip Studies (BHS)-4 cohort, a randomized controlled trial of a home-based exercise program in 180 community-dwelling older women (mean [SD] age 82.3 [7.0] years)with surgical repair of an incident non-pathologic hip fracture. Women were recruited and baseline data were acquired within 15 days of fracture. BMD of the whole body and contralateral hip (total hip and subregions) and grip strength were measured at baseline and 2, 6, and 12 months post fracture. Sarcopenia was defined at baseline as appendicular skeletalean muscle mass relative to height ≤ 5.67 kg/m2 and grip strength < 20 kg (n=138). At baseline 42% of the sample were sarcopenic; however, mean (SD) total hip BMD values did not differ significantly between those who were sarcopenic (0.625 (0.10) g/cm2) and those who were not (0.639 (0.11) g/cm2). Less than half the sample had sarcopenia at the time of fracture and just over half had sarcopenia at any time point over the 1 year post fracture. Baseline sarcopenic status was significantly associated with12-month total hip BMD ($p<.04$). A longitudinal analysis using a mixed effect model was performed. There was a trend for the time by sarcopenia interaction ($p<.08$) such that total hip BMD for those who were sarcopenic was lower at 12 months [(0.618 (0.01) vs. 0.628 (0.01)]. The fact that BMD did not differ by sarcopenic status at time of fracture, yet those with sarcopenia had lower BMD at 12 months highlights the possible longitudinal effects of muscle loss on BMD. More research is needed to understand whether interventions to increase muscle mass translate into reduction in BMD declines in such an at-risk group of hip fracture patients.

***Disclosures: Denise Orwig**, None.*

SU0314

Associations among Vitamin K Intake, Serum Osteocalcin Concentrations and Bone Traits in 37-to-47-year-old Caucasian Population - The PHOMI Study. Suvi Itkonen*[1], Lotta Juslin[1], Elisa Saarnio[1], Virpi Kemi[1], Merja Kärkkäinen[1], Heini Karp[1], Minna Pekkinen[2], Harri Sievänen[3], Kaisa Ivaska[4], Christel Lamberg-Allardt[1]. [1]University of Helsinki, Finland, [2]Folkhälsan Institute of Genetics, University of Helsinki, Finland, [3]UKK Institute for Health Promotion Research, Finland, [4]University of Turku, Finland

Vitamin K (VitK) is required in the carboxylation reaction of osteocalcin (OC). Low serum concentrations of undercarboxylated OC have been associated with hip fractures and lower bone mineral density (BMD). However, the role of dietary vitK in bone health remains unclear. The aim of the study was to investigate the associations among vitK intake, serum total OC concentrations and tibial BMD and bone mineral content (BMC) and bone strength indices in a cross-sectional Caucasian population in Finland.

A sample of 364 37-to-47-year-old pre-menopausal females who participated in the PHOMI Study was included in the analyses. Fasting blood samples were collected, as well as habitual dietary intake by 3-day food records and background data by a questionnaire. Serum total OC and some other biomarkers related to bone metabolism were analysed. BMD and BMC from distal and proximal sites of tibia were measured with peripheral quantitative computed tomography (pQCT). The data was analysed by correlation analysis and partial correlation analysis as T-scores of bone traits, adjusted for height, weight, physical activity, dietary calcium intake, smoking and serum 25-hydroxy vitamin D concentrations.

Dietary vitK correlated positively with distal tibia total area ($r=0.128$, $p=0.015$) but correlations with other bone traits were non-significant ($p>0.05$). After adjusting for covariates, no correlations among VitK intake and any bone traits existed ($p>0.05$). No correlation was observed between vitK intake and serum OC ($p>0.05$) neither in unadjusted nor adjusted models. Serum total OC correlated negatively with BMC ($r=-0.164$, $p=0.002$), BMD ($r=0.218$, $p<0.001$), bone strength index (BSI) ($r=0.204$, $p<0.001$), and stress-strain index (SSI) ($r=-0.127$, $p=0.016$) in distal tibia and in cortical strength index (CSI) ($r=-0.115$, $p=0.030$) in proximal tibia. After adjustment, statistically significant negative correlations existed between OC and distal tibial BMC ($r=-0.122$, $p=0.023$), BMD ($r=-0.157$, $p=0.003$) and BSI ($r=-0.140$, $p=0.009$), as well as proximal tibial BMD ($r=-0.160$, $p=0.003$). No significant correlations were found between OC and other bone traits ($p>0.05$).

In conclusion, we did not find associations between vitK intake and bone health in the adjusted model in the current study but serum OC was negatively correlating with some bone traits.However, there is a need for analysis of the role of different forms of vitK in the bone metabolism.

Keywords: vitamin K, osteocalcin, bone mineral density, bone mineral composition, bone strength

***Disclosures: Suvi Itkonen**, None.*

SU0315

Associations of Protein Intake and Protein Source with Bone Biomarkers, Bone Mineral Density and Fracture Risk in a Canadian Population-based Study. Lisa Langsetmo*[1], Claudie Berger[2], Nancy Kreiger[3], David Goltzman[4], Susan Barr[5], Stephanie Kaiser[6], Jerilynn Prior[5], Robert Josse[7], Elham Rahme[8], David Hanley[9], Alexandra Papaioannou[10], Jonathan Adachi[11], Christopher Kovacs[12]. [1]Canandian Multicenter Osteoporosis Study, Canada, [2]CaMos, McGill University, Canada, [3]University of Toronto, Canada, [4]McGill University, Canada, [5]University of British Columbia, Canada, [6]Dalhousie University, Canada, [5]University of British Columbia, Canada, [7]St. Michael's Hospital, University of Toronto, Canada, [8]University of McGill, Canada, [9]University of Calgary, Canada, [10]Hamilton Health Sciences, Canada, [11]St. Joseph's Hospital, Canada, [12]Memorial University of Newfoundland, Canada

Background: High dietary protein has been hypothesized to lead to high dietary acid load causing bone resorption, increased calcium loss, and increased risk of fracture; but not all studies support this hypothesis.

Objective: To determine the association between total protein intake, and protein intake by source (dairy, non-dairy animal, plant-based) with biomarkers of bone/mineral metabolism [25-hydroxy vitamin D (25OHD), parathyroid hormone (PTH), insulin-like growth factor 1 (IGF1)], bone mineral density (BMD), and osteoporotic fracture.

Methods: Canadian Multicentre Osteoporosis Study participants completed a food frequency questionnaire at Year 2 (1997-99). Protein intake was assessed as percent of total energy intake (TEI) for 1919 men and 4591 women. At Year 5 participants had BMD measured and a subset had fasting blood samples taken. Participants were contacted annually up to Year 15 to ascertain incident fracture. Cox proportional hazards and multiple linear regression models were used to assess association between protein and incident main fracture (hip, spine, forearm, humerus), biomarkers and BMD. Hazard ratios (HR) or betas were adjusted for confounders and reported with 95% confidence intervals (CI).

Results: Among women 50+y, higher dietary protein (%TEI) was associated with higher serum 25OHD, lower serum PTH, higher IGF1, and higher total hip BMD (Table 1-2);similar but non-significant (NS) relationships were found in men. Higher dairy protein (%TEI) was associated with increased serum 25OHD in both women and men 50+y. Plant-based protein (%TEI) was associated with lower BMD at all sites in women 50+y, with similar but NS relationships in other groups. In men 50+y, higher dairy protein (%TEI) was associated with higher BMD at all sites, with similar but NS relationships in other groups. In subjects 50+y, moderate protein intake (15%TEI) was associated with lowest risk of main fracture; with HR= 1.76 (95% CI: 1.03-3.02) for 10%TEI vs 15%TEI in women and HR=4.16 (95% CI: 1.29-13.4) for 10%TEI vs 15%TEI in men, while protein intake greater than 15%TEI was associated with a NS trend of increased main fracture risk. There was no heterogeneity by source of protein.Conclusion: In contrast to hypothesized risk of high protein, we found that for adults 50+y, low protein intake (below 15% TEI) may lead to changes in serum biomarkers, low bone mass and increased fracture risk. Source of protein was a determinant of BMD, but not fracture risk.

Table 1: Association between protein intake (as a percentage of total intake) with the biomarkers 25-hydroxy vitamin D (25OHD), parathyroid hormone (PTH) and insulin like growth hormone 1 (IGF1)

	25OHD (nmol/L)	PTH (log-scale)	IGF1 (log-scale)
Women 25-49 y			
%Total protein	-0.8 (-5.5, 3.9)	-0.012 (-0.084, 0.060)	-0.002 (-0.078, 0.073)
% Dairy protein	-2.9 (-7.3, 1.5)	-0.007 (-0.074, 0.061)	-0.004 (-0.074, 0.067)
% Non-dairy animal protein	-2.0 (-7.6, 3.7)	0.036 (-0.051, 0.123)	-0.095 (-0.186, -0.004)
% Plant protein	0.0 (-3.6, 3.7)	-0.033 (-0.089, 0.024)	0.002 (-0.053, 0.057)
Men 25-49 y			
% Total protein	3.6 (-2.2, 9.5)	0.041 (-0.061, 0.143)	0.035 (-0.031, 0.100)
% Dairy protein	3.5 (-1.8, 8.7)	0.068 (-0.020, 0.156)	0.029 (-0.035, 0.094)
% Non-dairy animal protein	-0.7 (-7.5, 6.1)	0.058 (-0.056, 0.172)	0.029 (-0.043, 0.100)
% Plant protein	-0.5 (-6.3, 5.3)	-0.050 (-0.148, 0.047)	0.037 (-0.036, 0.109)
Women 50+ y			
% Total protein	3.0 (1.2, 4.8)	-0.032 (-0.064, 0.000)	0.039 (0.011, 0.067)
% Dairy protein	2.8 (1.1, 4.5)	-0.003 (-0.033, 0.027)	0.006 (-0.020, 0.031)
% Non-dairy animal protein	0.0 (-2.1, 2.1)	-0.033 (-0.069, 0.003)	0.016 (-0.015, 0.046)
% Plant protein	0.8 (-1.0, 2.5)	-0.016 (-0.047, 0.016)	0.027 (0.001, 0.054)
Men 50+ y			
% Total protein	1.8 (-1.1, 4.7)	-0.030 (-0.080, 0.020)	0.018 (-0.025, 0.060)
% Dairy protein	2.9 (0.3, 5.5)	0.034 (-0.018, 0.085)	0.022 (-0.022, 0.065)
% Non-dairy animal protein	-2.7 (-5.9, 0.5)	0.036 (-0.027, 0.098)	0.011 (-0.031, 0.052)
% Plant protein	0.5 (-2.5, 3.5)	0.004 (-0.055, 0.064)	-0.016 (-0.055, 0.023)

*Estimates (95% confidence intervals). Shading indicates confidence interval excludes null value.

Table 1

Table 2: Association between protein intake (as a percentage of total intake) with bone mineral density (BMD) at the total hip, lumbar spine, and femoral neck.

	Total Hip BMD (g/cm²)	Lumbar Spine BMD (g/cm²)	Femoral Neck BMD (g/cm²)
Women 25-49 y			
% Total protein	-0.001 (-0.011, 0.010)	-0.002 (-0.013, 0.009)	-0.001 (-0.010, 0.009)
% Dairy protein	0.009 (-0.001, 0.019)	0.009 (-0.002, 0.021)	0.006 (-0.003, 0.015)
% Non-dairy animal protein	-0.004 (-0.015, 0.006)	-0.012 (-0.024, 0.000)	-0.003 (-0.012, 0.007)
% Plant protein	-0.010 (-0.020, 0.000)	-0.001 (-0.012, 0.011)	-0.009 (-0.018, 0.000)
Men 25-49 y			
% Total protein	0.004 (-0.012, 0.019)	-0.001 (-0.016, 0.015)	0.006 (-0.006, 0.018)
% Dairy protein	0.013 (-0.002, 0.028)	0.019 (0.004, 0.035)	0.013 (0.001, 0.026)
% Non-dairy animal protein	-0.001 (-0.015, 0.013)	-0.011 (-0.026, 0.003)	0.000 (-0.012, 0.011)
% Plant protein	-0.006 (-0.019, 0.008)	-0.005 (-0.018, 0.009)	-0.004 (-0.015, 0.007)
Women 50+ y			
% Total protein	0.005 (0.000, 0.010)	0.003 (-0.004, 0.009)	0.004 (-0.001, 0.008)
% Dairy protein	0.006 (0.001, 0.010)	0.002 (-0.004, 0.008)	0.004 (0.000, 0.008)
% Non-dairy animal protein	0.004 (-0.001, 0.009)	0.010 (0.003, 0.016)	0.003 (-0.001, 0.007)
% Plant protein	-0.006 (-0.011, -0.001)	-0.010 (-0.016, -0.003)	-0.004 (-0.008, 0.000)
Men 50+ y			
% Percent protein	0.007 (-0.002, 0.016)	0.007 (-0.004, 0.018)	0.008 (0.001, 0.016)
% Dairy protein	0.014 (0.006, 0.023)	0.013 (0.002, 0.025)	0.013 (0.005, 0.020)
% Non-dairy animal protein	-0.002 (-0.011, 0.007)	0.000 (-0.011, 0.011)	0.001 (-0.007, 0.008)
% Plant protein	-0.006 (-0.015, 0.002)	-0.008 (-0.019, 0.003)	-0.005 (-0.012, 0.003)

* Estimates (95% confidence intervals). Shading indicates confidence interval excludes null value.

Table 2

***Disclosures: Lisa Langsetmo**, None.*

This study received funding from: Canadian Agri-Science Clusters Initiative, Dairy Research Cluster (Dairy Farmers of Canada, Agriculture and Agri-food Canada, Canadian Dairy Commission)

SU0316

Development of a Simplified Self-Questionnaire for Evaluation of Calcium Intake in Osteoporosis Prevention: a Study from the Workgroup SOLIDOS.

Florence Levy-Weil*[1], Eric Lespessailles[2], Catherine Beauvais[3], Dominique Aubraye[4], Francoise Debiais[5], Christelle Sordet[6], Corinne Thevenot[7], Didier Poivret[8], Patrice Fardellone[9], Anne-Christine Rat[10]. [1]Centre Hospitalier Victor Dupouy, France, [2]Centre Hospitalier Regional, France, [3]Service de Rhumatologie, CHU Saint-Antoine, France, [4]Service de Rhumatologie, Centre hospitalier Victor Dupouy, France, [5]Hopital Jean Bernard, France, [6]Service de Rhumatologie, CHRU Strasbourg, France, [7]Médecine Interne et Spécialité, CH Laon, France, [8]Service de Rhumatologie, CHR Metz-Thionville, France, [9]Service de rhumatologie, CHU Hôpital Nord, France, [10]Lorraine Universié Ea 4360 Apemac, Cic-Ec Cie6 et Rhumatologie, CHU Nancy-Brabois, France

Background: An adequate supply of calcium and vitamin D is essential for bone health. An assessment of calcium intake is necessary among patients with bone loss for correct adjustment.

Calcium intake measures are usually imperfect because validated questionnaires are few or too complex to be used in daily practice. The aim of the study was to develop a shorter form of the validated calcium intake self-questionnaire (the Fardellone questionnaire (FQ)) currently used in France (1).

Methods: The FQ is based on 20 different types of food with a high calcium content and/or frequently eaten in France (hereafter called items). The first stage was to update the existing FQ to be more suited with the current French diet (mainly by adding new mineral waters). In stage two, based on this updated FQ, we implemented a step-by-step approach in which we progressively reduced the number of answering modalities, the number of items based on their maximal daily calcium intake and we simplified the weight (calcium content) used to calculate the score of calcium intake. Analyses were based on equivalence tests with a limit of equivalence set at 100 mg (table 1).

Results: 717 in or outpatients from 7 hospitals completed the FQ throughout 2012. Mean age was 62 years (±12), 90% were women and 34% had a diagnosis of osteoporosis. All the obtained selected scores were equivalent except for the one including only the dairies (table 2). Finally, the questionnaire with 13 items was retained because it was easily and quickly completed by the patients and it still remained equivalent to the validated FQ. In this new questionnaire, we simplified the answering modalities, the number of items by deleting all foods containing less than 150mg of daily calcium intake and we simplified the weight to calculate the score.

Conclusion: The new 13 items self-questionnaire is equivalent to the French reference FQ. It has the advantage to be easy to use and quick to fill. Thus, it can be accessible to a large majority of patients in clinical practice. The validity of this short form will need further assessment by performing comparison with calcium intake as measured by a detailed diet survey. Thereafter, this new questionnaire can be applicable to other countries provided that food habits are similar.

(1) Fardellone and al. Rev Rhum Mal Osteoartic 1991

Table 1: Scores of the different short forms developed from the Fardellone questionnaire

Different short forms developed from the Fardellone questionnaire	Mean	95% confidence intervals
Fardellone	748,6	(726,8 ; 770,4)
Updated Fardellone	775,9	(753,5 ; 798,3)
Simplification of the answering modalities	778,5	(756,9 ; 800,0)
+ Deletion of the food with a maximal daily intake < 100mg	709,7	(687,7 ; 731,7)
+ Simplification of the weights (calcium content)	710,0	(687,9 ; 732,2)
+ Deletion of the food with a maximal daily intake < 150mg	688,0	(665,9 ; 710,1)
Dairy products only	464,8	(447,5 ; 482,0)

Table 1

Table 2: Differences between the Fardellone questionnaire and different short forms

Different short forms compared with the Fardellone questionnaire	Mean	95% confidence intervals
Comparison with the Fardellone questionnaire		
Updated Fardellone	-27,3	(-32,6 ; -22,0)
Comparison with the updated Fardellone questionnaire		
Simplification of the answering modalities	-29,9	(-35,1 ; -24,6)
+ Deletion of the food with a maximal daily intake < 100mg	66,2	(59,9 ; 72,5)
+ Simplification of the weights (calcium content)	65,9	(59,0 ; 72,7)
+ Deletion of the food with a maximal daily intake < 150mg	90,1	(82,9 ; 97,2)
Dairy products only	**313,3**	**(300,6 ; 326,0)**

Table 2

***Disclosures: Florence Levy-Weil**, None.*

SU0317

Early Postmenopausal Dietary Patterns and Markers of Bone Formation, but not Bone Resorption, Predict Bone Mineral Density 10 Years On.

Helen Macdonald*[1], Adrian Wood[2], Ania Gryka[2], Antonia Hardcastle[3], Lorna Aucott[2], Alison Black[4], William Fraser[2], David Reid[5]. [1]University of Aberdeen Musculoskeletal Research, United Kingdom, [2]University of Aberdeen, United Kingdom, [3]University of East Anglia, United Kingdom, [4]Woolmanhill Hospital Aberdeen Osteoporosis Research Unit, United Kingdom, [5]University of Aberdeen, GBR

The role of diet in bone health during adulthood is unclear. There is concern that by focusing on only one or two nutrients (eg calcium) the diet may become unbalanced to the detriment of other important nutrients, as their intake or gastrointestinal absorption may be reduced. As many nutrients have common food sources, associations attributed to a single nutrient may be spurious, as intakes for that nutrient may be a marker for a different nutrient. Investigating dietary patterns may be more appropriate. The aim of this study was to determine what dietary pattern consumed by early postmenopausal women predicted bone mineral density (BMD) ten years on.

We used dietary data collected from food frequency questionnaires from 3239 women (mean age 54y) at visit 2 (1997-2000) of the Aberdeen Prospective Osteoporosis Screening Study (APOSS) to generate dietary patterns using principal components analysis. At that visit, bone markers (urinary pyrridinoline cross-links expressed relative to creatinine, DPD/Cr, PYD/Cr; and serum pro-peptide of type 1 collagen P1NP) were measured. At visit 3 (2009-2012) 2099 women (mean age 66 y) returned for BMD measurements of the hip and spine (Lunar iDXA) of whom 1850 had dietary data at visit 2.

The third principal component at visit 2, reflecting a dietary pattern marked by high intakes of carbohydrates and fat, and low spirits (liquor) consumption, was associated with lower BMD at the hip and spine at visit 3. This remained significant after adjustment for visit 2 age, weight, height, physical activity and menopausal status. No other dietary pattern predicted BMD. Bone formation markers and not bone resorption markers at visit 2 predicted lower BMD at visit 3. There were small incremental changes for some nutrients with increasing quintile of this dietary pattern, but the dominant characteristic was alcohol intake, where the bottom quintile (10.8 g/d) had > twice the mean alcohol intake of the top quintile (4.1 g/d). Further examination of food groups showed that all classes of alcoholic drinks (beer, wine and spirits) decreased with increasing quintile of this diet.

Care needs to be taken when interpreting dietary patterns, but they provide data that are not subjected to the problems of co-linearity as with nutrient intakes. Our data are consistent in indicating that alcoholic drinks are protective for bone health. Early postmenopausal markers of bone formation may predict future bone health better than bone resorption.

	n	BMD hip visit 3 Pearson r (p)		BMD spine visit 3 Pearson r (p)
Dietary pattern visit 2	1791	-0.079 (0.001)	1850	-0.073 (0.002)
Adjusted*	1768	-0.076 (0.001)	1833	-0.069 (0.003)
P1NP visit 2	1412	-0.168 (<0.001)	1462	-0.181(<0.001)
DPD/Cr visit 2	1643	0.026	1693	-0.002
PYD/Cr visit 2	1643	0.000	1693	-0.046

Table. Dietary pattern and bone turnover marker predictors of BMD

***Disclosures: Helen Macdonald**, None.*

SU0318

Bone Mineral Density (BMD) Loss May Predict Fracture Differently in Older Adults According to Fall History. Sarah Berry*[1], Robert McLean[2], Marian Hannan[3], L. Adrienne Cupples[4], Douglas Kiel[5]. [1]Hebrew SeniorLife/Beth Israel Deaconess Medical Center, USA, [2]Hebrew SeniorLife Institute for Aging Research & Harvard Medical School, USA, [3]HSL Institute for Aging Research & Harvard Medical School, USA, [4]Boston University School of Public Health, USA, [5]Hebrew SeniorLife, USA

Purpose: It is important to identify clinical factors that inform the decision of whether a repeat BMD screening test should be performed. The purpose of our study was to determine whether BMD loss over 4 yrs affects the risk of hip and non-vertebral fracture differently according to an individual's history of falls or recurrent falls.

Methods: Participants included 492 women and 310 men in the Framingham Original Cohort Study with baseline and second BMD measures at the femoral neck (mean interval: 3.7 yrs) and no prior hip fracture. Falls were ascertained by self-report at time of second BMD measure, and categorized as recent fall (any fall during past yr) or recurrent falls (≥ 2 falls in past yr). Hip fractures were confirmed with medical records, whereas other non-vertebral fractures were self-reported. Cox regression models were used to calculate hazard ratios (HR) for the association between annual percent BMD change (per SD loss) and risk of fracture adjusting for baseline BMD, age, sex, BMI, and history of fracture. Separate models were used for history of recent fall and recurrent falls. Interactions were tested by including 'fall history * BMD change' in the models.

Results: Mean age was 79 yrs (± 4 yrs). 28% of participants reported a recent fall, and 11% reported recurrent falls (range: 2-21 falls/yr). Over a median follow-up of 9.6 yrs, 76 hip and 175 non-vertebral fractures occurred. BMD loss was associated with a modest increased risk of hip (HR 1.4, 95% CI 1.2, 1.8) and non-vertebral fractures (HR 1.2, 95% CI 1.0, 1.4). The association between BMD loss and hip fracture was similar regardless of fall history (Table 1: p for interactions ≥ 0.2). For non-vertebral fractures there was a suggestion that BMD loss was associated with fracture among individuals without a recent fall (HR 1.3, 95% CI 1.1, 1.6), but not among individuals with falls (HR 0.9, 95% CI 0.7, 1.3; p for interaction =0.07).

Conclusion: Our results suggest that when predicting non-vertebral fractures, individuals without a history of falls may benefit from repeating a BMD screening test, whereas individuals with a fall may not. These surprising findings could be explained if BMD change contributes less to fracture risk when a strong risk factor for fracture, such as falls, is present and unrelated to bone health. Replication of these findings is needed before recommending that fall status be used to determine whether a repeat BMD screening test should be performed.

Table 1. Effect of BMD loss on risk of hip and non-vertebral fracture over 12-years as characterized by history of falls: the Framingham Osteoporosis Study

	Hip fracture			Non-vertebral fracture		
	Multivariate adjusted HR*	95% confidence intervals	p-value for interaction	Multivariate adjusted HR*	95% confidence intervals	p-value for interaction
Recent fall	1.4	0.9, 2.2	0.6	0.9	0.7, 1.3	0.07
No recent fall	1.5	1.2, 1.9		1.3	1.1, 1.6	
Recurrent falls (≥ 2)	1.1	0.6, 2.2	0.2	0.7	0.4, 1.2	0.2
No recurrent falls	1.5	1.2, 1.9		1.3	1.1, 1.5	

* Models include age, sex, BMI, history of fracture, and baseline BMD

Table 1

***Disclosures: Sarah Berry**, None.*

SU0319

Changes In Femoral Shaft Cortical Thickness In Older Women: the Study of Osteoporotic Fractures. Dennis Black*[1], Katherine Peters[2], Kristine Ensrud[3], Nicola Napoli[4], Jane Cauley[5]. [1]University of California, San Francisco, USA, [2]California Pacific Medical Center, USA, [3]Minneapolis VA Medical Center / University of Minnesota, USA, [4]University Campus Biomedico, Italy, [5]University of Pittsburgh Graduate School of Public Health, USA

Background: The 2010 ASBMR definition of atypical femur fractures (AFF) includes cortical thickness (CT) at the femoral shaft as a "minor" feature. However, there has been little systematic study of femoral shaft CT nor its relationship to AFF. We recently showed that in bisphosphonate naïve women in the Study of Osteoporotic Fractures (SOF), thicker cortices were associated with lower, not higher, risk of subtrochanteric fractures. In this analysis, we analyze changes in CT over 8 years in SOF.

Methods: Using baseline pelvic radiographs obtained at baseline and follow-up (about 8 years later) from women in the SOF study, we measured CT at the top of the femoral shaft in a random sample of 394 women. Women were > age 65 (mean 71) at the start of SOF in 1986. We analyzed two parameters at the femoral shaft: total CT (medial plus lateral) and total bone width (BW) (both averaged across the right and left sides). We looked at changes in these two parameters over time and predictors of these changes.

Results: On average, total CT was 1.34 cm at baseline and decreased by 0.26 (+ SE=0.01) cm (to 1.09 cm) over the 8 yrs. Overall bone width increased by 0.21(+ 0.01) cm from 3.69 to 3.89cm.

Changes in total CT were only weakly related to age: decreases were only somewhat higher in the oldest women (0.23cm in age 65-70 vs 0.29 cm in those >80, p=0.18). The only other risk factor with a trend toward significance was current estrogen use (HT current users had slower decrease in CT with age, p=0.12). Walking for exercise and smoking were not related to changes in CT.

Age was more strongly related to changes in BW. Among younger (65-70 yrs) women, BW increases were larger (0.24 cm) compared to older women (0.1 cm in those over age 80, p=0.03). Those with excellent or good self-reported health also showed larger increases in bone width than those with poorer self-reported health, although this did not reach statistical significance (p=0.12). Other variables did not predict changes in BW.

Conclusions: We found that femoral shaft CT decreased and BW increased over time in women over age 65. Our findings at the femoral shaft confirm other studies showing increased BW and decreased TC with age at other anatomical sites at the hip. The slowing of BW increases after age 80 may help explain the exponential increase in risk of subtrochanteric and diaphyseal fractures with age.

***Disclosures: Dennis Black**, None.*
This study received funding from: CT measurements funded by Merck

SU0320

Prevalent Vertebral Fractures Predict Risk of Vertebral and Non-Vertebral Fractures in Older Men: the MrOS Study. Dennis Black*[1], Katherine Peters[2], Peggy Cawthon[3], Jane Cauley[4], Steven Cummings[5], Eric Orwoll[6], Kristine Ensrud[7], Howard Fink[8], Lynn Marshall[6], Neeta Parimi[9], Deborah Kado[10], Marcia Stefanick[11], John Schousboe[12]. [1]University of California, San Francisco, USA, [2]California Pacific Medical Center, USA, [3]California Pacific Medical Center Research Institute, USA, [4]University of Pittsburgh Graduate School of Public Health, USA, [5]San Francisco Coordinating Center, USA, [6]Oregon Health & Science University, USA, [7]Minneapolis VA Medical Center / University of Minnesota, USA, [8]GRECC, Minneapolis VA Medical Center, USA, [9]California Pacific Medical Center, USA, [10]University of California, San Diego, USA, [11]Stanford University School of Medicine, USA, [12]Park Nicollet ClinicUniversity of Minnesota, USA

Background: Prevalent vertebral fractures in women have been shown to be strongly predictive of future vertebral as well as non-vertebral fractures. However the ability of prevalent vertebral fractures to predict future risk of various types of fractures in men has been less well studied.

Methods: Prevalent vertebral fractures were defined from baseline X-rays in men from the MROS study, a longitudinal cohort study in men over age 65. Baseline prevalent vertebral fractures (PVfx) were defined as a semi-quantitative (SQ) grade fracture >=2 and incident vertebral fractures by a change of SQ>=1 between baseline and follow-up radiographs. The analysis included 4389 men with both baseline and follow-up x-rays and was restricted to follow-up time prior to repeat x-ray (mean=4.5 years). We examined presence and number of PVfx to predict incident spine fracture as well as non-spine (any non-spine, hip and wrist) fractures. Adjustments for age, site, BMD and other risk factors used multivariable models (logistic or PH)

Results: Over 4.5 years, there were 197 incident spine and 157 non-spine fracture (including 23 hip and 34 wrist fractures). After age adjustment, men with PVfx (7%) were at more than 5 times risk of incident radiographic vertebral fracture (OR=5.7, p<.0001). Among those with PVfx, risks of non-spine fractures were also significantly increased (any non-spine, RH=2.2, p<.001) as was risk of hip (RH=3.3,p=.02) and

wrist fracture (RH=4.1, p=0.001). Relative risk for each fracture type increased strongly with number of PVfx (see figure). Defining PVfx by SQ>=1 increased prevalence but attenuated the associations. Adjustment for BMD, history of non-vertebral fracture or other factors only slightly attenuated the association for incident spine fracture (OR=3.4,p<0.001). The associations for non-spine fractures were more strongly attenuated: the RH for non-spine and wrist fracture remained marginally significant (p=0.003 and 0.02, respectively) but the relationship to hip fracture was no longer significant (p=0.33).

Conclusion: PVfx were strongly predictive of incident spine as well as non-spine fractures. PVfx in men may reflect some aspect of bone quality not assessed by BMD or other risk factors and therefore may play an important independent role in future fracture risk assessment, particularly for incident vertebral fracture.

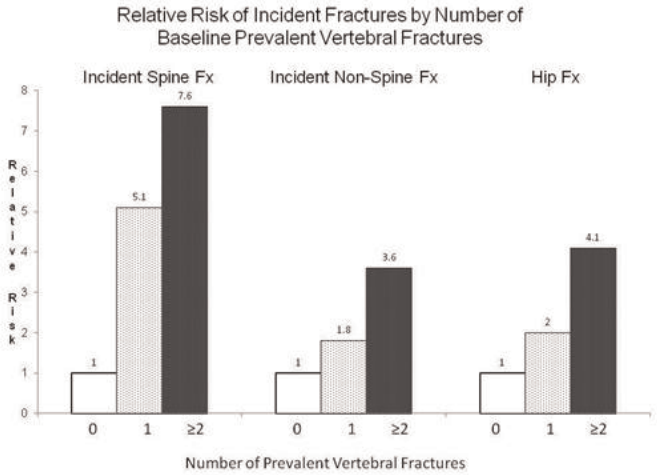

Figure

***Disclosures: Dennis Black**, None.*

SU0321

Concordance and Discordance between Incident Radiographic Vertebral Fractures and Clinical Vertebral Fractures in Older Men. Kristine Ensrud*[1], Terri Blackwell[2], Howard Fink[3], Jie Zhang[4], Jane Cauley[5], Peggy Cawthon[2], Dennis Black[6], Douglas Bauer[6], Jeffrey Curtis[4], Eric Orwoll[7], Elizabeth Barrett-Connor[8], Deborah Kado[8], John Schousboe[9]. [1]Minneapolis VA Medical Center / University of Minnesota, USA, [2]California Pacific Medical Center Research Institute, USA, [3]GRECC, Minneapolis VA Medical Center, USA, [4]University of Alabama at Birmingham, USA, [5]University of Pittsburgh Graduate School of Public Health, USA, [6]University of California, San Francisco, USA, [7]Oregon Health & Science University, USA, [8]University of California, San Diego, USA, [9]Park Nicollet ClinicUniversity of Minnesota, USA

Prior studies in older women have reported that 1/4 to 1/3 of incident vertebral fractures identified on the basis of radiographs alone (radiographic vfxs) are also clinically diagnosed as fracture events (clinical vfxs), but there is a lack of data in men. Among 4398 men aged ⩾65 years enrolled in MrOS, we determined the proportion of incident radiographic vfxs also diagnosed as incident clinical vfxs and vice-versa. Incident radiographic vfxs were identified by comparing baseline and follow-up lateral and thoracic spine study films (average 4.6 years between films) using a semiquantitative (SQ) method and defined as those with a change in SQ reading of ⩾1 at a given vertebral level from baseline to follow-up radiograph (for incident radiographic vfxs with grade 1 severity, endplate depression also required). Men were queried every 4 months after baseline about clinical fracture events (>99% of follow-up contacts completed). Incident clinical vfxs were those reported by participants and confirmed by the study radiologist, who used the SQ method to establish that the community imaging study showed a new deformity of higher grade than was present in the same vertebra on the baseline study film.

197 men (4.5%) had 237 incident radiographic vfxs identified by comparison of study films, whereas 31 men (0.7%) experienced 37 incident clinical vfxs. For men with incident clinical vfxs, back pain was the presenting complaint in 84% of cases. Of the 237 incident radiographic vfxs, 29 (12.2%) were also clinically diagnosed at the same vertebral level, with clinical diagnoses made for 14.4% of incident radiographic vfxs with SQ change ⩾2 compared with 8.3% of incident radiographic vfxs with SQ change = 1. Of the 37 confirmed incident clinical vfxs, 29 (86.5%) were also identified as incident radiographic vfxs at the same vertebral level, most of them (22 of 29) with SQ change ⩾2. Using an alternative definition of concordance (fxs identified at same vertebral level ±1 level) did not substantially alter these results.

In this study of older men, less than 1/7 of incident radiographic vfxs were also clinically diagnosed as new vfxs; the proportion clinically diagnosed was somewhat higher for more severe radiographic vfxs. Most, but not all, incident clinical vfxs were also identified as incident radiographic vfxs. These results in men complement those in women and suggest a complex relationship between clinical and radiographic vfxs in older adults.TBD

***Disclosures: Kristine Ensrud**, Merck Sharpe & Dohme, 2*

SU0322

Construction validity of the ICECAP-O index amongst people with non-traditional low trauma fractures. Yu Zhang*[1], Mark Kotowicz[2], Julie Pasco[3], Kerrie Sanders[4]. [1]University of Melbourne, Australia, [2]Deakin University School of Medicine, Australia, [3]Deakin University, Australia, [4]NorthWest Academic CentreThe University of MelbourneWestern Health, Australia

Osteoporotic fractures could affect patients' health related and general quality of life (QoL). The IcePop Capability Index (ICECAP-O) is a relatively new tool that measures individuals' general QoL using five attributes [1]: attachment (love and friendship), security (thinking about the future without concern), role (doing things that make you feel valued), enjoyment (enjoyment and pleasure) and control (feeling independent). Each attribute has four levels, allowing four a total of 4^5=1024 possible health states. Our aim was to investigate the construct validity of the ICECAP-O in patients who suffered a minimal trauma fracture at non-traditional/non-classical sites.

Patients with radiologically confirmed fractures, recruited from the Emergency Department and Imaging Department of the Geelong Hospital, were interviewed within two weeks after their first fracture-related healthcare visit. The interview included their demographic information (age, gender, income level, employment, and living conditions, activity level etc.), and measurements of health related QoL (HRQoL, measured using the EuroQol-5D instrument), anxiety and depression levels (measured using the Hospital Anxiety and Depression Scale, HADS) and overall ICECAP-O values. Measurements were repeated after 4 (phase II) and 12 months (phase III). A Kendall Taub's test was used to assess convergent validity. We hypothesized that patients' ICECAP-O values would correlate with their HRQoL and HADS values. Multivariate regression analysis was used to assess discriminant validity; confidence intervals obtained using bias corrected accelerated bootstrap method (10000 reps). We expected those who were inactive to have lower ICECAP-O scores.

Of the 778 fracture cases, 246 participants recruited at baseline, and information was obtained from 210 and 171 participants for phases II and III, respectively. Results for convergent validity are shown in tables 1 and 2. There were significant correlations between capabilities and HRQoL, both at phases II and III respectively. This was shown by the significant correlations between the ICECAP-O and the EQ5D and EQ-VAS scores. However, the correlations are not strong. Capabilities were also significantly correlated with the HADS scales, but again, the correlation was weak. For discriminante validity, regression analysis showed a positive association between ICECAP-O values and activity levels at both phases II (coefficient: 0.1, p<0.01 95%CI: 0.04-0.1) and III (coefficient: 0.1, p=0.01, 95%CI: 0.02-0.2).

The ICECAP-O uses different set of attributes to measure QoL than instruments that assesses HRQoL. Our results showed reasonable convergent and discriminant validity for ICECAP-O. Those with higher activity levels showed significantly higher ICECAP-O values.

1. Coast, J., et al., *Valuing the ICECAP capability index for older people.* Soc Sci Med, 2008. 67(5): p. 874-82.

Table 1: Results from Kendall Tabub's test at phase II, p-values less than 0.05 indicate significant association between the variables

	HADS	EQ-VAS	EQ-5D	ICECAP
HADS	1	-0.4 (p<0.001)	-0.4 (p<0.001)	-0.5 (p<0.001)
EQ-VAS		1	0.3 (p<0.001)	0.4 (p<0.001)
EQ-5D			1	0.4 (p<0.001)
ICECAP				1

Table 1: Results from Kendall Tabub's test at phase II, p-values less than 0.05 indicate significant

Table 2: Results from Kendall Tabub's test at phase III, p-values less than 0.05 indicate significant association between the variables

	HADS	EQ-VAS	EQ-5D	ICECAP
HADS	1	-0.3 (p<0.001)	-0.4 (p<0.001)	-0.5 (p<0.001)
EQ-VAS		1	0.3 (p<0.001)	0.4 (p<0.001)
EQ-5D			1	0.4 (p<0.001)
ICECAP				1

Table 2: Results from Kendall Tabub's test at phase III, p-values less than 0.05 indicate significan

***Disclosures: Yu Zhang**, None.*

SU0323

Dissecting the Relationship between High-Sensitivity Serum C-Reactive Protein and Increased Fracture Risk: the Rotterdam Study. Ling Oei*[1], Natalia Campos[2], Abbas Dehghan[2], Edwin Oei[2], Lisette Stolk[2], Joyce Van Meurs[1], Albert Hofman[2], Andre Uitterlinden[3], Oscar Franco[2], Carola Zillikens[2], Fernando Rivadeneira[1]. [1]Erasmus University Medical Center, The Netherlands, [2]Erasmus MC, The Netherlands, [3]Rm Ee 575, Genetic Laboratory, The Netherlands

Inflammatory diseases are associated with bone pathology, reflected in a higher fracture risk. Serum high-sensitivity C-reactive protein (CRP) is the most well-described inflammatory biomarker. Our aim was to investigate the relationship between CRP and bone health in the Rotterdam Study, a prospective population-based cohort. At baseline, bone mineral density (BMD) and hip bone geometry parameters were measured with dual-energy X-ray absorptiometry (DXA). For Mendelian randomization purposes, a weighted score for high CRP was computed including single nucleotide polymorphism (SNPs) (Illumina HumanHap550 Beadchip genotyping and HapMap imputation), which have previously been identified as associated with serum CRP levels. Models were adjusted for sex, age, BMI and other potential confounders and effect estimates reported per unit increase in log-transformed CRP. Linear regression was performed for continuous outcomes, logistic regression for radiographic vertebral fractures and Cox proportional hazard regression to estimate the risk of all other types of fracture. Complete data was available for 6,386 participants, of whom 1,561 persons sustained a fracture (mean follow-up: 11.6 years). CRP was significantly associated with all-type fracture risk (HR: 1.06; 95% CI: 1.01-1.12; P=0.03), including hip fractures (HR: 1.15; 1.03-1.27; P=0.009) and vertebral fractures (OR: 1.19; 1.06-1.34; P=0.003). The association seemed strongest in the lowest femoral neck (FN-) BMD tertile (0.39-0.80 g/cm^2: HR: 1.13; 1.04-1.23; P=0.002). The combined genetic risk score of CRP SNPs was significantly associated with serum CRP levels (P=9x10^{-56}), but not with fracture risk (HR: 1.00; 0.99-1.00; P=0.23). In conclusion, serum high-sensitivity CRP is associated with fracture risk, lower femoral neck width and bending strength. Mendelian randomization analyses did not yield evidence for this relationship being causal. Future studies might reveal what factors truly underlie the relationship between CRP and fracture risk.

***Disclosures: Ling Oei**, None.*

SU0324

Frequency of calcaneal insufficiency fracture in elderly patients. Koji Nozaka*, Naohisa Miyakoshi, Michio Hongo, Yuji Kasukawa, Hiroyuki Tsuchie, Kentaro Ohuchi, Hayato Kinoshita. Akita University Graduate School of Medicine, Japan

Background: Although a number of reports have examined insufficiency fracture of the calcaneus in elderly individuals, the frequency of this injury induced by bone fragility remains unclear.

Objective: To examine the frequency of calcaneal insufficiency fractures in the elderly.

Subjects: We investigated 123 patients (46 men, 77 women) ^{3}60 years old who visited the outpatient clinic due to calcaneal and calcaneus region pain without obvious external injuries and underwent calcaneus radiography between 2006 and 2010. Patients who clearly had a malalignment syndrome such as pes cavovarus or pes planovalgus were excluded from the study.

Results: The mean age of patients was 76.2 years (range, 60-100 years). The frequency of calcaneal insufficiency fracture was 8.1% (10 women). Of the 123 patients, 89 patients visited the clinic on their own without assistance of stretchers or wheelchairs. Fracture frequency in these 89 patients was 10.1% (9 of 89). None of the 10 patients with fracture had underlying diseases such as rheumatoid arthritis or diabetes, and none were taking steroidal medications. In addition, none were being treated for osteoporosis. Bone density tests were performed after injury in only 5 patients, and all five had a bone density <70% of the young adult mean (YAM) and subsequently started osteoporosis treatment medications. All 10 patients were successfully treated with conservative therapy on an outpatient basis. Eight patients received external fixation. Mean duration between onset of pain and initial visit was 17.4 days (range, 0-40 days). Osteosclerosis was observed on radiography performed on the initial visit in 2 patients. Definitive diagnosis of the fracture was made on magnetic resonance imaging (MRI) in 6 patients. In 2 patients, MRI was not performed due to various circumstances, but osteosclerosis was determined on radiography conducted during routine follow-up.

Discussion: Frequency of calcaneal insufficiency fracture in elderly individuals who had pain in the calcaneal region was 8.1%. This type of fracture cannot always be diagnosed solely by radiography on the initial visit, and MRI appears valuable for early diagnosis. This type of fracture can be treated using conservative therapy alone.

***Disclosures: Koji Nozaka**, None.*

SU0325

Genetic Risk Scores for the Prediction of BMD, BMD Loss and Fracture Risk in Elderly Subjects. Joel Eriksson*[1], Dan Evans[2], Jian Shen[3], Priya Srikanth[4], Carrie Nielson[3], Marc Hochberg[5], Shannon McWeeney[6], Peggy Cawthon[7], Beth Wilmot[8], Joseph Zmuda[9], Greg Tranah[10], Daniel Mirel[11], Sashi Challa[12], Michael Mooney[13], Andrew Crenshaw[14], Magnus Karlsson[15], Dan Mellström[16], Liesbeth Vandenput[17], Eric Orwoll[3], Claes Ohlsson[18]. [1]Centre for Bone & Arthritis Research, Sweden, [2]Department of Medicine, University of California, San Francisco, USA, [3]Oregon Health & Science University, USA, [4]Department of Public Health & Preventive Medicine, Oregon Health & Science University, Portland, OR, USA, USA, [5]University of Maryland School of Medicine, USA, [6]Oregon Clinical & Translational Research Institute, Oregon Health & Science University, Portland, OR, USA & Department of Biostatistics-Public Health & Preventative Medicine, Oregon Health & Science University, Portland, OR, USA, USA, [7]California Pacific Medical Center Research Institute, USA, [8]Department of Molecular & Medical Genetics, Oregon Health & Sciences University, Portland, OR, United States, USA, [9]University of Pittsburgh Graduate School of Public Health, USA, [10]Research Institute, California Pacific Medical Center, 185 Berry Street, Suite 5700, San Francisco, California 94107-1728, USA, USA, [11]Program in Medical & Population Genetics, Broad Institute, Cambridge, Massachusetts, United States of America, USA, [12]Oregon Clinical & Translational Research Institute, Oregon Health & Science University, Portland, OR, USA, USA, [13]Department of Medical Informatics & Clinical Epidemiology, Oregon Health & Science University, Portland, OR, USA, USA, [14]Broad Institute of MIT & Harvard, Cambridge, MA, 02142, USA, [15]Skåne University Hospital Malmö, Lund University, Sweden, [16]Center for Bone & Arthritis Research, Institute of Medicine, Sahlgrenska Academy, University of Gothenburg, Gothenburg, Sweden, Sweden, [17]University of Gothenburg, Sweden, [18]Center for Bone & Arthritis Research at the Sahlgrenska Academy, Sweden

Bone mineral density (BMD) is the most widely used predictor of fracture risk. Twin studies demonstrate that genetic factors play an important role for BMD and fracture risk. A recent large-scale meta-analysis identified 63 autosomal SNPs to be associated with BMD and 16 BMD-associated SNPs were also associated with fracture risk. Based on these findings two genetic risk scores (GRS63 and GRS16) were developed. The aim of the present study was to determine the clinical usefulness of these GRS for the prediction of BMD, BMD loss and fracture risk in elderly subjects.

Genotype data from two male (MrOS US and MrOS Sweden) and one female (SOF) well-powered cohorts of older subjects were evaluated against BMD (n=8,212), BMD loss (n=5,312), and incident fractures (n=8,067 including 2,185 incident fracture cases).

The GRS63 was significantly associated with BMD at both femoral neck (FN) and lumbar spine (LS) in all cohorts, with similar proportion of the variation in BMD explained (*FN*: MrOS Sweden 3.1%, MrOS US 3.2%, SOF 2.6%; *LS:* MrOS Sweden 3.3%, MrOS US 2.6%, SOF 3.2%). In contrast, the GRS63 was not significantly associated with BMD loss.

Although both the GRS63 and the GRS16 were associated with all fractures, the effect size for GRS63 (HR 1.16, 95% confidence interval (CI): 1.11-1.20, per SD increase) was larger than that for GRS16 (HR 1.06, 95% CI: 1.02-1.11, per SD increase). The GRS63 (HR 1.20, 95% CI: 1.11-1.30, per SD increase), but not the GRS16, was significantly associated with hip fractures. After adjustment for FN-BMD, the effect sizes between GRS63 and all fractures (-50%) and hip fracture (-64%) risk were substantially reduced.

Only minor improvements in C-statistics (AUC) for all fractures were seen when GRS63 was added to a base model including age, weight and height and no significant improvements in C-statistics were seen when GRS63 was added to a base model further adjusted for BMD (Fig). Net reclassification improvement (NRI >0) with the

addition of GRS63 to a base model was modest in all three cohorts and this improvement was substantially attenuated in BMD-adjusted models (Fig).In conclusion, the GRS63 predicts BMD, but not BMD loss, in elderly subjects, suggesting that the genetic determinants of the acquisition of BMD differ from those of BMD loss. As BMD is usually known, the clinical utility of the BMD-associated GRS63 for fracture prediction is limited in elderly subjects.

	Base model	+ GRS63		Reclassification	
	AUC	AUC	P	NRI	P
Age, Weight, Height					
MrOS Sweden	0.54	0.58	1.2E-01	0.26	3.8E-03
MrOS US	0.57	0.59	5.7E-02	0.12	1.9E-03
SOF	0.53	0.56	1.2E-02	0.18	2.6E-06
+ BMD					
MrOS Sweden	0.63	0.64	4.5E-01	0.22	1.6E-02
MrOS US	0.64	0.64	3.0E-01	0.06	1.5E-01
SOF	0.63	0.63	2.5E-01	0.11	4.6E-03

Figure 1

***Disclosures: Joel Eriksson**, None.*

SU0326

How well hip fractures can be captured using the postal enquiry?. Reijo Sund[1], Liisa Ollikainen[2], Risto Honkanen[2], Heikki Kroger*[3]. [1]National Institute for Health & Welfare, Finland, [2]University of Eastern Finland, Finland, [3]Kuopio University Hospital, Finland

The purpose of the study was to examine how well follow-up using postal enquiry can capture hip fractures.

Study population in the Kuopio Osteoporosis Risk Factor and Prevention (OSTPRE) study consisted the total population of 14220 women aged 47-56 years resident in the province of Kuopio in January 1989. The baseline postal enquiry was conducted in June-August 1989 and gave a high response of 92.8%. Follow-up enquiries have been sent every fifth year, i.e. in 1994, 1999, 2004 and 2009. Each enquiry contained question on occurred fractures. Self-reported fractures were verified from the medical records.

We used the Finnish Hospital Discharge Register to identify all hospitalizations with hip fracture diagnosis (ICD-9: 820, ICD-10: S72.0, S72.1, S72.2) during 1987-2011 for the OSTPRE population. A total of 1001 records for 384 persons with hip fracture diagnosis were found. After removing obvious follow-up hospitalizations there remained 470 records possibly indicating hip fracture. All these candidates for hip fractures were verified from the medical records.

After verification, the total number of hip fractures (excluding pathologic and periprothetic fractures) for the OSTPRE population during 1987-2011 turned out to be 363. Five hip fractures (1.4%) were not identified from the register with hip fracture diagnosis: one patient with only outpatient treatment for hip fracture was missing and four other had diagnosis of lower part of femur. More strikingly, only 122 hip fractures (33.6%) were captured using the postal enquiries. Obvious reasons for missed fractures were found for 110 (30.4%) cases. Failed reporting of hip fractures in 16 cases (4.4%) was surprising as hip fractures are typically major life events for individuals. Nonresponse was the main reason for missed fractures consisting of 115 cases (31.7%).

In conclusion, nonresponse and drop out have severe consequences for identification of hip fractures in postal inquiries. More than half of the hip fractures would have been missed without register-based data. Probably hip fractures and nonresponse are related to similar risk factors such as long-term care and increased comorbidity. Such major limitation must be kept in mind while utilizing purely self-reported (hip) fracture data.

Keywords: hip fracture, postal enquiry, registers

***Disclosures: Heikki Kroger**, None.*

SU0327

Impact of Vertebral Fractures on Hospitalization for Major Disease and Longterm Care Placement. Jane Cauley*[1], Li-Yung Lui[2], Misti Paudel[3], Lih-Wen Mau[4], Brent Taylor[4], Peggy Cawthon[2], Teresa Hillier[5], John Schousboe[6], Kristine Ensrud[7]. [1]University of Pittsburgh Graduate School of Public Health, USA, [2]California Pacific Medical Center Research Institute, USA, [3]Department of Epidemiology, University of Minnesota, USA, [4]University of Minnesota, USA, [5]Kaiser Center for Health Research, USA, [6]Park Nicollet ClinicUniversity of Minnesota, USA, [7]Minneapolis VA Medical Center / University of Minnesota, USA

Purpose: Vertebral fractures (VFx) are the hallmark of osteoporosis. Women with VFx have a higher risk of death, fracture and impaired function. The purpose of this analysis was to test the hypotheses that the impact of VFx extends to hospitalizations for major disease events and longterm care placement (LTC).

Methods: We studied 3603 Caucasian women enrolled in the Study of Osteoporotic Fractures (SOF) and merged SOF cohort data with Medicare claims. To be included in this analysis, women had to be enrolled in Medicare Fee for Service [(FFS), i.e. parts A and B but not C] as of 1/1/1992 and have radiographic information on VFx status at visit 3 (1990-91). VFx status was assessed using quantitative morphometry on lateral thoracic and lumbar spine radiographs obtained at visit 3 and defined as any height ratio >3 standard deviations below normal. Women were censored if they died or disenrolled in FFS. Hospitalizations with a primary diagnosis of congestive heart failure (CHF), myocardial infarction (MI), stroke, chronic obstructive pulmonary disease (COPD) and hip fracture were identified using ICD-9 hospital discharge diagnoses using Medicare data from inpatient files. Longterm (>100 days)or permanent placement in a LTC facility was also identified using claims data from inpatient and carrier (physician files). We used a Cox proportional hazards model to estimate the multivariable (MV) adjusted relative hazard (RH) [95% confidence interval (CI)] of hospitalization for one of the conditions listed above or LTC placement.

Results: The mean age of the women was 74.4 (68-95 yrs) and 810 (22.5%) had a VFx. Over an average of 10.4 ± 5.0 years of follow-up, 1676 (46.5%) were hospitalized for one of the major disease events and 825 (22.9%) were placed in a LTC facility. The MV adjusted RH (95% CI) for hospitalization for a major disease event among those with a VFx was 1.15 (1.02, 1.30) in comparison to women without a fracture, Table. Because VFx are major risk factors for hip fracture, we redid our analysis removing hip fracture as a hospitalization, MV adjusted RH, 1.12 (0.99, 1.28). VFx were also associated with LTC placement, MV adjusted 1.20 (1.02, 1.42). The association between VFx and hospitalization was especially strong for women with >2 VFx.

Conclusion: Our results extend the potential public health impact of radiographic VFx to include an increased risk of hospitalization for major diseases and placement in a LTC facility.

Table: Multivariate adjusted hazard ratio (HR) (95% confidence interval) for hospitalization or longterm care placement by vertebral fractures status. Referent=no vertebral fracture.

	Hospitalization[1]	Hospitalization[2]	Longterm care placement
Vertebral fracture (any)	1.15 (1.02, 1.30)	1.12 (0.99, 1.28)	1.20 (1.02, 1.42)
Vertebral fracture			
1	1.08 (0.93, 1.25)	1.08 (0.92, 1.26)	1.20 (0.99, 1.47)
>2	1.26 (1.07, 1.49)	1.19 (0.99, 1.43)	1.21 (0.95, 1.53)

[1] Hospitalization for CHF, MI, stroke, COPD and hip fracture.

[2] Hospitalization for CHF, MI, stroke, COPD.

MV model: age, height change since age 25, weight, fall in past 12 months, gait speed, number of impairments, takes walks for exercise, takes calcium supplements, health status.

Table

***Disclosures: Jane Cauley**, None.*

SU0328

Low Bone Mineral Density in Swedish Men with Distal Radius Fracture. Lisa Egund*[1], Fiona McGuigan[2], Kristina Akesson[1]. [1]Skåne University Hospital, Malmoe, Sweden, [2]University of Lund, Malmö, Skane University Hospital, Malmö, Sweden

A distal radius fracture is considered a predictor of future risk for osteoporosis and fragility fractures in women.Although men with this fracture type are known to have lower bone mineral density (BMD) the etiology has not been extensively studied. The purpose of this study was to evaluate on a large scale, the BMD of Swedish adult men of all ages with distal radius fracture and compare them to the background population.*Material* In this cross-sectional study, adult men presenting with a distal radius fracture and living in Malmö, Sweden, were recruited in two ways: All men who fractured during 1999-2000 (n=288) were invited to participate during 2003. Additionally, men who sustained a distal radius fracture from 2003-2007 (n=460) were invited to the prospective study-arm and followed during the first year post-fracture. A total of 233 patients were enrolled. Controls were chosen from a

preexisting database of individuals all randomly selected from the population registry and from the same geographical area. *Methods* BMD was measured using DXA at the femoral neck, total femur and lumbar spine. Medical history and other risk factors for health were obtained through questionnaire. Participants were grouped according to age at fracture: 20-44, 45-64 and >65yrs and in 10-yr age-bands to determine mean BMD levels.

Results The mean age of men with fracture of the distal radius was 52.2 ±16.7 and BMI was 26.5±3.9. The fracture distribution according to age group was 27%, 44% and 29%, respectively. The fracture group had significantly lower BMD ($p<0.001$) compared to controls at the femoral neck (45-64yrs: 0.930 vs 0.989 g/cm^2; >65yrs: 0.839 vs 0.939); Total hip (45-64yrs: 0.985 vs 1.048; >65yrs: 0.898 vs 1.019); Spine (45-64yrs: 1.153 vs 1.225, >65yrs: 1.109 vs 1.277). The corresponding difference in T-score at the femoral neck was 0.4-0.8 and at total hip 0.5-0.9.). At the hip sites, compared to controls, this equates to a 6.0% lower BMD for patients 45-64y and 11.9% for those 65y and above. The 3.1% lower BMD in those below 45 yrs was not significant. The proportions with osteoporosis were: 20-44yrs: 3.6% vs 1.0%; 45-64yrs: 5.5% vs 2.2%; >65yrs: 19.0% vs 5.5%. *Conclusion* In this study, to our knowledge the largest on men with distal radius fracture, those with fracture have significantly lower BMD at all sites. Interestingly, compared to controls the difference in BMD becomes more pronounced with increasing age, but is already evident from middle age.

***Disclosures: Lisa Egund**, None.*

SU0329

Outcomes in Patients with Atypical Femur Fractures: the Ontario AFF Cohort. Angela M. Cheung*[1], Aliya Khan[2], Robert Josse[3], Earl Bogoch[4], Lianne Tile[5], Robert Bleakney[6], George Tomlinson[7], Adrian Lau[7], Rowena Ridout[8], Heather McDonald-Blumer[7], Moira Kapral[5], Savannah Cardew[9], Khalid Syed[5], Nicholas Bellamy[10], Jessica Chang[5], Judite Scher[5], Hanxian Hu[5], Alexandra Papaioannou[11], Suzanne Morin[12], Jonathan Adachi[13]. [1]University Health Network-University of Toronto, Canada, [2]McMaster University, Canada, [3]St. Michael's Hospital, University of Toronto, Canada, [4]St. Michael's Hospital, Canada, [5]University Health Network, Canada, [6]Mount Sinai Hospital, Canada, [7]University of Toronto, Canada, [8]Toronto Western Hospital, Canada, [9]Women's College Hospital, Canada, [10]The University of Queensland, Australia, [11]Hamilton Health Sciences, Canada, [12]McGill University, Canada, [13]St. Joseph's Hospital, Canada

Background: Atypical femur fractures (AFFs) are associated with delayed healing and high morbidity. To better understand outcomes in patients with AFFs, we conducted a prospective cohort study to systematically assess health related quality of life (HR-QOL), pain, and functional disability post fracture.

Methods: Patients with AFFs were recruited through specialty clinics and orthopedic practices across Ontario. All AFF patients were assessed by at least one osteoporosis specialist (often two), and their plain radiographs were reviewed by the specialist(s) and a central musculoskeletal radiologist to confirm the diagnosis of AFF based on the ASBMR diagnostic criteria. Patients were asked to complete questionnaires on health related quality of life (HR-QOL,RAND SF-36), visual analogue pain scale (VAS), and the Western Ontario and McMaster Universities Arthritis Index (WOMAC) modified for use in the AFF population. They were asked to complete one set for the present and one set by recalling their experience 1 year prior to their AFF diagnosis.

Results: Of the 105 AFF patients in the Ontario AFF cohort, 100 were postmenopausal women and 5 were men. Mean age at time of fracture was 66.1 years (range18.8-87.0). 59% were Caucasians, 15% South Asians and 26% Oriental. 44% had fractures prior to their AFFs and 67% had bilateral AFFs. Of those with bilateral fractures (n=70), 2 (2.9%) had bilateral subtrochanteric fractures, 56 (80.0%) had bilateral mid-diaphyseal fractures, and 12 (17.1%) had one of each. Of those with unilateral AFFs (n= 35), 6 (17.1%) had subtrochanteric fractures and 29 (82.9%) had mid-diaphyseal fractures. Average duration of bisphosphonate use was 9.4 years (range 0-28 years). Mean serum 25-hydroxyvitamin D level was 97 nmol/L. Areal BMD T-scores ranged from 0.84 to -3.95 for lumbar spine, 0.82 to -3.53 for total hip, and 0.33 to -3.79 for femoral neck. Average time from first AFF to time of first survey was 2.5 years (range 0-10 years). Of the 110 femurs with surgical repair, 18 required surgical re-intervention. AFF patients had a much lower SF-36 physical composite score than their age and sex matched controls (mean physical component summary (PCS)=39.5, SD=11.5; mean mental component summary (MCS)=45.2, SD=12). Pain scores by VAS were 4.4 (2.8) and on the modified WOMAC, the mean (SD) scores were 3.1 (2.4) for pain, 3.7 (2.6) for weakness and 3.4 (2.6) for function.

Conclusions: Patients with AFFs have decreased HR-QOL, persistent disability and pain long after their initial fracture.

***Disclosures: Angela M. Cheung**, Eli Lilly, 9; Merck, 9; Eli Lilly, 5; Amgen, 9; Amgen, 6; Amgen, 5; Warner Chilcott, 2; Eli Lilly, 6; Merck, 6; Warner Chilcott, 5*

SU0330

Prediction of Fracture and Fracture-associated Outcomes. Tuan Nguyen*[1], Steven Frost[2], Nguyen Nguyen[1], Jacqueline Center[1], John Eisman[1]. [1]Garvan Institute of Medical Research, Australia, [2]University of Western Sydney, Australia

Background and Aim — A fragility fracture signals a series of adverse events, including recurrent fracture and mortality. Existing predictive models in osteoporosis have been developed to predict the risk of an initial fracture only, and do not predict the risk of subsequent fractures. In this study, we sought to examine the inter-relationships between an initial fracture, subsequent fracture, and mortality.

Methods — This study was based on a population-based cohort consisting of 757 men and 1224 women, aged 60 years and older, whose fracture status and health outcomes had been continuously monitored for up to 24 years. Fragility fractures were ascertained using X-ray report and circumstance of fracture. The incidence of mortality was obtained from individual participant during the follow-up period. Femoral neck bone mineral density and risk factors (eg lifestyle factors, physical activity, and concomitant illneses and medications) were also ascertained at the initial visit as well as during the study period. A multistate Markov style of the Cox's proportional hazards model was used to estimate the transition probabilities between three statuses (ie initial fracture, refracture, and mortality) with adjustment for competing risk of death.

Results — The average age of participants was 70 years (range: 60 to 101). Approximately 25% of women and 12% of men had osteoporosis (BMD T-scores <-2.5). Among women without a fracture, approximately 37% would remain fracture-free during the subsequent 10-year follow-up; 24% would suffer a fracture, and 8% went on to refracture, and another 32% would die during this 10-year period. Among women with an initial fracture, 56% died after within 10 years, and 60% died after a recurrent fracture. Among men without a fracture, 38% would remain fracture-free, 14% would sustain a fracture, and 45% would die during the next 10 years. Among men with an initial fracture, the risk of a recurrent fracture was 16%, and the risk of death was 76%. However, in both genders, the risks of subsequent fracture and mortality were increased with advancing age and reduced BMD (Table)

Conclusions — These results show that individuals with an initial fracture have an increased risks of subsequent fracture and mortality, and the risk of fracture-associated mortality in men is greater than in women. The strong effects of advancing age and reduced BMD on the three related events of fracture, refracture, and mortality allow an individualized approach to the risk assessment for a man and woman. Such an assessment can aid patients and doctors to reach an informed decision concerning treatment for individuals with an initial fracture to reduce fracture and mortality in the general population.

Predicted risk of fracture, refracture and mortality for men and women by age and bone density T-score.

Age	Femoral neck T-score	Women			Men		
		Initial fracture	Refracture	Death	Initial fracture	Refracture	Death
60	0	0.09	0.03	0.15	0.08	0.03	0.24
	-1	0.14	0.05	0.12	0.12	0.04	0.24
	-2	0.18	0.10	0.13	0.17	0.06	0.29
	-3	0.20	0.21	0.15	0.20	0.12	0.36
70	0	0.15	0.04	0.17	0.10	0.05	0.31
	-1	0.22	0.07	0.20	0.14	0.06	0.40
	-2	0.27	0.11	0.26	0.16	0.08	0.52
	-3	0.27	0.18	0.36	0.14	0.11	0.65
80	0	0.20	0.06	0.30	0.09	0.09	0.65
	-1	0.25	0.06	0.41	0.09	0.09	0.65
	-2	0.26	0.07	0.54	0.07	0.09	0.79
	-3	0.21	0.08	0.68	0.03	0.09	0.87

Prediction of fracture, refracture and mortality (table)

***Disclosures: Tuan Nguyen**, None.*

SU0331

Predictors of Re-fracture in Patients Managed within a Fracture Liaison Service: A 7-year Prospective Study. Kirtan Ganda*[1], Markus Seibel[2]. [1]Concord Hospital, Australia, [2]Bone Research Program, ANZAC Research Institute, University of Sydney, Australia

Background: Effective fracture liaison services (FLS) increase treatment initiation rates and adherence amongst patients with incident osteoporotic fracture, and significantly reduce the risk of subsequent fracture. Predictors of re-fracture have been well documented in untreated populations but not in patients managed long-term within the setting of secondary fracture prevention programs. Based on 7 years of continuous follow-up data we identified predictors of re-fracture amongst a specialist-managed population.

Methods: The analysis included 212 subjects who at baseline presented with an incident osteoporotic fracture and were treated for at least 4 years since then. All patients were managed within the well-established Concord FLS (Sydney, Australia). Relevant anthropometric, clinical and technical data were documented at each six-monthly visit. Predictors of re-fracture were identified by logistic regression analysis before and after adjustment for potential confounders.

Results: The mean duration of follow-up was 5.57 years (range: 4.02-7.51). At baseline, mean age (SD) was 72.4 (12.7) years, 79% of subjects were female and 38% had prevalent fractures at the time of the index fracture. The mean (SD) total hip T-score was -1.2 (1.2) SD. Adherence to osteoporosis therapy was high throughout. During the study period, 24% of treated subjects re-fractured. Re-fracture rates in a population of similar composition were reported at 35-46% over 2-6 years. In unadjusted analyses, predictors of re-fracture were female gender, use of oral steroids, significant co-morbidities (>3), gastro-oesophageal reflux, cardiovascular disease, body weight < 66.4kg, total hip T-score <-1.65 SD, previous falls, maternal history of hip fracture, sunlight exposure of <30 min/d, and >2 prevalent fractures. After adjusting for confounders female gender (OR 7.3, 95%CI 1.6-33.8, p=0.01), comorbidity (OR 4.1, 95%CI 1.9-9.1, p<0.01), total hip T-score <-1.65 SD (OR 3.9, 95%CI 1.8-8.3, p<0.01), and ⩾1 fall within the last year (OR 2.2, 95%CI 1.0-4.8, p=0.04) remained significantly associated with re-fracture. Prevalent fracture status and age were not associated with re-fracture.

Conclusion: Female patients with low hip BMD, a history of recent falls and significant comorbidity are at heightened risk of re-fracture even when managed by a dedicated FLS. This sub-group at patients require intensive management including falls reduction strategies.

***Disclosures: Kirtan Ganda**, None.*

SU0332

Changes in Frailty-Related Characteristics of the Hip Fracture Population and their Implications for Healthcare Services: Evidence from Quebec, Canada. Mohammad Auais*[1], Suzanne Morin[2], Lyne Nadeau[3], Lois Finch[3], Nancy Mayo[3]. [1]Ivey International Centre for Health Innovation, Can, [2]McGill University, Canada, [3]McGill University Health Centre, Canada

Purpose To estimate secular changes in the prevalence of selected frailty-related characteristics among the hip fracture population in Quebec (2001-2008) and the potential impact of these changes on healthcare services.

Methods The Quebec hospitalization database was used to identify non-traumatic hip fractures for the purposes of calculating age- and sex-specific rates. Also estimated were time trends for selected frailty-related characteristics and discharge destinations.

Results A significant decline in fracture rates was evident for all age groups except for those <65; sex differences were also observed. Almost all frailty-related characteristics increased over time, ranging from 2% to 14% per year, which translates to an estimated increase from 16 to 112%, over the study period. For those whose prior living arrangement was LTC, rates declined significantly (women OR= 0.93; 0.91-0.95; men OR=0.97; 0.94-0.99). In-hospital mortality and discharge to in-patient rehabilitation decreased while discharges back to community and to LTC increased.

Conclusions Although hip fracture rates decreased for older hip fracture patients, the absolute number and prevalence of specific frailty-related characteristics increased. Policy-makers should review care models to ensure adequate resources are provided to the community to offset the expected increase in demand arising from ongoing changes in patients' characteristics.

***Disclosures: Mohammad Auais**, None.*

SU0333

Serum Pentosidine and its Decoy Receptor, endogenous secretory receptor for Advanced Glycation End Products, Predict Fragility Fractures in Elderly Men: the Fujiwara-kyo Osteoporosis Risk in Men (FORMEN) Study. Junko TAMAKI*[1], Katsuyasu KOUDA[1], Yuki FUJITA[1], Masayuki IKI[1], Akiko YURA[1], Eiko KADOWAKI[1], Masakazu MIURA[2], Yuho SATO[3], Nozomi OKAMOTO[4], Norio KURUMATANI[4]. [1]Department of Public Health, Kinki University Facluty of Medicine, Japan, [2]Hokuriku University Faculty of Pharmaceutical Sciences, Japan, [3]Department of Human Life, Jin-ai University, Japan, [4]Department of Community Health & Epidemiology, Nara Medical University School of Medicine, Japan

Objectives: The aim was to evaluate the ability of serum pentosidine (PEN) and the endogenous secretory receptor for advanced glycation end products (esRAGE) to predict fragility fractures in community-based cohort study of elderly men. Methods: We analyzed 1,290 Japanese men in FORMEN Study which baseline survey was conducted in 2007-2008 as part of Fujiwara-kyo study, and followed during 5-year period. The outcome was the initial fracture event defined as clinical fractures of the hip, vertebra, forearm, proximal humerus, clavicle, rib, proximal and distal cubitus, and pelvis that occurred without strong external force and diagnosed with radiographic reports. Bone mineral density (BMD) at femoral neck (FN) and at lumbar spine (LS) was measured at baseline (QDR4500A, Hologic, USA). The multiple logistic regression analysis was used to estimate the odds ratio (OR) per 1 standard deviation (SD) increase of the log-transformed PEN and esRAGE values at baseline measured using the FSK pentosidine ELISA kit, and the B-Bridge esRAGE ELISA Kit, respectively. Receiver operating characteristics (ROC) curves analysis with expected probabilities for fragility fractures was performed, and cut-off values were determined by Youden's index which gives maximum difference between sensitivity and false-positive rate. Results: The mean age at the baseline was 73.1 $\pm$ 5.1 years. The twenty-six men suffered incident fractures and were significantly older and had significantly lower BMD values and higher proportions of type 1 diabetes mellitus or high glycemic status with fasting glucose ⩾ 160 mg/dl or with HbA1c(NGSP) ⩾ 8.4%, and higher PEN (p=0.019) and lower esRAGE (p=0.128) levels than those without fractures. The age-adjusted ORs per 1SD increase of PEN and esRAGE were 1.50 [95% confidence interval (CI): 1.03-2.17, p=0.033], and 0.70(0.48-1.01, p=0.058), respectively. The ORs per 1SD increase for PEN and esRAGE were 1.54(1.05-2.28), 0.66(0.45-0.97), respectively, adjusted for age, FN BMD, type 1 diabetes mellitus, and high glycemic status. The area under ROC curve (AUC) of the expected probabilities obtained by the model was 0.72(0.61-0.84) with 61.5% sensitivity and 79.0% specificity at a cutoff determined by Youden's index. The adjusted ORs of PEN and esRAGE obtained by the model in which LS BMD substituted for FN BMD were 1.60(1.07-2.37), 0.64(0.43-0.95), respectively, with AUC value of 0.78(0.68-0.87), 61.5% sensitivity, and 85.0% specificity. Conclusions: Higher serum pentosidine and lower serum esRAGE values were associated with an increased risk of fragility fractures independently of BMD among Japanese elderly men over a 5-year follow-up period.

***Disclosures: Junko TAMAKI**, None.*

SU0334

Interaction of a single genotype and body mass index for prediction of hip fracture risk: a prospective cohort study. Joshua Lewis*[1], Karol Estrada[2], Andre Uitterlinden[3], Fernando Rivadeneira[4], Richard Prince[5]. [1]University of Western Australia, Sir Charles Gairdner Hospital, Australia, [2]Analytic & Translational Genetics Unit, Massachusetts General Hospital, USA, [3]Rm Ee 575, Genetic Laboratory, The Netherlands, [4]Erasmus University Medical Center, The Netherlands, [5]Sir Charles Gairdner Hospital, Australia

To date, studies on the genetic determinants of fracture risk adjust for environmental and nutritional influences but have not tested the relationship of these factors with the genetic polymorphisms associated with fracture. To study this further, we undertook a proof of principle study on the interaction between body mass index (BMI) and the six polymorphisms that reached genome wide significance in osteoporotic fracture prediction (Estrada K et al. Nat Genet 2012;44:491-501) in 1,316 women enrolled in the Calcium Intake Fracture Outcome study (CAIFOS) who were genotyped as part of the GEFOS GENOMOS consortium study. The participants were aged 70-85 at baseline and provided complete 10-year hip fracture data from the WA Hospital Morbidity Database and Mortality Registry.

In logistic regression, modifiers of the association of genotype on 10-year hip fracture risk were analysed including age and BMI (PASW, IBM). In the first analysis, the six polymorphisms association with hip fracture was studied. Only the rs4727338 polymorphism (SLC25A13) was associated with an increased the risk of 10-year of hip fracture (GG 17/166, 10.2%; CG 34/575, 5.9% and CC 28/575, 4.9%; OR per copy of the risk allele 1.46 (1.05-2.01), P = 0.022) which remained significant after adjustment. Interaction testing for the rs4727338 genotype and each of these factors was undertaken. For tertiles of BMI but no other covariates an additive interaction between the rs4727338 C→G polymorphism and BMI was identified for 10-year hip fracture, P = 0.005. In women in the lowest tertile of BMI (below 24.9 kg/m^2) per copy of the rs4727338 risk allele (G) there was an increased risk of 10-year of hip fracture in unadjusted analysis; (GG 11/58, 19.0%; CG 16/186, 8.6% and CC 7/191, 3.7%; OR per copy of the risk allele 2.48 (1.51-4.08), P < 0.001. However in the two higher tertiles of BMI (24.9-28.7 and >28.7 kg/m^2) there was no association with the risk allele and hip fracture (P = 0.849 and P = 0.659 respectively). Whilst genes in this locus have been associated with split-hand/foot malformations, the biological mechanism in which these variants are increasing fracture in combination with low/normal BMI is yet to be explored. In conclusion the rs4727338 G allele is associated with an increased hip fracture risk and an additive interaction between this polymorphism and body mass index may be responsible for underestimation of the reported genetic association of this polymorphism.

***Disclosures: Joshua Lewis**, None.*

SU0335

Testing reported SNPs for cortical and trabecular vBMD for hip and spine in the Age, Gene/Environment Susceptibility-Reykjavik Study. Tamara Harris*[1], Albert Smith[2], Thomas Lang[3], Kristin Siggeirsdottir[1], Gudny Eiriksdottir[2], Vilmundur Gudnason[4]. [1]Intramural Research Program, National Institute on Aging, USA, [2]Icelandic Heart Association, Iceland, [3]University of California, San Francisco, USA, [4]Icelandic Heart Association Research Institute, Iceland

Introduction: As bone exists in two primary compartments, the cortical and trabecular, it might be expected that these might have different genetic associations. Paternoster et al. (PLOS Genetics 9(2):e1003247) reported GWAS results for cortical volumetric BMD (vBMD) and trabecular vBMD based on values from the tibia. As the hip and spine are the main sites of osteoporotic fracture, we extended the published results by examining the association between the identified loci and measures of cortical vBMD in the hip and spine as well as fractures.

Methods: We used volumetric QCT scans of the hip and spine from the Age, Gene/Environment Susceptibility-Reykjavik Study (AGES-Reykjavik). We defined cortical vBMD and trabecular vBMD using standardized analytic protocols for the total femur, neck and trochanteric areas and the average of L1 and L2. From genotype data on 3,200 participants, we created an unweighted cortical BMD genetic risk score using the four loci for cortical vBMD reported by Paternoster et al.: RANLK, rs1021188; LOC285735, rs271170; OPG, rs783959; and ESR1/C6orf97, rs6909279. Paternoster et al. reported only one SNP for trabecular BMD, FMN2/GREM2, rs9287237. We used regression models for vBMD that adjusted for age, gender, the log of weight, and height. For fractures, we used data that has been compiled into a Fracture Registry as well as reports of fracture from recent hospitalizations categorized with specific ICD codes for location of fracture.

Results: The cortical vBMD score was strongly related to trochanteric cortical vBMD (1.37×10^{-10}), neck cortical vBMD (7.691×10^{-4}), and total femoral cortical vBMD (2.947×10^{-10}) and to vertebral cortical vBMD (3.03×10^{-4}). The cortical vBMD score was also associated with trochanteric trabecular vBMD (2.282×10^{-4}), which may be due to a correlation of .51 between the cortical and trabecular measures. There was no association of all fractures with the cortical vBMD score. The trabecular SNP was associated with femoral trabecular bone, but associations were weaker (trochanteric vBMD=.005; neck vBMD=.03; total femoral trabecular vBMD=.025 and that for vertebral trabecular vBMD was not significant (P=.07). There was no significant association with fracture.

Conclusion: SNP's identified for volumetric cortical bone showed a strong association with cortical vBMD at the hip and spine in our cohort while associations for an independent SNP for trabecular bone were much weaker. Further examination and analysis is needed to understand the contribution of these risk alleles to fracture risk.

***Disclosures: Tamara Harris**, None.*

SU0336

TNSALP Mutation Analysis in Women with Atypical Femoral Fracture and Bisphosphonate Therapy for Osteoporosis. Melissa Sum*[1], Margaret Huskey[1], Kathryn Diemer[1], Roberto Civitelli[1], Michael Gardner[1], Christopher McAndrew[1], William Ricci[1], Michael Whyte[2], Steven Mumm[2]. [1]Washington University, USA, [2]Shriners Hospital for Children-Saint Louis, USA

Hypophosphatasia (HPP) is caused by loss-of-function mutation(s) in the tissue non-specific alkaline phosphatase gene (*TNSALP*), resulting in low serum alkaline phosphatase (ALP) activity and inorganic pyrophosphate (PPi) accumulation extracellularly. PPi is a substrate for TNSALP and inhibits mineralization, thus providing a mechanism for the impaired bone matrix calcification and consequent femoral diaphyseal pseudofractures typical of adult HPP. Bisphosphonates (BPs) are analogs of PPi and can also inhibit mineralization. Since atypical subtrochanteric and diaphyseal femoral fractures (ASFFs) associated with long-term BP use for osteoporosis clinically resemble the pseudofractures seen in adult HPP, we hypothesized that carrying a *TNSALP* mutation, or having a mild form of HPP, predisposes to ASFFs with BP exposure. Indeed, one such case (Sutton et al. 2012) has been published. Here, we report prospective *TNSALP* mutation analysis of 11 patients with ASFFs and BP use. We sequenced all coding exons and adjacent splice sites of *TNSALP* in these individuals, and found a mutation in one patient. This heterozygous single-base change (c.648+1G>A) alters the mRNA splice donor site (GT) at the 3' end of exon 6, likely preventing normal splicing. This mutation has been reported once in a severe perinatal HPP case involving a second *TNSALP* mutation (Mornet et al. 1998). In our 66-year-old patient, serum ALP was 33 and 40 U/L on BPs (Nl: 35-129) compared to 86 IU/L (mean) in the 10 subjects with ASFF but without a *TNSALP* mutation. Low serum ALP levels are consistent with being a carrier of a loss-of-function *TNSALP* mutation, and this patient was never diagnosed with HPP. Based on DXA, she had "osteopenia". She suffered one ASFF while receiving BP therapy. Thus, we have prospectively identified 1 out of 11 women with BP-associated ASFF who is a carrier of a *TNSALP* mutation. Although the precise prevalence of *TNSALP* mutations in the general population is unknown, our results support the hypothesis that *TNSALP* mutation may contribute to ASFFs in some women exposed to BPs. If our hypothesis is validated in studies of larger populations, identification of such carriers before treatment might help to reduce the incidence of ASFFs.

***Disclosures: Melissa Sum**, None.*

SU0337

Gastrointestinal Events and Osteoporosis Treatment Initiation among Elderly Women with Medicare Part D Coverage. Ethel Siris[1], Jingbo Yu*[2], Ankita Modi[2], Mitch Dekoven[3], Anshu Shrestha[4]. [1]Columbia University College of Physicians & Surgeons, USA, [2]Merck & Co, Inc., USA, [3]IMS Health, USA, [4]Precision Health Economics, LLC, USA

Objectives: To examine the association of gastrointestinal (GI) events with osteoporosis (OP) treatment initiation among elderly osteoporotic women with Medicare Part D drug coverage.

Methods: This was a retrospective cohort study using the Medicare 20% medical and pharmacy claims (Part D) from 2006-2009. Patients were included if they were female; ⩾66 years old; had a diagnosis for OP (ICD-9-CM 733.0x; 1st diagnosis date as index date); no prior OP treatment; and no Paget's disease, malignant neoplasm diagnosis, or estrogen use in the 12 month pre-index. GI event was defined as having a diagnosis or procedure for a GI condition between OP diagnosis and treatment initiation or end of 12 month follow-up, whichever occurred first. OP treatment initiation was defined as use of any pharmacological OP medication within 1 year post-index, including bisphosphonates (BIS) and non-BIS. Descriptive and multivariate analyses were conducted. Cox proportional hazard regression was used to model association of GI events and treatment initiation and logistic regression was used to model GI events and type of initial therapy (BIS vs. non-BIS) among those treated, adjusting for age, use of glucocorticoid, GPA and NSAID, and comorbidities.

Results: 126,188 women with newly-diagnosed OP were included in the analysis. Of them, 72.1% did not receive any OP medication within 1 year of diagnosis, 41.6% had pre-index and 40.4% had post-index GI events. Compared with those without post-index GI, patients who had post-index GI were less likely to start OP treatment (14.3% vs. 37.1%, $p<0.001$), and were less likely to be on BIS vs. non-BIS upon treatment initiation (10.1% vs. 29.4%). Patients with post-index GI had a 68.8% lower hazard among those with pre-index GI (HR=0.312, $p<0.001$) and a 74.6% lower hazard among those without pre-index GI (HR=0.254, $p<0.001$) to initiate treatment than those without post-index GI, controlling for covariates. Treated patients with a post-index GI event had 12% lower odds ($p<0.001$) of starting with BIS vs. non-BIS, compared with patients without a post-index GI event, controlling for pre-index GI and other covariates.

Conclusions: Among women with Medicare Part D coverage who were newly diagnosed with OP, about 40% of them had GI events between OP diagnosis and treatment initiation within 1 year. The presence of a GI event was associated with a higher likelihood of not being treated and increased likelihood of being treated with a non-BIS vs BIS.

***Disclosures: Jingbo Yu**, Merck & Co., Inc, 2*
This study was funded by Merck & Co. Inc

SU0338

Objectively Measured Physical Activity and Bone Health in Frail Older Adults. Hyuntae Park*, Hiroyuki Shimada, Hyuma Makizako, Daisuke Yoshida, Yuya Anan, Takehiko Doi, Kazuki Uemura, Kota Tsutsumimoto, Sangyoon Lee, Tadashi Ito, Takao Suzuki. National Center for Geriatrics & Gerontology, Japan

Age-related bone loss and decline in physical activity are a serious public health problem, especially in frail populations. Previous study [1] shows significant associations between bone characteristics and yearlong physical activity in healthy older adults, with better health in those taking >7,000 steps/day and/or spending >15 min/day of moderate to vigorous physical activity (MVPA, >3 METs). Despite this finding, it remains unclear the relationship between the habitual physical activity and bone health in frail older adults. The present study examines these relationships. A cross-sectional study of 239 older adults with frailty (mean [SD] age: 73.2 [5.1] y, 105 men) in a sub study of the Obu Study of Health Promotion for the Elderly (OSHPE). Frailty was defined according to the criteria developed by Fried et al. in participants of the OSHPE, a cohort of 5,104 community-dwelling older adults. Daily physical activity was measured using a triaxial accelerometer on 30 consecutive days and duration of MVPA and daily step counts were calculated. Bone mineral density (BMD) in lumbar spine 2-4 and total hip were measured by dual energy X-ray absortiometry. Linear regressions showed that after controlling data for age and/or sex, BMD was associated with physical activity, more closely for the femur values than for the lumbar spine, and for duration of MVPA than for step count. Multivariate logistic models with control for potential confounders (age, BMI, alcohol and drug intake, tobacco, nutritional status) confirmed the risk of osteoporosis was related to both measures of physical activity (step count and MVPA) in both men and women. These relationships, however, were stronger for the duration of MVPA than for step count. After adjusting for confounders, men and women in the lowest quartile of step count and in the two lowest quartiles of moderate-exercise duration showed, respectively, 1.5 and 1.8, and 1.7.–2.2 and 2.1–2.8 times greater risk of osteoporosis than those in the highest quartile. The direction of causation cannot be inferred from a cross-sectional study and further prospective research is required to clarify this. Nevertheless, we suggest that from the viewpoint of the prevention of osteoporosis, frail older adults should be encouraged to engage in low- and moderate-intensity habitual physical activity, taking >5,800 steps/day with a duration >10 min/day at moderate to vigorous intensity. [1] Park H, et al. Osteoporos Int, 2007; 18: 285–293.

***Disclosures: Hyuntae Park**, None.*

SU0339

Physical Activity in Midlife Is Associated with Peripheral Bone Density and Microarchitecture in Later Life: The Framingham Osteoporosis Study. Kerry Broe*[1], Marian Hannan[2], Elizabeth Samelson[3], Robert McLean[4], Ching-An Meng[1], Mary Hogan[1], Danette Carroll[1], Xiaochun Zhang[1], L. Adrienne Cupples[6], Mary Bouxsein[7], Douglas Kiel[8]. [1]Institute for Aging Research, Hebrew SeniorLife, USA, [2]HSL Institute for Aging Research & Harvard Medical School, USA, [3]Hebrew SeniorLife, Harvard Medical School, USA, [4]Hebrew SeniorLife Institute for Aging Research & Harvard Medical School, USA, [6]Department of Biostatistics, Boston University School of Public Health, USA, [7]Beth Israel Deaconess Medical Center, USA, [8]Hebrew SeniorLife, USA

The intensity of physical activity (PA) during childhood and adolescence may have lasting effects on bone health. Less is known about the effects of PA in midlife on later bone health. PA has modest associations with traditional measures of areal BMD in older adults but has not been studied with regard to bone microarchitecture. Our objective was to determine the association between PA, assessed in midlife, on subsequent bone density and microarchitecture in a community-based sample of middle-aged adults.

Study participants included 185 Framingham Offspring participants who had PA assessed in 1996-2001 (mean age 57 ± 7 yrs, 57% female) and bone density and microarchitecture of the tibia and radius evaluated in 2012, on average 14 ±1 yrs later. PA was measured using the Physical Activity Scale for the Elderly (PASE), a validated activity summary score. Bone density and microarchitecture parameters were measured using high-resolution peripheral quantitative computed tomography (HR-pQCT, Scanco Medical AG). We focused on six bone parameters: cross sectional area (CSA, mm2), total bone density (Dtot, mg/ccm), trabecular density (Dtrab, mg/ccm), trabecular number (TbN, 1/mm), cortical thickness (CtTh, mm), and cortical porosity (CtPo,%). Linear regression was used to assess the association between PASE and bone density and microarchitecture. PASE was categorized into sex-specific tertiles to assess least squares means of bone density and microarchitecture by PASE category. All analyses were adjusted for sex, age, height, and weight.

Average PASE was 163 ±79 and ranged from 12 to 402. At the tibia, higher PASE was significantly associated with greater adjusted Dtot and CtTh and lower CSA. At the radius, higher PASE was associated with greater adjusted Dtot, Dtrab, and CtTh. PASE was not associated with TbN or CtPo at either site. Similar patterns of higher bone measures with higher PASE were observed with bone microarchitectural parameters by PASE tertiles (Table1). At the tibia, significant positive trends were observed between PASE tertiles and adjusted Dtot, Dtrab, and CtTh. At the radius, positive trends were observed with Dtrab (all p-trend ≤ 0.04).

In conclusion, PA in midlife years had a positive effect on subsequent bone density and microarchitecture parameters at peripheral sites, more so at the weight-bearing tibia than the radius. Thus, PA at midlife may confer protective benefits on bone density and microarchitecture at older ages.

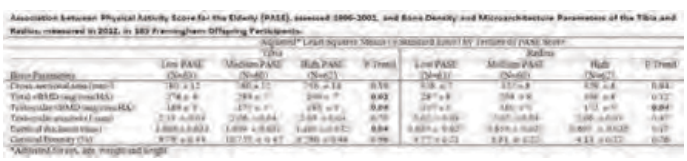

Physical Activity and Bone Microarchitecture: The Framingham Osteoporosis Study

***Disclosures: Kerry Broe**, None.*

SU0340

A Randomized Controlled Trial Evaluating Appropriate Osteoporosis Treatment by Family Physicians in Response to FRAX® versus CAROC Reports. Karen Beattie*[1], George Ioannidis[1], Alexandra Papaioannou[2], Joy MacDermid[1], Ruby Grewal[3], Jonathan Adachi[4], Anthony Hodsman[5]. [1]McMaster University, Canada, [2]Hamilton Health Sciences, Canada, [3]University of Western Ontario, Canada, [4]St. Joseph's Hospital, Canada, [5]Western University, Canada

Introduction: Current Canadian clinical practice guidelines recommend the use of either the FRAX® or the Canadian Association of Radiologists and Osteoporosis Canada (CAROC) fracture risk assessment tools to report 10-year fracture risk in an individual. The CAROC tool includes sex, age and femoral neck BMD as risk factors. Prevalent fragility fractures and corticosteroid use are incorporated as step-wise categorical modifiers of baseline fracture risk. While the CAROC tool reports fracture risk as low <10%, moderate 10-20%, or high >20%, FRAX® provides a precise estimate of risk in percent. It is unknown whether one reporting system is more effective in helping family physicians (FPs) identify individuals who should be considered for treatment than the other. Thus, compared to the CAROC-based BMD report (hereafter referred to as the BMD report), we hypothesized that the FRAX® report would result in better identification of patients who should be treated by FPs.

Methods: Individuals ⩾50 years old with a distal radius fracture were included provided they had no previous osteoporosis diagnosis and were not taking any osteoporosis medication. Participants underwent a DXA scan and answered questions about fracture risk factors. Each participant's FP was randomized to receive either a FRAX® or a BMD report. The FRAX® report, which was pilot tested with 8 FPs, included statements regarding treatment recommendations as per clinical guidelines. There were no such treatment recommendations on the BMD report. After 3 months, participants were called and asked if they were contacted by their FP and if they were treated. FPs' treatment decisions were compared to recommendations of a rheumatologist (osteoporosis expert).

Results: Sixty non-consecutive participants were enrolled (n=31 FRAX®; 11 low, 16 mod, 4 high risk; n=30 BMD; 22 mod, 9 high risk). Of clinical significance is that 45.2% of FRAX® group participants were contacted by their FPs to discuss their results compared to 28.2% of BMD report group participants. Kappa statistics of agreement in treatment recommendation between the rheumatologist and FPs were 0.64 for FRAX® and 0.32 for BMD group participants. The FRAX® report was preferred by FPs.

Conclusions: FRAX® reporting resulted in better post-fracture follow-up and treatment recommendations that substantially agree with a specialist in osteoporosis care. Treatment recommendations stated on the FRAX® report may have been an important factor in helping FPs make treatment decisions.

***Disclosures: Karen Beattie**, None.*

SU0341

Association of Waist Circumference with Bone Mineral Densities in Middle- and Old-aged Men and Women: The Dong-gu Study. Lian-Hua Cui[1], Sun-Seog Kweon[2], Jin-Su Choi[2], Hae-Sung Nam[2], Jane Cauley[3], Min-Ho Shin*[4]. [1]Department of Preventive Medicine, Qingdao University Medical college, China, [2]Department of Preventive Medicine, Chonnam National University Medical School, South Korea, [3]University of Pittsburgh Graduate School of Public Health, USA, [4]Chonnam National University Medical School, South Korea

Several studies have examined the association between waist circumference as the index of abdominal fat and BMD and inconsistent results have been reported. Our study included a total of 8981 Korean (3592 men and 5389 women) community-dwelling individuals aged 50 years and over enrolled between 2007 and 2010. BMD were measured by dual-energy X-ray absorptiometry at lumbar spine and femoral neck skeletal sites. Multiple linear regression analysis was used to evaluate the relationship between the quartiles of waist circumference and BMD, adjusting for age, height, weight, and body fat percent. After adjusting for age, height and weight, there was a negative linear association between waist circumference and BMD at femoral neck and lumbar spine sites in both men and women. Waist circumference was more strongly associated with BMD in men than in women. These associations were slightly attenuated but remained significant after further adjustment for body fat percent. We found that waist circumference was inversely associated with BMD. Our results suggest that the waist circumference is a likely predictor of osteoporosis in middle- and old-aged Korean men and women.

Table Difference in bone mineral density by quartiles of waist circumference

		Quartile of Waist Circumference					
		1st	2nd	3rd	4th	P for trend	P for interaction
Number (men/women)		912/1322	991/1219	961/1318	728/1530		
Range (cm)		57.0-82.4	82.5-87.9	88.0-93.4	93.5-130.1		
Model 1	Lumbar spine						
	Men	0 (reference)	0.010 (-0.010 to 0.029)	0.042 (0.019 to 0.064)	0.082 (0.052 to 0.112)	<0.001	
	Women	0 (reference)	0.006 (-0.006 to 0.018)	0.021 (0.009 to 0.034)	0.036 (0.021 to 0.052)	<0.001	0.002
	Femoral neck						
	Men	0 (reference)	0.010 (-0.002 to 0.022)	0.033 (0.019 to 0.047)	0.060 (0.042 to 0.079)	<0.001	
	Women	0 (reference)	0.004 (-0.003 to 0.012)	0.009 (0.001 to 0.017)	0.025 (0.015 to 0.035)	<0.001	0.018
Model 2	Lumbar spine						
	Men	0 (reference)	0.005 (-0.015 to 0.024)	0.035 (0.012 to 0.058)	0.073 (0.041 to 0.104)	<0.001	
	Women	0 (reference)	0.004 (-0.008 to 0.016)	0.019 (0.006 to 0.032)	0.034 (0.018 to 0.049)	<0.001	0.002
	Femoral neck						
	Men	0 (reference)	0.003 (-0.009 to 0.015)	0.025 (0.008 to 0.037)	0.047 (0.028 to 0.066)	<0.001	
	Women	0 (reference)	0.001 (-0.006 to 0.009)	0.005 (-0.003 to 0.014)	0.021 (0.010 to 0.031)	<0.001	0.036

Values are mean difference with 1st quartile group in g/cm² with 95% confidence interval, adjusted for age, height and weight (model 1) or age, height, weight, and body fat percent (model 2).

Table

***Disclosures: Min-Ho Shin**, None.*

SU0342

Associations of Overweight and Obesity with Incident Major Osteoporotic and Hip Fractures: A Large Clinical Cohort Study of Women and Men. Carrie Nielson*[1], Eric Orwoll[1], Suzanne Morin[2], Sumit Majumdar[3], William Leslie[4]. [1]Oregon Health & Science University, USA, [2]McGill University, Canada, [3]University of Alberta, Canada, [4]University of Manitoba, Canada

Although underweight is a known risk factor for hip fracture, many fractures occur in overweight and obese older adults – a rapidly growing segment of the population. Understanding fracture associations with higher BMI and potential differences according to sex is important.

Methods: 51,313 women and 4689 men age ⩾50 years at the time of baseline DXA testing (Lunar DPX or Prodigy; GE Healthcare) were identified in a clinical database from Manitoba, Canada. Height and weight were used to calculate BMI at the time of DXA testing, and classified according to WHO critera (Figure). Major osteoporotic fractures (MOF), including clinical vertebral, hip, humerus, and wrist fractures, were obtained by linkage to a population-based repository. Multivariable Cox proportional hazards models were used to study the independent contributions of BMI on fracture risk, with and without hip BMD adjustment; normal weight was the reference group for all analyses.

Results: Most women were overweight or obese (60%), as were most men (68%), while only 2% of women and 1% of men were underweight. During a mean follow-up of 5 years, incident MOF occurred in 3721 women and 276 men (1027 female and 75 male hip fractures). Most female (51%) and male (59%) MOF occurred in those who were overweight or obese. Adjusting for age and clinical variables, there was an apparent protective effect of higher BMI on MOF in women (Figure, left panel); however, these associations were attenuated and not significant after BMD adjustment (right panel). Similar but weaker associations were seen in men. While a similar pattern in proportions of hip fractures across BMI categories was observed, protective effects of higher BMI were stronger and persisted in obese categories after BMD adjustment. For example, with age and clinical variable adjustments, the HR for obese I was 0.53 (CI: 0.42-0.66) in women. After BMD adjustment, the HR was attenuated to 0.79 (CI: 0.63-0.99). No statistically significant sex interactions were observed.Discussion: In a clinical cohort of more than 50,000 people, a protective association for MOF with higher BMI was explained by BMD in both men and women. However, a protective association of higher BMI with hip fracture in women was only partially explained by BMD. Our findings suggest a substantial burden of fracture in older adults with high BMI. The factors not related to BMD that conferred lower risk of hip fracture in Manitoba women deserve further study.

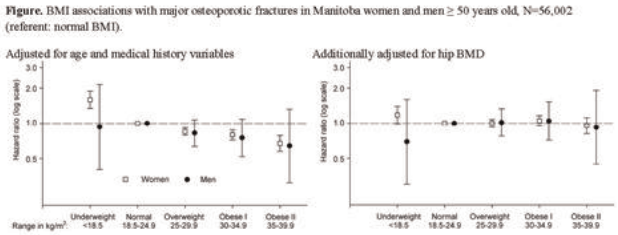

Figure. BMI associations with major osteoporotic fractures

***Disclosures: Carrie Nielson**, None.*

SU0343

Withdrawn

SU0344

Changes in the Prevalence of Osteoporosis in the United States After Inclusion of the Long Term Care Population. Nicole Wright*[1], Bess Dawson-Hughes[2], David Redden[1], Jeffrey Curtis[1], Susan Randall[3], Kenneth Saag[1]. [1]University of Alabama at Birmingham, USA, [2]Tufts University, USA, [3]National Osteoporosis Foundation, USA

Purpose: The National Health and Nutrition Examination Survey (NHANES) is the source used for estimating the prevalence of osteoporosis (OP) and low bone mass (LBM) in the United States (US). However, NHANES requires participants to be community dwelling, thus excluding those living in nursing homes or other long term care (LTC) facilities. There is a larger reported prevalence of OP in LTC than the general population. However, it is not known how the inclusion of the LTC population alters the overall prevalence of OP in the US.

Methods: We conducted a literature search to evaluate the reported prevalence of OP in LTC populations. We used mixed-linear models as a meta-analytical technique to generate an overall OP prevalence estimate in the LTC population. We applied this prevalence to the number of US residents in LTC facilities based on the 2010 American Community Survey (ACS), a yearly census like survey that provides information on factors such as living arrangements to help communities plan investments and services. We estimated how including those in LTC alters the overall NHANES OP prevalence estimate.

Results: We found six North American articles that reported OP prevalence in LTC settings, with prevalence ranging from 12-75%. Based on the meta-analysis results, we estimated an OP prevalence estimate of 42.4% (18.2%, 66.7%). The ACS reports that 1,397,107 US residents 50 years and older are in LTC facilities. Using our meta-analysis OP prevalence, we estimate that 592,793 residents over 50 years of age in LTC have OP, with lower and upper bounds of 254,234 and 931,352 individuals, respectively. NHANES reports the most recent overall prevalence of OP in US adults 50 years and older is 9.0%, resulting in 8.9 million adults over the age of 50 with OP based on the 2010 Census. However, when the meta-analytic estimates of OP in the LTC population are taken into account, the new overall prevalence becomes 9.5% (9.1%, 9.8%), resulting in an estimated 9.5 million adults over the age of 50 with OP.

Conclusions: Although the prevalence of OP ranges significantly in the published literature, the overall meta-analysis prevalence of OP is high in LTC settings. The addition of this population produces a somewhat larger overall OP prevalence estimate than reported by NHANES. Additional work examining the statistical significance of the differences and how the addition of LTC potentially alters age, gender, and race/ethnic specific prevalence is needed.

***Disclosures: Nicole Wright**, None.*
This study received funding from: National Osteoporosis Foundation

SU0345

Predicting Osteoporosis Knowledge and Perceived Susceptibility and Seriousness of Osteoporosis. Nicole Wright*[1], Stephanie Edmonds[2], Mollie Giller[2], Peter Cram[2], Kenneth Saag[1]. [1]University of Alabama at Birmingham, USA, [2]University of Iowa, USA

Purpose: Adherence to oral osteoporosis (OP) medications is low. While perceived side effects and costs are well known contributors to poor adherence, the roles of OP knowledge and perceived susceptibility are less certain. We used data from the Patient Activation After DXA Result Notification (PAADRN) study to examine factors associated with OP knowledge, perceived susceptibility and perceived seriousness in a regionally diverse cohort of patients undergoing DXA testing.

Methods: We administered the "Osteoporosis and You" Knowledge Scale, a 10 item scale a 5-point Likert response set to 3,860 patients presenting for DXA in 2012-2013 at three clinical sites (University of Iowa, University of Alabama at Birmingham, and Kaiser Permanente Georgia). Based on the scale scoring system, we recorded "correct" answers for those with "agree or strongly agree" responses and "incorrect" answers to all other response categories. We used the proportion correct as the OP knowledge outcome. For those not reporting OP at baseline, we administered the "Susceptibility" and "Serious" subscale questions of the "Osteoporosis Health Belief" Scale, 10 items with a 5-point Likert response sets. We conducted marginal linear regression analyses with a series of demographic, lifestyle characteristic, and co-morbidity variables. Variables significant at the $p<0.10$ level were included into one model. We used a combination of backward elimination and forward addition techniques to produce the final models for each outcome (final terms with $p < 0.05$).

Results: Our cohort was 83% women, 78% White, 20% Black, and had a mean age of 67 years. The mean (SD) Osteoporosis & You knowledge score was 75% (19%). Of the 2,869 participants without OP, the mean (SD) susceptibility score was 11.8 (17.3) out of a range of 4-20 and seriousness score was 17.3 (3.6) out of a range of 6-30. Factors including location, sex, race, prior fracture history, smoking status, and general health were significantly associated with the outcomes in the marginal analyses. The Table provides selected factors associated with a significant increase or decrease in knowledge, perceived susceptibility and seriousness from the final models.

Conclusions: We identified several demographic and lifestyle factors associated with OP knowledge, perceived susceptibility and seriousness. Increasing OP knowledge and correcting potential misconceptions about OP susceptibility and seriousness may improve adherence to medications.

Table. Factors Associated with Osteoporosis Knowledge, Perceived Susceptibility and Seriousness of Osteoporosis*

	Knowledge Coef. (95% CI)	Susceptibility Coef. (95% CI)	Seriousness Coef. (95% CI)
Women vs. Men	0.29 (0.11, 0.47)	0.56 (0.27, 0.86)	-
Black vs. White	-0.94 (-1.09, -0.78)	-0.45 (-0.73, -0.17)	-
Age, yrs	-0.03 (-0.04, -0.02)	-0.04 (-0.05, -0.03)	-
Prior Fx vs No Fx	0.19 (0.06, 0.32)	0.401(0.14, 0.67)	-
Ever vs. Never Smoked	-0.22 (-0.34, -0.10)	-0.29 (-0.52, -0.07)	-
General Health			
Excellent	Ref.	Ref.	Ref.
Very Good	-0.10 (-0.28, 0.09)	0.10 (-0.24, 0.44)	0.02 (-0.40, 0.45)
Good	-0.24 (-0.43, -0.05)	0.70 (0.35, 1.05)	0.64 (0.21, 1.06)
Fair	-0.33 (-0.56, -0.10)	1.27 (0.84, 1.70)	0.83 (0.31, 1.34)
Poor	-0.39 (-0.74, -0.05)	1.48 (0.81, 2.14)	1.96 (1.18, 2.73)
Location of Healthcare			
Iowa	Ref.	-	-
UAB	-0.32 (-0.48, -0.16)		
KPG	0.12 (-0.04, 0.29)		

*Selected factors from outcome
Coef. = Beta coefficient from regression model, Fx = Fracture, UAB = University of Alabama at Birmingham, KPG = Kaiser Permanente of Georgia

Table

***Disclosures: Nicole Wright**, None.*

SU0346

Increased Risk of Hip Fracture Among Spouses. Effect of Homogamy?. Dan Mellstrom*[1], Valter Sundh[2], Cecilie Hongslo Vala[2], Magnus Karlsson[3], Bjorn Rosengren[3], Claes Ohlsson[4], Mattias Lorentzon[5], John Kanis[6], Boo Johansson[7], Anders Odén[8]. [1]Sahlgrenska University Hospital, Sweden, [2]Geriatric Medicine, Department of Internal Medicine & Clinical Nutrition. Center for Bone & Arthritis Research (CBAR) at Sahlgrenska Academy, Sweden, [3]Skåne University Hospital Malmö, Lund University, Sweden, [4]Center for Bone & Arthritis Research at the Sahlgrenska Academy, Sweden, [5]Geriatric Medicine, Center for Bone Research at the Sahlgrenska Academy, Sweden, [6]University of Sheffield, Belgium, [7]Department of Psychology, University of Gothenburg, Sweden, [8]Department of Biostatics, Chalmers University, Gothenburg., Sweden

Hip fracture among parents is an established risk factor for hip fracture. Genetic factors have importance for variation of bone density and fracture risk. However, also lifestyle factors like physical activity, smoking and nutrition are related to bone density and fracture risk. The aim of this study was to investigate if there is an increased risk for hip fracture among spouses.

We studied all patients with hip fracture n=218.285 in the national inpatient register in Sweden from 1987 to 2002. Each patient included in the register had both ICD codes for hip fracture and ICD codes for surgical procedure related to the hip fracture. Only the first hip fracture was recorded. This register was coordinated with the multi generation register, the register of causes of deaths, the national census register from 1970-1990 and the register of the total population in Sweden. We studied all married couples in Sweden (n=1.281.857) born 1902-1951 and married for at least 5 years. The married population was followed for 17.961.850 person-years. The hip fracture risk was estimated with a Poisson regression model.

During the period 1987-2002 hip fracture occurred among both spouses in 4226 married couples. In 7 couples hip fracture occurred in both spouses within 3 days. The HR for hip fracture in a married woman after a hip fracture in husband was 1.13 (95% CI 1.082-1.176). The corresponding HR for a married man was 1.19 (CI 1.145-1.239). The risk was significant from the age of 60 to 90 years. The HR for hip fracture in married women aged 60-70 was 1.35 (CI 1.058-1.712) after a hip fracture in husbands. The higher risk for hip fracture among spouses was consistent after adjustments for income, education, latitude and urbanisation.

We show for the first time an increased risk for hip fracture among spouses. The reason might be common social and life style factors but also assortative mating.

***Disclosures: Dan Mellstrom**, None.*

SU0347

Low thyrotropin levels as a predictor of major osteoporotic fractures in 260,783 adult men and women - The *OPENTHYRO* register cohort. Bo Abrahamsen*[1], Henrik Jørgensen[2], Anne Sofie Laulund[2], Mads Nybo[3], Thomas Brix[4], Laszlo Hegedüs[4]. [1]University of Southern Denmark, Denmark, [2]Bispebjerg Hospital, Denmark, [3]Odense University Hospital, Dept of Clin Biochemistry, Denmark, [4]Odense University Hospital, Dept of Endocrinology, Denmark

Background: Though previous studies have linked hyperthyroidism to an increased risk of osteoporotic fractures in women, recent work from the MrOs study suggests that fracture risk in men with low TSH levels is not increased. We have conducted a population-based assessment of the association between low TSH and major osteoporotic fractures.

Subjects and Methods: All TSH measurements performed in Funen County, Denmark (pop 484,346), between 1995 and 2010 were extracted for analysis, including tests from primary practice. We identified 260,783 individuals with at least one TSH measurement. All measurements were performed at the same laboratory. Using national health registers, we retrieved information on all hospital contacts, prescriptions filled and date of death/emigration. Individuals taking thyroid medications or having a record of thyroid surgery or radioiodine prior to the first TSH measurement were excluded.

Results: The risk of major osteoporotic fractures (16,874 persons) was significantly increased in subjects with TSH levels below reference (N=13,541), unadjusted Hazard Ratio (HR) 1.96 (1.87-2.07), p<0.0001, adjusted HR 1.18 (1.12-1.24), p<0.0001. The adjusted HR for hip fracture was 1.20 (1.02-1.42), p=0.03, in men and 1.28 (1.18-1.39), p<0.0001, in women. For major osteoporotic fractures, the adjusted HR was 1.20 (1.07-1.36) in men and 1.16 (1.09-1.22) in women.

Conclusions: Low TSH (<0.3 IU/L) was associated with an increased risk of major osteoporotic fractures, including hip fractures, with similar relative effect sizes in both genders.

Incident fracture	HR (unadjusted) and 95% CI	HR (adjusted[1]) and 95% CI
Hip (N=6,166)	2.66 (2.48-2.86), p<0.0001	1.24 (1.15-1.34), p<0.001
Spine (N=1,792)	1.56 (1.32-1.84), p<0.0001	1.03 (0.87-1.22), p=0.72
Forearm (N=7,835)	1.62 (1.50-1.75), p<0.0001	1.15 (1.07-1.25), p<0.001
Humerus (N=3,562)	1.94 (1.74-2.16), p<0.0001	1.16 (1.04-1.29), p<0.01

Fracture risk (both genders together). Cox PH model. [1]Adjusted for age, gender, Charlson index.

Table 1

***Disclosures: Bo Abrahamsen**, None.*

SU0348

Mild to Moderate Chronic Kidney Disease is Associatedwith Vertebral Fracture Independent of Albuminuria or Bone Mineral Density in Patients with Type 2 Diabetes Mellitus. Masahiro Yamamoto*[1], Toru Yamaguchi[1], Shozo Yano[1], Mika Yamauchi[1], Toshitsugu Sugimoto[2]. [1]Shimane University Faculty of Medicine, Japan, [2]Shimane University School of Medicine, Japan

Purpose: Patients with type 2 diabetes mellitus (T2DM) have an increased risk of vertebral fractures (VFs) compared to non-T2DM controls independent of bone mineral density (BMD) (JBMR 2009). In non-T2DM, a creatinine clearance rate (Ccr) below 65 ml/min is associated with an increased fracture risk, suggesting that the progressive stage of chronic kidney disease (CKD) is a risk factor for fracture. However, it is unclear whether renal dysfunction and urine albumin (uAlb) are associated with bone fragility in T2DM patients. The aim of this study is to clarify these relationships in T2DM men and women.

Methods: We divided 367 Japanese T2DM men over 50 years old and 326 postmenopausal T2DM women into 3 groups based on their calculated Ccr (using the Cockcroft-Gault equation): ?90 (stage 1: S1), 89–60 (S2), and 59–30 ml/min (S3). All of their creatinine levels were within normal range. Logistic regression analyses were performed to assess the relative VF risk of CKD S2 and S3 to S1.

Results: Men and women who experienced VFs were significantly older than those without VFs (68 *vs*. 64 years old, $P<0.01$; 70 *vs*. 65 years old, $P<0.01$, respectively), and had a lower Ccr (83 *vs*. 92 ml/min, $P<0.01$; 79 *vs*. 87 ml/min, $P<0.05$, respectively). There was no significant difference in the uAlb levels in either sex. As the CKD stage advanced from S1 to S3, prevalence VFs rate were significantly elevated in both men (30, 39, 58%, respectively, $P<0.01$) and women (24, 37, 41%, respectively, $P<0.01$), and BMD values were concomitantly and significantly decreased at femoral neck in men (0.792, 0.757, 0.737 g/cm^2, respectively, $P<0.01$) and women (0.713, 0.621, 0.543 g/cm^2, respectively, $P<0.01$) as well as at spine of women (0.946, 0.851, 0.816 g/cm^2, respectively, $P<0.01$). In contrast, uAlb levels were not significantly different among the three CKD stages. The VF risk relative to S1 was 1.8 (95%CI 1.1–3.0, $P<0.05$) for S2 and 4.8 (2.3–9.8, $P<0.01$) for S3 in men and 2.9 (1.2–6.8, $P<0.01$) for S3 in women, after adjustments for BMI, HbA1c, duration of T2DM, uAlb, and spine BMD Z score. The same relationships were observed in men, when these analyses were performed using the estimate GFR instead of Ccr.

Conclusion: CKD stages 2 and 3 were risk factors for VFs in T2DM patients. These associations were independent of uAlb or BMD, suggesting that the progression of CKD, but not albuminuria, may cause bone fragility and enhance VF risk due to deterioration in bone quality inT2DM.

***Disclosures: Masahiro Yamamoto**, None.*

SU0349

Modified "Osteoporosis Questionnaire" of FRAX is sufficient tool for screening of osteoporosis patients. Shinya Tanaka*[1], Sawako Moriwaki[2], Kiyoshi Tanaka[3], Syunpei Niida[2]. [1]Saitama Medical University, Japan, [2]Biobank-Omics, National center for geriatrics & gerontology, Japan, [3]Kyoto Women's University, Japan

Objective; In Japan, a revised version of diagnosis criteria of primary osteoporosis was published in 2012. Although medication of osteoporosis is effective approach, the knowledge of osteoporosis has not widely spread around the general population. To improve the screening efficiency of osteoporosis patients, we assessed the simple "Osteoporosis Questionnaire" composed of the age and the six factors extracted from the fracture risk assessment tool (FRAX), and compared the results with those of FRAX.

Materials and Methods; Total 99 women, age from 43- to 75-y-o, living in a local governments in Aichi, Japan, were included in this study. They took FRAX examination, were analyzed bone mineral density from the 2nd to the 4th lumbar spine and left femoral neck, and was took X-ray of the thoracic and lumbar spine. Osteoporosis was diagnosed in accordance with a 2012 revised version of primary osteoporosis of Japan. Usefulness of probabilities of major osteoporosis fracture of FRAX or the Osteoporosis Questionnair to discriminate subjects with either osteoporosis or non-osteoporosis was made sure by making receiver operating characteristic (ROC) curve or calculating sensitivity and specificity. The Osteoporosis Questionnair was constituted of age points and 6 CRF points, 1 point was given to every CRF and 1 point was given to person who were 59-y-o or below, 2 points was

given to person 60- to 64-y-o, 3 points was given to person 65- to 74-y-o, and 4-points was given to person 75-y-o or above.

Results: The area under ROC curve of FRAX in distinct osteoporosis patient was 0.760. And, if inhabitants who were 3 point or above in the Osteoporosis Questionnair was diagnosed as osteoporosis, sensitivity was 60.5% and specificity was 63.9%.

Conclusion; Both FRAX and "Osteoporosis Questionnaire" are useful for screening osteoporosis patients in group examinations.

***Disclosures: Shinya Tanaka**, None.*

SU0350

Multiple Gene Polymorphisms can Improve Prediction of Non-vertebral Fracture in Postmenopausal Women. Seung Hun Lee*[1], Seon Woo Lee[2], Seong Hee Ahn[1], Taehyeung Kim[2], Beom-Jun Kim[3], Eun-Hee Cho[4], Sang-Wook Kim[4], Tae-Ho Kim[5], Ghi Su Kim[1], Shin-Yoon Kim[6], Changwon Kang[2], Jung-Min Koh[3]. [1]Asan Medical Center, University of Ulsan College of Medicine, South Korea, [2]Department of Biological Sciences, Korea Advanced Institute of Science & Technology, South Korea, [3]Asan Medical Center, South Korea, [4]Department of Internal Medicine, Kangwon National University College of Medicine, South Korea, [5]Kyungpook National University School of Medicine, South Korea, [6]Kyungpook National University Hospital, South Korea

Clinical risk factors (CRFs), with or without bone mineral density (BMD), are used to determine the risk of osteoporotic fracture (OF), which has a heritable component. This study investigated whether genetic profiling can additionally improve the ability to predict OF. Using 1,229 unrelated Korean postmenopausal women, 39 single-nucleotide polymorphisms (SNPs) in 30 human genomic loci were tested for association with osteoporosis-related traits, such as BMD, osteoporosis, vertebral fracture (VF), non-vertebral fracture (NVF), and any fracture. To estimate the effects of genetic profiling, the genetic risk score (GRS) was calculated using five prediction models: (model I) GRSs only; (model II) BMD only; (model III) CRFs only; (model IV) CRFs and BMD; and (model V) CRFs, BMD and GRS. A total of 21 SNPs within 19 genes associated with one or more osteoporosis-related traits and were included for GRS calculation. GRS associated with BMD before and after adjustment for CRFs ($P = <0.001$ to 0.018). GRS associated with NVF before and after adjustment for CRFs and BMD ($P = 0.017$ to 0.045), and with any fracture after adjustment for CRFs and femur neck BMD ($P = 0.049$). In terms of predicting NVF, the area under the receptor-operator characteristics curve (AUC) for model I was 0.55, which was lower than the AUCs of models II (0.60), III (0.64), and IV (0.65). Adding GRS to model IV (in model V) increased the AUC to 0.67, and improved the accuracy of NVF classification by 11.5% ($P = 0.014$). In terms of predicting any fracture, the AUC of model V (0.68) was similar to that of model IV (0.68), and model V did not significantly improve the accuracy of any fracture classification ($P = 0.39$). Thus, genetic profiling may enhance the accuracy of NVF predictions and help to delineate the intervention threshold.

***Disclosures: Seung Hun Lee**, None.*

SU0351

Parathyroid Hormone and Bone Mineral Density as Independent Risk Factors for Mortality in Community-Dwelling Older Adults: the São Paulo Ageing & Health Study (SPAH). Diogo Domiciano*[1], Luana Machado[1], Camille Figueiredo[1], Jaqueline Lopes[2], Valéria Caparbo[1], Liliam Takayama[1], Eloisa Bonfa[1], Rosa Pereira[2]. [1]University of São Paulo, Brazil, [2]Faculdade De Medicina Da Universidade De São Paulo, Brazil

Objectives: Previous studies have shown a relationship between osteoporosis and increased risk of death. Moreover, secondary hyperparathyroidism has been linked to mortality amongst frail older hip fractures patients. However, none of these studies performed a concomitant evaluation of the parathormone (PTH)-calcium-vitamin D-axis and bone mass, and this is essential to determine more accurately the contribution of each of these parameters to survival in community-dwelling older subjects. Thus, the aim of this study was to investigate the association between iPTH, calcium, vitamin D and bone mineral density (BMD), and all-cause mortality in a prospective, population-based study of community-dwelling older adults. Methods: 839 community-dwelling subjects (516 women and 323 men), aged over 65 years, were prospectively studied. Clinical data (including history of osteoporotic fractures and cardiovascular events) were assessed by specific questionnaire. Serum 25(OH)D, iPTH, total calcium, phosphorus, creatinine, and alkaline phosphatase were measured. BMD of the lumbar spine and hip were evaluated by DXA. All analysis was done at baseline (2005-2006). Mortality was recorded during follow-up. Multivariate Cox regression analysis was used to compute hazard ratios for all-cause mortality. Results: After a mean 4.1 ± 1.1 years of follow-up, there were 132(15.7%) deaths. In multivariate Cox proportional model, age (HR:1.06 95% CI:1.03–1.09,$P<0.001$), male sex (HR:1.91 95% CI:1.31–2.77,$P<0.001$), history of falls in the last year (HR:1.45 95% CI:1.02–2.07,$P=0.04$), *diabetes mellitus* (HR:2.17 95% CI:1.49-3.16,$P<0.001$), low score of physical activity (HR:2.77 95% CI:1.15-2.73, $P=0.009$), history of any cardiovascular event (HR:1.70 95% CI:1.14-2.52, $P=0.009$), total hip T-score (HR:1.43 95% CI:1.19–1.74, $P<0.001$, per each 1SD reduction in BMD) and iPTH (HR:1.054 95% CI:1.051-1.056, $P<0.001$, per 10pg/ml iPTH) were independently associated to all-cause mortality. Subjects in the highest quartile of iPTH were at higher risk of death (HR 2.90, 95% CI: 1.29-6.50, $P = 0.009$) compared to subjects in the lowest quartile.

Conclusion: Lower BMD and higher iPTH were significantly associated with mortality in community-dwelling older adults. These findings support the notion that a careful screening of bone parameters may help to improve the outcomes in older individuals.

***Disclosures: Diogo Domiciano**, None.*

SU0352

Parental Divorce or Death Is Associated with Lower Adult Bone Strength: The Midlife in the U.S. Study. Carolyn Crandall*[1], Arun Karlamangla[1], Sharon Stein Merkin[2], Neil Binkley[3], Deborah Carr[4], Gail Greendale[1], Teresa Seeman[2]. [1]University of California, Los Angeles, USA, [2]UCLA, USA, [3]University of Wisconsin, Madison, USA, [4]Rutgers University, USA

Background. Because peak bone mass is acquired during childhood, bone health may be susceptible to environmental adversity in childhood. It is not known whether a childhood experience of separation from a parent due to death or divorce or being raised in a single mother family is associated with lower adult bone strength.

Methods. Using DXA data from 627 participants (ages 37-86 years, mean 56.3 years) in the Midlife in the United States Biomarker Project, we examined the associations of composite indices of femoral neck bone strength relative to load (in three failure modes: compression, bending, and impact) in adulthood with the experience of parental death or divorce in childhood and with being raised in a single mother family, adjusting for gender, race, age, menopausal transition stage (for women), body mass index, childhood and current smoking, pack-years of smoking, physical activity (in high school, during young adulthood, and currently), education, childhood socioeconomic status, adult financial status, and peak alcohol intake level.

Results. 110 participants experienced parental death or divorce during childhood (median age 5 years). After adjustment for covariates, participants who experienced a parental death or divorce before the age of 5 years had lower values for each of the composite indices (Table). Exposure to parental death or divorce between ages 5 and 16 years or being raised by a single mother was not associated with femoral neck strength indices (Table).

Conclusions. When experienced in early childhood, parental death or divorce is associated with lower adult bone strength, and this association is not explained by socioeconomic conditions and life style choices in childhood or adulthood.

Table. Adjusted associations of parental death or divorce, and single mother household, with composite indices of femoral neck bone strength relative to load[1]

	Bending Strength Index, SD units (95% CI) (N=627)	Compression Strength Index, SD units (95% CI) (N=627)	Impact Strength Index, SD units (95% CI) (N=627)
Parental death or divorce under age 5 years (n = 42)	-0.347 (-0.561, -0.133)**	-0.228 (-0.422, -0.035)*	-0.211 (-0.446, 0.025)~
Parental death or divorce between ages 5 and 16 years (n = 68)	0.049 (-0.154, 0.251)	0.206 (-0.115, 0.527)	0.089 (-0.088, 0.267)
Single mother and no parental death or divorce before age 16 years (n = 26)	0.163 (-0.230, 0.557)	0.167 (-0.271, 0.407)	0.142 (-0.251, 0.535)
No parental death or divorce before age 16 years, and two-parent family (n = 491)	Ref	Ref	Ref

*p-value 0.05-0.01; ** 0.01-0.001; ***<0.001; ~0.05-0.

[1] Presented as standardized regression coefficients, adjusted for race, site, menopausal transition stage, age, gender, age interactions with men over age 60 and post-menopausal women, BMI, BMI squared, BMI*gender, pack years of smoking, recreational sports at ages 14-18, competitive sports at ages 14-18, physical activity at ages 20-35, current physical activity, education, financial advantage, childhood socioeconomic advantage, whether started smoking ≤ age 18 (vs. never smoked or started >age 18), heavy drinker at period of peak alcohol consumption

Table

***Disclosures: Carolyn Crandall**, None.*

SU0353

Patients with Rheumatoid Arthritis Receiving High Doses of Prednisolone Tended to Fall More Frequently than Healthy Individuals: the TOMORROW study. Tatsuya Koike*[1], Masahiro Tada[2], Yuko Sugioka[3], Tadashi Okano[3], Kenji Mamoto[3], Kentaro Inui[3]. [1]Search Institute for Bone & Arthritis Disease (SINBAD), USA, [2]Department of Orthopaedic Surgery, Osaka City University Medical School, Japan, [3]Osaka City University Medical School, Japan

Purpose Patients with rheumatoid arthritis (RA) who have muscle weakness and stiff or painful joints might be at increased risk of falling and vertebral fractures. The present study prospectively determines the incidence of falls and associated risk factors in patients with RA in the TOMORROW study (UMIN000003876) that started in 2010.

Methods We evaluated muscle volume, bone density, thoracolumbar spine X-rays and disease activity in 202 consecutive patients with RA (54% using biological agents) and 202 age- and sex-matched healthy individuals as controls and then assessed the incidence of falls for 2 years.

Results The incidence of having at least one fall during the 2-year period did not significantly differ between the patients and controls (29.7% vs. 26.7%, NS). However, the patients fell significantly more often than controls (2.37 vs.1.56 falls; p = 0.03) and had a higher prevalence of vertebral fractures (45.5% vs. 30%) and semiquantitative (SQ) grade ⩾2 (15% vs. 5%) than the controls. After adjusting for risk factors of falls such as age, gender, smoking and BMI, multiple logistic regression analysis identified that a history of falls was the most significant parameter associated with the incidence of falls (odds ratios: all, 2.44, p < 0.001; patients, 2.40, p = 0.014; controls, 2.72, p = 0.015; Table 1). Existing vertebral fractures and SQ grade ⩾2 did not correlate with the incidence of falls (Table1). Multiple regression analysis revealed that the number of falls experienced by patients with RA was associated with doses of prednisolone (PSL; β = 0.188, P = 0.010,) and matrix metalloproteinase-3 (MMP-3; β = 0.156, P = 0.028).Conclusion A history of falls was an independent risk factor for any fall in all participants. Patients with RA receiving high doses of PLS or MMP-3 tended to fall more frequently than healthy individuals.

***Disclosures: Tatsuya Koike**, None.*

SU0354

Evaluation of Patients' Response Toward an Automated Osteoporosis Intervention Program. Matt Varacallo*[1], Edward Fox[2], Emmanuel Paul[3], Susan Hassenbein[3], Pamela Warlow[4]. [1]Penn State Hershey, Canada, [2]Pennsylvania State Hershey Medical Center, USA, [3]Penn State Hershey Department of Orthopaedics, USA, [4]Penn State Hershey, USA

INTRODUCTION: Osteoporosis is overshadowed in an era of chronic illnesses and a care gap exists between physicians and patients. Methods for improving the care gap via various intervention programs have yielded modest success. The aim of this study was to determine the effectiveness of implementing an automated system for identifying and sending a letter to patients at high-risk for developing osteoporosis.

METHODS: Penn State Hershey Medical Center (PSHMC) fracture patients 50 years of age and older were tagged with a diagnostic ICD-9 code upon the ER visit, identifying fractures at osteoporosis risk. Hospital encounter screening identified these codes and subjects were pre-screened to exclude cases involving trauma/MVA, repeats in the database, and individuals already being treated for osteoporosis. 103 subjects comprised the final intervention group.

Computer generated letters were sent out to each subject up to 3 months after the initial visit to the ER indicating that he or she was at risk for osteoporosis, and these individuals were urged to schedule an appointment with their PCP or with the bone health clinic at HMC. The control group was not sent a letter, but were contacted via telephone up to 3 months out after the initial injury to determine whether or not they had any follow-up.

RESULTS: For the control group, 84 individuals out of the total 98 (85.71%) did not have any follow-up evaluation after being treated for their fracture, and 14 out of the 98 (14.29%) had some sort of follow-up. For the intervention group, 62 out of 103 (60.19%) did schedule follow-up, while the remaining 41 out of 103 (39.81%) did not seek follow-up. The data were analyzed using the chi-squared test, yielding a p-value of <0.0001.

DISCUSSION: Current literature has demonstrated the low rate of follow-up care received by patients experiencing fragility fractures (1-25% without intervention). Research has shown the effectiveness of various types of intervention programs for improving the continuum of care for these high-risk patients, but many of these programs are non-automated and can have a multitude of human related system failures in the patient identification process. The results of our study are very similar to the current literature demonstrating the benefits of these osteoporosis intervention programs, and we report the success of our automated system that is able to be applied to any hospital with minimal cost and resources.

***Disclosures: Matt Varacallo**, None.*

SU0355

The Performance of FRAX® According to Different Levels of Socioeconomic Status. Sharon Brennan*[1], William Leslie[2], Lisa Lix[2], Helena Johansson[3], Anders Oden[4], Eugene McCloskey[5], John Kanis[6]. [1]The University of Melbourne, Australia, [2]University of Manitoba, Canada, [3]Swedish University of Agricultural Sciences, The Biomedical Center, Sweden, [4]World Health Organization (WHO) Collaborating Centre, University of Sheffield, United Kingdom, [5]University of Sheffield, United Kingdom, [6]University of Sheffield, Belgium

Background: FRAX® was constructed to predict 10-year major osteoporotic fracture (MOF) and hip fracture risk. Social factors may independently affect fracture risk. Therefore, we investigated FRAX calibration and discrimination according to socioeconomic status.

Methods: Women aged ⩾50years with baseline femoral neck BMD measured 1996-2011 were identified from the Manitoba Bone Density Program, Canada (n=51,327). Mean household income was extracted from 2006 census files, and categorized into quintiles. 10-year fracture probabilities were calculated using FRAX Canada. Incident fractures (excluding trauma codes) from population-based administrative data were studied in relation to income quintile in Cox proportional hazards models that adjusted for age and other covariates. To assess calibration, we compared observed *vs.* predicted fractures using a competing mortality framework.

Results: During mean 6.2±3.7 years of follow up there were 6,392 deaths, 3,723 women with ⩾1 MOF and 1,027 with hip fractures. Lower income was associated with higher risk for death, MOF and hip fracture in age and FRAX covariate-adjusted models (all *p* for linear trend <0.005 Table). More women in income quintile 1 (lowest) *vs.* income quintile 5 died (19% *vs.* 8%), or had a MOF (10% *vs.* 6%) or hip fracture (3.0% *vs.* 1.3%) (all $p \leq 0.001$). Adjustment for competing mortality mitigated the effect of socioeconomic status on FRAX calibration such that good calibration was observed for both income quintile 1 (lowest) and income quintile 5 (Figure). FRAX provided significant fracture discrimination for MOF and hip fracture within each income quintile (all $p<0.001$). Area under the curve (AUC) was slightly lower for income quintile 1 *vs.* quintile 5 for FRAX with BMD to predict MOF (0.68, 95%CI 0.66-0.70 *vs.* 0.71, 95%CI 0.69-0.74; $p=0.04$) and hip fracture (0.79, 95%CI 0.76-0.81 *vs*. 0.87, 95%CI 0.84-0.89; $p \leq 0.001$). Similar differences were seen for FRAX without BMD (MOF $p=0.04$, hip fracture $p \leq 0.001$). In contrast, femoral neck BMD performed equally for MOF and hip fracture in income quintiles 1 *vs.* 5 ($p \geqslant 0.4$).

Conclusions: Socioeconomic adversity independently modulates risk for death and fracture. Increased fracture risk in individuals of lower income is offset by increased mortality. Thus, under a competing mortality framework, FRAX provides robust fracture prediction and calibration regardless of socioeconomic adversity.

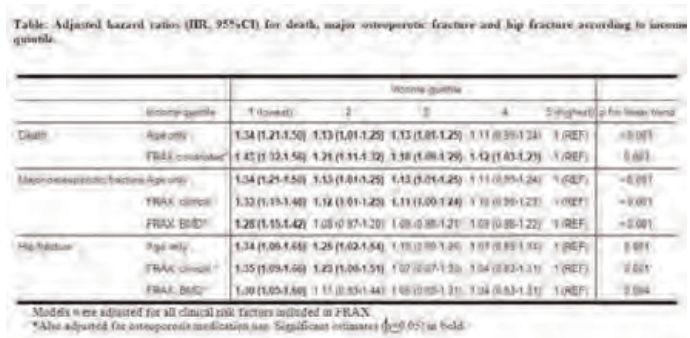

Adjusted hazard ratios (HR, 95%CI) for death, major osteoporotic fracture and hip fracture according

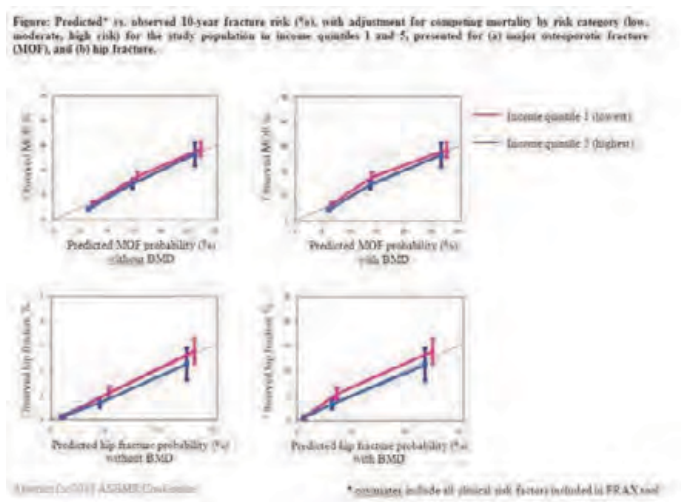

Predicted* vs. observed 10-year fracture risk (%), with adjustment for competing mortality by risk c

***Disclosures: Sharon Brennan**, None.*

SU0356

The Risk of Fractures after Initiating Antihypertensive Medications: Results from the National Claim Registry. Hyung Jin Choi*[1], Chanmi Park[2], Young-Kyun Lee[3], Yong-Chan Ha[4], Sunmee Jang[5], Chan Soo Shin[6]. [1]Chungbuk National University Hospital, South Korea, [2]Health Insurance Review & Assessment Service, South Korea, [3]Seoul National University Bundang Hospital, South Korea, [4]Chung-Ang University Hospital, South Korea, [5]College of Pharmacy Inje University, South Korea, [6]Seoul National University College of Medicine, South Korea

Several studies have investigated effects of antihypertensive medications on bone metabolism and fracture. We examined the relative risk of fractures among subjects who initiated antihypertensive medications using the nationwide database of medical and pharmacy claims in South Korea. Among 8,315,709 subjects with antihypertensive prescriptions, 527,500 subjects aged 50 years and older, who initiated single-drug antihypertensive medications from January 2008 to June 2011, were analyzed. Based

on medication possession ratio data, subjects were classified as a non-user, calcium channel blocker (CCB), angiotesin-receptor blocker (CRB), beta blocker (BB), angiotensin converting enzyme (ACE) inhibitor and diuretic users. The outcome measure was the first occurrence for a vertebral fracture or a non-vertebral fracture. The incidence of fracture was analyzed controlling for age, gender, comorbidity score, diagnosis of diabetes, diagnosis of osteoporosis, osteoporosis treatment, and osteoporosis related diseases. Total of 16,765 fractures were observed among 527,500 subjects during the observation period. Fracture rate per 10,000 person-years varied significantly across type of antihypertensive medications, with non-user group having the lowest rate [152.2, 95% confidence interval (CI) 148.7-155.7] and ACE inhibitor group having the highest rate (254.0, 95% CI 225.0-286.7). In models adjusting for all confounding factors, ACEI users (HR=1.68), diuretics users (HR=1.45), CCB users (HR=1.23) and BB users (HR=1.15) showed significantly increased risk of fractures compared with non-users (P<0.05). Only the fracture risk of ARB users (HR=1.00, 95% CI 0.95-1.05) was not significantly different from the non-users. These findings suggest that use of anti-hypertensive agents, except for the ARB, is significantly associated with increased risk of fracture although the relative risk varies depending on the type of medications.

***Disclosures: Hyung Jin Choi**, None.*

SU0357

Vertebral and Nonvertebral Fractures Depend on Physical Activity of Osteoporosis Patients. Hans-Christof Schober*[1], Johanna Torner[2], Reimer Andresen[3]. [1]Klinikum Südstadt RostockKlinik Für Innere Medizin I, Germany, [2]Klinikum Südstadt ostock, Germany, [3]Westküstenklinikum, Germany

Introduction: There is a certain relationship between bone health and physical activity level of patients with Osteoporosis. Until now no specific markers were made out that describe the risk of fracture.

Objective:Our aim was to investigate how physical activity in detail influences the number of vertebral and non-vertebral fractures in patients with Osteoporosis.

Patients and Methods:Data of 179 patients with Osteoporosis, aged 32 to 92 years, were retrospectively analyzed. The appearance of peripheral and vertebral fractures, as being the main variable, was documented by questionnaire or medical imaging.Height, weight, body fat percentage, body muscle percentage, abdominal girth and visceral fat were measured during consultation- hour. BMI was calculated.Parameters of physical activity like time in tandem stand, chair rising test and gait speed were measured by stopwatch (manually). Hand grip strength on the right and left side were measured by hand dynamometer.Patient's medication was documented by questionnaire. We divided all mentioned drugs into three groups, concerning their influence on bone health.To examine the influence of age we used the model of medication's relationship to the number of fractures and defined ''age'' as being a co-variable. We once calculated this model with the average age and twice for an age of 50 years.The classification of all patients was realized as follows: group 1(without fractures), group 2(only non-vertebral fractures), group 3(only vertebral fractures) and group 4(both, vertebral and non-vertebral fractures).The statistical calculation was accomplished using Spearman Correlation Coefficients and Glimmix Procedure.

Results:Our calculations showed, that hand grip strength on the left side correlates significantly (p<0,05) negatively with number of non-vertebral fractures.The effects on vertebral fractures were different: Visceral fat correlates positively to this number. Gait speed correlates strongly negatively (p<0,01) to vertebral fractures. Patients who receive drugs with verifiably negative effect on bone health do have significantly more non-vertebral fractures (p<0,05) than patients without any ''negative drugs''. Regarding vertebral fractures, especially patients treated with ''Osteotropica'', do have significantly more fractures (p<0,05) than patients without any osteoporotic treatment.

Conclusion:Gait speed and hand grip strength should be used in order to detect patients at risk for fractures.

***Disclosures: Hans-Christof Schober**, None.*

SU0358

Concurrently Lower Chance of Diabetes but Higher Chance of Osteoporosis in Elderly Women with Elevated Osteocalcin. Kyoung Min Kim*[1], Eun Young Lee[2], Ju Mi Lee[3], Young Mi Yun[4], Yoosik Youm[5], Hyeon Chang Kim[3], Chang Oh Kim[2], Yumie Rhee[6]. [1]Seoul National University Bundang Hospitatl, South Korea, [2]Department of Internal Medicine, Yonsei University College of Medicine, South Korea, [3]Department of Preventive Medicine, Yonsei University College of Medicine, South Korea, [4]Medical Research Center, Yonsei University College of Medicine, South Korea, [5]Department of Sociology, Yonsei University, South Korea, [6]Department of Internal Medicine, College of Medicine, Yonsei University, South Korea

Recent animal studies have suggested a new regulatory circuit between bone and energy metabolism via osteocalcin (OCN). Both increased bone remodeling and insulin resistance are major degenerative changes with aging. The aim of this study was to examine the association between serum OCN and metabolic profiles in women aged 64 and over. This is a community-based, cross-sectional study and 616 healthy ambulatory elderly women were enrolled. Serum OCN levels had significant negative correlations with fasting plasma glucose (FPG), HbA1c, insulin and HOMA-IR after adjusting for age and BMI (r=-0.186, -0.162, -0.147 and -0.166. p<0.001 respectively). After dividing the subjects into 3 tertiles by OCN levels, FPG, HbA1c, insulin and HOMA-IR varied inversely with the OCN tertiles (p<0.05, respectively). The prevalence of metabolic syndrome was significantly lower in the women with highest OCN with OCN tertiles (p<0.05 analyzed with linear by linear association). In contrast, those in the higher tertiles of OCN had lower bone mass in the lumbar spine and hip (p<0.05, respectively). In a multiple logistic regression analysis, the OCN level was inversely associated with the development of diabetes, but positively related with risk of osteoporosis after adjusting for the confounding factors (OR, 0.70; 95% CI, 0.54-0.86, p=0.028 for diabetes, OR, 1.28; 95% CI 1.19-1.37, p=0.01 for osteoporosis). Increased OCN level is associated with improved glucose tolerance, but decreased bone strength, which supports a potential link between bone and energy metabolism in elderly Korean women.

Table 1. Stepwise multiple logistic regression of OCN for diabetes and osteoporosis

	Diabetes				Osteoporosis			
	OR per 1SD increase of OCN	95% CI		p-value	OR per 1SD increase of OCN	95% CI		p-value
Crude	0.57	0.44	0.69	<0.001	1.31	1.23	1.40	0.00
Model 1	0.57	0.45	0.70	<0.001	1.33	1.24	1.42	0.00
Model 2	0.58	0.45	0.71	<0.001	1.30	1.21	1.39	0.00
Model 3	0.70	0.54	0.86	0.028	1.29	1.19	1.38	0.01
Model 4	-'	-'	-'	-'	1.28	1.19	1.37	0.01

Model 1: age adjusted

Model 2: as Model 1 and body mass index (BMI) adjusted

Model 3: as Model 2 and FPG adjusted for diabetes, 25-hydroxyvitamin D adjusted for osteoporosis

Model 4: as Model 3 and parathyroid hormone adjusted

Table 1. Stepwise multiple logistic regression of OCN for diabetes and osteoporosis

***Disclosures: Kyoung Min Kim**, None.*

SU0359

Glycemic Control in Relation to High Bone Mineral Density and Fracture Risk Among Postmenopausal Women: The CEOR Study. Mohammed-Salleh Ardawi*[1], Mohammed Qari[2], Abdulrahim Rouzi[3], Sharifa Al-Sibiani[4], Nawal Al-Senani[4], Bader Mustafa[5]. [1]Center of Excellence for Osteoporosis Research & Faculty of Medicine, Saudi Arabia, [2]Center of Excellence for Osteoporosis Research & Department of Haematology, Faculty of Medicine & KAU Hospital, King Abdulaziz University, Saudi Arabia, [3]Center of Excellence for Osteoporosis Research & Faculty of Medicine, Saudi Arabia, [4]Center of Excellence for Osteoporosis Research & Department of Obstetrics & Gynecology & KAU Hospital,Faculty of Medicine, King Abdulaziz University, Saudi Arabia, [5]Center of Excellence for Osteoporosis Research, King Abdulaziz University, Saudi Arabia

Background: Subjects with type 2 diabetes (T2DM) show increased fracture risk despite higher bone mineral density (BMD). Our objective was to examine the influence of glycemic control on BMD and the risk of fractures among postmenopausal women.

Methods: Data of 3015 postmenopausal women of the Center of Excellence for Osteoporosis Research (CEOR) Study, a prospective population-based cohort, were available (mean follow-up 6.2 $\pm$ 1.3 years). At baseline, 412 women with T2DM were classified by glycemic control (according to HbA1c%), resulting in three comparison groups: well- controlled diabetes (WCD; n=198; HbA1c $<$ 7.5%), poorly-controlled diabetes (PCD; n=214; HbA1c $\geqslant$ 7.5%) and no diabetes (n=2603). Cox proportional hazard regression analysis adjusted for age, BMI, and BMD [neck femur and lumbar spine (L_1-L_4)] were used to test for differences in bone variables and fracture risk (hazard ratio [HR] [95% CI]).

Results: Women in the PCD group had an increased fracture risk compared with WCD group (HR 1.66 [1.26-2.17]) and those without diabetes (1.94 [131-2.87)]; whereas those with WCD had an HR of (0.81 [0.60-1.11]) as compared with women without diabetes. PCD group showed 1.2-5.8% higher BMD, 4.9-6.2% thicker cortices, and -1.3 to 2.1% narrower neck femur than WCD and women without diabetes, respectively.

Conclusions: Poor glycemic control in postmenopausal women with T2DM is associated with fracture risk, high BMD, and thicker femoral cortices in narrower bones. We suggest that osteofragility in apparently ''healthy'' bones in PCD can result from micro-fragility accumulation and/or cortical porosity, reflecting impaired bone repair processes.

***Disclosures: Mohammed-Salleh Ardawi**, None.*

SU0360

Bone Turnover Markers and Calcium Metabolism in Young Men With Hyperthyroidism. Ana Paula Barbosa*[1], Mário Rui Mascarenhas[2], Ana Gonçalves[3], Vera Simões[4], António Gouveia de Oliveira[5], Manuel Bicho[6], Isabel do Carmo[3]. [1]Endocrinology, Santa Maria Hospital & Faculty of Medicine, Portugal, [2]Lisbon's Faculty of Medicine, Santa Maria University Hospital, CHLN,EPE, Portugal, [3]Endocrinology, Diabetes & Metabolism Department, Santa Maria Hospital, CHLN-EPE, Portugal, [4]CEDML - Endocrinology, Diabetes & Metabolism Clinic, Lda., Portugal, [5]Biostatistics Department, FCMUNL, Portugal, [6]Metabolism & Endocrinology Center, Genetics Laboratory (FMUL), Portugal

Hyperthyroidism is a known risk factor for reduced bone mineral density (BMD), osteoporosis and fragility fractures, even in young populations. Bone turnover markers can be impaired as well as calcium and the hormones involved in the control of bone metabolism.

Purpose: To evaluate the relationships between the bone turnover markers plasma levels, the hormones affecting calcium metabolism and BMD, in young men with hyperthyroidism.

MATERIAL AND Methods: A group of 48 men aged ≤ 50 years was divided and paired in hyperthyroid (n= 24) and control (n=24) groups. The plasma osteocalcin, CTX, and bone alkaline phosphatase (BAP), as well as the thyroid hormones, TSH, PTH, calcium, and 25(OH)vitamin D blood concentrations were measured.

The BMD (g/cm^2) at the lumbar spine (L_1-L_4), at the proximal femur, at the distal radius and at the whole body and the total body soft tissues composition (lean and fat masses, Kg) were evaluated by dual X-ray absorciometry, using the Hologic QDR Discovery W densitometer.

No patient was previously treated for hyperthyroidism and/or OP.

Descriptive and regression tests were used and statistical significance was considered for P <0.05.

RESULTSThe anthropometric data were similar between the groups; in the hyperthyroidism group, the BMD in all skeletal sites (except at the distal radius), the lean mass and the PTH were decreased, while the bone formation markers were increased (*Table 1*).

In the control group, there were significant relations between PTH and TSH plasma levels and between the BMD at distal radius and the BAP; in the hyperthyroidism group, significant relations were detected between PTH and BMD at the femoral neck.

CONCLUSIONS: The results of this study may suggest that the bone turnover markers and some of the hormones involved in bone metabolism are already modified and associated to an increased bone turnover, even in the youngest hyperthyroid men. Thus, both the diagnosis and therapy of the hyperthyroidism and an increase in calcium intake and sun exposure, should be precociously instituted, in order to minimize the bone mass loss and the possible increase of osteoporotic fractures risk.

GROUPS Variables	CONTROL	HYPERTHYROIDISM	P
Age *years*	**35.9** (±8.3)	**37.6** (±7.0)	NS
Total lean mass *kg*	**60.5** (±6.2)	**55.6** (±8.0)	0.0244
BMD L_1-L_4 *g/cm²*	**1.072** (±0.15)	**0.988** (±0.11)	0.0367
BMD fem neck *g/cm²*	**0.964** (±0.17)	**0.862** (±0.16)	0.0374
Osteocalcin *ng/ml*	**13.9** (±4.9)	**32.4** (±19.5)	0.0037
BAP *mcg/l*	**15.0** (±5.4)	**29.4** (±21.6)	0.0352
PTH *pg/ml*	**50.4** (±20.1)	**31.0** (±17.3)	0.0047

Table 1

***Disclosures: Ana Paula Barbosa**, None.*

SU0361

Influence of vitamin D status on the effect of statins on bone mineral density and bone turnover markers. Jesus Gonzalez-Macias*[1], José L. Hernández[1], Josefina Martínez[1], Sheila Ruiz[1], Jose Olmos[2]. [1]Department of Internal Medicine, Hospital Universitario Marqués de Valdecilla-IFIMAV, Universidad de Cantabria. RETICEF, Spain, [2]Hospital Universitario M. Valdecilla, Spain

Aim: To analyze whether the association between statin use and bone mineral density (BMD) and bone turnover markers (BTM) is influenced by serum 25OHD levels in postmenopausal women.

Methods: Some 1352 postmenopausal women were recruited from the Camargo Cohort after excluding those with any known medical disorder or drug that might affect bone metabolism, apart from statin use and low 25OHD serum levels. Participants were divided into four groups: group 1, women without statin treatment and 25OHD < 20 ng/ml; group 2, women on statin treatment and 25OHD > 20 ng/ml; group 3, women on statin treatment and 25OHD < 20 ng/ml; group 4, women without statin treatment and 25OHD > 20 ng/ml. BMD at lumbar spine (LS), femoral neck (FN) and total hip (TH) was measured by DXA (Hologic, QDR 4500). Bone turnover markers (CTX and P1NP) and 25OHD were determined by automated method (Elecsys, Roche). Multivariate analyses were performed to compare BMD and BTM in groups 2-4 vs. group 1. Adjustement for age, BMI, years since menopause, GFR, dairy calcium intake, exercise, family history of hip fracture, smoking and alcohol intake, diabetes and season was performed.

Results: Results are shown in table 1. Women in groups 3 and 4 did not show significant differences compared to group 1. However, women in group 2 had greater BMD at the FN and TH, and lower CTX, than women in group 1 (p=0.004, 0.035 and 0.05 respectively).

Conclusions: Women on statins and 25OHD above 20 ng/ml have less bone resorption and greater hip BMD than those in which both factors are absent. Differences, however, are not significant in women with only one of them. Vitamin D and statins seem to have a positive interaction in their effects on bone.

	n	DMO CL	DMO CF	DMO TH	CTX	P1NP
Statins - 25D<20	422	0.910 (0.906-0.922)	0.718 (0.708-0.728)	0.840 (0.830-0.850)	0.418 (0.399-0.437)	51.14 (49.13-53.15)
Statins + 25D>20	143	0.937 (0.914-0.960)	0.750 (0.732-0.768)	0.869 (0.851-0.887)	0.367 (0.333-0.401)	46.47 (42.85-50.07)
Statins + 25D<20	117	0.930 (0.904-0.956)	0.730 (0.710-0.750)	0.849 (0.828-0.869)	0.418 (0.379-0.457)	50.80 (46.76-55.06)
Statins - 25D>20	675	0.919 (0.908-0.930)	0.722 (0.713-0.730)	0.852 (0.844-0.861)	0.405 (0.389-0.421)	50.29 (48.55-52.01)

Table 1

***Disclosures: Jesus Gonzalez-Macias**, None.*

SU0362

Oxytocin, A New Determinant of Bone Mineral Density and Bone Turnover in Post-menopausal Women: Analysis of the OPUS Cohort. Veronique Breuil*[1], Patricia Panaia-ferrari[2], Eric Fontas[3], Christian Roux[4], Sami Kolta[5], Richard Eastell[6], Hedi Ben Yahia[7], Claude Laurent Benhamou[8], Liana Euller-Ziegler[9], Ez Zoubir Amri[10]. [1]Chu De Nice, France, [2]laboratoire d'hormonologie - CHU de Nice, France, [3]statistical department - CHU de Nice, France, [4]Hospital Cochin, France, [5]Centre D'Evaluation, Des Maladies Osseuses, France, [6]University of Sheffield, United Kingdom, [7]Laboratoire d'Hormonologie CHU de Nice, France, [8]CHR ORLEANS, France, [9]Rheumatology Department CHU de Nice, France, [10]CNRS UMR7277, F-06108, University of Nice Sophia Antipolis, France

Introduction: Oxytocin (OT), a neurohypophysial hormone regulated by estrogen, leptin and alcohol, may play a role in bone metabolism in humans as suggested by animal studies. The aim of our study was to assess the relationship between OT and bone status in a large population of post menopausal women.

Subjects and Methods: Subjects were included in the Osteoporosis and Ultrasound study (OPUS), a 6-yr prospective study of osteoporosis related factors, conducted in a population-based cohort from five European cities. Final visit data were used for the present cross-sectional study. OT, leptin and estradiol serum levels were measured in 1097 post-menopausal women and compared with BMD (lumbar, femoral neck and hip), fractures and bone remodeling (PINP, bone ALP and CTX).

Results: The median age of this population was 70.8 years (66 – 76.9), 16% were osteoporotic (OP), 48% osteopenic, 36% had normal BMD and 29% had at least 1 fragility fracture. Univariate analysis showed a positive association between OT serum level and BMD at all sites: femoral neck ($p < 0.0001$), hip ($p < 0.0001$) and spine ($p < 0.0002$). After adjustment for age, estradiol, leptin, BMI, alcohol, tobacco use, parental history of hip fracture and steroid use, the association was no longer significant. However, in women with low estradiol serum levels (≤ 11.79 pg/ml, 89% of the population), after adjustment on all others parameters, OT was positively associated with hip BMD (g/cm^2, p=0.05), and this relation was stronger in women with higher leptin (>19.1 ng/ml) (p=0.001) or higher BMI (> 22 kg/m^2 known to be associated with lower risk of OP)(p=0.01). Univariate analysis showed a negative association between OT serum levels and bone markers: PINP (p<0,0001), bone ALP (p=0.01) and CTX ($p < 0,0001$), and this relation remained significant in women with undetectable estradiol. There was no significant relationship between OT and prior fractures.

Conclusion: High OT levels are associated with high BMD at the spine and hip. The mechanism may be explained by the effect of OT on bone turnover; high OT levels are associated with low bone turnover markers.

***Disclosures: Veronique Breuil**, amgen, 6; Roche, 6*
This study received funding from: amgen - roche

SU0363

Role of Wnt antagonists (sclerostin and Dkk-1) on bone turnover markers and bone mass in patients with complete spinal cord injury. Preliminary results. Laia Gifre*[1], Joan Vidal[2], Sílvia Ruiz-Gaspà[3], Enric Portell[2], Ana Monegal[4], África Muxí[5], Núria Guañabens[4], Pilar Peris[6]. [1]Hospital Clinic Barcelona, Spain, [2]Spinal Cord Unit. Neurorehabilitation Institute Guttmann, Badalona, Spain, [3]CIBERehd. Hospital Clínic of Barcelona, Spain, [4]Rheumatology Department. Metabolic Bone Diseases Unit. Hospital Clinic of Barcelona., Spain, [5]Nuclear Medicine Department. Hospital Clínic of Barcelona, Spain, [6]Hospital Clínic of Barcelona, Spain

Background: Spinal cord injury (SCI) has been associated with a marked increase in bone loss and bone remodelling. The absence of mechanical load seems to be one of the most important factors related to bone loss. However, the pathogenesis and clinical management of this condition remains unclear.

Objectives: To analyze the effect of Wnt signalling antagonists (sclerostin and DKK-1) and their relationship with bone turnover markers and bone mineral density (BMD) evolution in patients with a recent SCI.

Methods: Patients with a recent complete motor SCI (AIS A)(<6 months) were prospectively included.Bone turnover markers (Bone formation: P1NP, bone AP; Bone resorption: sCTx), Wnt antagonists (serum sclerostin and Dkk-1, determined by ELISA, Biomedica Gruppe, Austria) and BMD were assessed in all patients at baseline and at 6 months. The results were compared with 15 healthy individuals of similar age and sex.

Results: 23 men with a mean age of 38±15 years (range18-64) were included at 105±32 days of SCI onset (AIS 23A). 52% had paraplegia. 11 patients were assessed at 6 months of follow-up. Patients with SCI showed a significant increase in bone turnover markers compared to controls (P1NP 191±90 ng/ml vs. 50±9, $p<0.001$; sCTx 1.39±0.49 ng/ml vs. 0.52±0.19, $p<0.001$) and increased levels of sclerostin and Dkk-1 (40.7±15.3 vs. 31.2±17.9 pmol/L, p=0.038; 64.7±32.5 vs. 42.4±16.7 pmol/L, p=0.036). At 6 months, bone turnover markers decreased (P1NP -33%, p=0.008 and sCTx -24%, p=0.021) and BMD decreased about 12% at total femur (p=0.003) compared to baseline. Sclerostin levels increased significantly (40%, p=0.013), whereas Dkk-1 levels significantly decreased (-35%, p=0.041). Changes in Dkk-1 levels were positively correlated with changes in total femur BMD (r=0.6, p=0.05), while changes in sclerostin were negatively correlated with bone AP change (r=-0.668, p=0.025).

Conclusions: Patients with complete SCI have a marked increase in bone turnover markers and early bone loss over 10% at femur. Wnt signalling antagonists seem to be related to bone loss in acute SCI.

***Disclosures: Laia Gifre**, None.*

SU0364

The Association between Bone Turnover Markers and Kyphotic Status in Community-dwelling Older Adults. Corinne McDaniels-Davidson*[1], Donna Kritz-Silverstein[2], Mei-Hua Huang[3], Gail Laughlin[2], Elizabeth Barrett-Connor[2], Deborah Kado[2]. [1]SDSU/UCSD Joint Doctoral Program in Public Health (Epidemiology), USA, [2]University of California, San Diego, USA, [3]UCLA School of Medicine, USA

Bone turnover markers reflect the dynamic process of bone formation and resorption, and have been shown to be associated with several bone disorders. Hyperkyphosis, an accentuated curvature of the thoracic spine, is estimated to affect up to 40% of older adults and is associated with negative health outcomes and mortality in the elderly. This study examined the association between serum levels of bone turnover markers and kyphotic status in a large sample of community-dwelling older men and women.

Between 2003 and 2006, 760 participants in the Rancho Bernardo Study age 60 and older (308 men and 452 women) had blood drawn and were assessed for kyphotic status at a research clinic. Serum was assayed for collagen type 1 cross-linked N-telopeptide (NTX), a marker of bone resorption, and procollagen type 1 n-terminal propeptide (PINP), a marker of bone formation. Kyphotic status was assessed as the number of 1.7cm blocks, placed under each participant's head, required to achieve a neutral supine position. Analyses were stratified by sex and estrogen therapy (ET) use. Multivariate logistic regression modeled odds of normal (0-1 block) kyphotic status for each one-SD change in log markers adjusting for age, obesity, and smoking history.

Mean age was 75 years (range=60-100); 49% of non-ET using women, 59% of ET-using women, and 25% of men had normal kyphotic status. Among non-ET using women, higher log PINP and serum NTX were associated with increased odds of normal kyphotic status in fully-adjusted models (PINP OR=1.4, 95% CI=1.1-1.7, p=.007; NTX OR=1.5, 95% CI=1.2-1.8, p=.001). Among ET-using women and men, no significant associations were found between bone turnover markers and kyphotic status ($p>.05$).

Higher bone turnover was associated with normal kyphotic status in non-ET using women, suggesting that increased osteoclast and osteoblast activity may be a compensatory mechanism against developing hyperkyphosis.

***Disclosures: Corinne McDaniels-Davidson**, None.*

SU0365

Skin Wound Trauma after Low-dose Gamma-ray Exposure Exacerbates Cancellous Bone Loss in Mice. Joshua Swift*[1], Matthew Allen[2], Joan Smith[1], Juliann Kiang[3]. [1]Armed Forces Radiobiology Research Institute, USA, [2]Indiana University School of Medicine, USA, [3]Armed Forces Radiobiology Research Institute, Uniformed Services University of the Health Sciences, USA

Low doses of ionizing radiation result in significant and deleterious effects on numerous physiological systems, including skeletal tissue. However, the effects of a low dose of ionizing radiation combined with another trauma (i.e. non-lethal skin wounding) on bone quantity/quality and biomarkers of bone metabolism have not been elucidated. To determine the timing and extent of damage to skeletal tissue after radiation injury (RI), skin wounding (W), and combined injury (CI; RI +W), 16-week-old B6D2F1/J female mice were exposed to a single dose of 1 Gy gamma rays (Co^{60}, 0.4 Gy/min) immediately followed by skin wound trauma (W and CI groups only; 15-20% total body skin surface area). Distal femur bone properties and serum biomarkers were assessed 3, 7, 30, and 120 days post-irradiation and compared to sham controls. RI significantly lowered cancellous bone volume (BV/TV) and trabecular number (Tb.N), -11% and -12% (vs. SHAM), respectively, by day 7 and recovered to SHAM levels 120 days post-irradiation. Skin wounding (W) resulted in significantly lower BV/TV (-17%) and Tb.N (-14%) compared to SHAM mice. CI demonstrated greater negative effects on BV/TV (-18%), trabecular thickness (Tb.Th; -13%), and Tb.N (-20%) by day 7 (vs. RI), which continued to decline through day 30 and recovered to SHAM levels 120 days post-CI. Femur cortical bone geometry was not affected by RI, W, or CI at any time point. RI increased circulating serum TRAP 5b on day 7 (+34%) and reduced osteocalcin by day 3 (-59%) vs. SHAM. TRAP 5b stabilized by day 30, but osteocalcin remained suppressed through day 30. Wounding increased TRAP 5b on day 3 (+34%) and day 7 (+57%), and reduced osteocalcin by day 3 (-73%) vs. SHAM. CI further increased TRAP 5b (+25 to +39%) from days 3 to 7 as compared to RI. In addition, osteocalcin was reduced on days 3 (-27%), 7 (-53%), and 30 (-49%) vs. RI mice. Altogether, these data indicate that skin wound trauma exacerbates bone loss after radiation exposure as low as 1 Gy and as early as 7 days post-injury. Although the exact mechanisms have not been elucidated, it appears that skeletal tissue damage after radiation and skin wounding may arise from early increases in bone resorption and reductions in formation activity, which persist for at least 30 days post-injury.

***Disclosures: Joshua Swift**, None.*

SU0366

Vitamin D supplementation on calcium absorption in young women. Prachi Jindal*[1], J. Christopher Gallagher[1], Lynette Smith[2]. [1]Creighton university medical center, USA, [2]university of nebraska medical center, USA

Background: 1,25 dihydroxyvitamin D ($1,25(OH)_2D$) is the major hormone that controls intestinal calcium absorption. Serum $1,25(OH)_2D$ decreases when serum 25 hydroxyvitamin D (25OHD) falls below <10ng/ml but it is not known at what serum 25OHD level malabsorption of calcium can occur. Based on cross sectional data, one study suggested that a threshold for normal calcium absorption occurred at a serum 25OHD level of 30 ng/ml but in another study it was 5-10ng/ml. We performed a longitudinal study of different doses of vitamin D on absorption to measure the effect on calcium absorption and look for a threshold effect.

Methods: 198 Caucasian and African American women, ages 25-45 years, were randomized to a 12 month double blind study of vitamin D3 - 400, 800, 1600, 2400 IU, or placebo. Calcium intake was increased to 1200-1400mg/day from an average of 655 mg/day. Main inclusion criteria was - serum 25OHD level < 20ng/ml. Exclusion criteria were – medical illness or medications known to affect calcium absorption. Calcium absorption was measured at baseline and after 12 months using a single isotope method with 100 mg calcium and 5 microcuries Ca^{45}, serum Ca^{45} was corrected for weight or BMI. Serum 25OHD and $1,25(OH)_2D$ were measured by immunoassay (Diasorin). Multivariate regression was conducted to predict final calcium absorption with race, age, dietary calcium intake, weight, baseline calcium absorption, serum 1,25OH2D3 and baseline and final serum 25OHD.

Results:128 women completed the study.Mean baseline serum 25OHD was 14.6 ng/ml (39nmol/L) in Caucasians and 11.6 ng/ml in African Americans. In the longitudinal study mean serum 25OHD increased to 40 ng/ml, and there was no difference in final serum 25OHD between groups. There was no increase in 12-month calcium absorption compared to baseline on any dose of vitamin D in either Caucasians or African Americans. In the baseline analysis, serum 25OHD < 20ng/ml was divided into 4 groups of 5ng/ml increments. There was no difference in absorption nor in serum $1,25(OH)_2D$ amongst serum 25OHD groups (ANOVA p 0.86,0.12)

Conclusions:Vitamin D did not increase calcium absorption up to a dose of 2400IU daily or mean serum 25OHD of 41ng/ml. No threshold level of serum 25OHD for calcium absorption was found at baseline or in the longitudinal study suggesting that the threshold for decreased calcium absorption occurs at a very low serum 25OHD level < 5ng/ml.

Key words: Calcium absorption, 25 hydroxy vitamin D

***Disclosures: Prachi Jindal**, None.*
This study received funding from: Department of defence

SU0367

Relationship between Dexamethasone Suppressed Cortisol levels, Bone Mineral Density and Vertebral Fractures in Postmenopausal Women. Miguel Debono*, Selina Simpson, Margaret Paggiosi, Fatima Gossiel, John Newell-Price, Richard Ross, Richard Eastell. University of Sheffield, United Kingdom

Background: Patients with adrenal incidentalomas and cortisol excess are at an increased risk of vertebral fractures. As adrenal incidentalomas are commonly found in the elderly population and up to 50% have dexamethasone cortisol >50nmol/l, we designed a study to assess whether we could commonly find cortisol excess secondary to adrenal incidentalomas in patients with vertebral fractures.

Methods: In a cross-sectional, observational study we recruited 30 postmenopausal women with vertebral fractures and a hip or spine T-score <-1.0 (Group1). In addition two sex-, BMI- and age-matched control groups each consisting of 30 women were studied; one group was BMD matched (Group2) whilst the other had normal BMD (Group3). A 1mg overnight dexamethasone suppression test (ONDST) to assess for excess cortisol, a BMD by DXA scan of the spine and hip with VFA, and high resolution peripheral quantitative computed tomography (HR-pQCT) scans of the tibia and radius were performed. Fractures were confirmed by spinal x-rays using the algorithm-based qualitative method.

Results: By ANOVA there was a significant difference in hip ($p<0.001$) and spine ($p<0.001$) T-scores between the groups. Post-hoc Scheffe tests revealed that Group1 and 2 had similar hip T-scores (mean(SD) Group1: -1.6 (0.9), Group2: -1.1(0.8)) and spine T-scores (Group 1: -2.4(0.8), Group 2: -2.2(0.7)) whilst Group3 T-scores (hip: 0.3(0.8), spine: 0.3(0.9)) differed significantly from both Group 1 and 2 ($p<0.001$). Similarly, measures of bone architecture, as assessed using HR-pQCT, for Group3 were significantly different to those for the other two groups. In Group 1, 2/30 patients (7%) failed the ONDST. Dexamethasone cortisol levels in the rest of the women were similar (Group1: 27 (6) nmol/l, Group2: 28 (7) nmol/l, Group3: 26 (10) nmol/l).

Conclusion: In this analysis we have identified two patients with an ONDST cortisol >50nmol/l and both had a vertebral fracture. This study suggests that hypercortisolism might be identified occasionally in postmenopausal women with vertebral fractures and treatable causes should be investigated and treated; mild elevations in cortisol when screened using a 1mg ONDST are not consistently found among patients with vertebral fracture.

***Disclosures: Miguel Debono**, None.*

SU0368

Increased Cortical Porosity in Older Men with Low 25-OH-Vitamin D. Dan Mellstrom[1], Daniel Sundh[2], Magnus Karlsson[3], Anna Nilsson[4], Claes Ohlsson[5], Mattias Lorentzon*[6]. [1]Sahlgrenska University Hospital, Sweden, [2]Geriatric Medicine, Dept. of Internal Medicine & Clinical Nutrition, Sahlgrenska Academy, University of Gothenburg, Gothenburg, Sweden., Sweden, [3]Skåne University Hospital Malmö, Lund University, Sweden, [4]Sahlgrenska University Hospital, Sweden, [5]Center for Bone & Arthritis Research at the Sahlgrenska Academy, Sweden, [6]Geriatric Medicine, Center for Bone Research at the Sahlgrenska Academy, Sweden

The relationship between low serum levels of 25-OH-vitamin D and areal bone mineral density (aBMD) has been established, but whether this relationship is due to affected bone geometry or microstructure of the cortical or trabecular bone has been less studied. Bone loss at peripheral sites after age 65 is mainly cortical and involves an increase in cortical porosity, but the relationship between this bone trait and 25-OH vitamin D has not been previously reported. The aim of the present study was to investigate the association between serum levels of 25-OH-vitamin D and cortical and trabecular microstructure in 445 80-year-old men.

High Resolution Peripheral Computed Tomography (HRpQCT, Scanco) was used to scan the distal tibia and DXA (Hologic) was used to measure aBMD of the spine and hip, while 25-OH-vitamin D was measured with a competitive RIA (Diasorin). Men were divided into quartiles (Q1-Q4) according to 25-OH vitamin D (Q1 41.0 ± 8.2, Q2 55.8 ± 3.3, Q3 67.6 ± 3.7, Q4 85.3 ± 10.5 nmol/l). Men in the lowest vs. the highest quartile of 25-OH-vitamin D were slightly older (80.9 ± 3.2 vs. 79.5 ± 3.5 years) while no differences in height, weight, calcium intake, physical activity, or smoking were found. Cortical porosity at the distal tibia was 13% higher (12.5 ± 4.3 vs. $10.9\pm4.1\%$) while cortical volumetric BMD (4.6%; 757 ± 75 mg/cm^3 vs. 792 ± 74, $p<0.01$), thickness (11.2%; 0.91 ± 0.3 mm vs. 1.02 ± 0.3; $p<0.05$) and femoral neck aBMD (5.2%; 0.74 ± 0.11 mg/cm^2 vs. 0.78 ± 0.13, $p=0.01$) were lower in men in Q1 than in men in Q4. There were no differences between quartiles in spine aBMD or trabecular bone volume fraction. A linear regression model with age, weight, height, daily calcium intake, physical activity (walking distance per day), smoking (yes/no), 25-OH-vitamin D adjusted for season was used to determine the independent predictive role of serum vitamin D on bone variables. In this model, 25-OH-vitamin D independently predicted cortical porosity (standardized β= -0.11, $p=0.02$), thickness (β= 0.15, $p<0.01$), and cortical vBMD (β= 0.16, $p<0.01$) of the tibia as well as aBMD of the femoral neck (β= 0.17, $p<0.01$).

In conclusion, serum 25-OH-vitamin D levels independently predicted cortical porosity, thickness and density as well as aBMD of the femoral neck, a mainly cortical bone site, in older men. Our results suggest that bone fragility due to low vitamin D levels could mainly be due to affected cortical bone, at least partly mediated by increased porosity.

***Disclosures: Mattias Lorentzon**, None.*

SU0369

Impact of Traumatic Brain Injury on Bone in a Mouse Model. Hongrun Yu*, Heather Watt, Subburaman Mohan. Jerry L. Pettis Memorial VA Medical Center, USA

The impact of traumatic brain injury (TBI) especially mild TBI on public health is significant. There are 1.7 million cases of TBI reported annually in the United States, and approximately 85% are mild cases. While it is well established that the brain produces hypothalamic hormones and neuropeptides that influence skeletal metabolism, the impact of TBI on bone is not known. Based on the recognition from clinical studies that there is an association between TBI and long-term hypothalamic pituitary dysfunction, we have proposed the hypothesis that TBI including mild TBI exerts a negative impact on skeletal growth and maintenance. To evaluate this hypothesis, we used a recently established mouse model of human repetitive TBI (Kane et al., 2012) which utilized the weight drop method to create a closed head injury. A 72 g weight was dropped at a 1.5 m height onto anesthetized five week old female C57BL/6J mice, once per day for four consecutive days. Control mice underwent anesthesia only. All mice were euthanized two weeks after the first impact. Bone densitometry (DEXA) measurements revealed that total body bone mineral content (BMC), bone area (B area) and bone mineral density (BMD) were reduced 15% ($P < 0.01$), 10% ($P < 0.01$) and 5% ($P < 0.05$), respectively in the impacted mice compared to the controls. Similar reductions were also observed in individual skeletal sites at the femur, tibia and vertebra. Micro-CT analysis of cortical bone at the tibial mid-diaphyseal region indicated 16% and 4% reductions ($P < 0.01$) in total and cortical volumetric BMD (vBMD) of the impacted mice. Accordingly, there was a 33% reduction ($P<0.01$) in breaking strength of the cortical bone as measured by 3-point bending. Micro-CT analysis of trabecular (Tb) bone at the tibial metaphysis revealed a 42% reduction ($P<0.01$) in BV/TV, which was caused by a significant reduction in Tb number (20%, $P < 0.01$) and thickness (8%, $P < 0.01$), and increased Tb separation (26%, $P < 0.01$). Real time RT-PCR analysis showed that mRNA levels of osteocalcin in the femur of the impacted mice was reduced by 37% ($P < 0.05$) while that of osteoclast derived TRAP was unchanged, suggesting that reduced bone formation is the cause for reduced bone mass. In conclusion, repetitive TBI produced a negative impact on both cortical and trabecular bone mass accrual by inhibiting bone formation.

***Disclosures: Hongrun Yu**, None.*

SU0370

Skin color measurement and serum 25OH Vitamin D level: A comparison in young Caucasian and African American women. SRI HARSHA TELLA*[1], Prachi Jindal[2], J. Christopher Gallagher[2]. [1]Creighton University School of Medicine, USA, [2]Creighton university medical center, USA

Background: Vitamin D is essential for bone health and its level depends on dietary intake and on sunlight which generates vitamin D from 7-dehydrocholeterol in the skin through the effect of ultraviolet-B light (290-315 nm). Dietary intake is usually low, less than 150-200 IU daily, thus, sunlight exposure becomes a major source of vitamin D in most people. Certain groups may be at higher risk for a lower UV-B effect on skin synthesis of vitamin D, such as veiled women or women with darker skin color. The main objective of this analysis is to make quantitative assessments of skin color and its relation to serum 25 OHD.

Design: We recruited 198 young women for a 1-year trial of the effect of vitamin D on serum 25OHD. There were 119 Caucasian and 79 African American women, ages 25-45 years. The main inclusion criterion was vitamin D insufficiency, defined as a serum 25OHD level < 20ng/ml (50nmol/l). Exclusion criteria were sun screen use, medical illness or medications known to affect calcium and vitamin D metabolism. In this study we analyzed the baseline results of skin color measurement with reflectance spectrometry, the dietary intake of vitamin D from 7-day food diaries and the screening serum 25OHD levels. Skin color was measured 3 times on an exposed site – lower forearm and on a clothed area- inside of upper arm.

Results: The mean age for Caucasian women was 37.7 years ($\pm$ 5.58) and for African Americans was 35.1 ($\pm$ 5.94) years. The mean baseline serum 25OHD in African American was 11.6 ng/ml ($\pm$4.19)and 14.4 ng / ml($\pm$4.30) in Caucasians ($p=0.79$). Mean 7 day dietary vitamin D intake was 103 IU/d in Caucasians and 96 IU/d in African Americans ($p=0.53$). The mean forearm skin color in the Caucasian women was 68.28($\pm$ 2.16) and in African American women was 48.09($\pm$6.68) ($p<0.005$). Linear regression analysis showed a significant correlation between serum 25OHD and lower forearm skin color ($r= 0.37$, $p<0.01$) but no correlation with upper arm skin color ($r=0.04$, $p=0.567$). After Vitamin D supplementation for 12 months, there was no correlation between forearm skin color and Vitamin D levels($r=0.05$, $p=0.676$).

Conclusion: The results show that serum 25OHD levels are correlated with skin color only in the exposed skin area. Vitamin D intake was very low in both groups. The results suggest that in women with vitamin D insufficiency serum 25OHD is dependent on exposed skin and is lower in African American women because of darker skin.

Keywords: Skin Color, reflectance spectrometry, 25OHD, African American, Caucasian

***Disclosures: SRI HARSHA TELLA**, None.*
This study received funding from: Department of Defence

SU0371

Changes in Serum Undercarboxylated/Carboxylated Osteocalcin Ratio in Daily vs. Weekly Teriparatide Therapy for Vertebral Compression Fracture.
Yoichi Kishikawa*. Kishikawa Orthopedics, Japan

Background: At ASBMR 2012, we reported facilitated fracture union and increases in serum bone metabolism markers after 4 months of daily teriparatide (Forteo) injections in 26 vertebral compression fracture patients who were kept at a defined level of rest during early post-fracture stages. Percent changes in tartrate-resistant acid phosphatase (TRACP) 5b, undercarboxylated osteocalcin (ucOC) and carboxylated osteocalcin (OC) levels were 205%, 858% and 313%, respectively, resulting in a significant increase in ucOC/OC ratio by 240%. Meanwhile, a weekly teriparatide product (Teribone) has become available and clinically used in Japan since the end of 2011. Unlike the daily product, it is a chemically synthesized form of parathyroid hormone (PTH) and requires weekly subcutaneous injections of 56.5 μg, approximately 2.8 times the recommended dose of the daily product (20 μg).

Methods: Twenty-two patients with vertebral compression fracture were kept at a defined level of rest during early post-fracture stages and received weekly teriparatide. Changes in serum TRACP 5b, ucOC, OC and ucOC/OC at 4 months were compared to those in patients on daily teriparatide. Alfacalcidol (0.25 μg) was also used in both groups of patients.

Results: After 4 months of weekly doses of teriparatide, TRACP 5b, ucOC, OC and ucOC/OC changed by 96%, 237%, 129% and 145%, respectively.

Discussion: Although the two products are essentially identical in the PTH structures, their differences in dosage and dosing interval resulted in considerably different % changes in bone metabolism markers after only 4 months of treatment. In contrast to the dramatic increases in TRACP 5b, ucOC and OC by daily teriparatide, no change in TRACP 5b and mild increases in OC and ucOC were observed with weekly teriparatide. It is of future interest to examine whether the observed % changes in ucOC/OC would be affected by concurrent administration of vitamin K. An Animal study have shown that daily teriparatide leads to increased cortical porosity; the result of this studies suggest a possible association between ucOC/OC and the effects of the two products on bone quality.

***Disclosures: Yoichi Kishikawa**, None.*

SU0372

Forteo Voluntary Patient Registry: 3-Year Progress on a Prospective Osteosarcoma Surveillance Study.
Nicole Kellier*[1], Kelly Krohn[2], Alicia Gilsenan[3], David Harris[3], Elizabeth Andrews[3], Daniel Masica[1]. [1]Eli Lilly & Company, USA, [2]Lilly USA, LLC, USA, [3]RTI Health Solutions, USA

Background: In rat toxicology studies, teriparatide, the active ingredient in Forteo, when given for the entire rodent lifespan caused increases in bone mass and a dose-dependent increase in the incidence of osteosarcoma, a rare primary bone cancer. Among adults aged ⩾18 years, the human incidence of osteosarcoma is 2.7 cases per million persons per year. As part of a long-term 12-year surveillance program for a possible signal of osteosarcoma in treated patients, the voluntary Forteo Patient Registry was launched in July 2009 to complement an ongoing retrospective case finding study.

Objective: To describe study progress of the Forteo Patient Registry, designed to estimate the incidence of osteosarcoma in patients treated with Forteo, and to enhance healthcare provider awareness of the progress of the Registry after 3 years.

Methods: Patients who complete a brief pre-enrollment form are sent a registration packet. After completing a one-time registration and consent, patients are considered enrolled. An annual linkage is performed by participating state cancer registries using a standardized linkage algorithm with the Forteo Patient Registry database to identify cases of osteosarcoma potentially associated with Forteo treatment. Linkage variables include name, birth date, sex, address, telephone number, race, ethnicity, and last 4 digits of social security number.

Results: The third annual linkage, performed in September 2012, including a total of 38 state cancer registries covering 86% of the US population linked 26,810 patients from the Forteo Patient Registry with 1,641 adult osteosarcoma cases diagnosed since January 1, 2009. No matches were identified. As of December 2012, of the 30,758 registrants, the distribution by pathway of recruitment was medication packaging (61%), starter kit (26%), study toll-free number (6%), patient brochure (3%), physician tear pad (2%), direct pharmacy mail (2%), and study website (1%).

Conclusion: Evaluation of the first 3 years of data, detected no signals of a possible association between Forteo treatment and osteosarcoma. The most frequent pathway for patient recruitment to date is information about the voluntary patient registry in product packaging. Patient respondent burden is kept to a minimum. Healthcare provider encouragement of Forteo treated patients to consider enrolling in the Registry can contribute to the scientific advancement of this surveillance study.

***Disclosures: Nicole Kellier**, Eli Lilly & Company, 3*

SU0373

Monthly Cycles of Teriparatide and Raloxifene Increase BMD Comparable to Continuous Teriparatide: Is it Possible to "Open the Anabolic Window?".
Neil Binkley*, Jessie Libber, Gretta Borchardt, Diane Krueger, Bjoern Buehring. University of Wisconsin, Madison, USA

Osteoporosis therapies reduce fractures by only ~50%; better medications or alternatively, different approaches with current agents are needed. The anabolic window paradigm has been advanced to indicate a period of time during which teriparatide (TPD) produces bone anabolism prior to a coupled increase in resorption. We hypothesized that initial formation stimulation by TPD promptly followed by modest resorption suppression with raloxifene (RLX) then repeated in a cyclic manner may allow ongoing formation without concomitant increased resorption. This 6-month pilot study evaluated the effect of cyclic TPD/RLX compared to continuous TPD on BMD and bone turnover in postmenopausal osteoporotic women.

Community-dwelling postmenopausal women (n = 26) with osteoporosis (T-score ≤ -2.5 and/or prior fragility fracture) were randomly assigned to receive open-label TPD 20 mcg by daily sc injection or to alternating cycles of TPD for 1 mo followed by 1 mo of daily RLX 60 mg/day for 6 mo. All participants received ~1000 mg of calcium from diet and supplements if needed and 1000 IU of vitamin D_3 daily. Fasting serum was obtained at baseline and mo 1, 1.5, 2, 2.5, 3, 4, 5 and 6 to evaluate CTX and P1NP. BMD was measured at the L-spine by QCT (baseline and 6 mo) and at the L-spine, proximal femur and .3 radius by DXA at baseline and after 3 and 6 mo. L-spine trabecular bone score (TBS) was determined from the DXA images. Baseline group comparisons were performed by unpaired T-test with change over time evaluated by repeated measures ANOVA.

Participant mean age, BMI and lowest T-score was 67.0 years, 26.0 kg/m^2 and -2.7; no between group differences in demographics, serum chemistries, 25(OH)D or BMD were observed. No between group differences in BMD change (all $p > 0.10$) were observed (Table).

TBS values were unchanged at 6 months in both groups with no between-group difference. Serum CTX and P1NP increased progressively with TPD; mean increase was 188% and 298% respectively at 6 months. In the TPD/RLX group an undulating pattern in CTX and P1NP was observed with a decrease seen during the RLX treatment months; at 6 months mean CTX was numerically 4% lower and P1NP 21% higher than baseline.

In conclusion, 6 months of cyclic TPD/RLX increases L-spine BMD comparable to daily TPD. Temporal effects on bone turnover markers consistent with an antiresorptive effect of RLX were observed. This pilot work supports feasibility of opening the anabolic window.

BMD mean (SD) % change at 6 months

Group	L-spine (DXA)	L-spine (QCT)	Total proximal femur	.3 radius
TPD	+5.0 (2.8)	13.0 (7.1)	-0.3 (2.5)	-2.5 (3.5)
TPD/RLX	+4.9 (2.3)	9.4 (4.9)	+1.0 (1.3)	-1.4 (2.8)

Anabolic window table

***Disclosures: Neil Binkley**, Merck, 2; Lilly, 2; Lilly, 6; Amgen, 6; Merck, 6*

SU0374

Safety of Concomitant Use of 20 μg Teriparatide Once-Daily Subcutaneous Injection with Active Vitamin D Focusing on Calcium Levels.
Masako Nakano*[1], Mika Tsujimoto[2], Hideaki Sowa[3]. [1]Eli Lilly Japan K.K., Japan, [2]Asia Pacific Statistical Science, LRL DCOE Asia Pacific Eli Lilly Japan K.K, Japan, [3]Lilly Research Laboratories Japan, Eli Lilly Japan K.K., Japan

Objective: Teriparatide once-a-day subcutaneous injection, which stimulates bone formation, is globally approved for treatment of osteoporosis with high risk of fracture. Although it is recommended in Japan package insert of teriparatide to avoid a concomitant use with active vitamin D due to a theoretical risk that serum calcium level may increase, no reports that evaluated the risk in Japanese have been published. Meanwhile, active vitamin D is a common treatment for osteoporosis in Japan. Therefore, we evaluated the safety, including teriparatide's effects on serum and urinary calcium levels, when teriparatide and active vitamin D were coadministered to Japanese patients with osteoporosis. Methods: The trial was conducted at a clinical pharmacology institution under Good Clinical Practice. A total of 30 Japanese female patients (aged 71 years, median) with osteoporosis entered in this post-marketing clinical trial that consisted of 14-day lead-in, 28-day cotreatment, and 7-day follow-up periods (ClinicalTrials.gov identifier: NCT01430104). Patients were orally administered alfacalcidol 1 μg/day and calcium aspartate 600 mg/day during all periods. Teriparatide 20 μg/day was administered during the cotreatment period. Patients self-injected teriparatide after an introductory training. Serum calcium levels were measured at predose and 2, 4, 6, 16, and 24 hours postdose on Days 1, 7, 14, and 28 of the cotreatment period. Daily urinary calcium excretion was also measured by 24-hour urine collection. Adverse events (AEs) were evaluated throughout the trial. Results: No patients had exceeded albumin-corrected serum calcium levels or daily

urinary calcium excretion amounts beyond the predefined maximum limit of 11 mg/dL or 0.30 g/day, respectively (max: 10.3 mg/dL or 0.23 g/day, respectively). No hypercalcaemia or hypercalciuria was reported. Adverse events occurred in 5 patients (17.2%), and no serious AEs occurred during the trial. All AEs were of mild severity, except for one moderate positional vertigo that resulted in her study withdrawal. There were no reports of AEs that were not expected from the safety profile of teriparatide. Conclusion: The results suggest that teriparatide 20 µg/day can be safely coadministered with active vitamin D to the Japanese patients with osteoporosis. However, further experience of coadministration in actual clinical practice will be necessary.

***Disclosures: Masako Nakano**, Eli LIlly Japan.K.K., 3*
This study received funding from: Eli LIlly Japan K.K.

SU0375

Anti Resorptive Drugs Related Osteonecrosis of the Jaw: Epidemiology, Risk Factors and Evolution. Alice Pham Quang Hai*[1], Bernard Cortet[2], Guillaume Penel[3], Jean Michel Maes[4], Jacques Bonneterre[5], Marie Helene Vieillard[1]. [1]Rheumatology department Lille Hospital, France, [2]Service de Rhumatologie, France, [3]Surgical dental department Lille Hospital, France, [4]Stomatology department Lille Hospital, France, [5]Oncology Oscar Lambret Center Lille, France

Background: Osteonecrosis of the jaw (ONJ) is a rare but serious adverse event. In bisphosphonate (BP) treatment, the incidence is evaluated to 0.6-6.2% in breast cancer, 1.7-15% in multiple myeloma (MM), and 0,028-4,3% in osteoporosis. The aim of our study was to evaluate risk factors, clinical and radiological features and the evolution of ONJ.

Methods: Our study included 83 patients from January 2005 to November 2012. Patients were followed up in multidisciplinary consultation in Lille university hospital. Patients were evaluated regularly every 3 or 6 months according to their clinical symptoms and using our previously published classification. All ONJ completed task force definition.

Results: BP were administrated in 20 cases of osteoporosis, 17 cases of MM and 46 cases of bone metastasis (BM). The average age was 65 years [11]. The follow up median duration was 33 months [1-94]. The average duration between the beginning of BP and the first signs of ONJ was 38 months [35]; 77 months [36] in osteoporosis, 27 months [35] in malignant disease. Tooth extraction was reported in 54%.

In malignant disease, the average duration of treatment was 20 months [14] with zoledronate (ZA) and 21 [19] with pamidronate (Pam).The average cumulative dose of BP was 85mg [63] for ZA and 1600mg [1679] for Pam.

In BM, the average duration of ZA was 28 months [14] and 59 months [19] for Pam.

In MM, the average duration of ZA was 66 months [13] and 33 months [19] for Pam. 94% of patient received chemotherapy, 92% corticotherapy, 60% hormonotherapy and 19 % anti angiogenic treatment.

The time between BP and ONJ seems to be shorter when patients were treated with anti angiogenic (14.5 months [9-84] vs 24 months [1-96] without anti angiogenic treatment ns p=0.09). BP were stopped in 65% of cases.

In osteoporosis, the average duration of alendronate (Al) was 81 months [51]. The average cumulative dose of Al was 24629 mg [15462]. We noted 40% glucocorticoid induced osteoporosis.

According to our clinical classification, 36% of patients were improved (15% of patients were healed), 23% were worsened, and 23% remained in stable stage.

Conclusion: Physicians must be careful in case of association of anti-resorptive drugs, corticotherapy and anti angiogenic treatment. In osteoporosis, ONJ often appears after 6 years of BP treatment, or in case of association with corticotherapy. When ONJ occurred, symptomatic treatment and BP disruption could allow good evolution of ONJ.

***Disclosures: Alice Pham Quang Hai**, None.*

SU0376

Changes in Low Back Pain and Upper Gastrointestinal Symptoms in Japanese Osteoporotic Patients after Switching to Once-monthly Oral Minodronate from Daily or Weekly Bisphosphonates. Nobukazu Okimoto*[1], Akinori Sakai[2], SATOSHI IKEDA[3], Toru Yoshioka[4], Kitau Teshima[5], Shinobu Arita[6], Masato Nagashia[7], Hidehiro Matsumoto[8], Fumio Fukuda[9], Yuichi Okazaki[10], Hiroshi Tsurukami[11]. [1]Okimoto Clinic, Japan, [2]University of Occupational & Environmental Health, Japan, [3]Ken-Ai Memorial Hospital, Japan, [4]Saka Midorii Hospital, Japan, [5]Teshima Orthopaedic Clinic, Japan, [6]Obase Hospital, Japan, [7]Katsuki Neurosurgery & Orthopaedic Clinic, Japan, [8]Sanzai Hospital, Japan, [9]Kitakyushu General Hospital, Japan, [10]Makiyama Central Hospital, Japan, [11]Tsurukami Clinic of Orthopedics & Rheumatology, Japan

Introduction: Minodronate, a new-generation bisphosphonate (BP), is the first BP available as a once-monthly oral regimen in Japan. Aside from being a highly potent inhibitor of bone resorption, minodronate has been shown to possess antagonistic action against the P2X2/3 receptor, which has an important role in nociceptive transmission. The purpose of this study was to investigate the analgesic effects of once-monthly oral minodronate (MIN50mg) on low back pain (LBP) associated with osteoporosis. We also evaluated the changes in upper gastrointestinal (GI) symptoms (common adverse effects with the use of BPs) after switching from daily or weekly BPs to MIN50mg. Methods: We conducted a prospective multicenter study involving 11 institutions in Japan. A total of 397 patients (374 females) using BPs for the treatment of osteoporosis were enrolled. Participants completed a self-administered questionnaire to investigate patient preference for monthly dosing regimens, and were assigned to either the MIN50mg (n=264) or their current BP (n=133) according to their preference. Upper GI symptoms were self-assessed using a six-point symptom severity scale, and LBP was evaluated using a horizontal 100-mm visual analogue scale (VAS), for a period of six months. Results: LBP VAS scores were significantly reduced in the MIN50mg-switched group at one month post-treatment and after ($p<0.001$); however, no significant changes were seen in the previous BP-continued group. Upper GI symptom scores of heartburn, epigastralgia and epigastric fullness in the MIN50mg-switched group were all significantly improved early at one month after switching, and the improvement in epigastralgia was significantly superior compared with the previous BP-continued group ($p<0.05$). Conclusion: MIN50mg significantly improved LBP in patients previously treated with other BPs, and upper GI symptoms were significantly reduced after switching to MIN50mg. These QOL-related benefits of MIN50mg, together with the dosing convenience, may improve treatment adherence, thereby optimizing outcomes.

***Disclosures: Nobukazu Okimoto**, None.*

SU0377

Comparative Gastrointestinal Safety of Bisphosphonates: A Network Meta-analysis. Mina Tadrous*[1], Lindsay Wong[1], David Juurlink[2], Murray Krahn[3], Linda Lévesque[4], Muhammad Mamdani[5], Suzanne Cadarette[1]. [1]University of Toronto, Canada, [2]Sunnybrook Health Sciences Centre, Canada, [3]Toronto Health Economics & Technology Assessment Collaborative, Canada, [4]Queen's University, Canada, [5]St. Michael's Hospital, Canada

Title: Comparative Gastrointestinal Safety of Bisphosphonates: A Network Meta-analysis

Background: Bisphosphonates are first line treatment for primary osteoporosis. Gastrointestinal (GI) adverse events (AEs) are cited as a primary reason for non-adherence with therapy. Little is known about the comparative GI safety of bisphosphonates.

Objective: To use published clinical trial data to assess the comparative GI safety of bisphosphonates.

Methods: We completed a systematic review of all English language clinical trials that assessed bisphosphonate safety and/or efficacy in primary osteoporosis. Randomized, blinded, and controlled studies were eligible. Extension, open-label, and studies not reporting AEs were excluded. The primary outcome was any GI-related AE. Subanalyses were completed for upper GI, serious GI, nausea, esophageal-related events, and discontinuation due to AEs. A Bayesian based network meta-analysis was completed using WINBUGS and GeMTC to allow for indirect comparisons.

Results: We identified 51 studies eligible for analysis: 33 alendronate, 12 risedronate, 5 etidronate, 7 zoledronic acid, and 44 placebo. Zoledronic acid had the highest probability (91%) of causing the greatest number of any GI AEs and highest probability (70%) of the greatest incidence of nausea. Etidronate (70%) and zoledronic acid (28%) had the highest probability of the greatest attrition due to AEs. Etidronate also had the highest probability (56%) of having the greatest number of upper GI symptoms among oral bisphosphonates. Only risedronate and alendronate had data on both serious GI and esophageal related AEs with no significant difference between drugs or compared to placebo.

Conclusion: Zoledronic acid had the highest probability of having the greatest number of GI AEs. Discontinuation due to AEs may be a more clinically relevant outcome, with the highest probability of greatest occurrence found with etidronate and zoledronic acid. These results question the assumption that annual zoledronic acid will translate into better long-term adherence to bisphosphonate therapy . More research into real-world implications of the comparative safety of bisphosphonates is needed.

***Disclosures: Mina Tadrous**, None.*

SU0378

Comparison of bone mass in lumbar vertebral segmentation and femoral area after treatment of novel intravenous alendronate in Japanese women with osteoporosis. Keiko Kobayashi, Akio Kanezashi, Serita Ikuro, Norihiko Kato*. otomi orthopedic clinic, Japan

Oral alendronate (ALN) administrations are currently preferred therapy for the treatment of osteoporosis. On the other hand, the efficacy and safety of the new intravenous ALN was reported. However, bone volume of spinal segmentation and femoral area after intravenous ALN administration is uncertain. The aim of this study is to evaluate the changes bone volume in AP lumbar spine from 1, 2, 3, 4 vertebrae and femoral area after treatment of novel intravenous ALN on BMD measurements. In 59 Japanese women (age 52-89 years) with osteoporosis, Intravenous ALN 900

micro-g every 4 weeks for 20 weeks was infused over 30 minutes. The intravenous formulation was a soft bag of 100 ml saline/citrate buffer solution containg 900 micro-g of ALN. The efficacy endpoint was percentage BMD by DXA change from baseline in AP lumbar spine (L1, L2, L3, L4, L1-4) and Ward's triangle (Ward), trochanter (Troch), femoral neck (Neck), total hip after intravenous ALN treatment. Percentage BMD change from baseline in L1, L2, L3, L4, and L1-4 at week 20 were $3.81 \pm 0.076\%$, $3.62 \pm 0.051\%$, $2.87 \pm 0.046\%$, $4.1 \pm 0.08\%$, and $3.7 \pm 0.038\%$. Percentage change in BMD in Ward, Troch, Neck, and total hip at 20 weeks after treatment were $0.33 \pm 0.083\%$, $2.06 \pm 0.05\%$, $0.41 \pm 0.046\%$, and $1.49 \pm 0.035\%$. Thus, Treatment of intravenous ALN in short duration significantly increased bone mass in L4 of vertebrae and trochanter of femur. The present study gives BMD change at anatomical sites in Japanese patients with osteoporosis after new intravenous ALN treatment. Our observation on the treatment of intravenous ALN may provide a clue to develop novel options for the treatment of osteoporosis.

***Disclosures: Norihiko Kato**, None.*

SU0379

Early Response to Once-monthly Oral Minodronate after Switching from Daily or Weekly Bisphosphonates in Japanese Osteoporotic Patients. Akinori Sakai*[1], SATOSHI IKEDA[2], Nobukazu Okimoto[3], Kitau Teshima[4], Shinobu Arita[5], Hidehiro Matsumoto[6], Hiroshi Tsurukami[7], Yuichi Okazaki[8], Masato Nagashima[9], Fumio Fukuda[10], Toru Yoshioka[11]. [1]University of Occupational & Environmental Health, Japan, [2]Ken-Ai Memorial Hospital, Japan, [3]Okimoto Clinic, Japan, [4]Teshima Orthopaedic Clinic, Japan, [5]Obase Hospital, Japan, [6]Sanzai Hospital, Japan, [7]Tsurukami Clinic of Orthopedics & Rheumatology, Japan, [8]Makiyama Central Hospital, Japan, [9]Katsuki Neurosurgery & Orthopaedic Clinic, Japan, [10]Kitakyushu General Hospital, Japan, [11]Sakamidorii Hospital, Japan

Introduction: Minodronate, a highly potent, new-generation bisphosphonate (BP), is the first BP available as a once-monthly oral regimen in Japan. The aim of the present study was to investigate the effects of once-monthly oral minodronate on bone turnover markers (BTM) and bone mineral density (BMD) in osteoporotic patients previously using daily or weekly BPs in real clinical practice.

Methods: We conducted a prospective multicenter study involving 11 institutions in Japan. A total of 397 patients (374 females) using BPs for the treatment of osteoporosis were enrolled. Participants were divided into two groups depending on their preference for dosing regimens as follows: MIN50mg group (n=264) were switched to once-monthly minodronate (50mg), and d/wBP group (n=133) continued their current daily or weekly BP. Serum TRACP-5b, a bone resorption marker, was measured at baseline and 1, 2 and 6 months post-treatment. Serum P1NP, a bone formation marker, was measured at baseline and 2 and 6 months post-treatment. BMD of lumbar spine, total hip, and/or 1/3 distal radius were measured at baseline and 6 months post-treatment.

Results: In MIN50mg group, significant reductions were seen in TRACP-5b at 1 month post-treatment (-10.2%, $p<0.001$) and onward, and in P1NP at 2 months post-treatment (-8.4%, $p<0.001$) and onward, while remaining within the reference range for a healthy young adult throughout the study period of 6 months. BMD in the MIN50mg group was significantly increased at lumbar spine (+1.5%, $p<0.001$) and 1/3 distal radius (+1.1%, $p<0.01$) at 6 months after therapy; however no significant changes were seen in the d/wBP group.

Conclusion: Once-monthly minodronte after switched from daily or weekly BPs demonstrated prompt BTM suppression within the normal reference range and superior BMD gains compared with continuing previous BPs. Thus, once-monthly minodronate provides an effective and convenient alternative to current BP therapies.

***Disclosures: Akinori Sakai**, None.*

SU0380

Effect of One Year Alendronate Administration on the Bone Strength, Soft Tissue Mass and Biochemical Markers of Bone Metabolism. Shigeharu Uchiyama*[1], Shota Ikegami[2], Mikio Kamimura[3], Hiroyuki Kato[2]. [1]Shinshu University, School of Medicine, Japan, [2]Department of Orthopaedic Surgery, Shisnhu University School of Medicine, Japan, [3]Kamimura Clinic, Japan

[Hypothesis] It is assumed that alterlation of skeletal conditions by ALN administration can cause secondary effect on the other structures, such as skeletal muscle or adipose tissue in the muscle. We hypothesized that ALN administration would increase not only BMD, but also in the skeletal muscle mass, along with little effect on biochemical markers of bone quality.

[Methods] We enrolled 24 female patients (76 years) without a history of any osteoporotic treatment. At the time of enrollment. QCT analysis of the femoral neck was performed with Mindways QCT-PRO BIT software. Total cross sectional area(CSA), cortical CSA, average cortical thickness were measured as geometrical parameters, and CSMI, section modulus, and buckling ratio, were calculated as measurements of bending strength and risk of buckling. BMD of the proximal femur and lumbar spine derived from DXA was also taken. QCT analysis of soft tissue was also performed using Mindways Tissue Composition Module software. CSA of the skeletal muscle and intramuscular fat at the proximal thigh were calculated. As biochemical markers of bone metabolism, serum BAP, OC, ucOC, serum and urine pentosidine, plasma homocysteine, whole PTH, 1,25(OH)2D, 25(OH)D, TRACP-5b, urinary DPD, and urinary NTX were measured. Oral ALN (35mg/week) was administered and continued for 1 year. Then, the same examinations described above were repeated and each parameter was compared between before and after ALN administration, using a paired t-test.

[Results] DXA-derived BMD of the proximal femur and lumbar spine significantly increased after one year. However, BR, SM and CSMI were not significantly different. Skeletal muscle CSA and fat CSA did not differ. BAP, urine NTX, DPD, and TRACP-5b were significantly decreased. Serum and urinary levels of pentosidine and serum homocysteine did not change significantly. 1,25-(OH)2 vitamin D and 25-(OH)D levels did not significantly differ between before and after ALN administration. (Table).

[Summary points] BMD of the femoral neck increased after one year ALN administration. But this increase was not accompanied by increase in skeletal muscle mass or decrease in fat. This was because such a small increase in BMD may not be large enough to increase bone strength parameters derived from QCT so that its interaction with skeletal muscle may remain the same as before treatment.

Table. Parameters before and after ALN treatment

		Before Treatment	After a year of ALN	P value
DXA	Total Hip BMD g/cm²	0.641 (0.102)	0.655(0.095)	0.0002
	FN BMD g/cm²	0.572 (0.104)	0.587 (0.094)	0.006
	Lumbar Spine BMD g/cm²	0.843 (0.117)	0.892 (0.124)	< 0.0001
QCT Bone	FN cortical BMD mg/cm³	516(54)	517 (44)	n.s.
	FN trabecular BMD mg/cm³	114 (17)	118(19)	0.0048
	FN total CSA cm²	8.6 (1.2)	8.7(1.3)	n.s.
	FN cortical CSA cm²	1.2 (0.4)	1.2 (0.4)	n.s.
	FN cortical thickness mm	1.4 (0.6)	1.5 (0.5)	n.s.
	FN Max. CSMI cm⁴	1.03 (0.27)	1.00(0.24)	n.s.
	FN Section modulus cm³	0.79 (0.12)	0.78(0.13)	n.s.
	FN Buckling Ratio	13.7 (6.7)	13.1 (7.1)	n.s.
QCT Soft Tissue	Fat mass g	4.5 (1.7)	4.6 (1.6)	n.s.
	Fat area cm²	9.4 (3.5)	9.3 (3.2)	n.s.
	Skeletal muscle mass g	46.4 (10.1)	46.6 (6.5)	n.s.
	Skeletal muscle area cm²	82.6 (12.5)	83.7 (11.1)	n.s.
Serum	BAP μg/L	16.1 (6.5)	9.9 (3.8)	<0.0001
	TRACP-5b mU/dL	461(192)	216(106)	<0.0001
	Osteocalcin ng/mL	7.1 (2.4)	4.2 (1.6)	< 0.0001
	ucOC ng/mL	4.6 (3.0)	2.1 (1.6)	< 0.0001
	Pentosidine μg/mL	0.031(0.014)	0.030 (0.019)	n.s.
	Whole PTH pg/mL	28.1 (17.1)	24.1 (8.9)	n.s.
	1·25(OH)₂D pg/mL	58.9 (14.2)	60.3 (21.0)	n.s.
	25(OH)D ng/mL	21.3 (8.4)	22.6 (7.3)	n.s.
	Homocysteine nmol/mL	9.6 (2.8)	9.6 (3.1)	n.s.
Urine	NTx nmolBCE/nmol·CRE	41.4 (23.2)	17.0 (10.0)	<0.0001
	DPD nmol/mmol. CRE	6.7 (2.9)	4.4 (2.0)	0.0035
	Pentosidine μg/mg. CRE	0.070(0.096)	0.051(0.05)	n.s.

Table

***Disclosures: Shigeharu Uchiyama**, None.*

SU0381

MIV-711, a Highly Selective Cathepsin K Inhibitor, First in Man Study – Safety, Pharmacokinetics and Pharmacodynamics of Multiple Ascending Oral Doses in Healthy Subjects. Urszula Grabowska[1], Markus Jerling[2], Disa Böttiger[2], Torbjörn Larsson[2], Kerstin Danielson[2], Erik Lindström[2], Charlotte Edenius*[2]. [1]Medivir, United Kingdom, [2]Medivir, Sweden

Introduction: Excessive resorption associated with bone diseases such as osteoporosis and osteoarthritis, can be regulated by cathepsin K inhibition. Cathepsin K, a cysteine protease expressed in the osteoclast, is necessary for bone matrix resorption. Non-clinical studies have demonstrated that MIV-711, a highly selective cathepsin K inhibitor, successfully attenuates bone resorption. This abstract presents results for multiple dosing over seven days as part of a First in Man study with MIV-711.

Aim: To determine the safety, tolerability, pharmacokinetics and pharmacodynamics of the cathepsin K inhibitor MIV-711 during multiple oral dosing.

Methods: A double-blind, placebo-controlled, randomized study in 27 healthy subjects of both genders. Multiple ascending doses of 50, 100 or 200 mg given in fasting state, once daily for 7 days were investigated for adverse events, clinical chemistry and haematology, vital signs, ECG parameters, pharmacokinetics, and biomarkers both in serum and urine.

Results: MIV-711 was well tolerated with no apparent effect on haematology, clinical chemistry, vital signs, or ECG parameters. Adverse events included skin reactions at ECG electrode sites which appeared both after active drug and placebo, headache, gastrointestinal symptoms and muscle pain. Drug exposure increased linearly with dose. MIV-711 significantly reduced serum CTX-I levels compared to placebo-treated subjects. The reductions in CTX-I compared to baseline levels were consistent after the first dose and after multiple doses for 7 days. At 24 h after dose, 50 mg MIV-711 reduced serum CTX-I levels by 49% and 40% after the first dose and last (seventh) dose, respectively. The corresponding CTX-I reductions in response to 100 mg MIV-711 were 44% (first dose) and 54% (last dose), while for 200 mg MIV-711, CTX-I levels were reduced by 59% (first dose) and 55% (last dose). At 48 h after the seventh (last) dose, serum CTX-I levels were approaching initial baseline levels in most groups indicating reversible efficacy.

Conclusions: Multiple doses of MIV-711 up to 200 mg administered once daily to healthy subjects for 7 days were safe and well tolerated and displayed linear pharmacokinetics over the investigated dose range. Serum CTX-I levels were suppressed by up to 55% at 24 h after last dose.These data suggest that the cathepsin K inhibitor, MIV-711 may be developed as an effective therapeutic agent for diseases characterised by excessive bone resorption.

***Disclosures: Charlotte Edenius**, Medivir, 3*
This study received funding from: Medivir

SU0382

Patient Preference and Adherence to Once-monthly Oral Minodronate in Japanese Osteoporotic Patients Previously Using Daily or Weekly Bisphosphonates. SATOSHI IKEDA*[1], Akinori Sakai[2], Nobukazu Okimoto[3], Yuichi Okazaki[4], Fumio Fukuda[5], Shinobu Arita[6], Kitau Teshima[7], Masato Nagashima[8], Hidehiro Matsumoto[9], Hiroshi Tsurukami[10], Toru Yoshioka[11]. [1]Ken-Ai Memorial Hospital, Japan, [2]University of Occupational & Environmental Health, Japan, [3]Okimoto Clinic, Japan, [4]Makiyama Central Hospital, Japan, [5]Kitakyushu General Hospital, Japan, [6]Obase Hospital, Japan, [7]Teshima Orthopaedic Clinic, Japan, [8]Katsuki Neurosurgery & Orthopaedic Clinic, Japan, [9]Sanzai Hospital, Japan, [10]Tsurukami Clinic of Orthopedics & Rheumatology, Japan, [11]Saka Midorii Hospital, Japan

Introduction: Bisphosphonates (BPs) are currently the mainstay of treatment in osteoporosis; however, the complex dosing regimens might interfere with long-term adherence, which provided the rationale to develop BPs with less-frequent dosing schedules. Minodronate, a highly potent new-generation BP, is the first BP available as a once-monthly oral regimen in Japan. The aim of the present study was to investigate patient preference for, and adherence to, once-monthly oral minodronate (MIN50mg) in Japanese osteoporotic patients previously using daily or weekly BPs.

Methods: We conducted a prospective multicenter study involving 11 institutions and 397 patients (374 females) in Japan. At enrollment, participants completed a self-administered questionnaire to see whether they were willing to switch to MIN50mg or continue taking their current BP. According to their preference, subjects were assigned to either MIN50mg or their current BP. Treatment adherence was monitored for six months, and patient satisfaction levels with the therapy were assessed at six months.

Results: Of the 397 patients using daily or weekly BPs, 264 patients (66.5%) were willing to switch to MIN50mg, mainly because they expect less-frequent dosing would be more convenient. Significantly more patients, who were dissatisfied with their current BP (e.g., insufficient efficacy) or who have ever missed taking any doses of their current BP, were more willing to switch to MIN50mg than continuing their current BP ($p<0.001$). Treatment adherence at six months was significantly higher in the MIN50mg-switched group compared with the previous BP-continued group (89.8% vs. 79.0%, $p<0.01$). After six months, patients who switched and persisted with MIN50mg all preferred MIN50mg rather than their prior BP.

Conclusion: Once-monthly dosing of MIN50mg was associated with better medication adherence than daily or weekly dosing during a six-month observation period. MIN50mg may provide patients with a more convenient treatment option and enhance compliance and long-term persistence with therapy.

***Disclosures: SATOSHI IKEDA**, None.*

SU0383

Preliminary results of a randomized head to head study between Denosumab and Zoledronic Acid in severe osteoporotic women. Marco Invernizzi*[1], Stefano Carda[2], Alessio Baricich[3], Carlo Cisari[3]. [1]University of Eastern Piedmont, Novara, Italy, [2]Department of Neurorehabilitation & Neuropsychology, Centre Hospitalier Universitaire Vaudois (CHUV), Switzerland, [3]Physical & Rehabilitation Medicine, Department of Health Sciences, University of Eastern Piedmont "A. Avogadro", Italy

Introduction: Denosumab and Zoledronic Acid (ZOL) are currently used for osteoporosis treatment. The efficacy of these two powerful antiresorptive agents in increasing BMD and reducing fracture risk in osteoporotic postmenopausal women has been demonstrated in numerous clinical trials; however,at present time the effects of these drugs on Bone Turnover Markers (BTM) have not been compared yet.

AIM: to determine the effects on BTM of Denosumab 60mg vs. 5mg intravenous ZOL after multiple administration in severe osteoporotic patients.

Methods: 104 severe osteoporotic post-menopausal woman were enrolled and randomly divided in two groups: 55 were treated with Denosumab 60mg subcutaneously every 6 months and 49 with 5mg of intravenous ZOL once yearly. The inclusion criteria were: age > 70, presence of at least one vertebral or femoral osteoporotic fracture, a T-score at vertebral or hip site <-3. Previous treatment for osteoporosis were recorded. BMT (serum CTX, OC and B-ALP) were assessed at baseline, 1 month after treatment and 1 year after treatment in both groups. Moreover BMT were also assessed in DENOS group at second treatment (6 months) and 1 month after the second treatment. Tolerability was evaluated by adverse experience (AE) reporting.

Results: One month after the first Denosumab treatment were found decreases of OC (-17,1%), serum CTX (-80,3%; $p<0.01$ vs. baseline) and B-ALP (-10,2%) compared to baseline values. Similar trends occured for CTX, OC, and B-ALP after second and third Denosumab treatment. One month after ZOL infusion we observed a decrease in OC (-11%), serum CTX (-41,1%; $p<0.01$ vs. baseline; $p<0.05$ vs. Denosumab group) and B-ALP (-6,4%) compared to baseline values.The percentage of treatment naive patient was 44,1% in Denosumab group an 47,5% in ZOL group respectively. Treatment-Naive patients in both groups showed no significant differences in BTM compared to previously treated patients. 5 patients (9%) experienced moderate self-limiting AE (myalgia) after Denosumab, while 25 patients (51%) experienced a self-limiting acute phase reaction after ZOL.

Conclusions: Denosumab treatment resulted in greater suppression of BTM compared with ZOL. This result is maintained also after the second and third administration. Moreover, Denosumab reported less AE than ZOL. The greater and earlier effect of Denosumab on BTM compared to ZOL may have clinical implications for therapeutic choices in severe osteoporotic patients.

***Disclosures: Marco Invernizzi**, None.*

SU0384

Relationship between Response to Treatment with Risedronate and Baseline TRACP-5b Activity -Subanalysis of Japanese Risedronate 75mg Phase III Trial-. Taro Mawatari*[1], Ryoichi Muraoka[2], Yukihide Iwamoto[3]. [1]Hamanomachi Hospital, Japan, [2]Ajinomoto Pharmaceuticals Co, Ltd., Japan, [3]Department of Orthopaedic Surgery, Kyushu University, Japan

Risedronate increases bone mineral density (BMD) and reduces fracture risk. However, the response to treatment may depend on the baseline state of bone turnover, or more specifically, the degree of bone resorption. We analyzed the results of the Japanese Phase III clinical trial (OMP3) of risedronate 75 mg monthly to examine this question. The subanalysis was performed for 850 subjects whose baseline levels of TRACP-5b activity were measured before risedronate treatment without vitamin D supplementation for 48 weeks in the OMP3 trial. Patients were divided into three groups according to their baseline TRACP-5b level: a low-activity group with TRACP-5b $<$ 379 mU/dL (n = 282), a medium-activity group with TRACP-5b $\geqslant$ 379 mU/dL and $<$ 504 mU/dL (n = 283), and a high-activity group with TRACP-5b $\geqslant$ 504 mU/dL (n = 285). The percentage change and change from baseline in BMD due to treatment with risedronate were evaluated for each group. One-way analysis of variance showed that both the percentage change and change in BMD were greater in the group with high baseline TRACP-5b activity than in the other two groups (One-way ANOVA: $P < 0.0001$). BMD was increased by risedronate treatment in each of the three groups stratified by low, medium, and high baseline TRACP-5b activity, but the response was greater in patients with higher baseline TRACP-5b activity, demonstrating a positive correlation between the increase in BMD and baseline TRACP-5b activity. The degree of BMD increase by the treatment with risedronate may differ according to the state of bone turnover at baseline.

***Disclosures: Taro Mawatari**, None.*

SU0385

Risk factors for incident vertebral fractures treated with bisphosphonates in glucocorticoid-induced osteoporosis. Mari Ushikubo*[1], Ikuko Tanaka[2], Harumi Kuda[1], Sayaka Kubo[1], Keisuke Izumi[1], Kumiko Akiya[3], Shigenori Tamaki[2], Hisaji Oshima[1]. [1]Tokyo Medical Center, Japan, [2]NAGOYA Rheumatology Clinic, Japan, [3]National Tokyo Medical Center, Japan

Background) Although bisphosphonate (BIs) is one of the most preferred treatments in glucocorticoid-induced osteoporosis (GIO), some patients treated with Bis still have incident fractures. Porpose) To clarify risk factors for incident fracrures in patients with Bis in GIO. Patients and Methods) Patients (n = 137) with connective tissue disease other than rheumatoid arthritis were recruited and observed for 2 years. The means of age, disease duration, total predonisolone (PSL) dosage and daily PSL dosage during the study period were 61 ± 15 (SD), 12 ± 11 years, 34 ± 34g and 8 ± 6 mg/day, respectively. Prevalent vertebral fractures were seen in 44% of the patients. Agents used for prevention and treatments of GIO were Bis (54%), active vitamin D3 (7%) and vitamin K2 (6%). Bone mineral densities (BMD) were measured with DXA at the distal radius. Results) 1) Incident vertebral fractures determined with deterionating grades by the SQ method were seen in 64 patients (47%). 2) Logistic regression analysis showed the age (1.43 (OR)/5yo), total PSL dosage (1.09/5g), daily PSL dosage (2.36/5mg) and BMD (1.25/5% decrease) as independent risk factors, and

treatments with Bis (0.02) and vitamin K2 (0.06) as preventing factors ($p<0.05$). 3) Analysis of 74 patients with Bis, incident fractures, the age was higher and the BMD was lower than those without incident fractures. Multivariable analysis with logistic regression revealed the presence of prevalent fracture (3.6), ther higher daily PSL dosage during the study period (1.7/5mg) and ther lower BMD (1.6/5%) as independent risk factors. Conclusions) Patient treated with Bis in GIO, the presence of prevalent fractures, the higher daily PSL dosage, and the lower BMD were risk factors for incident vertebral fractures. An further treatment may be needed in those patients.

***Disclosures: Mari Ushikubo**, None.*

SU0386

Safety and Tolerability of Monthly i.v. Ibandronate Injections: MOVER Study 3-Year Analysis. Toshitaka Nakamura*[1], Tetsuo Nakano[2], Masako Ito[3], Hiroshi Hagino[4], Junko Hashimoto[5], Masato Tobinai[5], Hideki Mizunuma[6]. [1]National Center for Global Health & Medicine, Japan, [2]Tamana Central Hospital, Japan, [3]Nagasaki University Hospital, Japan, [4]Tottori University, Japan, [5]Chugai Pharmaceutical Corporation Limited, Japan, [6]Hirosaki University, Japan

Purpose: The randomized, double-blind MOVER (MOnthly intraVenous ibandronatE versus daily oral Risedronate) study is the first head-to-head comparison of the anti-fracture efficacy and safety of monthly i.v. ibandronate (IBN) with daily oral risedronate (RIS) in female and male Japanese patients (pts) with primary osteoporosis. We present the 3-year safety analysis.

Methods: Ambulatory pts aged ≥60 years, with fragile bone fracture, bone mineral density of the lumbar spine L2–L4 or proximal femur <80% of the young adult mean, and 1–5 vertebral fractures in the thoracic and lumbar spine were randomized to receive i.v. IBN 0.5 or 1 mg/month + oral daily placebo, or oral RIS 2.5 mg/day (licensed Japanese dose) + monthly i.v. placebo. Calcium 305 mg and vitamin D 200 IU/day were also given. Adverse events (AEs) were recorded during the study and for up to 15 days of follow-up.

Results: Of 1265 pts randomized, 37 were not treated, leaving 1228 pts in the safety population (IBN 0.5 mg n=411, IBN 1 mg, n=411, RIS n=406). The groups were balanced with respect to baseline patient characteristics. The study met its primary endpoint, showing non-inferiority for both doses of IBN to RIS with respect to the risk of vertebral fractures (non-inferiority limit 1.55): 0.5 mg, hazard ratio (HR) 1.09 (95% CI 0.77–1.54); 1 mg, HR 0.88 (95% CI 0.61–1.27). The incidence of AEs, serious AEs, and AEs leading to death/withdrawal was similar across the treatment groups. A similar proportion of pts in each group had renal disorder AEs (2.9% IBN 0.5 mg, 2.7% IBN 1 mg, 2.0% RIS) and most of these AEs were mild in all treatment groups. Change from baseline in serum creatinine was similar between the groups. More pts had acute phase reaction (APR) AEs with IBN (9.0%, 0.5 mg; 11.2%, 1 mg) than with RIS (4.9%); most occurred after the first dose of study drug, were mild, transient, and decreased with each subsequent dose. No APR-related AEs led to treatment discontinuation. Gastrointestinal (GI) AEs occurred at a similar incidence in all groups, but there were more GI-related AEs with causality linked to RIS (6.4%) than to IBN (3.4%, 0.5 mg; 1.9%, 1 mg). There were no cases of hypocalcemia, osteonecrosis of the jaw, or atypical fracture of the femur.Conclusions: Monthly i.v. ibandronate injections were well tolerated by Japanese pts with osteoporosis; the safety profile and nature/severity of AEs was similar to studies in Western pts.

***Disclosures: Toshitaka Nakamura**, Asahi Kasei Pharma Corp, Astellas Pharma Inc, Banyu Pharmaceutical Co. Ltd, Chugai Pharmaceutical Co. Ltd, Daiichi Sankyo Inc, Eisai Co. Ltd, Eli Lilly Japan K. K., Ono Pharmaceutical Co Ltd, Takeda Pharmaceutical Co Ltd, and Teijin Pharma Ltd, 2; Belongs to Japan Ministry of Health, Welfare and Labor as a councillor for hospital admissions and social medical insurance,*
This study received funding from: Chugai Pharmaceutical Co. Ltd, Japan

SU0387

Short term safety and Acute Phase Reaction assessment of Postmenopausal Osteoporosis patients within 4 weeks after Zoledronic Acid treatment in China. Fuxing Pei*[1], Xun Liu[2]. [1]Department of Orthopaedics, West China Hospital, Sichuan University, China, [2]Novartis Pharmaceuticals (China), Peoples Republic of China

Objectives: The study was aimed to observe the post-infusion safety and APR assessment in clinical practice during the first 4 weeks post Zoledronic Acid (Zol) infusion in PMO patients of mainland China.

Patients and Methods: This was a 4-week, prospective, multicenter, open-label, non-interventional study, enrolling 945 PMO patients (mean age: 67.84±9.97 years). All patients received a single 15' infusion of Zol, and were followed at the infusion day, 1-3 d, 4-7 d, 2 weeks and 4 weeks post infusion. The fever and body pain were primary outcomes. Other adverse events (AE) were secondary outcomes.

Results: Data from 917 patients with complete body temperature were analyzed, 239 (26.06%) patients had a fever (temperature increase 1℃ compared with baseline) within the 1st week (236 and 3 patients at 1-3 d and 4-7d post infusion, respectively). For the 239 patients, the median onset time to fever was one day; the median duration was one day. At the 1st fever day, 19, 113, 103 and 4 patients had temperature ≥39℃, 38.1~39℃, 37.1~38℃ and ≤ 37℃, respectively.

At baseline 513 (54%) patients had body pain. Within the 1st week, 225 (23.8%) patients pain severity aggravated, including 156 patients who had no pain at baseline, (151 and 5 patients at 1-3 d and 4-7 d post infusion respectively), 69 patients with pain at baseline (66 and 3 patients at 1-3 d and 4-7 d post infusion respectively). For the 156 patients the median onset time to pain was one day; the median duration was 3 days. However, 343 more patients felt no pain at the 14th day than at baseline (82.3% vs. 46% respectively). There were 77 patients with pain category information, which were 55 myalgias, 9 arthralgias, 6 headaches, 2 chest pains, 2 stomach aches, 2 backaches and one leg pain.

Except fever and body pain, 50 (5.29%) patients experienced 101 AEs, of which 93 were mild or moderate, 69 AEs resolved without medication. Nausea (1.59%), vomiting (0.95%), dizziness (0.85%), fatigue (0.63%), chest distress (0.53%) were AEs with frequency >0.5%. There was 1 serious AE, not considered drug-related. The patient had pneumonia 9 days post infusion and died of respiratory failure at the 18 days.

Conclusion: APR in Chinese patients was generally mild or moderate. The most frequent symptoms were fever and body pain, which happened mostly within 3 days post infusion, and relieved within the 1st week. Zol treatment is associated with a generally safety profile, with manageable APR symptom.

***Disclosures: Fuxing Pei**, None.*
This study received funding from: novartis pharmceuticals (China)

SU0388

The Instructive Effects of Minodronate on Prevention of New Vertebral Fractures at the Higher Fracture Risk of Japanese Patients with Osteoporosis. Hiroshi Hagino*[1], Masataka Shiraki[2], Masao Fukunaga[3], Tetsuo Nakano[4], Kunio Takaoka[5], Yasuo Ohashi[6], Toshitaka Nakamura[7], Toshio Matsumoto[8]. [1]Tottori University, Japan, [2]Research Institute & Practice for Involutional Diseases, Japan, [3]Kawasaki Medical School, Japan, [4]Tamana Central Hospital, Japan, [5]Hanwa Joint Reconstruction Center Hospital, Japan, [6]University of Tokyo, Japan, [7]University of Occupational & Environmental Health, Japan, [8]University of Tokushima Graduate School of Medical Sciences, Japan

Minodronate is a potent nitrogen-containing bisphosphonate that was launched in 2009 in Japan for oral daily administration of osteoporosis, and then monthly administration was launched in 2011. Previous in vitro and in vivo preclinical studies demonstrated that minodronate is about ten times as potent as alendronate in inhibiting bone resorption. In clinical study, a randomized placebo-controlled trial was conducted to examine the effect of daily oral 1 mg minodronate on vertebral fractures in 704 postmenopausal women with established osteoporosis for 24 months. Subjects were 55 to 80 years old with 1 to 5 fragility fractures between the T4 and L4 vertebrae, and BMD <80% of the young adult mean. A total of 704 subjects were randomized to take minodronate 1 mg (n = 359) or placebo (n = 345) once a day for 24 months. Daily 1 mg minodronate showed a significant reduction in the risk of new vertebral fractures by 58.9% compared with that in the placebo group. In subgroups analysis of this study, minodronate reduced the risk of new vertebral fractures by 59.1% in patients aged 75 years or older at higher fracture risk population, in the same way as in patients aged less than 75 years. Besides, the relative risk reductions of new vertebral fractures by minodronate treatment were 45.2%, 61.1%, and 64.2%, for patients with one, two, and three or more prevalent vertebral fractures, respectively, and 87.8%, 64.6%, and 50.1%, for patients with mild, moderate, and severe grades of prevalent vertebral fractures, respectively. On the other hand, the results of this study showed that the number and severity of prevalent vertebral fractures had significant relationships with the risk of subsequent vertebral fractures. The number of prevalent vertebral fractures was an independent risk factor for incidence of vertebral fractures in multivariate analysis. In conclusion, minodronate reduced the fracture risk even in Japanese patients with osteoporosis at higher risk of fracture.

***Disclosures: Hiroshi Hagino**, ONO PHARMACEUTICAL CO., LTD., 2*

SU0389

The Prevalence of Major Radiographic Features of Atypical Femoral Fractures in Thai Patients. Aasis Unnanuntana[1], Sittichai Luangkittikong*[2]. [1]Hospital for Special Surgery, Siriraj Hospital, Thailand, [2]Siriraj hospital, Mahidol University, Thailand

Introduction: The ASMBR described major radiographic features for diagnosing atypical femoral fracture (AFF) including noncomminuted, transverse or short oblique fracture configurations with medial cortical spike. This study's objectives were to evaluate the prevalence of AFF based on the ASBMR major radiographic criteria and compare clinical characteristics between patients with these criteria who had fractures after low- and high-energy trauma.

Methods: We retrospectively reviewed plain radiographs of 734 patients who were diagnosed with subtrochanteric/femoral shaft fractures from January 2002 to May 2011 at Siriraj Hospital, Bangkok, Thailand. Patients with inadequate radiographs, multiple or pathological or periprosthetic fractures were excluded. From a total of 378 cases, only those who had major radiographic features of AFF according to the ASBMR criteria were included. AFF were then divided into 2 groups based on mechanism of injury: low-energy and high-energy fractures. Low-energy fracture was

defined as fracture after fall from a standing height or less. Comparative analyses were made to compare clinical variables between low- and high-energy AFF.

Results: From a total of 378 patients, 76 (20.1%) had the ASBMR major radiographic criteria of AFF. Of 76 patients, 17 (22.4%) occurred after sustaining a low-energy trauma. Low-energy AFF occurred more at the subtrochanteric region (64.7% VS 3.4% of low- and high-energy AFF, respectively). Patients with low-energy AFF were older, more females, associated with higher scores of Charlson comorbidity index and higher rate of bisphosphonates use ($p<0.01$). Forty seven percent of patients with low-energy AFF had history of bisphosphonates use while none in the high-energy AFF group used bisphosphonates. The odds ratio of bisphosphonates use in low-energy AFF was 106.5 (95%CI, 5.7 to 2000.5).

Conclusions: The prevalence of low-energy AFF in Thai patients at a single institution was 4.5%. The majority of patients with the ASBMR major radiographic features (77.6%) had high-energy trauma. Therefore, these major radiographic criteria are not specific for diagnosing a low-energy AFF. Future refinement of the current ASBMR criteria for AFF should be considered.

***Disclosures: Sittichai Luangkittikong**, None.*
This study received funding from: Faculty of Medicine, Siriraj hospital, Mahidol University

SU0390

Undercarboxylated osteocalcin and vitamin K nutritional status in postmenopausal osteoporotic women during bisphosphonate treatment. Jun Iwamoto*. Keio University School of Medicine, Japan

Bisphosphonates reduce serum undercarboxylated osteocalcin (ucOC) levels as well as bone turnover marker levels in patients with osteoporosis. The high ucOC level (>2.6 ng/mL) is reported to be an independent risk factor for incident fractures in Japanese osteoporotic patients during bisphosphonate treatment. The purpose of this study was to reveal the association between serum ucOC levels and vitamin K nutritional status in postmenopausal osteoporotic Japanese women during bisphosphonate treatment. One hundred and six postmenopausal women with osteoporosis (range: 47–90 years) were initiated bisphosphonate treatment (weekly alendronate, weekly risedronate, or monthly minodronate) in our out-patient clinic. Osteoporosis was diagnosed based on the thoracic and lumbar spine radiographs and speed of sound (SOS) measured using a quantitative ultrasound (QUS) device. The treatment was continued for 6 months and serum calcium, phosphorus, alkaline phosphatase (ALP) levels and urinary cross-linked N-terminal telopeptides of type I collages (NTX) levels were monitored during this period. After 6 months of treatment, serum ucOC levels were measured and vitamin K nutritional status was evaluated using the simple vitamin K intake questionnaire developed by Uenishi (Osteoporosis Japan 2011; 19: 513-518). This questionnaire evaluates vitamin K nutritional status using scores based on *natto* (fermented soy bean) and green vegetable intakes. The patients were divided into two groups according to the serum ucOC level: the high ucOC (>2.6 ng/mL) group and the normal ucOC (≤2.6 ng/mL) group, and all parameters were compared between the two groups. Sixteen patients discontinued bisphosphonate treatment during the 6 months of period due to acute phase reaction (n=1), gastric pain (n=2), drug allergy (n=1), tooth extraction (n=2), and noncompliance (n=10). Eighty-four patients were processed for analyses (n=30 in the high ucOC group and n=60 in the normal ucOC group). There were no significant differences in baseline parameters (age, height, body weight, body mass index, serum calcium, phosphorus, ALP, and urinary NTX) and changes in these parameters during the 6 months of period. However, vitamin K nutritional intake score was significantly lower in the high ucOC group than in the normal ucOC group. These results suggest that one-third of postmenopausal osteoporotic patients treated with bisphosphonates are at a higher risk of incident fractures with higher serum ucOC levels due to inadequate vitamin intake despite the reduction in bone turnover similar to those with normal serum ucOC levels.

***Disclosures: Jun Iwamoto**, None.*

SU0391

***Own the Bone*: A system-based intervention to improve osteoporosis care after fragility fractures.** Andrew Bunta[1], Beatrice Edwards*[2], William Macaulay[3], Kyle Jeray[4], Laura Tosi[5], Clifford Jones[6], Deborah Sietsema[7], John Kaufman[8], Sarah Murphy[9], James Goulet[10], Gary Friedlander[11], Mark Swiontkowski[12], Douglas Dirschl[13]. [1]Northwestern University Feinberg School of Medicine, USA, [2]MD Anderson Cancer Center, USA, [3]Columbia University, USA, [4]Greenville Hospital System, USA, [5]Children's National Medical Center, USA, [6]Orthopaedic Associates of Michigan; Michigan State University, USA, [7]Orthopaedic Association of Michigan, USA, [8]Henry Mayo Newhall Memorial Hospital, USA, [9]American Orthopaedic Association, USA, [10]University of Michigan, USA, [11]Yale University, USA, [12]University of Minnesota, USA, [13]University of Chicago, USA

Objective: Approximately 2 million individuals sustain an osteoporosis-related fracture in the United States each year, at an estimated annual cost of more than $19 billion to the Medicare system. The occurrence of fracture seldom triggers osteoporosis assessment and treatment. Thus, the purpose of this study is to evaluate the success of the American Orthopaedic Association's - Own the Bone program for secondary prevention of recurrent fractures in patients 50 years of age and older.

Design: A retrospective pre-intervention (a pilot study) and postintervention study.

Setting: Sixty-three academic and community hospitals or orthopaedic outpatient centers participating in the program between June 1, 2009, and September 30, 2012. Patients: Patients aged 50 years or older presenting with fragility fractures (n=7065) were enrolled in the Own the Bone web registry.

Interventions: Physicians recommended calcium and vitamin D supplementation, increased exercise, fall prevention, smoking cessation, limited alcohol intake, bone mineral density (BMD) testing, and osteoporosis medications and sent letters to the patient and the patient's primary care physician (PCP) explaining these recommendations

Main Outcomes Measures: The percentage of physicians recommending each quality measure and communicating with PCP as well as patient compliance with BMD testing, compared with pilot study data.

Results:All quality measures improved compared with the pilot study ($p = 0.001$), including calcium and vitamin D intake (95.6%vs. 80%);exercise (95.5% vs. 87%), fall prevention (96.6% vs. 80%), smoking cessation (82.2% vs. 81.8%), osteoporosis medication (85.7% vs. 5%), and BMD testing recommendations (67.6% vs. 11%). BMD testing was completed in 43.5%of patients (compared with 5% in the pilot study), and letters were sent to 86.8% of patients (vs. 77%) and to primary care physicians for 82.8% of patients (vs. 75%). After a 90-day follow up, the percentage of MD's recommending or initiating therapy ranged from 30 - 78%.

Conclusions and Relevance: The Own the Bone intervention has succeeded in improving the behaviors of participating orthopaedic surgeons, medical specialists and PCP's in the areas of bone health and osteoporosis counseling, coordination of care, BMD testing, and recommendations for or initiation of pharmacotherapy for patients who have experienced a fragility fracture.

***Disclosures: Beatrice Edwards**, None.*
This study received funding from: Merck, Novartis, Eli Lilly, Amgen, Synthes

SU0392

Change in osteoporosis treatment rates after implementation of an electronic consult service for patients with recent fracture. Richard Lee*[1], Kenneth Lyles[2], Megan Pearson[3], Karen Barnard[4], Cathleen Colon-Emeric[2]. [1]Duke University, USA, [2]Duke University Medical Center, USA, [3]Durham VA Medical Center, USA, [4]Duke University Medical Center, Durham VAMC, USA

Background: According to the Office of the Inspector General, less than 9 percent of Veterans received a prescription for an osteoporosis medication within 6 months after an index fracture. An electronic consult (E-consult) service was implemented at 2 Veterans Affairs Medical Centers (VAMCs) and affiliated outpatient clinics to facilitate identification of and to recommend management for patients with recent fracture.

Method: The E-consult service identified Veterans with osteoporotic fractures from inpatient and outpatient encounter data, based on ICD9 diagnosis codes (800-829) from the central data warehouse. Patients were excluded if they were deceased, receiving palliative care, under 50 years, had no primary provider assigned, or if fracture management was already addressed by the primary provider. The medical record of an eligible patient was reviewed by a metabolic bone specialist, and an electronic consult note was sent to the patient's primary provider that specified recommendations for further management. Recommendations were initiated per the provider's discretion.

Results: Prior to implementation of the E-consult service, the rate of osteoporosis treatment at the intervention sites, among patients with recent fractures, was 4.7% for bisphosphonates and 12.3% for vitamin D. After implementation of the program, the treatment rate increased to 5.9% ($P = 0.43$) for bisphosphonates and 17.6% ($P = 0.01$) for vitamin D. The change in treatment rates was not significantly different than the concurrent change among VAMCs without the E-consult service, -1.8% ($P = 0.12$) and +1.5% ($P = 0.10$), respectively.

Conclusion: Implementation of an E-consult service was not able to significantly increase the rate of osteoporosis treatment among patients with a recent fracture. These results suggest an electronic service is feasible, but a program with more direct patient interaction is likely required to significantly improve treatment rates.

***Disclosures: Richard Lee**, None.*

SU0393

Management of Fragility Fracture: An Integrated Interdisciplinary Approach. Marie-Claude Beaulieu*[1], Hélène Corriveau[1], Gilles Boire[2], François Cabana[3], Earl Bogoch[4], Pierre Dagenais[5], Suzanne Gosselin[1], Diane Theriault[6], Bernard Burnand[7], Sonia Jean[8], Johanne Filiatrault[9], Sophie Laforest[9], Marie Rochette[10], Alvine Fansi[1], Isabelle Gaboury[1]. [1]Université de Sherbrooke, Canada, [2]Centre Hospitalier Universitaire De Sherbrooke, Canada, [3]CHUS, Canada, [4]St. Michael's Hospital, Canada, [5]INESS, Canada, [6]Dartmouth General Hospital, Canada, [7]CHUV, Switzerland, [8]INSTITUT NATIONAL DE SANTÉ PUBLIQUE DU QUÉBEC, Canada, [9]Université de Montréal, Canada, [10]MSSQ, Canada

In most Canadian provinces, governmental and community organizations provide fall prevention or fragility fracture (FF) prevention programs; however, none fully integrates fall prevention with post-fracture management. It is increasingly accepted that the success of fall prevention and post-fracture screening and treatment programs is mediated by the context in which interventions occur within the local healthcare system and with primary care practitioners.

A secondary FF prevention model is currently under implementation in the province of Québec (Canada). The program is complemented by a research project which aims to 1) compare the performance of these integrated programs to results from conventional care, using a pragmatic study design; 2) identify barriers as well as factors that improve effectiveness across different implementation milieus; and 3) develop and engage in active knowledge transfer activities with clinicians.

The program relies on a collaborative process between secondary healthcare (orthopaedic surgeons and bone specialists), primary care physicians (PCPs), and local and provincial fall prevention programs. This is orchestrated by a program coordinator. The 3192 expected participants are identified for recruitment as outpatients in orthopaedic clinics, inpatients with hip fracture, and from administrative discharge data from the emergency departments and hospital wards. An integrated approach (pharmacological intervention, promotion of healthy habits and fall prevention program) is offered to the intervention group. The research program measures different short-, intermediate-, and long-term outcomes over a 18-month period, including: recurrent fractures, initiation and compliance with osteoporosis treatment, time to first subsequent fall, number of falls, FF-related death, practice of physical activities, participant's quality of life, FF related costs, and perception of care integration.

This novel integrated FF prevention program will help health professionals to improve patient-centered care, and promote chronic disease prevention and management, including interprofessional collaboration and communication between both primary and secondary healthcare practitioners. Lastly, the pragmatic evaluative design of this project will provide estimates of the effectiveness of a FF prevention program in different geopolitical contexts.

***Disclosures: Marie-Claude Beaulieu**, None.*
This study received funding from: IRSC

SU0394

A Successful Knowledge Translation Intervention in Long-Term Care: Results from the Vitamin D and Osteoporosis (ViDOS) Cluster Randomized Trial. Alexandra Papaioannou*[1], Courtney Kennedy[2], George Ioannidis[2], Lora Giangregorio[3], Lehana Thabane[2], Suzanne Morin[4], Richard Crilly[5], Sharon Marr[2], Robert Josse[6], Lynne Lohfeld[2], Laura Pickard[2], Mary-Lou van der Horst[7], Jackie Stroud[8], Glenda Campbell[8], Lisa Dolovich[2], Anna Sawka[9], Lynn Nash[2], Ravi Jain[10], Carly Skidmore[2], Jonathan Adachi[11]. [1]Hamilton Health Sciences, Canada, [2]McMaster University, Canada, [3]University of Waterloo, Canada, [4]McGill University, Canada, [5]University of Western Ontario, Canada, [6]St. Michael's Hospital, University of Toronto, Canada, [7]Ontario Osteoporosis Strategy for Long-Term Care, McMaster University, Hamilton Health Sciences, Canada, [8]Medical Pharmacies Group Limited, Canada, [9]Toronto General Hospital, Canada, [10]Osteoporosis Canada, Canada, [11]St. Joseph's Hospital, Canada

Background: Meta-analyses demonstrate that vitamin D reduces falls, and calcium and vitamin D reduce fractures in LTC residents. The objective of the ViDOS trial was to evaluate the feasibility and effectiveness of a knowledge translation (KT) intervention aimed at integrating evidence-based osteoporosis/fracture prevention strategies in Long-term Care (LTC) homes.Methods: We randomized 40 LTC homes in Ontario, Canada to intervention (n=19) or control (n=21) arms. Interdisciplinary teams (physicians, nurses, pharmacists, dietitians) in intervention homes participated in a 12-month multifaceted program. Key components were 3 interactive sessions facilitated by an Expert Opinion Leader (via webinar), audit and feedback, point-of-care tools, and action planning for quality improvement. Control homes received toolkits and optional webinars offered to all Ontario LTC homes. Primary outcomes were the proportion of residents prescribed vitamin D ⩾800 IU/day (primary) and ⩾500 mg/day of elemental calcium at 12-months. We examined differences between intervention arms in the proportion of all residents prescribed vitamin D/calcium using the generalized estimating equations technique assuming an exchangeable correlation structure. Unit of analysis was the resident; unit of inference was the LTC home. Analyses were age-sex adjusted. Prescribing rates and odds ratios (95% CI's) are reported. Results: After randomisation, 7 LTC homes in the intervention group declined to participate (operational issues); they were excluded. 4660 residents [mean 84.5 (SD 10.7) years] resided in the remaining 33 LTC homes [mean size= 180 beds (SD 80)] and at baseline the proportion of residents prescribed vitamin D (⩾800 IU/day) and calcium (⩾500 mg/day), respectively, were: 38.8%, 32.7% of residents in intervention homes and 41.9%, 34.8% in control homes. At 12-months, vitamin D (⩾800 IU/day) was prescribed to 72.4% of residents in the intervention arm versus 49.4% in the control arm (OR 3.14, 95% CI: 2.23, 4.41); and calcium (⩾500 mg/day) was prescribed to 45.5% of residents in the intervention arm versus 37.5% in the control arm (OR 1.59, 95% CI: 1.12, 2.25). Conclusion: This study demonstrated that an interdisciplinary, multifaceted knowledge translation intervention significantly improved prescribing of appropriate vitamin D and calcium in the LTC setting.

***Disclosures: Alexandra Papaioannou**, Amgen, Eli Lilly, Merck Frosst Canada, Novartis, Warner Chilcott, 6; Amgen, Eli Lilly, Merck Frosst Canada, Novartis, Warner Chilcott,; Amgen, Eli Lilly, Merck Frosst Canada, Novartis, Warner Chilcott, 2*
This study received funding from: Canadian Institutes of Health Research (CIHR)

SU0395

Effect of a Mixture of Calcium, Vitamin D, Inulin and Soy Isoflavones on Bone Metabolism in Post-Menopausal Women: A Retrospective Analysis. Giorgio Gandolini[1], Maurizio Bevilacqua*[2], Matteo Alemanni[3]. [1]IRCCS S. Maria Nascente - Don C. Gnocchi Foundation - Milan, Italy, [2]Ospedale L. Sacco - Polo Universitario, Italy, [3]Medical Affairs, Medical Department, Bayer SpA – Pharmaceuticals, Milan, Italy, Italy

Objectives.

Aging might affect the effectiveness of the sole supplementation of calcium and vitamin D in post-menopausal women, due to the development of vitamin D resistance in the gut, which limits calcium absorption. Thus, we wanted to test the efficacy of a mixture of calcium (500 mg), serum 25-hydroxyvitamin D (25(OH)D; 300 UI), inulin (3 g) and soy isoflavones (40 mg), present on the Italian market (Calcidon Menopausa), to improve calcium absorption in this type of population.

Study design.

A retrospective study on otherwise healthy post-menopausal women. Main outcome measures The following parameters were evaluated at baseline and after three months of supplementation: daily calciuria – as an indirect marker of calcium absorption – serum 25(OH)D, parathormone, insulin-like growth factor 1 (IGF-1) as a marker of bone anabolism, collagen telopeptide and osteocalcin as markers of bone resorption.

Results.

Twenty-eight women (median age 67 years) were included in the analysis. The supplementation markedly increased daily calciuria (+60%; $p = 0.00009$), while reducing parathormone levels (-18%; $p = 0.02$) and leaving 25(OH)D unaltered. An increase in IGF-1 (+16%; $p = 0.01$) and a reduction in collagen telopeptide (-17%; $p = 0.04$) were observed, too, as well as a modest trend towards osteocalcin reduction, although not significant. Conclusions.

These results suggest that the considered mixture improved intestinal calcium absorption and bone metabolism in postmenopausal women. Since the amount of supplemented calcium was relatively low and 25(OH)D levels were unchanged, the observed effects are likely due to the combined contributions of inulin and soy isoflavones.

***Disclosures: Maurizio Bevilacqua**, None.*

SU0396

Efficacy of Continuing with Alendronate or Risedronate after Long-term use can be Improved by Adding Alfacalcidol Instead of Plain Vitamin D in Postmenopausal and Male Osteoporosis. Johann D. Ringe*[1], Erich Schacht[2]. [1]West-German Osteoporosis Center, Klinikum Leverkusen (University of Cologne) Leverkusen, Germany, [2]Zurich Osteoporosis Research Group (ZORG), Zollikerberg, Switzerland, Switzerland

Background: Oral once weekly bisphosphonates (BP) are the leading treatment for osteoporosis, but the optimal duration of application has not been defined. A recent publication suggests periodically re-evaluating of such patients and to discontinue in case of low risk and continuation in patients still at high risk (1).

Patients and methods: In our study based on retrospective chart analysis we followed 214 patients (167 female, 47male) still at a significantly increased fracture risk after an average of 4.3 years of oral once weekly BP. 145 had taken alendronate (ALN), 69 risedronate (RIS). We compared continuation of the same BP plus either plain vitamin D as before (group A, n=106) or switching to the active D-hormone analog alfacalcidol (group B, n=108) over 2 more years. Primary endpoint was changes in BMD at the lumbar spine (LS) and femoral neck (FN). Further endpoints were falls, back pain, fractures and adverse events.

Results: The two groups were well matched in terms of age, BMI and severeness of osteoporosis. The respective proportions of males and females and patients with ALN or RIS intake did not differ between the 2 groups. BMD at LS and FN did not change significantly over 2 years in group A, but increased significantly with BP plus alfacalcidol. The average number of falls per patient-year was reduced by 12% in A

(ns) and by 44% in B ($p<0.03$). There was a significant decrease in average back pain score with BP plus alfacalcidol vs. BP plus plain vitamin Vit. D after two years ($p<0.02$). The number of patients with new vert. fractures did not significantly differ between A and B while we found a significantly lower rate of non-vert. fractures with alfacalcidol ($p<0.05$). The pattern of adverse events (AE) did not differ between groups.

By subgroup analysis we could show that men were on the average significantly younger than women (67 vs. 72 years) and had a relatively higher proportion of RIS takers (43% vs. 29%). Nevertheless the overall superiority of the combination BP plus alfacalcidol vs. plain vitamin D in all endpoints was also true for females and males alone and for patients on ALN or RIS once weekly. While the advantage of combining ALN with alfacalcidol had been shown in different previous studies this is the first trial to prove that also RIS plus alfacalcidol is advantageous (2).

Ref.:
(1) Whitaker M et al. 10.1056/NEJMp1202619 (2012)
(2) Schacht E, Ringe J. Arzneim Forsch. Drug Res. 2011; 61(1): 40-54

***Disclosures: Johann D. Ringe**, Amgen, Novartis, Merck, Teva, 2*

SU0397

Potassium Citrate Supplementation Results in Sustained Improvement in Calcium Balance in Older Men and Women. Kendall Moseley*[1], Connie Weaver[2], Lawrence Appel[3], Anthony Sebastian[4], Deborah Sellmeyer[5]. [1]Division of Endocrinology, Johns Hopkins Bayview Medical Center, USA, [2]Purdue UniversityDept of Nutrition Science, USA, [3]Johns Hopkins University, USA, [4]University of California San Francisco, USA, [5]The Johns Hopkins Bayview Medical Center, USA

The dietary acid load created by the typical Western diet may adversely impact the skeleton by disrupting calcium metabolism. Whether neutralizing dietary acid with alkaline potassium salts results in sustained improvements in calcium balance remains controversial. In this randomized, double blind, placebo controlled study, 52 men and women (mean age 65.2 + 6.2 years) were randomly assigned to potassium citrate 60 mmol, 90 mmol or placebo daily with measurements of bone turnover markers, net acid excretion, and calcium metabolism including intestinal fractional calcium absorption and calcium balance obtained at baseline and six months. At six months, net acid excretion was significantly lower in both treatment groups compared to placebo and negative, meaning subjects' dietary acid was completely neutralized (-11.3 mmol/day, 60 mmol/day; -29.5 mmol/day, 90 mmol/day, $P < 0.001$ compared to placebo). At 6-months, 24-hour urine calcium was significantly reduced in persons taking potassium citrate 60 mmol (-46 $\pm$ 15.9 mg/day) and 90 mmol (-59 $\pm$ 31.6 mg/day) daily compared with placebo ($p<0.01$). Fractional calcium absorption was not changed by potassium citrate supplementation. Net calcium balance was significantly improved in participants taking potassium citrate 90 mmol/day compared to placebo (142 $\pm$ 80, 90 mmol vs. -80 $\pm$ 54, placebo; $p = 0.02$). Calcium balance was also improved on potassium citrate 60 mmol/day, but this did not reach statistical significance ($p=0.18$). Serum C-telopeptide decreased significantly in both potassium citrate groups compared to placebo (-0.03 + 0.04 nmol/L , 90 mmol/d, $p=0.05$; -0.07 + 0.04 nmol/L , 60 mmol/day, $p=0.02$) while bone specific alkaline phosphatase did not change. Intact parathyroid hormone was significantly decreased in the 90 mmol/day group ($p=0.01$). Readily available, safe, and easily administered in an oral form, potassium citrate has the potential to improve skeletal health. Longer term trials with definitive outcomes such as bone density and fracture are needed.

***Disclosures: Kendall Moseley**, None.*

SU0398

Role of Vitamin D Status on Strontium Absorption after a Strontium Ranelate Oral Overload Test and its Influence on Parathyroid Hormone (PTH) Levels. Tatiane Vilaca*[1], Marilia Camargo[1], Olguita Rocha[2], Marise Lazaretti Castro[3]. [1]Unifesp, Brazil, [2]CETEC, Brazil, [3]Escola Paulista de Medicina, Brazil

Strontium ranelate (SrR) is a drug used to treat osteoporosis in many countries. Calcium (Ca) and strontium (Sr) have common features and are absorbed by the same pathways and it is well established that vitamin D is important for Ca intestinal absorption. We aimed to evaluate whether vitamin D status is determinant for Sr absorption and to investigated the PTH behavior after this Sr overload. For this, 25 postmenopausal women with vitamin D deficiency (25OHD<50nmol/L) and 25 women with sufficiency (25OHD>75nmol/L) were submitted to an oral Sr overload test. After that, deficient patients were treated until reaching adequate vitamin D levels (25OHD>75nmol/L) and the Sr test was repeated. Sr absorption was evaluated as the fraction of the absorbed dose and the area under the curve. Blood PTH, $1,25(OH)_2$ D and Sr were measured. One gram of SrR (Protos^{TM}, Servier) was dissolved in 200 mL of deionized water and administered orally. Blood was drawn for Sr and PTH determinations at 30, 60, 120 and 240 minutes. Sr concentrations increased similarly in both groups, no matter the Vitamin D status. No differences were found in any Sr absorption parameters between the vitamin D deficient and sufficient groups. Moreover, no difference in Sr absorption was found in the deficient group before and after treatment. Nevertheless, the correction of vitamin D status in deficients resulted in a significant increase in 1,25(OH)2D (25.0$\pm$4.6 to 34.6$\pm$9.1 pg/mL $p<0,001$) and a reduction in PTH (73.9$\pm$37.5 to 58.2$\pm$20.1 pg/mL $p=0,006$). The Sr increment on blood was followed by a significant decrease in PTH levels. The mean PTH decrement was 27.7% for sufficient, 23.8% for deficient and 26.6% after Vitamin D correction. Interestingly, this decrease was transient, despite crescent concentrations of Sr, with most patients reaching a nadir at 60 min. In conclusion, Vitamin D status seems not to be determinant for strontium ranelate absorption. In fact, all patients had 1,25(OH)2D within the normal range, regardless of their vitamin D status. This finding is in agreement with the idea that, in the absence of kidney failure, vitamin D deficiency must be very severe to cause deficiency in 1,25(OH)2D. Strontium ingestion causes a variation in PTH levels. The anabolic effect on bone of a pulse elevation of PTH is well known but the effects of the acute decrease are not described. More studies need to be performed to evaluate the effects of this PTH oscillation on bone metabolism.

***Disclosures: Tatiane Vilaca**, None.*
This study received funding from: Servier

SU0399

"Is this exercise safe?" - Building consensus around responses to common questions about physical activity posed by people with osteoporosis. Lora Giangregorio*[1], Maureen Ashe[2], Kathy Shipp[3], Angela M. Cheung[4], Ari Heinonen[5], Alexandra Papaioannou[6], Stuart McGill[1], Judi Laprade[7], Ravi Jain[8], Heather Keller[1], Norma MacIntyre[9], John Wark[10]. [1]University of Waterloo, Canada, [2]University of British Columbia, Canada, [3]Duke University Medical Center, USA, [4]University Health Network-University of Toronto, Canada, [5]Department of Health Sciences, University of Jyväskylä, Finland, [6]Hamilton Health Sciences, Canada, [7]University of Toronto, Canada, [8]Osteoporosis Canada, Canada, [9]McMaster University, Canada, [10]University of Melbourne Department of Medicine, Australia

Background: There is little evidence to guide responses to questions commonly asked by individuals with osteoporosis about safe and effective physical activity for health benefits, or safety around activities of daily living.

Objective: The Too Fit To Fracture (2F2F) initiative will create exercise recommendations for people with osteoporosis with or without vertebral fracture, by synthesizing evidence and expert consensus. We report findings from step two in hte Too Fit To Fracture initiative, a consensus process designed to address questions often asked by patients.

Methods: The 2F2F expert panel identified researchers and clinicians with expertise in exercise and osteoporosis, and stakeholder groups (e.g., Osteoporosis Canada, National Osteoporosis Foundation). We used FluidSurveys to deliver a modified RAND/UCLA Delphi survey to 75 invitees. We presented three clinical cases (moderate risk, one vertebral fracture, multiple vertebral fractures/hyperkyphosis/pain) and asked about assessment and exercise prescription; questions included those commonly asked by patients. Descriptive statistics were used to summarize participant characteristics and responses. Content analyses of free text responses were performed by two expert panel members, and merged.

Results: Of 75 invitees, 39 participated (52% response rate). In cases with prevalent vertebral fractures , there was less confidence that existing physical activity guidelines were appropriate (Table 1). There was consensus in the following areas: 1) the importance of resistance and balance training e; 2) spinal extension exercises should be performed; 3) those with vertebral fractures should receive instruction on safe movement and body mechanics, especially in the presence of pain or kyphosis. Regarding activities considered risky, (e.g., golf, yoga), patients with a history of the activity or strong preference may be able to do it with modification, e.g., for yoga controlled twisting in supine, where the spine is least loaded. Other areas of consensus emerged around activities of daily living and safe movement.

Conclusions: Using patient questions to inform the process has generated a number of recommendations that will make the development of exercise recommendations more comprehensive and patient-centred. Further, the process has highlighted a number of gaps that can inform future research.

Table 1: Responses to the question "Do you think that the physical activity guidelines detailed above* (CSEP, ACSM, WHO) are appropriate for this case?" Presented as a % of total respondents (n=39)

	Moderate risk	High risk (1 vertebral fracture)	High risk (1 vertebral fracture, pain, hyperkyphosis)
Yes	54%	31%	25%
No	36%	49%	62%
I don't know	4%	10%	22%
Missing	0	10%	15%

*We provided a summary of the guidelines in the survey. CSEP = Canadian Society for Exercise Physiology, ACSM = American College of Sports Medicine, WHO = World Health Organization

Table 1

***Disclosures: Lora Giangregorio**, None.*
This study received funding from: Osteoporosis Canada

SU0400

Effect of Denosumab Treatment on Bone Histology and Histomorphometry in Men With Low Bone Mineral Density. David Dempster*[1], David L Kendler[2], Jesse Hall[3], Steven Boonen[4], Michael Bolognese[5], Roland Chapurlat[6], Stefan Goemaere[7], Lars Hyldstrup[8], E Michael Lewiecki[9], Paul Miller[10], Yu-Ching Yang[3], Rachel B Wagman[3], Bente Langdahl[11]. [1]Columbia University, USA, [2]University of British Columbia, Canada, [3]Amgen, Inc., USA, [4]Leuven University, Belgium, [5]Bethesda Health Research Center, USA, [6]Hopital Edouard Herriot, France, [7]Ghent University Hospital, Belgium, [8]Hvidovre Hospital, Denmark, [9]New Mexico Clinical Research & Osteoporosis Center, USA, [10]Colorado Center for Bone Research, USA, [11]Aarhus University Hospital, Denmark

Purpose: In the phase 3 ADAMO trial in men with low bone mineral density (BMD), 1 year of denosumab (DMAb) treatment significantly increased BMD compared with placebo.[1] Consistent with DMAb's mechanism of action, DMAb-treated subjects had reduced bone resorption as measured by serum C-terminal telopeptide. It has been shown that transiliac crest bone biopsies from women with postmenopausal osteoporosis (PMO) treated with DMAb for up to 5 years demonstrated normal bone quality and decreased remodeling at the tissue level.[2,3] Here, we report the effects of DMAb on bone histology and histomorphometry after 1 year of treatment in a subset of ADAMO subjects.

Methods: Following labeling with tetracycline or demeclocycline, transiliac crest bone biopsy was performed as a substudy of the phase 3 ADAMO trial ≤ 30 days before the year-1 visit. For biopsies with only single labels in trabecular bone within the measurable field (20 mm^2), mineral apposition rate was imputed as 0.3 μm/day.

Results: A total of 29 subjects (17 DMAb; 12 placebo) participated in the bone biopsy substudy. Demographics for this subset were comparable with that of the overall ADAMO population. Mean (SD) number of months from the last dose of DMAb to the first dose of label was 5.0 (0.5) months. Qualitative bone histology, assessed in all samples, was unremarkable, showing normally mineralized lamellar bone. Structural indices, including cancellous bone volume and trabecular number and surface, were similar between treatment groups (Table). Consistent with the mechanism of action, bone remodeling was decreased in DMAb-treated subjects. A total of 12/17 (71%) DMAb- and 12/12 (100%) placebo-treated subjects had specimens with double labels in trabecular and/or cortical compartments; 6 DMAb- and 12 placebo-treated subjects were evaluable for dynamic trabecular bone parameters. Static and dynamic remodeling indices were lower in DMAb- than placebo-treated subjects, consistent with reduced bone turnover with DMAb therapy.

Conclusions: Treatment of men with low BMD with DMAb for 1 year resulted in qualitatively normal bone with reduced bone turnover. These findings are consistent with those from women with PMO treated with DMAb for 1, 2, 3, or 5 years.

1. Orwoll E, et al. *J Clin Endocrinol Metab.* 2012;97(9):3161-3169
2. Reid I, et al. *J Bone Miner Res.* 2010;25(10):2256-2265
3. Brown JP, et al. *J Bone Miner Res.* 2012;27(suppl 1):S44

Table. Cancellous Bone Histomorphometry after 12 months of DMAb or Placebo

Index	n	Denosumab (N = 17)	n	Placebo (N = 12)
Structural and static parameters				
Trabecular bone volume (BV/TV), %	16	7.730 (5.710, 13.320)	12	10.625 (5.985, 13.295)
Trabecular number, 1/mm	16	0.725 (0.405, 0.980)	12	0.835 (0.600, 1.045)
Osteoid volume, %	16	0.040 (0.010, 0.215)*	12	0.375 (0.240, 1.495)
Osteoid surface, %	16	0.495 (0.275, 1.86)*	12	3.735 (2.015, 8.200)
Osteoid width, μm	16	5.300 (3.885, 6.985)	12	7.555 (5.915, 9.910)
Eroded surface (ES/BS), %	16	0.00 (0.000, 0.060)*	12	0.325 (0.025, 0.585)
Dynamic parameters†				
Mineral apposition rate, μm/day	6	0.695 (0.430, 1.040)	12	0.725 (0.580, 0.850)
Mineralization surface, %	6	0.755 (0.500, 1.670)	12	2.075 (1.100, 5.280)
Bone formation rate, %/year	6	3.675 (1.080, 11.060)	12	10.100 (5.320, 28.010)
Activation frequency, year^{-1}	6	0.0421 (0.0152, 0.1129)	12	0.1270 (0.0640, 0.4540)

N = number of subjects enrolled. n = number of subjects with observed data.
Data are median (Q1, Q3). *$P < 0.02$ compared with placebo; Wilcoxon rank sum test.
†Of the 17 biopsies obtained from DMAb-treated subjects, 7 had double labels, 1 had single label, and 9 had no label in the trabecular compartment. Of the 8 evaluable samples, 2 samples with double labels were excluded (1 had label outside the measured field and 1 was only evaluable for cortical width).

Table. Cancellous Bone Histomorphometry after 12 months of DMAb or Placebo

***Disclosures: David Dempster**, Amgen, 2; Amgen,*
This study received funding from: Amgen Inc.

SU0401

Effect of TNF inhibitors on BMD in patients with ankylosing spondylitis- a systematic review and meta-analysis. Nisha Nigil Haroon*[1], Jeevitha Srighanthan[2], Angela M. Cheung[3], Robert.D. Inman[4], Nayef Al Ghanim[5]. [1]University of Toronto, Canada, [2]Osteoporosis Program, University Health Network, Canada, [3]University Health Network-University of Toronto, Canada, [4]Rheumatology division, University Health Network, Canada, [5]UHN Toronto Western Hospital, Canada

Background: Patients with ankylosing spondylitis (AS) are susceptible to osteoporosis (OP) and have high fracture risk. Currently, no specific strategies are established to treat OP in these patients. TNF inhibitors are now increasingly used for treating AS. If TNF inhibitors are shown to prevent or reverse bone loss, use of OP medications like bisphosphonates can be avoided. Thus, we did a systematic review and meta-analysis to study the effect of TNF inhibitors on spine and hip BMD in patients with AS.

Methods: 2 authors searched MEDLINE, EMBASE & Cochrane databases (inception to February, 2013), reviewed abstracts,read selected articles in full and extracted data. Discrepancies were resolved by a 3rd author. Studies included had at least 70% of subjects satisfying Modified New York AS criteria and a minimum follow-up of 1 year. Case reports &studies on children and adolescents were excluded. The quality of the studies was assessed by Newcastle–Ottawa Quality Assessment Scale. Primary outcomes (BMD at spine, total hip &femoral neck) were analyzed at 1 and 2 years, to reflect the time points used in our abstracted literature. BMD was expressed as the percent change from baseline. Publication bias was assessed by Funnel plots comparing weight & effect size. Statistical heterogeneity was assessed using Q statistic. The overall summary estimate was determined using the random effects model, which was weighted by the inverse variance of the effect size.

Results:Our search retrieved 5207 articles which were narrowed down to 7 studies (6 observational studies &1 randomized controlled trial; N = 285 at 1 year, 394 at 2 years). 76-92% of subjects were men. Bisphosphonate use was negligible (n=12). Little data was available on intake of calcium /vitamin D. The use of TNF inhibitors led to significant improvement in spine and total hip BMD after 1 and 2 years when compared to baseline (Table).Femoral neck BMD remained stable at 1 year. The BMD gain was also significant in those treated with TNF inhibitors when compared to controls. In a RCT (TNF inhibitors vs. placebo), the gain in BMD was significantly higher in those treated with TNF inhibitors for 2years versus those treated with placebo for the initial 6 months.Conclusions: Treatment with TNF inhibitors is associated with improvement in spine and hip BMD in patients with AS. More studies of longer duration and larger sample sizes are needed to better understand the effect of TNF inhibitors on fracture risk.

Table: Summary estimates of the effect of TNF inhibitors on BMD in patients with AS

Duration of follow up (years)	Lumbar spine Mean difference,% (95% CI)	Total hip Mean difference,% (95% CI)	Femoral neck Mean difference,% (95% CI)
1 year	5.05 (4.01-6.09)	1.77 (1.03-2.52)	0.73 (-0.78-2.23)
2 years	8.71 (6.71-10.72)	2.45 (1.92-2.98)	Insufficient data

Table

***Disclosures: Nisha Nigil Haroon**, salary support from grant from Amgen, 6*

SU0402

A Novel ^{41}Ca Assay to Measure Short and Long-term Mineral Kinetics in Patients Undergoing Cancer Therapy. Susanta Hui*[1], Luke Arentsen[1], Thanasak Sueblinvong[1], Levi Downs[1], David Potter[1], Gary Grammens[1], Rahel Ghebre[1], Sharon Allen[1], Anne Minenko[1], Yang Zhang[2], Chap Le[1], Jerry Froelich[1], George Jackson[3], Maryka Bhattacharyya[4], Douglas Yee[1]. [1]University of Minnesota, USA, [2]Creighton University, USA, [3]Purdue University, USA, [4]Georgia Health Sciences University, USA

Cancer survivors have an increased risk of osteoporotic fractures. *We report here a new isotope* ^{41}Ca *(measured by ultra-sensitive accelerator mass spectrometry) to study bone mineral kinetics in* cancer patients undergoing anti-cancer therapy and prevention of bone loss. *Patients with estrogen positive* breast cancer, ovarian cancer, endometrial cancer receive microdose (below background) of ^{41}Ca during on initial visit to clinic. 4-8 weeks later Patients undergo standard treatment: Aromatase inhibitor for breast cancer, chemotherapy (platinum- and taxane-based regimen) for Ovarian cancer, Chemo and pelvic radiation (45-50 Gy in 25-28 fractions) ± high dose rate brachytherapy (5-18 Gy) for endometrial cancer. 200-400 ml of urine is collected at frequently for 30 days to establish initial excretion rate prior to treatment and later once in two months for one year. For low bone density group, bisphosphonate drug is used as intervention and followed with ^{41}Ca assay. DXA, QCT, were performed. Rapid excretion of ^{41}Ca, following quasi steady state. In breats patients, with 3 patients maintaining and 7 patients increasing their levels of bone remodeling (Figure 1A). The maintenance or loss of bone was confirmed in all patients who are far enough along in the study to have received a follow-up DECT and DXA measurement. The onset of *increased bone remodeling (elevated ^{41}Ca/Ca) is associated with the start of aromatase inhibitor (AI) at day 60.*

Oophorectomy and chemotherapy show elevated excretion of ^{41}Ca/Ca in region II (Figure 1B). This pilot study also helped us perfect our techniques, including timing for ^{41}Ca injection in the hospital, and demonstrates the feasibility of this approach. We observed (Figure 1C) a rapid response to antiresorptive (mainly ZA) treatment intervention using the ^{41}Ca/Ca assay with a) a rapid decrease within 30 days from the start of the BP intervention, b) a slow decrease between 30-60 days and c) a trend to a quasi-steady state. We measured a statistically significant ($p<0.0001$, general linear mixed models) decrease in ^{41}Ca/Ca from the baseline (pre-intervention) at 90 days post BP initiation. The clinical advantage of using ^{41}Ca assay in the intervention is that it may allow us to obtain an early measure of response to BP intervention on bone, thus allowing us to optimize treatment dose or guide alternative drug selection.

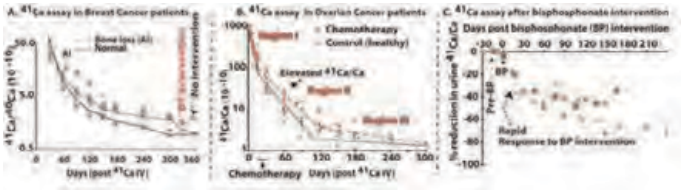

Figure 1. 41Ca detection

***Disclosures: Susanta Hui**, None.*

SU0403

Evaluation of QOL and Fracture Probability Using FRAX in Japanese Postmenopausal Women with Osteoporosis Treated with Raloxifene. Kousei Yoh*[1], Etsuro Hamaya[2], Masanori Taketsuna[3], Hisashi Urushihara[4], Kiyoshi Tanaka[5]. [1]Department of Orthopedic Surgery, Hyogo College of Medicine Sasayama Hospital, Japan, [2]Eli Lilly, Japan, [3]Eli Lilly Japan K.K., Japan, [4]Eli Lilly Japan K.K. & Ethics Committee, Graduate School & Faculty of Medicine, Kyoto University, Japan, [5]Kyoto Women's University, Japan

Kanis et al.* analyzed the data from a global large-scale clinical trial and found that raloxifene hydrochloride (RLX) significantly reduced the risks of all clinical and morphometric fractures regardless of the FRAX risk, that is the 10-year probability of major osteoporotic fractures estimated with the fracture risk-assessment tool (FRAX® version 1.3). Previously, we reported on QOL improvement in Japanese patients with postmenopausal osteoporosis treated with RLX. To date, however, no report that assessed QOL with the fracture risk at baseline using FRAX in Japanese patients treated with RLX has been published. In this study, we investigated changes in QOL in Japanese postmenopausal women treated with RLX in relation to the FRAX risk. Patients with postmenopausal osteoporosis (diagnosed based on the diagnostic criteria for primary osteoporosis, 2000 version) participated in this study and were administered RLX for 24 weeks. The FRAX risk was assessed before RLX administration. QOL improvement by 24-week RLX treatment was evaluated by changes from baseline in each score of QOL instruments (SF-8, EQ-5D, VAS and Japanese osteoporosis quality of life questionnaire [JOQOL] 2000). Subgroup analyses based on the FRAX risk $<15\%$ and $\geqslant 15\%$ were conducted with the patient (aged $\geqslant 50$ and <75 years) data for the primary evaluation. Of the 536 enrolled patients, 506 were included in the analysis (mean age: 70.7). The mean FRAX risk level for 411 patients utilized in the subgroup analyses was $15.96 \pm 9.66\%$ at baseline. The baseline scores in EQ-5D, VAS, and JOQOL2000 showed significant differences between the FRAX risk $<15\%$ and $\geqslant 15\%$ groups (p=.006 to .001). At 24 weeks, all QOL instruments at both groups, except for SF-8 mental component of the FRAX risk $\geqslant 15\%$ group (p=.061), significantly improved in scores compared to baseline (p=.001) with the mean changes from baseline in JOQOL2000 of 3.5 ± 9.1 for the FRAX risk $<15\%$ group and 7.4 ± 9.1 for the $\geqslant 15\%$ group. No significant differences in changes from baseline between the groups were shown in physical and mental component summary of SF-8 and EQ-5D (p=.153, .647, and .155, respectively). Meanwhile, in VAS and JOQOL2000, there were significant differences between the groups (p=.001 and .045, respectively). In conclusion, the results suggest that QOL improved in Japanese patients with postmenopausal osteoporosis treated with RLX, regardless of major osteoporotic fracture probability.

* Kanis JA et.al. Bone. 2010;47(4):729-35.

Table QOL scores and mean changes from baseline at Week 24 by the FRAX risk level of <15% and ≥15%

Subscales with the FRAX risk level (%)		Baseline n	Baseline Mean	Baseline SD	Baseline p-value*	QOL scores Week 24 n	Week 24 Mean	Week 24 SD	Change from baseline n	Change from baseline Mean	Change from baseline SD	Change from baseline p-value*	p-value**
SF-8 (Physical component summary)	<15	203	43.490	7.465	.560	188	46.251	6.614	182	3.004	7.150	.153	.001
	≥15	55	42.880	7.350		55	47.009	6.885	52	4.681	8.361		.001
SF-8 (Mental component summary)	<15	203	48.979	6.666	.151	188	50.946	5.875	182	1.650	6.580	.647	.001
	≥15	55	47.485	8.285		55	49.297	6.319	52	2.150	8.092		.061
EQ-5D	<15	203	0.7464	0.1608	.006	188	0.7994	0.1627	182	0.0562	0.1569	.155	.001
	≥15	56	0.6764	0.1740		56	0.7703	0.1660	54	0.0917	0.1725		.001
VAS	<15	198	3.32	2.36	.001	184	2.57	2.13	175	-0.72	2.44	.001	.001
	≥15	54	4.61	2.56		55	2.51	2.21	52	-2.09	2.54		.001
JOQOL2000	<15	162	72.0	14.1	.001	113	74.9	14.9	90	3.5	9.1	.045	.001
	≥15	43	63.6	18.2		31	72.6	13.2	29	7.4	9.1		.001

EQ-5D, Euro-QOL 5 single-item Dimensions; JOQOL, Japanese osteoporosis quality of life questionnaire; QOL, quality of life; SD, standard deviation; SF-8, Short Form-8 Health Survey; VAS, visual analog scale.
*: Two-sample t-test.
**: Paired t-test.

Table QOL scores and mean changes from baseline at Week 24 by the FRAX risk level of <15% and >=15%

***Disclosures: Kousei Yoh**, None.*
This study received funding from: Eli Lilly Japan K.K.

SU0404

Osteoporosis Assessment Questionnaire-Physical Function (OPAQ-PF): a Psychometrically Validated Osteoporosis-Specific Patient Reported Outcome Measure of Daily Activities of Physical Function. April Naegeli[1], Annabel Nixon[2], Helen Doll[3], Sarah Shingler[3], Katie Breheny[3], Russel Burge*[1], Stuart Silverman[4], Deborah Gold[5]. [1]Eli Lilly & Company, USA, [2]Oxford Outcomes, an ICON plc., United Kingdom, [3]Oxford Outcomes, United Kingdom, [4]Cedars-Sinai/UCLA, USA, [5]Duke University Medical Center, USA

This study aimed to evaluate the measurement properties of the Osteoporosis Assessment Questionnaire-Physical Functioning (OPAQ-PF), a new 15-item scale modified from the OPAQ (Silverman, 2000) to measure the impact of osteoporosis on daily activities of physical functioning.

A prospective psychometric validation study of the OPAQ-PF was conducted in a sample of 141 post-menopausal women with moderate to severe osteoporosis (T-score $\leq$-2.5) or a history of a fragility/non-traumatic fracture, 37 of whom had experienced a recent fragility fracture (<6 weeks). Participants completed the SF-36, QUALEFFO-41, WOMAC and four performance based measures (PBMs) at baseline, to assess the construct validity of the OPAQ-PF. Patients without a recent fracture completed the OPAQ-PF and global items 2 weeks after baseline to assess test-retest reliability. Patients with a recent fracture completed the same measures 12 and 24 weeks post-baseline to assess ability to detect change and identify a meaningful change score. Dimensionality of the OPAQ-PF was evaluated by exploratory and confirmatory factor analysis (EFA, CFA).

The OPAQ-PF had a good distribution of scores for recent fracture patients: scores ranged across almost the entire spectrum of the 0-100 scale; median score 58.7. EFA identified a single factor explaining the majority of the variance in the data (75% on principal component extraction). CFA confirmed a total OPAQ-PF score best represents the underlying construct. The OPAQ-PF had good internal consistency (α=0.974) and stability over a two week period amongst patients reporting no global change (ICC range 0.92 - 0.95). The OPAQ-PF differentiated between patients with and without recent fracture, and by severity of osteoarthritis (WOMAC $\geqslant$40). As predicted, the OPAQ-PF correlated strongly with physical and physical function domains of the WOMAC, the SF-36, the QUALEFFO-41 and with performance-based measures ($r>0.3$, $p<0.001$). High correlations were observed between changes in OPAQ-PF score and changes in global concept scores in patients with a recent fracture ($r\geqslant 0.6$, 24-week change). Effect sizes of OPAQ-PF score change increased by level of global change at 12 and 24 weeks ($p<0.001$). Anchor-based methods identified an OPAQ-PF change of >10 at an individual level as meaningful to patients.

The OPAQ-PF has been developed and evaluated following regulatory guidelines for measuring treatment benefit in clinical trials, and has strong psychometric properties.

***Disclosures: Russel Burge**, Eli Lilly and Company, 7*
This study received funding from: Eli Lilly and Company

SU0405

***In Vivo* Bone Dynamic Imaging Reveals Increased Bone Formation and Inhibited Bone Resorption in Rat Tibia in Response to Combined Alendronate (ALN) and PTH Treatment.** Chantal De Bakker*, Allison Altman, Wei-Ju Tseng, Mary Beth Tribble, Beom Kang Huh, Abhishek Chandra, Ling Qin, Xiaowei Liu. University of Pennsylvania, USA

Anti-resorptive and anabolic agents, such as ALN and PTH, each improve bone quality. However, the effects of combined therapy are controversial, partly due to the inability of standard CT and histology to assess the dynamic process of bone remodeling. We developed a novel *in vivo* bone dynamic imaging technique to evaluate the effects of combination and monotherapy and hypothesized that combined PTH and ALN therapy would increase bone formation while inhibiting resorption.

3-mo-old rats were treated with 60μg/kg PTH (n=6), 50μg/kg ALN (n=6), saline (Veh, n=5), or PTH+ALN (n=7) by daily injection over a 12-day period. Calcein was injected at d3 and d10. The proximal tibia was scanned at 10.5μm (Scanco vivaCT40) at d4 and d12. The two scans were registered and subtracted to identify formation and resorption sites (Fig1). 3D μCT-based bone formation rate: BFR/BS=formation volume/(days*bone surface), mineral apposition rate: MAR=thickness of newly formed bone/days, bone resorption rate: BRR/BS=resorption volume/(days*bone surface), and mineral erosion rate: MER=thickness of resorbed bone/days were quantified. Standard BFR/BS, MAR, osteoblast number (Ob.N), and osteoclast number (Oc.N) were measured by histology, and serum resorption marker TRAP was assessed for a subset of specimens.

In vivo μCT- and histology-based identification of formation sites (Fig 1) as well as BFR/BS ($r=0.8$, $p<.0001$) and MAR ($r=0.6$, $p<.005$) yielded excellent agreement with each other. Compared to d0, PTHALN caused a greater increase in bone volume fraction (BV/TV) than PTH over 12 days (45% *vs.* 33%). μCT-based analysis indicated that PTHALN had 300% greater BFR/BS and 110% greater MAR than both Veh and ALN, while PTH had 300% greater BFR/BS than Veh, which were consistent with increased histology-based BFR/BS, MAR, and Ob.N in both PTH and PTHALN compared to Veh (Table 1). μCT-based resorption measures show that BRR/BS was 50% lower in PTHALN and tended to be lower (35%) in ALN than Veh. PTH resulted in 92% greater MER than ALN. Serum analysis indicated that ALN treatment lowered PTH-induced TRAP activity as compared to PTH monotherapy.*In vivo* bone dynamic imaging provides longitudinal, 3D evaluation of bone formation and resorption. Reduced μCT-based BRR/BS and elevated BFR/BS and MAR in

PTHALN indicate that combined therapy increases bone formation while inhibiting resorption, which partially explains the additive effect of combined PTHALN therapy over monotherapy.

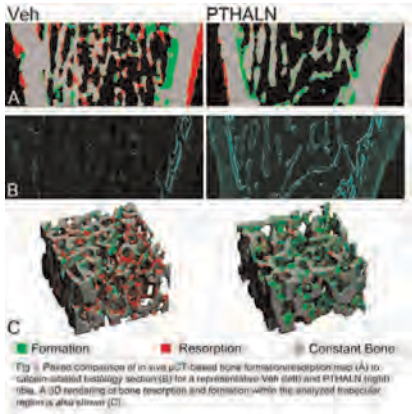

Figure 1

Table 1. Comparison of treatments. Values are shown as mean ± 1SD. Values significantly different from PTHALN are indicated by *, those significantly different from PTH are indicated by # ($p < 0.05$)

	Veh	ALN	PTH	PTHALN
CT-based parameters				
BV/TV (% change over 12 days)	5.7 ± 8.7*#	12.5 ± 3.3*#	32.5 ± 15.3*	45.1 ± 18.5
BFR/BS (μm/day)	0.31 ± 0.06*#	0.40 ± 0.03*	1.24 ± 0.22	1.45 ± 0.24
MAR (μm/day)	1.41 ± 0.17*	1.43 ± 0.18*	2.82 ± 0.23	2.97 ± 0.15
BRR/BS (μm/day)	0.40 ± 0.08*	0.26 ± 0.09	0.35 ± 0.12	0.20 ± 0.12
MER (μm/day)	1.56 ± 0.26	1.28 ± 0.21*#	2.46 ± 0.23	1.86 ± 0.33
Histology-based parameters				
BFR/BS (μm/day)	0.05 ± 0.02*#	0.05 ± 0.03*#	0.22 ± 0.05	0.18 ± 0.06
MAR (μm/day)	1.17 ± 0.26*#	1.35 ± 0.72*#	2.48 ± 0.37	2.11 ± 0.16
N.Ob/BS (1/μm)	5.06 ± 1.32#	7.13 ± 0.99	15.45 ± 5.74	10.27 ± 3.67
N.Oc/BS (1/μm)	1.03 ± 0.38	1.02 ± 0.21	1.13 ± 0.31	1.04 ± 0.36
Serum-based parameters				
TRAP (U/L)	2.29 ± 1.06	0.70 ± 0.35	3.60 ± 1.03*	0.40 ± 0.25

Table 1

***Disclosures: Chantal De Bakker**, None.*

SU0406

A Closer Look at the Immediate Trabeculae Response to Combined Parathyroid Hormone and Alendronate Treatment. Allison Altman*, Beom Kang Huh, Wei-Ju Tseng, Abhishek Chandra, Ling Qin, Xiaowei Liu. University of Pennsylvania, USA

Combined anti-resorptive and anabolic treatments, such as alendronate (ALN) and parathyroid hormone (PTH), were expected to exert an additive effect compared to PTH monotherapy but conflicting results were found in both clinical and animal studies. A shorter treatment time in rats (<2 wk) may be more clinically relevant to the short PTH treatment window in humans (<2 yr). We hypothesized that combined treatment would result in a greater improvement in trabecular bone structure and strength than PTH monotherapy by immediately enhancing bone formation on the trabecular surface.

Saline (Veh, n=6), PTH (60μg/kg, n=9), ALN (50μg/kg, n=6), or combined PTHALN (n=9) was injected daily to 3-mo rats for 12 days. The right proximal tibia was scanned every 4 days by Scanco vivaCT 40 at 10.5 μm resolution for PTH and PTHALN groups, and days 0 and 12 for VEH and ALN groups. Microstructure and finite element analysis were performed on registered trabecular bone images (Fig. 1). The left tibia was scanned by Scanco MicroCT 35 at 3.5 μm resolution for tissue mineral density (Tb.TMD) analysis.

PTH caused 7%, 19%, and 33% increase in BV/TV at day 4, 8, and 12 compared to baseline, while PTHALN resulted in 9%, 25%, and 45% increase. Similar increases in Tb.Th were observed for both PTH (7-35%) and PTHALN (8-35%) over 12 days. In contrast, little or no change in Tb.Th or BV/TV was detected in the Veh and ALN groups. Tb.N showed no difference between groups or over time. SMI suggests a 15% and 27% increase in plate-like structures in the PTH and PTHALN groups, respectively, compared with a 6% increase in the ALN group and no change in the Veh group. At day 12, the PTHALN group had 9% and 13% greater BV/TV and plate-like structure than the PTH group. Overall, compared to the baseline, treatment by ALN, PTH, and PTHALN achieved 25%, 68%, and 103% increases in stiffness, respectively. On the bone surface, PTH and PTHALN groups had reduced mineralization (4.5% and 3.0%), possibly due to the new bone formation, when compared to VEH and ALN respectively.

We demonstrated an additive effect of combined PTH and ALN therapy over monotherapy on trabecular microstructure and strength in rats over 12 days. The improvement in SMI indicates that PTHALN may further strengthen bone by filling perforated plates. We conclude that rather than blunting the formation stimulated by PTH, the addition of antiresorptive treatment exerts an additive beneficial effect by inhibiting bone resorption.

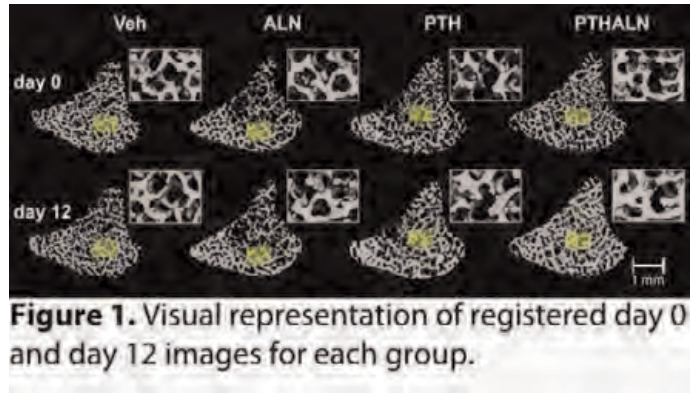

Figure 1. Visual representation of registered day 0 and day 12 images for each group.

Figure 1

Table 1. Variables of interest shown as mean percent change at day 12 compared to day 0 (%SD), and for Tb.1MU at day 12 mean (SD). * indicates significant ANOVA result, post-hoc analyses detailed in text.

	Veh (n = 6)	ALN (n = 6)	PTH (n = 8)	PTHALN (n = 9)
BV/TV (%Δ)*	5.7 (8.7)	12.5 (3.2)	32.5 (15.3)	45.1 (18.5)
Tb.Th (%Δ)*	8.5 (6.3)	9.8 (1.5)	35.4 (9.6)	34.9 (14.4)
SMI (%Δ)*	-0.9 (6.0)	-6.4 (2.6)	-14.6 (7.5)	-26.6 (9.0)
Stiffness (%Δ)*	9.2 (24.6)	25.0 (13.4)	68.5 (32.5)	102.8 (50.8)
Tb.TMD (mgHA/ccm)*	985.8 (26.7)	1007.2 (9.8)	943.0 (23.0)	978.0 (25.7)

Table 1

***Disclosures: Allison Altman**, None.*

SU0407

An Evaluation of Calcilytic Effects on Parathyroid Hormone and Bone Mineral Density Response Using a Physiologically-Based, Multiscale Systems Pharmacology Model. Kyle Baron*[1], Matthew Riggs[1], Ryoko Sawamura[2], Takako Shimizu[2], Fumihiko Okada[2], Jin Zhou[3], Takahiro Shibayama[3], Mendel Jansen[4]. [1]Metrum Research Group LLC, USA, [2]Daiichi Sankyo Co., Ltd., Japan, [3]Daiichi Sankyo Pharma Development, USA, [4]Daiichi Sankyo Development Ltd., United Kingdom

Recent research involving Ca receptor (CaR) antagonists (calcilytics) has focused on assimilating transient spikes in PTH observed with subcutaneous PTH (1-34, 1-84) administration. The goal has been to provide a 'by mouth' osteoporosis treatment comparable to PTH without invasive dosing. Investigations have yet to achieve this target profile, with typical BMD elevations of no more than 2-3% and often notably elevated serum calcium. A model-based approach to quantify the physiologic response to calcilytics was undertaken to support development of DS-9194b, an orally administered investigational calcilytic. An existing physiologically-based, multiscale systems pharmacology mathematical model (MSPM) [Bone2010;46:49–63] was expanded to include a capacity-limited PTH release pool. Pharmacokinetic (PK) and PTH data [ronacaleret (R), JTT-305 (J)] were used for this further MSPM model development. Results indicated a limit to the maximum achievable peak PTH response and described the characteristic persistent PTH elevation.

The MSPM results were coupled with a modeled relationship between peak PTH and BMD (Fig 1); results suggested that mean PTH peak (~20 pM) from the investigated calcilytics equated to a mean BMD increase <3%, as typically observed for these agents; whereas a PTHmax >30pM was considered necessary to provide appreciable BMD increase.

PK, PTH and Ca data were prospectively collected from a single-dose, first-in-human study including DS-9194b administration [0-100 mg]. PTHmax reached an apparent plateau (~30pM) as doses increased above 15mg (Fig 2); this peak was well described by the MSPM as were the prolonged elevations at higher doses. Urine Ca excretion decreased with increased DS-9194b dose (Fig 3); this effect was included in the MSPM through PTH effects on urine Ca excretion. A maximal 12-month 4~5% BMD increase was predicted for DS-9194b based on the prior modeling; only the single-dose clinical data was required to support this prediction and suggests potential for DS-9194b as a future osteoporosis treatment option.

Overall, the modeling indicated that BMD elevation with calcilytic administration routines evaluated is possible but the magnitude of BMD elevation is unlikely to match that seen with exogenous PTH. The MSPM provided a physiologic explanation of maximal PTH response due to capacity-limited PT gland pool of PTH. Results can

guide future considerations for calcilytic-related therapies for osteoporosis or other PTH-related disorders.

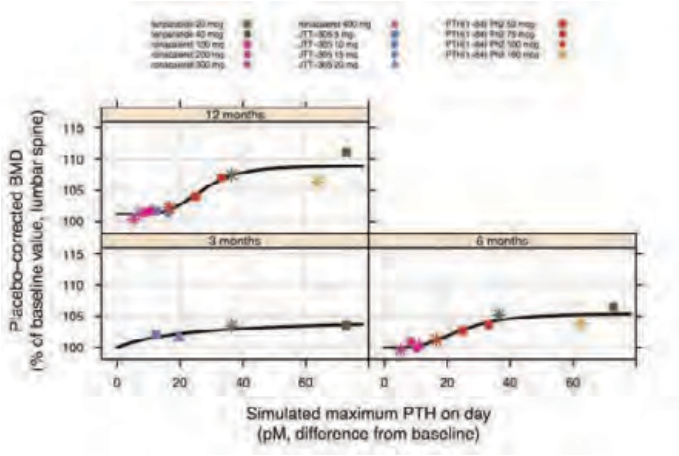

Relationship between BMD change and maximum PTH elevation

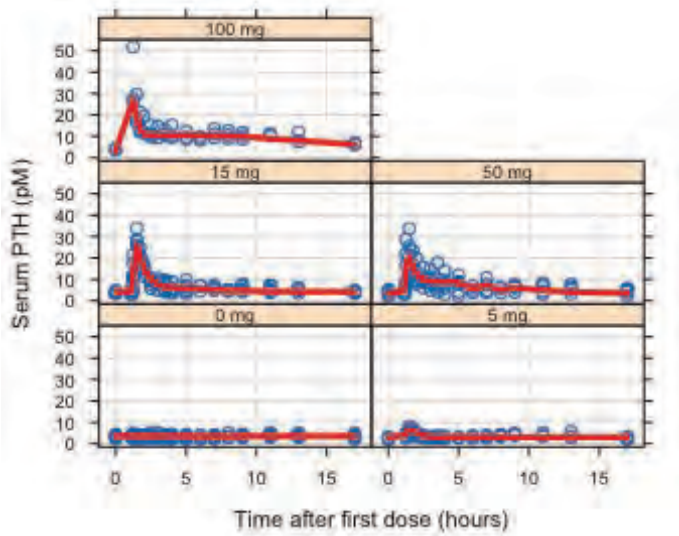

Observed (circles) and median MSPM-predicted (red line) serum PTH after single oral DS-9194b dose

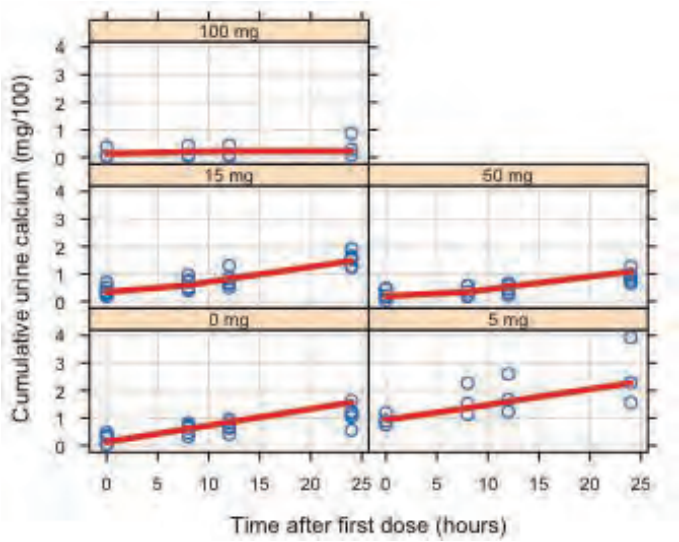

Observed (circles) and median predicted (red line) urine Ca following single-dose DS-9194b

***Disclosures: Kyle Baron**, Daiichi Sankyo, 2*
This study received funding from: Daiichi Sankyo

SU0408

Ecdysterone, a Main Component from Chinese Herb, Achyranthes Root, Prevents Glucocorticoid-induced Bone Loss by Preserving Osteogenesis and Osteocyte Autophagy. Weiwei Dai*[1], Evan Lay[2], Li Jiang[2], Sarah Amugongo[3], Nancy Lane[4], Wei Yao[4]. [1]Department of Biochemistry, Integrative Medicine Discipline, Shanghai University of Traditional Chinese Medicine, China, [2]UC Davis Medical Center, USA, [3]University of California, Davis, USA, [4]University of California, Davis Medical Center, USA

Introduction. Ecdysterone (Ecd), a main component from Chinese herb, achyranthes root (niu xi), is reported to have some beneficial effects on preserving trabecular bone and cartilage following ovariectomy (OVX) (Kapur et al., 2010). We previously demonstrated that glucocorticoids excess (GC) alters osteocyte cell viability through autophagy or apoptosis and that GC treatment dose-dependently alter gene expression for autophagy, an intracellular degradative mechanism to remove the dysfunctional organelles to keep the cells alive, or apoptosis. Lower GC dose (0.7-2.1mg/kg/d) activating autophagy, while higher dose (5.6mg/kg/d) decreased autophagy but increased apoptosis. The purpose of this study was to evaluate the effects of Ecd on osteogenesis, osteocyte viability (autophagy and apoptosis) and bone loss following GC excess.

Methods. Two-month-old male Swiss-Webster mice received either placebo (PL) or prednisolone (5.6mg/kg/d) and then treated immediately with Ecd (400μg sc 5x/wk) for three weeks. Trabecular bone volume and surface based bone turnover were measured at the distal femurs (DF), lumbar vertebral bodies (LVB) and mid-femoral shafts (FS) by μCT and bone histomorphometry. Osteocyte autophagy and apoptosis were measured at the LVB as well as on FS by western blotting.

Results. We first evaluated the effects of Ecd on osteogenesis in vitro found that Ecd stimulated mesenchymal stem cells towards osteogenesis. Trabecular bone volume (Tb, BV/TV) measured at the DF and LVB were 20% and 30% lower in GC – treated groups as compared to PL, which were accompanied by 30-50% lower mineralizing surface (MS/BS) and bone formation rate (BFR/BS). Cortical bone volume (Ct) was 20% lower in GC-treated mice with almost diminished bone formation at both the periosteal and endocortical surfaces. Ecd completely prevented the decreases in Tb BV/TV, BFR and partially prevented cortical bone loss by maintaining bone formation at the periosteal surface. GC reduced autophagic related protein (ATG-7, ATG-16L and LC3-II) expression by more than 50% and increase expression of caspase 3, corresponding to increased apoptosis. Ecd preserved osteocyte viability by preserving autophagy and preventing apoptosis.

Conclusion. Our data prompt the potential application of Ecd as a treatment option for preventing the detrimental effects of GC on bone via preservations of osteogenesis and osteocyte viability by maintaining the level of autophagy and bone formation.

***Disclosures: Weiwei Dai**, None.*

SU0409

Effect of Sclerostin Antibody on the Osteocyte in a Glucocorticoid -Induced Osteopenia. Zahra Achiou[1], Stephane Pallu[2], Hechmi Toumi[3], Michael Ominsky[4], Hugues Portier[3], Eric Lespessailles*[5], Claude Laurent Benhamou[6]. [1]EA4708 I3MTO Université d'Orleans, France, [2]EA 4708 - I3MTO Orléans, France, [3]EA4708 I3MTO University of Orleans, France, [4]Amgen Inc., USA, [5]Centre Hospitalier Regional, France, [6]CHR ORLEANS, France

INTRODUCTION: Glucocorticoid-induced bone loss is characterized by decreased bone formation and promotion of osteocyte apoptosis. We have previously demonstrated that modulation of the Wnt signaling pathway using the administration of a sclerostin neutralizing monoclonal antibody (Scl-Ab) prevented deleterious microarchitectural bone changes and limited osteocyte apoptosis in a rodent glucocorticoid-induced osteopenia model (GIO). In the current study, we further investigated the effects of the Scl-Ab on the osteocyte in this animal GIO model to assess possible effects on gene expression, lacunar area and occupancy. METHODS: Thirty male Wistar rats, 4 month-old, were randomly assigned to 3 groups. (C) control group subcutaneously injected 5 days a week with vehicle, (M) group subcutaneously injected 5 days a week with 5 mg/kg methylprednisolone and (M+S) group injected with both methylprednisolone and Scl-Ab (Scl-AbVI, 25 mg/kg/day, 2 days a week) for 9 weeks. Twenty out of the 30 rats (C, n=6; M, n=7; M+S, n=7) were randomly selected for analysis. Decalcified, 1μm thick tibia diaphyseal sections were stained with Toluidine blue, and lacunar density (number per mm^2), lacunar area (area per lacuna in μm^2), and osteocyte lacunar occupancy (% of total lacunae) were calculated. RESULTS: Between the groups, there were no significant differences in mean lacunar area (ranged from 28.5 $\pm$ 2.4 to 34.6 $\pm$ 3.6 μm^2) or mean lacunar density (ranged from 634 $\pm$ 37 to 660 $\pm$ 63 /mm^2). Methylprednisolone caused a significant decrease in osteocyte lacunar occupancy (42% $\pm$ 3.8 vs 53 $\pm$ 4.1 % for C group), that was prevented by coadministration of Scl-Ab (60% $\pm$ 3.2 M+S vs 42 % $\pm$ 3.8 for M group). These changes in lacunar occupancy were inversely correlated with the fractional number of apoptotic osteocytes previously reported ($r = -0.74$; $p=0.001$). CONCLUSION: These data have shown that Scl-Ab prevents the decrease in osteocyte lacunar occupancy and the increase in osteocyte apoptosis caused by methylprednisolone treatment in rats, suggesting an improvement in osteocyte viability.

Keywords: Osteocyte, Glucocorticoid, Osteopenia, Sclerostin antibody

***Disclosures: Eric Lespessailles**, None.*

SU0410

Parathyroid hormone improves skeletal status of rats with type 2 diabetes mellitus. Christine Hamann*[1], Ann-Kristin Picke[2], Graeme Campbell[3], Martina Rauner[4], Ricardo Bernhardt[5], Claus-C Glueer[3], Gerd Huber[6], Klaus-Peter Günther[1], Michael Morlock[6], Lorenz Hofbauer[2]. [1]Dresden Technical University Medical Center, Germany, [2]Dresden University Medical Center, Germany, [3]Christian-Albrechts Universität zu Kiel, Germany, [4]Medical Faculty of the TU Dresden, Germany, [5]Technische Universität Dresden, Germany, [6]Institute of Biomechanics, Hamburg University of Technology, Germany

The pathogenesis of low bone mass and increased skeletal fragility in diabetes mellitus is unclear, and efficient therapies are limited. ZDF rats with type 2 diabetes mellitus display low bone mass and delayed bone defect healing due to impaired osteoblast function. We tested the hypothesis whether human parathyroid hormone (PTH 1-84) increases bone mass, strength and defect regeneration in diabetic rats. A subcritical femoral defect was created in 11 weeks old diabetic ZDF (fa/fa) and non-diabetic ZDF (+/+) rats. PTH (75 µg/kg) or vehicle was administered subcutaneously five days per week over 12 weeks. The non-operated femur, the lumbar vertebra, and the filling of the femur gap were analyzed by µCT. Three-point bending was performed at the mid-diaphysis of the non-operated femora. In addition, dynamic histomorphometry and serum markers of bone turnover were analyzed. µCT analysis of the femur revealed asignificant reduction in distal metaphyseal BV/TV (-50%) and tBMD (-41%), as well as mid-diaphyseal Ct.Th (-16%) and MOI (-16%) in the untreated diabetic group compared to the control. Treatment with PTH resulted in 59% higher BV/TV and 36% higher tBMD in the diabetic animals, but had no effect on Ct.Th, cBMD or MOI. The diabetic rats showed a significant reduction in extrinsic stiffness (-17%), yield (30%) and ultimate load (-23%), work to yield (-38%), and failure (-23%). PTH treatment improved the work to failure (+28%) and modulus of toughness (+28%) in the wild-type, but not in diabetic rats. While non-diabetic rats filled 63% of the femoral defect, diabetic rats filled only 31%. PTH-treatment increased defect regeneration in the diabetic and non-diabetic groups by 11% and 12%, respectively. Dynamic histomorphometry of the lumbar spine demonstrated an increased BFR by 55% (diabetic rats) to 230% (non-diabetic rats) in response to PTH treatment. Intermittent PTH treatment resulted in increased serum levels of osteocalcin by 33% and 10% in diabetic and non-diabetic animals, respectively, and lower serum levels of CTX (-49% and -19%), consistent with a marked bone-anabolic effect. In conclusion, intermittent PTH therapy is capable of reversing the adverse effects of type 2 diabetes mellitus on bone mass and delayed bone defect regeneration in rats.

***Disclosures: Christine Hamann**, None.*
This study received funding from: Nycomed

SU0411

Retreatment With Sclerostin Antibody Increased Bone Formation and Bone Mass in Ovariectomized Rats. Xiaodong Li*, Kelly S Warmington, Qing-Tian Niu, Denise Dwyer, Chun-Ya Han, Marina Stolina, Andreas Grauer, Hua Zhu Ke. Amgen, Inc., USA

Treatment with sclerostin antibody (Scl-Ab) resulted in transient increases in bone formation markers and sustained decreases in bone resorption markers, leading to substantial bone mass gains. Here we explored the effects of Scl-Ab retreatment on bone formation and bone mass in ovariectomized (OVX) rats after an initial treatment and withdrawal phase.

Seven-month-old OVX rats (11 wks post-OVX) were treated with vehicle (Veh) or Scl-Ab (Scl-Ab VI, 5 mg/kg, SC, 2x/wk) for 12 wks (initial treatment), followed by treatment with Veh for 12 wks (withdrawal). Thereafter, 1 group of Scl-Ab-treated OVX rats received Scl-Ab and the other group received Veh for 6 wks (n=8/group, retreatment). All groups were evaluated for serum P1NP and BMD. In addition, bone histomorphometry was evaluated in Veh- and Scl-Ab-treated OVX rats at wks 6, 12, 24, and 30 (n=8/group).

During the initial treatment phase, P1NP increased significantly in the Scl-Ab group at wks 2 and 4 and gradually returned to OVX control levels at wk 10; it then remained at OVX control levels during the withdrawal phase (through wk 24). During the retreatment phase, Scl-Ab treatment resulted in increases in P1NP comparable to those observed after the initial treatment. Lumbar spine BMD increased continuously throughout Scl-Ab treatment and peaked at wk 14, 2 wks after withdrawal, gradually returning to sham control levels at wk 24 (Figure). After 6 wks of retreatment, BMD had significantly increased again to the peak level initially observed at wk 14. Trabecular (Tb), endocortical (Ec), and periosteal (Ps) bone formation rate (BFR/BS) peaked at wk 6 in the Scl-Ab group and then returned to OVX controls at wk 24, but Tb and Ec BFR/BS were significantly greater in the Scl-Ab group than OVX controls at wk 12. During the retreatment phase, the increases in Tb and Ec BFR/BS with Scl-Ab retreatment were similar to those following initial treatment; there were significant increases in Ps BFR/BS. For Tb and Ec eroded surface (ES/BS), similar decreases were observed in the Scl-Ab group compared with Veh during initial and retreatment phases. After treatment withdrawal, Tb ES/BS increased to levels above OVX controls and Ec ES/BS returned to OVX control levels.

In conclusion, Scl-Ab retreatment reproducibly increased bone formation and BMD, and decreased bone resorption, as seen during initial treatment in OVX rats. These results suggest that retreatment with Scl-Ab could be a viable way to increase bone mass.

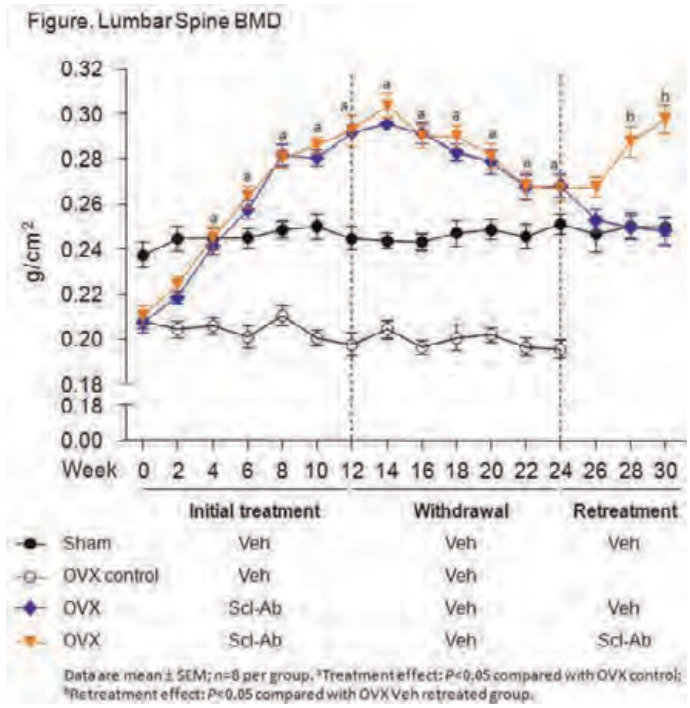

Figure. Lumbar Spine BMD

***Disclosures: Xiaodong Li**, Amgen, 7; Amgen, 3*
This study received funding from: Amgen Inc. and UCB Pharma

SU0412

Romosozumab (Sclerostin Antibody) Improves Bone Mass and Bone Strength in Ovariectomized Rats After 12 Months of Treatment. Michael S Ominsky*[1], Aurore Varela[2], Susan Y Smith[2], Elisabeth Lesage[2], Sabina Buntich[1], Rogely W Boyce[1]. [1]Amgen, Inc, USA, [2]Charles River Laboratories, Canada

Romosozumab, a sclerostin antibody, is a bone-forming agent under clinical investigation for the treatment of osteoporosis. To examine the effects of romosozumab on bone quality over the duration of proposed clinical treatment, bone mass and strength were assessed at cortical and cancellous sites in ovariectomized (OVX) rats treated for 12 months.

Six-month old SD rats were OVX and, beginning at 8 months of age, treated with weekly subcutaneous injections of either vehicle (Veh), or 3, 10, or 50 mg/kg romosozumab (n=10-15/group) for 12 months; a Sham control group treated with Veh was also included. Bone mass was evaluated in vivo by DXA and pQCT, and ex vivo by pQCT and microCT after termination at month 12. Bone strength was assessed at the femur midshaft (in 3pt bending), femur neck (in shear), and L4 and L5 vertebra (in compression).

Bone mass was dose-dependently increased throughout the skeleton, with DXA BMD increases >40% over baseline at the lumbar spine and whole femur at the 50 mg/kg/wk dose. At the tibia diaphysis, cortical thickness was significantly increased by pQCT at all doses compared to OVX controls, due to geometric changes on both periosteal and endocortical surfaces. Romosozumab also resulted in significant increases in ex vivo bone area and bone strength parameters at the femur midshaft, femur neck, and lumbar vertebra at all doses tested. Peak load was significantly dose-dependently increased by romosozumab at the femur midshaft (41-121%), femur neck (33-46%), and lumbar vertebra (150-268%) (all doses/sites $P<0.05$ vs Veh). These improvements correlated positively with the bone mass at these sites, with r^2 values of 0.92, 0.41, and 0.94 at the femur shaft, femur neck, and lumbar vertebra, respectively, across groups. Material properties calculated at the femur shaft suggested that romosozumab improved ultimate strength and toughness while elastic modulus remained unaffected by treatment.

These data demonstrate that 12 months of romosozumab treatment in OVX rats resulted in marked improvements in bone mass, cortical geometry, and bone strength. Bone quality assessment by regression analysis and calculated material properties demonstrated that long-term romosozumab treatment resulted in bone matrix that had normal-to-improved bone strength. These results support the bone efficacy and safety profile of romosozumab and suggest that treatment-related improvements in BMD should yield greater bone strength in patients with osteoporosis.

***Disclosures: Michael S Ominsky**, Amgen, 7; Amgen, 3*
This study received funding from: Amgen Inc. and UCB Pharma

SU0413

Sclerostin-Antibody is More Effective Than Dkk1-Antibody for Augmenting Bone Mass in Adult Rice Rats. Carley Trcalek*[1], Jose Aguirre[1], Kathleen Neuville[1], Donald Kimmel[2], Thomas Wronski[1]. [1]University of Florida, USA, [2]Kimmel Consulting Services, USA

Sclerostin (Scl) and Dickkopf-1 (Dkk1) are well known antagonists of Wnt signaling, which results in negative regulation of bone formation. Therefore, treatment with neutralizing antibodies to inhibit Scl (Scl-Ab) and Dkk1 (Dkk1-Ab) is thought to be a promising approach for increasing bone mass in osteoporotic patients. The purpose of this study is to compare the effects of monotherapy with Scl-Ab or Dkk1-Ab on bone mass in adult rats.The experimental animals were rice rats (*Orozomys palustris*), which are more genetically diverse than conventional outbred strains of rats used for biomedical research. At 22 weeks of age, groups of male rice rats (N=10-12) were treated SC twice weekly with vehicle, Scl-Ab, or Dkk1-Ab at a dose of 25 mg/kg for 8 weeks. At 30 weeks of age, the left tibia and femur were collected from each rat for bone histomorphometric and pQCT analyses, respectively. Due to high variability of bone parameters in rice rats, some data were not normally distributed, and the nonparametric Kruskal Wallis test was used for statistical comparisons. Data are expressed as the mean ± SEM.Treatment of rice rats with the Scl-Ab or Dkk1-Ab for 8 weeks did not affect body weight. In comparison to vehicle-treated rats, cancellous bone volume in the proximal tibial metaphysis was significantly increased by nearly 3-fold in Scl-Ab-treated rats (4.2 ± 1.8% vs. 12.1 ± 3.1%, $P<0.05$), but not by treatment with the Dkk1-Ab (4.2 ± 1.2%). This augmentation of cancellous bone mass in rats treated with the Scl-Ab was associated primarily with increased trabecular width (23.4 ± 2.0 μm vs. 42.0 ± 4.0 μm, $P<0.001$) rather than increased trabecular number. Compared to vehicle-treated rats, osteoblast surface was increased by at least 50% in rats treated with Scl-Ab or Dkk1-Ab, but these trends indicative of increased cancellous bone formation did not achieve statistical significance. In the distal femoral metaphysis, pQCT analyses revealed that total BMD was significantly increased in Scl-Ab-treated rats (657.6 ± 32.5 mg/cm^3, $P<0.02$) compared to both vehicle-treated rats (556.5 ± 33.0 mg/cm^3) and Dkk1-Ab-treated rats (541.7 ± 17.0 mg/cm^3). In the femoral diaphysis, cortical thickness was significantly increased in Scl-Ab-treated rats compared to both vehicle-treated rats (0.63 ± 0.01 mm vs. 0.55 ± 0.02 mm, $P<0.001$) and Dkk1-Ab-treated rats (0.59 ± 0.01 mm, $P<0.02$). These findings indicate that, in genetically diverse adult rice rats, the Scl-Ab was more effective than the Dkk1-Ab for augmentation of bone mass.

***Disclosures: Carley Trcalek**, None.*
This study received funding from: Amgen Inc.

SU0414

Combination Therapy with Ibandronate and Eldecalcitol Enhances Bone Strength via Elevation of BMD in Aged Ovariectomized Rats. Sadaoki Sakai*[1], Satoshi Takeda[1], Masanori Sugimoto[2], Masaru Shimizu[3], Koichi Endo[3]. [1]Chugai Pharmaceutical Co., Ltd., Japan, [2]Molecular Function & Pharmacology Laboratories, Taisho Pharmaceutical Co., Ltd, Japan, [3]Chugai Pharmaceutical Co., Ltd., Japan

Ibandronate [IBN; 1-hydroxy-3-(methylpentylamino)-propylidene bisphosphonate] is an intravenously injected anti-osteoporosis medicine. Eldecalcitol [ED-71, ELD; 1α,25-dihydroxy-2β-(3-hydroxypropyloxy) vitamin D_3], an active vitamin D_3 derivative, is superior to alfacalcidol, a prodrug of active vitamin D_3, in preventing bone fractures in postmenopausal osteoporotic patients. However, there are no reports on the effects of combined IBN and ELD treatment for osteoporosis.

In this study, we examined the effects of combination treatment with IBN and ELD on the lumbar vertebrae and femur in aged ovariectomized rats. Eight-month-old Wistar-Imamichi rats were ovariectomized and treated for 12 weeks with either vehicle, IBN (3 μg/kg/month, s.c., monthly), ELD (15 ng/kg/day, p.o., daily), or a combination of IBN and ELD. Serum and urine were collected every 4 weeks. BMD and bone strength of the lumbar vertebrae and femur were measured after 12 weeks of treatment.

Urinary deoxypyridinoline (DPD), a bone resorption marker, was significantly reduced in each monotherapy group. The combination therapy group showed further decreases in DPD compared to each monotherapy group at 4, 8, and 12 weeks of treatment. Osteocalcin, a bone formation marker, in each of the 3 therapy groups was not lower than the level in the sham group throughout the experimental period.

Lumbar (L2–L4) BMD after 12 weeks was significantly higher in the IBN and ELD monotherapy groups than in the vehicle control group, and BMD was higher in the combination group than in either monotherapy group. A compression test showed the mechanical strength of L5 was improved in each monotherapy group and in the combination group compared with the vehicle control group. The maximum load was higher in the combination group than in the IBN monotherapy group. BMD of the proximal, middle, and distal femur was increased in the IBN and ELD monotherapy groups, and was significantly higher in the combination therapy group than in either monotherapy group. In the 3-point bending test, the maximum load of the femur was slightly, but not significantly, higher in each monotherapy group than in the vehicle control group and was significantly higher in the combination therapy group.

5This study demonstrates the additive effect of IBN and ELD combination therapy on the mechanical strength of the lumbar vertebrae and femur. This effect may be induced by increased BMD via reduction of bone resorption without suppression of bone formation.

***Disclosures: Sadaoki Sakai**, Chugai Pharmaceutical Co., Ltd., 3*

SU0415

Effects of Odanacatib on Early and Late Stage Fracture Healing in an Adult Rabbit Radial Osteotomy Model. Tara Cusick*[1], Rana Samadfam[2], Le Thi Duong[3]. [1]Merck & Co., Inc., USA, [2]Charles River Laboratories, Canada, [3]Merck Research Laboratories, USA

Cathepsin K (CatK), a lysosomal cysteine protease highly expressed by osteoclasts, degrades de-mineralized bone matrix proteins. Odanacatib (ODN) is an orally active and reversible CatK inhibitor in development for the treatment of postmenopausal osteoporosis. Fracture (Fx) healing is a complex process that involves both bone resorption and formation. Various preclinical models of skeletal repair have evaluated agents that alter these processes. Here, we characterized effects of ODN on Fx repair in the rabbit radial osteotomy model during the reparative (6wks) and remodeling (25wks) phases. Skeletally-mature female rabbits (n=150, 6 mo-old) were randomized by radii/ulnae DXA-based aBMD into four groups and pretreated for 12wks prior to radial osteotomy with: vehicle (Veh), ODN in food at ~ 1.7-fold (1.5mg/kg/d or 12μM-24hr) and 7-fold clinical exposure (6mg/kg/d or 50μM-24hr), or alendronate (ALN, 0.3mg/kg/wk, sc). The ALN dose was previously shown to fully prevent bone loss in ovariectomized rabbit. Post-surgery, ODN groups were further divided into continued (ODN/ODN) or discontinued (ODN/Veh) groups and maintained on the same treatment for an additional 6 or 25wks. Study endpoints included longitudinal radiography, histopathology, pQCT and biomechanical testing. Rates of radiographic healing among all groups were comparable based on callus initiation (p=0.20), radiographic bridging (p=0.80) and radiographic union (p=0.41). Histopathology of the Fx callus in ODN/ODN, ODN/Veh, ALN groups were not different from that in Veh. ODN/ODN and ALN increased pQCT-based total vBMD at 6wks (9-10%, $p<0.01$) and 25wks (26-33%, $p<0.001$) without altering total callus area vs Veh. Moreover, ODN/ODN enhanced mature (mineralized) callus vBMC by 15-18% ($p<0.05$) at 6 wks and 49-69% ($p<0.01$) at 25wks vs Veh. Mature callus vBMC in the ALN group was unaltered at 6wks and increased 9-18% ($p<0.05$) at 25wks vs Veh. Biomechanical tests of fractured and intact radii in all treatment groups at 6wks were not different from Veh. However, at 25wks, while peak load across the healing sites in ODN/Veh and ALN groups were the same as that in Veh, peak load in ODN/ODN groups increased by 18% (1.5mg/kg, p=0.11) and 25% (6mg/kg, $p<0.05$), reaching intact contralateral levels. Taken together, in the rabbit radial osteotomy model of fracture repair, ODN treatment did not delay fracture union and callus remodeling while at the same time tended to improve callus mineralization and strength.

***Disclosures: Tara Cusick**, Merck & Co., 3*
This study received funding from: Merck & Co.

SU0416

Introduction of a New Class of Cathepsin K Inhibitor with Peptidomimetic Structure, SI-591. Toshiaki Fujii*, Yoshitaka TANAKA. SEIKAGAKU CORPORATION, Japan

We have synthesized and developed a series of unique peptidomimetic compounds with hydrophilic and neutral properties, which potently inhibit the activity of the lysosomal cysteine protease, cathepsin K. SI-591 is a prototype compound in this chemical class and possesses a superior pharmacological activity *in vitro* and *in vivo* with orally bioavailable characteristics.

In an enzyme inhibition assay, SI-591 inhibited human cathepsin K with an IC_{50} value of 1.4 nM, which was 8- to 320-fold more selective for cathepsin K than other members of the human cathepsins.

In an *in vitro* assay, osteoclast-like cells were cultured with various doses of SI-591 on dentin slices in the presence of RANKL and M-CSF for 6 days. The C-terminal cross-linking telopeptide of Type I collagen (CTX-I) released into the culture medium was measured as a bone resorption marker. Resorption pits formed on the slices were stained with Mayer's hematoxylin. SI-591 (0.01-10 μM) dose-dependently inhibited the release of CTX-I and significantly decreased the formation of the resorption pits.

To study the preventative effects of SI-591 on the ovariectomized (OVX) rat as a model of postmenopausal osteoporosis, adult female F344 rats underwent OVX surgery and were treated with a vehicle or SI-591 (0.26-10 mg/kg p.o., b.i.d.) for 4 weeks from the day following surgery. SI-591 dose-dependently inhibited urinary CTX-I release and prevented bone mineral density (BMD) loss at the lumbar vertebrae and femur. To further investigate the therapeutic effect of SI-591, OVX rats were treated with a vehicle or SI-591 (4-25 mg/kg p.o., b.i.d.) for 12 weeks from 12 weeks following surgery. SI-591 dose-dependently inhibited urinary deoxypyridinoline release and prevented BMD loss in the lumbar vertebrae and femur. In addition, to evaluate the long-term preventive effects of SI-591 on the OVX model, cynomolgus monkeys (aged 9-16 years) underwent OVX surgery and were treated with a vehicle or SI-591 (4-36 mg/kg p.o. b.i.d.) for 6 months from the day following surgery. SI-591 inhibited the urinary N-terminal cross-linking telopeptide of type I collagen (NTX) release and prevented BMD loss in the lumbar vertebrae and the body as a whole.SI-591 remarkably prevented bone resorption in *in vitro* and *in vivo* assays.

In conclusion, our results support that our second generation cathepsin K inhibitor, SI-591, may have a therapeutic potential in the treatment of postmenopausal osteoporosis.

***Disclosures: Toshiaki Fujii**, None.*

SU0417

Treatment with Odanacatib Increases Bone Mass and Maintains Normal Biomechanical Properties in Orchidectomized Male Rabbits. Brenda Pennypacker*[1], Charles Chen[2], Tara Cusick[2], Rana Samadfam[3], Le Thi Duong[1]. [1]Merck Research Laboratories, USA, [2]Merck & Co., Inc., USA, [3]Charles River Laboratories, Canada

Odanacatib (ODN) is a selective Cathepsin K (CatK) inhibitor in development for the treatment of postmenopausal osteoporosis. We evaluated the effects of long-term ODN treatment on bone quality in the lumbar vertebrae (LV) and femur of orchidectomized (ORX) male rabbits, a model of male osteoporosis. Adult male rabbits (age 11 mo.) were sham-operated (N=20) or ORX (N=24/group) for 7.5 months prior to the start of treatment. ORX rabbits were randomized by LV BMD into the following treatment groups: vehicle (Veh), ODN (1.5 or 6mg/kg/d, in food), or alendronate (ALN) (300μg/kg/wk, sc) for 14 mo. *Ex vivo* endpoints included DXA- and pQCT-based BMC and BMD and strength testing. ORX resulted in ~9% bone loss in LV3-4 aBMD vs. Sham ($p<0.01$). ODN dose-dependently increased LV aBMD by 21% and 26%, respectively ($p<0.001$), compared to ALN (9.9%, $p<0.01$) vs. Veh. pQCT-based LV5-6 trabecular (Tb) vBMC and vBMD were increased in ODN groups (up to 88%, $p<0.001$) vs. Veh. Similarly, ALN increased Tb.vBMC and BMD by 11% and 8% ($p<0.05$ for both), respectively. ODN at both doses increased Tb thickness (32-51%, $p<0.001$). Significant increases in strength parameters (peak load, apparent strength, yield load, and yield stress, stiffness) of LV5-6 were noted for the comparison between ALN to Veh and ODN to Veh or Sham. From compression testing of LV, peak load from all groups was positively correlated with pQCT-vBMC ($R=0.9383$, $p<0.001$). ODN also dose-dependently increased aBMD of the total hip and distal femur, but did not change central femur (CF) aBMD compared to Veh. However, ODN 6 mg/kg increased cortical thickness and area by ~7% ($p<0.01$), and reduced endocortical perimeter by 4% ($p<0.05$) vs. Veh. ODN-treated CF trended to have higher peak load and significant increases in work-to-failure (25%, $p<0.05$) and toughness (29%, $p<0.01$) vs. Veh. No significant changes in biomechanical parameters of CF were noted in the ALN group. CF peak load vs. pQCT-vBMC was highly correlated ($R=0.7555$, $p<0.001$). Taken together, ODN treatment for 14 months increased bone mass and strength in the lumbar spine to levels above Veh and Sham, as well as maintaining biomechanical properties at femoral sites of ORX male rabbits. These findings support the clinical evaluation of the CatK inhibitor ODN for the treatment of osteoporosis in men.

***Disclosures: Brenda Pennypacker**, Merck and Co., 3*

SU0418

Effects of Fructus Ligustri Lucidi Extract and Its Fractions on Renal Calcium Reabsorption and Trabecular Bone Structure in Type 1 Diabetic Mice. Yan Zhang*[1], Teng-Yue Diao[2], Man-Sau Wong[1]. [1]The Hong Kong Polytechnic University, Hong Kong, [2]University of Shanghai for Science & Technology, China

Our previous study demonstrated that the alterations of vitamin D metabolic enzymes expression and the increase in urinary Ca excretion as a result of the decrease in renal Ca transporters expression contributed to the deteriorations of bone properties in type 1 diabetic mice. Our previous study indicated that Fructus Ligustri Lucidi (FLL), one of kidney-tonifying herbs, could improve Ca balance in mature and aged rats through its ability to modulate circulating levels of calciotropic hormones as well as intestinal Ca absorption and renal Ca wasting. This study was conducted to determine if FLL exert the beneficial effects on bone health via its actions on calcium homeostasis in type 1 diabetic mice induced by streptozotocin (STZ). The diabetic dba/2J mice after 1 week of STZ injection were divided into 4 groups with 8 mice in each group, and treated with vehicle (DOP, diabetic osteoporosis), ethanol extract of FLL (EF), ethyl acetate-soluble fraction of EF (EA), and water-soluble fraction of EF (WF) for 6 weeks on a medium-Ca diet (0.6% Ca), and one additional group without any treatment was used as non-diabetic control. There was no statistical difference of serum Ca level among groups, while, EA and WF could both increase serum parathyroid hormone level ($P < 0.05$). Compared to normal control, the urinary Ca level climbed up significantly in DOP group ($P < 0.01$), and EF, EA and WF could effectively reversed the high urinary excretion to the normal level. EF and EA could up-regulate renal 25-hydroxyvitamin D-1a-hydroxylase mRNA expression, in contrary, WE could down-regulate the mRNA expression of 25-hydroxyvitamin D-24-hydroxylase (24-OHase) and calcium-sensing receptor (CaSR) in kidney of DOP mice. Micro-CT analysis of trabecular bone parameters at tibial proximal metaphysis showed that WF could markedly inhibit the decrease in trabecular bone number and connectivity density and the increase in trabecular bone separation. However, the improvement of EF and EA on trabecular bone properties was not statistically different as compared to those of DOP mice. Therefore, our present study suggested that the biological targets, including renal 24-OHase and CaSR, might, at least partially, contribute to the improvement of urine Ca excretion and bone loss in WF group, and this underlying mechanism might be different from those of EF and EA on diabetic mice.

***Disclosures: Yan Zhang**, None.*

SU0419

Prevention and Restoration of Bone Loss by n-3 fatty acids in an Ovariectomized Mouse Model. Jameela Banu*[1], Gabriel Fernandes[2]. [1]University of Texas-Pan American, USA, [2]University of Texas Health Science Centre, USA

Recently, there have been many reports about the benefits of n-3 fatty acids (n-3 FA) on bone. n-3 FA decrease bone resorption and protect bone from ovariectomized bone loss in preclinical studies. However, there is very little information on the preventive and restorative properties of n-3 FA on bone. We used a mouse model to determine if n-3 FA are more beneficial as preventive agents or can restore bone loss after established bone loss.

Two experiments were conducted. Experiment 1 – Prevention studies. Ten months old, C57BL/6, retired breeder mice were started on a diet regimen containing lab chow (LC) or fish oil (FO) for 3 months before they were either ovariectomized or sham operated. The different groups were: Group 1. LC sham (LC S); Group 2. LC ovariectomized (LC O); Group 3. FO sham (FO S); Group 4. FO ovariectomized (FO O). Mice were fed LC or 10% FO respectively and maintained in the respective diet regimens for another 3 months and sacrificed. The long bones were subjected to micro-architectural analyses. Experiment 2 – Restoration studies. Ten months old, C57BL/6, retired breeder mice were either sham operated or ovariectomized and left for 3 months. The different groups were: Group 1. LC S; Group 2. LC O; Group 3. FO S; Grouop 4. FO O. Mice were fed either LC or FO (10%). The LC and FO fed groups were kept in the respective diet regimens for the next 3 months, at the end of which they were sacrificed. Long bones were subjected to micro-architectural analyses.

Experiment 1: In the DFM, ovariectomy caused significant decreases in the trabecular thickness (Tb Th) and trabecular width (Tb W) and FO prevented this decrease. Trabecular number (Tb N) increased in sham and ovariectomized mice fed FO. Trabecular separation (Tb Sp) increased in the ovariectomized mice (LC and FO) and FO decreased this to a lesser extent. In the PTM, however, FO did not protect trabecular bone.

Experiment 2: In the DFM, there were significant decreases in Tb N and Tb Th of LC O mice, compared to LC S mice. FO O mice had significantly higher Tb N and Tb Th compared to those of LC O. Tb W decreased in the LC O mice by 14% and by 4% in the FO O compared to the respective sham mice. Tb Sp increased only in the LC O, not in the FO O compared to their respective shams. In the PTM, again there was no effect of FO.

In conclusion, FO could prevent and restore trabecular bone in the DFM and did not have any effect on the PTM in a rodent model for bone loss.

***Disclosures: Jameela Banu**, None.*

SU0420

Eldecalcitol Increases Bone Mineral Density and Improves Trabecular Structure and Biomechanical Properties of the Lumbar Spine in Streptozotocin-Induced Diabetic Rats. Satoshi Takeda*, Sadaoki Sakai, Koichi Endo. Chugai Pharmaceutical Co., Ltd., Japan

It is well known that type 1 diabetes mellitus (DM) increases the risk of fragility fractures owing to low bone mineral density (BMD) and deteriorated bone quality. Eldecalcitol (ELD), an active vitamin D_3 analog, is reported to reduce the risk of fractures in osteoporotic patients; however the effects of ELD on fragility fractures in DM patients have not been fully examined. In the present study, we evaluated the efficacy of ELD on bone metabolism including biomechanical properties of lumbar spine in type 1 DM rats.

Male Sprague-Dawley rats (12-weeks old) were injected intravenously with streptozotocin (STZ) (35 mg/kg). From 1 week after STZ injection, ELD (10, 20 and 40 ng/kg) was administered orally 5 times a week for 12 weeks. Urinary deoxypyridinolin (DPD) and serum osteocalcin (OC) were measured every 4 weeks after ELD treatment began. After 12 weeks of treatment, lumbar (L2-L4) BMD and biomechanical properties of the L5 vertebra were assessed, and bone histomorphometry was performed using the L3 vertebra.

DM was confirmed by the development of hyperglycemia (blood glucose >250 mg/dL) after 1 week of STZ injection. After 12 weeks of treatment, blood glucose levels in the ELD-treated groups were not significantly different from those in the disease control (DC) group. In the DC group, urinary DPD tended to increase, while serum OC significantly decreased compared with that in the normal control group during the treatment period. ELD decreased urinary DPD in all doses but did not change serum OC. ELD inhibited the decrease in lumbar BMD observed in the DC group. Although DM induced a significant reduction in bone volume at the L3 vertebra, accompanied by a decrease in trabecular thickness and an increase in trabecular separation, ELD improved this deterioration in trabecular architecture. In the compression test of the L5 vertebral body, max load, stiffness and ultimate stress decreased in the DC group, and ELD improved max load and ultimate stress. These results suggested that treatment with ELD increased lumbar BMD and improved trabecular architecture, resulting in an increase in biomechanical strength of lumbar vertebra in type 1 DM rats. ELD may be useful in preventing vertebral fragility fractures in DM patients.

***Disclosures: Satoshi Takeda**, Chugai Pharmaceutical Co.,Ltd., 3*

SU0421

High prevalence of vitamin D insufficiency in older community people: the role of season, diabetes, parathormone, female gender and age. The Sao Paulo Ageing & Healthy Study (SPAH). Camille Figueiredo*[1], Jaqueline Lopes[2], Georgea Fernandes[1], Liliam Takayama[3], Valeria Caparbo[3], Rosa Pereira[4]. [1]Hospital das Clinicas da Faculdade de Medicina da USP, Brazil, [2]Hospital das Clínicas da FMUSP, Brazil, [3]Faculdade de Medicina da USP, Brazil, [4]Faculdade de Medicina da Universidade de São Paulo, Brazil

Purpose: To estimate the prevalence and analyze the risk factors associate to hydroxyvitamin D insufficiency (25OHD< 20ng/mL) in community-dwelling older people.

Methods: This cross sectional study included 750 (506 women and 244 men) older subjects (> 65 years old) living in São Paulo, Brazil. The serum concentration of 25-hydroxyvitamin D was measured using a radioimmunoassay technique. Anthropometrical data and information about lifestyle habits, physical activity and comorbities were obtained. Bone mineral density (BMD) was measured by DXA. Other laboratory tests were also determined. Multiple logistic regression models were designed 25OHD<20ng/mL as the dependent variable and all other parameters as the independent ones.

Results: The prevalence of 25OHD<20ng/mL was of 57.9% (95% CI 54.4 - 61.4). The main factors associated with 25OHD<20ng/mL were age, body mass index, female gender, diabetes, season (winter/spring), alkaline phosphatase, phosphorus, intact parathormone (iPTH), creatinine clearance and Total femur T-score. After adjustment for these variables, the logistic regression analyses revealed that age (OR = 1.04, 95%CI 1.01 - 1.07, p = 0.024), iPTH (OR = 1.01; 95% CI 1.01 – 1.02; p = 0.003), female gender (OR = 1.45; 95% CI 1.06 – 2.0; p = 0.020), diabetes (OR = 1.84; 95%CI 1.23–2.76; p = 0.003), and season (winter/spring) (OR = 3.63, 95% CI 2.65 - 4.97; p<0.001) remains as independent factors for 25OHD<20ng/mL.

Conclusions: Our results suggest that the vitamin D insufficiency is common in Brazilian community-dwelling older and age, iPTH, female gender, diabetes and season (winter/spring) are major risk factors associated. The clinical use of these parameters can be help to design and target appropriate interventions in the public health for vitamin D insufficiency in older population.

***Disclosures: Camille Figueiredo**, None.*

SU0422

12/15-LO But Not 5-LO is Critical For Denervation-Induced Bone Loss In Mice. Md Rahman*, Arunabh Bhattacharya, Sabia Marian, Rasel Mohiuddin, Amanda Jernigan, Holly Van Remmen. University of Texas Health Science Center, USA

Unloading or skeletal immobilization-induced osteoporosis is a critical issue in paralyzed, bed-ridden patients and astronauts. Skeletal immobilization or disuse induces bone loss resulting from increased bone resorption and decreased bone formation. However, a rapid surge in bone resorption due to significant increase in the number of osteoclasts is considered to be the key reason in skeletal immobilization associated bone loss. Unloading bone loss can be induced in animals by denervation of sciatic nerve. This study examines the role of 5- and 12/15-lipoxygenase (LO) lipid metabolic pathways in denervation-induced bone loss. In the left leg, surgical sciatic nerve transection was performed in 6 month old wild-type, *12/15-LO*$^{-/-}$ and *5-LO*$^{-/-}$ male mice. In addition, wild-type mice were injected with either vehicle control or 12/15-LO specific inhibitors, PD146176, and Baicalein or 5-LO specific inhibitor, Zileuton (4 mg/kg, i.p.) in mice subjected to nerve transection. Tibias were collected 7 days post-denervation and analyzed by dual energy x-ray absorptiometry (DXA). Wild-type mice exhibited significant bone loss in the denervated leg as compared to contralateral control leg. While 12/15-LO$^{-/-}$ mice and both 12/15-LO inhibitors treated wild-type mice were protected against denervation-induced bone loss, genetic or pharmacological inhibition of 5-LO did not confer any protection against denervation-induced bone loss. These data indicate a specific role for 12/15-LO and its downstream mediators in denervation-induced bone loss. Our *in vitro* study in RAW264.7 cell and bone marrow cell cultures subjected to osteoclast differentiation (with RANKL and M-CSF) in the presence of 12/15-LO and 5-LO specific inhibitors corroborated our *in vivo* findings. Both PD146176 and Baicalein dose-dependently inhibited osteoclast differentiation, whereas Zileuton had no effect. Our preliminary findings support a role for 12/15-LO in osteoclastogenesis and indicate that 12/15-LO may be an important therapeutic target in diseases associated with excessive osteoclastogenic bone resorption.

***Disclosures: Md Rahman**, None.*

SU0423

Effects of a carbon-containing polyhedral boron-cluster compound BA321 on bone loss due to sex steroid deficiency by AR- and ER-dependent mechanism. Chiho Matsumoto, Masaki Inada, Michiko Hirata, Chisato Miyaura*. Tokyo University of Agriculture & Technology, Japan

Carboranes are a class of carbon-containing polyhedral boron-cluster compounds having exceptional hydrophobicity, and their features may allow a new medical application as a biologically active molecule that interact with steroid hormone receptors. We have reported carborane compound BE360 having carborane structure with two phenols, binds to estrogen receptor and exhibits estrogenic action in bone but not in uterus as selective estrogen receptor modulator (SERM). On the other hand, we have designed carborane compounds having affinity with androgen receptor (AR) and synthesized them to search effective compounds for osteoporosis in the male. Among several carborane compounds, we noticed two compounds, BA321 and BA341, as a putative AR antagonist, in which a benzene ring with electron-withdrawing group (-NO2, -CN) and a hydroxyl group are placed at the opposite vertices of the hydrophobic carborane cage. In the competitive binding assay, BA321 and BA341 exhibited binding affinity to AR, and their affinities are 10-fold higher than that of hydroxyflutamine. In NIH3T3 cells transfected with AR, both BA321 and BA341 exhibited anti-androgenic activity in reporter gene assay. To examine the effects of BA321 and BA341 in bone, male mice were orchidectomized (ORX) and some of the mice were treated with BA321 and BA341 (10, 30, 100 μg/head/day) subcutaneously for 4 weeks using a mini-osmotic pump. Orchidectomized (ORX) mice showed severe bone loss due to androgen deficiency measured by femoral BMD and micro-CT, and the bone loss was completely recovered by the treatment with BA321. BA341 significantly restored the bone loss in ORX mice, but the potency of BA341 was relatively less than that of BA321. The weight of seminal vesicle was reduced in ORX mice, and not influenced by the treatment of BA321, indicating that BA321 does not exhibit androgenic action in sex organ in the male. On the other hand, BA321 bound to ER, and prevented the bone loss due to estrogen deficiency in ovariectomized female mice. BA321 may selectively bind to AR and ER, and act on bone tissues as selective androgen receptor modulator (SARM) or selective estrogen receptor modulator (SERM).

***Disclosures: Chisato Miyaura**, None.*

SU0424

Preclinical Assessment of mesenchymal stromal cell (MSC) transplantation to treat type II (age-related) osteoporosis. Jeffrey Kiernan*[1], John E Davies[1], William Stanford[2]. [1]University of Toronto, Canada, [2]Ottawa Hospital Research Institute, Canada

Osteoporosis and low BMD affects over 52 million people in the United States and Canada, and represents a substantial economic burden. In the USA and Canada approximately 1 in 3 women, and 1 in 5 men, will suffer an osteoporotic fracture in their lifetime with a cost to the system in excess of 22 billion dollars annually. While therapies targeting type I (post-menopausal) osteoporosis are well developed, those targeting type II (age-related) osteoporosis remain underdeveloped. Our lab has generated a Sca-1 null mouse model of human type II osteoporosis. Sca-1 null mice display decreased mesenchymal stromal cell (MSC) self-renewal and expansion capabilities. This model strongly suggests that defects in MSC function can contribute to age-related osteoporosis. Therefore, we wished to increase the MSC pool in Sca-1 null mice, by transplantation of wild-type (WT) bone marrow derived MSC, and assess the putative therapeutic potential of this approach. Donor MSCs were highly clonogenic, devoid of hematopoietic cell contamination, and retained a high osteogenic capacity. Short-term engraftment of 2x10^6 DiR labeled MSCs transplanted via intravenous injection display successful engraftment into hind limbs of Sca-1 null mice for at least 14 days. Flow cytometry of nucleated cells flushed from marrow shows engraftment of between 1:1000 to 1:3000 cells. To assess long-term engraftment, we transplanted 2x10^6 eGFP+ MSCs from male donor mice into 2.5-month-old Sca-1 null females. At approximately 8.5 months of age, mice were sacrificed and engraftment was assessed. Sca-1 null mice that received the eGFP+ MSC transplant display low-level engraftment beyond 8.5 months of age. Bone micro-architecture assessed in 8.5-month-old mice via Micro CT displayed improved trabecular connectivity density in mice transplanted with 2x10^6 WT MSCs vs Sca-1 null controls ($p \leq 0.05$). Further, trabecular number, bone volume/total volume, trabecular spacing, and trabecular degree of anisotropy showed trends towards improvement ($0.1 \geqslant p \geqslant 0.05$). These results show that a single systemic transplanted dose of MSCs is capable of engrafting into the bone marrow of osteoporotic mice and protects against progressive bone loss and reduction in bone quality for at least 6 months. Ongoing experiments including mechanical testing and histological analysis will further investigate the efficacy of MSC transplantation to treat osteoporosis in our preclinical model of type II osteoporosis.

***Disclosures: Jeffrey Kiernan**, None.*

SU0425

Therapeutic Potential of Adipose-derived Stromal Cells (ASCs) for the Treatment of Osteoporosis. Ali Mirsaidi*[1], Jolanda Vetsch[2], Matthias Arlt[3], Ralph Müller[3], Sandra Hofmann[2], Peter Richards[1]. [1]CABMM, Zurich University, Switzerland, [2]ETH Zurich, Institute for Biomechanics, Switzerland, [3]Balgrist University Hospital, Switzerland

We have previously confirmed that unlike bone marrow-derived stromal cells, adipose-derived stromal cells (ASCs) isolated from osteoporotic senescence-accelerated mouse prone 6 (SAMP6) mice retain their osteogenic potential when cultured under standard two-dimensional (2D) conditions. As such, ASCs may represent an alternative therapeutic approach for enhancing bone quality in patients with osteoporosis. In the present report, we have extended these studies to examine the influence of 3D-culture conditions on the osteogenic potential of ASCs from SAMP6 mice in an attempt to better assess their suitability as a cell-based therapy for treating osteoporosis. ASCs were isolated from subcutaneous inguinal fat pads by collagenase digestion and stem cell purity determined by fluorescence-activated cell sorting (FACS). Cells were grown in 3D-cultures either as scaffold-free microtissues (ASC-MTs) or in silk fibroin scaffolds. Osteogenic differentiation of ASCs was determined at selected time points using molecular, histological and micro-computed tomography (micro-CT) analyses. Bone morphogenetic protein 2 (*Bmp2*) and osteopontin (*Spp1*) expression levels were significantly upregulated in a time dependent manner in ASC-MTs in response to osteogenic stimuli. Mineral deposition was also apparent in osteogenic ASC-MTs as determined by Alizarin Red staining, and could be detected after only 6 days of differentiation. Silk fibroin scaffolds seeded with ASCs were cultured in bioreactors for up to 42 days, and mineral formation monitored by micro-CT. The bone volume fraction (BV/TV) was significantly elevated in silk fibroin scaffolds seeded with ASCs as compared to scaffolds alone. Silk fibroin scaffolds seeded with ASCs also stained positive for Alizarin Red, and expressed high levels of both *Bmp2* and *Spp1*. Preliminary *in vivo* studies confirmed that fluorescent-labeled isogenic ASCs could be injected directly into the tibial bone cavity of SAMP6 mice without any adverse effects and could be identified within the bone marrow after 24 hours. In conclusion, ASCs harvested from osteoporotic mice have the potential to undergo efficient osteogenic differentiation in a 3D-microenvironment resulting in the formation of a mineralized matrix. Adipose tissue may therefore represent a promising autologous cell source in the development of novel stem cell-based therapeutic strategies for the treatment of osteoporosis

***Disclosures: Ali Mirsaidi**, None.*

SU0426

Differential effects of calorie restriction on the skeleton implicate marrow adipose tissue as an independent adipose tissue depot. Casey Doucette*[1], Erica Scheller[2], Ormond MacDougald[3], Mark Horowitz[4], Clifford Rosen[5]. [1]Maine Medical Center Research Institute, USA, [2]University of Michigan, USA, [3]Department of Molecular & Integrative Physiology, University of Michigan Medical School, USA, [4]Yale University School of Medicine, USA, [5]Maine Medical Center, USA

The role of marrow adipose tissue (MAT) in the regulation of bone formation and resorption is largely unknown. Many studies have indicated an inverse relationship between bone mass and MAT content; humans with anorexia nervosa show increased levels of MAT and decreased BMD compared to healthy control subjects. Marrow fat content also increases with age along with age-related bone loss. Here, we investigate the role of MAT in the regulation of bone remodeling and energy homeostasis during a period of caloric deprivation in adolescent and aging mice. In cases of reduced energy intake, we hypothesized that MAT volume increases but is protective of bone. We took advantage of the innate differences between the C57BL/6J (B6) and C3H/HeJ (C3H) strains, which have diverse bone phenotypes; male C3H mice display significantly higher bone density and MAT volume than B6. Male B6 and C3H mice were fed a 30% calorie restricted (CR) diet for a period of 12 weeks from either 3-15 weeks of age (adolescent) or 40-52 weeks of age (aging). Littermate controls from each strain were given control (CTRL) diet *ad libitum*. As expected, adolescent CR mice had significantly lower trabecular BV/TV in the distal femur by μCT analysis in both strains ($n=10$, $p<0.001$), due to the detrimental effect of CR on bone formation during peak acquisition. Tibial MAT content, quantified by osmium staining, was significantly increased with CR in B6 ($n=5$, $p<0.01$) but not C3H mice compared to controls, while body composition by DEXA showed that adolescent C3H mice lost a greater percentage of body fat with CR than B6. CR in aging C3H mice led to significantly reduced cortical and trabecular BV/TV in the femur ($n=10$, $p<0.01$) as compared to CTRL-fed mice; remarkably, aging B6 CR mice were resistant to loss of bone mass, suggesting that CR is protective of skeletal mass in aging B6 but not C3H mice. Whole-body DEXA analysis showed that aging B6 mice lost a greater percentage of body fat with CR than C3H, while quantification of tibial MAT content from these mice showed significant increases in MAT volume in both strains with CR ($n=9$, $p<0.03$). Our results demonstrate that CR has strain-dependent effects on bone mass and adipose tissue depots and that MAT is an independent adipose depot that may serve distinct purposes within the skeletal niche depending upon age, energy status, and genotype. The previous tenet that MAT is purely a filler in response to reduced trabecular bone volume is no longer tenable.

***Disclosures: Casey Doucette**, None.*

SU0427

Effects of opioid substitution therapy with diacetylmorphine or methadone on bone health: a controlled study. Lisa Strahm*[1], Christoph Senn[1], Robert Haemmig[2], Kurt Lippuner[1]. [1]Department of Osteoporosis, University Hospital & University of Berne, Switzerland, [2]University Psychiatric Departement Addiction Therapy Unit, Switzerland

Introduction: Opioids, and thus opioid substitution treatment (OST), may have deleterious effects on bone mass leading to increased fracture risk. Whether long term OST with either diacetylmorphine (DAM) or methadone (MET) have different effects on bone is unknown.

Methods: Cross-sectional controlled study with 55 men in three groups: former heroin addicts on OST with DAM (n=19) or MET (n=17), and healthy controls (n=19). All patients on OST had been substituted for at least five consecutive years. Patients with known confounders in regard to bone health apart from smoking and non-cirrhotic viral hepatitis were excluded. BMD was assessed at the lumbar spine (LS), total hip (TH), femoral neck (FN), and tibial epiphysis (T-EPI) and diaphysis (T-DIA) using Dual X-ray Absorptiometry (DXA). Fractures history was recorded and prevalent spine fractures were assessed by Vertebral Fracture Assessment (VFA) during DXA acquisition.

Results:Patients substituted with DAM or MET, had a significantly lower Z-score than controls at T-EPI (-0.8 and -0.5 vs. 0.3, with p=0.001 and 0.015, respectively). Patients substituted with DAM, but not MET, had a significantly lower Z-score than controls at LS, -1.6 vs. -0.6 (p=0.016) and TH, -0.5 vs. 0.1 (p=0.049). Prior fractures at any localization were reported by 16 patients on DAM (38 fractures), 10 patients on MET (22 fractures), and 12 controls (24 fractures). Prior fractures during adulthood were detected in 10 patients on DAM (24 fractures), 7 patients on MET (13 fractures) and 6 controls (8 fractures). VFA detected two vertebral fractures (one severe on DAM and one moderate on MET).

*Conclusion:*Former heroin addicted men under long term OST have lower BMD than healthy controls, with numerically worse Z-scores at all measurement sites, and significantly lower Z-scores at the LS (DAM) and T-EPI (DAM and MET). Fractures were also numerically more frequent in these patients.

***Disclosures: Lisa Strahm**, None.*

SU0428

Abnormal Microarchitecture and Stiffness in Postmenopausal Women Treated with Glucocorticoids. Stephanie Sutter[1], Kyle Nishiyama[2], Anna Kepley[1], Thomas Nickolas[3], Adi Cohen[1], Bin Zhou[2], X Guo[2], Elizabeth Shane[3], Emily Stein*[3]. [1]Columbia University Medical Center, USA, [2]Columbia University, USA, [3]Columbia University College of Physicians & Surgeons, USA

Patients treated with glucocorticoids (GCs) are more likely to fracture than untreated patients with similar areal bone mineral density (aBMD), suggesting that GCs increase fragility via mechanisms distinct from their effects on bone density. This study used high resolution peripheral computed tomography (HRpQCT) and micro finite element (μFE) analyses to characterize bone microarchitecture and stiffness in postmenopausal women on GCs. We hypothesized that women using GCs would have disrupted microarchitecture and lower stiffness compared to controls, and that abnormalities would be more prominent in the trabecular compartment, as GC-related fractures traditionally occur at primarily trabecular sites. 27 postmenopausal women using oral GCs for >3 months were matched 1:2 with 54 controls of the same ethnicity and age. All had aBMD of lumbar spine, total hip, femoral neck, 1/3 and ultradistal radius (UDR) by DXA. Trabecular (Tb) and cortical (Ct) volumetric BMD, and Tb microarchitecture were measured by HRpQCT (voxel size ~82 μm) of the distal radius and tibia. Whole bone stiffness was estimated by μFE. Mean age of subjects was 68 ± 9 years (67% Caucasian). BMI and menopausal age were similar between groups. GC subjects were more likely to be using bisphosphonates (33% vs. 6%;$p<0.01$). Among GC subjects, 74% had rheumatologic diseases. Mean daily dose of prednisone was 7.8 mg and duration of use 3.4 years. Mean T-scores both groups were in the osteopenic range and did not differ significantly at any site. There were substantial microarchitectural differences between groups by HRpQCT (Table). At the radius, GC subjects had lower total and Tb density and Tb thickness. Ct thickness tended to be lower, and Tb separation higher among GC subjects (representative HRpQCT images are shown in Figure). At the tibia, GC subjects had lower total, Ct and Tb density. Tb thickness was lower and network heterogeneity was greater. Ct thickness tended to be lower among GC subjects. Differences remained significant after adjustment for aBMD. Whole bone stiffness was lower in GC subjects at both sites. In summary, postmenopausal women using GCs had microarchitectural and biomechanical deterioration at both radius and tibia compared to controls, despite similar aBMD by DXA. As hypothesized, Tb abnormalities, particularly Tb thinning, were most marked. These abnormalities in microarchitecture and stiffness may be important determinants of skeletal fragility in patients using GCs.

Microarchitecture in GC subjects vs. Controls (% difference)

	RADIUS	p-value	TIBIA	p-value
Total Density	-12	<0.03	-15	<0.003
Ct Density	-3	0.20	-5	<0.03
Ct Thickness	-10	0.08	-12	0.09
Tb Density	-18	<0.03	-17	<0.005
Tb Number	-9	0.13	-4	0.45
Tb Thickness	-9	<0.05	-14	<0.003
Tb Separation	+26	0.09	+10	0.12
Network Heterogeneity	+46	0.15	+33	<0.03
Stiffness	-15	<0.02	-12	<0.02

GC Table

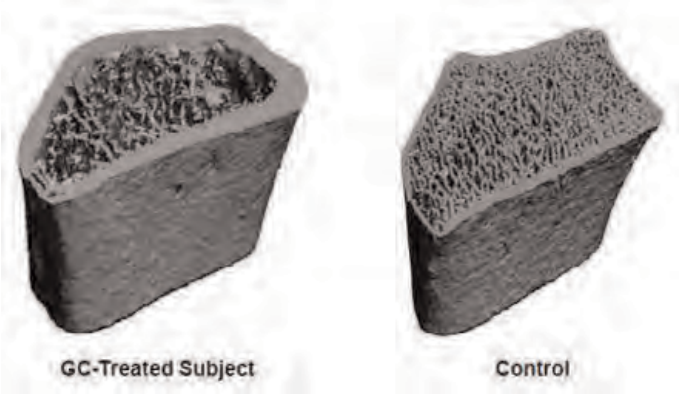

HRpQCT images from GC and Control Subjects

***Disclosures: Emily Stein**, None.*

SU0429

Altered Cortical Microarchitecture and Bone Metabolism in Patients with Monoclonal Gammopathy of Undetermined Significance. Joshua Farr*[1], Wei Zhang[1], Richard Jacques[2], Alvin Ng[1], Louise McCready[1], Matthew Drake[3]. [1]Mayo Clinic, USA, [2]University of Sheffield, United Kingdom, [3]College of Medicine, Mayo Clinic, USA

Monoclonal gammopathy of undetermined significance (MGUS) is associated with increased fracture risk. Recent evidence shows that MGUS patients have altered trabecular microarchitecture but no differences in bone turnover markers as compared to controls (Blood 118:6529, 2011). However, whether MGUS patients have deficits in cortical microarchitecture or bone strength is unknown. Furthermore, no study in MGUS patients has simultaneously considered the complementary processes of bone balance and turnover, using the ''bone marker plot'' (Eur J Clin Invest 39:220, 2009). Thus, we used HRpQCT and micro-finite element analysis to assess bone microarchitecture and strength of the distal radius in a case-control study of 50 men and women (age 49–88 yrs) with MGUS and 100 age-, sex-, and BMI-matched (1:2 ratio) controls. Serum levels of Dickkopf-related protein 1 (DKK1) and markers of bone formation and resorption were also measured. Compared to controls, MGUS patients had significantly altered cortical microarchitecture at the radius [i.e., higher cortical porosity (+16.8%; $P<0.05$); lower cortical volumetric BMD (–4.5%; $P<0.001$)], while also having greater endocortical and periosteal circumferences (+5.7% and +4.2%, respectively; $P<0.01$). In addition, radial apparent modulus (stiffness corrected for cross-sectional area) was significantly lower (–8.9%; $P<0.05$) in MGUS patients relative to controls. When all MGUS patients were combined, bone balance and turnover were not different between MGUS patients and controls. However, MGUS patients with higher monoclonal protein levels (>2.0 g/dL) showed a significant shift towards a reduced bone turnover rate in bone marker plot analyses (Figure; P=0.022). In addition, these patients tended to have higher DKK1 levels.

In conclusion, despite their larger radial bone size, MGUS patients have compromised cortical microarchitecture and bone strength as compared to controls. Furthermore, MGUS patients with higher monoclonal protein levels have reduced bone turnover. Given the critical role of DKK1 as an inhibitor of Wnt signaling in bone cells, the higher DKK1 levels observed in these patients may reflect suppression of bone formation. Our findings point to the need to further define the factors that regulate bone microarchitecture and metabolism in MGUS in order to better identify patients at risk for skeletal complications and to develop appropriate treatment strategies to reduce the increased fracture risk in these patients.

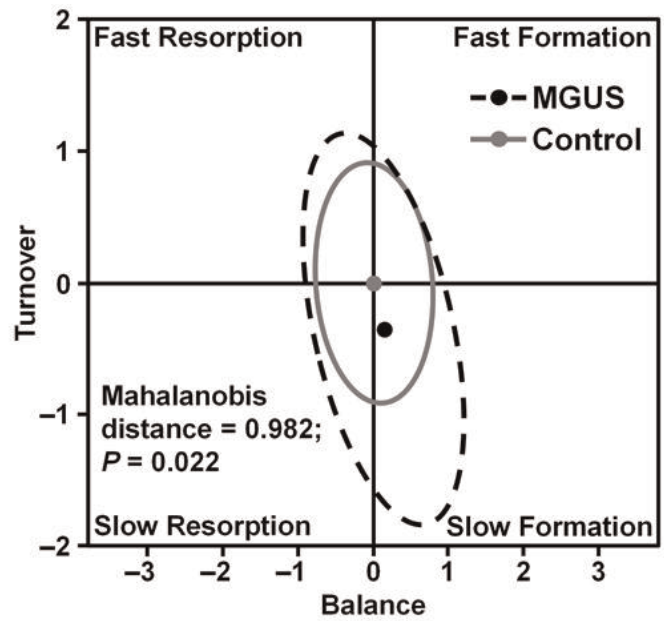

Figure

***Disclosures: Joshua Farr**, None.*

SU0430

Bone density and bone material strength measured by microindentation ten years after kidney transplant. Laia Vilaplana[1], Maria José Pérez-Sáez[2], Daniel Prieto-alhambra[3], Elisa Torres-Del-Pliego[4], Leonardo Mellibovsky[5], Marta Crespo[2], Roberto Güerri-Fernández[5], Julio Pascual-Santos[2], Xavier Nogues[6], Adolfo Diez-Perez*[7]. [1]Internal Medicine Department, Parc de Salut Mar, Universitat Autònoma de, Spain, [2]Nefrology Department, Parc de Salut Mar, Universitat Autònoma de Barcelona, Spain, [3]University of Oxford, United Kingdom, [4]Internal Medicine Department, Hospital del Mar, Barcelona, Spain, [5]Internal Medicine Department, Parc de Salut Mar, Universitat Autònoma de Barcelona, Spain, [6]Institut Municipal D'Investigació Mèdica, Spain, [7]Autonomous University of Barcelona, Spain

Background: Kidney transplant recipients (KTR) suffer an increased fracture risk in the months following the procedure that later on comes back to background population rates. However, no data is available on the bone status several years after the transplant. We assessed bone strength related parameters in a cohort of KTR ten years after the procedure.

Methods: Consecutive series of patients with over 10 years of kidney transplant and recovery of kidney function (MDMD 42.6+14.3 ml/min). BMD was measured using DXA. Vertebral fractures were assessed in dorsal and lumbar lateral spine radiography. BMS was measured by microindentation in the anterior midtibia with an Osteoprobe® device (Active Life Scientific, Santa Barbara, CA) applying a 20N force with a test probe, standardized as the ratio to a PMMA phantom. Statistical analyses were performed by ANOVA.

Results: A total of 27 KTR cases and 41 controls have been studied. Average BMD T-score at lumbar spine (-1.3 + 1.33) and total hip (-1.45 + 0.99) in transplant patients where within osteopenia range. BMS values were 81.01 + 7.40 in KTR and 84.62 + 6.17 in controls (p=0.65 after adjusting by age, sex and BMI). In 10 KTR cases vertebral fractures were detected (40% over 25 cases with X-rays). No differences in BMS were seen between KTR cases with (80.70+8.27) and without (81.26+7.33) prevalent fractures (p=0.69 after adjustment by age, gender and BMI). All variables expressed as mean + SD. No significant correlation was observed between BMS and BMD at any location.

Conclusions: Ten years after kidney transplant bone parameters are normal, as assessed by densitometry and microindentation. The high prevalence of vertebral fractures may be related with increased bone fragility in the period after the procedure. In these patients, with recovery of kidney function, there are no detectable long-term skeletal abnormalities and our results suggest a full recovery.

***Disclosures: Adolfo Diez-Perez**, None.*

SU0431

Bone Density Changes after Lower Limb Amputation. Debra Bemben*[1], Vanessa Sherk[2], Michael Bemben[1]. [1]University of Oklahoma, USA, [2]University of Colorado - Denver, USA

Cross-sectional studies have reported that lower limb amputees have compromised bone health. Recently, we found that areal BMD (aBMD) for the hip sites was lower in the amputated side compared to the intact side. The purpose of this longitudinal study was to assess changes in total body, hip and spine areal BMD occurring in the early stages after lower limb amputation. Six participants (1 premenopausal female, 5 males), ages 23 to 53 years were enrolled in the study immediately prior to their amputation surgery. They all were traumatic unilateral amputees (1 above knee, 5 below knee) who had undergone the Ertl procedure. BMD variables (total body, lumbar spine, dual proximal femur) and body composition were assessed by DXA (GE Lunar Prodigy) after amputation prior to prosthesis fitting (pre-ambulatory baseline), at 6 months walking with prosthesis, and at 12 months walking with prosthesis. Participants gained body weight ($p < 0.05$) from baseline to the 6 month time point. There were no significant changes in total body or spine (L1-L4) aBMD at either ambulatory time point compared to pre-ambulatory baseline. One participant had a spine T-score ≤ -1.1 at each time point. There were significant ($p < 0.01$) side, time, and side × time interaction effects for the total hip and femoral neck sites. Total hip aBMD significantly decreased from baseline to 6 months ($p = 0.001$) and 12 months ($p = 0.003$) with prosthesis for the amputated side but not for the intact side (Table 1). Similarly, the femoral neck aBMD for the amputated side significantly decreased, however, the intact side also significantly ($p = 0.008$) decreased from baseline to 6 month time points. The % decreases were -15.8% and -14.9% for the amputated side total hip and femoral neck sites. None of the participants were osteopenic or osteoporotic for the amputated or intact side hip sites at baseline. By 6 months, 2 participants were osteopenic at the total hip for the amputated side and by 12 months, 3 (below knee) participants were osteopenic and 1 (above knee) was osteoporotic for the amputated side total hip. In conclusion, large decrements occurred in the amputated hip aBMD by 6 months walking with prosthesis and was maintained at the 12 month time point. These findings suggest that bone losses resulting from unloading with amputation were not regained with prosthesis use.

Table 1. Total Hip aBMD (n=6)

	Amputated Side	Intact Side
	(g/cm²)	(g/cm²)
Baseline	1.122 ± 0.031	1.145 ± 0.032
6 Months with Prosthesis	0.956 ± 0.031**	1.136 ± 0.036
12 Months with Prosthesis	0.944 ± 0.039**	1.136 ± 0.034

** p<0.01 vs. baseline

Disclosures: Debra Bemben, None.
This study received funding from: DOD-MRAA

SU0432

Bone Health in Postmenopausal Women with Breast Cancer Receiving Aromatase Inhibitors. Vit Zikan*[1], Martina Zimovjanova[2], Luboš Petruželka[2], Jana Přibylová[2], Michaela Cabinakova[3], Maria Raskova[1]. [1]3rd Department of Medicine - Department of Endocrinology & Metabolism, First Faculty of Medicine, Charles University in Prague & General University Hospital in Prague, Czech Republic, [2]Department of Oncology, First Faculty of Medicine, Charles University in Prague & General University Hospital in Prague, Czech Republic, [3]Department of Oncology, First Faculty of Medicine, Charles University in Prague & General University Hospital in Prague, Dominican Republic

Aromatase inhibitors (AIs) are the standard of care for the treatment of most postmenopausal women with early stage hormone-receptor-positive breast cancer (EBC). However, one side-effect of AIs on bone is a decrease in bone mineral density (BMD) and an increased risk of fracture. Early identification of women with poor bone health offers opportunities for interventions aimed at reducing fracture risk. In this study we investigated bone health in a prospective cohort of patients recruited prior to adjuvant AIs therapy, with the aim of establishing potential AIs impact on bone loss and fractures. Methods: Eighty-one postmenopausal women (mean age: 61.4 years) who have been considered for adjuvant AIs therapy for EBC were enrolled for the study. BMD was measured by dual-energy X-ray absorptiometry (DXA). Clinical risk factors and FRAX algorithm were evaluated. Bone remodeling was assessed using circulating concentrations of type 1 collagen cross-linked C-telopeptide (CTX) and N-terminal propeptide of type I procollagen (PINP). In addition, we examined the prevalence of vitamin D deficiency. Results: Twelve patients (14.8%) met the criteria for osteoporosis and thirty six patients (44.5%) for osteopenia. The mean 25 (OH) D level was 21.9 ± 11.1 ng/ml (range 4.6-47.3 ng/ml). Of the 53 patients, 7 patients (13.2 %) had vitamin D deficiency (< 10 ng/ml), 34 patients (64.2 %) had an insufficiency (10 to 30 ng/ml) and 12 patients (22.6 %) had normal values (> 30 ng/ml). Conclusion: Low BMD and vitamin D insufficiency were highly prevalent among patients considered to adjuvant AIs for EBC. Therefore, it is important to assess BMD and 25 (OH) D levels before starting AIs therapy. However, factors other than BMD levels alone may influence fracture risk and a combined fracture risk assessment (eg, FRAX algorithm) will probably more accurately identify breast cancer patients who require bone-protective therapy. Longitudinal study is currently underway.

Keywords: aromatase inhibitors, breast cancer, osteoporosis

Disclosures: Vit Zikan, None.

SU0433

Endosteal Resorption and Worsening Cortical Porosity after Roux-en-Y Gastric Bypass Surgery. Elaine Yu*[1], Melissa Putman[2], Mary Bouxsein[3], Adam Roy[1], Nicolas Derrico[1], Joel Finkelstein[1]. [1]Massachusetts General Hospital, USA, [2]Massachusetts General Hospital, Children's Hospital Boston, USA, [3]Beth Israel Deaconess Medical Center, USA

Purpose: We have previously reported discordance between reported effects of Roux-en-Y gastric bypass (RYGB) on BMD when assessed by DXA versus QCT, likely due to imaging artifact related to large weight loss at central sites. High-resolution peripheral quantitative computed tomography (HR-pQCT) may provide more accurate estimates of skeletal changes after RYGB.

Methods: We assessed cortical and trabecular volumetric BMD (vBMD) and bone microarchitecture at the distal radius and tibia in 50 severely obese adults (30 undergoing RYGB surgery + 20 non-surgical controls) using HR-pQCT (Scanco, Basserdorf, SZ) at 0 and 12 months. Specialized software was used for more detailed assessment of cortical bone, including cortical porosity, and to estimate bone strength by microfinite element analysis (mFEA).

Results: The RYGB and control groups were well matched at baseline. Body weight fell 37 ± 2 kg in the RYGB group versus 3 ± 2 kg in the controls ($p<0.0001$). In the RYGB group, total vBMD declined significantly at the radius and the tibia ($p<0.001$ for both sites, see Table). The decline at the radius was largely due to a fall in trabecular vBMD whereas the decline at the tibia was largely due to a decrease in cortical vBMD (Table). Cortical porosity increased by 27 ± 11% at the radius and by 31 ± 8% at the tibia though only the latter value was significantly different from controls (Table). After RYGB, cortical area and cortical bone volume declined with a parallel increase in trabecular area at both sites ($p<0.03$ for all, Table), consistent with endosteal resorption and "trabecularization" of cortical bone. Changes in trabecular microarchitecture were not significantly different between RYGB and control groups. Estimated failure load declined significantly at the tibia but not at the radius in the RYGB group compared with controls (Table). There were no significant associations between changes in vBMD, microarchitectural or mFEA parameters and changes in weight, PTH, or 25OHD in the RYGB group. Lastly, declines in total vBMD at the radius and tibia after RYGB were not associated with changes in spine or hip BMD by DXA or QCT.

Conclusions: Volumetric BMD at both the distal radius and tibia decreases after RYGB, accompanied by increased endosteal resorption. At the tibia, these changes are primarily due to increased cortical porosity and lead to a decrease in estimated strength. The long-term consequences of the early skeletal changes after RYGB need to be assessed.

Percent change in HR-pQCT parameters from 0 to 12 months

	RADIUS		TIBIA	
	RYGB	Controls	RYGB	Controls
Total vBMD	-3.0 ± 0.7%*	1.7 ± 0.6%	-3.3 ± 0.7%*	-0.4 ± 0.2%
Cortical vBMD	-0.5 ± 0.4%	-0.1 ± 0.5%	-2.4 ± 0.6%*	0.1 ± 0.5%
Trabecular vBMD	-1.7 ± 0.7%*	0.5 ± 0.8%	-0.7 ± 0.9%	-1.6 ± 0.5%
Cortical Porosity	27 ± 11%	6 ± 17%	31 ± 8%*	-8 ± 4%
Cortical Area	-3.3 ± 1.0%*	3.0 ± 1.2%	-2.7 ± 1.1%*	0.3 ± 0.6%
Trabecular Area	1.0 ± 0.4%*	-1.1 ± 0.6%	0.7 ± 0.3%*	-0.1 ± 0.1%
Failure Load	-0.8 ± 1.1%	0.0 ± 0.8%	-1.4 ± 0.8%*	1.4 ± 0.7%

*p-value <0.05 for difference between RYGB vs. controls

Table

Disclosures: Elaine Yu, None.

SU0434

Genetic determinants of bone mineral density loss in Aromatase inhibitors treatment. MARIA RODRIGUEZ-SANZ[1], Daniel Prieto-alhambra[2], Sonia Servitja-Tormo[3], Elisa Torres-Del-Pliego[4], Leonardo Mellibovsky[4], Laia Garrigós[3], Natalia Garcia-Giralt[1], Adolfo Diez-Perez[5], Ignacio Tusquets[3], Xavier Nogues*[6]. [1]IMIM, Spain, [2]University of Oxford, United Kingdom, [3]Medical Oncology Department, Parc de Salut Mar, Barcelona, Spain, Spain, [4]URFOA-IMIM, Red Temática de Investigación Cooperativa en Envejecimiento y Fragilidad (RETICEF), Instituto de Salud Carlos III FEDER, Barcelona, Spain, Spain, [5]Autonomous University of Barcelona, Spain, [6]Institut Municipal D'Investigació Mèdica, Spain

Purpose: Therapy with Aromatase inhibitors (AI) for estrogen receptor-positive breast cancer in postmenopausal women results in bone mineral density (BMD) loss and fractures. This study aims to identify genetic variants associated with BMD in the first year of AI treatment.

Methods: Single nucleotide polymorphisms (SNPs) were selected in genes potentially involved in: 1.Vitamin D and estrogen signaling pathways, 2.described association with BMD and fractures in a GWAs study (Estrada K et al, Nature Genetics, 2012), and/or 3.AI CYP450 metabolizer subunits. Selected SNPs were genotyped in 280 Caucasian, postmenopausal women with early breast cancer, starting adjuvant treatment with AI as recommended by ASCO guidance. Outcome was absolute (baseline minus 1-year BMD [in gr/cm2]) BMD loss at 1 one year of therapy as measured using DXA scan at three sites: Lumbar spine (LS), femoral neck (FN) and total hip (TH).

Paired T-tests were used to measure AI-related BMD loss. Multivariate linear regression models were fitted to test the association between the selected SNPs and absolute BMD loss after 1 year of follow-up. All models were adjusted for body mass index, years since menopause and baseline BMD. For the analyses of the SNPs involved in vitamin D signaling, we further adjusted for baseline vitamin D concentrations.

Results: After 1 year of AI therapy, participants experienced a significant 1.42 % [95 % CI 0.93–1.91 %] BMD loss at LS (0.014 g/cm2 [0.009–0.019], $P < 0.0001$), 1.16 % [95 % CI 0.62–1.70 %] at FN (0.009 g/cm2 [0.005–0.013], $P < 0.0001$), and 0.72 % [95 % CI 0.30–1.14 %] at TH (0.007 g/cm2 [0.003–0.010], $P = 0.01$).

Under the hypothesis of Vitamin D and estrogen signaling, rs2544037 in VDR gene and rs6013897 in CYP24A1 reached significant p-values (P=0.04 and P=0.01 respectively) for the association with LS BMD loss. The same SNP in VDR (P=0.02), as well as rs11907350 in CYP24A1 were associated (P=0.02) with FN BMD loss. For the analyses of genes previously associated with BMD, rs7851693 in FUBP3 showed a significant association (P=0.01), and rs163879 in DCDC5 yielded a borderline p-value (P=0.06) for the association with LS BMD loss. Finally, rs4986894 in CYP2C19 gene and rs9332982 in CYP4A11 gene, both involved in AI metabolization, obtained significant results in the association with LS BMD loss (P=0.01 and P=0.004 respectively).

Conclusions: SNPs in VDR, CYP24A1, FUBP3, DCDC5, CYP4A11 and CYP2C19 genes appeared significantly associated with BMD loss in the first year of AI treatment. None of the three postulated hypothesis stood out amongst the others, suggesting that BMD loss during AI therapy is determined by an interaction of genes involved in several metabolic pathways: Vitamin D and estrogens signalling, AI-metabolization by CYP450, genetic determinants of BMD and fracture risk.

***Disclosures: Xavier Nogues**, None.*

SU0435

HIV+ male patients receiving fluoride, present in an antiretroviral therapy (TRUVADA®), have an improved trabecular bone density and micro-architecture at the tibia. Pierre Sellier[1], Hervé Trout[2], Corinne Collet[3], Amanda Lopes[1], Karine Champion[1], Guy Simoneau[1], Agnès Ostertag[3], Sylvie Fernandez[3], Jean-Dominique Magnier[1], Marie-Christine De Vernejoul*[4], Jean-François Bergmann[1]. [1]Service de Medecine interne A, Hopital Lariboisiere, Assistance Publique-Hopitaux de Paris, France, [2]Pharmacie : medicaments et laboratoires, Hopital Lariboisiere, Assistance Publique-Hopitaux de Paris, France, [3]INSERM U 606 & University Paris Diderot, Service de rhumatologie, Hopital Lariboisiere, Assistance Publique-Hopitaux de Paris, France, [4]Fédération De Rhumatologie Et INSERM U606, France

Background: HIV+ patients are considered at risk for excessive bone fragility. Several factors could contribute: age, low body mass index (BMI), HIV infection *per se* and antiretroviral treatment (particularly tenofovir, a reverse transcriptase inhibitor). Tenofovir is used with [TRUVADA®] or without [VIREAD®] emtricitabine (FTC). FTC is 5-fluorinated to increase bioavailability and half-life of the drug; the daily intake of fluoride in patients treated with TRUVADA® is 15.4 mg. Fluoride induces bone formation by stimulating osteoblasts. The aim of our study was to investigate if this fluoride supplementation impact on bone.

Methods: We have included in this retrospective cross-sectional study 35 HIV+ male patients treated with TRUVADA® for more than 60 months. We compared them to 18 HIV+ male patients treated with VIREAD® who had never received TRUVADA® and were matched to the TRUVADA® group for age, ethnic origin, BMI, total HIV+ duration and tenofovir exposure. Fluoride metabolism was studied by measurement of fluoride in blood, bone formation by measurement of serum P1NP. Dual X-ray absorptiometry was used to determine the areal bone mineral density (aBMD) of the lumbar spine, femoral neck and distal radius. Volumetric BMD (v-BMD) and micro-architecture of distal radius and tibia were studied using a HR-pQCT scan (Xtreme, Scanco).

Results: The age of the patients (50 ± 9 vs. 49 ± 8 yrs, p=0.57), the disease duration (13 ± 6 vs. 15 ± 5 yrs, p=0.27) and the total tenofovir exposure (78 ± 19 vs. 77 ± 11 months, p=0.83) of TRUVADA® and VIREAD® groups were not different. The two groups did not differ significantly regarding the mean fluoride in blood, the mean P1NP (47 ± 15 vs. 41 ± 11 ng/ml, p=0.21), the a-BMD of the lumbar spine, femoral neck and distal radius (assessed by Z-scores, after adjustment on age and ethnic origin). Micro-architectural parameters at the radius were not different between groups. At the tibia, trabecular v-BMD (171 ± 39 vs. 143 ± 41 mg HA/cm^3 $p< 0.05$), BV/TV (0.14 ± 0.03 vs. 0.12 ± 0.03, $p<0.05$), trabecular number (2.0 ± 0.3 vs. 1.7 ± 0.4, $p<0.01$) were significantly higher in the TRUVADA® group, whereas trabecular separation was reduced (0.45 ± 0.08 vs. 0.56 ± 0.14 mm, $p<0.01$). There was no difference in any cortical parameters.Conclusions: The improved trabecular bone parameters observed in HIV+ male patients chronically treated by TRUVADA®, compared to those receiving VIREAD® were compatible with a positive action of small amount of fluoride on trabecular bone.

***Disclosures: Marie-Christine De Vernejoul**, None.*

SU0436

Longitudinal Change in Bone Mineral Density Among Adult Patients with Malignant Lymphoma Receiving Chemotherapy. Julien Paccou*[1], Isabelle Henry-Desailly[1], Lavinia Merlusca[1], Said Kamel[1], Daciana Ursu[1], Rachel Desailloud[1], Jean-Pierre Marolleau[1], Patrice Fardellone[2], Gandhi Damaj[1]. [1]Université De Picardie Jules Verne, France, [2]Service de rhumatologie, CHU Hôpital Nord, France

The time course of bone mineral density (BMD) loss is poorly characterized in malignant lymphoma patients. The present study was designed to measure the extent of bone loss assessed by BMD in a cohort of adult patients with known malignant lymphoma receiving chemotherapy.

This was a single-center, prospective, longitudinal study. Inclusion criteria: Patients aged ⩾18 years with previously confirmed malignant lymphoma treated by chemotherapy. Exclusion criteria: Patients with low baseline vertebral or hip BMD defined as T-score ≤ -2.5 and/or history of osteoporotic fractures. BMD was measured at baseline before initiating chemotherapy with final BMD testing one year later. BMD in the lumbar spine, total hip and femoral neck using pencil-beam dual energy X-ray absorptiometry, and clinical, biochemical, and anthropomorphic changes were assessed. Predictive factors of BMD loss and factors associated with an unfavourable outcome (death or no remission) were investigated. Osteoporotic fractures were also assessed at baseline and at the end of follow-up.

Forty-one patients with malignant lymphoma receiving chemotherapy were enrolled. No patients were lost to follow-up, but 6 died before one year and 3 required treatments with bisphosphonates during the first month of the study. The characteristics of the remaining 32 patients at baseline and 12 months later are shown in Table. Mean absolute BMD changes were -0.027 g/cm^2 ± 0.042 for lumbar spine (-2.7 $\pm 3.9\%$), -0.021 g/cm^2 ± 0.067 for femoral neck (-2.2 $\pm 7.6\%$) and -0.026 g/cm^2 ± 0.043 for total hip (-2.6 $\pm 4.5\%$). Predictive factors of BMD loss at lumbar spine were female gender (-6.1 $\pm 4.0\%$) versus male (-1.7 $\pm 3.5\%$) (P=0.009), International Prognostic Index (IPI) score=3-4 (-6.2 $\pm 5.3\%$) versus IPI=0-2 (-2.0 $\pm 3.1\%$) (P=0.03) and WHO score=1-2 (-4.7 $\pm 4.9\%$) versus WHO score=0 (-1.7 $\pm 3.1\%$) (P=0.04). No predictive factors of BMD loss at femoral neck or total hip were found. Factors associated with an unfavourable outcome in multivariate analyse were WHO score with OR = 19.8 (95% CI: 11.59 - 247.01; P=0.02) and chemotherapy duration with OR = 16.59 (95% CI: 1.31 - 209.82; P=0.03). Four patients developed osteoporotic fractures during follow-up.

In conclusion, adult patients with known malignant lymphoma receiving chemotherapy experienced significant bone loss as assessed by BMD at the lumbar spine, total hip and femoral neck. Moreover, BMD loss in the lumbar spine was influenced by female gender, IPI and WHO scores.

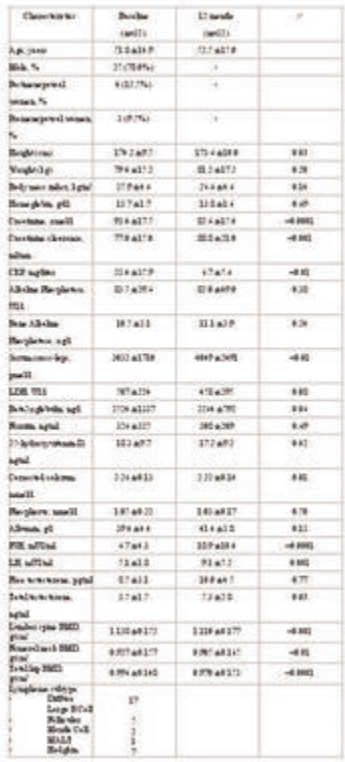

LYMPHOS

***Disclosures: Julien Paccou**, None.*

SU0437

Pregnancy Associated Osteoporosis with Vertebral Fractures: Report of a Case with 5-Year Follow-Up. Gulseren Akyuz*[1], Ozun Bayindir[2], Beyhan Eren[3]. [1]Marmara University, Turkey, [2]MD, Department of Physical Medicine & Rehabilitation, School of Medicine, Marmara University, Turkey, [3]MD, Physical Medicine & Rehabilitation Clinic, Mersin State Hospital, Turkey

Pregnancy associated osteoporosis (PAO) is a rare clinical condition that may affect women during third trimester of pregnancy or after the delivery. Little is known about the prevalence, reasons, risk factors and prognosis of PAO. It can cause severe or prolonged back pain with one or more vertebral fractures and loss of height. Herein we report a case of PAO in a 32 year-old female who presented with severe back pain with multiple vertebral fractures 1 month after delivery. There were delayed menarche and low dietary calcium intake in history. The radiological examinations have shown compression fracture of 8th thoracic vertebra and wedging of 11th and 12th thoracic vertebrae and lumbar spine. In the bone mineral density (BMD) total lumbar spine T-score and Z-score were -2,8 while femoral neck T-score and Z score were -1,2 and -1,1, respectively. There were no abnormality in laboratory findings except mild alkaline phosphatase elevation and 25-hydroxy vitamin D insufficiency. Three months after delivery for pain reduction T8 kyphoplasty was applied. Along 5-year follow-up vitamin D_3, calcium, calcitonin, bisphosphonate, GABA anologs, analgesics, physical agents, dry needling were used for treatment. Back pain decreased with all kind of treatments significantly (VAS decreased from 10 to 3 point) but localized pain around kyphoplasty area have been continued even if low level pain severity (VAS 3 point) along 5-year follow-up. There were no new fractures and marked recovery of spine BMD was observed during the same period. Her activities of daily living improved permenantly. As a conclusion, when back pain occurs at last trimester of pregnancy or early postpartum period, PAO should be considered in differential diagnosis and long term treatment should be planned for the patient's well being.

***Disclosures: Gulseren Akyuz**, None.*

SU0438

Bone Density and Vitamin D Status in Liver Transplant Patients 12 Years After the First Assessment. Elena Segal*[1], Yacov Baruch[1], Rimma Kramsky[1], Marina Nodelman[2], Marina Hefetz-Kustanovich[1], Sophia Ish-Shalom[1]. [1]Rambam Health Care Campus, Israel, [2]Western Galilee Hospital, Israel

Twelve years ago we evaluated 29 liver transplant patients. Nineteen (65.5%) had decreased bone mass, 11 (37.8%) were osteoporotic, 28 (96.5%) had serum level of 25(OH)D<20 ng/ml, mean 12.52±3.19, mean PTH 59.67±29.78 pg/ml. None was treated with calcium or vitamin D supplements, in spite of low calcium intake and low or suboptimal 25OHD serum level. The patients received letters containing the diagnosis and treatment recommendations.

Now we re-evaluated patients' charts. Nineteen patients continued follow-up at the Liver Unit, 9 men, 10 postmenopausal women, aged 58.8±15.8. Ten patients died, none of them had fractures. Twelve fractures were reported following transplantation, 10 (83.3%) within the first year, 2 in the following years, both were traumatic.

Second BMD results were available for 8 (42%) patients, two (25%) were osteoporotic, 6(75%) - osteopenic. 13 patients (68.4%) received 600 mg of elemental calcium, 400-1600 IU of vitamin D daily, 2 (10.5%) received bisphosphonates.

Plasma PTH ranged from 32-71 pg/ml, mean 61.9±26.42 , 25OHD range was 14-22, mean 24.72±9.49 ng/ml; increased form the 12 years ago assessment PTH 59.67±29.78 pg/ml, 25OHD 12.52±3.19 ng/ml; p=0.068 and p=0.003 respectively

Since the first evaluation, 20 new post liver transplant patients joined the Rambam Liver Unit. They were not evaluated in the Bone Metabolism Unit. According to the information retrieved from the patients' charts, 7 of them had BMD evaluation, one woman was in the osteoporotic range, 6 –osteopenic, PTH was 82.83±67.01 pg/ml, 25OHD was 23.95±8.7 ng/ml.

Nine (45%) of them are treated at present with calcium 600 mg/day and vitamin D, 400-2000 IU/day, r two are treated with oral bisphosphonates. No fractures were reported by these patients since the time of transplantation.

In the whole group of post liver transplant patients PTH was 71.82±49.64 pg/ml, 25OHD 25.11±9.31ng/ml.

Conclusions: Osteoporotic fractures in liver transplant patient occurred during the first postransplantation year. No osteoporotic fractures were observed during subsequent long term follow-up. Vitamin D deficiency and low calcium intake were actively treated and secondary hyperparathyroidism was not observed during long term follow-up. BMD follow-up was not routinely performed in all patients. No significant change in BMD was observed during long term follow-up in the tested group.

***Disclosures: Elena Segal**, None.*

SU0439

Case-control Study of the *SQSTM1/P392L* Post-zygotic Mutation in Paget's disease of Bone. Sabrina Guay-Bélanger*[1], Edith Gagnon[2], Jean Morissette[2], Jacques P. Brown[2], Laetitia Michou[4]. [1]Centre de recherche du CHUQ-CHUL, Canada, [2]CHU de Québec Research Centre, Canada, [4]Université Laval, Canada

Purpose: Paget's disease of bone (PDB) is a uni or plurifocal metabolic bone disorder transmitted, in one third of cases, in an autosomal-dominant mode of inheritance with incomplete age-dependent penetrance. The germinal *SQSTM1/P392L* mutation is the most common mutation, present in 40% of patients with a familial form of PDB, and 8% of unrelated patients. Given the focal nature of PDB, some authors have suggested that somatic mutations in *SQSTM1* gene could occur in pagetic lesions in absence of germinal mutation. The objective of this study was to search if *SQSTM1/P392L* post-zygotic mutations can occur in peripheral blood of PDB patients. Methods: Since PCR-clamping method has been reported to be effective to detect post-zygotic mutations in fibrous dysplasia, we optimized this PCR method to detect the *SQSTM1/P392L* post-zygotic mutation in PDB patients. We used a LNA specific for the *SQSTM1/P392L* mutation, which blocks the wild-type allele amplification. We analyzed 217 unrelated PDB patients, and 289 individuals without diagnosis of PDB based on a questionnaire and total alkaline phosphatase measurement, all without any germinal *SQSTM1/P392L* mutation. We then compared PDB patients with post-zygotic mutation (n=11) to unrelated patients with a germinal mutation (n=23) and without any germinal nor post-zygotic mutation (n=207) for age at diagnosis and number of affected bones. Results: Among the PDB patients, eleven (5.1%) were carrier of a *SQSTM1/P392L* post-zygotic mutation and, surprisingly, we identified this post-zygotic mutation in three a priori healthy individuals (1.0%) (p=0.011, OR=5.08 [1.32; 28.71]). PDB patients with a post-zygotic mutation tended to have a lower number of affected bones than patients carrying a germinal mutation (1.91±0.83 vs. 4.45±3.42 respectively, p=0.059). However, we found no association with age at diagnosis in this rather small sample. Conclusion: This study confirms that PCR-clamping increases considerably the sensitivity to detect *SQSTM1/P392L* mutations in the French-Canadian population. The detection of *SQSTM1/P392L* post-zygotic mutation in individuals a priori healthy has possibly led to the identification of individuals with asymptomatic undiagnosed PDB, which we plan to verify with bone imaging. This post-zygotic mutation would less likely act like a polymorphism.

***Disclosures: Sabrina Guay-Bélanger**, None.*

SU0440

Environmental Factors are Associated with Paget's Disease of Bone or with the *SQSTM1/P392L* Mutation Carriage. Marie-Claude Audet*[1], Claudia Beaudoin[2], Jeannette Dumont[2], Jacques P. Brown[3], Laetitia Michou[4]. [1]CHU de Québec, Canada, [2]Centre de recherche du CHU de Québec, Canada, [3]CHU de Québec Research Centre, Canada, [4]Université Laval, Canada

Background: Several publications have demonstrated that the most frequent mutation in Paget's disease of bone (PDB), *SQSTM1/P392L,* leads to some of the phenotypic characteristics of PDB, but this single mutation is seemingly unable to result in the complete pagetic phenotype, suggesting that other mechanisms such as environmental factors may play a role.

Purpose: To identify environmental factors associated with PDB or with the *SQSTM1/P392L* mutation in the French-Canadian population.

Methods: We investigated environmental factors through a questionnaire in 176 French-Canadian patients with PDB and 185 healthy controls. This questionnaire relied on socio-demographic and physical characteristics, tobacco exposure, diet, residency, work, leisure, and contact with animals, during childhood/adolescence and adulthood. We searched for associations with PDB phenotype, or with the *SQSTM1/P392L* mutation (86 individuals carried the mutation and 275 were non carrier), independently of the PDB status. We performed Chi-squared or Fisher exact tests when appropriate for nominal values and t test for continuous variables. Odds ratio (OR) and 95% confidence interval were calculated.

Results: We found an association of PDB with tobacco exposure (p=0.02), which was stronger in individuals who smoked >20 cigarettes per day (p=0.005, OR =2.12 [1.25-3.58]) or for 20 years (p=0.01). PDB was also associated with rural residency in adolescence (p=0.02), residency close to a farm (p=0.02), and wood-fired heating during childhood/adolescence (p=0.001, OR=2.14 [1.37-3.36]). The carriage of the *SQSTM1/P392L* mutation was associated with loss of weight 10kg in 6 months (p=0.04), wood-fired heating during adulthood (p<0.001, OR=3.76 [2.04-6.94]), residency close to a mine (p=0.005, OR=3.21 [1.36-7.58]), work on a farm (p=0.001, OR=2.24 [1.36-3.68]), and contact with dog and bovine during childhood/adolescence (p=0.003, OR=2.22 [1.29-3.81] and p=0.009, OR=1.92 [1.17-3.14], respectively).

Conclusions: The variables most strongly associated with PDB phenotype were smoking 20 cigarettes per day and exposure to wood-fired heating during childhood/adolescence; whereas those most strongly associated with the *SQSTM1/P392L* mutation were exposure to wood-fired heating during adulthood, living close to a mine as well as having worked on a farm and contact with domestic animals during childhood/adolescence. Multivariate analyses should be done to confirm these associations.

***Disclosures: Marie-Claude Audet**, None.*

SU0441

Valosin containing protein is a key link between autophagy and osteoclastogenesis in Paget disease of bone (PDB). Milka Budnik-Zawilska*. University of East Anglia, United Kingdom

Dominant mutations in the N-domain of the valosin containing protein (VCP) give rise to the complex disease syndrome known as Inclusion body myopathy with Paget disease of the bone and frontotemporal dementia (IBMPFD). VCP plays a key role in the ubiquitin-proteasome dependent protein degradation although mutations in VCP result in a late stage autophagy defect. There is also an enhanced activation of NFκB pathway involved and osteoclast precursors containing VCP mutations are hyper-responsive to RANKL. This suggests that under normal homeostasis VCP plays an important role in regulating the response of osteoclasts to bone microenvironment. However, the mechanisms by which VCP mutations stimulate osteoclast differentiation in Paget disease of the bone (PDB) are not completely understood. To investigate this further we examined the role of VCP in autophagy and the role of autophagy on osteoclastogenesis. We used immunofluorescence to evaluate whether VCP co-localises to autophagic components such as p62 (sequestosome) and LC3. We also tested any direct interaction of VCP with p62 and LC3 by co-immunoprecipitation. We assessed the effect of initiating autophagy on osteoclastogenesis by treating RAW264.7 cells with either Rapamycin or Torin 1 at different time point during osteoclastogenesis. Expression of VCP mutants in cell culture results in the increased expression of autophagic markers p62 and LC3. By using immunofluorescence we observe that VCP, p62 and LC3 all co-localize to pathogenic polyglutamine (Q79) inclusions which are degraded by autophagy. In cells expressing poly(Q)-79 both VCP and p62 surround large, perinuclear inclusion bodies, suggesting that VCP is directly involved in the aggresome formation. In contrast, in cells expressing non-pathogenic control polyglutamine repeat (Q35), there's no VCP-positive perinuclear inclusion bodies. We show that VCP co-immunoprecipitates with p62 in the autophagy-dependant manner. Initiation of autophagy in RAW264.7 cells in the presence of RANKL results in marked reduction in osteoclast formation, regardless of the time point at which the treatment begun. These data together with the already existing knowledge on VCP, and the link with PDB, suggest that modulation of the autophagy pathway by VCP may represent a major regulator of bone remodelling and maintenance. We show that autophagy has direct effect on the fate of osteoclast progenitor cells and is thus a key process underlying the pathogenesis of PDB.

***Disclosures: Milka Budnik-Zawilska**, None.*

SU0442

Glucocorticoids antagonize RUNX2 during osteoblast differentiation in a locus and concentration-dependent manner. Theodora Koromila*[1], Anthony Martin[1], Jian Xiong[2], Yae Sam Song[2], Sanjeev Baniwal[1], Baruch Frenkel[1]. [1]University of Southern California, USA, [2]Department of Biochemistry & Molecular Biology, Institute for Genetic Medicine, Keck School of Medicine of the University of Southern California, USA

A common side effect of glucocorticoids (GC) treatment for autoimmune and inflammatory diseases is GC-induced osteoporosis (GIO). One of the mechanisms contributing to GIO is inhibition of the bone master regulator RUNX2 in osteoblast precursors. To address the hypothesis that GCs inhibit RUNX2-mediated stimulation of gene expression in a locus-dependent manner, we employed ST2/Rx2^{dox} cells, a bone marrow stroma-derived pluripotent cell line, engineered to expresses RUNX2 in response to doxycycline (dox). Cells were treated with 500 μg/ml dox either alone or along with 10 nM or 1 μM dexamethasone (dex). Runx2-induced osteoblast differentiation was confirmed by histological staining for alkaline phosphatase (ALP) activity. Expression of RUNX2-responsive genes was measured by RT-qPCR and cell proliferation was assessed by MTT assays. Each assay was performed in triplicate and repeated at least twice. Differences between groups were considered significant when $p<0.05$ using Student's t-test. Dox-mediated induction of RUNX2 was associated with a 3- to 12-fold increased mRNAs levels of all RUNX2-target genes tested including those related to osteoblast differentiation (Bsp, Bglap, Alp) and those related to osteoblast-driven osteoclastogenesis (Sema7a, Tnc, OPG, Hey1, Cdk5rp, Enfb1). Dex antagonized RUNX2-mediated stimulation of all the genes tested. This antagonism, however, was strongly dependent on the target gene and the dex concentration. Whereas 10 nM dex antagonized RUNX2-mediated stimulation of most genes tested, the RUNX2-mediated stimulation of Alp and Efnb1 was resistant to 10 nM Dex. In contrast, 1 μM Dex antagonized RUNX2-mediated stimulation of all genes tested. Consistent with the Alp mRNA results, histological staining demonstrated inhibition of RUNX2-induced ALP activity by 1 μM, but not 10 nM Dex. MTT assays showed no significant alterations in cell proliferation. The locus-dependent antagonism of RUNX2 by increasing dex concentrations offers an opportunity to discern RUNX2 target genes relevant to GIO. Specifically, the inhibitory effects of GCs at most RUNX2 target genes is likely irrelevant to GIO because these genes are strongly affected at low GC concentrations, which inhibit neither osteoblast differentiation in vitro nor bone formation in vivo. Genome-wide analysis of the concentration-dependent interactions between RUNX2 and GCs in osteoblast progenitor cells will facilitate identification of GIO-relevant RUNX2 target genes.

***Disclosures: Theodora Koromila**, None.*

SU0443

Glucocorticoids Promote a Greater Decrease of VEGF, RANKL, Bone Turnover, Vasculature, and Material Properties in the Murine Femoral Head as Compared to the Distal Femur or Lumbar Vertebra: New Insights into the Pathogenesis of Osteonecrosis. Robert Weinstein*, Erin A. Hogan, Stuart B Berryhill, Stavros Manolagas. Central Arkansas VA Healthcare System, University of Arkansas for Medical Sciences, USA

Glucocorticoids (GC) are the most common cause of nontraumatic osteonecrosis of the femoral head but the reason for the susceptibility of this site is unexplained, the cellular and molecular mechanisms responsible remain unidentified, and the sequential pathological changes are unknown. We report that in C57Bl/6 mice, expression of both the receptor activator of nuclear factor-κB ligand (RANKL) and vascular endothelial growth factor (VEGF), and the bone formation rate were higher in the cancellous bone of the femoral head than in the distal femur or lumbar vertebra (L5). Fourteen days after prednisolone administration, cancellous bone volume of the femoral head began to decrease and was markedly lower than placebo after 28 days, well before significant changes were detected in the distal femur or L5. Osteocalcin, RANKL, and VEGF expression in the femoral head decreased after GC, but RANKL and VEGF did not change in the distal femur or L5. Surprisingly, the material density of the femoral head increased similar to the radiographic sclerosis typical of clinical osteonecrosis; nonetheless, GC reduced the strength and toughness of the femoral head. In addition, the dendritic pattern of the vasculature of the femoral head, as determined by infusion of lead chromate, was converted to lakes, in distinction to the femoral diaphysis and L5 where vessel volume decreased but dendritic morphology was preserved. The abnormal vascular pattern was verified histologically and was reminiscent of the increased water signal detected by magnetic resonance imaging in patients with osteonecrosis. GC also decreased canalicular fluid as determined by reduced cancellous fluorescence after injection of procion red, perhaps accounting for the decreased strength in spite of increased material density. Finally, in line with clinical evidence that repeated delivery of large doses of GC is associated with a greater risk of osteonecrosis than with steady-state dosage, sequential high GC administration induced a unique and profound increase in femoral head cortical and cancellous porosity and in osteoclast number. These results validate the mouse as a model of glucocorticoid-induced osteonecrosis of the femoral head that replicates the progression of the human disorder. Furthermore, they suggest that the susceptibility of the load-bearing femoral head to osteonecrosis may be due to the high bone turnover of this site and the abrupt remodeling imbalance caused by GC administration.

***Disclosures: Robert Weinstein**, None.*

SU0444

Treatment of aged rats with methylprednisolone decreases bone mass accrual by suppression of bone formation. Rana Samadfam*, Elisabeth Lesage, Susan Y. Smith. Charles River Laboratories, Canada

The objective of this study was to investigate the effects of methylprednisolone (3 mg/kg/day) on bone when administered to aged rats (19 weeks old female Wistar Hannover) with an inactive growth plate, for a period of 13 weeks. The effects on bone densitometry and bone geometry were evaluated using pQCT at baseline and at Weeks 4 and 13. In addition, body weight, food consumption, selected urine and serum biochemistry, bone turnover markers, PTH and 1, 25 dihydroxyvitaminD were also evaluated to add perspective to mechanisms underlying the effects on bone. A sharp decrease in body weight was noted one week following treatment compared to the baseline with no further loss for the remaining of the treatment period. Steady weight gain for controls over the treatment period along with lack of gain (or loss during the first week) resulted in marked differences between treated and controls. Trends for increases in food consumption were noted compared to controls. At the proximal tibia metaphysis the mean BMC (bone mineral content) and BMD (bone mineral density) were significantly lower compared to vehicle controls. Slightly lower values were also noted for total slice area. At the diaphysis, significantly lower BMC was noted with lower bone diameter indices, indicating smaller bones. Lower bone geometry indices at the diaphysis (total slice area, periosteal circumference) along with shorter bone length were consistent with the lower body weights and slower or lack of growth. Growth suppression was consistent with decreases in bone formation markers (osteocalcin and P1NP) most notably at Week 4/5. No effect was noted on the bone resorption markers. No effect was noted on PTH with a trend for decreases in VD3 at week 4. No effects were noted on serum biochemistry including phosphrous and calcium. Statistically significant increases in urinary calcium were noted over the study period compared to controls. Lack of any significant effects on bone resorption along with increases in urinary calcium suggests an increase in the GI absorption of calcium. Slight increases in food consumption (in spite of lower body weight) are in agreement with this observation. These data collectively indicate that treatment with methylprednisolone is associated with decreases in bone formation resulting in lower values for bone densitometry indices.

***Disclosures: Rana Samadfam**, None.*
This study received funding from: Novartis

SU0445

Gene Expression Profiling of Avian Osteoclasts Treated with Estrogen for Exploring Unidentified Action(s) of Estrogen in Bone. Shinji Hiyama*[1], Yumiko Kadoyama[2], Mineo Watanabe[1], Takashi Uchida[1]. [1]Hiroshima University Institute of Biomedical & Health Sciences, Japan, [2]Hiroshima University, Faculty of Dentistry, Japan

Medullary bone (MB), a calcium reservoir for egg-shell formation, in the bone marrow cavity of female birds is remodeled under the powerful control of estrogen. A single injection of estrogen causes the formation of MB even in male birds and subsequent activation of bone resorption by osteoclasts with diminished circulating estrogen levels. Estrogen induces osteoclast apoptosis, which may be implicated in postmenopausal bone loss. This hormone, however, does not induce apoptosis in MB osteoclasts, while their activity and morphology were affected. Clarifying the difference between avian and mammalian osteoclast responses to estrogen may be valuable to identify additional roles of estrogen in bone. We, then, provided a comprehensive analysis of the estrogen-dependent gene expression in the avian medullary bone osteoclastogenesis model. Male Japanese quails were given a single injection of 17b-estradiol (E2). After a couple of days, bone marrow cells were collected and cultured with or without E2 in the presence of RANKL/M-CSF for a week. Total RNA was extracted and subjected into DNA microarray analysis (Chicken oligoDNA). In parallel with these cultures, we estimated the effects of E2 on osteoclast formation and activity by TRAP staining and pit assay, respectively. As described before, E2 did not change the number of osteoclasts, while it decreased their resorption activity. Of the genes displaying significant changes (more than 4-fold) in expression levels, 108 genes were up-regulated and 42 genes were down-regulated in response to E2. We found that 13 genes (up, 10 genes; down, 3 genes) were identical to functional genes in mammalian osteoclasts. Amongst these, 11 genes are involved in osteoclastogenesis and 3 genes are associated with bone resorption, e.g., NHA2, CTLA-4 and ATG7. Further, remainders (137 genes) included common genes with unknown functions in bone and avian-specific genes, such as multimerin 1, GAL7 and TICAM1. We are exploring functional genes involved in both avian and mammalian osteoclasts by siRNA-meidated gene silencing.

***Disclosures: Shinji Hiyama**, None.*

SU0446

Oxidative Stress Induced CD4 T Cell Activation Plays A Critical Role in Estrogen Deficiency Induced Bone Loss Mediated via Bmi1. Jinbo Li*[1], Qian Wang[1], Dengshun Miao[2]. [1]Nanjing Medical University, China, [2]Nunjing Medical University, Peoples Republic of China

Role of CD4 T cell activation in estrogen-deficiency induced bone loss has been well studied; however, it is unclear whether oxidative stress mediates such role. To answer this question, we examined the effect of ovariectomy (OVX) on oxidative stress, CD4 T cell activation and RANKL production. Results revealed that ROS levels were raised, whereas expression levels of antioxidant enzyme genes including SOD2, GSR and GPX1 were down-regulated, the percentage of activated T cells and RANKL production were increased significantly in CD4 T cells from OVX mice compared those from sham mice. Moreover, oxidative stress induced by H_2O_2 increased activated CD4 T cells when con-cultured with macrophages. Previous studies have demonstrated that Bmi1 deficiency resulted in increasing oxidative stress and bone loss. To explore whether Bmi1 involves estrogen-deficiency induced bone loss by regulating oxidative stress, we examined the effect of OVX on Bmi1 expression and found that Bmi1 expression at both mRNA and protein levels were down-regulated dramatically in CD4 T cells from OVX mice. Furthermore, we found that alterations of oxidative stress, CD4 T cell activation, RANKL production related parameters in Bmi1 deficient mice were closely resembled those occurred in OVX mice. In contrast, the alterations of those parameters were reversed in Eμ-Bmi1 transgenic (Eμ-Bmi1) mice with overexpression of Bmi1 in lymphocytes. To further determine whether oxidative stress mediates CD4 T cell activation in estrogen-deficiency and Bmi1 deficiency induced bone loss, OVX mice and $Bmi1^{-/-}$ mice were treated with antioxidant N-acetylcysteine (NAC, 1mg/ml) in their drinking water and compared them with untreated OVX and $Bmi1^{-/-}$ mice, respectively. NAC supplementation of OVX mice and $Bmi1^{-/-}$ mice decreased ROS levels, inhibited CD4 T cell activation and reduced RANKL production in CD4 T cells. Consequently, BMD, cortical and trabecular volume were increased significantly, whereas TRAP positive osteoclast surface was reduced significantly in NAC-treated OVX and $Bmi1^{-/-}$ mice compared to untreated ones. To determine whether Bmi1 mediates estrogen deficiency induced bone loss, we created estrogen deficient Eμ-Bmi1 (Eμ-Bmi1+OVX) mice and found that those alterations occurred in OVX mice were rescued in Eμ-Bmi1+OVX mice. These results indicate that oxidative stress induced CD4 T cell activation plays a critical role in estrogen deficiency induced bone loss mediated via Bmi1.

***Disclosures: Jinbo Li**, None.*

SU0447

Duodenal Ca Absorption Increases to Compensate for the Loss of Vitamin D Receptor (VDR) from the Large Intestine and Kidney of Mice. Perla Reyes*, James Fleet. Purdue University, USA

Habitual consumption of low dietary Ca increases renal 1,25 dihydroxyvitamin D (1,25D) production to stimulate vitamin D receptor (VDR)-mediated regulation of genes that increase Ca absorption efficiency in intestine, Ca reabsorption in the kidney, and bone resorption. Our previous research suggests that 1,25D-mediated Ca absorption in the lower bowel contributes significantly to whole body Ca homeostasis. Our goal was to determine the impact of large intestinal VDR deletion on Ca/bone metabolism. We used the CDX2P9.5 promoter-Cre transgenic mice to delete floxed VDR alleles throughout the caudal region of the mouse. This was confirmed by detection of Cre recombinase activity in multiple tissues, including kidney, ileum, and colon. Weanling $CDX2\text{-}Cre^{+/-}$,$VDR^{fl/fl}$ (CDX2-VDRKO) and control littermates ($CDX2\text{-}Cre^{-/-}$,$VDR^{fl/fl}$, WT) mice were fed low (0.25%) or normal (0.5%) Ca diets until 10 weeks of age. Serum and urinary Ca, vitamin D metabolites, bone parameters (by μCT), and gene expression in kidney, duodenum, ileum and colon were analyzed. Serum 1,25D was increased by low Ca intake but was not different between genotypes while CDX2-VDRKO mice had serum PTH levels 67% lower than WT mice ($p<0.001$). CDX2-VDRKO mice had renal mRNA levels consistent with those previously seen in global VDR KO mice, i.e. low calbindin D_{9k} (CaBPD9k, -85% WT $p<0.001$), high TRPV5 (+49%, $p<0.005$), and no change in CaBPD28k mRNA levels. In addition, urinary Ca/creatinine ratio was 10-fold higher ($p<0.001$) in CDX2-VDRKO mice. As expected, TRPV6 mRNA levels (a marker of active Ca absorption) were low in the proximal (-92% WT, $p<0.001$) and distal colon (-88% WT, $p<0.001$) where the VDR was deleted in CDX2-VDRKO mice. Despite elevated urinary Ca loss and reduced TRPV6 expression in the lower bowel, CDX2-VDRKO mice had normal femoral cancellous and cortical bone density. However, duodenal TRPV6 mRNA expression was 4-fold higher in CDX2-VDRKO compared to WT mice ($p<0.001$), suggesting that there is up-regulation of duodenal Ca absorption that protects bone and contributes to increased urinary Ca loss. These data support the hypothesis that large intestine VDR significantly contributes to whole body Ca metabolism but suggests that duodenal adaptation can prevent the consequences of VDR deletion from large intestine and kidney.

***Disclosures: Perla Reyes**, None.*

SU0448

Effect of Vitamin D Receptor Gene Polymorphism on Associations between Serum 25-hydroxyvitamin D and Biochemical Parameters in Young Adults.
Rieko Tanabe*[1], Yuka Kawamura[1], Naoko Tsugawa[2], Mayu Haraikawa[1], Natsuko Sogabe[3], Toshio Okano[2], Takayuki Hosoi[4], Masae Goseki-Sone[5]. [1]Department of Food & Nutrition, Faculty of Human Sciences & Design, Japan Women's University, Japan, [2]Kobe Pharmaceutical University, Japan, [3]Department of Health & Nutrition Sciences, Faculty of Human HEalth, Komazawa Women's University, Japan, [4]National Center for Geriatrics & Gerontology, Japan, [5]Japan Women's University, Japan

Several genes have been implicated as genetic determinants of osteoporosis. Vitamin D receptor (VDR) is an intracellular hormone receptor that specifically binds to the biologically active form of vitamin D, 1-alpha, 25-dihydroxyvitamin D_3 [1, $25(OH)_2D$], and mediates its effects. One of the most frequently studied single nucleotide polymorphisms is the restriction fragment length polymorphism (RFLP) *Fok-I* (rs2228570). The presence of a *Fok-I* site, designated f, allows protein translation to initiate from the first ATG. An allele lacking the site (ATG>ACG: designated F), initiates from a second ATG site. Thus, translation products from these alleles are predicted to differ by three amino acids with the f variant elongated. In the present study, we explored the effect of the VDR *Fok-I* genotype on associations among serum bone-specific alkaline phosphatase, 25-hydroxyvitamin D_3 [25(OH)D], 1, $25(OH)_2D$, intact parathyroid hormone (PTH), and the dietary nutrient intake in healthy young Japanese subjects (n=193). Dietary nutrient intakes were calculated based on 3-day food records before the day of blood examinations. Quantitative ultrasound (QUS) parameters at the right calcaneus were measured. The study protocol was approved by the Institutional Review Board of Japan Women's University, and written informed consent was obtained from all study subjects. As the results, the mean ($\pm$SD) levels of serum bone-specific alkaline phosphatase, 25(OH)D, 1, $25(OH)_2D$, and intact-PTH were 26.9 ± 7.8 U/l, 20.1 $\pm$ 6.9 ng/ml, 50 ± 17 pg/ml, and 43 ± 13 pg/ml, respectively. The allele frequencies were 0.622 for the F allele and 0.378 for the f allele in all subjects. Grouped by the *VDR* genotype, a significant positive correlation between the levels of serum bone-specific alkaline phosphatase activity and 25(OH)D was observed in the FF-type (38% of the study population) (p=0.005) and Ff-type (48% of the study population) (p=0.004), but not in the ff-type (14% of the study population). In addition, there was a significant positive correlation between the level of serum 25(OH)D and osteo-sonoassessment index (OSI) in the FF-type (p=0.008). There was no such significant positive correlation between the level of serum 25(OH)D and OSI in the ff-type. These results suggest that the level of circulating 25(OH)D is an important factor when assessing the VDR *Fok-I* polymorphism to prevent osteoporosis.

***Disclosures: Rieko Tanabe**, None.*

SU0449

Gender-related differences in the skeletal phenotype of aged Vitamin D Receptor Knockout mice.
Jackson Ryan*[1], Howard Morris[2], Paul Anderson[3]. [1]University of South Australia, Australia, [2]SA Pathology, Australia, [3]Musculoskeletal Biology Research, University of South Australia, Australia

Global VDR deletion in a mouse model (VDR-/-) demonstrates features typical of vitamin D-dependent rickets type II unless weanling mice are fed a 'rescue' diet containing high levels of calcium (2%) and phosphorus (1.25%). This diet prevents the development of hypocalcemia and secondary hyperparathyroidism and is sufficient to normalise mineralization of bone at 10 weeks of age. However, at 17 weeks of age male VDR-/- exhibit marked osteopenia associated with decreased osteoblast number and mineral apposition rate, despite no induction of osteoclast activity (Panda, et. al. 2004). The role for VDR in bone appears to be complex and dependent on the physiological context, with reports of both inhibitory and enhancing roles of VDR in bone in both *in vitro* and *in vivo* studies[1-3]. To clarify the role of VDR in maintaining skeletal health in aged animals, male and female VDR-/- mice were fed a rescue diet containing 2% calcium and 1.25% phosphorus from weaning until 26 weeks of age and compared to VDR+/- litter mate controls fed the same diet. At time of death, femora and tibia were collected for histomorphometric analyses. Consistent with previously reported data[4], in male VDR-/- mice, metaphyseal BV/TV% declined (36%; p=0.06) due to decreased Tb.Th (p=0.03). Cortical bone volume and width were also decreased (23%, p=0.003; 10% p=0.006) when compared to control. However, in female VDR-/- mice metaphyseal BV/TV% increased 2-fold (p=0.04), largely due to increased Tb.N (p=0.009), compared to control mice. No significant differences were seen in cortical bone volume or width of female mice. These data suggest that there exist significant gender-related differences with regards to the role of VDR in maintenance of bone mineral volume in aged animals. Furthermore, quantitation of calcium content of trabecular bone was performed using back-scatter electron microscopy. Male VDR-/- mice display a significant increase in calcium width (24%; p=0.004), with no changes to overall wt% calcium within trabecular bone, suggesting greater heterogeneity of the mineralisation state in male VDR-/- mice compared to control mice. Taken together, these data suggest that VDR is required to maintain both bone quantity and bone quality and these effects are dependent on age and gender.

1. Gardiner, E, et al. (2000) *FASEB* (14) 1908-1916
2. Matsumoto, T, et al. (1991) *Bone* (12) 27–32
3. Lieben, L, et al. (2012) *JCI* (4), 1-13
4. Panda, D, et al. (2004) *Biochemistry 279*(16) 16754 -16766

***Disclosures: Jackson Ryan**, None.*

SU0450

Mechanism of Hyponatremia-Related Vitamin D Deficiency in Rats.
Julia (Julianna) Barsony*[1], Qin Xu[2], Aifen Wang[2], Joseph Verbalis[2]. [1]Georgetown University Hospital, USA, [2]Georgetown University, USA

Chronic hyponatremia is frequent in the aging population due to medication use and the syndrome of inappropriate antidiuretic hormone secretion (SIADH), and has been associated with increased fall risk and fracture frequency in patients, and with high bone resorption and loss of bone mineral density (BMD) in a rat model of SIADH. Chronically hyponatremic old and young male and female rats all displayed features of vitamin D deficiency, including reduced serum 25OHD and $1,25(OH)_2D$ levels. It is difficult to isolate causes of vitamin D deficiency in elderly patients; therefore we used our rat model to explore how hyponatremia might lead to abnormal vitamin D metabolism. In two experiments, 12-month-old male and female F44BN rats (8 per group) were infused with desmopressin at 5 ng/h and fed a liquid diet to generate hyponatremia (serum $[Na^+]=114 \pm 8$ mmol/L) for 3 months; controls were pair-fed with the same liquid diet but did not receive desmopressin infusions (serum $[Na^+]=147 \pm 1$ mmol/L). All rats received defined vitamin D3 in the liquid diet (75 IU/day) in the first experiment, and received10-fold higher vitamin D3 in the diet (750 IU/day) in the second experiment. In both experiments, urine 25OHD losses were increased in hyponatremic rats, in proportion to the vitamin D intake. Urine vitamin D binding protein (DBP) and albumin were significantly increased in the hyponatremic rats, more so in males than females. Serum albumin was significantly reduced in both male and female hyponatremic rats, and DBP was slightly reduced. Serum $1,25(OH)_2D$ were reduced and PTH and alkaline phosphatase were moderately increased in hyponatremic groups (males more than females), which may have contributed to the bone loss observed by DXA and micro-CT. Analysis of mRNA expression from kidneys revealed that hyponatremia did not significantly influence VDR expression, but it increased 1alpha-hydroxylase (CYP27b1) and reduced 24-hydroxylase (CYP24a1) expression. The increased urinary vitamin D metabolite clearance was associated with 2-fold reduced megalin (LRP2) mRNA expression ($p<0.01$) in the kidneys from hyponatremic rats; this finding was corroborated by reduced kidney megalin protein expression by immunohistochemistry. Our studies demonstrated for the first time that hyponatremia caused vitamin D deficiency in a rat model of SIADH by inhibiting renal megalin expression, thereby causing increased urinary clearance of vitamin D metabolites along with DBP and albumin.

***Disclosures: Julia (Julianna) Barsony**, None.*

SU0451

Ratio of 25-OH-D_3:24,25-$(OH)_2D_3$ is a Novel and Sensitive Measure of Predicting Vitamin D Deficiency.
Martin Kaufmann*[1], J. Christopher Gallagher[2], Munro Peacock[3], Glenville Jones[1]. [1]Queen's University, Canada, [2]Cheighton University Medical School, USA, [3]Indiana University Medical Center, USA

Background: Normal healthy women were recruited for a vitamin D supplementation study; the inclusion criteria included serum 25-hydroxyvitamin D (25-OH-D)< 20ng/ml threshold and no condition that affected calcium and vitamin D metabolism. Because serum 25-OH-D plateaued at the 4,000 IU/day dose level, we explored the role of 25-OH-D_3-24 hydroxylase (CYP24A1) in the regulation of serum 25-OH-D.

Methods: Subjects: 273 healthy Caucasian & African American postmenopausal women age 57-90 years, randomized to 6 doses of vitamin D ranging from 400-4800 IU/day or placebo for 1 year; and 190 young Caucasian and African American women (25-45 years). The primary outcomes of the study were serum 25-OH-D & parathyroid hormone (PTH) levels. A secondary outcome was measurement of serum 24,25-$(OH)_2D_3$. Serum 25-OH-D & 24,25-$(OH)_2D_3$ were measured by liquid chromatography-tandem mass spectrometry using a Waters Xevo TQ-S instrument after derivatization.

Results: Serum 25-OH-D ranged between 5-85 ng/mL; serum 24,25-$(OH)_2D_3$ ranged between 0.1-15 ng/mL; the ratio of 25-OH-D_3: 24,25-$(OH)_2D_3$ ranged between 4-75. After vitamin D supplementation, there was a curvilinear increase in serum 25-OH-D best described by a quadratic model and plateauing at 40-45 ng/ml, showing that serum 25-OH-D is more closely regulated than previously expected. Serum 24,25-$(OH)_2D_3$ increased from a mean value of 1.18 ng/ml to 5.35 ng/ml reaching a plateau at about the 4000 IU dose and showed the same curvilinear increase as the serum 25-OH-D curve. Women with baseline values for 25-OH-D in the 5-12 ng/mL range showed the highest serum 25-OH-D_3: 24,25-$(OH)_2D_3$ ratios of 20-75.

Conclusion: In normal subjects treated with increasing doses of vitamin D there is a wide range of serum 25-OH-D_3 values and a similar curvilinear increase in serum 25-OH-D_3 and serum 24,25-$(OH)_2D_3$ that reaches a plateau on vitamin D doses of about 4000 IU/day. Since CYP24A1 is documented to be the most responsive vitamin D-dependent gene in the human genome, we would expect that CYP24A1 expression to be suppressed in vitamin D deficiency and serum 24,25-$(OH)_2D_3$ levels to decline. We

conclude that a 25-OH-D_3:24,25-$(OH)_2D_3$ ratio less than 25 is a sensitive indicator of vitamin D deficiency & insufficiency and may be a more sensitive measure than PTH. In summary, we found the ratio of 25-OH-D_3: 24,25-$(OH)_2D_3$ is a sensitive predictor of vitamin D deficiency and insufficiency.

***Disclosures: Martin Kaufmann**, None.*

SU0452

Redistribution of the hormone binding protein catalase by 24,25-dihydroxyvitamin D_3. Ilka Nemere*, Yang Zhang. Utah State University, USA

The vitamin D metabolite, 24,25-dihydroxyvitamin D_3 (24,25D_3) is made in vitamin D replete animals, and has been shown by our lab to act as an inhibitor of 1,25-dihydroxyvitamin D_3 with regard to abolishing rapid, pre-genomic responses such as enhanced calcium or phosphate uptake in intestinal cells. We subsequently identified catalase as the binding protein for 24,25D_3 in chick intestinal cells. Upon binding the steroid, catalase activity is decreased and the subsequent increase in H_2O_2 levels oxidizes the 1,25D_3-MARRS receptor, thereby inhibiting the action of 1,25D_3. Catalase is classically thought of as a peroxisomal enzyme. A subset of catalase has been reported to be at the cell surface or complexed with the transcription factor STAT 3. In this study we used confocal microscopy to determine catalase localization in the absence and presence of steroid. Intestinal cells isolated by citrate chelation were cultured on coverslips overnight and then treated with vehicle, 300 pM 1,25D_3, 6.5 nM 24R,25D_3, or 200 pM 24S,25D_3 for varying times prior to fixation, permeabilization, and immunostaining. We found that in permeabilized, vehicle-treated cells, punctate staining for catalase was visible, but diminished rapidly after 15 minutes treatment with 1,25D_3 or 25 minutes treatment with 24S,25D_3, but not with 24R,25D_3. Since 1,25D_3 does not compete with 24,25D_3 for binding to catalase, its effects may be due to the 1,25D_3-MARRS receptor causing actin depolymerization (Sterling and Nemere, unpublished observations). 24R,25D_3 treatment also increased nuclear staining of catalase after 15 min. In unpermeabilized cells treated wtih 200 pM 24S,25D_3 or 6.5 nM 24R,25D_3, we observed both a significant decrease in catalase activity compared with vehicle treated cells, with a p-value less than 0.05. Additional studies are on going in unpermeabilized cells to see what effects these steroids have on cell surface catalase.

***Disclosures: Ilka Nemere**, None.*

SU0453

Studies in Mice with Transgenic Expression of the Vitamin D Receptor (VDR) Exclusively in the Distal Intestine of VDR Knockout Mice Provide Evidence for a Critical Role of Intestinal Epithelial Cells in the Suppression of Inflammatory Bowel Disease by 1,25$(OH)_2D_3$/VDR. Ran Wei*, Puneet Dhawan, Sylvia Christakos. University of Medicine & Dentistry & New Jersey - New Jersey Medical School, USA

Inflammatory bowel disease (IBD) is a chronic disorder of the GI tract that includes ulcerative colitis and Crohn's disease. Although immune dysfunction has been implicated in the development of the disease, its pathogenesis is still poorly understood. Previous studies reported a link between vitamin D deficiency and IBD and VDR knock out (KO) mice develop more severe IBD. The enhanced severity of IBD in VDR KO mice has been associated with increased numbers of IL-17 and IFNγ secreting T cells. However T cell deficient mice develop IBD, suggesting that other pathways may also be involved in the enhanced susceptibility of VDR KO mice to IBD. In this study VDR KO mice with transgenic expression of VDR exclusively in the distal intestine (distal ileum, cecum and colon) provided a unique model to determine whether the enhanced susceptibility of VDR KO mice to IBD can be entirely caused by a lack of VDR in intestinal epithelial cells. We previously reported the generation of mice expressing VDR exclusively in distal intestine [serum PTH and serum calcium are similar to wild type (WT) and VDR dependent rickets is rescued]. WT, VDR KO mice and mice from two KO transgenic lines (KO/TG [1] and KO/TG [2] which express levels of VDR in distal intestine equivalent to WT) were administered 3.5% dextran sodium sulfate (DSS) in the drinking water. VDR KO mice began to die by the 7th day post DSS administration. Diarrhea, rectal bleeding and loss of body weight preceded mortality of the VDR KO mice. WT mice and KO/TG [1] and [2] mice did not die and showed mild diarrhea and bleeding. DSS treatment that caused a mild form of colitis in WT and KO/TG mice resulted in extensive mucosal damage and blood in the colon of VDR KO mice. In one transgenic line (KO/TG3), which showed low VDR expression, DSS treatment resulted in more severe symptoms than those observed in the other transgenic lines but not as severe as in VDR KO mice. 1,25$(OH)_2D_3$ treatment (0.5 ng/g bw/day) significantly improved symptoms of DSS colitis in WT mice as well as in all 3 transgenic lines and was associated with an induction in colonic expression of E-cadherin. These findings indicate for the first time that VDR expressed only in intestinal epithelial cells can control susceptibility to IBD. Since VDR is absent from immune cells in KO/TG mice, our findings suggest a critical role of intestinal epithelial cells and maintenance epithelial cell integrity in the suppression of IBD by 1,25$(OH)_2D_3$/VDR.

***Disclosures: Ran Wei**, None.*

SU0454

Two-step immunoassay for free 25 Hydroxy Vitamin D. Leon Swinkels, Ernst Lindhout*, Niels Donnelly, Gregg Mayer, Mike Martens. Future Diagnostics, The Netherlands

The objective of this study was to assess the characteristics of a two-step immunoassay for free 25 Hydroxy Vitamin D [25(OH)VitD].

Recent studies suggest that the level and genotype of Vitamin D binding protein (DBP) are important factors that determine the bioavailability of 25(OH)VitD in serum. It has been suggested that measurement of free, non-protein bound 25(OH)VitD in serum, may provide more relevant diagnostic information than total 25(OH)VitD, for instance in bladder cancer and pancreatic cancer (1), or in hemodialysis patients (2).

We have developed a two-step enzyme-linked immunosorbent assay (ELISA) for the determination of free 25(OH)VitD assay. In this assay an anti-vitamin D antibody is coated on a microtiterplate. Free 25(OH)VitD is captured by the antibody during a first incubation. After washing, a biotin-labeled 25(OH)VitD analog is allowed to react with the non-occupied antibody binding sites in a second incubation. After washing and incubation with a streptavidin-peroxidase conjugate, the bound enzyme is quantitated using a colorimetric reaction. The intensity of the signal is inversely proportional to the level of free 25(OH)VitD in the sample. The assay was calibrated against a symmetric dialysis method.

The calibrator range was 0.0 – 35.0 pg/ml. The LOB of the assay was 1.1 pg/ml; the LOD was 1.7 pg/ml. Total assay precision was 5.7% at 6.3 pg/ml, 3.8% at 15.9 pg/ml and 4.8% at 24.8 pg/ml. The antibody in this assay cross-reacts with 25(OH)VitD2 for 60%.

A better inverse correlation was found between PTH and free 25(OH)VitD than between PTH and total 25(OH)VitD in a set of random patient samples that were sent in for measurement of total 25(OH)VitD.

We have developed an assay that reproducibly determines the level of free 25(OH)VitD. The assay can be used as a tool in studies to establish the clinical relevance of bioavailable 25(OH)VitD .

1. Weinstein SJ, Stolzenberg-Solomon RZ, Kopp W, Rager H, Virtamo J, Albanes D. Impact of circulating vitamin D binding protein levels on the association between 25-hydroxyvitamin D and pancreatic cancer risk: a nested case-control study.
Cancer Res. 2012 Mar 1;72(5):1190-8.

2. Bhan I, Powe CE, Berg AH, Ankers E, Wenger JB, Karumanchi SA, Thadhani RI. Bioavailable vitamin D is more tightly linked to mineral metabolism than total vitamin D in incident hemodialysis patients.
Kidney Int. 2012 Jul;82(1):84-9.

***Disclosures: Ernst Lindhout**, Future Diagnostics, 3*
This study received funding from: Future Diagnostics

SU0455

Vitamin D Levels in HIV Infected Adults and its Relation with Immunologic and Virologic Status. Exploratory Study. Silvina Mastaglia*[1], Natalia Bello[2], Vanesa Fridman[2], Daniel Stecher[2], Beatriz Oliveri[3]. [1]Laboratorio de Enfermedades Metabólicas Oseas, Instituto de Inmunología, Genética,y Metabolismo (INIGEM), Hospital de Clínicas, CONCET-UBA. * Researcher of the National Council on Scientific & Technical Research (CONICET)., Argentina, [2]División Infectologia, Departamento de Medicina Interna, Hospital de Clínicas, Universidad de Buenos Aires, Argentina, [3]Centro De Osteopatías Médicas, Argentina

Vitamin D has strong immunomodulting properties. The nuclear vitamin D receptor is expressed in various immune cell lines which locally convert vitamin D to its active form 1,25-dihydroxyvitamin D (1,25[OH]2 D). Under infection condition 1,25[OH]2 D stimulate the production in monocytes and macrophages the antimicrobial peptide, cathelicidin. In vitro studies demonstrate cathelicidin's ability to inhibit HIV replication in CD4+ T cell and macrophages. Aim: evaluated the relationship between 25-hidroxyvitamin D (25OHD), CD4 and HIV viral load. Fifty six clinical records from patients with diagnostic HIV/AIDS attending to the Division of Infectology, Department of Internal Medicine, Clinical Hospital, Buenos Aires University. The data of clinical record as predictors of low vitamin D metabolite were the following: age, gender, ethnicity, duration of HIV infection, hepatic and renal diseases, diagnostic of osteopenia or osteoporosis, vitamin D supplementation and season in that 25OHD was measured. The biochemical parameters were: 25OHD [RIA-DIASORIN], CD4 cell count (absolute number and percentage) and HIV viral load. We considered for this study 25OHD levels sufficient that $\geq$30ng/ml, insufficient: 21-29ng/ml, inadequate $\leq$20ng/ml and deficient $\leq$10ng/ml. Results: In the table 1 showed characteristics of the 56 patients according to 25OHD levels. We observed that 76% of the patients with HIV/AIDS showed 25OHD levels below 30ng/ml (insufficient 28%; inadequate: 30% and deficient: 20%). Our results are consistent with others HIV cohorts recent report[1-3]. A weak negative lineal correlation was observed between 25OHD levels deficient and HIV load, log10 ($r=-0.591$; $p<0.05$) but there are no correlations between 25OHD and CD4 (absolute number/%). Conclusion: Vitamin D deficiency was common in this HIV population, as seen in other HIV cohorts. Vitamin D deficit may affect the immune responder to HIV viral load. Future studies are required to understand the vitamin D metabolism in the HIV/AIDS infection.[1]AIDS 2010; 24:1127-1134; [2]Clin Infect Dis.2011; 52:396-405, [3]AIDS 2011; 25:1305-1315.

Table 1: Characteristics of the patients according to 25OHD levels (mean ±SD)

	25OHD (ng/ml) levels			
Characteristics	Sufficient(≥30) (n=13)	Insufficient(21-29) (n=15)	Inadequate (≤20) (n=17)	Deficient(≤10) (n=11)
Age(years)	49.4±15	53.2±12	50.6±13	58.0±14
Sex: F/M (%)	85/15	60/40	65/35	64/36
Season: WS/SO (n)	10/3	9/6	12/5	7/4
CD4(cells/ml)	630.58±349	554.66±242	446.11±216	615.45±299
CD4 (%)	28.2±10	26.7±9	23.7±9	27.6±11
HIV viral load,log10	1.6±0.3	1.7±0.3	1.7±0.6	1.6±0.2
25OHD (ng/ml)	43.8±12*	24.9±1.2	14.6±2.3	8.17±1.9

F: female; M: masculine; W-S: winter-spring; S-O: summer-autumn

*p<0.000

Table 1

***Disclosures: Silvina Mastaglia**, None.*

SU0456

Are BMP4 and Runx2 more prevalent in malignant canine mammary tumors?. Kristi Milley*[1], Barbara Bacci[2], Stewart Ryan[2], Janine Danks[3]. [1]RMIT University, Australia, [2]The University of Melbourne, Faculty of Veterinary Science, Australia, [3]School of Medical Sciences, RMIT University, Australia

Recently in humans, the presence of a group of proteins traditionally associated with bone and cartilage formation have been demonstrated in breast cancers. These genes include bone morphogenetic protein 4 (BMP4) and Runt related transcription factor 2 (Runx2).

There is limited data on the role of BMP4 in breast cancer in humans. It is known that BMP4 is expressed at low levels in normal tissue whilst tumors have significantly increased expression levels. BMP4 positive breast cancers that are positiveare associated with reduced proliferation rates but also associated with increased recurrence (Alarmo et al. Mod Pathol. 26:10, 2013).

Runx2 has been demonstrated to play a role in human breast cancer progression, particularly in hormone receptor negative cancers and is an independent prognostic factor (Onodera et al. Cancer Sci. 101:2670, 2010). Consequently, the presence of this protein in canine mammary tumours (CMT) is important as the majority are hormone receptor negative and could be used as a prognostic marker.

CMTs are similar to human breast cancers in many crucial respects including hormone dependency, onset age and tumour kinetics (Uva et. al. BMC Genomics 10:135, 2009). Genome-wide comparative analysis of the main pathways involved in breast cancer has shown that transcriptional changes are conserved between both dogs and humans.

We have collected more than 250 CMTs that consist of benign, mixed and malignant mammary tumors. They were classified histopathologically and immunohistochemistry with antibodies to Runx2 and BMP4 completed. Preliminary data has demonstrated the presence of BMP4 and Rnux2 in benign mixed mammary tumours (ASBMR 2012). This was the first demonstration of the presence of BMP4 and Runx2 in canine mammary tissue or tumor. We demonstrated BMP4 and Runx2 in the nucleus of normal ducts but they were preferentially localized in the cytoplasm of tumor cells. In addition, both markers were localized in metaplastic cartilage present and the tumor cells within bone.

We have localized of BMP4 and Runx2 in 90 samples of normal mammary tissue and 80 samples of CMT. This has demonstrated that BMP4 and Runx2 are associated with different grades of breast cancer subtypes and may help to predict survival of our canine patients. These results demonstrate that both proteins could be useful prognostic markers for malignant canine mammary tumours.

***Disclosures: Kristi Milley**, None.*

SU0457

Beneficial Effects of Combined Therapy of Halofuginone and Zoledronic Acid on Breast Cancer Bone Metastases and Normal Bone Remodeling. Patricia Juarez*[1], Pierrick Fournier[1], Khalid Mohammad[1], Ryan C Mckenna[2], Desiree Lane[1], Sreemala Murthy[1], Maryla Niewolna[1], Alexander Robling[1], Larry Suva[3], John Chirgwin[1], Theresa Guise[1]. [1]Indiana University, USA, [2]University of Virginia, USA, [3]University of Arkansas for Medical Sciences, USA

Breast cancer frequently metastasizes to the skeleton causing bone destruction. Halofuginone (Hfg), a plant alkaloid derivate, reduces osteolytic bone metastases through inhibition of TGFβ and BMP signaling, both regulators of bone remodeling. Thus we seek to determine the effects of Hfg on normal bone unaffected by cancer and whether current therapies could correct Hfg effects.

Female-nude mice (n=15) were treated with Hfg (1-5mg/d) for 4 wks. Hfg (5mg) significantly decreased whole body BMD (20 ± 3 vs $12\pm2 g/cm^2$, $p<0.01$), as well as spine, tibia, and femur BMD. mCT analysis showed that Hfg (5μg) significantly decreased trabecular bone volume. This was associated with increased osteoclast number as well as decreased osteoblast number, mineralizing surface and bone formation rate.

We then tested whether Hfg-induced bone loss can be prevented by the anti-resorptive zoledronic acid (ZA). Hfg (5mg/d) and ZA (5mg/kg/3x per wk) alone or combined were administrated to female-nude mice over 4 wks. Mice treated with Hfg alone had lower BMD, as described earlier, as well as reduced whole bone stiffness measured by femoral 3-pt bending test. Concomitant treatment with ZA completely rescued the osteopenia (40 ± 3 vs $10\pm2 g/cm^2$, $p<0.01$) and bone stiffness deficiencies caused by Hfg.

We next tested the effect of Hfg (5mg/d) and ZA (5mg/kg/3x per wk) alone or combined in nude mice with MDA-MB-231 breast cancer bone metastases in a preventive treatment. Hfg or ZA alone significantly reduced osteolytic area compared with vehicle ($1.9\pm.9$ vs $3.5\pm.2 mm^2$, $p<0.001$ and $1.3\pm.4$ vs $3.5\pm.2 mm^2$, $p<0.001$, respectively). Combined treatment with Hfg and ZA was significantly more efficient at reducing osteolysis area in mice than either treatment alone ($0.4\pm 0.1 mm^2$, $p<0.001$).

In conclusion, Hfg reduces breast cancer bone metastases in mice, and this effect is enhanced when Hfg is combined with ZA. Our data show that Hfg induces bone loss and should be used in combination with anti-resorptive agents such as ZA to prevent this. Hfg completed Phase II trials in sarcoma patients and could rapidly be brought to the clinic for the treatment of bone metastases in breast cancer patients. However, due to its effects increasing osteoclast activity and reducing bone mass, Hfg should be combined with anti-resorptive therapy.

***Disclosures: Patricia Juarez**, None.*
This study received funding from: Susan Komen Foundation (P. Juárez and T. A. Guise)

SU0458

Osteolytic Bone Lesions in Breast Cancer Cause Local and Systemic Alterations in Bone Composition. Xiaohong Bi*[1], Jeffry Nyman[2], Julie Sterling[3], Daniel Perrien[2], Anita mahadevan-jansen[4]. [1]University of Texas Health Science Center at Houst, USA, [2]Vanderbilt University Medical Center, USA, [3]Department of Veterans Affairs (TVHS)/Vanderbilt University Medical Center, USA, [4]Vanderbilt Univ, USA

Pathological fracture is a common and severe complication in breast cancer metastasis to bone, which is thought to be caused by an increase in osteoclast activity as evidenced by the significant architectural disruption in microCT studies. While the material properties of bone are key determinants of bone strength they have not been investigated. To study tumor effects on bone composition, we examined tumor-bearing bones from a mouse model of breast cancer-induced bone disease using Raman spectroscopy (RS) and quantitative microCT, and examined the relationship between tumor-induced changes in material properties and bone architecture.

Five-week-old female nude mice were inoculated intracardically with MDA-MB-231 breast cancer cells (n = 15) or PBS (n = 15), and sacrificed 4 weeks later. Lesion area was calculated from radiographs. Excised tibiae were analyzed by microCT and RS. Raman spectra were acquired every 500 um from the metaphysis to the mid-shaft of tibiae. Spectral measures such as collagen mineralization, carbonate substitution, mineral crystallinity, and hydroxyproline content were calculated.

Radiographs of tumor-bearing bones primarily displayed osteolytic lesions in the metaphysis. Significant decrease in bone volume fraction and trabecular number, and increase in trabecular space from microCT analysis indicated bone loss and architecture disruption caused by tumor. Raman derived measures from pooled spectra showed significantly higher mineralization, carbonation, mineral crystallinity as well as hydroxyproline content in the cortical bone from the tumor-bearing group than the control. When the data were sorted by the collection location, the increases in mineralization and mineral crystallinity were only present at the metaphysis where the osteolytic lesions are dominant. The carbonation and hydroxyproline, however, showed significant increases at all the locations along the tibiae. The carbonation level at the metaphysis was positively correlated with the lesion area in the bone.

Overall, RS is a valuable tool for analyzing compositional changes in bone resulting from tumor burden. Results from our study indicate an increase in mineralization at the metaphyseal cortex, suggesting a possible compensatory

response in the tissue. Furthermore, the universal changes in carbonation and hydroxyproline content suggested a possible systemic effect of tumor on bone microenvironment, which requires further investigation.

***Disclosures: Xiaohong Bi**, None.*

SU0459

Zoledronic Acids Inhibits Epithelial-mesenchymal Transition (EMT) of Breast Cancer Cells in Bone via Ubiquitin/Proteasome System. Toshiyuki Yoneda*[1], Soichi Tanaka[2], Kenji Hata[3], G. David Roodman[4], Riko Nishimura[3]. [1]Indiana University School of Medicine, USA, [2]Osaka University, Japan, [3]Osaka University Graduate School of Dentistry, Japan, [4]Indiana University, USA

Epithelial-mesenchymal transition (EMT) is a program through which epithelial cancer cells transdifferentiate to mesenchymal cancer cells with enhanced aggressiveness that allows colonization in distant organs. Recent accumulating evidence showed EMT is regulated by the microenvironment in which cancer cells colonize. Since breast cancer preferentially spreads to bone, we examined whether bone microenvironment promoted EMT of breast cancer cells. MCF-7 human breast cancer cells expressing GFP (MCF-7/GFP) were inoculated into the mammary fad pad (MFP) and tibial bone marrow (TBM) of female nude mice and examined for the expression of the mesenchymal marker Snail and epithelial marker E-cadherin. Real-Time PCR showed MCF-7/GFP tumors in the MFP expressed high E-cadherin and low Snail mRNA levels. In contrast, MCF-7/GFP tumors in TBM demonstrated increased Snail and decreased E-cadherin expression, suggesting that the bone microenvironment promoted EMT. Of note, zoledronic acid (ZA) down-regulated Snail expression in tumors in TBM, thus ZA inhibited EMT in bone. ZA blocked the TGFβ-induced Snail increase and E-cadherin decrease and reversed TGFβ-induced mesenchymal shape into epithelial. These in vitro results suggest ZA inhibits EMT not only in osteoclast-dependent but also -independent mechanisms. Since Snail is a target of proteasomal degradation, we next examined whether ZA affected proteasomal degradation of Snail. The proteasome inhibitor MG132 restored ZA-decreased Snail expression, suggesting ZA decreases Snail via the ubiquitin/proteasome system. Differential microarray using mammary tumors in TBM isolated from untreated and ZA-treated mice identified the de-ubiquitinating enzyme, ubiquitin-specific enzyme 45 (USP45), as a candidate molecule involved in proteasomal degradation of Snail. ZA significantly inhibited USP-45 expression and activity, which in turn decreased Snail expression. Finally, to determine the biological significance of ZA inhibition of EMT of breast cancer in bone, the effects of ZA on mammary tumors in TBM were determined. ZA inhibited not only tumor progression but also distant metastasis to lung and liver from bone. In conclusion, our results suggest the bone microenvironment promotes EMT in breast cancer. ZA inhibits EMT via stimulation of proteasomal degradation of Snail by suppressing the de-ubiquitinating enzyme USP-45. EMT inhibition by ZA leads to suppression of aggressive behaviors of breast cancer in bone.

***Disclosures: Toshiyuki Yoneda**, None.*

SU0460

Acidic conditions epigenetically repress the TRAIL receptor DR4 in myeloma cells to confer their resistance to TRAIL. Ryota Amachi*[1], Masahiro Abe[2], Masahiro Hiasa[3], Keiichiro Watanabe[4], Shiro Fujii[5], Takeshi Harada[5], Hirokazu Miki[5], Shingen Nakamura[5], Itsuro Endo[6], Eiji Tanaka[7], Toshio Matsumoto[6]. [1]Dept. of Medicine & Bioregulatory Sciences, Tokushima Univ. /) Dept. of Orthodontics & Dentofacial Orthopedics, Tokushima Univ., Japan, [2]University of Tokushima, Japan, [3]University of Tokushima Graduate School, Japan, [4]Tokushima University Hospital, Japan, [5]Dept. of Medicine & Bioregulatory Sciences, Tokushima Univ., Japan, [6]University of Tokushima Graduate School of Medical Sciences, Japan, [7]Dept. of Orthodontics & Dentofacial Orthopedics, Tokushima Univ., Japan

TRAIL-mediated immunotherapy is an attractive anti-tumor maneuver because of its tumor-specific cytotoxic activity. In osteolytic lesions in myeloma (MM), MM cells and osteoclasts (OCs) create an acidic milieu by protons produced by OCs and lactate by MM cells, which confers drug resistance in MM cells. We found that acidic conditions blunted TRAIL-mediated apoptosis in MM cells. In the present study, we explored the mechanisms of MM cell resistance to TRAIL in acidic conditions. DR4 expression was markedly reduced at mRNA and protein levels in MM cells cultured in acidic media or cocultured with acid-producing OCs. Acidic conditions suppressed H3 and H4 acetylation in MM cells, while enhancing the nuclear localization of Sp1, a transcription factor for HDACs, and thereby HDAC1 and HDAC2 expression in MM cells. Furthermore, the acetylation of H3K9 in a DR4 promoter was found to be suppressed in acidic conditions; treatment with the HDAC inhibitor valproate restored the DR4 expression in MM cells in acidic conditions, indicating HDAC-mediated repression of DR4 in an acidic environment. Acidic conditions also induced Akt phosphorylation in MM cells; the inhibition of the PI3K-Akt pathway by LY294002 or the Akt inhibitor Akt-in (Calbiochem) abrogated the suppression of the histone acetylation and restored the DR4 expression in MM cells in acidic conditions. Although the anti-MM effects of the anti-DR4 agonistic antibody R1-B12 were blunted in acidic conditions, the Akt or HDAC inhibition sensitized MM cells to R1-B12. From these results, an acidic milieu in MM bone lesions is suggested to confer the resistance in MM cells against TRAIL-mediated immunotherapy through the PI3K-Akt-mediated epigenetic repression of DR4 expression.

***Disclosures: Ryota Amachi**, None.*

SU0461

Autoregulation of RANK Ligand Expression in Oral Squamous Cell Carcinoma Tumor Cells. Yuvaraj Sambandam*[1], Kumaran Sundaram[2], William Ries[1], Sakamuri Reddy[2]. [1]Medical University of South Carolina, USA, [2]Charles P. Darby Children's Research Institute, USA

Head and neck squamous cell carcinoma is the most common malignant neoplasms estimated to be 40,000 cases annually in the US. RANK ligand (RANKL) is an essential bone resorbing osteoclastogenic factor in the bone microenvironment. We previously demonstrated high levels of RANKL expression in oral squamous cell carcinoma (OSCC) tumor cells. Also, OSCC cells stably transfected with RANKL-luc reporter construct showed a significant increase in luciferase activity with tumor growth in athymic mice. Therefore, we hypothesize that RANKL promotes OSCC tumor progression and invasion of bone. Immunohistochemical staining demonstrated high levels of RANKL and its receptor, RANK expression in tumor specimens from human subjects compared to normal adjacent tissues. Confocal microscopic analysis further confirmed RANK expression in OSCC cells (SCC1, SCC12 and SCC14a). Western blot analysis of total cell lysates obtained from OSCC cells stimulated with RANKL revealed a dose-dependent (0-125 ng/ml) increase in RANKL expression. Also, real-time PCR analysis of total RNA isolated from OSCC cells stimulated with RANKL in the presence and absence of RANKL inhibitor, OPG suppress RANKL mRNA expression in these cells. These results suggests an autoregulation of RANKL expression in OSCC cells. We next examined the RANKL capacity to increase OSCC cells proliferation. Interestingly, RANKL stimulation dose-dependently increased OSCC tumor cell proliferation in vitro. Also, RANKL stimulated OSCC cells demonstrated an increased levels of proliferating cell nuclear antigen (PCNA) expression. Furthermore, RANKL dose-dependently increased MMP-9 expression in SCC14a cells. Conditioned media obtained from SCC1 and SCC14a cells treated with different concentrations of RANKL (0-50 ng/ml) subjected to gelatin zymogram analysis showed elevated levels of MMP-9 activity suggesting a functional role for RANKL in tumor invasion of bone. Western blot analysis of total cell lysates obtained from OSCC cells treated with RANKL demonstrated a significant increase in the levels of TRAF-6 expression. We further identify that RANKL treatment significantly increased the levels of phospho-IKK and IkB expression in these cells. Thus, our results implicate RANKL autoregulation plays an important role in OSCC tumor progression and bone destruction.

***Disclosures: Yuvaraj Sambandam**, None.*

SU0462

Denosumab an innovative and effective treatment for Giant Cell Reparative Granuloma. Alicia Dean Ferrer[1], Francisco Alamillos[1], Juan José Ruiz Masera[1], Cristina Navarro Valverde[2], Jose Manuel Quesada gómez*[3]. [1]Servicio de Cirugía Maxilofacial. HU Reina Sofía, Spain, [2]Servicio de Endocrinología, Spain, [3]Servicio de Endocrinología.HU Reina Sofía, Spain

Giant Cell Reparative Granuloma (GCRG) is an expansive eand destructive lesion of the jaw, positive for osteoclast markers, which affects children and young adults (female-male ratio 2:1). The fast growing lesions, despite their innocent histological appearance, have a dramatic aggressive behavior, mimicking a malignant lesion. Conventional management consists of surgical enucleation and curettage, with a recurrence rate of 15-20% (treatment may need to be aggressive even with an ''in block'' resection). Medical treatment such as intralesional steroid injections, calcitonin, or alpha interferon sc. injections have shown limited efficacy. Denosumab is a fully human monoclonal antibody that binds and inhibits RANKL, thereby preventing the activation of the RANK pathway. We tested the possibility to counteract osteoclast activation in GCRG and prevent the potential physiopathological role of RANK pathway. Denosumab has demonstrated its therapeutic potential and safety for Giant-cell tumor of bone.

We hereby report the first therapeutic use of denosumab in two young patients with recurrent GCRG of the jaw (aged 20 and 21 yrs.) after failure of tumor resection and intralesional steroid injections. Compassionate use of Denosumab was approved by Reina Sofía Hospital Ethics Committee, and administrated at a dose of 60 mg sc every three months and 1000 mg of calcium & 1000 IU vitamin D every day. Shortly after initiation therapy both patients recovered from severe pain and mandibular swelling disappeared. After a year of treatment no side effects of denosumab were observed, and both orthopantomography and computed tomography showed near-total tumor regression in on case and complete tumor regression in the second case, with adequate recalcification in both patients. Perforation of mandibular cortical disappeared and it was fully covered with new bone.

Denosumab could represent a medical treatment option for patients with GCRG to prevent dramatic disfiguring destruction of the jaw even without surgery.

***Disclosures: Jose Manuel Quesada gómez**, None.*

SU0463

Immunomodulatory Role of Mechanical Signals in Regulating the Expansion of Hematopoietic Precursors in a Murine Model of Multiple Myeloma. Gabriel Pagnotti*[1], Benjamin Adler[1], M. Ete Chan[1], Clinton Rubin[2]. [1]Stony Brook University, USA, [2]State University of New York at Stony Brook, USA

Cancer progression, often complicated by a decline in bone quantity and quality and an increased risk of fracture, negatively impacts the bone marrow (BM) niche, disrupting hematopoietic stem cell populations that are critical for immune regulation and control of inflammation. Exercise, recognized as a non-pharmacologic strategy for preserving bone strength, also serves to suppress inflammation. We have demonstrated low intensity vibration (LIV) to be anabolic to bone in an ovarian cancer model by forcing mesenchymal stem cells through osteoblastogenesis without compromising longevity. To investigate the modulatory role of mechanical signals during the early onset of a primary blood cancer in the marrow, 2E6 U266β1 Hu-myeloma cells were injected intravenously into an immunocompromised mouse strain (NSG). Mice were divided into 3 groups (n=10) at 5w of age: diseased (MM), diseased mice treated with LIV, and age-matched control (AC). LIV mice were subject to 15m/d, 5d/w on a vertically oscillating vibrating platform (0.3g @ 90Hz). Pathologies indicative of disease, including lung nodules, splenomegaly, and enlarged kidneys, were significantly observed in MM and LIV. At sacrifice and as compared to AC, flow cytometric analysis of BM from the left femur of MM revealed a +30% ($p<0.001$) and a +27% (ns) increase in hematopoietic precursor stem cells (KLS: C-kit+, Lin-, Sca-1+) and T-cells (CD3+, B220-), respectively, in MM as compared to AC. This inflammatory response was significantly reduced in LIV mice, with KLS (-15%; $p<0.01$ relative to MM) and CD3+ cells (-29%; p=0.06 relative to MM). Natural killer cells (NK1.1+, CD3-) from the left femur were +88% higher in MM relative to AC, while these cells decreased by -20% in LIV compared to MM. These data suggest that induction of U266 cells into the circulation significantly affects hematopoietic outcomes, elevating an immune response to the instigation of myeloma cells, manifested by the elevation of early-stage hematopoietic KLS cells as well as immature T-lymphocytes. Though preliminary, this evidence suggests that induction of disease has incited an apparent increase in immune response at multiple levels of the hematopoietic lineage. Interestingly, this immune response appears somewhat mitigated following 8w exposure to mechanical signals, suggesting a potential immunomodulatory effect on the bone marrow microenvironment.

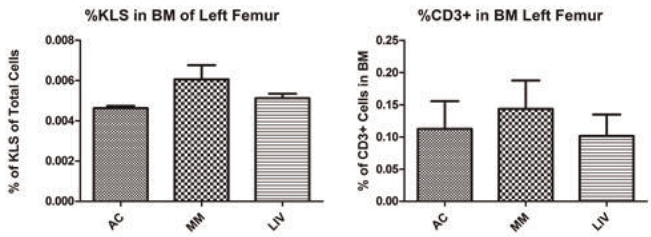

Immune Response

***Disclosures: Gabriel Pagnotti**, None.*
This study received funding from: National Institutes of Health

SU0464

Loss of Parafibromin Immunoreactivity in Sporadic Ossifying Fibroma. Jessica Costa-Guda*[1], Andrew Arnold[2]. [1]University of Connecticut Health Center, USA, [2]University of Connecticut School of Medicine, USA

Hyperparathyroidism jaw-tumor syndrome (HPT-JT) is an autosomal dominant disorder consisting of a predisposition to benign and/or malignant parathyroid tumors, jaw tumors most often characterized as ossifying, cementifying or cemento-ossifying fibromas and a variety of kidney and uterine lesions. Inactivating mutations of the *HRPT2* (also called *CDC73*) tumor suppressor gene, encoding parafibromin, were identified as the genetic cause of HPT-JT in the majority of affected kindreds. Subsequently, examination of sporadic parathyroid carcinomas revealed germline and/or somatic mutations of *HRPT2* and loss of parafibromin protein expression in the majority of patients. Somatic mutations of *HRPT2* have also been reported in a subset of sporadic renal tumors. Germline and somatic mutations of *HRPT2* were identified in a subset of sporadic ossifying fibromas but aberrant protein expression, even in cases with *HRPT2* mutation, could not be demonstrated. In this study, we examined a series of 9 ossifying fibromas, including ossifying, cemento-ossifying and juvenile active variants, for parafibromin protein expression via immunohistochemistry. Four ossifying fibromas showed a complete absence of nuclear parafibromin expression; loss of parafibromin expression was coupled with aberrant cytoplasmic parafibromin expression in one case. These results provide novel evidence at the level of protein expression for the suggestion that loss of *HRPT2*/parafibromin may play an important role in the pathogenesis of ossifying fibroma. Further studies are needed to determine the extent of involvement of *HRPT2*/parafibromin abnormalities in these tumors, and to identify additional molecular contributors to the pathogenesis of ossifying fibroma.

***Disclosures: Jessica Costa-Guda**, None.*

SU0465

Lung Cancer Stem-Like Cells (CSC) Display a Retarded Osseous Prometastatic Activity. Anne-Marie Bleau*[1], Carolina Zandueta[1], Miriam Redrado[1], Susana Martinez-Canarias[1], Alfonso Calvo[1], Fernando Lecanda[2]. [1]Center for Applied Medical Research, Spain, [2]Foundation for Applied Medical Research, Spain

Current evidence indicates that a fraction of cells within tumors, called Cancer Stem Cells (CSC), display stem cell–like properties and overt chemoresistance. To enrich for CSC, *in vivo* limited dilution and spheres cultures have been widely used as assays for stem cell properties. These structures present a heterogeneous population of cells, containing a mixture of quiescent CSC together with highly proliferative cells. At present, the extent to which CSC also display prometastatic activity remains poorly understood.

Sphere cultures (SC) derived from a mouse lung adenocarcinoma (LACUN3) showed higher levels of CSC markers including a 5-fold increase in ALDH and a 4-fold increase in Sca-1 (Ly-6A/E), as compared to adherent cultures (non-SC). Consistent with their quiescent phenotype, SC displayed a marked cell cycle arrest in G_0/G_1 phase that was translated into a 15-fold reduction in *in vitro* growth kinetics as compared to the other conditions. More importantly, the evaluation of quiescence by fluorescent-dye retention was 80% higher in SC than in non-SC. As expected, SC presented a 6-fold higher colony formation activity in soft agar assay, as well as a 40% increase in resistance to paclitaxel. All these experiments were repeated with the human lung cancer cell line H460, where SC overexpressed ALDH and ABCG2 markers and were also endowed with quiescent properties.

To delineate the metastatic activity of SC, upon intracardiac inoculation into nude mice, bioluminescence imaging (BLI) showed a dramatic delay in the appearance of bone metastatic lesions as compared to non-SC. At day 21 postinoculation, BLI in SC-injected animals showed a striking decrease in osseous metastatic tumor burden as compared to non-SC mice. Analogous delay was observed when SC were disaggregated and cultured as adherent cells before inoculation. Similar results were obtained when *in vivo* experiments were repeated with other cell lines.

Interestingly, using subcutaneous injection, tumor growth was similar (SC vs non-SC). In contrast, assessment of osseous colonization activity by intratibial injection of SC cells showed a six-fold decrease in bone tumor burden as compared to non-SC injected mice.

Taken together, these data suggest that differentiation of CSC in the target organ might be required for the emergence of cell variants with high prometastatic activity. We postulate that microenvironmental factors imposed by each target metastatic organ might be crucial in this process.

***Disclosures: Anne-Marie Bleau**, None.*

SU0466

Ras Activation Mediates WISP-1 Induced Increases in Cell Motility and Matrix Metalloproteinase Expression in Human Osteosarcoma. Yi-chin Fong*, Chih-Hsin Tang. China Medical University, Taiwan

WISP-1 is a cysteine-rich protein that belongs to the CCN (Cyr61, CTGF, Nov) family of matrix cellular proteins. Osteosarcoma is a type of highly malignant tumor with a potent capacity to invade locally and cause distant metastasis. However, the effect of WISP-1 on migration activity in human osteosarcoma cells is mostly unknown. In this study, we first found that the expression of WISP-1 in osteosarcoma patients was significantly higher than that in normal bone and corrected with tumor stage. Exogenous of osteosarcoma cells with WISP-1 promoted cell motility and matrix metalloproteinase (MMP)-2 and MMP-9 expression. In addition, the Ras and Raf-1 inhibitor or siRNA abolished WISP-1-induced cell migration and MMPs expression. On the other hand, activation of the Ras, Raf-1, MEK, ERK, and NF-κB signaling pathway after WISP-1 treatment was demonstrated, and WISP-1-induced expression of MMPs and migration activity were inhibited by the specific inhibitor, and mutant of MEK, ERK, and NF-κB cascades. Taken together, our results indicated that WISP-1 enhances the migration of osteosarcoma cells by increasing MMP-2 and MMP-9 expression through the integrin receptor, Ras, Raf-1, MEK, ERK, and NF-κB signal transduction pathway.

***Disclosures: Yi-chin Fong**, None.*

SU0467

Transcriptome Signatures of Mesenchymal Stem Cells and their Osteogenic Offspring after Contact with Myeloma Cells. Julia Dotterweich*[1], Beate Geyer[1], Katrin Schlegelmilch[1], Alexander Keller[2], Norbert Schuetze[1], Franz Jakob[1]. [1]University of Wuerzburg, Orthopedic Center for Musculoskeletal Research, Germany, [2]University of Wuerzburg, Biocenter, DNA-Analytics, Germany

Multiple myeloma (MM) is a hematological malignancy with 90% of all patients developing myeloma bone disease characterized by osteolytic lesions. This bone disease is accompanied with an increased mortality and is caused by a disordered bone remodeling with enhanced bone resorption and impaired bone formation. Insufficient osteoblastogenesis is a consequence of humoral and direct cell-cell interaction between mesenchymal stem cells (MSC) and myeloma cells. To elucidate the alterations of bone-forming cells in the tumor microenvironment, global gene expression analysis for MSC and osteogenic precursor cells was performed after myeloma cell contact.

The global gene expression analysis was performed by using Affymetrix gene chip HG-U133 2.0 Plus Array. MSC were co-cultured with the myeloma cell line INA-6 for 24 h. To separate the co-culture by FACS sorting, INA-6 cells were stained with CellTracker® Green CMFDA before culturing. Same procedure was performed for osteogenic precursor cells. Osteogenic precursor cells were generated by incubating MSC with osteogenic differentiation media for 14 days. Osteogenic differentiation was checked with histological staining for alkaline phosphatase and alizarin red for calcified extracellular matrix. RNA of five independent experiments was used for gene expression analysis, whereas the according MSC or osteogenic precursor cells were used as control. The evaluation was performed by software R (normalization: RMA; filter: $-0{,}5 \leq \log \text{Fold change} \geqslant 0{,}5$, AFFX). Target genes were validated by semiquantitative RT-PCR and analysed by densitometry.

The direct co-culture of INA-6 cells with MSC resulted in 991 differential expressed probe sets (718 genes/86 NA) whereas the contact with osteogenic precursor cells led to 552 differential expressed probe sets (397 genes/32 NA). Both conditions share 161 up-regulated (107 genes/5 NA) and 20 down-regulated (15 genes/2 NA) probe sets. The regulation of target genes was confirmed by semiquantitative RT-PCR. Regulated targets include important angiogenic factors like VEGF-A, chemokines like CCL28, and adhesion molecules like ICAM-1.

We further aim to elucidate candidate genes on protein level in *in vitro* culture with primary myeloma cells and in tumor tissues. Altered surface molecules on bone marrow cells in case of disease will preferentially be looked at to provide a tool for novel therapeutic approaches and diagnostic markers.

***Disclosures: Julia Dotterweich**, None.*

MO0001

Anti-dementia glutaminergic NMDA and Acetylcholine esterase inhibitor inhibits osteoclastogenesis. Charles Inderjeeth*[1], Jiake Xu[1], Dian Teguh[2], Bay Sie Lim[2]. [1]University of Western Australia, Australia, [2]University of WA, Australia

Background: Alzheimer's dementia (AD) and osteoporosis (OP) are common and parallel ageing and frequently coexist in an ageing population. Low BMD appears related to increased risk of AD. Various clinical conditions have been shown to alter Acetylcholine (Ach) signalling and affect bone. Ach Receptor (AchR) subunits and Ach Esterase (AchE) are expressed in bone. We demonstrated an in vitro effect of acetylcholine esterase inhibitors (AchEI) on osteoclast (abstract ECTS 2013). We demonstrated at equimolar concentrations Donepezil inhibit, whereas Galantamine enhances osteoclastogenesis. Memantine, uncompetitive antagonist at glutaminergic NMDA receptors, are also effective in treating AD. NMDA receptors have also been identified in bone. We hypothesised that, given the parallels with ageing in AD and OP and effect of AchEI, NMDA may be a useful target as well.

Methods: BMMs are seeded at 6×10^3 cells/well in 96-well plate. Prior to RANKL stimulation, cultures were incubated with the drugs Memantine, Donepezil and Galantamine at equimolar concentrations of 0.1 to 5.0μM. Control plates were incubated with and without RANKL only for comparison.

Results: At equimolar concentrations Memantine and Donepezil inhibit, whereas Galantamine enhances osteoclastogenesis. Memantine and Donepezil inhibited osteoclastogenesis at the lowest concentration of 0.1μM. IC50 for Donepezil is estimated at 0.35 uM and for Memantine, it is estimated to be 0.75 uM..

Conclusion: This data suggests Ach and glutaminergic neurotransmission may both be important in bone biology. This may have important implications for osteoporosis management in older and dementia populations who have both conditions coexist.

***Disclosures: Charles Inderjeeth**, None.*

MO0002

Characterization of Age-related Skeletal Muscle Regenerative Function and Gait Performance Recovery in Hindlimb Injured Fibroblast Growth Factor-2 Null Mice. Toru Nishikawa*[1], Collin Homer-Bouthiette[1], Liping Xiao[1], Marja Marie Hurley[2], Morgan Carlson[1]. [1]University of Connecticut Health Center, USA, [2]University of Connecticut Health Center School of Medicine, USA

Recent evidence suggests an age-dependent role for FGF2 in muscle satellite stem cell quiescence and self-renewal. We examined the impact of Fgf2 knockout on muscle regenerative capacity, and in a cross-age comparative analysis of gait performance following acute injury. *Approach*: The numbers of Pax7-expressing satellite cells were determined in uninjured muscle harvested from 2, 10-12 and 18 months WT and Fgf2KO mice. Ventral plan videography was used to assess whether Fgf2KO resulted in enhanced loss of muscle homeostasis and physiological performance.WT and Fgf2KO mice of different ages walked on a transparent treadmill belt at baseline day 0, and 3 and 5-days post-hindlimb muscle injury. At 5-days post-injury, total numbers of newly-generated myofibers were determined in isolated gastrocnemius by hematoxylin and eosin (H&E) and immunohistochemical staining for embryonic myosin heavy chain (eMyHC). *Results*: Analysis of uninjured muscle from WT and Fgf2KO mice revealed a significant and progressive decline in the number of Pax7 and M-cadherin positive satellite cells with age and genotype. Gait analysis showed no difference at base line in hindlimb propulsion duration (an indicator of muscle strength) between WT and Fgf2KO mice. However, at 3days post-injury propulsion was decreased in both genotypes returning to baseline at 5days post-injury in WT (202.6 ± 13.6ms) but remaining significantly shorter in Fgf2KO (122.8 ± 24.5ms; $p<0.05$). Stride length was similar in both genotypes at day 0 and at 3 days post-injury, returning to baseline in WT at day 5 post-injury (4.1 ± 0.1cm), but remained significantly reduced in Fgf2KO (2.6 ± 0.3cm; $p<0.05$). Stride frequency was similar between genotypes at days 0 and 3 post-injury but was significantly increased at day 5 post-injury in Fgf2 KO (4.9 ± 0.7Hz), compared with WT (2.5 ± 0.1Hz $p<0.05$). Since gait dysfunction was observed in Fgf2KO mice at 5 days post-injury, we determined muscle regenerative responses by quantifying production of de novo myofibers. There was a significant reduction in myofiber density in Fgf2KO (55.6 ± 7.2) compared with WT (77.5 ± 8.8 $P<0.05$). Further analysis revealed fewer active-Notch1 positive satellite cells present in 5 days post-injury Fgf2KO mice. These results demonstrate an age-associated negative impact of FGF2KO on skeletal muscle regenerative capacity, suggesting that losses in endogenous FGF2 signaling with age, may contribute to functional impairment of the muscle stem cell compartment.

***Disclosures: Toru Nishikawa**, None.*

MO0003

Inducible Conditional Inactivation of FGFR3 in Collagen II Expressing Cells at adult stage Leads to Early-Onset Degeneration of the Intervertebral Disc. Yangli Xie*[1], Siru Zhou[1], Wei Xu[1], Junlan Huang[1], Xiaolan Du[1], Lin Chen[2]. [1]Trauma Center, Daping Hospital, Third Military Medical University, Peoples Republic of China, [2]Daping Hospital, Peoples Republic of China

Although Fibroblast Growth Factor Receptor 3 (FGFR3) signaling plays a critical role in regulating bone development and homeostasis, its roles in the maintenance of intervertebral disc (IVD) remain poorly understood. FGFR3 knockout mice showed skeletal defects including kyphosis, scoliosis, crooked tails and overgrowth of long bones and vertebrae. Mice with conditional deletion of FGFR3 in collagen2-expressing cells using Col2a1-Cre mice also showed kyphosis, scoliosis and bone overgrowth, suggesting the role of FGFR3 in the development and maintenance of IVD. To distinguish the role of FGFR3 in the early development and adult stage maintenance of IVD, we inducibly inactivated FGFR3 in collagen2-expressing cells including inner annulus fibrosus cells and endplate chondrocytes by injecting tamoxifen (TM) into mice with both floxed FGFR3 alleles and Col2a1-CreERT^2 allele (hereafter referred to as $Fgfr3^{Col2ER}$). $Fgfr3^{Col2ER}$ mice and controls ($Fgfr3^{flox/flox}$) were injected with TM at 2-month (1mg/10 g BW, × 5 days, i.p.), and were examined at 3- and 4- month old. Disc tissue specimens were analyzed by micro-computed tomography, histologic analysis, and real-time PCR.

FGFR3 protein was expressed in the cells of annulus fibrosus and endplate cartilage of IVD and growth plates of WT mice, but not in the nucleus pulposus cells. Compared to WT mice, $Fgfr3^{Col2ER}$ mice showed no significant gross phenotype. The vertebral body height and disc space also showed no remarkable changes. Histologically, $Fgfr3^{Col2ER}$ mice developed early-onset of aging related cartilage loss and had bony tissue in the endplates at 3- and 4-month old. The histology of bone-like tissues resembled those found in ectopically formed bone, containing bone marrow, osteoclasts and mineralized osteoblasts. Immunohistochemical analysis demonstrated a notable reduction in Collagen 2 level and a significant increase in Mmp13 and Collagen 10 expression in the IVD of $Fgfr3^{Col2ER}$ mice. Gene expression analysis of IVD demonstrated that inactivation of FGFR3 led to enhanced Collagen10, Mmp13 and Adamts5 expression and depressed Col2, aggrecan expression.

These results indicate that deletion of FGFR3 in chondrocytes leads to early-onset degeneration of endplate regions, which is similar to changes of early stage IVD degenerative in humans. These findings may provide experimental data for further mechanism studies, and for screening of therapeutic approaches for human disc degeneration.

***Disclosures: Yangli Xie**, None.*

MO0004

Selective Amino Acid Supplementation Can Exacerbate or Prevent Low Protein-Induced Bone Loss in the Aged Animal. Kehong Ding[1], Qing Zhong[2], Bryce Wyatt[3], Jarrad Rowse[3], Xing-Ming Shi[1], Jianrui Xu[3], Mona El Refaey[3], William Hill[4], Wendy Bollag[3], Mohammed Elsalanty[1], Nicole Howie[3], Karl Insogna[5], Norman Chutkan[3], Monte Hunter[3], Mark Hamrick[1], Carlos Isales*[3]. [1]Georgia Health Sciences University, USA, [2]Medical College of Georgia, USA, [3]Georgia Regents University, USA, [4]Georgia Regents University & Charlie Norwood VAMC, USA, [5]Yale University School of Medicine, USA

Epidemiologically, low protein diets have been shown to be associated with a higher incidence of hip fractures in the elderly. We have previously reported that L-type amino acids bind to extracellular receptors on bone marrow-derived mesenchymal stem cells, osteoblasts and osteoclasts and modulate their activity depending on the amino acid type. In addition we have demonstrated that a low protein (8%), as compared to a normal protein (18%), diets induces bone loss in the aged (24 month) but not the mature (12 month) C57Bl6 mouse. Low protein diet-induced bone loss can be prevented by supplementing the diet with only three aromatic amino acids (tyrosine, tryptophan and phenylalanine or TTP) up to the 18% protein levels. We wished to extend the previous study and examine the effects of other amino acid supplements in order to determine the selectivity of the aromatic amino acid effects. Three amino acid groups were selected in this IACUC approved study: (1) aromatic amino acids, based on previous data demonstrating them to have the most potent anabolic effects on osteoblasts in vitro; (2) the branched-chain amino acids, valine, leucine and isoleucine (VLI), based on previous data demonstrating them to have no anabolic effects on osteoblasts; and (3) serine, threonine and valine (STV), based on data demonstrating them to have the greatest potency in stimulating osteoclastic activity. We divided 24-month old C57Bl6 mice into five dietary groups (n=12/group): (1) standard protein (18%); (2) low protein (8%); (3) low protein + TTP; (4) low protein + VLT; and (5) low protein + STV. Animals were sacrificed at the end of eight weeks, blood obtained by cardiac puncture and bones removed for micro-CT, DXA, biomechanical, histomorphometric, and biochemical studies. We report that the low protein diets resulted in significant bone loss, decreased biomechanical strength and increased biochemical markers of bone breakdown and decreased bone formation rates. In contrast, (1) supplementing the low protein diets with TTP prevented the low protein-induced bone loss; (2) VLI supplements had no impact on the low protein diets; and (3) STV supplements significantly exacerbated the low protein-elicited bone loss. Taken together we conclude that amino acid supplements have specific effects on bone turnover in the aged animal

***Disclosures: Carlos Isales**, None.*

MO0005

Association of Sarcopenia with Muscle Strength and Quality of Life in Postmenopausal Women with or without Osteoporosis. Michio Hongo*, Naohisa Miyakoshi, Yuji Kasukawa, Yoichi Shimada. Akita University Graduate School of Medicine, Japan

Introduction: The purpose of this study was to evaluate the association of sarcopenia with muscle strength and quality of life in postmenopausal women. Methods: A total of 167 postmenopausal women with an average age of 68 years were enrolled in this study. Participants underwent dual energy x-ray absorptiometry for whole body, lumbar spine, and total hip. Relative skeletal muscle mass index (RSMI) was calculated by sum of appendicular muscle mass from whole body scan divided by the square of the height. Sarcopenia was defined as RSMI more than 2 standard deviations below the average of normative data. The diagnosis of osteoporosis was defined by bone mineral density at lumbar spine or hip. Back extensor and grip strength, Roland-Morris questionnaire (RDQ), Short-form-36 (SF-36), and Japanese osteoporosis quality of life score (JOQOL) were measured. Participants were categorized into 4 groups according to the presence of osteoporosis (OP) and sarcopenia (SP): (1) OP+/SP+, (2) OP+/SP-, (3) OP-/SP+, and (4) OP-/SP-. Each measurement was compared among the groups. Results: The prevalence of sarcopenia was 34 women (20%) in this study population. There were 22 (13%) women in OP+/SP+ group, 80 (48%) in OP+/SP-, 12 (7%) OP-/SP+, 53 (32%) OP-/SP-. There was no significant difference in age among the groups. JOQOL scores in OP+/SP+ group showed significantly lower in domains for physical activity, social activity/recreation, posture/figure, fall, and total score compared with other groups. JOQOL scores in OP+/SP- also showed significantly lower in domains for posture/figure and fall compared with OP-/SP- and OP-/SP+. Back extensor strength of OP+/SP- and OP+/SP+ was significantly lower than those of OP-/SP-. However, there was no significant difference between sarcopenia and non-sarcopenia. Grip strength, SF-36 except for mental health status, and pain measurements from RDQ and JOQOL showed no significant difference among the groups. Conclusions: Decreased quality of life in individuals with combination of both osteoporosis and sarcopenia were influenced by poorer physical activity, aggravated posture, or fear of fall, suggesting the importance of detecting patients with combination of both. Although grip strength has been widely used for evaluating sarcopenia, there was no association of muscle strength with the presence of sarcopenia. Identifying sarcopenia with measuring muscle strength is limited for diagnosis and combination with other tools will be needed.

***Disclosures: Michio Hongo**, None.*

MO0006

Choice of Reference Population Radically Affects Sarcopenic Obesity Prevalence. Bjoern Buehring*, Ellen Fidler, Jessie Libber, Diane Krueger, Neil Binkley. University of Wisconsin, Madison, USA

Saracopenic obesity (SO) can be defined as a relative excess of fat mass in comparison to lean mass. SO impairs health more than either sarcopenia (SP) or obesity independently. However, there is no current consensus definition of SO; until such consensus is reached, SO will not receive needed clinical recognition. Multiple potential definitions of SO have been advanced. We hypothesized that SO prevalence will vary among the definitions and cut-offs used. This study examines different definitions that include fat and lean mass as measured by DXA. Cut-offs for these parameters were based on either an ''ideal'' or a ''regular'' population. The main outcome parameter was SO prevalence based on various definitions in a cohort of older adults.SP was defined by ALM/ht^2 (Baumgartner et al). SO parameters included %body fat, total fat/leg lean mass ratio and leg fat/leg lean mass ratio. Two standard deviation (SD) cut-offs were examined based on an ''ideal'' population (college athletes) and a ''regular'' population (20-29 year olds from NHANES 1999-2004 cohorts) and a published cut-off for %body fat (Dufour et al, M>30%, F>40%). Definitions and cut-offs were applied to a cohort of community dwelling older adults. The prevalences of different SO definitions and the prevalence of the combination of SP and SO were compared.

The reference population cohorts included 326 (150F/176M) athletes and >10,000 DXA data points from 2,116 (999F/1,117M) 20-29 year old individuals in NHANES. The cohort of older adults consisted of 97 (49F, 48M) adults age ⩾70. Two SD cut-offs for %body fat, total body fat/leg lean mass ratio, leg fat/lean mass ratio were higher in the NHANES cohort compared to athletes. Prevalence of SP by low ALM/ht^2 was 24%. SO prevalence varied based on comparison population and SO measure selected and ranged from 1 to 77% (66-77% based on athlete parameters versus 1-6% based on NHANES). Prevalence of SO combined with SP varied from 1 to 16.5%. Percentages based on athlete cut-offs were higher compared to NHANES cut-offs ($p<0.5$).

In conclusion, the prevalence of SO and the combination of SP and SO varies widely depending on the choice of fat and lean mass measures and reference population to define ''normal.'' SO prevalence based on an ''ideal'' (athlete) cut-off is several fold higher compared to a ''regular'' (NHANES) cut-off. These results highlight the need to base SP and SO definitions on health outcomes such as falls and fractures rather than reference populations.

***Disclosures: Bjoern Buehring**, None.*

MO0007

Defining Osteosarcopenic Obesity and Identifying its Prevalence in Women Across a Wide Age-range. Julia E. Inglis*[1], Lynn B. Panton[2], Michael J. Ormsbee[2], Owen J. Kelly[3], Jasminka Z. Ilich[2]. [1]Florida State University Dept. of Nutrition, Food, & Exercise Science, USA, [2]Florida State University, USA, [3]Abbott Nutrition, USA

Sarcopenia and sarcopenic obesity have been recognized in the last decade, however, a condition to include the loss of muscle and the loss of bone (osteopenia) with coexistence of adiposity (osteopenic obesity), may be prevalent but has not been defined or adequately studied. Here we consolidate *osteopenic obesity* with the already existing and more familiar term, sarcopenic obesity, and delineate the resulting combined condition assigning it the term *osteosarcopenic obesity*. Further, we examine a population of 602 healthy Caucasian women between 18 and 88 (mean ± SD 49.4 ± 16.2) years to determine the prevalence of osteosarcopenic obesity. Body compostition and BMD of the total body, spine, and femur were measured by iDXA. Obesity was determined based on % body fat, taking >30% as a cutoff for obesity. Sarcopenic obesity was identified using a linear regression (as proposed by Newman et al. 2003) to derive the association between appendicular skeltal muscle mass (obtained from iDXA) with height and fat mass. Negative residuals from the linear regression indicated the obese individuals who had lower appendicular skeletal muscle mass than the expected value and therefore were identified as having sarcopenic obesity. Osteopenic obesity was also identified using the linear regression by comparing BMD of total hip and/or spine to height and fat mass in the obese. Similarly, negative residuals identified those individuals whose BMD was less than the expected value in the presence of obesity, indicating osteopenic obesity. Results identified 492 (82%, ages 18-83 y) obese individuals; 250 (42%, ages 20-80 y) with sarcopenic obesity; 251 (42%, ages 22-83 y) osteopenic obesity; and 148 (25%, ages 22-79 y) presenting with osteosarcopenic obesity. These findings suggest that osteosarcopenic obesity is a relevant health condition for women of all ages, where compromised bone and muscle tissues are combined with excess of adiposity, exacerbating each of these conditions and is not limited just to older individuals. However, this combined condition has not been previously identified or recognized. Further research is warranted to identify prevalence of osteosarcopenic obesity, whether in the newly created studies, or by re-examining existing data-bases.

***Disclosures: Julia E. Inglis**, None.*

MO0008

Effects of Age and Caloric Restriction on the Expression of Leptin in Peripheral Tissues. Phonepasong Arounleut[1], Sunil Upadhyay[2], Xing-Ming Shi[3], William Hill[4], Carlos Isales[2], Mark Hamrick*[3]. [1]Georgia Regents University (formally Georgia Health Sciences University), USA, [2]Georgia Regents University, USA, [3]Georgia Health Sciences University, USA, [4]Georgia Regents University & Charlie Norwood VAMC, USA

Leptin, the product of the obese gene (ob), is known to be secreted by fat cells (adipocytes). Leptin then crosses the blood-brain barrier to bind its receptors in the hypothalamus where it regulates food intake and energy balance. Recent data also show that leptin receptors are abundant in peripheral tissues such as bone and skeletal muscle, and these same tissues are also reported to be sources of leptin itself. Leptin-deficiency is associated with decreased hindlimb muscle and bone mass in ob/ob mice and in food-restricted mice, and so we tested the hypothesis that age-related muscle and bone loss may be associated with reductions in leptin secreted from these peripheral tissues. ELISA assays were utilized to quantify leptin levels in the femur, quadriceps femoris muscle, inguinal fat pads, and liver of mice aged 12 months and 20 months fed ad-libitum (AL) and mice aged 20 months on caloric restriction (CR). We also treated mice aged 20 months on caloric restriction with recombinant mouse leptin for 10 days at 10 mg/kg body weight to examine the response of peripheral tissues to exogenous leptin. Data show that in all groups leptin levels are highest in skeletal muscle, both absolutely and relative to total protein. Leptin levels are slightly lower in the liver and in fat, and lowest in bone. Aging does not significantly alter leptin levels in any of these tissues, but caloric restriction (CR) significantly reduced leptin levels in bone (- 20%) and fat (-45%) of aged mice. Exogenous leptin significantly reduces leptin levels in all tissues of aged CR mice, and this effect is most dramatic in the liver where there is a 10-fold decrease in leptin following leptin treatment. These data suggest that the regulation of local and circulating leptin levels is complex and involves multiples tissues and organ systems. Funding for this research was provided by the National Institute on Aging (P01 AG 036675).

***Disclosures: Mark Hamrick**, None.*

MO0009

Identification of a single nucleotide polymorphism in the 5'-flanking region of *PRDM16* gene as a novel susceptibility marker for low lean body mass. Tomohiko Urano*[1], Masataka Shiraki[2], Yasuyoshi Ouchi[3], Satoshi Inoue[3]. [1]UMIN, Japan, [2]Research Institute & Practice for Involutional Diseases, Japan, [3]The University of Tokyo, Japan

Loss of skeletal muscle mass and function is a common disorder in the elderly. Sarcopenia is a common skeletal muscle disease characterized by low lean body mass of muscle tissue, leading to decreased skeletal strength and increased susceptibility to fracture. Low lean body mass has a strong genetic component, with heritability ranging over 50%. However, specific genes underlying the variation in low lean body mass are largely unknown. Rapid technological advances have made it feasible to pursue genome-wide association studies (GWAS). A number of GWAS have found novel single-nucleotide polymorphisms (SNPs) associated with complex diseases or traits, including bone mineral density, fat content, and body mass index. By performing a GWAS for SNPs associated with lean body mass by using SNP arrays, we have focused on a SNP located in the 5'-flanking region of the PRDM16 (PRD1-BF-1-RIZ1 homologous domain containing protein 16) gene. We demonstrated that PRDM16 gene polymorphism was significantly associated with lean body mass in 1,081 postmenopausal Japanese women. The SNP was located in the 5'-flanking region of the PRDM16 gene. A luciferase assay using the C2C12 myoblast-like cells revealed that the genomic region has differential transcriptional activity depend on the SNP genotype. Thus, human genetic analyses demonstrated the importance of the PRDM16 gene in the regulation of lean body mass in human.

***Disclosures: Tomohiko Urano**, None.*

MO0010

Osteocalcin and Musculoskeletal Health in Older Women. Itamar Levinger*[1], David Scott[2], Geoffrey Nicholson[3], Gustavo Duque[4], Thomas McCorquodale[5], Amanda Stuart[6], Peter Ebeling[2], Markus Herrmann[7], Kerrie Sanders[8]. [1]Victoria University, Australia, [2]The University of Melbourne, Australia, [3]The University of Queensland, Australia, [4]Ageing Bone Research Program, University of Sydney, Australia, [5] Nepean Clinical School, University of Sydney, Australia, [6]Department of Clinical & Biomedical Sciences, The University of Melbourne, Barwon Health, Australia, [7]Royal Prince Alfred Hospital, The University of Sydney, Australia, [8]NorthWest Academic Centre, The University of MelbourneWestern Health, Australia

Exercise increases total osteocalcin (TOC) and undercarboxylated OC (ucOC) and improves glucose control[1]. We investigated associations between TOC, ucOC and ucOC/TOC ratio (ucOC%) and indices of both muscle and bone health. We hypothesized that in N=90 women aged 70+ years (1) ucOC and ucOC% is associated with increased muscle strength of the lower-limbs and (2) TOC, but not ucOC, is associated with other bone turnover markers and the heel ultrasound measures speed of sound (SOS), broadband ultrasound attenuation (BUA) and stiffness index (SI).

A chemiluminescence immunoassay (DiaSorin) was used to quantify TOC, with hydroxyapatite pre-treatment for ucOC. Lower-limb muscle strength was measured using the Manual Muscle Testing System (SI Instruments, Australia). Peak isometric force at the hip flexors, hip abductors and quadriceps were assessed. Regression statistics were used for analysis.

ucOC% was associated with all three strength tests (age-adjusted; $p<0.05$). The association for both quadriceps and hip abduction strength remained significant following further adjustment for BMI and 25(OH)D or PTH. Neither TOC, nor P1NP or CTx were associated with any of the strength tests (p=0.15 to 0.72). The muscle inflammatory marker, alpha-1-antichymotrypsin (α-ACT), was inversely associated with ucOC% (p=0.03) only. PTH was associated with both TOC and ucOC (p=0.001 and 0.017 respectively). TOC was positively associated with both P1NP and CTx ($p<0.001$), while ucOC% tended to be negatively associated with both P1NP and CTx (both p = 0.06). For each per unit increase in TOC (μg/L) there was a corresponding lower BUA, SOS and SI (β-co-efficient -0.28; -0.23 and -0.23; all $p<0.04$). BUA remained associated with TOC after adjustment for age and BMI, however, all three indices were not significant after adjustment for 25(OH)D or PTH (p= 0.15 to 0.9).

An association between ucOC% (but not TOC) and muscle strength is novel and supports a distinct metabolic musculoskeletal role for ucOC in humans. This and the negative correlation between ucOC% and a-ACT is consistent with improved glucose control mediated through a musculoskeletal interaction. The results confirm that TOC is associated with bone health and provide a potential link whereby TOC, ucOC% and ucOC are all related to falls and fracture risk.

(1) Levinger et al, Osteoporos Int, 2011

***Disclosures: Itamar Levinger**, None.*

MO0011

Alterations of Bone Quantity and Quality of the Periarticular and Non-Periarticular Bone in Patients with Rheumatoid Arthritis. Roland Kocijan*[1], Stephanie Finzel[2], Matthias Englbrecht[2], Axel Hueber[2], Jürgen Rech[2], Georg Schett[2]. [1]St. Vincent Hospital Vienna, Austria, [2]Friedrich-Alexander University Medical School, Germany

Purpose: Rheumatoid arthritis (RA) is a chronic inflammatory joint disease characterized by local and systemic bone loss. Thus, RA is an independent risk factor for osteoporosis and fracture. The purpose of this study was to investigate bone quantity and bone quality of the appendicular skeleton in RA patients.

Methods: 90 RA patients (60 women, mean age 52.6 ± 13.9 years and 30 men, mean age 55.8 ± 10.1 years) were included into the study and compared to healthy, age matched female (n=40, mean age 50.0 ± 10.9 years) and male (n=30, mean age 55.5 ± 14.2 years) controls, respectively. HR-pQCT measurements (Xtreme-CT, Scanco) were carried out at the distal radius (DR; non-periarticular) and the ultra-distal radius (UDR; periarticular). 110 slices (voxel size 82 μm) were measured in the DR and the UDR to determine volumetric bone mineral density (vBMD) and trabecular and cortical bone microstructure.

Results: Female and male patients with RA did not differ in age and body mass index from female and male controls, respectively. Less than 10% of RA patients used glucocorticoids with doses over 7.5 mg prednisolone equivalent and none of them was treated with doses of more than 10 mg prednisolone equivalent. Total ($p<0.05$), trabecular ($p<0.001$) and cortical ($p<0.001$) vBMD were significantly lower at DR and UDR sites in female and male RA compared to female and male controls, respectively. At the DR, significantly reduced bone volume fraction (BV/TV, p=0.001), trabecular number (Tb.N, $p<0.05$), trabecular thickness (Tb.Th, $p<0.05$) and cortical thickness ($p<0.05$) were found in both sexes of RA patients as compared to controls. Furthermore, trabecular separation (Tb.Sp, p=0.001) and inhomogeneity ($p<0.005$) were significantly increased in female RA patients compared to controls. No differences were found regarding cortical porosity. At the UDR, BV/TV ($p<0.001$) and Tb.N ($p<0.001$) were significantly decreased in female RA, whereas BV/TV (p=0.001) and Tb.Th ($p<0.005$) were decreased in male RA compared to the respective sex-matched controls.

Conclusions: Both, trabecular and cortical bone is severely affected in RA. Trabecular bone loss is mainly caused by a decrease in trabecular number in female RA, and trabecular thinning in male RA patients. Thus, our data suggest that bone quantity and quality are significantly decreased in the appendicular skeleton of RA patients at both, periarticular and non-periarticular sites.

***Disclosures: Roland Kocijan**, None.*

MO0012

Control of cartilage maintenance and degeneration by Twist1 and Runx1 transcription factors. Rosa Guzzo*[1], Jason Gibson[1], Douglas Spicer[2], Gregory Polkowski[1], Hicham Drissi[1]. [1]University of Connecticut Health Center, USA, [2]University of New England, USA

There remains a critical gap in our understanding of the molecular signals that control articular cartilage maintenance and degeneration. We previously established the chondrogenic effects of the transcription factor Runx1 in vitro and in vivo. Conversely, we and others demonstrated the anti-chondrogenic and anti-hypertrophic effects of the bHLH factor Twist1. The dichotomy between the functions of these two factors during chondrocyte differentiation led us to examine their expression and function in articular chondrocytes. Within the native murine knee joint, we detected abundant Twist1 and Runx1 protein expression in chondrocytes at the articular surface. This pattern of expression was also observed in human articular cartilage where Twist1 and Runx1 proteins were co-expressed in articular chondrocytes at the superficial zone, with little to no expression in deep zone chondrocytes. In vitro studies using human articular chondrocytes isolated from normal cartilage demonstrated that the expressions of Twist1 and Runx1 declined as chondrocytes undergo hypertrophy, suggestive of a mutual function for these factors within immature cartilage. In human osteoarthritic cartilage, the expressions of Twist1 and Runx1 proteins are activated in cartilage cell clusters near fissures or clefts in the upper articular cartilage layer. To gain insight into the functional roles of these factors in modulating the progression of osteoarthritis (OA), we generated chondrocyte-specific Twist1 gain of function (Col2a1-Cre) and Runx1 loss of function mouse models. Using these two models, we performed surgical destabilization of the medial meniscus (DMM) to induce the development of OA. Micro-CT analyses of wild type joints showed the presence of osteophytes at 12 weeks post-surgery, while little to no evidence of osteophyte formation was observed in the surgical joints of Twist1 transgenic mice at 12 weeks post-surgery. Whereas extensive cartilage erosion was detected in the surgical knee joints of wild type mice, the cartilage surface remained well preserved in Twist1 transgenic mice at 12 weeks post-surgery. We observed advanced cartilage erosion within the surgical knee joints of Runx1 haploinsufficient mice at 8 weeks post-surgery. In vitro experiments indicated a lack of transcriptional cross-regulation between Twist1 and Runx1. We speculate that Twist1 and Runx1 synergistically confer protection against cartilage erosion through independent mechanisms.

***Disclosures: Rosa Guzzo**, None.*

MO0013

Degenerative Changes in Knee Joints and Joint Pain in Surgically and Chemically Induced Rat Models of Osteoarthritis. Jukka Morko*, ZhiQi Peng, Jukka Vääräniemi, Katja Fagerlund, Jukka Rissanen, Jenni Bernoulli, Jussi Halleen. Pharmatest Services Ltd, Finland

Several experimental animal models have been developed for osteoarthritis (OA) and used to study the preclinical efficacy of disease and symptom modifying OA drugs. The preclinical efficacy has been determined by various microscopic scoring systems. Recently, the OARSI histopathology initiative presented recommendations for histological OA assessment in order to standardize preclinical efficacy studies. In this study, we performed a systemic characterization of knee joints in rat OA models using OARSI rat scoring system and pain assessments. The study was conducted using male Lewis rats. Unilateral OA was induced in their knee joints at 3 months of age using the following four rat models: 1) intra-articular monoiodoacetate (MIA) at the dose of 1 mg/kg, 2) medial meniscal tear (MMT) + medial collateral ligament transection (MCLT), 3) anterior cruciate ligament transection (ACLT) + partial medial meniscectomy (pMMx), 4) ACLT. Body weight, static weight bearing and static mechanical allodynia were followed during the study. Knee joints were harvested and digital radiographs of the joints were obtained at two time points in each model. Histological OA assessment was performed in medial tibial plateau following the OARSI recommendations. Static weight bearing decreased in operated knee joints during the first week and paw withdrawal threshold decreased in operated and MIA-injected knee joints during the first week and at end of the study. These results indicated operation-related joint discomfort and OA-related joint pain. Histological OA assessment demonstrated degenerative changes in medial tibial plateau in all models. Mild to moderate changes were observed in MIA and ACLT models and moderate to severe changes in MMT+MCLT and ACLT+pMMx models. Degenerative changes included the loss of chondrocytes, proteoglycans and collagen matrix in superficial layer of articular cartilage. These changes exacerbated down to intermediate layer at 4 weeks in MIA model and down to tidemark at 10 weeks in ACLT model, at 4 weeks in ACLT+pMMx model, and at 3 weeks in MMT+MCLT model. These changes in articular cartilage were associated with moderate to large osteophytes and minimal synovial inflammation in ACLT model and with large osteophytes and mild synovial inflammation in MMT+MCLT and ACLT+pMMx models. Results obtained in this study can be used to evaluate and select rat OA models for testing the preclinical efficacy of disease and symptom modifying OA drugs.

***Disclosures: Jukka Morko**, Pharmatest Services Ltd, 3*

MO0014

Withdrawn

MO0015

Identification of osteoarthritis patients with chronic tissue inflammation whom may benefit from anti-inflammatory treatment. Anne Sofie Siebuhr*[1], Kristian Kjær Petersen[2], Lars Arendt-Nielsen[2], Line Egsgaard[3], Thomas Eskehave[3], Claus Christiansen[4], Ole Simonsen[5], Hans Christian Hoegh[3], Morten Karsdal[4], Anne-Christine Bay-Jensen[6]. [1]Nordic Bioscience, Herlev, Denmark, Denmark, [2]Center for Sensory-Motor Interaction (SMI), Department of Health Science & Technology, Faculty of Medicine, Aalborg University, Denmark, [3]Center for Clinical & Basic Research, Denmark, [4]Nordic Bioscience A/S, Denmark, [5]Aalborg University Hospital, Orthopaedic Surgery Research Unit, Denmark, [6]Nordic Bioscience, Denmark

Purpose: It is evident that a subset of osteoarthritis (OA) patients has chronic tissue inflammation. These patients may benefit from anti-inflammatory treatment prescribed in inflammatory arthritis. C-reactive protein (CRP) has shown limited use in predicting disease severity, progression or response to anti-inflammatory treatment. The aim was to segregate patients in groups based on the present or absence of systemic and/or chronic tissue inflammation and describe them by serological markers.

Methods: A cross-sectional study of 342 OA patients: 281 patients had symptomatic knee OA and 61 underwent total knee replacement (TKR). Serum biomarkers were measured by ELISA: high sensitive CRP (hsCRP), CRP degradation fragment (CRPM, chronic tissue inflammation), matrix metalloproteinase-mediated degradation fragments of type I, II and III collagen; C1M (connective tissue), C2M (cartilage) and C3M (synovium). Associations between biomarkers and KL were investigated: KL0, Mild, n=12; KL1-2, Moderate, n=202; KL3-4, Severe, n=57; and TKR, KL3-4, n=61. Patients were divided in quartiles (Q) based on cut-off values of CRP and CRPM (mean+2SD of controls). Biomarker reference values were recorded for healthy controls. Data are shown as mean [95%-CI].

Results: hsCRP was elevated in TKRs compared to controls. In contrast, the mean levels of the CRPM were twice as high in all OA groups (10-14ng/mL) compared to controls (5ng/mL). C1M and C2M were elevated in TRKs compared to Moderate and Severe ($P<0.001$), but no difference in C3M. Patients in Q4 (fig) had higher KL compared to patients in Q1 ($P<0.0001$), Q2 ($P=0.017$) and Q3 ($P<0.0001$). C1M, C2M and C3M were lower in Q1 compared to the other quartiles. Comparing Q2 with Q3 showed that C1M was higher ($P=0.0005$) in Q3, but C3M was lower ($P=0.019$). Thus, patients identified by the chronic tissue turnover marker were significantly different compared to that of traditional acute inflammation markers.

Conclusion: OA patients had surprisingly high levels of chronic tissue inflammation. OA patients could be divided in quartiles or 2 groups: i) those who may benefit from anti-inflammatory treatment (Q3, Q4) and ii) those eligible for a tissue centric treatment (Q1, Q2). Patients with high chronic tissue inflammation (Q2 and Q4) had higher levels of tissue degradation (C1M and C2M) suggesting elevated tissue turnover. TKR patients had even higher levels of the tissue turnover markers, suggesting a distinct TKR serological phenotype.

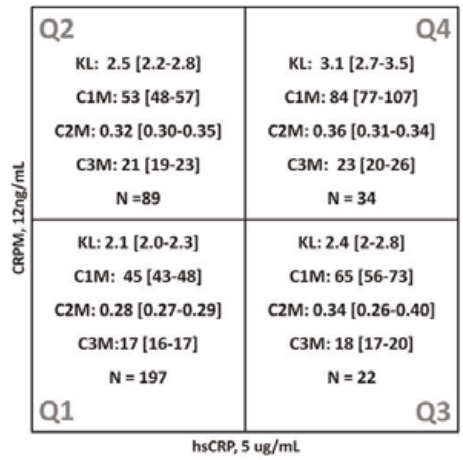

Identification of the patients with systemic and/or chronic tissue inflammation by CRP and CRPM

***Disclosures: Anne Sofie Siebuhr**, Full time employee at Nordic Bioscience, 3*

MO0016

Inhibition of TGF-β Signaling in Articular Chondrocytes Leads to Activation of MMP13 and Adamts5, OA-like Pathological Defects and Pain-Related Behavior Change in Mice. Jia Li*[1], Jie Shen[2], Jeffrey Kroin[1], Guozhi Xiao[3], Hee-Jeong Im[1], Di Chen[3]. [1]Rush University, USA, [2]University of Rochester, USA, [3]Rush University Medical Center, USA

TGF-β signaling plays an important role in chondrocyte differentiation and development of osteoarthritis (OA). However the downstream target genes of TGF-β signaling during OA development remain undefined. In this study, we investigated TGF-β target genes in OA development using mouse genetic approach. *Tgfbr2* conditional knockout ($Tgfbr2^{Col2ER}$) mice were generated by breeding *Tgfbr2-flox* mice with *Col2-CreER* transgenic mice. Deletion of the *Tgfbr2* gene was achieved by administration of tamoxifen into 2-week-old $Tgfbr2^{Col2ER}$ mice. Changes in histology, gene expression and pain-related behavior were analyzed. Deletion of the *Tgfbr2* gene in articular chondrocytes resulted in up-regulation of *Runx2*, *Mmp13*, *Adamts5* and *ColX* expression. Histological analysis showed articular cartilage degradation, increased hypertrophic chondrocyte numbers, early osteophyte formation, and increased subchondral bone mass in 3-month-old $Tgfbr2^{Col2ER}$ mice. Loss of entire articular cartilage, formation of extensive osteophytes, and substantially increased subchondral bone mass were observed in 6-month-old $Tgfbr2^{Col2ER}$ mice. Histomorphometric analysis of changes in articular cartilage volume or evaluation with histological scoring system recommended by Osteoarthritis Research Society International (OARSI) showed a significant decrease in articular cartilage area in $Tgfbr2^{Col2ER}$ mice. Significant reduction in spontaneous rearing activity and ambulation counts were also observed in 4-, 5-, 6-, 7-, and 8-month-old $Tgfbr2^{Col2ER}$ mice. To determine if up-regulation of *Mmp13* and *Adamts5* expression is responsible for $Tgfbr2^{Col2ER}$-induced OA development, we generated *Tgfbr2*/*Mmp13* and *Tgfbr2*/*Adamts5* double KO mice. Deletion of the *Mmp13* gene significantly alleviates OA-like pathological changes observed in 3- and 6-month-old $Tgfbr2^{Col2ER}$ mice. In contrast, deletion of the *Adamts5* gene only reversed OA-like phenotype in 3-month-old $Tgfbr2^{Col2ER}$ mice. These changes were further confirmed by histomorphometric analysis and by evaluation with OARSI scoring system. Treatment of $Tgfbr2^{Col2ER}$ mice with MMP13 inhibitor (CL82198, 10 mg/kg) for 2 months decelerated OA progression in 3-month-old $Tgfbr2^{Col2ER}$ mice. In this study, we demonstrate that inhibition of TGF-β signaling in articular chondrocytes leads to a progressive OA-like phenotype in mice. *Mmp13* and *Adamts5 are* critical downstream target genes of TGF-β signaling during OA development.

***Disclosures: Jia Li**, None.*

MO0017

Inhibition of TGFβ signaling in Mesenchymal Stem Cells Prevents Onset of Osteoarthritis. Gehua Zhen*[1], Xu Cao[2]. [1]The Johns Hopkins Hospital, USA, [2]Johns Hopkins University, USA

Osteoarthritis (OA) is a highly prevalent and debilitating joint disorder. Currently there is no effective disease modifying treatment due to limited understanding of its pathogenesis. Clinically, changes in the subchondral bone precede cartilage degeneration. Therefore, we investigated the cell signaling mechanism that results in subchondral bone changes, studying the subchondral bone-articular cartilage as a functional unit. We detected high levels of active TGFβ1 in the subchondral bone of human OA knee joints. Using an anterior cruciate ligament transaction (ACLT) mouse model, we were able to replicate the findings of elevated levels of active TGFβ in subchondral bone. High levels of TGFβ in the subchondral bone marrow led to increased numbers of mesenchymal stem cells (MSCs) and osterix^{+} osteoprogenitors post ACLT. Over time, bone formation became uncoupled, angiogenesis increased, and articular cartilage was damaged. To confirm the pathological role of high levels of active TGFβ in the subchondral bone, we analyzed an osteoblast tissue-specific TGFβ1 transgenic mice. Overexpression of active TGFβ1 in the transgenic mice resulted in a similar phenotype with increased osteoblast progenitors and angiogenesis in the subchondral bone preceding the development of OA. We then examined whether inhibition of TGFβ activity in the subchondral bone could prevent OA development. Systemic injection of TGFβ type I receptor (TβRI) inhibitor improved subchondral bone structure and decreased angiogenesis, but only partially attenuated articular cartilage degeneration as TGFβ signaling directly in articular cartilage has protective effects. Direct administration of TGFβ antibody in the subchondral bone resulted in an even better outcome in preventing articular cartilage degeneration. Moreover, deletion of TGFβ type II receptor (TβRII) specifically in nestin^{+} MSCs using an inducible nestin-CreER mouse model prevented osteoarthritic changes seen post ACLT, demonstrating that MSCs are the target cell population for high levels of TGFβ and contribute to the pathological changes at the onset OA in subchondral bone. Therefore, inhibition of TGFβ in subchondral bone prevented OA progression and could be an effective therapy of OA.

***Disclosures: Gehua Zhen**, None.*

MO0018

K/BxN Mouse Serum–Induced Arthritis Is Aggravated in Mice with Tamoxifen-Induced Chondrocytic Glucocorticoid Receptor Knockout. Jinwen Tu[1], Yaqing Zhang[1], Shihani Stoner[1], Edgar Wiebe[1], Tazio Maleitzke[1], Ulrike Baschant[2], Di Chen[3], Jan Tuckermann[4], Markus Seibel[1], Hong Zhou*[1]. [1]Bone Research Program, ANZAC Research Institute, University of Sydney, Australia, [2]Institute of General Zoology & Endocrinology, University of Ulm, Germany, [3]Rush University Medical Center, USA, [4]University of Ulm, Germany

Background: Exogenous glucocorticoids (GCs) are widely used in the treatment of rheumatoid arthritis (RA), however, the function of endogenous GCs in RA remains unclear. This study aimed to investigate the impact of cartilage-specific glucocorticoid receptor knockout (GRKO) on joint inflammation, cartilage damage, and bone metabolism in the K/BxN mouse serum transfer model of autoimmune arthritis.

Methods: GRKO mice were generated by breeding GRflox mice with tamoxifen inducible Cre (Col2a1-CreER^{T2}) mice. K/BxN arthritis was induced in 8-week-old male Col2a1-CreER^{T2}, GR$^{fx/fx}$ (KO) mice and their Cre-negative GR$^{fx/fx}$ littermates (WT) by injection of K/BxN serum ("KO-K/BxN" and "WT-K/BxN"). KO and WT mice receiving PBS served as controls (CTR). Paw swelling was assessed daily from induction (day 0) to day 14. Micro-CT and histomorphometry of the tibiae were employed to assess for bone morphological changes. Semiquantitative histological scores were used to determine the degree of joint inflammation, cartilage degradation, and bone erosion.

Results: Both KO-K/BxN and WT-K/BxN mice developed acute arthritis. However, the peak inflammatory response was significantly more pronounced in KO-K/BxN mice (Fig. A). In keeping with this phenoptype, histological analysis revealed significantly increased inflammatory activity and greater bone erosions in KO-K/BxN than WT-K/BxN mice (Fig. B). Micro-CT and histomorphometry showed reduced tibial bone volume (BV/TV) in both groups of arthritic mice compared to CTR, with increased osteoclast activity observed in KO-K/BxN compared to WT-K/BxN mice. In addition, spleen weight was significantly increased in KO-K/BxN mice compared to CTR, while no difference was observed between WT-K/BxN and CTR mice.

Conclusion: Disruption of endogenous glucocorticoid signaling in cartilage aggravates K/BxN serum-induced arthritis. Our data suggests that chondrocytes modulate local inflammation via a GR-dependent pathway.

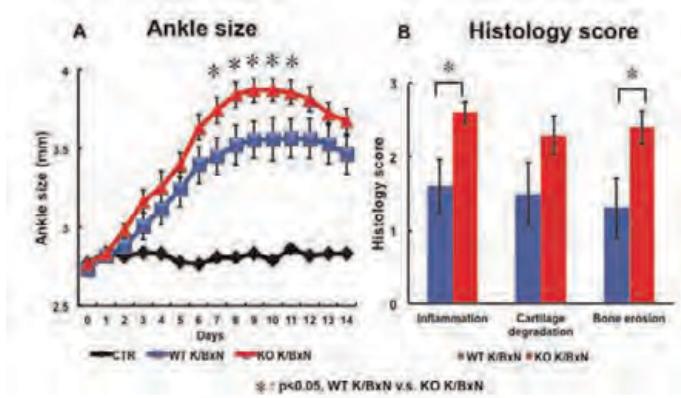

Figure

***Disclosures: Hong Zhou**, None.*

MO0019

The development of articular cartilage thickness, impeded by obesity, is protected by low magnitude mechanical signals. Tee Pamon*[1], M. Ete Chan[1], Denis Nguyen[1], Clinton Rubin[2]. [1]Stony Brook University, USA, [2]State University of New York at Stony Brook, USA

Obesity is a contributing factor to osteoarthritis, a pathology characterized by thinning of uncalcified cartilage (UC) and expansion of the calcified cartilage (CC) zone. This degeneration in the obese is typically attributed to ablation of articular cartilage (AC) by excessive load bearing. Considering the disruption of osteoblastogenesis by obesity, it is possible that chondroblastogenesis is simultaneously interrupted, thus contributing to an inferior bearing surface. Further, in light of recent evidence that low intensity vibration (LIV) has been shown to protect mesenchymal stem cell lineage selection towards the formation of higher order connective tissues, we sought to determine if these mechanical signals could protect the formation of AC in spite of the obese phenotype. C57BL/6 male, 5w mice were separated into 3 groups: Regular diet (RD), High fat diet (HF), and High fat diet + LIV (HFv). Phase I of the protocol consisted of 2w of high fat diet for HF and HFv , and through the 6w of Phase II, HFv were also subject to LIV (90Hz, 0.2g, 30 min/d, 5 d/w). At sacrifice, HF and HFv were 12% and 13% heavier, respectively, than RD mice ($P<0.01$). The left knee joints were sectioned in the sagittal plane and stained with Safranin-O/fast green. Average thickness of the UC and CC regions were measured with IMAGE J across 0.2 mm of the central region of the tibial lateral condyle. Following 8w of a high fat diet, UC thickness in HF mice was 20% lower than RD, while CC thickness was 24% higher in HF compared to RD mice. LIV protected the AC of HFv mice, as evidenced by an 8.4% higher total AC thickness compared to HF mice ($p<0.01$), preserving thickness exhibited in RD mice (nsd). Looking at the individual regions, the HFv displayed a 22.6% higher uncalcified cartilage thickness and a 12.1% reduction in calcified cartilage zone thickness compared to HF. These results suggest that the osteoarthritis that parallels obesity may, to a degree, be a result of a disrupted cartilage formation driven by interrupted chondroblastogenesis rather than excessive loading on the joint surface. Considering that there were no differences in body weight between HF and HFv mice, the protection of the articular surfaces appears to be achieved by the mechanical enhancement of the cartilage development, rather than the mechanical ablation of the tissue.

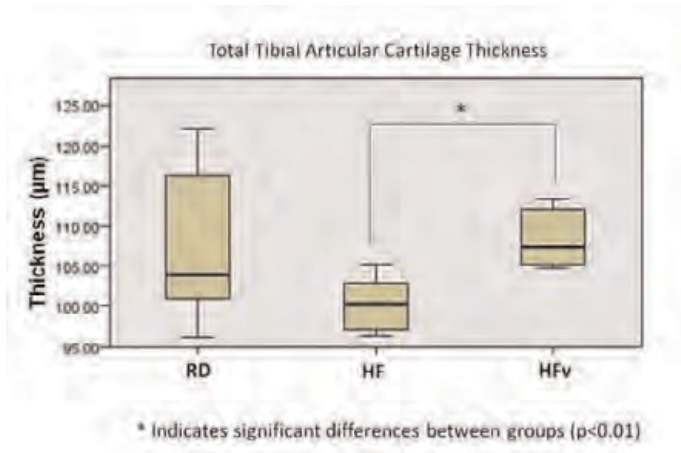

Total Tibial Articular Cartilage Thickness

***Disclosures: Tee Pamon**, None.*

MO0020

TRAF3: A potential biomarker of anti-TNF treatment response in rheumatoid and psoriatic arthritis. Yan Xiu*[1], Christopher Ritchlin[2], Lianping Xing[2], Brendan Boyce[1]. [1]University of Rochester Medical Center, USA, [2]University of Rochester, USA

Rheumatoid arthritis (RA) and psoriatic arthritis (PsA) are characterized by inflammation-induced joint damage mediated in large part by TNF, which also stimulates synovial expression of RANKL, a central mediator of joint destruction. TNF receptor-associated 3 (TRAF3) limits RANKL-induced osteoclast (OC) formation by proteasomally degrading NF-kB-inducing kinase. Thus, TRAF3 could limit resorption in inflammatory bone diseases if its level is increased in OC precursors (OCPs). Anti-TNF treatments (ATTs) have greatly reduced joint inflammation in RA and PsA, but up to 40% of patients are inadequate responders, and we lack biomarkers to predict potential responders from non- responders. We hypothesize that cellular levels of TRAF3 may reflect the responsiveness of peripheral blood monocytes (PBMCs) to extracellular TNF and that RA and PsA patients with high TRAF3 expression in PBMCs will preferentially respond to ATTs. To examine this hypothesis, we compared TRAF2, 3 and 6 protein levels in CD-11b$^+$ OCPs from TNF-Tg and WT mice by Western blotting and found that TRAF3 levels were 5-fold higher than other TRAFs in these cells. In contrast, OCP TRAF3 levels in mice with auto-antibody-induced arthritis were increased far less than in TNF-Tg cells, suggesting that increased TRAF3 elevation is associated with TNF stimulation. Further, FACS analysis revealed higher TRAF3 mean fluorescence intensity (MFI) levels in PBMCs of TNF-Tg mice than in WT littermates. These data support the concept that high TRAF3 levels in PBMCs from RA and possibly PsA patients may serve as a marker of responsiveness to ATTs. To examine this possibility, we stained PBMCs from 5 healthy controls, 10 RA and 10 PsA patients not on ATT with a mixture of labeled cell-specific markers and anti-TRAF3 antibodies and subjected them to FACS to determine their TRAF3 levels. We found that mean/SD TRAF3 MFI levels in CD14$^+$/CD16$^-$ PBMCs were 345/110 (range 224-466) from 5 normal subjects, 520/191 (range 239-740) in 10 RA patients, and 4309/2527 (range 235-7603) in 10 PsA patients. TRAF3 levels were elevated in the PBMCs of ~60% of these patients and low in the remaining 40%, corresponding to the % of RA and PsA patients who respond to ATTs in clinical trials. The relationship between PBMC TRAF3 levels in these patients and their subsequent responses to ATTs are under investigation to determine if TRAF3 is a potential biomarker to predict which RA and PsA patients will respond to ATTs.

***Disclosures: Yan Xiu**, None.*

MO0021

Lifestyle therapy preserves bone quality, reduces visceral fat inflammation and bone marrow adipogenic signals in obese old mice. Xavier DeLeon*[1], Lina Aguirre[2], Alexander Proctor[3], Dennis Villareal[4], Reina Armamento-Villareal[4]. [1]Biomedical Research Institute of New Mexico, USA, [2]BRINM, USA, [3]Active Life Scientific, USA, [4]University of New Mexico School of Medicine, USA

Purpose: Weight loss-induced bone loss may exacerbate age-related bone loss and worsen existing osteopenia in the elderly which can be attenuated by exercise. Recent reports of increased fractures in obese patients suggest poor bone quality in these patients. Thus, weight loss in obese elderly may lead to further deterioration in bone quality. In this study, we evaluated the independent and additive effects of weight loss and exercise on bone quality in obese old mice. Secondarily, we evaluated the independent and additive effects of weight loss and exercise on inflammation which may have an important role in bone loss with aging and obesity, in the visceral fat and bone marrow.

Methods: Thirty-two 15-mo old male C57BL6 mice were fed high-fat diet for 12 wks to 18 mo (n=8/grp). Afterwards, mice were assigned to high fat diet (HFD), Diet, Exercise (EX) and Diet+Exercise (Diet-EX). Controls were lean age-matched mice. Diet was by caloric restriction to induce weight loss of 15 to 25% of baseline bw and exercise was treadmill running for 15 min, speed 10cm/sec 3x/wk x 12 wks.

Results: Diet and Diet-EX lost 18% to 24% of bw. Exercise tolerance improved in both EX and Diet-EX (232 $\pm$ 70 and 271 $\pm$ 60 sec) relative to HFD and Diet (-27 $\pm$ 88 and -44 $\pm$ 67 sec), ($p<0.05$). Volumetric BMD by pQCT showed bone loss at the tibial midshaft in HFD and Diet (Fig. 1). BMD on explanted bone showed higher total tibial midshaft BMD in EX (677 $\pm$ 50 mg/cm3) relative to HFD and Diet (545 $\pm$ 40 and 519 $\pm$ 34 mg/cm3) ($p<0.05$), while Diet-EX was lower (565 $\pm$ 30 mg/cm3) but not different from EX. Sclerostin was lowest in EX (327 $\pm$ 11pg/ml), highest in Diet (547 $\pm$ 114pg/ml), and intermediate Diet and EX (422 $\pm$ 181pg/ml) for Diet-EX, p=0.06. Bone biomechanics by Reference Point Indentation showed indentation distance increase and total indentation distance were lower in Diet, EX and Diet-EX compared to HFD (see Fig.2) Visceral fat TNF-α/100gm tissue release was lower in EX relative to Diet and Diet-EX (Fig 3). Bone marrow PPARγ gene expression normalized to GAPDH was suppressed in Diet (0.07 $\pm$ 0.04) compared to EX (1.9 $\pm$ 1.4) and Diet-EX (0.68 $\pm$ 0.4) ($p<0.05$). IL-6 and TNF-α expressions were similar among the groups.

Conclusion: Bone quality is preserved with or without exercise in Diet and Diet-EX, despite bone loss. Exercise is effective in reducing inflammation in the visceral fat. In the bone marrow, lifestyle therapy has no effect on inflammation, but Diet is effective in reducing adipogenic signals.

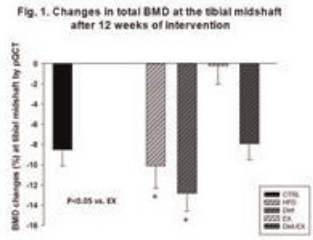

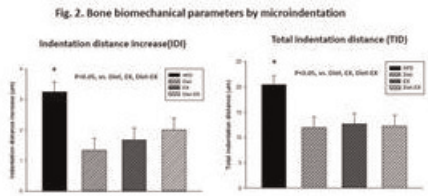

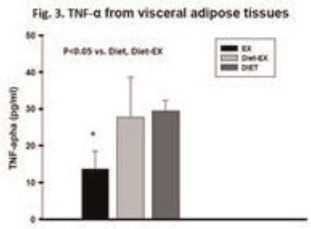

Figures_Lifestyle therapy_bone quality_inflammation

***Disclosures: Xavier DeLeon**, None.*

MO0022

Withdrawn

MO0023

Healthy Black and White Children Show No Difference in the Relationship between Change in Serum PTH and Change in Serum 25-Hydroxyvitamin D with Oral Vitamin D_3. Kathleen Hill Gallant*[1], George McCabe[2], Linda McCabe[2], Berdine Martin[2], Emma Laing[3], Dorothy Hausman[3], Connie Weaver[4], Richard Lewis[3], Munro Peacock[5]. [1]Indiana University School of Medicine, USA, [2]Purdue University, USA, [3]The University of Georgia, USA, [4]Purdue University, Dept of Nutrition Science, USA, [5]Indiana University Medical Center, USA

Background: The inverse curvilinear relationship between serum PTH and 25 OH vitamin D (25D) found in adult populations is frequently used as an indicator of vitamin D insufficiency with values of serum 25D above maximal suppression of PTH used to determine vitamin D sufficiency. In healthy children, it is unclear if this relationship occurs or whether it differs between whites and blacks who have higher serum PTH and lower 25D than whites. Aim: To examine the relationship between serum PTH and 25D in a sample of white and black healthy children. Methods: Black and white boys and girls (n=318) who participated in randomized placebo-controlled trial of oral vitamin D3 supplementation during winter had fasting serum 25D and PTH measured at baseline and 12 weeks. Results: Blacks (n=162) had higher serum PTH and lower 25D compared with whites (n=156) (PTH mean 29.7 (9.9-70.5) pg/mL [blacks] and 24.9 (10.8-62.0)pg/mL [whites] $p < 0.0001$; 25D mean 24.1 (10.2-42.5) ng/mL [blacks] and 32.0 (17.9-46.0) ng/mL [whites] $p < 0.0001$). Serum PTH was negatively related to serum 25D ($r=-0.37$, $p <0.0001$) and there was no difference in this relationship between blacks and whites. After 12 weeks, serum 25D was higher than baseline in both blacks and whites (mean 33.6 (9.7-92.4) [blacks] and 42.5 (12.7-95.1) ng/mL [whites] $p < 0.0001$). Increasing serum 25D caused minimal change in serum PTH (doubling serum 25D results in a 10% decrease from baseline in serum PTH) and this was not different between races (figure). Conclusion: These results indicate 1) that increasing serum 25D in winter through vitamin D3 supplementation minimally reduces serum PTH in healthy adolescents, and 2) the response does not differ between blacks and whites.

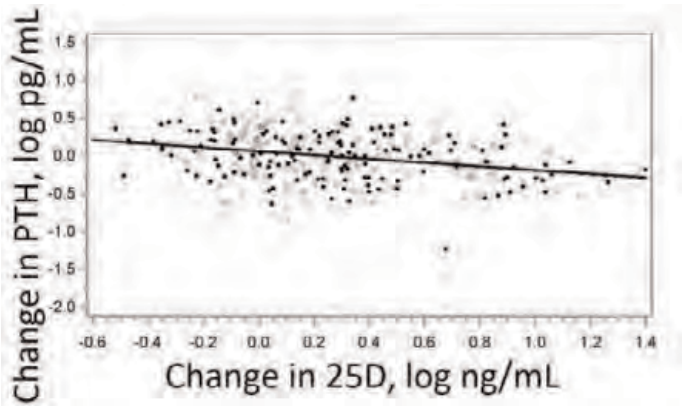

Figure

***Disclosures: Kathleen Hill Gallant**, None.*

MO0024

Inclusion of Anthropometric Parameters in the Creation of Reference Curves for Pediatric Bone Mineral Density and Bone Mineral Content: Impact on Classification of Below-Normal Individuals. Thomas Hangartner*[1], David Short[1], Vicente Gilsanz[2], Heidi Kalkwarf[3], Joan Lappe[4], Sharon Oberfield[5], John Shepherd[6], Babette Zemel[7], Karen Winer[8]. [1]Wright State University, USA, [2]Children's Hospital Los Angeles, USA, [3]Cincinnati Children's Hospital Medical Center, USA, [4]Creighton University Osteoporosis Research Center, USA, [5]Columbia University Medical Center, USA, [6]University of California, San Francisco, USA, [7]Children's Hospital of Philadelphia, USA, [8]National Institutes of Health, USA

The goal of this study was to assess the implication of including relevant anthropometric variables in the creation of reference curves for areal bone mineral density (aBMD) and bone mineral content (BMC) in pediatrics.

Analysis of the dual-energy x-ray absorptiometry (DXA) data collected as part of the Bone Mineral Density in Childhood Study[1], including 2012 boys and girls, 5-22 y old, with a total of 10,525 visits, resulting in aBMD and BMC observations at the lumbar spine, hip (neck and total), forearm and whole body (total body and total body less head). Multivariate statistics were used to rank order the influence of the independent variables age, gender, race (black/non–black), height, weight, percent body fat (%fat) and sexual maturity. Two different models were created for each aBMD and BMC parameter, the practical model containing age, gender, race, height and weight as well as the full model, adding %fat. We compared the number of subjects that fell below 2 standard deviations in our models with those below the same limit of the currently standard LMS model[2], which is based on age, sex and race, and of the height adjusted Z-scores[3].

Between 50% and 82% of subjects identified as below normal (<-2 SD) based on the LMS model were not classified as being below normal in our practical model. Using the full model, misclassification increased for all aBMD and BMC parameters, ranging from 49% to 92%. Height-adjusted Z-scores reduced the misclassifications to 33-60% in comparison to the practical model and to 41-73% in comparison to the full model. For both the practical and the full model, misclassifications in comparison to the LMS model were worse for BMC than for BMD at all sites with the exception of the femoral neck. Considering that BMC is more heavily influenced by bone size than BMD, inclusion of body height and weight in the model reclassifies small, underweight subjects away from the lower tail of the distribution, which is not done by the LMS model, as this model takes care of body size only through the surrogate of age.

The traditional comparison of pediatric BMD and BMC data against age-, sex- and race-matched controls can be refined if anthropometric parameters are taken into account.

[1] Sponsored by the National Institute for Child Health and Human Development
[2] Zemel BS et al., J Clin Endocrinol Metab 96:3160-3169, 2011
[3] Zemel BS et al., J Clin Endocrinol Metab 95:1265–1273, 2011

***Disclosures: Thomas Hangartner**, None.*

MO0025

A Pediatric Bone Mass Scan has Poor Ability to Predict Adult Bone Mass - A 28-Year Prospective Study. Bjorn Rosengren*, Christian Buttazzoni, Magnus Karlsson. Skåne University Hospital Malmö, Lund University, Sweden

Purpose: The correlation between bone mass in childhood and adulthood is not fully understood. This includes the correlation between relative accrual of bone mineral and relative gain in bone size since both these traits independently contribute to bone mineral density (BMD).We conducted a long-term prospective observational study as to determine if a pediatric bone mass scan is useful to predict adult bone mass and evaluate in there are similar relative gain in bone mineral and bone size during growth.

Methods: We measured cortical bone mineral content (BMC; g), bone mineral density (BMD; g/cm^2) and bone width (cm) longitudinally in the distal forearm by single photon absorptiometry in 120 boys and 94 girls with a mean age of 10 years (range 3–17) and mean 28 years (range 25–29) later. We calculated individual bone mass Z-scores, using all participants at each measurement as reference and evaluated correlations between the measurements at baseline and follow-up with Pearson's correlation coefficient. Individual Z-scores were also stratified in quartiles to register movements between quartiles from childhood to adulthood and to calculate sensitivity and specificity.

Results: BMD in childhood and adulthood correlated in both boys ($r=0.35$; $p<0.0001$) and girls ($r=0.50$, $p<0.0001$) and in both children $\geq$10 years at baseline (boys $r=0.43$ and girls $r=0.58$, both $p<0.0001$) and in children <10 years at baseline (boys $r=0.26$ and girls $r=0.40$, both $p<0.05$). 93/211 (44%) of the participants had a proportionally higher accrual of BMC than gain in bone size and 118/211 (56%) a proportionally higher gain in bone size than accrual of BMC.

A pediatric bone scan in the lowest quartile had a sensitivity of 48% (95% CI 27%, 69%) and a specificity of 76% (95% CI 66%, 84%) to predict an adults value in the lowest quartile. Among the children in the lowest quartile of BMD, 58% had left the lowest quartile in adulthood due to a higher than average accrual in bone mineral (Δ BMC Z-score 0.5; 95% CI 0.2, 0.9) and a lower gain in bone size (Δ bone width Z-score -0.3, 95% CI -0.7, 0.0).

Conclusions: Childhood BMD explained in men 12% of the variance in adult BMD and in women 25%. A pediatric distal forearm BMD scan has poor ability to predict adult bone mass since the accrual in bone mineral and the gain in bone size during growth differ between individuals.

***Disclosures: Bjorn Rosengren**, None.*

MO0026

A Pre-Pubertal Bone Mass Scan has Poor Ability to Predict Peak Bone Mass - A 12-Year Prospective Study in 121 Children. Bjorn Rosengren*[1], Magnus Dencker[2], Jan-Åke Nilsson[2], Magnus Karlsson[1]. [1]Skåne University Hospital Malmö, Lund University, Sweden, [2]Inst of Clinical Sciences, Skane University Hospital, Lund University, Sweden

Purpose: The correlation between bone mineral density (BMD) in childhood and at peak bone mass (PBM) is unclear. Furthermore, among those who have a higher than average gain in BMD during growth, that is leave the lower regions, it is unclear if this is the result of a relative high accrual in bone mineral or a relative low gain in bone size.

We conducted a prospective study to determine if a pre-pubertal bone mass scan is useful to predict bone traits at PBM. In individuals with an initially low BMD but with a favorable gain during puberty we also evaluated if this was the result of a higher than average gain in BMC or a lower than average gain in bone size. We chose femoral neck (FN) as region of interest as data in our cohort shows that PBM is reached there in girls at age 17-18 and in boys at age 18-19.

Methods: We measured BMC (g), BMD (g/cm^2) and bone area (cm^2) longitudinally in FN by DXA in 65 boys and 56 girls, all in Tanner stage I and aged 6-8 years at baseline, and mean 12 years later when they were 18-19 years and all in Tanner stage V. We calculated individual Z-scores, using all participants at each measurement as reference and estimated correlations between the measurements at baseline and follow-up with Pearson's correlation coefficient. Individual Z-scores were also stratified in quartiles in order to visualize movements between quartiles between the pre-pubertal period and PBM.

Results: There was a correlation between pre-pubertal FN BMD and FN BMD at PBM ($r=0.57$; $p<0.001$), but also for BMC ($r=0.65$; $p<0.001$) and bone area ($r=0.37$; $p<0.001$). 47% of the participants had a proportionally higher accrual of BMC than gain in bone size and 53% a proportionally higher gain in bone size than accrual of BMC.

A pre-pubertal FN BMD value in the lowest quartile had a sensitivity of 44.8% and a specificity of 82.8% to predict a FN PBM in the lowest quartile. Among the 29 children in the lowest quartile, 44.8% had left the lowest quartile at PBM (ΔBMD Z-score 0.9 (95% CI 0.6, 1.1). Their gain in BMD was driven by a higher than average accrual in bone mineral (ΔBMC Z-score 0.4; 95% CI 0.1, 0.7) but not from a lower gain in bone size (Δ bone area Z-score -0.1, 95% CI -0.8, 0.4).

Conclusions: A pre-pubertal FN BMD explained 32% of the variance in FN PBM. A pre-pubertal FN BMD scan has poor ability to predict FN PBM since the relative accrual of bone mineral and the gain in bone size vary between subjects.

***Disclosures: Bjorn Rosengren**, None.*

MO0027

Body Composition and Physical Activity During Childhood and Adolescence: Relations to Biomechanical Bone Strength. Joshua Farr*[1], Shreyasee Amin[1], L. Joseph Melton[1], Salman Kirmani[1], Louise McCready[1], Elizabeth Atkinson[1], Sundeep Khosla[2]. [1]Mayo Clinic, USA, [2]Mayo Clinic College of Medicine, USA

Numerous studies have examined the influences of body composition and physical activity (PA) on bone development, but none have used micro-finite element analysis (μFEA) from HRpQCT scans. Thus, in 150 healthy 8- to 15-yr old boys (n=85) and girls (n=65), we investigated the relations of appendicular skeletal muscle mass (ASM), total body fat mass (TBFM) and PA to distal radius and tibia biomechanical bone strength (failure load), using μFEA. We determined relative ASM and TBFM from whole-body DXA scans. PA strain score (related to mechanical loading) and time spent in vigorous-intensity PA was quantified from a validated questionnaire. Results were similar in analyses stratified by sex; thus, we present analyses from the boys and girls combined. Relative ASM was positively associated with bone strength of the distal radius (r=0.55, P<0.001; Fig. A) and tibia (r=0.61, P<0.001; Fig. B) after adjusting for bone-age, sex, fracture history, relative TBFM and PA. By contrast, after adjustment for the same covariates, substituting relative TBFM for relative ASM, a significant inverse association was observed between relative TBFM and bone strength of the distal radius (r=–0.30, P<0.001), while no correlation was seen at the distal tibia (r=–0.01, P=0.91). In addition, after adjustment for bone-age, sex, fracture history, height and weight, time spent in vigorous-intensity PA was positively associated with bone strength (r=0.28, P<0.01) at the distal tibia only, while PA strain score was significantly associated with greater bone strength of the distal radius (r=0.16, P<0.05) and tibia (r=0.24, P<0.01).

These data thus highlight the importance of skeletal muscle mass and PA for optimizing bone strength during growth. Furthermore, fat mass has differential influences on bone strength at weight-bearing versus non-weight-bearing skeletal sites in children and adolescents. At the distal tibia, fat mass is not associated with bone strength, whereas fat mass is negatively associated with bone strength at the distal radius after adjusting for bone-age, sex, fracture history, skeletal muscle mass and PA. These observations suggest that the strength of the distal radius does not commensurately increase with excess gains in adiposity during growth, which may result in a mismatch between bone strength and the load experienced by the distal forearm during a fall. These findings may, in part, explain why obese children are over-represented in distal forearm fracture cases.

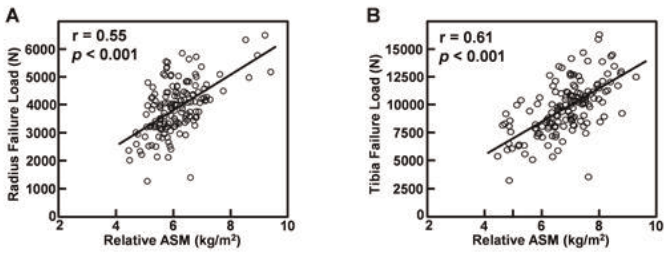

Figure

***Disclosures: Joshua Farr**, None.*

MO0028

Bone formation markers during growth hormone treatment in short prepubertal children. Diana Swolin-Eide*[1], Björn Andersson[1], Per Magnusson[2], Berit Kriström[3], Kerstin Albertsson-Wikland[4]. [1]The Queen Silvia Children's Hospital, Sweden, [2]Linkoping University,Sweden, Sweden, [3]Institute of Clinical Sciences, Department of Pediatrics, Umeå University, Sweden, [4]Institute of Clinical Sciences, Sahlgrenska Academy, University of Gothenburg, The Queen Silvia Children's, Sweden

Purpose: Growth hormone (GH) promotes longitudinal growth and bone remodeling and it is therefore of interest to study bone formation markers during GH treatment.

Method: This study comprised 128 Swedish short prepubertal children (boys=90, girls=38) mean (±SD) age 7.31±2.0 years. The bone formation markers alkaline phosphatase (ALP), bone-specific ALP (BALP), osteocalcin and intact amino-terminal propeptide of type 1 procollagen (PINP) were measured using the IDS-iSYS automated system (Immunodiagnostic Systems). One third received standard GH dose (43 μg/kg/day). The individualized GH dose (mean 49; range 17–100 μg/kg/day) comprised one of six different doses calculated using a prediction model that considers the estimated GH sensitivity for the child corresponding to the same biological dose. The maximum peak GH secretion (GH_{max}) ⩾ 32 mU/L ('old 10 μg/l'), estimated by arginine–insulin tolerance test or by spontaneous GH secretion over a 24 h period, was used to classify the patients as having either idiopathic short-stature (ISS) (n=89) or short stature due to GH deficiency (GHD) (n=39).

Results: All bone markers increased rapidly during the first 3 months of treatment and remained approximately at the same level or decreased slightly after 2 years of treatment, however, still higher than at baseline (Table 1). No significant differences were found between the ISS and GHD subgroups or between individual and fixed dosages of GH at any time point. At start, ALP and BALP correlated with the 2-year growth response to GH treatment (r=0.26, p=0.002; r=0.17, p=0.03, respectively). After 3 months and after 1 year of GH treatment, significant correlations were found with longitudinal growth for ALP (r=0.42, p<0.0001; r=0.41, p<0.0001, respectively), BALP (r=0.37, p<0.0001; r=0.49, p<0.0001), and PINP (r=0.45, p<0.0001; r=0.50, p<0.0001). Multiple regression analysis showed that osteocalcin and BALP, together with PINP at 3 months and BALP and PINP at 1 year, predicted the 2-year growth response with high accuracy (R^2=0.40, p<0.0001). Using only osteocalcin at start and ALP and PINP at 3 months resulted in R^2=0.28, p<0.0001.

Conclusion: Only ALP showed an association with growth at start of GH treatment. However, after 3 months and after 1 year of GH treatment, significant correlations were found for ALP, BALP and PINP with longitudinal growth.

Table 1. Bone markers during 2 years of GH treatment

	Start	3 months	1 year	2 years	P
Osteocalcin	76±30	129±38	131±45	128±44	<.0001[a,b,c]
ALP	3.3±0.9	4.5±1.3	4.2±1.5	4.1±1.2	<.0001[a,b,c]
BALP	70±23	104±37	113±40	105±36	<.0001[a,b,c]
PINP	517±140	900±255	830±248	814±228	<.0001[a,b,c,e]
Vitamin D	69±19	73±22	64±21	63±18	<.001[c,d,e]

[a]0y vs 3m, [b]0y vs 1y, [c]0y vs 2y, [d]3m vs 1y, [e]3m vs 2y, [f]1y vs 2y

Table 1

***Disclosures: Diana Swolin-Eide**, None.*
This study received funding from: Immunodiagnostic Systems

MO0029

Does Bone Resorption Stimulate Periosteal Expansion? A Cross-sectional Analysis of β-C-telopeptides of Type I Collagen (CTX), Genetic Markers of Resorption, and Periosteal Circumference as Measured by pQCT. John P Kemp[1], Adrian Sayers[2], David M Evans[1], Lavinia Paternoster[1], Kevin Deere[1], Mattias Lorentzon[3], Terho Lehtimäki[4], Joel Eriksson[5], Mika Kähönen[6], Olli Raitakari[7], Marika Laaksonen[8], Harri Sievänen[9], Jorma Viikari[10], Leo-Pekka Lyytikäinen[6], William D Fraser[11], Liesbeth Vandenput[5], Claes Ohlsson[5], Jonathan H Tobias*[12]. [1]MRC Centre for Causal Analyses in Translational Epidemiology, School of Social & Community Medicine, University of Bristol, United Kingdom, [2]School of Social & Community Medicine, University of Bristol, United Kingdom, [3]Geriatric Medicine, Dept. of internal medicine & clinical nutrition & The Center for Bone & Arthritis Research, Institute of Medicine, Sahlgrenska Academy, University of Gothenburg, Sweden, [4]Department of Clinical Chemistry, Fimlab Laboratories, University of Tampere & Tampere University Hospital, Finland, [5]Centre for Bone & Arthritis Research, Institute of Medicine, Sahlgrenska Academy, University of Gothenburg, Sweden, [6]Department of Clinical Physiology, University of Tampere & Tampere University Hospital, Finland, [7]Research Centre of Applied & Preventive Cardiovascular Medicine, University of Turku & the Department of Clinical Physiology & Nuclear Medicine, Turku University Hospital, Finland, [8]Department of Food & Environmental Sciences, University of Helsinki, Finland, [9]The UKK Institute for Health Promotion, Finland, [10]Department of Medicine, University of Turku & Turku University Hospital, Finland, [11]Norwich Medical School, University of East Anglia, UK, United Kingdom, [12]School of Clinical Sciences, University of Bristol, United Kingdom

Aim: Bone size increases across puberty more rapidly in peripubertal males compared to females, in whom bone resorption markers are also higher. Hence in childhood, bone resorption may act to stimulate periosteal expansion and increase bone strength. To address this hypothesis, we examined whether bone resorption, as reflected by serum *β*-C-telopeptides of type I collagen (CTX), is positively associated with periosteal circumference (PC), in contrast to inverse associations with parameters related to bone remodelling such as cortical bone mineral density (BMD_C). To examine the causal nature of this relationship, we analysed whether SNPs within key osteoclast regulatory genes, known to reduce BMD, conversely increase PC.

Methods: CTX and mid-tibial pQCT scans were available in 1130 adolescents (mean age 15.5 years) from the Avon Longitudinal Study of Parents and Children (ALSPAC). Analyses were adjusted for age, gender, tanner stage, lean mass, fat mass and height. Genetic variants were identified within or proximal to *RANK, RANKL* and *OPG*, and previously reported to be associated with areal/cortical BMD in genome wide meta-analyses. To confirm their relationship with bone resorption, we examined associations with CTX (n=2379). Subsequently, we examined associations

between these SNPs and PC, based on a genome-wide meta-analysis involving ALSPAC (n=3382); Gothenburg Osteoporosis and Obesity Determinants (GOOD) (n=938) and the Young Finns Study (YFS) (n=1558).

Results: CTX was positively related to PC [β= 0.19(0.13, 0.24)] (coefficient=SD change per SD increase in CTX, 95% CI)], but inversely associated with BMD_C [–0.46(–0.52,–0.40)] and cortical thickness [β=–0.11(–0.18, –0.03)]. CTX was positively related to bone strength as reflected by SSI [β=0.09(0.03, 0.14)]. 15 *RANKL*/*RANK*/*OPG* SNPs were identified by literature search to be robustly associated with BMD. Supporting the assumption that these associations reflect altered bone resorption, six of these 15 alleles that were previously reported to be inversely related to BMD were positively related to CTX in ALSPAC (P<0.05 cut-off). In our subsequent genome-wide meta-analysis, eight of these 15 alleles were positively related to PC (five based on P<0.05 cut-off, and three P<0.1).

Conclusion: Despite having lower BMD, individuals with a genetic predisposition to higher bone resorption have greater bone size, suggesting that bone resorption represents an important positive stimulus for periosteal expansion.

***Disclosures: Jonathan H Tobias**, None.*

MO0030

Estradiol Dependent Accrual of Bone Mass in Young Growing Rats is not Amplitude–Modulated. Ingrid Kantner*[1], Hartmut Blode[2], Kerstin Gude[3], Reinhold Erben[4]. [1]Vetmeduni Vienna, Austria, [2]Bayer Healthcare Global R&D Centre, China, [3]Bayer Healthcare AG, Germany, [4]University of Veterinary Medicine, Austria

There is evidence suggesting that use of low dose monophasic oral contraceptives may impair bone mass accrual in young women. One possible explanation could be that the response of bone to estrogen may be modulated by recurrent episodes of higher estrogen levels found in the preovulatory phase of the natural cycle, i.e., bone may respond to estrogenic amplitude modulation. Constant low doses of estrogen might not be the optimal stimulus for physiological accrual of bone mass in women. It was the aim of the current study to test this hypothesis by comparison of a continuous and a cyclical estradiol dosing regimen administered to growing ovariectomized (OVX) rats over 4 months. Two-month-old female Fischer 344 rats were either OVX or sham-operated. OVX rats allocated to the continuous regimen received 0.15, 0.5, 1.5, or 2.5 µg 17β-estradiol/kg per day subcutaneously (s.c.) 7 times per week throughout the experiment. Using the same mean doses averaged over a 5-day treatment period, cyclical estradiol treatment was achieved by s.c. injection with half of the mean dose over 3 days, followed by 1 day with the 1.5-fold mean dose, and 1 day with the 2-fold mean dose, thus imitating the natural rat 4 - 5-day cycle. This cyclical 5-day administration regimen was repeated over the 4-month treatment period. Controls received vehicle (10% ethanol in saline s.c.) alone. Treatment of OVX rats with estradiol in a continuous or cyclical fashion dose-dependently protected against the development of tibial and vertebral osteopenia as measured by peripheral quantitative computed tomography (pQCT). In addition, bone formation and bone resorption was dose-dependently suppressed by continuous and cyclic estradiol as evidenced by bone histomorphometry in lumbar vertebrae and proximal tibiae, and by measurement of biochemical bone markers at the whole body level. However, regardless of the endpoint the main determinant of the skeletal response to estradiol was the mean dose administered, independent of a continuous or cyclical administration regimen. Thus, the current experiment suggests that estrogen dependent accrual of bone mass is not amplitude-modulated in young growing rats.

***Disclosures: Ingrid Kantner**, None.*
This study received funding from: Bayer Healthcare AG

MO0031

In Growing Girls, Muscle Functional Indices and Activity Dose Are Robust Predictors of Upper Extremity Bone Outcomes, but Less Consistent as Predictors of 1- Year Growth Velocities. Alex Skwirz[1], Jodi Dowthwaite*[2], Carol Sames[3], Melissa Zajdel[4], Paula Rosenbaum[3], Tamara Scerpella[5]. [1]Syracuse University, USA, [2]SUNY Upstate Medical University; Syracuse University, USA, [3]SUNY Upstate Medical University, USA, [4]Princeton University, USA, [5]University of Wisconsin, USA

Purpose: It is unclear whether muscle force and impact affect bone growth independently. Muscle functional indices (MFI), activity dose and impact exposure were tested as predictors of bone outcomes in young, female gymnasts (GYM) and non-gymnasts (NON).

Methods: Repeated annual measures for 28 GYM & 23 NON yielded 1 year velocities for predictors and bone outcomes (v: T1 to T2 interval= 0.85-1.15yrs). Whole body and forearm DXA yielded non-dominant arm and distal radius data (Arm, UD (ultradistal), 1/3; Hologic Discovery A). For MFI, grip strength (Takei) and elbow/shoulder flexion/extension peak torques were measured (Biodex). Semi-annual questionnaires assessed maturity (pre-puberty, puberty/pre-menarche, post-menarche) and organized non-aquatic activity dose (pre-DXA annual means; OPA, h/wk). Backward linear regression built predictive models. Base models entered maturity, height and all MFI. Activity models added OPA and GYM status to maturity, height and all MFI. For velocities, relative change in maturity level was evaluated; height and MFI velocities were entered (change/time).

Results: Baseline age ranged from 8 to 15 years. NON were taller than GYM (T2); GYM OPA was higher than NON (T1 & 2)(p<0.05). Activity level tracked across time (r=0.85, p<0.05). At Time 1, MFI were positively associated with all bone outcomes (p<0.05), except 1/3 BMD; MFI associations with Arm & 1/3BMC changed after adding activity factors. Time 1 OPA was positively associated with radius BMC & BMD (1/3 & UD, p<0.05 except UDBMD p=0.07). At Time 2, various MFI were associated with bone outcomes (p<0.05), except 1/3BMD. MFI were significant predictors in Time 2 activity models, except 1/3BMD; Time 2 OPA was positively associated with bone outcomes (p<0.05), except 1/3Area. For velocities, vMFI were associated with vArmBMC, v1/3BMC, v1/3BMD (p<0.05). In activity models, vMFI results were similar after adding activity factors. T2 OPA was positively associated with vArmBMC (p<0.10) & vUDBMC (p<0.05). GYM status was associated with higher T1ArmBMC, T1UDBMD and lower vUDBMC (p<0.05).

Conclusion: Muscle peak torque and activity dose varied as predictors of bone outcomes by time, muscle group, skeletal site and bone metric. High physical activity doses were associated with benefits for most bone outcomes at single time points. Tracking of predictors during growth may have limited detection of associations between activity exposure and bone growth velocities.

***Disclosures: Jodi Dowthwaite**, None.*

MO0032

Leptin Blunts the Starvation-Induced Increase in Bone Marrow Adiposity. Maureen Devlin*[1], Christine Conlon[2], Miranda Van Vliet[2], Leeann Louis[2], Lamya Karim[2], Clifford Rosen[3], Mary Bouxsein[2]. [1]University of Michigan, USA, [2]Beth Israel Deaconess Medical Center, USA, [3]Maine Medical Center, USA

Starvation induces both high bone marrow adiposity and low bone mass in humans, suggesting common mechanisms may underlie these effects. Here we test the role of the adipokine leptin in mediating increased bone marrow adiposity and impaired skeletal acquisition due to caloric restriction. Prior studies have shown leptin increases bone mineral content and decreases bone marrow adiposity in the leptin-deficient ob/ob mouse (Hamrick et al., 2005). Thus we hypothesized that starvation-induced hypoleptinemia may contribute to bone marrow fat accumulation and impaired skeletal acquisition, and that leptin replacement during caloric restriction (CR) would reduce marrow adiposity and improve bone mass. We tested this hypothesis in female C57Bl/6J mice fed a 30% calorie restricted (CR) or normal (N) diet from 5-10 wks of age, with daily injections of vehicle, 1 mg/kg/day leptin, or 2 mg/kg/day leptin (N=6-8/group). Outcomes included daily body mass (BM, g) and food intake, serum leptin, %body fat, whole body bone mineral content (BMC, g) via pDXA, cortical (Ct) and trabecular (Tb) bone architecture at the midshaft and distal femur via µCT, and marrow adiposity via osmium staining. Overall, CR mice had lower body mass, %body fat, and Ct bone area fraction, and higher Tb bone volume fraction and connectivity density vs. N mice (p<0.05 for all). Fasting serum leptin levels (~16h post-injection) were lower in CR vs. N (p<0.05) and did not differ across leptin treatments within either diet. However, within each diet, leptin altered body composition and skeletal acquisition. Leptin-treated CR mice gained less body fat and gained more BMC/BM vs. CR controls, although BMC/BM remained lower vs. N controls (p<0.05 for all). Leptin-treated N mice had lower %body fat (p<0.05) but similar BMC/BM vs. N controls. Importantly, while vehicle-treated CR mice had 354% greater marrow fat in the proximal tibia compared to N, leptin-treated CR mice had only a 113% increase (Figure). Leptin treatment had no effect on bone marrow adiposity in N mice. In conclusion, these data demonstrate that leptin replacement during CR inhibits bone marrow fat formation and increases bone mass acquisition compared to controls, supporting the hypothesis that hypoleptinemia contributes to starvation-induced bone marrow adiposity and low bone mass.

Caloric restriction, female, leptin, bone, marrow adiposity, mouse

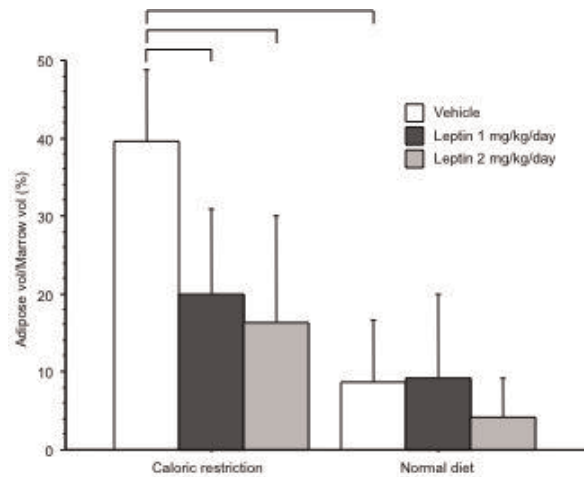

Figure

***Disclosures: Maureen Devlin**, None.*

MO0033

Novel implemental roles of the NF-κB subunit RelB in osteoblastogenesis: intrinsic antagonism of the classical NF-κB pathway by RelB. Masahiro Hiasa*[1], Masahiro Abe[2], Toshio Matsumoto[3], Naozumi Ishimaru[2]. [1]University of Tokushima Graduate School, Japan, [2]University of Tokushima, Japan, [3]University of Tokushima Graduate School of Medical Sciences, Japan

Although the activation of the classical NF-κB pathway suppresses bone formation, the role of the non-classical NF-κB pathway in osteoblastogenesis remains largely unknown. In the present study, we therefore explored the role of the non-classical NF-κB subunit relB in the classical NF-κB signaling activation and osteoblastogenesis. TNF-α suppressed mineralized nodule formation by MC3T3-E1 preosteoblastic cells and bone marrow stromal cells at 100 pg/ml but not at 10 pg/ml. However, TNF-α was able to suppress mineralized nodule formation even at 1 pg/ml by these cells upon treatment with RelB siRNA or by bone marrow stromal cells from $RelB^{-/-}$ mice, suggesting the potentiation of the suppressive effects of TNF-α on bone formation in the absence of RelB. Furthermore, the RelB knockdown facilitated the nuclear localization of the classical NF-κB subunits p65/p50 and their DNA binding in MC3T3-E1 cells in the presence of TNF-α at 10 pg/ml. However, inhibition of the classical NF-κB pathway by IMG-2001 or SN50, inhibitory peptides for the nuclear translocation of p65/p50, restored the mineralized nodule formation under the RelB knockdown in the presence of TNF-α, and was also able to resume fracture healing in $RelB^{-/-}$ mice in which the fractured bones were otherwise not united. Interestingly, the mRNA expression of *RelB* but not other NF-κB subunits, *p50*, *p52*, *p65* and *c-Rel*, was up-regulated in fractured bones in wild-type mice. Similarly, TNF-α enhanced the expression of RelB but not other NF-κB subunits, suggesting the intrinsic mitigation of the classical NF-kB pathway by RelB. Therefore, RelB appears to be indispensable for bone repair, and play an implemental role in osteoblastogenesis at least in part through antagonzing classical NF-κB signaling.

***Disclosures: Masahiro Hiasa**, None.*

MO0034

RANKL, OPG, and Exercise Dose in Overweight and Obese Children. Norman Pollock*, Haidong Zhu, De-Huang Guo, Catherine Davis. Georgia Regents University, USA

Our understanding of bone turnover has increased considerably with the discovery of the key molecular drivers of osteoclastogenesis, receptor activator of nuclear factor-κB ligand (RANKL) and osteoprotegerin (OPG). It was demonstrated that binding of RANKL to its receptor, RANK, promotes osteoclast differentiation and bone resorbing activity. OPG, a member of the TNF receptor superfamily, acts as a decoy receptor to RANKL, and therefore inhibits osteoclast activation and bone resorption. The roles of RANKL and OPG in bone have been confirmed by mouse models and by exogenous administration of these molecules. A number of clinical reports on serum RANKL and OPG in musculoskeletal pathology have been published; however, interpretation of these data has been elusive. To increase our understanding of this relationship, it would be desirable to have pediatric data under controlled conditions with no musculoskeletal pathology. Therefore, we investigated the dose-response effect of exercise training on circulating concentrations of RANKL, OPG, and the RANKL/OPG ratio in children. Associations of RANKL, OPG, and RANKL/OPG with bone turnover markers were also determined. Overweight children (n=222, aged 7-11 years, 42% male, 58% black, 85% obese) were randomly assigned to 3 experimental conditions: low-dose (20 min/d, n=71) or high-dose (40 min/d, n=73) aerobic exercise program (13 weeks, 5 d/wk) or a control condition (usual physical activity, n=78). Fasting serum samples were taken at baseline and posttest and concentrations of total RANKL and OPG were quantified together with measures of bone formation [osteocalcin (OC)] and resorption [C-terminal telopeptide of type 1 collagen (CTX)]. A significant linear downward trend indicating dose-response to exercise was observed for OPG (P=.04). A dose-response effect was also observed for RANKL/OPG and OC, as indicated by significant upward trends (both P<.04). There was no effect of exercise on RANKL or CTX. Multiple linear regression adjusting for age, sex, and race revealed that changes in both OPG and RANKL/OPG were associated with changes in OC (both P<.05). Changes in RANKL were not associated with changes in OC or CTX. In overweight children, aerobic exercise training influenced serum OPG, RANKL/OPG, and OC in a dose-dependent manner. The increase in bone formation along with the decrease in OPG might reflect an increase in OPG binding to RANKL, which could explain the beneficial exercise training effect on bone.

***Disclosures: Norman Pollock**, None.*

MO0035

Norepinephrine reuptake is required for acquisition of a normal peak bone mass. Yun Ma*[1], Jeffry Nyman[2], Maureen Hahn[1], Florent Elefteriou[1]. [1]Vanderbilt University, USA, [2]Vanderbilt University Medical Center, USA

A large body of evidence supports the role of post-synaptic beta 2 adrenergic receptor (β2AR) signaling in the regulation of bone remodeling. Stimulation and blockade of β2AR signaling indeed cause bone loss and bone gain in mice, respectively, however, the contribution of endogenous norepinephrine released by sympathetic nerves to these processes remains unclear. We show here that differentiated osteoblasts (but not immature osteoblasts), like neurons, express the norepinephrine transporter (NET), whose role is to control duration and intensity of sympathetic signals following action potential. NET expression by osteoblasts was detected at both RNA and protein levels by qPCR, Western blot and immunocytochemistry analyses. Specific NE uptake activity, measured by [^{3}H]NE uptake assays, was observed in differentiated osteoblasts. Moreover, by analyzing the expression of enzymes of the NE synthetic and catabolic pathways, we show that differentiated osteoblasts can catabolize, but cannot generate, NE. Chronic pharmacological blockade of NET by the NET blocker reboxetine for 2 months induced bone loss in growing mice. In addition, lack of extracellular norepinephrine (NE) reuptake in *Norepinephrine transporter* (*Net*)-deficient mice led to reduced bone formation and increased bone resorption, resulting in suboptimal peak bone mass and weakened mechanical properties, in the context of low sympathetic outflow and high plasma NE levels. These findings suggest that the response of differentiated osteoblasts to sympathetic outflow and serum NE levels is controlled by the activity of NET in sympathetic neurons or differentiated osteoblasts and support the notion that the control of endogenous NE release and reuptake is an important component of the complex homeostatic machinery by which the central nervous system control bone remodeling. In addition, they suggest that patients prescribed NET blockers for the treatment of ADHD or depression may be at risk for premature osteoporosis and more susceptible to bone fracture.

***Disclosures: Yun Ma**, None.*

MO0036

***In Vivo* Evaluation of Skeletal Development in Non-Clinical Pediatric Studies in Rabbits.** Rana Samadfam*, Nancy Doyle, Aurore Varela, Susan Y. Smith. Charles River Laboratories, Canada

In recent years there has been an increased emphasis placed on nonclinical pediatric drug testing, with a focus on effects on growth and development of several organ systems including the skeleton (FDA guidance 2006, EMEA guideline 2008). The aim of this study was to establish procedures to evaluate the effects of drugs on skeletal development and bone density in non-clinical pediatric studies in rabbits. A wide variety of techniques are potentially available to assess skeletal development. Feasibility of using some of these techniques including radiography, DXA and pQCT was examined. These imaging techniques were performed repeatedly on the same animals, from juvenile (4 weeks of age) to adulthood (6 months of age).

Animal were anesthetized for in vivo scanning. DXA scans were obtained at the lumbar spine, femur and/or whole body and provided measurements for area, bone mineral content (BMC) and bone mineral density (BMD). Peripheral QCT scans were acquired at the proximal tibia and provided volumetric measurements of area, BMC and BMD of the total slice, trabecular and cortical compartment as well as geometry parameters. Radiographs were used for bone length measurements at the lumbar spine and long bones. In vivo radiograph measurements showed increases in bone length with age. At each time points, the measurements were reproducible with CV lower than 5 %. The results for whole body (area, BMC and BMD), Lumbar spine (L1-L4, area, BMC and BMD) and femur (global and subregional area, BMC and BMD at 24-25 days old and global parameters at 8 weeks old) were reproducible with CV ranging between 1.2-5%. Appropriate positioning and feasibility of tibia for pQCT scanning was also confirmed. The results for total and cortical parameters were reproducible CV lower than 5%. Trabecular parameters were more variable likely due to small amount of trabecular bone at this site. The results of these investigations indicate that in vivo radiography, DXA and pQCT provide safe, reproducible and repeated non-invasive measurements of skeletal growth in skeletally immature rabbits at axial and appendicular sites. These techniques provide a comprehensive set of assessments for the evaluation of the potential effects of drugs on the developing skeleton.

***Disclosures: Rana Samadfam**, None.*

MO0037

Pamidronate use in Children with Osteogenesis Imperfecta at Boston Children's Hospital: Retrospective Cohort Study. Paulina Ortiz-Rubio*[1], Ingrid Holm[2], Nina Ma[1]. [1]Boston Children's Hospital, USA, [2]Children's Hospital Boston, USA

Osteogenesis imperfecta (OI) is a collagen disorder resulting in bone fragility, progressive deformity and chronic pain. Bisphosphonate therapy, specifically with pamidronate, has been shown to be beneficial in children with severe OI by reducing fracture rate and improving bone mineral density (BMD). Currently, however, there is no standardized approach to treating children with OI using pamidronate, and regimens vary widely in dose and frequency between institutions.

We therefore performed a retrospective cohort study of children with severe OI who were treated with intravenous pamidronate infusions at Boston Children's Hospital during the past fifteen years. Subjects included were those who received a standardized protocol of pamidronate infusions for a single day every four (0.5-0.75mg/kg/dose) or six (1mg/kg/dose) weeks depending on age. Comparisons were made regarding measures of efficacy before and after treatment, and safety data was collected and reported.

Of the 32 children with OI treated with pamidronate, 11 received the 4-6 week standardized regimen and had complete data available. Children ranged from 2 to 15 years old and were treated for 3.73 ±1.89 (mean ±SD) years. Growth data showed

no significant change in height ($p > 0.180$) and weight ($p > 0.267$) z-scores from before to after treatment. Adverse events related to treatment included a mild acute phase reaction after the first pamidronate infusion (45.5%), post-infusion hypocalcemia (9.1%) and delayed fracture healing during treatment (9.1%). Of 11 patients, 8 (72.7%) reported significant improvement in strength and activity, 11 (100%) reported improvement in fracture rate and, of 8 patients complaining of significant pain prior to treatment, 7 (87.5%) reported marked decrease in pain. There was a mean annualized percent change in BMD of +48.24% ± 19.53, and BMD z-scores improved from -3.81 ± 1.93 before to -0.918 ± 1.66 after treatment ($p < 0.001$).

In conclusion, children with severe OI treated with single day pamidronate infusions every 4 to 6 weeks showed significant clinical and radiographic improvement. There was no evidence of a detrimental effect on growth related to pamidronate therapy, which has been a concern raised by clinicians. Lastly, patients should be counseled regarding acute phase reaction symptoms following the first administration of pamidronate and calcium levels should be monitored following infusions as there is risk of hypocalcemia.

***Disclosures: Paulina Ortiz-Rubio**, None.*

MO0038

Age and Sex Dependence of Baboon Proximal Femur Composite Traits Determined Using Statistical Shape and Density Modeling. Todd Bredbenner*[1], Arthur Nicholls[1], Donald Moravits[1], Jennifer Harris[2], Shayna Levine[2], Lorena Havill[2], Daniel Nicolella[1]. [1]Southwest Research Institute, USA, [2]Texas Biomedical Research Institute, USA

The structural integrity of bone in any mechanical loading environment is an integrative function of a multitude of complex and interrelated characteristics, including microstructural organization, macroscopic bone morphology, and, of course, bone density. In ongoing work utilizing a pedigreed baboon model, we hypothesize that bone traits functionally co-vary in a complex multivariate manner to produce sufficient structural integrity for routine daily loading; however, some bone structures will perform poorly under non-habitual loading conditions, such as those encountered in a fall.Using microCT, we imaged 74 baboon left proximal femurs obtained at routine necropsy, along with a density calibration phantom, in order to investigate the dependency of variation in geometry and bone mineral density distribution on sex and age. To date, volumetric femur models describing geometry and spatial BMD distribution were created for 74 animals (31 males, 43 females; age: 18.8 ± 3.9 years, developmentally equivalent to 56.4 ± 11.8 human years). Each 3D model consisted of 31,874 variables (i.e. spatial location and density at each mesh node located at corresponding anatomic positions for all femurs). Statistical shape and density modeling (SSDM), based on Principal Component Analysis, was used to describe variation in 3D bone geometry and BMD distribution within the set of 74 individual femurs by reducing the ~32,000 highly correlated variables for each model to a set of 73 uncorrelated and independent principal components (e.g. composite geometry and BMD traits) without loss of information. Two-way unbalanced analyses of variance were used to test the principal component weighting factors for dependence on sex and age, where animals were grouped into young (age < 15 years), old (> 22 years), and middle-aged (others). Four of the 74 weighting factors were significantly associated with sex and 2 of the 74 were associated with age grouping. Principal components defined using SSDM identify complex combinations of structural bone traits (e.g. geometric and BMD distribution traits) that vary with sex and age. In ongoing work, we are characterizing these bones with a comprehensive suite of bone traits and we expect that comprehensive description of bone sample variation will allow investigation of important structural differences that differentiate between strong and weak bones under routine loading (i.e. single-leg stance) and abnormal loading (i.e. fall-type loading).

***Disclosures: Todd Bredbenner**, None.*
This study received funding from: NIH

MO0039

Bone microstructure characteristics in high fat diet induced fatty liver disease mice. Shen Qu[1], Ran Cui*[1], Yunzi Liu[2], Chunlei Jiang[2]. [1]Shanghai Tenth People's Hospital of Tongji University, School of Medicine, China, [2]The Second Military Medical University, China

Purpose: It has been proved that non-alcoholic fatty liver disease (NAFLD) had detrimental effect on bone mineral density (BMD) in both adults and adolescents. However, most of the evidence was from clinical studies, which cannot ensure the adverse effect. Thus, we performed an animal experiment to certify this phenomenon.

Methods: 46 C57 male mice, 8-10 weeks old, average body weight 15-20g at the beginning of the experiment, were enrolled and divided into two groups, feeding for 12 weeks either standard chow (control; N = 21) or high-fat diet (HFD; N = 25). Femur, Tibia and liver samples were collected after sacrifice. The bone samples were scanned using a micro-CT system (mCT-80; Scanco Medical AG) in a high-resolution scanning mode (a voxel size and slice thickness of 20 mm). In HFD group, 20 mice were proved with fatty liver by liver biopsy. Tissue mineral density (TMD), total bone volume fraction (BV/TV), trabecular thickness (Tb.Th), trabecular number (Tb.N), trabecular separation (Tb.Sp), connectivity density (Conn.D) and structure model index (SMI) were compared between control and HFD groups.

Results: Compared to control group, HFD had a lower level of TMD (59.741 ± 23.038 vs. 112.196 ± 54.940, P=0.028), BV/TV (0.017 ± 0.003 vs. 0.068 ± 0.044, P=0.007), and Tb.Th (0.050 ± 0.006 vs. 0.063 ± 0.006, P<0.001) in femur. For tibia, HFD also had a lower level in TMD (25.078 ± 19.822 vs. 85.462 ± 34.011, P=0.021), BV/TV (0.023 ± 0.012 vs. 0.068 ± 0.017, P<0.001), Conn.D (0.359 ± 1.688 vs. 8.522 ± 6.458, P=0.023), Tb.Th (0.048 ± 0.007 vs. 0.061 ± 0.007, P=0.004), while a higher level of SMI (3.428 ± .412 vs. 2.529 ± .454, P=0.002) and Tb.Sp (0.636 ± 0.158 vs. 0.441 ± 0.145, P=0.022).Conclusion: Our results convinced the adverse effect on bone microstructure of high fat diet induced fatty liver mice. However, further study was needed to investigate the mechanism.

***Disclosures: Ran Cui**, None.*
This study received funding from: High Density Lipoprotein Metabolism Regulation by Beta Chain of ATP Synthetase on the Surface of Hepatic Cells

MO0040

Can lost bone be recovered after 12 weeks of reduced energy availability? Corinne Metzger*[1], Kaleigh Camp[1], Sibyl Swift[2], Mary Jane DeSouza[3], Evelyn Yuen[1], Florence Lima[1], Susan Bloomfield[1]. [1]Texas A&M University, USA, [2]Armed Forces Radiobiology Research Institute, USA, [3]The Pennsylvania State University, USA

Reduced energy availability due to restricted caloric intake leads to bone loss; however, less is known about the impact of exercise during reduced energy availability and recovery from a period of reduced energy intake. We hypothesized that bone loss would be minimized, and that recovery of any losses would be enhanced, in animals achieving reduced energy availability (EA=energy intake minus energy expenditure from exercise) with exercise as well as caloric restriction. Virgin female Sprague-Dawley rats (5-mo-old) were acclimated to AIN-93M purified diet for 8 weeks and then randomly assigned into sedentary (Adlib-SED) and exercising (Adlib-EX) adlib-fed controls or sedentary (-25EA-SED) and exercising (-25EA-EX) energy restricted groups. Sedentary -25EA were fed 40% less energy with all other nutrients maintained at 100%. Exercising -25EA received 30% less energy from the diet and achieved another 10% energy reduction by treadmill running 4 days/week for 90-100 min (~60% VO_{2max}). Following 12 weeks of reduced EA, -25EA-SED animals exhibited significantly decreased fat mass ($p<0.0001$) and cancellous volumetric BMD (Canc-vBMD, by pQCT; $p< 0.006$) at the PTM compared to Adlib-SED mice; declines in lean mass did not reach significance. By contrast, 25EA-EX animals' lean mass and PTM Canc-vBMD values were not different from Adlib-EX controls, although fat mass was significantly reduced ($p =0.0014$). Serum leptin concentrations were lower in the -25EA-SED vs. Adlib-EX and AdLib-SED ($p<0.005$), while serum IGF-1 concentrations were lower in -25EA-SED vs. only Adlib-EX ($p=0.005$). Cancellous bone formation rate (BFR) declined in both EA groups relative to their adlib fed controls, but did not reach statistical significance. During recovery from reduced EA, all rats were fed adlib and running exercise volume was halved for 12 weeks. After 12 weeks, lean mass, proximal tibia Canc-vBMD and serum leptin and IGF-1 concentrations recovered to adlib-fed controls' values in both EA groups. Cancellous BFR in both EA groups was recovered to the same values as adlib-fed control values after 12 weeks of recovery. In conclusion, we found decreased EA produces bone loss and a decrease in BFR; however, if the reduced EA is achieved in part by exercise, bone loss and decreases in BFR are minimized. Deficits in bone with reduced EA appear to be reversible by 12 weeks in both exercising and sedentary energy-restricted animals if energy balance is achieved and maintained during recovery.

***Disclosures: Corinne Metzger**, None.*

MO0041

Comparative Experimental Study of the Effect of Osteoprotegerine and Testosterone on the OPG/RANKL System in an Animal Model of Male Castrate Rats. Marta Martín-Fernández*[1], Mónica Sánchez-Sánchez[1], Manuel Díaz-Curiel[2], Concepción De la Piedra[3]. [1]Instituto de Investigación Sanitaria Fundación Jiménez Díaz, Spain, [2]Medicina Interna. Instituto de Investigación Sanitaria Fundación Jiménez Díaz, Spain, [3]Bioquímica Investigación. Instituto de Investigación Sanitaria Fundación Jiménez Díaz, Spain

Lack of androgens leads to a loss of bone mass and bone quality in general. The administration of either Osteoprotegerin (OPG) or testosterone is capable of preventing the negative effects on bone of a lack of androgens. In a previous work we have observed that osteopenia due to ORX was reverted with OPG-Fc administration (totally) and with testosterone administration (partially) to ORX male rats. The aim of this work was to evaluate if OPG-Fc and testosterone treatment act through the OPG/RANKL system.

Sixty 3-month-old male Wistar rats were used and divided into 4 groups: SHAM: n=15, simulated intervention; ORX: n=15, orchidectomized; ORX+TEST: n=15, orchidectomized and treated with testosterone cypionate (1.7 mg/Kg) i.m. every week; ORX+OPG: n=15, orchidectomized and treated with OPG-Fc (a recombinant RANKL inhibitor with rat cross-reactivity) (10 mg/Kg) s.c. twice a week. The treatment was started immediately after orchidectomy, and was maintained for 8 weeks. Total RNA was isolated from the rat femur and reverse-transcribed. Quantitative RT-PCR was performed to evaluate the expression of OPG and RANKL, using GAPDH gene as constitutive control. Results are expressed as the mean ± SEM.

RANKL expression was significantly increased in the ORX group with respect to SHAM group. OPG-Fc and testosterone treatments produced a decrease in RANKL expression although no statistical differences were observed. OPG-Fc treatment produced a significant decrease in OPG expression with respect to all other groups. It

is important to note that testosterone treatment produced a significant increase in OPG/RANKL ratio with respect to ORX group. That could explain the increase observed in femoral BMD when rats were treated with testosterone. Exogenous OPG-Fc (which produced an increase in systemic OPG) but not endogenous femoral expression of OPG could explain the increase in BMD observed in OPG-Fc treated rats.

***Disclosures: Marta Martín-Fernández**, None.*

MO0042

Correlating FTIRI and Raman Parameters using Iliac Crest Biopsies. Adele Boskey*[1], Lyudmila Spevak[1], Gurjit Mandair[2], Susan P. Bare[3], Robert Recker[3], Michael Morris[4]. [1]Hospital for Special Surgery, USA, [2]University of Michigan, Department of Chemistry, USA, [3]Creighton University, USA, [4]University of Michigan, USA

Fourier transform infrared imaging (FTIRI) and Raman microspectroscopy (RS) have widely been used to probe the physicochemical and microstructural changes in aged or diseased bone for the past decade. Earlier studies in cortical bone have shown that, as expected from theory, parameters measured by FTIRI correlate with those measured by RS. Some parameters, on the other hand, are based on different molecular vibrations in FTIRI and RS, and are not necessarily correlated. In this study, using a small subset (n=20) of a larger study, examines the correlations between select FTIRI and RS parameters of "bone quality" using iliac crest biopsies obtained from age-matched postmenopausal women with and without fractures. Embedded and sectioned biopsies were initially mapped by RS and then by FTIRI using adjacent 1 um-thick sections. The following FTIRI parameters were calculated for cortical and cancellous bone: Mineral/Matrix (Min/Mat), Carbonate/Phosphate (C/P), Collagen maturity (XLR), and Crystallinity (XST). Cortical FTIRI parameters were derived from the thinner side of the iliac crest (cortex b). Each FTIRI parameter was then correlated with a blind set of one of the closest matching RS parameters: Phosphate/Proline, Phosphate/Phenylalanine (Phe), Phosphate/Amide I, 1070/Phosphate, or 1045/ Phosphate. In this correlative FTIRI and RS study, we demonstrate agreement with cancellous bone parameters but not always with cortical bone parameters as measured in the thinner (cortex b) or thicker (cortex a) cortex, or a combination of both (cortex a+b) for FTIRI with RS parameters (Table). Accepting an R^2 value greater than 0.22 as a reportable correlation between FTIRI vs. RS parameters, we report significant correlations (with $p<0.05$) for cancellous Min/Mat vs. Phosphate/Proline, cancellous and cortical Min/Mat vs. Phosphate/Phe, and cancellous C/P vs. 1070/Phosphate. Although the study was not powered to address differences between fracture and control cases, we found that in general that crystallinity and collagen maturity parameters as measured by FTIRI for cancellous and cortical bone tended to be increased in cases relative to controls.

Correlation coefficients (R^2) between FTIRI vs. RS parameters of Bone Quality

Parameter (FTIRI vs. RS)	Cancellous bone	Cortical bone
Min/Mat vs. Phosphate/Proline	0.24	0.054 (cortex b)
Min/Mat vs. Phosphate/Phe	0.28	0.38 (cortex b)
Min/Mat vs. Phosphate/Amide I	0.23	0.28 (cortex b)
C/P vs. 1070/Phosphate	0.55	0.04 (cortex b)
Crystallinity vs. 1045/Phosphate	0.36	0.10 (cortex a+b)

Table

***Disclosures: Adele Boskey**, None.*

MO0043

Cx43 Hemichannels Involves in TMJ Cartilage Degradation Induced by Biomechanical Dental Stimulation. Mei-Qing Wang*[1], JIng Zhang[2], Mian Zhang[2], Min Guo[2], Min Guo[2], Ting Yang[2]. [1]School of Stomatology, Fourth Military Medical University, Peoples Republic of China, [2]FMMU, China

Temporomandibular joint (TMJ) is a site that frequently suffers osteoarthritis (OA). It has a biomenchanical association with dental occlusion so that OA like lesions could be induced in TMJ when tdental occlusion is disorderedly altered. Connexin 43 (Cx43) hemichannels and P2 receptors is a putative mechanoreceptor complex that expressed on the surface of articular chondrocytes and involves in the primary cilium. In recent, we developed a rat TMJ OA model by installing a pair of metal tubes onto the left pair of incisors. In present work we used this rat TMJ OA model to explore the role of Cx43 hemichannels in TMJ cartilage degradation. Cartilage from TMJs of Sprague-Dawley rats were sampled for *in vivo*, *ex vivo* and *in vitro* studies. Histomorphometric and micro-CT analysis, real time PCR and immunohistochemistry were used to test the histomorphological changes in cartilage and subchondral bone of TMJs, and also in the expression of Cx43 and molecules related to cartilage degenerative changes, and also to the osteoblastogenetic and osteoclastogenetic activities. In vitro methods like cell shear stress, dye uptake, siRNA, ELISA and western blot were performed on the rat primary chondrocytes and ATDC-5 cell line. Cartilage degradation and condylar subchondral bone loss were observed which changes were more serious with growing of the experimental time. Micro-CT analysis revealed the significant decreased BMD and BV/TV ($P<0.05$). The mRNA expression of RANKL, RANKL/OPG, RANK, TRAP and cathepsin K were significantly increased while the expression of osterix?RUNX2?ALP?osteocalcin?DMP-1 and VEGF decreased initially followed by an significantly increase ($P<0.05$). Aberrant calcification was found at the osteochondral interface. The expression of Cx43 and the synthesis and secretion of PGE_2 increased ($P<0.05$). In vitro data showed that fluid flow shear stress promoted the expression of Cx43 and the synthesis of PGE_2 in primary chondrocytes of rat TMJ cartilage. Mechanical strain could open Cx43 hemichannels, then the release of intracellular PGE_2 increased, and the increased release of PGE_2 could be blocked by the hemichannel inhibitor ($P<0.05$). The similarly changes could be found in ATDC-5 cell line with the shear stress stimulation. In addition, the secretion of PGE_2 decreased due to the effect of siRNA on Cx43 expression ($P<0.05$). All these data indicates that the biomechanical dental stimulation, as well as the stimulation of shear stress, increased the expression of Cx43 and intracellular PGE_2, and opened Cx43 hemichannels in chondrocytes. Then the increased release of PGE_2 through Cx43 hemichannels led to cartilage degradation. Conclusively, Cx43 play a key role in TMJ OA cartilage degradation induced by biomechanical dental stimulation.

***Disclosures: Mei-Qing Wang**, None.*
This study received funding from: NSFC No.81271169

MO0044

Does Reference Point Indentation Assess the Fracture Toughness of Human Cortical Bone?. Mathilde Granke*[1], Sasidhar Uppuganti[1], Alexander Makowski[2], Ahbid Zein-Sabatto[1], Andrew J Schultze[1], Jack M Whitehead[1], Jeffry Nyman[1]. [1]Vanderbilt University Medical Center, USA, [2]Department of Veterans AffairsVanderbilt University, USA

There is a need for diagnostic tools that accurately assess age- and disease-related changes in fracture risk. Reference point indentation (RPI) is one promising tool capable of measuring material properties directly from the patient's tibia. However, this site is not a typical site of fragility fracture nor do RPI measures encompass all contributions of bone's hierarchy to fracture resistance. Therefore, to help establish clinical utility, we assessed the relative contribution of RPI measures and intracortical porosity to fracture toughness.

Cadaveric femurs were acquired from an extensive dataset of 51 human donors (22 female, age = 61±20 [29-101]; 29 male, age = 64±24 [21-98]). We cut single-edge notched beam specimens from the lateral quadrant of each mid-diaphysis, obtained its porosity by μCT, and its initiation toughness K_{Ic} by propagating a crack normal to osteon direction. In order to mimic clinical measurements, we performed RPI (Biodent, Active Life Scientific) on the medial quadrant of the midshaft, below the periosteum.The average value of 10 indents (20 cycles at 2 Hz, 10N maximal force) was recorded to ensure an acceptable confidence interval on the mean values of RPI parameters despite their inherent intra-specimen variablity.

Age-adjusted analysis of covariance showed a significant influence of gender (r^2 = 0.17, $p<0.01$) on K_{Ic}. Including gender as a covariate, regressions on K_{Ic} identified parameters that explain the variance in fracture toughness better than age: porosity (r^2 = 0.43, $p<10^{-5}$), total indentation distance (TID) (r^2 = 0.20, $p<0.01$), average creep indentation distance (avgCID) (r^2 = 0.22, $p<0.001$), average energy dissipation (avgED) (r^2 = 0.20, $p<0.01$), and first indentation distance (ID1) (r^2 = 0.21, $p<0.01$). Of multivariate regressions in which gender and porosity were significant covariates, TID, avgCID, and ID1 significantly improved the explanation of variance in K_{Ic} (table 1). Porosity, TID, avgCID and ID1 contributed negatively to K_{Ic} but did not account for gender difference.

Since microcracking below the indenter tip could dictate RPI parameters, RPI may be a local measure of tissue fracture toughness. Indeed, total, initial and creep indentation at the bone surface explain age-related changes in the fracture toughness at the millimeter scale even when microscopic porosity is a co-determinant.

Table 1. Coefficients (and standard error) from the final mutivariate regression models on K_{Ic} after removing the non-significant interactions

RPI variable / covariate	TID	avgCID	ID1
porosity	-0.082** (0.014)	-0.081** (0.017)	-0.081** (0.017)
sex.women	0.55** (0.19)	0.64** (0.19)	0.55** (0.19)
RPI variable	-0.028* (0.014)	-1.42* (0.60)	-0.033* (0.017)
constant	8.35** (1.19)	8.21** (0.96)	8.47** (1.25)
adjusted-r^2	0.46	0.48	0.47

*p<0.05, **p<0.01

Table 1

***Disclosures: Mathilde Granke**, None.*

MO0045

DPP4 Inhibition Attenuates Bone Loss in Diabetic Rats. Lorenzo Glorie*[1], Geert Behets[2], Lesley Baerts[3], Ingrid De Meester[3], Patrick D'Haese[2], Anja Verhulst[2]. [1]Universiteit Antwerpen, Belgium, [2]Laboratory of Pathophysiology, Belgium, [3]Laboratory of Medical Biochemistry, Belgium

Dipeptidyl peptidase 4 (DPP4) modulates activity of proteins by removing two aminoterminal amino acids. DPP4 inhibitors are currently being used to improve glucose tolerance in type 2 diabetes patients by increasing the halflife of DPP4 substrates. It has been shown that these substrates do not only increase pancreatic insulin secretion, but also influence the activity of bone cells. The potential therapeutic effect of DPP4 inhibition on bone metabolism is thus worth being investigated. In the present study, we evaluated the effect of the DPP4 inhibitor sitagliptin (SG) on bone structure in the streptozotocin (STZ)-induced diabetic rat.

This study included 64 male Wistar rats (age 10 weeks), divided into 4 groups (n=16): 2 diabetic and 2 control groups. One diabetic and one control group received SG through drinking water (2g/L). Rats were scanned every 3 weeks using an in vivo micro-CT scanner. After 6 & 12 weeks, rats were sacrificed after tetracyclin labeling for bone histomorphometric analysis of static and dynamic bone parameters. Mechanical properties of femora were assessed using a three-point bending test.

STZ-treated (diabetic) rats had significantly increased blood glucose and reduced body weight compared to controls, which was not influenced by SG. SG however significantly decreased diuresis and food consumption in diabetic rats. In vivo DPP4 inhibition of 89% was achieved in both SG-treated groups. Trabecular bone volume & bone over tissue volume ratio in the tibia was significantly lower in STZ-treated rats compared to untreated rats, but was normalized through SG treatment (significant at week 9 & 12). Trabecular thickness was decreased and trabecular spacing was increased in diabetic rats. SG treatment also in resulted in partial but significant recovery of these trabecular parameters in diabetic rats. Cortical bone volume stabilized after 3 weeks in diabetic rats, but kept increasing steadily in SG-treated diabetic rats. Although nonsignificant, the SG-treatment resulted in increased presence of osteoid in diabetics. In a three-point bending test performed on femora of rats sacrificed after 12 weeks, applied ultimate load in SG-treated diabetic rats was significantly higher than in non-treated diabetic rats.

Results show an attenuation of diabetic bone loss through DPP4 inhibition. Exact effect of DPP4-inhibitors on the activity of bone cells remains to be elucidated through histomorphometric and biochemical analyses of acquired samples.

***Disclosures: Lorenzo Glorie**, None.*

MO0046

Evaluating the Precision of Compressive Failure Tests of the Murine Tibia Using 3D Printing. Lillian Chatham*, Vanessa Sherk, Dana Carpenter. University of Colorado, Denver, USA

Compressive axial loading of the murine tibia has proven to be a valuable model for investigating the effects of mechanical loading on bone functional adaptation [1,2]. One possible endpoint of studies using this model is the experimentally measured strength of the tibia. Three- and 4-point bending tests provide useful measurements of tibial strength, but the loading in these tests is quite different from the axial compressive loading to which the bone adapts in vivo. To determine the precision of tibial strength measurements in a load direction similar to that applied in vivo, we performed a set of compressive failure tests of the murine tibia using 3D printed models. A model of a murine tibia was developed from micro computed tomography data (voxel size=0.02 mm^3). Twenty replicate models were printed on the 3D printer. Two trays with 0.5 $in.^3$ cubic wells were used for potting the model tibiae. To hold the samples upright during potting, holes were drilled into an acrylic plate and aligned with each cube in the trays. The holes were 0.125 in. in diameter, which was sufficient for the tibiae to pass through, but small enough to provide support during potting. Urethane was used to pot each end of the tibia. After curing, samples were removed from the trays and loaded to failure in compression at a speed of 6 mm/min, and the fracture force was recorded. Finite element (FE) models were developed to recreate the mechanical tests. The experimentally measured failure force for each FE model was applied in the axial direction. The average von Mises stress was computed at a mid-diaphyseal cross-section, just proximal to the junction of the tibia and fibula. Due to slipping during testing, three samples were discarded. Therefore, 17 samples were taken into account for calculating the mean, standard deviation, and coefficient of variation (standard deviation/mean) of the measurements. The average experimentally-measured fracture force was 48.01 $\pm$ 3.57 N, and the average FE-based von Mises stress was 43.64 $\pm$ 3.24 MPa. The coefficients of variation of the failure force and the von Mises stress values were both calculated to be 7.43%. The results of these tests suggest that the precision of our mechanical testing method and FE analysis technique will be sufficient for measuring changes in tibial strength and stress magnitudes that occur due to applied mechanical loading.

References: 1. De Souza RL et al., Bone, 2005. 37: 810-8. 2. Fritton JC, Bone, 2005. 36: 1030-8.

***Disclosures: Lillian Chatham**, None.*

MO0047

Exercise During Recovery Between Two Hindlimb Unloading Exposures Enhances Cancellous Bone Microarchitecture and Mechanical Properties. Yasaman Shirazi-Fard*[1], Andrea Kwaczala[2], Stefan Judex[2], Susan Bloomfield[1], Harry Hogan[1]. [1]Texas A&M University, USA, [2]Stony Brook University, USA

Bone response to repeated disuse exposures has been a concern for astronauts and clinical patients experiencing periods of non-weightbearing. The goal of the current experiment was to assess effects of resistance exercise during recovery between two bouts of disuse at the proximal tibia metaphysis (PTM) in the adult hindlimb unloaded rat model. We hypothesized that exercise would not only enhance recovery but would also mitigate impact of the 2nd disuse.

Adult male Sprague-Dawley rats (6 mo.) were assigned to age-matched control (AC) and hindlimb unloaded (HU) groups by body weight and total (integral) vBMD. HU animals were exposed to 4 wk of hindlimb unloading (HU), followed by 8 wk of recovery (HU+R), and then a 2nd HU exposure (2HU). Subsets of HU animals performed progressive resistance exercise during recovery for 7 wk (3d/wk) (HU+EX), and were exposed to a second HU exposure (2HU+EX). Bones were analyzed by in vivo pQCT at baseline and every 4 wk. Animals (n=15/group) were euthanized at baseline, after initial HU, after recovery/exercise, and after 2nd HU. Changes in bone mechanical properties were estimated through FEM on ex vivo μCT scans and measured by mechanical testing of cancellous bone.With exercise added following the 1st HU, both Total BMC and vBMD increased significantly (17% & 11.6%, resp.) and even exceeded AC levels, but losses for the 2nd HU were not significant pre-to-post whether exercise was included or not. After the 1st HU exposure, BV/TV and Tb.Th were significantly lower (-31% and -13%, resp.) than AC, but they recovered to AC after 4 wk of reloading without exercise. Exercise had no additional effect on BV/TV, but it was strongly anabolic for Tb.Th, which was significantly higher (25%) than AC and non-exercise levels at the end of recovery and after 2nd HU. Unloading had no effect on Tb.N, but HU+EX and 2HU+EX were significantly lower (-23%) than HU+R and 2HU. With exercise added, PTM cancellous bone ultimate stress and elastic modulus for HU+EX increased significantly (74% & 127%, resp.) but HU+R were not different from post-HU values. When loaded to 1N in a constrained compression test in axial direction using FEM, metaphyseal bone failure load for HU+EX was significantly higher (9%) than HU+R.In summary, exercise benefits were more potent in the cancellous bone of the PTM (compared to integral cortico-cancellous) and were most prominent in mechanical properties and Tb.Th despite no appreciable effect on BV/TV.

***Disclosures: Yasaman Shirazi-Fard**, None.*

MO0048

Human Ossicles Adapt their Tissular Bone Quality to their Biomechanical Function. François Duboeuf*[1], Brigitte Burt-Pichat[1], Delphine Farlay[1], Paul Suy[2], Eric Truy[3], Georges Boivin[1]. [1]INSERM UMR 1033; Université de Lyon, France, [2]Hôpital Edouard Herriot, Département d'ORL, Lyon, France, [3]Hôpital Edouard Herriot, Département d'ORL, Université de Lyon, France

Bone quality of the middle ear bones was never studied. These tiny bones are subjected to vibrations transmitted from the tympanic membrane through the cavity of the middle ear up to the oval window of the internal ear. We have characterized bone quality and mechanical properties of ossicles (malleus and incus) using a pluri-methodological approach. Ten malleus and 9 incus were obtained from 11 patients [9 cholesteatoma (54$\pm$20 yrs), 1 chronic otitis (30 yrs), 1 external ear cancer (66 yrs)]. Two malleus and 2 incus from a control (80 yrs) were taken at necropsy. Results were also compared to human cortical bone from 1 femoral and 9 iliac samples. Ossicles were analyzed by μCT then embedded in methyl methacrylate for histological study. Microhardness Vickers (Newton/mm^2) was calculated on blocks (10 indentations in lamellar tissue and 10 in woven tissue)[1]. FTIRM was done in 4 pathological ossicles of various ages and in control ossicles to assess mineral maturity, index of crystallinity and mineralization, carbonation and collagen maturity[2-3]. μCT showed that half of the ossicles were morphologically degraded. Mean density of pathological and control ossicles was higher than in human cortical bone. Significant correlation was found between incus density and age (p=0.001,r=0.82). The mean porosity of pathological ossicles was higher than in both control ossicles and human cortical bone. Histology showed a vascularized compact bone, well calcified with mainly a lamellar texture; area of woven tissue persisted. Osteoclasts and osteoblasts were not observable; some areas were rich in periosteocytic lacuna sometimes empty. The calcified tissue was lined with a thick fibrous organic tissue, rarely with a true osteoid tissue. Microhardness of all ossicles was higher than in human cortical bones, and identical in both woven and lamellar tissues. In ossicles compared to human cortical bone, index of mineralization was higher, mineral maturity was lower, and crystallinity,

carbonation and maturity of the collagen were similar. Finally, pathological ossicles showed important bone destruction compared to the control ossicles. Density, microhardness, and index of mineralization were higher than in human cortical bones. These variables reflect a bone quality well adapted to the specific function of the ossicles, i.e., transmission of vibrations.[1]*Boivin et al. 2008, Bone, 43:532 ;* [2]*Farlay et al. 2011, PLoS ONE 6(12):e287;* [3]*Farlay et al. 2010, J Bone Miner Metab 28:433*

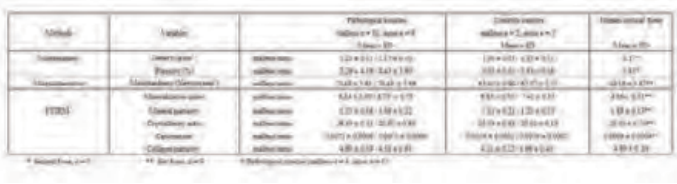

Table. Variables assessed in Human ossicles

***Disclosures: François Duboeuf**, None.*

MO0049

Intensive Treadmill Running Induces Microstructural Deterioration in Mouse Femoral Trabecular Bone. Allison Altman*[1], Klyde Breitton[1], Guangyi Zhao[2], Beom Kang Huh[1], Wei-Ju Tseng[1], James H-C Wang[2], Xiaowei Liu[1]. [1]University of Pennsylvania, USA, [2]University of Pittsburgh, USA

Weight-bearing exercise has been shown to strengthen bone in both clinical and experimental settings in human and rodent models. However, intensive endurance running is associated with a reduced bone mineral density (BMD) and a high risk of stress fractures. We hypothesized that in addition to stimulating bone formation, intensive exercise may induce excessive resorption beyond the stimulated formation in mouse femoral bone resulting in a net bone loss.

Twenty-eight 3-month old female C57BL/6 mice were divided into three groups: control (CTL, n=9), moderate treadmill running (MTR, n=9), or intensive treadmill running ITR: n=10). Both MTR and ITR groups ran on the treadmill 5 days/week for 3 weeks at a speed of 13 m/min, after one week of acclimatization to treadmill running. The MTR group ran 50 min/day for 3 weeks and the ITR group ran 3 hr/day, 4 hr/day and 5 hr/day on the 1st, 2nd, and 3rd weeks respectively. Following treadmill running the femurs were scanned at 6 μm using a Scanco MicroCT 35. A 1.2 mm section from the distal femur and a 0.6 mm section from the femur midshaft were analyzed using standard microstructural analysis. Kruskall-Wallis non-parametric ANOVA were performed on all variables of interest.

As shown in Table 1 there were no differences in trabecular bone volume fraction (BV/TV), trabecular number (Tb.N*), trabecular spacing (Tb.Sp*) or polar moment of inertia (pMOI) of the cortex. Structural measures indicated a 21% reduction ($p = 0.02$) in connectivity density (Conn.D) and a 12% increase ($p = 0.07$) in structure model-index (SMI) in the ITR group when compared to the MTR group. There was a 6% increase ($p = 0.04$) in trabecular thickness (Tb.Th*) in the ITR group compared to the MTR group, and a trend towards reduced cortical thickness (Ct.Th) by 4% ($p = 0.09$) in the MTR group compared to the CTL group.

These results demonstrate that intensive treadmill running exercise results in a less connected trabecular network and more rod-like trabecular structure in mouse femoral trabecular bone. The increased Tb.Th* in the ITR group indicates elevated bone formation on the bone surface; however, intensive running may also stimulate resorption, which may have exceed the new formation, leading to lost trabecular structural integrity. This may ultimately lead to injury or reduced BMD with longer training periods. Therefore, we conclude that intensive treadmill running induces microstructural deterioration in mouse femoral bone.

Table 1. Variables of interest shown as mean *(SEM)*. $ indicates significantly different from the MTR group ($p<0.05$), and * indicates statistical trend with respect to MTR group ($p<0.1$).

	CTL (n = 9)	MTR (n = 9)	ITR (n = 10)
BV/TV (%)	10.9 *(0.3)*	11.0 *(0.5)*	10.1 *(0.6)*
Tb.N*	4.07 *(0.05)*	4.10 *(0.07)*	3.90 *(0.08)*
Tb.Sp* (μm)	240 *(2.9)*	238 *(4.4)*	252 *(5.0)*
pMOI (mm^4)	0.33 *(0.01)*	0.32 *(0.01)*	0.32 *(0.01)*
Conn.D ($1/mm^3$)	211 *(9)*	203 *(12)*	160 *(12)*$
SMI	5.04 *(0.03)*	4.99 *(0.09)*	5.22 *(0.07)*$*
Tb.Th* (μm)	43.1 *(0.7)*	41.7 *(0.4)*	44.2 *(0.8)*$
Ct.Th (μm)	165 *(2.4)**	156 *(3.2)*	160 *(2.0)*

Table 1

***Disclosures: Allison Altman**, None.*

MO0050

Modeling Reference Point Indention in Equine Cortical Bone with Finite Elements and Mechanical Testing Data. Kevin Hoffseth*, Connor Randall, Paul Hansma, Henry Yang. University of California, Santa Barbara, USA

This study is aimed at investigating cortical bone mechanical properties through minimally invasive in-vivo measurement, which is of value to the community concerned with skeletal health, ranging from the elderly concerned with bone quality degradation, to the equine field concerned with training and diet, to name just two examples. For this purpose, equine cortical bone properties are examined by a recently developed Reference Point Indentation technique (Bridges et al, Rev Sci Instrum 2012), finite element simulation, and mechanical testing data. A broad attempt is made to connect the reference point indentation depth measurement to the cortical bone mechanical properties using the same donor material, with focus on yield strength and inelastic deformation.

Cortical bone tissue from the third metacarpal bone of an equine donor was prepared for testing, and depth was measured by Reference Point Indentation using two different geometry tips. The tips consisted of a sharp 90˚ cone with tip radius less than 15 μm, and a blunt 90˚ cone with tip radius of approximately 35 μm. Material from the same bone was also tested in both axial compression (4 samples) and four-point bending (8 samples) to obtain mechanical property data. Finite element simulations using a Drucker-Prager yield criterion were built to simulate indentation response using mechanical property data as input.

Reference Point Indentation measurement of indentation depth gave values of 159 ± 12 μm for sharp tip and 151 ± 8 μm for blunt tip. Critical mechanical property values from testing were Young's Modulus of 10 GPa, Average Compressive Yield Strength of 89 MPa, and Average Tensile Yield Strength of 48 MPa. Finite element simulations using the mechanical property data were able to replicate indentation depth readings to within 10% for both tip geometries in this study.

These results help show the direct connection in cortical bone between indentation depth, measured through Reference Point Indentation, and important mechanical properties. We also can conclude that, up to a respectable degree, using a Drucker-Prager yield criterion is a reasonably accurate model to study the deformation in cortical bone, acknowledging the certain cracking and microfracture taking place and viewing them as a form of pseudo plasticity.

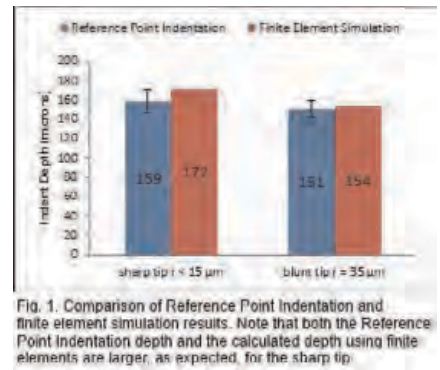

Fig. 1. Comparison of Reference Point Indentation and finite element simulation results. Note that both the Reference Point Indentation depth and the calculated depth using finite elements are larger, as expected, for the sharp tip

Fig. 1

***Disclosures: Kevin Hoffseth**, None.*

MO0051

Mouse Femoral Neck Architecture Determined by MicroCT Reflects Skeletal Architecture Observed at Other Bone Sites. Robert Brommage*, Sabrina Jeter-Jones, Wendy Xiong, Rose Champ, Jeff Liu. Lexicon Pharmaceuticals, USA

Mouse femoral neck architecture is seldom examined in genetic, physiology and pharmacology studies. Using a Scanco μCT40, we developed a microCT scanning protocol providing reproducible values for total area (diameter), bone area, BV/TV and BS/BV. Careful positioning of the bones in the sample holder to obtain vertical orientation of the neck is critical. The entire neck (~150 slices) is scanned using 6 micrometer voxel dimensions, an X-ray tube voltage of 55 keV, a current of 145 microamperes, an integration time of 200 milliseconds and an analysis threshold of 240. From standard 2-D analysis, the slice having the lowest total area is identified. A 3-D analysis is performed using a total of 20 consecutive slices with the middle slice having the lowest total area in the 2-D analysis. To avoid subjective bias, no attempt is made to distinguish trabecular from cortical bone. Femoral neck architecture consistently reflects results from microCT analyses of LV5 vertebral body trabecular bone and midshaft femur cortical bone. Consistent with findings in femur shaft, femoral neck diameter is higher in male than female C57BL/6J mice and higher in C57BL/6J mice compared to 129SvEv and BALB/c mice. BV/TV declines as mice reach 2 years of age. Femoral neck diameter is elevated in Sost and Sfrp4 knockout (KO) mice but reduced in Lrp5 KO mice. BV/TV is increased, unaffected and reduced with KO of Sost, Lrp5 and Sfrp4, respectively. Reflecting increased trabecular but reduced cortical bone at other sites, femoral necks from Sfrp4 KOs show increased trabecularization, as indicated by a high BS/BV ratio. Bone loss with aging is greater in Sfrp4 KOs. Femoral neck BV/TV is reduced following ovariectomy but increased

with teriparatide treatment. Bones from mice undergoing spontaneous wheel running have increased BV/TV and diameter. Loss of BV/TV occurs during lactation and this loss is greatly increased when lactating rats are fed a low (0.1%) Ca diet. Dramatic gains in bone mass occur during the first 6 weeks post-lactation. These results demonstrate the feasibility of measuring bone mass and architecture in the mouse femoral neck. Several groups successfully determine mouse femoral neck breaking strength. Since this site is particularly important in human osteoporosis, the ability to assess femoral neck architecture in mice may provide insights on the efficacy of potential treatments.

***Disclosures: Robert Brommage**, Lexicon Pharmaceuticals, 3*
This study received funding from: Lexicon Pharmaceuticals

MO0052

Notch1 and Notch2 receptors show opposite patterns of expression and differing effects on osteoblastogenesis in murine and human mesenchymal stem cells. Fengchang Zhu*, Kurt Hankenson, Michael Dishowitz, dereck dopkin, Patricia Mutyaba. University of Pennsylvania, USA

Our previous work has demonstrated that canonical Notch signaling, activated by the Jagged1 ligand, is potently induce osteogenic differentiation in human mesenchymal stem cells (hMSC). However, in stark contrast, canonical Notch signaling in murine MSC (mMSC) inhibits terminal osteoblast differentiation (F Zhu *et al*, *Stem Cells*, 2013 Feb). We hypothesized that this pronounced difference in osteoblastogenic response to canonical signaling could be associated with differing Notch receptor utilization in hMSC compared to mMSC.

We first investigated the expression of Notch1 and Notch 2 in multiple donor-lines of primary hMSC and mMSC using quantitative PCR. The results show that Notch2 expression level is 40-fold greater than Notch1 in undifferentiated hMSC, while in mMSC the expression level of Notch2 is much lower than that of Notch1 (0.15-fold decrease). This elevated Notch1 relative to Notch2 is similar in mouse cortical bone (0.2-fold Notch2 relative to Notch1); however, when bone is injured, during the course of healing, the levels of Notch2 increase relative to Notch1 temporally. Thus, the NICD2/NICD1 ratio is increased to 0.4 at day 5 post-fracture, 2.0 at day 10 post-fracture, and 4.0 at day 20 post-fracture.

Next we evaluated the impact of overexpressing the active intracellular domains of Notch1 (NICD1) and Notch2 (NICD2) in both primary mMSC and hMSC using retrovirus. NICD1 and NICD2 overexpression in either mMSC or hMSC significantly upregulated the canonical Notch target gene Hey1. Both NICD1 and NICD2 are sufficient to induce osteoblast gene expression and mineralization in hMSC. In contrast, overexpression of NICD1 inhibits osteoblast gene expression and mineralization in mMSC, while NICD2 overexpression in mMSC shows no negative effects on osteoblastogenesis.

Collectively, our study shows that Notch1 and Notch2 show opposite patterns of expression in primary mouse and human MSC. Particularly, Notch1 is dominant in mMSC while Notch2 is dominant in hMSC. During fracture healing in mice, Notch1 and Notch2 expression shift during the osteogenic phase of bone regeneration. Intriguingly, when NICD1 is overexpressed in mMSC, it has the same deleterious effect on osteoblastogenesis as we previously observed when mMSC were plated on Jagged1. This suggests that the Notch1 expression dominance in mMSC may limit osteoblastogenesis when cells are exposed to Jagged1.

***Disclosures: Fengchang Zhu**, None.*

MO0053

The Effect of Bone Tissue Ductility on Vertebral and Femoral Strength. Shashank Nawathe*[1], Haisheng Yang[1], Aaron Fields[2], Mary Bouxsein[3], Tony Keaveny[1]. [1]University Of California at Berkeley, USA, [2]University of California at San Fracisco, USA, [3]Beth Israel Deaconess Medical Center, USA

While the ability of bone tissue to deform in a ductile manner can decrease with aging and disease, the influence of tissue-level ductility on whole-bone strength, either at the hip or spine, remains poorly understood. Addressing this issue, we performed biomechanical testing and high-resolution micro-CT-based finite element analysis on 12 human thoracic (T9) vertebrae (mean ± SD, age 77 ± 11 years) and 14 human proximal femora (age 76 ± 10 years). The simulations enabled us to directly compare whole-bone strength for two hypothetical situations: fully ductile tissue behavior, in which the trabecular and cortical bone tissue can fail but never fracture (plastic-like behavior); and fully brittle behavior, in which the tissue fractures as soon as it begins to fail (glass-like behavior). Bones were first imaged at ~ 60 micron resolution and then mechanically tested to measure whole-bone strength (compression for the spine; fall loading for the hip). Using massively parallel, non-linear finite element analysis (~ 60 micron element size), we computed the whole-bone strength for compression loading for the spine, and both fall and stance loading for the hip. All analyses were done for two distinct cases of tissue-level post-yield failure behaviors: fully ductile vs. fully brittle. We found that when the assumed tissue-level failure behavior was changed from fully ductile to fully brittle, the whole-bone strength decreased by 40–60% (Figure). This negative effect on strength was relatively uniform across all specimens but at the hip was larger for fall than stance loading. Further, measures of whole-bone strength correlated well between experiment and model — both for the ductile and brittle simulations — despite for each simulation using the same tissue-level ductile or brittle material properties in all specimens (hip: ductile $R^2 = 0.90$, brittle $R^2 = 0.86$; spine: ductile $R^2 = 0.85$, brittle $R^2 = 0.87$). These results suggest that the general ability of bone tissue to deform in a fully ductile manner can substantially influence whole-bone strength. However, the strong correlation between experiment vs. model (brittle or ductile) suggests that typical between-person variations in tissue-level ductility may not be sufficiently large to appreciably alter whole-bone strength. This study therefore highlights the need to better characterize real population variations in tissue-level ductility and to determine the extent to which such variations affect overall strength.

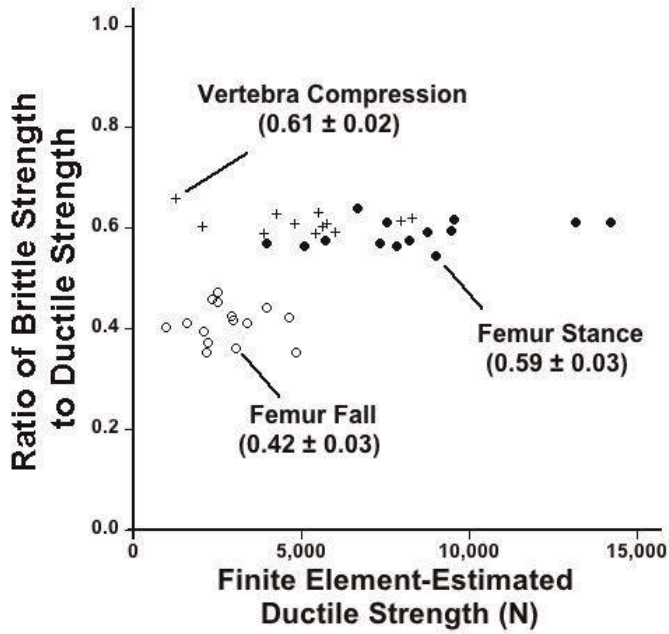

Figure

***Disclosures: Shashank Nawathe**, None.*
This study received funding from: The study was supported in part by a research grant from Merck.

MO0054

The Optimization and Effect of a Platinum Catalyst on the Mechanical and Handling Properties of Novel Silorane Bone Cements while maintaining Osteogenic Capacity. Kathleen Kilway*[1], Rachel Weiler[1], Lianxiang Bi[1], J. David Eick[1], Bradley Miller[1], Thomas Schuman[2], Lynda Bonewald[1]. [1]University of Missouri – Kansas City, USA, [2]Missouri University of Science & Technology, USA

Commercially available bone cements, however widely used, still have issues, which include toxicity, high polymerization temperatures and shrinkage, all of which can be attributed to polymethylmethacrylate and its polymerization, a major component of bone cements. Our group has developed a novel biomaterial based on a silorane resin filled with modified glasses in order to address the negative attributes of commercialized bone cements previously listed. Our biomaterial also includes a four-component dual initiation system that contains Lamoreaux's catalyst (LMC) and does not require irradiation. We were able to improve the biomechanical properties by optimizing the amount of catalyst needed in the dual initiation system. We hypothesized that the more LMC used for the dual initiation system would result in very fast polymerization leading to a brittle material. On the other hand, a lower amount of LMC would result in a material that polymerized too slowly, if at all, resulting in a low strength material. We used two methods to test the mechanical properties of our material in a dry environment: the 4-pt bend test and a mimic of the traditional pull-out test. We also tested the biocompatibility using the Trypan Blue Assay.

The 4-pt bend was used to test the effect of amount of catalyst (0.46 vs. 0.60 wt%) on flexural strength and modulus on the resulting material. We found that the higher amount of catalyst affected the flexural strength (MPa) (M12-ECHE (0.46% LMC), 19.20±5.86; M12-ECHE (0.60% LMC), 23.27±12.03) but not the modulus (GPa) (M12-ECHE (0.46% LMC), 2.52±0.36; M12-ECHE (0.60% LMC), 2.61±0.54). Using a pull-out mimic test, we measured the strength (MPa) using a LMC range from 0.16 to 0.80 wt% (M12-ECHE (0.16% LMC), 5.71±0.42; M12-ECHE (0.32% LMC), 5.14±0.06; DY5-1TOSU (0.32% LMC), 3.77±0.18; DY5-1TOSU (0.56% LMC), 4.06±0.28; DY5-1TOSU (0.80% LMC), 0.79±0.07). It was found that pull-out strength was not only dependent on the amount of catalyst but also on the type of filler and its modification. These tests revealed that there is an optimal amount of catalyst needed to provide good biomechanical strength, 0.32 wt% of LMC, for the average formulation, independent of filler or filler modification.

The amount of LMC used did not significantly affect the biocompatibility (% dead cells) of our material (DY5-1TOSU (0.46% LMC), 2.9±0.8; DY5-1TOSU (0.80% LMC), 3.2±0.3) thereby maintaining bone cell function while improving mechanical strength.

***Disclosures: Kathleen Kilway**, None.*

MO0055

Thoracic vertebral fracture is associated with a localized increase in spine curvature at the fracture site that exceeds the observed increases in global thoracic kyphosis. Alexander Bruno*[1], Dennis Anderson[2], Brett Allaire[2], M. Clara De Paolis Kaluza[2], Douglas Kiel[3], Elizabeth Samelson[4], Mary Bouxsein[2]. [1]Harvard-MIT, USA, [2]Beth Israel Deaconess Medical Center, USA, [3]Hebrew SeniorLife, USA, [4]Hebrew SeniorLife, Harvard Medical School, USA

Prior studies have found an association between vertebral fracture (VF) and increased thoracic kyphosis (T4-T12 Cobb angle (CA)). However, the extent to which the presence of a VF directly increases curvature is unclear, given that hyperkyphosis in the absence of VF is common and likely caused by non-skeletal degeneration. In this study, we sought to determine: i) if the presence of a thoracic VF is associated with a *local* increase in curvature at the fracture site, and ii) whether this *local* increase in curvature accounts for any *global* increase in curvature (T4-T12 CA). We hypothesized that subjects with a single VF in the mid-thoracic region (T6-T8), but not outside this region, would have greater local curvature (T6-T8 CA) as well as greater global thoracic curvature (T4-T12 CA) relative to subjects with no thoracic VF, but that the curvature of the thoracic spine outside the local region would not differ between cases and controls. Subjects were selected from the Framingham Heart Study CT cohort. Cases were 13 men and 19 women with a single VF at T6, T7, or T8 (all VF were grade SQ1), but no other VF between T4 and T12. Controls were 359 men and 397 women with no VF between T4 and T12. The T4-T12 CA and the T6-T8 CA were measured on lateral CT scout views using SpineAnalyzer software (Optasia Medical), and the curvature outside the local VF region was calculated by subtracting the T6-T8 CA from the T4-T12 CA. Multiple regression analysis was used to test for differences between cases and controls in the total sample, and in men and women separately, after adjusting for age, height, and weight. Relative to controls, cases had a significantly higher T4-T12 CA ($36.4^\circ \pm 8.8^\circ$ vs $30.6^\circ \pm 8.9^\circ$, $P<0.05$), and a higher T6-T8 CA ($21.0^\circ \pm 5.0^\circ$ vs $13.7^\circ \pm 4.8^\circ$, $P<0.05$), but similar curvature outside the local region ($15.4^\circ \pm 7.3^\circ$ vs $16.9^\circ \pm 6.8^\circ$, $P=0.15$) (Table 1). The difference in local curvature between cases and controls was numerically greater than the difference in global curvature, indicating that the presence of a VF fully accounts for the greater T4-T12 CA in subjects with VF, and that the increased curvature is localized to the VF site. A trend toward lower curvature outside the local region in cases could indicate compensation for increased local curvature by straightening the remainder of the thoracic spine. In this case, the T4-T12 CA may underestimate the local effects of VF on curvature and mechanical loading of the spine.

Table 1: Cobb angles (mean ± SD) in degrees for cases and controls.

	All Subjects		
	Control, N=756	Case, N=32	Diff
T4 to T12 (Deg)	30.6±8.9	36.4±8.8*	5.8
T6 to T8 (Deg)	13.7±4.8	21.0±5.0*	7.3
T4 to T12 - T6 to T8 (Deg)	16.9±6.8	15.4±7.3	-1.5
	Men		
	Control, N=359	Case, N=13	Diff
T4 to T12 (Deg)	28.8±8.0	36.2±12.1*	7.4
T6 to T8 (Deg)	13.0±4.6	22.1±5.9*	9.2
T4 to T12 - T6 to T8 (Deg)	15.8±6.4	14.1±9.0	-1.7
	Women		
	Control, N=397	Case, N=19	Diff
T4 to T12 (Deg)	32.2±9.4	36.5±6.1	4.4
T6 to T8 (Deg)	14.3±5.0	20.2±4.2*	5.9
T4 to T12 - T6 to T8 (Deg)	17.8±7.0	16.3±5.9	-1.5

* p<0.05 VF cases vs. controls

Table 1

***Disclosures: Alexander Bruno**, None.*

MO0056

Trabecular Plates Have Different Elastic Modulus and Tissue Mineral Density (TMD) from Trabecular Rods in Human Trabecular Bone. Eric Yu*[1], Ji Wang[1], Bin Zhou[1], Zhang Zhendong[2], X Guo[1]. [1]Columbia University, USA, [2]Department of Orthopedic Surgery, First Affiliated Hospital of the Medical College, China

Our previous studies have demonstrated that trabecular (Tb) plates play dominant roles in determining mechanical properties of Tb bone and osteoporosis is hallmarked by a remarkable conversion from Tb plates to rods. We have also observed that Tb plates have significantly higher TMD than Tb rods. However, mechanical properties of individual Tb plates and rods have not yet been measured and co-localized with TMD measurements. In this study, we hypothesized that Tb plates have different tissue elastic modulus than Tb rods and these microscopically determined tissue elastic moduli correlate with co-localized TMD.

Nine cylindrical human Tb bone samples from proximal femurs were imaged with five hydroxyapatite calibration phantoms at 25 μm using μCT (Scanco VivaCT40). Individual Tb plates and rods were segmented using individual trabecula segmentation (ITS) technique (Fig1.A). Samples were embedded and polished for micro-indentations. Microscopic images of the indentation surface were registered with 3D μCT image such that 12 indentation locations were selected for longitudinal plate (LP), transverse plate (TP), longitudinal rod (LR), and transverse rod (TR), respectively (Fig1.C). Microindentations were performed to determine tissue elastic modulus under wet condition. The point-by-point co-localized grayscale values of the μCT image at the indentation site were measured and converted to calculate TMD using calibration phantom (Fig1.D).

The Tb plate tissue modulus was significantly higher than that of Tb rods, which corresponded well with the significantly higher TMD in Tb plates ($p<0.001$, Fig. 2A). No significant differences in either the tissue modulus or TMD were detected between LP and TP. In contrast, modulus and TMD in TR were 28.7% and 19.4% lower than those in LR (*$p<0.001$, Fig.2B*). In addition, both tissue modulus and TMD in TP were significantly higher than those in TR (*$p<0.05$*). Furthermore, Tb tissue moduli determined by microindentation were strongly correlated with μCT measured TMD (*$R^2=0.58$*).

The study reported novel findings in mechanical properties of individual Tb plates and rods. The results suggest that Tb plates are not only distinctly different morphological elements in human Tb, but also have significantly different microscopic mechanical properties. Since Tb plates are the major biomechanical components in human Tb bone, these findings may have significant implications in osteoporosis and its related bone fragility.

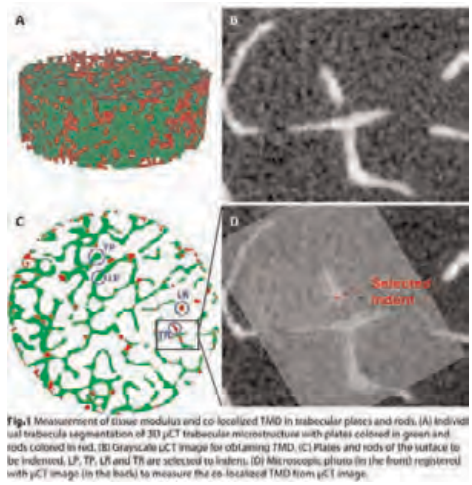

Fig.1 Measurement of tissue modulus and co-localized TMD in trabecular plates and rods. (A) Individual trabecula segmentation of 3D μCT trabecular microstructure with plates colored in green and rods colored in red. (B) Grayscale μCT image for obtaining TMD. (C) Plates and rods of the surface to be indented. LP, TP, LR and TR are selected to indents. (D) Microscopic photo (in the front) registered with μCT image (in the back) to measure the co-localized TMD from μCT image.

Fig1. Measurement of tissue modulus and co-localized TMD in Tb plates and rods

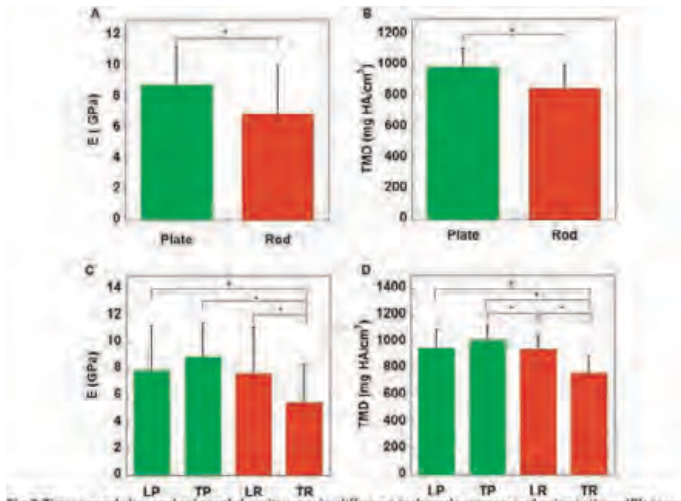

Fig.2 Tissue modulus and mineral density vary in different trabecular types and orientations (Plates: n=54; Rods:n=54; LP:n=27; TP:n=27; LR:n=27; TR:n=27, n is the number of indentation points). (A) Plates have higher tissue modulus than rods. *p<0.001. (B) Plates have higher TMD than rods. *p<0.001. (C) TR has lower tissue modulus than LP, TP and LR. *p<0.001. (D) TR has lower TMD than LP, TP and LR. *p<0.001

Tissue modulus and TMD vary with Tb type and orientation

***Disclosures: Eric Yu**, None.*

MO0057

Transitional Zones Displacement at the Subchondral Bone Layers in an Experimental Model of Osteoporosis and Osteoarthritis. Santos Castañeda*[1], David Guede[2], Jose R Caeiro[3], Jorge A Roman-Blas[4], Raquel Largo[5], Gabriel Herrero-Beaumont[5]. [1]Rheumatology Department, Hospital de la Princesa, IIS-Princesa, Spain, [2]Coordinator I+D+ i. Trabeculae, Empresa de Base Tecnológica, S.L., Spain, [3]Orthopaedic Surgery Department, Spain, [4]Bone & Joint Research Laboratory, IIS-FJD, Fundación Jiménez Díaz, Spain, [5]Bone & Joint Research Laboratory, IIS-FJD, Spain

INTRODUCTION: Subchondral bone (SB) plays a crucial role in osteoarthritis (OA) pathogenesis. In previous animal experiments, we have confirmed that increased SB remodeling may account for the aggravation of cartilage damage in OA rabbits with previous osteoporosis (OP).

OBJECTIVE: To analyze the microstructural characteristics of the different SB layers and transitional zones (TZ) at the SB in our OP-OA model in the rabbit.

METHODS: Experimental OA was induced in 12 female NZ white rabbits (8 months old; weight 3.5-5 kg) by anterior cruciate ligament transection and partial medial meniscectomy (OA knees) in the left knees. In 6 of them, OP was previously induced by bilateral oophorectomy and subsequent prednisolone administration 1 mg sc/kg/d for 5 wks (OPOA knees). Right knees of OPOA were used as OP knees, while right knees of OA group were used as healthy knees. After sacrifice, cylindrical samples of SB (4 mm in diameter by 9 mm in length) were extracted from femoral condyles. The microarchitectural characteristics of the samples were studied using micro-CT with a SkyScan 1172 (Bruker micro-CT NV). Statistical analysis was performed using the Kruskal-Wallis H test and post-hoc analysis by Dunn's test.

RESULTS: According to the bone area fraction (B.Ar/T.Ar) profile, 3 SB layers were characterized: the SB plate, a dense trabecular bone of mixed characteristics (trabecular SB) and the subarticular trabecular bone. Furthermore, 2 different TZ between these 3 layers could be distinguished. Decreased thickness of SB plate was seen in both OP and OA knees with respect to healthy knees ($p<0.05$ in both cases). OPOA group revealed a deeper reduction of SB plate thickness vs. other groups ($p<0.05$). Other variables analyzed, such as Tb.Th, Tb.Sp, Tb.N, polar moment of inertia and Tb.Pf showed the same behavior. The dispersion curves of these parameters showed a consistent displacement of the TZ toward the joint surface in all experimental groups.

CONCLUSIONS: These data confirm the existence of at least 3 different microstructural layers at SB and 2 different TZ between them. Furthermore, there was a concordant TZ displacement toward more superficial areas, transforming the biomechanic properties of SB, that might partially explain the OA aggravation in rabbits with previous OP. These findings could be of great interest for future therapeutic approach of patients with OA and associated OP.

***Disclosures: Santos Castañeda**, None.*
This study received funding from: Fondo de Investigacion Sanitaria (FIS); The Spanish Ministry of Science and Innovation

MO0058

Effects of Spaceflight and Sclerostin Antibody on Femoral Neck Strength in Estimated by Finite Element Analysis in Mice flown on Space Shuttle Flight STS-135. Lindsay Sullivan*[1], Alicia Ortega[2], Ted Bateman[3], Andrea Hanson[4], Eric Livingston[1], Travis Pruitt[5], Colin Smith[6], Angelica de Rosa[1], Eric Lai[1], Louis Stodieck[7], Laura Bowman[8], Rachel Ellman[9], Jordan Spatz[10], Kelly Warmington[11], HL Tan[11], Dave Hill[11], Rachel Paietta[2], Andrew Cureton[2], Chris Paszty[11], Mary Bouxsein[9], Virginia Ferguson[7], Anthony Lau[8]. [1]University of North Carolina-Chapel Hill-Biomedical Engineering, USA, [2]University of Colorado-Boulder-BioServe/ Department of Mechanical Engineering, USA, [3]Univesity of North Carolina, USA, [4]Wyle Science, Technology & Engineering Group, USA, [5]Clemson Universeity, USA, [6]North Carolina State University-Department of Mechanical & Aerospace Engineering, USA, [7]University of Colorado, USA, [8]University of North Carolina at Chapel Hill, USA, [9]Beth Israel Deaconess Medical Center, USA, [10]Harvard-MIT Division of Health Sciences & Technology (HST), USA, [11]Amgen Inc, USA

Skeletal unloading during spaceflight reduces bone volume and bone mineral density; however, how this loss translates to functional changes in strength and stiffness in the proximal femur is not well understood. This study uses finite element modeling (FEM) that replicates mechanical testing of the femoral neck in mice flown on STS-135 to assess changes in bone stiffness from spaceflight and sclerostin antibody (Scl-Ab).

Thirty mice were flown on Space Shuttle Flight STS-135 for 13-days (FL). Half the mice were treated with vehicle (n=15) and half were treated with a Scl-Ab (n=15). Corresponding ground control (GC) groups were similarly treated. In this study, subject specific FE models were meshed from microCT images from the same mice (down sampled from 10 to 20μm resolution) for a 3.25mm segment of the proximal femur, which was taken from the top of the femoral head. Bone was segmented using the identical threshold previously used in the microCT analysis of the STS-135 femurs. All bone elements were modeled as linear elastic (E=10GPa, ν=0.3). A downward displacement of 50μm was applied to the entire femoral head (Figure) and the femoral neck bending stiffness was calculated from the measured load at 50μm.

FEM of the proximal femur found a 10% decrease in stiffness in the FL mice compared to the GC mice. Scl-Ab treatment resulted in an increased stiffness by 20% in the FL and 23% in the GC. Linear regression found significant correlations ($P<0.01$) between the FEM stiffness and the femoral neck stiffness, fracture load, and force at max load found from mechanical testing. While the FEM correlated well with the mechanical testing, the absolute stiffness values from FEM were greater than those obtained with mechanical testing. These results are expected because the mechanical testing configuration causes large deformations of the femoral head, including a 2 mm tall region directly underlying the greater trochanter, when it loads the femoral neck. This deformation did not occur in the FEM because of the boundary conditions used (Figure).

Conclusion: The unloading environment of microgravity caused a significant loss of femoral neck stiffness in the proximal femur. Scl-Ab prevented the loss of bone strength, and increased femoral neck stiffness in both FL and GC mice. FEM had significant correlation to the previously performed mechanical testing, which makes it a viable alternative to mechanical testing, especially with complex boundary conditions.

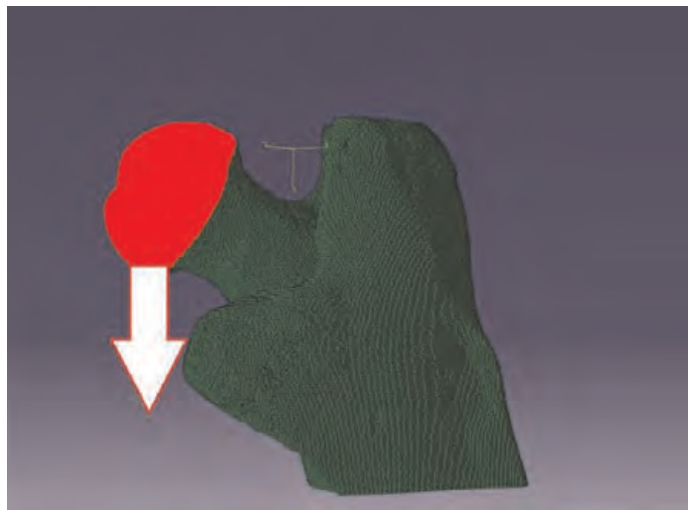

FEM of Proximal femur. Boundary condition (red) applied isolates load/deformation to femoral neck

***Disclosures: Lindsay Sullivan**, None.*
This study received funding from: Amgen Inc

MO0059

Finite Element Analysis of the Dynamically Loaded Mouse Forearm. Ganesh Thiagarajan*[1], Yunkai Lu[1], Mark Dallas[1], Mark Johnson[2]. [1]University of Missouri - Kansas City, USA, [2]University of Missouri, Kansas City Dental School, USA

The mouse forearm compression loading model is widely used to study bone formation in response to mechanical loading. Using standard finite element analysis (FEA) models with uniform strain field distributions, no correlation in magnitude or type of strain and β-catenin signaling in a subpopulation of osteocytes within 1 hour of loading. Therefore, we built models incorporating osteocyte lacuni into the matrix of the ulna and radius and performed simultaneous strain gaging of both the ulna and radius. In addition we have included loading caps that are used in *in vivo* loading for the numerical analysis, and simulated dynamic loading in our computer based numerical studies. Segmented images obtained from microCT of the mouse forearm were imported into GeoMagic Studio 9 and FEA meshes were created using automated tetrahedron mesh creation software (ABAQUS CAE). Mesh convergence was investigated using both 4- and 10-node tetrahedrons. Contact boundary conditions at the wrist and olecranon were included in the model with caps to simulate the experimental loading. Displacement and strain contours resulting from simulated loads of 2 N/3.5 N at 2 Hz/0.2 Hz were calculated using LS-DYNA and compared with experimental values. The maximal compressive strain on the ulna was found to occur at about 3.5 mm from the distal end and on the radius, about 2.5 mm from the proximal end. The magnitude of the maximal compressive strain under dynamic load of 2 N was around 5200 με for the ulna and 1750 με for the radius. These values were much higher than their counterparts (2000 με in the ulna and 1650 με in the radius under 2 N load) using static analysis in which static load with the same magnitude was applied. Under dynamic load of 3.5 N, the corresponding magnitudes increased to 9700 με for the ulna and 3700 με for the radius. In the dynamic models using 4-node tetrahedrons, 72% of the total applied load was sustained by the ulna while only 65% of the load was carried by the ulna in the corresponding static model. These data show that the dynamic ulna/radius FEA model is a superior approach to traditional static models. These models predict a very heterogeneous pattern of strain distributions and are being used to determine the biological strain thresholds required for β-catenin signaling in osteocytes in response to mechanical loading.

***Disclosures: Ganesh Thiagarajan**, None.*

MO0060

FSTL3 Mediates Exercise Driven Bone Formation. Sudha Agarwal[1], Derrick Knapik*[2], Alisa Blazek[2], Beth Lee[3], Lai-Chu Wu[2], JIn Nam[4]. [1]The Ohio State University, USA, [2]Wexner Medical center Ohio State University, USA, [3]Department of Physiology & Cell BiologyOhio State University, USA, [4]University of California at Riverside, USA

Introduction. Exercise promotes bone remodeling, a process involving bone resorption and bone deposition. How exercise drives mechanoresponsive bone remodeling is still elusive. Here, we provide evidence that Follistatin-like3 (*Fstl3*) could be a mechanosensitive protein that takes part in exercise-driven bone formation. Methods: Wild-type rats/mice and FSTL3-/- mice were exercised by treadmill walking (TW) and following 0, 2, 5 or 15 days of exercise, sacrificed and distal femurs analyzed by qrtPCR, Western blots, or immunohistochemistry. Bone mineral apposition rates (MAR) of mice were assessed using Calcein and Alizarin complexones injected on day 3 and 12, respectively. On day 15, femurs were excised, sectioned, and subjected to fluorescence microscopy to examine bone remodeling. Statistical analysis was performed by one-way ANOVA with Tukey's post hoc or T-test. Results: TW dramatically stimulated a ~6 fold increase in *Fstl3* mRNA expression in trabecular bone and bone marrow cells on day 2 and declining by day 5. A robust increase in *Fstl3* was observed in osteocalcin positive cells adjacent to trabecular bone and in osteocytes present in the trabecular bone. *Fstl3*+/+ or *Fstl3*-/- mice subjected to TW for 15 consecutive days and injected with Calcein and Alizarin, revealed significant increase in bone deposition on the endosteal surface of the femur and increase in the total MAR. However, bone deposition in both groups of non-exercised controls was limited. Similar treatment failed to induce exercise-induced bone formation and MAR increase in *Fstl3*-/- mice. *Fstl3*-/- mice also exhibited weaker and brittle femurs and tibias. FSTL3 treatment of osteoblasts induced a rapid and transient induction of BMP-7 and BMP-2 in WT but not in *Fstl3*-/- mice. Conclusions: Our data suggest that *Fstl3* is a novel molecule identified that might be critical for load driven bone formation and strengthening. This is evident by observations that genomic deletion of *Fstl3* abolishes load-dependent bone formation, weakening bones with failure to upregulate genes associated with bone deposition. The identification of *Fstl3* as a mechanoresponsive protein provides a new paradigm for investigating exercise-driven bone formation and to understand bone diseases.

***Disclosures: Derrick Knapik**, None.*

MO0061

Hedgehog pathway inhibitor GDC-0449 impairs the woven bone healing response to stress fractures in the rat ulna. Jennifer McKenzie*[1], Nikolas Kazmers[1], Fanxin Long[2], Matthew Silva[3]. [1]Washington University in St. Louis, USA, [2]Washington University School of Medicine, USA, [3]Washington University in St. Louis School of Medicine, USA

Hedgehog signaling (Hh) is critical in developmental osteogenesis, and more recent studies suggest it is also involved in regulating osteogenic gene expression in the post-natal setting. However, there is a void of studies directly assessing the effect of Hh inhibition on post-natal osteogenesis. In this study we utilized our previously-described, ulnar stress fracture model (WBF loading) to induce woven bone formation in adult rats. Our objectives were to characterize the temporal profile of Hh signaling after WBF loading and to determine whether Hh signaling contributes to osteogenesis during stress fracture healing. Following creation of a stress fracture by cyclic forelimb compression, rats (F344 males, 5 months age) were given GDC-0449 (Vismodegib, 50mg/kg orally twice daily), a small molecule compound that selectively inhibits the Hh pathway by binding to the smoothened receptor, or vehicle. Based on qPCR assessment of Gli1 and Ptch1 gene expression, upregulation of Hh signaling was noted in vehicle-treated ulnae 72h after WBF loading (Gli1 increased by 31%, Ptch1 increased by 41%), with respect to the contralateral non-loaded ulna. Treatment with Hh inhibitor GDC-0449 significantly decreased Hh signaling 72h after loading; Gli1 and Ptch1 expression decreased to 5.8% and 20.1%, respectively, of vehicle expression levels. Expression of Hh ligands Dhh, Ihh and Shh were unchanged in response to GDC-0449 at 24h, but Shh expression was decreased by 26.4% at 72h ($p<0.05$). Hh inhibition decreased the woven bone callus volume (4.21 vs 2.64 mm^3, $p<0.05$) and density (367 vs 314 mg HA/cm^3, $p<0.05$) as measured by microCT 7 days after WBF loading (Figure). Importantly, stress fracture crack length did not differ between the two groups, indicating equivalent levels of damage. Dynamic histomorphometry revealed that the day 7 callus was composed predominately of woven bone in both the vehicle and inhibition groups (Figure). Furthermore, lamellar bone formation was also inhibited by GDC-0449. Analysis of lamellar bone from the loaded limb (directly adjacent to the woven bone callus) revealed a significant decrease in mineral apposition rate (3.13 vs 2.60 micron/day, $p<0.05$). In the non-loaded limb there was a significant decrease in mineralizing surface (49 vs 37%, $p<0.05$), indicating Hh signaling was required for normal bone modeling. In conclusion, Hh signaling plays an important role in post-natal bone formation in the setting of stress fracture healing.

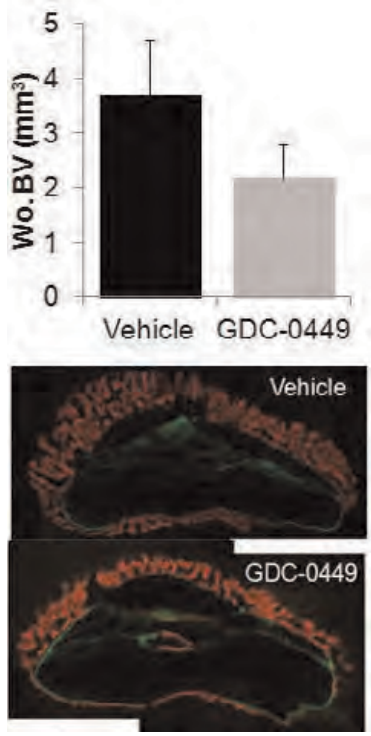

Hh inhibition with GDC-0449 treatment impairs stress fracture healing.

***Disclosures: Jennifer McKenzie**, None.*

MO0062

Response and Adaption of Bone Cells to Mechanical Stimulation. Airong Qian*, Hu Lifang, Wang Yang, Shang Peng. Northwestern Polytechnical University, China

Mechanical stimulation is necessary for bone growth and development. Bone loss is a negative balance course especially occurred after long-term space flight for astronauts under weightlessness [1]. Bone remodeling is a dynamic process that requires the coordinated interaction of osteocytes, osteoblasts, and osteoclasts, collaborating in basic multicellular units (BMUs)[2].

In this study, we investigated the effects of different mechanical stimulation, including diamagnetic levitation, random position machine (RPM) or different substrate stiffness on proliferation, morphology, mineralization, cytoskeleton architecture, cell cycle and apoptosis in bone cells (Osteocytes MLO-Y4 and osteoblasts MC3T3-E1) and its mechanism.

The results showed that diamagnetic levitation or RPM condition significantly affected osteoblast proliferation, morphology, mineralization, cytoskeleton and Ca2+/Calmodulin. 24 h treatment of simulated microgravity (SM) significantly inhibited the mineralized nodules formation compared with 1 g condition. In addition, the alkaline phosphatase (ALP) activity was significantly decreased and the expression of OC, Col Iα1 and DMP1 was all down-regulated by 24 h treatment of simulated microgravity. Diamagnetic levitation or RPM condition also influenced osteocyte morphology, cytoskeleton related proteins distribution and expression, and induced cytoskeleton reorganizing and apoptosis. Conditioned medium (CM) of osteocytes cultured in RPM for 48h stimulated proliferation of MC3T3-E1 cells. Cell spread area was inhibited in MC3T3-E1 cells cultured on soft substrate and soft substrate was not conducive to MC3T3-E1 cells proliferation and mineralization.

Our findings indicate that the morphology, cytoskeleton and functions of bone cells are changed under diamagnetic levitation, RPM or different substrate stiffness conditions. It suggests that bone cells are sensitive to alteration of mechanical environment.

ACKNOWLEDGMENTS

This work was supported by the National Basic Research Program of China (2011CB710903) and the National Natural Science Foundation of China (No.30970706).

REFERENCES

[1] Graebe A., Schuck E.L., Lensing P., Putcha L. and Derendorf H. (2004) J Clin Pharmacol 44, 837-853.

[2] Roberto C (2008). BBRC 473,188-192.

***Disclosures: Airong Qian**, None.*

MO0063

The Ability of Human Mesenchymal Stem Cells to Differentiate between Vertical and Horizontal Vibrations in Vitro Depends on the Intensity of the Signals. Suphannee Pongkitwitoon*, Stefan Judex. Stony Brook University, USA

Vibrations can serve as a growth factor to the skeleton but the underlying mechanisms have not been elucidated. In vitro studies have demonstrated that both vertical and horizontal vibrations can be sensed in 2D cell cultures but it is unknown whether cells are preferentially sensitive to one loading direction and whether interactions between the two loading directions may exist. Considering that the mechanical environment of cells in the culture dish is directly dependent on the direction of the applied vibration, data on loading direction sensitivity may provide important cues about a physical transduction mechanism. Here, we exposed human mesenchymal stem cells (hMSCs) to either horizontal, vertical, or a combination of horizontal and vertical vibrations and hypothesized that the efficacy of horizontal and vertical vibrations to enhance mineralization is similar. This hypothesis was tested with two different signal combinations; 30Hz at 1g and 100Hz at 0.15g. These two combinations were selected to produce low shear (0.04Pa at 100Hz/0.15g) and high shear (0.94Pa 30Hz/1g) during horizontal vibrations. During vertical vibrations, shear is at least 10-fold smaller for both mechanical signals due to the restricted motion of the fluid. Osteogenesis was induced in hMSCs and cells were exposed to 30min of either vertical, horizontal, or 15min of vertical followed by 15min of horizontal vibrations. After 16d of 30Hz/1g vibrations, levels of mineralization were 3.7-fold greater in all experimental groups independent of loading direction. In contrast to the 30Hz/1g signal, loading direction played a role in the increase in mineralization in the 100Hz/0.15g group. While vertically vibrated cells experienced a 2.2-fold increase in mineralization, horizontal vibration generated a 3.8-fold increase ($p<0.05$). Interestingly, the combination of horizontal and vertical vibrations further enhanced the levels of mineralization (4.2-fold, $p<0.05$). These data demonstrate that vibration direction can influence ossification at specific signal combinations. Considering the similarity in increased mineralization between groups with greatly different levels of shear, they also emphasize that shear per se did not influence mineralization. The temporal sequence of vertical and horizontal vibrations produced the greatest increase in mineralization under low-intensity (shear) conditions may suggest that mechanotransduction may not be identical between horizontal and vertical vibrations.

***Disclosures: Suphannee Pongkitwitoon**, None.*
This study received funding from: NASA

MO0064

Vibrations Increase Osteocyte Gap Junctional Communication Independent of the Level of Fluid Shear. Gunes Uzer*[1], M. Ete Chan[2], Suphannee Pongkitwitoon[2], Stefan Judex[2]. [1]University of North Carolina, USA, [2]Stony Brook University, USA

When applied at high frequencies, bone can sense and respond to mechanical signals of extremely small magnitude. However, the mechanical cues regulating the vibration response are yet to be identified. Computational studies revealed that during the application of vibrations, cell populations within the bone will be subjected not only to acceleratory motions but also to fluid shear as a result of fluid-cell interactions at the bone surface. Mechanosensitive osteocytes can sense local mechanical signals within bone and communicate with other cells, in-part through gap junctions that connect intracellular domains of adjacent cells. Here, we hypothesized that vibrations will increase osteocyte gap junctional intracellular communication (GJIC) and will not require fluid shear as a mechanical input. Applied vibration parameters were selected to vary accelerations between 0.15g to 1g and frequencies between 30Hz to 100Hz, thereby creating fluid shear stresses between 0.04 and 0.94Pa. Osteocyte like MLO-Y4 cells were vibrated at four different vibration frequency/acceleration combinations and the role of fluid shear on GJIC was investigated by parachuting calcein stained donor cells onto unstained osteocytes. All four vibration treatments showed significantly increased GJIC between osteocytes with the largest increase in the 30Hz-1g group ($33.2\% \pm 4.9$, $p<0.001$). Interestingly, increases in GJIC were not different between the four distinct vibration groups despite the large differences in generated fluid shear, suggesting that vibration induced fluid shear does not serve as critical regulatory input. Blocking connexin 43 (Cx43) function with 18α-GA effectively blocked GJIC ($p<0.0001$). In contrast, vibrations did not alter Cx43 mRNA expression levels indicating that vibrations modulate Cx43 function but not its transcription. Spatially enhanced cellular communication was further demonstrated by the greater distance of calcein stained cells from donor cells after vibration treatment. Our data show that vibrations affected GJIC independent of fluid shear stress by directly modulating gap junction function but the specific mechanism by which vibrations can alter Cx43 function is yet to be identified. By not only activating cell mechanotransduction but also providing increased communication between cells, vibrations may have the potential to enhance the efficacy of anabolic signals in bone.

***Disclosures: Gunes Uzer**, None.*

MO0065

Effect of Body Size on the Quantification of Bone Mineral Density From QCT Images Using a Novel Anthropomorphic Hip Phantom. Serena Bonaretti*[1], Isra Saeed[2], Andrew Burghardt[1], Lifeng Yu[3], Michael Bruesewitz[3], Sundeep Khosla[4], Thomas Lang[1]. [1]University of California, San Francisco, USA, [2]UC San Francisco, USA, [3]Mayo Clinic, USA, [4]Mayo Clinic College of Medicine, USA

Beam hardening associated with variations in body size and skeletal density affect the measurements of bone mineral density (BMD) from quantitative computed tomography (QCT) images. In this study we aimed at evaluating the effect of body size on BMD quantification using a novel anthropomorphic hip phantom, evaluating four CT scanners at two centers.

The hip phantom consists of anthropomorphic hips and pelvis of known amount of hydroxyapatite-equivalent material. The two hips have different neck compositions. One hip contains a *calibration* neck made of three concentric cylinders, with densities spanning typical values of integral, cortical and trabecular compartments. The other hip contains a *test* neck made of an outer ellpise for cortical bone, and an inner cylinder for trabecular bone. Two *test* necks were created, one representing the BMD of a young subject, and the other simulating the BMD of an old subject. Each *test* neck was associated to correspondent pelvis-shaped elements, i.e. with higher density for the young subject and with lower density for the old subject. Hips and pelvis are positioned in a tank filled with water, and which represents the dimensions of a small adult female. Two different girdles can be placed concentrically over the tank, creating a maximum body size that corresponds to a 95% adult male (Figure 1).

We scanned the phantom in four different scanners, two GE VCT 64 systems, one Siemens Biograph and one Siemens Definition. For each machine, the phantom was scanned in 6 different configurations, i.e. combining young/old neck with no/small/large girdle. Each acquisition was performed with a calibration standard underneath the phantoms, used to calibrate the acquired image to units of hydroxyapatite concentration. We measured the cortical BMD of the test neck, and the linear slope relating the nominal BMD of the concentric rings of the calibration neck to the measured values.

For each scanner, we found that the BMD measures in the test femoral neck systematically decreased with increasing phantom size (Table 1), and that the slope measured from the calibration neck systematically increased with increasing phantom size (Figure 2).In conclusion, our phantom simulation shed light on the quantitative effects of beam hardening due to increasing body size. Methodological studies in this area will be important for using QCT to understand the effect of obesity and weight loss on skeletal health.

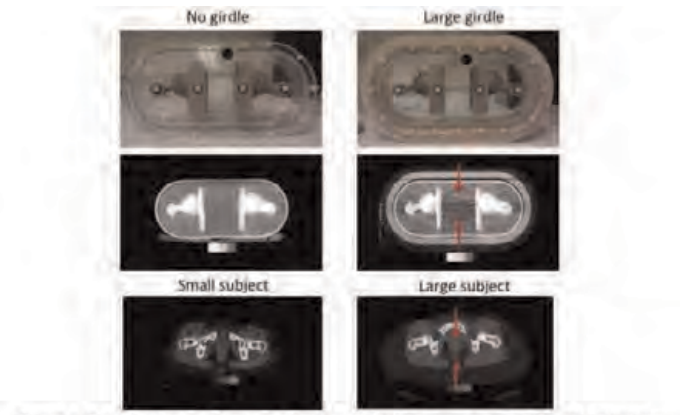

Figure 1. Beam hardening effects on phantom and subject images with different body size. The first row shows the phantom without and with large ring, and the second row shows the corresponding CT images acquired for the two phantom configurations. The final row shows images of larger and smaller subjects. In the CT images of large girdle phantom and fat subject, the beam hardening effect is visible between the two hips.

Figure 1

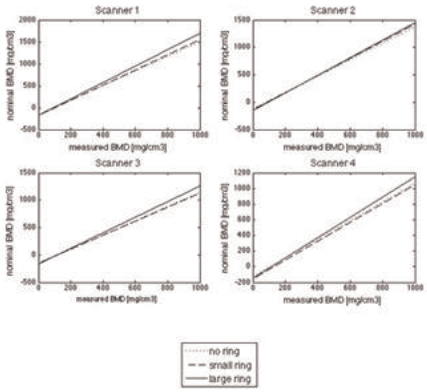

Fig. 2 Calibration line for the *test* neck of the young configuration for the four different scanners. The slope of the calibration line systematically increases with increasing phantom size.

Figure 2

	no ring [mg/cm³]	small ring [mg/cm³]	large ring [mg/cm³]
Scanner 1	430.53	374.60	312.43
Scanner 2	443.61	416.11	405.80
Scanner 3	553.83	528.91	460.22
Scanner 4	579.05	561.97	487.19

Table 1. Measured values of cortical BMD of the *test* neck for no, small and large tissue rings. For each of the different scanners, the cortical BMD decreases systematically with increasing phantom size.

Table 1

***Disclosures: Serena Bonaretti**, None.*

MO0066

Pre- and post-yield mechanical properties are altered in multiple myeloma patients with fractures as assessed by qCT-based finite element models of the vertebral body. Graeme Campbell*[1], Sarah Giravent[2], Christian Graeff[3], Claus-C Glueer[1]. [1]Christian-Albrechts Universität zu Kiel, Germany, [2]Universitätsklinikum Schleswig-Holstein, Germany, [3]University Clinic Schleswig-Holstein, Germany

Multiple myeloma (MM) is associated with bone destruction and high fracture incidence. Surgical necessity is currently determined by the examination of lesion size or number, but this does not consider bone biomechanics. Nonlinear finite element (FE) models simulate mechanical loading and examine both the pre- and post-yield behavior of the bone structure, which may give a more reliable prediction of fracture risk. The purpose of this study was to test the hypothesis that biomechanical properties of the vertebrae, as assessed by non-linear QCT-based FE models, can distinguish between groups of MM patients with and without fracture.

Quantitative computed tomography (QCT) scans of the thoracic vertebrae were evaluated in 48 MM patients, 23 with fracture and 25 without. In-house software was used to generate FE meshes with isotropic tetrahedral elements from the images. The elemental stiffness, yield stress and post-yield behavior were calculated from the local BMD according to relations from Keyak et. al., 1998. Uniaxial compression was simulated (Calculix v.2.5, www.calculix.de) to 1mm and the reaction force-displacement data was determined. The apparent level stiffness, yield and ultimate load and work to yield and failure were calculated. T-tests were used to compare the mechanical parameters between fracture and non-fracture groups. Standardized Odds Ratios (ORs) normalized to standard deviation (SD) and adjusted for age as well as 95% confidence intervals were determined.

Significant reductions in vertebral body stiffness (-23%, p=0.013), yield load (-36%, p=0.003), ultimate load (-35%, p=0.004), work to yield (-48%, p=0.002), and work to failure (-43%, p=0.006) were observed in the fracture compared to non-fracture group. The age-adjusted logistic regression revealed an OR per SD of 2.13 (1.05-4.33) for stiffness, 2.75 (1.24-6.12) for yield load, 2.65 (1.20-5.84) for ultimate load, 3.37 (1.33-8.51) for work to yield, and 2.80 (1.18-6.68) for work to failure.

Reductions in the mechanical properties determined by nonlinear FE were associated with fracture prevalence. These properties had significant Odds Ratios, indicating that FE methods, in particular those that simulate yield and post-yield behavior, may give insight into the susceptibility of fracture in MM patients. Future work will examine prospective datasets to determine the ability of this model to predict fracture.Keyak, J. H., et al. (1998). *J Biomech*, *31*(2), 125–133.

***Disclosures: Graeme Campbell**, None.*

MO0067

Quantitative 3D microcrack imaging for weak and strong bones assessed by reference point indentation. Philipp Schneider*[1], Paul Hansma[2], Connor Randall[3], Ralph Müller[4]. [1]Institute for Biomechanics, ETH Zurich, Switzerland, [2]University of California, Santa Barbara, USA, [3]Department of Physics, University of California at Santa Barbara, USA, [4]ETH Zurich, Institute for Biomechanics, Switzerland

Recently, reference point indentation (RPI) has been introduced for microindentation of human bone [1], which allows *in vivo* assessment of bone mechanical properties at the tissue level, for instance by the indentation distance increase (IDI). Moreover, RPI can discriminate between patients with and without fractures [2]. It was suggested that this ability of RPI to detect bone fragility differences is due to a negative correlation between IDI and crack growth toughness [2] measuring bone's crack-growth resistance. However, there is a lack of microcrack characterization close to the indentation site for bones of distinct IDI. Therefore, the aim of the study was to assess and quantify microcracks in 3D close to the indentation site for weak and strong bones with high and low IDI, respectively. Cylindrical human bone biopsies (diameter = 1.7 mm) were obtained from the tibial midshaft of two male donors (74 and 23 y/o) with high and low IDI, respectively. Specimens were assessed at the TOMCAT beamline of the Swiss Light Source using synchrotron radiation-based computed tomography (SR CT) at a voxel size of 740 nm for quantitative morphometry of the intracortical bone microstructure [3]. Microcracks, canals, and osteocyte lacunae were quantified by crack volume density (Cr.V/Ct.TV), lacuna volume and number density (Lc.V/Ct.TV and N.Lc/Ct.TV) as well as mean lacuna volume (<Lc.V>) [4]. 3D views of the bone tissue after indentation and morphometric results are provided in Figure 1 and Table 1. Cr.V/Ct.TV was more than five times smaller for high IDI vs. low IDI, where more (N.Lc/Ct.TV) and smaller (<Lc.V>) lacunae were found at comparable Lc.V/Ct.TV. The decreased crack formation for weaker vs. stronger bones (higher vs. lower IDI) is against our expectations to find more microcracks in weaker bones, commonly associated with reduced crack-growth resistance [2]. It may be that the microcracking around the indentation site is actually a way that stronger bone distributes the indentation energy to a greater volume of bone and thus, leaving less energy to deepen the indentation. To clarify the relation between bone fragility, microindentation results, and microcrack behavior, further biomechanical imaging studies are needed, which combine RPI and high-resolution 3D imaging, such as SR CT.

[1] Hansma P *et al* 2008, Rev Sci Instrum 79:064303.
[2] Diez-Perez A *et al* 2010, JBMR 25:1877-85.
[3] Voide R *et al* 2009, Bone 45:164-73.
[4] Schneider P *et al* 2007, JBMR 22:1557-70.

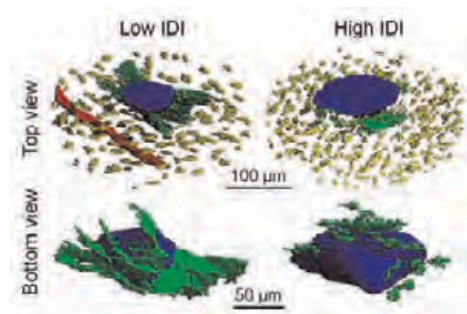

Figure 1: 3D view of indentation. Indent (blue), canal (red), lacunae (yellow), microcracks (green)

	Cr.V/Ct.TV [%]	Lc.V/Ct.TV [%]	N.Lc/Ct.TV [mm^{-3}]	<Lc.V> [µm^3]
Low IDI	0.64	0.99	24907	399
High IDI	0.12	1.12	48991	228

Table 1: Quantitative bone morphometry of microcracks (Cr) and osteocyte lacunae (Lc)

***Disclosures: Philipp Schneider**, None.*

MO0068

Relationships of Bone Stiffness, Bone Structure, Muscle, and Fat. Edward Colt*[1], Muhammad Akram[2], Xavier Pi Sunyer[2]. [1]Columbia University & St. Luke's-Roosevelt Hospital, USA, [2]Columbia University, USA

This study was done to see how increasing BMI affects bone structure and stiffnes smeasured by high resolution peripheral quantitative computerized tomography (HR-pQCT) of the ankle and wrist. We studied 49 healthy pre-menopausal women aged 18 – 45 - BMI from 18 to 47; they were also studied by whole body DXA. Stiffness of the wrist and ankle was estimated from HR-pQCT by finite element analysis (FEA). The correlation of BMD measured by DXA with BMI was higher than the correlation of bone density parameters measured by HR-pQCT with BMI – which were non-significant. There were high correlations of geometric parameters measured by HR-pQCT with BMI. BMD of the tibia measured by DXA was correlated with fat (r = 0.57) and muscle (r = 0.57) in the legs. BMD of the radius was correlated with fat (r = 0.82) and with muscle (r = 0.83) in the arms. There were correlations of bone cross sectional area with fat and muscle around the tibia (r = 0.49 and r = 0.67) and the radius (0.47 and 0.63). The highest correlations of bone stiffness were with trabecular bone volume fraction in the tibia (r = 0.76) and radius (r = 0.73) . Stiffness of the tibia and radius were correlated ($p < 0.001$) with several parameters in both radius and tibia, including sl area, trabecular thickness, BMD, muscle, fat, average bone density by HR-pQCT, weight (W), and BMI. Geometry changed with increasing obesity – differently in the tibia compared with the radius, suggesting that weight bearing may have effects on bone stiffness independent of obesity.

CONCLUSION: Bone stiffness at the wrist and ankle was correlated with muscle and fat in the extremities. Increasing obesity was associated with increased muscle around both tibia and radius. Bone stiffness of the tibia and radius was more highly correlated with the amount of muscle than with the amount of fat around the bone. It seems likely that in our population there muscle, fat, and bone are inherited together; Livshits et al found that 6 genomic variants were most likely associated with body mass as a composite phenotype. Thus our findings might be one reason that fractures are less common in obese than in lean subjects. We found no correlation between bone density measured by HR-pQCT and BMD measured by DXA. BMD measured by DXA is influenced by the amount of soft tissue (muscle and fat) around and within the bone.

KEY WORDS: BMI, DXA, HR-pQCT, Bone Stiffness, Muscle, Fat

Correlations of stiffness with bone parameters. BV/TV bone volume/total volume, BMD, D100 Average Bone Density by HR-QCT, TbN Number of trabeculae, Tb Th Trabecular thickness (mm), Sl ar Slice area of bone enclosed by perimeter, Tb 1/N SD) Standard deviation of 1/TbN: inhomogeneity. Tb Sp Trabecular separation

Tib stiff	parameter	r	p	Rad stiff	parameter	r	p
	BV/TV	0.76	<0.001		BV/TV	0.73	<0.001
	BMD	0.74	<0.001		Th Th	0.70	<0.001
	Leg muscle	0.52	<0.001		BMD	0.66	<0.001
	D100	0.51	<0.001		Arm muscle	0.55	<0.001
	Tb N	0.50	<0.001		D100	0.52	<0.001
	Tb Th	0.47	<0.001		W	0.50	<0.001
	W	0.43	<0.01		BMI	0.47	<0.001
	Sl area	0.41	<0.01		Arm fat	0.43	<0.001
	BMI	0.38	<0.01		H	0.31	<0.05
	H	0.34	<0.05		Sl area	0.24	ns
	Leg fat	0.30	<0.05		Tb N`	0.09	ns
	Tb 1/NSD	-0.50	<0.001		Tb 1/NSD	-0.16	ns
	Tb Sp	-0.57	<0.001		Tb Sp	-0.21	ns

Relationships of Bone Stiffness, Bone Structure, Muscle, and Fat

***Disclosures: Edward Colt**, None.*

MO0069

Risedronate Slows or Partly Reverses Microarchitecture Deterioration Depending on Whether Remodelling Is Perturbed or in Steady State. Yohann Bala*[1], Roland Chapurlat[2], Dieter Felsenberg[3], Thierry Thomas[4], Michel Laroche[5], Edward Morris[6], Jose Ruben Zanchetta[7], Angela M. Cheung[8], Ali Ghasem-Zadeh[9], Roger Zebaze[9], Ego Seeman[9], Rene Rizzoli[10]. [1]University of Melbourne, Dept. of Medicine, Australia, [2]E. Herriot Hospital, France, [3]Charité - Campus Benjamin Franklin, Germany, [4]Hôpital Nord - CHU de St-Etienne, France, [5]Centre de Rhumatologie, CHU Purpan, France, [6]Department of Obstetrics & Gynaecology, Norfolk & Norwich University Hospitals, United Kingdom, [7]Instituto de Investigaciones Metabolicas (IDIM), Argentina, [8]University Health Network-University of Toronto, Canada, [9]Austin Health, University of Melbourne, Australia, [10]Geneva University Hospitals & Faculty of Medicine, Switzerland

In young adulthood, remodelling is slow and in steady state; equal numbers of basic multicellular units (BMUs) excavate and refill on the endosteal surface. Remodelling is balanced; equal bone volumes are excavated and replaced by each BMU. In early menopause, steady state is perturbed, remodelling rate increases, the number of resorbing BMUs increases and exceeds the low number now refilling (activated before menopause). BMU balance becomes negative so bone loss accelerates. Later, steady state is restored at a high remodelling rate; the numbers of BMUs resorbing and filling again is equal but the negative BMU balance causes bone loss but more slowly than in early menopause (Figure). We hypothesized that risedronate slows structural deterioration when administered in early menopause and partly reverses it later.

Risedronate (RIS, 35 mg/week) or placebo (PLB) were given to younger (Group 1, n=161: 53 yr, range: 44-55) and older (Group 2, n=163, 61yr, range: 55-76) postmenopausal women, in a double blind placebo controlled study with 2:1 randomization. High resolution-peripheral computed tomography was used to measure distal tibia and radius volumetric bone mineral density (vBMD, g/cm^3) and cortical porosity (%) quantified using StrAx 1.0[1].

At the distal tibia, in group 1, PLB had a $1.1 \pm 0.4\%$ (p=0.007) decrease in cortical vBMD due to a $3.4 \pm 0.9\%$ (p=0.001) increase in compact-appearing cortex porosity. RIS blunted the decrease in cortical vBMD and blunted the increase in porosity by 60%, (p=0.06 vs. PLB). In group 2, there were no changes in PLB. RIS increased cortical vBMD by $0.5 \pm 0.2\%$ (p=0.007 vs. PLB) and trabecular vBMD by $0.4 \pm 0.2\%$ relative to baseline (NS vs. PLB) and decreased cortical porosity by $0.7 \pm 0.3\%$ relative to baseline (p=0.005 vs. PLB). Trends were similar at the distal radius.

Risedronate slows the appearance of porosity in compact cortex following menopause and partly reverses it in older women. These changes likely account for the anti-vertebral and non-vertebral fracture efficacy of risedronate.

Reference: 1) Zebaze *et al.,* Bone 2013 (54):8-20

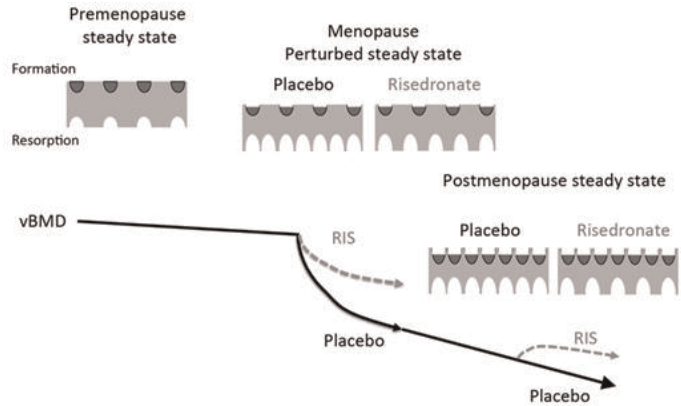

Figure

***Disclosures: Yohann Bala**, None.*
This study received funding from: Warner Chilcott

MO0070

Trabecular Plate Deficiencies in Young Men Infected with HIV Early in Life. Bin Zhou*[1], Michael Yin[1], Stephen Arpadi[2], Ji Wang[1], Kyle Nishiyama[1], Emily Broun[2], Jayesh Shah[2], Chiyuan Zhang[1], Marc Foca[2], Natalie Neu[2], John Nelson[2], David Bell[2], Elizabeth Shane[3], X Guo[1]. [1]Columbia University, USA, [2]Columbia University Medical Center, USA, [3]Columbia University College of Physicians & Surgeons, USA

HIV infection and antiretroviral therapy early in life may result in inadequate bone acquisition and abnormal bone microarchitecture, which contributes to bone strength. We conducted a cross-sectional study using high-resolution peripheral quantitative CT (HRpQCT) at the distal radius and tibia in 30 HIV-infected and 15 HIV-uninfected black or Latino Tanner stage 5 men aged 20-25 years. Among HIV-infected men, 15 were perinatally-infected, 15 were infected during adolescence, and all were on stabile antiretroviral regimens. Standard HRpQCT evaluation protocols were used to analyze geometric and microstructural parameters including cortical porosity. Individual trabecula segmentation (ITS) morphological technique was applied to segment trabecular bone network into individual trabecular plates and rods and to examine in-depth the microstructural characteristics. We also estimated bone stiffness using micro finite element analysis. Cross-sectional area and cortical porosity did not differ between the two groups at the radius or tibia. Total vBMD, trabecular vBMD, and cortical thickness were 6-19% lower in the HIV-infected at both sites ($p<0.05$). By ITS analysis, plate bone volume fraction (pBV/TV), plate-rod ratio (PR ratio), plate number (pTb.N), plate thickness (pTb.Th), plate surface (pTb.S), plate-plate junction density (P-P Junc. D) and axial bone volume fraction (aBV/TV) were 29%, 31%, 8%, 5%, 7%, 17% and 23% lower in HIV-infected than controls at the radius ($p<0.05$). Similarly, plate-related parameters pBV/TV, pTb.N, pTb.Th, pTb.S, P-P Junc. D and aBV/TV were 24%, 7%, 4%, 5%, 17% and 20% lower in HIV-infected than controls at the tibia ($p<0.05$). No differences were found in the rod-related parameters at radius or tibia. Differences in microstructure were reflected in the estimated mechanical properties: HIV-infected had 17% and 14% lower whole bone stiffness at the radius and tibia, respectively, and 24% lower trabecular bone stiffness at the radius than controls.

In conclusion, at an age by which young men have typically acquired approximately 95% of peak bone mass, men infected with HIV perinatally or during adolescence who are on stable antiretroviral regimens have profound deficiencies in trabecular plate, (not trabecular rod) microstructure and decreased trabecular bone stiffness. Compromised bone strength due to trabecular plate deficiencies in young adults infected with HIV early in life may place them at higher risk for fractures as they age.

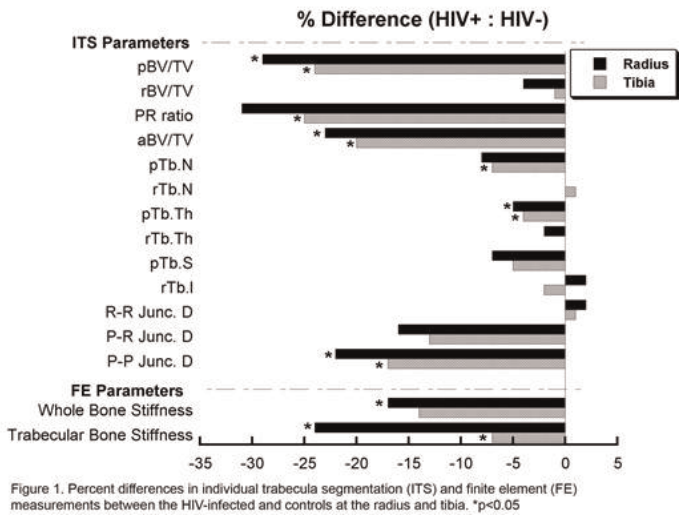

Figure 1. Percent differences in individual trabecula segmentation (ITS) and finite element (FE) measurements between the HIV-infected and controls at the radius and tibia. *p<0.05

Figure 1

***Disclosures: Bin Zhou**, None.*

MO0071

Women With and Without Fragility Fractures: The Bone Quality By TBS. Mário Rui Mascarenhas*[1], Ana Paula Barbosa[2], Ana Gonçalves[3], Vera Simões[4], Didier Hans[5], Isabel do Carmo[3]. [1]Lisbon's Faculty of Medicine, Santa Maria University Hospital, CHLN,EPE, Portugal, [2]Endocrinology, Santa Maria Hospital & Faculty of Medicine, Portugal, [3]Endocrinology, Diabetes & Metabolism Department, Santa Maria University Hospital, CHLN-EPE, Portugal, [4]CEDML - Lisbon's Endocrinology, Diabetes & Metabolism Clinic (Osteoporosis Unit), Portugal, [5]Lausanne University Hospital, Switzerland

Bone strength depends mostly on bone mass (bone mineral density, or aBMD, accessed by DXA) and on bone microarchitecture. The extreme fragility of the bones produced by low mass and deterioration of bone microarchitecture may have, as major consequence, an augmented risk of osteoporotic fractures, mainly at the distal radius, at the spine, at the proximal femur and humerus.

The DXA scan is currently the gold standard to measure BMD, in order to diagnose preciously osteoporosis and estimate fracture risk. The decrease in the BMD is related to an increased risk of osteoporotic fracture.

TBS, a novel gray-level measurement of lumbar spine DXA image texture, is related to microarchitecture and fracture risk independently of BMD. Although some studies were already performed in women, the data about the bone microarchitecture are scarce in women with and without osteoporotic fractures.

Objective: The aim of this study is to compare the lumbar spine bone microarchitecture as estimated by TBS with the spine BMD as well as the correlation between spine TBS and BMD in women with and without fragility fractures.

Material and Methods: The BMD (g/cm^2) at the lumbar spine was measured by DXA (Discovery W, Hologic Inc., USA) in 79 women [mean age 66.0 ($\pm$8.9) years] with osteoporotic fractures (fracture group) and in 76 osteoporotic women [mean age 65.7($\pm$9.2) years] without fractures (no fracture group). Site matched spine TBS was derived for each spine DXA scan (TBS iNsight software, Medimaps, France). Adequate statistical tests were used with the significance level at P<0.05.

ResultsNo significant difference was found between the two groups for all the anthropometric parameters. The mean TBS was lower in the fracture group, as compared with the other group; nevertheless, the mean BMD was not significantly different between these groups of women (Table 1).

There was no significant relationship between spine TBS and BMD, in the fracture group.

Conclusions: The spine TBS was significantly reduced in the osteoporotic fracture group of women, but there was an overlap of the BMD values in both groups, without a clear differentiation of women with and without osteoporotic fractures.These data further suggest that this new diagnostic tool nicely complement the BMD and improve osteoporosis management.

Groups	FRACTURE	NO FRACTURE	P
Spine			
BMD g/cm²	0.860 (±0.1)	0.905 (±0.2)	ns
TBS	1.255 (±0.1)	1.320 (±0.1)	0.0003

Table 1. The mean spine TBS and BMD in the women with and without fractures groups

***Disclosures: Mário Rui Mascarenhas**, None.*

MO0072

Characterizing Micro-architectural Changes at the Distal Radius and Tibia in Postmenopausal Women Using HR-pQCT. Chantal Kawalilak*[1], James Johnston[1], Wojciech Olszynski[2], Saija Kontulainen[1]. [1]University of Saskatchewan, Canada, [2]College of Medicine; University of Saskatchewan, Canada

Introduction. There is little longitudinal evidence of bone micro-architectural changes in postmenopausal women; a population highly susceptible to osteoporotic fracture. When interpreting (or designing) longitudinal studies, it is essential to know the monitoring time interval (MTI) required to significantly detect measured changes (Glüer et al. JBMR 1999). MTI has not been defined for HR-pQCT derived bone measures. Our objective was to characterize annual changes in bone density, area, and micro-architecture at the distal radius and distal tibia in postmenopausal women and to define MTI in this population.

Methods. Distal radius and tibia were measured using HR-pQCT at baseline and 1-year follow-up in 51 women (mean age$\pm$SD: 78$\pm$7 years) from the Saskatoon cohort of the Canadian Multicentre Osteoporosis Study (CaMos). We determined the mean and median annual rate of change, and MTI for bone density, area, and micro-architecture. Paired samples *t*-tests or Wilcoxon sign tests were used for to compare bone outcomes between baseline and follow-up; significance was set at $P<0.05$.

Results. At the radius, total and cortical density decreased (-1.5% and -0.7%, respectively), while trabecular area increased (0.4%). Trabecular number decreased (-3.3%). At the tibia, total and cortical density decreased (-1.4% and -1.8%, respectively). Cortical area and thickness decreased (both -3.3%), while trabecular area increased (0.8%). At the radius, change can be measured in approximately 4 years for cortical and trabecular area, total and cortical density, cortical thickness, bone volume fraction, trabecular number, thickness, and heterogeneity (Table 1). At the tibia, change can be measured in less than 3 years for cortical and trabecular area, total and cortical density, cortical thickness and bone volume fraction (Table 1).

Discussion. Observed changes in bone area, density, and micro-architecture suggest trabecularization of the cortex may have occurred at both measured sites and support earlier evidence from cadavers (Zebaze et al. Lancet 2010). Based on the MTIs, 1-year change in HR-pQCT derived bone properties can be monitored reliably for distal tibia cortical area, density and thickness, as well as bone volume fraction at both sites. However, at least 2 years are needed to monitor change for the other skeletal parameters at the distal tibia and at the distal radius.

Table 1. Annual means at baseline and 1-year follow-up scans and significance, the least significant change (LSC), percent median annual change, and the monitoring time interval [LSC/(Median annual change)] for the HR-pQCT derived bone outcomes at the distal radius and tibia.

		Baseline Scan± SD	Follow-up Scan± SD	*P*- value	LSC	Median Annual Change (%)	MTI (Years)
Radius (n=44)							
Area							
Cortical	(mm²)	39.7± 13.8	39.0± 13.4	0.045	8.0	-1.8	4.4
Trabecular	(mm²)	237.6± 45.1	238.4± 44.6	0.004	1.2	0.3	4.0
Density							
Total	(mg HA/cm³)	253.8± 59.1	249.6± 57.7	0.009	3.5	-1.2	2.9
Cortical	(mg HA/cm³)	781.5± 86.8	775.5± 86.2	0.022	3.0	-1.3	2.4
Trabecular	(mg HA/cm³)	135.2± 39.8	133.9± 40.2	0.505	3.4	0.3	12.2
Meta	(mg HA/cm³)	190.0± 36.6	188.9± 36.0	0.489	4.5	0.1	40.2
Im	(mg HA/cm³)	97.3± 43.8	96.0± 45.1	0.557	3.2	0.0	0.0
Micro-architecture							
Ct.Th	(µm)	549.1± 200.0	539.5± 19.3	0.081	8.4	-2.0	4.2
BV/TV	(%)	11.3± 3.3	11.2± 3.4	0.517	3.2	0.0	0.0
TbN	(1/mm)	1.8± 0.5	1.7± 0.4	0.012	16.0	-3.5	4.5
TbTh	(µm)	61.9± 9.5	64.2± 10.1	0.050	15.0	4.6	3.3
TbSp	(µm)	560.0± 360.8	575.8± 321.8	0.071	16.2	3.3	4.9
TbSpSD	(µm)	315.5± 317.7	329.4± 294.6	0.007	18.3	6.7	2.7
Tibia (n=51)							
Area							
Cortical	(mm²)	81.3± 27.3	78.9± 27.4	<0.001	3.0	-2.8	1.1
Trabecular	(mm²)	627.2± 111.5	628.8± 111.7	<0.001	0.4	0.3	1.5
Density							
Total	(mg HA/cm³)	240.9± 51.1	237.6± 51.2	<0.001	2.7	-1.0	2.6
Cortical	(mg HA/cm³)	765.3± 76.8	752.0± 78.3	<0.001	0.7	-1.6	0.4
Trabecular	(mg HA/cm³)	155.9± 34.9	155.8± 35.2	0.857	3.6	0.1	55.9
Meta	(mg HA/cm³)	226.2± 29.9	226.1± 30.5	0.910	3.1	-0.2	20.6
Im	(mg HA/cm³)	108.1± 39.7	108.0± 40.0	0.786	5.3	0.1	37.5
Micro-architecture							
Ct.Th	(µm)	772.8± 273.7	750.4± 27.6	<0.001	3.8	-2.8	1.3
BV/TV	(%)	13.0± 2.9	13.0± 2.9	0.853	3.6	0.0	0.0
TbN	(1/mm)	1.7± 0.4	1.8± 0.4	0.214	18.7	1.3	14.7
TbTh	(µm)	76.9± 14.8	74.9± 14.5	0.129	17.3	-2.3	7.5
TbSp	(µm)	542.4± 204.4	530.8± 205.2	0.327	19.0	-1.7	11.3
TbSpSD	(µm)	308.8± 341.9	306.5± 362.8	0.469	17.4	-1.4	12.8

Table 1

***Disclosures: Chantal Kawalilak**, None.*

MO0073

Withdrawn

MO0074

Atypical Femoral Fractures are Associated with High Cyclic Tensile Strain Regions During Walking. Saulo Martelli*[1], Peter Pivonka[2], Mariana Kersh[1], Peter Ebeling[3], Marcus Pandy[1]. [1]Department of Mechanical Engineering, The University of Melbourne, Australia, [2]Australian Institute for Musculoskeletal Science, The University of Melbourne, Australia, [3]The University of Melbourne, Australia

Atypical femoral fractures (AFF) are rare low-energy stress fractures progressing from the lateral aspect of the subtrochanteric and diaphyseal region to complete and predominantly transverse fractures. AFFs have been associated with bisphosphonate treatment, which may also result in a bone mineralisation increase, narrowed bone mineralisation density distribution, and a reduction in bone remodeling. AFFs may also be associated with abnormal femur geometry, being more common with femur bowing and in Asian populations (J. Bone Miner Res. 25:11, 2010). We examined the physiological loading environment to test the hypothesis that AFF onset in femoral sub-regions is associated with high cyclic tensile strains occurring during daily activities. We computed the femur tensile strain distribution during walking for ten postmenopausal women using the finite-element (FE) method. Ten volunteers underwent a computed-tomography (CT) and gait analysis. The femur FE model was created using the bone geometry and the material properties extracted from the CT images (J Biomech. 40:13, 2007). A generic musculoskeletal model was scaled on the volunteers' anthropometry. The joint net moments driving a selected stance of walking were calculated using the body motion and the ground reaction forces recorded during gait analyses. The muscle and the hip reaction forces were calculated using published algorithms (IEEE Trans Biomed Eng. 54:11, 2007). FE analyses were performed applying the calculated muscle and hip reaction forces and using a full constraint condition distally. Five phases (Fig. 1, phase A, B, C, D, and E) of walking including heel-strike (A), the first (B) and the second (D) peak of the hip reaction force, mid stance (C) and toe-off (E) were studied. Results for one volunteer are shown in Fig. 1. The peak tensile strains corresponded with the two peak values of the hip reaction force magnitude (Fig. 1, B and D). For both peaks, high tensile strains were located on the lateral femur diaphysis across its entire length. The maximum tensile strain value was 0.4%, corresponding with the second peak of the hip reaction force (4.5 body-weight). In conclusion, AFFs may be initiated in a femur sub-region (lateral femur diaphysis) subjected to high cyclic tensile strains where bone micro-cracks may progress to fracture due to a combination of a) high cyclic tensile strain inducing a significant crack opening and b) altered material properties and reduced bone remodeling.

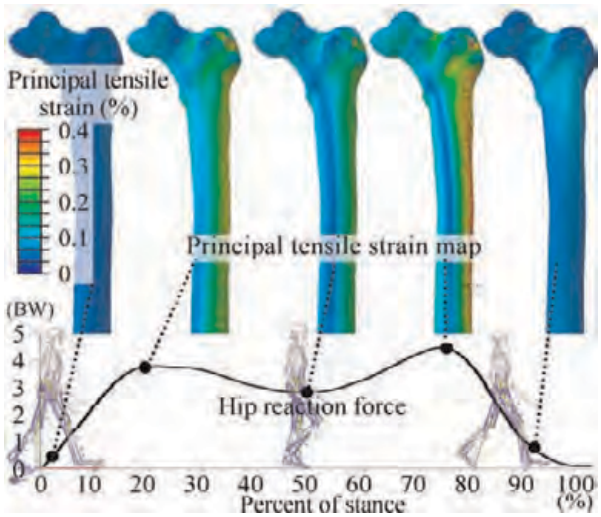

Fig. 1. The tensile strain pattern in the femur during the stance phase of walking

***Disclosures: Saulo Martelli**, None.*

MO0075

Physically Active Women Have Denser Bones and May Be Less Responsive to a Mechanical Loading Intervention. Karen Troy*, Breanna Johnson, Mary Lou Bareither. University of Illinois at Chicago, USA

Physical activity produces mechanical strains within bone that are known to be osteogenic. Several studies have illustrated a positive association between mechanical loading history and bone mass and structure. Loading history is often quantified using one of two bone-specific survey instruments: the Bone Loading History Questionnaire (BLHQ) and Bone Physical Activity Questionnaire (BPAQ). These surveys weight activities based on ground reaction forces, with validations focused on lumbar spine or hip bone mineral density (BMD). The degree to which these survey measures reflect upper extremity loading is not known.

We have developed an *in vivo* upper extremity loading protocol in which women apply a force to their distal radius, resulting in measurable changes to bone. Our purpose was to determine whether physical activity surveys were related to baseline measures of, and changes to, distal radius bone mineral following our loading protocol. We hypothesized that survey scores would be related to baseline measures, and that subjects with high scores would be less responsive to loading, based on the concept that bone adaptation is "error signal" driven.

Twenty-one women age 22 ± 3 years participated in a 6 month loading protocol where a force of 300N was applied to the palm of the hand, 50 cycles/day, 3 days/week. Quantitative computed tomography was performed at baseline and at 6 months to measure bone mineral content (BMC) and density (BMD) of the total and ultra-distal (UD) radius. Subjects completed two physical activity surveys: the BLHQ, and the BPAQ. Upper extremity versions of the surveys were created by scoring the subset of activities that would be expected to produce forces on the hands or arms; e.g., volleyball but not soccer.

Pearson correlations were used to compare survey scores with baseline and 6-month change measures of bone. BPAQ scores were positively correlated with BMD at baseline, but negatively correlated with change in total BMC (Table 1). The positive association at baseline is consistent with previous reports. The upper extremity versions of the surveys were not better predictors of baseline or change values than the full versions. This may be because the surveys used weighting factors for each activity based on ground reaction forces, which are irrelevant to the radius. This research may help us prospectively identify individuals who would most benefit from our mechanical loading intervention targeting the distal radius.

Table 1: Correlations (r) between baseline and change values for bone versus physical activity. *p<0.05

	Baseline values				Change values			
	UD BMC (g)	UD BMD (g/cm^3)	Total BMC (g)	Total BMD (g/cm^3)	UD BMC (g)	UD BMD (g/cm^3)	Total BMC (g)	Total BMD (g/cm^3)
BPAQ - past activities	0.338	0.546*	0.367	0.553*	0.534*	-0.362	-0.614*	-0.512*
BPAQ - current activities	0.168	0.222	0.092	0.233	-0.31	0.097	0.038	0.314
BPAQ - total	0.404	0.619*	0.377	0.632*	0.249	-0.246	-0.502*	-0.228
Upper Extremity BPAQ past	0.371	0.566*	0.383	0.586*	0.541*	-0.349	-0.570*	-0.485*
Upper Extremity BPAQ current	0.478	0.249	0.428	0.091	-0.505*	-0.247	-0.204	-0.261
Upper Extremity BPAQ total	0.429	0.601*	0.435	0.603*	0.490*	-0.381	-0.599*	-0.520*

Table 1

***Disclosures: Karen Troy**, None.*

MO0076

Comparison of Raman spectroscopic mapping and histological characterization of heterotopic ossification. Nicole Crane*[1], Eric Elster[2], Benjamin Potter[3], Jonathan Forsberg[1]. [1]Naval Medical Research Center, USA, [2]Uniformed Services University of Health Sciences, USA, [3]Walter Reed National Military Medical Center, USA

Over 60% of patients with major combat-related extremity injuries develop radiographically apparent heterotopic ossification (HO), the formation of mature lamellar bone in the soft tissues. Nearly a third of patients that develop HO require surgical excision of persistently symptomatic lesions, a procedure that is fraught with complications and delays or regresses functional rehabilitation in many cases. Due to the high prevalence and the morbidity of surgical removal, prophylaxis would be much preferred to treatment. The exact etiology of HO, however, remains unknown. We asked whether Raman spectral changes, also known as Raman spectro-histopathology, mapped across tissue sections correlated with histologic evidence (serial sections of tissue stained with H&E, Alcian blue, Masson's trichrome, S-100, and UCP-1) of the earliest signs of HO formation using tissue biopsies from the wounds of combat casualties. In doing so, we compared tissue biopsies from ten combat-wounded patients, five of whom developed HO after wound closure and five of whom did not. Raman spectroscopic features extracted from mineral and matrix components of tissue biopsies demonstrated strong associations with histologic findings. Raman spectroscopic mapping further demonstrated utility as an adjunct technique by providing information beyond standard histological analysis including evaluation of mineral quality. Raman spectroscopy may therefore prove a useful, non-invasive diagnostic modality to detect and characterize early HO formation, potentially at a time point when primary prophylaxis or selective early excision remains practicable.

***Disclosures: Nicole Crane**, None.*

MO0077

High-Precision Analysis of Subchondral Sclerosis as an Early and Progressive Marker of Post-Traumatic Osteoarthritis Using Micro-Computed Tomography. Joseph Temple*[1], Lara Longobardi[2], Tieshi Li[2], Timothy Myers[3], Alessandra Esposito[4], Anna Spagnoli[2]. [1]University of North Carolina at Chapel Hill Department of Biomedical Engineering, USA, [2]University of North Carolina at Chapel Hill, USA, [3]University of North Carolina, USA, [4]University of North Carolina at Chapel Hill Department of Pediatrics, USA

Purpose: It has recently been proposed that subchondral sclerosis (SCS) is an early marker for osteoarthritis (OA). This marker is evident histologically (Fig. 1a-b, dashes), but histological scoring emphasizes cartilage pathology and cannot quantitatively evaluate SCS. The purpose of this study was to localize and evaluate SCS using high-resolution micro-computed tomography (uCT) analysis within rigorously defined volumes of interest (VOIs). This study was aimed at quantifying SCS as an early and progressive marker in a post-traumatic OA mouse model.

Methods: 10-week (W) old male C57BL/6 mice underwent destabilization of the medial meniscus (DMM) or SHAM survival surgery to induce post-traumatic OA. Two, 4, 12, and 20W after surgery, mice were euthanized and tibiae were dissected. Bones were fixed, immersed in Cysto-Conray 2 (24h) to visualize cartilage, and scanned (SCANCO, 55 kVp, 145 μA, 6 μm voxel). Samples were rinsed, decalcified (10% EDTA, 14d), and coronally sectioned for Safranin-O/Fast Green staining.

We developed an algorithm to precisely isolate the VOI where SCS is localized (Fig. 1e, red borders). Axial uCT slices were reconstructed, realigned, and resliced based on the midsagittal plane containing three anatomically invariant landmarks (Fig. 1e, arrows): the tibial tuberosity (blue), the anterior border of the intercondylar notch (AIN, white), and the origin of the posterior cruciate ligament (green). The VOI (Fig. 1e, red dashes) was bordered by this plane (laterally), the coronal plane with the AIN (anteriorly), and the growth plate (inferiorly). The VOI was evaluated for bone morphometric analysis.

Statistics: A two-tailed *t*-test was used to compare DMM and SHAM SCS. Longitudinal comparison was performed with one-way ANOVA. Significance was set at $p < 0.05$.

Results: As early as 4W after DMM surgery, SCS was visible in the medial tibial plateau by both histology (Fig. 1a-b) and uCT (Fig. 1c-d) in the VOI. As shown in Table I, uCT quantified SCS, and DMM VOIs had greater bone density, mineral density, and trabecular thickness than SHAM controls as early as 4W post-surgery. Remarkably, both uCT and histology showed that cartilage was still intact (Fig. 1a-d, arrows), indicating the relevance of SCS as early OA marker. SCS increased longitudinally in DMM mice. These results suggest that SCS is both an early and progressive marker in murine post-traumatic OA and that high-resolution uCT provides a valid means to quantify SCS.

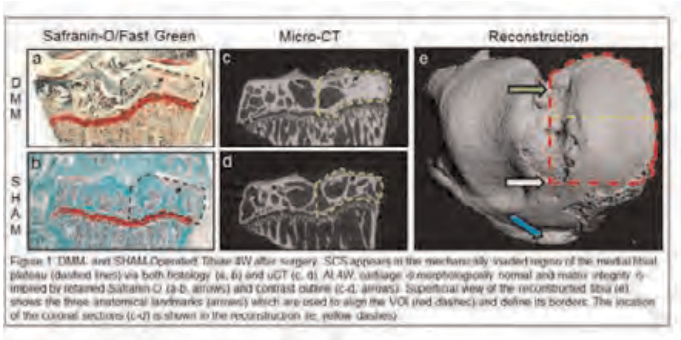

Figure 1. DMM- and SHAM-Operated Tibiae 8W after surgery. SCS appears in the mechanically loaded region of the medial tibial plateau (dashed lines) via both histology (a, b) and uCT (c, d). At 4W, cartilage is morphologically normal and matrix integrity is implied by retained Safranin O (a-b, arrows) and contrast outline (c-d, arrows). Superficial view of the reconstructed tibia (e) shows the three anatomical landmarks (arrows) which are used to align the VOI (red dashes) and define its borders. The location of the coronal sections (c-d) is shown in the reconstruction (e, yellow dashes).

Figure 1

Time	Surgery	BV/TV	mg HA/TV	Tb. Th. (mm)
2W	DMM	0.456 ± 0.058	631.9 ± 50.3	0.120 ± 0.014*
	SHAM	0.373 ± 0.050	564.4± 38.6	0.058 ± 0.009
4W	DMM	0.582 ± 0.023*†	773.8 ± 18.9*	0.119 ± 0.019*
	SHAM	0.394 ± 0.031	575.9 ± 25.6	0.062 ± 0.010
12W	DMM	0.621 ± 0.026*†	776.2 ± 29.6*	0.121 ± 0.006*
	SHAM	0.381 ± 0.023	562.0 ± 33.5	0.065 ± 0.011
20W	DMM	0.680 ± 0.036*†	803.4 ± 37.3*	0.161 ± 0.009*
	SHAM	0.415 ± 0.012	566.4 ± 24.2	0.069 ± 0.004

Table I. Bone morphometric analysis (mean ± standard deviation) of the SCS VOI in DMM- and SHAM-operated mice 2, 4, 12, and 20W after surgery (n = 3 per group). At 4, 12, and 20W, DMM mice had significantly greater bone density (BV/TV), Hydroxylapatite (HA) density, and trabecular thickness (Tb. Th.) than SHAM counterparts (*$p < 0.05$ compared to SHAM). One-way ANOVA of these variables in DMM mice suggested an increase in SCS longitudinally (†$p < 0.05$ compared to DMM 2W).

Table I

***Disclosures: Joseph Temple**, None.*

MO0078

Joint Bleeding in Factor VIII Deficient Mice Causes an Acute Loss of Trabecular Bone and Calcification of Joint Soft Tissues, Which is Prevented with Aggressive Factor Replacement. Anthony Lau*[1], Junjiang Sun[2], William Hannah[2], Eric Livingston[3], Dominique Heymann[4], Ted Bateman[5], Paul Monahan[6]. [1]University of North Carolina at Chapel Hill, USA, [2]University of North Carolina-Chapel Hill-Gene Therapy Center, USA, [3]University of North Carolina-Chapel Hill-Department of Biomedical Enginering, USA, [4]INSERM U957, University of Nantes, France, [5]Univesity of North Carolina, USA, [6]University of North Carolina-Chapel Hill-Gene Therapy Center & Department of Pediatrics, USA

Adults and children with hemophilia experience both reduced bone density and joint damage from hemarthrosis. The goal of this study is to characterize the acute 1) bone loss and 2) joint damage response from an induced joint bleed in hemophilic mice, and determine the efficacy of aggressive factor replacement treatment. Male 22-week old Factor VIII knock-out mice were used and treated with or without recombinant Factor VIII just prior to and after injury. Mice were subjected to knee joint hemorrhage induction by instilling 5 microliters of saline into the left knee joint space. Thirty minutes prior to inducing joint hemorrhage, mice received an intravenous dose of human recombinant factor VIII 250IU kg^{-1}(n=9) or placebo dose of saline (n=9). This dose was repeated at 4, 24, 48, 72 and 96 hours after bleed induction. Two weeks post-injury, the mice were euthanized and hind limbs were collected and scanned with microCT at 10μm resolution.

For the bone loss goals of the study, microCT analysis was performed on proximal tibia trabecular bone, inferior to the growth plate. Comparing the injured joint against the contralateral un-injured joint found that hemarthrosis resulted in significant reduction of trabecular bone of proximal tibia BV/TV (-25%), trabecular connectivity density (-20%) and thickness (-13%), bone tissue mineral density (-5%), and volumetric bone mineral density (-27%), which was mitigated by aggressive FVIII replacement (Figure 1).

In addition to loss of bone in the proximal tibia, gross degradation of the joint tissues was observed. Analysis of the morphology of this degradation suggests that what the literature has typically described as joint erosion, is actually mineralization of the joint soft tissues. Joint bleeding resulted in mineralization of the articular surface, joint ligaments and tendons, as well as the patella and patellar tendon (Figure 2). Treatment with factor VIII prevented this soft-tissue mineralization. The rapid mineralization of the joint two-weeks post injury alters the joint soft tissue mechanical properties, which could lead to improper joint function, accelerating joint degradation. The finding of rapid mineralization of the joint soft tissues has implications for both the fields of osteoarthritis, and regenerative medicine.

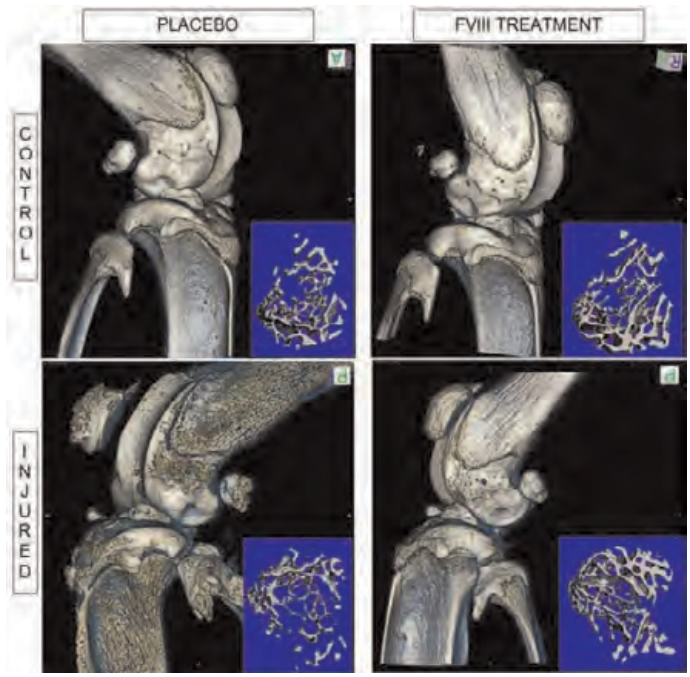

Figure 1: 3D Rendering of Control and Injured Joints from Placebo and FVIII treated mice

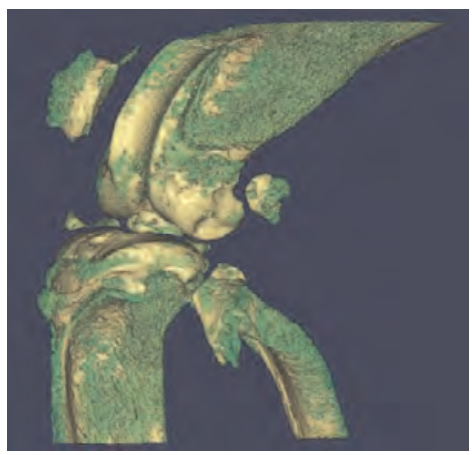

Figure 2: MicroCT rendering of injured joint showing mineralization (green) of joint soft tissues

***Disclosures: Anthony Lau**, None.*
This study received funding from: Baxter Health Care

MO0079

Evidence that Perichondrial Cells are derived from Chondrocytes. Stephan Spath*[1], Michael Chau[2], Ola Nilsson[2]. [1]NIH, USA, [2]NICHD, USA

Background: During early bone formation, mesenchymal stem-cells condense and differentiate into collagen type 2-expressing chondrocytes which form the cartilaginous bone anlagen. This anlage becomes enclosed by the perichondrium. The perichondrium consists of two layers, the inner cambium layer containing chondrocyte- and osteo-precursor cells and the outer fibrous layer important for mechanical and structural support.

Aim: To explore the cellular origins of perichondrium.

Methods: Perichondrium-specific markers were identified by microarray and real-time PCR analysis of microdissected perichondrium. High-density chondrocyte pellets were produced by isolating chondrocytes from rat epiphyseal cartilage and centrifugation. During the dissection, the perichondrium was carefully removed and its absence was confirmed by histological examination and by real-time PCR for perichondrium markers. Differentiation of pellet cultures was studied using real-time PCR and *in situ* hybridization for chondrocyte and perichondrium markers.

Results: Cultured chondrocyte pellets developed a surrounding perichondrium-like tissue. This surrounding tissue did not express chondrocyte markers, collagen 2 or 10, as assessed by *in situ* hybridization. Instead, perichondrium markers Dickkopf 3 (Dkk3), Pleiotrophin (Ptn), Periostin (Postn), Roundabout 2 (Robo2), Protein Tyrosine Phosphatase Receptor Type Z 1 (Ptprz1), Cadherin 2 (Cdh2), L-galectin (Lgals), Thrombospondin 4 (Thsb4) were upregulated during the formation of the perichondrium-like tissue by real-time PCR. Interestingly, molecular markers for the cambium (Dkk3, Lgals and Thsb4) and not the fibrous layer (Collagen 14 and Decorin) were upregulated in cultured chondrocyte pellets.

Conclusions: These results suggest that epiphyseal chondrocytes of postnatal animals are not terminally differentiated, but still retain the potential to transdifferentiate into perichondrial cells, and thus support previous cell-lineage tracing studies suggesting that the perichondrium is formed from collagen 2 expressing chondrocytes in the periphery of the bone anlagen.

***Disclosures: Stephan Spath**, None.*

MO0080

Bio-Adhesive for Tissue Integration and Construction of Bone and Cartilage Interface. Hyunji Cho*[1], Changhwan Kim[1], Sung Hyun Kim[2], Seungwoo Nam[1], EunAh Lee[3], Youngsook Son[1]. [1]Lab of Tissue Engineering, Department of Genetic Engineering, College of Life Science, Kyung Hee University, South Korea, [2]Materials Research Center for Information Display, College of Engineering, Kyung Hee University, South Korea, [3]Kyung Hee University, South Korea

Recent advances in tissue engineering made it possible to apply chondrogenic graft to cartilage-defect area. However, successful regeneration of cartilage depends on the integration of transplanted tissue with surrounding natural tissue. In the case of tissue engineering approach for articular cartilage, subchondral bone comprises the surrounding tissue. In the aim of developing bio-adhesive that can acts at the bone-cartilage interface, the surface of hydroxyapatite microcrystals were chemically modified with linker molecules to confer adhesive property. The linker molecules that can participate in chemical reaction to form covalent bonding with the chemical groups on natural tissues were chosen based on the biocompatibility of the reaction. Grafted linker molecules were chemically confirmed and characterized by chromogenic reaction and FTIR analysis. Thereby comprised bioadhesive was names as 'stickyapatite'.

As an *in vitro* attachment test, chondrogenic graft composed of BMSCs or chondrocytes were attached to the surface of rabbit tibia using stickyapatite, and checked for their attachment after 1 hour. While commercial hydroxyapatite showed attachment only in 25%, the stickyapatite showed attachment in 75% of the applied chondrogenic graft. As an in vivo attachment test, chondrogenic grafts composed of chondrocytes were transplanted to full-thickness articular cartilage defect of rabbit autologous chondrocyte implantation (ACI) model with or without stickyapatite. After 6 weeks upon transplantation, coverage of articular cartilage was measured by image analysis, and the attachment interface was subjected to histological analysis. The newly formed cartilage induced by transplanted chondrocytes were covering about 74% of the defect area in stickyapatite treated group, while the control group showed much lower coverage of defect with so much variation in each case indicating that chondrocytes were lost on the transplanted surface.

Being a powder-type bio-adhesive, those 'sticky apatite' exhibited advantageous trait showing no insulation around the interface of attached tissues which was confirmed based on the fact that stickyapatite-induced newly formed cartilage did not show discrete line between the subchondral bone and the transplanted cartilage. This research was supported by a grant from Korean Ministry of Health and Welfare given to Youngsook Son (A040003) and a grant from National Research Foundation of Korea given to EunAh Lee (2011-0009391).

***Disclosures: Hyunji Cho**, None.*

MO0081

Choline Kinase Beta is an Important Regulator of Endochondral Bone Formation. Zhuo Li*[1], Gengshu Wu[1], Roger Sher[2], Kayla Rumack[3], Gregory Cox[4], Michael Doschak[1], Monzur Murshed[5], Frank Beier[3], Dennis Vance[1]. [1]University of Alberta, Canada, [2]University of Maine, USA, [3]University of Western Ontario, Canada, [4]The Jackson Laboratory, USA, [5]McGill University, Canada

Choline kinase converts choline to phosphocholine and is the first enzyme in the choline pathway to generate phosphatidylcholine. Choline kinase has two isoforms encoded by the genes *Chka* and *Chkb*. Inactivation of *Chka* results in embryonic lethality, whereas *Chkb* mutant mice display neonatal forelimb bone deformation. To understand the mechanisms of the bone deformation phenotype, we characterized the major long bones in the forelimb. We found that the deformation is specific to the radius and ulna and the deformation occurs during the late embryonic stage. We also found that the radius and ulna in mutant mice display abnormal chondrocyte cell morphology, unorganized proliferative columns and expanded hypertrophic zones in their growth plates as well as delayed formation of primary ossification centers. We then quantified the choline metabolites by Mass Spectrometry. No change in phosphatidylcholine was observed but the amount of phosphocholine is decreased by approximately 60% in mutant chondrocytes. To further understand these phenotypes, we examined chondrocyte differentiation, proliferation, apoptosis, and cartilage extracellular matrix (ECM) degradation events. We found that mutant chondrocytes have impaired differentiation. They also have a decreased rate of cell proliferation and apoptosis. In addition, the cartilage in mutant mice has diminished ECM degradation by matrix metalloproteinase 9 and 13. Taken together, our data suggests that choline kinase beta plays an important role in endochondral bone formation through regulation of growth plate chondrocyte physiology.

***Disclosures: Zhuo Li**, None.*

MO0082

Evaluation of osteoarthritis based on second harmonic generation microscopy. Hiroshi Kiyomatsu*[1], Yusuke Oshima[2], Atsuhiko Hikita[3], Hiromasa Miura[4], Takeshi Imamura[4]. [1]Ehime University Hospital, Japan, [2]Translational Research Center, Ehime University Hospital, Japan, [3]Ehime University, Japan, [4]Ehime University Graduate School of Medicine, Japan

Osteoarthritis restricts daily activities of patients and significantly decreases their quality of life. There is no fundamental treatment other than an invasive surgical treatment at the late stage of the disease, because articular cartilage can't be regenerated and early detection of disease is quite difficult. Quantitative and sensitive methods for diagnosis and evaluation of osteoarthritis must be established to develop new treatments by clarifying the nature of the disease in animal studies and to detect subtle changes from the early phase of the disease. Second harmonic generation (SHG) imaging make it possible to observe non-centrosymmetric molecular assemblies such as collagen fibers without staining. The cartilage matrix consists mainly of type II collagen. The SHG signal reflects the localization and orientation of the fibrous structure of the collagen molecule, and thus enables us to detect its minute changes at the molecular level. Several groups have reported SHG imaging of articular cartilages, but these studies were not done in vivo.To establish a new method for the evaluation of the degenerative articular cartilages in living animal and clinical setting, we performed SHG and two-photon excited fluorescence imaging of articular cartilage matrix and chondrocytes of H2B-GFP mice which express green fluorescence protein in nuclei. Firstly, time-course measurements of drug-induced degeneration of mouse articular cartilage were performed ex vivo. SHG signals was significantly reduced after collagenase treatment, which suggests that SHG signal reduction is associated with the degeneration of the cartilage. Dislocation of chondrocytes from articular cartilage was also observed, which showed the breakdown of the structures of extracellular matrices. Next, hyalronidase treatment of articular cartilage was done in a same manner, but no significant change in the intensity of SHG from articular cartilage was observed.We also developed a cartilage defect model to evaluate the regeneration of cartilage by using MPEM imaging in vivo. We generated this model by removing cartilage of patella groove in mice and observed postoperative change in living mice. We found that SHG signal intensity and distribution were significantly changed.Although further development of this assay and quantitative analysis would be required for establishment of diagnostics and fundamental treatments, SHG imaging of cartilage matrix is promising technique for osteoarthritis study.

***Disclosures: Hiroshi Kiyomatsu**, None.*
This study received funding from: Core Research for Evolutional Science and Technology

MO0083

Genes significantly highly expressed in synovium derived stromal cells than in bone marrow derived cells are conserved both in mouse and human, and may contribute to higher potential for chondrogenic differentiation. Yoichi Ezura*[1], Tadayoshi Hayata[2], Takuya Notomi[3], Ichiro Sekiya[4], Masaki Noda[4]. [1]Tokyo Medical & Dental University, Medical Research Insititute, Japan, [2]Medical Reserach Institute, Tokyo Medical & Dental University, Japan, [3]GCOE, Tokyo Medical & Dental University, Japan, [4]Tokyo Medical & Dental Univerisyt, Japan

Stromal progenitor cells resident in various adult tissues possess multi-potency to differentiate, and thus are called as mesenchymal stem cells (MSCs). Basic characterization of these cells indicates shared common features. Previously, we have shown that there were consistent differences between the synovium derived human MSCs (SMSCs) and bone marrow (BM) derived MSCs (BM-MSCs) in global gene expression, possibly contributing to their potency for chondrogenic differentiation. To investigate if the differences are conserved among diverse species, we examined expression profiles of mouse synovium derived stromal cells (m-SSCs) and mouse bone marrow derived stromal cells (m-BMSCs). Regression analysis of the relative expression levels of about 10,000 genes that were shared in mouse and human microarray platform indicated that the relative expression of those genes in mouse SSCs v.s. mouse BMSCs were positively correlated with those of human SMSCs vs. human BM-MSCs ($r=0.17$, $p=6.6 \times 10^{-42}$). Importantly, we found that many transcription factors known to be required for chondrogenic differentiation or maturation, including Sox5, Nkx3.2, Zfp521, and Zeb1 were significantly expressed more highly in mouse SSCs or human SMSCs than in mouse BMSCs or human BM-MSCs. In addition, we found many genes encoding extracellular matrix proteins preferentially expressed in cartilage, such as Asporin, Comp, Prg4 were more highly expressed in synovium derived cells than in BM derived cells. A list of 226 genes significantly expressed more highly in synovium derived cells than in bone marrow derived cells both in mouse and human may provide new insight into the differentiation potential of mesenchymal progenitor cells to chondrocytes, and thus would contribute to develop novel diagnostic or therapeutic methods for human osteoarthritis or related diseases.

***Disclosures: Yoichi Ezura**, None.*

MO0084

Ihh Directly Regulates ColX Expression by PTHrP-independent Mechanisms via Runx2/Smad Interaction during Limb Development. Katsuhiko Amano*[1], Michael Densmore[1], Riko Nishimura[2], Toshiyuki Yoneda[3], Mikihiko Kogo[2], Beate Lanske[1]. [1]Harvard School of Dental Medicine, USA, [2]Osaka University Graduate School of Dentistry, Japan, [3]Indiana University School of Medicine, USA

Indian hedgehog (Ihh) expressed in pre- and hypertrophic chondrocytes is essential for skeletal bone formation. Ihh has been shown to form a negative feedback loop with parathyroid hormone- related protein (PTHrP) to regulate the rate of chondrocyte differentiation. We and others previously reported that Ihh promotes Collagen type X (ColX) expression, chondrocyte maturation and calcification independently of PTHrP, however, the molecular mechanism for this was still unknown. We hypothesized that Ihh signaling directly regulates ColX expression and transcription and have performed *in vitro* and *in vivo* analyses to address this question. First, we tested the effect of hedgehog-induced transcription factors Gli1/2 on ColX promoter activity and determined that Gli1/2 upregulated the promoter activity. Using ColX promoter deletion constructs and sequence analysis, we identified a Gli1/2 binding site in the basic ColX promoter region (250bp). Further studies with oligo pull-down assays indicated that Gli1/2 physically interacted with this site. We then examined the interaction of Gli1/2 with Runx2/Smads since these are important factors in late chondrocyte differentiation and could show that both interacted with these proteins using binding and ColX Luc promoter assays. To confirm our findings *in vivo*, we generated a *Prx1-Cre;Ihh$^{fl/fl}$* mouse to delete Ihh during development from limb mesenchyme. This model allowed us to analyze the long bone phenotype from embryogenesis to postnatal life. We observed initiation of ColX expression in mutant long bones at E15.5 which then decreased over time, and was completely lost in long bones of *Prx1-Cre;Ihh$^{fl/fl}$* mice at P10. The remaining chondrocytes found close to the distal ends of the mutant bones strongly expressed Collagen type 2 and PTHrP, but ColX expression was completely lost suggesting that Ihh is required to specifically maintain ColX expression. In summary, our data suggest that Ihh directly regulates ColX transcription through Gli1/2 interaction with Runx2/Smads and that Ihh is essential to maintain postnatal ColX expression *in vivo.*

***Disclosures: Katsuhiko Amano**, None.*

MO0085

Indispensable Role of Thyroid Hormone in Secondary Ossification via a Novel Mechanism Involving Transdifferentiation of Chondrocytes into Osteoblasts. Subburaman Mohan*[1], Shaohong Cheng[2], Weirong Xing[3], Heather Watt[4], Sheila Pourteymour[4], Catrina Alarcon[4], Jon Wergedal[1]. [1]Jerry L. Pettis Memorial VA Medical Center, USA, [2]VA Loma Linda Health Care Systems, USA, [3]Musculoskeletal Disease Center, Jerry L. Pettis Memorial Veteran's Admin., USA, [4]Jerry L Pettis VA Medical Center, USA

Our recent studies using genetic mouse models that are deficient in thyroid hormone (TH) and/or growth hormone (GH) have provided unequivocal evidence that there is an important window of time, prior to puberty, when the effects of GH are surprisingly small and TH plays a critical role in the regulation of skeletal growth. In terms of mechanisms for TH regulation of bone accretion, we focused on the secondary ossification center (SOC), since the time of appearance of SOCs in several species (mice, rats, humans) coincides with the time when peak levels of TH are attained. Accordingly, μCT evaluation of femurs and tibias at day 21 in TH-deficient and control mice revealed that endochondral ossification of SOCs is severely compromised (>75% reduction in BV/TV) due to TH deficiency and that TH treatment for 10 days rescued this phenotype fully. Staining of cartilage and bone in the epiphysis of TH deficient Tshr$^{hyt/hyt}$ and control mice at postnatal day 3, 7, 10, 14, 17 and 21 revealed that while all of the cartilage is converted into bone in the control mice, this conversion failed to occur in the TH-deficient mice. Accordingly, the Col2 mRNA level was increased (30%, $P<0.05$) while Col10, ALP and osteocalcin (OC) mRNA levels were decreased (>70%, $P<0.01$) in the epiphysis of TH deficient mice (day 7). These changes were rescued by TH treatment of Tshr$^{hyt/hyt}$ mice. Immunohistochemistry studies revealed that TH treatment of Tshr$^{hyt/hyt}$ mice induced expression of osterix (Osx) in Col2 expressing chondrocytes (CCs) in the SOC at day 7 which subsequently transdifferentiate into Col10/OC expressing chondro-osteoblasts at day 14. Consistent with these data, treatment of serum-free tibia cultures from 3-day old mice with 10 ng/ml TH for 1, 3 and 10 days increased expression of Osx, Col10, ALP and OC in the epiphysis by 6-60 fold (all $P<0.01$). Furthermore, knockdown of the TH-induced increase in Osx expression using lentiviral Osx shRNA significantly blocked TH-induced ALP and OC expression in CCs, thus suggesting that the TH effect on chondro-osteoblast differentiation is mediated via increased Osx expression. By contrast, knockdown of Runx2 did not block TH-induced OC expression in CCs. Based on our findings, we conclude: 1) TH is indispensable for initiation and progression of the SOC. 2) TH acts via a novel mechanism in which TH acts on Col10 expressing CCs to induce Osx expression to transdifferentiate them into bone matrix producing osteoblasts.

***Disclosures: Subburaman Mohan**, None.*

MO0086

Inhibiting calcineurin activity promotes chondrogenic differentiation through induction of Dkk1. Seungwoo Han*[1], Eun-Ju Lee[2], Youn-Kwan Jung[2], Min-su Han[2], Gun-Woo Kim[3], Hye-Ri Park[2], Je-Yong Choi[4]. [1]Daegu Fatima Hospital, South Korea, [2]Laboratory for Arthritis & Bone Biology, Fatima Research Institute, South Korea, [3]Department of Internal Medicine, Daegu Fatima hospital, South Korea, [4]Kyungpook National University, School of Medicine, South Korea

The differentiation of mesenchymal cells into chondrocytes is a multistep process and the precise mechanism is still unclear. In this study, we investigated the role of calcineurin on early chondrogenic differentiation from mesenchymal cells. E11.5 limb bud cells were cultured as high-density 10-μl drops containing 2.5×10^5 cells in chondrogenic media and treated with 100 ng/ml and 1000 ng/ml of FK-506. The inhibition of calcineurin by FK-506 promoted chondrogenesis with increased absorbance of alcian blue staining in dose-dependent manner. Along with alcian blue staining, the m-RNA expression of chondrogenic markers like Sox9, Col2a1 and aggrecan was significantly increased. To investigate the mechanism of FK-506-mediated upregulation of chondrogenesis, Wnt signaling pathways were activated with Wnt3a or Wnt5a (50 ng/ml) together with FK-506. FK-506-mediated chondrogenic differentiation was attenuated by activation of canonical Wnt signaling, but not by non-canonical pathway. With respect to the expression of Wnt pathway components, FK-506 increased Wnt5a, the major ligand of non-canonical Wnt pathway, and Axin2 and Lef1, the major adaptor molecules of canonical Wnt pathway, as well. However, the inhibitory effect in co-treatment experiment suggested that the canonical Wnt pathway may not be involved in FK-506-induced chondrogenic differentiation. Interestingly, FK-506 significantly increased Dkk1, but not Dkk2. When Dkk1 function was blocked by Dkk1-neutralizing antibody in micromass culture, FK-506-mediated upregulation of chondrogenesis was diminished. Collectively, the inhibition of calcineurin/NFAT signaling with FK-506 increases chondrogenic differentiation, which may largely depend on Dkk1 induction resulting in attenuation of canonical Wnt signaling.

***Disclosures: Seungwoo Han**, None.*

MO0087

IRE1α Dissociates with BiP and Inhibits ER Stress-mediated Apoptosis in Cartilage Development. Fengjin Guo*[1], Xiaofeng han[2], yanna Liu[2]. [1]Chongqing Medical University, Peoples Republic of China, [2]Department of Cell Biology & Genetics, Core Facility of Development Biology, Chongqing Medical University, China

BMP2 (bone morphogenetic protein 2) is known to activate unfolded protein response signaling molecules, including XBP1S, BiP and IRE1α. ER (Endoplasmic Reticulum) stress is induced in chondrogenesis and activates IRE1α signal pathway, which is associated with ER stress-mediated apoptosis. However, the influence on IRE1α and BiP in BMP2-induced chondrocyte differentiation have not yet been elucidated, the molecular mechanism remains unexplored.

In this study, we demonstrate that IRE1α interacts with BiP in unstressed cells and dissociates from BiP in the course of cartilage development. Induction of ER stress-responsive proteins (XBP1S, IRE1α, BiP) was also observed in differentiating cells. IRE1α inhibition ER stress- mediated apoptosis lies in the process of chondrocyte differentiation. Furthermore, knockdown of IRE1α expression by way of the RNAi approach accelerates ER stress-mediated apoptosis in chondrocyte differentiation induced by BMP2, as revealed by enhanced expression of Cleaved Caspase3, CHOP and p-JNK; and this IRE1α inhibition effect on ER stress-mediated apoptosis is required for BiP in chondrogenesis.

Collectively, the ER stress sensors were activated during apoptosis in cartilage development, suggesting that selective activation of ER stress signaling was sufficient for induction of apoptosis. These findings reveal a novel critical role of IRE1α in ER stress-mediated apoptosis and the molecular mechanisms involved. These results suggest that activation of p-JNK, Caspase3 and CHOP were detected in developing chondrocytes and that specific ER stress signaling leads to naturally occurring apoptosis during cartilage development.

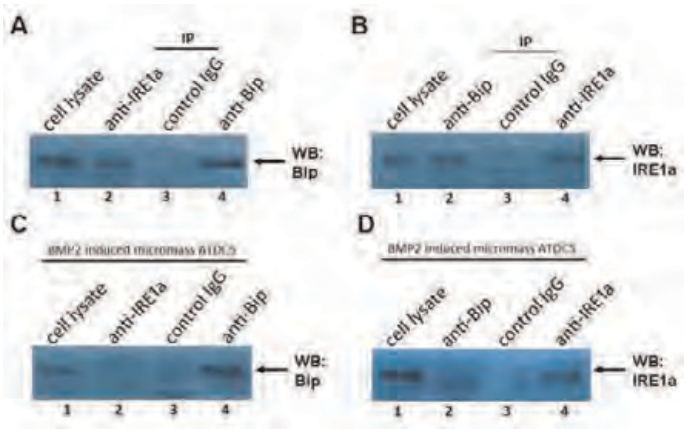

Fig.1. BiP dissociates with IRE1a in chondrogenesis while binds to IRE1a in chondrocyte

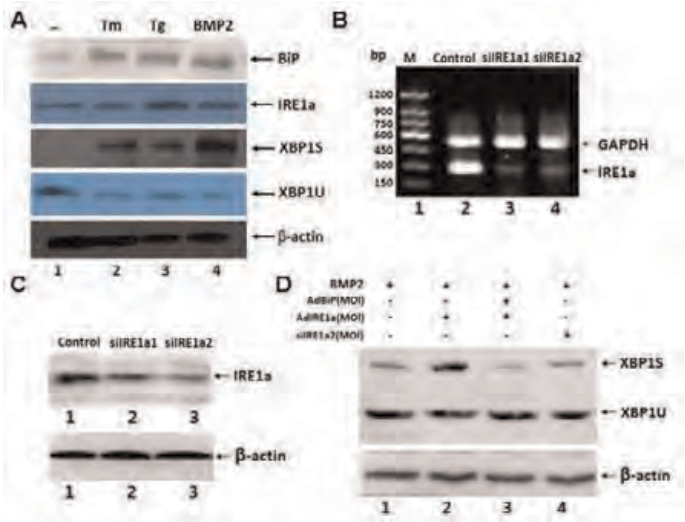

Fig.2. Determination on si-IRE1a inhibits rate and the kinetics of IRE1a influenced by BMP2 and BiP

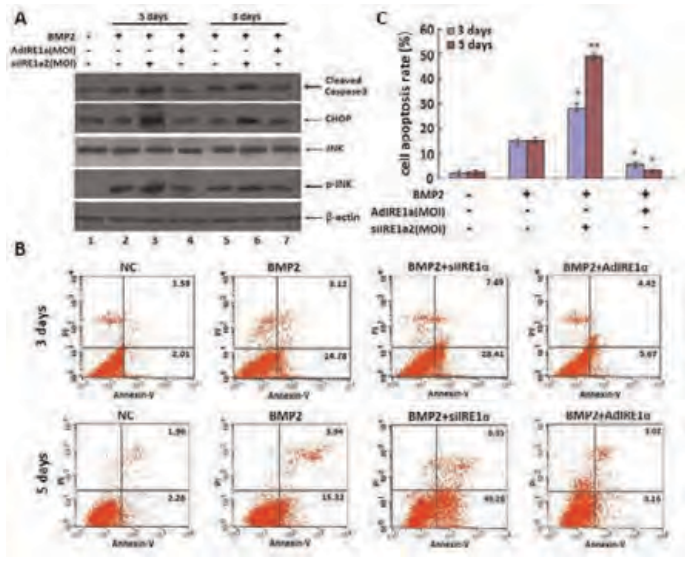

Fig.3 The effects of IRE1a on the expression of ERS associated molecules in ATDC5 induced by BMP2

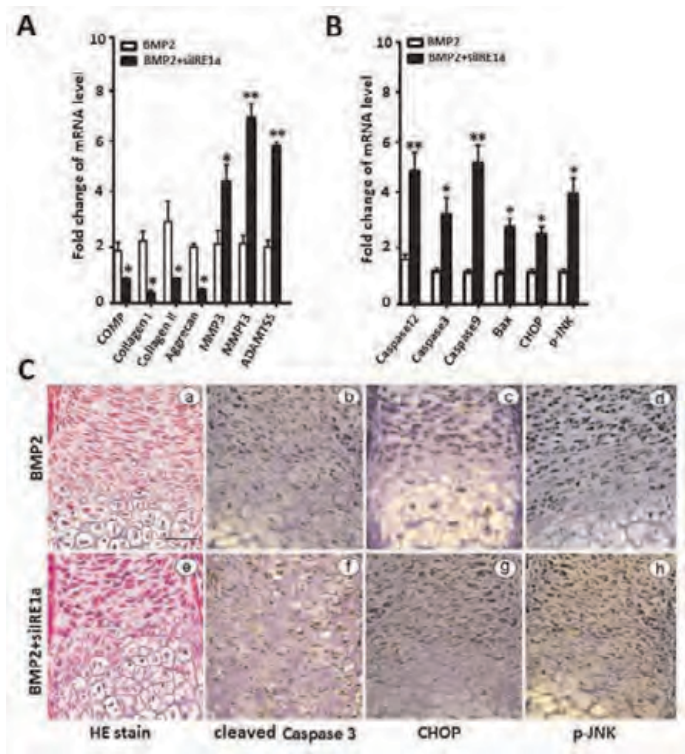

Fig.4 siIRE1a increases ERS-mediated apoptosis molecules and matrix degrading proteases expression

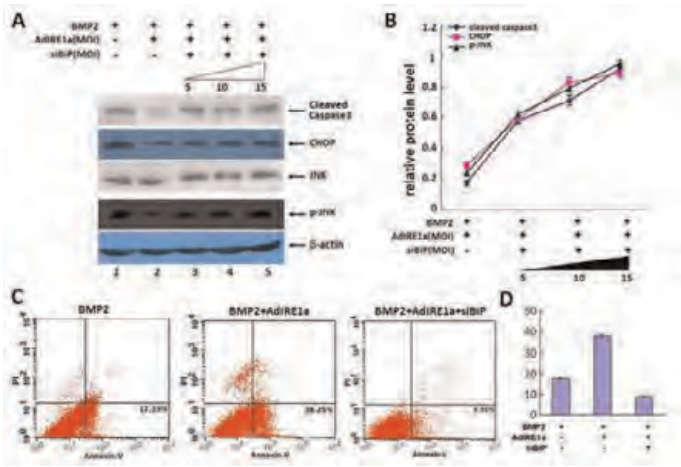

Fig.5 The expression of ERS associated molecules in BMP2-induced ATDC5 influenced by IRE1a and BiP

***Disclosures: Fengjin Guo**, None.*
This study received funding from: NSFC81171697

MO0088

Runx2 is required for early stages of endochondral ossification but delays final stages of bone repair in Axin2-deficient mice. Meghan McGee-Lawrence*[1], Elizabeth Bradley[1], Wei Hsu[2], Jane Lian[3], Andre Van Wijnen[1], Jennifer Westendorf[1]. [1]Mayo Clinic, USA, [2]University of Rochester Medical Center, USA, [3]University of Vermont, USA

Runx2 and Axin2 are key regulators of skeletal development. We recently reported that Runx2 represses Axin2 transcription to promote osteoblast maturation, and double mutant *Runx2*$^{+/-}$*:Axin2*$^{-/-}$ mice do not have the craniosynostosis phenotype associated with *Axin2*-deficiency, indicating that Runx2 is essential for enhanced calvarial bone formation in *Axin2*$^{-/-}$ mice. Primary osteoblasts from double mutant mice resembled WT cultures, intermediate in phenotype between the extreme low and high osteogenic activity of *Runx2*$^{+/-}$ and *Axin2*$^{-/-}$ cells, respectively. Interestingly, more in depth analyses revealed persistent cartilage in the frontal suture of double mutant animals, exacerbating the cleidocranial dysplasia phenotype found in *Runx2*$^{+/-}$ mice. To better understand this phenomenon, we analyzed chondrocyte development in growth plates and primary cells from wildtype (WT), *Runx2*$^{+/-}$, *Axin2*$^{-/-}$, and *Runx2*$^{+/-}$*:Axin2*$^{-/-}$ mice. Despite relatively normal growth plate morphology, chondrocyte maturation was impaired in the double mutant mice, as chondrocytes arrested at intermediate stages of differentiation and failed to produce a calcified matrix in vitro. We then functionally tested the regulation of bone formation by *Axin2* and *Runx2* using endochondral fracture and intramembranous defect repair models. Pin-stabilized, closed femoral fractures (endochondral repair) or single femoral cortex, 0.7 mm diameter defects (intramembranous repair) were created in mice from each genotype. MicroCT, torsional testing, histology, and molecular analyses were used to quantify healing rates and tissue differentiation patterns. Consistent with the in vitro chondrocyte cultures, both *Runx2*$^{+/-}$ and double mutant mice had larger calluses than WT and *Axin2*$^{-/-}$ mice at early stages of endochondral fracture healing, confirming the dominance of Runx2. However, by day 28 after fracture, double mutant animals diverged from the *Runx2*$^{+/-}$ mice, showing smaller callus size and differences in torsional strength indicative of more rapid healing as seen in the *Axin2*$^{-/-}$ mice. The intramembranous repair model confirmed our earlier osteoblastic results, as double mutant mice showed an intermediate bone volume fraction in the mending defect as compared to *Runx2*$^{+/-}$ or *Axin2*$^{-/-}$ mice after 21 days of healing. Taken together, our data suggest a dominant role for Runx2 in chondrocyte maturation, but implicate Axin2 as an important modulator of the terminal stages of endochondral ossification.

***Disclosures: Meghan McGee-Lawrence**, None.*

MO0089

Sclerostin Is Up-regulated In Articular Chondrocytes Exposed To Simulated Microgravity. Liliana Mellor*, Minoti Hiremath, Lindsey Catlin, Travis Baker, Julia Oxford. Boise State University, USA

The skeletal system responds to mechanical changes by remodeling bone tissue, a process orchestrated between osteoblasts and osteoclast activity. During unloading conditions such as the one experienced by astronauts during space missions or prolonged bed rest, osteocytes respond by secreting a protein called sclerostin, which is an inhibitor of the Wnt signaling pathway. Sclerostin has been shown to inhibit bone formation by binding to the LRP5/6 receptors and reducing osteoblast proliferation and differentiation. Clinical trials using a sclerostin antibody have shown promising results in preventing bone loss in unloading conditions. Although bone density loss in space is a growing field of interest, little is know about the possible effects of microgravity on the adjacent articular cartilage. Similar to bone, articular cartilage of the synovial joints are constantly exposed to mechanical forces produced by daily activities here on Earth, and it requires a balance between synthesis and degradation of extracellular matrix components to maintain tissue homeostasis. Our goal is to study the effects of simulated microgravity on articular cartilage using chondrocyte cell lines and articular cartilage explants in a Rotating Wall Vessel (RWV) bioreactor, which models reduced gravity.

Our results show a significant increase in sclerostin expression both at the RNA and protein level. Interestingly, RT-PCR data shows down-regulation of LRP5/6 receptors when sclerostin expression is up-regulated, suggesting that sclerostin may be associated with LRP5/6 turnover. Although cartilage is responding to simulated microgravity in a similar way bone tissue does, little is known about the effects of sclerostin in articular cartilage. A recent study detected sclerostin expression in osteoarthritic cartilage, but believes sclerostin prevents cartilage degradations because it decreases expression of matrix degrading genes such as MMPs and ADAMTSs. This suggests that sclerostin has opposite effects on adjacent bone and articular cartilage tissues, and therapeutic targeting against sclerostin needs to be further investigated.

Our study is the first to detect sclerostin up-regulation in articular cartilage in response to simulated microgravity and to identify Wnt signaling as a potential therapeutic target to prevent cartilage degradation during prolonged bed rest and lack of gravity during spaceflight missions.

***Disclosures: Liliana Mellor**, None.*

MO0090

Skull growth anomalies in *fgfr3*$^{Y367C/+}$ mice explain craniofacial malformation of achondroplasia. Laurence Legeai-Mallet*[1], Martin Biosse Duplan[2], Catherine Benoist-Lasselin[3], Nabil KACI[3], Arnold Munnich[3], Federico Di Rocco[3]. [1]INSERM U781 - Paris Descartes university, Necker hospital, France, [2]Faculté de Chirurgie DentaireUniversité Paris DescartesAP-HP, France, [3]INSERM U781, France

Activating fibroblast growth factor receptor 3 (FGFR3) mutations in humans are responsible for both the most frequent dwarfism, achondroplasia (ACH) and the most frequent syndromic craniosynostosis, Muenke-Lajeunie (MLS) syndrome. This receptor induces cartilage and bone anomalies in endochondral and membranous ossification. The characteristic features of ACH include an enlarged head with a prominent forehead, midface hypoplasia and severe malocclusion while in MLS the patients exhibit a coronal craniosynostosis. In order to understand how FGFR3 affects membranous ossification (vault) and endochondral ossification (skull base) in FGFR3 related diseases, we studied the skull formation of a mouse model expressing an activating FGFR3 mutation (fgfr3Y367C/+). As expected, the analysis of fgfr3Y367C/+ skull mice shows anomalies of the skull characterized by a domed macrocephalic skull associated to severe brain alteration seen with MRI, a stenotic craniovertebral junction seen with µCT, and an inverted bite. We observed in Fgfr3Y367C/+ mice a loss of the clivo-sphenoid synchondrosis where differentiation of the chondrocytes was disrupted, suggesting a defect in endochondral ossification. The size of the foramen magnum in fgfr3Y367C/+ mice was reduced as in ACH and MLS patients. These data show that endochondral ossfication is modified in both ACH and MLS and that fgfr3Y367C/+ mice mimic these defects. We next focused on areas of the skull that are formed by membranous ossification. Studying the calvaria bones of the vault, we observed a decrease in size in frontal bone, an increase size of the interparietal bone and a wide calvaria frontal defect characterized in fgfr3Y367C/+ mice. Abnormal coronal sutures were also present in mutant mice thus suggesting a possible premature fusion of the suture. Interestingly, when the calvaria were separated from the base, we observed a decrease of the calvaria frontal defect and a modification of the sutures.

In conclusion, anomalies of the skull base and vault were observed in fgfr3Y367C/+mice thus indicating that activating FGFR3 mutations affect both endochondral and membranous ossification.

***Disclosures: Laurence Legeai-Mallet**, None.*

MO0091

TGF-β1 inhibits maturation of chondrogenic cell line ATDC5 by impeding canonical hedgehog signaling through direct down-regulation of ciliary component gene Ift88. Makiri Kawasaki*[1], Tetsuya Nakamoto[1], Takuya Notomi[2], Tadayoshi Hayata[3], Yoichi Ezura[4], Masaki Noda[1]. [1]Tokyo Medical & Dental University, Japan, [2]GCOE, Tokyo Medical & Dental University, Japan, [3]Medical Reserach Institute, Tokyo Medical & Dental University, Japan, [4]Tokyo Medical & Dental University, Medical Research Insititute, Japan

Chondrocytes play crucial role in endochondral ossification, and their proliferation and differentiation are tightly regulated by various cytokines such as Indian hedgehog (Ihh). Recent studies have demostrated that Ihh signaling takes place in primary cilium for its signal transduction and thus primary cilium is essential for endochondral ossification. Primary cilia have Intraflagellar transport (IFT) sytem where IFT complex transport proteins bidirectionally between proximal and distal end of cilia. IFT88 is one of the major components of IFT complex and its lack leads

disappearance of primary cilia. It has been reported that conditional knockout mice lacking IFT88 specifically in early limb bud exhibited severe dwarfism and aberrant endochondral ossification accompanied with decreased Ihh signaling.

Preveiously we observed that TGF-β1 dose-dependently decreased Ift88 expression in chondrogenic cell line ATDC5, while TGF-β1 increased type 2 collagen (Col2) expression and decreased type 10 collagen (Col10) expression. To know if TGF-β1 directly down-regulates Ift88 expression, we treated ATDC5 with TGF-β1 in the presence of Cycloheximide (CHX) or D-ribofuranosylbenzimidazole (DRB). The down-regulation of Ift88 expression by TGF-β1 treatment was observed both in the presence of CHX and DRB, suggesting that TGF-β1 directly regulates the transcription and mRNA stability of Ift88. We next treated ATDC5 with TGF-β1 under the attenuated expression level (about 70%) of Ift88 by RNAi and observed that Gli1 expression was enhanced with TGF-β1 treatment under the down-regulation of Ift88 expression. On the other hand, Smoothened Agonist (SAG) treatment markedly down-regulated Gli1 expression when Ift88 was knockdowned in ATDC5 suggesting that Hh signaling through Smoothened is impeded. SAG treatment up-regulated Runx2 expression but its action was ineffective under the attenuated level of Ift88 expression.These data indicate that TGF-β1 inhibits maturation of ATDC5 by suppressing canonical Hh signaling through down-regulation of Ift88 expression.

***Disclosures: Makiri Kawasaki**, None.*

MO0092

Thyroid Hormone Interacts with Alpha$_{2A}$ Adrenergic Receptor to Regulate Longitudinal Bone Growth. Marcos Silva*[1], Manuela Rodrigues[1], Marilia Teixeira[1], Patrícia Brum[2], Cecilia Gouveia[3]. [1]Department of Anatomy, Institute of Biomedical Sciences, University of Sao Paulo, Brazil, [2]School of Physical Education & Sport, University of Sao Paulo, Brazil, [3]University of Sao Paulo, Institute of Biomedical Sciences, Brazil

It is well known that thyroid hormone (TH) regulates bone development and growth. Hypothyroidism (HYPO) causes a generalized delay in endochondral and intramembranous ossification, in addition to important alterations in the epiphyseal growth plates (EGPs), such as reduced thickness, disorganized columns of chondrocytes, and impaired differentiation of hypertrophic chondrocytes, resulting in reduced growth and skeletal abnormalities. On the other hand, hyperthyroidism (HYPER) results in accelerated skeletal maturation, with premature closure of the EGPs and subsequent decrease in the longitudinal bone growth (LBG). There are evidences that TH has direct actions in the EGPs, acting mainly via its nuclear receptors (TRs), however, the mechanisms through which TH regulates the LBG are still poorly understood. We recently found protein expression of α_{2A} and α_{2C} adrenoceptors (α_{2A}AR and α_{2C}AR) in the EGPs of mice, a decrease in the length of long bones in α_{2A}-AR and α_{2C}-AR single knockout mice and that the double inactivation of these receptors (α_{2A}/α_{2C}-AR$^{-/-}$) leads to resistance to the thyrotoxicosis-induced reduction in the LBG in mice. To investigate if TH interacts with the sympathetic nervous system (SNS), via α_{2C}-AR, to control LBG, we evaluated the effect of 30 days of HYPO (induced by methimazole and sodium perchlorate treatment) and HYPER (induced by daily i.p. injections of 20 times the physiological dose of triiodothyronine = 7μg/100 g body weight / day) on the bone growth of 21-day old female wild-type (WT = C57BL/6J) and α_{2C}-AR$^{-/-}$ mice. As expected, both HYPO and HYPER significantly impaired LBG in the femur, tibia, fourth lumbar vertebra (L4), radius and humerus. Surprisingly, the femur, L4 and humerus of α_{2C}-AR$^{-/-}$ mice were resistant to the negative effects of HYPO and HYPER on bone growth. Only a slight negative effect of HYPO was observed in the LBG of the tibia and radius, while HYPER promoted a slight increase in the length of these two bones. Altogether, these findings suggest that TH interacts with the SNS, via a_{2C}-AR, to control LBG.

***Disclosures: Marcos Silva**, None.*

MO0093

Defining Mesenchymal Stem/Stromal Cell Subpopulations With Variable Differentiation and Immunomodulatory Potential. Sally James*, Farinaz Afsari, Jennifer Dyson, James Ashmore, Charlotte Knight, Peter Ashton, Paul Genever. University of York, United Kingdom

Mesenchymal stem/stromal cells (MSCs) can differentiate into bone, cartilage and fat tissues. They have also been shown to have immunomodulatory properties and are prime candidates for cell-based therapy in orthopaedics. However, MSCs lack selective markers and often consist of heterogeneous mixtures of cells that are likely to contain different MSC types of varying potency. To identify functional variance in MSC subpopulations, we isolated >100 clonal MSC lines following immortalisation by human telomerase (hTERT) transduction. From these lines, our interest centred on four clones of hTERT-MSCs (C101, C102, C201 and C202) with different behavioral traits. All lines were positive for typical MSC markers CD29, CD44, CD73, CD90, CD105 and CD166, and CD34/CD45-negative. C101 and C201 were capable of trilineage differentiation and C101 spontaneously differentiated towards osteogenesis with prolonged confluency. C102 and C202 showed no evidence of skeletogenic differentiation. Applying principal component analysis and clustering algorithms to the global gene expression datasets showed grouping of C101 and C201, closest to primary MSCs, whilst C102 and C202 clustered independently. Over 6,000 transcripts were differentially expressed between the four lines and parental MSCs ($P<0.05$, >2-fold) with highly significant differences in gene sets, ontologies and pathways representative of cell-ECM interactions, RTK signalling, adipogenesis and endochondral ossification. Furthermore, C101 and C201 (plus primary MSCs) were enriched in genes representative of typical mesodermal MSCs (PRRX1, PDGFRA, KITLG, GDF5, NGFR) whereas C102/202 were enriched in angiohematopoietic genes (FLT1, KDR, TEK, EDN1, EDN2, VWF, MCAM). Strikingly, immunomodulatory gene sets such as cytokine/inflammatory responses, and interferon/TNF signalling were enriched in the non-differentiating lines. Flow cytometry confirmed >3-fold higher levels of ICAM1 surface expression in C102/C202 versus C101/C201. In samples of primary MSCs, selected only by plastic adherence, we identified a wide range of low to high ICAM1-expressing populations. Finally, expression of nestin, a putative in vivo marker of bone marrow MSCs, was >10-fold higher in C201 compared to the other lines using QPCR. These findings demonstrate the presence of multiple MSC subpopulations in bone marrow, some with typical MSC differentiation ability and others that play a resident immune-regulatory role in bone marrow stroma.

***Disclosures: Sally James**, None.*

MO0094

Epigenetic Regulation of Age-Dependent *Sox9* Expression in Mouse Articular Cartilage. Mingcai Zhang*[1], Qinghua Lu[1], James Bernard[1], Andrew Miller[1], Jinxi Wang[2]. [1]Department of Orthopedic Surgery, University of Kansas Medical Center, USA, [2]University of Kansas Medical Center, USA

Purpose: Transcription factor *Sox9* is essential for the differentiation of mesenchymal progenitor cells into chondrocytes during embryonic development. Mice with cartilage-specific inactivation of *Sox9* at the postnatal stages display a loss of proteoglycans in articular cartilage. However, the collagen II protein persists in articular cartilage, with no histopathological signs of osteoarthritis (OA) even at 18 months of age. It remains unclear why deficiency of *Sox9*, the master regulator of cartilage formation, does not cause OA or loss of collagen II in adult mice. This study aimed to test our hypothesis that *Sox9* expression in articular chondrocytes decreases in adult mice and that the age-dependent expression of *Sox9* is mediated by epigenetic mechanisms.

Methods: Joint tissues were harvest from wild-type BALB/c mice at the age of embryonic day 16.5 (E16.5), postnatal day 1 (1-day), and 2, 6, 12, and 18 months for histology and immunohistochemistry (IHC). Total RNA, genomic DNA, and chromatins obtained from femoral and humeral head cartilage at those ages were used for gene expression assay by qPCR, methylated DNA immunoprecipitation (MeDIP), and chromatin immunoprecipitation (ChIP), respectively.

Results: qPCR revealed that *Sox9* mRNA expression in articular cartilage was highest at E16.5 and 1-day, but significantly declined at 2 months and maintained at a lower level until 18 months (Figure 1). IHC showed a similar age-dependent expression pattern of the *Sox9* protein. Epigenetic studies revealed that DNA methylation levels of the 5 islands in the *Sox9* promoter region were low at the developmental stages, elevated at 6 and 12 months, but not significantly changed at 18 months. ChIP assay showed that histone 3 lysine 4 dimethylation (H3K4me2, an epigenetic code for transcriptional activation) was highest at E16.5 and significantly reduced after 2 months (Figure 2); whereas the histone 3 lysine 9 dimethylation (H3K9me2, an epigenetic code for transcriptional repression) was lowest at E16.5 and significantly increased after 2 months of age.

Conclusion: These results indicate that *Sox9* expression in articular chondrocytes decreases after the completion of skeletal development in mice and that the age-dependent expression of *Sox9* is mediated by epigenetic mechanisms. The data suggest that the demand for *Sox9* expression in adult articular cartilage diminishes with possible changes in the regulatory role of *Sox9* in articular chondrocyte function.

Keywords: Epigenetics, *Sox9*, cartilage

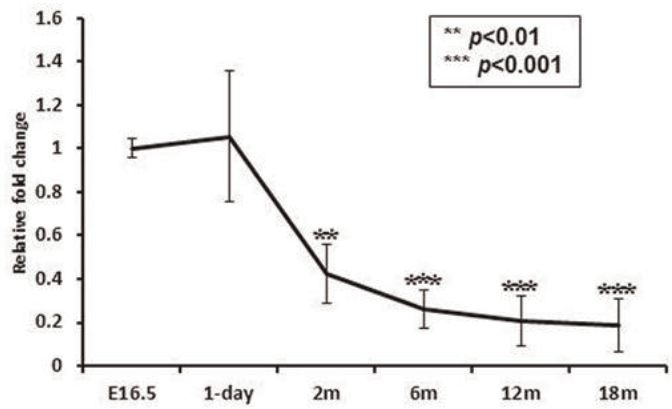

Figure 1. Age-dependent expression of Sox9 mRNA in mouse articular cartilage

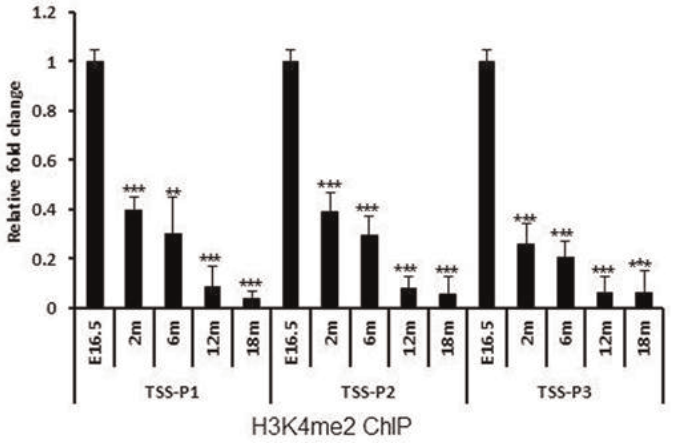

Figure 2. Age-dependent changes of histone methylation in Sox9 promoter region.

***Disclosures: Mingcai Zhang**, None.*

MO0095

Transcriptome Profiling Reveals that Postmenopausal Osteoporosis and Bone Density Correlate with Fat Metabolism but not Adiposity. Sjur Reppe*[1], Ole K. Olstad[2], Simon J. Cockell[3], Paul Sanderson[4], Vigdis T. Gautvik[5], Kaare M. Gautvik[6], Harish Datta[7]. [1]Oslo University Hospital, Ullevaal, Norway, [2]Oslo University Hospital, Norway, [3]Faculty of Medical Sciences, Newcastle University, United Kingdom, [4]The Royal Victoria Infirmary, United Kingdom, [5]Institute of Basic Medical Sciences, University of Oslo, Norway, [6]University of Oslo, Oslo University Hospital, Lovisenberg Deacon Hospital, Norway, [7]Newcastle University, United Kingdom

The negative relationship between adiposity and bone mineral density has been explained in terms of increased rate of mesenchymal stems cells (MSC) differentiation into adipocytes, adversely affecting the osteoblast pool and thereby reducing bone formation capability. Whether marrow adiposity is a cause or consequence of postmenopausal bone loss and ageing, and the underlying molecular mechanisms are unclear. We performed genome-wide gene expression profiling of transiliacal trabecular bone biopsies derived from an unbiased cohort of Caucasian postmenopausal women. The cohort comprised healthy controls, osteoporotics (T-score <-2.5) plus one or more fragility fractures, and a group with intermediate bone mass. The data analysis showed that transcripts associated with fat metabolism were negatively correlated with osteogenic activity (as measured by expression levels of ACSL3, PPARA, FABP3, PHKB, ACADM, ACADSB, LPIN1, PDK4, ABCA1, HADHB, PRKAA2) and areal bone mineral density (aBMD). Furthermore, the transcripts associated with fat metabolism showed higher expression in osteoporotics than controls. However, mRNAs associated with adiposity (PRARG, FAB4, SLC2A4 (GLUT4)) had no correlation with aBMD or elevated expression in an osteoporotic cohort. The importance of metabolic stress playing a critical role in the pathogenesis of postmenopausal osteoporosis was underlined by a strong negative association of BMD of key microRNAs, including miR-378, with an established role in lipid metabolism.

***Disclosures: Sjur Reppe**, None.*

MO0096

Trps1 Regulates Mineralization in a Context-Dependent Fashion. Maria Kuzynski[1], Callie Mobley[2], Tony Winters[2], Manisha Yadav[3], Anne Poliard[4], Odile M.C. Kellerman[5], Jose Luis Millan[6], Dobrawa Napierala*[7]. [1]University of Alabama at Birmingham, USA, [2]Institute of Oral Health Research, Department of Oral & Maxillofacial Surgery, School of Dentistry, University of Alabama at Birmingham, Birmingham, AL, USA, [3]Burnham Institute for Medical Research, USA, [4]Faculté de Chirurgie Dentaire, et UMR-S 747, Université Paris Descartes, France, [5]UMR-S 747 INSERM, France, [6]Sanford-Burnham Medical Research Institute, USA, [7]University of Alabama At Birmingham School of Dentistry, USA

Trps1 is a transcriptional repressor that belongs to the GATA family of transcription factors. A number of *in vitro* and *in vivo* studies demonstrate the involvement of Trps1 in the development of skeletal and dental tissues as well as the mineralization process. The importance of *TRPS1* in tooth formation and mineralization is underscored clinically by dental and skeletal manifestations in two distinctive human disorders caused by different mutations of *TRPS1*: tricho-rhino-phalangeal syndrome (TRPS) and Ambras syndrome. In our previous studies of a mouse model of TRPS ($Trps1^{\Delta GT}$ mice), we uncovered that *Trps1* deficiency leads to premature mineralization of the perichondrium. In turn, overexpression of *Trps1* from the 2.3kb fragment of *Col1a1* promoter results in severe impairment of dentin formation. Interestingly, both $Trps1^{+/\Delta GT}$ and *Col1a1-Trps1* mice present with age-related osteopenia, suggesting that the role of *Trps1* in mineralizing tissues is context-dependent. To understand the molecular consequences of Trps1 deficiency and upregulation in the development and function of cells producing mineralized matrix, we used the 17IIA11 cell line as a cellular model of mineralization. We generated *Trps1*-deficient and *Trps1*-overexpressing cell lines and analyzed their mineralization and expression of osteogenic genes prior to and during the mineralization process. We performed a series of analyses including alizarin red staining and quantification, tissue non-specific alkaline phosphatase activity, qRT-PCR, and western blot analysis. We discovered that downregulation of *Trps1* results in loss of mineralization potential associated with decreased expression of genes critical for the initiation of mineralization. In contrast, upregulation of *Trps1* results in delayed mineralization as well as reduced expression of phosphate homeostasis genes during the propagation phase of mineralization. Based on these data we have concluded that *Trps1* is required for the maturation of cells destined to produce mineralizing matrix and therefore *Trps1* supports the initiation of mineralization. However, in mineralized-matrix producing cells, *Trps1* represses the extent of extracellular matrix mineralization, thus acting as a repressor of mineralization in mature cells.

***Disclosures: Dobrawa Napierala**, None.*

MO0097

***Sostdc1*, a paralog of *Sost*, is Involved in Bone Maintenance and Fracture Repair.** Nicole Collette*[1], Cristal Yee[2], Salustra Urbin[1], Liqin Xie[3], Aris Economides[4], Gabriela Loots[5]. [1]Lawrence Livermore National Laboratory, USA, [2]University of California, Merced, USA, [3]Regeneron Pharmaceutical company, USA, [4]Regeneron Pharmaceuticals, Inc., USA, [5]Lawrence Livermore National Laboratory, UC Merced, USA

Sostdc1 (Sclerostin domain-containing-1, Sost-Like, Wise, Ectodin, USAG-1) is a paralog of Sclerostin (Sost) that modulates both BMP and WNT signaling. Previously it has been shown that loss of *Sostdc1* causes tooth defects, resistance to kidney disease, and abnormal hair follicles. It is expressed in the developing limb, and we have previously shown that *Sost; Sostdc1* double knockouts display preaxial polydactyly through SHH misregulation and ectopic activation of Sox9 in the digit 1 field. Sostdc1 binds to BMP4 and -7 to antagonize BMP signaling, and to LRP4 and -6 WNT co-receptors to modulate WNT signaling, acting as a WNT activator or antagonist in a context-dependent manner. Recently, a genome-wide linkage analysis identified a quantitative trait locus for femoral neck bone mineral density (BMD) on chromosome 7p21.1. Subsequently, strong association was found between SNPs in *Sostdc1* intron and BMD in Chinese women, suggesting that Sostdc1 may participate in skeletal development or maintenance. Unlike *Sost*, *Sostdc1* is not expressed in osteocytes, trabecular osteoblasts, or osteoclasts; however *Sostdc1* expression is high in the periosteum, vasculature, and connective tissues. Because the periosteum is rich in osteoblasts and osteoprogenitor cells that build and repair bone, we examined whether $Sostdc1^{-/-}$ mice have altered bone mass or fracture repair. Micro-CT analysis revealed that $Sostdc1^{-/-}$ mice have a higher total bone volume (TV) in the femoral cortex ($p<0.01$), distal femur, proximal tibia, and lumbar vertebra ($p<0.005$) compared to C57Bl/6 controls (*WT*). We also found significantly increased BMD in long bones ($p\leq0.05$). In the femoral mid-shaft cortex, the pMOI and BMD was increased ($p<0.05$) suggesting increased biomechanical strength. Despite these improved bone qualities, $Sostdc1^{-/-}$ show a defect in fracture repair, with 1/3 of fractures failing to form unions by 28 days post-injury in a closed Einhorn model, compared to the 100% union rate for control mice. During early fracture repair, *Sostdc1* expression shows a dynamic pattern: in periosteum and surrounding soft tissues (muscle/vasculature) the pool of *Sostdc1* positive cells rapidly expands and migrates into the callus at 3-days post fracture, but the expression diminishes as healing progresses. By 14-days post fracture *Sostdc1* positive cells are no longer visible in the callus. These data suggest that Sostdc1 plays a role in bone maintenance and repair.

This study received funding from NIH DK075730 and LLNL LDRD ER (11-ERD-060). This work was conducted under the auspices of the USDOE by LLNL (DE-AC52-07NA27344) LLNL-ABS-633635.

***Disclosures: Nicole Collette**, None.*

MO0098

Application of Silver Nanoparticle-based Materials in Orthopedic Surgery. Zhong Zheng*[1], Ching-Yun Hsu[1], Yulong Zhang[1], Omar Velasco[1], Kevin S. Lee[1], Todd Rackohn[1], Ching Shen[1], Thua Thang Ngo[1], Benjamin Wu[1], Xinli Zhang[2], Kang Ting[2], Chia B Soo[1]. [1]UCLA, USA, [2]University of California, Los Angeles, USA

Purpose: Infection of surgically-implanted materials accounts for nearly 1 million cases of nosocomial infections in the U.S. per year, which exhaust healthcare resources and create an enormous economic burden. This project focuses on engineering multifunctional silver nanoparticle (Ag^{NANO})-based orthopedic devices with sustained antimicrobial and osteoinductive activities. Methods: Ag^{NANO}-based porous PLGA graft was used to induce bone regeneration in a well-documented

grossly contaminated rat femoral segmental defect (FSD) model. Ag^{NANO}/PLGA-coating was used to prevent biofilm formation on orthopedic devices and subsequent implant-related infection. Gram-positive vancomycin-resistant, methicillin-intermediate *Staphylococcus aureus* Mu50 and Gram-negative opportunistic pathogen *Pseudomonas aeruginosa* PAO1 were used as infectious agents. Antimicrobial activity was assessed by bacterial colonization evaluation, microplate proliferation assay, and Taylor-modified Brown and Brenn Gram staining. MC3T3-E1 pre-osteoblasts were used to determine cytotoxicity and osteoinductivity of these Ag^{NANO}-based materials *in vitro*. *In vivo* bone formation was evaluated by radiography, 3D micro-computed tomography, and histological and immunohistological staining. Results: Ag^{NANO}-based materials exhibited strong antibacterial properties *in vitro* and *in vivo* without significant cytotoxicity against osteoblasts. A 6-mm critical-sized FSD (total volume ~ 75 ml) infected with 10^8 CFU bacteria (~10^9 CFU/ml bacteria, which far exceeds the typical 10^5 CFU/ml criteria for invasive tissue infection) and implanted with BMP2-coupled Ag^{NANO}/PLGA graft healed in 8 weeks without evidence of residual bacteria, while the control implanted with non-Ag^{NANO}-containing graft failed to result in new bone formation due to the presence of continued bacterial infection. Additionally, Ag^{NANO}/PLGA-coated stainless steel alloy exhibited strong osteoinductive and antibacterial properties and resulted in bone formation around the alloy without bacterial survival *in vivo*. Moreover, Ag^{NANO}/PLGA-coated titanium also presented antimicrobial properties. Conclusions: Our results indicate that Ag^{NANO} of defined particle size is bactericidal without discernible osteoblast toxicity or negative effects on BMP2 osteoinductivity, making it an ideal antimicrobial and osteoinductive agent for bone regeneration in infected wounds. In addition, Ag^{NANO}/PLGA can be used for coating implants to prevent secondary infection.

***Disclosures: Zhong Zheng**, None.*

MO0099

Atorvastatin Increases Biomechanical Strength of Repaired Rotator Cuff Tendon Via a Cyclooxygenase-2 Dependent Mechanism. Oleg Dolkart*[1], Ofir Chechik[2], Tamar Liron[3], Dalia Somjen[2], Tamar Brosh[4], Yankel Gabet[5], Eran Maman[2]. [1]Orthopedic Surgery Division, Tel-Aviv Medical Center & Bone resarch lab. the Sackler Faculty of Medicine, Tel-Aviv University, Tel-Aviv, Israel, [2]Orthopedic Surgery Division, Tel-Aviv Medical Center & the Sackler Faculty of Medicine, Tel-Aviv University, Tel-Aviv, Israel, [3]Bone research laboratory, Department of Anatomy & Anthropology, Sackler Faculty of Medicine, Tel-Aviv University, Tel-Aviv, Israel, [4]Biomechanics Laboratory, School of Dental Medicine, Tel-Aviv University, Tel-Aviv, Israel, [5]Sackler School of Medicine, Tel Aviv University, Israel

Statins are lipid-lowering drugs with many pleiotropic effects, part of which are associated with the stimulation of cyclooxygenase (COX)-2.COX-2 inhibitors of are commonly prescribed in orthopedic patients. Here we investigated whether post-operative Atorvastatin (ATV) administration improves tendon healing by stimulating COX-2 and whether COX-2 inhibitors have a detrimental effect.

Following experimental rotator cuff (RC) tear and suturing, 48 Wistar rats were randomly allocated into four groups: ATV 20 mg/kg, celecoxib (CEL, COX-2 inhibitor) 20 mg/kg, ATV+CEL or saline alone (S). Animals were sacrificed after 3 weeks and evaluated biomechanically by tension testing. Primary tenocytes were obtained from the supraspinatus tendon under sterile conditions. Cells cultures were treated with therapeutic dosage of ATV, CEL, ATV+CEL or prostaglandin E2 (PGE-2). Cell migration (wound healing assay) and proliferation (thymidin incorporation) were evaluated. Expression of the PGE-2 receptors (EP) was determined by qRT-PCR.

Significantly higher maximal load and stiffness were demonstrated in the ATV group as compared to S (+35% and +74%, respectively; $p<.001$) and CEL group (+34% and +50%, respectively; $p<.005$). Importantly, CEL alone did not affect tendon healing ($p=.88$). Tenocytes treated with ATV demonstrated significantly higher proliferation and migration rates whereas CEL alone had no effect. In line with the in vivo biomechanical results, the mitogenic effect of ATV on tenocytes was abrogated by CEL. However, PGE-2 treatment stimulated tenocyte proliferation even in the presence of CEL. Among the four PGE-2 receptors, tenocytes mainly expressed EP-4, suggesting that this receptor mediates PGE-2 signaling in tenocytes.

These results indicate that statin administration enhances tendon repair in vivo while COX-2 inhibitors have an opposing effect. The statin-induced biomechanical strengthening of the repaired tendon is likely due to the stimulation of tenocyte proliferation and migration via increased COX-2 activity and auto/paracrine PGE-2 signaling. Although chronic inflammation contributes to the development of tendinopathy, our results advocate for a positive role of PGE-2 in tendon healing during the acute inflammatory phase that follows tendon surgical repair. We therefore conclude that the use of post-operative COX-2 inhibitors should be carefully considered while statin administration may improve tendon healing.

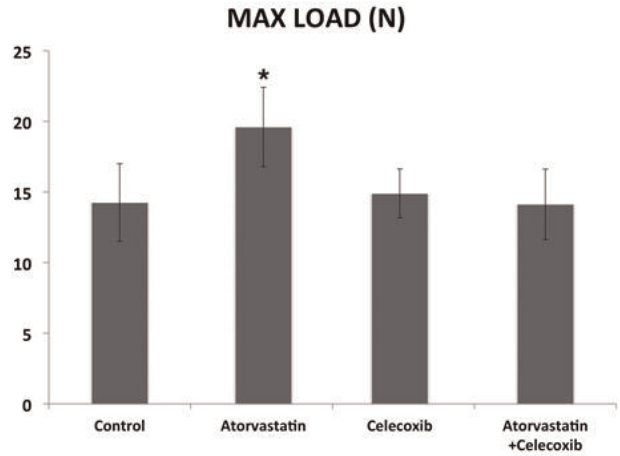

Biomechanical testing of rotator cuff, 3 weeks post-surgery showed that Atorvastatin stimulation of tendon repair is blocked by Celecoxib. *, vs. control (saline), p<.005.

Biomechanical testing results

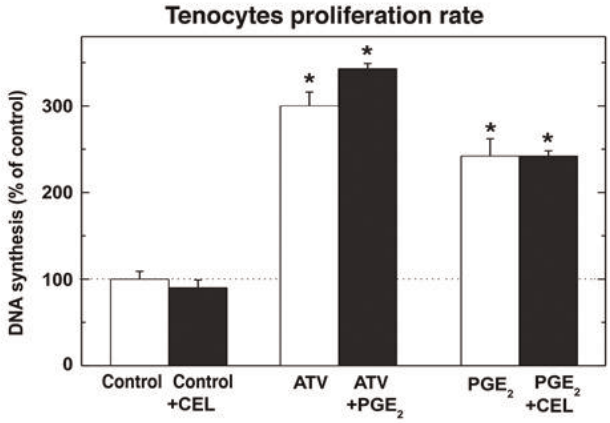

Tenocytes proliferation rate following saline (C), atorvastatin (ATV), celecoxib (CEL) and/or PGE-2 administration. ATV significantly increased tenocyte proliferation rate. This effect was abrogated by CEL addition and was reinstated by PGE-2 treatment even in the presence of CEL. *, vs. control (saline), p<.005.

Tenocyte proliferation results

***Disclosures: Oleg Dolkart**, None.*

MO0100

Epigenetic Transcriptional Silencing of ZIC1 in Human Trabecular Bone Is Associated with Promoter Hypermethylation. Harish Datta*[1], Marianne Kringen[2], Ole K Olstad[2], Sjur Reppe[3], Vigdis T Gautvik[4], Paul Sanderson[5], Kaare M Gautvik[6]. [1]Newcastle University, United Kingdom, [2]Oslo University Hospital, Norway, [3]Oslo University Hospital, Ullevaal, Norway, [4]Institute of Basic Medical Sciences, University of Oslo, Norway, [5]The Royal Victoria Infirmary, United Kingdom, [6]University of Oslo, Oslo University Hospital, Lovisenberg Deacon Hospital, Norway

The zinc finger protein of cerebellum 1 (ZIC1), a neural developmental transcription factor, has a demonstrated role in shear flow mechanotransduction in osteocytes. A transcriptome analysis that compared gene expression in human bone biopsy samples taken from lumbar spine and iliac crest analysis revealed that Zic1 was among the most up-regulated genes in the lumbar spine in comparison with the iliac crest. To determine whether ZIC1 is silenced by promoter hypermethylation, we compared the expression of ZIC1 mRNA in iliac crest (IC) (n=7) and the lumbar spinal vertebrae (LS) (n=25) using Affymetrix expression analysis and validation by qRT-PCR. The methylation pattern of twenty CpG sites in the ZIC1 promoter was measured using pyrosequencing with bisulfite treated genomic DNA as template. To investigate the relationship between ZIC1 expression and promoter hypermethylation, we correlated ZIC1 mRNA expression and degree of CpG site methylation in LS and

IC, respectively. The ZIC1 expression was found to be 47-fold higher in the L5 than IC (P=2.90E-09). The most intensely methylated CpG site had a 55% higher degree of methylation in IC than in the LS (49.2 vs 31.8; p<0.001). All but one of the twenty CpG methylation sites in the ZIC1 promoter region showed strong significant negative correlation between the extent of methylation and ZIC1 expression (Pearson r = -0.43 to -0.79, p= 2.4E-06 to 3.0E-02)). The hypomethylated bone sites, apart from having higher ZIC1 expression, had higher overall bone turnover as reflected by an increased expression of respective genes characteristically associated with osteoblast (Col1a1, BGLAP, SPP1, SPARC, IBSP), osteoclast (CTSK, ACP5) and osteocyte (SOST, DMP1, FGF23). Whilst our findings cannot exclude possible involvement of other mechanisms in silencing of ZIC1, they do however suggest that in human bone promoter CpG methylation is the predominant mechanism for ZIC1 down-regulation at low turnover skeletal sites.

***Disclosures: Harish Datta**, None.*

MO0101

FOXO1 Deletion in Dendritic Cells Leads to Bacteria Induced Osteoclastogenesis and Periodontitis. Wenmei Xiao*[1], Sandra Pacios[1], Maher Alnammary[1], Dana Graves[2]. [1]University of Pennsylvania Dental School, USA, [2]University of Pennsylvania, School of Dental Medicine, USA

Introduction: The host response plays both a protective and destructive role in periodontitis, the most common osteolytic disease in humans. The goal of this study was to establish the contribution of DC to activating a protective lymphocyte response in periodontal disease by limiting DC activation by deletion of the transcription factor FOXO1.

Materials and Method: Conditional deletion of FOXO1 was achieved by breeding FOXO1L/L mice with mice that expressed Cre recombinase under control of CD11c to generate experimental (CD11c.Cre+.FOXOL/L) and the control littermates (CD11c.Cre−.FOXO1L/L). Periodontitis was induced by inoculation of P. gingivalis and F.nucleatum. Mice were euthanized 6 weeks later the periodontium including molar teeth were examined by histomorphometric analysis and three color immunofluorescence and the gingiva adjacent to boneby real-time PCR.

Results: The number of dendritic cells the migrated to the periodontal tissue was ~40% lower in the CD11c.Cre+.FOXOL/Lgroup compared to littermates that did not have FOXO1 deleted (P<0.05).The activation of DC measured by DC produced IL-12 determined by immunofluorescence was reduced by more than 50% by FOXO1 deletion in the experimental mice. CD11c.Cre+.FOXOL/Lmice with FOXO1 deletedin DC had 20-30% more bone loss than the corresponding CD11c.Cre-.FOXOL/Lmice (P<0.05). In addition the experimental micehad 36% increase in osteoclasts and 55% more eroded bone surface (P<0.05). Greater bone loss in the experimental mice was accompanied by 2 fold higher levels of IL-1β and IL-17 (P<0.05).

Conclusion: This study demonstrates that FOXO1 expression in DC is required to generate a protective response to bacteria induced periodontitis. In the absence of FOXO1 there was reduced migration of DC to periodontal tissues and decreased DC activation. This caused an increase in expression of IL-17 and IL-1β along with increased osteoclastogenesis, eroded bone surface and bone loss.

***Disclosures: Wenmei Xiao**, None.*

MO0102

Glycated Osteocalcin. Grazyna Sroga*, Deepak Vashishth. Rensselaer Polytechnic Institute, USA

Non-enzymatic glycatio is a spontaneous biochemical reaction occuring *in vivo* and *in vitro* between reducing sugars and proteins that leads to the formation of crosslinks known as advanced glycation end products (AGEs) [1]. Typically, sugars attach to the functional groups of such amino acids as arginine, lysine, valine and cysteine. Accumulation of AGEs is most pronounced in long-lived proteins such as bone-matrix collagen. In addition to collagen, several non-collagenous bone matrix proteins play an important role in mechanical properties of bone [2, 3]. Osteocalcin (OC) is the second major component of bone matrix accounting for 10-20% of noncollagenous proteins and 2% of total bone proteins. As a matrix protein, OC deposited in the skeleton is only replaced with newly synthesized material during bone remodeling. Among 49 amino acids that compose human OC, there are four arginines and five tyrosines that can undergo glycation. Thus, similarly to collagen, OC in bone could become post-translationally glycated to a variable extent depending upon the age and the local glucose concentration. In the present study, we have quantified the extent of glycation in human OC that was modified *in vitro* using glucose. The extent of OC glycation was measured using the total fluorescent AGE assay as well as ultrahigh liquid pressure chromatography (UPLC) [4].

We established that similarly to other long-lived proteins, OC undergoes glycation, which leads to the production of different AGEs. Interestingly, analysis of acidic hydrolysates of OC using UPLC revealed the presence of pentosidine, a clinically relevant AGE [2], and it has not yet been shown that PEN can form as one of the AGE modifications of OC.

[1] Knott & Bailey, *Bone*, 1998
[2] Sroga & Vashishth, *Curr Osteop Rep*, 2012
[3] Poundarik et al., *PNAS USA*, 2012
[4] Sroga & Vashishth, *J Chromatogr B*, 2011
Funding source: NIH/NIA AR049635

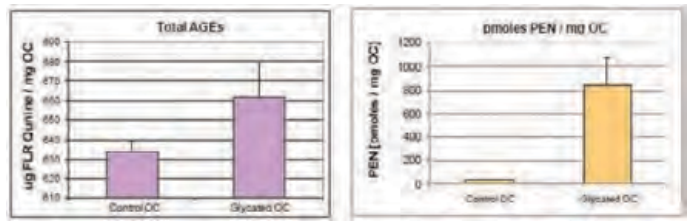

Figure

***Disclosures: Grazyna Sroga**, None.*

MO0103

Heterozygous Inactivation of Gnas Induces Heterotopic Ossification and Impairs Normal Skeletal Development. Girish Ramaswamy*[1], Deyu Zhang[1], Frederick Kaplan[2], Robert Pignolo[1], Eileen Shore[1]. [1]University of Pennsylvania, USA, [2]University of Pennsylvania Hospital, USA

Progressive osseous heteroplasia (POH), Albright hereditary osteodystrophy (AHO), osteoma cutis (OC), and pseudohypoparathyroidism 1a/1c (PHP) form a spectrum of disorders that are caused by heterozygous inactivating mutations in *GNAS*, a gene that encodes multiple transcripts including the α-subunit of the stimulatory G-protein ($G_s\alpha$) of adenylyl cyclase. All these disorders exhibit subcutaneous heterotopic ossification (HO); however, POH is the most severe form and is characterized by HO progression into deeper connective tissues including muscle and fascia. The *GNAS* gene shows genomic imprinting and POH is associated with paternal inheritance of the mutation. Mice with paternal inheritance of heterozygous deletion of exon 1 (Gnas $Ex1^{+/-}$) have lower body weight and length, and develop subcutaneous ossifications with age. But whether reduced Gnas expression leads to alterations in the formation or quality of skeletal bone remains undetermined. To investigate the effects of Gnas mutation on skeletal development, we performed μCT and histological analyses to examine the effects of paternal allele inactivation of Gnas on developing bone and cartilage. At postnatal days 1 (P1) and 14 (P14), $Ex1^{+/-}$ mice weighed significantly less than wild-type (wt) littermates. Tibiae from $Ex1^{+/-}$ mice at these ages were significantly shorter in length (15% ± 4). Trabecular bone parameters, analyzed through μCT scans of the distal epiphyseal region in P14 mice, revealed dramatic reductions in bone volume (36% ± 11) and bone volume fraction (20%±12). Microarchitecture of trabeculae was altered with a significant decrease in trabecular thickness and a concomitant increase in the structure model index, suggesting that trabecular bone is more rod-like in these mutants than wt littermates. μCT analyses of the femoral mid-diaphysis region showed reduced cortical thickness (20%±10) and cortical bone volume (35%±8) in P14 mutants. Histology of hindlimb sections from P14 mice showed a marked decrease in the length of the hypertrophic zone of the growth plates of $Ex1^{+/-}$ mice. The calvaria of P1 and P14 heterozygous mutants were reduced in size in both antero-posterior and medial-lateral dimensions. Taken together with our previous findings, heterozygous paternal allele inactivation of Gnas not only alters post-natal progenitor cells to form heterotopic ossification, but also adversely affects normal skeletal development that impacts both endochondral and intramembranous bone formation.

***Disclosures: Girish Ramaswamy**, None.*

MO0104

The mineral dissolution function of osteoclasts is dispensable for hypertrophic cartilage resorption during the development and growth of long bones. Heiani Touaitahuata*, Gaelle Cres, Virginie Vives, Anne Blangy. CNRS CRBM Montpellier University, France

During long bone growth, the initial cartilaginous model of the skeleton is progressively replaced by bone to allow long bone development and growth. This process is known as endochodral ossification. It involves in particular the resorption of the mineralized cartilage produced by hypertrophic chondrocytes and its replacement by bone. This results in the formation of trabecular bone. Trabecular bone is then remodeled throughout life by alternation of bone resorption and bone formation cycles. Osteoclasts are multinucleated macrophages specialized for mineralized tissue degradation with the combined ability to solubilize hydroxyapatite and to degrade extracellular matrix proteins. We reported previously that osteoclasts lacking Dock5, an activator of the GTPase Rac, are defective for bone resorption due to abnormal podosome organization and absence of sealing zone formation (Vives et al., JBMR. 2011, 26(5):1099-110). As a consequence, $Dock5^{-/-}$ adult mice have increased bone mass. We used $Dock5^{-/-}$ mice to further investigate the implication of osteoclasts resorption function during endochondral bone formation. In $Dock5^{-/-}$ mouse bones, we found normal expression of MMP9 and MMP13 metalloproteases, which are necessary for hypertrophic cartilage formation and resorption. $Dock5^{-/-}$ osteoclasts secrete normal amounts of MMP9, TRAP and CtsK but they are unable to solubilize minerals. Cartilage and primary spongiosa are unaffected in $Dock5^{-/-}$ mouse bones. Conversely, starting from P7 and remaining until adulthood, the secondary spongiosa in $Dock5^{-/-}$ mice showed increased BV/TV as compared to $Dock5^{+/+}$ animals, with normal trabecular numbers but increased trabecular thickness and

reduced trabecular separation. These observations reveal that contrarily to bone resorption, the sealing zone and the ability of osteoclasts to dissolve minerals is dispensable for the removal of hypertrophic mineralized cartilage and the building of the trabecular network geometry during endochondral bone formation.

***Disclosures: Heiani Touaitahuata**, None.*

MO0105

Zfp521 in conjunction with the NuRD complex and Tgm3 regulates mesenchymal stem cell lineage determination and induced pluripotency. Harikiran Nistala*[1], Ken-ichi Takeyama[2], Hsu-Hsin Chen[1], Bernard Boback[2], Francesca Gori[3], Roland Baron[4]. [1]Harvard University, USA, [2]Harvard School of Dental Medicine, USA, [3]Harvard School of Dental Medicine, Massachusetts General Hospital, USA, [4]Harvard School of Medicine & of Dental Medicine, USA

A portfolio of cell fate choices along with the ability for self-renewal is the hallmark of pluripotency in stem cells. Regulatory programs involving master transcription factors and epigenetic regulators mediating chromatin remodeling have been identified in the maintenance of pluripotency. How interactions between transcription factors and chromatin remodeling proteins maintain pluripotency and regulate differentiation remains unclear.

Zinc finger protein 521 (Zfp521) has been implicated in lineage determination of mouse ES cells and in the maintenance of precursor cells within the neuronal, mesenchymal and hematopoietic lineages. Zfp521 regulates chondrocyte and osteoblast maturation and represses adipocyte lineage determination (Hesse et al., 2010;Kang et al., 2013;Kiviranta et al., 2013). In a separate study, proteomic analyses revealed Zfp521 to be part of NuRD complex in a novel configuration that includes nuclear transglutaminases (Tgm1 and 3) in HEK293 cells. The NuRD complex has a dual role, silencing differentiation genes in pluripotent states, as well as pluripotency genes during differentiation, whereas nuclear transglutaminases induce a post-translational modification involving a ε-(γ-glutamyl) lysine cross-link between core histones.

In this study, we validated endogenous interactions between Zfp521, Tgm3 and NuRD components within H3 enriched nuclear fraction in MEFs. These findings led us to hypothesize that Zfp521 along with Tgm3 and NuRD forms an effector complex (Zfp521-Tgm3-NuRD) that regulates transcriptional programs leading to cell-lineage determination. To test this hypothesis in germ layer specification and induced pluripotency we used teratoma formation and the somatic cell reprogramming assay, respectively. Immunocytochemical and gene expression profiling of the explanted teratomas established the inhibitory role of Zfp521 and Tgm3 in mesoderm specification. Despite an increase in $Desmin^+$ mesodermal precursors, loss of Zfp521 or Tgm3 led to impaired osteo-chrondro commitment and increased adipogenesis. In addition, loss of Zfp521 or Tgm3 significantly impaired formation of iPS cells, as evidenced by reduced $SSEA1^+$ or AP^+ colonies. These results underscore the requirement of both Zfp521 and Tgm3 in the maintenance of induced pluripotency. Taken together these results further demonstrate the regulatory role of Zfp521, now in conjunction with NuRD and Tgm3, in mesenchymal cell-fate determination and maintenance of pluripotency.

***Disclosures: Harikiran Nistala**, None.*

MO0106

Development of a WISP2/CCN5-specific immunoassay. Alexander Noll[1], Katrin Schlegelmilch[2], Susanne Duncker*[1], F. Armbruster[1], Norbert Schuetze[3]. [1]Immundiagnostik AG, Germany, [2]Universität Würzburg, Germany, [3]University of Wuerzburg, Orthopedic Center for Musculoskeletal Research, Germany

Introduction: WISP2 (Wnt-inducible signaling pathway protein-2)/CCN5 is a member of the CCN family of matricellular proteins that modify signaling of other molecules, in particular those associated with the extracellular matrix. WISP2/CCN5 is expressed in human bone, muscle, skin, and in the synovium of rheumatoid arthritis patients. Furthermore, WISP2 is differentially regulated during tumor progression. The aim of this study was to develop an immunoassay for the quantification of mature full length WISP2/CCN5 protein in biological fluids.

Material and Methods: Recombinant human WISP2/CCN5-flag protein was expressed in HEK293-EBNA cells and purified from cell culture supernatant by affinity chromatography. The purified protein was used to generate polyclonal antibodies against WISP2/CCN5 in rabbits. A sandwich ELISA for the quantitative detection of WISP2/CCN5 was established and validated. WISP2/CCN5 was measured in serum samples of 192 healthy persons, ages 0-70 years, in order to establish a reference range.

Results: Immunization of rabbits resulted in the generation of a specific antiserum against WISP2/CCN5, with no cross reactivity to related proteins albumin (0.78%), CYR61 (0.01%), CTGF (1.9%), NOV (0.16%), WISP1 (0.01%), and WISP3 (3.2%). The limit of blank was determined to be 0.993 ng/ml. The mean coefficient of variation was < 8 % for intraassay and <9 % for interassay variance. In a healthy population WISP2/CCN5 serum levels increased with age, and there was no significant difference between males and females of each age group. Using this ELISA, it was also possible to determine WISP2/CCN5 in other sample matrices such as EDTA, heparin, and citrate plasma as well as in synovial fluid.

Discussion: We have established a specific and sensitive immunoassay for the detection of WISP2/CCN5 in biological fluids. This ELISA could serve well in future investigations on the function of WISP2/CCN5 in normal and pathological states, maybe even for diagnostics or therapeutic monitoring of arthritic diseases.

***Disclosures: Susanne Duncker**, Immundiagnostik AG, 3*
This study received funding from: Immundiagnostik AG

MO0107

Fibrillin-1 is an extracellular component of the Bone Marrow Stem Cell niche. Francesco Ramirez, Silvia Smaldone*. Icahn School of Medicine at Mount Sinia, USA

Fibrillin-1 is a structural component of the bone matrix that also regulates osteoblastogenesis by calibrating the bioavailability of TGFβ and BMP molecules. Mice under-expressing fibrillin-1 ($Fbn1^{mgR/mgR}$ mice) display reduced bone mass (osteopenia) associated with accelerated osteoblast maturation, greater osteoblast-dependent osteoclast activity, and abnormally high TGFβ and BMP signaling. As $Fbn1^{mgR/mgR}$ mice die from ruptured aneurysm at ~3 month of age, osteopenia progression was studied in mice with conditional inactivation of the Fbn1 in the developing limbs ($Fbn1^{Prx-/-}$ mice). Examination of $Fbn1^{Prx-/-}$ femurs by micro-computed tomography (μCT) documented a relatively greater bone loss between 3 and 6 months of age than between 1 and 3 months age. Ex-vivo experiments correlated these in vivo findings with higher and lower than normal clonogenic potential (as evidenced by the CFU-F assay) of marrow aspirates from 3 and 6 month old $Fbn1^{Prx-/-}$ mice, respectively. The additional finding that 3 month-old $Fbn1^{Prx-/-}$ mice have fewer mesenchymal stem cells (MSC) but more osteoprogenitors suggested a premature depletion of the MSC pool. Indeed, the number of osteoprogenitors was dramatically less in 3 month-old $Fbn1^{Prx-/-}$ mice treated with 5-Fluorouracil. As we also found that marrow cultures from $Fbn1^{Prx-/-}$ mice exhibit higher TGFβ activity, 1 month-old mutant mice were systemically treated with pan-TGFβ neutralizing antibodies (1D11) for 8 weeks. The treatment normalized the number of MSCs with the result of preventing bone loss in $Fbn1^{Prx-/-}$mice. Altogether, our data demonstrate that fibrillin-1 is an extracellular component of the bone marrow niche that regulates stem cell lineage commitment by modulating local TGFβ signaling.

***Disclosures: Silvia Smaldone**, None.*

MO0108

Fibronectin Splice Variation in Human Knee Cartilage, Meniscus and Synovial Membrane and Association with Osteoarthritis. Carla Scanzello[1], Dessislava Markova[2], Ana Chee[1], Sherrill Adams[3], D. Greg Anderson[2], Howard An[1], Yejia Zhang*[4]. [1]Rush University Medical Center, USA, [2]Thomas Jefferson University, USA, [3]University of Pennsylvania School of Dental Medicine, USA, [4]Rush University Medical CTR, USA

Purpose: Osteoarthritis (OA) is characterized by extracellular matrix degradation of cartilage and meniscus, and low-grade synovial membrane (SM) inflammation. Fibronectin (FN) is a widely expressed molecule that can participate in these pathological processes. Multiple alternatively spliced isoforms of FN exist which have functional consequences, but splicing in joint tissues other than cartilage has not been well studied. The present study compares FN splice variation in human cartilage, SM and meniscus.

Methods: Joint tissues were collected from a non-arthritic organ donor, and from patients undergoing surgery. Total RNA was amplified by PCR using primers flanking alternatively spliced FN Extra Domain A (EDA), Extra Domain B (EDB) and Variable (V) regions.

Results: The FN EDB+, EDB- and EDA- variants were present in cartilage, SM, and meniscus, while the EDA+ variant was detected in only one SM specimen. V+ variants were present in all three tissues, and synovial expression varied with degree of cartilage degeneration. In addition, two V- isoforms, previously described as specifically expressed in cartilage, were present in SM and meniscus as well.

Conclusions: Fibronectin splice variation in meniscus and SM bears striking resemblance to that of cartilage, including expression of isoforms previously described as "cartilage-specific". While the EDB+, EDB- and EDA- variants are present in all tissues examined, EDA+ variants were largely undetectable. Synovial V+ forms were expressed at higher levels in patients with mild to moderate osteoarthritic changes. V+ FN should be investigated as a potential biomarker of disease stage or progression in larger OA patient populations.

***Disclosures: Yejia Zhang**, None.*

MO0109

Osteopontin as a Novel Substrate for Proprotein Convertase 5/6 (*PCSK5*) in Bone. Betty Hoac[1], Delia Susan-Resiga[2], Rachid Essalmani[2], Edwidge Marcinkiewicz[2], Nilana Barros[3], Nabil Seidah[2], Marc McKee*[1]. [1]McGill University, Canada, [2]Clinical Research Institute of Montreal, Canada, [3]Federal University of Sao Paulo, Brazil

Seven proprotein convertases (PCs) cleave the basic consensus sequence K/R-X_n-K/R ↓ (where n = 0, 2, 4 or 6 variable amino acids) to activate precursor proteins. Despite similarities in substrate specificity, basic amino acid-specific PCs have a distinct tissue distribution allowing for enzymatic actions on tissue-resident substrates. The proprotein convertase PC5/6 (*PCSK5*) exists as soluble PC5/6A or membrane-bound PC5/6B isoforms. *Pcsk5* is highly expressed in mouse bone development, but cellular localization and a substrate for PC5/6 have not been described in this tissue. *Pcsk5*-knockout mice die at birth with a bone phenotype that includes small size, retarded ossification and additional thoracic segments and ribs. Osteopontin (OPN) is an abundant bone extracellular matrix protein with roles in mineralization, cell adhesion and migration, and it has two consensus sequence sites for cleavage by PC5/6A which might modify its functions. We aimed to determine whether OPN is a substrate for PC5/6A. *In situ* hybridization was performed on sections of normal mouse bone using *Pcsk5, Opn*/*Spp1* and *Dmp1* anti-sense and control sense cRNA probes. Quantitative RT-PCR for *Pcsk5* was performed on mouse RNA extracts from the osteoblastic MC3T3-E1 cell line and from primary osteoblast and osteoclast cultures. Enzyme-substrate assays using recombinant human PC5/6A and OPN were performed along with gel electrophoresis to visualize cleavage products. Immunoblotting for OPN was performed after SDS-PAGE of long-bone extracts from *Pcsk5*$^{A1/A1}$ (knockout) E18.5 embryos and wild type (WT) littermates. E18.5 embryos were also analyzed by micro-computed tomography. *In situ* hybridization and quantitative RT-PCR showed expression of *Pcsk5* and *Dmp1* in bone-forming cells (similar to *Opn* expression) but not in osteoclasts. Cell-free *in vitro* digestions showed that PC5/6A efficiently cleaved OPN. Consistent with this finding, immunoblotting of mouse bone extracts confirmed an OPN fragment appearing at ~15 kDa in WT bone that was not present in PC5/6-deficient bone. By micro-computed tomography, PC5/6-knockout embryos had delayed skeletal mineralization. In conclusion, we show that *Pcsk5* is expressed in OPN- and DMP1-producing bone-forming cells, and that OPN is a novel substrate for PC5/6A. Cleavage of OPN by PC5/6A could modify the function of OPN in bone leading to the bone phenotype, and/or it could contribute to downstream sequential processing of OPN by other enzymes. *Supported by CIHR.*

***Disclosures: Marc McKee**, None.*

MO0110

Role of Fibromodulin and Biglycan in Periodontal Development and Homeostasis. Le Wang*[1], Brian Foster[2], Vardit Kram[3], Francisco Nociti[2], Brendan Lopez[4], Anne Tran[2], Kanako Nagatomo[4], Marian Young[5], Martha Somerman[6]. [1]NIAMS/NIH, USA, [2]National Institute of Arthritis & Musculoskeltal & Skin Diseases (NIAMS), USA, [3]National Institute of Dental & Craniofacial Research (NIDCR), USA, [4]University of Washington School of Dentistry, USA, [6]National Institutes of Health, USA, [7]NIDCR, USA

Background: The periodontal apparatus (PA), which includes the periodontal ligament (PDL), and surrounding mineralized tissues, cementum and alveolar bone, is essential for tooth function. A better understanding of key regulators controlling development and homeostasis of the PA is necessary for improved periodontal regenerative therapies. Small-leucine rich proteoglycans (SLRPs) are extracellular matrix (ECM) proteins suggested to regulate collagen organization and cell-cell signaling. Mice with double-deficiency (dKO) in two SLRPs, fibromodulin (Fmod) and biglycan (Bgn), acquire ectopic calcification of tendons, and severe osteoarthritis. However, the role(s) of SLRPs in regulating the PA remain undefined. Results: Radiographic and histologic analyses showed that teeth of dKO mice were fully erupted with normal morphology. Polarized light studies demonstrated abnormal collagen fibrils and defective remodeling of alveolar bone of dKO mice. Immunohistochemistry revealed increased staining of SLRPs, asporin (Asp), lumican (Lum) and decorin (Dcn), in PDL of dKO mice, indicating compensatory mechanisms enhancing expression of alternative SLRPs. Although expression of mature osteoblast/cementoblast markers, bone sialoprotein and osteopontin, remained unchanged, dentin matrix protein-1 (DMP1), a mechanosensory osteocyte marker, was increased markedly in dKO PDL. Disruption of homeostasis of dKO PDL was further supported by increased expression of osteoclast-promoting receptor activator of nuclear factor-kB ligand (RANKL) and elevated numbers of tartrate resistant acid phosphatase (TRAP) positive osteoclasts (~20 fold at 4 wks and ~2 fold at 8 wks). To elucidate the underlying mechanisms, we analyzed PDL tissues by PCR array and found there was hyperactive TGFß/BMP signaling in dKO, further confirmed by dramatically elevated staining of phosphorylated SMAD5 (second messenger for TGFß/BMP) in dKO PDL. Dysregulated TGFß/BMP signaling in the dKO was further confirmed in studies using primary PDL cells, where exogenous BMP2 increased Asp and Dcn gene expression in WT, but decreased both in dKO. Conclusions: We demonstrated the importance of the SLRPs in maintaining homeostasis of PA, identifying Fmod and Bgn as key players in regulating the TGFß/BMP signaling pathway for ECM turnover and collagen organization. These novel findings increased our understanding of PA development and function with application toward designing new periodontal regenerative therapies.

***Disclosures: Le Wang**, None.*

MO0111

In Vitro Mechanobiological Studies of Tenocyes. David Musson*, JungJoo Kim, Karen Callon, Dorit Naot, Iain Anderson, Vickie Shim, Jillian Cornish. University of Auckland, New Zealand

The musculoskeletal system experiences severe mechanical strain, often causing trauma; this has led to increased studies evaluating mechanical strain on musculoskeletal cells. Most studies use devices where levels of strain applied do not correspond to that experienced by the cell. Furthermore, nearly all studies use fibronectin (FN)-coated culture surfaces to enhance cell attachment. However, recent studies suggest that FN increases cell turnover, DNA damage, while FN fragments cause extracellular matrix degradation - all indicative of musculoskeletal disease. We employed a novel cell stretching device where strain is evenly distributed across the culture surface and to the cell, with two aims: to validate the device and to determine how different substrate coatings affect cell behaviour.

To mimic an experiment looking at collagen synthesis following 1h of knee extension (Miller et al, 2005), primary rat tenocytes were cultured on collagen type I coated silicone and exposed to 4% strain for 1h. Sirius red staining and real-time PCR were performed over 72h to measure collagen gene expression and protein deposition. In addition, primary rat tenocytes cultured on collagen type I or FN-coated silicone were exposed to 2% and 4% strain for 12h. Calcein staining and alamarBlue® assays were used to evaluate cell morphology and viability, while differential gene expression of tenocyte and inflammatory markers was determined using real-time PCR.

Collagen type III gene expression peaked at 48h and collagen type I was highest 72h post-stretching. This differs from that seen by Miller et al, who saw a peak at 24h, although levels were still elevated at 72h, as seen in our study. We also found a marked difference in tenocyte response to strain with different substrate coatings. FN-coated cultures showed greater attachment and growth compared to collagen-coated cultures; and calcein staining suggested cells cultured on FN had a more tenocytic morphology. However, at the gene expression level, cells stretched 2% on collagen had a 2-fold increase in the expression of the matrix protein tenascin-C, and a 3-fold increase in COX-2 expression, a key mechanotransduction mediator. FN coating did not show similar effects on gene expression.

This study suggests that our novel device is a useful tool in mechanobiological studies and is capable of mimicking in vivo studies, while collagen type I coating appears to be a better substrate for studying tenocyte response to strain.

***Disclosures: David Musson**, None.*

MO0112

Determination and Modulation of Total and Surface Calcium-sensing Receptor Expression in Monocytes in vivo and in vitro. Julien Paccou*[1], Cédric Boudot[1], Aurélien Mary[1], Said Kamel[1], Tilman Drueke[1], Patrice Fardellone[2], Ziad Massy[1], Michel Brazier[3], Romuald Mentaverri[4]. [1]Université De Picardie Jules Verne, France, [2]Service de rhumatologie, CHU Hôpital Nord, France, [3]University of Picardie, France, [4]INSERM U1088, Fra

Expression of the calcium-sensing receptor (CaSR) has previously been demonstrated in human circulating monocytes (HCM). The present study was designed to measure both total and surface CaSR expression in HCM and to examine its potential modulation by pro-inflammatory cytokines and/or Ca2+ and/or vitamin D sterols in U937 monocytic cell line.

Twenty healthy volunteers underwent blood sampling with subsequent isolation of peripheral blood mononuclear cells (PBMC) at 3 visits. Flow cytometry analysis (FACS) was performed initially (Visit 1=V1) and 19 days later (Visit 2=V2) to examine intra- and intersubject fluctuations of total and surface CaSR expression in HCM and 15 weeks later (Visit=V3) to study the effect of oral vitamin D supplementation. Serum biochemistry parameters were measured at each visit. Moreover, *In vitro* experiments were conducted to assess the effects of pro-inflammatory cytokines (TNFα and IL6), calcidiol, calcitriol and Ca2+ on CaSR expression in U937 monocytic cell line.

By FACS analysis, more than 95% of HCM exhibited cell surface CaSR staining. In contrast, CaSR staining failed to detect surface CaSR expression in other PBMC. After cell permeabilization, total CaSR expression was observed in more than 95% of all types of PBMC. Both total and surface CaSR expression in HCM showed a high degree of intra-assay reproducibility (<3%), an approximately 10% variation from V1 to V2 and a moderate intersubject fluctuation observed at V1, V2 or V3. In response to oral vitamin D supplementation, there was no significant change for both total and surface CaSR expression. In the *in vitro* study, U937 cells showed strong total and surface CaSR expression, and both were moderately increased in response to calcitriol exposure. Neither total nor surface CaSR expression was modified by increasing Ca2+ concentrations. Total CaSR expression was dramatically and concentration-dependently decreased by TNFα exposure. For IL6 stimulation, no clear-cut trend was observed for both total and surface CaSR expression.

In conclusion, CaSR expression can be easily measured in circulating monocytes and could potentially represent an accessible biomarker. It could be of particular interest to follow patients and see how pathological conditions such as osteoporosis modify CaSR expression. In the *in vitro* study, total and surface CaSR expression in U937 monocytic cell line were increased by calcitriol but total CaSR expression was decreased by TNFα stimulation.

***Disclosures: Julien Paccou**, None.*

MO0113

Effect of adriamycin on mineral metabolism of Pi loaded and vitamin D depleted C57BL/6J mice. Masanori Takaiwa*[1], Kunihiko Aya[2], Kosei Hasegawa[3], Hiroyuki Tanaka[4], Yoichi Kondo[1], Tsuneo Morishima[3], Nobuyuki Kodani[1]. [1]Department of Pediatrics, Matsuyama Red Cross Hospital, Japan, [2]Department of Pediatrics, Kurashiki Chuou Hospital, Okayama, Japan, [3]Department of Pediatrics, Okayama University Graduate School of Medicine, Dentistry & Pharmaceutical Sciences, Japan, [4]Okayama Saiseikai General Hospital, Japan

FGF23 is associated with progression and mortality of CKD. Meanwhile, FGF23 might compensate the aberrant mineral metabolisms in the early CKD. It is also likely that FGF23 potentially prevents the progression of hyperparathyroidism at least in early CKD. However the significance of FGF23 in the parathyroid of early CKD has not been clarified. C57BL/6J mice are relatively resistant against nephrotoxicity of adriamycin (ADR). Hence ADR could be a potent means to create a model of early CKD using C57BL/6J mice. Upon making 3 experimental groups, control group; a group fed a 1.5% Pi diet containing 2200IU/kg of cholecalciferol (VD), VD deficient group; a group fed a VD deficient 1.5% Pi diet, ADR group; a group fed the VD deficient diet, 12-week-old male C57BL/6J mice were weekly administered either serine (the control and VD deficient groups) or ADR (the ADR group, 5mg/kg/dose, ip) for 4 weeks. After the treatment, the ADR group weighed 21.3±0.8g and significantly smaller that the control (28.4±0.1g) and the VD deficent group (28.1±0.3g). Serum creatinine of the ADR group was 5.03±0.69mg/dl and markedly higher than the control (0.90±0.06mg/dl) and VD deficient groups (1.63±0.59mg/dl). ADR group showed significant hyperphosphatemia (10.27±0.25mg/dl) compared with the control (8.12±0.14mg/dl) and the VD deficient group (8.02±0.79mg/dl). Serum intact FGF23 of the control, the VD deficient and the ADR groups were 247.0±19.0, 338.1±19.8 and 368.8±30.9pg/ml, respectively. Serum PTH 1-84 of the control, the VD deficient and the ADR groups were 472.4±64.0, 579.7±202.1 and 598.3±269.2, respectively. Histological studies of kidney showed mild to moderate interstitial and glomerular injuries in the ADR group. The difference in the parathyroid of these 3 groups was not confirmed using the light microscopy. It was indicated that the weekly ADR injection caused chronic renal failure and hyperphosphatemia indicating that ADR treated C57BL/6J could be used as a CKD animal model. Deprivation of cholecalciferol was designed to enhance the aberrant mineral metabolisms of CKD and for further application using animal carries impaired FGF23 signaling. It is suggested that elevations in the FGF23 and PTH 1-84 among these 3 groups were due to dietary Pi and cholecalciferol intake than to the ADR nephropathy. Hence, although further examinations were required, our protocol could be the reasonable platform to examine the significance of FGF23 in the early stage of CKD.

***Disclosures: Masanori Takaiwa**, None.*
This study received funding from: the Kidney Foundation, Japan

MO0114

FGF23 Reduces Endothelium–Dependent Vasorelaxation and Nitric Oxide Bioavailability. Neerupma Silswal*[1], Dorothy Daniel[1], Chad Touchberry[1], Lynda Bonewald[2], Jason Stubbs[3], Jon Andresen[1], Michael Wacker[1]. [1]University of Missouri-Kansas City School of Medicine, USA, [2]University of Missouri - Kansas City, USA, [3]University of Kansas Medical Center, USA

Fibroblast Growth Factor 23 (FGF23) is a 32-kDa protein that is secreted primarily by osteocytes. Normal serum concentrations of FGF23 are app. 50 pg/ml but can be elevated 1000 fold during chronic kidney disease (CKD). Recent clinical studies have shown that elevated levels of FGF23 are independently associated with endothelial dysfunction and arterial stiffness in CKD patients; however, the direct effects of FGF23 on vascular smooth muscle and endothelial function have not yet been examined. We have detected expression of all four subtypes of FGF receptors in C57BL/6 male mouse aortas (10-12 week old) using real time RT-PCR. FGFR1 was highly expressed while FGFR4 and the co-receptor Klotho were expressed at low levels (n=4). We then examined the vascular effect of different concentrations of exogenous FGF23 (9, 90, 900, 9000 pg/ml) on aortas using isometric tension myography. FGF23 did not induce significant contraction from baseline and did not relax aortic rings precontracted with $PGF_{2\alpha}$ (10^{-5} M) ($P>0.05$; n=5). However, preincubation with FGF23 at 9000 pg/ml caused a 27.6% inhibition of endothelium-dependent relaxation elicited by acetylcholine (Ach) in precontracted aortic rings ($P<0.05$ vs. vehicle; n=5). This inhibition was rescued by preincubation with the FGF receptor antagonist, PD166866 (50nM) ($P<0.05$; n=5). FGF23 pretreatment of vessels did not alter relaxation caused by addition of sodium nitroprusside (SNP) suggesting that the impaired response was endothelium-specific. To further explore this mechanism, total nitrates produced after Ach treatment of aortic rings were measured using a nitrate/nitrite colorimetric assay kit. In FGF23 (9000 pg/ml) pretreated rings, nitrate production was reduced by 53.1% compared to vehicle levels ($P<0.05$; n=5). Therefore, our data suggest that acute exposure of FGF23 can cause endothelial dysfunction by inhibiting nitric oxide bioavailability in mouse arteries. Together, these data provide evidence that high levels of FGF23, as occurs in CKD, may play a role in cardiovascular dysfunction. These data also provide further evidence for crosstalk between kidney, bone, and the cardiovascular system and suggest that therapeutic strategies for treatment of CKD need to take this interplay into consideration.

***Disclosures: Neerupma Silswal**, None.*

MO0115

Iron Status Regulates Serum C-terminal FGF23 in Healthy Adult Women. Erik Imel*[1], Siu Lui Hui[1], Amie Gray[1], Dena Acton[1], Anthony Acton[1], Leah Padgett[1], Munro Peacock[2], Michael Econs[1]. [1]Indiana University School of Medicine, USA, [2]Indiana University Medical Center, USA

Purpose: Fibroblast growth factor 23 (FGF23) is secreted as N- and C-terminal fragments and intact protein. Low iron status increases serum FGF23 in the setting of genetic mutations impairing normal FGF23 cleavage. We hypothesized that in healthy women iron status would also influence both C-terminal and intact FGF23 concentrations independently of serum phosphorus (Pi) or 1,25(OH)2D.

Methods: Serum iron, creatinine, Pi, 1,25(OH)2D, and FGF23 were measured in stored fasting samples from healthy white women (n= 974, age 20-55 years). Serum FGF23 was measured with an ELISA specific for intact FGF23 and an ELISA detecting both intact and C-terminal fragments of FGF23. FGF23 was log-transformed. Variables were analyzed with Pearson correlations and multiple regression analyses.

Results: Age correlated negatively with Pi ($p<0.0001$) and positively with C-terminal FGF23 (r= 0.167) and intact FGF23 (r= 0.131)($p<0.001$), but not iron. Creatinine was not related to age, Pi, 1,25(OH)2D or FGF23. Intact and C-terminal FGF23 log-concentrations correlated positively (r= 0.165, $p<0.0001$). Intact FGF23 was negatively related to 1,25(OH)2D (r= -0.111, $p<0.01$), and positively to Pi (r= 0.067, $p<0.05$). C-terminal FGF23 had no relationship with Pi or 1,25(OH)2D.

C-terminal FGF23 was most strongly related to iron (r= -0.254) and iron saturation (r= -0.231, both $p<0.0001$). Thus, subjects with iron <50mcg/dl had higher log-C-terminal FGF23 than those with iron ⩾50 mcg/dl (1.41 ± 0.40 versus 1.13 ± 0.27 RU/ml, $p< 0.0001$). Intact FGF23 was not related to serum iron. Pi did correlate negatively with iron (r= -0.078, P=0.015) and iron saturation (r=-0.128, $p<0.0001$).

Iron status influenced C-terminal FGF23 concentration independently of other variables including age, Pi, and intact FGF23 (R2= 0.112, $p<0.0001$). 1,25(OH)2D did not predict C-terminal FGF23. High Pi decreased the influence of iron on C-terminal FGF23 ($p<0.05$ for interaction of iron and Pi); iron regression slopes became smaller at higher Pi levels.

Conclusion: In healthy women, C-terminal FGF23 was most strongly related to iron status. However, this relationship was blunted at higher Pi level. In contrast, intact FGF23 was not related to iron status, but was related to Pi and 1,25(OH)2D. Thus when low iron status increases FGF23 production, increased cleaving of FGF23 into fragments allows maintenance of normal intact FGF23 and Pi. Further study of the physiologic interaction of iron and FGF23 is needed.

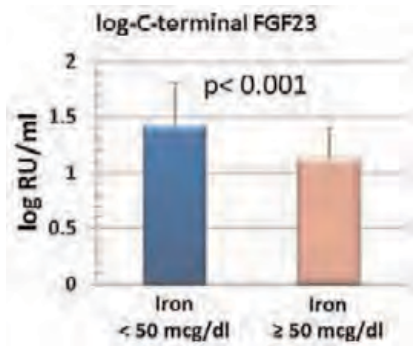

Figure 1

***Disclosures: Erik Imel**, Kyowa Hakko Kirin Pharma, Inc., 6; Kyowa Hakko Kirin Pharma, Inc., 2*

MO0116

PHEX Substrate Protein Osteopontin and its ASARM Peptide Decrease *NaPT2A* Expression. Gabrielly Chiarantin[1], Raquel Neves[1], Betty Hoac[2], Adriana Carmona[1], Marc McKee[2], Nilana Barros*[1]. [1]Federal University of Sao Paulo, Brazil, [2]McGill University, Canada

X-linked hypophosphatemia (XLH/HYP) is the most prevalent form of inherited rickets in humans, occurring as a consequence of inactivating mutations in the *PHEX* gene (phosphate-regulating gene with homologies to endopeptidases on the X chromosome). XLH is characterized by growth retardation, rickets and osteomalacia leading to hypomineralized bones that deform, and soft tooth dentin prone to infection and abscesses. Associated with XLH and causing hypophosphatemia are defects in renal phosphate reabsorption and vitamin D metabolism. *In vivo* mouse studies have shown that the absence of PHEX leads to the release of a circulating factor(s) that decreases mineralization by inhibiting the sodium/phosphate co-transporter NaPT2A which mediates reabsorption of phosphate in the kidneys. Recently we demonstrated that the mineral-binding bone extracellular matrix protein osteopontin (OPN) is a physiologically relevant substrate for PHEX, whose inactivation by PHEX normally promotes bone mineralization. However, in PHEX-deficient Hyp mouse bone, OPN and its fragments accumulate to inhibit mineralization locally in the extracellular matrix. In the present study, we have extended these observations to show that OPN and a derived OPN fragment

(ASARM peptide; acidic serine- and aspartate-rich motif) affect *Napt2a* expression. Using the supernatant from cultures of a constructed *PHEX*-deficient human osteoblast cell line (MG-63 osteoblasts treated with shRNAi-*PHEX*) we show that, in the absence of PHEX, a secreted factor found in the MG-63 osteoblast supernatant decreased *NaPT2A* mRNA and protein expression in human kidney (HK-2) proximal tubule epithelial cell cultures. Based on this observation and on the fact that OPN is essentially completely degraded by PHEX, we investigated the effects of exogenous OPN and its ASARM peptide on HK-2 cell *NaPT2A* expression. RT-PCR and cell sorting (FACs) analyses revealed that both OPN and its ASARM peptide significantly decreased *NaPT2A* expression. In conclusion, these results provide new insight into circulating humoral factors that might influence phosphate handling in the kidney whose alterations contribute to the osteomalacic XLH phenotype, and they suggest that OPN and its ASARM peptide may be involved in this process. *Supported by FAPESP.*

***Disclosures: Nilana Barros**, None.*

MO0117

Sympathetic Activation Induces Skeletal *Fgf23* Expression in a Circadian Rhythm Dependent Manner. Masanobu Kawai*[1], Saori Kinoshita[1], Shigeki Shimba[2], Keiichi Ozono[3], Toshimi Michigami[1]. [1]Osaka Medical Center & Research Institute for Maternal & Child Health, Japan, [2]School of Pharmacy, Nihon University, Japan, [3]Osaka University Graduate School of Medicine, Japan

Phosphorus is a pivotal nutritional factor involved in energy and skeletal metabolism, and has been implicated to possess a circadian profile in the circulation; however, the precise mechanisms how phosphate metabolism is regulated by circadian clock network remain largely unknown. In the current study we postulated that skeletal *Fgf23* expression was controlled by sympathetic activity in a circadian rhythm dependent manner. Skeletal *Fgf23* expression exhibited greater levels during dark phase (DP) when food intake was active in mice. To further analyze the association between food intake and *Fgf23* expression, mice were fed exclusively during light phase (LP). Interestingly, *Fgf23* expression pattern showed a peak expression during LP. To determine the mechanisms by which circadian expression of *Fgf23* is regulated by food intake, we analyzed urine epinephrine levels as a marker for sympathetic tone because food ingestion is known to enhance sympathetic activity. As expected, amount of urine epinephrine was greater during DP in mice fed ad lib, whereas it was elevated during LP in mice under LP-restricted feeding conditions. To determine whether sympathetic tone activates *Fgf23* expression, we administered beta-adrenergic agonist, isoproterenol (ISO) into mice at different time points of the day and found it enhanced skeletal *Fgf23* expression only when administered at ZT8 and 12. *In vitro* reporter assays revealed that ISO trans-activates *Fgf23* promoter through a cAMP-response element in osteoblastic UMR-106 cells. To analyze the reason why *Fgf23* induction by ISO is restricted to ZT8 and 12, we tested our hypothesis that Cryptochrome1 (Cry1), a circadian clock gene, suppressed ISO-induced *Fgf23* expression since Cry1 has been shown to inhibit some of G protein-coupled receptor signaling pathways. Cry1 expression was lower at ZT8 and 12, and over-expression of Cry1 in UMR-106 cells inhibited the phophorylation of CREB by ISO. To further understand the role of circadian clock system in ISO-induced *Fgf23* expression, we utilized mice deficient in *Bmal1*, a core clock gene, where Cry1 expression was enhanced. In these mice, ISO-induced *Fgf23* expression was decreased compared to that in WT mice. These lines of evidence indicate that regulation of skeletal *Fgf23* expression by sympathetic activity is dependent on circadian clock system and may shed light on new regulatory networks of FGF23 which could be important for understanding the physiology of phosphate metabolism.

***Disclosures: Masanobu Kawai**, None.*

MO0118

Depolarizing Membrane Potential by PTH and VD_3 Regulates RANKL-intracellular Transportation; A Novel Mechanism of PTH- and VD_3-induced Osteoclastogenesis. Takuya Notomi*[1], Miyuki Kuno[2], Yoichi Ezura[3], Masaki Noda[4]. [1]GCOE, Tokyo Medical & Dental University, Japan, [2]Osaka City University, Japan, [3]Tokyo Medical & Dental University, Medical Research Insititute, Japan, [4]Tokyo Medical & Dental University, Japan

The PTH and VD_3 are not only osteogenic reagents but also major regulator for osteoclastogenesis. These molecules transiently increase bone resorption by increment of the expression level of RANKL, whereas their mechanism of RANKL-intracellular transportation (RANKL-iTP) remains unclear. The RANKL-iTP depends on lysosomal vesicles whose fusion is related to increment of intracellular Ca^{2+} concentration ($[Ca^{2+}]_i$) following depolarizing membrane potential (MP). Thus, MP could regulate osteoblastic function and RANKL-iTP. So far little is known about the role of MP on bone cells, because it is hard to control temporal patterns of MP. Here, by novel system of light-responsive osteoblastic MP, we show that the transiently increasing $[Ca^{2+}]_i$ following depolarization regulates PTH- and VD_3- induced RANKL-iTP.In membrane fraction of RANKL-GFP expressed MC3T3-E1 cell, PTH and VD_3 increase membrane-bound RANKL (mbRANKL) at 10 min (more than 300% increment compared to control), however those mRNA expression level were unchanged at same time. Confirming by time-lapse imaging, the addition of PTH and VD_3 translocated RANKL-GFP to cell membrane within 10 min. In previous reports, PTH and VD_3 transiently increase $[Ca^{2+}]_i$ following depolarization. The $[Ca^{2+}]_i$ spike was diminished by depolarization-activated Ca^{2+} channel blocker (Diltiazem: Dil) or ER-dependent $[Ca^{2+}]_i$ blocker (Thapsigargin: Tg). The increment of mbRANKL by PTH and VD_3 was also decreased by Dil and Tg. These results showed that depolarization-dependent change of $[Ca^{2+}]_i$ affected PTH- and VD_3-induced RANKL-TPi.To address whether depolarization controls RANKL-TPi, we developed a novel system of light-responsive osteoblastic MP by channel-rhodopsin wide receiver (ChWR). MPs in ChWR stably expressed cell were depolarized immediately (<20 msec) after light-stimulus (ΔMP: 16.3 $\pm$ 1.1 mV) and were returned to the pre-stimulus potential after the off-stimulus. Light induced depolarization increase $[Ca^{2+}]_i$ and mbRANKL at 10 min in similar to addition of PTH and VD_3. In co-culture of RAW267 and RANKL-GFP expressed MC3T3-E1 cell, TRAP activities were increased 4- fold by light stimulus and the development of mature osteoclasts was observed.We showed that depolarizing MP is related to osteoblastic function. Our results indicates that RANKL-iTP is regulated by $[Ca^{2+}]_i$ following depolarization of MP. The mechanism of PTH- and VD_3-induced RANKL-iTP would have benefits for developing PTH- and VD_3-like medicine.

***Disclosures: Takuya Notomi**, None.*

MO0119

Parathyroid hormone (PTH) mediated down-regulation of dentin matrix protein 1 (*Dmp1*) expression. Anne Tran[1], Mudita Patel*[2], Francisco Nociti[2], Kamila Kantovitz[2], Le Wang[2], Brian Foster[3], Martha Somerman[4]. [1]National Institutes of Health, USA, [2]NIAMS/NIH, USA, [3]National Institute of Arthritis & Musculoskeltal & Skin Diseases (NIAMS), USA, [4]NIDCR, USA

Objective: Parathyroid hormone (PTH) plays a critical role in bone remodeling and mineral homeostasis. PTH interacts with PTH1R, a G-protein coupled receptor that activate adenylyl cyclase and phospholipase C, producing cAMP which activates protein kinase A and C pathways. Other key regulators of mineralization 1, 25 dihydroxyvitamin D_3 (Vit. D) and ?broblast growth factor 23 (FGF23), interact with and regulate PTH in a complex feedback loop. FGF23 is, in turn, regulated by dentin matrix protein (DMP1), an extracellular matrix protein, and phosphate regulating endopeptidatse (PHEX). The effect of PTH on DMP1 and the pathway(s) through which they interact has yet to be determined, and was the focus of our *in vitro* studies. Methods: Murine cementoblasts (OCCM.30), expressing DMP1, were exposed to PTH (1-34) in dose-response (10^{-6}M-10^{-8}M) and time--course (1, 3, 12, and 24 hrs) experiments. Activators of the PKA (forskolin, 10^{-6}M) and PKC pathway (phorbol dibutyrate, 20nM), and an antagonist of the PKA pathway (H-89: 2,10, 20 µM), were used to analyze pathways. cAMP was measured in cells treated with 3-isobutyl-1-methylxathine (IBMX, 1mM) and PTH (1-34) using ELISA. Actinomycin D and cycloheximide were used to determine *Dmp1* mRNA stability and protein synthesis requirement, respectively. Gene expression of *Dmp1* and other mineralization markers were analyzed by RT-qPCR. Results: Cells exposed to PTH (1-34) decreased *Dmp1* mRNA expression at all time points, 83% at 10^{-7}M PTH and 90% at 3 hours. The addition of PTH (1-34) to cells pre-treated with actinomycin D showed no acceleration of *Dmp1* mRNA degradation by PTH. There was partial recovery of *Dmp1* mRNA when cycloheximide was added to the cells by 3 fold, suggesting that protein synthesis is required. Treatment with PTH (1-34) increased intracellular cAMP levels by 4-fold. Forskolin decreased *Dmp1* mRNA and H-89 partially recovered the PTH inhibition of *Dmp1*, implicating cAMP/PKA pathway involvement. Conversely, a PKC agonist slightly up-regulated *Dmp1* mRNA, suggesting that PTH (1-34) regulates *Dmp1* mRNA stability through the PKC pathway. Conclusions: For the first time, these data indicate that the cAMP/PKA pathway mediates the PTH (1-34) mediated down-regulation of *Dmp1* mRNA expression in cementoblasts *in vitro*. Elucidating the relationship between PTH and DMP1 provides new insights on phosphate homeostasis and skeletal mineral metabolism.

***Disclosures: Mudita Patel**, None.*

MO0120

PTH Alters Cartilage Callus Remodeling in a Model of Delayed Osteotomy Repair. Jiliang Li*[1], Masahiko Sato[2], Yanfei Ma[3], Evan Himes[1], Matthew Hamang[2], Jonathan Lucchesi[2], David Rowe[4]. [1]Indiana University Purdue University Indianapolis, USA, [2]Lilly Research Labs, USA, [3]Eli Lilly & Company, USA, [4]University of Connecticut Health Center, USA

Previously, intermittent hPTH (1-34) enhanced the rodent skeleton in models of osteoporosis and bone healing; however, the mechanistic basis to the latter has not been fully elucidated. To better understand PTH efficacy on formation and remodeling of the cartilage callus and outer cortical shell, we utilized triple-GFP reporter mice expressing a SMA-RFPchry (red), Col3.6-GFPcyan (blue), hOC-GFPtpz (green), which reflect different stages in osteoblastic differentiation. Mice (2 months old) were divided into vehicle and PTH 40 µg/kg/d groups. Bilateral femoral osteotomies were performed, and internally fixed using a sterilized carbon fiber pin (0.8 mm). Animals received EdU (3 mg/kg) and alizarin (30 mg/kg) one day before necropsy. Mice were euthanized at days 7, 14, 21 and 28 day post-surgery, and frozen sections of right femora were obtained for multi-channel fluorescence microscopy. After 4 weeks, µCT (6 mm ROI centered to the fracture plane) showed that PTH induced a 77% larger fracture callus (TV) that contained 57% more bone (BV), 53% higher BMC, 100% more BS, 25% more BS/BV, with 82% greater connectivity, but no increase in overall BMD compared to vehicle. No obvious difference in EdU labeling,

myofibroblast migration into the fracture site, mineralization or expression of Col3.6 or hOC reporters was appreciated at any time point. At day 7, neither group had bridging and had cartilage cores consistent with severe periosteal damage. However by day 14, a cartilage callus was seen in both. A greater proportion of the core had become hypertrophic cartilage with extensive osteoclastic activity in controls than with PTH. More striking was the reduction of osteoclastic activity at the interface between the invading osteogenic front and hypertrophic cells and on the outer cortical shell of the PTH group. By 3 weeks, controls had replaced the cartilage core with bone marrow and a well-formed inward-modeling cortical shell; but the PTH group showed the cartilage was replaced with a highly trabeculated bone undergoing osteoclastic remodeling, with less osteoclastic activity of a trabulated outer cortical surface. These unanticipated results suggest that the larger callus and greater bone volume found by μCT in the PTH treated animals reflects a change in the tempo and intensity of cartilage core removal, and the formation and inward modeling of the outer cortical shell. Analyses are underway to ascertain how these changes ultimately affect the quality of the repaired bone.

***Disclosures: Jiliang Li**, Lilly Research Labs, 6*
This study received funding from: Lilly Research Labs

MO0121

Signal Transduction Pathways Associated with PTHrP-induced Proliferation of Colon Adenocarcinoma Cells. Maria Julia Martin, Natalia Calvo, Ana Russo De Boland*, Claudia Gentili. Universidad Nacional del Sur, Argentina

Parathyroid Hormone-related Peptide (PTHrP, also known as its tumoral analog) was initially identified through its role in humoral hypercalcemia of malignancy, one of the most frequent paraneoplastic syndromes. Subsequently, the protein was found to be distributed in most fetal and adult tissues, including intestinal mucosa. It has been observed that its expression correlates with the severity of colon carcinoma and that its overexpression increases cell proliferation in certain intestinal cell lines. However, so far the role of exogenous PTHrP in Caco-2, a cell line derived from human colorectal adenocarcinoma, is not known. This study examined, whether extracellular PTHrP induces proliferation of Caco-2 cells and whether regulates cell proliferation via the MAP kinases and Akt signaling pathways. Using different cell proliferation assays we found that PTHrP (10^{-8} M) increased the number of live Caco-2 cells. Furthermore, Western blot analysis revealed that the PTH analog stimulates the phosphorylation of ERKs as well as the α isoform of p38 MAPK and Akt without affecting their protein expression levels and the phosphorylation/activation of JNK. Fluorescence microscopy studies indicated that extracellular PTHrP induces the translocation of ERK1/2, p38α and Akt into the nucleus of these intestinal cells. PTHrP also stimulates the phosphorylation of ATF-1 and CREB transcription factors in a biphasic manner, the second phase being partially dependent on MAP kinases activation. Moreover, the peptide induces the translocation of β-catenin into the nucleus of Caco-2 cells and increases the amounts of positive cell cycle regulators c-Myc and Cyclin D. In addition, use of specific inhibitors of ERK 1/2, p38 MAPK and Akt signaling pathways indicate that both MAPKs and Akt participate in PTHrP-induced colonic cell proliferation The present work provides, to our knowledge, the first evidence demonstrating that exogenous PTHrP induces the proliferation of Caco-2 cells and identifies, at least in part, the signaling pathways that are involved in the mitogenic effect of PTHrP on these intestinal cells

***Disclosures: Ana Russo De Boland**, None.*

MO0122

The Cell Cycle Inhibitor p27 Mediates the Regulation of Dental and Mandibular Development by Parathyroid Hormone-Related Peptide. Wen Sun*[1], Hong Liu[2], Rong Wang[2], David Goltzman[3], Andrew Karaplis[3], Dengshun Miao[4]. [1]Nanjing Medical University, The Research Center for Bone & Stem Cells, Peoples Republic of China, [2]Nanjing Medical University, China, [3]McGill University, Canada, [4]Nunjing Medical University, Peoples Republic of China

Our previous study showed that mice deficient in the nuclear localization sequence (NLS) and C-terminus of parathyroid hormone related protein (PTHrP) (Pthrp KI) displayed severe defects in dental and mandibular development, however underlying mechanisms remain largely unknown. Previous studies have demonstrated that the cell cycle inhibitor p27 serves as a down-stream target to regulate the proliferation of vascular smooth muscle, however, it is unclear whether p27 is involved in the regulation by PTHrP of dental and mandibular development in vivo. To answer this question, we examined the protein expression levels of p27 in mandibles from Pthrp KI and their wild-type (WT) littermates.We found that the expression levels of p27 were up-regulated 5 fold in Pthrp KI mice relative to WT littermates. We then compared mandible and tooth phenotypes of compound mutant mice which are homozygous for both p27 deletion and the Pthrp KI mutation ($p27^{-/-}$Pthrp KI) with $p27^{-/-}$, Pthrp KI, and WT littermates. At 2 weeks of age, the mandible size and mineral density and the alveolar bone formation parameters including alveolar bone volume, osteoblast numbers, ALP and type I collagen positive bone areas, and the dental formation parameters including the dental volume and dentin sialoprotein (DSP) immunopositive areas in the incisor and 1st molar and the percentage of Ki67 positive cells in the nuclei of cells of Hertwig's epithelial root sheath (HERs) were increased significantly in $p27^{-/-}$ mice, and reduced significantly in both Pthrp KI and $p27^{-/-}$Pthrp KI mice compared to WT mice, however these parameters were increased significantly in $p27^{-/-}$Pthrp KI mice compared to Pthrp KI mice. In contrast, the ratio of predentin or biglycan immunopositive dentin areas relative to total dentin area, and the percentage of TUNEL positive cells in HERs were decreased in $p27^{-/-}$ mice, and increased in both Pthrp KI and $p27^{-/-}$Pthrp KI mice compared to WT mice. Nevertheless these parameters were reduced significantly in $p27^{-/-}$Pthrp KI mice compared to Pthrp KI mice. Our results demonstrate that dental and mandibular development were accelerated by the deletion of p27, and were impaired by the deletion of PTHrP NLS and C-tuminus, whereas the deletion of p27 in Pthrp KI mice can partially rescue defects in dental and mandibular development. This study therefore indicates that the p27 pathway may function downstream in the action of PTHrP to regulate dental and mandibular development.

***Disclosures: Wen Sun**, None.*

MO0123

The Remarkable Voyage of the MCL. Meina Wang*[1], Steven Tommasini[2], Ali Nasiri[1], Arthur Broadus[3]. [1]Yale University, USA, [2]Yale School of Medicine, USA, [3]Yale University School of Medicine, USA

One of the most curious examples of modeling of the cortical surface of a long bone during linear growth is the migration of tendon/ligament insertion sites along its periosteal (PO) surface. The tibial insertion of the medial collateral ligament (MCL) is a poster-child of this process, yet the details of how the MCL attaches to and migrates along the tibial PO surface are unknown. We studied this process in CD-1 and PTHrP-lacZ ($PTHrP^{lacZ/+}$) mice during development and linear growth. At birth, MCL fibers are attached to the PO near the epiphyseal end of the tibia. By day 8 (D8), the insertion has migrated to the distal end of the bone bark, and its fibers intermingle with the peripheral osteoblasts (OBs) of the bark and become incorporated into the forming cortical bone in this region (confirmed by calcein labeling at D8). By D12-16, the MCL insertion has migrated into the tibial metaphysis well distal to the bone bark and contains a mixed population of PO osteoclasts (OCs) that excavate and PO OBs that fill in a definable enthesis structure. By D21, the MCL enthesis is fully excavated and contains abundant OCs and OBs in a prototypical pattern of coupled OC/OB activities. At this time (3 weeks), the PO underlying the free-standing MCL immediately above the insertion site contains a ''cutting-cone'' of PO OCs that initiates excavation of the so-called migratory canal. From 3-9 weeks, this PO surface lengthens by 7-to-10 fold and contains an army of OCs and not a single OB, a pattern of completely uncoupled OCic bone resorption. This process forms the migratory canal during growth and doubles as the cortical depression that houses the MCL in adulthood. Both the insertion site and the PO surface overlying the migratory canal express abundant PTHrP/lacZ. This presumably reflects growth-induced loading of the MCL insertion as well as the metaphyseal PO, which is itself anchored to the bone bark above and the MCL insertion below.We conclude that anchoring the MCL insertion to the distal bone bark/proximal metaphysis during the first postnatal week is a key developmental event that enables the MCL insertion to subsequently travel south coincident with linear growth. This anchoring tethers the ligament and also the subjacent PO in such a fashion that growth-driven loading induces PTHrP, RANKL, and OCs that mediate the excavation of the MCL enthesis as well as the migratory canal.

***Disclosures: Meina Wang**, None.*

MO0124

Hypocalcemic myopathy in a 16 -year old boy with pseudohypoparathyroidism. Stepan Kutilek*[1], Pavla Bebova-Mala[2], Kristyna Hasenohorlova[2]. [1]Pardubice Hospital; Faculty of Health Studies; University of Pardubice, Czech Republic, [2]Dept. of Pediatrics, Pardubice Hospital, Czech Republic

Introduction: Calcium plays a key role in muscle contraction and metabolism. Myopathy can be a rare manifestation of hypocalcemia of various origin.

Case Report: A 16-year old previously healthy boy was admitted because of 3 minutes convulsions. Upon admission Glasgow coma scale was 12 points. He had hypocalcemia (total S-Ca<1.0 mmol/L), hyperphosphatemia (S-P 2.8 mmol/L), hypomagnesemia (S-Mg 0.64 mmol/L). Serum creatinkinase (S-CK) activity was 32 μkat/L (normal 0.57-2.45 ukat/L) He immediately received i.v. infusion of 10%calcium gluconate (1.5 ml/kg/hour). His total calcemia improved within 5 hours to 1.25 mmol/L and S-Mg to 0.88 mmol/L, however, S-CK increased to 38 μkat/L. Further he received also oral calcium (3000 mg/day) and oral cholecalciferol (20 000 IU/day) for the following two weeks. There was a gradual improvement in S-Ca (1.6 and 1.7 mmol/L on days 3 and 5, respectively), reaching 1.9 mmol/L on day 14. However, S-CK was initially further on rise (131 μkat/L and 222 μkat/L on days 3 and 4, respectively). Since day 5, S-CK began to drop from 186 μkat/L through 104 μkat/L to 60 μkat/L on days 6, 7 and 9, respectively, to 7.2 μkat/L on day 14. There were no myalgias nor clinical sings of myopathy. Due to hypocalcemia, there was a prolonged QTc interval of 0.47 sec on ECG, with no signs of myocardial damage. Echocardiography was normal, with normal contractility, without calcifications. Serum levels of creatinine and alkaline phosphatase activity (S-ALP) were normal (66 μmol/L and 2.2 μkat/L, respectively). The serum level of parathyroid hormone was repeatedly high (10.3 and 12 pmol/L; normal 0.7-5.5). These findings ruled out vitamin D deficiency and osteomalacia and were compatible with the diagnosis of pseudohypoparathyroidism (PHP). Discussion: In animal experiments hypocalcemia may lead to

cardiac decompensation, but heart failure from hypocalcemia is quite rare in clinical practice. Dilated cardiomyopathy and cardiac failure can occur in children with severe vitamin D deficency and hypocalcemia. Myopathy with extremely elevated S-CK has been very rarely encountered in patients with severe hypocalcemia, due to hypoparathyroidism or PHP. Our patient presented with hypocalcemia due to PHP, manifest tetany, very high S-CK with normal cardiac function and without severe myopathy. Conclusion: Mild myopathy with very high S-CK can occur in hypocalcemic patients with PHP and usualy resolves with normalization of hypocalcemia.

***Disclosures: Stepan Kutilek**, None.*

MO0125

Leptin-independent Regulation of Bone Homeostasis by ΔFosB in the Ventral Hypothalamus Contrasts with its Leptin-dependent Effects on Energy and Glucose Metabolism. Kazusa Sato*[1], Anna Idelevich[2], Glenn Rowe[3], Francesca Gori[4], Roland Baron[5]. [1]Harvard School of Dental Medicine, USA, [2]Harvard University, USA, [3]Harvard Medical School, USA, [4]Harvard School of Dental Medicine, Massachusetts General Hospital, USA, [5]Harvard School of Medicine & of Dental Medicine, USA

The hypothalamus plays a pivotal role in bone homeostasis as well as energy balance and glucose metabolism through endocrine and neuronal pathways, but the exact relationship between these three systems is still only partially understood.

Mice in which the expression of ΔFosB, a naturally truncated isoform of FosB that antagonizes AP-1, is driven by the ENO2 promoter in bone, adipose tissues, and the ventral hypothalamus (VHT), develop increased bone mass and energy expenditure and decreased fat mass. ENO2-ΔFosB mice also exhibit increased glucose tolerance and insulin sensitivity despite lower levels of leptin. Moreover, viral-mediated expression of ΔFosB in the VHT phenocopies both the bone and energy phenotypes of ENO2-ΔFosB mice, demonstrating the critical role of the VHT.

The present study was performed to determine whether expression of ΔFosB in the VHT also regulates glucose metabolism, and to evaluate the contribution of leptin to ΔFosB-mediated regulation of these three systems. To this end, C57BL/6 mice were stereotaxically injected in the VHT with AAV encoding ΔFosB (AAV-ΔFosB) or GFP (AAV-GFP) as control. Intraperitoneal glucose (GTT) and insulin (ITT) tolerance tests were performed. ΔFosB transgenic model in leptin deficient ob/ob (ΔFosB-ob/ob) mice were also generated.

AAV-ΔFosB mice had markedly improved glucose tolerance despite lower insulin response to a glucose bolus compared to AAV-GFP mice during GTT, suggesting increased insulin sensitivity. ITT indeed revealed that AAV-ΔFosB mice were more insulin-sensitive and this effect was observed even before their body and fat mass fell behind those of AAV-GFP mice. Elevated insulin signaling was observed in peripheral tissues (muscle and brown fat) but not in bone tissue in AAV-ΔFosB mice, excluding the possibility that the bone phenotype is the result of increased insulin signaling in bone. In contrast, ΔFosB expression in ΔFosB-ob/ob mice did not correct the obesity or decreased energy expenditure yet it made ΔFosB-ob/ob mice glucose tolerant compared to ob/ob mice due to compensatory hyperinsulinemia. Importantly, leptin deletion in ΔFosB-ob/ob mice did not affect the increased bone mass seen in ENO2-ΔFosB mice.Taken together, these results suggest that VHT signaling downstream of ΔFosB affects separately bone homeostasis and energy/glucose metabolism: bone homeostasis is leptin-independent whereas the energy and glucose phenotypes are leptin-dependent.

***Disclosures: Kazusa Sato**, None.*

MO0126

Altered Behavior of Bone Marrow Mesenchymal Stem Cells in the *Crtap* Murine Model of Osteogenesis Imperfecta. Roberta Besio*, Milena Dimori, Katrin Gruenwald, Roy Morello. University of Arkansas for Medical Sciences, USA

Bone disease is often associated with alterations in extracellular matrix (ECM) composition and/or properties with potential impact on mineralization. Recent evidence suggests that the ECM is an important contributor to the establishment of the mesenchymal stem cell (MSC) niche and the maintenance of MSCs pluripotency in the bone marrow. Collagens are a major component of all ECMs, and our studies have demonstrated that dysregulation of collagen post-translational modifications, including prolyl 3-hydroxylation, cause severe skeletal dysplasia. Mutations in components of the prolyl 3-hydroxylation complex, including Crtap, P3h1 and Cyclophilin B, cause recessive osteogenesis imperfecta (OI) in humans and osteochondrodysplasia with severe osteopenia in mice. Both human and murine *Crtap-KO* osteoblasts/fibroblasts deposit less collagen with fibrils of larger diameter in the ECM, and the bone matrix has altered mineralization kinetics. To determine if such alterations in matrix affect the bone marrow microenvironment and, specifically, the differentiation of osteoblasts from MSCs, we analyzed bone marrow MSCs from *Crtap-KO* and WT mice. MSCs derived from *Crtap-KO* mice and cultured towards osteoblasts showed significantly increased numbers of both alkaline phosphatase (CFU-AP) and alizarin red (CFU-OB) positive colonies compared to controls. This suggests an enhanced capacity of MSCs to be recruited to the osteoblastic lineage and to terminally differentiate into matrix-mineralizing osteoblasts in *Crtap-KO* mice. Moreover, the total number of colony forming unit-fibroblast (CFU-F) was also elevated in *Crtap-KO* mice, suggesting an overall increase in the number and/or proliferation of MSCs in this murine model of OI. Concomitantly, mRNA of the early osteoblastic marker *Sp7* (Osterix) was significantly up-regulated in CFU-F and adult calvaria from *Crtap-KO* compared to control mice. These findings suggest that a MSC adaptation response to abnormal matrix ultimately results in an increased commitment toward the osteoblastic lineage. Because *in vivo* osteoblast numbers are not increased in *Crtap-KO* mice, ongoing studies are addressing the terminal differentiation and mineralization capacity of *Crtap-KO* osteoblasts. Interestingly, the osteoblastic differentiation potential of *Crtap-KO* MCSs is opposite to that described in the BrtlIV mouse model of OI and may reflect different cell adaptation and cell lineage response to distinct and unique bone matrix alterations.

***Disclosures: Roberta Besio**, None.*

MO0127

Withdrawn

MO0128

Bone from Low Capacity Running Rats Exhibit Altered Mitochondrial Gene Expression Compared to High Capacity Running Rats after an Exhaustive Bout of Exercise. Anamaria Antolic*[1], Adeel Safdar[2], Steven Britton[3], Mark Tarnopolsky[1], Gregory Wohl[1]. [1]McMaster University, Canada, [2]Harvard Medical School, USA, [3]University of Michigan, USA

BACKGROUND: Aerobic exercise capacity is linked to longevity and decreased disease susceptibility. At the cellular level, increased abundance of mitochondria and higher mitochondrial oxidative enzyme capacity provide the basis for enhanced aerobic capacity. These adaptations have been shown in multiple tissues including, liver, fat depots, heart and brain. The Koch-Britton rat model of low capacity and high capacity runners (LCRs and HCRs respectively) has demonstrated that selection for low and high running capacity led to a divergence in mitochondrial content and function between these two groups. Mechanical strain in the form of exercise has been shown to play a key role in regulating bone health, however underlying mechanisms are still being described. The untrained status and differences in aerobic capacity allow for the elucidations of bone adaptations to exercise.

PURPOSE: To investigate the effect of an acute endurance run to exhaustion on mitochondrial gene expression and enzyme activity in LCR and HCR rats.

METHODS: LCR and HCR rats (30 wk old, n=40; ?=20, ?=20) underwent a graded running exercise. A speed ramped running protocol was used starting at 10m/min (elevation of 15°) and increased 1m/min every 2 min until exhaustion. Upon completion of the test the LCR and HCR rats were randomly assigned for sacrifice three hours (n=20) or three days (n=20) after the exhaustive bout. Femoral, tibial, and lumbar vertebral bones were collected for biomechanical testing, protein content, enzyme activity and gene expression. Acute gene expression at 3 hr was normalized to expression at 3 d after exercise and compared between HCR and LCR groups by MANOVA with Tukey post-hoc.

RESULTS: LCR rats were heavier than HCR rats ($p<0.05$) and ran 75% less than HCR rats ($p<0.05$). LCR rats demonstrated lower citrate synthase activity, an indicator of lower mitochondrial content ($p<0.05$). Exhaustive exercise increased mitochondrial (*Tfam and Cox.iv;* $p<0.05$) and *Vegf* ($p<0.05$) gene expression in the LCR rats compared to HCR at 3 hr. Foxo1 was significantly upregulated in HCR bone at 3 hr, but not in LCR bones ($p<0.05$).CONCLUSION: LCR rat bones exhibited significantly greater mitochondrial and VEGF expression compared to HCR bones following an exhaustive bout of exercise, but changes in osteogenic gene expression were not different between LCR and HCR. These data indicate that the intrinsic aerobic capacity influences bone mitochondrial changes in response to exercise

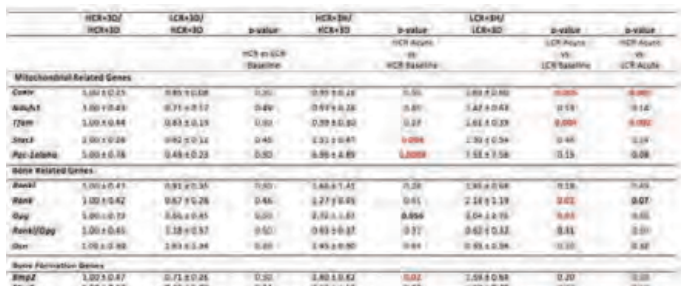

Table

***Disclosures: Anamaria Antolic**, None.*

MO0129

Change of Phenotypic in a Patient with Hypophosphatasia with the Onset of Renal Failure. Tim Cundy*[1], Toshimi Michigami[2], Kanako Tachikawa[3], John Collins[4], Michael Dray[5]. [1]Faculty of Medical & Health Sciences University of Auckland, New Zealand, [2]Osaka Medical Center & Research Institute for Maternal & Child Health, Japan, [3]Department of Bone & Mineral Research, Osaka General Medical Center, Japan, [4]Renal Medicine, Auckland City Hospital, New Zealand, [5]Department of Pathology, Waikato Hospital, New Zealand

Hypophosphatasia is a recessively inherited disorder with a wide phenotypic manifestation ranging from lethality in neonates to asymptomatic in adults. The severity of the phenotype is largely determined by the nature of the *ALPL* mutations. We describe a previously asymptomatic adult whose phenotype dramatically changed after he developed renal failure. A 50 year old man was diagnosed with IgA nephropathy. At age 52 (eGFR 50ml/min) he suffered his first metatarsal fracture. A DXA scan showed osteopenia, and he was prescribed alendronate. His renal failure progressed and he began dialysis (CAPD) at age 55. Prior to and after starting CAPD he suffered multiple non-traumatic fractures affecting metatarsals, vertebrae and ribs. Alendronate treatment was stopped. Further investigation showed low serum PTH levels 1.8-5.2 pmol/L (N 1-7) and discordance between the bone formation markers Alkaline Phosphatase (ALP) 56 U/L (N 40-120) and Procollagen-1 N-peptide 180ug/L (N 20-85). The ALP levels had been low (26-32 U/L) before starting alendronate. A bone biopsy showed osteomalacia, reduced cellular activity and negative staining for aluminium. Genetic analysis showed compound heterozygosity for missense mutations in *ALPL* (T117H and G438S). Expression plasmids for the mutant ALPs fused to green fluorescent protein were transfected into COS7 cells, and the cell lysates were harvested to assay enzymatic activity. The T117H mutant had almost no enzymatic activity, but the G438S mutant retained similar activity to wild-type ALP. Six months treatment with teriparatide produced an increase in ALP activity and histological improvement in bone, but significant side effects. After the restoration of renal function by transplantation there was complete symptomatic resolution. It is probable that as the patient developed renal failure, phosphate retention inhibited his residual ALP enzyme activity, resulting in a marked clinical deterioration – an interesting example of a reversible genotype-environment interaction affecting phenotype

***Disclosures: Tim Cundy**, None.*

MO0130

Combination Therapy with Bone Morphogenetic Protein 2 (BMP-2) and Zoledronic Acid (ZA) Improves Posterolateral Spinal Fusion in a Mouse Model of Neurofibromatosis Type 1. Justin Bobyn*[1], Anton Rasch[2], Kathy Mikulec[2], Aaron Schindeler[3], David Little[1]. [1]Sydney University, Australia, [2]Childrens Hospital Westmead, Australia, [3]The Children's Hospital at Westmead, Australia

Introduction: Bone morphogenetic proteins (rhBMPs) are being increasingly utilized to treat the orthopedic complications associated with neurofibromatosis type 1 (NF1). Correction of scoliotic deformities associated with NF1 can be extremely challenging and these individuals exhibit a high rate of spinal pseudarthrosis. As excessive bone resorption is also reported to be problematic in NF1, we hypothesized that BMP-induced fusion could be improved using co-treatment with the bisphosphonate zoledronic acid (ZA).

Materials and Methods: NF1-deficient mice have been reported to show reduced bone healing. A published murine posterolateral lumbar spine fusion technique was applied to 16 wild type (*Nf1*+/+) mice and 16 NF1 deficient (*Nf1*+/-) mice. Fusion surgery involved the delivery of 10μg rhBMP-2 delivered bilaterally via collagen sponge (20μg total). N=8 mice of each genotype received s.c. saline or s.c. 0.02 mg/kg ZA twice weekly for 3 weeks. Mice were culled at 3 weeks and spines harvested for analysis.

Bone volume (BV; mm^3) and total bone mineral content (TMD; mg/mm^3) of the fusion mass were then calculated via CTan software.

Results: μCT images of harvested mouse vertebrae obtained at 3 weeks were reconstructed (Fig 1). Striking increases in bone volume were noted ($p<0.01$) in WT and *Nf1*+/- mice treated with ZA, bone volumes of 131.9 $\pm$15.4 mm^3 and 100.2 $\pm$21.7 mm^3 respectively, compared with WT and *Nf1*+/- mice which did not receive ZA, with volumes of 40.5 $\pm$4.5 mm^3 and 36.6 $\pm$6.9 mm^3. Similarly significant ($p<0.01$) increases in bone mineral density (BMD; mg/mm^3).

Bioquant analysis of TRAP stained sections revealed a significant ($p<0.05$) increase in the osteoclast surface area to bone surface area ratio (OcS/BS) in *Nf1*+/- samples relative to wild type controls. Co-treatment with rhBMP-2 and ZA treatment led to a significant reduction in OcS/BS in both groups.

Discussion: We have described a novel approach for mouse lumbar spine fusion that is safe, efficient, and analogous to contemporary human surgery. This model has shown that dual treatment with BMP and ZA is superior to treatment with BMP alone. ZA increased the fusion mass bone volume by 3-fold with an associated increase in bone density. Even with ZA treatment, *Nf1*+/- mice yielded smaller, less dense fusion masse compared to wild type counterparts. Nevertheless, the ZA-induced increase in bone led to a superior result in *Nf1*+/- mice compared to BMP alone in wild type mice.

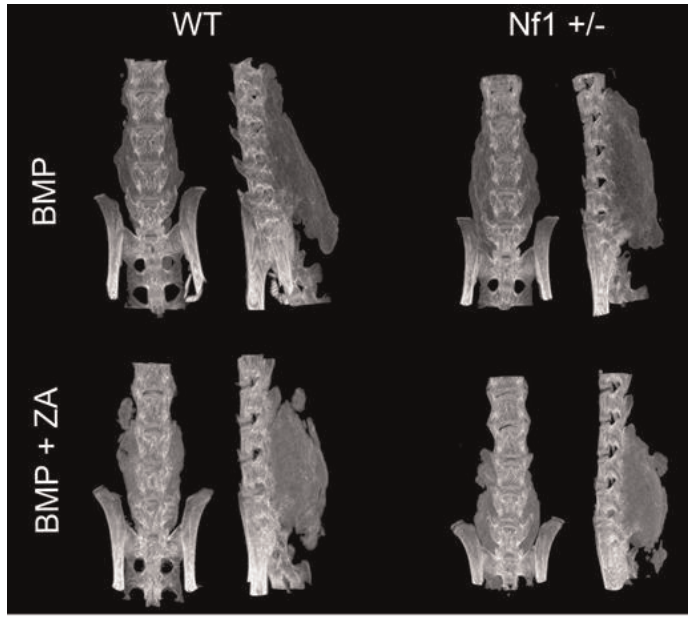

Fig 1. μCT reconstructions of harvested spines demonstrating increased size and mass density in ZA-treated groups over BMP only.

Figure 1

***Disclosures: Justin Bobyn**, None.*

MO0131

Deletion of osteopontin rescues the skeletal deformities observed in *Phospho1*$^{-/-}$ mice. Manisha Yadav*[1], Carmen Huesa[2], Sonoko Narisawa[3], Alain Moreau[4], Colin Farquharson[5], Jose Luis Millan[3]. [1]Burnham Institute for Medical Research, USA, [2]The Roslin Institute & R(D)SVS, University of Edinburgh, Easter Bush, Midlothian EH25 9RG, United Kingdom, [3]Sanford Burnham Medical Research Institute, USA, [4]Sainte-Justine Hospital Research Center, Canada, [5]Roslin Institute, University of Edinburgh, United Kingdom

PHOSPHO1, a phosphatase with specificity for phosphoethanolamine and phosphocholine, plays a functional role in the initiation of calcification. *Phospho1*$^{-/-}$ mice display stunted growth, spontaneous fractures, bowed long bones, osteomalacia, and scoliosis. *Phospho1*$^{-/-}$ mice, as well as their isolated cells and matrix vesicles, display increased output of the mineralization inhibitor PP_i, a situation highly reminiscent of *Alpl*$^{-/-}$ mice, where elevated PP_i levels explain the rickets/osteomalacia characteristic of hypophosphatasia (HPP). Correcting PP_i levels in *Alpl*$^{-/-}$ mice prevents the development of all skeletal and dental abnormalities. Osteopontin (OPN), encoded by the *Spp1* gene, is another potent inhibitor of mineralization whose plasma and tissue levels we have shown changes in parallel to changes in PP_i. *Alpl*$^{-/-}$ mice, not only display elevated plasma PP_i but also elevated OPN levels and we showed that the *Alpl*$^{-/-}$ phenotype is only partially corrected in [*Alpl*$^{-/-}$; *Spp1*$^{-/-}$] double knockout mice while the elevated PP_i concentrations remain unresolved, suggesting that increased OPN contributes in part to the *Alpl*$^{-/-}$ bone phenotype independently of the mineralization inhibitory action of PP_i. *Phospho1*$^{-/-}$ mice display moderately increased levels of plasma PP_i and we have observed particularly high OPN expression in the spine, by immunohistochemistry and qPCR. While the transgenic overexpression of TNAP normalized plasma PP_i, no correction of the skeletal phenotype was observed in *Phospho1*$^{-/-}$ mice. However, here we show that the ablation of *Spp1* leads to the complete rescue of the scoliosis and long bone phenotype characteristic of *Phospho1*$^{-/-}$ mice. Von Kossa/van Gieson staining of vertebral and femoral sections showed decreased unmineralized osteoid in [*Phospho1*$^{-/-}$; *Spp1*$^{-/-}$] mice at 1 month of age and complete absence at 3 months of age. MicroCT analysis also showed improved BV/TV, BMD and trabecular thickness in the double knockout mice. Mineralization assay from chondrocytes harvested from the double KO mice also concur with the histology and μCT results. Thus, while both the *Alpl* and *Phospho1* deficiencies lead phenotypically to skeletal hypomineralization and similar changes in the expression levels of PP_i and OPN, there is a clear dissociation in the hierarchical roles of these potent inhibitors of mineralization, with elevated PP_i being the culprit in HPP while elevated OPN levels appears to be the main determinant of the *Phospho1*$^{-/-}$ skeletal phenotype.

***Disclosures: Manisha Yadav**, None.*

MO0132

Genetic Analysis of Serum Sclerostin. Allison Kuipers*[1], Yingze Zhang[2], Shibing Yu[3], Candace Kammerer[1], Cara Nestlerode[2], Yanxia Chu[2], Clareann Bunker[2], Alan Patrick[4], Victor Wheeler[4], Iva Miljkovic[2], Joseph Zmuda[1]. [1]University of Pittsburgh Graduate School of Public Health, USA, [2]University of Pittsburgh, USA, [3]University of Pittsburgh Medical Center, USA, [4]Tobago Health Studies Office, Trinidad & tobago

Sclerostin, encoded by the *SOST* gene, is a Wingless (Wnt) inhibitor that regulates bone mineralization and is a potential therapeutic target for bone mineral disorders. Genome-wide association studies have implicated the *SOST* locus as a candidate for osteoporosis. Because little is known about the factors influencing inter-individual variation in serum sclerostin levels, we assessed the genetic and non-genetic factors associated with serum sclerostin in 446 Afro-Caribbean men and women aged 18+ from 7 large, multigenerational families (mean family size: 64; 3840 relative pairs). Thirty-six common single nucleotide polymorphisms (SNP) were genotyped within a 100 KB region encompassing *SOST*. Genetic and non-genetic factors were tested for association with serum sclerostin using variance component linear regression methods. Mean serum sclerostin was 41.3 pmol/l and was greater in men than women ($P<0.05$). Greater serum sclerostin was associated with greater age and body weight, male sex, diabetes and lower glomerular filtration rate, which collectively accounted for 25.4% of its variation. Residual genetic heritability of serum sclerostin was 0.393 ($P<0.0001$). Nine SNPs were significantly associated with sclerostin, of which three (rs851056, rs41455049 and rs9909172) accounted for 7.8% of the total phenotypic variation in serum sclerostin. Thus, in this African ancestry population, known and unknown genetic factors account for more variation in serum sclerostin than do known non-genetic factors. These results highlight the potential importance of genetic evaluation with regard to individual assessment of serum sclerostin in bone mineral disorders.

***Disclosures: Allison Kuipers**, None.*

MO0133

Genotype-Phenotype Correlations and Pharmacogenetic Studies in 152 Swedish Families with Osteogenesis Imperfecta. Katarina Lindahl*[1], Carl-Johan Rubin[2], Eva Åström[3], Barbro Malmgren[4], Andreas Kindmark[5], Osten Ljunggren[5]. [1]Endocrinology, Sweden, [2]Uppsala University, Sweden, [3]Department of Woman & Child Health, Division of Pediatric Neurology, Karolinska Institutet, Sweden, [4]Department of Clinical Science, Intervention & Technology, Division of Paediatrics, Karolinska University Hospital, Sweden, [5]Uppsala University Hospital, Sweden

Objective: Osteogenesis imperfecta (OI) is a rare heterogeneous disease leading to bone fragility, spanning from mild to lethal osteoporosis in severity. Over 1000 mutations causing OI have been described in the genes encoding collagen type I. As *COL1A1* and *COL1A2* are large genes, there are still many codon positions where no mutations have been reported and only a fraction of theoretically possible glycine substitutions have been discovered. Here mutations causing OI in Sweden were investigated with respect to genotype-phenotype correlations and pharmacogenetics.

Method: 152 families (204 individuals) with OI participated; 92 type I, 38 type IV and 23 type III. Extensive clinical data was collected and sequencing of *COL1A1* and *COL1A2* performed.

Results: A total of 119 typical OI mutations were detected, while no mutation was present in 29 families. In *COL1A1* 51 quantitative and 34 qualitative mutations were found and in *COL1A2* 33 qualitative mutations were discovered. 53 of the qualitative mutations had been reported to the collagen database (www.le.ac.uk/ge/collagen/) on average 7.1 times previously. New mutations were found in regions reported to be exclusively lethal, saturating the phenotypic map of *COL1A1* and *COL1A2* mutations. Only 13/66 quantitative mutations were formerly reported. Four families carried two separate mutations, one being a typical OI causing mutation. In two families previously unpublished mutations of unclear significance were discovered.

Delta lumbar BMD Z-score response to bisphosphonate treatment was calculated for the initial two treatment years and for the entire available treatment period. No difference was seen in treatment response in different OI types; in qualitative vs. quantitative collagen defects or *COL1A1* vs. *COL1A2* mutations. A significant increase in delta BMD ($p= 0.03$) for qualitative vs quantitative mutations in *COL1A1* was observed the initial two treatment years, but this effect was not preserved over longer treatment time (mean 5.7 years for quantitative and 6.9 years for qualitative).

Conclusion: The spectrum of mutations causing OI described in this Swedish cohort is of the expected type. It is notable that 79% of qualitative mutations have been reported previously, supporting theories of mutational hotspots or sequencing bias. Pharmacogenetic data does not support a mutation dependent response to bisphosphonate treatment in OI and subsequently all patients may be expected to increase BMD on treatment.

***Disclosures: Katarina Lindahl**, None.*

MO0134

Metabolomics Signature and Risks of Osteoporosis: A Systems Biology Approach by Integrating Bone Tissue-Specific Metabolomics and Transcriptomics in Postmenopausal Caucasian Women. Yi-Hsiang Hsu*[1], Sjur Reppe[2], Chin-Lin Chi[3], David Karasik[4], Joseph Brain[5], Douglas Kiel[6], Kaare Gautvik[7]. [1]Hebrew SeniorLife Institute for Aging Research & Harvard Medical School, USA, [2]Oslo University Hospital, Ullevaal, Norway, [3]Medical Informatics Center, Harvard Medcial School, USA, [4]Hebrew SeniorLife; Bar Ilan University, USA, [5]Dept. Envrionmental Health, Harvard School of Public Health, USA, [6]Hebrew SeniorLife, USA, [7]Department of Medical Biochemistry, Oslo University Hospital, Norway

Metabolomics is the quantitative measurement of dynamic metabolic response to pathophysiologic stimuli or genetic modification making metabolome quintessence of biological processes. To identify metabolite signatures for osteoporosis and to understand its underlying biological implication, we measured ~500 metabolites in bone tissue and serum from osteoporosis patients (OP with at least one fragility fracture and low BMD) and age-matched normal-BMD controls. Bone tissues were obtained from trans-iliac biopsies in 84 post-menopausal Caucasian women. Transcriptome profiling of bone biopsies was measured by Affymetrix microchips. Metabolites were measured by LC-MS/MS (+ESI), LC-MS/MS (-ESI) or GC-MS. MS signatures of metabolites were matched to a small-molecule library. Age, BMI, estrogen use, cigarette smoking, menopause age and medication were collected and used in statistical analyses. To find metabolite signature, we applied a support vector machine algorithm with a nonlinear classification and identified 12 endogenous metabolites significantly differed between OP and controls. These 12 metabolites are involved in fatty acid amides; lipid oxidation; bile acid metabolism; tryptophan metabolism and redox homeostasis. Among them, significant accumulation of 5 dicarboxylic fatty acids (2~4 fold higher in OP) suggests potentially suppressed mitochondrial ß-oxidation in OP. Higher levels of the cannabinoid (CB) receptors agonist, oleamide, were observed in OP, indicating a disruption of CB signaling. Serotonin (5HT) was also higher in OP. To further characterize underlying mechanisms, we performed regression analysis between transcriptome and these 12 metabolites, adjusted for covariates described above. The expression of 71 genes was associated with these 12 metabolites at $p < 5x10^{-5}$. *AR*, *FGF2*, *PRKAA2* and several *G-protein coupled receptors* expressions associated with oleamide, providing supportive evidence of the involvement of CB receptors in OP. A pathway enrichment analysis pointed out three distinct cellular functional pathways (synaptic transmission; skeletal development of cortical bone and dystrophy of muscle). In summary, we identified a "signature" of 12 endogenous metabolites associated with osteoporosis in postmenopausal Caucasian women. We used the transcriptome to further characterize their functional implications. A replication study of metabolite signatures in ~1,000 Framingham Study participants is underway to further validate these findings.

***Disclosures: Yi-Hsiang Hsu**, None.*

MO0135

Mutant ALK2 receptors found in patients with typical and variant fibrodysplasia ossificans progressiva are activated by different BMP type II receptors through phosphorylation at Thr203. Mai Fujimoto*[1], Satoshi Ohte[2], Arei Miyamoto[1], Sho Tsukamoto[3], Kenji Osawa[1], Takato Mizuta[1], Shoichiro Kokabu[1], Naoto Suda[4], Takenobu Katagiri[1]. [1]Saitama Medical University Research Center for Genomic Medicine, Japan, [2]Harvard School of Dental Medicine, USA, [3]Saitama Medical University RCGM, Japan, [4]Division of Orthodontics, Meikai University School of Dentistry, Japan

BMPs are important growth factors for bone formation. BMP signaling is transduced by two types of Ser/Thr kinase receptors, type I and type II receptors. Although type II receptors are constitutively activated Ser/Thr kinases, type I receptors are inducible kinases via phosphorylation by type II receptors in response to BMPs. The ligand-dependent BMP signaling is deregulated in patients with fibrodysplasia ossificans progressiva (FOP), which is a rare hereditary disorder characterized by progressive heterotopic ossification in skeletal muscle. Patients with typical FOP, who show early-onset heterotopic bone formation in childhood, a mutation (R206H) in a BMP type I receptor, ALK2. ALK2(R206H) induces BMP signaling without BMPs and is activated by the presence of BMPR-II, which is one of BMP type II receptors. A substitution mutation at Thr203 in ALK2(R206H) blocked the activation by BMPR-II. Recently, we found that BMPR-II failed to activate a novel mutant ALK2, G325A, which has been identified in a variant of FOP, who showed late-onset heterotopic ossification in adulthood. Thus, we examined molecular mechanisms of the activation of ALK2(G325A). Cellular localization and protein

levels of ALK2 were not distinguishable among WT, G325A and R206H. Overexpression of G325A or R206H in C2C12 cells activated BMP-specific luc reporter, induced ALP activity and, increased phosphorylation levels of FLAG-Smad1. The stimulatory activity of G325A was weaker than that of R206H and was blocked by adding LDN-193189, a specific inhibitor for the Smad phosphorylation by BMP receptors. ActR-IIB, another BMP type II receptor, synergistically increased the ALP activity in cooperation with G325A, although kinase activity-deficient ActR-IIB did not activate G325A, suggesting that ActR-IIB phosphorylates ALK2. ALK2 has nine potential Ser/Thr residues in the intracellular GS domain. In G325A, substitutions of the eight residues except Thr203 by Ala/Val (G325A-8AV) still allowed the activation by ActR-IIB, but, a substitution of Thr203 with Val (G325-T203V) blocked that. These findings suggest that G325A is a novel mutation of ALK2, which is activated by ActR-IIB, but not BMPR-II, through the phosphorylation at Thr203. Interestingly, it has been reported that the patient with G325A did not have heterotopic bone formation even after muscle injury. The sensitivity of mutant ALK2 to BMP type II receptors may change the clinical features of patients with FOP.

***Disclosures: Mai Fujimoto**, None.*

MO0136

Mutations in *WNT1* cause different forms of bone fragility. Katharina Keupp[1], Filippo Beleggia[1], Hülya Kayserili[2], Aileen Barnes[3], Magdalena Steiner[4], Oliver Semler[5], Ekkehart Lausch[6], Stefan Breer[7], Eckhard Schoenau[5], Thorsten Schinke[8], Bernhard Zabel[6], Stefan Mundlos[4], Michael Amling[9], Joan Marini[10], Uwe Kornak*[11], Bernd Wollnik[12]. [1]Center for Molecular Medicine Cologne (CMMC), University of Cologne, Germany, [2]Medical Genetics Department, Istanbul Medical Faculty, Istanbul University, Turkey, [3]Bone & Extracellular Matrix Branch, NICHD, NIH, USA, [4]Institute of Medical Genetics & Human Genetics, Charité-Universitaetsmedizin Berlin, Germany, [5]Children's Hospital, University of Cologne, Germany, [6]Children's Hospital, Division of Genetics, University of Freiburg, Germany, [7]Department of Osteology & Biomechanics, University Medical Center Hamburg-Eppendorf, Germany, [8]Department of Osteology & Biomechanics University Medical Center Hamburg Eppe, Germany, [9]University Medical Center Hamburg-Eppendorf, Germany, [10]National Institute of Child Health & Human Development, USA, [11]Charité-Universitaetsmedizin Berlin, Deu, [12]Center for Molecular Medicine Cologne (CMMC), University of Cologne, Germany

We report that hypofunctional alleles of *WNT1* cause autosomal recessive osteogenesis imperfecta, a congenital disorder characterized by reduced bone mass and recurrent fractures. In consanguineous families we identified five homozygous mutations in *WNT1*. In addition, in a family with dominantly inherited early onset osteoporosis, a heterozygous *WNT1* missense mutation was identified in affected individuals. Initial functional analysis revealed that mutant WNT1 proteins failed to activate the canonical LRP5-mediated WNT/β-catenin signaling. Furthermore expression analysis on mRNA and protein level indicates a switch from a neuronal to a skeletal expression pattern during prenatal development and increasing expression levels with advancing osteoblast differentiation. This indicates an unexpected role of the "neuronal" WNT1 in bone development and homeostasis. Our findings might also have relevance for more common forms of age-related osteoporosis.

***Disclosures: Uwe Kornak**, None.*

MO0137

Primary Cilia are Essential for Determination of Dentin Thickness. Courtney Haycraft*, Michael B. Chavez. Medical University of South Carolina, USA

Primary cilia are solitary organelles found on most eukaryotic cells. Despite their nearly ubiquitous presence, their function on many cell types has yet to be fully investigated, but a growing number of human genetic disorders have been shown to be related to defects in the formation or function of this organelle. Orpk mutant mice have a partial loss of function of the gene Ift88 and homozygous mutants develop pathologies in multiple organs including renal cysts, hydrocephalus, and polydactyly. In addition to these pathologies orpk mutant mice develop supernummary molars due to alterations in signaling pathways essential for tooth patterning including Sonic hedgehog. Despite the known defects in molar patterning, no information regarding the morphogenesis of the molars has been reported. The objective of the current study was to examine the morphology of the first molar in orpk mutant mice to determine the role primary cilia play in the later stages of molar development. We examined molars from orpk mutant and control mice using microCT imaging and analysis. All first molars contained the same number of cusps in control and orpk mutants suggesting that patterning of the cusps is unaffected despite the reduced size of the molars and presence of a supernummary molar in the mutants. Orpk mutant first molars contained significantly less dentin than controls at 30 days of age (P30) through 120 days of age (P120). The volume of dentin relative to the total volume (DV/TV) showed a significant reduction in the oprk mutant molars. Although dentin volume fraction was significantly decreased, we did not observe an increase in predentin thickness at any age examined suggesting that the reduction in mineralized dentin is not due to alterations in the mineralization process. Despite the decreased volume fraction of dentin in orpk mice, enamel volume not altered at P30. Primary cultures of isolated molar mesenchyme from orpk and control mice showed a reduction in the number of mutant cells expressing primary cilia in vitro. Overall our results show that primary cilia are essential for proper molar morphogenesis specifically the volume of dentin. We are currently investigating whether the reduced amount of dentin found in the orpk mutant first molars is due to changes in odontoblast differentiation or matrix secretion.

***Disclosures: Courtney Haycraft**, None.*

MO0138

Role of endothelial cells in heterotopic ossification using FOP iPS cells. Emilie Barruet*[1], Christopher Schlieve[1], Hannah Kim[1], Mark White[2], Christina Theodoris[2], Deepak Srivastava[2], Ashley Urrutia[1], Edward Hsiao[1]. [1]Institute for Human Genetics & the Division of Endocrinology & Metabolism, University of California, San Francisco, USA, [2]Gladstone Institute of Cardiovascular Disease, San Francisco, USA

Musculoskeletal disorders affecting the bones and joints are major health problems for children and adults. Unfortunately, treatments for skeletal diseases are still rudimentary. The recent advent of human induced pluripotent stem cells (hiPSCs) provides an unparalleled opportunity to identify novel therapies for human skeletal diseases. One major regulatory pathway in bone formation involves bone morphogenetic proteins (BMPs). Patients with mutations in the Activin A Type I receptor (ACVR1), a BMP receptor, develop the debilitating disease fibrodysplasia ossificans progressiva (FOP). They show progressive ossification of muscle and tendon. The majority of ACVR1 mutations occur in a single amino acid (R206H) that may increase ACVR1 signaling activity. Recent data suggest that human endothelial cells carrying the ACVR1 R206H mutation may contribute to the formation of FOP lesions. Our overall hypothesis is that activated BMP signaling in endothelial cells increases heterotopic bone formation by increasing osteogenesis. In this study, we use a series of human iPSCs created from normal control and FOP donors. We previously showed that the FOP iPSCs not only demonstrate increased mineralization and enhanced chondrogenesis but also increased levels of gene expressed by endothelial cells (CD31) when cultured in osteogenic conditions. To determine if the ACVR1 R206H mutation leads to increased endothelial cell production, we used a recently-developed protocol to create human iPSC-derived endothelial cells. We successfully derived endothelial cells from our iPS lines. We found a yield of 25% phenotypic endothelial progenitors ($CD31^+/KDR^+$) from control and FOP iPS lines. After sorting they yield more than 95% $PECAM^+/VE\text{-}CAD^+$ cells. Since there was no significant difference in endothelial cell production, we are now testing if the altered BMP signaling in FOP endothelial cells affects their osteogenic properties. These studies use iPSCs created from patients with FOP, a rare and dramatic disease of massive heterotopic ossification, to establish a robust *in vitro* model of human skeletal tissue formation that may be extended to iPSCs created from other skeletal conditions. The cellular mechanistic insights gained from these studies will establish a solid foundation for understanding the roles of non-bone tissues such as endothelial cells in skeletal formation and for identifying new therapies not only for FOP but also other diseases of abnormal skeletal formation.

***Disclosures: Emilie Barruet**, None.*

MO0139

Withdrawn

MO0140

The genetic basis of cross-phenotype correlation with bone fracture risk: the GEFOS consortium. Ling Oei*[1], Peter Nordström[2], Evangelia Ntzani[3], Hou-Feng Zheng[4], Karol Estrada[5], Emma Duncan[6], Carolina Medina-Gomez[7], Stephen Kaptoge[8], Yi-Hsiang Hsu[9], Jian Yang[10], Carrie Nielson[11], Unnur Styrkarsdottir[12], Paul Ridker[13], Melissa Garcia[14], Aaron Aragaki[15], Anke Enneman[16], Terho Lehtimäki[17], Tõnu Esko[18], Stella Trompet[19], Joel Eriksson[20], Najaf Amin[16], Annie Kung[21], Konstantinos Tsilidis[3], Gudmar Thorleifsson[22], Lynda Rose[23], Joseph Zmuda[24], Ching-Ti Liu[25], Albert Vernon-Smith[26], Priya Srikanth[27], Scott Wilson[28], Graeme Clark[29], Jorma Viikari[30], Evelin Mihailov[18], Alireza Moayyeri[31], Guo Li[32], Candace Kammerer[24], Mattias Lorentzon[33], Natalia Rivera[16], Sumei Xiao[34], Gregory Tranah[35], Dan Evans[35], Kristin Siggeirsdottir[36], Edwin Oei[16], Kari Stefansson[22], Ville Aalto[37], Dana Willner[29], Nicholas Wareham[38], Ryan Minster[39], Joshua Bis[32], Cornelia van Duijn[16], Alan Boyle[40], Michael Snyder[40], Lizbeth Herrera[16], L. Adrienne Cupples[25], Thor Aspelund[26], Olli Raitakari[37], Paul Leo[29], Kay-Tee Khaw[41], John Robbins[42], Yongmei Liu[43], Stephan Breda[16], Robert Luben[41], Jane Cauley[24], Alice Arnold[32], Sjur Reppe[44], Matthew Hibbs[45], Lisette Stolk[16], Julie Pasco[46], Elin Grundberg[47], Kaare Gautvik[48], Cheryl Ackert-Bicknell[45], Vijay Yadav[49], Kwangbom Choi[50], Jeroen van de Peppel[16], Johannes Van Leeuwen[51], Huibert Pols[51], Albert Hofman[16], Jian Shen[11], Joyce van Meurs[16], Biljana Atanasovska[16], Pak Sham[52], Claes Ohlsson[53], Bruce Psaty[32], Tamara Harris[54], Jonathan Reeve[55], J. Wouter Jukema[19], Andres Metspalu[18], Mika Kahonen[56], Nathalie van der Velde[16], Matthew Brown[57], Vilmundar Gudnason[26], John Ioannidis[40], Andre Uitterlinden[58], Steven Cummings[59], Tim Spector[31], Douglas Kiel[60], Rebecca Jackson[61], Unnur Thorsteinsdottir[22], Daniel Chasman[23], Eric Orwoll[11], David Karasik[62], Maria Zillikens[63], Evangelos Evangelou[3], Brent Richards[4], Peter Visscher[10], Karl Michaelsson[64], Fernando Rivadeneira[51], the GEFOS consortium[65]. [1]Erasmus University Medical Center, The Netherlands, [2]Umeå University, Sweden, [3]University of Ioannina Medical School, Greece, [4]McGill University, Canada, [5]Analytic & Translational Genetics Unit, Massachusetts General Hospital, USA, [6]Royal Brisbane & Women's Hospital, Australia, [7]Erasmus Medical Center, The Netherlands, [8]University of Cambridge Bone Research Group, United Kingdom, [9]Hebrew SeniorLife Institute for Aging Research & Harvard Medical School, USA, [10]Queensland Institute of Medical Research, Australia, [11]Oregon Health & Science University, USA, [12]Decode Genetics, Iceland, [13]Brigham & Women's Hospital, USA, [14]NIA, NIH, USA, [15]Division of Public Health Sciences, Fred Hutchinson Cancer Research Center, USA, [16]Erasmus MC, Netherlands, [17]University of Tampere & Tampere University Hospital, Finland, [18]University of Tartu, Estonia, [19]Leiden University Medical Center, Netherlands, [20]Centre for Bone & Arthritis Research, Sweden, [21]Dr. Kung-Wai Chee Clinic, Hong Kong, [22]deCODE Genetics, Iceland, [23]Brigham & Women's Hospital, USA, [24]University of Pittsburgh Graduate School of Public Health, USA, [25]Boston University School of Public Health, USA, [26]Icelandic Heart Association & University of Iceland, Iceland, [27]Oregon Health & Science University, USA, [28]University of Western Australia, Australia, [29]University of Queensland Diamantina Institute, Australia, [30]University of Turku & Turku University Hospital, Finland, [31]King's College London, United Kingdom, [32]University of Washington, USA, [33]Geriatric Medicine, Center for Bone Research at the Sahlgrenska Academy, Sweden, [34]The University of Hong Kong, Peoples Republic of China, [35]Research Institute, California Pacific Medical Center, USA, [36]Icelandic Heart Association, Iceland, [37]Research Centre of Applied & Preventive Cardiovascular Medicine, University of Turku, Finland, [38]Medical Research Council (MRC) Epidemiology Unit, United Kingdom, [39]Graduate School of Public Health, University of Pittsburgh, USA, [40]Stanford University, USA, [41]University of Cambridge, United Kingdom, [42]University of California, Davis Medical Center, USA, [43]Wake Forest University School of Medicine, USA, [44]Oslo University Hospital, Ullevaal, Norway, [45]The Jackson Laboratory, USA, [46]Deakin University, Australia, [47]McGill University, Canada, [48]Institute of Basic Medical Sciences, Norway, [49]Sanger Welcome Trust Institute, United Kingdom, [50]The Jackson Laboratory, USA, [51]Erasmus University Medical Center, The Netherlands, [52]The University of Hong Kong, Hong Kong, [53]Center for Bone & Arthritis Research at the Sahlgrenska Academy, Sweden, [54]Intramural Research Program, National Institute on Aging, USA, [55]University of Oxford, United Kingdom, [56]University of Tampere & Tampere University Hospital, Tampere, Finland, Finland, [57]Diamantina Institute of Cancer, Immunology & Metabolic Medicine, Australia, [58]Rm Ee 575, Genetic Laboratory, The Netherlands, [59]San Francisco Coordinating Center, USA, [60]Hebrew SeniorLife, USA, [61]The Ohio State University, USA, [62]Hebrew SeniorLife; Bar Ilan University, USA, [63]Erasmus Mc, The Netherlands, [64]Uppsala Clinical Research Center, Sweden, [65], USA

Introduction: Fracture risk has a multifactorial etiology with a significant heritable component. We estimated how much of the variance in fracture risk could be explained by known genetic variants for phenotypes correlated with fracture risk. Methods: The GEFOS consortium fracture (age >18 years, any bone) GWAS meta-analysis discovery phase included 19,414 cases (total 102,873 participants; 24 GWAS). SNP lists were drawn from published GWAS meta-analyses for correlated phenotypes: 1) bone mineral density (BMD), at femoral neck and lumbar spine measured by DXA); 2) height; 3) type 2 diabetes mellitus (T2DM); 4) C-reactive protein (CRP); 5) vitamin D. Inverse variance fixed-effects logistic regression models were meta-analyzed adjusted for sex, age, height and weight (2,483,202 SNPs). Independent signals for fracture association were clumped by PLINK (distance>250kb; $r^2<0.50$). The variance explained was summed from per-SNP (V_{SNP}) calculations dependent on minor allele frequency (MAF) and the effect estimate for fracture risk from the meta-analysis ($\beta_{fracture}$): $V_{SNP}=2*(\beta_{fracture})^2*MAF*(1-MAF)$. Analyses were performed per trait and as a composite score (independent signals $r^2<0.1$). To determine whether sets of SNPs for the correlated traits explained more phenotypic variance in fracture risk than expected by chance, P-values were derived from random sampling cumulative distributions. Results:The top-associated genome-wide significant signals ($P<5x10^{-8}$, 3 SNPs) explained 1% of variance of fracture risk; a more lenient significance threshold ($P<5x10^{-6}$) resulted in genetic variants (24 SNPs) explaining 5.1%. BMD SNPs explained 3.9% (63 SNPs in 56 loci, $P=2x10^{-4}$), height SNPs 2.5% (180 SNPs in 180 loci, P=0.04), T2DM SNPs 0.7% (68 SNPs in 65 loci, P=0.4); CRP SNPs 0.3% (29 SNPs in 29 loci, P=0.4) and vitamin D SNPs 0.04% (3 SNPs in 3 loci, P=0.26). The composite score explained 6.7% of fracture risk (322 SNPs in 322 loci, P=0.002). Conclusion: Prioritized fracture SNPs explain ~5% of variance in our discovery sample. However, SNPs associated with traits correlated with fracture risk still explain more, validating these traits as important contributors overall. Finding genetic determinants of fracture independently from the known clinically contributing traits is relevant, but will require very large sample sizes for sufficient power. The GEFOS and GENOMOS consortia replication phase is ongoing and our prediction studies should be validated in independent studies.

***Disclosures: Ling Oei**, None.*

MO0141

Transcriptional Induction of ADAMTS5 by an NF-κ Family Member RelA/p65 in Chondrocytes during Osteoarthritis Development. Hiroshi Kobayashi*[1], Makoto Hirata[2], Shozo Itoh[2], Taku Saito[3], Ung-Il Chung[4], Hiroshi Kawaguchi[5]. [1]The University of Tokyo Hospital, Japan, [2]The University of Tokyo, Japan, [3]University of Tokyo, Graduate School of Medicine, Japan, [4]University of Tokyo Schools of Engineering & Medicine, Japan, [5]University of Tokyo, Faculty of Medicine, Japan

ADAMTS5 (aggreacanase-2) is a crucial proteinase that degrades articular cartilage during osteoarthritis (OA) development. To elucidate the molecular network as a therapeutic target of OA, this study attempted to identify transcripion factors to induce ADAMTS5 expression and examined the underlying mechanism. Exhaustive comparison of the genomic sequences of 5'-end flanking regions of human, macaca, and mouse *Adamts5* genes revealed that the 1.4 kb region upstream of the transcriptional start site was highly conserved among the species. The sequence search in this region predicted the consensus binding motifs of NF-κB, C/EBP, GATA, RUNX, AP-1, OCT, SOX, STAT, and HIF. Among the transcription factors that are known to bind to these sites, an NF-κB family member, RelA/p65, most strongly stimulated the luciferase activity containing the 1.4 kb human *ADAMTS5* gene fragment. In the *ADAMTS5* genes, there were three NF-κB binding motifs: −1,196/−1,187, −896/−887, and −424/−415 bp, in which deletion, mutagenesis, and tandem-repeat analyses of the luciferase assay identified the core responsive regions of RelA/p65 to be the two upstream motifs. Electrophoretic mobility shift assay revealed the binding of nuclear extracts of RelA/p65-overexpressed COS-7 cells with the two NF-κB motif oligonucleotide probes. The specificity of the binding was verified by the cold competition with excess amount of the unlabelled wild-type probe and by the supershift with an antibody to RelA/p65. Retroviral overexpression of RelA/p65 markedly increased the *Adamts5* mRNA level in ATDC5 cells. The endogenous *Adamts5* induction by IL-1β, a putative NF-κB inducer, was suppressed by the knockdown of *RelA* through its specific siRNA transfection. The *Adamts5* expression was inhibited by the *Rela* deletion through adenoviral transfection with Cre in primary articular chondrocytes from $Rela^{fl/fl}$ mice. In the *ex vivo* culture of femoral head cartilage from *Prx1*-Cre;$Rela^{fl/fl}$ mice, the aggrecan fragment release induced by IL-1β was significantly lower than that in the culture from $Rela^{fl/fl}$ mice. Finally, in the OA model by surgical induction of instability in the knee joints of 8-week-old mice, Adamts5 and RelA/p65 were co-localized in chondrocytes of the degraded articular cartilage. In conclusion, we identified RelA/p65 as a potent transcriptional activator of ADAMTS5 in chondrocytes. The molecular network related to the RelA/p65-ADAMTS5 axis may thus represent a therapeutic target for OA.

***Disclosures: Hiroshi Kobayashi**, None.*

MO0142

Genome-wide association identifies *Wnt4* as a regulator of osteoblast activity. Cheryl Ackert-Bicknell*[1], Gina Calabrese[2], Dana Godfrey[1], Kathryn Shultz[1], Charles Farber[2]. [1]The Jackson Laboratory, USA, [2]University of Virginia, USA

Osteoporotic fracture and fracture-related traits, such as bone mineral density (BMD), are highly heritable. BMD has become the trait of choice for genetic studies of osteoporosis due in part to its high heritability; however, BMD is not an ideal phenotype for genetic studies. Bone mass is the net product of formation and resorption and each of these processes is influenced by a myriad of complex factors. This makes it challenging to translate the discovery of novel BMD genes into a better understanding of bone biology. As an alternative, we have focused on the genetics of osteoblast activity. Osteoblast activity was defined as the ability of osteoblasts to form mineralized modules *in vitro*. Primary calvarial osteoblasts from 22 inbred strains of mice were cultured in differentiation media for 10 days, after which the degree of mineralization was assessed by alizarin red staining. For 16 of these strains, BMD data was also available and we found that mineralized nodule formation was positively correlated with BMD in both females (r=0.35; P=0.17) and males (r=0.54; P=0.03), indicating that this *in vitro* phenotype is physiologically relevant. Using genome-wide association (GWA) analysis we identified three genome-wide significant loci (permutation-derived significance threshold P=2.53 x 10^{-6}) associated with mineralized nodule formation. The most significant (P= 5.25 x 10^{-8}) locus was located on mouse chromosome 4. Mineralized nodule formation was twice as high for strains homozygous for the reference (C57BL/6J) allele (0.89 $\pm$ 0.04 mM, N=16) as compared to strains homozygous for the non-reference allele (0.43 $\pm$ 0.04 mM, N=6). The associated haplotype spanned ~200 Kbp (from 136.65 to 136.88 Mbp) and contained only the *Wnt4* gene, a gene previously implicated in human BMD GWA studies. By examining gene expression across osteoblastogenesis using RNA-seq, we determined that expression of *Wnt4* is highest in pre-osteoblasts, after which expression falls to a low but consistent baseline level. The DBA/2J strain is homozygous for the non-reference allele at this locus and expression of *Wnt4* was 7.3 fold higher in osteoblasts from DBA/2J mice as compared to C57BL/6J (P =0.01). These data suggest that the genetic analysis of physiologically relevant cellular phenotypes is a powerful alternative to complex organismal-level traits and that *Wnt4* is a regulator of osteoblast activity.

***Disclosures: Cheryl Ackert-Bicknell**, None.*

MO0143

BMP3 Expression by Osteoblasts Is Regulated by Canonical Wnt Signaling. Shoichiro Kokabu*[1], Laura Gamer[1], Jonathan Lowery[1], Tsuyoshi Sato[2], Tetsuya Yoda[2], Takenobu Katagiri[3], Vicki Rosen[1]. [1]Harvard School of Dental Medicine, USA, [2]Saitama Medical University, Japan, [3]Saitama Medical University Research Center for Genomic Medicine, Japan

Bone morphogenetic protein 3 (BMP3), the most abundant BMP in bone matrix, is produced by osteoblasts and osteocytes in the adult skeleton. Targeted disruption of *Bmp3* in mice results in increased trabecular bone formation and high bone mass, while transgenic overexpression of BMP3 in skeletal progenitors leads to delayed mineral deposition during endochondral ossification and spontaneous fracture. BMP3 suppresses BMP-induced osteoblast differentiation and subsequent maturation through an interaction with the type II BMP/activin receptor, activin receptor 2b (Acvr2b). Thus, BMP3 is regarded as a negative regulator of bone formation.Recently we identified the minimal promoter region of mouse *bmp3* and determined that this region contains several putative canonical Wnt responsive elements. Here we report that canonical Wnt signaling stimulates BMP3 expression in osteoblasts. First, we observed elevated BMP3 expression by calvarial osteoblasts isolated from DKK1 heterozygous knockout mice, a model of increased canonical Wnt signaling. Next we found that when calvarial osteoblasts harvested from wild-type mice were treated with recombinant Wnt3a, BMP3 mRNA levels were strongly increased. Based on these findings, we used primary osteoblasts obtained from mice carrying a LacZ knock-in allele to the *Bmp3* locus as a system to monitor BMP3 production. We find that treatment with Wnt3a and other canonical Wnts greatly increased BMP3 production, as did treatment with LiCl, an inhibitor of GSK3-beta. In contrast, treatment with Wnt5a, an activator of non-canonical Wnt signaling, had no effect on BMP3 expression. Taken together, these data suggest that the BMP and Wnt signaling pathways interact at the level of BMP3. The importance of canonical Wnt signaling in bone is well documented and in general, increasing canonical Wnt signaling correlates with enhanced bone formation through increased differentiation and maturation of osteoblasts. Based on these results, we hypothesize Wnt signaling not only induces bone formation but also regulates osteogenic BMP activity in vivo via induction of BMP3.

***Disclosures: Shoichiro Kokabu**, None.*

MO0144

Evaluation of muscle derived stem cells combined with a sustained release of BMP2 coacervate for bone regeneration. Hongshuai Li*[1], Noah Johnson[2], Xueqin Gao[1], Yadong Wang[2], Johnny Huard[3]. [1]University of Pittsburgh, USA, [2]Dept. of Bioengineering, University of Pittsburgh, USA, [3]Orthopaedic Surgery, USA

Introduction:Muscle-derived stem cells, (MDSCs) can be isolated from the skeletal muscle via a modified preplate technique [1], which is a promising cell source for bone tissue engineering [2-4]. However, without the transduction of BMPs the cells do not differentiate towards an osteogenic lineage. We report here the efficacy of a unique growth factor delivery platform comprised of native heparin and a polycation, poly(ethylene argininylaspartate diglyceride) (PEAD) incorporated with BMP2 (BMP2 coacervate) that can stimulate mouse and human MDSCs to differentiate into an osteogenic lineage and form viable bone. Methods:Mouse andhuman MDSCs were isolated via a modified pre-plated technique. The BMP2 coacervate was prepared as previously described [5]. The osteogenic effects that the delivered BMP2 had on the MDSCs were evaluated both in vitro and in vivo at an ectopic site and in a critical sized calvarial defect which were compared with MDSCs that were transduced with a lenti-BMP2 viral vector. Results:Prolonged release of loaded BMP2 was observed and BMP2 coacervate significantly stimulated the expression of ALP and mRNA levels of Col-1 and osteocalcin compared to the free BMP2. Micro-CT analysis showed significantly more ectopic bone in the BMP2 coacervate+MDSC group compared with free BMP2+MDSC group. In the calvarial defect model, significantly higher bone volume in the BMP2 coacervate+MDSC group was observed compared to the free BMP2+MDSC group; and there was no significant difference between the BMP2 coacervate+MDSC and BMP2 transduced MDSC groups (Fig. 1). Alizarin red and von Kossa staining revealed calcified osteoid matrix in the transplanted area containing MDSCs with BMP2 coacervate. Immuno-histological staining of GFP and human specific MHC-1 demonstrated the presence of donor cells throughout and at the edge of the osteoid, which suggests that the MDSCs were not only present within the osteoid but were active in the new bone formation. Conclusion:This study demonstrated that a dual muscle cell and growth factor delivery approach may be a viable therapy for bone regeneration. The implantation of non-genetically modified MDSCs to the injury site with an effective BMP delivery system is a practical option for patients in terms of both safety and long term results.

References:1. Nat Protoc. 2008;3:1501-9. 2. Blood Cells Mol Dis. 2001;27:924-33. 3. J Cell Biol. 2002;157:851-64. 4. Bone. 2004;34:982-92. 5. Biotechnol Prog. 2012;28:257-64

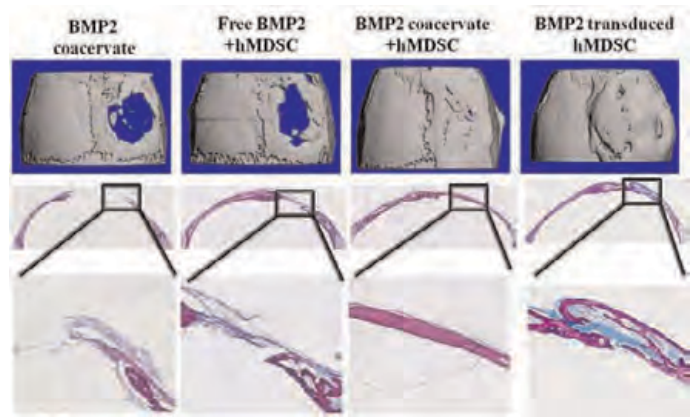

Fig. 1 Representative Micro-CT and histological (Herovici staining) images of bone formation at week

***Disclosures: Hongshuai Li**, None.*

MO0145

The BMP Type I Receptor Alk2 is a Key Regulator of Chondrogenesis. Andria Culbert*, Salin Chakkalakal, Edwin Theosmy, Linda Wang, Eileen Shore. University of Pennsylvania, USA

Bone morphogenetic protein (BMP) signaling is a critical regulator of cartilage differentiation and endochondral ossification. Suppression or hyper-activation of BMP signaling results in delayed maturation and expansion of cartilage elements respectively. ALK2 (activin receptor-like kinase 2) is a highly conserved bone morphogenetic protein (BMP) type I receptor that responds to exogenous ligand to mediate downstream BMP signaling. Gain-of-function mutations in ACVR1/ALK2 cause the rare genetic disorder fibrodysplasia ossificans progressiva (FOP), characterized by progressive heterotopic (extra-skeletal) endochondral ossification, suggesting that the Alk2 receptor mediates signaling in progenitor cells to regulate chondrogenic cell fate decisions. To test this hypothesis, mouse embryonic fibroblasts (MEFs) were used as a mesenchymal progenitor cell model. MEFs from $Alk2^{R206H/+}$ knock-in and Alk2 knock-out ($Alk2^{KO}$) embryos were used to examine enhanced and absent Alk2 signaling respectively. $Alk2^{R206H/+}$ MEFs showed increased BMP signaling, relative to wild-type cells, as detected by Smad1/5/8 phosphorylation and

increased expression of BMP responsive genes in both the absence and presence of BMP ligand. BMP-induced Smad1/5/8 phosphorylation and BMP-responsive transcripts are reduced in Alk2KO MEFs; the remaining BMP signaling in these cells is mediated by Alk3 and Alk6 BMP type I receptors. BMP-induced chondrogenic differentiation is accelerated in $Alk2^{R206H/+}$ MEFs but suppressed in $Alk2^{KO}$ MEFs, despite BMP signaling through Alk3 and Alk6. We determined that Alk2 mRNA expression is highest in undifferentiated MEFs and decreases rapidly upon differentiation. Depletion of Alk2 at early stages of chondrogenic induction (within 48 hours), but not later stages, impairs chondrogenesis. By contrast, stimulating differentiation of either wild-type or $Alk2^{R206H/+}$ MEFs with BMP for only the initial 48 hours is sufficient to promote differentiation and maintain the enhanced differentiation of $Alk2^{R206H/+}$ MEFs. Our data show that Alk2 in mesenchymal progenitor cells enhances chondrogenic differentiation with specific and key roles during commitment and/or early chondrogenesis.

***Disclosures: Andria Culbert**, None.*

MO0146

Determining the role of FGF on osteogenic and adipogenic differentiation and conversion in mesenchymal stem cells. Meike Simann*[1], Solange Le Blanc[2], Franz Jakob[3], Norbert Schuetze[1], Tatjana Schilling[4]. [1]University of Wuerzburg, Orthopedic Center for Musculoskeletal Research, Germany, [2]Universitat Wurzburg, Germany, [3]Orthopedic Center for Musculoskeletal Research, Germany, [4]University of Wuerzburg, Germany

Osteoporosis is commonly accompanied by an accumulation of fat tissue in the bone marrow, referred to as fatty degeneration. Thus, trabecular bone is replaced by adipose tissue. Moreover, adipocytes and osteoblasts emerge from the same origin, the mesenchymal stem cell (MSC), which can differentiate into the adipogenic or the osteogenic lineage. Consequently, there is an inverse relationship between bone and fat. Besides the differentiation of bone marrow MSC (BM-MSC) into adipocytes the conversion of osteoblasts into adipocytes is a major cause of fatty degeneration. To our knowledge, to date common therapeutics do not address this issue. Therefore, our aim is to find and explore factors inhibiting adipogenic differentiation and conversion in order to contribute to a novel approach for osteoporosis therapy and prevention.

So far, we have demonstrated in vitro that human BM-MSC-derived pre-osteoblasts can be converted into adipocytes (adipogenic conversion) and vice versa (osteogenic conversion). Differentiation/conversion status was approved by histological stainings and RT-PCR of adipogenic and osteogenic markers. A global gene expression analysis displayed regulated signaling factors during the onset of adipogenic and osteogenic conversion. Strongly and inversely regulated genes were found in FGF (fibroblast growth factor), IGF (insulin-like growth factor) and G-protein signaling cascades. Members of the FGF family were upregulated in osteogenic conversion and downregulated in adipogenic conversion, hinting at downstream control points favoring osteogenesis while preventing adipogenesis.

Recently, we showed that different promising members of the FGF family strongly inhibit both, the adipogenic differentiation of MSC and the adipogenic conversion of pre-osteoblasts into adipocytes. Furthermore, the addition of a selective FGFR (FGF receptor) inhibitor abolished the inhibitory effect. The relevant FGFR isoform was identified via RNA interference using a stable lentiviral transduction system. Next, we want to address the dose dependency of the inhibitory process. Furthermore, we aim to elucidate the intracellular signaling mechanisms crucial for the onset of conversion and their involvement within either established or so far unknown pathways.

Taken together, our results could aid to prevent the fatty degeneration of bone marrow as well as bone loss in elderly and osteoporotic patients by enhancing osteogenesis and inhibiting adipogenesis at the same time.

***Disclosures: Meike Simann**, None.*

MO0147

Differential Fracture Healing in FGF2KO and FGF2 Transgenic Mice is Associated with Altered Periosteal Progenitor Proliferation. Collin Homer-Bouthiette*[1], Liping Xiao[1], Marja Marie Hurley[2]. [1]University of Connecticut Health Center, USA, [2]University of Connecticut Health Center School of Medicine, USA

FGF2 is decreased in osteoblasts of aged mice and FGF2 knockout (Fgf2KO) mice have impaired bone formation. In contrast, mice overexpressing low molecular weight FGF2 (18kDaFGF2Tg) in osteoblast progenitors have increased bone mass. We hypothesized that fracture healing would be impaired in Fgf2KO but not 18kDaFGF2Tg mice due to modulation of periosteal progenitor proliferation in the early post fracture period. *Approach:* Femur fracture healing was examined in 2m and 24m WT and Fgf2ko mice, as well as 18kDaFGF2Tg and control mice. To assess periosteal cell proliferation, femur fracture was performed on 6m WT and Fgf2KO mice. Immediately after fracture, mice were S.C injected with 100ug/kg (body weight) FGF2 or Vehicle. Mice were sacrificed on day 2 post fracture. 24 hours prior to sacrificing mice were injected intraperitoneally with EdU (5-ethynyl-2'-deoxyuridine) 3ug/gram (body weight) to assess proliferation. Fractured femurs were harvested and frozen sections were stained for EdU, and counterstained with 4'6-diamidino-2-pheynlindole (DAPI) to identify nuclei. Similar assessment of periosteal cell proliferation was performed in 12m 18kDaFGF2Tg and vector mice, however these mice were not treated with FGF2. *Results:* At day 14 post fracture, x-rays showed that calluses were less mineralized in 24m WT type mice as well as in 2 and 24m Fgf2ko mice compared with 2m WT. Quantitative analysis showed that the ratio of bony/total callus area was decreased in 24m WT compared with 2m WT. In addition bony/total callus area was decreased at all ages in Fgf2KO compared with 2m WT. Decreased labeling with EdU was observed in cells of the periosteal surface of the vehicle treated Fgf2KO femur compared with WT, which was partially rescued by exogenous FGF2 treatment. When compared to Fgf2KO mice, utilizing radiography, micro-CT and histology, 18kDaFGF2Tg mice displayed enhanced femur fracture healing. Micro-CT and histology also showed more complete bridging of the femur fracture callus in 18kDaFGF2Tg mice while remodeling was continuing in femurs of Vector mice. Enhanced fracture healing was associated with increased EdU labeling of cells of the periosteal surface of the cortical bone in 18kDFGF2Tg compared with Vector. Thus enhanced periosteal cell proliferation could contribute to the enhanced fracture healing in these mice. These data suggest that endogenous FGF2 is necessary for normal bone regeneration and the 18kDa isoform displays increased fracture healing.

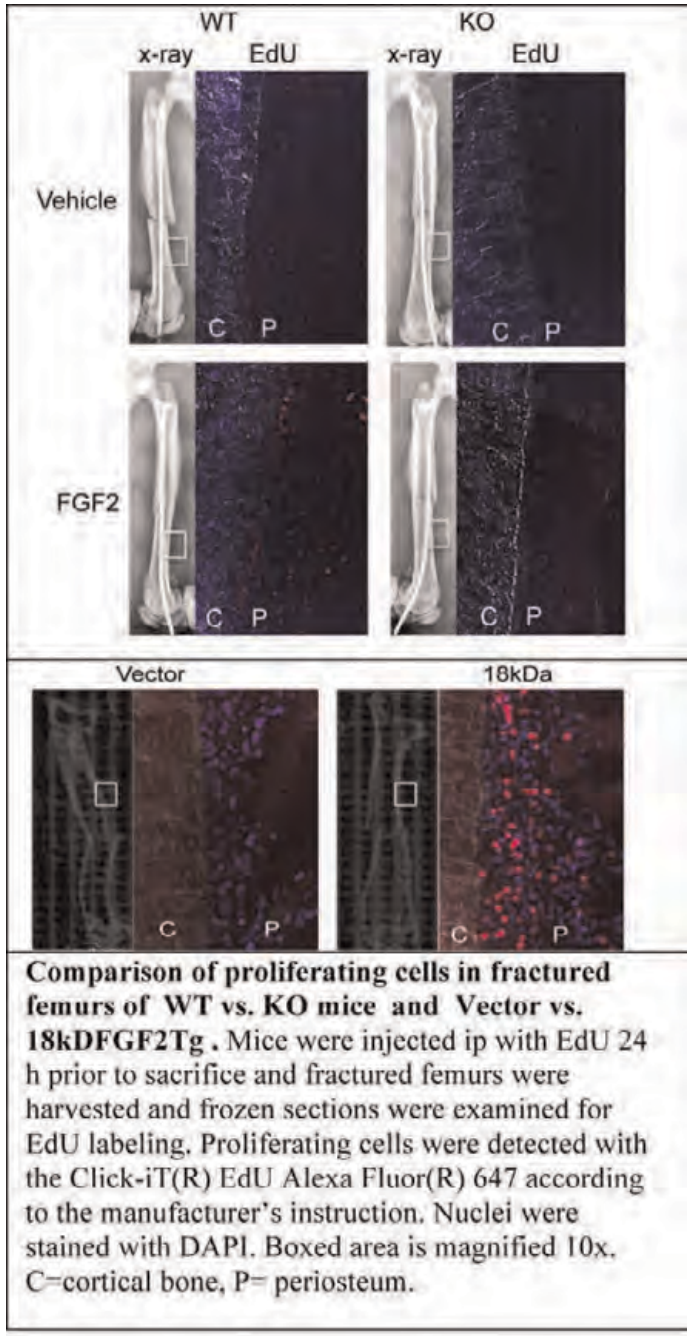

Comparison of proliferating cells in fractured femurs of WT vs. KO mice and Vector vs. 18kDFGF2Tg . Mice were injected ip with EdU 24 h prior to sacrifice and fractured femurs were harvested and frozen sections were examined for EdU labeling. Proliferating cells were detected with the Click-iT(R) EdU Alexa Fluor(R) 647 according to the manufacturer's instruction. Nuclei were stained with DAPI. Boxed area is magnified 10x. C=cortical bone, P= periosteum.

Figure 1

***Disclosures: Collin Homer-Bouthiette**, None.*

MO0148

Bone metastatic melanoma promotes angiogenesis with the production of prostaglandin E2 by host stromal cells. Kenta Watanabe[1], Satoshi Yokoyama[2], Chiho Matsumoto[1], Michiko Hirata[1], Masaki Inada[1], Chisato Miyaura*[1]. [1]Tokyo University of Agriculture & Technology, Japan, [2]Tokyo, Japan

Bone metastasis of malignant melanoma is accompanied by severe bone destruction with increased bone resorption. We reported that sequential pathway of osteoblastic prostaglandin E (PGE) biosynthesis in bone, which is mediated by an inducible PGE synthase, membrane-bound PGE synthase-1 (mPGES-1). *In vivo* mouse cancer injection model, malignant melanoma (B16) proliferation and metastasis were dramatically increased. In the present study, we investigated the mechanisms of PGE associated neo-vascularization with promotion of tumor proliferation and metastasis using mPGES-1-/- mice (mPGES-/-). When B16 cells were injected intravenously into wild-type mice (WT), numerous metastasized locus were found in various tissues including bone, lung, liver, and kidney. In mPGES-/-, however, the number of metastasized locus was markedly suppressed at all. In the laser imaging for *in vivo* detection of neo-vascularization, a red fluorescent labeled polyethyleneglycol particle was used to detect angiogenesis, since the particle was able to incorporate specifically into growing endotherial cells. In WT, the fluorescent signals of neo-vascularization were strongly detected in B16 metastasized foci, but not in mPGES-/-. In the experiments of subcutaneous injection of B16 cells to WT and mPGES-/-, the neo-vascularization was only found in WT. To further elucidate the roles of host-stromal cell derived PGE2 in neo-vascularization for tumor, skin stromal cells from WT and mPGES-/- were co-cultured with fixed-B16 cells. In the co-cultures, stromal cells from WT, but not from mPGES-/-, markedly produced PGE after cell-to-cell interaction with B16 cells. WT derived stromal cells produced vascular endothelial cell growth factor (VEGF)-A and basic fibroblast growth factor (bFGF), and the production of these factors was enhanced by the treatment with PGE. On the other hand, VEGF-A and bFGF production was dramatically decreased in mPGES-/-derived stromal cells. These results suggest that PGE2 produced by host stromal cells promotes VEGF-A and bFGF production, which leads the angiogenesis at the site of melanoma metastasis. The blockage of PGE2 signaling such as PGE receptor antagonist is a candidate for therapy of bone cancer that associate with angiogenesis.

***Disclosures: Chisato Miyaura**, None.*

MO0149

Effect of Foxo1 Deletion in Dendritic Cells on Developing Antibody Levels and Bone Loss in Periodontal Model. Yu Wang*[1], Wenmei Xiao[2], Sandra Pacios[2], Marisa Reason[2], Guangyu Dong[2], Dana Graves[3]. [1]University of Pennsylvania, USA, [2]University of Pennsylvania Dental School, USA, [3]University of Pennsylvania, School of Dental Medicine, USA

Background: Periodontitis is the most common osteolytic disease, is induced by inflammation and characterized by loss of supporting connective tissue and bone. While the host response participates in osteoclastogenesis it also provides essential protection against periodontal pathogens. We determined whether expression of the transcription factor FOXO1 in dendritic cells (DC) played an essential role in protecting alveolar bone from bacteria-stimulated osteolysis or enhanced bone loss.

Methods:FloxedFOXO1 was deleted in dendritic cells *in vivo* by CD11c driven Cre recombinase(CD11c .Cre+.FoxoL/L). Periodontitis was induced in mice by inoculation of P. *gingivalis* and F.*nucleatum* while controls received vehicle alone (2% methylcellulose). Periodontal bone was examined by microCT, antibody level (IgG1) against P. gingivalis was measured by ELISA and migration of dendritic cells was analyzed in vitro in a transwell migration assay. Expression of selected genes that regulate migration was examined by real-time PCR.

Result: Bone loss was observed following infection in both wild type and Foxo1 deletion mice ($P<0.05$). Bone loss in the Foxo1 deletion group compared with wild type was 37% greater in the maxilla and 33% in the mandible. Anti-P. gingivalis IgG1 peaked at 2 weeks after infection was ($P<0.05$) and Foxo1 deletion reduced anti-P. gingivalis IgG1 levels by 51%. Deletion of FOXO1 in dendritic cells decreased CCL21 stimulated migration by 47% ($P<0.05$). FOXO1 deletion reduced mRNA levels of Itgav, Itgb2,Itgb3,CCR7,CXCR4 by 40-60%.

Conclusion: FOXO1 expression in DC is required to protect alveolar bone from periodontal infection that induces bacteria-induced osteolysis. This protection involves regulation of target genes that control DC migration, which is needed to induce an antibody response.

***Disclosures: Yu Wang**, None.*

MO0150

Identification of Novel Small Molecules That Bind to the Loop2 Region of Sclerostin –An *In Silico* Computational Analysis. Karthikeyan Muthusamy*[1], Subburaman Mohan[2], Selvaraman Nagamani[1], Chandrasekhar Kesavan[2]. [1]Dept. of Bioinformatics, Alagappa University, India, [2]Jerry L. Pettis Memorial VA Medical Center, USA

Targeted deletion of sclerostin, a Wnt antagonist, in mice resulted in high bone mass due to a massive increase in the bone formation rate. Furthermore, antibody-based sclerostin inhibition has been used in various studies to reverse bone loss caused by ovariectomy or immobilization and to improve fracture healing. Because of the established importance of sclerostin for the treatment of low bone mass diseases, we screened for novel antagonists against sclerostin using an in *silico* approach. Computational analyses were carried out on a Red hat 5.1 Linux platform. The crystal structure of human sclerostin protein (PDB id -2k8p) was selected as a reference structure (Veverka et al. 2009), in particular loop 2 regions for a molecular docking analysis, as this region is predicted to be involved in binding to Wnts. Screening of a Zinc database containing 99,800 compounds against the active site of sclerostin using virtual workflow revealed 9 potential molecules binding to the loop 2 region of sclerostin. The ADME/T properties predicted by the Qikprop program revealed that the partition coefficient (QPlogPo/w) and water solubility (QPlogS) that provide estimates of absorption and distribution of drugs within the body, ranged between ~ -2.69 to ~ -6.88 and ~ -1.05 to ~ 0.53, respectively, for all nine compounds suggesting that the pharmacokinetic parameters and physicochemical properties are within the acceptable range defined for human use. Compounds 30160056 and 56871042 showed the highest docking score. Density functional theory analysis (an approach that determines the molecular property and biological activity of the compound by using HUMO, LUMO and MESH analysis) showed the best score for compounds 30160056, 56871042 and 72112226 among the 9 molecules. Subsequently, biological activity spectrum analysis (PASS prediction, represents the complex of pharmacological effects, physiological and biochemical mechanism of action results from compound interaction with the biological compound) revealed a best activity score for compounds, 30160056, 56871042 and 72112226 (Table 1). In conclusion, *in silico* analysis revealed nine compounds of which three compounds demonstrated a high binding affinity for sclerostin.

Zinc database Compound[a] ID	DOCKING			ADME		DFT		PASS	
	Glide docking score[b]	Glide docking energy[c]	Prime (ΔG bind)[d]	QPlog Po/w[e]	QPlogS[f]	HOMO[g]	LUMO[h]	Pa[j]	Pi[k]
30160056	-9.56	-47.19	-43.25	-6.69	0.53	0.14	0.20	0.096	0.053
56871042	-8.36	-41.95	-43.85	-6.87	0.20	0.18	0.18	0.135	0.083
72112226	-7.78	-33.83	-45.85	-6.88	-0.17	0.16	0.17	0.153	0.066

TABLE 1. Prediction of activity spectra for compounds [a]Compound id: all the listed compounds are from the Zinc database ; [b]Docking score; [c]Docking energy ; [d]Binding free energy ; [e]Predicted octanol/water partition coefficient (Acceptable range – 2.0 – 6.5); [f]Predicted aqueous solubility, log S. S in mol dm^{-3} is the concentration of the solute in a saturated solution that is in equilibrium with the crystalline solid (Acceptable range -6.5 – 0.5); [g]Highest Occupied Molecular Orbital energy; [h]Lowest Unoccupied Molecular Orbital energy; [j]Estimates of probability being active with 1 being most active; [k]Estimates of probability being inactive with 0 being inactive.

Table 1

***Disclosures: Karthikeyan Muthusamy**, None.*

MO0151

miR-125a, a Pro-inflammatory microRNA that Enhances NF-kB Signaling, Is Elevated with Age in Human Bone Marrow Microvesicles. Sunil Upadhyay*[1], Sudharsan Periyasamy-Thandavan[2], William Hill[2], Carlos Isales[1], Randy Ruark[1], Norman Chutkan[1], Jay Hinson[1], Raymond Corpe[1], Mary Anne Park[1], Candelario Laserna[1], Mark Hamrick[3]. [1]Georgia Regents University, USA, [2]Georgia Regents University & Charlie Norwood VAMC, USA, [3]Georgia Health Sciences University, USA

Cell-derived microvesicles are now acknowledged to play important roles in cell-cell communication. These lipid-based carriers are also known to shuttle microRNAs (miRNAs) between cells, delivering their miRNAs to various cell types via endocytosis and membrane fusion. Microvesicle- derived transport of miRNAs therefore represents one cellular and molecular pathway for epigenetic reprogramming of target cells. We therefore tested the hypothesis that microvesicles isolated from the bone marrow microenvironment transport specific miRNAs, and that these miRNAs change with age. To evaluate this hypothesis we obtained bone marrow samples from young (30-50 y.o.) and older (60-70 y.o.) knee and hip arthroplasty patients. Microvesicles were isolated from bone marrow supernatants (interstitial fluid) using a process of sequential ultracentrifugation and filtration. Presence of microvesicles was validated using PKH67 staining and flow cytometry, and western blotting for Alix and TSG101, well-established markers of exosomes derived from multivesicular bodies. MicroRNA arrays were then used to identify miRNAs whose expression was significantly altered with age. Seven miRNAs were identified from the arrays as showing a greater than two-fold change with age, and PCR validation of these

miRNAs showed that expression of miR125a was increased more than three-fold in samples from the older patients. This miRNA is known to enhance NF-kB signaling in macrophages, and is generally regarded as a pro-inflammatory miRNA. These data suggest that miRNAs derived from exosomes and microvesicles may play a key role in age-related bone loss. Funding for this research was provided by the National Institute on Aging (P01 AG 036675).

***Disclosures: Sunil Upadhyay**, None.*

MO0152

Oxy133, An Osteogenic Oxysterol, Promotes Healing In A Rat Femoral Defect Model. Scott Montgomery*[1], Michael Daubs[1], Haijun Tian[1], Gil Weintraub[1], Elisa Atti[1], Bayan Aghdasi[1], Akinobu Suzuki[1], Trevor Scott[1], Jeffrey Wang[1], Farhad Parhami[2]. [1]UCLA, USA, [2]University of California, Los Angeles, USA

Proteins and small molecules are commonly used in orthopaedics and neurosurgery to stimulate bone growth, augment fracture healing, and promote spine fusion. We have previously demonstrated the ability of Oxy133, an analogue of naturally occurring oxysterols, to promote bone formation in a rat model of spine fusion. Oxy133 was selected among over one hundred and fifty oxysterol analogues based on its potency in inducing alkaline phosphatase activity and its ability to induce the in vitro expression of osteogenic markers in osteoprogenitor cells. Although Oxy133 has been found to successfully promote spine fusion in rats, efficacy of osteogenic oxysterols has not yet been demonstrated in a femoral defect model, which often demands higher doses of BMP2 to achieve healing compared to that used in spine fusion. The current study further investigated the ability of Oxy133 to heal critical sized rat femoral defects. A 6 mm defect was created in the femurs of twenty-four male Lewis rats and a collagen sponge carrying 40 mg Oxy133, 10 ug BMP2, or buffer solution was implanted at the defect site (n=8 per group). Xrays were performed at 4, 6 and 8 weeks. All animals were killed at 8 weeks and the femurs were dissected out and underwent micro-CT and histological analysis. Callus formation bridging the femoral defect was observed on plain radiographs in 7/8 animals treated with 40 mg Oxy133 and 8/8 in the BMP2 group, compared to 1/8 in the control group. Micro-CT confirmed healing of the defect in 87.5% of femurs treated with Oxy133. Oxy133, which we have previously shown to induce spine fusion in a rat model with equivalent efficacy to BMP2, is also capable of healing a critical sized femoral defect in a rodent model with similar success to BMP2. This pre-clinical data suggests significant promise for the use of Oxy133 in clinical scenarios requiring bone formation, such as spine fusion and fracture healing.

***Disclosures: Scott Montgomery**, None.*

MO0153

PDGF Induces Development of Vascularized Bone Grafts by Adipose-Derived Stem Cells. Daphne Hutton*[1], Erika Moore[1], Jeffrey Gimble[2], Xiaofeng Jia[1], Warren Grayson[1]. [1]Johns Hopkins University, USA, [2]Pennington Biomedical Research Center, USA

Vasculature is essential to the functional integration of a tissue-engineered bone graft to enable sufficient nutrient delivery and viability after implantation. Native bone and vasculature develop through intimately coupled, tightly regulated spatiotemporal cell-cell signaling. The complexity of these developmental processes has been a challenge for tissue engineers to recapitulate, resulting in poor co-development of both bone and vasculature within a unified graft. To address this, we cultured adipose-derived stromal/stem cells (ASCs), a clinically relevant, single cell source that has been previously investigated for its ability to give rise to vascularized bone grafts, and studied the effects of initial spatial organization of cells, the temporal addition of growth factors, and the presence of exogenous platelet-derived growth factor-BB (PDGF-BB) on the co-development of bone and vascular tissue structures.

Human ASCs were aggregated into multicellular spheroids via the hanging drop method prior to encapsulation and subsequent outgrowth in fibrin gels. Cellular aggregation substantially increased vascular network density, interconnectivity, and pericyte coverage compared to monodispersed cultures. To form robust vessel networks, it was essential to culture ASCs in purely vasculogenic medium for at least 8 days prior to the addition of osteogenic cues. Physiologically relevant concentrations of exogenous PDGF-BB (20 ng/ml) substantially enhanced both vascular network stability and osteogenic differentiation (Fig. 1). Comparisons with bone morphogenetic protein-2 (BMP-2), another pro-osteogenic and pro-angiogenic growth factor, indicated that this potential to couple the formation of both lineages might be unique to PDGF-BB. Furthermore, the resulting tissue structure demonstrated the close association of mineral deposits with pre-existing vascular structures that have been described for developing tissues.This combination of a single cell source with a potent induction factor used at physiological concentrations can provide a clinically relevant approach to engineering robust vascularized bone grafts with greater efficiency and potential for subsequent viability. In on-going studies, we are growing ASCs in 3D-printed PCL scaffolds to engineer vascularized bone grafts and will evaluate their integration and functionality with native tissues *in vivo*.

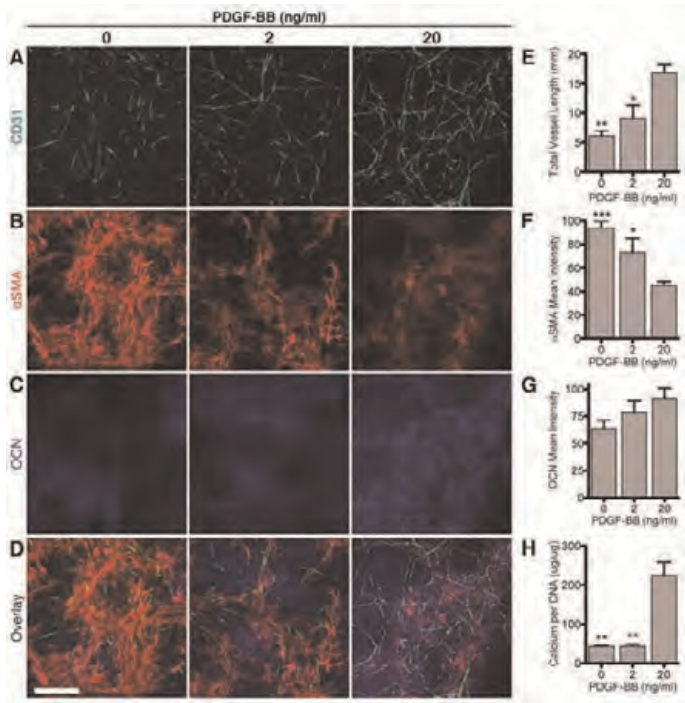

Figure 1. Effects of PDGF-BB on vascular morphogenesis & mineral deposition

***Disclosures: Daphne Hutton**, None.*

MO0154

Progranulin protects against titanium particle induced inflammation and inflammatory osteolysis. Qingyun Tian*[1], Yunpeng Zhao[2], Chuanju Liu[2]. [1]NYU Hospital for Joint Diseases, USA, [2]New York University, USA

It is well known that TNFα play an important role in wear debris induced inflammatory osteolysis, which is a major cause of periprosthetic loosening. We previously reported that Progranulin (PGRN) antagonized TNFα action via binding to TNF receptors and protected against bone erosion in inflammatory arthritis (Tang W, et al, Science, 2011). The goal of this study is to determine whether PGRN plays a protective role in titanium particle induced inflammatory osteolysis. To do so, we took advantage of both in vitro RAW647.3 cells and two in vivo well-accepted mice models. Ti particle dramatically induced expression of endogenous PGRN in RAW647.3 cell and in the mice models. In addition, recombinant PGRN attenuated Ti particle induced inflammation and inflammatory osteolysis in RAW647.3 cell, calvaria explant and mice models, as the elevation of inflammatory biomarkers were significantly impaired, osteoclastogenesis was suppressed and bone erosion of calvaria was protected by PGRN. Furthermore, recombinant PGRN repressed activation of NF-κB signaling pathway by Ti particle. Collectively, PGRN is a novel molecule that inhibits Ti particle induced inflammation, probably through interacting with TNF-α/NF-κB signaling pathways. These findings not only provide novel insights into the role of PGRN in Ti particle induced inflammation reaction, but may also lead to the development of novel therapeutic intervention strategies for periprosthetic loosening.

***Disclosures: Qingyun Tian**, None.*

MO0155

Vasopressin Negatively Regulates Bone Mass. Roberto Tamma*[1], Concetta Cuscito[1], Michelangelo Corcelli[1], Graziana Colaianni[1], Adriana Di Benedetto[1], Maria Grano[1], Silvia Colucci[1], Jianhua Li[2], Tony Yuen[2], Li Sun[2], Mone Zaidi[3], Alberta Zallone[1]. [1]University of Bari Medical School, Italy, [2]Tount Sinai School of Medicine, USA, [3]Mount Sinai Medical Center, USA

Several pituitary hormones, namely TSH, FSH, ACTH, oxytocin (OT) and prolactin, are now known to regulate bone remodeling and bone mass directly. Specifically, a direct anabolic action of the neurohypophseal peptide OT on the skeleton has been demonstrated (Tamma et al., *PNAS,* 2009). Because Arg-vasopressin (AVP) differs from OT by only two amino acids and displays related functions in the brain, we investigated whether AVP directly affects bone and bone cells. We find that the deletion of one of the two AVP receptors, AVPR-1a, in mature mice was sufficient to induce an increase in bone mass, which we documented through micro-CT and by 2D histomorphometry performed at both cortical (femur diaphysis) and trabecular (vertebrae) sites. *Ex vivo* cultures of bone marrow stromal cells obtained from *AVP-1a*$^{-/-}$ mice showed increased expression of osteoblast differentiation genes encoding bone

matrix proteins, and transcription and growth factors (qPCR and Western blotting). *Ex vivo* alkaline phosphatase-positive Cfu-f formation (day 10) and von Kossa-positive Cfu-ob (day 21) formation were also strongly increased in cultures from *AVP-1a*$^{-/-}$ mice. In contrast, TRAP-positive osteoclast formation and resorption of mineralized substrate were both reduced in bone marrow cell cultures from *AVP-1a*$^{-/-}$ mice compared with wild type control cultures, as was the expression (qPCR) of several osteoclast-specific genes. Treatment *in vitro* of both calvarial osteoblasts and bone marrow stromal cells with AVP resulted in reduced mineralized Cfu-ob formation. In contrast, AVP expectedly enhanced the expression of proteins involved in osteoclastogenesis and resorptive activity, namely RANK, c-fms, cathepsin K, TRAP, and the calcitonin receptor. These findings suggest that AVP, through its action on the AVPR-1a, opposes the effect of OT on the skeleton, primarily by decreasing osteoblast differentiation and enhancing osteoclastogenesis and resorption. We also show that both OT and AVP are produced by bone marrow osteoblasts. We believe that mechanisms that control the autocrine production of, and cross-talk between, OT and AVP, as well as those that determine their relationship to the systemic secretion of the two neuropeptides by hypothalamic nuclei, is worthy of further investigation.

***Disclosures: Roberto Tamma**, None.*

MO0156

Delayed bone fracture healing in mice due to Tamoxifen-induced knockout of IGF1R gene in chondrocyte. Zhiqiang Cheng*[1], Hanson Ho[2], Fuqing Song[3], Nathan Liang[3], Alfred Li[3], Rachel Roston[3], Christian Maria[3], Yongmei Wang[4], michael you[3], Chia-ling Tu[3], Daniel Bikle[5], Wenhan Chang[6]. [1]University of California, San Francisco, USA, [2]VAMC, USA, [3]UCSF, USA, [4]Endocrine Unit, University of California, San Francisco/VA Medical Center, USA, [5]Endocrine Research Unit, Division of Endocrinology UCSF & VAMC, USA, [6]Endocrine Unit, VA Medical Center, University of California, San Francisco, USA

Fracture healing in callus recapitulates all stages of endochondral bone formation that is initiated by chondrocyte differentiation. To investigate the role of IGF1R in chondrocytes in regulating bone fracture healing, we performed unfixed tibial mid-shaft fractures by 3-point bending on Tamoxifen-inducible chondrocyte-specific IGF1R knockout (KO) mice and control (Cont) littermates at 3 months of age. Calluses were analyzed at day 10 and 28 post-fracture by histomorphometry, micro-computed tomography (μCT) and quantitative PCR (qPCR). The ablation of IGF1R gene in the cartilage of KO callus was confirmed by genomic DNA analyses and the lack of protein expression by immunohistochemistry. We previously reported that at day 10 post-facture chondrocyte differentiations in the calluses of KO mice was profoundly delayed and this appeared to block the transition from the chondrogenic phase to the osteogenic phase of fracture healing. In the present study, we investigated whether the delayed chondrocyte differentiation impacts the osteogenic phase of fracture healing. At day 28 post-fracture, the sizes of KO and Cont calluses were comparable. There was no visible cartilage present in the calluses of both KO and WT mice, indicating that the calluses have entered osteogenic phase of differentiation. Histomorphometric analysis showed comparable ratio of trabecular bone volume (Tb.BV) over total callus volume (TV) (Tb.BV/TV) in both groups, but revealed significantly increased ratios of bone surface over BV (BS/BV) and ratios of osteoid volume (OV) over BV (OV/BV) and increased ratio of osteoid surface (OS) over BS (OS/BS) in the KO calluses, indicating delayed matrix mineralization. This concept is confirmed by uCT data that showed increased Tb.BV/TV, Tb.CD, and Tb.N with reduced bone mineral density in the KO vs WT calluses. These histomorphometric and μCT data indicated a delay in progression of osteogenesis in the calluses lacking IGF1R in their chondrocytes. This notion is further supported by the reduced expression of markers of mature osteoblast (osteocalcin; by 30%) and osteocyte (dentin matrix protein 1; by 50%) in the KO callus. Together our data suggest that IGF1R signaling in chondrocytes is essential for chondrocyte differentiation, cartilage development, and timely bone formation during fracture healing.

***Disclosures: Zhiqiang Cheng**, None.*

MO0157

Withdrawn

MO0158

Skeletal IGF-1 signaling impacts glucose and energy metabolism. Muriel Babey*[1], Chak Fong[2], Monique O'Leary[3], Emmeline Academia[3], Yongmei Wang[4], Candice GT Tahimic[5], Brian Kennedy[3], Pankaj Kapahi[3], Daniel Bikle[5]. [1]UCSF, Division of Endocrinology, USA, [2]UCSF, USA, [3]Buck Institute, USA, [4]Endocrine Unit, University of California, San Francisco/VA Medical Center, USA, [5]Endocrine Research Unit, Division of Endocrinology UCSF & VAMC, USA

Insulin and insulin-like growth factor (IGF), their receptors, and IGF-binding proteins are important in the hormonal control of many metabolic and growth-related processes. Surprisingly, studies from mouse strains lacking the insulin receptor in two classical insulin target tissues, muscle and white fat, failed to demonstrate an impact on whole body glucose homeostasis, whereas deletion of the insulin receptor from osteoblasts did. In osteoblasts the IGF-1 receptor and insulin receptor show reciprocal cross talk interactions, leading us to evaluate whether deletion of the IGF-1 receptor from osteoblasts would also alter whole body glucose homeostasis and energy balance. Our results indicate that it does and in a reciprocal fashion to deletion of the insulin receptor from these cells. With consumption of a regular diet, glucose clearance was significantly increased in mice lacking the IGF-1 receptor in osteoblasts (IGF-1R OBKO, Cre-Recombinase driven by the 2.3 kb Collagen (α)I Type I promoter) compared to control mice. Glucose clearance was faster in the female than in the male group. However, with the ingestion of a high fat diet, the differences in glucose clearance were not significant between IGF-1R OBKO mice and control mice for either gender. Oxygen consumption, CO_2 production and energy expenditure were increased in female IGF-1R OBKO mice compared to control mice ingesting a normal diet. However, the high fat diet increased these parameters in the control females, but not control males or any of the KO mice. These results indicate that osteoblasts have an important role in regulating both glucose and energy metabolism, a role mediated at least in part by IGF-1 signaling. The metabolic effects of IGF-1 signaling in osteoblasts are more pronounced in the female than in the male group in a diet dependent manner. Further ongoing metabolic evaluation will determine whether these effects are due to changes in endocrine factors such as insulin and osteocalcin and/or to alterations in physical activity, food intake or thermogenesis.

***Disclosures: Muriel Babey**, None.*

MO0159

Bone cells govern T lymphopoiesis by regulating thymic emigrants from bone marrow. Vionnie Yu*[1], Borja Saez[2], Sutada Lotinun[3], Colleen Cook[2], Rushdia Yusuf[2], Marc Raajimakers[2], Joy Wu[4], Henry Kronenberg[2], Roland Baron[5], David Scadden[2]. [1]Massachusetts General Hospital/Harvard University, USA, [2]Massachusetts General Hospital, USA, [3]Harvard School of Dental Medicine, USA, [4]Stanford University School of Medicine, USA, [5]Harvard School of Medicine & of Dental Medicine, USA

Mesenchymal cell direction of parenchymal cell activity is hypothesized to be critical for adult tissue function, but remains poorly defined. We examined how specific subsets of osteolineage mesenchymal cells affect parenchymal hematopoietic cells in the bone marrow by a method of selective cell depletion. Unexpectedly, mature bone cells expressing osteocalcin (Ocn+) were found to be critical for T lymphopoiesis through the modulation of cells destined for thymic emigration. Specific depletion of Ocn+ cells reduced the number of adult bone marrow T-lymphoid biased progenitors by reduced endosteal DLL4 production and hematopoietic progenitor Notch activation. Thymic emigrants were compromised in association with reduced CCR7 expression, yet were capable of normal T lineage differentiation upon adoptive transfer to the thymus. B cell, myeloid progenitor cell and hematopoietic stem cell numbers were unperturbed. Therefore, mature osteolineage cells have a highly constrained hematopoietic cell specific effect, altering T cell production by regulation of thymic emigrants and their ability to translocate to the site of maturation. These data suggest a new role for bone in the homeostasis of the immune system.

***Disclosures: Vionnie Yu**, None.*

MO0160

IDR-1018: A Synthetic Host Defense Peptide that Decreases Infection of Orthopaedic Implants. Hyonmin Choe*[1], David Corn[1], Ashley Rettew[1], Joscelyn Tatro[1], Steve Marshall[2], Aaron Weinberg[1], Zhenghong Lee[1], Robert Bonomo[2], Edward Greenfield[1]. [1]Case Western Reserve University, USA, [2]Louis Stokes Cleveland VA Medical Center, USA

Orthopaedic implant infection is a serious complication that is becoming more difficult to treat due to the increased prevalence of multiple drug resistant bacteria. IDR-1018 is a 12 amino acid, synthetic host defense peptide that reduces soft tissue infections. IDR-1018 is less likely to induce drug resistance because it acts primarily by recruiting macrophages to the infection site rather than directly killing the bacteria. In the current study, we first confirmed that IDR-1018 is not potently bactericidal in physiological solutions (>30-fold higher minimal inhibitory concentration for *Staphylococcus aureus* in PBS than in bacterial broth, 128 ug/ml vs 4 ug/ml). We therefore determined the effects of IDR-1018 in a novel murine model of orthopaedic implant infection. For this purpose, bioluminescent *S. aureus* (Xen36 strain, Caliper Life Sciences) were adhered to titanium alloy implants (1 mm diameter, 3.2 mm length) before insertion into pilot holes in the mid-diaphysis of the femur of 7-week old mice. IDR-1018 (200ug/injection) was administrated i.p. 4 hours before and 24 and 48 hours after implant insertion. Bioluminescence imaging (Xenogen IVIS 200 system) demonstrated that IDR-1018 decreased the bacteria levels by 2- to 4-fold ($p<0.05$) at 1, 3, and 7 days after implant insertion. The decreased bacterial burden induced by IDR-1018 led to increased implant osseointegration as measured by biomechanical pull-out testing. Thus, ultimate force was increased 12-fold ($p<0.05$) and stiffness was increased 15-fold ($p<0.05$). We hypothesized that IDR-1018 would primarily affect bacteria that had spread into the surrounding bone rather than the bacteria adherent to the implant because bacteria in biofilms are protected from macrophages. Consistent with our hypothesis, IDR-1018 decreased the number of colony forming units in the surrounding bone by 10-fold ($p<0.05$) and the amount of bacterial DNA measured by real-time PCR by 6-fold ($p=0.15$) without affecting the

number of bacteria adherent to the implants. These results suggest that application of IDR-1018 may be especially effective in combination with removal of the implant, which is the standard of care for infected orthopaedic implants in patients.

***Disclosures: Hyonmin Choe**, None.*

MO0161

Lectin-like Oxidized Low-density of Lipoprotein Receptor-1 Is Involved in RANKL-production Elevated by Lipopolysaccharide-injection on Mouse Calvaria and thereby Contributes to Inflammatory Bone Destruction. Mai Nakayachi*[1], Junta Ito[1], Mari Okayasu[2], Chiyomi Hayashida[1], Takuya Sato[1], Naoto suda[1], Tatsuya Sawamura[3], Yoshiyuki Hakeda[1]. [1]Meikai University School of Dentistry, Japan, [2]The University of Tokyo Hospital, Japan, [3]National Cerebral & Cardiovascular Center, Japan

We have demonstrated that osteoclastogenesis is associated with the extracellular level of low-density lipoprotein (LDL) and that LDL receptor deficiency causes impaired osteoclastogenesis and increased bone mass in mice because of defect in osteoclastic cell-cell fusion. Here, we used scavenger receptor class A (SRA) and lectin-like oxidized LDL recptor-1 (LOX-1) knockout (KO) mice to elucidate the role of oxidized LDL in regulating osteoclastogenesis and inflammatory bone destruction. Although RANKL-induced osteoclast formation from SRA KO osteoclast precursors was equivalent to that from wild-type (WT) cells, the osteoclastogenesis from LOX-1 KO precursors was increased and the multinucleated cells formed in culture contained more nuclei than WT cells, indicating the increase in cell-cell fusion. These phenotypes were contrast to osteoclastogenesis of LDL receptor KO mice. However, RANKL-induced expression of osteoclastogenesis-related proteins such as c-fos, NFATc1, cathepsin K and TRAP did not alter between LOX-1 KO and WT osteoclasts. Regarding osteoclast differentiation signals, RANKL-induced Erk activation level was also equivalent between the both genotypes. However, Akt phosphorylation evoked by RANKL in LOX-1 KO osteoclast precursors was greater than that in WT cells. When inflammation was induced by subperiosteal injection of lipopolysaccharide (LPS) on calvaria *in vivo*, gene expression of RANKL mRNA in the injected region was elevated equivalently in WT and SRA KO mice. Consistently with the elevation of RANKL mRNA expression, TRAP, cathepsin K and NFATc1 mRNA levels were comparably increased in the both mice. In contrast, the elevation of RANKL gene expression in LOX-1 KO mice was smaller than that of WT and SRA KO mice, whereas level of RANK gene expression did not change among the three genotypes. These *in vivo* results suggest that osteoclast formation following the induction of RANKL production caused by local inflammation depends on LOX-1. Osteoblats and activated T-cells are RANKL-producing cells in inflammation sites. Although mRNA levels of ALP and CD4 were augmented in WT calvariae injected by LPS, the augmentation in LOX-1 KO calvariae was smaller, suggesting an involvement of LOX-1 in RANKL production by osteoblasts and/or activated T-cells. In conclusion, although LOX-1 is potentially a negative regulator in osteoclastogenesis, LOX-1 may contribute to the inflammatory bone destruction.

***Disclosures: Mai Nakayachi**, None.*

MO0162

Osteoimmmunology deregulation in the osteopetrotic grey-lethal mouse. Marie Mutabaruka*[1], Monica Pata[1], Nathalie Labrecque[2], Jean Vacher[1]. [1]Institut de Recherches Cliniques de Montréal, Canada, [2]Maisonneuve-Rosemont Hospital Research Center, Montreal, Qc, Canada, Canada

Mutations affecting the *Ostm1* gene are responsible for the most severe form of autosomal recessive osteopetrosis both in humans and in the grey-lethal (*gl/gl*) mouse. This osteopetrotic phenotype is associated with increased population of non-functional osteoclasts, obliteration of marrow space and major lymphopoietic defects leading to death at ~3weeks of age. The *gl/gl* T-lymphoid lineage is characterized by an altered distribution of the double and single positive $CD4^+$ and $CD8^+$ T cells, suggesting a role for Ostm1 in T-cell differentiation program. To investigate whether Ostm1 may have a direct role in the T cell lineage, expression of *Ostm1* was evaluated in the various T-cell differentiation stages from early T cells progenitors (ETPs), double negative (DN) precursors and mature single positive ($CD4^+$, $CD8^+$) T cells. Quantification of the various T-cell populations demonstrated significant reduction in the ratio of early T cells progenitors (ETPs) in *gl/gl* thymus compared to controls. Consistent with Ostm1 expression pattern, *gl/gl* mice display early impaired T-cell differentiation by lower c-kit expression level in the DN1 subpopulation that led to the altered distribution of double negative and double positive ($CD4^+CD8^+$) T-cells. Characterization of the *gl/gl* T-cell populations with mature TCRβ and CD69 markers showed normal expression and indicated that intrathymic mechanisms of selection and production were unaffected. Further, ex-vivo co-culture assays of gl/gl ETPs cells showed a faster differentiation kinetic in comparison to controls. This phenotype suggests that Ostm1 play a role during early T-cell differentiation. To assess whether *Ostm1* has an intrinsic role in thymic homeostasis, transgenic mice were generated by targeting *Ostm1* expression, under the control of the CD2 gene regulatory sequences, from early progenitor to mature T cells. Transgenic CD2-*Ostm1* progenies mice had no lymphoid alteration. Importantly, all CD2-*Ostm1 gl/gl* transgenic mice displayed full rescue of the thymic distribution of ETPs, DN as well as of double and single $CD4^+$ $CD8^+$ positive T cells. Since, these mice still have defective osteoclasts and develop osteopetrosis, the T-cell lineage by itself do not play a role in Ostm1 osteopetrosis. Taken together, our study provides the first evidence of an early cell-autonomous role for the *Ostm1* gene in T-cell lineage and thymus homeostasis independently of the myeloid osteoclast lineage.

***Disclosures: Marie Mutabaruka**, None.*

MO0163

Inhibition of MCP-5 Signaling Decreases Osteoarthritic Lesions in a Murine Model of Post-traumatic Osteoarthritis. Lara Longobardi*[1], Huseyin Ozkan[2], Joseph Temple[1], Tieshi Li[1], Alessandra Esposito[1], Timothy Myers[3], Anna Spagnoli[1]. [1]University of North Carolina at Chapel Hill, USA, [2]Gulhane Military Academy, Dept. Orthopedics & Traumatology, Turkey, [3]University of North Carolina, USA

In previous studies we found that down-regulation of the chemokine MCP5 by TGF-β Type II receptor (TβRII) signaling is required for joint development. A balance between cytokines and anabolic growth factors is critical to maintain proper tissue homeostasis. MCP-5, its human homologous MCP-1 and their sole common receptor CCR2, are increased in the inflamed joints of patients with arthritis and in rodent models of arthritis. We found that increasing MCP5 expression levels correlate with OA severity in a murine model of osteoarthritis (OA) (destabilization of medial meniscus, DMM). By using a *Tgfbr2-β-Gal-GFP-BAC* mouse, containing β-gal and GFP reporters for TβRII expression, we have recently reported that TβRII expressing cells ($T\beta RII^+$) localize in specific niches that are maintained through development and postnatal life. Our previous studies demonstrated that intra-articular implants of $T\beta RII^+$ cells into DMM knees were able to abolish MCP-5 up-regulation (Longobardi et al., ASBMR 2012). Our *in-vivo* studies are aimed at determining whether blockade of MCP-5 signaling during DMM affected OA progression. For this purpose we followed two approaches: 1) mice subjected to DMM were treated with RS504393 (an antagonist of the MCP5 receptor CCR2) 1, 4 and 8 weeks after DMM; 2) FACS sorted $T\beta RII^+$ cells from *Tgfbr2-β-Gal-GFP-BAC* limb buds were injected in the intra-articular space of DMM knees 1, 4 and 8 weeks after DMM ($25X10^3$ cells/15µl PBS) to inhibit MCP-5 expression in articular cartilage. In both approaches, mice were euthanized 12-weeks after DMM and knees were subjected to Safranin-O/Fast green staining and graded following the OARSI scoring system for mouse. We found that inhibition of MCP5 signaling by both approaches was able to decrease OA lesions when RS504393 treatment or $T\beta RII^+$ cell implants were performed at an early stage of OA development (1 or 4 weeks after DMM), but not at later stages (8 weeks after DMM). In a parallel study conducted in our group we found that micro-CT analysis of DMM posterior medial tibia show an increased mineralization of endochondral bone compared to sham control (Temple et al, abstract submitted). Interestingly, we observed that the endochondral bone mineralization in the posterior medial tibia subjected to DMM was decreased in mice treated with RS504393, compared to untreated. Our findings suggest a potential role for TβRII/MCP-5 axis during early stage of OA development and open new perspective for OA treatment.

***Disclosures: Lara Longobardi**, None.*

MO0164

A Randomized, Double-Blind, Placebo-Controlled study to evaluate the effects of Alendronate (ALN) on bone mineral density (BMD) and bone remodeling in perimenopausal women with low BMD. Aliya Khan*[1], Sacha Dubois[2], Zohair Rahman[3], Christine Derzko[4]. [1]McMaster University, Canada, [2]LakeHead University, Canada, [3]McMaster, Canada, [4]St. Michael's Hospital, Canada

Introduction: Bone loss in association with the menopausal transition begins approximately 2 years before the last menstrual period. This study evaluated the efficacy of alendronate (ALN) in comparison to placebo in preventing bone loss in perimenopausal women with low BMD.

Methods: Women (40-55 years of age; experiencing at least 5 menstrual cycles per year; confirmed FSH level of $>$ 20 iu/L and lower than 40 iu/L ; reduced BMD T $<$ -1.0 at LS, TH or FN) were randomly assigned to treatment (70 mg ALN and 2800 IU cholecalciferol once per week for one year) or control (a placebo tablet, identical in appearance and taste). All patients also received 500 mg of supplemental carbonate daily.

BMD was measured by Dual-energy X-ray absorptiometry at LS,FN, and TH sites. Biochemistry tests at baseline and 12 month follow-up included: bone specific ALP, creatinine, random urine creatinine, and N-telopeptide (NTX) in serum and urine. Analysis of covariance was used to compare 12 month differences on BMD and biochemical markers by group (ALN versus placebo).

Results: At 12 month follow-up, the ALN group mean LS BMD increased by 3.66% (µd= 0.32; ±0.0081 SE) at 12 months versus a reduction of -3.33% (µd= -0.03; ±0.0084 SE) in the control group ($F(1,36) = 25.45$, $p < .001$). The ALN group FN mean BMD increased by 2.07% (µd= 0.014; ±0.0090 SE) at 12 months versus a reduction of -1.87% (µd= -0.014; ±0.0081 SE) in the control group ($F(1,36) = 4.28$, $p = .046$). In the ALN group, bone-specific alkaline phosphates was reduced by 37.79% (µd= -9.90; ±1.92 SE) compared to a 2.46% (µd= 0.56; ±1.79 SE) increase in the control group ($F(1,35) = 13.65$, $p < .001$)). Similarly, N-telopeptide Urine was also reduced in the ALN group (-27.21%; µd= -11.68; ±4.80 SE) compared to an increase of 21.21% (µd= 9.79; ±5.15 SE) in the control group ($F(1,35)=15.44$, $p<.001$).

Discussion: This is the first study conducted in perimenopausal women evaluating the effect of an antiresorptive agent on BMD and bone remodeling. In perimenopausal women treatment with ALN over 12 months lowered bone remodelling and increased BMD. Bone loss was evident in the placebo group. Early intervention with a bisphosphonate for 12 months in the menopausal transition may be effective in maintaining BMD and microarchitectural integrity.

***Disclosures: Aliya Khan**, AMGEN, Merck, NPS, 6*

MO0165

Bone mineral density predicts fractures in men and women with chronic kidney disease. Sarah West*[1], Charmaine Lok[2], Angela M. Cheung[3], Sophie Jamal[1]. [1]The University of Toronto, Canada, [2]Toronto General Hospital, Canada, [3]University Health Network-University of Toronto, Canada

The clinical utility of bone mineral density (BMD) testing by dual energy x-ray absorptiometry to predict fractures in men and women with chronic kidney disease (CKD) is unclear. Indeed, current clinical practice guidelines do not recommend BMD testing to assess fracture risk in CKD. We determined if BMD at the lumbar spine, femoral neck, and ultradistal radius could predict incident fractures (clinical low trauma and morphometric spine fractures) over one year in 161 subjects with stages 3 to 5 CKD. Subjects were recruited from predialysis renal clinics in the greater Toronto area. The mean age was 62.5 $\pm$ 16.3 years, the mean weight 78.1 $\pm$ 18.1 kg, over half the subjects were men (n=94; 58%), and subjects were equally divided between stages 3, 4 and 5 CKD. The most common cause of CKD was diabetes. One third of subjects reported a fall in the past year and one third had a prevalent fracture at study entry. Over the one year follow-up there were 26 new fractures - 6 self-reported clinical low trauma fractures and 20 morphometric spine fractures. We used linear regression models adjusted for age and weight to determine if there were differences in BMD at baseline by incident fractures. We found that those with fractures had a statistically significant lower BMD at the ultradistal radius compared to those without fractures [0.41 g/cm^2 (95% Confidence Intervals: 0.37 to 0.44) vs. 0.44 g/cm^2 (95% CI: 0.43 to 0.46)]. As well, there was a trend towards a lower BMD at the femoral neck in those with fractures than those without [0.68 g/cm^2 (95% CI: 0.63 to 0.74) vs. 0.74 g/cm^2 (95% CI: 0.71 to 0.76)]. There was no significance difference in BMD at the lumbar spine by incident fractures. Our findings, while limited by the small number of incident fractures during follow-up, suggest that BMD testing, particularly at the ultradistal radius may be a useful clinical test to identify men and women with CKD who are at increased fracture risk.

***Disclosures: Sarah West**, None.*

MO0166

Cortical and Trabecular Bone Mass are Severely Compromised in Rats with Renal Failure and Secondary Hyperparathyroidism. Subburaman Mohan[1], Cheryl Sanchez-Kazi*[2]. [1]Jerry L. Pettis Memorial VA Medical Center, USA, [2]JLP VA Medical Center, USA

While chronic kidney disease (CKD) is known to result in phosphate retention secondary hyperparathyroidism (SHPT) and increased bone fragility, the molecular causes that contribute to skeletal changes are poorly understood. Based on evidence that FGF23, a regulator of phosphate homeostasis, is a key player of disordered mineral metabolism in CKD, we tested the hypothesis that elevated FGF23 is associated with SHPT in a nephrectomized model of renal failure. At 4 wks of age, 27 rats underwent 2-stage 5/6 nephrectomy (Nx) while 12 rats underwent sham Nx (Intact-control). Nx rats were fed either a standard rodent diet (Nx-control, N=13), or a high phosphorus diet to induce advanced SHPT (Nx-phos, N=14). There were no differences in femur length or gain in body length/weight between the 3 groups. Serum creatinine levels were elevated 2-fold ($P<0.01$) in the Nx groups. Serum iPTH levels were 50% and 180% higher ($P<0.03$) in Nx-control and Nx-phos compared to Intact-control at 12 days post Nx. After 25 days post Nx, iPTH levels further increased (5.7 and 1.6 fold, $P<0.04$) in the Nx-phos and Nx-control compared to Intact-control. Serum FGF23 levels were elevated in the Nx-phos compared to Intact-control at 12 days and correlated highly ($r=0.71$, $P<0.01$) with iPTH, thus suggesting that elevated FGF23 could in part contribute to SHPT in Nx-phos. MicroCT measurements of cortical bone at femoral mid-diaphysis revealed 3.9% ($P=0.06$) and 9% ($P<0.01$) reductions in total vBMD in the Nx-control and Nx-phos, respectively, compared to Intact-control. Analyses of trabecular (Tb) bone at the femoral metaphysis revealed a 16% ($P= 0.3$) and 37% ($P<0.001$) reduction in Tb bone volume adjusted for total volume in Nx-control and Nx-phos, respectively. The significant reduction in Tb. bone mass in Nx-phos is caused by a 36% reduction in Tb number ($P=0.01$) and a 29% increase in Tb. separation ($P=0.01$). Accordingly, connectivity density was decreased by 41% in the Nx-phos compared to Intact-control. Furthermore, Tb bone volume changes showed significant negative correlations with both iPTH ($R=-0.66$, $P<0.01$) and FGF23 ($r=-0.55$, $P<0.01$) levels, suggesting that the acute changes in serum iPTH and/or FGF23 contributed to changes in Tb bone mass. Based on these data, we conclude that the initial rise in FGF23 may contribute to PTH elevation that leads to significant loss of cortical bone and increased turnover of Tb bone resulting in deterioration of trabecular architecture in CKD.

***Disclosures: Cheryl Sanchez-Kazi**, None.*

MO0167

Two-year bisphosphonate treatment of renal osteodystrophy in a dialysis patient with chronic kidney disease. Jerzy Przedlacki*[1], Kamilla Nawrot-Wawrzyniak[2], Andrzej Sawicki[3], Paul Roschger[4], Andrzej Dębiński[5], Monika Staszków[6], Ireneusz Nawrot[6], Joanna Matuszkiewicz-Rowińska[6], Klaus Klaushofer[7]. [1]Medical University of Warsaw, Poland, [2]Ludwig Boltzmann Institute of Osteology, Austria, [3]Synexus Poland, Poland, [4]L. Boltzmann Institute of Osteology, Austria, [5]Medical Centre Synexus, Poland, [6]Warsaw Medical University, Poland, [7]Hanusch HospitalLudwig Boftzmann Institute of Osteology, Austria

KDIGO group suggests administration of, e.g., bisphosphonates in dialysis patients with chronic kidney disease with an increased risk for bone fractures only after excluding adynamic bone disease (ABD) on bone biopsy because of their antiresorptive action. The objective of the study was to assess the effectiveness and safety of a two-year alendronate treatment in a 49-year old man receiving a 30-year dialysis course sustaining four low-energy fractures (left and right hip, left metacarpal bone and one rib, the last one 10 days before starting treatment) during last 8 years. After excluding ABD and diagnosing osteomalacia by means of a transiliac bone biopsy, alendronate was started at a weekly oral dose of 70 mg. Simultaneously, daily oral administration of calcium carbonate (3x1.0) and alfacalcidol (0.25 μg) was continued. The alendronate tolerance was good, bone pain decreased, the patient's physical fitness had improved. No new fracture occurred during the therapy. Bone biopsy performed after 1 year of treatment showed recurrent osteomalacia without ABD. There was an increased bone volume, increased trabecular number and thicknesss, decrease of osteoid volume and surface. The bone matrix mineralization density distribution measured by quantitative backscattered electron imaging exhibited: mean and mode calcium content was increased; the width of the distribution was reduced; the fraction of low mineralized bone areas were reduced and that of high one was increased. BMD of radial ultradistal site sustained markedly reduced during 2 years of treatment (Z-score -4.0 to -3.9) but BMD of the shaft was increased for 5.6% (from 0.479 g/cm2, Z-score -6.0 to 0.506 g/cm2, Z-score -5.4) at the end of the second year. Serum osteocalcin significantly decreased from 33.0 ng/ml to 21.2 ng/ml (35.8%) after 6 months and to 4.57 ng/ml after 2 years (86.2%); bone alkaline phosphatase activity remained unchanged up to the end of the first year but significantly decreased after the second year: from 111 IU/l to 39 IU/l (reduction of 64.9%); CTX increased at the end of the first year, from 2.82 ng/ml to 4.5 ng/ml (increase of 59.6%) but returned to the basic value in the end of the second year (2.37 ng/ml). Serum PTH was in optimal range during treatment. In summary, the two-year alendronate treatment of the haemodialysis patient with chronic kidney disease has been effective and safe and is being continued.

***Disclosures: Jerzy Przedlacki**, None.*

MO0168

An Unusual Discrepancy in Bone Density in a Case of Congenital Hypophosphatemic Rickets. Aren Skolnick*[1], Stuart Weinerman[2], Dennis Carey[3]. [1]North Shore-LIJ Health System, USA, [2]Division of Endocrinology, USA, [3]Cohen Children's Medical Center of New York, USA

Background: Hypophosphatemic rickets (HR) is characterized by renal phosphate wasting and defective bone mineralization, resulting in short stature and skeletal abnormalities. It is most commonly caused by an X-linked mutation in the phosphate-regulating endopeptidase gene (PHEX). It has been established that bone mineral density (BMD) results appear to be site-specific with elevated BMD at the lumbar spine and low BMD at the radius. This pattern is felt to be due to secondary hyperparathyroidism. We present a case of congenital HR with a large discrepancy in bone density between the spine and proximal radius in a patient with a normal, intact parathyroid hormone (PTH) on long-term oral phosphate and calcitriol supplementation.

Case: A 20-year-old male was referred for evaluation of HR. He was initially diagnosed as a child with bone deformities, taking calcitriol and sodium potassium phosphorous since diagnosis, with subsequent normal growth and development. Family history was insignificant. Examination revealed a well-nourished male with height 70 inches, weight 111 kg and a body mass index of 35 kg/m. General medical exam was unremarkable with normal dentition and no rachitic rosary. Biochemical investigations revealed total calcium: 9.1 mg/dL, phosphorus: 2.2 mg/dL, albumin: 4.7 g/dL, creatinine: 1.03 mg/dL alkaline phosphatase: 171 U/L, bone specific alkaline phosphatase (BSAP) 54mcg/l(0-20), 1,25-dihydroxyvitamin D: 43.3 pg/ml, 25-hydroxyvitamin D 15.5 ng/mL (PTH): 47 pg/mL, fibroblast growth factor (FGF)23: 84 RU/mL (<180 RU/ml).

BMD revealed a markedly elevated T-score in the spine at +7.2 and total hip +4.1, but -2.6 at the proximal radius. He was given 50,000 IU of ergocalciferol weekly; a 24-hour urine for calcium and phosphorus and genetic testing are planned.

Conclusion: This unusual case is the first reported of a discrepancy of almost 10 standard deviations between the spine and proximal radius BMD in a patient with a normal PTH and FGF-23. The bone turnover appears elevated, based on the high BSAP despite a normal PTH. It is possible that this patient may have an alternative form of HR such as a disorder of the sodium-dependent phosphate transporter in the kidney. The BMD pattern in other HR syndromes has not been studied. Further genetic testing may help establish a specific diagnosis.

References:
Rosenthall L. DEXA bone densitometry measurements in adults with X-linked hypophosphatemia. Clin Nucl Med. 1993;18:564–566.
Cheung M, Roschger P, Klaushofer K, Veilleux L, Roughley P, Glorieux F, Rauch F. Cortical and Trabecular Bone Density in X-Linked Hypophosphatemic Rickets. J Clin Endocrinol Metab. 2012; 1210:1-8.

Keywords: Hypophosphatemic Rickets; Bone Density; Genetics

***Disclosures: Aren Skolnick**, None.*

MO0169

Expansile Ankylosing Skeletal Disease: Phenotype Delineation and Identification of the *IFITM5* Mutation That Causes Osteogenesis Imperfecta, Type V. Michael Whyte*[1], James Aronson[2], William McAlister[3], Robert Weinstein[4], Deborah Wenkert[5], Karen Clements[6], Alexander Pruitt[7], Gary S Gottesman[1], Katherine Madson[1], Horacio Plotkin[8], Steven Mumm[9]. [1]Shriners Hospital for Children-Saint Louis, USA, [2]University of Arkansas for Medical Sciences at Arkansas, Children's Hospital, USA, [3]Mallinckrodt Institute of Radiology at St. Louis Children's Hospital, USA, [4]Central Arkansas VA Healthcare System, Univ of Arkansas for Medical Sciences, USA, [5]Amgen, Inc., USA, [6]Shriners Hospital for Children, USA, [7]Northwest Iowa BOne, Joint & Sports Surgeons, USA, [8]Genzyme, USA, [9]Washington University School of Medicine, USA

In 2003, we briefly reported the unique osteopathy of a 12-year-old boy who beginning in infancy suffered recurrent fractures with hypertrophic callus formation and extraordinary bone expansion followed by skeletal fusion [JBMR 18 (Suppl 2): S286]. We called this "expansile ankylosing skeletal disease" (EASD). In utero, his femurs were short. At age two months, the first of many extremity fractures accompanied this sequence. By age 10 years, the major bones of the lower limbs and pelvis were a single structure. Skin, but almost no other soft tissue, covered the widened bones. Computed tomography revealed shell-like bones that could be cystic and fat-filled with hyperdense cortical areas. Marked hyperphosphatasemia followed major fractures. Bone turnover markers indicated accelerated skeletal remodeling. Histological examination of the cortical and medullary regions of major long bones demonstrated woven bone, cartilage, and fibrovascular tissue with little overlying muscle, fascia, or subcutaneous fat. A brief course of alendronate therapy improved the radiographic appearance of small tubular bones in his hands, but not the generalized pain in his expanded bones. At age 22 years, amputation of a leg showed joint structures encased by bone. Mutation analysis was negative for RANKL, RANK, OPG, SQSTM1, ANKH, GNAS1, and ENPP1. Then, we characterized EASD lifelong in an unrelated woman who succumbed at age 51 years to sepsis from her profound skeletal deformities. Our patients shared with osteogenesis imperfecta, type V (OI-V), calcification of forearm interosseous membranes, dislocation of radial heads, wormian bones, and densely packed osteocytes. In 2012, when OI-V was discovered to be caused by heterozygous mutation (c.-14C>T) of the 5′-UTR of *IFITM5* encoding interferon-induced transmembrane protein 5, we documented this identical mutation in both EASD patients. Here, we delineate the clinical, radiologic, biochemical, and histopathological features of EASD.

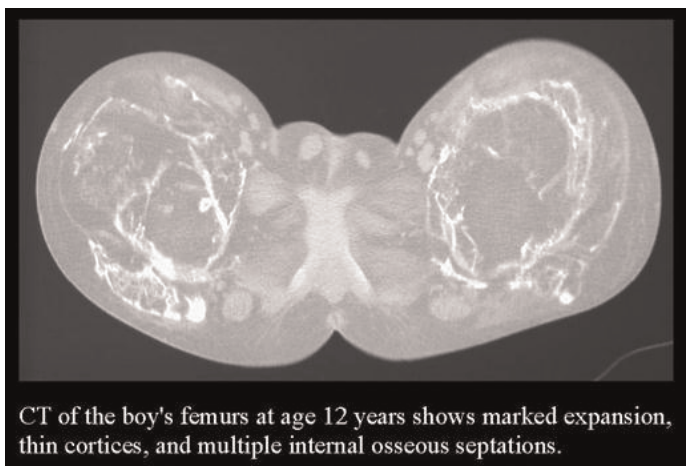

CT of the boy's femurs at age 12 years shows marked expansion, thin cortices, and multiple internal osseous septations.

Figure 1

***Disclosures: Michael Whyte**, None.*

MO0170

Osteopathia Striata with Cranial Sclerosis – A rare osteosclerotic bone disorder. Mariana Marin*[1], Bridget Sinnott[2]. [1]UT Southwestern, USA, [2]UTSW Dallas, USA

We present a case of osteopathia striata with cranial sclerosis (OS-CS) in an 18 year old female who presented to our clinic for evaluation of cranial sclerosis (CS).

The diagnosis of CS followed work-up for sensorineural hearing loss, which revealed bilateral internal auditory canal stenosis. On presentation, she complained of daily frontal headaches, weekly migraines and right knee pain. Medical history was remarkable for a cleft palate, delayed dental eruptions, hearing loss necessitating hearing aids and irregular menses. She had not sustained any fractures. Family history was negative for bone disorders, neurological disorders or endocrinopathies.

Examination revealed a well-nourished female below the mid-parental height who was normocephalic with evidence of a prominent jaw, blue sclera and hypertelorism. Musculoskeletal exam was remarkable for scoliosis and shortened 4th and 5th metacarpals. Neurologic exam was remarkable for myopia and deafness. She had a normal intellect.

Work-up revealed normal bone specific alk phos, TRAP, calcium, phosphate, PTH and IGF-1 levels. 24 hr urine calcium studies were normal. Vitamin D level was 21ng/ml.

Head CT imaging revealed diffuse osteosclerosis of the calvarium and the skull base with osseous encroachment of the bilateral middle ear cavities. There was hypopneumatization of the mastoid, maxillary and sphenoid sinuses. DXA scan showed Z scores of: 4.1 at lumbar spine, 2.0 at left total hip, 4.7 at left femoral neck and -1.5 at 1/3 radius. Thoracic spine X-ray showed mild scoliosis. Radiographs of the femurs revealed vertically orientated sclerotic striations extending from the metaphysis to the diaphysis. Radiographs of the pelvis revealed radiating striations extending into the iliac crests.

OS-CS, also known as Horan-Beighton syndrome, is a rare X-linked dominant sclerosing bone dysplasia, characterized by dense linear striations of long bones & pelvis, CS and extra-skeletal anomalies such as congenital heart disease, respiratory & renal tract abnormalities. It is caused by a mutation in the WTX (Wilm Tumor on X chromosome) gene and is often lethal in males (1). Patients may remain asymptomatic or present with complications secondary to CS, namely cranial nerve entrapment. It is important to make a diagnosis of OS-CS to enable appropriate genetic testing and enable further testing for extra-skeletal anomalies.

(1) Zicari AM et al. WTX R353X mutation in a family with OS-CS. Ital J Pediatr; 2012: 38: 27

***Disclosures: Mariana Marin**, None.*

MO0171

Rapid Response to Denosumab in Fibrous Dysplasia of Bone: Report of Two Cases. Kirtan Ganda*[1], Markus Seibel[2]. [1]Concord Hospital, Australia, [2]Bone Research Program, ANZAC Research Institute, University of Sydney, Australia

Purpose: Fibrous dysplasia (FD) of bone is a non-heritable genetic condition characterized by bone pain, skeletal deformities and pathological fractures. So far, the only treatment shown to significantly alleviate pain, suppress bone turnover and improve radiological features in FD has been bisphosphonate therapy. We here report on clinical and biochemical outcomes in two patients with active polyostotic FD treated with the RANKL inhibitor, denosumab, following unsatisfactory responses to prior long-term bisphosphonate therapy.

Patient and Methods: A 44-year-old female who had received a cumulative dose of 20mg zoledronic acid over 2.5 years, and a 48-year-old male who had received a cumulative dose of 45mg zoledronic acid over 8 years both experienced minimal reductions in pain scores and markers of bone turnover. Following initiation of denosumab 60mg s.c., changes in bone pain, bone turnover (assessed by serum amino-terminal propeptide of type I collagen (PINP) and urinary deoxypyridinoline (DPD)) and whole body radioisotope bone scans were monitored over a period of 14 and 6 months in the female and male patient, respectively.

Results: Following administration of denosumab, both patients demonstrated a rapid and pronounced biochemical response. Within 4-7 weeks, bone turnover markers fell to levels within the respective reference range. The female patient experienced a reduction in pain whilst the male demonstrated a reduction in tracer uptake on bone scan. Dosing intervals varied significantly between the two patients, depending on disease activity at baseline.

Conclusions: Our observations suggest that denosumab is a potential therapeutic option for fibrous dysplasia, particularly in patients who respond insufficiently to treatment with bisphosphonates.

***Disclosures: Kirtan Ganda**, None.*

MO0172

Prevalence of Hypercalcemia of Malignancy in the United States. Victor Gastanaga*[1], Rajul Jain[1], Melissa Pirolli[2], David Quach[2], Jane Quigley[2], Scott Stryker[1], Alexander Liede[1]. [1]Amgen, USA, [2]IMS, USA

Background: Hypercalcemia of malignancy (HCM; CTCAE grade ⩾1, CSC >10.7 mg/dL) is a serious metabolic complication whose prevalence has not been quantified. Rates of HCM differ by tumor type, with highest rates reported in multiple myeloma (MM) and lowest among prostate cancer patients (pts). This analysis estimates HCM prevalence in the US.

Methods: This retrospective study used the Oncology Services Comprehensive Electronic Records (OSCER) warehouse of electronic health records (EHR) including laboratory values from >640,000 pts treated at 525 oncology outpatient sites. OSCER data were projected to the national level by linking EHR to claims data. Cancer pts included were ⩾18 years, and had serum calcium (Ca) and albumin (for corrected serum Ca [CSC]) records. Period prevalence was estimated by HCM CTCAE grade, tumor type, and year (2007-2011). Estimates were adjusted to capture pts diagnosed with HCM outside oncology practices using a subset of pts linkable to office/hospital data.

Results: The analysis included 50912 (2007) to 100449 pts (2012), projected to 3.3 to 3.6 million cancer pts. In 2012, pts with HCM had a median of 5 Ca tests, 54% had chemotherapy, and 35% had bone modifying agents. HCM rates were highest for MM (7.6-10.7%), lowest for prostate (1.4-1.8%). Estimated annual 2007-2012 (adjusted) prevalence of HCM was 72382, 86213, 103746, 105119, 98058, and 98997, respectively. HCM is estimated to have affected 2.7% of cancer pts in 2011.

Conclusions: This study of EHR data from oncology practices across the US found that HCM was more common among MM and lung cancer pts. Approximately 100,000 U.S. cancer pts are affected by HCM each year. These pts would benefit from additional treatment options.

***Disclosures: Victor Gastanaga**, Amgen, 3*
This study received funding from: Amgen

MO0173

Increased Frequency of Renal Stones and Nephrocalcinosis in Heterozygous and Homozygous Carriers of Sequence Variations in SLC34A3/NPT2c. Clemens Bergwitz*[1], Monica Reyes[2], Amita Sharma[2], Thomas Carpenter[3], Marco Janner[4], Andrew Biggin[5], Shamir Tuchman[6], H. Jorge Baluarte[7], Shoji Ichikawa[8], Craig Munns[5], Harald Jueppner[2]. [1]Massachusetts General Hospital & Harvard Medical School, USA, [2]Massachusetts General Hospital, USA, [3]Yale University School of Medicine, USA, [4]University Children's Hospital, Switzerland, [5]The Children's Hospital at Westmead, Australia, [6]Children's National Medical Center, USA, [7]The Children's Hospital of Philadelphia, USA, [8]Indiana University School of Medicine, USA

Homozygous and compound heterozygous mutations in *SLC34A3*, the gene encoding the sodium-dependent co-transporter NPT2c, cause hereditary hypophosphatemic rickets with hypercalciuria (HHRH), a disorder characterized by renal phosphate-wasting resulting in hypophosphatemia, elevated $1,25(OH)_2$ vitamin D (1,25D) levels, hypercalciuria, and rickets/osteomalacia. Similar albeit less severe biochemical changes are also observed in heterozygous carriers, which are furthermore indistinguishable from those encountered in idiopathic hypercalciuria (IH). We here report three HHRH kindreds, in which novel *SLC34A3* mutations were found (c.1304delG in exon 12, c.1357delTTC p.F453del, and c.G1369A p.G457S in exon 13). Review of the clinical records suggests that individuals with mutations in the current and previously reported kindreds affecting one or both *SLC34A3* alleles have a significantly increased risk for the formation of renal stones or nephrocalcinosis (17% (p=0.26) and 50% (p=0.0009), respectively) compared to normals (6%). Prevalence of renal calcifications was associated with increased urinary calcium excretion (p=0.047) due to increased serum levels of 1,25D (p=0.0042), which appears to be a biomarker of adequate oral phosphate supplementation (Yu et. al., Bone, 2012). Urine calcium/creatinine of stone carriers was furthermore inversely correlated with serum parathyroid hormone (PTH) levels (p=0.032). Careful adjustments of oral phosphate therapy on the basis of serum 1,25D and PTH levels may be important for carriers of *SLC34A3* mutations to prevent formation of renal calcifications and possibly chronic kidney disease.

***Disclosures: Clemens Bergwitz**, None.*

MO0174

Quantifying Tissue Mineralization In Vivo for Diagnosing Osteomalacia. Cherie Chiang*[1], Jeffrey Zajac[2], Yu Peng[3], Xiao-Fang Wang[4], Yohann Bala[5], Ali Ghasem-Zadeh[6], Roger Zebaze[6], Ego Seeman[6]. [1]Austin Health, Australia, [2]Austin Hospital, Australia, [3]Straxcorp, Australia, [4]University of Melbourne, Austin Health, Australia, [5]University of Melbourne, Dept. of Medicine, Australia, [6]Austin Health, University of Melbourne, Australia

Purpose: Vitamin D deficiency is the most common cause of osteomalacia worldwide, but whether a circulating level of 25(OH)D of <30 ng/ml is associated with bone disease, and so justifying this diagnostic threshold, is unknown due to lack of studies with bone biopsy evidence of osteomalacia . We hypothesized that non-invasive imaging can be used to quantify tissue under-mineralization associated with osteomalacia.

Methods: We applied a novel nonthreshold based image analysis method (StrAx1.0) to images acquired using high resolution peripheral quantitative computed tomography (HR-pQCT) scans of distal radius, tibia and fibula to quantify tissue mineralization in vivo in 3 kindreds with Vitamin D resistant rickets and 6 age and sex matched healthy controls. Attenuation of voxels containing only void (porosity), only bone matrix at varying degrees of mineralization, or both, was quantified as reported (Zebaze et al 2013). Mineralization level was calculated as the ratio of attenuation by mineralized bone matrix to that produced by 1200 mgHA/cc (maximally mineralized bone matrix) and expressed as a Z-score (standard deviation, SD) away from the mean of age and sex matched controls. Analysis was made of voxels with > 80% maximum attenuation which excludes porosity (as porosity will lower the attenuation to <80% of maximum) and so allows unambiguous assessment of tissue mineralization heterogeneity.

Results: Distal radius mineralization level in the cases was 2.7 to 12 SD lower than controls. In the 25 year old patient with biopsy proven rickets, the voxels within the compact-appearing cortex with attenuation 90-100% of fully mineralized bone matrix was 0.003% compared to 5.38% in the controls. The void-bone matrix curves of the patient illustrates a shift to the left (Fig 1) which could be due to increased porosity, decreased mineralized tissue mass, or decreased level of mineralization of that tissue. After confining analysis to voxels with >80% maximum attenuation (to avoid confounding by porosity), a distinct separation of the patient and control's mineralization distribution was consistent with the presence of matrix under-mineralization. (Fig 2) Data in the tibia and fibula were similar.Conclusions: StrAx1.0 analysis of HR-pQCT images permits identification of undermineralized bone in osteomalacia without the need for invasive bone biopsy.

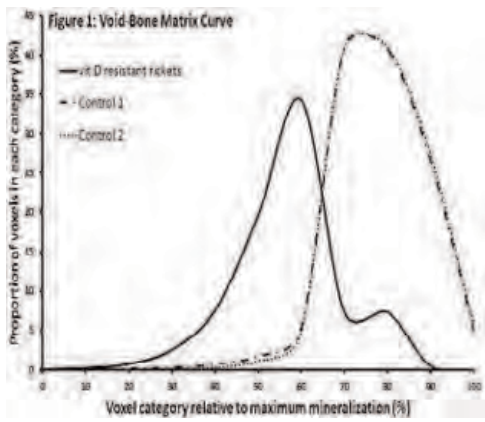

Fig 1

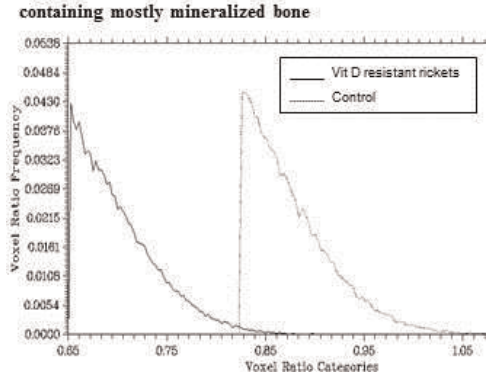

Fig 2

***Disclosures: Cherie Chiang**, None.*

MO0175

Skeletal Fluorosis Progression Revealed by the Analysis of Bone Biopsies. Case Report. Louis-Georges Ste-Marie*[1], Natalie Dion[1], Delphine Farlay[2], Algis V. Jovaisas[3], Georges Boivin[2]. [1]CHUM, Canada, [2]INSERM, UMR1033; Université De Lyon, France, [3]University of Ottawa, Canada

This study describes the progressive development of skeletal fluorosis in a 60-year-old white woman. Thirty years ago, elevated levels of fluoride were found in serum and urine of this patient. In 1983 and 1994, she underwent posterior iliac biopsies which revealed bone quality alterations due to idiopathic fluorosis. In 2008, further investigation on bone remodelling status was initiated by performing a transiliac bone biopsy for histomorphometric analysis. In addition to osteoporosis, the histomorphometric pattern confirmed a mild fluorosis shown by hyperosteoidosis, presence of woven bone and focal mineralization impairment. Moreover, the fluoride content in bone ashes was 4X the upper level of normal (cf Table 1;NI: 0.10 ±0.07). Recently, after sustaining a fragility fracture, a second transiliac biopsy was performed and confirmed the development of the bone disorder which correlates with the accumulation of fluoride content in bone ashes reaching 9X the upper level of normal (cf Table 1). Microhardness analysis (Hv;Table 2) revealed that Hv was first high then decreased to normal values in cancellous (Cc) and total (cortical + cancellous) bone. Characteristics of bone mineral at tissue and crystal levels are in progress to precise the impact of fluoride. Taken together, these results suggest that if the source of fluoride is not found and removed, bone alterations will continue to progress with impaired bone matrix quality leading to decreased bone strength. This could lead to the establishment of a severe osteoscleorosis comparable to a case we presented at the ASBMR meeting in 1995 (Ste-Marie LG *et al*., JBMR 1995; 10 (Supp. 1):S499, Abstract #T580) where fluorosis was induced by the regular and prolonged ingestion of toothpaste.

Biopsies	BV/TV %	OV/BV %	OS/BS %	ES/BS %	MS/BS %	Fluoride % ashes
2008	15.0	7.4	38.9	5.6	2.6	0.39
2012	21.9	6.6	49.1	4.8	1.5	0.90
1995	41.4	12.4	92.9	5.5	NM	0.93

NM: not measured

Table 1. Histomorphometric Analysis and Bone Fluoride Content

Biopsies	Cc Hv Newton/mm^2	Total Hv Newton/mm^2
2008	59.9	59.7
2012	48.3	47.5
1995	60.8	56.2
Normal values in women = 49.7 ± 2.0 (Boivin *et al*. Bone 2008; 43:532-8)		

Table 2. Microhardness Analysis

***Disclosures: Louis-Georges Ste-Marie**, Eli Lilly, 6; Merck, 2; Genzyme, 6; Eli Lilly, 2; Novartis, 2; Servier, 6; Warner Chilcott, 2; Amgen, 6; Novartis, 6; Amgen, 2; Servier, 2; Alliance for better bone health, 6*

MO0176

X-linked hypophosphatemia in adults and rheumatological manifestations: cross-sectional survey of the Bone Section of the French Society of Rheumatology SFR-OS. Rose Marie Javier*[1], Karine Briot[2], Martine Cohen-Solal[3], Bernard Cortet[4], Capucine Eloy[5], Michel Laroche[6], Pierre Lafforgue[7], Marie-Christine De Vernejoul[8]. [1]University Hospital, France, [2]Paris Descartes University, Cochin hospital, Rheumatology Hospital, France, [3]Centre Viggo Petersen, France, [4]Service de Rhumatologie, France, [5]University Hospital Lille, France, [6]University Hospital Toulouse, France, [7]Hôpital Sainte-Marguerite, France, [8]Fédération De Rhumatologie Et INSERM U606, France

X-linked dominant hypophosphatemia (XLH) is the most common (prevalence 1:20,000) heritable vitamin D resistant rickets. It is caused by mutations in the PHEX gene. In children, the classic triad (shortness of stature, deformities of the lower limbs, hypophosphatemia) allows the diagnosis. Since the end of the 1970s, early and systematic treatment (phosphate derivatives and 1-hydroxylated vitamin D) partially corrects mineralization disorders, leg deformities with improvement of adult height but without modifying the evolution of osteoarticular complications (early osteoarthritis, enthesopathies). Continued treatment in adults is not systematic. Sometimes the discovery is made in adulthood, mainly during a rheumatologic consultation for osteomalacia or osteoarthritis.

The purpose of this study is to 1) describe and determine the frequency of rheumatological disorders (location, pain intensity) in adults XLH ; 2) better manage these adult patients.

MATERIALS AND METHODS: This study was conducted by members of the Bone Section of the French Society of Rheumatology who included adults XLH consulting in a rheumatology department for any reason. Questionnaires including body schema of painful areas, visual analogic scale (VAS) score for pain and fatigue, current and past treatments, X-rays datas, were delivered to the patients.

RESULTS: Forty-three adults XLH (74.4% women, average age of 42 years [21-80years]) were included. Twenty-six patients (60%) (including young patients treated during childhood) reported pain in the last 6 months (mean pain VAS: 5.9 / 10 [1.2 to 10]). Analgesic treatments were prescribed in about 50% of patients with (most often mild analgesics of level 1 or NSAIDs). Most of this painful symptoms were osteoarticular, located with decreasing frequency in knees (54%), hips (50%), lumbar spine (41%), the rest of the lower limbs (ankles) often with limitation in motion. X-rays showed features of early osteoarthritis and calcified enthesopathies. Significant fatigue (VAS fatigue 5.6 / 10 [0.2 to 9.2]) was present in 58% of patients. Most patients did not receive phosphate and / or derivatives 1-hydroxylated vitamin D.

CONCLUSION: XLH adult patients have frequent disabling skeletal pain secondary to articular and pararticular involvement.

***Disclosures: Rose Marie Javier**, None.*

MO0177

Changes in Bone Microarchitectural Texture Assessed by Trabecular Bone Score After Parathyroidectomy in Primary Hyperparathyroidism. Barbara Silva*[1], Natalie Cusano[2], Chiyuan Zhang[3], Alice Abraham[3], Stephanie Boutroy[4], Wen-Wei Fan[1], Didier Hans[5], John Bilezikian[2]. [1]Columbia University Medical Center, USA, [2]Columbia University College of Physicians & Surgeons, USA, [3]Columbia University, USA, [4]INSERM U1033 & Université de Lyon, France, [5]Lausanne University Hospital, Switzerland

Following parathyroidectomy (PTX), BMD improves in patients with primary hyperparathyroidism (PHPT), but little is known about changes in bone microarchitectural texture by trabecular bone score (TBS). We have recently shown that TBS is associated with HRpQCT measures of bone microstructure in PHPT. Moreover, TBS predicts fracture risk, independent of BMD. In this study, we investigated whether TBS improves over time after PTX in a group of men and women with PHPT, and examined the sex-specific differences in TBS changes after surgery.

We studied 17 subjects with PHPT followed for at least 6 and up to 12 months after successful PTX. Site-matched spine TBS was extracted from the DXA image (Hologic) using TBS iNsight software. Linear mixed model for repeated measures was performed to assess the % change in TBS relative to the baseline over 12 months. Sex-specific differences were evaluated by using sex as a covariate in the model.

The mean age was 65±14 yrs. Only 3 subjects had nephrolithiasis (n=2) and/or fragility fracture (n=2). At baseline, mean serum calcium level was elevated at 10.8±0.6 mg/dl. All subjects became and remained normocalcemic at 6 and 12 months after PTX. Men (n=5) and women (n=12, 11 postmenopausal) did not differ in age, BMI or serum calcium levels. Men had a shorter duration of the disease (0.8±0.3 vs 11±10 yrs; p=0.006). At baseline, the mean TBS was low at 1.218±0.158 (normal ⩾1.35). TBS was lower in men than in women (1.024±0.038 vs 1.299±0.108; p<0.001). In the entire cohort, there was an increase in TBS after 6 months (+2.9±7.0%; p=0.04), which was sustained at 12 months (+2.8±11.1%; p=0.1). Sex was a predictor of the % change in TBS over time (p<0.001). Between-sex differences in the % change of TBS were seen at 6 (p=0.003) and 12 (p=0.005) months. While TBS markedly improved at 6 (+10.4±9.5%; p<0.001) and 12 (+10.3±15.2%; p<0.001) months post PTX in men, it did not change in women (-0.3±6.1%; p=0.8 at 6 months; and -0.6±10.4%; p=0.7 at 12 months) (Fig). There was no correlation between the % change in TBS and the % change in aBMD or HRpQCT measures at any site or time point.

These data demonstrate that TBS increases after PTX in men, while it does not change in women over a 12-month period. The results not only confirm the previous findings by histomorphometry and HRpQCT of similar or better trabecular microstructure in PHPT after PTX, but also reveal marked differences between men and women not described before.

Figure: Percent change in TBS in men and women at 6 and 12 months after PTX (Mean ± SEM; *p<0.01 from baseline, #p<0.01 men *vs* women)

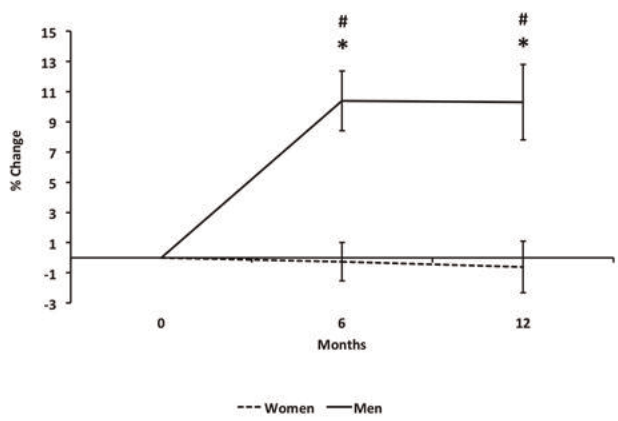

Figure

***Disclosures: Barbara Silva**, None.*

MO0178

Continuous Infusion of PTH is superior to PTH Injections in the Treatment of Severe Hypoparathyroid Neuromuscular Symptoms. Erik Fink Eriksen*[1], Helen Dahl-Hansen[2], Lena Seland[1], Daysi Duarte-Sosa[1]. [1]Oslo University Hospital, Norway, [2]Norwegian hypoparathyroidism organisation, Norway

Most patients with hypoparathyrodism achieve normocalcemia on conventional treatment with Vitamin D analogues combined with magnesium and calcium supplementation. PTH once daily or on alternate days has recently been introduced as a new treatment option, but neither this new modality, nor conventional treatment improve neuromuscular symptoms (in particular painful muscle cramps) accompanying the disease,. In this study we tested whether continuous infusions of PTH to mimic physiological PTH secretion more closely would provide better symptomatic relief in patients with severe hypoparathyroid symptoms.

We studied 4 patients with severe postoperative hypoparathyroidism (undetectable PTH for more than 2 years, and severe neuromuscular symptoms despite stable S-calcium at the lower range of normal). The patients were first switched to PTH(1-84) (Preotact®) injections every or every other day due to either severe subjective symptoms or in one case due to progressive renal insufficiency, while on Rocaltrol. None of the patients experienced significant symptomatic relief after the switch to PTH injections (Fig. 1), but renal function returned to normal in the patient with renal insufficiency. In order to test the effects of continuous PTH infusions the patients were equipped with an insulin pump (Omnipod® or Dana®), where the infusion syringe was loaded with PTH extracted from the (PTH(1-84) ampules (0.25 ml diluted in 1.5 ml of NaCl). Infusion rates were adjusted to achieve S-Ca in the lower to mid-range of normal (usually 20-30 IU/24h).

Infusions caused significant relief of neuromuscular symptoms after a few weeks. Muscle pain/cramps VAS was reduced from 8-9 to 2-3 within 3 months (Fig. 1), and fatigue improved significantly too. The symptoms were all assessed during normocalcemia.

Thus, in this short term study on a small subset of patients with severe hypoparathyroidism, we found that continuous PTH infusions provided better symptomatic relief than conventional treatment or PTH injections. This observational study warrants a larger randomized study and suggests that the neuromuscular symptoms are intimately related to low concentrations of PTH, rather than being adverse effects of hypocalcemia

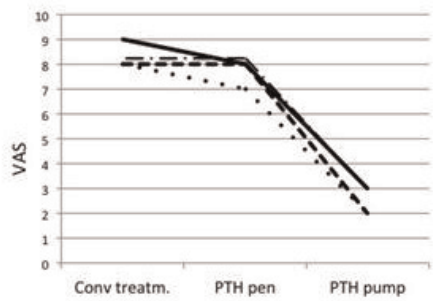

Fig. 1. VAS scores during conventional treatment, PTH injections and PTH infusions (pump)

***Disclosures: Erik Fink Eriksen**, None.*

MO0179

Effect of Long Term Stable Hypercalcemia on Kidney Function in the Elderly. Sharon Lahiri, Tarlisha Eskridge, Manjari Devidi, Sudhaker Rao*. Henry Ford Hospital, USA

Background: Advancing age is a well known risk factor for declining renal function, but the additional effect of stable hypercalcemia due to primary hyperparathyroidism (PHPT) is unknown. It is argued that elderly patients are less likely to receive parathyroidectomy (PTX) because of concerns about surgical risk. Accordingly, we retrospectively reviewed the effect of chronic stable moderate to severe hypercalcemia on renal function as assessed by serum creatinine (Cr) in the elderly.

Materials & Methods: Twenty three patients, all women, >75 years (mean age of 80 ± 4 years), were followed for at least 10 years. They represented 25% of all patients with PHPT seen in 2003 and 40% of those >75 yrs. Serum calcium (Ca; adjusted for albumin), ionized Ca (iCa), PTH, and Cr were measured periodically to monitor the disease. Three of the 23 had failed surgeries (1-3 PTXs) in expert hands and refused further surgery; the others 20 did not want PTX believing that they were "well and did not need surgery". None of the 23 had kidney stones or bone fractures despite moderate to severe PHPT and low bone density.

Results: The mean serum Ca at entry was 11.0 ± 0.65 mg/dl, iCa 1.45 ± 0.11 mmol/l, Cr 1.05 ± 0.26 mg/dl and PTH 84 ± 37 pg/ml with no regression of serum Cr on serum Ca, iCa or PTH, or age. None developed any of the known complications traditionally associated with PHPT or hypercalcemic crisis. All were on adequate calcium and vitamin D supplements (mean serum 25-OHD was 34.3 ± 11.9 ng/ml). After 10 years of follow-up without PTX (or failed PTX in 3), mean serum Ca was 10.7 ± 0.75 mg/dl, Cr 1.09 ± 0.32 mg/dl (p=ns), and PTH 118 ± 58 pg/ml (p=ns for all). The mean lowest BMD T-score (spine or femoral neck) at entry was -2.4 ± 1.3 SD. Five patients died of unrelated causes during follow-up mostly related to advanced age as each of these 5 patients was older than 80 years at entry in 2003.

Conclusions: Despite the traditional concerns, there appears to be no adverse effects of hypercalcemia on renal function in the elderly. Our study is limited by relatively small sample size and lack of more sensitive measures of renal function. Adequate Ca and vitamin D supplements during follow-up may have mitigated some of the adverse effects. Finally, there appears to be no compelling reason to recommend PTX in asymptomatic PHTP elderly patients since the benefits of surgery may not outweigh the potential risks in these elderly subjects, especially after failed PTX.

***Disclosures: Sudhaker Rao**, None.*

MO0180

Increased Incidence of Primary Hyperparathyroidism in Rochester, Minnesota after 1997: An Update on the Changing Epidemiology of the Disease. Marcio Griebeler*[1], Ann Kearns[2], Eujung Ryu[1], Matthew Hatchcock[1], L. Joseph Melton[2], Robert Wermers[2]. [1]Mayo Clinic Rochester, USA, [2]Mayo Clinic, USA

Purpose: Introduction of automated serum calcium measurements in the early 1970s resulted in a dramatic rise in primary hyperparathyroidism (PHP) incidence, followed by a decrease afterwards. Recent studies from North America and Europe report an increasing PHP incidence. Our objective was to evaluate secular trends in the incidence of PHP.

Methods: In this population-based descriptive study, residents from Rochester, MN who met previously defined diagnostic criteria for PHP from Jan 2001 through Dec 2010 were identified through the medical record system of the Rochester Epidemiology Project and added to our historical cohort beginning in 1965. Incidence was calculated per 100,000 person-yrs using age and sex distribution of the 2010 US white population and differences between groups were tested using Pearson chi-square test for categorical and t-test for continuous variables.

Results: 391 residents were newly diagnosed with PHP from 2001 to 2010 for a total of 1152 patients since 1965. As shown in the figure, two peaks were observed, one in 1974 (121.7 per 100,000 person-yrs) associated with the introduction of automated serum calcium measurements and a second one beginning in 1998 (101.2 per 100,000 person-yrs). To better understand differences in patient profiles, two time periods were analyzed (group 1: 1985-1997: 194 pts vs group 2: 1998-2010: 523 pts). There was no significant difference in sex (73% women in group 1 vs 78% group 2) but significant differences in mean age (55.4 yrs vs 60.1 yrs), symptoms/signs associated with the diagnosis (9% vs 31%), PHP surgery (22% vs 35%) and diagnosis in patients older than 55 yrs (54% vs 67%). Although more patients had surgery in 1998-2010, the mean serum calcium of 10.9 mg/dL wasn't significantly higher than in the preceding era (10.8 mg/dL). In addition, more subjects were diagnosed on the basis of inappropriately elevated parathyroid hormone (25% vs 50%) and histological evidence (25.7% vs 34.9%) in the most recent period.

Conclusions: A second sharp rise in PHP incidence in our community, similar to observations in 1974, has occurred since 1998 in a population that is older with more PHP complications. The abrupt increase in both men and women is inconsistent with several potential etiologic causes (e.g., estrogen discontinuation, increasing obesity, and systemic changes in vitamin D or calcium intake or sufficiency) and suggests a change in PHP epidemiology possibly related to case ascertainment bias.

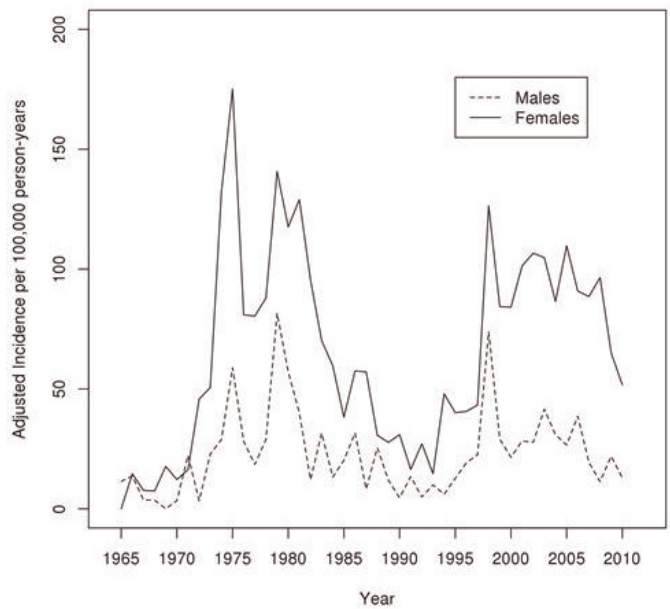

Secular trends in PHP incidence among Rochester, Minnesota residents, 1965-2010

***Disclosures: Marcio Griebeler**, None.*

MO0181

Muscle Function and Quality of Life in Primary Hyperparathyroidism. Lars Rolighed*[1], Anne Kristine Amstrup[1], Niels Frederik Breum Jakobsen[2], Tanja Sikjaer[3], Leif Mosekilde[4], Peer Christiansen[5], Lars Rejnmark[4]. [1]Aarhus University Hospital, Denmark, [2]Dept. of Endocrinology & Metabolisb MEA, Denmark, [3]Department of Medicine & Endocrinology, MEA Aarhus University Hospital, Denmark, [4]Aarhus University Hospital, Denmark, [5]Dept. of Surgery P, Denmark

Introduction: In spite of the frequent encounter of ''asymptomatic'' primary hyperparathyroidism (PHPT), the patients often describe various relevant improvements postoperatively suggesting a subclinical biological effect of elevated PTH or hypercalcaemia.

Materials and Methods: To evaluate muscle function, postural stability, and quality of life (QoL) in untreated PHPT, we assessed maximal isometric muscle strength in upper and lower extremities, time of 10 repeated-chair-stands (RCS), time to walk 3 m and back (TTW), balance function, and questionnaires of QoL in 58 untreated PHPT patients and 58 controls matched on age, sex, and menopausal status.

Results: Patients and controls had a mean age of 59 years and 47 (81%) were women. We found marked differences between groups in PTH (13.9 vs. 4.8 pmol/l) and ionized calcium levels (1.45 vs. 1.24 mmol/l), whereas plasma creatinine and 25(OH)D levels did not differ. In PHPT, the SF-36 questionnaire showed a lower QoL in all 8 domains ($p<0.05$) and the WHO-5 index showed a reduced well-being ($p<0.001$). Postural stability was impaired in PHPT during normal standing with eyes open ($p<0.05$) and eyes closed ($p<0.001$). Female patients spent significantly longer time on performing the RCS- and TTW-tests, and had a lower muscle strength in upper ($p<0.01$) and lower extremities ($p<0.001$) compared with female controls. In men, muscle function and strength did not differ between groups.

Conclusions: In PHPT, constantly elevated PTH and calcium levels seem to have deleterious effects on muscle strength, muscle function, postural stability and QoL. The increased risk of fracture in PHPT may therefore both be related to a decreased BMD and a reduced postural stability and muscle strength.

***Disclosures: Lars Rolighed**, None.*

MO0182

Two-years effects of PTH (1-84) on bone microstructure in post-menopausal women with hypoparathyroidism. Silvia Chiavistelli*[1], Barbara Silva[2], Mishaela Rubin[3], Natalie Cusano[4], Aline Costa[3], Chiyuan Zhang[3], James Sliney jr[2], Laura Beth Anderson[3], Didier Hans[5], John Bilezikian[4]. [1]Azienda Ospedaliera Pisana, Italy, [2]Columbia University Medical Center, USA, [3]Columbia University, USA, [4]Columbia University College of Physicians & Surgeons, USA, [5]Lausanne University Hospital, Switzerland

Hypoparathyroidism (HypoPT), an uncommon disorder of parathyroid hormone (PTH) deficiency, is characterized by hypocalcemia and abnormal structural and dynamic skeletal properties. We previously found in a combined cohort of HypoPT men, pre- and postmenopausal women that PTH therapy is associated with increased areal bone mineral density (aBMD) at the lumbar spine (LS) and reduction at the 1/3 radius. Yet, little is known about the effects of PTH on trabecular and cortical microarchitecture in HypoPT. To address this question, we used 3 different imaging modalities to better characterize changes in areal and volumetric densities and bone microstructure in a homogenous cohort of PTH-treated postmenopausal women. Postmenopausal HypoPT women (n=23, mean age 63 ± 7.8 yrs; 12.6 ± 7.5 yrs since menopause) were treated with PTH(1-84) for up to 2 yrs. aBMD was assessed by DXA (Hologic); cortical (Ct) and trabecular (Tb) volumetric density (vBMD) and microstructure were evaluated by high resolution peripheral quantitative computed tomography (HRpQCT; Scanco); trabecular bone score (TBS) was extracted from the LS DXA image (TBS iNsight software). At 12, 18, and 24 months, aBMD at the 1/3 radius fell by -2.2%, -3%, and -3.7% respectively ($p<0.001$ for all). Ultradistal radius aBMD also declined with the same trend ($p<0.001$ for all). LS aBMD increased at 18 (1.44%, p=0.01) and 24 (2.52%, p=0.025) months. An increase in TBS became apparent at 18 months (+3.1%, p=0.03), which tended to remain above baseline at 2 yrs (+2.6%, p=0.09). By HRpQCT at the radius, declines in total (-0.5%, p=0.008) and Ct area (-5%, p = 0.015) were noted at 24 months. Ct vBMD also decreased (-3.8%, p=0.004) at 2 yrs, while Tb vBMD increased (4.9%, p=0.012). Ct thickness (Ct Th) fell progressively, to -6% by 18-24 months (p=0.03), whereas Tb bone volume fraction (BV/TV) increased (5%, p=0.01) at 2 yrs. By HRpQCT at the tibia, total area fell by 1 and 2 yrs, as did Ct area, total vBMD, Ct vBMD, and Ct Th ($p<0.05$ for all), while Tb vBMD was unchanged. In summary, PTH therapy in postmenopausal HypoPT women was associated with increases in trabecular indices by HRpQCT and TBS, consistent with improvements in aBMD at the LS. In contrast, there was a decrease in cortical measures by HRpQCT at the radius and tibia, as well as aBMD at the cortical 1/3 radius site. Future studies are necessary to determine how these changes alter bone strength in HypoPT.

***Disclosures: Silvia Chiavistelli**, None.*

MO0183

Vertebral Bone Marrow Fat Associated with Lower Bone Mass in Primary Hyperparathyroidism. Francisco Jose De Paula*[1], Maira Mendonça[2], Carlos Salmon[3], Marcello Nogueira-Barbosa[2]. [1]School of Medicine of Ribeirao Preto - USP, Brazil, [2]School of Medicine of Ribeirao Preto, University of Sao Paulo, Brazil, [3]University of Sao Paulo, Brazil

Recently, a remarkable advance occurred on the knowledge about the molecular and cellular action of parathyroid hormone (PTH) on bone, while scarce progress was observed regarding the physiological role of PTH on bone mass development and maintenance. In primary hyperparathyroidism (PHPT), bone catabolism occurs in trabecular and cortical bone. Recently, bone marrow fat content has been associated negatively with bone mass and positively with visceral fat. There is no data about the bone marrow fat in patients with PHPT. The present study was designed to evaluate bone marrow fat in lumbar spine (L3) in PHPT patients and its relationship with bone mass and bone remodeling.

Material and Methods: the study comprises 11 PHPT patients (4 Males and 7 females), and 11 controls (CG, 5 Males and 6 Females) matched for age ($C=48.8\pm8.5$ vs $HPTP=48.9\pm8.8$years), weight ($C=82.1\pm14.5$ vs $HPTP=80.6\pm21.5$ kg), height ($C=1.67\pm0.1$ vc $HPTP=1,61\pm0.1$ m) and body mass index (BMI: $C=28.9\pm3.2$ vs $PHPT=31.1\pm5.6$ kg/m^2). Laboratory measurements included calcium, phosphorus, creatinine, PTH, 25-OHD, IGF-I, osteocalcin and CTX. Bone mineral density was determined in L1-L4, femoral neck, total hip, 1/3 forearm, total body, and vertebral morphometry. Bone marrow fat was estimated by magnetic resonance spectroscopy.

Results: PHPT patients exhibited normal serum levels of creatinine ($1.04\pm0,3$ mg/dl). Serum levels of calcium ($C=9.4\pm0.6$ vs $PHPT=11.6\pm0.9$ mg/dl) and PTH ($C=43.3\pm13.8$ vs 304.1 ± 278.2) levels were increased in PHPT patients $p<0.05$. BMD was significantly higher in control group in lumbar spine ($C=0.995\pm0.09$ vs $PHPT=0.876\pm0.16$ g/cm^2, $p<0.05$) and 1/3 radius ($C=0.700\pm0.057$ vs $PHPT=0.606\pm0.113$ g/cm^2). BMD in femoral neck was not different ($C=0.936\pm0.17$ vs $PHPT=0.799\pm0.19$). Bone marrow fat was slightly increased in PHPT patients ($C=52.4\pm20.1$ vs $PHPT=57.2\pm29.6$ %). There was a negative correlation between bone mass in lumbar spine with bone marrow fat in L(3) in PHPT group, $p<0.05$, $r=-0.65$. Remarkably, a patient with a severe bone disease showing fragile fracture exhibited very high bone marrow fat.

Conclusion: Previous studies have showed a negative association between bone marrow fat and bone mass in young females. Recently, higher bone marrow fat has been associated not only with lower trabecular BMD but also with prevalent fracture. We originally demonstrated that bone marrow fat is negative associated with lumbar spine BMD in patients with primary hyperparathyroidism.

***Disclosures: Francisco Jose De Paula**, None.*

MO0184

Impact of High Calcium Intake from Calcium Carbonate or Dairy on Cardiovascular Function and the Progression of Coronary Artery Disease in Ossabaw Miniature Swine. Alyssa Phillips*[1], Mikaela McKenney[2], Martin Bahls[3], Sean Newcomer[4], Berdine Martin[5], William Van Alstine[6], Scott Radcliffe[7], Meryl Wastney[8], George Jackson[9], Michael Sturek[2], Connie Weaver[1]. [1]Purdue University, Department of Nutrition Science, USA, [2]Indiana University School of Medicine Department of Cellular & Integrative Physiology, USA, [3]Purdue University Department of Health & Kinesiology, USA, [4]California State University San Marcos Department of Kinesiology, USA, [5]Purdue University, USA, [6]Purdue University Department of Comparative Pathobiology, USA, [7]Purdue University Department of Animal Sciences, USA, [8]Metabolic Modeling Services, USA, [9]Purdue University Department of Physics, USA

Calcium supplements have been regarded as safe and effective in promoting bone health. However, recent secondary analyses have linked calcium supplementation to increased risk for heart attack and cardiovascular-related death in older, healthy adults. One putative mechanism is that an acute spike in circulating calcium following excessive intake leads to increased calcium deposition in the coronary arteries and subsequent cardiovascular dysfunction. However, evidence to support this hypothesis is lacking. The Ossabaw swine model mimics human metabolic syndrome and coronary artery disease (CAD) when fed an atherogenic diet. The aim of this study was to investigate the impact of high calcium intake from calcium carbonate or dairy on cardiovascular function and the progression of CAD utilizing Ossabaw swine. All pigs (n=24) were fed an atherogenic diet and randomized to control calcium (0.5%Ca by weight), high calcium from calcium carbonate (2%Ca), or high calcium from dairy (2%Ca) diets. Conscious systolic and diastolic blood pressures did not differ among dietary groups. After 6 months of dietary intervention, simultaneous Positron Emission Tomography Computed Tomography (PET-CT) was performed to assess cardiac function and soft tissue calcification. Stroke volume and ejection fraction did not vary among groups. Uptake of 18F-NaF was measured as standard uptake values (SUVs) utilizing PET-CT. SUV in all tissues did not differ among diet groups and there was no significant SUV in the heart; suggesting no evidence of calcification in the heart soft tissues. Intravascular ultrasound was performed to quantify CAD and showed no difference in plaque wall coverage of the left anterior descending artery (LAD) among groups. Following euthanasia, segments of LAD were excised and mounted on an *in vitro* wire myograph. Endothelium-dependent and –independent

responses were assessed with increasing doses of bradykinin and sodium nitroprusside, respectively. Endothelial-dependent and –independent vasodilation were similar among groups. These data suggest calcium intake below the upper limit recommended by the Institute of Medicine is not likely to adversely impact cardiovascular health and function. Prospective data assessing the impact of calcium intake on vascular calcification using sensitive ^{41}Ca kinetic modeling in the Ossabaw swine will further contribute to our understanding of the relationships between calcium intake and cardiovascular health.

***Disclosures: Alyssa Phillips**, None.*
This study received funding from: Dairy Research Institute, Pharmavite, Kraft, Nestle, and Fonterra

MO0185

Up-regulation of Osteocyte Markers by Muscle Secreted Factor(s) but Lack of any Effect on Osteoblast proliferation/differentiation. Ning Zhao*[1], Matthew Prideaux[1], Marco Brotto[1], Leticia Brotto[2], Lynda Bonewald[1]. [1]University of Missouri Kansas City, USA, [2]School of Nursing, university of missouri kansas city, USA

The spatial proximity and co-ordinated actions of bone and muscle during exercise led to the hypothesis that communication between bone and muscle cells play an important role in regulating bone modeling. We have previously shown that muscle secreted factors preserve osteocyte viability. In this study we examined the effect of muscle factors on osteoblast proliferation, viability, and differentiation and the expression of osteocyte biomarkers, Dmp1, E11/gp38, and sclerostin. The MC3T3 osteoblasts and the IDG-SW3 cell line were used, the IDG-SW3 as a model of osteoblasts that can fully differentiate into mature osteocytes. Conditioned media from C2C12 myotubes (MT-CM) and ex-vivo contracted mouse EDL and SOL muscle (10%) was added to IDG-SW3 cultures every 3 days for up to 28 days of culture. Non-conditioned media was used as a control. No effect was observed on osteoblast (either MC3T3 or IDG-SW3 cell) proliferation, metabolic activity using the MTT assay, nor mineralization. However, MT-CM (1%) increased expression of Dmp1- GFP in IDG-SW3 cells by over 3-fold ($P<0.001$) after 14 days. E11/gp38 and sclerostin were not only elevated in IDG-SW3 cells by MT-CM, but also by 10% EDL or SOL CM at 28 days. These data suggest that a factor(s) secreted by muscle cells influences osteoblast to osteocyte differentiation or can influence mature osteocyte function while having no effects on osteoblast proliferation or mineralization.

***Disclosures: Ning Zhao**, None.*

MO0186

Exploring the Relationship between Changes in Bone Mineral Density, Lean Body Mass, and Hormones in Active, Adult Males with Osteopenia after a 12-month Exercise Intervention. Melissa Carter*, John Thyfault, Tim Sinak, Peggy Nigh, Lynn Eaton, Jun Jiang, Pamela Hinton. University of Missouri, USA

Weight-bearing exercise may positively affect bone via muscle contractions, impact forces, and hormonal changes; however, the relative importance of these factors remains controversial. We examined the effects of 12-months of resistance training (RT, 2x/wk, N= 10) or plyometric exercise (PLY, 3x/wk, N= 10) on bone mineral density (BMD) and hormones (testosterone, TEST; free testosterone, fTEST; estradiol, E2; and insulin-like growth factor-1, IGF-1) in physically active (≥4hr/wk), osteopenic, but otherwise healthy men between 25 and 60y (mean: 42 ± 9.7y) who were provided daily supplemental calcium (1200 mg) and vitamin D (10 μg). We examined relationships between percent changes (%Δ) in lean body mass (LBM), hormones, and BMD of the whole body (WB), weight-bearing (leg, hip) and non-weight-bearing (arm) sites. LBM and BMD were measured using dual-energy X-ray absorptiometry, and plasma hormone concentrations were assessed using ELISA. Effects of RT or PLY on changes in WB and regional (i.e., arm and leg/hip) LBM and BMD and hormone concentrations were evaluated using 2x2 repeated measures ANOVA (time, group). Relationships between %Δ in LBM or hormones and BMD were assessed using Pearson's product moment correlations. WB (time, p= 0.025) and leg (time, p= 0.024) BMD significantly increased post-intervention with no differences between RT and PLY. By contrast, hip BMD increased in RT, but remained unchanged in PLY (group x time, p= 0.068). Whole body and leg LBM did not change significantly after RT or PLY; arm LBM significantly decreased in PLY and remained unchanged in RT (group x time, p= 0.080). The %Δ in WB LBM was positively correlated with %Δ in leg (r= 0.581, p= 0.039) and hip BMD (r= 0.565, p= 0.044) in PLY only. The %Δ in arm LBM was positively correlated with %Δ in arm BMD (r= 0.577, p= 0.047) in RT only. There were no significant changes in TEST, fTEST, or E2; IGF-I increased in both RT and PLY with a greater increase in RT vs. PLY (group x time, $p<0.001$). %Δ in the hormones was not associated with increases in BMD in either RT or PLY. In conclusion, weight-bearing exercise that elicits either high-muscle-contraction forces or high-impact forces may positively affect whole body and leg BMD, while hip BMD increased following high-muscle-contraction force exercise in physically active men with osteopenia.

***Disclosures: Melissa Carter**, None.*

MO0187

From GWAS to cell-based studies in search of common pleiotropic pathways for bone-muscle crosstalk. Jian Huang*[1], Chenglin Mo[1], Yi-Hsiang Hsu[2], Eduardo Abreu[1], Dauglas P kiel[3], Lynda Bonewald[1], Marco Brotto[1], David Karasik[4]. [1]University of Missouri-Kansas City, USA, [2]Hebrew SeniorLife Institute for Aging Research & Harvard Medical School, USA, [3]Hebrew Senior Life, USA, [4]Hebrew SeniorLife; Bar Ilan University, USA

Sarcopenia and osteoporosis are among the most serious and costly public health problems and normally occur concurrently. A bivariate genome-wide association study (GWAS) using meta-analysis data from two consortia of mostly Caucasian cohorts identified *METTL21C* as a suggestive pleiotropic gene for bone and muscle phenotypes. METTL21 methylates chaperone proteins involved in the etiology of both Inclusion Body Myositis and Paget's Disease. To validate GWAS results, using siRNA to silence *METTL21C* in murine C2C12 myoblasts and osteocyte-like cell line MLO-Y4 was conducted. After 24h of transfection, quantitative real-time PCR revealed that *Mettl21C* expression was reduced by 36.1 ± 4.0% in the siRNA-treated cells (siRNA-cells). In addition, 3 days after the onset of myoblast differentiation into myotubes, a significantly reduced number of myocytes aligning/organizing for fusion in the siRNA-cells (30.8 ± 3.6/per random image area, PRIA) was observed compared to control-cells (61.8 ± 7.4/PRIA) ($p < 0.05$). At day 5 of differentiation, both fewer and smaller early myotubes were observed in the siRNA-cells (51.5 ± 6.9/PRIA) compared to control-cells (79.8 ± 8.0/PRIA) ($p < 0.05$). By day 7, fully matured and developed myotubes were observed in the control but not in the siRNA-cells. These results were also confirmed by double staining of myosin heavy chain and nuclei. Since intracellular calcium (Ca) homeostasis is essential for both muscle and bone function, at day 5 of differentiation, we measured intracellular Ca using Fura-2, and found that the maximal amplitude peak Ca response to 20mM caffeine decreased by approximately 500nM, and the time of return from peak levels to basal Ca levels was 20% shorter in the siRNA-treated cells, suggesting that less Ca is available for release after partial silencing of *METTL21C*. In siRNA-treated MLO-Y4 cells, no obvious morphological phenotypic charges were detected, but when, MLO-Y4 cells were treated with dexamethasone 48 hours after transfection, the percentage of cell death induced with dexamethasone significantly increased in siRNA-cells (18.2 ± 1.4%) compared to control-cells (13.1 ± 1.2%) ($p < 0.05$). These results suggest that *Mettl21C* plays previously unrealized roles in bone and muscle cells. These results warrant additional cell based studies to advance our understanding of the functions of Mettl21C in musculoskeletal biology and provide solid rationale for cellular and molecular validation of GWAS studies.

***Disclosures: Jian Huang**, None.*

MO0188

Muscle microstructure: a new point of view on osteoporosis-related muscle atrophy. Umberto Tarantino*[1], Monica Celi[2], Jacopo Baldi[1], Francesca Mastrangeli[1], Federico Maria Liuni[1], Giulia Di Pietro[3], Elena Gasbarra[1], Silvia Capuani[3]. [1]Università degli Studi di Roma Tor Vergata, Italy, [2]University of Rome Tor Vergata, Italy, [3]Università degli Studi di Roma "La Sapienza", Italy

Osteoporosis and sarcopenia are considered two of the hallmarks of the aging process. Aim of this study was to investigate the microstructural features in muscles of osteoporotic and osteoarthritic women by using Magnetic Resonance (MR) diffusion tensor imaging (DTI). Towards this goal we examined in vitro at 9.4T the vastus lateralis biopsy of osteoporotic and osteoarthritic subjects (extracted during a surgical operation of femoral head replacement) by measuring mean diffusivity (MD), fractional anisotropy (FA), the three eigenvalues (l_1 l_2 l_3) of muscles and assessing associations between DTI parameters, subjects age, subjects bone mineral density (BMD) and subjects body mass index (BMI). Moreover we performed an histological evaluation of muscle fibers pattern using anti-slow skeletal myosin and anti-fast skeletal myosin immunohistochemistry reaction.

After informed consent, we performed vastus lateralis biopsy in 10 women with osteoporosis (mean-age=82.3±4.5) underwent primary Total Hip Arthroplasty (THA) for hip fracture, and 10 age-matched women (mean-age=75.0±5.5) underwent surgery for hip osteoarthritis. A 9.4T MR system with a micro-imaging probe was used to investigate muscle samples. Each muscle of 2cm in length was stored in a 4%-paraformaldeyde and PBS. The DTI protocol with b-values = 400 and 700 s/mm2 was applied, using a PGSTE-imaging sequences (TE/TR=14.5/2500ms, diffusion delay D=40ms, diffusion gradient pulse duration δ=2ms, field-of-view FOV= 0.75cm, number of average NS=4, slice thickness, ST=1mm, twelve axial slices). Mean values and standard deviation were obtained for each variable for osteoporotic and osteoarthritic subjects. Between-group comparisons to assess group differences and Pearson correlation analysis were performed. P values<0.05 were considered statistically significant.

FA was significantly higher in OA compared to OP subjects while MD, l_2 and l_3 were lower in OA compared to OP subjects (P=0.039, P=0.040 P=0.022, respectively). A significant linear correlation was found between FA and BMI in OP subjects only. No significant correlation was found between DTI parameters, BMD and age.

Our in vitro preliminary results highlight differences in DTI parameters of OP patients: DTI images show the loss of the typical longitudinal orientation of muscle fibers confirming previous histological evidences. This data encourages further analysis of muscle microstructure investigation by means of MR imageing.

***Disclosures: Umberto Tarantino**, None.*

MO0189

Radiation Exposure Prevents Recovery of Cancellous Bone in Mouse Vertebrae following Partial Weightbearing. Ray Boudreaux*[1], Katherine Elmer[1], Corinne Metzger[1], Brandon Macias[2], Matthew Allen[3], Leslie Braby[1], Harry Hogan[1], Susan Bloomfield[1]. [1]Texas A&M University, USA, [2]UC San Diego, USA, [3]Indiana University School of Medicine, USA

We have previously demonstrated that partial weightbearing (PWB) in simulated Lunar gravity (1/6th-g) does not protect against disuse bone loss seen with tail suspension simulating 0-g. Further, high energy radiation simulating galactic cosmic radiation leads to dramatic reductions in cancellous bone mass. Since exercise is a well-known osteogenic stimulus via strains imparted upon the skeleton by contracting muscles, the purpose of this study was to investigate whether resistance exercise could enhance the recovery of bone lost during 21-d of PWB with and without previous low-dose, high-energy radiation exposure.

Female BALB/cByJ mice (4-mo-old) were assigned to age-matched cage controls (CC) or PWB (G/6). Half were then assigned to acute 0.5 Gy 56Fe, 1 GeV/n radiation (RAD) or SHAM exposure applied 3-d prior to PWB. After 21-d PWB, two G/6 groups were allowed 21-d recovery with normal activity (No EX) or with tower climbing resistance exercise (EX), 5 days/wk. EX mice performed repeat climbs of a 1-m vertical wire-mesh tower with progressively heavier weights attached to the tail. Micro-computed tomography (μCT) and axial compression of L4 spine were performed to assess recovery of bone properties lost from 21-d PWB.

Exercise during recovery from 21-d PWB in non-irradiated mice (EX SHAM) resulted in increased cancellous BV/TV (+21%) and trabecular thickness (Tb.Th)(+16%) over 21-d of recovery. Exercising mice previously exposed to radiation (EX RAD) experienced absolute declines in cancellous BV/TV (-8.9%) and Tb.Th (-11%). Trabecular number, spacing, and connectivity density were not significantly affected by either EX or No EX recovery. Ash weights of L5 vertebrae increased during recovery except in EX RAD mice. There was also a main effect of radiation: after 21-d recovery, SHAM exposed animals had higher ash weights than did EX RAD mice. Mechanical compression testing results follow similar trends as ash weight, but inter-group comparisons did not reach significance.

Radiation exposure caused a decline in measures of bone volume and mineralization in lumbar vertebrae (with and without exercise) after 21-d of PWB and recovery. Based on these data, we conclude that resistance exercise effectively stimulates bone recovery following PWB but not PWB coupled with RAD. Future studies should address how simulated GCR impairs osteoblast responsiveness to mechanical loading imposed by high-intensity muscle contractions during resistance exercise.

***Disclosures: Ray Boudreaux**, None.*
This study received funding from: National Space Biomedical Research Institute via NASA Cooperative Agreement NCC 9-58

MO0190

The Effect of a Single High Dose of Cholecalciferol on Oxidative Stress in Post-Menopausal Women: a Double Blind Randomized Study. Marcia Regina Scalcon[1], Manuela Sangoi[2], Aline Cocco[3], Priscila Borges[3], Lucas Zottele[3], Karen Koff da Costa[3], Giovani Sartori[3], Jose Mainardi[4], Rafael Moresco[5], Melissa Premaor*[4]. [1]Pos-graduacao em Farmacologia - Universidade Federal de Santa Maria, Brazil, [2]Pos-graduacao em Farmacia - Universidade Federal de Santa Maria, Brazil, [3]Department of Clinical Medicine - Federal University of Santa Maria, Brazil, [4]Federal University of Santa Maria, Brazil, [5]Programa de Pós-Graduação em Farmacologia - Universidade Federal de Santa Maria, Brazil

Vitamin D has been shown to reduce oxidative stress in vitro. Moreover, observational studies have found reduced oxidative stress in individuals with vitamin D deficiency. We hypothesized that a high dose of cholecalciferol might be able to improve oxidative stress in healthy subjects. The aim of our study was to evaluate the effect of a single high dose of cholecalciferol on oxidative stress markers in healthy post-menopausal women. We carried out a double blind randomized clinical assay in 40 post-menopausal women. Women aged >= 60 were recruited from the Catholic Church parish member lists. Those with acute diseases, cancer, renal diseases, and bone diseases, were excluded. Each group (20 subjects) was randomized to receive a single dose of cholecalciferol 300,000 UI (vitD) or placebo (P). Oxidative stress was evaluated by ischemia modified albumin (IMA) and advanced oxidation protein product (AOPP). The outcomes were assessed at days 0, 30, 60, and 90. The variables were transformed to their natural logarithm (LN). Generalized linear model was used to evaluate the differences between the groups. There were no baseline differences between the groups [mean(SD); vitD vs. P, respectively]: age 67.5(4.7) yrs vs. 66.7(6.1) yrs, BMI 27.9 (4.0) kg/m2 vs. 27.8 (4.8) kg/m2, LN IMA -0.64(0.2) vs. -0.61(0.2), and LN AOPP 2.40(0.6) vs. 2.52(0.7). Thirty-nine women completed the study (P=20 and vitD=19) and there were no effects on LN IMA (p=0.99). Nevertheless, LN AOPP was significantly lower at the vitD group (p=0.11) during all the evaluation and at the last visit [0.46(1.2) vs. 1.25(1.2), p=0.03]. In conclusion, a high dose of vitamin D was able to reduce oxidative stress evaluated by AOPP on healthy post-menopausal women.

***Disclosures: Melissa Premaor**, None.*

MO0191

A Novel Mouse Model of Heterotopic Ossification with Spinal Cord Injury. Xuhui Liu*[1], Heejae Kang[2], Alexis Dang[1], Hubert Kim[1], Robert Nissenson[3], Bernard Halloran[4]. [1]University of California, San Francisco, USA, [2]San Francisco Veterans Affairs Medical Center, USA, [3]VA Medical Center & University of California, San Francisco, USA, [4]VA Medical Center (111N), USA

Introduction: Heterotopic ossification (HO) is a frequent complication following spinal cord injuries (SCI). The prevention and treatment of HO after SCI are challenging. A major barrier to the development of more effective prevention and treatment methods for SCI-induced HO is the lack of clinically relevant animal models. In this study, we sought to develop a novel mouse model of HO by introducing an intramuscular injection of a sub-threshold dose of bone morphogenetic protein-2 (BMP-2) to mice after SCI.

Methods: 3-month-old male C57/BL6 mice were divided into 3 groups: the control group (dorsal midthoracic spine process removal); the laminectomy group (dorsal midthoracic laminectomy); and the spinal cord injury (SCI) group (dorsal midthoracic spinal cord contusion). The animals received 0.5 μg or 0.25 μg of BMP-2 injections in the bilateral quadriceps muscles immediately after surgery/treatment. Two weeks later, animals were sacrificed and the hindlimbs were harvested for μCT scans to evaluate ectopic bone formation.

Results: The mean ectopic bone volumes for the control, laminectomy, and SCI groups received 0.5 μg BMP-2 were 0.1463 mm^3, 1.219 mm^3, and 1.116 mm^3 respectively. One-way ANOVA and Tukey's HSD post-hoc tests showed significant difference between the control and laminectomy groups (p=0.012) and between the control and SCI groups (p=0.021), but not between the laminectomy and SCI groups (p=0.956). In the mice receiving 0.25 μg of BMP-2, no HO was observed in the control group. The mean ectopic bone volumes for laminectomy and SCI groups were 0.615 mm^3 and 0.505 mm^3 respectively. T-test showed no significant difference between these two groups (P=0.808).

Discussion: In this study, we have successfully developed a novel mouse model of SCI-induced HO. This novel murine model will serve as a powerful tool to devise effective prophylactic measures and treatment for HO. One interesting finding in this study is that the mice with laminectomy have significantly increased HO compared to the control mice. Though no functional deficiency was observed, laminectomy may cause neuroinflammation at the midthoracic region of spinal cord. This result implies that neuroinflammation alone may induce HO by sensitizing soft tissues to BMP-2 signaling.

***Disclosures: Xuhui Liu**, None.*

MO0192

Autocrine role of PGE_2 Signaling in Cell Cycle Regulation of C2C12 Myogenic Differentiation. Chenglin Mo*[1], Lori Wetmore[2], Lynda Bonewald[1], Orisa Igwe[1], Marco Brotto[1]. [1]University of Missouri-Kansas City, USA, [2]William Jewell College, USA

Previously we have shown that addition of exogenous PGE_2 in amounts similar to osteocyte conditioned media (~10 nM) dramatically enhanced C2C12 myogenic differentiation via EP1 and EP4 receptors. Inhibition of these two receptors significantly attenuates myotube development and myotube fusion in C2C12 cells. Cell cycle progression during myoblast proliferation and cell cycle withdrawal after the onset of myogenic differentiation are two important steps in skeletal muscle repair or regeneration. To investigate whether PGE_2 signaling regulates C2C12 proliferation, dose-response studies were performed using five different concentrations of PGE_2 (10nM to 10μM), EP1 agonist 17-phenyl trinor PGE_2 (10nM to 2.5μM), and EP4 agonist CAY10598 (10nM to 2.5μM). The MTT assay confirmed that all these treatments did not alter C2C12 proliferation, since optical densities at 570nm were between $86.9 \pm 5.5\%$ and $101 \pm 3.5\%$ compared with control at 48h of proliferation. However, treatment with EP1 antagonist SC 51322 or EP4 antagonist L161,982 inhibited C2C12 growth by 30% at 48h. Flow cytometry was then used to study the mechanism(s) behind the inhibitory effect of SC 51322 and L161,982. C2C12 cells were first serum-starved with Dulbecco's Modified Eagle Medium (DMEM) containing 1% fetal bovine serum (FBS) for 24h to synchronize cells in G0/G1, which effectively translated into 75-80% cells stuck in G0/G1 phase. Cells were then switched to a complete growth medium (DMEM with 10% FBS) to reinitiate proliferation resulting in the reduction of percentage of cells in G0/G1 phase to 45% at 12h. However, treatment with SC 51322 or L161,982 increased the percentage of cells in the G0/G1 phase by 12% and 10%, respectively. These data suggest that autocrine PGE_2 signaling is important for cell cycle progression from G0/G1 phase. On the other hand, withdrawal from cell cycle (G0/G1 phase arrest) is critical for transition from proliferation to myogenic differentiation. After 24h in differentiation medium (DMEM with 2.5% horse serum), the relative percentages of C2C12 cells in G0/G1 were approximately 75% for control, SC 51322, and L161,982 treated groups, suggesting PGE_2 signaling may not be involved in the regulation of cell cycle withdrawal. In conclusion, whereas exogenous PGE_2 such as from mechanically loaded osteocytes stimulates myogenic differentiation, endogenous low level (~1nM) PGE_2 plays an important role in maintaining C2C12 myoblast proliferation.

***Disclosures: Chenglin Mo**, None.*

MO0193

Distribution of reference values for components of sarcopenia among postmenopausal women – results from the OSTPRE study. Samu Sjöblom*[1], Juha Suuronen[1], Toni Rikkonen[1], Risto Honkanen[1], Heikki Kröger[2], Joonas Sirola[3]. [1]University of Eastern Finland, Finland, [2]University of Eastern Finland & Kuopio University Hospital, Finland, [3]University of Eastern Finland / Kuopio, Finland

Abstract

PURPOSE: The aim of the study was to determine the distribution of measures of sarcopenia among postmenopausal women.

METHODS: The present study was based on 1) Young reference population (YRP), 197 healthy women aged 20 to 40 years (mean 27.4, SD 6.4) and 2) postmenopausal women from the population-based OSTPRE study (N=397), aged 63 to 75 years (mean 68.6 years, SD 2.9). Both samples underwent weight, height, grip strength (GS), quadriceps strength (QS) and total body DXA (TBDXA) measurements. Upper body muscle quality (UMQ) and lower body muscle quality (LMQ) were determined as upper/lower body muscle strength divided by upper/lower body appendicular muscle mass. Relative skeletal muscle index (RSMI) was determined as appendicular muscle mass divided by square of height. Based on the distributions (SD) of the indices in the YRP, the distributions of GS, QS, MQ and RSMI were determined in the OSTPRE sample. Both study populations were divided into three groups (A<-3SD, -3SD<B>-2SD C > -2SD) based on the distribution of the measures in the YRP.

RESULTS: In the YRP sample, the mean (SD) values were: RSMI 6.5 (0.74) kg/m^2, GS 35.0 (5.0) kPa, QS 466.5 (92.2) Nm, UMQ 8.6 (1.0) kPa/kg and LMQ 34.1 (6.6) Nm/kg, while in the OSTPRE sample these were: RSMI 6.6 (0.8), GS 24.7 (6.0), QS 290.7 (9.9), UMQ 6.1 (1.5) and LMQ 23.3 (8.5), respectively.The cut-off points based on the YRP data .The distribution of the population in the YRP and OSTPRE are presented in table 1. Consequently, the UMQ was mostly affected among the postmenopausal women (30.1% in comparison to 0% in the YRP).

CONCLUSIONS: Among postmenopausal women, upper body muscle quality is mostly deteriorated. UMQ may provide to be a new tool for diagnostics of sarcopenia.

Table 1. The distribution of measure values of YRP and OSTPRE study population, respectively.

The distribution of measures of YRP and OSTPRE respectively-3 SD -3 SD to -2 SD

RSMI 0.0%/0.5% 1.5%/1.0%

GS 0.5%/22.1% 0.5%28.3%

QS 0.0%/10.3% 2.5%/32.1%

UMQ 0.0%/30.1% 1.0%/30.9%

LMQ 0.0%8.4% 3.0%/24.2%

***Disclosures: Samu Sjöblom**, None.*

This study received funding from: Academy of Finland, Kuopio University Hospital EVO grant, Finnish Ministry of education and culture

MO0194

Relationships between Leptin, Muscle Fat, and Muscle Strength in Healthy Children. Richard Kremer*[1], Nicole Mueske[2], Arutyun Pogosyan[2], Patricia C. Aggabao[2], Jing Lian[1], Skorn Ponrartana[2], Vicente Gilsanz[2], Tishya Wren[2]. [1]McGill University, Royal Victoria Hospital, Canada, [2]Children's Hospital Los Angeles, USA

Levels of circulating leptin are positively related to body weight and recent studies suggest a negative association between leptin and muscle strength in elderly men and women. We prospectively examined the relation between leptin, muscle fat, and muscle strength in healthy children; 47 girls ages 11.8 $\pm$ 3.1 years; 47 boys ages 11.4 $\pm$ 3.1 years. Measures of leptin were determined using a commercially available RIA kit (Linco Research, Inc., St. Charles, MO); calf musculature density (surrogate of muscle fat) was measured using computed tomography (CT) (Hilite Advantage; GE Medical Systems, Milwaukee, WI); and jumping mechanography was used to measure maximum jumping height as an index of muscle strength using 3D motion capture technology (Vicon Motion Systems, Oxford, UK). As expected, there was a positive relation between leptin and measures of fatness (weight, BMI, % body fat) overall (r's = 0.46, 0.71, 0.79), in boys (r's = 0.46, 0.75, 0.82) and girls (r's = 0.61, 0.76, 0.74), and between leptin and insulin in all children (r = 0.69), in boys (r = 0.76) and girls (r = 0.61); all P's $\leq$ 0.001. As hypothesized, a significant negative correlation was observed between muscle density and leptin and between maximum jumping height and leptin (r's = -0.49 and -0.53, respectively; both P's $<$ 0.0001) which were independent of gender, age, BMI %, and insulin (see table below). These results provide strong evidence that in healthy boys and girls, higher levels of circulating leptin are strongly related to increases in muscle fat and decreases in muscle strength. Although prior studies have shown that muscle strength diminishes in response to muscle fat accumulation, further studies are needed to determine whether the positive association between leptin and muscle fat is mechanistically related.

Predictors of muscle density and muscle strength in 94 children

	β	SE	P-value	R^2
Muscle Density (HU)				
Gender	1.162	0.939	0.220	0.40
Age (yr)	-0.423	0.149	0.006	
BMI%	-0.069	0.020	0.0007	
Insulin (pmol/L)	0.036	0.020	0.076	
Leptin (pg/mL)	-2.323E-4	7.473E-5	0.003	
Max. Jumping Height* (cm)				
Gender	-1.950	0.697	0.006	0.44
Age (yr)	0.382	0.111	0.0009	
BMI%	-0.027	0.015	0.069	
Insulin (pmol/L)	-0.007	0.015	0.658	
Leptin (pg/mL)	-1.645E-4	5.543E-5	0.004	

*normalized to height

Predictors of muscle density and muscle strength in 94 children

***Disclosures: Richard Kremer**, None.*

MO0195

The Effect of Vitamin D Supplementation on Physical Performance and Activity in non-Western Immigrants. Mirjam Oosterwerff[1], Rosa Meijnen*[1], Natasja van Schoor[2], Dirk Knol[2], Mark Kramer[1], Mireille van Poppel[3], Paul Lips[4], Elisabeth Eekhoff[4]. [1]Department of Internal Medicine, Endocrine Section, VU University Medical Center, Netherlands, [2]Department of Epidemiology & Biostatistics, VU University Medical Center, Netherlands, [3]Department of Public & Occupational Health, EMGO Institute for Health & Care Research, VU University Medical Center, Netherlands, [4]VU University Medical Center, The Netherlands

Objective: Physical inactivity has been identified as the fourth leading risk factor for global mortality, while overweight and obesity are in the fifth place. Both factors are more prevalent among non-western immigrants in the Netherlands, compared to the indigenous population. Vitamin D deficiency, associated with poor physical performance, is highly prevalent in non-western immigrants. The aim of this study was to assess the supplementation effect of vitamin D on physical performance, exercise capacity and daily physical activity in vitamin D deficient, overweight non-western immigrants.

Methods: A randomized, double-blind, placebo-controlled trial primarily designed for glucose tolerance parameters was conducted. Eligibility criteria included overweight (BMI $>$ 27 kg/m^2), 25-hydroxyvitamin D (25(OH)D) $\leq$ 50 nmol/l, age 20- 65 yr, an impaired fasting glucose (IFG 5.6-6.9 mmol/l) and/or impaired random serum glucose (IRG: 7.8-11 mmol/l). A total of 130 participants received 1200 IU vitamin D3 or placebo. All participants received 500 mg calcium as calcium carbonate per day for four months. Change in physical performance score, six minutes walk test and average daily physical activity by questionnaire and accelerometer were measured. Intention-to-treat analyses were performed for each follow-up moment using linear mixed models. Next, per-protocol analyses were conducted.

Results: There was no significant effect on physical function. There was, however, an (non-significant) improvement of 7 meter in the distance walked on the 6-minutes walk test in the intervention group, compared to the placebo group. This difference increased to 14 meter in per-protocol analysis (p=0.17). The percentage of participants meeting international physical activity guidelines was extremely low.

Conclusions: Vitamin D supplementation did not significantly improve physical performance, exercise capacity or physical activity. However, especially in per protocol analysis, we found an (non-significant) improvement of exercise capacity. A promising result, since all participants were overweight and did not improve their overall activity levels.

Keywords: randomized controlled trial, vitamin D supplementation, obesity, overweight, non-western immigrants, 6-minutes walk test, Physical Activity Questionnaire, walking test, chair stands test, tandem stand test, accelerometry, physical activity, physical performance

***Disclosures: Rosa Meijnen**, None.*

MO0196

Wnt Signaling Regulates Osteoblast Growth through miR-27a. Mohammad Hassan[1], Bhaskar Roy*[2]. [1]University of Alabama, USA, [2]School of Dentistry, University of Alabama, USA

MicroRNA (miR) are evolutionarily conserved non-coding RNA of ~22 nucleotides that regulate gene expression by facilitating translational repression and mRNA degradation. Recently, several groups reported that miR-27a is a key miRNA in controlling cell proliferation and several forms of cancer pathogenesis. Wnt-β-catenin cellular signaling is also equally important in regulating numerous biological processes, including cellular growth and cancer. However, the mechanism(s) of

miR-27a regulation for cell growth is not clear. In this study we observed that Wnt signaling directly upregulates miR-27a expression and over expression of miR-27a in MC3T3-E1 also enhanced the expression of Wnt activators TCF and LEF but suppressive for GSK3β, DKK1 and APC expression, the potential antagonists of Wnt pathway. These findings reinforce a positive proliferative ambience involving both miR-27a and Wnt signaling. MiR-27a gain of function in pre osteoblast MC3T3-E1 cells increases RB1 phosphorylation that promotes G1-S cell cycle transition and activates cell growth while miR-27a loss of function decreases RB1 phosphorylation leading to cell cycle arrest. Immunoblot analysis of miR-27a stable MC3T3 cells showed enhanced expression for CyclinD1 and c-Myc. Increased association of histone H3K4 (activating) and decreased recruitment H3K27 (repressive) on c-Myc promoter, suggesting a significant enhancement of c-Myc gene transcription in miR-27 overexpressed cells. Cell cycle synchronization assay with nocodazole block and release in miR-27a stable cell lines revealed that c-Myc, Cyclin D1 expression peaked around 6hr after release. Western blot analysis with anti phospho RB1 antibody indicates a sharp increase at 6hrs after release. Therefore, our findings suggest that miR-27a gain of function induces the cell to progress from G1 to S phase by CyclinD1 induced Rb1 phosphorylation where c-Myc is maintaining increased level CyclinD1 expression. Taken together, our results establish a key role for Wnt signaling-miR-27a regulatory circuit to promote osteoblast cell cycle during proliferation by RB1 phosphorylation and c-Myc amplification. A feed forward and feedback loop between Wnt and activated miR-27a most probably inducing c-Myc and CyclinD1 expression to promote Rb1 phosphorylation and releasing E2F from Rb1 sequestration that constantly propels and maintains the cells in proliferation.

***Disclosures: Bhaskar Roy**, None.*

MO0197

Adipogenic and osteogenic differentiation/conversion in 3D collagen gels as a model for osteoporosis research. Solange Le Blanc*[1], Meike Simann[2], Norbert Schuetze[2], Tatjana Schilling[3]. [1]Universitat Wurzburg, Germany, [2]University of Wuerzburg, Orthopedic Center for Musculoskeletal Research, Germany, [3]University of Wuerzburg, Germany

It has been suggested that one factor contributing to the bone loss and the accumulation of fat tissue in bone marrow of osteoporotic patients is the misregulation in the differentiation processes of bone marrow mesenchymal stem cells (BM-MSCs). An increase of adipogenesis in BM-MSCs as well as the conversion of pre-osteoblasts into adipocytes may contribute to this fatty degeneration and bone loss. There is increasing evidence that the characteristics and behaviour of cells may greatly differ in 3D versus 2D environments and therefore the need to move from 2D culture systems to 3D is becoming more relevant. Since type I collagen is the major component of the extracellular matrix of bone, 3D culture using collagen could better mimic the native bone marrow environment, allowing the study of factors that modulate adipogenesis and osteogenesis of BM-MSCs in conditions closer to the native physiology.

In this work, we investigated the adipogenic and osteogenic differentiation of primary human BM-MSCs embedded in 3D type I collagen gels, as well as the conversion capacity of the population after switching of the differentiation cocktail. Two different formats were studied, floating and attached collagen gels. Differentiation/conversion was analysed by histochemical staining with Oilred O and Alizarin Red S.

As expected, in the presence of adipogenic cocktail BM-MSCs cultured in type I collagen gels underwent adipogenesis as confirmed by Oilred O staining of lipid droplets. Similarly, after osteogenic induction BM-MSCs produced mineralized matrix stained by Alizarin Red S. Conversion was also possible in collagen gels, i.e. adipocytes were detected in BM-MSCs previously induced to differentiate into osteoblasts and vice versa.

Despite reports on type I collagen enhancing osteogenesis and inhibiting adipogenesis in BM-MSCs, our study shows that floating and attached 3D type I collagen gels allow for osteogenesis and adipogenesis of BM-MSCs under chemical induction as well as for conversion. Our *in vitro* 3D models of BM-MSC cultivation better mimic the spatial tissue environment and will therefore aid to understand the osteoporosis-associated misregulation of osteogenesis and adipogenesis *in vivo*.

***Disclosures: Solange Le Blanc**, None.*

MO0198

Analysis of Human *SOST* Gene Expression Using Large Minigenes Reveals the Potential for Multiple Enhancers. Hillary St John*, Sydney Hansen, Nancy Benkusky, Mark Meyer, J. Pike. University of Wisconsin-Madison, USA

Sclerostin (SCL) is an osteocyte-derived negative regulator of bone formation. Transcribed from the *SOST* gene, SCL inhibits osteoblastogenesis via blockade of LRP5/6 co-receptors and antagonism of the Wnt pathway. SCL is a promising therapeutic target for low bone mass diseases and several neutralizing antibody therapies that suppress SCL are in development. Physiologically, the anabolic effects of both mechanical strain and PTH (and forskolin) are known to be involved in suppression of SCL levels. In the studies presented here, we conducted a high throughput screen to identify novel regulators of *SOST* expression and then characterized the distal enhancer regions that mediated the regulation by several of these compounds. We first created a series of stable cell lines that contained either the full-length or enhancer-mutated minigene versions of the *SOST* gene locus in a MC3T3-E1 cell host. Each minigene contained an IRES luciferase reporter/neomycin selectable marker cassette inserted into the 3' UTR. As anticipated, the full-length minigene was upregulated by BMP-2 and downregulated by forskolin, both known regulators of *SOST*. A screen of the full length *SOST* minigene stable MC3T3-E1 cell line with over 2000 compounds revealed regulators with both positive and negative activity. Negative-regulatory compounds for *SOST* included Wnt3a, $1,25(OH)_2D_3$, OSM, and $TGF\beta_1$, as well as a number of natural and synthetic glucocorticoids. To explore the mechanisms by which these compounds regulated *SOST* expression, we examined their ability to induce or suppress *SOST* mutant minigenes containing deletion of the promoter proximal enhancer (-1/-2 kb), ECR2, or ECR5, or two point mutations in the MEF2 binding site of ECR5 (ECR5/MEF2). Previous reports suggest that both PTH and $TGF\beta_1$ effects of *SOST* are mediated through ECR5 and that the action of PTH is mediated specifically via the MEF2 binding site at ECR5. Consistent with these reports, the suppressive effects of forskolin were abrogated following both ECR5 deletion and ECR5/MEF2 mutation. In contrast, we found that $TGF\beta_1$ negatively regulated *SOST* and that neither ECR5 nor ECR5/MEF2 was involved. Surprisingly, none of these four mutations abrogated the suppressive effects of Wnt3a, $1,25(OH)_2D_3$, OSM, dexamethasone, or $TGF\beta_1$, or the positive effects of BMP-2. These data suggest that with regard to regulation it is clear that in order to understand the effects of regulators other than PTH we need to move beyond ECR5.

***Disclosures: Hillary St John**, None.*

MO0199

Clopidogrel enhances periodontal repair through decreased inflammation. Denise Spolidorio*[1], Joao Paulo Steffens[2], Carlos Rossa Junior[2], Dana Graves[3], Luís Carlos Spolidorio[2], Leila Coimbra[4]. [1]Araraquara Dental School, São Paulo State University-UNESP, Araraquara, Brazil, [2]Araraquara Dental School, São Paulo State University-UNESP, Brazil, [3]University of Pennsylvania, School of Dental Medicine, USA, [4]University of São Paulo State, Brazil

Platelet degranulation causes the release of an array of biological mediators including chemokines, cytokines and growth factors that can modulate the repair process. We hypothesized that platelet inactivation induced by drugs might interfere with periodontal repair in experimental periodontitis by suppressing the release of biological mediators from platelets at the site of injury. To evaluate the effects of antiplatelet drugs on experimental periodontal repair 60 rats were randomly assigned to 6 groups (n=10) and ligatures were placed around lower first molars of three groups. The other three groups were not subjected to the induction of periodontal disease and were used as negative controls. Ligatures were removed after 10 days of periodontitis induction and aspirin (Asp) (30 mg/kg) or clopidogrel (Clop) (75 mg/kg) was given intragastrically once daily for 3 days. Periodontal tissue was assessed by the measurement of CXCL12, CXCL4, CCL5 and PDGF by ELISA; histomorphometric analysis of PMN infiltration, attachment loss, bone loss and osteoclast numbers and quantification of blood vessels by imunnohistochemistry.

During periodontal repair gingival content of CCL5 was significantly decreased and CXCL12 increased when compared to negative control groups. Asp and Clop decreased CXCL12 expression but only Clop decreased CXCL4 and PDGF-AB content. Clop treatment appears to have improved the repair process as shown by an increase in blood vessel number (Factor VIII+), a reduced polymorphonuclear leukocyte (PMN) count, and decreased attachment and bone loss. Clop also impaired bone resorption demonstrated by a significant decrease in the osteoclast number (TRAP+) in animals submitted or not to periodontal repair.Systemic administration of Clop during 3 days improved the repair process associated with experimental periodontal disease.

***Disclosures: Denise Spolidorio**, None.*
This study received funding from: The State of São Paulo Research Foundation (FAPESP) and National Council for Scientific and Technological, Development (CNPq)

MO0200

Demineralized Bone Matrix Concurrently Induces Vascular Tissue Formation and Endochondral Bone Formation Adjacent to the Periosteum. Beth Bragdon*[1], Sherif Aly[2], Anthony De Giacomo[2], Elise Morgan[3], Louis Gerstenfeld[1]. [1]Boston University School of Medicine Department of Orthopaedics, USA, [2]Boston University School of Medicine, USA, [3]Boston University, USA

Introduction: The osteoinductive property of demineralized bone matrix (DBM) is believed to arise from bone morphogenetic proteins (BMPs) that drive osteogenesis in mesenchymal stem cells (MSCs). It is thought that the MSCs express vascular endothelial growth factor A (VEGFA), which in turn attracts endothelial cells that further promote BMP expression. However, the exact molecular factors in DBM that are needed for *de novo* bone growth and crosstalk between osteogenesis and angiogenesis during DBM-induced bone formation are poorly understood.

Methods: HumanDBM was obtained with an MTA from Medtronics Inc. Fifty milligrams was implanted adjacent to the periosteal surface of the femur of B6,129S7-$Rag1^{tm1/MOM}$/J. Ectopic bone formation was followed for 31 days. Micro-CT quantified new bone formation, and vascular tissue was assessed by Microfil perfusion followed by micro-CT. RNA was isolated from the implant, femur, and surrounding

muscle at various time points (2-31 days). RT-qPCR was used to quantify mRNA expression describing stem cell recruitment (Nanog, Oct4, Sox2), chondrocyte (Aggrecan and Collagen10a), osteoblast/osteocyte (Osteocalcin and SOST), and vascular (VEGFA, Ve-Cadherin, and SMA) development.

Results: Extensive *de novo* bone and vascular tissues were induced by the DBM implant (Fig. 1). The volume of mineralized tissue increased from day 12 to day 24, after which the levels were constant. Blood vessel formation was detected within the DBM implant. Molecular assessment (Fig. 2) showed peak expression of stem cell markers at the implant within the first 4 days, followed by peak expression for chondrocytes at day 8 and osteoblasts/osteocytes at day 16. VEGFA and SMA expression were concurrent with the expression of the stem cell markers, while endothelial cell markers showed peaks at 2 and 8 days. In contrast to this dynamic mRNA expression for the various stages for endochondrogenesis in the implant, only basal levels of mRNA expression were observed in the femur itself.

Discussion: DBM implanted on the femur concurrently initiated vascular and endochondral bone development. Interestingly the femur itself did not respond to the DBM; rather, stem cells appear to arise from the periosteum. The implant site appeared to be the source for VEGFA. These data suggest a population of SMA-positive cells express VEGFA, facilitating the invasion of endothelial cells into the implant site, with blood vessels developing within the *de novo* ectopic bone.

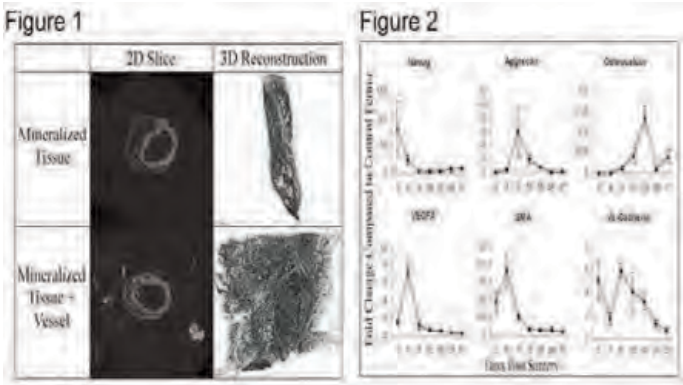

Figure 1. Micro-CT 2D slice (left) and 3D reconstructed (right) image at day 24. Top panel shows the 2D slice of the native and *de novo* bone. 3D reconstruction shows only the newly formed mineralized tissue (cortex removed from the image). Bottom panel depicts the blood vessels and the native and *de novo* bone. **Figure 2.** Expression of selected genes across time at the implant site.

Figures 1-2

***Disclosures: Beth Bragdon**, None.*
This study received funding from: National Institutes of Health (NIH) and Musculoskeletal Transplant Foundation

MO0201

Enhanced bone healing with local delivery of a GSK3β inhibitor. Masahiko Sato*[1], Nicoletta Bivi[2], Matthew Hamang[3], Lowell Gibson[2], Qing Qiang Zeng[2], Ricky Cain[3], Mary Adrian[3], Jonathan Lucchesi[3], Thomas Engler[2], Christian Clarke[2], Timothy Richardson[2], Yanfei Ma[2]. [1]Lilly Research Labs, USA, [2]Eli Lilly & Co., USA, [3]Musculoskeletal Research, Lilly Research Laboratories, USA

GSK3β inhibitors were shown previously to increase bone mass and to enhance fracture repair in rodents; therefore we explored the feasibility of local delivery bone healing with a bisarylmaleimide as a strategy to enabling skeletal efficacy while minimizing toxicity. The GSK3β inhibitor was shown to potently enhance mineralization in a dose-dependent manner until 0.32 nM when rat bone marrow stromal cells were cultured in osteogenic media containing ascorbate and β-glycerophosphate for 5 days. However, at doses above 1.6 nM, reduced mineralization was observed. Quantification of DAPI-stained nuclei showed no reduction in cell number at the higher doses; however, viability assays based on the dye formazan suggested cytotoxicity concerns. The bisarylmaleimide was then formulated in PLGA to control the rate of inhibitor release in 2 rat cortical defect models. Cancellous bone healing was evaluated in young (14 week old) male rats (Sprague-Dawley) which had 2 mm holes drilled through the secondary spongiosa of both proximal tibia before injection of 3, 10, or 30 μg of bisarylmaleimide in 50% PLGA/50%NMP, using positive displacement pipettes. After 3 weeks post-surgery, μCT analyses showed dose-dependent increases in cancellous BMD, cortical BMC, and total BMD relative to vehicle controls. Cortical bone healing was evaluated of the same formulations in mature (8 month old) osteopenic (Ovx at 6 months) rats in which 2 mm holes were drilled into both femura before pipetting of compounds into the cortical defect. Longitudinal μCT analyses showed that the high dose increased whole femur BMC at the cortical defect site from 3 to 5 weeks post-surgery. Interestingly, whole femur BMD decreased as marrow area, cortical area and total area increased faster than BMC. μCT confirmed considerable bone formation activity, but outside the confines of the cortical defect. In summary, these data taken together suggest interesting potential for local delivery of a GSK3β inhibitor at bone healing sites to significantly enhance repair efficacy while reducing systemic exposure and safety concerns.

***Disclosures: Masahiko Sato**, Eli Lilly and Co., 3*
This study received funding from: Eli Lilly and Co.

MO0202

Frizzled-4 expression by the mature osteoblast is required for normal trabecular bone acquisition. Ryan Riddle*[1], Julie Leslie[2], Jeremy Nathans[1], Thomas Clemens[2]. [1]Johns Hopkins University School of Medicine, USA, [2]Johns Hopkins University, USA

Initiation of Wnt/β-catenin signaling requires the interaction of Wnt ligands with a seven trans-membrane frizzled (Fzd) receptor. The specific biological roles of these receptors in bone, however, remain poorly defined, despite the well-accepted role of Wnt signaling in skeletal development. To begin to define the contribution of individual frizzled proteins to osteoblast function, we profiled the expression of all 10 mammalian receptors in calvarial osteoblasts. While the expression of Fzd8 and Fzd9 increased modestly during *in vitro* differentiation, Fzd4 was the most highly up-regulated, with mRNA levels increasing more than 7-fold as cells matured. To determine the function of this receptor in bone, mice lacking Fzd4 (ΔFzd4) in mature osteoblasts were generated by crossing $Fzd4^{flox}$ mice with mice expressing Cre-recombinase under the control of the human osteocalcin promoter. Trabecular bone architecture in young ΔFzd4 mice (3weeks) was comparable to control littermates, but the mutant mice failed to acquire normal amounts of trabecular bone, as bone volume in the distal femur was reduced by approximately 25% when compared to controls at both 6 and 12 weeks of age. By contrast, cortical bone morphology was unaltered in Fzd4 mutants. Osteoblast numbers per bone perimeter were higher in ΔFzd4 mice relative to controls, but the mineralizing surface was decreased and the mineralization lag time was increased, suggestive of a defect in the mineralization process. Consistent with this idea, matrix calcification was impaired in cultures of primary calvarial osteoblasts rendered deficient for Fzd4 and the expression levels of markers of osteoblast maturation, including Runx2, Sp7, and Bglap, were uniformly decreased when compared to cultures of control osteoblasts. Despite a compensatory increase in the expression of other frizzled receptors, including Fzd8, which acts redundantly with Fzd4 in other tissues, Fzd4-deficient osteoblasts also exhibited an impaired ability to respond to Wnt ligands. In this regard, the ability of Wnt3a to inhibit β-catenin phosphorylation and stimulate Axin2 expression was reduced in the mutant osteoblasts relative to controls. To our knowledge, these data represent the first attempt to examine the function of a Fzd receptor in bone in a tissue-specific manner, and suggest that Fzd4 exerts envelope-specific effects on bone structure that are indispensible during the acquisition of trabecular bone mass.

***Disclosures: Ryan Riddle**, None.*

MO0203

IGF-1 enhances osteoblastic function by stimulating oxidative phosphorylation: Insights from a spontaneous mutation in the *Irs1* gene. Anyonya Guntur*[1], Victoria Demambro[1], Clifford Rosen[2]. [1]Maine medical center research institute, USA, [2]Maine Medical Center, USA

We previously showed that Insulin Like growth factor -1 (IGF1) and its downstream signaling system play a key role in osteoblast differentiation. To understand the potential mechanisms involved in IGF1 induced differentiative function we studied a spontaneous mouse mutant that has a single nucleotide deletion in Insulin receptor substrate 1 (*Irs1*) a key adaptor protein involved in IGF1 signaling. The characterization of the metabolic and skeletal phenotype of this mutant was done on two different genetic backgrounds in mice C3-$Irs1^{sml}/Irs1^{sml}$ and B6-$Irs1^{sml}/Irs1^{sml}$. Mice with this mutation have decreased body weight, lower % fat mass and decreased energy expenditure. Comprehensive skeletal phenotyping revealed that mutant mice have very low bone mass and reduced bone formation by histomorphometry despite equal numbers of osteoblasts compared to wildtype (WT) mice. Developmentally the bones that form through endochondral and intramembranous ossification of the mutant mice are smaller. Both the hindlimbs and the skull base have shorter bones with smaller hypertrophic zones. We could identify a loss of IRS1 protein in both osteoblasts and chondrocytes suggesting that the defects are because of loss or attenuation of IGF1 signaling in the mutant limbs. Since the bone formation rates in the mutant mice are low despite adequate numbers of osteoblasts (which is similar to deletion of the IGF1R in late osteoblasts), we examined the metabolic activity of calvarial osteoblasts by studying their oxygen consumption rates (Oxidative phosphorylation,OCR) using the Seahorse XF24. Calvarial osteoblasts from both WT strains (i.e. *C3H/HeJ* and *C57BL/6J*) have increased OCR during differentiation compared to non differentiating cells. On the other hand, mutant calvarial osteoblasts have a markedly blunted OCR response during differentiation compared to WT calvarial osteoblasts. Mechanistically, we observed a decrease in IGF1 induced protein synthesis in the mutant osteoblasts as evidenced by decreased pAKTser473 and pP70S6K in response to IGF1 stimulation. In sum these data suggest that an intact IGF1 signaling pathway is necessary not only for osteoblast differentiation but also for the "work" required to induce collagen synthesis and matrix mineralization.

***Disclosures: Anyonya Guntur**, None.*

MO0204

In vivo Microenvironment pH of biomaterials influence their performance in osteoporotic bone defect repair. Wenlong Liu*[1], Haobo Pan[2], Ting Wang[1], Jianbin Wu[3], Jiang Chang[4], William Lu[1]. [1]The University of Hong Kong, Hong Kong, [2]Shenzhen Institutes of advanced technology, Chinese academy of sciences, China, [3]The University of Hong Kong Shenzhen Hospital, China, [4]Shanghai Insitute of Ceramics, Chinese Academy of Sciences, China

Traditional characterization methods to evaluate the performance of orthopedic biomaterial in repairing bone defect mainly focus on mechanical behavior, degradation properties, surface chemistry and so on. However, though researchers have realized that the degradation products of implants should be non-toxic, the changes and influence of in vivo microenvironment pH (Micro-pH) brought by their degradation on bone remodeling has often been neglected. The aim of this study is to monitor the relationship between the repairing performance of implants and its Micro-pH, and propose the new idea to take Micro-pH as a new evaluation index.

Different biomaterials powders are filled into rat models of osteoporotic bone defect. The Micro-pH surrounding biomaterials-biology interface was monitored with needle combination pH microelectrodes, at different phases of healing. Micro-CT scanning, goldner's trichrome and TRAP staining were employed to detect the performance of specific implants. However, besides Micro-pH, other parameters, such as beneficial element, would influence in vivo performance of implants. So, the in vitro experiments with strickly controlled variables were performed to examine the effect of pH on oBMSCs and RAW 264.7 cells.

After TCP, CS and Sr-CS implantation, the Micro-pH surrounding bone defect area increased immediately (TCP: 7.77 ± 0.15; CS: 8.17 ± 0.06; Sr-CS:9.16 ± 0.10; n=4). CS and Sr-CS showed higher initial Micro-pH compared with TCP group (Fig.1). A higher osteoid formation activity and late response of TRAP-positive cells in vivo were observed in CS and Sr-CS groups. In vitro results shows that, alkaline environment inhibit oBMSCs proliferation activity, while stimulates their osteogenesis differentiation potential. On the other hand, the proliferation efficiency of RAW 264.7 osteoclast precursor, and their capability of forming multi-nucleus osteoclasts were inhibited under alkaline culture condition.

Our results indicate that, though other parameters would influence the performance of orthopedic implants, weak microenvironment pH is also an indispensible factor, which is vital to ameliorate the imbalance between bone formation and absorption under osteoporotic bone remodeling microenvironment. Besides, needle combination pH microelectrode can be employed to detect biomaterials in vivo Micro-pH, and could help to find specific suitable Micro-pH condition for specific biomaterials.

***Disclosures: Wenlong Liu**, None.*

MO0205

Osteoblastic p38alpha MAPK Signaling Mediates Ovariectomy-Induced Bone Loss by Stimulating Interleukin-6 Expression. Cyril Thouverey*, Joseph Caverzasio. Service of Bone Diseases - Dpt of Internal Medicine Specialties - University Hospital of Geneva, Switzerland

Selective p38alpha inhibitors were found to prevent bone loss induced by estrogen deficiency but implicated mechanisms remained to be identified. The p38 MAPK pathway was suggested to influence bone resorption at different regulatory levels. In osteoblasts, p38alpha was reported to stimulate the production of osteoclastogenic interleukin-6 and Rankl in response to various bone-resorptive agents *in vitro*. Therefore, we investigated whether p38alpha in osteoblasts may contribute to ovariectomy-induced bone loss in mice.

Mice lacking *p38alpha* in osteoblasts (*Ocn-Cre;p38alpha$^{f/f}$*) and their control littermates (*p38alpha$^{f/f}$*) were either sham-operated or ovariectomized at 12 weeks of age. Their bone phenotypes were assessed 6 weeks after operations by dexa, microCT, histomorphometry and gene expression analyses (n=7 per group). Data were analyzed by two-way ANOVA and *post hoc* analyses were performed using the Holm-Sidak method.

Ovariectomy caused a decrease in bone mineral density in the spine (-13.1 %; $p<0.001$ versus sham) and to a lesser extent in the femur (-1.8 %; $p<0.001$ versus sham) of control mice but not in *Ocn-Cre;p38alpha$^{f/f}$* mice (+12.7 % in the spine; +8.1 % in the femur; $p<0.01$ versus *p38alpha$^{f/f}$*). Ovariectomy decreased vertebral cancellous bone volume (-45.8 %; $p<0.01$ versus sham), trabecular thickness (-16 %; $p<0.01$) and trabecular number (-20.6 %; $p<0.01$) in control mice but not in *Ocn-Cre;p38alpha$^{f/f}$* mice, indicating that mice lacking *p38alpha* in osteoblasts were protected from ovariectomy-induced bone loss. Consistent with this, ovariectomy caused significant increases in osteoclast surface (4-fold), osteoclast number (3-fold) and serum level of CTX (1.4-fold) in *p38alpha$^{f/f}$* mice but not in *Ocn-Cre;p38alpha$^{f/f}$* mice. Moreover, ovariectomy induced a 2-fold increase in interleukin-6 expression in the long bones of *p38alpha$^{f/f}$* mice ($p<0.05$), whereas expression of this osteoclastogenic cytokine remained unchanged in *Ocn-Cre;p38alpha$^{f/f}$* mice. Finally, tumor necrosis factor alpha, interleukin-1 and CD40 ligand which are overproduced in the bone marrow under estrogen deficiency, stimulated interleukin-6 expression in control osteoblasts but not in those lacking *p38alpha in vitro*.

Our findings indicate that the p38alpha MAPK signaling in osteoblasts mediates ovariectomy-induced bone loss by upregulating interleukin-6 expression.

***Disclosures: Cyril Thouverey**, None.*

MO0206

Protein Tyrosine Kinase 7 (PTK7): A Novel "Molecular Switch" Regulating Differentiation Fate of Human Skeletal (Mesenchymal) Stem Cells into Osteoblasts versus Adipocytes. Abbas Jafari*[1], Majken S. Siersbæk[1], Kenneth Larsen[2], Matthias Dobbelstein[3], Moustapha Kassem[1]. [1]Odense University Hospital, Denmark, [2]Syddansk Universitet, Denmark, [3]Göttingen Center of Molecular Biosciences, Faculty of Medicine, University of Göttingen, Germany

Intracellular signaling proteins (kinases) that act as molecular switches regulating human skeletal (mesenchymal) stem cells (hMSC) differentiation into osteoblasts (OB) versus adipocytes (AD) are not known. Thus, we performed RNAi-based screening of the human Kinome, using Silencer® V3 Human Kinase siRNA Library against 800 known kinases (n=3 siRNA per individual kinase) and identified Protein Tyrosine Kinase 7 (PTK7) as regulating hMSC differentiation, with no effects on cell proliferation. In the follow up experiments, siRNA knock-down of PTK7 in hMSC enhanced OB differentiation upon *in vitro* OB induction, evidenced by increased alkaline phosphatase (ALP) activity, gene expression of osteoblastic markers: ALP, osteocalcin, and collagen type I and *ex vivo* matrix mineralization. On the other hand, PTK7-deficient hMSC exhibited impaired AD differentiation when cultured under AD induction, evidenced by reduced expression of adipogenic markers: PPARγ, C/EBPα, PLIN, ADN, and AP2 as well as reduced formation of mature adipocytes. Stable over-expression of PTK7 in hMSC, led to opposite effects with reduced osteoblast differentiation and enhanced adipocyte differentiation. To identify down stream targets, PTK7-deficient hMSC exhibited increased canonical Wnt signaling, measured by TCF dual luciferase reporter assay, that was associated with increased expression of Wnt target genes: CCND1 and NKD1. In contrast, decreased Wnt signaling and CCND1 and NKDI gene expression were observed in PTK7-overexpressing hMSC. To test the effect of *in vivo* targeting of PTK7 in a pre-clinical *in vivo* bone formation model, shRNA-based PTK7-deficient hMSC exhibited increased bone formation when implanted subcutaneously in immune deficient mice. Our results demonstrate that PTK7 is a molecular switch regulating hMSC differentiation balance between OB and AD through changes in canonical Wnt signaling and can be targeted to enhance *in vivo* bone formation.

***Disclosures: Abbas Jafari**, None.*

MO0207

Role of Menin in Bone Development. Ippei Kanazawa*[1], Lucie Canaff[2], Aarti Angrula[2], Jingjing Li[2], Monzur Murshed[2], Geoffrey Hendy[3]. [1]Shimane University Faculty of Medicine, Japan, [2]McGill University, Canada, [3]McGill University, Royal Victoria Hospital, Canada

Background: The tumor suppressor menin is widely expressed including in bone. Homozygous *Men1* inactivation in mice is embryonic lethal at 12 days and the small fetuses exhibit cranial and facial defects consistent with a role for menin in bone formation. The heterozygous *Men1* phenotype mirrors that of the human multiple endocrine neoplasia type 1 (MEN1) with normal development and endocrine tumors developing later in life. Although previous *in vitro* studies showed that menin has important roles in the osteoblast lineage, little is known about the *in vivo* role of menin in the skeleton. Methods and Results: We conditionally inactivated *Men1* in osteoblasts by crossing *Osteocalcin*-Cre mice with those having a floxed *Men1* gene to generate mice lacking menin in differentiating osteoblasts. Nine-month-old *Men1$_{ob}^{-/-}$* mice displayed significant reduction in bone mineral density by dual-energy X-ray absorptiometry and in trabecular bone volume and cortical bone thickness by micro-computed tomography (μCT) compared to their control littermates. By histomorphometry, bone volume/total volume, osteoblast and osteoclast number, as well as mineral apposition rate (MAR) were significantly reduced whereas osteocyte number was increased. Primary calvarial osteoblasts of *Men1$_{ob}^{-/-}$* mice proliferated more quickly but had deficient mineral apposition and alkaline phosphatase activity. The expression of osteoblast marker genes, BMP-2, Runx2, Osterix, Dlx5, type I collagen, and osteocalcin was all decreased with reduced responsiveness to TGF-β and BMP-2 defined by promoter/reporter assay. Moreover, cyclin-dependent kinase inhibitor expression was reduced, whereas cyclin dependent kinase expression was increased. The gene expression of Phex and sclerostin was significantly increased, while that of RANKL was decreased. In contrast to the *Men1$_{ob}^{-/-}$* mice, 12-month-old transgenic mice specifically overexpressing a human menin cDNA in osteoblasts had a gain of bone mass by μCT and histomorphometry with increased MAR and osteoblast number. Conclusion: Taken together, depletion of menin in the osteoblast leads to decreased bone formation by reducing TGF-β/BMP-2 responsiveness and increasing sclerostin expression as well as impaired bone remodeling, resulting in a reduction in trabecular and cortical bone whereas overexpression increases bone mass by enhancing bone formation. Therefore, maintenance of menin expression and function in the osteoblast is important to avoid decreased bone mass.

***Disclosures: Ippei Kanazawa**, None.*

MO0208

Syndecan-2 Controls the Fate of Osteoblast and Osteoclast Precursors Cells in the Bone Marrow and Modulates Wnt Signaling in Mice. Rafik MANSOURI*[1], Caroline Marty[2], Pierre Marie[3], Dominique Modrowski[2]. [1]INSERM, France, [2]INSERM U606, France, [3]Inserm Unit 606 & University Paris Diderot, France

Syndecan-2 (Sy2) is a proteoglycan that modulates growth factor activity as well as attachment to and assembly of the matrix. We previously showed that Sy2 controls apoptotic pathways in osteosarcoma cells. To determine the role of Sy2 in normal bone, we analyzed the effects of 2.3 kb Col1A1 promoter-driven Sy2 overexpression on the bone phenotype in transgenic (TG) mice. Sy2 overexpression was found in mature osteoblasts and bone marrow (BM) stromal cells. TUNEL staining showed that the number of apoptotic cells was increased in BM of TG mice compared to wild type (WT) mice. Histomorphometric analyses showed that the number of TRAP+ cells was strongly decreased in TG compared to WT mice. Ex vivo studies showed that the number of TRAP+ cells in TG BM-derived cells was lower than normal when cultured in the presence of RANKL and M-CSF to promote osteoclast differentiation, or when cultured in the presence of vitamin D and ascorbic acid to promote osteoblast-mediated osteoclast differentiation, demonstrating a defect in osteoclast precursor differentiation in the BM of TG mice. Interestingly, the fibroblast-like layer was missing in TG BM cell cultures, suggesting an alteration of the stromal cell population. In support of this hypothesis, RT-qPCR analyses showed a striking decrease in RANKL mRNA in BM of TG mice compared to WT mice. Additionally, BM cell viability and proliferation were reduced in TG mice compared to WT mice, as assessed by crystal violet and BrdU incorporation, and the number of fibroblast-like colony-forming units. However, the in in vitro osteoblastic differentiation capacity of BM cells, and the activity of mature osteoblasts (mineral apposition rate) were unchanged in TG mice. Collagen type 1, RUNX2 and alkaline phosphatase mRNA expression also did not differ in bone marrow of TG and WT mice. In contrast, the expression of Wnt effectors was altered. The expression of Wnt3a, Wnt11 and bcatenin were down-regulated and DKK1 was increased. Consistently, crossing TG mice with mice bearing the Wnt reporter system (TOP-GAL mice) demonstrated that Sy2 overexpression decreased Wnt/βcatenin signaling. Altogether, these results show that Sy2 overexpression in osteoblastic cells induces the death of proliferating osteoblast precursors and thereby alters RANKL-mediated osteoclast precursor cell differentiation. Furthermore, the Sy2-mediated alteration of the osteoblast precursor fate is related to alteration of Wnt/βcatenin signaling.

***Disclosures: Rafik MANSOURI**, None.*

MO0209

Systemic Sclerostin Antibody Treatment Reduces Alveolar Bone Loss in Rice Rats with Active Periodontitis. Jose Aguirre*[1], Donald Kimmel[2], Mohammed Akhter[3], Kathleen Neuville[1], Carley Trcalek[1], Alicia Leeper[1], Alyssa Williams[1], Mercedes Rivera[4], Lakshmyya Kesavalu[4], Hua Zhu (David) Ke[5], Min Liu[5], Thomas Wronski[1]. [1]University of Florida, USA, [2]Kimmel Consulting Services, USA, [3]Creighton University Osteoporosis Research Center, USA, [4]Department of Periodontology & Oral Biology, College of Dentistry, UF, USA, [5]Amgen Inc., USA

Inhibition of Sclerostin (Scl), a negative modulator of the Wnt/β-catenin pathway, by a neutralizing antibody (SAB) stimulates bone formation and increases bone mass. Moderate or worse periodontitis (PD) is prevalent in one-third of dentate US adults. Mechanical debridement is the principal method proven to slow PD-related alveolar bone loss (ABL). No known bone-active systemic medication reduces the rate of ABL in animals or humans with active PD. Rice rats (*Oryzomys palustris*) develop spontaneous PD that requires no local manipulation, and is accelerated by a high sucrose/casein (HSC) diet. We hypothesize that systemic treatment with SAB reduces PD-related ABL in rice rats. At age 28 days, male rats (n=12-16/grp) were fed standard (STD) or HSC diets during an 18wk PD-establishment period (PEP). Rats then began an 8wk PD-treatment period (PTP). During the PTP, rats continued their PEP diets (STD-STD and HSC-HSC). In addition, half that were fed HSC during the PEP were switched to STD (HSC-STD) to remove the acceleratory stimulus for PD. The STD-STD, HSC-HSC and HSC-STD groups were divided in half and treated SC with vehicle (Veh) or SAB [ratized Scl-AbIII (Amgen, Inc.), 25mg/kg, 2X/wk]. At necropsy, femurs were collected to measure BMD. Mandibles were used to study vertical (v) ABL by histomorphometry and MicroCT, and overall PD status by qualitative histology [PD Score (0-4; 4 = worst)].(1) vABL was assessed as the distance from the cemento-enamel junction to the alveolar bone crest between the first and second, and the second and third molars.

BMD values verified expected SAB bioactivity in all rats. As shown by two-factor ANOVA, diet significantly affected PD score and vABL. SAB treatment also had a significant effect on both PD score and vABL. Student's t-test revealed that all SAB treatment groups had at least a strong trend for slower vABL compared to their respective Veh-treated controls fed the same diet regimen. Our data suggest that systemic treatment with SAB, a powerful bone formation stimulator, reduces vABL in rice rats with active mild, moderate, or severe diet-induced periodontitis. Combined systemic bone-active medication and long-proven standard mechanical therapy for periodontitis, that may act by independent mechanisms, could save periodontally-compromised teeth by increasing alveolar bone support more than is now possible.

1. Aguirre JI et al. 2012 Oral Dis 18:459-468

Table 1. Systemic sclerostin antibody treatment reduces alveolar bone loss in rice rats with active periodontitis

Group	N	Mandibular PD Score	vABL (MicroCT) M1-M2 (mm)	vABL (Morph) M1-M2 (mm)	vABL (Morph) M2-M3 (mm)
Veh/STD-STD	16	3.45±0.28	0.92±0.13	0.71±0.11	0.81±0.09
SAB/STD-STD	15	2.79±0.22[a]	0.68±0.10[a]	0.54±0.06	0.48±0.06[b]
Veh/HSC-HSC	10	2.90±0.39	1.26±0.22	0.93±0.19	0.91±0.20
SAB/HSC-HSC	10	1.85±0.33	0.71±0.14[b]	0.44±0.10[b]	0.36±0.10[b]
Veh/HSC-STD	10	3.59±0.23	1.57±0.25	1.26±0.12	1.13±0.11
SAB/HSC-STD	10	3.00±0.42[a]	1.12±0.22[a]	0.96±0.16	1.05±0.18
SAB effect	P=	0.006	0.017	0.003	0.000
Diet Effect	P=	0.033	0.034	0.002	0.000
Interaction	P=	0.714	0.645	0.254	0.398

PD. Peridontitis; vABL. Vertical alveolar bone loss; Morph. morphometric measurement.
Data presented as Mean±SEM. [a] 0.1>P>0.05. [b] P<0.05 vs. appropriate Veh group.

Table 1. Aguirre et al. Systemic sclerostin antibody treatment reduces alveolar bone loss in rice rats

***Disclosures: Jose Aguirre**, Amgen Inc., 6*
This study received funding from: Amgen Inc.

MO0210

The HtrA1 and DDR2 pathway is activated during mechanical instability and impairs bone formation during Fracture Healing. Paul Fanning*[1], Marie Walcott[1], Christopher Raskett[1], John Wixted[2], David Ayers[3]. [1]University of Massachusetts Medical School, USA, [2]University of Massachusetts, USA, [3]UMass Memorial Medical Center, USA

There is a clinical need to understand the relationship between mechanical stability and pathological nonunion. The transition from chondroid to bone is critical for normal healing and is influenced by mechanical rigidity at the fracture site. The molecular mechanisms that mediate cartilage turnover in varying states of mechanical stability in fracture healing are not understood. We hypothesize that expression of HtrA1, an antagonist of TGFb and BMP signaling, and a chondrocyte mechanoreceptor, DDR2 contributes to nonunion during fracture healing. Reproducible transverse femur fractures were generated using controlled injury level in 8-week old C57BL/6 male mice using rigid (normal healing) or flexible (nonunion) fixation. On sacrifice days 5, 7, 10 and 14, the fracture callus was dissected and total RNA isolated. Relative transcript levels were measured (qPCR) and normalized to 18S RNA levels. Vasculature formation was assessed by μCT using a Scanco μCT 40 system, following perfusion with a lead chromate radiopaque silicone compound. Morphometric analysis of the callus, revealed that both total and percent cartilage areas were increased in unstable fractures at all time points. Calluses also showed delayed expression of cartilage formation markers (Col2a1; Acan) in flexible- vs. rigid-fixed fractures. HtrA1 mRNA levels were increased in flexibly-fixed fractures at all time points following the initial inflammatory phase. Ddr2 was expressed at a significantly higher level in flexibly-fixed fractures at day 10, the peak day of cartilage formation. Vegf-A, an angiogenic marker was significantly decreased at all time points following the initial inflammatory phase. μCT similarly showed significantly reduced vascular formation at day 17. These data suggest that the mechanically unstable fracture callus reaches the cartilage stage however, it is not resorbed, persisting as a prolonged chondrogenic phase, preventing osseous bridging. Neovascularization is also delayed allowing reduced recruitment of osteogenic cells to the fracture site. HtrA1 activation via the Ddr2 mechanoreceptor in unstable fractures concomitant with antagonism of bmp molecules arising from the callus and the vascular cells antagonism could impair bone formation. In summary, our data proposes that an increase of this HtrA1-Ddr2 signaling pathway is associated with the mechanically unstable fracture environment, prolonging the chondrogenic phase and delaying bone repair.

***Disclosures: Paul Fanning**, None.*

MO0211

The Role of TGR5 Receptor in Bile Acid-mediated Bone Metabolism. Hyojung Park*[1], Jae-Yeon Yang[1], Sun Wook Cho[2], Jung Hee Kim[1], Seung Hye Kim[1], Mi Gyeong Jang[1], Sang Wan Kim[1], Mijung Yim[3], Chan Soo Shin[1]. [1]Seoul National University College of Medicine, South Korea, [2]National Medical Center, South Korea, [3]Sookmyung Women's University, South Korea

Bile acids have established as hormones involved in the regulation of various metabolic processes including glucose and lipid metabolism. Previously, we have demonstrated that several endogenous bile acids play positive roles in osteogenesis. However, their mechanisms are still elusive. The aim of this study was to investigate the role of TGR5, a G protein-coupled receptor for bile acids, in bone metabolisms. To verify the physiologic role of TGR5 in bone tissues, we first demonstrated the endogenous expressions of TGR5 in osteoblasts. Interestingly, mRNA expressions of TGR5 genes were significantly increased by chenodeoxycholic acid (CDCA) treatments in calvarial cells. Additionally, TGR5 gene expressions were also increased during osteoblastic differentiation of mesenchymal stem cells (C3H10T1/2 cells), suggesting functional roles of TGR5 in osteoablasts. To further evaluate the role of TGR5 in osteoblast differentiations, natural agonist, oleanolic acid (OA) and synthetic agonist, Isoxazolecarboxamides were used. When C3H10T1/2 cells were differentiatied with osteogenic medium with both TGR5 agonists, alkaline phosphatase (ALP) activities were significantly increased compared to vehicle-treated group. Moreover, this positive effect of Isoxazolecarboxamides in osteoblastic differentiation was significantly attenuated by knockdown of TGR5 with siRNA. These results validated that TGR5 involved in osteoblast differentiation. To examine the effect of TGR5 in osteoclast differentiation we used mouse bone marrow macrophages. Osteoclasts formation from BMMs was significantly decreased by OA or Isoxazolecarboxamides in a dose dependant manner and osteoclast marker gene expression was inhibited notably. Furthermore, knockdown with TGR5-siRNA increased osetoclasts formation and this increase was inhibited by Isoxazolecarboxamides treatment. In molecular insight, the expression of NFATc1 and c-fos, a master regulator of osteoclast differentiation, was attenuated by OA or Isoxazolecarboxamides. Consistent with in vitro results, Isoxazolecarboxamides blocked LPS-induced osteoclast formation in mouse calvaria. Taken together, these results suggest that TGR5 play a pivotal role in bone metablolism through regulating both arms of bone remodeling, ie. bone formation and resorption. These findings provide a better mechanistic understanding of bile acid actions in bone metabolism.

***Disclosures: Hyojung Park**, None.*

MO0212

TRIP-TRAP Interactions Control Spatial Coupling During Remodeling. J. Edward Puzas*[1], Diana Metz-Estrella[2], Tzong Jen Sheu[1]. [1]University of Rochester School of Medicine, USA, [2]Hospital for Special Surgery, USA

Introduction: TRIP-1 is a 36 kDa protein with a dual function in cells. It is part of the initiation complex for protein synthesis (eIF3i) as well as a substrate for the type II TGF beta (where it is known as TGF beta receptor-interacting protein). Its function as either a regulator of translation or gene transcription is modulated by its phosphorylation state which also determines whether it can be found in the nucleus or cytoplasm.

We have previously shown that TRIP-1 has an extremely high affinity for the catalytic region of type 5 tartrate resistant acid phosphatase (TRAP). Our early hypothesis is that TRAP can de-phosphorylate TRIP-1 and prepare it for translocation into the nucleus.

In this work we show that loss of function of TRIP-1 compromises osteoblast activity and treatment of osteoblasts with TRAP activates them. We have also characterized the movement of TRIP-1 between the nucleus and cytoplasm and correlated it with its phosphorylation state.

Methods: Isolated osteoblasts from calvaria and marrow as well as bone cell lines were used for these experiments. Phosphorylation state for TRIP-1 was evaluated with Western blot analysis after using phospho-enrichment protocols. Sub-cellular localization was performed with con-focal microscopy.

Results: Ablation of TRIP-1 in osteoblasts using siRNA methodology led to a decrease in gene expression for alkaline phosphatase, Runx 2, type 1 collagen, osteopontin and osteocalcin. Overall protein synthesis was not affected as evidenced by a lack of change in beta actin levels.

TRIP-1 levels were themselves decreased by dexamethasone and increased by vitamin D and PTH.

Phosphorylation of TRIP-1 occurred rapidly (15 min.) after treatment of the cells with TGF beta. This activation is consistent with TRIP-1's role in the immediate preparation for new protein synthesis after TGF beta treatment. Virtually, all of the phosphorylated TRIP remains in the cytoplasm. However, within 30 min. TRIP-1 is dephosphorylated and appears to migrate into the nucleus where we believe it becomes a co-factor for Smad signaling.Conclusion: As osteoblasts are known to endocytose TRAP via M-6-P receptors and the catalytic domain of TRAP binds avidly to TRIP-1 we speculate that the TRAP-coated resorption pit provides the key dephosphorylation step for activating TRIP-1. This could explain, in part, why osteoblasts form bone only on prior resorbed surfaces during normal remodeling.

***Disclosures: J. Edward Puzas**, None.*

MO0213

A Novel Lipidoid-MicroRNA Conjugate Promotes Osteogenic Differentiation. Lei Sui*[1], Leilei Zheng[1], Qianqian Han[1], Lan Zhang[1], Liming Yu[1], Qiaobing Xu[2], Qisheng Tu[1], Jake Jinkun Chen[1]. [1]Tufts University School of Dental Medicine, USA, [2]Tufts University, USA

We have shown that the microRNA (miR)-335-5p plays an important role in regulating bone development (JBMR 26:1953-63, 2011). It activates Wnt signaling pathway and promotes osteogenic differentiation by down-regulating Dickkopf-related protein 1 (DKK1). However, reliable delivery of microRNAs to specific cell types remains a concern. Although viral and commercial lipid delivery systems are available, the safety and efficiency of these vectors are still questionable. Thus, we created a combinatorial library of lipidoid nanoparticles as the amphiphilic nature of lipids enables them to penetrate through various cellular barriers. Therefore, lipidoids are an ideal carrier to facilitate the miR-335-5p delivery in promoting osteogenic differentiation. Briefly, miRNA at an initial concentration of 10 mg/mL was added to empty liposomes at a weight ratio of 10:1 total lipids-miRNA for particle characterization. After primary and secondary screening, we found the lipidoid with a specific structure, tightly packed with miR-335-5p, showed the highest transfection efficiency compared with other lipidoids as well as Lipofectamine 2000. Thus we used this particular lipidoid-miR-335-5p conjugate in this study. Transfection of the conjugate into ascorbic acid-induced C3H10T-1/2 murine mesenchymal stem cells significantly increased the expression levels of major osteogenic transcription factors Runx2, Osx, and Satb2. Our real-time RT-PCR analyses also indicated increased ALP and Col-1 expressions in these cells. The transfection was conducted in the presence of serum, which simulated an *in vivo* environment. Throughout the induction and transfection procedure, C3H10T-1/2 cells showed normal morphological characteristics. No obvious cytotoxicity of the lipidoid-miR-335-5p conjugates was observed. This study represents the first attempt to deliver microRNA using a lipidoid carrier and suggests that lipidoid conjugates are a promising system to implement the modulating function of specific microRNAs in osteogenic differentiation. To determine the feasibility and efficiency of this system in clinical application, lipidoids with multiple osteogenic miRNAs are currently used to enhance osteoblast differentiation and promote bone wound healing in animal models.

***Disclosures: Lei Sui**, None.*

MO0214

Alendronate Alters Single Cell Gene Expression of Cortical Osteoblast Lineage Cells in an Estrogen Deficiency Model of Bone Loss. James Flynn*[1], Ryan Murphy[1], Steven Spusta[1], Clifford Rosen[2], Simon Melov[1]. [1]Buck Institute for Research on Aging, USA, [2]Maine Medical Center, USA

Because of bone's mineralized cellular matrix it is often difficult to define specific cell populations or examine the biology within cortical bone using traditional molecular methods. Through the use of single cell genomics, we are able to analyze the gene expression profiles of individual cells from specific cell populations. In this study, we examined single cortical osteoblasts derived from femur shafts of female C57BL/6 mice. The mice used were either sham surgical controls, ovariectomized mice undergoing estrogen depletion bone loss, or ovariectomized mice treated with an anti-resorptive bisphosphonate drug (100 µg/kg alendronate) via weekly I.P. injections. A subset of these mice were euthanized at 4, 8, and, 16 weeks post-surgery at which point bone tissues were preserved for later molecular analysis (n=10 mice per treatment per timepoint). Cortical bone cells of these femurs were isolated via serial collagenase digestion, and the osteoblast lineage cells were enriched via FACS selection for $CD31^{-}/CD45^{-}/Alkaline\ Phosphatase^{+}$ cell markers. Subsequently, over 100 individual osteoblastic cells from each treatment group were analyzed via nanofluidic qPCR arrays for simultaneous detection of 82 bone specific transcripts. The resulting expression data revealed the single cell differential gene expression between the control mice and mice suffering bone loss. This was further confirmed via whole body *in vivo* microCT scans at 35 micron and *ex vivo* femur scans at 9 micron resolution. The alendronate treated mice demonstrated a unique expression signature in a subset of the osteoblastic cells. Single cell gene expression analysis reveals a unique genetic signature within cell populations undergoing bone loss. The analysis of these cell populations at the single cell level may reveal a greater understanding of the effects of anti-resorptives on cell populations derived from bone.

***Disclosures: James Flynn**, None.*
This study received funding from: Supported by Merck IISP # 50196 (SM) and Glenn Foundation Fellowship (JF)

MO0215

Endothelin Signaling Promotes Osteogenesis via Changes in the miRNA Environment which Induces IGF-1 and PGE2 while Derepressing Wnt Signaling. Michael Johnson*[1], Jasmin Kristianto[2], Anne Gustavson[1], Kathryn Konicke[2], Baozhi Yuan[1], Robert Blank[1]. [1]University of Wisconsin, USA, [2]University of Wisconsin–Madison, USA

Endothelin promotes the growth of osteoblastic breast and prostate cancer metastases, an effect previously shown to be due in part to derepression of canonical WNT signaling. Conversion of big ET1 to mature ET1, catalyzed primarily by endothelin converting enzyme 1 (ECE1), is necessary for ET1's biological activity. We previously identified *Ece1*, encoding ECE1, as a positional candidate gene for a pleiotropic quantitative trait locus affecting femoral biomechanics. To test the hypothesis that ET1 signaling regulates osteogenesis in the normal state as well as in cancer. We exposed TMOb osteoblasts to 25 ng/ml big ET1 prior to and over the course of *in vitro* differentiation. Cells were grown for 6 days in growth medium and then switched to mineralization medium for an additional 15 days, by which time they form mineralized nodules. Cells were harvested every three days following the switch to mineralization medium. We measured mRNA levels of genes involved in the ET1 signaling axis, production of paracrine factors involved in osteogenesis, and miRNA expression. TMOb cells exposed to big ET showed greater mineralization than control cells ($N = 6$, $p = 0.008$). The mineralization difference was specific to ET1 signaling, as it was blocked by pharmacological inhibition of ECE1 or endothelin receptor A. Under normal mineralization conditions, *Ece1* mRNA expression showed no change over the course of mineralization, ET1 was repressed and endothelin receptor A was induced. Addition of big ET1 repressed expression of all three genes. IGF-1 levels were significantly (1.3-1.8X) higher over time in the presence of big ET ($p<0.001$). PGE2 levels were significantly increased over time (1.2-1.4X) in the presence of big ET-1 while DKK1 and SOST production were repressed over time by 30-40% by big ET-1 ($p<0.001$). Big ET1 repressed anti-osteogenic miRNAs including miRNA 335-5p, which targets *Igf1*. MiRNAs that target proteins involved in bone catabolism were induced by big ET1 exposure. Modulation of canonical WNT signaling could not fully account for ET1's osteogenic effects, as big ET1 produced a greater mineralization than treatment with LiCl. Conclusion: Our data show that osteoblasts express all elements needed for ET1 signaling differentiation and that ET1 signaling promotes mineralization. Moreover, they suggest that ET1's osteogenic effects are mediated in part via IGF-1 and PGE2 induction, potentially through changes in miRNA expression, previously unrecognized ET1 osteogenic mechanisms.

***Disclosures: Michael Johnson**, None.*

MO0216

Genome-wide changes in DNase-hypersensitivity during osteoblastogenesis reveal differential usage of DNA motifs: New perspectives in gene regulation. Phillip Tai*[1], Hai Wu[2], Troy Whitfield[3], Jonathan Gordon[4], Andre Van Wijnen[5], Jane Lian[2], Gary Stein[6], Janet Stein[7]. [1]University of Vermont, College of Medicine, Department of Biochemistry, USA, [2]University of Vermont, USA, [3]Dept. of Biochemistry & Molecular Pharmacology, University of Massachusetts Medical School, USA, [4]University of Vermont, Department of Biochemistry, USA, [5]Mayo Clinic, USA, [6]University of Vermont, College of Medicine, USA, [7]University of Vermont Medical School, USA

Gene regulation during the process of osteoblastogenesis has been well-described, yet the discovery of novel regulatory regions has been limited by how we currently predict the locations of functional *cis*-regulatory modules (CRMs). Historically, the *de novo* identification of sequences critical for the control of gene expression relied primarily on sequence conservation in promoters, querying for binding motifs based on position weight matrices of known transcription factors, and the identification of disease causing, non-coding mutations near critical genes. However, we now must consider that regulatory elements also rely on 3-dimensional chromosomal interactions between far-distal regions, epigenetic chromosomal modifications, and RNA:DNA interactions. Traditionally, DNaseI-hypersensitivity assays have been used for the identification of regulatory regions via preferential digestion at chromatin depleted or displaced of nucleosomes, as a result of transcription factor occupancy. With the advent of new sequencing technologies, we probed DNase hypersensitivity on a genome-wide scale, to determine whether differentiation and/or bone-related gene regulation is marked by the presence of commonly utilized DNA motifs within active CRMs. We thus sought to evaluate the gain or loss of motif representation within hypersensitive regions during osteoblastogenesis, from day-0 (growth-phase) to day-28 (mineralizing) MC3T3 cultures. We find that differentiation is marked by an increased enrichment of NFkB-p65, MEF2, and bHLH/E-box motifs within hypersensitive regions, while CTCF, NF1, TEAD, and AP1 motifs decrease. Furthermore, grouping hypersensitive regions based on genomic positioning (promoters, introns, exons, and far-distal regions) revealed significant differences in motif abundance in first introns versus other genomic positions. This finding suggests that the regulation conferred within first intron sequences may be somewhat distinct. Interestingly, the majority of motifs that were enriched regardless of genomic position or differentiation time-point, were not completely matched to currently known transcription factor motifs curated in the JASPAR database. Taken together, the changes in DNase-hypersensitive regions during osteoblastogenesis and the enrichment of distinct motifs within these regions indicate that osteoblasts utilize unique sets of motif rules for transcription factor binding or that regulatory control operates through undiscovered factors.

***Disclosures: Phillip Tai**, None.*

MO0217

Genomic Occupancy of Runx2 Combined with Global Expression Profiling Identifies Novel Mechanisms Regulating Osteoblastogenesis. Hai Wu*[1], Troy Whitfield[2], Jonathan Gordon[3], Jason Dobson[2], Phillip Tai[4], Andre Van Wijnen[5], Janet Stein[6], Jane Lian[1], Gary Stein[7]. [1]University of Vermont, USA, [2]University of Massachusetts Medical School, USA, [3]University of Vermont, Department of Biochemistry, USA, [4]University of Vermont, College of Medicine, Department of Biochemistry, USA, [5]Mayo Clinic, USA, [6]Universityof Vermont Medical School, USA, [7]University of Vermont, College of Medicine, USA

Proliferation and differentiation of osteoblasts are highly regulated during bone development and formation, as well as normal turnover and repair in the adult skeleton. The epigenetic and transcriptional program leading to osteoblastogenesis, necessary for bone formation is coordinated through genomic occupancy of Runx2. While numerous Runx2 gene targets are known, here we have identified a broad spectrum of Runx2 functions by global analysis of Runx2 binding. ChIP-Seq was performed to characterize genome-wide Runx2 occupancy during commitment and stages of osteoblast differentiation in bone marrow stromal cells (BMSCs) and pre-osteoblasts (MC3T3-E1s). Using a peak-calling algorithm, we discovered close to 80,000 statistically confident Runx2 binding events throughout the mouse genome. These binding events revealed distinct spatiotemporal patterns during osteoblast differentiation that occur across the genome including proximal promoters but with a large percentage in upstream, introns, exons, transcription termination sites (TTSs), and intergenic regions. This result implicates these regions in Runx2-mediated gene regulation of osteogenesis which was further supported by reporter assays of non-promoter regulatory domains. Moreover, Runx2 binding patterns correlate in functional clusters, relating to biological changes in osteoblast differentiation. Using Affymetrix expression profiling of differentiating osteoblasts depleted of Runx2, we identified novel, primary Runx2 targets in a broad spectra of functional categories such as extracellular matrix remodelers (Adamts4), Vdr signaling components (Crabp2), epigenetic regulators (Ezh2), JAK-STAT signaling pathways (Stat1), Wnt signaling pathways (Dkk2), and immune-responsive genes with as of yet, unknown functions in osteoblasts (Stat2, Mitf, Irf7). Thus, combining ChIP-Seq data with gene expression profiling, we uncovered a comprehensive regulatory network by Runx2 of transcription corresponding to Runx2 binding events. Our data establishes that Runx2 interactions with chromatin across the entire genome reveals novel mechanisms for the control of phenotypic gene expression contributing to osteoblastogenesis.

***Disclosures: Hai Wu**, None.*

MO0218

Pin1-mediated conformational change of Runx2 is required for skeletal development. WON JOON Yoon*[1], Rabia Islam[2], Woo Jin Kim[3], Young-Dan Cho[4], Toshihisa Komori[5], Gary Stein[6], Jane Lian[7], Je-Yong Choi[8], Hyun-Mo Ryoo[9]. [1]SEOUL NATIONAL UNIVERSITY, Rok, [2]School of Dentistry, Seoul National University, South Korea, [3]Seoul National University, Rok, [4]Seoul National University, South Korea, [5]Nagasaki University Graduate School of Biomedical Sciences, Japan, [6]University of Vermont, College of Medicine, USA, [7]University of Vermont, USA, [8]Kyungpook National University, School of Medicine, South Korea, [9]Seoul National University School of Dentistry, South Korea

Haploinsufficiency of RUNX2 is the genetic cause of cleidocranial dysplasia (CCD) that is characterized by hypoplastic clavicles and open fontanels. CCD is inherited as a completely penetrant trait with variable expressivity of the RUNX2 mutation. Previous reports have indicated that the Runx2 mRNA levels are directly related to the penetrance and to the expressivity of CCD phenotypes in mice. In this study, Pin1 mutant mice developed a range of CCD phenotypes similar to those of the Runx2+/- mice. We found that Pin1 interacts with the Runx2 C-terminus following a phosphorylation event. Pin1-mediated proline isomerization stabilizes the Runx2 protein by enhancing its acetylation and stimulating its transactivation activity. Importantly, Runx2 is a master transcription factor of osteogenesis. Thus, CCD phenotypes observed in the Pin1 mutant mice could be indirectly resulted from a decrease in the Runx2 protein stability and transactivation activity caused by Pin1 deficiency. Hence, the structural modification of Runx2 by Pin1 could be a novel therapeutic target for osteogenesis.

***Disclosures: WON JOON Yoon**, None.*

MO0219

Post-transcriptional Control of the Lineage Commitment Factor Runx2 During Mitotic Division of Osteoprogenitors via its MicroRNA Dependent 3' Untranslated Region. Ozkan Aydemir[1], Hatem Elif Kamber[1], Rodrigo Grandy[2], Martin Montecino[3], Jennifer Westendorf[4], Jane Lian[2], Janet Stein[2], Gary Stein[5], Mario Galindo[6], Andre Van Wijnen*[4]. [1]University of Massachusetts Medical School, USA, [2]University of Vermont, USA, [3]Universidad de Concepcion, Chile, [4]Mayo Clinic, USA, [5]University of Vermont, College of Medicine, USA, [6]University of Chile, Chile

Expression of the bone-related master regulator Runx2 is tightly regulated during the cell cycle to control its osteogenic activity in expanding mesenchymal progenitor populations. Runx2 mRNA is upregulated prior to mitotic division in the G2 phase, but Runx2 protein accumulates only in progeny cells early during the ensuing G1 phase. Here, we characterized post-transcriptional mechanisms that regulate Runx2 protein levels during the cell cycle. Runx2 mRNA has an unusually long 3' untranslated region (UTR), which is targeted by multiple microRNAs (miRNAs) through both functional and predicted seed sequences. This 3'UTR is more easily detected during mitosis than in interphase relative to Runx2 coding mRNA sequences, suggesting that processing or stability of the 3'UTR varies depending on the cell cycle stage. The levels of at least 16 distinct miRNAs that are known or predicted to target the 3'UTR are constitutively expressed during the cell cycle. Hence, inhibitory interactions between miRNAs and the Runx2 3' UTR are restricted by the availability of Runx2 mRNA and the accessibility of seed sequences in the 3'UTR, but not by miRNA levels. Reporter/3'UTR assays in live cells using a destabilized enhanced green fluorescent protein (deGFP) reveal that the Runx2 3'UTR decreases deGFP expression by 40-70%. This suppression is more effective in G2 or M phases than during G1 or G0 phases. Thus, Runx2 protein expression is induced in early G1 phase in osteoprogenitors by relieving cell cycle dependent suppression of its miRNA dependent 3' UTR.

***Disclosures: Andre Van Wijnen**, None.*

MO0220

Role of DGCR8 inactivation in immature osteoblast during bone formation. Young-jin Choi*[1], Seon-Ae Jeon[1], Je-Yoel Cho[2]. [1]Seoul National University, South Korea, [2]College of Veterinary Medicine, Seoul National University, South Korea

MicroRNAs are known to significantly contribute to bone formation by post-transcriptional regulation of gene expression. Most of microRNAs occur in the study of canonical microRNAs that require two sequential cleavages by the Drosha/Dgcr8 heterodimer and Dicer to generate mature products. On the other hand, in the non-canonical pathway, miRNAs are generated by only one cleavage of Dicer. For the study of DGCR8 functions in osteogenesis, we generated mice of which DGCR8 is conditionally deleted in osteoprogenitor cells by Col1a1-Cre. We discovered increase of bone mass in long bones and vertebrae in mice of postnatal to 8-month old. Similar level of activity increase of both osteoblasts and osteoclasts has been detected. It has been already reported by other researchers that the deletion of Dicer at same period of Col1a1-Cre activation induces embryonic lethal. However, cKO DGCR8 mice did not show embryonic lethal and any bone deformity. From this result, it seems that the generations of most abundantly expressed bone microRNAs are dependent on both Dicer and DGCR8. In conclusion, our result shows that the importance of DGCR8 dependent microRNAs during the osteogenesis, especially Col1a1 period of bone formation. Further study for the specific miRNA discovery and validation of its functions might be needed for the deeper understanding of miRNA involvement in osteogenesis.

***Disclosures: Young-jin Choi**, None.*

MO0221

Rorβ, a Novel Regulator of Runx2, Modulates Bone Mass in Mice. Kristy Nicks*[1], Daniel Fraser[1], Matthew Roforth[1], Sundeep Khosla[2], David Monroe[3]. [1]Mayo Clinic, USA, [2]Mayo Clinic College of Medicine, USA, [3]Mayo Foundation, USA

The regulation of osteoblast (OB) differentiation requires the coordinate activities of numerous transcription factors. Although few are essential (Runx2/osterix), others act to fine-tune in response to external cues. Previously, we identified retinoic acid receptor-related orphan receptor beta (Rorβ) as a novel regulator of OB differentiation (JBMR (4):891, 2012). Rorb expression decreases during OB differentiation and sustained expression inhibits mineralization. Rorβ also increases in the pre-osteoblastic bone marrow cell population in aged mice and in bone biopsies from old compared to young women. Furthermore, we have demonstrated that Rorb antagonizes the transcriptional activity of Runx2. Therefore, we hypothesized that mice lacking Rorb would exhibit a high bone mass. Using a Rorb knockout (KO) model, we characterized the skeletal phenotype of Rorβ-KO mice (Rorb-/-) and littermate controls (Ror+/+; WT) in both genders at 12 weeks. Total aBMD was determined at the spine and femur using DXA, whereas measurement of cortical and trabecular bone parameters at the tibia was determined using pQCT. There were no observed differences in the anthromorphometric parameters in either gender, as body and gonad weights were similar. In Rorb-/- male mice, aBMD was decreased at the femur (-8.2%; p=0.007) and vertebrae (-8.1%; p=0.031), when compared to WT mice. In female Rorb-/- mice, no significant difference was found at the femur, however a decrease in vertebral aBMD (-7.0%; p=0.017) was observed. Total density (-4.9%; (p=0.008), cortical density (-2.6%; p=0.017), cortical thickness (-11.6%; (p=0.003) and cortical area (-14.8%; p=0.004) were decreased at the tibia diaphysis of Rorb-/- male mice. Similar decreases were observed in cortical parameters at the tibial diaphysis of Rorb-/- female mice: total density (-4.6%; p=0.021), cortical density (-2.4%; p=0.004), cortical thickness (-7.0%; p=0.008) and cortical area (-8.2%; p=0.011). In summary, we demonstrate that Rorβ loss results in decreased bone parameters, particularly in cortical bone. Although contrary to our initial hypothesis, we believe loss of Rorβ results in increased Runx2 activity and results in decreased bone mass, similar to what is observed in Runx2 transgenic models. Therefore, Rorβ may represent an important modulator of bone mass by optimizing Runx2 activity. Further characterization of Rorβ function in osteoblasts may define it as a potential clinical target to treat age-related bone loss.

***Disclosures: Kristy Nicks**, None.*

MO0222

Smad8 is a novel type regulator of BMP signaling. Sho Tsukamoto*[1], Satoshi Ohte[2], Mai Fujimoto[3], Takato Mizuta[3], Arei Miyamoto[3], Kenji Osawa[3], Shoichiro Kokabu[3], Eiko Murata[4], Eijiro Jimi[5], Takenobu Katagiri[3]. [1]Saitama Medical University RCGM, Japan, [2]Harvard School of Dental Medicine, USA, [3]Saitama Medical University Research Center for Genomic Medicine, Japan, [4]Saitama Medical University, Health & Medical Care, Japan, [5]Kyushu Dental College, Japan

Smad1 through Smad8 are critical transcription factors for bone formation regulated by BMPs. Smads are classified in 3 subgroups according to their functions: Smad1, Smad5 and Smad8 are phosphorylated at C-terminal SVS motif by BMP receptors (R-Smads). Smad4 acts as a co-activator of the phosphorylated R-Smads to regulate transcription of target genes. Smad6 and Smad7 directly bind to BMP receptors and competitively inhibit the phosphorylation of R-Smads, thus they are classified in I-Smads. Recently, we have established constitutively active forms of Smad1, Smad5 and Smad8 and found that Smad8 is less active than other BMP-regulated R-Smads, owing to a deletion in the linker region. In the present study, we further examined the functions of Smad8 using C2C12 myoblasts. At the basal condition, real-time PCR analysis showed that C2C12 cells express abundant mRNAs of Smad1 and Smad5, but negligible Smad8. When the cells were treated with BMP-4, the BMP target genes, such as Id1 and osterix, were induced within 1 h and 3 h, respectively. During the induction, Smad8 mRNA was also induced within 3 h without changing mRNA levels of Smad1, Smad5 or Smad4. The time-course changes in Smad8 mRNA were similar to those of Smad6 and Smad7. The BMP-specific luc reporter activated by a constitutively active BMP receptor was inhibited by the over-expression of not only Smad7 but also Smad8. Moreover, Smad8 inhibited the luc activity activated by a constitutively active Smad1, suggesting that Smad8 targets downstream of BMP receptors. Smad8 formed a complex with Smad4 and bound to a BMP-responsive element in EMSA as R-Smad, but Smad8 showed much weaker transcriptional activity than Smad1 or Smad5. The expression of Smad8 mRNA was induced by BMP signaling similar to I-Smads. In contrast to I-Smads, however, Smad8 did not target BMP receptors and inhibited R-Smad activity. Taken together, our findings suggest that Smad8 is a novel type regulator of BMP signaling that is phosphorylatable by BMP receptors and represses BMP signaling through affecting other Smads.

***Disclosures: Sho Tsukamoto**, None.*

MO0223

Withdrawn

MO0224

SUMOylated αNAC Potentiates Transcriptional Repression by FIAT. Bahareh Hekmatnejad*[1], Omar Akhouayri[2], Rene St-Arnaud[3]. [1]Shriners Hospitals for Children - Canada, Canada, [2]Ibn Tofail Sciences Faculty, Morocco, [3]Shriners Hospital for Children & McGill University, Canada

The transcriptional coregulator αNAC (Nascent polypeptide associated complex And Coregulator alpha) and the transcriptional repressor FIAT (Factor Inhibiting ATF4-mediated Transcription) interact but the biological relevance of this interaction remains unclear. The activity of αNAC is extensively modulated by post-translational modifications (PTMs). We identified a novel αNAC PTM through covalent attachment of the Small Ubiquitin-like MOdifyer, SUMO1. Recombinant αNAC was a SUMO1 target in *in vitro* SUMOylation assays and we confirmed that αNAC is conjugated to SUMO1 in cultured osteoblasts and in calvarial tissue. The amino acid sequence of αNAC contains one copy of the composite 'phospho-sumoyl switch' motif that couples sequential phosphorylation and SUMOylation. We found that αNAC is selectively SUMOylated at lysine residue 127 within the motif and that SUMOylation is enhanced when a phosphomimetic mutation is introduced at the nearby serine residue 132. SUMOylation did not alter the subcellular localization, protein stability,

or DNA-binding capacity of αNAC. The S132D, hyper-SUMOylated αNAC mutant specifically interacted with histone deacetylase-2 (HDAC2) and enhanced the inhibitory activity of FIAT on ATF4-mediated transcription from the *Osteocalcin* gene promoter. This effect required binding of SUMOylated αNAC to the target promoter. We propose that maximal transcriptional repression by FIAT requires its interaction with SUMOylated, HDAC2-interacting αNAC.

***Disclosures: Bahareh Hekmatnejad**, None.*

MO0225

The Endogenous Bmp2 Gene Is required for α-SMA Positive Bone Marrow Stromal Cells to Form Bone In Vivo and Osteoblast Differentiation In Vitro. Stephen Harris*[1], Yong Cui[2], Marie Harris[1], Xiao-Dong Chen[1], Ivo Kalajzic[3]. [1]University of Texas Health Science Center at San Antonio, USA, [2]UTHSCSA, USA, [3]University of Connecticut Health Center, USA

Using the α-SMA-CreERt2 model, we deleted the Bmp2 gene in α-SMA+BMSC that has been shown by lineage studies to be at least one major pool of mesenchymal stem cells.. We activated the Cre at 5-6 days after birth with administration of Tamoxifen (Tam) at 100μg/gm. Bmp2 conditional knock-outs in the α-SMA+ cells leads to thinner long bones with reduced cortical thickness and reduced trabecular bone. One injection at 7 days with Tam and assayed at 17 days also leads to a significant reduced size of the bones and reduced trabecular structures. We then expanded bone marrow stromal cells from Bmp2fx/Bmp2fx mice on a special extracellular matrix (XC-marrowECM, stembiosys.com) that maintains the Mesenchymal Stem Cell (MSC) phenotype. These cells are over 85% α-SMA positive and have high capacity to form a well mineralized matrix within 7-10 days (α-SMA+BMSC$^{bmp2fx/bmp2fx}$); and addition of recombinant Bmp2 greatly accelerates their differentiation process. When the endogenous Bmp2 gene is removed by Adenovirus-Cmv-Cre pretreatment or control pretreatment with Adenovirus-Cmv-GFP, the Cre treated cells fail to differentiate to mineralizing osteoblasts and have greatly reduced expression of Osterix, Col1a1, Osteocalcin, Dmp1, and VegfA. The control α-SMA+BMSC$^{bmp2fx/bmp2fx}$ cells differentiate normally with increased levels of Bmp2, Col1a1, Dmp1, Osteocalcin, and respond to rBmp2. These data suggest a model in which Bmp2 from mature cells activate the Bmp2 gene in MSC that functions in an intracrine fashion , since the addition of rBmp2 could not rescue the deletion of the endogenous Bmp2 in these α-SMA+ BMSC.

***Disclosures: Stephen Harris**, None.*

MO0226

Zinc finger protein 521 recruits the NuRD complex together with transglutaminases and regulates mesenchymal stem cell differentiation. Ken-ichi Takeyama*[1], Harikiran Nistala[1], Steven Gygi[2], Bernard Boback[1], Francesca Gori[3], Roland Baron[4]. [1]Harvard school of dental medicine, USA, [2]Harvard Medical School, USA, [3]Harvard School of Dental Medicine, Massachusetts General Hospital, USA, [4]Harvard School of Medicine & of Dental Medicine, USA

Zinc finger protein 521 (Zfp521) represses the activity of several transcription factors (TFs) to regulate the differentiation of mesenchymal stem cells into osteoblasts or adipocytes, respectively (Hesse et al, 2010; Kang et al., 2013; Kiviranta et al., 2013). It has been suggested that Zfp521 associates with Nucleosome Remodeling and Deacetylation (NuRD) complex components, including HDACs and MTAs, to induce transcriptional silencing and possibly chromatin organization. How Zfp521 interacts with NuRD components and how this interaction modifies the molecular functions of both partners is however still largely unknown.To further elucidate the molecular roles of Zfp521, mass spectrometry was performed after purification by immunoprecipitation and size fractionation of nuclear extracts from human embryonic kidney 293A cells stably expressing Zfp521. We found that Zfp521 forms a tight complex with all the core components of NuRD. Most importantly, this Zfp521-NuRD complex also contained novel subunits, i.e. the transglutaminase (TGM) 1 and 3, enzymes that catalyze the formation of a covalent bond between a free amine group and the gamma-carboxamid group of protein-bound glutamine. These findings were validated by purification of TGM3 and confirmed by affinity purification of endogenous Zfp521 in mouse mesenchymal stem cells. In vitro pull-down analysis showed that Zfp521 binds to NuRD through direct interaction with RBBP4, a NuRD component, mediated by the N-terminal 13 amino acids of Zfp521. TGM3 also directly binds to RBBP4, but not to Zfp521, suggesting that the complex formation of Zfp521 with TGM3 and the NuRD complex is mediated by RBBP4. Furthermore, the Zfp521-NuRD-TGM complex exhibits not only HDAC activity, but also transglutaminase activity. Considering the fact that RBBP4 also provides histone H4 binding ability and that Zfp521 acts as a gene silencer during cell differentiation, we propose that the formation of a Zfp521 complex with NuRD and TGM3 leads to a particular set of post translational modifications and epigenetic regulation resulting in gene silencing. Indeed, depletion of Zfp521 or TGM3 leads to alterations of germ layer determination in teratoma assays and altered pluripotency in mesenchymal cells reprogramming. Thus, the mechanisms by which Zfp521 regulates mesenchymal cell lineage determination between bone and fat through repression of TFs such as Ebf1 and PPARg, may involve the recruitment of this novel complex.

***Disclosures: Ken-ichi Takeyama**, None.*

MO0227

Activation of Hedgehog signaling by loss of Gαs causes heterotopic ossification. Deepti Malhotra*[1], Jean Regard[2], Jelena Gvozdenovic-Jeremic[3], Min Chen[4], Lee Weinstein[5], Eileen Shore[6], Frederick Kaplan[7], Yingzi Yang[3]. [1]NHGRI, NIH, USA, [2]National Institutes of Health, USA, [3]NIH, USA, [4]NIDDK, USA, [5]National Institute of Diabetes & Digestive & Kidney Diseases, USA, [6]University of Pennsylvania, USA, [7]University of Pennsylvania Hospital, USA

Bone formation is exquisitely controlled in space and time. Heterotopic ossification (HO), the pathologic formation of extra-skeletal bone, occurs as a common complication of trauma or in rare genetic disorders, and is highly disabling and lethal. However, there are no good treatments since, the molecular mechanisms that spatially restrict bone formation remain unknown. While our previous work in the bone deformation disorder, fibrous dysplasia (FD) showed that gain of function mutations in the G protein, Gαs leads to pathological upregulation of Wnt/β-catenin signaling; here, we demonstrate another fundamental role of Gαs in spatially restricting bone formation to the normal skeleton by inhibiting Hedgehog (Hh) signaling in mesenchymal progenitor cells. We find that in the human disease progressive osseous heteroplasia (POH), which results from null mutations of *GNAS* that encodes Gαs, Hh signaling is upregulated in ectopic osteoblasts and progenitor cells. We further show that ectopic activation of Hh signaling is sufficient to induce HO, while genetic or pharmacological inhibition of Hh signaling blocks HO in animal models. Our findings identify Gαs signaling as centrally important in regulating osteoblast differentiation from mesenchymal progenitors by maintaining a delicate balance between the two key signaling pathways: Wnt/β-catenin and Hh. These findings further suggest that the Hh signaling inhibitors developed for cancer therapy may also be applied to treat HO spectrum disorders.

***Disclosures: Deepti Malhotra**, None.*

MO0228

Blockade of Receptor Activated Gi Signaling in Osteoblasts Enhances the Anabolic Effect of PTH. Liping Wang*[1], Dylan O'Carroll[2], Theresa Roth[2], Robert Nissenson[3]. [1]VA Medical Center, San Francisco, USA, [2]Endocrine Unit, VA Medical Center & Departments of Medicine & Physiology, University of California, USA, [3]VA Medical Center & University of California, San Francisco, USA

Intermittent PTH is the only FDA approved anabolic therapy for osteoporosis. PTH is presumed to increase Gs signaling and activate cAMP-dependent pathways in osteoblasts (OBs). In contrast, Gi signaling in OBs is believed to antagonize Gs-mediated increases in cAMP. Previous studies have demonstrated that endogenous Gi signaling in OBs restricts bone formation in adult mice and blockade of receptor activated Gi signaling in OBs achieved by target expression of pertussis toxin (PTX) increases both trabecular and endocortical bone formation and prevents age-related bone loss. Therefore, we hypothesized that effectiveness of PTH as an anabolic agent in aged mice would be markedly enhanced by blocking of endogenous Gi signaling in OBs. We examined the effects of intermittent injection of PTH (1-34) on bone metabolism in 4.5 month old female littermate wild type (WT) and Col12.3.PTX mice in which expression of PTX gene is driven by an inducible (tet-off) 2.3 kb Collagen I α promoter (Col12.3). Two weeks after induction of PTX expression, PTH (80μg/kg body weight/day, 5 days/week, s.c.) or solvent vehicle was given to the Col12.3PTX and WT mice for 4 weeks. The distal femur and tibiofibular junction were assessed by μCT in vivo. Compared with age-matched, vehicle treated WT mice, PTH treatment resulted in a 40% ($p<0.01$) increase in cancellous bone fractional volume (BV/TV), a 13.6 % ($p<0.01$) increase trabecular number (Tb.N), and a 12 % ($p<0.05$) decrease in trabecular separation (Tb.SP) in WT mice. There were no significant changes in bone structure in Col2.3.PTX mice treated with vehicle alone. However, PTH treatment increased cancellous BV/TV by 92% ($p<0.001$), increased Tb.N by 33.5% ($p<0.001$), increased trabecular thickness by 11.1 % ($p<0.05$), and decreased Tb.SP by 23 % ($p<0.001$) in Col12.3.PTX mice. PTH increased cortical bone thickness by 5% ($p<0.05$) in Col2.3PTX, not in WT, mice. Thus, PTH produced a significantly greater anabolic effect in Col2.3PTX compared to WT mice. Serum analysis showed that PTH treatment did not affect levels of Ca and P, but increased alkaline phosphatase (ALP) by 11.6% ($p>0.05$) in WT and by 24.3% ($p<0.05$) in Col12.3PTX mice. In conclusion, our results demonstrate that blockade of Gi signaling in osteoblasts greatly enhances the anabolic response to PTH, suggesting a new therapeutic approach for osteoporosis.

***Disclosures: Liping Wang**, None.*

MO0229

Direct Actions of Adiponectin on Mature Osteoblasts May Contribute to Negative Regulation of Skeletal Homeostasis. Marcia Abbott*[1], Dylan O'Carroll[1], Liping Wang[2], Theresa Roth[1], Robert Nissenson[3]. [1]University of California, San Francisco, USA, [2]VA Medical Center, San Francisco, USA, [3]VA Medical Center & University of California, San Francisco, USA

Epidemiological studies show that high circulating levels of the adipokine adiponectin (APN) are associated with low BMD and increased fracture risk. It is unclear if the skeletal effects of APN are site-specific due to local production by marrow adipocytes and if these effects are direct on osteoblasts. To address these issues, we compared the skeletal phenotype of 3 mo old female wild type (WT) mice and transgenic mice in which secretion of endogenous APN is increased by adipocytes (AdTg), provided by Philipp Scherer, UT Southwestern. Increases in circulating APN in AdTg mice was verified (WT 31.9 ± 6.6 vs AdTg 52.5 ± 8.6 ug/ml; $p<0.05$). MicroCT analysis showed 16% decrease ($p<0.05$) in fractional bone volume (BV/TV) in AdTg mice at the proximal tibia with no reduction in BV/TV at the distal femur when compared to WT mice. Histomorphometric analysis revealed 22% reduction ($p<0.05$) in BV/TV in the proximal tibia of AdTg mice. Cortical thickness at the TFJ was 4% smaller ($p<0.05$) in AdTg mice when compared to WT mice. Both the femurs (WT 15.33 ± 0.58 vs AdTg 13.88 ± 0.14 mm) and tibiae (WT 18.89 ± 0.25 vs AdTg 17.20 ± 0.08) from AdTg mice were shorter ($p<0.05$) and the growth plates appeared disorganized when compared to bones from WT mice. H&E staining showed more adipocytes in the proximal tibia in AdTg mice when compared to WT mice. APN concentration in the marrow from the tibia was higher when compared to marrow from the femur isolated from AdTg mice (9.9 vs 4.3 ug/ml/ug protein). Bone marrow stromal cells (BMSCs) from AdTg mice had the same propensity to differentiate into either osteoblasts or adipocytes as WT BMSCs. Treatment of WT BMSCs with APN (2.5 ug/ml) from day 14-28 of osteoblastic differentiation resulted in a reduction of colony formation and mineralized nodules. With the APN treatment mRNA of osterix, runx2, alkaline phosphatase, Col1, and osteocalcin were reduced ($p<0.05$). Surprisingly, APN treatment resulted in an increase ($p<0.05$) in mRNA of PPARγ and C/EBPα and an increase in lipid droplet size and colony formation, as visualized by Oil Red O, in the osteoblastic cells. These data show a negative role for APN in regulating trabecular bone volume in a site specific manner. APN may stimulate cellular plasticity of osteoblasts towards adipocytes both in vivo and in vitro. These data indicate that the negative association between APN and BMD in humans may be at least in part due to direct effects of APN to alter the phenotype of mature osteoblasts.

***Disclosures: Marcia Abbott**, None.*

MO0230

Elucidating the Role of O-GlcNAcylation on RUNX2-Mediated Transcriptional Programs in Bone-Marrow Derived Mesenchymal Stem Cells. Alexis Nagel*, Lauren Ball. Medical University of South Carolina, USA

The *runt*-related transcription factor 2 (RUNX2) activates osteogenic transcriptional processes key to bone development, and its function is modulated by post-translational modifications such as phosphorylation and acetylation. A single study [Kim *et al.* (2007) Biochemical and Biophysical Research Communications, vol. 362, pp. 325-329] suggests that RUNX2 is modified by O-linked N-acetylglucosamine, a post-translational mechanism which modulates cellular nutrient- and stress-induced transcriptional pathways. In addition to identifying a number of O-GlcNAcylated proteins in differentiating osteoblasts, we confirm O-GlcNAcylation on exogenously expressed RUNX2. Further supporting a role for O-GlcNAc in the regulation of osteogenesis, we observe enhanced activity of the matrix marker alkaline phosphatase (ALP) in osteogenic bone marrow mesenchymal stem cells (bmMSCs) cultured in the presence of Thiamet G, a selective inhibitor of the O-GlcNAcase (OGA) cycling enzyme. Continuing studies are focused on elucidating exact sites of RUNX2 Ser/Thr O-GlcNAcylation, determining upstream factors which modulate the extent of RUNX2 glycosylation in bmMSCs, and the impact of RUNX2 O-GlcNAcylation on pathways supporting osteogenesis. This work is supported by NIH/NIDCR grant nos. RO1-DE020925-01A1 and T32-DE017551-05.

***Disclosures: Alexis Nagel**, None.*

MO0231

Osteolineage Jagged1 is a critical component of the PTH activated hematopoietic stem and progenitor cell niche. Rialnat Lawal*[1], Laura Calvi[2], Alexandra Goodman[3], Benjamin Frisch[3]. [1]University of Rochester Medical Center, USA, [2]University of Rochester School of Medicine, USA, [3]University of Rochester, USA

Hematopoietic stem and progenitor cells (HSPCs) have vast regenerative potential, which is vital for transplantation therapies in bone marrow failure and hematopoietic malignancies. However, HSPC numbers are limited, therefore strategies for their expansion are needed. We previously demonstrated that osteoblastic cells expressing a constitutively active parathyroid hormone receptor (PTH-receptor) or systemic PTH treatment expands HSPCs. Activation of Notch signaling in HSPCs was required for this action of PTH. Moreover, PTH increased expression of the Notch ligand Jagged1 in osteolineage cells. However, the role of Jagged1 up-regulation in PTH-dependent HSPC expansion is only partially understood. To determine if osteoblastic Jagged1 mediates PTH-dependent HSPC expansion, we utilized genetic mouse models with Cre –loxP- mediated inactivation of the Jagged1 gene. In this model, the Cre recombinase is driven by Prx1, targeting it to mesenchymal progenitors. Mice with osteolineage Jagged1 inactivation (*Prx1-cre;Jag1$^{fl/fl}$* mice) showed a significant decrease of Jagged1 mRNA with qRT-PCR ($p<0.0001$) compared to control littermates. At baseline, *Prx1-cre;Jag1$^{fl/fl}$* mice were viable and fertile. There were no differences between *Prx1-cre;Jag1$^{fl/fl}$* mice and control littermate in phenotypic HSPC frequency by flow cytometric analysis, peripheral blood counts by HESKA analyses and bone phenotype by micro-CT. These data demonstrate that osteoblastic Jagged1 is not essential at homeostasis for maintaining hematopoiesis, HSPCs and bone growth. However, PTH treatment of *Prx1-cre;Jag1$^{fl/fl}$* mice failed to recapitulate the PTH-dependent expansion in phenotypic HSPCs (lin- Sca1+ cKit + frequency: 0.0644 ± 0.00428 vs 0.07367 ± 0.006458 % Vehicle vs PTH $p=0.2338$ $N \geqslant 6$ mice/group) as seen in wild-type littermates (0.0581 ± 0.00530 vs 0.1250 ± 0.0209 % Vehicle vs PTH $p = 0.0028$ $N \geqslant 5$ mice/group), with a significant decrease in LSK frequency in PTH- treated *Prx1-cre;Jag1$^{fl/fl}$* mice compared to wild-type littermates ($p<0.05$). However, the bone anabolic effect of PTH is maintained. Thus, osteolineage Jagged1 is necessary for PTH-dependent phenotypic HSPC expansion. Moreover, these data support a central role of osteolineage cells in activating the HSPC niche. Together, these data suggest that the PTH initiated increase of Jagged 1 in osteolineage cells is critical as a microenvironmental regulator of HSPCs. Therefore these data identify Notch ligand Jagged1 as an essential component of the PTH stimulated HSPC niche and a potential therapeutic target for pharmacologic HSPC expansion.

***Disclosures: Rialnat Lawal**, None.*

MO0232

The Effects of OA Signaling Pathways on Osteoblast Differentiation and Migration. Fayez Safadi, Gregory Sondag*, Omar Ali, Samir Abdelmagid. Northeast Ohio Medical University, USA

Osteoactivin (OA) is a type I transmembrane protein (576 amino acids) that stimulates osteoblast differentiation and function. Our lab has previously shown that there are two isoforms of Osteoactivin, transmembrane and secreted forms. In addition, we also showed that overexpression of Osteoactivin in MC3T3-E1 increases osteoblast differentiation and matrix mineralization. In this study, we tested the effects of the recombinant Osteoactivin (rOA) on osteoblast function and determined the signaling pathways responsible for OA function in osteoblasts . MC3T3-E1 osteoblast-like cells and primary mouse osteoblasts were used in this study. Cells were treated with different concentrations of rOA and cell proliferation and survival were evaluated using CyQuant and MTT assays, respectively. rOA had no significant effects on cell proliferation or survival. Next, we examined the effects of OA treatment on osteoblast differentiation and function. Osteoblast treated with rOA showed significant increase in mRNA expression of osteoblast differentiation markers (Runx2, Osterix, Osteocalcin (OC) and Type I Collagen (Col1))at days 7 and 14. In addition, we tested the effects of rOA on osteoblast migration using a modified boyden chamber and scratch assay. rOA significantly induces osteoblast cell migration in a dose- and time-dependent manner,. Various signaling molecules including Src, MAPK, AKT, and FAK have been shown to be involved in various stages of osteoblast differentiation and function. Therefore, we examined differentsignaling pathways that mediate OA function in osteoblasts. rOA treatment showed a time-deponent increase in Src, MAPK, AKT, and FAK activation using Western Blot analysis. . Furthermore, using MAPK and AKT specific inhibitors, we showed that OA effects on osteoblast differentiation and function is MAPK-dependent and it effects of cell migration is AKT-dependent. Taken together, these data suggest that OA stimulates osteoblast differentiation and migration independent of cell proliferation.

***Disclosures: Gregory Sondag**, None.*
This study received funding from: NIH

MO0233

A comparative study of the bone regeneration capacity of human muscle derived stem cells and bone marrow mesenchymal stem cells. Xueqin Gao*[1], Arvydas Usas[1], Ying Tang[1], Aiping Lu[1], Jian Tan[1], Johannes Schneppendahl[1], Nicholas Oyster[1], Bing Wang[1], James Cummins[1], Johnny Huard[2]. [1]University of Pittsburgh, USA, [2]Orthopaedic Surgery, USA

Introduction: Human muscle-derived stem cells (hMDSCs) possess multi-lineage differentiation capacity in vitro and form bone in vivo when transduced with BMP2. In order to test whether hMDSCs are as effective as human bone marrow mesenchymal stem cells (hBMMSCs) for bone regeneration, we compared hMDSCs and hBMMSCs for their in vitro osteogenesis and in vivo bone regeneration in a mouse calvarial defect model. Methods: (1) 4 populations of hMDSCs and hBMMSCs were isolated using an established protocol. (2) Both hMDSCs and hBMMSCs were infected with lenti-BMP2 virus and the cells were then selected with 10μg/ml blasticidin for 24hrs. BMP2 secretion levels were measured using ELISA. (3) Comparison of gene expression via RT-PCR. Alkaline phosphatase (ALP) staining

was performed. (4) In vitro osteogenesis were compared using pellet culture. (5) Comparison of in vivo bone regeneration of hMDSC and hBMMSC without or with lenti-BMP2 transduction in critical size calvarial bone defect model using fibrin sealant as the scaffold. (6)MicroCT scans was performed biweekly.(7) Herovici's staining was used to identify type I collagen. Results: (1) The BMP2 secretion levels were: 2.8, 1.2, 0.48, 0.3 ng/million/24hrs for 4 populations of hMDSC respectively and 29.9, 12.7, 14.1, 14.1 ng/million/24hrs for 4 hBMMSCs respectively. (2) hMDSCs exhibited similar expression level of BMPR2,BMPR1b, COX-2 and SOX-9 as hBMMSCs. Lenti-BMP2 transduction increased COX-2 expression in both cell groups. ALP was expressed in a small percentage of hMDSCs and hBMMSCs and was slightly increased after lenti-BMP2 transduction. (3)MicroCT and von Kossa staining indicated both hMDSCs and hBMMSC undergo osteogenesis and enhanced by lenti-BMP2 transduction. (4) Both hMDSC and hBMMSC formed limited bone without gene transduction in vivo. (5) hMDSCs displayed equal bone defect repair capacity as the hBMMSCs when transduced with lenti-BMP2 as shown by the newly formed bone volume and bone defect coverage. (6) Histological analysis revealed formation of the main bone matrix-type I collagen in the defect area in both the hMDSC and hBMMSC groups.

Conclusion: Our results indicated that the hMDSCs exhibited equal capacity as hBMMSCs of osteogenesis in vitro and bone regeneration in vivo. Genetically modification with lent-BMP2 is required for efficient in vivo bone repair for both hMDSC and hBMMSC. Therefore, hMDSCs could be used as an alternative source of human adult stem cells for bone repair.

***Disclosures: Xueqin Gao**, None.*

MO0234

Dexamethasone shifts bone marrow mesenchymal stem cell differentiation to favor adipocyte lineage over osteoblast lineage through C/EBPalpha promoter methylation mechanism. Jiao Li*[1], Ning Zhang[1], Kerong Dai[2], Xiaoling Zhang[1]. [1]The Key Laboratory of Stem Cell Biology, Institute of Health Sciences, Shanghai Institutes for Biological Sciences (SIBS), Chinese Academy of Sciences (CAS) & Shanghai Jiao Tong University School of Medicine (SJTUSM), China, [2]Shanghai Key Laboratory of Orthopaedic Implant, Department of Orthopaedic Surgery, Shanghai Ninth People's Hospital, Shanghai Jiao Tong University School of Medicine (SJTUSM), China

Dexamethasone (Dex), a potent synthetic member of the glucocorticoid (GC) class of steroid drugs, is widely used as an immune suppressor. However, chronic Dex therapy is clearly associated with side effects, including bone loss, low bone mineral density (BMD), and increased fracture risk, which has been described as the most severe complication of long-term GC therapy. Till now, no effective method exists to treat these side effects of Dex. Clinical investigation has shown that Dex-induced osteoporosis is accompanied by increased bone marrow adiposity, Osteoblasts and adipocytes both arise from the same progenitor cells and bone marrow mesenchymal stem cells (BMSCs); a reciprocal relationship exists between osteoblast and adipocyte differentiation, so BMSCs differentiating into one lineage gradually lose the ability to differentiate to the other. Decreased bone formation and increased marrow adiposity increase the possibility that the differentiation balance between osteoblast and adipocyte is shifted by Dex, but the underlying mechanisms are still unknown. To test this hypothesis, we established a Dex-induced osteoporotic mouse model, and found that BMSCs from Dex-treated mice are more likely to differentiate into adipocyte than those from control mice, even under the induction of bone morphogenetic protein-2 (BMP2). We also discovered both in vitro and in vivo that the expression level of adipocyte regulator CCAAT/enhancer-binding protein alpha (C/EBPalpha) is significantly up-regulated in Dex-induced osteoporotic BMSCs during osteoblastogenesis by a mechanism that involves inhibited DNA hypermethylation of its promoter, Dex up-regulated C/EBPalpha expression level by preventing DNA methyltransferases 3a and 3b (Dnmt 3a/3b) from binding to C/EBPalpha promoter, thereby inhibiting its hypermethylation during osteoblast differentiation. Knockdown of C/EBPalpha in Dex-induced osteoporotic cells rescues their differentiation potential, suggesting that Dex shifts BMSC differentiation by inhibiting C/EBPalpha promoter methylation and up-regulating its expression level. We further found that the Wnt/beta-catenin pathway is involved in Dex-induced osteoporosis and C/EBPalpha promoter methylation, and its activation by LiCl rescues the effect of Dex on C/EBPalpha promoter methylation and osteoblast/adipocyte balance. This study revealed the C/EBPalpha promoter methylation mechanism and evaluated the function of Wnt/beta-catenin pathway in Dex-induced osteoporosis, providing a useful therapeutic target for this type of osteoporosis.

***Disclosures: Jiao Li**, None.*

MO0235

Differential Intracellular Processing Of Fluorescently-Labeled Bisphosphonate In Human Bone Mesenchymal Stem Cells. Pinky Salat, Frank Stefano, Kathleen Boesze-Battaglia, Sunday Akintoye*. University of Pennsylvania School of Dental Medicine, USA

Objectives: Bisphosphonates and denosumab used to control skeletal cancer metastasis have been associated with osteonecrosis of the jaws (ONJ). A common ONJ pathophysiologic theory relates to actions of antiresorptives on osteoclast-osteoblast balance. Bone mesenchymal stem cells (MSCs) are postnatal stem cells that repopulate osteoprogenitors vital for home healing but orofacial/jaw MSCs (OFMSCs) are disproportionately more sensitive to nitrogen-containing bisphosphonates (nBP) than MSCs from non-oral bones. If the jaw is disparately targeted by ONJ, disproportionate nBP uptake by OFMSCs with consequent apoptosis will reduce jaw osteoprogenitors essential for bone healing and homeostasis. We tested the hypothesis that MSC bisphosphonate uptake and internalization is skeletal site dependent.

Methods: Normal human OFMSCs and iliac crest MSCs (ICMSCs) from same individuals were exposed to 0.25mg/ml fluorescently labeled pamidronate (FL-nBP) [OsteoSense®680, Perkin Elmer, Boston MA]. Live cell imaging was used to visualize cellular components and track FL-nBP intracellular uptake. Nuclei, lysosomes and plasma membrane were visualized with Hoechst 33342 [2μM], Lysotracker Green DND26 [50nM] and Wheat Germ Agglutinin (WGA) [5μg/ml] respectively. Nikon A1R Laser Scanning Confocal microscope was used to capture images every 2 minutes for 3 hours at 37℃, 5% CO2 and constant humidity in four channels using these probes: Blue (405nm)- Nuclei; Green (488nm)-Lysotracker; Red (561nm)-WGA and Far Red (640)- FL-nBP. In parallel experiments, cells were pre-cultured with and without monodansyl cadaverine [MDC, 100μM] for 3 hours before exposure to FL-nBP to assess the role of fluid-phase endocytosis on differential FL-nBP uptake by OFMSCs and ICMSCs.

Results: FL-nBP was internalized within 8 minutes by ICMSCs and OFMSCs. Total FL-nBP uptake displayed dual peak pattern at 15 and 40 minutes in ICMSCs and 40 and 120 minutes in OFMSCs. Lysosomal localization of FL-BP was rapid in ICMSCs but a delayed gradual increase was displayed by OFMSCs. There were no differences in the plasma membrane permeability and adsorptive endocytosis based on uptake of WGA. However, inhibition of fluid-phase endocytosis with MDC demonstrated 10% and 50% increase in lysosomal FL-nBP in ICMSCs and OFMSCs respectively.

Conclusion: Internalized nBP is differentially processed by OFMSCs and ICMSCs.

Acknowledgement: This study was supported by grant R21DE022826-01 from DHHS/NIH/NIDCR Bethesda MD.

***Disclosures: Sunday Akintoye**, None.*

MO0236

Differentiation Stage- and Cell Type-Specific Expression of Claudin Family Members During In Vitro Differentiation of Osteoblasts and Osteoclasts. Fatima Alshbool*[1], Shin-Tai Chen[2], Subburaman Mohan[3]. [1]Loma Linda University, USA, [2]Jerry L. Pettis VA Medical Center, USA, [3]Jerry L. Pettis Memorial VA Medical Center, USA

Claudins (Cldns), a family of 24 known transmembrane proteins, represent major components of tight junctions. The canonical function of Cldns involves regulation of paracellular permeability of ions and small molecules. In a recent study, we found that Cldn-18 is a novel negative regulator of bone resorption and acts non-canonically to modulate RANKL-induced osteoclast (OC) differentiation. In this study, we examined the hypothesis that the expression of Cldns is differentiation stage- and cell type-dependent in bone. The expression of Cldns were examined during ascorbic acid (AA)-induced differentiation of fetal calvarial cells into osteoblasts (OBs) at days 0, 4, 6 and 8 and RANKL-induced differentiation of bone marrow precursors into OCs at days 0, 1 and 6 by real-time PCR. Expression of several of the Cldns (-1, -2, -5, -8, -10, -11, -13 and -14) were increased more than 10-fold ($P<0.01$) during OB differentiation with some showing peak expression at day 6 while others at day 8. By contrast, expression levels of Cldn-4, -12, -15 and -22 were decreased significantly ($P<0.01$) during OB differentiation. Surprisingly, several of the Cldns including -1, -7, -11 and -15 were significantly down regulated at day 1 of OC differentiation. Only expression of Cldn-6 was increased at day 1. At day 6, however, expression of Cldn-1, -2, -3, -5, -6, -12, -13, -15 and -22 were increased 3 to 7-fold compared to day 0 cultures. Because Cldn-1 expression was increased by >15-fold during OB differentiation and targeted knockout of Cldn-1 results in perinatal lethality, we determined the consequence of lentiviral shRNA mediated knockdown of Cldn-1 expression on differentiation of MC3T3-E1 osteoblasts. Cldn-1 expression was increased by 3-fold ($P<0.01$) by AA treatment at day 6 in MC3T3-E1 cells and was blocked by 60% by Cldn-1 shRNA. Furthermore, ALP and BSP mRNA levels were reduced by 90% ($P<0.01$) in lentiviral Cldn-1 shRNA vs control shRNA treated cultures. We next determined if Cldn-1 regulated expression of Runx2 and osterix, master transcription factors of osteoblast differentiation. We found that expression levels of both Runx2 and osterix mRNA was reduced significantly as a consequence of Cldn-1 knockdown. Conclusions: 1) Regulation of expression of Cldn family members during bone cell differentiation is complex and involves cell type and differentiation stage-dependent regulation. 2) Cldn-1 is a positive regulator of osteoblast differentiation.

***Disclosures: Fatima Alshbool**, None.*

MO0237

Withdrawn

MO0238

Effects of Therapeutic Radiation on the Differentiation Potential of Human Embryonic Stem Cell Derived Mesenchymal Stem Cells. Mohammad Islam*[1], Melissa Stemig[1], Yutaka Takahashi[2], Susanta Hui[1]. [1]University of Minnesota School of Dentistry, USA, [2]University of Minnesota, USA

Human embryonic stem derived mesenchymal stem cells (hESMSC) have been shown to have similar properties of bone marrow MSCs (BMMSC). The purpose of this study was to learn the effects of therapeutic radiation on the hESMSC. We used human embryonic stem cell line WA-09 and differentiated them in presence of 15% serum. hESMSCs were isolated based on CD73 expression using magnetic sort. Cells were irradiated as follows: 0 Gy (no radiation), 2 Gy, 4 Gy and 16 Gy using Varian Linear accelerator at the dose rate (400 cGy/min) commonly used for patient treatment. Cells were analyzed at post radiation day 1 and day 5. We studied 1. the expression of MSC specific cell surface markers; 2. cell cycle profile; 3. the expression of osteoblastic, adipogenic and oxidative stress related genes and 4. osteogenic and adipogenic differentiation potential of irradiated hESMSCs. Bone marrow MSCs were used as control cells. Radiation did not significantly affect the expression of MSC specific CD90, CD105 and CD146 in irradiated and non-irradiated cells. We observed accumulation of cells in G2/M phase at higher radiation doses, compared to no radiation group. This observation was consistent in post radiation day 1 and day 5 groups. Starting at post radiation day 1 and day 5, differentiation towards osteogenic and adipogenic lineage (for 2 to 3 weeks) showed that cells were differentiating in lineage specific manner when treated with 2 Gy and 4 Gy, but not with 16 Gy. Adipogenic oil red O staining showed fat cells formed in clusters in the culture, different from adipogenesis in BMMSCs. We found that radiation changes the expression of osteoblast lineage specific Runt related transcription factor 1 (RUNX2) and adipogenic Peroxisome proliferator-activated receptor Gamma (PPARG) expression. Oxidative stress related superoxide dismutase 1 (SOD1) expression was inversely related to the ratio of PPARG and RUNX2 expressed in irradiated cells. This pattern was observed in both day 1 and day 5 post radiation studies. We conclude that, at different radiation doses hESMSCs retain properties of MSCs. Radiation induced gene expression changed the lineage specific gene expression pattern in the culture.

***Disclosures: Mohammad Islam**, None.*

MO0239

Identification of differentiation-stage specific molecular markers for the osteoblastic phenotype. Natalie Twine*[1], Chi Pang[1], Li Chen[2], Marc Wilkins[1], Moustapha Kassem[3]. [1]NSW Systems Biology Initiative, University of New South Wales, Australia, [2]Medical Biotechnology Center (MBC), Denmark, [3]Odense University Hospital, Denmark

The phenotype of osteoblastic (OB) cells in culture is currently defined using a limited number of markers of low sensitivity and specificity which belong mostly to extracellular matrix proteins. Also, for clinical use of human skeletal (mesenchymal) stem cells (hMSC) in bone regeneration, there is a need to identify predictive markers for *in vivo* bone forming capacity.

Thus, we employed Illumina RNA sequencing (RNASeq) to examine changes in gene expression across 8 time points between 0-12 days of *ex vivo* OB differentiation of hMSC. We identified a subset of expressed genes as potentially sensitive markers of *ex vivo* differentiating OB (n=123) based on: i) identified in literature and/or had the Gene Ontology (GO) category: 'osteoblast differentiation' ii) exhibited significant changes in expression (> 2 Fold Change (FC), FDR <0.1) at any one time point during OB differentiation.

Pearson's correlation of the 123 expression profiles, followed by hierarchical clustering, resulted in 4 groups of markers: early differentiating OB markers (n= 28), which had a peak expression during 0-24 hours and were enriched for GO 'extracellular matrix organisation' e.g. *COL1A1, LOX, SERPINH1*; middle stage differentiating OB markers (n=20), which had a peak expression during 3-6 days and were enriched for GO 'extracellular matrix' and 'skeletal system development' e.g *BMP4, CYP24A1, TGFBR2*; late stage differentiating OB markers (n=27), which had a peak expression 9-12 days and enriched for GO 'bone development/osteoblast differentiation' e.g. *BMP2, IGF2* and a pleitropic group of marker genes (n=13) with peak expression during early and late time points that included growth factors e.g. *VEGFA, PDGFA, FGF2*.

In addition, a subset of these OB markers (n=21) e.g. *CLEC3B, SMAD6, BMP4, NRP3, DLX5* were able to predict hMSC *in vivo* bone forming capacity as they were upregulated by more than 1.5 FC in hMSC-derived clones with high bone forming capacity compared to low bone forming clones. Interestingly, 33 OB markers were significantly up-regulated (>2FC, FDR<0.1) in cultured hMSC obtained from patients with osteoporosis (n=5) compared to age-matched control (n=4).

Using RNA-seq and cluster analysis, we identified a set of stage-specific molecular markers that define the progression of OB phenotype during *ex vivo* culture of hMSC, predict *in vivo* bone formation capacity of hMSC and can be employed to study the mechanisms of impaired bone formation in patients with osteoporosis.

Keywords: osteoblast differentiation, molecular marker, human mesenchymal stem cell, RNA sequencing

***Disclosures: Natalie Twine**, None.*

MO0240

Intravital imaging of osteogenesis and angiogenesis in repair and regeneration. Xinping Zhang*[1], Chunlan Huang[1], Vincent Ness[1], Edward B Brown[2]. [1]University of Rochester Medical Center, USA, [2]University of Rochester, USA

Bone defect healing is a progenitor cell-driven tissue morphogenetic process marked by coordinated osteogenesis and angiogenesis at the site of repair. The progenitor cells dynamics and spatiotemporal regulation of bone defect repair remain poorly understood, largely due to the lack of an animal model that permits high resolution and non-destructive analyses of progenitors and the surrounding microenvironment at the site of repair. We have recently established a chronic cranial defect window chamber model in mice that permits high-resolution, dynamic tracking of progenitors and their surrounding neovasculature via two-photon microscopy. By simultaneously probing the intrinsic optical signatures of collagen matrix from new bone via second harmonic generation (SHG) and fluorescence-labeled osteoblasts via 2.3kb collagen type I promoter driven GFP (Col2.3GFP), we showed that angiogenesis preceded osteogenesis. Differentiation of osteoblasts was initiated at the edge of the defect in close proximity of the invading blood vessels. The expansion and migration of the osteoblastic cells were closedly associated with microvessels less than 10 mm in diameter during the first 4 week of healing. Quantitaive and histomorphometric analyse showed that vessel length and volume were markedly increased at week 1, peaked at week 3 and reduced at week 6, coincided with early expansion and migration of the osteoblasts. By week 9, volume of $Col2.3^{+}GFP$ cells were markedly reduced, yet SHG continued to climb suggesting that late stage collagen fiber assembly could be independent of osteoblasts. Similar spatiotemporal interaction between Col2.3GFP cells and neovascularization was observed when bone marrow stromal cells isolated from Col2.3GFP mice were implanted into the cranial defect window chambor model. The surviving $Col2.3GFP^{+}$ cells were found in colonies surrounded by microvessels. Longitudinal tracking of the cells and collagen matrix revealed formation of criss-crossing collagen fiber arrays which served as a porous template for bone regeneration. Taken together, the cranial defect window chambor model provided a live imaging platform for tracking and quantitative analyses of spatiotemporal cordination of osteogenesis and angiogenesis at a microscopic resolution. The establishment of the model could aid in the development of material-based approaches to engineering suitable microenvironment to modulate progenitor cell behavior for enhanced bone repair and reconstruction.

***Disclosures: Xinping Zhang**, None.*

MO0241

Phenotypic and Functional Characterization of an Osterix-Cherry+ Bone Marrow Cell Population. Sara Strecker*[1], Peter Maye[2]. [1]University of Connecticut, USA, [2]University of Connecticut Health Center, USA

Objectives: Osterix is a zinc finger transcription factor, which functions as a master regulator of osteoblast differentiation. We created Osterix-Cherry reporter mice, which revealed the marking of a bone marrow cell population retaining low Osterix reporter expression (referred to as LORE cells). The goal of this study was to determine whether LORE cells are a multipotent bone marrow stromal cell (BMSC) population.Methods: In order to resolve Osterix expression in the context of the skeletal lineage, we intercrossed our Osterix-Cherry mice with *Connective Tissue Growth Factor* (CTGF)- eGFP, *Bone Sialoprotein* (BSP)- Topaz and *Collagen 3.6* (Col 3.6) Cyan reporter mice. We carried out *in vitro* differentiation studies of sorted cells to confirm the multipotency of this LORE population in the context of other skeletally specific reporters. Immunostaining studies and flow analysis have been used to determine the localization and identity of these LORE cells within the marrow.

Results: Osterix reporter expression proceeds both BSP and Col 3.6 and appears to co-localize with CTGF. Both CTGF+ and Osterix+ populations are multipotent *in vitro*, differentiating into bone, fat, and cartilage. LORE cells isolated from the marrow first express Col 3.6 then express BSP in culture. LORE cells localize near, but are not on, the bone surface. Immunostaining and flow suggests that these cells are similar to reticular cells. This data suggests that the LORE cell is marking an uncommitted skeletal progenitor population. The Osterix-Cherry mouse is the first skeletally specific reporter mouse to show a distinct, multipotent, reporter positive population within the bone marrow.

Conclusions: We observed a LORE cell population in the bone marrow which marks an early osteoprogenitor that is required for supporting postnatal skeletal growth and bone maintenance. Osterix reporter mice may provide us with a means to isolate and study the earliest cells of the osteoblast cell lineage, which remain poorly understood.

***Disclosures: Sara Strecker**, None.*

MO0242

Repeated Osteoblast Depletion Decreases Osteogenic Potential of Bone Marrow Stromal Cells in Mice. Adeline Ng*[1], Gurpreet Baht[2], Marc Grynpas[3], Benjamin Alman[2]. [1]University of Toronto Samuel Lunenfeld Research Institute, Canada, [2]Program in Developmental & Stem Cell Biology, Hospital for Sick Children, Canada, [3]Samuel Lunenfeld Research Instituteof Mount Sinai Hospital, Canada

Background: Literature has suggested factors that sustain stem cell levels in the bone marrow decline with age and this deficit may be related to age-associated bone loss. Using the Col2.3Δtk (DTK) transgenic mouse, we investigated the consequences of repeated ablation of differentiated osteoblasts on osteogenic progenitor cells in the bone marrow. The DTK transgenic mouse takes advantage of the HSV-tk (herpes simplex virus thymidine kinase)/GCV (ganciclovir) system to conditionally ablate differentiated osteoblasts.

Methods: 4-month old DTK mice were treated with ganciclovir (GCV) to conditionally ablate differentiated osteoblasts or treated with saline control. Bone marrow from GCV-treated donors was transplanted into treated- or control-recipients and vice versa. Bone marrow transplant recipients were sacrificed at the end of a 12-week engraftment period. At sacrifice, bone marrow stromal cells (BMSCs) were harvested for cell culture and whole bones were excised for bone quality assessment. Colony forming unit (CFU) assays were conducted to investigate BMSC osteogenic potential. RNA was extracted from cell culture to assess the expression of genes defining BMSC lineage. *Ex vivo* bone quality assessments included bone histomorphometry, TRAP-staining, dual energy x-ray absorptiometry, microcomputed tomography, and biomechanical testing.

Results: There were no differences in CFU-F (fibroblast) counts between any of the treatment groups. However, GCV-treated animals had lower CFU- ALP (alkaline phosphatase and CFU-VK (von Kossa) counts, indicative of decreased osteoblast activity. Interestingly, there were no statistical differences in bone mineral density (vertebrae and femurs) between any of the treatment groups despite differences in BMSC osteogenic capacity *in vitro*. Furthermore, histological analyses showed no differences in bone formation or bone structure.

Discussion: This study aims to connect *in vitro* cell culture data with *in vivo* skeletal phenotypes. Early results suggest that the number of healthy bone marrow stromal cells (BMSCs) do not decline with depletion of differentiated osteoblasts; however, the osteogenic potential of BMSCs decline significantly with repeated osteoblast ablation. This decline is only partially rescued with bone marrow transplantation into healthy recipients. We are currently investigating the mechanisms responsible this decrease in osteogenic potential and its effects on skeletal phenotype.

***Disclosures: Adeline Ng**, None.*

MO0243

Sex and Genetic Factors Determine Bone Remodeling and Osteoblastogenesis. Stefano Zanotti*[1], Ivo Kalajzic[2], Ernesto Canalis[1]. [1]St. Francis Hospital & Medical Center, USA, [2]University of Connecticut Health Center, USA

Sex determines cancellous bone mass of C57BL/6 mice and the differentiation of bone marrow stromal cells toward the osteoblastic lineage. To explore the mechanisms that mediate the effects of sex on bone mass, cancellous bone of femurs from 1 to 6 month old C57BL/6 mice was analyzed by histomorphometry. Trabecular bone volume was comparable between sexes at 1 month of age but it declined rapidly in maturing female mice whereas it remained stable in maturing male littermates. Osteoclast number and bone resorption declined as mice of both sexes matured but were always higher in female than in male mice. Moreover, whereas osteoblast number declined in male mice, it increased in maturing female mice. A limited number of tropism for Friend leukemia virus-B mice were available for study and showed similar trends, but differences between male and female mice were not statistically significant. The results indicate that female mice remodel at a higher rate than male littermates and consequently lose cancellous bone. Since the increase in osteoblast number was not sufficient to prevent the decline in bone mass, we questioned whether sex determines the potential for osteoblastic differentiation of mesenchymal progenitor cells. To this end, bone marrow stromal cells from C57BL/6 mice where the *a*-smooth muscle actin (*aSma*) promoter, active in mesenchymal progenitors, directs green fluorescent protein (GFP) expression (*aSmaGFP*) were cultured. Fluorescence activated cell sorting revealed fewer GFP expressing cells in cultures from female than from male *aSmaGFP* littermates. Furthermore, *Runx2*, *Alpl*, *Osteocalcin* and *Osteopontin* expression was higher in GFP expressing cells from male mice than from female littermates. To test whether genetic factors modify the impact of sex on osteoblastogenesis, bone marrow stromal cells from C3H/HeJ and BALB/c mice were cultured. Mineralization and *Alpl* expression and activity were lower in cultures from female than from male littermates of both genetic backgrounds. *Osteocalcin* expression was lower in cells from female than from male C3H/HeJ, but not BALB/c, littermate mice. In conclusion, cancellous bone declines in maturing female mice because of increased bone remodeling and reduced potential for osteoblastogenesis in comparison to male littermates and genetic factors determine the magnitude of these effects.

***Disclosures: Stefano Zanotti**, None.*

MO0244

Study of Mesenchymal Stem Cells and Endothelial Progenitor Cells in Osteonecrosis of the Femoral Head. Myrielle Mathieu[1], Delphine Spruyt[1], Sabrina Rigutto[1], Aude Ingels[1], Nadia Stricwant[1], Valentina Albarani[2], Joanne Rasschaert[3], Enrico Bastianelli[2], Valerie Gangji*[4]. [1]Université Libre de Bruxelles, Belgium, [2]Bone Therapeutics, Belgium, [3]Laboratory of Bone & Metabolic Biochemistry, Belgium, [4]Hôpital Erasme, Université Libre de Bruxelles, Belgium

Introduction: Osteonecrosis of the femoral head (ONFH) is a painful disorder of the hip affecting young active patients. The disease is characterized by a necrosis of the osteomedullary tissue leading to subchondral bone collapse and joint destruction. We postulated that alterations in the number, proliferation and function of mesenchymal (MSCs) and endothelial progenitor cells (EPCs) might play a role in the pathophysiology of ONFH. Moreover, we analyzed the serum levels of growth factors and chemokines involved in their recruitment, proliferation and differentiation. Methods: Fifty-two osteonecrosis patients (ONFH) and eighty healthy volunteers (HV) were included in this study. The number, morphology phenotype and biological activity of bone marrow-derived MSCs and circulating EPCs were compared between groups. Serum levels of growth factors and chemokines were assessed by ELISA.Results: In ONFH patients, the pool of hMSCs was decreased (25.2 ± 7.2 CFU-F in ONFH vs 51.8 ± 7.6 CFU-F in controls, $p < 0.05$) and their proliferation delayed ($5.3\% \pm 1.5\%$ in ONFH vs $13.7\% \pm 2.3\%$ in HV, $p < 0.05$). Once committed, hMSCs from ONFH mineralized less than hMSCs from HV as observed by ARS scoring (0.44 ± 0.19 in ONFH vs 1.21 ± 0.23 in HV, $p < 0.05$). Moreover, the number of early outgrowth EPCs was not affected while the frequency of late outgrowth EPCs was increased in ONFH patients. Granulocyte colony-stimulating factor (G-CSF, $p < 0.05$), interleukin-8 (IL-8, $p < 0.001$), and interleukin-6 (IL-6, $p < 0.05$) were increased and leptin tended to be increased ($p = 0.06$) in ONFH as compared to controls. Platelet-derived growth factor-BB (PDGF-BB, $p < 0.005$), and insulin like growth factor binding protein 3 (IGF-BP3 $p = 0.006$) were decreased and angiopoietin-1 tended to be decreased (Ang-1, $p = 0.05$) in ONFH. Conclusion: ONFH patients showed an increased pool of late outgrowth EPCs, a decreased pool, proliferation and function of hMSCs in ONFH patients. These altered progenitor cells and function were associated with altered serum chemokines, and cytokines that suggest a negative interplay between endothelial cell function and mesenchymal cell function. We showed an altered endothelial cell function associated with an altered endocrine environment that could be detrimental to MSCs recruitment, migration and function.

***Disclosures: Valerie Gangji**, None.*

MO0245

Withdrawn

MO0246

Visualization of Osteoblast-Derived Trabecular and Endosteal Bone Lining Cells. Marc Wein*[1], Forest Lai[2], Henry Kronenberg[1]. [1]Massachusetts General Hospital, USA, [2]MGH, USA

Intermittent administration of parathyroid hormone (PTH) leads to a net osteoanabolic effect associated with increased numbers of osteoblasts. The precise molecular and cellular mechanisms whereby this occurs remain to be determined. Our laboratory investigated whether PTH might convert quiescent bone lining cells into active osteoblasts. In a previous report, dual transgenic mice expressing tamoxifen-inducible DMP1-Cre and a Cre-activated ROSA26R X-gal reporter were studied. When these animals were analyzed 3 weeks after tamoxifen administration, flat X-gal positive bone lining cells were observed in the periosteal surfaces of the calvariae and tibiae. Brief intermittent PTH treatment converted these flat quiescent cells into active osteoblasts. However, only periosteal osteoblasts were labeled with this approach. In order to study endosteal and trabecular bone lining cells at additional skeletal sites, we now have generated dual transgenic mice expressing tamoxifen-inducible osteocalcin-Cre and floxed-stop tdTomato Cre reporter transgenes. These dual transgenic mice were treated with tamoxifen at 6 weeks of age to label osteocalcin-expressing cells. The subsequent behavior of these labeled cells was then analyzed over time using fluorescence microscopy. As expected, 3-4 days after tamoxifen administration, many red "plump" cuboidal cells on trabecular, endosteal, and (to a lesser extent) periosteal surfaces of the tibiae and vertebrae were observed. In the tibia, after 2, 4, and 6 weeks of chase, the majority of these labeled cells disappeared. Red osteocytes did appear over this interval, along with labeled endosteal and trabecular cells with a distinct, flat morphology. In the vertebrae, the rate of decay of "plump", cuboidal cells over the same chase period was much less pronounced than in the appendicular skeleton. Studies are now underway to determine the effects of intermittent PTH administration on endosteal and trabecular bone lining cells.

***Disclosures: Marc Wein**, None.*

MO0247

Novel Therapeutic Effects Of Endoxifen In Pre-Clinical Models Of Type 1 Osteoporosis. Anne Gingery*[1], Malayannan Subramaniam[2], Kevin Pitel[2], Laurence Lindenmaier[3], James Ingle[4], Matthew Goetz[4], Russell Turner[3], Urszula Iwaniec[3], Thomas Spelsberg[2], John Hawse[4]. [1]Mayo Clinic School of Medicine, USA, [2]Mayo Clinic, USA, [3]Oregon State University, USA, [4]Mayo Clinic College of Medicine, USA

Endoxifen is a selective estrogen receptor modulator (SERM) currently being developed as a novel breast cancer therapy. Since SERMs are approved for the treatment and prevention of osteoporosis, it was of interest to characterize the effects of endoxifen on the skeleton. As a first step, we analyzed the effects of endoxifen (50mg/kg/day, for 30 days) on the mouse skeleton using ovariectomized (OVX) C57BL/6 mice. Total body bone mineral density (BMD) and content (BMC) were significantly elevated in the endoxifen treated group as were numerous trabecular and cortical parameters in the vertebrae and long bones. Histomorphometric analysis of the L5 vertebrae revealed significant increases in both osteoblast and osteoclast perimeter per tissue area in endoxifen treated animals which correlated with a nearly 2-fold increase in the serum levels of P1NP and CTX-1. To expand upon these observations, we next employed a pre-clinical rat model to study the effects of endoxifen in both intact and ovariectomized animals. Briefly, four month old Sprague-Dawley rats (n=40) underwent either sham or OVX surgeries and were randomized to placebo or endoxifen (10mg/kg/day, for 35 days). Micro-CT analysis of the proximal tibial metaphysis revealed that BV/TV, connectivity, density, and trabecular number were significantly greater, while trabecular spacing was significantly lower, in endoxifen treated OVX rats compared to placebo treated controls. Interestingly, BV/TV and trabecular thickness were also significantly greater in sham operated ''premenopausal'' animals treated with endoxifen compared to placebo. This observation is in stark contrast to other SERMs, where in the ''premenopausal setting'', SERMs induce bone loss. Endoxifen treatment had no impact on serum levels of P1NP and CTX-1 in sham operated rats but significantly repressed both of these markers in OVX animals. Interestingly, endoxifen treatment also repressed serum sclerostin levels in both the intact and OVX setting. These studies are the first to examine the *in vivo* impact of endoxifen on the skeleton and suggest that endoxifen functions differently than tamoxifen and raloxifene. Based on these data, endoxifen may represent a novel and effective therapy for the prevention and treatment of osteoporosis and/or other bone related disorders.

***Disclosures: Anne Gingery**, None.*

MO0248

Prevention of Glucocorticoid Induced-apoptosis of Osteoblasts and Osteocytes by Protecting Against Endoplasmic Reticulum (ER) Stress. Amy Sato*, Lilian Plotkin, Teresita Bellido. Indiana University School of Medicine, USA

Increased oxidative stress, such as with excess of glucocorticoids (GC) or during aging, has been associated with endoplasmic reticulum (ER) stress, due to accumulation of misfolded or unfolded proteins, leading to cellular apoptosis. The double-stranded RNA-activated protein kinase-like ER kinase (PERK) is activated to alleviate ER stress and phosphorylates the eukaryotic translation initiation factor 2 alpha subunit (eIF2α). Phosphorylated eIF2α in turn inhibits global protein translation to provide time to the ER to recover from the unfolded protein load, promoting cell viability. We hypothesized that the pro-apoptotic effect of GC on osteoblasts and osteocytes are at least in part due to induction of ER stress. To test this hypothesis, we used MLO-Y4 osteocytic cells, OB-6 osteoblastic cells, and primary osteoblastic cells derived from neonatal murine calvaria. We found that the synthetic GC dexamethasone (DEX) significantly increased the percentage of apoptotic cells in cultures of MLO-Y4, OB-6, and primary osteoblastic cells. Similarly, the specific ER-stress inducing agents brefeldin A, an inhibitor of ER-golgi apparatus vesicle transport, and tunicamycin, a protein glycosylation inhibitor, significantly increased OB-6 cell apoptosis. We then tested the effect of salubrinal, an agent that protects against ER stress by inhibiting the dephosphorylation of eIF2α, on bone cell apoptosis. Salubrinal blocked apoptosis induced by the ER stressors brefeldin A and tunicamycin in OB-6 cells. Salubrinal was also effective in blocking apoptosis induced by DEX in MLO-Y4, OB-6 and primary osteoblastic cells. Optimal responses were found at 10 μM salubrinal, after either 6 or 24 h. Guanabenz, another inhibitor of eIF2α dephosphorylation, also blocked DEX and tunicamycin-induced apoptosis of primary osteoblastic cells. Furthermore, addition of DEX to mineralizing OB-6 or primary osteoblastic cells markedly decreased mineral deposition and hydroxyapatite formation. In contrast, treatment with guanabenz increased mineralization of OB-6 cell cultures and prevented the inhibitory effect of DEX. We conclude that part of the pro-apoptotic actions of GC on osteoblastic cells are mediated through ER stress and that interventions that prevent dephosphorylation of eIF2α could potentially prevent the deleterious effects of GC on bone.

***Disclosures: Amy Sato**, None.*

MO0249

Cathepsin K null mice exhibit altered frequency of hematopoietic precursors in the bone marrow and in the periphery. Christian Jacome[1], Do Soung*[1], Maureen Pickarski[2], Le Thi Duong[3], Joseph Lorenzo[1], Hicham Drissi[1]. [1]University of Connecticut Health Center, USA, [2]Merck & Co., Inc., USA, [3]Merck Research Laboratories, USA

Cathepsin K (CatK) is a lysosomal cysteine protease, highly expressed by osteoclasts (OC), that is important for degrading bone matrix during bone resorption. In humans, mutations in the *CatK gene (Ctsk)* causes pycnodysostosis, characterized by osteopetrosis due to impaired OC bone resorption. Gene-targeted disruption of Cat K in mice produces a similar bone phenotype. Differentiation of myeloid hematopoietic precursors into OCs, macrophages or dendritic cells, depends on the stimuli it is exposed to. We investigated whether the lack of CatK modulated the number of OC precursors versus other hematopoietic cells. We utilized two mouse models that lack functional CatK protein, a gene-targeted knock-out ($CatK^{-/-}$) that results in the absence of the protein and a knock-in mouse model in which *Ctsk* is replaced by the *cre recombinase*. In both models, the bone resorbing activity of individual OC is decreased. However, the number of non-resorbing OC on bone significantly increases. In the bone marrow, we found that hematopoietic stem cells ($Lineage^{-}c\text{-}Kit^{+}Sca\text{-}1^{+}$, LKS) and early OC precursors defined as PIV, PV and PVI (Jacquin et al., JBMR 2006) were unchanged in $CatK^{cre/cre}$ and $CatK^{-/-}$ compared to wild type (WT) mice. However, we found an increase in CD11b+ (% committed OC precursors) and decreased F4/80+ (% committed macrophages) and CD11c+ (% committed dendritic cells). However, in the spleen we found a significant increase in LKS and a decrease in OC precursors defined as $B220^{-}CD3^{-}NK1.1^{-}CD11b^{hi}Ly\text{-}6C^{hi}CD115^{+}$ (Jacome-Galarza et al., JBMR 2012) in CatK null mice vs. WT. We also found an increase in F4/80+ but no changes in CD11c+ cells. In addition, circulating OC precursors was decreased in the CatK null mice. In conclusion, the high bone mass phenotype in the CatK null mice was not associated with changes in early hematopoietic precursors or early OC precursors, but was associated with an increase frequency of committed OC precursors (CD11b+) in the bone marrow, increased LKS in the spleen and a decreased frequency of peripheral OC precursors. Taken together the absence of functional CatK limits the number of committed peripheral OC precursors migrating to bone marrow. Hence, this contributes to the increased number of TRAcP+ multinuclear osteoclasts that are observed on bone surfaces in the CatK null mice.

***Disclosures: Do Soung**, None.*
This study received funding from: Merck

MO0250

Withdrawn

MO0251

Absence of interleukin-22 interferes with the progression of periapical inflammation and bone loss related to endodontic infection. Raquel Silva*[1], Katharina de Oliveira[2], Sandra Fukada[3], Andiara De Rossi[4], Lea Silva[2], Paulo Nelson-Filho[2]. [1]School of Dentistry of Ribeirao Preto - University of Sao Paulo, Brazil, [2]University of Sao Paulo - School of Dentistry of Ribeirao Preto, Brazil, [3]University of Sao Paulo -School of Pharmaceutical Sciences of Ribeirão Preto, Brazil, [4]Faculty of Dentistry of Ribeirão Preto, University of São Paulo, Bra

The aim of this study was to characterize the lesions related to endodontic infection experimentally induced in interleukin-22 knockout mice (IL-22 KO) compared to wild-type (WT) animals. The lesions were induced in the inferior first molars of the mice and, after the periods of 7, 21 and 42 days, the animals were euthanized in a CO2 chamber. Sections were subjected to histotechnical processing and stained with: (1) hematoxylin and eosin (HE) for description of the pulp tissue, apical and periapical regions in conventional optical microscopy and measurement of the area of periapical lesions in fluorescence microscopy; (2) histoenzimology for osteoclasts (TRAP); (3) Brown & Brenn staining (presence/abscence of bacteria); and (4) immunohistochemistry (for osteoclastogenesis markers). The numerical results of the morphometric analysis of the area of the periapical lesions and the number of osteoclasts were subjected to statistical analysis one-way ANOVA and Bonferroni's post-test (level of significance of 5%). Concerning the microscopical analysis, the group of WT mice showed a statistically significant difference between 7 and 42 days and between 21 and 42 days ($p<0.05$), with a gradual increase in the size of periapical lesions and number of osteoclasts. In the group of IL-22 KO animals, an increase in lesion size and number of osteoclasts between 7 and 21 days was observed, followed by a decrease of these parameters between 21 and 42 days, with significant differences between 7 and 21 days ($p<0.05$). Moreover, when comparing the two types of animals, significant differences were found ($p<0.05$) related to the size of the lesions and number of osteoclasts at 42 days, without differences in localization of bacteria and immunolocalization of the osteoclastogenesis markers. This study showed that the absence of IL-22 in mice interfered with the progression of periapical inflammation and bone loss related to endodontic infection suggesting the involvement of this cytokine in host's immune and inflammatory response to the infection of the tooth.

***Disclosures: Raquel Silva**, None.*

MO0252

Comparative Analysis of Osteoclastic Gene Expression in Mucosal Tissues with Aging and Periodontitis in Nonhuman Primates. Sudha Gudhimella[1], Sreenatha Kirakodu[1], Luis Orraca[2], Janis Gonzalez Martinez[3], Sarandeep Huja*[1], Jeffrey L Ebersole[1], Octavio A. Gonzalez[1]. [1]University of Kentucky, USA, [2]University of Puerto Rico, Puerto Rico, [3]Caribbean Primate Research Center, Puerto Rico

Osteoclastic activity plays a vital role in physiologic bone remodeling. Currently we know little about the complex molecular interactions that occur within the gingival milieu with aging and during bone destruction which is the hallmark of periodontitis.The objective of this study was to use a systems biology approach to determine age-related changes in osteoclastic gene expression profiles in gingival tissues with aging and in naturally occurring periodontitis.The study groups included 34 (14 F: 20 M) systemically healthy *Macaca mulatta* grouped as follows: Healthy - young (<3 y, n=5), adolescent (3-7 y, n=5), adult (12-15 y, n=7) and aged (18-22 y, n=6); Periodontitis – adult (n=5) and aged (n=6). Interdental papilla (2nd premolar/1st molar) from maxilla or mandible were excised and subjected to RNA extraction and microarray analysis (Rhesus Macaque Genome Array, Affymetrix). The expression levels of 84 genes involved in osteoclast regulation were evaluated. For each gene, statistical differences were determined between healthy aged tissues and all other groups or between periodontitis tissues and all healthy tissues. Additionally, a linear regression model compared expression levels using age as a continuous variable. A $p \leq 0.05$ was used to identify significant differences and correlations. Among the 84 evaluated genes approximately 13 were altered in healthy aging tissues and 31 in periodontitis tissues with only 7 overlapping genes. Substantial up-regulation (>2-fold) was noted in periodontitis with CASP9, c-Fos, IL-17A, IL-1β, IL-20, IL-6, RAC2, SPP1, DC-STAMP, MMP9 and MMP1. Moreover, IL-6 ($r=0.59$, $p=0.003$,), IL-17A ($r=0.48$, $p=0.020$), MAP2K1 (MEK1; $r=0.72$, $p<0.0001$), ARPC3 ($r=0.56$, $p=0.003$) and M-CSF (CSF1; $r=0.53$, $p=0.009$) showed significant positive correlations with age. While various genes related to up-regulation of osteoclast functions were observed in healthy gingival tissues with aging, the profile of numerous genes that would mitigate the osteoclast functions or enhance osteoblast activities was also found in these healthy tissues. Thus, this transcriptome environment may reflect a more general osteogenic homeostasis. In contrast, alterations in gene expression in periodontitis particularly in aged animals, was skewed towards creating an environment with substantial osteoclastogenic potential consistent with bone resorption in periodontitis.

***Disclosures: Sarandeep Huja**, None.*

MO0253

Expression of C-C chemokine ligands for osteoclastogenesisinduced by hyperocclusion. Takashi Tsutsumi*, Hiroshi Kajiya, Kazuko Goto, Yutaka Takahashi, Koji Okabe. Fukuoka Dental College, Japan

BACK GROUND: Excessive mechanical stress (MS) is a representative invasive factor in tooth and periodontal tissues in oral and periodontal diseases. It is well known that excessive MS in hyperocclusion resulted in destruction of alveolar bone. We hypothesized that MS induces expression of osteoclastogenesis-associated chemokines, resulting in alveolar bone destruction during occlusal traumatism. We have previously reported that MS induced expression of C-C chemokine ligand (CCL) 2 in periodontal ligament (PDL), resulting in MS-dependent alveolar bone resorption. Therefore, we examined that the effect of ablation of CCL2 and it receptor CCR2 signaling pathway on MS-dependent osteoclastogenesis, using *in vivo* and *in vitro* hyperocclusion models with wild-type (WT), CCL2-deficient ($CCL2^{(-/-)}$)and CCR2-deficient ($CCR2^{(-/-)}$) mice.

MATERIAL AND METHODS: All animal experiments and procedures followed guidelines of the Animal Care Committee, Fukuoka Dental College, Japan. *In vivo* model: The stainless steel wire (diameter 0.3mm) was bonded on the occlusal surfaces of the right maxillary molars in 5 week old mice for a week. After fixation and decalcification for 2 weeks the specimens were prepared 6μm thickness tissue and stained for TRAP staining, HE staining and immunohistostaining. The bone morphological analysis was photographed and analyzed by micro-CT. *In vitro* model: The first molar in mandibular bone was extracted and treated with trypsin for 2 h. PDL cells were cultured in a silicone chamber and subjected to stretching MS until 7days. CCL expression was detected by RT-PCR, western blotting and ELISA analysis.

RESULTS AND DISCUSSION: *In vitro* hyperocclusion model stretching MS increased significantly expression of CCL2, but slightly CCL3 in PDL cells isolated from WT mice. *In vivo* hyperocclusion model, MS increased dominantly the expression of CCL2 in PDL and the number of TRAP positive cells in the alveolar bone in WT mice. In contrast, the expression of CCL3 and the number of TRAP positive cells were spontaneously more in $CCL2^{(-/-)}$ and $CCR2^{(-/-)}$ mice than WT mice. Furthermore, MS significantly increased the number of TRAP positive cells and bone resorption in all types of mice. The results are suggested that CCL2 has a significant role in MS-induced osteoclastogenesis. If CCL2 signaling pathway was suppressed the expression of CCL3 was significantly increased in PDL, leading to compensatory role for osteoclastogenesis.

***Disclosures: Takashi Tsutsumi**, None.*

MO0254

Autophagy Is Impaired in Osteoclasts from Osteopetrotic Mice with the V-ATPase a3 R740S Mutation. Elena Bajenova[1], Noelle Ochotny[2], Celeste Owen[3], Irina Voronov*[2]. [1]Faculty of Dentistry, University of Toronto, Canada, [2]University of Toronto, Canada, [3]Centre for Modeling Human Disease, Samuel Lunenfeld Research Institute, Mt Sinai Hospital, Canada

Vacuolar H^+-ATPases (V-ATPases) are multisubunit enzymes necessary for acidification of intracellular and extracellular compartments. Mice with an R740S mutation in the V-ATPase a3 subunit have defective V-ATPase activity resulting in mild osteopetrosis in heterozygous (+/R740S) and severe osteopetrosis in homozygous (R740S/R740S) animals. We previously demonstrated that +/R740S osteoclasts (OCs) have increased lysosomal pH and impaired *in vitro* OC differentiation. Furthermore, +/R740S OCs had decreased NFATc1 nuclear translocation. This inhibition was due, in part, to accumulation of regulator of calcineurin 1 (RCAN1), an endogenous NFATc1 inhibitor. Upon signaling, RCAN1 is degraded via the autophagic-lysosomal pathway, suggesting impairment of this pathway in +/R740S OCs. Based on these results, we hypothesized that autophagy is inhibited in +/R740S OCs.

To test our hypothesis, +/R740S and +/+ bone marrow-derived OCs were differentiated in the presence of M-CSF and RANKL for 4 or 6 days. To assess the state of autophagy in the cells, we looked at protein expression of two key molecules, microtubule-associated protein light chain 3 (LC3) and sequestosome 1 (p62/SQSTM1). LC3 is necessary for formation of autophagosomal membranes and is cytosolic; upon induction of autophagy, LC3-I is lipidated to the LC3-II form which associates with the autophagosomal membrane. p62 is a scaffold protein that targets ubiquitinated proteins for degradation via autophagy; it is degraded within an autophagosome and is used as an indicator of autophagic protein degradation.

Immunoblotting demonstrated that the LC3-II/LC3-I ratio was consistently increased in +/R740S compared to +/+ cells, both at day 4 and day 6. The levels of p62 were also increased in +/R740S cells. Immunofluoresence confirmed higher LC3 expression in +/R740S OCs; furthermore, the pattern of LC3 expression was punctate in +/R740S cells compared to a more diffuse cytosolic staining in +/+ OCs. +/+ OCs treated with chloroquine, known to increase lysosomal pH, demonstrated a similar punctate LC3 staining pattern.

Accumulation of LC3 and p62 in +/R740S OCs is consistent with a block in late stages of autophagy, supporting our hypothesis. Future experiments will look at precise mechanisms of this inhibition, as well as at the induction of autophagy via mTOR signaling pathway in OCs with R740S mutation. These studies will help to elucidate precise roles of the V-ATPases and autophagy in OC differentiation.

***Disclosures: Irina Voronov**, None.*

MO0255

Bisphenol A reduces differentiation and stimulates apoptosis of osteoclasts and osteoblasts. Ho-Yeon Chung*[1], Kwan Hee Min[1], Kyoung Hee Choi[1], You Cheol Hwang[1], In-Kyung Jeong[1], Kyu Jeung Ahn[1], Hyoung-Moo Park[2]. [1]Kyung Hee University, South Korea, [2]Chung-Ang University, South Korea

Bisphenol A, a known endocrine-disrupting chemical, is a major component of the epoxy resins used in protective coatings. This compound binds to estrogen receptors. We examined the direct effects of bisphenol A on in vitro osteoclast and osteoblast culture systems. We evaluated the effects of bisphenol A on osteoclast formation using bone marrow-derived macrophage and RAW 264.7 cells and osteoblast differentiation using MC3T3-E1 cells. Bisphenol A significantly inhibited RANKL-induced TRAP-positive multinucleated cell formation in bone marrow-derived macrophages and RAW 264.7 cell cultures in a dose-dependent manner (0.5 uM to 12.5 uM). The suppression of ERK, JNK, AKT, and p38 mitogen-activated protein kinases engaged by RANK were observed in Western blotting after bisphenol A treatment in RAW 264.7 cells. Furthermore, bisphenol A suppressed Bcl-2 (anti-apoptotic) and stimulated Bax (pro-apoptotic) protein expression in RAW 264.7 cells. Bisphenol A also significantly suppressed ALP activities and bone nodule formation in MC3T3-E1 cell cultures. Specifically, the expression of Bcl-2 protein was decreased, but the expression of caspases 3, 8, and 9 were increased by bisphenol A treatment in MC3T3-E1 cells. We found that cell death was stimulated with BPA in a dose-dependent manner. These results demonstrate that bisphenol A may cause toxicity through anti-differentiation and pro-apoptosis in bone cells through MAPK cascades and death receptor pathways.

***Disclosures: Ho-Yeon Chung**, None.*

MO0256

C/EBPα Is a Novel Regulator in Osteoclast Lineage Commitment and Regulates Both Bone Resorption and Bone Formation Synchronously. Guochun Zhu*[1], Wei Chen[2], Mengrui Wu[2], Joel Jules[2], Liang Hao[1], Yi-Ping Li[2]. [1]Department of Pathology, University of Alabama at Birmingham, USA, [2]University of Alabama at Birmingham, USA

Current osteoclast inhibitors used to treat osteoclast-related bone diseases display the negative side effects (*e.g.* jaw osteonecrosis and increased bone fragility). It is thus crucial to identify novel therapeutic targets that can regulate both bone resorption and bone formation synchronously. To search for such a regulator, we mapped the critical cis-regulatory elements (CCREs) in the promoter of *Cathepsin K (Ctsk)*, which is expressed specifically in osteoclasts (OCs). We found that CCAAT/enhancer binding protein α (C/EBPα) is the critical cis-regulatory element binding protein. Our results indicate that C/EBPα is highly expressed in pre-OCs, OCs and osteoblasts. The combined presence of M-CSF and RANKL significantly induces C/EBPα expression. Surprisingly, *C/EBPα*$^{-/-}$ newborn mice have a bone volume increase of approximately 450%. Our results show that *C/EBPα*$^{-/-}$ newborn mice exhibit the severe osteopetrosis due to impaired osteoclastogenesis. Interestingly, although osteoclast formation is reduced to less than 10% *in vivo* and is completely blocked *in vitro* compared to wild-type, monocyte/macrophage development is not affected. This indicates a unique role for *C/EBPα* in osteoclast lineage commitment. The impaired osteoclastogenesis of *C/EBPα*$^{-/-}$ mouse bone marrow (MBM) cells can be rescued by *c-fos* overexpression, suggesting that *c-fos* is the major downstream targeted gene of *C/EBPα*. Ectopic expression of C/EBPα in MBM cells and monocyte/macrophage cells (in the absence of RANKL) induces expression of *RANK, c-fos, Nfatc1*, and *Ctsk*, and reprograms monocyte/macrophage cells to OC-like cells. These data indicate that *C/EBPα* is the downstream gene of RANKL signaling and the key transcription factor that regulates osteoclast lineage commitment. Our results demonstrate that C/EBPα directly upregulates *c-fos* expression at the transcriptional level. Importantly, C/EBPα$^{+/-}$ mice exhibit about a 40% increase in bone density, a 26% increase in the number of osteoblasts per bone surface, and a 40% decrease in the number of osteoclasts per bone surface, compared to the C/EBPα$^{+/+}$ control. Notably, C/EBPα$^{+/-}$ mice with Haploinsuffciency for C/EBPα exhibited significant protection against ovariectomy-induced osteoporosis. These discoveries establish C/EBPα as a key transcriptional regulator that regulates both bone resorption and formation synchronously, providing a unique therapeutic target for diseases of excessive bone resorption such as osteoporosis and arthritis.

***Disclosures: Guochun Zhu**, None.*

MO0257

CD97 Expression on Osteoclasts Enhances Osteoclastogenesis and Regulates Bone Mass. Hee Yeun Won*[1], SeHwan MUN[2], Sun-Kyeong Lee[1]. [1]University of Connecticut Health Center, USA, [2]Department of Medicine, University of Connecticut Health Center, USA

Receptor activator of nuclear factor κB ligand (RANKL) induces osteoclast formation by stimulating the fusion of mononuclear osteoclast precursor cells. CD97 is a member of the epidermal growth factor-seven transmembrane (EGF-TM7) family of adhesion receptors. It was identified as an early T cell activation marker and a ligand for CD55 (decay accelerating factor, DAF) that is expressed on myeloid cells at high levels. We found that CD97 was selectively induced by RANKL in FACS sorted murine bone marrow osteoclast precursor cells. To elucidate the functions of CD97 in bone, we examined osteoclastogenesis in bone marrow cultures from WT and CD97-deficient (CD97 KO) mice and compared their bone mass.

RANKL induced CD97 mRNA and protein expression in bone marrow macrophage (BMM) by 6.7 fold and 9.9 fold, respectively ($p<0.01$). Furthermore, reducing CD97 expression using CD97 targeted siRNA in BMM cells inhibited osteoclastogenesis. Conversely, CD97 protein (30 ng/ml) enhanced OCL formation in BMM cultures that were treated with M-CSF (30 ng/ml) and RANKL (30 ng/ml). Trabecular bone volume measured by μCT in the femurs of CD97 KO female mice was increased by 33% ($p<0.05$) compared to WT mice and was associated with a decrease in osteoclast number *in vivo* (49%, $p<0.05$). BM and BMM cells from CD97 KO mice that were stimulated with M-CSF and RANKL at 30 ng/ml each had significantly fewer OCL (22% and 20%, respectively) compared to WT cells ($p<0.05$) without differences in proliferation rates. Furthermore, OCL that formed from CD97KO mice were significantly smaller in size (20%, $p<0.01$) and had drastically reduced (67%, $p<0.01$) bone resorption activity by pit assay compared to cells from WT mice. In addition, the number of CFU-GM and osteoclast precursor population in bone marrow of CD97 KO mice was 26% and 18% less ($p<0.05$) than in WT mice, respectively. Deletion of CD97 in BMM cells also resulted in a significant attenuation of NFATc1 and macrophage fusion receptor (MFR) expression, indices, respectively, of osteoclast differentiation and fusion.

These results demonstrate that CD97 is a positive regulator of OCL differentiation and function. Bone marrow cell cultures from CD97 KO mice had a decreased capacity to form osteoclasts and resorb bone. Furthermore, CD97 KO mice had significantly increased trabecular bone mass, which is consistent with decreased osteoclast activity. We conclude that CD97 enhances osteoclastogenesis and regulates bone mass *in vivo*.

***Disclosures: Hee Yeun Won**, None.*

MO0258

Genome-wide Comprehensive Epigenetic Analysis Reveals that TGF-beta Works as an Essential Mediator for RANKL-induced Osteoclastogenesis Cooperating with c-FOS. Yasunori Omata*[1], Tetsuro Yasui[1], Yuho Kadono[1], Takumi Matsumoto[1], Hironari Masuda[1], Jun Hirose[2], Naoto Tokuyama[1], Hisataka Yasuda[3], Yuuki Imai[1], Hiroyuki Aburatani[1], Kozo Nakamura[1], Sakae Tanaka[1]. [1]The University of Tokyo, Japan, [2]Research Hospital, The Institute of Medical Science, The University of Tokyo, Japan, [3]Oriental Yeast Company, Limited, Japan

Previous studies found that TGF-beta promotes RANKL-induced osteoclastogenesis. However the molecular mechanism remains unclear. We employed chromatin immunoprecipitation sequencing (ChIPseq) method and comprehensively analyzed the genes regulated by TGF-beta. Smad2/3 work as transcription factors in TGF-beta signal transduction. To identify Smad2/3 binding sites globally, the immunoprecipitates were subjected to massively parallel DNA sequencing and the obtained data were mapped to the genome. After treating BMMs with 2 ng/ml TGF-beta for 1.5 hrs, cells were collected and chromatin immunoprecipitation using anti-Smad2/3 antibody was performed. 2,786 Smad2/3 binding sites were detected, and 992 of them (903 genes) existed around the promoter regions of RefSeq genes. Microarray analysis demonstrated that the expression of the Smad2/3 target genes was significantly up-regulated by TGF-beta. The analysis of the Smad binding motif revealed that the *AP-1* binding motifs well existed close to the Smad binging sites. c-Fos plays an essential role in osteoclast differentiation, and the nuclear translocation of c-Fos during the osteoclastogenesis was promoted by TGF-beta and also confirmed that Smad and c-Fos were co-localized in the immunocytochemistry assay and Smads bind to c-Fos in the immunoprecipitate assay. The proximity ligation assay which enables the visualization of protein-protein interaction in the immunocytochemistry revealed that the two molecules located close in the nucleus during the RANKL stimulation with TGF-beta, on the other hand no proximity spot was detected in nucleus during the inhibition of TGF-beta receptor using SB431542. Furthermore the ChIPseq method demonstrated that Smad bind to the promoter region of *NfatC1* which is a master key regulator of osteoclastogenesis, and the region was close to an *AP-1* site. In addition, the histone modification profiles at the Smad binding site was converted from H3K4me3/K27me3 bivalent to H3K4me3 monovalent by TGF-beta, indicating that the gene is in a state of up-regulation. These results suggest that TGF-beta promotes the osteoclastogenesis via Smad's cooperation and support to the nuclear transinduction of c-Fos. In summary, we performed the comprehensive analysis using the novel ChIPseq method and revealed a mechanism that TGF-beta mediates RANKL-induced osteoclastogenesis. Here is a new insight that Smads play an essential role by binding and cooperating with c-Fos to promote osteoclastogenesis.

***Disclosures: Yasunori Omata**, None.*

MO0259

Hydrogen Sulfide Inhibits Osteoclast Differentiation Through NRF2 Activation and Reduced ROS Signaling. Francesco Grassi*[1], Laura Gambari[2], Cristina Manferdini[2], Andrea Facchini[2], Gina Lisignoli[2]. [1]Istituti Ortopedici Rizzoli, Italy, [2]Istituto Ortopedico Rizzoli, Italy

Hydrogen Sulfide (H_2S) is a gaseous molecule long known as a toxic agent for living organisms. Even so, H_2S is released endogenously in mammalian tissues within the so called 'transsulfuration pathway' by two pyridoxal-5'-phosphate-dependent enzymes both responsible for the metabolism of L-cysteine: cystathionine b-synthase (CBS) and cystathionine g- lyase (CSE). H_2S has been recently shown to play a critical role in the regulation of organs and tissues and several correlations were described between low levels of plasmatic H_2S, reduced activity of H_2S-generating enzymes and diseases such as diabetes, GI-tract irritations, cancer. However, the role of H_2S in the regulation of bone cells is still elusive. Here we investigated whether H_2S can modulate differentiation and function of human osteoclasts (OC) in vitro. CD11b+ OC precursor cells were obtained by immunomagnetic positive selection of human PBMC isolated from healthy donors. Mature OC were then obtained by stimulation with M-CSF (10ng/ml) and RANKL (75ng/ml) in the presence or absence of a common H_2S-donor, NaHS, added to cell cultures at concentrations ranging from 50 to 300mM. Pit assays were performed to assess OC activity, NaHS dose-dependently decreased OC differentiation and activity ($p<0.01$ at 200 and 300 mM NaHS). Attesting to specificity, NaHS did not affect viability of OC precursors as measured by annexinV/PI and LDH cytotoxicity assay after 24 or 72h of stimulation.

As H_2S works predominantly as a reducing agent within cells, we investigated whether NaHS stimulation can affect RANKL-dependent ROS signaling in OC precursors, a key step in OC differentiation. ROS were measured within 30 minutes of RANKL stimulation by dichlorodihydrofluorescein diacetate (DCF) staining, and found that pre-stimulation of OC precursors with NaHS (50-300mM for 10') dose-dependently inhibited RANKL-dependent increase in intracellular ROS. Furthermore, NaHS stimulation significantly increased activation and nuclear translocation of NRF-2, the master regulator of antioxidant response and ROS inhibition in cells. To establish if NRF2 is required for NaHS inhibition of OC, siRNA were used to silence NRF2 expression in OC precursors throughout osteoclastogenic differentiation. NRF2-silencing completely prevented the ability of NaHS to inhibit OC differentiation, suggesting that NRF-2 antioxidant response is critical to OC inhibition by NaHS. In conclusion, H_2S inhibits OC differentiation by blunting ROS and triggering an antioxidant response in OC precursor cells.

***Disclosures: Francesco Grassi**, None.*

MO0260

OC Fusion: Regulation through Collagen and Mineral Contacts at the Marrow/Bone Interface? Kent Soe*[1], Thomas Andersen[2], Jean-Marie Delaisse[2]. [1]Vejle Hospital, University of Southern Denmark, Denmark, [2]Vejle Hospital, IRS, University of Southern Denmark, Denmark

Mono-nucleated pre-osteoclasts (preOCs) move from the bone marrow to the bone surface where they fuse to form multinucleated OCs. PreOCs situated in the bone marrow are obviously in contact with a very distinct extracellular matrix (ECM) compared with fusing OCs on a mineralized bone surface. Since fusion occurs only on the bone surface, it is possible that contact of the preOC with the respective ECMs of the bone surface and the bone marrow may induce different fusion competent states and thereby favor fusion.

First, we performed immunofluorescent staining of human iliac crest biopsies for collagen type I and $TRAcP^+/OSCAR^+$ cells, and found that 75% of $TRAcP^+/OSCAR^+$ preOCs in the bone marrow are in direct contact with collagen type I fibers while 95% are within two cell layers distance. Next we tested the influence of collagen (demineralized bone slices) or mineral (NaOCl treated bone slices) on the fusion of preOCs generated from $CD14^+$ human peripheral blood monocytes. We found that contact with collagen for 24 or 48 hrs stimulated fusion of preOCs compared to mineral. The average number of nuclei per OC ($\geqslant$2 nuclei) after 48 hrs was found to be 1.6 to 2.3 fold larger on collagen compared to mineral. Actually, it appears that fusion is slowed down dramatically on mineral since the average number of nuclei per OC did not increase from 24 to 48 hrs but clearly did on collagen. Expression levels of factors known to be involved in OC fusion were tested in preOCs by Q-RT-PCR 2 hrs after seeding on either mineral or collagen and proved to be different in these two conditions. On collagen the expression of IL1β was increased by 3.5-fold and TNFα was increased 12-fold compared to mineral. Furthermore, preliminary results suggest that also syncytin-1 and ASCT2 were induced on collagen while DC-STAMP and OSCAR did not seem to be induced.

Our data can lead to the following model: preOCs in contact with collagen in the marrow are put in a fusion competent state so that upon arrival to the bone surface they function as a ''fusion donor'' while the OCs on mineral serve as a ''fusion acceptor''. The existence of fusion acceptors and donors is already established for other fusing cell types such as trophoblasts and myoblasts. Our findings may help to understand the site restricted fusion of OCs in vivo.

***Disclosures: Kent Soe**, None.*

MO0261

RBP-J imposes a requirement for ITAM-mediated co-stimulation of RANKL and TNF signaling during osteoclastogenesis. Susan Li*, Xiaoyu Hu, Lionel Ivashkiv, Baohong Zhao. Hospital for Special Surgery, USA

Osteoclastogenesis requires not only RANK signaling but also co-stimulatory signals from immunoreceptor tyrosine-based activation motif (ITAM) -containing receptors/adaptors, predominantly DAP12 and FcRγ in osteoclast precursors. The mechanisms by which co-stimulatory signals are regulated and integrated with RANK signaling are not well understood. We recently identified RBP-J as a key inhibitory regulator of inflammatory osteoclastogenesis and bone resorption. In the present study, we investigated whether RBP-J regulates ITAM-mediated co-stimulation and controls the crosstalk between ITAM and RANK signaling. To address these questions, we generated DAP12 and RBP-J double knockout (KO) mice (R-DKO) and DAP12, FcRγ and RBP-J triple KO mice (TKO). Strikingly, we found that the osteopetrotic bone phenotype shown in DAP12 KO mice or DAP12/ FcRγ DKO mice was rescued by RBP-J deficiency in R-DKO or TKO mice due to significantly recovered osteoclast formation. Thus, RBP-J deficiency relieves the requirement for ITAM-mediated co-stimulation in osteoclastogenesis during homeostatic bone remodeling. RBP-J deficiency almost completely rescued osteoclast differentiation in DAP12 and FcRγ deficient osteoclast precursors in vitro, resulting in formation of TRAP positive multinuclear cells and induction of osteoclastogenic genes, such as TRAP, cathepsin K and β3 integrin. Mechanistically, RBP-J deficiency allowed the induction of key osteoclastogenic factors NFATc1, Blimp1 and c-Fos in DAP12/ FcRγ DKO cells in response to RANKL or TNF-α stimulation. RBP-J suppressed induction of NFATc1 and Blimp1 by downregulating PLCγ expression and downstream calcium-CaMKK-PyK2 signaling during osteoclastogenesis. These results indicate that RBP-J plays an important role in suppressing ITAM-mediated co-stimulation, thereby limiting crosstalk between ITAM and RANK signaling. In addition, RBP-J deficiency resulted in increased TNF-α induced multinuclear osteoclast formation and NFATc1/Blimp1 expression in vitro, and increased inflammatory bone resorption in vivo in DAP12 deficient mice. Our findings identified RBP-J as an important factor in restraining the crosstalk between RANK/ TNFR signaling and co-stimulatory signals. Environmental cues attenuating RBP-J expression or activity can bypass the requirement for co-stimulation in osteoclastogenesis.

***Disclosures: Susan Li**, None.*

MO0262

Specific Modulation of NEMO SUMOylation Regulates Osteoclastogenesis and Bone Resorption. Yousef Abu-Amer[1], Kyuhwan Shim*[2]. [1]Washington University in St. Louis School of Medicine, USA, [2]Washington University school of medicine, USA

IKKγ/NEMO is the regulatory subunit of IκB kinase complex and regulates NF-κB activation. Expression and function of NEMO itself is tightly regulated by poly-ubiquitination (pUB) and SUMOylation events. *Nemo* is X-linked, and certain mutations in this gene result in Incontinentia Pigmenti and skeletal defects in human hemizygous females suggesting that NEMO regulates bone metabolism. To elucidate the role of NEMO in the skeleton, we used myeloid conditional deletions of *nemo* floxed mice. Phenotypic and molecular analyses showed that NEMO-deficiency in the myeloid compartment caused osteopetrosis owing to defective osteoclastogenesis. The function of NEMO is governed by post-translational modifications, primarily UB and sumoylations at multiple lysine residues which appear to be cell and signal specific. To this end, several viral constructs representing strategic point mutations at key residues in coiled-coil-2 and leucine zipper domains were utilized to examine their osteoclastogenic potential in NEMO deficient osteoclast precursors (OCPs). Of these mutants, K270A-NEMO (K270 SUMOylation-deficient) elicited higher osteoclastogenesis in NEMO-null compared to wild type cells. In contrast, expression of the mutant K319A NEMO into NEMO-null cells was lower and failed to restore osteoclastogenesis, indicating that K319-modification is essential for NEMO stability and function. To further investigate the physiological significance of K270-mediated osteoclastogenesis, we utilized the SUMO inhibitor ginkgolic acid (GA). SUMOylation of NEMO has been known as important for localization of NEMO in the nucleus, and SUMO-free NEMO is directed to the cytosol where it stages IKKβ activation. GA showed enhanced osteoclastogenesis *in vitro* compared to DMSO (carrier)-treated control. The nuclear form of NEMO was approximately 14kDa higher in molecular mass due to SUMOylation compared to the cytosolic form. Upon treatment of OCPs with GA for two hrs, the nuclear form of NEMO-SUMO was diminished, probably due to inhibition of NEMO SUMOylation. These results support our previous finding that SUMO-free K270A NEMO shows higher stability. We also tested the in vivo effects of GA on mouse bone remodeling and osteolysis. TRAP-stained histological sections of tibia indicated that the GA-treated mice showed significant increase in osteoclast number along the growth plates and decrease in trabecular bone mass. Thus, NEMO SUMOylation is crucial for regulation of osteoclasts and bone loss.

***Disclosures: Kyuhwan Shim**, None.*

MO0263

Steap4 is Critical for Osteoclast Differentiation via Regulating Cellular Iron/ ROS and CREB Activation. Jian Zhou*[1], Shiqiao Ye[2], Toshifumi Fujiwara[3], Stavros Manolagas[2], Haibo Zhao[2]. [1]UAMS, USA, [2]Central Arkansas VA Healthcare System, Univ of Arkansas for Medical Sciences, USA, [3]Center for Osteoporosis & Metabolic Bone Diseases, University of Arkansas for Medical Sciences & the Central Arkansas Veterans Healthcare System, Little Rock, AR, USA

Iron overload causes loss of bone mass and fractures in patients with hemochromatosis, hemosiderosis, thalassemia, and also accelerates bone loss in postmenopausal women. Iron overload leads to an imbalance in bone remodeling caused by an increase in osteoclastic bone resorption and a decrease in osteoblastic bone formation. It has recently been shown that iron uptake via the transferrin/transferrin receptor (Tf/TfR1) pathway, in concert with the peroxisomes proliferator-activated receptor-γ 1β (PGC-1β), regulates mitochondrial biogenesis, the generation of reactive oxygen species (ROS), and CREB activation during osteoclastogenesis. However, the molecular mechanisms controlling cellular iron metabolism in osteoclast lineage cells remain largely unknown. Mammalian cells acquire iron mainly through the Tf cycle, in which ferric iron (Fe^{3+})-loaded Tf binds to TfR1 on the cell surface, and the complex is then internalized via receptor-mediated endocytosis. Fe^{3+} is released from Tf due to acidic pH in endosomes. Before Fe^{3+} can be transported across the endosomal membrane to the cytoplasm for cellular utilization, it must be reduced to ferrous iron (Fe^{2+}). In this study, we have elucidated that expression of Steap4, an endosomal ferrireductase of the six-transmembrane epithelial antigen of prostate (Steap) family proteins, is increased during osteoclast differentiation, as revealed by both gene-array analysis and quantitative real-time PCR. Knocking down Steap4 expression by lentivirus-mediated shRNAs in macrophages inhibits osteoclast formation, as determined by TRAP staining, TRAP activity measurements, and quantitative expression of osteoclast marker genes. Loss of Steap4 in osteoclast lineage cells resulted in reduced ferrous iron level, decreased ROS generation, as measured by fluorescent dyes, PG SK and dichlorodihydrofluorescein, respectively. In line with previous reports, CREB activation was decreased in Steap4-deficient osteoclast precursors. Moreover, the induction of PGC1-β/ mitochondrial mRNA expression, two downstream pathways regulated by CREB, was attenuated in the absence of Steap4. In conclusions, our results indicate that Steap4 is the major endosomal ferrireductase in osteoclasts. Coupled with the up-regulated Tf/TfR pathway, Steap4 enhances cellular iron uptake and utilization, and therefore may play a critical role in osteoclast development and activation under physiological and pathological conditions.

***Disclosures: Jian Zhou**, None.*

MO0264

Withdrawn

MO0265

TMEM178 is a novel negative regulator of osteoclastogenesis and inflammatory bone loss via specific modulation of the RANKL- NFATc1 axis. Corinne Decker*[1], Deborah Novack[2], Roberta Faccio[2]. [1]Washington University in St. Louis, USA, [2]Washington University in St. Louis School of Medicine, USA

Although pro-osteoclastogenic mechanisms are well-defined, relatively few negative regulators of osteoclast (OC) formation and function have been described. Here we show that transmembrane protein 178 (TMEM178), a previously unstudied and uncharacterized integral membrane protein, acts in a negative feedback loop to restrain osteoclastogenesis (OCG) in basal and pathological conditions. By quantitative RT-PCR, we found that TMEM178 induction in response to RANKL treatment is dependent on the lipase PLCγ2, thus positioning TMEM178 downstream of RANKL-PLCγ2 pro-osteoclastogenic signaling pathways. In opposition to the osteopetrotic phenotype of PLCγ2-/- mice however, unmanipulated 16-week old TMEM178-/- mice show a surprising 25% loss in trabecular bone volume and significant cortical thinning compared to WT controls, suggesting that TMEM178 is actually a negative regulator of the OC. Indeed, TMEM178 ablation accelerates OC formation *in vitro* in a RANKL dose-dependent manner; OC markers including TRAP, β_3 integrin, DC-STAMP, and calcitonin receptor are induced earlier and to higher levels in TMEM178-/- OC compared to WT. Consistent with increased number of OC, resorptive pit area is nearly doubled in TMEM178-/- OC cultures on bone slices *in vitro*. To assess inflammatory bone loss *in vivo*, we utilized supracalvarial LPS and K/BXN serum-transfer arthritis. LPS induced 3.5 times the amount of eroded area and increased OC number in TMEM178-/- mice compared to WT. Similarly, TMEM178-/- mice suffer more bone loss correlated to a significant increase in TRAP+ OC during arthritis. To uncover the mechanism of TMEM178 activity, we examined RANKL signaling cascades. Strikingly, TMEM178-/- OC display dramatically elevated NFATc1 protein levels throughout OCG while NFκB and MAPK activation are remarkably unaffected. Moreover, ratiometric imaging of Fura-2-loaded cells shows significantly higher $[Ca^{2+}]_i$ in TMEM178-/- preOC compared to WT, further implying that TMEM178 explicitly antagonizes RANKL-induced Ca^{2+} fluxes to restrain NFATc1 activation and amplification. In sum, our results define TMEM178 as a critical mediator of a novel negative feedback loop specifically targeting the RANKL-Ca^{2+}-NFATc1 pathway and establish the importance of TMEM178 *in vivo* for maintenance of normal bone mass and protection from pathological bone loss.

***Disclosures: Corinne Decker**, None.*

MO0266

Zinc inhibits Osteoclast Differentiation by Suppression of Ca^{2+}-Calcineurin-NFATc1 Signaling Pathway. Kwang Hwan Park*[1], Jae Hyuck Shim[2], Jin Woo Lee[1], Jae Myun Lee[1]. [1]Yonsei University College of Medicine, South Korea, [2]Weill Cornell Medical College, USA

Zinc, an essential trace element, has been found to inhibit osteoclast differentiation in vitro and in vivo. The molecular mechanism for the inhibitory effect of Zinc , however, has been poorly understood. The purpose of this study was to investigate the effect of Zinc and its molecular mechanism on the receptor activator of NF-κB ligand (RANKL)-induced osteoclastogenesis in mouse bone marrow-derived monocyte cells (BMMs) and RAW264.7 cells.

In BMMs, Zinc treatment during osteoclast differentiation decreased RANKL-induced osteoclast formation in a dose dependent manner. We showed that Zinc suppressed the mRNA levels of the nuclear factor of activated T-cells, cytoplasmic 1 (Nfatc1). Zinc also dose-dependently accumulated phospho-Nfatc1 (p-Nfatc1) in the cytosol and inhibited the translocation of Nfatc1 to the nucleus in RAW264.7 cells. Zinc suppressed the activities of Nfatc1 in the nucleus without changing the activities of NF-κB in RAW264.7 cells. On the other hand, the calcineurin activity was decreased due to Zinc but its protein level was unchanged. Moreover, RANKL-induced Ca^{2+} oscillations were inhibited by Zinc treatment, but phospho-phospholipaseCγ1 (p-PLCγ1), the upstream signaling molecule of the Ca^{2+} oscillations was not affected.

Taken together, this study, for the first time, demonstrates that the inhibitory effect of Zinc during osteoclastogesis is caused by suppressing Ca^{2+}-Calcineurin-NFATc1 signaling pathway. Thus, Zinc may be a useful candidate of therapeutics for the prevention of bone loss caused by NFATc1 activation in osteoclasts.

***Disclosures: Kwang Hwan Park**, None.*
This study received funding from: the National Research Foundation of Korea

MO0267

Effects of alendronate binding to bovine bone slices and smear layer removal on cultured mouse marrow-derived osteoclasts. Vivian Bradaschia-Correa*, Giovanna Ribeiro-dos-Santos, Victor Arana-Chavez. University of São Paulo - School of Dentistry, Brazil

Most *in vitro* resorption assays employ bone slices for supplying the mineralized substrate on which cultured osteoclasts are tested. However, the cutting procedures for obtaining the bone slices result in the formation of a smear layer (SL), which is not present during in vivo conditions. It is possible that the presence of SL may interfere with the osteoclast behavior. Based on this premise, the present study aimed to analyze whether the presence of SL interferes on the resorptive activity of mouse marrow-derived osteoclast-like cells. Additionally, it was analyzed whether the SL removal may affect the binding affinity of the bisphosphonate alendronate (ALN) to bone slices, osteoclast differentiation, viability and survival. Disk-shaped 0.1mm-thick slices with 0.5mm diameter were prepared from freshly obtained bovine bones by using an Isomet 1000 slow-speed precision saw equipped with a diamond-impregnated disk under refrigeration with copious water. They were treated with 1% sodium hypochlorite solution followed by 4.13% ethylidenediaminotetraacetic acid, rinsed thoroughly with deionized water and air dried. The SL removal was confirmed by scanning electron microscopy (SEM) examination. Bone slices were treated in O-phthalaldehyde-labeled ALN solutions at varied concentrations (1μM – 10mM) for 24h. The initial and final concentrations in media were analyzed by spectrophotometry. Marrow cells obtained from 30 days-old Balb c mice were cultured in α-MEM supplemented with calcitriol onto bone slices with or without SL for 5 days, and bone resorption was analyzed by SEM. Additional mouse marrow cells were cultured onto ALN-saturated SL-free bone slices during 3 days and bone resorption was analyzed by SEM; the cells that remained on the plate were incubated for TRAP, TUNEL and submitted to MTT assay. The resorbed areas decreased in SL-free samples, while SL did not affect the binding affinity of the bone slices to ALN. Bone slices in both conditions were saturated by 1mM ALN. SL removal followed by ALN treatment did not interfere in the number of TRAP positive cells and cell viability, but the resorbed area significantly reduced, while TUNEL positive cells increased compared to controls. It is concluded that the presence of SL on the bone substrate increases the in vitro resorptive activity of osteoclat-like cells, whereas the presence of ALN decreases cell viability and resorption activity.

***Disclosures: Vivian Bradaschia-Correa**, None.*

MO0268

H_2O_2 Production in Osteoclast Mitochondria Promotes Bone Resorption and Mediates the Effects of Estrogen Deficiency. Shoshana Bartell*[1], Li Han[1], Aaron Warren[1], Julie Crawford[1], Semahat Serra Ucer[2], Stavros Manolagas[1], Maria Jose Almeida[1]. [1]Central Arkansas VA Healthcare System, Univ of Arkansas for Medical Sciences, USA, [2]University of Arkansas for Medical Sciences, USA

Osteoclastogenesis requires mitochondrial biogenesis and H_2O_2, and catalase is a critical enzyme for the elimination of H_2O_2. Estrogens attenuate osteoclastogenesis and promote osteoclast apoptosis, at least in part, via anti-oxidant mechanisms. Furthermore, the anti-resorptive effects of estrogens on cancellous and cortical bone mass are mediated by distinct mechanisms: cell autonomous effects in the former and indirect effects via osteoblast progenitors in the latter. We have tested here the hypothesis that mitochondria-derived H_2O_2 in cells of the osteoclast lineage is an important mediator of bone resorption. To do this, we generated transgenic mice expressing human catalase targeted to the mitochondria in cells of the monocyte/macrophage lineage, using the LysM-Cre strain. We found that the number of osteoclasts formed in bone marrow cultures from MitoCat;LysM-Cre (mitoCAT) mice was lower as compared to LysM-Cre littermate controls, due to an increase in macrophage and osteoclast apoptosis. Consistent with the decreased lifespan, the activation of the pro-survival kinases Akt and Erk in response to M-CSF or RANKL was attenuated in osteoclasts from the mitoCAT mice. Under basal conditions, both male and female mitoCAT mice had higher cancellous bone volume due to an increase in trabecular number and decreased trabecular separation as determined by micro-CT. MitoCAT mice also had increased femoral cortical thickness due to decreased endosteal resorption as well as a decrease in the number of osteoclasts per cancellous bone perimeter. Six weeks following ovariectomy (OVX) of 3 month old mice, oxidative stress was increased and DEXA BMD was decreased at the spine and femur in the LysM-Cre littermate controls. All of these changes were abrogated in the mitoCAT mice. Furthermore, the mitoCAT mice were protected against the OVX-induced cortical bone loss and porosity, but not the loss of cancellous bone, as determined by micro-CT. These results demonstrate that H_2O_2 is required for optimal signaling by both RANKL and M-CSF and that H_2O_2 formation in the mitochondria promotes osteoclast generation and survival, and thereby bone resorption. In addition, they show that estrogens decrease bone resorption at the endocortical, but not the cancellous, surface via an anti-oxidant mechanism. Mitochondria H_2O_2 production, therefore, represents a potentially important pharmacotherapeutic target for the treatment of diseases caused by increased bone resorption.

***Disclosures: Shoshana Bartell**, None.*

MO0269

Individual and Combining Effects of Anti-RANKL Monoclonal Antibody and Teriparatide in Ovariectomized Mice. Naoto Tokuyama*[1], Hironari Masuda[1], Jun Hirose[2], Yasunori Omata[1], Yuho Kadono[1], YURIKO FURUYA[3], Hisataka Yasuda[3], Nobuyuki Udagawa[4], Hiroshi Takayanagi[5], Sakae Tanaka[1]. [1]The University of Tokyo, Japan, [2]Research Hospital, The Institute of Medical Science, The University of Tokyo, Japan, [3]ORIENTAL YEAST CO., LTD, Japan, [4]Matsumoto Dental University, Japan, [5]The University of Tokyo, Department of Immunology, Japan

Introduction: Receptor activator of nuclear factor-kappaB ligand (RANKL) is a member of the tumor necrosis factor (TNF) superfamily cytokines and an essential mediator of osteoclast formation, bone-resorbing function and survival. RANKL plays a major role in the pathogenesis of postmenopausal osteoporosis and other diseases associated with bone loss. Antiresorptive agents such as bisphosphonates have been most commonly used for osteoporosis therapy. However, previous studies showed that combining alendronate with teriparatide rather attenuated the anabolic effect of teriparatide. In this study, we examined the individual and combined effects of teriparatide and anti-RANKL monoclonal antibody in ovariectomized mice.

Materials and Methods: Three-month-old female C57BL/6 mice were ovariectomyzed (OVX) or sham operated. Four weeks after OVX, they were assigned to 3 different groups to receive anti-RANKL mAb alone (5 mg/kg single injection at 4 weeks after OVX, Ab group), teriparatide alone (80 μg/kg daily injection for 4 weeks from 4 weeks after OVX, PTH group), or mAb plus teriparatide (Ab+PTH group). Mice were sacrificed 8 weeks after OVX. Bone mineral density (BMD) was measured at the femur and lumber spine. Hind limbs were subjected to histological and immunohistological analysis. Bone marrow cells were analyzed with a flow cytometer to evaluate the quantity of osteoclast precursors. Serum osteocalcin and CTX-I levels were measured to investigate the bone turnover.

Results: Compared with Ab group, Ab+PTH group showed a significant increase in BMD at distal femur, femoral shaft and lumber spine. Cancellous bone volume reached a maximum after 4 weeks of Ab injection and gradually decreased thereafter. Cortical bone volume was significantly increased in Ab+PTH and PTH groups compared with Ab group. Bone turnover in Ab+PTH group was suppressed to the same degree as in Ab group. The number of TRAP-positive multinucleated cells was markedly reduced in Ab group, while it was maintained in Ab+PTH group. The number of osteoclast precursors was increased in Ab group compared with other groups as determined by immunohistochemical analysis and flow cytometric analysis. These results suggest that combined treatment of teriparatide with anti-RANKL antibody had additive effects on BMD in OVX mice compared with individual treatment.

***Disclosures: Naoto Tokuyama**, None.*

MO0270

Losartan increases bone mass by direct inhibition of osteoclasts: evidence from murine and human data. Shan Chen*[1], Tarek Sibai[1], Nahid Rianon[2], Tao Yang[3], Jennifer Black[4], Elda Munivez[1], Terry Bertin[1], Brian Dawson[1], Yuqing Chen[1], Brendan Lee[5]. [1]Baylor College of Medicine, USA, [2]UTHealth The University of Texas Medical School at Houston, USA, [3]Van Andel Research Institute, USA, [4]Department of Pathology, Microbiology & Immunology, Vanderbilt University, USA, [5]Baylor College of Medicine & Howard Hughes Medical Institute, USA

Introduction: Osteoporosis and hypertension are two major chronic diseases of advanced age. Although traditionally these diseases are viewed as separate entities, increasing evidence suggests an overlapping etiology. One important determinant for both hypertension and osteoporosis is renin-angiotensin signaling. Inhibition of this signaling pathway lowers blood pressure and has demonstrated potential for bone loss prevention. We investigated the molecular mechanism underlying regulation of bone mass by the renin-angiotensin pathway through both animal and human studies.

Methods: Wild type mice were treated with Losartan, an antihypertensive drug that inhibits the angiotensin type 1 receptor, from birth until 6-weeks of age, after which bones were collected for microCT and histomorphometry analyses. Elderly hypertensive women treated with Losartan were examined by DXA and serum P1NP, N-UTX levels at 6 and 12 months after the onset of treatment. Osteocalst culture and Western blot assays were performed to determine the effects of Losartan on osteoclast differentiation and RANKL-induced ERK1/2 signaling.

Results: Losartan increased trabecular bone volume vs. tissue volume (a 98% increase) and cortical thickness (a 9% increase) in 6-week old wild type mice. The bone changes were attributed to decreased osteoclastogenesis as demonstrated by reduced osteoclast number per bone surface in vivo and suppressed osteoclast differentiation in vitro. At the molecular level, RANKL-induced ERK1/2 phosphorylation was attenuated by Losartan, suggesting a convergence of RANKL and angiotensin signaling at the level of ERK1/2 regulation. This also suggests that Losartan acts on ERK1/2, the essential mediator of RANKL signaling, and influences osteoclast differentiation. In the two women (Age 81 and 74) were prospectively treated for idiopathic hypertension with Losartan. Interestingly, both showed evidence of decreased bone resorption as measured by the urinary N-telopeptide.

Conclusion: Inhibition of the angiotensin pathway by Losartan has beneficial effects on bone beyond reducing blood pressure. Our study adds evidence to support the relationship between angiotensin receptor blockers (Losartan) and age-related bone loss that increases the risk of fractures in the elderly.

***Disclosures: Shan Chen**, None.*

MO0271

Pin1 regulates osteoclast fusion through the suppression of the master regulator of cell fusion DC-STAMP. Rabia Islam*[1], Won-joon Yoon[2], Kyung-Mi Woo[2], Jeong-Hwa Baek[3], Hyun-Mo Ryoo[3]. [1]School of Dentistry, Seoul National University, South Korea, [2]Seoul National University, South Korea, [3]Seoul National University, School of Dentistry, South Korea

Cell fusion is a fundamental biological event and an essential process for the development of multinucleated cells such as osteoclasts which originate from bone marrow hematopoietic precursors of the monocyte lineage. Fusion failure leads to accumulation of dense and fragile bone such as in osteopetrosis, demonstrating the importance of fusion in osteoclast maturity and bone remodeling. Previously, we discovered a role of Pin1, a peptidyl-prolyl isomerase catalyzing cis-to-trans conformational switches of target proteins presenting the Ser/Thr-Pro motif, in regulation of osteoblastogenesis and bone development. To explore its role in osteoclast formation and bone resorption we examined an in vivo mouse genetic model and found that mice null for Pin1 have low bone mass and increased amount of TRAP staining in histological sections of the upper metaphyseal region of the tibia, compared to Pin1 wild type mice; but *in vitro* culture of Pin1 deficient bone marrow-derived osteoclasts did not show a significant amount of increase in the number of TRAP positive multinucleated cells except in case of cells which have more than thirty nuclei. Pin1 deficient osteoclasts are larger than wild type osteoclasts and have higher nuclei number indicating higher fusion rate. Pin1 deficient foreign body giant cell formation was also highly increased both *in vitro* and *in vivo*. Among the known fusion proteins only DC-STAMP was highly increased in Pin1 null osteoclasts during osteoclastogenesis. DC-STAMP expression was also seen to be highly increased by immunohistochemistry in upper tibial section of Pin1 KO mice. With real time PCR we also found that mRNA of genes known to be regulated by DC-STAMP like *ACP5* and *CD9* were highly increased in Pin1 null osteoclasts after four days of culture in RANKL and MCSF supplemented media, compared to wild type osteoclasts. We found that DC-STAMP is post-translationally modified by proline directed serine threonine phosphorylation and Pin1 binds and isomerizes DC-STAMP affecting its stability and localization at the plasma membrane. Taken together our data, derived using a genetic approach, indicate that Pin1 is a determinant of bone mass through its regulation of osteoclast fusion protein DC-STAMP. The identification of Pin1 as a factor involved in cell fusion contributes to the understanding of osteoclast-associated diseases, including osteoporosis and opens new avenues for therapeutic targets.

***Disclosures: Rabia Islam**, None.*

MO0272

The Link module from Human TSG-6 is a Potent Inhibitor of Osteoclast-Mediated Bone Resorption; Towards a Novel Therapy for Osteoporosis. Jennifer Thomson*, Caroline Milner, Anthony Day. University of Manchester, United Kingdom

The TSG-6 protein has been identified as an endogenous protector of tissues during acute inflammation, e.g. in the context of inflammatory arthritis (see [1]). We showed previously that full-length recombinant human TSG-6 (rhTSG-6) is a potent inhibitor of RANKL-mediated osteoclastic bone resorption and works in synergy with OPG [1,2]; the isolated Link module from human TSG-6 (Link_TSG6) was found to be less active that rhTSG-6 and showed no synergistic effect. We also found that TSG-6 produced by osteoclasts in response to inflammatory cytokines (e.g. TNFα) acts as an autocrine regulator of their activity [1]. rhTSG-6 was found to inhibit F-actin ring formation, but had no measurable effect on the foramtion of TRAP-positive multinucleated cells from osteoclast precursors [1,2]. This suggests that TSG-6 mediates its inhibitory effect at the level of osteoclast activation, in contrast to OPG, which also suppresses osteoclast formation. In light of its anti-resorptive effects, TSG-6 represents a target for the development of novel treatments for conditions, such as osteoporosis, that are associated with excessive osteoclast-mediated bone loss. Even though Link_TSG6 may be less potent that rhTSG-6 *in vitro* [2], its greater ease of production (in *E. coli*) could make it more suitable for clinical development. Therefore, the aim of this study was to further compare the anti-resorptive activities of Link_TSG6 and rhTSG-6 and their mechanism of action.

Here we have shown (surprisingly) that Link_TSG6 has a similar potency to rhTSG-6 at inhibiting lacunar resorption of dentine by osteoclasts derived from human $CD14^+$ mononuclear cells (in the presence of M-CSF/RANKL); e.g. with ⩾90 %inhibition at 0.85 nM. Link_TSG6 also suppressed the resorptive activity of osteoclasts derived from mouse bone marrow, whereas rhTSG-6 did not. Like rhTSG-6 [1], Link_TSG6 was found to inhibit F-actin ring formation, providing a mechanism for its anti-resorptive properties.

Thus, Link_TSG6 might have therapeutic potential and work is now in progress to determine its efficacy in experimental models of osteoporosis and develop a scalable manufacturing process for this recombinant domain.

[1] Mahoney DJ, Swales C, Athanasou NA, Bombardieri M, Pitzalis C, Kliskey K, Sharif M, Day AJ, Milner CM & Sabokbar A (2011) *Arthritis Rheum.* 63: 1034-43.
[2] Mahoney DJ, Mikecz K, Ali T, Mabilleau G, Benayahu D, Plaas A, Milner CM, Day AJ & Sabokbar A. (2008) *J. Biol. Chem.* 283:25952-62.

***Disclosures: Jennifer Thomson**, None.*

MO0273

Trapidil, a platelet-derived growth factor antagonist, prevents osteoclastogenesis by down-regulating Ca^{2+}-NFATc1 axis and suppressed bone loss in mice. Sun-Don Kim*[1], Ha-Neui Kim[1], Zang Hee Lee[2]. [1]School of Dentistry, Seoul National University, South Korea, [2]Seoul National University School of Dentistry, South Korea

Trapidil, a platelet-derived growth factor antagonist, originally developed as a vasodilator and anti-platelet agent and has been used to treat patients with ischemic coronary heart, liver and kidney disease. In addition, Trapidil has been reported to inhibit glioma cell proliferation. In this study, we investigated effects of Trapidil on osteoclastogenesis and elucidated possible mechanism of Trapidil by RANKL stimulation in osteoclast precursors BMMs. Trapidil strongly inhibited osteoclast formation in co-culture of bone marrow cells and osteoblast without affecting RANKL and OPG expression in osteoblasts. In addition, Trapidil suppressed the RANKL-induced osteoclast formation from osteoclast precursors BMMs. Trapidil reduced the RANKL-induced NFATc1expression, a master transcription factor, in BMMs, whereas those of NF-kB and c-Fos, which are also transcription factors involved in osteoclast differentiation, were not affected. Ectopic expression of constitutively active form of NFATc1 reversed the Trapidil-induced anti-osteoclastogenic effect. Trapidil inhibited RANKL-induced phosphorylation of CREB, which is necessary for osteoclast differentiation. In addition, we found that Trapidil decreased formation inactive form of GSK3β, modulator of NFATc1 in osteoclast differentiation. Furthermore, Trapidil reduced protein level of TRPV5 calcium channel, which is involved in Ca^{2+} influx on osteoclast and significantly inhibited calcium influx by RANKL stimulation. Consistent with the in vitro anti-osteoclastogenic effect, Trapidil had potent inhibitory effect on osteoclast formation and bone resorption and induced by IL-1 in an animal model. Taken together, our data demonstrate that Trapidil may influence Ca^{2+} entry through TRPV-5 calcium channel, resulting in down-regulation of NFATc1 and CREB phosphorylation involved in osteoclast formation and bone resorption in osteoclasts.

***Disclosures: Sun-Don Kim**, None.*

MO0274

Vascularendothelial cells inhibit osteoclastogenesis by netrin 4 through DSCAM receptor. YUICHIRO ENOKI*[1], Tsuyoshi Sato[1], Masahito Matsumoto[1], Shoichiro Kokabu[2], Masahiko Okubo[1], Takanori Iwata[3], Michihiko Usui[4], Toru Fukuda[5], Shu Takeda[6], Yuuki Imai[7], Shinya Tanaka[1], Hiromi Oda[1], Tatsuo Suda[8], Tetsuya Yoda[1]. [1]Saitama Medical University, Japan, [2]Harvard School of Dental Medicine, USA, [3]The Institute of Advanced Biomedical Engineering & Science, Japan, [4]Kyushu Dental College, Japan, [5]Keio University School of Medicine, Japan, [6]Keio University, Dept. of Nephrology, Endocrinology & Metabolism, Japan, [7]Ehime University, Japan, [8]Research Center for Genomic Medicine Saitama Medical School, Japan

Bone is organized by several organs through the endocrine and nervous systems. Since bone is a highly vascularized organ, angiogenesis is a vital process during skeletal development. Recent studies demonstrated that the interaction of osteoblasts and endothelial cells has been essential for bone fracture repair. However, the role of vascular system in bone metabolism is not fully elucidated. Here we investigate whether vascular endothelial cells communicate with osteoclasts directly. We found that osteoclast differentiation was inhibited in the co-culture system of vascular endothelial cells and bone marrow macrophages under RANKL stimulation. Then we examined the expression of netrin family, which vascular endothelial cells robustly express, and found that vascular endothelial cells expressed netrin 4 and osteoclast expressed the receptors for netrin family. We showed that TRACP positive cells were significantly reduced and gene expression of osteoclast differentiation markers was significantly decreased in osteoclasts treated with netrin 4, suggesting that netrin 4 inhibited osteoclast differentiation. Next we examined gene expression of netrin receptors of osteoclast in the co-culture system and found that Down syndrome cell adhesion molecule (DSCAM), which was one of the netrin receptors, was strongly up-regulated in osteoclasts co-cultured with vascular endothelial cells. Moreover, the blockade of osteoclast differentiation by netrin 4 produced from vascular endothelial was neutralized with treatment with anti-netrin 4 antibody, resulting in the augmentation of osteoclast differentiation. Finally, immunostaining revealed that netrin 4-positive cells were consistent with PECAM 1-positive cells. Our results demonstrated that netrin 4 derived from vascular endothelial cells inhibit osteoclast differentiation via DSCAM receptor of osteoclasts.

***Disclosures: YUICHIRO ENOKI**, None.*
This study received funding from: Saitama Internal Grant

MO0275

Age Effects on Bone Microarchitecture and Osteocyte Sensing of Skeletal Loading. Teri Cline*[1], Matthew Stern[1], Mark Van Dyke[2], Christopher Bergman[3], Ying Liu[1], Amber Stern[1]. [1]University of Missouri - Kansas City, USA, [2]Virginia Tech, USA, [3]Wake Forest Institute for Regenerative Medicine, USA

At the cellular level, bone adaptation is controlled by osteocytes. Studies have shown that in the absence of mechanical loading, osteocytes send signals of bone resorption. Understanding the microarchitecture of bone is essential to the study of the mechanotransduction of these signals within the osteocyte lacanocanalicular network. The purpose of this study was to analyze the effect of age on the microarchitecture of bone and its role in strain transmission to the osteocyte.

Ten murine femur bone samples were studied; 5 old (2-yr-old), and 5 young (5-mo-old). Each sample was resin-embedded, acid etched, and imaged using Scanning Electron Microscopy (SEM). ImageJ was utilized to analyze the samples and quantitatively assess changes in canaliculi number, canaliculi diameter, lacunar size, and lacunar density. The samples were also analyzed based on the location of the osteocyte within the bone: periosteal versus endosteal regions. All results reported are significant based on t-tests ($p<0.05$). Representative finite element (FE) models of the bone microarchitecture were then created.

The microarchecture of young bone was found to be significantly different than that of old bone. Differences were also found between the endosteal and periosteal regions. The number of canaliculi/lacuna were found to decrease with age, while a greater number of canaliculi were found the periosteal regions of the young bone samples when compared to the endosteal regions. The diameter of the canaliculi increased with age. The canaliculi diameter also increased in the periosteal region from young to old. In the old murine bone samples, the canaliculi diameter decreased from the periosteal to the endosteal regions. The lacunar size decreased in the periosteal region from young to old. Lacunar size also decreased from the endosteal to the periosteal regions in the young bone. The overall lacunar density was found to increase with age. The resulting FE models predicted lower levels of strain being transmitted to osteocytes in the old bone and also those located in the endosteal region.

These results provided the necessary data to create a more anatomically accurate parametric FE analysis to study the microscopic strains sensed by osteocytes *in vivo*. Osteocytes in old murine bone experience lower strain levels than their young bone counterparts. Additionally, murine bone may remodel differently than primate bone, as the lacunar density was significantly higher in the old bone.

Summary of Properties	Young	Old
Canaliculi Count	73	63*
Canaliculi Diameter (um)	0.2641	0.2771*
Lacunar Cross sectional area (um^2)	92.7	88.6*
Density (lacunae/mm^2)	1345	1492*
* p<0.05		

Summary of Properties

***Disclosures: Teri Cline**, None.*

MO0276

Age Effects on the Macromechanical and Micromechanical Properties of Bone. Craig Meers*[1], Mark Johnson[2], Ying Liu[1], Thomas Register[3], Amber Stern[1]. [1]University of Missouri - Kansas City, USA, [2]University of Missouri, Kansas City Dental School, USA, [3]Wake Forest School of Medicine, USA

It is known that bone remodels itself in response to changes in its mechanical environment, with osteocyte mechanotransduction playing a major role. It has been shown that the modulus of the perilacunar region has an effect on the force transmitted to the embedded osteocyte. As the modulus increases, the bone deforms less to an applied force and less force is perceived by the osteocyte. This study examines bone microstructure directly around the lacunae in the perilacunar region and how its biomechanical properties change with age and the resulting effects on the osteocyte.

Femurs from 6 young (4-mo-old) and 5 old (24-mo-old) female mice (C57Bl/6) were harvested. Right femurs were used to determine overall bone biomechanical properties via 3-point bending. Nanoindentation was performed on the left femurs every 1 μm for 20 μm radially out from 3 mid-shaft lacunae/femur in the endosteal and periosteal directions (figure below). Additionally, lacunae from 10 female non-human primate (NHP) (vervet) femurs, 5 young and 5 old, were used for nanoindentation. Student's t-tests for paired/unpaired samples were conducted ($p<0.05$). All results reported are statistically significant.

The 3-point bending experiments resulted in a modulus in the young bones of 4.68 ± 0.37 GPa and 2.24 ± 0.17 GPa for the old and an ultimate strength of 14.10 ± 0.2 MPa for young and 8.66 ± 0.39 MPa for the old. A difference between young and old perilacunar and non-perilacunar regions were seen in both species. Mice had a perilacunar modulus of 21.5 ± 0.42 GPa for young and 22.1 ± 0.47 GPa for old while NHPs had a perilacunar modulus of 30.6 ± 0.40 GPa for young and 31.3 ± 0.37 GPa for old. The moduli in the endosteal direction were significantly higher than in the periosteal direction.

Overall bone strength deteriorated with age with decreases in both modulus and ultimate force for the whole bone. However, the nanoindentation results revealed that there was actually an increase in modulus surrounding the lacunae in the old bone. By applying these values to a finite element model created for an individual lacuna, we have also shown that the forces imposed on the embedded osteocyte are lower for the older animals than that of the younger. If the osteocytes are not experiencing the same loading signals as they age, they may not be reaching the signaling threshold required to initiate bone remodeling, leading to the deterioration of bone strength and unresponsiveness to exercise with age.

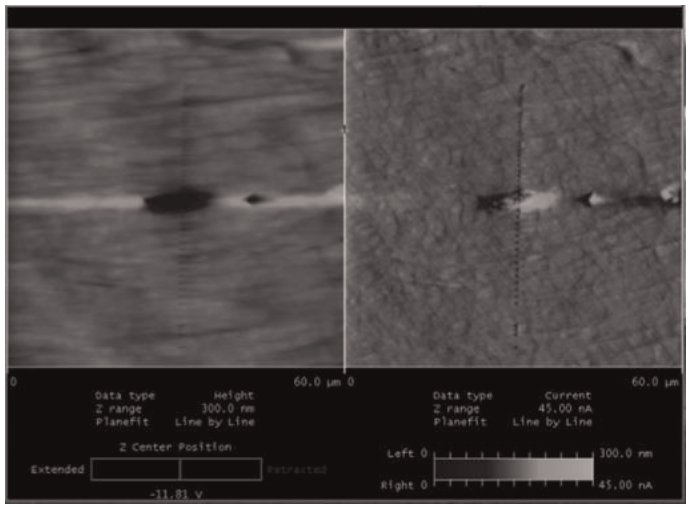

Nanoindentation/AFM of Osteocyte Lacuna

Disclosures: ***Craig Meers****, None.*

MO0277

Feasibility Studies on In Situ Imaging-Based Quantification of the Density of Osteocyte Pericellular Matrix. Xiaohan Lai*, Christopher Price, Liyun Wang. University of Delaware, USA

Osteocytes are believed to detect external mechanical loads through sensing the interstitial fluid flow through their pericellular matrix (PCM), which can be deformed under load-induced fluid flow, like trees bent in wind. The PCM also can modulate the transport of signaling molecules and nutrients in bone. Despite its physiological importance, quantitative study of the PCM *in situ* and *in vivo* is challenging, since the PCM is encased in the mineralized matrix, is extremely thin, is very fragile, and often damaged by histological techniques. Our lab has recently developed an approach combining fluorescence recovery after photobleaching (FRAP) and mathematical modeling to quantify the osteocyte PCM. However, in our previous one-tracer FRAP approach (Wang et al., 2012 JBMR doi: 10.1002/jbmr.1804), velocities of fluid and solute were measured individually in different bone samples, which introduced variability from both anatomical and loading inconsistency. To address these limitations, we propose a novel dual-colored FRAP approach, which allows simultaneous measurements of both fluid and solute velocities.

In this study, the feasibility of dual-colored FRAP in detecting changes in PCM ultrastructure was tested using mathematical simulations. Using a three-compartment model developed previously (*Fig 1, Table 1*), we examined the ratio of transport rates for two differently sized tracers (sodium fluorescein, radius 0.5nm; parvalbumin, radius 1.3nm) under dynamic loading as we parametrically varied the PCM fiber density (0.5% to 50% fiber volume fraction) and the anatomical parameters (lacunar size and spacing and canalicular number) at 50%, 100%, and 200% of mean values obtained in adult B6 tibiae. The tracer diffusivities in the PCM were estimated from their free diffusivities in water using Monte-Carlo simulation (*Fig 2*). Load-induced flow velocities were obtained from a previous tissue-level poroelasticity model.

We found that the transport ratio of larger to smaller probe monotonically decreased with increasing PCM fiber density. The transport ratio was also affected by mechanical loading magnitude and the lacunar spacing, but was insensitive to the lacunar size and canalicular number (*Figs 3, 4*). The results suggest that dual-colored FRAP could be feasible in detecting changes in PCM ultrastructure, which may account for the genetic- and site-specific bone sensitivity to mechanical loading.

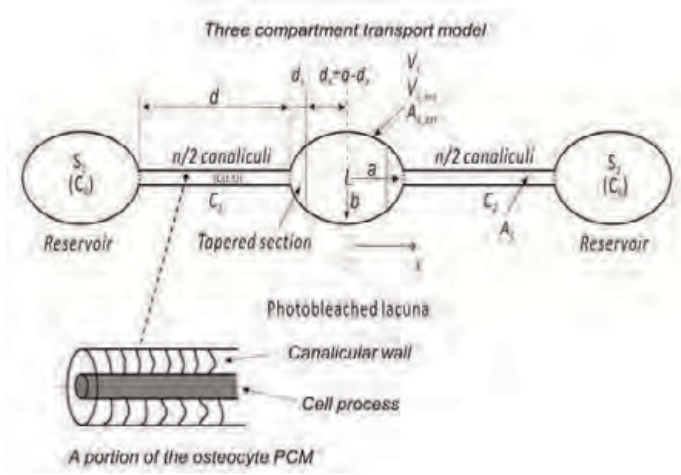

Figure 1. The three-compartment LCS transport model with an enlarged sketch of PCM

Table 1. Parameters used in the LCS transport model

Lacunar major radius *a* (µm)	Lacunar minor radius *b* (µm)	Total Canalicular number	Canalicular length *d* (µm)	Free diffusivity of sodium fluorescein (µm²/s)
6.7	3.9	68	20.06	540
Canalicular wall radius (nm)	**Canalicular cell process radius (nm)**	**Fiber radius r_f (nm)**	**Loading frequency (Hz)**	**Free diffusivity of parvalbumin (µm²/s)**
160	76	2	0.5	197

Table 1. Parameters used in the LCS transport model

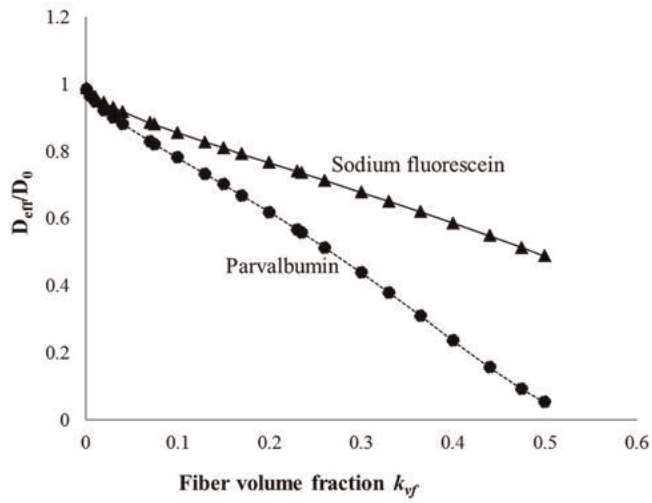

Figure 2: The influence of the PCM fiber volume fraction (kvf) on the change in diffusivity

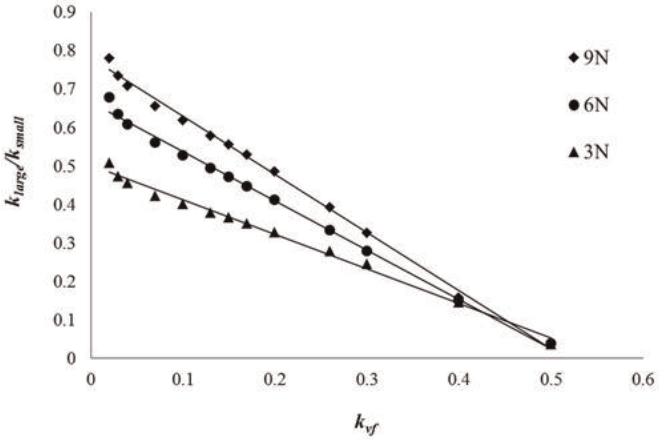

Figure 3: The relationship between transport ratio and fiber volume fraction under different loads

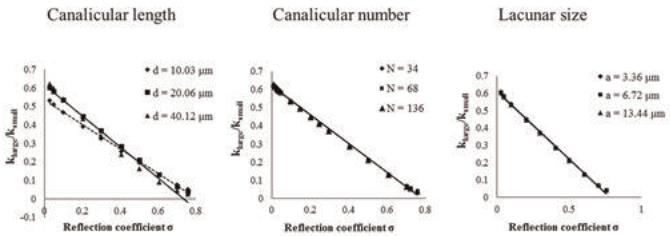

Figure 4: The influence of anatomical parameters on the transport ratio

***Disclosures: Xiaohan Lai**, None.*

MO0278

Sclerostin Directly Abrogates Mechanical Loading-Induced Bone Formation in an Ex Vivo Bovine Bone Model. Masakazu Kogawa*, Kamarul Khalid, Asiri Wijenayaka, David Findlay, Gerald Atkins. University of Adelaide, Australia

Sclerostin is expressed exclusively by mature osteocytes in bone. Our recent findings indicate that sclerostin targets pre-osteocytes/osteocytes to regulate bone mineralization(1), osteoclast activity(2) and also osteocytic osteolysis(3). Sclerostin expression *in vivo* is associated with the osteocyte response to mechanical loading/unloading(4). The aim of this study was to examine the direct effects of sclerostin on loading-induced bone growth *ex vivo*.

Bovine sternum trabecular bone cores were perfused with osteogenic media at 37℃ for up to 3 weeks in individual bone culture chambers. The cores were divided into 3 groups; a) mechanically loaded (300 cycles, 4000 μstrain, 1 Hz/day), b) identical loading regime with continuous perfusion of 50 ng/ml recombinant human sclerostin and c) unloaded controls. Loading was accomplished using a second-generation Zetos bone loading system. Daily measurements of bone stiffness, media pH and ionic calcium concentrations were made. Histomorphometric assessment, including fluorochrome labelling analysis, was made of resin-embedded, non-decalcified samples at the end of the experiment. Gene expression in the bovine bone was examined by real-time RT-PCR.

Bone stiffness increased with daily mechanical loading. This increase in stiffness was blocked by the co-addition of sclerostin. Sclerostin also induced bone acidification and a net release of bone calcium, indicated by the decrease in media pH and the relative increase in ionic calcium concentrations in the presence of sclerostin. Sclerostin also completely abrogated loading-induced calcium/calcein uptake. Sclerostin induced an increase in the expression of the bone resorption genes, tartrate resistant acid phosphatase (TRAP), carbonic anhydrase and cathepsin K. Consistent with osteocyte involvement in this effect, osteocyte lacunar size was significantly increased in SCL-treated loaded bone cores.

Together, this study demonstrates that sclerostin directly antagonizes mechanical loading induced bone growth and is consistent with loading induced reduction of endogenous sclerostin expression being essential for a growth effect.

1. Atkins GJ, et al. 2011 J Bone Miner Res 26(7):1425-1436.
2. Wijenayaka AR, et al. 2011 PLoS One 6(10):e25900.
3. Kogawa M, et al. 2012 J Bone Miner Res 27(Suppl 1) http://www.asbmr.org/Meetings/AnnualMeeting/AbstractDetail.aspx?aid=f2827d72-7a35-40bb-a89e-3666ad97b27f.
4. Robling AG, et al. 2008 J Biol Chem 283(9):5866-5875.

***Disclosures: Masakazu Kogawa**, None.*

MO0279

Dichotomy in osteocyte regulation of anabolic action of mechanical loading challenge and that of bone repletion after a low dietary calcium challenge. Matilda Sheng*[1], Kin-Hing William Lau[2], Xiao-Dong Zhou[1], Denise Rodriguez[1], Adam Finck[1], David Baylink[1]. [1]Loma Linda University, USA, [2]Jerry L. Pettis Memorial VA Medical Center, USA

Skeletal tissue has 2 major skeletal anabolic functions apart from fracture healing: 1) anabolic response to mechanical loading and 2) anabolic repletion of bone after a period of calcium deficiency. Numerous recent publications suggest that osteocytes are pivotal in both mechanisms. Recently we developed mice with conditional knockout (KO) of IGF-I in osteocytes, which showed marked reduction in immunohistochemical staining of IGF-I in osteocytes but not in osteoblasts. These mutant mice displayed an almost complete resistance to the anabolic effects of mechanical loading. Accordingly, a progressive increase in loading strain from 2,000 to 5,000 με on the tibia showed a dose-dependent increase in anabolic endosteal bone formation in the wild-type (WT) animal but no anabolic response in the conditional osteocyte IGF-I KO mice (1.26 ± 0.30 vs. 2.42 ± 0.43 mm^2 x 10^{-3}/day in WT, 1.02 ± 0.30 vs.1.08 ± 0.29 mm^2 x 10^{-3}/day in KO; Fig. 1). We then sought to use this mouse model to test the hypothesis that the regulation of bone formation by mechanical loading and bone repletion after a low calcium dietary challenge is independent of each other. In sharp contrast to mechanical loading response, both WT and KO animals showed an increase in endosteal bone formation ($+40 \pm 2$% of control in WT vs. $+50 \pm 5$% in KO, p=N.S.; Fig. 1) attended by a sharp reduction in osteoclast number (-63 ± 8% of control in WT vs. -56 ± 8% in KO, p=N.S.), at 1 week calcium repletion following 2 weeks of dietary calcium restriction. Consistent with the bone repletion response, dietary calcium restriction also did not cause significant differences in the WT and KO mice, as similar decrements in serum calcium (-9.9 ± 1.5% of control in WT vs. -8.1 ± 1.8% in KO) and similar increments in serum PTH ($+301 \pm 32$% of control in WT vs. $+380 \pm 54$% in KO). There was also no significant difference in the increase in endosteal/trabecular osteoclast number in response to calcium deficiency (+25% in WT vs. +9% in KO, p=N.S.). In conclusion, 1) there is a dichotomy between the mechanisms necessary for anabolic responses to mechanical loading and the regulatory hormonal and anabolic skeletal repletion following low dietary calcium challenge. 2) Osteocyte-derived IGF-I is essential for anabolic bone response to mechanical loading but not for bone repletion after a low calcium challenge.

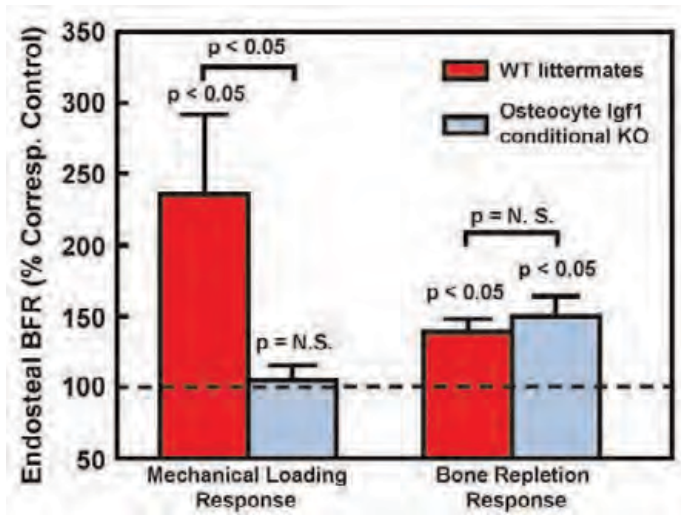

Figure 1

***Disclosures: Matilda Sheng**, None.*

MO0280

Initial Activation of β-catenin Signaling in Osteocytes is Prostaglandin Dependent. Nuria Lara*[1], Mohamed Kamel[1], Behzad Javaheri[2], Mark Johnson[3]. [1]University of Missouri - Kansas City, USA, [2]The Royal Veterinary College, United Kingdom, [3]University of Missouri, Kansas City Dental School, USA

Bone increases its mass in response to mechanical loading. Activation of the Lrp5/Wnt/β-catenin signaling pathway has been shown to be critical for this process. Previously we have shown using the TOPGAL (β-catenin reporter) mouse that after forearm loading there is a rapid activation of the β-catenin signaling pathway in osteocytes and eventually to cells on the bone surfaces. Moreover, we observed that cells activate the Wnt/β-catenin pathway even in the presence of the two well-known Lrp5/6 inhibitors, sclerostin and Dkk1. We have shown that the prostaglandin signaling pathway can crosstalk with β-catenin signaling through Akt mediated inhibition of GSK-3β *in vitro*. In this study we sought to determine if production of prostaglandin is required for the initial activation of β-catenin signaling pathway and

if Akt is a key mediator of this activation. *In vivo* mechanical loading of the forearm was performed on anesthetized TOPGAL mice using compression loading of the right forearm (100 cycles, 2 Hz, 2500 μ?) with the left arm as non-loaded control. Mice were euthanized at 24 hours post loading and activation of the β-catenin signaling was monitored by β-gal staining. Mice were treated with the COX-2 inhibitor Carprofen (5mg/Kg) or vehicle three hours prior to forearm loading. For *in vitro* loading studies, MLO-Y4 cells were subjected to flow fluid shear stress (2 dynes/cm^2) for 2 hours in the presence or absence of Akti (an Akt inhibitor), immunocytochemistry was used to detect β-catenin translocation to the nucleus. Activation of β–catenin signaling in osteocytes reaches a peak at 24 hours and reaches basal levels by 72 hours. At 24 hours post-load the number of β-catenin activated osteocytes increased to 176% of unloaded ulnae in vehicle treated mice, but in Carprofen treated mice there was no increase in the number of activated osteocytes in loaded versus unloaded ulnae ($p<.01$, n=4). In our *in vitro* model of loading, there was an increase in the translocation of β-catenin to the nucleus by 196%, but in the presence of Akti this effect was reduced to static, non-flow treated levels ($p<0.05$, n=3); indicating that β-catenin translocation to the nucleus in response to mechanical loading can be blocked by inhibiting the Akt pathway. These data support our hypothesis that prostaglandins play an important role in the early activation of the β-catenin/Wnt pathway and can activate signaling even in the presence of the Lrp5/6 inhibitors, sclerostin and Dkk1.

***Disclosures: Nuria Lara**, None.*

MO0281

MMP13-mediated osteocyte remodeling during glucocorticoid induced osteonecrosis. Faith Hall-Glenn*, Aaron Fields, Ellen Liebenberg, Jeffery Lotz, Thomas Vail, Tamara Alliston. University of California, San Francisco, USA

The maintenance of subchondral bone is essential for articular cartilage health. Osteonecrosis (ON) is a painful progressive joint disorder in which subchondral bone sclerosis and failure leads to the collapse of the overlying cartilage. Although glucocorticoid (GC) treatment and vascular defects have been implicated in ON, many questions remain about the cellular mechanisms that lead to the deposition of the disorganized, hypermineralized subchondral bone matrix in this disease. Nor is it known how these cellular defects can be reversed to prevent ON progression. We recently found that matrix metalloproteinase-13 (MMP-13) is essential for the ability of osteocytes to maintain cortical bone matrix composition, organization and function through a process called perilacunar remodeling (PLR). MMP-13-deficient bone shows hallmarks of defective PLR including disorganized collagen matrix, hypermineralization, and degeneration of the canalicular network that facilitates osteocyte nourishment, cellular communication and mechanosensation. Based on similarities between bone from MMP-13-deficient mice and human ON femoral heads, we hypothesized that osteocyte mediated PLR remodeling is required for subchondral bone health and is disrupted in ON. To that end, outcomes of PLR were examined in subchondral bone from human ON femoral heads from hip arthroplasties, as well as in an established mouse model of GC-induced ON. MMP-13 and TRAP expression, and canalicular organization were evaluated histologically. Mineralization was assessed by micro-CT and collagen organization by second harmonic generation microscopy. MMP-13 mRNA expression was evaluated in mouse tibiae and in murine osteocyte-like (MLO-Y4) cells treated with GC for 24 hours. Each outcome measure showed that PLR was disrupted in subchondral bone of ON human femoral heads, with hypermineralization, collagen disorganization, degenerated canaliculi, and abnormal MMP-13 expression. Similar defects were apparent in bone from GC-treated mice relative to control littermates. GC repressed MMP-13 RNA and protein expression in mice and in MLO-Y4 cells. These studies suggest that osteocyte-mediated PLR is deregulated in ON, and further, that this deregulation may result from GC-mediated repression of the essential PLR enzyme MMP-13. Elucidation of the role of PLR in ON may reveal novel ON therapeutic targets.

***Disclosures: Faith Hall-Glenn**, None.*

MO0282

Strontium Ranelate accelerates MLOY4 osteocyte lineage wound healing. Hechmi Toumi[1], Priscilla Aveline[2], Chloé Leduc[3], Eric Lespessailles*[4], Chantal Pichon[3], Claude Laurent Benhamou[5]. [1]EA 4708 I3MTO, France, [2]Centre Hospitalier Régional D'Orléans, France, [3]CBM Orléans, CNRS UPR4301, France, [4]Centre Hospitalier Regional, France, [5]CHR ORLEANS, France

Since pre-osteocyte wound healing may play an indirect but important role in bone fracture or microcrack repair. We have recently settled a wound healing experiment on in vitro cell culture. This experiment permits subsequent study of cell proliferation and migration during the healing process. Strontium Ranelate (SrRan) is known to act on the bone forming lineage. Purpose: The aim of the present study was to investigate the wound healing process on MLOY4 cell culture with or without SrRan.Method: Osteocyte woung healing was analysed by a MLOY4 cell culture in 24-well plates each containing inserts (Wound healing assay kit, Cell Biolabs). Cells were incubated 3 days with or without SrRan (0, 0.1, 1 and 5mM) before removing insert to generate a wound field. 2 pictures per well were taken every hour during 72h. Changes in cells density between T0h and T48h were avaluated by counting the number of cells per well.Results: MLOY4 cells were multiplied by 5.7 and 4.8 at T48h compared to T0h respectively for 0 and 0.1mM groups and by 3.4 for both 1 and 5mM groups. Concerning MLOY4 culture healing, all wound fields with SrRan were closed at T35h after baseline. While, the control group (0mM) was not completely haeled at T35h nor at T48h. The healing kinetics showed a dose effect of SrRan.Conclusions: SrRan has a positive dose dependent effect on wound healing and negative dose response on cell density in MLOY4 cell cultures. Whether this effect is related to proliferation or migration (or change in their balance) remains to be evaluated.

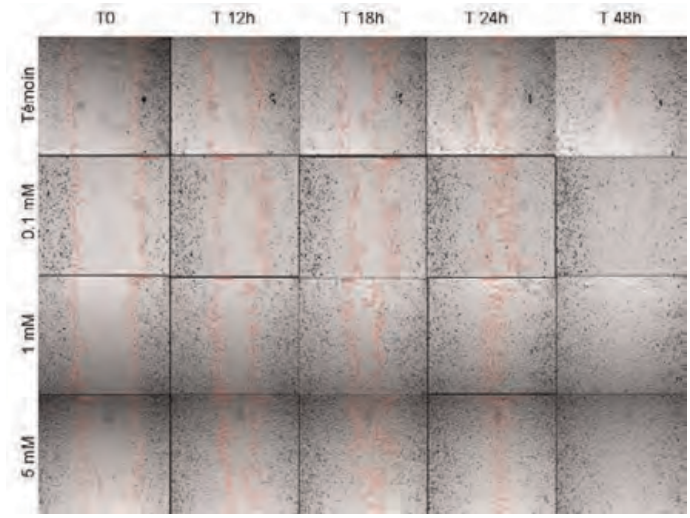

Figure

***Disclosures: Eric Lespessailles**, None.*
This study received funding from: Laboratoires Servier

MO0283

Deletion of Cx43 in osteocytic cells increases autophagy: a potential mechanism for accumulation of empty lacunae in mice lacking Cx43 in osteoblastic cells. Rafael Pacheco Da Costa[1], Iraj Hassan*[2], Wonjin Kim[3], Rejane D Reginato[4], Teresita Bellido[5], Lilian Plotkin[5]. [1]Indiana University/Universidade Federal de Sao Paulo - Brazil, Brazil, [2]Dept. Anatomy & Cell Biology, USA, [3]College of medicine, Yonsei university, South Korea, [4]Department of Morphology & Genetics, Federal University of São Paulo, Brazil, [5]Indiana University School of Medicine, USA

Mice lacking connexin (Cx) 43 in osteoblasts/osteocytes or only in osteocytes exhibit high prevalence of osteocyte apoptosis and accumulation of empty lacunae, features that resemble the consequences of aging in bone from rodents and humans. Empty lacunae accumulation in Cx43 deficient mice contrasts with other models of increased osteocyte apoptosis, i.e. sex steroid deficiency or glucocorticoid excess in which lacunae remain occupied by the apoptotic osteocytes. We hypothesized that osteocyte disappearance from their lacunae in Cx43 deficient mice is due to elevated autophagy, a catabolic mechanism that involves degradation of cellular components and can be associated with apoptosis. To test this hypothesis, we used MLO-Y4 osteocytic cells in which Cx43 expression was silenced by shRNA [Cx43(-) cells]. Cultured Cx43(-) MLO-Y4 cells exhibit spontaneous loss of viability, demonstrating that apoptosis is a cell autonomous outcome of Cx43 deletion. In addition, Cx43 shRNA lead to 3-fold higher expression of p62/SQSTM1, a mediator of autophagy, compared to scramble-shRNA transfected cells. Further, the percentage of cells with LC3 in the autophagic compartment (a marker of autophagy visualized by punctuated LC3-GFP expression) was 2-fold higher in Cx43(-) MLO-Y4 cells compared to scramble-transfected cells. Conversely, the percentage of Cx43-naïve HeLa cells exhibiting punctuated LC3-GFP is reduced by Cx43 transfection. In addition, autophagy is increased in scramble- and Cx43-silenced MLO-Y4 cells treated with 30nM rapamycin, 0.1μM dexamethasone, or serum-starved, all known to increase cellular autophagy. Since autophagy can increase or decrease cell death depending on the cell type and intensity of the proautophagy stimuli, we tested whether rapamycin, a specific autophagy inducer, affected apoptosis of MLO-Y4 osteocytic cells. Rapamycin further increases the already elevated levels of apoptosis in Cx43(-) MLO-Y4 cells, whereas it did not affect scramble-shRNA cells. Our results demonstrate that Cx43 deficiency increases osteocyte autophagy and that autophagy exacerbates osteocytic cell death. We conclude that accumulation of empty lacunae in bones from Cx43-deficient mice might result from concomitant increases in osteocyte apoptosis and autophagy. Because Cx43 expression is reduced in bones from old mice, these findings raise the possibility that Cx43 deficiency could contribute to accumulation of empty lacunae and increased fragility with skeletal aging.

***Disclosures: Iraj Hassan**, None.*

MO0284

Kalirin: Novel Role in Osteocyte Function and Bone Cell Signaling. Kornchanok Wayakanon*, Pierre Eleniste, Su Huang, Matthew Allen, Angela Bruzzaniti. Indiana University School of Dentistry, USA

Communication between bone cells is important for the maintenance of bone mass. Although osteocytes are embedded within the mineralized matrix, they play an essential role in the regulation of osteoblast and osteoclast (OC) function. However, the intracellular proteins that control the morphology and function of osteocytes, and their ability to communicate with other bone cells are still unknown. Kalirin is a novel GTP exchange factor (GEF) protein that activates Rac1 and RhoA. Recently, micro-CT analysis of 14 week old female Kalirin knockout (Kal-KO) mice revealed a 45% decrease in trabecular bone density, as well as significantly lower cortical area, perimeter, thickness and polar cross-sectional moment of inertia (-12.6%, -7.2%, -7.6% and -21.9%, respectively, $p<0.05$), compared to WT mice. Moreover, we found a 42% increase in TRAP-stained OCs/bone surface in femoral trabecular bone *in vivo*, as well as increased OC differentiation with RANKL and MCSF *in vitro*. However, the function of Kalirin and its mechanisms of action in bone cells are still unclear. In this study we examined the role of Kalirin on the morphology and function of osteocytes. Primary osteocytes were isolated by sequential collagenase digestions from long bones (femurs and tibias) of 10-week old female WT and Kal-KO mice. Quantitative real-time PCR demonstrated that the expression RANKL mRNA, which is important for OC differentiation, was increased 5.4 ± 3.0 fold in Kal-KO mice compared with WT mice ($p<0.05$), whereas the expression of OPG was unchanged. In contrast, the expression of SOST, which is important for controlling Wnt signaling and bone formation by osteoblasts, was decreased (0.6 ± 0.2 fold, $p<0.05$) in Kal-KO mice. Microscopic analysis of primary osteocytes isolated from long bones of Kal-KO and WT mice revealed 50% fewer cytoplasmic processes ($n=100$ cells, $p<0.01$) in Kal-KO osteocytes, compared with WT cells. Moreover, using the osteocytic cell line MLO-Y4, we demonstrated that activation of Rac1-GTP and RhoA-GTP, which are substrates of Kalirin, led to an increase in the length of osteocyte cytoplasmic processes. Together, these results suggest that Kalirin may control osteocyte function and signaling to OCs by regulating RANKL secretion, leading to an increase in osteoclastogenesis. Kalirin deficient osteocytes may also alter the balance of bone formation via the Wnt signaling pathway in osteoblasts.

***Disclosures: Kornchanok Wayakanon**, None.*

MO0285

Sclerostin Exerts a Coordinated Pro-osteoclastogenic Effect via its Action in Osteocytes. Asiri Wijenayaka*[1], Masakazu Kogawa[1], Lynda Bonewald[2], David Findlay[1], Gerald Atkins[1]. [1]University of Adelaide, Australia, [2]University of Missouri - Kansas City, USA

Sclerostin (SCL) is a product of mature osteocytes and a potent negative regulator of bone formation.(1) Our recent study showed that SCL affects osteoblasts in an anti-anabolic manner.(2) However, studies employing a neutralising antibody against SCL have reported decreased bone resorption markers,(3) indicating that SCL may also have a catabolic action. In recent studies, osteocyte expression of RANKL has been shown to be critical for osteoclastic remodelling of bone.(4) We have reported that SCL stimulated RANKL expression in human bone, in human primary osteocyte-like cultures and in MLO-Y4 cells. SCL stimulated osteoclast activity in a dose-dependent manner in co-cultures of MLO-Y4 cells and osteoclast precursors.(5) The aim of the current study was to further examine the pro-osteoclastogenic effect of SCL in this latter model.

To examine the individual contributions of osteocytes and osteoclast precursors, MLO-Y4 cells were co-cultured with human peripheral blood mononuclear cells (PBMC) in the absence or presence of human recombinant sclerostin (rhSCL). We used species-specific PCR primers to amplify osteocyte or osteoclast-derived markers. Human bone samples were obtained from patients undergoing hip arthroplasty and cultured in the absence or presence of rhSCL; total RNA was extracted and histology conducted to study the effects of rhSCL on human bone. Since SCL has shown to bind to three known low density lipoprotein receptor-related protein (LRP) receptors, we also performed siRNA knockdown of *Lrp4*, *Lrp5*, and *Lrp6* respectively in MLO-Y4 cells to elucidate which receptor or receptors were important for the pro-osteoclastogenic effect.

Interestingly, rhSCL was capable of inducing mRNA levels of a number of pro-osteoclastogenic mediators, such as *Rankl, Csf1* and *Il6* in MLO-Y4 cells in co-cultures. In the osteoclast fraction *CA2, ACP5* (TRAP) and *CATK* mRNA increased with rhSCL treatment. Human bone treated with rhSCL also had increased expression of *RANKL* and *CSF1* mRNA. siRNA knockdown studies indicated that all of LRP4, LRP5 and LRP6 receptors were required for the pro-osteoclastogenic response to SCL in MLO-Y4 cells. Together, these findings suggest that sclerostin exerts a coordinated pro-osteoclastogenic effect via its action on the osteocyte, in a manner consistent with inhibition of Wnt signalling.

1. Li X, et al. 2009 J Bone Miner Res 24:578-588.
2. Atkins GJ, et al. 2011 J Bone Miner Res 26:1425-1436.
3. Padhi D, et al. 2010 J Bone Miner Res 26:19-26.
4. Nakashima T, et al. 2011 Nat Med 17:1231-1234.
5. Wijenayaka AR, et al. 2011 PLoS One 6:e25900.

***Disclosures: Asiri Wijenayaka**, None.*

MO0286

Tartrate-Resistant Acid Phosphatase (TRAP) Co-localize with Receptor Activator of NF-κ Ligand (RANKL) in Osteoblasts and Osteocytes: a Potential Role for TRAP in Regulation of Osteoclast Differentiation. Lene Solberg*[1], Espen Stang[1], Sverre-Henning Brorson[1], Goran Andersson[2], Finn Reinholt[3]. [1]University of Oslo & Oslo University Hospital, Norway, [2]Karolinska Institute, Sweden, [3]University of Oslo, Norway

TRAP is a well known osteoclast marker with several biological abilities in bone; i.e., dephosphorylation of osteopontin, bone sialoprotein and osteonectin as well as dephosphorylation of Man-6-P recognition marker on lysosomal proteins and bone matrix degradation via generation of reactive oxygen species. In addition to osteoclasts, osteoblasts and osteocytes in discrete bone areas show TRAP protein expression and enzyme activity. The origin and function of TRAP in these cells are debated however; demonstration of TRAP mRNA implies some endogenous production. The most prominent hypothesis has been that osteoclasts initiate TRAP expression in osteoblasts and osteocytes. Alternatively, it has been suggested that osteoblast-like cells engulf osteoclastic TRAP for inactivation. Recent data indicate that TRAP is involved in osteocytic osteolysis under specific metabolic conditions, e.g. lactation. TRAP+ vesicles have been observed in osteoblasts *in vivo* indicating that TRAP could either be excreted from the cell, involved in lysosomal processes or internalized from the matrix. In order to explore the function of TRAP in osteoblasts and osteocytes, we used long bones from 3 days old rats. Undecalcified sections from tibia metaphysis and diaphysis were subjected to immunogold labeling and immunofluorescence. Transmission electron microscopy demonstrated TRAP in osteoblasts and osteocytes in electron dense vesicles (200-500nm). LAMP1 was observed in the vesicle membrane (A) indicating that the TRAP+ vesicles may be late endosomes, degradative lysosomes or secretory lysosomes. TRAP and RANKL were found co-localized in the vesicles in both osteoblasts and osteocytes; confocal fluorescence microscopy demonstrated co-localization of TRAP and RANKL in osteocytes (B). Our results do not support the notion that the TRAP+ vesicles represent late endosomes since RANKL is produced for secretion by osteoblasts and osteocytes. Recent studies have demonstrated that the majority of RANKL in osteoblasts and osteocytes is sorted to secretory lysosomes with stimulation dependent release to the cell surface. We propose that the TRAP+ vesicles observed in osteoblasts and osteocytes *in vivo* may either represent lysosomes involving TRAP in intracellular degradation of RANKL, or secretory lysosomes suggesting a regulatory role for TRAP in the secretion of RANKL or in the early stage of osteoclast differentiation and activation.

Keywords: TRAP, RANKL, Osteoblast, Osteocyte, Rat

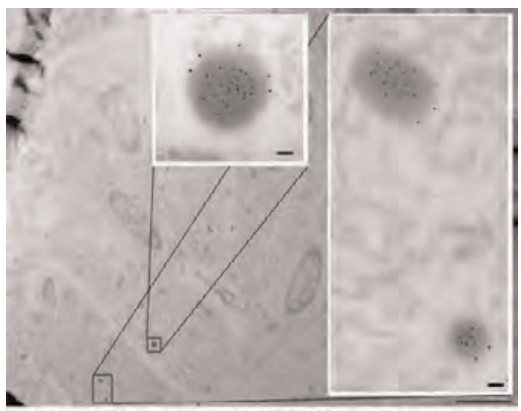

A) TRAP (10nm gold) and LAMP1 (15nm gold) in vesicles in metaphyseal osteoblasts (scalebars 5μm, 100nm)

A

B) TRAP and RANKL co-localize in diaphyseal osteocytes (yellow)

B

***Disclosures: Lene Solberg**, None.*

MO0287

The "unfolded protein response" stimulates RANKL production: a potential mechanistic link between osteocyte apoptosis and cortical porosity. Robert Jilka*, Kanan Vyas, Michela Palmieri, Yu Liu, Charles O'Brien, Stavros Manolagas. Central Arkansas VA Healthcare System, Univ of Arkansas for Medical Sciences, USA

Cortical bone porosity increases with advancing age in humans and mice, but the underlying molecular and cellular mechanisms are unknown. Earlier work in rodents indicated that osteocyte apoptosis is associated with increased RANKL synthesis by neighboring osteocytes, induction of intracortical remodeling, and the development of cortical porosity, raising the possibility that the same intracellular signaling pathways involved in regulation of osteocyte apoptosis may modulate the expression of RANKL. To elucidate a mechanistic link between osteocyte apoptosis and RANKL production, we have investigated the role of the unfolded protein response (UPR) to endoplasmic reticulum (ER) stress, a mechanism by which cells adapt to a variety of toxic conditions including oxidative stress and hypoxia. The UPR increases synthesis of proteins that reduce ER stress and thereby prevents apoptosis. If stress is not alleviated, the UPR stimulates the production of pro-inflammatory cytokines and activates pro-apoptotic pathways. We report that the ER stress-inducing agent tunicamycin increased UPR transcripts such as Xbp-1s within 4 h in cultures of osteoblastic/osteocytic cells obtained from neonatal murine calvaria. These changes were associated with increased expression of RANKL, the pro-apoptotic transcription factor CHOP, and induction of apoptosis as measured by caspase-3 activation. Tunicamycin, as well as hypoxia, also activated the UPR and stimulated the expression of TNF and RANKL in neonatal calvaria organ cultures. OPG expression was unaffected. Treatment of calvaria with tunicamycin for 4 hours per day for 4 days increased osteoclastogenesis as indicated by cathepsin K expression and secretion of TRAPase, and stimulated bone resorption as evidenced by release of calcium into the culture medium. Moreover, a single injection of tunicamycin to 3-mo-old female C57BL/6 mice increased expression of UPR transcripts and RANKL in osteocyte-enriched femoral bone, and increased the number of osteoclasts within 7 days. Based on these findings, we propose that an increase in the intensity and/or duration of the UPR in osteocytes with advancing age may contribute to the development of cortical bone porosity by stimulating the production of pro-inflammatory cytokines like TNF, leading to the local synthesis of RANKL.

***Disclosures: Robert Jilka**, None.*

MO0288

A Single PTH Administration Induces Bone Mineral Dissolution around Capillary Vessels Entrances at the Endosteal Surface. Nobuhito Nango*[1], Shogo Kubota[1], Wataru Yashiro[2], Atsushi Momose[2]. [1]Ratoc System Engineering Co., Ltd., Japan, [2]Institute of Multidisciplinary Research for Advanced Materials, Tohoku University, Japan

Parathyroid hormone (PTH) is known to promote bone resorption, and to increase Ca2+ concentration in blood when continuously administered. On the other hand, intermittent administration of PTH promotes bone formation and is used to treat osteoporosis. However, its mechanism of action remains unclear. Using synchrotron X-ray microscope, we previously reported that osteocytes dissolve bone mineral through their canaliculi. In this report, we examined the impact of a single PTH administration that might dissolve mineral through osteocytes and canaliculi. Sixty seven wild-type male mice were divided into the control (placebo) groups and PTH-treated groups. PTH dosage was 160μg/kg. The tibial bone specimens were isolated at 0, 6, 9, and 12 hours after placebo or PTH treatment. Each group was represented by 3 ~ 8 mice. Bone mineral density (BMD) and three dimentional bone morphometry of proximal tibia were measured using μCT. Hydroxyapatite calibration phantom was also scanned. Furthermore, synchrotron multi-scan X-ray microscope was built at SPring-8, and the BMD around osteocytes and osteocytic canaliculi were quantified. The figure shows a cross section of μCT images of mouse tibia. The image contrast represents the mineral density. Left shows the endosteal surface of tibia before PTH administration, and Right shows 6 hours after administration. Capillary vessels of the mouse before administration were not much outstanding, whereas these of the mouse 6H after PTH treatment stand out as many black dots (arrow heads) on the endosteal surface. These are capillary vessels appearing to bone marrow from the endosteal side. The contrast indicates that the BMD around capillary vessels was decreased at the endosteal space to marrow. Compared with before administration, trabecular bone BMD significantly decreased 2% after 6 hours, recovered after 9 to 12 hours. BV/TV tended to decreased 10~15% by 6 to 12 hours. As we reported at the last ASBMR meeting, osteocytes dissolve mineral through canaliculi. On the other hand, osteocytes are connected with the capillary vessels in bone through canaliculi. The phenomenon of bone mineral dissolution around capillary vessels at the endosteal surface after single PTH treatment indicates that bone mineral dissolution by the osteocyte is related to the action of PTH. We will report the action of PTH and involvement of osteocyte and canaliculi in this phenominon.

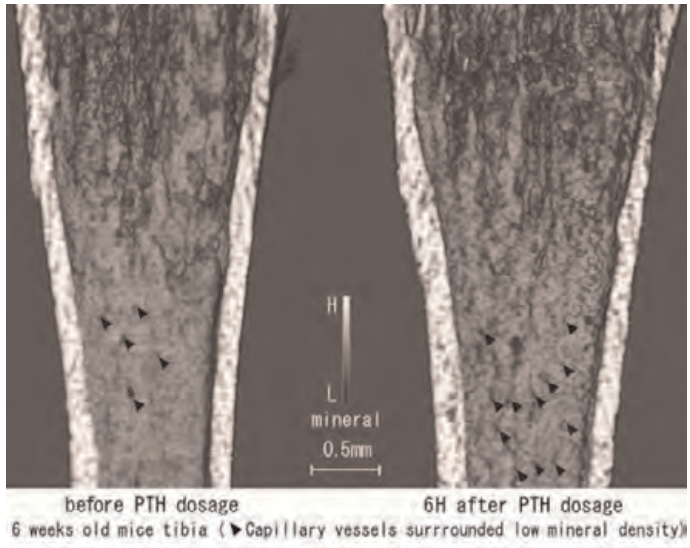

A Single PTH Administration Induces Bone Mineral Dissolution around Capillary Vessels

***Disclosures: Nobuhito Nango**, None.*

MO0289

Circulating Periostin: a novel serum marker of cortical bone structure in human. Nicolas Bonnet*[1], Claire Durosier[2], Patrick Garnero[3], Serge Ferrari[4], Rene Rizzoli[4]. [1]University Geneva Hospital-Department of Internal Medecine Specialities, Switzerland, [2]Division of Bone Diseases, Geneva University Hospital & Faculty of Medicine, Switzerland, [3]INSERM Research Unit, France, [4]Geneva University Hospital & Faculty of Medicine, Switzerland

Periostin is a matricellular protein, which is mainly expressed by periosteal cells and osteocytes in bone. Periostin down-regulates Sost gene expression and is necessary for the cortical bone response to loading and to PTH treatment. We previously reported that circulating periostin levels (cPostn) correlate with periosteal bone formation and cortical thickness (CtTh) independently of bone turnover in mice treated with PTH. In the present study, we investigated the relationship between cPostn and cortical structure in human healthy subjects.

We measured cPostn, bone turnover markers, aBMD by DXA, bone trabecular (Tb) and cortical (Ct) parameters at the distal radius and tibia by HRpQCT (XtremeCT) in 242 healthy women and 59 men, aged 64.9±1.4SD years. To test the association between cPostn and bone parameters, we divided the subjects into 3 tertiles of cPostn (low: 1277±148, medium: 1636±94, high: 2140±311 ng/ml), and applied an ANOVA and ANCOVA with adjustment for gender. Multiple regressions were used to assess the relation between cPostn, bone mineral mass, microstructure and turnover markers.

Mean cPostn was 1633±410 ng/ml (min. 814, max 3490 ng/ml). cPostn was higher in men than women (+8.6%, $p<0.01$), whereas P1NP and CTX were lower in men than women (-20% and -21%, $p<0.01$). Distal radius total bone area, cortical area (Ct.area) and perimeter were higher in the highest vs lowest cPostn tertile (+6.4%, +7.7% and +3.8%, $p<0.05$; p=0.12-0.34 after adjustment for gender). BV/TV was higher in the highest tertile (+12.4% vs low tertile, $p<0.01$) and disappeared after sex-adjustment. cPostn positively correlated with Ct.area and Ct. perimeter of distal radius (r=0.12, $p<0.05$, both) and tibia (r=0.15, $p<0.05$, both). These correlations remained significant after adjusting for P1NP, CTX or whole body bone mineral mass, but not for gender. There was no difference in whole body bone mineral mass, spine and proximal femur aBMD, PTH, P1NP and CTX between cPostn tertiles. Separate analyses per tertile in men and women indicated similar, but non-significant trends. cPostn was associated with PTH levels, but only in the subgroup of subjects with higher PTH levels (>6.3pM, $r^2=0.09$, $p<0.01$).These results recorded in a homogeneous population of healthy 65-year old subjects indicate a positive correlation of cPostn with cortical bone structure, independently of bone turnover markers as previously observed in mice, but likely through a sex-dependent effect.

***Disclosures: Nicolas Bonnet**, None.*

MO0290

Vitamin D Status in Obesity: Evaluation of Free 25(OH)D. Amy Evans*[1], Fatma Gossiel[1], Kim Naylor[2], Jennifer Walsh[3], Richard Eastell[3]. [1]Academic Unit of Bone Metabolism, University of Sheffield, United Kingdom, [2]The University of Sheffield, GBR, [3]University of Sheffield, United Kingdom

Obese individuals have lower circulating 25(OH)D levels than normal weight individuals. The binding proteins vitamin D binding protein (DBP) and albumin are important determinants of vitamin D action, namely free 25(OH)D. Parathyroid hormone (PTH) is increased in response to 25(OH)D deficiency. We aimed to investigate total and free 25(OH)D, DBP and PTH levels in obese individuals.

In September 2012, fasting serum samples were obtained from 99 men and women aged 55 to 75 years. 54 individuals (48% women, 52% men) were obese (BMI ⩾30 kg/m^2) and 45 (49% women, 51% men) were lean (BMI 18.5-24.9 kg/m^2). Total 25(OH)D was measured by automated immunoassay (Cobas e411, Roche Diagnostics). Free 25(OH)D index was determined using the equation (Free 25OHD = total 25OHD/1+ (6*103 *albumin) + (7*108*DBP)) (Powe et al). PTH was measured by automated immunoassay (IDS-iSYS), albumin by automated immunoassay (Cobas c311, Roche Diagnotics) and DBP by immunoassay (R&D Systems). Standard deviation scores were calculated by standardising the mean difference between lean and obese groups against the standard deviation of the lean group. Independent samples t-tests were used to determine significant differences ($p<0.05$) between lean and obese groups.

Total 25(OH)D was lower in obesity (mean difference (95% CI) -0.47 (-1.05 to 0.11) SD scores in men, -0.71 (-1.40 to -0.02) in women)). There was no significant difference in free 25OHD index between groups. No difference in DBP was observed in obesity (mean difference (95% CI) -0.33 SD scores (-0.98 to 0.32) in men, -0.28 (-0.93 to 0.37) in women). Albumin was significantly lower in obese women (mean difference (95% CI) -0.91 (-1.71 to 0.10) SD scores) but not in obese men (mean difference (95% CI) -0.41 (-0.97 to 0.15) SD scores). No differences in PTH were observed between the groups.

25(OH)D levels are low in obesity and yet there is no increase in PTH. This is most likely because free 25(OH)D is not low and this is because serum albumin, a binding protein for 25(OH)D, is low in obesity.

		Mean (SD) Lean	Mean (SD) Obese	Standardised Difference
Total25(OH)D, nmol/L	Men	71.24 (27.75)	52.53 (19.85)	-0.469**
	Women	68.20 (29.07)	51.36 (29.24)	-0.712**
DBP, µmol/L	Men	2.50 (0.63)	2.21 (0.74)	-0.329
	Women	2.59 (0.86)	2.31 (0.67)	-0.282
Free 25(OH)D index, nmol/L	Men	0.0043 (0.0017)	0.0036 (0.0014)	-0.229
	Women	0.0040 (0.0015)	0.0042 (0.0043)	0.115
Albumin, g/L	Men	50.21 (2.68)	49.28(2.04)	-0.409
	Women	49.64 (2.09)	47.88 (2.97)	-0.909*
PTH, ng/L	Men	69.26 (42.30)	56.72 (27.25)	-0.324
	Women	72.54 (57.71)	70.67 (46.22)	0.227
				[*p<0.05, **p<0.01, ***, p<0.001]

Mean (SD) and Standardised Difference Values

***Disclosures: Amy Evans**, None.*
This study received funding from: Department of Health, England

MO0291

A Comparison of Two Methods for Analyzing Change in Trabecular BMD from QCT Spine Scans over 2 Years of Treatment. Dennis Black*, Lucy Wu, Lisa Palermo. University of California, San Francisco, USA

Background: Unlike DXA BMD, QCT of the spine and hip can provide separate assessments of trabecular and cortical bone density and structure. Therefore, QCT of bone is frequently used in clinical trials of medications in order to gain insight into mechanisms of action for new treatments. There are several different programs available for analysis of QCT spine and hip scans but they have not been compared with respect to changes seen in treatment.

Methods: We used spine QCT scans from the PTH and alendronate (PaTH) trial which compared 4 different combinations of PTH(1-84) and alendronate over two years (1). A total of 187 women had QCT scans obtained at baseline and during follow-up. For this analysis, we used the 2 year follow-up scans only. The original analysis of QCT was done using software developed at UCSF (2). For this re-analysis, the scans were analyzed using Mindways software (Austin, Tx). Results from Mindways analyses were compared to those from the original analysis.

Results: For trabecular BMD at the spine, there was a strong correlation between the original measurements and the reanalyzed values at baseline ($r=0.92$, $p<.0001$). Similarly, 2 year % change was strongly correlated by the two methods ($r=0.89$, $p<.0001$). Within treatment groups, the estimates of % change were generally similar when the different methods were used (see table). While the statistical significance of the differences across treatment were similar for the two methods, the mean % differences across treatments varied somewhat.

Conclusions: Analysis of QCT spine scans in treatment studies should yield similar treatment effects, regardless of which of these two programs are used. However, small differences suggest caution should be used in comparing mean % change across trials when different methods for QCT analysis at the spine have been used.

References
1. Black DM, Rosen CJ, et al. 2004 J Bone Miner Res 19:S26
2. Lang TF, Li J, Harris ST, et al. 1999 J Com Assist Tomogr 23:130-137

Table: Comparison Mean % Change of Trabecular Spine BMD by Original and Reanalysis (Mindways) of PaTH QCT scans (2 year changes by treatment)

	Treatment in Year 1 (Y1) and Year 2 (Y2)			
	Y1: PTH; Y2: PLB	Y1: PTH; Y2: ALN	Y1: PTH/ALN; Y2: ALN	Y1: ALN; Y2: ALN
N	46	48	45	48
Original Analysis (Lang method)	13%	34%	11%	8%
Reanalysis (Mindways)	16%	30%	11%	7%

Table

***Disclosures: Dennis Black**, None.*
This study received funding from: Mindways reanalysis: Merck

MO0292

Agreement of Distal Femur Bone Mineral Estimates From Two Different Procedures in Adults with Spinal Cord Injury. Michael Porter*[1], Therese Johnston[2], Ralph Marino[3], Christopher Modlesky[4]. [1]Department of Kinesiology & Applied Physiology, University of Delaware, USA, [2]Department of Physical Therapy, Thomas Jefferson University, USA, [3]Department of Rehabilitation Medicine, Thomas Jefferson University, USA, [4]University of Delaware, USA

Conditions that result in loss of ambulatory status, such as spinal cord injury, are associated with low bone loss and a high rate of fracture in the lower extremities, especially the distal femur. Different procedures for assessing areal bone mineral density (aBMD) in the distal femur using dual-energy X-ray absorptiometry (DXA) have been proposed. The aim of this study was to assess the agreement in aBMD, bone mineral content (BMC) and bone area between two different DXA procedures in individuals with complete spinal cord injury. A second aim was to assess the validity of the aBMD measurements using magnetic resonance imaging as a comparison. Sixteen adults with complete spinal cord injury and were recruited for the study. aBMD, BMC and bone area in the distal femur were determined using DXA (Delphi C; Hologic Inc) and two different procedures on the same day during the same test session. Procedure 1 involved the spine protocol with the participants lying in the supine position. Procedure 2 involved the forearm protocol with the participants lying in on their side. Apparent bone volume to total volume (appBV/TV) of the distal femur was determined using magnetic resonance imaging (MRI; 1.5 T, GE) at the same site as evaluated using DXA. There were moderate-to-strong relationships between aBMD ($r = 0.85$), BMC ($r = 0.81$) and bone area ($r = 0.72$) from procedure 1 vs. procedure 2 (all $p < 0.01$). However, aBMD was 15 % lower, BMC was 39 % higher and bone area was 64 % higher using procedure 1 vs. procedure 2 (all $p < 0.001$). Furthermore, aBMD determined using procedure 1 vs. procedure 2 was not as strongly related to appBV/TV from MRI ($r = 0.72$, $p = 0.002$ vs. 0.85, $p < 0.001$, respectively). The findings suggest that bone measurements from DXA are strongly dictated by the procedure used to collect the data. The procedure using the forearm protocol with participants lying on their side vs. the procedure using the spine protocol and participants lying supine may provide better estimates of bone mineral.

***Disclosures: Michael Porter**, None.*

MO0293

Assessing Age, Sex, and Racial Differences in Cortical Porosity Requires Adjustment for Site-Specific Variation in the Selected Region of Interest. Ali Ghasem-Zadeh*[1], Roger Zebaze[1], Ashild Bjornerem[2], Xiao-Fang Wang[3], Yohann Bala[4], Ego Seeman[1]. [1]Austin Health, University of Melbourne, Australia, [2]University of Tromsø, Norway, [3]University of Melbourne, Austin Health, Australia, [4]University of Melbourne, Dept. of Medicine, Australia

High-resolution peripheral quantitative computed tomography (HR-pQCT) measures micro-architecture in a region of interest (ROI) at the distal radius and tibia. Bone width and micro-architecture vary slice by slice along the length of a bone so differences in micro-architecture by age, pubertal stage, sex and racial group may be the result of differences in the placement of the ROI rather than the characteristics of the subjects. To assess the slice-by-slice variation in cortical porosity we used images of the distal tibia, fibula and radius acquired by HR-pQCT and assessed cortical porosity using Strax 1.0 software in 69 women aged 40 to 61 years. The mean (SD) cortical porosity at the distal tibia, fibula and radius were 57.6% (5.4), 38.1% (7.3) and 46.9% (6.2).Each 1 mm (12 slices) more distal ROI increased porosity as shown: Tibia Fibula Radius

Mean ±SE Mean ±SE Mean ±SE Total 1.22%±0.06 0.89%±0.06 2.43%±0.09
Compact cortex 1.27%±0.06 0.68%±0.09 2.01%±0.08
Outer transitional zone 0.67%±0.11 0.51%±0.12 1.25%±0.08
Inner transitional zone 0.16%±0.05 0.58%±0.10 0.34%±0.05

We infer that a more distal ROI has a significant effect on cortical porosity which may result in erroneous age, sex and racial differences being reported. This variation needs to be considered when interpreting data in persons who differ in bone length.

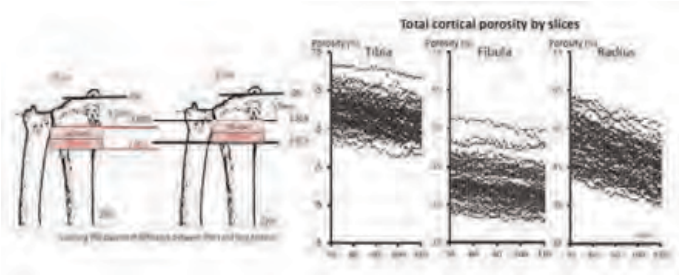

Figure

***Disclosures: Ali Ghasem-Zadeh**, None.*

MO0294

Associations between Birth Weight and Bone Microarchitecture in the Radius and Tibia of Older Adults from the Hertfordshire Cohort Study. Mark Edwards*[1], Kate Ward[2], Camille Parsons[1], Jennifer Thompson[2], Ann Prentice[2], Elaine Dennison[1], Cyrus Cooper[1]. [1]MRC Lifecourse Epidemiology Unit, University of Southampton, United Kingdom, [2]MRC Human Nutrition Research, United Kingdom

Evidence is accruing that environmental factors in early life have a critical influence on the magnitude of peak bone mass achieved, and on later risk of fracture. To date, no studies have investigated the relationship between birth weight and bone microarchitecture in human populations. High resolution peripheral quantitative computed tomography (HRpQCT) scanners permit the non-invasive assessment of cortical and trabecular structure; we used HRpQCT to investigate the relationship between birth weight and bone macro- and micro- architecture and volumetric BMD (vBMD) in older age in the Hertfordshire Cohort Study. 198 men and 178 women born between 1931 and 1939 were studied. Birth weight was obtained from birth records. Ages at the time of scanning ranged from 72.1 to 81.4 years. HRpQCT images (voxel size 82μm) of the non-dominant distal radius and tibia were acquired with an Xtreme scanner (Scanco Medical). Standard morphological analysis was performed for assessment of macrostructure, vBMD, cortical porosity and trabecular microarchitecture. Anthropometric measurements were taken and information on demographics, lifestyle, and comorbidities were obtained from study questionnaires. The mean(SD) age of participants was 76.1(2.5) and 76.5(2.6) years in men and women respectively. There was a positive association between birth weight and bone area (total and trabecular) in men and women at both the radius and tibia ($p<0.05$). In women, birth weight was negatively associated with trabecular BMD (β(95%CI) radius -16.8(-29.4,-4.2)mg/cm^3/kg; tibia -12.5(-24.3,-0.8)mg/cm^3/kg) and trabecular thickness (β(95%CI) radius -3.47(-6.63-0.32)μm/kg; tibia -6.09(-9.56,-2.63)μm/kg) ($p<0.05$ for all). With the exception of radial trabecular thickness, these associations were robust to adjustment for adult height and weight. There was no evidence of an association between birth weight and cortical area, vBMD or porosity in either sex. In summary, we have observed relationships between early life and bone area in both men and women in their eight decade. Associations between birth weight and trabecular architecture were identified in women and all but radial trabecular thickness were maintained after adjustment for body size. This may suggest an estrogen dependent effect. Further work in larger groups is indicated to reproduce these findings, and to relate their significance to fracture incidence.

***Disclosures: Mark Edwards**, None.*

MO0295

Automated Scan Prescription For HR-pQCT: A Multi-Atlas Prospective Registration Approach. Julio Carballido-Gamio*[1], Serena Bonaretti[2], Margaret Holets[3], Isra Saeed[2], Louise McCready[3], Sharmila Majumdar[2], Thomas F. Lang[2], Sundeep Khosla[3], Andrew J. Burghardt[2]. [1]University of California, San Francisco, USA, [2]Musculoskeletal & Quantitative Imaging Research Group, Department of Radiology & Biomedical Imaging, University of California, San Francisco, USA, [3]Division of Endocrinology, Metabolism & Nutrition, Department of Internal Medicine, College of Medicine, Mayo Clinic, USA

Bone density and geometry vary dramatically along the distal radius. Consequently, the prescription of a scan by an operator introduces a significant—but underappreciated—source of variability in HR-pQCT measurements, increasing the scatter in cross-sectional and normative datasets, and complicating the translation of HR-pQCT to multicenter studies. To address this issue, we developed an automatic technique to *prospectively* prescribe patient HR-pQCT scans by automatically mapping scanning landmarks of a set of reference atlas radiographs of the forearm to their scout radiographs.

Scan-reposition-rescans of 60 radii of adult men and women from two different imaging centers were used to quantify root mean square coefficients of variation (RMSCVs) of integral BMD, Ct.Th and Tb.N, and slice-wise offsets between baseline and repeat scans for subvolumes identified by manual prescription in the scouts, and by the default *post hoc* slice-matching registration method—assumed to reflect ideal positioning. Repeat 330-slice scans of 5 cadaveric radii were used to validate the subvolume identification using the prospective method and similar metrics. Five atlases were generated, each based on ten scout radiographs randomly selected from a normative population. The automatic positioning of the scanning landmarks was computed with affine and nonlinear transformations between the scout radiographs and the atlases (Fig. 1A-E). Sub-volumes for bone quantification were identified by retrospectively applying the registrations to the scout radiographs.

Based on RMVCVs and mean slice offsets, a single atlas performed better than the others, however, values were also calculated for different atlas combination strategies. The ex vivo manual mean slice offset was 0.5 mm (93% overlap), with RMSCVs exceeding 9% for Ct.Th. The prospective mean slice offset was 0.1 mm (99% overlap) with RMSCVs equivalent to slice-matching (Fig. 1F).True precision errors (in vivo and ex vivo) for BMD and Ct.Th in HR-pQCT are greater than previously reported (Fig. 1F) once variability due to operator positioning is considered. Results indicate that scan prescription by prospective atlas-based image registration can minimize this error and potentially improve standardization of HR-pQCT acquisitions. While mainly advantageous for cross-sectional studies, standardized positioning would also benefit longitudinal studies where periosteal bone changes make the default slice-matching method undesirable.

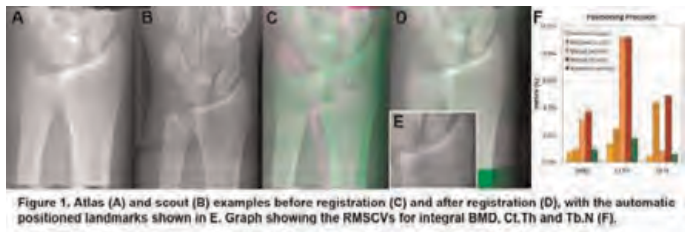

Figure 1. Atlas (A) and scout (B) examples before registration (C) and after registration (D), with the automatic positioned landmarks shown in E. Graph showing the RMSCVs for integral BMD, Ct.Th and Tb.N (F).

Figure 1

***Disclosures: Julio Carballido-Gamio**, None.*

MO0296

Comparison of Incident Clinical Vertebral Fracture Identified Using Medicare Administrative Claims and from Self-report Confirmed by Medical Record Review. Jie Zhang*[1], Elizabeth Delzell[1], Kristine Ensrud[2], John Schousboe[3], Brent Taylor[4], Misti Paudel[4], Cora Lewis[1], James Shikany[1], Peggy Cawthon[5], Jeffrey Curtis[1]. [1]University of Alabama at Birmingham, USA, [2]Minneapolis VA Medical Center / University of Minnesota, USA, [3]Park Nicollet ClinicUniversity of Minnesota, USA, [4]University of Minnesota, USA, [5]California Pacific Medical Center Research Institute, USA

Purpose: The definition and complete ascertainment of incident clinical vertebral fracture is challenging. We used data from the Osteoporotic Fractures in Men (MrOS) study participants, a cohort of men aged > 65 years, to examine the agreement between incident clinical vertebral fractures identified using Medicare claims vs. those self-reported to the study and confirmed with medical record review.

Methods: We conducted a retrospective cohort study among MrOS participants linked to their Medicare claims between 2000 and 2007. The study period was the time when a participant had Medicare fee-for-service coverage and was under active follow-up in the MrOS study. The claims-based algorithm required at least one of the following: vertebral fracture diagnosis as the primary discharge diagnosis from a hospitalization, on a physician evaluation & management claim preceded by spinal imaging <= 10 days, or on a kyphoplasty or vertebroplasty claim. In the MrOS study, participants were queried by mail and/or phone every 4 months and self-reported fractures were confirmed by comparing spine film obtained from medical record to the baseline study spine film. We examined the proportion of concordant cases (men identified to have had an incident clinical vertebral fracture from both the claims-based algorithm and from radiographically confirmed self-report) and discordant cases (from only one method and not the other).

Results: We identified 3,601 men eligible for the current analysis. During the study period, 58 men had one or more self-reported radiographically confirmed clinical vertebral fracture in MrOS study and 95 from the claims-based algorithm. We identified 36 concordant cases, which accounted for 62% of the 58 men with self-reported radiographically confirmed fractures and for 38% of the 95 men identified from the claims-based algorithm. When an expanded definition was used (any claim with a diagnosis of vertebral fracture), claims identified 85% of self-reported radiographically confirmed fractures.

Conclusions: Our findings suggest that relying on one method for identification of incident clinical vertebral fracture would likely have missed a significant proportion of cases. Despite the limitation that fractures identified from the claims are not validated unlike those from the self-report, future studies that also include participant consent to obtain Medicare claims might aid more complete study endpoint ascertainment.

***Disclosures: Jie Zhang**, Amgen and Genentech, 6*

MO0297

Detection of Incomplete Non-displaced Atypical Femur Fractures by Densitometer. Angela M. Cheung*[1], Robert Bleakney[2], Harry Genant[3], Rowena Ridout[4], Heather McDonald-Blumer[5], Diana Yau[6], Lianne Tile[6], George Tomlinson[5]. [1]University Health Network-University of Toronto, Canada, [2]Mount Sinai Hospital, Canada, [3]UCSF/Synarc, USA, [4]Toronto Western Hospital, Canada, [5]University of Toronto, Canada, [6]University Health Network, Canada

Background: Complete atypical femur fractures (AFFs) are rare, but patients often have prodromal symptoms for months to years prior to a complete break. Recent studies suggest that incomplete AFFs are more common and imaging with plain radiographs may detect them prior to a complete break. We conducted a cross-sectional study to test the diagnostic characteristics of high definition single energy scans by densitometer (HD-DXA) to detect incomplete AFFs.

Methods: We recruited from two cohorts of patients, the Ontario AFF Cohort and from bone density laboratories. From the AFF cohort, we recruited patients with unilateral or bilateral femurs with no surgical hardware who may or may not have abnormal radiographic findings consistent with incomplete AFFs. From the second cohort, we recruited postmenopausal women or women over age 50 with pain, discomfort or weakness in their leg who had been on 5 or more years of bisphosphonate therapy. All patients received a HD-DXA scan using Hologic Discovery A densitometers, scanning from above the lesser trochanter to the medial condylar flare, and a plain radiograph of the affected femur. Two musculoskeletal radiologists, blinded to patient identifiers, read the HD-DXA scans and the radiographs independently. Using plain radiographs as the reference standard, the diagnostic accuracy of HD-DXA (sensitivity, specificity, positive and negative predictive values, positive and negative likelihood ratios) was assessed separately for each reader and then averaged. For each abnormal finding (generalized cortical thickening, focal cortical thickening, endosteal thickening, lucent cleft, cortical beaking), inter-rater agreement on HD-DXA and plain radiographs were measured with the kappa statistic.

Results: A total of 61 subjects with 86 femurs were included in this study. Using HD-DXA for the identification of any bone abnormality, the average sensitivity was 75% and the average specificity was 92%. The average positive and negative predictive values were 87% and 81.9%. The average positive and negative likelihood ratios were 9.3 and 0.28. For HD-DXA, kappa was highest for the presence of lucent cleft [0.63, 95% CI (0.37 to 0.90)], followed by focal cortical thickening [0.55, 95%CI (0.38 to 0.72)]. For plain radiographs, kappa was highest for focal cortical thickening [0.59, 95%CI (0.41-0.76)], followed by endosteal thickening [0.53, 95%CI (0.30 to 0.76)].

Conclusions: HD-DXA is a promising point-of-care diagnostic tool for detecting incomplete AFFs.

***Disclosures: Angela M. Cheung**, Eli Lilly, 5; Merck, 6; Merck, 9; Eli Lilly, 6; Amgen, 6; Warner Chilcott, 2; Warner Chilcott, 5; Amgen, 5*

MO0298

Differences in Bone Geometry, Mass and Microarchitecture between Asian and Caucasian Young Men. Anna Kepley*[1], Chiyuan Zhang[2], Bin Zhou[2], Donald McMahon[3], X Guo[2], Elizabeth Shane[3], Thomas Nickolas[3]. [1]Columbia University Medical Center, USA, [2]Columbia University, USA, [3]Columbia University College of Physicians & Surgeons, USA

Chinese-American and Caucasian premenopausal women have similar areal BMD (aBMD) by DXA, but different bone microarchitectural properties by high resolution peripheral quantitative CT (HRpQCT). At the radius and tibia, Chinese-American premenopausal women have lower total area, and higher cortical and trabecular density and thickness. To investigate whether Asian men differ from Caucasian men in a pattern similar to women, we evaluated 62 healthy Asian (n=24) and Caucasian (n=38) men between ages 25 and 35 with aBMD by dual energy X-ray absorptiometry (DXA) of the lumbar spine (LS), total hip (TH), femoral neck (FN), 1/3- and ultra-distal radius (1/3R and UDR, respectively). HRpQCT was used to assess bone geometry, mass and microarchitecture at the distal radius and tibia. Results are expressed as Means $\pm$ SD. Univariate comparisons were made with Students T-Test; multivariate comparisons were made with generalized linear models adjusted for differences in height, weight and their first order interaction. Asians were shorter ($p<0.0001$) and lighter ($p<0.001$) than Caucasians, but did not differ by age or BMI (*Table*). In uni- and multi-variate models, there were no between group differences in aBMD. By HRpQCT at the radius, univariate models demonstrated that Asians had smaller total ($p<0.001$) and trabecular area ($p=0.0001$), fewer trabeculae ($p<0.05$), but greater cortical density ($p<0.001$), thicker cortices ($p<0.05$) and trabeculae ($p<0.05$), and more trabecular heterogeneity ($p<0.01$). In multivariate models, race remained a significant predictor of differences in total and trabecular area, cortical density and thickness, and trabecular network heterogeneity, but racial differences in total density, and trabecular thickness and number were no longer significant. At the tibia, in univariate models Asians had smaller total ($p<0.01$) and trabecular area ($p<0.01$), but thicker cortices ($p<0.05$). In multivariate models between group differences were no longer significant. In conclusion, Asian men have smaller bones with thicker and denser cortices, differences that could lead to greater bone strength. These cortical differences were similar to those previously reported for Chinese-American women, but trabecular characteristics may differ between men and women. Further studies are needed to elucidate genetic, biochemical and metabolic factors that could lead to differences in skeletal structure between Asians and Caucasians

Table. Univariate comparisons using Students T-Test. Multivariate comparisons using a generalized linear model adjusted for weight, height and height-weight interactions.

	Asian (n=24)	Caucasian (n=38)	Univariate p-value	Adjusted p-value
Age (years)	28.7±2.8	28.4±2.6	NS	-
Height (cm)	174.2±4.1	181.6±7.4	<0.0001	-
Weight (kg)	72.0±8.3	81.2±10.4	<0.001	-
BMI (kg/m^2)	23.7±2.6	24.6±2.5	NS	-
BMD by DXA				
Lumbar Spine (g/cm^2)	1.094±0.132	1.076±0.106	NS	NS
Total Hip (g/cm^2)	1.042±0.115	1.094±0.117	NS	NS
Femoral Neck (g/cm^2)	0.936±0.113	0.971±0.131	NS	NS
1/3R (g/cm^2)	0.804±0.065	0.816±0.055	NS	NS
Ultradistal Radius (g/cm^2)	0.538±0.060	0.534±0.047	NS	NS
HRpQCT: Radius				
Total Area (mm^2)	312±49	371±65	<0.001	<0.05
Cortical Area (mm^2)	73±11	68±12	NS	NS
Trabecular Area (mm^2)	240±50	303±71	0.0001	<0.05
Total Density (mg HA/cm^3)	375±49	340±55	<0.05	NS
Cortical Density (mg HA/cm^3)	892±30	851±51	<0.001	<0.05
Trabecular Density (mg HA/cm^3)	205±33	205±31	NS	NS
Cortical Thickness (mm)	0.963±0.149	0.821±0.190	<0.01	<0.05
Trabecular Thickness (mm)	0.086±0.013	0.079±11	<0.05	NS
Trabecular Number (1/mm)	2.0±0.3	2.2±0.3	<0.05	NS
Network Heterogeneity (mm)	0.179±0.036	0.155±0.027	<0.01	<0.05
HRpQCT: Tibia				
Total Area (mm^2)	882±105	974±136	<0.01	NS
Cortical Area (mm^2)	155±29	143±28	NS	NS
Trabecular Area (mm^2)	727±109	831±148	<0.01	NS
Total Density (mg HA/cm^3)	329±46	314±50	NS	NS
Cortical Density (mg HA/cm^3)	859±34	845±37	NS	NS
Trabecular Density (mg HA/cm^3)	213±34	217±31	NS	NS
Cortical Thickness (mm)	1.3±0.3	1.2±0.3	<0.05	NS
Trabecular Thickness (mm)	83±14	80±9	NS	NS
Trabecular Number (1/mm)	2.2±0.3	2.3±0.3	NS	NS
Network Heterogeneity (mm)	0.173±0.034	0.159±0.033	NS	NS

Table

***Disclosures: Anna Kepley**, None.*

MO0299

Fracture discrimination is improved by combiningMicro-architectural Texture analysis as assessed by H or TBS and Spine or hipBMD. Jerome Touvier*[1], Renaud Winzenrieth[2], Helena Johansson[3], Hech Toumi[1], Jean-Paul Roux[4], Jean Chaintreuil[5], Didier Hans[6], Eric Lespessailles[7]. [1]EA4708 - I3MTO - Orleans University, France, [2]Med-imaps, Hôpital X. Arnozan, PTIB, Pessac, France, [3]Swedish University of Agricultural Sciences, The Biomedical Center, Sweden, [4]INSERM, UMR 1033, Université de Lyon, France, [5]R&D department, D3A, France, [6]Lausanne University Hospital, Switzerland, [7]Centre Hospitalier Regional, France

Purpose: The aim of the study was to assess the clinical performance of a model combining bone mineral density (BMD) and microarchitectural texture (spine TBS and Calcaneus H) for the detection of the osteoporotic fractures at the spine and hip joints.

Method: Trabecular Bone Score was assessed in 272 women aged 40 yrs, who had a lumbar spine (LS) and total Hip (TH and FN) DXA scan as well as texture analysis of the calcaneus as assessed by H. Ninety six women had prevalent fragility fractures. The additional clinical values of BMD and TBS or H combinations were evaluated using a 2 steps classification tree approach based on BMD T-score stratification followed by a TBS or H or by the minimum of TBS or H (Min_TBS_H) tertile classification. Combinations add-values were evaluated using the Net Reclassification Index approach (NRI).

Results: Women with prevalent fracture were older (71 ± 10 vs. 62 ± 10 yrs, $p<0.001$), had lower TBS (1.165 ± 0.11 vs. 1.270 ± 0.10, $p<0.001$), H (0.607 ± 0.03 vs. 0.630 ± 0.03, $p<0.001$),Spine BMD (0.842 ± 0.14 vs. 0.931 ± 0.14, $p<0.001$) and TH BMD (0.736 ± 0.13 vs. 0.855 ± 0.12, $p<0.001$) than women without fracture. No significant difference was found in BMI. Correlation between BMD versus texture parameters were modest (range from 0.3 to 0.5) while TBS was poorly correlated to H ($r = 0.29$). Age-adjusted ORs per SD decrease (95% CI) were 1.73 (1.27-2.35), 1.68 (1.16-2.44) and 1.98 (1.35-2.90) for spine, neck and TH BMD respectively and 2.22 (1.58-3.11) and 1.86 (1.35-2.54) for TBS and H respectively. Both TBS and H remained significant after additional adjustment for TH BMD : OR=2.09 (1.43-3.06)

and 1.48 (1.03-2.13) respectively. When using BMD T-score of -2.5 (TH-BMD) combined with lowest TBS tertile (model 1) or lowest H tertile (model 2) thresholds, NRI of the model 1 or 2 were significantly improved in comparison with BMD (+32% and +31% respectively). Combining TH-BMD and Min_TBS_H lowest tertile (model 3), NRI reached +37%. Although the NRI increase was slight, model 3 significantly improved fracture detection since 73% of the overall fracture were in the first tertile (vs. 48 and 52% for model 1 and 2) and 2% were in the 3rd tertile (vs. 20 and 15% for model 1 and 2).

Conclusions: Both H and TBS have a significant clinical add-value over the BMD for osteoporotic fracture detection. H and TBS combination in addition to the BMD improve fracture detection compared with their combination with BMD alone.

	Two-sided p-value	OR per 1 SD (95% CI)	
TH BMD	0.0093	1.69 (1.14 - 2.51)	Adjusted for age and TBS
TBS	<0.001	2.09 (1.43 - 3.06)	Adjusted for age and TH BMD
TH BMD	0.012	1.68 (1.12 - 2.52)	Adjusted for age and H
H	0.033	1.48 (1.03 - 2.13)	Adjusted for age and TH BMD

Table 1

***Disclosures: Jerome Touvier**, None.*

MO0300

In Vivo Characterization of Cortical Bone at Distal Tibia Using Multi-Detector CT Imaging – Validation and Results of Application in Healthy Young Adults. Cheng Li*, Dakai Jin, Elena Letuchy, Trudy Burns, Kathleen Janz, James Torner, Steven Levy, Punam K. Saha. University of Iowa, USA

Cortical bone plays an important role in determining bone strength and fracture risk. Segmentation of cortical bone is needed for its volumetric and structural analyses. This task is nontrivial for *in vivo* multi-row detector CT (MD-CT) imaging due to limited resolution and partial volume effects. An automated cortical bone segmentation algorithm for *in vivo* MD-CT imaging of the distal tibia is presented and its accuracy and reproducibility are examined using cadaveric ankle specimens. The algorithm is applied in a pilot study evaluating volumetric and structural differences in cortical bone among healthy male and female young adults.

Three repeat MD-CT scans of fifteen cadaveric ankle specimens were acquired on a 128 slice Siemens Flash scanner at 120kV, 200mAs, pitch: 1, 0.3mm slice-thickness and 10cm scan-length. A Gammex calibration phantom was used to transform CT Hounsfield units into BMD (mg/cc). Cortical bone thickness and porosity were measured using the new cortical bone segmentation algorithm. Accuracy of the algorithm was defined as the percentage of agreement between manual and automatic segmentations of cortical bone. Repeat scan reproducibility of cortical bone measures was evaluated. Forty-five pairs of age similar (18 to 23 year old) height order-matched healthy male and female pairs who had MD-CT scans were selected from the Iowa Bone Development Study (IBDS) cohort.

In the cadaveric study, the agreement between manual and automatic segmentations of cortical bone showed a mean accuracy of 95.1%, and a repeat MD-CT scan intraclass correlation coefficient of 98.2%. Application of the segmentation algorithm to MD-CT scans for one of the age- and height-order matched representative IBDS (male-female) pairs (Figure 1) suggests that the male IBDS cohort member has thicker, but more porous cortex as compared to the female. In fact, a pairwise t-test comparing the 45 healthy male-female IBDS pairs showed that, on average, males had 16.3% thicker cortex but 4.7% increased porosity.

MD-CT imaging, together with an advanced segmentation algorithm, is suited for volumetric and structural analyses of cortical bone *in vivo*. The human study indicates that, on average, bones for males are substantially larger with thicker cortical shell than for females. The relatively higher porosity in males may increase big bone flexibility such as bending strength.

This study was funded by NIH grants: R01-AR054439, R01-DE012101, UL1-RR024979, and UL1-TR044206.

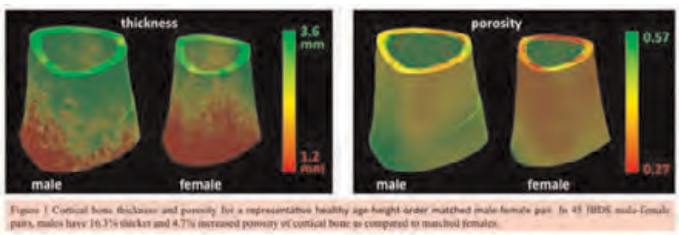

Figure 1

***Disclosures: Cheng Li**, None.*
This study received funding from: National Institutes of Health (NIH)

MO0301

Precise 3D Localisation of Cortical Defects Associated with Subcapital, Trans-cervical and Trochanteric Hip Fractures in Life. Kenneth Poole*[1], Graham Treece[1], Karen Blesic[1], Paul Mayhew[1], Thomas Turmezei[1], Fjola Johannesdottir[1], Madhavi Vindlacheruvu[1], Simon Donell[2], Jan Vaculik[3], Pavel Dungl[3], Martin Horak[4], Jan Stepan[5], Andrew Gee[1]. [1]University of Cambridge, United Kingdom, [2]University of East Anglia, United Kingdom, [3]Charles University Prague, Czech Republic, [4]Homolka Hospital, Czech Republic, [5]Charles University, Czech Republic

The precise distribution of cortical bone is likely to determine the location and type of hip fracture sustained during a trip, stumble or fall. Since osteoporosis medications and exercise also enhance cortical bone in key areas (Poole et al 2011), each person may need a tailored hip fracture prevention strategy depending on their existing bone structure. We applied 3D cortical bone mapping to ordinary clinical CT scans in order to identify average focal bone defects in women with the three commonest types of acute hip fracture versus healthy controls without fracture. By extending recruitment to our case-control studies in England and the Czech Republic, we could pinpoint systematic differences and visualise the magnitude of the differences in cortical bone between each fracture type and controls with a colour map displayed on an average femur model.We analysed Siemens or GE CT scans from 144 older women volunteers with acute fracture and 124 age-matched controls from both the Prague Study of Hip Joint in Trauma and the UK FEMCO study. Fractures were diagnosed using the Muller AO classification of fractures into trochanteric (code AO31-A, n=53), transcervical (AO31-B2, n=37) or sub-capital (AO31-B1,B3, n=54) before creating cortical thickness maps of the unfractured contralateral hip. After non-rigid registration to an average femur shape and statistical parametric mapping (SPM), we were able to pinpoint statistically significant foci of lower cortical mass and thickness associated with each fracture type. The generalised linear SPM model allowed for age, weight and country.The major finding was a marked difference between women with trochanteric fractures, who had an extensive trochanteric cortical defect (fig. 1a) compared with controls, and those with intracapsular fractures (fig 1b & 1c) who had cortical defects located on the superior femoral neck. Closer examination of the two intracapsular fracture types reveals a subtler difference in that the principal cortical defect in transcervical fractures is mostly confined to the upper neck, whereas the defect in subcapital fractures spreads across the anterior femur.Alongside recent evidence that osteoporosis treatments and exercise have focal effects on the proximal femoral cortex, these results suggest that hip fracture prevention strategies may need to be tailored to improve the focal cortical deficits which are characteristic of each fracture type.

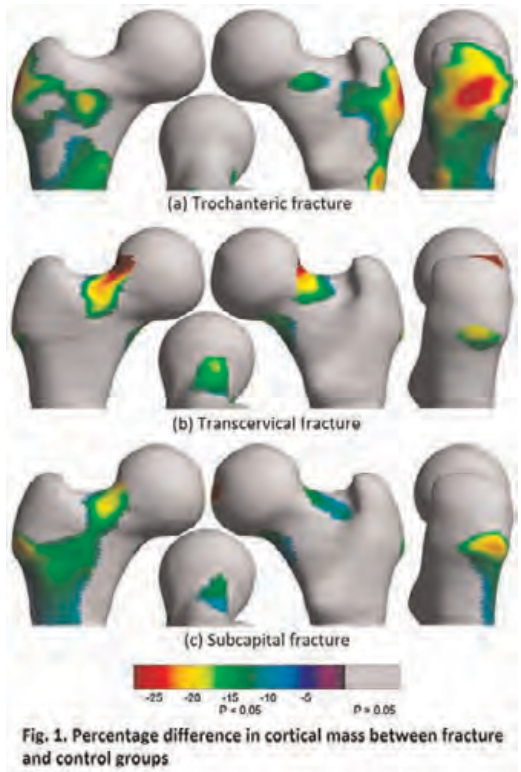

Fig. 1. Percentage difference in cortical mass between fracture and control groups

Figure 1

***Disclosures: Kenneth Poole**, Patent - GB0917524.1 , 9*

MO0302

Reading Between the Lines of Bone Mineral Density: the Significance of Changes in BMD of Individual Lumbar Vertebrae. Sumiaki Okamoto*[1], Hitoshi Noguchi[2], Hiroyuki Suzuki[3], Akira Itabashi[4], Sumitada Okamoto[1]. [1]Okamoto Clinic SORF, Japan, [2]Noguchi Thyroid Clinic & Hospital Foundation, Japan, [3]Suzuki Orthodontic Office, Japan, [4]Saitama Center for Bone Research, Japan

As previously reported, bone mineral density (BMD) of individual vertebrae from L1 through L4 sequentially increase in young healthy controls and the disruption of this sequence implies vertebral fracture. A refinement of this observation and a potential new arsenal in the analysis of vertebral fracture is presented. We first took lumbar DXA measurements of 20 young volunteers, aged 22-28, and found that L1 had lower BMD than L2 in all subjects , L2 had lower BMD than L3 in 16 of 20 subjects (80%), L3 had lower BMD than L4 in 12 subjects (60%) and the BMD of L3 was never higher than L4 by more than 5%. L1toL2, L2 toL3 andL3 toL4 ratios in average were 0.90, 0.95 and 0.99, respectively. Aberration from this norm was studied in 1680 patients of osteoporosis who were examined by DXA and three dimensionally analyzed by CT under fully informed consent. We present a series of cases in which the disruption in the sequence of BMD in the lumbar vertebrae was verified for vertebral fracture by CT. The diagnostic value of the sequence is diminished, however, when every vertebrae is equally compromised. But sudden changes in the sequence may alert the astute observer of newly formed fractures. Sudden increase of BMD is often seen after new lumbar vertebral fracture often followed by false rapid decrease of apparent BMD in the same vertebrae. The sudden increase is the product of the compaction of the vertebrae and attendant decrease of the region of interest (ROI), callus formation and sclerotic change of the vertebral rim, angle induced mixing of the posterior element of the vertebrae into the ROI area and the formation of traction spurs or sclerosis due to the instability of the vertebrae after fracture. The false decrease of BMD is the product of the parting of the spinous process following kyphosis resulting in the removal of the spious process from the ROI area. Also, the unloading at the posterior intervertebral joint may result in the absorption of sclerotic changes or inflammatory high density lesions. As we had reported, Osteophytes and vertebral selerosis are found in more than 99% of spines, with equal frequency to osteoporosis in elderly women. Even minor indentations of vertebra might induce falsely high BMD scores, which will be followed by the false decrease. Misinterpreting non-responders by vertebral BMD might occur, when these phenomenons are not fully understood.

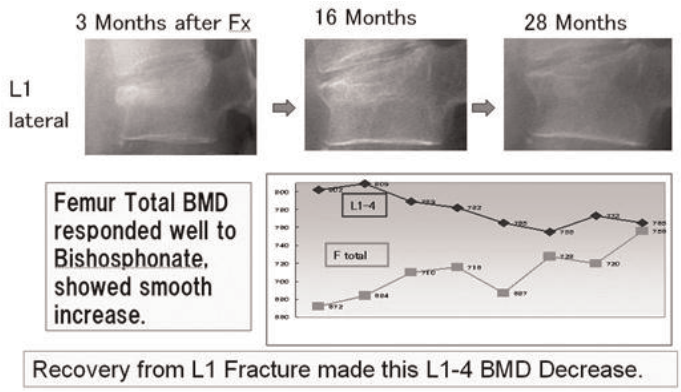

Figure 1

***Disclosures: Sumiaki Okamoto**, None.*

MO0303

Sensitivity, specificity and accuracy improvement by combining TBS and spine BMD: The Eastern European Study. Jelena Vasic[1], T Petranova[2], Carmen Gabriela Barbu[3], Vladyslav Povoroznjuk[4], F Gojkovic[1], Renaud Winzenrieth*[5], Didier Hans[6], J Elez[1], V CulaficVojinovic[1], Catalina Poiana[3], R Rashkov[2], Aleksandar Dimic[7]. [1]Bone Diseases, Railway Healthcare Institute, Serbia, [2]Rheumatology Clinic, the Medical University, Bulgaria, [3]Department of Endocrinology, Carol Davila University of Medicine & Pharmacy, Romania, [4]Department of Clinical Physiology & Pathology of Locomotor Apparatus, Institute of Gerontology AMS, Ukraine, [5]Med-imaps, Hôpital X. Arnozan, PTIB, Pessac, France, [6]Lausanne University Hospital, Switzerland, [7]Institute for Treatment & Rehabilitation ''NiskaBanja'', Serbia

The aim of the study was to assess the clinical performance of the model combining bone mineral density (BMD) at spine and microarchitecural texture (TBS) for the detection of the osteoporotic fracture.

The Eastern European Study (EES) is a multicenter study (Serbia, Bulgaria, Romania and Ukraine) evaluating the role of TBS in routine clinical practice as a complement toaBMD. All scans were acquired on Hologic Discovery and GEHC Prodigy densitometers in a routine clinical manner. Lumbar spine TBS (TBS iNsight®) was derived from each spine DXA examination blinded to clinical parameters and outcomesby the University of Lausanne (Switzerland). Age- and BMI-adjusted odds ratios (OR) per standard deviation decrease are reported for aBMD and TBS. The correlation between aBMD and TBS was calculated. The additional clinical values of aBMD and TBS were analyzed using2 steps classification tree approach (aBMD followed by TBS tertiles) for all type of osteoporotic fracture (All-OP Fx). Sensitivity, specificity and accuracy of fracture detection as well as the Net Reclassification Index (NRI) were calculated.

We recruited 1762 women from routine clinical practice, of whom 1253 were deemed eligible: mean age 63.3±8.8 y, BMI 26.3±3.9, aBMD 0.894±0.171, TBS 1.199±0.127. No significant differences between centers in baselines characteristics were found. As such data were merged. As expected, aBMD and TBS were only moderately correlated (r^2=0.15). Prevalence rate forAll-OP Fxwas 29% (mainly forearm and clinical vertebral fractures). Age and BMI-adjusted ORs were 1.48 (1.29-1.70) for aBMD and 1.55 (1.35-1.78) for TBS. TBS remained significant after additional adjustment for Spine BMD: OR=1.41(1.21-1.63).When using aBMD T-score of -2.5 and the lowestTBS tertile thresholds, both BMD and TBS were similar in terms of sensitivity (38% vs. 43%), specificity (76% vs. 78%) and accuracy (62% vs. 66%). When combined, a significant improvement in sensitivity was observed (+28% and +22%, in comparison with 2.5 aBMD T-score and first TBS tertile thresholds). NRI of the combined model compared with BMD and TBS alone exhibit a significant improvements of +38% and +31% respectively.

In a multi-centre Eastern European cohort, we have shown that combining TBS and BMD significantlyimproves the sensitivity and overall accuracy of osteoporotic fracture detection, even after adjusting for age and BMI.

***Disclosures: Renaud Winzenrieth**, None.*

MO0304

Simplified Criteria for Selecting Patients for VFA Imaging. Tamara Vokes*[1], John Schousboe[2], Harold Rosen[3]. [1]University of Chicago, USA, [2]Park Nicollet Clinic, University of Minnesota, USA, [3]Beth Israel Deaconess Medical Center, USA

Purpose: We have previously shown that among women referred for BMD testing selection of patients who should have VFA is best achieved using a multivariate regression model[1]. Similarly, the 2007 ISCD position development conference (PDC) proposed accurate but complicated criteria for selecting patients for VFA[2], which included different combinations of cut-off points for age and height loss, use of glucocorticoids, prior fractures, diseases and medications known to cause bone loss (http://www.iscd.org/official-positions/2007-iscd-official-positions-adult/). We now examine whether simpler criteria could be equally effective in identifying patients with prevalent vertebral fractures (VFx).

Methods: We compared the discrimination between those with and without VFx using 3 different models: 1. previously reported ''Full model'' (age, T-score, height loss, self-reported vertebral fracture, history of non-vertebral fracture, and glucocorticoid use)[1] at cut-off corresponding to 10% VFx prevalence, 2. ISCD PDC2007 indications[2], and 3. ''Simple criteria'' where VFA is indicated if T-score<-1 plus any of the following: age over 70 in women or 80 for men; height loss>4 cm, self-reported vertebral fracture, glucocorticoid use.

Results: Among 860 female densitometry patients 163 (19%) had VFx. The ''Full model'' performed slightly better likely because it was derived and tested in the same population. Overall the measures of performance were similar for the 3 models and simple criteria were no worse than the more complicated PDC2007 indications (Table).

Conclusion: Selecting patients for VFA using simplified criteria (age, height loss, self-reported vertebral fractures, glucocorticoid use) performed as well as the more complex models in identifying densitometry patients with VFx.

[1]Vokes et al OI (2010) 21:2083; [2]Schousboe et al JCD (2008) 11:92

	Full model[1]	PDC2007[2]	Simple criteria
% PRVFX captured	87%	91%	85%
% Screened	49%	61%	53%
Yield*	33%	28%	30%
Area under ROC curve	0.73 (0.70, 0.76)	0.69 (0.66, 0.72)	0.70 (0.66, 0.73)
Sensitivity	87% (81, 92)	91% (86, 95)	85% (79, 90)
Specificity	59% (56, 63)	46% (42, 50)	54% (50, 58)
Positive predictive value	33% (29, 38)	28% (25, 33)	30% (26, 35)
Negative predictive value	95% (93, 97)	96% (93, 98)	94% (91, 96)
NRI vs. Full model		-0.091, p<0.001	-0.074, p<0.001
NRI vs. PDC2007			0.016, p=0.48

*percent of those screened who had VFx; NRI – net reclassification index (Pepe method)

Table

***Disclosures: Tamara Vokes**, None.*

MO0305

Trabecular Bone Score is Associated With Vertebral and Non Vertebral Fracture in Men - The STRAMBO Study. Stephanie Boutroy*[1], Didier Hans[2], Renaud Winzenrieth[3], Roland Chapurlat[4], Pawel Szulc[5]. [1]INSERM U1033 & Université de Lyon, France, [2]Lausanne University Hospital, Switzerland, [3]Med-imaps, Hôpital X. Arnozan, PTIB, Pessac, France, [4]E. Herriot Hospital, France, [5]INSERM UMR 1033, University of Lyon, Hopital E. Herriot, Pavillon F, France

Areal BMD (aBMD) is a less powerful predictor of fracture in men than in women. TBS, a gray-level measurement derived from lumbar spine DXA image texture, is related to microarchitecture and fracture risk in women independently of BMD. Our goal was to assess the ability of TBS to improve discrimination of prevalent vertebral and peripheral fractures in men, over aBMD.

TBS was assessed in 886 men aged 50 yrs and over from the STRAMBO cohort, who had a lumbar spine (LS) DXA scan (Hologic Discovery A) at baseline. 164 men had prevalent fragility fractures (vertebral = 70, peripheral = 74, both = 20).

Men with prevalent fracture were older (73 ± 8 vs. 70 ± 9 yrs, $p<0.001$), had lower LS_TBS (-5.5%, -0.6 SD, $p<0.001$), LS_aBMD (-7.9%, -0.5 SD, $p<0.001$) and total hip (TH) aBMD (-8.1%, -0.6 SD, $p<0.001$) than men without fracture. After adjustment for age, height, weight and treatment, the magnitude of association with peripheral, vertebral and all types of fracture jointly was similar for LS_TBS, LS_aBMD and TH_aBMD with OR per 1SD decrease [95% CI] of 1.7 [1.4;2.0], 1.5 [1.3;1.7] and 2.0 [1.6;2.5] respectively. In multivariate analysis including the above covariables as well as LS_aBMD and/or TH_aBMD, LS_TBS remained significantly associated with an increased prevalence of peripheral and vertebral fracture alone and in combination (OR = 1.7 [1.3;2.1], 1.6 [1.2;2.1] and 1.6 [1.3;1.9] respectively).

When using the WHO classification, 13.4% of fractures occurred in osteoporotic (fracture rate=42.3%), 57.3% in osteopenic (fracture rate=23.4%) and 29.3% in men with T-score>-1 (fracture rate=11.1%). 44.5% of fractures occurred in the lowest quartile of LS_TBS, regardless of BMD. By combining osteoporotic men with osteopenic men in the lowest quartile of TBS, we were able to depict three times as many fractures as in the osteoporotic men alone (40.9% vs. 13.4%) with a rather small decrease of the fracture rate: 38.3% vs. 42.3%.

In conclusion, LS_TBS is a useful tool to discriminate men with and without prevalent fracture, even in addition to aBMD measured either at the lumbar spine or total hip. Its use in prospective studies in men should confirm its ability to predict fracture independently of aBMD.

***Disclosures: Stephanie Boutroy**, None.*

MO0306

Trabecular Bone Score: A Tool for Identification of Severe Spinal Osteoporosis. Kawtar Nassar[1], Simon Paternotte[1], Sami Kolta[1], Jacques Fechtenbaum[1], Christian Roux[1], Karine Briot*[2]. [1]Paris Descartes University, Cochin Hospital, Rheumatology Department, France, [2]Paris Descartes University, Cochin hospital, Rheumatology Hospital, France

Vertebral fractures (VFs) are the hallmark of osteoporosis and are more predictive of future fracture than areal Bone Mineral Density (aBMD). Number and severity of VFs are related to bone microarchitecture deterioration. Trabecular Bone Score (TBS), derived from the texture of the DXA image, has been shown to be related to bone microarchitecture and fracture risk. Our objective was to evaluate performance of TBS, alone or added to aBMD, in the prediction of the presence of VFs and of the severity of these fractures.

Patients and methods: Patients were selected from the Fracture Liaison Service of our department, aiming at providing assessment of osteoporosis to patients over the age of 50 years who had sustained low trauma fractures. aBMD and Vertebral Fracture Assessment (VFA) were performed one week to 3 months after the fracture using DXA. VFs were classified using the Genant's semiquantitative evaluation and severity was assessed using the spinal deformity index (SDI), i.e. the sum of number and grades of VFs. TBS was obtained after re-analysis of DXA lumbar spine (L2-L4) scans. Performance of TBS, BMD and their combination was assessed using Receiver operator characteristic (ROC) and areas under receiver operating characteristics curves (AUCs).

Results: 362 patients (77.3% women; mean age 74.3 ± 11.7 years) were analysed; 182 (50.3%) had hip fractures and 49 (13.5%) received an anti-osteoporotic treatment. Prevalence of VFs by VFA was 36.7%; 189 (52.2%) patients were osteoporotic (T score≤-2.5 at at least one site). TBS was lower in the patients with VFs than in patients without VFs in the whole population (1.156 ± 0.11 vs 1.227 ± 0.11, $p<0.0001$) and in non osteoporotic patients (1.187 ± 0.12 vs 1.253 ± 0.10, $p=0.001$). In whole population, performance of TBS (AUC=0.677) was similar to lumbar spine (LS) BMD (AUC= 0.669) and hip BMD (AUC= 0.692) for the identification of VFs. However combination of TBS and LS BMD improves the discrimination as compared to LS BMD alone (AUC=0.707, $p=0.043$). In the non osteoporotic population (n=173), AUC of TBS for the discrimination of VFs was higher than AUC of LS BMD (0.67 0vs 0.541, $p=0.035$). There was a negative correlation between TBS and SDI: r= -0.31 ($p<0.0001$).

Conclusion: in a population of patients with a recent non traumatic fracture, TBS added to lumbar spine aBMD improves the detection of patients having vertebral fracture, thus receiving spine imaging.

***Disclosures: Karine Briot**, None.*

MO0307

Using Body Composition Phantoms to Validate Performance of Dual Energy X-Ray Absorptiometry (DXA) instrument. Colin Miller*[1], Hui Jing Yu[1], Blaine Horvath[1], Jessie Libber[2], Diane Krueger[2], Neil Binkley[2]. [1]BioClinica, Inc., USA, [2]University of Wisconsin-Madison, USA

BACKGROUND: The purpose of this study was to assess the use of Dual Energy X-Ray Absorptiometry (DXA) phantoms as part of the validation process of a newly installed iDXA instrument. METHODS: An in vitro calibration was carried out using four DXA phantoms: the GE (Lunar) encapsulated spine phantom, the Hologic encapsulated spine phantom, the Bona Fide Phantom (BFP, BioClinica, Inc., Newtown, PA), and the BioClinica Body Composition Phantom (BBCP, BioClinica, Inc., Newtown, PA). Each phantom was scanned 30 times consecutively on an existing iDXA instrument, with 15 minutes wait between each scan series. Total Bone Mineral Density (BMD) values for L1-L4 were calculated for the Lunar phantom, Hologic phantom and BFP, and total BMD values for whole body were calculated for the BBCP. This was repeated on a newly installed iDXA instrument. The coefficient of variation (%CV) was calculated for each of the scan series. A Pearson Correlation plot was used to calculate the degree of agreement between the two instruments for each phantom. The mean difference between the two instruments was also calculated. RESULTS: There was a systematic increase in %CV observed for the new iDXA instrument when compared to the existing iDXA instrument. The %CVs for the new iDXA were 0.19% for Lunar phantom, 0.33% for Hologic phantom, 0.21% for BFP, and 0.46% for BBCP, whereas the %CV for the old iDXA were 0.12% for Lunar phantom, 0.20% for Hologic phantom, 0.18% for BFP, and 0.27% for BBCP. BMD measured on the new iDXA instrument was approximately 1% higher than the existing instrument for L1-L4 and about 2% higher for whole body measure, although the correlations were not statistically significant between the two instruments. Moreover, similar findings were observed for Total Fat Mass and Total Lean Mass when comparing the two instruments using the BBCP. Subsequently, these results were sent to GE for evaluation. GE staff confirmed the scanner requires adjustment, and adjustments were made to the new instrument. DISCUSSION: This study demonstrated the importance of performing repeated phantom analyses for in vivo BMD calibration and validation activity with new scanners before replacing any existing instruments in the clinic or clinical trials.

***Disclosures: Colin Miller**, None.*

MO0308

Alterations in Lean Mass Predict Development of Trabecular Bone Density and Cortical Bone Size in Young Adult Men. ROBERT RUDANG*[1], Dan Mellstrom[2], Claes Ohlsson[3], Mattias Lorentzon[4]. [1]INSTITUTE OF MEDICINE, SAHLGRENSKA ACADEMY, Sweden, [2]Sahlgrenska University Hospital, Sweden, [3]Center for Bone & Arthritis Research at the Sahlgrenska Academy, Sweden, [4]Geriatric Medicine, Center for Bone Research at the Sahlgrenska Academy, Sweden

Increased body weight has been associated with higher bone mineral density (BMD), but whether alterations in lean mass (LM) or fat mass (FM) predict the development in bone size and volumetric BMD (vBMD) is unclear. The aim of this study was to longitudinally investigate the associations between changes in LM and FM and the development of cortical and trabecular parameters of the radius and tibia in a 5-year longitudinal population-based study of 828 young men (18-20 years (baseline)). Areal BMD (aBMD) of the total hip and lumbar spine, and total body LM and total body FM were assessed using Dual-photon X-ray Absorptiometry (DXA). Trabecular vBMD, and cortical cross-sectional area (CSA) were obtained using peripheral quantitative computed tomography (pQCT) at the radius and tibia, respectively. Physical activity was obtained as hours/week using a standardized questionnaire.

The mean 5-year increase in LM was 2.3% (interquartile range -1.0% to 5.0%) and in FM 38,2% (3.4% to 61.0%). Changes in LM and FM were weakly correlated ($r=-0.1$, $p<0.01$). Using a stepwise linear regression model, including age at baseline, 5-year change in LM and FM, and 5-year change in height and physical activity as independent predictors, the 5-year change in LM was positively associated with aBMD of the total hip ($R^2=20.6\%$, $p<0.001$) and lumbar spine ($R^2=20.0\%$, $p<0.001$). The 5-year change in FM was only weakly positively associated with aBMD of the total hip ($R^2=0.6\%$, $p<0.05$). Using the same model, the change in LM was also positively associated with the 5-year development of CSA and trabecular vBMD at the radius (R^2 =6.8%, $p<0.001$, and $R^2=3.3\%$, $p<0.001$, respectively) and tibia ($R^2=8.3\%$, $p<0.001$, and $R^2=4.3\%$, $p<0.001$, respectively), whereas FM was only weakly associated with trabecular vBMD development at the tibia ($R^2=1.3\%$, $p<0.001$).

We conclude that alterations in lean mass predict the development of aBMD, bone size and trabecular vBMD in young adult men, indicating that lean rather than fat mass increments are beneficial for optimal bone development in young men.

***Disclosures: ROBERT RUDANG**, None.*

MO0309

Association between Metabolic Syndrome and Bone Mineral Density in a Community-dwelling Older Women: the São Paulo Ageing & Health Study (SPAH). Luana Machado*[1], Diogo Domiciano[1], Jaqueline Lopes[2], Camille Figueiredo[1], Valéria Caparbo[1], Liliam Takayama[1], Rosa Pereira[2]. [1]University of São Paulo, Brazil, [2]Faculdade De Medicina Da Universidade De São Paulo, Brazil

Purpose:Recent studies have shown a link between metabolic syndrome (MS) and bone mass. However, these results are uncertain about the positive/negative effect of the components of MS on bone mineral density (BMD) and risk of fragility fractures. Furthermore, the higher prevalence of MS among subjects with higher body mass index (BMI) is a confounding factor, since previous findings have demonstrated that obesity could be a protective factor against bone loss. In this way, the aim of this study was to evaluate the prevalence of MS in a community-dwelling older women with high frequency of overweight/obesity and its association with bone parameters.

Methods: 343 women aged over 65 years were evaluated by specific questionnaire (including history of clinical fractures and cardiovascular risk factors). Lumbar spine, femoral neck and total hip BMD were evaluated by DXA. Laboratory tests, including calcium, phosphorus, creatinine, lipid profile and glucose were also performed. Thoracolumbar spine X-rays were assessed to identify vertebral fractures. National Cholesterol Education Program-Adult Treatment Panel III (NCEP-ATPIII) criteria were used to define MS. Logistic regression models were used to analyze the relationship between MS and bone parameters.

Results:The prevalence of MS was high (62.1%). Women with MS had higher BMI (30.7 ± 4.9 vs. $27.2 \pm 4.9 kg/m^2$, $P<0.001$), body fat percentage (37.7 ± 5.0 vs. $34.9 \pm 6.5\%$, $P<0.001$), lumbar spine BMD (0.881 ± 0.171 vs. $0.837 \pm 0.178 g/cm^2$, $P=0.025$), femoral neck BMD (0.684 ± 0.120 vs. $0.629 \pm 0.121 g/cm^2$, $P<0.001$) and total hip BMD (0.814 ± 0.131 vs. $0.743 \pm 0.140 g/cm^2$, $P<0.001$) compared to women without MS. After adjustments for BMI, logistic regression analyses demonstrated that hip BMD remained as an independent factor associated with MS (OR:10.73 95% CI:1.33-86.55, P=0.026). No significant difference concerning the prevalence of vertebral or nonvertebral fractures was observed between the two groups.

Conclusion: A positive association between total hip BMD and MS was found, even after adjustment for BMI. Nevertheless, the frequency of vertebral and nonvertebral fractures was similar in women with and without MS. Taken together, these results suggest that higher BMI per se does not explain the positive association between higher BMD and MS and does not protect against osteoporotic fractures. Further studies are necessary to elucidate the effect of MS on bone mass and fracture risk, possibly related to bone quality.

***Disclosures: Luana Machado**, None.*

MO0310

Bone Mineral Density (BMD), Vertebral Marrow Fat, and Markers of Metabolism in Older Men and Women: Results from the AGES-BMA study. Trisha Hue*[1], Xiaojuan Li[1], Clifford Rosen[2], Vilmundur Gudnason[3], Sigurdur Sigurdsson[4], Kristin Siggeirsdottir[4], Gunnar Sigurdsson[5], Gudný Eiríksdóttir[4], Tamara Harris[6], Lisa Palermo[1], Thomas Lang[1], Ann Schwartz[1]. [1]University of California, San Francisco, USA, [2]Maine Medical Center, USA, [3]Icelandic Heart Association Research Institute, Iceland, [4]Icelandic Heart Association, Iceland, [5]Landspitali University Hospital, Iceland, [6]Intramural Research Program, National Institute on Aging, USA

Higher levels of marrow fat (MF) are associated with osteoporosis, but little is known about the mechanisms governing MF accumulation. Endocrine factors involved in metabolic regulation may play a role in both MF accrual and bone density/strength. Ghrelin stimulates appetite, as well as osteoblast activity and affects adipogenesis, while preadipocyte factor-1 (pref-1), an inhibitor of differentiation, has been associated with increased MF and low bone mineral density (BMD). Insulin-like growth factor-1 (IGF-1), which responds to available energy from diet and body reserves, has also been found to be involved in bone formation, in contrast to insulin-like growth factor binding protein-2 (IGFBP-2), which is elevated with poor energy status and associated with increased MF and low BMD.

We assessed the relationship between markers of metabolism, MF and BMD in older men and women in the Bone Marrow Adiposity, Bone and Body Composition (BMA) study. BMA is a cross-sectional ancillary study to Age Gene/Environment Susceptibility-Reykjavik (AGES-Reykjavik), an ongoing population-based cohort study in Iceland. This analysis excluded those who reported current bone-active medication use (n=44), diabetes (n=17), or had inadequate serum (n=2). Blood was drawn fasting and serum was stored at -70˚C until batched assays for IGF-1, IGFBP-2, pref-1, and ghrelin were performed at the end of the study. Vertebral (L1-L4) MF content was measured with single voxel proton magnetic resonance spectroscopy. Other measures included: areal-BMD assessed by dual-energy X-ray absorptiometry, volumetric-BMD by quantitative computed tomography, and body mass index (BMI).

In this cohort of older adults, vertebral MF was modestly correlated with ghrelin in women (r=0.21, p=0.07), but not in men. The other markers were not correlated with MF. Pref-1 was positively correlated with BMD in men, ghrelin was inversely correlated with BMD in women, and IGFBP-2 was inversely correlated with BMD in men. IGFBP-2 was also inversely correlated with BMI in both men and women. We found no significant correlations (not shown) between IGF-1 and BMD.

With the exception of ghrelin in women, there was no evidence of an association between these markers of energy status and MF in older adults. These data also show that ghrelin, pref-1 and IGFBP-2 have gender-dependent patterns of association with trabecular and cortical bone density.

	Men			Women		
Mean age (years)	80.0			78.6		
	IGFBP-2 (n=111)	pref-1 (n=111)	ghrelin (n=63)	IGFBP-2 (n=127)	pref-1 (n=127)	ghrelin (n=75)
Vertebral marrow fat (%)[1]	-0.06	0.03	0.07	-0.04	0.05	0.21
Areal BMD (g/cm^2)						
spine	-0.21*	0.04	-0.01	0.02	-0.06	-0.10
femoral neck	-0.15	0.22*	0.07	-0.18*	-0.08	-0.19
total hip	-0.17	0.25*	0.03	-0.29*	-0.09	-0.31*
Volumetric BMD (g/cc)						
spine: trabecular	-0.20*	0.21*	-0.08	0.01	-0.03	-0.09
femoral neck: integral	-0.05	0.26*	0.07	-0.12	-0.08	-0.26*
femoral neck: trabecular	-0.22*	0.19	-0.07	-0.00	-0.04	-0.15
femoral neck: cortical	-0.08	0.11	0.15	-0.06	-0.02	-0.20
total hip: integral	-0.10	0.28*	-0.03	-0.18	-0.15	-0.28*
total hip: trabecular	-0.19	0.29*	-0.09	-0.12	-0.14	-0.23
total hip: cortical	0.08	0.21*	0.05	-0.15	-0.11	-0.29*
Body mass index (BMI, kg/m^2)	-0.43**	-0.01	-0.15	-0.37**	0.12	-0.29*

[1]Percent vertebral marrow fat = mean (L1-L4 fat content/ (L1-L4 fat content + water content) x 100)
*p value ≤ 0.05; **p value ≤ 0.001

Spearman Correlations of Marrow Fat and Bone Mineral Density with Markers of Metabolism

***Disclosures: Trisha Hue**, None.*

MO0311

The Effect of Bone-Active Medication Use on Bone Mineral Density Post-Hip Fracture. Denise Orwig[1], Emma G. Sheldon*[2], Rasheeda Johnson[1], Marc Hochberg[2], William G. Hawkes[2]. [1]University of Maryland, Baltimore, USA, [2]University of Maryland School of Medicine, USA

Bone-active medications (BAMs), including prescription (RxBAM), calcium and vitamin D, have been shown to increase bone mineral density (BMD) and reduce the risk of fractures, yet utilization rates post hip fracture are still low. Studies examining the overall benefit of this group of medications on BMD in a hip fracture population are lacking, aside from a single specific randomized trial of zolendronic acid which has not translated as yet into standard clinical care. This study sought to identify trends in BAM use and determine if BAMs impact BMD in women during the 1-year post hip fracture period. Participants were 180 community-dwelling women aged 65 and older with surgical repair of an incident non-pathologic hip fracture from the fourth cohort of the Baltimore Hip Studies (BHS-4) that tested an in-home exercise intervention. Participants reported medication use and BMD at the total hip was measured within 22 days of fracture and at 2, 6, and 12 months post fracture. RxBAMs assessed were those available during the study time period (1998-2004) including: estrogen, etidronate, calicitonin, alendronate, and risendronate. Prior to the hip fracture, 85 (47%) took calcium/vitamin D only, 5 (3%) took RxBAM only, 50 (28%) took both calcium/vitamin D and RxBAM, and 39 (22%) took neither. Over 12 months post fracture, only 29 (16%) participants took RxBAMs during the entire study period. Of those who were using RxBAMs at any time post fracture (81) only 26 (32%) were new users while many participants started and stopped treatment or never started. A longitudinal analysis using a mixed effect model was performed. A two way interaction between BAM use and time was statistically significant ($p<.05$). While BAM users had lower total hip BMD at baseline [0.645 (0.01) vs. 0.657 (0.01) gm/cm2] compared to nonusers, BAM users had higher BMD at 12 months [0.635 (0.01) vs. 0.619 (0.01) gm/cm2]. These results show the beneficial effect of BAMs post fracture in preserving BMD over time.

***Disclosures: Emma G. Sheldon**, None.*

MO0312

Hip fracture incidence is much higher in Hong Kong Chinese women than Beijing Chinese women despite higher bone density in Hong Kong women: Major implications for hip fracture prevention. Rick Chung*[1], George Qin[2], Peng Cheng Ha[2], Edith Lau[1]. [1]Center for Clinical & Basic Research (CCBR) (Hong Kong), Hong Kong, [2]Center for Clinical & Basic Research (CCBR), China

Back ground and objectives: Hong Kong has the highest incidence of hip fracture in Asia, while mainland China still has very low incidence of hip fracture. However, it has been predicted there will be a major epidemic of hip fracture in China. The objective of the current study is to compare the bone mineral density at the hip between a large population sample of Hong Kong and mainland Chinese women, so that insight can be gained into the etiology of hip fracture.

Subjects and Methods: 7130 ambulatory Hong Kong Chinese women and 7037 mainland Chinese women living in Beijing (aged 50 to 96) were recruited from the community. They volunteered for the study. BMD was measured by Lunar Prodigy Advance Whole Body Bone Densitometers. Cross calibration was carried out by a phantom. The prevalence of osteoporosis was calculated according to the World

Health Organization criteria. BMD at the total spine and femoral neck were adjusted for age, height and weight and compared between the 2 populations.

Results: According to published data, the incidence rate of hip fracture was 465/100,000 in Hong Kong Chinese women and 229/100,000 in Beijing Chinese women. The prevalence of osteoporosis at the total hip in our study was 24.8% in Hong Kong Chinese women and 20.0% in Beijing Chinese women, but these did not account for difference in weight and height. After adjustment for age, height and weight, the BMD of Hong Kong Chinese women was 2.8% higher at the hip and 1.5% higher at the femoral neck than Beijing Chinese women. This implies that BMD is a poor measurement of bone strength, and also that there are many extraskeletal factors causing hip fracture.

Conclusion: The difference in hip fracture incidence between Hong Kong Chinese and Beijing Chinese women cannot be explained by difference in BMD. Further research should focus on better measurement of bone strength in Chinese women, as well as extraskeletal factors for hip fracture, so that recommendations can be made to prevent the imminent epidemic of hip fracture in mainland China.

		Mean (g/cm²)		
Total hip	Age group	Hong Kong (n=7130)	Beijing (n=7037)	P Value by t-test
	50-64	0.907	0.886	<0.05
	≥65	0.806	0.780	<0.05
	All	0.838	0.815	<0.05
Femoral neck BMD	50-64	0.834	0.824	<0.05
	≥65	0.737	0.722	<0.05
	All	0.767	0.756	<0.05

Bone mineral density (BMD) with adjustment for age, height and weight at the hip in subjects from Beijing and Hong Kong.

Figure 1

***Disclosures: Rick Chung**, None.*

MO0313

Increased Bone Loss is Associated with Post-Fracture Mortality. Dana Bliuc*, Nguyen Nguyen, Tuan Nguyen, John Eisman, Jacqueline Center. Garvan Institute of Medical Research, Australia

Background: Mortality risk is increased following all major osteoporotic fractures, however the mechanism of this risk is unknown. Bone loss, a risk factor for osteoporotic fracture is associated with mortality in the general population. However, the role of bone loss in mortality risk post-fracture is unknown. This study aims to examine the effect of bone loss on post-fracture mortality.

Methods: Women and men aged 60+ from Dubbo Osteoporosis Epidemiology Study with incident fractures followed prospectively from April 1989 to December 2012. Bone density at the hip was measured at baseline and 2-yearly. Bone loss was assessed by linear regression for each participant. Quartiles of bone loss were assessed using Kaplan-Meier survival curves. Bone loss was also assessed as a continuous variable using Cox Proportional Hazards Models.

Results: 462 women and 149 men with incident fracture and at least 2 BMD measurements were included. Women and men had a similar age and fracture distribution. The rate of bone loss was similar for women and men (women: mean -0.75%/year and highest quartile: -1.38%/yr; men: mean -0.74%/yr and highest quartile: -1.34%/year). Using Kaplan-Meier analysis, survival was lowest for the highest quartile of bone loss for both women and men (women, p<0.005; men, p=0.05). When analysed by fracture type, the association of bone loss with mortality was observed for vertebral (highest quartile vs. lower 3 quartiles of bone loss, women p=0.03 and men p=0.03) and non-hip non-vertebral fractures (highest quartile vs. lower 3 quartiles of bone loss, women p=0.03 and men p=0.05), but not for hip fractures (highest quartile vs. lower 3 quartiles of bone loss, women p=0.5 and men p=0.7).

When bone loss was assessed as a continuous variable in a Cox Proportional Hazards Model, a decrease in bone mass by 1%/per year was associated with 13% increased mortality risk in women [HR: 0.87 (95% CI, 0.80- 0.94)] and 8% in men [HR 0.92 (95% CI, 0.80- 0.98)]. The effect of bone loss on mortality risk was maintained after adjusting for age in women [age-adjusted HR 0.87 (95% CI, 0.80- 0.96)] but not in men [age-adjusted HR 0.91 (95% CI, 0.80- 1.39)].

Conclusion: In this study bone loss was associated with increased mortality risk in both women and men, particularly for vertebral and non-hip non-vertebral fractures. The effect of bone loss on mortality was less clear for hip fractures.

***Disclosures: Dana Bliuc**, None.*

MO0314

Ethnic Difference in Lumbar Spine TBS Between White, Black and Asian Women: Towards Explaining a Paradox?. William Leslie*[1], Olivier Lamy[2], Didier Hans[3]. [1]University of Manitoba, Canada, [2]University Hospital, Switzerland, [3]Lausanne University Hospital, Switzerland

Asian women have lower fracture rates than White women despite lower areal BMD. Black women have lower fracture rates than both White and Asian women but also have higher areal BMD. Both Asian and Black women tend to have stronger cortical parameters than White women at the axial site, but little is known about axial trabecular microarchitecture. TBS, a novel gray-level measurement of lumbar spine DXA image texture, is related to microarchitecture and fracture risk independently of BMD. Our aim was to evaluate ethnic difference in lumbar spine TBS.

41 147 White, 739 Asian and 152 Black women age ⩾50 years at the time of baseline hip (femoral neck) and spine (L1-4) DXA were identified from a database containing all clinical results for the Province of Manitoba, Canada. Spine TBS (TBS iNsight®) was derived from each spine DXA examination blinded to clinical parameters and outcomes. ANCOVA models were used to estimate least squares mean (LSM) ethnic TBS and BMD adjusted for FRAX variables (age, BMI, prior fracture, parental hip fracture, COPD, recent glucocorticoid use, rheumatoid arthritis, alcohol/substance abuse diagnosis), prior osteoporosis treatment, and bone area. Health service records were assessed for incident non-traumatic fracture codes after BMD testing.

Mean age of the women was 65.4 ± 9.2 y. Spine and hip BMD LSM showed significant between-ethnicity differences: Black > White > Asian (all p<.001). Spine TBS LSM showed a different pattern: Asian = White > Black (p<.01). Ethnic differences were unaffected by further adjustment for spine or hip bone area. During mean 5.6 y of follow up major osteoporotic fractures (MOF) occurred in 2626 (6.4%) White versus 22 (3.0%) Asian women (p<.001), despite similar estimated fracture risk from FRAX with BMD: MOF White 10.8% (±7.1) versus Asian 10.2% (±6.5), p=0.027; hip fracture White 2.6% (±4.2) versus Asian 2.5% (±3.6), p=0.425.

In conclusion, we observed significant ethnic differences in spine TBS, a correlate of trabecular bone structure. These differences were unrelated to skeletal size, BMI or other covariates and showed a different pattern from BMD differences. Our results suggest that TBS may be useful for assessing ethnic differences in bone quality, and may be less sensitive to skeletal size differences than areal BMD. The finding of lower spine TBS in Black women was unexpected, and requires confirmation. Studies in larger populations with more fracture events and greater ethnic diversity are warranted.

Ethnicity	Hip BMD T-score	p-value vs White	Spine BMD T-score	p-value vs White	Spine TBS unitless	p-value vs White
Adjusted for FRAX covariates and prior treatment						
Asian	-1.72	<.001	-1.48	<.001	1.232	0.466
White	-1.44		-1.15		1.235	
Black	-0.81	<.001	-0.89	0.022	1.210	0.007
Adjusted for bone area, FRAX covariates and prior treatment						
Asian	-1.65	<.001	-1.32	<.001	1.211	0.308
White	-1.45		-1.15		1.236	
Black	-0.77	<.001	-0.82	<.001	1.200	0.013

Table: Least square means in BMD and TBS (adjusted ANCOVA models)

***Disclosures: William Leslie**, None.*

MO0315

Associations among Dietary Phosphorus Intake and Bone Turnover Markers in 37-to-47-year-old Caucasian Population - The PHOMI Study. Suvi Itkonen*[1], Elisa Saarnio[1], Virpi Kemi[1], Heini Karp[1], Merja Kärkkäinen[1], Minna Pekkinen[2], Juha Risteli[3], Marja-Kaisa Koivula[4], Kaisa Ivaska[5], Christel Lamberg-Allardt[1]. [1]University of Helsinki, Finland, [2]Folkhälsan Institute of Genetics, University of Helsinki, Finland, [3]University of Oulu, Finland, [4]NordLab Oulu & Department of Clinical Chemistry, Institute of Diagnostics, University of Oulu, Finland, [5]University of Turku, Finland

Phosphorus (P) intake in Western countries is high due to abundant intake of animal protein and also because of the expanding use of highly absorbable P salts as food additives. In short-term studies high P intake has had negative effects on bone metabolism but the long-term effects are unknown. The aim of the study was to investigate the associations among dietary P intake and bone turnover markers in a cross-sectional Caucasian population in Finland.

A sample of 370 37-to-47-year-old pre-menopausal females who participated in the PHOMI Study was included in the analyses. Fasting blood samples were collected, as well as habitual dietary intake by 3-day food records and background data by a questionnaire. Serum osteocalcin (OC) and intact pro-collagen type I amino-terminal propeptide (iPINP) (both characteristics of bone formation), bone resorption marker collagen type 1 cross-linked C-terminal telopeptide (CTX) and some other biomarkers related to bone metabolism were analysed. The data was statistically analysed by analysis of variance (ANOVA) and analysis of covariance (ANCOVA) in tertiles of P intakes using different combinations of covariates (contraceptive use (CU), age, 25-hydroxy vitamin D (25OHD), smoking, weight). Linear trends were tested by contrast analyses.

In unadjusted analyses, P intake was inversely associated with iPINP and CTX over the tertiles (p=0.003 and p=0.049, ANOVA), and between P intake and OC existed a negative linear trend (p=0.034). In the covariate-adjusted models the most significant results were found using CU, age, smoking and 25OHD as covariates: P intake was adversely associated with iPINP (p=0.005, ANCOVA), between P intake and CTX existed a negative linear trend (p=0.020), and between P intake and OC an almost statistically significant negative linear trend was found (p=0.057). When weight was introduced as a covariate among above-mentioned ones, the significance weakened: between P intake and iPINP a negative linear trend (p=0.005) was found while the results between P intake and CTX or OC were non-significant (p>0.05).

High P intake seems to be associated with lower concentrations of iPINP, a linear trend towards lower concentrations of CTX was found, and a tendency towards a linear trend to lower concentrations of OC emerged, altogether indicating lower bone turnover with higher P intake.

Keywords: phosphorus, phosphate, osteocalcin, iPINP, CTX, bone turnover markers

***Disclosures: Suvi Itkonen**, None.*

MO0316

Associations between Serum Concentrations of Vitamin B12, Folate and Iron, and Body Composition in Adults Aged ⩾ 45 years: An Analysis of NHANES 1999-2002. Maryam Hamidi*[1], Jeevitha Srighanthan[1], Angela M. Cheung[2]. [1]University Health Network, Canada, [2]University Health Network-University of Toronto, Canada

Background: There is evidence that vitamin B12, folic acid and iron can influence lipid, bone and muscle metabolism by different mechanisms. However, very few studies have examined the associations between serum concentrations of B12 (sB12), folate (sFol) and iron (sFe) and body composition.

Objectives: To examine the associations between serum concentrations of sB12, sFol and sFe, and body composition (measured by dual energy X-ray absorptiometry (DXA)), BMI and waist circumference (WC) among men and women aged ⩾ 45 years in a population-based study.

Methods: We used cross-sectional data from the National Health and Nutrition Examination Survey (NHANES) 1999-2002. Weighted survey procedures with adjustments for age, ethnicity, physical activity, nicotine exposure and income were used for all analyses. The study sample included 666 postmenopausal women and 1326 men who were not taking hormones, steroids or medications that may affect body composition; and were free from kidney and liver disease, cancer and rheumatoid arthritis. DXA was used to measure trunk and total body fat and lean mass (g), trunk and total body fat percent, and BMD of lumbar spine and sub-total body (total body BMD-head BMD).

Results: Mean age for men and women was 56.8 ± 0.33 and 64.78±0.51 years, respectively. We found significant negative associations between sB12 and fat mass variables ($p < 0.05$) in women and men. In women, there were also significant negative associations between both sB12 and sFol, and WC and BMI ($p<0.05$). In men, sFe had significant positive associations with lean mass variables and sub-total body BMD ($p<0.05$).

Conclusions: To our knowledge, this is the first population-based study that examined the associations between sB12, sFol and sFe and body composition. Our results suggest that high sB12 may be associated with low fat mass in men and women; also that the associations between sFol and sFe, and body composition may be different between men and women. Further investigations into the associations between sB12, sFol and sFe, and body composition are warranted.

***Disclosures: Maryam Hamidi**, None.*

MO0317

Dietary Fatty Acid Intake Does Not Interact with the Association between Tumor Necrosis Factor-α Soluble Receptors and Incident Hip Fracture in The Women's Health Initiative. Steven Ing*[1], Tonya Orchard[1], Andrea Lacroix[2], Charles Kooperberg[2], Aaron Aragaki[2], Martha Belury[1], Bo Lu[1], Rebecca Jackson[1]. [1]The Ohio State University, USA, [2]Fred Hutchinson Cancer Research Center, USA

Background: Inflammatory biomarkers, tumor necrosis factor-a soluble receptor (TNFa-sR) 1 and 2 are positively associated with incident hip and total fracture. Polyunsaturated fatty acids (PUFA) are inversely associated with these markers of inflammation and could modify this association.

Methods: A nested case-control study from the Women's Health Initiative Clinical Trial and Observational Study of hip fracture cases and matched controls (400 pairs matched on age, year of enrollment, randomization to hormone therapy or self-reported hormone use). The outcome variable was centrally adjudicated incident hip fracture. Predictors were baseline serum TNFa-sR1 and TNFa-sR2 concentration. Candidate effect modifiers were dietary intake of fatty acids determined by baseline Food Frequency Questionnaire: saturated fatty acids, mono-unsaturated fatty acids (MUFA), poly-unsaturated fatty acids (PUFA), total n-3 fatty acids, total n-6 fatty acids, eicosapentaenoic acid (EPA), docosahexaenoic acid (DHA), and alpha linoleic acid (ALA). Data were analyzed using logistic regression models accounting for the paired design. Models were adjusted for hip fracture risk (composite FRAX score), other nutritional variables (total calcium intake, total vitamin D intake, total energy intake, total protein intake, multivitamin use) and factors impacting inflammation (NSAID use, arthritis, depression).

Results: Highest quartile of TNFa-sR1 and TNFa-sR2 were associated with greater risk of incident hip fracture in the fully adjusted base model (Table). The sample size decreased from the initial 400 pairs after exclusion of subjects with missing data and the consequent occurrence of partial pairs, yielding a final sample of 290 and 285 pairs for TNFa-sR1 and TNFa-sR2, respectively. These associations were confirmed using tests for linear trend (p for trend, 0.0069 and 0.0010 for TNFa-sR1 and TNFa-sR2, respectively). Testing the association of incident hip fracture using log TNFa-sR1 and log TNFa-sR2 as predictor also showed significant results (p=0.0055 and p=0.0034, respectively). Addition of fatty acid intakes into the fully adjusted model did not alter quartile-specific hip fracture risk (all changes <10%).

Conclusion: Highest baseline quartiles of TNFa-sR1 and TNFa-sR2 were associated with greater adjusted risk of incident hip fracture, but dietary fatty acid intakes did not modulate this association, perhaps related to limited narrow range of fatty acid intakes.

Table. Multivariate-adjusted OR of hip fracture based on quartiles of TNFα-sR1and TNFα-sR2[1,6]

		TNFα-sR1			TNFα-sR2		
	Q1	Q2	Q3	Q4	Q2	Q3	Q4
Base Model	1	1.298 (0.752, 2.241)	1.472 (0.850, 2.548)	2.340* (1.269, 4.318)	1.491 (0.853, 2.606)	1.715 (0.962, 3.060)	2.913* (1.559, 5.446)
n-6/n-3	1	1.260 (0.729, 2.178)	1.468 (0.845, 2.547)	2.270* (1.226, 4.202)	1.466 (0.838, 2.566)	1.697 (0.950, 3.033)	2.907* (1.551, 5.449)
EPA&DHA	1	1.290 (0.747, 2.229)	1.462 (0.844, 2.535)	2.284* (1.220, 4.276)	1.490 (0.852, 2.608)	1.699 (0.950, 3.037)	2.870* (1.528, 5.391)
ALA	1	1.295 (0.750, 2.236)	1.473 (0.850, 2.550)	2.341* (1.269, 4.318)	1.486 (0.850, 2.598)	1.716 (0.962, 3.063)	2.916* (1.560, 5.449)
SFA	1	1.270 (0.732, 2.205)	1.442 (0.830, 2.507)	2.285* (1.231, 4.243)	1.472 (0.840, 2.580)	1.700 (0.952, 3.034)	2.896* (1.546, 5.424)
MUFA	1	1.286 (0.744, 2.222)	1.463 (0.845, 2.535)	2.290* (1.235, 4.247)	1.479 (0.845, 2.591)	1.710 (0.959, 3.049)	2.893* (1.544, 5.423)
PUFA	1	1.299 (0.752, 2.241)	1.472 (0.850, 2.548)	2.333* (1.263, 4.308)	1.490 (0.852, 2.606)	1.715 (0.962, 3.059)	2.911* (1.557, 5.444)

[1] Odds Ratios (95% confidence interval) are obtained from logistic regression models
[2] Quartile 1 is the reference strata; OR=1
[3] n = 290 pairs for TNFα-sR1, 285 pairs for TNFα-sR2
[4] *P<0.05 relative to Q1
[5] Base model matched on age, year of enrollment, randomization to hormone therapy or self-reported hormone use; adjusted for composite FRAX score, nutritional variables (total calcium intake, total vitamin D intake, total energy intake, total protein intake, MVI use), and factors impacting inflammation (NSAID use, arthritis, depression)
[6] Interquartile cut points for TNFα-sR1: 1292.4, 1504.4 1800.9;TNFα-sR2: 2784.8, 3179.6, 3670.2 pg/ml

Table. Multivariate-adjusted OR of hip fracture based on quartiles of TNFa-sR1and TNFa-sR2

***Disclosures: Steven Ing**, None.*

MO0318

Higher Dairy Intakes are Associated with Improved Bone Health in a Population-based Study - CaMos. Claudie Berger*[1], Lisa Langsetmo[2], Susan I Barr[3], Jonathan Adachi[4], David Hanley[5], Jerilynn Prior[3], Christopher Kovacs[6], Elham Rahme[7], Stephanie Kaiser[8], Robert Josse[9], Alexandra Papaioannou[10], Nancy Kreiger[11], David Goltzman[7]. [1]CaMos, McGill University, Canada, [2]Canandian Multicenter Osteoporosis Study, Canada, [3]University of British-Columbia, Canada, [4]St. Joseph's Hospital, Canada, [5]University of Calgary, Canada, [6]Memorial University of Newfoundland, Canada, [7]McGill University, Canada, [8]Dalhousie University, Canada, [9]St. Michael's Hospital, University of Toronto, Canada, [10]Hamilton Health Sciences, Canada, [11]University of Toronto, Canada

Background: Calcium and vitamin D are essential for bone health. Dairy products are sources of both nutrients, but associations between dairy products and the primary measures of bone health remain to be elucidated.

Objective: To determine associations between total dairy intake (milk, milk dessert, yogurt, cheese, cream soup) and bone health outcomes (blood biomarkers, bone mineral density [BMD], incident fracture).

Methods: We used data from 984 youth aged 16-24 years (y), 1625 adults aged 25-49 y, and 6937 adults aged >50 y from the Canadian Multicentre Osteoporosis Study, a prospective population-based cohort. Youth and adult (>25 y) participants had an interviewer-administered questionnaire with clinical assessments including BMDs at baseline, Year 2 in youth and Years 5 and 10 in adults. A subgroup of each cohort had fasting blood drawn. Participants were contacted annually to ascertain incident fracture up to Year 15. Hierarchical models (over 2 y in youth and 10 y in adult), multiple linear regression (baseline and over 2 and 10 y) and Cox proportional hazards (over 15 y) were used to assess the association of total dairy intake with biomarkers (25-Hydroxyvitamin D [25OHD],parathyroid hormone [PTH], bone specific alkaline phosphatase [BSAP], C-terminal telopeptide of type I collagen [CTX], Insulin-like growth factor-1 [IGF-1]), BMDs and incident main fracture (hip, clinical spine, forearm, humerus). All analyses were adjusted for possible confounders.

Results: *Biomarkers*: Using hierarchical models and data available at all interviews, higher total dairy intake per day was associated with higher 25OHD levels in men 16-24, women 25-49 y, and women and men >50 y (Table 1). Higher total dairy intake was also associated with a lower PTH levels in men 25-49 y; higher IGF-1 in women 25-49 y; and lower BAP and CTX in women and men >50 y.

BMDs: Higher baseline total dairy intakes were associated with higher baseline total hip and/or femoral neck BMD in men 25-49 y and in women and men > 50 y (Table 2).

Fractures: Among men >50 y, overall higher dairy intake was associated with a lower risk of incident main fracture with HR=0.80 (95% CI: 0.64; 0.99). In contrast, among women >50 y, overall dairy intake was not associated with risk of main fracture.

Conclusion: Higher total dairy intake is associated with apparent better bone health as reflected by improved blood biomarkers, maintenance of or increased BMD, and reduced risk of fracture in men over age 50.

Table 1: Hierarchical models (using data available at all interviews) assessing associations among total dairy intakes per day with the Vitamin D (25OHD), Parathyroid Hormone (PTH) levels, growth factors (IGF-1) and bone turnover biomarkers: bone specific alkaline phosphatase (BSAP) and C-telopeptide (CTX) in men and women in the youth (ages 16-24) and adult (ages ≥25) cohorts of the Canadian Multicentre Osteoporosis Study.

Estimates and 95% C.I.	25(OH)D (nmol/L)	PTH (log-scale)	IGF-1 (log-scale)	BSAP (log-scale)	CTX (log-scale)
Women 16-24					
>500 to 1000 ml	-0.2 (-10.1; 9.5)	0.073 (-0.068; 0.215)	0.004 (-0.131; 0.121)	0.022 (-0.100; 0.141)	-0.063 (-0.187; 0.061)
> 1000 ml	4.8 (-6.8; 16.3)	0.016 (-0.149; 0.180)	0.018 (-0.118; 0.152)	0.048 (-0.094; 0.185)	0.031 (-0.105; 0.173)
Men 16-24					
>500 to 1000ml	2.5 (-7.1; 11.7)	0.089 (-0.063; 0.242)	-0.084 (-0.187; 0.022)	0.049 (-0.114; 0.217)	0.107 (-0.052; 0.257)
> 1000 ml	**14.5 (3.3; 25.5)**	0.033 (-0.125; 0.191)	-0.50 (-0.169; 0.069)	-0.061 (-0.252; 0.132)	0.043 (-0.120; 0.201)
Women 25-49					
>500 to 1000ml	1.8 (-2.3; 5.9)	0.010 (-0.070; 0.090)	**0.060 (0.002; 0.112)**	-0.003 (-0.065; 0.060)	-0.027 (-0.132; 0.077)
> 1000 ml	**5.1 (0.1; 10.2)**	-0.031 (-0.132; 0.070)	0.061 (-0.010; 0.132)	-0.012 (-0.090; 0.067)	0.041 (-0.088; 0.171)
Men 25-49					
>500 to 1000ml	-0.1 (-5.0; 4.9)	-0.048 (-0.161; 0.068)	-0.042 (-0.107; 0.024)	0.002 (-0.074; 0.078)	-.014 (-0.113; 0.087)
> 1000 ml	0.9 (-5.8; 7.8)	**-0.150 (-0.300; 0.000)**	-0.023 (-0.117; 0.070)	0.044 (-0.062; 0.151)	-0.032 (-0.172; 0.106)
Women ≥50 y					
>500 to 1000ml	**2.0 (0.1; 4.0)**	0.024 (-0.012; 0.061)	--	-0.001 (-0.032; 0.030)	0.010 (-0.042; 0.063)
> 1000 ml	**5.6 (3.1; 8.3)**	0.024 (-0.026; 0.073)	--	-0.012 (-0.055; 0.031)	-0.053 (-0.124; 0.018)
Men ≥50 y					
>500 to 1000ml	**3.8 (0.7; 6.9)**	-0.019 (-0.077; 0.041)	--	**-0.065 (-0.120; -0.011)**	**-0.135 (-0.205; -0.063)**
> 1000 ml	**5.6 (1.3; 10.0)**	-0.025 (-0.107; 0.054)	--	**-0.085 (-0.161; -0.011)**	**-0.122 (-0.220; -0.023)**

*The reference category is ≤ 500 ml. Results excluding 0 in their 95% C.I. are in bold.

Table 1: Total dairy intake and biomarkers

Table 2: Association of baseline total dairy intake per day with baseline bone mineral density (BMD, g/cm^2) in men and women in the youth (ages 16-24) and adult (ages ≥25) cohorts of the Canadian Multicentre Osteoporosis Study.

Estimates and 95% C.I.	Total hip BMD	Femoral neck BMD	Lumbar spine BMD
Women 16-24 y			
>500 to 1000ml	-0.006 (-0.036; 0.024)	-0.006 (-0.033; 0.021)	-0.010 (-0.037; 0.017)
> 1000 ml	-0.021 (-0.056; 0.014)	-0.014 (-0.045; 0.018)	-0.028 (-0.060; 0.004)
Men 16-24 y			
>500 to 1000ml	-0.034 (-0.074; 0.007)	-0.028 (-0.067; 0.010)	0.004 (-0.032; 0.040)
> 1000 ml	0.021 (-0.017; 0.058)	0.006 (-0.030; 0.042)	0.012 (-0.022; 0.045)
Women 25-49 y			
>500 to 1000ml	0.006 (-0.011; 0.022)	0.013 (-0.002; 0.029)	0.001 (-0.018; 0.019)
> 1000 ml	0.001 (-0.021; 0.022)	0.007 (-0.012; 0.027)	-0.009 (-0.033; 0.015)
Men 25-49 y			
>500 to 1000ml	0.003 (-0.019; 0.024)	0.006 (-0.013; 0.025)	-0.002 (-0.026; 0.022)
> 1000 ml	0.024 (-0.003; 0.050)	**0.032 (0.009; 0.056)**	0.023 (-0.006; 0.053)
Women ≥50 y			
>500 to 1000ml	0.006 (-0.001; 0.013)	**0.006 (0.000; 0.012)**	0.003 (-0.006;0.013)
> 1000 ml	**0.017 (0.007; 0.026)**	**0.017 (0.009; 0.026)**	0.011 (-0.003; 0.024)
Men ≥50 y			
>500 to 1000ml	-0.013 (-0.045; 0.018)	0.006 (-0.006; 0.017)	0.012 (-0.005; 0.029)
> 1000 ml	0.012 (-0.029; 0.052)	**0.015 (0.000; 0.029)**	0.009 (-0.012; 0.031)

*The reference category is ≤ 500 ml. Results excluding 0 in their 95% C.I. are in bold.

Table 2: total dairy intake and BMD

***Disclosures: Claudie Berger**, None.*
This study received funding from: Dairy farmers of Canada

MO0319

Prediction Model for Normal Vitamin D in Elderly Women. Thomas Merlijn*, Petra Elders, Coen Netelenbos. VU medical center, The Netherlands

Introduction: Vitamin D insufficiency is common in elderly and results in increased risk of falls and fractures. Several guidelines advise suppletion of vitamin D in elderly. Possibly not all elderly women are at risk for vitamin D insufficiency or deficiency.

Goal: The goal of this study is to develop a model to distinguish elderly women with normal serum 25-hydroxyvitamin D levels (> 50nmol/l).

Methods: For modelling we used data of the participants of the first included regions of the SOS-trial. This is a primary care population of women ⩾65 years with at least one risk factor for osteoporosis. All women completed a questionnaires and subsequently bone densitometry and laboratory tests (including 25-hydrxoyvitamin D, Diasorin) were performed. Vitamin D levels and other variables were categorized or dichotomized. Multiple logistic regression with backward selection was applied to select the predictors for the model. The model will be validated in two extern populations.

Results: Data of 2301 women were available for modelling. The AUC of the model was 0,737. Table 1 shows the predictors and a risk score. Table 2 shows the results at different cut-off points.

Discussion

We formulated a model to predict normal vitamin D levels. This model shows the important role of the seasons. All elderly women without vitamin D suppletion, even in absence of risk factors, are at risk for vitamin D insufficiency in winter.

Table 1. Predictors in the model and risk score

Risk factor	Score
Age> 75 years	2
BMI >kg/m2	1
Length < 160cm	1
Smoking	1
Actual prescriptions≥ 7 /day	1
Time outdoor in summer < 1hour/day	2
Walking aid	2
Season spring/ autumn (Nov, Dec, Jan, May, June)	2
Season winter (Feb, March, April)	4
Vitamin D,prescription	-7
Vitamin D, self administered	-2
Multivitamin use	-2

Table 2. Positive predictive value of the total risk score

Cut-off	≤-2	≤-1	≤0	≤1	≤2	≤3	≤4	≤5	≤6	≤7
N	142	215	364	616	823	1135	1375	1680	1878	2032
PPV Vit D >50	85,9%	84,2%	79,4%	74,4%	71,6%	65,0%	62,0%	57,7%	55,1%	52,5%
PPV Vit D >30	2,1%	2,3%	2,5%	3,7%	4,4%	6,4%	7,5%	9,9%	11,0%	11,9%

Table 1 and 2

***Disclosures: Thomas Merlijn**, None.*

MO0320

Vitamin D Levels and Calcium Supplementation One-Year Follow up in Osteopenic Patients in West Bohemia. Vaclav Vyskocil*[1], Tomas Pavelka[2]. [1]Center for Metabolic Bone Diseases, Czech Republic, [2]Department of Orthopaedic Surgery, Czech Republic

Authors observed the group of 2900 patients in age between 18 - 91, who were examined by DXA in period from February 2011 to February 2012. All patients had at any of the measured points BMD lower than -2.0 SD.

The aim of the study was to determine vitamin D saturation according to preselected age categories and simultaneously determine existing relation between vitamin D level and bone density. In the second phase we planned to evaluate calcium and vitamin D intake from supplementation and food in order to confirm effect on study results.

Patients were divided into age groups: 18-25 years (15 patients), 26-55 (307 patients), 56-80 (1469 patients), 81 and more (112 patients).

Vitamin D levels were significantly higher in summer months in patients between 18-25 years, mostly in women. Increased values in summer season were also detected in the 26-55 year category and in patients between 56-80 years were the vitamin D values constant.

Lower level of vitamin D (25(OH)D<50 nmol/l) was present in 80% of patients in the group 18-25 years, 71% in the group of 26-55 years, 64.7% in the group of 56-80 years and only 59.5% in the group of older than 80 years.

Our analysis of more than 2000 patients confirmed the effect of insolation on vitamin D levels in summer months in the group 18-25 years and a partial effect on the group 26-55 years.

Further we found strong deficiency of 10-40 nmol/ml vitamin D in men older than 80 years, whereas in other age groups were the values sufficient, average value about 80 nmol/ml.Calcium and vitamin D intake was evaluated by questionnaire. We collected above mentioned parameters in 2000 patients. We evaluated the effect of supplementation on vitamin D level in those patients one year after initial measurement. Patient with low level of vitamin D were divided into 2 groups according to BMI (BMI ≤25 and BMI ⩾ 30). Effect on vitamin D level was corrected with respect to different BMI. Higher doses of vitamin D were required to normalize vitamin D level in obese patients. Higher calcium intake correlated with higher BMD increase in lumbar spine.

***Disclosures: Vaclav Vyskocil**, None.*

MO0321

Updated Non-hip to Hip Fracture Ratios in Canadian Men and Women with Potential Implications for FRAX Calibration: A Population Based Analysis.

William Leslie*[1], Lisa M Lix[1], Marina Yogendran[1], Anna Lam[1], Suzanne Morin[2], Colleen Metge[1], Sumit Majumdar[3]. [1]University of Manitoba, Canada, [2]McGill University, Canada, [3]University of Alberta, Canada

Background: FRAX tools are calibrated from country-specific fracture epidemiology, but data on non-hip fractures are difficult to collect. Where accurate non-hip fracture information is lacking, rates can be estimated assuming that a similar relationship with hip fractures exists as in 1987-1994 data from Malmo, Sweden (Kanis: OI 2000;11:669). Evidence to support this assumption in other populations is limited and ratios may have changed given secular changes in hip fractures which are declining in North America.

Objective: To examine ratios of osteoporotic fractures in the Province of Manitoba, Canada and compare these to older Swedish ratios.

Methods: We used 2000-2007 data from the Manitoba Population Health Research Data Repository to identify incident major osteoporotic fractures using definitions that approximate population-based Canadian rates from CaMos (Lix: BMC Public Health 12:301, 2012). Age (5 year subgroups) and sex specific ratios in fracture counts (clinical vertebral, forearm, humerus versus hip) with 95% confidence intervals were calculated and compared with the equivalent Swedish ratios.

Results: During 7-years of observation, 14 191 incident fractures were identified (men versus women: 1611 / 3285 vertebral, 1090 / 4387 forearm, 844 / 2699 humerus, 1373 / 3820 hip). All non-hip/hip ratios decreased with age for both sexes (Figure). Men and women showed similar vertebral/hip ratios (all $p > 0.1$, odds ratios [ORs] 0.80-1.31). Forearm/hip ratios were significantly lower among men than women for all ages (all $p < 0.001$, ORs 0.31-0.57), and also significantly lower in eight of nine age subgroups for humerus/hip (ORs 0.45-0.65, NS for age 80-84 years). A similar pattern was observed for any non-hip/hip ratios which were significantly lower among men than women in seven of nine age subgroups (ORs 0.45-0.83, NS for age 80-84 years and 90+ years). Compared to Swedish ratios, Canadian ratios were significantly higher among younger age subgroups in both men and women, but showed closer agreement for older age subgroups.

Conclusions: All non-hip to hip fracture ratios decreased with age in both sexes, with non-vertebral to hip fracture ratios significantly greater in women than men. Non-hip to hip fracture ratios were higher in younger Canadian men and women than ratios computed from previously reported Swedish data. FRAX tools calibrated using these older ratios may underestimate fracture risk in younger individuals.

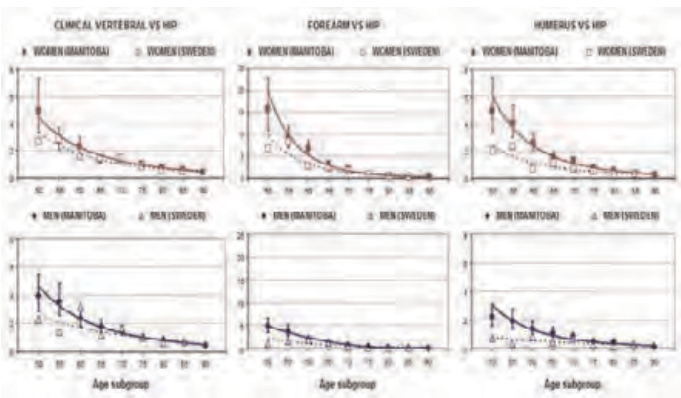

Figure: Non-hip to hip fracture ratios by age and sex

***Disclosures: William Leslie**, None.*
This study received funding from: Amgen Canada

MO0322

Withdrawn

MO0323

Can we improve the reproducibility of vertebral fracture assessment (VFA) readings?An exploratory study based on the OsteoLaus Cohort.

Bérengère Aubry-Rozier*[1], Katia Iglesias[2], Marc-Antoine Krieg[1], Olivier Lamy[1], Bernard Burnand[2], Didier Hans[1]. [1]Center for Bone Diseases. Lausanne University Hospital, Switzerland, [2]Département de médecine sociale et préventive, Lausanne University Hospital, Switzerland

Osteoporotic vertebral fractures are highly prevalent and a major cause of morbidity and mortality in industrialized countries. The *vertebral fracture assessment* (VFA), obtained with bone mineral density testing via dual energy X-Ray absorptiometry (DXA) has been validated for vertebral fracture diagnosis in clinical settings. The International Osteoporosis Foundation (IOF) and the International Society of Clinical Densitometry (ISCD) both proposed specific guidelines for VFA interpretation. But the reproducibility of VFA reading is not known in population based cohort screening. The aim of this study was to estimate the benefits of using IOF/ISCD guidelines for VFA reading and to estimate the level of reproducibility within and between raters for VFA in a population based cohort. To assess these estimations, two statistical tolls were used: Cohen's and uniform kappa coefficients.

360 women were randomly selected from the larger cohort OsteoLaus. We calculated inter- and intra-reading reproducibility of the two kappa statistics both before and after applying an IOF/ISCD adapted guideline (IIR). All readings were performed independently by two osteoporosis experts with extensive experience reading VFA but no prior training in the IOF/ISCD courses.Overall, 12% of vertebrae were unreadable, with this percentage as high as 48% for levels T4 and T5. Depending on the reader, the prevalence of VF varied from 3% to 4% with 3 to 4% grade 1, 0.6 to 1.3% grade 2 and 0.03% to 0.2% grade 3 VF. Before IIR application, inter-reader reproducibility with Cohen's kappa was 0.35 to 0.71 and 0.74 to 0.98 with the uniform kappa coefficient for all criteria. After applying the IRR recommendations, inter-reader reproducibility was 0.28 to 0.68 and 0.70 to 0.99, respectively. All the results were better for lumbar spine as for dorsal spine. We concluded that kappa uniform is better adapted for the screening in a population-based cohort (events rare and repartition not uniform) than kappa of Cohen. The uniform kappa statistic is more accurate as a measure of reproducibility than Cohen's kappa for VFA reading. Moreover the IOF/ISCD guidelines did not increase reproducibility in VFA reading when readers are already experts in osteoporosis

***Disclosures: Bérengère Aubry-Rozier**, None.*

MO0324

Characteristics Influencing Quality of Life in Women 6 Months After Suffering a Fragility Fracture.

Claudia Beaudoin*[1], Sonia Jean[2], Louis Bessette[3], Louis-Georges Ste-Marie[4], Jacques P. Brown[3]. [1]Centre de recherche du CHU de Québec, Canada, [2]INSTITUT NATIONAL DE SANTÉ PUBLIQUE DU QUÉBEC, Canada, [3]CHU de Quebec Research Centre, Canada, [4]CHUM, Canada

Purpose: To identify the socio-demographic and clinical characteristics associated with a decrease in quality of life in a cohort of women $\geq$ 50 years who suffered a fragility fracture (FF). Methods: In the Recognizing Osteoporosis and its Consequences in Quebec Programme, women who suffered a FF were recruited from hospitals and an administrative database-generated list. Women were contacted 6-8 months after a FF to complete a questionnaire detailing personal and clinical characteristics related to osteoporosis (diagnosis, treatment, comorbidities, risk factors, etc.). An EQ-5D health questionnaire was also sent to women to assess their health-related quality of life (HRQoL). In this questionnaire, 5 dimensions of health were covered (mobility, self-care, usual activities, pain/discomfort, and anxiety/depression) and collected data were used to construct a global index of health score ranging from -0.59 to 1 (0=dead, 1=full health). General perception of health was also evaluated with a visual analogue scale where 0 represents the worst health and 100, perfect health. To identify the characteristics associated with HRQoL, linear regression models were constructed using the health perception and global index scores as dependent variables as well as the socio-demographic and clinical characteristics as independent variables. Differences in the EQ-5D index score ranging from 0.03 to 0.07 were considered to be the minimal clinically important differences, as proposed by previous studies. Results: 1979 women completed both questionnaires. The characteristics associated with a decrease in the EQ-5D index score were: having suffered a hip/femur or humerus fracture, history of fractures after 40 years, kyphosis, comorbid conditions, being underweight or obese, being retired, unemployed, homemaker or disability, smoking tobacco, living alone, early menopause, and having received a diagnosis or treatment for osteoporosis (Table 1). Except for a history of fractures, the same characteristics were associated with a decrease in the health perception score (Table 2). Regular use of medications that decrease bone mineral density was also associated with a decrease in the health perception score. Conclusions: Hip, femur or humerus fractures have a significant influence on HRQoL 6-8 months after the event. Other characteristics related to bone health such as history of fracture after 40 years and having a kyphosis are also associated with a significant reduction in HRQoL.

Variable	Modality	Estimate (SD)	P-value
Intercept	-	0.78 (0.04)	<.0001
Age	-	0.003 (0.001)	<.0001
Fracture site	Forearm, elbow, wrist	Ref	<.0001
	Ankle, tibia/fibula, foot	-0.03 (0.01)	
	Humerus	-0.05 (0.02)	
	Hip, femur	-0.11 (0.02)	
Number of fractures after 40 years	0	Ref	<.0001
	1	-0.03 (0.01)	
	2	-0.04 (0.02)	
	3 and +	-0.11 (0.03)	
Kyphosis	No	Ref	<.0001
	Yes	-0.08 (0.01)	
Comorbidity (Charlson index)	0	Ref	<.0001
	≥1	-0.08 (0.01)	
Body mass index	Underweight	-0.06 (0.04)	<.0001
	Normal	Ref	
	Overweight	-0.02 (0.01)	
	Obesity	-0.08 (0.01)	
Employment status	Full-time, part-time or student	Ref	<.0001
	Retired, unemployed, …	-0.06 (0.01)	
Tobacco	Non-smoker	Ref	0.0003
	Ex-smoker	-0.01 (0.01)	
	Smoker	-0.06 (0.02)	
Living with another adult	No	-0.04 (0.01)	0.0002
	Yes	Ref	
Early menopause	No	Ref	0.0003
	Yes	-0.04 (0.01)	
Diagnosed or treated for osteoporosis	No	Ref	0.0271
	Yes	-0.02 (0.01)	

Table 1: Characteristics associated with a decrease in the EQ-5D index score (N=1743)

Variable	Modality	Estimate (SD)	P-value
Intercept	-	78.80 (3.35)	<.0001
Age	-	0.15 (0.05)	0.0029
Fracture site	Forearm, elbow, wrist	Ref	<.0001
	Ankle, tibia/fibula, foot	-0.87 (0.86)	
	Humerus	-3.38 (1.14)	
	Hip, femur	-7.29 (1.24)	
Kyphosis	No	Ref	<.0001
	Yes	-5.67 (0.85)	
Body mass index	Underweight	0.01 (2.51)	<.0001
	Normal	Ref	
	Overweight	-1.67 (0.86)	
	Obesity	-6.51 (0.97)	
Comorbidity (Charlson index)	0	Ref	<.0001
	≥1	-6.25 (0.77)	
Tobacco	Non-smoker	Ref	0.0029
	Ex-smoker	-1.21 (0.79)	
	Smoker	-3.79 (1.11)	
Employment status	Full-time, part-time or student	Ref	0.0002
	Retired, unemployed, …	-3.41 (0.91)	
Use of medications that decrease BMD	No	Ref	0.0005
	Yes	-2.82 (0.81)	
Early menopause	No	Ref	0.0016
	Yes	-2.55 (0.81)	
Living with another adult	No	-2.25 (0.76)	0.0032
	Yes	Ref	
Diagnosis and treatment for osteoporosis	Not diagnosed and treated	Ref	0.0189
	Diagnosed, but not treated	-3.05 (1.40)	
	Diagnosed and treated	-1.87 (0.83)	

Table 2: Characteristics associated with a decrease in the EQ-5D health perception score (N=1616)

***Disclosures: Claudia Beaudoin**, None.*
This study received funding from: Merck, sanofi-aventis, Warner Chilcott, Amgen, Eli Lilly, Novartis

MO0325

Could Fracture Risk Assessment in Elderly Men Be Improved by Adiponectin? Mr Os Sweden. Helena Johansson*[1], Anders Odén[2], Magnus Karlsson[3], Eugene McCloskey[4], John Kanis[5], Claes Ohlsson[6], Dan Mellström[7]. [1]Swedish University of Agricultural Sciences, The Biomedical Center, Sweden, [2]WHO Collaborating Centre, University of Sheffield, United Kingdom, [3]Skåne University Hospital Malmö, Lund University, Sweden, [4]University of Sheffield, United Kingdom, [5]University of Sheffield, Belgium, [6]Center for Bone & Arthritis Research at the Sahlgrenska Academy, Sweden, [7]Centre for Bone & Arthritis Research (CBAR), Sahlgrenska Academy, University of Gothenburg, Sweden, Sweden

Several studies suggest that high serum adiponectin is associated with an increased risk of fracture in elderly men. The aim of the present analysis was to determine the impact of serum adiponectin on the 10 year probability of fracture.

The 10 year probability of osteoporotic fracture was computed in 989 elderly men recruited to the MrOS study in Gothenburg, Sweden. Baseline data included clinical risk factors for fracture, femoral neck BMD and serum adiponectin. Poisson regression was used to model the hazard function for osteoporotic fracture and death. By using the hazard functions and extrapolation in time, the 10 year probability of fracture was calculated.

Men were followed for up to 7.4 years (average 5.3 years), during which 124 (13%) men sustained one or more osteoporotic fractures. The risk of fracture (adjusted for age and BMD) increased by 40% for each SD increase in serum adiponectin (gradient of risk =1.40; 95% CI = 1.16-1.68). The ten year probability of osteoporotic fracture was 21% for a man aged 75 years with a BMD T-score of -2.0 SD and an adiponectin value of 5.6μg/ml (10^{th} percentile). When adiponectin was 20.1μg/ml (90^{th} percentile) for the same age and BMD the probability was 39%. There was, however, a significant interaction between adiponectin and time since baseline (p=0.026), such that the longer time since baseline the lower the GR. When using this interaction in the calculation of 10 year probability of fracture, the ten year probabilities of osteoporotic fracture were almost identical in the examples above (probability was 32% for an adiponectin value of 5.6μg/ml and 33% for an adiponectin value of 20.1μg/ml).

Serum adiponectin is a risk factor for fracture, at least in the short term, but its predictive value attenuates with time. Its use for fracture risk assessment in the long term (10 years) is questionable. This study underlines the importance of testing the long term stability of potential risk factors in risk assessment.

***Disclosures: Helena Johansson**, None.*

MO0326

Exome chip analysis for osteoporotic fracture: Results from the CaMos/ ManMc consortium. Hou-Feng Zheng*[1], Vincenzo Forgetta[1], William Leslie[2], David Goltzman[1], Alexandre Montpetit[1], Mark Lathrop[1], Brent Richards[1]. [1]McGill University, Canada, [2]University of Manitoba, Canada

Background: Genome-wide association studies (GWAS) have identified loci associated with bone mineral density. However the influence of coding variation on osteoporotic fracture has not been systematically interrogated using standardized genotyping arrays.

Aim: To examine the effect of coding variants on the risk of osteoporotic fracture.

Methods: Using the Illumina HumanExome BeadChip we genotyped 1,202 osteoporotic fracture cases (83.5% occurring at distal forearm) and 862 controls at 247,870 coding variants. Cases had sustained x-ray or surgically confirmed osteoporotic fractures and controls were followed prospectively for ten years without sustaining any type of fracture. Accuracy of genotyping was assessed using duplicate samples, which had an average concordance rate of 99.99%. Population stratification was assessed using SmartPCA. After quality control, 1102 cases and 818 controls assayed at 244,030 variants remained for analysis. We tested for trait-SNP associations assuming an additive genetic model using a linear mixed model to correct for relatedness as implemented in the GEMMA software package. Given power considerations, only variants with a minor allele frequency greater than 0.5% (N = 41,263) were assessed.

Results: 133,207 (54.59%) variants were monomorphic in the studied individuals, 69,560 (28.5%) variants had a MAF <0.5%, 14,637 (6%) had a MAF between 0.5% and 5% and the remaining variants were common. We identified one missense variant to be genome wide significant for risk of fracture at C16orf71 (MAF=0.04, P= 1.74x10-8, OR=3.37) and two variants to be genome-wide suggestive ($P < 5x10-6$) at gene MDC1 (MAF=0.01, P= 5.13x10-7, OR=8.42), and at HLADPB1/HLADPA1 (MAF=0.22, P= 1.22x10-6, OR=1.51).

Conclusion: While replication of these findings are on-going, this study demonstrates the utility of exome array genotyping to identify coding variants contributing to osteoporotic fracture—a clinically relevant osteoporotic outcome.

***Disclosures: Hou-Feng Zheng**, None.*

MO0327

In men, bone microarchitecture measured by high resolution pQCT improves fracture prediction - the prospective STRAMBO study. Pawel Szulc*[1], Stephanie Boutroy[2], Roland Chapurlat[3]. [1]INSERM UMR 1033, University of Lyon, Hopital E. Herriot, Pavillon F, France, [2]INSERM UMR 1033, Université de Lyon, France, [3]E. Herriot Hospital, France

Areal bone mineral density (aBMD) measured by DXA is a suboptimal fracture predictor in older men, because low aBMD identifies only about 20% of men who will sustain subsequently a fragility fracture. Our aim was to assess the value of bone microarchitectural parameters for the fracture prediction in older men.

Bone microarchitecture was assessed at the distal radius and distal tibia by high resolution peripheral quantitative computed tomography (HR-pQCT, XtremeCT device, Scanco Medical AG, Brüttisellen, Switzerland) in a cohort of 819 men aged 60 to 87 yrs. During the average follow-up of 4.9 years, 76 men sustained at least one vertebral or peripheral fracture. Lower total volumetric BMD (vBMD), trabecular vBMD (Tb.vBMD, including Tb.vBMD assessed separately in the central and subendocortical compartments) and trabecular number (Tb.N) as well as higher separation (Tb.Sp) and distribution (Tb.Sp.SD) were associated with higher risk of fracture. After adjustment for age, weight, fall history and prior fracture, HR varied from 1.29 to 1.61 per SD change according to the parameter ($p<0.05$ to $p<0.001$). The trends were similar for both skeletal sites. After additional adjustment for ultradistal radius aBMD, Tb.N, Tb.Sp and Tb.Sp.SD of the distal radius remained

significantly associated with higher fracture risk (e.g., Tb.N: HR= 1.61 per SD decrease, 95%CI: 1.23-2.13, p<0.001). After additional adjustment for total hip aBMD, lower central Tb.vBMD and higher Tb.Sp.SD of the distal tibia remained associated with a significantly higher risk of fracture (e.g., central Tb.vBMD: HR= 1.38 per SD, 95%CI: 1.03-1.86, p<0.05). Cortical thickness and vBMD (assessed using the standard algorithm) as well as trabecular thickness did not predict fractures. In comparison with the lowest quartile of ultradistal radius aBMD, the lowest Tb.N quartile improved the sensitivity of the identification of fractures (46 vs 33%) without influencing specificity and better identified men at high risk of fracture (p<0.05). Similar results were obtained in the analyses limited to the fragility fractures (68 men) and low trauma fractures (69 men).

This is the first prospective analysis showing that assessment of bone microarchitecture by HR-pQCT may improve the fracture prediction in older men in comparison with DXA.

***Disclosures: Pawel Szulc**, None.*

MO0328

Long-Term Proton Pump Inhibitor Therapy: Large Effects on Falls and Fractures in Elderly Women. Joshua Lewis*[1], Deka Barre[2], Kun Zhu[1], Jeff Hughes[2], Richard Prince[3]. [1]University of Western Australia, Sir Charles Gairdner Hospital, Australia, [2]Curtin University, School of Pharmacy, Australia, [3]Sir Charles Gairdner Hospital, Australia

Proton pump inhibitors (PPIs) are widely used in the elderly. Recent studies have suggested long-term PPI therapy is associated with hip and spine fractures, however the mechanism remains unknown. We sought to determine the association between long-term PPI therapy greater than one year for fracture outcomes and fracture risk factors including bone structure, falls and balance-related function. The initial study was a post hoc analysis of a longitudinal prospective cohort of 1,025 elderly women followed for 5 years from 2003 (baseline) to 2008 with a pre-planned replication in a second prospective 9-month study of falling in 686 elderly postmenopausal women (replication study).

In Study 1 the adjusted odds ratio (AOR) for 5-year falls and fracture-related hospitalizations in participants on long-term PPI therapy (n = 120) compared to no long-term use at baseline (n = 905) was 2·168; 95% CI, 1·248-3·766; P = 0·006 and 1·947; 95% CI, 1·201-3·157; P = 0·007 respectively. In the replication study, long-term PPI therapy (n= 132) compared to no long-term PPI therapy (n = 554) was also associated with increased risk of falling, AOR, 1·509; 95% CI, 1·002 -2·273; P = 0·049. The number needed to cause harm (NNH) with long-term PPi therapy for injurious fall or fracture-related hospitalizations over the 5-year period in Study 1 was 11 and 14 respectively, while in the replication study the NNH was 11. Using mediation analyses the association of long-term PPI for fracture outcomes was completely mediated by the observed increased falling. Regarding mechanism in Study 1, bone structure determined from heel ultrasound, hip DXA and total body DXA did not differ by PPI use category, however falls associated metrics assessed by questionnaire and objective clinical measurements including; fear of falling indoors and outdoors, dizziness, numbness of the feet, timed up and go test and Romberg eyes closed test were all significantly impaired in long-term PPI users. In conclusion, long-term PPI therapy at baseline in elderly women doubled the risk of falling and fracture over 5 years compared to those with no long-term PPI use at baseline. PPI therapy was also associated with impaired balance, dizziness, numbness of the feet and increased fear of falling.

This substantial increase in risk of falls and fracture in individuals, already at high risk of falling, should be considered when prescribing PPI therapy in this patient group.

***Disclosures: Joshua Lewis**, None.*

MO0329

Mortality After a Hip Fracture in the United Kingdom: 2000 – 2011. Corinne Klop*[1], Paco Welsing[2], Cyrus Cooper[3], Johannes Bijlsma[4], Hubert Leufkens[1], Frank de Vries[1]. [1]Utrecht Institute for Pharmaceutical Sciences, Division of Pharmacoepidemiology & Clinical Pharmacology, Utrecht University, Netherlands, [2]Julius Center for Health Sciences & Primary Care, University Medical Center, Netherlands, [3]University of Southampton, United Kingdom, [4]Department of Rheumatology & Clinical Immunology, University Medical Center, Netherlands

Purpose: There are limited data on recent trends in mortality risk after hip fracture and this risk is often not adjusted for co-morbidities, medication use and lifestyle factors. Aims of this study were to examine trends in all-cause one-year mortality after hip fracture from 2000 to 2011 and to report on gender differences in cause-specific mortality.

Methods: A cohort study was conducted within the Clinical Practice Research Datalink (CPRD), which is the world's largest primary care database including more than 5 million patients in the United Kingdom. Patients with a first hip fracture between April 1st 2000 and March 31st 2011 (n=32,031) were matched to up to four controls (n=118,637) by age, sex, index date, and practice. Changes in all-cause one-year mortality in hip fracture patients and relative to control subjects were evaluated using Cox regression. Hazard Ratios [HRs] were adjusted for age, co-morbidities, lifestyle factors (body mass index, smoking status, alcohol use) and medication use. In order to estimate adjusted HRs of cause-specific relative mortality the CPRD database was linked to death certificates for 57% of all patients to assess the primary cause of death.

Results: As compared to 2000 – 2001, the all-cause one-year mortality risk after hip fracture tended to be lower for men in 2008 – 2009 (adj. HR 0.79, 95% Confidence Interval [CI]: 0.63 – 1.00) and was significantly decreased in 2009 – 2010 (adj. HR 0.79, 95% CI: 0.63 – 0.98) and 2010 – 2011 (adj. HR 0.68, 95% CI: 0.54 – 0.86). In contrast, no decrease in mortality risk was observed for women. The decline in men was attributable to patients aged 75 – 84 years and ⩾ 85 years with a decrease in cumulative mortality of respectively 26% (31% in 2000 – 2008, 23% in 2008 – 2011) and 17% (from 46% to 38%). Because of increased survival in the controls, the relative all-cause mortality risk remained stable for men and was slightly increased for women. Finally, the cause-specific relative mortality risk was significantly higher for men as compared to women for respiratory infections, non-infectious respiratory diseases, cardiovascular diseases, malignant neoplasms, and diseases of the musculoskeletal system.

Conclusions: In the United Kingdom, all-cause one-year mortality rates after hip fracture have declined in men but not in women. This may be related to better treatment of postoperative complications such as heart failure and chest infection for which male gender is a risk factor.

***Disclosures: Corinne Klop**, None.*

MO0330

Obese Older Adults Have a Lower Adjusted Risk of Incident Hip Fracture. Jennifer Lloyd*[1], Dawn Alley[1], William Hawkes[1], Marc Hochberg[2], Shari Waldstein[1], Denise Orwig[1]. [1]University of Maryland, Baltimore, USA, [2]University of Maryland School of Medicine, USA

Higher body mass index has been associated with lower risk of hip fracture, but recent studies have documented a growing prevalence of hip fracture among overweight and obese persons, who make up the majority of the older population. The objective of this study was to determine the risk of hip fracture among overweight and obese older adults in a nationally representative sample of U.S. older adults. Data from 2,790 adults age >= 65 examined in the National Health and Nutrition Examination Survey (NHANES) III from 1991-1994 were linked to Medicare claims data (1991-2007) to assess incident hip fractures [ICD-9 codes (820.*xx*) of first hip fracture from Medicare claims]. Subjects were defined as overweight and obese based on BMI of 25.0 to 25.9 and >=30.0 kg/m^2, respectively. Cox proportional hazard models were used to test whether risk for incident hip fracture differed by body mass index (BMI) categories [measured during NHANES III, kg/m^2], controlling for baseline measures of sociodemographic factors, low bone mineral density (BMD), physical activity, chronic conditions, prior hip fracture, fall frequency, self-reported health status, cognition, bone-related vitamins and medications, performance measures, current smoking status, and alcohol use. Effect modifiers such as age, sex, race, and low BMD [femoral neck DXA at baseline] were also examined. The majority of subjects were either overweight (40%) or obese (23%). Hip fractures occurred in 13% during follow-up. The crude risk of hip fracture for overweight (Hazard Ratio [HR] =0.99, 95% confidence interval [CI]: 0.91, 1.08) and obese (HR=0.93, 95% CI: 0.85, 1.03) older adults were not significantly different than for normal weight older adults. Obese older adults did have an adjusted 15% lower risk of hip fracture (HR=0.85, 95% CI: 0.76, 0.96) compared to normal weight older adults; the adjusted risk in overweight participants did not differ from risk in normal weight older adults (HR=0.94, 95% CI: 0.85, 1.04). The relationship between BMI categories and hip fracture did not differ by age, gender, race, or low BMD (all interaction terms were not-significant). Adjusted study results confirm obesity is protective against risk of hip fracture and that this effect is mediated, in part, by higher BMD. Findings from this study add to the literature with results from a nationally representative, U.S. sample.

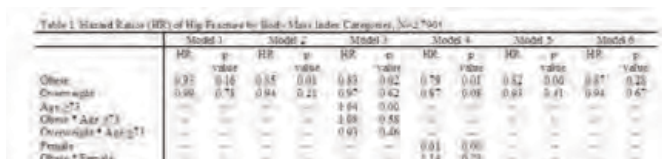

Table 1. Hazard Ratios (HR) of Hip Fracture by Body Mass Index Categories, N=2,790

***Disclosures: Jennifer Lloyd**, None.*

MO0331

Outcomes of an Orthopaedic Post Fracture Bone Health Assessment Program. Victoria Elliot-Gibson*[1], Earl Bogoch[1], Dorcas Beaton[2], Robert Josse[3]. [1]St. Michaels Hospital, Canada, [2]Keenan Research Centre, St Michael's Hospital, Canada, [3]St. Michael's Hospital, University of Toronto, Canada

Purpose: To present the outcomes of a coordinator based post fracture osteoporosis (OP) intervention program in an orthopaedic unit. Methods: A university teaching hospital implemented an OP Exemplary Care Program to improve OP recognition and intervention rates in patients with a fragility fracture. A coordinator screens Fracture Clinic outpatients and orthopaedic inpatients: males ⩾ 50 years; females ⩾ 40 years; fracture sites: wrist, shoulder, hip and spine. Patients receive OP education and may be referred for further investigation/treatment. Data were from self-report questionnaires, coordinator chart notes and general chart audits. Results: Data presented are from the period December 1, 2002 to November 30, 2011. There were 2511 patient identified in which 1803/2511 (71%) were not prescription medication for their bone health at baseline and are the focus of this report. There were 497 males, mean age 70.4 (SD 11.9) years, and 1306 females, mean age 70.2 (SD 14.6) years. There were 679 hip, 719 wrist, 368 shoulder and 37 vertebral fractures. Outpatient referrals to a specialist or family doctor for secondary bone health assessment was recommended for 1206/1803 (67%) patients; the orthopaedic surgeon initiated treatment for 44 (2%); and 227 (13%) received an inpatient assessment by a specialist . The overall bone health assessment rate was, 1173/1803 (65%), which represents 79% of those who had an assessment recommended. Bone mineral density (BMD) testing was recommended for 1323/1803 (73%) of patients with an overall BMD testing rate of 1102/1803 (61%) which represents 83% of those who had BMD testing recommended. Of the 1803, 689 (38%) were prescribed a specific anti OP therapy in addition to Vitamin D and calcium; 112 (6%) patients were not prescribed medication due to contraindications; 661 (37%) of patients were recommended adequate vitamin D and calcium as their definitive treatment; 2 (<1%) enrolled in a clinical trial; and 339 (19%) were unavailable/unable to participate in follow up had the recommendation for Vitamin D and calcium at baseline. Conclusions: This program has found that a dedicated coordinator, and an engaged orthopaedic and metabolic bone disease unit has bone health assessment, BMD testing and treatment post fracture that is comparable to other published programs.

***Disclosures: Victoria Elliot-Gibson**, None.*

MO0332

Subsequent Fracture Risk and Mortality in the Glasgow Fracture Liaison Service: an 8-year Follow-Up Study. Tineke Van Geel*[1], Dana Bliuc[2], Piet Geusens[3], Jacqueline Center[2], Geert-Jan Dinant[1], John Eisman[2], Joop Van Den Bergh[4], Alastair McLellan[5]. [1]Maastricht University, The Netherlands, [2]Garvan Institute of Medical Research, Australia, [3]University Hasselt, Belgium, [4]VieCuri MC Noord-Limburg & Maastricht UMC, The Netherlands, [5]Western Infirmary, United Kingdom

Purpose: The Glasgow Fracture Liaison Services (FLS) is a model of care for fracture assessment. In this study, the risk of re-fractures and mortality over an 8-year follow-up period was evaluated in patients aged 50 years and over who attended the Glasgow FLS.

Method: Between 1999 and 2007, patients with a low trauma fracture were identified by nurse practitioners and invited to attend the FLS. Their treatment recommendations were based on national osteoporosis guidelines. The present study evaluated the risk of re-fracture and mortality risk.

Results: The 9394 patients with a non-vertebral fracture (mean age: 71.9 ± 12.1, 77.8% women) were categorised according to the following FLS outcome groups: A. 5081 (54.1%) were assessed by FLS incl. DXA; B. 497 (5.3%) were assessed by FLS without DXA - review previous treatment; C. 1794 (19.1%) were assessed by FLS without DXA - for calcium and vitamin D; and D. 2022 (21.5%) declined or were not assessed by FLS. The distribution within these groups, particularly into group A, related to their longer expected survival. In group A, 659 (13.0%) patients re-fractured, and 601 (11.8%) patients died. In group B, 49 (9.9%) patients re-fractured and 99 (19.9%) patients died. In group C, 196 (10.9%) patients re-fractured and 773 (43.0%) patients died. In group D, 175 (8.7%) patients re-fractured and 417 (20.6%) patients died.

In all groups, longer survival was associated with higher re-fracture rates. More than half of these occurred within 24 months after the initial fracture. Mortality, as expected, differed by group but also by time. For group A, half of the 12.8% who died did so within 30 months; for group B half of the 19.9% who died did so within 18 months; for group C half of the 43% who died did so within 12 months; and group D half of the 20.6% who died did so within 24 months (Figure 1).

Conclusion: Re-fractures and mortality occur soon after the initial fracture. Over an 8 year follow-up period, more than 50% of the re-fractures occurred within 2 years of follow-up, regardless of the FLS outcome group. However, mortality was substantially less and later in the group who were selected for active assessment and intervention. It remains to be shown to what extent this mortality difference reflects the effect of treatment versus the selection process.

Keywords: Fracture Liaison Service, Re-Fractures, Mortality

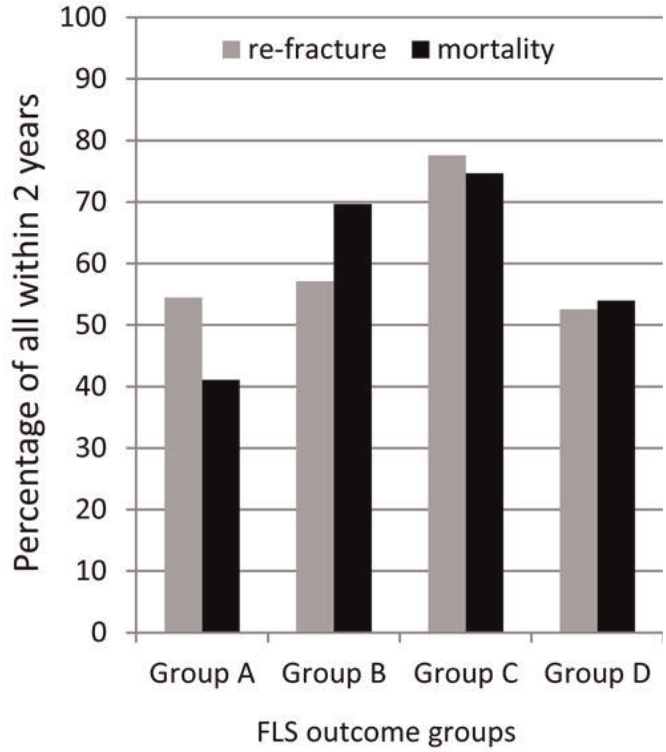

Percentage of all re-fractures and mortality within 2 yrs per FLS outcome group

***Disclosures: Tineke Van Geel**, None.*

MO0333

Withdrawn

MO0334

"Such terrible bone":weight-bearing orders following hip fracture surgery. Leslie Carlin*[1], Kathryn Sibley[2], Pia Kontos[2], Susan Jaglal[1]. [1]University of Toronto, Canada, [2]Toronto Rehabilitation Institute, Canada

OBJECTIVES: Immediate weight-bearing (IWB) following hip fracture surgery is associated with decreased mortality, fewer complications, improved recovery, and is deemed best practice. However, IWB has yet to be systematically implemented in Canada. In this qualitative study, we explore barriers and facilitators to IWB prescription by orthopedic surgeons. APPROACH: Twenty orthopedic surgeons and 8 physical therapists from across Canada participated in semi-structured interviews conducted by one researcher (LC), by phone or in person. Topics varied for the two populations, but included the role of weight-bearing in decisions about surgical procedure, influences on post-operative weight-bearing orders, implementation of the orders, and attitudes toward evidence-based 'best practice' with respect to weight-bearing. Interviews were professionally transcribed and each read by two or more of the authors. Thematic codes were created using an iterative, phenomenological approach and used as units of analysis. Data analysis informed the development of a survey currently underway, targeting all orthopedic surgeons in Canada who perform hip fracture surgery. RESULTS: While almost all surgeons interviewed agreed that IWB is indeed best practice for hip fracture repair or replacement, they each had a rubric for 'rules to break the rule' that allowed them to avoid or delay weight-bearing for certain patients in order to protect the surgeon's repair. Factors that influenced them included 1) 'weak bones' (osteoporosis); 2) the fracture pattern (comminuted, displaced); 3) expectations of recovery for that patient, considering age and mental status, and 4) surgeons' own experience of having seen a repair fail. 'It taints you,' said one doctor; another described walking 'a fine balance' between IWB and repair failure.' Most surgeons reported having no data on patient outcome by weight-bearing orders for their own institution. Physical therapists, conversely, felt that IWB was always appropriate because 'the weight actually helps with the healing'. They expressed frustration about surgeons' limitations on weight-bearing. CONCLUSIONS: Surgeons fear repair failure and its cost to their patients, whereas the benefits to bone healing and to general patient welfare from immediate weight-bearing are more 'visible' to the physical therapists. Institutional chart audits tracking patient outcome based on their weight-bearing orders may prove helpful.

***Disclosures: Leslie Carlin**, None.*

MO0335

A web repository and browser to search results of Genome-wide association studies (GWAS) for multiple musculoskeletal aging phenotypes. Yi-Hsiang Hsu[1], Chia-Ho Cheng[2], Jason Rightmyer[2], Douglas Kiel[3], Joanne Murabito[4], David Karasik*[5]. [1]Hebrew SeniorLife Institute for Aging Research & Harvard Medical School, USA, [2]IFAR HSL, USA, [3]Hebrew SeniorLife, USA, [4]Boston University, USA, [5]Hebrew SeniorLife; Bar Ilan University, USA

GWAS are successful in identifying loci associated with common disorders. However, to date, investigators are able to access only the top GWAS results that are published, while less significant associations with the millions of single-nucleotide polymorphisms (SNPs) are usually not available. Furthermore, it is not possible to easily interrogate SNPs that may be important for more than a single phenotype. Therefore, we developed a web repository and browser to search GWAS results on musculoskeletal aging phenotypes. This database is called GWAS Resource for Aging-related Traits (''GREAT'').

The resource was developed using open source Web, database and analytical technologies (Linux, PHP, MySQL) and is hosted on secure infrastructure. The system is HIPAA-compliant as it contains only aggregate statistics (mostly from meta-analyses) and hyperlinks to gene and variant annotation resources (e.g. NCBI dbSNP, UCSC genome browser etc.) The GWAS data are transferred from the respective coordinating centers from large consortia to us for uploading. Access to the data requires approval of the Research Steering Committee (RSC) consisting of a 5-person multidisciplinary panel of researchers and technical experts. The RSC reviews the investigator's application and IRB approval. In turn, users can provide feedback on the database to enhance the search function and allocate resources according to the need. Querying is available for multiple traits from several major musculoskeletal phenotypes: e.g. whether a SNP related to a BMD trait is also associated with a trait in another domain, such as lean mass, to identify shared genetic determinants for BMD and lean mass. In addition, GREAT will be incorporating information, such as expression quantitative trait loci and functional annotation for the associated SNP, obtained from a variety of private databases. We plan to add software for multivariate analyses, to provide the user with the opportunity to identify potentially pleiotropic genetic loci.

In conclusion, the ''GREAT'' resource provides a user-friendly interface for searching, filtering, and visualizing the results from GWAS meta-analyses of musculoskeletal aging-related phenotypes. Importantly, the GREAT system is inherently scalable, given sufficient storage and processing capacity. The generation of the GREAT resource has the potential to provide a unique platform for exploring and sharing multiple GWAS results and their functional interpretation.

Supported by Glenn Foundation

Screen shot of a start page from the GREAT database

***Disclosures: David Karasik**, None.*

MO0336

Association of GC and CYP2R1 Genetic Variants and Serum Vitamin D Concentrations in Chinese Postmenopausal Women. Weibo Xia*[1], Wen Xu[2], Jing Sun[2], Wenbo Wang[3], Xiran Wang[4], Yan Jiang[2], Wei Huang[5], Xin Zheng[6], Qiuping Wang[7], Yu Pei[8], Zhiwei Ning[9], Mei Li[2], Ou Wang[10], Xiaoping Xing[2], Ling Xu[11]. [1]Peking Union Medical College Hospital, Department of Endocrinology, Peoples Republic of China, [2]Department of Endocrinology, Key Laboratory of Endocrinology, Ministry of Health, Peking Union Medical College Hospital, Chinese Academy of Medical Sciences, China, [3]Department Endocrinology, Peking University Shougang Hospital, China, [4]Department of Cadre Unit, General Hospital of the second Artillery Force, China, [5]Department of Endocrinology BeiJing Haidian Hospital, China, [6]Department of Endocrinology, China Rehabilitation Research Center, China, [7]Department of Endocrinology, Beijing Liangxiang Hospital, China, [8]Department of Geriatric Endocrinology, Chinese PLA General Hospital, China, [9]Department of Endocrinology, Beijing Chaoyang Hospital, China, [10]Peking Union Medical College Hospital, Chinese Academy of Medical Sciences, Peoples Republic of China, [11]Department of Gynaecology & Obstetrics, Key Laboratory of Endocrinology, Ministry of Health, Peking Union Medical College Hospital, Chinese Academy of Medical Science, China

Purpose: To determine if GC and CYP2R1 genetic variants have association with serum 25-OHD_3 level, BMD, or bone turnover markers in Chinese postmenopausal women.

Methods: We randomly selected 1494 postmenopausal women of Han ethnic group from 7 communities in Beijing. BMD of L2-4, FN and total hip was determined by DXA; Serum bone turnover markers and 25-OHD_3 were measured by automated Roche electrochemiluminescence system; Genotypes of GC and CYP2R1 were detected by TaqMan allelic discrimination assay. Multiple statistic methods were used to test the associations of SNP genotypes andVitamin D levels.

Results:In our sample 1338 women had vitamin D deficiency and another 146 women had vitamin D insufficiency, accounting for 89.6% and 9.8% of total sample, respectively. The variants of rs222020 (P=0.003) and rs2298849 (P=3.73×10^{-4}) at GC were significantly associated with serum 25-OHD_3 level. Allele C of rs222020 and allele G of rs2298849 might be protective for serum 25-OHD_3 level. Among the haplotypes of rs222020-rs2298849, CG (β=0.138,P=0.001) and TA (β=-0.118,P=0.002) corresponded to increasing and decreasing serum 25-OHD_3 concentrations, respectively. We didn't find significant association between CYP2R1 polymorphisms and serum 25-OHD_3 level. No significant association was found between GC polymorphisms and β-CTX, P1NP or BMD of L2-4, FN, and total hip. CYP2R1 polymorphisms had similar results except its significant association with β-CTX and P1NP.

Conclusions: We found that GC variants had significant association with serum 25-OHD_3 level among postmenopausal women of Han ethnic group in Beijing while CYP2R1 variants weren't found significant. Association of CYP2R1 genetic variants with β-CTX and P1NP needed to be proven.

Keywords: GC, CYP2R1, 25-OHD_3, bone turnover markers

***Disclosures: Weibo Xia**, None.*

MO0337

Gene by genome-wide interactions on femoral neck BMD in MrOS and SOF: a synergistic effect of polymorphisms in the alkaline phosphatase (*ALPL*) and lecithin retinol acyltransferase (*LRAT*) genes. Carrie Nielson*[1], Priya Srikanth[1], Joseph Zmuda[2], Jian Shen[1], Robert Klein[3], Eric Orwoll[1]. [1]Oregon Health & Science University, USA, [2]University of Pittsburgh Graduate School of Public Health, USA, [3]Portland VA Medical Center, USA

Gene-by-gene interactions are expected to account for some of the unexplained variability in bone mineral density in humans. We analyzed interactions between single nucleotide polymorphisms (SNPs) in a gene known to affect mineralization, *ALPL*, with SNPs in the rest of the genome in two cohorts of older adults.

Methods: 4,704 non-Hispanic white men in the Osteoporotic Fractures in Men (MrOS) cohort and 3,625 women in the Study of Osteoporotic Fractures (SOF) cohort (ages ⩾65) had femoral neck BMD measured by DXA and genome-wide genotyping data from the Illumina Human Omni1-Quad, for 699,502 SNP genotypes with minor allele frequency ⩾5%. 38 SNPs in the *ALPL* gene were tested for epistatic interactions with all remaining SNPs in the genome-wide dataset, for a total of ~25 million tests. Meta-analysis of interaction terms was performed on models adjusted for age, BMI, and principal components for population stratification. SNP combinations that resulted in fewer than 30 participants in any cell of the cross-tabulation of genotypes were excluded. R^2 were calculated for linear regression models containing each SNP alone and compared to the R^2 for models containing both SNPs and their interaction term.

Results: In MrOS, the mean BMD was 0.84 g/cm^2 (SD = 0.13), and in SOF, mean BMD was 0.73 (SD = 0.11). We observed an interaction between a SNP in *ALPL* (rs12145027) and a SNP in *LRAT* (rs201821), a gene involved in retinoic acid metabolism (meta-p for interaction = 1.08×10^{-8}). For those participants who were

homozygote wild type or heterozygous at the *ALPL* SNP there was little effect of *LRAT* genotype on BMD. However, for those who were homozygous for the *ALPL* SNP minor allele, the additive effect of the *LRAT* SNP minor allele was -0.03 g/cm^2 (meta-p = 0.004). Neither SNP had a main additive effect on BMD (meta-p $\geq$ 0.13), and R^2 for each SNP separately was $\leq$ 0.07%. However, the R^2 for the interaction between the two SNPs was 0.32% in MrOS and 0.48% in SOF.

Discussion: An interaction between a SNP in the *ALPL* first intronic region and an intronic SNP in the *LRAT* gene resulted in a synergistic effect on BMD in two cohorts of older men and women. The interaction is plausible due to the presence of a retinoic acid response element in the promoter region of *ALPL*, which may be marked by the SNP. Retinoic acid effects on *ALPL* expression or function may be a source of heritable BMD variation in older adults.

***Disclosures: Carrie Nielson**, None.*

MO0338

Genome-Wide Association Study Meta-Analysis Identifies the *SOAT1/AXDND1 Locus* To Be Associated With Hip and Forearm Fracture Risk. Ulrika Pettersson-Kymmer*[1], Samuel Handelman[2], Joel Eriksson[3], Ulrica Bergstrom[4], Beatrice Melin[5], Carl Wibom[5], Liesbeth Vandenput[7], Preetha Rajaraman[8], Patricia Hartge[9], Stephen Chanock[9], Goran Hallmans[11], Andrea Lacroix[12], David Duggan[13], Charles Kopperberg[14], Aaron Aragaki[14], Maria Nethander[15], Andre Uitterlinden[16], Fernando Rivadeneira[17], Rebecca Jackson[18], Claes Ohlsson[19]. [1]Clinical Pharmacology, Sweden, [2]Mathematical Biosciences Institute, The Ohio State University, USA, [3]Centre for Bone & Arthritis Research, Sweden, [4]Umea University Hospital, Sweden, [5]Radiation Sciences, Oncology Umeå University, Sweden, [7]University of Gothenburg, Sweden, [8]Center for Global Health, US National Cancer Institute, USA, [9]Division of Cancer Epidemiology & Genetics, National Cancer Institute, NCI, USA, [11]Public Health & Clinical Medicine, Umea University, Sweden, [12]Fred Hutchinson Cancer Research Center, USA, [13]Translational Genomics Research Institute, USA, [14]Public Health Sciences, Fred Hutchinson Cancer Research Center, USA, [15]Bioinformatics Core Facility, Sahlgrenska Academy, University of Gothenburg, Sweden, [16]Rm Ee 575, Genetic Laboratory, The Netherlands, [17]Erasmus University Medical Center, The Netherlands, [18]The Ohio State University, USA, [19]Center for Bone & Arthritis Research at the Sahlgrenska Academy, Sweden

Hip- and forearm fractures are the two most clinically important non-vertebral fractures. Twin studies have demonstrated a high heritability of these fractures and this heritable component is largely independent of bone mineral density (BMD).

To identify common genetic variants associated with hip and forearm fractures, we performed a genome-wide association study (GWAS ~ 2.5 million SNPs) meta-analysis of two large fracture data sets within the well-characterized Umeå Fracture and Osteoporosis (UFO) cohort (UFO-forearm; 1,060 forearm fractures and 1,055 controls, and UFO-hip; 1,014 hip fractures and 862 controls). All fractures were confirmed through radiographic reports. Replication was performed in the Women's Health Initiative (WHI) cohort (1,845 hip fractures verified by blinded review of medical records and 2,120 controls).

We identified one single nucleotide polymorphism (SNP), within the *SOAT1/AXDND1 locus* (1q25.2) that was associated with fracture risk at genome wide significance (OR per G allele = 1.33; P = 3.1 x 10^{-8}) in the UFO discovery meta-analysis. This SNP was associated with fracture risk both in the WHI replication cohort (OR 1.16, P = 2.2 x 10^{-3}) and in the combined analyses comprising 7,956 subjects (3,919 cases and 4,037 controls; OR = 1.24, P = 4.8 x 10^{-10}). It was significantly associated with fracture risk in both genders and with a similar magnitude at both hip and forearm.

The *SOAT1/AXDND1 locus* has been implicated in cholesterol metabolism and cognition but this loci and the identified SNP has not been reported to be associated with BMD in previous GWAS. To further explore whether the association of the SNP in the *SOAT1/AXDND1 locus* is independent of BMD, we generated a genetic risk score (GS) which includes 63 SNPs previously identified to be reproducibly associated with BMD. Although this GS, was significantly associated with both hip (p=7.9 x 10^{-4}) and forearm (p=8.6 x 10^{-5}) fractures, models including both the SNP in the *SOAT1/AXDND1 locus* and the GS demonstrated that the impact of the SNP in the *SOAT1/AXDND1 locus* on fracture risk was independent of the BMD-associated GS.

In summary, we have identified a non-BMD associated genetic variant in the *SOAT1/AXDND1 locus* associated with hip and forearm fractures.

***Disclosures: Ulrika Pettersson-Kymmer**, None.*

MO0339

Reduced Serum Osteocalcin Concentrations Are Associated with Type 2 Diabetes Mellitus and the Metabolic Syndrome Components in Postmenopausal Women: The Crosstalk between Bone and Energy Metabolism. Rajib Bhattacharya*[1], Kamyar Asadipooya[2], Iraj Nabipour[3], Ali Movahed[3], Bagher Larijani[4], Mohammadreza Kalantarhormozi[3], Katayoun Vahdat[3], Samad Akbarzadeh[3], Maryam Farrokhnia[3], Majid Assadi[3], Roya Amirinejad[3], Afshar Bargahi[3], Zahra Sanjdideh[3]. [1]KU Medical Center, USA, [2]University of Kansas Medical Center, USA, [3]Bushehr University of Medical sciences, Iran, [4]Tehran University of Medical Sciences, Iran

Introduction: Although it has been shown that osteocalcin functions as a regulatory hormone in glucose metabolism and fat mass, few population-based study to date has addressed serum osteocalcin levels in relation to energy metabolism concurrent with bone metabolism in postmenopausal women.

Materials and Methods: This study measured cardiovascular risk factors, high-sensitivity C-reactive protein (hs-CRP), osteoprotegerin, receptor activator of nuclear factor-jB ligand, osteocalcin, CrossLaps, alkaline phosphatase, and bone mineral density (BMD) at the lumbar spine (L2–L4) and the proximal femur were measured in 382 Iranian postmenopausal women.

Results: In multiple logistic regression analysis, lower osteocalcin (lower than median) and CrossLaps (less than 0.242 ng/ml) levels were associated with a higher odds ratio (OR) of having type 2 diabetes mellitus when adjustments were made for age, hs-CRP, cardiovascular risk factors, BMD, and markers of bone metabolism [OR 5.17, CI (2.66–10.04), p\0.0001 and OR 2.51, CI (1.37–4.61), p = 0.003, respectively]. However, lower alkaline phosphatase levels were associated with a lower OR of having type 2 diabetes mellitus [OR 0.28, CI (0.15–0.52), p<0.0001] in regression analysis. No significant difference was found between serum osteocalcin levels of those with and without metabolic syndrome. Among the metabolic syndrome components, low osteocalcin levels had significant associations with elevated blood glucose [OR 1.89, CI (1.16–3.07), p = 0.010] and elevated waist circumference [OR 2.53, CI (1.13–5.67), p = 0.024] in multivariate analyses.

Conclusion: Serum osteocalcin was independently associated with glucose intolerance and increased waist circumference and type 2 diabetes mellitus in postmenopausal women. Since CrossLaps andalkaline phosphatase levels were independently associated with the presence of type 2 diabetes mellitus, the uniquecontribution of osteocalcin in glucose metabolism could not be concluded.

***Disclosures: Rajib Bhattacharya**, None.*

MO0340

High cardiorespiratory fitness is associated with reduced risk of osteopenia and osteoporosis in women: Cooper Center Longitudinal Study. Chwan-Li Shen*[1], Laura Defina[2], David Leonard[3], Benjamin Willis[2], Carolyn Barlow[2], Marjorie Jenkins[1], Barbara Pence[1], Yan Zhang[1], Ming-Chien Chyu[4], E. Michael Lewiecki[5]. [1]Texas Tech University Health Sciences Center, USA, [2]The Cooper Institute, USA, [3]UT Southwestern Medical Center, USA, [4]Texas Tech Univeristy, USA, [5]University of New Mexico School of Medicine, USA

Current common belief is that all types of physical activity are beneficial to bone health of women, including reducing risk for bone loss. However, there is no conclusive scientific evidence demonstrating that women with higher cardiorespiratory fitness (CRF) levels have lower risk for bone loss. This study was to determine the association between the CRF level and risk for osteopenia or osteoporosis in women (age $\geq$ 40 years) using existing Cooper Center Longitudinal Study data. A cohort of 3353 predominately healthy Caucasian women (50.8 $\pm$ 7.9 years) who underwent a preventive medical examinations that included CRF by maximal Balke treadmill exercise testing and femoral neck bone mineral density (FN-BMD) by DXA. CRF was defined as a continuous variable expressed as total time achieved on a treadmill in minutes and also categorized into quintiles of CRF (1-5 with 1 being low fit). Logistic regression was used to characterize the association between CRF and osteopenia or osteoporosis adjusting for age, weight, physical activity level, resistance activity level (defined by number of days/week), menopausal status, and smoking status. Overall the mean BMI for all subjects was 24.5 $\pm$ 4.5 kg/m^2. However, in the moderate fit group, the average BMI was in the overweight range and in the low fit group, in the obese range. The prevalence of osteopenia and osteoporosis was greatest in the low fit group at 33.7% and 3.4%, respectively. Fully adjusted logistic regression models showed an inverse association between CRF and osteopenia (moderate, OR 0.45, 95% CI 0.31-0.65); high, OR 0.31, 95% CI 0.21,0.46). A similar relationship was seen with osteoporosis (moderate, OR 0.25, 95% CI 0.09-0.70; high, OR 0.25 95% CI 0.10-0.65). As expected, in both osteopenia and osteoporosis, age and weight had the expected relationship. Menopause had a inverse relationship with osteopenia (OR 1.52 95% CI 1.23-1.88). Furthermore, resistance activities did not show a significant relationship with osteopenia (OR 0.95, 95% CI 0.80-1.13) or osteoporosis (OR 0.74, 95% CI 0.39-1.39). In summary, CRF levels are inversely associated with the reduce risk for osteopenia and osteoporosis for women aged 40 years and older. Although prior research suggests that strength training is of great importance in the prevention of osteoporosis, in this cohort the association of resistance activity with the outcomes was attenuated in the fully adjusted model. Further prospective studies are warranted.

***Disclosures: Chwan-Li Shen**, None.*

MO0341

Impact of Lifestyle Factors on Fracture Risk in Older Patients with Cardiovascular Disease and Diabetes: A Prospective Cohort Study of 26,335 Individuals from 40 Countries. Alexandra Papaioannou*[1], Alexandra Papaioannou[2], Salim Yusuf[3], Joshua Barzilay[4], Peggy Gao[5], Philip Joseph[3], Koon Teo[3], Andrew Mente[3]. [1]Hamilton Health Sciences, Canada, [2]Department of Clinical Epidemiology & Biostatistics, McMaster University, Canada, [3]Population Health Research Institute, McMaster University & Hamilton Health Sciences, Canada, [4]Kaiser Permanente of Georgia & Emory University School of Medicine, USA, [5]Population Health Research Institute, Canada

Introduction: Fractures are a major health concern among the elderly and are associated with morbidity and mortality. The impact of common modifiable lifestyle risk factors on incident fracture risk has not been evaluated in patients with cardiovascular disease and diabetes.

Objectives: The aim of this study is to assess the individual and combined effect of the common modifiable risk factors (smoking, alcohol consumption, and physical activity) on fracture risk in a large sample of older (≥ 55 years) individuals with cardiovascular disease or diabetes with end organ damage.

Methods: Observational analyses of 26,335 women and men (mean age of 66.5 years) without any previous fracture and enrolled in two randomized trials (ONTARGET and TRANSCEND). Lifestyle factors were assessed by questionnaire. The effect of lifestyle factors (current smoking, alcohol intake of >3 in men and >2 in women), and less than 5 days of physical activity) was assessed individually and in combination, on incident fracture risk using logistic regression analyses adjusting for age, sex, trial enrolment, region, and other known potential risk factors for fractures. The predictive model was internally validated by bootstrapping.

Results: During the 56 month follow up, 1,079 incident fractures occurred; 508 (6.51%) occurred among women and 571 (3.08%) occurred among men. Smoking (relative risk [RR]: 1.46, 95% confidence interval [CI]: 1.22-1.76) and low physical activity (RR: 1.17, 95%CI: 1.03-1.33) were associated with an increased risk of any fracture, while high alcohol intake showed a directional but nonsignificant relationship with fracture risk (RR: 1.12; 95%CI: 0.65-1.92). Compared to participants with no lifestyle risk factors, those having two or three risk factors had an increased risk of a future fracture (RR: 1.64, 95%CI: 1.31-2.07 for two risk factors; and RR: 2.30; 95%CI: 0.83-6.40 for three risk factors; p for trend<0.001). The pattern of effects was similar for osteoporotic fractures (RR: 1.76, 95%CI: 1.34-2.31 for two risk factors; and RR: 2.68; 95%CI: 0.83-8.69 for three risk factors; p for trend<0.001). An estimated 10.2 (95% CI: 2.9-18.2) events could be prevented for every 100 fractures occurring in the population if every person followed a healthy lifestyle.

Conclusions: A healthier lifestyle advocated reducing the risk of cardiovascular disease and diabetes could be associated with a significant and graded reduction in fracture risk.

***Disclosures: Alexandra Papaioannou**, None.*

MO0342

Measuring Compliance with Oral Bisphosphonates: Potential Impact of Days Supply Errors in Pharmacy Data. Andrea Burden*[1], J. Micheal Paterson[2], Andrea Gruneir[3], Suzanne Cadarette[1]. [1]University of Toronto, Canada, [2]Institute for Clinical Evaluative Sciences, Canada, [3]Women's College Research Insititute, Canada

Background: Days supply (DS) values are commonly used to identify drug utilization, estimate drug exposure and quantify adherence to therapy. We recently identified potential reporting errors in DS values for weekly, monthly, and cyclical osteoporosis medications, particularly in long-term care (LTC).

Objectives: To examine the potential impact of DS reporting errors on measurement of compliance with oral bisphosphonate therapy.

Methods: We identified all oral bisphosphonate prescriptions for osteoporosis dispensed through the Ontario public drug plan for seniors (66+ years) from April 2000 to March 2011. DS values were examined by dosing regimen, and illogical values for weekly, monthly and cyclical regimens (e.g., 1 DS for weekly regimens) were flagged for data cleaning. DS values were cleaned using dose specific algorithms (e.g., 7 DS value was imputed if 1 DS value was observed for a weekly regimen). Compliance with therapy was estimated using the proportion of days covered (PDC), calculated as the total DS in 1-year divided by 365 days. Mean PDC and proportion with high compliance (PDC ⩾80%) were compared using the observed and cleaned DS values. Results were examined separately for patients residing in LTC and community.

Results: A total of 356,134 eligible new users were identified, 25% in LTC. Among LTC users, mean PDC increased from 60% to 77% following data cleaning, and the proportion identified with high compliance (PDC⩾80%) increased from 48% to 79%. Fewer DS errors were noted in the community setting; mean PDC increased from 79% to 81%, and high compliance increased from 60% to 65% after data cleaning.

Conclusions: Results suggest that compliance with oral bisphosphonate therapy is underestimated in LTC. With 25% of oral bisphosphonates dispensed in LTC, careful attention to potential exposure misclassification is important. For example, differential exposure misclassification would exaggerate the association between better compliance and drug effectiveness since oral bisphosphonate exposure is underestimated in LTC patients, who are also more likely to experience a hip fracture than community-dwelling patients. Similarly, the safety of oral bisphosphonate exposure (e.g., esophageal cancer) may be underestimated if more common among LTC patients. Better understanding of potential errors in the DS field in pharmacy claims data is needed to inform pharmacoepidemiologic analyses of the safety and effectiveness of oral bisphosphonates.

***Disclosures: Andrea Burden**, None.*

MO0343

Undertreatment with Anti-osteoporosis Medications among Women Diagnosed with Osteoporosis in the United States Medicare Population. Ethel Siris[1], Ankita Modi[2], Jingbo Yu*[2], Renee Arnold[3], Katalin Bognar[4]. [1]Columbia University College of Physicians & Surgeons, USA, [2]Merck & Co., Inc., USA, [3]IMS Health, USA, [4]Precision Health Economics, USA

Objective: To describe characteristics and treatment initiation among women diagnosed with osteoporosis (OP) in the Medicare population

Material and Methods: A retrospective cohort study using the 20% Medicare claims data from the Centers for Medicare and Medicaid Services (CMS) from January 1, 2006 to December 31, 2009 (study period) was conducted. Women 66 years of age or older, who had a first diagnosis of OP (Index date) found in outpatient or inpatient claims during 2007 to 2008, who were continuously enrolled in Medicare parts A, B and D for at least one year pre-index (baseline) and one year post-index date (follow-up), and who were naïve to OP medication in the baseline period, were included. Those who had a claim of Paget's disease or estrogen use during the baseline period, or a diagnosis of malignant neoplasm during the baseline or follow-up periods, were excluded. OP medications were identified based on NDC and HCPCS codes and included pharmacological treatment such as: alendronate, ibandronate, risedronate, calcitonin, raloxifene, zoledronic acid, and teriparatide. Subjects were characterized as 'treated' if they received at least one OP medication within the follow-up period. The proportion of individuals receiving OP medication was determined in this population. Patient characteristics such as age, Charlson comorbidity index, OP fracture history, gastrointestinal problem history, renal disease history, glucocorticoid use, estrogen use and NSAID use in the baseline period were assessed for all patients.

Results: Among 126,188 patients meeting study criteria with a mean [SD] age of 78.5 [7.9] years, 72.1% of patients did not receive any pharmacological treatment within the one-year following OP diagnosis. 21.6% of patients initiated treatment with bisphosphonates and 6.3% initiated a form of treatment other than bisphosphonates. The mean [SD] time to any OP treatment initiation was 75.4 [88.9] days from the Index date. Approximately 12.1% of the patients had a history of OP fractures and 41.6% of women had a history of gastrointestinal problems during the baseline period.Conclusion: This analysis showed that a large proportion of elderly women with osteoporosis did not receive any pharmacological treatment after their diagnosis, suggesting a need for further understanding of the reasons for non-treatment despite diagnosis.

***Disclosures: Jingbo Yu**, Merck & Co, Inc, 2*
This study received funding from: Merck & Co., Inc

MO0344

Differences In Osteocalcin Between Osteoporosis Patients In An Ambulatory Clinic Without Fracture And Hospitalized Trauma Patients With Fractures. Matthew Hnatow*[1], Catherine Ambrose[2], Milan Sen[2], Nahid Rianon[3]. [1]Univeristy of Texas Health Science Center at Houston - Medical School, USA, [2]University of Texas Health Science Center at Houston, USA, [3]UTHealth The University of Texas Medical School at Houston, USA

Fractures are devastating consequences of osteoporosis. Despite known risk factors, the ability to predict a fracture remains elusive and is a public health concern. Osteocalcin (OC), a bone turnover marker, has been correlated with bone mineral density and other secondary risk factors of fracture. Whether or not OC can predict fracture in patients with osteoporosis is unknown. We compared serum OC between ambulatory patients visiting our osteoporosis clinic and hospitalized patients temporarily bed-bound with an acute fracture from low-impact trauma to identify a possible predictor of fracture.

The ambulatory group consisted of 27 patients diagnosed with osteoporosis who were seen in an outpatient geriatric-osteoporosis clinic between September 2011 and November 2012. The hospitalized group consisted of 37 trauma patients admitted with fracture and were treated under an ''Own the Bone'' protocol implemented by the orthopaedic trauma team to reduce post-fracture morbidity and mortality between June and December 2011. Serum OC was obtained as part of osteoporosis work up. An independent sample t-test was used to compare OC between the two groups. Multivariate regression adjusted for age, height, weight, sex, race, serum calcium, magnesium, phosphate, parathyroid hormone, 25-hydroxy vitamin D, glomerular filtration rate and bisphosphonate (BP) use (usage defined as current or past usage and no usage) confirmed an association between low osteocalcin level and positive fracture status.

The mean (SD) age were 82.7 (7.6) years (86% women) for the ambulatory and 77.6 (13.2) years (71% women) for the trauma group. The most frequent fractures in the trauma group were proximal femur (41%) and distal femur (16%). Ambulatory patients reported no fractures; 3 reported current and 21 reported previous BP use. In the trauma group, 6 reported current and 4 reported past BP use. There was

significant difference in serum OC levels between the groups ($p<0.01$) with mean (SD) 25.8 (19.8) ng/mL for the ambulatory and 16.1 (9.8) ng/mL for the trauma patients. Low OC was associated with positive fracture state (regression coefficient -11.06, 95% CI -20.76 to -1.35). In stratified models, t-test remained significant only for those who used BP. Small sample size limited further multivariate regression with stratified model by BP use.

Lower serum OC in fracture patients indicates the need to continue investigation to see if osteocalcin can be used as a predictor of fracture.

***Disclosures: Matthew Hnatow**, None.*

MO0345

Does a Hip Axis Length Assessment Alter the T-score Based Treatment Strategy. Cesar Graf[1], Walter Rial[1], Marcelo Obai[1], Pedro Rial[1], Cesar Wouterlood[1], Cecilia Sprengel[1], Giorgina Cavello[1], Tom Sanchez*[2]. [1]ITEO SRL, Argentina, [2]Norland - A Cooper Surgical Company, USA

Hip Axis Length (HAL) has been proposed as a significant parameter in fracture risk with Faulkner and associates (J Bone Mineral Res. 9:1065, 1994) noting that a HAL of 11.5cm is associated with a 4X greater hip fracture risk than a HAL of 10.5cm. We examined how consideration of HAL in a population might change the clinical recommendation of a DXA study based on a T-score only.

The study included 1,620 women between 21 and 79 years of age with HAL assessments grouped into three risk defined groups based on the Faulkner and associates report—HAL <10.75cm associated with a low risk, a HAL between 11.0 and 11.749cm associated with a moderate risk , and a HAL >11.749cm associated with a high risk. A WHO based Femur Neck T-score grade of Normal, Osteopenic or Osteoporotic was also assessed for each subject. The study then determined how many subjects saw a shift to increase treatment strategy from the T-score based treatment strategy as a result of HAL risk estimate.

The table below details the number of subjects in each HAL risk level and the number of subjects that based on T-score would have entered a particular treatment strategy. Based on these numbers, 559 (34.5%) of the subjects would not see a HAL-based change from T-score based treatment strategy while 98 (6.0%) subjects would see their T-score based strategy elevated to a more aggressive treatment strategy and 115 (7.1%) subjects would see their T-score based strategy elevated to a preventive treatment strategy. Agreement between the HAL based classification and the T-score based classification was poor with a Kappa value of 0.0247. T-score

HAL Normal Osteopenic Osteoporotic

<10.75cm 238 502 213

11-11.749cm 115 275 133>11.749cm 27 71 46

HAL based risk assessment has poor agreement with Femur Neck T-score value based assessment and, to the extent that HAL can be considered a significant factor in hip fracture, the present survey suggests that a HAL assessment should be included when developing a treatment strategy for the patient.

***Disclosures: Tom Sanchez**, None.*

MO0346

Effect of Walking Difficulty on Bone Mass and Bone Turnover in Japanese People Aged 40 Years and Over. Yasuyo Abe*, Kiyoshi Aoyagi, Kazuhiko Arima. Nagasaki University, Japan

Low bone mass and accelerated bone turnover contribute to osteoporotic fractures. However, the effect of walking difficulty on bone mass or bone turnover has not well been studied.

We studied 1097 community-dwelling Japanese people aged 40 years and over (379 men and 718 women) to examine the association of walking difficulty, which is defined as having difficulty walking 100-meter on a level surface, with calcaneal stiffness index (bone mass) measured by quantitative ultrasound, and with urinary N-terminal cross-linking telopeptide of type-I collagen (NTx) devided by creatinine (Cre), a marker of bone resorption.

Stiffness index significantly decreased with age in both sexes (p for trend<0.001), and the decline was steeper in women than in men. Urinary NTx/Cre did not differ among age groups in men (p for trend=0.25), but significantly increased in women 50 years and above (p for trend<0.001).

The prevalence of walking difficulty was significantly higher in women than in men (7.4% vs. 3.4%, p=0.011), and significantly increased with age in men (p for trend=0.02) and women (p for trend<0.001).

In univariate analysis, men and women with walking difficulty were older ($p<0.001$) and had lower stiffness index ($p<0.001$) compared to those without walking difficulty. Among women, individuals with walking difficulty had significantly higher urinary NTx/Cre than those without walking difficulty ($p<0.001$), but not among men (p=0.41).

Multiple regression analysis adjusting for age and BMI showed significant association between walking difficulty and lower stiffness index in men ($\beta=-14.2$, p=0.002) and women ($\beta=-4.5$, p=0.007). In women, walking difficulty was significantly associated with higher NTx/Cre ($\beta=12.6$, p=0.001), but not in men ($\beta=6.5$, p=0.17).

In conclusion, walking difficulty may contribute to low bone mass in both sexes, but might affect bone turnover only in women.

***Disclosures: Yasuyo Abe**, None.*

MO0347

Effects of Escitalopram on Biochemical Markers of Bone Turnover: A Randomized Controlled Trial. Susan Diem*[1], Hadine Joffe[2], Joseph Larson[3], Katherine Guthrie[3], Joy Tsai[2], Andrea Lacroix[3], Kristine Ensrud[4], Benjamin Leder[5]. [1]University of Minnesota, USA, [2]Massachusetts General Hospital, USA, [3]Fred Hutcinson Cancer Research Center, USA, [4]Minneapolis VA Medical Center / University of Minnesota, USA, [5]Massachusetts General Hospital Harvard Medical School, USA

Some, but not all, observational studies have reported that use of selective serotonin reuptake inhibitors (SSRIs) is associated with higher rates of bone loss and increased fracture risk. To date, findings are limited to observational studies, which are limited by the potential for residual confounding.

To determine the effect of SSRIs on markers of bone metabolism, we measured serum carboxy-terminal collagen crosslinks (CTX) and serum amino-terminal propeptide of type I collagen (P1NP) in healthy peri- and post-menopausal women enrolled in a placebo-controlled randomized controlled trial (RCT) of the SSRI escitalopram (10-20 mg/day) for the treatment of vasomotor symptoms (VMS).

141 peri- or post-menopausal non-depressed women (mean age 53.7 $\pm$ 4.1) enrolled in the RCT with baseline and 8 week follow-up serum specimens were included in the study. 69 women were assigned to escitalopram, 72 to placebo. The between-group differences in the change in sCTX and P1NP from baseline to Week 8 were compared by a repeated measures linear model after adjustment for race, clinical center, and baseline measurement.

Treatment groups were balanced across baseline characteristics, including age, race, BMI, smoking status, and levels of 25-OHD and TSH.

There were no between-group differences in mean change in serum CTX (p=0.24) or serum P1NP (p=0.65) over the 8-week treatment period. Results were similar when the analysis was restricted to those women whose adherence to study medication was $\geqslant$ 70% (N=127).

In this randomized, placebo-controlled 8-week trial of escitalopram in healthy peri- and post-menopausal women with VMS, there was no evidence of an effect on biochemical markers of bone formation or resorption. These results demonstrate that escitalopram has no short-term effect on markers of bone metabolism and, if confirmed in trials evaluating other SSRIs, would suggest that reported adverse effects of these medications on skeletal health may be largely due to confounding influences.

	Escitalopram		Placebo		Difference	
Bone Turnover Marker	N	Mean (95% CI)	N	Mean (95% CI)	Mean (95% CI)	P value
CTX						0.24
Baseline	69	0.44 (0.40, 0.48)	72	0.43 (0.39, 0.46)	0.01 (−0.04, 0.07)	
Week 8 – baseline	69	−0.02 (−0.05, 0.01)	72	0.00 (−0.02, 0.02)	−0.02 (−0.06, 0.02)	
PINP						0.65
Baseline	69	53.31 (48.52, 58.10)	72	58.68 (52.83, 64.54)	−5.38 (−12.91, 2.16)	
Week 8 - baseline	69	−1.02 (−5.2, 3.1)	72	−1.88 (−4.82, 1.06)	0.86 (−4.18, 5.90)	

Mean change in CTX and P1NP by treatment group

***Disclosures: Susan Diem**, None.*

MO0348

Factors Associated with Osteoporosis Treatment Following Fragility Fracture. Cynthia O'Malley*[1], Akhila Balasubramanian[1], Douglas Dirschl[2], Pei-Ran Ho[1], Joseph Lane[3], Laura Tosi[4]. [1]Amgen Inc., USA, [2]University of Chicago Medicine & Biological Sciences, USA, [3]Hospital for Special Surgery, USA, [4]Children's National Medical Center, USA

Introduction: Despite guidelines for post-fracture osteoporosis (OP) care, treatment rates after a fragility fracture remain low. To explore why most subjects were not treated, we assessed patient and clinical characteristics associated with OP treatment initiation post-fracture.

Methods: Using 2000-2010 data from a large US commercially-insured population, community-dwelling individuals aged $\geqslant$50 years with a newly diagnosed fragility fracture and no evidence of OP treatment or fragility fracture in 12 months pre-fracture baseline were identified. Baseline demographics, health services utilization and clinical characteristics were evaluated as predictors of OP treatment in the 12 months post-fracture. Multivariable logistic regression was used to derive odds ratios (OR) and 95% confidence intervals (CI) to assess the association of risk factors with treatment initiation.

Results: Only 18.6% of the 88,571 women and 9.6% of the 41,984 men initiated treatment post-fracture; rates of treatment declined significantly over the study period (Table1). Subjects with hip or spine fractures were 1.8 and 3.8 times more likely to be treated, respectively, than those with wrist fractures. Compared to women, men were less than half as likely to be treated (OR=0.40, CI 0.38-0.41).The odds of treatment increased with age and with increasing number of other medications. Liver disease, rheumatoid disease, steroid use $\geqslant$90 days and hyperthyroidism were associated with increased treatment likelihood as was having a dual-energy x-ray absorptiometry (DXA) test pre-fracture. Diabetes, renal failure and paralysis were associated with decreased odds of treatment.

Conclusion: While those with certain high risk factors for fracture such as older age, rheumatic disease and steroid use were more likely to receive treatment, most

subjects did not receive treatment despite being at high risk for repeat fracture. Moreover, treatment rates decreased significantly over time. Disparities by gender and fracture site were glaring. DXA prior to fracture was a strong predictor of treatment initiation after fracture, suggesting that a fracture in the setting of an on-going OP evaluation may be more likely to trigger treatment. Our results highlight the need for greater recognition of secondary fracture risk and for quality improvements in post-fracture treatment, particularly since treatment rates declined significantly over the last decade.

Table 1.Multivariate associations of selected baseline risk factors with post-fracture OP treatment in subjects with fragility fractures.[1]

		Odds Ratio	Wald 95% CI
Year of index fracture	2000-2003	1.00	--
	2004-2006	0.77	(0.74, 0.80)
	2007-2009	0.62	(0.59, 0.64)
Fracture site	Spine	3.80	(3.63, 3.99)
	Hip	1.75	(1.66, 1.84)
	Wrist	1.00	--
	Humerus	0.93	(0.87, 0.99)
Sex	Female	1.00	--
	Male	0.40	(0.38, 0.41)
Age group (years)	50-54	0.47	(0.43, 0.51)
	55-64	0.71	(0.68, 0.75)
	65-74	1.00	--
	75-84	1.10	(1.05, 1.14)
	85+	0.98	(0.93, 1.03)
Rheumatic disease	No	1.00	--
	Yes	1.56	(1.41, 1.73)
COPD	No	1.00	--
	Yes	1.08	(1.02, 1.14)
Diabetes	No	1.00	--
	Yes	0.78	(0.75, 0.82)
Liver disease	No	1.00	--
	Yes	1.35	(1.06, 1.70)
Chronic renal failure	No	1.00	--
	Yes	0.74	(0.66, 0.83)
Paralysis	No	1.00	--
	Yes	0.66	(0.50, 0.86)
Hyperthyroidism	No	1.00	---
	Yes	1.43	(1.05, 1.94)
Number of concomitant medications	0	0.41	(0.39, 0.44)
	1-5	0.91	(0.87, 0.95)
	6-10	1.00	--
	11+	1.06	(1.02, 1.10)
Steroid use	No	1.00	--
	Yes	2.25	(2.08, 2.45)
DXA scan during baseline	No	1.0	--
	Yes	1.54	(1.45,1.61)

[1] Simultaneously adjusted for geographic region of residence, congestive heart failure, cerebrovascular disease, hypertension, number of hospitalizations and antidepressant use.
Rheumatic disease includes SLE, Systemic Sclerosis, Rheumatoid arthritis, Polymyalgia rheumatica and Polymyositis.
COPD=chronic obstructive pulmonary disease. Steroid use= glucocorticoid use for 90 days or more.

Predictors of Post-fracture treatment Table

***Disclosures: Cynthia O'Malley**, Amgen, Inc, 3; Amgen, Inc, 7*
This study received funding from: Amgen, Inc.

MO0349

FRAX Calculator and Garvan Nomogram in Male Osteoporotic Population.
Wojciech Pluskiewicz*[1], Piotr Adamczyk[2], Edward Franek[3], Ewa Sewerynek[4], Piotr Leszczynski[5], Hanna Wichrowska[3], Luiza Napiórkowska[3], Michał Stuss[4], Aleksandra Ptaszek[4], Tomasz Kostyk[6], Krzysztof Golba[7], Wioleta Garbacz[8], Bogna Drozdzowska[9]. [1]Medical University of Silesia, Katowice, Poland, [2]Dept. & Clinic of Paediatrics, Medical University of Silesia, Katowice, Poland, [3]Dept. of Endocrinology, Medical Res. Centre, Polish Academy of Science, Warsaw, Poland, [4]Dept. of Endocrine Disorders & Bone Metabolism, Medical University, Lodz, Poland, [5]Dept. of Physiotherapy, Rheumatology & Rehabilitation, Medical University, Poznan, Poland, [6]Dept. of Rheumatology & Osteoporosis, Hospital J. Strusia, Poznan, Poland, [7]Dept. of Cardiology, Medical University of Silesia, Katowice, Poland, [8]Military hospital, Gliwice, Poland, [9]Dept. of Pathomorphology, Medical University of Silesia, Katowice, Poland

Purpose. The aim of the study was the analysis of osteoporotic fracture prediction in men.

Methods. Eight hundred and one (801) patients of four outpatient osteoporotic clinics were examined. The mean age was of 70.8 ± 9.31 years. A ten-year fracture prediction period was established, using the FRAX calculator and Garvan nomogram.

Results. The mean value for any and hip fracture probabilities, calculated by the FRAX method, were 7.26 ± 5.4% and 3.68 ± 4.25%, respectively and 26.44 ± 23.83% and 12.02 ± 18.1%, respectively in Garvan nomogram. Assuming the threshold of 20% (any fracture) and 3% (hip fracture), the mean conformity between both methods for any and hip fracture prediction was 55.8% and 79.65%, respectively. A ROC analysis showed the following areas under the ROC curves (AUC) for any fractures: FRAX 0.808 and Garvan nomogram 0.843 (p=0.059). The AUC values for hip fractures were 0.748 and 0.749 for Garvan nomogram and FRAX, respectively, thus showing no differences.

On the basis of the ROC data, cut-off values were established for fracture prediction by both methods, giving 20.2% for any fracture by the Garvan method and 7.6% by FRAX, while for hip fracture, the respective results were 4.9% and 3.8%. The conformity between the two methods was 72.5% for any and 77.7% for hip fractures, taking into account the thresholds from ROC analysis.

Conclusion. The conformities between FRAX and Garvan methods with regards to hip fracture prediction were acceptable for the threshold of 3% and the thresholds, derived by ROC analysis, while for any fracture, it is recommended to use the thresholds from ROC analysis. This may suggestive of some misleading character of the 'universal' cut-off points. It is necessary to establish a cut-off point, according to the results of the sensitivity-specificity analysis, separately for each method and each population.

***Disclosures: Wojciech Pluskiewicz**, None.*

MO0350

Incidence and characteristics of atypical femoral fractures.
Zeineb Mahjoub*[1], Sonia Jean[2], Jean-Thomas Leclerc[3], Jacques P. Brown[4], Dominic Boulet[3], Stephane Pelet[3], Charlotte Grondin[1], Jeannette Dumont[5], Etienne Belzile[1], Laetitia Michou[3]. [1]CHU de Québec, Canada, [2]INSTITUT NATIONAL DE SANTÉ PUBLIQUE DU QUÉBEC, Canada, [3]Université Laval, Canada, [4]CHU de Québec Research Centre, Canada, [5]Centre de recherche du CHU de Québec, Canada

Introduction: Many publications have reported the emergence of atypical subtrochanteric or shaft femoral fractures (AFF). Such fractures are characterised by a unique fracture line, generally affecting the proximal third of the femur, a medial bone spike and a localised periosteal reaction of the lateral cortex. The objective of this study was to estimate the incidence of AFF on a 18 month period in Quebec City, and to collect all clinical characteristics likely to constitute an AFF risk factor.

Methods: We reviewed medical records of patients hospitalised for hip or femoral fracture, in Quebec City between June 1st, 2009 and December 31st, 2010. We selected AFF according to the ASBMR task force criteria, and calculated their incidence. We collected all data likely to influence an AFF occurrence, from medical, pharmacological records, proximal femur measurements on X-rays and patient interviews. For each variable, data analysis consisted of comparing patients with an AFF during the last five years (including the observation period for the incidence estimation), with two controls with hip or femoral osteoporotic fracture or traumatic fracture, paired for age and gender.

Results: We identified 36 atypical fractures during the observation period, corresponding to an AFF incidence of 0.034 [0.024-0.047] case per 1000 persons-years. We collected 56 AFF in the last five years, including the observation period, and we found a significant association with the use of bisphosphonates: p = 0.0001, OR = 29.03 [6.98-120.84], of proton pump inhibitors: p = 0.02, OR = 2.33 [1.12-4.84], of statins: p = 0.03, OR = 2.05 [1.06-3.97]. There was a significant association with a personal history of osteoporosis: p = 0.0002, OR = 5.16 [2.20-12.08], and a higher body mass index: p = 0.03, OR = 1.18 [1.02-1.36] (Table 1). Patients with AFF had excessive femoral offset (43.0 vs 38.3, p=0.0009), proximal femoral varus (129.1 vs 133.8, p=0.0001) and greater proximal cortical thickness (Table 2).

Conclusion: The incidence of AFF in our city was similar to others reported in the literature. Our retrospective study showed a significant association between AFF and exposure to bisphosphonates and pump proton inhibitors. Surprisingly, we observed an association of AFF with statins intake, although these drugs are known to have a protective effect against osteoporotic fractures. The proximal femoral geometry may play an important role in the AFF occurrence.

Variable	Cases (N=56) % (N)	Controls (N=112) % (N)	OR (95% CI)	P
Mean BMI (±SD)	26.2 (5.1)	23.6 (6.2)	1.18 (1.02-1.36)	0.0314
Previous fracture	45.4 (20)	23.7 (23)	2.6 (1.13-5.96)	0.0243
Personal history of osteoporosis	70.6 (36)	35.7 (40)	5.16 (2.2-12.08)	0.0002
Bisphosphonate use	94.3 (49)	28.8 (32)	29.03 (6.98-120.84)	0.0001
Statin use	49.0 (25)	29.1 (32)	2.05 (1.06-3.97)	0.0322
Proton pomp inhibitor use	55.1 (27)	33.9 (37)	2.33 (1.12-4.84)	0.0228

Table 1: Comparison of the main clinical characteristics between cases and controls

Femoral measurements on X-rays	Cases N	Cases Mean (SD)	Controls N	Controls Mean (SD)	P
Femoral Offset (mm)	51	43.0 (8.1)	104	38.3 (7.7)	0.0009
Angle CDH (degree)	51	129.1 (7.0)	104	133.8 (6.9)	0.0001
Femoral neck width	51	35.7 (3.6)	103	37.5 (3.9)	0.0060
Lateral cortical thickness 50 mm below the lesser trochanter (mm)	51	7.7 (2.0)	103	6.9 (1.3)	0.0062
Medial cortical thickness 50 mm below the lesser trochanter (mm)	51	8.1 (1.7)	103	7.1 (1.4)	0.0018
Medial cortical thickness at the level of the lesser trochanter (mm)	51	5.1 (2.8)	103	2.9 (3.0)	<0.0001
Lateral cortical thickness at the level of the lesser trochanter (mm)	47	4.3 (1.2)	103	3.8 (1.1)	0.0297

Table 2: Comparison of the main radiographic characteristics between cases and controls

***Disclosures: Zeineb Mahjoub**, Amgen, 2; Bristol-Myers-Squibb, 2; Bristol-Myers-Squibb, 6*

MO0351

Incidence of subtrochanteric and femoral shaft fractures in 3 French centers. Thomas Funck-Brentano*[1], Agnes Ostertag[2], Francoise Debiais[3], Patrice Fardellone[4], Louis-Etienne Gayet[5], Patrice Mertl[5], Remy Nizard[5], Philippe Orcel[6], Martine Cohen-Solal[7]. [1]Department of rheumatology, hopital Lariboisiere, France, [2]INSERM U606, France, [3]Hopital Jean Bernard, France, [4]Service de rhumatologie, CHU Hôpital Nord, France, [5]department of orthopedic surgery, France, [6]University Paris Diderot, France, [7]Centre Viggo Petersen, France

Purpose: Subtrochanteric and femoral shaft (ST/FS) fractures are rare fragility fractures. Atypical ST/FS fractures have been reported in patients with long duration of bisphosphonate use although they can be observed in osteoporotic patients independently of any treatment. We here assessed the incidence of atypical and typical ST/FS fractures in orthopedic departments of 3 academic hospitals and analyzed the associated risk factors and treatments in these populations. Methods: We first retrieved the files in the databases from 3 French using ICD-10 codes (S72.2 for ST and S72.3 for ST/FS) from January 2007 to December 2010. Characteristics of ST/FS fractures (atypical or non-atypical) were identified in X-Rays obtained before surgery. Information on age, sex, weight, height, history of diseases, falls and treatments were collected. The use of bone-related treatments was confirmed by patient phone calls. Results: ST/FS fractures (S72.2 / S72.3) were initially declared for 389 patients. Among them, 179 (46%) occurred in the presence of materials (prosthesis or nails), 89 (22%) were traumatic, pathologic or misclassified fractures. Finally, low trauma ST/FS fractures were found in 121 patients (mean age: 78 $\pm$ 11 years), in particular 14 (12%) were atypical fractures while 107 (88%) were typical fractures. Several associated diseases were present at the time of the fractures, but there were no difference in the prevalence of hypertension, diabetes, cognitive function, troubles of rhythm and lipid diseases. Nine patients with atypical and 102 patients with typical fractures were naïve of any bone treatment. Atypical fractures occurred in 5 patients (5/14; 36%) treated with alendronate (n=3), strontium ranelate (n=1) and raloxifene (n=1) while typical fractures occurred in 5 patients (5/107; 5%) treated with alendronate (n=3), risedronate (n=1), zoledronic acid (n=1) (Fisher exact test, $p<0.01$). Conclusions: ST/FS fractures are rare events and frequently occur in the presence of materials. They are mostly typical fractures and can be observed in the absence of any treatment for bone. However, atypical fractures characterized by ASBMR features are more frequent in patients receiving anti-fracture treatment.

***Disclosures: Thomas Funck-Brentano**, None.*

MO0352

Increased fracture risk among women with diabetes mellitus is not mediated by increased falls risk or decreased functional status. Richard Lee*[1], Cathleen Colon-Emeric[2]. [1]Duke University, USA, [2]Duke University Medical Center, USA

Background: Prior studies have shown that despite having a higher average bone mineral density (BMD), persons with diabetes mellitus type 2 (DM2) have a 1.5 to 2-fold increase in the risk of fracture, compared to those without DM2. The underlying mechanism for this paradoxical observation may result from increased fall risk and decreased functional status among persons with DM2.

Method: This is a secondary analysis of the Women's Health Initiative Clinical Trial cohort. The analysis was limited to those women who had BMD testing during the trial period (N =4644). Falls risk and functional status were determined in the annual and semi-annual questionnaires. Increased falls risk was defined as 2 or more falls in the preceding year. Decreased functional status was determined by self-reported difficulties in activities of daily living including bathing and transferring, as well as physical performance including bending/stooping, carrying groceries, and moving large objects. The association between DM2 and the incidence of any clinical fracture was determined, controlling for multiple factors including falls risk and functional status.

Results: Compared to women without DM2, the risk of any clinical fracture during the study period was increased among women with DM2, after controlling for age, race/ethnicity, and body mass index (HR 1.40, 95% CI 1.08 - 1.80). After controlling for medications and BMD at the hip and spine, the increased risk in fracture among persons with DM2 remained significant (HR 1.48, 95%CI 1.09-2.01). Inclusion of falls risk and functional status did not significantly change the association between DM2 and the risk of any clinical fracture (HR 1.44, 95% CI 1.06-1.95).

Conclusion: Women with DM2 are at increased risk of clinical fractures, independent of BMD. The increased risk is not mediated by increased falls risk or by decreased functional status in these persons.

***Disclosures: Richard Lee**, None.*

MO0353

Insulin-like Growth Factor Binding Protein 1 (IGFBP-1), FRAX and the prediction of hip fractures. Hans Lundin*[1], Maria Saaf[2], Lars-Erik Strender[3], Sven Nyren[2], Sven-Erik Johansson[3], Helena Salminen[1]. [1]Karolinska Institutet, Sweden, [2]Department for Molecular Medicine an Surgery, Karolinska Institutet, Sweden, [3]Centre for Family Medicine, Karolinska Institutet, Sweden

Insulin-like growth factor binding protein 1 (IGFBP-1)is a serum protein which binds circulating insulin-like growth factor 1 (IGF-1) and thereby decreases its bioavailability. IGF-1 has been shown to stimulate bone formation and a low serum concentration of IGF-1, adjusted for BMI and bone mineral density (BMD), has been shown to increase the risk of a future osteoporotic fracture. IGFBP-1 is inversely correlated to body mass index (BMI) and a low BMI is a well established risk factor for both low BMD and for osteoporotic fractures, including hip fractures. To our knowledge there are no previous studies published on the relation between IGFBP-1 and fractures.

FRAX is the most used fracture prediction tool worldwide. It was developed by WHO and it is freely available on the Internet.

This is a population-based prospective cohort study on 351 Swedish women aged 69-79 years at inclusion. These women were tested for serum IGFBP-1 and with FRAX including bone mineral density (BMD) at inclusion between 1999-2001. Follow up was performed ten years later through Swedish medical records. The main outcome was a hip fracture.

The aims of this study were to evaluate whether IGFBP-1 could predict hip fractures and further to compare predictive ability of IGFBP-1 with the standard method FRAX.No participant was lost to follow up. The data was analyzed with Cox regression.

The relation between IGFBP-1 and the risk of a hip fracture was found to be positively linear. The age-adjusted risk of a hip fracture increased significantly by 2% for every unit increase in IGFBP-1 (Hazard ratio (HR) 1.020, 95% CI 1.004-1.036). This HR was not significantly altered by further adjusting for either BMI, the serum concentration of IGF-1 or for BMD of the femoral neck (Figure 1). The age-adjusted IGFBP-1 had a Harrells c of 0.63 compared to 0.59 for FRAX which indicates that IGFBP-1 has a predictive ability similar to that of FRAX. Harrell's c is the equivalent to the area under curve (AUC) used in logistic regression, but designed for Cox regression models. For a model combining IBFBP-1 with FRAX, Harrell's c was 0.64.

In conclusion, IGFBP-1 could predict hip fractures as good as FRAX and the relation could not be explained by differences in BMI, IGF-1 or BMD of the femoral neck.Keywords: Hip fractures, Insulin-Like Growth Factor Binding Proteins, Insulin-Like Growth Factor Binding Protein 1, Risk assessment, Osteoporosis.

	Hazard Ratio for hip fracture (95% CI)
IGFBP1 adjusted for age	1.020 (1.004- 1.036)
IGFBP1 adjusted for age and BMI	1.023 (1.006-1.041)
IGFBP1 adjusted for age and IGF-1	1.023 (1.006-1.039)
IGFBP1 adjusted for age and BMD of the femoral neck	1.013 (0.995-1.031)

Table 1 IGFBP-1, FRAX and the prediction of hip fractures

***Disclosures: Hans Lundin**, None.*

MO0354

Is lower income associated with an increased likelihood of qualification for treatment for osteoporosis in Canadian women?. Sharon Brennan*[1], William Leslie[2], Lia Lix[3], Helena Johansson[4], Anders Oden[5], Eugene McCloskey[6], John Kanis[7]. [1]The University of Melbourne, Australia, [2]University of Manitoba, Canada, [3]Department of Community Health Sciences, University of Manitoba, Canada, [4]Swedish University of Agricultural Sciences, The Biomedical Center, Sweden, [5]World Health Organization (WHO) Collaborating Centre, University of Sheffield, United Kingdom, [6]University of Sheffield, United Kingdom, [7]University of Sheffield, Belgium

Background: Lower income has been associated with increased fracture risk. We examined whether lower income in women was associated with an increased likelihood of treatment qualification determined by Canada FRAX®.

Methods: We calculated 10-year FRAX probabilities in 51,327 Canadian women aged ⩾50years with baseline femoral neck BMD measured by dual energy x-ray absorptiometry 1996-2011, identified from the Manitoba Bone Density Program, Canada. Mean household income was extracted from 2006 Canada Census public use files and the population was categorized into quintiles. Age, weight and height were recorded at the time of DXA. Medically diagnosed conditions prior to BMD testing (rheumatoid arthritis, and prior fracture since 1987) were ascertained through a combination of hospital discharge abstracts. A diagnosis of chronic obstructive pulmonary disease was used as a proxy for smoking status, and a diagnosis of alcohol or substance abuse was used as a proxy for high alcohol intake. Prolonged glucocorticoid use was obtained from a province-wide retail pharmacy system. Adjustments were made for incomplete history of parental hip fracture using age- and sex-specific adjustment factors. FRAX probabilities for hip fracture ⩾3% or major osteoporotic fracture (MOF) ⩾20% were used to define treatment qualification. Logistic regression analyses were used to model associations between income and treatment qualification.

Results: Percentages of women who qualified for treatment based upon high hip fracture probability (defined with BMD) in income quintiles 1 (lowest income) through 5 (highest income) were 34.6%, 28.2%, 24.9%, 19.9% and 17.3%, respectively. Similar negative linear associations were observed for MOF, where percentages ranged from 13.5% in quintile 1 to 5.8% in quintile 5 ($p<0.001$). Compared to the highest income quintile, women in the lowest income quintile had a 2.5-fold greater likelihood of treatment qualification based upon high hip fracture probability (adjusted odds ratio [OR] 2.47, 95%CI 2.32-2.63 without BMD, and OR 2.53, 95%CI 2.37-2.71 with BMD in FRAX calculation) (Figure 1). Similar results were observed for MOF probability (Figure 2).

Conclusions: FRAX identifies a larger proportion of lower income women as qualifying for treatment than higher income women. The strong negative linear associations between income and treatment qualification has implications for clinical practice and public health outcomes.

HIPC File Number: 2012/2013-15

Figure 1: Logistic regression analysis results for the association between income quintile and treatment qualification based upon high 10-year probability of hip fracture (=3%) defined with and without BMD. Results are presented as odds ratios (ORs) with error bars indicating 95% CI. Quintile 5 (highest income) is the referent.

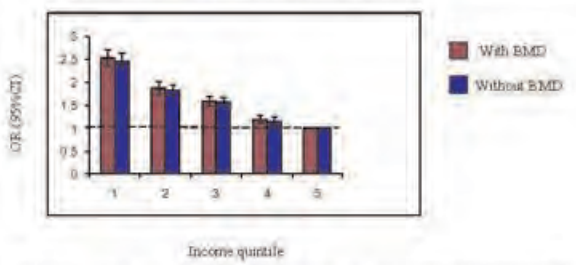

Figure 2: Logistic regression analysis results for the association between income quintile and treatment qualification based upon high 10-year probability of major osteoporotic fracture (=20%) defined with and without BMD. Results are presented as odds ratios (ORs) with error bars indicating 95% CI. Quintile 5 (highest income) is the referent.

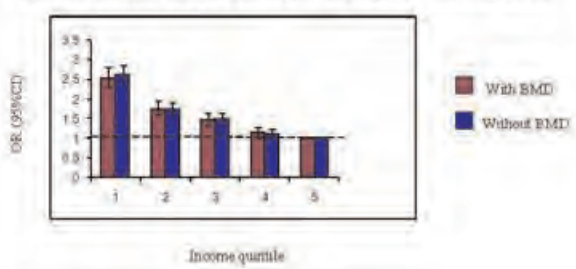

Associations between income quintile and treatment qualification for hip fracture and MOF

***Disclosures: Sharon Brennan**, None.*

MO0355

Racial/ethnic Differences in Bone Microarchitecture among Middle-aged and Elderly Men. Andre Araujo*[1], Gretchen Chiu[1], Benedetta Bartali[1], Thomas Travison[2], Joseph Zmuda[3], Mary Bouxsein[4]. [1]New England Research Institutes, USA, [2]Brigham & Women's Hospital, USA, [3]University of Pittsburgh Graduate School of Public Health, USA, [4]Beth Israel Deaconess Medical Center, USA

Although there are known differences in rates of osteoporotic fractures and bone mass among racial/ethnic groups, few studies have examined the relationship between race/ethnicity and bone microarchitecture, especially among men. We obtained cross-sectional data from the BACH/Bone Survey, a population-based cohort study of racially diverse men aged 38-86y. Microarchitecture at the distal radius (N=459) and tibia (N=487) was measured by high-resolution peripheral quantitative computed tomography (HR-pQCT, XtremeCT, Scanco). Outcomes considered were trabecular volumetric bone mineral density (vBMD), trabecular number, cortical vBMD, cortical thickness, and total area in the distal radius and tibia. Multivariable linear regression was used to examine the associations of race/ethnicity with these outcomes, controlled for age, household income, smoking, self-rated health, diabetes, physical activity, and BMI. Mean(SD) age was 58.0(11.6)y, with Black, Hispanic, and White men representing 30.9%, 29.5%, and 39.6% of the sample, respectively. Most radius parameters (except trabecular number and total area) were lower with increased age; whereas only cortical vBMD and cortical thickness were associated with age at the tibia. Furthermore, we found cross-sectional age-related differences varied significantly by race/ethnicity for trabecular vBMD (p=.006) and trabecular number (p=.02); these particular age-related differences were more than two times greater in Hispanic men. Controlled for covariates, racial/ethnic differences were evident in both the radius and tibia (3%-17%), with a larger number of differences in tibia parameters (Table). While cortical parameters were higher in minority vs. White men, trabecular parameters were generally lower in minority men. In conclusion, cross-sectional racial/ethnic differences in bone microarchitecture are most evident in the weight-bearing tibia (even after adjustment for BMI), which is consistent with the important role of mechanical loading in determining potential racial/ethnic differences in bone strength. In addition, the relative advantage of Blacks and Hispanics in cortical density and microarchitecture appears consistent with reported racial/ethnic differences in non-vertebral fracture rates.

Table. Multivariable-adjusted mean (SE) in bone microarchitectural parameters by race/ethnicity. Column Ns are no. subjects with complete radius and covariate data.

Site	Parameter	Black (N=138)	Hispanic (N=141)	White (N=180)
Radius	Tb.vBMD (mg/ccm)	130(11.4)	122(11.5)	123(11.6)
	Tb.N (1/mm)	1.70(0.08)	1.65(0.08)	1.70(0.08)
	Ct.vBMD (mg/ccm)	766(22)	784(22)*	764(22)
	Ct.Th (mm)	0.53(0.07)	0.56(0.07)*	0.50(0.07)
	Total Area (mm²)	404(23)**	363(23)	377(24)
Tibia	Tb.vBMD (mg/ccm)	121.9(11.4)*	111.3(11.5)***	131.1(11.5)
	Tb.N (1/mm)	1.31(0.10)**	1.18(0.10)***	1.40(0.10)
	Ct.vBMD (mg/ccm)	799(16)***	817(16)***	773(16)
	Ct.Th (mm)	0.66(0.09)**	0.67(0.09)**	0.57(0.09)
	Total Area (mm²)	837(46)	747(46)***	818(46)

*p<.05, **p<.01, ***p<.001 (vs. White)

Table

***Disclosures: Andre Araujo**, None.*
This study received funding from: NIH

MO0356

The Association between Higher Serum Ferritin Level and Lower Bone Mineral Density is Prominent in Women ⩾ 45 Years of Age (KNHANES 2008-2010). Beom-Jun Kim*[1], Seung Hun Lee[2], Jung-Min Koh[1], Ghi Su Kim[2], Seong Hee Ahn[3]. [1]Asan Medical Center, South Korea, [2]Asan Medical Center, University of Ulsan College of Medicine, South Korea, [3]University of Ulsan, Asan Medical Center, South Korea

Introduction: Despite extensive in vitro and in vivo studies showing the detrimental effects of iron on bone metabolism, the clinical studies relating to osteoporosis-related phenotypes have not been evaluated extensively. In the present study, we investigated and compared the association between serum ferritin and bone mineral density (BMD), depending on the stratified age groups in both genders.

Methods: This is a population-based, cross-sectional study from the Korea National Health and Nutrition Examination Surveys, including 14,017 Koreans (6,817 men and 7,200 women) aged 10-80 years. BMD was measured using dual X-ray absorptiometry, and osteoporosis was diagnosed by the WHO definition.

Results: Initially, we divided the subjects into three age groups, based on the patterns of age-related BMD changes in this national cohort (i.e., ≤ 24, 25–44, and ⩾ 45 years old). Serum ferritin concentrations were inversely associated with BMD values at all measured sites after adjustment for confounders, only in women ⩾ 45 years of age (P = 0.041 to <0.001). Furthermore, when we divided these women into serum ferritin quartiles, the odds for prevalent osteoporosis and fractures were

1.55-fold (95% CI = 1.09–2.23) and 1.52-fold (95% CI = 1.02–2.27) higher, respectively, in subjects in the highest quartile compared with those in the lowest quartile.

Conclusions: These results provide the first clinical evidence that the associations between serum ferritin level and bone parameters could be the most prominent in women ⩾ 45 years of age.

***Disclosures: Beom-Jun Kim**, None.*

MO0357

The Effect of Anticholinergic Medications on Fracture Risk, Bone Mineral Density, and Falls over a Ten Year Period. Lisa-Ann Fraser*[1], Jonathan Adachi[2], William Leslie[3], David Goltzman[4], Robert Josse[5], Stephanie Kaiser[6], Nancy Kreiger[7], Christopher Kovacs[8], Tassos Anastassiades[9], Alexandra Papaioannou[10]. [1]Western University, Canada, [2]St. Joseph's Hospital, Canada, [3]University of Manitoba, Canada, [4]McGill University, Canada, [5]St. Michael's Hospital, University of Toronto, Canada, [6]Dalhousie University, Canada, [7]Division of Epidemiology, Dalla Lana School of Public Health, Canada, [8]Memorial University of Newfoundland, Canada, [9]Queen's University, Canada, [10]Hamilton Health Sciences, Canada

Purpose: Many medications used in older adults have strong anticholinergic (ACH) properties. There has been concern that these medications may increase the risk of falls and fractures in this already vulnerable population; although results of studies have not been definitive.

Methods: We examined a large population-based Canadian cohort, the Canadian Multicentre Osteoporosis Study, over 10 years. Use of oral medications with previously proven strong ACH effects (as per Ancelin BMJ 2006; Rudolph ArchIntMed 2008) were identified at baseline, year 5, and year 10. Cross sectional regression analyses of the cohort were performed at years 0, 5, and 10 to examine associations between ACH medication use and falls. Time-dependent Cox-Regression was used to prospectively examine time-to-first non-traumatic fracture; and differences in the mean change in BMD over 10 years was examined in ACH medication users compared to non-users. Analyses were adjusted for potentially confounding variables.

Results: Strongly ACH medications were used by 614 of 9423 participants (6.5%) at study baseline, 596 of 7652 (7.8%) at year 5, and 361 of 5569 (6.5%) at year 10. Unadjusted, ACH medications were found to be associated with falls at study baseline (OR=1.47, 95% CI 1.10-1.96, p=0.009) but the association was lost after adjustment. Similar results occurred at years 5 and 10, with an association present prior to adjustment (OR=1.52, CI 1.27-1.82, p<0.001; OR = 1.45, CI 1.16-1.82, p=0.001, respectively), but not after. ACH medication use was associated with an increased incident fracture rate (HR=1.35, CI 1.08-1.69, p=0.01) but not after adjustment. Parkinson's disease was strongly associated with both falls (OR=4.02, CI 1.71-9.48, p=0.001, at baseline) and incident fracture (HR=5.58, CI 2.98-10.46, p<0.001). Mean (SD) change in femoral neck BMD T-score over 10 years, in those using ACH medications at both years 0 and 5, was -0.599(0.631) in ACH users vs. -0.503(0.454) in non-users (p=0.056).

Conclusions: In this Canadian cohort, we did not find strongly ACH medications to be independently associated with an increased risk of falling, fractures, or BMD loss. Instead, underlying conditions associated with ACH medication use (eg. Parkinson's disease) were independently associated with increased falls, which may explain why previous studies have found an association between ACH medications and falls.

***Disclosures: Lisa-Ann Fraser**, None.*

MO0358

Which Patients with Ankle Fractures Are at Risk for Recurrent Fragility Fractures? Results from the OPTIMUS Initiative. François Cabana[1], Nathalie Carrier[2], Marie-Claude Beaulieu[3], Michèle Beaulieu[4], Sophie Roux[5], Gilles Boire*[6]. [1]Division of Orthopaedics, Centre hospitalier universitaire de Sherbrooke, Canada, [2]Division of Rheumatology, Centre hospitalier universitaire de Sherbrooke, Canada, [3]Université de Sherbrooke, Canada, [4]Merck Canada Inc, Canada, [5]University of Sherbrooke, Canada, [6]Centre Hospitalier Universitaire De Sherbrooke, Canada

Introduction. Some but not all guidelines consider ankle fractures as fragility fractures (FF). Objectives. To analyze the characteristics of patients with low-trauma ankle fractures presenting new low-trauma fractures during follow up. Methods. The OPTIMUS study is an ongoing prospective cohort of men and women over 50 years of age, designed to increase the rate of initiation and persistence of osteoporosis treatment after a FF leading to an orthopaedic consultation. The occurrence of novel FF was collected during regular phone follow-ups up to 48 months after inclusion. FRAX scores were calculated without BMD at the time of the ankle fracture, without accounting for this fracture. Ankle x-rays were reviewed and classified as unimalleolar (lateral (Weber A, B or C) or medial), bimalleolar or trimalleolar. Results. 265 patients (190 women; median (IQR) age 61 (55-69); median (IQR) BMI 27.0 (24.6-30.1)) with low-trauma ankle fracture were included. New low-trauma fractures occurred in 11 (4.2%) patients over 716 patient-years of observation, at hip (1), vertebra (1), knee (1), shoulder (2), wrist (2), ankle (2) and other sites (2). 55% of ankle fractures were uni-, 18% bi-, and 27% trimalleolar with rates of recurrent FF of 1.4, 1.4, and 2.2 / 100 patient-years, respectively. Of the 11 recurrent FF, 8 occurred in women (Relative Risk (RR) 1.05 [0.29-3.86], NS), 6 in patients with FF prior to the ankle fracture (RR 6.72 [2.15-20.97], p=0.001) and 7 in patients at high risk according to pre-ankle fracture FRAX (RR 5.98 [1.81-19.74], p=0.003). Incidence of recurrent FF (per 100 patient-years) was highest in patients with FF prior to the ankle fracture (4.90), intermediate in patients without previous FF but with a High risk FRAX score (1.87), and lowest in patients without previous FF and with Low or Moderate risk (0.62). Conclusions. Most recurrent fractures occurring in older individuals after low-trauma ankle fractures are at typical sites of FF. Recurrent fractures occur at about 1.5 per 100 patient-years, with highest rates (4.90) in patients with previous FF, and lowest rates (0.62) in those without previous FF and with pre-fracture Low or Moderate risk. Gender, BMI and severity of bone damage were not predictors for recurrent fractures. Low-trauma ankle fractures represent clinical opportunities to identify patients with previous FF and patients with FRAX estimated high risk, two groups in need for preventive treatment.

***Disclosures: Gilles Boire**, None.*
This study received funding from: Merck Canada, Alliance for Better Bone Health, Amgen Canada, Novartis Canada, Warner Chilcott, Eli Lilly Canada, Servier Canada

MO0359

Bone Mineral Distribution in the Tibiae of Stroke Survivors During the First Year of Recovery: A pQCT Study. Norma MacIntyre*[1], Arpita Parmar[1], Gregory Wohl[1], Brenda Brouwer[2]. [1]McMaster University, Canada, [2]Queen's University, Canada

Purpose: Spatial adaptation of volumetric cortical bone density (CoD) in the paretic limb of stroke survivors has not been reported. This study describes and contrasts spatial distribution (polar divisions, radial divisions), CoD and resistance to torsion (Strength Strain Index, SSI) at the 66% site of the tibia in the paretic and nonparetic limbs of subacute stroke survivors followed for one year after a unilateral stroke.

Methods: Adults being discharged from a rehabilitation hospital following their first hemispheric stroke were recruited. Bilateral images were acquired bilaterally at the tibial 66% site at baseline, 6 mo and 12 mo using pQCT (XCT 2000L, Stratec). Image analysis was conducted using BoneJ (www.bonej.org), to quantify total CoD, distribution in 36 equal polar subdivisions (10° each) and radial divisions (endocortical, mid, periosteal), and SSI. Mineral distribution in the 36 polar subdivisions were characterized by calculating mean CoD for 4 polar anatomic divisions: posterior (0-5,33-35), anterior (15-23) lateral (6-14), and medial (24-32) as shown in Fig. 1. Descriptive statistics were used to characterize the bone variables in each limb at each timepoint. To minimize the difference in variance in paretic limb measures, the main effect of time was determined for between-limb differences (paretic-nonparetic) using RM ANOVA. To contrast distribution within the polar and radial divisions over time, 2-way RM ANOVAs were used. Significance level was set at $p \leq 0.05$

Results: Data were obtained for 17 subjects (mean age: 61.2(9.9)y; sex: 13M/4F; Paretic Limb: 9 right/8 left). Table 1 summarizes the bone outcomes. No main effect due to time was observed for CoD ($F(2, 32)=1.14$, $p=0.33$), mineral distribution in polar divisions ($F(2, 32)=0.325$, $p=0.73$) or radial divisions ($F(2, 32)=0.57$, $p=0.57$), or SSI ($F(2,32)=1.10$, $p=0.34$). Mineral was not significantly redistributed within the polar ($F(2,48)=0.587$, $p=0.63$) or radial ($F(2,32)=0.214$, $p=0.81$) divisions. Observed power for all contrasts ≤ 0.23.Conclusions: This study is the first to describe spatial distribution of bone mineral at the 66% site of the tibiae in stroke survivors. Our study is underpowered to detect changes during the first year following a unilateral stroke. On average, the paretic limb had insignificantly lower values for all bone outcomes at 6 mo; this trend was not observed at 12 mo. Changes in mobility ability over the 1y study may explain these results.

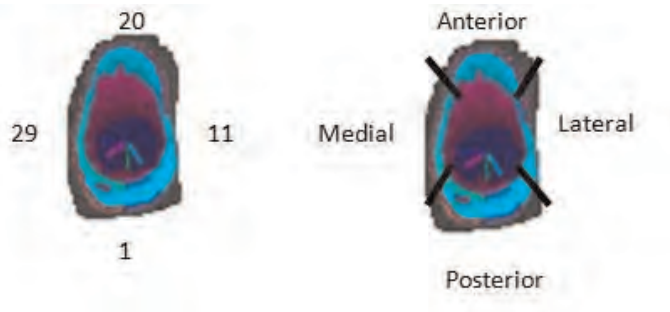

Figure 1. Tibial cross sectional images demonstrating the 4 anatomical polar divisions

Bone Outcome	Baseline (n=17)			6 Months (n=17)			12 Months (n=17)		
	Paretic	Non Paretic	Diff	Paretic	Non Paretic	Diff	Paretic	Non Paretic	Diff
Total CoD, mg/cm³	1109.7 (34.1)	1104.9 (34.7)	4.787 (14.70)	1103.3 (44.7)	1108.9 (29.5)	-1-580 (12.78)	1106.1 (45.1)	1107.8 (36.6)	-1.639 (25.65)
Polar Divisions, mg/cm³									
Posterior	1177.0 (42.2)	1170.2 (41.9)	6.793 (24.55)	1175.8 (36.3)	1175.0 (36.7)	0.764 (27.82)	1171.0 (49.2)	1164.4 (43.3)	6.530 (38.81)
Anterior	1127.9 (45.9)	1125.6 (40.2)	2.284 (18.63)	1127.0 (45.5)	1131.4 (45.3)	-4.404 (20.03)	1125.6 (52.2)	1132.4 (42.4)	-6.833 (27.95)
Lateral	1193.6 (30.9)	1196.3 (34.6)	-2.628 (22.48)	1191.3 (31.5)	1192.2 (32.1)	-0.933 (21.22)	1192.6 (37.6)	1186.7 (37.7)	5.839 (32.51)
Medial	1184.0 (33.2)	1181.9 (39.3)	2.025 (22.26)	1181.6 (38.7)	1185.0 (34.0)	-3.390 (36.28)	1183.0 (47.7)	1188.1 (50.6)	-5.130 (27.16)
Radial Divisions, mg/cm³									
Endosteal	1111.2 (34.1)	1110.4 (37.9)	0.821 (22.52)	1108.2 (35.1)	1113.3 (35.1)	-5.104 (16.92)	1110.2 (46.6)	1108.1 (42.6)	2.096 (27.09)
Middle	1196.9 (31.7)	1194.8 (29.6)	2.097 (13.13)	1196.6 (34.8)	1200.0 (28.8)	-3.389 (15.27)	1194.3 (43.4)	1198.5 (36.5)	-4.190 (25.45)
Periosteal	1203.9 (26.4)	1200.4 (27.7)	3.438 (11.96)	1202.0 (22.7)	1203.0 (21.7)	-1.080 (14.96)	1199.9 (37.3)	1200.7 (31.7)	-0.808 (26.00)
SSI, mm³	2562.1 (488.4)	2547.6 (486.9)	14.454 (123.3)	2554.2 (485.4)	2561.7 (490.5)	-7.457 (120.1)	2553.5 (482.6)	2540.0 (497.2)	13.538 (135.9)

Table 1. Mean (SD) values for total cortical bone density (CoD), mineral distribution, and strength

***Disclosures: Norma MacIntyre**, None.*

MO0360

Is Low Bone Mineral Density a Reason for Schmorl's Node?. Sevinc Kulekcioglu*[1], Alp Cetin[2]. [1]Specialist of Physical Medicine & Rehabilitation Sevket Yilmaz Education & Research Hospital, Turkey, [2]Proffessor of Physical Medicine & Rehabilitaion, Hacettepe University Medical School, Turkey

Inroduction: Schmorl's node is described as intravertebral herniation of intervertebral disc tissue. It can be considered that any process which weakens the subchondral trabeculae of the vertebra results with development of these nodes. One of the reason for this weakness is osteoporosis. As far as our knowledge the role of bone mineral density (BMD) on development of schmorl's node has not been studied yet. So the aim of this study was to investigate if there is any relation between bone mineral density and schmorl's node development.

Materials and Methods: Thirtysix patients (23 female, 13 male, mean age 49.3 $\pm$ 15.2) who had schmorl's node on magnetic resonance inaging (MRI) examination were included in this study. Control group consisted of 35 (22 female, 13 male, mean age 46.5$\pm$14.4) subjects without any schmorl's node on MRI. Bone mineral densities of both groups were measured with dual energy X-ray absorptiometry (DXA) at lomber spine and proximal femur.

Results: Ages and other demographic parameters of study and control groups were similar. Both, proximal femur (0.763 ± 0.109g/cm^2 vs 0.830 ± 0.141g/cm^2 for femoral neck, p=0.026 and 0.835 ± 0.106g/cm^2 vs 0920 ± 0.116g/cm^2 for femur total and p=0.010) and lomber spine (0.859 ± 0.116g/cm^2 vs 0.989 ± 0.140g/cm^2 for L1-L4 and p=0.000) BMD values in patients with Schmorl's node were significantly lower than control group. BMD difference was more marked at lomber spine.

Conclusion: The results of this preliminary study showed that development of schmorl's node might be related with low BMD. These findigs supports the hypothesis that weakness of subcondral trabeculae of the vertebra is related with schmorl's node.

***Disclosures: Sevinc Kulekcioglu**, None.*

MO0361

Higher Serum Osteocalcin is Associated with Metabolic Syndrome Severity in Men from the MINOS Cohort. Cyrille Confavreux*[1], Pawel Szulc[2], Romain Casey[3], Annie Varennes[4], Joelle Goudable[5], Roland Chapurlat[6]. [1]INSERM UMR1033 - Universite de Lyon, France, [2]INSERM UMR 1033, University of Lyon, Hopital E. Herriot, Pavillon F, France, [3]OFSEP-Université de Lyon, France Hospices Civils de Lyon, France, [4]Université de Lyon, Central Biochemical Laboratory, Hospices Civils de Lyon, France, [5]INSERM U1060 – Université de Lyon, France, [6]E. Herriot Hospital, France

Objectives. Recently bone has emerged as an endocrine organ that regulates energy metabolism through the secretion of osteocalcin favoring insulin secretion and insulin sensitivity. Several epidemiological studies reported a negative association between osteocalcin level and the presence of metabolic syndrome (MetS). Therefore, we evaluated whether osteocalcin may be quantitatively associated to MetS severity in men.

Material and methods. We included 798 men aged 51-85 with fasting serum total osteocalcin measurement. MetS diagnosis was based on the presence of at least 3 out of the 5 criteria of the current consensus definition (Alberti Circulation 2009). The number of criteria (3, 4 or 5) was used to define MetS severity. We used a polytomous logistic regression model to assess the relationship between gravity of MetS and osteocalcin.

Results. Thirty percent of the cohort (n= 247) had MetS. After adjustment for age, 25OHD, testosterone, physical activity, smoking and alcohol consumption, in logistic regression model, higher serum concentrations of osteocalcin were associated with lower MetS prevalence (OR=0.75 per 10 ng/ml increase, 95%CI: 0.58-0.97; p=0.028). In the stepwise logistic regression including the previously used variables and bone turnover markers (BTM: PINP, Bone ALP, serum CTX-I), osteocalcin was the first BTM retained in the model (OR= 0.81 [0.67-0.97], p=0.02).

In patients with MetS, the higher the number of the MetS traits were present, the lower was the average osteocalcin level (0-2 criteria: 551 men:19.5 ng/ml, 3 criteria, 155 men: 19.3ng/ml, 4 criteria, 72 men: 17.3ng/ml, 5 criteria, 20 men: 15.0 ng/ml; adjusted p for trend=0.02). In polytomous logistic regression model after adjustment on the variables specified above, higher osteocalcin (by 10 ng/ml) level was associated with a lower prevalence of MetS proportionally to the MetS severity: OR=0.93 [0.70-1.24] for 3 criteria, 0.54 [0.34-0.84] 4 criteria and 0.28 [0.10-0.82] 5 criteria; p=0.008.

Conclusion. Total osteocalcin level was associated with MetS severity in older Caucasian men. MetS was associated with osteocalcin more strongly than with other BTM, which suggests a specific link independent of the general bone turnover rate. These data suggest that osteocalcin might be an indicator of global health outcome.

***Disclosures: Cyrille Confavreux**, None.*

MO0362

Suppression of autophagy in Osx1-Cre-expressing cells causes low bone mass and spontaneous fractures in mice. Marilina Piemontese*[1], Melda Onal[2], Yiying Wang[1], Jinhu Xiong[3], Priscilla Baltz[1], Rajamani Selvam[1], Stuart Berryhill[1], Li Han[3], Stavros Manolagas[3], Charles O'Brien[3]. [1]University of Arkansas for Medical Sciences, USA, [2]university of wisconsin, USA, [3]Central Arkansas VA Healthcare System, Univ of Arkansas for Medical Sciences, USA

Autophagy is a stress-activated pathway that maintains cellular health and viability by recycling intracellular components, such as damaged proteins and organelles, via a lysosomal pathway. Previous studies have shown that genetic suppression of autophagy in mature osteoblasts and osteocytes using a Dmp1-Cre transgene caused low bone mass and strength associated with increased oxidative stress in the bone marrow microenvironment. However, whether autophagy plays an important role in osteoblast progenitors remains unknown. To address this question, we deleted the Atg7 gene, which is essential for autophagy, using Osx1-Cre transgenic mice. Female conditional knockout mice (Osx1-Cre;Atg7f/f), and their control littermates (Atg7f/f, Osx1-Cre, or wild-type) were subjected to serial BMD measurements from 8 to 24 weeks of age and then euthanized. Femoral, vertebral, and total BMD were low in conditional knockout mice compared to control groups at all time-points, with no differences in body weight between Osx1-Cre;Atg7f/f and Osx1-Cre, which were both slightly smaller than wild-type controls consistent with previously reported effects of the Osx1-Cre transgene on body weight. Abundance of the loxP-flanked Atg7 exon was significantly reduced in genomic DNA isolated from cortical bone but not spleen, demonstrating the specificity of deletion. Cancellous bone volume was low in the femur and spine of Osx1-Cre;Atg7f/f mice compared to controls, as was femoral cortical thickness. Consistent with this, bone strength was low at both sites as revealed by compression and 3-point bending analysis. Moreover, 48% of Osx1-Cre;Atg7f/f mice, but not controls, displayed healed or healing fracture calluses in the tibia, indicative of spontaneous fractures and a profound loss of bone strength. Lastly, reactive oxygen species levels in the bone marrow and phosphorylation of the p66shc protein in L4 vertebra, both markers of oxidative stress, were elevated in Osx1-Cre;Atg7f/f mice compared with Atg7f/f mice. The similarity of the low bone mass phenotype in this model with that observed after deletion of Atg7 using a Dmp1-Cre transgene suggests that autophagy in post-mitotic osteoblast-lineage cells is largely responsible for the low bone mass. However the presence of spontaneous fractures in the Osx1-Cre;Atg7f/f mice indicates that failure of autophagy in osteoblast progenitors may have additional deleterious effects on bone quality, the composition of bone cells, or both.

***Disclosures: Marilina Piemontese**, None.*

MO0363

Increased Cortical Porosity in Older Men with Fracture. Mattias Lorentzon*[1], Daniel Sundh[2], Magnus Karlsson[3], Claes Ohlsson[4], Dan Mellstrom[5]. [1]Geriatric Medicine, Center for Bone Research at the Sahlgrenska Academy, Sweden, [2]Geriatric Medicine, Dept. of Internal Medicine & Clinical Nutrition, Sahlgrenska Academy, University of Gothenburg, Gothenburg, Sweden, [3]Skåne University Hospital Malmö, Lund University, Sweden, [4]Center for Bone & Arthritis Research at the Sahlgrenska Academy, Sweden, [5]Sahlgrenska University Hospital, Sweden

Cortical porosity increases with ageing and experimental studies have reported that this bone trait is highly correlated to bone strength but whether it contributes to fracture risk has not been reported. The aim with the present study was to investigate whether cortical porosity was associated with x-ray verified fractures in older men.

The MrOS Gothenburg study is a prospective population based study from which a sub population consisting of 457 men, 80.1±3.5 (mean±SD) years, with available High Resolution pQCT (XtremeCT, Scanco Medical) measurements at the follow up exam (45 (15-73) months after study inclusion), was used in the present study. DXA (Hologic) was used to measure areal BMD of the hip. Fractures during the 45-month study were X-ray verified and information concerning physical activity, calcium intake and smoking was collected using questionnaires at the follow up exam.

During the study period 50 (10,9%) men had suffered a fracture. There were no differences in age, height, or weight between men with and without prevalent fractures at the end of study.

Using independent samples T-test, men with fracture during the study period had 10.0% lower areal BMD of the femoral neck (0.71±0.14 vs. 0.79±0.13 g/cm^2; $p<0.01$), 9.5% lower trabecular bone volume fraction (13.6±2.7 vs. 15.0±2.8 %; $p<0.01$), 20.6% thinner cortices (1.01±0.30 vs. 0.80±0.33 mm; $p<0.01$) and 21.0% higher cortical porosity (13.9±5.1 vs. 11.5±3.8 %; $p<0.01$) than men without fracture.

The independent associations between the above bone variables and fracture were tested using a logistic regression model with age, height, weight, calcium intake, smoking, physical activity and time in study as covariates. Cortical porosity (Odds Ratio 1.76 (95% CI 1.32-2.35) per SD increase), cortical thickness (OR 2.25 (1.51-3.20) per SD decrease), trabecular bone volume fraction (OR 1.65 (1.19-2.28) and femoral neck aBMD (OR 1.99 (1.32-3.00)) were independently associated with fracture. When entering all microstructure variables simultaneously in the model, cortical porosity and thickness remained independently associated with fracture. When adding femoral neck aBMD to the model, only cortical porosity (OR 1.63 (1.20-2.23)) and femoral neck aBMD (OR 1.80 (1.22-2.34)) were significantly related to fracture.

In conclusion, cortical porosity was associated with fracture independently of femoral neck BMD, suggesting a substantial contribution of cortical porosity to bone strength and fracture risk.

***Disclosures: Mattias Lorentzon**, None.*

MO0364

Loss of BromoDomain2 Function Leads to the Development of Sex-Linked Osteoporosis. Elise Morgan[1], Beth Bragdon[2], Robert Burns[3], Patrick Diviney[3], Amelia Baker[3], Anna Belkina[3], Gerald Denis[3], Andre Van Wijnen[4], Jennifer Schlezinger[5], Louis Gerstenfeld*[3]. [1]Boston University, USA, [2]Boston University School of Medicine Department of Orthopaedics, USA, [3]Boston University School of Medicine, USA, [4]Mayo Clinic, USA, [5]Boston University School of Public Health, USA

Osteoporosis is age and sex dependent and is exacerbated by obesity. Mice with reduced expression of the transcriptional regulator, bromodomain 2 (BrD2), are obese but do not develop insulin resistance. These mice provide an excellent model to assess the effects of obesity on bone loss, not confounded by Type II diabetes.

Methods: Male and female C57BL6 (WT) and BrD2lo mice, ages 3-18 months, were studied (N=4-7/group). Trabecular bone in the right tibia and L5 vertebra was assessed by microCT. Immunohistology for perilipin was used to assess marrow fat. RNA was isolated from the humeri, and the expression of mRNAs for osteoblasts/osteocytes (RUNX2, osteocalcin, DMP1 and SOST), and adipocytes (PPARγ, Adipsin, FABP4, Perilipin) was quantified by qRT-PCR. Primary bone marrow stromal cells (BMSCs) were cultured from the remaining hindlimb long bones to assess osteogenic and adipogenic potential. BrD2 expression was assessed in human adipose-derived MSCs.

Results: From 3 to 18 months of age, trabecular bone volume fraction (BV/TV) decreased by ~50% in both WT and BrD2lo males (Fig. 1). In contrast, both WT and BrD2lo females started with ~30% lower BV/TV than the males, and then exhibited age-related bone loss dependent on BrD2 activity. While BV/TV declined by only ~25% by 18 months in WT females, BV/TV in the BrD2lo females dropped to only ~45% and ~30% of the BV/TV in age-matched females and males, respectively. Both WT and BrD2lo females had greater fat content in the marrow (Fig. 2). Peak expression of osteoblast markers was seen in males and females at 6 months, with the females always showing the highest levels (Fig. 3). Levels of fat-associated genes were very low in the WT males, were much higher in the females, and were higher in BrD2lo vs. WT. Low BrD2 expression had no effect on bone gene expression in females but produced a marked increase in males. BMSCs from WT females maintained these sex- and genotype-specific differences in gene expression (Fig. 4). Both sets of lineage markers were greatly diminished in BrD2lo female cultures compared to WT female, WT male, and BrD2lo male cultures. In human adipose-derived MSCs, expression of BrD2 was 2- to 5-fold higher than that of any other family member.Conclusions: Maintenance of BrD2 expression is protective against bone loss in females. The expression of BrD2 in human adipose MSCs suggests that this transcriptional regulator may have functional importance in sex-linked bone loss in humans.

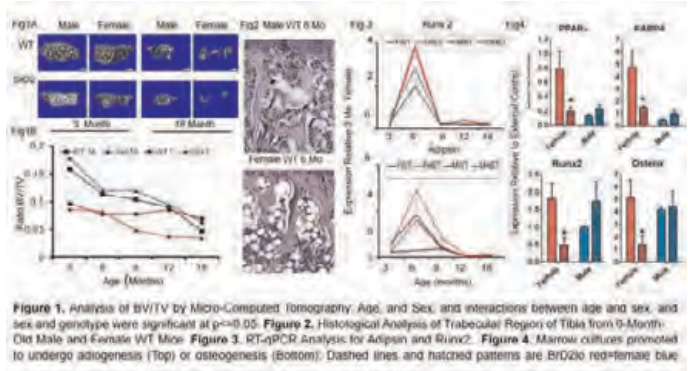

Figure 1. Analysis of BV/TV by Micro-Computed Tomography. Age, and Sex, and interactions between age and sex, and sex and genotype were significant at p<=0.05. **Figure 2.** Histological Analysis of Trabecular Region of Tibia from 9-Month-Old Male and Female WT Mice. **Figure 3.** RT-qPCR Analysis for Adipsin and Runx2. **Figure 4.** Marrow cultures promoted to undergo adipogenesis (Top) or osteogenesis (Bottom). Dashed lines and hatched patterns are BrD2lo red=female blue

Figures 1-4

***Disclosures: Louis Gerstenfeld**, None.*
This study received funding from: Ellison Foundation Grant

MO0365

Trabecular Bone Loss is Underestimated in Postmenopausal Women. How to Improve the Assessment. The OFELY Study. Rafaa Ellouz*[1], Roland Chapurlat[2], Elisabeth Sornay-Rendu[1], Pawel Szulc[3], Stephanie Boutroy[4]. [1]INSERM UMR 1033, Université de Lyon, France, [2]E. Herriot Hospital, France, [3]INSERM UMR 1033, University of Lyon, Hopital E. Herriot, Pavillon F, France, [4]INSERM U1033 & Université de Lyon, France

Definition of cortical and trabecular compartments is crucial for bone loss assessment, especially in longitudinal studies. Age-related cortical thinning produces cortical remnants that are artefactually considered as trabecular bone. In longitudinal studies, accurate assessment of cortical and trabecular bone loss in their original compartments would permit to determine true bone loss.

Our goal was to compare cortical and trabecular bone loss assessed by HRpQCT at the distal radius over 6 years, using the standard procedure and baseline-defined compartments after 3D registration.

Forty-six postmenopausal women (60±7 yrs) were measured by HRpQCT at the distal radius at baseline and after 6 years. The longitudinal analysis was performed using three methods: 1. standard software which identifies the volume of interest (VOI) based on cross-sectional area (CSA) matching and involves Laplace-Hamming filtering and thresholding to separate cortical from trabecular bone. 2. VOI based on CSA matching and double contouring of the cortical compartment and 3. VOI based on 3D registration and double contouring of the baseline compartment used for both baseline and follow-up scans.

Trabecular bone compartment (Tb.TV) increased with both CSA-based matching algorithms (2.6 and 2.1%, $p<0.001$ for both) which confirms that, over a 6 years period, cortical remnants are considered as trabecular bone. Trabecular volumetric BMD (Tb.vBMD) decreased by -4% and -3% with standard and double contouring method respectively ($p<0.005$) but was not significantly different between the two methods. Albeit both significant ($p<0.001$), decrease in cortical thickness was lower using double contouring than with the standard software (-6% vs -15%; $p<0.001$). When Tb.TV was kept constant with 3D registration, the decrease in Tb.vBMD was markedly higher than those obtained using CSA matching and either standard or double contouring procedure (-10% vs -4% and -3% respectively, $p<0.01$). Moreover, the increase in cortical porosity (Ct.Po) was greater (92 vs 65 %, $p<0.01$) and consistent with a greater decrease in cortical vBMD (-6% vs -5%; $p<0.01$) than that obtained with double contouring based on CSA matching VOI.

In conclusion, we have shown that with an accurate registration technique (3D registration) trabecular and cortical bone loss can be assessed in their original compartments, therefore precluding the artefactual underestimation of trabecular bone loss and Ct.Po increase observed with standard procedures.

***Disclosures: Rafaa Ellouz**, None.*

MO0366

Alternative Methods to Measure Fractional Intestinal Magnesium Absorption (FMA). Karen Hansen*[1], Andrea Nabak[1], Rachael Johnson[1], Martin Shafer[2], Steven Abrams[3]. [1]University of Wisconsin, USA, [2]Wisconsin State Lab of Hygiene, USA, [3]Baylor College of Medicine, USA

Animal and human studies, though few in number, link low magnesium intake to osteoporosis pathogenesis. A major barrier to more conclusive research on the relationship between magnesium status and osteoporosis relates to challenges in

measuring fractional intestinal magnesium absorption (FMA), which requires use of dual isotopes and a 72-hour urine collection. We evaluated alternative methods of measuring FMA, hypothesizing that shorter or spot urine collections or serum isotope values would provide data similar to 72-hour FMA values.

We administered two stable magnesium isotopes to 15 postmenopausal women with 25(OH)D levels between 16 and 25 ng/mL. Subjects fasted from midnight until 0700 when they arrived on the research ward and consumed breakfast along with ~23 mg ^{26}Mg orally and ~11 mg ^{25}Mg intravenously. We measured magnesium isotope levels in a 72-hour urine collection (collected as three 24-hour urine specimens), in spot urine samples at 36, 48, 60 and 72 hours and in serum samples collected 1, 3 and 5 hours after isotope dosing. We calculated FMA using the fraction of the oral divided by iv tracers from the 72-hour urine isotope values (J Nutr 1994;124:674-682). The fraction label was the [volume (urine or serum) x magnesium concentration in the sample x delta-excess label], divided by the tracer dose. The delta-excess label for each day was 100 x [observed isotope ratio – natural abundance ratio]/natural abundance ratio.

Among 15 Caucasian women ages 62 $\pm$ 7 years with an average dietary magnesium intake of 345 $\pm$ 70 mg per day, FMA based on the gold-standard 72-hour urine collection was 0.28 $\pm$ 0.08. 72-hour FMA correlated most highly with 24-hour urine values (rho 0.95, $p<0.001$) and the average of the 24-hour urine and 5-hour serum isotope values (rho 0.96, $p<0.001$, Table). FMA values based on the 24-hour urine collection and a formula (Value x 0.958 + 0.05 = FMA) explained 93% of the variance in 72-hour FMA values. The average of the 24-hour urine and 5-hour serum isotope levels (Value x 0.953 – 0.008 = FMA) explained 95% of the variance in 72-hour FMA values.

Our results suggest that FMA can be accurately measured using a 24-hour urine collection. Validation is underway; if confirmed in an additional sample of subjects, the new method could provide a more convenient option for researchers to measure FMA.

Table: Relationship Between Gold-Standard and New Measurements of Fractional Intestinal Magnesium Absorption

	New Method	Fractional Magnesium Absorption	Spearman Correlation Coefficient	p-value	Bland-Altman Bias	p-value	Linear Regression Equation	R^2
Urine Values	24-hour Urine Collection	0.24 ± 0.08	0.95	<0.001	-0.039	<0.001	**Value x 0.958 + 0.050 = FMA**	**0.93**
	36-hour Spot Urine Sample	0.36 ± 0.08	0.79	<0.001	0.081	<0.001	Value x 0.837 - 0.023 = FMA	0.75
	48-hour Spot Urine Sample	0.37 ± 0.10	0.84	<0.001	0.090	<0.001	Value x 0.706 + 0.020 = FMA	0.77
	60-hour Spot Urine Sample	0.38 ± 0.07	0.68	0.007	0.093	<0.001	Value x 0.897 - 0.054 = FMA	0.62
	72-hour Spot Urine Sample	20.18 ± 55.62	-0.26	0.340	19.895	0.029	Value x -0.001 + 0.292 = FMA	0.03
Serum Values	1 Hour Serum Sample	0.08 ± 0.04	0.63	0.014	-0.206	<0.001	Value x 1.167 + 0.193 = FMA	0.23
	3 Hour Serum Sample	0.30 ± 0.08	0.82	<0.001	**0.019**	**0.063**	Value x 0.874 + 0.019 = FMA	0.80
	5 Hour Serum Sample	0.37 ± 0.08	0.93	<0.001	0.085	<0.001	Value x 0.848 - 0.029 = FMA	0.86
	3 Hour Serum/1 Hour Serum	0.17 ± 0.05	0.78	<0.001	-0.113	<0.001	Value x 1.331 + 0.057 = FMA	0.71
	5 Hour Serum/1 Hour Serum	0.15 ± 0.05	0.63	0.014	-0.133	<0.001	Value x 0.360 + 0.130 = FMA	0.34
	5 Hour Serum/3 Hour Serum	0.27 ± 0.07	0.54	0.039	**-0.017**	**0.298**	Value x 0.737 + 0.087 = FMA	0.43
Averaged Values	24-Hour Urine, 3 Hour Serum	0.27 ± 0.08	0.93	<0.001	**-0.010**	**0.128**	Value x 0.953 + 0.023 = FMA	0.90
	24-Hour Urine, 5 Hour Serum	0.31 ± 0.08	0.96	<0.001	0.023	<0.001	**Value x 0.953 - 0.008 = FMA**	**0.95**
	24-Hour Urine, 5 Hour/3 Hour Serum	0.26 ± 0.07	0.83	<0.001	-0.028	0.009	Value x 0.989 + 0.031 = FMA	0.78
	1 Hour Serum, 3 Hour Serum	0.19 ± 0.05	0.82	<0.001	-0.093	<0.001	Value x 1.240 + 0.048 = FMA	0.71
	1 Hour Serum, 5 Hour Serum	0.22 ± 0.05	0.94	<0.001	-0.060	<0.001	Value x 1.389 – 0.026 = FMA	0.87
	3 Hour Serum, 5 Hour/3 Hour Serum	0.28 ± 0.07	0.77	0.001	**0.001**	**0.936**	Value x 0.921 + 0.022 = FMA	0.70

We used dual stable isotopes and a 72-hour urine collection as the gold-standard method to measure intestinal magnesium absorption (mean ± SD = 0.28 ± 0.08) in 15 subjects. We summarize new methods to estimate magnesium absorption above, with all comparisons to the gold-standard measurements. All data exhibited a normal distribution except for the spot 72-hour urine level (median -8.87, range -20.97 to 147.93).

Table

***Disclosures: Karen Hansen**, None.*

MO0367

Definition and determinants of a normal reference range for 24-hour urine calcium for caucasian and african american women. Prachi Jindal*[1], J. Christopher Gallagher[1], Munro Peacock[2], SRI HARSHA TELLA[3], Lynette Smith[4]. [1]Creighton university medical center, USA, [2]Indiana University Medical Center, USA, [3]Creighton University School of Medicine, USA, [4]University of nebraska medical center, USA

Background- Different recommendations exist for a normal range for 24-hour urine calcium that varies from 50-300mg.

Objective- The objective of this analysis is to establish a normal range in older women for 24-hour urine calcium and examine the relationship between calcium intake, vitamin D metabolites and calcium absorption and 24h urine calcium.

Design-In two randomized, prospective trials we collected at baseline 24 hour urine calcium and creatinine, 7 day food diary for calcium, serum 25-hydroxyvitamin D (25OHD) and 1,25dihydroxyvitamin D ($1,25(OH)_2D$. In study 1(STOP IT) there were 489 normal women, age 65-77 years. In Study 2(ViDOS) there were 163 Caucasian (C) and 110 African American (AA) women, age 57-90 years. The main inclusion criterion for study I was normal femoral neck bone density for age and for study II a serum 25OHD < 20ng/ml (50nmol/l) and 24h urine calcium< 300mg. Serum and 24 hour urine were collected at baseline.

Methods- Urine calcium was measured on Roche Auto analyzer. Calcium absorption was a single isotope method. In study 1 Serum 25OHD and $1,25(OH)_2D$ were measured by competitive protein binding assay and in study 2 by radio-immunoassay RIA(Diasorin). The 24-hour urine calcium did not fit a normal distribution,, the 95% reference interval (RI) was found using non-parametric methods and 90% non-parametric confidence intervals (CI) are provided for the endpoints of the RI. SAS software was used to estimate the normal range. P-values < 0.05 were significant.

Result (Table)-Age range for both studies was 57-90 years. There was no difference in the reference range for 24h urine calcium for two Caucasian studies so the data were combined for 652 women. The reference range was 37 to 275mg. The reference range for African American women was 7-225mg, with mean 24h urine calcium significantly lower than Caucasians, $p< 0.001$. In Caucasians the correlations for24h urine calcium with serum $1,25(OH)_2D$ was r=0.2 ,$p< 0.001$; serum 25OHD r=0.07, p=0.066; calcium intake r=0.124,p=0.0018 and calcium absorption r=0.141, p=0.0008. In African Americans the correlation for24h urine calcium with serum 25OHD was r=0.11, p=0.28 and calcium intake was r=0.17, p=0.078.

Conclusion- 24h urine calcium was correlated with calcium intake, calcium absorption, serum $1,25(OH)_2D$ but not serum 25OHD. In the combined data the normal reference interval for 24-hour urine calcium for Caucasian women is 37-275mg and for African American women is 7- 225mg.

Key words- 24-hour urine calcium, normal reference interval, calcium absorption, Vitamin D metabolites, Caucasian, African American

Reference Interval for 24h urine calcium (mg)
C=Caucasian, AA= African American

	24h Urine calcium		
Study	Reference Interval	90% CI for lower value	90% CI for upper value
STOP IT(C)	37 – 275	29 – 49	263 – 282
VIDOS(C)	39 – 274	17 – 43	266 – 304
Overall(C)	37 – 275	31 – 40	266 – 282
AA	7-225	2-10	216-270

table

***Disclosures: Prachi Jindal**, None.*
This study received funding from: National Institute of health

MO0368

Importance of serum 25(OH)D2 levels as a risk factor for incident vertebral fractures in glucocorticoid-induced osteoporosis in Japan. Ikuko Tanaka*[1], Mari Ushikubo[2], Shigenori Tamaki[1], Harumi Kuda[2], Sayaka Kubo[2], Keisuke Izumi[2], Kumiko Akiya[2], Hisaji Oshima[2]. [1]Nagoya Rheumatology Clinic, Japan, [2]Tokyo Medical Center, Japan

Background: Serum 25-hydroxyvitamin D (25(OH)D) assay is now a highly reliable method for evaluating vitamin D stores in individual patients. A critical review of available evidences indicates that a relationship exists between sufficient vitamin D status and bone fracture. However, Japanese population showed ethnic difference even in bone fracture. In this study, we evaluated serum 25(OH)D2 as a risk factor for incident vertebral fractures in glucocorticoid-induced osteoporosis in Japan

Patients and Methods: Subjects with connective tissue disease except rheumatoid arthritis were 15 males and 71 females, showing 60$\pm$15 y.o. of mean age, 11$\pm$10 years of mean disease duration, 36$\pm$34 g (predonisolone; equivalent) of mean total glucocorticoid medication, and 9$\pm$6 mg of mean daily dose. Prevalent vertebral fractures were seen in 37 % of the patients. Other medications were bisphosphonate (59 cases) and menatetrenone (vitamin K analog) (2 cases). 25 subjects had no medication. None of subjects had a medication of natural vitamin D. In this 2-year longitudinal study, an incident vertebral fracture was diagnosed with a conventional spine radiography using semiquantitative criteria by Genant (JBMR, 1993). Bone mineral density (BMD) was assessed by the radial DXA.

Results: 1) 32 subjects (37%) had an incident vertebral fracture. 2) The distribution of serum 25(OH)D2 concentration was 5.9-36 pg/ml and the mean was 17.5$\pm$7.2 pg/ml. 3) There was no significant difference in the serum level of 25(OH)D2 between subjects with a incident fracture and subjects without fracture. 4) The decrease of serum 25(OH)D2 concentration was an independent risk factor for an incident vertebral fracture with statistical significance (OR 1.2/2pg, $P<0.01$), after adjustment for age, total glucocorticoid dosage, mean daily glucocorticoid dosage, BMD, previous fracture, and therapeutic agents. The decrease of serum 25(OH)D2 was a significant independent risk factor (OR 2.4/2pg, $P<0.05$) in the cases with fracture progression of SQ 2 and over.

Conclusions: These data suggests that the decrease of serum 25(OH)D2 level is an independent risk factor and the severity of incident fractures in Japanese subjects with glucocorticoid-induced osteoporosis. In further study, clinical utility of 25(OH)D3 should be evaluated.

***Disclosures: Ikuko Tanaka**, None.*

MO0369

Bone Phenotype of Casp2-/- mice is Defined by Gender and Genetic Background. Ramaswamy Sharma*[1], Difernando Vanegas[2], Clair Martin[2], Diane Horn[2], Roberto Fajardo[3], Sherry Werner[2], James Lechleiter[2], Brian Herman[5]. [1]University of Texas Health Sciences Center At San Antonio, USA, [2]University of Texas HSC at San Antonio, USA, [3]UT Health Science Center, San Antonio, USA, [5]UT HSC San Antonio, USA

Genetic determinants of bone mineral density (BMD) are not fully known. Such knowledge is critical for the diagnosis and treatment of osteoporosis. We have previously shown that ablation of the apoptotic cysteine aspartate protease, caspase-2, in mice with mixed genetic background resulted in significant decreases in BMD, bone volume, trabecular number, cortical thickness and bone mechanical strength in old (24-27 month) but not young or middle-aged male *Casp2*$^{-/-}$ mice. Herein, we show that male and female *Casp2*$^{-/-}$ mice on pure C57Bl/6 background exhibit significant bone loss at younger ages. Specifically, male *Casp2*$^{-/-}$ mice exhibited significant bone loss from 5 months onwards whereas female *Casp2*$^{-/-}$ mice exhibited consistently decreased BMD from 2-3 months. Further characterization of female *Casp2*$^{-/-}$ mice by dual X-ray absorptiometry (DXA) indicated decreases in BMD in tibia, femur, lumbar vertebrae and total body. Micro-CT measurements of tibial trabecular bone in 4 month old female *Casp2*$^{-/-}$ mice showed significantly decreased trabecular bone volume (BV/TV) and trabecular number (Tb.N). Micro-indentation analyses showed increased indentation distance increase (IDI), suggesting material changes in bone. Female *Casp2*$^{-/-}$ femoral bone length was significantly shorter in young (4 month) and old (16 month) female mice. To determine if the observed trabecular bone loss was related to decreased bone formation or increased bone resorption, we performed histomorphometric counts of osteoblasts and osteoclasts on 4 month bones. A significant decrease in osteoblast numbers (OB/mm bone surface) was observed. Serum levels of 1, 25 (OH) vitamin D were also significantly decreased in young female *Casp2*$^{-/-}$ mice. Surprisingly, female mice overexpressing caspase-2 in osteoclasts exhibited higher BMD at young and older ages, perhaps due to indirect effects on osteoblast-osteoclast interactions. In conclusion, our data highlight the influence of genetic background and gender in determining the bone phenotype observed due to deficiency of caspase-2.

***Disclosures: Ramaswamy Sharma**, None.*

MO0370

Replicative senescence of circulating osteogenic cells in young men with perinatal HIV infection. John Manavalan*[1], Stephen Arpadi[1], Jayesh Shah[1], Jannine Chan[1], Liana Greer[1], Marc D. Foca[1], Natalie M. Neu[1], David Bell[1], C.Amy Zhang[1], Stavroula Kousteni[2], Michael Yin[1]. [1]Columbia University, USA, [2]Columbia University Medical Center, USA

HIV infection is characterized by chronic T cell activation and proliferation, leading to senescence of immune cells. We hypothesize that chronic HIV infection is also associated with accelerated replicative senescence and exhaustion of the cellular proliferative capacity of bone cell precursors, which may negatively impact bone formation, especially in children infected with HIV early in life.A cross-sectional study was performed in 30 HIV-infected, on stable ART, and 15 HIV-uninfected men aged 20-25 years utilizing dual-energy x-ray absorptiometry (DXA) and flow cytometry to identify circulating ostegeogenic cells in peripheral blood mononuclear cells (PBMCs). Among HIV-infected men, 15 were perinatally-infected (PNI) and 15 were infected during adolescence (ADI). *Runx2*, osteocalcin (OCN) and CD34 antibodies, were used to identify specific osteogenic cell populations in lineage (LIN) negative PBMCs enriched for stem and progenitor cells. Our previous studies suggest that OCN+CD34- cells are more mature osteogenic cells than OCN+CD34+ cells, since they have lost the hematopoietic CD34 marker and express higher mRNA levels of *Runx2* and alkaline phosphatase. Relative average telomere length was measured in sorted osteogenic cells (LIN-/OCN+/Runx2+) using qPCR, and expressed as the relative ratio of telomere (T) to nuclear DNA (S) copies.DXA derived aBMD Z scores were 0.4-1.2 lower in HIV-infected men at the spine, femoral neck, total hip and radius (all $p<0.05$). The percentage of circulating osteogenic cells (LIN-/OCN+/*Runx2*+) in PBMCs, was significantly lower in both the PNI group (0.15+0.10%) and the ADI group (0.22+0.12%) than in uninfected controls (0.39+0.26%; $p<0.05$); but did not differ between HIV-infected groups. In contrast, the PNI group had a significantly lower percentage of mature osteogenic cells (LIN-/OCN+/*Runx2*+/CD34-; 55.6+27.3%) than both the ADI group (73.2+11.4%; $p<0.05$) and uninfected controls (67.2+6.8%; $p<0.05$). Similarly, the PNI group had shorter telomere lengths (T/S ratio: 2.3+0.2) in LIN-/OCN+ cells than both the ADI group (T/S ratio: 2.5+0.2; $p<0.05$) and uninfected controls (T/S ratio: 2.6+0.4; $p<0.05$).These data suggest that HIV infection, especially perinatal infection, is associated with replicative senescence, decreased numbers and maturation of circulating osteogenic cells, which may result in decreased number and function of osteoblasts at the bone, contributing to the observed decreased BMD in HIV-infected individuals.

***Disclosures: John Manavalan**, None.*

MO0371

The Postprandial Response of Bone Turnover Markers in Patients with Inflammatory Bowel Diseases. Maria Yavropoulou*[1], Ioannis Karatzoglou[2], Maria Pikilidou[3], George Germanidis[2], John Yovos[3]. [1]Aristotle University of Thessaloniki, Greece, [2]Department of Gastrenterology, AHEPA Univ. Hospital, Aristotle University of Thessaloniki, Greece, [3]Department of Endocrinology & Metabolism, AHEPA Univ. Hospital, Aristotle University of Thessaloniki, Greece

Inflammatory bowel diseases (IBD) disturb bone metabolism through multiple mechanisms, such as malnutrition, corticosteroid treatment and disease-related inflammation. The exact underlying pathophysiology, however, is still not completely understood and data on the physiological skeletal responses, as is the postprandial reduction of bone resorption, in these patients are missing. To address this issue we studied the effect of oral glucose in bone turnover markers in patients with ulcerative colitis (UC) and Crohn's disease (CD).

Thirty patients with UC, 59 patients with CD and 45 healthy individuals matched for age and BMI were included in the study. Activity of the disease was assessed by calculation of the CD activity index (CDAI) and Mayo score for patients with CD and UC, respectively. All participants underwent an oral glucose tolerance test (OGTT) and serum levels of procollagen type 1 amino-terminal propeptide (P1NP) and β-carboxy-terminal cross-linking telopeptide of type I collagen (β-CTX) were measured at 0, 60 and 120 min.

Serum β-CTX was significantly lower in patients with UC compared to controls (278 $\pm$ 18 pg/ml vs. 380 $\pm$ 28 pg/ml p=0.004, respectively), while patients with CD had significantly higher values of serum β-CTX and P1NP compared to controls (β-CTX: 573 $\pm$ 24 pg/ml vs. 380 $\pm$ 28 pg/ml, and P1NP: 57 $\pm$ 6 ng/ml vs. 45 $\pm$ 4 ng/ml, $p<0.001$, respectively). Nevertheless, serum β-CTX was significantly correlated with serum P1NP levels in both patient groups (UC: r=0.439, p=0.015, CD: r=0.271, p=0.038) (Figure 1).

Oral glucose significantly suppressed β-CTX levels in patients and controls. Despite the significant differences in baseline values, the percentage decrease of serum β-CTX at 2h after glucose load did not differ significantly between patients with UC or CD and the controls (41.7% and 40% vs. 43.9%, respectively). Disease activity was significantly related to the degree of β-CTX suppression 2h after oral glucose in both diseases (r=0.913, $p<0.001$ in CD and r=0.953, $p<0.001$ in UC).

The physiological skeletal response of postprandial reduction of bone resorption is preserved in patients with IBD and is strongly related to the activity of the disease, probably reflecting a compensatory mechanism of the skeleton against the negative effects of IBD in bone metabolism.

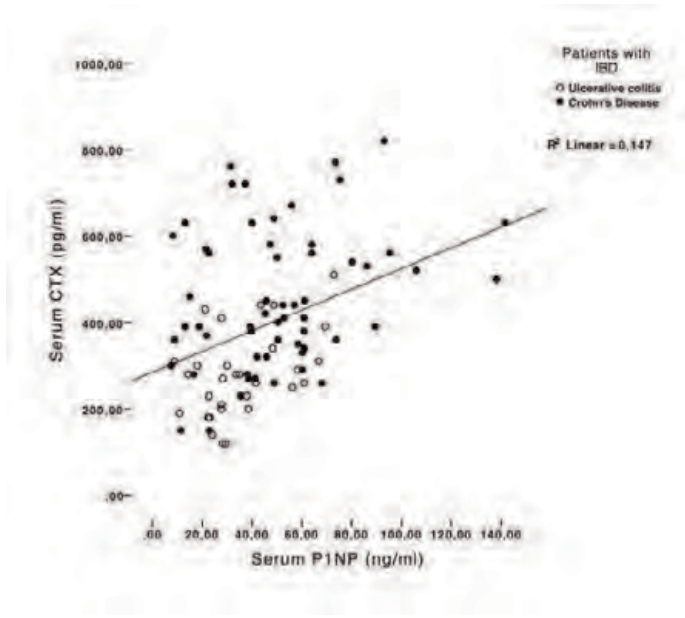

Figure 1

***Disclosures: Maria Yavropoulou**, None.*

MO0372

Effectiveness of Teriparatide in the Treatment of Osteoporosis, Data from Real-World Clinical Practice. George Tsoukas[1], Philippe Tsoukas[2], George O. Tsoukas*[3], Louise Ullyatt[3]. [1]McGill University Health Center, Canada, [2]Department of Medicine, University College Dublin, Ireland, [3]Division of Endocrinology,McGill University Health Center, Canada

Objective: Although the efficacy of teriparatide in bone metabolism has been demonstrated in multiple controlled clinical trials, data from longitudinal observational studies are limited. Such studies are essential in understanding the real-world effectiveness of therapeutic interventions. In this study, we aim to demonstrate true population-based benefits of teriparatide in a clinical practice setting.

Methods: We conducted a retrospective chart review on patients treated with teriparatide for osteoporosis. Data was obtained from four endocrine clinics specialized in the treatment of osteoporosis. Patients were treated according to Canadian osteoporosis guidelines. We specifically examined interval changes in BMD, osteocalcin, total alkaline phosphatase, and type 1 collagen C-terminal telopeptide in patients treated with teriparatide for a mean of 18 or 24 months. Statistical analysis was performed using linear mixed model with repeated measures.

Results: A total of 286 patients were included in our analysis with a mean age of 71 years. Among these, 253 (88%) were female and 33 (12%) were male. At baseline, 65% of all patients had a documented history of two or more fractures. Vertebral fractures represented 60% of all prevalent fractures at baseline. Prior to initiating teriparatide, 70% of all patients had been treated with bisphosphonates. At baseline, the mean T-score was -3.7 for spine (L1-L4) and -2.3 for the hip (femoral neck). Duration of treatment varied with 60% of the patients receiving teriparatide for 18 months and 40% for 24 months. After an 24-month course of teriparatide, there was a net increase in BMD of 9% at the spine and 5% at the hip, corresponding to a change in T-score of +1.0 at the spine and no change at the hip. The results was maintained at 24 months. The total alkaline phosphatase, osteocalcin, and C-terminal telopeptide increased by 26.5%, 110.6%, and 105.9%, respectively, at 18 months. Compliance to therapy was reported to be 85% at 18 months.

Conclusions: Our results suggest that treatment with teriparatide for a mean duration of 18 months and 24 months significantly increased BMD of the spine in patients with osteoporosis. Changes in bone turnover markers were positively associated with BMD changes, indicating bone formation. Our findings are consistent with larger controlled clinical trials. We are currently examining fracture outcomes in these patients.

***Disclosures: George O. Tsoukas**, McGill University Health Center, 3*

MO0373

Effects of Recombinant Human Parathyroid Hormone on the Anabolic Window and Lower Extremity Stress Fracture Healing in Premenopausal Women: A Pilot Study. Ellen Almirol*[1], Lisa Gao[1], Shelley Hurwitz[1], Bharti Khurana[1], Jennifer Baima[1], Eric Bluman[1], Christopher Chiodo[1], Meryl Leboff[2]. [1]Brigham & Women's Hospital, USA, [2]Brigham & Women's HospitalProfessor of Medicine, Harvard Medical School, USA

Stress fractures are the most common overuse injuries of the lower extremities and are 5 times more common in women than men. Although the anabolic therapy Teriparatide (TPTD) has advanced osteoporosis care, there are no approved systemic therapies for stress fractures. In this pilot study, we evaluated whether TPTD compared to placebo: increased markers of bone formation in advance of resorption, creating an anabolic window and hastened stress fracture healing on MRI.

Premenopausal women (aged 21-45 years) with lower extremity stress fractures diagnosed within 1 month of screening were eligible. Bone formation markers amino terminal propeptide of type 1 collagen (P1NP) and osteocalcin (OC), and resorption markers serum C-telopeptide (CTX) and urinary N-telopeptide (NTX) were measured at baseline, 4 and 8 weeks. To assess stress fracture severity, we used a MRI grading system. Grade 4 was most severe with a low-signal fracture line, while Grade 0 showed no edema or bone lesions. Groups were compared using the Wilcoxon Rank-Sum Test or Chi Square test, where appropriate.

Among 101 women screened, 13 women were randomized to TPTD, 20 μg s.c./d (n=6) or daily placebo injection (n=7) for 8 weeks. In the TPTD-treated group at 4 and 8 weeks, P1NP increased by 133.6 and 179.6% and OC by 409.6 and 859.1%, respectively. In contrast, the placebo-treated group at 4 and 8 weeks showed a smaller increase in P1NP of 8.5 and 15.2% ($p \leq 0.01$) and OC of 20.4 and 25.9%, ($p \leq 0.03$), respectively. There were no significant differences between groups in changes of bone resorption markers. The anabolic window was defined as the area between P1NP and CTX over the duration of the study. In the TPTD-treated groups vs. the placebo-treated group, the anabolic window was significantly greater (mean area $\pm$SEM of 145.82 ± 50.24 vs. 5.99 ± 18.30, $p \leq 0.05$) [Fig. 1]. According to the MRI grading scale at 8 weeks, 83.3% of the TPTD group and 57.1% of the placebo-treated group had improved or healed stress fractures with changes in MRI grading of $m=2.17 \pm 0.8$ vs. 1.86 ± 0.9, respectively ($p=0.31$); these differences were not significant.

In summary, use of TPTD compared to placebo in premenopausal women with lower extremity stress fractures resulted in early and robust rises in bone formation markers and a larger anabolic window. While the changes in bone healing are promising, larger prospective, controlled studies are needed to fully assess the potential effects of TPTD on stress fracture healing.

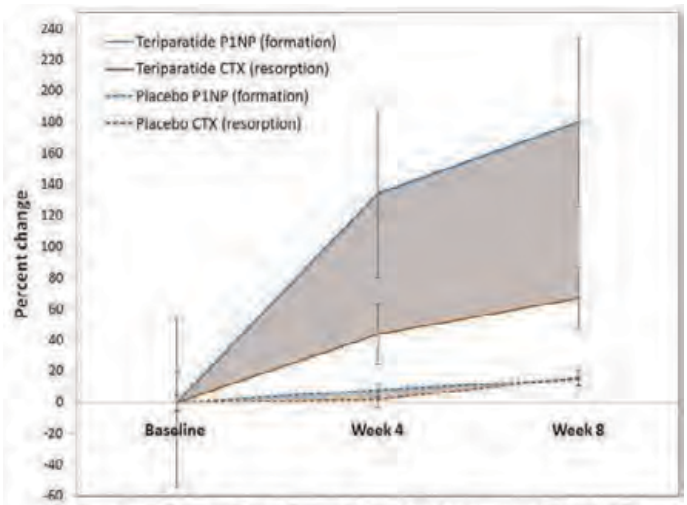

Figure 1: Mean Percent Change in Formation Marker P1NP and Resorption Marker CTX for Teriparatide and Placebo. Shaded Area between P1NP and CTX over 8 weeks indicate an anabolic window.

Figure 1

***Disclosures: Ellen Almirol**, None.*

MO0374

Enhanced Bioavailability of a Nasal Formulation of Teriparatide with CriticalSorb™ Compared to a Subcutaneous Injection: A Non -invasive Approach for the Treatment of Osteoporosis. Faron Jordan*[1], Gareth King[2], Allan Williams[3], Richard Pearson[4], Alan Perkins[4], Tahir Masud[5]. [1]Critical Pharmaceuticals Ltd, United Kingdom, [2]Critical Pharmaceuticals, United Kingdom, [3]University of Nottingham, Vanuatu, [4]University of Nottingham, United Kingdom, [5]Nottingham University Hospitals NHS Trust, United Kingdom

Parathyroid Hormone (PTH) is an effective treatment for osteoporosis and unlike other therapies that reduce bone resorption, PTH increases bone formation resulting in greater bone mineral density. The biological activity of PTH resides in the N-terminal sequence with the 34 amino acid peptide (PTH1-34), [teriparatide]. Currently administration requires a subcutaneous injection and an intranasally delivered formulation would potentially improve patient convenience and may improve efficacy. In certain patient groups, it has been shown that nasal delivery is preferred over injections (Illum *et al.*, 2012).

CriticalSorb is an advanced nano-enabled nasal delivery system that facilitates the absorption of macromolecules across biological membranes. We have used this technology to develop CP046, a nasal spray formulation of teriparatide. Solutions of CriticalSorb and teriparatide were prepared and administered intranasally to Sprague Dawley rats and New Zealand white rabbits. The animals also received a subcutaneous injection of teriparatide in order to compare bioavailability. Blood samples were collected for up to 6 hours after administration and teriparatide concentrations in the plasma were analysed by LCMS/MS.

CriticalSorb proved to be highly effective at enhancing the transport of teriparatide across the nasal mucosa in both rats (Fig 1) and rabbits with a relative bioavailability of 79 and 64% respectively. When teriparatide was administered intranasally to rats without CriticalSorb the bioavailability was below 6%.

In conclusion, CriticalSorb is an effective absorption promoter for the systemic delivery of teriparatide via the nasal cavity and offers a non-invasive route for delivery. The pulsatile pharmacokinetics obtained following nasal delivery of teriparatide may further improve efficacy. Proof of concept has been demonstrated in animal models and a clinical trial is being carried out in post menopausal women to assess nasal deposition and clearance using gamma scintigraphy and to provide pharmacokinetic data comparing nasal and subcutaneous delivery in humans.

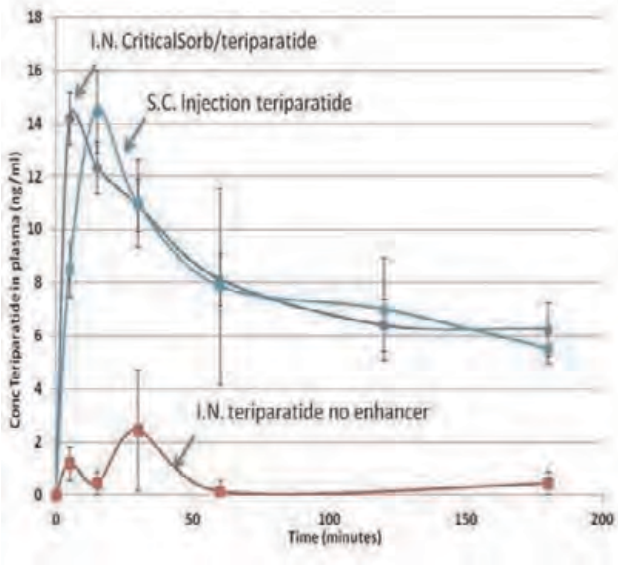

Fig 1 Teriparatide plasma levels after intranasal administration of teriparatide with CriticalSorb

***Disclosures: Faron Jordan**, None.*

MO0375

Higher Rates of Union in Older Patients with Type 2 and Type 3 Odontoid Fractures Treated with Teriparatide. Debra Sietsema*[1], Michael Merrick[2], Casey Smith[2], Tan Chen[3], Scott Russo[4], Clifford Jones[1], James Stubbart[1]. [1]Orthopaedic Associates of Michigan; Michigan State University, USA, [2]Grand Rapids Medical Education Partners, USA, [3]Michigan State University, USA, [4]Orthopaedic associates of Michigan, USA

Purpose: High rates of morbidity and mortality are a major concern in older patients with odontoid fractures. Teriparatide is an anabolic drug approved for use in patients with osteoporosis at high risk for fracture. The only published evidence of teriparatide use in patients with odontoid fractures is a case report of three patients who went on to union after delayed healing. The purpose of this study was to determine the effect of teriparatide on union rates in older patients with odontoid fractures.

Methods: Between 2002 and 2011, 97 consecutive patients, age 65 years and over, with type 2 and type 3 odontoid fractures were treated at a single Level I trauma center, were followed in a single private practice, and retrospectively evaluated. Eight patients were treated with teriparatide for osteoporosis and were at high risk for a subsequent fracture. Radiographs were reviewed and fusion was determined by flexion/extension x-rays, CT scan, or both. Twenty-three mortalities were excluded from the union analysis and one patient was lost to follow-up prior to fusion evaluation.

Results: Of the 8 patients receiving teriparatide, there were 2 males and 6 females with an average age of 79 (range 67-88) and body mass index (BMI) of 25.9 (range 19.9-34.0). In the non teriparatide group, there were 29 males and 36 females with an average age of 80 (range 65-93) and BMI of 27.1 (17.1-37.5). The Charlson score was 1.5 (range 0-3) in the teriparatide group as compared to 2.0 (range 0-9) in the non teriparatide group. Odontoid classification was six Type 2 and two Type 3 in the teriparatide group and 49 Type 2 and 16 Type 3 in the non teriparatide group. Operative treatment was performed in 3 (38%) of the teriparatide group and in 19 (29%) of the non teriparatide group. The T-score in the teriparatide group averaged -3.2 (-2.4 to -3.9) compared to -2.4 (-1.0 to -4.9) in the non teriparatide group. Patients treated with teriparatide had a higher rate of union (7/8, 87.5%) compared to patients who did not receive teriparatide (45/65, 69.2%). The time from initiating teriparatide to fusion averaged 97 days (range 36-206 days).

Conclusion: Teriparatide may lead to higher union rates in type 2 and type 3 odontoid fractures. Teriparatide should be considered as a supplemental treatment in the elderly with odontoid fractures at high risk for subsequent fracture. More studies with larger sample sizes including other contributing factors are needed to confirm this finding.

***Disclosures: Debra Sietsema**, Lilly USA,*

MO0376

Progression of Vertebral Compression Fractures during Anti-Osteoporotic Therapy: Bone Turnover Markers and Radiographic Evidences in the First Six Months. Costantino Corradini*[1], Cesare Verdoia[2]. [1]State University of Milan, Italy, [2]Orthopaedic Clinic University of Milan, Italy

Introduction: In postmenopausal women with vertebral compression fractures (VCF) the mechanisms regulating healing processes and an anti-osteoporotic treatment are not completely clarified. The aim of this prospective study was the evaluation of bone turnover markers, bone mineral density and radiographic progression of one or more VCF during assumption of risedronate, strontium ranelate or teriparatide. Materials and methods: Women with recent osteoporotic VCF verified through magnetic resonance were assigned to receive either risedronate (RIS group, n = 19) or strontium ranelate (SR group, n= 16) or teriparatide (TPTD group, n = 24) following guidelines of Italian regulatory agency. Serum and urinary bone turnover markers and lateral thoraco-lumbar spine X-rays were obtained at 0, 1, 3 and 6 months of therapy. Lumbar BMD was measured by DEXA before and 6 months after treatment initiation. Results: At time 0 serum markers of bone formation alkaline phosphatase (ALP), osteocalcin (OC) and of bone resorption desoxipiridoline (DPD) but also osteoprotegerin (OPG) were around higher level of normality, while sclerostin (SOST) was substantially unchanged. Between 1st and 3rd month within the consolidation process OC peaked in TPTD group while those in RIS group and SR group remained significantly lower. In the same period ALP levels decreased in RIS group, unchanged in SR group and increased in TPTD group. DPD remain high in TPTD group; while in all groups were significantly and constantly reduced in 6 month. Serum OPG levels remained unchanged in RIS group and SR group while reduce in TPTD group. SOST was significantly increased 6 months in RIS group, whereas remained statistically unaffected in the TPTD group. Lumbar BMD increased at 6 month in all groups and significantly in TPTD group. An inconstant progression in VCF on radiograms were detected in RIS and SR groups. Some levels were more involved of others.Conclusions: In recent osteoporotic VCF a divergence between the formation and resorption markers has been revealed between anti-osteoporotic therapies with a different radiographic progression. The clinical relevance is the possibility of choice different anti-osteoporotic treatments on radiographic and metabolic behaviour of VCF. Bibliography: Corradini C. Aging Clin Exp Res. 2011;23(2 Suppl):45-6.

***Disclosures: Costantino Corradini**, None.*

MO0377

Bisphosphonates and Alveolar Bone with Reference to Bone Mineral Density and Osteoporotic Fracture. Takuo Fujita*[1], Yoshitomo Takaishi[2], Mutsumi Ohue[1], Takami Miki[3], Yoshio Fujii[4], Tsuyoshi Jotoku[5]. [1]Katsuragi Hospital, Japan, [2]Takaishi Dental Clinic, Japan, [3]Osaka City University Medical School, Japan, [4]Calcium Research Institute Kobe Branch, Japan, [5]Department of Orthopedic Surgery, Osaka Medical College, Japan

Background: Osteoporosis and periodontal disease tend to occur in parallel. Alveolar bone mineral density (al-BMD) measured by computed densitometry (Bone Right) was reported to be more closely associated with osteoporotic fracture than widely used lumbar bone mineral density (LBMD). In view of the high al-BMD at the site of jaw bone necrosis on Bisphosphonate (BP) use (Takaishi et al 2010), BP effect on alBMD was studied.

Methods: Among 148 women consulting the Osteoporosis and Osteoarthritis Clinic of Katsuragi Hospital, BP (etidronate, alendronate, risedronate and minodronate) were given in 83 (mean age $\pm$SD, 68 $\pm$7), but not in 65 others (63 $\pm$11). Except for the higher age, no significant difference was seen between the two groups as to al-BMD, LBMD, FNBMD and fracture frequency (47.6% in N and 47.0% in B).

Results: Significant positive correlation was found between the duration of BP treatment and al-BMD (r=0.225, p=0.0428), LBMD(r=0.256, p=0.0185) and FNBMD (r=0.204, p=0.0367). ROC curves constructed to assess the predictability of facture stayed similar regardless of the use of BP as to LBMD and FNBMD, but markedly differed for al-BMD. On the use of BP (Group B), predictability for fracture almost disappeared with he AUS-0.5 value of 0.15 exhibiting a drastic fall from 0.148, contrasted to the corresponding values indicating fluctuations from 0.118 to 0.158 for LBMD and 0.123 to 0.146 for FNBMD. BMD fall along with fracture was 9.9% for BR, evidently higher than -1.7% for LBMD, and 2.7% for FNBMD. A possible explanation is a marked sensitivity of alveolar bone to BP with sustained increase of al-BMD compared with other sites, interfering with the evaluation of BMD-fracture relationship. One way analysis of variance revealed significantly greater rise of BR in response to BP than LBMD (p=0.0040) and FNBMD (p=0.0031). Compared with the group without BP treatment, only the subgroup treated with etidronate for more than 6 months achived a significantly higher al-BMD, but not LBMD or FNBMD, suggesting a role of etidronate augmenting the action of N-containing BP.

Conclusion: Decrease of al-BMD seems to be more intimately associated with fracture than that of LBMD and FNBMD without, but not with BP treatment. Alveolar bone appear to respond to BP differently from LBMD and FNBMD with more pronounced and sustained increase.

***Disclosures: Takuo Fujita**, None.*

MO0378

Comparison of the Efficacy, Adverse Effects and Cost of Zoledronic Acid and Denosumab In the Treatment of Osteoporosis. Kellen Sheedy*[1], Isabel Camara[2], Pauline Camacho[3]. [1]Loyola University Stritch School of Medicine, USA, [2]University of Notre Dame, USA, [3]Loyola University of Chicago, USA

Injectable osteoporosis drugs are increasing in popularity due to their efficacy and convenient administration. There are currently two injectable osteoporosis treatments administered in an outpatient setting, denosumab (Prolia®) and zoledronic acid (ZA, Reclast®). In this first direct comparison of these two treatments, we aimed to determine and compare the efficacy and tolerability of denosumab and zoledronic acid.

Patients who received denosumab and ZA at Loyola University Medical Center were included in this retrospective study. The charts of both groups were reviewed and adverse events were noted. Of primary interest were myalgias, flu-like symptoms, back pain, and fractures. A questionnaire regarding the efficacy, tolerability and cost of treatment supplemented this chart review in a subset of the study participants. Statistical analysis was used to compare bone mineral density changes, bone turnover markers, and questionnaire results.

The study cohort consisted of 107 patients, 51 patients in the denosumab group and 56 patients in the ZA group. A subset of 29 patients responded to the questionnaire. The denosumab group had a greater mean increase in spine BMD at one year of 0.060g/cm^2 than the ZA group, 0.021g/cm^2 (p=0.04, two sample t-test). The change in femur T-score and BMD, and change in spine T-score at one year were not significantly different between the two groups. The ZA group had a significantly greater incidence of mild flu-like symptoms compared to the denosumab group (29% ZA group, 0% D group; p=0.04, Fisher's exact test). No significant differences in bone specific alkaline phosphatase, back pain, muscle pain, or patient satisfaction were observed. Of the questionnaire respondents, all of the ZA treatments were covered by insurance and only two participants had a copayment ($150 and $1500); 93% of the denosumab treatments were covered by insurance and three participants had a copayment ($70, $200, and $1800 for two treatments).

The denosumab group had a higher mean increase in spine BMD, and the ZA group had a higher incidence of flu-like symptoms, but the two study groups were statistically similar in patient satisfaction. Since denosumab is still a relatively new therapy, there were a limited number of patients with post-treatment data available for comparison. As more post-therapy data becomes available, the categories that were significantly different can be further investigated.

***Disclosures: Kellen Sheedy**, None.*

MO0379

Denosumab is here – do intravenous bisphosphonates still have a role?. Rosaleen Lannon*[1], Michael O'Callaghan[2], Nessa Fallon[2], Miriam Casey[2], James Bernard Walsh[3]. [1]St James's Hospital, Ireland, [2]Bone Health Unit, St James's Hospital, Ireland, [3]Trinity College Dublin, The University of Dublin, Ireland

Denosumab is here - do intravenous bisphosphonates still have a role?

Background: Denosumab is available to treat severe osteoporosis in Ireland for 30 months. Prior to release our options with regard to patients who were intolerant, non complaint or unresponsive to oral therapies were recombinant parathyroid hormone therapy or intravenous bisphosphonates. The former has certain specific indications and is costly leaving the later to ''fill the gap'' so to speak; that is until the introduction of denosumab.

Method: We reviewed our rates of first prescription of iv zoledronic acid and denosumab since the introduction of denosumab in late 2010 in our specialist bone clinic. We compared this to the rate of first prescription of iv zoledronic acid in the one year prior.

Results: Rate of prescription of iv zolendronic acid has declined significantly as denosumab use has increased. However iv zoledronic acid still plays a major role in our treatment of osteoporosis. In 2010 iv zoledronic acid was prescribed for the first time in 267 patients. Denosumab was prescribed 7 times towards the end of the year. In 2011 iv zoledronic acid was prescribed 211 times with denosumab issued 80 times. In 2012 iv zolendronic acid was prescribed 146 times with denosumab prescribed 153 times. Interestingly use of drugs combined remains similar over these two years.

Conclusion: Denosumab is a very useful addition to the treatments for osteoporosis which is convenient and cost effective as it can be administered in the community rather than a day ward setting. It has led to a 46% reduction in use of iv zoledronic acid in our service. It is also well tolerated. No dose adjustment is necessary and it is suitable for patients with chronic kidney disease. Nevertheless iv zoledronic acid remains available as a potent antiresorptive. It is the treatment of choice in complex medical patients attending our service such as those with transplants or autoimmune conditions as well as useful in augmenting the gains of 2 years of anabolic treatment with recombinant PTH. Denosumab has emerged as a competitor in this domain.[1] We conclude that iv zoledronic acid remains pivitol in our treatment options for osteoporosis.

[1]The Effects of Combined Denosumab and Teriparatide Administration on Bone Mineral Density in Postmenopausal Women: The DATA (Denosumab and Teriparatide Administration) Study. Leder B, Uihlein A, Neer R et al. J Bone Miner Res. 2012;27 (Suppl 1)

***Disclosures: Rosaleen Lannon**, None.*

MO0380

Development of a Claims-based Algorithm to Identify Prolia Use in Medicare Data. Nicole Wright*, Rui Chen, Tarun Arora, Huifeng Yun, Elizabeth Delzell, Jeffrey Curtis. University of Alabama at Birmingham, USA

Purpose: Prolia, a new biologic agent for osteoporosis (OP) launched May 26, 2010, was originally billed in Medicare Part B with non-specific Healthcare Common Procedure Coding System (ns-HCPCS) codes. These codes do not uniquely identify the drug being administered. Our objective was to develop a claims-based algorithm to identify Prolia and distinguish it from other injection or infusion medications using ns-HSCPS codes in Medicare data.

Methods: We used 2010 Medicare Part B data from a cohort of beneficiaries with OP age 65 years and older with at least one month of Medicare Parts A, B, and D coverage, without Medicare Advantage. We selected Part B claims with ns-HCPCS codes from launch date to 12/31/2010. We reviewed information such as service date, units given, allowed amount, submitted amount, and associated diagnosis codes from claims with the specific Prolia HCPCS code, in limited use since 10/2010, to derive the algorithm. We evaluated claims for two other agents with attributes similar to Prolia using ns-HSPCS in 2010 (tocilizumab (TCZ) & Ozurdex (OZD)). The final algorithm classified each ns-HCPCS claim as Likely, Probably, Possibly, or Unlikely Prolia. We evaluated differences in characteristics between the groups, focusing on the Likely and Unlikely claims.

Results: Our study included 89,581 beneficiaries with 197,043 claims with ns-HCPCS codes. We identified 11,557 duplicate/redundant claims, 1,610 TCZ, and 296 OZD claims. Algorithm development used 1,061 Prolia claims with the specific HCPCS code. Our final algorithm identified 10,438 Likely, 483 Probably, 134 Possibly, and 174,381 Unlikely Prolia claims. A larger proportion of Likely claims had an OP diagnosis code on the same claim than the Unlikely claims (99.4% vs 8.5%). Similarly, the proportion of Likely claims (85.3%) with the appropriate Prolia allowed amount, $874.50-$874.80, was larger than that of the Unlikely claims (0.0%).

Conclusions: Our algorithm appeared successful at identifying Prolia users in Medicare with good internal validity. An external source to examine the sensitivity and specificity of the algorithm is needed for further validation.

***Disclosures: Nicole Wright**, Amgen, 6*
This study received funding from: Amgen

MO0381

DEVIDE-Study: DEnosumab Versus Intravenous Ibandronate – a 24 months retrospective head to head real life study - Study Design. Astrid Fahrleitner-Pammer*[1], Christian Muschitz[2], Heinrich Resch[3], Doris Wagner[4], Karin Amrein[5], Stefan Pilz[5], Andreas Tomaschitz[5], Thomas Pieber[5], Hans Dimai[1]. [1]Medical University Graz, Austria, [2]St. Vincent's Hospital, Austria, [3]Medical University Vienna, Austria, [4]Department for Transplantation, Medical University Graz, Austria, [5]Medical University Graz, Department for Internal Medicine, Austria

Purpose: Effective treatment of postmenopausal osteoporosis (PMO) is frequently compromised by poor persistence and adherence to short-term (≤ 1-monthly) medications. Several head to head trials comparing the efficacy of Denosumab with that of oral Bisphosphonates (BP) are available so far, indicating a superior effect of Denosumab on bone markers and BMD (STAND, DECIDE, TTR, TTI). All of these studies have been conducted as randomized controlled clinical trials and compare the effect of an oral with a parenteral therapy. Aim of this study which has been performed in a real-life setting, is to investigate the effect of parenteral ibandronate (IBN) compared to denosumab treatment in a cohort of IBN pretreated PMO patients.

Methods: In a retrospective analysis, a total of 808 patients with PMO were analyzed. All women are regularly monitored at the osteoporosis outpatient clinic at the Medical University of Graz (Austria) or the St. Vincent Hospital of Vienna (Austria). All patients had received parenteral IBN therapy due to intolerance or contraindications to oral BP therapy. After Denosumab was launched for treatment of OPO, 366 women were switched to receive this therapy due to their own or their physician's decision, whereas the remaining 442 stayed on IBN intravenously every three months. Effectiveness in terms of fracture incidence, BMD, BTM, as well as adherence and safety of these two parenteral therapies are analyzed.

Results: Mean age of the population at baseline was 66 + 7 years. All patients had primary PMO, and were treated with quarterly IBN injections for a median time period of 27 + 6 months. BMD readings, fracture status, age, body mass index, bone turnover markers (BTM) as well as safety laboratory parameters were comparable among the two treatment groups. Laboratory testing, recording of adverse events was done every 6 months, and BMD readings, spinal X- ray and fracture assessment were performed at baseline as well as after 12 and 24 months of IBN or Denosumab therapy.

Conclusion: The results of this study not only will provide clinicians with insight into persistence with denosumab in comparison to IBN therapy, but will also compare the effect of denosumab with a parenteral administered BP.

***Disclosures: Astrid Fahrleitner-Pammer**, None.*

MO0382

Evaluation of odanacatib in subjects with hepatic insufficiency. Stefan Zajic[1], Michelle Trucksis[2], Graig Garrett[2], Anish Mehta[2], Patrice Auger[3], Nancy Wang[3], Daria Stypinski[3], Anne Hohnstein[3], Megan Kozisek[3], Bruce DeGroot[3], Gautam Baheti[4], Cindy Dempsey[3], Richard A. Preston[5], Aubrey Stoch*[6]. [1]Merck Research Laboratories, USA, [2]Merck Sharp & Dohme Corp., USA, [3]Celerion, USA, [4]Parexel, USA, [5]University of Miami, USA, [6]Merck Sharp & Dohme, USA

Objectives: Hepatic elimination is an important metabolic pathway for odanacatib, a cathepsin-K inhibitor in development for the treatment of osteoporosis. We conducted 2 clinical studies to determine the effect of hepatic insufficiency (HI) on the pharmacokinetics (PK) of odanacatib.

Methods: Two open-label studies compared the PK of single-dose odanacatib 25 mg (Study 1) and single-dose 50 mg (Study 2) in subjects with HI versus healthy matched control subjects. Study 1 evaluated mild HI subjects (score of 5-6 on Child-Pugh's scale) and matched control subjects in Part I after dosing with odanacatib 25 mg; if data demonstrated acceptable tolerability and PK levels, subjects with moderate HI (score of 7-9 on Child-Pugh's scale) and matched control subjects were evaluated after dosing with odanacatib 25 mg. Study 2 evaluated moderate HI subjects after dosing with odanacatib 50 mg. The primary PK measurement was $AUC_{0-\infty}$. Blood and urine samples were analyzed for serum CTx and urine NTx/Cr in Study 1. Vital signs and adverse events (AE) were monitored throughout the studies.

Results: Subjects –Study 1 included 40 male and female subjects (ages 41-62 years), 10 with mild HI, 10 with moderate HI and 20 healthy matched control subjects. Study 2 included 17 male and female subjects, 8 with moderate HI and 9 healthy matched control subjects. In Study 1, the $AUC_{0-\infty}$ geometric mean ratio (GMR) (90% CI) was 0.95 (0.68, 1.31) for mild HI/healthy controls and 0.81 (0.62, 1.06) for moderate HI/healthy controls after administration of odanacatib 25 mg. In Study 2, the $AUC_{0-\infty}$ GMR (90% CI) was 0.85 (0.61, 1.19) for moderate HI/healthy controls after administration of odanacatib 50 mg. Biomarker data in Study 1 showed that, at 168 hours postdose (odanacatib 25 mg), the LS Mean (95% CI) change in serum CTx was -63.7 (-75.1, -47.2) in mild HI subjects and -41.0 (-59.5, -13.9) in healthy controls, while LS Mean (95% CI) change in serum CTx was -62.2 (-73.0, -47.2) in moderate HI subjects and -39.8 (-56.7, -16.3) in healthy controls; Urine NTx results were consistent with those observed for serum CTx. There was one subject with serious AEs (sinusitis, mastoiditis, otitis followed by pneumococcal meningitis) in Study 1. There were no serious AEs in Study 2.

Conclusions: The $AUC_{0-\infty}$ of odanacatib 25 mg and 50 mg was not meaningfully altered in subjects with mild or moderate HI. The slightly decreased PK in moderate HI subjects may reflect differences in odanacatib plasma protein binding in this group. Preliminary biomarker data (serum CTx, urine NTx/Cr) demonstrate comparable pharmacodynamic efficacy with odanacatib in patients with mild or moderate HI when compared to healthy matched controls. Odanacatib was generally well tolerated.

***Disclosures: Aubrey Stoch**, Merck, 3*
This study received funding from: Merck sponsored the study

MO0383

Intravenous Ibandronate Increases Femoral and Vertebral Strength Measured by Finite Element Analysis in Male Patients with Idiopathic Osteoporosis and Fragility Fractures. Christian Muschitz*[1], Dieter Pahr[2], Michael Kinzl[2], Benoit Luiser[2], Afrodite Zendeli[3], Roland Kocijan[4], Judith Haschka[4], Wolfgang Schima[5], Heinrich Resch[6]. [1]St. Vincent's Hospital, Austria, [2]Institute of Lightweight Design & Structural Biomechanics University of Thechnology, Austria, [3]The VINFORCE Study Group - St. Vincent Hospital - Medical Department II, Austria, [4]St. Vincent Hospital Vienna, Austria, [5]Institute of Radiology - St. Vincent Hospital, Austria, [6]Medical University Vienna, Austria

Purpose: Male idiopathic osteoporosis (MIO) is a metabolic bone disease characterized by low BMD, micro structural alterations, reduced mineralization of cortical structures resulting in increased fracture risk in otherwise healthy men. The evidence of antiresorptive treament for MIO is lower than those for postmenopausal osteoporosis. Volumetric BMD measurements and strength predictions using voxel-based finite element (FE) simulations of the vertebral body and the proximal femur predict alterations in strength and stiffness. The hypothesis of this study was to test if ibandronate (IBN) improves biomechanical properties of femoral and vertebral bone in MIO.

Methods: 13 treatment naïve MIO patients from a prospective paired biopsy study - mean age 53.0 [44.5; 57.0] years - with prevalent fragility fractures and low BMD received 3mg intravenous IBN for 24 months quarterly. QCT (baseline/month 24) of Th12 and hip were assessed to compare BMC, vBMD, BV/TV, areal bone volume fraction (aBMD), stiffness and ultimate force by using FE simulations for fall (femur) and compressive (vertebra) loading.

Results: At the proximal femur the average strength increase (%) was 4.9 ± 8.9 (range -8.4 to 16.5, $p<0.01$; 3 patients below 0). Pronounced increases were observed for trochanteric aBMD (2.9 ± 2.6) and BV/TV of FE models (3.7 ± 1.7, $p<0.05$), with less effect in the neck region (0.7 ± 1.5). Most hip fracture types observed by FE simulated side-fall scenarios were discovered in the trochanteric region. Regressions between strength increase and vBMD increases showed no correlation for BMC, BMD, BV/TV or aBMD ($R2<0.04$). In the vertebral body the mean strength increase was 7.3 ± 9.2 (range -2.7to 31.9, 2 patients below 0) with most pronounced increase for BMC ($9.4 \pm 10.5\%$); BV/TV distributions increased both at cortical shell and trabecular center ($p<0.01$). A strong correlation was found for increase in strength and BV/TV ($R2=0.80$) and between BV/TV, BMD and BMC ($R2>0.65$). Predicted fracture locations based on damage patterns by FE simulation were similar between baseline and follow up.

Conclusions:

This study clearly shows decisive positive effects of intravenous IBN treatment on biomechanical properties at the hip and spine in patients with MIO comparable postmenopausal osteoporosis. FE simulations are more sensitive and provide improved detailed insight than BMD measures alone, especially for side-fall simulations, since the fracture position and the local BMD increase can be considered.

***Disclosures: Christian Muschitz**, None.*

MO0384

Lycopene Supplementation Improved the Response of Postmenopausal Women With Osteoporosis to Alendronate Therapy: A 12-Month Follow-Up Study. Mohammed-Salleh Ardawi*[1], Mohammed Qari[2], Abdulrahim Rouzi[1], Sharifa Al-Sibiani[3], Nawal Al-Senani[3], Bader Mustafa[4]. [1]Center of Excellence for Osteoporosis Research & Faculty of Medicine, Saudi Arabia, [2]Center of Excellence for Osteoporosis Research & Department of Haematology & KAU Hospital,Faculty of Medicine, King Abdulaziz University, Saudi Arabia, [3]Center of Excellence for Osteoporosis Research & Department of Obstetrics & Gynecology, Faculty of Medicine & KAU Hospital, King Abdulaziz University, Saudi Arabia, [4]Center of Excellence for Osteoporosis Research, King Abdulaziz University, Saudi Arabia

Background: Alendronate (ALN),a potent inhibitor of bone resorption, has been shown to be very effective in the treatment of osteoporosis. Lycopene is a potent antioxidant. No information is available on the combined effects of ALN therapy with lycopene supplementation. We studied the effect of lycopene supplementation on ALN therapy in relation to bone mineral density (BMD) and bone turnover markers among postmenopausal women with osteoporosis.

Methods: This is a randomized prospective study with a 12-month follow-up. A total of 180 postmenopausal women (aged 61.2 ± 5.5 years) with osteoporosis were randomized into two groups: ALN-Lyco (70 mg/week) and lycopene (30 mg/day) (n=90) as compared with ALN only (70 mg/week) (n=90). All women were supplemented with calcium (600 mg) and vitamin D3 (400 IU) daily. BMD (measured by DXA) and levels of bone turnover markers (BTMs) including: serum osteocalcin (s-OC), serum procollagen type 1 N-terminal (s-P1NP), serum bone-specific alkaline phosphatase (s-bone ALP), plasma cross-linked C-terminal telopeptide of type 1 collagen (p-CTX), urinary N-telopeptide of type 1 collagen (u-NTX) were measured at baseline and at 3, 6 and 12 months of therapy. BMD and BTMs were compared between the baseline and the end of therapy, and the changes in BMD and BTMs were also compared between the two treatment groups.

Results: After 12-month therapy, ALN-Lyco group showed significantly higher percentage increases in BMD at lumbar spine (L_1-L_4), neck femur and total hip (5.35%, 4.12% and 3.74%, respectively) as compared with ALN therapy group (4.92%, 3.81% and 3.22%, respectively; $P<0.001$, each). Relative to baseline, by 12 months the ALN-Lyco group had greater reductions in s-OC (-46% vs -136%), s-bone-ALP (-58% vs -42%), s-P1NP (-65% vs -45%), p-CTX (-75.2% vs -58.5%), u-NTX (-66.1% vs -49.2%) compared with ALN group, respectively ($P<0.001$, each). There was no difference between groups and those who experienced falls or fractures, and adverse events were similar among the two groups.

Conclusions: Lycopene supplementation with ALN therapy produced greater gains in BMD and greater reductions in BTMs than ALN treated group. We suggest the addition of lycopene supplementation to antiresorptive therapy in postmenopausal women with osteoporosis.

***Disclosures: Mohammed-Salleh Ardawi**, None.*

MO0385

Randomized Trials Show Greater Bone Mineral Density Increase on Estrogen plus Progestin Versus Estrogen Alone—progestin effect on bone formation?. Jerilynn Prior*, Shirin Kalyan. University of British Columbia, Canada

Progesterone and progestins including medroxyprogesterone (MPA) sit on osteoblast receptors and increase osteoblast numbers and proliferation. However, progesterone and non-androgenic progestins do not suppress bone resorption, the more rapid phase of human bone remodelling and thus alone are ineffective osteoporosis therapy. Current bone-formation stimulating osteoporosis therapy is via daily injection and expensive. However, if co-therapy of an antiresorptive plus progesterone increased areal bone mineral density (aBMD) more than the antiresorptive alone, this co-therapy might provide effective fracture prevention at a lower cost. Purpose: to review randomized controlled trials (RCT) of estrogen alone (CEE) versus co-therapy with MPA (CEE-MPA) on annual change in spinal aBMD. Methods: Data from all RCTs including an estrogen and an estrogen-MPA arm were reviewed (PEPI, Women's Hope, Liu NIH progestin-bone, Adachi and Gallagher trials). Results: Of these six, five showed numerically greater co-therapy spinal aBMD

increases over CEE alone and two reported significant differences (See*in Figure). The PEPI intent-to-treat analysis also showed significantly greater aBMD increases on CEE-low dose MPA than CEE alone. These RCTs tested full dose CEE (0.625 mg/d) or estradiol plus 2.5 mg/d MPA vs. estrogen alone (PEPI, Women's Hope, Liu) except for CEE 0.3 in the negative trial (Gallagher). The Women's HOPE RCTs showed significantly greater 2-y L2-4 aBMD gains on combined CEE 0.625 mg/MPA 2.5 mg vs. CEE 0.625 therapy alone (3.5% vs. 2.4%, P=0.03); CEE 0.45/MPA was also significant. Co-therapy with both full-dose CEE or estradiol and MPA (10 mg) caused 44% and 77% greater aBMD gains respectively in the Adachi and Liu studies but did not reach significance due to a lack of power. Summary: combined CEE-MPA therapy appears to increase lumbar aBMD more than CEE alone. Additionaltrials are needed that combine antiresorptives such as bisphosphonates [SK1] with physiological progesterone that assess changes in aBMD and bone strength.

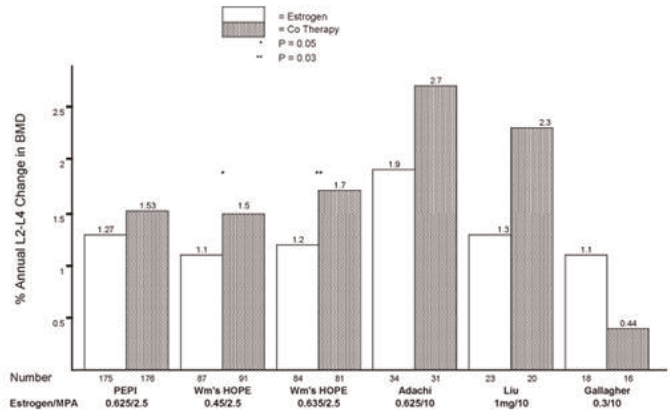

n this Figure estrogen-only therapy is shown in open boxes and estrogen-MPA co-therapy in the stippl

***Disclosures: Jerilynn Prior**, None.*

MO0386

Results of Secondary Fracture Prevention Program in Patients with Severe Osteoporosis in Rambam Health Care Campus. Sophia Ish-Shalom*[1], Elena Segal[1], Marina Nodelman[2], Marina Hefetz-Kustanovich[1], Doron Norman[1]. [1]Rambam Health Care Campus, Israel, [2]Western Galilee Hospital, Israel

The risk of additional osteoporotic fractures in a patients that underwent a fragility fractures is at least 6 fold higher than in age and gender matched adults. Treatment strategies should be directed to provide intensive fracture prevention treatment to patients with osteoporotic fractures.

A collaborative (ortopedics and bone metabolism) fracture prevention program for patients that were hospitalized with osteoporotic fractures was initiated in Rambam Health Care Campus in 2008. All patients that were hospitalized with fractures were offered fracture prevention treatment after surgical fracture repair.

Results: 1647 patients, aged median 78 (range 23-103), 1165 (71%) women aged 78 (33-100) and 482 (29%) men aged 77 (23-103) were enrolled in the program between 2008 – 2013. Proximal femoral fractures were sustained by 1115 (68%) of all patients: 769 (66%) of women and 346 (72%) of men; 256 (16%) of patients died during the study period, 152 (13%) of women and 104 (22%) of men; in hip fracture patients 123 (16%) of women and 89 (26%) of men. The relative risk (RR) of men to die after a hip fracture was 1.61 (95% CI 1.26-2.05) compared to women. The major predictors of death in women were greater age, number of medications, creatinine and lower albumin; in men, greater age, number of medications, and creatinine. 264 (23%) of all women and 10 (2%) of all men were treated for osteoporosis before admission and 171 (22%) of women with hip fractures and 6 (2%) of all men with hip fractures. After discharge 404 (35%) of all women and 42 (9%) of all men received treatment; of hip fracture patients, 247 (32%) of women and 31 (9%) of men received treatment. While no factors were related to increased likelihood of men being treated, women were more likely to be treated if they had any previous fractures, previous treatment, higher vitamin D or albumin, and lower creatinine. Treatments distribution in all patients was: 319(19.3%) received oral bisphosphonates, 73 (4.45%) IV bisphosphonates (Zoledronate), 2 (0.12%) pamidronate), 47 (2.87%) teriparatide, 5(0.31%) raloxifen.

We conclude that in spite of a marked increase in the rate of patients that were treated after an index fracture, in a hospital initiated collaborative treatment program, it is still unsatisfactory . The use of of IV bisphosphonates, approved as first line therapy after hip fracture in Israel, is still very low.

***Disclosures: Sophia Ish-Shalom**, None.*

MO0387

Risedronate Improves Proximal Femur Bone Mineral Density and Geometry Parameters Over 5 Years in Patients with Osteoporosis or Osteopenia and Clinical Risk Factors of Fractures: A Practice-Based Observational Study. Masayuki Takakuwa[1], Jun Iwamoto*[2]. [1]Takakuwa Orthopedic Nagayama Clinic, Japan, [2]Keio University School of Medicine, Japan

Advanced Hip Assessment (AHA) software installed in a dual-energy X-ray absorptiometry (DXA, GE-Lunar) can be used to evaluate bone strength indices as well as bone mineral density (BMD) of the proximal femur. In particular, Femur Strength Index (FSI) is calculated using structural geometric properties, neck shaft angle, height, and body weight. The purpose of this study was to investigate the 5-year effects of risedronate treatment on AHA parameters of the proximal femur and BMD of the lumbar spine and proximal femur in patients with increased risk of fractures. In total, 181 patients (mean age: 68.1yrs; 172 females and 9 males) with osteoporosis or osteopenia and clinical risk factors of fractures were treated with risedronate for 5 years in our outpatients clinic. AHA parameters of the proximal femur and BMD of the proximal femur and lumbar spine (L1-L4) were evaluated every 1 year over 5 years. The mean percentage changes from baseline in FSI after 12 months of risedronate treatment were 7.9% ($p<0.001$) for the right femur and 7.0% ($p<0.001$) for the left femur. The respective values for the right femur after 24,36,48 and 60 months of treatment were 12.3%, 14.5%, 10.9% and 11.0% ($p<0.001$) and those for the left femur were 10.8%,13.3%, 18.8 ($p<0.001$)% and 9.7% ($p<0.01$). Cross-sectional moment of inertia (CSMI : right femur 9.3%, left femur 13.0% after 60months $p<0.001$), cross-sectional area (CSA), mean neck width(d3) in the femoral neck, and BMD of the right and left proximal femur and BMD of the lumbar spine also continued to increase during 5 years of treatment. The increases in FSI and CSMI in the proximal femur at each time point were apparently greater than those in the proximal femur and lumbar spine BMD. These results suggest that risedronate treatment may more significantly improve femoral strength parameters than BMD of the proximal femur and lumbar spine over 5 years. Thus, it has been demonstrated that risedronate dose not only increase lumbar spine and proximal femur BMD, but also more significantly improves bone strength indices of the proximal femur in patient with increased risk of fractures.

***Disclosures: Jun Iwamoto**, None.*

MO0388

The change of serum osteocalcin is not associated with the changes of insulin secretion or resistance in osteoporotic patients treated with bisphosphonate. Deog-Yoon Kim*[1], Seong-Hun Hong[2], Jin Kyung Hwang[2], You-Cheol Hwang[2], In-Kyung Jeong[2], Kyu Jeong Ahn[2], Ho-Yeon Chung[3]. [1]Kyung Hee University Hospital, South Korea, [2]Kyung Hee University School of Medicine, South Korea, [3]Kyung Hee University, South Korea

Osteocalcin, a protein secreted by osteoblasts and released from the bone matrix during osteoclastic bone resorption, has been found to control blood glucose levels by increasing insulin production and sensitivity. Bisphosphonate is used in osteoporosis treatment to repress osteoclast activity, which then decreases levels of osteocalcin. The question addressed by this study is whether decreasing osteocalcin by bisphosphonate treatment can provoke a change in glucose homeostasis.

Eighty-four patients with osteoporosis were treated with once-weekly risedronate 35 mg and cholecalciferol 5600 IU. We measured fasting plasma glucose, insulin, and undercarboxylated and carboxylated osteocalcin at baseline and after 16 weeks. To estimate insulin sensitivity and β-cell function, HOMA-IR and HOMA-B% were calculated, respectively.

The mean fasting plasma glucose of all subjects increased significantly from 5.3 to 5.5 mmol/L, but no changes in blood glucose were noted in 24 subjects with impaired fasting glucose. The levels of undercarboxylated and carboxylated osteocalcin declined significantly after treatment. However, no correlation was observed between changes in osteocalcin and changes in glucose after multiple regression analysis.

Bisphosphonate treatment for osteoporosis reduced osteocalcin and this change was not associated with changes in glucose metabolism.

***Disclosures: Deog-Yoon Kim**, None.*

MO0389

The Effect of Calcitonin Therapy on Postoperative Rehabilitation in Patients with Femoral Neck/Trochanteric Fractures. Tetsuo Nakano*[1], Shinya Tanaka[2]. [1]Tamana Central Hospital, Japan, [2]Saitama Medical University, Japan

Introduction: Management of a bedridden state and depressed walking ability due to femoral neck/trochanteric fractures involves a complex, long-term system of therapy comprising surgical intervention, perioperative management, rehabilitation, etc., all of which are necessary for avoiding an unfavorable prognosis. Regarding rehabilitation, studies on the training methods and influence of timing of initiation and frequency of rehabilitation have been reported; however, few studies concerning the effects of pharmaceutical therapy on rehabilitation have been conducted.

Subjects and Methods: A total of 352 patients with femoral neck/trochanteric fractures surgically treated at this hospital were classified into two groups, of which only one group received calcitonin in a dose of 20 units intramuscularly once a week during hospitalization. Other treatments and rehabilitation were provided in the same manner in the two groups.

Results: Of all the patients treated, a total of 242 patients were included in the data analysis. A further analysis was made on these eligible patients divided into the following 3 groups according to pre-injury walking ability (independent outdoor walking group, independent indoor walking group, dysbasia group).

The percentage of patients achieving improvement in walking ability over time was compared between these two groups. The calcitonin-treated group exhibited a significant improvement of walking ability at Weeks 2 and 3 post-operation. The same assessment parameter was compared among the 3 groups classified according to degree of pre-injury walking ability. In the independent outdoor walking group, patients who were treated with calcitonin showed a significant improvement of walking ability at Weeks 2 and 3 post-operation, as was the case with the whole population analysis.

Discussion: Calcitonin has a pain-relieving effect mediated by the central serotonergic nervous system. Depression of cognitive function is a representative factor contributing to inhibition of rehabilitation in patients with femoral neck/trochanteric fractures, and pain is also considered a noticeable inhibitory factor. Assuagement of painfulness may therefore improve the rehabilitation of fracture patients. The present results demonstrate the usefulness of calcitonin therapy during early postoperative rehabilitation only in patients had had high pre-injury walking ability before fracture.

***Disclosures: Tetsuo Nakano**, None.*
This study received funding from: Japan Osteoporosis Foundation

MO0390

The Effects of Intravenous Aminobisphosphonates on Carotid Atherosclerosis could Be Influenced by the Changes in FGF23 Serum Levels. Stefano Gonnelli*, Carla Caffarelli, Loredana Tanzilli, Maria Dea Tomai Pitinca, Alice Cadirni, Barbara Lucani, Maria Beatrice Franci, Ranuccio Nuti. University of Siena, Italy

Some, but not all studies have reported a positive effect of aminobisphosphonates on atherosclerotic lesions. However, no convincing explanations exist regarding this finding. Recently it has been reported that the levels of FGF23 are positively related to the progression of atherosclerosis and to the calcification of atherosclerosis plaque.

Sixty postmenopausal osteoporotic women (mean age: 66.4 ± 7.6 years), not previously treated with drugs for osteoporosis and with normal levels of 25OHvitamin D, were randomly allocated to receive zoledronate 5 mg i.v. annually or ibandronate 3 mg i.v. every 3 months.

At baseline and at month 12 we measured serum lipids, bone isoenzyme of alkaline phosphatase, parathyroid hormone, 25-hydroxy-vitamin D, the terminal fragment of collagen type 1, the fibroblast growth factor-23 (FGF23) and osteocalcin. Patients with impaired renal function were excluded from the study. Bone Mineral Density (BMD) at lumbar spine and at femur (neck and total sub regions) and total body were also measured (DXA method, Prodigy GE Lunar, USA). An ultrasound examination of carotid vessels was performed to assess intima-media-thickness (IMT), presence of plaque and the degree of calcification.

Patients with atherosclerotic plaques were found to have significantly lower BMD values ($p < 0.05$) than those without plaques. Serum levels of FGF23 were reduced in osteoporotic women who presented with carotid plaques but without reaching any statistical significance (26.6 ? 14.6 vs 18.9 ? 8.1 RU/ml). Also serum levels of osteocalcin were reduced in women with carotid plaques (4.3 ? 2.5 vs 4.7 ? 1.2 ng/ml; p=n.s.). Both FGF23 and osteocalcin were negatively correlate with IMT (r =-0.42 $p < 0.05$ and r =-0.35 $p < 0.05$, respectively). In addition the serum levels of FGF23 were significantly correlated with BMD at all femoral subregions ($p < 0.05$).

At month 12 a significant increase in HDL-cholesterol and HDL/LDL-cholesterol ratio was observed. Moreover at month 12 both zoledronate and ibandronate induced a reduction in IMT (-4.73% $p<0.05$; and -1.75% p=n.s. respectively). FGF23 serum levels showed a significant decrease with respect to baseline in both zoledronate (-40.2% $p<0.01$) and ibandronate (-31.2% $p<0.05$) groups.

Our findings seem to support a crosstalking between bone and atherosclerotic lesions, however, further studies are warranted to confirm as to whether FGF23 may play an important role in this.

***Disclosures: Stefano Gonnelli**, None.*

MO0391

The Occurrence of Renal Insufficiency and Hypocalcemia after Zoledronic Acid Infusion. Laurae Hicks*[1], Pauline Camacho[2]. [1]Loyola University, USA, [2]Loyola University of Chicago, USA

Zoledronic acid (ZA) is an effective injectable bisphosphonate medication that was approved by the FDA for treatment of osteoporosis in 2007. In the United States, osteoporosis is a major concern, impacting almost 44 million people; 80% of these are post-menopausal women. The incidence is likely to increase as the population ages. Although zoledronic acid has been found to reduce the risk of vertebral fracture by 70% and hip fractures by 41% in affected patients, there are potential side effects, such as renal insufficiency and hypocalcemia. In this study, we aimed to determine the incidence of renal insufficiency and hypocalcemia after ZA infusion for osteoporosis treatment. 237 charts of osteoporotic patients were reviewed; 141 patients had 2 zoledronic acid infusions and 58 had 3. McNemar's Test revealed no significant difference between pre- and post- eGFR for all infusions (p= 0.07, 0.41, and 0.41). Paired t-test between pre- and post-creatinine clearance values showed no significant difference (p= 0.4269, 0.2742, 0.8949). In regards to hypocalcemia, paired t-test of 244 pre- and post- corrected serum calcium levels (corrected with plasma albumin) and 86 pre- and post- ionized calcium levels showed a significant difference with the 1st infusion, but not the 2nd or 3rd (p= <0.0001, mean = -0.1739 for corrected calcium and p= 0.0272, mean = -0.0143 for ionized calcium). Overall results indicate that use of zoledronic acid does not significantly alter renal function. During the first infusion, however, significant changes in serum calcium occurred, but serious hypocalcemia was not seen in this vitamin D replete population.

Keywords: zoledronic acid, osteoporosis, renal, hypocalcemia

Infusion	Average Age	Males	Females	Total Number
1	69.97	27	210	237
2	70.74	11	130	141
3	71.98	7	51	58

Table 1. Demographic information for each of the three infusions

Table 1.

Infusion 1			
pre-eGFR	post-eGFR		
	≤60	>60	Total
≤60	52	21	73
>60	13	144	157
Total	65	165	230
		p value	*0.17*
Infusion 2			
pre-eGFR	post-eGFR		
	≤60	>60	Total
≤60	32	8	40
>60	5	96	101
Total	37	104	141
		p value	*0.41*
Infusion 3			
pre-eGFR	post-eGFR		
	≤60	>60	Total
≤60	15	4	19
>60	2	37	39
Total	17	41	58
		p value	*0.41*

Table 2. McNamer's Test for all three infusions shows no significant change in eGFR values before and after infusions.

Table 2

Infusion	Difference	Number	Mean Difference	Pre-Mean	Post-Mean	P Value
1	PostCorrectedCa2+ PreCorrectedCa2+	138	-0.1739	9.5729	9.3871	<.0001
2	PostCorrectedCa2+ PreCorrectedCa2+	73	0.0687	9.5728	9.5056	0.0963
3	PostCorrectedCa2+ PreCorrectedCa2+	33	0.0764	9.5544	9.4672	0.2347
1	PostIonizedCa2+ PreIonizedCa2+	70	0.0143	1.2333	1.2096	0.0272
2	PostIonizedCa2+ PreIonizedCa2+	13	0.00462	1.2280	1.2206	0.6364
3	PostIonizedCa2+ PreIonizedCa2+	3	0.01	1.2225	1.2270	0.7852
1	PostCreatinine PreCreatinine	232	0.00853	0.9110	0.9047	0.4269
2	PostCreatinine PreCreatinine	141	0.0157	0.8875	0.8718	0.2742
3	PostCreatinine PreCreatinine	58	0.00293	0.8990	0.9019	0.8949

Table 3. Paired -T tests for pre- and post- infusion differences show a significant change in calcium levels for the 1st infusion, but not the 2nd, 3rd, or any of the creatinine values.

Table 3.

***Disclosures: Laurae Hicks**, None.*

MO0392

Vitamin D Repletion in Korean Postmenopausal Women with Osteoporosis. Yoon-Sok Chung*[1], Han-Jin Oh[2], Il Hyung Park[3], In-Ju Kim[4], Jung-Min Koh[5], Moo-Il Kang[6], Sung-Kil Lim[7], Yong-Ki Min[8], Yil-Seob Lee[9], Barbara Kravitz[10], Brian Waterhouse[10], Lorraine Fitzpatrick[10], Antonio Nino[10]. [1]Ajou University School of Medicine, South Korea, [2]Cheil General Hospital, Kwandong University, South Korea, [3]Kyungpook National University Hospital, South Korea, [4]Pusan National University Hospital, South Korea, [5]Asan Medical Center, South Korea, [6]Seoul St. Mary's Hospital, South Korea, [7]Yonsei University College of Medicine, South Korea, [8]Samsung Medical Center, South Korea, [9]GlaxosmithKline Pharmaceuticals, South Korea, [10]GlaxosmithKline Pharmaceuticals, USA

Purpose: To assess the effect of daily, oral vitamin D supplementation in Korean postmenopausal women with osteoporosis with serum levels of vitamin D 25(OH)) < 50 nmol/L during a clinical trial.

Methods: Korean postmenopausal women aged 60-90 years were screened for study participation in a randomized, double-blind trial with denosumab in osteoporosis patients. Participants were required to have vitamin D levels ⩾ 50 nmol/L for randomization. Repletion with 1000 IU capsules of vitamin D was allowed. For those subjects whose vitamin D levels were < 50 nmol/L, the investigator determined the dose, frequency, and duration of the vitamin D repletion for the subject. When the repletion regimen completed (maximum 75 days were allowed), a second blood sample was obtained and tested for 25(OH) vitamin D levels. All sites obtained approval from their Ethics Committees and all subjects signed informed consent.

Results: Of 371 subjects screened, 191 subjects needed repletion because of serum levels of 25(OH) vitamin D <50 nmol/L. Of the subjects who required repletion,168 (88%) were successfully repleted and 77 met study entry criteria and were randomized. Fourteen subjects did not reach 50 nmol/L and no sample was available for 9 subjects. An additional 180 subjects did not require repletion as their baseline vitamin D level was ⩾50 nmol/L; of these, 58 subjects met study entry criteria and were randomized. Repletion results are presented (Table 1). Mean time to successful repletion was 31 days (SD 8.4; Min 11 days, Max 48 days). Median dose of vitamin D for successful repletion was 2000 IU daily (min 1000 IU and max 9000 IU daily).

Conclusions: Successful vitamin D repletion in Korean postmenopausal women with osteoporosis was achieved to levels of ⩾ 50 nmol/L by a maximum observed 48 days using daily doses of oral vitamin D ranging from of 1000 to 9000 IU with a median dose of 2000 IU daily.

This study was sponsored by GlaxoSmithKline Pharmaceuticals.

Table 1 Vitamin D Laboratory Assessments by Status at Initial Screening

Subjects with serum level vitamin D ≥50 nmol/L at initial screening

Lab Test	Status	N	Visit	n	Mean	SD
25(OH) vitamin D (nmol/L)	Randomized	58	Screening 1	58	71.5	15
	Non-randomized	122	Screening 1	115	52.6	22.91

Subjects with serum level of vitamin D <50 nmol/L at initial screening and achieved levels of ≥50 nmol/L after repletion

Lab Test	Status	N	Visit	n	Mean	SD
25(OH) vitamin D (nmol/L)	Randomized	77	Before repletion	77	29.7	9.75
			After repletion	77	71.4	15.38
	Non-randomized	91	Before repletion	90*	29.4	10.56
			After repletion	91	70.4	15.82

* One patient was discontinued for repletion in error, their vitamin D level was >50 nmol/L

Subjects with serum levels of vitamin D <50nmol/L at initial screening, received vitamin D repletion, and did not reach ≥50 nmol/L or did not have a second assessment

Lab Test	Status	N	Visit	n	Mean	SD
25(OH) vitamin D (nmol/L)	2nd lab sample available	14	Before repletion	14	22.8	9.25
			After repletion	14	40.8	9.65
	2nd sample not available	9	Before repletion	9	32.8	11.22

Vitamin D Laboratory Assessments by Status at Initial Screening Visit

***Disclosures: Yoon-Sok Chung**, None.*
This study received funding from: GlaxoSmithKline Pharmaceuticals

MO0393

In Patients with Different Forms of Osteoporosis Excellent Adherence to 6-Monthly Denosumab Injections Can be Achieved by Positive Feedback Based on 6 and 12 Months BMD Increases and Rare Adverse Events. Johann D. Ringe*, Parvis Farahmand. West German Osteoporosis Center (WOC), Klinikum Leverkusen, University of Cologne, Germany

Introduction: More than 50% of osteoporosis patients discontinue bisphosphonate therapy within the first year of treatment. Denosumab's (Dmab) longer dosing interval with its s.c. administration every 6 months might result in a better real life treatment adherence and persistence than weekly or monthly oral bisphosphonate treatment regimen.

Methods: In an open investigator-initiated prospective observational study in routine clinical practice we aimed to assess whether a careful medical explanation of treatment results 6 and 12 months after the first Dmab injection focussing on no or only mild and probably not drug related AEs, changes in back pain and on significant BMD increases have effects on patients' drug perception and future adherence with further Dmab injections. We included 142 patients (69 with postmenopausal, 42 with male, and 32 with GC-induced osteoporosis).

Results: At onset almost all patients had concerns about possible AEs, but 93% reported no negative changes in their health condition at all after two injections of Dmab, and only 7.0% reported AEs. These were all mild to moderate, disappeared without intervention and were obviously not drug related. Besides this good tolerability patients were very impressed by demonstrating and carefully explaining to them the original DXA-protocols showing a significant increase in lumbar spine (LS) and/or total hip (TH) BMD. The therapeutic effect of Dmab on BMD did not differ between the three different types of osteoporosis. The mean increase rates at month 6 were +4.7% at the LS site and +2.1% at the TH area and at month 12 +7.8% at the LS site and +3.7% at the TH area, respectively. There were only 5 vertebral and 4 non-vertebral fractures during the 142 patient years follow-up. The back pain score measured by VAS 0-10 decreased in all 3 groups significantly after 6 and 12 months. This clinical effect together with the scarcity of AEs and the positive feedback of a rapid BMD-increase at both sites resulted for 141 (99%) patients after 6 months and 139 (97%) after 12 months in a willingness to accept a further injection.Conclusion: Results indicate that the convenient treatment regime together with back pain improvements, rarity of adverse events and the consistency of rapid and highly significant BMD-increases after 6 and 12 months of Dmab therapy used as a positive reinforcement had a significant, positive impact on patient's adherence to continue with the 6-monthly s.c. Dmab injections.

***Disclosures: Johann D. Ringe**, None.*

MO0394

Long-term (up to 5 years) persistence with different anti-osteoporosis medications in Catalonia (Spain): a population-based cohort study. Cristina Carbonell*[1], Aina Pages-Castella[2], Pilar Estrada[2], Xavier Nogues[3], Adolfo Diez-Perez[4], Daniel Prieto-alhambra[5]. [1]Facultat de Medicina Universitat de Barcelona, Spain, [2]GREMPAL Research Group (USR Barcelona), IDIAP Jordi Gol, Universitat Autònoma de Barcelona, Spain, [3]Institut Municipal D'Investigació Mèdica, Spain, [4]Autonomous University of Barcelona, Spain, [5]University of Oxford, United Kingdom

Purpose: Although reports from different countries suggest very low persistence with oral bisphosphonates, there is a scarcity of data regarding other anti-osteoporosis (OP) medications. Our aim is to compare persistence to all available outpatient oral anti-OP drugs up to five years after therapy initiation.

Methods: We conducted a population-based retrospective cohort study using data from primary care computerized records in SIDIAP (www.sidiap.org). SIDIAP includes clinical information (diagnoses, referrals, etc) recorded by GPs together with pharmacy invoice data. We included all SIDIAP participants starting an anti-OP drug at anytime between 1/1/2007 and 30/06/2011. Users of any of these drugs in the previous 2 years were excluded. We analysed persistence, rate of discontinuation and switching to alternative therapies at up to 5 years follow-up. Fine and Gray survival modelling was used to estimate risk of therapy discontinuation (sub-hazard ratios = SHR) for each drug compared to weekly alendronate, after adjustment for the following confounders: age at therapy initiation, gender, fracture history, Charlson co-morbidity Index, use of oral glucocorticoids, use of aromatase inhibitors, smoking, alcohol drinking, and body mass index.

Results: We identified 124,827patients who started any anti-osteoporotic drug in the study period. The most commonly prescribed drug was weekly alendronate (N=55,399). Persistence at five years ranged from 26.7% (monthly risedronate) to 9.3% (strontium ranelate). Only monthly risendronate had better persistence than weekly alendronate at 5 years: adjusted SHR 0.80 [95%CI 0.86-0.92]. Conversely, daily drugs were the ones with worst persistence: adjusted SHR 1.45 95%CI 1.42-1.47), 1.46 [95%CI 1.42-1.48], and 1.73 [95% CI 1.57-1.87] for strontium ranelate, daily raloxifene, and daily risedronate respectively. [Table 1]

Conclusions: Persistence at five years with available therapies for Osteoporosis is very low, ranging from 9% to 27%. There are significant differences in persistence at 5 years of treatment: whilst only monthly risedronate has 20% lower discontinuation rates, all daily drugs have 45% to 70% lower persistence than weekly ALN.

TABLE. MULTIVARIABLE ADJUSTED SUB HAZARD RATIOS (SHR) FOR THERAPY DISCONTINUATION ACCORDING TO DRUG USED

Therapy	Number of drug users	N (%) Discontinued	Adjusted SHR (95%CI)
weekly alendronate	53,317	36,460 (68.2%)	REF
weekly risedronate	25,312	17,646 (69.5%)	1.16 (1.15-1.16)
monthly ibandronate	13,270	9,596 (64.79%)	1.03 (1.00-1.05)
monthly risedronate	5,100	2,564 (50.27%)	0.80 (0.77-0.82)
daily alendronate	497	359 (61.97%)	1.33 (1.20-1.47)
daily risedronate	430	307 (71.40%)	1.73 (1.53-1.97)
raloxifene	10,377	8,057 (77.66%)	1.46 (1.42-1.49)
ibandronate	551	328 (59.53%)	1.15 (1.04-1.26)
strontium ranelate	14,173	10,501 (74.09%)	1.45 (1.43-1.47)

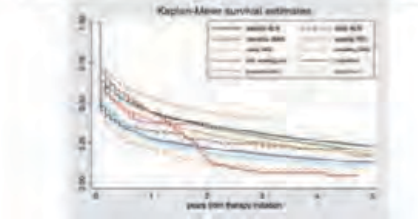

table, figure

***Disclosures: Cristina Carbonell**, None.*

MO0395

Predictors of Medication Use in Australian Men and Women Following a Low Trauma Fracture. Kerrie Sanders*[1], Julie Abimanyi-Ochom[2], Jennifer Watts[3], Catherine Shore-Lorenti[4], Geoffrey Nicholson[5], Amanda Stuart[6], Yu Zhang[7], Ego Seeman[8], Sandra Iuliano-Burns[8], Richard Prince[9], Lynn March[10], Marita Cross[10], Tania Winzenberg[11], LL Laslett[12], Gustavo Duque[13], Peter Ebeling[14], Fredrik Borgstrom[15]. [1]NorthWest Academic Centre, The University of Melbourne, Western Health, Australia, [2]Deakin University, Australia, [3]Health Economics, Deakin University, Australia, [4]The University of Melbourne, Department of Medicine, NorthWest Academic Centre, Australia, [5]The University of Queensland, Australia, [6]Deakin University, Barwon Health, Australia, [7]Department of Medicine, The University of Melbourne, Australia, [8]Austin Health, University of Melbourne, Australia, [9]Sir Charles Gairdner Hospital, Australia, [10]Royal North Shore Hospital, University of Sydney, Australia, [11]Menzies Research Institute Tasmania, Australia, [12]Menzies Research Institute Tasmania, Musculoskeletal Unit, Australia, [13]Ageing Bone Research Program, University of Sydney, Australia, [14]The University of Melbourne, Australia, [15]Karolinska Institutet, Medical Management Centre, Sweden

Access to appropriate medication following a low trauma fracture (LT Fx) is critical to preventing further LT Fx in adults but treatment rates are frequently low. We aim to identify predictors of commencing bone-related medication (bone-meds) including calcium and vitamin D supplements (CaD) following a LT Fx in adults aged 50+ years.

The AusICUROS study is part of an international cost and outcomes study. Medication use was collected 4-months post-Fx in 796 participants treated at 8 Australian teaching hospitals. Bone-meds commenced as a consequence of the Fx were recorded from patient and hospital data. Other medical and demographic data were also collected. Binary logistic regression was used to identify predictors of commencing bone-meds.

Outcomes were any bone-meds including CaD (Y/N) with a sub-analysis of bisphosphonates (Y/N). Predictors tested were age, Fx type (hip, wrist, vertebral, other), income (low, medium, high), education (4 levels), Fx in last 5 years (Y/N) and gender.

Participant profile was: 69 years (IQR: 59 to 78 years) 76% female; 18% had a previous Fx in last 5 years and few were on bone meds. Fx type at study entry were: hip 21% (171); wrist 36% (288); vertebral 10% (80); other 32% (257). Only 35% (n=275/796) commenced any bone-meds; 27% (215) commenced CaD; 9% (74) bisphosphonates; 5% (38) strontium. Odds ratios (OR) for the final model predictors were: female 2.1 [95% CI: 1.4, 3.1] and Fx type hip 1.7 [CI: 1.1, 2.5]; wrist 0.6 [CI: 0.4, 0.9]; vertebral 2.1 [CI: 1.3, 3.6]. Final predictors for bisphosphonates were: age 1.04 [CI: 1.01, 1.06] and Fx type: hip 2.2 [CI: 1.1, 4.5], vertebral 4.3 [CI: 2.0, 9.3].

Our findings demonstrate that medical treatment post LT Fx remains suboptimal. Only a third of LT Fx patients were commenced on any bone-meds and less than half of these commenced specific anti-osteoporosis medications with proven efficacy for secondary fracture prevention. Importantly, we also identified subgroups at higher risk of not receiving appropriate treatment, namely males, and those with wrist Fx, and for bisphosphonates, younger age. Of concern, those with a past Fx were not more likely to commence meds despite being at increased Fx risk. The analysis does not account for those already on bone meds prior to this Fx. These gaps in the management of osteoporosis in a high risk population need to be urgently addressed, including highlighting the need to treat men, those with wrist and multiple Fx and younger people.

***Disclosures: Kerrie Sanders**, MSD; Sanofi-Aventis,*

MO0396

Treatment of Osteoporosis at an Academic Center in a Major Metropolitan Area. Lance Freeman*[1], Phillip Orlander[2], Nahid Rianon[3]. [1]University of Texas Health Science Center at Houston, Medical School, USA, [2]University of Texas Houston Health Science Center, Medical School, USA, [3]UTHealth The University of Texas Medical School at Houston, USA

Endocrinology is considered the main specialty involved in the study and treatment of osteoporosis. However, the chronic nature of this disease combined with an aging population, has created a chasm between the number of Endocrinologist and the number of patients with osteoporosis requiring treatment. This gap has of course been filled by many different types of physicians from non-endocrine backgrounds such as Internist, Family Physicians, Geriatricians, Rheumatologists and Gynecologists to name a few. As a disease entity, osteoporosis and its main complication of fractures have staggering health care implications. Given the multitude of physicians treating osteoporosis, and all that is at stake for patients and the health care system, quality assurance is a necessity as we move forward. Identifying treatment differences among specialties and standardizing proper treatment protocols will prove beneficial for all involved. We investigated differences in patient characteristics and types of treatment for patients being treated by endocrinologist and non-endocrine physicians in an academic institution at the University of Texas Medical School at Houston (UT).

Retrospective chart review identified patients seen in all UT clinics in December 2012 for osteoporosis or related fractures. Data for 35 patients from an ongoing project were analyzed. Patient characteristics and prescribed treatment were described by treating specialty [Endocrinology vs. non-endocrinology].

Mean $\pm$ SD of patients were 66 ± 13 (range 43 to 90) years. Only 9% were male and 63% were treated by Endocrinologists. All Patients managed by Endocrinologists also had concomitant diabetes mellitus ($P<0.01$), 90% had hypothyroidism ($p<0.01$) and 83% had a history fracture ($p=0.24$) as compared with those managed by other services. Despite no significant differences, about 60% and 30% of patients treated by all physicians were not taking calcium or vitamin D supplements, respectively. There were no differences in types of medications and osteoporosis status by T-score between patients being treated by endocrinologists and other physicians.

Physicians are not consistently treating at risk patients with calcium and vitamin D supplementation which are recommended by the Institute of Medicine as essential for optimum bone health. The data also indicates that the majority of patients with a previous fracture, diabetes and hypothyroidism are in fact being funneled to Endocrinologist for more specialized care.

***Disclosures: Lance Freeman**, None.*

MO0397

Dietary Calcium versus Calcium Supplementation on Vascular and Bone Health in Postmenopausal Women; Preliminary Results of a Pilot Study. Rouba Hadad[1], Hope Weiler[2], Michelle Wall[3], Stella S Daskalopoulou[1], David Goltzman[1], Suzanne Morin*[1]. [1]McGill University, Canada, [2]McGill University, USA, [3]McGill University Health Center Research Institute, Canada

Background: There are reports thatcalcium supplementation, with or without vitamin D, is associated with increased rates of cardiovascular events. However, whether calcium intake from supplements has similar effect to that from dietary sources on vascular and bone health markers is unknown.

Objectives: A 12-month randomized trial was piloted to estimate the effect of dietary calcium intake versus supplemental calcium on vascular and bone health in postmenopausal women. Feasibility of the study was assessed by examining the ability of the participants to adhere to the study interventions. The objectives were to examine 1) associations between baseline anthropometry, vascular markers and dietary calcium and vitamin D intakes and 2) whether a short nutrition education session followed by monthly telephone contacts successfully modified dietary intakes between groups and compared to baseline.

Methods: Healthy post-menopausal women, not on calcium or vitamin D supplement, were randomized to dietary (DI) intake of 1200 mg Ca + 400 IU supplemental vitamin D or a supplemental (S) intake 750 mg supplemental $CaCO_3$ (and of 450 mg dietary Ca) + 800 IU supplemental vitamin D. Correlations were conducted to determine associations between dietary intakes, anthropometry and vascular markers (arterial stiffness and carotid intima-media thickness measured via ultrasound) at baseline. Using repeated measures ANOVA, between- groups differences in dietary calcium, vitamin D intakes were measured at baseline and up to 5 months.

Results: Thus far, we have recruited12 participants (63 SD 2 years, BMI 24.7 SD 0.9 kg/m^2; WC 81.8 SD 2.3 cm; body fat 31.5 SD 1.4 %, systolic BP 112 SD 4 mmHg; diastolic BP 74 SD 3 mmHg). Using food frequency questionnaire we estimated baseline energy 2379 ± 178 kcal and calcium 1134 ± 70 mg; vitamin D 553 ± 90 IU intakes. There were no between group differences. No associations were found between calcium and vitamin D intake and baseline vascular measures. At every month post-randomization, higher dietary calcium and vitamin D intake was observed in the DI group compared with the S group (Figure 1). Compliance with calcium and vitamin D supplements at 5 months was found to be 85% overall.

Conclusion: A brief education session and monthly contacts were effective in changing dietary calcium intake and ensuring compliance with the study interventions, supporting the feasibility of this trial.

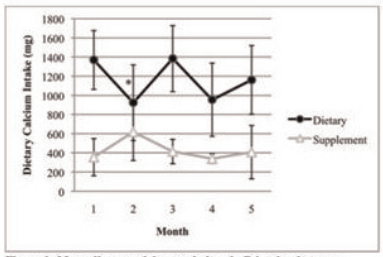

Figure 1: Mean dietary calcium and vitamin D intakes between intervention groups (24 hr recall)
All between group comparisons: p<0.05 except for * where p=0.26

Figure 1 Mean dietary calcium and vitamin D intakes between intervention groups (24 hr recall)

***Disclosures: Suzanne Morin**, None.*

MO0398

Uptake of Evidence-based Osteoporosis Practices in Canadian Long-term Care (LTC). Courtney Kennedy*[1], George Ioannidis[1], Lehana Thabane[1], Denis O'Donnell[2], Lora Giangregorio[3], Jonathan Adachi[4], Alexandra Papaioannou[5]. [1]McMaster University, Canada, [2]Medical Pharmacies Limited, Canada, [3]University of Waterloo, Canada, [4]St. Joseph's Hospital, Canada, [5]Hamilton Health Sciences, Canada

Background: Knowledge translation of best practices in long-term care (LTC; i.e. nursing homes) presents unique challenges. These include applying practice guidelines not developed for the frail elderly and physicians who are frequently off-site and rely on the multidisciplinary healthcare team to monitor residents. In 2007, the Ontario Osteoporosis Strategy for Long-term Care initiated a program of outreach activities across the province (approximately 630 LTC homes) to increase uptake of evidence-based osteoporosis and fracture prevention strategies (www.osteoporosislongtermcare.ca). At that time, an environmental scan revealed a wide spectrum of prescribing practices between LTC homes likely reflecting the lack of standardized guidelines. The objective of the present study was to describe osteoporosis prescribing practices across Ontario LTC homes in 2012. Methods: Individual-level, de-identified medication/demographic data were downloaded from Medical Pharmacies, a pharmacy provider for approximately one-third of Ontario LTC homes. After excluding 40 LTC homes participating in the Vitamin D and Osteoporosis (ViD*OS*) trial, we analyzed data for 166 unselected LTC homes. For each LTC home, we calculated the proportion of residents receiving 1) Vitamin D (⩾800 IU/day), 2) calcium supplements (⩾500 mg/day), and 3) osteoporosis medication. Mean [95% confidence interval (CI)] LTC home prescribing rates and ranges are reported. Results: The analysis cohort was 21,699 residents, mean age 83.5 (SD: 10.7) years, 70% women. Fifty-seven percent of LTC homes were for-profit, 45% affiliated with a corporate chain, 61% had ⩾100 residents. Overall, there were 967 physician prescribers. Mean LTC home prescribing rates were 59.9% (95% CI: 57.2, 62.6) for vitamin D, 32.2% (95% CI: 30.2, 34.2) for calcium, and 18.5% (95% CI: 17.4, 19.7) for osteoporosis medications. Home-level prescribing rates were normally distributed and ranged from 22.3-94.9% for vitamin D, 1.6-78.4% for calcium, and 0-55.9% for osteoporosis medications (Figure 1). Discussion: Although there was a range in prescribing between LTC homes, our results indicate that wide-scale implementation of outreach activities resulted in uptake by many LTC homes, particularly for Vitamin D, with half the homes prescribing at approximately 60% or better. Currently, osteoporosis consensus guidelines for LTC are being developed and will be the focus of future knowledge translation activities.

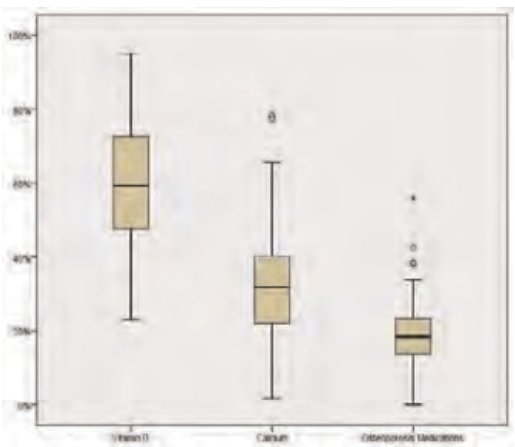

Figure 1: Box plot of the distribution of mean prescribing rates in 166 LTC homes

***Disclosures: Courtney Kennedy**, None.*

MO0399

Significant Reduction of Osteoporosis Fracture-related Hospitalization Rate Due to an Intensified, Multimodal Treatment - Results from the Integrated Health Care Network Osteoporosis North Rhine / Germany. Christopher Niedhart*[1], Anne Preising[2], Christoph Eichhorn[3]. [1]Germany, [2]AOK Northrhine, Germany, [3]Practice, Germany

Introduction: Osteoporosis is known as undertreated in Germany. Aim of the integrated health care model osteoporosis" was the improvement of patient care by multimodal treatment within an integrated health care network. This paper shows the results of the accompanying evaluation.

Methods: A retrospective cross-sectional analysis was performed using routine data from the AOK Rheinland/Hamburg fort the years 2007-2010. Patients were included, if they were 50-89 years old and had a diagnosis of osteoporosis (ICD 10 M80 or M81) and at least two presciptions of osteoporosis-specific medication/year. Data were analysed separately for integrated health care and regular health care.

Results: 22.040 patients were detected, thereof 3.173 patients in the integrated health care group (IV). The hospitalization rate for hip fractures was significantly lower in the IV group: 5.93/1.000 patient years versus 22.96/1.000 patient years (-74 %, $p<0.05$). Also the hospitalization rate of all other osteoporosis-related fractures was 73 % reduced: 46.92/1.000 patient years versus 172.88/1.000 patient years ($p<0.05$). Osteoporosis-related medication costs were doubled in the IV group, while total medication costs were lower in the IV group (1438 € vs. 1702 €).

Discussion: This observational, cross-sectional study shows, that an intensified, multimodal treatment of osteoporosis within an integrated health care network of highly qualified physicians can reduce the hospitalisation rate due to osteoporosis-associated fractures and simultaneously reduces direct costs even in the short run.

***Disclosures: Christopher Niedhart**, None.*

MO0400

Nasal Salmon Calcitonin prevents bone microstructure alterations in early postmenopausal women. Rene Rizzoli*[1], Anne Sigaud[2], Moise Azria[3], Francois Herrmann[2]. [1]Geneva University Hospitals & Faculty of Medicine, Switzerland, [2]Geneva University Hospitals, Switzerland, [3]Novartis Pharma AG, Switzerland

Calcitonin decreases bone resorption, by reducing osteoclast activity. At a dose of 200 IU/day, nasal salmon calcitonin (NSC) has been shown to lower vertebral fracture risk by 33%, with an only 1.5% increase in spine BMD. This suggests that, in addition to BMD, NSC may also influence microstructure, as another determinant of bone strength. In a randomized, double-blind, placebo-controlled, two-year duration trial (ClinTrial. Gov : NCT00372099), we investigated the effects of 200 IU/day NSC on bone microstructure, areal BMD and bone turnover markers in early postmenopausal women. All received 880 IU vitamin D and 1000 mg calcium daily. Distal radius and tibia bone microstructure variables were quantified by HR-pQCT (XtremeCT, Scanco Medical). Mean age was 57.6 ± 0.8 (± SEM) and 57.4 ± 0.7 in the NSC group (n=45) and placebo controls (n=45), respectively. Femoral neck T-Score was -1.23 ± 0.07 and -1.01 ± 0.10, with 4% prevalent vertebral fracture in each group. More than 67% of the subjects had 25-hydroxyvitamin D levels above 50 nmol/l. By 1 year, 91 and 89% of subjects were still in the trial, and 73 and 87% by 2 years, in the NSC and placebo groups, respectively. By 6 and 12 months, serum CTX decreased by -17.3 ± 6.2% and -19.1 ± 6.6% (both $p<0.05$, vs baseline) on NSC, respectively, vs +3.6 ± 4.6 and -6.0 ± 3.7% in the controls (NS vs baseline). By 2 years, distal radius total density changes vs baseline were -2.1 ± 0.6 in NSC group and -4.4 ± 0.7% in controls (between group: $p<0.05$). The 2-year distal radius and tibia cortical thickness decrease of -3.7 ± 1.0 and -2.4 ± 0.5% in the controls ($p<0.05$ vs baseline for both), did not occur in the NSC group (NS). At distal tibia, BV/TV decreased by -1.7 ± 0.6% in the placebo ($p<0.05$ vs baseline), but not in NSC group (-1.1 ± 0.6, NS) by 1 year. Corresponding values were -2.5 ± 0.7 and -1.4 ± 0.6% (both : $p<0.05$ vs baseline, between group: NS) by 2 years. There was no difference in areal BMD changes between NSC and controls. The -0.1% decrease in height in controls, did not occur in the NSC group. Two fractures were recorded in controls and 1 in NSC group. NSC was well tolerated, with a lower incidence of arthralgia (14 vs 26 in placebo, $p<0.05$). One cancer was recorded in each group. Thus, the degradation of bone microstructure in early postmenopausal women, was attenuated or prevented by 200 IU/day nasal salmon calcitonin, together with a lowering of bone resorption, and less arthralgia.

***Disclosures: Rene Rizzoli**, None.*
This study received funding from: Novartis

MO0401

Retrospective study of the nephrotoxicity of Pamidronate in CKD. Wael Taha, Basel Taha*, Ali Achira. Wayne State University, USA

Background: Bisphosphonates are anti-absorptive agents that reduce the rate of bone turnover and are also first line drugs for the treatment of cancer related hypercalcemia, Pagets' disease and osteoporosis. However, their usage is restricted due to the prevailing concern regarding their nephrotoxicity.

Objectives: To study the safety of intravenous Pamidronate in patients with Chronic Kidney Disease (CKD) with estimated Glomerular Filtration Rate (eGFR) ≤ 50

Methods: Our study is a retrospective review of patients, aged 18 to 80 years, with chronic kidney disease with eGFR $\leq$ 50 mL/min/1.73m2 based on the MDRD formula, who were treated in Detroit Medical Center with IV Pamidronate between 2007 to 2012. We excluded patients who were on dialysis before the treatment, who had nephrotoxic treatment and who had insufficient data to analyze. We compared creatinines at up to 12 months before and 1 to 6 months after treatment with IV Pamidronate. The baseline renal function is defined as the best one (up to 12 months) before the admission date. The post treatment creatinine is considered the highest in the period of one to six months of the infusion. We considered a minimum of 10 mL/min/1.73m2 change of eGFR to be significant. We consider acute renal failure if Cr is $\geqslant$ 15% from baseline.

Results: We found 358 patient who were treated with pamidronte. So far we reviewed 123 charts, of which, 9 patients had eGFR of $\leq$ 50 and had enough data for analysis (average eGFR 38.7). None of which had significant decrease in eGFR in the 12 month period before the infusion. The rest were excluded due to eGFR $>$ 50, or not available at baseline. All 9 patients had hypercalcemia.

Five of these nine (the first group, 55.6%) had maintained stable, or had some improvement of creatinine levels. This five patients had average baseline eGFR of 37.4 (range 20-50). Three of them were diagnosed with acute on chronic renal failure at the infusion time.

The second group were four patients (44.4%) had increased creatinine levels, eGFR dropped by range of 10 to 18. The latter group had average eGFR of 40.25 at baseline (range 25-50). Two of this group had acute on chronic renal failure.

Conclusion: Whether IV pamidronate causes deterioration of renal function to patients with advance CKD patients is not clear. Other factors that play a role need to be studied such as the calcium levels and the cause of hypercalcemia (i.e. malignancy)

***Disclosures: Basel Taha**, None.*

MO0402

Strontium Ranelate Effect on Bone Mineral Density is Modified by Previous Bisphosphonate Treatment. Lucas Ricardo Brun[1], Ana María Galich[2], Laura Maffei[3], Valeria Premrou[4], Eduardo Vega*[5], Helena Salerni[6], Marcelo Alfredo Sarli[7], Pablo Costanzo[6], Paula Rey[7], María Silvia Larroude[8], María Susana Moggia[9], María Lorena Brance[10], Ariel Sánchez[11]. [1]Laboratorio de Biología Ósea. Facultad de Ciencias Médicas. Universidad Nacional de Rosario., Argentina, [2]Servicio de Endocrinología del Hospital Italiano de Buenos Aires., Argentina, [3]Consultorios Associados De Endocrinologia, Argentina, [4]Consultorios Asociados de Endocrinología Dra. Laura Maffei., Argentina, [5]CESAN, Buenos Aires. Instituto de la Mujer, Campana, Argentina, [6]Consultorios de Investigación Clínica Endocrinológica y del Metabolismo Óseo (CICEMO)., Argentina, [7]Instituto de Investigaciones Metabólicas, Dr. Zanchetta., Argentina, [8]Hospital César Milstein, Argentina, [9]Centro Tiempo, Argentina, [10]Consultorios de Reumatología, Argentina, [11]Centro de Endocrinología., Argentina

Strontium ranelate (SrR) is an effective treatment for osteoporosis that reduces the incidence of vertebral and non-vertebral fractures. The aim of this study was to evaluate the effect of SrR on bone mineral density (BMD) and bone turnover markers after 1 year of treatment in clinical practice conditions. Additionally, the effect of SrR in bisphosphonate-naïve patients (BP-naïve) compared to patients previously treated with bisphosphonates (BP-prior) was analyzed. This retrospective study analyzed records from 482 postmenopausal women treated with SrR (2 g/day) for 1 year in eleven Argentine centers; 41 patients were excluded due to insufficient data, while 441 were included. All patients received calcium (1000 mg/day) and vitamin D (800 U/day). BMD (g/cm^2) was measured by dual-energy X-ray absorptiometry (DXA) GE Lunar Prodigy. Data are expressed as mean$\pm$SEM, and changes were analyzed with Mann-Whitney test or Wilcoxon signed rank test as appropriate. Results: the whole population main characteristics were: age (years): 67.20$\pm$0.50; body mass index (kg/m^2): 24.55$\pm$0.18; serum calcium (mg/dl): 9.36$\pm$0.02; serum phosphate (mg/dl): 3.97$\pm$0.03; 25(OH)vitamin D (ng/ml): 32.04$\pm$1.0; PTH (pg/ml): 51.00$\pm$3.11; total alkaline phosphatase (tAP, UI/L): 59.70$\pm$1.36; serum osteocalcin (BGP, ng/ml): 17.02$\pm$0.98; serum C-telopeptide (s-CTX, ng/l): 331.10$\pm$16.03. After 1 year of treatment with SrR, tAP (65.76$\pm$1.57) and BGP (22.93$\pm$1.46) as bone formation markers, were increased ($p<0.0001$), while s-CTX (305.60$\pm$16.31) as bone resorption marker, was decreased (p=0.0579). SrR after 1 year of treatment increased BMD at the lumbar spine (LS), femoral neck (FN) and total hip (TH) ($p<0.0001$). The change in BMD was: LS= 3.73$\pm$0.26%, FN= 2.00$\pm$0.24% and TH= 1.54$\pm$0.24%. These increments were significant ($p<0.0001$) both among BP-naïve (n=86) and BP-prior (n=320) patients; 35 patients were not included in this analysis because the use of other drugs different as BP or insufficient data. Interestingly, the change in BMD after 1 year of SrR treatment was higher in BP-naïve patients: LS: BP-naïve= 4.58$\pm$0.62%; BP-prior = 3.37$\pm$0.30% (p=0.0686). FN: BP-naïve= 2.61$\pm$0.55%; BP-prior= 1.72$\pm$0.28% (p=0.0961). TH: BP-naïve= 2.77$\pm$0.50%; BP-prior= 1.22$\pm$0.26% (p=0.0011). In conclusion, SrR treatment increased BMD and bone formation markers and decreased bone resorption markers in the whole group with better response in patients BP-naïve, suggesting that SrR could be considered as first-line treatment.

***Disclosures: Eduardo Vega**, None.*

MO0403

Responsiveness of the Japanese Osteoporosis Quality of Life Questionnaire to Raloxifene Treatment in Women with Postmenopausal Osteoporosis. Kousei Yoh[1], Etsuro Hamaya*[2], Masanori Taketsuna[3], Hisashi Urushihara[4], Kiyoshi Tanaka[5]. [1]Department of Orthopedic Surgery, Sasayama Medical Center, Hyogo College of Medicine, Japan, [2]Eli Lilly, Japan, [3]Eli Lilly Japan K.K., Japan, [4]Eli Lilly Japan K.K.and Ethics Committee, Graduate School & Faculty of Medicine, Kyoto University, Japan, [5]Kyoto Women's University, Japan

Objective: The Japanese Osteoporosis Quality of Life Questionnaire (JOQOL) is a disease-specific QOL measure of osteoporosis developed by the Japanese Society for Bone and Mineral Research. The psychometric properties of the overall JOQOL total score have been investigated in part (Kumamoto *et al*. 2010). However, responsiveness, an important psychometric property required for a patient-reported outcome measure, of each JOQOL subdomain to treatment has yet to be assessed. Using data from a previously reported QOL study in Japanese women receiving raloxifene treatment for postmenopausal osteoporosis (Yoh *et al*. 2012), we examined responsiveness of each domain of the JOQOL questionnaire to treatment changes related to raloxifene administration.

Method: A total of 506 eligible patients (mean age: 70.7 years) were stratified into those who did or did not achieve a minimal clinically important change (MCIC) in pain, as assessed by Visual Analog Scale for pain reduction ($\geqslant$ 20 mm or $<$ 20 mm). Summary statistics and Standardized Response Mean (SRM) for changes in JOQOL domain scores over 24 weeks were compared. The correlation of changes in JOQOL domains with those of Short Form-8 Health Survey (SF-8) and European Quality of Life Instrument (EQ-5D) were also assessed.

Results: The mean changes of several JOQOL domains (pain, activities of daily living, overall health, falls/psychological factors) and total score in patients who achieved MCIC were significantly larger than those who did not ($p<.001$, Student t-test). Moderate to large (0.5-0.9) SRM values in patients who achieved MCIC were seen for domains with significantly larger changes, indicating adequate responsiveness of these domains to treatment. SRMs were close to 0 (0.1-0.2) for those domains that were not significantly different (recreation/social activity, posture/physique). The SRMs and mean changes of SF-8 subscales and EQ-5D indicated sufficient responsiveness of these reference instruments. Correlation analysis with the reference instruments supported responsiveness of some of the JOQOL domains (r=0.3-0.5).

Conclusion: Some of the JOQOL domains showed adequate responsiveness to treatment changes in postmenopausal women with osteoporosis. Further scrutiny of JOQOL domains may be warranted to ensure adequate validity.

References:

Kumamoto K et al. *J Bone Miner Metab*. 2010;28:1-7.

Yoh K et al. *Curr Med Res Opin*. 2012;28:1757-1766.

***Disclosures: Etsuro Hamaya**, None.*

This study received funding from: Eli Lilly Japan K.K.

MO0404

The National Bone Health Alliance: An Instrumental Force in Improving the Nation's Bone Health Through Partnership. David Lee*. National Bone Health Alliance, USA

The U.S. National Bone Health Alliance (NBHA) is a public-private partnership launched in 2010 that brings together the expertise and resources of its member organizations to collectively promote bone health and prevent disease; improve diagnosis and treatment of bone disease; and enhance bone research, surveillance and evaluation.

NBHA membership currently includes 50 members (35 non-profit organizations and 15 companies) as well as liaisons representing the CDC, FDA, NASA and NIH. ASBMR is among NBHA's founding members.

The operations and major activities of NBHA are funded through financial support from its members, which may include but are not limited to corporations, academic and medical institutions, professional and membership organizations, associations, advocacy groups and non-profit and philanthropic organizations.

NBHA is implementing three major initiatives in 2013:

1. Fracture Prevention CENTRAL Resource Center

NBHA is advocating for the widespread implementation of a fracture liaison service (FLS) model of care in which a FLS coordinator ensures that individuals who suffer a fracture receive appropriate diagnosis, treatment and support. NBHA launched Fracture Prevention CENTRAL (www.FracturePreventionCENTRAL.org) in March 2013, a resource center for institutions interested in implementing a FLS.

2. 2Million2Many Awareness Campaign

In April 2012, NBHA launched the 2Million2Many campaign. Its centerpiece Cast Mountain is a thought-provoking 12-foot tall by 12-foot wide installation representing the 5,500 bone breaks that every day in the U.S. (totaling 2 million bone breaks annually). Cast Mountain has traveled to several events across the country and the campaign has been featured in online and print stories through national media outreach activities. Learn more at www.2Million2Many.org.

3. Bone Turnover Marker Standardization Project

NBHA is leading the U.S. effort to standardize bone turnover marker assays to improve their use in clinical laboratories to help monitor osteoporosis treatment and assess future fracture risk. The project team published a position paper in Osteoporosis International in 2012 that describes the next steps in the standardization project, which is now underway.

In addition to these projects, NBHA convenes a rare bone working group and provides a platform for its collective voice to weigh in on subjects important to bone health, particularly vitamin D, calcium, and DXA reimbursement and utilization.

***Disclosures: David Lee**, None.*

MO0405

Development of a Novel Prostaglandin EP4 Agonist Which Stimulates Local Bone Formation *in vivo*. Jim O'Malley*[1], Adam Uzieblo[2], Bradlee Germain[2], Andrei Kornilov[2], Joseph Colombo[2], James Kramer[2], Gregory Endres[2], Stephen Barrett[2], Thomas Owen[1]. [1]Myometrics, LLC, USA, [2]Cayman Chemical Company, Inc., USA

Prostaglandin E1 (PGE1) and prostaglandin E2 (PGE2) are produced from arachidonic acid through the actions of cyclooxygenases in many cell types. These molecules interact with four G-protein coupled cell surface receptors (EP1-EP4) with equal affinity, producing a multitude of effects on a wide range of cells and tissues. Both PGE1 and PGE2 have been long known to stimulate bone formation both *in vitro* and *in vivo*. This stimulation was first observed in humans and its mechanism of action has been widely studied in a variety of species including rats, dogs, and humans. It has been well established that it is stimulation of the EP2 and EP4 receptor subtypes which leads to bone formation while stimulation of the EP1 and EP3 subtypes leads to unwanted effects on animals such as induction of pain and diarrhea. EP4 and EP2 receptors agonists have previously been developed for treatment of osteoporosis. However these agents also lead to decreased blood pressure, preventing their use as systemic bone anabolic agents. We have therefore focused on developing an EP4 agonist for stimulating bone formation following local delivery to specific bone sites. Our novel EP4 agonist demonstrates potent and specific binding to the EP4 receptor, stimulation of cAMP formation in cell culture, and stimulation of osteoblastic differentiation as demonstrated by a dose-dependent increase in alkaline phosphatase activity and mineralized colony formation in a rat bone marrow assay system. This agonist was used *in vivo* in several bone repair models including the critical calvarial defect in rats. Following treatment of the rats at the time of surgery, images were obtained at weekly intervals using a cone-beam CT scanner and bones were processed for histological analysis at the end of the studies. In these models, our agent demonstrated repair rates approximately four-fold that of controls and equal to those of BMP-2 delivered in the same matrix.

***Disclosures: Jim O'Malley**, Myometrics, LLC, 8*
This study received funding from: Myometrics LLC, Cayman Chemical

MO0406

Effects of anti-resorptive agents on ovariectomised (OVX) rat cortical bone: Raman spectroscopy and multivariate analyses. Xiaomei Yao*[1], Wei Yao[2], Xinyan Bai[1], Amber Stern[1], Mark Johnson[3], Yong Wang[1], Nancy Lane[2]. [1]University of Missouri-Kansas City, USA, [2]University of California, Davis Medical Center, USA, [3]University of Missouri, Kansas City Dental School, USA

Osteoporosis is a syndrome of extreme skeletal fragility frequently resulting from estrogen deficiency and aging. Patients are often cycled through these different types of bone active medications for a number of years such as anti-resorptive (AR) agents and more recently the anabolic therapeutic, hPTH. The prolonged effects of these agents on bone quality is unknown. In this study, we utilized Raman microspectroscopy and multivariate analysis methods to evaluate the influence of cyclical therapies on cortical bone structural changes based on the organic and mineral molecular composition.

Six-month old female SD rats were either OVX or sham operated. The OVX rats were untreated for two months to develop osteopenia then treated with SQ injections of either vehicle (OVX) 0.1ug/kg,3x/wk; hPTH (1-34)(PTH) 20ug/kg/d,3x/wk; alendronate (Ale) 0.5ug/kg/2x/wk; or Raloxifene (Ral) 5mg/kg, po 3x/wk. We studied four sequential treatment regimens in three 90 day cycles (Veh-Veh-Veh,PTH-Veh-Veh, Ale-Ale-Ale, Ral-Ral-Ral) (n=3). The Raman spectra were recorded from 877 to 1785 cm^{-1} range, allowing acquisition of peaks attributed to the bone mineral and proteins. Two osteocyte lacunae per sample were chosen from the tibial midshaft. For each lacuna, four line mappings with 1 μm steps were acquired from the edge of the lacuna, and 16 spectra were used. The integrated area ratios of the hydroxyapatite peak (960 cm^{-1}) to matrix amide I peak (1630 cm^{-1}) were measured. The datasets of 240 Raman spectra were built in and normalized. Multivariate data analyses using principal component analysis (PCA) and discriminant analysis in combination with MANOVA were performed to distinguish among the groups. Mechanical testing was performed on the cortical bone and whole bone strength was measured.

The mineral/matrix ratios and mechanical testing corresponding to the five groups were not significantly different. However, using the more powerful PCA-discriminant analyses of the cortical bone, the Sham group was different from OVX group (Figure below). Also, based on scatter plots, the Ale and Ral groups were more closely associated with the Sham group, while the PTH and OVX groups were more similar, indicating different treatment effects on the combined parameters.

Mulitvariate analysis of the Raman spectroscopy data detected changes in the chemical compositional of the cortical bone after various treatments with bone active agents.

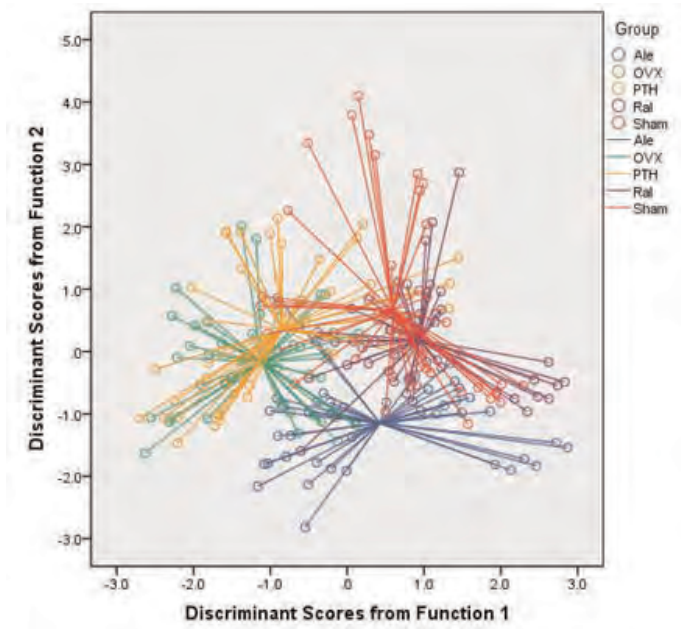

Figure

***Disclosures: Xiaomei Yao**, None.*

MO0407

Endothelial Cell Removal Completely Eliminates Vasodilation of Bone Arteries to PTHrP While Slight Vasodilation Remains in Response to PTH 1-34. Rhonda Prisby*[1], Ashley Bice[2]. [1]University of Delaware, USA, [2]University of Delaware, Department of Kinesiology & Applied Physiology, USA

BACKGROUND: Vasodilation of the femoral principal nutrient artery (PNA) to PTHrP is augmented in comparison to PTH 1-84 and PTH 1-34 (Benson et al., 2012). Moreover, inhibition of NO production with L-NAME reduced vasodilation by 81%, 92% and 54% in response to PTH 1-84, PTH 1-34 and PTHrP, respectively. Recently, we demonstrated that vasodilation to PTH 1-84 peaked at 5% of the maximal diameter in the PNA following endothelial cell removal (Benson & Prisby 2013). These data indicate that vasodilation to PTH 1-84 is completely reliant upon the vascular endothelium. Thus, we sought to determine whether vasodilation of the PNA to PTHrP and PTH 1-34 is also exclusively reliant upon vascular endothelial cells. *METHODS:* Right femoral PNAs were isolated from male Wistar rats (4-5 months, 558 $\pm$ 33g; n=6), cannulated on glass micropipettes and denuded (i.e., removed of the endothelial cells). PNAs were considered adequately denuded if they dilated $\leq$ 5% to a bolus does of acetylcholine ($5x10^{-5}$ M). Vasodilation to PTHrP (10^{-13} – 10^{-8} M) and PTH 1-34 (10^{-13} – 10^{-8} M) was assessed in the presence of 1) PSS buffer, 2) PSS buffer with L-NAME, and 3) PSS buffer with L-NAME + indomethacin (Indo; a cyclooxygenase inhibitor). To ensure that the smooth muscle cells were not damaged during endothelial cell removal, endothelium-independent vasodilation to sodium nitroprusside (SNP; 10^{-10} – 10^{-4}) was determined. *RESULTS:* Vasodilation to cumulative doses of PTHrP and PTH 1-34 peaked at 2% and 16%, respectively, of maximal diameter. Inhibition of NO and prostacyclin production with L-NAME and L-NAME + Indo, respectively, did not alter vasodilation in response to PTHrP or PTH 1-34 alone. Vasodilation to SNP of denuded PNAs rose to 57% of maximal diameter and did not differ from vasodilation of intact PNAs, indicating that smooth muscle cell responsiveness was not altered with endothelial denudation. *CONCLUSION:* Vasodilation of the bone resistance vasculature in response to PTHrP occurs via endothelium-dependent, rather than endothelium-independent signaling pathways. Further, even though vasodilation was dramatically impaired in response to PTH 1-34, some dilatory capacity remained following endothelial cell removal. In totality, data suggest that vasodilation of the bone resistance vasculature to the endogenously produced peptide and hormone (i.e., PTHrP and PTH 1-84) relies exclusively on vascular endothelial cells.

***Disclosures: Rhonda Prisby**, None.*

MO0408

Fixation Stiffness Modulates the Efficacy of Sclerostin-Neutralizing Antibody Treatment during Bone Healing. Bettina Kruck*, Georg Duda, Sophie Damerow, Florian Wichlas, Serafim Tsitsilonis, Bettina Willie. Charité – Universitätsmedizin Berlin, Germany

Bone healing is influenced by mechanical strain. Inhibition of SOST/sclerostin may be partially responsible for the anabolic action of mechanical loading. The protein sclerostin is thought to reduce bone formation by inhibiting Wnt signaling and decreasing osteoblast function. We examined the efficacy of sclerostin neutralizing antibody (Scl-Ab) to enhance bone healing and the influence of interfragmentary movement on the healing response to Scl-Ab.

A 0.5mm femoral osteotomy was performed on 26wk old female C57BL/6J mice, stabilized with a rigid or semi-rigid external fixator, allowing different magnitudes of interfragmentary movement at the osteotomy during weight bearing. Scl-Ab VI or vehicle was administered (25 mg/kg), twice per week by subcutaneous injection, starting one day post-op. Bone healing was assessed by in vivo microCT (n=10-12 mice) after 3, 7, 14, and 21d for mineralized callus volume (BV), total callus volume (TV), mineralized callus volume fraction (BV/TV), callus tissue mineral density (TMD), and bone/calcified cartilage mineral density (BMD). After 21 days, osteotomized and contralateral femurs (n=6-8 mice) underwent torsion testing to determine ultimate torque, stiffness, and energy to failure. At 7, 14, 21d osteotomized femurs (n=7-12 mice/time point) were decalcified, paraffin embedded and analyzed for bony bridging and callus tissue area (bone, cartilage, fibrous tissue formation, bone marrow). Effects of treatment, fixation stiffness and interactions were assessed by ANOVA.

Scl-Ab significantly enhanced BV, BV/TV, TMD, (14, 21d), and bone area (21d) compared to vehicle treated groups with both rigid and semi-rigid fixation (Table 1, 2). Rigid fixation enhanced BV/TV, BMD, TMD, bone area (14, 21d), BV (14d), bone marrow area (7, 14, 21d), and decreased cartilage and fibrous tissue area (7, 14, 21d). Neither fixator stiffness, nor Scl-Ab influenced mechanical properties of osteotomized femurs at 21d, although intact femurs treated with Scl-Ab had significantly greater mechanical properties. The rigidly fixed Scl-Ab group had the greatest number of bridged cortices (63% vs. 43%) at day 14, although the rigidly fixed vehicle group was similar at 21d (46% vs.44%, Table 2). In summary, fixation stiffness modulated the healing response to Scl-Ab. Scl-Ab under more rigid fixation appeared to accelerate healing (14d). By 21 days, rigidly fixed vehicle and Scl-Ab groups had similar healing, although the Scl-Ab group exhibited more bone.

Parameter/Time point	Rigid-SclAb	Rigid-Vehicle	SemiRigid-SclAb	SemiRigid-Vehicle
BV/TV (mm³/mm³)				
3d	0.125 ± 0.029	0.117 ± 0.031	0.104 ± 0.024	0.125 ± 0.034
7d	0.172 ± 0.097	0.136 ± 0.030	0.142 ± 0.021	0.126 ± 0.020
14d*†	0.386 ± 0.117	0.294 ± 0.112	0.257 ± 0.089	0.194 ± 0.044
21d*†	0.528 ± 0.200	0.336 ± 0.120	0.343 ± 0.080	0.226 ± 0.084
BV (mm³)				
3d†	0.166 ± 0.062	0.147 ± 0.038	0.108 ± 0.025	0.135 ± 0.063
7d	0.248 ± 0.203	0.174 ± 0.037	0.168 ± 0.045	0.135 ± 0.047
14d*†	0.718 ± 0.372	0.525 ± 0.275	0.384 ± 0.075	0.202 ± 0.064
21d*	1.115 ± 0.715	0.584 ± 0.321	0.841 ± 0.522	0.549 ± 0.279
TV (mm³)				
3d†	1.292 ± 0.208	1.273 ± 0.211	1.086 ± 0.302	1.041 ± 0.275
7d†	1.344 ± 0.269	1.294 ± 0.174	1.175 ± 0.254	1.059 ± 0.269
14d†	1.740 ± 0.470	1.702 ± 0.395	1.666 ± 0.758	1.035 ± 0.257
21d	1.897 ± 0.730	1.622 ± 0.452	2.419 ± 1.224	2.396 ± 1.036
TMD (mg HA/cm³)				
3d	353 ± 37	349 ± 35	333 ± 28	354 ± 45
7d	358 ± 41	355 ± 41	371 ± 17	354 ± 35
14d*†	540 ± 83	473 ± 81	457 ± 67	414 ± 29
21d*†	643 ± 157	496 ± 90	511 ± 55	431 ± 65
BMD (mg HA/cm³)				
3d	942 ± 82	915 ± 24	926 ± 46	907 ± 40
7d	910 ± 28	913 ± 22	918 ± 27	932 ± 69
14d†	948 ± 38	941 ± 31	910 ± 24	917 ± 34
21d†	1004 ± 42	1000 ± 28	940 ± 14	924 ± 23

Table 1: Mean ± SD of MicroCT data, *treatment; †fixation stiffness; #interactions effects

Time point/Parameter	Rigid-SclAb	Rigid-Vehicle	SemiRigid-SclAb	SemiRigid-Vehicle
7d	n=7	n=7	n=10	n=9
Total callus area (mm²)*†	1.647 ± 0.160	1.388 ± 0.265	1.893 ± 0.307	1.571 ± 0.289
Bone area (mm²)	0.053 ± 0.034	0.041 ± 0.037	0.063 ± 0.040	0.051 ± 0.075
Cartilage area (mm²)*†#	0.001 ± 0.004	0 ± 0	0.054 ± 0.042	0.006 ± 0.007
Fibrous connective tissue area(mm²)*†	1.457 ± 0.159	1.183 ± 0.227	1.760 ± 0.290	1.508 ± 0.323
Bone marrow area (mm²)†	0.136 ± 0.099	0.159 ± 0.107	0.016 ± 0.032	0.007 ± 0.011
Total % bridging (peri+intracortical)	0%	0%	0%	0%
14d	n=8	n=7	n=10	n=12
Total callus area (mm²)†	1.643 ± 0.123	1.488 ± 0.172	2.061 ± 0.316	2.086 ± 0.519
Bone area (mm²)†#	0.430 ± 0.118	0.271 ± 0.150	0.144 ± 0.083	0.208 ± 0.121
Cartilage area (mm²)†	0.076 ± 0.109	0.054 ± 0.053	0.356 ± 0.372	0.282 ± 0.318
Fibrous connective tissue area(mm²)†	0.825 ± 0.182	0.850 ± 0.291	1.535 ± 0.269	1.592 ± 0.295
Bone marrow area (mm²)†	0.311 ± 0.243	0.307 ± 0.159	0.005 ± 0.013	0.004 ± 0.007
Total % bridging (peri+intracortical)	63%	43%	3%	8%
21d	n=7	n=8	n=7	n=7
Total callus area (mm²)†	1.656 ± 0.299	1.553 ± 0.188	1.866 ± 0.149	1.877 ± 0.135
Bone area (mm²)*†	0.486 ± 0.217	0.245 ± 0.133	0.277 ± 0.120	0.217 ± 0.114
Cartilage area (mm²)†	0.003 ± 0.008	0.010 ± 0.024	0.051 ± 0.086	0.214 ± 0.270
Fibrous connective tissue area(mm²)†	0.826 ± 0.294	0.938 ± 0.394	1.514 ± 0.182	0.1.394 ± 0.237
Bone marrow area (mm²)†	0.341 ± 0.180	0.365 ± 0.304	0.023 ± 0.022	0.051 ± 0.060
Total % bridging (peri+intracortical)	46%	44%	4%	14%

Note: total percent of mice within each group with bony bridging was calculated as [medial periosteal + lateral periosteal + medial intracortical + lateral intracortical bridging/(number of mice in the group * 4 cortices)]*100.

Table 2: Mean ± SD of histomorphometry data, *treatment; †fixation stiffness; #interaction effects.

***Disclosures: Bettina Kruck**, None.*

MO0409

LLP2A-Ale Directs Mesenchymal Stem Cells to Bone to Reverse Bone Loss in Ovariectomized Rats. Wei Yao*[1], Li Jiang[2], Evan Yu-An Lay[2], Weiwei Dai[3], Sarah Amugongo[4], Nancy Lane[1]. [1]University of California, Davis Medical Center, USA, [2]UC Davis Medical Center, USA, [3]Shriner's Hospital for Children, USA, [4]University of California, Davis, USA

Aging is associated with a reduction in the number of mesenchymal stem cells (MSCs) and with a decrease in their osteogenic potential that may be responsible for reduced bone formation. However, systemic MSCs tranplantation had limited sucess for bone regeneration as they fail to home to the bone surface. Our research group has developed a compound, LLP2A-Ale that has high affinity for both the activated α4β1 integrin on the MSC surface and hydroxyapatite, and alendronate (Aln) that directs the MSCs to the bone surface. We have previously reported that LLP2A-Ale directed transplanted MSCs to bone and increases the retention of the transplanted MSCs in bone in multiple in vivo mouse models that included estrogen deficiency and aging. The purpose of these studies were to evaluate the effects of LLP2A-Ale in the combination of MSC transplantation in an osteopenic rat model.

Four-month-old ovariectomized (OVX) rats were allowed to develop bone loss for two months and then treated with PBS, LLP2A-Ale (200μg/kg, IV/month), MSC (3x105, GFP and luciferase transduced, IV at day 0), hPTH (1-34) (25 μg/kg, 5x/wk x 4 wks), LLP2A-Ale + MSC or one IV LLP2A-Ale + MSC followed by PTH (1-34) from day7 (25 μg/kg, 5x/wk x 3 wks). The dose of LLP2A-Ale was chosen from a prior dose-finding study ranging from 50-300 μg/kg in 6-month-old OVX rats. After 4 weeks of treatment, BV/TV loss at the proximal tibiae was 40% ($p<0.01$ from baseline) in the OVX and OVX+MSC groups. Treatment with LLP2A-Ale, LLP2A-Ale + MSC or PTH increased the PTM BV/TV by 35, 53, and 70%, compared to the OVX-PBS; and BV/TV was increased by nearly 200% with LLP2A-Ale + MSC followed by PTH treatment compared to OVX + PBS ($p<0.01$). PTH, LLP2A-Ale +MSC or LLP2A-Ale + MSC followed by PTH treatment also increase tibial cortical bone thickness by 2%, 2% and 8%, respectively, as compared to OVX group that was primary the results of the periosteal expansion.

In summary, LLP2A-Ale by itself prevented and partially restored trabecular bone loss in an acute estrogen deficiency model. Treatment with one IV LLP2A-Ale + MSC transplantation and daily PTH injections for four weeks had similar gains in bone volume. Greater gains in bone bone volume was obtained with one treatment of IV LLP2A-Ale + MSC transplantation was followed by three weeks of daintly PTH injections. Additional studies that quantitate the efficacy of MSC homing and their contributions to bone formation and strength are currently in progress.

***Disclosures: Wei Yao**, None.*

MO0410

Nmp4/CIZ-knockout Mice Are Hyperresponsive to Anabolic Agonists But Susceptible to Ovariectomy-induced Bone Loss. Paul Childress, Marta Alvarez, Joseph Bidwell*. Indiana University School of Medicine, USA

Disabling Nmp4/CIZ ('Nmp4') in mice enhances the skeletal response to anabolic agonists; these mice are also resistant to unloading-induced bone loss. The untreated *Nmp4*-null phenotype includes a modest but significant increase in cancellous and cortical bone as well as expanded populations of bone marrow CD146+/nestin+ mesenchymal stem cells and CFU-F(alk phos+) cells. Null mice exhibit a small increase in CFU-GM cells, precursors to osteoclasts, and an augmented number of marrow-derived osteoclasts. The purpose of this study was to determine the susceptibility of *Nmp4*-KO mice to ovariectomy (ovx)-induced bone loss. Virgin female *Nmp4*-KO mice and their wild-type (WT) littermates were sorted into four treatment groups by body weight at 12wks of age (8-12 mice/group) and ovx or sham-operated. Additional mice (8-10/genotype) were used for baseline analysis. At 4wks post-op mice were euthanized and femurs prepared for micro-computed tomography analysis including bone volume/total volume (BV/TV), connectivity density (Conn D), structure model index (SMI), trabecular number (Tb N), thickness (Tb Th), and spacing (Tb Sp). For statistical analysis a 2-way ANOVA was employed using genotype and treatment as the independent variables followed by a Tukey HSD if a genotype x treatment interaction was indicated. Statistical significance was set at $p \leq 0.05$. Both the ovx WT and *Nmp4*-KO mice gained body weight compared to the sham-operated animals. There was a strong treatment effect as both genotypes exhibited significant ovx-induced bone loss as indicated by changes in BV/TV, Conn D, SMI, Tb N, and Tb Sp. A strong genotype effect was observed for all parameters since the null mice had significantly more cancellous bone throughout the study. The parameter Conn D showed a genotype x treatment interaction (Prob >ItI 0.005) since the decrease in this parameter was greater in the null mice. Similarly, the genotype x treatment interaction term approached significance for BV/TV (Prob > ItI 0.06). We conclude that disabling Nmp4 does not protect mice from ovx-induced bone loss as it does for disuse-associated osteopenia. The *Nmp4*-null mice show a very modest heightened sensitivity to ovx for some parameters. This phenomenon may derive from the small surplus of null osteoclast precursors. These results raise the question as to whether ovx *Nmp4*-KO mice exhibit an enhanced response to therapeutic PTH like the intact null mice.

***Disclosures: Joseph Bidwell**, None.*

MO0411

Sclerostin Antibody Prevented Severe Bone Loss in Ovariectomized Rats with Concurrent Mechanical Unloading. Dongye Zhang*[1], Minyi Hu[1], Liangjun Lin[2], Xiaodong Li[3], Hua Zhu (David) Ke[3], Yi-Xian Qin[2]. [1]Stony Brook University, USA, [3]State University of New York at Stony Brook, USA, [3]Amgen, Inc., USA

Osteoporosis most often occurs with aging populations that have significantly reduced physical activities and diminished load to their skeletons. Sclerostin antibody (Scl-Ab) increases bone formation and bone mass, and decreases bone resorption in animal models of bone loss due to either estrogen deficiency (ovariectomy; OVX) or immobilization. The objective of this study was to evaluate the effect of Scl-Ab in a bone loss model from both estrogen deficiency and immobilization (OVX rats with concurrent hindlimb suspension (HLS)). Four-month-old female Sprague Dawley rats were divided into 7 groups (n=11 per group) as shown in Figure 1, HLS was introduced 2 weeks after sham and OVX. Scl-Ab (25 mg/kg) or vehicle was injected sc twice weekly for 5 weeks starting at the time of HLS. The metaphyseal trabecular bone of the distal femurs was analyzed with micro-CT (μCT). Four-point bending mechanical testing was performed at the midshaft of the femur. HLS or OVX alone resulted in significant loss of trabecular bone volume (BV/TV, -29% and -71%, respectively) compared to sham control (Fig. 1a), whereas the OVX+HLS resulted in the greater bone loss at 87%. Scl-Ab fully preserved BV/TV in rats with HLS or OVX (Fig. 1a, 2), and partially prevented trabecular bone loss in rats with combination of OVX plus HLS (Fig.1a, 2). Tb.Th was increased to similar extent in HLS, OVX and OVX plus HLS rats treated with Scl-Ab. HLS or OVX+HLS was associated with significantly lower stiffness as compared with Sham controls (Fig. 1c). Scl-Ab prevented the decrease in stiffness due to HLS, OVX or OVX+HLS. Ultimate load was not significantly lower in HLS, OVX or OVX plus HLS as compared with Sham controls, but it was significantly greater in Scl-Ab-treated HLS or OVX rats as compared with respective vehicle controls and sham group (Fig. 1d). Scl-Ab-treated HLS plus OVX showed increased ultimate load, but not significant compared with OVX control. In summary, Scl-Ab prevented the loss of trabecular bone mass and cortical bone strength in OVX rats with concurrent immobilization. The data suggested that sclerostin inhibition may represent a therapeutic option for the osteoporosis with concurrent immobilization or decreased skeletal loading.

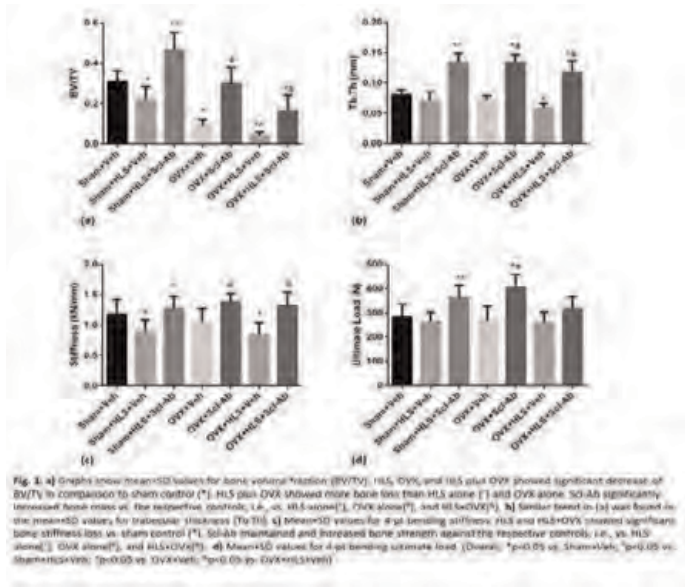

Fig.1

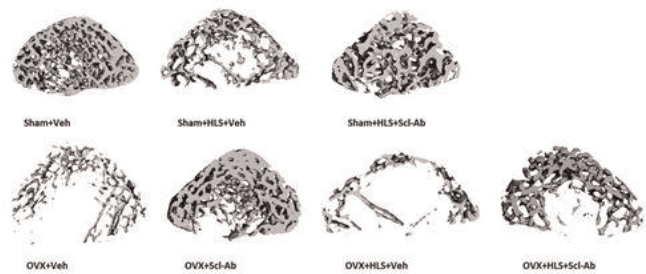

Fig.2. 3-D Micro-CT reconstruction image of trabecular area of distal femur of rats.

Fig.2

***Disclosures: Dongye Zhang**, None.*
This study received funding from: NIH, Amgen

MO0412

Simvastatin Prodrug Promotes Bone Fracture Repair in a Closed Fracture Mouse Model. Yijia Zhang*[1], Zhenshan Jia[1], Hongjiang Yuan[1], Ke Ren[1], Aaron Daluiski[2], Edward Fehringer[1], Steven Goldring[2], Dong Wang[1]. [1]University of Nebraska Medical Center, USA, [2]Hospital for Special Surgery, USA

Purpose. Though known for their bone anabolic effect, statins have not been used clinically for metabolic skeletal diseases due to the lack of tissue specificity to the skeleton. Recently, we have developed a novel micelle-forming macromolecular prodrug of simvastatin (SIM). When administered systemically, the prodrug formulation would passively target to the fracture site and provided a potent and locally sustained bone anabolic effect in an osteotomized mouse model. In the present study, the prodrug formulation was further optimized and evaluated in a closed fracture mouse model.

Method. The simvastatin-containing prodrug, SIM-mPEG was synthesized and further formulated into micelles loaded with free SIM (SIM/SIM-mPEG). Unilateral transverse femoral closed fracture wascreated by a three-point bending device. Forty male CD-1 mice were fractured and randomly assigned into four groups (n = 10): SIM/SIM-mPEG (equiv. SIM 3 mg/kg/d, weekly i.v.), SIM (equiv. SIM 3 mg/kg/d, daily i.p.), SIM-H (high dose SIM, equiv. SIM 6 mg/kg/d, daily i.p.) and saline treated control group (CON). The treatments were initiated on day 2 post-op and the mice were euthanized on day 22. The fractured femurs were processed for μ-CT analysis. The data were analyzed for the histomorphometric parameters of the longitudinal fracture callus.

Results. μ-CT morphometric parameters, such as callus volume (Cl.V), callus surface (Cl.S), connective density (Conn.Dn) and mean polar moment of inertia (MMI) values of the SIM/SIM-mPEG group were all significantly higher than the CON mice ($p<0.003$), suggesting enhanced callus formation, organization and strength. For SIM group, these parameters (except Conn.Dn) were significantly lower than SIM/SIM-mPEG treated group ($p<0.05$). No significant difference was found

between SIM and CON. Comparing to CON, SIM-H could only significantly increase Cl.S and Conn.Dn, while a significant body weight decline ($p < 0.05$) was found during the treatment in this group suggesting the potential toxicity of SIM-H.*Conclusions*. Passive-targeting of SIM to fracture site using the SIM/SIM-mPEG formulation provides potent local bone anabolic effect and accelerates the healing of closed fracture without any noted side effect. This outcome suggests the potential benefits of this nanomedicine formulation in clinical management of impaired fracture healing.

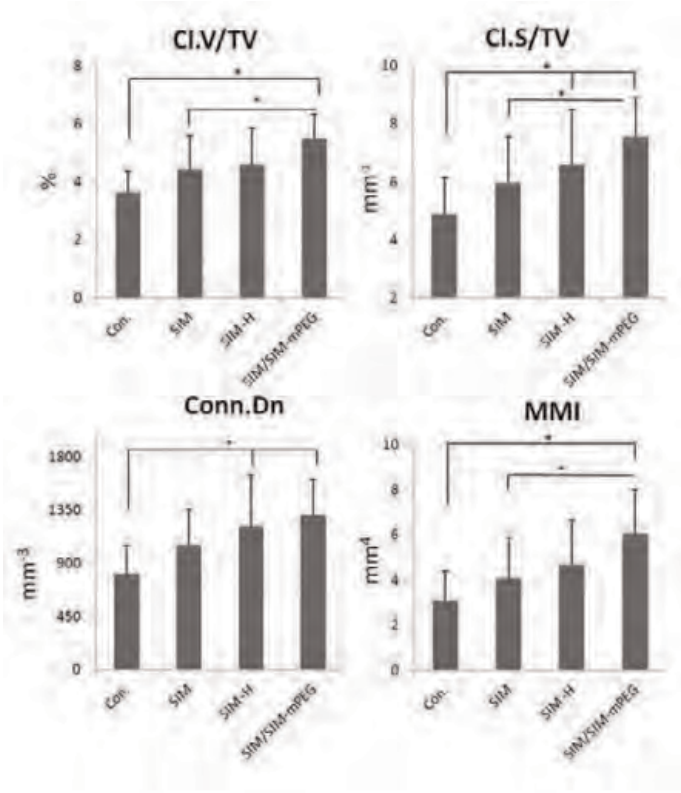

Simvastatin Prodrug Promotes Bone Fracture Repair in a Closed Fracture Mouse Model

***Disclosures: Yijia Zhang**, None.*

MO0413

Subcutaneous and Intravenous Single Dose Pharmacokinetics of PTH(1-34) and PTH-CBD, a Long-Acting Parathyroid Hormone Analog, in Sprague Dawley Rats. Tulasi Ponnapakkam*[1], Ranjitha Katikaneni[2], Robert Stratford[3], Joshua Sakon[4], Robert Gensure[2]. [1]Childrens Hospital at Montefiore, New York/Albert Einstein College of Medicine, USA, [2]Childrens Hospital at Montefiore/Albert Einstein College of Medicine, USA, [3]Xavier University, USA, [4]University of Arkansas, USA

PTH-CBD is a novel hybrid protein of PTH(1-33) and a bacterial collagen binding domain designed to accumulate in collagen rich areas such as bone. PTH-CBD has been shown in rodents to have a sustained (6-9 month) anabolic action in bone after a single subcutaneous injection, which we hypothesize is the result of prolonged retention in the bone rather than a depot effect. We previously reported subcutaneous single dose pharmacokinetics of PTH-CBD and PTH(1-34) at molar equivalent doses (320 ug/kg and 80 ug/kg, respectively). Both drugs showed similar bioavailability using a one-compartment model with 1st order absorption. While the initial phase half-lives were similar, the terminal phase half-life of PTH-CBD was 3 times greater. This together with lower peak levels suggested there was prolonged absorption. PTH-CBD was not completely eliminated by the last (6 hr) time point in this study, but the model predicted that it would be completely eliminated by 24 hours. We next conducted a longer term study to test this prediction. The results showed the expected high levels of serum PTH-CBD at 1 hour, and levels remained elevated above the normal range at 6 hours, similar to the initial study. At 12 hours, PTH-CBD levels had fallen to within the normal range. At 24 hours, there was no detectable PTH-CBD in the serum, as predicted. To determine if prolonged absorption or slower elimination was responsible for the longer terminal phase half life of PTH-CBD observed in the subcutaneous studies, we bypassed any absorptive effects by comparing IV single-dose pharmacokinetics of PTH(1-34) and PTH-CBD, again at molar-equivalent doses. PTH(1-34) and PTH-CBD had similar terminal-phase half lives, and both were completely eliminated by 6 hours after IV dosing, thus confirming that the increased terminal phase half-life seen after subcutaneous dosing was indeed the result of prolonged absorption. There was no hypercalcemia observed in any of our studies. Importantly, the overall pharmacokinetic analysis show that subcutaneously administered PTH-CBD (vs. PTH(1-34)) shows lower peak and only mildly prolonged elevated serum PTH levels which do not result in sustained hypercalcemia. As the number of injections required to achieve an anabolic bone effect is also markedly reduced with PTH-CBD, this would result in a reduced overall systemic exposure to PTH during the course of therapy, presumably corresponding to a reduced risk of any systemic side-effects.

***Disclosures: Tulasi Ponnapakkam**, BiologicsMD, 7*

MO0414

***In vivo* assessment of skeletal biomechanical properties reveals beneficial effects of combination anti-remodeling drug treatment.** Jason Organ*[1], Maxime Gallant[1], Mohammad Aref[1], Joseph Wallace[2], David Burr[1], Christopher Newman[1], Drew Brown[1], Matthew Allen[1]. [1]Indiana University School of Medicine, USA, [2]Indiana University Purdue University Indianapolis (IUPUI), USA

Pharmaceutical agents used to treat osteoporosis significantly reduce fracture risk via different mechanisms. Bisphosphonates, such as alendronate (ALN), increase bone volume and density, whereas raloxifene (RAL) improves material-level properties. This study was designed to assess whether combination treatment improves mechanical properties more than either monotherapy. Skeletally mature female dogs (n=24) were treated with vehicle, ALN, RAL, or ALN+RAL at clinical doses used for treating post-menopausal osteoporosis. After 6 months of daily treatment, all animals underwent *in vivo* biomechanical assessment using reference point indentation (RPI) on the anterior tibial cortex. Indentation distance increase (IDI), a measure of cyclic indentation resistance of the bone, was significantly lower in animals treated with RAL monotherapy (-17%) and ALN+RAL (-26%) compared to vehicle-treated animals, whereas ALN alone had no significant effect. Reductions in IDI represent an improvement in material-level mechanical properties. All three treatment groups exhibited significantly reduced first cycle indentation distance (ID) (-30-40%), total ID (-28-40%), and first cycle energy absorption (-20-28%) compared to vehicle-treated animals. These data suggest that RAL, and its combination with ALN, improves bone resistance to damage initiation and propagation. Results also indicate that RPI can detect treatment-induced alterations in skeletal mechanical properties *in vivo* – something previously restricted to *ex vivo* assessment.

***Disclosures: Jason Organ**, None.*
This study received funding from: Active Life Scientific

MO0415

Can Bisphosphonates extend Life Span? Effects on Stem Cell survival, DNA Repair and Tissue Regeneration. Juhi Misra*[1], Sindhu T Mohanty[2], Sanjeev Madan[3], James A Fernandes[3], Frank H Ebetino[4], Henry Roehl[5], R Graham Russell[6], Ilaria Bellantuono[1]. [1]Mellanby Centre for Bone Research; CIMA, The MRC-Arthritis Research UK Centre for Integrated research into Musculoskeletal Ageing, Dept. of Human Metabolism Medical School, University of Sheffield, United Kingdom, [2]Mellanby Centre for Bone Research, Dept. of Human Metabolism, Medical School, University of Sheffield, United Kingdom, [3]Department of Paediatric Orthopaedic & Trauma Surgery, Sheffield Childrens Hospital, United Kingdom, [4]Structural Genomics Consortium, University of Oxford, United Kingdom, [5]Dept. of Biomedical Science, MRC Centre for Developmental & Biomedical Genetics, University of Sheffield, United Kingdom, [6]University of Oxford, United Kingdom

Several lines of experimental and clinical evidence have recently raised the intriguing possibility that bisphosphonates (BPs) may extend life span. The observations include a pronounced extension of life span with a combination of zoledronate (Zol) and statins in a murine progeria model of accelerated aging (Varela et al 2008, 10.1038/nm1786), a 28% reduction in mortality in the Zol Horizon study in osteoporotic patients (Lyles et al 2007, 10.1056/NEJMoa074941), and several observational studies suggesting that alendronate and other BPs reduce cardiovascular events and deaths (eg Center et al 2011, 10.1210/jc.2010-2730; Wolfe et al 2012, 10.1002/jbmr.1792; Kang et al 2012, 10.1007/s00198-012-2213-5). In studies designed to explore potential underlying mechanisms, we have now found that BPs have hitherto unknown effects on stem cell survival, DNA repair and tissue regeneration.

We used human bone marrow mesenchymal stem cells (hMSC) and showed that Zol extended the life span of hMSC cultures (n=3) in vitro by more than 30% at 1μM, and significantly enhanced their clonogenic ability. Moreover Zol significantly enhanced repair of DNA damage (γH2AX) foci in hMSCs induced by cellular ageing or by gamma irradiation (1-5Gy; n=3) by as much as 84% at 1Gy; 40% at 3Gy and 19% at 5Gy that resulted in rescue of their proliferation and differentiation ability within 4-48 hours. In an in vivo model utilising Zebrafish embryos Zol significantly restored tail regeneration following amputation and irradiation (1-5Gy; n=15). All these effects appear to be mediated by inhibition of the mevalonate pathway, since they could be reversed by adding back appropriate isoprenoid metabolites (eg farnesol or geranylgeraniol), and the effects of other N-containing BPs were related to their known potencies as inhibitors of farnesyl pyrophosphate synthase in this pathway.

Downstream mechanisms were dependent on inhibition of TORC1 and TORC2 mediated mTOR signalling, leading to increased nuclear translocation of FOXO-3a and phosphorylation of ATM resulting in an activated DNA damage response.

In conclusion these remarkable effects of BPs on stem cell aging and survival and on DNA repair and tissue regeneration may help to explain some of the observations already made about non-skeletal effects of BPs. Furthermore, they open up a range of exciting new potential applications for utilizing these novel effects in repair of damaged tissues, and more widely in biology and medicine.

***Disclosures: Juhi Misra**, None.*

MO0416

Intermittent Minodronic Acid Treatment with Sufficient Bone Resorption Inhibition Prevents Reduction in Bone Mass and Strength in Ovariectomized Rats with Established Osteopenia Comparable with Daily Treatment. Makoto Tanaka*[1], Aishi Kimoto[2], Masamichi Mori[2], Kazutoshi Nozaki[3], Shinji Fukushima[2], Hiroshi Mori[1], Tsutomu Shiroya[4], Toshitaka Nakamura[5]. [1]ONO Pharmaceutical Co., Ltd., Japan, [2]Pharmacology Research Laboratories, Drug Discovery Research, Astellas Pharma Inc., Japan, [3]Medical Affairs, Astellas Pharma Inc., Japan, [4]Discovery Research Laboratories, Ono Pharmaceutical Co., Ltd., Japan, [5]University of Occupational & Environmental Health, Japan

This study examined to compare the effects of four-week intermittent and daily administrations of minodronic acid, a highly potent nitrogen-containing bisphosphonate, on bone mineral density (BMD), bone strength, bone turnover, and histomorphometry on established osteopenia in ovariectomized (OVX) rats.

Female rats were OVX or sham-operated. At 12 weeks post surgery, minodronic acid was orally administered once every 4 weeks at 0.2, 1, and 5 mg/kg and once daily at 0.006, 0.03, and 0.15 mg/kg for 12 months. The total dosing amount was comparable between two dosing regimens. The levels of bone turnover markers were measured. BMD as assessed via DXA, bone structure and dynamical changes in vertebral trabecular and biomechanical properties were measured ex vivo at 12 months. Minodronic acid ameliorated the decrease in BMD of lumbar and the femur in both treatment regimens similarly. Minodronic acid suppressed elevated urinary deoxypyridinoline levels, a bone resorption marker, and reduced serum levels of osteocalcin, a bone formation marker. In the mechanical test at 12 months, minodronic acid ameliorated the reduction in bone strength in femur and vertebral body. There is no significant difference in parameters between two regimens except maximal load of lower doses in lumbar vertebral body and absorption energy of middle doses in femur. These parameters with significant difference, values in intermittent regimen were significantly lower than that in daily repeated regimen. Bone histomorphometric analysis showed that minodronic acid significantly ameliorated the decrease in bone mass, trabecular thickness and number, and increased in trabecular separation, bone resorption indices, and bone formation indices in both regimens. Minodronic acid suppressed OVX-induced increases in bone turnover at the tissue level and ameliorated all structural indices, thereby improving the deterioration in bone quality under osteoporotic disease conditions regardless of the regimen.In conclusions, four-week intermittent treatment of minodronic acid suppressed increased bone resorption as daily treatment when considering the total administered dose. The improvement of microarchitectural destruction in low dose of intermittent treatment was weaker than that observed in a daily repeated regimen; however the effect in high and middle doses of intermittent treatment were equivalent with that observed in a daily repeated regimen accompanied sufficient bone resorption inhibition.

***Disclosures: Makoto Tanaka**, ONO Pharmaceutical Co.,Ltd., 3*

MO0417

Periprosthetic Bone Response to Mechanical Loading with Administration of an Anti-Catabolic Agent, Osteoprotegerin (OPG). James Sutherland*[1], Hayden-William Courtland[1], Chad Ishmael[2], Joseph Choi[1], Kirsten Stoner[1], Alex Sarkisian[2], Joe Nguyen[1], Marjolein Van Der Meulen[3], F. Patrick Ross[1], Mathias Bostrom[1]. [1]Hospital for Special Surgery, USA, [2]Weill Cornell Medical College, USA, [3]Cornell University, USA

Osseointegration is crucial to the success of implant fixation in uncemented total joint arthroplasty and depends on the integrity and quantity of periprosthetic bone. Mechanical loading has been proven to increase periprosthetic cancellous bone volume, thereby enhancing osseointegration. However, while mechanical loading is a known anabolic therapy, the contribution of osteoblast-osteoclast coupling to its anabolic effect is not well understood. Recent findings reveal that osteoclasts not only degrade bone but also secrete anabolic factors. Thus, we hypothesized that the inhibition of bone resorption with an anti-catabolic agent (osteoprotegerin, OPG) may diminish the beneficial effects of mechanical loading on cancellous bone volume. A porous titanium disc and mechanical loading device were bilaterally implanted on cancellous bone in the distal femurs of adult rabbits (n=28). The right femur was loaded daily, while the left femur received a sham loading device. Half of the rabbits received OPG (10 mg/kg, weekly), and half received saline (daily). Periprosthetic cancellous bone was harvested at 7 and 14 days for microcomputed tomography. At 14 days, mechanical loading significantly increased periprosthetic cancellous bone volume within 500 μm of the implant interface, with and without OPG treatment (29% and 35% respectively, p = 0.008). No effect of OPG was observed on any outcome parameters, and no synergistic effects of combined OPG and loading treatment were observed. Inhibition of bone resorption with an anti-catabolic agent (OPG) neither diminished nor enhanced the beneficial effects of mechanical loading on cancellous bone volume. This finding suggests that mechanical loading increases bone volume by upregulation of new bone formation, not by maintenance of bone mass through the inhibition of resorption.

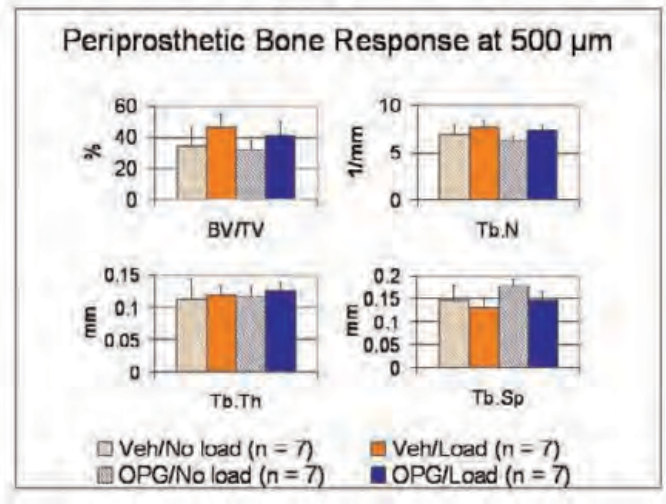

uCT Parameters

***Disclosures: James Sutherland**, None.*

MO0418

Switching from Alendronate to RANKL Blockade alters Bone Properties after 14 Weeks of Therapy in the *oim/oim* Mouse. Josephine Marino*[1], Nancy Pleshko[2], Steve Doty[1], Erin Carter[1], Adele Boskey[1], Cathleen Raggio[1]. [1]Hospital for Special Surgery, USA, [2]Temple University, USA

The purpose of this study was to determine whether Osteogenesis Imperfecta(OI) patients entering adulthood should continue bisphosphonate therapy or would benefit from switching to a RANKL blockade therapy. To address this question, we used a mouse model of type III OI.

METHODS: Animal studies were performed under IACUC approval. OI(*oim/oim*) and wild-type(WT) mice were treated from 2-26 weeks with 1)Saline; 2)Alendronate(ALN; 0.21 mg/kg/dose weekly); or 3)ALN from 2-14 weeks followed by 1.5 mg/kg/dose biweekly RANK-Fc from 14-26 weeks(ALN+RANK-Fc). Fracture number was calculated from high-resolution faxitrons obtained in the anterior-posterior and medial-lateral planes at 14 weeks and sacrifice. Femurs were analyzed by microcomputed tomography using a Scanco μCT 35 system(Scanco Medical, Basserdorf, Switzerland). A subset of femora were embedded in poly methyl methacrylate and sectioned at 2 μm for Fourier transform infrared imaging analysis. Nine images of cortical and trabecular bone were taken from each femur using a Perkin Elmer Spotlight Imaging Spectrometer and ISys(Malevern Instruments) software. Results are statistically significant $p<0.05$ by two-way ANOVA(SigmaStat).

RESULTS: At 14 weeks, both *oim/oim* treated groups had fewer fractures compared to saline. At 26 weeks, both treatment groups had fewer fractures compared to saline. There were no differences between treatment groups at either time-point and no new fractures after 14 weeks in either group(fig1).

There were no differences in cortical bone in any parameters studied. Trabecular number was increased in *oim/oim* for both treatment groups compared to saline(fig2). ALN+RANK-Fc increased trabecular number compared to ALN. Trabecular spacing decreased and bone volume fraction increased in both treated *oim/oim* groups compared to saline. Changes in WT mirror *oim/oim*.

oim/oim trabecular bone: ALN treatment increased mineral:matrix ratio compared to saline and both treatment groups increased collagen maturity compared to saline(fig3). *oim/oim* cortical bone mineral:matrix ratio was increased in ALN compared to ALN+RANK-Fc treatment. WT cortical bone: ALN+RANK-Fc treatment resulted in more perfect crystals compared to saline.DISCUSSION Based on our current data, treatment with ALN or ALN+RANK-Fc comparably reduces fracture number, increases bone quantity, and alters bone quality in *oim/oim* mice. Mechanical testing will be essential in determining the implication of these changes on patient life.

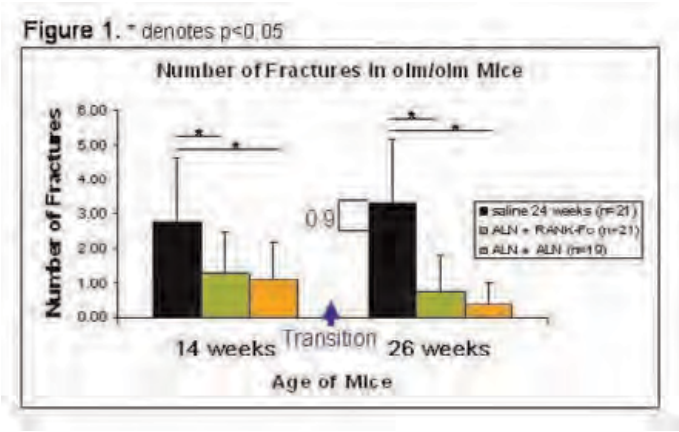

Figure 1

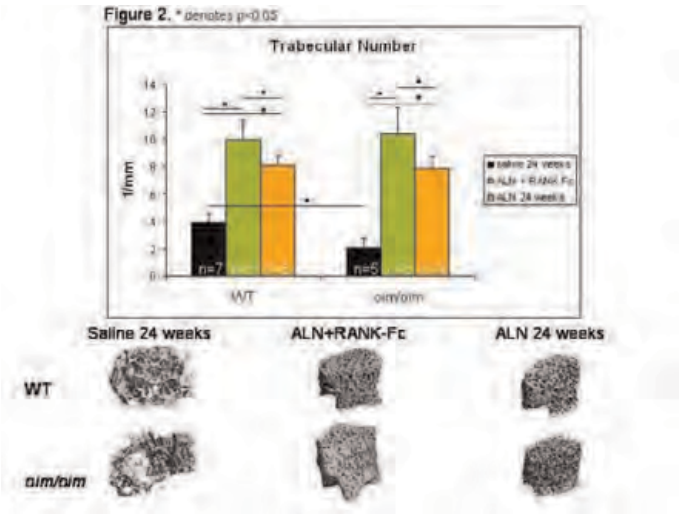

Figure 2

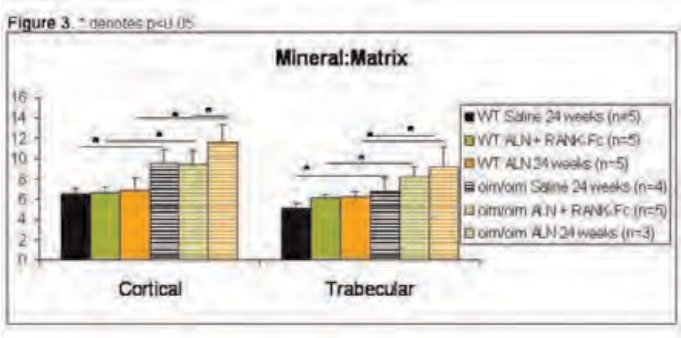

Figure 3

***Disclosures: Josephine Marino**, None.*
This study received funding from: Amgen

MO0419

Probiotics Protect Mice from Ovariectomy Induced Bone-Loss. Klara Sjogren*[1], Cecilia Engdahl[2], Frida Fåk[3], Annica Andersson[4], Sara Windahl[2], Helen Farman[5], Sofia Moverare Skrtic[6], Ulrika Islander[4], Claes Ohlsson[6]. [1]Centre for Bone & Arthritis Research, Sweden, [2]Center for Bone & Arthritis Research, Sahlgrenska Academy, Sweden, [3]Applied Nutrition & Food Chemistry, Department of Food Technology, Engineering & Nutrition, Lund University, Sweden, [4]Centre for Bone & Arthritis Research, Institute of Medicin, Sahlgrenska Academy at University of Gothenburg, Sweden, [5]University of Gothenburg, Sweden, [6]Center for Bone & Arthritis Research at the Sahlgrenska Academy, Sweden

Absence of gut microbiota in germ-free mice leads to increased bone mass in combination with decreased osteoclastogenesis and altered immune status in bone marrow suggesting that the gut microbiota can regulate bone mass[1]. Probiotic bacteria are defined as live microorganisms which when administered in adequate amounts confer a health benefit on the host and are believed to alter the composition of the gut microbiota.

The purpose of this study was to test if probiotic treatment, via its effects on gut microbiota, could protect mice from ovariectomy (ovx) induced bone-loss. The probiotic strains were selected based on their anti-inflammatory properties in an earlier study[2]. Mice were treated with either a single Lactobacillus (L) strain, L. paracasei DSM13434 (L. para) or a mixture of three strains, L. paracasei DSM13434, L. plantarum DSM 15312 and DSM 15313 referred to as L. mix during 6 weeks, starting two weeks before ovx to study the preventive effect of probiotic treatment on ovx induced bone-loss. The L. strains were given in the drinking water at a concentration of 10^9 colony-forming units/ml while control mice only received tap water with vehicle. Ovx resulted in an expected increased body weight (16%, $p<0.01$) compared to sham mice that was similar for all treatments. Cortical bone parameters were measured by peripheral quantitative computed tomography (pQCT) in the mid-diaphyseal region of femur. In the vehicle treated mice, ovx decreased the cortical bone mineral content and cortical cross sectional bone area by 11% ($p<0.01$) and 7% ($p<0.01$), respectively. In contrast, ovx did not reduce corresponding cortical bone parameters in the L. para or the L. mix treated mice. Cortical bone mineral content was higher in both L. para ($p<0.05$) and L. mix ($p<0.05$) treated ovx mice compared to veh treated ovx mice.

In conclusion, these data show that probiotic bacteria in the drinking water prevents ovx induced cortical bone-loss suggesting a therapeutic potential for probiotics in the treatment of postmenopausal osteoporosis. In addition, this study supports a role of the gut microbiota for the regulation of bone mass.

1. Sjogren, K., et al. The gut microbiota regulates bone mass in mice. Journal of bone and mineral research : the official journal of the American Society for Bone and Mineral Research 27, 1357-1367 (2012).

2. Lavasani, S., et al. A novel probiotic mixture exerts a therapeutic effect on experimental autoimmune encephalomyelitis mediated by IL-10 producing regulatory T cells. PloS one 5, e9009 (2010).

***Disclosures: Klara Sjogren**, None.*

MO0420

The Efficacy of Dried Plum's Bioactive Components in Reversing Bone Loss. Jennifer Graef*, Elizabeth Rendina, Pitipa Chongwatpol, McKale Davis, Sandra Peterson, Stephen Clarke, Edralin Lucas, Brenda Smith. Oklahoma State University, USA

Dietary dried plum supplementation has been shown to be effective at preventing and reversing bone loss in animal models of osteoporosis, but the bioactive components that are responsible for these osteoprotective effects remain in question. Much of the focus has been on the phenolic compounds in dried plum due to their anti-inflammatory and antioxidant properties as well as non-digestible carbohydrates such as inulin that may lower colonic pH and increase calcium absorption. Therefore, the purpose of this study was to determine whether synthetic forms of the major chlorogenic isomers found in dried plum with or without inulin exert a similar beneficial effect on bone as dried plum in a model of postmenopausal osteoporosis. Twelve-week-old female C57BL/6 mice (n=50) were either sham-operated or ovariectomized (OVX) and allowed to lose bone two weeks prior to beginning an 8 wk treatment period in one of the following groups: Sham-control (Sham-CON), OVX-control (OVX-CON), OVX- 25% w/w dried plum (OVX-DP), OVX- synthetic phenolics (OVX-SP), or OVX- synthetic phenolics plus inulin (OVX-SP+I). DXA was used to assess whole body bone mass/density and microCT scans were performed to assess trabecular bone structure of the 4th lumbar vertebra and distal femur metaphysis and cortical bone structure of the femur mid-diaphysis. In agreement with previous findings, bone in the OVX-DP group was restored to the level of the Sham-CON as indicated by whole body bone densitometry measures (BMD, BMC, and BMA) and trabecular bone volume, trabecular number, and trabecular separation of the L4 vertebra and distal femur metaphysis. No effect on trabecular bone was observed in the OVX-SP and OVX-SP+I treatment groups. However, the OVX-SP treatment restored cortical thickness and cortical area to the level of the OVX-DP group and the cortical area was comparable to the Sham-CON group by the end of the study period. In conclusion, the OVX-SP with and without inulin did not restore trabecular bone properties in a manner comparable to dried plum, but the OVX-SP

group did experience some improvement in cortical bone parameters. This response was not enhanced with the addition of inulin. Further studies are needed to determine the mechanism involved in the restoration of cortical bone with the supplementation of these synthetic phenolic compounds and to identify the bioactive components in dried plum exerting osteoprotective effects on trabecular bone.

***Disclosures: Jennifer Graef**, None.*

MO0421

Long-Term Effect of Diet on the Ovariectomy Response in the Rat Model of Osteoporosis. Aurore Varela*, Elisabeth Lesage, Susan Y. Smith. Charles River Laboratories, Canada

Diet composition, restrictions or supplements have been proven to impact prevention and bone loss treatment. The study purpose was to compare long-term effects of two diets on bone turnover, mass and strength over a 12-month period in aged ovariectomized rats. Six months old rats were fed with PMI certified rodent chow 5CR4 (14% protein) or 5002 (21% protein) *ad libitum*. The effects of OVX vs. diets were monitored using body weight (BW), food consumption (FC), bone markers, DXA (whole body, lumbar spine), pQCT (proximal tibia metaphysis and diaphysis) and biomechanics. Eighteen females/group underwent OVX or Sham surgery (Sx).

Within 2/3 weeks after Sx, OVX rats gained BW vs. Sham (+15%). With 5CR4, BW differences stabilized after 6 months to +10%, whereas with 5002, BW differences continued to increase up to +22% 8 to 12 months after Sx up to 12 months. Sham controls fed with 5002 gained 20% more BW over 52 weeks, 5002 OVX gained FC was 10% larger in 5002 sham vs. 5CR4 sham and 22 % in OVX. Due to larger BW, cage size was 290 in^2 for 5002 rats vs. 180 in^2 for 5CR4 rats. Marker values were generally higher for 5002 Sham vs. 5CR4 Sham rats, therefore, differences were more marked between Sham and OVX in 5CR4 vs. 5002 fed rats. Differences between Sham and OVX were 2-fold higher in 5CR4 rats for osteocalcin and depxypyridinoline, and 25% higher in 5CR4 rats for C-telopeptide, vs. 5002 fed rats. Sham controls fed with 5002 had larger increases in DXA lumbar spine BMC and BMD during the second part of the study, after 6/8 months, vs. 5CR4 fed Sham rats. Also decreases in trabecular BMC and BMD at tibia metaphysis were less marked in 5002 vs. 5CR4 fed Sham rats. In OVX animals, the overall bone loss observed during the course of the study was generally similar in 5002 vs. 5CR4 fed OVX rats. This resulted in greater differences between Sham and OVX in terms of bone loss for 5002 (-46%) vs. 5CR4 fed rats (-18%) (tibia metaphysis trabecular BMD at the end of the study) and bone strength, -14 vs. -45% (peak load, vertebral compression).

These data suggested that diet and BW can influence the effects of aging and the OVX response in rats as evidenced by changes in bone turnover and bone mass measured by densitometry techniques. The influence of diet, calorie intake and BW should be taken into consideration in this model to better discriminate potential bone anabolic or anti-catabolic agents in the preclinical evaluation of potential anti-osteoporosis agents.

***Disclosures: Aurore Varela**, None.*

MO0422

***L. reuteri* treatment suppresses osteoclast activity and bone loss in ovariectomized mice.** Laura McCabe*, Narayanan Parameswaran, Regina Irwin, Darin Quach, Laura Schaefer, Jing Zhang, Taehyung Lee, Robert Britton. Michigan State University, USA

Estrogen deficiency increases bone resorption and is a major risk factor for osteoporosis. Half of women over the age of 50 will experience an osteoporosis related fracture in their lifetime, thus novel therapies are needed to combat post-menopausal bone loss. Recent studies suggest an important role for the intestinal microbiota in bone health. The probiotic Lactobacillus reuteri ATCC PTA 6475 (L. reuteri) produces immunomodulatory factors as well as an antimicrobial compound, therefore we hypothesized that L. reuteri modulation of the gut microbiota and systemic and bone inflammation may suppress ovx-induced bone loss. As expected, Ovx caused significant bone loss compared to non-Ovx mice. Strikingly, L. reuteri treated Ovx mice did not display bone loss. Osteoclast markers and activators (Trap5 and RANKL) were decreased after L. reuteri treatment, suggesting that L. reuteri suppresses bone resorption. Consistent with this, Ovx-induced increase in bone marrow CD4+ T-cells (which promote osteoclastogenesis) were suppressed in L. reuteri treated Ovx mice. Furthermore, L. reuteri secreted factors directly suppress osteoclastogenesis in vitro. Finally, associated with these changes in the bone, the gut microbiota was distinct between the different groups of mice (ovx vs non-ovx $\pm$ L. reuteri). Taken together, our studies demonstrate that L. reuteri treatment modifies the gut microbiota and is capable of suppressing bone loss associated with estrogen deficiency, likely through suppression of osteoclastogenesis. Thus, L. reuteri treatment may be a straightforward and cost-effective approach to reduce post-menopausal bone loss.

***Disclosures: Laura McCabe**, None.*

MO0423

Brief Daily Low Intensity Vibrations (LIV) Promote Osteoblast Activity in an Estrogen-Deficient Murine Model of Osteoporosis. Divya Krishnamoorthy*[1], Danielle Frechette[2], Benjamin Adler[2], M. Ete Chan[2], Clinton Rubin[3]. [1]SUNY Stony Brook University, USA, [2]Stony Brook University, USA, [3]State University of New York at Stony Brook, USA

The significant bone loss following ovariectomy (OVX) is considered a direct result of estrogen depletion and the downstream imbalance of bone remodeling. The lack of estrogen also results in a dramatic change in the bone marrow environment, disrupting the proliferation and differentiation of resident mesenchymal (MSCs) and hematopoietic (HSCs) stem cells. In addition to an impaired bone phenotype, OVX also leads to increased adiposity, not only in visceral depots, but also within the marrow cavity. Low intensity vibrations (LIV), representing a surrogate for exercise, may serve as an osteogenic mechanical signal by biasing the fate of MSCs away from adipogenesis and towards osteoblastogenesis. This study investigates the use of LIV as a non-invasive means to protect the bone phenotype in osteoporotic OVX mice. Eight week old female C57BL/6 mice underwent ovariectomy or SHAM surgery (AC); 2w later, ovariectomized mice were subject to 6w of LIV (0.3g at 90Hz, 15 min/d, 5 d/wk) (V) or SHAM LIV (O). Based on microCT evaluation of the proximal tibia, both O and V animals exhibited severe osteopenia compared to AC (-36% and -42%, respectively; $p<0.05$). OVX also caused a marked suppression of bone turnover markers, including osteoclast-specific tartrate-resistant acid phosphatase (TRAP5b; -32%, $p<0.05$) and osteoblast-specific alkaline phosphatase (ALP; -15%, $p>0.05$) suggesting decreased osteoclast and osteoblast activity. In contrast, V exhibited significantly greater ALP activity (26%, $p<0.05$) compared to O, suggesting increased osteoblast activity. Furthermore, TRAP5b concentrations of V were comparable to that of O, implicating that LIV is more anabolic than anti-catabolic in ovariectomized mice. The increase in ALP maybe a result of MSCs being driven towards osteoblastogenesis, leaving behind fewer stem cells in the marrow and increasing osteoblast number and therefore activity; however this hypothesis needs to be tested further. While the biologic responses evidenced here are encouraging, it may take longer-term studies to determine if mechanical signals can ultimately protect the skeleton from the harmful effects of estrogen deficiency. In conclusion, the results of this study corroborate the severe insult to bone as a result of estrogen depletion, while providing evidence of the ability of mechanical signals (LIV) to restore normal bone remodeling activity by promoting an osteogenic effect.

***Disclosures: Divya Krishnamoorthy**, None.*

MO0424

Effects of anti-diabetic drugs alone or in combination with risedronate on bone mass and architecture in Goto-Kakizaki rats, a spontaneous non-obese model of type 2 diabetes. Tetsuo Yano*[1], Mei Yamada[1], Makoto Shiozaki[2], Daisuke Inoue[3]. [1]Ajinomoto Pharmaceuticals Co., LTD, Japan, [2]Ajinomoto Pharmaceuticals, Japan, [3]Teikyo University Chiba Medical Center, Japan

Background/Aim: Patients with type 2 diabetes exhibit decreased bone strength and increased fracture risk in part independently of bone mineral density (BMD). However, molecular basis of the bone fragility and specific treatment for such diabetes-associated osteoporosis remain to be established. We previously demonstrated that risedronate (RIS) improved both bone mass and quality in Goto-Kakizaki (GK) rats, a spontaneous non-obese model of type 2 diabetes. In the present study, we examined effects on BMD and bone architecture of treatment with anti-diabetic drugs, each alone or in combination with RIS using GK rats.

Methods: GK rats and control Wistar rats at 48 weeks of age were used. Vehicle or RIS was administered subcutaneously, twice a week. And vehicle, metformin (Met), pioglitazone (Pio) or a DPP-4 inhibitor, sitagliptin (Sita) was administered orally, once a day. After 16 weeks of treatment, bone architecture in lumber vertebrae (L4) was evaluated by micro CT, measuring trabecular BMD, bone volume fraction, structure model index (SMI), trabecular number (TbN), trabecular separation and trabecular thickness (TbTh).

Results: At the start of treatment, blood glucose concentration was significantly increased in GK rats compared with Wistar rats both under fasting condition and after oral glucose load. Met and Sita significantly decreased the area under the curve of blood glucose concentration on after glucose load. Bone architecture in GK rats significantly deteriorated with the progression of diabetes, compared with that in Wistar rats, exhibiting decreased BMD, TbN and TbTh. RIS in combination with Met significantly decreased trabecular separation (-13.1%) and SMI (-9.1%) compared with vehicle, showing the best effect among the tested groups. In contrast, Pio was further detrimental to bone in GK rats as expected, and addition of RIS was minimally effective. Effect of Sita was more or less in between.

Conclusion: The results suggest that treatment with RIS in combination with Met is among the best therapeutic maneuvers of osteoporosis associated with type 2 diabetes, maintaining both bone mass and quality as well as good glycemic control.

***Disclosures: Tetsuo Yano**, Ajinomoto Pharmaceuticals, 3*

MO0425

Low-intensity pulsed ultrasound lessons therapeutically bone loss on overiacteomized mice. Yoshitsugu Kojima*[1], Hiroki Yazawa[1], Takayuki Watanabe[1], Kazuki Terada[2], Nobuo Izumo[2], Yoshihiro Nishimura[1]. [1]Nippon Sigmax Co., Ltd, Japan, [2]Yokohama College of Pharmacy, Japan

Low-intensity pulsed ultrasound (LIPUS) has been widely used for bone fracture treatment. The recent studies have reported the usefulness of LIPUS on bone fracture site. However, mechanism of LIPUS on osteoporosis is less elucidated. In previous study, we demonstrated the protective effects of LIPUS on osteoporotic bone loss in ovariectomized (OVX) model mouse. In this study, we tested therapeutic recovery effects of LIPUS for existing bone loss in osteoporotic model.

Nine-week-old female ICR mice were ovariectomized or sham operated and allow for 8weeks to develop osteoporotic bone loss. OVX mice were divided into ultrasound exposed group and unexposed group before LIPUS irradiation. LIPUS condition was 2.0 MHz, duty 20%, 30mW/cm^2 for 20min/day and 5days/week for 8 weeks.Then the mice were sacrificed to collected ovaries and femora. The bone mineral density (BMD) and bone mineral content (BMC) of femora were measured with micro-CT (LCT-100Lite, Hitachi Aloka Medical, Ltd).Ovary weight was significantly decreased to 24% of sham group on both OVX group and OVX-LIPUS group. Although BMD and BMC were significantly decreased on OVX group against sham group (Fig. 1), BMD on trabecular bone of OVX-LIPUS group was significantly increased by 8.8% against OVX group.

In this study, we demonstrated the effects of LIPUS on Bone density even after osteoporotic bone loss. Our next step is to elucidate the mechanism of osteogenic responses of LIPUS through western blot analysis and real-time PCR analysis.

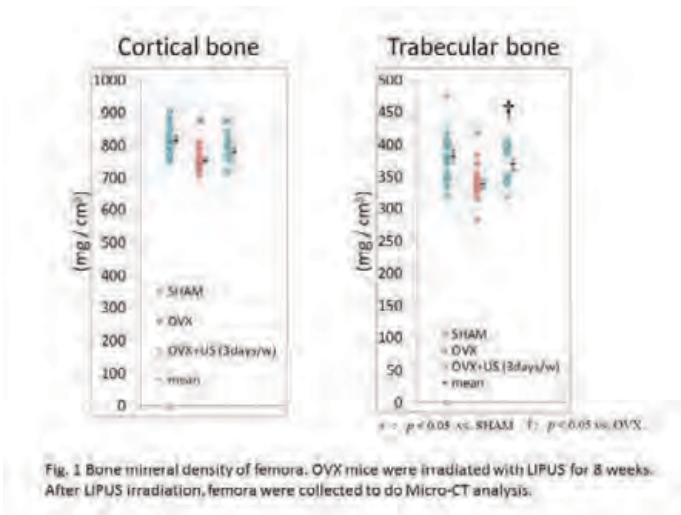

Fig. 1 Bone mineral density of femora. OVX mice were irradiated with LIPUS for 8 weeks. After LIPUS irradiation, femora were collected to do Micro-CT analysis.

Fig1 Femoral BMD

***Disclosures: Yoshitsugu Kojima**, None.*

MO0426

Molecular Basis of the Dual Effects of Thiazolidinediones (TZDs) on Osteoclastogenesis. Dongfeng Zhao*[1], Zhenqi Shi[2], Amy Warriner[1], Xu Feng[1], Yongjun Wang[3]. [1]The University of Alabama At Birmingham, USA, [2]University of Alabama, USA, [3]Longhua Hospital, Shanghai University of Traditional Chinese Medicine, China

Thiazolidinediones (TZDs) are synthetic peroxisome proliferation-activated receptor γ (PPARγ) agonists that have been used for treating Type 2 Diabetes Mellitus (T2DM). Accumulating clinical data indicate that TZD treatments augment the risk of bone fractures in T2DM patients. Moreover, emerging evidence supports the notion that PPARγ induces bone loss in part, if not primarily, by modulating osteoclastogenesis. However, the effect of TZDs on osteoclastogenesis is currently controversial. While a number of groups demonstrated that TZDs exert inhibitory effect on osteoclastogenesis, one study showed that TZDs stimulate osteoclastogenesis. To address this discrepancy, we further investigated the role of TZDs in osteoclastogenesis. As reported in last year's ASBMR meeting, we found that RANKL-mediated lineage commitment dictates the effect of TZDs on osteoclastogenesis. Specifically, while both rosiglitazone and pioglitazone dose-dependently inhibit osteoclastogenesis in tissue culture dishes and on bone slices from primary bone marrow macrophages (BMMs) freshly isolated from 6- to 8-week old C57BL/6 mice with complete inhibition of osteoclastogenesis at 40uM/ml of either TZD, the inhibitory effect of TZDs on osteoclastogenesis was significantly impaired when BMMs were pretreated with 100ng/ml RANKL for as short as 24 hours. Here, we report our new studies which aim to elucidate the molecular mechanism by which TZDs exert the dual effects on osteoclastogenesis. First, we determined the effect of rosiglitazone and pioglitazone on known RANK signaling pathways in fresh BMMs. We found that both agents at 40uM/ml exert no effect on the activation of the ERK, p38, JNK and I?B pathways. However, rosiglitazone and pioglitazone impair RANKL-induced expression of NFATc1 and four osteoclast genes (cathepsin K, matrix metalloproteinase 9, carbonic anhydrase 2 and tartrate acid resistant phosphatase) in freshly isolated BMMs. Next, we repeated the assays with BMMs pretreated with RANKL for 48 hours. Our data indicate that the ability of rosiglitazone and pioglitazone to suppress the expression of NFATc1 and the four osteoclast genes was significantly reduced in BMMs pretreated with RANKL for 48 hours. These findings demonstrate that RANKL-mediated lineage commitment determines the effect of TZDs on osteoclastogenesis through modulating the expression of NFATc1, a master transcriptional regulator of osteoclastogenesis.

***Disclosures: Dongfeng Zhao**, None.*

MO0427

Analysis of BMD, Hip Geometry and Trabecular Bone Score in Relation to Body Composition and Biochemical Markers in Adult Females with Severe Anorexia Nervosa. Judith Haschka*[1], Janina Patsch[2], Roland Kocijan[1], Didier Hans[3], Christian Muschitz[4], Afrodite Zendeli[5], Christina Bittighofer[1], Angela Trubrich[6], Julia Wild[1], Peter Weiss[4], Heinrich Resch[2]. [1]St. Vincent Hospital Vienna, Austria, [2]Medical University of Vienna, Austria, [3]Lausanne University Hospital, Switzerland, [4]St. Vincent's Hospital, Austria, [5]The VINFORCE Study Group - St. Vincent Hospital - Medical Department II, Austria, [6]BHS, Austria

Purpose: Anorexia nervosa (AN) is a psychiatric eating disorder associated with reduced body mass, estrogen deficiency, malnutrition and amenorrhea. The aim of the study was to investigate differences in hip geometry (HSA) and spinal bone microarchitecture as measured indirectly by trabecular bone score (TBS) in relation to body composition in patients with AN. TBS, a new texture measurement that can be applied to X-ray images and DXA, quantifies local variations in gray level and characterizes bone microstructure. HSA, derived from DXA, provides information about hip geometry and biomechanical strength.

Methods: DXA scans of femoral neck, lumbar spine and body composition (lean body mass [kg], body fat percentage [%], BMC [kg]) and HSA (CSMI cross-sectional moment of inertia, CSA cross-sectional area) were assessed by iDXA (GE Lunar) in 34 patients with AN (23.5 $\pm$ 4.5y, BMI 14.7 $\pm$ 1.3) and 26 controls (24.4 $\pm$ 2.5y, BMI 23.5 $\pm$ 3.7). The raw data of spinal DXA (L1-L4) were extracted and analysed with TBS iNsight software (v1.9, Medimaps SA, France). Serum parameter for bone formation (P1NP) and bone resorption (CTX), sclerostin levels (Scl), 25(OH)Vit.D, estradiol and cortisol were assessed.

Results: In patients with AN BMD was significantly decreased at all sites (femoral neck 0.850$\pm$0.14 vs 1.068$\pm$0.11; L1-L4 0.973$\pm$0.15 vs 1.292$\pm$0.15, $p<0.001$). Consequently mean TBS spine was significantly lower in AN (1.35$\pm$0.12 vs 1.56$\pm$0.08, $p<0.001$). CSMI (7.6$\pm$1.8 vs 10.8 $\pm$2 .7) and CSA (121.2$\pm$21.7 vs 161.6$\pm$19.7) were significantly lower in AN ($p<0.001$ for both). Body composition showed significantly lower BMC (2.0$\pm$0.3 vs 2.5$\pm$0.5), lean body mass (32.7$\pm$4.0 vs 42.6$\pm$5.1) and body fat percentage (14.1$\pm$8.0 vs 36.1$\pm$5.2, $p<0.001$ for all) in AN. In AN, lean body mass, BMC and hip BMD correlated positive with CSMI and CSA. Patients with AN had significantly higher Scl (41.7$\pm$17.7 vs 28.8$\pm$11.9, $p<0.05$) and CTX (0.767$\pm$0.4 vs 0.446$\pm$0.2, $p<0.001$) levels, while there was no difference in P1NP and cortisol. Vit.D (26.7$\pm$11.0 vs 32.9$\pm$9.5) and Estradiol (25.9$\pm$25.6 vs 75.4$\pm$81.1, $p<0.05$ for both) were significantly lower in patients with AN.

Conclusion: Apart of the expected significant decreased body composition, patients with AN show significantly reduced BMD, TBS, hip geometry and biomechanical strength compared to age-matched controls which may be partly explained by the elevated Scl expression and uncoupling in bone turnover.

***Disclosures: Judith Haschka**, None.*

MO0428

A Model for Assessment of Vitamin D_3 Deficiency & Implementation of Vitamin D_3 Regimen in a Skilled Nursing Facility. F. Michael Gloth*[1], Jennifer Coates[2], Kim Adams[3], Elizabeth Hidlebaugh[4]. [1]John Hopkins University School of Medicine, USA, [2]Moorings Park Healthy Living, Inc, USA, [3]The Chateau at Moorings Park, USA, [4]Hope College, USA

Purpose: To determine the prevalence of nursing home residents at high risk for vitamin D deficiency and to describe a process for implementing Vitamin D supplementation acceptable in the highly regulated nursing home environment demanding individualized care.

Design: A chart review of skilled nursing home patients was performed with the goal of identifying those at high risk for Vitamin D deficiency.*Setting*: The Chateau of Moorings Park in Naples, FL.

Subjects: Seventy Long-term Care nursing home resident.

Methods: During the chart review, risk factors such as hours of sunlight/day, skin pigment, inflammatory bowel disease diagnosis, fat malabsorption syndromes, obesity, kidney disease, Vitamin D rich foods, muscle weakness, muscle pain, osteoporosis diagnosis, history of bone fractures, bone pain, and menopause were collected. Data were also collected on whether or not the patient had been given a Vitamin D deficiency diagnosis, treated with Vitamin D and what dosage, and if there were 25-OH Vitamin D measures. A teleconference was conducted with the nursing

home regulartory agency for the State of Florida to discuss the prospect of writing a facility-wide order for all residents to receive vitamin D supplementation. Subjects with a diagnosis of vitamin D toxicity were excluded.

Results: Seventy charts were reviewed representing all long-term care residents of the nursing home. Hours of sunlight per day (60%), menopause (54%), and muscle weakness (69%) were found to be the most common risk factors present in this population and every patient met at least one risk factor beyond age (all residents were >70 y.o.). Also, prior to the assessement process, four patients had Vitamin D deficiency (defined by 25-OH Vitamin D blood concentration < 30 ng/mL) diagnosed and twenty patients were taking Vitamin D (2 or 3) of some dosage.

Conclusion: All long-term care residents in a representative nursing home in Florida were at high risk for vitamin D deficiency. Vitamin D supplemenation was provided for all. Further testing in additional facilities is warranted and, if results are similar, implementation of supplementation for all residents can be recommended without jeopardizing the individualization of care plans.

***Disclosures: F. Michael Gloth**, None.*

MO0429

Bone Material Strength by Microindentation in Patients Initiating Glucocorticoids and Effect of Treatments. Elisa Torres-Del-Pliego[1], Leonardo Mellibovsky[2], Xavier Nogues[3], Robert Guerri Fernandez[4], Laia Vilaplana[2], Fernando Mellibovsky[5], Daniel Prieto-alhambra[6], Adolfo Diez-Perez*[7]. [1]Internal Medicine Department, Hospital del Mar, Barcelona, Spain, [2]Servicio de Medicina Interna. Hospital del Mar, Spain, [3]Institut Municipal D'Investigació Mèdica, Spain, [4]Fundacio IMIM, Spain, [5]Engineer. Universidad Politecnica de Cataluña, Spain, [6]University of Oxford, United Kingdom, [7]Autonomous University of Barcelona, Spain

Fracture risk increases very early after starting glucocorticoids (GC) well before bone mineral density (BMD) shows any change. Microindentation can detect changes in Bone Material Strength (BMS) of bone tissue, related with bone fragility and fracture independent of BMD. We assess early changes in BMS in patients initiating glucocorticoids and the response to treatment.

A series of 26 consecutive patients were included in the study at the time of starting glucocorticoids (polymyalgia rheumatica/Horton arteritis 11, sarcoidosis 6, myasthenia gravis 2, rheumatoid arthritis 1, scleroderma 1, pemphigus 1, serositis 1, systemic vasculitis 1, adult Still's disease 1). A general laboratory workup, BMD by DXA, and BMS measurement at the anterior midtibia were performed with an Osteoprobe® (Active Life Scientific Sta Barbara CA) device. Measurements were performed at baseline and after 7+1.5 weeks of treatment with either calcium + vitamin D3 (Ca+D3) alone, bisphosphonates (BP) plus Ca+D3 or teriparatide (TPTD) plus Ca+D3 for the different risk categories, according to the official guidelines of the Spanish Bone and Mineral Society (SEIOMM). Median age for the different groups were: Ca+D3: 55.9+14.9, BP: 80+6, PTH: 62.2+27.6. Age adjusted no differences between groups. For the 14 patients treated with Ca+D3, BMS significantly declined from baseline (81.8+5.3) to the follow up visit (72.8+8.1, $p<0.001$). Non-significant increase was observed for the 6 cases treated with bisphosphonates (78.7+6.6 to 81.9+12.4) while teriparatide-treated patients (6 cases) significantly increased BMS from baseline to week 7 (72.8+7.5 vs. 85.2+4.9, $p<0.001$). No changes in BMD between baseline and follow up were observed in any of the groups. The main results are displayed in the figure1. Further follow up is underway at week 20.

We conclude that microindentation can detect very early changes in bone material strength at a tissue level induced by GC. Effect of different treatments iuis diverse in these cases and can be tracked prematurely. The effect of GC and the different treatments in bone tissue properties, related with fracture propensity, might offer an opportunity for monitoring changes induced by GC and their treatments well beyond what BMD currently allows.

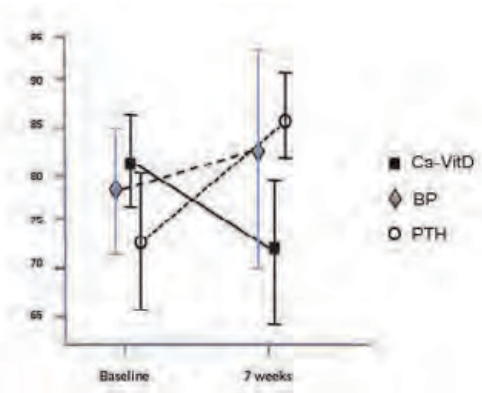

Figure 1. Bone material strenght changes in different treatment

***Disclosures: Adolfo Diez-Perez**, None.*

MO0430

Bone Microarchitecture in Young Adults with Cystic Fibrosis: Differential Mechanisms of Fragility in Weight Bearing and Non-Weight Bearing Bone. Melissa Putman*[1], Nicholas Derrico[2], Leonard Sicilian[3], Ahmet Uluer[4], Allen Lapey[5], Catherine Gordon[6], Mary Bouxsein[7], Joel Finkelstein[8]. [1]Massachusetts General Hospital, Children's Hospital Boston, USA, [2]Endocrine Unit, Massachusetts General Hospital, USA, [3]Pulmonary & Critical Care Medicine, Massachusetts General Hospital, USA, [4]Division of Pulmonary & Respiratory Diseases, Boston Children's Hospital, USA, [5]Pediatric Pulmonary Medicine Massachusetts General Hospital for Children, USA, [6]Hasbro Children's Hospital & Brown University, USA, [7]Beth Israel Deaconess Medical Center, USA, [8]Massachusetts General Hospital, USA

Purpose: Young adults with cystic fibrosis (CF) are at risk for low bone density and fractures, but the underlying alterations in bone microarchitecture are currently unknown. High-resolution peripheral quantitative computed tomography (HR-pQCT) can provide detailed information regarding volumetric bone mineral density (vBMD), cortical and trabecular microarchitecture, and estimates of bone strength using microfinite element analysis (μFEA).

Methods: We performed HR-pQCT scans (Scanco Medical AG) of the radius and tibia in 22 young adults with CF ages 18-30 years to assess cortical and trabecular vBMD, bone microarchitecture, and bone strength by μFEA. Areal BMD measures by DXA of the hip, spine, and total body were also obtained. CF subjects were compared with 44 healthy volunteers matched by age (±3 years), gender, and race.

Results: Subjects with CF were 24.4±3.5 years old, and 59% were female. Most recent FEV1 was 73.1±28.9% predicted, and a broad range of cystic fibrosis transmembrane regulator (CFTR) genotypes were represented. Subjects with CF had a lower BMI than controls (20.7 vs 25.0 kg/m^2, $p<0.01$) and 37.5% reported a history of fracture. CF subjects reported adequate calcium (2162±1868 mg/day) and vitamin D intake (2050±1950 IU/day). Areal BMD was significantly lower at the femoral neck, total hip, and PA spine in CF compared to healthy volunteers ($p<0.05$ for all). At the distal radius, CF subjects had lower total area and cortical area ($p<0.05$ for all), but the remainder of vBMD and bone microarchitectural measures were similar to normals. At the tibia, CF subjects had lower total vBMD, cortical area and volume, trabecular vBMD, and trabecular number, along with higher trabecular separation and heterogeneity vs controls ($p<0.05$ for all). Cortical porosity of the radius and tibia did not differ between groups. μFEA revealed significantly lower stiffness and failure load at both the radius and tibia in CF subjects ($p<0.05$ for all).

Conclusions: Young adults with CF have compromised bone microarchitecture and estimated bone strength at both the radius and tibia. At the non-weight bearing radius, reductions in total and cortical area predominate, whereas trabecular microarchitecture and trabecular vBMD were compromised in addition to lower cortical area at the weight-bearing tibia. Further studies are needed to understand the underlying pathophysiology and clinical implications of these bone alterations.

Table 1: HR-pQCT Results (mean ± SD)

	Radius		Tibia	
	CF Subjects	Healthy Volunteers	CF Subjects	Healthy Volunteers
Total Area (mm^2)	268 ± 38*	299 ± 75	656 ± 147	729 ± 157
Total vBMD (mgHA/cm^3)	316 ± 61	328 ± 52	297 ± 60*	336 ± 48
Cort Area (mm^2)	53.6 ± 11*	60.4 ± 11	110 ± 25*	125 ± 25
Cort Volume (mm^3)	458 ± 102	497 ± 100	924 ± 195*	1053 ±197
Cort vBMD (mgHA/cm^3)	948 ± 31	951 ± 35	936 ± 60	957 ± 36
Cort Thickness (mm)	0.84 ± 0.18	0.87 ± 0.16	1.20 ± 0.23	1.25 ± 0.20
Cort Porosity (%)	1.03 ± 0.56	1.36 ± 0.79	3.66 ± 2.97	3.15 ±1.72
Trab vBMD (mgHA/cm^3)	175 ± 44	187 ± 41.5	170 ± 45*	207 ± 42
Trab Number (mm^{-1})	2.07 ± 0.23	2.08 ± 0.28	1.79 ± 0.25*	2.09 ± 0.38
Trab Thickness (mm)	0.07 ± 0.01	0.07 ± 0.01	0.079 ± 0.017	0.083 ± 0.012
Trab Separation (mm)	0.42 ± 0.08	0.41 ± 0.07	0.49 ±0.10*	0.41 ± 0.09
Trab Distribution (μm)	0.17 ± 0.06	0.17 ± 0.04	0.22 ±0.09*	0.18 ± 0.6
Stiffness (N/mm)	76224 ± 22511*	93694 ± 32488	202382 ± 57166*	246353 ± 55360
Failure Load (N)	3857 ± 1097*	4556 ± 1394	10214 ± 2786*	12358 ± 2765

*p<0.05 comparing CF subjects with age, gender, and race-matched healthy controls

Table 1

***Disclosures: Melissa Putman**, None.*

This study received funding from: Vertex Pharmaceuticals Investigator Initiated Studies Grant

MO0431

CTX as an early prediction on bone loss in women on aromatase inhibitors: the B-ABLE cohort study. Elisa Torres-Del-Pliego[1], Daniel Prieto-alhambra[2], Sonia Servitja[3], Raquel Soriano-Tomas[4], Iria González-Maeso[3], Natalia Garcia-Giralt[5], Maria Rodríguez-Sanz[6], Adolfo Diez-Perez[7], Ignacio Tusquets[3], Xavier Nogues*[8]. [1]Internal Medicine Department, Hospital del Mar, Barcelona, Spain, [2]University of Oxford, United Kingdom, [3]Medical Oncology Department, Parc de Salut Mar, Spain, [4]Internal Medicine Department, Parc de Salut Mar, Spain, [5]IMIM, Spain, [6]URFOA-IMIM Red Temática de Investigación Cooperativa en Envejecimiento y Fragilidad (RETICEF), Instituto de Salud Carlos III FEDER, Spain, [7]Autonomous University of Barcelona, Spain, [8]Institut Municipal D'Investigació Mèdica, Spain

Purpose: According to results from RCTs, the use of aromatase inhibitors (AI) in the adjuvant treatment of breast cancer results in decreased bone mineral density (BMD) and increased fracture risk. However, there is variability in the intensity of AI-related bone loss, making it difficult for the clinician to decide on who to treat with anti-resorptives based on other than baseline BMD measurements.

To address this issue, we analyzed the association between levels of C-telopeptide (CTX) at 3 months post-therapy initiation and bone loss at one year..

Methods: B-ABLE is a prospective cohort study including a consecutive sample of postmenopausal women at the time when they are started on AI treatment for hormone-sensitive early breast cancer. As recommended by current guidelines, women with a T score <-2.0 or with any clinical risk factor received oral bisphosphonates and Calcium and Vitamin D supplements. All others received only Calcium and Vitamin D supplementation. The latter were included for this study. A random sample of these women had CTX measured at baseline and 3-months, and all participants had a DXA scan at baseline and 1 year follow-up.

Main exposure was change in CTX at 3 months (ΔCTX3m) defined as 3-month CTX minus baseline. Main outcome was absolute bone loss at 1 year (ΔBMD1y), defined as Lumbar Spine (LS) BMD (in gr/cm2) at baseline minus 1-year BMD. We tested for the association between ΔCTX3 and ΔBMD using linear regression.

Results: 121 participants had CTX measurements available. Baseline and 3-months mean (SD) CTX levels were 0.472(0.244) and 0.565(0,265) ng/ml respectively. Similarly, LS BMD was 0.955(0.113) g/cm2 at baseline, and 0.942(0.115) after 1 year of AI therapy. ΔCTX3m was significantly associated with ΔBMD1y: beta 0.04 g/cm2 per 1 ng/ml [95%CI 0,0068-0,0180].

Conclusions: In women starting AI therapy for early breast cancer who do not require anti-resorptive treatment, 3-month CTX increments can be used to predict 1-year bone loss. This could be used to target patients with highest bone loss rates, who could potentially benefit from early preventative interventions to reduce fracture risk.

***Disclosures: Xavier Nogues**, None.*

MO0432

Decreased exercise capacity negatively affects bone mass in patients with acute decompensated heart failure. Yumie Rhee*[1], Jong-Chan Youn[2], Seok-Min Kang[2]. [1]Department of Internal Medicine, College of Medicine, Yonsei University, South Korea, [2]Division of Cardiology, Severance Cardiovascular Hospital, Yonsei University College of Medicine, South Korea

Heart failure is associated with increased risk of osteoporosis. However, the prevalence and predictors of osteoporosis in patients with acute decompensated heart failure (ADHF) are not well investigated. Fifty male patients with ADHF (60 ± 16 years, mean ejection fraction 28.0 ± 11.5%) were prospectively and consecutively enrolled. Quantitative CT scans for volumetric bone mineral density (vBMD) as well as biochemical, echocardiographic and cardiopulmonary exercise tests were evaluated. Sixteen patients (32%) had osteopenia (lumbar vBMD of 80-120 mg/cm^3) and six patients (12%) had osteoporosis (vBMD < 80 mg/cm^3). C-telopeptide of type I collagen (0.564 ± 0.323 ng/mL) was within normal range, however osteocalcin (18.7 ± 23.2 ng/mL) and 25-hydroxyvitamin D (13.8 ± 7.0 ng/mL) were low, while parathyroid hormone (65.3 ± 41.0 pg/mL) was increased. Lumbar vBMD was lower in ischemic patients than non-ischemic patients (107.9 mg/cm^3 *vs.* 144.7 mg/cm^3, p=0.007). Multivariate regression analysis revealed peak VO_2, which is a well known prognostic marker in ADHF, independently predicted low lumbar vBMD when controlled for age, BMI, etiology of heart failure (β=0.487, p=0.022, Figure 1). In conclusion, low bone mass is prevalent in ADHF patients, especially more in ADHF due to ischemia. The exercise capacity independently predicted low lumbar vBMD in patients with ADHF. These findings may explain the novel relationship between exercise capacity and BMD in ADHF patients.

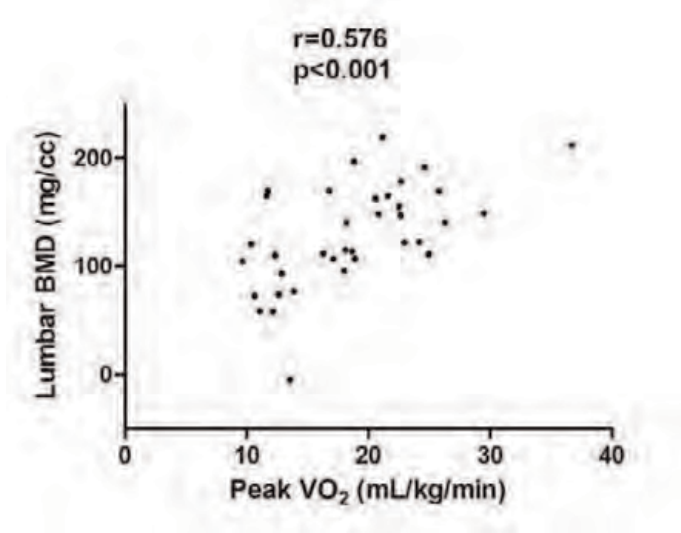

Figure 1

***Disclosures: Yumie Rhee**, None.*

MO0433

Determination of the Role Autophagy on Bone Metabolism and Structure during the Initiation and Progression of Type 2 Diabetes. Elizabeth Rendina*[1], Jennifer Graef[1], McKale Davis[1], Jeffrey Gimble[2], Stephen Clarke[1], Edralin Lucas[1], Brenda Smith[1]. [1]Oklahoma State University, USA, [2]Pennington Biomedical Research Center, USA

Type 2 diabetes mellitus (T2DM) is a major public health problem affecting approximately 26 million Americans. Patients with T2DM have demonstrated a 1.5 - 3.5 fold increase in fracture incidence despite no change or an increase in bone mineral density (BMD). Although there has been a growing interest in the field, the mechanism associated with this disconnect has remained elusive. Macroautophagy, hereafter referred to as autophagy, is regulated by the signaling cascade downstream of the insulin receptor and cellular glucose availability. Metabolic changes occurring during the initiation and progression of T2DM may alter autophagy in osteoblasts and osteoclasts activity. To determine whether autophagy plays a role in the dysregulation of bone metabolism associated with T2DM, 4-week old, male C57BL/6 mice were fed a control or high fat diet (HFD) for 2, 8, and 16 wks. Animals on the HFD experienced an increase in body weight after 1 week and maintained a significantly higher body weight throughout the remainder of the study. Consistent with impaired insulin signaling, animals on the HFD demonstrated elevated blood glucose despite increased plasma insulin after 16 wks. The HFD resulted in impaired glucose tolerance which was exacerbated over time. Whole body BMD, determined by dual energy x-ray absorptiometry (DXA; PixiMUS GE Lunar), was decreased after 8 and 16 wks on the HFD. Micro-computerized tomography (μCT; SCANCO Medical) analyses revealed that the animals on the HFD had a lower trabecular bone volume (BV/TV) in the distal femur metaphysis and femoral neck at 8 and 16 wks. No changes were observed in trabecular bone of the vertebra at any time point. Cortical thickness and area of the femoral diaphysis was decreased only at the 8 wk time point in response to the HFD. PCR array sought to determine whether alterations in insulin signaling corresponded to transcriptional regulation of autophagic machinery in the bone marrow and mineralized portion of the flushed femur. Preliminary array results suggest alterations in genes associated with the down-regulation of autophagy (*i.e., Dram1* and *Tgfb*) occur after 2 wks on a HFD. However at 8 and 16 wks genes involved in autophagy, such as *Rb1*, *Becn1, Gabarapl2, Sqstm1*, and *Ulk1* were up-regulated. Further investigation of how autophagy alters osteoblasts and osteoclasts during the advancement of T2DM is warranted and could lead to innovative therapeutic options to reduce fracture risk.

***Disclosures: Elizabeth Rendina**, None.*

MO0434

Does The Choice Of Surgical Technique Affect Bone Turnover Changes After Bariatric Surgery?. Kaisa Ivaska*[1], Minna Soinio[2], Jarna Hannukainen[3], Pauliina Salminen[4], Pirjo Nuutila[2], Riku Kiviranta[5]. [1]University of Turku, Finland, [2]Department of Medicine, University of Turku & Turku PET Centre, Finland, [3]Turku PET Centre, Finland, [4]Department of Surgery, Turku University Hospital, Finland, [5]Department of Medical Biochemistry & Genetics & Department of Medicine, University of Turku, Finland

Bone and adipose tissue interact at multiple levels. Adipokines secreted by the fat tissue control both energy homeostasis and the skeleton while bone is also recognized as an endocrine organ that is capable of regulating energy metabolism. Bariatric surgery by either gastric bypass or sleeve gastrectomy has become a worthy option to treat severe obesity. It results in rapid weight loss often accompanied with normalization of plasma glucose levels in patients with type 2 diabetes (DM2), both of which have implications for bone health. Our aim was to evaluate the changes in bone turnover, particularly osteocalcin, in response to gastric bypass or sleeve gastrectomy.

23 morbidly obese subjects (mean BMI 43.1 +/- 3.7 kg/m2, 14 with DM2) underwent either gastric bypass (n=13) or sleeve gastrectomy (n=10). An oral glucose tolerance test (OGTT, 120 min) and hypersinsulinemic euglycemic clamp were performed and fasting serum samples collected before and 6 months after the operation. A panel of bone turnover markers, adipokines and cytokines were analyzed. Ten healthy subjects with normal body weight (BMI 23.7 +/- 1.8 kg/m2) were recruited as a reference group.

Bariatric surgery resulted in significant weight loss (mean -23.1 +/- 6.2 %) and a decrease in circulating leptin ($p<0.01$). Diabetes was in remission in 9 of the 14 diabetics after surgery.. All bone markers increased significantly after surgery, ranging from +65% to +270% depending on the marker ($p<0.01$ for all). There were no significant differences in weight loss, glucose or leptin values between the two procedures ($p>0.05$), but the increase in bone turnover was more pronounced in subjects that underwent gastric bypass ($p<0.05$ for PINP and CTX; $p<0.01$ for osteocalcin). Patients with DM2 before the operation had significantly lower osteocalcin values than the control group ($p<0.01$). Post-surgery increases in bone markers did not correlate with insulin sensitivity but appeared to be most pronounced in those whose DM2 was in remission after surgery, although the differences were not statistically significant.

Bone turnover is increased in response to bariatric surgery. The increase in turnover is more pronounced when proximal small intestine is bypassed in addition to reducing the stomach size, and in subjects with DM2 that achieve remission after surgery. Thus both diabetes status and the choice of surgical technique may affect the changes in bone turnover after bariatric surgery.

***Disclosures: Kaisa Ivaska**, None.*

MO0435

Lean Mass And Not Fat Mass Is Associated With Measures Of Better Bone Health In Type 2 Diabetes Mellitus. Indira Maisnam*[1], Deep Dutta[2], Anubhav Thukral[2], Rajesh Jain[2], Satinath Mukhopadhyay[2], Subhankar Chowdhury[2]. [1]IPGMER & SSKM Hospital, India, [2]IPGMER, India

Background

The fracture risk in type 2 diabetes mellitus is high. Studies have shown increased, decreased or normal bone mineral density (BMD) in type 2 diabetes compared to controls. This heterogeneity could be due to body composition (lean vs. fat mass), which may affect bone health differently. Type 2 diabetes is frequently associated with obesity and accelerated lean mass loss.

Purpose of the study

To compare the BMD and bone mineral content (BMC) in obese and non-obese type 2 diabetes; and to evaluate the relationship between fat mass and lean mass with BMD and BMC in type 2 diabetes

Methods: Cross-sectional observational study, conducted between January 2011 and January 2013. Type 2 diabetes 35 to 55 years were recruited. Conditions that may affect bone health were excluded from the study. Patient were obese if body mass index (BMI) was $\geqslant 25 kg/m^2$ (based on Indian criteria). Dual Energy X- Ray Absorptiometry (DXA) done with a GE Lunar DPX NT densitometer was used to measure BMD at the lumbar spine& both femur, BMC, lean and fat mass. Statistical analysis was done with SPSSv20.

Results: There were age-matched 76 type 2 diabetes and 44 controls. Obese controls and obese diabetes had significantly higher BMD at all sites compared to non-obese controls and non-obese diabetes respectively (Tables 1 and 2). Non-obese diabetes had similar BMD compared to non-obese controls except at one site (left femur) where non-obese diabetes had higher BMD (Table 3). Obese diabetes had similar BMD compared to obese controls except at one site (lumbar spine) where obese diabetes had higher BMD (Table 4). We looked for correlation between lean mass and fat mass with BMD and BMC. In diabetes there was a significantly positive strong correlation between BMI and BMC, and a stronger correlation of lean mass with BMC that persisted after adjusting for height, however there was no significant correlation between fat mass and BMC (Table 5). Also in diabetes, BMD positvely correlated with lean mass at both femur but not with fat mass. In controls lean mass and not fat mass positively correlated with BMC; and both lean mass and fat mass correlated with BMD at some sites (Table 5).

Conclusion: The positive correlation between body weight with BMD and BMC in type 2 diabetes was due to lean mass and not fat mass. Controls too had a positive correlation of lean mass with BMD and BMC. But the correlation was stronger and more significant in type 2 diabetes mellitus compared to controls.

Table 1: Table showing comparison of the various parameters between non-obese and obese type 2 diabetes mellitus

Parameter	Non-obese T_2DM (45)	Obese T_2DM (31)	p value
BMI (kg/ m^2)	22.3±1.67	27.8±2.10	<0.001
WC (cm)	84.5±7.87	96.8±7.86	<0.001
BMD(Right femur) (g/cm^2)	0.95±0.125	1.11±0.15	<0.001
BMD(Left femur) (g/cm^2)	0.97±0.11	1.13±0.13	<0.001
BMD (Lumbar spine) (g/cm^2)	1.05±0.12	1.22±0.16	<0.001
Fat mass (g)	16288±3948.74	27058±7485.99	<0.001
Lean mass (g)	34722±7093.28	36918±7481.12	0.226
BMC (g)	2169±319.14	2495±402.76	0.001

T_2DM: Type 2 Diabetes Mellitus , BMI: Body Mass Index, WC: Waist Circumference, BMD: Bone Mineral Density, BMC: Bone Mineral Content

p value < 0.05 considered significant

Table 1

Table 2: Table showing comparison of the various parameters between non-obese and obese controls

Parameter	Non-obese Controls(n=12)	Obese Controls (n=32)	P value
BMI (kg/ m^2)	21.9±1.50	28.2±2.65	<0.001
WC (cm)	79.3±3.50	98.2±6.04	<0.001
BMD(Right femur) (g/cm^2)	0.9±0.11	1.07±0.17	0.01
BMD(Leftt femur) (g/cm^2)	0.88±0.11	1.08±0.18	0.001
BMD (Lumbar spine) (g/cm^2)	1.01±0.05	1.14±0.15	0.007
Fat mass (g)	18169±1945	30729±6846	<0.001
Lean mass (g)	35823±7662	36207±7313	0.87
BMC (g)	2278±361	2579±626	0.12

T_2DM: Type 2 Diabetes Mellitus , BMI: Body Mass Index, WC: Waist Circumference, BMD: Bone Mineral Density, BMC: Bone Mineral Content

p value < 0.05 considered significant

Table 2

Table 3: Table showing comparison of the various parameters between non-obese controls and non-obese type 2 diabetes mellitus

Parameter	Non-obese control (n=12)	Non-obese T_2DM (n=45)	p value
BMI (kg/ m^2)	21.9±1.50	22.3±1.67	0.399
WC (cm)	79.3±3.50	84.5±7.87	0.058
BMD(Rightt femur) (g/cm^2)	0.9±0.11	0.95±0.125	0.258
BMD(Left femur) (g/cm^2)	0.88±0.11	0.97±0.11	0.028
BMD (Lumbar spine) (g/cm^2)	1.01±0.05	1.05±0.12	0.274
Fat mass (g)	18169±1945	16288±3948.74	0.120
Lean mass (g)	35823±7662	34722±7093.28	0.646
BMC (g)	2278±361	2169±319.14	0.39

T_2DM: Type 2 Diabetes Mellitus, BMI: Body Mass Index, WC: Waist Circumference, BMD: Bone Mineral Density, BMC: Bone Mineral Content

p value < 0.05 considered significant

Table 3

Table 4: Table showing comparison of the various parameters between obese controls and obese type 2 diabetes mellitus

Parameter	Obese control (n=32)	Obese T_2DM (n=31)	p value
BMI (kg/m^2)	28.2±2.65	27.8±2.10	0.569
WC (cm)	98.2±6.04	96.8±7.86	0.427
BMD(Rt femur) (g/cm^2)	1.07±0.17	1.11±0.15	0.119
BMD(Lt femur) (g/cm^2)	1.08±0.18	1.13±0.13	0.263
BMD (Lumbar) (g/cm^2)	**1.14±0.15**	**1.22±0.16**	**0.048**
Fat mass (g)	**30729±6846**	**27058±7485.99**	**<0.05**
Lean mass (g)	36207±7313	36918±7481.12	0.711
BMC (g)	2579±626	2495±402.76	0.545

T_2DM: Type 2 Diabetes Mellitus, BMI: Body Mass Index, WC: Waist Circumference, BMD: Bone Mineral Density, BMC: Bone Mineral Content

p value < 0.05 considered significant

Table 4

Table 5: Table showing correlation of the various parameters in controls and type 2 diabetes mellitus

Controls				Type 2 Diabetes Mellitus			
Parameter 1	Parameter 2	Pearson Correlation co-efficient	P value	Parameter 1	Parameter 2	Pearson Correlation co-efficient	P value
BMC	BMI	0.019	0.902	**BMC**	**BMI**	**0.440**	**<0.001**
BMC	Fat Mass	0.195	0.204	BMC	Fat Mass	0.162	0.191
BMC	**Lean Mass**	**0.756**	**<0.001**	**BMC**	**Lean Mass**	**0.827**	**<0.001**
BMC*	**Lean Mass***	**0.524**	**<0.001**	**BMC***	**Lean Mass***	**0.623**	**<0.001**
BMD (Rt)	**Lean Mass**	**0.565**	**<0.001**	**BMD (Rt)**	**Lean Mass**	**0.484**	**<0.001**
BMD (Lt)	**Lean Mass**	**0.535**	**<0.001**	**BMD (Lt)**	**Lean Mass**	**0.440**	**0.009**
BMD (LS)	**Lean Mass**	**0.482**	**0.001**	BMD (LS)	Lean Mass	0.179	0.146
BMD (Rt)	Fat Mass	0.277	0.068	BMD (Rt)	Fat Mass	0.305	0.012
BMD (Lt)	**Fat Mass**	**0.401**	**0.007**	BMD (Lt)	Fat Mass	0.315	0.009
BMD (LS)	Fat Mass	0.350	0.02	BMD (LS)	Fat Mass	0.280	0.022

*after correcting for height

BMC: Bone Mineral Content, BMD (Rt): Bone Mineral Density Right Femur, BMD (Lt): Bone Mineral Density Leftt Femur, BMD (LS): Bone Mineral Density Lumbar Spine

Correlation coefficient >0.4 suggests positive correlation, p value < 0.05 considered significant

Table 5

***Disclosures: Indira Maisnam**, None.*

MO0436

Low Bone Density and Fractures Associated with Cannabis Use – A Population Based Prospective Study. Antonia Sophocleous*[1], James McKenzie[1], Roy Robertson[2], Stuart H Ralston[1]. [1]Rheumatic Disease Unit, Centre for Molecular Medicine, Institute of Genetics & Molecular Medicine, University of Edinburgh, United Kingdom, [2]Centre for Population Health Sciences, University of Edinburgh, United Kingdom

Preclinical studies have shown that the endocannabinoid system of ligands and receptors play a key role in the regulation of bone mass and bone turnover. Mice with targeted inactivation of the type 1 cannabinoid receptor have increased peak bone mass and are protected against ovariectomy induced bone loss due to reduced osteoclastic bone resorption. Conversely, cannabinoid receptor agonists have been found to increase osteoclast differentiation *in vitro*. Together these observations raise the possibility that cannabinoid receptor agonists might be detrimental for bone health. In this study therefore, we investigated the effects of recreational cannabis use on bone mineral density and fracture risk. The study was conducted in 113 regular cannabis users and 78 controls recruited from the local community. Cannabis use was quantified in terms of "joint-years", where 1 joint-year was defined as smoking 365 cannabis-containing cigarettes. The controls were selected on the basis that they smoked cigarettes but did not smoke cannabis. Information was collected on age, gender, tobacco smoking, alcohol, diet, weight, height and fractures. Bone mineral density was measured by DEXA at the lumbar spine and total hip. Heavy cannabis users (>57 joint-years) had a significantly lower total hip bone density Z-score than controls (-0.11 ± 0.83 *vs.* +0.41±0.95; p=0.007) with intermediate values (+0.18 ± 1.05) in the moderate users (≤57 joint-years). Cannabis users were about 10 years younger than controls (39.5 ± 9.8 *vs.* 49.6 ± 9.3 years; p<0.001). There was no difference between groups in spine Z-score values. Heavy cannabis users had a lower body mass index than controls (25.7 ± 5.8 *vs.* 29.6 ± 6.9; p=0.003) whereas values in moderate users were similar to controls (28.9 ± 7.4). Heavy cannabis users had a significantly higher dietary calcium intake than controls (1464 ± 1022 *vs.* 896 ± 439mg/day; p<0.001) with intermediate values in moderate users (1039 ± 609mg/day). There was no difference in cigarette smoking or alcohol intake between groups. There was a preponderance of males in the heavy cannabis users group (61.4%). Fractures were more common in cannabis users (56% *vs.* 43%; p=0.09), and multiple fractures (3 or more) were significantly more common (13.3% *vs.* 1.3%; p=0.014). We conclude that heavy cannabis use impacts negatively on bone health and is associated with reduced body mass index and an increased risk of multiple fractures.

***Disclosures: Antonia Sophocleous**, None.*

MO0437

Study of Very Long Term (> 25 years) L-Thyroxine Suppressive Therapy in Postmenopausal Women With Differentiated Thyroid Cancer: Effect on Bone Mineral Density and Bone Turnover Markers. María Luísa de Mingo Domínguez*[1], Guillermo Martinez Diaz-Guerra[1], Sonsoles Guadalix Iglesias[1], Gonzalo Allo Miguel[1], Mercedes Aramendi[1], Federico Hawkins[2]. [1]University Hospital 12 De Octubre, Spain, [2]Hospital Universitario, Spain

Background: After initial therapy (thyroidectomy with or without radioiodine), all patients with differentiated thyroid cancer (DTC) are treated with high doses of L-thyroxine (LT4) aimed at suppressing thyrotropin (TSH) levels. However, there is uncertainty about the potential adverse effects of long-term suppressive therapy, particularly in relation to increased risk of developing osteoporosis. The objective of this study is to investigate the effects of very long-term treatment with LT4 on bone mineral density (BMD) and bone remodeling.Methods: 30 postmenopausal women (age 64.5± 10.2 years) with DTC were studied. All of them had undergone total thyroidectomy followed by radioiodine ablative therapy and were on TSH suppressive treatment for a median period of 27.8 ± 3.1 years. BMD was measured by dual energy X-ray absorption (DXA) at baseline and at the present time at lumbar spine (LS), Total hip (TH), femoral neck (FN), ultradistal radius (UDR), midradius (MDR) and distal third radius (1/3DR). Bone turnover markers (β-CTX and osteocalcin) and calcitropic hormones (PTH and 25OH vitamin D) were measured. For comparisons, patients were classified according to their menopausal status at baseline: premenopausal (group 1) or postmenopausal (group 2). For statistical analysis SPSS v.21 was used.Results: Group 1: n=17, age 57.6 ± 6.1; Group 2: n=13, age 73.6 ± 6.8 . Compared with baseline, we found a statistically significant decrease in BMD at LS (p=0.000), FN (p= 0.000) and 1/3DR (p=0.02) in group 1 . No significant changes were found in group 2. Percentage of BMD variation were: Group 1: LS -11.7± 9.0%; FN -12.8 ± 9.7%; TH -0.3 ± 12.1%; UDR -3.3 ± 10.0%. Group 2: LS 4.6 ± 19.7%; FN -6.9 ± 12.0%; TH 2.2 ± 5.3%; UDR 8.4 ± 4.3%. At the second DXA, group 2 had lower TH (p=0.02), UDR (p=0.047), MDR (p=0.002) and 1/3DR BMD (p=0.017) than group 1. Osteoporotic women were 46.7% (total), 29.4% (group 1) and 69.2% (group 2). No correlation was found between BMD and TSH, free T4, or LT4 dose (either total or adjusted per body weight). Only osteocalcin showed a weak negative correlation with UDR BMD (r= -0.46, p < 0.01).Conclusion: Very long-term LT4 suppressive therapy in postmenopausal women with DTC does not adversely affect bone mineral density. Estrogen deprivation appears to be the most important factor for bone loss in previous premenopausal women with DTC

***Disclosures: María Luísa de Mingo Domínguez**, None.*

MO0438

The Association of Serum Osteocalcin with Glucose Control, Pancreatic Function and Insulin Resistance in Type Two Chinese Diabetes Patients. Hui Sheng*[1], Xuefei Rui[2], Chunping Pan[2], Junlei Su[2], Chenyu Zhan[2], Shen Qu[3]. [1]Shanghai, Fudan University, Peoples Republic of China, [2]Department of Endocrinology & Metabolism, Shanghai Tenth People's Hospital, Tongji University School of Medicine, China, [3]Tongji University School of Medicine, Peoples Republic of China

This study is to investigate the association between serum osteocalcin and glucose control, pancreatic function and insulin sensitivity in the type 2 diabetes mellitus (T2DM) Chinese patients.

1019 T2DM patients were recruited (Male:432, Female:587, Average age: 65.96 ± 13.11 years). After measured BMI, the fasting plasma glucose(FPG), insulin(FINS), C peptide(F-CP), postprandial blood glucose (2hPBG) and C peptide (2hC-P), HbA1C and osteocalcin were determined. Homeostasis model assessment of β cell function (HOMA-β) and homeostasis model assessment of insulin resistance (HOMA-IR) were calculated based on the above parameters.

The difference in osteocalcin levels between male and female are significant [(13.51±12.37)ng/mL vs (16.22±10.40)ng/mL, P<0.001]. After adjustment for age and BMI, serum osteocalcin was negatively correlated with HbA1C, FPG and 2hPBG (P<0.05), and positively correlated with fasting C peptide (FC-P), 2h C peptide (2hC-P) and HOMA-β (P<0.05). In male, after adjustment for age and BMI, serum osteocalcin was negatively correlated with 2hPBG (P<0.05), and positively correlated

with FC-P, 2hC-P and HOMA-β (P<0.05). In female, after adjustment for age and BMI, serum osteocalcin was negatively correlated with HbA1C, FPG (P<0.05). Multivariable liner regression analysis showed that serum osteocalcin was the independent related factor in influencing HOMA-β and HOMA-IR in male, and it was also the independent related factor in influencing HOMA-IR in all subjects (P<0.05).

In T2DM, osteocalcin was negatively associated with glucose, implying osteocalcin could lower blood glucose. And osteocalcin was positively associated with FC-P, 2hC-P and HOMA-β, supporting the idea that osteocalcin might improve glucose control through promoting insulin secretion of pancreatic islet.

***Disclosures: Hui Sheng**, None.*

MO0439

Trabecular Bone Assessment in Type 2 Diabetes Mellitus. Mishaela Rubin*[1], Ankit Shah[1], Chiyuan Zhang[1], Serge Cremers[1], Elzbieta Dworakowski[1], Laura Beth Anderson[1], Didier Hans[2], Shonni Silverberg[1]. [1]Columbia University, USA, [2]Lausanne University Hospital, Switzerland

Type 2 diabetes mellitus (T2D) is associated with increased fracture risk despite greater bone mineral density (BMD). The reason for this paradox is not fully understood. Trabecular bone score (TBS) provides information independent of BMD by extracting variations in the spine DXA image, with more heterogeneity giving a lower score. TBS was recently shown to reflect skeletal fragility in T2D (Leslie et al JBMR 2013). We sought to confirm and extend these data by assessing the association of TBS with trabecular heterogeneity by high resolution pQCT (HRpQCT) and with changes in biochemical markers of bone turnover (BTM) in T2D. Postmenopausal T2D (n=14; duration T2D: 9 ± 2 yr; Hgb A1c: 9.3 ± 0.6%) and Controls (C; n=21; Hgb A1c: 5.6 ± 0.1%; p<0.001) of similar age (T2D: 58 ± 2 vs C: 58 ± 1 yr) and non-black race were compared. All had normal renal function and were on no bone-active medications or TZDs; 3 T2D and 4 Cs had prior fractures. TBS data were extracted from the Hologic DXA image using TBS iNsight software; HRpQCT data were obtained by XtremeCT (Scanco, Switzerland). Because weight was greater in T2D (T2D: 81 ± 5 vs C: 68 ± 3 kg; p=0.02), general linear models were used to compare T2D and Cs with the effect of weight removed. BMD by DXA did not differ at the spine, hip or forearm. Despite similar lumbar spine BMD (T2D: 0.920 ±0.03 vs C: 0.938 ± 0.03 gm/cm^2; p=0.68), TBS was significantly lower in T2D (T2D: 1.146 ± 0.04 vs C: 1.270 ± 0.02; p=0.01). Consistent with this, trabecular heterogeneity (SD of 1/Tb Number) at the tibia was greater in T2D (T2D: 0.397 ± 0.05 vs C: 0.259 ± 0.04; p=0.05). Other HRpQCT parameters did not differ. Weight adjusted biochemical indices showed that T2D had lower 25(OH)D (T2D: 18.2 ± 5 vs. C: 33.9 ± 4 ng/ml; p=0.02) and P1NP (T2D: 45.6 ± 3 vs. C: 63.2 ± 7 ng/ml; p=0.06) levels, but higher BAP (T2D: 50.6 ± 4 vs C: 34.7 ± 3 U/l; p=0.003). Osteocalcin, TRAP-5b and sCTx did not differ. In T2D, TBS correlated inversely with BAP (r=-0.69, p=0.04), while TBS was not associated with BTM in Cs. In summary, while BMD does not differ from controls in T2D, TBS is worse and is consistent with the greater trabecular heterogeneity seen on HRpQCT. The lower TBS may be associated with a defect in mineralization, as suggested by the low 25(OH)D and high BAP. Despite normal DXA measurements, these data suggest that abnormalities in trabecular bone could contribute to the observed increase in fracture risk in T2D.

***Disclosures: Mishaela Rubin**, None.*

MO0440

Severe alterations in cortical and trabecular bone microarchitecture in lung transplant recipients. Alexander Valentinitsch*, Lukas Fischer, Matthew DiFranco, Claudia Schueller-Weidekamm, Franz Kainberger, Georg Langs, Janina Patsch. Medical University of Vienna, Austria

Organ transplant recipients often suffer from impaired bone strength arising from a combination of pre-existing secondary osteoporosis and disease aggravation in the post-transplant phase caused by various factors such as immunosuppressive therapy. In lung transplant (LUTX) recipients, the post-transplant drug regimen is particularly intense and fracture rates are high. Although, low bone mineral density [1] and altered states of bone turnover [2] have been described after LUTX, bone microarchitecture status has not been investigated in depth. After recovery from surgery, 46 patients (female:n=28,male:n=18;age=43.9±13.7yrs), and 46 healthy, age, and gender-matched controls (Co) underwent high resolution peripheral quantitative computed tomography (HR-pQCT) of the ultradistal radius. Scans were analysed with the standard and cortical analysis software of the manufacturer, and a 3D texture-based clustering method for trabecular bone (TMAC)[3]. Based on 3D morphology, TMAC defined three types of trabecular bone: TMAC1 contained thick trabeculae with low intertrabecular spacing, TMAC2 was characterized by trabeculae of intermediate morphometric quality, and TMAC3 was defined as regions with thinner, inhomogeneous trabeculae. Paired t-tests were used to compare mean differences between LuTX and Co. Compared with healthy women, female LUTX patients had higher cortical porosity (+51.5%,p=0.034), cortical pore diameter (+10.9%,p=0.009), diameter heterogeneity (+18.3%,p=0.021) and a higher volume fraction of morphologically poor trabecular bone (TMAC3; +41%,p=0.05). Compared with healthy men, male LUTX patients had lower cortical thickness (-18.9%,p=0.003), trabecular bone density (-23.3%,p=0.001), trabecular thickness (-14.4%,p=0.003), and trabecular number (-13%,p=0.028). TMAC3 was higher (+86.3%, p=0.02) and TMAC2 lower (-21.2%, p=0.001) than in healthy men. Our results indicate that cortical integrity and trabecular bone microarchitecture are both severely impaired in lung transplant recipients. Although, the morphologic pattern seems to vary with gender, men and women are affected by significant deficits in peripheral bone microarchitecture. Thinning and porosity of cortical bone might thus be crucial factors leading to disproportionally high risk of fragility fractures in lung transplant recipients. [1] Trombetti et al.(2000) J Heart Lung Transplant.19;736–743. [2] Aringer et al. (1998) Bone.23;485–488. [3] Valentinitsch et al. (2013) Bone.54;133–140.

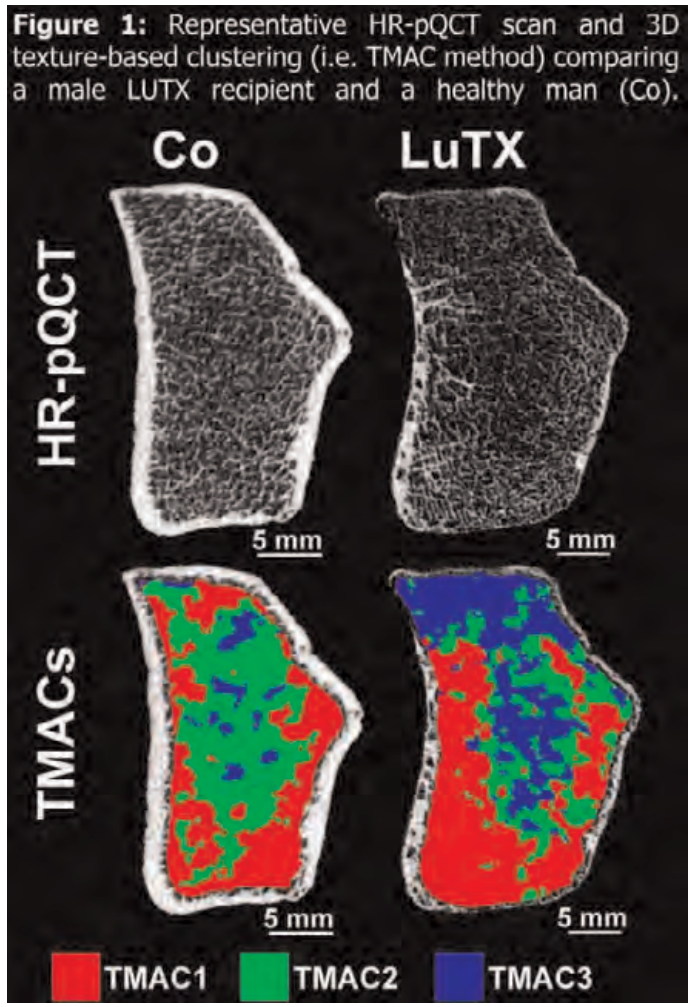

Example for HR-pQCT and texture clustering in LUTX

***Disclosures: Alexander Valentinitsch**, None.*

MO0441

Vitamin D Supplementation Decreases The Occurrence Of Acute Phase Response Following Intravenous Bisphosphonate Treatment In Paget's Disease Of Bone. Daniela Merlotti*[1], Luigi Gennari[1], Beatrice Franci[2], Barbara Lucani[2], Stella Campagna[2], Laura Cresti[2], Konstantinos Stolakis[2], Stefano Rotatori[2], Ranuccio Nuti[1]. [1]University of Siena, Italy, [2]Dept. Medicine Surgery & Neurosciences, University of Siena, Italy

Acute phase reaction (APR) is the most frequent side effect following the infusion of intravenous nitrogen-containing bisphosphonates (N-BPs), occurring in up to 40% of cases at the first infusion. A recent observation in postmenopausal women treated with N-BPs for osteoporosis evidenced a negative association between 25(OH)D levels and the development of APR, likely due to immuno-modulatory effects of vitamin D on gdTcells. However, this association remains to be demonstrated in patients with Paget's disease of bone (PDB). Moreover whether vitamin D supplementation is able to prevent the occurrence of APR has not yet been demonstrated. We initially performed a retrospective analysis of 205 consecutive patients treated with intravenous N-BPs (neridronic acid 200mg or zoledronic acid 5mg) for PDB. Overall APR occurred in 31% of cases and was more frequent in previously untreated patients (43%). Neither gender nor disease severity nor use of other drugs (i.e. statins or nonsteroidal anti-inflammatory drugs) apart previous N-BP treatment was associated with the occurrence of APR. Consistent with the previous report in osteoporotic women, 25(OH)D levels at the time of treatment were lower in PDB cases with APR than in patients who did not experience APR after infusion (16.4±7 vs 28.6 ±3 ng/ml, p<0.0001). Following this observation we performed a prospective study in 30 patients at the time of PDB diagnosis. Hypovitaminosis D was common in this cohort

of patients (mean 18.0±5 ng/ml; with 63% of cases below 20 ng/ml). All patients received oral vitamin D3 (7000 UI/week) for 60 days before N-BPs infusion with either zoledronic acid 5mg (16 pts) or neridronic acid 200mg (14 pts). Moreover a single oral dose of 25000 UI was given at baseline to all patients with 25(OH)D levels below 20 ng/ml. All adverse events occurring within the first week of the administration of the 2 N-BPs were listed. Of interest, APR occurred in 2/16 (12.5%) patients treated with zoledronic acid and 1/14 (7%) patients treated with neridronic acid (overall incidence rate 10%). In 2 of these cases 25(OH)D levels at the time of infusion were within the normal range (30.7 and 33.0 ng/ml) while in the third case remained below the range (18.8 ng/ml). These results suggest that APR following N-BPs infusion for PDB is a common event particularly in patients with hypovitaminosis D and that vitamin D supplementation prior bisphosphonate infusion is able to reduce the occurrence of this complication.

***Disclosures: Daniela Merlotti**, None.*

MO0442

Zoledronic Acid (ZA) Therapy in the Treatment of Patients with Paget's Disease of Bone (PD) Resistant to Prior Bisphosphonate Therapy or with an Unsustained Response of One Year or Less. Joseph Tucci*. Boston University School of Medicine, USA

The primary objective of this investigator initiated study supported by Novartis Pharmaceuticals was to evaluate the effect of (ZA) in patients previously treated with other bisphosphonates (etidronate, pamidronate, alendronate, risedronate) who had failed to respond or had remissions of ≤12 months. Patients included 7 males and 7 females who were 64-90 years of age. Three had been treated with intravenous pamidronate, 2 with risedronate, and 9 with 2, 3 or 4 bisphosphonates. Screening tests included chemistry profile, CBC, and serum PTH and 25-OHD. Serum alkaline phosphatase (SAP) and urine NTx creatinine ratios were measured before infusion of ZA and at 3,6,9, and 12 months, and thereafter at 4 monthly intervals for at least 3 years or until the offset of effect. Serum calcium was measured at baseline and 10-12 days after the infusion of ZA. At baseline, SAP ranged from 141-1009 U/L (normal 25-100). In all but 1 of 14 patients, SAP fell to normal following ZA. ZA effected remissions in 5 patients who had not had remissions with prior bisphosphonates and effected a more prolonged remission in the other 8 patients. Five patients withdrew from the study while in remission for 12,20,36,36, and 48 months. One patient was in remission at 24 months when she died following a stroke. One patient has remained in remission for 48 months and 2 others for 60 months. Normalization of SAP occurred in 1-9 months. Reactivation of (PD) occurred in one patient at 12 months who had previously failed to respond to alendronate and risedronate and in 3 patients at 24,36, and 40 months. ZA failed to induce a remission in 1 of the 14 patients despite a 74% decrease in SAP and failed to induce a remission followed a 2nd infusion. Serum calcium remained within normal limits 10-12 days after therapy in all but 2 asymptomatic patients in whom levels fell to 8 and 7.9 mg/dl. There were no other adverse clinical or biochemical effects that occurred during the 3 or more years of observation. In summary, ZA therapy was effective in 13 of 14 patients with PD in inducing remissions in 5 patients who had not had remissions with prior bisphosphonate therapy and in inducing more prolonged remissions in those who previously had remissions of ≤12 months. Our experience with 1 patient in whom a remission was not induced despite 2 courses of therapy is evidence of a continuing therapeutic challenge for some patients with a more resistant form of PD.

***Disclosures: Joseph Tucci**, None.*

MO0443

Dexamethasone Affects GR and GILZ Expression in Mesenchymal Stem Cells from Osteonecrosis Patients. Azeb Haile[1], Dongqing Wang[1], Aaron Johnson[2], Robert Pivec[3], Michael Mont[3], Lynne Jones*[4]. [1]Johns Hopkins University, USA, [2]University of Maryland, USA, [3]Sinai Hospital of Baltimore, USA, [4]Johns Hopkins University School of Medicine, USA

Purpose: High dose corticosteroid therapy is a major risk factor for osteonecrosis. The aim of this study was to test whether bone marrow stromal cells (MSCs) from osteonecrosis patients respond differently to dexamethasone than MSCs from healthy controls regarding protein expression of the GR (glucocorticoid receptor) and GILZ (the glucocorticoid induced leucine zipper) proteins.

Methods: IRB approval and informed consent were obtained. hMSCs were isolated from bone marrow aspirates from 10 osteonecrosis patients (5 men, 5 women) undergoing total hip arthroplasty. The mean age was 43 years (range, 23-57). Comorbidities included corticosteroids (n=3), sickle cell disease (n=4), and other (n=3). Bone marrow aspirates (3-8ml) were collected in tubes containing 25U/ml heparin. Cells from 2 healthy donors were obtained from Texas A&M Health Science Center. Cells at passage 3 were cultured until 80% confluent. Dexamethasone was added at concentrations ranging from 10^{-8}-10^{-6}M and cells incubated for 48 hrs. GR and GILZ were detected from cell lysates using Western blots (Fig1).

Results: No significant differences were noted between the baseline levels (no dex) of GR and GILZ between the ON patient and control cells. However, the mean baseline level was the highest for the corticosteroid-associated patients for both proteins. GR levels decreased when the MSCs were exposed to dexamethasone (Fig2) ($p<.05$); the response of GR was similar for patient and control cells. The response of GILZ to dexamethasone was more variable between patients. Dexamethasone treatment resulted in increased expression of GILZ for 7/10 ON patients and control cells (#2) (Fig3). This increase was significant for the osteonecrosis patients for all doses ($p<.05$), especially for the non-steroid patients ($p<.02$).

Conclusions: Following corticosteroid treatment, protein expression of GR decreased while expression of GILZ increased. Wang et al. identified GILZ as a target gene for GR (1), and Shi et al. reported an antagonistic relationship between GILZ and GC-induced adipocytes differentiation (2). Studying the effect of corticosteroids on the expression and post-translational modification of the multiple hGR isoforms will help define the molecular mechanisms of corticosteroid-associated bone diseases and the inter-patient variability in corticosteroid responses that exist.

References:
1. Wang et al., PNAS 2004; 101: 15603-15608.
2. Shi et al., EMBO reports.2003; 374-380.

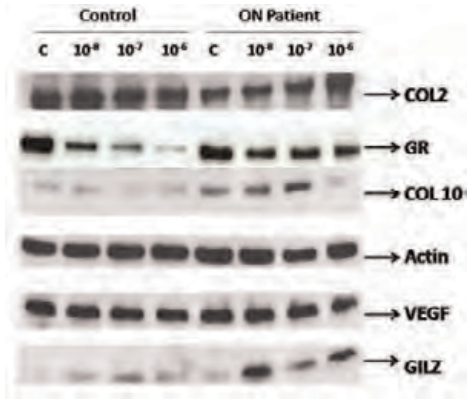

Figure 1

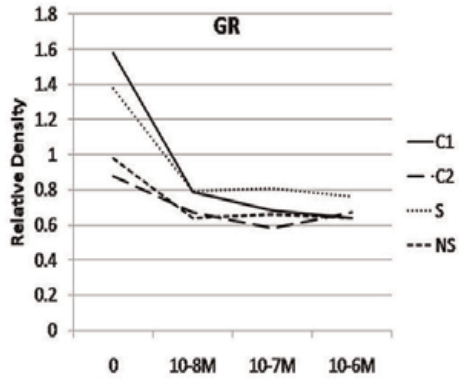

Figure 2

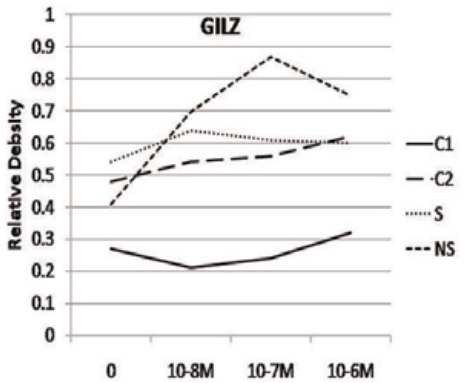

Figure 3

***Disclosures: Lynne Jones**, None.*

MO0444

Estrogen-mimicking isoflavone Genistein prevents the bone loss due to hypoxia in a rat model of Obstructive Sleep Apnea-Hypopnea Syndrome. Lige Song*[1], Yun Zhou[2], Xiao Liang[3]. [1]Tongji Hospital, Tongji University School of Medicine, Peoples Republic of China, [2]Dept.of Endocrinology, Tongji Hospital, Tongji University School of Medicine, China, [3]School of Basic Medical Sciences, Fudan University, China

The incidences of Obstructive Sleep Apnea-Hypopnea Syndrome (OSAHS) have been on rise in general population, in part, due to increasing obesity. The incidences are 2-fold higher in postmenopausal women, further exacerbating their risk of osteoporosis and fractures. Anoxia and other systemic complications of OSAHS including oxidative stress and metabolic abnormalities have been shown to cause detrimental effect on osteoblast proliferation and differentiation and also increase osteocalsts activity. In this study, we investigate whether an estrogen-mimicking isoflavone, Genistein, could reverse the decreased bone mass by intermittent hypopnea in ovariectomied rat. To mimic OSAHS, rats were housed in hypoxia chambers infused with nitrogen and normal air alternatively every 15 seconds, 8 hours per day, 5 days per week for 5 weeks. The air circulation was controlled by a time-lapse solenoid valve such that an oxygen concentration of 1% was maintained as assessed by a digital oxygen meter. The ovariectomied (OVX) rats had a significantly decreased vertebral bone mineral density (BMD) as compared to control rats (0.2546 ± 0.010 vs. 0.2684 ± 0.013, n=8, $p<0.05$). The simulated OSAHS in addition to ovariectomy (OVX + OSAHS) further significantly decreased the BMD compared to OVX alone rats (0.2454 ± 0.0173, n=8, $p<0.05$). Treatment with Genistein of the OVX + OSAHS rats significantly improved the BMD as compared to OVX + OSAHS group alone (0.2588 ± 0.012, n=8, $p<0.05$). Bone histomorphometry revealed a significant decrease in percentage trabecular area (Tb.Ar) in OVX as compared to controls (29.32 ± 6.98 vs. 31.14 ± 5.98, n=8, $p<0.05$). Tb.Ar was further decreased in OVX + OSAHS rats (28.41 ± 7.90, n=8, $p<0.05$) but was normalized in Genistein treated OVX + OSAHS rats (29.15 ± 6.89, n=8, $p>0.05$) as compared to OVX alone rats. Similar significant trends were observed in the measurement of trabecular thickness and trabecular spacing. Mechanical strength of the bone, as assessed by 3-point bending of femur, was not significantly changed in OVX vs control rats; although, it was significantly decreased in OVX + OSAHS rats compared to OVX alone (116.47 ± 15.32 vs. 126.57 ± 13.35, n=8, $p<0.05$). Genistein treatment of the OVX + OSAHS rats restored the mechanical strength of the femur to the level of OVX and control rats (124.81 ± 22.58, n=8, $p>0.05$). Taken together, this data suggest that the estrogen-mimicking action of Genestein can prevent OSAHS-induced bone loss in postmenopausal women.

***Disclosures: Lige Song**, None.*
This study received funding from: Ganquan New Star of Tonji Hospital

MO0445

Sex Steroid Hormones and Kyphosis in Older Men: The Osteoporotic Fractures in Men (MrOS) Study. Deborah Kado*[1], Mei-Hua Huang[2], Corinne McDaniels-Davidson[3], Gail Laughlin[4], Jane Cauley[5], Eric Orwoll[6], Nancy Lane[7], Marcia Stefanick[8], Elizabeth Barrett-Connor[1], Peggy Cawthon[9]. [1]University of California, San Diego, USA, [2]UCLA School of Medicine, USA, [3]SDSU/UCSD Joint Doctoral Program in Public Health (Epidemiology), USA, [4]UCSD, USA, [5]University of Pittsburgh Graduate School of Public Health, USA, [6]Oregon Health & Science University, USA, [7]University of California, Davis Medical Center, USA, [8]Stanford University, USA, [9]California Pacific Medical Center Research Institute, USA

In men, hyperkyphosis, or increased thoracic spine curvature, tends to progress with age and is associated with poor physical and pulmonary function, injurious falls, and premature mortality. Although closely associated with osteoporosis, only 1/3 of older persons with the worst degrees of kyphosis have underlying vertebral fractures. Rodent models of kyphosis suggest a link between sex steroid hormones and hyperkyphosis. To test the hypothesis that low sex steroid hormone levels are associated with kyphosis, we studied 996 men from the Osteoporosis Fractures in Men Study (MrOS) aged 65 – 99 years (mean age 72.9) who had baseline measures of total and bioavailable testosterone, total and bioavailable estradiol, sex hormone binding globulin (SHBG) and Cobb angle of kyphosis (calculated from lateral spine x-rays). Using multivariable linear regression, we examined the correlation between each sex-steroid hormone and kyphosis. Men had an average kyphosis of 38° (SD = 11.3) and 4.2% had a prevalent vertebral fracture. All sex hormones were normally distributed. Men had a mean testosterone level of 423.7 ng/dL (SD = 160.4), mean bioavailable testosterone of 216.4 ng/dL (SD = 70.6), mean total estradiol of 18.1 pg/mL (SD = 6.3), mean bioavailable estradiol of 12.3 pg/mL (SD = 4.5), and mean SHBG of 48.9 nmol/L (SD =19.7). Adjusting for age and clinic site, only total and bioavailable estradiol were significantly associated with kyphosis. Further adjustment for body mass index, prevalent vertebral fracture, hip BMD and degenerative disc disease did not materially change the results (see Table – each row represents a different fully adjusted model).

We considered additional potential confounders that included co-morbidities and health behaviors such as physical activity, alcohol use, and smoking, but adjustment for these factors made no difference in our findings. Confirming reports from the animal literature in a large epidemiological study, we report that older men with higher levels of total and bioavailable estradiol tend to have less kyphosis than men with lower estradiol levels. Of the sex hormones, estrogen appears to be the most important factor in determining both bone density and degree of kyphosis in older men.

Hormones	Beta-estimate (per SD)	95% Confidence Interval	P value
Total Estradiol (pg/mL)	-1.14	-1.83, -0.45	0.001
Bioavailable Estradiol (pg/mL)	-1.19	-1.92, -0.46	0.006
Total Testosterone (ng/dL)	0.11	-0.59, 0.81	0.75
Bioavailable Testosterone (ng/dL)	-0.09	-0.82, 0.64	0.81
SHBG (nmol/L)	0.51	-0.20, 1.23	0.16

Table

***Disclosures: Deborah Kado**, None.*

MO0446

The bone sparing effects of 2-methoxyestradiol are mediated via estrogen receptor alpha. Anna-Lena Eriksson*[1], Anna Wilhelmson[2], Johan Bourghardt-Fagman[2], Åsa Tivesten[2], Claes Ohlsson[3]. [1]University of Gothenburg, Sweden, [2]Wallenberg Laboratory for Cardiovascular Research at the Sahlgrenska Academy, Sweden, [3]Center for Bone & Arthritis Research at the Sahlgrenska Academy, Sweden

2-methoxyestradiol (2me2), a naturally occurring metabolite of 17β-estradiol (E2), exerts bone sparing effects in animal models. *In vitro*, 2me2 has a very low affinity for estrogen receptors (ERs). ERα (ESR1) is crucial for the bone sparing effect of estradiol. We here assessed the involvement of ESR1 in the bone sparing effects of 2me2 in an *in vivo* model.

Nine-week-old wild type and ESR1 knockout (ESR1 KO) mice were orchidectomized and treated for 28 days with 6.66μg of 2me2 per day, or with placebo. Bone parameters were assessed using peripheral quantitative computed tomography (pQCT) and μCT.

2me2 preserved trabecular and cortical bone in WT mice. Trabecular vBMD was $64 \pm 20\%$ and trabecular BV/TV was $60 \pm 20\%$ higher in the metaphyseal region of the femur in the group treated with 2me2, compared with the placebo group ($p<0.01$). This was due to an increase in trabecular number ($41 \pm 10\%$, $p<0.01$) as well as trabecular thickness ($13 \pm 4\%$, $p<0.01$). In the ESR1 KO mice, treatment with 2me2 had no effect on trabecular bone (vBMD $5 \pm 5\%$, and BV/TV $6 \pm 18\%$ increase in the treatment group compared with the placebo group, non-significant)

Cortical bone mineral content in the diaphyseal region of the femur was $31 \pm 3\%$ higher in the 2me2 treatment group compared with placebo ($p < 0.001$). This was due to a $23 \pm 3\%$ larger cortical area and a $7 \pm 1\%$ higher cortical vBMD ($p<0.001$) compared with placebo. Cortical bone was not affected by 2me2 treatment in the ESR1KO mice (Cortical bone mineral content $2 \pm 2\%$ increase in the treatment group compared with the placebo group, non-significant).

In conclusion, our data show that the bone sparing effects of 2me2 on both trabecular and cortical bone parameters are mediated via ESR1. 2me2 may exert these bone sparing effects directly via ESR1 but given the low affinity of 2me2 for ESR1 this seems less likely. Alternatively, 2me2 might have been back transformed to E2, which in turn binds to ESR1. Further research is needed to clarify the mechanism underlying the ERα mediated bone-sparing effects of 2me2.

***Disclosures: Anna-Lena Eriksson**, None.*

MO0447

Dietary vitamin D is reflected in a dose-response manner in circulating 25-hydroxyvitamin D and its C-3 alpha epimer as well as the 24,25 dihydroxyvitamin D metabolite in adult Sprague-Dawley rats. Christina Bianchini*[1], Hope Weiler[2]. [1]McGill University, Canada, [2]McGill University, USA

The C-3 α epimer (3-epi-25(OH)D) of 25-hydroxyvitamin D (25(OH)D) is present in high concentrations in infant serum samples and commonly present in adult serum. However the source the epimer and biological function in vivo remain unknown. The objectives were to: (1) establish a dose-response of 25(OH)D in response to increasing dietary cholecalciferol (2) describe the dose-response of other vitamin D metabolites including 24,25(OH)2D3 and 3-epi-25(OH)D (3) determine the biological response of bone to varied cholecalciferol and 3-epi-25(OH)D supplementation. Adult Sprague Dawley rats (12 weeks, n=36 female n=36 male) were randomized to: control AIN93-Mdiet (1 IU vitamin D3/g food) or experimental diets for 8 weeks: cholecalciferol 2 and 4 IU/g food, 3-epi-25(OH)D at 0.5 and 1 IU/g food and a 25(OH)D group (0.5 IU/g food) reference group. Body weights and food consumption were measured weekly. Blood samples were collected at as well as whole body dual-energy X-ray absorptiometry (DXA) at beginning, mid-point and end of study and in vivo micro-computed tomography (μCT) was performed at baseline and end of study. Vitamin D metabolites; 25(OH)D3, 24,25(OH)2D3, 3-epi-25(OH)D were quantified using liquid chromatography tandem mass spectrometry. Differences were tested using a mixed model ANOVA with post-hoc testing and Bonferroni adjustment. There were no significant differences among groups for weight or dietary intake throughout the

study. Plasma 25(OH)D followed a clear dose-response as did the 3-epi-25(OH)D and 24,25(OH)2D in response to increasing intake of cholecalciferol (Table). No significant differences were detected in bone mineral density among diet groups based on DXA and in vivo μCT scanning after post-hoc adjustments for multiple comparisons. These data are to our knowledge the first to describe several key vitamin D metabolites that respond in a positive dose-response manner to dietary vitamin D when provided at and up to four times above the recommendation for rodents. The Institute of Medicine recently set the target for 25(OH)D at 20 ng/ml for bone health in humans. Our data demonstrate that the AIN-93M control diet for rodents was not sufficient to achieve a 25(OH)D concentration of 20 ng/mL as measured using gold-standard LC-MS/MS. Longer-term studies are required to confirm the response of bone to higher intakes of vitamin D and the biological generation of 3-epi 25(OH)D.

Metabolites (ng/ml)	Diets					
	Control	2 IU Cholecalciferol	4 IU Cholecalciferol	0.5 IU 25(OH)D	0.5 IU 3-epi-25(OH)D	1 IU 3-epi-25(OH)D
25(OH)D	12.5±0.9	13.8±0.6	19.7±0.8[a]	17.00±1.0[a]	4.92±0.6[a]	7.24±1.1[a,b]
3-epi-25(OH)D	6.1±0.7	10.7±2.1	23.3±6.0	4.36±1.0	80.6±3.6[a,b]	112±17.6[a,b]
3-epi-25(OH)D/25(OH)D	0.5±0.2	0.8±0.2	1.25±0.34	0.26±0.06	19.1±5.05[a,b]	14.1±10.6[a,b]
24,25(OH)2D	11.7±0.4	14.2±0.5	23.0±1.2[a]	13.8±0.8[a]	4.18±0.1[a,b]	7.1±1.1[a,b]
24,25(OH)2D/25(OH)D	0.9±0.03	1.03±0.03	1.2±0.05	1.07±0.03	0.75±0.1[a]	0.12±0.1

Means ± S.E.M main effect of diet at 8 weeks shown, n=12/dietary group
[a]Significantly different from control group p<0.05 [b]Significantly different from reference 0.5 IU 25(OH)D group p<0.05

Table: Vitamin D Metabolite Concentrations

***Disclosures: Christina Bianchini**, None.*

MO0448

Ethnic and racial disparities in innate and adaptive immunity following vitamin D supplementation. Philip Liu*[1], Rachel Reyes[2], Andy Hur[3], Brandon Rafison[2], John Adams[1], Robert Modlin[2], Peter Joyce[2]. [1]Univeristy of California, Los Angeles, USA, [2]UCLA, USA, [3]Andy Hur, USA

A role for vitamin D and its metabolites in the human immune response has become increasingly clear via laboratory experiments. However, little is known regarding the levels of circulating 25-hydroxyvitmain D (25D) needed to facilitate the immune response in humans. We have previously demonstrated that innate (Toll-like receptor 2.1) and adaptive (IFN-γ) immune signals converge on a common vitamin D-dependent antimicrobial pathway in the human macrophage resulting in i) upregulation of the CYP27B1-hydroxylase, ii) conversion of prohormone 25D to the active metabolite 1,25-dihydroxyvitamin D (1,25D), iii) activation of the vitamin D receptor (VDR), iv) induction of antimicrobial peptides, cathelicidin (CAMP) and human beta defensin 4 (DEFB4), and v) antimicrobial activity. While increasing $25D_3$ levels of deficient sera during macrophage activation *in vitro* resulted in recapitulation of the antimicrobial response, it is unclear if modulation of 25D levels *in vivo* will have the same effect. To address this, we measured expression of CAMP and CYP27B1 from primary cultures of human monocyte-derived macrophages, preconditioned with sera from 25D deficient subjects before and after vitamin D repletion *in vivo*, then stimulated with TLR2/1 ligand or IFN-γ *in vitro*. Serum was collected prospectively and tested from 11 African American black, 34 Hispanic/Latino and 25 non-Hispanic white individuals who were vitamin D-insufficient/deficient (8-29ng/ml) and treated with 500,000 IU vitamin D_3. The total serum 25D levels of all individuals increased significantly by an average of 2.5 fold following vitamin D_3 treatment, with a 3.3 fold, 3.0 fold and 1.8 fold in the African American black, Hispanic/Latino and non-Hispanic white groups respectively. However, induction levels of CAMP via TLR2/1 or IFN-γ activation correlated with conditioning serum 25D levels only in the non-Hispanic white group (R=0.489, P<0.002 and R=0.501, P<0.002., respectively). In contrast, induction levels of CAMP via TLR2/1 or IFN-γ correlated with co-induction of CYP27B1 only in the Hispanic/Latino group (R=0.357, P<0.005 and R 0.419, P<0.001, respectively). These results demonstrate an ethnic/racial disparity in response to vitamin D supplementation and suggest that host genetics should be given consideration when determining the total 25D levels needed to reconstitute vitamin D-dependent immune responses.

***Disclosures: Philip Liu**, None.*

MO0449

Expression of Cardiovascular System-Related Genes in Vitamin D Receptor Knockout Mice. Toshio Okano*, Naoko Tsugawa. Kobe Pharmaceutical University, Japan

Introduction: 1α,25-Dihydroxyvitamin D_3 (1α,25-D_3) is thought to play an important role in controlling cardiovascular functions. In human studies, vitamin D deficiency has been shown to increase myocardial contractility and fibrosis. In animal studies, vitamin D deficiency has been reported to induce hypertension and cardiac hypertrophy. The well-known function of 1α,25-D_3 is to maintain calcium homeostasis and to promote bone mineralization. However, apart from these classical actions, vitamin D has potent non-calcemic actions such as anti-proliferative, differentiation-inducing and immune-modulatory actions. To determine whether cardiovascular abnormalities caused by vitamin D deficiency are dependent or independent of calcium metabolism, we examined the expression of cardiovascular system-related genes in vitamin D receptor knockout (VDR-KO) mice fed a normal diet or a rescue diet to normalize serum calcium levels. Methods: Wild-type (WT) and VDR-KO littermates were divided into two groups, respectively. After weaning they were fed a normal diet or a rescue diet (2% Ca, 1.25% Pi, and 20% lactose) for 7 weeks before sacrifice. Serum calcium levels were measured. The mRNA levels of atrial natriuretic peptide (ANP), brain natriuretic peptide (BNP), α-actin, α- or β-myosin heavy chain (α- or β-MHC) of the hearts and aorta were measured by real-time PCR. In WT and VDR-KO mice fed a normal diet or a rescue diet for 32 weeks after weaning, blood pressure (BP) was measured using a noninvasive computerized tail-cuff system. Results: The mRNA expression of ANP, BNP, α-actin, α-MHC, and β-MHC in the hearts and the mRNA expression of ANP in the aorta of VDR-KO mice fed a normal diet were significantly lower than those of WT mice. On the other hand, there was no significant difference in the mRNA expression levels of the above cardiovascular parameters between WT and VDR-KO mice fed a rescue diet. VDR-KO mice fed a normal diet for 32 weeks after weaning exhibited significantly higher systolic BP, diastolic BP, and mean BP compared with WT mice fed a normal diet for 32 weeks after weaning. However, there was no significant difference between the WT and VDR-KO mice fed a rescue diet for 32 weeks after weaning. Conclusion: Although vitamin D deficiency is a risk factor for cardiovascular abnormalities, the decreased ANP, BNP, and MHCs expression in the heart resulting in hypertension may be largely due to an impaired calcium homeostasis caused by vitamin D deficiency.

***Disclosures: Toshio Okano**, None.*

MO0450

Higher levels of $25(OH)D_2$ and $1,25(OH)_2D_2$ are associated with lower levels of $25(OH)D_3$ and $1,25(OH)_2D_3$ in older men. Christine Swanson*[1], Carrie Nielson[1], Smriti Shrestha[1], Steven Cummings[2], Elizabeth Barrett-Connor[3], Ivo Jans[4], Steven Boonen[5], Roger Bouillon[6], Dirk Vanderschueren[7], Eric Orwoll[1]. [1]Oregon Health & Science University, USA, [2]San Francisco Coordinating Center, USA, [3]University of California, San Diego, USA, [4]KU Leuven Labs, Belgium, [5]Center for Metabolic Bone Disease & Division of Geriatric Medicine, Bel, [6]Katholieke Universiteit Leuven, Belgium, [7]Catholic University of Leuven, Belgium

Vitamin D_2 has commonly been used as a supplement in the US, but the associations of serum vitamin D_2 with other vitamin D metabolites are unclear.

Sensitive, specific liquid chromatography-tandem mass spectrometry methods were used to measure vitamin D_3 and D_2 metabolites in archived serum (collected 2000-01) from 679 community dwelling men aged > 65 yrs randomly selected from those enrolled in the MrOS Study (>99% with GFR>30). The limit of quantification was 4 ng/ml for $25(OH)D_2$, 2 ng/ml for $25(OH)D_3$, 4.3 pg/ml for $1,25(OH)_2D_2$ and 6 pg/ml for $1,25(OH)_2D_3$. Spearman correlations were used to examine the associations among vitamin D metabolites. Supplement use was identified using a questionnaire at baseline.

$25(OH)D_2$ and $1,25(OH)_2D_2$ were detectable in 189 (28%) and 149 (26%) of the men respectively; 141 (21%) had detectable levels of both D_2 metabolites. 57.9% of the men reported using vitamin D supplements at baseline and they more often had detectable levels of $25(OH)D_2$ than those that did not report supplement use (43.6% vs. 2.5%). $25(OH)D_3$ was detectable in all (range 3.13 – 55.8 ng/mL); the median total 25OHD level was 25 ng/mL (range 3-56ng/mL). In the original 679 men, levels of total 25OHD were correlated with total $1,25(OH)_2D$ (r = 0.39, p<0.0001). Among the 141 men who had detectable levels of all metabolites (Table 1), $25(OH)D_2$ and $25(OH)D_3$ were strongly correlated with $1,25(OH)_2D_2$ & $1,25(OH)_2D_3$, respectively. However, men with higher levels of $25(OH)D_2$ had lower levels of $25(OH)D_3$ and $1,25(OH)_2D_3$ (Table 1), but higher $1,25(OH)_2D_2$ levels were not associated with lower levels of $1,25(OH)_2D_3$ (r =-0.043, p=0.61). Whereas higher $25(OH)D_3$ was associated with higher total $1,25(OH)_2D$, men with higher $25(OH)D_2$ tended to have lower total $1,25(OH)_2D$ levels.

Measures of vitamin D metabolites in a large cohort of men reveal that $25(OH)D_2$, a form of vitamin D derived exclusively from food and medical supplements, is associated with increased $1,25(OH)_2D_2$ levels, but decreased levels of both $25(OH)D_3$ and $1,25(OH)_2D_3$. The cause of the decrease in D_3 metabolite levels in the presence of D_2 is unclear, but may involve effects on 25-, 1α-, or 24,25- vitamin D hydroxylases. From a population perspective it appears that vitamin D_2 supplementation may reduce vitamin D_3 availability. The reasons for these relationships need further investigation and may have implications for the role of various forms of vitamin D supplementation.

Unadjusted correlations among vitamin D metabolite levels among 141 men with measurable levels of all metabolites

	Total 25OHD	$25(OH)D_2$	Total $1,25(OH)_2D$	$1,25(OH)_2D_2$	$1,25(OH)_2D_3$
$25(OH)D_2$	0.20	-0.26	-0.14	0.59	-0.32
p-value	<0.02	0.002	0.09	<0.001	<0.001
$25(OH)D_3$	0.88		0.49	-0.50	0.65
p-value	<0.001		<0.001	<0.001	<0.001

Table 1

***Disclosures: Christine Swanson**, None.*

MO0451

Inhibition of Methicillin-resistant Staphylococcus aureus (MRSA)-induced cytokines mRNA synthesis in human bone marrow derived mesenchymal stem cells (hMSCs) by 1,25-dihydroxyvitamin D3. Aparna Maiti*[1], William Jiranek[2]. [1]Virginia Commonwealth University, USA, [2]Department of Orthopaedic Surgery, Virginia Commonwealth University School of Medicine, USA

Staphylococci, particularly *Staphylococcus aureus* are the predominant cause of bone infection worldwide. Toll like receptors (TLRs) are an important segments of host response to bacterial infection and are expressed by a variety of immune and non-immune cells. Human mesenchymal stem cells (hMSCs) are multipotent cells found in many tissues of our body, can differentiate into stromal tissue such as bone. MSCs are known to expresses TLRs to recognize pathogenic particle and play important role in defense mechanism. 1,25-dihydroxyvitamin D_3 [$1,25(OH)_2D_3$] has direct effects on immunity modulated by vitamin D receptor (VDR) present in immune cells. Binding of ligand-activated VDR to its responsive element induces expression of antimicrobial peptides. The aim of this study was to explore the anti-inflammatory mechanism of 1,25-dihydroxyvitamin D_3 [$1,25(OH)_2D_3$] to inhibit *Staphylococcus aureus* infection mediated TLRs activation and downstream cytokine production in hMSCs via direct inhibition of transcription factor nuclear factor-?B (NF-?B) and affect global level of histone H3 lysine 9 trimethylation (H3K9me3) mark for transcriptional repression. Our data revealed that methicillin-resistant *Staphylococcus aureus* (MRSA)-infection predominantly induces TLRs 1-2, and 6 expressions in human MSCs as detected by qRT-PCR. MRSA-mediated TLR ligands reduced osteoblast differentiation and increase hMSCs proliferation, which indicated that *Staphylococcus aureus* as TLR ligands disrupted the multipotency function of hMSCs. 1,25-dihydroxyvitamin D_3 treatment followed by MRSA treatment inhibit nuclear translocation of p65-NF?B and reduced cytokines (IL-6, IL-8, and TNFα) mRNA levels along with NR4A2 in hMSCs. Finally, $1,25(OH)_2D3$ activated VDR restores the global level of H3K9me3 to repress MRSA-stimulated inflammatory cytokine IL-8 expression.

***Disclosures: Aparna Maiti**, None.*

MO0452

Local production of 1,25-dihdydroxyvitamin D3 in breast tumors of the pYMT mouse model regulates lipid metabolism as determined by imaging mass spectrometry and gene array analysis. Ami Grunbaum*[1], Jiarong Li[1], Richard Kremer[2], Pierre Chaurand[3]. [1]McGill University, Canada, [2]McGill University, Royal Victoria Hospital, Canada, [3]University of Montreal, Canada

Introduction: Mounting evidence suggests important protective roles for vitamin D in malignancies. Exploring the hypothesis that local production of 1,25-dihdydroxyvitamin D3 is protective, we are studying mouse breast cancer models in which localized deficiency has been induced by conditionally knocking out mammary expression of 1-alpha-hydroxylase. MALDI imaging mass spectrometry (I-MS) is becoming a method of choice to characterize the molecular content of biological tissues. Employing a systems biology approach, we are using I-MS in combination with gene microarray analysis of KEGG pathways of lipid biosynthesis to compare the lipid composition of breast tumors in 1-alpha-hydroxylase ablated (knockout) versus functional 1-alpha-hydroxylase (wildtype) mice.

Methods: Wildtype & knockout mouse (pYMT strain) breast tumors were harvested. Profiling and imaging MS of the tumors were performed by MALDI MS. To identify differentially expressed signals, spectra from each tissue section were compared by PCA & ANOVA. Lipids were identified by comparing accurate mass measurements with the LIPIDMAPS database and confirming by MS/MS. For gene analysis, tumors were analyzed by DNA microarray. Differentially expressed genes involved in lipid metabolism were mapped onto KEGG pathways of lipid biosynthesis.

Results: In a proof of principle pilot study, we have identified differences in lipid profiles of knockout compared to wildtype mouse breast tumors. Several classes of differentially expressed lipids were demonstrated, including phosphatidylinositol, phosphatidylethanolamine & phosphatidylcholine. Validation of our preliminary findings will require study of a larger well defined tissue cohort and comparison with an independent platform.

Initial analysis of our gene array data demonstrated up-regulation of several enzymes involved in sulfatide formation (serine palmitoyl transferase, galactosyl ceramide transferase) and down-regulation of sulfatide degrading enzymes (aryl sulfatase, cerebroside sulfatase). Further analysis by focussed PCR analysis of lipid pathways will improve the sensitivity and specificity of these findings.

Discussion: Currently, there is a lack of information concerning the role of lipids in cancer progression. Studies such as this will help in the discovery of lipid biomarkers to assist in the classification, diagnosis & prognosis of similar tumors. It will also enable the elucidation of metabolic pathways & potential therapeutic targets.

***Disclosures: Ami Grunbaum**, None.*

MO0453

Local Synthesis of 1,25D Promotes Osteocyte Maturation. Andrew Turner*[1], Maarten Hanrath[2], Gerald Atkins[3], Paul Anderson[1], Howard Morris[4]. [1]Musculoskeletal Biology Research, University of South Australia, Australia, [2]University of Utrecht, Netherlands, [3]University of Adelaide, Australia, [4]SA Pathology, Australia

The local synthesis of active vitamin D (1,25D) by the enzyme CYP27B1 within osteoblasts has been previously shown to act in an autocrine manner to regulate cell proliferation and differentiation. Thus, in the current study we focused on the local metabolism of 1,25D within osteocyte-like cells. To do so we utilized the mouse cell lines MC3T3-E1, MLO-A5 and MLO-Y4 which represent increasingly mature stages of the osteoblast/osteocyte lineage, and are capable of further differentiation in culture. Our data confirm that expression of Cyp27b1 mRNA is a feature of the osteoblast lineage as cells transition to an osteocyte phenotype. Furthermore, osteocyte-like cells supplemented with 25D produce detectable levels of 1,25D in the media, sufficient to induce Cyp24A1 mRNA in all 3 cell lines studied. MC3T3-E1 cells, cultured for up to 4 weeks in osteogenic media, expressed low levels of FGF-23 mRNA under basal conditions, but expression was elevated 10-fold in the presence of 100nM 25D. Similarly, chronic 25D supplementation (100nM) increased osteocalcin (Ocn) mRNA by approximately 50% in cultures at Day 21 ($P<0.05$), however this effect was reversed in more mature cultures (44% decrease in Ocn mRNA at Day 28) suggesting that the role of locally synthesized 1,25D on activities such as mineralization may depend on the stage of maturation. Consistent with this observation, 25D exposure upregulated Ocn, Col-I and Alk Phos mRNA in MLO-A5 pre-osteocyte cells, but decreased Ocn and Phex in more mature MLO-Y4 osteocyte cells. This repression of Ocn and Phex by 25D in MLO-Y4 cells was exacerbated by transfection with a plasmid vector that increased transcription of a human Cyp27b1 transgene. Taken together, our findings suggest that the local synthesis of 1,25D within osteocytes promotes the maturation of less mature cells, and may regulate osteocyte gene expression and function in temporally dependent manner.

***Disclosures: Andrew Turner**, None.*

MO0454

Lower Vitamin D Status is More Common among Saudi Adults with Type 1 Diabetes Mellitus than Non-Diabetics. Nasser Al-Daghri*. King Saud University, Saudi Arabia

Objectives: To determine vitamin D status among Saudi individuals with type 1 diabetes mellitus (T1DM) adults.

Methods: A group of 60 Saudi adults with T1DM and Diabetes Clinics, and 60 healthy controls. We measured serum 25-hydroxy vitamin D (25OHD), calcium Cholesterol, Glucose, HDL, Triglyceride in those patients, and compared the results between T1DM group and control subjects.

Results: Both T1DM and healthy groups has vitamin D deficiency. The mean levels of 25OHD were significantly lower in the T1DM adults compared to the controls (28.1 ± 1.4 nmol/l versus 33.4 ± 1.6 nmol/l). In the T1DM adults, 66.7% were mildly, 31.7% were moderately, and 3.3% were severely vitamin D deficient as compared with 41.7% (mildly), 31.7% (moderately), and 5% (severely) in the control group. Overall, 100% of the T1DM children, and 78% of the healthy children were vitamin D deficient.

Conclusion: Prevalence of vitamin D deficiency in diabetic adults is relatively high. Therefore, screening for vitamin D deficiency and supplementation of adults with low vitamin D levels should be warranted.

***Disclosures: Nasser Al-Daghri**, None.*

MO0455

The Effect of Vitamin D Supplementation on Metabolic Phenotypes in Thais with Prediabetes. Hataikarn Nimitphong*, Rattanapan Samittarucksa, Sunee Saetung, Nuttapimon Bhirommuang, Laor Chailurkit, Boonsong Ongphiphadhanakul. Medicine department, Ramathibodi Hospital, Mahidol University, Thailand

Background: There have been inconsistent data about the benefit of vitamin D supplementation in cardiometabolic phenotypes. Moreover, reports regarding the issue in Asian populations are scant. In the present study, we investigated the effect of vitamin D supplementation for 3 months on anthropometric and glucose homeostasis measures in Thai adults with impaired fasting glucose (IFG) and/or impaired glucose tolerance (IGT).

Methods: Forty-seven IFG and/or IGT subjects completed the study. Subjects were randomized into 3 groups; control (n=18), vitamin D_2 weekly (n=19) or vitamin D_3 weekly (n=10). To raise total 25-hydroxyvatamin D [25(OH)D] levels to comparable levels with vitamin D_2 or D_3, vitamin D_2 20,000 IU or D_3 15,000 IU weekly were used. Anthropometric variables were obtained at baseline and at 3 months. Oral glucose tolerance test was performed at baseline and at 3 months. Total serum 25(OH)D, $25(OH)D_3$ and $25(OH)D_2$ were measured by LC-MS/MS. Insulin resistance (HOMA-IR) and insulin secretion index (HOMA%B) were calculated by the homeostasis model assessment.

Results: Total 25(OH)D levels significantly increased from baseline in both the vitamin D_2 and the vitamin D_3 groups; (D_2: Δ total 25(OH)D =12.8±3.6 ng/mL, $p <$ 0.01, D_3 13.1 ±4.1 ng/mL, $p = 0.05$) while there was no change in the control group (table 1). D_3 supplementation raised $25(OH)D_3$ significantly (+13.7 ± 4.9 ng/mL, $p <0.001$) while D_2 increased $25(OH)D_2$ levels (+25.9 ± 4.2 ng/mL, $p <0.01$) but with a decrease in $25(OH)D_3$ (−13.1 ± 3.1 ng/mL, $p <0.01$). Subjects were then classified into 2 groups, i.e., control and D_2 or D_3 supplementations. After 3 months of vitamin D supplementation, body weight (BW), waist circumference (WC) and systolic blood pressure (SBP) significantly decreased (table 2). HOMA-IR (p=0.09) and body mass index (BMI, p=0.06) also tended to decrease (table 2). Using robust regression analysis to examine the differences in changes in metabolic phenotypes after D_2 as compared to D_3, it was found that the use of D_3 was associated with a larger decrease in WC (coefficient = -3.5, $p < 0.001$) independent of the change in total 25(OH)D and baseline BMI. No difference between D_2 and D_3 was observed for other metabolic measures.

Conclusion: Weekly supplementations of vitamin D_2 (20,000 IU) or vitamin D_3 (15,000 IU) improve metabolic phenotypes in subjects with prediabetes. D_3 supplementation may decrease waist circumference more than D_2 supplementation.

Table 1 total 25(OH)D, $25(OH)D_2$ and $25(OH)D_3$ at baseline and at 3 month in control, vitamin D_2 and vitamin D_3 group

		Control (n=18)	Vitamin D_2 20,000 IU/wk (n=19)	Vitamin D_3 15,000 IU/wk (n=10)	p value (between group)
Age (yr)		57.9±13.3	61.2±7.6	63.0±12.9	NS
F/M (n)		9/9	15/4	8/2	0.07
Total 25(OH)D(ng/mL)	Baseline	26.3±6.1	25.2±5.3	26.3±3.9	NS
	3 mo	25.6±5.8	38.0±5.0	39.3±5.7	<0.001
	p value (between baseline and 3 mo)	NS	<0.01	0.05	-
$25(OH)D_2$(ng/mL)	Baseline	0.6±0.2	0.9±0.9	1.3±2.1	NS
	3 mo	0.6±0.3	26.8±4.7	0.7±1.0	<0.001
	p value (between baseline and 3 mo)	NS	<0.01	0.02	-
$25(OH)D_3$(ng/mL)	Baseline	25.8±6.0	24.3±5.3	25.0±4.3	NS
	3 mo	25.0±5.8	11.2±3.4	38.7±5.3	<0.001
	p value (between baseline and 3 mo)	NS	<0.01	0.05	-

Data was presented as mean±SD

Table 1

Table 2 Metabolic characteristic between baseline and 3 month of subjects in control and vitamin D group

		Control (n=18)	Vitamin D_2 or D_3 (n=29)	p value (between group)
Age (yr)		57.9±13.3	61.8±9.5	NS
F/M (n)		9/9	23/6	0.06
BW (kg)	Baseline	72.0±15.3	64.6±10.2	0.07
	3 mo	71.9±15.0	64.1±10.4	0.05
	p value (between baseline and 3 mo)	NS	0.05	-
BMI (kg/m^2)	Baseline	29.0±5.0	27.1±3.2	NS
	3 mo	28.9±4.8	26.8±3.5	NS
	p value (between baseline and 3 mo)	NS	0.06	-
WC (cm)	Baseline	97.7±11.7	94.7±9.8	NS
	3 mo	97.7±11.7	93.3±9.5	NS
	p value (between baseline and 3 mo)	NS	0.012	-
SBP (mmHg)	Baseline	127.2±14.3	126.9±11.1	NS
	3 mo	124.3±11.3	122.3±13.0	NS
	p value (between baseline and 3 mo)	NS	0.05	-
DBP (mmHg)	Baseline	82.6±8.8	76.9±8.9	0.07
	3 mo	78.6±9.0	78.3±9.0	NS
	p value (between baseline and 3 mo)	NS	NS	-
FPG (mg/dL)	Baseline	104.50±11.2	104.1±11.2	NS
	3 mo	104.0±15.2	103.5±10.9	NS
	p value (between baseline and 3 mo)	NS	NS	-
PP 2 h (mg/dL)	Baseline	161.4±13.9	149.5±29.3	NS
	3 mo	155.0±28.4	154.5±39.1	NS
	p value (between baseline and 3 mo)	NS	NS	-
HOMA%B	Baseline	112.1±61.5	104.3±31.2	NS
	3 mo	113.8±61.1	100.2±34.5	NS
	p value (between baseline and 3 mo)	NS	NS	-
HOMA-IR	Baseline	1.9±1.0	1.8±0.8	NS
	3 mo	1.8±0.8	1.7±0.9	NS
	p value (between baseline and 3 mo)	NS	0.09	-
Disposition index (HOMA%B/ HOMA-IR)	Baseline	62.0±14.4	64.3±22.9	NS
	3 mo	64.3±19.9	66.3±21.7	NS
	p value (between baseline and 3 mo)	NS	NS	-

Table 2

***Disclosures: Hataikarn Nimitphong**, None.*

MO0456

The vitamin D receptor is required for activation of the canonical Wnt and Hedgehog signaling pathways in keratinocytes. Thomas Lisse*[1], Hilary Luderer[2], Francesca Gori[3], Marie Demay[1]. [1]Massachusetts General Hospital & Harvard Medical School, USA, [2]Massachusetts General Hospital, USA, [3]Harvard School of Dental Medicine, Massachusetts General Hospital, USA

Alopecia (hair loss) in vitamin D receptor (VDR) knockout mice is due to impaired cyclic regeneration of the hair cycle, however the molecular basis for this phenotype remains unclear. Initiation of a new hair cycle requires activation of the canonical Wnt (cWnt) signaling pathway, leading to induction of Hedgehog signaling. Previous studies demonstrated that the VDR interacts with Lef1, an effector of the cWnt signaling pathway. To determine if the VDR is required for induction of cWnt and Hedgehog target genes, wild type (WT) and *vdr*$^{-/-}$ primary keratinocytes (KCs) were treated with Wnt3a conditioned media (cm) or a Hedgehog agonist (SAG, smoothened agonist). Gene expression was evaluated via rt-qPCR. In WT KCs, *Axin2* and *Gli1* transcript levels were induced 4.1±0.8 and 4.7±2.3 fold, respectively, three hours post Wnt3a-cm treatment compared to control-cm. Induction of *Axin2* and *Gli1* after three hours of Wnt3a-cm was impaired in *vdr*$^{-/-}$ KCs (2.3±0.2 and 1.8±0.4 respectively; p=0.001 and 0.03 vs. WT KCs), demonstrating abnormalities in early cWnt responses in *vdr*$^{-/-}$ cells. SAG treatment (50nM, 6hrs) induced expression of *Gli1* (2.7±0.6) in WT, but not *vdr*$^{-/-}$ KCs. Chromatin immunoprecipitation (ChIP) analyses were performed to evaluate VDR occupancy of the regulatory regions of the *Gli1* and *Axin2* genes. In WT KCs, the VDR was enriched 4.4±1.0 fold on *Gli1* sequences and 2.5±0.4 fold on *Axin2* regulatory regions. VDR was not enriched in these regions in *lef1*$^{-/-}$ KCs. However, the VDR was enriched at the *osteocalcin* (OC) vitamin D response element in both WT and *lef1*$^{-/-}$ KCs (2.4±0.3 and 2.9±1.2, respectively). These data demonstrate that the VDR is required for optimal induction of cWnt and Hedgehog target genes in primary keratinocytes. Furthermore, they demonstrate that absence of Lef1 impairs occupancy of the VDR at regulatory regions in cWnt and Hedgehog target genes, but does not impair interactions of the VDR with a classic VDRE. These studies suggest that impaired Lef1/VDR interactions are the molecular basis for impaired induction of cWnt and Hedgehog target genes during initiation of post-morphogenic hair cycles in *vdr*$^{-/-}$ mice.

***Disclosures: Thomas Lisse**, None.*

MO0457

Vitamin D and Interferon beta Cooperate to Suppress Inflammatory Cytokines and to Ameliorate Disease Severity in Experimental Autoimmune Encephalomyelitis, the Murine Model of Multiple Sclerosis. Tanushree Samanta*[1], Robert Axtell[2], Sneha Joshi[1], Puneet Dhawan[1], Cheng Sun[1], Lawrence Steinman[2], Sylvia Christakos[1]. [1]University of Medicine & Dentistry & New Jersey - New Jersey Medical School, USA, [2]Stanford School of Medicine, Stanford University, USA

There is a high prevalence of vitamin D deficiency in multiple sclerosis (MS) patients and early maintenance of vitamin D sufficiency is associated with decreased risk of MS. However the immunosuppressive activity of vitamin D in MS has not been clearly defined. Interferon beta is the most popular first line treatment of MS but only reduces relapse rate by 30%. Therefore clinical trials using vitamin D or $1,25(OH)_2D_3$ analogs in combination with interferon beta would be a first consideration. In this study we examined the mechanisms by which vitamin D protects against neuroinflammation and whether vitamin D and interferon beta act synergistically to attenuate experimental autoimmune encephalomyelitis (EAE), the murine model of MS. In vivo treatment of mice with ongoing EAE with $1,25(OH)_2D_3$ was found to reverse paralysis and reduce IL-17 secreting CD4+T cells in the periphery and the central nervous system. The mechanism of $1,25(OH)_2D_3$ suppression of IL-17 was found to be transcriptional and to involve blocking of NFAT, recruitment of histone deacetylase, sequestration of Runx1 by the vitamin D receptor and induction of Foxp3. In addition, $1,25(OH)_2D_3$ was found to synergize with interferon beta to reduce IL-17 expression and transcription. Synergistic effects between interferon beta and $1,25(OH)_2D_3$ were also observed in inhibition of GMCSF and interferon gamma expression. Mice fed high dose vitamin D (20,000 IU/kg diet) were found to have significantly reduced EAE compared to mice fed the control diet (1,500 IU/kg). The combination of high dose dietary vitamin D and interferon beta (10,000 U every other day from 9 to day 17) was more effective than either high dietary vitamin D alone or interferon beta alone in ameliorating disease severity in mice with ongoing EAE. Although previous studies have shown that $1,25(OH)_2D_3$ can prevent EAE, this is the first study demonstrating that high dose of the hormone precursor, vitamin D, can cooperate with interferon beta to ameloriate disease severity in mice with ongoing EAE. From these studies we conclude that vitamin D and interferon beta have cooperative immunomodulatory effects and cooperate to diminish paralysis in ongoing EAE. These findings result in new concepts with regard to the mechanisms involved in the interaction of the vitamin D endocrine system and the immune system and provide a rationale for trials combining vitamin D and interferon beta.

***Disclosures: Tanushree Samanta**, None.*

MO0458

A Novel Factor Derived From Resorbing Bone *In Vitro* Potently Stimulates C-Fos Expression In Breast Cancer Cells. Jane Dillon*[1], Peter Wilson[1], Alison Gartland[2], Robert Hipskind[3], James Gallagher[1]. [1]University of Liverpool, United Kingdom, [2]The Mellanby Centre for Bone Research, The University of Sheffield, United Kingdom, [3]Institut de Génétique Moléculaire de Montpellier, France

Metastasis to bone is a devastating development in cancer. When tumour cells disseminate to the skeleton, cancer becomes effectively incurable. Several factors found within bone are known to promote the growth of cancer cells but the complex interplay of host and tumour cells in the bone microenvironment remains to be elucidated. The overall aim of this project was to discover factors released during bone resorption that stimulate breast cancer cells. The specific objectives were to identify factors in conditioned medium from bone resorbing cultures that stimulate the key transcription factor, c-fos, as a biomarker of the metastatic activation of breast cancer cells.

Human osteoclasts were cultured on bone or dentine slices. The conditioned medium was harvested and added to cultures of Hs578T and T47D breast cancer cells which had been stably transfected with c-fos luciferase reporter gene constructs.

Conditioned medium from bone resorbing cultures produced a dose dependent induction in c-fos activity at dilutions 1:125 to 1:5. The stimulating activity correlated with the extent of resorption in the cultures from which it was isolated. There was a greater than 3 fold stimulation of c-fos with resorption conditioned medium, an effect larger than any other factors tested including dilutions of fetal calf serum, and candidate molecules. For example there was no induction of c-fos with TGFbeta or IGF1. EGF gave a significant stimulation up to 2 fold at doses between 20 and 200 ng/ml. PTHrP and purinergic receptor agonists also gave a stimulation but much lower than resorption conditioned medium. The activity could not be replicated by extracts of bone or dentine matrix or by conditioned medium from osteoclasts cultured on plastic. Collectively, these data strongly suggest that a previously unrecognised factor or cocktail of factors, in resorption conditioned medium was responsible for the induction of c-fos in the cell lines. Experiments are ongoing to identify the molecular entities contributing to the activating factor.In conclusion, we have identified a novel factor(s) derived from resorbing bone in vitro, which potently stimulates c-fos expression in breast cancer cells. The specific characteristics and potency of this factor(s) indicate that it cannot be ascribed to any of the known candidate molecules suggested to promote bone metastasis. This factor may provide a useful biomarker and a potential therapeutic target to prevent metastasis to bone.

***Disclosures: Jane Dillon**, None.*

MO0459

Development of a 3D In Vitro Co-Culture System to Model Bone Metastatic Prostate Cancer. Eliza Fong*[1], Olyver Yau[1], Nora Navone[2], Xinqiao Jia[3], Daniel Harrington[1], Mary Farach-Carson[1]. [1]Rice University, USA, [2]The University of Texas MD Anderson Cancer Center, USA, [3]University of Delaware, USA

Tumors originating in the prostate metastasize to bone and presence of skeletal lesions greatly reduces patient survival. Understanding survival and growth mechanisms used by metastatic prostate tumors (PCa) in the bone marrow microenvironment is key to the discovery of novel therapeutics targeting PCa in bone. However, study of cell-cell and cell-extracellular matrix (ECM) interactions is impeded by a lack of clinically relevant preclinical models. Xenograft tumor models, while valuable, lack some critical features of human tumors growing in bone. We developed an *in vitro* model of bone metastatic PCa to recapitulate the heterotypic cell-cell adhesion events that occur between bone marrow stromal cells (BMSC) and PCa cells engrafted in bone. A challenge is that PCa cells and BMSCs, cultured independently, grow best in hydrogels with different compositional and mechanical properties. Hyaluronan (HA) is a major component of bone marrow ECM, and HA hydrogels reflect the low modulus environment of the tissue. Having previously shown the ability of HA hydrogels to support PCa cell growth, we next sought to develop a system to co-culture both cell-types using a 3D HA-gelatin hydrogel system that could simulate cellular interactions in bone.

We evaluated if HA-gelatin hydrogels could support the growth of HS-27a cells, a human cell line representing structural marrow cells. Using bright-field microscopy (Fig. 1A), phalloidin staining (Fig. 1B) and evaluation of DNA content as an index of proliferation, HS-27a cell numbers remained static in hydrogels for about 10 days, after which cellularity increased, and was accompanied by formation of a reticular network in the 3D matrix, reminiscent of the architecture of bone marrow stroma. When co-cultured with BMSC, bone metastatic PCa cells seeded onto these stromal cell constructs actively adhered to the reticular network of stromal cells, highlighting the potential of this model to study homing mechanisms of PCa (Fig. 1C and D). Subsequent work developed a bilayered HA-based system to model the interface between PCa and the bone marrow stroma. This system consists of stacked layers of 6-mm discs of HA-gelatin hydrogels, one optimized for encapsulating BMSC and the other PCa cells. Preliminary studies indicate this system can support primary bone marrow cells as well as PCa cells directly seeded from xenografts. This engineered 3D system provides a novel tool to study bone metastatic PCa in a controlled, biomimetic system, overcoming some limitations of current models.

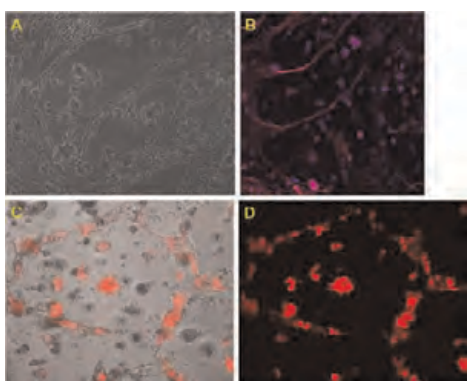

Figure 1

***Disclosures: Eliza Fong**, None.*

MO0460

Ectopic expression of twist-1 in breast cancer cells promotes bone metastasis formation. Martine Croset[1], Delphine Goehrig[1], Stephane Ansieau[2], Alain Puisieux[2], Philippe A.R. Clezardin*[3]. [1]INSERM, UMR1033, France, [2]INSERM, UMR 1052, France, [3]INSERM & University of Lyon, France

The basic helix-loop-helix transcription factor Twist-1 induces epithelial-mesenchymal transition and/or escape to the oncogenic-induced failsafe program, facilitating the intravasation of breast cancer cells in the systemic circulation and their dissemination to the lungs. Twist-1 is also expressed in breast cancer cells that disseminate in the bone marrow. Its involvement in breast cancer bone metastasis formation is however unknown. To address this question, we chose the human osteotropic MDA-MB-231/B02 breast cancer cell line which is devoid of Twist-1. MDA-MB-231/B02 cells were stably transfected with a Tet-inducible vector encoding for Twist-1, whose expression was specifically repressed in the presence of doxycycline (dox). Transfectants expressing Twist-1 or mock-transfectants were injected into the tail artery of immunodeficient mice. Radiographic analysis on day 32 after tumor cell injection revealed that the extent of osteolytic lesions in hind limbs of animals bearing Twist-1 tumors was increased, being 50% larger than that of animals bearing mock-transfected tumors. This difference was accompanied with a sharp reduction of the BV/TV ratio (indicating a higher bone destruction) and a 2-fold increase in the TuV/STV ratio (a measure of the skeletal tumor burden) compared with mice bearing mock-transfected tumors, as determined by histomorphometric examination. Twist-1 did not influence osteoclast-mediated bone destruction, as judged by the TRAP staining of osteoclasts at the bone/tumor interface in legs from animals bearing mock- or Twist1-expressing tumors. Importantly, the stimulatory effect of tumor-derived Twist-1 on bone metastasis formation was abolished in dox-fed animals, indicating that Twist-1 was responsible for enhanced in-vivo skeletal tumor growth. When breast cancer transfectants were injected orthotopically in female mice, Twist-1 expression induced a rapid tumor take compared with animals bearing mock-transfected tumors, whereas tumors grew at a similar rate, irrespective of Twist-1. Additionally, enhanced tumor take in animals bearing Twist-1 tumors was abrogated in dox-fed animals. In vitro, Twist-1 ectopic expression did not affect tumor cell proliferation and survival, nor their mesenchymal phenotype. By contrast, it promoted tumor cell invasion and enhanced microRNA-10b expression, a pro-invasive factor. Thus, our results strongly suggest that Twist-1 expression in breast cancer cells promotes bone metastasis formation.

***Disclosures: Philippe A.R. Clezardin**, None.*

MO0461

Estrogen Depletion by Ovariectomy or Aromatase Inhibitors Increase Breast Cancer Bone Metastases in Female Nude Mice. Ahmed Harhash*[1], Wende Kozlow[2], Chris McKenna[2], Holly Davis[2], Maria Niewolna[3], Khalid Mohammad[3], Theresa Guise[3]. [1]Indiana University- School of Medicine, USA, [2]University of Virginia, USA, [3]Indiana University, USA

Treatment of estrogen receptor positive breast cancer consists of blocking the estrogen receptor by Tamoxifen or decreasing estrogen production with aromatase inhibitors (AIs).The use of AIs was reported to accelerate bone loss and cause osteoporosis in postmenopausal women. We hypothesize that estrogen depletion generates a high bone turnover state, creating the fertile soil for the metastases to grow.

To study the effect of estrogen depletion on bone metastases, 4 week old athymic nude mice were randomized to ovariectomy (OVX) or sham surgery. 10 weeks after surgery, OVX mice had lower BMD at lumber spine ($P<0.0001$) and proximal tibia ($P<0.0001$). Mice were then inoculated (intra-cardiac) with MDA-MB-231 breast cancer cells. 4 weeks after inoculation, OVX mice developed more bone metastases than sham mice as assessed by histology ($P=0.06$). To determine if AIs have the same effect on bone metastases, fourweek old nude mice were randomized to receive daily letrozole or vehicle. Four weeks after treatment,mice were inoculated with MDA-MB-231 cells and treatment was continued. Letrozole-treated mice had more osteolytic lesions on x-ray ($P=0.06$), on histological analysis of the hind limbs, bone metastases tended to increase in Letrozole-treated mice.

To determine if letrozole efficiently depletes estrogen, we compared the degree of bone loss and the change in uterine weight in vehicle- treated OVX mice to letrozole-treated OVX mice. BMD was followed for 28 weeks by DXA. Letrozole-treated OVX mice had lower BMD compared to vehicle-treated OVX mice at the lumber spine ($P<0.0001$), proximal tibia ($P<0.0001$) and distal Femur ($P<0.0001$). Bone marrow culture showed that letrozole-treated OVX mice had higher number of colony forming unit (CFU)-osteoblast ($P=0.0002$), CFU-fibroblast($P<0.0001$) and tartrate resistant acid phosphatase (TRAP)+ multinucleated cells ($P=0.0012$) compared to vehicle-treated OVX mice.Our results show that OVX and letrozole together are necessary to completely deplete estrogen production in athymic nude mice. Combining both approaches is necessary to achieve complete estrogen depletion and to efficiently study the effect of estrogen depletion on the development of breast cancer bone metastases. This model will replicate the clinical situation of treatment for hormone-dependent breast cancer.

***Disclosures: Ahmed Harhash**, None.*

MO0462

Integrin αvβ3 and CD44 Pathways support osteoclastogenesis via a Runx2/Smad 5/Receptor Activator of NF-κB Ligand signaling axis in metastatic prostate cancer (PC3) cells. Aditi Gupta*[1], Meenakshi Chellaiah[2]. [1]University of Maryland, Baltimore, USA, [2]University of Maryland, Dental School, USA

Background:Skeletal complications such as bone loss and pathological fractures are developed as a result of androgen deprivation therapy and bone metastases in prostate cancer patients. Increased bone resorption by osteoclasts leads to bone loss. We have previously demonstrated that prostate cancer cells secrete receptor activator of NF-kB ligand (RANKL), a protein essential for osteoclast differentiation and activation. However, the mechanism(s) by which RANKL is produced remains to be determined. The objective of this study is to gain insight into the molecular mechanisms of RANKL expression by metastatic prostate cancer cells.

Results: We show here that phosphorylation of Smad 5 by integrin αvb3 and RUNX2 by CD44 signaling regulates the expression of RANKL in prostate cancer cells (PC3) derived from bone metastasis. Intranuclear targeting of RUNX2 is mediated by phosphorylation of Smad 5. Inhibition of Smad 5 phosphorylation by an inhibitor to αv reduced not only the nuclear localization of RUNX2 but also RANKL expression. Similarly knockdown of CD44 or RUNX2 by SiRNA attenuated the expression of RANKL. As a result, conditioned media from these cells failed to support osteoclast differentiation in vitro. Immunohistochemistry analysis of tissue microarray sections containing primary prostatic tumor (grade2-4) detected predominant localization of RUNX2 and phosphorylated Smad 5 in the nuclei. Immunoblotting analysis of nuclear lysates of prostate tumor tissue corroborates above observation.

Conclusions: In summary, we show here that CD44 signaling regulates phosphorylation of RUNX2. Localization of RUNX2 in the nucleus requires phosphorylation of Smad-5 by integrin αvb3 signaling. Our results suggest the possible integration of two different pathways in the expression of RANKL. These observations imply a novel mechanistic insight into the role of these proteins in bone loss when prostate cancer present in bone metastases.

***Disclosures: Aditi Gupta**, None.*

MO0463

Osteocytes promote prostate cancer bone growth. Joseph Sottnik*, Honglia Zhang, Evan Keller. University of Michigan, USA

Purpose: Osteocytes are the most abundant cell type in mineralized bone. Prostate, breast, and lung cancers frequently metastasize to bone. However, the role that osteocytes play in the development of bone metastases is unknown. In the presence of physical stimuli, osteocytes are known to produce HGF, IGF1, and VEGF, a potentially potent tumor promoting cocktail. The goal of this study is to determine if soluble factors produced by osteocytes can promote tumor activity.

Methods: Conditioned media (CM) was prepared from MLO-Y4 osteocyte-like cells and MC3T3 osteoblast cells. Viability of prostate, breast, and lung cancer cell lines in the presence of CM was measured using resazurin. Further investigation was performed using the CM on prostate carcinoma (PCa) cell lines. Apoptosis and cell cycle analysis were performed using flow cytometry and western blot. Invasion and migration towards CM using modified Boyden chamber assays were performed. Western blotting was used to determine activation of signaling pathways and alterations in phenotypic markers. Immunofluorescence was used to evaluate cell-cell interactions between MLO-Y4 or primary murine osteocytes and tumor cells *in vitro*.

Results: Incubation with osteocyte CM significantly increased viability in multiple cancer cell lines compared to incubation with control or osteoblast derived CM. No difference in apoptosis was observed across multiple assays. Increased proliferation of PCa cells, as measured by cell cycle and western blotting, was observed. Osteocyte CM led to a significant increase in the migration and invasion of PCa cells. Upregulation of proteins characteristic of EMT and promotion of a mesenchymal phenotype were observed. MLO-Y4 and primary osteocytes were found to form functional cell-cell interactions with PCa.

Conclusions: Osteocytes were found to significantly promote PCa proliferation, migration, invasion, and a mesenchymal phenotype compared to osteoblasts. These observations provide evidence that osteocytes are pro-metastatic. Exploration of osteocyte-tumor interactions will provide insight to the bone microenvironment and may produce novel targets for therapeutic development.

***Disclosures: Joseph Sottnik**, None.*

MO0464

Association of QCT bone mineral density and bone structure with vertebral fractures in patients with multiple myeloma. Jan Borggrefe*[1], Sarah Giravent[2], Asmus Wulff[3], Jaime Peña[2], Felix Thomsen[2], Martin Heller[3], Claus-C Glueer[2]. [1]Institut und Poliklinik für Diagnostische Radiologie, Uniklinik Köln, Germany, Germany, [2]Christian-Albrechts-Universtät zu Kiel, Germany, [3]UK-SH Campus Kiel, Germany

In patients with multiple myeloma (MM) computed tomography is used for staging and to detect pathological fractures. We investigated the association of prevalent vertebral fractures in MM patients with Quantitative Computed Tomography (QCT) based bone mineral density (BMD) and structure.

We evaluated a cohort of 123 MM patients (50 women, 73 men) from the OLYMP CT study who underwent low-dose whole body CT in clinical routine. The CT scans were acquired with 1.5 mm slice thickness, 120 kVp and appr. 100 mAs with INTable Calibration Pad (Image Analysis, KY). We analyzed vertebrae T11 and T12 excluding those with focal osteolytic changes. An in-house QCT software (Structural*Insight*) was used for BMD and structural analyses, including trabecular separation (Tb.Sp), bone volume fraction (BV/TV), trabecular number (Tb.N), trabecular thickness (Tb.Th), and cortical thickness (Ct.Th). Given the limited spatial resolution a prescript app. for *apparent* was used. Vertebral fractures were diagnosed by two radiologists in consensus based on Genant-criteria. Multivariate logistic regression models were calculated and t-test were performed for differences between subgroups.45% of the patients had prevalent vertebral fractures. Patients with and without fractures were comparable in age (65 vs. 63 years, $p > 0.3$). Comparing men and women, BMD and structural variables were similar, except for Tb.N. which was lower in women ($p = 0.03$). Trabecular BMD in patients with fractures of 168 ± 6.0 mg/cc (mean $\pm$SEM) was lower than in non fracture cases with 189 ± 6.6 mg/cc ($p = 0.023$). In age-adjusted logistic regression the OR per SD was 1.6 (1.1, 2.3) for BMD 1.7 (1.1, 2.6) for app.BV/TV, 2.0 (1.4, 3.0) for app.Tb.Sp and 2.1(1.4, 3.2) for app.Tb.N. No significant differences were observed for app.Tb.Th or app.Ct.Th. In multivariate models combining BMD and structural variables, app.Tb.Sp and app.Tb.N remained significant after adjusting for age and BMD. Cortical parameters did not provide significant predictive value for fracture events.

Low-dose whole body QCT investigation of MM patients permits the investigation of bone fragility status in clinical settings. Despite limitations of image resolution bone rarefication with an 8% reduction of app.Tb.N could be detected. This may reflect lytic processes not yet apparent visually which would provide added value for staging of MM disease.

***Disclosures: Jan Borggrefe**, None.*

MO0465

Cells of the Osteoblast lineage Hinder Acute Leukemia Progression in Murine Models: therapeutic implications. Maria Krevvata*[1], Barbara Silva[1], J. Sanil Manavalan[1], Aris Economides[2], Julie Teruya-Feldstein[3], Govind Bhagat[1], Ellin Berman[3], Stavroula Kousteni[1]. [1]Columbia University Medical Center, USA, [2]Regeneron Pharmaceuticals, Inc., USA, [3]Memorial Sloan-Kettering Cancer Center, USA

It is now appreciated that trabecular bone formation and establishment of hematopoiesis within the marrow are intimately coordinated. Osteoblasts influence homing of hematopoietic stem cells (HSCs) and are implicated in HSC lineage determination and expansion. In turn, deregulation of hematopoiesis is associated with hematological malignancies, which may in part be mediated by the microenvironment. The implication of cells of the osteoblast lineage in hematological disease recently came to light when deletion of the RNA processing *Dicer1* in osteoblast progenitors in mice induced myelodysplasia, a pre-leukemic condition in humans. We hypothesized that osteoblasts directly influence the fate of leukemic blasts. Consistent with this idea we found through genetic means that depletion of osteoblasts in syngeneic mouse models of acute myeloid or lymphoid leukemia increased circulating blasts and tumor engraftment in the bone marrow and liver or spleen leading to higher tumor burden and shorter survival. Myeloid activity was increased in the marrow and was coupled with a reduction in B-lymphopoiesis and compromised erythropoiesis suggesting that hematopoietic lineage progression was altered. In parallel studies in wild type mice, injection of the myelomonocytic leukemia cell line WEHI-3B or the lymphoblastic EL4 cells resulted in rapid, within 2 weeks, marked decrease in bone volume which was solely due to a decrease in the number of osteoblasts. Given this finding, we examined whether the course of leukemia could be ameliorated in mice by increasing their osteoblast numbers. Treatment of mice with acute myeloid or lymphoblastic leukemia with a pharmacological inhibitor for the synthesis of duodenal serotonin, a hormone suppressing osteoblast numbers, inhibited loss of osteoblasts in both models of leukemia. Mirroring the observations in mice lacking osteoblasts, maintenance of the osteoblast pool allowed for recovery of normal marrow function, hindered tumor burden and increased survival. Importantly, tumor burden inversely correlated with osteoblast numbers. Leukemia prevention was specifically due to maintenance of osteoblasts since selective inhibition of serotonin receptors in leukemia blasts did not affect leukemia progression in any of the two models. These results suggest that osteoblasts play a fundamental role in propagating leukemia in the bone marrow and that manipulating osteoblast numbers or function may be a potential target to treat leukemia.

***Disclosures: Maria Krevvata**, None.*

MO0466

Increased Expression of TAF12 in Myeloma Cells and the Bone Microenvironment Enhances Tumor Cell Growth and Osteoclast Formation. Noriyoshi Kurihara[1], Jumpei Teramachi[2], Yukiko Kitagawa*[1], John Chirgwin[1], G. David Roodman[1]. [1]Indiana University, USA, [2]The University of Tokushima, USA

Vitamin D (Vit.D) plays multiple roles in normal and malignant cellular function, including cell differentiation and proliferation, and is a key regulator bone homeostasis. Low Vit.D may play a role in the progression of lung cancer, breast cancer and prostate cancer as well as lymphoma and melanoma. However, the role of Vit.D in myeloma (MM) is much less clear. Vit.D insufficiency or deficiency has been documented in the majority of MM patients, but it is unclear if it affects disease activity. We previously found OCL precursors from patients with Paget's bone disease (PD) were hypersensitive to Vit.D and formed OCLs at physiologic concentrations of 1,25-(OH)2D3 (1,25-D3) rather than the pharmacologic concentrations of 1,25-D3 normally required for OCL formation. This enhanced sensitivity to 1,25-D3 was due to increased expression of a VDR co-activator, TAF12, a member of the TFIID transcription complex induced by IL-6. Since IL-6 levels also are increased in MM, we tested MM cells and marrow stromal cells (BMSC) for TAF12 expression. BMSC and CD138+ primary cells from MM patients expressed increased TAF12 levels compared to BMSC and CD138+ plasma cells from normal donors. MM cell lines (MM1.S, ANBL6, JJN3 and RPMI8266) expressed increased levels of VDR and TAF12 and were hyper-responsive to 1,25-D3. TNFα and IL-6 increased TAF12 expression in MM cells and BMSC. The increased TAF12 levels enhanced RANKL, VEGF, DKK1 and α4β1 integrin expression by CD138+ primary MM cells and MM cell lines in response to 10-10M 1,25-D3 and enhanced adhesive interactions between MM cells and BMSC to increase MM cell growth. To confirm the capacity of TAF12 to increase RANKL expression by MM cells in response to 1,25-D3, we made a stable TAF12 anti-sense JJN3 cell (AS-TAF12-JJN3). AS-TAF12-JJN3 cells had markedly decreased RANKL production, VDR content and CYP24A1 accumulation in response to 1,25-D3. Co-culture of JJN3 cells with BMSC treated with 1,25-D3 induced increased MM cell adhesion to BMSC that enhanced MM cell growth. In contrast, co-culture of BMSC with AS-TAF12-JJN3 cells resulted in decreased MM cell adhesion and growth. Further, 1,25-D3 treatment of human OCL precursors co-cultured with JJN3 cells, but not AS-TAF12-JJN3 cells, induced OCL formation which was blocked by OPG. These results suggest that increased expression of TAF12 in myeloma cells and their microenvironment allows low concentrations of 1,25-D3 to enhance tumor cell growth and osteoclast formation.

***Disclosures: Yukiko Kitagawa**, None.*

MO0467

Multiple Myeloma Cells Suppress Osteoblastogenesis by Upregulating Gfi1 via Activation of the ER Stress Transducer IRE1α. Feng-Ming Wang*[1], Hong-Jiao Ouyang[2], Deborah Galson[3], G. David Roodman[1]. [1]Indiana University, USA, [2]University of Pittsburgh, USA, [3]University of Pittsburgh School of Medicine, USA

Osteoblast suppression induced by myeloma cells is a major factor in the morbidity and mortality of multiple myeloma bone disease. Gfi1 is an important *Runx2* transcription repressor responsible for the osteoblast suppression induced by multiple myeloma cells. However, it remains unclear how *Gfi1* is upregulated by myeloma cells. In this study, we report that *Gfi1* is an endoplasmic reticulum (ER) stress response gene. Co-culture of myeloma cells with the pre-osteoblastic cell line MC3T3-E1 subclone 4 (MC4) induced the transcription of *Gfi1* along with the known ER stress target genes, *Grp78, Gadd34, Chop, Edem1*, in the MC4 cells. Similarly, treatment of MC4 cells with the ER stress stimulators tunicamycin and thapsigargin increased *Gfi1* mRNA and protein via transcriptional regulation. Consistent with this, inhibition of the endoribonuclease activity of the ER stress transducer Ire1α by 3-Ethoxy-5,6-dibromosalicylaldehyde strongly attenuated the induction of *Gfi1* in MC4 cells. The induction of *Gfi1* by ER stress did not occur in *Ire1α* deficient mouse embryonic fibroblasts (MEFs). Tunicamycin and thapsigargin treatment of *Xbp1* deficient MEFs revealed that Ire1α-mediated upregulation of *Gfi1* is only partly dependent on the known Ire1α endoribonuclease target Xbp1s. Further, over-expression of wild-type IRE1α induced *Gfi1* mRNA in NIH3T3 cells, whereas endoribonuclease deficient-IRE1α (K907A) and kinase deficient-IRE1α (K599A) did not, and the induction was predominantly dependent on the endoribonuclease activity. Finally, knockdown of *Ire1α* in MC4 cells by either siRNA transfection or shRNA lentivirus transduction prevented ER stressor and myeloma cell upregulation of *Gfi1*, and also prevented myeloma cell induced suppression of *Runx2* and osteoblast differentiation. These data suggest that ER stress upregulates *Gfi1* mRNA via activation of IRE1α in bone marrow stromal cells exposed to myeloma cells, resulting in osteoblast suppression. Therefore, the endoribonuclease activity of IRE1α in stromal cells may be a potential therapeutic target for reversing the protracted inhibition of osteoblast differentiation in multiple myeloma.

***Disclosures: Feng-Ming Wang**, None.*

MO0468

Osteoclasts from Multiple Myeloma Patients Are Highly Angiogenic. Rebecca Silbermann*[1], Dan Zhou[1], Wei Zhao[1], Courtney Tate[2], Wayne Blosser[2], Lisa Wyss[3], Louis Stancato[2], G. David Roodman[4]. [1]Indiana University School of Medicine, USA, [2]Eli Lilly & Company, USA, [3]Advanced Testing Laboratories, USA, [4]Indiana University, USA

Multiple myeloma (MM) bone disease is marked by increased osteoclast (OCL) formation and enhanced angiogenesis. Increased microvessel density in the MM bone marrow microenvironment (BMM) correlates with disease progression, and the apposition of OCL and endothelial cells in the BMM suggests that osteoclastogenesis and angiogenesis are linked. While MM cell, stromal cell, and endothelial cell interactions are known to produce angiogenic factors, OCL-conditioned media (CM) is also highly angiogenic, and the role of OCL themselves in MM angiogenesis has not been studied. We hypothesize that the angiogenic capacity of MM patient OCLs differs from healthy donor OCLs, and that MM OCL express different amounts of known angiogenic factors.

We cultured non-adherent bone marrow mononuclear cells from MM patients and healthy donors to induce OCL formation in the presence of mCSF and RANKL for 21 days. Purified, mature OCL populations were incubated in serum free media for 24 hrs. CM and OCL RNA were isolated and tested for angiogenic activity and expression of angiogenic genes. CM from healthy donor OCL and MM OCL significantly and dose-dependently increased human umbilical vein cell proliferation after 72 hrs. Endothelial cell cord formation was tested with adipose-derived stem cell / endothelial colony-forming cell co-cultures treated with each OCL-CM. Vascular networks were visualized with CD31 staining. Imaging and analysis were performed with the cord formation algorithm on the Thermo Fisher® ArrayScan® VTI. Both MM patient OCL-CM and healthy donor OCL-CM significantly increased cord formation, with dose-dependent increases in total tube area and connected tube area as compared with control. Direct comparison of MM patient OCL-CM with healthy donor OCL-CM, normalized for total protein concentration in the OCL cultures, demonstrated increased total tube area and connected tube area in the MM OCL-CM treated samples. Angiogenic gene expression in the MM and healthy donor OCL was compared using the Human Angiogenesis *Profiler* RT^2 PCR array. 30 of 84 genes screened had a 2 - 20 fold increased expression in the MM sample compared to the healthy donor. Highly expressed genes include ANG, CXCL12, PDGFB, and VEGFA.

These findings demonstrate that MM patient-derived OCL-CM is more angiogenic than healthy donor OCL-CM, and suggest that OCL may be major contributors to the increased angiogenesis seen in MM, in addition to their role in tumor growth and bone destruction.

***Disclosures: Rebecca Silbermann**, None.*

MO0469

Suppression of Osteoblastogenesis in Human MSCs Co-cultured with Human Multiple Myeloma Cells. Wei Zhang*[1], James Peterson[1], Moustapha Kassem[2], Matthew Drake[3]. [1]Mayo Clinic, USA, [2]Odense University Hospital, Denmark, [3]College of Medicine, Mayo Clinic, USA

Multiple myeloma (MM) is a malignancy of terminally differentiated clonal plasma cells. MM cells grow within the bone marrow (BM) cavity in close proximity to mesenchymal stem cells (MSCs), a dynamic population of self-renewing multipotent progenitor cells capable of osteoblastic differentiation. As most MM patients suffer from lytic bone destruction unmatched by bone formation, the interactions between MM cells and MSCs within the BM is likely crucial for MM bone disease.

To evaluate how MM cells impact MSC differentiation along the osteoblast (OB) lineage, we developed an *in-vitro* system in which the immortalized human MSC line hMSC-TERT was co-cultured in a transwell system separated by a 0.4 μm filter from the human MM cell lines RPMI8226 or U266. As a negative control, hMSC-TERT cells were co-cultured with hMSC-TERT cells. Following hMSC-TERT cell pre-differentiation with ascorbate and BGP for three days, MM cells were introduced and co-culture initiated. As expected, co-culture significantly reduced both AP activity and matrix mineralization in the hMSCs. Quantitative PCR results revealed that compared to control, hMSC-MM cell co-culture markedly suppressed the expression (by QPCR, n = 4-6, all $P < 0.01$) of OB differentiation marker genes in the hMSCs. Specifically, mRNA levels for AP decreased by 72-88%, col1α1 by 34-80%, and osteonectin by 54-81%. In contrast, hMSC expression of DKK1, a Wnt/beta-catenin pathway inhibitor with a well-recognized role in the pathogenesis of MM bone disease, was significantly increased by 52-100% ($P < 0.01$). Whole transcriptome sequencing is currently underway to evaluate for other hMSC genes impacted by co-culture. Given a recently described role for MSCs in regulating MM cell growth (J Clin Invest 123:1542, 2013), we also examined the effect of MSCs on proliferation markers in the MM cells. Consistent with these findings, MSC-MM cell co-culture markedly suppressed mRNA levels for cyclins A2 by 61-85%, B1 by 58-81%, and B2 by 55-84% (all $P < 0.01$) and Ki67 (-84% in RPMI 8226, $P < 0.01$; -36% in U266, $P = 0.057$).

In summary, using a co-culture system to simulate human MM cell/hMSC interactions, we found that MM cells significantly inhibited hMSC differentiation along the osteoblastic lineage; reciprocally, hMSCs suppressed MM cell proliferation gene expression. Future studies using this novel co-culture system will seek to understand the complex MM cell/hMSC interactions which underlie MM bone disease *in vivo.*

***Disclosures: Wei Zhang**, None.*

MO0470

Tumor-initiating Stem Cells are Regulated by α-CaMKII-induced VEGF in Human Osteosarcoma. Paul Daft*, Joan Cadillac, Majd Zayzafoon. The University of Alabama At Birmingham, USA

Osteosarcoma (OS) is among the most frequently occurring primary bone tumors, primarily affecting adolescents and young adults. Chemoresistance and disease recurrence are major challenges in the clinical management of OS and are thought to be caused by a small subpopulation of tumor-initiating stem cells (TISCs). Human OS TISCs are characterized by their expression of surface antigens $CD117^+$ and $Stro\text{-}1^+$, and the stem cell regulating transcription factors Sox2, Nanog, and Oct4. These OS TISCs are known to express high levels of receptors for vascular endothelial growth factor (VEGF). We have previously demonstrated that alpha-Ca^{2+}/Calmodulin kinase two (α-CaMKII) regulates VEGF and its autocrine signaling functions in human OS. Here, we examine whether OS TISCs are regulated by α-CaMKII-induced VEGF. Using fluorescence-activated cell sorting, we discovered that the pharmacological inhibition of α-CaMKII or VEGF in 143B OS cells by tamoxifen (1 μM) or bevacizumab (1 μM), respectively, decreases the population of $CD117^+$ and $Stro\text{-}1^+$ TISCs, and the gene expression (60%) and protein levels (80%) of Sox2, NANOG, and Oct4. Additionally, we developed a novel preclinical xenograft mouse model to examine the recurrence and metastasis of human OS. 143B OS cells were intratibially injected into mice, and tumors were allowed to grow for 2 weeks. Hind limbs-containing tumors were then amputated, and mice were confirmed to be tumor free by bioluminescent imaging 7 days post-surgery. Mice were randomized into four treatment groups: saline, tamoxifen (500μg/kg/day), and/or bevacizumab (5μg/kg twice weekly) and monitored monthly by bioluminescent imaging for the development of metastasis. The incidence of pulmonary metastasis/recurrence in saline treated mice was 100% two months after amputation. However, the incidence decreased to 38% in bevacizumab-treated mice, 12% in tamoxifen-treated mice, and 0% when both drugs were used. The levels of the TISCs subpopulation in pulmonary metastasis were determined by immunohistochemistry for Sox2, NANOG, and Oct4. We show that the number of TISCs were significantly increased in the recurrent metastatic pulmonary tumors when compared to primary amputated tumors. Furthermore, we show that treatment with tamoxifen and/or bevacizumab significantly decreases the number of TISCs when compared with saline treated mice. Taken together, our results demonstrate that α-CaMKII-induced VEGF controls the levels of TISCs both *in vitro* and *in vivo*.

***Disclosures: Paul Daft**, None.*

LATE-BREAKING ABSTRACTS

LB-SA01

A new *in vivo* methodology for quantifying intramuscular adipose tissue (IMAT) in the lower leg of women to define the relationship with BMD, strength, physical function and lifestyle variables. Janet Pritchard*[1], Sarah Karampatos[2], Karen Beattie[1], Lora Giangregorio[3], Stephanie Atkinson[1], Hertzel Gerstein[4], Zubin Punthakee[4], Jonathan Adachi[5], Alexandra Papaioannou[6]. [1]McMaster University, Canada, [2]Hamilton Health Sciences McMaster University, Canada, [3]University of Waterloo, Canada, [4]McMaster University, Canada, [5]St. Joseph's Hospital, Canada, [6]Hamilton Health Sciences, Canada

Introduction: Bone loss with age is linked to sarcopenia, defined as the aging-associated loss in muscle mass, strength and physical function. Muscle-bone interaction may also be influenced by fat infiltration of the muscle, known as intramuscular adipose tissue (IMAT). The primary aim of this study was to develop a reliable, non-invasive method of quantifying IMAT in the lower leg. The secondary aim was to determine the relationship between the amount of IMAT in the lower leg and BMD, strength, physical function, and other lifestyle variables.

Methods: This study included 28 postmenopausal women ⩾ 65 years of age with type 2 diabetes and 29 postmenopausal women without type 2 diabetes (control). All women were recruited from a diabetes outpatient clinic at Hamilton Health Sciences or the community. A 1-Tesla peripheral magnetic resonance imaging (MRI) system (OrthOne, GE) and fast spin echo sequence was used to acquire 10 sequential T1-weighted axial images of the non-dominant lower leg at the 66% site. Images were segmented with Slice-O-matic (Tomovision) using a threshold-based region growing technique to quantify IMAT area in each slice. The average cross-sectional area was calculated for each participant.19 participants' scans were analyzed in duplicate to assess intra-rater reliability, reported using root mean square coefficient of variation (RMSCV%) and type 2,1 intraclass correlation coefficient (ICC). Pearson correlation coefficients examined the relationships between IMAT and other variables.

Results: The relative intra-rater reproducibility of quantifying IMAT was good, with RMSCV% of 4.3% and ICC of 0.996 (95% confidence interval, 0.990-0.998). IMAT was related to lumbar spine and femoral neck BMD, timed-up-and-go result, grip strength, BMI, obesity, presence of type 2 diabetes, number of years since type 2 diabetes diagnosis, hip or knee OA and use of walking aid (Table 1).

Conclusion: This reliable method for measuring IMAT in the lower leg could be used in future studies to assess the interaction between muscle and bone quality. The positive relationship between BMD and amount of IMAT may be due to an interaction between BMI and IMAT, and skeletal loading. Lifestyle interventions may reduce the amount of IMAT and improve physical function and strength outcomes.

Table 1. Relationships between IMAT and BMD, strength, physical function and lifestyle variables.

	Pearson r	p-value
Lumbar spine BMD	0.273	0.042*
Femoral neck BMD	0.394	0.001*
Timed-up-and-go result	0.439	<0.001*
Grip strength	-0.268	0.048*
Amount of physical activity	-0.081	0.556
BMI	0.617	<0.001*
Participant in obese category (BMI ≥ 30 kg/m²) (yes/no)	0.499	<0.001*
Diet+supplement calcium intake	-0.208	0.125
Diet+supplement vitamin D intake	-0.059	0.666
Diagnosis of type 2 diabetes	0.428	<0.001*
# yrs since type 2 diabetes diagnosis	0.491	<0.001*
Diagnosis of hip or knee OA	0.336	0.011*
Use of walking aid	0.380	0.004*

** indicates statistical significance at p<0.05 level*

Table 1

***Disclosures: Janet Pritchard**, None.*

LB-SA02

Elevated Levels of Circulating Sclerostin in Hypophosphatemic Rickets. Telma Oliveira*[1], Francis Glorieux[2], Frank Rauch[3]. [1]Bone & Mineral Unit, Division of Endocrinology-UNIFESP, Bra, [2]Shriners Hospital for Children & McGill University, Canada, [3]Shriners Hospital for Children, Montreal, Canada

Background: Sclerostin is an antagonist of the Wnt signaling pathway and thereby is involved in the control of bone formation activity. The role of sclerostin in heritable metabolic bone disorders has not been studied in detail.

Objective: The objective of the study was to evaluate serum sclerostin levels in patients with osteogenesis imperfecta (OI) and X-linked hypophosphatemic rickets (XLH), and analyze the relationship of circulating sclerostin concentrations with bone mineral density and biomarkers of bone metabolism.

Materials and Methods: Serum sclerostin was quantified in 152 individuals, including 31 patients with XLH (14.7 ± 7.6 yr), 12 patients with OI type VI (26.8 ± 23.3 yr), 79 patients with other OI types (12.6 ± 4.8 yr) and 30 healthy subjects (20.8 ± 16.1 yr).

Results: Circulating sclerostin levels were higher in the XLH group (31.4 ± 17.8 pmol/l) than in healthy controls (22.6 ± 9.6 pmol/l ($p = 0.03$). Serum sclerostin levels were significantly higher in subjects with XLH than in OI subjects (21.84 ± 11.8 pmol/l), $p = 0.002$. In the XLH cohort, serum sclerostin levels were positively associated with the bone resorption marker serum NTX ($r = 0.84$) and with lumbar spine areal bone mineral density z-scores ($r = 0.71$; $p < 0.001$ in each case). Sclerostin levels were higher in boys (9 patients) with XLH than in girls (22 patients) 49.9 ± 18.7 vs. 23.9 ± 10.7 pmol/l, $p = 0.003$. Within the OI group, there was no significant difference in sclerostin levels between patients receiving bisphosphonates (n=31) and patients (n=45) who had never received bisphosphonates (21.2 ± 12.5 vs. 23.2 ± 12.7 pmol/l, $p = 0.48$).

Conclusion: Serum sclerostin levels are increased in XLH, a disorder with high bone mass. This can be interpreted as a mechanism that slows down bone formation and thus prevents a further increase in bone mass.

***Disclosures: Telma Oliveira**, None.*
This study received funding from: Shriners of North America, and the Fonds de Recherche Québec – Santé.

LB-SA03

Longitudinal modelling of fat and bone mass between aged 10 and 18 in a large cohort of boys: The Reciprocal Relationships between Bone Mass and Fat Mass. Adrian Sayers*[1], Emma Clark[1], J.H. Tobias[2], Kate Tilling[1], Fiona Steele[1]. [1]University of Bristol, United Kingdom, [2]Avon Orthopaedic Centre, United Kingdom

Introduction: Fat mass and bone mass are highly correlated, and to accurately study the dynamic relationships between these tissues across time, multiple measures in large numbers of people are required. We have investigated the relationship between fat mass and bone mass using longitudinal data from 9102 DXA scans in 2724 boys, aged 10 to 18 years, from the population-based cohort ALSPAC, the Avon Longitudinal Study of Parents and Children.

Methods: Fat mass and bone mass were measured using DXA at 5 time points: aged 10, 12, 14, 15.5 and 18 years. Bi-variate dynamic models were used to simultaneously assess the associations between fat and bone across the time points, and their associations with the previous measurements of bone and fat. Analyses were

standardised and adjusted for birth weight, crown heel length and maternal social economic status. For clarity, results are reported as regression coefficients, δ, with 95% confidence intervals where 0 equals no predictive ability and 1 indicates perfect prediction. These coefficients reflect the average predictive ability of the measurement across all time points.

Results: Measurements of fat at the previous time point were highly predictive of fat at the subsequent time point [$\delta_{fat,fat}$=0.97 (95%CI:0.96, 0.98), p<0.0001]. However, for bone the association was weaker [$\delta_{bone,bone}$ =0.72 (95%CI:0.70, 0.73) , p<0.0001]. There was a positive prospective association between fat and subsequent bone mass [$\delta_{bone,fat}$=0.043 (95%CI:0.019, 0.068) , p<0.0001] and also a positive prospective association between bone and subsequent fat mass [$\delta_{fat,bone}$ =0.046 (95%CI:0.032, 0.051), p<0.0001].

Conclusion: As expected there was a strong association between fat and previous fat, whereas the association between bone and previous bone was weaker. This suggests an important role of environmental influences on gain in bone mass across adolescence. Also, as expected, we report a positive prospective association between fat and bone. Uniquely, we also show a positive prospective association between bone and fat, of a similar strength to that seen between fat and bone, suggesting increased bone formation also results in increased in fat mass. This may be due to a direct effect of bone cells on adipose cells, or reflect the shared mechanisms of gain in bone and fat mass, perhaps because of their common mesenchymal origins. This study highlights new avenues for research in population cohorts.

***Disclosures: Adrian Sayers**, None.*

LB-SA04

Effects of Spaceflight on the "Non-Weight Bearing" L5 Vertebra Measured by Finite Element Analysis in Mice Flown on Space Shuttle Flight STS-135. Elizabeth Marshall*[1], Lindsay Sullivan[2], Eric Livingston[3], Andrea Hanson[4], Travis Pruitt[5], Louis Stodieck[6], Laura Bowman[2], Rachel Ellman[7], Jordan Spatz[8], Chris Paszty[9], Mary Bouxsein[7], Virginia Ferguson[6], Ted Bateman[10], Anthony Lau[2]. [1]Meredith College, USA, [2]University of North Carolina at Chapel Hill, USA, [3]University of North Carolina, USA, [4]Wyle, USA, [5]Clemson University, USA, [6]University of Colorado, USA, [7]Beth Israel Deaconess Medical Center, USA, [8]Harvard-MIT Division of Health Sciences & Technology (HST), USA, [9]Amgen, Inc., USA, [10]Univesity of North Carolina, USA

Skeletal unloading during spaceflight reduces bone volume and bone mineral density. How this loss translates to functional changes in strength and stiffness in the lumbar vertebrae is not well described. This study uses finite element modeling (FEM) of "non-weight bearing" L5 vertebrae in mice flown on STS-135 to assess the relationship between bone volume and bone stiffness from spaceflight and sclerostin antibody (Scl-Ab).

Thirty mice were flown on Space Shuttle Flight STS-135 for 13-days (FL). Half of the mice were treated with vehicle (n=15) and half were treated with a Scl-Ab (n=15). Corresponding ground control (GC) groups were similarly treated. Subject specific FE models were meshed from microCT, isolating a 1.50 mm tall segment of the L5 vertebral body starting at the superior endplate, excluding the pedicles. A downward displacement of 7.5 µm was applied to the superior face of the vertebral body to assess stiffness and structural efficiency (stiffness per amount of bone volume).

FEM of L5 vertebrae found a 20% decrease in stiffness and a 17% decrease in bone volume in the FL mice compared to the GC mice. Scl-Ab treatment resulted in increased stiffness by 75% and increased volume by 61% in the FL and increased stiffness by 65% and volume by 53% in the GC. Scl-Ab had a greater effect on bone volume and stiffness in both the FL and GC groups in comparison to the FE results of the proximal tibia or proximal femur ("weight bearing" bones) from the same mice. Bone structural efficiency changes were significant, but small compared to volume and stiffness, with a 4% decrease between GC and FL mice and a 9% increase and 8% increase respectively for the Scl-Ab treated FL and GC mice. Regardless, linear regression found a strong relationship between bone volume and stiffness of the L5 vertebrae among all test groups (P<0.01, R2=0.99). When examining the "weight-bearing" bones from the same mice, the changes in bone efficiency were larger between FL and GC, suggesting gravity has a greater effect on efficiency in "weight bearing" than in "non-weight bearing" vertebrae.

Regardless of treatment, bone volume was a good predictor of bone stiffness in the "non-weight bearing" L5 vertebrae, which was not observed in the "weight bearing" bones from the same mice. The unloading environment of microgravity caused a significant loss of L5 vertebrae stiffness in the vertebral body and treatment with Scl-Ab increased volume and stiffness in both FL and GC mice.

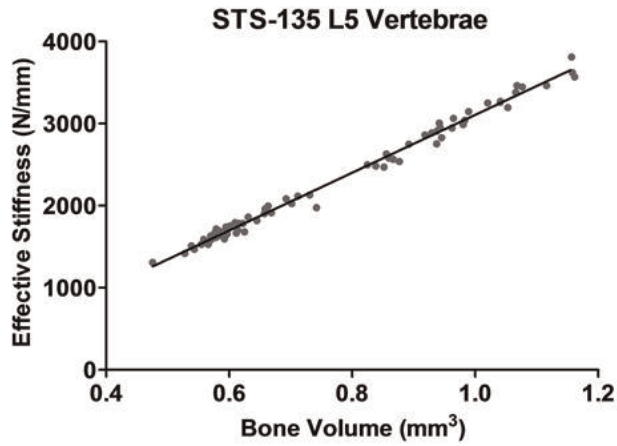

Regression shows linear relationship between bone volume and stiffness in L5 vertebrae (R2=0.992)

***Disclosures: Elizabeth Marshall**, None.*
This study received funding from: Amgen

LB-SA05

Passive Standing and Electrical Stimulation are Eligible Therapies for Preserving and Reverting the Loss of Bone Quality in Rats with Complete Spinal Cord Injury. Ariane Zamarioli[1], Daniel Maranho*[1], Francisco Jose De Paula[2], Leslie Morse[3], Ricardo Battaglino[4], Jose Volpon[1], Antonio Shimano[1]. [1]University of Sao Paulo, Brazil, [2]School of Medicine of Ribeirao Preto - USP, Brazil, [3]Harvard Medical School, USA, [4]The Forsyth Institute, USA

Objective: To assess the effects of passive standing (PS) and electrical stimulation (ES) on bone quality in rats with spinal cord injury (SCI).

Design: Seven-week-old male Wistar rats were divided into eight groups (n=7/group): (1) Sham33d; SCI33d; SCI+PS33d; SCI+ES33d; Sham63d; SCI63d; SCI+PS63d and SCI+ES63d. Complete SCI was generated by surgical transection of the cord at T10 level. ES and PS were performed 3days/week, 20minutes/day, for 30 days, whereas prevention was initiated three days after the surgery in the 33d groups and, treatment was started 33 days after SCI in the 63d groups. The following analyses were performed: biomechanical test, BMD analysis, H&E and Trap staining histology, microtrabecular quantification by Micro-CT in tibia, and serum markers for both formation (osteocalcin and OPG) and resorption (sclerostin and TRAP).

Results: SCI decreased bone quality in bones situated below injury level, which was more pronounced in long-term paraplegia (p<0.01). Thirty-three days of injury caused a reduction of 56% in mechanical strength, 72% in BMD, 61% in BV/TV, 50% in TbN, 60% in ConnDens, 20% in serum osteocalcin and 52% in serum OPG level. Whereas was observed an increase in serum levels of TRAP (47%), sclerostin (41%) and TbSp (133%), in comparison with SCI rats without treatment. These changes remained after 63 days of paraplegia, with some exacerbations as 67% in bone strength, 63% in TbN and 44% in osteocalcin. Regarding therapeutic modalities, both PS and ES preserved and reverted the bone loss following SCI (p<0.01) at varying degrees. PS increased BMD in 38%, bone mechanical strength in 48% (prevention) and in 96% (treatment), BV/TV in 40% (prevention) and in 75% (treatment), TbN in 100% (prevention) and in 117% (treatment), TbTh in 13%, ConnDens in 65% (prevention) and in 82% (treatment), osteocalcin in 75% (prevention) and in 176% (treatment) and OPG in 137%. Additionally, PS increased bone resorption in 43% (prevention) and in 63% (treatment) for TbSp and in 34% for sclerostin. ES also increased the bone quality of paraplegic rats, but to a lesser degree than PS; mechanical resistance in 35%, TbN and TbTh in 20%, osteocalcin in 40% and, decreased TbSp and TRAP in 22%.Conclusions*:* Passive standing and electrical stimulation have potential osteogenic effects as therapeutic modalities to both prevent and treat bone loss after spinal cord injury. Further investigation with the combination of both therapies may be performed.

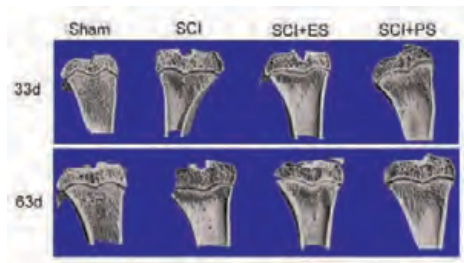

Micro-CT images

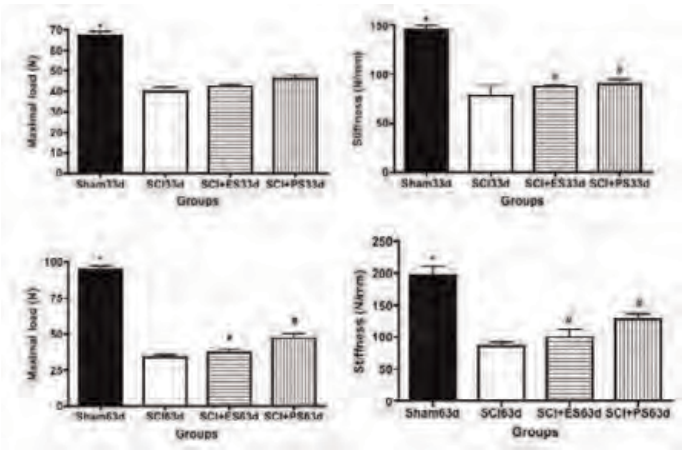

Biomechanical tests results

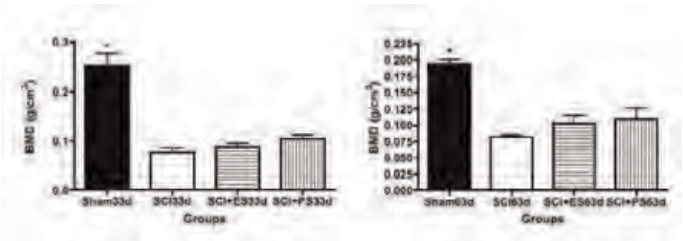

BMD results

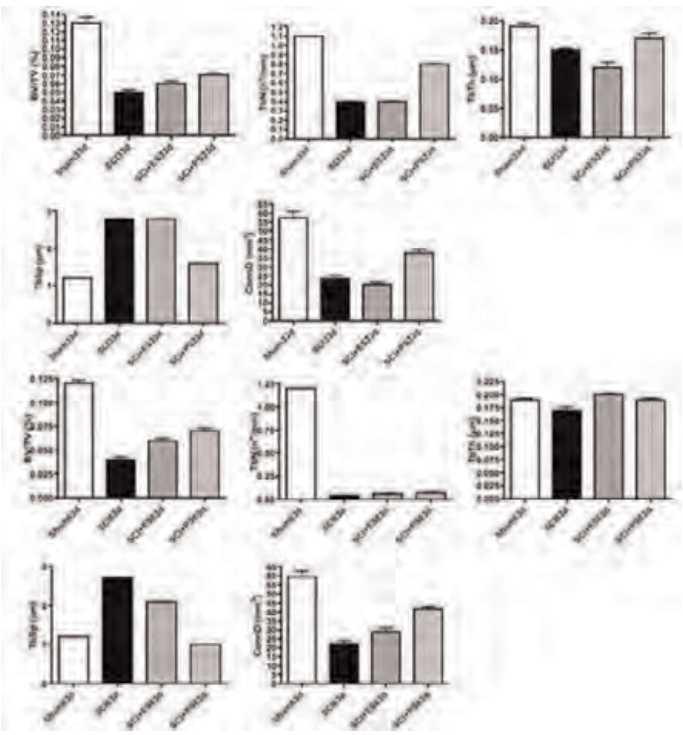

Micro-CT parameters results

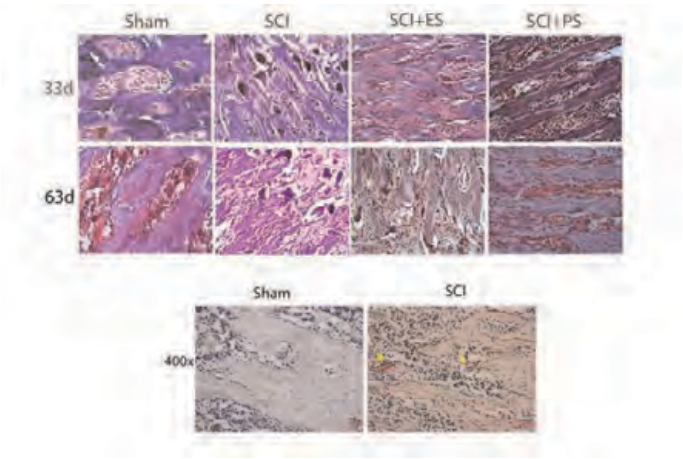

HE and trap staining histology.jpg

***Disclosures: Daniel Maranho**, None.*

LB-SA06

Alterations to Cortical Bone Fatigue Life Depend on Bisphosphonate Type.
Garry Brock*[1], Anthony Ingraffea[1], Jennifer MacLeay[2], Adele Boskey[3], Marjolein Van Der Meulen[1]. [1]Cornell University, USA, [2]Colorado State University, USA, [3]Hospital for Special Surgery, USA

Bisphosphonates (BP) are commonly prescribed for treatment or prevention of osteoporosis. Through osteoclast inhibition, BP suppress bone remodeling, preventing repair of damaged and aged tissue. Alendronate (ALN) treatment has been associated with increased microdamage in vivo[1] and shorter fatigue life[2] in cortical bone in the laboratory. Here we examined the fatigue life of cortical bone tissue treated with different generation BP and a SERM. Fatigue was chosen because atypical femoral fractures manifest as stress fractures.

In two experiments[3], skeletally mature sheep (n=25) were fed a metabolic acidosis (MA) diet to induce osteopenia[4] and then treated with ALN (n=2), zoledronate (ZOL n=6), raloxifene (SERM n=2) or vehicle (n=3 or 6 Table 1). Beams of cortical bone were cut from the medial region of the femoral diaphysis and anhydrously polished to a final cross section of 2 x 2 x 25mm. Beams were loaded cyclically to failure in four-point bending to generate surface strains of 400 to 4000με. Modulus degradation and cycles to failure were measured. Tissue mineral density (TMD) was measured by microCT.

Cycles to failure was similar across all groups except ALN, for which fatigue life was approximately an order of magnitude shorter ($p<0.01$ Figure 1). Differences in mineralization did not explain fatigue life and were not significant. SERM (+21.3%) and ALN (+7.7%) TMD were increased over their MA control, ZOL (+1.0%) was not.

These results suggest that the fatigue life of cortical bone is not altered by ZOL and is diminished by ALN. ZOL is a third generation BP with greater binding affinity for bone than ALN. Reduced fatigue life with ALN but not ZOL suggests repeated dosing, oral intake or chemical composition alters fatigue behavior of cortical bone. This study is limited by the small sample sizes for ALN and SERM; however, shorter fatigue life with ALN treatment was demonstrated previously[2]. Overall this study suggests that fatigue life of BP-treated cortical bone depends on the specific BP despite similar biologic mechanisms of action.

Table 1: Groups in this study. Osteopenia[4] induced in sheep with MA diet and treated with vehicle, ALN, ZOL or SERM. Red line indicates sheep euthanasia.

Figure 1: Cycles to failure (log scale) for all groups. ALN fatigue life shorter compared to all groups. Whisker plots show individual data points. Red line = grand mean.

Refs:[1]Mashiba+ JBMR 2000;[2]Geissler+ Trans ORS 2012;[3]Burket+ Bone 2012;[4]MacLeay+ CTI 2004

		Month												
	n	1	2	3	4	5	6	7	8	9	10	11	12	13	14
Control	6	Normal Diet												X	X
MA1	3	MA Diet						MA + Vehicle						X	X
SERM	2	MA Diet						MA + Raloxifene						X	X
ALN	2	MA Diet						MA + Alendronate						X	X
MA2	6	MA Diet								MA + Vehicle					
ZOL	6	MA Diet								MA + Zoledronate					

Table 1

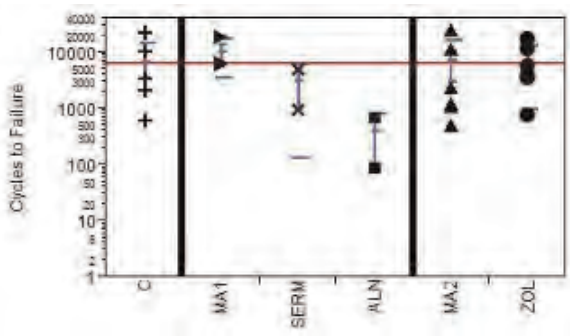

Figure 1

***Disclosures: Garry Brock**, None.*

LB-SA07

Nuclear Src Activity Functions to Suppress the Anabolic Response of Osteoblasts and Osteocytes to Fluid Shear Stress. Julia Hum*[1], Richard Day[1], Joseph Bidwell[1], Yingxiao Wang[2], Fredrick Pavalko[1]. [1]Indiana University School of Medicine, USA, [2]University of California San Diego, USA

Global deletion of Src kinase from mice results in increase bone mass. We tested the novel hypothesis that Src plays a previously unrecognized role in bone formation by regulating gene expression in osteoblasts and osteocytes, particularly in response to mechanical loading. Inhibition of Src activity using a pharmacologic inhibitor in MC3T3 osteoblasts and MLO-Y4 osteocytes led to an increase in expression of the anabolic bone gene osteocalcin. Mechanical stimulation of MC3T3 osteoblasts and MLO-Y4 osteocytes by fluid shear stress further enhanced expression of osteocalcin when Src activity was inhibited. Importantly, using a Src biosensor and nuclear fractionation, we report for the first time that Src activity in the nucleus increased in response to fluid shear stress. This study supports the idea that Src plays a nuclear role, suppressing expression of osteocalcin via a previously unrecognized function that limits the anabolic response of osteoblasts and osteocytes to fluid shear stress.

***Disclosures: Julia Hum**, None.*

LB-SA08

Ankle and forearm fractures are associated with similar low areal BMD and bone microstructural alterations in post-menopausal women. Emmanuel Biver*[1], Claire Durosier[1], Thierry Chevalley[2], François Herrmann[1], Serge Ferrari[1], René Rizzoli[1]. [1]Division of Bone Diseases, Geneva University Hospitals & Faculty of Medicine, Switzerland, [2]University Hospitals of Geneva Division of Bone Diseases, Switzerland

Ankle fractures are among the most common non-vertebral fractures. Previous studies have suggested that peripheral, but not axial areal(a) BMD predicted, though poorly, ankle fracture risk, in contrast to the well recognized association between forearm fractures and aBMD. Bone microstructure analysis may reveal alterations not captured by aBMD. To investigate the association between bone microstructure and ankle fractures, we determined distal radius cortical and trabecular bone microstructure by HRpQCT (XtremCT, Scanco Co, Bruttisellen, CH), together with aBMD by DXA, in 749 post-menopausal women aged 65.0 ± 1.4 ($x \pm SD$) years, with or without prevalent ankle or forearm fractures. Dietary protein and calcium intakes, and physical activity were evaluated by questionnaires.

Prevalent ankle and forearm fractures (having occurred after the age of 20) were found in 63 (8.0%) and 59 (7.8%) women, respectively. As compared with women without prevalent fracture, and after adjustment for height, weight, dietary intakes and physical activity, women with prevalent ankle fracture had lower aBMD (spine: -7.7%, $p<0.0001$; femoral neck: -6.4%, $p<0.001$; distal third radius: -4.1%, $p<0.01$), and lower distal radius total volumetric BMD (-10%, $p<0.001$), cortical thickness (-8.8%, $p<0.01$) and BV/TV (-13.2%, $p<0.001$). The corresponding values in women with prevalent forearm fracture were aBMD: -8.8%, $p<0.0001$; -6.8%, $p<0.001$; -3.4%, $p<0.025$; and distal radius microstructure: -16.3%, $p<0.0001$; -12.3%, $p<0.001$; -21.5%, $p<0.0001$. For 1 SD decrease, ORs for ankle and forearm fractures were 2.1 and 2.2 (both $p<0.0001$), 2.4 and 2.3 (both $p<0.001$), and 1.8 and 1.6 (both $p<0.01$) for spine, femoral neck and distal third radius aBMD, respectively. Similarly, ORs were 1.8 and 2.6 (both $p<0.001$), 1.6 and 1.7 (both $p<0.01$) and 1.8 and 2.9 (both $p<0.001$) for distal radius volumetric BMD, cortical thickness and BV/TV, respectively. There was no statistically significant difference in aBMD or bone microstructure values between women with prevalent ankle and forearm fracture.

These results highlight similar lower aBMD and bone microstructure values in postmenopausal women with prevalent ankle or forearm fracture. These alterations suggest that prevalent ankle fractures should be considered as a significant risk factor for subsequent fractures and taken into account in fracture risk assessment.

***Disclosures: Emmanuel Biver**, None.*

LB-SA09

The role of FoxA factors in the onset and development of Osteoarthritis. Andreia Ionescu*[1], Lin Xu[2], Elena Kozhemyakina[1], Yefu Li[2], Andrew Lassar[1]. [1]Harvard Medical School, USA, [2]Harvard School of Dental Medicine, USA

We have recently identified FoxA transcription factors as key regulators of chondrocyte hypertrophy in the developing skeleton (Dev.Cell 22(5),2012).Therefore, we next asked whether the Fox A family is involved in the onset and development of osteoarthritis (OA) in the adult cartilage.To evaluate the expression of FoxA2 in postnatal articular cartilage, we employed a tamoxifen-inducible Cre driver knocked-into the 3' UTR of the FoxA2 gene. After crossing this mouse line into the ROSA26 reporter line, we observed that FoxA2 expression was highest in the knee and the femoral cap articular cartilage of one-month old animals, it precipitously declined at 3 months of age and remained at this low level through at least 1 year. To evaluate whether FoxA family members are necessary for cartilage degradation, we conditionally deleted FoxA2 in the articular cartilage of FoxA3 -/- mice, using a tamoxifen-inducible CRE recombinase driven by the Prg4 (Lubricin) regulatory sequences. Subsequently, we performed surgical destabilization of the medial meniscus on either the tamoxifen treated *Prg4CreERT2/+;FoxA2fl/fl;FoxA3-/-* mice or control *C57BL/6* animals. While the wild-type *C57BL/6* mice that have undergone surgery developed significant cartilage degradation (OARSI score 5.87 ± 0.12), the tamoxifen treated *Prg4CreERT2/+;FoxA2fl/fl;FoxA3/-* mice showed very little sign of articular cartilage damage (OARSI score 1.45 ± 0.26). I next asked whether overexpression of FoxA2 in murine articular cartilage cells is sufficient to accelerate cartilage degradation. To drive exogenous FoxA2 expression in articular chondrocytes, I have generated mice containing the FoxA2 transgene driven by a reiterated reverse tetracycline transactivator (rtTA) response element (*TREtight-FoxA2*). This transgenic animal was in turn mated to a mouse containing rtTA knocked into the ROSA 26 locus downstream of a "floxed" STOP transcription cassette. Tissue specific expression of rtTA was achieved with the tamoxifen-inducible *Prg4CreERT2* line.Control mice, lacking the FoxA2 transgene, that have undergone surgery developed mild symptoms of the disease (OARSI score 1.37 ± 0.33). In contrast, triple transgenic mice that have undergone surgery developed far more cartilage damage with more lesions on the articular cartilage (OARSI score 2.63 ± 0.43). These findings imply that the FoxA transcription factors are crucial regulators of osteoarthritis following surgically induced joint destabilization.

***Disclosures: Andreia Ionescu**, None.*

LB-SA10

Detection and Partial Characterization of Bone Marrow Derived Cells in Periodontal Ligament. Masaru Kaku*, Asadullah Mohammad Edris, Megumi Kitami, Takako Ida, JM Rosales Rocabado, Katsumi Uoshima. Graduate School of Medical & Dental Science, Niigata University, Japan

It is well accepted that the substantial contribution of neural crest (NC) derived cells during the development of periodontal ligament (PDL). However the number of non-NC derived cells increases as PDL tissue development progresses. These observations suggest that non-NC cells are recruited to PDL from other cell sources during the tissue remodeling. Recent studies showed that bone marrow derived circulating mesenchymal stem cells (MSC) are found in peripheral blood vessels and are thought to contribute to tissue remodeling, especially to the tissues that undergo rapid remodeling. Considering the extremely high turnover rate of PDL tissue, it is possible that bone marrow derived MSCs reside in and contribute to the tissue maintenance of the PDL. The purpose of this study was to detect and partially characterize the bone marrow derived cells in developed PDL in vivo. Bone marrow stromal cells were collected from femur and tibia of Green Fluorescent Protein (GFP) rats (SD-Tg (CAG-EGFP)) and injected to the femur of the immuno-deficient rats (F344/NJcl-rnu). After 4 weeks of the GFP cell injection, tooth containing periodontal tissue, femur, skin, kidney and intestine were harvested, histology sections were prepared and subjected to immuno-histochemical analysis. GFP positive, femoral bone marrow derived cells were detected in PDL and the positive cell ratio was less than 0.1 %. The GFP positive cells have perivascular localization and some showed cluster like aggregate. While CD29, SSEA4, HNK1, αSMA and PDGFRβ positive cells were detected in PDL cells, only CD29 and SSEA4 positive cells were detected among GFP positive cells. The GFP positive cells were found not only in PDL, but also other mesenchymal tissues (i.e. cancerous bone surface of femur, connective tissue layer of skin, cortex of kidney and lamina propria of intestine). Our results clearly demonstrated that the GFP positive cells, which injected to femoral bone marrow cavity, were detected in PDL. The presence of GFP positive and MSC marker positive cells strongly indicates the supplementation of MSCs through the blood stream during the tissue remodeling of PDL. Furthermore, our observations strongly support the notion of circulating MSCs. Further studies are necessary to elucidate the significance of the bone marrow derived cells in PDL and mechanisms of delivery.

***Disclosures: Masaru Kaku**, None.*
This study received funding from: Grants-in-Aid for Scientific Research in JAPAN

LB-SA11

RANKL-Dependent and -Independent Mechanisms of Acute Calcemic Responses to PTH(1-34). Hila Bahar*[1], Akira Maeda[2], Monica Reyes[2], Thomas Dean[2], Ernestina Schipani[3], Paul Kostenuik[4], John Potts[2], Thomas Gardella[2]. [1]MGH & HMS, USA, [2]Massachusetts General Hospital, USA, [3]Indiana University School of Medicine, USA, [4]Amgen Inc., USA

Injection of Parathyroid Hormone (PTH) into animals or humans is well known to result in rapid (within 30 minutes) and robust (>10%) increases in blood ionized calcium (Ca^{++}) levels, but the molecular and cellular mechanisms underlying such an acute response are not fully understood. PTH regulates blood Ca levels largely by acting on both bone and kidney, but the PTH-induced increases in renal Ca reabsorption are likely to be too small and slow to account for the rapid calcemic responses observed with PTH injection. On the other hand, it is not clear whether an increase in the process of osteoclast (OC)-mediated bone resorption, which involves indirect activation of OCs by osteoblast/ocsteocyte-produced RANKL, could occur quickly enough to account for the rapid calcemic responses to PTH injection. To asses a possible role of RANKL-mediated activation of OCs in the acute calcemic response to PTH, we injected mice *iv* with PTH(1-34) (50 nmol/kg), either with or without the RANKL inhibitor, osteoprotegerin-Fc (OPG-Fc, 5 mg/kg), and assessed blood levels of Ca^{++} at times thereafter. We observed that the acute calcemic response to PTH(1-34) was markedly blunted by co-injection with OPG-Fc (PTH(1-34) vs. PTH(1-34)+OPG-Fc, $P<0.04$ and $P<0.000004$ at the 1 and 2 hour time points, respectively, n=6). These results suggest that at least some component of the mechanisms by which PTH induces a rapid calcemic response involves rapid activation of the RANKL/OC pathway of bone-resorption. We then assessed whether depletion of the OC cell populations would alter the calcemic response to PTH(1-34). To do this, we pre-treated mice for one week with OPG-Fc to block differentiation and activation of the OC pool, which is dependent on RANKL. Mice were thus injected *sc* with either vehicle (VEH) or OPG-Fc (5 mg/kg) on days 0, 3 and 6; then, on day seven, the mice were injected with either VEH or PTH(1-34) (50 nmol/kg) and acute calcemic responses were measured. Surprisingly, the acute calcemic response to PTH(1-34), assessed at 1 and 2 hours post-PTH injection, was not at all diminished in mice pre-treated with OPG-Fc, but rather was equivalent to that seen in the OPG-naive mice ($P>0.8$; n=8). There was a complete absence of TRAP-positive cells in the proximal tibia of the OPG-Fc-treated mice, versus an abundance of TRAP-positive cells in the VEH-pretreated controls. And, blood levels of TRAP-5b were significantly lower (85%) in the OPG-Fc-pre-treatment group, than in the VEH group ($P<0.001$), thus confirming that OPG-Fc pre-treatment strongly diminished OC cell function and numbers. The longer-term OPG-Fc treatment data thus suggest that PTH can act to mobilize Ca into blood via a heretofore unrecognized mechanism that is independent of RANKL and is induced or amplified by conditions that reduce or ablate OC populations. The possible roles of other cells types, such as osteocytes, in mediating this PTH-induced Ca mobilization need to be explored.

***Disclosures: Hila Bahar**, None.*

LB-SA12

Identification of Small Molecule Activators and Inhibitors of the Mutated $G_s\alpha$ Responsible for Fibrous Dysplasia of Bone by High-Throughput Screening; Results from the Secondary Screen using the Rat Pituitary GH3 cell-line model. Nisan Bhattacharyya*[1], Marek Kucka[2], Lesley A. Mathews[3], Marc Ferrer[3], Michael Collins[4]. [1]Csdb Nidcr Nih, USA, [2]NICHD, NIH, USA, [3]NCATS, NIH, USA, [4]National Institutes of Health, USA

Missense mutations in the α-subunit of the G-protein, Gsα, are directly correlated with the occurrence of fibrous dysplasia of bone/McCune-Albright syndrome (FD/MAS), a disease that is defined by skeletal abnormalities and as well as various forms of hyperfunctioning endocrinopathies. The biochemical outcome of these mutations (R201H or R201C) is constitutively active Gsα leading to increased levels of cellular cAMP. Clinically these patients can elicit ligand-independent hypersecretion of hormones in endocrine cells, (e.g., increased growth hormone and prolactin secretion by the pituitary) and age-dependent apoptosis of bone cells. In order to identify both small molecule activators and inhibitors of the mutated Gsα, high-throughput screening (HTS) was performed by measuring cAMP levels in Chinese hamster ovary (CHO) cells stably expressing the wild-type or mutant Gsα proteins. Chemical libraries comprised of more than 3X105 compounds in multiple doses were used and a total of 101 inhibitory and 129 stimulatory compounds were identified. The aim of this study was to develop a hormone-based rat pituitary cell culture model that would be useful in the secondary screening and identifying small molecule modulators specific for the mutant Gsα protein.

Several stable cell lines that overexpress either the wild-type (WT) or gsp (R201C or R201H) were prepared in the GH3 cells. Cell-lines were selected based for equivalent Gsα protein expression levels and high or low cAMP levels. Cells were treated with various concentrations of agonists and antagonists including known adenylyl cyclase activators and inhibitors as the controls. Prolactin levels were measured after 4 hours of incubation using a radioimmunoassay method. Results from inhibitor studies indicated that 36% of the selected inhibitors could inhibit prolactin secretion in GH3 cells expressing the wild-type or mutant Gsα. In fact, there were at least 7 compounds that resulted in reduced prolactin levels (down to 50% or more) at 10 μM concentrations. Results also showed that there were at least 3 compounds that could specifically inhibit the prolactin levels only in the cells expressing the mutant Gsα. In addition, secondary screening results from activator studies indicated that there 8 compounds that could increase prolactin levels in both wild-type and mutant protein expressing cells.

In conclusion, this secondary screening system for gsp activity we has confirmed that '36% of molecules identified in the earlier screens have inhibitory activity and that 3 compounds have selective activity on mutant Gsα. Results also indicated that there 8 of the 129 compounds identified in the stimulator screen have stimulatory activity. These compounds will be tested further in preparation for the development of drugs for the treatment of FD/MAS and other gsp-mediated diseases.

***Disclosures: Nisan Bhattacharyya**, None.*

LB-SA13

BMP2 Regulates CXCL12 in Endosteal Cells and their Commitment to Osteoblastic Differentiation. Timothy Myers*[1], Lara Longobardi[2], Helen Willcockson[1], Alessandra Esposito[3], Billie Moats-Staats[3], Ping Ye[3], Tieshi Li[2], Joseph Temple[3], Anna Spagnoli[2]. [1]University of North Carolina, USA, [2]University of North Carolina at Chapel Hill, USA, [3]UNC, USA

We have reported that bone marrow mesenchymal stromal (MSC) transplanted into fracture mouse models improve healing and thus provide a potential therapy to treat fracture non-unions. BMP2 is a critical component of the fracture healing process as it is expressed immediately after injury and mice lacking BMP2 in mesenchyme limb progenitor cells lack callus formation. We have previously shown that BMP2-expressing transplanted MSC localize along the endosteum of fractured bones and proper homing of transplanted cells depends on the CXCR4-CXCL12 signaling axis. To determine the interplay of BMP2 and CXCL12 in an *in vitro* model we used RT-PCR analyses of isolated endosteal cells from hindlimb bones of mice to measure changes in CXCL12 expression and the potential for osteoblastic differentiation. We measured CXCL12 expression in wild type (WT) endosteal cells, osteoblasts and MSC and compared them to Prx1Cre-BMP2-deficient cells and found that cells lacking BMP2 produce more CXCL12. Next we tested endosteal cells for the ability to differentiate into osteoblasts and found that WT cells had increasing osteoblastic markers over 14 days whereas BMP2-deficient endosteal cells expressed only low levels of the same markers. To test the effect of MSC on endosteal cells, we co-cultured endosteal cells with WT MSC. We found that CXCL12 expression significantly decreased in endosteal cells. However, in endosteal cells plus BMP2-deficient MSC cultures, endosteal CXCL12 remained highly expressed, suggesting a role for BMP2 in the regulation of endosteal CXCL12. To test a direct effect, endosteal cells were treated with BMP2 upon which endosteal cells differentiated into osteoblasts as determined by increases in osteoblastic markers, while CXCL12 expression decreased. BMP2 treatment also induced a downregulation in several factors expressed by endosteal cells (SCF, HGF, PECAM, CD164). To recapitulate the circumstances in our fracture model, endosteal cells from BMP2-deficient mice were co-cultured alone, or with either WT, or BMP2-deficient MSC. WT MSC induced a decrease in CXCL12 expression along with increases in osteoblastic markers that was not seen in BMP2-deficient MSC. Thus, in endosteal cells, osteoblastic differentiation and CXCL12 expression are closely related and can be regulated by BMP2 and this downregulation of CXCL12 could be a key switch for the allowance of endosteal cells to undergo osteoblastic differentiation.

***Disclosures: Timothy Myers**, None.*

LB-SA14

Putative Hematopoietic Progenitor Cells (HPCs) from Craniofacial Skeleton: Contrasting Long Bone Marrow Hematopoietic Stem/Progenitor Cells. Nan Jiang*[1], Jeremy Mao[2]. [1]USA, [2]PI, USA

Objective: Identify putative hematopoietic stem/progenitor cells (HSCs/HPCs) from craniofacial bones. Appendicular bone marrow is known to harbor two distinct stem-cell populations: hematopoietic stem cells (HSCs) and mesenchymal stem cells (MSCs). One of the fundamental hypotheses in stem cell biology is that MSCs, along with osteoblasts, form niches for HSCs in bone marrow. Whether craniofacial bones harbor HSCs is obscure.

Methods: Adult C57BL/6 mice were scarified to harvest mandibular bone-marrow contents and appendicular bones, the femur and tibia, as a positive control. Following established HSC isolation protocols, we subjected mandibular bone-marrow aspirates to centrifuging to form a density gradient. Mononucleated cells were aspirated from a thin cell-rich layer and subjected to Lin- selection by magnetic-activated cell sorting. Lin- cells were further sorted with CD34-, Sca1+ and c-kit+ antibodies by MoFlo, followed by additional characterization: colony-forming unit assay and flow cytometry. To appreciate whether mandibular marrow cells can be sustainably potentiated, cells were suspended in long-term culture media with 10-6 M hydrocortisone and cultured on irradiated bone marrow cells for 4 weeks at 33?C in 5% CO2. Upon 4-wk culture, cells were assayed and further isolated for clonogenic assay.

Results: A total of 1.5% Lin- cells from mandibular bone marrow were CD34-/low/c-Kit+ /Sca1+ cells (CD34-KSL cells) that represent a heterogeneous population of short-term repopulating HSCs, long-term repopulating HSCs and multi-potent progenitors. Mandibular CD34-KSL cells showed self-renewal over the tested 14 days and broad similarity to CD34-KSL cells isolated from appendicular bone

marrow of donor-matched mice. Interestingly, mandibular CD34-KSL cells differentiated into CFU-E/CFU-GM/CFU-GEMM, in contrast to BFU-E/ CFU-Pre B. Even following long-term culture, few mandibular bone marrow CD34-KSL cells differentiated into the lymphoid lineage, yielding only 0.5% CD45R/B220+ cells. Contrastingly, 57.2% CD45R/B220+ cells were isolated from appendicular bone marrow CD34-KSL cells following long-term culture.

Conclusion: The mandible harbors putative hematopoietic progenitor cells or CD34-KSL cells that show important differences from well-established HSC from appendicular bone marrow. Deficient lymphoid differentiation of mandibular HPCs suggests that appendicular HSCs may migrate to craniofacial bones and replenish the lymphoid lineage in the head.

***Disclosures: Nan Jiang**, None.*

LB-SA15

Fra1 deletion in B cells regulates bone homeostasis. Aline Bozec*[1], Bettina Groetsch[2], Dirk Mielenz[2], Erwin Wagner[3], Georg Schett[4]. [1]Deu, [2]1Medizinische Klinik 3 Rheumatologie und Immunologie, Friedrich-Alexander-Universitat Erlangen-Nurnberg, Germany, [3]Research Institute of Molecular Pathology, Austria, [4]Friedrich-Alexander University Medical School, Germany

Bone is crucial to maintain haematopoiesis as bone marrow spaces allow the interaction of bone and immune cells that functionally influence each other. The AP1 transcription factor is known to be essential for bone homeostasis and immune cell maintenance. Notably, Fra-1 was shown to regulate bone homeostasis by controlling osteoblast activity and the immune system by regulating plasma cell formation.

In addition of enhanced basal level of IgG1 and auto-antibodies observed in B cell specific Fra1 deficient mice, bone microCT analyses revealed a decreased bone volume in these mutant mice. Moreover, the histomorphometrie analyses revealed that the bone loss in mice with B cell specific deletion of Fra-1 was due to increase in osteoclast size and number.

Furthermore *in vitro* wild-type osteoclast assays supplemented with serum from mice Fra-1 deficient in B cell or with supernatant from Fra-1 deficient B cell cultures showed an increase in osteoclast differentiation, suggesting that Fra-1 expression modified the B cell secretome, which is increasing osteoclastogenesis. Interestingly, this effect was dependent of the presence of IgG in the supplemented serum. Finally, purified IgG from Fra-1 mutant serum further increased the number of polynucleated osteoclasts.

These findings indicate that Fra-1 expression in B cells acts on IgG level and pattern, which plays an important role in bone homeostasis. The identification of the molecular pathway will certainly lead to novel insights into the cross-talk between osteoclasts and B cells.

***Disclosures: Aline Bozec**, None.*

LB-SA16

Cortical and Trabecular Microarchitecture Impairment Correlates with Fibroblast Growth Factor-23 and Metabolic Acidosis in Men with Stages 3 and 4 of Chronic Kidney Disease. Francisco Paranhos Neto*[1], Guilherme Lima[2], Luciana Silva[2], Miguel Madeira[2], Inayá Lima[3], Maurilo Leite Junior[4], Carlos Gomes[4], Maria Lucia Farias[1]. [1]Federal University of Rio de Janeiro, Brazil, [2]Division of Endocrinology - University Hospital Clementino Fraga Filho, Federal University of Rio de Janeiro, Brazil, [3]Nuclear Instrumentation Laboratory, COPPE, Federal University of Rio de Janeiro, Brazil, [4]Division of Nephrology - University Hospital Clementino Fraga Filho, Federal University of Rio de Janeiro, Brazil

Chronic kidney disease (CKD) leads to disorders of mineral and bone metabolism described as CKD-Mineral and Bone Disorder (CKD-MBD). The discrepancies between the clinical picture, bone histomorphometry and bone densitometry raise doubts on the validity of this method in patients with CKD-MBD. High Resolution Peripheral Quantitative Computed Tomography (HR-pQCT) is a new and noninvasive method to assess bone microarchitecture that may help the evaluation of CKD-MBD. We investigated 46 men, 50 to 75 years, in stage 3 and 4 of CKD by HR-pQCT and correlated densities and structural parameters with biochemical changes. Patients on stage 4 exhibited a greater impairment of cortical and trabecular bone parameters, such as lower density and thickness associated with increased trabecular area and cortical perimeter, suggesting trabecularization of cortical bone. They also showed lower 25 hydroxyvitamin D [25(OH)D] and bicarbonate, and higher fibroblast growth factor 23 [FGF-23] and parathyroid hormone [PTH] serum levels. Estimated glomerular filtration rate [eGFR] correlated inversely with PTH and FGF-23 and positively with bicarbonate and 25(OH)D. FGF-23 correlated positively with PTH and negatively with 25(OH)D. PTH also correlated negatively with 25(OH)D. FGF-23 and metabolic acidosis were the only independent factors strongly associated with the bone impairment identified by HR-pQCT, suggesting the importance of these two biomarkers in the clinical management of these patients.

Keywords: HR-pQCT, CKD-MBD, metabolic acidosis, FGF-23, PTH, vitamin D, Renal Osteodistrophy

***Disclosures: Francisco Paranhos Neto**, None.*

LB-SA17

Cutaneous Skeletal Hypophosphatemic Syndrome: A new syndrome of FGF23 excess. Diana Ovejero*[1], Young Lim[2], Harald Jüppner[3], Michael Gottschalk[4], Cynthia Tifft[5], Rachel Gafni[6], Alison Boyce[7], Edward Cowen[8], Nisan Bhattacharyya[1], Lori Guthrie[1], William Gahl[5], Gretchen Golas[5], Keith Choate[2], Michael Collins[6]. [1]Skeletal Clinical Studies Unit, Craniofacial & Skeletal Disease Branch, National Institute of Dental & Craniofacial Research, National Institutes of Health, USA, [2]Department of Dermatology, Yale University School of Medicine, USA, [3]Pediatric Nephrology Unit & Endocrine Unit, Massachusetts General Hospital & Harvard Medical School, USA, [4]Pediatric Endocrinology, Rady Children's Hospital, San Diego & Departments of Pediatrics, University of California, USA, [5]NIH Undiagnosed Diseases Program, NIH Common Fund; Office of the Clinical Director, NHGRI, National Institutes of Health, USA, [6]National Institutes of Health, USA, [7]Children's National Medical Center, USA, [8]Dermatology Branch, Center for Cancer Research, National Cancer Institute, National Institutes of Health, USA

Pathologically elevated levels of fibroblast growth factor-23 (FGF-23), a bone-derived hormone that exerts a pivotal role in phosphate homeostasis, cause renal phosphate wasting, hypophosphatemia, and impaired skeletal mineralization. Rarely, elevated FGF-23 levels and hypophosphatemic rickets are found in association with congenital mosaic cutaneous disorders, such as epidermal and large congenital melanocytic nevi. In such cases, concomitant segmental dysplastic skeletal lesions are always observed. Furthermore, these disorders are variably associated with abnormalities in other organs such as the eye, brain and vasculature. Given the broad spectrum of cutaneous and systemic finidings, we have designated this disorder cutaneous-skeletal hypophosphatemia syndrome (CSHS). The source of the excess FGF23 production is to date unknown. In this report we describe 5 such individuals, 4 of which were affected with epidermal nevus, and one with large congenital melanocytic nevi. All of them presented extensive skin surface area involvement present since birth. The foci of dysplastic bone exhibited a variable distribution but typically were localized at same side as the skin lesions and exhibited a predisposition for the appendicular skeleton. Blood tests revealed in all cases hypophosphatemia associated with elevated or inappropriately normal FGF-23 levels, renal phosphate wasting, normocalcemia and no apparent abnormalities in the parathyroid function. Radiographic imaging studies revealed generalized ricketic changes and unhealed fractures in untreated patients. Histologic examination of dysplastic bone revealed fibroblast-like spindle-shaped cells surrounded by a relatively dense collagen matrix, an appearance consistent with cells in the osteogenic lineage. In addition, a number of other pathologic lesions were inconsistently observed in other tissues. These findings were consistent with somatic mosaicism for mutations contributing to multisystem disease. When treated adequately with phosphate and calcitriol, ricketic changes healed. However, unlike previous reports, none of the patients in our series who underwent ablative treatment of skin lesions showed improvement in phosphate metabolism. Given the involvement of skin and bone, tissues of ectodermal and mesodermal origins respectively, CSHS could be explained by a mutation in an early common progenitor. The underlying molecular mechanisms that drive this syndrome remain to be elucidated, but due to the phenotypic and metabolic similarities in all our subjects, we can assume that there is a common pathway implicated in all of them. Moreover, we can also infer from these observations, that the altered molecular events responsible for these disorders, may be involved in physiological FGF-23 regulation.

***Disclosures: Diana Ovejero**, None.*

LB-SA18

Minimally invasive parathyroidectomy versus bilateral neck exploration for primary hyperparathyroidism: a systematic review and meta-analysis. Omar Kreidieh*[1], Ghada El-Hajj Fuleihan[2], Hala Ahmadieh[3], Elie Akl[3]. [1]Lebanon, [2]American University of Beirut-Medical Center, Lebanon, [3]American University of Beirut, Lebanon

Objective: Compare the effects of Minimally Invasive Parathyroidectomy (MIP) and Bilateral Neck Exploration (BNE) on selected patient-important outcomes, in patients with sporadic primary HPTH undergoing surgery for the first time.

Methods: MEDLINE and EMBASE databases were searched up to January 2013 in order to conduct a Cochrane systematic review and meta-analysis of randomized controlled trials comparing BNE to MIP for the treatment of sporadic primary hyperparathyroidism. Primary outcomes were short (6 months) and long term (5 years) success rates (eucalcemia), total incidence of perioperative adverse events, all cause mortality, Health Related Quality of Life (HRQL), duration of surgery, and cosmetic satisfaction.

Data Collection and Analysis: Two independent reviewers screened titles, abstracts, full texts, extracted data from selected studies, and assessed risk of bias, with oversight from two senior investigators. The GRADE methodology to assess the quality of evidence was used.

Results: 5 trials with 264 adult participants were included; data was not extractable for HRQL and cosmetic satisfaction. Success rate in the MIP compared to BNE showed a RR= 0.98 [0.94;1.02] at 6 months (moderate quality of evidence), and of 0.94 [0.83; 1.08] at 5 years (low quality of evidence). The duration of surgery from 3

studies was shorter in the MIP group, RR= -18.32 [-30.69,-5.94] minutes, and the RR for the total incidence of peri-operative adverse events from 4 studies was 0.31 [0.09;1.1]. Both outcomes had a very low quality of evidence. One study found no difference in HRQL at one month and 6 months, with very low quality evidence. Mortality could not be adequately assessed. In 5 studies, peri-operative symptomatic hypocalcemia was significantly lower at two days, RR=0.55 [0.31;0.96], but not at six months, RR=0.3 [0.01;7.23]. The standardized mean difference postoperative pain score at 48 hours from 2 studies was -0.7 [-1.69;0.28], and the relative risk of vocal cord paralysis was 1.88 [0.47;7.47]. There was no reported difference in bleeding in 2 studies, nor in infection rate in one study. The conversion rate from MIP to BNE was 20% in 3 studies.

Conclusion: MIP and BNE had comparable success rates. Peri-operative hypocalcemia and post-operative pain were lower in the MIP group, while vocal cord paralysis was lower, in BNE. Our findings call for larger, prospective, randomized trials.

***Disclosures: Omar Kreidieh**, None.*

LB-SA19

Caloric Restriction during Growth, Serum Irisin and Bone Mass loss at Maturity. Vanessa Yingling, Tiffiny Butler*. Temple University, USA

Caloric restriction without malnourishment has maintained bone mass relative to bodyweight perhaps due to muscle mass maintenance. Muscle mass may increase bone mass due to loading or myokine secretion. Irisin is a myokine linked with bone mass maintenance mainly due to exercise. The long term effect of acute caloric restriction on bone mass at maturity remains elusive.

We set out to determine if 30% post pubertal food restriction during growth alters serum irisin and trabecular bone mass at maturity. Rats were assigned to groups: (n= 5-8), control (C), food restriction (FR), control recovery (RC), food restriction recovery (RFR), control ovariectomy (COVX) and food restricted ovariectomy (FROVX). A 6 week 30% food restriction protocol began at 65 days of age followed by a 10 week recovery period and then ovariectomy surgery (OVX) at 180 days of age. At sacrifice (108 days, 180 days and 227 days (47 days post OVX)) left femurs and L5 vertebrae were scanned using an ex vivo micro CT scanner. Serum assays for carboxy terminal collagen crosslinks (CTX), insulin like growth factor-1 (IGF-1) and irisin were performed. Student's t-tests determined significant differences between groups ($p< .05$). Linear regression was used to normalize percent trabecular bone volume (BV/TV) by body weight.

Normalized femur BV/TV was similar between groups. However, post OVX normalized vertebral trabecular BV/TV was greater in the FROVX group compared to COVX ($p<.05$). Lower serum CTX and IGF-1 were found in FR group following restriction. No differences in serum irisin were found between groups yet FR triceps surae muscle mass was lower than control ($p<.05$). During recovery, serum IGF-1 increased in RFR compared to RC with no difference in CTX or irisin ($p<.05$).

Food restriction during growth had no detrimental effect on BV/TV following 6 weeks of restriction and attenuated vertebral bone loss post OVX even though serum CTX levels were similar in COVX and FROVX groups. Lower resorption and formation resulting from restriction suggests a slowing of turnover. However during recovery serum IGF-1 increased resulting in a ''catch-up'' in trabecular BV/TV translating into bone loss attenuation following OVX. Irisin was similar between groups following restriction and recovery but FR animals had lower muscle mass on average suggesting more irisin per gram of muscle with restriction. No long term deficits in bone mass occur from caloric restriction during development.

***Disclosures: Tiffiny Butler**, None.*

LB-SA20

Early Behaviors of Transplanted Cells and the Effect of HSP27 on the Cell Survival. Megumi Kitami*, Masaru Kaku, Takako Ida, JM Rosales, Kastumi Uoshima. Graduate School of Medical & Dental Science,Niigata University, Japan

The combination of growth factors, scaffolds and cell transplantation, so called tissue engineering triad has been proposed as the gold standard of the tissue regeneration. Nonetheless, seeking more effective and less invasive application will still open up a new vista of the regenerative therapies. For instance, in Niigata University Medical and Dental Hospital, cultured periosteal cell sheet have been used for transplantation as a clinical trial of bone augmentation. Even though more than 50 cases of the trials have been carried out and appeared to be effective enough clinically, biological backgrounds of the transplanted cell behaviors are still unclear and there might be more efficient way of applications. The purpose of this study was to evaluate the fate of transplanted cells and the application of HSP27, an anti-apoptotic protein to the transplanted cells to explore a new way of cell transplantation. Primary human osteoblasts were cultured on a temperature responsive culture dish (UpCell, CellSeed Tokyo, Japan). After 3 weeks of culture, cell/matrix sheet was transplanted to the calvarial subperiosteal pocket of F344/NJcl-rnu immuno-deficient rats. The transplants were harvested after 1, 3, 5 days, paraffin embedded samples were prepared and immuno-histochemical analysis were performed. Neoangiogenesis was observed at the surface of transplants at days 3, and it was observed at the center of transplants at day 5. TUNEL-positive apoptotic cells were found at the ratio of 4.5%, 14.5% and 4.7% at day 1, 3 and 5 respectively. While PCNA-positive cells were rarely found at day 1 and 3, it became detectable at day 5 and the positive cell ratio was 4.6%. These results indicate that part of transplanted cells dead due to apoptosis at the initial stage of the transplantation. Then, we try to reduce the number of dead transplanted cells by introducing an anti-apoptotic protein HSP27. An HSP27 expression vector, pCMV-SPORT6-mHSP27 was transfected to osteoblast-like cell line MC3T3-E1. The H_2O_2 induced apoptosis was partially rescued by the over expression of HSP27. The over expression of HSP27 did not affect the cell proliferation and mineralization ability of MC3T3-E1 cells. These results suggests that transplanted cell death could be rescued by the over expression of HSP27 without affecting the mineralization ability. Further study will warrant the establishment of more effective cell transplantation protocol for the bone augmentation.

***Disclosures: Megumi Kitami**, None.*

LB-SA21

Roles of Histone Demethylase PHF8 in Osteogenic Differentiationand Bone Regeneration. Qianqian Han*, Qisheng Tu, Lan Zhang, Yin Tang, Jake Jinkun Chen. Tufts University School of Dental Medicine, USA

Epigenetic regulation of gene expression is a central mechanism that governs cell stemness, determination, commitment, and differentiation. It has been recently found that PHF8, a major H4K20/H3K9 demethylase, plays a critical role in craniofacial and bone development (*Nature466*, 503-7, 2010). As a nuclear matrix protein, special AT-rich sequence-binding protein 2 (SATB2) is expressed in branchial arches and in cells of the osteoblast lineage, therefore required for bone development and formation. However, our previous understanding of the modulation of SATB2 impedes our further insight into this important osteogenic transcription factor. In this study, we hypothesize that PHF8 promotes osteoblastogenesis by epigenetically regulating the expression of master gene SATB2. We performed a series of studies including real time PCR, Western blot, gain- and loss- functions, chromatin immunoprecipitation (ChIP) assays and *in vivo* animal models. Our results showed that expression levels of PHF8 and SATB2 in preosteoblast MC3T3-E1 and bone marrow stem cells (BMSCs) increased simultaneously during osteogenic induction. Overexpressing PHF8 in BMSCs and MC3T3-E1 cells with wild type PHF8 upregulated the expression of SATB2, Runx2 and osterix, and bone matrix proteins. Conversely, knockdown of PHF8 reduced the expression of SATB2 and other bone marker genes. Furthermore, using ChIP assays, we found that PHF8 specifically bound to the transcription start site (TSS) of the *Satb2* promoter, and the expression of H3K9me1 at the TSS region of Satb2 decreased in PHF8 overexpressed group. Our *in vivo* results indicated that PHF8 promoted the bone regeneration in critical-sized defects in mouse calvarias. Taken together, our results suggest, for the first time, that PHF8 enhances osteogenic differentiation via regulation of the SATB2 expression pattern by modulating histone methylation states and subsequently converting its chromatin into a transcriptionally active conformation.PHF8/SATB2 mediated epigenetic regulatory axis further harnesses BMSCs differentiation and facilitates bone tissue formation and regeneration.

***Disclosures: Qianqian Han**, None.*

LB-SA22

Anabolic Wnt-mTOR signaling enhances Integrated Stress Response via stimulation of Glutamine consumption. Courtney Karner*, Fanxin Long, Emel Esen. Washington University School of Medicine, USA

A defining feature of osteoblasts is their capacity to produce large amounts of extracellular matrix proteins. This increased capacity for protein synthesis is coupled with a heightened integrated stress response (ISR), commonly known as endoplasmic reticulum (ER) stress, in osteoblasts. Previous genetic studies have demonstrated the functional importance of ISR in normal bone formation in mice. However, whether ISR in osteoblasts is activated by unfolded proteins in the ER, or an alternative mechanism is not understood. Because Wnt proteins have emerged as potent inducers of bone formation, we have investigated the mechanism through which Wnt3a activates ISR during osteoblast differentiation in the mesenchymal progenitor ST2 cells. We find that Wnt3a induces ISR independent of Beta-catenin/Lef/TCF signaling, but critically dependent on mTORC1 activation that stimulates protein synthesis. Remarkably, however, inhibition of PERK, a critical activator of ISR in response to unfolded proteins in the ER, did not allay ISR induced by Wnt3a. In contrast, knockdown of GCN2, a kinase that is known to mediate ISR in response to amino acid deprivation, suppressed Wnt3a-induced ISR. Moreover, supplementation of glutamine, but not other amino acids, alleviated ISR in response to Wnt3a. Indeed, Wnt3a greatly stimulated glutamine consumption, at least partly due to the increase in anaplerosis to the tricarboxylic acid (TCA) cycle. Importantly, preventing glutamine anaplerosis alleviated ISR and osteoblast differentiation in response to Wnt3a. Thus, our results support a model in which Wnt signaling induces ISR necessary for osteoblast function through increased glutamine metabolism.

***Disclosures: Courtney Karner**, None.*

LB-SA23

Netrin1 is a critical autocrine factor for osteoclast differentiation. Aranzazu Mediero*[1], Bhama Ramkhelawon[2], Edward Purdue[3], Steven Goldring[4], Kathryn Moore[2], Bruce Cronstein[5]. [1]NYU SCHOOL OF MEDICINE, USA, [2]Leon H. Charney Division of Cardiology, Department of Medicine, NYU-Langone Medical Center, USA, [3]Caspary Research Building, Hospital for Special Surgery, USA, [4]Hospital for Special Surgery, USA, [5]NYU Medical School, USA

Netrins have been extensively studied for their role in axonal guidance during neural development. In addition, netrins are chemopulsants for a variety of non-neuronal cell types via binding to their receptors Unc5b and DCC. Although thought to suppress inflammation in several settings, netrin1, acting via Unc5b, inhibits macrophage migration directed by chemokines CCL2 and CCL19 to promote macrophage retention in and exacerbation of atherosclerotic plaque. We asked whether Netrin1 was expressed during osteoclast (OC) differentiation and whether it plays a role in OC differentiation.DXAscan and MicroCT analysis were performed on Netrin1 deficient mice (radiation chimeras) and wildtype (WT, radiation chimeras) littermates. OC differentiation was studied as M-CSF/RANKL-stimulated differentiation of murine bone marrow precursors to TRAP+/multinucleated cells, in the presence/absence of recombinant Netrin1 and Unc5b antibody. Netrin1, Unc5b and DCC expression were studied by RT-PCR and Western Blot in primary bone marrow-derived osteoclasts. Netrin1 immunostaining was performed in human tissue obtained following primary prosthesis implantation or after prosthesis revision. During OC differentiation cell-associated Netrin1 and Unc5b (but not DCC) protein expression increased by $30\pm2\%$ and $98\pm4\%$ respectively ($p<0.001$,n=4) and Netrin1 secretion increased by $66\pm2\%$ ($p<0.001$,n=4). Consistently, RANKL stimulates an increase in Netrin1 and Unc5b mRNA expression during OC differentiation (25 ± 4 and 3 ± 0.5 fold change respectively $p<0.001$,n=4). Moreover, in Netrin1-deficient marrow precursors OC differentiation was diminished by $65\pm2\%$ as compared to control ($p<0.001$,n=6), an effect reversed by addition of recombinant netrin1 to cultures ($121\pm5\%$ increased, $p<0.5$,n=4). An antibody to the netrin1 receptor Unc5b reduces OC formation by $57\pm6\%$ ($p<0.001$, =6) whereas an antibody to DCC had no effect on OC formation ($5\pm4\%$ reduction, p=NS vs. control,n=6). Finally, DXAscan and MicroCT analysis demonstrated an increase in bone mineral density (BMD), total volume (TV), bone volume (BV) and TV/BV in both cortical and trabecular bone in Netrin1 deficient mice when compared to WT ($p<0.01$ for all, n=5). Netrin1 immunostaining in human tissue biopsies reflect enhanced expression in tissue from implant revision when compared to primary implants.The chemorepulsant Netrin1 is required for osteoclast differentiation and stimulates OC differentiation by an autocrine mechanism. This finding suggests that Netrin1 may be a novel target to reduce OC-mediated bone resorption and to prevent joint prosthesis loosening.

***Disclosures: Aranzazu Mediero**, patent on use of adenosine A2AR agonists to prevent prosthesis loosening (pending)., 9*

LB-SA24

Direct Comparison of Pre- and Post-Contrast Enhanced Scans for Quantitative CT Bone Mineral Density Measurement at the Proximal Femur: Implications for Opportunistic Osteoporosis Screening. Alyssa Maciejewski[1], Timothy Ziemlewicz[1], Neil Binkley[2], Alan Brett*[3], Keenan Brown[3], Perry Pickhardt[1]. [1]University of Wisconsin School of Medicine & Public Health, USA, [2]University of Wisconsin, Madison, USA, [3]Mindways Software, Inc., USA

Objective(s): For patients undergoing routine contrast-enhanced MDCT exams, an opportunity exists for concurrent BMD screening without additional radiation exposure or patient time using quantitative CT (QCT) of the proximal femur. Previous studies have demonstrated equivalence between unenhanced CT and DXA for femoral neck BMD evaluation, but the impact of IV contrast requires further study. We investigated the effect of IV contrast enhancement on areal BMD measurement compared with the established DXA-equivalent pre-contrast QCT analysis (“CTXA”) at the hip.

Methods: Our cohort included 410 male and female adults (mean age, 65.3 ± 10.0 years; range, 49-95 years) who had standard CT urography (CTU) at $120kV_p$ (GE Healthcare, Waukesha, WI) between Aug. 2011 and May 2013. CTU exams represent an ideal protocol for this assessment as both pre-and post-contrast series are obtained, and the split-bolus contrast-injection technique effectively combines dynamic and delayed phases, resulting in excreted contrast in the urinary bladder. Areal BMD (aBMD) in g/cm^2 of the femoral neck was measured on both pre-and post-contrast CT series using QCT Pro Version 5.1 (Mindways, Austin, TX) with asynchronous phantom calibration. Constant bias and multiplicative factor corrections for the post-contrast series were derived from the Bland-Altman plot linear regression slopes.

Results: Mean pre- and post-contrast aBMD of the femoral neck was 0.68 ± 0.12 and 0.71 ± 0.12 g/cm^2, respectively. Although the estimated slope of a correction was significantly different from zero ($p<0.0001$), the SD of the distribution of residuals (SEE) for a constant bias and a multiplicative model correction were very similar at 0.0232 and 0.0231, respectively.. The constant bias correction associated with contrast enhancement was 0.032 ± 0.023 g/cm^2 which corresponds to 0.29 ± 0.21 T-score units using the CTXA young normal aBMD reference SD of 0.111 g/cm^2. T-score categorization changed between pre- and post-contrast series in 63 (15.4%) of 410 patients prior to simple correction, compared with 35 (8.5%) patients after correction.

Conclusion: For the purposes of opportunistic osteoporosis screening at routine post-contrast abdominopelvic CT scans, a simple offset correction of -0.3 T-score units for femoral neck BMD assessment appears to be appropriate. This simple additive measure could greatly enhance osteoporosis screening since it can be applied regardless of the clinical indication for CT scanning.

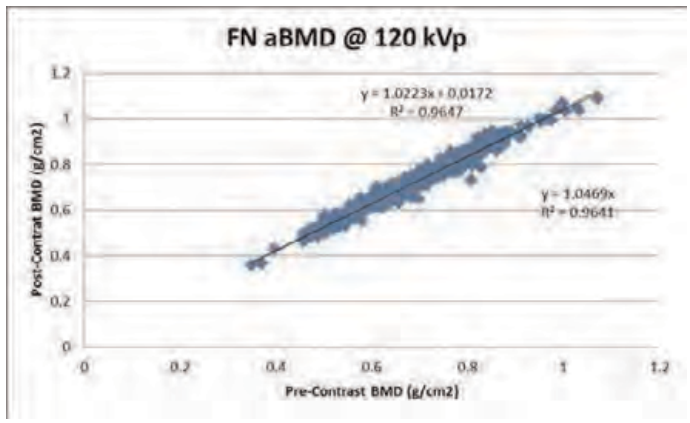

Comparison of areal BMD for Pre- and Post-Contrast CT

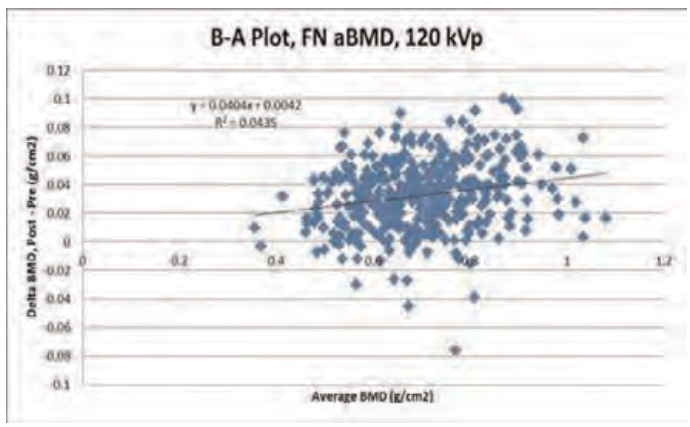

Bland-Altman Plot of Pre and Post-Contrast Change in BMD

***Disclosures: Alan Brett**, None.*

LB-SA25

Large-scale Whole Genome Sequencing Study for Bone Mineral Density: the UK10K Consortium. Hou-Feng Zheng*[1], Vincenzo Forgetta[1], Scott Wilson[2], Nicholas Timpson[3], Nicole Soranzo[4], Tim Spector[5], Brent Richards[1]. [1]McGill University, Canada, [2]University of Western Australia, Australia, [3]Bristol University, Canada, [4]Sanger institute, Canada, [5]King’s College London, United Kingdom

Aim: To identify genetic variants, including rare variants, associated with bone mineral density (BMD), we performed an association study using whole genome sequencing data within UK10K Consortium (http://www.uk10k.org/).

Methods: 3781 samples from TwinsUK (discovery study) and ALSPAC were whole genome sequenced in Sanger Institute. The haplotypes of sequenced individuals were then imputed into an additional 3896 TwinsUK GWAS samples (replication study), which are independent of the sequenced samples. We tested the association of TwinsUK samples at lumbar spine (L1-L4) (LS), femoral neck (FN) and forearm BMD separately in these two datasets. The phenotypes were standardized adjusting for age, age^2, weight and sex where appropriate. We undertook single variant tests, as well as a collapsing test of coding variants, with GEMMA and skatMeta, respectively. We then meta-analyzed the association results from the sequenced and imputed TwinsUK datasets. We set significant and suggestive thresholds for single variant test at $5x10^{-8}$, and $5x10^{-6}$, and set significance threshold for collapsing tests at $2.5x10^{-6}$ (0.05 over ~20,000 genes across the genome).

Results: In the single variant test meta-analysis of data from the discovery and replication studies for forearm BMD, 143 variants from *WNT16* locus were significant, and another 125 variants were suggestive. For LS and FN BMD, we identified 156 (including 11 *LRP5* variants) and 125 suggestive variants. In the skatMeta analysis of coding variants, we identified *WNT16* and *HSPB1* to be strongly associated with forearm BMD, however, when we excluded common variants (MAF>5%) in gene region, *WNT16* was no longer significant, suggesting common missense variants in *WNT16* drove the association signal. Nine rare coding variants in *HSPB1* were collapsed and had an association P-value of $9.8x10^{-7}$, and this association was largely driven by rs28708645 (MAF= 0.005, $P=9.4x10^{-8}$). We also identified 3 genes (including *LRP5*) and 11 genes for LS and FN BMD, respectively.

Conclusion: In this whole genome sequencing data analysis for BMD, we identified a novel, rare missense variant in a non-canonical *HSPB1* transcript (ENST00000447574) as an important genetic determinant of forearm BMD, and confirmed the association of variants in *WNT16* and *LRP5* with forearm and LS BMD, respectively, and highlighted other novel loci and genes. These variants will soon undergo replication in 44,057 additional samples.

***Disclosures: Hou-Feng Zheng**, None.*

LB-SA26

Associations of Serum Sclerostin and Polymorphisms in the *SOST* Gene with Bone Mineral Density and Markers of Bone Metabolism in Postmenopausal Chinese Women. Jin-Wei He*, Zhen-Lin Zhang. Shanghai Sixth People's Hospital affiliated with Shanghai Jiao Tong University, China

Objective: The aims of this study were to (1) evaluate the associations of serum sclerostin with bone mineral density (BMD) and markers of bone metabolism in postmenopausal Chinese women; (2) observe the relationships between the single nucleotide polymorphisms (SNPs) of the *SOST* gene with serum sclerostin, BMD and markers of bone metabolism.

Design: A cross-sectional study was conducted in 703 postmenopausal Chinese women (aged 50-94.5 years). Ten tagging SNPs (rs1234612, rs1513670, rs1634330, rs1708635, rs2023794, rs7220711, rs74252774, rs851057, rs851058, and rs865429) of the *SOST* gene were genotyped. Serum sclerostin and markers of bone metabolism were measured, including serum intact parathyroid hormone, 25(OH)D, procollagen type 1 Nterminal propeptide (PINP) and β-CrossLaps of type I collagen containing cross-linked C-telopeptide (β-CTX). BMD of the lumbar spine and proximal femur were measured by dual-energy X-ray absorptiometry.

Results: Serum sclerostin was positively correlated with BMD at lumbar spine, femoral neck, total hip and serum 25(OH)D (all $P<0.01$) but negatively correlated with β-CTX ($P<0.01$). The significance between BMD at lumbar spine, hip,serum β-CTX and serum sclerostin persisted even after adjustment for age, BMI and serum 25(OH)D (all $P<0.01$). But it exhibited no correlation with age and serum P1NP. SNPs (rs1513670, rs851057, rs851058, rs1708635 and rs1634330) in the SOST gene were significantly associated with serum P1NP. We failed to identify a significant association between the SNPs, haplotypes of *SOST* with BMD,serum sclerostin and other markers of bone metabolism.Conclusion: Our results suggested that serum sclerostin was positively correlated with BMD at lumbar spine, femoral neck, total hip, serum 25(OH)D and negatively correlated with serum β-CTX. Five SNPs in the *SOST* gene were associated with serum P1NP. Genetic polymorphisms in *SOST* may not be a major contributor to serum sclerostin or BMD in postmenopausal Chinese women.

***Disclosures: Jin-Wei He**, None.*

LB-SA27

Bone Marrow Adiposity is associated with Non-vertebral Fractures in Women. Luai Ahmed[1], Rajesh Shigdel[2], Ragnar Joakimsen[3], Petter Eldevik[3], Erik Fink Eriksen[4], Jacqueline Center[5], Roger Zebaze[6], Ashild Bjornerem*[7]. [1]Faculty of Health Sciences, University of Tromsø, Norway, [2]University of Tromso, Norway, [3]University Hospital of North Norway, Norway, [4]Oslo University Hospital, Norway, [5]Garvan Institute of Medical Research, Australia, [6]Austin Health, University of Melbourne, Australia, [7]University of Tromsø, Norway

The relationship between fat and bone is complex, but an increasing body of evidence suggests that increased marrow adiposity may signal a switch in stem cell differentiation towards adipogenesis and may be linked to bone loss. We therefore wanted to study whether marrow adiposity was associated with fracture risk.

In a nested case-control study in Tromsø, Norway, 162 postmenopausal women aged 54-94 years with fractures (hip, humerus and forearm) and 221 controls, had bone marrow fat proportion quantified as the proportion within the total bone with attenuation below that of water in QCT images of the subtrochanteric femur using StrAx 1.0 software. Femoral neck (FN) BMD was assessed using DXA. For the analysis we used linear and logistic regression analyses adjusted for age, height and weight.

Marrow adiposity increased by 0.20 and 0.29 SD for each SD increase in age and height, and by 0.14 and 0.48 SD for each SD decrease in weight and FN aBMD, respectively (all $p<0.01$). Women with fractures exhibited a higher proportion of marrow fat than controls; 31.2% (SEM 0.5) vs. 27.5% (SEM 0.4), $p<0.001$. Marrow adiposity was associated with fractures independently of FN aBMD, with OR of 1.55 (95% CI 1.17-2.04) for each SD increase in marrow adiposity, while each SD decrease in FN aBMD had OR of 1.72 (95% CI 1.26-2.33). Marrow adiposity significantly contributed to the variance in fracture risk (increment of R^2 was 0.02, $p=0.001$).

Our study suggests that marrow adiposity is an independent risk factor for bone loss and fracture.

***Disclosures: Ashild Bjornerem**, None.*

LB-SA28

Hyponatremia is associated with higher odds for fracture in hospitalized patient. Hussein Rajab*, Louis Loutrell. Medical University of South Carolina, USA

Backgrownd and Significance: Mild hyponatremia is the most common electrolye imbalance in older population, and has traditonally been considered begnign, but it may be associated with gait and attention deficit and an increased risk of fall. The association of mild hyponatremia and bone fracture is still unknown. Analysis of hospitalized patients records was conducted to evaluate the impact of hyponatremia on fracture risk.

Design: This study analyzed 145111 patient records from state of New Jerssey hopitlization records in 2010 using ICD 9 codes. Discharge diagnosis that might contriubute to hyponatremia, e.g., SIADH, CHF, hypothyroidism, pneumonia, liver cirrhosis, also, diagnosis that amight be assoicated with increase risk of fall and fracture, e.g., confusion, hypotension, osteoprosis, seizure, and gait abnormalities, were invistigated.

Results: Total records were 145111. Hyponatremia were present in 46409 (31%) patients . Out of these patients, mean age was 67 years, 25346 (54%) were female. 2258 (4.8%) had fracture, 3440 (7.4%) had osteoprosis, and 2835 (6.1%) had fall. Only 126 patients were diagnosed with SIADH according to the ICD9 codes. Hyponatremia were present in 70 % of those with versus 30 % of those with out a confirmed fracture ($P < 0.001$). On Multivariate logistic regression analysis controlling for age, sex, history of HTN, osteoprosis, confusion, pneumonia, hypothyroidisim, CHF, hyponatremia Na $<$ 135 versus Na $>$or= 135 mmol/L remained significantly and independently associated with fracture occurrence ($P < 0.01$).

Conclusion: Elderly patients with unsteady gait and/or confusion should be checked for the presence of mild hyponatremia and if present it should not be ignored. Hyponatremia can impair cognitive function and result in unsteady gait and falls. It can also produce bone impairment through osteo-porosis (due to increased bone resorption in order to mobilize sodium from the bone) or altered bone quality(through decreased bone microfracture repair). In elderly patients who take medications that cause hyponatremia, namely diuretics, antidepressants, and anticonvulsants. These medications should be avoided or carefully monitored. Patients with unsteady gait and/or confusion should be checked for the presence of mild hypona-tremia (Na $<$135 mEq/L) and if present, it should be treated.

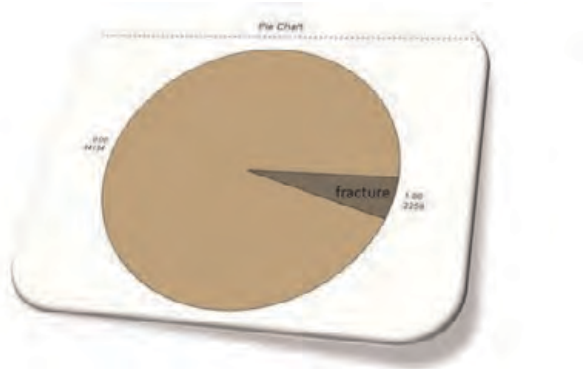

Hussein Rajab, Hyponatremia and Fracture risk 2

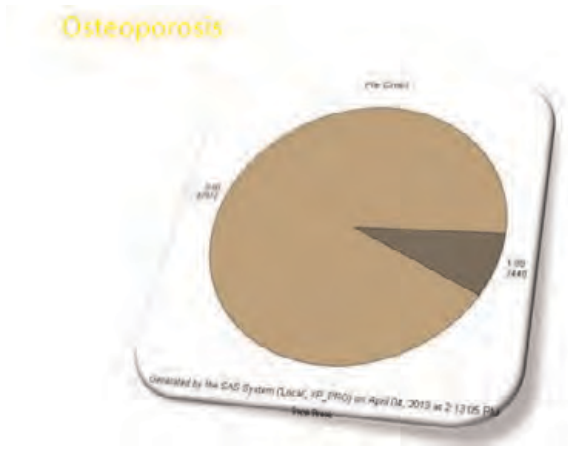

Hussein Rajab, Hyponatremia and Fracture risk 3

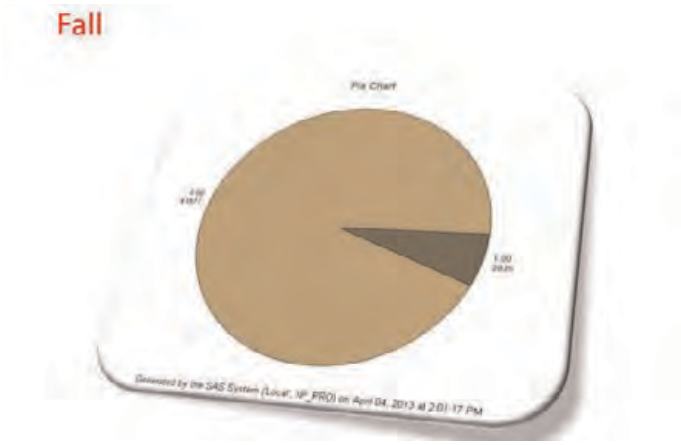

Hussein Rajab, Hyponatremia and Fracture risk 4

1	1	3112
2	0	141999

Probability modeled is Fracture=1.

NOTE: 7 observations were deleted due to missing values for the response or explanatory variables.

Model Convergence Status

Convergence criterion (GCONV=1E-8) satisfied.

Model Fit Statistics

Criterion	Intercept Only	Intercept and Covariates
AIC	30072.839	25943.223
SC	30082.725	26051.961
-2 Log L	30070.839	25921.223

Testing Global Null Hypothesis: BETA=0

Test	Chi-Square	DF	Pr > ChiSq
Likelihood Ratio	4149.6159	10	<.0001
Score	4589.0407	10	<.0001
Wald	3378.6572	10	<.0001

The SAS System 16:06 Tuesday, April 23, 2013 198

The LOGISTIC Procedure

Analysis of Maximum Likelihood Estimates

Parameter	DF	Estimate	Standard Error	Wald Chi-Square	Pr > ChiSq
Intercept	1	-6.9590	0.0911	5832.7811	<.0001
HypoNa	1	1.4219	0.0414	1181.3002	<.0001
AGE	1	0.0348	0.00126	768.7964	<.0001
FEMALE	1	0.1605	0.0406	15.6214	<.0001
HTN	1	0.0764	0.0381	4.0136	0.0451
osteoporosis	1	1.0120	0.0492	422.9446	<.0001
hypotension	1	-0.2363	0.1019	5.3746	0.0204
confusion	1	0.4289	0.1495	8.2275	0.0041
pneumonia	1	-0.8452	0.0850	98.7832	<.0001
hypothyroidism	1	-0.1584	0.0526	9.0839	0.0026
CHF	1	-0.5480	0.0513	114.1997	<.0001

Odds Ratio Estimates

Hussein Rajab, Hyponatremia and Fracture risk 1

Effect	Point Estimate	95% Wald Confidence Limits	
HypoNa	4.145	3.822	4.495
AGE	1.035	1.033	1.036
FEMALE	1.174	1.084	1.271
HTN	1.079	1.002	1.163
osteoporosis	2.751	2.496	3.030
hypotension	0.790	0.647	0.964
confusion	1.536	1.145	2.059
pneumonia	0.429	0.364	0.507
hypothyroidism	0.853	0.770	0.946
CHF	0.578	0.523	0.639

Association of Predicted Probabilities and Observed Responses

Percent Concordant	79.9	Somers' D	0.617
Percent Discordant	18.2	Gamma	0.629
Percent Tied	1.9	Tau-a	0.026
Pairs	441900888	c	0.809

Hussein Rajab, Hyponatremia and Fracture risk 5

***Disclosures: Hussein Rajab**, None.*

LB-SA29

Safety and Tolerability of BA058 Transdermal, a Novel Analog of hPTHrP Delivered via a Microneedle Patch: Results of a Phase 2 Clinical Trial. Louis Brenner*[1], Kris Hansen[2], Marcie Clarkin[3], Kyle Haraldsen[4], Bente Juel Riis[5], Michael Bolognese[6], Paul Miller[7]. [1]USA, [2]3M Drug Delivery Systems, USA, [3]Radius Health Inc., USA, [4]Radius Health, USA, [5]Nordic Bioscience, Denmark, [6]Bethesda Health Research, USA, [7]Colorado Center for Bone Research, USA

BA058 is a novel synthetic analog of hPTHrP (1-34) currently being developed as an osteo-anabolic therapy for the treatment of postmenopausal osteoporosis (PMO). Daily BA058 subcutaneous (SC) injection has produced promising safety and efficacy results thus far in Phase 1 and Phase 2 studies, and is completing treatment in a Phase 3 fracture prevention study. There is evidence of poor adherence and persistence with current osteo-anabolic agents available for the treatment of osteoporosis in clinical practice, with daily compliance in the Forteo® pivotal study ranging from 79 to 83%. Non-persistence and underuse may reduce the drugs' effectiveness, placing patients at increased risk of fractures with resultant negative outcomes. Thus, there is a significant need for an alternative to injection for delivery of osteo-anabolic agents that improves patient convenience and compliance. To achieve this, we have piloted the use of a microneedle patch (3M) for BA058 transdermal (TD) delivery. This was a randomized, double-blind, placebo controlled Phase 2 study of BA058 TD in healthy postmenopausal women with osteoporosis, conducted in 9 centers in the US (NCT#01674621) and EU. 250 subjects were enrolled and randomized to daily treatment with BA058 TD 50 µg, 100 µg, 150 µg, or TD placebo, or BA058 SC 80 µg for 24 weeks. At baseline, the mean age of the randomized subjects was 66.5 years and the mean t-score for spine and total hip were -2.33 and -1.47, respectively. Thirty-nine percent of randomized subjects had a history of fracture. A total of 32 (12.8%) subjects dropped out of the study, 27 (13.5%) who were randomized to the TD group and 5 (10%) who were randomized to the SC group. Compliance, based on subject diary reports and defined as the total number of administered daily doses/the total number of days on study * 100, for completed subjects was 99% in the TD groups. There were 12 serious adverse events (SAEs) reported in 9 subjects (3.6%); none of these events were considered to be related to study drug or route of administration. In conclusion, BA058 TD was well tolerated in this study population, with an SAE profile consistent with medical events in postmenopausal women. The BA058 TD compliance rate was on average higher than previous clinical trial experience with injectable osteo-anabolic drug delivery. The results of this study indicate that BA058 TD offers the potential of a new transdermal administration option for the osteo-anabolic treatment of PMO.

***Disclosures: Louis Brenner**, Radius Health, Inc, 3*
This study received funding from: Radius Health Inc

LB-SA30

The Effects of Oral Bisphosphonate Therapy on the Peripheral Skeleton in Postmenopausal Osteoporosis: The TRIO Study. Richard Eastell*[1], Margaret Paggiosi[1], Nicola Peel[2], Eugene McCloskey[1], Jennifer Walsh[1]. [1]University of Sheffield, United Kingdom, [2]Sheffield Teaching Hospitals, United Kingdom

Clinical trials of bisphosphonate therapy have usually examined changes in bone within central skeletal regions; few have assessed their effects on the peripheral skeleton.

We conducted a randomised, open-label, parallel, controlled trial of three bisphosphonates, orally administered at their licensed dose for two years, and examined their effects on the peripheral skeleton using multiple modes of measurement (NCT00666627). We studied 172 postmenopausal women (ages 53-84 years) who had either a BMD T-score of <-2.5 at the spine and/or total hip (stratum 1), or a BMD T-score of <-1.0 plus a previous low trauma fracture (stratum 2). Eligible participants were randomised to one of three treatment groups, either (i) alendronate 70 mg once a week, (ii) risedronate 35 mg once a week, or (iii) ibandronate 150 mg once a month; all were prescribed calcium (1200 mg) and vitamin D (800 IU) supplements over the two year study period. We also recruited 226 premenopausal women (ages 33-40 years) as controls, and studied them for up to 2 years.

Central skeletal assessments included DXA of the lumbar spine and total hip (Hologic Discovery A). Within the peripheral skeleton, we measured forearm and total body BMD using DXA, calcaneus BMD using DXL, radius and tibia total BMD (4% and 33% sites) using pQCT, finger BMD using radiographic absorptiometry (RA), and ultrasound variables of the fingers and calcaneus using QUS. Mixed model ANOVA was used to evaluate the effects of treatment by visit and any interaction of BMD change with treatment, using the ibandronate group as reference.

Measurements remained stable in the premenopausal controls over 2 years (Table 1). By 2 years, oral bisphosphonates resulted in significant increases ($p<0.05$) in BMD within the central skeleton and a few, but not all, of the sites in the peripheral skeleton. Responses were observed by DXA (total body BMD), by DXL (calcaneus BMD), by pQCT (33% total forearm BMD) and by QUS (QUS-2 BUA). There were treatment interactions in BMD change at the lumbar spine and total body (table).

Thus, we found that the calcaneus was the only site in the peripheral skeleton where changes similar to those found in the central skeleton occurred. This may help

to explain why the most striking effect of oral bisphosphonates is on fracture risk reduction within the central skeleton.

Table 1. Change in BMD over two years in response to 3 oral bisphosphonates

Site	Ibandronate (n=57)	Alendronate (n=57)	Risedronate (n=58)	Time effect, p-value	Controls (n=226)
Lumbar spine, %	6.7 (4.1)	6.8 (3.9)	3.0 (3.7)**	<0.001	0.1 (2.3)
Total hip, %	2.7 (2.4)	4.9 (3.5)	1.4 (2.5)	<0.001	0.1 (2.1)
Total body, %	1.9 (2.0)	2.2 (1.6)	1.1 (2.1)*	<0.001	0.1 (2.2)
Distal radius pQCT, %	1.1 (5.3)	1.3 (4.7)	-0.1 (7.8)	0.11	0.9 (4.5)
Distal tibia, pQCT, %	1.7 (2.7)	1.4 (4.6)	0.9 (2.2)	0.28	0.6 (2.4)

Mixed models ANOVA, effect of time on lumbar spine, total hip and total body; differences between ibandronate and risedronate, **, p=0.004, *, p=0.08.

Table 1

***Disclosures: Richard Eastell**, Merck, 2; Warner-Chilcott, 2*
This study received funding from: Warner-Chilcott

LB-SA31

Effects of a New Conjugate Drug in a Rat Model of Postmenopausal Osteoporosis. Careesa Liu*[1], Robert Young[2], Marc Grynpas[3]. [1]University of Toronto, Canada, [2]Simon Fraser University, Canada, [3]Samuel Lunenfeld Research Instituteof Mount Sinai Hospital, Canada

Prostaglandin E_2 (PGE_2) promotes bone formation in vivo, but has significant side effects when administered systemically. Since PGE_2 acts on bone via the EP4 receptor, we use a specific EP4 agonist (EP4a) to promote bone formation. Moreover, because bisphosphonates such as alendronate (ALN) target bone mineral, our approach reversibly conjugates ALN with EP4a via a linker (LK), such that the bone-binding property of ALN allows EP4a to be directly delivered to bone sites upon systemic administration of the ALN-LK-EP4a conjugate. Hydrolytic enzymes in the bone environment then gradually cleave the links to free both EP4a and LK, allowing EP4a to promote bone formation while leaving ALN bound to bone.

We investigated the in-vivo effects of ALN-LK-EP4a in a curative experiment, in which 3-month-old female Sprague-Dawley rats were ovariectomized (OVX), allowed to lose bone for 6 weeks, then treated for 6 weeks (n=9-12/group). Treatment consisted of conjugate in low dose (CL, 5mg/kg IV weekly) and high dose (CH, 25mg/kg IV week 1, 15mg/kg weeks 2, 4, 6), co-dosed unconjugated EP4a and ALN-LK (EA, 2.5mg/kg each IV weekly), vehicle for OVX (OV, IV weekly) and sham-operated rats (SV, subcutaneous daily), and PGE_2 (PG, 4mg/kg subcutaneous daily).

Histomorphometric analysis of the proximal tibial metaphysis shows that osteoid volume is dose-dependently increased under conjugate treatment. In addition, while CL exhibited increased MS/BS (35%), MAR (69%), and BFR/BS (131%) compared to OV, EA was decreased compared to CL. Micro-computed tomography (microCT) shows conjugate-induced dose-dependent increase in vertebral trabecular BV/TV with concomitant increase in Tb.N, and CL led to 63% recovery of OVX-induced bone loss while CH exceeded sham levels. Trabecular vBMD is dose-dependently increased, and the vertebral load-bearing ability under compression is improved but the material strength was unchanged.

MicroCT of the femoral shaft shows that conjugate treatment led to dose-dependent increase in both endocortical woven bone formation and cortical porosity. However, CH resulted in excessive remodeling that occluded the marrow cavity and increased the cortical porosity by 30X compared to OV. This enhanced the load-bearing ability but compromised the material strength.

These results indicate that conjugate treatment dose-dependently promotes bone formation and restores OVX-induced bone loss, with conjugation of the two components being crucial to the anabolic effect.

***Disclosures: Careesa Liu**, None.*

LB-SA32

Co-Administered 1,25-D Enhances the Direct Effect of Amino Acids on Total Transepithelial Calcium (Ca) Transport In Vitro. Jessica Bihuniak*[1], Jane Kerstetter[1], Karl Insogna[2]. [1]University of Connecticut, USA, [2]Yale University School of Medicine, USA

Nutrient-nutrient interactions that influence intestinal Ca transport are not well categorized. 1,25-dihydroxyvitamin D3, (1,25-D) is known to augment transcellular Ca transport. Increasing dietary protein in humans and rats has been shown to increase intestinal Ca absorption without affecting rates of bone formation or resorption. To examine the interaction between 1,25-D and dietary protein on gut Ca absorption, Caco-2 Bbe cells, a model of intestinal epithelia, were cultured in transwells for 25-26 days. At Time 0, Ca-45 was added to the upper chamber in the presence of: transport buffer (TB, control), a mixture of amino acids (AA) in TB at a final concentration twice that of normal growth media (2XAA), 100 nM 1,25-D or a combination of 2XAA and 100 nM 1,25-D. Total transepithelial Ca transport was estimated as the amount of Ca-45 appearing in the basolateral buffer at 6 hrs, expressed as a percentage of the total Ca-45 applied to the upper chamber at Time 0. For the two experimental conditions employing 1,25-D, the hormone was added 24 hrs before the study was begun, and continued for the subsequent 6 hrs. The osmolalities of all treatments were equivalent. A one-way ANOVA followed by Tukey's multiple comparisons was used to evaluate differences in Ca-45 flux.

As expected, treatment with 1,25-D increased transepithelial Ca flux (2.1 ± 0.2 vs. 4.1 ± 0.6%; 2-fold increase; $P \leq 0.05$), indicating that this model responds normally to vitamin D. Exposing Caco-2 cells to 2XAA for 6-hrs resulted in 6.3-fold and 3.2-fold increases in Ca flux compared to control and 1,25-D treatments, respectively ($P \leq 0.0001$). Combination treatment with 2XAA and 1,25-D induced a significantly greater increase in Ca flux than either 2XAA alone (1.3-fold increase compared to 2XAA; $P \leq 0.01$) or 1,25-D alone (4.2-fold increase compared to 1,25-D; $P \leq 0.0001$).

These data provide evidence for a direct effect of AA on transepithelial Ca flux. The observation that the effects of AA and 1,25-D on Ca transport are at least additive, supports a salutary interaction between these two nutrients. Whether 1,25-D and AA exert the majority of their effects via similar or different Ca absorption pathways remains to be determined.

Our data are consistent with a previous in vivo study that showed an enhanced effect of 1,25-D and L-lysine on Ca absorption in rats (Wasserman et al., J Nutr, 1957; 62:367-76).

***Disclosures: Jessica Bihuniak**, None.*

LB-SA33

Teriparatide increases bone formation and bone mineral density in adult women with anorexia nervosa. Pouneh Fazeli*[1], Irene Wang[2], Karen Miller[2], Joel Finkelstein[2], Mary Bouxsein[3], Anne Klibanski[1]. [1]Massachusetts General Hospital & Harvard Medical School, USA, [2]Massachusetts General Hospital, USA, [3]Beth Israel Deaconess Medical Center, USA

Anorexia nervosa (AN) is a psychiatric disorder characterized by self-induced starvation and low weight. Predominantly affecting women, the lifetime prevalence of AN approaches 2.2%. Bone loss is a major medical co-morbidity associated with AN, with nearly 90% of women with AN having bone mineral density (BMD) values more than one-standard deviation below an age-comparable mean. Importantly, AN is associated with a seven-fold increased risk of fracture, but there are no approved therapies for the low bone mass in these patients. Because bone formation is reduced in patients with AN, treatment with teriparatide [(hPTH-1-34), TPT], a potent anabolic agent, would appear to be a logical approach. However, TPT-induced bone formation requires local IGF-I synthesis, and IGF-I synthesis in response to growth hormone is reduced in patients with AN. Thus, to determine the effect of TPT on bone turnover and BMD in patients with AN, we randomized 21 women (mean age +/- SD: 47.0 +/- 7.9 yrs) who met DSM IV weight and psychiatric criteria for AN, to receive TPT (20 μg SC daily, n=10) or placebo (PBO) (n=11) for 6 months. We measured BMD of the spine and hip by dual energy x-ray absorptiometry and serum P1NP and CTX at baseline and six months. At baseline, both groups were of comparable BMI and BMD measurements of the spine and hip were similar (Table 1). CTX levels were also similar in both groups whereas P1NP levels were higher in TPT vs PBO (TPT: 63.0 +/- 24.6 ng/mL vs PBO: 37.4 +/- 20.8 ng/mL, p=0.02) (Table 1).

After six months of treatment, BMD increased significantly more with TPT than with PBO at the PA spine: (TPT vs PBO: 6.0 +/- 4.4% vs 0.2 +/- 2.3%, $p<0.01$) and lateral spine (TPT vs PBO: 10.5 +/- 7.8% vs -0.6 +/- 3.3%, $p<0.01$). The results remained significant after controlling for changes in weight and baseline P1NP level. Changes in FN (p=0.4) and total hip (p=0.8) BMD were similar in both groups. P1NP levels increased significantly more with TPT than with PBO (TPT vs PBO: 158 +/- 125% vs 8 +/- 35%, $p<0.01$) whereas changes in CTX levels in the two groups were comparable (p=0.3). TPT was well tolerated by all subjects.

In conclusion, six months of treatment with TPT selectively increases osteoblast activity in adult women with AN, which leads to significant increases in PA and lateral spine BMD. Further studies are needed to determine whether longer term treatment with TPT will increase BMD at other skeletal sites such as the proximal femur.

	Teriparatide (n=10)	Placebo (n=11)	*p*-value
BMI (kg/m²)	17.6 ± 1.3	16.6 ± 1.2	0.08
BMD of PA spine (g/cm²)	0.77 ± 0.08	0.81 ± 0.11	0.28
PA spine T-score	-2.6 ± 0.7	-2.1 ± 1.0	0.29
BMD of lateral spine (g/cm²)	0.53 ± 0.09	0.57 ± 0.05	0.22
Lateral spine T-score	-3.5 ± 1.1	-3.0 ± 0.6	0.24
BMD of total hip (g/cm²)	0.71 ± 0.14	0.69 ± 0.05	0.72
Total hip T-score	-1.9 ± 1.1	-2.0 ± 0.5	0.60
BMD of femoral neck (g/cm²)	0.60 ± 0.11	0.60 ± 0.05	0.70
Femoral neck T-score	-2.3 ± 1.0	-2.3 ± 0.5	0.57
P1NP (ng/mL)	63 ± 25	37 ± 21	0.02
CTX (ng/mL)	0.55 ± 0.35	0.53 ± 0.28	0.88

Mean ± SD

Table 1

***Disclosures: Pouneh Fazeli**, None.*
This study received funding from: Eli Lilly and Company

LB-SA34

Effects of 1α,25-Dihydroxyvitamin D3 on subcellular localization, VDR/RXRα interaction by Fluorescent resonance energy transfer (FRET) and nuclear mobility of RXRα by Fluorescent loss after photobleaching (FLIP). Sylvester Jusu*[1], John Presley[2], Loan Nguyen-Yamamoto[3], Benoit Ochetti[2], Richard Kremer[3]. [1]Canada, [2]McGill University, Canada, [3]McGill University, Royal Victoria Hospital, Canada

The Human Retinoid X receptor alpha (hRXRα) plays a critical role in DNA binding and transcriptional activity through its heterodimeric association with several members of the nuclear receptor superfamily including the human vitamin D receptor (hVDR). Several cancer cell lines have been shown to be resistant to the growth inhibitory action of 1,25(OH) $_2D_3$, the biologically active metabolite of vitamin D3. In the malignant HPK1*Aras* cells 10-100 fold higher concentrations of $1,25(OH)_2D_3$ are required than the non-malignant normal HPK1A cells to achieve comparable inhibition of cell growth. We previously showed that hRXRα phosphorylation on serine 260 was responsible for this resistance.

To obtain insight into the effects of hRXRα phosphorylation on the hVDR/hRXRα complex physiological function in living cells, we studied subcellular localization, hVDR- hRXRα interaction and nuclear mobility of GFP-tagged hVDR or hRXRα wt and the non-phosphorylatable hRXRα ala260 mutant in the presence of either 1, 25(OH) $_2D_3$, the MEK inhibitor UO126 or a combination of UO126 and 1, $25(OH)_2D_3$.

We show, through transfection of hVDR and hRXRα tagged constructs, that subcellular localization of both hVDR and hRXRα are localized to the nucleus in 1, 25(OH) $_2D_3$ treated HPK1A cells and HPK1Aras cells treated with UO126 or following transfection of the non- phosphorylatable hRXRα ala260 mutant.

Also, we demonstrate using FRET that hVDR and hRXRα interact in the absence of the ligand in both HPK1A and HPK1Aras cell lines. However, ligand addition increases their interaction in HPK1A cell but only in HPK1Aras cells treated with either UO126 or transfected with the non- phosphorylatable hRXRα ala260 mutant. This clearly demonstrates that heterodimerization of the hVDR / hRXRα complex and interaction in HPK1Aras cells can be improved and possibly reversed with the use of a non-phosphorylatable hRXRα ala260 mutant which completely abolishes hRXRα phosphorylation and restores the function of $1,25(OH)_2D_3$.

Lastly, we demonstrate using FLIP that the half time of dissociation of the receptor in the nucleus and residence time of the receptor within the nuclear compartments are significantly increased in HPK1Aras cells transfected with the non-phosphorylatable hRXRα ala260 mutant suggesting that binding of the hVDR/hRXRα complex to chromatin and therefore effective gene transcription or repression can be achieved with HPK1Aras cells transfected with non-phosphorylatable hRXRα ala260 mutant.

***Disclosures: Sylvester Jusu**, None.*

LB-SA35

Validation of The University of Connecticut Osteonecrosis Numerical Scale (UCONNS) for Risk Assessment of Osteonecrosis of the Jaws. Regina Landesberg*, Yana Stolyarov, Lisa Marie Di Pasquale, James Grady, Daniel Wakefield, Pamela Taxel. University of Connecticut Health Center, USA

Purpose: Osteonecrosis of the jaws (ONJ) is defined by exposed bone that fails to heal in 6 to 8 weeks. The ability to predict which patients will develop ONJ has remained elusive and the pathophysiology of ONJ remains ill-defined; a number of clinical risk factors have been implicated. Based on the current literature, we have developed an instrument to assess and risk-stratify co-morbidities that are critical for the development of ONJ, the UCONNS. This report describes an initial retrospective validation of this tool.

Methods: Information on 14 patients with documented ONJ was derived from a retrospective chart review of patients seen at UCHC OMFS Clinic. Information on 16 patients without documented ONJ, but who have cancer (breast, prostate, multiple myeloma, lung, ovarian) and/or were receiving bone-modifying medications was drawn from the UCHC Cancer Center. Data were extracted from medical records. These data included: Bone-modifying agents (including total accumulated dose), steroids, chemotherapy and immunomodulators, oral health and surgical procedures, medical conditions and co-morbidities. The UCONNS groups patients into three categories of risk for the development of ONJ; minimal (<10), moderate (10-15) and significant (>16). The group means for the UCONNS scores were compared using two group t-tests. The distribution of categorical variables was compared among the groups using exact chi-squared tests due to the small sample size. We used a two-sided alpha level of significance of 0.05 to assess statistical significance.

Results: The mean UCONNS score for the ONJ group was 23 +/- 8 and the mean score for the non-ONJ group was 14 +/- 4. Statistically significant risk factors ($p<0.05$) for ONJ included poor dental hygiene status, the presence of active oral infection, surgical procedures, and oral and/or IV steroid use within the past 12 months. The total bone-modifying agent use was significantly greater in the ONJ population (p=0.002); however, the cumulative dosage of zoledronic acid approached significance (p=0.07). The results of t-tests showed that the total UCONNS score was a sensitive predictor of ONJ status among at-risk patients. While the individual variables including medical co-morbidities (other than steroids) and smoking did not show significance, this may reflect the small sample size and distribution of these conditions. Future analysis on a larger population including benign conditions is warranted and may identify other critical risk factors for ONJ.

***Disclosures: Regina Landesberg**, None.*
This study received funding from: Connecticut Breast Health Initiative

LB-SU01

Hedgehog Signaling Regulates Expression of Cholesterol Biosynthetic Genes in Osteoarthritis. Shabana Ali*[1], Benjamin Alman[2], Heather Whetstone[2]. [1]Canada, [2]The Hospital for Sick Children, Canada

Osteoarthritis (OA) is a common degenerative disease of the joint that is characterized by degradation and calcification of articular cartilage, osteophyte formation, and subchondral bone changes. We previously found that Hedgehog (Hh) signaling is activated in human OA and murine models of OA. Since Hh signaling regulates Gli-mediated gene expression, we investigated whether the expression of Hh target genes in chondrocytes promotes OA pathogenesis by disrupting normal chondrocyte behavior. To identify Hedgehog target genes, microarray analyses were performed to detect changes in gene expression when the Hh pathway was inhibited in human OA cartilage samples. Results from the Affymetrix Human Gene 1.0 ST microarray were analyzed for differentially expressed genes, and were validated by real-time PCR. Using Ingenuity® Pathway analysis, several genes known to be involved in sterol homeostasis were found to be upregulated with Hh inhibition. To determine the function of these genes in OA, mice with cartilage-specific cholesterol accumulation were generated. Compared to wildtype littermates, these mice display skeletal dysplasia, including shortened bones and delayed development of the secondary ossification centre. With aging or surgically induced joint instability, these mice also developed typical phenotypic features of OA. They express markers that are associated with OA, such as type X collagen. Genetic manipulation of Hedgehog signaling in these mice suggests that Hh signaling is modulating the phenotype by regulating sterol homeostasis. Therefore Hh signaling regulates genes which modulate sterol biosynthesis and through this mechanism Hh activation drives cartilage degeneration. These data suggest that cholesterol dysregulation predisposes to OA, and provide support for pharmacologic correction of intra-articular sterol imbalance as a novel treatment for osteoarthritis.

***Disclosures: Shabana Ali**, None.*

LB-SU02

Prepubertal calcium supplementation alters the timing of adolescent skeletal growth and mineral accretion in boys. Kate Ward*[1], Tim J Cole[2], Yankuba Sawo[3], Ann Laskey[1], Ann Prentice[1]. [1]MRC Human Nutrition Research, United Kingdom, [2]MRC Centre of Epidemology for Child Health, United Kingdom, [3]MRC Keneba, Gambia

In rural Gambian prepubertal children with low mean daily calcium intakes (300mg/day) we reported positive effects, sustained for at least a year, on bone mineral content (BMC) after 12 months supplementation with calcium carbonate to international levels [1,2]. This group has been followed up regularly until the end of height growth. Results showed that boys in the calcium group (Ca) reached peak height velocity earlier and were taller in mid-adolescence, but stopped growing earlier and were shorter than the placebo (P) group[3] . Our aim was to determine whether the supplementation also altered the timing and rate of skeletal growth and mineral accretion.

80 prepubertal boys (8.0-11.9 years (y)) who participated in the RCT (1000mgCa/day, 5 days/week for 1 y) have been studied longitudinally for 13 years. DXA scans and anthropometry were performed 1y and 2y post-supplement and biennially thereafter. Outcomes were whole body (WB), spine and total hip BMC (g) and bone area (BA, cm^2), and lean mass. Within-individual changes over time and the effects of supplementation on the longitudinal profiles were analysed by the Superimposition by Translation and Rotation method (SITAR)[4]. Results are presented as mean differences ± SEM (months[mo]).

For the whole group mean age at peak velocity was: WBBMC=17.6y, WBBA=16.6y and lean mass=16.1y. Peak WBBA velocity preceded peak WBBMC velocity by 1.02 years ($p<0.0001$). This pattern of growth was similar to those reported in populations with moderate-high calcium intakes, but the ages of peak BMC and BA velocity were delayed in Gambian subjects.

As with height, Ca entered the skeletal growth spurt earlier than the P group, Ca-P peak accrual: WBBMC (6.8 ± 3.4mo, p=0.04), WBBA (6.1 ± 3.1mo, p=0.05), lean mass (4.4 ± 2.4mo, p=0.07). Similar BA results were found for spine (5.8 ± 3.1mo, p=0.06) and total hip (5.6 ± 3.0mo, p=0.07) but they did not reach statistical significance. There were no differences in the velocity of accrual of adult BMC or BA between the groups.

In conclusion, 12 mo of prepubertal calcium supplementation in Gambian boys with a low calcium intake increased BMC in the short-term and advanced the timing of the adolescent skeletal growth spurt. However, it was not associated with a sustained increase in BMC or bone size in young adult men.

[1]Dibba et al. Am J Clin Nutr 2000; 71; [2]Dibba et al. Am J Clin Nutr 2002; 76; [3]Prentice et al. Am J Clin Nutr 2012; 96; [4]Cole et al. Int J Epidemiol 2010; 39

***Disclosures: Kate Ward**, None.*

LB-SU03

Effects of Low-Magnitude High-Frequency Vibration on Bone Density, Bone Resorption and Muscular Strength in Ambulant Children Affected by Duchenne Muscular Dystrophy. Maria Luisa Bianchi*[1], Silvia Vai[1], Lucia Morandi[2], Giovanni Baranello[2], Barbara Pasanisi[2], Clinton Rubin[3]. [1]Istituto Auxologico Italiano IRCCS, Italy, [2]Fondazione Istituto Neurologico C. Besta IRCCS, Italy, [3]State University of New York at Stony Brook, USA

Some recent studies have demonstrated that low-magnitude high-frequency vibration (LMHFV) may increase bone density (BMD) or decrease bone loss in primary osteoporosis in adults and secondary osteoporosis in disabling conditions (e.g. cerebral palsy) in children.

This is the first prospective double-blind randomized placebo-controlled study to investigate the impact of LMHFV on BMD and muscular strength in children affected by Duchenne muscular dystrophy (DMD). We enrolled 21 ambulant children with DMD (mean age 9.3 $\pm$ 3.9 years). For at least 6 months before the study, all children were treated with glucocorticoids and calcifediol (0.7 mcg/kg/die), and took 100% of calcium RDA. The children were randomly assigned to either active LMHFV devices (delivering 0.3g, 30Hz; N=11, among them 2 brothers) or placebo devices (factory-transformed to produce no vibration; N=10). Children were instructed to use the platforms for 10 minutes a day for 1 year.

At baseline, bone age was evaluated (X-rays). At baseline, 6 and 12 months all children underwent auxological and neurological evaluation: muscular strength (measured by myometer at lower and upper limbs); BMD (by DXA): at spine (BMAD), hip, total body less head; auxological parameters: weight, height, Tanner stage; lab tests: calcium, phosphate, parathyroid hormone, 25-OH vitamin D, 1,25(OH)2 D; bone turnover markers: bone alkaline phosphatase (BSAP), osteocalcin, C- and N-terminal telopeptides (CTx, NTx).

Compliance was 79% (active group) and 75% (placebo group), and all children tolerated the treatment well. BMD significantly increased vs. baseline only in the active group (spine BMAD +7.9% $p<0.02$; TB +6.8% $p<0.02$; femoral neck +9.8% $p<0.01$). There was no change or a decrease in the placebo group (spine BMAD -2.9%, TB -3.9%, femoral neck -4.8%). Muscular strength did not change significantly in both groups.

25-OH D was within normal range in all children, as well as calcium, phosphate, PTH. Bone markers evaluation showed an increase in formation markers (BSAP and osteocalcin) and a significant reduction in resorption markers (CTx -12.3%, NTx -16.9%, $p<0.05$ vs. baseline for both) in the active group. An increase in resorption markers was observed in the placebo group (CTx +8.7%, NTx +10.6%, $p<0.05$ vs. baseline for both).

These data suggest that LMHFV can effectively improve BMD and bone turnover in ambulant DMD children, notwithstanding disease progression and chronic steroid use.

***Disclosures: Maria Luisa Bianchi**, None.*

LB-SU04

Mechanical Properties of Cancellous Bone from Normal, Osteoporotic and Treated Sheep. Gavriel Feuer*[1], Subrata Saha[2], James Bennett[3]. [1]USA, [2]State University of New York Downstate Medical Center, USA, [3]SUNY Downstate, USA

The purpose of the current study was to assess efficacy of a synthetic bone mineral (SBM) made of magnesium, zinc, and calcium phosphate with and without fluoride that could be used to prevent and treat osteoporosis. Twenty eight sheep were randomly allocated into one of four groups. Osteoporosis was induced in three of the four groups using a combination of ovariectomy (OVX), corticosteroid injections, and a low mineral diet. One group underwent a sham operation and served as a control for the study.

The sheep were sacrificed after 8 months. Cancellous bone cores (7.9 mm diameter, 2.8 mm thickness) were prepared from the distal end of the right femurs and their wet density was measured. A shear punch test was performed separately on the midpoint of the three distal samples. A load-deflection curve was generated for each slice and the shear stress of each sample was calculated by dividing the peak load by the shear area. The peak load, shear stress, stiffness, and density of the distal three samples for each core were averaged. Statistical analysis was performed using analysis of variance (ANOVA) to compare the means for each treatment group with Tukey adjustment for multiple comparisons.

The mean peak load of all the samples was 104.2 $\pm$ 34.1 N, the shear stress was 3.7 $\pm$ 1.6 MPa, the stiffness was 976.3 $\pm$ 378.7 N/mm, and the density was 1.148 $\pm$ 0.030 g/cc. As shown in Fig. 1 there was a significant increase in shear stress, peak load, stiffness and density between the SBM (F+) treated group and the OVX group. There was also a significant increase in shear stress, peak load and density between the SBM (+F) treated group and the sham operated group.

The current study showed a significant difference among the four treatment groups regarding the peak load, shear stress, stiffness, and density of the cancellous bone. There was a statistically significant improvement in the peak load, shear stress, and density when comparing the SBM (+F) group with the ovariectomized and sham-operated groups. In addition, there was a statistically significant improvement in the stiffness when comparing the SBM (+F) group with the ovariectomized group. These results suggest that although there was no significant difference between the SBM (+F) group and the SBM (-F) group, the SBM (+F) tended to be more effective at preventing loss of cancellous bone strength in osteoporosis.

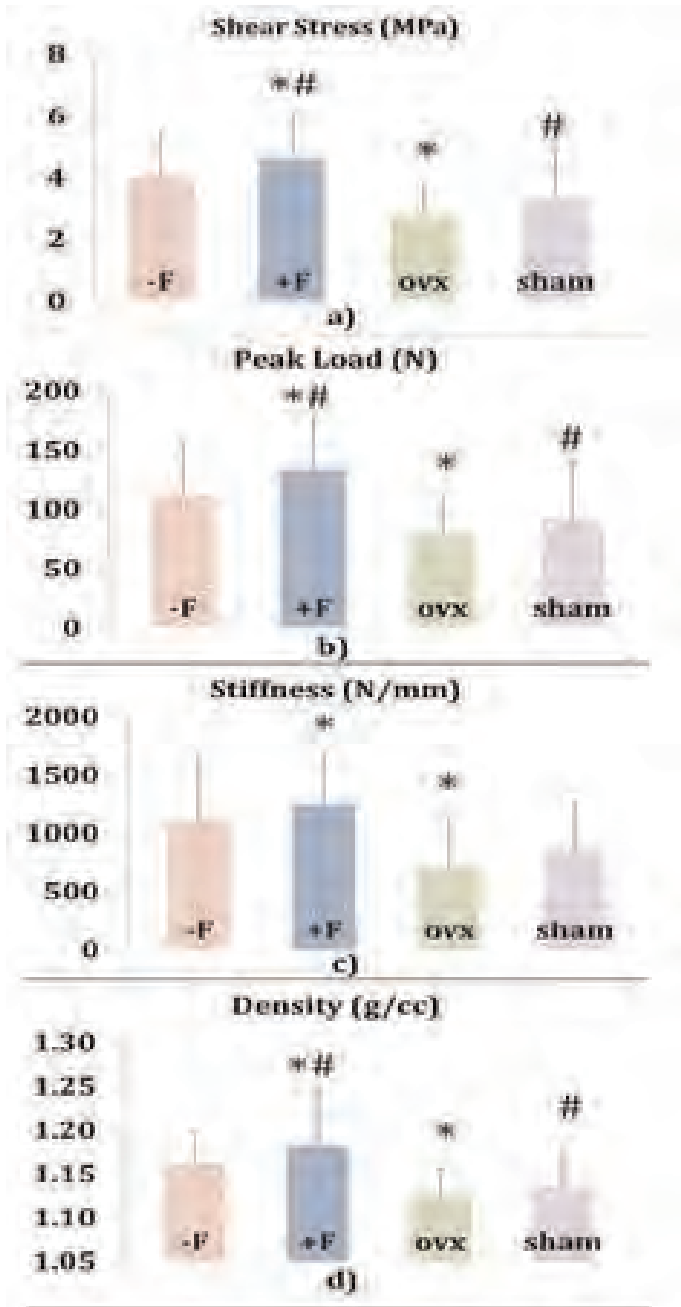

Figure 1: Mechanical and physical properties of sheep cancellous bone tested in shear (* and # denote statistical significance between groups)

Mechanical Properties

***Disclosures: Gavriel Feuer**, None.*

LB-SU05

Precision of Bone Mineral Density Calculation Utilizing Single X-Ray Absorptiometry (SEXA) versus Dual X-ray Absorptiometry (DEXA) in-vitro. Chester Lowe*[1], Li Sun[2], Jianhua Li[3], Yan Chen[1]. [1]KUB Technologies, Inc, USA, [2]Mt Sinai School of Medicine, USA, [3]Tount Sinai School of Medicine, USA

Abstract: Precision of Bone Mineral Density Calculation Utilizing Single X-Ray Absorptiometry (SEXA) versus Dual X-ray Absorptiometry (DEXA) in-vitro.

OBJECTIVE: To evaluate the precision of mouse bone mineral density (BMD) measurements by Brand P dual-energy X-ray absorptiometry (DEXA) versus Kubtec DIGICOM BMD single-energy absorptiometry(SEXA) in vitro.

METHODS: (1) The coefficients of variation (CV) for BMD measurements at various skeletal

regions were repeatedly determined by DEXA and SEXA in a preliminary study of mice weighing between 17.4 grams – 38.5 grams were analyzed on both machines. (2) Identical Regions of Interest, L3-L5, both sides of femurs and tibias, were visualized and the BMD calculated on both the SEXA and DEXA machines. And (3) resultant calculations were compared.

RESULTS: (1) The CVs of the preliminary BMD measurements in different regions of mice weighing between 17.4 grams to 38.5 grams by SEXA calculations versus the DEXA calculations were as follows, 135.52% for lumbar vertebra (L3-L5), 122.3% for left femur, 139.5% for right femur, 141% for left tibia, and 149.9% right tibia, respectively. (2) The BMD values in the 5 preliminary mice were (57.9 +/- 10.7 SEXA; 42.9 +/- 4.9 DEXA) mg/cm2 in lumbar vertebra (L4-6), (89.2 +/- 10.7 SEXA; 72.9 +/- 7.5 DEXA) mg/cm2 in left femur and (88.3 +/- 11.1 SEXA; 63.3+/- 8.3 DEXA;) mg/cm2 in right femur, (67.7 +/- 5.0 SEXA; 48.0 +/- 5.0 DEXA) mg/cm2 in left tibia and (65.2+/- 8.8 SEXA; 43.5+/- 4.5 DEXA;) mg/cm2 in right tibia, respectively., (3) The BMD values calculated and recorded were consistent between the SEXA and DEXA unit on the ROIs selected with variations between the 2 techniques being accounted for by the higher resolution and the 16-bit output of the SEXA detector versus the lower resolution and 8-bit output of the DEXA unit.

CONCLUSION: Measurement of MOUSE BMD in vitro by the Kubtec DIGICOM BMD SEXA is a useful method, it can produce repeatable results, and it can reflect the changes in mouse bone masses with good precision and as accurately as can Brand P utilizing DEXA.

***Disclosures: Chester Lowe**, KUB Technologies, Inc., 2*
This study received funding from: KUB Technologies, Inc.

LB-SU06

Sequential *in vivo* tracking of osteogenic stem/progenitor cells during fracture repair. Dongsu Park*[1], Charles Lin[1], David Scadden[2]. [1]Massachusetts General Hospital, USA, [2]Center for Regenerative Medicine, Massachusetts General Hospital, USA

Bone is highly regenerative following injury but the existence of osteogenic stem/progenitor cells have long been hypothesized and in vivo demonstration of such cells has only recently been attained. In particular, their in vivo identity and dynamics are not clearly understood. We recently defined that osteogenic stem/progenitor cells (OSPCs) can be genetically marked by transient activation of the myxovirus resistance-1 (*Mx1*) promoter. Here, we demonstrate in vivo characteristics of endogenous osteogenic stem/progenitor cells and their progeny in bone repair. Using osteo-lineage cell tracing models and intravital imaging of induced microfractures in calvarial bone, we found the relocation of endogenous OSPCs to fracture sites during the first few days after injury. Sequential in vivo imaging of OSPCs in the fracture site revealed that OSPCs increase in number and differentiate into bone forming osteoblasts. Notably, *Mx1* and *nestin* (a known MSC marker) double-labeled mice showed that Mx1+nestin- OSPCs rather than Mx1+nestin+ cells are the source of new osteoblasts during fracture healing in vivo. Our findings further define in vivo identification of skeletal stem/progenitor cells with physiological role in bone remodeling and regeneration and may offer a means of investigating the role of stem cells and their molecular regulators for bone repair.

***Disclosures: Dongsu Park**, None.*

LB-SU07

Mechanical Loading on Turkey Trabecular Bone Marrow Morphology. Quintin Eng*[1], Minyi Hu[1], Yi-Xian Qin[2]. [1]Stony Brook, USA, [2]State University of New York at Stony Brook, USA

Mechanical stimuli play an important role as a regulatory signal which allows the skeleton to recognize changes to its functional environment. Loading casues active bone remodeling by stimulating skeletal cells include osteoblasts, osteoclasts, osteocytes and osteoprogenitors. It would be vital to quantify the effects of mechanical stimuli on bone marrow. Medulla ossium rubra (red marrow), typically consists of mainly hematopoietic tissue; while medulla ossium flava (yellow marrow), mainly consists of adipocytic tissue. Red marrow is most prevalent at a young age and as time progresses; red marrow is converted to yellow marrow. Yellow marrow makes up the majority of bone marrow stroma, which contains mesenchymal stem cells (MSCs). Studying the effect of functional isolation with mechanical stimuli on bone marrow would give great insight into ways to promote bone growth. It was hypothesized that functionally isolated mechanically loaded bone can result in a higher red marrow content and lower yellow marrow content than normal functional bone.

An adult, one year old, skeletally mature male turkey's left ulnae was functionally isolated and mechanically loaded. Functional isolation and mechanical loading was achieved via two steel pins placed through drilled holes and a specially designed fluid loading device, performed by Dr. Yi-Xian Qin. The turkey was fed with a normal diet for one month and allowed to recover post-surgery then euthanized. Left and right ulnae were collected and proximal trabecular bones were then fixed in 70% ethyl alcohol before being embedded in paraffin. Microtone sections of 5 micron thick were collected. Each section was then stained with hematoxylin and eosin before photographed at a magnification of 10x using a Zeiss microscope. Image resolution was approximately one micron/pixel. ImageJ was used to analyze the images.

Analysis showed that sections of the loaded left ulnae contained a lower percentage of yellow bone marrow and higher red marrow content than the right ulnae. The amount of yellow marrow contained in loaded bone is lower than in unloaded bone. Yellow marrow contains MSCs which can differentiate into osteoblasts under functional loading; and leads to bone growth. A direct study of the number of osteoblasts and osteoclasts in functionally loaded and disuse bones would give important insight into ways of preventing and treating bone diseases such as osteoporosis and osteopenia.

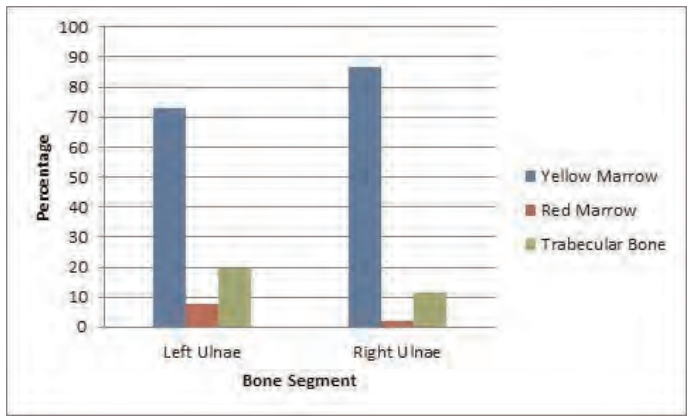

Left vs. Right Ulnae

***Disclosures: Quintin Eng**, None.*

LB-SU08

Reference Point Indentation Improves the DeXA-Derived BMD Prediction of Femoral Neck Strength. Adam Abraham*, Avi Agarwalla, Simon Tang. Washington University in St Lous, USA

Bone mineral density (BMD), as measured by DeXA, is the clinical gold standard for assessing fracture risk. BMD however is rather limited when diagnosing fragility in disorders involving diminished quality of the bone matrix. Reference point indentation (RPI), a novel tool for the direct minimally-invasive measure of bone material quality, discriminates between fracture vs non-fracture patients in BMD-matched cohorts, suggesting that bone quality is altered in fracture patients. Yet it is unknown whether RPI can assess the relative fracture risk, and whether the combined use of RPI-derived measures of bone quality and DeXA-derived BMD can more robustly predict the relative risk of fractures. Therefore, we aimed to determine the efficacy of RPI at discerning fracture risk and bone strength across the aging post-menopausal population.

Contralateral intact lower limbs from fourteen (ages: 58-97; 28 legs) fresh female cadavers were obtained from the Washington Univ. Femoral neck (FN) and total hip (TH) BMD were acquired using a clinical DeXA system (Hologic). RPI (BioDent Hfc) was performed *in situ* at the tibia mid-diaphysis for each leg through the skin and other surrounding soft tissues (15 sites/limb), and the parameter indentation distance increase (IDI) was averaged for each leg. Femoral neck strength was assessed by potting the proximal femur in PMMA and compressively loaded at the femoral head to failure at adduction 12° using an Instron 5866. Linear correlations were examined between the predictors BMD and IDI and response variables fracture load and work-to-failure.

BMD ranged from 0.39-0.94g/cm^2. FN and TH BMD were linearly correlated with failure load (FN:R^2=0.51, p<0.001; TH: R^2=0.55, p<0.001) and work-to-fracture (FN:R^2=0.35, p=0.002; TH: R^2=0.35, p=0.001). IDI was also linearly correlated with failure load (R^2=0.48, p<0.001) and work-to-fracture (R^2=0.36, p<0.001). More importantly, a multivariate model using TH-BMD and IDI yielded a significant improvement over the univariate correlations for both failure load (R^2=0.67, p<0.001) and work-to-fracture (R^2=0.47, p<0.001).

For the first time, we show that bone quality measured at the tibia by RPI can independently discern the relative risk of femoral neck fracture by predicting bone strength, and RPI may provide valueable clinical insights. Because fracture resistance is a culmination of both bone quantity and bone quality, utilizing both BMD and IDI may improve fracture risk assessment.

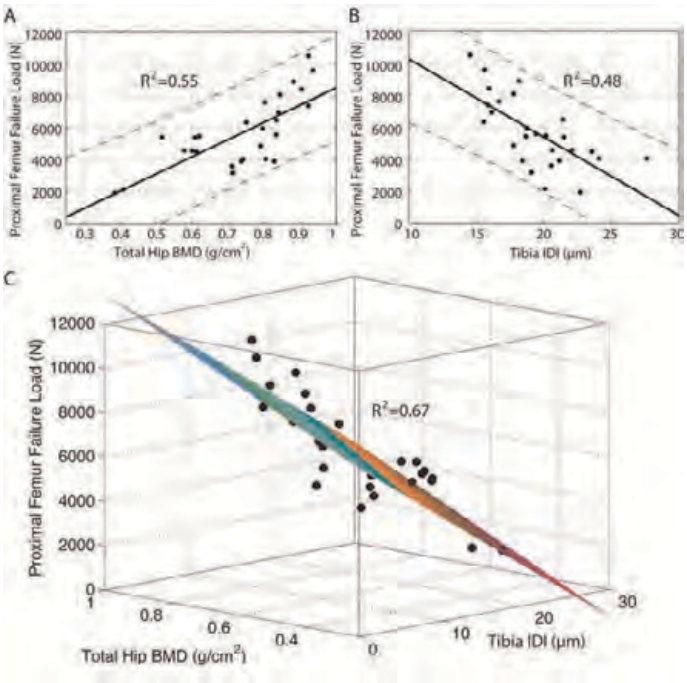

Fig 1: (A,B) BMD and IDI Predict FN Strength. (C) BMD and IDI combined better predicts FN Strength

***Disclosures: Adam Abraham**, None.*

LB-SU09

Cortical thickness and elastic modulus of trabecular bone assessed by a novel ultrasonic bone densitometry are associated with vertebral fracture in type2 diabetes. Takashi Mishima*[1], Koka Motoyama[1], Kae Hamamoto[1], Shinsuke Yamada[1], Nagato Kuriyama[2], Yasuo Imanishi[3], Masanori Emoto[1], Yoshiyuki Watanabe[2], Masaaki Inaba[1]. [1]Department of Metabolism, Endocrinology, & Molecular Medicine, Osaka City University Graduate School of Medicine, Japan, [2]Department of Neurology, Kyoto Prefectural University of Medicine, Japan, [3]Osaka City University Graduate School of Medicine, Japan

In patients with type 2 diabetes, bone fracture is one of well-recognized complications. Accumulated epidemiological studies have shown that patients with type 2 diabetes exhibited the higher bone fracture rate despite their bone mineral density. Further assessments of bone quality are required. Recently, an ultrasonic wave propagation phenomenon described as Biot's theory that focuses on two longitudinal waves (fast and slow waves) has been actively studied and adopted for the assessment of bone strength. The LD-100® system (Oyo Electric, Kyoto, Japan) is a newly developed ultrasonic bone densitometry based on the waves, which can non-invasively evaluate trabecular bone density, cortical thickness, and elastic modulus of trabecular bone. Cortical thickness and elastic modulus of trabecular bone are highly co-relate with grip strength suggesting these two parameters are valid as well as bone mineral density.We studied the associations of cortical thickness and elastic modulus of trabecular bone by LD-100® system with vertebral fractures in 174 type 2 diabetic patients. In the population of GFR≥60 ml/min/1.73m^2, elastic modulus of trabecular bone exhibited significant decrease in the fracture group despite bone mineral density did not. In the population of GFR<60 ml/min/1.73m^2, not only BMD but also cortical thickness and elastic modulus of trabecular bone were significantly decreased in the fracture group. Multivariate logistic regression model showed cortical thickness and elastic modulus of trabecular bone were independent risk factor for vertebral fractures despite bone mineral density was not.

In conclusion, cortical thickness and elastic module of trabecular bone evaluated by a novel ultrasonic bone densitometry were associated with bone fragility in type2 diabetes.

***Disclosures: Takashi Mishima**, None.*

LB-SU10

mTOR Promotes Embryonic Skeletal Growth through Stimulation of Protein Synthesis. Jianquan Chen*[1], Jeffrey Arbeit[2], Fanxin Long[3]. [1]Washington University, USA, [2]Department of Surgery, Washington University School of Medicine, USA, [3]Washington University School of Medicine, USA

Mammalian target of rapamycin (mTOR), an evolutionarily conserved serine/threonine kinase, integrates nutritional status and growth signals to regulate cell behavior via two separate protein complexes mTORC1 and mTORC2, each with distinct downstream effectors. To investigate the role of mTOR signaling during mouse embryonic skeletal development, we employed the Cre-LoxP technology to delete either mTOR, or the mTORC1-specific Raptor, or the mTORC2-specific Rictor, in the limb skeletogenous mesenchyme with Prx1-Cre. We find that *Prx1-Cre; mTOR$^{f/f}$* newborns exhibited normal limb skeletal patterning, but severe diminution of the limbs. Histological analyses revealed that at birth the mutant limbs remained a fully cartilaginous element, completely lacking a marrow cavity that is normally evident at this stage. In addition, approximately 50% of the mutants exhibited exencephaly. Interestingly, *Prx1-Cre;Raptor$^{f/f}$* embryos exhibited skeletal phenotypes resembling those of *Prx1-Cre; mTOR$^{f/f}$* embryos. In contrast, *Prx1-Cre; Rictor$^{f/f}$* embryos exhibited slightly shorter and narrower limbs than the control littermates, but they appeared otherwise normal. At the cellular level, loss of either mTOR or Raptor didn't affect chondrocyte survival or proliferation, but diminished the size of chondrocytes and the amount of cartilage matrix proteins. Direct measurement of protein synthesis rate reveals a notable deficit in chondrocytes with disrupted mTORC1 signaling. Thus, mTOR signaling through mTORC1 stimulates protein synthesis by chondrocytes to ensure the proper growth of the embryonic skeleton.

***Disclosures: Jianquan Chen**, None.*

LB-SU11

Runx1 and Runx3 are downstream effectors of Nanog in the promoted osteogenic differentiation of mesenchymal cells. Toru Ogasawara*[1], Tadahito Saito[2], Shinsuke Ohba[1], Takahiro Abe[3], Yoshiyuki Yonehara[2], Tsuyoshi Takato[3]. [1]The University of Tokyo, Japan, [2]Nihon University School of Dentistry, Department of Oral & Maxillofacial Surgery, Japan, [3]Department of Oral & Maxillofacial Surgery, Graduate School of Medicine, The University of Tokyo, Japan

The roles of transcription factors in the maintenance of stem cell pluripotency are important and as yet unknown. We previously reported that transcription factor Nanog, which maintains the self-renewal of embryonic stem (ES) cells, promotes the osteogenic differentiation of mouse mesenchymal cell line C3H10T1/2 cells through a genome reprogramming process (J. Cell. Physiol. 228:163-71, 2013). In the present study, in order to clarify the mechanism underlying the pluripotency of stem cells and to develop a novel approach to bone regenerative medicine, we tried to discover the downstream effectors of Nanog in the promoted osteogenic differentiation of mesenchymal cells. To this end, we performed a DNA microarray analysis between C3H10T1/2 cells constitutively expressing GFP and those expressing Nanog cultured with rhBMP-2. By forced Nanog expression, the expression levels of about 1000 genes showed a more than twofold increase (log2Ratio>1) or decrease (log2Ratio<0.5). We selected several of the upregulated genes (Runx1, Runx3, Sox4, Zfp235, Klf13, etc.) as candidates that could regulate the osteogenic differentiation of mesenchymal cells as downstream effectors of Nanog. Among these genes, we here focused on Runx1 and Runx3 in consideration of both the log2 Ratio (Runx1: 3.45; Runx3: 1.61) and findings gathered from the literature. Real-time quantitative RT-PCR analyses confirmed that there were dramatic upregulations of both Runx1 and Runx3 in Nanog-expressing cells compared with the levels in GFP-expressing cells. Next, to investigate the functional relevance of Runx1 or Runx3 to the osteogenic differentiation promoted by Nanog, we knocked down Runx1 or Runx3 mRNA in Nanog-expressing cells through small RNA interference (siRNA). Real-time quantitative RT-PCR analyses revealed that the expression levels of type I collagen mRNA were inhibited by both siRunx1 and siRunx3, though those of osteocalcin were not affected. These results indicate that Runx1 and Runx3 are the downstream effectors of Nanog, especially in the early and intermediate osteogenic differentiation of mesenchymal cells.

***Disclosures: Toru Ogasawara**, None.*

LB-SU12

FGF23 is a Naturally Phosphorylated Protein: FAM20C-mediated phosphorylation of Ser212 in human FGF23. Iris Lindberg[1], Kevin Li*[1], David Clark[1], Austin Yang[1], Lynda Bonewald[2]. [1]University of Maryland Medical School, USA, [2]University of Missouri - Kansas City, USA

Levels of serum phosphate are controlled by the peptide hormone FGF23, secreted from bone osteocytes. Elevated FGF23 has been shown to be responsible for hypophosphatemia and to play a role in cardiovascular outcomes in CKD. The posttranslational processing of this peptide hormone includes multi-site O-glycosylation, known to affect intracellular inactivation by proprotein convertases. The FGF23 protein also contains several casein kinase consensus sequences (S-X-D/E). It has

recently been shown that SIBLING proteins are phosphorylated at these consensus serines by the novel Golgi secretory kinase FAM20C. In this study, we asked whether FGF23 is also a substrate for secretory phosphorylation. We found that HEK cells transfected with plasmids encoding FGF23 and FAM20C, but not an inactive kinase mutant, were able to incorporate radiolabeled phosphate into immunoprecipitable 29 kDa FGF23 as well as into a 14 kDa C-terminal FGF23 fragment. Further work in the IDG-SW3 osteocyte model cell line showed that these cells are able to generate phosphate-labeled FGF23 and fragments in the absence of kinase transfection, suggesting endogenous FAM20C expression. Serine-to-alanine site-directed mutagenesis of four consensus sites was used to localize the site of phosphorylation to Ser212 (numbering according to wild-type human protein, including initiating methionine), though trace amounts of phosphorylation persisted in the Ser212Ala mutant. Since FAM20C is ubiquitously expressed, we asked whether commercially available recombinant FGF23, produced in NSO cells, is also phosphorylated. LC-coupled mass spectroscopy indicated the presence of phosphate at the homologous serine in recombinant R&D mouse FGF23. In support, a phosphopeptide-specific antibody raised against this site reacted preferentially with FGF23 secreted by FAM20C co-transfected HEK cells.

In conclusion, we have shown that FGF23 is naturally phosphorylated on the C-terminal fragment at Ser212 in a bone cell line; further, since FAM20C is widely expressed, it is likely that all commercially available recombinant FGF23 is also at least partially phosphorylated. The C-terminus of FGF23 is known to be involved in the interaction of Klotho with the FGF23 receptor; phosphorylation may play a role in this ternary interaction.

***Disclosures: Kevin Li**, None.*

LB-SU13

Role of Morphogenetic Proteins - FGF-23 and Klotho in the Vascular Calcification in Patients with Chronic Kidney Disease. Alexandra Plotnikova*[1], Ludmila Milovanova[2], Yurii Milovanov[3], Sergey Moisseyev[3], Lydia Kozlovskaya[4], Nikolay Mukhin[5], Daria Kryukova[6]. [1]PhD Student, investigator, Russia, [2]PhD, researcher, Russia, [3]M.D., PhD, supervisor of the research, Russia, [4]Professor, M.D., Russia, [5]Professor, M.D., the Head of Department, Russia, [6]PhD student, Russia

The aim of the study was to examine the relationship between changes in FGF-23/ Klotho levels in serum and diffuse arterial calcification in the patients with different stages of Chronic Kidney Disease (CKD).Materials and Methods: 70 patients with CKD 1-5D stage were included in the study: 41-with chronic glomerulonephritis, 22-tubulointerstitial nephritis and 7-hypertensive nephrosclerosis (30 men and 40 women, aged 20-65 years, mean age at enrollment was 41 $\pm$ 6,7 years). Serum FGF-23 levels (Human FGF-23 ELISA kit using monoclonal antibodies to the full FGF-23 molecule) and Klotho (Human alpha-Kl ELISA using anti-Klotho antibodies) were studied in these patients. The state of blood flow in the heart and large vessels (Doppler ultrasound), pulse wave velocity, calcifications presence (echocardiography) and vascular wall functional ability were studied. Results:In hypertensive CKD patients (n = 49), the degree of increasing Blood Pressure (BP) correlated positively with FGF-23 serum levels (r = 0,452; p <0,01) and inversely with Klotho levels (r = -0,687; p <0,01). In addition, in hypertensive patients (n = 49) was found the feedback between enhanced serum FGF-23 levels, reduced serum Klotho levels with increased left ventricular mass index (r=0,552; p<0,01 and r = -0,587 ; p <0,01). We also established the strong straight relationship of FGF-23 serum levels [r =0,492;p<0,01] and the reverse relationship of Klotho serum levels [r= -0,537; p<0,01] with the peripheral vascular resistance indices. In these patients increased FGF-23 levels and reduced Klotho levels have been associated with a higher frequency of calcification identification in the heart and large arteries [r=0,625;p<0,01 and r= -0,584;p<0.01].These correlations were strongest in the hypertensive patients who failed to achieve adequate blood pressure correction (n= 27). The patients who was a success to achieve and maintain target blood pressure level (120-130 mm Hg) had higher Klotho levels [r=0,509;p <0,01] and less pronounced degree of myocardial remodeling then those having uncorrected hypertension .This effect was more expressed in the patients who took nephroprotective means - angiotensin converting enzyme inhibitors or angiotensin receptor blockers for the hypertension correction. Conclusion.It was found the clear link between increased serum FGF-23 and decreased Klotho levels as increasing CKD severity, and diffuse arterial calcification, independent of traditional risk factors.

***Disclosures: Alexandra Plotnikova**, None.*
This study received funding from: I.M.Sechenov First Moscow State Medical University, Moscow, Russia

LB-SU14

Molecular insights into the RANKL-RANK interface using human protein expression models. Subhajit Das*[1], Janice Bramham[2], Angela Duthie[1], Julie Crockett[1]. [1]University of Aberdeen, United Kingdom, [2]University of Edinburgh, United Kingdom

The interaction of Receptor Activator of NFκB ligand (RANKL) with its cognate receptor RANK is crucial for osteoclast formation. The recent discovery of mutations in RANK that are associated with rare forms of osteopetrosis confirmed previous in vitro and mouse-model studies. We studied eight of these mutations within human RANK to gain mechanistic insights into the regulation of RANK signalling.

We investigated the role of the PreLigand Assembly Domain (PLAD or 'IVVY' motif) within the cytoplasmic region of RANK in rare cases of osteopetrosis. Immunoprecipitation showed that, by contrast to wild-type RANK, the absence of PLAD in two truncated, mutant RANK proteins (W434X and G280X) prevented ligand-independent but not ligand-dependent oligomerisation and, in the W434X mutant with an intact TRAF6 binding domain, NFκB signalling was normal. Hence, unlike other TNF receptors, removal of PLAD did not interfere with ligand-induced trimerisation and subsequent NFκB signalling, demonstrating that therapeutic targeting of PLAD in prevention of osteoporosis may not be as effective as previously proposed.

The structural importance of the four extracellular, cysteine-rich domains (CRD1-4) in RANK was highlighted in the crystal structure of the mouse RANK-RANKL complex. We studied six disease-associated, point mutations within this region of human RANK. Recombinant, wild-type and mutant his-tagged RANK proteins (residues 26-210) were expressed in mammalian cells and purified by Ni^{2+}-affinity, followed by size-exclusion chromatography. Surface plasmon resonance analysis confirmed the very high affinity interaction between human RANKL and wild-type RANK (K_d<1 nM). RANKL showed slightly weaker binding to four mutants (A134V, D148V and R170G in CRD3; and C175R in CRD4) and no binding at all to two mutants, G53R (in CRD1) and R129C (in the linker between CRD2 and CRD3), indicating the crucial role of the latter two amino acids; the equivalent residues in mouse RANK have previously been shown to significantly interfere with RANKL-RANK interaction. This study shows, for the first time, the effect of disease-associated mutations in RANK on the biophysical interaction of human RANK protein with human RANKL and highlights CRD1 and CRD3 as having crucial roles in the RANKL-RANK interaction.

Taken together, this work provides novel insights into factors influencing RANKL-RANK interaction and signalling, which will be important for the future development of osteoporosis drugs.

***Disclosures: Subhajit Das**, None.*

LB-SU15

Activin Expression During Osteoblastic Mice Embryonic Stem Cell Differentiation Induced by Bone Morphogenetic Protein. Bruno Camargos*[1], Aroldo Camargos[2], Fernando Reis[3], Rubens Tavares[3]. [1]Hospital Mater Dei, Brazil, [2]Menthor, Brazil, [3]Co-Menthor, Brazil

Embryonic stem cells (ESC) respond to molecular signals. Differentiation protocols of ESC into osteoblasts have been used successfully. Most protocols use bone morphogenetic protein (BMP) to induce osteoblast differentiation *in vitro*. Activin A is a growth factor that interacts with BMP and afects osteoblast proliferation and bone remodeling. Activin A may act through negative feedback on terminal osteoblastic differentiation stages. OBJECTIVE: evaluate Activin A expression during osteoblastic differentiation induced by BMP. MATERIAL / METHODS: a protocol for ESC differentiation into osteoblasts described by Kawaguchi was adapted. The cell culture in hanging drop method was substituted by suspension culture. Real time polimerase chain reaction (PCR) of cell indifferentiation markers (Oct-4, Nanog), osteoblastic differentiation markers (Osteocalcin, Runx2, Bone Specific Phospahtase) and Activin A were performed on key steps of the protocol. Immunocitochemistry targeted to Activin A documented it's expression along the differentiation process. RESULTS: the protocol adapted favoured osteoblastic differentiation. Bone markers and Activin A expression increased as the osteoblast differentiation protocol went through it's terminal stages compared to the indifferentiated cell samples. CONCLUSION: cell cultured in suspension demonstrated similar results to the hanging drop method originally described by Kawaguchi. Bone differentiation markers and Activin A expression increased during an osteoblastic differentiation protocol adapted.

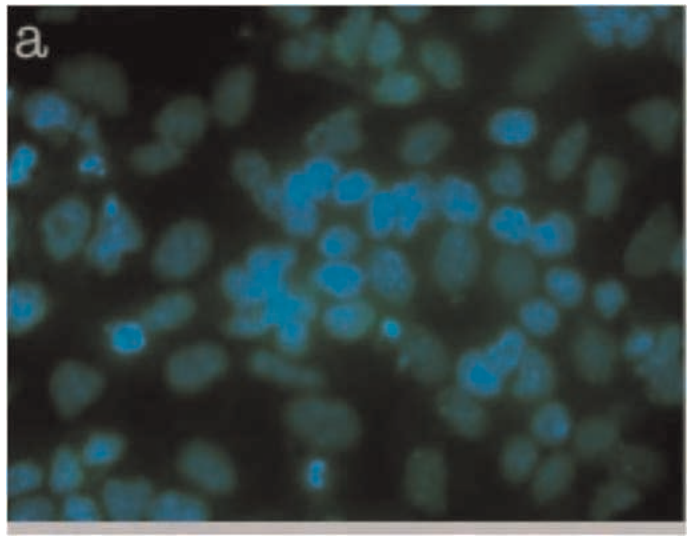

Activin A on Indifferentiated Stem Cells

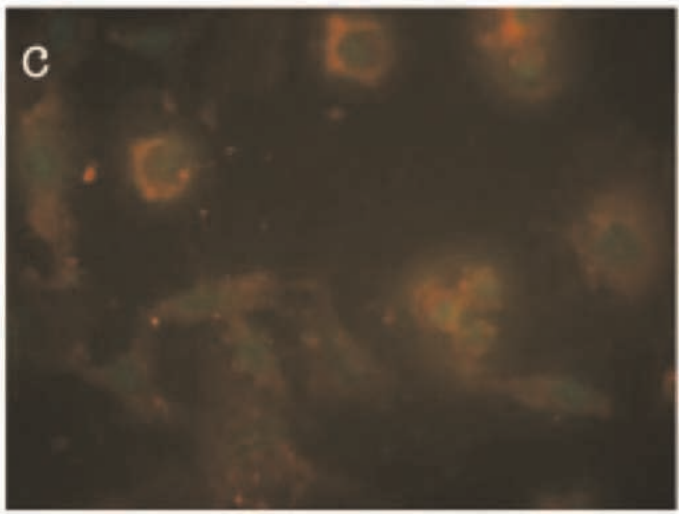

Activin A on Stem Cells Differentiated into Osteoblasts

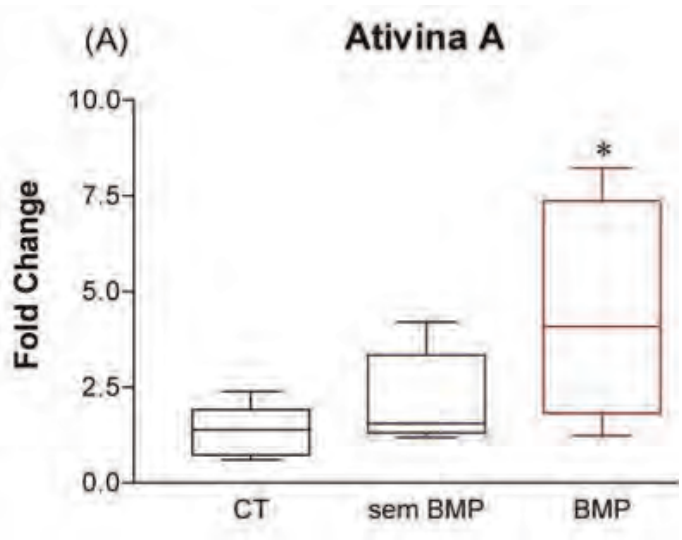

Activin A Expression on Different Steps of Differentiation Protocol

***Disclosures: Bruno Camargos**, None.*

LB-SU16

Osteoclastogenesis And Bone Degradation In Aseptic Loosening And Implant-Associated Infection. Ulrike Dapunt*[1], Felix Lasitschka[2], Matthias Gaida[2], Thomas Giese[3], Gertrud Maria Hänsch[3]. [1]Resident for Orthopaedic Surgery, Germany, [2]Heidelberg University, Department for Pathology, Germany, [3]Heidelberg University, Department for Immunology, Germany

Aim Although total joint replacements are a successful orthopaedic intervention, loosening of implants remains a severe complication of this procedure.Loosening can be the result of persistent local bacterial infection, or can be ''aseptic'' and caused by mechanical failure. Aim of this study was to investigate underlying cellular and molecular mechanisms, particularly with regard to the inflammatory response and the generation of osteoclasts.Materials and Methods From patients requiring surgery due to an implant-associated infection or because of aseptic loosening, tissue samples were taken directly from osteolytic sites and for comparison from adjacent sites, distant sites and from muscle. The tissue samples were evaluated a) histologically for cellular infiltrates and b) by RT-PCR for the presence of infiltrating cells, inflammation-related cytokines, and the osteoclast-typical gene cathepsin K. Results In aseptic loosening, high expression of cathepsin K and MMP-9 were found at sites with marked osteolysis. At these sites also proinflammatory cytokines (MCP-1, MRP14 and MIP2α) were highly expressed. Importantly, the expression of these parameters gradually decreased from sites of osteolysis to adjacent tissue, to distant tissue and further on to muscle tissue.The cellular infiltrate consisted mainly of mononuclear cells. In patients with infection, there was the high expression of IL-8, exceeding that seen in the aseptic patients by 10 to 20 fold. IL-8 was found at sites of osteolysis, but expression was even more pronounced in adjacent and distant tissues.To address the question of the possible source of IL-8, biopsies of patients with infection were examined. Infiltrating cells were positive for IL-8, but surprisingly the majority of IL-8 was seen in the tissue around blood vessels.Conclusion Aseptic loosening is associated with osteoclast generation, a prominent monocytic infiltrate, and occurs independently of the RANK/RANKL system, which is reported to be the main inductor of osteoclasts in diseases like rheumatoid arthritis or periodontitis. High expression of IL-8 is a hallmark of bacterial infection, and because it can induce osteoclasts, it is feasible that it provides the link between infection and bone resorption.Apparently, the endothelium is an important source of IL-8, which might be crucial for the recruitment of immune cells and thus for progression of the inflammatory response which is characteristic for implant-associated infections.

***Disclosures: Ulrike Dapunt**, None.*

LB-SU17

Pro-Resolving Mediators in the Bone Microenvironment Drive Macrophage Efferocytosis of Apoptotic Osteoblasts. Laurie McCauley*[1], Jesmond Dalli[2], Amy Koh[1], Nan Chiang[2], Charles Serhan[2]. [1]University of Michigan School of Dentistry, USA, [2]Brigham & Woman's Hospital, USA

Osteal macrophages reside in the bone marrow in sites of bone modeling and remodeling. Specialized pro-resolving mediators (SPMs) of inflammation promote wound healing via facilitating the specific phagocytosis of apoptotic cells by macrophages (termed efferocytosis). Little is known relative to the composition, regulation, and function of lipid mediators in the bone marrow. This study identified the profile of SPMs in the bone marrow and elucidated a novel role for resolvins in osteal macrophage efferocytosis. The profile of lipid mediators in the bone marrow and spleen was determined by mass spectroscopy. Metabololipidomic profiling revealed increased levels of the pro-resolving mediators resolvin D2 (RvD2), RvE1, and leukotriene B4 (LXB4) in the bone marrow versus the spleen. Parathyroid hormone (PTH) was administered via a single injection to mice, bone marrow harvested two hours later, and metabololipidomic profiling performed. PTH treatment resulted in significantly increased RvD1 and RvD2 levels in murine bone marrow versus controls. In ex vivo studies utilizing confocal microscopy and videography, primary murine bone marrow macrophages efferocytosed labeled apoptotic MC3T3-E1 osteoblasts in a temporal manner. Efferocytosis assays were performed using peripheral human blood mononuclear cells (PBMCs) induced to differentate to macrophages with the addition of M-CSF. Macrophages were treated with a dose response of RvD1 and RvD2, followed by incubation with apoptotic human osteoblastic cells (hFOB). There was a significant increase in efferocytosis in macrophage cultures treated with RvD1 (100pM-10nM) and RvD2 (100pM-100nM). These findings highlight a unique profile of specialized pro-resolving mediators in the bone marrow. PTH increased select SPMs including RvD1 and RvD2, both of which significantly increased macrophage efferocytosis of apoptotic osteoblasts. This work identifies a new resolution circuit in bone that is responsive to PTH and facilitates clearance of apoptotic cells.

***Disclosures: Laurie McCauley**, None.*

LB-SU18

Effects of endurance training on bone formation in a rat model of chronic kidney disease (CKD) related growth retardation. Daniel Landau*[1], Maayan Guterman[1], Ariel Troib[1], Ralph Rabkin[2], Yael Segev[1]. [1]Ben Gurion University, Israel, [2]Stanford University, USA

Objectives: CKD in children is associated with suppressed body growth. We have recently reported on suppressed epiphyseal growth plate (EGP) growth hormone receptor (GHR) signaling and reduced local IGF-I in a rat model of CKD related growth retardation. Physical activity has been previously shown to increase expression of IGF-I signaling in muscles of rats with CKD, but the effects of this intervention on bone tissue have not been investigated yet. The purpose of this study was to examine the effects of endurance training on CKD related bone disease.

Methods: Twenty-day old / 50g male rats underwent a 2 step subtotal nephrectomy (CKD) or sham surgeries (C). The animals were divided into 2 running (treadmill, 20 m/min, 0.5 hr/day, 5 days/wk) groups: control (Cr) and CKD (CKDr) and 2 non running groups: C and CKD. Food delivery was equal for all groups. The intervention lasted 4 weeks.

Results: Growth retardation (both longitudinal and weight gain) was well noticed in CKD Vs C. Exercise caused an increase in longitudinal growth and tibial length in Cr Vs C rats. However, CKDr rats did not grow better than CKD. CKDr rats consumed less food than CKD but grew to the same extent, hinting for better food efficiency. Total EGP width was increased in CKD Vs C, mostly at the expense of the hypertrophic zone. This effect was suppressed in CKDr Vs CKD. EGP cells were better organized in CKDr and showed less necrotic areas than CKD. Type II collagen was increased in CKD and decreased in CKDr. IGF-I mRNA and immunostainable IGF-I were increased in CKDr Vs CKD.

Conclusions: Endurance training did not rescue CKD somatic growth retardation, but longitudinal bone formation was better organized, associated with increased EGP IGF-I, supporting its positive role in bone health.

***Disclosures: Daniel Landau**, None.*

LB-SU19

Intracortical remodeling to meet mineral demands in X-Linked Hypophosphatemia (XLH). Carolyn Macica*[1], Richard Feinn[2], Steven Tommasini[3]. [1]Frank H. Netter School of Medicine Quinnipiac University, USA, [2]Frank H. Netter, M.D., School of Medicine at Quinnipiac University, USA, [3]Yale School of Medicine, USA

Hyp mice, a murine model of XLH, display increased porosity of cortical bone. However the etiology of changes in porosity is unknown. In addition, it is unclear how Hyp mice accommodate the increased mineral demands of pregnancy and lactation. As vitamin D biosynthesis is impaired in Hyp mice, and the highest density of mineral is in mature cortical bone, we hypothesized that mineral demand is met by intracortical remodeling, similar to that described in post-menopausal osteoporotic bone. Histochemical examination of Hyp cortical bone by von Kossa staining revealed that most intracortical pores were actually halos of demineralized bone, independent of osteocyte lacunae. Moreover, the central region of each halo stained positive for vascular markers. We therefore analyzed the femoral diaphysis by three-dimensional analysis using high resolution micro-CT (resolution = 1.55μm). Compared to C57BL6 controls, Hyp mice had a higher percentage of intracortical porosity (8.8% vs. 1.1%) due in part to a 9-fold increase in the percent volume of blood vessels (8.4% vs. 0.9%). This resulted in a 5-fold increase in intracortical surface area. Further, the percent volume of blood vessels and intracortical surface area increased in lactating Hyp compared to non-lactating Hyp controls. Taken together, these data suggest that so-called trabecularization of cortical bone serves as a means to create new bone resorption surfaces in the face of limited mineral availability. Consistent with this hypothesis is the finding of elevated type I collagen matrix degrading enzyme MMP-13 immunoreactivity and osteoclast activity detected by TRAP staining. We further characterized the matrix composition of cortical bone using FTIR analysis. Compared to C57BL6 controls, Hyp cortical bone had similar collagen cross-linking (2.77+0.14 vs. 2.83+0.14), significantly lower mineral/protein ratio (4.59+0.37 vs. 5.54+0.52, $p<0.05$), and significantly higher carbonate ion substitution (0.029+0.002 vs. 0.023+0.001, $p<.001$). Increased incorporation of carbonate into the hydroxyapatite lattice increases mineral matrix solubility and dissolution rate, making it possible to adsorb bone more readily. These data may provide insight into the mechanism of intracortical remodeling observed in osteoporosis and may have important implications in maintaining phosphate levels in the clinical management of XLH in adulthood during periods of high mineral demand.

***Disclosures: Carolyn Macica**, None.*

LB-SU20

The Role of Pigment Epithelium Derived Factor in Osteoblast Differentiation. Hadil Al-Jallad*[1], Frank Rauch[2], Marc McKee[3], Pierre Moffatt[4]. [1]Shriners Hospital for Children, McGill University, Canada, [2]Shriners Hospital for Children, Montreal, Canada, [3]McGill University, Canada, [4]Shriners Hospital for Children, Canada

Pigment epithelium derived factor (PEDF) is a secreted protein that is essential for bone metabolism. Absence of PEDF leads to osteogenesis imperfecta type VI, a severe heritable bone fragility disorder that is characterized by a mineralization defect in the presence of normal mineral metabolism. However, the precise role of PEDF in osteoblasts is unknown. In the present study, we therefore assessed the effects of PEDF knockdown and overexpression in the MC3T3-E1/M4 that we used as our *in vitro* model to study osteoblast differentiation. In PEDF deficient cells, collagen deposition was reduced and accompanied with delayed mineralization. Conversely, in PEDF overexpressing cells collagen deposition was significantly increased, with accelerated mineralization. PEDF deficient cells had 5- to 7-fold lower expression of osteoblast differentiation markers (tissue non specific alkaline phosphatase, osteopontin, osteocalcin, osterix/Sp7) and mineralization markers (Enpp1, Ank, Phex), whereas PEDF overexpression was associated with a significant up-regulation in the same markers. We conclude that lack of PEDF in osteoblasts primarily leads to an osteoblast differentiation problem, followed by delayed and decreased mineralization.

***Disclosures: Hadil Al-Jallad**, None.*

LB-SU21

Dlk1/FA1 Negatively Regulates Insulin-induced Osteoblast Differentiation and Osteocalcin Production In Mice. Basem Abdallah*[1], Moustapha Kassem[2]. [1]Odense University Hospital, University of South Denmark, Denmark, [2]Odense University Hospital, Denmark

Dlk1/FA1 (Delta like 1/ fetal antigen 1) is a known inhibitor of adipocyte differentiation and its increasing level of expression was shown to induce insulin resistance in mice. We have recently identified Dlk1/FA1 as a novel regulator of bone remodelling that function to inhibit bone formation and stimulate bone resorption. To study the potential involvement of Dlk1/FA1 in mediating the link between bone and energy metabolism, we investigated the regulatory role of Dlk1/FA1 in insulin signalling in osteoblasts using calvaria culture osteoblasts (OB) derived from osteoblast-specific-*Dlk1* over-expressing mice (Col1-Dlk1) and *dlk1*-deficient mice. Treatment of primary OB with insulin showed to inhibit dlk1 mRNA expression in a dose dependent manner during osteoblast differentiation. Insulin-induced osteogenesis was blocked in Dlk1-overexpressing calvaria cells (Dlk1-OB), while it was significantly stimulated in the absence of Dlk1/FA1 expression by *Dlk1*-/- OB. Studying the mechanism underlying the inhibitory effect of Dlk1/FA1 on insulin signalling in osteoblast by western blot analysis revealed the impairment of insulin-induced Akt phosphorylation in Dlk1-OB as compared to wild type OB or *Dlk*-/- OB. In addition, 70% of the insulin-signalling associated genes were significantly down-regulated in insulin-stimulated Dlk1-OB compared to WT-OB as assessed by supper-array pathway analysis. Interestingly, Dlk1/FA1 overexpression in OB significantly upregulated the expression of Twist1/2, (Runx2 inhibitor) in association with the down-regulation of runx-2 expression and its target osteocalcin gene in response to insulin stimulation. Consequently, the serum levels of osteocalcin were markedly reduced by 38.6% in Col1-Dlk1 mice as compared to wild type control mice. In conclusion, our data demonstrated Dlk1/FA1 as a downstream target of insulin signalling molecule that negatively regulates insulin-induced osteogenesis and osteocalcin production by suppressing Akt-dependent pathway and inhibiting Runx2 expression. Thus, Dlk1/FA1 is a novel factor that might function to regulate the link between bone, fat and energy metabolism.

Ref:
- Abdallah BM, et al., *J Bone Miner Res.* 2011 Oct;26(10):2548-51
- Abdallah BM, et al., *J Bone Miner Res*. 2011 Jul;26(7):1457-71.

***Disclosures: Basem Abdallah**, None.*

LB-SU22

Fate of Implanted Stem Cells in Tissue Engineered Bone. Donna Jones*[1], David Turer[2], Jesse Taylor[3]. [1]USA, [2]University of Michigan, USA, [3]Hospital of the University of Pennsylvania, USA

Bone tissue engineering typically provides a source of cells, the fate of which is not well understood. This study utilizes *gfp* labeled, adipose-derived stem cells (ASCs) in varying concentrations (null, $1x10^4$, $x10^6$ and $x10^8$ cells/mL). ASCs were harvested from globally expressing donor rats, expanded and transferred to cellulose sponge and placed with xenograft bone chips (4x2x2 mm) inside a pedicled, periosteal pouch elevated from the tibia of Lewis rats. Implants were left *in vivo* for four weeks, imaged with μCT, harvested, histologically examined and tested for *gfp* expression. All constructs grew new bone, but those with added cells grew significantly more than controls, regardless of initial cell concentration (Fig 1). The new bone was histologically healthy but less organized than cortical bone. *Gfp+* cells were visible in the three treatment groups and these were localized in the areas of new bone external to the xenograft chip and tibia (Fig 2). Biomechanical testing showed a loss of elasticity (Young's Modulous) and strength following implantation. Addition of stem cells did not affect elasticity or failure strength, although implantation altered both characteristics relative to both native bone and non-implanted chips (Fig 3). These data demonstrate that bone tissue engineering can be accomplished without added growth factors (e.g., bone morphogenic proteins), if done in the presence of periosteum (a bone morphogenic tissue). ASCs increased bone growth, but cell concentrations over $1x10^4$ provided no additional benefit.

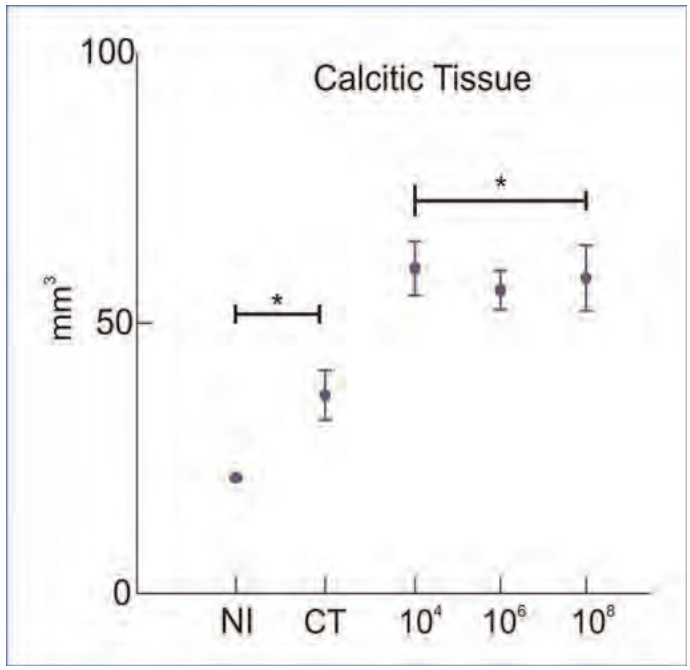

Figure 1

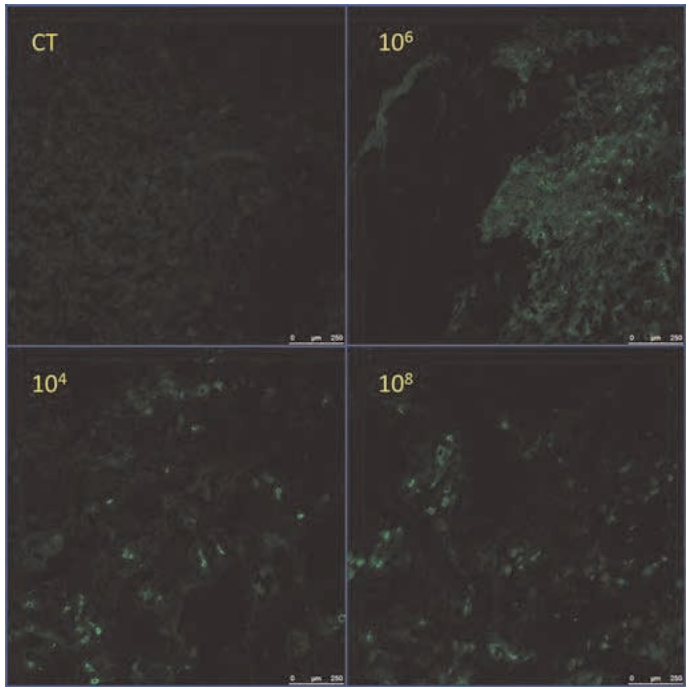

Figure 2

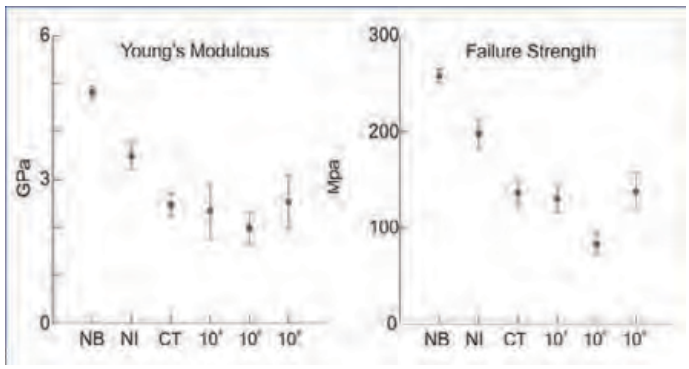

Figure 3

***Disclosures: Donna Jones**, None.*

LB-SU23

The combination of Cortical Porosity and FRAX improves the Diagnostic Sensitivity for Non-Vertebral Fractures in Women. Rajesh Shigdel*[1], Luai Ahmed[2], Ragnar Joakimsen[3], Petter Eldevik[3], Erik Fink Eriksen[4], Roger Zebaze[5], Ashild Bjornerem[1]. [1]University of Tromso, Norway, [2]Faculty of Health Sciences, University of Tromsø, Norway, [3]University Hospital of North Norway, Norway, [4]Oslo University Hospital, Norway, [5]Austin Health, University of Melbourne, Australia

The Fracture Risk Assessment Tool (FRAX), developed by the World Health Organization, helps to determine which patients may need medical treatment for bone fragility. The algorithm calculates the 10-year probability of a major osteoporotic fracture based on easily obtained clinical risk factors including femoral neck aBMD and has performed well in some cohorts but not in others. However, microarchitecture, particular cortical porosity is important for bone strength, and may improve fracture risk assessment, but is not included in FRAX. We therefore hypothesized that women with fractures are better distinguished from controls by the combination of cortical porosity and FRAX, than by either factor alone.

In a nested case-control design, 183 postmenopausal women aged 54-94 years with fractures (hip, humerus and forearm) and 210 age-matched controls from the Tromsø Study, Norway, had their 10-year probability of a major osteoporotic fracture assessed using FRAX including femoral neck aBMD, and simultaneously their cortical porosity was quantified in computed tomography images of the subtrochanteric femoral site using StrAx 1.0 software. The fracture risk was calculated as odds ratio (OR) using logistic regression analysis, and fracture sensitivity using the area under receiver operator curve (AUC).

Women with fractures exhibited higher mean cortical porosity than controls [43.8% (SEM 0.4) versus 40.3% (SEM 0.3)], and higher mean FRAX scores than controls [20.8% (SEM 0.6) versus 12.4% (SEM 0.4)] (both $p < 0.001$). Each standard deviation (SD) increase in cortical porosity increased the risk of fracture with OR of 2.20 (95% CI 1.72-2.81) $p < 0.001$ and the AUC was 0.69 (95% CI 0.64-0.74). Each SD increase in FRAX score increased the risk of fracture with OR of 4.57 (95% CI 3.25-6.42) $p < 0.001$ and AUC was 0.81 (95% CI 0.77-0.86). However, when cortical porosity was combined with FRAX the AUC increased by 0.03 (95% CI 0.003-0.05), $p = 0.03$, and the AUC for this combination was 0.84 (95% CI 0.80-0.88).

We infer that in this independent general population, a combination of cortical porosity and FRAX improve the diagnostic sensitivity.

***Disclosures: Rajesh Shigdel**, None.*

LB-SU24

Comparison of DXA and Quantitative CT Bone Mineral Density Measurement using Contrast Enhanced Scans at the Proximal Femur: Implications for Opportunistic Osteoporosis Screening. Alyssa Maciejewski[1], Timothy Ziemlewicz[1], Neil Binkley[2], Alan Brett*[3], Keenan Brown[3], Perry Pickhardt[1]. [1]University of Wisconsin School of Medicine & Public Health, USA, [2]University of Wisconsin, Madison, USA, [3]Mindways Software, Inc., USA

Introduction: For patients undergoing routine contrast-enhanced MDCT examinations, an opportunity exists for concurrent osteoporosis screening without additional radiation exposure or patient time using proximal femur quantitative CT (QCT) "CTXA". Previous studies demonstrated equivalence between unenhanced CT and DXA for femoral neck BMD evaluation; and have suggested a small BMD bias correction for enhanced CT studies. We investigated the effect of IV contrast enhancement on femoral neck CTXA T-score measurement compared with DXA.

Method: This cohort included 78 male and 277 female adults (mean age, 59.7 ± 13.3 years; range, 21-90 years) who underwent standard contrast-enhanced CT assessment including the pelvis at $120kV_p$ (GE Healthcare, Waukesha, WI) between November 2001 and December 2009. All subjects also had DXA BMD (GE Lunar, Madison, WI) assessment within 100 days of the CT study (mean 46 ± 30 days). DXA T-scores were calculated using the NHANES III female reference data. Areal BMD in g/cm^2 of the femoral neck was measured on the CT series using QCT Pro Version 5.1 (Mindways Software, Austin, TX) with asynchronous phantom calibration. QCT T-scores were derived using manufacturer's female reference data.

Results: Linear regression analysis showed good correlation between DXA and CTXA (R2 = 0.824 for both BMD and T-scores) and the SD of the distribution of residuals (SEE) was 0.063 g/cm^2 or 0.45 T-score units. A Bland-Altman plot of T-scores indicates no trend in differences between the two measurements and a small bias with DXA T-score +0.18 units higher than CTXA.

Conclusion: In this cohort, femoral neck T-scores obtained by CTXA and DXA are highly correlated. The SEE for BMD correlation compares favorably to that of a prior study comparing DXA and CTXA (0.053 g/cm^2) and may be higher due to variance in bias introduced by contrast enhancement in this study. The small bias between DXA and CTXA T-scores presented here may be due to differences in CT scanner calibration due to differences in CT table scan height and scanner type. In conclusion, for opportunistic osteoporosis screening at routine post-contrast abdominopelvic CT scans, CTXA produces T-scores similar to DXA. Femoral neck QCT BMD measurement is now included in the WHO FRAX® tool and this method could greatly enhance osteoporosis screening since it can be applied regardless of the clinical indication for CT scanning.

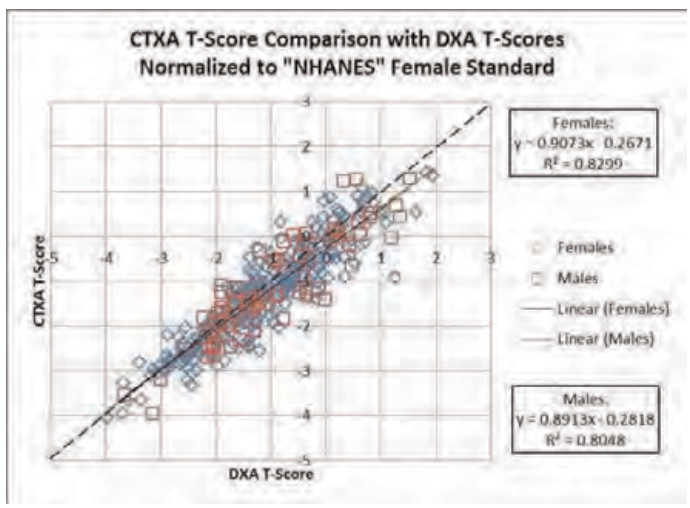

Post-contrast CTXA vs DXA femoral neck T-Scores

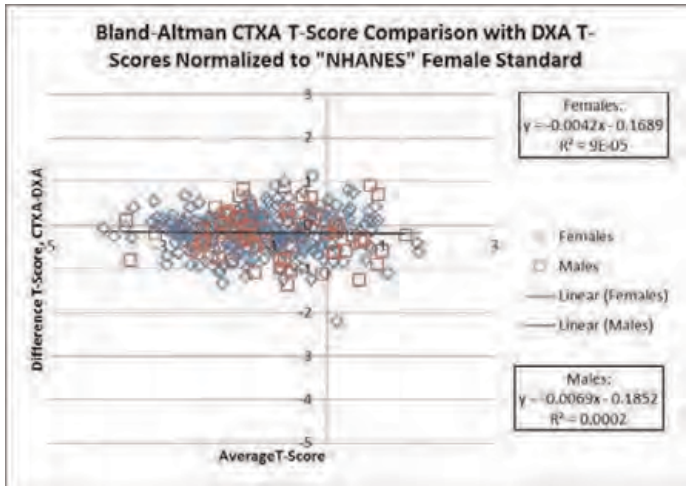

Bland-Atlman Plot of Post-contrast CTXA vs DXA T-Scores

***Disclosures: Alan Brett**, None.*

LB-SU25

Cortical Bone Defects Associated with Hip Fractures in Men. Fjola Johannesdottir*[1], Graham Treece[1], Andrew Gee[1], Karen Blesic[1], Madhavi Vindlacheruvu[2], Simon Donell[3], Kenneth Poole[1]. [1]University of Cambridge, United Kingdom, [2]Cambridge University Hospitals NHS Foundation Trust, United Kingdom, [3]Norfolk & Norwich University Hospital NHS Foundation Trust, United Kingdom

Background: Studies have shown that women who sustain hip fracture have a structural phenotype. Quantitative computed tomography (QCT) measurements of cortical bone in conventional regions of interest (ROI's) are associated with hip fracture in both men and women, especially cortical thinning superiorly in the femoral neck. Therefore, we aimed to study if a phenotype could be identified among male hip fracture cases, using cortical bone mapping.

Design, Setting and Participants: Participants in this case-control study included 20 British men (mean age 79yr, SD: 8) with a hip fracture and 24 British healthy controls (mean age 69yr, SD: 10). The cortical bone mapping technique was applied to clinical CT scans to identify locations where cortical bone in hip fracture cases differed, on average, from controls. This method involves non-rigid registration to an average femur surface and statistical parametric mapping to identify ROI's where clusters of values differ significantly, using Stradwin and Surfstat software. For cases, the non-fractured hip was used. Model effects were group (case*control), age, weight, height, and shape. The results are presented as percentage differences in cortical bone mass between cases and controls with a scaled colour map on an average femur model.

Results: Figure 1 displays the locations of significant ($p<0.05$) cortical bone mass differences associated with hip fracture; in the supero-lateral and inferior aspects of the femoral neck and lateral trochanteric region (red/yellow regions).Conclusion: Percentage differences in cortical mass were greatest superiorly in the femoral neck, with cases up to 40% lower in a patch where fractures may initiate. These patches in male hip fracture cases are similar to those found in women using voxel-based-morphometry, where there was loss of bone both at the superior cortex and the inferior cortex (Carballido-Gamio J Bone Miner Res 2013). These results indicate that women and men who sustain hip fracture might have a similar structural phenotype. This suggests that the mechanism causing cortical bone loss in 'at risk' individuals appears to be the same in men and women.

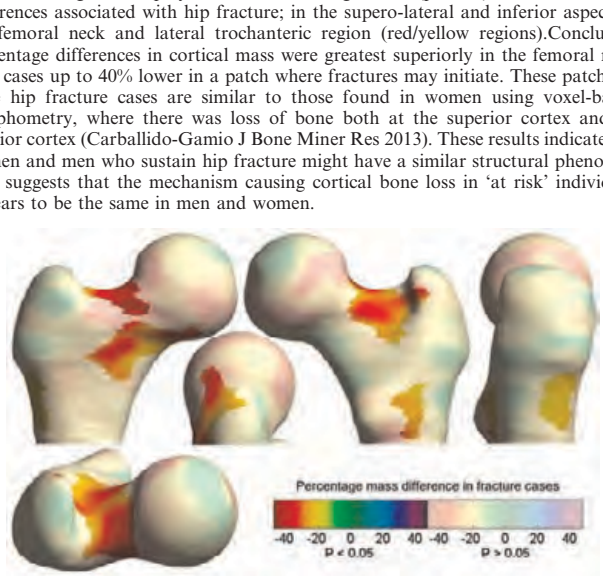

Percentage difference in cortical mass between controls and fracture cases (negative=fracture case)

***Disclosures: Fjola Johannesdottir**, None.*
This study received funding from: Arthritis Research UK

LB-SU26

Time to Major Fracture in Younger Postmenopausal Women According to Age and BMD T-score: the Women's Health Initiative (WHI). Margaret Gourlay*[1], Robert Overman[1], Guillaume Filteau[1], Jason Fine[1], Kristine Ensrud[2], Carolyn Crandall[3], Catherine Womack[4], Margery L.S. Gass[5], Erin LeBlanc[6], John Robbins[7], Karen Johnson[8], Andrea Lacroix[9]. [1]University of North Carolina, USA, [2]Minneapolis VA Medical Center / University of Minnesota, USA, [3]University of California, Los Angeles, USA, [4]University of Tennessee, USA, [5]The North American Menopause Society, USA, [6]Kaiser Permanente NW, USA, [7]University of California, Davis Medical Center, USA, [8]University of Tennessee Health Science Center, USA, [9]Fred Hutchinson Cancer Research Center, USA

The optimal approach for BMD screening to identify younger postmenopausal women who might benefit from osteoporosis treatment has not been established. We studied 4068 postmenopausal women aged 50 to 64 years at baseline in the placebo groups of the Women's Health Initiative Hormone Therapy, Calcium/vitamin D or Dietary Clinical Trial (WHI-CT) or in the WHI Observational Study (WHI-OS). Eligible participants were without a history of major (hip or clinical vertebral) fracture or use of pharmacologic treatment for osteoporosis at baseline, and had at least one DXA BMD test with femoral neck, total hip and lumbar spine measurements. We conducted a competing risk analysis to estimate the time for 1% of women to experience a first major fracture according to age group and the lowest of femoral neck, total hip or lumbar spine BMD T-score at baseline (T-score >-1.50; T-score -1.50 to -2.49; T-score <=-2.50). Hologic 4500 densitometers were used to determine BMD at 1 to 7 visits, and T-scores were calculated using white female normative values. For women without osteoporosis (T-score >-2.50) at baseline, the competing risks were incident osteoporosis, initiation of an FDA–approved agent for the treatment of osteoporosis (bisphosphonate, calcitonin, raloxifene or teriparatide) and death. For women with osteoporosis (T-score <=-2.50) at baseline, the competing risks were initiation of treatment and death. Follow-up time ranged from 23 days to 18.6 (mean 14.0) years. Parametric cumulative incidence curves for the time to major fracture were estimated from log logistic cumulative incidence models for interval censored data adjusting for age, BMI, race/ethnicity, current smoking, current estrogen use, current use of oral glucocorticoids, self-reported rheumatoid arthritis, parent with hip fracture, and WHI-CT vs. OS participation. The adjusted estimated time for 1% to transition to major fracture ranged from 16.57 (8.47, 32.43) years for women aged 50 to 54 with baseline T-score >-1.50, to 5.44 (2.82, 10.47) years for women aged 60 to 64 with baseline T-score <=-2.50. Eight of 336 (2.4%) women with osteoporosis at baseline had a major fracture before initiation of treatment during the study period. Postmenopausal women without a history of major fracture or treatment who had their first BMD screening test between age 50 and 64 had a very low incidence of major fracture before age 65. Optimal timing of subsequent DXA screens requires further exploration.

Baseline age range (years)	Baseline T-score range	Event N/ Group N (%)	Time for 1% of participants to have a first hip or clinical vertebral fracture	
			Unadjusted years (95% CI)	Adjusted years (95% CI)*
50-54	> -1.50	2/799 (0.25)	27.01 (10.24, 47.80)	16.57 (8.47, 32.43)
	-1.50 to -2.49	2/233 (0.86)	11.76 (6.77, 20.44)	14.01 (7.65, 25.66)
	<=-2.50	2/38 (5.26)	7.56 (3.72, 15.44)	8.47 (4.00, 17.96)
55-59	> -1.50	6/889 (0.67)	19.47 (11.36, 33.32)	12.73 (6.68, 24.23)
	-1.50 to -2.49	3/391 (0.77)	8.48 (4.89, 14.70)	10.76 (6.00, 19.29)
	<=-2.50	3/104 (2.88)	5.46 (2.69, 11.10)	6.50 (3.16, 13.38)
60-64	> -1.50	7/880 (0.81)	14.62 (9.01, 23.73)	9.76 (5.36, 17.77)
	-1.50 to -2.49	12/554 (2.17)	6.37 (3.98, 10.24)	8.25 (4.80, 13.91)
	<=-2.50	3/194 (1.55)	4.10 (2.16, 7.78)	5.44 (2.82, 10.47)

*estimated time to mjr or clinical vertebral fracture, based on a competing risks quantile regression (Peng and Fine, 2009), adjusted for the sample averages of the other covariates in the model. For women with T-score <=-2.50 at baseline, data were adjusted for age, BMI, race/ethnicity, current smoking, current estrogen use, current use of oral glucocorticoids, self-reported rheumatoid arthritis, parent with hip fracture, and WHI-CT vs. OS participation. For women with T-score > -2.50 at baseline, data were adjusted for continuous BMD and age term

GourlayWHIabstract799table

***Disclosures: Margaret Gourlay**, None.*

LB-SU27

Predictors of non-vertebral fracture in older Chinese men and women: MrOS and Ms Os (Hong Kong). Timothy Kwok*. Hong Kong

Kwok T MD, Khoo CC MPhil, Leung J MSc, Woo J MD

Introduction - A prospective cohort study was performed to identify clinical risk factors of non-vertebral fractures in older Chinese men and women

Methods - 4000 community-dwelling Chinese men and women with average ages of 72.4 and 72.6 years were followed up for an average of 6.5 and 8.8 years respectively. At baseline, they were interviewed by a structured questionnaire, underwent clinical measurements including total hip BMD measurements by dual X ray absorptiometry (DXA). The incidence of non-vertebral fractures was ascertained by self report and electronic medical record, and confirmed by X ray. Stepwise Cox regression models were used to identify risk factors of non-vertebral and fragility fractures.

Results - The incidence rates of non-vertebral fractures were 10.3 and 20.5 per 1000 person years in men and women respectively. 81.2% and 99.0% of fractures were

fragility fractures in men and women respectively. The age adjusted Hazard ratio (HR) of total hip BMD for non-vertebral fractures was 1.43(95% CI 1.19-1.70) and 1.40 (1.25-1.58) per SD decrease in men and women respectively. In the multivariable stepwise Cox regression model for non-vertebral fractures with total hip BMD as covariate in men, age?80, history of fall in the past year, fracture at or after age of 50 years or chronic obstructive pulmonary disease, impaired visual depth perception, and low physical health related quality of life (SF12) were the significant factors. In women, the corresponding factors were fracture at or after age of 50 years, low visual acuity and slow narrow walking speed. ROC curve areas predicted by BMD increased when clinical risk factors were included, especially in men.

Conclusion - Clinical risk factors have additive value to hip BMD in predicting non-vertebral fractures in older Chinese people, especially in men.

Key Words: Fracture, bone; Asian continental ancestry group; Aged; Risk factors.

***Disclosures: Timothy Kwok**, None.*

LB-SU28

Long term effects of higher dietary calcium intake on vertebral fractures and severe abdominal aortic calcification in older Australians. Peter Ebeling[1], Dallas English[1], Caryl Nowson[2], Robin Daly[3], Belal Khan*[1]. [1]The University of Melbourne, Australia, [2]School of Exercise & Nutrition Sciences, Deakin University, Australia, [3]Centre for Physical Activity & Nutrition Research, Deakin University, Australia

Introduction: Higher dietary calcium intakes (DCI) prevent age-related bone loss; however, data on fracture prevention are equivocal. Evidence on the influence of DCI on the association between vertebral fractures and abdominal aortic calcification (AAC) is scant. Vertebral fractures and bone mineral density (BMD) may both be associated with AAC due to a common pathogenesis.

Aims and Methods: We assessed the long-term associations between DCI and prevalent vertebral fractures and AAC, measured by lateral thoraco-lumbar radiographs, and hip and spine BMD, by DXA, in 407 men and women, followed for a mean (SD) of 17.7 (1.1) years, randomly selected from a large prospective cohort study (MCCS). DCI was assessed using a food frequency questionnaire at entry (1990-1994). During follow-up (2010-2011), vertebral fractures were graded using the semiquantitative(SQ)-method and AAC was quantified using a 24-point score. Fasting serum lipids and serum 25-hydroxyvitamin D (25D) were also measured.

Results: The mean (SD) baseline age was 53 (5.4) years. 103 (29.8%) participants had 172 prevalent vertebral deformities between T5-L4, while 229 participants (66.2%) had prevalent AAC between L1-L4. Compared with the low DCI group (<500 mg/d), the risk of vertebral deformities was significantly lower (OR 0.46; 95% CI, 0.27-0.78) in the high DCI group (≥1300 mg/d), and there was a non-significant 50% decrease in the risk of AAC (OR 0.50; 95%CI, 0.23-1.08). When only moderate/severe vertebral fractures (OR 0.31; 95%CI 0.12-0.78) or severe AAC (OR 0.35; 95%CI, 0.13-0.94) were considered, the risk of both was significantly decreased with high DCI. High DCI tended to be associated with higher spine and hip BMD, but was only significantly related to higher femoral neck BMD in women ($\beta_{FemoralNeck}$ 0.04; 95%CI, 0.01-0.07). Tertiles of AAC were also positively associated with vertebral deformity grades (OR 1.44; 95%CI, 1.05-1.97) and inversely associated with whole body BMD (β -1.05; 95%CI, -1.98 - -0.11) independent of age, sex, serum 25D, cholesterol:HDL and lean mass:fat mass ratios.

Conclusion: Higher dietary calcium intake is associated with decreases in both vertebral fracture risk and severe abdominal aortic calcification, and maintenance of hip BMD in postmenopausal women. More severe abdominal aortic calcification was also associated with higher grade vertebral fractures and lower whole body BMD supporting the concept of a common pathogenesis.

***Disclosures: Belal Khan**, None.*

LB-SU29

Sexual Dimorphism in Sirtuin1 Regulation of Skeletal Aging. Rivka Dresner-Pollak*[1], Hanna Artsi[2], Einav Cohen-Kfir[3], Irina Gurt[2], Alon Bajayo[4], Teresita Bellido[5], Gal Ben Shalom[2]. [1]Hadassah-Hebrew University Medical Center, Israel, [2]Endocrinology & Metabolism Hadassah-Hebrew University Medical Center, Jerusalem Israel, Israel, [3]HEBREW UNIVERSITY Medicine Faculty, Israel, [4]Bone Laboratory Hadassah-Hebrew University Medical Center, Jerusalem Israel, Israel, [5]Indiana University School of Medicine, USA

Bone loss is an inevitable consequence of ageing. Recent advances in aging research identified the sirtuins as key regulators of the aging process and age-associated conditions. Others and we reported that Sirt1 deficiency results in decreased bone mass in mice (*Endocrinology* 152:4514-4524, 2011, *JBMR* 28:960-969, 2013). To understand the role of Sirt1 in skeletal aging we investigated the changes in structural and cellular phenotype in 129Sv Sirt1 haplo-insufficient mice (*Sirt1* $^{+/-}$) with aging.

μCT analysis of L4 and femur was performed in 1, 3, 5, 7 and 12 month-old female mice and up to 2 years in male mice. Gene and protein expression were determined. Osteocyte apoptosis was determined by Tunnel staining.

Reduced trabecular and cortical peak bone mass (-30% and -10% respectively) was found in the spine and femur of Sirt1$^{+/-}$ female but not in Sirt1$^{+/-}$ male mice. The rate of trabecular and cortical bone loss was similar in Sirt1$^{+/-}$ and WT mice of both genders. Femoral cortical porosity was 50% higher in the femurs of 7-month-old Sirt1$^{+/-}$ compared to WT female mice. No increased porosity was detected in the femurs of Sirt1$^{+/-}$ males. Consistent with these findings, trabecular and cortical osteocyte apoptosis was more than double in Sirt1$^{+/-}$ female mice accompanied by decreased DMP1 and increased sclerostin level.

Gene expression analysis of brown adipocyte markers revealed a marked reduction in PGC1α, Dio2, β3AR and PRDM16 in whole bone extracts obtained from 5-month-old Sirt1$^{+/-}$ female mice.

To explore the underlying mechanism of the sexual dimorphism, estrogen receptor alpha (ERα) and the androgen receptor (AR) were studied. Indeed, Sirt1 positively regulated ERα and negatively regulated AR in C3HT101/2 cells, primary bone marrow-derived mesenchymal and osteoclast cultures and in whole femoral extracts obtained from 6-8 week-old female and male mice.

To understand the relevance of these findings to skeletal aging, Sirt1 level was determined in whole femur extracts obtained from 3-and 12- month-old WT female mice and was found to decline by 50%.

Sirt1 regulates peak bone mass acquisition in 129Sv mice in a gender specific manner. Sirt1 regulates key cells in skeletal aging: the osteocyte, the longest lived cell in bone and the marrow adipocyte. The sexual dimorphism in skeletal effects of Sirt1 maybe explained but its opposite effects on ERα and AR expression in marrow mesnchymal stem cells, osteoblasts, osteoclasts and osteocytes.

***Disclosures: Rivka Dresner-Pollak**, None.*

LB-SU30

International Consensus on Diagnosis and Management of Osteonecrosis of the Jaw. Aliya Khan*[1], Archie Morrison[2], David Hanley[3], Dieter Felsenberg[4], Laurie McCauley[5], Felice O'Ryan[6], Ian Reid[7], Sal Ruggiero[8], Akira Taguchi[9], Sotirios Tetradis[10], Nelson Watts[11], Maria Luisa Brandi[12], Ed Peters[13], Theresa Guise[14], Richard Eastell[15], Angela M. Cheung[16], Suzanne Morin[17], Basel Masri[18], Cyrus Cooper[19], Sarah Morgan[20], Barbara Obermayer-Pietsch[21], Bente Langdahl[22], Rana Al Dabagh[23], K. Shawn Davison[24], Juliet Compston[25]. [1]McMaster University, Canada, [2]Dalhousie University, Canada, [3]University of Calgary, Canada, [4]Charité - Campus Benjamin Franklin, Germany, [5]University of Michigan School of Dentistry, USA, [6]The Permanente Medical Group, USA, [7]University of Auckland, Nzl, [8]New York Center for Orthognathic & Maxillofacial Surgery, USA, [9]Matsumoto Dental University, Japan, [10]University of California, Los Angeles, USA, [11]Mercy Health Osteoporosis & Bone Health Services, USA, [12]University of Florence, Italy, [13]University of Alberta, Canada, [14]Indiana University, USA, [15]University of Sheffield, United Kingdom, [16]University Health Network-University of Toronto, Canada, [17]McGill University, Canada, [18]Jordan Hospital, Jordan, [19]University of Southampton, United Kingdom, [20]University of Alabama at Birmingham, USA, [21]Medical university of Graz, Austria, [22]Aarhus University Hospital, Denmark, [23]University of Toronto, Canada, [24]University of Victoria, Canada, [25]University of Cambridge School of Clinical Medicine, United Kingdom

An International Osteonecrosis of the jaw (ONJ) Task Force was formed in 2012 and formalized key questions addressing the diagnosis and management of ONJ in oncology and osteoporosis patient populations. Following a comprehensive literature review with critical appraisal of the evidence, the questions were addressed and recommendations developed based on international consensus. ONJ is associated with high-dose intravenous bisphosphonate or denosumab therapy in oncology patients. The incidence of ONJ in the osteoporosis patient population has been estimated largely from surveys and retrospective studies at 0.001-0.01%. This may be only slightly higher than the background incidence of ONJ in the general population. ONJ has been described to occur in the absence of antiresorptive therapy (lingual mandibular sequestration and ulceration) in which case it appears to be a self- limited condition. The staging of ONJ now includes stage 0, an early stage of presentation without evidence of exposed bone, but with signs and symptoms of ONJ. Radiographic evidence of osteosclerosis or thickening of the lamina dura on plain films are features of stage 0 disease. It is not clear if all patients at stage 0 will necessarily progress to osteonecrosis and this requires more study. New insights into the pathophysiology of ONJ include effects of bisphosphonates on osteoclast inhibition and gamma delta T-cells in addition to local infection, inflammation and necrosis. Denosumab may contribute by inhibiting osteoclast function as well as possible effects on monocyte and macrophage function. Advances in imaging include cone beam CT enabling assessment of architecture with minimal radiation exposure in addition to MRI, bone scanning and PET. Good oral hygiene is key for prevention of ONJ. There is currently no evidence that withholding antiresorptive therapy reduces the risk of ONJ or the progression of the disease in osteoporosis patients. In those individuals at high risk for the development of ONJ, including oncology patients, antiresorptive therapy should be withheld following dental surgery until soft tissue closure with well epithelialized mucosa. Management of ONJ is challenging and is based on the stage, lesion size, comorbidities and contributing factors. Conservative therapy includes topical antibiotic mouth rinses and systemic antibiotic therapy. Localized surgical debridement is indicated in advanced nonresponsive disease with successful resolution in most cases.

***Disclosures: Aliya Khan**, None.*

LB-SU31

Densitometry comparison after five years of therapy in patients with continuous bisphosphonates (BF) vs. sequential treatment: 3 years of bisphosphonates follow by 2 years of Strontium Ranelate (SrR). Carolina Pelegrin*[1], Malena Alvarellos[2], Maria Valeria Premrou[2], Laura Elena Maffei[2]. [1]Consultorios Asociados de Endocrinologia, Argentina, [2]coleague, Argentina

Introduction: Osteoporosis is a disease characterized by alteration of bone turnover with an increased bone resorption and decreased bone formation. The BP inhibits bone resorption and the SrR is a dual drug stimulating bone formation and inhibiting resorption.

Objectives: Evaluate densitometry response in patients (p) who had received five years of continued BP vs. patients who had received three years of BF treatment and then rotated to SrR.

Material and Methods: We retrospectively analyzed the medical histories of (p) treated at our center, evaluating densitometry changes in 4th and 5th year of BP treatment vs. SrR.

Results: We analyzed 79 women: 41 received continuous BP (74.1 ± 9 years), and 38 RS (70.2 ± 8.4).

Lumbar spine BMD (LS) to 3rd year in the SrR group 0.874 ± 0.116 36p , 0815 ± 37 BP group 0.088 (*p* 0.016). LS SrR group 4th year 0.861 ± 0.096 36 p and 0.876 ± 0.100 BP group (p 0.519).LS SrR group 5Th year in 30 p 0.901 ± 0.094 and 34 p BP group 0.868 ± 0.091(*p* 0.159).

Femoral neck BMD (FN) on 3rd year in 34 pat SrR group 0.666 ± 0.112 and 35 p BP group 0.719± 0.083 (*p* 0.03). FN on 4th year in 35 p SrR group 0,718 ± 0,100 and 34 p on po BP 0,716 ± 0,891 (*p* 0,926).FN on 5th year in 30 SrR p 0.739 ± 0.095 and 34 p on BP0.723 ± 0.084 (*p* 0.471).During 4th year of treatment improved 29 SrR p (82.8%) BMD increased 6.76 ± 4.92%, and 24 with BP (66.7%), increased 4.13 ± 2.64 (p 0,01).

We observed decrease in 6 SrR p (17.1%) and 12 with BP (33.3%) *p* 0.41.

This improvement was progressive with SrR after 5th year of treatment 26 p improved LS (89.7%) increased 8.90 ± 5.21 and 22 BP p (64.7%) increased 4.72 ± 3, 60 (*p* 0.003)

3 SrR p decreased (10.3%) vs. 12 BP p (35.3%) *p* 0020

After 5th years of treatment 24 SrR pat improved in FN (72.7%) inc 7,60± 8,31and 18 BP pat (52.9%) inc 2.61 ± 2 (p 0.009)

9 SrR pat decreased (27.3%) and 16 with BP (47.1%) After 5th year in FN 25 SrR pat (92.6%) inc 8.95 ± 9.5 and 22 with BP (64.7%) inc 2.71 ± 2.85 2 SrR pat decreased in FN(7.40%) and 12 with BP (35.3%)

Conclusions: Osteoporosis treatment is prolonged and it is often necessary rotate it to optimize the response or decrease adverse events. SrR showed a significant and progressive increase on BMD after BP administration in LS and FN, this response being higher than the continuous BP administration. Therefore we consider that BP-SrR sequential therapy is an attractive alternative in osteoporosis treatment.

***Disclosures: Carolina Pelegrin**, None.*

LB-SU33

Preosteoblasts are targets of hyperlipidemia-induced PTH resistance; a role of reactive oxygen species. Yin Tintut*[1], Xin Li[1], Jamie Garcia[1], Sidney Iriana[1], Jinxiu Lu[1], Ivo Kalajzic[2], David Rowe[2], Linda Demer[3]. [1]University of California, Los Angeles, USA, [2]University of Connecticut Health Center, USA, [3]David Geffen School of Medicine At University of California Los Angeles, USA

Lipid oxidation products initiate inflammatory reactions leading to pathogenesis of atherosclerosis. Evidence shows that they also contribute to bone loss by inhibiting differentiation and PTH receptor (PTH1R) expression in osteoblasts. We recently found that bone anabolic effects of PTH(1-34) are blunted in hyperlipidemic mice and that the PTH effects are restored by antioxidants. However, it is not clear which bone cell types are the targets of PTH(1-34) and/or inflammatory bioactive lipids. To investigate the effects of hyperlipidemia at the cellular level, hyperlipidemic *Ldlr*$^{-/-}$ mice were bred with Col3.6GFPtpz mice, in which preosteoblasts/osteoblasts carry a topaz fluorescent label, and with Col2.3GFPcyan mice, in which more mature osteoblasts/osteocytes carry a cyan fluorescent label. Daily PTH(1-34) treatment induced parameters of cortical bone growth, as expected, in Tpz-WT and Cyan-WT mice, but not in the Tpz-*Ldlr*$^{-/-}$ or Cyan-*Ldlr*$^{-/-}$ mice. Histological analyses of trabecular bone surfaces in femoral as well as calvarial bones showed that PTH(1-34) increased fluorescence intensity in WT-Tpz mice, but not in Tpz-*Ldlr*$^{-/-}$ mice. In contrast, PTH(1-34) did not alter fluorescence intensity in femoral cortical envelopes of either WT-Cyan or *Ldlr*$^{-/-}$-Cyan mice. To test the inhibitory mechanisms of bioactive lipids on PTH1R expression preosteoblasts, MC3T3-E1, were used. Treatment of cells with bioactive lipids induced intracellular oxidant stress and inhibited PTH1R expression, which was rescued by pretreatment with the antioxidant, Trolox. The inhibitory effects on expression of PTH1R as well as PTH-induced osteoblastic genes were mimicked by xanthine/xanthine oxidase, a known generator of reactive oxygen species. These findings suggest an important role of preosteoblasts as the target cells and downregulation of PTH receptor expression mediated by intracellular oxidant stress as the mechanisms in hyperlipidemia-induced PTH resistance.

***Disclosures: Yin Tintut**, None.*

LB-SU34

Osteoporosis Knowledge, Self-Efficacy, and Health Beliefs among Chinese Men and Women with HIV. Evelyn Hsieh*[1], Liana Fraenkel[1], Elizabeth Bradley[2], Weibo Xia[3], Qu Cui[4], Karl Insogna[5], Taisheng Li[4]. [1]Yale School of Medicine, Section of Rheumatology, USA, [2]Yale School of Public Health, USA, [3]Peking Union Medical College Hospital, Department of Endocrinology, Peoples Republic of China, [4]Peking Union Medical College Hospital, Department of Infectious Diseases, China, [5]Yale University School of Medicine, USA

Prior studies demonstrate reduced bone density and increased rates of fracture among patients with HIV. Validated scales exist for measuring knowledge, self-efficacy for behavioral change, and health beliefs related to osteoporosis, but have not yet been applied to populations with HIV. Better understanding of these factors can help increase the effectiveness of osteoporosis interventions.

Subjects were drawn from a multi-center trial in China comparing 3 antiretroviral regimens. Volunteers completed a questionnaire with 6 sections including: 1. Fracture risk assessment, 2. International Physical Activity Questionnaire (IPAQ), 3. Calcium and vitamin D intake scale, 4. Osteoporosis Knowledge Test (OKT), 5. Osteoporosis Self-Efficacy Scale (OSES), and 6. Osteoporosis Health Beliefs Scale (OHBS). Demographic data were obtained from the parent study.

In total 245 subjects participated (182 men, 63 women). Median age (37 yrs), and average BMI (21.7 ± 0.2 kg/m2) were similar for both sexes. Men were more educated and more likely to report smoking (51.2 v. 5.3%, p=0.000) and alcohol use (26.7 v. 12.3%, p=0.030) than women. Calcium and vitamin D supplement use was low for both sexes (7.6 v. 12.0%, p=0.294; 9.4 v. 6.9%, p=0.789). Moderate physical activity level was most common (41.1 v. 44.6%, p=0.643). On average subjects reported consuming calcium and vitamin D rich foods less than once a week. OKT scores were low for both sexes, yet OSES scores reflected self-confidence regarding ability to adopt behavioral change (Table 1). Subjects felt neutral regarding personal susceptibility to and seriousness of an osteoporosis diagnosis. Perceived benefits of exercise and calcium intake were high for all subjects, however men perceived fewer barriers to exercise and calcium intake compared with women. Both sexes reported high health motivation scores (Table 1). Multiple regression analysis adjusted for age, sex and BMI showed that intake of calcium and vitamin D rich foods was directly correlated with OKT and OSES calcium score, whereas physical activity correlated with higher OSES exercise score and lower education level, but not with OKT exercise score.

Knowledge regarding osteoporosis is low among Chinese men and women with HIV, and women perceive more barriers to behavioral change than men. Calcium and vitamin D intake and physical activity levels have unique predictors. Understanding these associations may aid in the development of targeted behavioral interventions.

Test	Men (N=182)	Women (N=63)	*p-value*
Osteoporosis Knowledge Test [a]			
Exercise *mean ± SEM*	6.2 ± 0.3	6.0 ± 0.5	0.769
Calcium *mean ± SEM*	6.5 ± 0.3	6.5 ± 0.4	0.990
Osteoporosis Self-Efficacy Test [b]			
Exercise *median (IQR)*	66.7 (41.7-85)	76.7 (53.3-91.7)	0.789
Calcium *median (IQR)*	66.7 (43-80)	80 (55-95)	0.760
Osteoporosis Health Beliefs Scale [c]			
Perceived susceptibility *median (IQR)*	16 (12-18)	17 (13-19)	0.305
Perceived seriousness *median (IQR)*	18 (16-21)	18 (16-21)	0.545
Perceived benefits - exercise *median (IQR)*	24 (19.5-24)	22.5 (18-25)	0.313
Perceived benefits - calcium *median (IQR)*	22 (19-24)	22 (18-24)	0.544
Perceived barriers - exercise *median (IQR)*	16 (12-18)	18 (15-19)	0.010
Perceived Barriers - calcium *median (IQR)*	16 (13-18)	18 (14-19)	0.005
Health Motivation *median (IQR)*	23 (19-24)	23 (20-25)	0.656

a. Scale range: 0 (lowest) to 16 (highest)
b. Scale range: 0 (not at all confident) to 100 (very confident)
c. Scale range: 6 (strongly disagree) to 30 (strongly agree)

Table 1. Osteoporosis Knowledge, Self-Efficacy, and Health Beliefs, by Sex

***Disclosures: Evelyn Hsieh**, None.*

LB-SU35

Macrophages support proliferation, invasion, and angiogenesis in thyroid cancer. Sun Wook Cho*[1], Sun Kyoung Han[2], Hyun Jin Sun[1], Ka Hee Yi[2], Young Joo Park[2]. [1]Department of Internal Medicine, National Medical Center, South Korea, [2]Department of Internal Medicine, Seoul National University College of Medicine, South Korea

Bone has an essential part in tumor progression by supplying numerous types of bone marrow cells to the tumor microenvironment. Among them, a subset of macrophages (tumor associated macrophages, TAMs) has been identified as having an important role in the progression of several human cancers. However, their characteristics and biological mechanisms still remain elusive. The purpose of this study was to determine the role of bone marrow-derived macrophages in thyroid cancer. First, we performed an in vitro experiment with a human thyroid cancer cell line (BHP10-3) and mouse primary bone marrow (BM) derived macrophages. Co-culture of BHP10-3 with the macrophages showed a significant increase in tumor cell survival and a decrease in cell apoptosis compared to a culture of BHP10-3 alone. Cell migration and invasion were enhanced in the BHP10-3/macrophage co-cultured group

compared to the BHP10-3 alone group. Furthermore, treatment with conditioned medium (CM) from the BHP10-3/macrophage co-culture group significantly enhanced tube formation potentials in human endothelial cells (HUVEC) compared to the control CM from the BHP10-3 alone group. Altogether, BM derived macrophages support tumor cell survival, invasion, and angiogenesis in vitro. Subsequently, we performed in vivo ectopic tumor implantation with nude mice. Co-transplantation of BHP10-3 and macrophages produced significantly bigger-sized tumors compared to the transplantation of BHP10-3 alone, which were attenuated by inducing the apoptosis of phagocytic cells by administrating clodronate liposomes. CD31 and VEGF-A gene expression correspondingly increased in tumors co-transplanted with macrophages compared to BHP10-3 cells transplanted alone. These changes were inhibited by the treatment of clodronate liposomes. Finally, to further characterize TMAs in thyroid cancer, macrophages (pre-stained with PKH26 dye) were sorted from tumor xenografts by flow cytometry, followed by gene expression analyses. Genes associated with alternatively activated macrophages (M2 type) (IL-10, IL-4, TGFβ, CD163), efferocytosis (clearance of apoptotic cells) (Scavenger receptor A, mannose receptor, Mer, Mer-6E) and angiogenesis (CD31, VEGF-A, MMP9) were up-regulated in macrophages from thyroid cancer xenografts compared to non-transplanted macrophages. In summary, BM derived macrophages promote tumor growth and angiogenesis in the thyroid cancer microenvironment through M2 polarization. These findings, herein, suggest a novel function of BM derived macrophages in a tumor microenvironment and a potential therapeutic target in human thyroid cancer.

***Disclosures: Sun Wook Cho**, None.*

LB-MO01

T-type Voltage Sensitive Calcium Channel (T-VSCC) Is a Key Player in Load-Induced Bone Mechanotransduction and a Novel Target for Osteoarthritis Treatment. Padma Srinivasan*[1], Andris Kronbergs[2], Christopher Price[1], Liyun Wang[1], Randall Duncan[1], Catherine Kirn-Safran[1]. [1]University of Delaware, USA, [2]IU School of Medicine, USA

Involvement of subchondral bone in osteoarthritis (OA) is well established, as indicated by the presence of osteophytes and subchondral bone sclerosis in late OA patients. It is known that soluble metabolites released from mechanically stimulated osteoblasts enhance catabolic changes in the adjacent cartilage tissue.

In this study, we used a genetically-engineered mouse model carrying a null mutation for the pore forming subunit of the T-type voltage sensitive calcium channel (T-VSCC, also known as Cav3.2) to demonstrate that reduced mechanosensitivity in T-VSCC subchondral bone is chondroprotective. In addition, we show that T-VSCC is essential for the anabolic response of bone cells to load. Selective inhibition of T-VSCC in murine osteoblastic cells (MC3T3) prior to fluid shear stress (FSS ~3.5 dynes/cm^2 for 2 hours) significantly reduced the expression of genes such as cyclooxygenase 2 (*Cox2*) and osteopontin (*Spp1*) that are known to be initiators of a pro-inflammatory response and bone formation. Additionally, treatment of chondrocytes with conditioned media (CM) obtained from sheared MC3T3 cells induced expression of markers of hypertrophy. This early osteoarthritic response was nearly abolished when primary chondrocytes were treated with CM obtained from MC3T3 cells sheared in the presence of a specific inhibitor of T-VSCC. These results indicate that T-VSCC is upstream to the release of catabolic factors from osteoblasts and therefore can serve as a target for blocking subchondral bone-induced cartilage degeneration in OA.

To understand the link between T-VSCC and OA, we compared OA damage in T-VSCC knockout and control mice using a load-induced OA model (Fig.1A&B) modified from Poulet et al., 2011 [1]. OA histological scores obtained in knees subjected to the loading regimen shown below (Fig. 1C) indicate that T-VSCC knockout mice exhibit smaller OA damage than the wild-type age-matched controls. Together our data strongly support the idea that T-VSCC plays an important role in the joint response to injury related to posttraumatic OA. Ongoing studies will determine whether pharmaceutical blocking of T-VSCC may be used as a novel therapeutic approach for treating patients at risk to develop OA, such as young adults who suffer from abnormal joint loading due to previous joint injury.

1. Poulet B et al., Arthritis Rheum. 63:137-47, 2011.

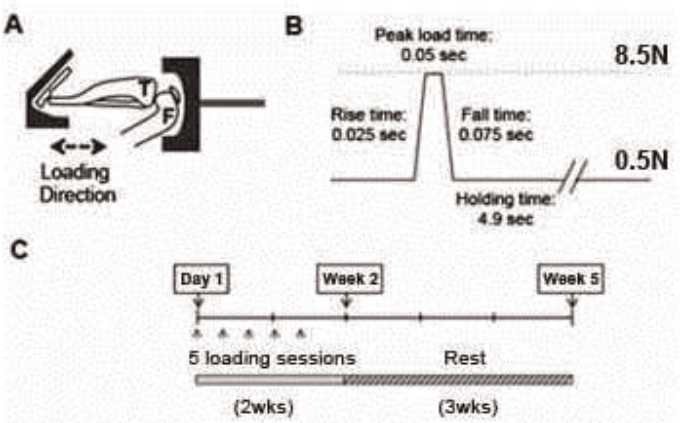

Figure 1: Loading model (A), pattern (B) and regimen (C)

***Disclosures: Padma Srinivasan**, None.*

LB-MO02

Maturity-Sensitivity of Physical Activity on Skeletal Growth: A 15-year Mixed-Longitudinal Analysis. Brittney Bernardoni*[1], Tamara Scerpella[2], Jodi Dowthwaite[3], Quefeng Li[1], Sijian Wang[4]. [1]USA, [2]University of Wisconsin, USA, [3]SUNY Upstate Medical University;Syracuse University, USA

PURPOSE: To examine the maturity-sensitivity of physical activity on site-specific bone acquisition during growth; to quantify maintenance of skeletal benefits to early adulthood.

METHODS: Female gymnasts and non-gymnasts provided >15y of longitudinal data. Gymnasts were divided into 2 maturational activity exposure groups: PERI, quit gymnastics -1 to +1y peri-menarche (-0.1 ± 0.4 y); and POST, quit >1.75y post-menarche (4.1 ± 1.9 y). Subjects underwent annual whole body and regional (forearm, hip, lumbar spine) DXA scans; anthropometrics, gymnastics exposure (gym hrs), physical activity (PA) and maturity were assessed simultaneously. Multilevel modeling analyzed group differences in bone growth, controlling for bone size, age at menarche and non-gymnastics organized PA; data was centered at menarche (men age=0).

RESULTS: 56 subjects (n=33 NON, n=10 PERI, n=13 POST) provided growth data from men age -2y to +8y. Mean gym hrs for PERI and POST did not differ except during +1 to 2y (as PERI were quitting gymnastics). Height and lean mass means differed only for +6 to 7y, when NON were taller than POST ($p < 0.05$).

At both radius and femoral neck, gymnastics participation produced advantages in geometry, bone mineral content (BMC) and strength from men age -2 to 8y; advantages were maintained to young adulthood (5-80%, men age +8y). Distal radius metaphyseal area was increased in PERI vs. NON, with no additional benefit for POST. With continued exposure, POST gained additional metaphyseal and diaphyseal BMC (advantage vs. PERI, men age +2y=7-10%, $p<0.05$), and tended to improve diaphyseal area (advantage over PERI, men age +1y=3.5%, p=0.06; men age +2y=4.5%, p=0.09). These adaptations yielded large skeletal strength advantages for POST vs. NON at +7 to 8y: UD IBS=11% ($p<0.01$) and 1/3 Z=74% ($p<0.0001$). Proximal femur narrow neck (NN) strength adaptations were a product of smaller NN width and endosteal diameter, yielding advantages in cortical thickness (CT), BMC and buckling ratio. PERI had 8% greater CT vs. NON at men age +4y (p=0.037). Continued exposure gave POST even greater advantages at men age +4y (8% BMC, 13% CT, 13.5% BR, $p<0.001$) and +8y (5% BMC, 11% CT, 14.4% BR $p<0.05$). We did not identify maturity-specific loading effects at lumbar spine or total body.

CONCLUSIONS: Skeletal advantages to exercise during growth are site-specific and maturity-sensitive. Advantages persist to early adulthood, even with peri-menarcheal activity cessation.

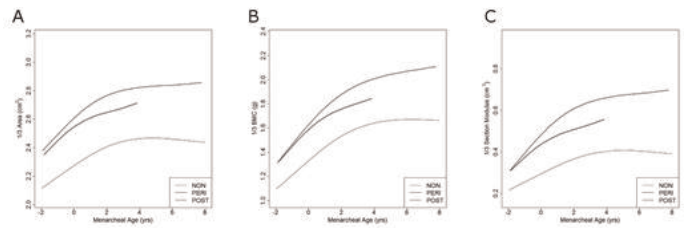

Diaphyseal Radius

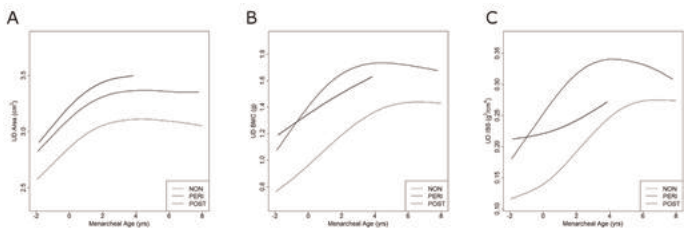

Metaphyseal Radius

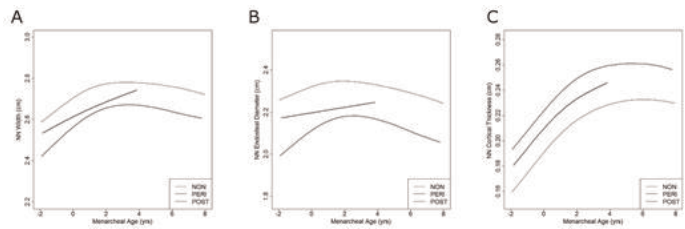

Femoral Neck

***Disclosures: Brittney Bernardoni**, None.*

LB-MO03

Could casein kinase-2 interacting protein-1 (CKIP-1) be postulated as a molecular target for promoting aged fracture repair in females?. Jin Liu*[1], Baosheng Guo[1], Yixin He[1], Lei Dang[1], Xiaohua Pan[2], Lingqiang Zhang[3], Aiping Lu[1], Ge Zhang[1]. [1]Institute for Advancing Translational Medicine in Bone & Joint Diseases, School of Chinese Medicine, Hong Kong Baptist University, Hong Kong SAR, China, Hong Kong, [2]Jinan University & Hong Kong Baptist University Joint Laboratory of Innovative Drug Development, Institute of Biomedicine (Guangzhou); Department of Orthopedics in Second Hospital of Medical College (Shenzhen), Jinan University, China, China, [3]Beijing Institute of Radiation Medicine, State Key Laboratory of Proteomics, Beijing Proteome Research Center, Beijing, China, China

Aim: CKIP-1 plays an important role in regulating BMP signaling through interacting with Smurf1 to enhance Smad1/5 degradation and its gene-deficient mice exhibit accelerated osteogenesis (Lu et al., Nat Cell Biol, 2008). The purpose of this study was to not only compare the difference in CKIP-1 within female callus between aged and adult fractured patients/mice, but also investigate the relationship between CKIP-1 and angiogenesis/osteogenesis during fracture across adult and aged mice.

Materials and methods: Callus specimens from 19 female fractured patients (Table 1) undergoing surgery to treat malreduction were collected and randomly divided into the aged group (65–80 years; n=11) and adult group (40–50 years; n=8). The specimens were subjected to western blotting for quantifying protein expression of CKIP-1, Smurf1 and Smad1/5. Radiographic/clinical union time of the fracture site was recorded, respectively. Bilateral femur transverse fractures were created in 20 female 15-month-old mice (aged group) and 20 female 15-week-old mice (adult group). At post-fracture week 2 and 4, ten mice in each group were sacrificed and all the calluses from left femurs were subjected to western blotting for quantifying protein expression of CKIP-1, Smurf1 and Smad1/5. 3-D Micro-CT analysis was performed on the callus specimens from right femurs in both groups for evaluating callus neovascularization at post-fracture week 2 and callus mineralization at post-fracture week 4.

Results: There was higher CKIP-1 expression and lower Smad1/5 expression in female callus from aged patients/mice when compared to adult ones, whereas no significant difference was found in Smurf-1 expression between aged and adult groups in patients and mice (Figure 1). The time of radiographic/clinical union was delayed in aged patients when compared to that in adult ones (Left, Figure 2). Micro-CT-based angiography showed fewer and smaller blood vessels in aged mice at early stage when compared to those in the adult mice. Reconstructed calluses showed lower bridging mineralization tissues within the gap in aged mice than adult mice at the later stage (Right, Figure 2). The CKIP-1 expression level was negatively correlated with the vessel volume and the bone mineral content (Figure 3).

Conclusions: CKIP-1 could be further postulated as a molecular target for promoting fracture repair in aged females.Key words: CKIP-1; Aged fracture repair

Table 1 Demography of Patients Included in This Study

Adult Group (n=8)			Aged Group (n=11)		
Gender	Age	Local.	Gender	Age	Local.
F	40	Humerus	F	76	Humerus
F	43	Humerus	F	73	Humerus
F	50	Humerus	F	80	Femur
F	49	Femur	F	71	Femur
F	50	Femur	F	65	Femur
F	42	Femur	F	68	Tibia
F	47	Tibia	F	75	Tibia
F	49	Tibia	F	69	Tibia
			F	77	Tibia
			F	78	Radius
			F	71	Radius

F, female. Local, fracture location.

Table 1

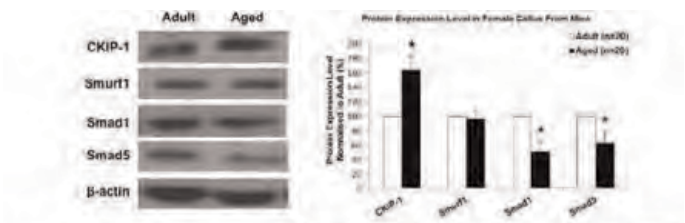

Figure 1 CKIP-1, Smurf1 and Smad1/5 expression levels in the female callus from adult and aged patients/mice. Representative electrophoretic bands for expression of CKIP-1, Smurf1 and Smad1/5 in female callus from adult and aged patients by western blots (left). Quantification of CKIP-1, Smurf1 and Smad1/5 in the callus from adult and aged female mice by western blot (right). The data from all the three patients in each respective group were pooled together for inter-group comparison. Representative electrophoretic bands for protein expression in mouse callus and quantitative data of protein expression in human callus not shown here. Note: *P < 0.05 for 'Adult' vs. 'Aged'.

Figure 1

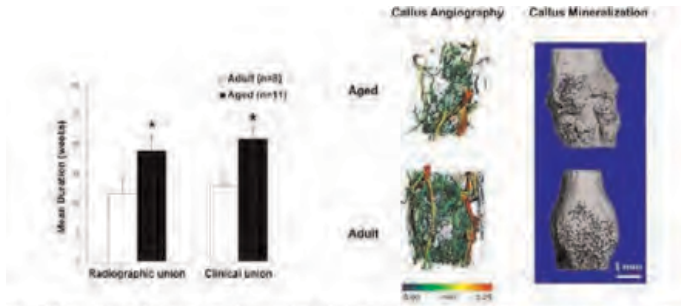

Figure 2 Different status of fracture healing between adult and aged patients/mice. The time of radiographic/clinical union in adult and aged patients (left). Representative images for micro-angiography at 2 weeks post fracture and callus mineralization at 4 weeks post fracture from adult and aged mice (Right). Note: *P<0.05 for 'Adult' vs. 'Aged'.

Figure 2

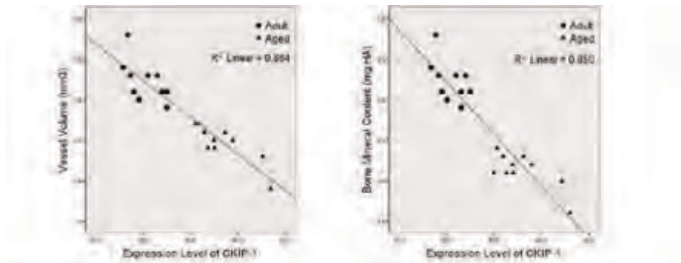

Figure 3 Correlation analysis between the CKIP-1 expression level and vessel volume (left) / bone mineral content (right) during fracture healing across adult and aged mice (P<0.001 for both).

Figure 3

***Disclosures: Jin Liu**, None.*

LB-MO04

The interaction of force and repetition on bone and cartilage in an operant rat model of work-related musculoskeletal disorders. Vicky Massicotte*[1], Steven Popoff[2], Sean Gallagher[3], Jeffrey Driban[4], Ann Barr-Gillespie[5], Mary Barbe[2]. [1]Temple University, USA, [2]Temple University School of Medicine, USA, [3]Auburn University, USA, [4]Tufts Medical Center, USA, [5]Pacific University, USA

The relationship of musculoskeletal risk factors (force and repetition) on bone and cartilage was examined for the first time using an operant rat model of repetitive reaching and pulling. We examined changes in the distal radial metaphysis and articular cartilage occurring with performance of a handle-pulling task for 12 weeks at one of four repetition and force levels: 1) low repetition low force (LRLF), 2) high repetition low force (HRLF), 3) low repetition high force (LRHF), or 4) high repetition high force (HRHF). Rats performed one of these tasks for 12 wks, 2 hrs/day, in four 30 min sessions/day, with 1.5 hr breaks between sessions, 3 days/wk. Results were compared between task groups and to age-matched controls. MicroCT of the radial metaphysis showed a force x repetition interaction effect (2-way ANOVA: $p<0.0001$), with a significant decrease in trabecular bone volume (BV/TV) in the radial metaphysis of HRHF rats ($p<0.01$, compared to the other groups), while the HRLF rats showed a trend towards an increase in trabecular bone volume. Serum CTX, measured using ELISA, showed a force x repetition interaction effect (2-way ANOVA: $p=0.04$), with increased levels in HRHF rats ($p<0.01$, compared to the other groups). Serum osteocalcin showed a force x repetition interaction effect (2-way ANOVA: $p<0.0001$), with increased levels in LRHF and HRLF rats ($p=0.05$ compared to the other groups). In the distal radius articular cartilage, histological Mankin scoring showed a force x repetition interaction effect (2-way ANOVA: $p=0.002$), with increased pathology in 12-week HRHF rats ($p=0.05$, compared to the other groups). These pathological changes included loss of proteoglycan content (reduced Safranin O staining), altered tidemark regions and presence of subchondral cysts. Taken together, these results show a significant interaction between the critical musculoskeletal risk factors of force and repetition, consistent with a fatigue failure process in musculoskeletal tissues. This is demonstrated by the catabolic responses in the bone and cartilage of the distal radius in response to 12 weeks of HRHF loading. Thus, high force tasks exhibit a rapid escalation in risk for musculoskeletal disorders when combined with high repetition. In contrast, the distal radial bone demonstrated an anabolic response to 12 weeks of HRLF and LRHF loading, a finding that indicates that bone can adapt to these moderate demand tasks.

***Disclosures: Vicky Massicotte**, None.*
This study received funding from: NIAMS/NIH and NIOSH

LB-MO05

Disuse sufficient to cause bone loss increases osteocytes' expression of sclerostin but has no effect on osteocyte RANKL. Peter Delisser*[1], Lee Meakin[1], Gabriel Galea[1], Lance Lanyon[2], Larry Suva[3], Joanna Price[1]. [1]University of Bristol, United Kingdom, [2]Royal Veterinary College, United Kingdom, [3]University of Arkansas for Medical Sciences, USA

The recent report[1] that, in mice at least, osteocytes are a major source of RANKL has led to the inference that it is by this means that these mechanically-responsive cells influence osteoclast recruitment, differentiation and activation in the processes of mechanically-related control of bone mass and architecture. This assumption appears to be supported by the finding that mice lacking RANKL do not show bone loss with tail suspension.

We attempted to relate changes in expression of RANKL and sclerostin in osteocytes with disuse-related bone loss associated in tibias of mice in limbs paralysed by unilateral sciatic neurectomy.

Seventeen week old female C57BL/6 mice underwent right sciatic neurectomy and left sham operation. They were sacrificed in groups; for qRT-PCR analysis for RANKL and SOST on day 3 (n=7) and day 14 (n=8), immunolocalisation of RANKL and sclerostin (n=4, day 4) and for microCT assessment of bone loss (n=8, day 21).

As expected, disuse as a consequence of sciatic neurectomy was associated with a significant loss of bone both in the proximal cancellous region (BV/TV -44.5%, $p<0.001$) and in the cortical compartment (-18.5% $p<0.001$ at 37% of their length from their proximal ends). Disuse had no effect on the periosteally enclosed area at this level (+2.7%, p=0.09), while cortical bone area was reduced (-11.6% $p<0.001$) and medullary area expanded (+29.3% $p<0.001$). The number of sclerostin immunopositive osteocytes was increased 4 days after neurectomy (+35.8% $p<0.01$) and osteocyte sclerostin mRNA expression elevated (+118% $p<0.05$) at day 14. In contrast, RANKL mRNA expression was unchanged between control and paralysed limbs at 3 and 14 days (+8.3%, p=0.76 and -21.2%, p=0.23). RANKL immunolocalisation was similarly unaffected (-0.2%, p=0.97 at 4 days).

These data support previous studies[2] showing that osteocytes respond to reduced loading in their surrounding matrix by increasing secretion of sclerostin.

The absence of any changes in RANKL with disuse suggests that RANKL is not involved in this resorption response, an observation that is incompatible with the view that RANKL derived from osteocytes is a necessary or universal influence in the recruitment, differentiation or activity of osteoclasts.

References:
1. Xiong J et al, Nat Med 17:1235-1241, 2011.
2. Moustafa A et al, Osteoporos Int Apr;23(4):1225-34., 2012.

***Disclosures: Peter Delisser**, None.*

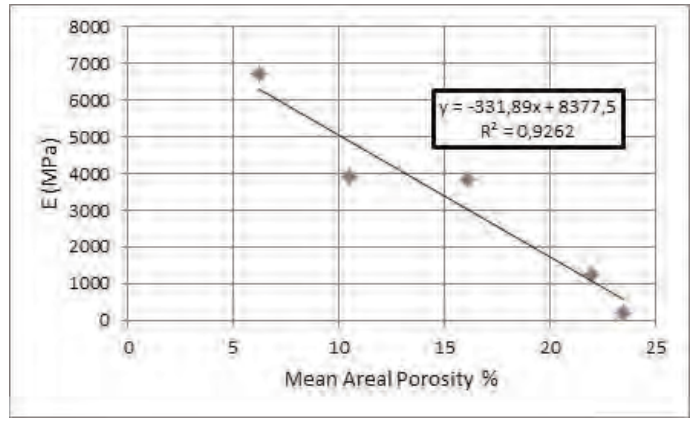

Young Modulus vs areal porosity

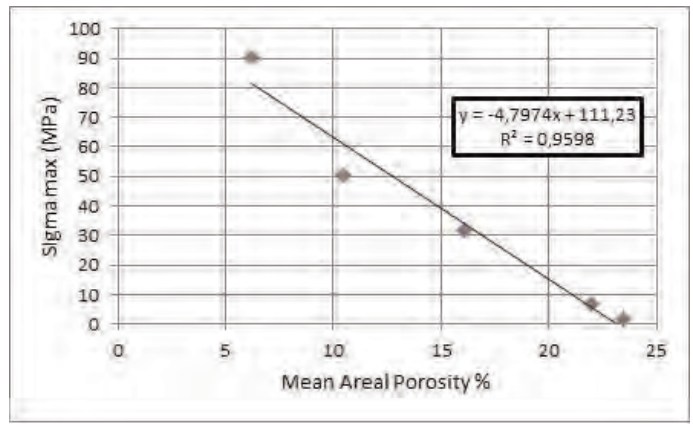

Ultimate stress vs areal porosity

***Disclosures: Wafa Skalli**, None.*

LB-MO06

Relationship between cortical bone porosity and mechanical properties in children with osteogenesis imperfecta : a preliminary study. Wafa Skalli*[1], Dominique Saletti[1], Clayton Adam[1], Vasiliki Vardakastani[1], Jean-Marc Allain[2], Pierre Mary[3]. [1]Arts et Métiers ParisTech, France, [2]Ecole Polytechnique, France, [3]Hôpital Armand Trousseau, France

Osteogenesis Imperfecta (OI) is a bone disease caused by abnormal type I collagen synthesis, resulting in increasing bone porosity and fragility. While subject specific biomechanical models could help in bone strength assessment for these patients, the necessary *in vivo* assessment of subject specific bone material properties is a major challenge, particularly for children. During surgery, very small bone fragments can be collected, allowing for mechanical testing at a mesoscopic (few millimeters) scale. In order to progress towards quantitative OI bone assessment in vivo, the aim of the current study is to search for correlations between cortical bone mechanical properties and microarchitecture.

Residual lower limb bone fragments were collected from 3 OI patients (age 3 to 7 years old, all under bisphosphonate treatment) after ethical committee approval and written consent. Fragments were wrapped in saline soaked gauze and fresh frozen at -18 ℃, then thawed at 6 ℃ and cut into parallelepiped samples. Depending on the initial fragment size, 1 to 3 samples per patient could be tested (total = 6), with dimensions varying from 5 to 7 mm in the longitudinal bone direction and from 1.3 to 4.3 mm in transverse directions. Compressive tests were performed at a strain rate of 0.1 $\%.s^{-1}$. Digital image correlation was used to quantify stress strain curves, Young modulus (E) and ultimate stress (σ_{max}). Specimens were then prepared for polarized light microscopy: fixation in 10% phosphate buffered formalin, dehydration, embedding in low viscosity resin, and milling to a thickness around 300 µm. Transmitted polarized light microscopy allowed characterization of collagen arrangement and pore size, and calculation of areal porosity.

Values for E and σ_{max} were highly variable, ranging respectively from 0.21 to 6.70 GPa (mean 2.89 GPa) and from 1.25 to 90.4 MPa (mean = 30.47 MPa). Mean areal porosity ranged from 9.2% to 14.5 %. Asymmetrical pores with dimensions often exceeding 100mm were observed. Strong correlations were found between porosity and both E ($r^2 = 0.9262$) and σ_{max} ($r^2 = 0.9598$).

These are preliminary results with only 6 samples. However for the first time, meso-scale mechanical properties of paediatric OI bone have been quantified, and a strong correlation found with porosity. The pore size often exceeds the resolution of existing in vivo pQCT technologies, which opens the way for in vivo quantification of OI bone and its subject specific modeling.

LB-MO07

Cortical Porosity in Perimenopausal Female Patients with Fragility Fractures. Heinrich Resch*[1], Teresa Stanek[2], Janina Patsch[3], Afrodite Zendeli[4], Judith Haschka[5], Roland Kocijan[5], Christian Muschitz[6]. [1]Medical University Vienna, Austria, [2]The Vinforce Study Group KH Barmherzige Schwestern Vienna, Austria, [3]Medical University of Vienna, Austria, [4]The VINFORCE Study Group - St. Vincent Hospital - Medical Department II, Austria, [5]St. Vincent Hospital Vienna, Austria, [6]St. Vincent's Hospital, Austria

Objectives: There is increasing evidence that cortical bone loss producing porosity starts before menopause. The relatively slow loss of cortical bone volume, which is four-fold larger than trabecular bone volume accounts for 70 percent of all bone loss and the occurrence of peripheral fractures in younger age. Aim of this study was to investigate bone micro structure, i.e. cortical and trabecular structure in perimenopausal patients with atraumatic peripheral fractures.

Materials and Methods: We consecutively investigated 26 treatment naive female patients (23-59 yrs) with atraumatic peripheral fractures and T-scores being above the threshold of -2.5 SD at lumbar spine and hip. Structural parameters of cortical and trabecular compartments were analysed by HR-pQCT (Xtreme CT, SCANCO Medical, Switzerland) at the distal radius and the distal tibia. These data were compared to a control group consisting of 38 healthy female individuals in the same age range (23-60 yrs).

Results: BMD values at hip and spine measured by DXA were similar in both groups. Structural analysis showed significant differences between patients and the healthy group in cortical parameters, both for the radius and the tibia. At the radius patients had increased cortical pore volume (Ct.Po.V [mm^3]) (7.74 $\pm$ 4.97 vs 5.29 $\pm$ 3.78; $p < 0.01$), increased cortical pore diameter (Ct.Po.Dm [µm]) (0.17 $\pm$ 0.03 vs 0.15 $\pm$ 0.02; $p < 0.01$) and an increased distribution of cortical pore diameters (Ct.Po.Dm.SD [µm]) (0.07 $\pm$ 0.03 vs 0.06 $\pm$ 0.01; $p < 0.01$). At the tibia in addition to Ct.Po.V (61.15 $\pm$ 30.66 vs 37.33 $\pm$ 20.85; $p < 0.01$) also cortical porosity (Ct.Po [%]) (7 $\pm$4 vs 4 $\pm$ 3; $p < 0.01$) was increased. The most striking significance was found at the radius for the cortical pore diameter and at the tibia in the cortical pore volume . The trabecular indices were similar in patients and controls. The strongest correlations were found within the healthy group between cortical porosity and age at the tibia (r = 0.87) and the radius (r = 0.74). In the patient group there was a significant correlation at the tibia between age and Ct.Po (r= 0.66) and Ct.Po.V (r = 0.68).

Summary: In perimenopausal women cortical bone is more dismantled than trabecular bone especially at the tibia. This increase of cortical porosity may be an explanation for the higher susceptibility to peripheral fragility fractures in younger females.

***Disclosures: Heinrich Resch**, None.*

LB-MO08

XBP1S, a BMP2-inducible transcription factor, Accelerates Endochondral Bone Growth by activating GEP Growth Factor. Fengjin Guo*, Xiaofeng Han, Peng Zhang, Zhangyuan Xiong, Meiling Li, Fei Xia. Chongqing Medical University, Peoples Republic of China

In this study,we report that XBP1S is a key downstream molecule of BMP2,and it is required for BMP2-mediated chondrocyte differentiation.XBP1S is upregulated during chondrocyte differentiation and demonstrates the temporal and spatial expression pattern during skeletal development,the expression profile of XBP1S is closely linked to the entire chondrogenic period(Fig.1).Overexpression XBP1S stimulates chondrocyte differentiation in vitro and endochondral ossification ex vivo.XBP1S significantly stimulated chondrocyte hypertrophy,mineralization,and bone length(Fig.2).The result of genome-wide DNA chip analysis showed that approximately 50 genes were up-regulated(2-fold) by BMP2,including XBP1S.The realtime PCR results showed that XBP1S mRNA is up-regulated 3-fold by BMP2.Besides,reductions of the endogenous XBP1S by siXBP1S adenovirus sharply decrease chondrogenic responses induced by BMP2,including ColII,ColX,SOX9 and RUNX2 expression.These results support the concept that XBP1S is a BMP2-inducible transcription factor and required for BMP2-mediated chondrocyte differentiation(Fig.3).In addition,XBP1S activates granulin-epithelin precursor(GEP) growth factor and induces GEP expressions in the process of chondrogenesis(-Fig.4).We next investigated whether endogenous GEP is required for XBP1S-induced chondrocyte development.Realtime PCR result showed that Ad-XBP1S can not promote BMP2-induced ColII,ColX and RUNX2 expression in GEP-/- BMSC cells,however,after infection with Ad-GEP,Ad-XBP1S can increase the expression of ColII,ColX and RUNX2 induced by BMP2 in GEP-/- BMSC cells.It was indicated that Ad-XBP1S activates BMP2-induced chongenesis through GEP. Besides,the effect of XBP1S-induced chondrogenesis and endochondral bone formation largely abolished in GEP-/- BMSC cells,however,it can be largely corrected in the presence of Ad-XBP1S+Ad-GEP.XBP1S recovered the potent stimulating effect of chondrocyte differentiation,mineralization and endochondral bone growth in GEP null growth plates rescued by GEP(Fig.5).Taken together,endogenous GEP is required for XBP1S-stimulated chondrocyte hypertrophy,mineralization,and endochondral bone formation.

In a word,XBP1S acts as a new GEP regulator and increases GEP-stimulated endochondral bone formation:(1)Overexpression of XBP1S stimulates chondrogenesis in vitro and endochondral bone growth ex vivo;(2)XBP1S is a downstream molecule of BMP2 and is required for BMP2 stimulation of chondrogenesis;(3)XBP1S increases GEP expression in chondrogenesis and enhances chondrogenesis through GEP;(4)XBP1S accelerates the chondroinductive activity of GEP.

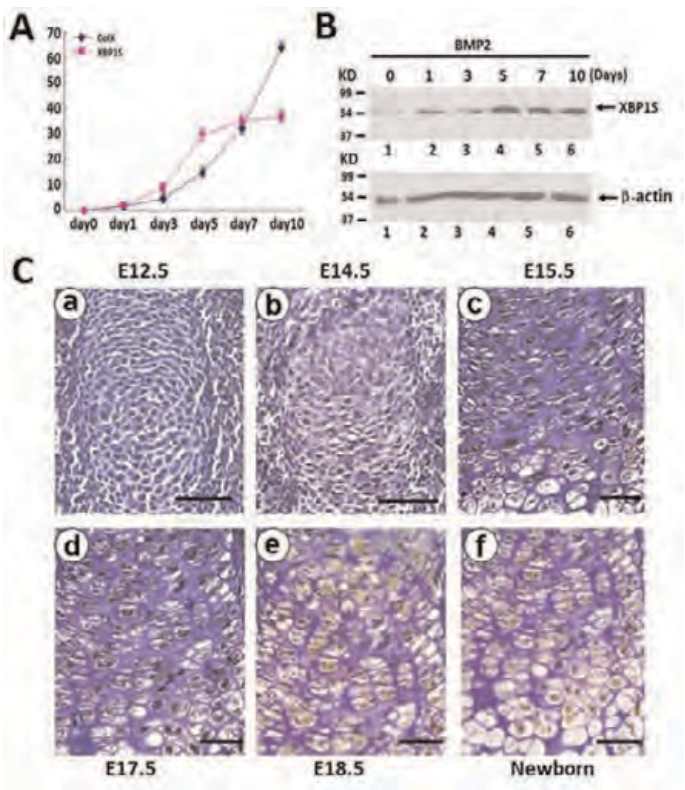

Figure 1. Expression of XBP1S in the course of chondrogenesis in vitro and in vivo

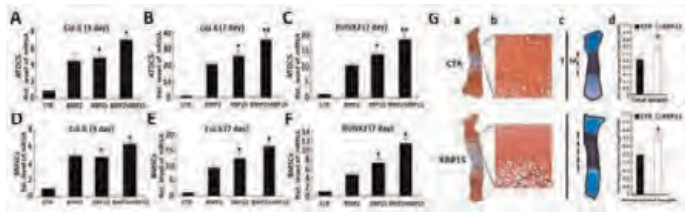

Figure 2. XBP1S stimulates chondrogenesis,mineralization,and endochondral bone growth in vitro

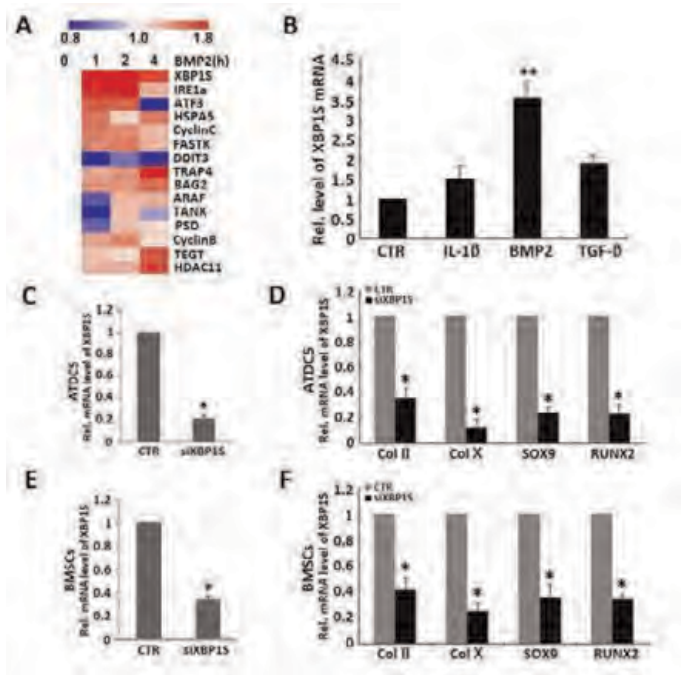

Figure 3. XBP1S is a downstream molecule of BMP2 and is required for BMP2-stimulated chondrogenesis

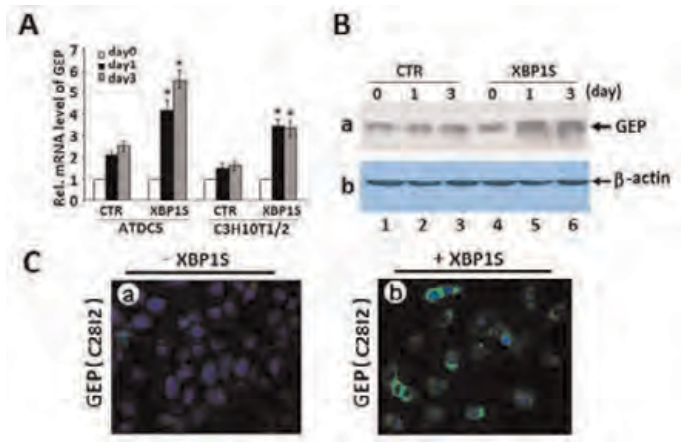

Figure 4. XBP1S induces the level of GEP mRNA and protein

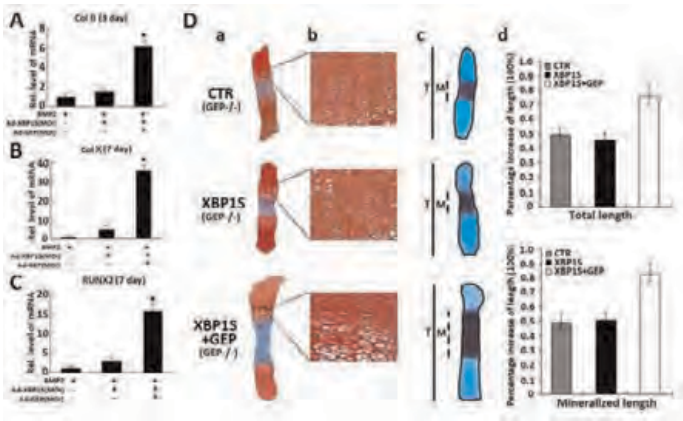

Figure 5.GEP is required for the XBP1S-induced chondrogenesis and endochondral bone formation

***Disclosures: Fengjin Guo**, None.*
This study received funding from: NSFC81171697;NCET-12-1090;

LB-MO09

Effects of Dynamic Hydraulic Flow Loading on Articular Cartilage Alteration against Functional Disuse. Sarah Moy*[1], Yi-Xian Qin[2], Minyi Hu[3]. [1]USA, [2]State University of New York at Stony Brook, USA, [3]Stony Brook University, USA

Introduction: Osteoarthritis patients exhibit a decrease in articular cartilage and the remodeling of the subchondral bone and the calcified cartilage [1]. Since dynamic hydraulic flow loading has been shown to mitigate the loss of bone due to disuse [2], it would be interesting to see how it could affect the thickness of the articular cartilage, which plays a vital role in protecting load-bearing joints. Thus, the objective of this study was to determine the effects of dynamic hydraulic stimulation (DHS) on uncalcified and calcified cartilage thickness in a rat hindlimb suspension (HLS) functional disuse model.

Materials and Methods: Five-month old Sprague-Dawley rats were divided into five groups: 1) baseline control (n=1), 2) age-matched control (n=1), 3) hindlimb suspension (HLS, n=1), 4) HLS+static-loading (n=1), and 5) HLS+2Hz DHS (n=1). Dr. Minyi Hu conducted the daily DHS loading in the mid-tibial region for ''10 minutes on, 5 minutes off, 10 minutes on,'' 5 days per week for a total of 4 weeks. The tibiae were then removed from the rats and embedded in poly-methyl methacrylate (PMMA). To analyze the articular cartilage, the embedded tibiae were sectioned at 5 microns and stained with Safranin O/Fast Green [3]. The stained samples were analyzed using ImageJ to quantify the thickness of the uncalcified (stained as darker red) and calcified cartilage.

Results: The HLS group had a smaller amount of uncalcified cartilage than the baseline group, though, it had a slight increase in calcified cartilage. This could be due to the remodeling of the subchondral bone plate [1]. HLS+2Hz DHS showed a decrease in uncalcified cartilage and an increase in calcified cartilage. However, the results could be heavily influenced by the small sample size per group.

Conclusions: The study does not currently show significance in terms of the effects of DHS on the thickness of articular cartilage. However, it is still an ongoing project which will increase the number of samples per group to increase the statistical power.

References:
[1] Hwang J. Increased hydraulic conductance of human articular cartilage and subchondral bone plate with progression of osteoarthritis. Arthritis Rheum. 2008; 58(12): 3831-3842.
[2] Hu M. Dynamic hydraulic flow stimulation on mitigation of trabecular bone loss in a rat functional disuse model. Bone. 2012; 51(4): 819-25.
[3] Center for Musculoskeletal Research. Safranin O/Fast Green Stain. University of Rochester Medical Center.2013. Web.

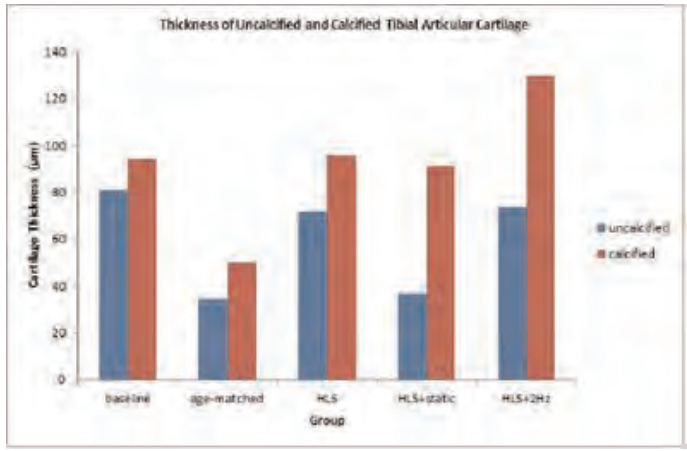

Results

***Disclosures: Sarah Moy**, None.*

LB-MO10

Role of Parathyroid Function and Phosphate Regulation in a Patient with Tumor-Induced Osteomalacia (TIO). Daniel Cadena*[1], Zinnia San Juan[2], Alan Burshell[3]. [1]USA, [2]Subinvestigator, USA, [3]Ochsner Clinic Foundation, USA

Phosphate regulation is affected by intestinal and renal phosphate handling as well as changes in bone fluxes. Well-known regulators include parathyroid hormone (PTH) and vitamin D. In more recent years, phosphaturia-inducing peptides have been identified as playing a role in both hypophosphatemic and hyperphosphatemic disorders.

A 79-year-old woman followed since age 32, initially presented with muscle weakness, soreness, bone pains, hip and clavicular fractures from 1968 to 1977. Evaluation in 1968 revealed hypophosphatemia (1.4-1.8 mg/dL [normal 2.7-4.5 mg/dL]), phosphaturia (tubular reabsorption of phosphate of 33% [n: 85%]), normal serum calcium (9.2 mg/dL [n: 8.7-10.5 mg/dL]), and elevated alkaline phosphatase (23.2-34.8 KAU [n: 4-12 KAU]). She was treated for hypophosphatemic osteomalacia with increasing doses of phosphate and vitamin D supplements with minimal improvement in phosphorus levels and symptoms. She developed tertiary hyperparathyroidism (serum calcium 10.2-10.8 mg/dL). In 1984, a bone biopsy showed osteomalacia and osteitis fibrosa cystica. Tertiary hyperparathyroidism was treated with parathyroidectomy in 1984 and also in 1998 with subsequent development of hypoparathyroidims. Interestingly phosphate levels normalized with hypoparathyroidsm and declined with tertiary hyperparathyroidsm. In 2009, FGF23 was found to be elevated at 4,850 RU/mL (n: 0-180 RU/mL). In April 2010 knee radiographs revealed a tibial tumor. The biopsy revealed a phosphaturic mesenchymal tumor, and was positive for FGF 23 mRNA by reverse transcription polymerase chain reaction (RT-PCR). The tumor was resected in July 2010. After surgery, calcitriol and phosphorus supplements were resumed, and cinacalcet started. Laboratory results showed normal PTH, calcium, and phosphorus levels and FGF 23 decreased to nadir of 507 RU/mL.

This case illustrates that serum phosphate levels appear to be inversely proportional to the parathyroid hormone in a patient with elevated FGF23 levels and TIO. Tertiary hyperparathyroidism has been reported in TIO and other FGF23 mediated diseases and occurred twice in our patient. Phosphate levels were below normal with tertiary hyperparathyroidism and normalized with surgical hypoparathyroidism on two occasions. Cinacalcet and calcitriol together normalized serum phosphate levels and inhibited PTH secretion. Medical and surgical parathyroidectomy are treatments for TIO and normalize the serum phosphate.

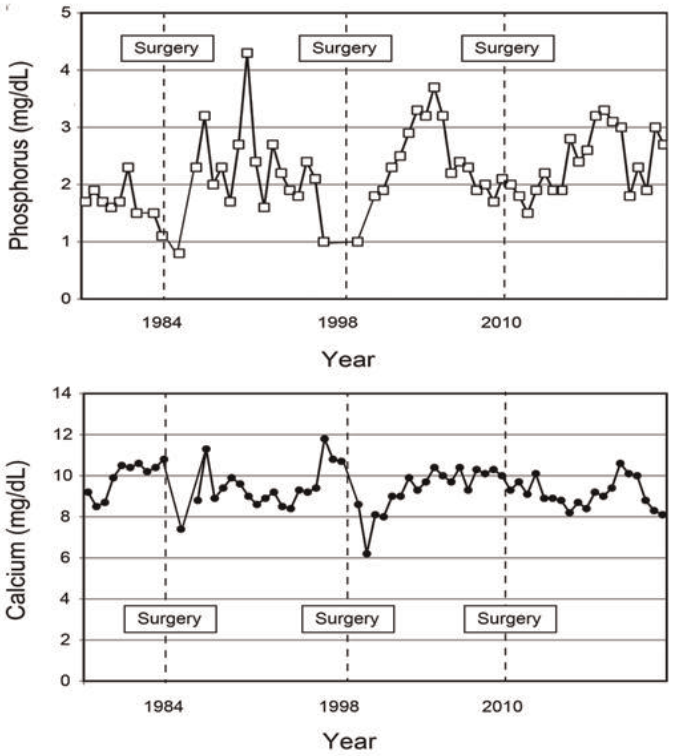

Serum phosphorus and serum calcium levels during surgical interventions

***Disclosures: Daniel Cadena**, None.*

LB-MO11

***Asxl1* Plays an Important Role in Bone Remodeling by Regulating both Osteoblasto- and Osteoclasto-genesis Through Histone Modification.** Feng-Chun Yang, Peng Zhang*. Indiana University, USA

Epigenetic mechanisms play an important role in the tissue-specific regulation of gene expression. Histone methylation is one of the most important epigenetic modifications. However, whether histone methylation underlies the physiology and pathophysiology of bone remodeling is not well established. *Additional sex combs* like 1 (*Asxl1*) has been shown to play an important role in both activation and silencing of *Hox* genes through interacting and regulating multiple histone modifying enzymes. Importantly, *ASXL1* is mutated in patients with Bohring-Opitz syndrome (BOS), characterized by severe bone deformities and other developmental deficits. Here, using an *Asxl1*-targeted mouse models, we challenged if deleting *Asxl1* dysregulates critical genes controlling osteoblasto-/osteoclasto-genesis, and bone remodeling through altered histone modifications.

Using qPCR and *Asxl1:GFP* reporter knock-in mice, we found that *Asxl1* is highly expressed in all mesenchymal stem cells (MSC) and preosteoclasts (preOCLs). $Asxl1^{-/-}$ mice are runt and have significantly lower BMD and less trabecular bone volume than WT littermates. $Asxl1^{-/-}$ mice had markedly decreased number of marrow MSCs with skewed differentiation favoring adipocytes, while away from osteoblasts. In contrast, $Asxl1^{-/-}$ preOCLs had increased OCL differentiation and bone resorptive capacity. To delineate the gene expression changes, microarray was performed with MSCs and preOCLs of $Asxl1^{-/-}$ and WT mice. A number of differentially expressed genes in $Asxl1^{-/-}$ MSCs (*Runx2*, *Sp7, Bglap1*) and in $Asxl1^{-/-}$ preOCLs (*Nfatc1*, *Acp5*, *Ctsk*) are implicated in the regulation of osteoblasto-/osteoclasto-genesis, respectively. Wnt5a and receptor tyrosine kinase-like orphan receptor (Ror), key members of non-canonical Wnt/β-catenin signaling pathway, are upregulated in both MSCs and preOCLs derived from $Asxl1^{-/-}$ mice. Furthermore, *Asxl1* loss dramatically reduced the H3K4me3 levels in MSCs and preOCLs. In addition, ChIP-qPCR in WT and $Asxl1^{-/-}$ MSCs and preOCLs showed that the dysregulated gene expression correlated with specifically altered histone methylation patterns across selected gene loci.These results indicate that deletion of *Asxl1* dysregulates histone methylation states and gene expression in MSCs and preOCLs, which in turn alters their differentiation program, leading to bone developmental defects. These results demonstrate a pivotal role of histone methylation in bone homeostasis.

***Asxl1* Plays an Important Role in Bone Remodeling by Regulating both Osteoblasto- and Osteoclasto-genesis Through Histone Modification**

Peng Zhang[1], Jiapeng Wang[1], Steven Rhodes[1], Sharmila Paul[1], Feng Pan[1], Yongzheng He[1], Linh Thi Thuy Nguyen[1], Mingjiang Xu[1,2], Feng-Chun Yang[1,3]

Departments of [1]Pediatrics, [2]Medical and Molecular Genetics, [3]Anatomy and Cell Biology, Indiana University School of Medicine, Indianapolis, IN

Epigenetic mechanisms play an important role in the tissue-specific regulation of gene expression. Histone methylation is one of the most important epigenetic modifications. However, whether histone methylation underlies the physiology and pathophysiology of bone remodeling is not well established. *Additional sex combs* like 1 (*Asxl1*) has been shown to play an important role in both activation and silencing of *Hox* genes through interacting and regulating multiple histone modifying enzymes. Importantly, *ASXL1* is mutated in patients with Bohring-Opitz syndrome (BOS), characterized by severe bone deformities and other developmental deficits. Here, using an *Asxl1*-targeted mouse models, we challenged if deleting *Asxl1* dysregulates critical genes controlling osteoblasto-/osteoclasto-genesis, and bone remodeling through altered histone modifications.

Using qPCR and *Asxl1:GFP* reporter knock-in mice, we found that *Asxl1* is highly expressed in all mesenchymal stem cells (MSC) and preosteoclasts (preOCLs). $Asxl1^{-/-}$ mice are runt and have significantly lower BMD and less trabecular bone volume than WT littermates. $Asxl1^{-/-}$ mice had markedly decreased number of marrow MSCs with skewed differentiation favoring adipocytes, while away from osteoblasts. In contrast, $Asxl1^{-/-}$ preOCLs had increased OCL differentiation and bone resorptive capacity. To delineate the gene expression changes, microarray was performed with MSCs and preOCLs of $Asxl1^{-/-}$ and WT mice. A number of differentially expressed genes in $Asxl1^{-/-}$ MSCs (*Runx2*, *Sp7, Bglap1*) and in $Asxl1^{-/-}$ preOCLs (*Nfatc1*, *Acp5*, *Ctsk*) are implicated in the regulation of osteoblasto-/osteoclasto-genesis, respectively. Wnt5a and receptor tyrosine kinase-like orphan receptor (Ror), key members of non-canonical Wnt/β-catenin signaling pathway, are upregulated in both MSCs and preOCLs derived from $Asxl1^{-/-}$ mice. Furthermore, *Asxl1* loss dramatically reduced the H3K4me3 levels in MSCs and preOCLs. In addition, ChIP-qPCR in WT and $Asxl1^{-/-}$ MSCs and preOCLs showed that the dysregulated gene expression correlated with specifically altered histone methylation patterns across selected gene loci.

These results indicate that deletion of *Asxl1* dysregulates histone methylation states and gene expression in MSCs and preOCLs, which in turn alters their differentiation program, leading to bone developmental defects. These results demonstrate a pivotal role of histone methylation in bone homeostasis.

***Disclosures: Peng Zhang**, None.*
This study received funding from: Department of Defense

LB-MO13

Type 2 receptor-level competition between BMP and Activin ligands regulates postnatal bone mass. Jonathan Lowery*, Giuseppe Intini, Laura Gamer, Karen Cox, Vicki Rosen. Harvard School of Dental Medicine, USA

Recent studies have demonstrated that postnatal bone mass is tightly controlled by the opposing actions of the canonical BMP (SMAD1/5/8) and Activin/TGFbeta (SMAD2/3) pathways: bone formation is increased by BMP signaling and decreased by Activin/TGFbeta signaling. However, the molecular mechanisms that allow these pathways to antagonize one another *in vivo* remain unclear. That the type 2 receptors for Activins (ACVR2A/B) also bind BMPs with high affinity led us to hypothesize that competition between BMPs and Activins at the type 2 receptor level plays a role in determining the balance of SMAD1/5/8 and SMAD2/3 activation *in vivo* and, in turn, regulates bone mass. Here we show that forcing all BMP and Activin signaling in bone cells to compete for ACVR2A/B by removing the BMP-specific type 2 receptor in *Bmpr2*-cKO mice leads to reduced Activin signaling in bone but has no effect on BMP signaling. *Bmpr2*--cKO mice have profoundly high bone mass by 2 months of age (>91% increase over littermates, $p<0.0001$) that is due to an increase in osteoblast (OB) activity and a higher bone formation rate (>101% over littermates, $p<0.02$) with no change in bone resorption. We confirmed the bone mass increase is due to reduced Activin signaling by systemically administering the ACVR2B-Fc receptor decoy, which has been demonstrated to sequester Activins and is currently under investigation as a clinical therapy. Five weeks of this treatment caused a >62% increase in bone mass in wild type mice ($p<0.007$) but had no effect on bone mass in *Bmpr2-cKO* mice, indicating that decreased SMAD2/3 signaling in these mice occurs at the level of pathway activation. Further, we identified MSC/osteoprogenitors as the cell type where receptor competition alters bone mass by comparing the phenotypes of mice lacking BMPR2 in OBs and osteocytes to those lacking BMPR2 in MSC/osteoprogenitors. Our findings suggest that increased utilization of ACVR2A/B by BMPs in osteoprogenitor cells comes at the expense of Activin signaling, providing the first mechanistic insight into the antagonism between SMAD1/5/8 and SMAD2/3 signaling in regulating postnatal bone mass. Our results are potentially informative to numerous human pathologies associated with changes in the balance of these two pathways, including pulmonary arterial hypertension, lung and kidney fibrosis, asthmatic airway remodeling, muscular dystrophy, osteosclerosis, and osteoporosis.

***Disclosures: Jonathan Lowery**, None.*

LB-MO15

Inflammation and Bone in Early Pubertal Black and White Children. Paige Berger*[1], Emma Laing[1], Stuart Warden[2], Kathleen Hill Gallant[3], Dorothy Hausman[1], Ralph Tripp[1], George McCabe[3], Connie Weaver[4], Munro Peacock[5], Richard Lewis[1]. [1]The University of Georgia, USA, [2]Indiana University, USA, [3]Purdue University, USA, [4]Purdue University, Dept of Nutrition Science, USA, [5]Indiana University Medical Center, USA

Inflammation is thought to influence bone properties, yet few studies have examined the relationships between inflammatory markers and bone in humans. The purpose of this cross-sectional study was to investigate the associations between serum inflammatory markers and serum markers of bone metabolism and cortical bone in black and white boys and girls. Fasting blood samples were collected from 314 healthy, early pubertal children (n=155 male; n=164 black). Luminex xMAP technology was used with a Milliplex Map immunoassay to analyze samples for markers of inflammation believed to influence bone turnover (monocyte chemoattractant protein-1 [MCP-1], interleukin-6 [IL-6], tumor necrosis factor-alpha [TNF-alpha], and vascular endothelial growth factor [VEGF]). ELISA was used to measure serum osteocalcin (OC) and bone alkaline phosphatase, RIA for 25-hydroxycholecalciferol (25[OH]D) and 1,25-dihydroxycholecalciferol (1,25[OH]2D), IRMA for parathyroid hormone (PTH), and a clinical analyzer was used for calcium (Ca) and creatinine (Cr). Peripheral quantitative computed tomography (pQCT) was used to assess cortical bone of the tibial diaphysis. Bivariate and partial correlations controlling for race and percent body fat were conducted among outcome variables. MCP-1 was positively associated with 25(OH)D ($r=0.28$, $P<0.0001$) and negatively associated with OC ($r=-0.13$, $P=0.03$) and PTH ($r=-0.15$, $P=0.01$). MCP-1 was also negatively associated with pQCT-derived cortical volumetric bone mineral density ($r=-0.22$, $P=0.0003$), endosteal circumference ($r=-0.13$, $P=0.03$), and polar strength-strain index ($r=-0.14$, $P=0.03$). IL-6 was positively associated with OC only ($r=0.18$, $P=0.003$). When race was added as a covariate, these relationships were no longer significant. There were no significant correlations between TNF-alpha or VEGF and bone biomarkers or cortical bone measures. Given the lack of research in the area of inflammatory markers and bone in humans, these relationships warrant further exploration.

***Disclosures: Paige Berger**, None.*

LB-MO16

Mutations in the *SLCO2A1* gene and primary hypertrophic osteoarthropathy: a clinical and biochemical characterization. Zeng Zhang*, Zhen-Lin Zhang. Shanghai Jiao Tong University Affiliated Sixth People's Hospital, China

Context:We previously demonstrated that deficiency of the prostaglandin transporter (SLCO2A1) is a cause of primary hypertrophic osteoarthropathy (PHO). However, its clinical and metabolic characteristics have not been well defined.

Objective: The objective of the study was to expand this mutational spectrum to better delineate the SLCO2A1 deficiency phenotype and investigate the clinical and metabolic characteristics of a cohort of subjects with PHO.

Design, Setting, Patients, and Main Outcome Measure: Eleven affected individuals and their available healthy family members from nine unrelated Chinese families with PHO (seven of which were previously undescribed) were clinically studied. The *SLCO2A1* gene was screened and analyzed. Urinary levels of PGE_2 and PGE-M were measured using competitive enzyme-linked immunosorbent assays. The serum levels of total testosterone, estradiol, sex hormone-binding protein, luteinizing hormone (LH), follicle-stimulating hormone (FSH) and fasting gastrin were detected.

Results: Nine different *SLCO2A1* mutations were identified in affected individuals in the seven previously undescribed families, seven of which (Glu165X, Ala286GlnfsX35, Gln356AlafsX77, Gly369Asp, Gly379Glu, Glu465Lys, and c.861+2T>C) were novel. The urinary levels of PGE_2 and PGE-M were much higher in the SLCO2A1-de?cient individuals and decreased with age. There was no relationship between sex hormones and PGE_2 or PGE-M. There was no significant difference in the levels of fasting serum gastrin between PHO patients with watery diarrhea and their relatives.Conclusions: The present findings broaden the allelic spectrum of *SLCO2A1* mutations. The urinary levels of PGE_2 and PGE-M in the SLCO2A1-de?cient individuals decreased with age. The measurement of excreted PGE_2 and PGE-M may have implications in the differential diagnosis, treatment and follow-up of PHO.

***Disclosures: Zeng Zhang**, None.*

LB-MO17

Circulating α-Klotho Levels Are Inversely Correlated to FGF-23 in TumourInduced Osteomalacia. Paul Zeun*[1], Jonathan Tang[2], Christopher Washbourne[2], Isabelle Piec[1], Emily Fisher[3], William Fraser[2]. [1]Dr., United Kingdom, [2]University of East Anglia, United Kingdom, [3]Miss, United Kingdom

Tumour induced osteomalacia is characterised by high circulating levels of fibroblast growth factor 23 (FGF23) due to ectopic secretion from mesenchymal tumors. An abundance of FGF23 drives the hypophosphatemia and low 1,25-dihydroxy vitamin D levels characteristic of this condition. The single-pass trans-membrane protein α-klotho is integral for FGF23-mediated receptor activation and its downstream effects. In addition, α-klotho may have a phosphaturic effect independent of FGF-23. The regulation of α-klotho in the face of high circulating FGF23 is currently unknown.

We investigated the relationship between circulating FGF23 and α-klotho in patients with TIO. We identified 15 consecutive plasma FGF-23 requests in subjects with confirmed TIO for testing. FGF-23 was measured using Immutopics C-term ELISA kit and soluble α-klotho was measured using the IBL ELISA kit. The group consisted of 7 males and 8 females with an age of 53 ± 20 years (mean ± SD). Only one subject was not on treatment for TIO at the time of sampling. The average circulating levels of FGF23 and α-klotho were 286 ± 244 RU/ml and 644 ± 309 pg/ml respectively. There was an inverse correlation between FGF-23 and α-klotho (Pearson coefficient - 0.28). This inverse correlation may suggest that increasing levels of FGF23 in TIO down-regulate α-klotho expression in the kidney and parathyroid glands leading to reduced circulating levels of α-klotho. Given α-klotho's role in mediating FGF23 signalling and that α-klotho may be a phosphaturic factor in its own right; such an adaptive mechanism would help partially reduce the renal phosphate wasting seen in TIO.In summary there is an inverse correlation seen between circulating levels of FGF23 and α-klotho in TIO. This may suggest there is a down-regulation of α-klotho expression to limit the phosphate wasting and resultant hypophosphatemia that is seen in TIO.

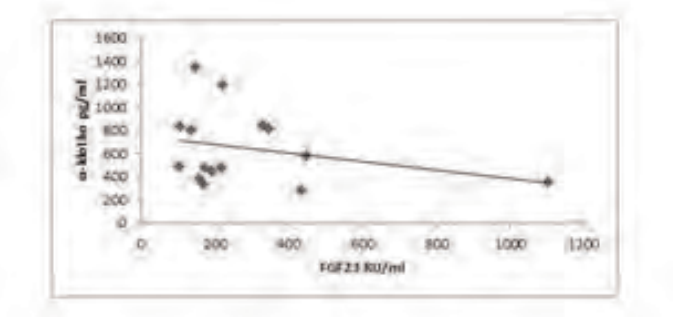

***Disclosures: Paul Zeun**, None.*

LB-MO18

Retinaldehyde (Rald) Increases Bone Mass by Repressing PPARγ, Increasing BMP2, and Stimulating Brown- like Adipogenesis: Implications for Treating Obesity and Osteoporosis. Shriram Nallamshetty*[1], Phuong Le[2], Hong Wang[1], Jorge Plutzky[1], Clifford Rosen[3]. [1]Brigham & Women's Hospital, USA, [2]Maine Medical Center Research Institute, USA, [3]Maine Medical Center, USA

New drugs to induce brown-like adipogenesis are being investigated for treating obesity and type 2 diabetes. However, a major off-target effect of such therapies (e.g. FGF-21, rosiglitazone, β3 agonists) is significant trabecular bone loss. Previously we showed that retinaldehyde (Rald), which is converted to retinoic acid by retinaldehyde dehydrogenase 1 (Aldh1a1), induces a thermogenic program in white adipose tissue (WAT) while increasing BMP2 expression in mesenchymal stromal cells (MSCs), thus promoting osteogenic differentiation. *Aldh1a1*$^{-/-}$ mice demonstrate high bone mass, resistance to diet-induced obesity, and ''browning'' of visceral fat *in vivo*. To understand Rald's unique effects on bone and fat, we examined: (1) *in vitro* actions of Rald and RAR/RXR modulators on osteoblast differentiation, and (2) *in vivo* effects of rosiglitazone (rosi) and a high fat diet (HFD) on bone mass, marrow adiposity, WAT, and BAT in Aldh1a1 deficiency. Rald (1 μM) induces alkaline phosphatase (ALP) in ST2 MSCs at day 2 even in the absence of ascorbic acid (AA) and beta glycerolphosphate (BGP). Furthermore, Rald's induction of ALP is blocked by an RAR but not an RXR antagonist. In contrast, Rald decreased ST2 MSC adipogenic differentiation by 80% through inhibitory effects on PPARγ and Cebpα expression. We next treated 18 week-old *Aldh1a1*$^{-/-}$ mice and WT B6 female mice with rosi (20 mg/kg/day for 12 weeks). Rosi increased visceral WAT in WT mice but not *Aldh1a1*$^{-/-}$ mice (50% reduction, $p<0.05$) with no effects on BAT. Similarly, when both strains were administered a HFD, there was a marked blunting in total body weight gain and fat accumulation in *Aldh1a1*$^{-/-}$ mice ($p<0.05$). *Aldh1a1*$^{-/-}$ mice challenged with rosi or HFD had significantly higher femoral BV/TV and less marrow adiposity than WT treated mice ($p<0.05$). Histomorphometry of the rosi-treated mice (n=5 per genotype) revealed an increase in Osteoblast number/Bone Area in the *Aldh1a1*$^{-/-}$ mice (WT: 45.84±16.54; *Aldh1a1*$^{-/-}$: 72.08±33.03; $p=0.15$) and a significant decrease in osteoclast number and OC surface/bone perimeter vs WT ($p<0.001$). In summary, Rald enhances osteogenesis *in vitro* and *in vivo*, reduces osteoclast activation *in vivo*, and protects against diet- induced obesity and rosi-induced marrow adiposity by impairing PPARγ transactivation. These findings support further studies of Rald and Aldh1a1 inhibition of Rald as potential therapies for obesity and osteoporosis.

***Disclosures: Shriram Nallamshetty**, None.*

LB-MO19

Ras Signaling Increases the Number of Osteoprogenitor Cells leading to Increased Bone Mass. Garyfallia Papaioannou*[1], Noriaki Ono[1], Simona Nedelcu[2], Jacqueline A Lees[2], Henry Kronenberg[1], Tatsuya Kobayashi[1]. [1]Massachusetts General Hospital, USA, [2]Koch Institute for Integrative Cancer Research, Massachusetts Institute of Technology, USA

Introduction: Ras signaling regulates cellular processes such as proliferation, differentiation and survival. However, its role in bone-lineage cells has not been fully understood. To determine the role of Ras signaling in bone-lineage cells in different differentiation stages, we overactivated the Ras signaling in mature osteoblasts, preosteoblasts and precursor cells of bone lineage using a tamoxifen-inducible, Cre-dependent overexpression system (CreERt). Methods : Mice harboring an expression construct containing a constitutively active mutant Kras gene preceded by a floxed "stop" sequence were crossed with mice expressing CreERt driven by a 3.2 kb-long type I collagen (Col1), an Osterix (Osx), or a type II collagen (Col2) promoter. The activation of the mutant Kras gene was achieved by tamoxifen injection at embryonic day (E) 18.5. Bone samples were analyzed at several time points. To trace the cells expressing Kras oncogene, a fluorescent reporter expressed only after cre activation was also bred in. Cellular proliferation was assessed by the BrdU assay. Results: A short chase experiment using the Col2-CreERt and Cre reporter mice suggested that a small number of Col2-positive cells were present in the bone marrow of perinatal mice. When Kras oncogene was activated in Col2-positive cells at E18.5, mice showed increased trabecular bone and modest growth plate shortening at 3 weeks of age. The number of stromal cells in the primary and secondary spongiosa was substantially increased. The stromal cells were mostly positive for the fluorescent reporter, indicating that they were descendants of Col2-positive cells. These results suggest that Col2-positive cells in the bone marrow are osteoblast progenitors and that overactivation of Ras signaling directly increases their number, leading to an increase in bone mass. The BrdU assay showed increased stromal cell proliferation, suggesting that Ras signaling positively regulates proliferation of bone progenitor cells. In contrast, activation of Kras in Col1-positive mature osteoblasts at E 18.5 did not cause a significant increase in bone mass. Activation of Kras in Osx-positive cells at E18.5 resulted in a bone phenotype similar to but milder than that of the Col2CreERt: Kras mice. Conclusions: Ras signaling increases the number of descendants of Col2-positive osteoprogenitor cells in the bone marrow in early differentiation stages to increase bone mass.

***Disclosures: Garyfallia Papaioannou**, None.*

LB-MO20

Effects of Calcium-independent Phospholipase A_2 on Differentiation and Activity of Cortical Bone derived Osteoblasts. Bill Hancock*[1], Jason Ashley[2], Gregory Clines[2], Sasanka Ramanadham[2]. [1]University of Alabama, USA, [2]University of Alabama at Birmingham, USA

Arachidonic acid and arachidonate metabolites are recognized mediators of bone modeling. These mediators can be generated by Phospholipases A(2) (PLA(2)) which hydrolyze the sn-2 fatty acid substituent from phospholipids. Most cellular Arachidonic acid is esterified in this position within membrane glycerophospholipids. Previously generated knockout mice, lacking the group VIA PLA(2) (iPLA(2)beta), exhibit an enhanced, age-related decline in cortical bone thickness, trabecular bone volume, and bone mineralizing surfaces. These mice lose mineral apposition by 6-months of age and gain lipid droplets in their bone marrow. Our new studies have shown that, relative to WT cells, osteoblasts differentiated from cortical bone mesenchymal stem cells of knockout mice express lower levels of Runx2 and Alkaline Phosphatase mRNA. This correlates with decreased osteoblastogenesis and osteoblast activity. These differentiated osteoblasts also exhibit reduced mineralization as detected by Alizarin Red staining and quantification. This reduction can be rescued by the treatment of osteoblasts with prostaglandin E2, a common metabolite of Arachidonic acid produced by cyclooxygenase metabolism. Prostaglandin E2 is known to increase osteoblast replication and differentiation. Our studies indicate that reduced differentiation factors and reduced mineralization are induced by knockout of iPLA(2)beta; further demonstrating the role of iPLA(2)beta in mesenchymal stem cell fate and bone remodeling.

***Disclosures: Bill Hancock**, None.*

LB-MO21

Post–Alendronate DXA Monitoring Strategy Based on 5-year Changes in BMD. Brian Mcnabb*[1], Eric Vittinghoff[2], Richard Eastell[3], Ann Schwartz[2], Douglas Bauer[2], Kristine Ensrud[4], Elizabeth Barrett-Connor[5], Dennis Black[2]. [1]San Francisco VA Medical Center, University of California, San Francisco, USA, [2]University of California, San Francisco, USA, [3]University of Sheffield, United Kingdom, [4]Minneapolis VA Medical Center / University of Minnesota, USA, [5]University of California, San Diego, USA

Context: Despite many women being candidates for therapy cessation after 5 years of alendronate, no information exists on how to monitor these women after therapy cessation.

Objective: To estimate the time until femoral neck BMD T-score (FNBMD-T) drops below -2.5 amongst women who have completed 5 years of alendronate therapy.

Design and Setting: Percent change in BMD over time functions were calculated using repeated measures models. These results were used to estimate the number of years until 10-50% of women with various baseline FNBMD-Ts crossed the prespecified FNBMD-T threshold of -2.5.

Participants: Four-hundred and four women who had received an average of 5.1 years of alendronate during the Fracture Intervention Trial (FIT) and were subsequently followed for 5 treatment-free years (on placebo) during the FIT Long Term Extension trial were used to derive functions for the percent change in BMD over time.

Results: Mean 5-year percent decline in BMD was 1.7% at the femoral neck and 3.6% at the total hip. The most rapid rate of bone loss occurred from baseline to year 2, with slower bone loss thereafter (test for this bone loss pattern versus linear bone loss pattern over 5-year period: $p = 0.0009$). For women with slightly higher BMD after stopping treatment, it took far longer for FNBMD-T to drop below -2.5. For example, for those with FNBMD-Ts of -2.1, it took over 5 years v. those with FNBMD-Ts of -2.3, it took 0.7 years for 20% of women to drop below -2.5.

Conclusions: When considering a retreatment threshold after alendronate discontinuation of FNBMD-T of -2.5, measuring BMD by DXA within 5 years of discontinuation is only likely to trigger a management change for women with FNBMD-T $<$ -2.1 at the time of discontinuation.

Table 1: Number of Years (95% CI)* Until 10 to 50% of Women with Femoral Neck T-scores of -2 to -2.4 Drop Below a T-score of -2.5, After 5 Years of Alendronate

Percentages of Patients	Starting T-Scores				
	-2	-2.1	-2.2	-2.3	-2.4
10%	4.9 (3.8 – > 5)	3.7 (2.2 – 4.2)	0.9 (0.5 – 2.1)	< 0.1 (N/A – 0.3)	--------
20%	--------	> 5 (4.4 – N/A)	4.2 (2.2 – 4.8)	0.7 (0.5 – 1.8)	-------
30%	--------	--------	> 5 (4.6 – N/A)	3.4 (1.1 – 4.7)	0.2 (0.1 – 0.5)
40%	--------	--------	--------	> 5 (3.5 – N/A)	0.9 (0.6 – 2.3)
50%	--------	--------	--------	--------	4.8 (1.1 – > 5)

Results are based on the mean and distribution of change in femoral neck BMD over time for women from the FLEX placebo group with femoral neck BMD T-scores +/- 0.25 T-scores from the starting T-score at baseline of the treatment-free period. Each 0.5 T-score window contains a mean of 117 women from the population of 404. The 95% CIs are derived from the bootstrapping method using 100 repetitions.
* Mean, lower, and upper bounds of 95% CI all > 5 or < 0.1 for blank entries.
Abbreviations: CI, Confidence Interval; BMD, bone mineral density; FLEX, Fracture Intervention Trial Long Term Extension trial.

Table1

***Disclosures: Brian Mcnabb**, DocMatter, 7*

LB-MO22

The 2nd Generation of HR-pQCT: Progresses in Bone Microstructure Assessment with 61çm Voxel Size *In Vivo* Scans. Nicolas Vilayphiou*, Stefan Hämmerle, Bruno Koller. Scanco Medical AG, Switzerland

We developed in 2004 a novel high resolution peripheral quantitative tomography (HR-pQCT) scanner dedicated to bone microstructure assessment at the ultradistal radius and tibia. This 1st generation scanner, XtremeCT (XT1, Scanco Medical AG, Bruttisellen, Switzerland), proposes a 2.8min scan over a 9.02mm region, with 82µm voxel size for radiation 3µSv dose [Laib et. al – Bone 1999]. Movement artifacts are known to affect XT1 scans, notably at the radius. They impact dramatically the reproducibility of the measurements, and reduce the number of valid scans in longitudinal studies on bone fragility or osteoporosis treatment efficacy [Pialat et. al – Bone 2011].

We are developing a new HR-pQCT scanner (XtremeCT 2 - XT2) to address the movement artifacts issue. Hardware improvements allow for scan time shortening with no cost on image quality, with 2 different scan protocols over 10mm. The basic protocol was specified to be compatible with XT1: 1.5min scan, 91µm voxel size and 4µSv dose. The 2nd protocol has better resolution and is still affordable for patient scans: 61µm voxel size, 2min scan time and 5µSv dose.

A forearm phantom (Radiology Support Devices, Long Beach, CA) was scanned to compare results across the different scan protocols. XT1 scan was the reference to address compatibility between the two scanners, whereas XT2 scan at native 30µm voxel size served as a gold standard to address the accuracy of all measurements. Lower resolution scans (82 and 91µm) were analyzed with the standard evaluation used in XT1. High resolution scans (61 and 30µm) were completely analyzed with direct transformation methods. Results are presented for Trabecular density (Tb.vBMD), number (Tb.N), thickness (Tb.Th) and bone volume fraction (BV/TV).

The basic XT2 scan gave similar results on trabecular bone as on XT1 excepted for Tb.N where it is lower. Both low resolution scans overestimated Tb.N and under-sestimated Tb.Th. The 61µm scan was more accurate with Tb.N=1.11 and Tb.Th=241, compared to 1.01 and 247 obtained at 30 µm. All results are detailed in the Table.

Reduced scan time should lead to significant improvements regarding movement artifacts on *in vivo* scans. Also a new forearm cast will help to limit patient mobility. Overall, studies on bone deterioration or on osteoporosis treatment efficacy should all benefit from this new scanner. Especially as XtremeCT 2 will make possible 61µm scans for the 1st time in clinical research.

	Scan parameters			Trabecular microarchitecture			
Scanner	Voxel size [µm]	Dose [µSv]	Scan Time [min]	Tb.vBMD [mgHA/ccm]	BV/TV [%]	Tb.N [1/mm]	Tb.Th [µm]
XT 1	82	3	2.8	239	19.9*	1.58	126*
XT 2	91	4	1.5	222	18.5*	1.26	147*
XT 2	61	5	2.0	235	20.9	1.11	241
XT 2	30	84	16.5	242	18.6	1.01	247

*derived from Tb.vBMD and Tb.N

Table

***Disclosures: Nicolas Vilayphiou**, Scanco Medical AG, 3*

LB-MO23

Adherence to Oral Bisphosphonates and the Risk of Subtrochanteric or Diaphyseal Femur Fractures among US Medicare Beneficiaries with Part D Coverage. John Wang*[1], Michael Ward[1], Timothy Bhattacharyya[1], Leighton Chan[2]. [1]Intramural Research Program, NIAMS/NIH, USA, [2]Rehabilitation Med Dept, Clinical Center, NIH, USA

Long-term use of oral bisphosphonates has been implicated in increased risks of atypical hip fractures located primarily in the subtrochanteric region of the diaphysis. We hypothesized that higher exposure to oral bisphosphonates was associated with an increase in the incidences of subtrochanteric or diaphyseal femur fractures. In this large national cohort study of Medicare fee-for-service female beneficiaries with at-least 24-month part D coverage from 2006-2010, we followed 522,287 new bisphosphonate users from their index prescription until a primary inpatient diagnosis of subtrochanteric/femur shaft (n=948) or typical hip (n=9,382) closed fracture, a switch to another bisphosphonate or different type of anti-osteoporosis medications, disenrollment, or end of the study. Adherence was measured as medication possession ratio (MPR: the proportion of days with prescription filled over days of follow-up), and classified according to: 1) MPR $<$ 1/3 as less compliant, 2) MPR$\geqslant$1/3 - $<$ 2/3 as compliant, and 3) MPR $\geqslant$ 2/3 as highly compliant. Survival analysis was used to determine the cumulative incidence of subtrochanteric/femur shaft fractures with typical hip fractures or mortality as a competing risk. There were dose-dependent increases in incidences of subtrochanteric/femur shaft fractures as the level of adherences increased (Figure, Gray's test, $p<0.0001$). Within the highly compliant group, the age-adjusted rate of subtrochanteric/femur shaft fractures increased from 56.7 per 100,000 person years in the first year to 175.1 in the fifth year, compared to an increase from 44.3 to 66.6 for the less compliant group during the same period. The adjusted hazard ratio for the highly compliant vs the less compliant was 1.23 (95% Confidence Interval: 1.06-1.43) overall, 1.09 (0.89-1.34) before and 2.09 (1.48-2.95) after 3 years of follow-up. Other risk factors included age, prior vertebral fractures, diabetes, inflammatory arthritis, comorbidity index, and statin use. These were also risk factors for typical hip fractures. However, age-adjusted incidence rates of typical hip fractures were significantly lower among highly compliant beneficiaries, compared to less compliant users (e.g., 873.8 vs 1,168.7 after four years, $p<0.03$). In conclusion, subtrochanteric/femur shaft fractures, unlike typical hip fractures, are positively associated with higher adherence to long-term ($\geqslant$ 3 years) prescription of oral bisphosphonates in the elderly female Medicare population.

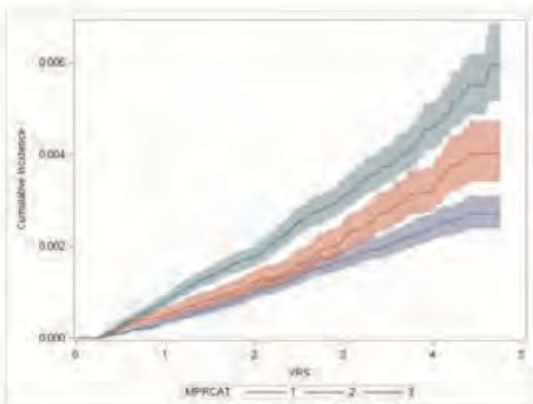

MPRCAT	YR=0	YR=1	YR=2	YR=3	YR=4
1: <1/3	214615	184416	134599	85754	38346
2: 1/3-<2/3	112556	88888	62394	39820	20004
3: ≥2/3	195116	142769	92236	53028	24524

Figure

***Disclosures: John Wang**, None.*

LB-MO24

A Frailty Index Predicts 10-Year Fracture Risk: Longitudinal Data from the Canadian Multicentre Osteoporosis Study (CaMos). Courtney Kennedy*[1], George Ioannidis[1], Lehana Thabane[1], Kenneth Rockwood[2], Jonathan Adachi[3], Susan Kirkland[2], Laura Pickard[1], Alexandra Papaioannou[4]. [1]McMaster University, Canada, [2]Dalhousie University, Canada, [3]St. Joseph's Hospital, Canada, [4]Hamilton Health Sciences, Canada

Purpose: Although the association between frailty and fractures is recognized, this relationship has not been well quantified across a frailty continuum. A Frailty Index is a continuous measure which considers the degree of frailty as proportional to the number of accumulated "health deficits" (symptoms, signs, diseases, and disabilities). This approach correlates well with other frailty measures and offers not only precision (i.e., the ability to differentiate different degrees of frailty), but also generalizability since the framework can be applied to most epidemiological data-sets. Using baseline data from the Canadian Multicentre Osteoporosis Study (CaMos), we created the 31-item CaMos Frailty Index and examined whether it was predictive of incident fractures over 10-years. Methods: CaMos is a prospective cohort study of 9423 randomly selected Canadians aged 25 years and older. Total CaMos Frailty Index scores were derived by summing the deficit score on individual variables (0=absent, 1=maximal expression of deficit) and dividing by the total number of variables (n=31), yielding a score between 0 and 1. We used a competing risk proportional sub-distribution hazards model to examine the association between baseline CaMos Frailty Index scores and 10-year fracture risk adjusting for age, sex, body mass index, education level, femoral neck t-score, and anti-resorptive therapy. Hazard Ratios (HR; *p-values*) are expressed for each 0.10 increase in baseline CaMos Frailty Index score [approximately one standard deviation (SD)]. Results: Our analysis cohort was CaMos participants 50 years and older (n=7753). At baseline, the mean age was 66.7 (SD 9.35) years, 71.8 % were women. The mean Frailty Index score was 0.14 (SD 0.11), ranging from 0 to 0.64. During a mean follow-up of 7.70 years (SD=3.17), 986 participants died before a fracture occurred and 1121 had a fracture. For every 0.10 increase in CaMos Frailty Index scores, the HR was 1.33 ($p=<0.001$) for hip fractures and 1.24 ($p=<0.001$) for all fractures (excluding face, cheek, skull, toe, finger). Conclusions: During the study period (up to ten-years of follow-up), for each 0.10 increase in baseline CaMos Frailty Index score, the risk of a hip fracture increased by 33% and all fractures by 24%. Irrespective of age and bone mineral density, the CaMos Frailty Index is an operational measure of frailty that was predictive of incident fractures.

***Disclosures: Courtney Kennedy**, None.*

LB-MO25

Mouse models of telomere dysfunction phenocopy skeletal changes found in human age-related osteoporosis. Tracy Brennan*[1], Robert Pignolo[2], Kurt Hankenson[2]. [1]University of Pennsylvania School of Medicine, USA, [2]University of Pennsylvania, USA

A major challenge in the elderly is osteoporosis and the associated high risk of fracture. Telomere dysfunction is a cause of cellular senescence and telomere shortening occurs with age in cells from most human tissues, including bone. Telomere defects contribute to the pathogenesis of two progeroid disorders characterized by premature osteoporosis, Werner syndrome and dyskeratosis congenital, and it is hypothesized that telomere shortening contributes to aging of bone. Using mice with disrupted telomere maintenance molecules, including mutants in the Werner helicase ($Wrn^{-/-}$), telomerase ($Terc^{-/-}$) and $Wrn^{-/-}$ $Terc^{-/-}$ double mutants, we evaluated the skeletal phenotypes as models for human bone aging. Compared to young wild-type mice, micro-computerized tomography (µCT) analysis revealed that young $Terc^{-/-}$ and $Wrn^{-/-}Terc^{-/-}$ mice have decreased trabecular bone volume, trabecular number, trabecular thickness, as well as increased trabecular spacing. In cortical bone, young $Terc^{-/-}$ and $Wrn^{-/-}Terc^{-/-}$ mice have increased cortical thinning, and increased porosity relative to age-matched wild-type mice. These trabecular and cortical changes were accelerated with age in the $Terc^{-/-}$ and $Wrn^{-/-}Terc^{-/-}$ mice compared to older wild-type mice. Histological quantification of osteoblasts in aged mice showed a similar number of osteoblasts in all genotypes. However, analysis of kinetic parameters of bone formation showed a significant decrease in mineralization surface and mineral apposition rate in older $Terc^{-/-}$ and $Wrn^{-/-}Terc^{-/-}$ bone, suggesting that osteoblast dysfunction is a prominent feature of precocious aging in these mice. Except in the $Wrn^{-/-}$ single mutant, osteoclast number did not increase in any genotype. Young $Wrn^{-/-}Terc^{-/-}$ mice had a statistically significant increase in bone marrow fat content compared to young WT, which remained elevated in aged double mutants. Overall, the bone phenotype of $Wrn^{-/-}Terc^{-/-}$ mutant mice is largely accounted for by the contribution of telomerase deficit rather than absence of the Wrn helicase. Taken together, our results suggest that $Terc^{-/-}$ and $Wrn^{-/-}Terc^{-/-}$ mutants recapitulate the human bone aging phenotype and are useful models for studying age-related osteoporosis.

***Disclosures: Tracy Brennan**, None.*
This study received funding from: National Institutes of Health/ National Institute on Aging

LB-MO26

Eight Years of Denosumab Treatment in Postmenopausal Women With Osteoporosis: Results From the First Five Years of the FREEDOM Extension.

Socrates Papapoulos*[1], Kurt Lippuner[2], Christian Roux[3], Jesse Hall[4], David Kendler[5], E. Michael Lewiecki[6], Maria Luisa Brandi[7], Edward Czerwiński[8], Edward Franek[9], Péter Lakatos[10], Carlos Mautalen[11], Salvatore Minisola[12], Jean Yves Reginster[13], Soren Jensen[14], Nadia Daizadeh[4], Andrea Wang[4], Michelle Geller[4], Rachel B. Wagman[4], Henry G. Bone[15]. [1]Leiden University Medical Center, The Netherlands, [2]Bern University Hospital, Switzerland, [3]Paris Descartes University, France, [4]Amgen Inc., USA, [5]University of British Columbia, Vancouver, Canada, [6]New Mexico Clinical Research & Osteoporosis Center, USA, [7]University of Florence, Italy, [8]Krakow Medical Center, Poland, [9]Central Clinical Hospital MSWiA, Poland, [10]Semmelweis University, Hungary, [11]Centro de Osteopatias Medicas, Argentina, [12]Sapienza University, Italy, [13]University of Liège, Belgium, [14]CCBR, Denmark, [15]Michigan Bone & Mineral Clinic, USA

Purpose: Denosumab (DMAb) is an approved therapy for the treatment of postmenopausal women with osteoporosis at high/increased risk for fracture. The effects of DMAb treatment for up to 10 years are being evaluated in the 3-year FREEDOM study and its 7-year extension. Here we report the 5-year results from the extension, representing up to 8 years of continued DMAb treatment.

Methods: During the extension, all subjects received 60 mg DMAb Q6M and daily calcium and vitamin D. In this analysis, subjects in the long-term group received 8 years of DMAb (3 years in FREEDOM followed by 5 years in the extension); subjects in the cross-over group received 5 years of DMAb (3 years of placebo in FREEDOM and 5 years of DMAb in the extension).

Results: Of 3046 subjects who continued to participate in the extension at the time of this submission, 88% (2678; 1382 long-term, 1296 cross-over) of subjects have completed dosing at year 8. Bone mineral density (BMD) data showed continued mean increases from FREEDOM baseline for cumulative 8-year gains of 18.5% (lumbar spine) and 8.2% (total hip) in the long-term group and continued to increase in the cross-over group with cumulative 5-year gains of 13.8% (lumbar spine) and 4.8% (total hip) (all $P < 0.05$ compared with FREEDOM and extension baseline; Figure). Serum C-telopeptide (CTX) was rapidly and similarly reduced after each DMAb dose with the characteristic attenuation of effect at the end of the dosing period. Incidence of new vertebral and nonvertebral fracture continued to remain low throughout the extension; hip fracture incidence during year 8 was 0.2% and < 0.1% for the long-term and cross-over groups, respectively. Overall incidences of adverse events (AEs) and serious AEs were consistent with data reported previously in the extension study.

Conclusions: DMAb treatment for up to 8 years was associated with persistent reduction of bone turnover, continued increases in BMD, and low fracture incidence. Modeling-based bone formation in cynomolgus monkeys in the context of maximal reduction of remodeling may help explain these clinical observations (Ominsky ASBMR 2013 submitted abstract). The benefit/risk profile for DMAb remains favorable.

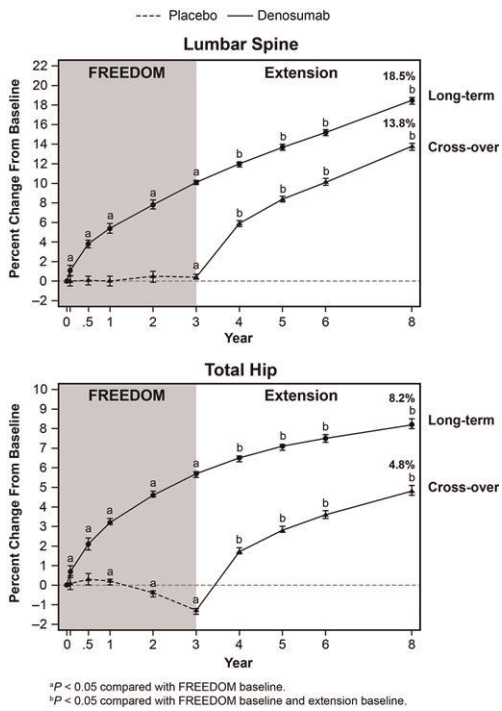

Figure

***Disclosures: Socrates Papapoulos**, Amgen Inc., Merck & Co., GSK, 5; Merck & Co., Novartis, 9; Amgen Inc., Merck & Co., GSK, Axsome, Gador, 2*

This study received funding from: Amgen Inc.

LB-MO27

BPS804, an anti-sclerostin monoclonal antibody, improves disease biomarkers and markers of bone formation in patients with adult-onset hypophosphatasia (HPP).

Lothar Seefried*[1], Jasmin Baumann[1], Sarah Hemsley[2], Shou-Ih Hu[3], Christine Halleux[2], Beate Kiese[4], Yue Huang[2], Steven Golieb[5], Simon Chivers[2], Marie-Anne Valentin[2], Babul Borah[3], Michaela Kneissel[6], Franz Jakob[7], Uwe Junker[2]. [1]Orthopedic Center for Musculoskeletal Research, Experimental & Clinical Osteology, Orthopedic Department, University of Würzburg, Germany, [2]Novartis Institutes for BioMedical Research, Switzerland, [3]Novartis Institutes for BioMedical Research Inc., USA, [4]Novartis Pharma AG, Switzerland, [5]Novartis Pharmaceuticals Corporation, USA, [6]Novartis Institutes for Biomedical Research, Che, [7]Orthopedic Center for Musculoskeletal Research, Experimental & Clinical Osteology, Orthopedic Department, University of Würzburg, Brettreichstraße 11, D-97074 Wuerzburg, Germany

Purpose: Previous case studies of adult-onset HPP patients treated with the bone anabolic molecule PTH1-34 (teriparatide, Forteo™) reported improvement in biochemical disease markers of HPP, bone pain, and accelerated fracture healing. Here, we report the tolerability, PK/PD and efficacy in a Phase 2A trial of the human anti-sclerostin monoclonal antibody BPS804 in patients with adult-onset HPP (ClinicalTrials.gov Identifier: NCT01406977).

Methods: Male and female patients age 18 to 75 years with clinical diagnosis of adult-onset HPP and confirmed *ALPL* genetic mutation were enrolled in this single center, open label trial. Patients received three escalating doses of BPS804 (5, 10, and 20 mg/kg i.v.) every two weeks and were followed for 3.6 months after the last dose. Primary endpoints were number of patients experiencing (serious) adverse events (AEs) and changes from baseline in the serum alkaline phosphatase (ALP) and bone-specific ALP (BSAP) enzymatic activity.

Results: Patients (N=8, mean age 47.8 years) had significantly below gender-matched normal levels of ALP and BSAP. Between days 2 to 29 after the 3rd infusion of BPS804, ALP and BSAP enzymatic activity increased vs. baseline by a mean of 37% (range 19-67%, $p<0.01$) and 30% (range 4-70%, $p<0.01$), respectively. BPS804 also increased bone biomarkers such as PINP, osteocalcin, and lumbar spine bone mineral density while it decreased CTX-1. BPS804 showed a typical PK profile for a human IgG2 lambda monoclonal antibody targeting a soluble ligand (T1/2 ~12 days), with no immunogenicity findings of clinical significance. One patient discontinued early from the study due to a serious AE deemed unrelated to BPS804. Most common AEs were affecting various organ systems (i.e., musculoskeletal and connective tissue, gastrointestinal, nervous system), were mild and transient in nature and mostly unrelated to study drug.Conclusions: BPS804 was generally well tolerated. BPS804 administration resulted in variable increases in ALP and BSAP activity and marked increases in bone formation biomarkers. As shown in this study, responsiveness to BPS804 treatment may vary considerably among adult-onset HPP patients. We hypothesize that osteoanabolic stimulation holds the potential as an effective treatment for bone loss, fragility fractures and fracture healing in genetically confirmed mild forms of HPP such as adult-onset HPP or odontohypophosphatasia, which has to be confirmed in larger clinical trials.

***Disclosures: Lothar Seefried**, None.*

This study received funding from: Novartis Pharma AG

LB-MO28

Comparison of Atypical Femoral Fracture Patients on Long term Bisphosphonates with Controls matched for age and duration of bisphosphonate therapy.

Deeksha Mehta*[1], Nazia Shamsuddin[1], Zehava S. Rosenberg[1], Renata L. Vieira[1], Nirmal C. Tejwani[1], Kenneth A. Egol[1], james S. Babb[1], Valerie Peck[2]. [1]NYU Langone Medical center, USA, [2]NYU School of Medicine, USA

To define the risk factors for atypical femoral fracture patients on long term Bisphosphonate (BP) therapy by comparison with controls matched for age and duration of bisphosphonate therapy.

Methods: Approval was obtained from the IRB. We have previously reported data on 25 patients on long term BPs with atypical femoral fractures without a corresponding control group. We now conducted a retrospective chart analysis of 55 subjects with complete subtrochantric or diaphyseal femoral fractures of which 29 with all relevant data available were selected (a part of this group has been reported before). We selected 29 controls from a prospective asymptomatic database, matched for age and duration of BP use. All subjects studied were on alendronate. Relevant clinical and demographic data including age, gender, height, weight, duration of BP use and prior use of hormone replacement therapy (HRT) were collected. Laboratory and imaging data including calcium, 25-hydroxy vitamin D (25-OHD), alkaline phosphatase, intact parathyroid hormone (PTH), serum c-telopeptide (CTX), urine n-telopeptide (NTX) and bone mineral density (BMD) were obtained.

Results: The age range was 46-86 years and duration of BP was 8.7 years in control group and 9.62 years in patient group, respectively (p=0.318). The mean T-score at the femoral neck was -1.69 and -2.36 in the patient and control groups respectively, which was statistically significant (p=0.004). Similar trend in mean T-score was seen at total hip, -1.22 and -1.93 in patient and control groups, respectively (p=0.005). The bone turnover marker CTX was higher in patients vs. controls (251 vs. 154, respectively; p=0.038), which is an expected finding after a fracture. No statistically significant

differences were seen in 25-OHD, calcium, PTH, alkaline phosphatase, height and weight parameters or prior HRT use between the 2 groups.

Conclusion: Patients with atypical bisphosphonate femoral fractures when compared with controls matched for age and duration of BP therapy were shown to have higher bone mineral density, in the non-osteoporotic range. Hence, early or unnecessary initiation of BP in patients with hip BMD in the non-osteoporotic range or continued therapy in patients with hip BMD in the non-osteoporotic range can be a risk factor for atypical femoral fractures.

***Disclosures: Deeksha Mehta**, None.*

LB-MO29

BA058, a Novel Human PTHrP Analog: Reverses Ovariectomy-Induced Bone Loss and Strength at the Lumbar Spine in Aged Cynomolgus Monkeys. Nancy Doyle[1], Aurore Varela[1], Susan Y. Smith[1], Robert Guldberg[2], Gary Hattersley*[3]. [1]Charles River Laboratories, Canada, [2]Georgia Institute of Technology, USA, [3]Radius, USA

BA058 is an analog of hPTHrP (1-34) undergoing clinical development for the treatment of osteoporosis. This study determined the effects of long-term (16 months) administration of BA058 on bone mineral density and strength in aged osteopenic, ovariectomized cynomolgus monkeys. Female cynomolgus monkeys, ⩾9 years of age, were randomly assigned to 5 groups based on whole body bone mineral content. Four groups of up to 16 animals were ovariectomized (OVX) and an additional group underwent Sham surgery. Treatment commenced after a 9-month bone depletion period. Animals received daily subcutaneously injection of either vehicle (Sham and OVX controls), or BA058 at 0.2, 1 or 5 µg/kg for 16 months. Lumbar vertebrae (L3 to L5) were retained for bone densitometry (DXA and pQCT) and biomechanical testing (vertebral body and core compression). As expected for osteopenic animals, decreases in BMD by DXA and pQCT (-19%) and bone strength parameters (yield load) were observed for lumbar vertebral cores (-30%) and vertebral body (-20%) in compression for OVX controls compared to intact Sham controls. Treatment with BA058 at 1 and 5 µg/kg/day resulted in complete reversal of the OVX-induced osteopenia at the lumbar spine with increased yield load of ~50% for the vertebral core and ~20% for the vertebral body compared to OVX controls. These changes were consistent with the increases in BMD of up to ~25%. At 1 and 5 µg/kg/day BA058 completely restored bone mass and bone strength (yield load) to values comparable to Sham control. At 0.2 µg/kg/day, there were partial gains in BMD and strength parameters. BA058 potentially offers important advantages as a new treatment for post-menopausal osteoporosis, including the ability to rapidly build new bone, sustain gains over time, and improve bone strength at clinically relevant sites.

***Disclosures: Gary Hattersley**, None.*
This study received funding from: Radius Health

LB-MO30

Continuous modeling-based bone formation: a novel mechanism that could explain the sustained increases in hip bone mineral density (BMD) with denosumab treatment. Michael Ominsky[1], Cesar Libanati[1], Rogely Waite Boyce[1], Paul Kostenuik[1], Roland Baron[2], Rachel Wagman[1], David Dempster*[3]. [1]Amgen Inc., USA, [2]Harvard School of Medicine & of Dental Medicine, USA, [3]Columbia University, USA

Denosumab administration in clinical studies is associated with continued increases in BMD and low fracture incidence through 8 years despite persistently low bone turnover markers and limited iliac crest tetracycline labeling[1]. We therefore hypothesized that, with persistently low bone remodeling, these BMD increases may result from a non-remodeling dependent mechanism to accrue bone matrix. To test this hypothesis, we examined the fluorochrome labeling pattern in proximal femur sections from ovariectomized (OVX) cynomolgus monkeys (cynos) treated with denosumab for 16 months.

Following OVX, mature 9+ year old cynos were treated with vehicle (n=20) or 25 mg/kg denosumab (n=14) QM for 16 months. Fluorochrome labels were administered at months 6, 12 and 16. Consistent with the potent anti-remodeling effect of this regimen (25x clinical dose), very low bone resorption and formation indices were observed histologically and by serum markers[2]. Despite these reductions, DXA BMD continued to rise at the femur neck in the denosumab group, from 5.9% at month 6 to 11.3% above baseline at month 16. Examination of proximal femur sections confirmed the low surface extent of label within the trabecular compartment of the denosumab group. In contrast, consistent and prominent labeling was observed in the cortex, primarily on both the superior endocortex (12 of 14 cynos) and the inferior periosteal surface (11 of 14 cynos), consistent with increasing cortical thickness. These regions typically contained multiple superimposed labels over smooth cement lines, often spanning months 6 to 16 (Figure), suggesting that modeling-based bone formation was continuous during denosumab administration.

Persistence of bone modeling on a background of maximal suppression of remodeling could explain the continued increases in BMD and mass observed with denosumab treatment. Importantly, this augmentation of bone mass occurred at biomechanically relevant sites on the superior and inferior aspects of the femur neck, and corresponded to significant increases in bone strength[3]. In conclusion, there is evidence in cynos that continual modeling-based bone formation occurs during denosumab therapy. This study provides the first histological evidence of a potential mechanism responsible for the clinical observations of continued BMD increases and low fracture rates with long-term denosumab administration in the FREEDOM Extension.

References: 1.Papapoulos 2013; 2.Kostenuik 2011; 3.Ominsky 2011

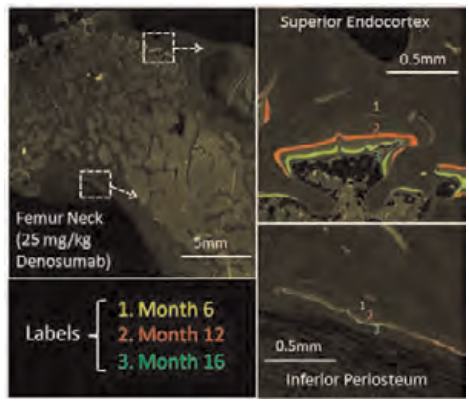

Figure: Epifluorescent micrograph from denosumab treated cyno

***Disclosures: David Dempster**, Amgen, 7; Amgen, 3*
This study received funding from: Amgen

LB-MO31

Co-treatment with *Fructus Ligustri Lucidi* and *Puerariae Radix* offsets their independent actions on bone/mineral metabolism in OVX rats. XL Dong[1], SS Cao[2], QG Gao[2], Haotian Feng*[3], Man-Sau Wong[1], Denney liya[4]. [1]Department of Applied Biology & Chemical Technology, The Hong Kong Polytechnic University, China, [2]The Hong Kong Polytechnic University, China, [3]Nestle Research Center Beijing, [4]Nestlé Research Centre, Switzerland

Accumulating evidences showed that *Fructus Ligustri Lucidi* (FLL) and *Puerariae Radix* (PR), two herbs long used in traditional Chinese medicine (TCM), could exert beneficial effects on bone and mineral metabolism individually. In this study, to further explore the potential of FLL and PR for bone protection, we aimed to evaluate therapeutic efficacies of cotreatment with FLL and PR on bone and mineral metabolism in ovariectomized (OVX) Sprague Dawley rats. Six-month-old OVX rats were used as postmenopausal osteoporotic models, and water extracts of PR and FLL were added to commercial diets individually or in combination and administrated to the OVX rats for 12 weeks. Bone properties, calcium and phosphorus absorption and bone biochemical markers were measured to investigate the potential interactions between the actions of PR and FLL on bone and mineral metabolism in OVX rats. PR treatment in this study did not significantly improve bone properties, but it greatly ameliorated the condition of secondary hyperparathyroidism induced by OVX in the animals. FLL significantly enhanced the intestinal Ca absorption rate and decreased the enlarged trabecular bone surface at the site of tibia metaphysics in OVX rats. However, the positive effects of FLL or PR alone on bone and mineral metabolism were diminished when OVX rats were co-treated with both FLL and PR. The results from the present study could provide insights for medical professionals to understand the potential negative impact of herb-herb interactions when combination of herbal mixtures is employed for the purpose of osteoporosis treatment & management.

***Disclosures: Haotian Feng**, None.*
This study received funding from: Nestle

LB-MO32

Effect of Aromatase Inhibition on Bone Density and Bone Turnover in Healthy Postmenopausal Women: Results of the International Breast cancer Intervention Study II (IBIS-II). Richard Eastell*[1], Ivana Sestak[2], Fatma Gossiel[1], Rajesh Patel[3], Glen Blake[4], Robert Coleman[1], Anthony Howell[5], Mitch Dowsett[6], John Forbes[7], Shalini Singh[2], Jack Cuzick[2]. [1]University of Sheffield, United Kingdom, [2]Queen Mary University, United Kingdom, [3]Imperial College London, United Kingdom, [4]King's College London, United Kingdom, [5]Paterson Institute for Cancer Research, United Kingdom, [6]Institute of Cancer Research, United Kingdom, [7]University of Newcastle, Australia

Background: The inhibition of aromatase in postmenopausal women with breast cancer has been associated with an increase in fracture risk, and this effect may be mediated by an increase in bone turnover and in the rate of bone loss. It has been difficult to estimate the magnitude of the effect of aromatase inhibitors on bone because the control arm is usually women treated with tamoxifen and this is known to have effects on bone. Here, we compare the effect of aromatase inhibition on bone in the International Breast cancer Intervention Study (IBIS-II), which is a randomised, placebo-controlled trial of anastrozole versus placebo in postmenopausal women at increased risk of breast cancer.

Methods: Measurements of bone turnover markers for the bone sub-study have been completed for a sub-set of postmenopausal women from the bone study, which included 1410 postmenopausal women aged 40 to 70 years at increased risk of breast cancer. Women were stratified by T-score at baseline; if the spine and hip T-score were both equal or above -1.0, women were not offered any bisphosphonate (Stratum I), but advised to take calcium and vitamin D supplementation. Bone resorption by N-telopeptide of type I collagen (NTX) expressed as a ratio to creatinine (from a second morning void urine sample) were measured at baseline, 6 months and year 1, and for 289 women bone turnover marker results were available for all three time points. Lumbar spine and total hip BMD were measured by dual-energy x-ray absorptiometry (Hologic or GE Lunar) at baseline, 1 and 3 years.

Results: 289 postmenopausal women with normal BMD at baseline (T-score $\geq$-1.0) were included in this analysis (Anastrozole=142, Placebo=147). A median increase in NTX/Cr between baseline and year 1 of 20% was observed for anastrozole and a median decrease of 7% for placebo and the difference was statistically significant (P<0.0001). The median annual rate of bone loss was much greater at the total hip (-1.3% vs. -0.4%) and lumbar spine (-1.3% vs. -0.2%) for women receiving anastrozole compared to placebo (P<0.0001) (Table 1). The baseline NTX/Cr and the change in NTX/Cr between baseline and year 1 were not significantly related to the rate of bone loss.

Discussion: This is the first report of a large placebo-controlled trial investigating an aromatase inhibitor to show a significant bone loss in women taking anastrozole, which is likely due to an increase in bone resorption.

Table 1: Annual median changes (IQR) between baseline and year 1 for NTX/Cr and between baseline and year 3 for BMD in spine and total hip according to treatment allocation.

	Anastrozole (N=142)	Placebo (N=147)	Difference between baseline and year 1 (95% CI)
Annual change in NTX/Cr, nmol BCE/mmol Cr	8.9 (-3.1 to 21.8)	-1.9 (-11.7 to 10.2)	10.8 (5.4 to 16.2)
Annual change in spine BMD, %/year	-1.3 (-2.17 to -0.44)	-0.2 (-1.0 to 0.9)	-1.1 (-1.5 to -0.7)
Annual change in hip BMD, %/year	-1.3 (-1.8 to -0.6)	-0.4 (-1.3 to 0.3)	-0.8 (-1.2 to -0.5)

*NTX=N-Telopeptide x, Cr=Creatinine, BCE=Bone Collagen Equivalent, BMD=Bone Mineral Density

Table

***Disclosures: Richard Eastell**, Aventis, 6; Astrazeneca, 6*
This study received funding from: Astrazeneca

LB-MO33

NFAM1 Signaling Modulates Osteoclast Differentiation in Paget 's Disease of Bone. Yuvaraj Sambandam*[1], Kumaran Sundaram[2], Sakamuri Reddy[2]. [1]Medical University of South Carolina, USA, [2]Charles P. Darby Children's Research Institute, USA

Paget's disease of bone (PDB) is a chronic focal skeletal disease that affects 2-3% of the population over 55 years of age. The primary abnormality in PDB is excess bone resorption by abnormal osteoclasts (OCLs) followed by abundant poor quality new bone formation. Recurrent mutations in SQSTM1/p62 ubiquitin associated domain (UBA) have been identified in PDB. Also, pagetic OCL contains paramyxoviral nuclear inclusions and nucleocapsid transcripts. We previously detected measles virus nucleocapsid protein (MVNP) transcripts in OCLs from patients with PDB. MVNP has been shown to induce pagetic phenotype in OCL. We showed that MVNP expression stimulates osteoclastogenesis by upregulating NFATc1, a critical transcription factor for OCL differentiation. We recently analyzed gene expression profiling by Agilent microarray and demonstrated MVNP significantly increased expression of several signaling molecules and cytokine/growth factors in normal human bone marrow derived preosteoclast cells. We thus identified MVNP upregulation (7-fold) of NFAT activating protein with ITAM motif 1 (NFAM1) expression. However, there is no change in NFAM1 expression in preosteoclast cells transfected with $p62^{WT}$ and $p62^{P392L}$. NFAM1 also known as CNAIP, is a ~30 kDa transmembrane glycoprotein that contains extracellular Ig domain and intracellular immunoreceptor tyrosine-based activation motif (ITAM) bearing region. We therefore hypothesize, that MVNP modulates NFAM1 signaling during pagetic OCL differentiation. Real-time PCR analysis showed that MVNP expression in human peripheral blood monocytes cells significantly increased (10-fold) NFAM1 mRNA expression without RANKL treatment. Cells transfected with a control empty vector (EV) and stimulated with RANKL showed a 3.0-fold increase in NFAM1 mRNA expression. Western blot analysis further confirmed that MVNP increased (4.8-fold) NFAM1 expression in these cells. NFAM1 has been shown to induce ITAM phosphorylation and Syk recruitment. Interestingly, MVNP expression resulted in increased ITAM phosphotyrosine activation (4.0-fold) and p-Syk (5.5-fold) levels in preosteoclast cells in the absence of RANKL. However, RANKL treatment alone increased ITAM activation (2.0-fold) and p-Syk (2.5-fold) levels in EV transfected preosteoclast cells. Furthermore, shRNA knockdown of NFAM1 suppresses MVNP induced NFATc1 expression in preosteoclast cells. Thus, our results suggest that NFAM1 modulates MVNP induced pagetic osteoclast development.

***Disclosures: Yuvaraj Sambandam**, None.*

LB-MO34

***CYP2R1* Gene Polymorphisms Are Associated With Variability In 25-Hydroxy Vitamin D Levels In The Elderly.** Asma Arabi*[1], Nathalie Khoueiry-Zgheib[2], Rami Mahfouz[3], Zainab Awada[2], Maya Rahme[1], Karim Firikh[1], Ghada El Hajj Fuleihan[1]. [1]Calcium Metabolism & Osteoporosis Program, American University of Beirut, Lebanon, [2]Department of Pharmacology & Toxicology, American University of Beirut, Lebanon, [3]Department of Pathology & Laboratory Medicine, American University of Beirut, Lebanon

Hypovitaminosis D is highly prevalent in the Middle East, although this region enjoys sunshine most days of the year. Genome wide association studies and candidate genes approaches have interrogated the role of genetic polymorphisms in the variability of 25 hydroxyvitamin D (25-OHD) levels in Western populations. The applicability of these studies to other races/populations is unclear.The cytochrome P450 2R1 (CYP2R1) plays a major role in the vitamin D hydroxylation in human. This study evaluated the association between variability in 25-OHD levels in Lebanese elderly and polymorphisms in 4 single nucleotides (SNP) of the CYP2R1 gene. Genotyping was performed for rs12794714, rs10741657, rs1562902, & rs10766197 SNPs in 250 subjects [109 men & 141 women] using Real-Time PCR. Blinded duplicate sample analyses were performed for all assays. Additional 10% of samples were repeated to verify reproducibility. Baseline 25-OHD levels were measured by chemiluminescent platform Liaison assay (DiaSorin).

The subjects' mean age was 71.0$\pm$4.7 yrs, mean BMI 30.0$\pm$4.5 kg/m^2 and mean 25-OHD level 18.4 $\pm$7.6 ng/ml. Genotype frequencies were in Hardy-Weinberg equilibrium.

There was a significant difference in 25-OHD levels between genotypes. For rs10741657 and rs1562902 SNPs, the mutant genotype had the highest 25-OHD levels compared to wild and heterozygous genotypes. Conversely, wild genotype had the highest 25-OHD levels for rs10766197 SNP [Table]. After adjustment for age, season, gender and BMI, mutant genotype had 25-OHD levels higher by 4.8 and by 4.3 ng/ml than wild genotype for rs10741657 SNP and for rs1562902 SNP respectively (p< 0.01). Conversely, for rs10766197 SNP, mutant and heterozygous genotypes had 25-OHD levels lower by 3.6 and by 2.7 ng/ml respectively compared to wild genotype (p< 0.01). Mutant genotype for rs12794714SNP had 25-OHD levels lower by 3 ng/ml compared to wild genotype (p=0.02) [Table]. Sub-group analyses by gender revealed comparable results for rs10741657 SNP in men and for rs1562902 and rs10766197 SNPs in women.

In conclusion, this study showed a significant difference in 25-OHD levels between CYP2R1 genotypes. This difference equates a daily supplementation of 200 to 400 IU vitamin D.

This study underscores possible genetic causes for the high prevalence of hypovitaminosis D in the Middle East. The impact on the response to vitamin D supplementation remains to be investigated.

Association between *CYP2R1* gene polymorphisms and OHD levels before & after adjustment for potential predictors

SNP/ Genotype (n)	25-OHD (ng/ml)**	p-value*	β (SE)[d]	p-value[d]
rs12794714				
Wild (70)	20.06 ± 9.01			
Heterozygous (119)	18.08 ± 6.84		-2.1 (1.1)	0.06
Mutant (61)	17.34 ± 7.27	0.09	-3.0 (1.3)	0.02
rs10741657				
Wild (122)	17.62 ± 7.11[a]			
Heterozygous (103)	18.6 ± 7.41[b]		1.1 (0.9)	0.2
Mutant (25)	21.94 ± 10.11[a,b]	0.03	4.8 (1.6)	0.003
rs1562902				
Wild (97)	17.38 ± 7.14[a]			
Heterozygous (114)	18.33 ± 7.27[b]		1.1 (1.0)	0.2
Mutant (39)	21.5 ± 9.23[a,b]	0.01	4.3 (1.4)	0.002
rs10766197				
Wild (70)	20.75 ± 9.19[a,b]			
Heterozygous (120)	17.86 ± 6.51[a]		-2.7 (1.1)	0.01
Mutant (59)	17.07 ± 7.34[b]	0.01	-3.6 (1.3)	0.007

*Unadjusted p-Value for difference between genotypes by ANOVA.
**Mean values with same superscript, within each SNP, were significantly different from each others in post hoc analyses
[d] Multivariate linear regression adjusted for age, gender, season and BMI.
Ref was wild genotype.

Table Arabi et al

***Disclosures: Asma Arabi**, None.*

LB-MO35

Control of Breast Cancer Growth and Dissemination By the Skeleton. Claire-Sophie Devignes*[1], Audrey Brenot[2], Amy-Jo Casbon[3], Audrey Devillers[1], Ying Yu[3], Zena Werb[3], Sylvain Provot[1]. [1]INSERM, France, [2]Washington University School of Medicine, USA, [3]UCSF, USA

Breast cancer is often associated with a poor prognosis largely due to its tendency to metastasize. Since Paget's ''seed and soil'' hypothesis from more than a century ago, it is known that bones constitute a very hospitable soil that attracts and allows breast cancer (BC) cells to thrive. Surprisingly, however, only a few studies have

addressed the role of the bone microenvironment in bone metastasis. We tested the possibility that osteoblasts (bone-making cells) could influence breast cancer metastasis to bone by inoculating a BC cell line (PyMT-FVB-Luc+ cells) either directly into the bloodstream, or into the mammary gland (fat pad) of syngeneic recipient mice presenting increased or decreased osteoblast numbers. Hypoxia and the Hypoxia inducible factor 1alpha (Hif-1alpha) play a fundamental role in bone development. Mice deficient for Hif-1alpha in osteoblasts (ΔHif-1alpha^{OB} mice, a Osx-Cre-mediated conditional knockout) present decreased number of osteoblasts and reduced bone mass. Conversely, mice deficient for von Hippel–Lindau (VHL, an E3 ubiquitin-ligase that targets Hif-1alpha for degradation) specifically in osteoblasts (ΔVHL^{OB} mice) present increased levels of Hif-1alpha protein in osteoblasts, and as a consequence, have a dramatic increase in osteoblast number and bone mass. Intracardiac injection of BC cells into these loss- or gain-of-function models reveals that osteoblasts directly or indirectly stimulate breast cancer metastasis to bone. Strikingly, our results also show that osteoblasts produce systemic changes, controlling breast cancer metastasis to several organs in addition to bones, as well as the growth of primary mammary tumors. Transplantation of BC cells in the mammary gland leads to larger primary tumors in ΔVHL^{OB} mice, and smaller tumors in ΔHif-1alpha^{OB} mice, compared to control mice. ΔVHL^{OB} mice also present increased disseminated tumors in multiple organs other than bones, both after tail vein (intravenous) and intracardiac injections of BC cells, or their transplantation in the mammary gland. Conversely, ΔHif-1alpha^{OB} mice present fewer disseminated tumors. Thus, osteoblasts can affect metastasis to distant tissues, well beyond the bone microenvironment. By providing the first evidence that the skeleton exerts a systemic control of breast cancer growth and dissemination, our study expands the biological importance of this organ, and our understanding of cancer biology.

***Disclosures: Claire-Sophie Devignes**, None.*

ADULT BONE AND MINERAL WORKING GROUP

WG1

Normocalcemic Familial Hypocalciuric Hypercalcemia: Loss of Function Calcium Sensing Receptor (CASR) Mutation in a Patient with Noraml Serum Calcium. Marcio L Griebeler[1], Stefan K Grebe[2], Robert A Wermers[1]. [1]Division of Endocrinology, Diabetes, Nutrition and Metabolism; [2]Department of Laboratory Medicine and Pathology, Mayo College of Medicine, Mayo Clinic, Rochester, MN, USA.

Familial hypocalciuric hypercalcemia (FHH) [OMIM #145980] is a autosomal dominantly inherited lifelong condition caused by inactivating mutations in the calcium sensing receptor (CASR) gene leading to calcium-hyposensitivity which is manifested biochemically as chronic hypercalcemia, inappropriately elevated parathyroid hormone (PTH) and a low fractional excretion of filtered calcium.

CASE HISTORY: A 37-year-old female presented with proximal muscle weakness, fatigue and mental sluggishness which began 10 years ago. Two years prior to presentation she developed facial pain and was treated with prednisone for possible trigeminal neuralgia and subsequently had a tooth extracted. She had a history of ankle and forearm fractures as a child. Her family history was pertinent for hypercalcemia associated with an elevated PTH in her mother. Physical exam was unremarkable.

LABORATORY DATA: Normal blood work included the following: CBC, sodium, potassium, ESR, AST, ALT, alkaline phosphatase, TSH, and cortisol. Her serum calcium was generally high normal associated with an intermittently elevated PTH. Her most recent serum calciums were 9.7 mg/dl and 10.1 mg/dL, phosphorus 3.1 mg/dL, PTH 44 pg/mL, magnesium 2.2 mg/dl and 25-hydroxyvitamin D 24.5 ng/mL. Her 24 hour urinary calcium was 141 mg with a calcium-clearance to creatinine-clearance ratio of 0.01.

OTHER STUDIES: A parathyroid scan and ultrasound of the neck were nonlocalizing. CASR gene testing revealed a c.1606delG frameshift mutation (p.Glu536ArgfsX91) resulting in loss of normal protein function. She was also heterozygous for R990G, a mild activating mutation linked to an increased renal calcium excretion.

CONCLUSION: Compensatory activating mutations resulting in increased renal calcium excretion may mask the lifelong hypercalcemia that is expected in FHH and result in normocalcemic variants.

WG2

Treating Familial Hypocalciuric Hypocalcemia Type-3 (FHH3) with Cinacalcet. Malachi J McKenna[1], Tom FJ King[1], Ciara M McDonnell[2], McMyra O'Keane[1], Michelle Morrin[1], Mark T Kilbane[1]. [1]Metabolism Laboratory, St. Vincent's University Hospital, and National Children's Hospital, Tallaght, Dublin, Ireland.

FHH is a rare cause of hypercalcemia that typically presents with mild hypercalcemia, inappropriately low urinary calcium excretion and a normal parathyroid hormone (PTH) level. There are three genetically distinct types: FHH1 in about 65% of cases with loss of function mutations in calcium sensing receptor (CaSR) (chromosome 3q21.1); FHH2 with mutation in G Protein Alpha subunit 11 (Gα11) (chromosome 19p); and FHH3 with mutation in adaptor protein-2 δ sub-unit (AP2S1)(chromosome 19q13.3)1. In FHH3, missense mutations affect Arg15 that seems to impair CaSR internalization1.

AIM: We report two cases with different but recently recognized mutations in FHH3, both of whom were treated with Cinacalcet.

CASE 1: A 34 year old woman was referred with lethargy, generalized pains and headaches. Her three children have subsequently been diagnosed with hypercalcemia, and all have symptoms including severe learning difficulties. Sequencing analysis of AP2S1 codon_Q.Arg15 showed that she was heterozygous for c.43C>T (p.Arg15Cys). She had previously undergone exploratory neck surgery which had revealed four normal parathyroid glands with no evidence of an adenoma. Results were as follows: ionized calcium = 1.52 mmol/L (N: 1.19–1.35 mmol/L); PTH = 42.5 pg/mL (N: 15–65 pg/ml); 24-hour urine calcium = 2.3 mmol (N: <6 mmol/24hr); calcium:creatinine ratio = 0.06 mmol/μmol (N: 0.07–0.41 mmol/μmol); 1,25(OH)2D = 15.4 pg/mL (N: 10–64 pg/ml); PTHrp <1.4 pmol/L. Following commencement of Cinacalcet, there was a reduction in both ionized calcium (1.34 mmol/L) and PTH (21 pg/mL). Response has been sustained over 3 years.

CASE 2: A 24 year man old presented with fatigue and rib pains, and he suffered from autistic spectrum disorder. His father, one of his three siblings, and a fraternal cousin had hypercalcemia. Sequencing analysis of AP2S1 codon_Q.Arg15 showed that he was heterozygous for c.44G>A (p.Arg15His). Results were as follows: ionized calcium 1.53 mmol/L (N: 1.19–1.35 mmol/L); PTH 65.1 pg/mL (N: 15–65 pg/ml); 24-hour urine calcium 4.1 mmol (N: <7.5 mmol); urine calcium:creatinine ratio 0.01 mol/μmol (N: 0.07–0.41 mol/μmol). Tc99m-sestamibi scan did not reveal any evidence of parathyroid adenoma; 18-fluorodeoxyglucose positron emission computed tomography imaging showed no metabolic hyperactivity in the parathyroid glands, or any other soft tissues or bony skeleton. He was treated with Cinacalcet 30 mg twice daily. Ionized calcium fell to 1.2 mmol/L and PTH to 11.1 pg/mL. Symptoms of bone pain and fatigue improved, and he became less withdrawn.

CONCLUSION: Cinacalcet is effective as treatment of symptomatic FHH3 with significantly lower of ionized calcium and PTH levels and with a sustained response. It may improve associated behavioral aspects.

REFERENCE:
1. Nesbit MA, Hannan FM, Howles SA, et al. Mutations in AP2S1 cause familial hypocalciuric hypercalcemia type 3. Nat Genet 2013;45:93–7.

WG3

Fibrogenesis Imperfecta Ossium (FIO): Clinical Aspects to Global Gene Expression Profiling of Bone Tissue. Sanjay Kumar Bhadada[1], Vandana Dhiman[1], Akhilesh Kumar[1], Yashpal Gogate[1], Kumardeep Chaudhary[2], Sameer Aggarwal[1], Anil Bhansali[1], D.S. Rao[3]. [1]Postgraduate Institute of Medical Education and Research, Chandigarh (160012), India; [2]Senior Research Fellow, Bioinformatics Centre, CSIR-Institute of Microbial Technology, Chandigarh, India; [3]Chief of Bone and Mineral Research Laboratory, Henry Ford Hospital, Detroit, USA.

Fibrogenesis imperfecta ossium (FIO) is an uncommon, crippling, relentlessly progressive metabolic bone disease characterized by multiple pseudo-fractures. The molecular pathogenesis and treatment stratification of FIO is not clearly known. Hence, present study is designed to identify genes putatively involved in the pathogenesis of FIO based on their expression profile.

METHODS: Trans-iliac bone biopsy was done in patient with clinical characteristic of FIO. The differential gene expression, compared to healthy control was studied using global microarray (AffymetrixGenechip. Human Primview) and analyzed using Gene Spring GX 12.1 software. We explored the topological characteristics of differentially expressed genes in the context of the human interactome and analyzed for pathway annotations using reactome and NCBI Gene bank database

RESULT: Bone remodeling is interplay between osteoclastogenesis, mediated by osteoclasts and osteoblastognesis, mediated by osteoblasts. We observed down regulation of SPARC (which encodes osteonectin) and BGLAP (which encodes osteocalcin). Both osteonectin and osteocalcin play an important role in bone formation. One of the actions of IGF-1on bone formation is through increasing osteocalcin. The patient responded to growth hormone therapy, further emphasizing the role of BGLAP (which encodes osteocalcin). Mineralization defect and the clinical finding of pseudo-fractures can be explained by down regulation of genes involved in mineralization, namely SPP-1 (which encodes osteopontin) and BGLAP (which encodes osteocalcin). The upregulation of SOST gene adds 'fuel to the fire' by inhibition of Wnt signaling, important osteoblast activation pathway. We also found up regulation of OSTM-1 gene, involved in osteoclastogenesis. Similarly, we also observed increase in collagen expression but decrease in expression of signaling molecules (MMP, ICAM) involved in assembly of these collagens fibrils leading to defective collagen synthesis.

CONCLUSION: This study is the first systematic network and pathway analysis of candidate genes in FIO, providing abundant important information about gene interaction and regulation in this rare bone metabolic disorder. The use of gene-expression profiling improves the molecular classification of FIO. The results suggest potential functional components underlying the molecular mechanisms of FIO and, thus, facilitate generation of novel hypotheses in this disease.

WG4

Hypercalcemia and Pneumocystis Pneumonia After Liver Transplantation: A Case Report. E Cong and E Shane. Division of Endocrinology, Columbia University Medical Center, New York, NY, USA.

Pneumocystis jirovecii pneumonia (PCP) is a potentially life threatening opportunistic infection that manifests in immunocompromised patients, such as those infected with human immunodeficiency virus (HIV) or receiving immunosuppressive therapy after solid organ transplant[1,2]. Chemoprophylaxis is recommended for the first six to twelve months after organ transplant because the highest risk of PCP is during the first post-transplant year[3]. PCP-induced hypercalcemia is a rare phenomenon, with fewer than ten reported cases, all in renal transplant patients and patients with HIV or leukemia[4]. We report the first case of PCP-induced hypercalcemia arising as a complication in a patient following liver transplant.

CASE HISTORY: A 61 year old Caucasian gentleman presented to Columbia University Medical Center with two months of fevers, chills, night sweats, weight loss, dry cough and gradually worsening dyspnea on exertion. He also had oxygen desaturation on exertion and required supplemental oxygenation. His past medical history was remarkable for orthotopic liver transplant 1.5 years prior to admission for hepatitis C and hepatocellular carcinoma, primary ocular lymphoma diagnosed three years prior to admission and now in remission, chronic kidney disease, steroid-induced diabetes and moderate aortic stenosis. His outpatient medications included prednisone 5 mg, tacrolimus, mycophenolic acid, valcyclovir, insulin, metoprolol and amlodipine, vitamin D 1200 IU and calcium 1500mg. His diet included 600mg calcium (total intake 2100 mg daily).

LABORATORY DATA: Serum calcium 15.4 mg/dl [8.7–10.2], ionized calcium 1.85 mmol/L [1.12–1.32], creatinine 2.7 mg/dl (baseline 1.8–2.3), GFR 24 mL/min/1.73 m^2, phosphorous 4.1 mg/dl [2.5–4.3], parathyroid hormone 16 pg/ml [8–51], $1,25(OH)_2$vitamin D >220 pg/ml [15–75], 25-OHvitamin D 32 ng/ml [30–80], alkaline phosphatase 464 U/L [33–96] and PTHrP 16 pg/ml [14–27]. The patient had no prior history of hypercalcemia or hypervitaminosis D.

OTHER STUDIES: Chest imaging showed bilateral diffuse ground glass opacities in lower lobes and was negative for pulmonary embolism. MRI of the brain, abdomen and pelvis, bone scan and ophthalmology exam were negative for recurrent ocular lymphoma. Bronchoscopy was negative for malignant cells and mycobacterium tuberculosis, and revealed *pneumocystis* jirovecii organisms by methenamine silver stain.

TREATMENT: Serum calcium remained markedly elevated despite 3L IVF daily and IV furosemide 20–40mg daily for the first five days (see Graph). Bisphosphonates were not administered because GFR declined to 12 mL/min/1.73 m^2. On day six, prednisone was initiated at 40mg twice daily together with trimethoprim-sulfamethoxazole for presumptive PCP. On day ten, calcitonin 4 IU/kg SQ was given every twelve hours for a total of four doses. Hypercalcemia and hypervitaminosis D began to improve on day ten, with repeat labs on day fourteen showing a calcium of 10 mg/dl (corrected calcium 10.5 mg/dl) and $1,25(OH)_2$vitamin D of 19 pg/ml. Six months later, the patient is normocalcemic off prednisone, renal function has returned to baseline, PCP has not recurred and his ocular lymphoma remains in remission.

CONCLUSION: We present a case of a patient who presented 1.5 years after liver transplantation with severe hypercalcemia and PCP with extraordinarily high serum $1,25(OH)_2$vitamin D concentration that responded to therapy with steroids and antibiotics. This case report suggests that the mechanism of PCP-induced hypercalcemia is similar to that seen in granulomatous diseases such as sarcoidosis. In these disorders, hypercalcemia results via interferon-mediated expression of extrarenal 1α-hydroxylase activity in macrophages within granulomas[5]. This case also highlights that hypercalcemia may be a harbinger for development of PCP in immunosuppressed patients, and that expeditious workup and therapy for PCP and prednisone therapy effectively correct the hypercalcemia.

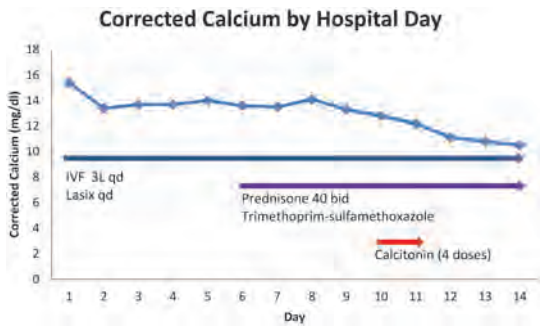

REFERENCES:

1. Thomas CF Jr, Limper AH. *Pneumocystis* pneumonia. N Engl J Med 2004; 350: 2487–2498

2. Fishman J.A. Infection in solid-organ transplant recipients. N Engl J Med 2007; 357: 2601–2614

3. Martin SI, Fishman JA. AST Infectious Diseases Community of Practice. *Pneumocystis* pneumonia in solid organ transplant recipients. Am J Transplant 2009; 9 (Suppl 4): S227–233

4. Chatzikyrkou C, Clajus C, Haubitz M, Hafer C. Hypercalcemia and *pneumocystis* pneumonia after kidney transplantation: report of an exceptional case and literature review. Transpl Infect Dis 2011; 13: 496–500

5. Barbour GL, Coburn JW, Slatopolsky E et al. Hypercalcemia in an anephric patient with sarcoidosis: evidence for extrarenal generation of 1,25-hydroxyvitamin D. N Engl J Med 1981; 305: 440–443

WG5

Osteoporotic Vertebral Fractures During Pregnancy: Be Aware of a Potential Underlying Genetic Cause. N Campos-Obando[1], L Oei[1], MEH Simon[2], MC Zillikens[1]. [1]Department of Internal Medicine, Erasmus Medical Center, Rotterdam; [2]Department of Clinical Genetics, Erasmus Medical Center, Rotterdam.

Although the baby growing in its mother's womb needs calcium for skeletal development, osteoporosis and fractures very rarely occur during pregnancy.

CASE HISTORY: A 27-year old woman in the 7th month of her first pregnancy contracted mid-thoracic back pain after lifting an object. The pain was attributed to her pregnancy, but remained post-partum. Her past medical history was uneventful, except for severely reduced vision of her left eye since birth. Family history revealed that her maternal grandmother had postmenopausal osteoporosis and her only brother had three fractures during childhood after minor trauma. Her height was 1.58 m, she had no blue sclerae or joint hyperlaxity.

LABORATORY DATA: Laboratory examination including serum calcium, phosphate, alkaline phosphatase, creatinine, bCTX, 25-hydroxyvitamin D and TSH was normal.

OTHER STUDIES: Multiple thoracic vertebral fractures were diagnosed on X-ray examination and DXA-scanning showed severe osteoporosis (T-score L2-L4: −5.7 SD, femur neck: −3.9 SD). DNA analyses revealed two compound heterozygous missense mutations in LRP5. Her mother carried one of the LRP5 mutations and was diagnosed with postmenopausal osteoporosis. Her brother, treated with cabergoline for a microprolactinoma, had osteopenia on DXA and carried the same LRP5 mutation.

TREATMENT: The patient was treated with risedronate for 2.5 years. BMD and back pain improved. She stopped bisphosphonate use 6 months before planning a second pregnancy.

CONCLUSION: Our patient was diagnosed with osteoporosis pseudoglioma syndrome/familial exudative vitreoretinopathy. Potentially underlying genetic causes should be considered in pregnancy-associated osteoporosis with implications for patients and relatives. More studies regarding osteoporosis treatment preceding conception are desirable.

WG6

Male Hypogonadism Impact in Bone Quality Assessed by Trabecular Bone Score (TBS). Mário Rui Mascarenhas[1-4], Ana Paula Barbosa[1-4], Ana Gonçalves[4], Vera Simões[2,3], David Santos Pinto[3], António Gouveia de Oliveira[5], Manuel Bicho[2], Didier Hans[6], Isabel do Carmo[1,4]. [1]Endocrine & Metabolic Diseases and [2]Center of Metabolism & Endocrinology, Genetic Lab. (FMUL); [3]CEDML – Clínica de Endocrinologia, Diabetes e Metabolismo de Lisboa, Lda.; [4]Endocrinology, Diabetes & Metabolism Department, University de Santa Maria Hospital, CHLN-EPE; [5]Biostatistic Department, FCMUNL, Lisboa, Portugal; [6]Center of Bone Diseases, Lausanne University Hospital, Lausanne, Switzerland.

OBJECTIVE: The high morbidity and mortality associated to osteoporotic fractures in men are important public health problems. Ageing and the tendency to fall are the main risk factors for reduced bone mineral density (BMD) in men. Male hypogonadism is a main secondary cause of low bone mass but the knowledge of bone microarchitecture is scant. The trabecular bone score (TBS) is determined from grey-level variation analysis of the AP spine DXA images using the experimental variogram concept to assess and qualify the bone microarchitecture.

AIMS: The purpose of this study is to compare the lumbar spine bone microarchitecture as estimated by TBS with the BMD at the L_1–L_4 as well as the correlation between spine TBS and BMD in hypogonadal and normal.

MATERIAL & METHODS: The BMD (g/cm^2) of the spine, proximal femur and distal forearm, as well as the total fat and lean body masses were measured by DXA in 108 hygogonadal (hypogonadal males group) and in 108 normal (control group) men. Site matched spine TBS was derived for each spine DXA scan (TBS iNsight software, Medimaps, France). Fasting blood was collected for LH, FSH, PRL, E2 and total testosterone measurements. The weight, height and BMI were also determined. Appropriate statistics were used with the significance level at $P<0.05$.

RESULTS: The mean age, weight and total body fat mass were identical, but the mean spine BMD, spine TBS and total body lean mass were significantly decreased in the hypogonadal men, as compared with the control group.

GROUP Technique	CONTROL	HYPOGONAL MEN	P
TBS L1-L4	1.350 (±0.1)	1.282 (±0.1)	0.0001
BMD L1-L4 g/cm²	1.074 (±0.2)	0.969 (±0.2)	0.0000
BMD HIP (total) g/cm²	1.067 (±0.1)	0.968 (±0.2)	0.0000

Significant negative correlation was found between the TBS and the age in the control group. A weak correlation between spine BMD and spine TBS was detected, validating this TBS is measuring different bone properties than BMD.

CONCLUSION: The study data show a significant decrease in both bone mass accessed by BMD and bone quality evaluated by TBS, thus suggesting an important negative impact in the bone strength in men with hypogonadism, which may be associated to an increased risk for osteoporotic fractures.

Conflict of Interest: Didier Hans is co-owner of the TBS patent and has corresponding ownership shares.

Acknowledgments: Medimaps (Medimaps, Bordeaux, France) and Radilan (Lisboa, Portugal) for the kind free access and use of the TBS iNsight software for this study

WG7

Hyperthyroidism in Young Women: Which Impact on Body Composition and Silent Vertebral Fractures Detected by VFA. Barbosa AP[1-4], Mascarenhas MR[1-4], Silva C[5], Távora I[5], Gonçalves A[4], Simões V[2,3], Bicho M[2], do Carmo I[1,4]. [1]Endocrinology University Clinic and [2]Metabolism and Endocrinology Center, Genetics Laboratory (FMUL); [3]CEDML - Endocrinology, Diabetes and Metabolism Clinic, Lda.; [4]Endocrinology, Diabetes and Metabolism Department, Santa Maria Hospital, CHLN-EPE; [5]Imagiology Department, Santa Maria Hospital, CHLN-EPE, Lisbon, Portugal.

Hyperthyroidism is a risk factor for reduced bone mineral density (BMD) as well as for osteoporotic fractures. Vertebral fractures are among the most frequent and are often silent. Only a third of them come to medical attention and up to 20% of patients with an incidental vertebral fracture experience a new one in the next year. Vertebral fracture assessment by dual-energy x-ray absorptiometry (VFA by DXA) is a radiological method of visualization of the spine, which confers more commodity for the patient and less radiation exposure than the conventional spine x-ray.

OBJECTIVE: To evaluate the BMD and the prevalence of silent vertebral fractures using VFA by DXA in patients with hyperthyroidism.

MATERIAL AND METHODS: In a group of 30 pre-menopausal women with hyperthyroidism, the body lean and fat masses (Kg) and the BMD (g/cm^2) at the lumbar spine (L_1–L_4), proximal femur, distal radius and whole body were evaluated by DXA (QDR Discovery, Hologic).

VFA was used to detect fractures and those were classified according to type (wedge, biconcave, crush) and severity (% of deformity) by Genant's semiquantitative method. Fast blood collection was also performed to measure the pituitary hormones levels. No patient was previously treated for hyperthyroidism, osteoporosis or low bone mass. The BMD was qualified by Z-score, according to the ISCD recommendations. Descriptive, Anova and regression analysis statistical tests were used.

RESULTS: The means (±SD) of the anthropometric data and of the BMD are described in table 1.

Table 1. The mean (±SD) anthropometric data, lean and fat body masses and the BMD at several skeletal sites.

Variables	Premenopausal women with hyperthyroidism *(n=30)*
Age *years*	40.8 *(±5.9)*
Height *m*	1.62 *(±0.05)*
BMI *kg/m²*	26.6 *(±4.6)*
Total body lean mass *kg*	40.7 *(±5.1)*
Total body fat mass *kg*	27.2 *(±8.1)*
BMD L_1-L_4 *g/cm²*	1.014 *(±0.1)*
BMD femoral neck *g/cm²*	0.812 *(±0.1)*
BMD distal radius *g/cm²*	0.696 *(±0.1)*
BMD whole body *g/cm²*	1.129 *(±0.1)*
Fractures *n (%)*	7 *(23.3%)*

BMD qualification: 1(3.3%)-osteoporosis, 9(30%)-reduced BMD and 20(66.7%)-normal BMD.

Significant relations were detected between total lean mass and femoral neck BMD. Regarding the vertebral fractures, we found 7 cases, 6 type wedge and 1 type crush, and all of them were grade 1.

CONCLUSION: The results of this study using VFA technology, may suggest that even in young women, the hyperthyroidism can originate reductions in the bone mineral density and also in the lean mass that can conjugate in the occurrence of asymptomatic vertebral fractures. These data also support the interest of VFA in the routine management of osteoporosis to detect precociously silent fractures and so, consider treatment as soon as possible.

WG8

SKELETAL FLUOROSIS DUE TO EXCESSIVE TEA DRINKING. Naveen Kakumanu, Saroj Palnitkar, Tarlsha Esridge, Robin Demuth, Sudhaker D Rao. Bone & Mineral Research Laboratory, Henry Ford Hospital, Detroit, MI, USA.

Skeletal fluorosis is prevalent in endemic areas of the world with high fluoride content in drinking water, but is rare in other parts of the world. Brewed tea is amongst the highest fluoride containing food products in the US.

CASE HISTORY: We describe a 47 year old woman who was referred to the Bone & Mineral Clinic for chronic diffuse bone pain and abnormal radiographs. She drank a pitcher of tea daily made from 100–150 tea bags for 17 years that she procured at the local dollar store. For the past 5 years she has developed pain in the lower back, arms, legs, and hips. Because of brittle teeth, her teeth were all extracted. Forearm radiographs demonstrated inter-osseous membrane calcifications, pathognomonic of skeletal fluorosis. Lumbar spine was uniformly osteosclerotic with rugger-jersey appearance, but without ligamentous calcifications.

LABORATORY DATA: Serum calcium (Ca) 9.6 mg/dl, creatinine 0.6 mg/dl, 25-hydroxyvitamin D 12 ng/ml, PTH 38 pg/ml, and fluoride level 0.43 mg/L (0.10 mg/L being the reporting limit). A 24-hour urine calcium was 112 mg/day.

OTHER STUDIES: BMD of the spine (L1–L4) was 2.244 g/cm2 (Z-score, +11.5), total hip 1.196 g/cm2 (Z-score, +2.5), femoral neck 1.05 g/cm2 (Z-score, +2.4), and forearm 0.772 g/cm2 (Z-score, +1.9). Bone histomorphometry showed slightly reduced cortical bone volume but increased cortical width. Calcellous bone volume and trabecular width were increased 1.5–2 fold. 3-D Micro-CT of the biopsy specimen showed low marrow space, and increased cortical and trabecular thickness. Bone formation could not be measured because of lack tetracycline labeling. However, osteoid indices were normal and there was no evidence of osteomalacia.

CONCLUSION: This case demonstrates an uncommon metabolic bone disease in the U.S. acquired from prolonged use of a common beverage. Other unusual features include: normal serum PTH, Ca, and alkaline phosphatase, despite vitamin D depletion and low Ca intake.. The skeleton accretes most of the fluoride burden and forms hydroxyl-fluoro-appetite. These crystals are more compact and stable than hydro-xyapatite and resist skeletal resorption resistant to PTH action; the latter leads to secondary hyperparathyroidism especially in endemic areas where vitamin D and calcium malnutrition is also endemic. The combination perpetuates further fluoride accumulation by increasing bone remodeling in the growing skeleton. Further insights and studies are needed to broaden our understanding of non-endemic skeletal fluorosis.

Numeric

A

B

C

D

E

F

G

H

I

M

Mineral metabolism, disorders

N

P

Q

R

S

T

U

W

X

Y

Z

(Key: 1001-1300 = Oral, FR = Friday Plenary poster, SA = Saturday poster, SU = Sunday poster, MO = Monday poster)

(Key: 1001-1300 = Oral, FR = Friday Plenary poster, SA = Saturday poster, SU = Sunday poster, MO = Monday poster)

C

(Key: 1001-1300 = Oral, FR = Friday Plenary poster, SA = Saturday poster, SU = Sunday poster, MO = Monday poster)

(Key: 1001-1300 = Oral, FR = Friday Plenary poster, SA = Saturday poster, SU = Sunday poster, MO = Monday poster)

D

(Key: 1001-1300 = Oral, FR = Friday Plenary poster, SA = Saturday poster, SU = Sunday poster, MO = Monday poster)

E

F

(Key: 1001-1300 = Oral, FR = Friday Plenary poster, SA = Saturday poster, SU = Sunday poster, MO = Monday poster)

G

(Key: 1001-1300 = Oral, FR = Friday Plenary poster, SA = Saturday poster, SU = Sunday poster, MO = Monday poster)

H

(Key: 1001-1300 = Oral, FR = Friday Plenary poster, SA = Saturday poster, SU = Sunday poster, MO = Monday poster)

I

J

(Key: 1001-1300 = Oral, FR = Friday Plenary poster, SA = Saturday poster, SU = Sunday poster, MO = Monday poster)

K

(Key: 1001-1300 = Oral, FR = Friday Plenary poster, SA = Saturday poster, SU = Sunday poster, MO = Monday poster)

(Key: 1001-1300 = Oral, FR = Friday Plenary poster, SA = Saturday poster, SU = Sunday poster, MO = Monday poster)

L

(Key: 1001-1300 = Oral, FR = Friday Plenary poster, SA = Saturday poster, SU = Sunday poster, MO = Monday poster)

M

(Key: 1001-1300 = Oral, FR = Friday Plenary poster, SA = Saturday poster, SU = Sunday poster, MO = Monday poster)

(Key: 1001-1300 = Oral, FR = Friday Plenary poster, SA = Saturday poster, SU = Sunday poster, MO = Monday poster)

N

O

P

(Key: 1001-1300 = Oral, FR = Friday Plenary poster, SA = Saturday poster, SU = Sunday poster, MO = Monday poster)

Q

R

(Key: 1001-1300 = Oral, FR = Friday Plenary poster, SA = Saturday poster, SU = Sunday poster, MO = Monday poster)

S

(Key: 1001-1300 = Oral, FR = Friday Plenary poster, SA = Saturday poster, SU = Sunday poster, MO = Monday poster)

(Key: 1001-1300 = Oral, FR = Friday Plenary poster, SA = Saturday poster, SU = Sunday poster, MO = Monday poster)

T

(Key: 1001-1300 = Oral, FR = Friday Plenary poster, SA = Saturday poster, SU = Sunday poster, MO = Monday poster)

U

V

(Key: 1001-1300 = Oral, FR = Friday Plenary poster, SA = Saturday poster, SU = Sunday poster, MO = Monday poster)

W

(Key: 1001-1300 = Oral, FR = Friday Plenary poster, SA = Saturday poster, SU = Sunday poster, MO = Monday poster)

X

Y

Z

(Key: 1001-1300 = Oral, FR = Friday Plenary poster, SA = Saturday poster, SU = Sunday poster, MO = Monday poster)

(Key: 1001-1300 = Oral, FR = Friday Plenary poster, SA = Saturday poster, SU = Sunday poster, MO = Monday poster)